Surgical Neuroangiography

A. BERENSTEIN
P. LASJAUNIAS
K. G. TER BRUGGE

2.1

Clinical and Endovascular Treatment Aspects in Adults

- Cerebral Ischemia
- Vascular Tumors of the Head and Neck
- Traumatic Arteriovenous Fistulae
- Aneurysms

Second Edition

Springer

Springer
Berlin
Heidelberg
New York
Hong Kong
London
Milan
Paris
Tokyo

The complete three-volume set consists of

Volume 1
Clinical Vascular Anatomy and Variations

Volume 2
Clinical and Endovascular Treatment Aspects in Adults

Volume 3
Clinical and Interventional Aspects in Children

A. Berenstein
P. Lasjaunias
K.G. ter Brugge

Surgical Neuroangiography

2.1 Clinical and Endovascular Treatment Aspects in Adults

- Cerebral Ischemia
- Vascular Tumors of the Head and Neck
- Traumatic Arteriovenous Fistulae
- Aneurysms

Second Edition
with 734 Figures in 2926 Separate Illustrations,
Some in Color and 155 Tables

Springer

Alejandro Berenstein, M.D.
Professor of Radiology and Neurosurgery
Albert Einstein School of Medicine, NY
Director of the Hyman-Newman Institute of Neurology and Neurosurgery,
and of The Center for Endovascular Surgery
Beth Israel Medical Center New York
170 East End Avenue at 87th Street, New York, NY 10128, USA

Pierre Lasjaunias M.D., Ph.D.
Professeur des Universités en Anatomie
Chef de Service de Neuroradiologie Diagnostique et Thérapeutique
Centre Hospitalier Universitaire de Bicêtre
78, rue du Général Leclerc, 94275 Le Kremlin Bicêtre, France

Karel G. ter Brugge, M.D.
Professor of Radiology and Neurosurgery
Head, Division of Neuroradiology University of Toronto /
University Health Network
Department of Medical Imaging, Toronto Western Hospital, FP3-210
399 Bathurst Street, Toronto, ON M5T 2S8, Canada

The second volume of the second edition of *Surgical Neuroangiography* combines the previous volumes 2, 4 and 5 in a two part volume.

ISBN 3-540-41668-4 Springer-Verlag Berlin Heidelberg New York

Cataloging-in-Publication Data applied for

Bibliographic information published by Die Deutsche Bibliothek
Die Deutsche Bibliothek lists this publication in the Deutsche Nationalbibliografie; detailed bibliographic data is available in the Internet at <http://dnb.ddb.de>.

This work is subject to copyright. All rights are reserved, whether the whole or part of the material is concerned, specifically the rights of translation, reprinting, reuse of illustrations, recitation, broadcasting, reproduction on microfilm or in any other ways, and storage in data banks. Duplication of this publication or parts thereof is only permitted under the provisions of the German Copyright Law of September 9, 1965, in its current version, and permission for use must always be obtained from Springer-Verlag. Violations are liable for prosecution under the German Copyright Law.

Springer-Verlag is a part of Springer Science+Business Media

springeronline.com

© Springer-Verlag Berlin Heidelberg 1987/1992, 2004

The use of general descriptive names, registered names, trademarks, etc. in this publication does not imply, even in the absence of a specific statement, that such names are exempt from the relevant protective laws and regulations and therefore free for general use.

Product liability: The publishers cannot guarantee the accuracy of any information about the application of operative techniques and medications contained in this book. In every individual case the user must check such information by consulting the relevant literature.

Cover design: E. Kirchner, Heidelberg, Germany
Typesetting: Fotosatz-Service Köhler GmbH, Würzburg, Germany

Printed on acid-free paper 21/3150/ih 5 4 3 2 1 0

Preface

Anatomy is a language and mastery of this language is in our opinion essential for physicians involved in the management of patients with vascular diseases of the central nervous system, head and neck, and spine and spinal cord. Understanding the clinicopathological aspects of vascular disease, its natural history, and the various therapeutic options is mandatory for optimal patient management.

Functional endovascular therapeutic strategies continue to expand and those that are currently available are discussed within the realm of the authors' combined experience. Our approach goes beyond today's technological advances and involves a new understanding of how vascular pathology is expressed, its impact on the structure of the vascular systems, and the possible repair mechanisms of the vascular system in various environments. The latest techniques that improve such therapeutic goals are illustrated in the individual chapters on the diseases and highlighted in the chapter on techniques.

The important field of occlusive vascular disease and our ability to reopen stenotic or even occluded vessels are revolutionizing Endovascular Neurosurgery. An in-depth study of occlusive vascular disease is a major addition to this second edition of *Surgical Neuroangiography (Vol. 2)*. Functional anatomical strategies and protocols are illustrated with the latest technological devices. As the rapid technological evolution continues, our approach and understanding will help guide us to the safest and most effective revascularization strategy.

Our new concepts with respect to aneurysms as a group of diseases of different etiologies and pathophysiologies alter the therapeutic indications for their management and therefore the role of specific treatment techniques.

Our experience in the management of patients with vascular disorders now extends over many decades and forms the basis for an approach to cerebral and dural vascular malformations that is both at the leading edge and well balanced. Management decisions based on a thorough understanding of these vascular pathologies, their natural history, as well as the risks associated with their treatment have been outlined in the text. This work is a reflection of the authors' ongoing commitment to balancing the exciting technological advances of the tools that have become available with thorough knowledge of vascular anatomy and an exhaustive understanding of vascular pathologies. It is this unique approach that facilitates ongoing progress in the safe management of patients with vascular disorders affecting the brain, the spine, and the head and neck.

December 2003 A. Berenstein, P. Lasjaunias, K.G. ter Brugge

Contents of Volumes 2.1 and 2.2

1	**Occlusive Vascular Disease**	1
1.1	*Introduction*	2
1.2	*Arterial Occlusive Disease*	3
1.2.1	Cerebrovascular Physiology	3
1.2.1.1	The Blood–Brain Barrier	3
1.2.1.2	Cerebral Blood Flow	4
1.2.1.3	Cerebral Autoregulation	5
1.2.1.4	Cerebral Blood Volume	7
1.2.1.5	Blood Viscosity	8
1.2.1.6	Metabolism in Cerebral Blood Flow	8
1.2.1.7	Carbon Dioxide Reactivity	9
1.2.1.8	Oxygen Reactivity	9
1.2.1.9	Nitrous Oxide in Cerebral Circulation	9
1.2.1.10	Other Factors	10
1.2.2	Arterial Ischemic Stroke	14
1.2.2.1	Definition	14
1.2.2.2	Neuronal Metabolism and Cerebral Ischemia	17
1.2.2.3	Selective Neuronal Vulnerability	18
1.2.2.4	Hemodynamic Effects of Ischemia	21
1.2.2.5	Nitrous Oxide and Cerebral Ischemia	21
1.2.2.6	Window of Opportunity	22
1.2.2.7	Neutrophil	23
1.2.3	Atherosclerosis	23
1.2.3.1	Introduction	23
1.2.3.2	Epidemiology	23
1.2.3.3	Pathogenesis	24
1.2.3.4	Mechanisms of Atherogenesis	24
1.2.3.5	Fatty Streak	27
1.2.3.6	Fibrous Plaque	28
1.2.3.7	Unstable Fibrous Plaques	28
1.2.3.8	Complicated Plaque	28
1.2.3.9	Carotid Atherosclerosis	29
1.2.3.10	Conclusion	29
1.2.3.11	Neuroimaging of Ischemic Stroke	30
1.2.4	Ischemic Stroke Treatment	31
1.2.4.1	Medical Treatment of Acute Stroke	31
1.2.4.2	Thrombolytic Therapy: Introduction	32
1.2.4.3	Thrombolytics (IV)	32
1.2.4.4	Recombined Tissue Plasminogen Activator	32

1.2.4.5 Streptokinase 33
1.2.4.6 Antiplatelets 34
1.2.4.7 Coumadin Versus Aspirin 39
1.2.4.8 Neuroprotective Agents 39
1.2.4.9 Pharmacological Properties of Neuroprotective Drugs . 40
1.2.4.10 Binding Properties 41
1.2.4.11 Angiographic Evaluation 41
1.2.4.12 Middle Cerebral Artery Stroke: Natural History 44
1.2.4.13 Local Intra-arterial Thrombolysis in the Anterior Circulation 45
1.2.4.14 Internal Carotid Artery Occlusion 52
1.2.4.15 Carotid Dissection 57
1.2.4.16 Central Retinal Artery Occlusion 67
1.2.4.17 Internal Carotid Artery Stenosis Above the Carotid Bulb 68
1.2.4.18 General Organization of a Stroke Emergency Team . . . 70
1.2.4.19 Evolving Treatment Strategies 72
1.2.5 Extracranial Carotid Artery Stenosis 73
1.2.5.1 Introduction 73
1.2.5.2 Natural History 73
1.2.5.3 Carotid Bruit 75
1.2.5.4 Imaging 75
1.2.5.5 Treatment 84
1.2.5.6 Symptomatic Carotid Stenosis 86
1.2.5.7 Asymptomatic Carotid Stenosis 86
1.2.5.8 Restenosis After Carotid Endarterectomy 89
1.2.6 Carotid Angioplasty and Stenting 90
1.2.6.1 Introduction 90
1.2.6.2 Techniques of Carotid Angioplasty and Stenting 93
1.2.6.3 Intimal Hyperplasia and Restenosis 93
1.2.6.4 Follow-up Monitoring 98
1.2.7 Posterior Circulation Stroke (Stroke Prevention) 98
1.2.7.1 Introduction 98
1.2.7.2 Clinical Presentation 98
1.2.7.3 Pretherapeutic Evaluation in Cerebral Vascular Insufficiency 99
1.2.7.4 Management of Posterior Circulation Insufficiency . . . 104
1.2.7.5 Basilar Thrombosis 110
1.2.7.6 Takayasu's Arteritis 115
1.2.8 Cerebral Angioplasty 116
1.2.8.1 Vasospasm 117

1.3 Venous Occlusive Disease 135
1.3.1 Etiology 135
1.3.2 Incidence 136
1.3.3 Clinical Presentation and Natural History 137
1.3.4 Imaging 138
1.3.5 Treatment 143
Appendix 147

2	**Dural and Bony Tumors**	153
2.1	***Introduction***	154
2.2	***Meningiomas***	154
2.2.1	Epidemiology	154
2.2.1.1	Origin	154
2.2.1.2	Incidence	154
2.2.1.3	Association of Meningiomas with Other Tumors	155
2.2.1.4	Sex Hormone Receptors in Meningiomas	156
2.2.1.5	Chromosomal Patterns in Meningiomas	156
2.2.1.6	Meningiomas in Children	156
2.2.1.7	Familial Occurrence	157
2.2.1.8	Meningioma Incidence, Prevalence, and Mortality	157
2.2.1.9	Etiology of Human Meningiomas	157
2.2.1.10	Oncogenic Viruses	158
2.2.2	Pathology	161
2.2.2.1	Growth and Spread	162
2.2.2.2	Malignant Meningioma	162
2.2.2.3	Angioblastic Meningioma and/or Hemangiopericytoma	165
2.2.2.4	Meningioangiomatosis	166
2.2.2.5	Meningeal Meningiomatosis	166
2.2.3	Clinical Presentation	166
2.2.3.1	Sites	169
2.2.3.2	Epidural Meningiomas	177
2.2.3.3	Meningiomas of the Orbit	177
2.2.3.4	Meningiomas Involving the Cavernous Sinus	178
2.2.3.5	Meningiomas in Other Unusual Sites	179
2.2.3.6	Intracranial Vascular Involvement	179
2.2.3.7	Peritumoral Edema in Meningiomas	181
2.2.4	Pretherapeutic Evaluation	181
2.2.4.1	CT Scanning in Meningiomas	181
2.2.4.2	MRI Scanning	182
2.2.4.3	Angiographic Investigation	184
2.2.4.4	Differential Diagnosis	187
2.2.5	Therapeutic Strategy and Clinical Objectives	187
2.2.6	Technical Aspects of Embolization	189
2.2.7	Special Considerations in Meningioma Embolization	192
2.2.7.1	Extracranial Tumor Extension	192
2.2.7.2	Recurrent Meningiomas	192
2.2.7.3	Internal Carotid Supply to Recurrent or Malignant Meningiomas After Radiation Therapy Has Failed	194
2.2.7.4	Pial Supply	194
2.2.7.5	Pre- and Postembolization Medical Management	194
2.2.7.6	Time of Operation	196
2.2.7.7	Complications of Embolization	196
2.3	***Other Bony and Dural Tumors***	198
2.3.1	Cerebral Tumors	198
2.3.2	Neurinomas	199
2.3.3	Esthesioneuroblastomas	199

3	**Nasopharyngeal Tumors**	201
3.1	***Juvenile Angiofibromas***	201
3.1.1	Macroscopic Pathology	201
3.1.2	Microscopic Pathology	204
3.1.3	Epidemiology	205
3.1.4	Pathophysiology	206
3.1.4.1	Juvenile Angiofibromas and Sex Hormones	206
3.1.4.2	Physiology and the Nasal Mucosa	206
3.1.4.3	Hormones and the Vascular System	207
3.1.4.4	Global Hypothesis for the Development of Juvenile Angiofibromas	207
3.1.5	Clinical Findings	210
3.1.6	Natural History	211
3.1.7	Pretherapeutic Evaluation	211
3.1.7.1	Computed Tomography	211
3.1.7.2	Magnetic Resonance Imaging	211
3.1.7.3	Angiography	211
3.1.8	Therapeutic Goals	214
3.1.8.1	Radiation Therapy	221
3.1.9	Technical Aspects of Embolization	221
3.1.10	Tumor Recurrence	223
3.2	***Other Nasopharyngeal Tumors***	224
3.3	***Conclusion***	226
4	**Paragangliomas**	227
4.1	***Introduction***	227
4.2	***Embryology***	228
4.3	***Epidemiology***	230
4.4	***Pathology***	232
4.4.1	Vascular Architecture	233
4.5	***Natural History***	235
4.6	***Clinical Aspects***	236
4.6.1	Tympanic Paragangliomas	236
4.6.2	Jugular Paragangliomas	238
4.6.3	Cervical Paragangliomas	238
4.6.4	Paragangliomas in Other Locations	244
4.6.5	Secretory Paragangliomas	245
4.6.6	Associated Lesions	246
4.7	***Differential Diagnosis***	246
4.8	***Pretherapeutic Evaluation***	250
4.8.1	Angiographic Protocol	252
4.8.2	Temporal Paragangliomas: Specific Features	252
4.8.3	Cervical Paragangliomas: Specific Features	257
4.9	***Therapeutic Strategies***	260
4.10	***Technical Aspects of Embolization***	261
4.11	***Complications of Embolization of Paragangliomas***	264

5	**Other Head and Neck Tumors**	265
5.1	*Thyrolaryngeal Tumors*	265
5.2	*Craniofacial Tumors*	270
6	**Traumatic Arteriovenous Fistulae**	277
6.1	*Introduction*	277
6.2	*Traumatic Carotid Cavernous Fistulae*	279
6.2.1	Etiology and Epidemiology	279
6.2.2	Clinical Aspects of Traumatic Carotid Cavernous Fistulae	285
6.2.2.1	Ophthalmological Symptoms	293
6.2.2.2	Corneal Ulcerations and/or Infections and Secondary Glaucoma	293
6.2.2.3	Diplopia	298
6.2.2.4	Cranial Nerve Involvement in Traumatic Carotid Cavernous Fistulae	298
6.2.2.5	Bruit	300
6.2.2.6	Arterial Steal	300
6.2.2.7	Hemispheric Arterial Insufficiency	300
6.2.2.8	Associated Traumatic Lesions	302
6.2.3	Pretherapeutic Evaluation	306
6.2.3.1	Location of the Fistula	308
6.2.3.2	Venous Drainage of the Fistula	314
6.2.4	Therapeutic Objectives and Strategy	321
6.2.4.1	Embolization	321
6.2.4.2	Emergency Treatment	322
6.2.4.3	Surgical Approach to Carotid Cavernous Fistulae	324
6.2.4.4	Conservative Treatment of Traumatic Carotid Cavernous Fistulae	325
6.2.5	Technical Aspects of Embolization	325
6.2.5.1	Balloon Selection	325
6.2.5.2	Manual Compression	332
6.2.5.3	The Use of NBCA in the Management of Carotid Cavernous Fistulae	332
6.2.6	Postembolization Care	333
6.3	*Other Traumatic Arteriovenous Fistulae*	334
6.3.1	Extracavernous Arteriovenous Fistulae	334
6.3.2	Vertebral Arteriovenous Fistulae	338
6.3.3	Common Carotid Fistulae	342
6.3.4	External Carotid Fistulae	342
6.3.5	Malignant Fistulae	354
6.3.6	Other Epistaxis	354
6.3.6.1	Coagulopathy	357
6.3.6.2	Spontaneous Epistaxis	357
6.3.6.3	Tumoral Epistaxis	357
6.3.6.4	Biopsy	359
6.3.6.5	Traumatic Epistaxis	362

7	**Aneurysmal Vasculopathies**	365
7.1	***From Aneurysm to Aneurysmal Vasculopathies***	366
7.1.1	General Perspectives	366
7.1.1.1	Medical Challenge	367
7.1.1.2	Decision-Making Challenge in Patients with Unruptured Aneurysms	370
7.1.1.3	Ethical Challenge	370
7.1.1.4	Academic and Nosological Challenges	371
7.1.2	Physiopathogenesis and Risks	371
7.1.2.1	Classification	374
7.1.3	Segmental Vulnerability	375
7.1.3.1	Embryological Origin	377
7.1.3.2	Age of Aneurysms	380
7.2	***Extradural Aneurysms***	382
7.2.1	Introduction	382
7.2.2	Extradural Internal Carotid Artery Aneurysms	382
7.2.2.1	Cervical Internal Carotid Aneurysms	384
7.2.2.2	Acute Spontaneous Dissection of the Carotid Artery	394
7.2.2.3	Petrous Internal Carotid Artery Aneurysms	399
7.2.2.4	Aneurysms of the Cavernous Segment of the Internal Carotid Artery	401
7.2.2.5	Cervical Fibromuscular Dysplasia	415
7.2.3	Internal Carotid Artery Occlusion in Extradural Internal Carotid Artery Aneurysms	417
7.2.3.1	Tolerance to Carotid Occlusion	418
7.2.3.2	Postembolization Care	420
7.2.4	Extradural Vertebral Aneurysms	420
7.2.5	Aneurysms of the External Carotid Artery	425
7.3	***Intradural Aneurysms***	431
7.3.1	Saccular Arterial Aneurysms and Associated Diseases	431
7.3.1.1	Polycystic Kidney Disease	431
7.3.1.2	Ehlers–Danlos Syndrome	434
7.3.1.3	Neurofibromatosis Type 1	435
7.3.1.4	Bourneville Disease	436
7.3.1.5	Fibromuscular Dysplasia	438
7.3.2	Saccular Arterial Aneurysms Without Diagnosed Associated Diseases	438
7.3.2.1	Nonsyndromic Familial Arterial Aneurysms	438
7.3.2.2	Multiple Saccular Arterial Aneurysms	440
7.3.2.3	Arterial Anatomy, Single, Mirror, and Twin Saccular Arterial Aneurysms	442
7.4	***Intradural Artery Dissections***	454
7.5	***Intradural Giant Saccular and Nonsaccular Arterial Aneurysms***	478
7.5.1	General Remarks	478
7.5.2	Giant Intracranial Aneurysms with Thrombosis	486
7.5.3	Nonsaccular Giant Arterial Aneurysms	497
7.5.3.1	Megadolicho Arteries and Serpentine Arterial Aneurysms	498

7.5.4 Multiple Giant Arterial Aneurysms and Mirror Giant Arterial Aneurysms 500

7.6 ***Infectious, Immune, and Inflammatory Intradural Aneurysms*** 502
7.6.1 Infectious Arterial Aneurysms 502
7.6.2 Intradural Fusiform Aneurysms in Patients with Immune Deficiencies 509
7.6.3 Inflammatory Diseases and Arterial Aneurysms 513

7.7 ***Flow-Related Arterial Aneurysms and Other Aneurysmal Vasculopathies*** 514
7.7.1 Intradural Traumatic Arterial Aneurysms 518
7.7.2 Arterial Aneurysms Associated with Proliferative Diseases 523
7.7.3 Arterial Aneurysms with Congenital Heart Disorders and Coarctation of the Aorta 524

7.8 ***Therapeutic Management*** 527
7.8.1 Introduction 527
7.8.2 Method 532
7.8.3 Results of the Endovascular Approach 538
7.8.4 Management of Multiple Arterial Aneurysms 549
7.8.5 Management of Giant Arterial Aneurysms 560

8 Dural Arteriovenous Shunts 565

8.1 ***Historical Review*** 566
8.2 ***Pathophysiology*** 570

8.3 ***The Osteodural–Venous Complex*** 571
8.3.1 Dural Venous Plexus 572
8.3.2 Transdural Veins 573

8.4 ***Classification*** 575

8.5 ***Clinical Presentation of Dural Arteriovenous Shunts*** . . 579
8.5.1 Cranial Nerve Symptoms 580
8.5.2 Tinnitus and Objective Bruits 581
8.5.3 Focal Neurological Deficits 582
8.5.4 Global Neurological Deficits 585
8.5.5 Intracranial Hemorrhage 587
8.5.6 Hormonal Influences 587
8.5.7 Associated Conditions and Multiplicity 590

8.6 ***Natural History*** 594
8.7 ***Progression of Symptoms*** 596
8.8 ***Pretherapeutic Evaluation*** 598

8.9 ***Therapeutic Aspects*** 598
8.9.1 Indications and Strategy 598
8.9.2 Topographic Considerations 602
8.9.3 Technical Aspects 605
8.9.4 Timing of Embolization 605
8.9.5 Results of Embolization 606

8.9.6 Complications of Embolization 606
8.9.7 Surgery 607

9 Cerebral Vascular Malformations: Incidence, Classification, Angioarchitecture, and Symptomatology of Brain Arteriovenous and Venous Malformations 609

9.1 Incidence of Cerebral Vascular Malformations 609
9.2 Principles of Classification 612

9.3 Classification of Cerebral Vascular Malformations . . . 614
9.3.1 Brain Arteriovenous Shunts 615
9.3.1.1 General Appearance of Arteriovenous Shunts 615
9.3.1.2 Multiple Brain Arteriovenous Malformations 618
9.3.1.3 Topographic Analysis of Brain Arteriovenous Malformations 625
9.3.1.4 Angioarchitecture of Brain Arteriovenous Malformations 631
9.3.1.5 Clinical–Angioarchitectural Correlation in Brain Arteriovenous Malformations 677
9.3.2 Venous Variations, Malformations, and Mixed Lesions . . 684
9.3.2.1 Developmental Venous Anomalies 685
9.3.2.2 Cavernous Hemangiomas 686
9.3.2.3 Cerebral Cavernous Malformations 687
9.3.2.4 Occult and Cryptic Malformations 690
9.3.2.5 Sturge–Weber Syndrome 691

10 Goals and Objectives in the Management of Brain Arteriovenous Malformations 695

10.1 Introduction 695

10.2 Indications for Treatment of Brain Arteriovenous Malformations 696
10.2.1 Age 700
10.2.2 Sex 701
10.2.3 Lifestyle and Occupation 701
10.2.4 Presenting Symptoms 703
10.2.4.1 Hemorrhage 703
10.2.4.2 Seizures 704
10.2.4.3 Headaches 704
10.2.4.4 Neurological Deficits 708
10.2.5 Location, Size, and Deep Venous Drainage 708
10.2.6 Brain Arteriovenous Malformations and Arterial Aneurysms 708

10.3 Therapeutic Management Strategy 715

10.4 Embolization 716
10.4.1 Partial (Targeted) Embolization 716
10.4.2 Partial (Palliative) Embolization 720

10.4.3 Curative Embolization 720
10.4.4 Preoperative Embolization 728
10.4.5 Intraoperative Embolization Therapy 729
10.4.6 Embolization Prior to Radiosurgery 729
10.4.6.1 Size Reduction 729
10.4.6.2 Targeted Embolization Prior to Stereotactic Radiosurgery 731
10.4.7 Staging of Embolization 732
10.4.8 Emergency Embolization 732
10.4.9 Contraindications for Endovascular Treatment 732
10.4.10 Embolization Results 734

11 Spinal Arteriovenous Malformations 737

11.1 Parachordal Arteriovenous Fistulae (Extracranial, Vertebro-Vertebral, Paraspinal, Extradural, and Extraspinal Arteriovenous Fistulae) 738
11.1.1 General Remarks 738
11.1.2 Cranial (Branchial) Arteriovenous Shunts 740
11.1.2.1 Maxillary Artery-to-Vein Arteriovenous Fistulae (Stapedial) 743
11.1.2.2 Ascending Pharyngeal-Internal Jugular Arteriovenous Fistulae (Hypoglossal) 743
11.1.3 Vertebro-Vertebral Arteriovenous Fistulae (Proatlantal and Intersegmental) 743
11.1.3.1 Vertebro-Vertebral Arteriovenous Fistulae 743
11.1.3.2 Clinical Findings 751
11.1.4 Paraspinal Arteriovenous Fistulae 752

11.2 Spinal Cord Vascular Lesions 758

11.3 Spinal Cord Arteriovenous Malformations 760
11.3.1 Classification of Spinal Cord Arteriovenous Malformations 767
11.3.2 Angioarchitecture 775
11.3.2.1 Arterial Features 775
11.3.2.2 Direct Arteriovenous Fistulae 784
11.3.2.3 High-Flow Angiopathy 786
11.3.2.4 Arterial Aneurysms in Spinal Cord Arteriovenous Malformations 786
11.3.2.5 Dural Supply 794
11.3.2.6 Nidus 794
11.3.2.7 Veins 802
11.3.3 Pretherapeutic Evaluation 808
11.3.3.1 Clinical Assessment 808
11.3.3.2 Noninvasive Imaging Modalities 808
11.3.3.3 Angiography 809

11.4 Spinal Cord Hemodynamics 810
11.4.1 Particular Forms of Spinal Cord Arteriovenous Malformations 811
11.4.1.1 Spinal Cord Intradural Arteriovenous Fistulae 811
11.4.1.2 Spinal Arteriovenous Metameric Syndromes 813

11.4.1.3 Associated Cerebral and Spinal Arteriovenous Malformations 822
11.4.2 Clinical Aspects 825
11.4.2.1 Natural History and Clinical Presentation 825
11.4.2.2 Prognosis 830
11.4.2.3 Aggravating Factors 831

11.5 Treatment of Vascular Lesions 833
11.5.1 Indications 833
11.5.2 Results of Spinal Cord Arteriovenous Malformation Embolization 839
11.5.3 Complications of Embolization 840
11.5.4 Surgery in the Treatment of Spinal Cord Arteriovenous Malformations 842
11.5.5 Radiotherapy of Spinal Cord Arteriovenous Malformations 843
11.5.6 Medical Therapy 843

12 Spinal Dural Arteriovenous Fistulae 849

12.1 Pathology 850
12.1.1 Macroscopic Appearance 851
12.1.2 Microscopic Appearance 853
12.1.3 Pathological Changes in the Spinal Cord 854

12.2 Pathophysiology 854
12.3 Clinical Presentation of Spinal Dural Arteriovenous Fistulae 858
12.4 Imaging of Spinal Dural Arteriovenous Fistulae 859

12.5 Treatment of Spinal Dural Arteriovenous Fistulae . . . 867
12.5.1 Indications 867
12.5.2 Embolization of Spinal Dural Arteriovenous Fistulae: Techniques 867
12.5.3 Results of Spinal Dural Arteriovenous Fistula Embolization 869
12.5.4 Surgery for Spinal Dural Arteriovenous Fistulae 871
12.5.5 Postoperative Follow-up 872

13 Tumors of the Spinal Column and Spinal Cord . . 873

13.1 Introduction 874
13.2 Spinal Angiography 874
13.3 Angiographic Protocol 875

13.4 Embolization 876
13.4.1 Cervical Tumors 877
13.4.2 Thoracic, Lumbar, and Sacral Tumors 877
13.4.3 Chemoembolization 877
13.4.4 Intralesional Embolization 880

13.5 Benign Tumors 883
13.5.1 Vertebral Hemangiomas 883
13.5.1.1 Associated Lesions 888

13.5.1.2 Pretherapeutic Evaluation . . . 888
13.5.1.3 Treatment . . . 889
13.5.1.4 Embolization . . . 889
13.5.2 Aneurysmal Bone Cysts . . . 890
13.5.2.1 Clinical Presentation . . . 890
13.5.2.2 Pretherapeutic Evaluation . . . 891
13.5.2.3 Angiography . . . 891
13.5.2.4 Differential Diagnosis . . . 891
13.5.2.5 Pathogenesis . . . 892
13.5.3 Other Benign Vascular Tumors . . . 893
13.5.4 Giant Cell Tumors . . . 893
13.5.4.1 Pathology . . . 893
13.5.4.2 Clinical Presentation . . . 893
13.5.4.3 Radiographic Findings . . . 893
13.5.4.4 Embolization . . . 895

13.6 Malignant Tumors . . . 895
13.6.1 Pretherapeutic Evaluation . . . 897
13.6.2 Embolization . . . 897

13.7 Spinal Cord Tumors . . . 898
13.7.1 Hemangioblastomas . . . 898
13.7.1.1 Histopathology . . . 898
13.7.1.2 von Hippel-Lindau Disease . . . 900
13.7.2 Pretherapeutic Evaluation of Hemangioblastomas . . . 904
13.7.2.1 Computerized Tomography . . . 904
13.7.2.2 Magnetic Resonance Imaging . . . 904
13.7.2.3 Angiography . . . 905
13.7.3 Feeding Arteries . . . 906
13.7.4 Draining Veins . . . 906
13.7.5 Treatment and Embolization . . . 906

13.8 Other Intradural Vascular Tumors and Spinal Hemorrhage 909

14 Technical Aspects of Surgical Neuroangiography . . 913

14.1 Introduction . . . 915

14.2 Patient Preparation . . . 917
14.2.1 Angiographic Equipment . . . 917
14.2.2 Preoperative Medications . . . 917
14.2.2.1 Corticosteroids . . . 918
14.2.2.2 Anticonvulsants . . . 918
14.2.2.3 Antiplatelets . . . 919

14.3 Anesthesia . . . 919
14.3.1 General Anesthesia . . . 919
14.3.2 Neuroleptic Analgesia . . . 920
14.3.3 Tracheostomy . . . 920
14.3.4 Local Anesthesia . . . 920
14.3.5 Input and Output Monitoring . . . 921
14.3.6 Arterial Line and Venous Line . . . 921
14.3.7 Heparinization . . . 923

14.3.8 Activated Coagulation Time Monitoring 924
14.3.9 Functional Evaluation 925
14.3.9.1 Somatosensory- and Motor-Evoked Potentials 925
14.3.9.2 Facial Nerve Monitoring 925
14.3.10 Pharmacological Testing 926
14.3.10.1 Amobarbital 926
14.3.10.2 Xylocaine 929
14.3.10.3 Mucocutaneous Territories 929

14.4 Arteriotomy Sites 929
14.4.1 Introducer Sheath 930
14.4.2 Closure Devices 932
14.4.2.1 Hemostasis of the Arteriotomy Site Closure 932
14.4.2.2 Internal Closure Devices 932

14.5 Catheters and Delivery Systems 933
14.5.1 Guiding Catheters 933
14.5.2 Microcatheters 934
14.5.3 Balloon Catheters 942
14.5.3.1 Tolerance Testing and Flow Control 942
14.5.3.2 Detachable Balloons 955
14.5.3.3 Angioplasty Balloon Catheters 958
14.5.3.4 Balloon-Mounted Stents 962
14.5.3.5 Stent Delivery Catheters 962

14.6 Guidewires 965
14.6.1 Microguidewires 965

14.7 Embolic Agents 969
14.7.1 Particulate Agents 969
14.7.1.1 Absorbable Materials 970
14.7.1.2 Nonabsorbable Particulate Materials 974
14.7.1.3 Flow-Directed Particle Embolization 980
14.7.1.4 General Principles in Aneurysm Treatment 1020
14.7.1.5 General Principles of Coil Treatment of Aneurysms . . . 1030
14.7.2 Nonabsorbable Liquid Agents 1059
14.7.2.1 Introduction 1059
14.7.2.2 Acrylates 1059
14.7.2.3 Sclerotherapy 1074
14.7.2.4 Ethylene-Vinyl Alcohol Copolymer 1083
14.7.3 EVOH in Brain Arteriovenous Malformation Treatment 1089

14.8 Opacifying Agents 1092
14.8.1 Tantalum Powder 1092
14.8.2 Iophendylate (Pantopaque) 1093
14.8.3 Iodized Oil 1093
14.8.4 Ethiodol 1093

14.9 Chemotherapy 1093
14.9.1 Intra-arterial Infusions 1093
14.9.2 Time-Released Microcapsules (Chemoembolization) . . 1094

14.10 Miscellaneous 1094
14.10.1 Syringes 1094

14.10.2 Stopcocks and Y-Adapters . . . 1095
14.10.3 Tray Containers . . . 1095
14.10.4 Flushing Solutions . . . 1095
14.10.5 Corticosteroids . . . 1096
14.10.6 Normal Physiology of the External Carotid Arteries . . . 1096

14.11 ***Flow Control*** . . . 1097
14.11.1 Introduction . . . 1097
14.11.2 Flow Control in the Craniofacial Area . . . 1097
14.11.2.1 Protection of an Endangered Anastomosis . . . 1101
14.11.2.2 Intralesional Flow Control . . . 1101
14.11.2.3 Occlusive Balloon Flow Reversal . . . 1102
14.11.2.4 Functional Rearrangement of the Supply to a Territory . 1104
14.11.2.5 Surgical Flow Control . . . 1104
14.11.3 Flow Control in the Meningeal Arcade and Dural Surfaces 1104
14.11.4 Flow Control in the Cerebral Circulation . . . 1104
14.11.4.1 Distal Catheterization . . . 1106
14.11.4.2 Flow Reversal . . . 1108
14.11.4.3 Flow Arrest . . . 1111
14.11.4.4 Systemic Hypotension . . . 1111
14.11.4.5 Catheter Withdrawal . . . 1111
14.11.5 Spine and Spinal Cord . . . 1113
14.11.5.1 Technical Aspects of Endovascular Treatment in the Spine and Spinal Cord . . . 1113

14.12 ***Postembolization Care*** . . . 1128
14.12.1 Head and Neck . . . 1128
14.12.2 Cerebral Arteriovenous Malformations . . . 1128
14.12.3 Intradural Aneurysms . . . 1128
14.12.4 Spinal Arteriovenous Malformations . . . 1129

14.13 ***Complications of Embolization*** . . . 1129
14.13.1 Complications of Head and Neck Embolization . . . 1129
14.13.1.1 Neurological Deficit . . . 1129
14.13.1.2 Cranial Nerve Deficit . . . 1129
14.13.1.3 Postoperative Swelling . . . 1130
14.13.1.4 Skin Necrosis . . . 1130
14.13.2 Complications of Cerebral Embolization . . . 1130
14.13.2.1 Medical Therapy for Acute Ischemic Stroke . . . 1130
14.13.2.2 Recanalization . . . 1131
14.13.2.3 Microcirculation Agents . . . 1132
14.13.2.4 Antiplatelets . . . 1132
14.13.2.5 Anticoagulation . . . 1132
14.13.2.6 Biorheological Factors . . . 1133
14.13.2.7 Antiedema and Pharmacological Protection Agents . . . 1134
14.13.2.8 Additional Measures . . . 1135
14.13.3 Hemorrhage . . . 1135
14.13.3.1 Generalities . . . 1135
14.13.3.2 Brain Arteriovenous Malformation Rupture . . . 1137
14.13.3.3 Aneurysm Rupture . . . 1141
14.13.3.4 Arterial Stenosis . . . 1143
14.13.3.5 Vasospasm . . . 1146

14.14 ***Follow-up*** 1146

14.15 ***Combined Endovascular Treatments*** 1146
14.15.1 Combined Endovascular Treatment in Aneurysm Therapy 1147
14.15.2 Combined Endovascular Treatment in Brain Arteriovenous Malformation Therapy 1147
14.15.3 Combined Endovascular Treatment in Occlusive and Hemorrhagic Vascular Disease 1147

14.16 ***Techniques of Carotid Angioplasty and Stenting*** 1152
14.16.1 Introduction 1152
14.16.2 Hemodynamic Disturbances During Stenting 1152
14.16.3 Premedication 1153
14.16.4 Vasoactive Medications 1154
14.16.5 Intervention 1154
14.16.6 Predilatation Angioplasty 1164
14.16.7 Stent Selection 1164
14.16.7.1 Self-Expandable Stents 1169
14.16.7.2 Nitinol 1169
14.16.7.3 Balloon-Expandable Stents 1171
14.16.7.4 Low-Profile Balloon-Expandable Stents 1171
14.16.7.5 GFX II 1171
14.16.8 Postdilatation Angioplasty 1173
14.16.8.1 Distal Cerebral Protection 1173
14.16.9 Mechanical Revascularization of Totally Occluded Brachiocephalic Vessels 1176
14.16.10 Complications of Mechanical Revascularization 1178
14.16.11 Stent Retrieval 1179

References 1183

Subject Index for Volumes 2.1 and 2.2 1259

Manufacturers 1271

Abbreviations

AA	Arterial aneurysm
ACAS	Asymptomatic Carotid Atherosclerosis Study
Ach	Acetylcholine
ACA	Anterior cerebral artery
AcomA	Anterior communicating artery
ACT	Activated coagulation time
ADC	Apparent diffusion coefficient
ADP	Adenosine diphosphate
AICA	Anterior inferior cerebellar artery
ASCA	Anterior superior cerebellar artery
ASD	Atrial septal defect
ATII	Angiotensin II
AVF	Arteriovenous fistula
AVM	Arteriovenous malformation
AVS	Arteriovenous shunt
BAVF	Brain arteriovenous fistula
BAVM	Brain arteriovenous malformation
BBB	Blood-brain barrier
BLC	Berenstein liquid coil
BP	Blood pressure
CAMS (1-3)	Cerebrofacial arteriovenous metameric syndrome
CAS	Carotid angioplasty and stenting
CBF	Cerebral blood flow
CBV	Cerebral blood volume
CCA	Common carotid artery
CCF	Carotid cavernous fistula
CEA	Carotid endarterectomy
CGRP	Calcitonin gene-related peptide
CMCC	Chronic macrocutaneous candidosis
CSF	Cerebrospinal fluid
CT	Computed tomography
CTA	Computer tomographic angiography
CVA	Cerebral vascular accidents
CVM	Cerebral vascular malformation
CVMS (1-3)	Cerebrofacial venous metameric syndrome
CVT	Cerebrovenous thrombosis

DAVF	Dural arteriovenous fistula
DAVS	Dural arteriovenous shunt
DBLC	Double lumen balloon catheters
DC	Direct current
DIC	Disseminated intravascular coagulation
DLBC	Double-lumen balloon tip catheters
DMSO	Dimetyl sulfoxide solvent
DSA	Digital subtraction angiography
DVA	Developmental venous anomaly
DWI	Diffusion-weighted imaging
EAA	Excitatory amino acid
ECASS	European Cooperative Acute Stroke Study
EC/IC	Extracranial to intracranial
ECST	European Carotid Surgery Trial
ED IV	Ehlers-Danlos syndrome type IV
EDRF	Endothelial-dependent relaxing factor
EDV	End diastolic velocity
ET-1	Endotheliin-1
EVAL	Ethylene-vinyl alcohol copolymer
EVOH	Ethylene-vinyl alcohol copolymer Onyx
F	French size
FGF	Fibroblast growth factor
FMD	Fibromuscular dysplasia
GDC	Guglielmi detachable coil
GPA	Glycoprotein GP IIb/IIIa receptor antagonists
GSA	Giant serpentine aneurysm
GVB	Gold valve balloon
HHT	Hereditary hemorrhagic telangiectasia
HITS	High-intensity transient signals
HMCAS	Hyperdense middle cerebral artery sign
HR	Heart rate
5-HT	Serotonin (5-hydroxytryptanine)
IBCA	Isobutyl-2-cyanoacrylate
ICA	Internal carotid artery
ICH	Intracranial hemorrhage
ICP	Intracranial pressure
ID	Inner diameter
IEL	Internal elastica lamina
ILT	Inferior lateral trunk
LIAT	Local intra-arterial thrombolysis
LDL	Low-density lipoprotein
LEI	Lamina elastica interna
LIAT	Local intra-arterial thrombolysis
LTICA	Left internal carotid artery
LTS	Cysteinyl leukotrienes

LTSA	Left subclavian artery
LTVA	Left vertebral artery
MAP	Mean arterial blood pressure
MCA	Middle cerebral artery
MCAO	Middle cerebral artery occlusion
MEPs	Motor evoked potentials
MRA	Magnetic resonance angiography
MRI	Magnetic resonance imaging
MSAS	Middle cerebral artery stenosis
NBCA	*N*-butyl-2-cyanoacrylate
NASCET	North American Symptomatic Carotid Endarterectomy Trial
NE	Norepinephrine
NF	Neurofibromatosis
NI	Neurological improvement
NIHSS	National Institutes of Health Stroke Scale
NK-1	Neurokenin-1 (NK-2, NK-3)
NMDA	*N*-methyl-D-aspartate
NO	Nitrous oxide
NOS	Nitric oxide synthase
NPY	Neuropeptide Y
OD	Outer diameter
OER	Oxygen extraction ratio
OVD	Occlusive vascular disease
PACAP	Pituitary adenylate cyclase-activating peptide
PAF	Platelet activation factors
PCA	Posterior cerebral artery
PcomA	Posterior communicating artery
PDGF	Platelet derived growth factor
PET	Positron emission tomography
PGs: PGD_2, PEG_2, PGF_{2a}	Prostaglandins
PGI_2	Prostacyclin
PHACE	Syndrome with posterior fossa malformations hemangiomas arterial anomalies coarctation of the aorta eye malformations
PHI	Peptide histidine isoleucine
PICA	Posterior inferior cerebellar artery
PKD	Polycystic kidney disease
PROCT II	Prolyse in Acute Cerebral Thromboembolism Trial II
PSAVMs	Paraspinal arteriovenous malformations
PSV	Maximal systolic velocity peak
PTT	Partial thromboplastin time
PVA	Polyvinyl alcohol
PWI	Perfusion-weighted imaging
PTA	Percutaneous transluminal angioplasty

rCBF	Regional cerebral blood flow
ROW	Rendu-Osler-Weber syndrome
RTCCA	Right common carotid artery
RTICA	Right internal carotid artery
RTSA	Right subclavian artery
RTVA	Right vertebral artery
r-TPA	Recombined tissue plasminogen activated
rUK	Recombined urokinase
SAH	Subarachnoid hemorrhage
SAMS (1-31)	Spinal arteriovenous metameric syndrome
SBE	Subacute bacterial endocarditis
SCA	Superior cerebellar artery
SD	Spontaneous dissections
SEPs	Somatosensory evoked potentials
SCAVMs	Spinal cord arteriovascular malformations
SP	Substance P
TIA	Transient ischemic attack
TIMI	Thrombolysis in myocardial infarction
TXA_2	Thromboxane A_2
UK	Urokinase
VBA	Vertebrobasilar artery
VCAM-1	Vascular endothelial addition molecule (vasodilator peptides)
VGAMs	Vein of Galen aneurysmal malformations
VHL	Von Hippel-Lindau disease
VIP	Vasoactive intestinal peptides
VP	Vasopressin
VVM	Venous vascular malformation
VVJ	Vertebrobasilar junction

1 Occlusive Vascular Disease

1.1 Introduction 2

1.2 Arterial Occlusive Disease 3
1.2.1 Cerebrovascular Physiology 3
1.2.1.1 The Blood–Brain Barrier 3
1.2.1.2 Cerebral Blood Flow 4
1.2.1.3 Cerebral Autoregulation 5
1.2.1.4 Cerebral Blood Volume 7
1.2.1.5 Blood Viscosity 8
1.2.1.6 Metabolism in Cerebral Blood Flow 8
1.2.1.7 Carbon Dioxide Reactivity 9
1.2.1.8 Oxygen Reactivity 9
1.2.1.9 Nitrous Oxide in Cerebral Circulation 9
1.2.1.10 Other Factors 10
1.2.2 Arterial Ischemic Stroke 14
1.2.2.1 Definition 14
1.2.2.2 Neuronal Metabolism and Cerebral Ischemia 17
1.2.2.3 Selective Neuronal Vulnerability 18
1.2.2.4 Hemodynamic Effects of Ischemia 21
1.2.2.5 Nitrous Oxide and Cerebral Ischemia 21
1.2.2.6 Window of Opportunity 22
1.2.2.7 Neutrophil 23
1.2.3 Atherosclerosis 23
1.2.3.1 Introduction 23
1.2.3.2 Epidemiology 23
1.2.3.3 Pathogenesis 24
1.2.3.4 Mechanisms of Atherogenesis 24
1.2.3.5 Fatty Streak 27
1.2.3.6 Fibrous Plaque 28
1.2.3.7 Unstable Fibrous Plaques 28
1.2.3.8 Complicated Plaque 28
1.2.3.9 Carotid Atherosclerosis 29
1.2.3.10 Conclusion 29
1.2.3.11 Neuroimaging of Ischemic Stroke 30
1.2.4 Ischemic Stroke Treatment 31
1.2.4.1 Medical Treatment of Acute Stroke 31
1.2.4.2 Thrombolytic Therapy: Introduction 32
1.2.4.3 Thrombolytics (IV) 32
1.2.4.4 Recombined Tissue Plasminogen Activator 32
1.2.4.5 Streptokinase 33
1.2.4.6 Antiplatelets 34
1.2.4.7 Coumadin Versus Aspirin 39
1.2.4.8 Neuroprotective Agents 39
1.2.4.9 Pharmacological Properties of Neuroprotective Drugs 40
1.2.4.10 Binding Properties 41
1.2.4.11 Angiographic Evaluation 41
1.2.4.12 Middle Cerebral Artery Stroke: Natural History 44
1.2.4.13 Local Intra-arterial Thrombolysis in the Anterior Circulation 45

1.2.4.14 Internal Carotid Artery Occlusion 52
1.2.4.15 Carotid Dissection 57
1.2.4.16 Central Retinal Artery Occlusion 67
1.2.4.17 Internal Carotid Artery Stenosis Above the Carotid Bulb 68
1.2.4.18 General Organization of a Stroke Emergency Team 70
1.2.4.19 Evolving Treatment Strategies 72
1.2.5 Extracranial Carotid Artery Stenosis 73
1.2.5.1 Introduction 73
1.2.5.2 Natural History 73
1.2.5.3 Carotid Bruit 75
1.2.5.4 Imaging 75
1.2.5.5 Treatment 84
1.2.5.6 Symptomatic Carotid Stenosis 86
1.2.5.7 Asymptomatic Carotid Stenosis 86
1.2.5.8 Restenosis After Carotid Endarterectomy 89
1.2.6 Carotid Angioplasty and Stenting 90
1.2.6.1 Introduction 90
1.2.6.2 Techniques of Carotid Angioplasty and Stenting 93
1.2.6.3 Intimal Hyperplasia and Restenosis 93
1.2.6.4 Follow-up Monitoring 98
1.2.7 Posterior Circulation Stroke (Stroke Prevention) 98
1.2.7.1 Introduction 98
1.2.7.2 Clinical Presentation 98
1.2.7.3 Pretherapeutic Evaluation in Cerebral Vascular Insufficiency 99
1.2.7.4 Management of Posterior Circulation Insufficiency 104
1.2.7.5 Basilar Thrombosis 110
1.2.7.6 Takayasu's Arteritis 115
1.2.8 Cerebral Angioplasty 116
1.2.8.1 Vasospasm 117

1.3 Venous Occlusive Disease 135
1.3.1 Etiology 135
1.3.2 Incidence 136
1.3.3 Clinical Presentation and Natural History 137
1.3.4 Imaging 138
1.3.5 Treatment 143

1.1 Introduction

Treatment of occlusive vascular diseases of the central nervous system (CNS) has become an important new discipline in the field of endovascular surgical neuroradiology. Over the past two decades, revascularization procedures of occlusive vascular lesions in the arterial or venous systems of the heart or peripheral circulation have become widely accepted. Advances in therapy for occlusive vascular disease of the CNS, however, have lagged behind because the potential for devastating complications prevented their implementation. Dramatic progress in device technology in combination with important pharmacological advances is now enabling us to perform cerebral revascularization with a high degree of safety and efficacy.

In view of the variety and frequency of occlusive vascular lesions, this chapter is divided into two major sections: arterial occlusive diseases and venous occlusive diseases.

1.2 Arterial Occlusive Disease

A review of cerebrovascular physiology is imperative to properly understand and manage occlusive vascular diseases.

1.2.1 Cerebrovascular Physiology

1.2.1.1 The Blood–Brain Barrier

In general, any lipid-soluble molecule that is very small (a radius <0.8 mm) can cross the intracerebral capillary walls freely. Larger polar molecules are, for the most part, unable to do so, except for a select group of metabolically important molecules such as glucose and amino acids. These, and other metabolically important molecules, cross the vessel wall by means of carrier mechanisms, which facilitate transfer, or by active processes and work against a concentration gradient. Trapping mechanisms within cytoplasm of endothelial cells prevent the unrestricted entry of catecholamines into the brain.

A mechanism for excluding toxic lipid-soluble molecules has been described. Capillaries in neural tissue possess an array of characteristics that restrict the passage of some molecules across the vessel wall, while enhancing the passage of others. The structural and functional features that are responsible for the permeability characteristics of the capillaries are collectively known as the blood–brain barrier (BBB).

The features of this barrier begin to develop very early in embryonic life but are not fully expressed until after birth. Currently available evidence suggests that these BBB features are expressed in neuron endothelium in response to active factors elaborated by the neural tissue environment.

Initially, the neural vessels are discontinuous, sinusoid-like vessels of large diameter, with fenestrated walls and interrupted tight junctions. The basement membrane is thin and discontinuous. These vessels are permeable to circulating solutes. They are surrounded by precursors of neural and glial tissues but have not yet formed the intimate association typically seen with mature neural tissue. Pericytes are present but cannot be identified because of the discontinuous nature of the basement membrane.

As development proceeds, neural vessels change both structurally and functionally. Fenestrations disappear, the luminal diameter and wall thickness decrease, probably due to vessel elongation. The basement membrane forms end-feet. Generally, around the time of birth, the tight junctions become continuous, the electrical resistance increases, and permeability to several blood-borne molecules decreases. Astrocytes differentiate and form end-feet associated with the capillary wall. Transport mechanisms in the fetus and newborn do not function as those in the adult. Rather, they change in an age-appropriate manner to meet the changing nutritional needs of the growing, developing brain.

The capillaries in the adult human brain average approximately 10 m^2 in area and 640 km in length. Blood–tissue exchange takes place almost exclusively across the wall of capillaries. These capillaries are highly spe-

cialized to control blood–tissue exchange within very restricted limits (Stewart 1997).

The small vessels in neural tissue are composed of a single layer of endothelial cells, pericytes, and a basement membrane. Astrocytic end-feet form an almost complete covering of the abluminal surface of the capillary wall. Pericytes are closely applied to the outer surface of the capillary wall and cover approximately 25% of the abluminal surface. They are enclosed within a common basement membrane along with the endothelial cells. Pericytes are believed to function as a backup mechanism for the BBB by phagocytosing substances that pass through the endothelial barrier. They are also smooth-muscle precursors.

Endothelial cells are connected to each other by a continuous row of complex tight junctions that effectively seal diffusion routes across the capillary wall. Contrary to typical highly permeable membranes, tight junctions lack intercellular fenestrations. Endothelial vesicles are believed to act as shuttling membranous structures that facilitate the transport of chemicals across the vessel wall, or by temporarily fusing, to form a patent transcellular channel.

1.2.1.2 Cerebral Blood Flow

The most significant consequence of decreased cerebral blood flow (CBF) from arterial occlusion is brain ischemia and subsequent infarction. Decreased cerebral perfusion may result from insufficient flow (i.e., hemodynamic insufficiency) or from vascular occlusion (i.e., embolic).

A brief review of CBF physiology and its relationship to perfusion, pressure, and metabolic demand will make it possible to ascertain when dangerous levels of decreased CBF require intervention. The functional and structural integrity of the brain requires adequate local CBF, which is normally between 50–60 ml/100 g per minute. Under normal conditions (normoxia and normocapnia), CBF is ample relative to the metabolic needs of the tissue.

The cerebrovascular circulation is capable of dynamic adjustments of the vascular caliber to various stimuli, or demands by different parts of the brain. A number of local and systemic, physical and chemical stimuli activate different mechanisms to change cerebrovascular resistance. The goal of these mechanisms is to accurately and rapidly match CBF to demands in local neuronal metabolic requirements and to provide adequate oxygen and glucose to the tissues, despite extreme degrees of hypotension or hypoxemia.

To calculate CBF, one needs to understand that the arterial vasculature is a living (dynamic) elastic structure. If the arteries were rigid tubes, perfusion pressure would be defined as the difference between cerebral vascular inflow and outflow pressures, divided by the in-parallel resistance to flow through the channels. The pressure–flow relationship could be expressed as Ohm's law:

$$F = P/R$$

where F is flow, P is pressure, and R is resistance.

Resistance to flow depends upon the caliber and length of the tube and the nature of the fluid that flows through it. If we assume that we are dealing with a Newtonian fluid with a laminar flow pattern at a steady rate, then flow can be expressed in the equation of Poiseuille:

$$F = Pir2\ (P\ in - P\ out)/8\ nL$$

where F is flow, r is vascular radius, P is pressure, n is viscosity, and L is length.

While these formulas may help us understand CBF, in reality blood is *not* a Newtonian fluid, flow is *not* linear, but it is parabolic: the effective length of the vascular bed varies as precapillaries open and close according to demands. The intravascular perfusing pressure is pulsatile, and the vessels are *not* rigid, but distensible and can actively contract (Miller and Dell 1987). Nevertheless, the fundamental relationship between flow, perfusion, pressure, and resistance in the intact mammalian cerebrovascular bed can be reasonably well approximated with these equations (Evans et al. 1977).

The caliber of the cerebral vessel has a marked effect upon the CBF because velocity of flow is proportional to the square of the vascular radius and that volume of flow is proportional to the fourth power of the vascular radius (Siegel et al. 1974).

CBF may be measured, and should be distinguished, as a volume flow rate (ml/min) for a specific tissue weight (ml/100 g per minute), or a velocity (cm/s), and as cross-sectional areas (cm^2).

According to Bernoulli's law, as blood passes from a wide to a narrow tube, the velocity of kinetic energy increases but the pressure falls. This effect may be amplified in a vessel narrowed by a pathological process.

1.2.1.3 Cerebral Autoregulation

The skull, a rigid container, encloses the entire cerebral vascular network with only very limited capability of external venting. In addition to the active and passive caliber changes in the cerebral vessels, the cerebral veins are collapsible. Therefore, extravascular pressure becomes important. The difference between intra-arterial pressure and extravascular pressure is the intracranial pressure (ICP), representing the arterial transmural pressure, which is the differential pressure that acts upon the walls of the arterial vessels (Miller and Bell 1987).

Cerebral perfusion pressure is the difference between intra-arterial pressure and the pressure in the thin-walled veins, which are collapsible at the point of entry into the venous dural sinuses. Venous pressure changes in parallel with ICP and is normally 2–5 mmHg higher than the ICP. Therefore, the driving pressure is calculated as the difference between mean arterial blood pressure (MAP) and cerebral venous pressure or ICP, whichever is higher.

Under normal conditions, ICP remains less than 15 mmHg and reflects the volume of three distinct compartments: (a) the brain parenchyma (1,200–1,600 ml in the adult human), (b) the extracellular CSF fluid (CSF, 100–150 ml), and (c) intravascular blood (100–150 ml). The pressure–vol-

ume relationship is exponential. To maintain the same ICP, an increase in volume of one compartment of the intracranial contents must be compensated by a decrease of an equivalent amount in the other intracranial compartment(s).

In contrast to all other organs, the vascular supply to the brain has the unique properties of constant blood flow, despite changes in blood pressure or ICP. Under normal physiological conditions, changes in cerebral perfusion pressure between 50 and 130 mmHg produce little or no change in CBF. To maintain constant CBF, despite an increase in perfusion (intra-arterial) pressure, the cerebrovascular bed must increase vascular resistance. Since the viscosity of blood and the length of the vascular network is not likely to change, a reduction in the caliber (vasoconstriction) of the small arteries and arterioles (principal resistant vessels), results in an increase in vascular resistance, thus preserving normal CBF. Conversely, reduction in the blood pressure within the autoregulatory range (50–130 mmHg) produces vasodilatation, resulting in a decrease in cerebrovascular resistance (Fog 1937, 1939; Forbes and Cobb 1938).

Contrary to popular belief, recent experimental measurements of the pressure gradient directly across different segments of the vascular bed indicate that the major source of vascular resistance is at the arteriolar level. Large extracranial vessels such as the cervical carotid arteries and vertebral arteries, in addition to the pial vessels, contribute roughly half of total cerebrovascular resistance. This phenomenon has been termed segmental vascular resistance (Hurn and Traystman 1997).

Cerebral vessels of different caliber respond to different threshold levels of arterial pressure. The larger vessels (>200 μm in diameter) start to dilate when mean arterial pressure falls to 90 mmHg, whereas arteries less than 70 μm in diameter do not dilate until the pressure falls below 60 mmHg. The larger arteries at the level of the circle of Willis and their immediate branches are also resistance vessels and buffer the more distal arterioles from systemic arterial pressure (Heistad et al. 1978). If arterial pressure remains constant, but ICP rises, cerebral perfusion pressure will also be reduced. In these circumstances, the same changes in the caliber of cerebral resistance arteries occur to maintain a constant CBF (Miller and Bell 1987).

The ability to compensate for pressure–flow variability has a limit beyond which cerebral vasodilatation or constriction can no longer maintain normal levels of CBF. At perfusion pressures below 40 mmHg, CBF will be reduced and ischemia will first be manifested at the watershed areas in a heterogeneous way. These watershed areas represent the critical hemodynamic threshold when systemic pressure falls (Abboud 1981; Miller and Bell 1987).

If systemic pressure exceeds 140 mmHg, CBF rises, and autoregulation may fail. Examination of pial vessels demonstrates leakage of intravascular tracers into the extravascular space (Kontos et al. 1978). In baboons, a continued and sustained rise in systemic pressure has been shown to produce petechial hemorrhage. This phenomenon is referred to as breakthrough of autoregulation (Strandgaard et al. 1974).

The upper and lower limits of autoregulation can be reset in different circumstances. In long-standing hypertension, a mean pressure above

150 mmHg can be well tolerated, without an increase in CBF (Strandgaard et al. 1975). However, in the same subject, the lower end of autoregulation (i.e., the point where ischemia can occur) has also shifted upwards on the pressure scale from the normal 60 mmHg to 80 mmHg. Under these circumstances, when ICP rises, the cerebrovascular system is less able to compensate (Miller and Bell 1987).

Conversely, in a normal cerebrovascular system, the lower threshold of perfusion pressure may be lowered (40 mmHg) by sympatholytics without producing cerebral ischemia. For example, pharmacologically induced hypotension during anesthesia (Fitch et al. 1975) or following bilateral sympathectomies (Miller and Bell 1987) may be well tolerated.

When the arteriolar transmural pressure is elevated by high intravascular pressure, stretching of the smooth muscle in the vessel wall leads to vasoconstriction, increasing resistance to flow. This explains pressure autoregulation to changes in both systemic blood pressure and subarachnoid venous pressure, since venous pressure is equal to extramural tissue pressure in the normal brain and represents the external pressure exerted on the arteriole wall. A rise in blood pressure increases the transmural gradient, resulting in vasoconstriction, while elevation of venous pressure, and hence tissue pressure, decreases the gradient and leads to vasodilatation.

Autoregulation can be abolished when overriding vasodilatation is induced by a variety of mechanisms such as high arterial pCO_2 or pO_2, seizures, opiate antagonists, or volatile anesthetics (Turner et al. 1984).

Autoregulation becomes impaired after a wide spectrum of insults, either local (cerebral) or systemic, including trauma and hypoxemia, as well as in the perimeter of tumors, in ischemia, infarction, and inflammatory lesions such as abscesses, and in diabetes (Miller and Bell 1987).

1.2.1.4 Cerebral Blood Volume

Intracranial blood volume is determined by CBF and the capacitance vessel diameter (i.e., small veins and venules). Cerebral blood volume (CBV) increases with vasodilatation and decreases with vasoconstriction. While for the most part CBV changes in the same direction as CBF, it may actually be inversely related in some normal circumstances (i.e., during autoregulation) or in some pathological conditions. Blood volume is not equally distributed throughout the brain; blood volume perfusion per unit of weight is greater in gray matter than in white matter, with further variations among the various nuclei. The average CBV in adult humans is 3–4 ml/100 g tissue.

The central volume principle (Meier and Zierler 1954) relates the volume that intravascular blood occupies within brain (CBV in milliliters) and the volume of blood that moves through the brain per unit time (CBF in ml/min).

Changes in vascular diameter will directly affect CBV, but not necessarily all the time. CBF varies simultaneously as mean transit time is altered. For example, during vasodilatation, as CBV increases, if blood viscosity correspondingly decreases, CBF may not change.

1.2.1.5 Blood Viscosity

Viscosity represents the internal frictional resistance of the transported fluid. According to Poiseuille's law, changes in blood viscosity will affect CBF, but as blood is not a Newtonian fluid, Poiseuille's law in effect does not precisely describe the relationship between CBF and blood viscosity, particularly in the microcirculation. Blood viscosity varies directly with the cellular elements of blood and the hematocrit. Blood viscosity also varies inversely with the shear rate (a parameter that describes the velocity gradient of laminar blood flow through a vessel), which is inversely proportional to vessel radius. Therefore, for a given blood velocity, shear rates are greater in smaller vessels than in larger vessels (e.g., 300–500 s^{-1} in arterioles vs. 50 s^{-1} in the aorta) and apparent viscosity is consequently lower in the microcirculation. The latter is called the Fahraeus-Lindqvist effect, where the viscosity is reduced by about 5% at 300-μm-diameter vessels and by 50% at 20-μm-diameter vessels relative to large bore tubes (Hurn and Traystman 1997).

Blood viscosity increases exponentially with increases in hematocrit and with elevation in gamma globulin and fibrinogen components of plasma protein. Furthermore, a fall in pH will increase red cell stiffness and further decrease flow, unless compensatory changes occur (Miller and Bell 1987).

When the hematocrit rises, flow decreases as the oxygen extraction ratio increases and less blood is required to deliver oxygen. Reduced flow increases viscosity further, producing a vicious circle until stasis occurs (Thomas 1982).

In normal physiological states, flow in the cerebral microcirculation frequently stops and starts; the force needed to restart flow is directly dependent upon hematocrit level. The autoregulatory mechanism to compensate for increase in blood viscosity is vasodilatation in response to the increase in cerebrovascular resistance.

As reviewed above, blood viscosity plays an important role at various stages in the physiology of ischemic states.

1.2.1.6 Metabolism in Cerebral Blood Flow

The average rate of metabolic glucose consumption in the brain is approximately 60 ml/100 g per minute and demonstrates considerable regional variation, being four to five times greater in the colliculi than in the basal ganglia. Oxygen is used at an average rate of 6 ml/100 g per minute in the cortex, and 2 ml/100 g per minute in the white matter (Frackowiak et al. 1980). If the oxygen supply is interrupted, tissue ATP reduces to zero in just 7 min (Siesjo 1984).

1.2.1.7 Carbon Dioxide Reactivity

Carbon dioxide (CO_2) has a profound effect upon the cerebral circulation and therefore upon CBF. Hypercapnia produces vasodilatation and hypocapnia results in vasoconstriction. These effects are reversible and are seen universally in all mammals and at all ages.

In man, inhalation of 5% CO_2 elevates CBF by 50%, and inhalation of 7% increases CBF by 100% (Kety and Schmidt 1948). All cerebral vessels respond to changes in CO_2. Hypocapnia vasoconstriction is size independent; however, hypercapnia dilates smaller-caliber vessels more so than larger-caliber vessels.

CO_2 freely diffuses between blood and CSF. As long as CO_2 remains constant, changes in blood pH have little effect upon extracellular pH or CBF (Miller and Bell 1987). The flow changes induced by alterations in arterial pCO_2 begin within 2 min and reach equilibrium within 12 min (Raper et al. 1971). As with other CBF parameters, prolonged changes in pCO_2 lead to chronic adaptation and after 36 h CBF will return to normal. CO_2 reactivity will become impaired by various physical insults, such as trauma, intracranial surgery, atherosclerosis, arterial hypotension, ischemia, and SAH (Miller and Bell 1987).

Where CO_2 reactivity is focally impaired, a rise in arterial pCO_2 will dilate the surrounding vessels and divert blood away from the damaged (ischemic) area. This paradoxical effect may further increase the ischemic area and has been termed intracerebral steal (Symon 1969).

Levels of arterial pCO_2 above 70 mmHg produce maximal vasodilatation and no additional increase in CBF, despite further increases in pCO_2. Lowering arterial pCO_2 below 20 mmHg produces no further decrease in blood flow once CBF goes below the 20 ml/100 g per minute threshold for normal neuronal function.

1.2.1.8 Oxygen Reactivity

Due to the shape of the oxygen dissociation curve of hemoglobin, pO_2 has less effect on CBF than pCO_2 and the CBF falls by only 10% when the subject is breathing 100% oxygen. CBF begins to rise when pO_2 falls below 50 mmHg, and at 30 mmHg the CBF will be doubled (Thomas and Crockard 1985).

1.2.1.9 Nitrous Oxide in Cerebral Circulation

Nitrous oxide (NO) is an inorganic membrane-permeable free-radical gas. It is synthesized in neurons, glial cells, perivascular nerves, cerebrovascular endothelium, macrophages, and white blood cells from the amino acid L-arginine and molecular oxygen by the enzyme, nitric oxide synthase (NOS) (Dawson and Synder 1994; Moncada et al. 1991). It is a powerful vasodilator and it is the endothelial-dependent relaxing factor (EDRF), which in turn activates guanylyl cyclase and initiates a cascade in the vascular smooth muscle, causing relaxation (Moncada et al. 1991).

Table 1.1. Nitric oxide synthase (NOS)

Constitutive neuronal	Chromosome 12	Ca^{2+}-dependent
Constitutive endothelial	Chromosome 7	Ca^{2+}-dependent
Inducible macrophages	Chromosome 17	Ca^{2+}-independent

At least three NOS isoforms have been identified: constitutive neuronal (chromosome 12); constitutive endothelial (chromosome 7); and an inducible isoform isolated from macrophages (chromosome 17) (Table 1.1).

The two constitutive isoforms (neuronal and endothelial) are activated by increases in intracellular calcium-calmodulin. The third type, the inducible isoform, is calcium insensitive and appears in tissue where its synthesis is stimulated by inflammatory substances such as endotoxin cytokinase. Constitutive NOS exists within cerebrovascular endothelium, perivascular nerves, neurons, and astrocytes. The role of NO in cerebrovascular hemodynamics includes flow augmentation during hypoxia and ischemia, cerebral autoregulation, hypercapnia, and flow metabolism coupling (Iadocola et al. 1994; Faraci and Brian 1994).

Nitrous oxide is involved in a variety of physiological functions such as regulation of blood pressure, platelet inhibition, inflammation, penile erection, and neurotransmission (Dawson and Synder 1994; Moncada et al. 1991; Iadocola et al. 1994).

Both neuronal and endothelial NO regulate vascular tone. Topical or systemic administration of NOS inhibitors constricts cerebral arteries and reduces regional cerebral blood flow (rCBF), suggesting that NO contributes to normal vascular tone. NO contribution to vascular tone varies among brain regions and amongst species. Thus, brain regions with higher NOS activity (for example, cerebellum and hypothalamus) show a greater decrease in cerebral blood flow (CBF) after NOS inhibition. Neuronally generated NO regulates rCBF responses to CO_2 inhalation.

NO is cytotoxic: macrophages kill bacteria in tumor cells by releasing high amounts of NO.

1.2.1.10 Other Factors

Extensive studies on the regulation of cerebral vessel tone conducted over the past 2 decades reveal a plethora of mediators that relax, contract, or modify cerebral vessel permeability and functions. These mediators are derived from sympathetic, parasympathetic, and sensory nerves that innervate the cerebral vessels (Table 1.2).

Investigations of cerebrovascular smooth muscle and blood–brain barrier (BBB) endothelium have elucidated the functional role of an array of vasoactive agents that govern the physiological coupling between regional cerebral blood flow, metabolism, and neuronal activity. This includes a host of diverse mediators, including vasoactive peptides, amines, lipids, phospholipids, and vasoactive gases. The precise role these factors play in maintaining cerebrovascular autoregulation in physiological conditions and in pathological conditions (such as cerebrovascular atherosclerosis,

Table 1.2. Vasoactive substances

	Vasoconstrictor	Vasodilator
Norepinephrine (NE) α_1- and α_2-adrenoreceptors		+
NE β_1- and β_2-adrenoreceptors		+
Serotonin (5-HT)	+ Large vessels +– Arterioles	+ Capillaries
Histamine	+	+– Depending on receptors (H1, H2, H3)
Dopamine (precursor of NE)		+ (Indirect)
Acetylcholine		+ (EDRF)
Prostacyclin		++
Thromboxane A_2	+	
Prostaglandins (PG_s: PGD_2, PEG_2, and $PGF2_\alpha$)		++
Cysteinyl leukotrienes (LTS)	++	
Platelet-activating factor (PAF)	+ Higher concentration	+ Low concentrations
Calcitonin gene-related peptide (CGRP)		++
Adrenomedullin		++
Substance P (SP)		+ EDRF/NO-mediated mechanism
Bradykinin B_1 receptors	+ Large arteries and large veins	
Bradykinin B_2 receptors		+ EDRF mediated arterioles and venules
Neuropeptide Y (NPY)	+++ (Prolonged)	
Angiotensin-II (AII)	+++ (Choroid plexus)	
Endothelium-1 (ET-1)	+++	
Vasopressin (VP)	+	
Adenosine		+
ADP and ATP		+
Carbon monoxide (CO)		+

ischemia, vasospasm, thrombosis, inflammation, and trauma) remains under intensive investigation. The cerebrovascular endothelium is a major contributor to cerebrovascular tone and autoregulation by the balanced actions of relaxing and contracting mediators (Feuerstein and Miller 1997).

The description of the ever-increasing number of mediators on neuronal metabolism and cerebral vessels, although important, is beyond the scope of this review. They are well reviewed by others (Miller and Bell 1987; Feuerstein and Miller 1997).

Briefly, we will enumerate critical aspects of the most important mediators.

Amines

Amines include the catecholamines (norepinephrine, epinephrine, and dopamine), serotonin, histamine, and acetylcholine.

Norepinephrine. Dense networks of perivascular norepinephrine (NE)-containing nerves are present in the walls of cerebral arteries, arterioles, capillaries and veins. The majority of these sympathetic fibers originate from the superior cervical ganglion. The vasodilator or vasoconstrictor's response to NE is a function of the balance between vascular α- and β-adrenoreceptors in different segments of the cerebrovascular tree. Noradrenergic-induced constriction of cerebrovascular smooth muscle cells is mediated by both α_1- and α_2-adrenoreceptors and is Ca^{2+} dependent. Cerebral arteries also possess β_1- and β_2-adrenoreceptors that mediate dilator responses, with isoproterenol being the most potent vasodilator, followed by epinephrine and lastly, the least potent, norepinephrine.

Serotonin. Cerebral vessels receive serotoninergic innervation originating from brainstem nuclei. The effect of serotonin (5-hydroxytryptanine, 5-HT) on the cerebral circulation depends on blood vessel size and the receptor subtype. At the major vessel level [i.e., internal carotid artery (ICA), middle cerebral artery (MCA)], 5-HT produces vasoconstriction, mediated in part by the release of NE and by prostaglandins, with increases in Ca^{2+} influx.

At the arteriolar level, depending on the preexisting vascular tone, 5-HT can produce either vasoconstriction or vasodilatation. At the capillary level, 5-HT produces vasodilatation and increases permeability. At the venular and venous level, 5-HT modulates venous caliber and vascular capacitance.

5-HT may be responsible for some headache syndromes such as migraine.

Histamine. Histamine can be found in neurons (predominately in the hypothalamus), endothelial cells and perivascular mast cells. While histamine is generally viewed as a vasodilator, depending upon the receptors (H_1, H_2, and H_3), it may mediate vasodilatation or vasoconstriction.

The vasodilatation effect of histamine on the cerebral vasculature is mediated via activation of H_2 receptors in the smaller distal arteries, which are the major contributors to cerebrovascular flow resistance. H_1 receptors act on the endothelial cells and are more common on the larger arteries.

Histamine increases the permeability of the BBB though H_2 receptors, probably by the release of substance P (Toda et al. 1985).

Dopamine. The effects of dopamine, a precursor of NE, are indirect. The use of dopamine antagonists in an experimental setting results in an increase in cerebral blood flow.

Acetylcholine. Acetylcholine (Ach) is secreted from parasympathetic innervations in cerebral arteries and is involved in the secretion of CSF from the choroid plexus (Branston 1995). Ach induces endothelium-dependent relaxation in the cerebral arteries and arterioles.

Lipid Mediators

The lipid mediators include the eicosanoids. The eicosanoids are a diverse group of substances derived from arachidonic acid. This group of mediators includes prostacyclin (PGI_2), thromboxane A_2 (TXA_2), prostaglandins and leukotrienes.

Eicosanoids are synthesized in the wall of cerebral arteries, capillaries and in the choroid plexus (Moskowitz and Coughlin 1981).

Prostacyclin is a potent vasodilator of cerebral vessels.

Thromboxane A_2 is a vasoconstrictor that also acts indirectly on platelets, causing platelet aggregation and thrombosis.

Prostaglandins (PGs: PGD_2, PEG_2, and $PGF2_\alpha$) are potent cerebral vasodilators.

Cysteinyl leukotrienes (LTS) include LTC_4 and LTD_4, which are potent vasoconstrictors to cerebral arteries.

Platelet-activating factor (PAF) is produced predominately by neutrophils, macrophages, and platelets, but also by endothelial and neuronal cells. PAF seems to have no direct effect on cerebral microvessels. At low concentrations, PAF may elicit endothelium-dependent relaxation, while at higher concentrations, PAF may induce vasoconstriction, in part via TXA_2 released from platelets.

Peptides

Vasodilator peptides include vasoactive intestinal peptides (VIP), peptide histidine isoleucine (PHI) and pituitary adenylate cyclase-activating peptide (PACAP).

Calcitonin gene-related peptide (CGRP), a potent vasodilator of cerebral vessels, is localized in sensory nerves on the large, medium, and small cerebral vessels. Adrenomedullin is a potent vasodilator of cerebral vessels in vitro and in vivo.

Substance P (SP) is the principal member of the tachykinin. SP is primarily localized in the perivascular sensory nerves, where it induces vasodilatation (although there were some exceptions to this effect). SP may be involved in vasodilatation and plasma extravasation in the extracerebral circulation and thereby mediates neurogenic inflammation. There are three types of tachykinin receptors designated as neurokenin-1 (NK-1), NK-2, and NK-3. SP is believed to induce vasodilatation by an endothelium-derived relaxing factor (EDRF)/NO-mediated mechanism.

Bradykinin. Bradykinin acts via B_1 and B_2 receptors that are present in cerebral vessels. B_1 receptors mediate contraction of large arteries and large veins, while B_2 receptors induce EDRF-mediated relaxation in arterioles and venules and increase permeability of endothelial cells and BBB.

Vasoconstrictor Peptides

Neuropeptide Y. Neuropeptide Y (NPY) is synthesized and released along with NE from sympathetic nerve innervations of cerebral vessels. It is a potent vasoconstrictor and its effect is prolonged.

Angiotensin II. Angiotensin II (ATII) receptors are potent vasoconstrictors; they potentiate the action of NE and are found in brain microvessels and most extensively in the vessels of the choroid plexus.

Endothelin-1. Endothelin-1 (ET-1) is a metalloprotease that induces a potent vasoconstriction of brain arteries, characterized by its slow onset but long-lasting effects. The presence of elevated levels of ET-1 in subarachnoid hemorrhage suggests that ET-1 may be involved in the pathogenesis of cerebrovascular spasm.

Vasopressin (VP) has a direct vasoconstricting effect on cerebral arteries and veins.

Purine Nucleotides

- Adenosine — Adenosine is a vasodilator, considered to serve as a link in coupling blood flow to oxidative metabolism and is responsible for hypoxia-induced vasodilatation.
- Adenosine diphosphate — Both adenosine diphosphate (ADP) and adenosine triphosphate (ATP) elicit relaxation of cerebral vessels by activation of purinergic P2 receptors.
- Carbon monoxide — Carbon monoxide (CO) is believed to serve as a mediator of cerebrovascular relaxation via an increase in CGMB. CO is much less potent than NO as a vasodilator agent, but like NO, may serve multiple neuronal functions.

1.2.2 Arterial Ischemic Stroke

1.2.2.1 Definition

Ischemic stroke is caused by a disruption in blood flow and results in a neurological deficit that persists longer than 24 h. In contrast, transient ischemic attacks (TIAs) are defined as brief episodes of neurological dysfunction resulting from cerebral ischemia. Typically, most TIAs last less than 15 min, but the classic description depicts episodes lasting less than 24 h.

Stroke is the most common life-threatening neurological disease (Table 1.3) and the third most common cause of death in the Western population (second in women), with an incidence in North America of over 500,000 strokes/year, of which 200,000/year are fatal (Table 1.3). In Western countries, there are 500 TIAs per year, and 2,400 strokes per year in a

population of 1 million inhabitants (Hankey 1999). Stroke, therefore, is more frequently disabling than lethal. It is the first cause of handicap and the second cause of dementia in Western countries.

The literature on stroke is extensive, and the epidemiology is beyond the scope of this chapter. The causes, location and impact of ischemic stroke (from prevention to treatment) will vary greatly between people of various races, genders, geographic areas, and socioeconomic statuses (Modan and Wagener 1992) (Table 1.4).

The prognosis for patients with ischemic stroke is worse than the prognosis of many types of cancer, with half of all strokes resulting in death or dependency after 1 year (Dyker and Lees 1998). The outcome is even bleaker for patients with severe stroke, with 96% of patients dead or dependent after suffering a major anterior or posterior circulation stroke (Dyker and Lees 1998).

The likelihood that arterial ischemia is the cause of a cerebral vascular accidents (CVA) increases with the patient's age (Table 1.5). Ischemia accounts for only 33% of events in patients under age 45, but 80% of events in those older than age 50 (Boosser and Mas 1988).

Stroke is a major health burden. Its impact and prevalence in the elderly and in those between 75 and 84 years of life makes stroke the leading cause of death (Table 1.6)

Table 1.3. Stroke in North America

Cerebral vascular accidents (CVAs)	500,000 patients/year
Average hospital stay	42 days
CVA death	200,000 patients/year
CVA cost	US $20 billion/year

Table 1.4. Stroke: race, sex, prevalence of location

Chinese	Intracranial
Japanese	Intracranial
African-American	Intracranial
White Americans	Extracranial and heart
White Scandinavians	Extracranial and heart

Male vs. female 30%> risk for cerebral vascular accident

Table 1.5. Stroke incidence per 100,000 population (USA)

All age groups	150
Under 40 years	3
Over 85 years	1,800

Table 1.6. Prevalence of major diseases in the elderly (%)[a]

Age	Stroke	TIA	MI	PAD	AA	AD	PD
55–64	2.0	0.9	2.6	0.9	1.2	0.2	0.3
65–74	4.2	1.7	5.6	2.0	2.5	0.9	1.0
75–84	7.8	2.3	6.2	2.9	4.7	7.4	3.1
85+	11.0	2.2	4.4	4.1	6.2	26.8	4.3

TIA, transient ischemic attack; MI, myocardial infarction; PAD, peripheral arterial disease; AA, aortic aneurysm; AD, aortic dissection; PD, pulmonary disease.

[a] Rotterdam study (1990–1999).

The risk of further cerebral ischemia after a stroke or TIA is highest immediately after the initial event. Results from the Oxford Community Stroke Project suggest that the absolute risk of a future cerebral ischemic episode is 4.4% during the first month and 8.8% during the first 2 months. The odds ratio of a stroke in these patients compared with age-matched controls without recent symptoms of cerebral ischemia is 80.0 within the first month and 27.0 within the second month. Thereafter, the odds ratio diminishes to 4.7 between 1 and 2 years (Dennis et al. 1990).

In a recent study, Johnston demonstrated the short-term risk of stroke and other adverse events after an emergency department diagnosis of TIA is substantial. Overall, 25.1% of the patients experienced a stroke or other adverse event within 90 days of the TIA diagnosis (Johnston et al. 2000).

The causes of ischemic stroke are various and are shown in Table 1.7. The risk factors associated with stroke are listed in Table 1.8.

Stroke risk increases with increasing carotid stenosis. With low-grade stenosis, the risk of stroke is relatively small. Conversely, high-grade stenosis (>75%) carries an annual stroke incidence of approximately 3%. When TIAs are included, the risk increases to approximately 10%, with the majority of events being referable to the ipsilateral stenosed artery (Norris et al. 1991). Carotid stenosis accounts for approximately 30% of CVAs (De Bakey 1996).

Table 1.7. Causes of stroke

Cerebral ischemia	80%
Large vessel atherosclerosis	20%
Cardiac emboli	20%
Small vessel occlusion	20%
Other definite causes	5%
Unknown	15%
Cerebral hemorrhage	20%

Table 1.8. Risk factors for ischemic cerebrovascular accident

Modifiable	Nonmodifiable
Arterial Hypertension	Gender Male
Hypercholesterolemia	Race Black Hispanic Asian
Smoking	Age
Diabetes mellitus	Family history
Alcohol	
Estrogen	
Migraine	
Transient ischemic attacks	
Other locations of atherosclerosis (CHD, PAD)	
Acute infections	
Sleep apnea syndrome	
Obesity	
APL antibodies	
Homocysteinuria	
Drug abuse	
Hypercoagulation states	
Sickle cell disease	

1.2.2.2 Neuronal Metabolism and Cerebral Ischemia

The functional and structural integrity of the brain requires adequate local CBF, which is normally between 50 and 60 ml/100 g per minute. Under normal conditions (normoxia and normocapnia), CBF is ample, relative to the metabolic needs of the tissue. At the normal range of autoregulation, brain tissue extracts between 35% and 40% of the delivered amount of oxygen, a value that can be doubled in order to avoid hypoxic symptoms. This increase in oxygen extraction ratio (OER) has been termed perfusion reserve.

When there is an occlusion to a cerebral artery resulting in insufficient CBF, a cascade of metabolic events takes place, depending upon the regional diminution of perfusion pressure distal to the occlusion. When the regional CBF is no less than about 20 ml/100 g per minute, the cerebrovascular bed first attempts to compensate by autoregulatory responses (vasodilatation). As distal blood pressure falls below approximately 60 mmHg, (lower threshold of autoregulation) and flow decreases, compensation occurs by increasing the OER. This compensation is adequate for moderate flow reductions down to about one-half the normal levels, in that the OER increases as flow decreases, preserving cerebral oxygen uptake and neuronal function.

When distal pressure falls below approximately 30 mmHg, the two compensatory mechanisms (autoregulation and perfusion reserve) become inadequate to prevent failure of oxygen delivery. As flow drops below the ischemic threshold around 20–23 ml/ 100 g per minute, symptoms of tissue hypoxia, referred to as ischemia, occur and tissue metabolic needs can no longer be supported, resulting in cerebrovascular insufficiency.

Ischemia refers to inadequate perfusion of tissues. There are two levels of ischemia, moderate and severe. Moderate ischemia occurs when regional CBF is between 10–23 ml/100 g per minute. This regional level of ischemia, resulting in paralysis or inhibition of function, but not in absent neuronal activity, is defined as penumbra, a tissue zone with partial or complete yet fully reversible ischemic paralysis (Astrup et al. 1981). Severe ischemia with flow below 10 ml/100 g per minute, if lasting for more than a few minutes, will result in an irreversible loss of neuronal function, and tissue necrosis (i.e., infarction) (Lassen 1982).

Based on electrophysiological observations following experimental MCA occlusion in baboons, the ischemic penumbra can be defined as a complete failure of the cortical evoked potentials at the level of the cortex, observed at a CBF threshold level of approximately 0.15 ml/g per minute (15 ml/100 g per minute). At this CBF threshold, extracellular potassium ion activity was only mildly elevated. With a further CBF reduction to the range of 0.06–0.10 ml/g per minute (6–10 ml/100 g per minute), massive increases in extracellular potassium occur and are associated with complete tissue infarction. Thus, the ischemic penumbra has been conceptualized as a region in which CBF reduction has exceeded the threshold for failure of electrical function but not that for membrane failure.

When correlating CBF autoradiographs with diffusion-weighted MR images and regional distribution of cerebral metabolites, the ischemic core region enlarges when adjacent, formerly penumbral areas undergo

irreversible deterioration during the initial hours of vascular occlusion. At the same time, the residual penumbra becomes restricted to the periphery of the ischemic territory and its fate may depend critically upon early therapeutic intervention. In the border zone of brain infarcts, marked uncoupling of local CBF and glucose utilization is consistently observed. The correlation with electrophysiological measurements shows that metabolism-flow uncoupling is associated with sustained deflections of the direct current (DC) potential, resembling transient depolarization. Such penumbral cell depolarization, which is associated with an increased metabolic workload, induces episodes of tissue hypoxia due to the constrained collateral flow, stimulates anaerobic glycolysis leading to lactacidosis, suppresses protein synthesis, and, finally, compromises energy metabolism. The frequency of depolarization correlates with the final volume of ischemic injury. Therefore, penumbral depolarization is regarded as an essential event in the pathogenesis of ischemic brain injury. *N*-methyl-D-aspartate (NMDA) and non-NMDA antagonists can suppress peri-infarct DC deflections and result in significant reduction of infarct size.

The histopathological sequelae within the penumbra consist of various degrees of scattered neuronal injury, termed incomplete infarction. The reduction of neuronal density at the infarct border is a flow- and time-dependent event, which is accompanied by an early response of glial cells. As early as 3 h after vascular occlusion, generalized microglial activation can be detected throughout the ipsilateral cortex. Astrocytic activation is observed in the intact parts of the ischemic hemisphere from 6 h after occlusion onwards. Thus, the penumbra is a spatially dynamic brain region of limited viability, which is characterized by complex pathophysiological changes involving neuronal function as well as glial activation in response to local ischemic injury (Back 1998).

1.2.2.3 Selective Neuronal Vulnerability

The pathophysiological process that leads to several discrete histological changes in the postischemic brain is related to various factors, including the distinct biochemical properties among various populations of brain cells and the spatial and the temporal dynamics of cerebral ischemia (Pulsinelli 1997).

Anatomically, cerebral ischemia may be classified as either focal, the loss or reduction of blood flow to a specific vascular territory, or global, the reduction of blood flow to the entire brain. The severity of brain ischemia is the product of the degree and duration of blood flow loss. In focal ischemia, which usually occurs following thromboembolic or atherothrombotic occlusion from extracranial or from intracranial cerebral vessel abnormalities, the histopathological outcome is directly influenced by the degree and duration of blood flow loss.

Global brain ischemia usually occurs following cardiac arrest and is uniformly severe and complete. Clinically relevant global brain ischemia is seen after no more than 5–10 min of blood flow loss in normothermic humans. Longer periods are incompatible with life. The histopathological changes and severity of the ischemia following cardiac arrest create a predictable and uniform type of histological brain injury.

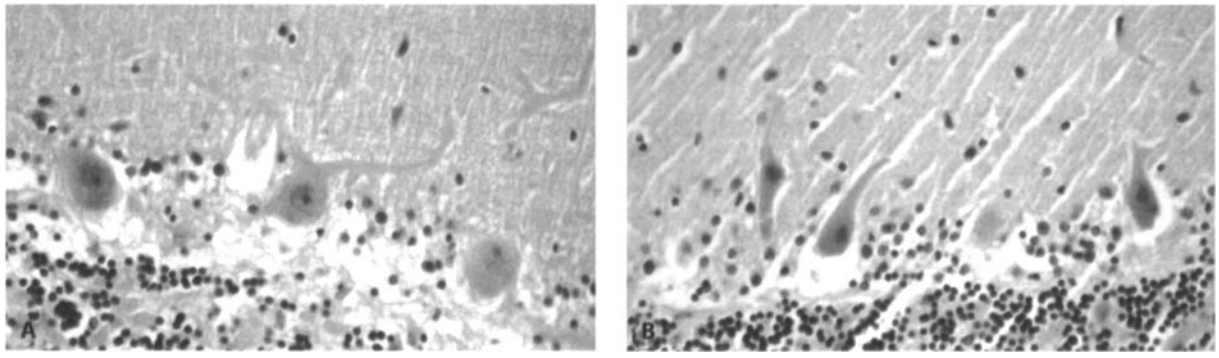

Fig. 1.1A, B. Selective vulnerability. Selective ischemic necrosis is characterized by irreversible injury limited to a specific population of brain neurons. Such vulnerable population includes Purkinje cells. **A** Normal Purkinje cells. **B** Selective loss of Purkinje cells with preservation of other neurons and glial cells

Ischemic depolarization is critical for the initiation of injury. The absolute blood flow reduction that causes ischemic depolarization varies among species. Increasing the duration of depolarizing ischemia is associated with progressively more severe histological changes. While early injury is reversible, sustained depolarizing ischemia results in a more severe form of ischemic brain injury, cerebral infarction.

Selective ischemic necrosis is characterized by irreversible injury limited to a specific population of brain neurons that have been empirically identified as vulnerable to hypoxia and ischemia (Graham 1992). Such vulnerable populations include the CA1 sector of the hippocampus, medium-size striatal neurons, and cerebellar Purkinje cells (Fig. 1.1). These highly vulnerable cells will suffer even if the injury is transient but severe, producing depolarization. In patients successfully resuscitated from cardiac arrest, one can see this type of depolarizing ischemia. Selective ischemic necrosis may also develop in transient focal brain ischemia, but such injury is infrequently encountered clinically, since there are no long-lasting neurological sequelae.

The histopathological characteristics of selective ischemic necrosis have classically been defined as a series of histological changes encompassed by the term ischemic cell change. Ischemic cell change begins with the stage called microvacuolization that is followed by incrustations, and finally, homogenizing cell change (Duchen 1992). Microscopically, one can see shrunken neuronal bodies, acidophilic staining of the neuronal cytoplasm, and darkly staining, pyknotic nuclei. Ultrastructural studies of cellular organelles reveal an early but reversible swelling of mitochondria that creates the microvacuolated appearance of ischemic neurons. Later, a dispersion of polyribosomes, a decrease in the amount of the endoplasmic reticulum, vesicular formation in the Golgi cisterns, and condensation of the nuclear chromatin occurs. Mitochondria vacuolization, which appears within minutes of cerebral reperfusion, is reversible, while the remaining stages of ischemic cell change that develop over a period of a few hours will be irreversible (Petito and Pulsinelli 1984). The stage of neuronal incrustations follows that of microvacuolization. Electromicroscopy shows that incrustations are dense packets of neuronal cytoplasm created

by swollen astrocytic processes that impinge upon the neuronal membrane. It is unclear whether homogenized cell change is an obligatory stage or develops in parallel with incrustations. It is a later stage of irreversible neuronal injury, which is characterized by homogenous, acidophilic, and what appears to be structureless cytoplasm and granular fragmentation of the nucleus and its membrane.

Various time-related properties of selective ischemic necrosis have been identified:

1. Ischemic sensitivity stage, the ischemic time interval required to trigger irreversible injury
2. Delayed interval stage, the time period after cerebral recirculation but before irreversible injury begins
3. Irreversible stage, the time it takes for irreversible injury to evolve once it has been initiated (Graham 1992; Pulsinelli et al. 1982; Kirino 1982)

As previously mentioned, ischemic sensitivity varies dramatically among different neurons. The CA1 zone of the hippocampus succumbs to periods of depolarizing ischemia lasting as little as 3 min, while periods of 15–20 min of severe ischemia are needed to create cell death in medium-size neurons in the striatum. Likewise, the interval between cerebral recirculation in the initiation of irreversible injury differs markedly among neuronal populations. The comparatively ischemia-resistant medium-size striatum neurons show signs of irreversible injury within 48–72 h of recirculation, while the onset of irreversible injury to the ischemia-sensitive CA1 hippocampal neurons occurs in 3 h. Once initiated, the time course for the evolution through the various stages of ischemic cell change may be constant (Pulsinelli et al. 1982; (Kirino 1982).

Neuropathologists define cerebral infarction as an area of pan-necrosis, where all cell types, including neurons, glial, and endothelial cells involving a defined vascular territory of the brain are dead. The histopathological appearance of the fully developed infarct is defined as coagulative necrosis affecting all cell types.

At the margins of the infarct, there is a transition zone containing irreversibly injured neurons but preserved glial and endothelial cells that separates the central area of pan-necrosis from normal brain. Since neuronal injury in this border zone involves all neurons and not only those identified to be selectively vulnerable, the term "generalized neuronal necrosis" is given.

Following both global and focal cerebral ischemia, there is delayed neuronal death found in areas directly exposed to ischemia. Following global cerebral ischemia, however, distant nonischemic areas remote from the original infarcts are also affected. In rats, one can see necrosis of the ipsilateral thalamus and ipsilateral substantia nigra a few weeks after occlusion of the ipsilateral middle cerebral artery (del Zoppo and Garcia 1995; Garcia et al. 1995). Since these areas lie outside the ischemic region, degeneration of these areas after middle cerebral artery occlusion obviously represents secondary ischemia or neuronal damage that takes longer to develop. Neuronal cell damage can develop not only via direct insult to the nerve cell body, as in the initial ischemic insult, but also (and most likely) result from degeneration of the axon. Therefore, two types of neuronal de-

generation are proposed as the cause of secondary degeneration in a remote area following a focal damage. The axon degenerates (Wallerian degeneration), along with its terminals and its surrounding myelin sheath. These changes are referred to as anterograde degeneration. Conversely, insult to an axon also causes the cell body of the affected neuron to react. This is termed retrograde degeneration. In addition, both types of degeneration may have an effect across the synapses: transneuronal antegrade and retrograde changes (Kelly 1985). Neurons require a certain amount of stimulation to survive, and there may be some trophic substances released by some synaptic terminals, which are necessary for neuronal survival.

Delayed neuronal degeneration in areas remote from the cerebral infarction can perhaps be prevented by the application of neurotrophic factors and/or neurotransmitter amino acid agonists. This may represent a potential therapeutic strategy in the future.

1.2.2.4 Hemodynamic Effects of Ischemia

In acute stroke, cerebral autoregulation is lost and local cerebral perfusion becomes dependent on systemic blood pressure. Changes in blood pressure (BP), may increase or reduce local cerebral blood flow. At present it is not known whether the cerebral hemodynamic changes are reproduced (or clinically relevant) in stroke patients. It is conceivable that increases in systemic blood pressure could lead to exacerbation of cerebral edema or even hemorrhagic transformation of infarction. However, it is equally possible that moderate increases in BP are beneficial to outcome by increasing local perfusion and improving blood flow. Delayed cerebral ischemia after subarachnoid hemorrhage is often treated with a combination of hypervolemia, hypertensive agents, and hyperventilation.

In the INWEST study (Wahlgren et al. 1994), administration of the calcium channel antagonist nimodipine, which in experimental circumstances exhibits neuroprotective activity, was associated with an increase in mortality and adverse stroke outcome. This poor outcome correlated directly with a fall in systemic BP observed in the actively treated group. Other drugs that result in a significant drop in the blood pressure are also likely to have an adverse effect in stroke treatment (Squire et al. 1995). The precise relationship between systemic BP and local cerebral perfusion in acute stroke is not yet fully understood.

1.2.2.5 Nitrous Oxide and Cerebral Ischemia

Within minutes (3–24 min) following MCA occlusion, NO levels dramatically increase. Constitutive NOS activity increases during ischemia due to an increase in intracellular Ca^{2+}. A late but sustained increase in NO levels may also occur due to the expression of inducible NOS (the Ca^{2+}-independent isoform) within the microglial following the inroad of inflammatory cells 24 h after the onset of ischemia.

During the period immediately following ischemic insult, an increase in NO production in vascular endothelium or perivascular nerves may

improve blood flow and be neuroprotective. Indeed, the infusion of NO precursor L-adenine, which dilates pial vessels and increases cerebral blood flow (in normal as well as in ischemic brain), reduces infarct size and leads to electrocorticographic recovery when blood flow enhancement exceeds the functional flow threshold (Dalkara et al. 1994).

Nonselective inhibition of NO synthesis in vascular endothelium and platelets by the administration of methyl-L-arginine following focal ischemia may obscure the neuroprotective effects of NOS inhibition in neurons.

Neuronal NOS knockout mice demonstrate resistance to transient focal ischemia (3 h ischemia and 24 h reperfusion) and develop less brain edema. A similar finding was seen in global ischemia models of neuronal NOS knockout mice. The opposite outcome, aggravation of the ischemic lesion, was observed in endothelial NOS knockout mice. Therefore, it appears that neuronal NO production contributes to the development of ischemic brain injury. Conversely, endothelial NOS seems to have a positive effect in the postischemic period. Since vascular nitrous oxide may favorably affect the outcome of cerebral ischemia, selective inhibition of the neuronal isoform may offer new therapeutic possibilities in brain ischemia (Dalkara and Moskowitz 1997) (Table 1.1).

1.2.2.6 Window of Opportunity

Evidence from animal models on stroke suggests that after an ischemic insult, neurological damage spreads out circumferentially from the central core of the infarct (Symon et al. 1974). If ischemia is present for over 1 h, the volume of the infarct gradually enlarges to its maximal size over a period of 3–4 h in rodents (Kaplan et al. 1991) and over a period 6–8 h in nonhuman primates (Ackerman et al. 1989). Evidence from human studies using positron emission tomography (PET) scanning suggests this time window may even extend up to more than 48 h in patients with stroke. This phase, termed misery perfusion, (i.e., locally reduced flow) is present in 100% of patients scanned within 9 h of the ischemic insult and in 30% of patients if scanned within 4 days of the event (Baron et al. 1981, 1983). Ischemic but viable tissue can be demonstrated for up to 48 h after the onset of stroke (Heiss et al. 1992). Consequently, there is a rationale for initiating and continuing neuroprotective treatment up to 48 h after stroke onset, although to date, no clinical trial has been able to show a beneficial effect in acute stroke.

Since regional blood flow abnormalities tend to resolve in most cases after 3–4 days, it is likely that these areas are reperfused via collateral vessels that develop, or mature in the intervening time. During this period, cerebral autoregulation is deranged and consequently constant perfusion levels in the face of fluctuating systemic BP cannot be maintained. Collateralization may simply lead to reperfusion injury. It therefore would seem logical to protect patients during this time of collateralization and cerebral autoregulation derangement (i.e., for 3–4 days after onset) (Back 1998).

1.2.2.7 Neutrophil

Neutrophil leukocytes play a major role in the development and maturation of cerebral infarction and are involved in certain aspects of reperfusion injury (del Zoppo et al. 1991). Neutrophil adhesion is mediated by specific adhesion molecules that are essential in initiating the release of cytotoxins and controlling cellular activation. Monoclonal antibodies to these adhesion molecules (i.e., anti-CD11 and anti-CD18) also reduce infarction volume, but are unsuitable for clinical use because of their immunogenicity (Clark et al. 1991; Chen et al. 1994; Chopp et al. 1994).

Neutrophil leukocytes may also aggravate the ischemic injury by the release of the NOS inducible isoform (Table 1.1).

1.2.3 Atherosclerosis

1.2.3.1 Introduction

Atherosclerosis involves the aorta more extensively and earlier than other vessels and the abdominal aorta is more widely involved than the aortic arch or the thoracic aorta. The pulmonary, renal, and mesenteric arteries are least susceptible. Upper limbs are less frequently involved than lower limbs. Fatty streaks (the earliest lesion of atherosclerosis) may be seen in the aorta in infancy and early childhood. Lesions in the vertebral and intracranial arteries appear much later in life.

What makes certain segments of the vascular tree more prone to developing atherosclerosis than others is not entirely known. Local hemodynamic factors and rheological factors have been thought to be responsible. Atherosclerotic plaques tend to form at areas of low sheer stress, with bifurcations being particularly vulnerable (Strong 1992). However, it is possible that the vasculogenesis of the brachiocephalic arteries plays a role in determining the specific distributions where atherosclerotic changes later occur (Vol. 1, Chap. 1, p. 24).

The lesions of atherosclerosis occur principally in large and medium-sized elastic and muscular arteries.

Mönckeberg disease, also referred to as medial calcified sclerosis in atherosclerosis, commonly affects medium-sized arteries such as the radial, ulnar, and tibial arteries. It is characterized by calcifications in the tunica media.

1.2.3.2 Epidemiology

Extracranial carotid artery disease is more common in Caucasians than in Afro-Americans, Hispanics, and Chinese or Japanese (Table 1.4). Intracranial MCA occlusive disease occurs in younger people and more frequently in females, Asians and Blacks. Hypertension and diabetes are risk factors for arteriosclerosis that result in proliferative and hyaline changes in the arterioles. Smoking induces relatively dense fibrotic lesions, whereas hypercholesterolemia causes largely fat additions (Caplan et al. 1986) (Table 1.8).

1.2.3.3 Pathogenesis

Atherosclerosis is considered an inflammatory disease (Ross 1999). The process of atherogenesis consists of the accumulation of lipids within the arterial wall. The lesions of atherosclerosis represent a series of highly specific cellular and molecular responses that can best be described collectively, as an inflammatory disease (Ross1986, 1993a, b; Ross and Glomset 1973, 1976)

The microscopic appearance of atherosclerosis is characterized by raised thickenings that present characteristic histological features and cellular changes, depending upon the composition, location, and extension at the site of the lesion.

The various abnormalities begin with the earliest type of lesion, the so-called fatty streak, which is a purely inflammatory lesion, consisting only of monocyte-derived macrophages and T lymphocytes (Stary 1994). In persons with hypercholesterolemia, the influx of these cells is preceded by the extracellular deposition of amorphous and membranous lipids (Napoli et al. 1997; Simionescu et al. 1986).

Multiple observations point to the hypothesis that atherosclerosis is a response to injury in which the first insult is denudation of the endothelium (Ross 1973a). The most recent version of this hypothesis, however, emphasizes endothelial dysfunction rather than denudation (Ross 1999). Possible causes of endothelial dysfunction leading to atherosclerosis include elevated and modified low-density lipoprotein (LDL); free radicals caused by cigarette smoking, hypertension, and diabetes mellitus; genetic alterations; elevated plasma homocysteine concentrations; and a combination of these or other factors. Recently, it has been demonstrated that atheromatous plaques removed from carotid arteries frequently harbor infectious microorganisms such as herpes viruses and *Chlamydia pneumoniae*, despite negative serology. The cause of this association remains speculative (Ross 1999; Grayston et al. 1995).

Furthermore, epidemiological studies have shown a link between fetal growth and cardiovascular disease, with the risk of carotid artery stenosis being greater in people who weighed 6.5 lb or less at birth (Martyn et al. 1998).

1.2.3.4 Mechanisms of Atherogenesis

Atherogenesis is multifactorial. LDL retention is both necessary and sufficient to initiate atherogenesis. The response to retention theory maintains that the rate of LDL entry into the arterial wall is no different in the lesion-prone aorta compared to the nonlesion prone aorta (Williams and Tabas 1995). What is different, however, is the degree of retention of LDL at these sites, rather than the increase permeability to LDL (Table 1.9).

Whichever process is at work, each characteristic lesion of atherosclerosis represents a different stage in a chronic inflammatory process in the artery that, if, left unabated and excessive, will result in an advanced, complicated lesion (Ross 1981, 1986, 1993a; Ross and Glomset 1973, 1976). The compensatory responses alter the normal homeostatic properties of the

Table 1.9. Mechanisms of atherogenesis

Fatty streak	Inflammatory lesion	Ma-Tl, foam cells	Chlamydia pneumoniae, herpes
			Endothelial dysfunction in LDL metabolism Smooth muscle cell migration and proliferation Platelet activation Blood flow
Intermediate lesion	Migration and proliferation of smooth muscle	Ma-Tl ++	
Remodeling	Arterial wall thickening and vasodilatation	Ma-Tl ++++ release hydrolytic enzymes	
Fibrous plaque	++ Foam cells, proliferation of smooth muscle cells	Collagenized	
Fibrous cap	Restructuring of the lesion	Ma-Tl ++++++ release hydrolytic enzymes – focal necrosis	
Unstable fibrous plaque	Erosion of fibrous cap; hemorrhage, thrombus formation, occlusion	Ma-Tl +++++++	
Advanced complicated lesion	Core of lipid and necrotic tissue, ulceration, thrombosis, Ca^{++}, cholesterol crystals, emboli	Loss of compensation and arterial stenosis	

Ma-Tl, macrophages–T lymphocytes.

endothelium, resulting in increased adhesiveness of the endothelium with respect to leukocytes and platelets, as well as increased permeability. The injury also induces the endothelium to have procoagulant instead of anticoagulant properties and to produce vasoactive molecules, cytokines, and growth factors. In addition, macrophages also play a vital role in this fibroproliferative process by secreting growth factors such as PDGF, tumor necrosis factor alpha, interleukin-1 and fibroblast growth factor (FGF).

If the inflammatory response does not effectively neutralize or remove the offending agents, it may continue indefinitely, stimulating migration and proliferation of smooth-muscle cells that become intermixed with the area of inflammation to form an intermediate lesion.

If the response continues unabated, arterial wall thickening and gradual compensatory vessel dilation occurs, which up to a certain point maintains the luminal diameter. This phenomenon is termed remodeling (Glagov et al. 1987).

Throughout every stage of the disease, the response is mediated by monocyte-derived macrophages and specific subtypes of T lymphocytes

(Jonasson et al. 1986; van der Wal et al. 1989). As for inflammatory cells, granulocytes are rarely present during any phase of atherogenesis (Stary 1996).

Continued inflammation results in increased numbers of macrophages and lymphocytes migrating from the blood and multiplying within the lesion. Activation of these cells leads to the release of hydrolytic enzymes, cytokines, chemokines, and growth factors (Libby and Ross 1996; Raines et al. 1996), which induces further damage and eventually leads to focal necrosis (Falk et al. 1996). Repeated cycles of these events lead to enlargement and restructuring of the lesion, which eventually becomes a fibrous cap overlying a core of lipid and necrotic tissue, the so-called advanced complicated lesion. At some point, the artery can no longer compensate by dilation; the lesion may then intrude into the lumen and alter the blood flow (Ross 1999).

Various cell types and circumstances play an important and synergetic role in the formation of the atherosclerotic lesion (Ross 1992; Manjo and Joris 1994; Kocher et al. 1988; Davies 1993; Davies and Hagen 1994; Stebens 1995).

Endothelial Cells

Endothelial cells produce vasoactive agents such as nitrous oxide and prostacyclin; they also elaborate thrombomodulin and tissue plasminogen activator, which maintain the nonthrombogenic nature of the vessel wall. Endothelial cells can modify LDL and transport it across the endothelial lining and make it available to the macrophages for phagocytosis. Presence of apolipoprotein (a) is probably responsible (at least in part) for the dysfunction in the metabolism of LDL by the endothelium and early atherogenesis. Other cells such as mast cells, which affect LDL ingestion by macrophages, have some role in atherogenesis.

The role of endothelial cell dysfunction in the adherence of leukocytes, has been shown to be mediated by both the vascular endothelial addition molecule (VCAM-1), selective for monocytes, and by the transportation of lipoproteins, which they modify by an oxidative process, making them available for macrophages. Endothelial cells also take part in the coagulation process and secrete a number of cytokinases that induce the expression of genes for various mitogens (e.g., PDGF, IL-1, etc.), most of which are important for the development and progression of fatty streaks.

Smooth Muscle

Smooth-muscle cells, under the influence of certain stimulants, also secrete growth factors and act as the main connective tissue component within the plaque. Monocytes, when activated, synthesize and secrete a variety of very active agents, including growth factors and mitogens that may act on other cell types within the lesion, and in addition, they may induce free-radical production. Platelets also contain several growth factors or mitogens and play a prominent role in the coagulation process (pro- and anticoagulants), resulting in hemorrhage or thrombosis within the

plaque. Lymphocytes, predominately T cells, when activated, play an important role in the immune or autoimmune response.

Platelets

Platelets are important in maintaining vascular integrity in the absence of injury and protect against spontaneous hemorrhage. Activated platelets can accumulate on the walls of arteries and recruit additional platelets into an expanding thrombus. An important component of the platelets is the glycoprotein IIb/IIIa receptors, which belong to the integrin superfamily of adhesion-molecule receptors and appear on the surface of platelets during platelet activation and thrombus formation. These receptors serve an important hemostatic function and antagonists to them prevent thrombus formation in patients who have had a myocardial infarction (Badimon et al. 1997).

Platelet adhesion and mural thrombosis are critical in the initiation and generation of the lesions of atherosclerosis (Ross 1993a). Platelets adhere to dysfunctional endothelium, exposed collagen, and macrophages. When activated, platelets release their granules, which contain cytokines, and growth factors, which together with thrombin may contribute to the migration and proliferation of smooth muscle cells and monocytes (Bombeli et al. 1998). Activation of platelets leads to the formation of free arachidonic acid, which can be transformed into prostaglandins such as thromboxane A, one of the most potent vasoconstricting and platelet-aggregating substances known, or lead to the formation of leukotrienes, which can amplify the inflammatory response.

Blood Flow

The nature of the blood flow (i.e., the presence of high shear stress or turbulence or decreased flow) appears to be important in determining whether lesions occur at the various vascular sites. Changes in flow alter the expression of genes that have elements in their promoter regions that respond to shear stress. For example, the genes for intercellular adhesion molecule-1 (Nagel et al. 1994), platelet-derived growth factor B (Resnick et al. 1993), and tissue factors (Lin et al. 1997) in endothelial cells have these elements, and their expression is increased by reduced shear stress (Mondy et al. 1997). Thus, alterations in blood flow appear to be critical in determining which arterial sites are prone to have lesions (Gotlieb and Langille 1996; McMillan 1985; Nakashima et al. 1998). Monocytes and T cells adhere at these sites, as a result of the activation of adhesion molecules on both the endothelium and the leukocytes.

1.2.3.5 Fatty Streak

Atherosclerosis develops as patches within the intima, often in the region of flow disturbances, especially near arterial bifurcations. Monocytes transform into macrophages and phagocytes, the lipid-forming foam cells. Simultaneously, there is migration of smooth-muscle cells from the media into the intima (under the influence of PDGF), where some cells

participate in the process of phagocytosis, while others remain activated or undergo myotrophic changes. Smooth-muscle cells may exist as one of two different phenotypes: the contractile or the proliferative form. The proliferative form is prominent in lesions, which are clinically irrelevant, but is a major problem after restenosis following revascularization and is responsible for intima hyperplasia (Pickering et al. 1993).

1.2.3.6 Fibrous Plaque

Once the fatty streak is formed, it may progress into a fibrous plaque, regress and disappear, or remain unchanged. As the lesion progresses, ongoing migration of lymphocytes and monocytes continues into the fatty streak. There is further accumulation of foam cells and proliferation of smooth-muscle cells. The lesion increases in size as collagen bundles, elastic fibers, and other matrix proteins are laid down in the lesion. Platelets may adhere to the endothelial layer and attain a subendothelial location. This lesion is referred to as a fatty plaque in its early stages and as a fibrous plaque as it becomes collagenized.

1.2.3.7 Unstable Fibrous Plaques

Rupture of the fibrous cap or ulceration of the fibrous plaque can rapidly lead to thrombosis. This usually occurs as a result of erosion or uneven thinning and rupture of the fibrous cap, often at the shoulders that cover the advanced lesion where macrophages enter, accumulate, and are activated, and where apoptosis may occur (Fuster 1994; Lee and Libby 1997). Thinning of the fibrous cap is apparently due to the continuing influx and activation of macrophages, which release metalloproteinases and other proteolytic enzymes. These enzymes cause degradation of the matrix, which may lead to hemorrhage from the vasa vasorum or from the lumen, which in turn may cause thrombus formation and occlusion of the artery.

Stable advanced lesions usually have uniformly dense fibrous caps. Potentially dangerous lesions are often nonocclusive and thus are more difficult to diagnose by angiography. At autopsy, active inflammation is evident by the accumulation of macrophages at sites of plaque rupture (Davies 1990).

1.2.3.8 Complicated Plaque

Complicated plaque refers to a more advanced lesion, with areas of ulceration and/or thrombosis, with or without calcium deposits. Calcified deposits will appear and may be accompanied by areas of necrosis, thrombosis, hemorrhage, and cholesterol crystals. Vascularization from the vasa vasorum may be present (WHO/ISFC 1997; Ross 1992; Manjo and Joris 1994).

The chemical composition of the plaque does not seem as important as plaque size, degree of stenosis, or plaque ulceration. A high incidence of microembolic events, as measured by Doppler ultrasonography, may occur with plaque ulceration. Plaque rupture occurs at the site of high ten-

sor stress, the junction of the fibrous cap, and the necrotic core with the surrounding normal intima. Following plaque rupture, a cascade of events may result in mural thrombosis, dislodgment of thrombi and/or multiple distal emboli. Following plaque rupture, the necrotic core is exposed and is highly thrombogenic, releasing various tissue factors. Various other hematological factors such as fibrinogen levels, blood viscosity, lipoprotein (a), and plasminogen activator inhibitors are also implicated in this process.

1.2.3.9 Carotid Atherosclerosis

The formation of atherosclerosis of the carotid arteries is multifactorial. In addition to the previously described factors, the development of atherosclerosis depends largely on the fluid dynamics within the carotid artery. Disease develops principally in the region where wall sheer stress is lowest (i.e., in the zone of flow separation), in relation to complex flow patterns associated with whirlpools, which form near the lateral wall of the bifurcation and extend into the carotid sinus. With time, the lesions progress, thicken, and often become complicated plaques, leading to severe stenosis, with or without ulceration. As the stenosis increases, the plaque becomes ulcerated and as thrombi form, the possibility of distal thromboembolic migration or obliteration of the carotid lumen increases, with potentially serious clinical consequences (Stebens 1995; Glasgov et al. 1988).

1.2.3.10 Conclusion

Cells involved in atherogenesis may express different constellations of genes and therefore vary phenotypically, depending on their environment. Newly developed techniques for DNA analysis should help identify which genes are expressed and in what patterns, information that should help us to decipher the complex nature of atherogenesis (Shalon et al. 1996; Ramsay 1998). Patterns of gene expression may vary between different people or between lesions at different sites in the same individual. Because atherosclerosis is a multifactorial disease, understanding patterns of gene expression may help to explain differences in susceptibility to agents that cause disease as well as differences in response to therapy.

Atherosclerosis is clearly an inflammatory disease and does not result simply from the accumulation of lipids. If we could selectively modify the harmful components of inflammation in the arteries and leave the protective aspects intact, we might create new avenues for management in the 50% of patients with cardiovascular disease who do not have hypercholesterolemia (Ross 1999).

Table 1.10. Summary of CT and MRI findings in atheroembolic infarction (from Montanera et al. 1998)

Time from symptom onset	CT	MRI
Hyperacute (<6 h)	Hyperdense middle cerebral artery	Diffusion-weighted MRI Perfusion abnormalities Absence of normal flow void Intra-arterial enhancement
Acute (<24 h)	Loss of gray-white matter differentiation Sulcal effacement	Hyperintensity on T2-weighted SE Cortical thickening Sulcal effacement
1–7 days	Wedge-shaped, hypodense	More conspicuously bright on T2-weighted SE
	Known vascular territory	Hypointense on T1-weighted SE
	Cortex and white matter	Bright cortical ribbon on T1-weighted SE
	Up to 20% hemorrhage	Mass effect more prominent
	Onset of patchy or gyral enhancement at 3–4 days Mass effect	
1–8 weeks	Gyral enhancement	Gyral enhancement may persist
	Mass effect has peaked, begins improving	Mass effect less prominent
		T1-weighted bright cortical ribbon begins to improve
Months to years	Lower attenuation	Encephalomalacia showing tissue loss and high T2-weighted signal
	Better defined margins	± Old blood products
	Loss of cerebral tissue volume	Wallerian degeneration
	Wallerian degeneration	

1.2.3.11 Neuroimaging of Ischemic Stroke

Imaging of stroke is beyond the scope of this volume; multiple examples are given throughout the book, and to avoid repetition the information is in the specific part of the text. Table 1.10 summarizes pertinent computed tomography (CT) and magnetic resonance imaging (MRI) findings in atheroembolic infarction. There are, however, a number of imaging techniques that will be addressed in this section.

Positron Emission Tomography

Presently, work is underway in a variety of fields to accurately measure human cerebral blood flow.

All evaluations of human cerebral blood flow and metabolism are based on the same principles. The accuracy of such measurements is de-

pendent upon the spatial and temporal resolution of the technique, as well as the sampling volume. Typically, in high-resolution techniques, spatial resolution and sampling volume are inversely related.

Positron emitting isotopes are usually produced in local cyclotrons. Their very short half-life, ranging from seconds to minutes, significantly limits their applications. The isotopes are chemically integrated into radiopharmaceuticals with known biological behavior. The resultant compounds are injected intravenously or inhaled, and data collected by the PET instrument is displayed as a 2-D or 3-D tomographic map.

Typical isotopes include oxygen-15, carbon-11, nitrogen-13, and fluorin-18.

At present, PET is used to measure cerebral metabolism, blood flow and volume, oxygen utilization, amino acid incorporation, neurotransmitter synthesis, and receptor binding (Mazziotta et al. 1997). However, PET is not universally available.

1.2.4 Ischemic Stroke Treatment

1.2.4.1 Medical Treatment of Acute Stroke

In the past, medical management with respect to ischemic stroke was primarily geared towards prevention, support, and rehabilitation. A new era, which uses a proactive approach to therapy, is evolving, and the healthcare community is starting to take a much more active role in the immediate diagnosis and treatment of acute ischemic stroke.

Until recently, the only therapy for patients who suffered an acute stroke was general supportive management. This included maintaining blood pressure, protecting the airways, achieving adequate oxygenation, avoiding dehydration and hyperglycemia, treating seizures, and reducing temperature. The decision to use anticoagulants depended upon the diagnostic imaging findings (presence of hemorrhage, large area of infarction, etc.) (Brandt et al. 1995).

A new era in acute stroke therapy began with the availability of recombined tissue plasminogen activator (r-TPA) in 1996. Data obtained from the National Institute of Neurological Disorders and Stroke (NINCDS) trial demonstrated that intravenously administered (IV) r-TPA within 3 h of the onset of stroke improved functional outcome at 3 months (NINCDS 1995), a duration that has now been extended to 1 year (Kwiatkowski et al. 1999). In order to treat patients in the limited therapeutic window, several mechanisms must be in place, including emergent patient evaluation and imaging, in addition to the availability of a monitored care setting with personnel trained in acute stroke management. Moreover, education is essential. The public needs to be able to recognize stroke symptoms in order to obtain emergency evaluation.

The role of IV versus intra-arterial (IA) treatment is evolving. While the IV route has the advantage of providing universal access, the indications for IA revascularization continue to increase.

A better understanding of the pathophysiology of stroke may offer opportunities beyond the hyperacute stage.

1.2.4.2 Thrombolytic Therapy: Introduction

One of the newest treatments during the acute phase of ischemic stroke is the use of thrombolytics. These agents can be administrated either by the IV or IA route or in combination.

While many additional agents are being developed, presently there are four primary agents: streptokinase, urokinase, recombined tissue plasminogen activator (r-TPA) and pro-urokinase. Their half-lives vary from 80 to 6 min.

The half-life of the various thrombolytic agents may play a role in deciding if and when a particular agent should be used. In cases in which recirculation would be counterproductive such as in patients with longer arterial occlusion time, streptokinase should not be employed, since recirculation may extend beyond 6 h. This may account for the high frequency of hemorrhagic complications in the MASTE trial (Theron et al. 1990).

With a 6-min half-life, r-TPA appears to be much more favorable in the lenticulostriate stroke group, when injected as a bolus rather than a slow infusion. In addition, it is particularly useful in the frequently encountered situation when treatment (IA thrombolysis) can only offered approximately 5 h after onset of symptoms (Table 1.11).

1.2.4.3 Thrombolytics (IV)

Despite recent encouraging results with IV r-TPA, there is presently no widely applicable treatment for the majority of patients with acute ischemic stroke, when they present 3 h after the onset of symptoms (NINCDS 1995).

1.2.4.4 Recombined Tissue Plasminogen Activator

The results of the NINDS r-TPA study support the use of this medication in patients who can be evaluated and treated within the first 3 h after the onset of stroke.

While intravenous r-TPA is not the ideal therapy for acute ischemic stroke, its beneficial effect should be characterized as more than just

Table 1.11. Thrombolytics

Agent	Administration	Half-life	Dosage
Streptokinase	IA	60–80 min	–
Urokinase	IA	9–12 min	1–2,000,000 IU
r-TPA	IV, IA	6 min	10 mg
Abciximab (ReoPro)	IV, IA	Long, 12 h	IV 10 mg bolus, IA 4 mg
Aspirin	PO, IV	15–20 min	–
Heparin	IV, SC	60 min	–
Coumadin	PO	1.5–2.5 days	–

IV, intravenous; IA, intra-arterial.

modest (NINCDS 1995). The study results indicate substantive relative differences between the treatment groups; 32%–55% of patients treated with r-TPA returned to normal or virtually normal clinical status 3 months after the ictus, an 11%–13% absolute increase compared to the control group (NINCDS 1995). This was a statistical improvement in outcome based on direct comparisons of the various parameters studied (National Institutes of Health Stroke Scale, modified Rankin Scale, Barthel Index, and Glasgow Outcome Scale). Analysis of the median National Institutes of Health Stroke Scale score 24 h after therapy revealed considerably better results ($p<0.002$) in patients treated with r-TPA. It is reasonable to assume that such early gains translate into more clinically relevant function 3 months later, and these improvements were sustained at 1 year (Kwiatkowski et al. 1999). Similar benefits were seen in the European Cooperative Acute Stroke Study (ECASS) (Hacke et al. 1955) when data were analyzed according to the NINDS r-TPA trial criteria. The increased risk of intracerebral hemorrhage when utilizing r-TPA was associated with several factors, including stroke severity, early changes indicative of infarction on baseline CT scans, and uncontrolled hypertension (Anonymous 1995; Hacke et al. 1995). While this risk of hemorrhage is of great concern, and while in the NINDS r-TPA trial more fatal hemorrhages occurred in the treated than in the placebo group (2.9% vs. 0.3%), the incidence of such hemorrhages was actually less than anticipated before the study began; despite this complication, the overall mortality rate at 3 months was slightly lower in the treated group than in the placebo group (17% vs. 21%, respectively) (Anonymous 1995).

There are substantial restrictions to the use of IV r-TPA treatment for acute ischemic stroke and r-TPA should not be given to every patient presenting to the emergency department with an acute stroke. In fact, this medication will be used infrequently if strict NINDS criteria are applied. Of 17,324 patients screened in the NINDS r-TPA trial, only 624 patients fulfilled the inclusion criteria (Boissel 1996; Hacke et al. 1997). Nonetheless, the positive risk–benefit ratio of the study (Anonymous 1995; Furlan and Kanoti 1997) indicates that for appropriately selected patients, IV r-TPA should be given.

1.2.4.5 Streptokinase

Streptokinase is no longer used in stroke management, due to its long half-life of 60–80 min and increased hemorrhagic complication rates. The relative fibrin-bound plasminogen specificity of r-TPA, as opposed to the circulating plasminogen activation of streptokinase, and r-TPA's shorter half-life (Verstraete and Collen 1986) have made the use of streptokinase problematic.

1.2.4.6 Antiplatelets

Platelets are important in maintaining vascular integrity in the absence of injury and protecting against spontaneous hemorrhage. Activated platelets can accumulate on arterial walls and recruit additional platelets into an expanding thrombus. Antiplatelet agents are a heterogeneous class of drugs that have been used successfully in stroke prevention for more than two decades.

Antiplatelet therapy for acute stroke, except for aspirin, has received little attention until very recently. There has been a general reluctance to employ any aggressive therapeutic strategy for the treatment of acute cerebral ischemia. This reluctance originates from the long-standing belief that the therapeutic window of opportunity for stroke was too short to realistically expect that any intervention could improve the natural history of the disease. This philosophy surfaced in the early 1960s when attempts to treat stroke with thrombolytics (streptokinase) and anticoagulants resulted in an increased mortality rate (Bednar and Gross 1999). An improved understanding of the pathophysiology of stroke, along with the development of stroke animal models, has permitted significant advancement in our understanding of various therapeutic options and their appropriate applications.

In the early 1980s, the concept of intensity–duration of cerebral ischemia was established. That is, the greater the intensity of the ischemic event the less time is necessary to demonstrate the same degree of permanent injury (Jones et al. 1981). The results of this study suggest the maximal time frame for treatment of acute ischemic stroke to be in the range of 6 h rather than the previously accepted time frame of 24–48 h. Antiplatelet agents (i.e., aspirin) and thrombolytics have been successfully used in the treatment of acute myocardial infarction (MI) and were shown to reduce mortality. The combined use of antiplatelet agents and thrombolytics was also found beneficial (Verstraete 1991; ISIS-2 1988). The success of these therapies in treatment of acute myocardial infarct suggests that they may play a major role in the treatment of ischemic stroke.

In experimental animals with acute cerebral ischemia, antiplatelet therapy has been recently combined with thrombolytics, and in humans it has been used in the treatment of MI (MAST-I 1995). Dual therapy of antiplatelets and thrombolytics improved the patency rate and reduced infarct size when compared with thrombolytic therapy alone (Umemura et al. 1993; Bednar and Gross 1999). The rationale for the use of adjuvant therapy in acute stroke is based upon the urgent need for treatment within the 3- to 6-h window of opportunity (IV or IA), as well as to prevent reocclusion.

Aspirin

Aspirin only partially inhibits platelet aggregation by inhibiting the production of the potent vasoconstrictor and platelet activator, thromboxane A (TXA) sub 2 relative to prostacyclin, a vasodilator and platelet inhibitor (Coller 1955).

Although aspirin therapy has been conclusively shown to reduce both the incidence of and mortality from MI, irrespective of the dose administered (Anonymous 1988), there is considerable controversy surrounding the optimal dose of aspirin for stroke prevention following TIAs (Barnett et al. 1996; Hart 1996; Dyken et al. 1992; CAPRIE Steering Committee 1996). Indeed, in some clinical studies, high-dose (15–20 mg/kg) aspirin therapy was more effective than low-dose aspirin in preventing stroke after TIA. Although there is some controversy concerning these studies (Bednar and Gross 1999), the effects of higher doses of aspirin on the arachidonic acid (AA) cascade are well accepted and include the complete inhibition of both TXA sub 2 and prostacyclin production.

Adenosine Receptor Antagonists

Ticlopidine hydrochloride and clopidogrel selectively inhibit the binding of adenosine diphosphate to its platelet receptor and block adenosine diphosphate-dependent platelet activation (Fitzgerald and Patrono 1998).

These platelet inhibitors inactivate only one pathway of platelet activation. Despite optimal inhibition of a specific pathway, platelet activation occurs through other pathways. Regardless of the stimulus for activation, platelet-to-platelet interaction and thrombus formation is ultimately regulated through the glycoprotein (GP) IIb/IIIa receptor complex. These observations provide the rationale for pharmacological intervention directed against the GP IIb/IIIa receptor.

Platelet Glycoprotein IIb/IIIa Receptor Antagonists

Platelets play a critical role in thrombus formation. Platelet function depends upon the interactions of membrane glycoproteins (GPs) that act as receptors for adhesive proteins and appear on the surface of platelets during platelet activation and thrombus formation. These receptors serve an important hemostatic function (Badimon et al. 1997). The most abundant receptors are the integrin superfamily of adhesion-molecule receptors, which include GP IIb/IIIa (fibrinogen), fibronectin, and vitronectin receptors. The integrins consist of heterodimeric molecules composed of α and β subunits (Hynes 1992). The surface of the resting platelet contains 50,000–80,000 copies of the GP IIb/IIIa (α-sub IIb and β-sub IIIa) receptor (Lefkovits et al. 1995; Marcus 1996). Agonists of platelet activation facilitate the configurational changes necessary for the receptor to become receptive to fibrinogen, Von Willebrand factor, and vitronectin (Plow et al. 1985). The ligands all contain the identical peptide sequence, arginine-glycine-aspartic acid (single-letter code, RGD). Fibrinogen is by far the most important ligand for IIb/IIIa, probably because of its high plasma concentration (Marcus 1996). Fibrinogen simultaneously binds to GP IIb/IIIa receptors on two separate platelets (Plow et al. 1987), resulting in platelet cross-linking critical to platelet aggregation (Table 1.12).

The platelet glycoprotein (GP) IIb/IIIa receptor is the final common pathway of platelet aggregation.

Table 1.12. Glycoprotein IIb/IIIa receptor

		Reversibility without platelets	Reversibility with platelets
Abciximab (ReoPro)	Monoclonal antibody	12 h	Yes
Eptifibatide	Peptide receptor antagonist	4–6 h	No
Tirofiban	Nonpeptide receptor antagonist	>4 h	No

Table 1.13. Glycoprotein IIb/IIIa antagonist

	Platelets bound half-life	Plasma half-life
Abciximab (ReoPro)	Long (hours)	Minutes
Eptifibatide	Short (minutes)	2.5 h
Tirofiban	Short (seconds)	1.8 h

The pathways of platelet activation indicate platelet-activating factors (PAF): adenosine diphosphate (ADP) → thromboxane A (TXA) → GP IIb/IIIa, glycoprotein IIb/IIIa; and epinephrine (Fuster et al. 1992).

Immediately (within 1–24 h) after spontaneous or mechanical injury, thrombosis with platelet deposition and fibrin formation begins. It is usually mural and subocclusive (Falk 1991). Plaque disruption activates the coagulation cascade leading to thrombin generation, and thrombin generated by arterial injury is a powerful platelet activator. Exposures of deeper components of atherosclerotic plaques (collagen, tissue necrosis factor, etc.) are also potent platelet stimuli. Foreign devices that damage the endothelium such as angioplasty balloons used for dilatation and/or stents will further stimulate platelet aggregation. These receptors serve an important hemostatic function, and antagonists to them prevent thrombus formation (Badimon et al. 1997).

Glycoprotein IIb/IIIa receptor antagonists include (a) the monoclonal antibody abciximab; (b) the peptide receptor antagonist eptifibatide; and (c) the nonpeptide receptor antagonists tirofiban and lamifiban. Numerous oral nonpeptide mimetics of the GP IIb/IIIa receptor antagonists are in clinical development and may replace present antiplatelet regimes used prior to endovascular interventions (Tables 1.12, 1.13) (Vorchheimer et al. 1999).

Present knowledge on the value of GP IIb/IIIa receptor antagonists comes from the cardiac literature. Individual experiences on the effectiveness of these antagonists used after embolic complications in the cerebral circulation appear to support its benefit in the management of cerebral ischemia and stroke (Connors 2000). Microvascular thrombosis occurs as an ongoing, dynamic process after the onset of stroke. Even if the site of major arterial occlusion is recanalized after the acute occlusion, thrombosis at the microvascular level may continue to occur at distal sites, reducing postischemic flow and contributing to ongoing neuronal

death. Choudhri and co-workers (1998) measured the effects of GP IIb/IIIa receptor antagonists (SDZ GPI 562) 23 h after reperfusion. These antagonists were administered before and after the onset of MCA occlusion in a murine stroke model for a duration of 45 min. When the antagonist was administered immediately before MCA occlusion, platelet accumulation was reduced by 48%, and fibrin accumulation was reduced by 47%. GPI 562 exhibited a dose-dependent reduction of cerebral infarct volumes, as well as improvement in postischemic cerebral blood flow. GPI 562 was shown to reduce cerebral infarct volumes by 70%. There was an increase in intracranial hemorrhage (ICH) at the highest doses tested when the antagonist was given immediately after the withdrawal of the MCA occluding suture. The cause may be the immediate reperfusion.

The efficacy of platelet IIb/IIIa inhibitor, when used for stenting, has been evaluated in the EPISTENT (coronary) trial of abciximab (ReoPro) in which 2,399 patients underwent elective coronary stenting. The primary end points (composite 30-day death, MI, or urgent need for revascularization) occurred in 10.8% of patients treated with stent plus placebo, but in only 5.3% of those in the stent plus abciximab group ($p<0.001$), and in 6.9% of those treated by balloon angioplasty plus abciximab ($p=0.007$; PARADIGM Investigators 1998). In this study, as in all others, treatment benefits were observed within hours following intervention and were sustained after 6–12 months, regardless of revascularization technique. These findings strongly suggest that treatment with glycoprotein IIb/IIIa receptor antagonists is beneficial in the setting of stent implantation at the coronary artery level.

The routine use of antiplatelets such as ticlopidine prior to carotid angioplasty and stenting (CAS) is well accepted. Although the effectiveness of GP IIb/IIIa is still anecdotal, the ability of these agents to revascularize at the time of occlusive complications (even when thrombolytics were unable to do so) has been very impressive. Many investigators involved in cerebral revascularization are therefore following the cardiac experience of prophylactic use of abciximab (ReoPro) (Lilly Research Laboratories, Indianapolis, IN, USA) in high-risk patients.

This group of drugs can also be used in selective cases where thrombus is forming at the site of an endovascular device (Fig. 14.101).

One of the most intriguing aspects undergoing investigation involves the choice of antiplatelet agent. Only aspirin was used in the CEA trials, and retrospective evidence suggests that the perioperative morbidity could have been reduced if high-dose aspirin (650 mg twice daily) had been used in all surgical patients. A combination of aspirin and ticlopidine has been shown to be even more effective than a combination of aspirin plus anticoagulation in coronary angioplasty and stenting (Mendelsohn et al. 1998). The value of the newer glycoprotein GP IIb/IIIa receptor antagonists (GPA) may be of even greater benefit.

Adjunctive Heparin. Heparin is administered routinely during interventional procedures. The low-dose, weight-adjusted regimen used in the EPILOG study [70 U/kg bolus, target activated clotting time (ACT) of over 200 s] was associated with the most favorable risk–benefit profile (Anonymous 1997).

In the absence of specific data regarding heparinization, this heparin regimen can also be used for patients undergoing interventional procedures treated with GP IIb/IIIa receptor antagonists (Anonymous 1994; Aguirre et al. 1995). The optimal parameters and duration of unfractionated heparinization to be used with GP IIb/IIIa receptor antagonists has not been determined. It is unknown whether low-molecular-weight heparin or other direct thrombin inhibitors would prove safer and more effective than unfractionated heparin in conjunction with GP IIb/IIIa receptor antagonists (Vorchheimer et al. 1999). Several coronary trials studied GP IIb/IIIa receptor antagonists used in conjunction with thrombolytics. These small pilot trials showed acceptable safety profiles and modest benefits in angiographic or electrocardiograph markers of reperfusion, but no differences in major clinical end points (Ohman et al. 1997; PAPADIGM Investigators 1998). More recent cardiac trials are studying the role of abciximab (ReoPro; Lilly Research Laboratories, Indianapolis, IN, USA) combined with lower-dose thrombolytic agents for MI patients in an ER setting. The results of abciximab plus half-dose (50 mg) accelerated tissue-type plasminogen activator showed no increase in complications or cerebral hemorrhage (Antman et al. 1998). We would like to caution the use of multiple agents and combination agents in neurological applications, until we learn more about the interaction and synergism of such combinations.

Safety of GP IIb/IIIa Receptor Antagonists. The safety of GP IIb/IIIa receptor antagonists has been evaluated and no increase in intracerebral hemorrhage has been observed. The majority of the reported bleeding events occurred at the vascular access puncture sites in patients undergoing percutaneous interventions. Reduction in the heparin dose to a level whereby the activated partial thromboplastin time (PT) would be between 2.0 and 2.5 times control is recommended at the time of percutaneous interventions. A target-activated partial thromboplastin time (PTT) of 70 s or an activated clotting time (ACT) of 300 s during percutaneous coronary interventions reduced the incidence of vascular access site complications to levels comparable to controls (Investigators 1997). In emergencies, the use of platelet transfusion may be life saving. However, the need for platelet transfusion to treat life-threatening bleeding is extremely uncommon (Vorchheimer et al. 1999).

For patients undergoing percutaneous interventions with abciximab plus low-dose heparin, platelet transfusions were required in 2.1% of patients in the CAPTURE study (Anonymous 1997).

Platelet transfusions may be required for patients treated with GP IIb/IIIa receptor antagonists undergoing urgent surgery. Thrombocytopenia as a side effect when using GP IIb/IIIa receptor antagonists appears to be higher (0.4%–1.4%). In a composite analysis of all abciximab trials, the incidence of thrombocytopenia increased from 0.35% to 1.0% in patients treated with GP IIb/IIIa receptor antagonists.

In patients receiving abciximab, platelet transfusions may be required. Since the onset of profound thrombocytopenia is generally acute, platelet counts should be measured within the first 2–4 h after a GP IIb/IIIa receptor antagonist has been administered and should be followed through-

out the course of therapy (Vorchheimer et al. 1999). It is unclear as to whether the abciximab antibody can be readministered without a significant increase in the incidence of immunological reactions (Coller 1997; Madan et al. 1997). Preliminary results of a prospective registry of 4,500 patients undergoing percutaneous coronary intervention, including approximately 500 patients receiving abciximab readministration, showed both a similar efficacy and incidence of hypersensitivity and anaphylaxis as compared to first-time abciximab recipients. There was also no significant increase in the incidence of severe thrombocytopenia (Tcheng et al. 1998).

1.2.4.7 Coumadin Versus Aspirin

The efficacy of warfarin versus aspirin for the prevention of major vascular events, including ischemic stroke, myocardial infarction, or sudden death, has been studied in the Warfarin Versus Aspirin Symptomatic Intracranial Disease Study. It included patients who were symptomatic with 50%–99% stenosis of a major intracranial artery (carotid; anterior, middle, or posterior cerebral; vertebral; or basilar). Kaplan–Meier analysis showed a significantly higher percentage of patients free of major vascular events among patients treated with warfarin (p=0.01). Five out of 88 patients (5.4%) treated with warfarin had a stroke over a mean 19-month follow-up, compared with 14.3% of patients treated with aspirin who suffered a stroke in the territory of the stenosis. An additional 9.5% suffered a stroke in a different territory than the stenosis, for a combined stroke rate of 23.8%.

Major hemorrhagic complications occurred in three patients on warfarin (including two deaths), during 166 patient-years of follow-up and in none of the patients on aspirin during 143 patient-years of follow-up. This study suggests a favorable risk–benefit ratio for warfarin compared with aspirin for the prevention of major vascular events in patients with symptomatic intracranial large-artery stenosis (Chimowitz et al. 1995).

1.2.4.8 Neuroprotective Agents

The role of neuroprotective agents is one of the more active areas of basic and clinical research in the treatment of ischemic stroke. We will review some of the principles and potential applications of these agents proposed for use at the time of ischemic brain management (Dyker and Lees 1998).

It is likely that the lack of efficacy of thrombolysis beyond 3 h results at least in part from reperfusion injury and the potential of hemorrhagic transformation of the infarcted tissue. Because both free-radical scavengers and leukocyte adhesion inhibitors may reduce reperfusion injury, they should be considered as possible adjuvant therapy in combination with thrombolytic treatment. Reperfusion promoted by thrombolytic drugs probably occurs within at most a few hours of drug administration, and spontaneous reperfusion may occur up to a few days after occlusive stroke. If combination therapy with a neuroprotective agent and a throm-

bolytic drug is contemplated, it should be sufficient to initially administer the drugs together and then maintain treatment with the neuroprotective agent for 2–3 days. The addition of neutrophil adhesion inhibitors such as certain antibiotics may be of benefit in intra-arterial treatment of stroke.

Cytotoxic injury following ischemic stroke evolves over at least 4 h in rodents and possibly beyond 48 h in humans. In addition, autoregulation and local cerebral perfusion are deranged for approximately 72 h in patients with stroke. At present, little is known about the effect of stroke on the integrity of the BBB, which is crucial in determining the penetration of less lipophilic compounds into the brain. In acute cerebral ischemia, hydrophilic compounds may cross the BBB and thus enter infarcted or ischemic tissue. Neuroprotection should probably be provided during this critical time. A number of neuroprotective compounds are in the advanced stages of clinical development after encouraging results from preclinical studies (Dyker and Lees 1998). There has been, however, no consistent approach to dosing schedules, optimal type of compound, or combinations for these novel treatments.

In animal models of stroke and in humans, the effects of cerebral ischemia are manifested on the cerebral metabolism rapidly, with a time scale measured in minutes or hours (Pulsinelli et al. 1982; Heiss 1983; Astrup et al. 1981).

Any form of potential neuroprotective treatment should therefore be given by the most rapidly effective route, which in practice means intravenously. In an ideal scenario, neuroprotective plasma and central nervous system levels of drugs would be attained immediately. This is widely recognized and is supported by the results of recent thrombolysis trials (NINCDS 1995; Hacke et al. 1995; Hommel et al. 1995; MAST-I Group 1995) and by meta-analysis of the nimodipine trial results (Mohr 1994). The outer therapeutic time limit will be established only by large-scale trials of a proven therapy that does not carry the risks associated with thrombolysis. Other questions that remain include how long and by what route adjuvant therapy should be administered.

The optimal duration and route of administration of treatment will depend on the individual pharmacokinetic properties of the neuroprotective compound, on the adverse-effect profile of the drug, and on the nature of the insult that gave rise to the stroke. For example, it would be desirable to maintain neuroprotection throughout recurrent episodes of cerebral ischemia, i.e., recurrent cardiac embolism. Neuroprotectives may play an important role in the endovascular suite, where some of these agents could be used prophylactically or at the time of an accidental vascular occlusion.

1.2.4.9 Pharmacological Properties of Neuroprotective Drugs

Ideally, any compound utilized in the treatment of stroke should adequately cross the BB in order to obtain therapeutic levels within brain tissue and the CSF. Highly lipid soluble drugs penetrate the cerebral tissues more rapidly and are cleared more slowly from neural tissue when compared to hydrophilic agents (Steinberg et al. 1994).

Although drugs with slow clearance from the brain tissue are more likely to accumulate and lead to toxic side effects if given by constant intravenous infusion, they will provide a longer protection than if given by single-bolus injection (Steinberg et al. 1994). There may be some advantages if they are given intra-arterially in appropriate circumstances.

1.2.4.10 Binding Properties

The mechanism of action at the cellular level of any particular agent will determine whether constant exposure to a drug is necessary or indeed desirable. Free radicals are thought to play a role in mediating ischemic neuronal damage and, in particular, reperfusion injury. The combination of ischemia, a rich supply of metal complexes (e.g., iron from hemoglobin) and a paucity of free-radical neutralizing enzymes (superoxide dismutase, catalase, and glutathione peroxidase) within the brain, predispose to free-radical-mediated neuronal damage. Tirilazad, a synthetic 21-aminosteroid, has free-radical scavenging activity, analogous to that of vitamin E. It also has antioxidant effects, inhibiting the generation of hydrogen peroxide and blocking the release of arachidonic acid from injured cell membranes. In animal models of stroke, tirilazad has reduced the volume of infarction after MCA occlusion in rats (Investigators 1996). Although extensive research is underway in this area, no definitive drugs or regimens are presently available.

Magnesium may block the influx of calcium into ischemic neurons and has been shown to be neuroprotective in animal models. It is inexpensive to produce and appears to be well tolerated in initial patient pilot studies (Wester et al. 1984; Muir and Lees 1995a, b). Magnesium has been used without ill effects in over 50,000 patients after acute myocardial infarction (Collins et al. 1995).

While tremendous research efforts are being made with respect to neuroprotective agents, no clinically applicable benefit has so far been demonstrated.

1.2.4.11 Angiographic Evaluation

A detailed angiographic examination of the vascular anatomy, including the collateral circulation at the circle of Willis and the leptomeningeal levels is performed and includes an analysis of the brain parenchyma vascularization (Theron et al. 1992)

An aortic arch study to demonstrate the status of the arch and the origin of the brachiocephalic vessels in two views (Fig. 1.2) can be very informative, as these cohort of vasculopathic patients usually have multifocal involvement.

A second arch injection is administered, centering on the neck; the brachiocephalic vessels are grossly visualized on the aortic arch study (Fig. 1.3, same patient as Fig. 14.150).

A third arch injection is administered, centering on the head, frontal, and lateral projections to look at the brain.

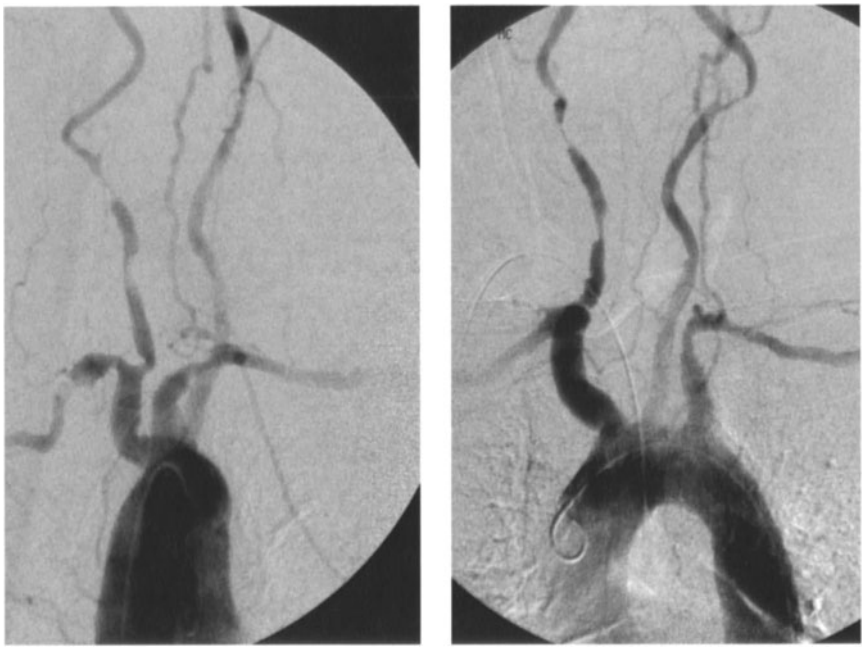

Fig. 1.2. Biplane aortic arch study to see the origin of the brachiocephalic vessels and include the portion of the cervical carotids

Fig. 1.3A–D. Aortic arch study with different centering and projections for anatomic and hemodynamic consideration. The patient's symptoms referred to the left hemisphere, left posterior fossa circulation, and left upper extremity. Same patient as Fig. 14.150. **A, B** Superimposition of an aortic arch study centering at the arch and in the cervical and upper intracranial portions in mid and late arterial phase. **C** Oblique arch demonstrates the better opacification of the right common carotid and right hemisphere. Note the retrograde visualization of the innominate artery stenosis (*arrow*), compare with Fig. 14.150. These global injections demonstrate lesser opacification of the vertebrobasilar system followed by the left carotid and left supratentorial circulation; note the collateral circulation in the cervical region attempting to collateralize the left vertebral artery and posterior fossa circulation. There is severe disease at the innominate artery and stenosis of the right common carotid artery. Same patient as Fig. 14.150. In this particular patient, this information is useful to decide first to attempt revascularization of the left subclavian artery (**D**) ▶

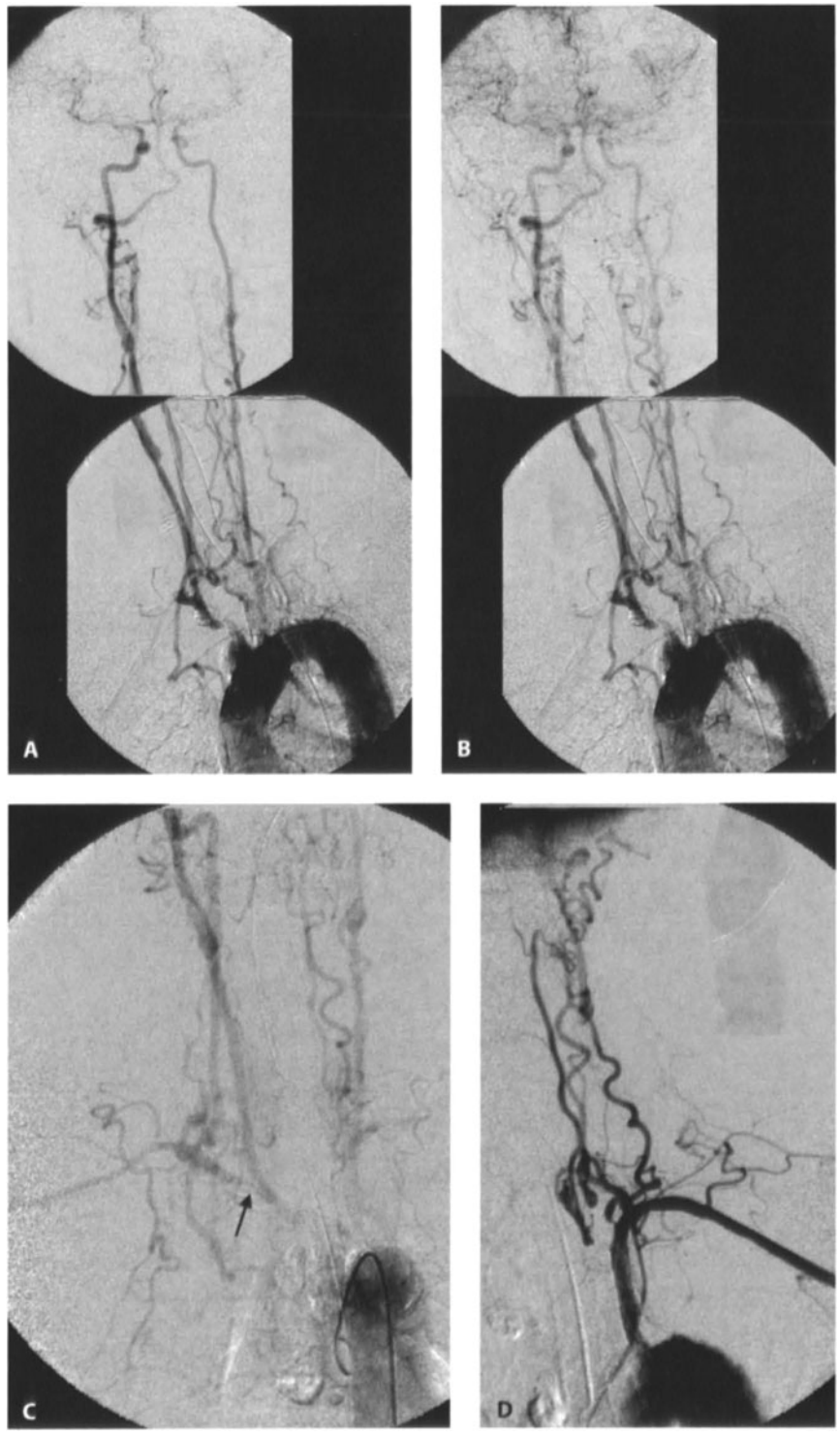

Fig. 1.3A–D.
Legend see p. 42

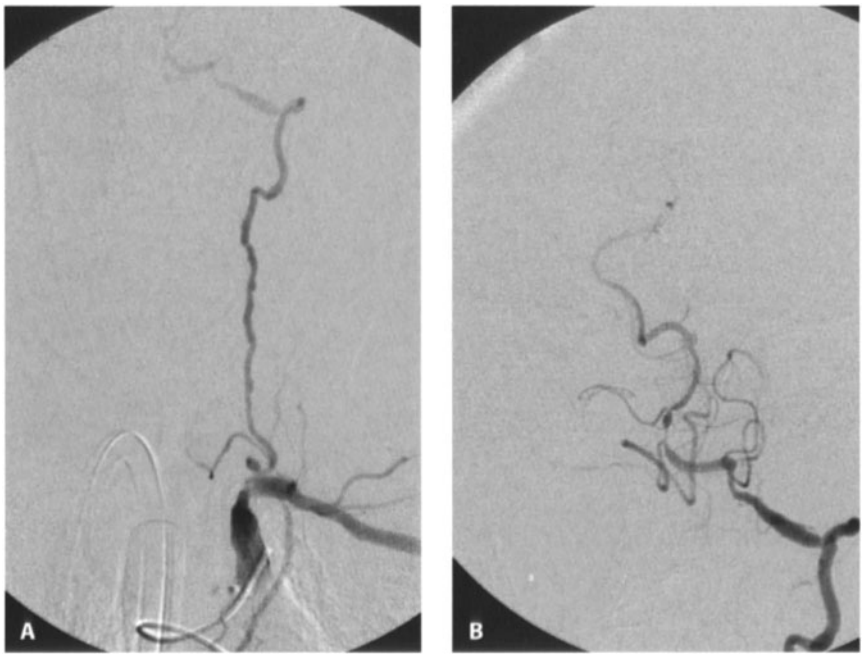

Fig. 1.4A, B. Selective catheterization of the subclavian artery to better clarify the status of the vertebrobasilar system, which cannot be assessed properly in the aortic arch study. **A** Selective injection of the subclavian artery with lower centering. There is severe disease at the subclavian artery as well as throughout the vertebral artery. **B** Note the severe stenosis just distal to the posterior inferior cerebellar artery and proximal to the anterior inferior cerebellar artery (AICA), with an additional stenosis at the AICA level

All brachiocephalic vessels are grossly visualized on the aortic arch study, with some hemodynamic global assessment, which will help in explaining the symptoms and assist in planning treatment (Fig. 1.3D)

More selective catheterization at the level of the subclavian, carotid and/or vertebral arteries that supply the ischemic territory is only done when there is a specific question concerning total occlusion of the internal carotid artery, the status of the vertebral or basilar arteries, the circle of Willis, etc. (Fig. 1.4), or in preparation for endovascular treatment.

1.2.4.12 Middle Cerebral Artery Stroke: Natural History

Bogousslavsky and co-workers (1986) reviewed 352 patients entered in the EC/IC bypass study with middle cerebral artery stenosis (MCAS, 53%) or middle cerebral artery occlusion (MCAO, 47%) secondary to atherosclerosis. Asian patients represented 58% of all patients entered in the EC/IC Bypass Study, 34% of the total were Black patients, and Caucasian patients represented 18% of all (Table 1.14).

Isolated TIAs were less frequent in MCAO (12%), because the vessel once occluded is less likely to embolize, than in MCAS (34%). Warning TIAs in the middle cerebral artery (MCA) distribution before a stroke occurred in one-third of the cases. Presentation with stroke or isolated TIA was not influenced by sex, age, and level of MCA obstruction, collateral circulation, or associated carotid disease.

In MCAS, no major difference in presentation was found between severe and moderate stenosis. Pure motor hemiparesis occurred in 15% and pure sensory stroke in 2% of the patients with stroke. In 30%, the MCA territory infarcts were small and limited to the lenticulocapsular area, suggesting that so-called lacunar infarcts may be due to large vessel disease.

Table 1.14. Middle cerebral artery (MCA) stroke

	All MCA stroke	MCA stenosis	MCA occlusion
Asian	58%		
African-American	34%		
White (USA)	18%		
Incidence	100%	53%	47%
TIAs	33%	34%	12%
Sex		No difference	No difference
Age		No difference	No difference
Hemiparesis motor		15%	–
Sensory stroke		2%	–
New TIA/stroke	11.7%/year	9.5%/year	10.1%/year
Ipsilateral stroke rate		7.8%	7.1%

During follow-up (42 months) of 164 medically treated patients, further cerebrovascular events (TIA and/or stroke) occurred in 11.7% of the patients per year. In MCAO, the stroke rate was 10.1% per patient-year and the ipsilateral infarct rate was 7.1% per patient-year. In MCAS, the stroke rate was 9.5% per patient-year and the ipsilateral stroke rate was 7.8% per patient-year.

Intracranial involvement by atherosclerosis varies in different populations, with up to 22.6% in Asians, with hemodynamically significant stenotic lesions as demonstrated during angiography (Gorelick et al. 1984). Intracranial disease usually presents with stroke rather than TIAs.

1.2.4.13 Local Intra-arterial Thrombolysis in the Anterior Circulation

The goal of intra-arterial thrombolysis is to limit the area of infarcted parenchyma and to enhance the survival of the functionally disabled parenchyma in the surrounding area of ischemic penumbra (Overgaard et al. 1993). In the rat stroke model, thrombolytic therapy has been shown to significantly reduce the volume of infarcted tissue.

Collateral circulation frequently revascularizes the ischemic penumbra inefficiently due to microemboli in the distal microcirculation (Figlos et al. 1988).

While local intra-arterial thrombolysis (LIAT) is an important addition to the treatment regimen of acute ischemic stroke, significant logistical limitations still exist, preventing this therapy from becoming universally employed. Two criteria must be satisfied for recanalization of acute ischemic stroke to be successful; the duration of the ischemia must be short, and the residual cerebral blood flow in the territory of the occluded vessels must be greater than the level at which viability of neuronal, glial, and vascular endothelial cells is lost.

Numerous experimental and clinical studies have addressed the issue of the optimal time window for LIAT to be performed. The consensus appears to be that 6 h is the maximum time period before infarction or hemorrhagic complications are likely to occur when treating middle cerebral artery territory occlusion.

Theron significantly advanced our understanding with respect to the time issue as it relates to different locations of occlusion and the patient's preexisting specific anatomical dispositions (Theron et al. 1998). Caplan reviewed the literature on thrombolytic therapy in 1997, at which time there were collectively over 200 patients treated with intra-arterial thrombolysis and over 250 patients treated with intravenous thrombolysis, all of whom were treated within 8 h of the onset of stroke and monitored angiographically (Caplan et al. 1997). There was effective recanalization in 67% of patients treated intra-arterially and 40% recanalization in patients treated intravenously. There was good outcome in 50% of patients treated intra-arterially versus 40% of those treated intravenously. Furthermore, brain hemorrhage occurred slightly more often with intravenous therapy (6.7%) than with intra-arterial therapy (5%) (Pessin et al. 1995).

Gonner et al. (1998) report an overall recanalization rate of 63% utilizing intra-arterial thrombolysis, with a 33% rate for patients with distal ICA occlusions and a 56% recanalization rate for patients with MCA occlusions. These figures are similar to other intra-arterial thrombolysis studies (average 64%, range 40%–100%, in a meta-analysis) (Boysen and Overgaard 1995). In acute MCA strokes, Bollaert and co-workers (1995) achieved 58% recanalization using intra-arterial urokinase, and Zeumer and co-workers (1993) report a 49% recanalization rate using intra-arterial r-TPA.

The Prolyse in Acute Cerebral Thromboembolism Trial II (PROACT II; Table 1.15) was the first double-blinded randomized trial conducted to evaluate the outcome of intra-arterial thrombolysis with recombined pro-urokinase (r-UK) in patients with angiographically proven MCA occlusion within 6 h after onset of stroke. The primary end point (modified Rankin Scale Score of 2 or less) at 90 days was achieved by 40% of patients treated with r-UK compared with 25% in the control group. The results demonstrated a 60% relative benefit with r-UK. In regards to symptomatic ICH, the r-UK group fared worse but the mortality rate at 90 days was similar in both groups. The recanalization rate at 2 h for TIMI (Table 1.16) grades 2 and 3 was 66% in the r-UK group versus 18% in the control group (del Zoppo et al. 1998).[1]

The techniques used for thrombolytic revascularization, including type of agent, dose, and route of administration, vary widely among reported studies (Adams et al. 1996; Theron et al. 1990; Jansen et al. 1995). The thrombolytic agent of choice has yet to be determined. Urokinase and r-TPA have been used most frequently. Recently introduced agents and regimens that may play a role in the future include recombined pro-urokinase (r-UK), combination regimens such as thrombolytics and GP IIb/IIIa receptor antagonists, and so-called cocktails, which include the addition of antioxidants, free-radical scavengers, and antineutrophils.

The maximum dose of urokinase is still not well established. Although there are reports of utilizing up to 2 million units, in our experience we

[1] In order to evaluate the reperfusion achieved with various thrombolytic regimens, the cardiology community adopted a simple grading system of coronary perfusion TIMI (thrombolysis in myocardial infarction). Although of only limited use in the cerebral circulation, most revascularization studies have investigated coronary circulation, and therefore we included it in this chapter.

Table 1.15. PROACT II: intra-arterial thrombolysis (Pro UK)

>12,000 Screened patients – 474 angiograms
180 Patients randomized
40% Good outcome vs. 25% for controls
66% Recanalization vs. 18% of controls
10% Symptomatic hemorrhage vs. 2% for controls

Table 1.16. Thrombolysis in myocardial infarction (TIMI)[a]

0	No perfusion	No distal opacification
1	Some flow	No distal opacification
2	Better flow	
3	Normal	Normal opacification

[a] The TIMI Study Group (1985) Phase I findings. New Eng J Med 312:932–936.

found that if the dose did not exceed 1 million units, the risk of hemorrhage is extremely small. This finding is supported by the experience gained with intravenous thrombolytic therapy, which also demonstrated that hemorrhagic complications were dose dependent.

The actual time required to perform intra-arterial thrombolysis is still a limiting factor (Barnwell et al. 1994; Brott et al. 1992). An investigation of the time needed to achieve repermeation using intra-arterial urokinase therapy alone, or in combination with mechanical clot disruption, demonstrated that the delay to open an occluded carotid and/or middle cerebral artery varied from 45 to 180 min. Thus, the time related to the performance of angiography and selective catheterization is an additional limitation of intra-arterial therapy and a potential advantage for intravenous therapy. Brott and Tomsick have used a technique that combines intravenous and intra-arterial therapy: intravenous thrombolysis is started immediately after the arterial puncture site is secured and then local intra-arterial therapy is given via superselective catheterization. This technique may have a long-term advantage, as it may have an impact on the local emboli at the site of occlusion as well as affect the distal microcirculation.

In Gonner's experience of 43 patients treated with local intra-arterial thrombolysis (LIAT), 60% had a good outcome (Gonner et al. 1998). Outcome was significantly related to the stroke severity as measured by the NIHSS score at admission. A large infarct associated with a high NIHSS score had a worse prognosis than a small stroke with a low NIHSS score.

Patients whose occluded vessels were recanalized had a better prognosis than patients whose vessels did not reopen. Neurological improvement (NI) within 24 h was an additional prognostic indicator for a good outcome and probably represents restoration of neuronal function in the penumbra.

The hyperdense middle cerebral artery sign (HMCAS) (Fig. 1.11A) on initial CT had no prognostic value in Gonner's patients. This is consistent with other stroke trials that showed no correlation or poor correlation between HMCAS and outcome, independent of treatment (Leys et al. 1992; Von Kummer et al. 1994; Wolpert et al. 1993; Moulin et al. 1996). On the other hand, Tomsick and co-workers (1996) observed generally poor clinical outcomes in patients treated within 90 min with intravenous r-TPA when HMCAS was present. However, in their series, the median baseline NIHSS score of HMCAS-positive patients was 19.5 compared to 10 in HMCAS-negative patients. This difference in baseline clinical status, rather than the presence or absence of HMCAS, may account for observed dif-

ferences in clinical outcome. In Gonner's series, HMCAS-positive and -negative patients had an NIHSS score on the same order. Von Kummer and co-workers (Von Kummer et al. 1994) found that the HMCAS per se was of low prognostic value. However, if on CT an extensive area of hypodensity was present in addition to the HMCAS, then extensive brain damage had already occurred and a fatal outcome could be predicted. There was no correlation between HMCAS and recanalization in our patients or in another series (Wolpert et al. 1993), which further underscores the low prognostic value of HMCAS.

Zeumer et al. (1993) reported fatal outcome in 59% and persistent severe neurological deficits in an additional 38% of patients with distal internal carotid artery "T" occlusions (Fig. 1.5). The recanalization rate was low (17%). In Gonner's series, recanalization was possible in three of their nine patients with ICA occlusion, and they all had a good outcome. Therefore, they concluded that LIAT in carotid occlusions is worth attempting, and that it has the potential to spare some patients from suffering a large stroke.

The site of occlusion and the potential to develop collateral flow plays an essential role in the outcome of stroke. Patients with internal carotid artery occlusion but with good collateral circulation via the ophthalmic and or the circle of Willis may be asymptomatic or may have fluctuating symptoms, representing hemodynamic perfusion abnormalities (Theron et al. 1998). If, however, the ICA occlusion extends towards the proximal MCA, patients tend to present with more severe neurological deficits and have poorer recanalization rates and worse outcomes than those with more distal (cortical) MCA occlusions.

Theron (Theron et al. 1998) reviewed a series of 142 patients, in whom the major goal had been to reduce the rate of hemorrhagic complications associated with thrombolysis and to best select patients that might benefit from LIAT.

In Theron's experience, when the angiographic work-up revealed occlusion involving the horizontal segment of the middle cerebral artery with extension towards the lenticulostriate arteries, successful thrombolysis was restricted to less than 6 h after onset of symptoms. This was also based on his previous experience that this group of patients had poor outcome and higher incidence of hemorrhage if thrombolysis was performed beyond 6 h. We have followed his recommendations, with good outcomes.

Fig. 1.5A–F. "T" carotid occlusion. **A** Late phase of the common carotid artery injection on the right lateral projection demonstrates the occlusion at the internal carotid artery proximal to the ophthalmic artery extending towards the bifurcation. **B** Frontal view of the left common carotid artery shows the occlusion to be a "T" lesion involving the A1 (*arrow*) and M1 segments. Note the leptomeningeal collaterals reconstituting the distal middle cerebral artery (MCA), the more proximal M1 segment is occluded. **C, D** The microcatheter is advanced through the internal carotid artery, which is totally occluded, without lysing the clot, but going through it. This shows the progressive recanalization of the MCA. **E, F** Final follow-up angiogram in **E** arterial and **F** venous phase shows the reconstitution of the A1 and M1 segments with excellent filling of the distal MCA. In the venous phase there is symmetry in the venous return. The patient made a full recovery ▶

Fig. 1.5A–F.
Legend see p. 48

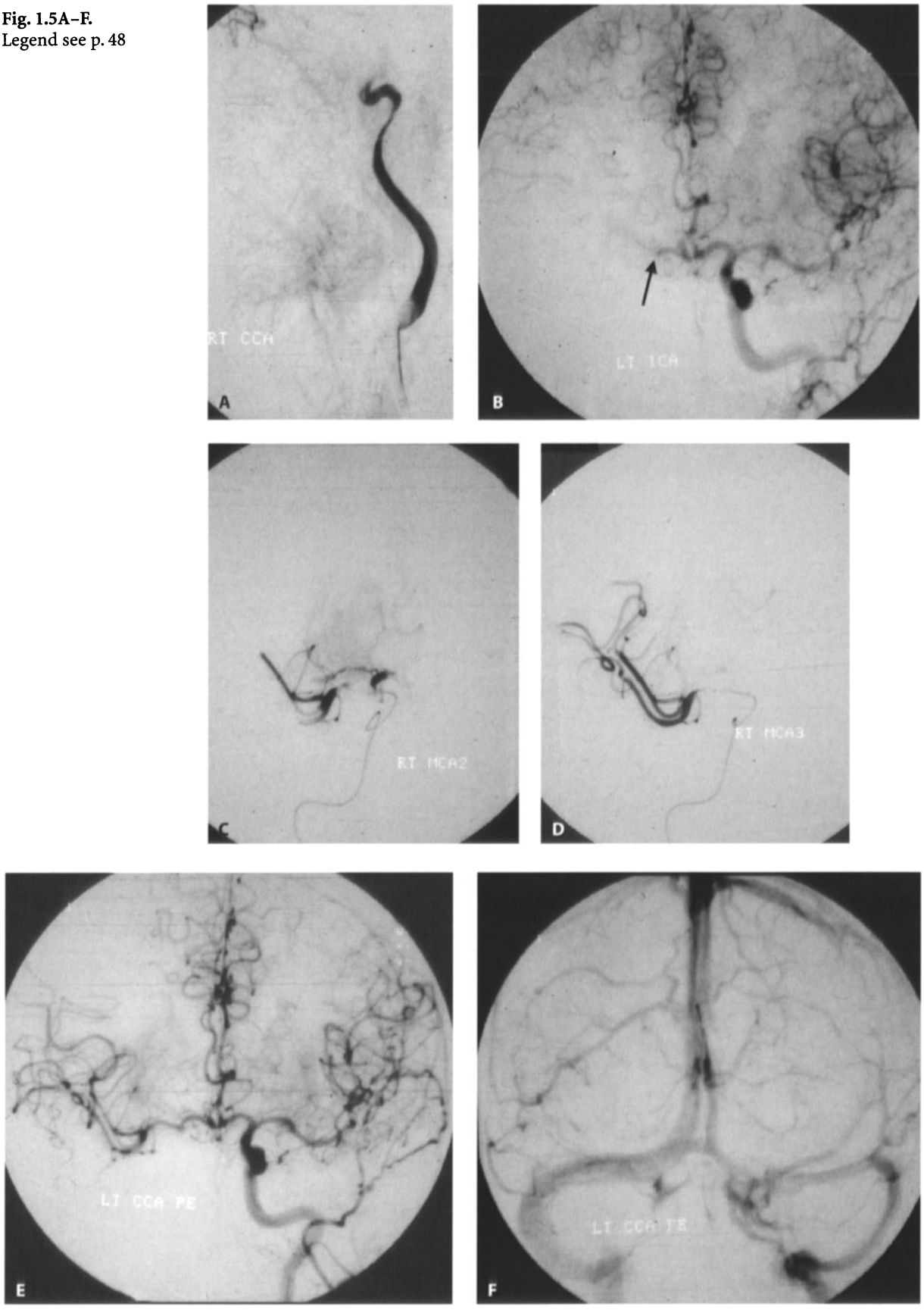

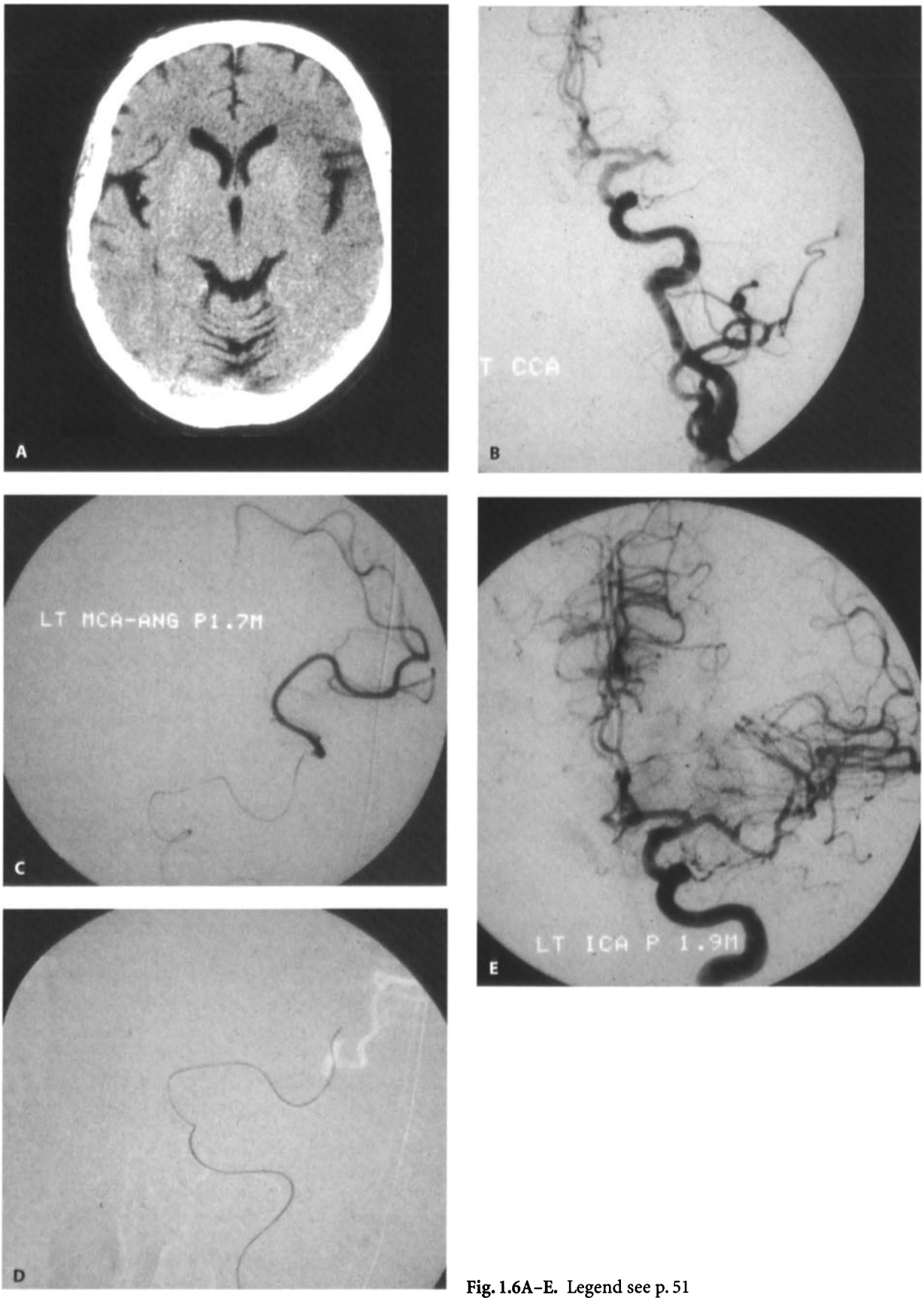

Fig. 1.6A–E. Legend see p. 51

In the appropriate clinical setting of ischemic stroke, we start with an immediate noncontrast head CT to rule out hemorrhage or other contraindication for LIAT (Fig. 1.6).

If the angiogram thus shows no involvement of the horizontal segment of the middle cerebral artery, including the lenticulostriate arteries and therefore primarily represented cortical branch occlusion, thrombolysis can be carried out up to 12 h after the occlusion (Theron et al. 1999).

Of the 142 patients reported by Theron, there were 61 cases in the cortical group, 71 cases of M1 occlusion involving the lenticulostriate perforators, eight cases with T lesions, and two patients with purely cervical ICA occlusion.

In experimentally occluded middle cerebral arteries that are opened after 6 h, the lenticulostriate arteries lose their ability to autoregulate and therefore are dependent on systemic BP. This was demonstrated by Kamijyo in cats (Kamijyo et al. 1977), Di Chiro in primates (Di Chiro et al. 1974), and confirmed in humans in Theron's first group of patients. Theron demonstrated a dramatic reduction in intraparenchymal hemorrhage when comparing his original series, in which there was a 16.6% hemorrhagic complication rate following thrombolysis, to his more recent series, in which this dropped to 0.7%, by avoiding those with lenticulostriate involvement (Theron et al. 1998).

It is believed that since lenticulostriate arteries have less efficient collateral circulation (thus called terminal arteries), they are particularly sensitive to ischemia. Ischemia not only damages neuronal and glial tissues, it also damages endothelial cells with loss of vascular integrity as their walls become weakened. Late revascularization increases the risk of rupture and parenchymal hemorrhage.

Theron also suggests that patients with a crescendo ischemic syndrome, involving the lenticulostriate artery territory should not undergo revascularization, because the risk of intraparenchymal hemorrhage is high in this group.

Symptomatic hemorrhages occurred in 4.7% of Gonner's patients. One of them (2.3%) bled 3 days after LIAT while under heparin, which may have caused the hemorrhage (Bollaert et al. 1995). The spontaneous bleeding rates were 1.2% in NINDS and 6.5% in European Cooperative Acute Stroke Study (ECASS) control groups with intravenous thrombolysis (Wardlaw et al. 1997; Hacke et al. 1995). The 4.7% bleeding rate in Gonner's series, while in the same range, is higher than the 0.7% reported by Theron and co-workers (1996); however, the latter group excluded patients with M1 occlusion.

◀ **Fig. 1.6A–E.** Occlusion of the horizontal segment of the left middle cerebral artery (MCA). **A** CT scan in the acute phase shows the subtle effacement of the white–gray interface. **B** Frontal digital subtraction angiogram within the first 4 h of the stroke demonstrate occlusion of the horizontal segment of the left MCA. There is one medial lenticulostriate artery preserved. **C** Superselective catheterization after reconstitution of the lateral branch of the middle cerebral artery. **D** Road map of the main angular branch, which is still occluded. Coaxial catheterization with a microcatheter and stirable microguidewire entering the occluded vessel. **E** Follow-up angiogram after revascularization of the MCA territory with good angiographic and clinical outcome

We concur with Theron that studies evaluating the efficacy of thrombolysis in stroke should not use the revascularization rate of the occluded artery as the sole outcome measure because an artery may be reopened without achieving efficient distal parenchymal revascularization.

Conversely, an artery may remain occluded and yet revascularization of the parenchyma will be achieved through recanalized collaterals.

The regime of combining intravenous and intra-arterial thrombolysis may improve the final outcome by acting at various levels. Several trials are being conducted to establish the validity of combined therapy.

Combining various therapeutic modalities such as chemical and mechanical repermeation will increase the number of treatment options in the future. In addition to thrombolysis, balloon angioplasty of the clot in the MCA may be of assistance to rapidly reopen the middle cerebral artery (Fig. 1.7). The use of thrombolysis and antiplatelet aggregation (chemical) with angioplasty and stenting (mechanical) may further enhance the long-term outcome of revascularization.

Based upon indirect comparisons of intravenous and intra-arterial thrombolysis, one may cautiously state that LIAT is at least as effective and safe as intravenous thrombolysis with r-TPA and has the advantage of a longer time window for successful application. In addition, LIAT has several other advantages over intravenous thrombolysis. Angiography performed prior to LIAT allows visualization of the individual vascular pathology and provides information on collateral flow. The thrombolytic agent can be administered directly into the thrombus, under visual control, and therefore the LIAT fibrinolytic dose needed for vessel recanalization is smaller than in systemic thrombolysis. In certain cases, the thrombus can be fragmented and dislodged mechanically with immediate reestablishment of blood flow in the larger vessel and an opportunity to perform LIAT more distally into the cortical branches (Theron et al. 1996a; del Zoppo et al. 1988; Jungreis et al. 1989; Barnwell et al. 1994; Casto et al. 1996; Ueda et al. 1997) (Fig. 1.6). In addition, the risk of symptomatic intracranial hemorrhage does not seem to increase, or at least not as much as in systemic thrombolysis. The significant remaining limitation of LIAT is the need for an appropriated team that has the expertise to perform LIAT.

1.2.4.14 Internal Carotid Artery Occlusion

ICA occlusion may be asymptomatic. Symptoms may be a result of incompetence of the collateral circulation, or more frequently distal embolization and associated distal occlusion of a perforator or perforators and/or cortical vessel(s). Unfavorable prognostic signs for outcome include MCA embolus (worse, if involving the M1 segment, i.e., a T lesion), poor collateral circulation, and profound neurological deficit.

The natural history of patients presenting with profound neurological deficit and acute carotid occlusion is dismal. A review of the literature by Meyer and co-workers revealed that 16%–55% of patients will die from infarction, 40%–69% will have severe neurological disability, and only 2%–12% will make a good recovery (Meyer et al. 1986).

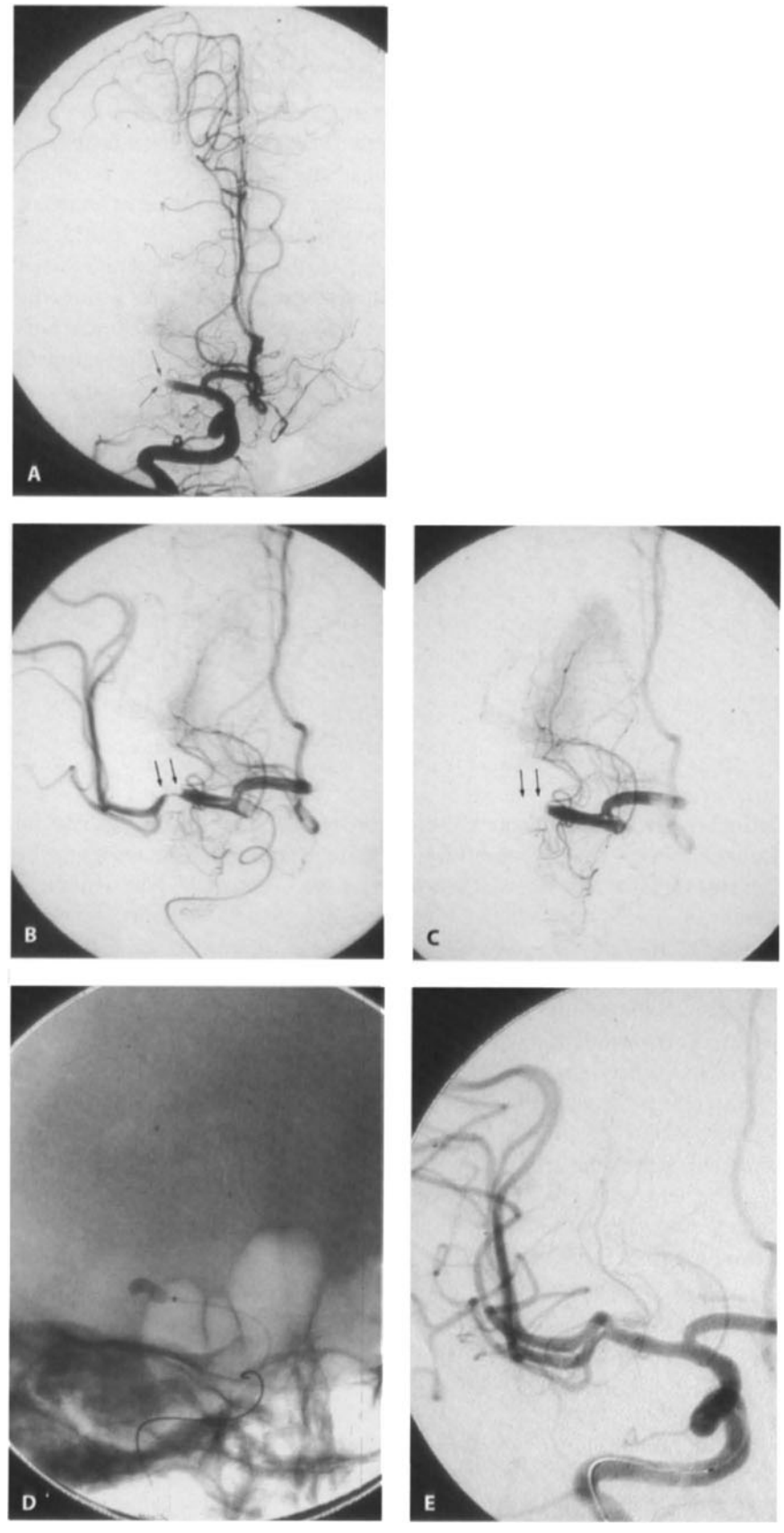

Fig. 1.7A–E. Combination of thrombolysis and mechanical angioplasty. Acute middle cerebral artery occlusion. **A** Right internal carotid artery shows the acute occlusion of the M1 segment (*arrows*). **B** Immediately after chemical thrombolysis, note the severe focal stenosis remaining (*arrows*). **C** Reocclusion occurred within minutes (*arrows*). **D** A mechanical angioplasty with a balloon tip catheter at the site of the focal stenosis was done. **E** Follow-up angiogram after balloon angioplasty. Note the excellent reconstitution of the M1 segment

A review of the surgical literature by Meyer et al. (1986) concerning the benefits of emergency surgical thromboendarterectomy in patients with totally occluded ICA and profound neurological deficit yielded variable results and remains controversial. In most experts' opinion, internal carotid artery occlusion with severe acute neurological deficit is considered a contraindication to surgery. An exception would be if it occurs in the hospital where the reestablishment of flow can be achieved in less than 1–2 h (Walters et al. 1987). The most optimistic study of carotid endarterectomy in patients with profound neurological deficits reported good outcome in 38.3% of patients, fair outcome in 29.4%, poor outcome in 11.8%, and a surgical mortality of 20.6% (Meyer 1986). The clinical outcome of patients who survived endarterectomy in that study group represents a significant improvement over the natural history of the disease, whereas the surgical mortality is similar to that of the natural history.

Theron divided patients who had carotid artery occlusion into three groups:

Group 1: Those with an internal carotid artery occlusion up to the ophthalmic artery, without infarction but possibly symptomatic due to hemodynamic factors

Group 2: Those with an internal carotid artery occlusion up to the ophthalmic artery, but who developed an area of infarction at the watershed area

Group 3: Those with occlusion of the internal carotid artery, extending towards the lenticulostriate arteries, similar to those previously described as T lesions

Patients with cortical arterial occlusion would have limited territorial damage, in view of the potential for leptomeningeal collaterals from the anterior and posterior cerebral arteries. The cortical group patients had results that were deemed to be very good (normal) or good (minimal deficit) in 80% of cases, and fair (significant disability) in 20% of cases. There were no deaths.

However, in patients with lenticulostriate arteries involvement, the results were considered very good or good in 57% of cases, fair in 20%, and vegetative or dead in 23%.

Patients in whom Theron opened an occluded cervical carotid artery, but who were symptomatic due to hemodynamic factors, all did well and returned to normal.

There were seven deaths (5%) in the 142 patients and all died from secondary vasogenic cerebral edema. All seven had various degrees of involvement of the lenticulostriate arteries and no significant improvement could be demonstrated on parenchymatography immediately after thrombolysis or on angiography on the following day. There was one hemorrhage (0.7%) in a case with occlusion of the lateral lenticulostriate arteries, which was interpreted as a cortical group and treated 7 h after the onset of symptoms.

Although in 12.7% of cases, hemorrhagic infarction was visualized on the CT scan done the following day, all these patients were clinically unchanged or markedly improved. Of the 18 cases that had a hemorrhagic transformation demonstrated by CT, 11 were in patients with involvement

of the lenticulostriate arteries. In the cortical group, six cases had a 24-h CT scan showing a hemorrhagic transformation. An intraparenchymal hemorrhage occurred 5 days after successful thrombolysis in one patient. This patient also had cardiac arrhythmia for which he was placed on heparin; he subsequently died.

To reduce hemorrhagic complications, patients with lenticulostriate artery occlusion for more then 6 h should probably not undergo thrombolysis. The report by Nesbit and co-workers (1996) utilizing endovascular IA revascularization of totally occluded ICA is very encouraging. They were able to catheterize the occluded carotid artery and go through the thrombi in three out of four cases. All four patients were considered poor candidates for thromboendarterectomy (given the profound neurological deficit, evidence of middle cerebral artery embolus, and lack of collateral circulation) and responded to endovascular revascularization with marked to moderate improvement in their clinical outcome. Nesbit's patients presented with a pretreatment mean NIH stroke score of 24±4 and demonstrated neurological improvement at 48 h with a mean NIH score of 12±5. All of his patients had significant improvement 3 months after treatment, with a mean NIH stroke score of 7±6. This improvement was statistically significant (p=0.03). There was a marked improvement in outcome when compared with that of the natural history of disease or surgical treatment. There was no associated morbidity or mortality (Nesbit et al. 1996). Probably the greatest advantage of the endovascular approach over endarterectomy is the ability to study and if needed also revascularize the distal territory.

Endo and co-workers (1998) were able to recanalize eight patients with a recently totally occluded internal carotid artery using intra-arterial local thrombolysis. Four of their patients had a good clinical outcome and four did not. Better outcome was related to the ability to obtain at least partial recanalization within 3 h of the event and subsequent opening of the lesion at the cervical internal carotid artery by transluminal angioplasty or carotid endarterectomy.

In their study, 29 of the 33 patients with major stroke and atherothrombotic internal carotid artery occlusion had a poor clinical outcome. These patients underwent urgent intravenous thrombolysis or unsuccessful intra-arterial thrombolysis, illustrating the devastating clinical course of this disease. However, the four patients in whom intra-arterial local thrombolysis was successful in at least partially recanalizing the vessel within 3 h had a good outcome.

In patients with total occlusion of the carotid artery, the initial assessment must be done rapidly and efficiently. It is our feeling that pancerebral angiography adds important information necessary to plan treatment. If there are good leptomeningeal collaterals with reconstitution of the distally occluded segment, and in addition there are good anterior and posterior communicating arteries, revascularization of the occluded carotid artery may not be necessary and may actually be dangerous. Conversely, if there is poor or absent collateral circulation and the occlusion includes the A1 or intracranial bifurcation of the ICA, then an attempt to reestablish flow through the occluded internal carotid becomes important.

If the internal carotid artery cannot be opened rapidly, but there are good collaterals at the circle of Willis, then a microcatheter can be passed through the occluded ICA and LIAT of the distal territory (such as in the MCA) can be performed. This would permit perfusion of the distal repermeated territory to occur through the circle of Willis (Fig. 1.5).

In Nesbit and Levy's series, the lack of collateral cerebral circulation produced reocclusion of the carotid artery, which required revascularization of the vessel (Nesbit et al. 1996; Levy 1998). In patients with recanalization of the internal carotid artery, a need exists to maintain patency of the carotid artery at the original site of the occlusion. If a stenotic lesion responsible for the occlusion is found, angioplasty and if possible stenting should be done to maximize durability of the vessel recanalization. It is important not only that flow is reestablished but also that the distal circulation is checked to guarantee the absence of distal emboli.

When evaluating an occluded internal carotid artery, the various etiological causes must be considered and determined whenever possible. While the presence of an atheromatous lesion is the most frequent cause of acute internal carotid thrombosis, cases of dissection may also be encountered.

When comparing the results of intra-arterial revascularization of the carotid artery with intravenous thrombolysis, the rate of recanalization with intravenous thrombolysis is extremely small, with only 11% of patients having the carotid recanalized, whereas local thrombolysis resulted in complete recanalization in 52% of cases (Sasaki et al. 1995). Significant work has been done in the development of more efficient techniques of recanalization, and we should expect this rate to be vastly improved (Fig. 1.8).

A review of multiple case reports by Nesbit and co-workers (1996), suggests that intra-arterial thrombolysis has a higher recanalization rate

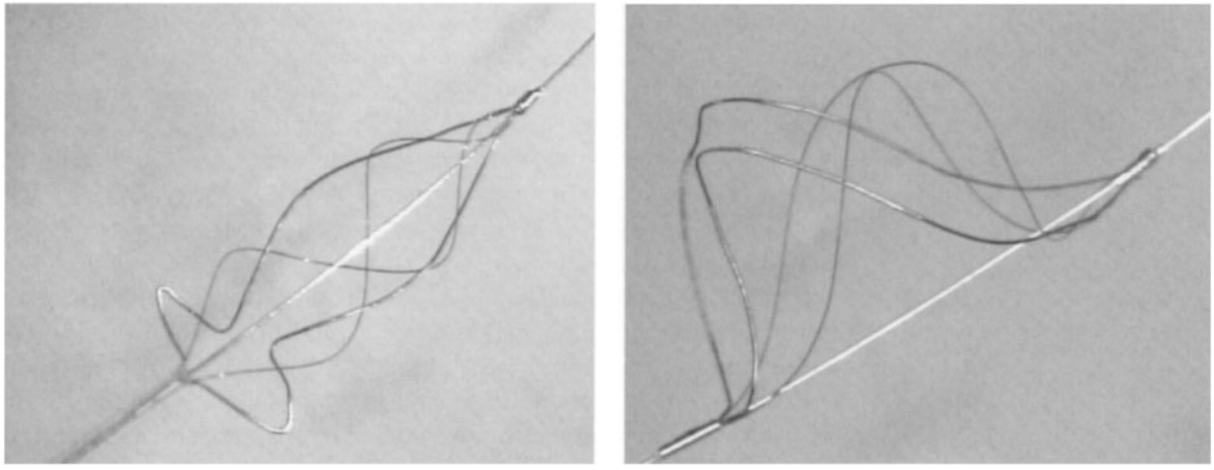

Fig. 1.8. Clot retrieval devices (also see coil retrieval devices Figs. 14.96, 14.97, 14.167). BSC/Target Loop Clot Retriever (Target Boston Scientific, San Jose, CA, USA). Over-the-wire design using 18 microcatheters, with an atraumatic, flexible tip using superelastic materials. When open, has off-center geometry for best engagement. The device is radio-opaque. Adaptable sizing to multiple vessel diameters, 2–5 mm; lengths, 1.5–3 cm

(58%–100%) and clinical improvement rate (53%–94%) than intravenous treatment (36%–89% and 26%–85%, respectively), without a significant increase in hemorrhagic transformation (Spearman et al. 1995; del Zoppo et al. 1992; Mori et al. 1992; Levy et al. 1994; Ueda et al. 1994; Sasaki et al. 1995).

Advancements in the local intra-arterial microcatheter delivery of high concentrations of thrombolytics, along with the assistance of mechanical disruption of the clot by catheter and/or guidewire manipulation, ballons, or by newer devices being introduced to remove large amounts of clot will further enhance the rate and speed of repermeation (Fig. 1.8). With the advent of various stents with increased flexibility, the possibilities for even better results are likely. A potential risk of opening a totally occluded carotid artery is thrombi dislodgment and distal embolization. Dislodgment of thrombus may also reocclude a distal middle cerebral artery after initial successful thrombolysis. Although Levy suggests urokinase infusion from the distal territory to the more proximal circulation, we prefer the reverse to prevent distal reocclusion while the proximal vessel is being opened. In this scenario, if distal embolization during proximal recanalization occurs, then it may still respond to the circulating thrombolytics used at the time of proximal thrombolysis. As an alternative, distal territories may first be mechanically revascularized to improve blood flow, then the more proximal area, and finally the distal territory is completed.

Many believe that the pathophysiological mechanism of distal thromboembolism associated with proximal internal carotid artery occlusion, results from the distal thrombosis of the internal carotid artery to its next major branch, usually the ophthalmic artery. Suggestions have also been made that a supraclinoid or middle cerebral artery embolus is the distal stump embolus that forms in the petrous or cavernous carotid artery. We concur with Nesbit that a more likely mechanism is that initially a nonocclusive embolus forms proximally and then embolizes to the distal territory. This embolization decreases flow in the territory beyond the original stenotic lesion, which worsens the flow proximally and results in internal carotid artery thrombosis, which then propagates to total occlusion.

The use of mechanical balloon angioplasty and or stenting will augment the recanalization of a stenotic segment following urokinase infusion, when thrombolysis is not sufficient. In cases with thrombosis, resulting from poor flow, angioplasty and/or stenting of the internal carotid artery has been shown to be useful (Spearman et al. 1995).

1.2.4.15 Carotid Dissection

Carotid dissection is one of the most common causes of ischemic stroke in people under 50 years of age (Guillon et al. 1998), with an incidence of 2.9 per 100,000 (Schievink et al. 1993). The pathogenesis is varied, including various types of trauma such as penetrating vessel injury or blunt trauma, with onset after jogging or weight lifting, or injury of iatrogenic origin (Fig. 1.9). Spontaneous dissection may be associated with preexisting arterial disease that predisposes cervical vessels to dissections, for example, fibromuscular dysplasia, type IV Ehlers-Danlos syndrome, Marfan syndrome, neurofibromatosis, cystic medial necrosis, idiopathic regressing ar-

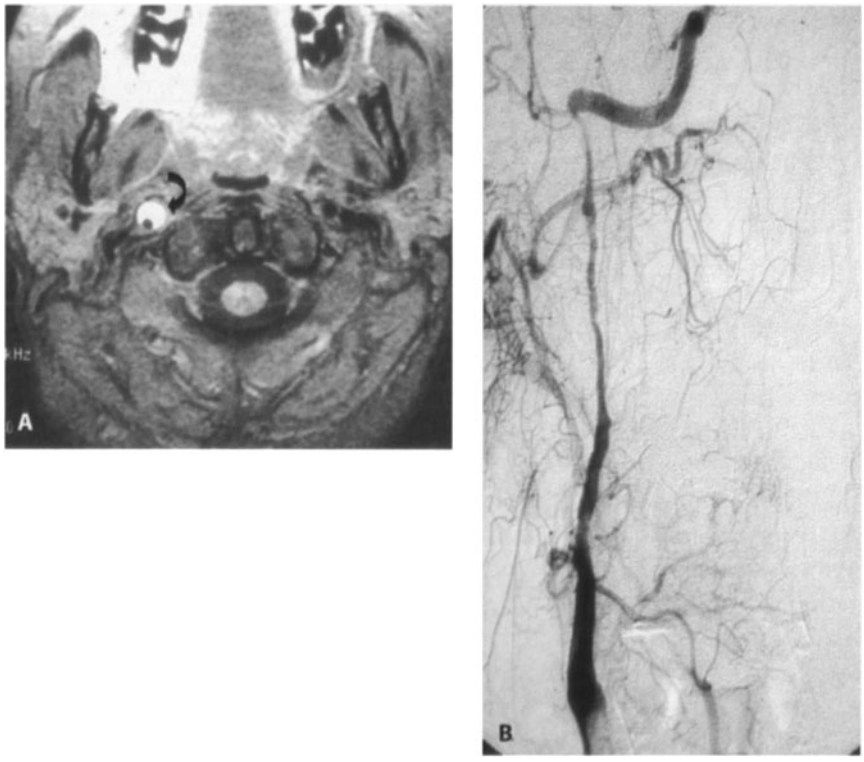

Fig. 1.9A, B. Right internal carotid artery dissection. **A** MRI following acute left hemiplegia demonstrates a hematoma in the wall of the internal carotid artery as an increased signal (*curved arrow*) with the small residual carotid lumen. **B** Frontal digital subtraction angiogram of the common carotid artery demonstrates the severe narrowing of the carotid lumen with a long segment extending from just distal to the carotid bulb to the petrous bone. A typical appearance of a carotid dissection of the spontaneous type

teriopathy, hypertension, and α_1-antitrypsin deficiency. Some reports also refer to ICA redundancy (Mokri et al. 1977; Barbour 1994; Schievink et al. 1994a, b). Some of these entities are also associated with aneurysms or dissection of other vessels (Schievink 1994a, b; see Sects. 7.2.2.2 and 7.4, Chap. 7, this volume).

Treatment is usually medical, with anticoagulants for 3–6 months. During the acute phase, full heparinization is preferred; it is effective and fast acting. It can easily be reversed if intervention is needed, and after establishing arterial access, the heparin can be reinstated. Complete recanalization in occluded vessels is seen in 62% of initially occluded vessels and 90% of initially stenosed arteries (Fig. 1.10) (Sturzenegger et al. 1995; Liu 1999).

In patients with persistent symptoms and/or recurrence of distal embolization, despite appropriate medical anticoagulation, intervention may be indicated for the symptomatic site, whereas dissection may respond to medical therapy (Fig. 1.11, p. 60). If the associated aneurysmal segment does not heal or expands, endovascular stenting has proven safe and effective and has become a therapeutic option (Fig. 14.92) (Geremia et al. 1994; Link et al. 1996; Massoud et al. 1995; Wakhloo et al. 1994; Marks et al. 1994). If the aneurysm sac is too large, then it may not thrombose, and the stent can be used as a protection for coil embolization (Fig. 14.144).

Extracranial carotid artery dissections may be bilateral, mostly after trauma, putting stress on the collateral circulation, and may be the reason for the apparent lack of response to anticoagulation. Symptoms may be caused by the added hemodynamic constraints (Fig. 1.12, pp. 61–64).

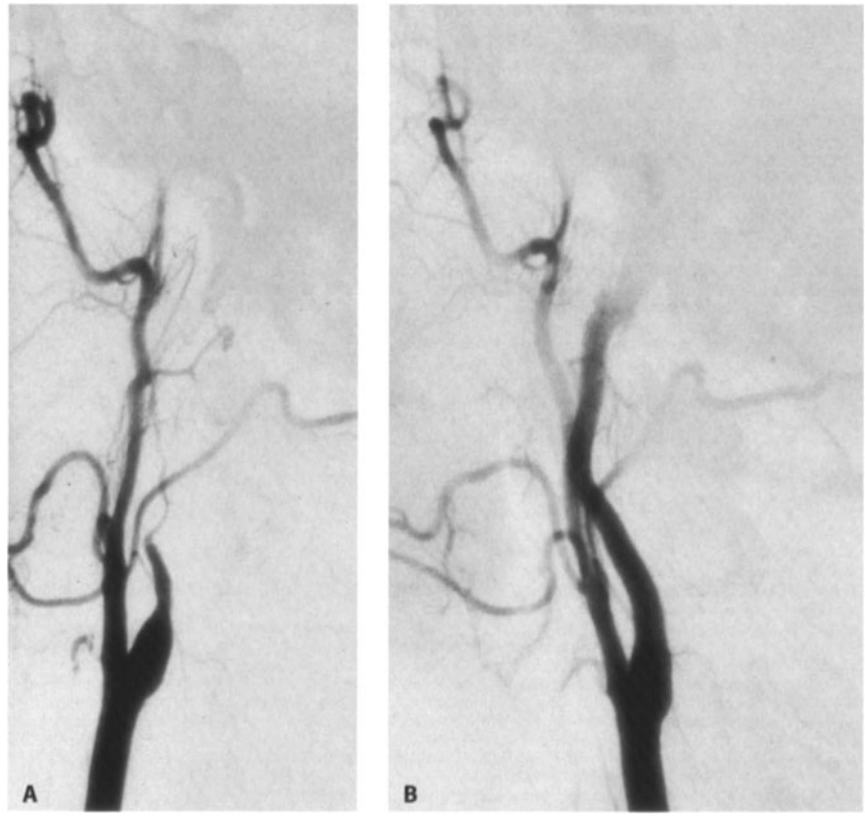

Fig. 1.10A, B. Carotid dissection 18 h after a cerebral vascular accident. **A** Before and **B** after 6 weeks of anticoagulation therapy, with resolution of the dissection, note a small residual aneurysm at the petrous entrance. Patient remained on antiplatelets

Alternatively, during iatrogenic dissection of the carotid artery, if the patient develops symptoms or has poor collateral circulation, one may want to immediately recanalize the damaged vessel (Fig. 1.13, p. 65). In the cervical carotid artery, the self-expandable stents are best, whereas the low-profile balloon-expandable stents are used in the distal petrous (Dorros 1998b) or cavernous carotid artery. In these types of cases, finding the true lumen may be problematic and we tend to explore and identify the true lumen with currently available neuromicrocatheters and neuromicroguidewires (Figs. 14.12, 14.13). When an associated post-traumatic aneurysm does not thrombose, one may consider supplementing the stent(s) with coiling of the aneurysm (Fig. 14.144), or introducing polymers into the aneurysm with the stent or a balloon acting as a neck bridge, to avoid the material from protruding into the vessel lumen or embolizing (Fig. 14.144) (Szikora et al. 1994; Mawad and Moret, personal communication). The development of cover stents (Fig. 14.42) may be of special value in these instances (Link et al. 1996). At present, however, their rigidity has been a limiting factor.

The majority of aneurysms will thrombose with the stents acting as a flow divertor, either acutely or in time. Marks, in 8 years of follow-up (with a mean of 3 years), reports excellent long-term results, with minimal intimal hyperplasia and no flow restriction (Hopkins 2000). In vessels with compromised lumen, the lumen returns to normal (Fig. 14.149). If long-term patency is good, stenting, with its low morbidity, may become the treatment of choice for larger vessel dissections, and in particular in the extracranial carotid and vertebral arteries, avoiding long-term commitment to anticoagulation.

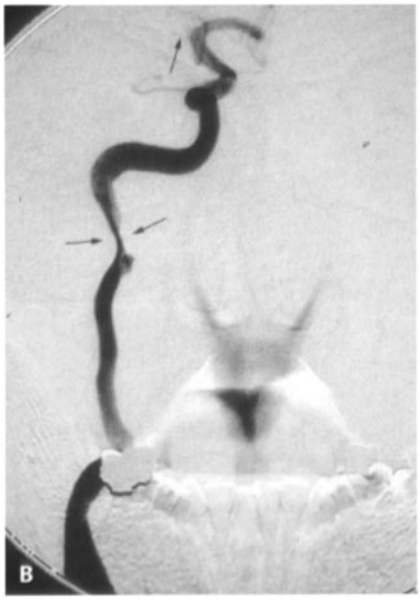

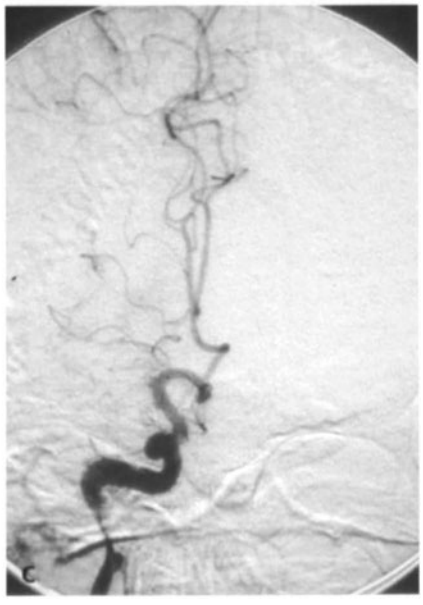

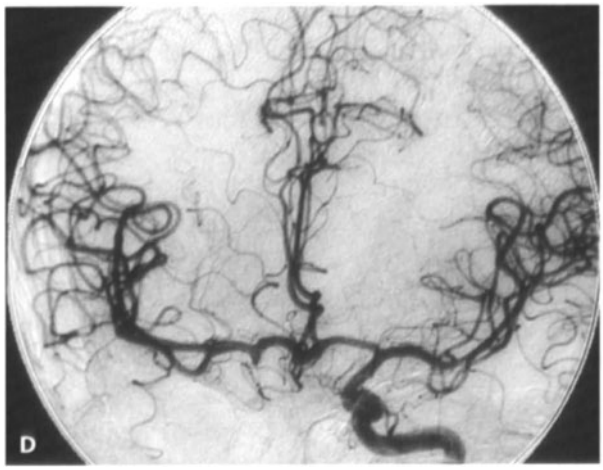

Fig. 1.11A–E. CT in acute cerebral vascular accident. **A** Hyperdense middle cerebral artery sign (HMCAS) (*arrow*), secondary to right internal carotid artery (RTICA) dissection **B** (*arrows*); note the irregularity at the entrance to the petrous bone, with occlusion of the M1 segment in **C. D** Left internal carotid artery (LTICA) follow-up after 1,000,000 U of urokinase selectively into the right middle cerebral artery with recovery. The RTICA closed after the thrombolysis. **E** RTICA after 6 weeks on heparin: there is reopening of the carotid artery, a residual dissecting aneurysm at the entrance into the petrous bone is seen. Conservative medical therapy was chosen with long-term antiplatelets. On follow-up there was no clinical or morphological change

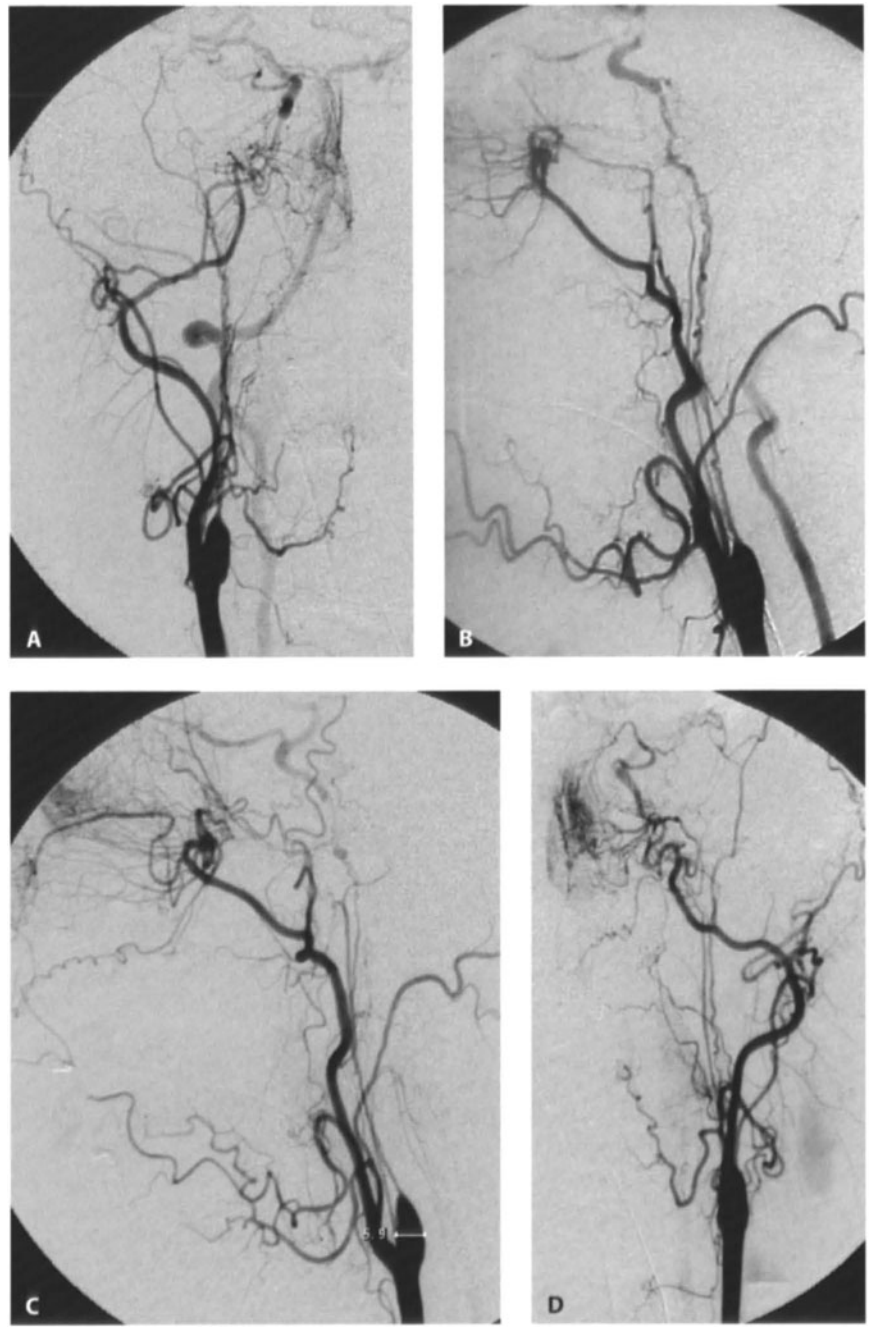

Fig. 1.12A–P. Bilateral carotid dissection. **A** Frontal and **B** lateral digital subtraction angiogram (DSA) of the right common carotid artery demonstrates irregular small channels reconstituting the internal carotid artery. Note preservation of the carotid bulb and extension of the lesion to the precavernous carotid artery in more than one channel. **C** Lateral and **D** frontal views of the left common carotid artery showing reconstitution of the internal carotid artery through the ascending pharyngeal artery to C5. Also see Fig. 14.149 for same patient. **E–P** see pp. 62–64

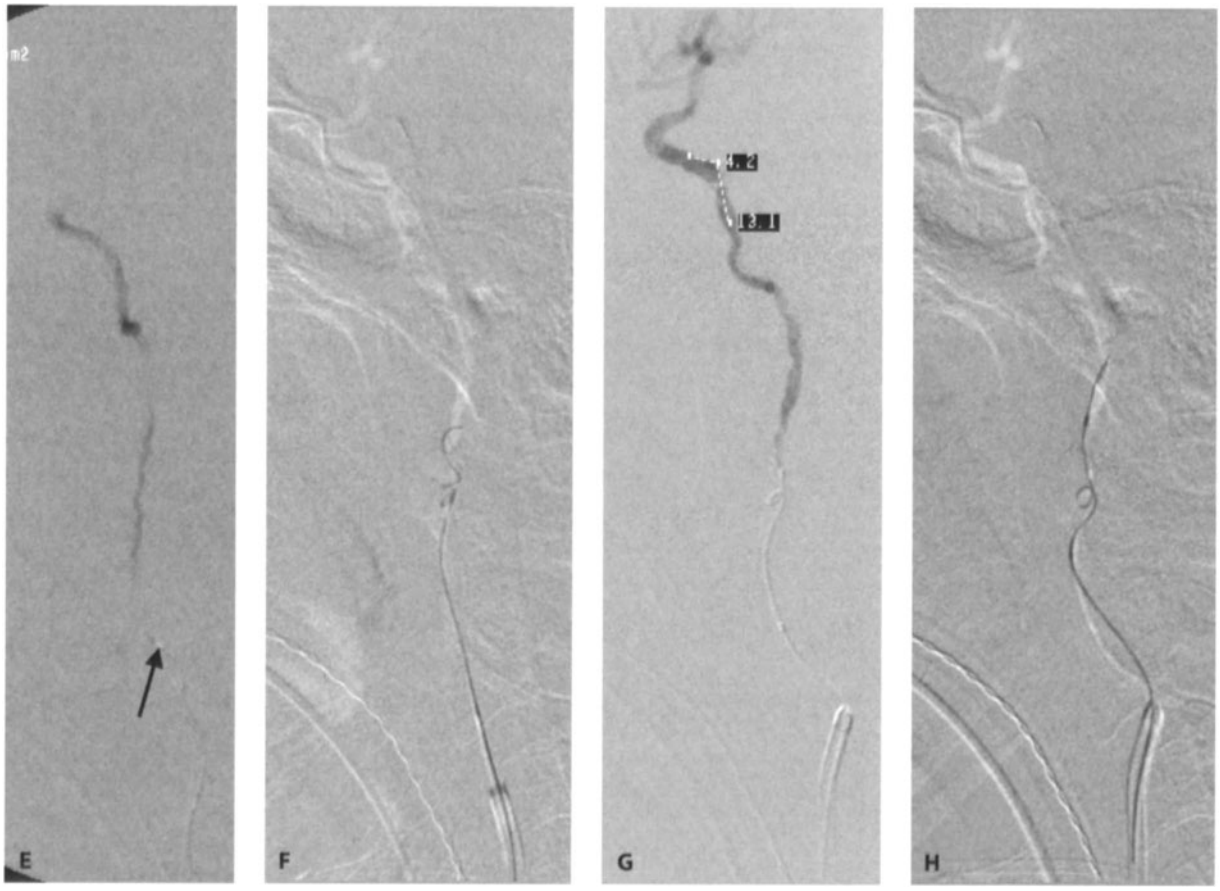

Fig. 1.12 (*continued*). **E–J** Road map images of the revascularization of the right carotid artery, previously thrombosed. A 0.01-in. microcatheter is engaged at the ostea of this tortuous multichannel lumen (*arrow*, **E**). **E** There is complete flow arrest but there is a continuous channel up to the precavernous carotid artery. **F** A neuromicroguidewire is advanced through the tortuosity. Once a more distal portion is reached, the guidewire is pulled back to straighten out the tortuosity, and the microcatheter is advanced (**G**, **H**). Also note the disease at the C5 segment of the carotid artery. **I** The microcatheter has reached the level of the ophthalmic artery, beyond the stenosis. Retrograde blood flow is obtained. This was then followed by replacing the neuromicroguidewire for a long (300-cm) stiffer exchange guidewire **J** and proceeded with a progressive balloon angioplasty **K**. Note the irregular recanalized lumen throughout the internal carotid artery (ICA). **L** This is then followed with stenting. A balloon-mounted flexible coronary stent (SX60) is advanced to the cavernous segment of the internal carotid artery representing the most proximal normal carotid artery; the balloon is inflated and the stent is deployed. **M** Frontal view of the entire carotid artery lined with the overlapping stents. The last stent is placed with approximately 2 mm of overlapping prior to balloon expansion. **I–P** see pp. 63, 64

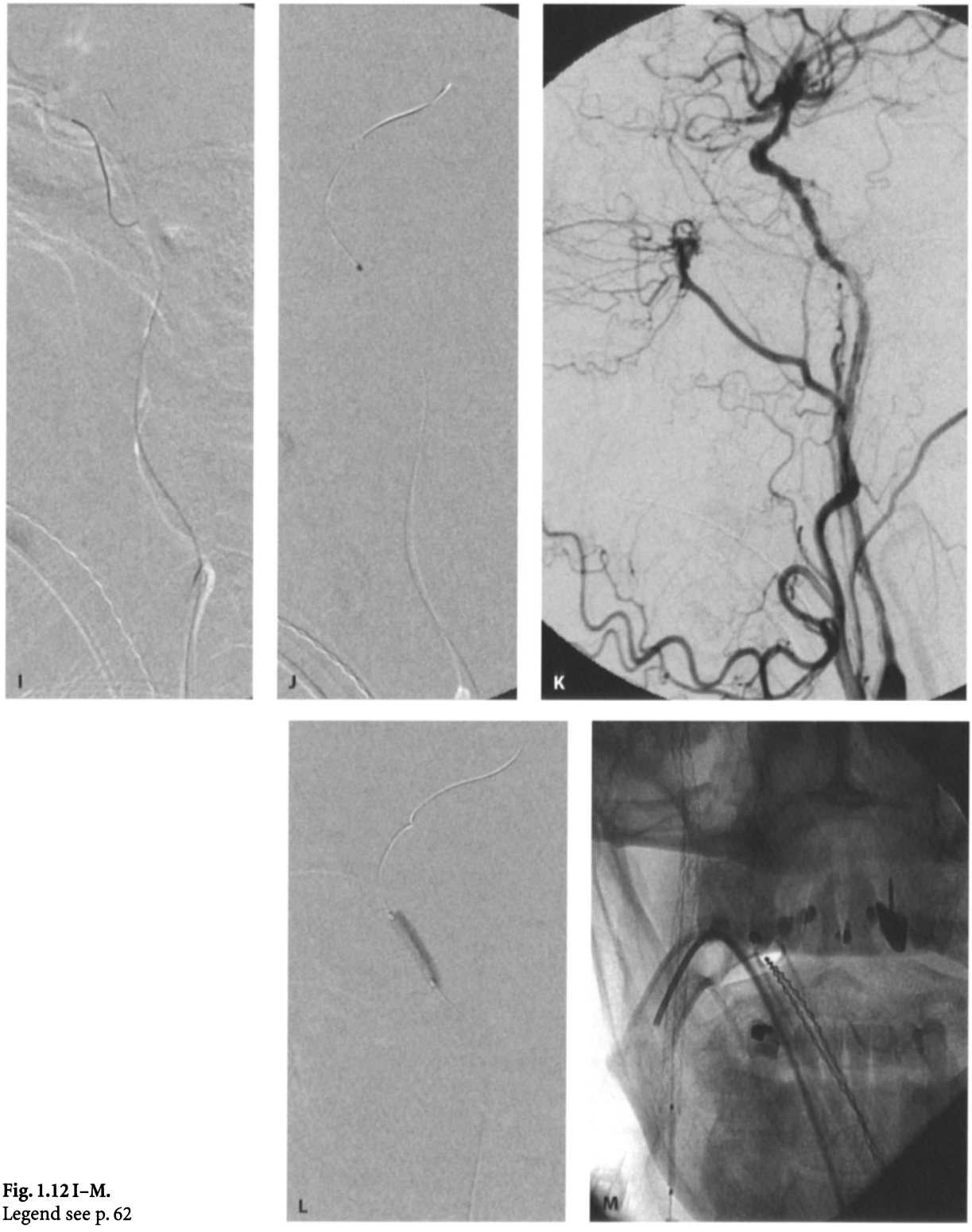

Fig. 1.12 I–M.
Legend see p. 62

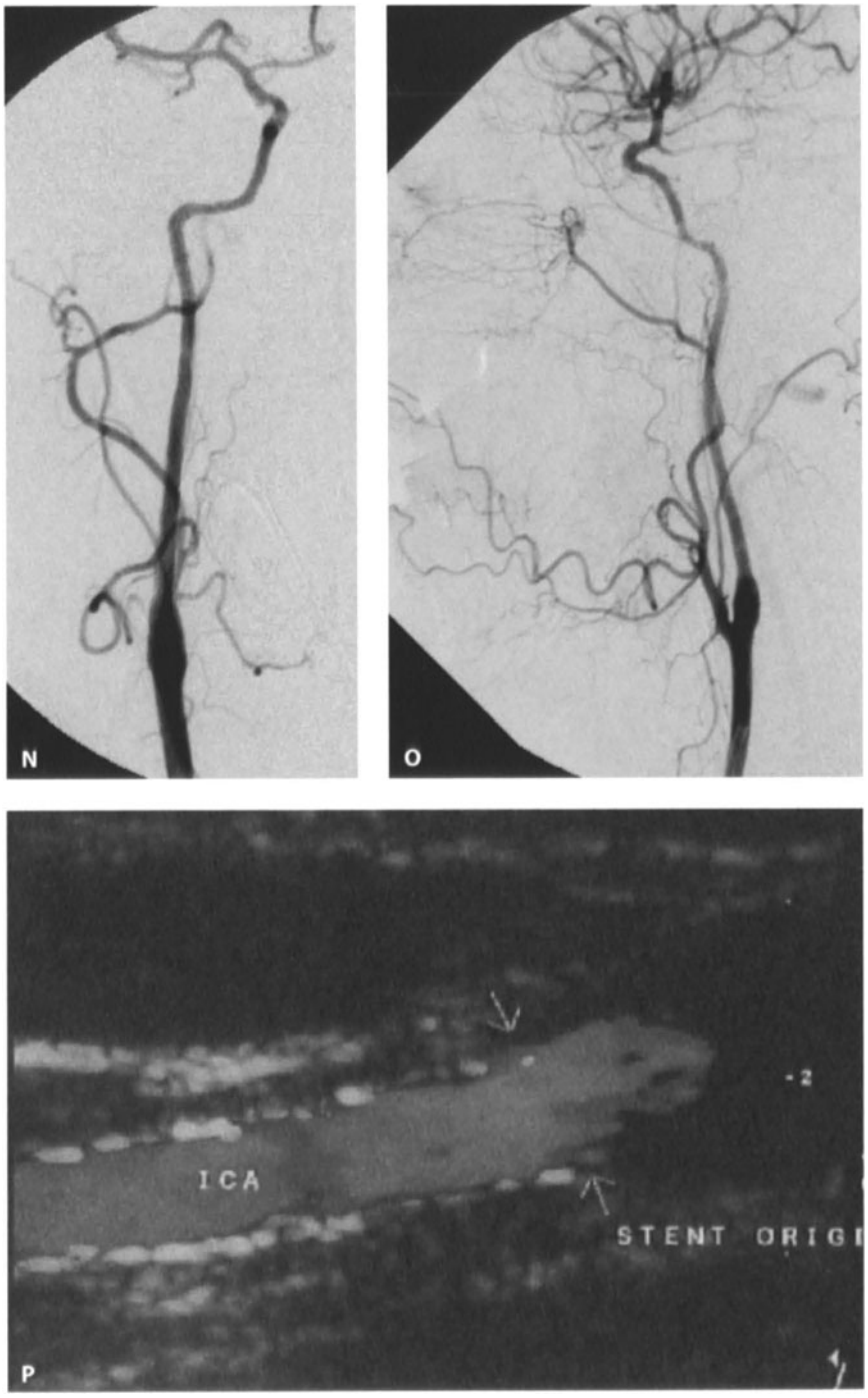

Fig. 1.12 (*continued*). **N** Frontal and **O** lateral DSA of the common carotid artery after total revascularization showing a nearly normal looking carotid artery, with excellent filling of the intracranial vessels. In the lateral view, antegrade flow through the posterior communicating artery can be seen. **P** Three months later, ultrasound shows the preserved patency of the ICA (*arrows*)

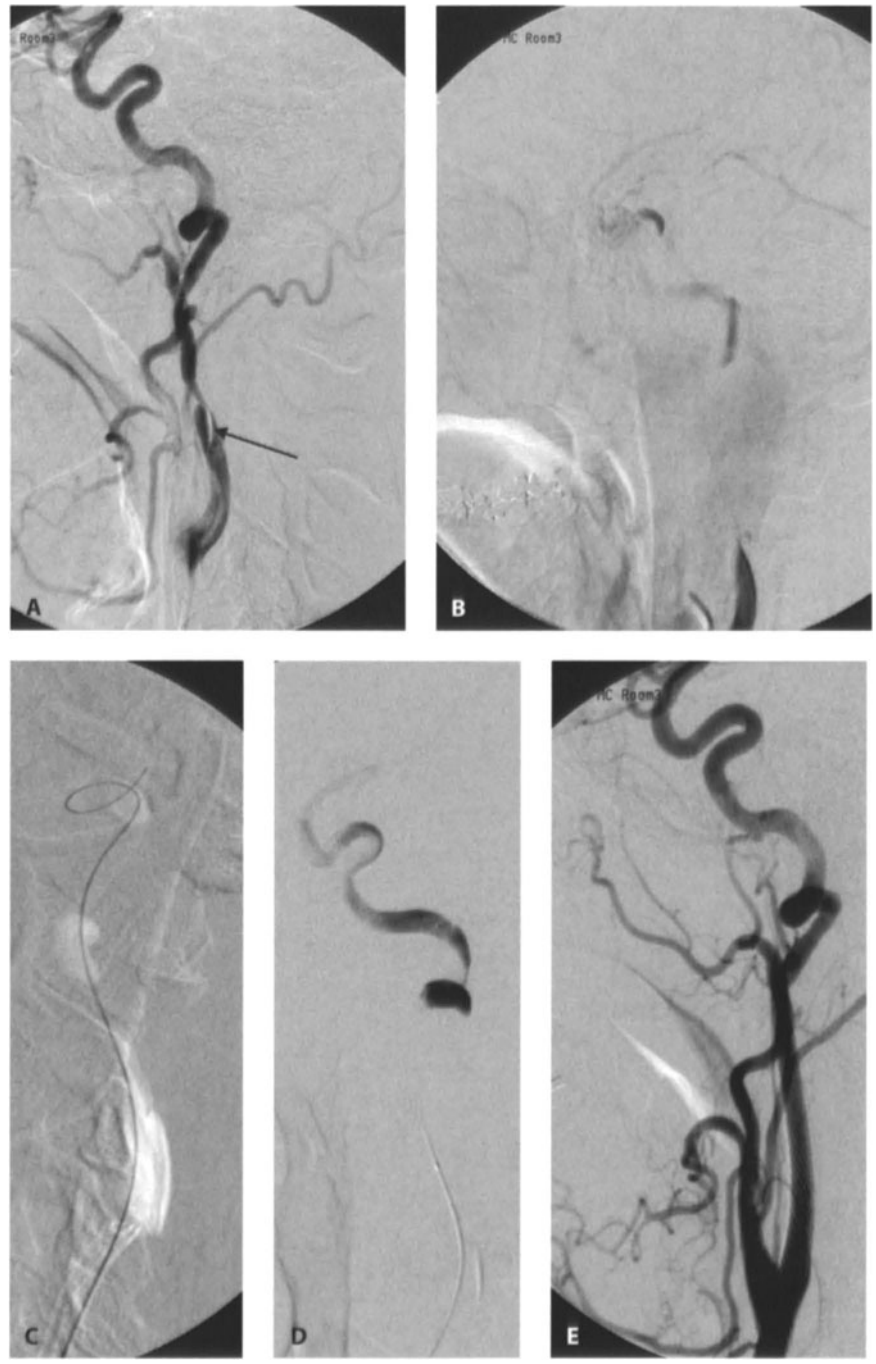

Fig. 1.13A–E. Iatrogenic internal carotid artery dissection with poor collateral circulation treated in emergency. **A** Lateral view of the common carotid artery during cerebral angiography demonstrates an iatrogenic dissection of the carotid artery. Note the lucency representing the dissection (*arrow*). **B** On the follow-up angiogram several minutes later, there is progressive occlusion of the carotid artery by the flap, despite full heparinization. **C, D** Emergency revascularization. **C** Road map image of the microcatheter with neuromicroguidewire crossing the lesion in the true lumen, which is confirmed on **D** following retrograde blood flow, confirming the intraluminal position of the microcatheter. At this point, an Exchange stiffer 300-cm guidewire is used to provide sufficient support to deploy a stent across the entire carotid artery, with an excellent final result. **E** The carotid artery has been repaired

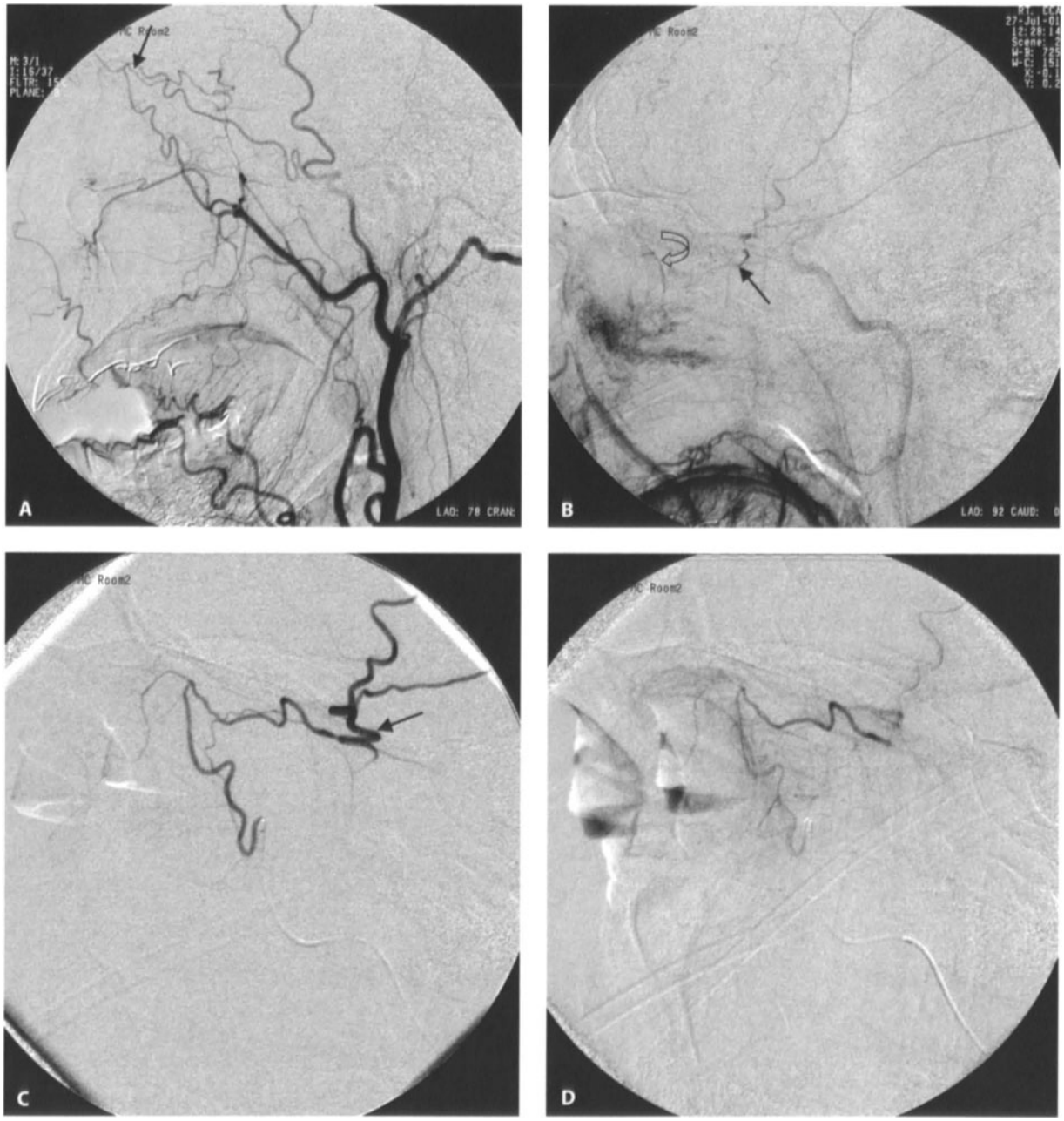

Fig. 1.14A–F. A 65-year-old patient presenting with 3.5 h of vision loss. **A** Lateral digital subtraction angiogram of the common carotid artery late arterial phase. There is no opacification of the internal carotid artery (*arrow*). **B** The anterior deep temporal artery anastomoses with the lacrimal artery (*arrow*) and opacifies the ophthalmic artery (*curved open arrow*). In the later phase, there is late opacification of the internal carotid artery but there is no filling of the ophthalmic artery origin. There is stagnation in the mid segment of the ophthalmic artery at the point of anastomosis from the middle meningeal artery, which originates from the ophthalmic artery itself (*arrow*). In the retinal blush only a small segment is visualized (*curved open arrow*). **C** Coaxial catheterization of the anterior deep temporal artery. Note, the injection of contrast material opacifies the variation of the ophthalmic origin of the middle meningeal artery (*arrow*) and then there is filling of the main ophthalmic trunk. The internal carotid artery does not opacify. **D** Legend and **E, F** see p. 67

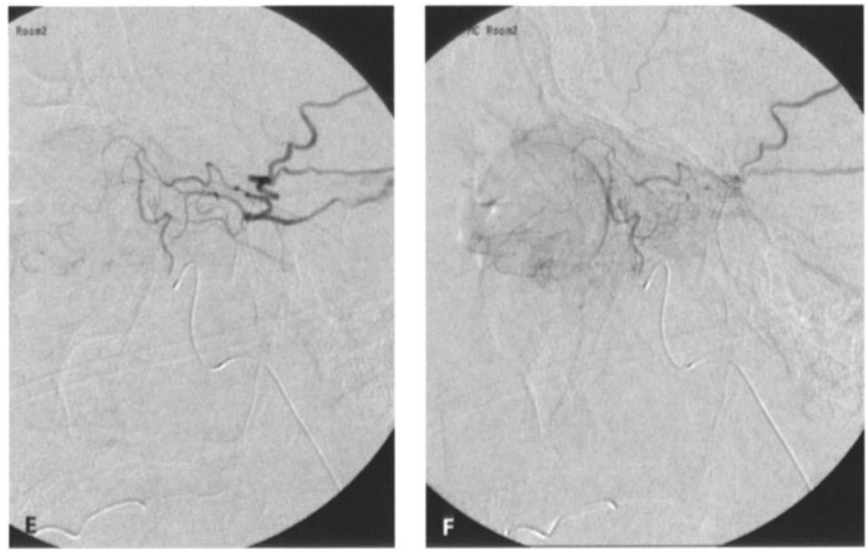

Fig. 1.14 (*continued*). **D** Late phase of the anterior deep temporal artery injection under flow control. Gentle injection of contrast material opacifies the ophthalmic artery anastomosis, with the middle meningeal artery reversing its flow towards the ophthalmic main trunk. This makes it possible to use the microcatheter and the anastomosis as an extension of the catheter tip, to deliver the recombined tissue plasminogen activator (r-TPA). **E** After 7 mg of r-TPA there is opacification of the ophthalmic artery in a retrograde fashion, with filling of the internal carotid artery. **F** Late phase of the same injection demonstrates better opacification of the retinal blush. The patient had partial recovery of vision

1.2.4.16 Central Retinal Artery Occlusion

Central retinal artery occlusion (CRAO) is a major ophthalmological event, usually resulting in blindness. Conventional therapeutic procedures, including ocular massage, carbohydrate inhibitors, and hemodilution are not very effective (Gold 1977; Simmonds 1962; Duker et al. 1991). According to Duker et al., only 33% of patients who underwent these different types of treatment experienced significant improvement in vision.

The role of superselective fibrinolysis, with high local concentration of fibrinolytic agents, is very promising, as was demonstrated by Schmidt et al. (1992), Schumacher et al. (1993), and Weber et al. (1997), and may be considered the treatment of choice for CRAO.

Most series have employed r-TPA in doses ranging from 40 to 70 mg, injected superselectively over a 1- to 3-h period. All reported patients have undergone similar regimes of systemic heparinization. The time interval between the onset of symptoms and the start of treatment is the most important factor in determining outcome in patients with CRAO. In fact, the clinical outcome was good in the majority of reported series if the treatment was performed within 6.5 h and in particular when performed less than 4.5 h from onset of symptoms (Padolecchia et al. 1999). Additionally, a better outcome is obtained when no severe retinal edema is present prior to treatment (Zeumer et al. 1992; Schmidt et al. 1992; Schumacher et al. 1993; Weber et al. 1997; Padolecchia et al. 1999).

For the most part, over-the-wire microcatheters were used, but flow-guided microcatheters have also been employed. Revascularization of the

Fig. 1.15A, B. Balloon angioplasty of the petrous internal carotid artery. **A** Lateral digital subtraction angiogram of the right internal carotid artery shows a discrete focal stenosis of the petrous segment. **B** Immediately after balloon angioplasty of the same segment with improvement in the flow. The deflated balloon markers can be seen

ophthalmic artery can be accomplished even in cases with total occlusion of the internal carotid artery. In such cases, the anastomosis from the internal maxillary artery and/or middle meningeal artery can be selectively catheterized to deliver the thrombolytic medication (Fig. 1.14, pp. 66, 67) (Schumacher et al. 1993; Padolecchia et al. 1999). Treatment is usually stopped as soon as improvement in vision is observed and retinal blood flow is reestablished.

1.2.4.17 Internal Carotid Artery Stenosis Above the Carotid Bulb

The natural history of intracranial ICA stenosis as reported by Marzewski et al. (1982) showed that cavernous stenosis is the most frequent location after the carotid bulb, followed by petrous lesions and supraclinoid stenosis.

Patients with intracranial ICA stenosis were followed up for an average of 3.9 years and divided into three groups depending upon outcome: TIA, stroke, or neither. In this group of patients, 12.1% had a TIA and 15.2% had a stroke, for an event rate of 27.3%. The rate of stroke in patients younger than 65 years of age with intracranial stenosis was 300 times the rate when compared to a matching normal population.

To date, the treatment of these patients has been difficult. The Extracranial to Intracranial Bypass Study was not favorable for the extracranial to intracranial (EC/IC) bypass operation, favoring medical therapy. Many of these patients suffer not only from strokes, but also from hypoperfusion symptoms and might benefit from balloon angioplasty, in the petrous carotid artery (Fig. 1.15), or preferably balloon-expandable stents (Fig. 14.160). There are cases of tandem lesions involving the carotid bulb and a more distal lesion such as the cavernous carotid artery, where endovascular revascularization has become the treatment of choice (Fig. 1.16).

Fig. 1.16A–E. Tandem lesions. **A** Common carotid artery (CCA) injection demonstrates a 70% narrowing of the carotid artery with a long plaque extending from the CCA to the distal carotid bulb. **B** 3-D image demonstrating the severe stenosis of the C5 segment of the internal carotid artery. **C** CCA after stenting the bifurcation. **D** The guidewire had crossed the distal lesion from the beginning. After repairing the bifurcation, a coronary stent was advanced into the C5 segment and the stent was deployed. **E** Follow-up angiogram after stent delivery shows excellent improvement in the lumen of the severely narrowed segment

1.2.4.18 General Organization of a Stroke Emergency Team

Modern global care of stroke victims requires the presence of a round-the-clock multidisciplinary team. This group includes the acute rescue team of paramedics and other health professionals, stroke nurse coordinator, and physicians of various disciplines, i.e., medicine stroke neurologists, intensivists, vascular surgeons, neurosurgeons, interventional neuroradiologists, and endovascular surgeons.

Information regarding the feasibility and importance of acute stroke treatment should be disseminated in paramedic and allied health professional journals. It should be stressed, not only at the professional level, but even more importantly to the public and to society as a whole, that acute stroke can and should be treated. Efficient therapeutic measures exist that may help or cure many stroke patients if they are promptly and accurately diagnosed and provided rapid access to dedicated stroke centers.

Experienced professionals have recommended a number of simple but very efficient timesaving maneuvers. Firstly, patients with a suspected stroke should be brought as soon as possible to a hospital that has 24-h access to CT and triage carried out by specifically trained professionals. CT will then be performed while the acute stroke team is alerted. In 20% of cases, a hemorrhage is found (Table 1.7), and the patient will then receive appropriate medical and surgical therapy. If the CT reveals no evidence of hemorrhage, then a neurologist will immediately examine the patient. Depending on the amount of time that has passed since the onset of symptoms, the neurological findings, and the amount of infarction already shown on CT, a decision will be made as to how best to proceed with the treatment. If the area of infarction is limited and corresponds to a cortical location, and if the time since onset has not exceeded 3 h, then IV r-TPA is considered the most appropriate treatment. If the time passed since onset is between 3 and 6 h, and the area of infarction represents less then one-third of the MCA territory, anesthesia is notified and the patient is immediately transferred to the angiographic suite for possible intra-arterial thrombolysis. If at all possible, depending on the time window available, the patient will have an immediate MRI examination prior to angiography, which will include diffusion-weighted imaging (DWI) and perfusion-weighted imaging (PWI). If the DWI and PWI match (Fig. 1.17), this means that there is no significant penumbra and most of the affected tissue is already infarcted. This will likely represent a contraindication for intra-arterial thrombolytic therapy, or at least the chances of salvageable tissue will be low. A DWI/PWI mismatch (Fig. 1.18) suggests the presence of a significant penumbra with potentially salvageable tissue. If so, consent for IA thrombolytic therapy will be obtained from the family while the patient is prepared for and undergoes diagnostic angiography with intent to treat. The angiogram will provide further information as to the anatomical area of occlusion, collateral circulation, and areas of cerebrovascular stenosis and/or anatomical variants that may be relevant to the decision-making process. If the angiographic findings are perceived to be favorable and the final neurological examination confirms lack of improvement in the clinical status, then the patient is fully anesthetized and superselective catheterization is carried out. A maximum of 20 mg of

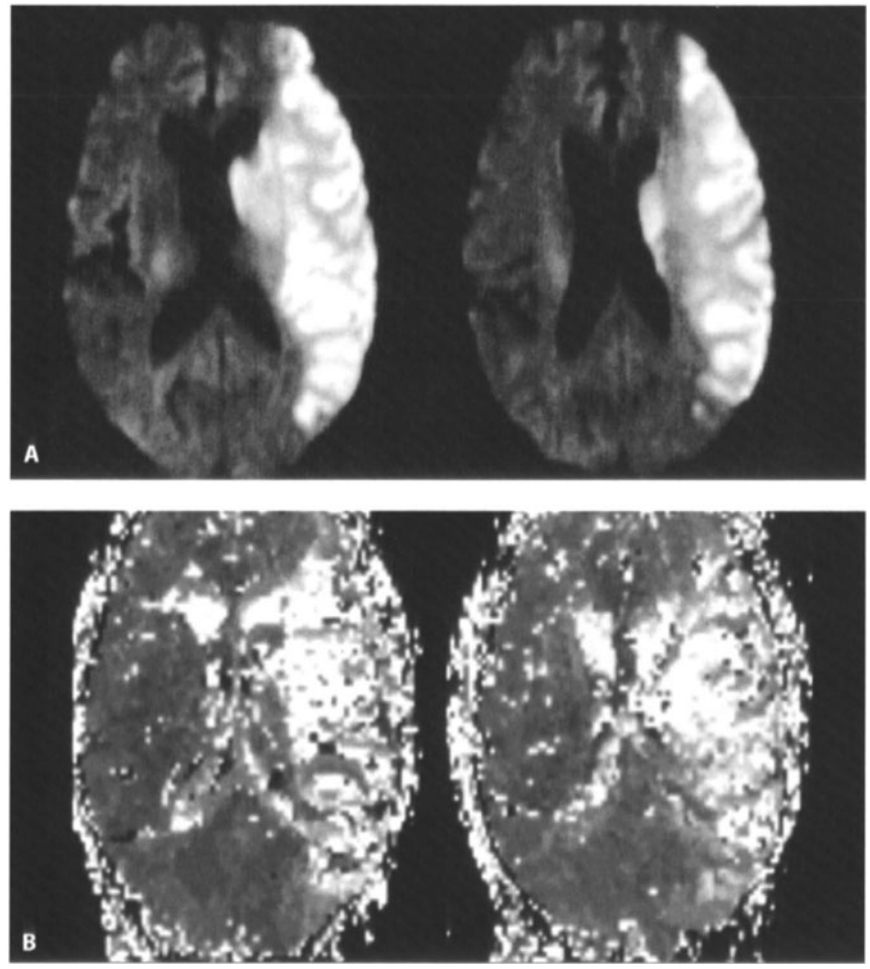

Fig. 1.17A, B. Diffusion and perfusion MRI matching. **A** Diffusion-weighted imaging (DWI) approximately 10 h after an acute stroke shows the extensive diffusion abnormality in the left hemisphere. **B** The DWI image matches the perfusion-weighted image (PWI) for lesion volume, suggesting that the tissue has already infarcted. This patient would not be a good candidate for thrombolysis

r-TPA is injected into the thrombosed segment over a 40-min period while a low dose of systemic heparinization is maintained intravenously during the treatment procedure. If following initial recanalization, reocclusion of the vessel occurs, then adjuvant therapy such as ReoPro should be considered as well as mechanical maneuvers such as balloon angioplasty, with or without stenting (Fig. 1.7), or a snare removal device (Chopko et al. 2000) may be tried.

Depending on the regional and local health care situation, two types of acute stroke care management strategies are proposed. In a given community, all acute stroke patients will be transported to one facility where all the above options are available (the stroke center). Alternatively, patients will be triaged at satellite centers, where they will be screened with CT and evaluated by a neurologist, who will provide intravenous therapy if indicated, and the patient will be transferred to the regional stroke center for possible intra-arterial therapy if appropriate.

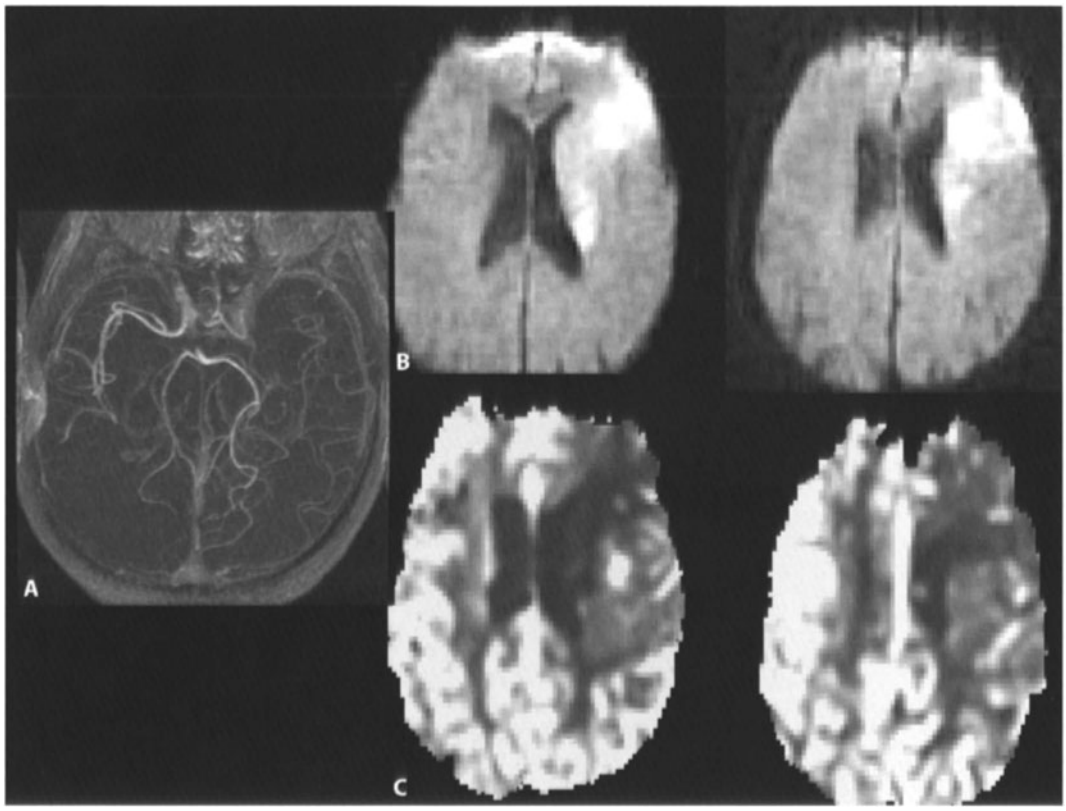

Fig. 1.18A–C. Diffusion-weighted–perfusion-weighted image mismatch. **A** Magnetic resonance angiogram demonstrates absence of the horizontal segment of the left middle cerebral artery. **B** Perfusion-weighted images demonstrate an area of perfusion abnormality extending in the frontal area. **C** Diffusion-weighted images demonstrate a significantly larger area of diffusion abnormality. This mismatch suggests an opportunity for significant salvageable tissue and is a good indication for intra-arterial thrombolysis

1.2.4.19 Evolving Treatment Strategies

Cocktail therapies combining thrombolytics, antiplatelets, free-radical scavengers, antioxidants, etc. will most likely be developed to treat various aspects of the ischemic insult. Cocktail therapies will be necessary because different cells may experience different levels of ischemic injury and chemical changes within a given cell vary depending upon time from the ischemic event. Unfortunately, the outcome of these adjuvant therapies, with the exception of the thrombolytics, has been somewhat disappointing, perhaps because they are not reaching their specific destinations in time. Treatment in the future may also be targeted towards a specific cell type (endothelial, glial, neurons, platelet, lymphocyte, etc.) and a specific pharmacological effect (cytokinins, etc.).

Treatments will also attempt to address the protection of the particular environment where the ischemia occurred and other related territories (i.e., global vs. focal area of ischemia).

The use of a combination of thrombolytics, with varying half-lives, as well as the utilization of other pharmacological agents that act upon

different cells of the coagulation cascade at different times may be important.

As IV thrombolysis and LIAT are being used more often, proper classification of the various ischemic stroke types is needed to evaluate their comparative efficacy. In addition to clinical assessment, such classification will need CT, MRI, as well as functional MRI, DWI and PWI MRI, and angiography. Research models for various therapeutic regimes will also be needed for evaluation of safety and efficacy of various treatments.

1.2.5 Extracranial Carotid Artery Stenosis

1.2.5.1 Introduction

Carotid artery stenosis, particularly involving the origin of the internal carotid artery, is a frequent clinical problem in Western populations. These stenoses are almost invariably due to atherosclerosis. It may be discovered as an asymptomatic bruit on physical examination or following one or more transient ischemic attacks related to thrombus embolization from the stenotic lesions. Carotid stenosis is responsible for 20% of all ischemic cerebral events.

The nature of the atherosclerotic plaque (see Sect. 1.2.3.4, "Mechanisms of Atherogenesis") and the mechanisms by which it results in symptoms (e.g., distal embolization) must also be kept in mind when designing and assessing any approach to carotid artery disease.

1.2.5.2 Natural History

The natural history of carotid artery stenosis may vary between different ethnic, socioeconomic, and gender groups. Within a given population, different life styles and/or diets may have an important influence in the epidemiology of carotid stenosis. The degree and type of stenosis as well as the absence or presence of symptoms will have an impact on the natural history of patients with carotid stenosis. As the severity of the stenosis increases, the rate of stroke increases. Norris et al. (1991) reported that in patients with carotid stenosis of 75%, the rate of stroke is 1.3% per year, and if the stenosis is greater than 75%, the stroke rate rapidly rises to 10.5% per year. Studies of large populations have found that patients with stenosis greater than 75% exhibit a 1st-year stroke rate of 2%–5% (Zarins 1996; Hennerici et al. 1987). The NASCET study demonstrated that symptomatic patients with 70%–99% carotid stenosis followed for 2 years had a 26% risk of ipsilateral stroke and 28% risk of any stroke (Hennerici et al. 1987).

The presence of an ulcerated plaque and/or extensive ulceration is associated with a stroke rate of 7.5% per year (Autret et al. 1987). Patients presenting with TIAs and a high-grade stenosis are at a 13% risk of stroke in the first year and 37% risk in the first 5 years following the onset of symptoms (Dennis et al. 1990). If the presenting symptom is an ischemic stroke, the chances for a recurrence are 59% during the first year and

Table 1.17. Presentation and risk of stroke

Presentation	1st year or yearly rate	5 years	NASCET at 2 years stroke
TIAs	13% 1st year	37.5% first 5 years	42%
Amaurosis fugax	2%/year		17%
Ulcerated plaque	7.5%/year	Two- to fourfold more events than smooth plaque	
Stroke	59% 1st year	45% at 5 years	

Table 1.18. Progression of stenosis[a] (ultrasound; modified from Johnson 1995)

% Stenosis	Symptomatic (7 years)	Asymptomatic (3 years)
<50	23% (3.2%/year)	–
50–79	50% (7.1%/year)	17% (5.6%/year)

[a] Progression to severe stenosis or total occlusion, with an annual stroke rate of 20.6%/year.

thereafter a cumulative risk at 5 years of 25%–45% (Sacco et al. 1982). Ulcerated heterogeneous lesions exhibit a reoccurrence two to four times greater than nonulcereted homogeneous lesions (Langsfeld et al. 1989; Sterpetti et al. 1988).

The initial symptom also has a prognostic implication of subsequent stroke. If the presenting symptom is a TIA or transient monocular blindness, then the annual rate of stroke is 2% (Jafar 1998). At 7 years, patients who presented with amaurosis fugax have a cumulative rate of stroke of 14%, compared to 27% in patients presenting with a hemispheric TIA (Table 1.17) (Jafar 1998). NASCET investigators reported a 2-year risk of fatal and nonfatal stroke of 17% after amaurosis fugax and a 42% risk after hemispheric TIA.

In 1995, Johnson et al. (1995) published a study of the natural history of 232 patients with mild (<50%) and moderate (50%–79%) carotid artery stenosis, who were followed up with annual carotid duplex ultrasonography for a mean of 7 years. They reported a progression of the stenosis in 23% patients, with 50% of these patients progressing to severe stenosis (80%–99%) or occlusion. The risk of progression to severe stenosis or occlusion of the carotid artery was greater in patients whose initial stenosis was moderate rather than mild (Table 1.18) (Johnson et al. 1995).

In asymptomatic patients with 50%–79% stenosis followed up with at least two serial ultrasound examinations for a mean of 38 months, progression of stenosis was noted in 17% of arteries. There was, however, a low incidence of ipsilateral stroke in this group of patients, with a rate of disease progression of 0.85% at 1 year, 3.6% at 3 years, and 5.4% at 5 years (Rockman et al. 1997).

As the degree of stenosis progressed up to 80%–99%, the annual rate of neurological events increased to 20.6%, even when these patients were originally asymptomatic (Bock et al. 1993).

Table 1.19. Carotid artery stenosis: risk factors of subsequent stroke (in decreasing order)

Ipsilateral stroke
TIA or amaurosis fugax
Severity of stenosis
Progression of stenosis
Carotid occlusion
Contralateral stroke
Heart disease
Plaque ulceration
Carotid bruit

In a retrospective review of 167 patients with carotid occlusion, 27% of whom had no history of symptoms, 43% had suffered a stroke and 17% had had a TIA, revealed on follow-up (mean, 39 months), 18% had developed a stroke, 67% of which were ipsilateral to the occlusion (Faught et al. 1993). Heart disease was the cause of death in 15% during follow-up. The rate of contralateral stroke was 33%, with a higher 5-year stroke incidence (77%) in patients with 50%–99% stenosis compared to patients with less severe (<50%) stenosis (94%) (p=0.082) (Faught et al. 1993).

An additional risk factor of subsequent stroke is plaque ulceration. The pathophysiological process of plaque rupture, foam cell infiltration, and thinning of the fibrous cap occurred more often in patients with symptomatic rather than asymptomatic carotid stenosis (Carr et al. 1996). In medically treated NASCET patients, plaque ulceration increased the risk of ipsilateral stroke over a 2-year follow-up, from 26.3% to 73.2%, as the degree of carotid stenosis progressed from 75% to 99%, respectively. In patients without plaque ulceration, the 2-year stroke risk rate was 21.3% regardless of the degree of stenosis (Eliasziw et al. 1994) (Table 1.19). Therefore, the risk of a neurological event nearly doubles in the face of ulceration and increasing severity of carotid stenosis.

Patients with carotid disease at locations other than the bifurcation may have a lower natural risk of stroke. Those who have other medical problems such as coexisting coronary disease may die or become disabled from these other conditions before the benefits of carotid endarterectomy (CEA) or carotid angioplasty and stenting (CAS) can be seen.

1.2.5.3 Carotid Bruit

While carotid bruits are common, they do not predict the severity of stenosis. Since carotid bruits are associated with an increased risk of subsequent stroke and cardiac death, all patients with carotid bruits should undergo carotid duplex ultrasound examination by a well-qualified vascular laboratory as well as an assessment for coronary artery disease. Once the degree of carotid stenosis has been determined, the risk of progression and subsequent neurological events can be determined.

1.2.5.4 Imaging

Carotid Ultrasound

Carotid duplex ultrasound has become the most frequently employed imaging modality in the diagnostic evaluation and follow-up of patients with suspected carotid artery disease. It is a noninvasive diagnostic imaging method with a high degree of sensitivity and specificity. Unless the degree of clinical suspicion suggests otherwise, there will be few reasons to proceed to catheter angiography (or other tests) when the ultrasound examination is normal.

Further diagnostic work-up for patients with carotid stenosis varies depending on extent of disease. In symptomatic patients with 30%–50% carotid stenosis, ultrasound testing should be repeated at least every

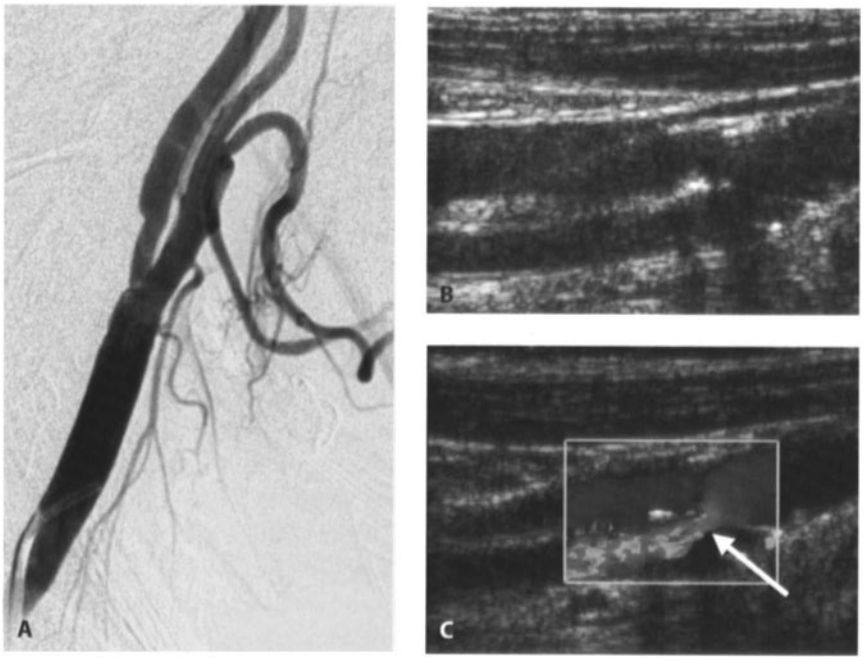

Fig. 1.19A–C. Ultrasound as a diagnostic modality. **A** Lateral digital subtraction angiogram of the right common carotid artery shows a 50% narrowing of the carotid artery lumen. **B** B-mode ultrasound showing the area of narrowing when comparing the internal to the external carotid artery. **C** Color Doppler, which clearly shows the internal carotid artery narrowing at the bifurcation (*arrow*)

6 months. In patients with carotid stenosis of 60% or more, ultrasound findings are usually corroborated with another noninvasive technique such as MRI or CTA. Presently, at most institutions, catheter angiography is rarely used in the diagnostic work-up, unless there is discordance between the various noninvasive imaging studies.

The reliability of ultrasound imaging is, however, very much operator dependent, and several factors, including the equipment utilized, may interfere with the accuracy of the results provided. In order to avoid making improper treatment decisions based on erroneous ultrasound reports, it is recommended to audit and validate the ultrasound laboratory versus catheter angiography obtained on the same group of patients (Fig. 1.19). Once the laboratory has been validated for the assessment of the degree of carotid stenosis, then audits should be carried out from time to time to ensure that their test results remain reliable.

Duplex scan and color-flow Doppler are noninvasive techniques with potential to assess both luminal features and arterial wall structure and are often used both before and after therapy. Duplex scanning is superior to other techniques such as catheter angiography in evaluating carotid plaque morphology. At present, if duplex ultrasound suggests total extracranial occlusion, angiography is still indicated because it is difficult to differentiate total occlusion from a high-grade stenosis by ultrasound. Ultrasound limitations also include the potential of missing skull base or intracranial arterial stenosis and intracranial aneurysms.

The role of transcranial Doppler as a complement to duplex ultrasonography is limited. It may be of assistance in determining flow patterns and direction of flow at the ophthalmic level, at the circle of Willis, or at the basilar level. Ultrasound is also of limited value in the evaluation of carotid dissection, while dissections in the vertebrobasilar territory are even more difficult to demonstrate.

Table 1.20. Carotid ultrasound: hemodynamic assessment

Carotid stenosis	PSV (cm/s)	EDV (cm/s)	Sensitivity (%)	Specificity (%)	Predictive value		Accuracy (%)
					+	–	
70–99	>140	>100	85%	98%	90%	96%	97%
50–69	>130	<100	92%	97%	93%	99%	97%
30–49	Not well established						

PSV, maximal peak systolic velocity; EDV, end diastolic velocity.

Some of the newer refinements in ultrasound imaging include color-coded Duplex, 3-D ultrasound, and double enhanced ultrasound. Added advantages include the ability to identify intraluminal thrombi loosely attached to the arterial wall, ulceration, and intramural hemorrhage (Alexandrov and Norris 1997).

Hemodynamic assessment by ultrasound utilizes the maximal peak systolic velocity (PSV) and the end diastolic flow velocity (EDV) measurements to quantify the degree of stenosis, by comparing the site of maximum stenosis to the diameter of the distal carotid artery.

For a 70%–99% carotid stenosis, a PSV of more than 140 cm/s and an EDV of more than 100 cm/s provides a sensitivity of 85% and a specificity of 98%, with a predictive positive value of 90%, and a negative predictive value of 96%, with an overall accuracy of 95%.

For a 50%–69% carotid stenosis, a PSV greater than 130 cm/s and an EDV of less than 100 cm/s proved to be the best combination, with a sensitivity of 92%, a specificity of 97%, a predictive positive value of 93%, a negative predictive value of 99%, and an accuracy of 97%.

For 30%–49% carotid stenosis, these criteria are less well established (Table 1.20).

The ratio of the peak systolic velocity in the ICA to the peak systolic velocity of the CCA, can accurately identify severe stenosis. An ICA/CCA systolic velocity ratio of 4 or greater predicts a stenosis greater than 70%, with a sensitivity of 91%, a specificity of 90%, a predictive positive value of 87%, a negative value of 94%, and an overall accuracy of 91%.

There are generally no accepted criteria to quantify stenosis with the color flow Doppler alone.

The presence of high-grade stenosis and certain plaque morphology in the cervical carotid artery is associated with increased risk of cerebral embolization events. Ultrasound can detect these potential emboli as high-intensity transient signals (HITS).

The risk–benefit ratio of treatment can be difficult to establish. Ultrasound, by characterizing the nature of carotid plaque and detecting HITS, may help determine which individuals are at greatest risk of cerebrovascular events. The risk–benefit ratio may become more accurate and meaningful if treatment options are adapted to individual patients, based in part upon these ultrasound findings.

Microemboli are most often detected beyond symptomatic carotid stenosis and the rate of microemboli is markedly reduced follow-

Table 1.21. Gerolakos and Nicolaides classification of plaque morphology (ultrasound)

Type I	Uniformly echolucent plaque with or without a thin echogenic cap
Type II	Predominantly echolucent plaques with less than 50% echogenic areas
Type III	Predominantly echolucent plaques with less than 50% echolucent areas
Type IV	Uniformly echogenic plaques
Type V	Plaques that cannot be classified due to calcifications producing acoustic shadows

ing endarterectomy. HITS are absent in control groups without carotid plaque.

The characterization of the structure of the plaque has been made possible with the advent of high-resolution B-mode ultrasound scanning, which may allow for a better correlation between plaque morphology and symptoms.

B-mode ultrasound scanning is able to differentiate the composition of carotid plaques. Fibrous or calcified material is more echogenic than lipid or intraplaque hemorrhage. It has been estimated that intraplaque hemorrhage is 1.6–6.7 times more common in symptomatic patients.

Lipid-filled and hemorrhagic plaques have a greater potential for ulcerating and embolizing. Plaque fracture over the site of the hemorrhage may lead to luminal thrombi formation. The most recent classification of plaque morphology is that of Gerolakos and Nicolaides (Table 1.21).

The visualization of ulceration in plaques is limited by size. An ulcer must be larger than 2 mm and deeper than 2 mm to be detected. Ulcerations are characterized by echocentric defects in the plaque, with smooth contours and abrupt margins. Use of 2-D and 3-D ultrasound should improve the ability to detect plaque ulceration.

A proper ultrasound report should describe the degree of stenosis, the analysis of the occluding material, and the integration of the stenosis into the context of the overall visualization of the vessel wall, as well as the clinical status of the patient (Luizy 1998; Alexandrov and Norris 1997).

Computer Tomographic Angiography

Computer tomographic angiography (CTA) provides excellent imaging of the cervical carotid arteries. When technically possible, it is a good way to image the carotid bifurcation, and the axial source images provide accu-

Fig. 1.20A–F. Computer tomographic angiography (CTA). Patient with a left hemispheric stroke was referred for endovascular treatment of the left carotid artery. The patient underwent CTA to demonstrate a long stenotic lesion of the left carotid artery. CTA of the left (**A**) and right (**B**) carotid arteries demonstrates a long segment of narrowing just distal to the carotid bifurcation on the left, and no significant disease on the right. Left common carotid artery digital subtraction angiogram of the neck (**C**), and the right common carotid artery neck (**E**), correlate well. However, films of the intracranial circulation on the left (**D**) and the right (**F**) demonstrate severe disease in the petrous and cavernous carotid arteries not visible on the CTA. This represents a contraindication for any type of carotid endarterectomy and severe limitations for endovascular treatment ▶

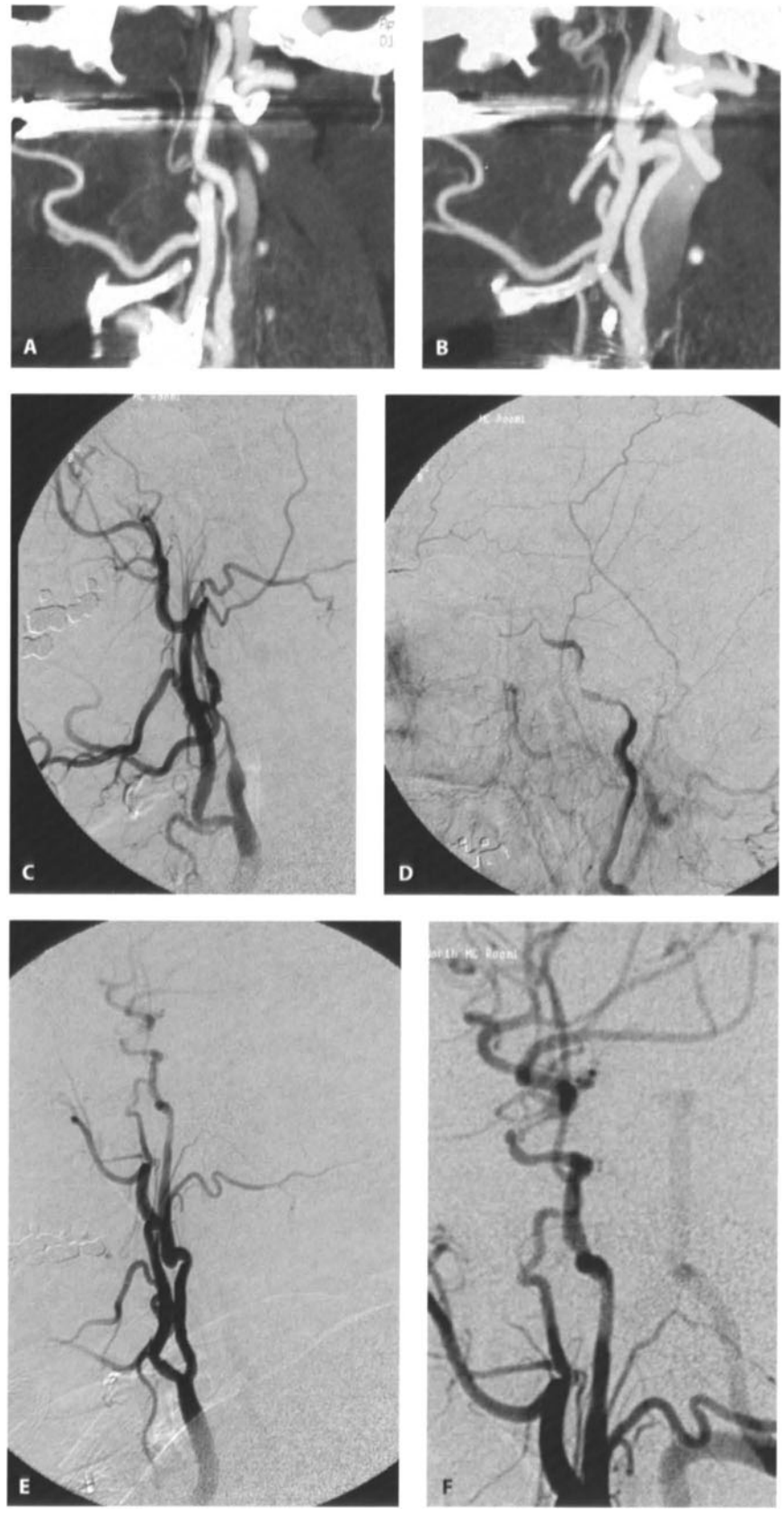

Fig. 1.20A–F.
Legend see p. 78

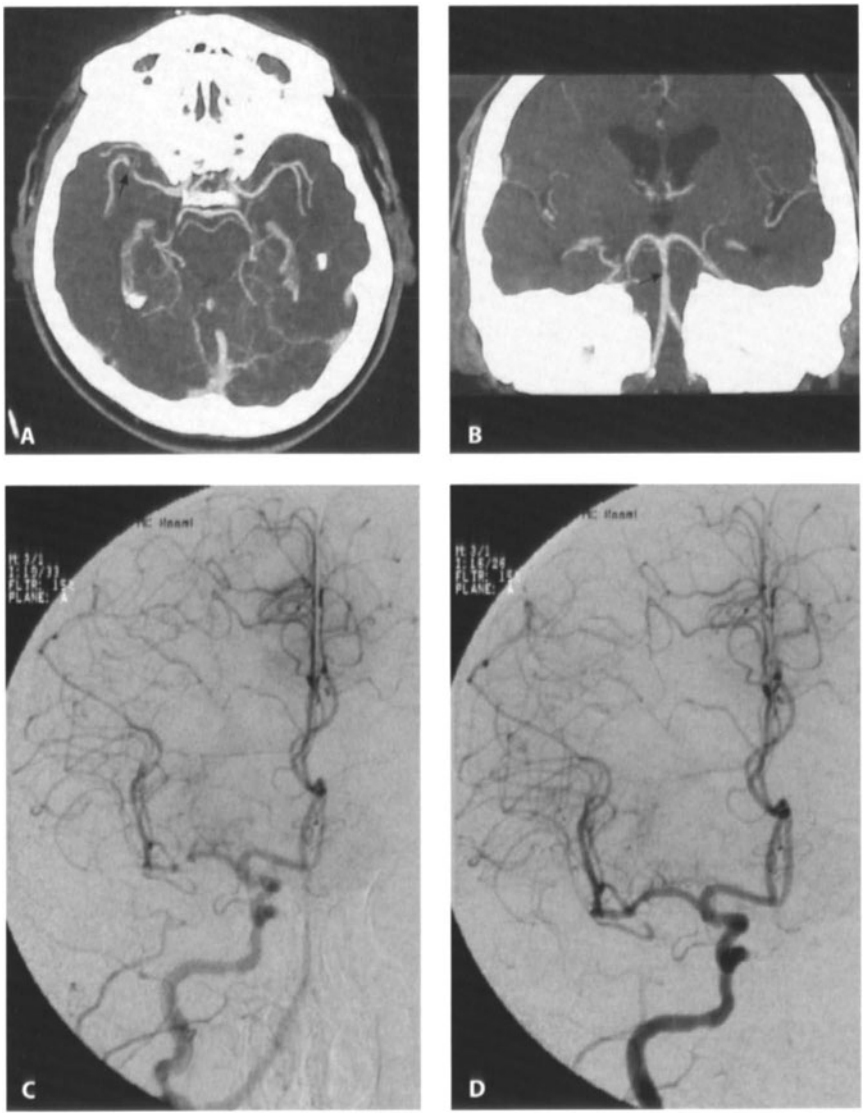

Fig. 1.21A–D. Intracranial computer tomographic angiography (CTA). **A** Axial CTA demonstrates stenosis of the right middle cerebral artery (RTMCA) (*arrow*). **B** Coronal CTA in the same patient demonstrates a stenotic lesion in the upper basilar artery (*arrow*). **C** Digital subtraction angiogram confirms the stenosis. **D** After balloon angioplasty

rate information regarding the cross-sectional degree of stenosis. Significant limitations include patient motion, short neck, and severe calcifications. However, the more problematic aspect of CTA, similar to ultrasound and to a certain degree MRA, is the limited information or lack of information on the vessels at the base of the skull and the status of the collateral circulation (Fig. 1.20).

CTA, however, is improving rapidly with the newer fast scanners, allowing noninvasive visualization of intracranial stenotic areas (Fig. 1.21)

Magnetic Resonance Imaging

Magnetic resonance imaging (MRI) is rapidly improving in its ability to accurately and noninvasively image the carotid arteries. Magnetic resonance angiography (MRA) has the advantage of imaging from the origin of the brachiocephalic vessels to the intracranial circulation (Figs. 1.22,

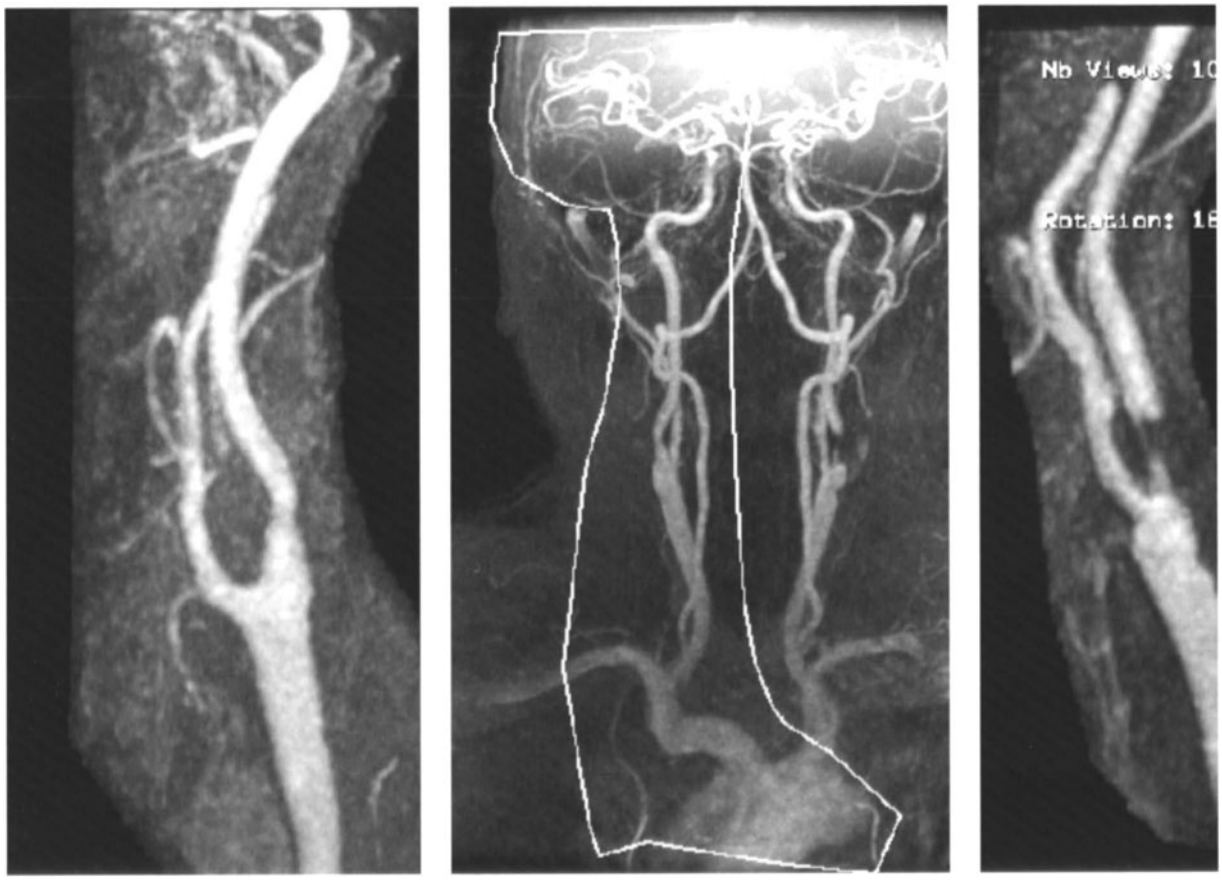

Fig. 1.22. Magnetic resonance angiography (MRA). The sophistication and ability of MRA to act as a noninvasive screening method of vascular assessment is increasing rapidly. Examples of 3-D time-of-flight central encoding MRI with gadolinium enhancement demonstrates the aortic arch, both carotid arteries with severe stenosis on the left carotid at the cervical bifurcation, and visualization of the intracranial circulation

1.23). Some of the limitations of MRA are related to patient motion, artifacts secondary to metal implants, and at the skull base MRA may exaggerate the severity of stenosis. The meaning of signal drop distal to a stenosis may have important implications in assessing the severity of such stenosis (Fig. 1.24). MRA, in combination with MRI, DWI, and PWI, is able to detect associated lesions such as multiple events, the age of lesions, and intracranial occlusive vascular lesions (Fig. 1.23). MRI has the additional advantage of showing parenchymal abnormalities and their result (Fig. 1.25). Functional information is also derived from MRI, with the detection of abnormalities in diffusion, perfusion, and their relationship (DWI/PWI mismatch) (Figs. 1.17, 1.18), the discovery of incidental aneurysms, multiplicity of insults at various circulations in conditions such as emboli from cardiac origin or vasculitis (Fig. 1.26), or other nonvascular pathology. In dissections, MRI has the great advantage of assessing the vessel wall as well as the lumen (Fig. 1.9). At present, there are multiple investigators attempting to use MRI spectroscopy to differentiate various plaque types, and correlate the type with the risk of distal em-

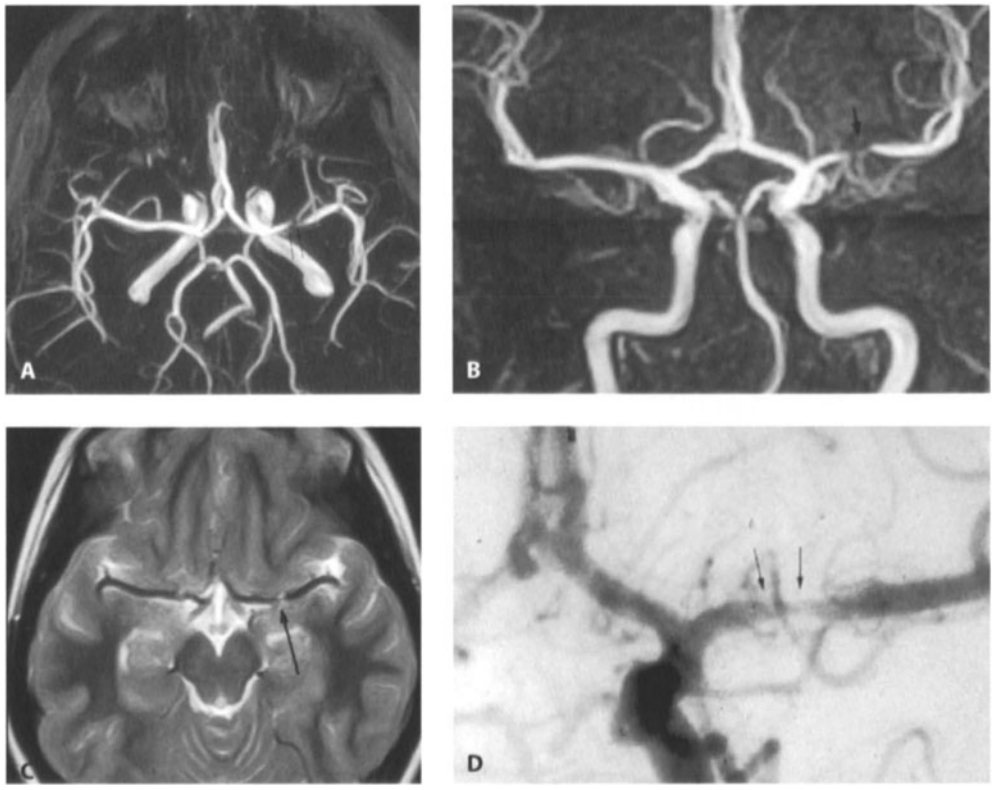

Fig. 1.23A–D. The value of magnetic resonance angiography (MRA). **A, B** MRA time-of-flight after contrast material in axial (**A**) and frontal (**B**) projections show a stenosis of the left M1 segment (*arrows*). **C** Axial T1-weighted image shows the area of stenosis (*arrow*). **D** Catheter angiography frontal view correlates the area of stenosis with the MRA and conventional MRI (*arrows*)

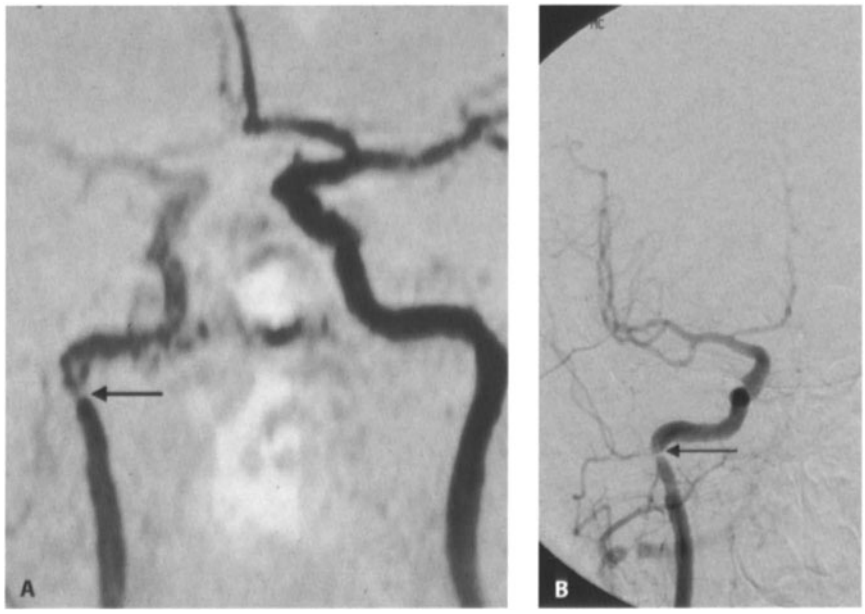

Fig. 1.24A, B. Signal drop in magnetic resonance angiography. **A** 3-D time-of-flight MRI frontal view shows an area of stenosis in the petrous segment of the internal carotid artery (*arrow*). Note the drop of signal in the distal right internal carotid artery including the A1 and M1 segments. **B** Conventional catheter angiography confirms the area of stenosis (*arrow*) and the poor circle of Willis

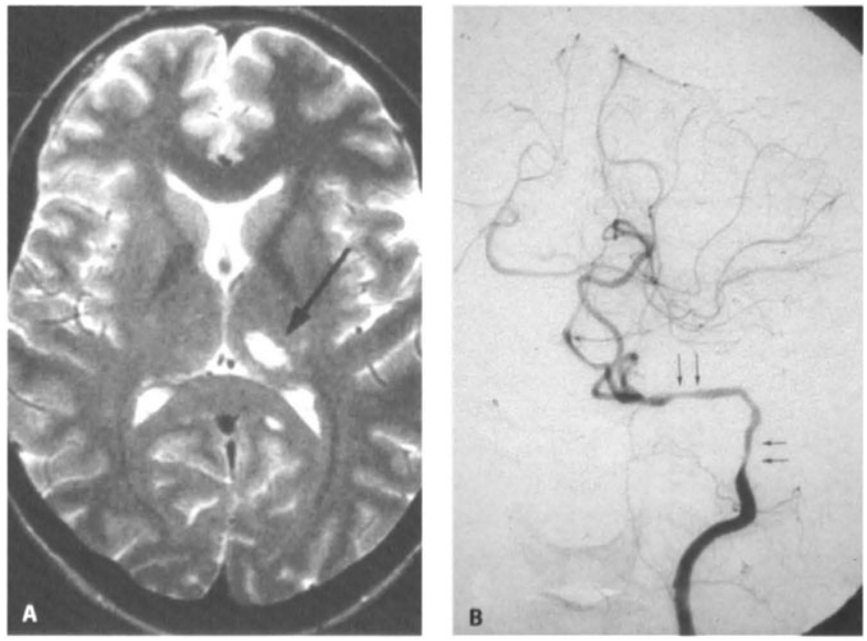

Fig. 1.25A, B. Embolic infarct secondary to left vertebral artery dissection. **A** T2-weighted MRI shows a posterior thalamic infarct (*arrow*). **B** Catheter angiography shows the dissection of the vertebral artery (*small arrows*)

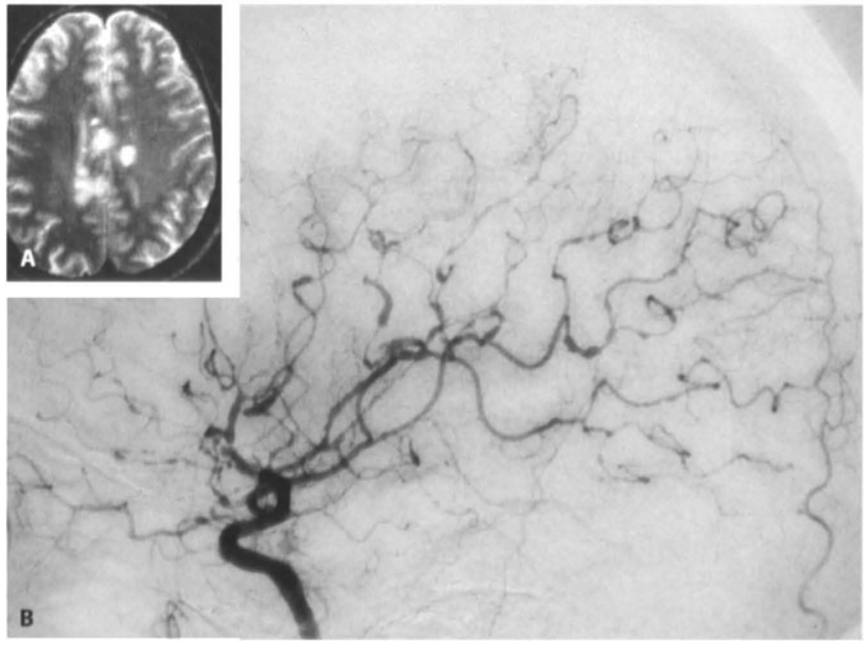

Fig. 1.26A, B. Vasculitis presented as multiple cerebral infarctions. **A** T2-weighted MRI shows multiple increased signals compatible with multiple events. **B** Lateral subtraction angiogram demonstrates the diffuse vasculitis throughout the opercular branches of the middle cerebral artery

bolization and natural history, with obvious implications. The addition of IV contrast material provides enhanced accuracy in cases of questionable flow in what appears to be an otherwise total occlusion.

In the near future, quantitative analysis of flow will further enhance the utility of MRI in patients with occlusive vascular disease.

Carotid Angiography

Nowadays carotid angiography is performed less and less as a primary method for investigation of patients presenting with cerebral ischemic events. The switch towards noninvasive imaging techniques can only be made when the laboratories performing these techniques have been validated locally for catheter angiography. Carotid angiography is now mostly reserved for specific situations, where the diagnosis is difficult or impossible to make with the less invasive studies or when such studies are in disagreement. Catheter angiography is still the gold standard for evaluating the status of the intracranial circulation and the presence of collateral circulation, and has a better spatial resolution than CTA or MRA. Angiographic imaging is evolving rapidly with the advent of three-dimensional (3-D) reconstruction from a rotational acquisition arterial injection. These images can be of great assistance, as they make it possible to visualize the vessels at any possible angle (Fig. 14.24), and in addition, one can acquire an "endoscopic" view of the lumen before and after treatment (Fig. 1.27)

Nevertheless we anticipate that diagnostic catheter angiography will be performed less frequently in the future and mostly be done in preparation for endovascular treatment.

1.2.5.5 Treatment

As the degree of carotid artery stenosis has become the main parameter for treatment decisions, we would like to emphasize that the best way to measure stenosis remains controversial (Table 1.22). Percent of stenosis assumes a standard method of measurement, comparing the narrowest lumen diameter at the bifurcation to the normal diameter of the internal carotid in a vertical distal segment (Grotta 1997). In our opinion, this is inadequate both because it fails to take into consideration the true cross-sectional degree of the stenosis and because the comparative measurement is done distal to a stenotic restrictive lesion. Nevertheless, the relative values of the NASCET measurements are probably comparatively valid.

Table 1.22. NASCET: risk of stroke vs. percentage of stenosis (see also Table 1.21)

Stenosis	Patients		Events (ipsilateral)		Risk		NTT	*P*
%	Med	Surg	Med	Surg	Abs	Rel		
70–99	331	328	26.1	12.9	13.2	51	8	0.00005
50–69	428	430	22.2	15.7	6.5	29	15	0.045
<50	690	678	18.7	14.9	3.8	20	26	0.16

Surg, surgical; Med, medical; Abs, absolute; Rel, relative.

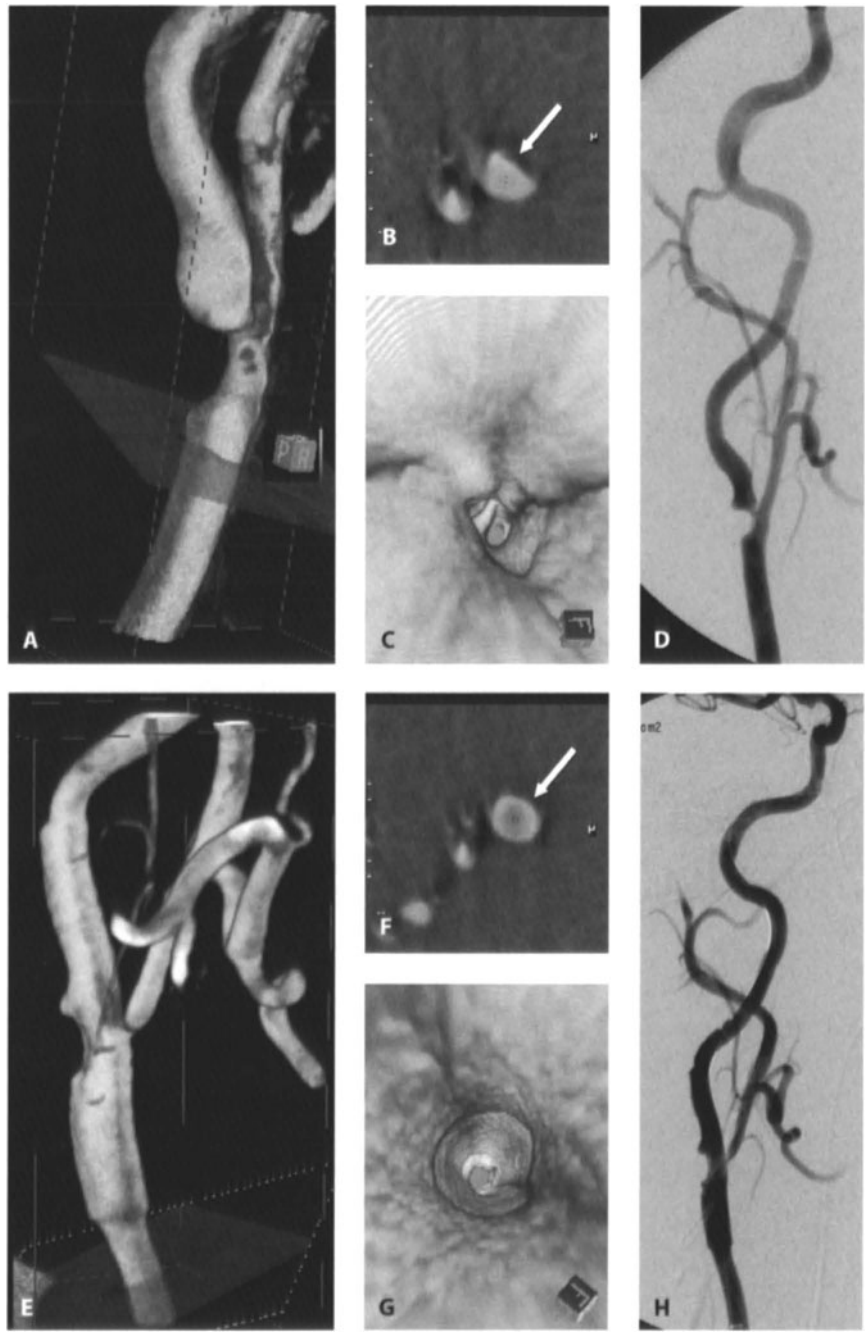

Fig. 1.27A–H. 3-D selective catheter angiography. **A** Reconstructed 3-D image of the common carotid artery showing the stenosis starting from the common carotid artery and extending into the origin of the internal carotid artery. **B** Source images from which the 3-D images were reconstructed show the impingement in the lumen of the internal carotid artery (*arrow*). **C** "Endoscopic" view shows the impingement in the internal carotid artery lumen with a larger external carotid visualized. **D** Conventional catheter angiography prior to endovascular stenting confirms the previously described findings. **E** 3-D reconstructed image after stenting shows the stent from the common carotid artery and in the internal carotid artery. **F** Source image shows the common carotid lumen in a circumferential fashion. **G** "Endoscopic" view shows the improvement in lumen at the common carotid artery. **H** Catheter angiography confirms the improvement in the internal carotid flow and the narrowing in the external carotid artery

1.2.5.6 Symptomatic Carotid Stenosis

At present, the primary treatment for symptomatic carotid stenosis greater than 70% is surgical carotid endarterectomy (CEA). The efficacy of CEA for extracranial carotid stenosis has now been unequivocally demonstrated. The publication of several large trials from around the world has provided valuable information on the management of patients at high risk of stroke, which includes patients with transient ischemic attacks (TIAs) or minor strokes that are referable to a high-grade stenosis at the carotid bifurcation.

This important work was the result of the cooperative efforts of neurologists, neurosurgeons, vascular surgeons, and neuroradiologists who addressed the issue of efficacy of CEA in various prospective randomized trials (NASCET 1991; ECST 1991, 1996; Mayberg et al. 1991).

The benefit of CEA in both studies assumes a perioperative risk of stroke or death of 6% or less at 30 days. In patients with TIAs or minor stroke, the CEA trials have provided a great deal of useful information:

- If the symptoms are referable to a 70% diameter stenosis at the carotid bifurcation, CEA reduces the risk of subsequent ipsilateral stroke from 26% during the first 2 years with optimal medical management to 9% with carotid endarterectomy, including the morbidity and mortality of CEA (NASCET 1991). This is a 65% risk reduction ($p<0.001$). The risk of a major stroke and death was 13.1% after medical treatment and 2.5% after CEA ($p<0.001$). The benefit of CEA becomes evident after 3 months, despite the risk of surgery.
- The risk of stroke without surgery is greater with increasing degrees of stenosis, reaching 30% during the first year for patients with 90%–95% stenosis (Tables 1.2, 1.22).
- CEA benefits patients with either hemispheric or retinal symptoms and in all relevant demographic subgroups.
- Surgery was found to be of no benefit for lesions with less than 50% stenosis.
- The risk–benefit of CEA for 50%–70% stenosis remains under investigation, although present discussions have suggested that if a risk of intervention (CEA or CAS) of less than 3% can be achieved, it may be of benefit.
- The ECST results are very comparable to those of the NASCET in those symptomatic patients with 70% or greater stenosis. The study reported a 16.8% risk of stroke after medical treatment, compared to 2.8% after endarterectomy ($p<0.001$; Table 1.23).
- In ECST, the benefit of surgical intervention in the 30%–69% stenosis group was uncertain.

1.2.5.7 Asymptomatic Carotid Stenosis

The benefit of CEA is small for patients with asymptomatic carotid stenosis of 60% or less: a 1% risk reduction per year for stroke. This is further qualified by the low risk of major stroke with either medical treatment or surgery in 1,662 asymptomatic patients and a possible lack of benefit in

Table 1.23. NASCET and ECST: risk of stroke at 2 years (see also Table 1.14)

		Stenosis %	Risk of stroke (2 years)	Risk stroke or death	Risk reduction		P
		Med	CEA[a]	Med	CEA		
NASCET	>70%[b]	26%	9%	13.1%	2.5%	65%	<0.001
ECST	>70%	16.8%	2.8%				

ECST, European Carotid Surgery Trial; NASCET, North American Symptomatic Carotid Endarterectomy Trial; CEA, carotid endarterectomy; Med, medical.

[a] CEA includes perioperative risk of stroke or death less or equal to 6% at 30 days.

[b] Stenosis of 90%–95%, 30% risk of stroke or death in the first year with medical therapy.

Table 1.24. Asymptomatic Carotid Atherosclerosis Study risk reduction

Stenosis %	Risk of stroke/death		Relative risk reduction (5 years)	P
	Medical	CEA[a]		
>60%	10.6%	4.8%	53% in males	<0.004
>60%			17% in females	Not significant
<60%			1% (per year)	Very low

CEA, carotid endarterectomy.

[a] CEA includes 2.3% perioperative risk of stroke or death at 30 days (as of 1994).

women (ACAS 1994) (Table 1.24). For stenosis greater than 60% over a period of 5 years, the risk of stroke was 10.6% following medical treatment and 4.8% after endarterectomy ($p<0.004$), hence a 53% risk reduction. It should be noted that in the 1994 ACAS trial, the perioperative risk of CEA was only 2.3%, as compared to 7.5% in the NASCET.

The benefits of CEA or carotid angioplasty and stenting (CAS) are critically dependent upon the rate of perioperative complications. If the complication rate goes up, the benefit of intervention is quickly lost.

In the Veterans Administration (VA) study of symptomatic patients with stenosis greater than 50%, the combined neurological perioperative morbidity and mortality of CEA was 5.8% (Mayberg et al. 1991). In the VA asymptomatic patients study, the risk of CEA was 4.3% (Hobson 1993).

Other non-CNS complications from CEA in the NASCET included myocardial infarction (0.9%), cranial nerve deficits (7.6%), hematoma (5.5%), and infection (3.4%) (Table 1.25).

When critically reviewing the results of all these large studies, one has to recognize that in both the NASCET and ACAS, all high-risk patients were excluded and therefore their results apply to a very select patient population. Patients with the following characteristics were excluded from these studies (Table 1.26):

Table 1.25. NASCET non-CNS complications from carotid endarterectomy

Complication	%
Myocardial infarction	0.9%
Cranial nerve deficit	7.6%
Hematoma	5.5%
Infection	3.4%

Table 1.26. NASCET exclusion: high-risk patients

Over 79 years of age
Severe cardiac, renal, hepatic disease, or patients suffering from cancer with a life expectancy of less than 5 years
Cardiac valve replacement or arrhythmia
Unstable angina or myocardial infarction less than 6 months old
Previous endarterectomy
Previous radical neck dissection
Previous radiotherapy
Patients with unstable angina or myocardial infarction within the preceding 6 months
Patients having undergone a major surgical procedure during the last 30 days
High cervical, petrous or cavernous carotid lesions
Contralateral carotid occlusion

Among these high-risk patients, the risk of CEA is significantly increased. Dyken and Pokra (1984) reported the risk of death in a patient with coronary artery disease to be between 4% and 18%, with a 2.8% mortality risk in 85,000 CEA procedures. Muuronen (1984) reported a mortality rate of 3.8% and a morbidity rate of 14.5% in a study of 110 cases with coronary artery disease. Thompson (1986) reported a mortality of 3.4% and morbidity of 2.7% associated with 748 CEAs in a similar group.

In a meta-analysis of 25 studies done since 1980 on the risk of stroke and death due to surgery, Goldstein and colleagues (Goldstein et al. 1997) estimated a 30-day complication rate of 3.35% for asymptomatic patients and a 5.18% rate for symptomatic stenosis.

The recorded risk of stroke and/or death was highest in studies in which patients were assessed by a neurologist after surgery (7.7%) and lowest (2.3%) in studies reported by a single author (surgeon) (Rothwell et al. 1996)

Table 1.27. Restenosis after carotid endarterectomy

Year	1st	2nd	3rd	Long term
	10%	3%	2%	1%/year

1.2.5.8 Restenosis After Carotid Endarterectomy

The patency rate reported following CEA is over 90% at 5 years and 90% at 10 years. The reported restenosis rate is 1.2%–23.9%, depending upon the operative technique and the mode of follow-up (Raithel 1996). The risk with reoperation is high and includes a higher chance of cranial nerve damage (Bergeron et al. 1996).

Fredricks et al. (1998) reviewed the literature to determine the incidence of recurrent stenosis after carotid endarterectomy. Although the collected data included several studies with widely ranging criteria, the review showed the risk of recurrent stenosis to be 10% in the first year, 3% in the second, and 2% in the third. Long-term risk of recurrent stenosis is about 1% per year (Table 1.27).

The reported relative risk of stroke in patients with recurrent stenosis compared with patients without recurrent stenosis varied widely, ranging from 10% to 0.10% (1:10–10:1).

It is clear that the risk of recurrent stenosis is highest in the first few years after carotid endarterectomy and very low subsequently. Increasing mean patient age was associated with a higher risk of ipsilateral stroke, and the use of a patch closure resulted in a lower risk.

In the absence of evidence to the contrary, the literature shows that many vascular surgeons reason by analogy. They assume that the secondary lesions of intimal hyperplasia and recurrent atherosclerosis carry the same increased risk of obstructive and thromboembolic ischemia as primary obstructive and atherosclerotic lesions, although the histopathology and physiopathology of the two lesions are very different. Until more reliable data become available, this reasoning by analogy will probably prevail.

Meyer et al. (1994) reported on the outcome of CEA for recurrent carotid stenosis in 82 patients. These patients suffered combined rates of major morbidity and mortality of 10.8%, with an additional minor ischemic event that recovered in 3.3%. In addition, cranial nerve damage was more frequent in reoperations.

1.2.6 Carotid Angioplasty and Stenting

1.2.6.1 Introduction

Since the development of balloon angioplasty for atherosclerotic lesions by Gruentzig in the early 1970s (Gruentzig and Hopff 1974), balloon angioplasty has gained wide acceptance for the treatment of atherosclerotic and other vascular stenosis in the cardiac and peripheral circulation. In various trials, involving many organ systems, percutaneous transluminal angioplasty (PTA) has been shown effective. Despite several large studies, there is still debate about its relative efficacy and applicability compared to surgery. This is primarily because long-term patency after PTA is only related to restenosis, which is well documented in the coronary, renal, and peripheral circulation (Currier and Faxon 1995; Lange et al. 1993; Blum et al. 1997).

Extracranial carotid PTA has been in use for nearly a decade (Theron et al. 1990; Mathias 1999; Dorros 1998b). As the cardiac and peripheral vascular experience has demonstrated, the use of endoluminal stents has proven to be safer and associated with better long-term outcome than angioplasty alone. Many published studies on carotid angioplasty and stenting also appear to favor balloon-assisted stenting versus balloon angioplasty alone (Theron et al. 1996; Iyer et al. 1997; Yadav et al. 1996).

Vascular stents have gained wide popularity over the last few years and many different types of stents are currently in clinical use or in varying stages of development. In almost all studies that directly compare PTA and stents, the patency rate with stenting has been better than that of angioplasty alone (Serruys et al. 1994; Fischman et al. 1994). So far, there has been no study completed that directly compares outcome of primary stent placement versus surgery in any vascular system.

Over the last years, there has been a great deal of interest in treating extracranial carotid stenosis with angioplasty supplemented by stent deployment, although only a few large studies have been reported.

From the various retrospective reports on CAS in mostly nonrandomized series of highly selected mostly high-risk patients, all series except one (Naylor et al. 1998) demonstrated favorable results. Actually, the results recorded were similar to those associated with CE in nonselected, non-high-risk populations, and the results were better than CE in the so-called high-risk group. Furthermore, the patients were treated with a variety of available stents (including balloon-expandable and self-expandable stents), not designed specifically for the carotid artery and without distal protection devices (see Chap. 14, Sect. 14.16, "Techniques of Carotid Angioplasty and Stenting," this volume).

In 1996, Roubin and co-workers (1996) reported 152 CASs in a group of patients in which over 80% of patients would have been excluded from NASCET. Technical success was achieved in 99% of cases. Stent thrombosis occurred in 0.6%. The 30-day mortality rate was 0.6%, major stroke occurred in 1.2%, there was a minor (nondisabling) stroke rate of 4.8%, a minor stroke (with residual weakness) stroke rate of 1.2%, and a follow-up TIA rate of 1.3%. Restenosis was seen in 5% of 74 patients eligible for follow-up. Interestingly, most restenoses were related to deformation of Palmaz stents.

Table 1.28. Carotid angioplasty and stenting

	No. of patients	Technical success	Stent thrombosis	30-day mortality	Major stroke	Minor stroke	F/U TIA	Restenosis[a]
Rubin 1996	152	99%	0.6%	0.6%	1.2%	6%	1.3%	5%
Iyer et al. 1996	543	97%	–	0.6%	3.3%	2.2%	–	–
Dietrich et al. 1996	110	99%	1.7%	0.9%	1.7%	–	4.3%	–
Wholey and Eles 1998	2048	98%	–	1.37%	1.32%	3.08%	–	4.8%
Naylor et al. 1998	7				5/7[b]			
Shawl 1998	124[c]	99%	–	0%	0.8%	2%		2%

F/U TIA, follow-up transient ischemic attack.
[a] Most related to deformation of Palmaz stent.
[b] Trial stopped because of poor results.
[c] High-risk patients.

Iyer et al. (1996) reviewed the results of a multicenter study that included 543 patients undergoing CAS, which demonstrated similar results. Technical success was achieved in 97%. Complications included a major stroke rate of 3.3%, a minor stroke rate of 2.2%, and a death rate of 0.6%.

Diethrich et al. (1996) reported on the results of CAS in 110 patients, with a technical success rate of 99%, a major stroke rate of 1.7%, TIA in 4.3%, and a stroke-related death rate of 0.9%). In three patients (2.6%), the procedure needed to be converted to CEA. Two (1.7%) cases of asymptomatic carotid artery thrombosis occurred. One other patient had restenosis from intimal hyperplasia at 7 months. No new neurological events occurred at 7 months, and one additional stented carotid thrombosed. Diethrich also used a number of different balloon-expandable stents.

In 1998, Wholey and co-workers (1998) surveyed the results of CAS throughout the world, with 24 major centers responding. 2,048 CAS procedures were collected, with a technical success rate of 98%. Complications during the procedure or within the first 30-day period following CAS included a major stroke rate in 1.32% and minor stroke rate in 3.08%. Death occurred in 1.37% of patients and there was a reported restenosis rate at 6 months of 4.80% (mostly after Palmaz stents). No distal protection was used (Table 1.28).

A large number of reports continue to appear with similar or better results (Horowitz and Purdy 2000). The only exception is the report by Naylor et al. (1998), in which five out of seven patients suffered a stroke from the procedure, prompting the trial to be stopped for safety and ethical reasons. The explanation for such poor results is difficult to understand and was almost certainly related to the technique used.

Shawl (1998) reported a series of high-risk patients in whom 124 carotid arteries were stented with a 99% technical success rate, a major stroke rate of 0.8%, and a minor stroke rate (that resolved within 7 days)

Table 1.29. Carotid endarterectomy (CEA) vs. carotid angioplasty and stenting (CAS) in high-risk patients

CEA	CAS	No. of patients	Major stroke	Minor stroke	30-Day mortality	Total stroke	Severe M and M
NASCET						14.3%	
Meyer 1994		82[a]		3.3% Transient			10.8%
	Shawl 1998	124	0.8%	2%	0%	2.8%	2.8%
	Mericel 1999	23[b]			0%	0%	
	Yadev 1996	25[a]					4%
	Berenstein 2000	60	0	1(2%)	0	1(2%)	0

M and M, morbidity and mortality.
[a] Restenosis after CEA.
[b] Severe stenosis and contralateral total occlusion.

of 2%. In 92 patients with a 6-month follow-up, only 2% had asymptomatic restenosis.

Mericle et al. (1999) treated 23 patients with severe carotid stenosis and contralateral carotid occlusion. Twenty-one stents were used. At 30 days, the stroke/death rate was 0%. This group fared very favorably when compared with a similar group of patients reported at the NASCET trial in which the stroke rate was 14.3%.

Yadav et al. (1996) reported on 25 carotid restenoses after CEA, retreated with CAS, with a 4% periprocedural complication rate. These results contrast with those of Meyer et al. (1994), who reported on the outcome of CEA for recurrent stenosis in 82 patients. This group of patients suffered a combined rate of major morbidity and mortality of 10.8%, and additional minor ischemic events that recovered in 3.3% (Table 1.29).

Our own experience consists of over 100 consecutive CASs, all in high-risk patients. Technical success was achieved in all attempted cases except one where the procedure was aborted because of tortuous anatomy. A minor MI occurred in a 91-year-old man, and there was one angiographically demonstrated distal embolization without clinical symptoms. No periprocedural neurological events occurred in any of our patients treated with CAS, despite multiple co-morbidities in most of the patients (Table 1.28).

However, before widespread clinical use of CAS as an alternative to CEA can be proposed, several important points must be considered.

The risks of diagnostic carotid angiography alone, particularly in patients with often widespread atherosclerotic disease, are not trivial. Although CAS adds catheter angiography to the procedure, it also provides us with a more accurate measurement of the degree of stenosis, presently not available with noninvasive methods, as well as invaluable information regarding intracranial circulation. Interestingly, during carotid angiography we have frequently noted an overestimation of the degree of stenosis by noninvasive imaging, and without angiography, these patients would probably have undergone CEA unnecessarily.

Unlike with coronary or iliac angioplasty, acute occlusion of the carotid artery after CAS may not be amenable to emergency surgical correction. Furthermore, if restenosis occurs after stenting, the standard surgical therapy may be either impossible or substantially more difficult to perform than on a virgin vessel. This is not true for percutaneous interventions in other vascular systems. In addition, while angioplasty for restenosis is usually relatively easy, more data is clearly needed to address this potential problem.

Carotid endarterectomy when performed by an experienced vascular surgeon is relatively safe and inexpensive and usually requires only a brief hospitalization. It can also be performed with good results using regional or local anesthesia, even in patients considered to be at high risk for other interventions. At a minimum, percutaneous CAS must approach CEA in safety and efficacy. Various prospective randomized trials are being proposed or are in progress in North America and Europe, and we believe they should in particular include those patients that were excluded from NASCET (Table 1.26). If CAS has similar results in this selected group of patients, then the only remaining question will be the long-term durability of the procedure. However, surgeons may be reluctant to enter "good" candidates into such a randomized trial, as they feel that the present standard of care (i.e., CEA) has already proven itself.

We believe that the present indications for CAS include symptomatic patients with severe carotid artery stenosis in whom CEA is considered difficult or anticipated to be associated with unacceptably high risk. These "difficult" patients have characteristics that are similar to the exclusion criteria of NASCET and ECST (Table 1.26).

Stent technology is continually evolving and the stents currently available will soon be replaced. Prospective studies should therefore also consider the inclusion of significant additional technological advances.

The relative technical ease of performing carotid angioplasty and stenting (CAS) has attracted considerable attention in the clinical community. A randomized multicenter clinical trial is in progress in the United Kingdom, sponsored by the Medical Research Council (CAVATAS 1996). In North America, the NIH has recently funded a randomized trial comparing CEA with CAS: the Carotid Revascularization Endarterectomy Versus Stenting Trial (CREST). This trial is designed with the same inclusion–exclusion criteria as NASCET, but with a registry for high-risk patients.

1.2.6.2 Techniques of Carotid Angioplasty and Stenting

See Chap. 14, Sect. 14.16, this volume.

1.2.6.3 Intimal Hyperplasia and Restenosis

Intimal hyperplasia remains a common long-term problem in all types of vascular interventions (Fig. 1.28). It is related to injury to the endothelium. It has been noted following arterial, as well as venous procedures, in anastomoses, bypass grafts and various types of endovascular interven-

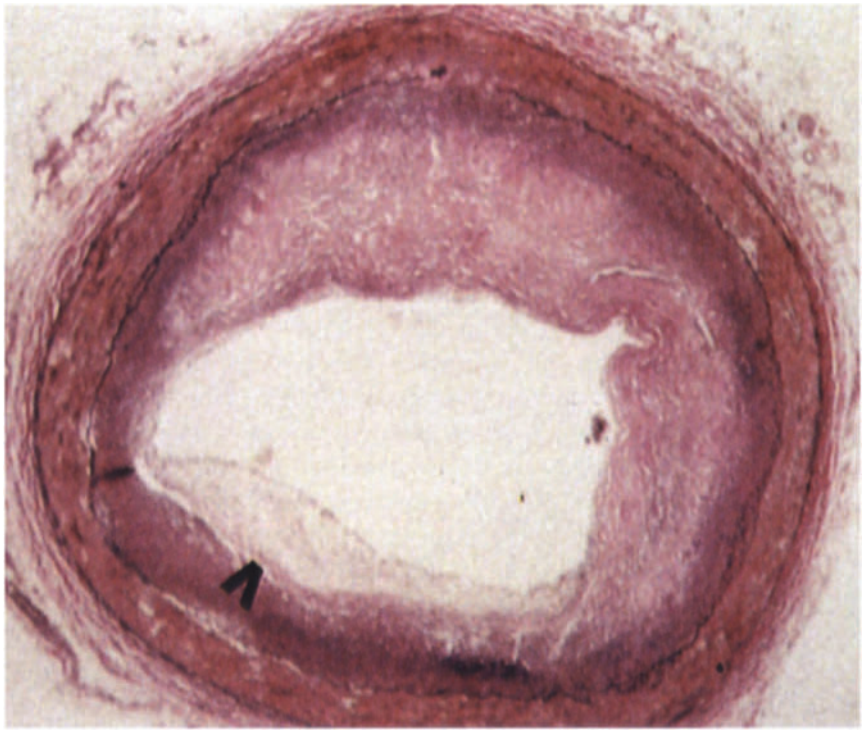

Fig. 1.28. Intimal hyperplasia. Cross section of a carotid artery after significant intimal hyperplasia ingrown into the vessel lumen

Table 1.30. Intimal hyperplasia following cervical carotid stenting

Rubin	5.3%
Higashida	5%
Porta	10%
Motarjeme	4%
Kachel	2%

tions (Figs. 1.29, 1.30). According to the reported series, intimal hyperplasia following carotid stenting appears to be in the 5% range, comparable to CEA (Table 1.30). We have seen it occur in only one case, in which it responded to balloon angioplasty (Figs. 1.29, 1.30). On occasion the development of a vasa-vasorum as collateralization may be seen, which will regress after distal flow is improved (Fig. 1.30).

In endovascular interventions, the goal is to produce as little damage to the intima as possible in order to avoid a chain of reactions that can subsequently result in endothelium damage.

Endothelium has an anionic surface charge that yields an antithrombotic environment, associated with the constant release of endothelium-derived relaxing factor (EDRF), with its potent antiplatelet effect. Damage to the endothelium exposes the subendothelial matrix to circulating blood. Having now lost its antithrombotic protection, the subendothelial matrix will induce platelet aggregation, initiating the thrombotic cascade. Groves, when examining rabbit aortas (Groves et al. 1979), and Wilenzt et al., in an experimental angioplasty model (Wilenzt et al. 1987), demonstrated that platelets are rapidly deposited at sites of intimal injury.

Fig. 1.29A–F. Intimal hyperplasia. **A** Lateral digital subtraction angiogram (DSA) of the common carotid artery shows a focal severe stenosis. **B** Following stenting with excellent angiographic and clinical result. **C** Six months of follow-up after ultrasonography suggests stenosis at the distal end of the stent and is confirmed with this DSA (*arrow*). Note the stenosis of the external carotid artery not present prior to stenting. **D** After balloon angioplasty there is improvement in the caliber. **E** Before and **F** after balloon angioplasty of the intimal hyperplasia, note the improvement in filling of the ipsilateral anterior cerebral artery

Fig. 1.30. Lateral angiogram of the common carotid artery in a patient who had a previous endarterectomy with restenosis (**A**) at both sites of surgical anastomosis (*arrows*), which was successfully treated with two separated stents (**B**), with a good anatomical and clinical result (**C**). **D** Six months later there was recurrent restenosis at the distal surgical anastomosis within the stent. Note the development of vasa vasorum in an attempt to collateralize flow (previously present prior to stenting seen in **A**). **E** Angiographic examination after balloon angioplasty. Note the reestablishment of flow and the disappearance or regression of the vasa vasorum

This progressive event will be completed within the subsequent 10 min. The more severe the intimal damage was, the more thrombosis occurred.

An additional downside of endothelium injury may be related to the degree of inflammation occurring after angioplasty. The interaction between the injured vessel wall and circulating blood components (the damaged endothelium, activated platelets, and neutrophils at the site of injury) generates reactive intermediary agents, as reported by Block (1994). Intimal injury will also affect the inhibiting role played by the endothelium on smooth-muscle cell migration and/or proliferation, resulting in intimal hyperplasia and late restenosis (Davies and Hagen 1994). Fuster and co-workers (1992) studied the role of vascular injury and smooth-muscle proliferation. Because of similarities in their pathology, intimal hyperplasia and spontaneous atherosclerosis are considered within the same spectrum of vascular diseases, the so-called accelerated atherosclerosis (Ip et al. 1990).

The EPIC study report on monoclonal antibody directed against the platelet glycoprotein IIb/IIIa receptors showed that decreasing vessel injury and decreasing platelet aggregation also decrease late restenosis. It is therefore likely that gradual balloon inflation results in fewer intimal tears, flaps, and dissections, as experienced by Connors (1999). If the dilatation is more traumatic, it likely has a higher degree of damage to the endothelium, with all its potential consequences.

Intense research is being conducted with respect to restenosis reduction. Local radiotherapy is being considered as promising (Koh 1996; Carter and Laird 1996; Fischell et al. 1996). We believe, however, that radiation may not be the right approach. Radiation is a factor that accelerates atherosclerosis. The endothelium is the most radiosensitive layer in the blood vessel wall, and therefore the one most likely to be damaged by radiation, resulting in restenosis. The stenosis may occur at the site of radiation or in the margins of the radiation field, where the radiation dose is not strong enough to damage the smooth muscle but will result in damage of the intima.

Additional efforts are being directed towards drug treatment against the proliferative phase of the cell cycle, with antineoplastic drugs used systemically, by coating stents with the eluding drug over time, or by premedicating the patients prior to stenting. We believe these approaches provide a more physiological approach to the problem (Grube et al. 2001; Dorros 1998b; Hiatt et al. 2002; Sousa et al. 2001).

Within the potential medications, probucol, a lipophilic-property drug that lowers cholesterol and has potent antioxidant properties, has been shown to have a beneficial effect in decreasing restenosis following coronary angioplasty. When compared with placebo, antioxidant multivitamins, or probucol and multivitamins, probucol versus no probucol provided significant results (p=0.003) (Tardif et al. 1997). It is possible that endothelial dysfunction affects the LDL metabolism and results in accelerated atherosclerosis and restenosis.

1.2.6.4 Follow-up Monitoring

Ultrasound is a good test for noninvasive follow-up. A baseline study is obtained shortly after the CAS, then repeated at 6 months, which appears to be the critical period for significant intimal hyperplasia restenosis (Roubin et al. 1996; Horowitz and Purdy 2000). Thereafter, we restudy the patients on a yearly basis with ultrasound (Bettmann et al. 1998).

1.2.7 Posterior Circulation Stroke (Stroke Prevention)

1.2.7.1 Introduction

One of the most difficult and challenging areas in the stroke field is the approach to patients with occlusive vascular disease of the posterior circulation. Such patients may present with rapidly evolving clinical symptoms with devastating consequences. While the approaches to diagnosis and treatment of carotid disease are widely appreciated, the treatment of vertebrobasilar disease has been limited in terms of therapeutic options. Recent advances have made it possible to accurately diagnose and effectively treat many more patients with posterior circulation occlusive vascular disease.

1.2.7.2 Clinical Presentation

The symptoms and clinical characteristics of posterior circulation ischemia have been recognized for over 50 years (Denny-Brown 1966). These include vertigo, ataxia, diplopia, bilateral weakness, and bilateral visual blurring. Glass has published an extensive review on this subject (Glass et al. 2002). In 1946, Kubik and Adams (reviewed in Glass et al. 2002) published an analysis of 18 patients with basilar artery occlusion that were studied clinically and at autopsy. They emphasized the clinical picture and suggested that this disorder could be diagnosed during life. This report brought the subject of basilar artery occlusion to the attention of the neurological community. During the next few years, others (Denny-Brown 1966) described similar patients who survived and suggested that symptoms were due to hemodynamic factors, leading to the use of the term "vertebrobasilar insufficiency." In many of these cases, this mechanism could not be established, as angiography was the only diagnostic technique to demonstrate these vessels and selective catheterization was not widely available. With advances in imaging and other diagnostic modalities, we now appreciate that ischemia in the posterior circulation is not a homogenous entity with a single mechanism. It is caused by the same factors that lead to stroke in the carotid territory (Table 1.7). These include cardioembolism, artery-to-artery emboli, small artery disease, thrombotic disorders, and large vessel occlusive disease. Strokes that occur as a result of progressive intracranial vertebrobasilar artery (VBA) occlusive disease can be devastating. Vertebrobasilar ischemic stroke accounts for approximately 20% of all ischemic strokes (Turney et al. 1984).

Almost half of the patients who present with posterior circulation TIAs have a stroke within 5 years (Whisnant et al. 1978; Glass et al. 2002). Patients identified with a stenosis of greater than 50% in the vertebrobasilar arterial system have a risk of stroke 17 times greater than the general (matched) population (Moufarrij et al. 1986; Bougousslavsky et al. 1986; Glass et al. 2002).

1.2.7.3 Pretherapeutic Evaluation in Cerebral Vascular Insufficiency

Coagulation Profile

In addition to routine laboratory and preliminary testing, a full coagulation profile is recommended on patients presenting with a stroke, and particularly those involving the posterior circulation.

Transesophageal Echocardiography

Transesophageal echocardiography (TE) makes it possible to detect sources of cardiogenic embolism in many more patients in whom standard transthoracic echocardiography does not. This technique uses an ultrasound transducer that is endoscopically positioned in the esophagus to provide clear and detailed images of the heart and aortic arch. It can reveal causes of stroke such as aortic arch atheroma, left atrial thrombi, and atrial septal defects, as well as other less common conditions. This technique has greatly reduced the number of strokes that were previously labeled cryptogenic.

At present, noninvasive diagnostic imaging has reached a high degree of accuracy, and in the majority of patients the diagnosis is derived from these work-ups.

Transcranial Doppler

Transcranial Doppler is an ultrasound technique also used to diagnose occlusive disease of the posterior circulation. A transducer is placed on the back of the neck to image through the foramen magnum. It is thus possible to detect stenosis of the intracranial vertebral arteries and of the proximal basilar artery. Retrograde flow can be detected and the patency of the posterior cerebral arteries can be demonstrated. The limitations of this technique include difficulty in examining the distal basilar artery and artifacts due to vessel tortuosity, which may make results unreliable. It is also a highly operator-dependent technique and takes significant experience to master. Some patients with large necks may be difficult to study.

Computer Tomographic Angiography

Computer tomographic angiography (CTA) is a very useful tool that has only recently come into more widespread use. It has been made possible by the speed of the newest generation of (helical) CT scanners (Figs. 1.20, 1.21). A bolus of intravenous contrast material is given over approximately 20 s and rapid scanning allows opacified vessels to be imaged. Comput-

erized reconstruction of axial sections provides angiographic images. CTA is capable of demonstrating the intracranial vertebral arteries and basilar system, including the posterior cerebral arteries, and has been shown to be useful in diagnosing basilar artery thrombosis. This tool is advantageous in that it is fast and can be used in patients who have pacemakers or are intubated. It cannot be used in patients with renal failure or allergies to iodinated contrast agents. Currently, CTA is only capable of demonstrating relatively short segments of the circulation, but this is rapidly improving. Its primary limitations are artifacts caused by dental or other metallic prostheses, calcifications, and imaging lesions at the skull base.

Magnetic Resonance Angiography

Until MRI scans arrived in the 1980s, adequate views of the brainstem and cerebellum were not obtainable. Magnetic resonance angiography (MRA) added the ability to visualize the intracranial and extracranial vasculature. This examination has the advantage of being noninvasive, easily repeatable, and capable of demonstrating a relatively large area. MRI and MRA can delineate the entire length of the vertebral artery and provide views of vessels surrounded by bone such as at the skull base (Fig. 1.31). MRI with contrast is able to image the aortic arch and great vessels with remarkable accuracy (Figs. 1.22, 1.23). The cross-sectional source images can visualize the lumen, vessel wall, and surrounding structures, and probably are best for dissections (Fig. 1.9). Diffusion-weighted imaging (DWI) MRI has contributed important information in patients suspected of having a CVA. Since DWI imaging is positive up to 2 weeks after an event, it is a particularly important diagnostic modality for patients with previous CVAs, when determining if a specific lesion correlates with the symptomatic territory, or if there are DW defects of different ages, newer events, as well as when determining the possible benefits of therapy (Fig. 1.31). MRA has limitations including the inability to image low flow states and the tendency to overestimate the grade of stenosis, particularly at the skull base. It is not able to directly image vessels with retrograde flow. Some imaging artifacts remain problematic, including those caused by swallowing or dental prostheses. MRA also cannot be performed in patients with a pacemaker or other MRI incompatible implants (certain aneurysm clips, etc.). The study of the intracranial vasculature remains limited, but with continued technical advancements, this will improve. Functional imaging will further advance the biological understanding of patients suffering from ischemic vascular disease.

Cerebral Angiography

Cerebral angiography is reserved for specific questions, where the diagnosis is difficult or impossible to make with the less invasive studies, which is more and more the exception. However, due to the new and more widespread use of endovascular revascularization, angiography is presently done primarily with the intent to treat.

When the symptoms are suggestive of cerebral vascular insufficiency, we include an aortic arch study that supplements the preliminary diag-

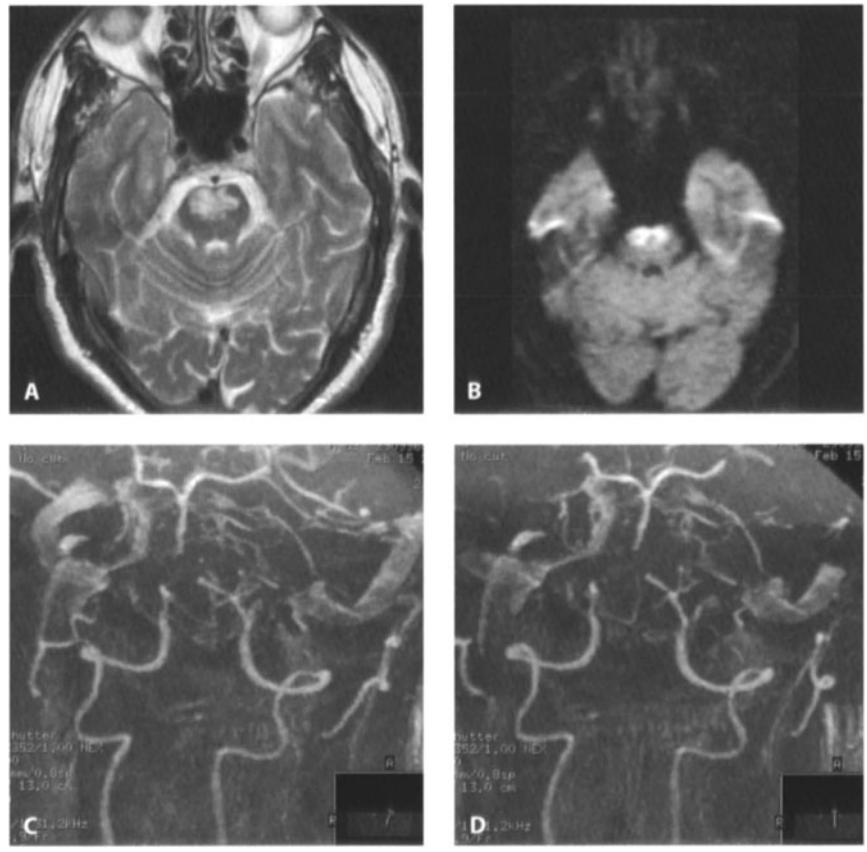

Fig. 1.31A–D. MRI in posterior circulation stroke. **A** T2-weighted axial MRI shows the increased signal in the midbrain. **B** Diffusion-weighted image (DWI) is more accurate in determining the event as well as the age of the stroke. Within the first 2 weeks of the event, the DWI will be positive. **C, D** Time-of-flight magnetic resonance angiograms showing the gap between the distal two vertebral arteries and the proximal basilar artery compatible with the level of the stroke

nostic imaging. One of the present authors also includes views of the neck and a global picture of cerebral perfusion. These injections are also used to compare the filling of the neck vessels and the circulation between both hemispheres (Figs. 1.2–1.4).

Road mapping of the arch may be used to grossly assess the status and origin of the brachiocephalic vessels prior to passing a guidewire or catheter. We prefer, however, a true study of the arch in at least two projections (Fig. 1.2).

Based on the preliminary diagnostic imaging and the angiogram, a decision is made as to the need for more selective studies to answer specific questions and/or if a therapeutic procedure is indicated. The goal of revascularization in patients with insufficiency is to do the minimum necessary to open the most accessible route that will improve distal perfusion or relieve a flow-restrictive, tight stenosis.

It is important to realize that cerebral vascular insufficiency may be due to inadequate blood flow related to lesions at a distance from the symptomatic region, anywhere from the aortic arch upwards (excluding a cardiac source). Finding the source requires the proper assessment of the collateral circulation at the level of the neck as well as at the circle of Willis and leptomeningeal collaterals (Fig. 1.32).

Fig. 1.32A–L. An 82-year-old female patient after axillary–axillary bypass who presented with ischemic symptoms referable to the posterior circulation and left cerebral hemisphere. **A** Aortic arch study demonstrates the proximal anastomosis from the right axillary artery towards the left axillary artery (*open arrow*). Note the absence of opacification of the left subclavian artery. **B–D** Views from a right subclavian artery injection demonstrates antegrade flow on the right vertebral artery towards the brain (*arrow*, **D**). The axillary bypass anastomoses the right subclavian (**B**) to the left subclavian artery (**C**). Note retrograde filling of the left subclavian towards the vertebral artery (*open curved arrow*, **C**). There is no opacification of the left vertebral artery. In **D**, frontal view of the right subclavian artery injection centering to the neck and head demonstrates filling of both posterior cerebral arteries. There is no left subclavian "steal", or filling of the left vertebral artery. **E** Parenchymatography of the aortic arch study demonstrates decreased opacification in the left parietal region. The right carotid artery has emptied and is in the capillary phase. There is delayed emptying of the left internal carotid artery and slow flow in the right vertebral artery. **F** Frontal and **G** lateral views of the right common carotid artery demonstrate in the frontal view filling of both posterior cerebral arteries from this injection. **E–L** see pp. 103, 104

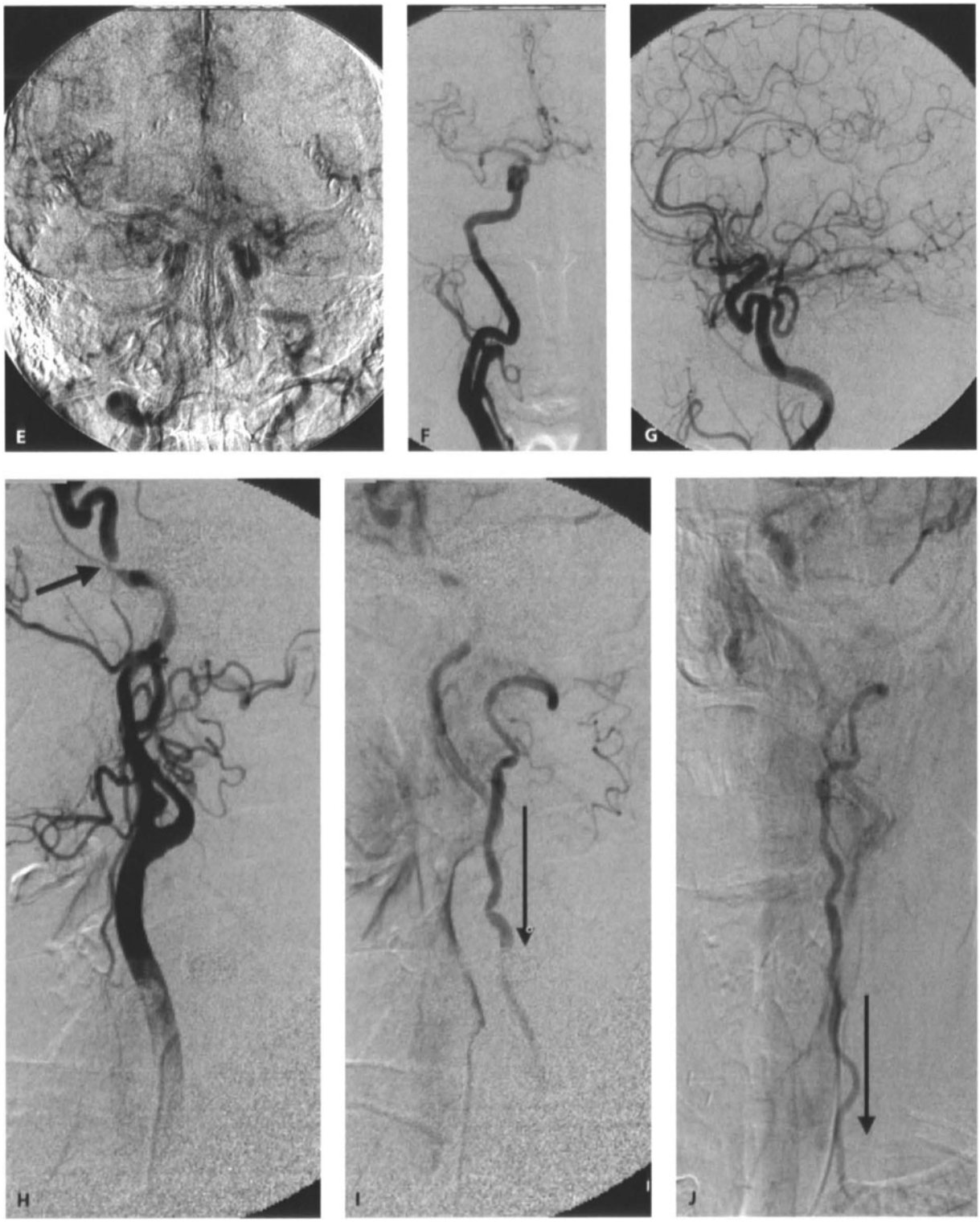

Fig. 1.32 (*continued*). **G** Note the presence of a trigeminal artery. **H** Late arterial phase and **I** late phase of the left common carotid artery, lateral view, shows prominent C1 and C2 collateral circulation, which then fills the vertebral artery on the left with a downwards flow towards the left subclavian artery (*arrow*). **J** Frontal view of the same injection shows downwards filling of the left vertebral artery (*arrow*). There is a tight stenosis in the petrous carotid artery (*arrow*, **H**). Lateral projection. **K, L** see p. 104

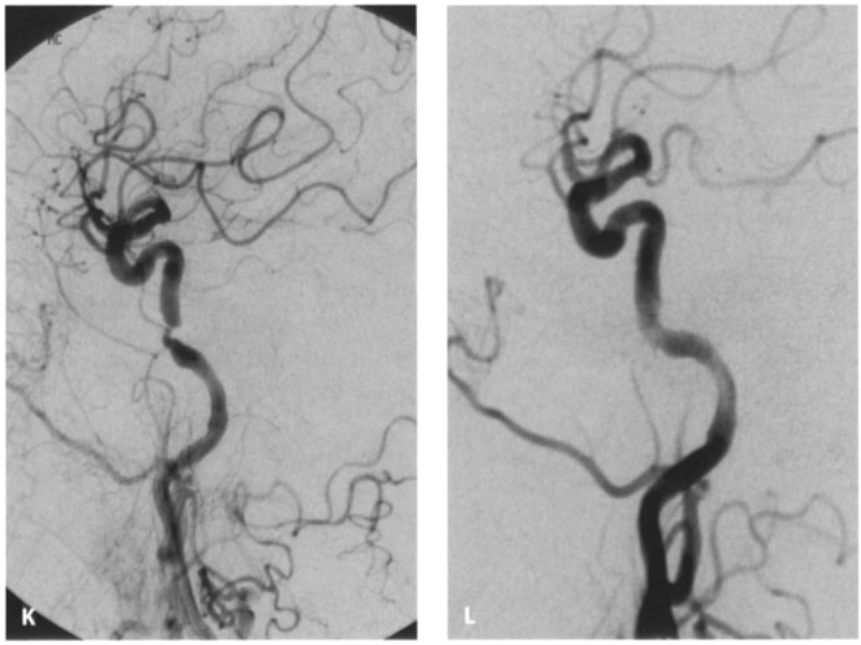

Fig. 1.32 (*continued*). **K** Before and **L** after stenting, with marked improvement in the lumen of the petrous carotid artery. Note the hemodynamic immediate filling of the posterior communicating and posterior cerebral artery from the left carotid artery improving perfusion to the left posterior hemisphere. (Same patient as Fig. 14.160)

1.2.7.4 Management of Posterior Circulation Insufficiency

The natural history of these patients remains poor (Hacke et al. 1988; Brandt et al. 1996; Archer and Horenstein 1977; Patterson and Grabois 1986). The present treatment of such patients depends on the underlying condition producing the symptoms. Frequently, the ability to improve the circulation is limited by our ability to repermeate the brachiocephalic vessels. Posterior circulation insufficiency may or may not be associated with embolic or perfusion strokes. If repetitive or prolonged, this will nearly always result in an adverse outcome.

Until recently, the only therapy for patients with large vessel occlusive disease of the posterior circulation was general supportive therapy for those who suffered an acute stroke. In particular, this included maintaining blood pressure, protecting the airways, achieving adequate oxygenation, and avoiding dehydration and hyperglycemia, treating seizures, and reducing temperature. The decision to use anticoagulants and/or antiplatelets or thrombolytics depends upon the diagnostic imaging findings (presence of hemorrhage, large area of infarction, etc.) (Brandt et al. 1995). Although anticoagulation continues to be in widespread use, it has never been demonstrated to be effective in any controlled trial. Patients with small vessel disease are generally treated with antiplatelet agents. In long-term management, stroke prevention is important, with long-term anticholesterol medication, diet, and behavioral modification. In many of these patients, long-term anticoagulants with or without antiplatelet medication will be required.

Revascularization

There is a subgroup of patients with persistent hemodynamic symptoms that do not respond to medical therapy. These patients may have repeated ischemic events that can usually be documented. With DWI MRI, some may be asymptomatic but will experience repeated and added insults that will eventually have poor prognosis. To improve perfusion, treatment has been limited to revascularization using microsurgical techniques such as bypass and/or endarterectomy (Ausman et al. 1982; Edwards and Mulherin 1980; Spetzler 1987a, b; Anson and Spetzler 1993). These treatments, however, are still restricted by their morbidity, limited access, and the required expertise needed to carry them out successfully. In addition, often these interventions are limited or not feasible due to the multiplicity of site involvement and complexity of the compensatory vascular circulation. New endovascular revascularization techniques can reach vessels at the base of the skull and have now made it possible to consider revascularization for selected patients. In appropriate cases, successful procedures can be performed with an acceptable level of risk. This technology is also undergoing rapid and continuing improvement. Even totally occluded vessels can be reopened, and this may be done in cases of hemodynamic steal such as a totally occluded subclavian artery in a patient with symptoms of subclavian steal syndrome (Fig. 14.164).

Revascularization for posterior circulation hypoperfusion requires planning a treatment that can improve distal flow from the origin of the brachiocephalic vessels to the basilar and carotid arterial systems. Careful analysis of the clinical vascular anatomy (i.e., collateral circulation in the neck and head, extracranial to intracranial anastomosis, and intracranial collateralization) will allow the endovascular surgeon to plan the specific procedure(s) with the best potential to improve distal perfusion, with the least possible number of interventions and morbidity. Creative revascularization strategies that combine endovascular revascularization and bypass procedures should be considered.

Endovascular revascularization in these patients will require the full spectrum of balloons and stents that are appropriate for lesions in both large- or small-caliber vessels located anywhere from the aortic arch to the very distal, small intracranial vessel. Accurate deployment is of utmost importance in these territories. At the aortic arch, the stent should not protrude into the arch, and at the same time, it must be of sufficient diameter so that there is satisfactory apposition with the vessel lumen to prevent distal migration (Fig. 1.3, same patient as Fig. 14.150). Constant movement in the chest due to cardiac and respiratory motion makes accurate placement more difficult. Since road mapping is of limited value in the arch, calcifications in the aorta often serve as the best landmark for accurate measurement and deployment. Similarly, in the origin of the vertebral artery (Fig. 14.150, or CCA origin, Fig. 14.159). Road mapping and bony landmarks are best for accurate deployment in the neck, at the skull base, or intracranially.

Occasionally, vascular access may have to be through atypical routes, particularly with total vascular occlusion. For example, an occluded subclavian artery may be approached from the femoral route, or from the brachial or radial root, or both (Fig. 14.150). During dilatation, caution

must be taken to avoid crushing the frequently encountered significant calcification at the origin of the brachiocephalic vessels, which may result in distal emboli or, if dilating at a vessel bifurcation, protrusion of plaque into a noninvolved branch. The use of guidewires is crucial to maintain vessel access and safety; one guidewire is placed across the lesion to be treated and a second wire is placed in the vessel to be protected (Fig. 14.150). If any compromise occurs in the noninvolved vessel, the guidewire is used to maintain the true lumen, which will make it possible, if necessary to repermeate that vessel. Alternatively, a balloon could be left inflated in the normal vessel while deploying a stent or while dilating at the level of the lesion.

Total occlusions can sometimes be safely recanalized. At the brachiocephalic level, the subclavian origin is frequently occluded and can be reopened with relative ease and safety. The main risk is vertebral artery embolization or dissection. To avoid complications, the guidewire is gently used as a probe, searching for the true lumen. A first attempt is usually made with a soft-tipped wire that has sufficient proximal pushability, or a soft 0.035-in. Terumo (Target Boston Scientific, Watertown, MA, USA) wire (Fig. 14.164). A variety of cardiac microguidewires or alternatively a neuromicroguidewire with a platinum distal end and hydrophilic coating, in conjunction with a neuromicrocatheter, can be used to find the true lumen (Figs. 14.149, 1.33I).

This technique for revascularization of total occlusions may also be used in more distal circulations such as in the distal vertebral or basilar artery, using low-profile flexible balloon-expandable stents, such as the GFX, S60, velocity, etc. (Fig. 1.33). The occluded lumen, even when long standing, tends to be softer than the vessel wall, and therefore gentle probing will usually identify the lumen. Forceful maneuvers should generally be avoided. Once the guidewire has been passed into the patent segment, depending on the length of the restrictive lesion and its relationship with the vertebral artery origin, it is exchanged for a stiffer guidewire. If an over-the-wire neuromicrocatheter technique is used, then the microcatheter is first passed across the lesion and is used for microguidewire exchange. If necessary, both guidewire techniques can be utilized as described above, with one wire protecting the vertebral artery.

To deliver the stent, a larger bore catheter is needed. To facilitate the catheter exchange, one may use one of the long, stiff exchange cardiac wires for support, or if necessary, a larger wire can be exchanged by repeating the wire–catheter maneuver with a 5F system and a 0.038-in. hydrophilic or stiffer guidewire. For best and more accurate stent delivery, the delivery catheter or sheath is passed across the stenosis to begin the stent delivery (Fig. 14.150).

If a dissection occurs, as long as the dissection and its extent are recognized, and the guidewire has remained in place, then it can easily be corrected with an additional stent deployment (Fig. 14.150). Angioplasties on dissections should probably be avoided. If the dissection is a spiral type and if the entrance of the dissection is apposed against the vessel wall by a stent or the catheter itself, most often the dissection will close (Fig. 14.165), or once the true distal lumen is found, a stent will solve the problem (Figs 1.13, 14.149).

Fig. 1.33A–L. Total occlusion of both vertebral arteries. **A** Frontal and **B** lateral digital subtraction angiogram (DSA) of the right vertebral artery injection shows total occlusion of the vertebral artery on the right. Note the prominence of the anterior spinal axis (*small arrows*) as it enters the contralateral (left) vertebral artery at the point where the posterior inferior cerebellar artery (PICA) is (*curved arrow*; see Vol. 1, Sect. 2.4, p.116 and Fig. 3.70). **C** Frontal and **D** lateral views of the left vertebral artery shows the occlusion of the left distal vertebral artery. The anterior spinal artery is again opacified through the artery of the cervical enlargement from the left side. **E–L** see pp. 108, 109

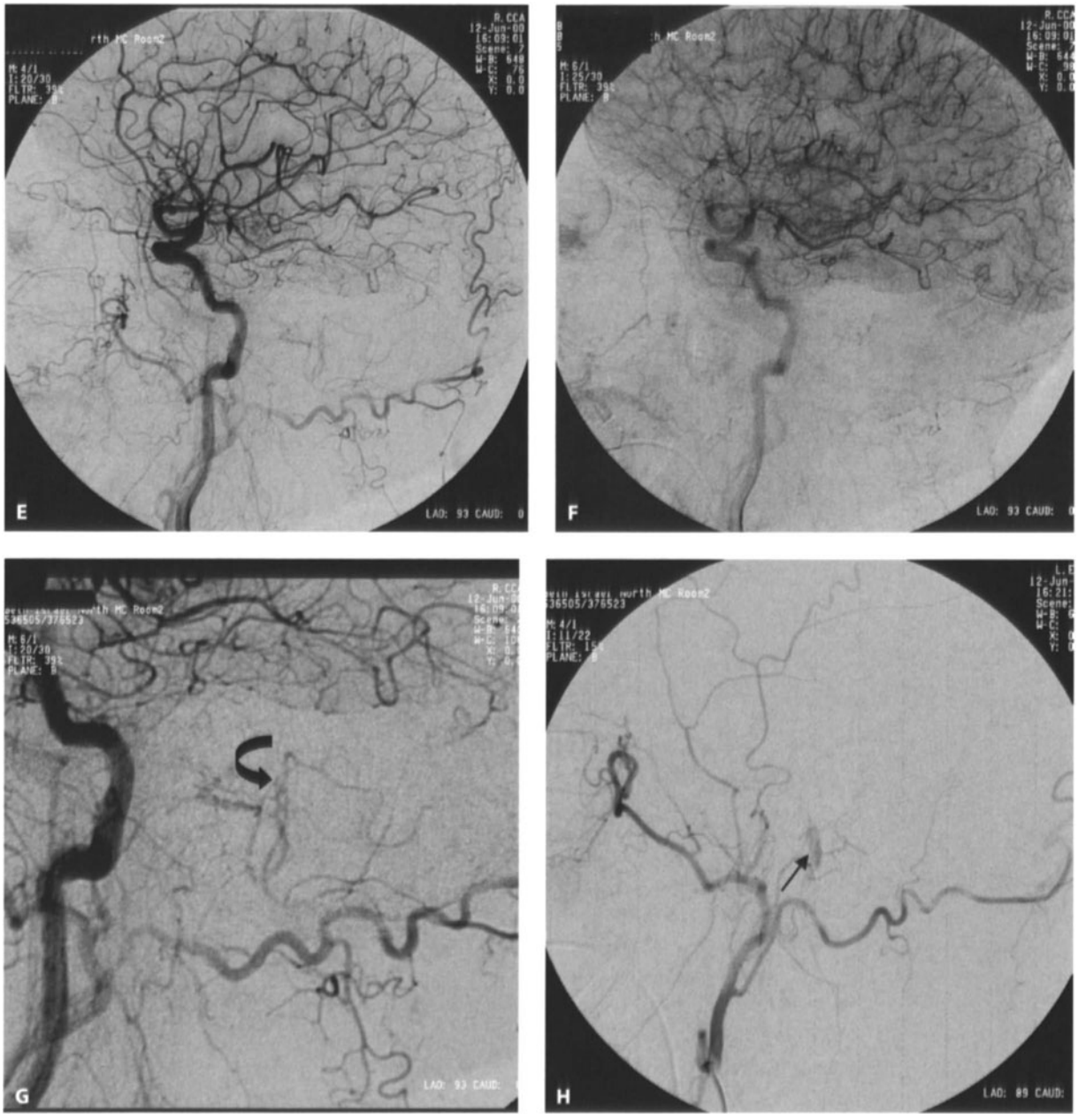

Fig. 1.33 (*continued*). **E** Lateral mid-arterial phase. **F** Late arterial phase of the right common carotid artery. Note the absence of a posterior communicating artery. The upper basilar segment and superior cerebellar arteries are filled in the late phase in **F** through anastomosis between the anterior choroidal and the posterior cerebral artery. This represents an inefficient collateral circulation. **G** Cone-down view of the right common carotid artery showing the meningeal reconstitution, probably through the ascending pharyngeal of the territory of the right PICA (*curved arrow*). **H** Left external carotid injections show the stylomastoid reconstitution of a mid-basilar segment (*arrow*). **I–L** see p. 109

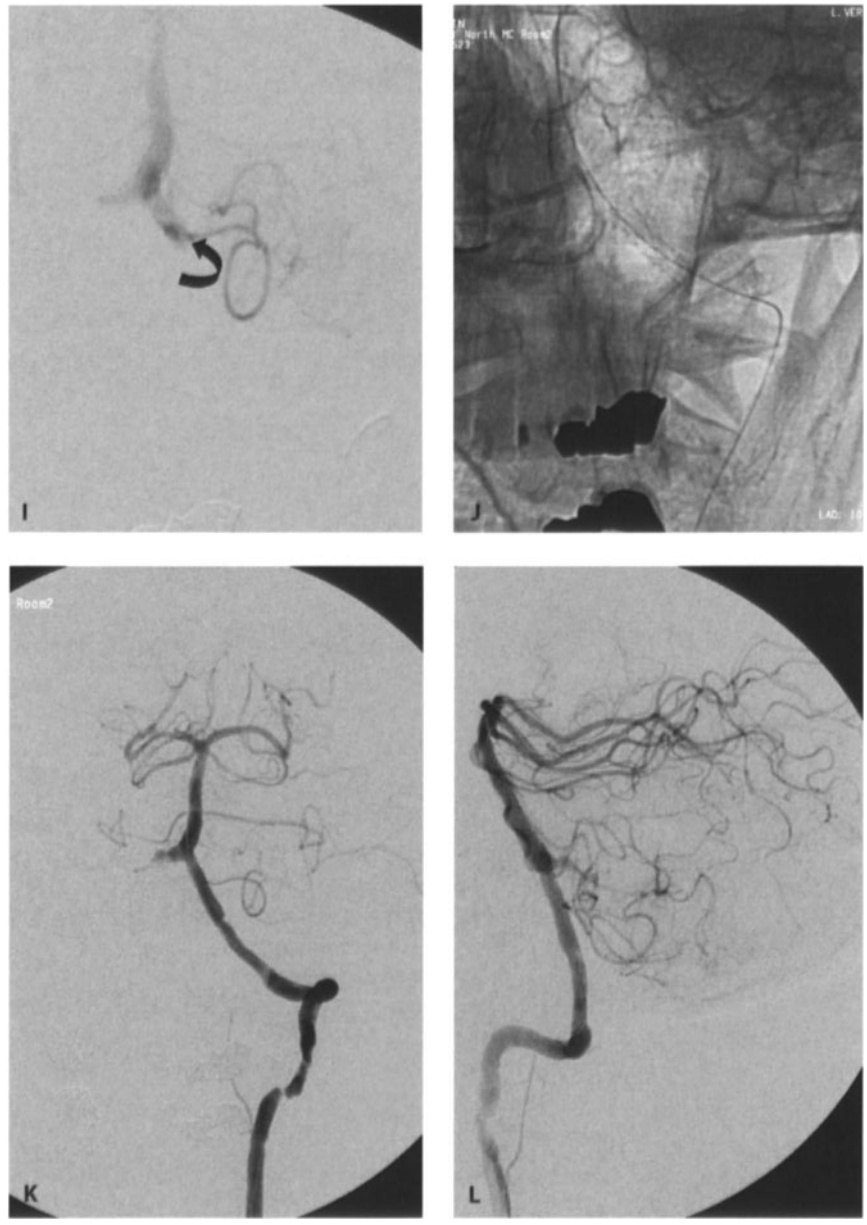

Fig. 1.33 (*continued*). **I** Cone-down view of the superselective catheterization of the left vertebral artery (LTVA) beyond the totally occluded segment. Utilizing neuromicrocatheter– microguidewire techniques of recanalization, the occluded segment is probed until the lumen distal to the occlusion is found. As expected, note the left PICA (*curved arrow*) as the microcatheter has crossed beyond the occlusion. Prior to contrast material injection, back flow is established. **J** Cone-down view of the guidewire with the deployed stent in the thrombosed segment. **K** Frontal and **L** lateral DSA of the LTVA after revascularization of the totally occluded segment

1.2.7.5 Basilar Thrombosis

Basilar artery occlusion remains a significant therapeutic challenge with very poor outcome. In multiple series, untreated basilar thrombosis had a severe morbidity and mortality, as high as 86%–100% (Hacke et al. 1988; Brandt et al. 1996; Archer and Horenstein 1977; Patterson and Grabois 1986).

Atherosclerosis is the underlying cause of 70% of cases of basilar thrombosis and thromboembolism is the etiology for approximately 10% of cases (Thomas 1997). The clinical presentation of patients with basilar artery thrombosis will depend on its anatomical location and its length. The collateral circulation at the circle of Willis, the leptomeningeal collaterals, and the collateral circulation between the posterior inferior cerebellar artery (PICA) and the anterior superior cerebellar artery (ASCA) (Vol. 1, Chap. 3, Fig. 3.70) may become an important bypass to a complete occlusion. The impact of a basilar thrombosis is therefore highly dependent on the quality of the collateral circulation. An older patient with atherosclerosis and progressive symptoms is more likely to develop efficient collaterals than a younger patient with sudden occlusion of the basilar artery from a cardiogenic embolus. Poor prognosis is also expected in patients with a falling level of conscious or with tetraparesis and in patients with large infarcts.

It is important to realize that many of these patients have had previous CVAs in different territories, and therefore the clinical picture and diagnostic imaging may not be as reliable as in patients during their first episode.

Local intra-arterial thrombolytic therapy (LIAT) improves the recanalization rate, giving those with successful recanalization a more favorable outcome and a significantly reduced mortality rate (Fig. 1.34). Brandt reported on 20 patients with basilar thrombosis: 60% had a good recovery on the Rankin scale, 20% had moderate long-term disability, and 20% did poorly (Brandt et al. 1995).

Five of Gonner's eight patients (63%) with occlusions in the basilar circulation could be recanalized and had a good outcome (Gonner et al. 1998). However, two patients who were comatose at admission died despite successful recanalization, suggesting that generally LIAT should be attempted only in noncomatose patients with BA occlusion (Zeumer et al. 1993; Hacke et al. 1988; Brandt et al. 1996). In Hacke's series, patients who were in coma for more than 4 h or those with cerebellar or brain stem lucencies on CT scan were excluded from the study, which probably accounts for the high survival rate of 73% in that series (Hacke et al. 1988). In 1999, Levy and co-workers (1999) conducted a meta-analysis in 164 patients composed of 154 cases from the literature and ten from their own experience. The data available limited the study to three independent variables: (a) presenting neurological condition, (b) clot location in the basilar artery, and (c) the degree of recanalization. Despite the limitations of retrospective literature reviews, it confirmed, as expected, that patients in coma at presentation had a significantly worse outcome, even if total recanalization was achieved. Location of the clot in the upper one-third of the basilar artery was associated with worse clinical outcome with LIAT

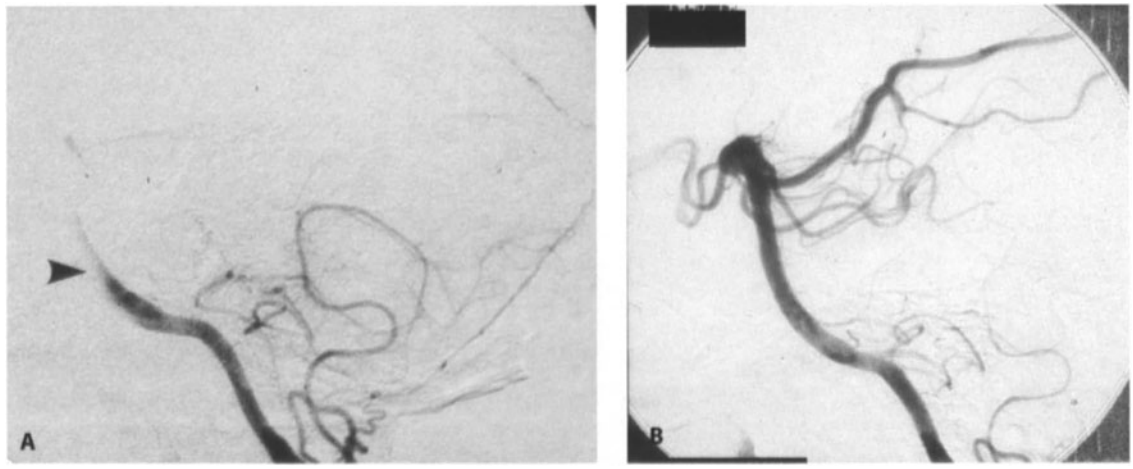

Fig. 1.34A, B. Acute basilar occlusion secondary to a distal emboli. **A** Lateral subtraction angiogram in the acute phase demonstrates occlusion of the mid basilar artery (*arrowhead*). **B** Lateral digital subtraction angiogram after 1,000,000 units of urokinase (UK) with total revascularization. The patient made a full recovery

as compared to a more proximal occlusion. Those with complete recanalization have a twofold better outcome than those with only partial recanalization.

With respect to the time window of LIAT in acute basilar thrombosis, several observations have been made. While in theory the same implications and restrictions apply as to the treatment of acute occlusions involving the anterior circulation (MCA), in reality the treatment window is often prolonged beyond the usual 6-h limit.

One reason that LIAT can be carried out beyond this time window is that the exact onset of symptoms at the posterior fossa level is often less well known. Symptoms may progress in a stuttering fashion, rather than abruptly, as in MCA distribution. As the clinical symptoms and signs progress further and become well established, the outcome without intervention is nearly universally poor or fatal. This has provided the rationale for LIAT beyond the 6-h window. In our experience, we were able to perform LIAT up to 12 h after onset of symptoms with favorable clinical outcome. However, it should be clearly understood that the chances of hemorrhagic conversion will become progressively worse with time. In the instances in which we were able to achieve recanalization even after 18 h, the clinical outcome invariably was poor, with a high incidence of hemorrhagic conversion (Fig. 1.35). We believe that at least a partial explanation of the hemorrhagic conversions may be necrosis involving the endothelial cells, loss of autoregulation, and malfunction of the tight junctions in the ischemic tissue. The use of thrombolytics in such an environment is probably a bad combination, and we believe that occlusions beyond a certain time should be treated with mechanical revascularization in an attempt to avoid thrombolytics (Fig. 1.36). We have used DWI and PWI MRI to guide us in these difficult circumstances, and if there was clear evidence on DWI of ischemic changes involving the brain stem and/or large areas of the cerebellum LIAT was withheld. Ethical issues and input from the patient's family become relevant in the decision-making process, since the patient's

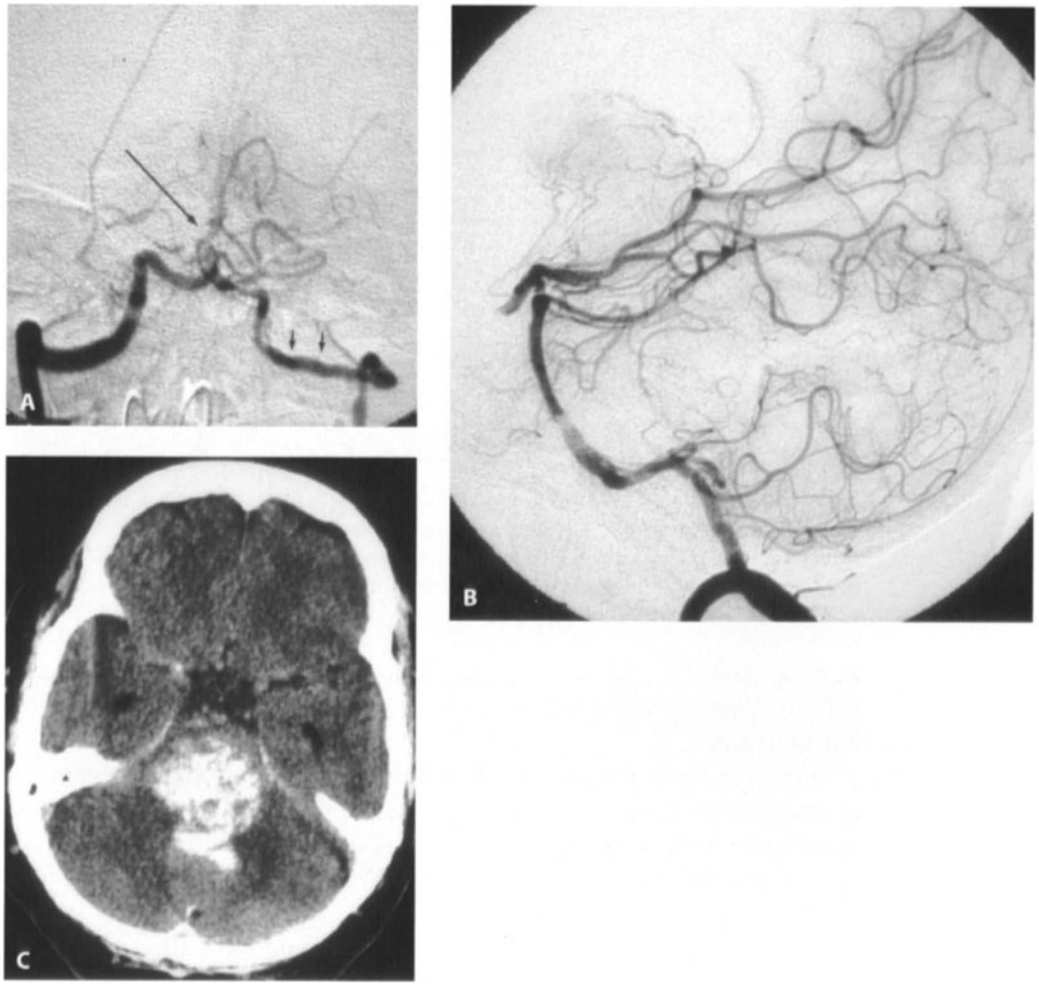

Fig. 1.35A–C. Recanalization of basilar artery occlusion. Acute event had occurred 18 h previously. **A** Frontal view of the right vertebral artery demonstrates the proximal basilar occlusion (*arrow*); note irregularities in the left vertebral artery (*small arrows*). **B** Lateral digital subtraction angiogram of the right vertebral artery after thrombolytic therapy with 1,000,000 units of UK with excellent recanalization of the basilar artery. **C** Three hours later there was a hemorrhagic conversion

quality of life can be significantly impacted by our ability to preserve life through revascularization, but possibly in a locked-in state. Good clinical judgment will therefore be more important than being able to create an excellent postrevascularization angiogram.

In cases of hemodynamic insufficiency, where the symptoms are positional and/or progressive, the lesion may be a stenosis and not thrombi. In such instances, balloon angioplasties with a less than perfect result may be enough to improve or resolve the symptoms (Fig. 14.38). As experience is gained in stenting techniques, and stents for the basilar artery become available, stenting may replace balloon angioplasty, as it has in most other circulations (Fig. 1.33).

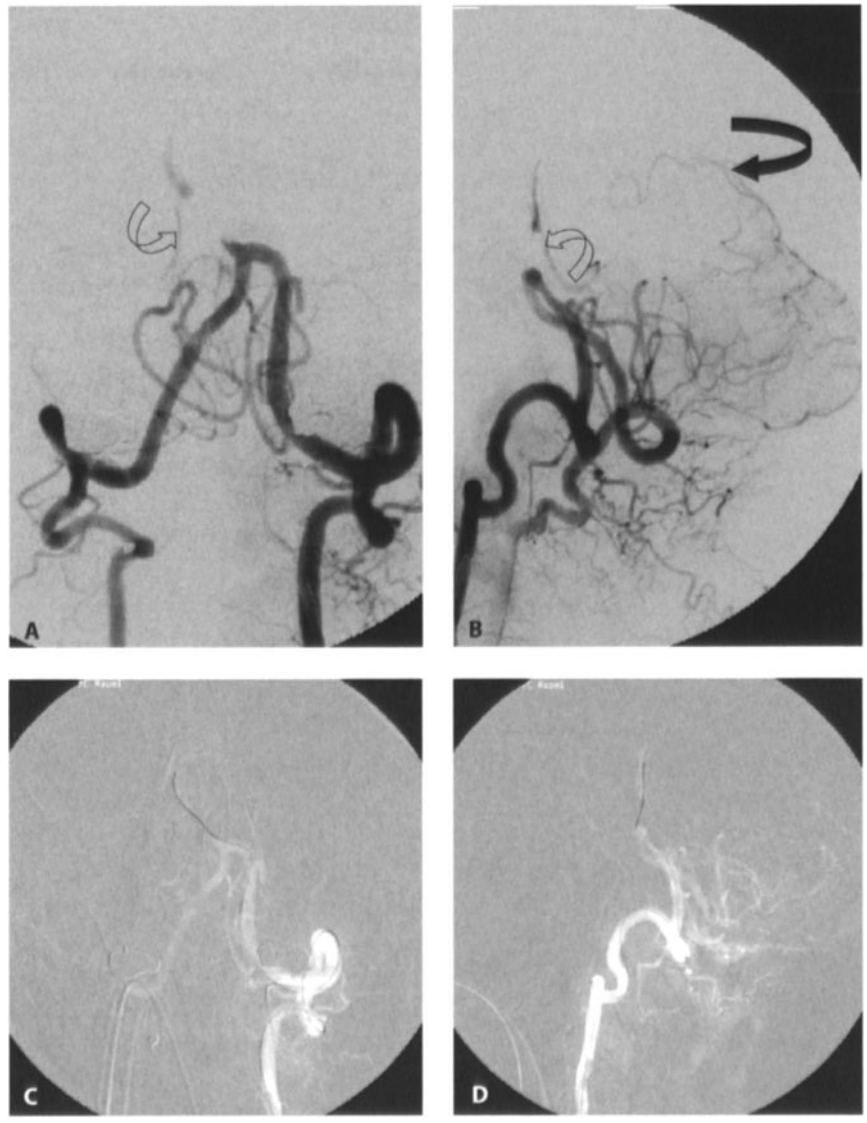

Fig. 1.36A–L. Acute total basilar occlusion. The patient presented approximately 12 h after an acute event of basilar occlusion. **A** Frontal digital subtraction angiogram of the left vertebral artery shows a total occlusion of the proximal basilar artery (*curved arrow*). **B** Lateral view of mid-arterial phase shows the basilar occlusion. Note the cerebellar arcade from the posterior inferior cerebellar to the superior cerebellar artery (*black curved arrow*), suggesting that a stenotic lesion or restriction of flow had been there for some time prior to the acute event. There is partial (inefficient) revascularization of the basilar artery above the occlusion, through a collateral channel paralleling the course of the basilar artery (*open curved arrow*). **C** Frontal and **D** lateral views of the mechanical recanalization of the totally occluded segment. **E–L** see p. 114

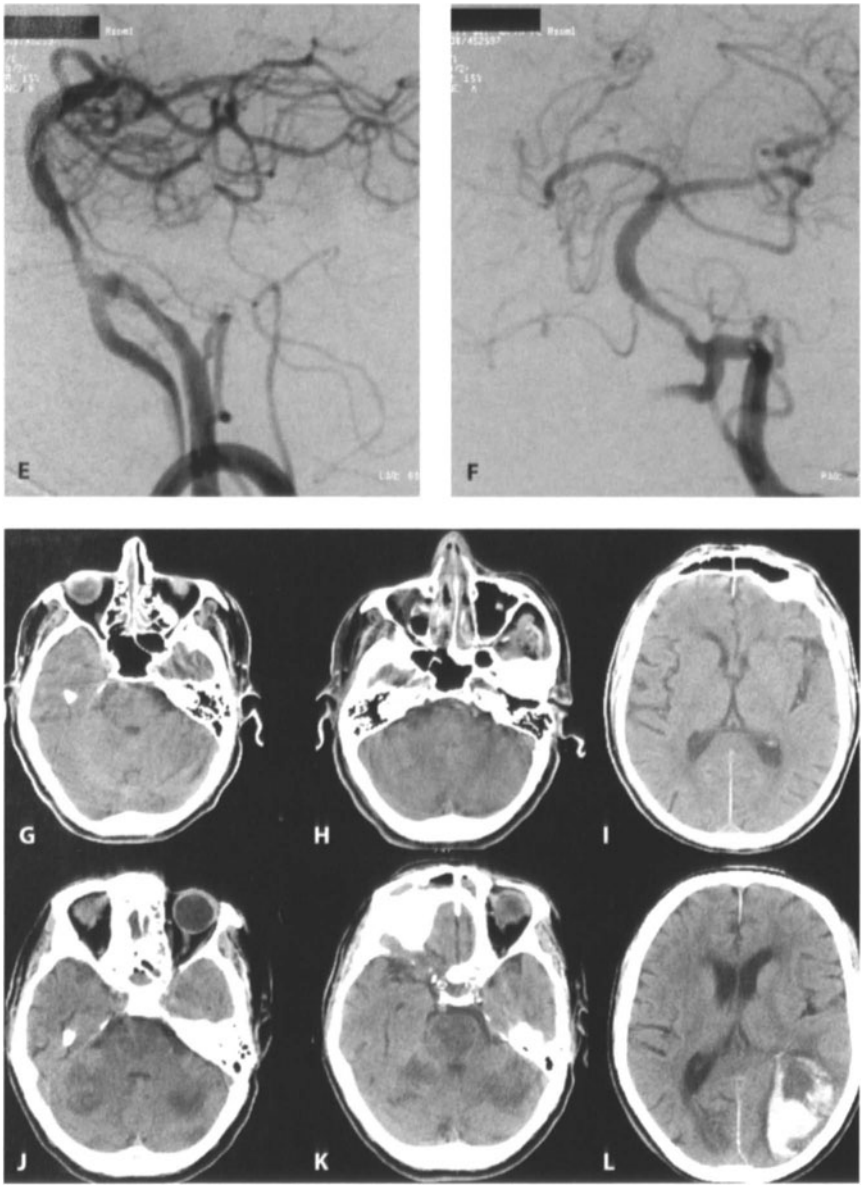

Fig. 1.36 (*continued*). **E** Frontal and **F** lateral views after mechanical recanalization with a good angiographic response. **G–I** CT scans at the time of acute stroke and prior to the mechanical revascularization demonstrate some lucencies within the cerebellar hemisphere on the left side and probably some changes in the brainstem. **J–L** CT scan 4 days after the revascularization. Note the bilateral areas of infarction in the cerebellum, as well as in the brainstem. There is a hemorrhagic conversion in the left occipital territory. The patient was kept on anticoagulants with heparin and antiplatelet medication. This probably represents a later complication at a distal embolic territory of the left posterior cerebral artery (PCLA)

1.2.7.6 Takayasu's Arteritis

Takayasu's arteritis is a chronic giant cell inflammation of the arterial wall of unknown cause. Associated conditions include rheumatic fever, streptococcal infections, tuberculosis, rheumatoid arthritis, and other collagen vascular diseases. There is evidence of an autoimmune process (Eichhorn et al. 1996). Takayasu's arteritis involves elastic arteries and predominantly involves large vessels such as the aorta and its branches (Matsunaga et al. 1997). The disease affects Asian populations and people from South America. There is a 96% preponderance of females over males in Asians, whereas more than 30% are males in India (Moriwaki et al. 1997). Interestingly, Japanese patients tend to present more often with symptoms referable to the aortic arch, including cerebral insufficiency and decreased or absent pulses in the upper extremities, often associated with pain. In Indians, the presenting symptoms tend to be related to involvement of the abdominal aorta, and result in renovascular hypertension and its complications. In India, China, Korea, Japan, and other Southeast Asian countries, Takayasu's arteritis is the most common cause of renovascular hypertension (Moriwaki et al. 1997).

Takayasu's arteritis is a disease that presents as a nonspecific syndrome of anorexia, weight loss, malaise, myalgias, etc., in young, mainly female patients (Ishikawa 1988).

The symptoms begin in childhood in one-third of patients. The average age of ischemic symptoms is 22 years. In the chronic stage, symptoms include coronary insufficiency, aortic regurgitation, hypertension, upper or lower extremity ischemia, and pain. In up to 50% of patients, there will be neurological symptoms, secondary to hypoperfusion or emboli, which may result in devastating stroke and are suggestive of a poor prognosis (Eichhorn et al. 1996).

Erythrocyte sedimentation rates, total serum protein levels, and serum albumin are usually elevated but do not correlate with the severity of the disease (Moriwaki et al. 1997; Ishikawa 1988).

The pathological features of the acute phase include mononuclear and giant cell infiltration of the adventitia and media, followed by intimal proliferation with fibrosis of the intima and adventitia. This leads to progressive stenosis and vessel occlusion. Less frequently, the involvement of the wall may lead to arterial ectasia and aneurysm formation (Moriwaki et al. 1997).The active phases of inflammation and stenosis may involve multiple arteries simultaneously. Even during inactive phases, biopsies of the arterial wall demonstrate inflammatory infiltration (Kerr et al. 1994).

Ishikawa noted an interesting pattern regarding the progression of the stenotic lesions: first, the left subclavian artery becomes involved, then the left CCA, and then the right subclavian artery. The left-sided brachiocephalic arteries are more severely affected than those on the right. In the left subclavian artery, most lesions are proximal to the vertebral artery, whereas in the right subclavian artery, 70% of the lesions are distal to the right vertebral artery origin. The common carotid arteries are involved in over 30% of cases (Eichhorn et al. 1996).

The frequency of orthostatic syncope and postural hypotension may reflect malfunction of the carotid sinus reflex, which has been reported to

be abnormal in Takayasu's arteritis (Takano et al. 1993). Bihemispheric hypoperfusion, vertebrobasilar insufficiency, or a combination of factors may all be responsible for symptoms, and differentiating the various etiologies is important in planning management.

Natural History

The natural history of Takayasu's arteritis is variable. In approximately 20% of cases, the disease may run a self-limiting course, with a single acute phase and spontaneous resolution. Alternatively, the disease will progress and carries significant morbidity; no accurate figures exist. Presentation at an early age has a poorer prognosis and is associated with all the morbidity resulting from the various hypoperfusion syndromes, making Takayasu's arteritis a severe condition: mortality is not negligible (Kerr et al. 1994). The causes of death include congestive cardiac failure, coronary ischemia, sudden cardiac death, stroke, aneurysm rupture, and the complications of hypertension.

Treatment

There is no specific treatment for Takayasu's arteritis. High-dose corticosteroids alone or in combination with immunosuppressive agents can be helpful in some cases, but relapses are frequent. Surgical techniques of revascularization and endovascular revascularization or a combination of revascularization techniques have only limited palliative effect (Stoodley et al. 2000). Since the disease is progressive, with inflammatory involvement of the arterial wall, procedures that mechanically interfere with the vessel wall may not resolve the problem. It may be of some value to utilize a combination of therapeutic strategies such as aggressive medical anti-inflammatory, immunosuppressive regimes, and revascularization procedures using newer stents. The recent introduction of stents that are able to deliver chemotherapeutic agents, to avoid intimal hyperplasia, may be of benefit to stop or slow down the inflammatory behavior in this condition. The revascularization should aim for less than optimal angiographic results, to decrease added insult to the arterial wall. Bypasses appear to be of some benefit, if placed in noninvolved arteries (EC/IC); however, aortobrachiocephalic procedures in this population should be avoided (Stoodley et al. 2000). It may be best to treat with revascularization at the brachiocephalic origins with endovascular techniques along with long-term use of combination antiplatelets and anticoagulants.

1.2.8 Cerebral Angioplasty

Cerebral angioplasty may be employed to mechanically dilate cerebral vessels narrowed by the vasospasm that follows subarachnoid hemorrhage or by stenotic lesions secondary to atherosclerosis, fibromuscular dysplasia, or other vascular pathology. Stenosis may also be iatrogenically induced, such as narrowing after aneurysm clipping (Figs. 1.37, 3.21, ICA clip, Vol. 5), or after endovascular devices including balloons (Figs. 1.38, 3.9, angioplasty balloon, Vol. 5).

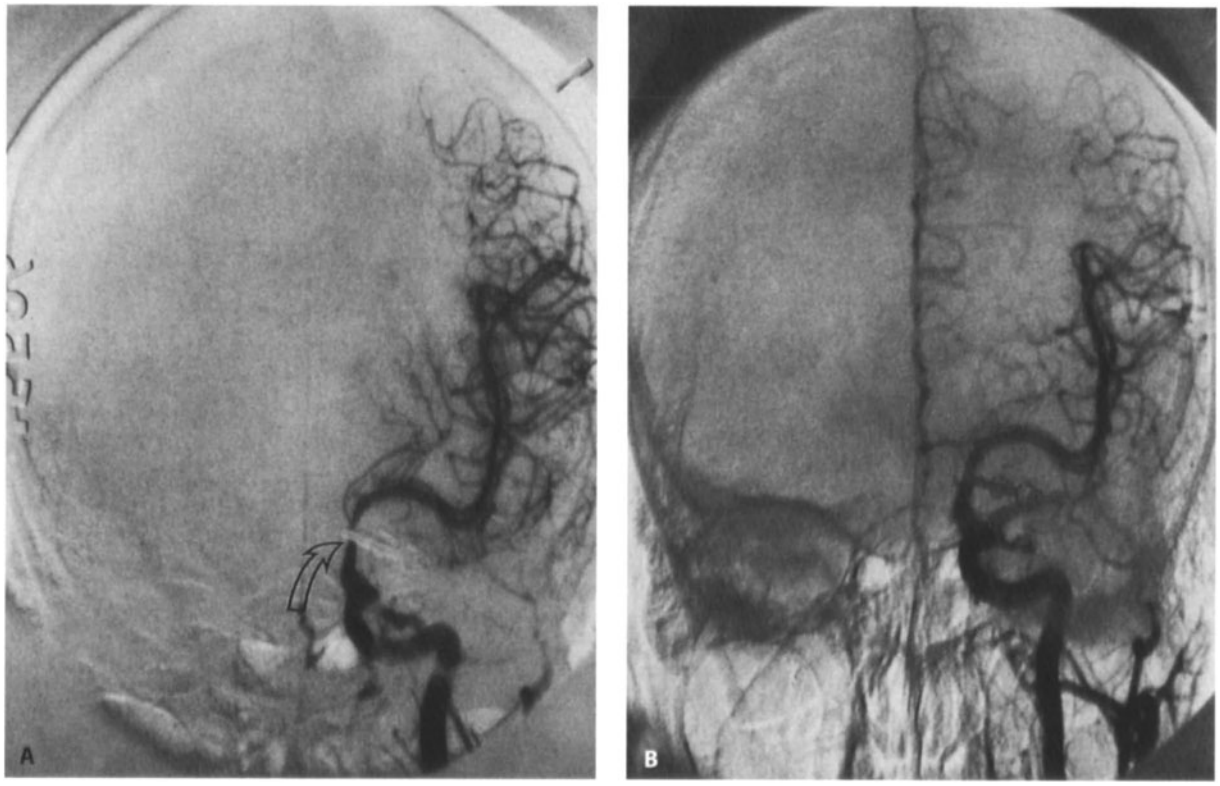

Fig. 1.37. A, B. Internal carotid artery dilatation. **A** Left internal carotid artery study in frontal projection. Note the vasospasm at the level of a posterior communicating artery aneurysm, which has been clipped (*curved open arrow*). **B** After angioplasty of the internal carotid artery with a Stealth balloon catheter (Target Boston Scientific; see Fig. 14.23). Note the improved caliber and filling of the anterior cerebral artery

1.2.8.1 Vasospasm

Delayed ischemic complications from arterial vasospasm that follows subarachnoid hemorrhage remain a major cause of morbidity and mortality despite a myriad of pharmacological agents and hemorheological maneuvers (Heros et al. 1983).

The introduction of mechanical balloon dilatation of cerebral arteries in the management of vasospasm was proposed by Zubkov et al. in 1984, and others (Higashida et al. 1989, l990c; Newell et al. 1989; Brothers and Holgate 1990; Bracard et al. 1990; Berenstein et al. 1990), with similar positive results and a very low morbidity rate. Over the past decade, angioplasty has become accepted as an effective and safe treatment for patients with symptomatic vasospasm.

Zubkov's Technique

Zubkov's technique consists of a single lumen catheter with a latex balloon introduced through direct carotid puncture; the materials are not commercially available.

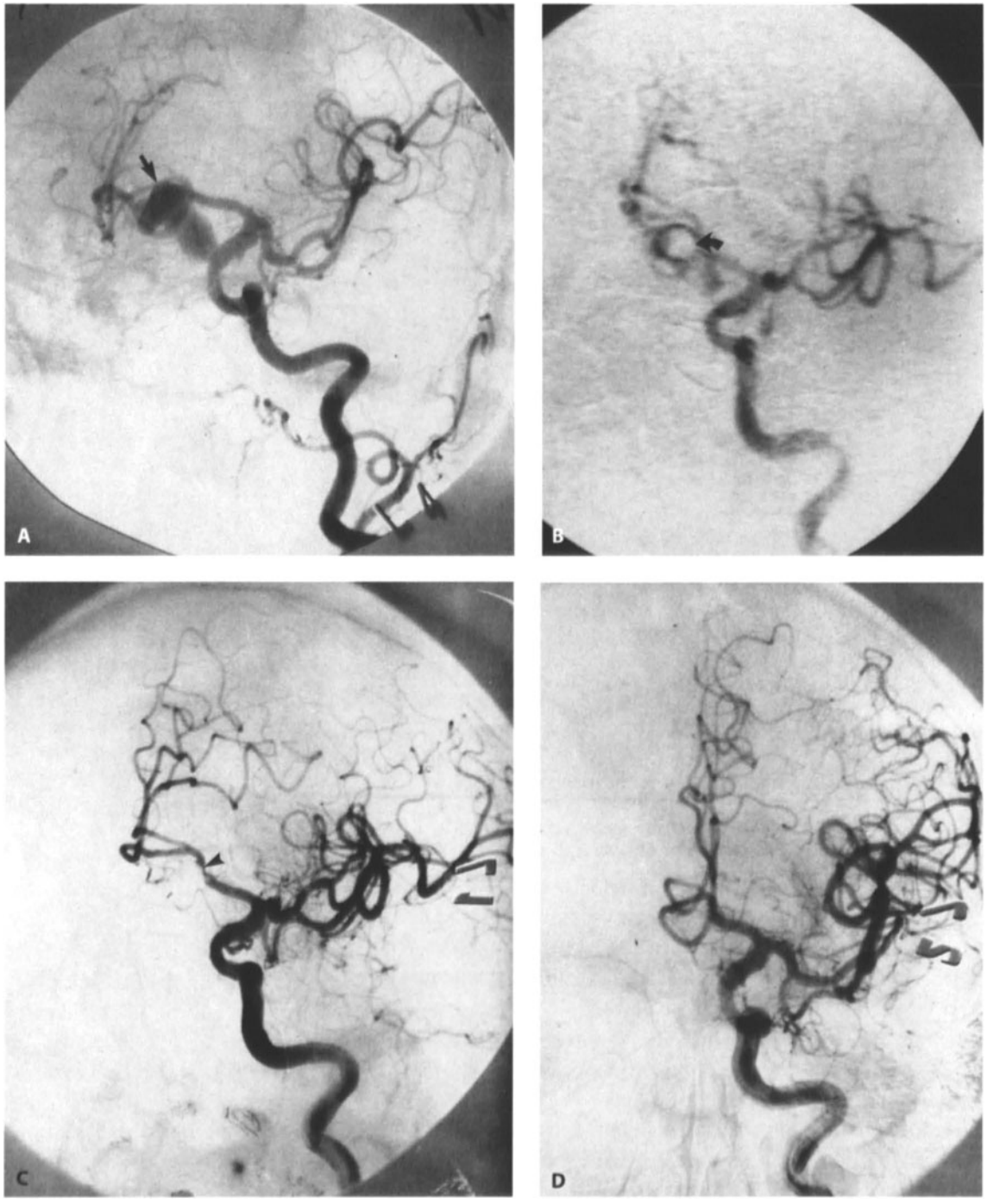

Fig. 1.38. A–E. Bilobed aneurysm of the anterior communicating artery treated with a Hieshima detachable balloon filled with HEMA. **A** Oblique view of the left common carotid artery demonstrates a large, partially thrombosed, bilobed aneurysm of the anterior communicating artery (*arrow*). **B** Digital subtraction angiogram as the balloon (*curved arrow*) is partially inflated to fill up the proximal dome and neck of the aneurysm. **C** Immediate postembolization control angiogram of the left internal carotid artery demonstrates obliteration of the aneurysm but narrowing of the anterior cerebral artery (*arrowhead*). **D** Frontal view after angioplasty of the narrow segment. Note reconstitution of the anterior cerebral artery without stenosis and no filling of the aneurysm. **E** see p. 119

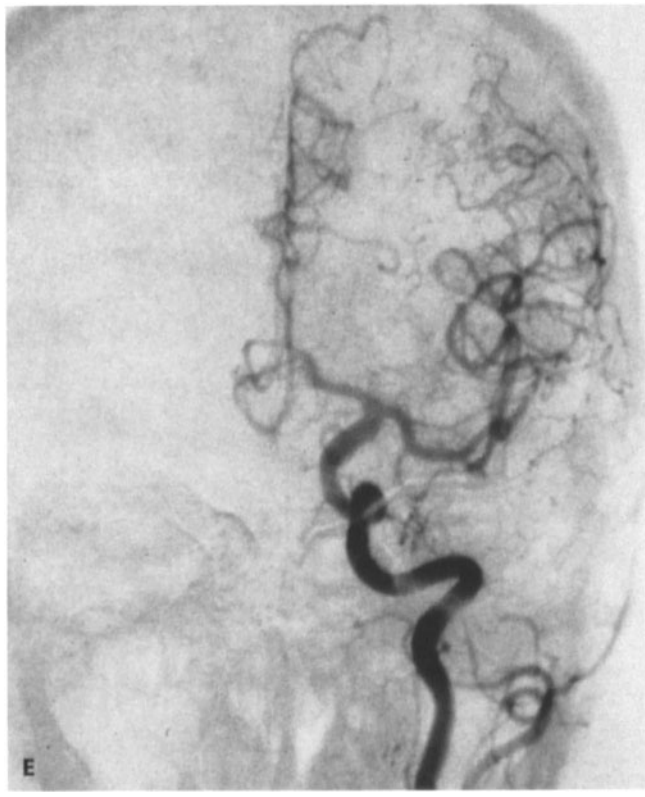

Fig. 1.38 (*continued*).
E A 1-year follow-up angiogram shows persistence of the occlusion without stenosis. If the neck of the aneurysm is occluded, the treatment is considered to be permanent

Higashida Balloon Catheter

The Higashida balloon catheter (Figs. 14.25, 3.22, Chap. 14; Target Boston Scientific) consists of a blind-ended silicone balloon attached to a 2F nontapered polyethylene catheter. Two different sizes of balloons have been described: (a) a 0.85 × 3.5-mm uninflated balloon with a capacity of 0.10 ml that will expand to 3.5 × 12.5 mm and (b) a larger balloon (1.5 × 3.9 mm) that accepts 0.50 ml and which will expand to 7.5 × 13.5 mm; this balloon is used for the internal carotid artery and vertebral artery.

The same balloon has been used by Newell et al. (1989) and by Brothers and Holgate (1990). The balloon is attached to a variable stiffness Tracker catheter (Target Boston Scientific), which facilitates navigation. The microcatheter also makes it possible to use deflecting guidewires within the balloon to deal with acute angulations such as catheterization of the anterior cerebral artery.

Calibrated Leak Techniques

Silicone Balloon. Brothers described a modification in the calibrated leak technique by making a hole in the balloon so a guidewire could pass through the silicone balloon while deflated, thus adding flexibility to the system.

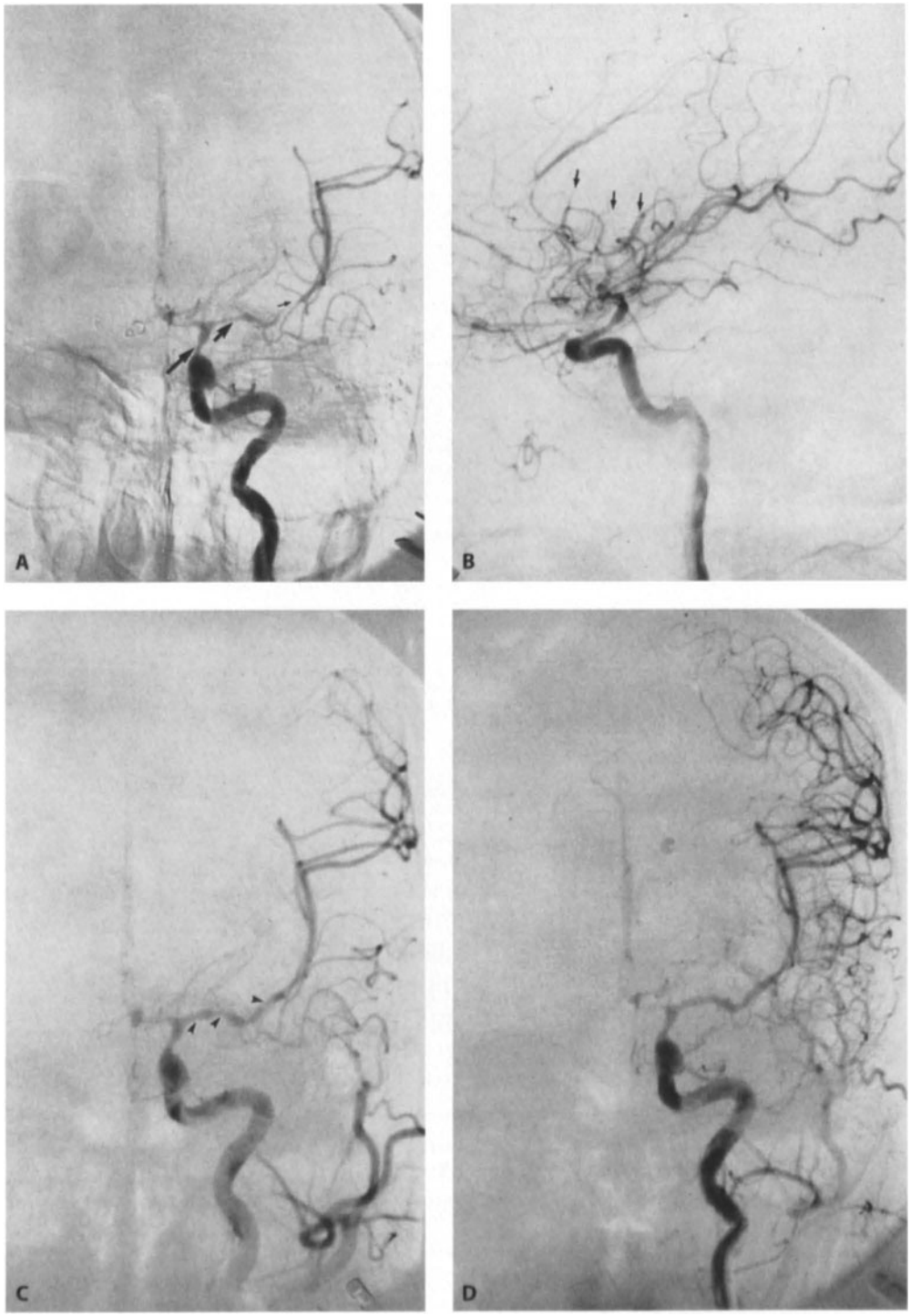

Fig. 1.39. A–H. Reversible deficit after dilatation in a 31-year-old man with cerebral vasospasm producing hemiplegia and aphasia. Latex calibrated leak technique (see text). **A** Frontal angiogram of the left internal carotid artery after clipping of an anterior communicating artery aneurysm. Note the spasm in the supraclinoid carotid M1 and M2 segments (*arrows*). There is also spasm of the A1 segment. **B** Lateral view of the same injection; later phase demonstrates absence of temporal branches in Broca's area (*small arrows*). **C** Frontal view of the left internal carotid artery after various segments have been dilated. Note the skip areas (*arrowheads*). **D** After those areas have been dilated there is a normal appearance to the middle cerebral artery (MCA). **E–H** see p. 120

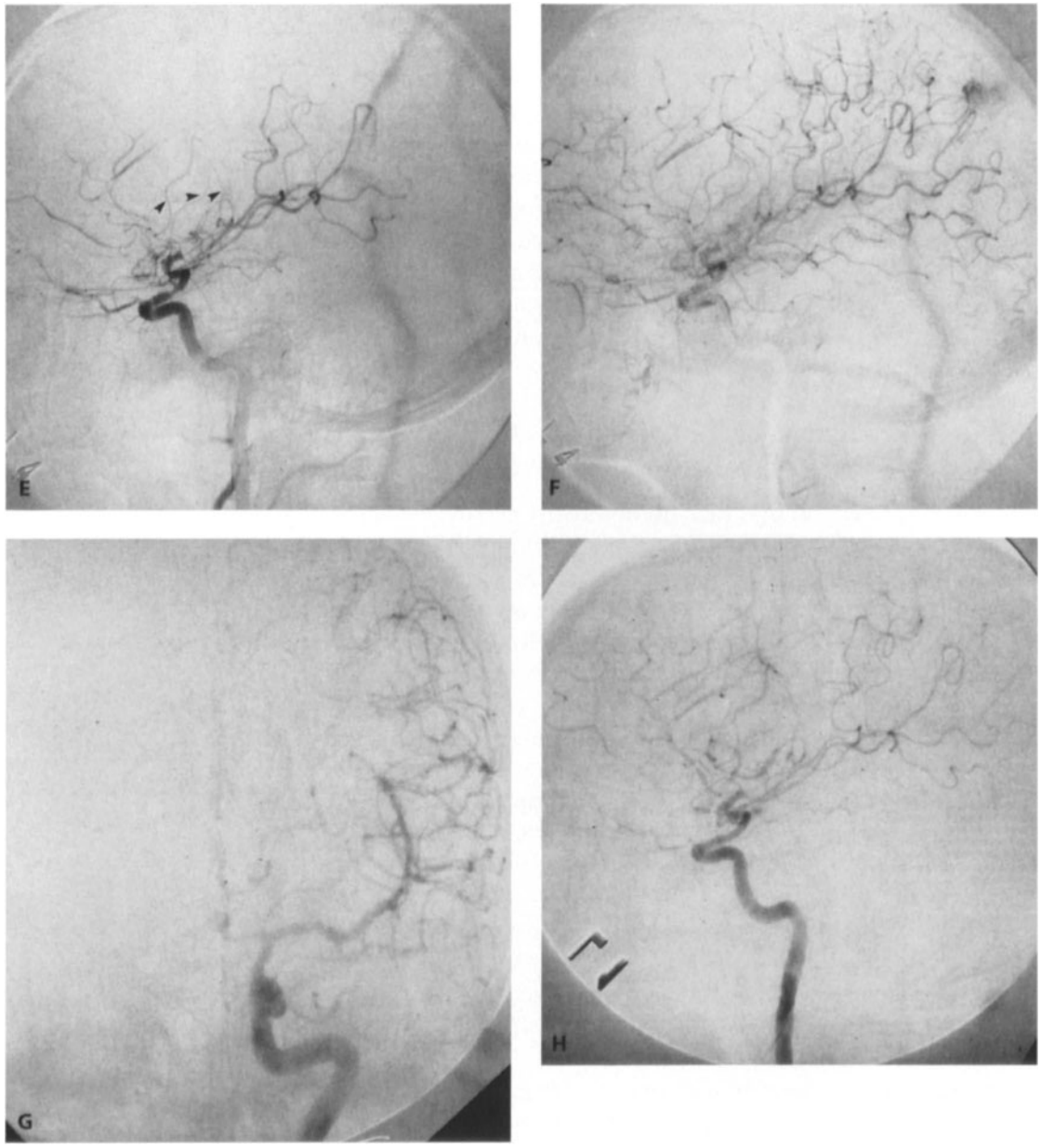

Fig. 1.39. (*continued*). **E** Lateral view in early arterial and **F** late phases following dilatation demonstrates filling of the temporal opercular branches of the MCA not opacified prior to MCA occlusion (*arrowheads*; compare to **B**). There is persistent spasm of the anterior cerebral and pericallostal arteries. **G, H** Follow-up angiogram 1 week later in frontal and lateral projections. The dilated segments remained dilated and have a normal appearance. There still is slight spasm in the nondilated anterior cerebral artery territory. There was clinical improvement and full recovery of arm movement and speech improvement, which was then followed by leg improvement, compatible with the territories treated

Latex Balloon. The latex balloon technique uses a latex, calibrated leak balloon attached to a variable-stiffness microcatheter (Figs. 14.25, 3.22 Vol. 5, and 14.37, 4.21, this volume) (Berenstein et al. 1990). The hole in the balloon should be large enough so that contrast material like heparin, thrombolytics, antispasmodics or other infusions, can be injected prior to balloon inflation. At present, we more often use the silicon balloon with a leak made externally with a 25- to 27-gauge needle (Fig. 14.25).

The use of a variable-stiffness microcatheter, as compared to polyethylene or other softer-type microcatheters, appears best, as they are soft enough to navigate but have sufficient rigidity to permit minor advancement or withdrawal in a very controlled manner. Thus, if skipped segments of stenosis remain, the balloon can be repositioned for additional dilatation (Figs. 1.39, pp. 120, 121).

In smaller, spastic, intracranial vessels, the calibrated leak system has multiple advantages over the blind-ended occlusive balloon technique:

1. There is inherent safety, which prevents early overdistension and vessel rupture. The balloon leak acts as a self-decompressive valve system.
2. The ability to inject distally makes it possible to continuously monitor the progress of dilatation. At the beginning of the procedure, stasis of contrast material is present. As spasm is relieved, distal washout of contrast material will be noted, which provides excellent and immediate feedback on the progression of the dilatation.
3. The initial mechanical force starting the dilatation is hydrostatic by the contrast material and confirms both the exact size of the spastic segment and the exact location of the balloon tip.
4. Instead of performing systemic heparinization, heparin can be locally injected. Vasoactive or thrombolytic agents can also be locally injected if needed.
5. Variable stiffness microguidewires can be passed through the leak of the balloon for distal navigation (Figs. 1.40). A curve can be performed to facilitate torque control, a feature that also adds support to advance the system. The guidewire is withdrawn as the catheter is being advanced.
6. The wire can also be used to accomplish the initial dilatation of severely vasoconstricted distal arteries. This is followed by advancing the deflated balloon to the narrow segment prior to dilatation while maintaining torque control (Figs. 1.41).

With all systems, balloon inflation is done with low pressure and for very short periods of 1–2 s. The narrowing of vasospasm is very easy to overcome, contrary to stenosis secondary to atherosclerosis. Therefore, the balloons (latex or silicone) must be very pliable and soft to be able to deform and follow the natural course and shape of the vessel's anatomy. Round balloons appear best, as they will be flattened when they reach the vessel wall, indicating the limit of inflation. As in the dilatation progresses, a more rounded configuration of the balloon is needed, which adds safety by preventing overdistension.

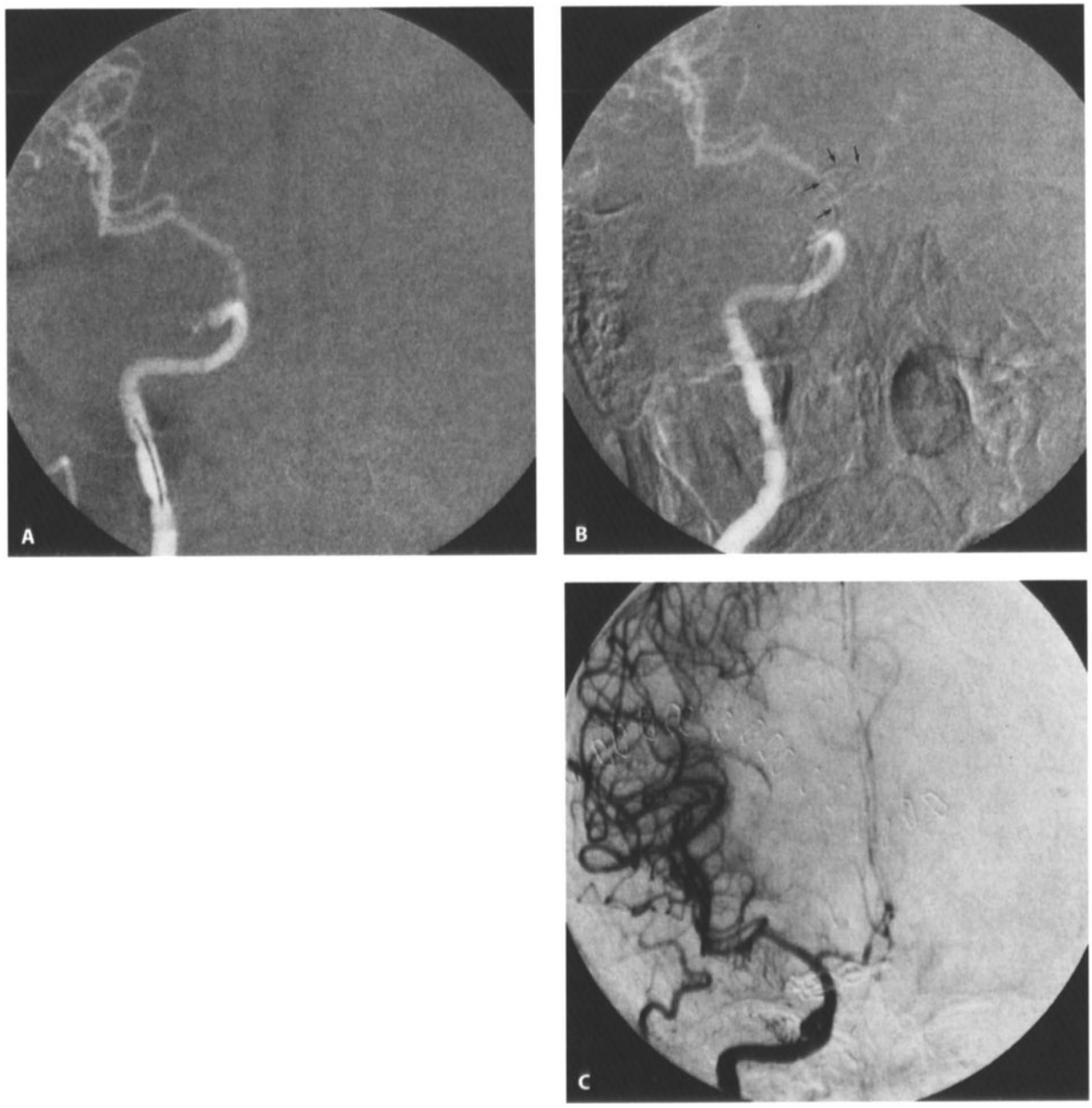

Fig. 1.40A–C. Guidewire through balloon technique. Angioplasty of the anterior cerebral artery. **A** Road mapping in frontal projection from the right internal carotid artery demonstrates no filling of the anterior cerebral artery. **B** Road mapping digital subtraction angiogram (DSA); the premounted curve guidewire is deflected towards the A1 segment (*arrows*). **C** Frontal DSA after angioplasty; note the filling of the anterior cerebral artery

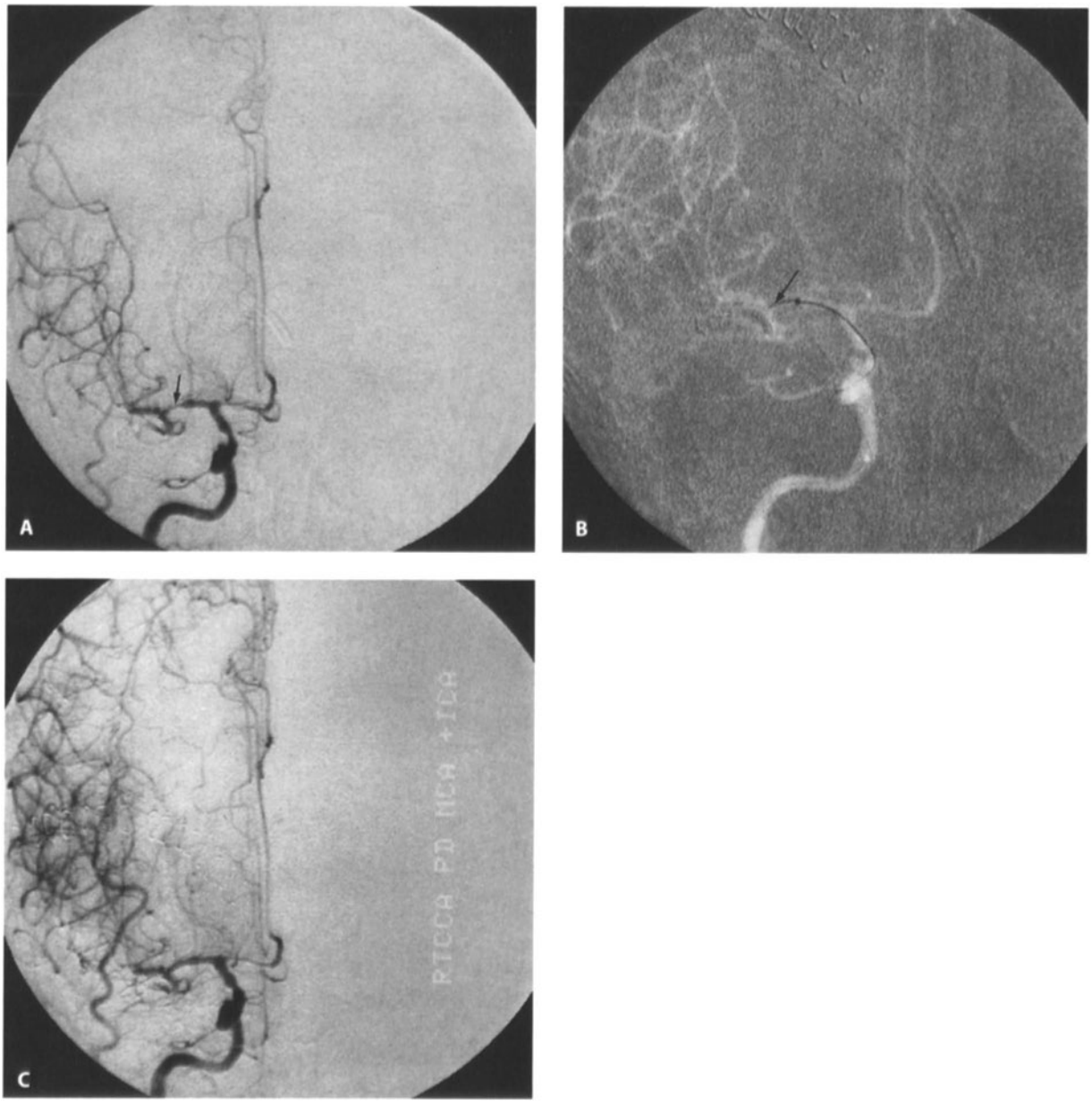

Fig. 1.41A–C. Guidewire through balloon technique. Initial dilatation with the wire. **A** Frontal digital subtraction angiogram (DSA) of the right internal carotid artery after dilatation of the proximal M1 segment shows a very narrow distal segment (*arrow*). **B** DSA road mapping image with the guidewire (*arrow*) as it passes the spastic segment, obtaining the initial dilatation. **C** After balloon dilatation of that segment

Over-the-Guidewire Balloon Tip Catheters

The Stealth (Target Boston Scientific), a single lumen angioplasty catheter that combines variable stiffness technology and a low profile, was developed by Berenstein. This catheter is designed for mechanical dilatation of atherosclerotic lesions of the vertebral artery, internal carotid artery (Figs. 14.23, 14.24), or vasospastic segments of the ICA (Figs. 1.37). The tractability of the variable-stiffness microcatheters makes it easy to reach the vessels at the base of the skull as well as the circle of Willis. Utilizing a special valve wire ball in the guidewire, the catheter tip is closed and an elongated balloon can be inflated. Deflation is easily accomplished by moving the microguidewire (Figs. 14.27) (Target Boston Scientific). Various sizes and lengths are available, depending on the vessel to be dilated.

The Stealth and fast Stealth have been used for vasospasm (Eskridge et al. 1991), long stenosis (Berenstein et al. 1990), and atherosclerosis (Ferguson 1990, personal communication). In vasospasm, it is used mainly in the proximal larger vessels such as the ICA (Figs. 1.37). However, with present technology, these catheters are primarily used for atherosclerotic lesions.

Use of softer compliant balloon-tip catheters such as the Sentry (Fig. 14.29) (Target Boston Scientific) and the Equinox (MTI, San Clemente, CA, USA) (Fig. 14.30) has the advantage of a single inflation obtaining a uniform dilatation over the length of the balloon, avoiding skip areas that require multiple inflations with the other balloons. The limitation, however, is their relatively large diameter, which limits their use to the more proximal M1 and P1 segments, and less so to the A1 (Fig. 1.42).

Small-profile double-lumen balloon-tip catheters such as the Comodor (Fig. 14.26) (Cordis Endovascular, Warren, NJ, USA) may play a role in cerebral angioplasty and have the advantage of a soft compliant balloon and a distal lumen for monitoring or infusion of vasoactive drugs, heparin, or thrombolytic agents.

Over-the-Guidewire Dotter Technique

In very distal spasm that does not respond to chemical dilatation, a Dotter-type technique can be used, using the microguidewire and microcatheter combination to dilate distal small arteries in a minimally traumatic fashion (Fig. 1.43).

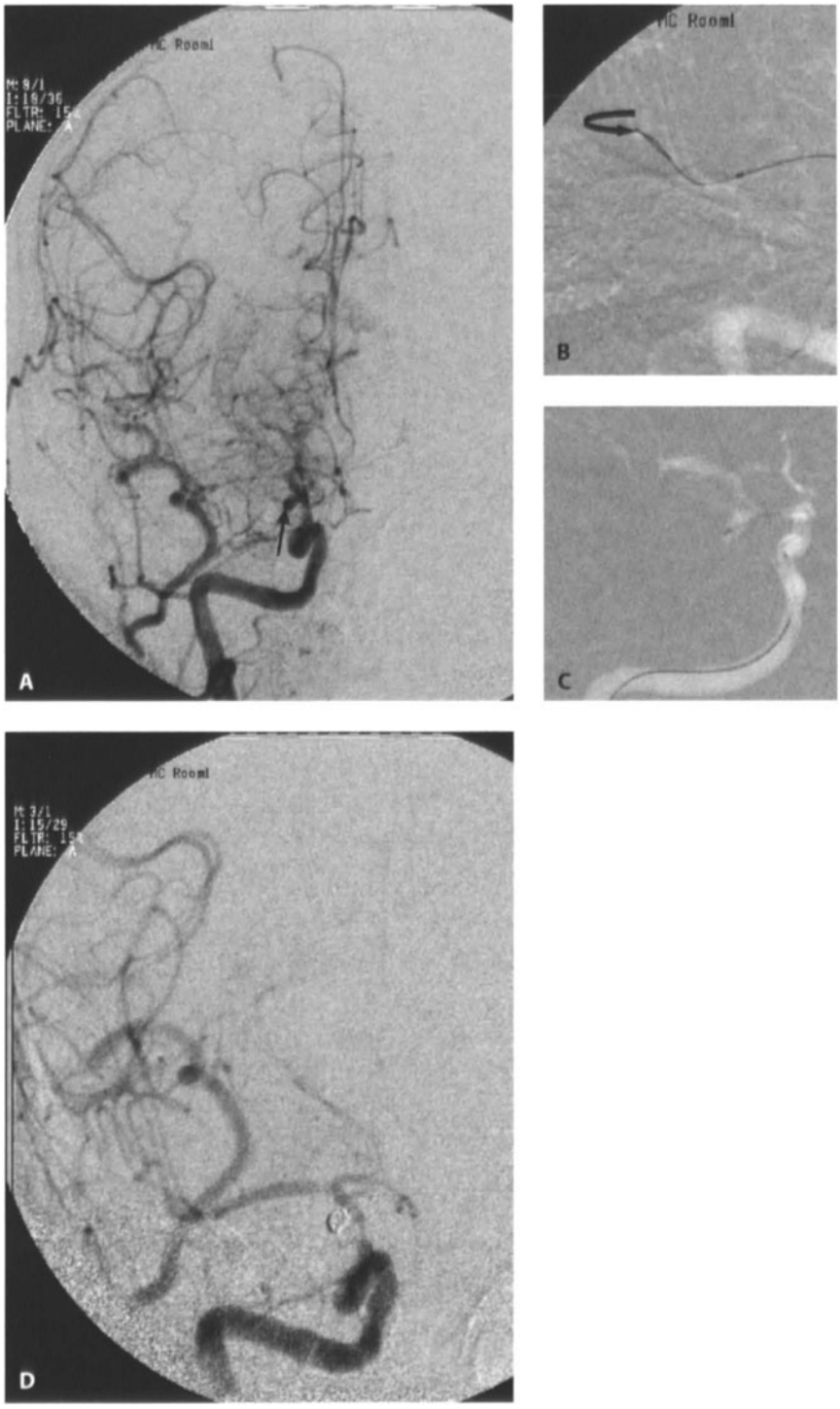

Fig. 1.42A–D. Balloon catheter angioplasty in the horizontal segment of the middle cerebral artery (MCA) for cerebral vasospasm following cerebral hemorrhage. **A** Frontal view of the right common carotid artery shows severe spasm of the horizontal segment of the MCA in a patient with a posterior communicating artery aneurysm (*arrow*). **B** Road map with the Sentry balloon-tipped catheter (Target Boston Scientific) to dilate the horizontal segment of the MCA in one inflation. Note the length of the balloon between the two *arrows*; the guidewire is distal to the tip of the balloon (*curved arrow*). **C** Following MCA angioplasty the aneurysm is catheterized. **D** Final angiogram after coiling the aneurysm and showing the improved flow in the MCA

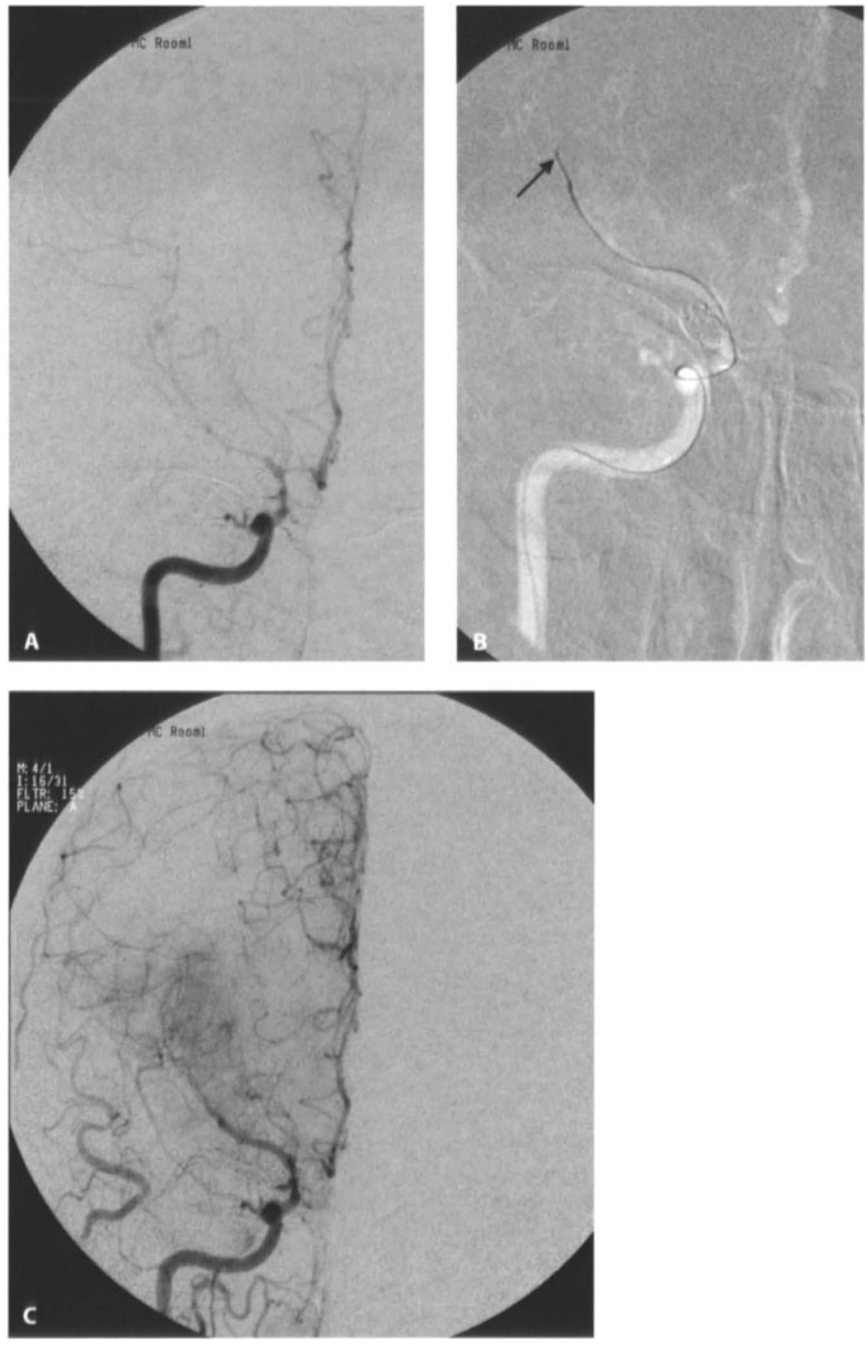

Fig. 1.43A–C. Over-the-guidewire catheter angioplasty (Dotter technique). **A** Frontal view of the right internal carotid artery after coiling a posterior communicating artery level aneurysm. Note the severe spasm of the middle cerebral artery extending into the more distal insular region. **B** Road map after the proximal MCA has been dilated with a calibrated leak balloon-tipped catheter. For the more distal MCA branches, the Dotter technique using a microcatheter and microguidewire is used to obtain a mechanical progressive dilatation of the more distal arteries. The tip of the guidewire (*arrow*) leads the tip of the catheter. **C** After angioplasty there is improved profusion of the MCA, which correlated with patient's clinical improvement

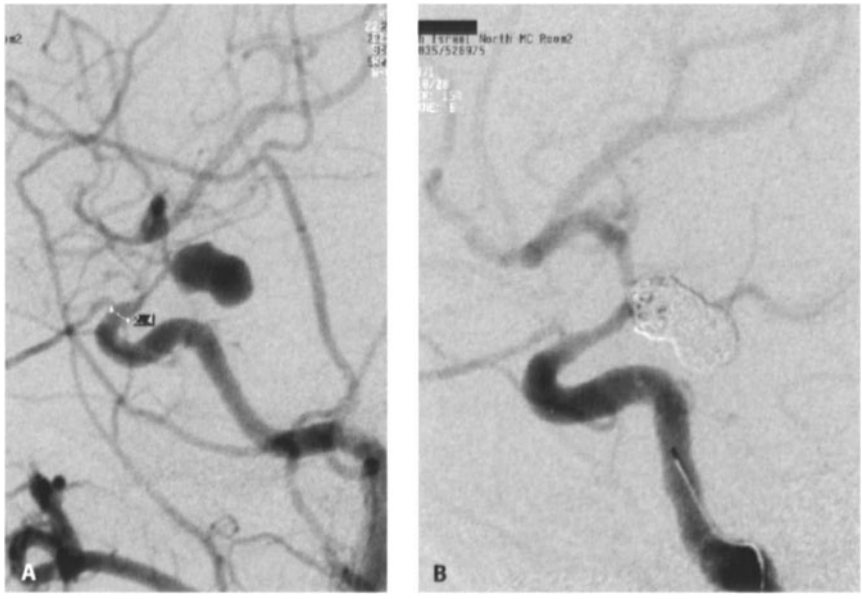

Fig. 1.44A, B. Cerebral angioplasty at time of coiling. **A** Lateral digital subtraction angiogram of the right common carotid artery demonstrates severe vasospasm in the supraclinoid internal carotid artery proximal to a large posterior communicating artery aneurysm. **B** At the end of the treatment, note the improved caliber of internal carotid artery: the aneurysm has been closed over 95%, and the posterior communicating artery now opacifies

Indications and Results of Angioplasty for Vasospasm

In the various series available, there has been an overall improvement in the patients' neurological condition. In Zubkov's experience in 33 patients (Zubkov et al. 1984), there was only one procedure that was not successful. Neurological improvement was noted in the other patients, although the exact number was not given. Among Higashida's patients, eight out of ten improved. In Newell's series, three out of four patients improved. In the four patients reported on by Brothers, early improvement was noted in three and arrest of progression occurred in the fourth patient. All five of Bracard's patients responded to angioplasty. In eight out of our nine patients, neurological improvement followed dilatation.

Eskridge et al. (1998) reported very good results in their first 50 cases, and in Rosenwasser's (1999) experience, patients treated within 2 h of the onset of vasospasm, with balloon angioplasty for the proximal spasm and papaverine infusion for the more distal spasm, did better in the long term than those patients treated later on and better than a similar cohort of patients treated medically.

Although there are no controlled studies, the nearly universal experience and available evidence for significant early benefits of angioplasty appears strong, especially if dilatation is instituted early. It is apparent that the various techniques available are effective and safe in obtaining mechanical dilatation of spastic cerebral arteries. It also appears that the earlier the angioplasty is done the better the outcome. The ease of the technique may justify the dilatation of angiographically spastic arteries at the time of the procedure even if not symptomatic. Such dilatation carries the potential of improving collateral circulation to distal territories (Brothers et al. 1990), especially in the presence of distal spasm.

There is a clear advantage to performing angioplasty at the time of endovascular treatment of an aneurysm (Fig. 1.44) that cannot be matched by intraoperative papaverine and clipping or by clipping and then sending the patient for dilatation.

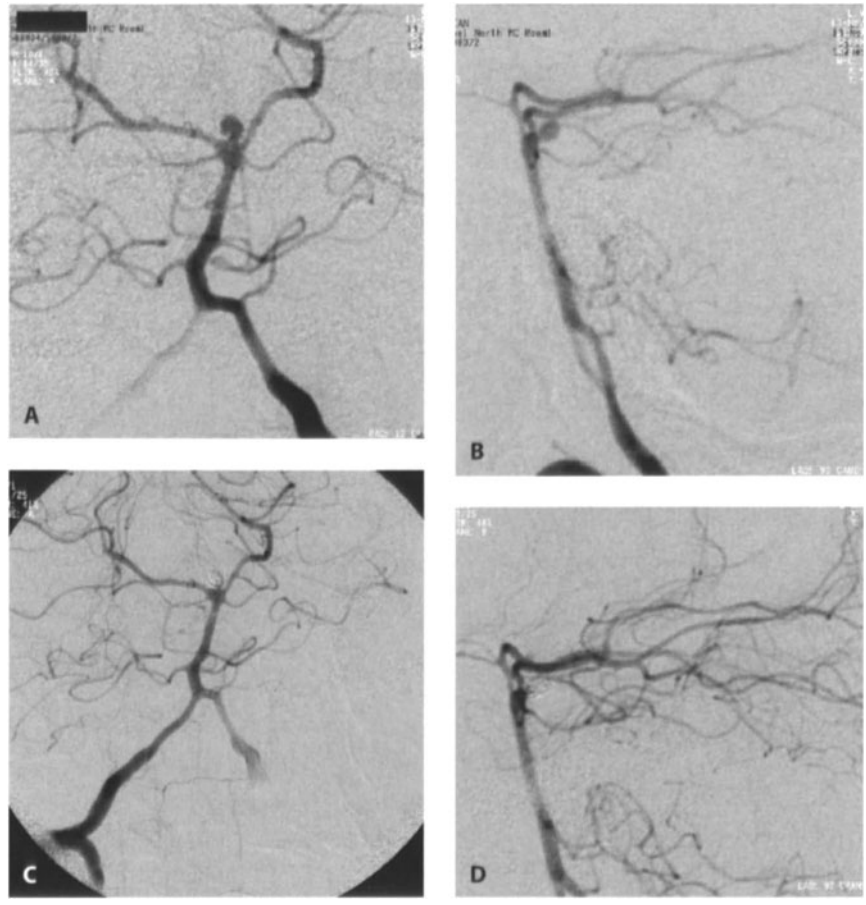

Fig. 1.45A–J. Delayed onset of spasm with global cerebral dysfunction. **A** Frontal, and **B** lateral digital subtraction angiogram (DSA) of the left vertebral artery (VA) shows a posteriorly pointing aneurysm. **C, D** Immediate DSA after endovascular coiling. **E–J** see p. 130

The limitations and contraindications are not clear. It may be prudent to avoid reperfusion of an extensively infarcted or hemorrhagic territory, as seen by preliminary CT or MRI. In small infarctions, however, angioplasty has been performed without apparent ill effects (Brothers et al. 1990). Partially ischemic territories can show decreased attenuation or lucencies on CT that may represent edematous tissue, which sometimes can be reversed by angioplasty. Bejjani (1998) found that patients treated as late as 24 h after the onset of symptoms of vasospasm had a favorable response. It is agreed, however, that early intervention is best. In questionable cases, if the CT fails to show a hemorrhagic transformation of an infarcted area or the development of hydrocephalous, angiography with intent to treat vasospasm, if present, has become the approach of choice in most centers where endovascular treatment is available.

In cases where the area of vasospasm correlates with the clinical findings, angioplasty of that area usually correlates with improvement. There are situations where the spasm is more global, and angioplasty of the various territories is done to improve overall cerebral perfusion (Fig. 1.45).

The question of vasodilatation prior to clipping of the aneurysm is probably not recommended, but it is not proven. Newell's patient, in whom a dilatation was done prior to clipping the aneurysm, died from rupture after dilatation. Zubkov, however, does not consider an unclipped aneurysm a contraindication. Angioplasty was performed on ten of his

Fig. 1.45 (*continued*). **E** Left VA angiogram 2 days later, following the patient's clinical deterioration, demonstrates severe vasospasm from the intradural portion of the left VA extending into the entire basilar territory and both proximal P1 segments. **F** After calibrated leak balloon angioplasty of the vertebral, basilar, and posterior cerebral arteries with excellent return to the normal caliber. **G** Lateral DSA of the right common carotid artery shows supraclinoid and middle cerebral artery (MCA) spasm. **H** DSA after angioplasty of the supraclinoid carotid and M1 segment with improvement in flow. **I** Lateral DSA of the left common carotid artery shows supraclinoid and MCA spasm. There is a small cavernous aneurysm. **J** Lateral DSA after angioplasty. The patient made a full recovery

patients prior to clipping; in six, vasodilatation was immediately followed by occlusion of the aneurysm by detachable balloons. Higashida had no complications in two patients after dilatation of the basilar artery in a superior cerebellar aneurysm, and in a basilar tip aneurysm. Both had unclipped lesions and both patients were operated on 2 days later.

We have experience in various settings of an unprotected aneurysm and spasm, where we first dilate the severe spasm prior to coiling (Fig. 1.44). In cases where there is severe vasospasm proximal to the aneurysm, the dilatation is first done chemically with papaverine or nitroglycerine, for example in the A1 origin, providing access to the aneurysm of the anterior communicating artery, securing the aneurysm with coils, and then infusing papaverine into the distal ACA territory, and subsequent angioplasty of the A1, with very good clinical results (Fig. 1.46).

The incidence of vasospasm following coiling versus clipping is not well established, although empirically it appears more frequent after clipping.

The concept of angioplasty prior to clipping the aneurysm is more controversial. If clipping must be done because the aneurysm cannot be coiled (even partially), then we recommend clipping the aneurysm first, followed by angioplasty under the same anesthesia.

Vessel rupture is a rare complication of angioplasty and has been reported in one instance (Higashida et al. 1989b). A delayed vessel occlusion was reported in one of Newell's patients, in whom a stiff balloon and guidewires were used. With our calibrated leak technique, we have not had vessel rupture, dissection, or occlusions.

The effect of angioplasty on the cerebral vessels and its mode of action is not well understood. The clinical improvement and resolution of neurological deficits has been maintained, suggesting that spasm does not recur after dilatation without an additional insult such as repeated hemorrhage. Follow-up angiograms in our patients showed persistent dilatation, a feature that has been observed by all other investigators (Figs. 1.39, 3.25 Vol. 5).

In vitro studies on the effect of mechanical dilatation in canine basilar arteries showed nonreactivity to vasoconstrictive pharmacological agents without intimal fracture (Pile-Spellman et al. 1987). In cadavers, Konishi et al. (1988) dilated middle cerebral artery branches to increase their lumen by 30% and showed compressed intima and stretched elastic laminas and media but no intimal tearing. In one of our patients who died from a blood transfusion, pathological examination, including electron microscopy, showed no structural damage. Significant work remains to properly understand how angioplasty affects the human cerebral vessels.

In canine cerebral arteries, Megyesi et al. (1997) demonstrated that vasospasm can be prevented if an angioplasty is done prior to the onset of vasospasm. They believed that it is due to disruption of normal response to the byproducts of SAH by the vessel wall.

Mechanical recanalization of cerebral arteries by other techniques such as laser energy (Choi et al. 1986) is still experimental.

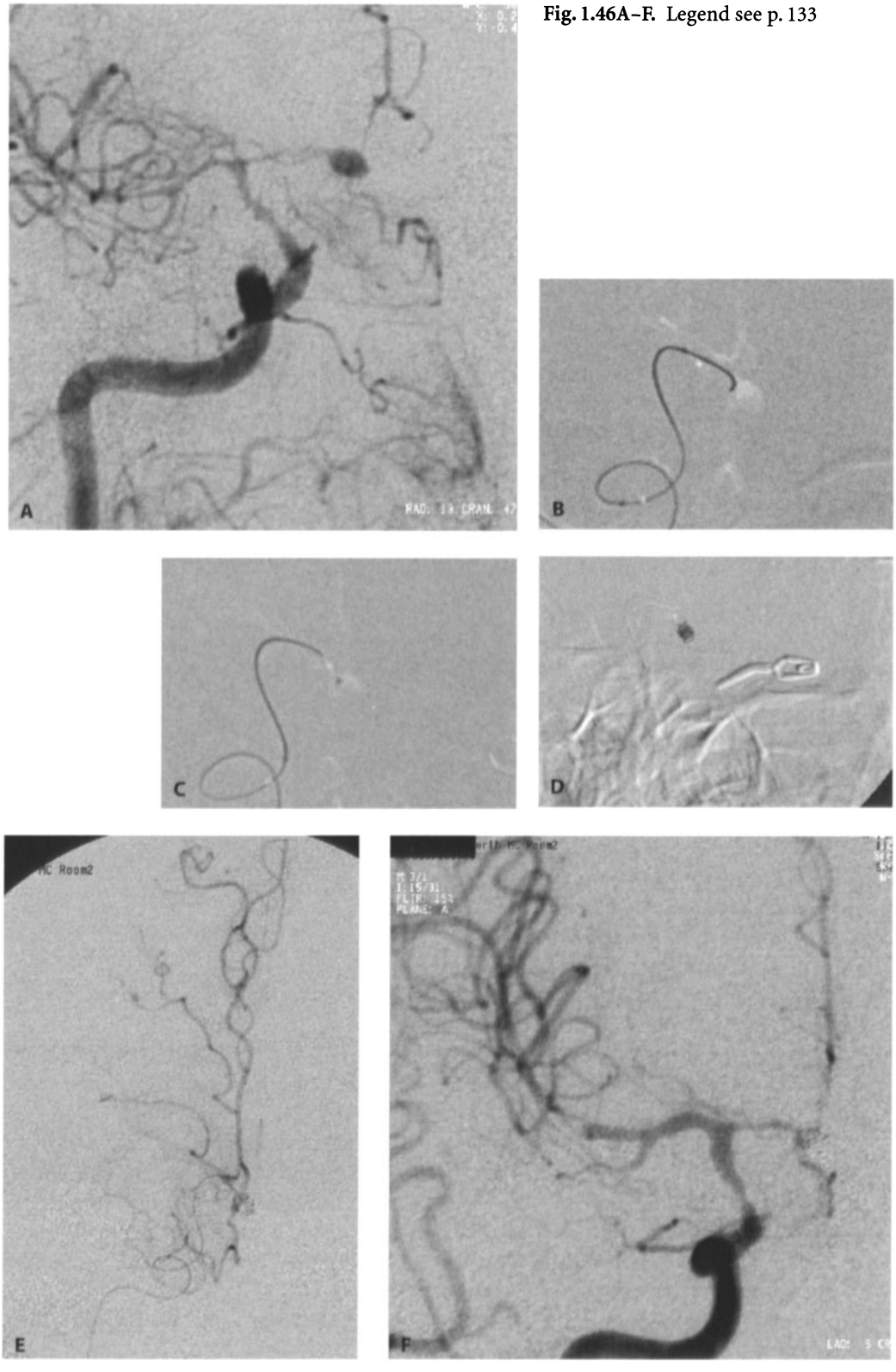

Fig. 1.46A–F. Legend see p. 133

◀ **Fig. 1.46A–F.** Combined chemical and mechanical angioplasty before and after coiling. **A** Frontal digital subtraction angiogram (DSA) of the right common cortical artery shows an anterior communicating artery aneurysm associated with severe vasospasm of the internal carotid artery, middle cerebral artery (MCA), and the anterior cerebral artery (ACA). **B** Frontal road map after papaverine injection into the ACA for catheterization of the aneurysm. The guidewire has entered the aneurysm and the tip of the catheter is later advanced. **C** Microcatheter tip is now inside the aneurysm. **D** Road map after the rapid placement of two coils within the sac of the aneurysm. **E** AP view after 95% coiling of the aneurysm with better circulation in time in the distal ACA following papaverine injection. **F** Frontal DSA after balloon angioplasty of the carotid, M1 and A1, and chemical angioplasty, using papaverine injection to the distal ACA, with significant improvement in flow

Chemical Treatment of Vasospasm

Papaverine. Papaverine has been the most frequently used agent, with only temporary results and the potential for increasing ICP (Eskridge et al. 1991).

We only use chemical angioplasty for catheterization of a spastic vessel leading to an aneurysm in the very distal territory (Fig. 1.46) or in spasm secondary to catheterization (Fig. 1.47).

The maximal dose is 300 mg, even when a good LD_{50} has not been established.

Nitroglycerin. Nitroglycerin at a dose of 100 μg is a very potent and an immediate vasodilator, and is used more and more in the spasm that can follow catheterization (Figs. 1.48, 14.83).

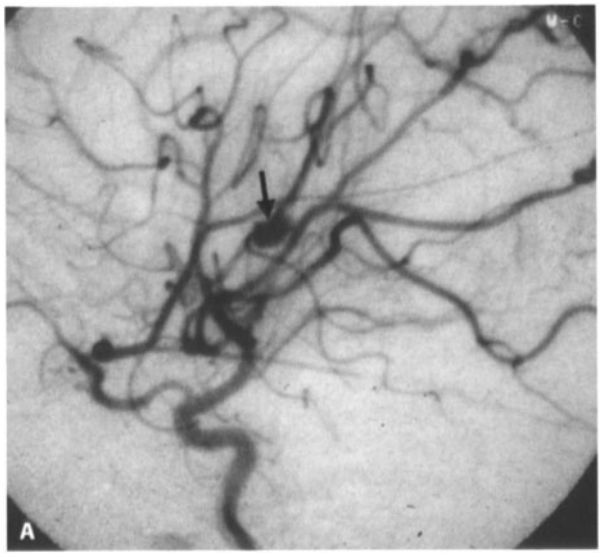

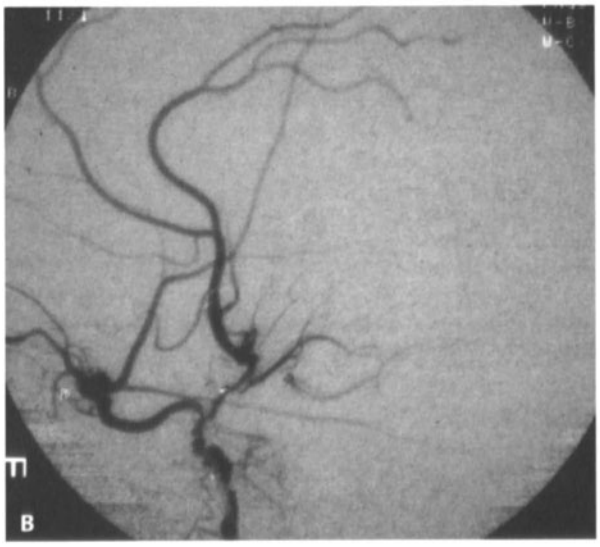

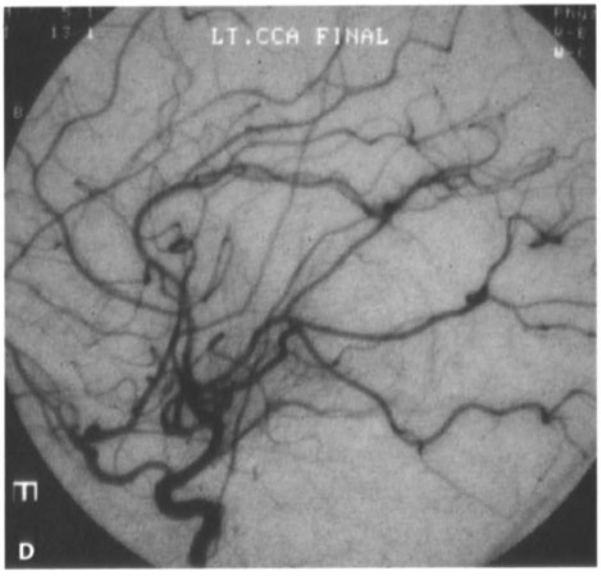

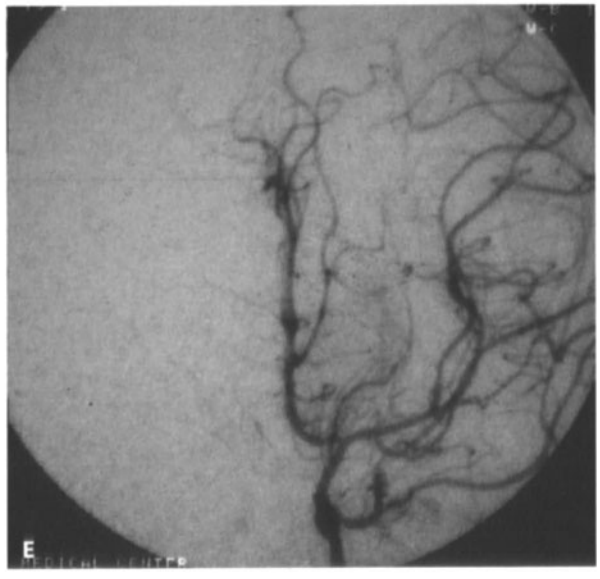

Fig. 1.47A–E. Legend see p. 135

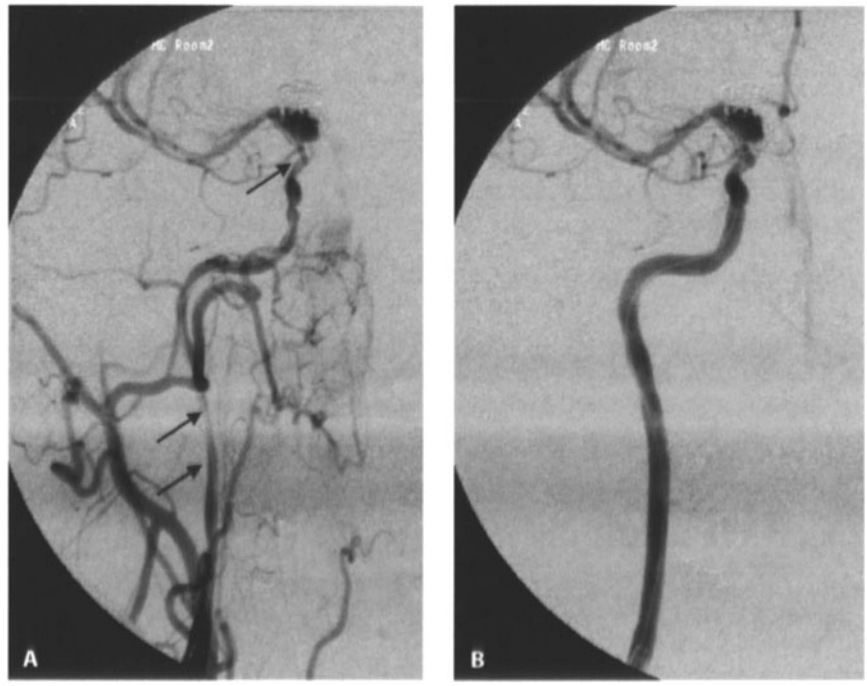

Fig. 1.48A, B. Nitroglycerin at a dose of 100 μg is a very potent and an immediate vasodilator, and is used for the spasm that can follow catheterization. **A** Note the severe vasospasm (*arrows*). **B** After 100 μg, note the immediate relief of the spasm

◀ **Fig. 1.47A–E. Iatrogenic vasospasm. Eight-month-old baby with a distal middle cerebral artery aneurysm after two hemorrhages. A** Lateral subtraction angiogram of the left internal carotid artery demonstrates a false aneurysm of the middle cerebral artery (*arrow*). **B** Lateral and **C** frontal digital subtraction angiogram (DSA) after the second coil has been placed in the aneurysm. Severe vasospasm occurred at the proximal internal carotid artery as well as distally; the vasospasm extends into the middle cerebral artery territory. **D** Lateral and **E** frontal DSA following three injections of papaverine demonstrate complete resolution of the vasospasm and obliteration of the aneurysm

1.3 Venous Occlusive Disease

1.3.1 Etiology

The first clinical description and autopsy findings of cerebral venous thrombosis was made by Ribes in 1825 in a 45-year-old man with disseminated malignancy, while in 1828 Abercrombie described intracranial dural sinus thrombosis occurring in a postpartum patient (puerperium).

These first descriptions already indicated what is now known: venous occlusive disease is a multicausal disorder that affects the venous aspect of the neurovascular tree and is related to certain hereditary and acquired predispositions. The incidence of venous thrombosis is therefore variable and will relate to multiple risk factors that are predominant in different age groups.

The risk factors that are known to be associated with venous thrombosis are tissue damage and stasis (trauma, surgery, and immobilization), dehydration, as well as congenital or acquired abnormalities associated with the hemostatic system (Table 1.31) (Seligsohn and Lubetsky 2001). De-

Table 1.31. Risk factors for cerebral venous thrombosis (from Lee et al. 2002a)

Infection	Paranasal sinusitis Intracranial infection: abscess, meningitis
Trauma	Head trauma Neurosurgical interventions Internal jugular catheter
Medical/surgical conditions	Dehydration Pregnancy and puerperium Coagulation disorders: Factor V Leiden (activated protein C resistance), protein C deficiency, protein S deficiency, antithrombin III deficiency, hyperhomocysteinemia, Antiphospholipid syndrome Hematological disorders: polycythemia, sickle cell disease, thrombotic thrombocytopenic purpura, polycythemia, paroxysmal nocturnal hemoglobinuria Malignancies, inflammatory bowel disease, nephrotic syndrome, dehydration, liver cirrhosis, collagen vascular diseases including systemic lupus erythematosus, Wegener's granulomatosis and Behçet syndrome Previous surgical procedures
Medication	Oral contraceptives, hormone replacement therapy, L-asparaginase, epsilon aminocaproic acid, corticosteroid

ficiency of protein C, protein S, antithrombin, and factor V Leiden carrier status or resistance to activated protein C are estimated to account for 25%–35% of all occurrences of venous thrombosis (Rosendaal 1997; de Visser et al. 1999). Hypercoagulable states related to the use of oral contraceptives, pregnancy/puerperium and malignancy represent another large group known to be associated with increased risk for venous thrombosis.

1.3.2 Incidence

The incidence of venous thrombosis between the ages of 1 month and 18 years was 0.7 per 100,000 per year in a Canadian stroke registry (de Veber et al. 2001) and 0.6 per 100,000 in a Dutch hospital discharge registry (Rosendaal 1997). In the first year of life, venous thrombosis frequently occurred in association with indwelling venous catheters or as renal vein thrombosis. Following a peak in the firsts year, the incidence becomes very low over the next 10 years and then gradually increases with age. In children, multiple risk factors for venous thrombosis can often be identified and are apparently required to produce symptomatic venous thrombosis.

The use of oral contraceptives (including third-generation contraceptives) is associated with a four- to sevenfold increase in the risk for venous thrombosis (Vandenbroucke et al. 2001). The absolute risk remains low with the base-line risk of less then 1 per 10,000 being increased to 3–4 per

10,000 person-years during the time when oral contraceptives are used. The risk for cerebral vein thrombosis increases 20-fold if oral contraceptives are taken by women who have an inherited disorder of the hemostatic system such as a mutation in the prothrombin gene (Martinelli et al. 1998) or 35-fold in women who were heterozygous for factor V Leiden (Seligsohn and Lubetsky 2001).

Pregnancy and puerperium increase the risk of venous thrombosis as much as fourfold. However, this risk is much greater shortly after delivery then during pregnancy, and per unit time the incidence of thrombosis is 25-fold higher postpartum then during pregnancy (Rosendaal 1997). In a woman below the age of 40 who presents with a cerebral ischemic event, the chance of it being caused by venous thrombosis is twice that of it being arterial in origin.

1.3.3 Clinical Presentation and Natural History

The clinical presentation of patients presenting with intracranial venous thrombosis will depend on the location and extent of the thrombosis (superior sagittal sinus, transverse sinus, straight sinus, cortical versus deep venous system) (Table 1.32). The clinical impact of the venous thrombosis will be worsened or diminished depending on the patient's venous anatomical disposition (collateral alternate pathways, Vol. 1, Chap. 7). Frequently the symptoms and signs of intracranial venous thrombosis are nonspecific, such as headaches and vomiting, and may continue for hours or days. This most likely reflects global increased venous pressure related to early dural sinus thrombosis. This type of presentation in association with new onset of seizures, papilledema, decreased mentation, and focal neurological deficit should raise a strong suspicion of venous occlusive disease affecting the cortical venous system secondarily to dural sinus thrombosis. Seizures may be focal or generalized and occur in about half of the patients. Stepwise slow progression of venous occlusive disease is expressed clinically by accumulative symptoms and signs, sometimes extending over days or even weeks. Rapid clinical progression may occur in

Table 1.32. Clinical presentation of cerebral venous thrombosis[a] (from Lee et al. 2002a)

Symptoms	Headache
	Double vision
	Blurred vision
	Altered consciousness
	Nausea, vomiting
	Seizures
Signs	Papilledema
	Focal neurological deficit
	Cranial nerve palsies
	Nystagmus

[a] Clinical presentation of cerebral venous thrombosis is dependent on the location and extent of the thrombosis.

a smaller subgroup leading to status epilepticus, progressive loss of consciousness and a comatose state, which without treatment is associated with 70% mortality (Einhaupl et al. 1991). With recent advances in imaging and increased clinical awareness, this poor outcome has resulted in earlier medical therapy and decreased mortality rates of less then 10% (Brucker et al. 1998; Bousser 1999, 2000).

Simultaneous venous occlusive disease involving other body parts is not rare and pulmonary embolism has been demonstrated in up to 11% of patients with dural sinus thrombosis (Diaz et al. 1992).

1.3.4 Imaging

Clinical suspicion of the diagnosis of cerebral venous thrombosis will greatly facilitate the radiological interpretation of subtle abnormalities that may be visualized in early venous occlusive disease. In addition, the radiological findings interpreted with an awareness of this clinical condition may result in an early diagnosis despite the still nonspecific clinical symptomatology. Frequently, however, early diagnosis is not made because of a lack of clinical or radiological suspicion. CT, MRI, and angiography have all been used for the purpose of investigating patients suspected of having cerebral venous thrombosis.

CT, because of its easy access, is probably used in most instances as the first imaging modality and it may demonstrate a variety of findings depending on the localization of the venous thrombosis and its impact on the surrounding brain. Clot may be demonstrated within the dural sinus as an elongated area of increased density in the transverse or straight sinus on plain CT. Clot mass may also be shown following intravenous contrast enhancement as a triangular filling defect (empty delta sign) in the superior sagittal sinus or the torcula. Bilateral areas of decreased density may be present parasagittal in location in case of superior sagittal sinus thrombosis or may involve the basal ganglia and thalamic regions in case of deep cerebral venous thrombosis with involvement of the straight sinus

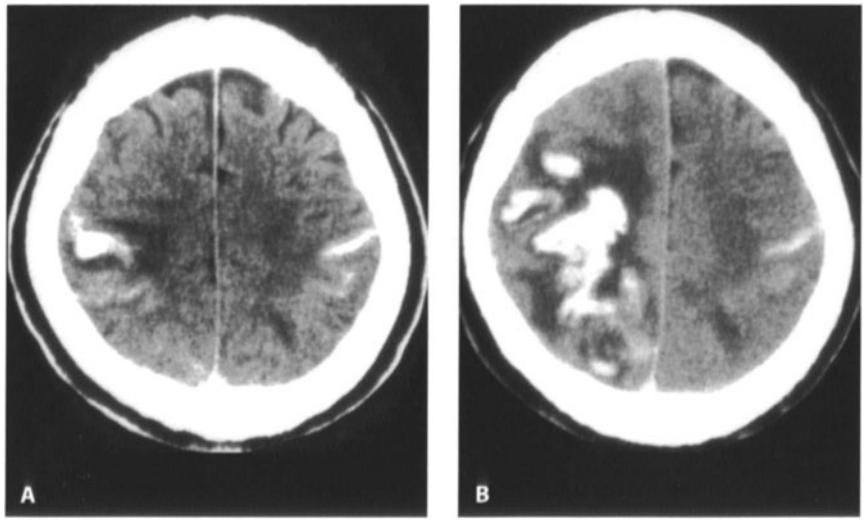

Fig. 1.49A, B. A 32-year-old woman on birth control medication presented with new onset of seizure and sudden headaches. Unenhanced CT (**A**) at presentation showed small bilateral cortical areas of increased and decreased density, which 48 h later on unenhanced CT (**B**) showed characteristic findings of bilateral hemorrhagic venous infarction associated with superior sagittal sinus thrombosis

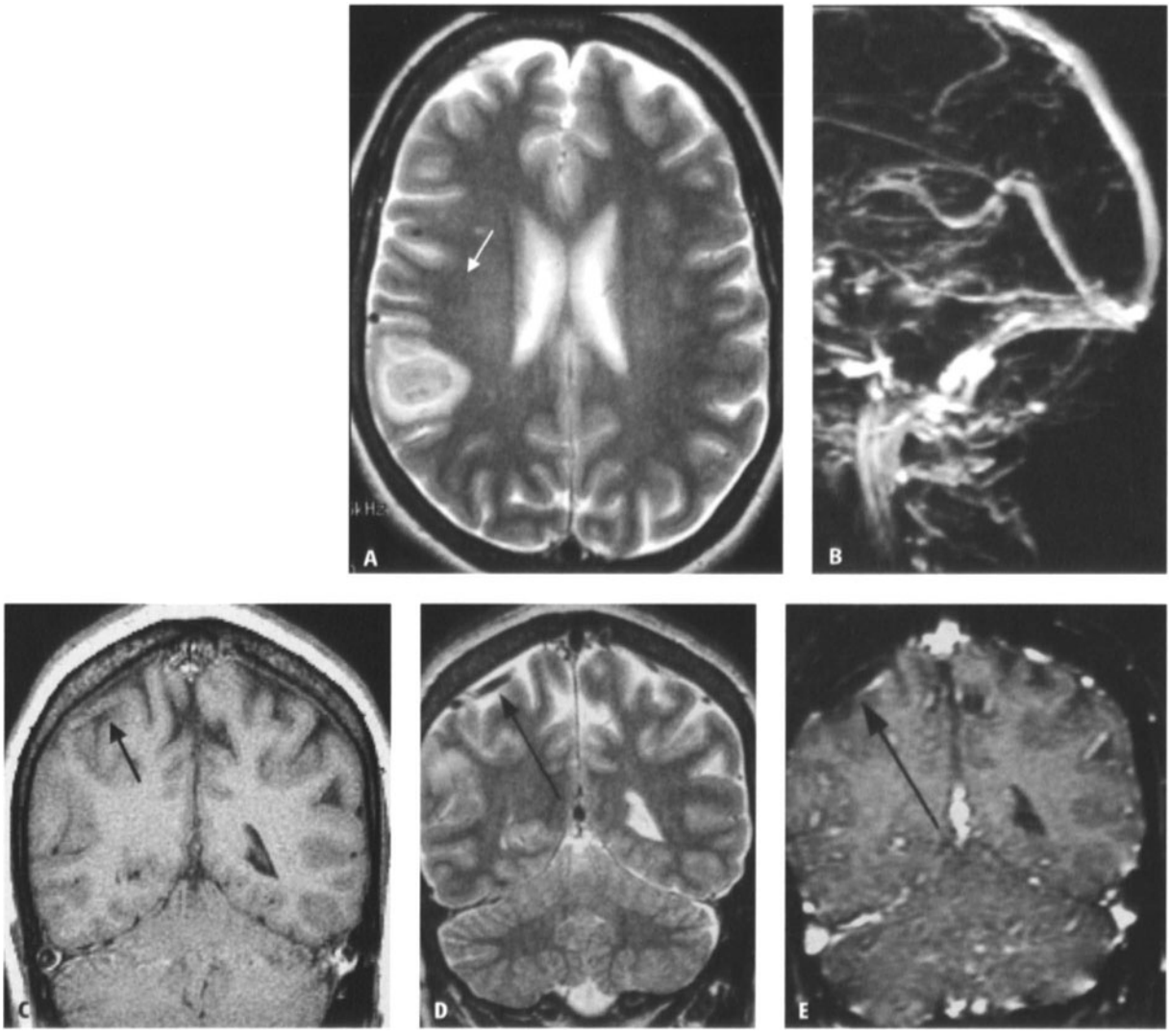

Fig. 1.50. A 40-year-old woman presenting with a postpartum seizure shows a mixed signal intensity lesion within the right parietal lobe on T1-weighted MRI (*arrow*, **A**). The MRI venogram in sagittal view (**B**) shows the major dural sinuses, including the superior sagittal sinus, to be patent. T1-weighted MRI in coronal view (**C**) shows a tubular structure over the surface of the right parietal lobe cortex to be iso-intense in signal (*arrow*). T2-weighted MRI in the coronal view (**D**) shows the same tubular structure to be low signal (*arrow*), simulating flow void. Source images from gadolinium-enhanced MRI venogram in coronal view (**E**) demonstrates nonenhancement of this tubular structure (*arrow*), indicating an isolated cortical vein thrombosis. Anticoagulation therapy resulted in reversal of the clinical symptoms

(Brown 1993). Unilateral areas of decreased density involving the temporal lobes in a nonarterial distribution are seen with transverse sinus thrombosis. As the venous cerebral ischemia is prolonged, hemorrhagic conversion occurs and becomes readily visible on plain CT (Fig. 1.49).

MRI has proven to be the modality of choice and has surpassed cerebral angiography in its ability to demonstrate dural sinus thrombosis and venous ischemia (Tsai et al. 1995). Conventional MRI sequences will demonstrate clot within cortical veins or dural sinuses with different sig-

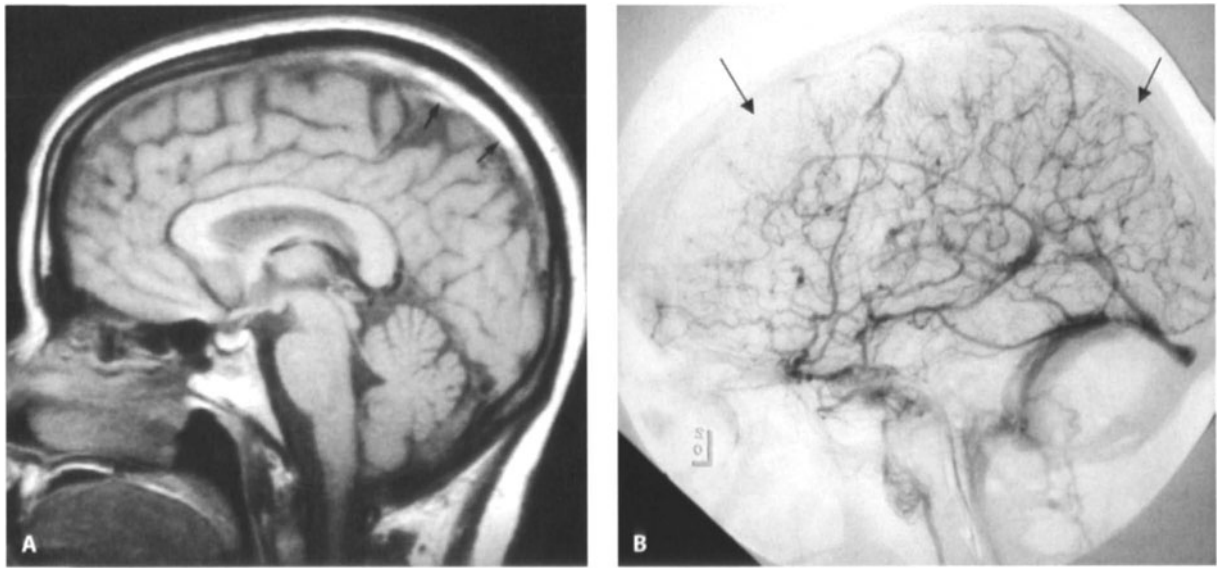

Fig. 1.51A, B. A 46-year-old man with 1-week history of intermittent but progressive headaches and blurred vision and 1-day history of nausea and vomiting. T1-weighted MRI (**A**) shows increased signal within the superior sagittal sinus (*arrows*), indicating subacute thrombosis which was confirmed at carotid angiogram lateral view (*arrows*, **B**). Anticoagulation therapy resulted in reversal of clinical symptoms

nal characteristics, depending on the age of the clot. T1-weighted images will show iso-signal intensity and hypointense signal is seen on T2-weighted images (Fig. 1.50). About 3–7 days later, it is easier to recognize the thrombus on MRI. The thrombus will show high signal intensity on T1-weighted images (Figs. 1.51, 1.52). Special sequences can be used in combination with contrast enhancement to best demonstrate the venous vascular structures (Fig. 1.53) (Farb et al. 2003), obviating the need for conventional angiography. Careful analysis of the MRI scan (including the source images) is required to be able to decode the various signal characteristics associated with the evolution of the clot within the venous channels and the developing venous congestion and infarction.

The impact of venous ischemia on the brain parenchyma is well demonstrated with MRI.

Diffuse low attenuated lesions on CT or high signal intensity lesions on T2-weighted images on MRI that do not correspond to the arterial territories are highly suggestive imaging findings of cerebral venous thrombosis (CVT). About 40% of symptomatic CVT patients showed CT evidence of hemorrhage and almost all CVT patients demonstrated T2-weighted high signal intensity of the lesion (Ducreux et al. 2001; Forbes et al. 2001). DWI and the apparent diffusion coefficient (ADC) may help predict the possibility of permanent neurological deficit in arterial infarction. These imaging techniques have also been used to differentiate reversible ischemic tissue from irreversible ischemic tissue in CVT (Fig. 1.54). Preliminary results have shown the potential to predict the prognosis of the CVT (Manzione et al. 2000). Recent investigations have also revealed that the mixed signal intensity of DWI in CVT suggested mixed cytotoxic and vasogenic edema. Interestingly, the reduced ADC value in CVT did not correlate with permanent neurological deficit (Ducreux et al. 2001).

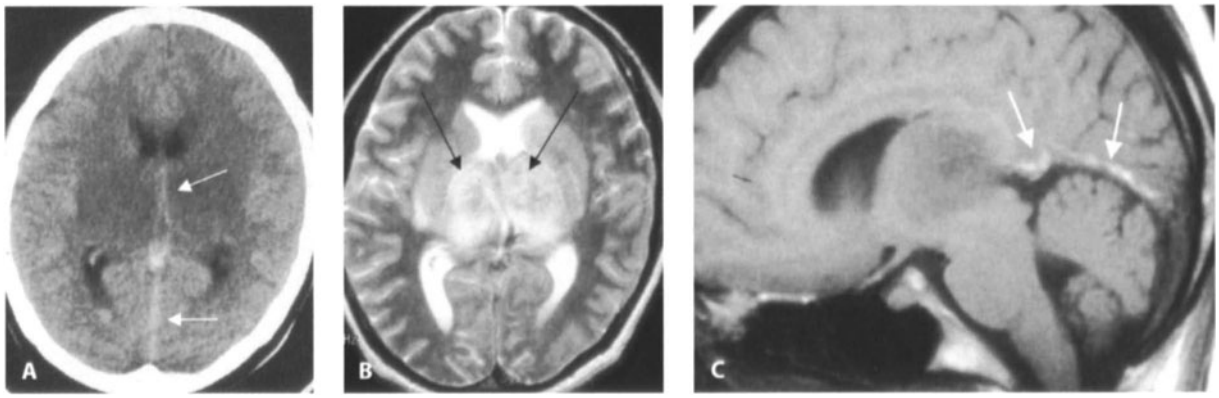

Fig. 1.52A–C. A 27-year-old female patient presented with headache, nausea, and vomiting and in 24 h progressed to aphasia and a decreased level of consciousness. Axial noncontrast CT (**A**) shows an increased density within the internal cerebral veins and straight sinus (*arrows*) as well as decreased density in the thalami on both sides; a small hemorrhage is seen in the right lateral ventricle. T2-weighted MRI (**B**) demonstrates bilateral basal ganglia and thalamic increased signal changes (*arrows*). **C** T1-weighted MRI in sagittal view demonstrates subacute thrombus in the vein of Galen and straight sinus (*arrows*). The patient was subsequently proven to have antiphospholipid antibody syndrome

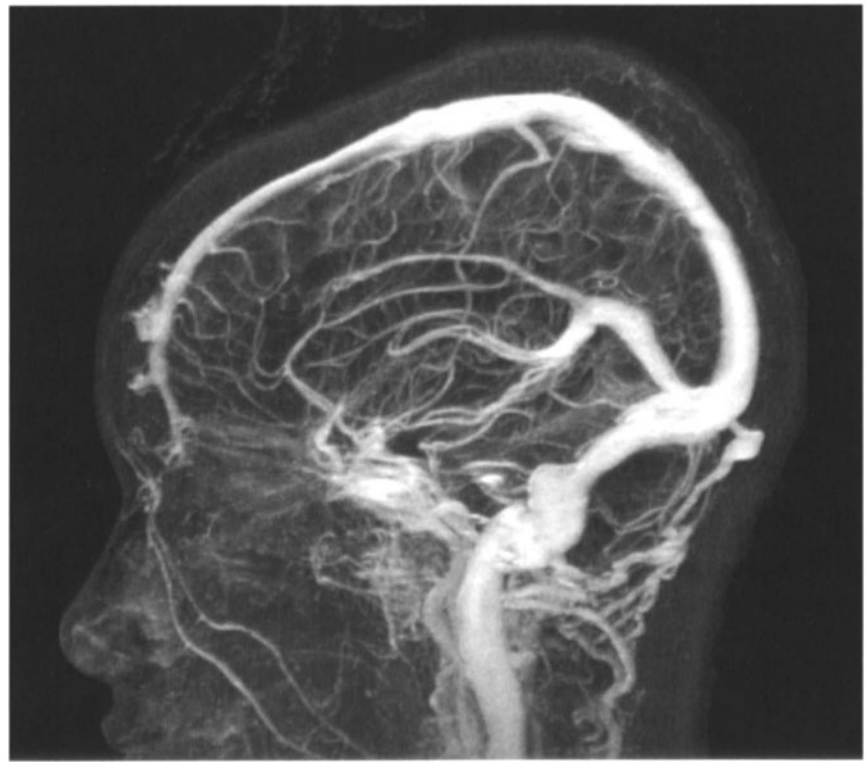

Fig. 1.53. Example of normal cerebral venous anatomy as shown by special contrast-enhanced MRI technique. (Farb et al. 2003)

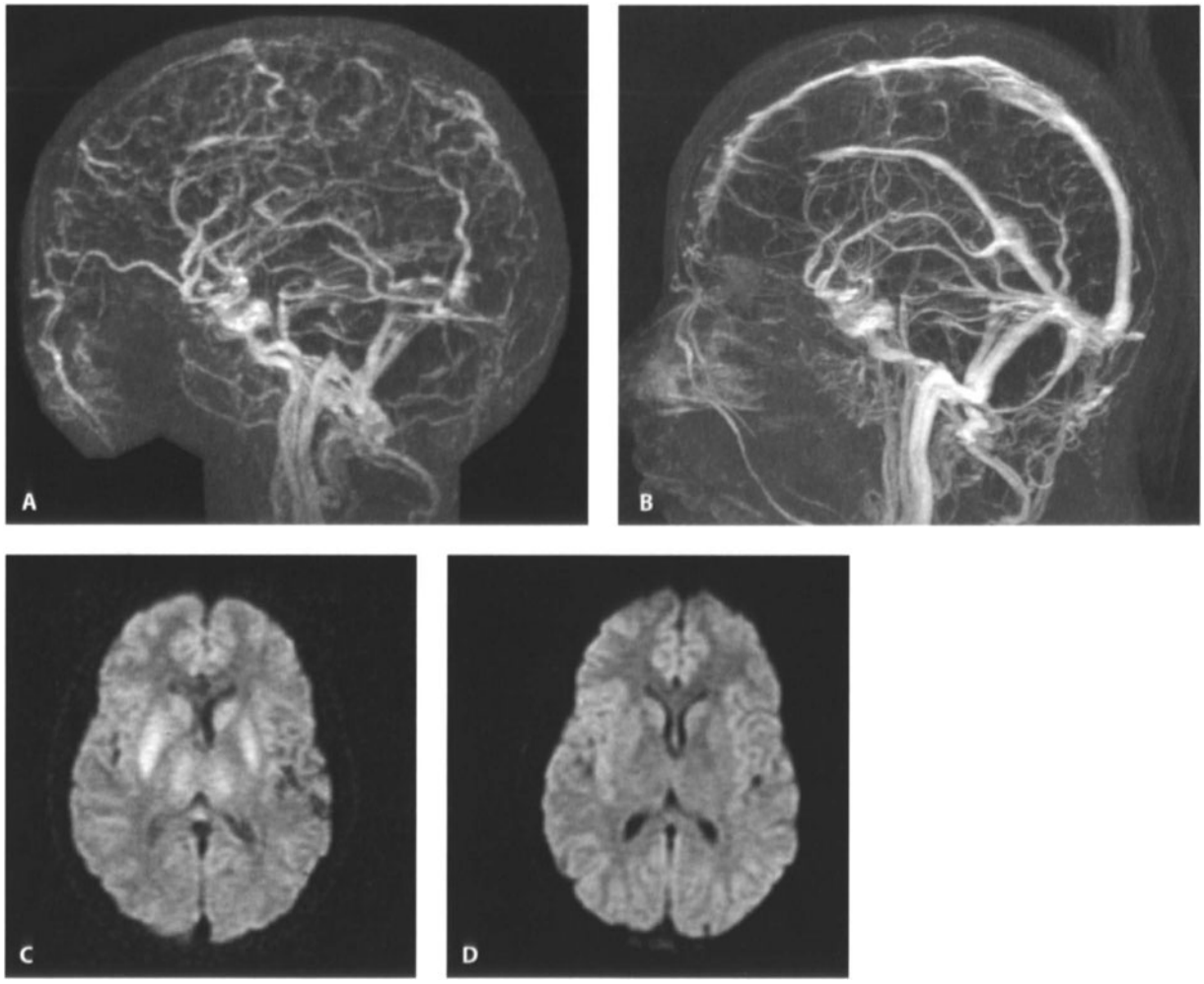

Fig. 1.54. A 23-year-old woman presented with a 5-day history of headache, nausea and vomiting, demonstrating thrombosis of the deep venous system as well as the superior sagittal sinus on contrast enhanced MRI (**A**). Repeat contrast-enhanced MRI 3 months later, following institution of anticoagulation therapy, demonstrates recanalization of the dural sinuses and deep venous system (**B**). Patient made an excellent clinical recovery with reversal of the abnormal signal changes involving the basal ganglia and thalamic regions shown on DWI at presentation (**C**) with normalization on follow-up 3 months later (**D**)

Thus, a decrease in ADC in the CVT patient might not have the same prognostic value as those following an arterial stroke and imply the reversibility of ischemic brain tissues despite its decreased ADC value.

Magnetic resonance venography (MRV) demonstrates venous anatomy exquisitely, and is a very useful screening imaging technique (Fig. 1.52), and cerebral angiography is nowadays rarely used to make the diagnosis of venous thrombosis. However, angiography can provide significant additional information, by showing the circulation of the contrast material through the vascular bed, thereby demonstrating the individual host response to the presence of venous thrombosis and possibly showing alternate (collateral) venous pathways being used (Andeweg 1996). This type of physiological response to the presence of venous thrombosis may

explain the individual differences (clinical presentation and outcome) of patients presenting with intracranial venous thrombosis; this information, shown by angiography, cannot be demonstrated on CT or MRI.

1.3.5 Treatment

Treating patients with intracranial venous thrombosis is dependent on the ability to clinically suspect and radiologically confirm this diagnosis, which continues to be the biggest challenge. Timely diagnosis is critical for effective management. Once the diagnosis is made, medical therapy is started, which includes hydration, systemic anticoagulation, and anticonvulsant therapy. Purdon Martin and Sheehan (1941) were the first to propose anticoagulation therapy for dural sinus thrombosis. Anticoagulation therapy has been used routinely for the treatment of intracranial venous thrombosis for the past 15 years.

A randomized, blinded placebo-controlled study in 20 patients demonstrated that anticoagulation with dose-adjusted intravenous heparin (unfractionated heparin, bolus dose of 3,000 IU and continuous infusion of 25,000–65,000 IU/day) was an effective treatment in patients with dural sinus thrombosis and showed that associated hemorrhage was not a contraindication to heparin in these patients (Einhaupl et al. 1991). The trial was stopped after 20 patients because of the dramatic difference in outcome in the two groups. The statistically significant beneficial effect of heparin treatment was seen after 3 days of therapy and confirmed at every subsequent examination up to 3 months after the start of treatment. Systemic heparin does not appear to initiate hemorrhage and prevents propagation of clot. Even in the presence of hemorrhagic infarction, the great majority of patients respond well to a regimen of medical therapy that includes anticoagulation.

A second randomized trial investigating the role of low-molecular-weight heparin (LMWH) in the management of cerebral venous thrombosis demonstrated the safety of anticoagulant therapy (de Bruyn et al. 1999). In this study, 20% of patients in the heparin treatment group and 24% in the placebo group had a poor outcome after 3 weeks, and 13% in the treatment and 21% in the placebo group had a poor outcome after 12 weeks. The definition of poor outcome was death or a Barthel Index Score under 15. This study did not demonstrate statistically significant clinical outcome improvement differences between the heparin treatment group and the control group. However, it revealed that LMWH treatment followed by oral anticoagulation showed favorable outcome compared to the control group and the safety of anticoagulation, even in the case of cerebral hemorrhage.

Patients in this trial were treated earlier and their conditions were less severe as compared to the first trial.

A meta-analysis of the two available trials shows an absolute risk reduction for mortality of 14% and 15% for dependency, with relative risk reductions of 70% and 56%, respectively (de Bruyn et al. 1999). This strongly reinforces the use of heparin as the first-line treatment for cerebral venous thrombosis. It is expected that about 70% of patients with

cerebral venous thrombosis affecting the dural sinuses will make a complete recovery with anticoagulation therapy alone (Bousser 1999; Bousser et al. 1985) (Fig.1.54). In exceptional circumstances, heparin treatment may worsen the thrombosis by inducing thrombocytopenia (Lee et al. 2002a)

However, the effect of heparin, which can usually be seen within the first days of treatment, may be too slow to help a subgroup of patients with rapidly progressing thrombosis that involves large parts of the cerebral venous system and rapidly leads to diffuse brain swelling and multiple hemorrhages, resulting in an overall mortality rate of 10%. It is this subgroup that should be considered for thrombolytic therapy, as it is the only possible treatment method that can prevent catastrophic outcome. It has been our practice to await the impact of anticoagulation therapy for at least 24 h and to consider thrombolytic therapy if clinical symptoms continue to worsen during that time period. Vines and Davis (1971) were the first to propose thrombolytic therapy (urokinase) in the management of cerebral venous thrombosis, followed by Di Rocco et al. (1981), who used intravenous urokinase in combination with heparin treatment.

Local urokinase infusion into the dural sinus was first used as treatment in 1988 (Scott et al. 1988). Subsequently, several reports demonstrated the feasibility of infusion of thrombolytic agents into the thrombosed dural sinus via the direct percutaneous or retrograde transvenous approach (Higashida et al. 1989; Barnwell et al. 1991; Tsai et al. 1992; Horowitz et al. 1995). With improved catheter technology, it also became possible to access the deep venous system via the straight sinus and infuse thrombolytic therapy (Holder et al. 1997; Spearman et al. 1997; Smith et al. 1994). Local administration of thrombolytic therapy generally avoids the systemic hemorrhagic effects caused by high-dose intravenous delivery.

The dose, method, and type of thrombolytic therapy has changed over the past decade, from prolonged infusions with a low dose of urokinase to more rapid pulse spray techniques using recombined tissue plasminogen activator (r-TPA). The duration and dose has ranged from 2 to 244 h to infuse 0.5–20 million units of urokinase and from 2–43 h to administer 50–300 mg of r-TPA (Barnwell et al. 1991; Tsai et al. 1992; Smith et al. 1994; Kim and Suh 1997; Chaloupka et al. 1999). Local injection of r-TPA in combination with heparin appears to carry a higher risk for worsening the intracerebral hemorrhage than heparin alone in patients with pretreatment hemorrhagic infarction. The overall outcome was improved in the absence of such pretreatment hemorrhage when using intravenous heparin in combination with local r-TPA treatment (Frey et al. 1999). They showed flow restoration in 75% of the patients in 29 h after r-TPA treatment. They also demonstrated that clinical recovery was closely related to the degree of flow restoration. For example, the complete flow restoration group showed complete clinical recovery in 83% of patients, while the partial recanalization group had symptomatic recovery in 66%, but in the nonrecanalized group, only 33% demonstrated functionally independence. This study also showed 16.7% neurological complications such as enlargement of intracranial hematoma and 33.3% nonneurological complication related to r-TPA treatment (one groin hematoma and three with neck pain related to catheterization). From these observations, one can

conclude that local infusion of r-TPA in CVT was technically feasible, that flow restoration after r-TPA treatment was important for future clinical outcome, and that r-TPA local infusion had a relatively high nonneurological complication rate and worsening of intracranial hemorrhage after r-TPA treatment.

In the CVT patients without obvious pretreatment hemorrhage, endovascular treatment seems to be safe and improves clinical outcome through rapid restoration of flow. It is important to keep in mind that currently no scientifically proven regimen of endovascular therapy exists with inclusion or exclusion criteria, dosage of thrombolytic agent, duration of treatment, concomitant usage of heparin and radiological end point of the interventional procedure. It has been our experience to perform endovascular treatment in patients who show clinical deterioration despite 24-h heparin therapy, and we use the rapid-pulsed direct infusion technique with up to 30–50 mg r-TPA through a microcatheter for 40–60 min (Fig. 1.55). We use concomitant intravenous heparin, and our angiographic end point is not the total absence of thrombus in the dural sinus but rather the reestablishment of antegrade flow within the dural sinus. In our experience, reestablishment of antegrade flow with continued anticoagulation is sufficient to facilitate clinical improvement (Fig. 1.56) (Lee et al. 2002b).

As the amount of clot can be prohibitive in the venous dural sinuses, other solutions to more rapidly reopen the venous channels have been explored in combination with thrombolytic therapy. They include mechanical disruption using guidewires, rheolytic thrombectomy catheters, transluminal balloon angioplasty, as well as balloon angioplasty and stenting, and surgical thrombectomy (Ekseth et al. 1998; Chaloupka et al. 1999; Malek et al. 1999; Scarrow et al. 1999). While these methods are being explored, it is important to keep in mind that the absolute end point of thrombolytic therapy is often unclear. While we prefer total absence of clot in the dural sinuses at the end of the procedure, this may in fact not be necessary, and, in our experience, reestablishment of antegrade flow is often sufficient to facilitate clinical improvement (Fig. 1.56). Continued anticoagulation will prevent propagation of clot, and in time, the full lumen of the sinus will become reestablished.

Venous thrombosis of the dural sinuses can also be part of the dynamic progression of patients with intracranial dural arteriovenous malformations and fistulas as well as being associated with the syndrome of pseudotumor cerebri. The role of endovascular reopening of the dural sinuses using transvenous thrombolytic therapy as well as retrograde transvenous angioplasty and stent placement is currently being explored for those patients demonstrating a relentless, progressive neurological deterioration and has shown promising results in selected cases (Vilela et al. 2001a; Kollar et al. 2001).

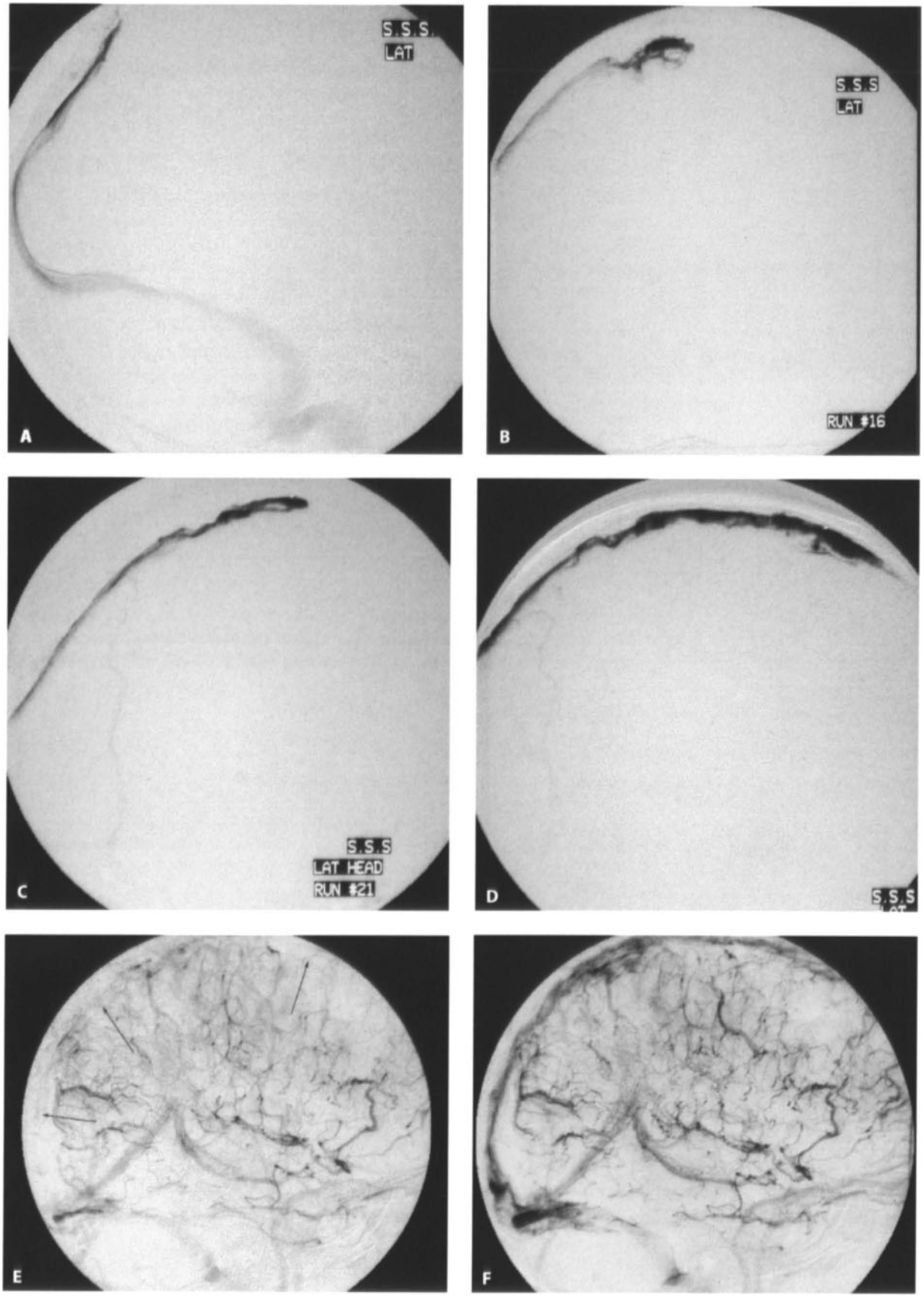

Fig. 1.55A–F. Legend see p. 147

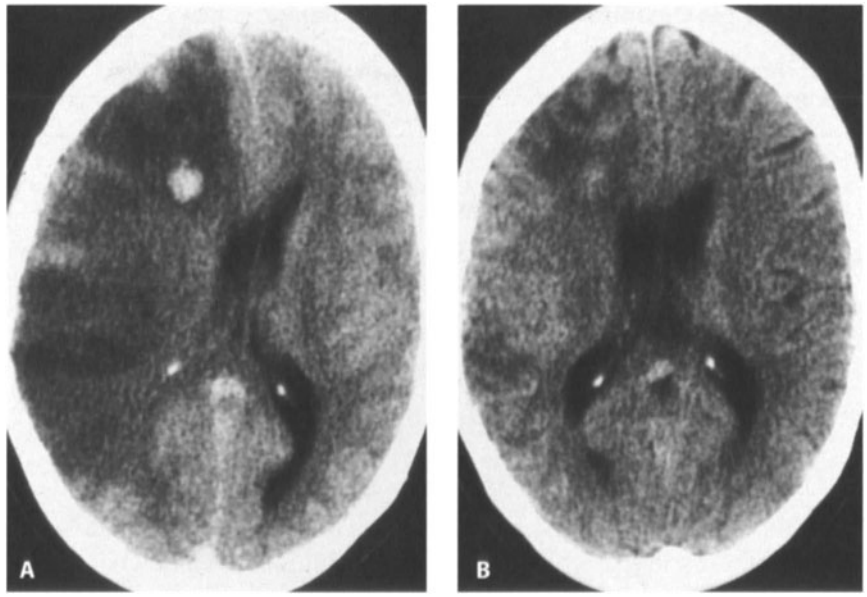

Fig. 1.56A, B. A 28-year-old female patient who had presented with superior sagittal sinus thrombosis and continued to worsen clinically despite anticoagulation therapy was then additionally treated with retrograde transvenous thrombolytic therapy. Unenhanced CT (**A**) prior to treatment and 10 days after combination of anticoagulation and local transvenous thrombolytic therapy (**B**) demonstrates dramatic reversal of the low-density changes paralleling the clinical recovery which continued over several weeks to eventually stabilize with minor neurological deficit

◀ **Fig. 1.55A–F.** Patient presenting with superior sagittal sinus thrombosis failed to respond to anticoagulation therapy and retrograde venous catheterization of superior sagittal sinus (SSS) was performed for local injection of thrombolytic therapy. Progressive opening of SSS with local thrombolytic therapy was demonstrated on sequential venograms in lateral views (**A–D**) performed progressively more forward into the SSS. Preretrograde (**E**) and immediately postretrograde transvenous thrombolytic therapy internal carotid angiograms in lateral view, venous phase (**F**) demonstrated partial reopening of the SSS and was associated with excellent clinical recovery

Appendix

GOS Rating Scale (Glasgow Outcome Scale)

Score

1 Dead
2 Vegetative state
  Unable to interact with environment; unresponsive
3 Severe disability
  Able to follow commands; unable to live independently
4 Moderate disability
  Able to live independently; unable to return to work or school
5 Good recovery
  Able to return to work or school

Hunt and Hess Classification of Subarachnoid Hemorrhage

Grade[a]	Description
0	Unruptured aneurysm
1	Asymptomatic or mild headache and slight nuchal rigidity
1a	No acute meningeal/brain reaction, but with fixed neurological deficit
2	Cranial nerve palsy, moderate to severe headache, nuchal rigidity
3	Mild focal deficit, lethargy or confusion
4	Stupor, moderate to severe hemiparesis, early decerebrate rigidity
5	Deep coma, decerebrate rigidity, moribund appearance

[a] Add one grade for serious systemic disease (e.g., hypertension, diabetes, severe atherosclerosis, chronic obstructive pulmonary disease) or severe vasospasm on angiography.

Modified Rankin Scale

0 No symptoms at all
1 No significant disability despite symptoms: able to carry out all usual duties and activities
2 Slight disability: unable to carry out all previous activities, but able to look after own affairs without assistance
3 Moderate disability: requiring some help, but able to walk without assistance
4 Moderate to severe disability: unable to walk without assistance, and unable to attend to own bodily needs without assistance
5 Severe disability: bedridden, incontinent, and requiring constant nursing care and attention
6 Death

NIH Stroke Scale

1a. Level of consciousness:	0. Alert 1. Not alert, but arousable with minimal stimulation 2. Not alert, requires repeated stimulation to attend 3. Coma
1b. Ask patient the month and their age	0. Answers both correctly 1. Answers one correctly 2. Both incorrect

1c. Ask patient to open and close eyes	0. Obeys both correctly 1. Obeys one correctly 2. Both incorrect
2. Best gaze (only horizontal eye movement)	0. Normal 1. Partial gaze palsy 2. Forced deviation
3. Visual field testing	0. No visual field loss 1. Partial hemianopia 2. Complete hemianopia 3. Bilateral hemianopia (blind including cortical blindness)
4. Facial paresis (ask patient to show teeth or raise eyebrows and close eyes tightly)	0. Normal symmetrical movement 1. Minor paralysis (flattened nasolabial fold, asymmetry on smiling) 2. Partial paralysis (total or near total paralysis of lower face) 3. Complete paralysis of one or both sides (absence of facial movement in the upper and lower face)
5. Motor function – arm (right and left) Right arm Left arm	0. Normal (extends arms 90° or 45° for 10 s without drift) 1. Drift 2. Some effort against gravity 3. No effort against gravity 4. No movement 9. Untestable (joint fused or limb amputated)
6. Motor function – leg (right and left) Right leg Left leg	0. Normal (hold leg 30° position for 5 s) 1. Drift 2. Some effort against gravity 3. No effort against gravity 4. No movement 9. Untestable (joint fused or limb amputated)
7. Limb ataxia	0. No ataxia 1. Present in one limb 2. Present in two limbs
8. Sensory (use pinprick to test arms, legs, trunk and face; compare side to side):	0. Normal 1. Mild to moderate decrease in sensation 2. Severe to total sensory loss
9. Best language (describe picture, name items, read sentences)	0. No aphasia 1. Mild to moderate aphasia 2. Severe aphasia 3. Mute

10. Dysarthria (read several words)	0. Normal articulation 1. Mild to moderate slurring of words 2. Near unintelligible or unable to speak 9. Intubated or other physical barrier
11. Extinction and inattention	0. Normal 1. Inattention or extinction to bilateral simultaneous stimulation in one of the sensory modalities 2. Severe hemi-inattention or hemi-inattention to more than one modality

- Peer Review Status: Government Publication and Internal Review
- Harold Adams, M.D.
- Patricia Davis, M.D.
- James Torner, Ph.D.
- Karla Grimsman, R.N.
- Jeff Van de Berg, M.S.

Barthel Index

Score	Activity
	Feeding
0	Unable
5	Needs help cutting, spreading butter, etc., or requires modified diet
10	Independent
0 5 10	
	Bathing
0	Dependent
5	Independent (or in shower)
0 5	
	Grooming
0	Needs to help with personal care
5	Independent face/hair/teeth/shaving (implements provided)
0 5	
	Dressing
0	Dependent
5	Needs help but can do about half unaided
10	Independent (including buttons, zips, laces, etc.)
0 5 10	

Score	Activity
	Bowels
0	Incontinent (or needs to be given enemas)
5	Occasional accident
10	Continent
0 5 10	
	Bladder
0	Incontinent, or catheterized and unable to manage alone
5	Occasional accident
10	Continent
0 5 10	
	Toilet use
0	Dependent
5	Needs some help, but can do something alone
10	Independent (on and off, dressing, wiping)
0 5 10	
	Transfers (bed to chair and back)
0	Unable, no sitting balance
5	Major help (one or two people, physical), can sit
10	Minor help (verbal or physical)
15	Independent
0 5 10 15	
	Mobility (on level surfaces)
0	Immobile or <50 yards
5	Wheelchair independent, including corners, >50 yards
10	Walks with help of one person (verbal or physical) >50 yards
15	Independent (but may use any aid; for example, stick) >50 yards
0 5 10 15	
	Stairs
0	Unable
5	Needs help (verbal, physical, carrying aid)
10	Independent
0 5 10	
Total 0–10	

Patient name: _____ Rater: _____

Date: / /

The Barthel ADL Index: Guidelines

1. The index should be used as a record of what a patient does, not as a record of what a patient could do.
2. The main aim is to establish degree of independence from any help, physical or verbal, however minor and for whatever reason.
3. The need for supervision renders the patient not independent.
4. A patient's performance should be established using the best available evidence. Asking the patient, friends/relatives and nurses are the usual sources, but direct observation and common sense are also important. However, direct testing is not needed.
5. Usually the patient's performance over the preceding 24–48 h is important, but occasionally longer periods will be relevant.
6. Middle categories imply that the patient supplies over 50% of the effort.
7. Use of aids to be independent is allowed.

2 Dural and Bony Tumors

2.1 Introduction 154

2.2 Meningiomas 154
2.2.1 Epidemiology 154
2.2.1.1 Origin 154
2.2.1.2 Incidence 154
2.2.1.3 Association of Meningiomas with Other Tumors 155
2.2.1.4 Sex Hormone Receptors in Meningiomas 156
2.2.1.5 Chromosomal Patterns in Meningiomas 156
2.2.1.6 Meningiomas in Children 156
2.2.1.7 Familial Occurrence 157
2.2.1.8 Meningioma Incidence, Prevalence, and Mortality 157
2.2.1.9 Etiology of Human Meningiomas 157
2.2.1.10 Oncogenic Viruses 158
2.2.2 Pathology 161
2.2.2.1 Growth and Spread 162
2.2.2.2 Malignant Meningioma 162
2.2.2.3 Angioblastic Meningioma and/or Hemangiopericytoma 165
2.2.2.4 Meningioangiomatosis 166
2.2.2.5 Meningeal Meningiomatosis 166
2.2.3 Clinical Presentation 166
2.2.3.1 Sites 169
2.2.3.2 Epidural Meningiomas 177
2.2.3.3 Meningiomas of the Orbit 177
2.2.3.4 Meningiomas Involving the Cavernous Sinus 178
2.2.3.5 Meningiomas in Other Unusual Sites 179
2.2.3.6 Intracranial Vascular Involvement 179
2.2.3.7 Peritumoral Edema in Meningiomas 181
2.2.4 Pretherapeutic Evaluation 181
2.2.4.1 CT Scanning in Meningiomas 181
2.2.4.2 MRI Scanning 182
2.2.4.3 Angiographic Investigation 184
2.2.4.4 Differential Diagnosis 187
2.2.5 Therapeutic Strategy and Clinical Objectives 187
2.2.6 Technical Aspects of Embolization 189
2.2.7 Special Considerations in Meningioma Embolization 192
2.2.7.1 Extracranial Tumor Extension 192
2.2.7.2 Recurrent Meningiomas 192
2.2.7.3 Internal Carotid Supply to Recurrent or Malignant Meningiomas After Radiation Therapy Has Failed 194
2.2.7.4 Pial Supply 194
2.2.7.5 Pre- and Postembolization Medical Management 194
2.2.7.6 Time of Operation 196
2.2.7.7 Complications of Embolization 196

2.3 Other Bony and Dural Tumors 198
2.3.1 Cerebral Tumors 198
2.3.2 Neurinomas 199
2.3.3 Esthesioneuroblastomas 199

2.1 Introduction

Because of the rich blood supply of the dura and bone, tumors involving these structures are frequently hypervascular. The unique dual function of the dura as the periosteum of the inner table of the skull and as a protective covering for the central nervous system, makes tumors affecting the dura and/or bone of particular interest. Presenting complaints may involve central nervous system manifestations, or, if the lesion grows outward, local changes in the bone, muscle, or skin.

2.2 Meningiomas

2.2.1 Epidemiology

2.2.1.1 Origin

The term "meningioma" was introduced by Harvey Cushing in his 1922 Cavendish Lecture on tumors arising from the meninges. Although known to exist for many decades, they had previously been called by a variety of names.

Meningiomas originate from cell elements that form the meninges, usually the arachnoid cells, packing the arachnoid villi, which protrude as fingerlike projections into the walls of the dural veins and sinuses. They may also arise from dural fibroblasts and pial cells (Rubinstein 1972).

The most frequent sites of origin of these tumors are, therefore, those where the arachnoid villi are normally the most numerous, i.e., the major dural sinuses and along the root sleeves of the existing spinal nerves.

Meningiomas may, however, originate anywhere along the arachnoid membrane. Rarely, they may arise from stromal cells in the spaces that surround the perforating blood vessels or the intracerebral extensions of the leptomeninges as they form the villi interposita and the stroma of the choroid plexus, giving rise to intraventricular meningiomas. There are also rare extracalvarial or ectopic meningiomas, which are believed to arise from ectopic arachnoid cell inclusions.

2.2.1.2 Incidence

Meningiomas account for 13%–18% of all primary intracranial tumors and 20%–25% of intraspinal tumors (Rubinstein 1972). They occur at any age, but typically affect adults between 20 and 60 years of age, with a peak incidence at age 45. In adults, intracranial meningiomas are more frequent in females, with a female-to-male ratio of 2.5:1 (Kepes 1982). It is interesting to note that this female predominance applies primarily to symptomatic middle-aged adults. At the extremes of life one does not find these features.

Deen et al. (1982), in their review of meningiomas in patients under 20 years of age, found a female-to-male ratio of 1:1. The rapid growth of meningiomas during pregnancy was noted as early as 1929 by Cushing.

Tumors in these women are most frequent near the sella turcica, and their clinical behavior is probably related to their proximity to the optic nerve and chiasm; the changes in visual acuity produced by tumor growth are quickly noticed by the patients.

As with other tumors, the relationship of sex hormones to tumor growth is a very interesting and puzzling phenomenon. One may argue that the changes that occur are secondary to direct hormonal activity of the tumor, such as occurs with breast or endometrial cancers, or that they are due to swelling with vacuolization, suggesting tissue edema. It is difficult to estimate the relative importance of tumor enlargement by hormonal factors versus the role of cerebral edema during the hyperemia of pregnancy. Michelsen and New (1969) demonstrated a decrease in mass effect of a frontal meningioma after pregnancy was terminated. Unfortunately this was reported before the era of computed tomography (CT), and the reduced mass effect documented by serial angiography may have been due to a decrease in white matter edema and not tumor size. Even in carcinoma of the breast or endometrium, where estrogens are thought to play a role in the formation or growth rate of the tumor, these effects are believed to be slow and cumulative. Probably some combination of hormonal stimulation and hydropic swelling contribute to the growth of meningiomas and the edema that is frequently associated.

2.2.1.3 Association of Meningiomas with Other Tumors

Breast Carcinoma

There are numerous reports of patients suffering from both of these tumors. Schoenberg et al. (1975), in his analysis of a possible relationship between nervous system tumors and primary cancers in other sites, found a statistically significant correlation only between meningiomas and breast carcinoma. Fenyes and Kepes (1956) reported a patient with carcinoma of the breast and a cerebellar metastasis, who at autopsy was found to have multiple meningiomas; one of these harbored a tumor embolus from the carcinoma. This association between meningioma and breast cancer is of clinical importance: patients with known breast cancer who develop symptoms and signs of an intracranial mass must be evaluated very carefully, as the cerebral lesion may be a curable lesion rather than a metastasis (Haar and Patterson 1972).

Multiple meningiomas occur incidentally in 1%–2% of cases (Kepes 1982) but are typically associated with the central form of von Recklinghausen's neurofibromatosis, which also has a high incidence of neurinomas and gliomas. The occurrence of gliomas or other central nervous system tumors in association with meningiomas in other patients is felt to be coincidental (Russell and Rubinstein 1989).

2.2.1.4 Sex Hormone Receptors in Meningiomas

Donnell et al. (1979) demonstrated estrogen receptors in four out of six meningiomas, at a high level in two. Interestingly, one of the four patients with a positive tumor was a male. Poisson et al. (1980) studied 22 meningiomas: they found estrogen receptors in 59% and receptors for progesterone in all 22 cases. This may explain why meningiomas appear to grow more rapidly during pregnancy. Schnegg et al. (1981) found androgen receptors in two of ten patients with meningiomas: both were postmenopausal females.

These sex hormone receptors may be important in cases of nonresectable, partially resected, or in malignant meningiomas, as some form of hormonal therapy may play a role in the management of these patients in the future.

2.2.1.5 Chromosomal Patterns in Meningiomas

The relationship between chromosomal abnormalities and meningiomas has interested many investigators. Robbins and Cotran (1979) states that most human cancers are aneuploid. Zang and Singer (1967) reported eight meningiomas cultured for 4–9 days. The karyotypes showed loss of a chromosome from the 22nd pair in the G group (monosomy G), suggesting a tendency for meningiomas to lose chromosomes during their karyotypic evolution. Benedict et al. (1970), in studying recurrent meningiomas and their incidence of malignancy, suggest that this karyotypic aberration may prove useful in the future prediction of malignancy (see Sect. 2.2.2.2).

2.2.1.6 Meningiomas in Children

Meningiomas occur infrequently in children; they represent between 1.1% (Taptas 1961) and 2.3% (Crous and Berg 1972) of all meningiomas and less than 2% of all intracranial tumors in children (Kepes 1982).

Congenital meningiomas are even rarer, but a few cases have been reported (Kepes 1982).

Childhood meningiomas have a number of special characteristics:

1. Higher incidence of malignancy: a 33%–38% incidence of meningiosarcomas has been reported by Crouse and Berg (1972), Russell and Rubinstein (1989) (Fig. 2.1, p. 158, 159)
2. Relatively high incidence of intraventricular tumors
3. High incidence of cyst formation within the tumor
4. No sex predilection
5. High incidence of association with the central form of neurofibromatosis (NF 2) (Deen 1982)
6. High incidence (39%) of tumor recurrence (Figs. 2.1, 2.21) (Deen et al. 1982)
7. Decreased 15-year survival (68%) (Deen et al. 1982)
8. Relatively poor surgical results reported even in the presence of benign tumors (Kepes 1982)

2.2.1.7 Familial Occurrence

It has long been recognized that patients with neurofibromatosis, a hereditary autosomal dominant condition, are susceptible to meningiomas that are often multiple. However, there have been reports of multiple occurrences of meningiomas in families without stigmata of von Recklinghausen disease (Kepes 1982). In most cases, however, it is probably justified to assume the presence of neurofibromatosis with incomplete expression in these families.

2.2.1.8 Meningioma Incidence, Prevalence, and Mortality

Benign meningiomas are not infrequently found incidentally at autopsy. The larger symptomatic tumors are usually removed during life and will therefore fail to show up in postmortem statistics. Choi et al. (1970), in their epidemiological study of central nervous system neoplasms, found that only 6.8% of patients dying from brain tumors had meningiomas.

2.2.1.9 Etiology of Human Meningiomas

It is probably accurate to say that the etiology of most naturally occurring meningiomas is as yet unknown. Nevertheless, there are some factors that may play a role in their occurrence:

Genetic factors: As we have seen in the central form of neurofibromatosis, there is a definite genetic factor.

Trauma: Cushing and Eisenhardt (1938) introduced a theory linking head trauma and meningiomas, but this association has not since been substantiated and is not felt to be valid.

Radiation: There is definitely an increased incidence of meningiomas in patients who have received either high-dose irradiation for other neoplasms (Kepes 1982) or low-dose radiation to the scalp for the treatment of tinea capitis (Modan et al. 1974). Furthermore, Soffer in 1983 demonstrated that postirradiation meningiomas have distinctive characteristics. They typically occur at the site of maximal irradiation and demonstrate the following differences from spontaneous meningiomas:

1. More rapid growth and aggressive biological behavior
2. Higher incidence of calvarial locations
3. Higher proportion of multiplicity
4. Higher recurrence rate
5. Higher proportion of histological malignancy

The time interval between radiation therapy and the clinical manifestation of meningiomas has been reported to be from 5 to 25 years (Kepes 1982). We have seen a mesenchymal chondrosarcoma of the petrous cavernous area in a young female 4 years after radiation therapy, which

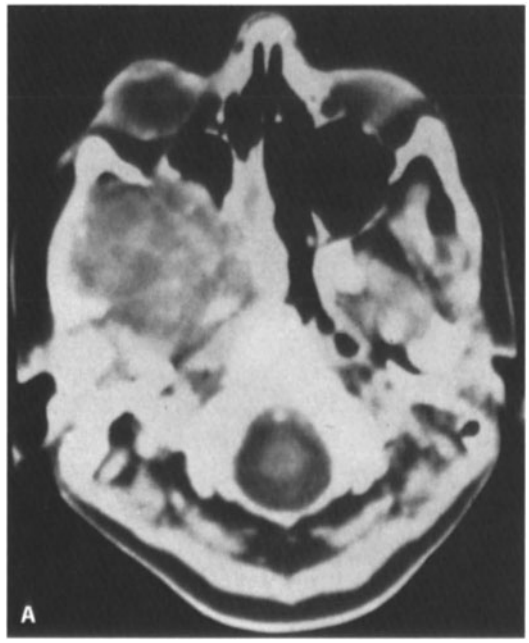

Fig. 2.1A–E. A 16-year-old female patient with a recurrent malignant meningioma with extracranial extension into the subtemporal fossa and face. **A** Axial CT after intravenous administration of contrast material. Note the extension to the right subtemporal and pterygoid region of a homogenously enhancing lesion. **B** Lateral subtraction angiogram in late arterial phase demonstrates the marked tumor hypervascularity, its intracranial, epidural extension into the middle cranial fossa, parasellar, and cavernous area (*small arrows*), as well as its downward and anterior extension to the face. **C** Lateral subtraction angiogram of the distal internal maxillary artery (*arrow*) shows the tumor hypervascularity to best advantage. Note the inhomogeneous stain with some puddling but no arteriovenous shunting. Note flow reversal in the collateral circulation via the ascending palatine, buccal and infraorbital arteries (*curved arrows*). **D** Postembolization (polyvinyl alcohol preoperative) follow-up angiogram of the ascending palatine artery (*arrow*) demonstrates filling of the ascending palatine and buccal arteries (*curved arrows*) in an antegrade fashion. There is no opacification of the tumor. **E** Eight months later there was significant recurrence of the tumor. (Same patient as Fig. 2.21) ▶

rapidly increased its rate of growth (Fig. 2.2). This tumor was considered a nonresectable meningioma and was radiated without a tissue diagnosis, but the possibility of malignant transformation of a benign lesion must also be considered.

2.2.1.10 Oncogenic Viruses

Oncogenic viruses have been used with success to induce meningeal tumors in animals. However, there is no conclusive evidence that oncogenic viruses play a role in the induction of these tumors in humans (Kepes 1982).

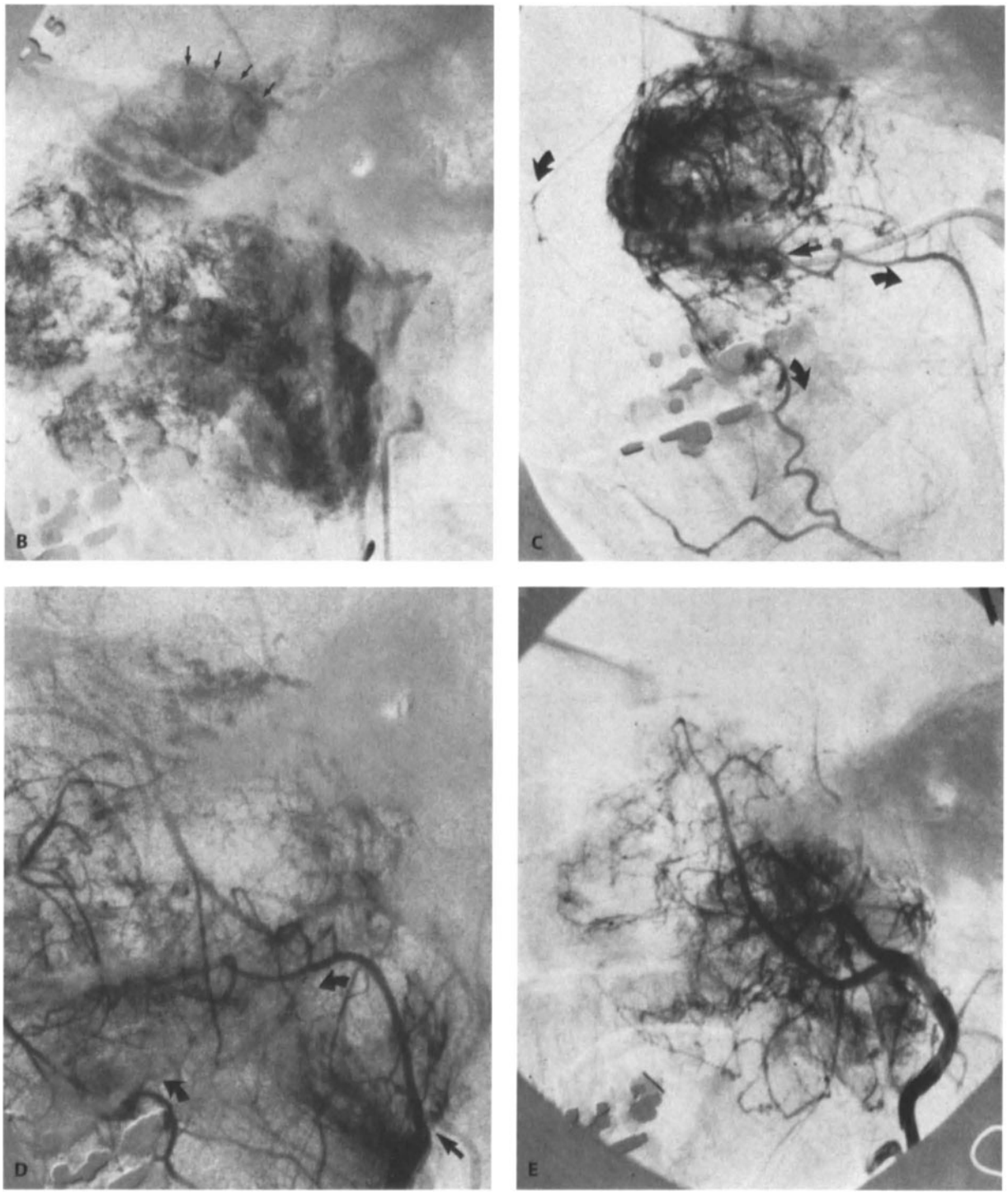

Fig. 2.1B–E. Legend see p. 158

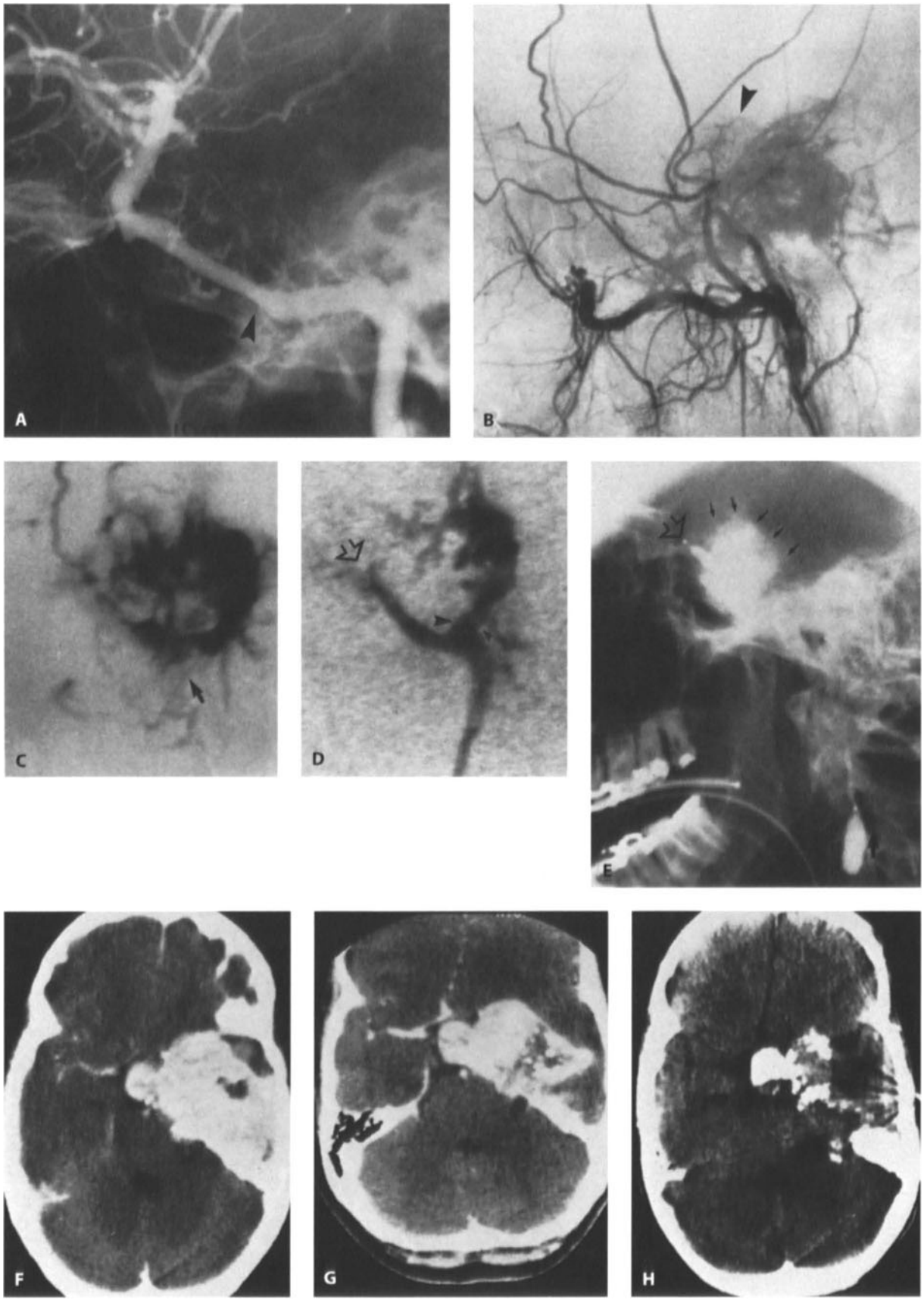

Fig. 2.2A–H. Legend see p. 161

◀ **Fig. 2.2A–H.** A 23-year-old female patient, who in 1980 presented with a vascular tumor in the cavernous-petrous area and was treated with radiation therapy at that time. Proven mesenchymal chondrosarcoma (1984). **A** Lateral carotid angiogram from 1980 demonstrates narrowing of the internal carotid artery starting in its precavernous segment (*arrowhead*) with some hypervascularity. **B** Lateral subtraction angiogram of the distal external carotid artery in 1980 demonstrates only minimal hypervascularity from the petrosal branch of the middle meningeal artery (*arrowhead*). **C** Four years later the patient was referred to us because of rapid increase in the size of the tumor. Lateral angiogram of the middle meningeal artery (*arrow*). Note the marked change in the tumor hypervascularity. **D** Lateral angiogram of the left internal carotid artery after a balloon (*open arrowhead*) has been detached distal to the cavernous branches to protect the brain. Note the development of a malignant fistula between the petrous segment of the internal carotid artery and the tumor (*arrowheads*). This tumor fistula eroded both the petrous carotid and middle meningeal arteries, producing an unusual anastomosis. **E** Lateral film of the skull following 95% ethanol infusion of the tumor bed after the distal internal carotid artery was protected by a detachable balloon (*open arrow*). A second balloon was placed more proximally to trap the carotid artery (*arrow*). Note the stagnant alcohol metrizamide mixture in the tumor bed (*small arrows*). The middle meningeal (C), accessory meningeal, and ascending pharyngeal supply was also treated with ethanol (not shown). **F** Contrast-enhanced CT prior to ethanol infusion shows tumor filling the temporal fossa, and suprasellar cistern and invading the petrous bone. **G** CT 1 week after ethanol treatment. Note the significant reduction in size of the infused area. **H** Follow-up CT 16 months later (contrast could not be given for technical reasons). The patient underwent partial resection of tumor which was mostly necrotic and remained stable. There has been subsequent calcification in most of the remaining tumor

2.2.2 Pathology

Meningiomas are characteristically well-circumscribed globular or lobulated tumors that are clearly demarcated from the brain. They are firm, tough, grayish, or pinkish gray and rather homogeneous. They may compress adjacent structures, but do not infiltrate neural tissue, with the exception of the very rare sarcomatous type. Calcium, bone, or rarely cartilage can be found in them. In general, necrosis is not present in meningiomas, except in the rare malignant type, and spontaneous hemorrhage and cyst formation within the tumor are also unusual. Arachnoidal entrapments may occur at the periphery of the tumor. Hyperostosis of the adjacent skull may be the presenting features; it represents extensive new bone formation which may or may not be associated with invasion of the marrow spaces by meningioma cells (Rubinstein 1972).

The microscopic appearance is highly variable. The fundamental cell of origin, however, is the meningothelial arachnoid cell.

The histological variants have been designated by the different structural patterns. Two major classifications exist: that adapted by Russell and Rubinstein (1989) (Table 2.1) and a more comprehensive one proposed by the WHO (Kleihues et al. 1993) (Table 2.2).

Table 2.1. Classification of meningiomas (Russell and Rubinstein 1989)

Syncytial
Transitional
Fibroblastic
Angioblastic
Malignant

The various histological variants exemplify the multipotentiality of the arachnoid cell from which these are derived.

Except for the rare atypical examples (the papillary type) and possibly the angioblastic type), no prognostic significance can be attached to these histological variants. A description of these variants is beyond the scope

Table 2.2. WHO classification of tumors of meningeal and related tissues (Kleihues et al. 1993)

A. Meningioma
1. Meningiothelioma (endotheliomatous, syncytial arachnotheliomatous)
2. Fibrous (fibroblastic)
3. Transitional (mixed)
4. Psammomatous
5. Angiomatous
6. Hemangioblastic
7. Hemangiopericytic
8. Papillary
9. Anaplastic (malignant) meningioma
B. Meningeal sarcomas
1. Fibrosarcoma
2. Polymorphic cell sarcoma
3. Primary meningeal sarcomatosis
C. Xanthomatous tumors
1. Fibroxamthoma
2. Xanthosarcoma (malignant fibroxanthoma)
D. Primary melanotic tumors
1. Melanoma
2. Meningeal melanomatosis
E. Others

of this text. With the possible exception of the angioblastic or hemangiopericytoma type (Fig. 2.3), the different histological patterns do not have distinguishing radiological or angiographic features.

2.2.2.1 Growth and Spread

Meningiomas are characteristically benign. They are slow growing, circumscribed, and do not invade the compressed brain, but may infiltrate or invade other supportive mesodermal tissues. They may invade the tissues on both sides, dural sinuses and their tributaries, the bone marrow, or when they extend outside of the cranial cavity, the pericranial musculature, other tissues, including the skin, may be involved. Inferior frontal meningiomas invade the optic nerve sheath and infiltrate the extraocular muscles.

2.2.2.2 Malignant Meningioma

The rare highly invasive meningioma may be considered to be sarcomatous (Fig. 2.1) and cannot always be differentiated from the primary meningeal sarcoma. This unusual tumor, although circumscribed and grossly similar to other meningiomas, may have atypical cytological features and in some patients gives rise to extracranial metastasis. In many cases, the future behavior of an individual tumor cannot be predicted by its histological appearance. As stated previously, cytogenetic studies may

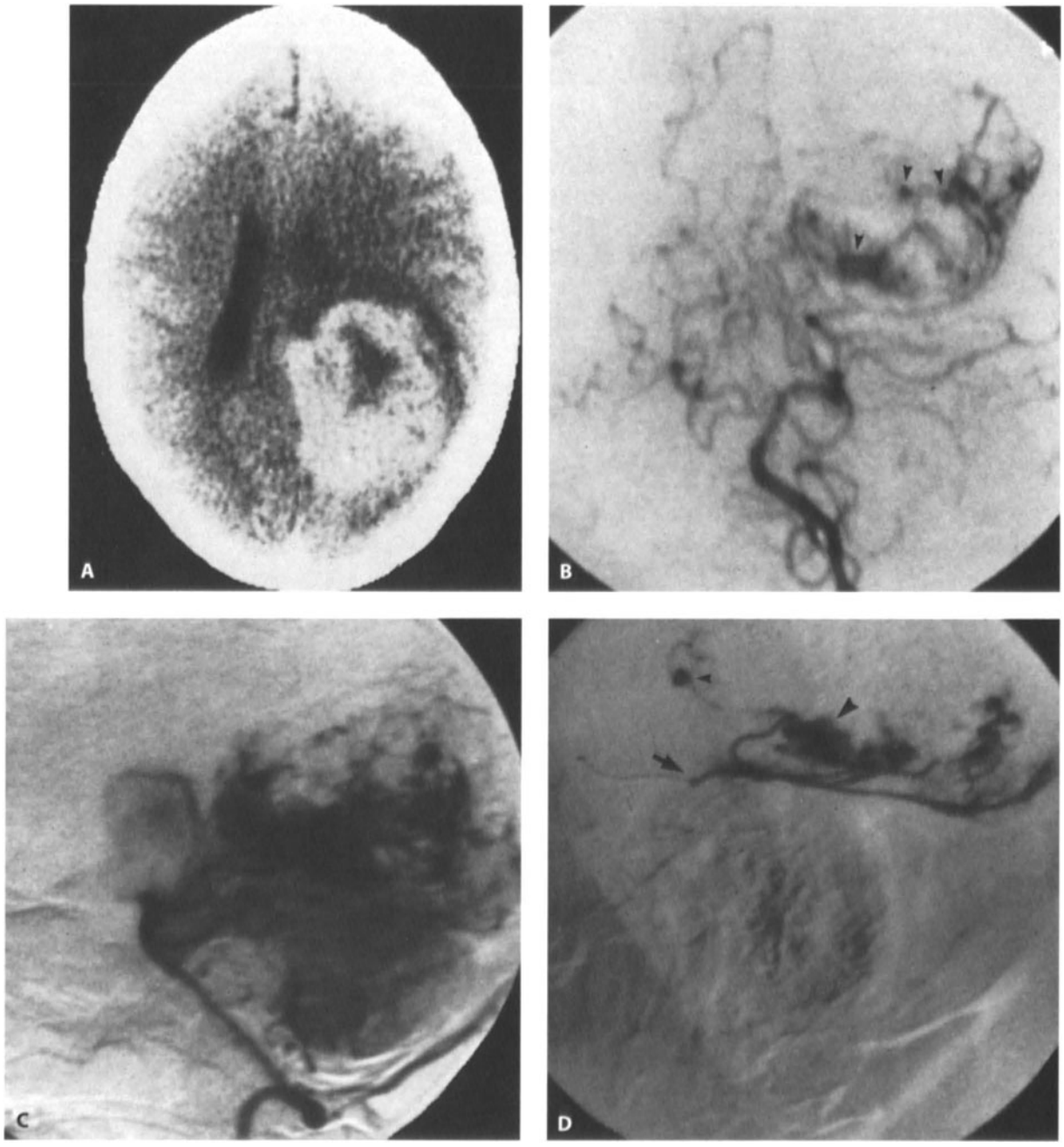

Fig. 2.3A–D. A 42-year old-female patient presented with relatively rapid onset of severe headaches, papilledema, and a homonymous hemianopsia. Histologically proven hemangiopericytoma. **A** Axial CT after intravenous administration of contrast material. Note the lobulated irregular tumor with a central area of decreased absorption coefficient suggesting necrosis, and the peritumoral edema. **B** Angiogram of the left vertebral artery in frontal view, mid-arterial phase. Note the two branches of the posterior cerebral artery supplying a hypervascular tumor that demonstrates some puddling (*arrowheads*). **C** Late arterial phase of the left vertebral artery injection in lateral projection showing the inhomogeneous tumor blush. **D** Lateral view of one of the two posterior cerebral branches supplying the tumor using microballoon catheter (*arrow*). The feeding vessels are not markedly hypertrophied and show the tumor puddling to best advantage (*arrowheads*). For management (see Fig. 2.24), additional dural supply from the left occipital artery was present (not shown)

prove useful in the future to distinguish those tumors that will behave aggressively (Thomas et al. 1981). At present, however, one must still rely on clinical and pathological criteria; malignancy is presumed in the presence of a history of rapid recurrence rather then histological anaplasia and metastases. Mitotic figures are exceptional in typical meningiomas and if present in large number indicate aggressive growth. Although any histological variant may behave aggressively, the angioblastic and/or hemangiopericytoma type is particularly likely to do so (Fig. 2.3). Papillary formation or transformation to a papillary form of meningioma has been recognized as a reliable sign of malignancy or malignant transformation (Kepes 1982) and carries a poor prognosis, with a high incidence of local recurrence and distal metastasis.

In general, features suggestive but not specific for malignancy include necrosis, mitosis, increased cellularity, invasion of small blood vessels within the tumor, anaplasia, and cerebral invasion (Kepes 1982).

The presence of distant metastasis is irrefutable evidence of malignancy, although patients with distal metastasis may live for years.

Kepes (1982) tabulated 85 recorded cases and demonstrated metastasis within the neural axis to be even less common. Most metastatic tumors have histological hallmarks of malignancy, although a few of them appear histologically benign, both in the primary tumor and their metastasis.

Three possible mechanisms of spread have been postulated:

1. Seeding via the CSF. This is very rare and only 12 cases of such spread have been reported (Kepes 1982); nine had histological features of malignancy, whereas three did not. Conceivably, surgical intervention could mobilize clusters of tumor cells and cause subarachnoid seeding. Eight of these 12 reported patients had previous surgery, but four did not. Six (50%) had additional extraneural implants. If one considers the thousands of surgical interventions for these tumors, the role of surgical mobilization of tumor cells can hardly be considered important. Meningioma cells are generally not found in the cytological analysis of CSF of patients with meningiomas (Kepes 1982).
2. Extraneural metastasis. There is a slight male predominance of 1.2:1, and although as a whole metastases are more frequently seen in adults; they proportionally are more common in children. The site of the primary tumor is of limited significance, as is the history of previous surgery. However, invasion of the scalp by the primary tumor may facilitate metastasis to cervical lymph nodes. Invasion of major dural sinuses has a questionable role, as this phenomenon is so frequent in benign meningiomas. The most common sites for distal metastasis are the lungs, liver, lymph nodes, bone, pleura, kidney, pancreas, thyroid, mediastinum, breast, urinary bladder, thymus, superior vena cava, heart, stomach, colon, skin, vulva, thigh, finger, ocular fundus, and adrenal gland. Most but not all patients who were reported with metastatic meningiomas also had local recurrence.
3. Local recurrence. Although not classified as metastasis, local recurrence is the most common presentation of malignant meningiomas and occurs far more frequently than distal metastasis.

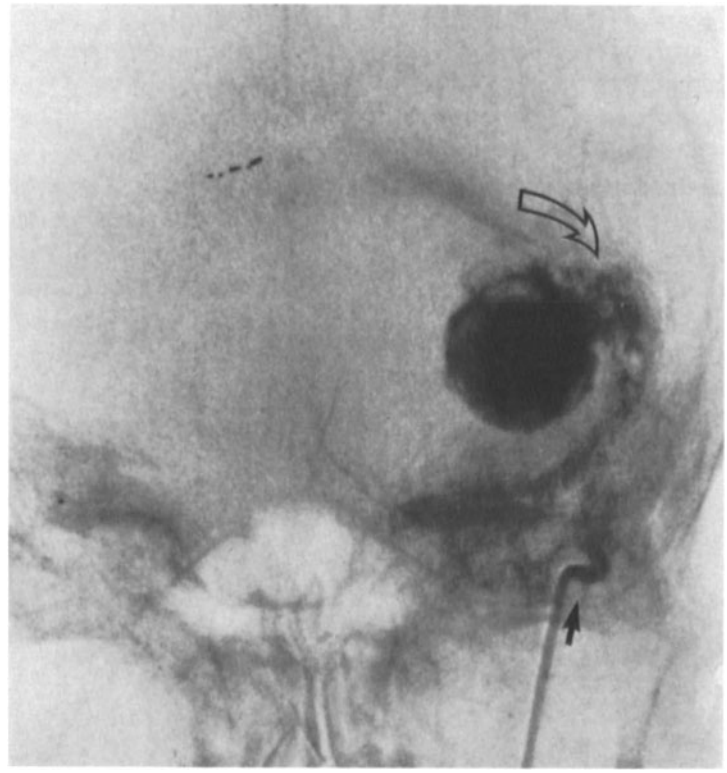

Fig. 2.4. Angioblastic meningioma, sometimes called hemangiopericytoma, in the posterior fossa with extension into the sigmoid sinus. Frontal selective angiogram of the occipital artery (*arrow*). Late arterial phase. A well-circumscribed highly vascular tumor is seen attached to the inferior border of the sigmoid sinus, with some tumor blush extending into the sinus (*open curved arrow*), confirmed at surgery. The patient was embolized with Gelfoam powder and the tumor was surgically removed

2.2.2.3 Angioblastic Meningioma and/or Hemangiopericytoma

Some controversy exists regarding the inclusion of the meningeal hemangiopericytoma in the meningioma group (Kepes 1982; Rubinstein 1972). All authors, however, concur that this group of meningeal tumors exhibits the most malignant behavior of the meningioma-like tumors. Jaaskelainen (1985) reviewed their experience in 21 patients with hemangiopericytomas. He found an incidence of 1.9% among his 936 meningiomas; a comparable figure of 1.6% was reported in Jellinger and Slowik's series (1975), with a higher incidence in males (1.4:1) and a younger mean age of 38 years. In this series, 86% were supratentorial, and there was a higher incidence of occipital lesions. They were frequently attached to the sinus (Fig. 2.4) and bled profusely at operation. All 21 primary tumors were solitary, but two patients had multiple recurrences. The recurrence rate was 19% after the first operation and 43% after the second operation in Jaaskelainen's series. An 80% recurrence rate was reported in 1975 by Jellinger. Operative mortality was as high as 24% due to uncontrollable bleeding. Distant metastases occurred in 14% of Jaaskelainen's series and in up to 23% in Jellinger's series. Radiotherapy, although not proven, is thought to be of some value. None of the three hemangiopericytomas reported by Hayword et al. (1983) had progesterone receptors; this is in contrast to the almost constant presence of these receptors in all other histological types of meningiomas.

Marc et al. (1975) and Jaaskelainen (1985) reviewed the angiographic features of hemangiopericytomas and found a high incidence of dual sup-

ply from the meningeal and cortical arteries, a hypervascular network of small corkscrew tumor vessels, an intense persistent blush, and absence of early venous drainage (Fig. 2.3). This angiographic pattern is best appreciated by superselective angiography of both dural and pial vessels (Fig. 2.3), with numerous capillaries being responsible for the intense tumor stain and thin-walled channels that show up as corkscrew vessels.

Preoperative irradiation is felt to be indicated primarily because the vascular supply from cortical vessels make these tumors unfavorable for embolization. It is possible to superselectively catheterize and embolize some of these cortical branches (Fig. 2.3). Embolization of hemangiopericytomas would provide a major benefit, as the effect of radiation therapy on these tumors remains controversial. Yamakama et al. (1980) reported positive tumor response to radiation therapy; however, Enzinger and Smith (1976) felt that a significant number of these tumors do not respond. Jaaskelainen in 1985 reported that only one of three tumors responded to radiation therapy. Major disadvantages of preoperative radiation therapy include the risk of skin atrophy, which impairs wound healing, risk of secondary induced neoplasms, and the length of time necessary before the effect on the local blood vessels occurs.

2.2.2.4 Meningioangiomatosis

This is a rare condition in which a portion of the cerebral cortex is diffusely involved with an ingrowth of both meningothelial cells and blood vessels, with a variable ratio of the two. These lesions do not behave in a malignant fashion, and they are probably more a hamartomatous than a true neoplastic lesion (Kepes 1982) and are frequently but not always associated with the central form of neurofibromatosis (Rubinstein 1972). It presents in the second or third decade of life, frequently with focal epilepsy, and may show cortical calcification on CT. The frontal and temporal gyri are most frequently involved.

2.2.2.5 Meningeal Meningiomatosis

Meningeal meningiomatosis is a multifocal neoplastic disease that involves the leptomeninges diffusely without the presence of a mass (Fig. 2.5); it presents mainly in infants and children and clinically resembles the course of meningoencephalitis. It is frequently accompanied by small nodules of subarachnoid tumor at various sites along the cerebral spinal axis. Microscopically they may be indistinguishable from the polymorphic type of intracranial sarcoma.

2.2.3 Clinical Presentation

Meningiomas, for the most part, are slow-growing neoplasms. Earle and Richany's (1969) review of the Frazier-Grant collection showed the average length of time between the onset of symptoms and the diagnosis of tumor to be 2.5 years.

Headaches, visual impairment, and focal seizures are the most common complaints, in that order; seizures are usually the first symptom of meningiomas involving the convexity.

Most of the clinical symptoms and signs in patients with meningiomas are caused by local effects of the tumor mass, except perhaps with "en plaque" meningiomas. There is always some pressure on the underlying tissues with resulting damage to the cortex or other parts of the brain.

The tumor may be large enough or may grow rapidly enough to produce increased intracranial pressure. Other effects include vascular occlusion, either venous or arterial, and hemorrhage or cyst formation in adjacent tissue. Meningiomas may also affect more distant portions of the brain, e.g., incisural obstruction with resultant hydrocephalus.

Some indirect effects may be due to local pressure on the pituitary gland or hypothalamus, with endocrine dysfunction (Korsgaard et al. 1976) or diencephalic syndromes of emaciation in children (Campiche and Oberson 1972).

Distant effects that are derived from the mere presence of the tumor or its chemical constituents may be seen. Mahaley et al. (1977) found some degree of immunological energy in 17 patients with meningiomas that

Fig. 2.5A–D. Meningiomatosis. **A** Representative CT scan in coronal view, after intravenous administration of contrast material, demonstrates marked thickening of the free margin of the tentorium (*arrows*), left cavernous area (*arrowhead*) as well as multiple areas of thickening and nodularity along the convexity dura (*open arrowhead*). There was involvement of the sinuses by tumor (*asterisk*). Biopsy of dural and tentorial surfaces demonstrated meningeal infiltration. **B** Lateral angiogram of the left vertebral artery in late venous phase demonstrates multiple collateral venous pathways with complete obliteration of the occipital portion of the superior sagittal sinus and confluent sinus by tumor invasion. **C, D** see p. 168

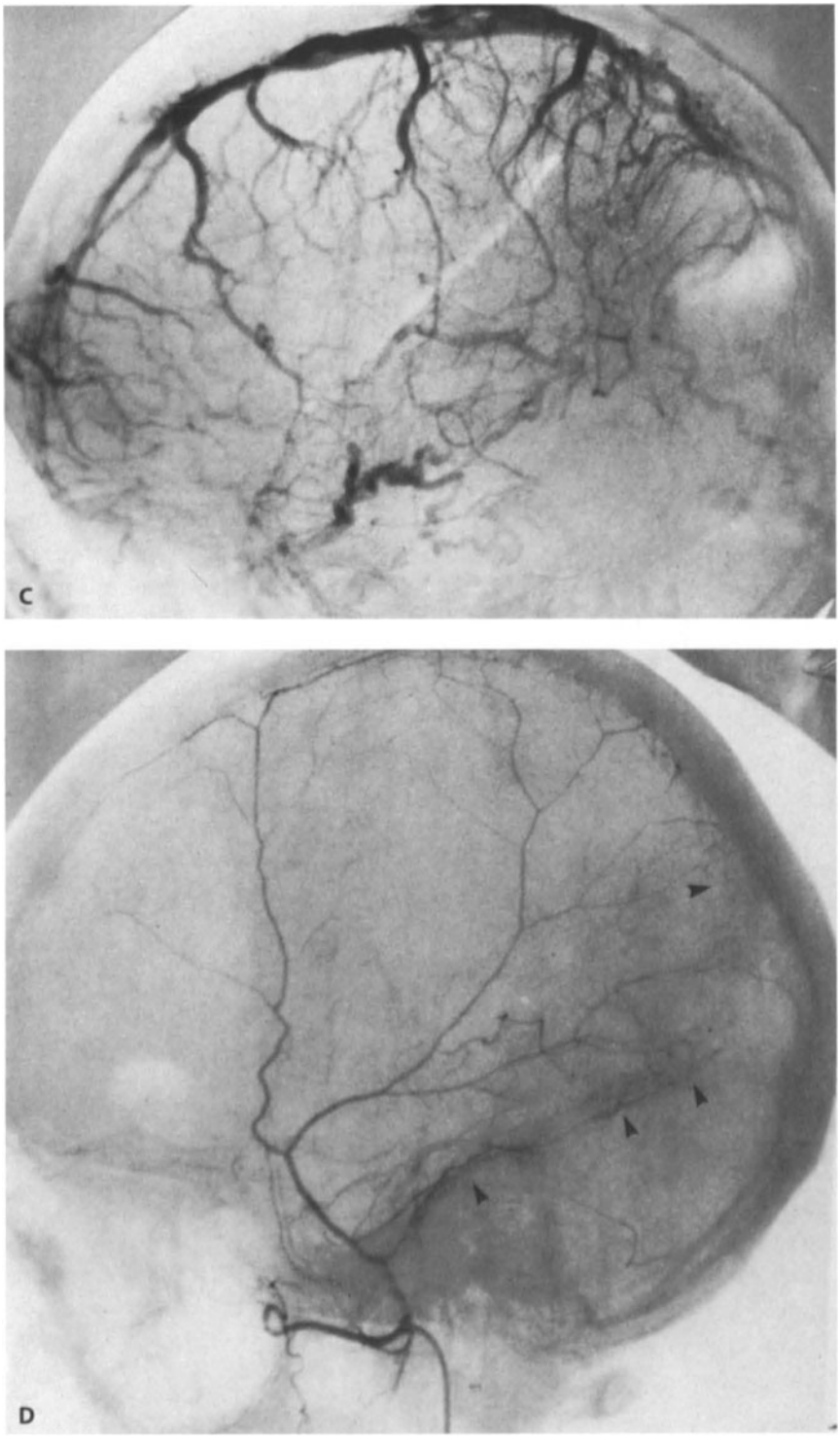

Fig. 2.5 (*continued*). **C** Lateral angiogram of the left internal carotid artery of the posterior portion of the superior sagittal sinus, with collateral venous drainage towards cavernous sinus. **D** Lateral angiogram of the middle meningeal artery demonstrated tumor blush in the region of the torcular and the sigmoid sinuses (*small arrowheads*)

did not improve after removal of the tumor. In the same group of patients, lymphopenia and a decrease in humoral antibodies was also present. Mazzei et al. (1976) found tetany and hypocalcemia in one patient, which disappeared after removal of the tumor. The significance of these distant manifestations (Kepes 1982) is beyond the scope of this text.

Significant symptoms related to the specific locations of these tumors may occur. We will therefore review the sites of presentation without reviewing the obvious symptoms that they will produce; however, in specific sites important diagnostic features will be pointed out.

2.2.3.1 Sites

The most frequent site of intracranial meningiomas is the parasagittal region (Figs. 2.6, 2.7, 2.16), followed by the lateral cerebral convexity (Fig. 2.8). A significant number of tumors arise from the falx cerebri and these may extend laterally on both sides of the dura, or anteriorly into the orbit to form the so-called dumb-bell tumor (Fig. 2.9). Another frequent location is the sphenoid ridge (Fig. 2.10) and tuberculum sellae. Other sites include the olfactory groove, cerebellopontine angle, petrous ridge (Fig. 2.11) (this may be at the cavum of Meckel, which presents clinically with a fifth nerve dysfunction) or the peritorcular area. Less frequently seen are those on the lower surface of the tentorium cerebelli, the cerebellar convexity in the posterior fossa, and the foramen magnum (Fig. 2.12) and clivus (Fig. 2.13).

With the exception of the malignant form and hemangiopericytoma, meningiomas more often involve the anterior half of the cranial cavity than the posterior half.

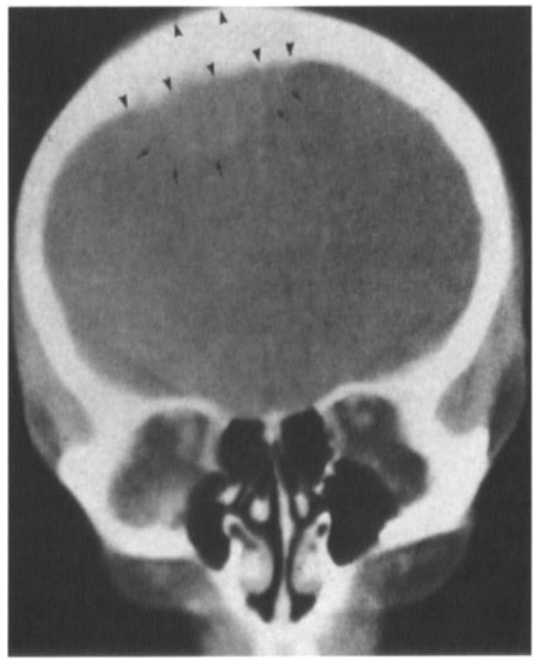

Fig. 2.6. Parasagittal meningioma. Axial CT with bony window demonstrates a parasagittal tumor (*arrows*) with bony hyperostosis that crosses the midline and extends into the extracranial soft tissues (*arrowheads*)

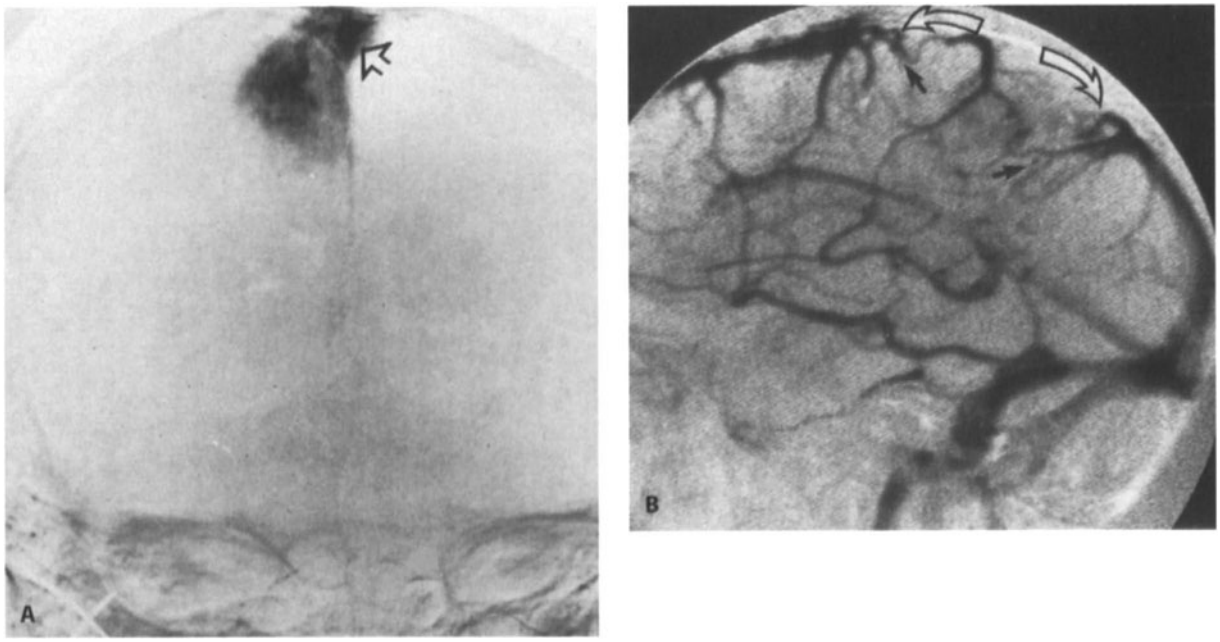

Fig. 2.7A, B. Parasagittal meningioma in another patient. **A** Frontal angiogram of the left middle meningeal artery in late phase shows a right parasagittal tumor. Note the tumor blush on the right side as well as a dense tumor blush in the superior sagittal sinus (*open arrowhead*). **B** Lateral angiogram demonstrating occlusion of the parietal portion of the superior sagittal sinus (*open curved arrows*) with collateral venous bridges (*arrows*). To properly document sinus occlusion, filling of both carotid arteries is necessary, either by high-volume angiography or manual compression. In addition, collateral bridging veins to explain cerebral venous drainage have to be documented

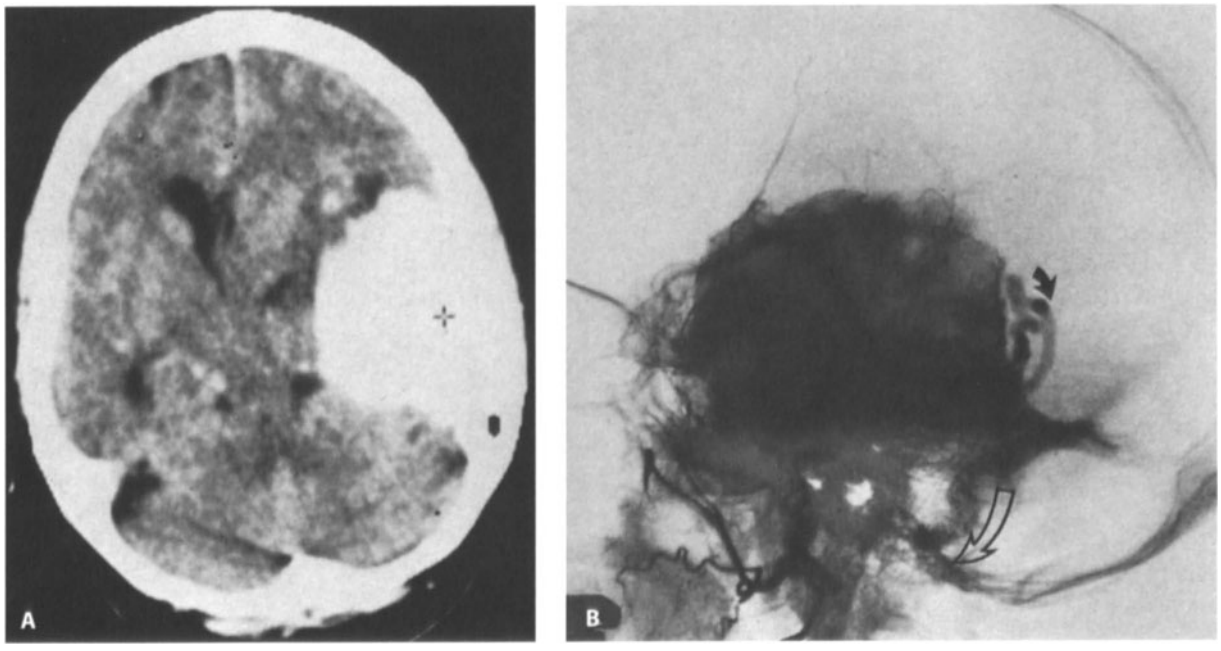

Fig. 2.8A, B. Legend see p. 171

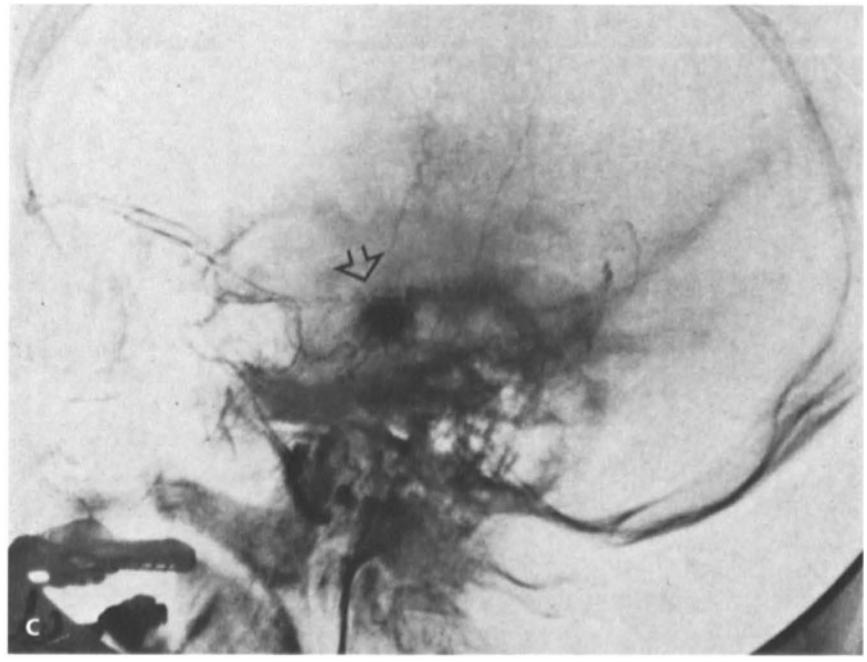

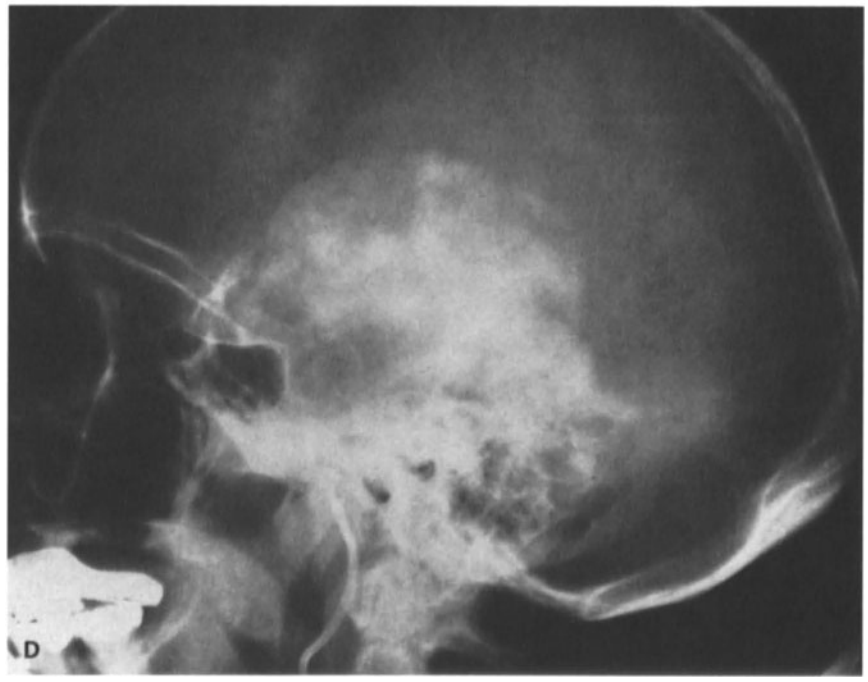

◀ **Fig. 2.8A–E.** Convexity meningioma. **A** Contrast-enhanced axial CT demonstrates a relatively well-circumscribed homogeneously enhancing hyperdense lesion (+) associated with minimal irregularity in its most anterior medial portion and a moderate amount of surrounding edema. Note the significant shift of midline structures. **B** Lateral angiogram of the middle meningeal injection, late phase. The tumor was exclusively supplied by the middle meningeal artery. Note the homogeneous tumor blush similar to the CT findings. Note a dural venous structure draining the tumor (*curved arrow*) and filling the sigmoid sinus (*open curved arrow*). **C** Lateral angiogram after embolization with Gelfoam powder; 95% of the tumor blush has disappeared. Note a small area of stasis (*open arrowhead*). **D** Plain film of the skull in lateral view shows the stagnant Gelfoam powder and contrast-material mixture casting the embolized tumor (compare to **B**). **E** see p. 172

Fig. 2.8 (*continued*). **E** CT scan 12 h after embolization. Note the intratumoral lucencies and decrease in midline shift. At surgery, a completely avascular necrotic, well-circumscribed tumor was found

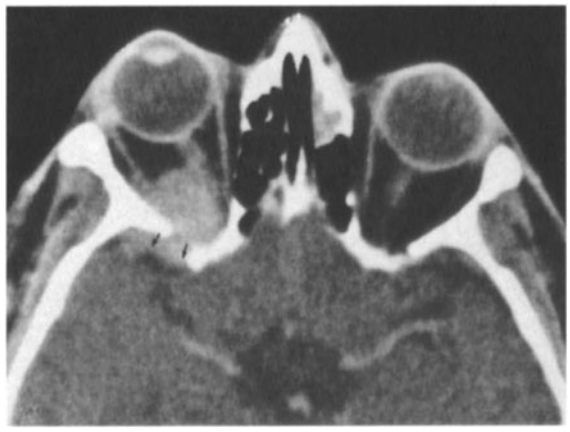

Fig. 2.9. Dumb-bell orbital tumor. Axial CT at the level of the orbits demonstrates a well-circumscribed homogenously enhancing mass, which is primarily in the orbit with extension into the middle cranial fossa in a "dumb-bell" shape (*small arrows*). Supply to this tumor location is usually ophthalmic in its intraorbital part, but the middle meningeal artery may reach part of the intracranial extension

In all locations, the tumor tends to be related to a major dural venous sinus (Figs. 2.4–2.7). Those arising in the convexity abut the sagittal sinus in about 50% of cases (Figs. 2.6, 2.7, 2.16).

En plaque meningiomas are a special group with some specific characteristics. They have a marked predilection for females, even more so than other meningiomas. They usually provoke hyperostosis of neighboring bony structures. For the most part, they do not compress the adjacent brain or produce increased intracranial pressure (Fig. 2.14). When present in the pterional region or when the sphenoid bone is involved (Fig. 2.10), they often present with exophthalmos. Cranial hyperostosis is caused by a diffuse process that does not spare the midline structures (Fig. 2.6) if it develops near the sagittal plane. This is an important sign in the differential diagnosis with hyperostosis frontalis interna, which does not cross the midline.

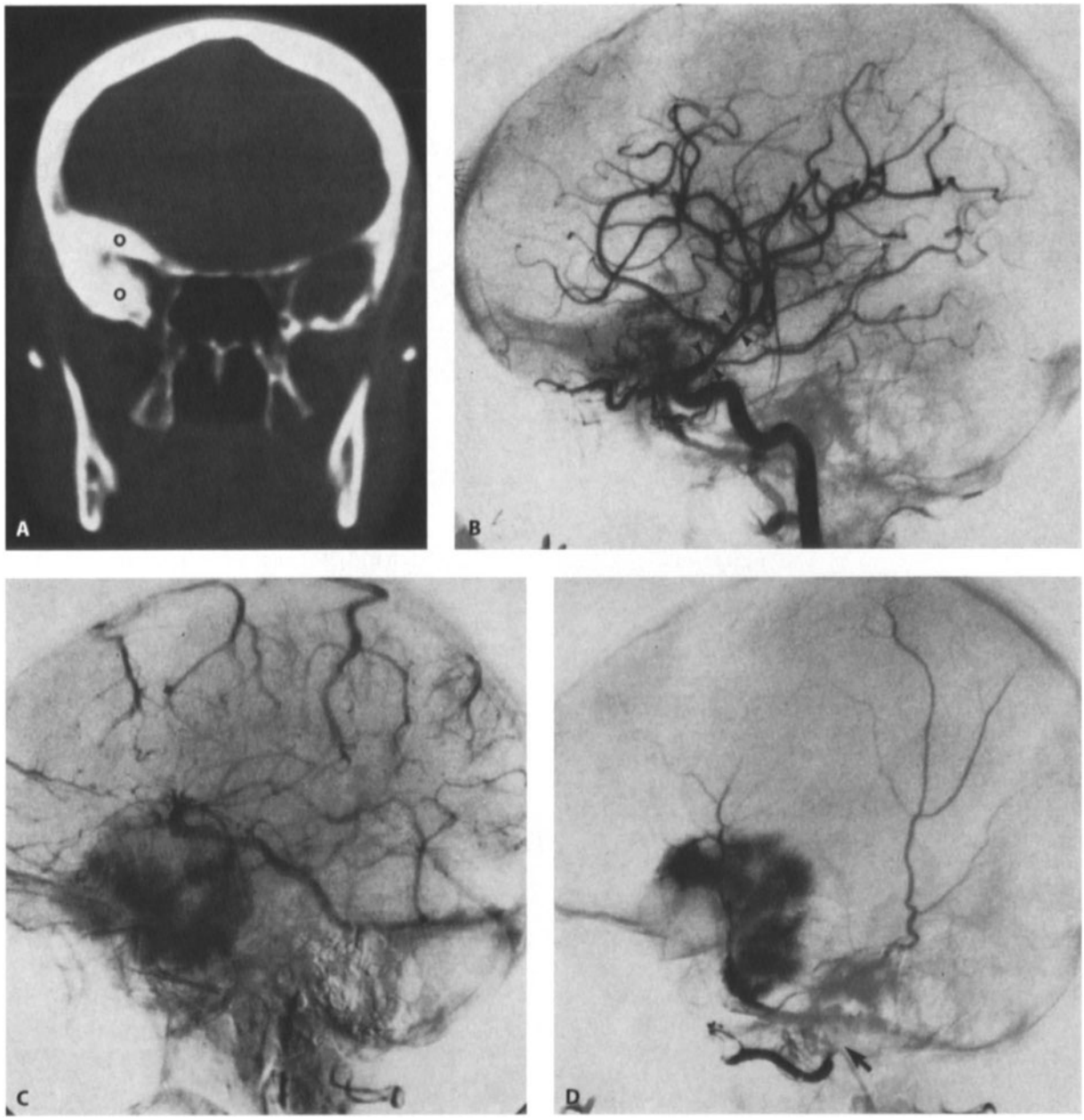

Fig. 2.10A–D. Sphenoid region meningioma with marked hyperostosis and narrowing of the superior orbital fissure with exophthalmos and ophthalmoplegia. **A** Axial CT with bony windows demonstrates the encroachment of the fissure by marked hyperostosis of bone (*O*). Significant intracranial extension was seen in the conventional axial CT with soft tissue window (not shown). **B** Lateral angiogram of the internal carotid artery in mid-arterial phase. Note the significant narrowing of the supraclinoid carotid artery (*arrowheads*). Tumor blush could be seen anterior, posterior, medial, and lateral to the carotid artery. An important consideration is to differentiate compression from encasement. **C** Late phase of the common carotid injection demonstrating the homogeneous tumor stain lasting far into the venous phase without arteriovenous shunting. **D** Lateral angiogram of the middle meningeal artery (*arrow*). Note the different compartment opacified by the middle meningeal artery. The most anterior medial portion was supplied by the inferior lateral trunk and ethmoidal arteries as shown in **B**

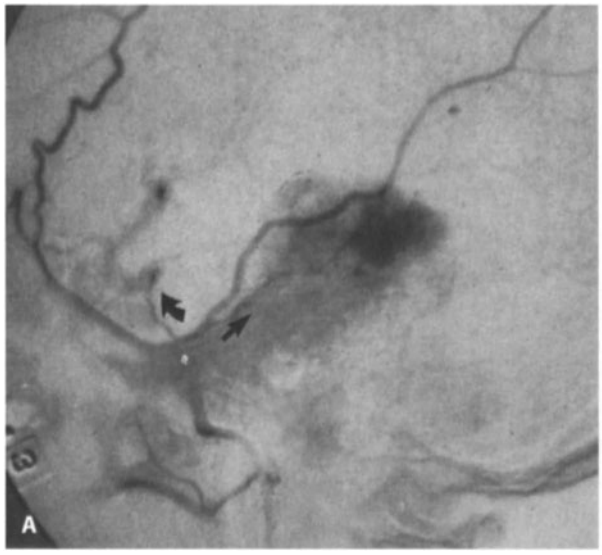

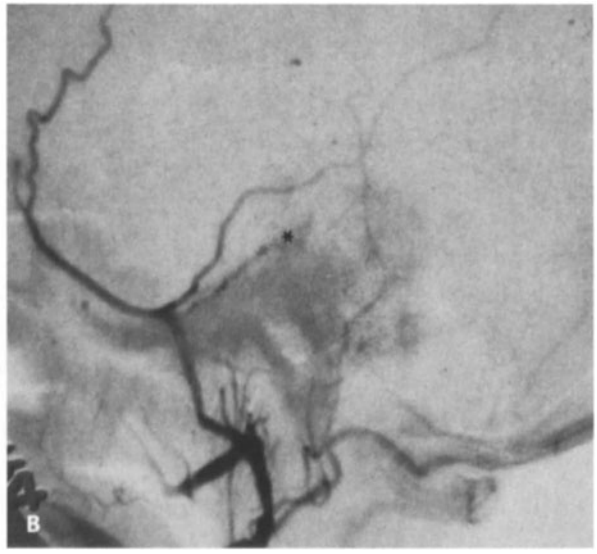

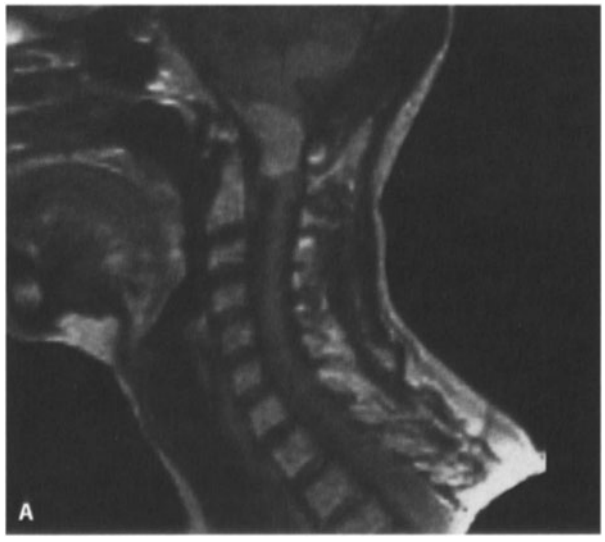

Fig. 2.11A, B (*above*) and
Fig. 2.12A–C (*below*). Legends see p. 175

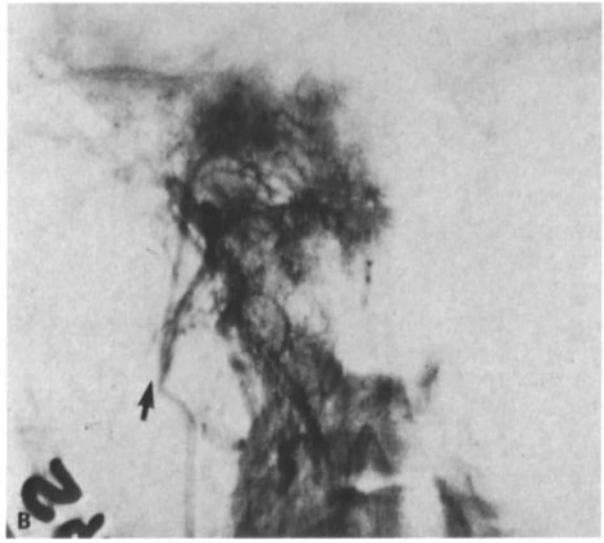

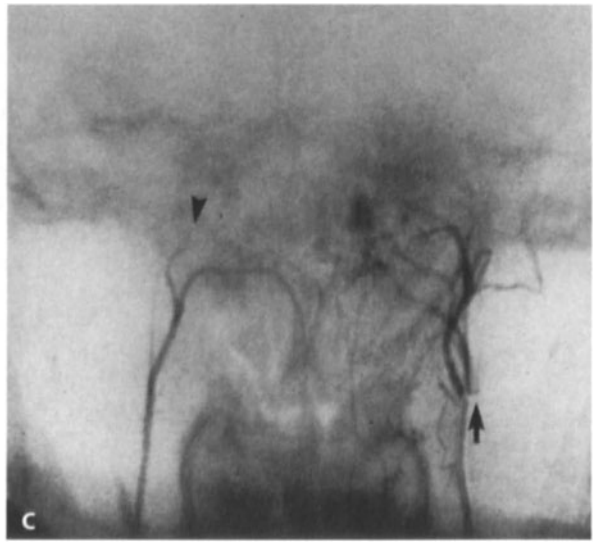

◀ **Fig. 2.11A, B** (*above*). Petrous meningioma. **A** Lateral angiogram of the middle meningeal artery. Note the filing of the internal carotid artery via the inferior lateral trunk (*curved arrow*) and filling of the petrosal branch of the middle meningeal artery supplying the tumor (*arrow*). This represents a danger for microembolization unless flow control to induce reversal of flow in the inferior lateral trunk can be accomplished. **B** Lateral angiogram after microparticle embolization under flow control by gentle hand injection, with microparticles larger than the anastomosis. Note complete devascularization of the tumor (*asterisk*)

◀ **Fig. 2.12A–C** (*below*). Foramen magnum meningioma, MRI scan. **A** T1-weighted image demonstrating a well-circumscribed extra-axial mass with a broad basal attachment on the anterior dural surface. Note in the T1-weighted image the multiple areas of void signal (*black*), which represent hypervascularity. **B** Frontal angiogram of the right ascending pharyngeal artery (*arrow*) demonstrates the main supply to the tumor. **C** Control left ascending pharyngeal injection (*arrow*) in frontal view, demonstrates tumor supply from the left ascending pharyngeal artery. Refilling of the contralateral ascending pharyngeal artery via the clival arcade demonstrates the point of occlusion following embolization of the right ascending pharyngeal artery (*arrowhead*). The left ascending pharyngeal artery was also embolized with microparticles. (Polyvinyl alcohol, 250 μm, low concentration)

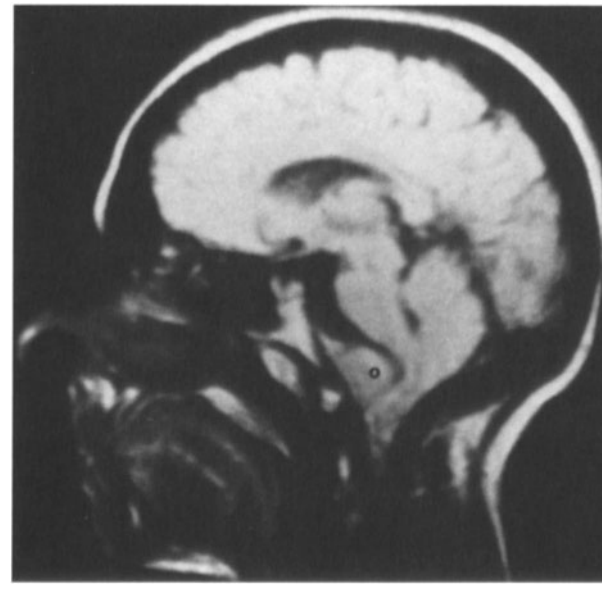

Fig. 2.13. Clival meningioma, MRI scan on T2-weighted image demonstrates posterior displacement of the brain stem by extra-axial mass effect, produced by a clival meningioma. Note the similar signal given in the T1-weighted image by meningioma and normal brain. This may make tumors in the convexity more difficult to detect

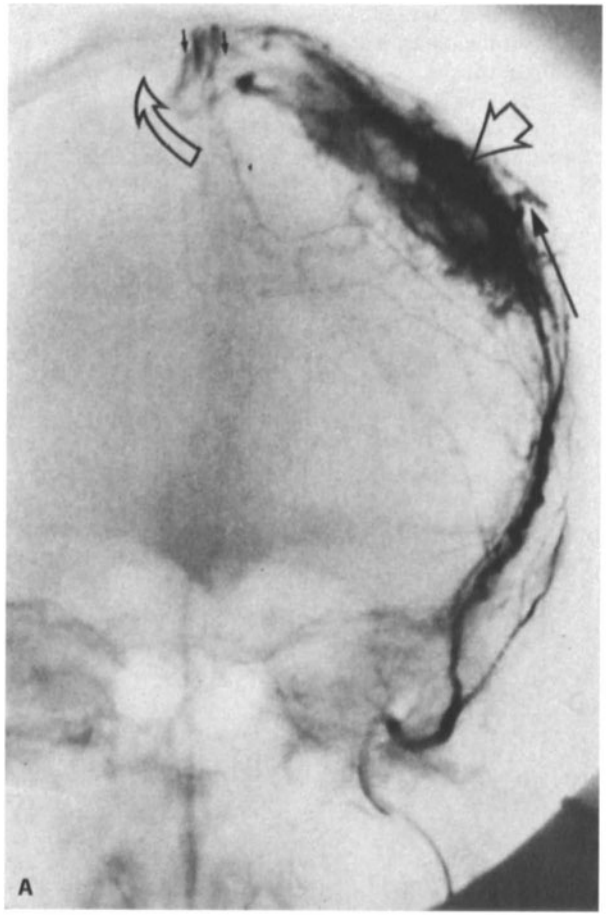

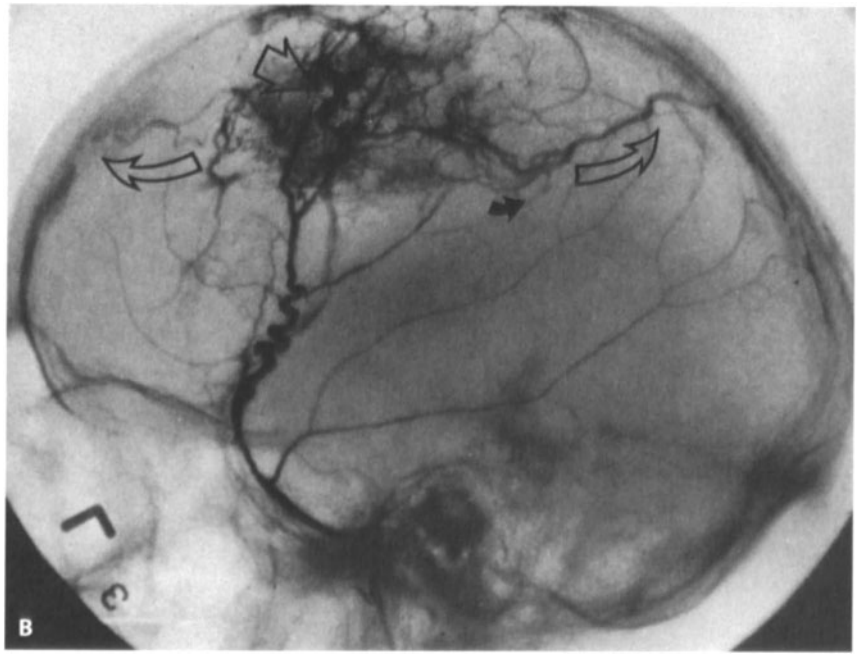

Fig. 2.14A–C.
Legend see p. 177

◀ **Fig. 2.14A–C.** En plaque meningioma of the left parietal region in a 36-year-old man who presented with seizures. **A** Frontal angiogram in late arterial phase of the left middle meningeal artery. The en plaque meningioma is seen following the convexity of the brain but without compression. There are transbony emissary veins (*arrow*), diploic (*open arrowhead*), dural (*small arrows*), and cortical (*open curved arrow*) venous drainage. **B** Lateral angiogram of the same patient. Note the dural-to-cortical venous anastomosis (*small curved arrow*) draining into a cortical vein (*curved open arrows*). The diploic venous lake (*open arrowhead*) is well visualized. Embolization will not be successful in stopping the venous bleeding from this diploic drainage. **C** Frontal skull radiogram of the same patient following glue embolization. Note the excellent cast of the en plaque tumor (*open curved arrow*). The outer table is not involved (compare with **A**). Facial nerve palsy occurred following embolization and resolved in 3 months

Meningiomas may also occur without dural attachment (pial forms) in the depth of major fissures (such as the sylvian fissure). Intraventricular meningiomas arise either from the tela choroidea or from the stroma of the choroid plexus. Although they may occur in any ventricle, there is a distinct preference for the lateral ventricle in general, and the left lateral ventricle in particular. Intraventricular meningiomas are more frequent in children.

2.2.3.2 Epidural Meningiomas

By far, most cranial meningiomas develop deep to the dura mater, with or without attachment to the membrane. Some can grow right through it. Much less frequently, the main bulk of the tumor is in the epidural space, and therefore in the bone itself (Fig. 2.15). These may grow through the bone and into the soft tissues of the scalp. These epidural tumors are frequently associated with hyperostosis and may be palpable on examination. In some cases, a purely intraosseous tumor may be found without involvement of the dura, the so-called primary intraosseous meningioma. These may or may not involve the diploic space (Kepes 1982).

2.2.3.3 Meningiomas of the Orbit

Reese (1976) found meningiomas to account for 3% of expanding lesions of the orbit. There is a higher incidence in younger people, especially young white females below 20 years of age (25%; Karp et al. 1974); 16% of these patients have the central form of neurofibromatosis.

Meningiomas present in the orbit by three mechanisms. The most frequent type invades the orbit as an extension from an intracranial tumor, usually but not exclusively from the middle cranial fossa through the optic foramen and superior orbital fissure.

Meningiomas also originate from the anterior portion of the optic nerve sheath. They may develop in the optic foramen region and form a dumb-bell-shaped tumor with intracranial extension (Fig. 2.9). Finally, rarely the tumor may arise from ectopic arachnoid nests in the orbital tissues.

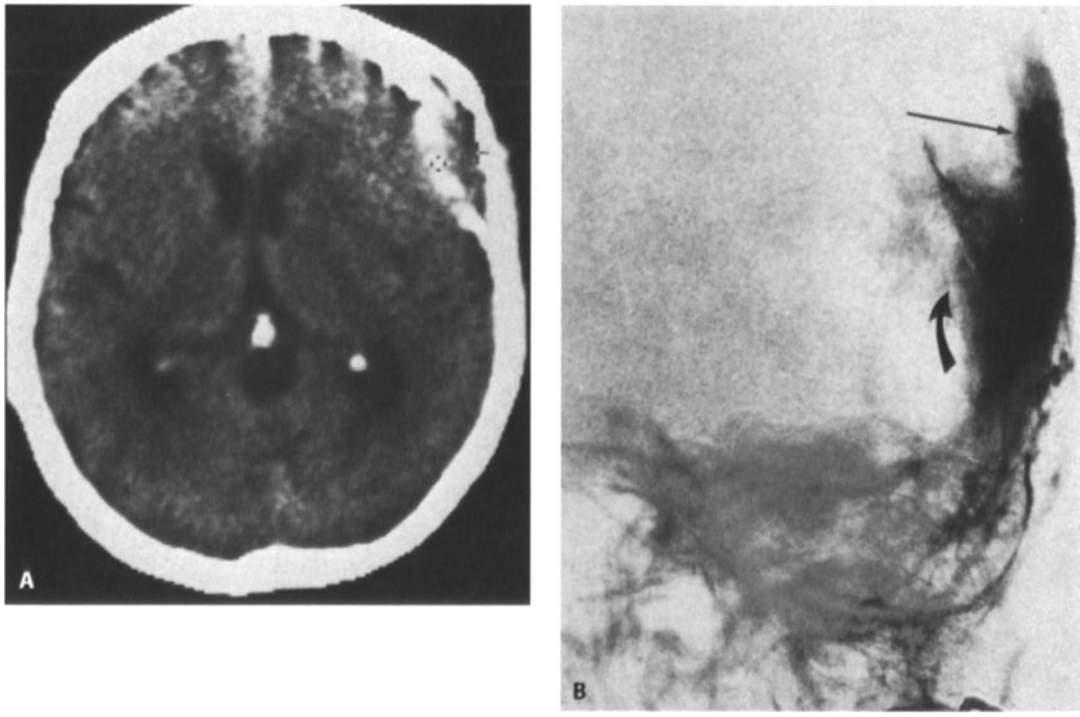

Fig. 2.15A, B. Epidural meningioma. **A** CT scan with bony windows demonstrates splaying of the outer and inner table. **B** Frontal angiogram in late phase of the left middle meningeal artery demonstrates the diploic (*long arrow*) and epidural (*curved arrow*) tumor

Ocular signs may be related to impingement on the optic canal and obstruction of the superior orbital fissure. En plaque meningiomas (or tumor invasion; Fig. 2.10) of the pterion can cause exophthalmos secondary to tumor growth or hyperostosis and may endanger vision. Optic nerve sheath meningiomas usually lead to severe optic atrophy (Karp et al. 1974). Additional ocular circulatory problems may be caused by the shunting effect of ectatic opticociliary veins that develop in patients with orbital meningiomas (Zakka et al. 1979). Rarely, the tumor will penetrate the globe and invade the choroid and the retina (Henderson and Campbell 1977). Tumors near the optic canal cause prechiasmal optic nerve compression with slowly progressive loss of vision characterized by near normal acuity, but poor color perception, and Marcus Gunn pupils, but with a normal appearance of the disc. This is important in the differential diagnosis with optic nerve gliomas.

2.2.3.4 Meningiomas Involving the Cavernous Sinus

These tumors, in view of their difficult location for surgical removal, have a relatively high incidence of oculomotor palsies and recurrences. On occasion, a good embolization alone may provide relief of cranial nerve dysfunction.

2.2.3.5 Meningiomas in Other Unusual Sites

This group of tumors is considered separately in view of its relative infrequency, and its clinical importance to surgeons and radiologists who may be involved in the diagnosis and treatment.

1. Meningiomas can originate from extracranial and extraspinal arachnoid cells in or near the foramina that serve as exit points for cranial nerves.
2. Most meningiomas arising in the parapharyngeal region are related to cranial nerves, particularly the sixth nerve. Additionally the ninth, tenth, 11th, and 12th cranial nerves may be the site of origin. Those arising from the base of the skull usually occur in association with spinal nerves (Harkins and Reed 1969) or sympathetic nerve roots (Wilson et al. 1979).
3. Truly ectopic meningiomas without obvious connection to foramina or nerves can occur at remote sites. These originate from embryonic rests of arachnoid. They may arise from the outer table of the skull, particularly the frontal or temporal bone. In the orbit they are seen without involvement of the optic nerve (Lloyd 1982).

The most frequent location for ectopic meningiomas is the paranasal sinus and nasal-oral cavity (Geoffrey et al. 1984; see Chap. 3).

Ectopic meningiomas have been reported at multiple sites (Farr et al. 1973), including those reviewed and also in the parathyroid glands, ear, mediastinum, and skin (Kepes 1982).

In 1974, Lopez et al. reported 25 cases of cutaneous meningiomas; he divided them into three types.

1. Those in the scalp, face, and paravertebral skin. These are most frequently seen in children and are usually benign.
2. Those in the skin near the sensory organs.
3. Meningiomas originating intracranially or intraspinally may reach the skin by growing through the bone or through a bony defect; these have the poorest prognosis (Figs. 2.1, 2.2).

2.2.3.6 Intracranial Vascular Involvement

Infarcts or hemorrhage may be included in the differential diagnosis of meningiomas, and may actually be the presenting symptom of these tumors (Moore 1954). Massive hemorrhage as a complication of a meningioma has been reported by Skultety (1968), but this is rare. When meningiomas do cause hemorrhage, it may be intracerebral, subdural, subarachnoid, or intratumoral (Modesti et al. 1976). The majority of reported hemorrhagic complications in meningiomas have been found in tumors that are highly vascular at histology.

The subdural hematomas seen with meningiomas may be caused by growth of tumor into the subdural space, producing rupture of bridging veins or by direct hemorrhage from the tumor into the subdural space.

Meningiomas involving the choroid plexus of the lateral ventricle may present with subarachnoid hemorrhage, which can also be seen with tumors outside the ventricular system (Kepes 1982).

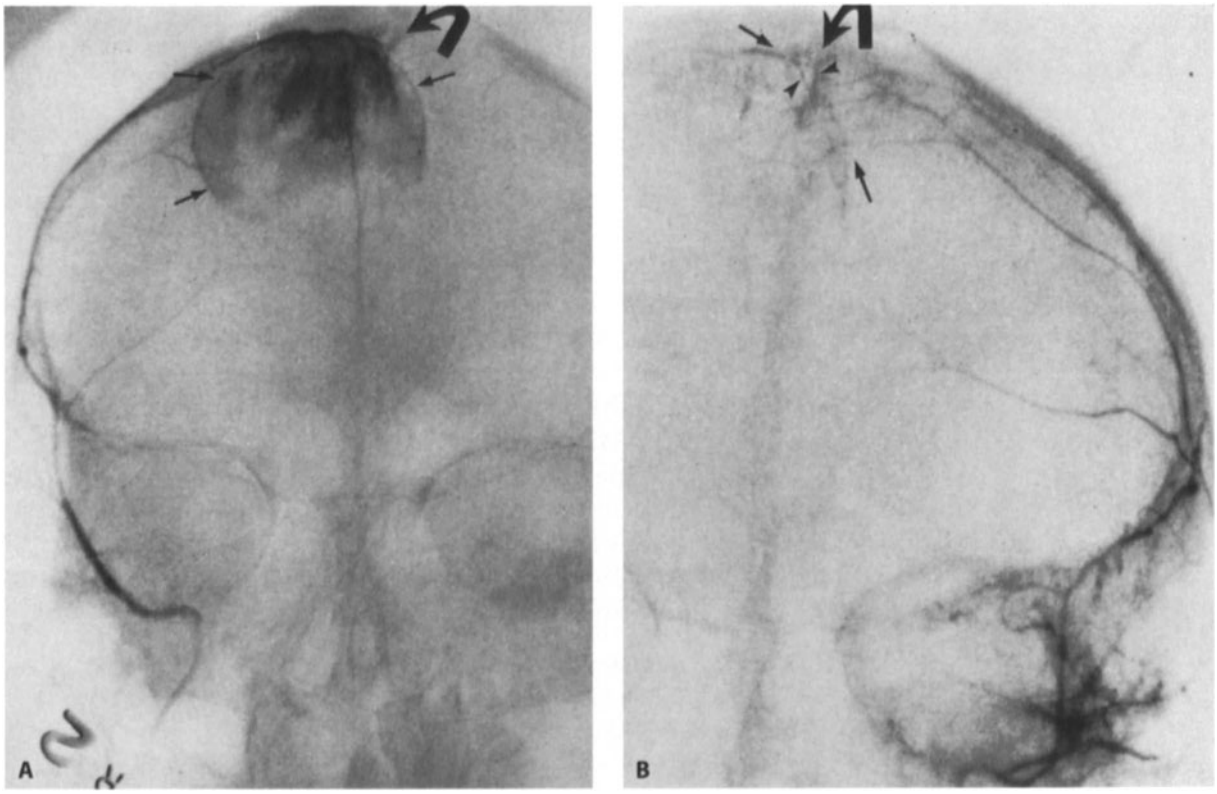

Fig. 2.16A, B. Functional compression of the superior sagittal sinus in a parasagittal meningioma. **A** Frontal angiogram of the right middle meningeal artery. The catheter is at the level of the foramen spinosum. Note the well-circumscribed tumor (*arrows*). The superior sagittal sinus is pushed medially (*curved arrow*) but is not invaded (compare with Fig. 2.7). **B** Frontal angiogram of the left middle meningeal artery after right-sided embolization. The meningeal artery shows the wall of the sinus, with a characteristic triangle configuration and is shown compressed, but free of tumor (*arrowheads*). Note the filling of the same capsular artery as in **A** (*arrows*), but no tumor visualization, confirming the ability of Gelfoam powder microparticles to enter the tumor angioarchitecture. Furthermore, proximal larger particle embolization of the right middle meningeal artery would not have devascularized the tumor. Closure of this left middle meningeal artery is also advisable in preparation for surgery to avoid the need of opening the left side and maximize the effect of devascularization

Intratumoral hemorrhage may be present as an acute and even fatal episode due to rapid enlargement of the tumor mass (Helle and Conley 1980). Venous occlusions occur more frequently, usually in the presence of meningiomas that arise near a major sinus occluded either by extrinsic pressure (Fig. 2.16) or actual tumor invasion. If this occurs slowly (as is usually the case) it will be tolerated, due to the development of bridging or collateral pathways of drainage (Fig. 2.7). Rapid occlusion of a major sinus may cause a venous infarction.

Another complication of venous occlusion is increased intracranial pressure and papilledema.

Arterial occlusion is less frequent, but may occur secondary to tumor encasement of an artery (Fig. 2.10).

2.2.3.7 Peritumoral Edema in Meningiomas

The presence of cerebral edema in association with meningiomas is well known, and its cause has been a topic of great interest to many investigators. Multiple theories have been proposed (Tamiya et al. 2001); however, none has been conclusive. Therefore, we will only describe the pertinent and practical aspects of this phenomenon. The edema of meningiomas is of vasogenic origin (Klatzo 1967). Stevens, in 1983, analyzed the literature and his own experience with peritumoral edema in meningiomas, based on CT scans in 160 patients (Stevens et al. 1983). Edema was present in 46% of cases; it occurred most frequently in the centrum semiovale and the deep white matter around the ventricular trigone and frontal horns, reflecting the size of the interstitial spaces adjacent to the tumor. Edema usually resolved within 3 months after surgery, except in very large lesions. Atrophy in the underlying cortex was related to tumor size and not the edema. Increased edema after surgery could nearly always be ascribed to a definable complication. He found a statistically significant positive correlation between edema production and tumors of large surface area, tumors that were flat and lobulated, tumors that spread across the midline, those located in the anterior parasagittal region, those involving the sinus, and those with a short clinical history. Significant negative correlations were found with small tumors, presence of Ca^{++}, and relatively low vascularity. Although the exact cause of the edema is still unclear, he believed hydromechanical factors to be predominant.

2.2.4 Pretherapeutic Evaluation

At present, CT scanning and magnetic resonance imaging (MRI) are the best imaging studies for diagnosis and the proper localization of a suspected meningioma.

2.2.4.1 CT Scanning in Meningiomas

This topic has been well reviewed by various authors. A brief review of the CT findings is pertinent.

On the noncontrast scans, the lesions are hyperdense compared to brain in over 55% of cases, isodense in 20%, hypodense in about 10%, and calcified in approximately 14%. Surrounding edema is noted in 46% and associated cyst-like spaces are seen in about 20% of cases (Stevens 1983).

Following intravenous administration of contrast material, the lesions usually show well-circumscribed borders and marked enhancement as compared to normal brain; this enhancement measures in the range of 25–40 HU. Tumor enhancement is homogeneous in over 85% of cases (Figs. 2.8, 2.9). Russell found that 14% of lesions had atypical features such as areas of lucency, which seemed to correlate with more aggressive behavior (Fig. 2.3). Tumor necrosis is also unusual and is suggestive of aggressive behavior.

Meningiomas are found near dural surfaces, usually with their broadest margins abutting it (Figs. 2.3, 2.6). Signs of an extra-axial origin can usually be detected, including buckling of the white matter, which is very useful in evaluating large lesions.

Bony window imaging is necessary to detect hyperostosis (Figs. 2.6, 2.10) and/or bone expansion, which is suggestive of marrow involvement or frank destruction (Fig. 2.15). Soft tissue windows are useful to detect extracranial or extraorbital (Fig. 2.9) extension of the tumor, including subtemporal and zygomatic fossa involvement. En plaque meningiomas or epidural tumors are best seen with the higher windows.

Although CT is excellent in determining the site of origin and/or attachment of most tumors, this may be impossible to determine for very large lesions. In these cases superselective angiographic studies may provide this information. Sinus invasions and/or thrombosis can often be predicted from CT, although it is best documented by vascular studies (Figs. 2.7, 2.16).

Additional pertinent information such as mass effect, ventricular size, presence of additional tumors, areas of intratumoral hemorrhage, or the presence of associated lesions such as extra-axial or intra-axial collections (subdural, intracerebral, or subarachnoid hemorrhage) can be assessed.

Although CT findings in meningiomas are usually characteristic, in some rare exophytic intra-axial tumors, the diagnosis is not obvious, and for these, superselective vascular studies usually resolve the diagnostic dilemma.

2.2.4.2 MRI Scanning

Meningiomas have a homogeneous appearance with a signal similar to brain on T1-weighted images (Fig. 2.13) and therefore sometimes can be indistinct from normal parenchyma, especially if no edema is present. MRI scans can detect vascularity within the tumor, which will appear on T2-weighted images (Fig. 2.17) as focal areas of signal void due to the flow phenomena. Calcifications within the meningioma may mimic these flow voids. The relationship of the meningioma to the major cerebral arteries and veins is best examined using MRI with the contrast enhancement technique (Farb et al. 2002) and should be performed to assess patency of the dural sinuses. In addition, MRI is of greater value in detecting meningiomas along the skull base [cavernous area, clivus (Fig. 2.13), foramen magnum (Fig. 2.12), etc.], where CT is less useful due to its inherent inability to differentiate bony structures from tumor. The so-called dural tail sign was initially believed to be characteristic for the presence of meningioma, but was subsequently noted to be a rather nonspecific finding of enhancement along the dura, caused by a multitude of pathologies.

The ability of MRI to demonstrate the marrow spaces of the skull may make it possible to differentiate between diploic involvement by tumor and reactive hyperostosis.

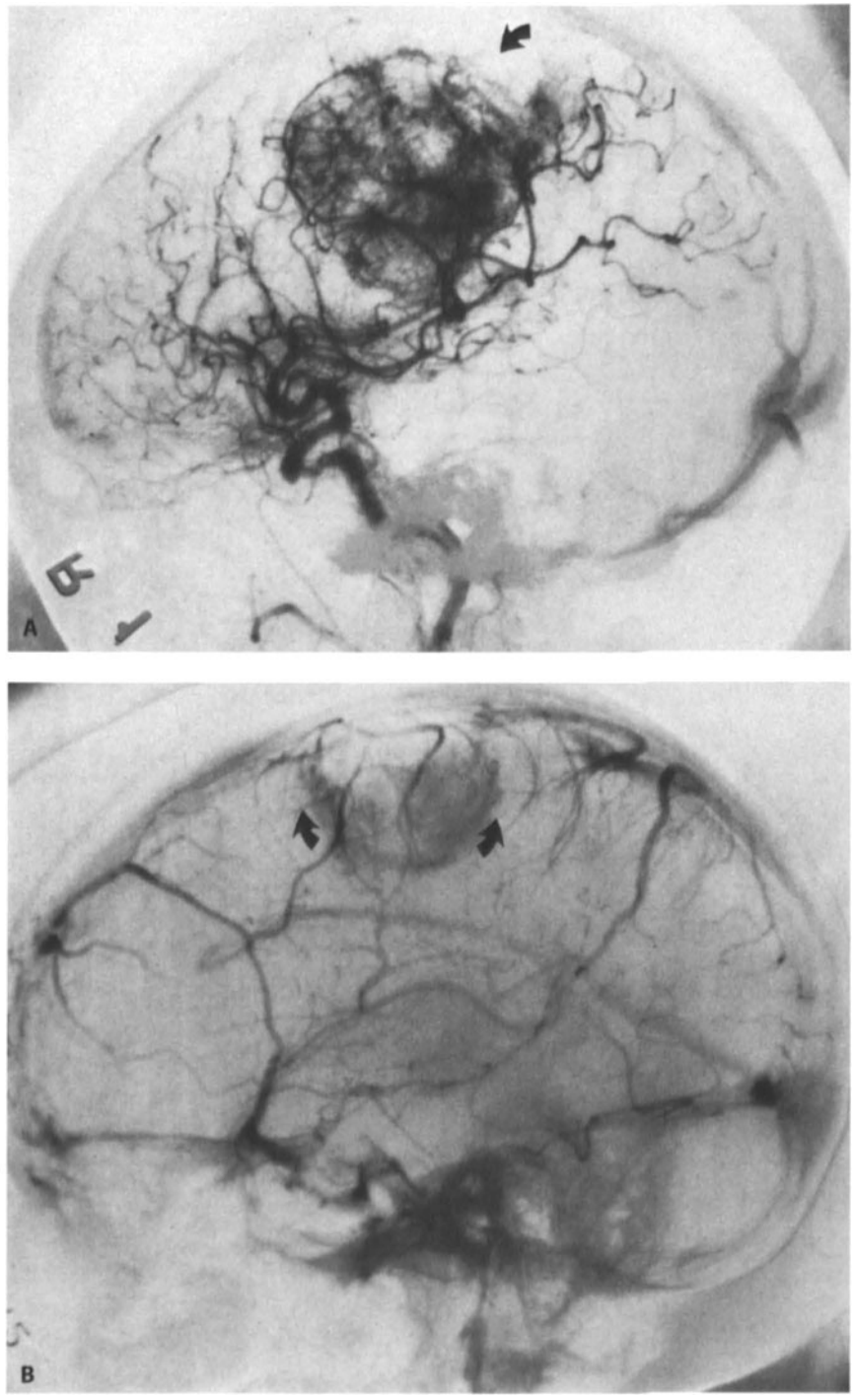

Fig. 2.17A, B. True pial supply versus compressed parenchyma. **A** Lateral subtraction angiogram of the right internal carotid artery demonstrates pial supply to a hypervascular parietal convexity meningioma. The middle cerebral pial supply corresponds to the more central portion of the tumor. The dural supply from middle meningeal artery (MMA) (not shown) corresponds to the areas of lucency in the most peripheral portion (*curved arrow*). **B** Lateral angiogram in late venous phase in another patient demonstrates a smooth homogeneous capsular blush, which represents compressed parenchyma. No pial supply was confirmed at surgery. Note that there is occlusion of the superior sagittal sinus; therefore part of the blush may represent some outflow congestion in the compressed parenchyma

Table 2.3. Information provided by angiography of meningiomas

1. Arterial supply (dural and/or pial) Tumor vascularity Site of tumor attachment Differential diagnosis
2. Arterial displacement and relationships
3. Arterial encasement
4. Collateral circulation to the brain
5. Venous displacements
6. Cortical venous arrangement (congenital disposition or collateral venous circulation)
7. Status and patency of major sinuses
8. Possibility of endovascular embolization

2.2.4.3 Angiographic Investigation

The contributions of the angiographic investigation of meningiomas are listed in Table 2.3.

With the availability of CT and MRI scans, the tumor location is usually known prior to the angiographic investigation; therefore, one can plan the angiographic protocol accordingly.

Meningiomas arise from arachnoid villi in the meninges; therefore, they receive their main supply from dural branches and initially are fed exclusively by the meningeal arteries. However, as they enlarge they can acquire additional supply from pial vessels (Fig. 2.17). The involvement of cerebral arteries, however, does not necessarily mean that the brain has been invaded. In cases with a dual supply, the center and dural base of the tumor (site of attachment) are supplied by meningeal arteries, whereas the peripheral portion of the tumor is supplied by cerebral arteries. Therefore, there may be limitations to what can safely be embolized (Figs. 2.3, 2.24). It is important to differentiate true pial supply from the smooth homogeneous blush of compressed parenchyma (Figs. 2.17, 2.18).

Intraventricular meningiomas are supplied by choroidal arteries, most frequently from the carotid and/or posterior cerebral circulation and for the most part they are not amenable to embolization; the main thrust of angiography is to suggest the diagnosis of a curable lesion.

The resectability of a given tumor, as predicted from CT and MRI, will determine the need and extent of the subsequent therapeutic angiography. The angiographic evaluation may reveal features that predict a difficult surgical resection. For example, evidence of carotid or other cerebral artery encasement (Fig. 2.10) may be an indication for extracerebral–intracerebral (EC–IC) bypass prior to tumor resection. Tumor supply from the cerebral arteries (Figs. 2.3C, 2.17) will require close consultation between the surgeon and the interventional neuroradiologist to modify the aggressiveness during embolization (Figs. 2.3, 2.24).

As previously alluded to (Table 2.3), proper assessment of venous anatomy and patency is of utmost importance in the planning of surgery for meningiomas that are at or near a major sinus. The venous drainage of the tumor correlated with the drainage of the normal cerebral circulation

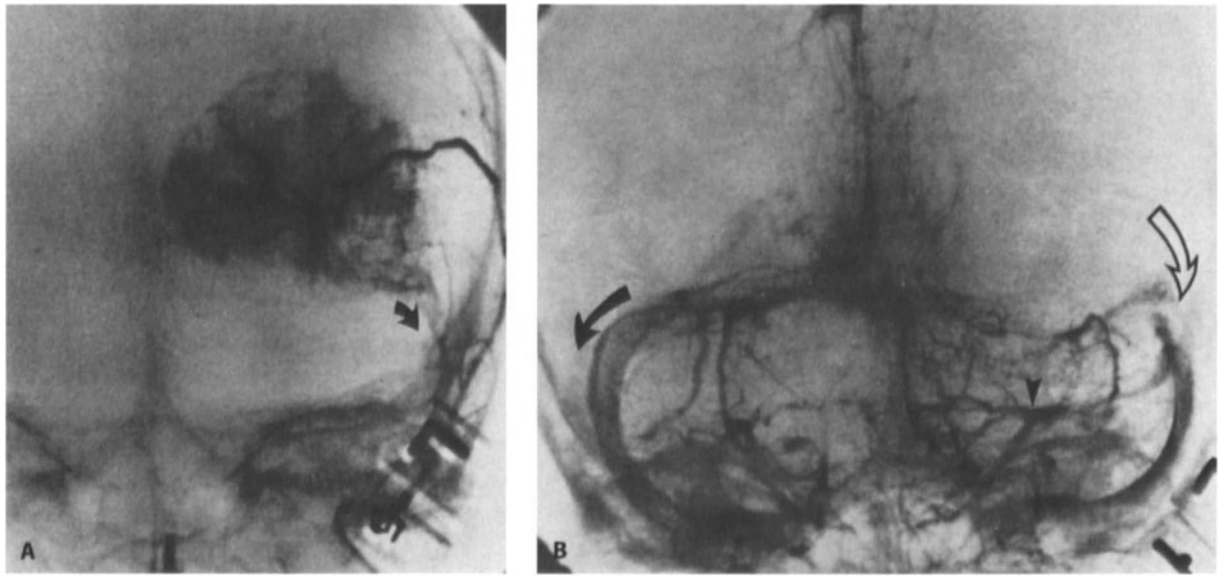

Fig. 2.18A, B. Tumor drainage towards the sigmoid sinus. **A** Frontal subtraction angiogram of the left middle meningeal artery demonstrates a hypervascular meningioma draining towards the left sigmoid sinus and compressing the transverse sinus. **B** Frontal angiogram of the left vertebral artery, venous phase. Note the lack of opacification of the left transverse sinus which is compressed, but not invaded by tumor. The filling defect in the proximal sigmoid sinus (*open curved arrowhead*) represents the diluted blood draining the tumor (*curved arrow* in **A**). There is good opacification of the right transverse-sigmoid sinuses (*curved arrow*). Collateral venous circulation in the left cerebellar hemisphere is noted with primary drainage towards the superior petrosal vein (*arrowhead*). Compare venous drainage of tumor towards the sinus with invasion of the sinus by tumor (Figs. 2.4, 2.7)

must be assessed to determine the effects of sinus resection and ensure the safety of complete tumor removal.

In our experience, drainage through cortical veins (Fig. 2.14) has been associated with tumors that infiltrate adjacent brain without a cleavage plane. Drainage through diploic (Fig. 2.15) or superficial veins may indicate bone or soft tissue involvement. Supply from the superficial temporal artery may indicate extension to extracranial soft tissues or bone or may be present via transosseous anastomoses with intracranial tumor without extracranial or bony involvement (Fig. 2.19). In this situation, significant osseous bleeding may be expected at the time of surgery.

The assessment of resectability in a given case will depend on the skills and experience of an individual surgeon or team.

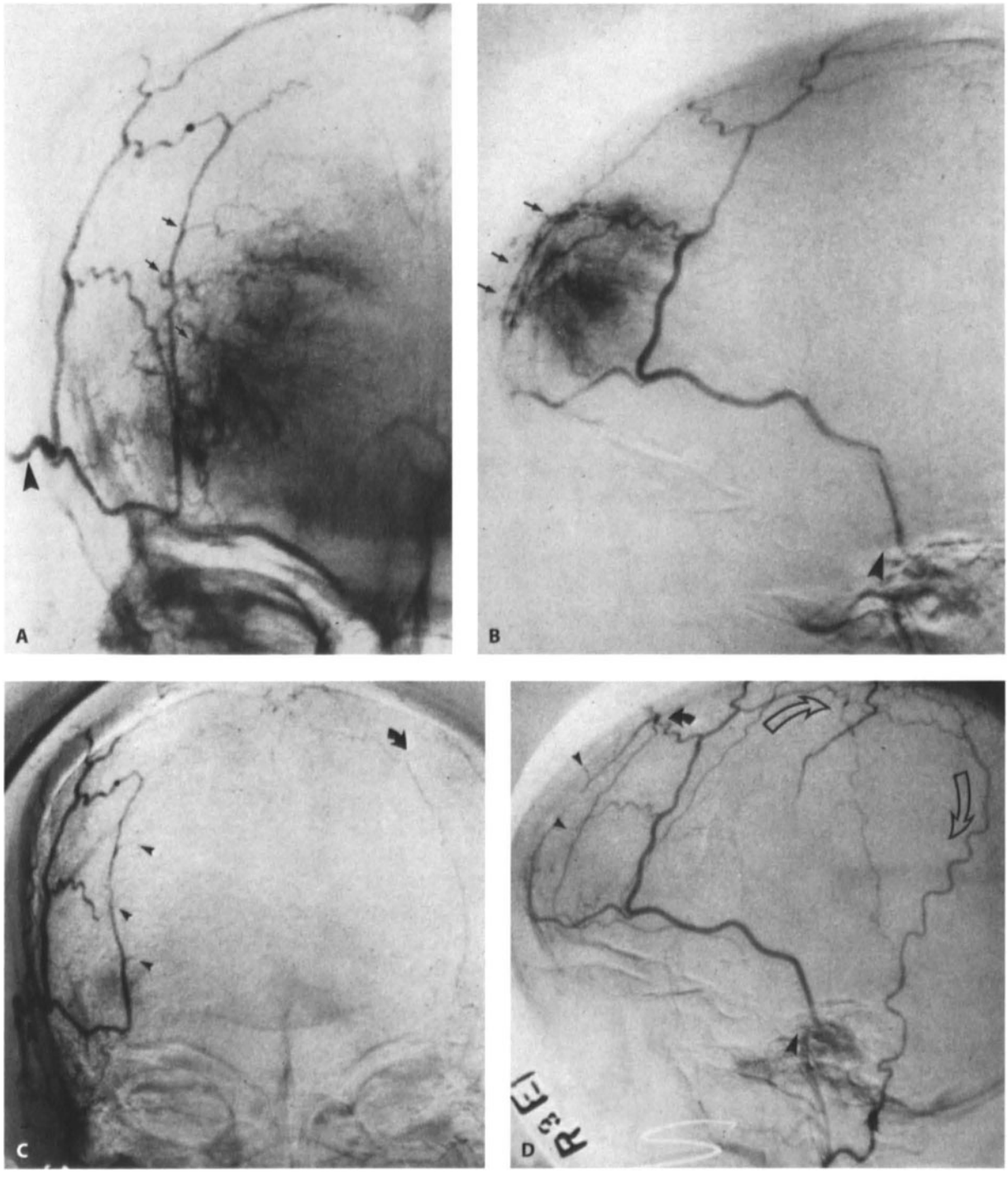

Fig. 2.19A–D. Transosseous superficial temporal supply to an intracranial meningioma. **A** Frontal and **B** lateral angiogram of the right superficial temporal artery (*arrowhead*), supplying a frontal convexity meningioma via transosseous anastomosis (*arrows*). The bone is not involved. **C** Frontal and **D** lateral postembolization angiograms demonstrating the ability of flow-directed diluted microparticles to reach exclusively the abnormal vessels by preferential flow, sparing normal tissue to prevent unwanted skin problems following surgical excision. The transosseous anastomosis has been blocked (*arrowheads*). Note the excellent preservation of microanastomosis filling the contralateral superficial temporal artery (*curved arrow*) and the collateral circulation towards the posterior auricular artery (*open curved arrow* in **D**)

Table 2.4. Other bony tumors with invasion and/or supply from dural or scalp arteries

Cerebral tumors (intra-axial)	Glioblastoma Astrocytoma Oligodendroglioma Optic glioma Oflactory neuroblastoma Medulloblastoma Metastatic carcinoma Retinoblastoma Cranial nerve schwannoma Melanoma Pituitary adenoma Ependymoma Hemangioblastoma Pinealoma	Melanoma	
Neuroinoma		Chondrosarcoma	
Esthesioneuroblastoma		Fibrosarcoma	
Rhabdomyosarcoma		Plasmacytoma	
Primary neurogenic tumors	Neurilemmoma Ganglioneuroma Ganglioblastoma Neuroblastoma Malignant schwannoma Neurofibrosarcoma	Metastatic	Carcinoid Kidney Thyroid Adrenal carcinoma Multiple myeloma Prostatic
Osteoblastoma		Bony dysplasias	Fibrodysplasia Paget's
Osteosarcoma		Squamous cell carcinoma	
Osteochondroma		Giant cell tumor	
		Hemangioendothelioma	
		Chordoma	

2.2.4.4 Differential Diagnosis

The differential diagnosis of meningiomas varies according to the location. Table 2.4 lists other tumors that may receive dural supply and therefore could be confused with meningiomas. Usually the CT appearance or multiplicity of lesions (Fig. 2.20) will suggest the diagnosis.

In the parasellar region, the most important consideration to exclude is a vascular lesion such as a giant carotid aneurysm.

2.2.5 Therapeutic Strategy and Clinical Objectives

Most meningiomas are benign and curable tumors, so that every effort must be made to properly diagnose and treat them. The best available cure is offered by total surgical excision, and the surgical neuroradiologist may contribute towards this goal. There is some controversy as to the value of preoperative embolization of meningiomas over the convexity, or those in which the blood supply can be easily reached during surgery. The value of preoperative embolization in these situations is difficult to assess and will depend on the philosophy of the surgeon and his or her operative tech-

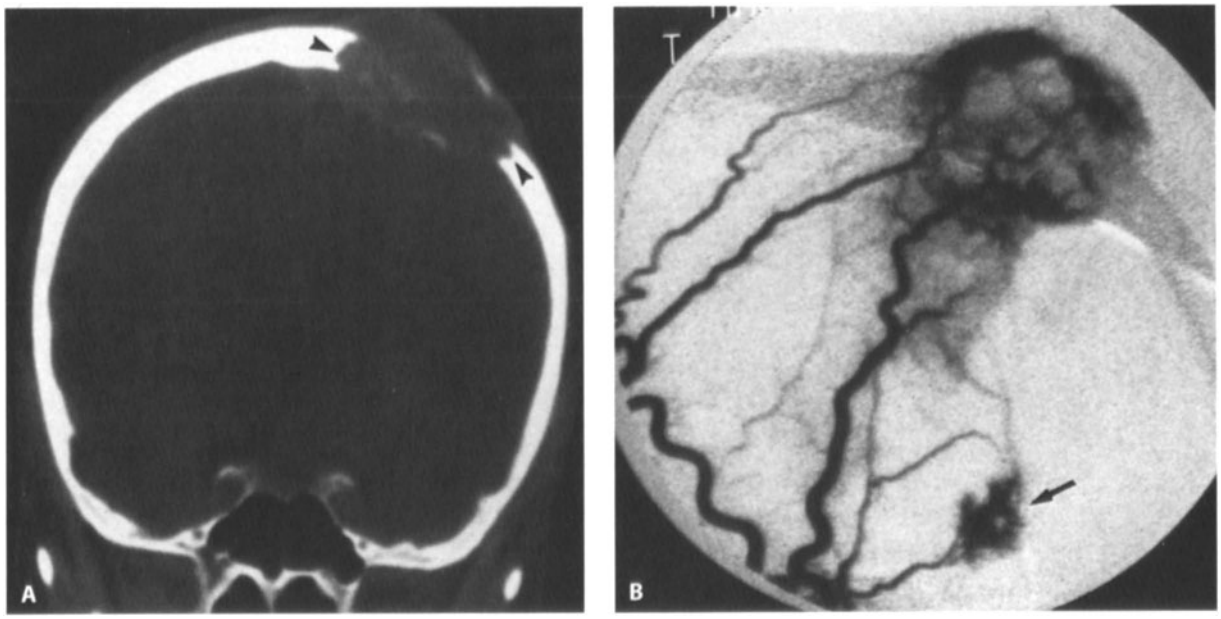

Fig. 2.20A, B. Metastatic hypernephroma. **A** Coronal CT with window level demonstrates the pathological irregular expansion of the diploic space (*arrowheads*) with marked bone destruction and with soft tissue and intracranial extension. This appearance is more characteristic of an aggressive malignant lesion such as metastasis. **B** Coned-down view of a lateral angiogram demonstrates the marked tumor hypervascularity as well as a secondary metastasis (*arrow*). This metastasis was treated by superselective ethanol infusion for palliation with good and lasting relief of pain

nique. Although it is true that ligation of the meningeal arteries as they enter the tumor would permit adequate hemostasis and proper tumor excision, some additional advantages are derived from preoperative microembolization in hypervascular convexity tumors. More recently there has been a general consensus that depending on the location of the tumor and the anticipated arterial supply, embolization is a useful and safe method that enhances the surgical ability to remove such neoplasms (Macpherson 1991; Nelson et al. 1994; Oka et al. 1998; Gruber et al. 2000a).

1. Microemboli can enter the tumor angioarchitecture and devascularize the lesion, irrespective of collateral circulation (Figs. 2.1, 2.8, 2.17, 2.20).
2. Bilateral dural devascularization is easy to accomplish and will obviate the need for exposure of the contralateral side during resection of tumors involving the falx or parasagittal region (Fig. 2.16).
3. Tumor necrosis will occur with a decrease in mass effect, giving more latitude during surgical manipulation (Fig. 2.8) (Tymianski et al. 1994).
4. Even in hypervascular tumors, devascularization will allow the surgeon to amputate the tumor in a dry field and remove it from the inside out with minimal brain retraction.
5. The operative time is shortened.

In tumors involving the base of the skull, preoperative embolization is most effective in blocking the supply from surgically inaccessible feeding arteries. Obvious care must be taken while embolizing skull base lesions,

to avoid dangerous anastomoses and the supply to the transcranial nerves (Fig. 2.11).

During the pretherapeutic evaluation and the planning of the angiographic and therapeutic strategy for a given meningioma, one must consider the tumor extension beyond the intracranial cavity (subtemporal, facial extension, cavernous sinus, etc.), as it will require further angiographic delineation and may be an indication for a more aggressive endovascular treatment. Likewise, meningiomas presenting in patients below the age of 20, if recurrent or if frankly malignant, should probably be treated more aggressively, in view of their poorer prognosis (see Sect. 2.2.1.6).

2.2.6 Technical Aspects of Embolization

Preoperative embolization of meningiomas is an easy procedure, and in our practice it is performed at the same session as the angiographic examination. In most cases, embolization is limited to the external carotid branches supplying the tumor. Midline lesions require bilateral assessment of dural supply (Fig. 2.16).

The goal of the endovascular approach will therefore be the same as in presurgical devascularization for other lesions:

1. To reach the tumor capillary bed (Fig. 2.8)
2. To preserve arteries to the regional normal tissues, thereby facilitating healing in the postoperative period

At angiography, meningiomas demonstrate variable enlargement of the dural arteries with a radial or sunburst pattern of tumor vessels. Although a tumor capillary barrier does exist and no fistulization is present, early filling veins are seen in approximately 40% of cases with superselective injections, usually related to the tumor hypervascularity. The tumor vascularity may vary from one histological type to another, with the highest vascularity seen in the angioblastic type of meningioma, and in the hemangiopericytoma variant (Figs. 2.3, 2.4). For the most part, the angiographic pattern is nonspecific, but can be suggestive of a more or less aggressive lesion based on the degree of vascularity, the irregularity of the tumor vessels, intensity of the blush, and presence or absence of pathological venous lakes (Fig. 2.3). On the other hand, there is some controversy regarding the correlation between tumor vascularity as seen in conventional angiography and that found at surgery. We believe that a lot of this depends on the type of angiography, i.e., global versus superselective studies.

Our technique consists of superselective catheterization of meningeal arteries followed by an angiographic study to look for dangerous anastomoses between the dural arteries of the internal maxillary system and the inferolateral trunk, ophthalmic, and pial arteries. The contribution of the petrosal branch of the middle meningeal artery in the supply to the seventh cranial nerve is an important consideration, especially if liquid emboli are to be used.

In our experience, when particle emboli above 140 μm in size are used, facial nerve palsies may occur but are almost always transient, usually lasting only hours and seldom more than 2 days.

Presurgical embolization of meningiomas, we believe, should be done with the smallest possible particles, which will then enter the tumor bed. Wakhloo et al. (1993) demonstrated that the efficacy of embolization with 50–150-μm size polyvinyl alcohol (PVA) was better than the 150- to 300-μm size, as shown on MRI by improved size reduction and increased tumor necrosis.

If in the preliminary superselective study or during the course of the embolization a large anastomosis in seen, one would change the particle size to one larger than the anastomosis. As discussed in Chap. 14 of this volume, particle embolization and flow control filling of an anastomosis is a function of various factors:

1. Presence or absence of the anastomosis
2. Size of the anastomosis
3. Pressure of injection (Fig. 2.10)

Therefore the main focus of attention should be the catheter tip position (level, wedging) and flow (washout). Even if no anastomosis has been previously documented, if there is no significant washout it is advisable to stop the microparticle embolization, as undetected anastomosis may open. It is also advisable to close the proximal middle meningeal artery with larger particles (or Gelfoam) at the end of the embolization, to reduce bleeding during the operative approach.

We have also used the aid of temporary balloon occlusion of the internal carotid artery to assist in delivering small particles to branches of the internal carotid artery, which were the main supply to a skull base meningioma but were insufficient in size to allow for superselective catheterization with excellent outcome (Tymianski et al. 1994).

When embolizing cutaneous branches of the scalp such as the superficial temporal artery, microparticles are used. In the majority of cases, the catheter tip is at a distance from the target and one should then use preferential flow to carry the particles distally. No attempt should be made to force the emboli, as they may occlude normal scalp vessels and impair postoperative healing. The main trunk is left open, in contrast to middle meningeal artery embolization (Fig. 2.19).

Fig. 2.21A–H. A 39-year-old female patient presented with new onset seizures, and MRI (not shown) demonstrated high convexity left-sided meningioma. Presurgical embolization was preformed and superselective catheterization of the anterior division of middle meningeal demonstrated characteristic tumor blush (**A**). Embolization with liquid embolic material (Onyx) was performed and penetrated the tumor bed with reflux upstream into posterior dural supply (*arrow*) (**B**). Residual dural supply from posterior division of the middle meningeal artery (**C**) was also embolized with Onyx (**D**). Pre-embolization internal carotid angiograms, early (**E**) and late venous phase (**F**) demonstrated slight tumor blush (*arrows*), indicating pial supply to the meningioma. Following embolization of the external carotid supply to the tumor with liquid embolic material, the internal carotid angiogram in lateral view, early (**G**) and late venous phase (**H**) no longer demonstrated evidence of the tumor blush (*arrows*) ▶

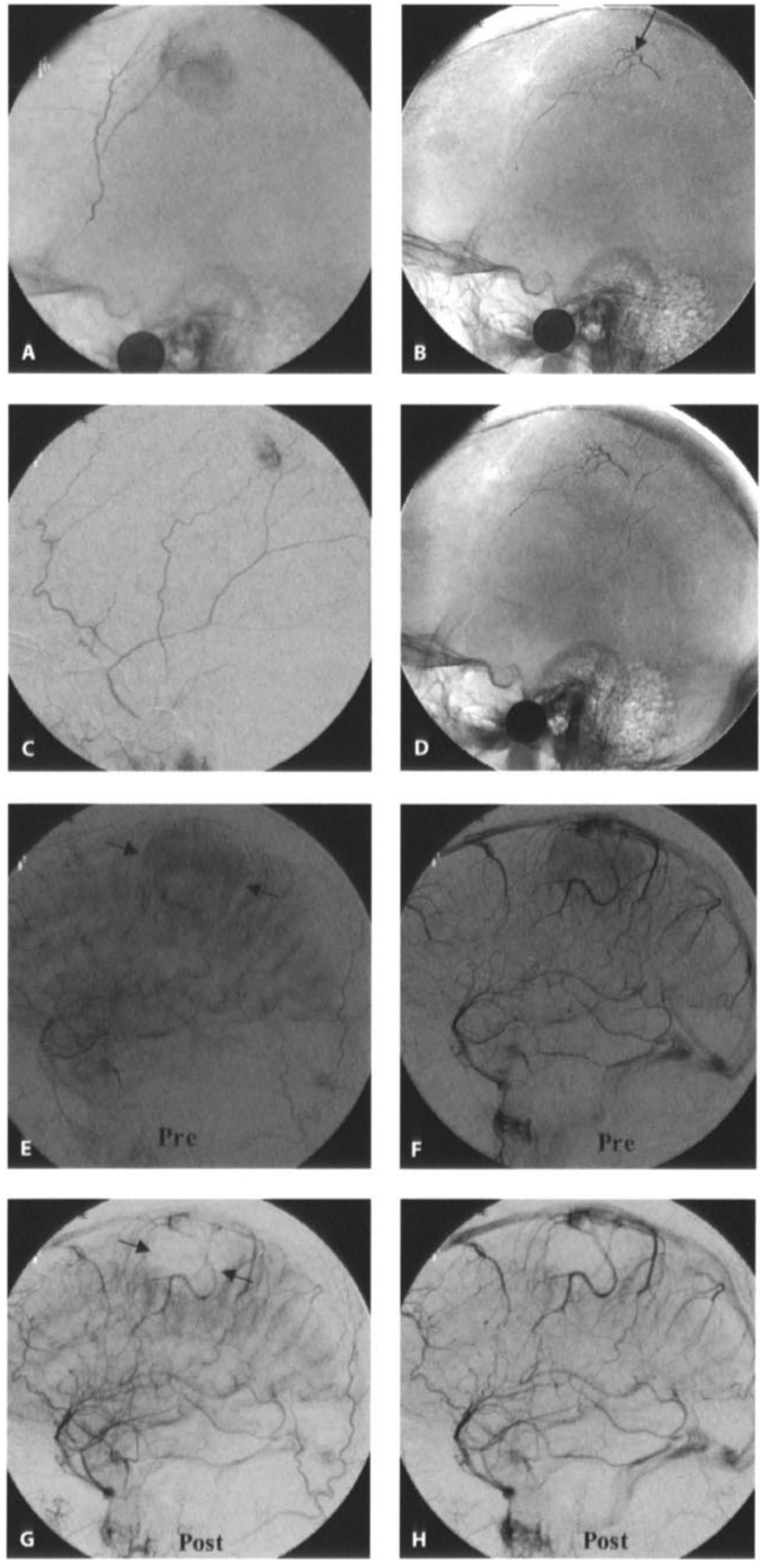

Fig. 2.21A–H.
Legend see p. 190

In the occipital artery, two main points of caution must be considered:

1. Anastomosis with the vertebral artery at the C1 and C2 levels
2. Avoidance of microparticles to normal cutaneous territories

In the ascending pharyngeal territory, one must be careful with the collateral circulation to the vertebral system at the third cervical level or internal carotid artery at its C5 portion, as well as take into consideration the supply to the ninth, tenth, 11th, and 12th cranial nerves.

Factors that limit what can be accomplished in presurgical devascularization relate to the internal carotid (C4–C5), ophthalmic, and/or cerebral arteries supplying these tumors. In general, these arteries are not embolized in benign, de novo lesions and should only be considered in special situations (see Sect. 2.2.2.2).

While we favor the use of small particles as the embolic material of choice for presurgical embolization of meningiomas, the role of newer liquid embolic materials is currently being explored (Fig. 2.21).

2.2.7 Special Considerations in Meningioma Embolization

2.2.7.1 Extracranial Tumor Extension

Extracranial tumors, as discussed previously, usually occur in young patients and have a more aggressive behavior; therefore, if de novo, embolization with 40- to 140-μm particles of either PVA or Gelfoam powder is suggested. The main feeding pedicle is then closed with a strip of Gelfoam. In the case of tumor recurrence, which in our experience is not unusual (Fig. 2.1), or if the histological diagnosis is reported as malignant, we still have an avenue for infusion embolization with ethanol (Fig. 2.2) and/or a chemotherapeutic protocol, which, although experimental, may offer the only alternative after repeated attempted resections and/or radiotherapy have failed (Fig. 2.22).

2.2.7.2 Recurrent Meningiomas

This group of patients may present specific problems:

1. Altered vascular anatomy
2. Pial recruitment of dural or cutaneous vessels, which will supply normal brain and/or tumor
3. More aggressive type of tumor
4. Pure pial blood supply, not accessible to embolization

The most important aspect to be recognized is the participation of dural or scalp vessels in the supply of normal brain, which carries important consequences for subsequent embolization and surgery.

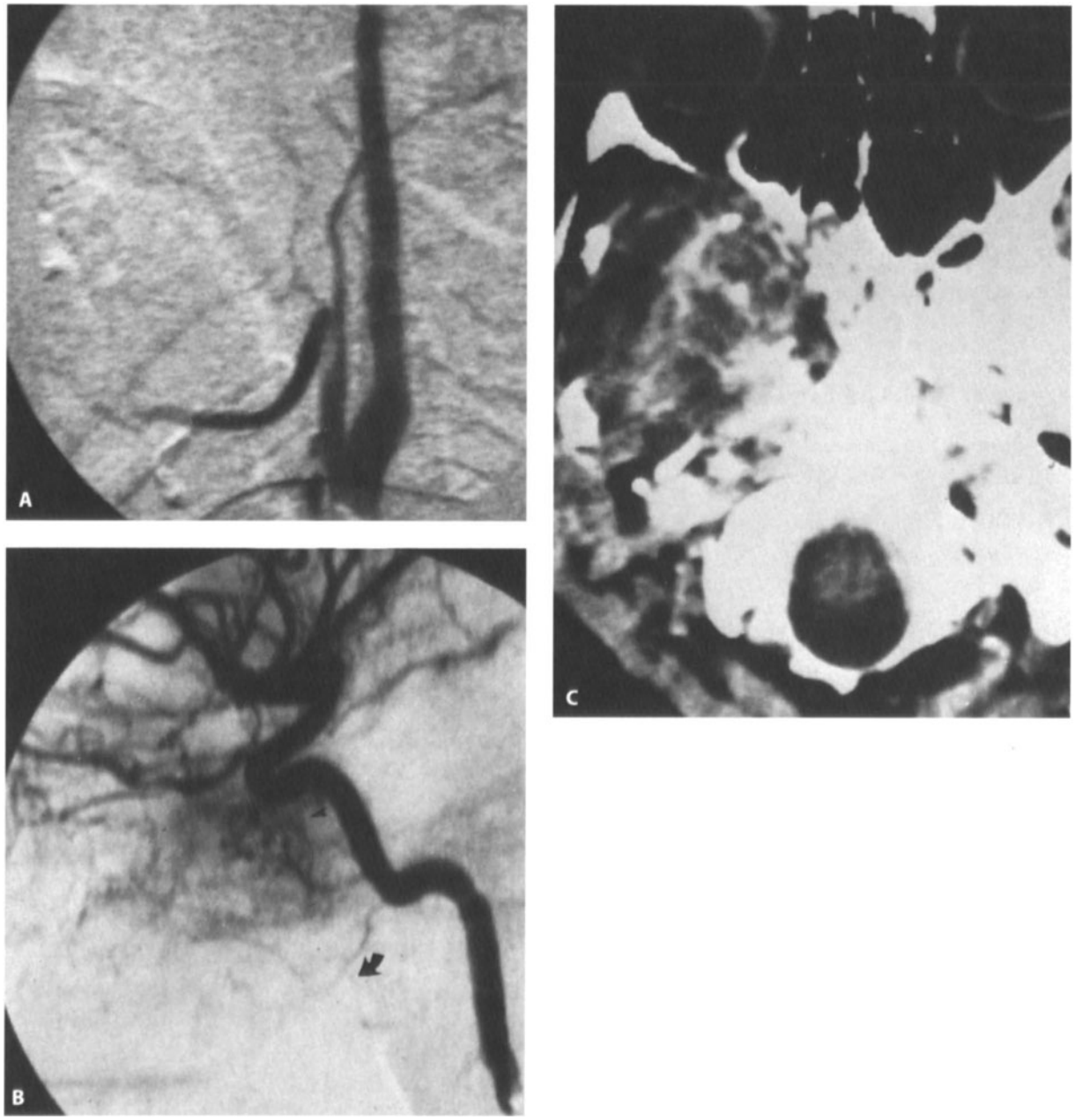

Fig. 2.22A–C. Same patient as Fig. 2.1. Recurrent meningiosarcoma: Chemotherapeutic infusion (cisplatinum, 60 mg/mm^2) superselectively in the internal maxillary artery, ascending palatine and main trunk of the external carotid artery was performed in that order and divided into proportional doses. The superficial temporal and occipital arteries were blocked proximally with a strip of Gelfoam prior to infusion to prevent alopecia. **A** Lateral digital subtraction angiogram (DSA) of the common carotid artery at the time of the second course of treatment, 6 weeks later. The superselectively injected vessels and distal external carotid artery have thrombosed. **B** DSA of the ipsilateral (right) internal carotid artery at the same time as **B**, demonstrates no evidence of tumor reconstitution via the mandibular (*arrow*), or inferior lateral trunk (*arrowhead*) branches, which did supply the tumor previously (not shown). The contralateral (left) sphenopalatine artery was the only minor contributor to the tumor. **C** Axial contrast-enhanced CT scan at this time showed nonhomogeneous enhancement, suggesting tumor necrosis. The only significant enhancement probably represents the supply from opposite (left) sphenopalatine artery. The patient has since received two additional courses of intravenous chemotherapy with complete arrest of tumor growth

Fig. 2.23A–E. A 29-year-old man with a massive recurrent aggressive esthesioneuroblastoma treated with 95% ethanol infusion. **A** Representative contrast CT demonstrates the massive enhancing tumor, which is now compromising the left optic nerve. **B** Lateral angiogram (DSA) of the right internal carotid artery demonstrates a large hypervascular tumor that shows irregular vessels with puddling. The angiographic appearance is more that of a hemangiopericytoma or malignant type of lesion. The main vascular contribution is seen to come from the ophthalmic artery; additional supply also comes from cavernous (*white arrow*) and mandibular branches (*curved black arrow*). Similar supply arose from multiple branches of the internal maxillary and ascending pharyngeal arteries (not shown). **C** Superselective ophthalmic catheterization using a calibrated leak microballoon catheter (*curved arrow*). **D** Immediate postinfusion carotid angiogram. The ophthalmic infusion had to be stopped due to significant slowing in flow, to prevent reflux. There is a substantial decrease in the vascularity as compared with **A**; the cavernous and mandibular supply is grossly unchanged. **E** Significant improvement occurred in the intervening 4 weeks. Lateral DSA 1 month later prior to any new infusion demonstrates a remarkable decrease in the abnormal vascularity and caliber of the ophthalmic artery. Note the significant decrease in the supply in the cavernous portion with a lesser decrease in the mandibular one. These two territories were reached via the maxillary and pharyngeal systems. The patient underwent surgical excision with plastic reconstruction. His visual loss has improved on the left side and he remains stable 18 months later ▶

2.2.7.3 Internal Carotid Supply to Recurrent or Malignant Meningiomas After Radiation Therapy Has Failed

In these aggressive lesions, the surgical neuroradiologist may be the last alternative, and therefore, the goal is different from preoperative devascularization. The need to sacrifice an internal carotid artery (ICA) (Fig. 2.2) and/or an ophthalmic artery (Fig. 2.23) must be considered seriously and an assessment of the circle of Willis is therefore indicated. Once this has been done, a balloon is placed distal to the tumor, to protect the brain circulation either permanently (Fig. 2.2) or temporarily (Jungreis 1991; Tymianski et al. 1994) so as to use microparticles of the smallest size available, 95% ethanol, or chemotherapeutic agents.

2.2.7.4 Pial Supply

Consideration of embolization of pial supply should be reserved for cases where the preliminary study is highly suggestive of the malignant (hemangiopericytic) type of tumor or the hypervascularity of pial origin is such that surgical excision is an obvious hazard with significant morbidity and mortality. Although not always successful, as the pathological vessels are not as hypertrophied as those supplying arteriovenous malformations, it can be of significant assistance to the surgeon and to the patient (Figs. 2.3, 2.24) (Kaji et al. 1999).

2.2.7.5 Pre- and Postembolization Medical Management

It is recommended that patients with intracranial lesions be placed on corticosteroids and anticonvulsant medications.

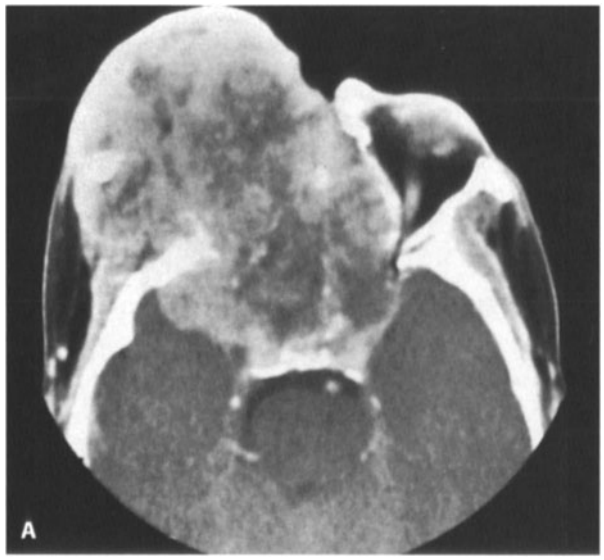

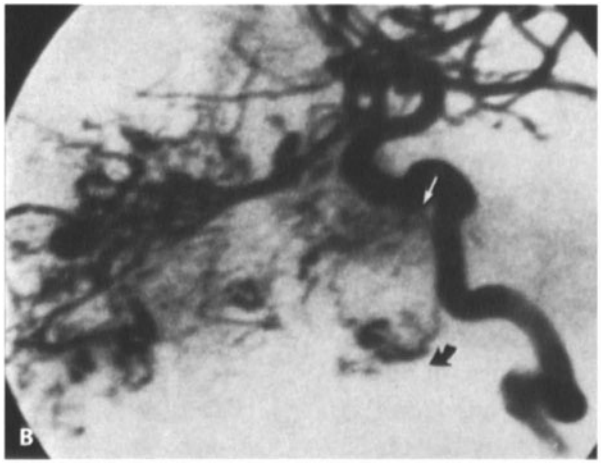

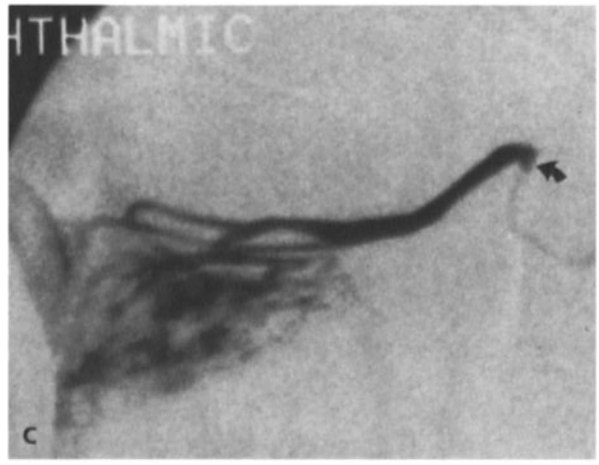

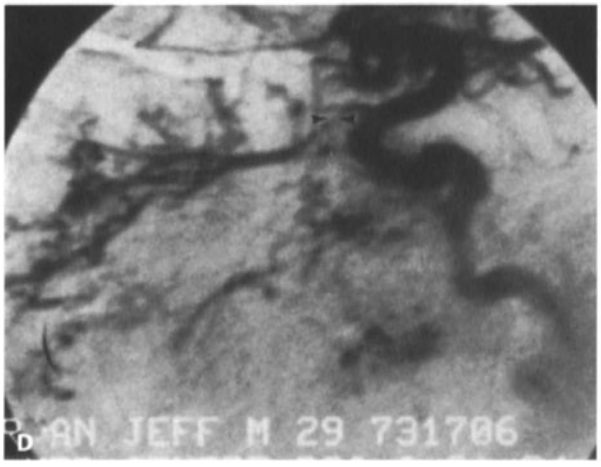

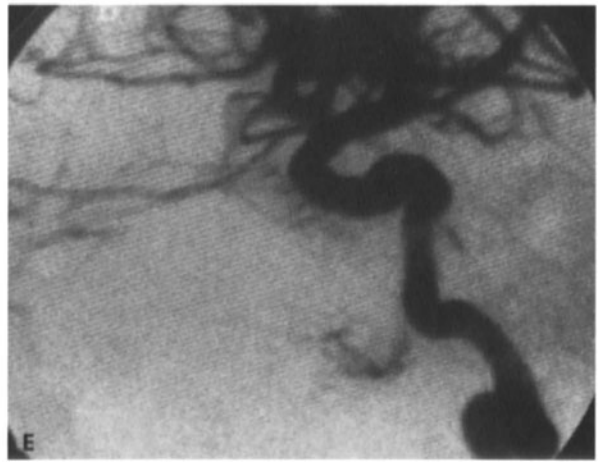

Fig. 2.23A–E. Legend see p. 194

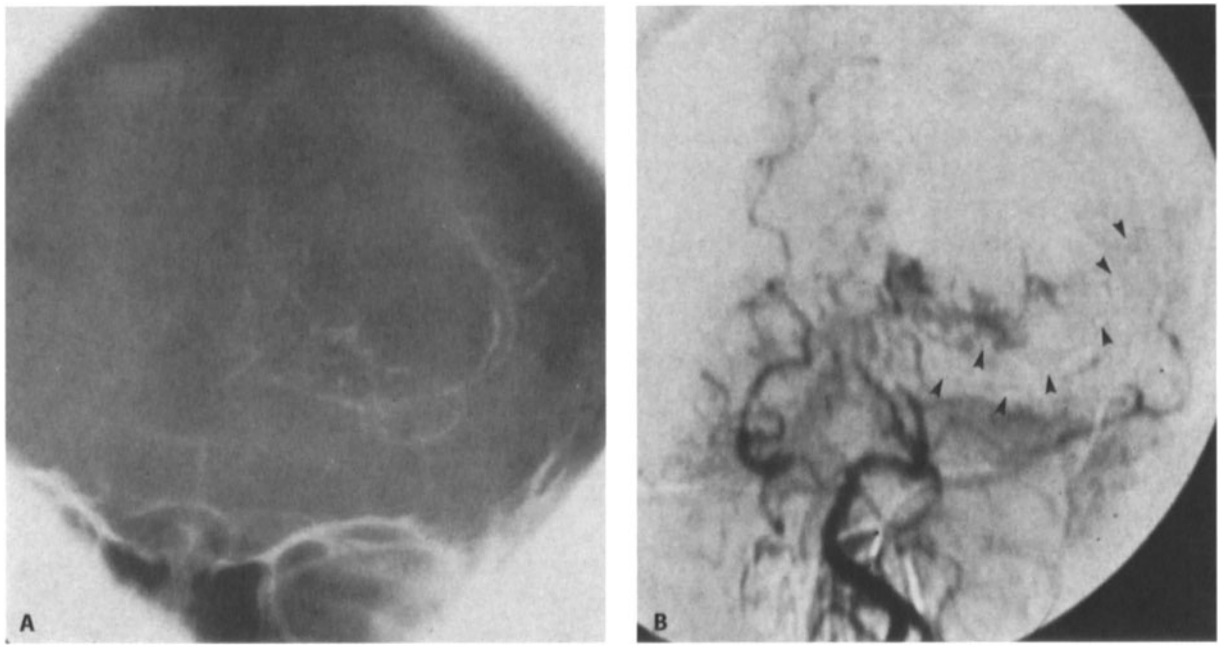

Fig. 2.24A, B. Superselective embolization of pial vessels in a hemangiopericytoma. Same patient as in Fig. 2.3. **A** Frontal view of the radiopaque glue cast obtained after embolization of the two main posterior cerebral feeders to the tumor (compare with Fig. 2.3B). **B** Frontal angiogram of the left vertebral artery after embolization. The *arrowheads* point to the subtracted cast. Note the marked reduction in vascularity (compare to Fig. 2.3B)

2.2.7.6 Time of Operation

It has been our practice to wait at least 24–48 h before proceeding to surgery, as further thrombosis of the embolized territory occurs during this time. CTs done within 12 h after embolization show lucencies within the tumor bed or even a decrease in mass effect (Fig. 2.8). MRI has also proven to be a valuable method to assess the efficacy of embolization, enabling assessment of tumor size and necrosis (Grand et al. 1993; Tymianski et al. 1994). Kai et al. (2002) demonstrated greatest tumor softening occurred 7–9 days after embolization, and after 10 days no further softening occurred. They recommended an optimal time for surgery of 7–9 days after embolization. On the other hand, we believe that waiting more than 10 days may be disadvantageous, as some recanalization and/or collateral circulation may occur.

It is most unusual to have an increase in mass effect and/or aggravation of neurological symptoms from swelling or intratumoral hemorrhage.

2.2.7.7 Complications of Embolization

Many complications reported in the literature are related to poor technique, primarily reflux, or they represent a disregard of the EC–IC anastomoses, and should for the most part be avoidable. In our own experience in more than 500 patients embolized for meningiomas, we have had

Table 2.5. Complications of embolization of meningiomas (Berenstein's experience in 185 patients)

	Permanent	Transitory	Mortality
Cerebral	1 (0.5%)	–	
Ophthalmic	2 (1.08%)	–	
Cranial nerves	–	5 (VII nerve) 2.7%	0
Total	3 (1.6%)	5 (2.7%)	0

two permanent meningeal-to-ophthalmic embolizations with permanent blindness but not stroke, both at the beginning of our experience. One patient experienced right hemiparesis and aphasia 4 h after we occluded the internal carotid artery for a recurrent angioblastic meningioma.

In retrospect, the ipsilateral middle cerebral artery was significantly compromised by the tumor, and a prophylactic EC–IC bypass was probably indicated prior to carotid occlusion. Five transient seventh nerve palsies occurred and lasted less than 48 h in all except one patient in whom it lasted 3 months. This patient was treated with glue (Fig. 2.14), whereas the remaining four were treated with PVA and/or Gelfoam powder (Table 2.5).

More recently, we have seen extravasation of contrast material towards the subarachnoid space occurring in the immediate postembolization follow-up angiogram in one patient (Fig. 2.25). The patient developed immediate focal seizures that progressed to focal status within 10 min, was treated with immediate intubation, intravenously administered barbiturates, corticosteroids, the episode was controlled, and the patient operated on 3 days later without sequelae. Although extravasation is unusual, it can occur in head and neck embolization, primarily with tumors such as paragangliomas. It is generally related to overembolization and is usually of no consequence. In patients with intracranial lesions, extravasation obviously may be more significant (Kallmes et al. 1997).

When performing postembolization angiograms through the embolized vessel, one should take into consideration the degree of flow remaining, especially if the catheter is wedged in the vessel, and diminish the injection pressure accordingly. Follow-up angiograms through the collateral circulation, however, are done with high-volume high-pressure injections.

Trismus is a relatively infrequent and transitory complaint. It is usually seen when normal branches of internal maxillary artery have been occluded and was more prevalent in our early experience; it has been reported by others (Manelfe et al. 1975). With superselective middle meningeal artery catheterization and occlusion of only abnormal arteries, trismus is usually avoided. In 1975, Manelfe et al. also reported two instances of symptomatic middle cerebral arterial embolization: both were felt to be due to reflux of embolic material. Other reported complications stem from technical mistakes of excessive embolization or a lack of attention to extracerebral–intracerebral anastomosis. Current knowledge of the vas-

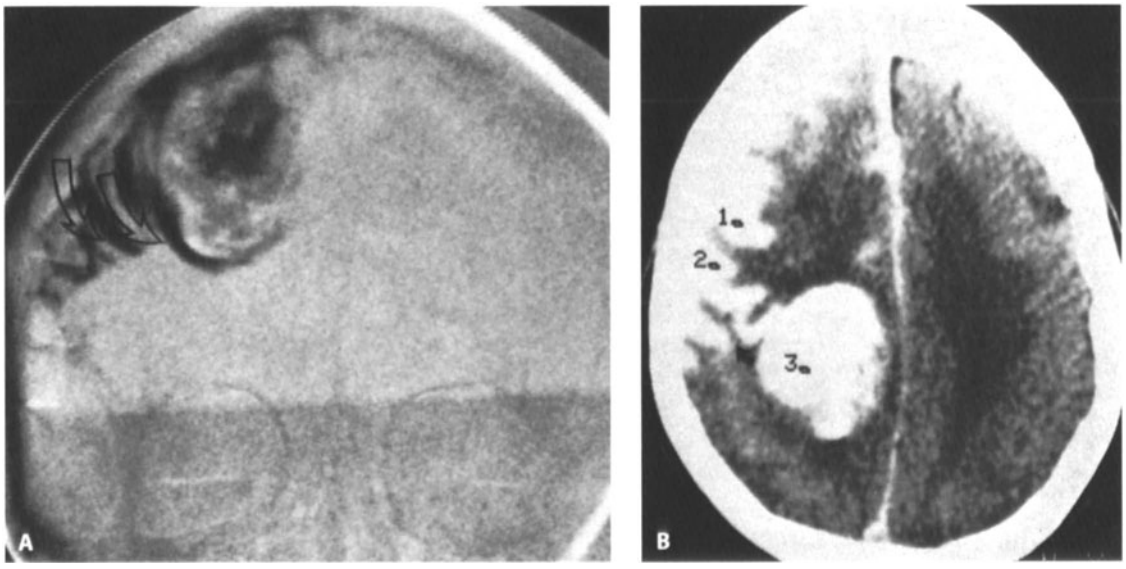

Fig. 2.25A, B. Extravasation of contrast material during follow-up angiography after embolization. **A** Frontal angiogram late phase. Note, the extravasated contrast material following the sulcal pattern (*open curved arrows*). The patient developed immediate focal seizures, which rapidly progressed to focal status epilepticus, despite intravenously administered Diazepam. Immediate intubation and deep barbiturate and intravenously administered Dilantin controlled the seizures. **B** CT confirmed the extravasation but no edema or increased mass effect. On the third day moderate edema was noted and surgical excision was opted for. The tumor was completely avascular and necrotic and was very easily removed without sequelae

cular anatomy and availability of microcatheter technique have resulted in very low risk associated with embolization of meningiomas (Gruber et al. 2000b).

2.3 Other Bony and Dural Tumors

A variety of tumors may arise or invade the bony calvaria or meninges and therefore pick up meningeal supply from the adjacent vessels (Table 2.4).

2.3.1 Cerebral Tumors

Primary cerebral tumors may penetrate the pial barrier and invade the meninges and these may appear to be of dural pial origin. They can produce a desmoplastic reaction of meningeal fibroblasts that may resemble a tumor of the meninges. Invasion of the meninges is probably more related to the proximity of the tumor to the meninges than to histology, as it occurs with a variety of different tumors (Table 2.4). Dural supply of a hemangioblastoma without previous surgery rarely occurs. Hemangioblastomas may, in rare circumstances, also involve the optic nerves (Ginzburg et al. 1992), and, depending on the origin of the ophthalmic artery, supply to these structures may be dural based.

2.3.2 Neurinomas

Neurinomas are extra-axial tumors that are hypervascular in 68% of cases, and they receive meningeal supply in up to 35% of cases, as reported by Moscow and Newman (1975). Theron and Lasjaunias (1976) reported partial or complete supply by meningeal branches of the external carotid artery in each of six patients with acoustic neurinomas, demonstrated by superselective angiography and routine injection of the ascending pharyngeal artery.

The angioarchitecture of these tumors may be indistinguishable from meningiomas or even some intra-axial malignancies. However, some neurinomas have a distinctive vascular pattern that includes the presence of capsular vessels, an inhomogeneous blush characterized by interspersed areas of hypervascularity and nonvascularity with puddling of contrast material and persistence of the blush into the late venous phase. The feeding arteries are usually normal or only moderately enlarged. An early filling vein may occasionally be seen.

The embolization goals and principles are similar in these tumors to those described for meningiomas.

2.3.3 Esthesioneuroblastomas

Esthesioneuroblastomas are rare neurogenic tumors of the olfactory region (Bataskis 1979). They originate from the basal cell layer of the olfactory epithelium in the upper third of the nasal septum (superior and supreme nasal turbinates of the nasal cavity and cribriform plate) as well as the lateral nasal wall. There is a slight male predominance; two-thirds of the patients are between 10 and 34 years of age, but these tumors may be present from the first to the eighth decades of life.

The symptoms are those of any slow growing intranasal neoplasm.

They are locally invasive and will grow into the base of the skull, producing headaches, diplopia, proptosis, signs and symptoms of a frontal, extra-axial mass, or they may grow as a mass in the malar region. The neoplasms that originate from the olfactory mucosa are composed of nerve cells, either neurocytes or neuroblasts. Intracranial extension, as well as systemic metastases, will invariably recur following inadequate local or block excision. Local recurrences occur in nearly 50% of patients; distal metastases have been reported in 20%, most frequently to lymph nodes and lung. Both the tumors and the metastasis are moderately responsive to radiation therapy, with a 52% 5-year survival.

We have studied six such tumors by angiography; five were hypervascular with a very fine small-vessel pattern, a persistent tumor blush, and no early filling veins. One recurrent massive tumor showed some puddling, similar to that seen in hemangiopericytomas (Fig. 2.23). The goals, principles, and precautions of embolization are as described for other tumors. We have treated these recurrent tumors according to our protocol for recurrent and/or malignant meningiomas using ethanol (Figs. 2.2, 2.23) with promising results.

Other tumors that can involve the calvaria and/or the dura with external carotid supply are listed in Table 2.4. For the most part, we are called upon to assist in the management of those in which a biopsy and/or previous intervention has demonstrated a highly vascular lesion.

Our present philosophy in cases of malignant hypervascular tumors is aggressive devascularization, usually with liquid agents such as ethanol and glue or superselective infusion of chemotherapeutic agents (Fig. 2.22). The goal of such embolization is to stop local growth, relieve pain or bleeding, and permit excision if possible, as cure of malignant tumors remains an ongoing challenge.

3 Nasopharyngeal Tumors

3.1 Juvenile Angiofibromas 201
3.1.1 Macroscopic Pathology 201
3.1.2 Microscopic Pathology 204
3.1.3 Epidemiology 205
3.1.4 Pathophysiology 206
3.1.4.1 Juvenile Angiofibromas and Sex Hormones 206
3.1.4.2 Physiology and the Nasal Mucosa 206
3.1.4.3 Hormones and the Vascular System 207
3.1.4.4 Global Hypothesis for the Development of Juvenile Angiofibromas 207
3.1.5 Clinical Findings 210
3.1.6 Natural History 211
3.1.7 Pretherapeutic Evaluation 211
3.1.7.1 Computed Tomography 211
3.1.7.2 Magnetic Resonance Imaging 211
3.1.7.3 Angiography 211
3.1.8 Therapeutic Goals 214
3.1.8.1 Radiation Therapy 221
3.1.9 Technical Aspects of Embolization 221
3.1.10 Tumor Recurrence 223
3.2 Other Nasopharyngeal Tumors 224
3.3 Conclusion 226

3.1 Juvenile Angiofibromas

Juvenile angiofibromas (JAFs) are benign vascular tumors that usually develop in the nasopharynx in young males around the time of puberty.

3.1.1 Macroscopic Pathology

The juvenile angiofibroma is a benign nonencapsulated fibrovascular mass lesion. It usually originates from the superolateral aspect of the choana, but may also arise more medially, near the vomer, from the pharyngeal roof where it involves the body of the sphenoid bone, or from the adjacent pterygoid plates. The tumor has a base that is attached to these osseous structures, but it does not invade the bone tissue itself. It extends submucosally into the adjacent open spaces and passages and for that reason often has a lobulated shape. Typically, the JAF is reddish-gray or red-purple and has a firm rubbery consistency. Patterns of extension are illustrated in Figs. 3.1 and 3.2 and correspond to the local invasion of the tumor.

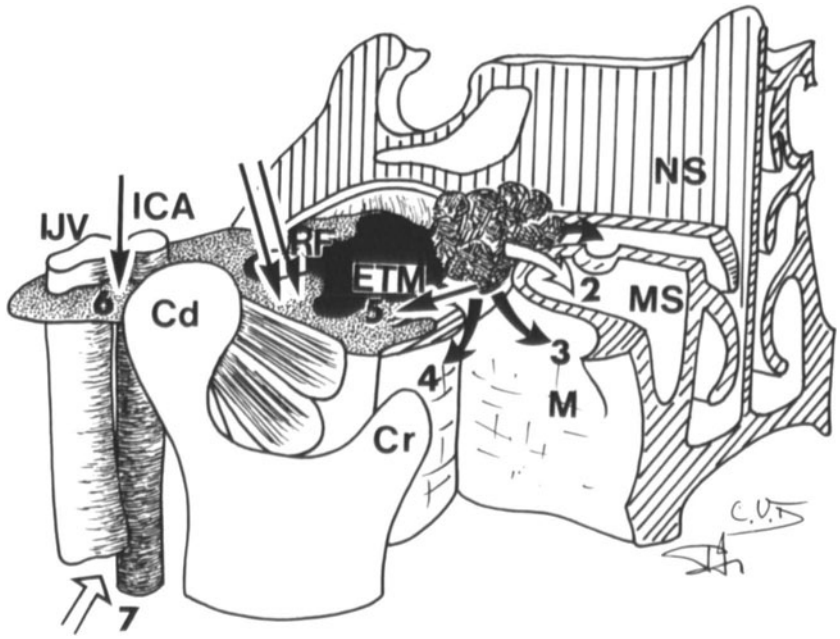

Fig. 3.1. Nasopharyngeal tumor: patterns of invasive extracranial extension. *1*, Nasal; *2*, sinusal (maxillary); *3*, maxillomalar and facial below the inferior orbital fissure; *4*, infratemporal; *5*, pharyngeal and parapharyngeal (*double arrow*); *6*, retropharyngeal below skull base (*arrow*); *7*, carotid. *ETM*, eustachian tube meatus; *RF*, Rosenmüller fossa; *Cr*, coronoid process; *Cd*, condyle process; *NS*, nasal septum; *M*, maxillary bone; *MS*, maxillary sinus

Table 3.1. Patterns of extension of juvenile angiofibromas (JAF)

JAF extension	Waldman 1981 10 Cases	Wilson 1969 16 Cases	Hollman 1965 (Not mentioned)
Nasal fossa	100%	100%	100%
Sphenoid sinus	70%	61%	68%
Pterygopalatine and infratemporal areas	70%	89%	93%
Ethmoidal cells	40%	35%	25%
Maxillary sinus	30%	43%	62%
Intracranial	0%	0%	37%

The most frequent extensions are listed in Table 3.1. Considering all the bony landmarks and barriers in the deep maxillofacial region and adjacent skull base, it is of interest to note that JAFs do not usually invade the bony structure, but successively displace, thin, erode, and finally destroy them. These characteristics are seen best on computed tomography (CT) axial or coronal images with bone windows at the level of the nasal septum and pterygoid plates (Fig. 3.4).

Usually, the lesions extend in continuity; multifocal tumors have never been reported. Intracranial extension is infrequent (Table 3.1) and is usually encountered in older patients. Tumors with intracranial extension are generally the most advanced, either large at the time of diagnosis or recurrent. Intracranial invasion is usually extradural, involving the parasellar (extra- or intracavernous) or the intrasellar area. Subarachnoid spread may occur, but is seen only with recurrence. Likewise intraorbital

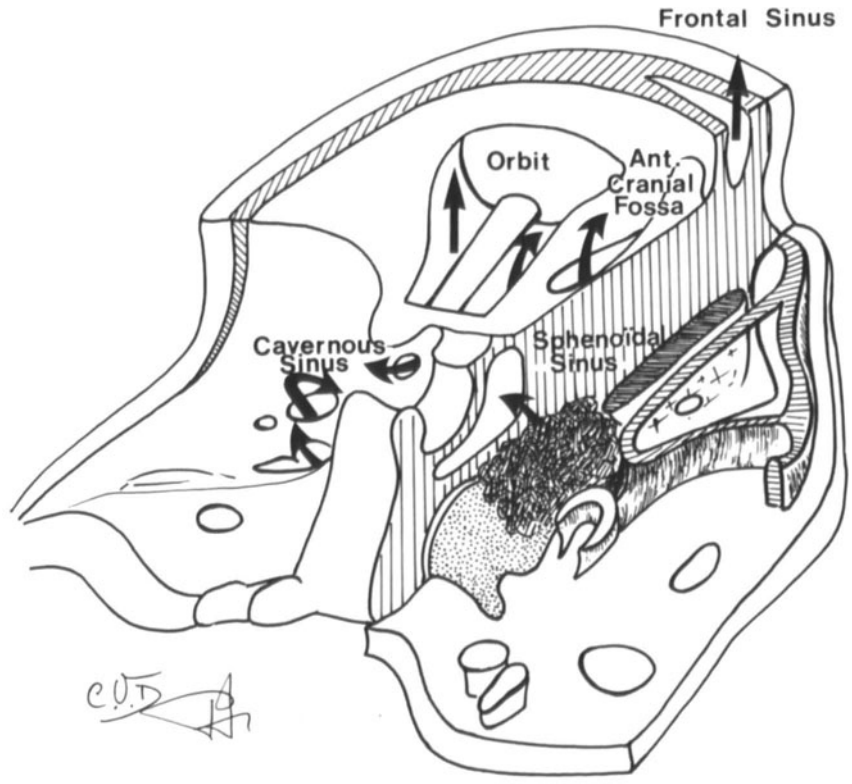

Fig. 3.2. Nasopharyngeal tumor, pattern of invasion: intracranial and orbital extensions

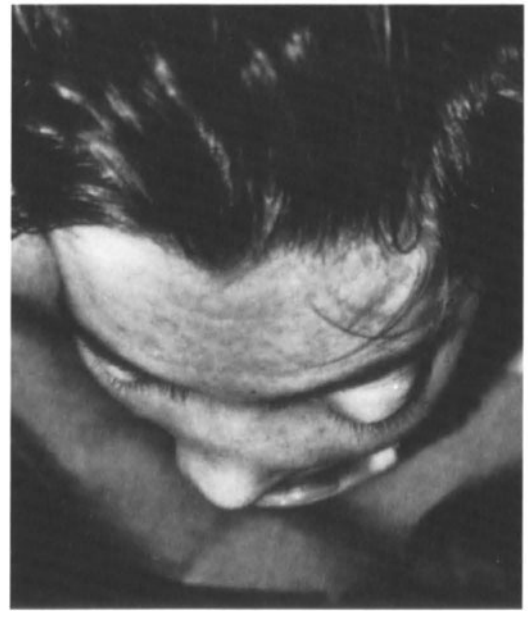

Fig. 3.3. A 16-year-old male patient with a recurrent juvenile angiofibroma following surgery without prior embolization. Note the left exophthalmos and mass effect at the left nasal fold

invasion most often remains extracapsular and extraconal for a long time (Figs. 3.1–3.3).

Paranasal sinus invasion occurs frequently but must be differentiated from serous or purulent sinusitis related to occlusion of the sinus ostia by tumor in the ipsilateral nasal fossa.

Although the tumor initially arises from one of the areas mentioned above, with a topographically predictable vascular pedicle, it recruits additional blood supply as it extends locally. The recruitment of new vascular supply is probably related to production of an angiogenic factor (Brem 1976); similar activity has been noted with other tumors and has been studied at angiography. It is thought to express the local invasiveness of some types of juvenile angiofibroma (Schiff 1959).

3.1.2 Microscopic Pathology

The lesion is nonencapsulated and consists of fibrovascular stroma. The fibrous cells correspond to a type of fibroblast (myofibroblast) that produces collagen and elastin fibers and can transform into a smooth muscle cell; it can therefore be impossible to differentiate the stromal fibroblasts from the cells of a vascular wall. The proportion and type of fibrous tissue is variable and is probably not related to the age of the patient. It may range from an almost myxomatous fibromatosis to an erectile-like tissue (Batsakis 1979). The vascular components, although also variable, are typically of two different types:

1. Thin-walled vascular spaces, which form endothelialized cavities without muscular layers in their walls.
2. A true arteriocapillary tree with normal muscular layers and some subintimal cushions in the vessel walls. Electron microscopy has not yet completely classified the function of the stroma. However, it has confirmed the origin of the smooth-muscle cells of the vascular walls to be from the fibroblasts of the stroma.

Various authors have tried to show a correlation between the spectrum of histopathological findings and the variable clinical presentations. For example, the highly vascular tumors theoretically are more invasive and present with hemorrhage, while those that are clinically silent are more likely to have a high proportion of fibrous tissue (Batsakis 1979).

Osborn and Friedman in 1959 and 1976, respectively, suggested that repeated hemorrhages within the tumor could stimulate the formation of granulation tissue and a fibrous reaction. This would account for some cases of so-called spontaneous regression and provide a rationale for tumors seen after adolescence, which tend to have a slower rate of growth, a higher proportion of fibrous tissue, and less tendency to bleed (Maurice and Milad 1981). The relationship between these evolutive forms and the sex hormones will be discussed with physiopathology. Complete spontaneous regression of these tumors should not be expected and treatment should not be delayed.

JAFs do not have malignant potential, but can manifest highly aggressive behavior. Several authors have reported cases of sarcomatous transformation, most of them following radiation therapy. In 1969, Hormia described regional lymph node invasion. We agree with Batsakis's statement that "this complication of angiofibroma must be considered negligible." The full potential of a given lesion is difficult to assess using histochemical methods. At the base of the skull, JAFs have local invasive potential,

similar to paragangliomas and most meningiomas. In 1973, Girgis and Rahny suggested that JAFs might arise from nonchromaffin paraganglionic cells located at the level of the distal internal maxillary artery. In our series, in 1980, we reported a 16-year-old male patient with a very aggressive JAF and a permanent decrease in the urinary levels of 17 ketosteroids and 17 hydroxysteroids, without modification of the secondary sexual characteristics. While the behavior of the lesion may have been related to the abnormal sex hormone levels in this unusual case, it is, in general, impossible to confirm such a relationship. For the time being, there is still no biological test or definitive angiographic pattern that allows us to predict the real aggressiveness of a given tumor.

3.1.3 Epidemiology

The term "juvenile angiofibroma" has been applied because the tumor typically develops in young males at puberty. In our series, the age ranged from 8 to 23 years, with a peak at 14–17 years, identical to the figures reported by Neel et al. (1973) and Batsakis (1979).

However, the term "juvenile" is not always appropriate, as up to 20% of the tumors are diagnosed after the age of 20 (Fu and Perzin 1974). JAFs have been reported in 49- and 52-year-old men (Goncalves and Briant 1978; Hiranandani et al. 1967, respectively). In every reported series, almost all patients are male, but JAFs occurring in females have been described (Osborn and Sokolovski 1965; Fitzpatrick and Rider 1973; Lasjaunias et al. 1980; Ewing and Shively 1981). In fact, Albrecht (1959), who accumulated 452 published cases from the literature, reported that 6% of JAFs occurred in females. Although some of these patients may have had angiomatous polyps, most appear to have had true angiofibromas. Apostol and Frazel (1965) have recommended chromosome analysis in all females in whom JAF is diagnosed.

Hora and Brown (1962) found that JAFs represented 0.5% of the head and neck tumors diagnosed in 6,000 admissions before 1962. Out of 256 nonepithelial tumors of the nasal and paranasal cavities, Fu, in 1974, diagnosed 38 (15%) JAFs. We found no obvious geographic predominance in our series, although Batsakis mentioned a higher incidence in Egypt, India, Southeast Asia, and Kenya as compared to the United States and Europe. Tapia Acuna (1965), in Mexico, who saw 279 cases in 22 years and diagnosed 15 new cases in the first 3 months of 1970, suggested the presence of an unidentified epidemiological factor. Angiofibromas remote from the nasopharynx seem to occur in a slightly older age group with a higher percentage of females. Most of the tumors occurring late or in females are thought to be more fibrous, leading to the diagnosis of either silent evolutive forms or angiomatous polyps. This differentiation does not in general seem to interfere with the practical management of these lesions but they should be considered as separate entities (Ali and Jones 1982).

3.1.4 Pathophysiology

Certain unusual characteristics of JAFs have stimulated a great deal of discussion in the literature. Several aspects must be considered:

- The relationship between JAF and sex hormones
- The physiology of the nasal fossa mucosa with regard to sex hormone levels
- The effect of sex hormones on the vascular system
- A global hypothesis for the development of this tumor

3.1.4.1 Juvenile Angiofibromas and Sex Hormones

Johns et al. (1980) discussed the relationship between the behavior of tumor and sex hormones. Their results can be summarized as follows:

1. Reduction in size is observed after exogenous estrogen therapy (diethylstilbestrol 15 mg per day for 1 month).
2. Increase in size occurs following testosterone treatment.
3. The results of biological testing of the pituitary–gonadal axis are normal.

Specific receptors for testosterone, but not for estrogen, have been demonstrated (Johns et al. 1980). Following diethylstilbestrol therapy, histological examination has shown partial thrombosis of the vessels as well as significant wall thickening due to an increase in the quantity of elastic and collagen fibers (Batsakis 1979). No changes seem to occur at the level of the endothelial cells, which are known to possess specific estrogen receptors. Walike and Mackay (1970) also reported the stimulation of fibrosis, leading to regression of the angiofibroma after diethylstilbestrol treatment. Finally, it should be noted that JAFs treated with exogenous hormones react in the same way as cultures of healthy tissue. Therefore, the tumor vessels could be considered to have a normal hormonal response.

3.1.4.2 Physiology and the Nasal Mucosa

The effects of sex hormone levels or cycles on the nasal mucosa are well known (Melon 1974; Toppazada et al. 1981, 1982). There are interesting similarities in the histological appearances of the nasal mucosa, the genital erectile tissue, and vascular spaces of the JAF. However, most of the data concerning hormonal changes in the nasal fossa have been obtained from pregnant and nonpregnant females (Toppazada et al. 1981, 1982), and little work has been devoted to the nasal mucosal responses in males.

It is felt that when nose bleeds precede menses, they are not related to estrogen levels (which are low during that period), but rather to a substance called menotoxin, which is released as the estrogen level decreases. This substance shares many properties with prostaglandins of the E group, especially the inhibition of fibrinogen formation, which contributes to menstrual bleeding.

Table 3.2. Effects of sex hormones on the normal vascular wall (from Cox 1978; Drouet 1980; Schiff 1959; Johns et al. 1980; Lasjaunias 1980)

Endrogenous estrogens	Δ	Androgens
↓		↓
Endothelial cells effects	Protein synthesis	No endothelial cell
↓		↓
Catabolism of fibers (compliance)		Anabolism of fibers (rigidity)
↓		↓
Reduction of smooth muscle Cells (thinner)		Increase of smooth muscle Cells (thicker)

3.1.4.3 Hormones and the Vascular System

The action of hormones on the vascular system is complex and sometimes nonspecific. The following information is taken from the Cox and Fisher's (1978) and Drouet's (1980) research (Table 3.2).

Endogenous estrogens act in a specific manner at the endothelial cell level via specific receptors. They stimulate the synthesis of protein, particularly of prostaglandin (PG_{12}), an inhibitor of platelet aggregation. Their action on the smooth-muscle cells is nonspecific and affects their multiplication; estrogens reduce the number of smooth muscle cells in the wall and thus its thickness. Their action on collagen results in a reduction of fiber in the arterial wall, which in turn results in a more compliant and elastic wall.

Androgens and testosterone appear to have opposite effects compared to those of endogenous estrogens, particularly on collagen synthesis: testosterone increases the number of collagen fibers in the vascular wall. Exogenous estrogens and progesterone also have effects opposite those of endogenous estrogens: they increase the fiber content of the arterial wall but in addition increase the number of smooth-muscle cells, producing a hypertrophic pattern. Finally, they act at the level of the endothelial cells to increase their number and reduce synthesis of proteins, particularly the prostacyclins.

3.1.4.4 Global Hypothesis for the Development of Juvenile Angiofibromas

In 1948, Martin stated that development of JAFs could be related to a deficiency in androgens with an overactivity of estrogens. Schiff (1959) proposed that the tumor growth was related to the vascular component while the connective tissue content corresponded to the activity of the sex-hormone-sensitive tissue, following a disturbance of pituitary activity (Table 3.3). In fact, most apparently contradictory explanations are not

Table 3.3. Pathophysiological hypothesis for juvenile angiofibroma (JAF) development

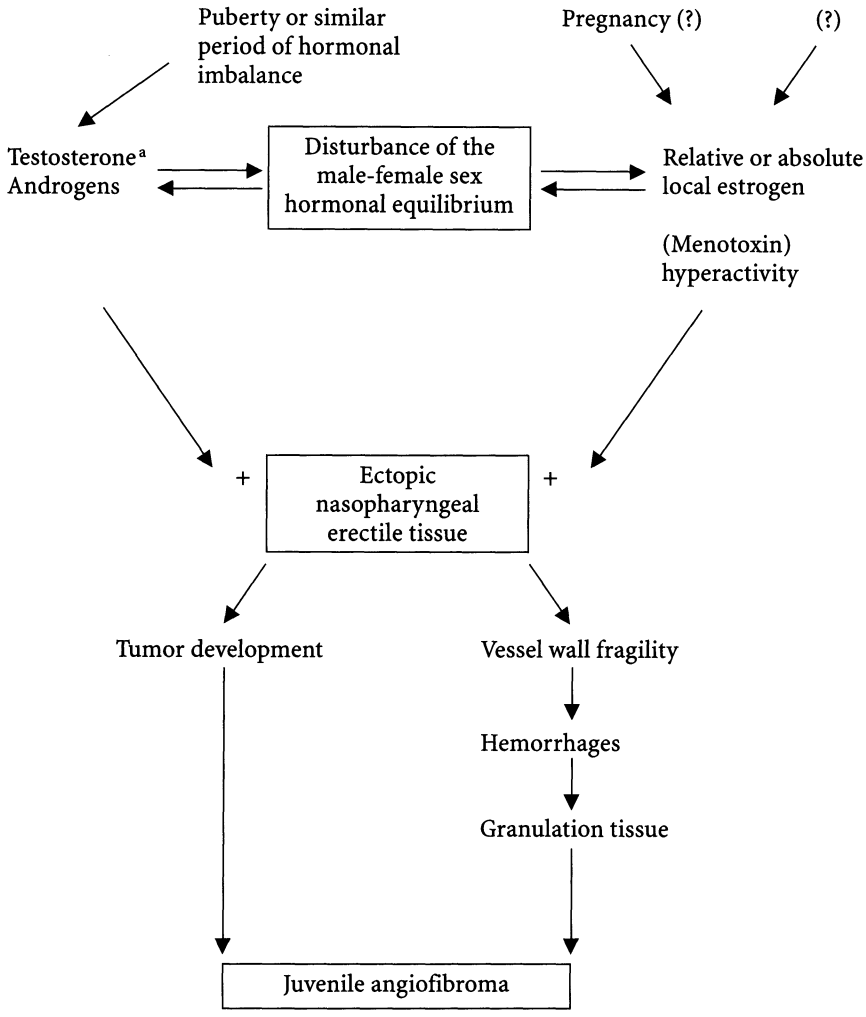

[a] Systemic hormone levels may be inferior to usual normal values, but local levels may be high to produce adverse effect (i.e., proximity of the venous system of the pituitary gland to the nasopharynx?).

mutually exclusive, since they focus either on the vascular aspect of the lesion or on its fibrous component. Johns et al. (1980) introduced the notion of target cells, located in the nasopharynx and dormant before puberty. These testosterone-sensitive cells would become activated with the maturation of the pituitary–gonadal axis at puberty. In 1981, based on pathological studies of JAF tumors and penile cavernous tissue, Maurice found enough similarities to support the concept that ectopic genital erectile tissue in the choanal region indicated the same target cells. He postulated that the muscularized vascular channels were the remnant of the original erectile tissue, which gave rise to the tumor, while the thin-walled nonvascularized spaces resulted from the formation of granulation tissue around hemorrhages. Therefore, one can suggest that simultaneously, testosterone stimulation and estrogenic hypersensitivity (direct or via

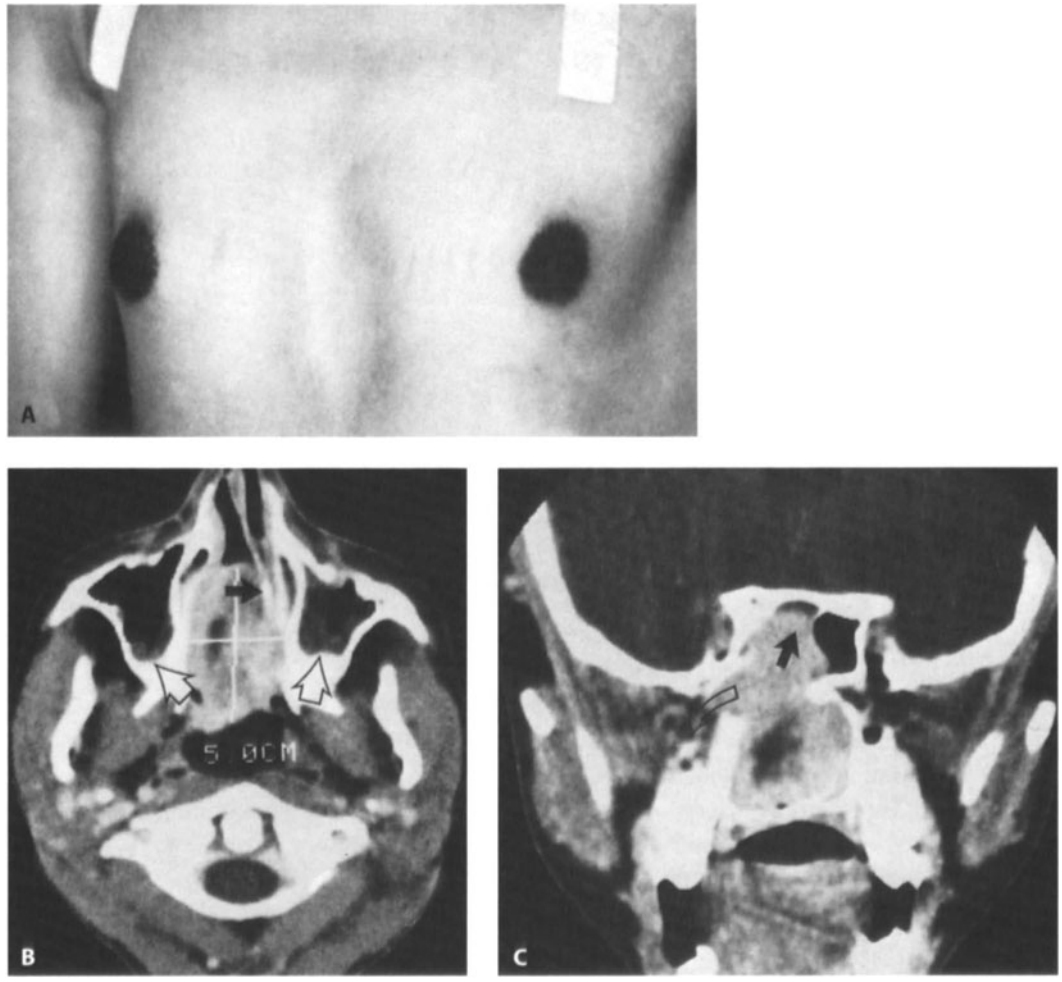

Fig. 3.4. A 14-year-old boy presented with bilateral nasal obstruction with gynecomastia (**A**) and epistaxis for 4 months. CT axial (**B**) and coronal (**C**) images demonstrate a typical enhancing right nasopharyngeal mass, extending into the sphenoid sinus (*solid arrow*) and the soft palate, displacing the septum towards the opposite side. The pterygopalatine fossa is free of tumor (*open curved arrow*) and no intracranial extension is seen. Note the nonneoplastic reaction in both maxillary sinuses (*open arrows*). The arterial supply arose exclusively from the external carotid system (not shown)

menotoxin) could stimulate this erectile genital nasopharyngeal tissue and, following estrogen-induced bleeding, transformed its original pure erectile aspect into a combination of erectile and granulation fibrous tissue. It is impossible to know whether this dual hyperactivity is simultaneous or whether a primary phenomenon induces the other. However, it seems to provide a satisfactory explanation for most of the hormonal effects observed, provided we recall that exogenous estrogens have vascular effects antagonistic to endogenous estrogens. In practice, most of the cases reported have not been studied in enough detail to support this pathophysiological hypothesis. Kumagami (1993) showed that in all five cases of JAF, progesterone and estradiol levels were positive, and in three out of five cases, dihydrotestosterone was positive.

Three of our cases were also peculiar and emphasize the dual hormonal background in which some cases of JAF are diagnosed:

1. In one woman, JAF was discovered during the last trimester of her second pregnancy.
2. A young man had exceptionally aggressive JAF, with a permanent decrease in the urinary levels of 17-keto and 17-hydroxysteroids.
3. A young man presented with typical JAF and gynecomastia (Fig. 3.4).

3.1.5 Clinical Findings

The symptomatology of a JAF is related to its size and direction of extension. The most typical presenting symptoms are nasal obstruction and epistaxis.

Nasal obstruction is usually the first symptom to appear and frequently produces serous sinusitis by obstruction of the ostia of the ethmoidal, sphenoidal, and maxillary sinuses and less frequently will produce otitis by obstruction of the eustachian tube meatus. Infection then leads to intermittent purulent rhinorrhea and/or otorrhea and systemic manifestations of infection. Decreased hearing may result from long-standing otitis (serous or purulent) and is usually preceded by ipsilateral tinnitus. Further superior extension produces anosmia, usually associated with bilateral nasal obstruction and a nasal voice.

Recurrent hemorrhage is a constant symptom of JAF. Moderate spontaneous epistaxis may even occur at night and can lead to anemia.

Life-threatening massive hemorrhage can occur and is often incompletely controlled with nasal packing; it requires rapid diagnosis of the cause of the hemorrhage in addition to compensation for blood loss. Emergency ligation of the distal internal maxillary artery or other branches of the external carotid artery should be avoided as this compromises the definitive treatment of the tumor. Facial (Fig. 3.3) swelling, proptosis, and extraoculomotor nerve palsy usually indicate infratemporal, temporal, orbital, or cavernous extension of the tumor (Figs. 3.1, 3.2). However, these extensions may also exist without obvious clinical manifestations. On the other hand, overestimation of the subclinical extension of the tumor may incorrectly suggest that the lesion is nonresectable. Therefore, the topography of the tumor extent must be accurately analyzed with various imaging methods.

The clinical examination of the cavum usually reveals a reddish or grayish tumor bulging into the nasopharynx, sometimes inferiorly or even displacing the soft palate. The tumor may bleed on contact; there is usually no ulceration and the surrounding areas do not show any evidence of malignancy (biopsy should be avoided, as the clinical history and the appearance of the tumor should be sufficient to make the clinical diagnosis).

Further detailed examination should be directed to detecting sex hormone deficits and signs of secondary sex organ development (Fig. 3.4).

In practice, the diagnosis of JAF is usually simple, even though it is a rare tumor.

3.1.6 Natural History

The natural history of these tumors is controversial, as already discussed, and spontaneous stabilization of the lesion cannot be expected given that JAFs observed in older patients are rare and less aggressive. In our experience, a significant regression from an aggressive to a stable form has not been demonstrated. On the contrary, spontaneous extension into the adjacent areas is to be expected. Treatment should not be delayed since true subclinical intracranial extension may occur during the period of observation, transforming what was easily curable JAF into an inoperable case. The possibility of malignant degeneration has been discussed, but it should be remembered that most cases reported in the literature were secondary to radiation therapy.

3.1.7 Pretherapeutic Evaluation

3.1.7.1 Computed Tomography

CT examination should be performed with proper soft tissue and bone windows, before and after contrast administration, in axial and coronal planes. Direct coronal imaging following contrast enhancement provides the best anatomical information, especially regarding bone and soft tissue involvement at the level of the skull base. Plain skull radiographs do not provide further useful information, although if they are obtained early in the evaluation of the patient they may help to distinguish between a benign category of tumor including JAF, which typically thins and displaces bony structures such as the pterygoid plates, and malignant tumors, common in children, such as rhabdomyosarcoma, which typically destroy adjacent bone.

3.1.7.2 Magnetic Resonance Imaging

Magnetic resonance imaging (MRI) is particularly important in the evaluation of intracranial and transdural extension of the tumor. This is best accomplished by assessment of the coronal and sagittal planes following intravenous contrast enhancement (Fig. 3.5). MRI is also the method of choice to distinguish tumor extension into the sinuses from sinusitis. Contrast enhancement and tissue signal characteristics will be different on MRI and an accurate diagnosis can be made using this technique.

3.1.7.3 Angiography

True Intracranial Extension

At angiography, intracranial extension corresponds to a blush projecting above the base of the skull on AP and/or lateral views. This blush is seen during internal carotid, ascending pharyngeal, or proximal internal max-

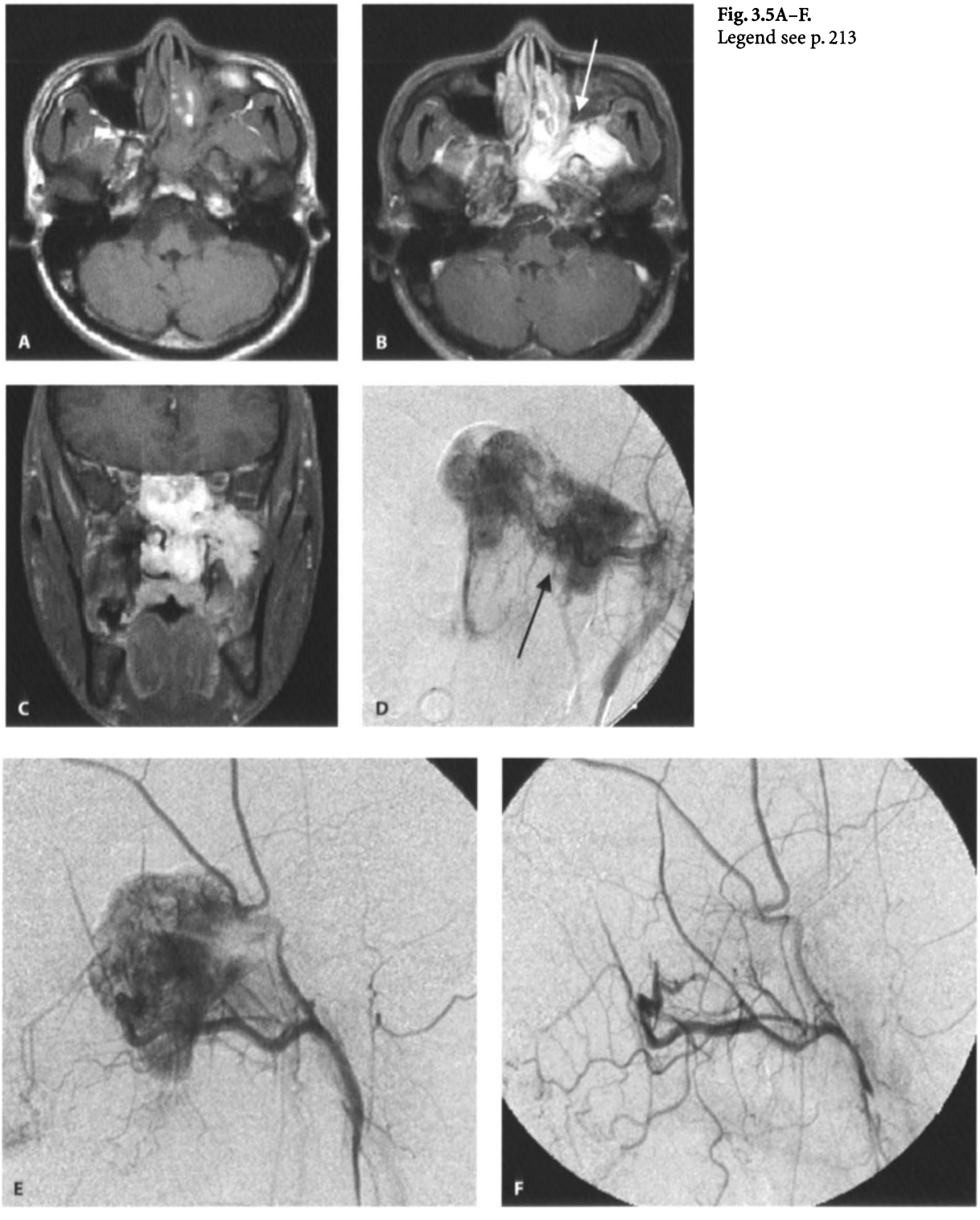

Fig. 3.5A–F.
Legend see p. 213

◀ **Fig. 3.5A–F.** A 20-year-old man presented with a 3-month history of stuffy nose. MRI T1-weighted axial views without (**A**) and after contrast enhancement (**B**) showed evidence of soft tissue mass arising from the posterior aspect of nasopharynx on the left side with extension towards the pterygopalatine fossa and deep temporal fossa (*arrow*, **B**). Coronal MRI, T1-weighted, showed the enhancement to be contained within the sphenoid sinus without evidence of dural or transdural extension (**C**). The extension towards the deep temporal fossa corresponds to the tumor blush at distal external carotid angiogram in AP view (*arrow*, **D**). The distal external carotid angiogram in lateral view before (**E**) and after embolization (**F**) shows devascularization of the tumor following particle embolization (150–250 μm) and facilitated subsequent total surgical removal with less then 200-cc blood loss

illary artery injections. A frontal view, in transorbital projection, makes it possible to differentiate between, intrasellar, intracavernous and extracavernous extension. Subarachnoid extension typically recruits arterial supply from cerebral arteries and therefore is easily diagnosed. The late phase of the internal carotid angiogram will demonstrate the patency of the cavernous venous plexus and completes the study of the parasellar area.

False Intracranial Extension

Recognizing false intracranial extension is extremely important so that potentially curative surgery is not incorrectly rejected. The erroneous diagnosis of intracranial tumor extension is usually based on the visualization of a blush during internal carotid angiography. Careful examination of the films reveals that this blush projects outside of the cranial cavity. It is produced by tumor supply from extradural internal carotid artery branches (intrapetrous or intracavernous) that leave the cranial cavity via their respective foramina and supply the tumor, which is adjacent to the skull base but is extracranial. The cavernous sinus venous plexus is normal in these cases, if the cerebral venous anatomical disposition permits its visualization on the late phase of the internal carotid angiogram. Similarly, false angiographic intraorbital extension may be diagnosed. This corresponds to tumor invasion of posterior ethmoidal cells, which are superimposed on the orbit in the lateral projection. A frontal view (in Caldwell projection) will exclude orbital tumor infiltration. When present, orbital involvement is usually clinically evident but CT and MRI examinations will give a very accurate demonstration of its extent.

Recognition of these arterial characteristics is important, as they affect surgical resectability. These territories are supplied by branches of the internal carotid arteries as well as the internal maxillary and ascending pharyngeal arteries and may be used for embolotherapy. Sacrifice of the internal carotid artery to reach the portion of tumor supplied by siphon branches may be considered if it can facilitate radical removal of a large tumor, but it requires proper functional testing.

Two surgical classifications have been proposed to stage the various patterns of tumor extension and predict the surgical resectability (Table 3.4).

Table 3.4. Topographical classification of juvenile angiofibromas

Fisch et al. 1984	Class I	Class II	Class III	Class IV
	Nasopharynx and nasal cavity no bone destruction	Pterygopalatine fossa and paranasal sinuses with bone destruction	Infratemporal, orbit and extracavernous Intracranial extension	Cavernous sinus pituitary fossa optic chiasm

Table 3.5. Effects of embolization (E) on intraoperative blood loss (modified from Wlaman 1981)

Series		Number of cases	E°	Average blood replacement (ml)
Conley and Fairmont	1977	34	–	1,850
Jafek et al.	1973	34	–	2,700
Christiansen et al.	1974	29	–	1,700
Ward et al.	1974	12	–	1,300
Pletcher	1975	16	–	2,387
		7	+	1,177
Roberson et al.	1979	12	+	800
Lasjaunias et al.	1980	53	+	<1,000
Waldman et al.	1981	10	+	775

3.1.8 Therapeutic Goals

The therapeutic goal for JAFs should be the eradication of the tumor. Surgical removal of the lesion is still the best available technique (Ungkanont et al. 1996; Paris et al. 2001); however, two factors may limit the resection: intraoperative bleeding and the size and extent of the tumor.

Three modalities may help in diminishing these two factors:

1. Embolization carried out by an experienced team carries no significant morbidity or mortality. Reported complications or unsatisfactory results are likely related to insufficient training or knowledge or poor judgment during the procedure itself. We have found this technique to be safe and helpful in preparation for surgery (Table 3.5).
   Percutaneous embolization of JAFs with liquid embolic material such as glue or alcohol has been proposed for those lesions that are mostly supplied by branches of the internal carotid artery (Casasco et al. 1994; Tranbahuy et al. 1994). However, subsequent experience with this method has shown the potential for significant complications (Casasco et al. 1999), making this technique problematic for routine use.
2. Radiation therapy can be expected to produce partial regression or at least an arrest in the tumor growth of the angiofibroma (Reddy et al. 2001); however, functional morbidity, as well as the significant long-term hazard of secondary neoplastic induction, places this form of treatment in a secondary role. Its role will be limited to rare circum-

stances of unresectable neoplasms with intracranial extension. Radiation has no demonstrable effect on the cellular portion of this benign tumor; its effect is felt to be secondary to postradiation vasculitis.

3. Exogenous estrogens have produced positive effects on the operative bleeding rate. However, the morbidity caused by the dosage required for a clinically significant effect is very high considering that we are dealing with adolescent males. The effects of estrogens were confirmed at pathology by Delarue et al. (1956). The side effects of this type of treatment on gonadal development and function, given the population involved, make it an undesirable choice.

In 1980, Cummings analyzed the relative risk factors in the treatment of JAFs (Cummings 1980). Although no reference was made to embolization nor to the respective efficacy of the available therapeutic modalities, the author demonstrated that surgery and radiation therapy carried the same treatment risk of 1% mortality. The results of surgery alone are a function of the technical skills of the surgeon and, therefore, it is difficult to predict the results possible in each medical center. Based on the classification of Fisch et al. (1984), most surgeons in the international literature tend to operate on stages I and II, some on stage III, and a few on stage IV.

The overall mortality of JAF is thought to be 3% (Batsakis 1979) and the rate of recurrence varies from 12% to 35% (Ungkanont et al. 1996; Lloyd et al. 1999; Paris et al. 2001).

Our own strategy favors presurgical embolization and embolization alone (or associated with estrogens) if the lesion is not surgically resectable; sacrifice of the internal carotid artery can be discussed on an individual basis in patients with intracavernous extension (Fig. 3.6). Radiation therapy should be reserved for bilateral cavernous sinus involvement and for the situation where adequate surgical or therapeutic angiographic teams are not available in a given geographic location.

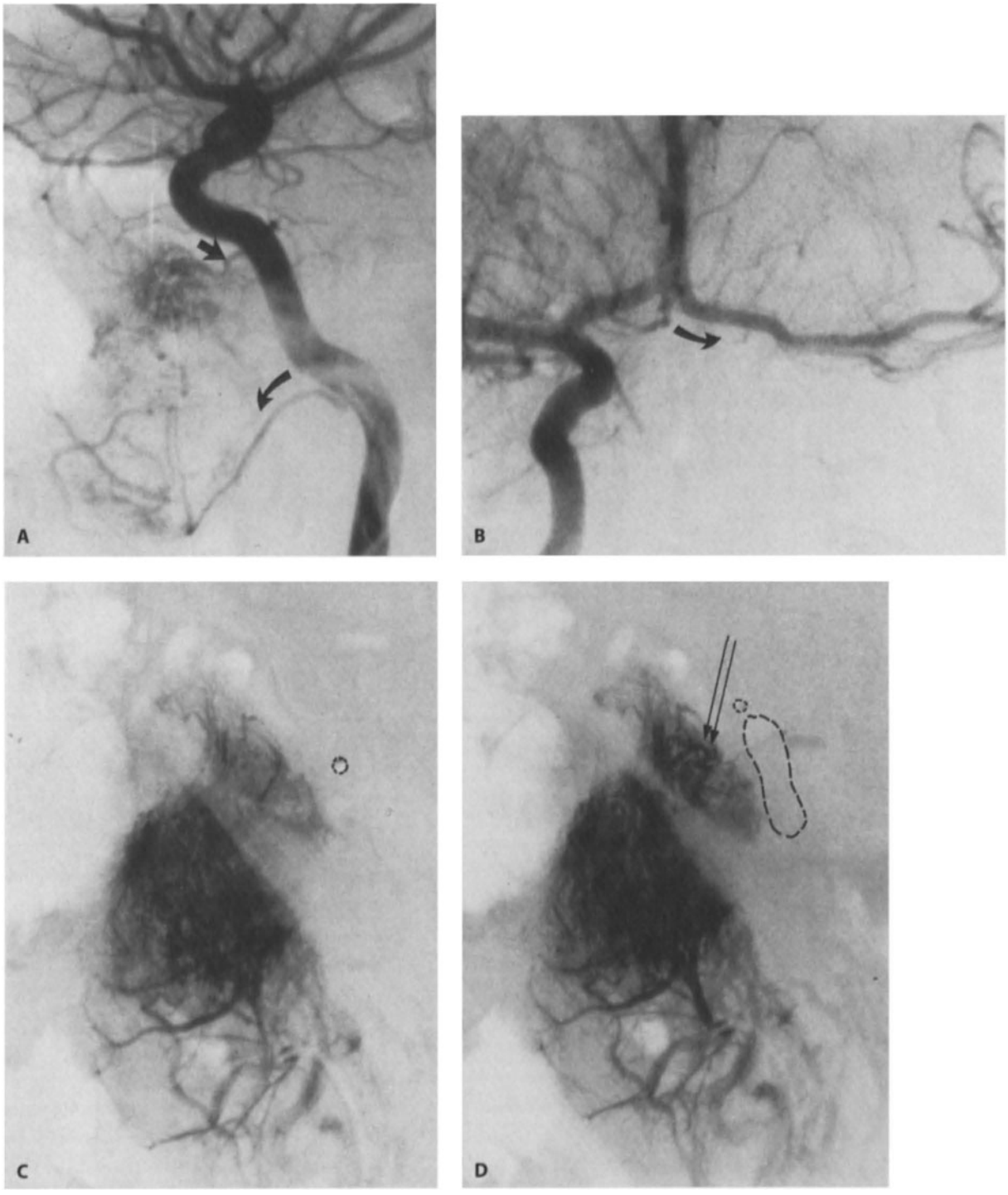

Fig. 3.6A–R. An 18-year-old male patient presented with a 1-month history of nasal obstruction and epistaxis. **A** Extracavernous middle cranial fossa tumor extension is primarily supplied by the inferior lateral trunk (ILT) (*arrow*) from the left internal carotid artery siphon. The mandibular artery (*curved arrow*) arises from the intrapetrous portion of the same internal carotid artery and vascularizes the nasopharyngeal portion of the lesion. In an attempt to preserve the internal carotid artery, we tried to reach the intracranial extension via its external carotid supply, by transiently occluding the internal carotid artery at the level of the ILT and mandibular artery. **E–R** see pp. 217–220

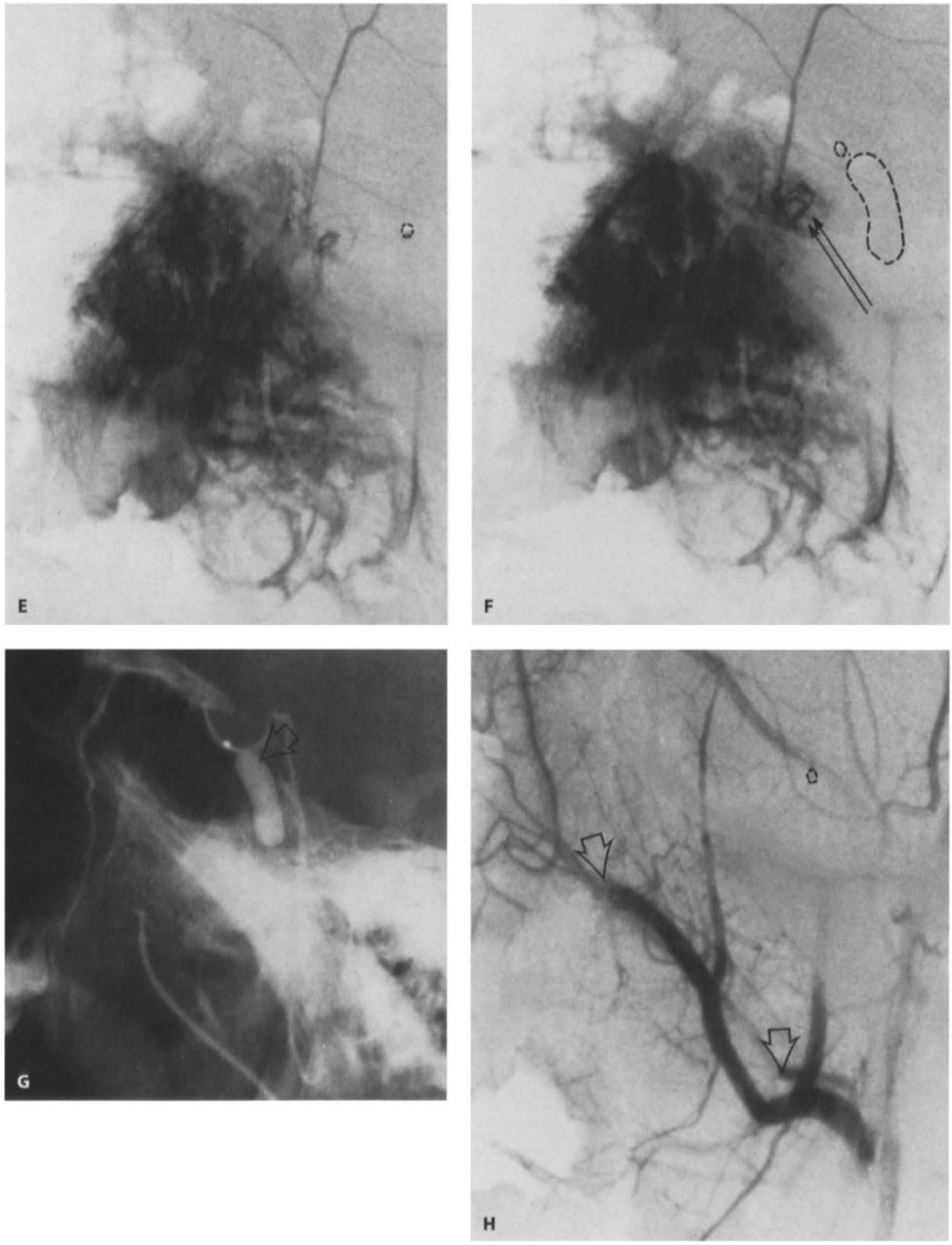

Fig. 3.6 (*continued*). Morphological (**B**) and functional testing of the circle of Willis was first carried out under neuroleptanalgesia, and successively the left accessory meningeal artery (**C, D**), the distal internal maxillary artery (**E, F**), and the anterior branch of the ascending pharyngeal artery (**J, K**) were injected with the balloon inflated and then deflated in the siphon. **I–R** see pp. 218–220

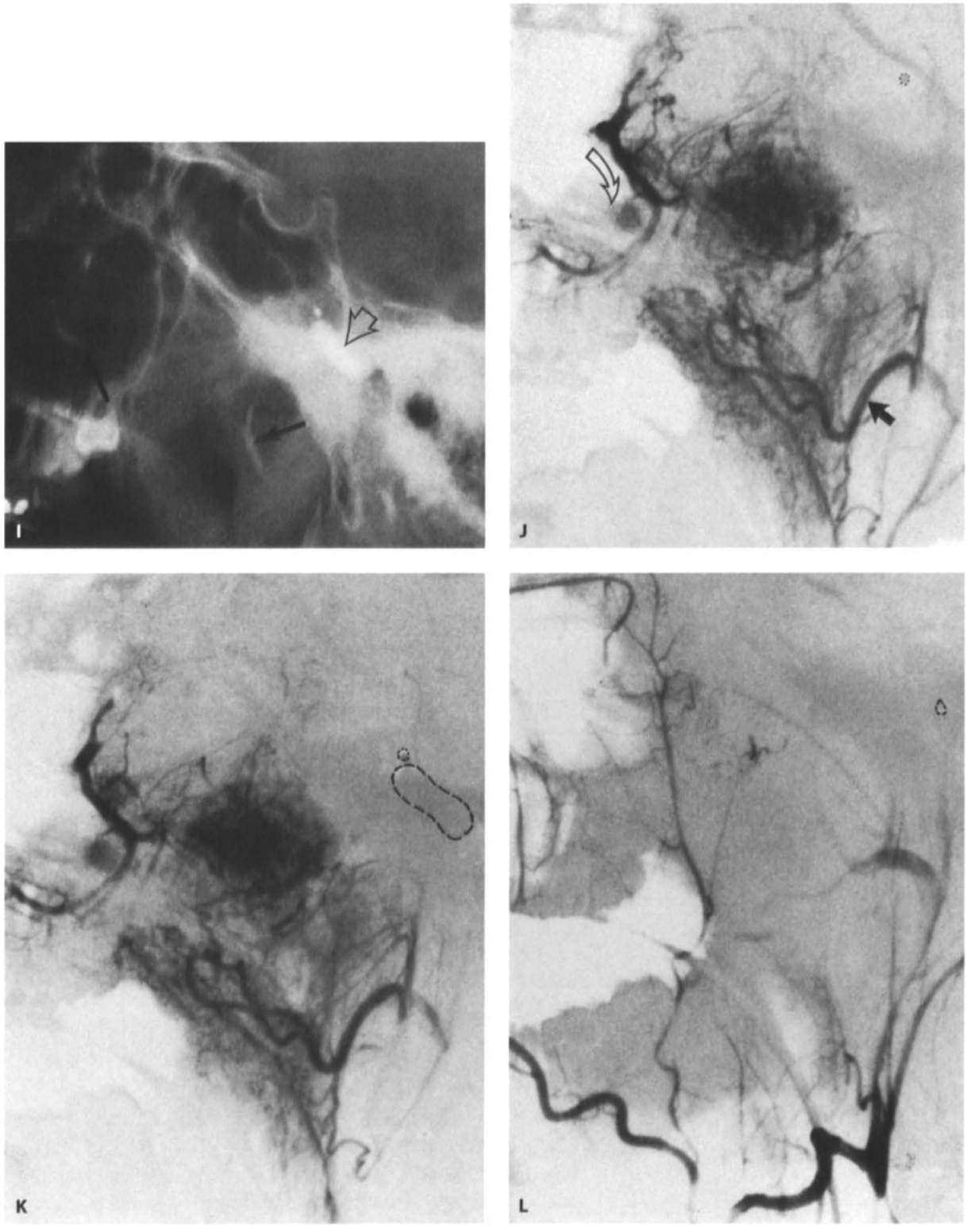

Fig. 3.6 (*continued*). Although changes in the quantity of intracranial tumor supplied by the external carotid artery were minimal (*double arrow*), embolization of these arteries was carried out with polyvinyl alcohol with the balloon inflated in the internal carotid artery siphon (*open arrow, dotted lines around balloon*). Follow-up angiograms performed in the external carotid systems following each embolization (**H, L**) showed satisfactory occlusion of the tumor feeders. Stagnation of contrast material in the embolized vessels (*arrow*) was seen on plain skull X-rays (**I, G**). **M–R** see pp. 219, 220

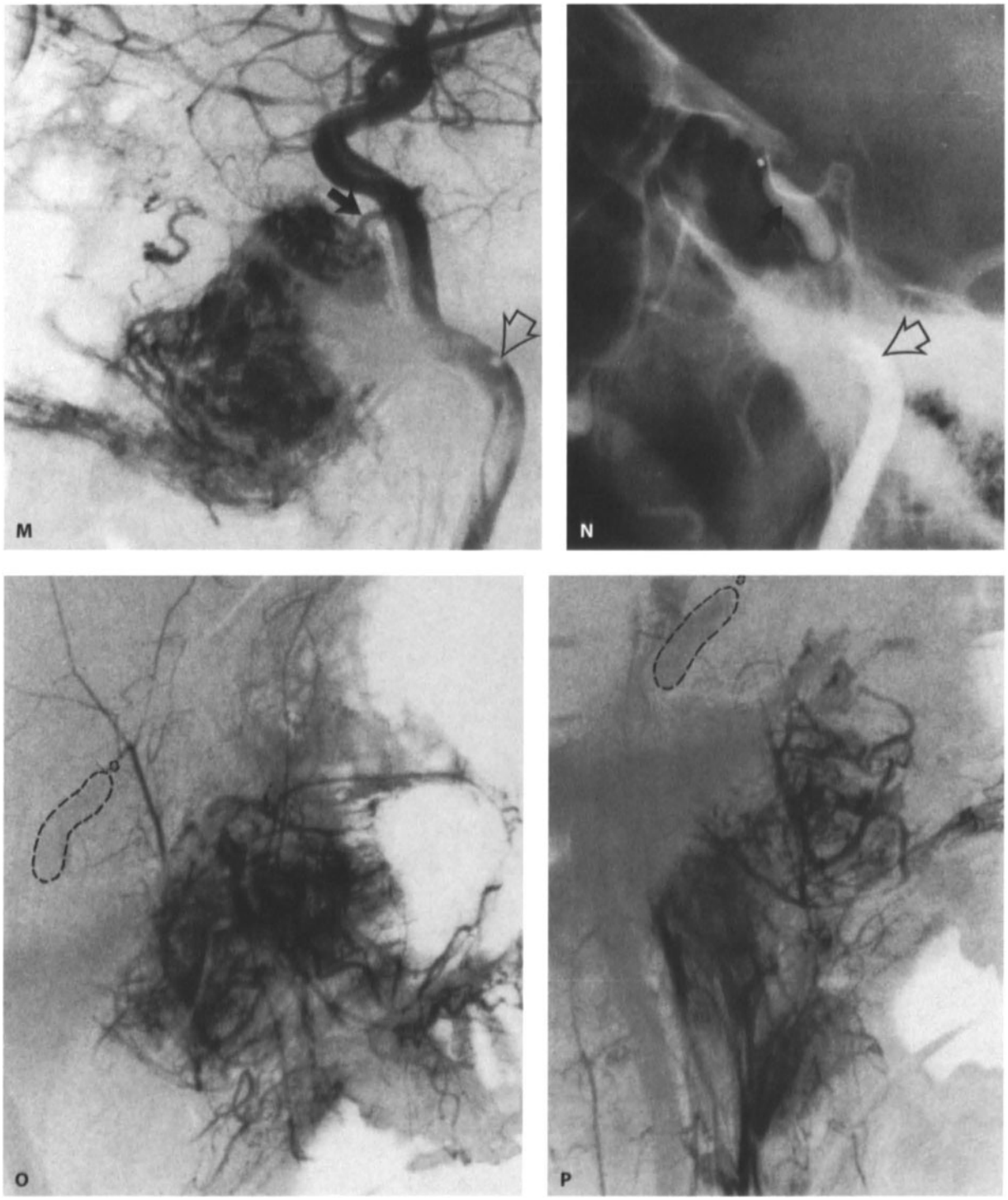

Fig. 3.6 (*continued*). However, the supply from the internal carotid artery persisted and had even increased slightly (**M**); only the mandibular artery territory appeared to have been controlled. As the morphological and functional patency of the circle of Willis had been tested previously, the siphon was occluded by means of a detachable latex balloon (Debrun's type, no. 16 Ingenor), below the ipsilateral ophthalmic artery (*arrow*, **N**); a second one was detached at the level of the origin of the mandibular artery (*arrowhead*, **N**). Contralateral distal internal maxillary (**O**) and ascending pharyngeal (**P**) arteries were then embolized. **Q, R** see p. 220

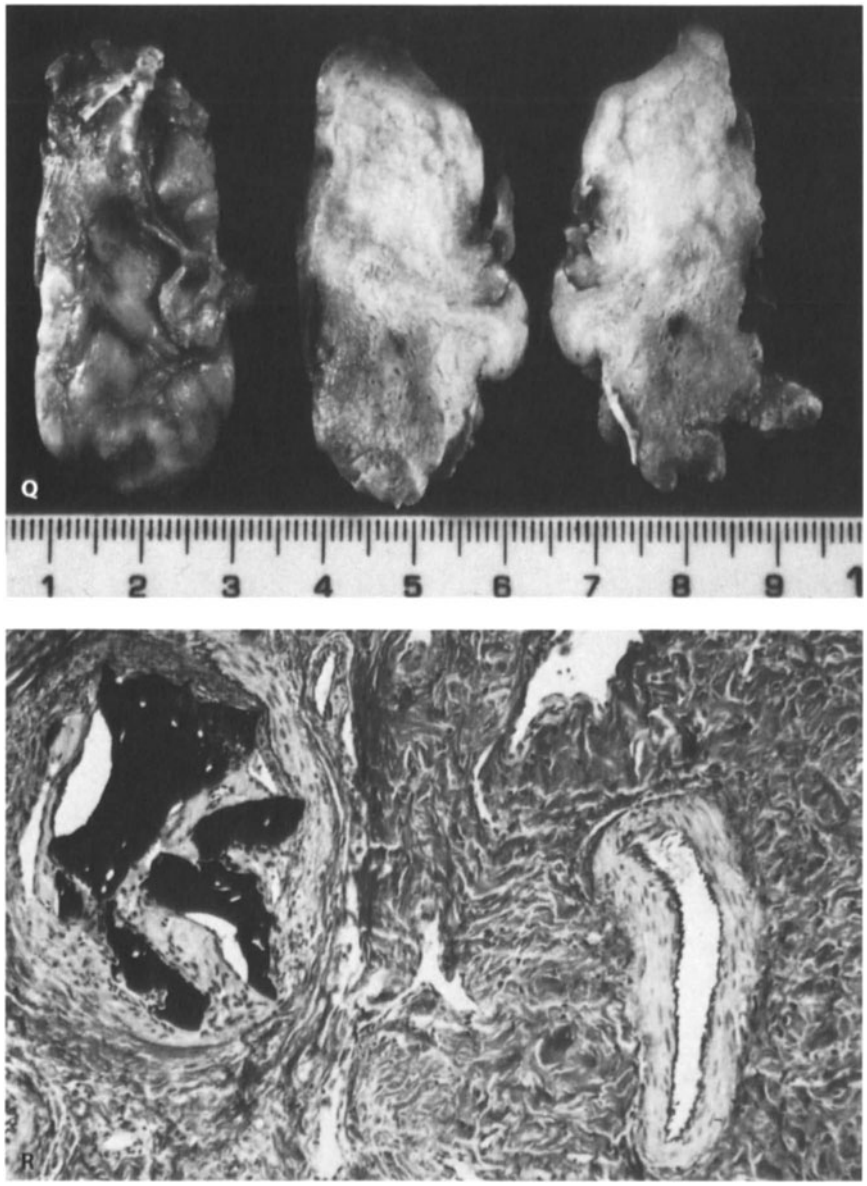

Fig. 3.6 (*continued*). The tumor was removed en bloc (**Q**) 1 week later with minimal blood loss. Emboli can be seen within the tumor specimen (**R**). In this particular case, careful attention should be paid to the opening of the internal maxillary–ophthalmic artery anastomosis, following internal carotid artery balloon occlusion before and during embolization. As pointed out in the text, the blood pressure and fluid balance must be monitored in the hours following embolization to avoid any hypovolemia or hypotension, which would change the status of the circle of Willis from what was tested, with a high risk of stroke

Table 3.6. Primary treatment of juvenile angiofibromas

Series Type of treatment	Number of cases treated	Number of recurrences	Number of repeated recurrences
Surgery alone (Sergent 1968; Muller 1971)	49	21	11
Surgery alone (Biller 1974)	43	16	Not mentioned
Embolization and surgery (Lasjaunias 1980) Group II	41	3	1
Embolization and surgery (Waldman 1981)	10	0	0
Radiation therapy and surgery (Cummings 1984)	55	11	2

3.1.8.1 Radiation Therapy

The results of radiation therapy as the primary treatment of JAFs were reviewed by Cummings in 1984. In over 55 patients followed up from 3 to 26 years, the overall results were considered to be very good. Eighty percent had tumor control; however, 20% (11 patients) presented with recurrence following radiation, eight of which were reradiated with good results. Although these figures may appear to be satisfactory, two patients developed malignant tumors (thyroid and skin). Two cataracts (one in the patient presenting with the skin cancer) and one case of clinical hypopituitarism were also noted. Most patients developed mucositis during the radiation therapy.

One can consider the results of radiation therapy alone or in association with surgery to be almost as good as those of embolization with surgery in comparable series. However, the 5% morbidity of the former includes induced cancer, while the latter has no associated late morbidity. Therefore, our preference is embolization combined with surgery each time both teams are available in a given place (Table 3.6).

3.1.9 Technical Aspects of Embolization

Presurgical embolization of JAFs is a simple procedure in most cases; the tumor is supplied exclusively by external carotid artery branches, which most of the time can be easily catheterized.

The goals of the endovascular approach will therefore be:

1. Reaching the capillary bed (it is a tumor)
2. Devascularizing the region

Angiographic patterns are predictable in most cases. The location of the arterial feeders depends on the site of origin of the lesion; they are usually only moderately enlarged. The parenchymal blush is intense, without arteriovenous shunting, and no early venous return (Fig. 3.5).

Certain specific characteristics may make the procedure more difficult: anastomoses between branches of the internal maxillary and ascending pharyngeal arteries and the intracranial or intraorbital arteries, and internal carotid artery supply to the tumor.

JAF differs from other lesions in that it demonstrates a strong correlation between the angiographic blush and the true extent of the tumor. Therefore, the angiographic appearance following embolization is a reliable indication of the adequacy of the procedure.

Generally, the limiting factors are sought first: internal carotid artery supply in particular. Therefore we start with angiography of the opposite internal carotid artery with cross compression in the AP projection (Caldwell view), followed by ipsilateral internal carotid artery injection in the lateral projection (with or without Caldwell view, as necessary). These injections will show existing ethmoidal, sphenoidal, and middle cranial fossa extensions.

The next step is the successive catheterization and embolization of the external carotid artery feeders to the tumor. All extracranial feeders can be predicted accurately from CT and MRI examination if one has a clear understanding of the territorial vascular anatomy. In general, the distal internal maxillary arterial branches, the accessory meningeal artery, the superior pharyngeal division of the ascending pharyngeal artery, and the ascending palatine artery (or its equivalent) are the most constant suppliers to the JAF and must be reached consecutively.

We prefer to perform selective catheterization and embolization using a specific sequence. If several branches of the external carotid artery must be embolized, one should always try to embolize the most distal one first, to avoid later loss of access caused by vasospasm. The second or next artery to be catheterized should give an indication of the quality of the embolization achieved; it should, therefore, be one of the possible sources of collateral circulation to the region embolized and provide an alternate route to reach the territory, in case the embolization was too proximal.

By personal choice, we start with the ipsilateral distal internal maxillary artery, followed by the accessory meningeal, the ascending pharyngeal, and the ascending palatine arteries. On a given side, the final verification angiogram will be done in the facial artery. Sequential catheterization and embolization of feeding vessels from the opposite side should be carried out in almost all cases, in the same order. However, it may require a less aggressive approach than the dominant side, depending on the midline extension and contralateral collateral circulation.

For many years, we have used 150- to 250-μm polyvinyl alcohol (PVA) particles to embolize the tumor bed. Schroth et al. (1996) demonstrated that up to 95% of PVA particles measuring less then 50 μm may pass trough the tumor bed and will embolize to the lungs. We usually complete the particle embolization of the tumor bed by an injection of two or three large pieces of Gelfoam (3 mm in caliber, 1 cm in length). The objective of this part of the embolization procedure is to produce a transient devascularization of the region adjacent to the tumor, as well as increase in the distal thrombosis within the tumor itself. This technique is used in all of the feeders, bilaterally if necessary.

Table 3.7. Hazards of embolization of specific vessels

Distal internal maxillary artery	Orbital and cavernous ICA anastomoses
Accessory meningeal artery	Intracavernous ICA anastomoses and cranial nerve blood supply
Ascending pharyngeal	Intrapetrous and intracavernous ICA anastomoses, cranial nerves, and vertebral artery anastomoses

ICA, internal carotid artery.

The management of intracranial extension or large nonresectable tumors may require the use of:

1. Fluid agents (NBCA, alcohol, or others), with flow control in the internal maxillary or ascending pharyngeal branches
2. Temporary or permanent occlusion of the internal carotid artery siphon

Each of these two methods of embolization carries its own risks, which must be carefully analyzed before they are undertaken (Table 3.7). Cerebral functional testing should always be carried out before sacrifice of the internal carotid artery. Shrinking of the tumor is observed both radiologically and clinically (breathing is improved often with return of nasal patency), usually within 12 h of the embolization. Using our technique, the effect of embolization on the ease of surgical resection is consistently excellent, and we believe it justifies the rejection of more aggressive embolic agents in most patients. To our knowledge, the use of intra-arterial injection of sex hormones or cytotoxic drugs in nonsurgical cases has not yet been reported.

3.1.10 Tumor Recurrence

The rate of recurrence varies in the literature, but can reach up to 30% with surgery. Symptomatic recurrence usually occurs during the first 12 months but can occur up to 5 years after surgery, with an average of 2.5 years in 19 patients. This relatively high recurrence rate usually reflects incomplete removal of the lesion (Lloyd et al. 1999). Most of the recurrences encountered occurred when surgery was done without prior embolization or because of posterior extension along the pterygoid canal, with invasion of the sphenoid bone.

Some recurrences may be asymptomatic and discovered during a late follow-up or during imaging examinations done for other reasons. The therapeutic strategy will then depend on the experience of the team. We would still recommend removal of the recurrent tumor, if possible, as future growth is unpredictable and further subclinical extension might occur.

3.2 Other Nasopharyngeal Tumors

The angiographic and therapeutic protocols described for JAFs are readily applicable to other benign hypervascular tumors of this region. Embolization with particles usually does not alter the tumor architecture so much that it interferes with making a subsequent histological diagnosis. Therefore we feel comfortable using this type of embolization prior to diagnostic biopsy or radical removal. In the adult population, benign nasopharyngeal tumors are less common than malignant ones.

Paragangliomas may occur in this region. Clinically they may simulate malignant lesions. They are most often benign hypervascular lesions that are locally invasive. Malignant and metastatic paragangliomas do exist in this region but are rare. Paraganglioma management will benefit from presurgical embolization, similar to the protocol described for JAFs. More recently, percutaneous embolization techniques have been described (Casasco et al. 1994, 1999), with liquid embolic material injected directly into the tumor bed. The results of this approach appear to be encouraging and could lead to embolization techniques being the only treatment providing local in-situ deposition of specific antitumor agents.

Other benign vascular lesions that can occur in the nasal fossa include neuroblastomas, esthesioneuroepitheliomas, hemangiopericytomas, hemangioendotheliomas (most of which are considered malignant), and what Aufdemorte (1981) has named hemangiopericytoma-like tumors. This separate entity is encountered in adults between the ages of 14 and 79 years, with a mean age of 53 years (Compagno 1976). The benign course of the lesion, following surgery, is remarkable considering its local invasiveness (25%–50% recurrence) and the potential for metastasis (12%–60%) (Enzinger and Smith 1976). More recently, Batsakis et al. (1983) reported the electron microscopic study of the biological and histological low-grade character of hemangiopericytomas in the nasal cavity. He outlined the difference between the low-grade true hemangiopericytoma and the hemangiopericytoma-like tumors (Fig. 3.7). Similarly, Cole (1982) collected 14 cases of hemangioendotheliomas of the nose and nasal cavity and paranasal sinuses. The ages of the patients ranged from 3 months to 71 years of age. Four of them were in the pediatric group. The mean age was 42 years for male patients and 40 for females. Only three of them died from their disease, nine are still alive (eight without recurrence), and two were lost to follow-up. These tumors are all highly vascular and in this specific area have a relatively benign course. We feel that they should undergo radical surgery whenever possible and will therefore also benefit from presurgical embolization.

Extracranial meningiomas are rare in this region and usually develop in the parapharyngeal space. They represent only 1% of overall meningiomas (Geoffray et al. 1984).

In their review, Geoffray et al. (1984) collected 94 cases of meningioma involving the head and neck region: 39 in the paranasal sinuses and the nasopharyngeal cavity, 15 of which had documented intracranial extension. In addition to these, 19 were in the para- and retropharyngeal space.

Tumors developing in the parapharyngeal space were reviewed by Work and Hybels (1974), who reported 80% of the tumors to be benign and the majority of salivary gland origin.

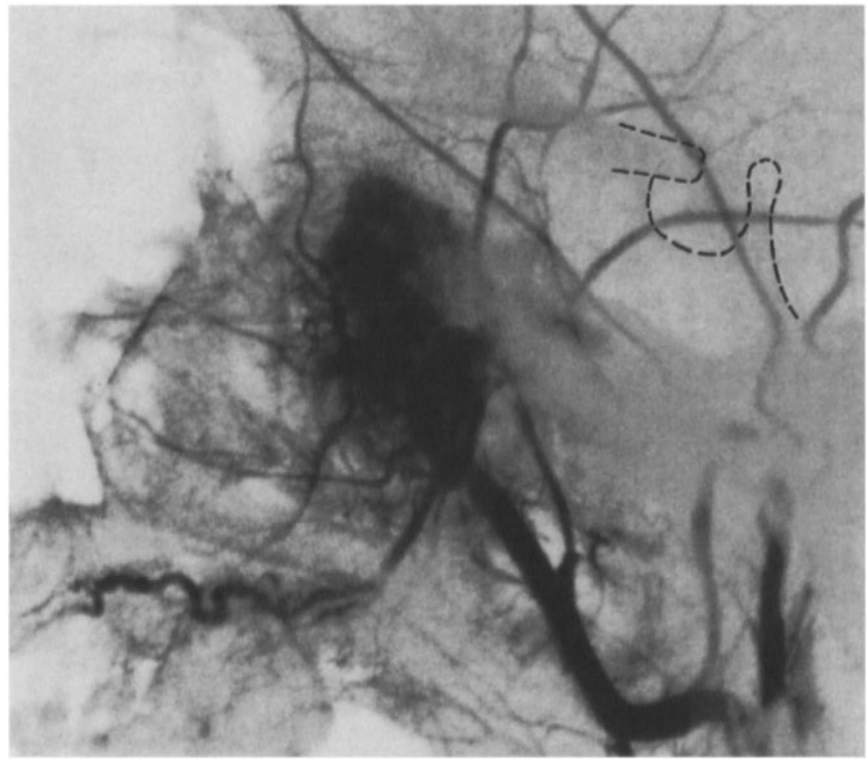

Fig. 3.7. A 14-year-old female patient presented with epistaxis. Rhinoscopy disclosed a reddish tumor. Distal internal maxillary angiogram demonstrates tumor blush fed by the sphenopalatine branches. Ipsilateral facial, internal carotid, and contralateral internal maxillary artery angiograms (not shown) were normal. The lesion was embolized and subsequently removed. Pathological diagnosis was hemangiopericytoma

In other series, neurogenic tumors were the most frequent benign lesions encountered in the parapharyngeal space (Conley and Clairmont 1977; Ferlito et al. 1984). Schwannomas are encountered in the nasal fossa and the paranasal sinuses (Khalifa and Bassyouni 1981; Mahe et al. 1983), maxillary sinus (Agarwall et al. 1980), and sphenoid sinus (Calcaterra 1974).

The angiomatous polyp is a rare benign lesion. Som et al. (1982) described five cases, three of which were biopsy proven. These lesions have histological findings similar to JAF and may bleed profusely at the time of biopsy. Most patients with these lesions present in a similar fashion to those with JAF, and therefore are referred for presurgical angiography and embolization. At angiography, they are less vascular than the typical JAF, probably because they contain more fibrous tissue, but since they also have a high potential for intraoperative hemorrhage, they will benefit from preoperative embolization.

In 1982, Ali reported a 28-year-old woman with an extranasopharyngeal angiofibroma in the tonsillar area and reviewed the literature extensively. Over 36 cases have been reported since 1936, with a mean age of 22 years (Ali and Jones 1982; Neel et al. 1973). Among these 36 cases of extranasopharyngeal angiofibromas, 44% were between 10 and 20 years of age at the time of the discovery of the lesion, compared to 80% of patients with nasopharyngeal JAF.

Thirty-one percent of the extranasopharyngeal angiofibromas occurred in females. Because of these differences in site of origin, sex ratio, and age, Lucas in 1976 and Ali in 1982 felt that although the structural aspect and clinical presentation and benign course are identical, extranasopharyngeal angiofibromas and the usual type of juvenile nasopharyngeal angiofibromas should be considered as two different entities.

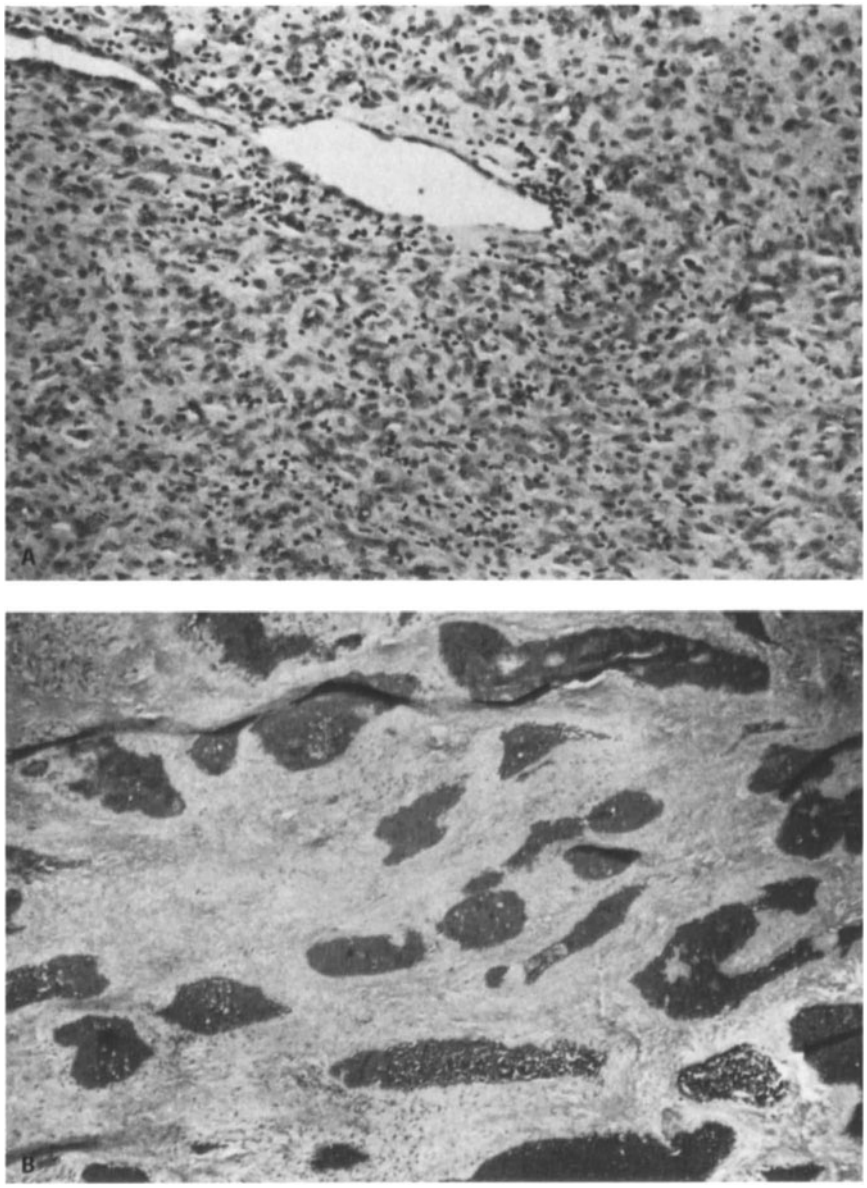

Fig. 3.8A, B. A 16-year-old male patient with a nasopharyngeal juvenile angiofibroma. **A** Pathological specimen from surgery performed a few days after Gelfoam embolization. Note the intense cellularity. **B** Pathological specimen obtained following the second surgery for recurrence of the tumor 8 months later. Silicone fluid embolization was performed a few weeks before this resection. Note the fibrotic transformation of the tumor and the organized thrombi into the vascular lumen. No recurrence on 11-year follow-up

3.3 Conclusion

We feel that benign vascular tumors such as JAFs, angiomatous polyps, extranasopharyngeal angiofibromas, nasal, paranasal, and nasopharyngeal paragangliomas, meningiomas, hemangiomas, hemangiopericytomas, esthesioneuroblastomas, and hemangioendotheliomas can all benefit from preoperative embolization. Their location at the base of the skull, the frequency of recurrence following incomplete surgery, and the potential long-term side effect of radiation therapy are all factors that support the use of embolotherapy prior to their surgical removal. The role of in-situ deposition of embolic materials (Fig. 3.8), including antineoplastic agents using percutaneous image-guided techniques, is expected to grow and in the future may very well obviate the need for surgical resection and or radiation therapy for vascular neoplasms involving the head and neck region.

4 Paragangliomas

4.1 Introduction 227

4.2 Embryology 228

4.3 Epidemiology 230

4.4 Pathology 232
4.4.1 Vascular Architecture 233

4.5 Natural History 235

4.6 Clinical Aspects 236
4.6.1 Tympanic Paragangliomas 236
4.6.2 Jugular Paragangliomas 238
4.6.3 Cervical Paragangliomas 238
4.6.4 Paragangliomas in Other Locations 244
4.6.5 Secretory Paragangliomas 245
4.6.6 Associated Lesions 246

4.7 Differential Diagnosis 246

4.8 Pretherapeutic Evaluation 250
4.8.1 Angiographic Protocol 252
4.8.2 Temporal Paragangliomas: Specific Features 252
4.8.3 Cervical Paragangliomas: Specific Features 257

4.9 Therapeutic Strategies 260

4.10 Technical Aspects of Embolization 261

4.11 Complications of Embolization of Paragangliomas 264

4.1 Introduction

Paragangliomas occur in a variety of sites in the head and neck, with almost one-half arising in the temporal bone (Tables 4.1, 4.2). Although tumors of the middle ear occur infrequently, paragangliomas are the most common in this location.

If one considers all tumors of the temporal bone, paragangliomas are second in frequency to neurogenic tumors (Spector et al. 1973).

Paragangliomas best represent the multidisciplinary therapeutic strategy and technical aspects involved in the treatment of benign neoplasms of the cervical and temporal regions.

The considerable interest generated by these lesions is apparent from the 2,000 cases reported in the literature, even though they represent only 0.012% of tumors in the pathology files of large centers (Lack et al. 1977).

The interesting features of paragangliomas include their multicentricity and their frequent association with other neural crest tumors.

Table 4.1. Neural crest derivates (modified from Turpin 1978)

Mesenchymal cells	Ectodermal cells	Ectomesenchymal cells after endodermic settlement (argentaffin cells)
Muscular, osseous cartilaginous, etc. structures of the head and neck	Ganglion cells (autonomic nervous system; cranial and spinal nerves	
Odontoblasts	Neural coverings and stroma (microglia leptomeninges)	
	Secretory cells • Chromaffin cells • "Non-chromaffin" paraganglions (brachial etc.) • Melanoblasts • Hypothalamic cells • Pineal cells	Compact endocrine system (thyroid, pituitary; parathyroid) Disseminated endocrine system (pancreas) Diffuse endocrine system (GI tract)

Cells oft the APUD system are included in the box.

Table 4.2. Locations of head and neck paragangliomas in order of frequence (from Zak and Lawson 1982)

Temporal { Tympanic	Temporalis muscle
Temporal { Jugular	Buccal mucosa
Carotid	Tongue
Vagal	Soft palate
Laryngeal	Pterygopalatine fossa
Orbital	Mandible
Nasopharyngeal	Nasal fossa
Tyroid, parathyroid	Cervical esophagus
Face, ear, submastoid area, parotid	Intracranial (sphenoid sinus, parasellar region, intrasellar, epithalmic)

Glomic tumors, chemodectoma, nonchromaffin paraganglioma, and neurocristopathic tumor are the most common names given to the benign neuroendocrine neoplasms that arise from the neural crest derivatives.

4.2 Embryology

The neural crest gives rise to three types of cells (Table 4.1; Rosenwasser 1968; Louvel and Abelanet 1979): mesenchymal, ectomesenchymal, and ectodermal.

Ectomesenchymal cells migrate to colonize the endodermal derivatives (hypophysis, thyroid gland, thymus, digestive tract) and belong to the so-called argentaffin cell group (from which the serotonin-secreting carcinoid tumors develop). Argentaffin cell derivatives are further categorized

into two subgroups depending on their chromaffin reaction: those that react positively are termed enterochromaffin cells, while those with a negative reaction are argyrophilic cells. The argyrophilic cells are very different from the cells giving rise to the paragangliomas, and although they can both release serotonin, their initial embryonic pattern of migration results in different patterns of differentiation.

The ectodermal group gives rise to leptomeningeal cells, microglial cells, ganglion cells (for the spinal nerves, autonomic nervous system, and sensory cranial nerves), and special secretory cells. The secretory cells are divided into two subgroups depending on the chromaffin reaction. The chromaffin-positive subgroup includes the cells of the adrenal medulla (pheochromocytes, adrenalin secreting) and the para-aortic cells (chromaffin paraganglion cells, which release noradrenalin). The nonchromaffin cells extend throughout most of the body, where they have both receptive and secretory functions. The hormones released include catecholamines and serotonin, with no relation to cellular topography. Some groups of cells are, however, more consistently located in the same areas: branchial and aortic, for example.

In the past, Glenner and Grimley (1974) and Zak and Lawson (1982) emphasized that the chromaffin reaction of the cells may not be a satisfactory test to differentiate these subgroups.

For example, catecholamine secretion by both extra-adrenal chromaffin tumors and adrenal nonchromaffin tumors has been described. Therefore, the term "branchial paraganglion" most appropriately describes the specific group of neural crest cells in the head and neck regions that give rise to the tumors to be described in this section: the paragangliomas (Table 4.2).

The use of the name "glomus tumor" should be reserved for those tumors that actually develop in the glomus of Masson, a vascular structure located in the finger tips. These glomi have two types of cells – endothelial cells and pericytes – with smooth muscle cells and amyelinic nerve fibers. The tumors developing from the glomus of Masson are painful benign neoplasms which occur in young patients and have the potential to transform into hemangiopericytomas.

The term "apudoma" refers to the neoplasms that are derived from the amine precursor uptake and decarboxylation (APUD) system described by Pearse (1977).

They consist of cells that can produce polypeptides and fluorogenic amines (catecholamines, serotonins, etc.). This category includes the cells of the ectomesenchymal and ectodermal groups, both of which have endocrine activity regardless of their chromaffin response.

Branchial paragangliomas also belong to this group, as do tumors that release calcitonin, MSH, ACTH, parathormone (compact endocrine system); insulin, glucagon, gastrin, somatostatin, thymin (disseminated endocrine system); and secretin, enteroglucagon, motilin, pneumokinin (diffuse endocrine system).

This embryologic overview supports three possible conclusions.

A dysgenetic lesion derived from the neural crest can include several cells of the same subgroup or of different subgroups of the APUD system, with the potential for multifocality and polymorphism. Clinical manifes-

tations are illustrated by the association of single or multiple unilateral tumors or bilateral paragangliomas, and other tumors such as abdominal pheochromocytoma.

The neural crest cells carry the potential of producing different types of polypeptides; therefore, a clone of tumor cells within a paraganglioma may mature toward cells that release a different hormone (single paraganglioma with polymorphic secretory activity). This characteristic is illustrated in the case reported by Farrior in 1980 of a carcinoid tumor within a temporal paraganglioma.

The early polymorphic potentiality of each cell is preserved until migration is complete. Therefore, ectopic tumors and hormonal release can be found. Most of the ectopic paragangliomas reported are located in the head and neck areas. It is important to note that most of the head and neck paragangliomas in the usual location develop from a preexisting normal paraganglion (Table 4.2). However, head and neck paragangliomas have been reported to occur in areas where normal paraganglions have not been observed, and these should be considered ectopic tumors.

4.3 Epidemiology

Paragangliomas are unique in that the tumor that brings the patient to the physician may be part of a complex disease (neurocristopathy). Therefore, the epidemiology of the single paraganglioma may appear too restrictive.

For practical purposes we shall consider that the most common branchial paragangliomas can be differentiated by their location: tympanic, jugular, carotid, vagal, laryngeal, nasopharyngeal, and orbital. In fact, pure tympanic and pure jugular paragangliomas are not frequent; also, since their clinical manifestations are similar, they are usually classified as a single entity: temporal paragangliomas.

In 1982, Zak and Lawson reviewed about 2,000 cases and discussed the problems arising from paragangliomas in the head and neck territory.

Table 4.3 displays the age and sex distribution of the paragangliomas. One can note two groups: the branchial paraganglioma with a female pre-

Table 4.3. Epidemiology of paragangglomas (from Zak and Lawson 1982)

Location	Number of patients	Benign tumors			Malignant tumors		
		Age range	Mean age (yrs)	Female (%)	Total (%)	Mean age (yrs)	Female (%)
Temporal	507	18–25	46	71	3	45	70
Carotid body	370	5–89	44	52	10–15	32	59
Vagal	115	18–79	48	72	10	45	81
Laryngeal	34	14–71	47	55	18	58	83
Orbit	17	3–69	44	52	3 reported cases		
Nose and pharynx	16	8–92	44.5	75	none reported		
Total	1059						

dominance of 2.5:1 (temporal, vagal, nasal, and nasopharyngeal) and the branchial paraganglioma with no sex predominance (carotid, laryngeal, orbit). For almost all locations, the mean age is in the fifth decade, with a range from 6 months (Wosnessenski 1923) to 89 years. The youngest and oldest patients both had carotid body tumors. There is no significant relationship between sex hormones and the clinical presentation or progression of the tumor in any of the groups mentioned above, although rare cases have shown some symptomatic changes during menses or pregnancy (Mirizzi 1935). The duration of symptoms before diagnosis is related to the medical environment and cultural habits of the patient. Branchial paragangliomas are usually considered to be slowly growing benign neoplasms, but in younger patients they may develop rapidly and tend to be larger and more endocrinologically active and to produce more rapid cranial nerve impairment. There is no definitive racial nor geographic distribution, but in 1973 Saldana found that branchial paragangliomas (carotid) were ten times more frequent in high-altitude (2,500–4,500 m) dwellers in the Peruvian Andes than in sea-level residents. Hypoxia, present from birth, was thought to be the stimulating factor for chronic hyperplasia leading to further tumor development. These observations were confirmed by a few other reports but were not supported by large series. Our review of personal cases did not disclose any patient in this group.

Although paragangliomas appear to be neoplasms, there is evidence of a familial distribution, which is not restricted exclusively to branchial paragangliomas tumors but applies to all apudomas. In familial cases, the inheritance is autosomal dominant with strong penetrance, but variable expression. Each offspring carries the disorder, but the disease may not be revealed in a given patient. Among a group of 46 patients with paragangliomas, nine (20%) revealed a family history of this tumor (Netterville et al. 1998). Between 40% and 80% of patients with familial forms have multifocal disease, while this multifocality occurred in 23% of patients with nonfamilial paragangliomas (McCaffrey et al. 1994; Netterville et al. 1998). Multicentric familial paragangliomas have the same epidemiological distribution as multicentricity encountered in the spontaneous form.

Multifocality can be expressed in many ways, including bilateral and unilateral multiple lesions and multiple lesions in the same tumoral mass (Zak and Lawson 1982; Moret and Lasjaunias 1986). Vagal and carotid paragangliomas are more likely to be multifocal than those in other locations (Table 4.4). The number of tumors and the possible endocrine activity are also variable. In a series of over 2,000 patients, Zak estimated that 1% had tumors with secretory activity. This subgroup had no sex dominance, but 40% were below 25 years of age, whereas only 15%–20% of patients with secretory paragangliomas are below 25 years of age. Clinically functioning tumors were noted in 17% of the patients reported by Somasunder et al. (2000) and their typical presentation was uncontrolled hypertension. Multicentricity and secretory activity can be observed with malignant paragangliomas (Strauss 1983). The malignant character of the lesion is difficult to assess at pathology (see Sect. 4.4), and only lymph node involvement or metastasis can be considered reliable indicators. The incidence of malignant forms is probably underestimated.

Table 4.4. Multicentricity of paragangliomas

Topography	Incidence (%)
Carotid	15
Jugular	2
Vagal	10
Number of tumors	
2 tumors	84%
3 tumors	13%
4 tumors	2%
5 tumors	1%

Vagal, carotid, and laryngeal paragangliomas have a malignant potential estimated at between 10% and 18%, while those in the temporal region have a lower incidence at 3% (Table 4.3).

4.4 Pathology

The macroscopic appearance of branchial paragangliomas is usually typical. The tumor is encapsulated, polypoid, brown or frankly purple, with an inflammatory appearance. Depending on the location, the tumor may be lobulated or oval in shape. At histology, the findings are those of a paraganglion with epithelial cells and a highly vascular stroma. Usually, the lesions appear to be true neoplasms, showing no normal relationship between the nerve fibers and the cells, unlike either a hyperplasia or a hamartoma. The degree of vascularity is variable; the most vascular lesions may be almost cavernous, including fenestrated endothelium. The epithelial cells have clear cytoplasm with eosinophilic granules. Unfortunately, it is impossible to correlate the histological differences, the clinical symptoms, the catecholamine storage, or the type of secretion with the appearance or the number of granules seen in electron microscopic studies. Neurons and ganglion cells can also be seen within the tumor, with no particular significance.

The histological diagnosis of malignancy is not definitive, but the following minor findings may cause suspicion of malignancy in any given branchial paraganglioma: rupture or absence of the capsule, invasion of vessel wall by tumor cells, vacuolization of the cytoplasm, and increased mitotic activity. Although mitotic activity is usually minimal, variations in its appearance may be related to changes induced by therapy. Folpe et al. (2001) have proposed a new classification scheme and criteria for atypical and malignant glomus tumors: malignant glomus tumor, symplastic glomus tumor, glomus tumor of uncertain malignant potential, and gangliomatosis. Using this classification scheme, metastases were observed in 38% of tumors fulfilling these criteria for malignancy.

The differential diagnosis of the histological findings includes hemangiopericytomas, carcinoid tumors, alveolar sarcomas, metastasized thyroid carcinomas, some neurogenic tumors, and granular cell myoblastomas.

Ectopic paragangliomas, especially intracranial ones, are a diagnostic challenge. Some meningiomas labeled angioblastic, transitional, or neuroepithelial often show glomic patterns and may be mislabeled, (Zak and Lawson 1982); more rarely, cerebellar hemangioblastomas, pineal tumors, metastatic hypernephromas, and cauda equine tumors may be misdiagnosed as paragangliomas.

4.4.1 Vascular Architecture

Small arteries are present in the capsules and septa of branchial paragangliomas; the stroma, as mentioned above, contains sinusoidal spaces. In some areas, these spaces appear to be all that separates the tumor cells from the blood stream (Pettet et al. 1937). In 1955, Willis and Birell showed a complex arterial arrangement within carotid body tumors with a centripetal distribution: the arteries often have a normal proximal caliber of about 90 μm and enlarge deep within the tumor, where they may reach a caliber of 300–600 μm. These vessels, called paracapillaries, metacapillaries and medium-caliber vessels, have anastomoses with each other as well as with the veins and the sinusoids.

From these observations and the angiographic findings in branchial paragangliomas, several remarks can be made.

Moret et al. (1986), describing lesions in the temporal region and in the cervical area, showed the compartmental arrangements of paragangliomas in which an artery, superselectively injected, will opacify a segment of the lesion with a specific venous drainage. The tumor can therefore be rebuilt like pieces of a puzzle. Two types of puzzles can be identified: unicompartmental masses (with only one "puzzle piece") and multicompartmental masses (with two or more puzzle pieces); each puzzle piece can be visualized by the injection of one or more than one artery.

This analysis has theoretical and practical implications: multicentric lesions can be bilateral or unilateral and can be close together. Therefore, multicompartmental masses could, theoretically, constitute multiple adjacent tumors that are macroscopically not separable. The second implication of this theoretical analysis is practical. The existence of a capillary bed and of arteriovenous communications explains the rapid venous filling seen on angiographic studies and the efficiency of small-particle embolization.

Two characteristic patterns of involvement of the large vessels of the neck by branchial paragangliomas should be emphasized. The development of the jugular paraganglioma within the lumen of the jugular vein is a very specific feature compared to the extrinsic vascular compression produced by other branchial paragangliomas and other cervical masses.

The irregular narrowing of the internal carotid artery seen in some cervical paragangliomas is similar to encasement by tumors and is probably not specific.

The role of the vascular system in the development of branchial paragangliomas is very interesting. In 1973, Spector pointed out the possible role played by neovascularization, preceding tumor invasion regardless of its site. This concept is supported by Folkman's work on the tumor angio-

genic factor (TAF). We have observed this phenomenon twice and will discuss it further with the pretherapeutic evaluation.

Finally, the angiographic analysis of the vascular architecture of these branchial paragangliomas provides some additional insight into their pathology. Clinically, tympanic and jugular paragangliomas are seldom multifocal (2% vs. 15% for other locations). Analysis of the surgical results of large paragangliomas (Fisch types C2 and D2) of the temporal bone (Table 4.8) shows that in type C2 (petrous extension), their carotid arteries are sacrificed or repaired in 10% of cases and all of the lower cranial nerves remain intact. In type D2 (intradural extension larger than 2 cm), although the carotid artery is preserved in l00% of cases, the lower cranial nerves are constantly impaired.

These two groups seem to represent the extreme forms of two different branchial paragangliomas. The C type appears to evolve from a tympanic paraganglioma, and the D type evolves from a jugular paraganglioma. Coexistence of both types raises the possibility of multicentricity within the temporal bone itself. Angiographic analysis supports this theory. Typically because they are encapsulated, branchial paragangliomas do not recruit arterial feeders from adjacent territories like other types of invasive or nonencapsulated tumors. For example, the jugular paraganglioma, which extends within the jugular vein, occupies an angiographically isolated compartment that can only be occupied by the neuromeningeal branch of the ascending pharyngeal artery. In our experience, large paragangliomas of the temporal bone that extend into the tympanic cavity and the jugular vein do not correspond to a single vascular territory but to two, fed by the tympanic arteries and the jugular branch of the neuromeningeal division of the ascending pharyngeal artery. We feel that even though grossly these lesions appear to be a single mass, they may actually be two separate tumors. The significance of the vascular supply pattern did not receive sufficient attention and has led to underestimating the multifocality of the tympanic and jugular paragangliomas in the past (Fig. 4.1).

Several authors have reported surgical evidence of separate tumors within the temporal bone, further supporting the possibility of multicentricity in the tympanic–jugular location (Berg 1950; Buckingham et al. 1959; Samy and Hashem 1962; Rosenwasser 1968, 1974).

Retrospective analysis of the origin of tumors reported before the mid-1970s is difficult, because the lesions tended to be diagnosed after they were advanced, and the radiological techniques used were not sufficiently sophisticated to provide the answers to the questions asked now.

The ascending pharyngeal artery is a unique link between paragangliomas in the tympanic, jugular, vagal, carotid, and laryngeal locations, as each of these territories is supplied by a different branch of this artery.

Other branchial arteries, the internal maxillary artery more rostrally and the superior and inferior laryngeal arteries more caudally, primarily supply paragangliomas that develop in their respective territories.

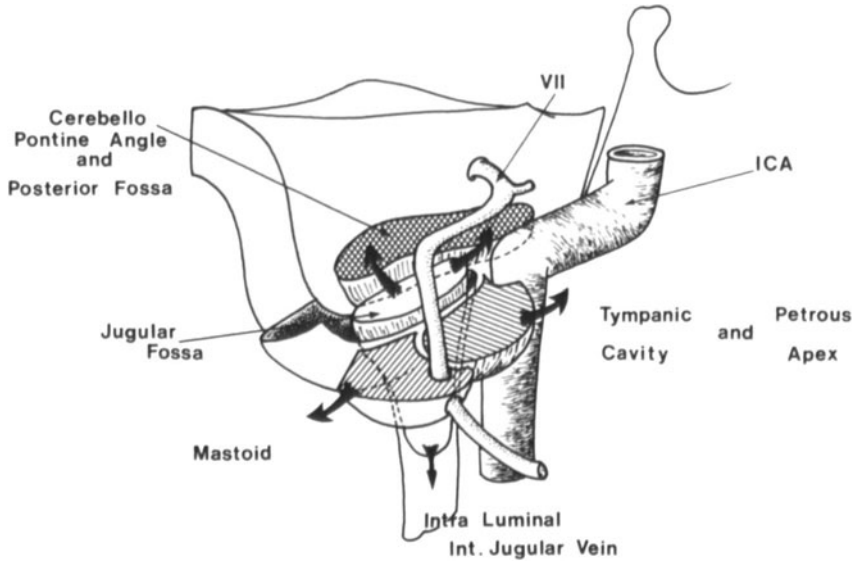

Fig. 4.1. Tympanojugular paraganglioma: patterns of invasion

Table 4.5. Evolutive classification of temporal paragangliomas (from Alford and Guilford 1962)

	Presenting symptoms	Additional clinical findings
Stage 0	Hearing loss and/or pulsatile tinnitus	Discolored tympanic membrane conductive hearing loss
Stage 1	+ Discharge (otorrhea (otorrhagia	+ Bulging or polypoid mass in the EAC
Stage 2	+ VII – aural pain +	Perceptive hearing loss
Stage 3	+ IX nerve neuralgia	+ Palsy IX, X, XII, ± XI
Stage 4	+ Intracranial symptoms (ataxia)	+ Complete cranial nerve paralysis from III to XII • Papilledema • Metastasis

Comments: Metastasis is presented as a predictable evolution of the tumors. Could they be malignant at stage 1 or 2? Could they remain benign? EAC, external auditory canal.

4.5 Natural History

Spontaneous regression of paragangliomas has never been reported. The growth is generally slow, but it can be rapid or associated with additional tumors in other territories.

The therapeutic strategy will also be based on the answers to the following questions: is the lesion malignant? Can a paraganglioma become malignant?

If Alford and Guilford's staged classification (1962) is true, any paraganglioma (Table 4.5) will eventually become malignant (stage 4), if their local invasion does not compromise the life of the patient first.

Table 4.6. Life expectancy of patients with temporal paragangliomas (from Harrison 1974; personal survival statistics)

71% of patients alive and well at 5 years
29% of patients alive and well at 10 years
17% of patients alive and well at 15 years
10% of patients alive and well at 20 years

According to Harrison's (1974) series of paragangliomas of the temporal area (Table 4.6), the mean age of the patients presenting with this so-called benign tumor is 45 years (see Sect. 4.3), and their life expectancy is 34 years. It is, however, important to note that only 10% of patients presenting with a temporal paraganglioma are alive and well 20 years after the discovery of their tumors.

Therefore, since we consider that lymph node invasion and metastasis are the only manifestations of malignancy, every reasonable attempt to totally remove the lesion should be made and any incomplete treatment discouraged. Delay in radical treatment while waiting for symptoms such as cranial nerve involvement to justify an aggressive approach should be avoided. Pretherapeutic evaluation will endeavor to find the safest way to cure the patient of the tumor and to disclose an existing but asymptomatic associated lesion.

4.6 Clinical Aspects

Two clinical aspects of branchial paragangliomas should be considered: the tumor itself and the neurocristopathy.

The symptoms of paragangliomas are related to the primary location of the tumor. Schematically, three syndromes can be described: tympanic, jugular and caroticovagal. The symptomatology (mass, bruit, cranial nerve palsies, pain), is usually progressive (typically neoplastic) but may be fluctuating, acute, or even regressive (pseudovascular). Gaillard et al. (1978) related this phenomenon to possible intratumoral hemorrhage or peritumoral inflammatory reaction.

4.6.1 Tympanic Paragangliomas

Tympanic paragangliomas are often considered as a unique entity because they are usually already large at the time of diagnosis (Tables 4.7, 4.8). However, specific features can be recognized.

The most prominent symptom is the presence of pulsatile tinnitus, which usually increases during effort, and often decreases with the Valsalva maneuver or cervical vascular compression. It is present early in the history of the disease because of bone conduction at the promontory; it may be intermittent but progressively more intense and intolerable. Typically unilateral, it is always related to the arterial pulsation. Tinnitus is usually not associated with headaches.

Table 4.7. Temporal paragangliomas: presenting symptoms

Hearing loss (perceptive or conductive)	Vertigo
Pulsatile tinnitus	Hemorrhage (otorrhagia)
VIIth nerve palsy	Lower cranial nerve palsy
Discharge	Mass effect (EAC, pharyngeal, mastoid)
Pain	

Table 4.8. Classification of temporal paragangliomas (72 patients over 12 years) (from Fisch et al. 1982 and Valavanis et al. 1983)

Type a 6 (8%)	Tumor limited to the middle ear cavity	Surgery (tympanoplastic techniques)
Type B Mastoid 16 (22%)	Tumor limited to the tympanomastoid (without infralabyrinthic extension)	Surgery (tympanoplastic techniques)
Type C Petrous pyramid extensions 33 (47%)	C1 and C2 destroy the jugular foramen and ascending portion of carotid canal C3 extension to the petrous pyramid.	Surgery (infratemporal techniques) ICA: 10% suture or ligature 90% intact Lower cranial nerves: IX lost in CI IX, X lost in C2 IX, X, XI lsot in C3
Type D Intracranial Intradural 17 (23%)	D1 < 2 cm D2 > 2 cm D3 inoperable intracranial Extension (?)	Surgery (infratemporal) ± Neurosurgery ICA: 100% intact Lower cranial nerves: IX, X, XI lost
Comments:	– Extradural extension although intracranial does not affect the classification. – No reference is made to: exocranial extension, jugular vein occlusion and lateral sinus patency, false intracranial extension.	

Any subjective bruit described as a buzzing or roaring is unlikely to be due to a tympanic paraganglioma. As the tumor evolves, the disappearance of tinnitus indicates cochlear destruction.

Conductive hearing loss, otorrhagia, seventh nerve palsy, and reddish or bluish bulging of the tympanic membrane complete the typical presentation of a tympanic paraganglioma.

In 30% of cases, seventh nerve palsies occur acutely (Spector 1973). They can regress spontaneously, thus leading to the incorrect diagnosis of Bell's palsy. They are thought to be related to transient arterial steal following activation of arteriovenous shunt within the tumor. Further growth of the tumor will lead to its extension towards the mastoid cells, with retroauricular pain, and mass effect in the external auditory canal, parapharyngeal space, and petrous apex.

Medial extension toward the inner ear will cause additional symptoms such as perceptive deafness and vertigo. Posteromedial growth toward the jugular bulb and pars nervosa will produce other cranial nerve manifes-

tations. In general, when one considers the diagnosis, tympanic paragangliomas can be recognized and treated at an early stage when the tumor is still small, preserving hearing function.

4.6.2 Jugular Paragangliomas

Jugular paragangliomas typically present with a jugular foramen syndrome (Vernet's syndrome), which includes paralysis of the fourth, fifth, and 11th cranial nerves. At this stage, they are already large tumors.

Jugular paragangliomas can produce minimal symptoms such as hypoglossal neuralgia (sore throat without infection) for an extended period of time. Intermittent pulsatile tinnitus is often neglected, even at the stage of cranial nerve involvement, but is remembered by the patient after embolization, when it disappears and is replaced by what is described as complete silence. The tinnitus may be nonpulsatile and is probably related to slightly turbulent jugular vein circulation from the intraluminal tumor extension. Retroauricular pain can also be encountered when lateral expansion of the tumors occurs. Later, when the lower cranial nerves are impaired, cough due to aspiration, hoarseness, uvular displacement, and sternocleidomastoid and trapezoid muscle paralysis will be noted.

The venous occlusion of the internal jugular vein and retrograde adjacent extension in its tributaries, either by the tumor or induced thrombosis, usually has no specific clinical manifestations. However, vertigo and hearing loss may occur without obvious inner ear extension of the tumor.

A 12th nerve palsy is usually combined with facial nerve involvement, following progressing tumor growth, but it may occur before the 11th nerve palsy. In our experience, function of the 11th nerve is often preserved for a long time.

In this location, further extension occurs toward the tympanic cavity (i.e., local multicentricity) and intracranially. Although they usually remain extradural for a long time, large jugular paragangliomas have also been reported in the intradural cerebellopontine angle (D type, Fisch's classification), where they produce cerebellar symptoms and increased intracranial pressure. Forty percent of jugular paragangliomas were thought by Glenner and Grimley (1974) to have an intracranial extension. Only one of 37 patients in our experience had intracranial extension; however, four had either a false angiographic extension or strictly extradural spread (Fig. 4.2). Compression of the motor pathways in the posterior fossa and subarachnoid hemorrhage occur rarely (Moody et al. 1976).

4.6.3 Cervical Paragangliomas

Cervical paragangliomas have in common a cervical mass effect, but some specific findings can help to differentiate the vagal from the carotid forms (Fig. 4.3).

Carotid paragangliomas present as pulsatile expansile masses and when they occur as single, isolated lesions are usually associated with few other symptoms (Fig. 4.4). However, although the mass is typically cervical, it may extend into the parapharyngeal space (10% in Zak and Law-

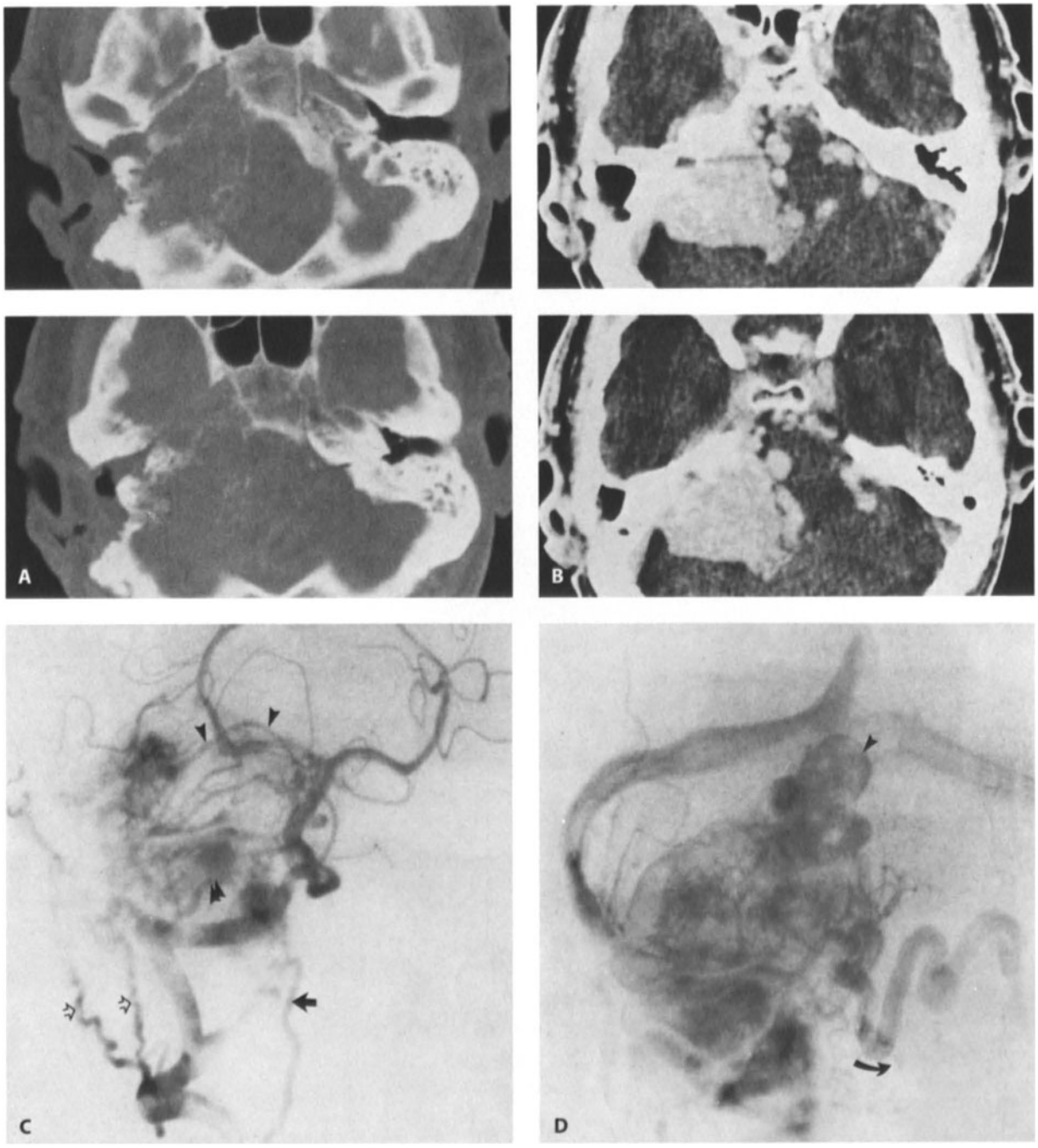

Fig. 4.2A–D. A 56-year-old man with a right recurrent jugular paraganglioma and seventh to 12th cranial nerve palsies and long tract deficits (motor and cerebellar). Note on the CT sections (**A, B**) the bone destruction and cerebral venous drainage. On the right vertebral angiogram (**C, D**), note the extradural extension fed by the odontoid arterial arch (*arrow*) and the occipital branches (proximally ligated during the previous surgical attempt) (*open arrow*). The cerebellopontine extension recruits intradural supply from anterior inferior cerebellar artery displaced superiorly (*arrowheads*), and posterior inferior cerebellar artery inferiorly (*double arrowhead*). Note the bilateral venous drainage of the tumor (*curved arrow*), and the upper venous ectasia (*arrowhead*)

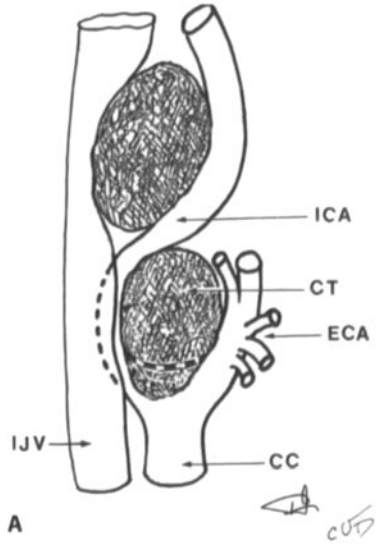

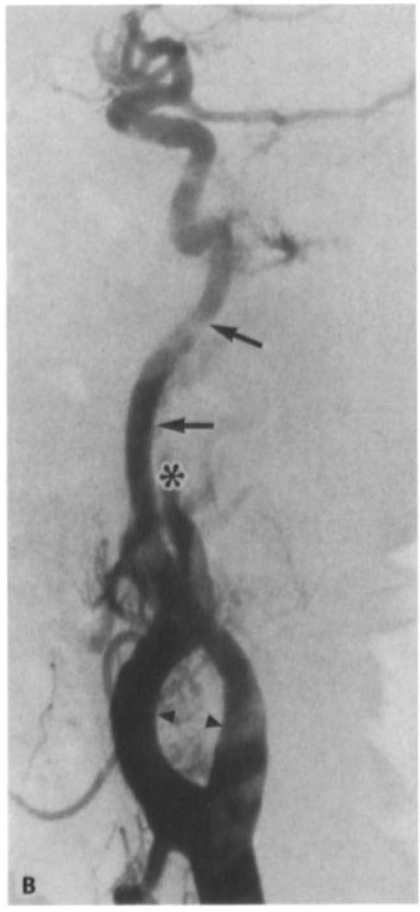

Fig. 4.3. **A** Diagrammatic illustration of the relationship between vagal (*VT*) and carotid (*CT*) tumors and the large vessels of the neck. *CC*, common carotid artery; *ECA*, external carotid artery; *ICA*, internal carotid artery; *IJV*, internal jugular vein. **B** Left carotid angiogram in a 50-year-old woman with a left temporojugular, vagal, and carotid body paraganglioma following polyvinyl alcohol embolization of the external carotid branches (*asterisk*). Note the displacement of the vessels related to the vagal (*arrows*) and carotid (*arrowheads*) tumors

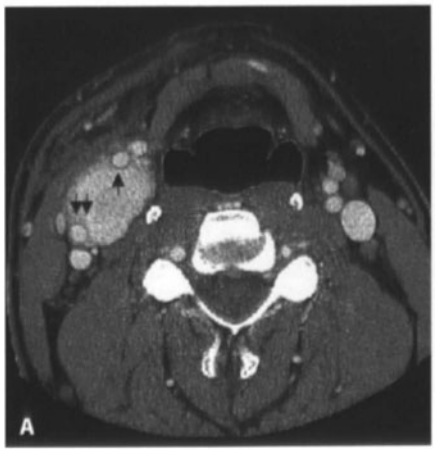

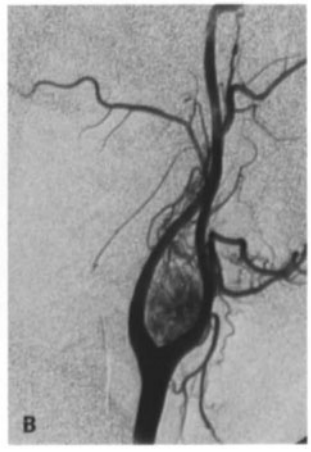

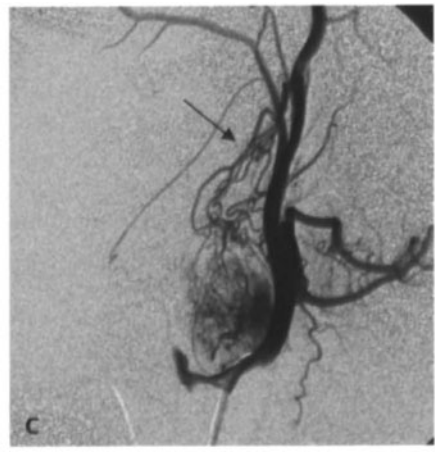

Fig. 4.4A–C. A 37-year-old woman presented with a 2-month history of fullness of the right side of the neck. On enhanced CT, there was (**A**) evidence of a homogeneously enhancing mass lesion that was displacing the external carotid artery forward (*arrow*) and the internal carotid artery posteriorly (*double arrows*). Common carotid angiogram (**B**) and proximal external carotid angiogram (**C**) in lateral views confirm this displacement by a mass lesion at the crotch of the carotid bifurcation receiving most of its supply from the ascending pharyngeal artery (*arrow*), which was embolized with medium-sized particles of polyvinyl alcohol and subsequently removed surgically without difficulty

Table 4.9. Carotid paragangliomas: clinical presentation in over 254 patients (from Zak and Lawson 1982)

Symptoms	
Pain	19%
Dysphagia	11%
Syncope	9%
Hoarseness	8%
Horner's syndrome	7%
XIIth nerve deficit	2%

son's review) (Table 4.9) or even into the oral cavity or larynx. This apparently contradictory behavior, extensive regional spread at the time of diagnosis of a slow-growing lesion, may be explained by the multicentric origin of the various components of the mass.

Cranial nerve involvement is rare with isolated carotid paragangliomas and has been reported in patients with large (or multicentric) lesions. Typically, the superior laryngeal nerve (leading to the hoarseness perceived by the patient) and the descending branch of the 12th nerve are affected. The unilateral hemiatrophy and tongue fasciculation produced by the involvement of the 12th nerve are generally not noticed by the patient.

Horner's syndrome and cerebral infarction may result from local invasion, the latter caused by internal carotid artery occlusion following tumor extension into the arterial wall.

Vagal paragangliomas demonstrate some characteristic features related to the site of origin of the mass within the neurovascular bundle of the neck, adjacent to the pharyngeal wall and high in the cervical space. The most frequent presenting symptom is a mass in the cervical (78%) or pharyngeal (44%) spaces (Fig. 4.5).

Table 4.10. Vagal paragangliomas: peripheral nervous system involvement

Symptoms	
X	24%
XII	14%
IX	11%
XI	8%
Horner's syndrome	11%

Thirty percent of patients have cranial nerve impairment (Table 4.10), which frequently manifests by neck hypoesthesia and pharyngeal pain. The high incidence of symptoms of peripheral cranial nerve involvement is probably related to the tight neurovascular compartment in which the tumor arises.

In our experience, a female in her 40s with a painful pharyngeal mass, associated with tenth and 12th nerve impairment, has a very high chance of having a vagal paraganglioma; tumors in this location and population are more likely to be malignant (3/37 vagal tumors in our series were malignant; all were in female patients 16, 40 and 45 years of age) (Fig. 4.5).

Vagal paragangliomas may arise from paraganglions in two locations: intravagal at or below the ganglion nodosa and extravagal. Those arising from intravagal paraganglions rapidly produce vagal nerve impairment and generally do not permit preservation of the nerve during tumor resection, while with tumors arising from extravagal paraganglions, the vagal nerve can often be preserved even when the tumor is large. As with paragangliomas in other locations, further growth results in extension to the base of the skull or intracranial contents. Again, it is difficult to know whether this pattern reflects multicentric origin or malignant expression, as is classic for jugular tumors with destruction of the base of the skull (Rosenwasser 1958).

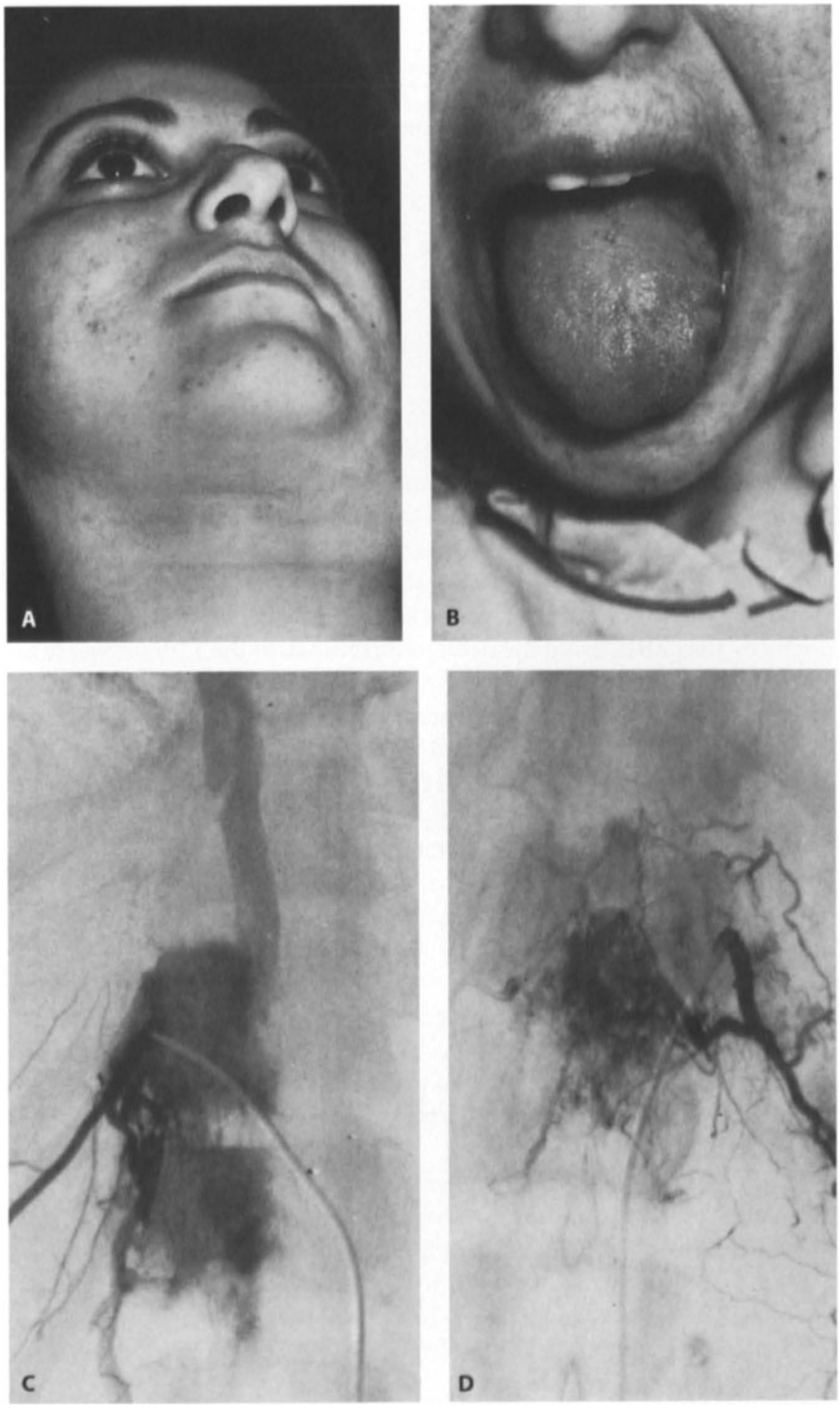

Fig. 4.5. A 16-year-old female patient presenting with a left cervical mass (**A**) and ipsilateral 12th nerve palsy (**B**). A vagal paraganglioma was embolized and removed entirely. However, 6 months later, the patient was readmitted for progressive paraplegia. Spinal angiography (**C–G**) demonstrates metastases in the low thoracic spine (**C**), mid-thoracic epidural space (**D**), cervical space (**E**), and paraspinal tissue (**F**). **G** Displacement of the artery of Adamkiewicz due to an intraspinal metastasis as well as extraspinal disease ▶

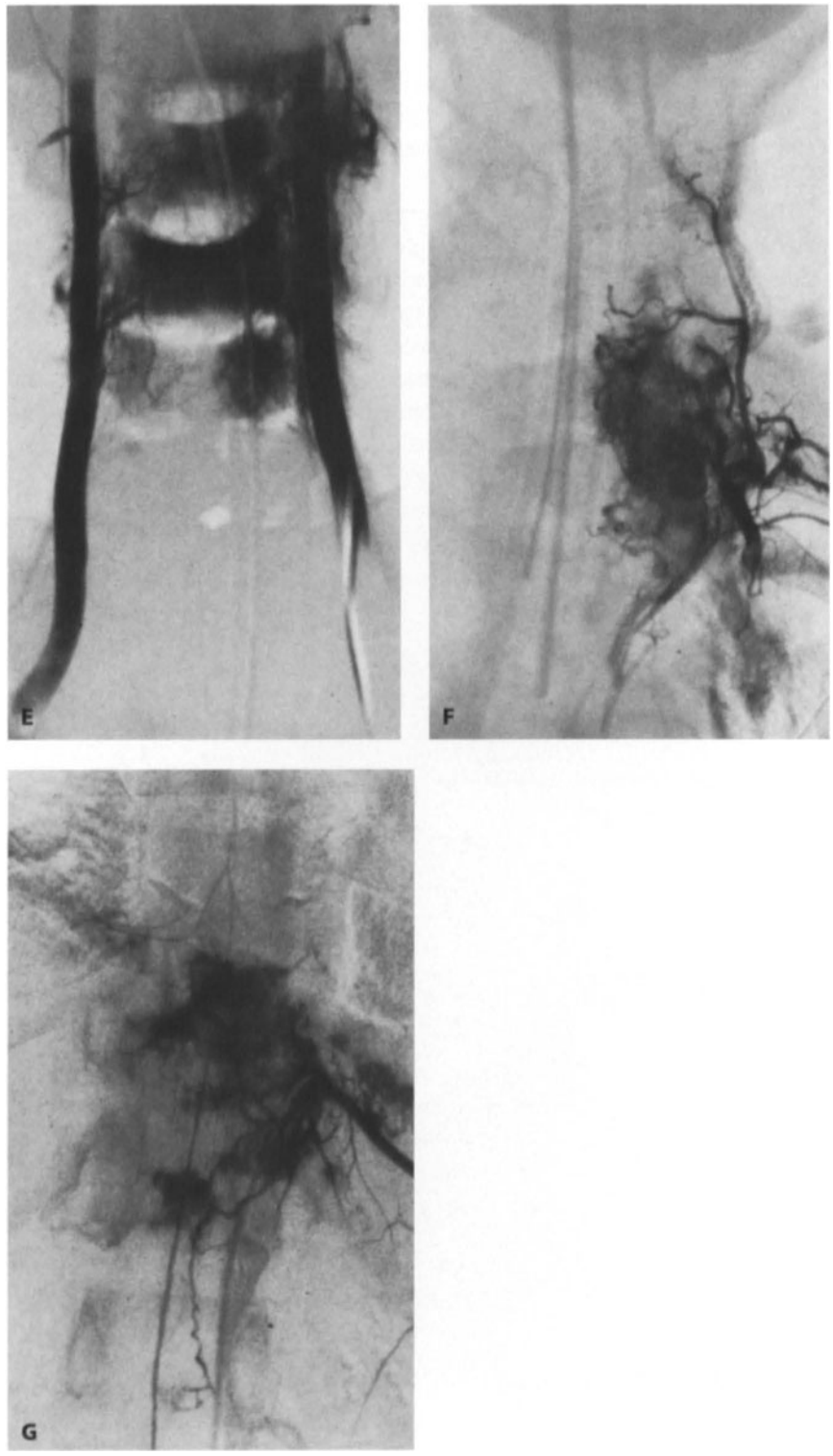

Fig. 4.5E–G.
Legend see p. 242

4.6.4 Paragangliomas in Other Locations

Paragangliomas that arise in atypical locations within the head and neck regions are much more difficult to diagnose and generally require biopsy. Delay in specific diagnosis, unfortunately, frequently leads to delay in appropriate treatment.

Those that present in the nasopharynx are frequently misdiagnosed as pharyngeal carcinomas, as they develop in the same age group. Unfortunately, some may even be irradiated without a diagnostic biopsy. These lesions are infrequent, so it is difficult to characterize their clinical features.

Prabhaker (1984) reported a 7-year-old girl with a sellar paraganglioma who presented with a skull base syndrome involving most of the left cranial nerves and recurrent episodic reversible ophthalmoplegia. The computed tomography (CT) findings were those of a solid mass containing a cystic (or necrotic) lucency (Fig. 4.6).

Laryngeal paragangliomas are also rare, but can be diagnosed early due to their localizing symptomatology: hoarseness (70%), dyspnea (43%)

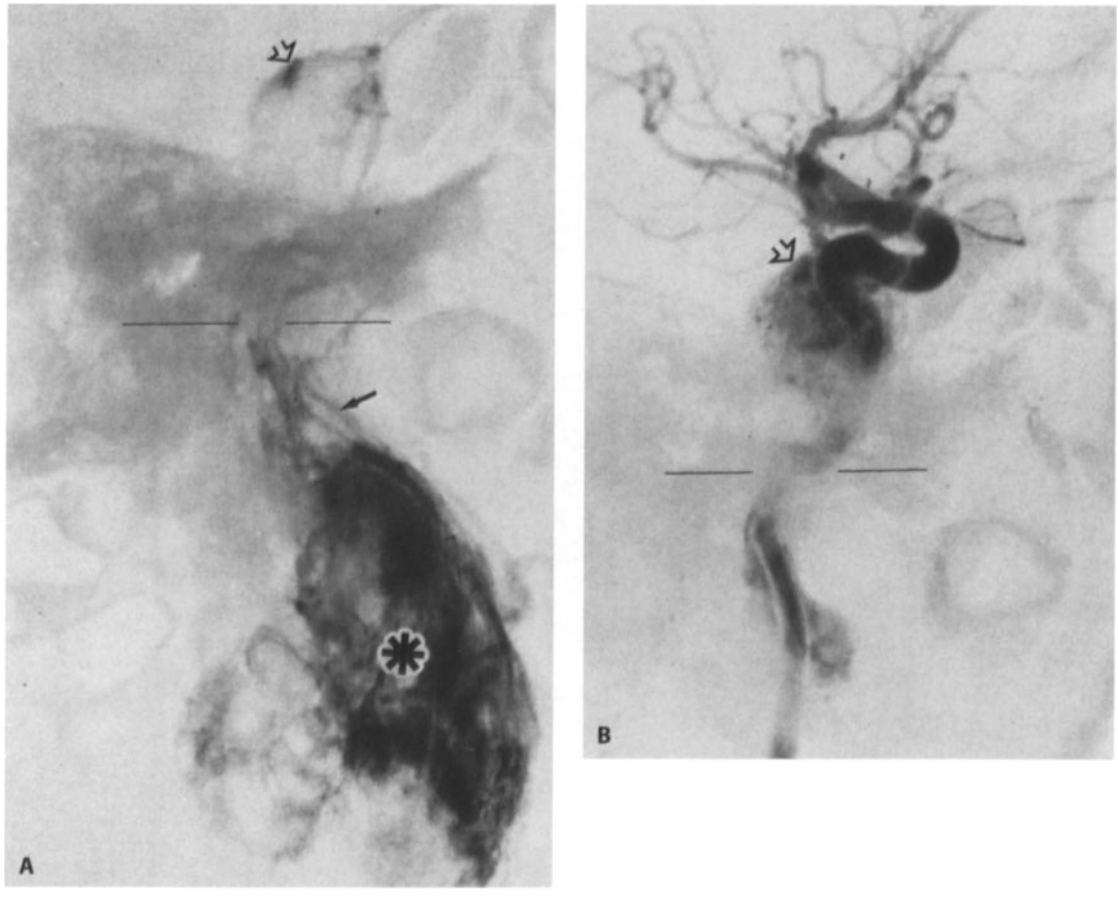

Fig. 4.6. Right ascending pharyngeal (**A**) and internal carotid (**B**) angiograms, in a 65-year-old patient complaining of a moderately painful chronic parapharyngeal mass. A large vagal paraganglioma (*asterisks*) was associated with an asymptomatic clival localization (*open arrow*). Note the normal appearance of the pharyngeal artery (*arrow*) and the discontinuity between the extra- and intracranial tumor masses

and pain. Like other paragangliomas, they can be endocrinologically active, multicentric, and malignant (see Chap. 5, this volume).

Orbital paragangliomas are intraconal and present with nonpulsatile proptosis and decreased vision. Unfortunately, they produce no specific symptoms that differentiate them from other orbital tumors and require histological examination for diagnosis. Zak, after analyzing the cases reported in the literature, emphasized the local invasiveness of orbital paragangliomas and their tendency to recur and metastasize.

4.6.5 Secretory Paragangliomas

The endocrine activity of some paragangliomas may infrequently produce additional symptoms, although uncontrolled hypertension was reported in 17% of patients described by Somasundar et al. (2000), with biochemical screening in 40 out of 128 patients (17%) demonstrating hyperfunctional tumors in a series reported by Erickson et al. (2001) (Table 4.11).

Table 4.11. Secretory activity: clinical manifestations

Headache
Hypertension
Palpitation
Diaphoresis
Anxiety

Manipulation of some secretory tumors, either by massage or during surgery, may produce hypertensive crisis requiring the pre- and intraoperative use of α-adrenergic receptor-blocking agents and/or nitroprusside (Strauss 1983). Elders (1962) reported a 12-year-old boy with a carotid body paraganglioma in whom massage of the tumor produced hypertension, sweating, and pallor. Its removal resulted in intractable hypotension and death.

Less commonly, tumor manipulation may result in hypotension with black-out spells (Strauss 1983). Although we have noted no evidence of release of catecholamines or serotonin during presurgical embolization procedures, blood pressure fluctuations usually stop once devascularization of the tumor is completed. In our experience, systolic blood pressure frequently decreases by 20 mmHg following embolization, even when no evidence of secretory activity was noted prior to treatment.

Hypertensive crises have been reported to occur during angiography of secretory paragangliomas and require urgent therapy. This complication may be secondary to hypertonic contrast agents. If possible, secretory activity should be assessed prior to angiography and embolization, and appropriate antihypertensive agents should be readily available.

Twenty functional paragangliomas included in Zak's series were distributed as follows: carotid (5), temporal (7) laryngeal (1), vagal (1) and ectopic (6). At histochemical examination, 12 were nonchromaffin and three were chromaffin tumors. A high level of the following substances was detected in samples of blood, urine, or tumor: total catecholamines, normetanephrine, and homovanillic acid.

Strauss (1983) pointed out that malignant carotid and laryngeal paragangliomas were more likely to have endocrine manifestations. Unfortunately, in this series, only metastatic tumors were included so that the relationship between secretion and malignancy could not be accurately assessed.

We have observed three patients with hypertension, suggesting endocrine activity in which biological evidence could not be obtained by

laboratory assays. In one of these, a 20-year-old woman with episodes of Bouveret tachycardia, a surgical attempt to remove a carotid paraganglioma had to be interrupted because of fluctuating blood pressure. She then underwent embolization and reoperation with complete removal of the tumor, with no additional hemodynamic manifestations.

We have wondered about a possible relationship between endocrine activity and the influence of a local angiogenic factor on the development of tumors. However, in two patients who demonstrated a peritumoral blush at angiography, we were not able to confirm the presence of a true abnormality underlying the blush, either at the time of postoperative follow-up angiography in one patient or at histological examination in the other.

4.6.6 Associated Lesions

Theoretically, numerous syndromes can be distinguished, depending upon the combination of paraganglioma and other tumors involving the cells of the APUD system.

Carcinoid tumors, pheochromocytomas, pituitary adenomas, thyroid carcinomas, other secretory tumors, and neurofibromatosis have all been reported in association with paragangliomas.

Albores et al. (1968) pointed out a parallel between the association of (a) carotid paragangliomas and thyroid adenomas and (b) papillary or follicular carcinomas and the more classic association of medullary thyroid carcinoma and pheochromocytoma.

In individual patients, these associations do not alter the diagnostic or therapeutic approach to the paraganglioma. They do, however, emphasize the need to consider all of the possible causes of symptoms in individuals with these tumors and the need to thoroughly investigate these patients prior to treatment. Regardless of the presence of additional lesions, radical surgical removal (following embolization) of the paraganglioma is still the treatment of choice.

4.7 Differential Diagnosis

The differential diagnosis of the symptoms and/or mass aspect of paragangliomas include a variety of anatomical variations and nonneoplastic diseases, listed in Tables 4.12 and 4.13.

Normal anatomical vascular variants such as aberrant internal carotid flow in the tympanic cavity, persistent stapedial artery, osteodural arteriovenous shunts, and ectopic jugular bulb may all mimic the presence of a paraganglioma (van den Berg et al. 2002).

A dominant jugular bulb may produce pulsatile tinnitus, partly because it receives a normally pulsating venous flow from the inferior petrosal tributaries, which drain the cavernous sinus (Buckwalter et al. 1983). Aside from this entity, all other causes of objective pulsatile tinnitus are produced by arterial flow (Noyek et al. 1983).

Moderate ectasia of the internal carotid bulb or dolicho-carotid artery may be associated with local pain, parapharyngeal mass effect, and even

Table 4.12. Differential diagnosis of jugular-tympanic paraganglioma (modified from Zak and Lawson 1982)

Prominent jugular bulb
Intratympanic course of internal carotid circulation
Stapedial artery persistance
Granuloma (tympanic)
Neurogenic tumor (cochlear nerve, Jacobson's nerve)
Meningiomas (temporal bone)
Metastasis (jugular foramen)
Hemangiomas (osseous, tympanic)

Table 4.13. Differential diagnosis of carotid paragangliomas (modified from Zak and Lawson 1982)

Lymphadenitis
Branchial cleft cyst
Metastasis (thyroid cancer[a], lymphoma, or Hodgkin's disease)
Neurogenic tumors
Aneurysms
Dolicocarotid sinus

[a] Thyroid carcinoma can be associated with cartoid body paragangliomas whereas medullary cancer of the thyroid is associated with pheochromocytoma.

lower cranial nerve palsies, and may be mistaken for small carotid body tumors. Likewise, internal carotid artery aneurysms may simulate carotid, vagal, or tympanic paragangliomas by producing dysphagia, mass effect, cranial nerve palsies, and pulsatile tinnitus (Fig. 4.7) (Margolis et al. 1972). Among 20 patients with aneurysms of the internal carotid artery reported by Margolis et al. (1972), five were atherosclerotic, seven were congenital, six were traumatic, and two were secondary to local infection (mycotic). They may be associated with other aneurysms or vascular lesions, and the associated lesions may be the underlying cause of the symptoms (subarachnoid, hemorrhage, traumatic carotid cavernous fistulae, etc.).

Postoperative symptomatic scar tissue, which is difficult to diagnose, may cause recurrence of symptoms. Lastly, nonneoplastic lesions such as enlarged lymph nodes or branchial cysts may transmit carotid pulsations, simulating pulsatile tinnitus.

The congenital vascular anomalies can be assessed or predicted from a careful study of the foramina using high-resolution CT. The carotid and dominant vertebral artery injections with proper analysis of the venous phase provide definitive confirmation of any of the congenital or acquired vascular causes of tinnitus.

Because of the importance of establishing the correct diagnosis, we still recommend selective angiography as the method of choice for confirmation or exclusion of the diagnosis, despite improvements in magnetic resonance imaging (MRI) technology.

The discovery of a congenital anatomical variant or other vascular abnormality during the investigation of a symptomatic patient, in whom one has anticipated the presence of a surgically treatable tumor, often

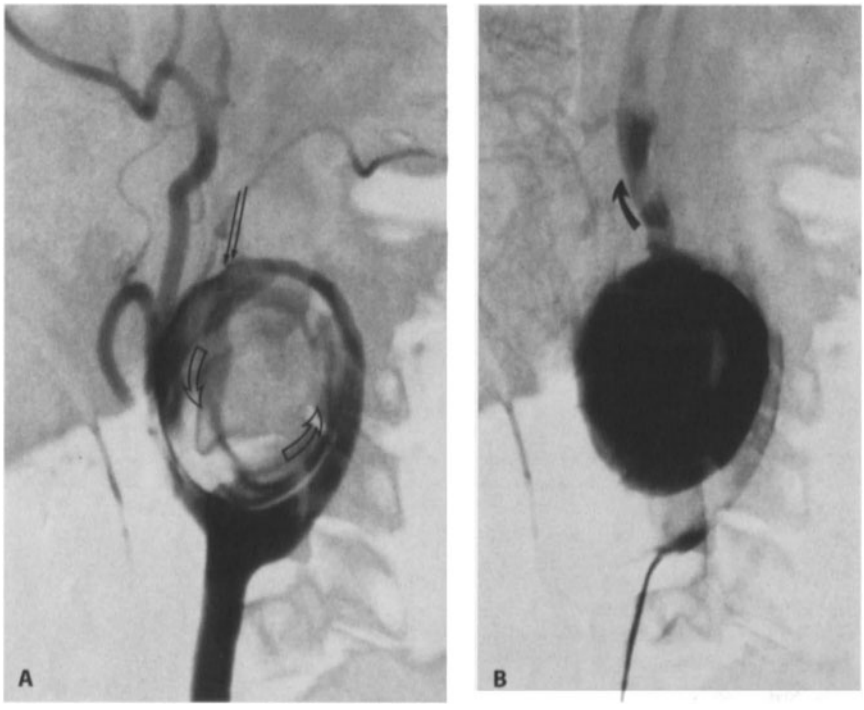

Fig. 4.7. Left common carotid angiogram, (**A**) early and (**B**) late phases, in a 32-year-old female patient presenting with a painful cervical pulsatile mass, thought to be a carotid body tumor. Note the giant aneurysm of the cervical internal carotid body (*double arrow*). Turbulent flow in the pouch (*open curved arrow*) is followed by filling of the distal cervical internal carotid artery (*curved arrow*)

leads to confusion regarding the most appropriate management. One must be careful to avoid the temptation of overly aggressive treatment.

Other tumors that enter the differential diagnosis of paragangliomas are listed in Tables 4.14 and 4.15. The final diagnosis rests with the histological findings in the surgical specimen.

Metastatic disease involving the jugular and carotid lymph nodes may simulate paragangliomas, especially when they are hypervascular at angiography and the primary tumor is not appreciated.

Meningiomas that are purely tympanic in location may be mistaken for paragangliomas, even at histological examination, but can be distinguished from them at angiography. On the other hand, their therapeutic management is the same with embolization followed by surgical resection (Fig. 4.8).

Neurogenic tumors are fairly common in the parapharyngeal space; less commonly they can occur at the jugular or hypoglossal foramina. In the few cases we studied, the tumors were all supplied by the ascending pharyngeal artery but were less vascular than most paragangliomas. The clinical features may be helpful in distinguishing these lesions, as they tend to have early neurological deficits (Fujiwara et al. 1980; Chang and Schi 1984). Similarities to cervical paragangliomas include hoarseness, dysphasia, and pulsation. These tumors may be malignant and are radioresistant, thus their management also includes embolization and surgical resection (Fig. 4.9).

Primary malignant tumors or metastases can be highly vascular and a specific diagnosis at angiography may not be possible. Cerebellopontine angle tumors such as acoustic neurinomas and hemangioblastomas may be supplied by the external carotid artery, but generally have a different angiographic blush compared to paragangliomas.

Table 4.14. Primary lesions involving the petrous apex (from Flood 1984)

Epidermoid cyst
Mesenchymal tumor
Eosinophilic granuloma
Primary mucocele

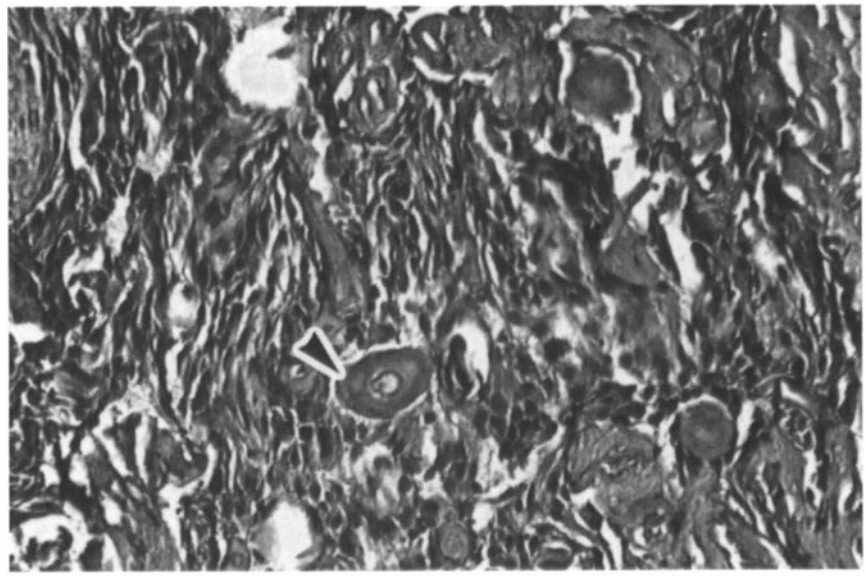

Fig. 4.8. A 48-year-old female patient presented with progressive deafness related to a strictly intratympanic meningioma. Note the typical psammoma (*arrowhead*) on the pathological section

Fig. 4.9. A 55-year-old woman presenting with progressive deafness of the right ear, related to an intratympanic neurofibroma involving Jacobson's nerve. Note the cutaneous manifestations of von Recklinghausen's disease (neurofibromatosis)

Table 4.15. Secondary lesions involving the petrous apex (from Flood 1984)

Osteomyelitis	Secondary to mastoiditis Secondary to malignant external otitis
Direct tumor spread	Nasopharyngeal carcinoma of the clivus. Paraganglioma Neurogenic tumors (V–XII) Meningioma
Erosion by disseminated tumor	Metastatic carcinoma Lymphoma
Other osteolytic process	Sphenoid mucocele Aneurysm of the internal carotid artery

One of our patients was referred to us with the diagnosis of tympanojugular paraganglioma on the basis of lower cranial nerve palsies and low cerebellopontine angle tumor associated with bluish discoloration of the tympanic membrane. Increased intracranial pressure due to the size of the mass led to ventricular shunting. Pulsatile tinnitus could not be expected since the patient had deafness related to the cerebellopontine angle lesion. Clinical examination revealed a bluish discoloration of the external ear, including the helix and external auditory canal. Aside from these latter findings, the features were felt to be consistent with the diagnosis of a branchial paraganglioma. However, tympanic tumors do not produce discoloration of the helix and this abnormality was found to be caused by a venous vascular malformation, present since birth. The cerebellopontine angle tumor was a malignant melanoma.

Most bone tumors have CT findings that distinguish them from paragangliomas, although vascular malformations involving the bone may have some features in common (Glasscock et al. 1984).

Ascending pharyngeal angiography will nearly always confirm or rule out the diagnosis of a suspected branchial paraganglioma. Absence of the typical appearance of the tumor blush seen with paragangliomas essentially excludes that diagnosis. Other branchial lesions that may occur, in order of decreasing angiographic tumor vascularity, include metastases, hemangiomas, meningiomas, neurogenic tumors, and lymphatic neoplasia.

4.8 Pretherapeutic Evaluation

Although the clinical presentation is often strongly suggestive of the diagnosis of a branchial paraganglioma, CT examination is useful and necessary in demonstrating or ruling out vascular variants that may simulate paragangliomas and in demonstrating the topography of large masses (Figs. 4.2, 4.10). As with other mass lesions, the examination should be performed with and without contrast enhancement and should be filmed or at least viewed at bone as well at soft tissue windows. Direct coronal images are indispensable in the presence of cervical or base of the skull mass lesions, and thin (1.0–3.0 mm) sections are necessary to evaluate the petrous temporal bones. The following structures should be specifically examined: the carotid canal, inner and middle ear, cerebellopontine angle, mastoid process, cervical vessels, and pterygoid muscles, as involvement of these structures will modify the surgical and embolization approaches (Figs. 4.2, 4.10). On MRI, small areas of signal void can be identified within the soft tissue mass lesion, and intense homogeneous enhancement of the paraganglioma occurs following contrast administration. The extension towards the venous system as well as transdural intracranial extension is often best demonstrated with enhanced MRI examination while the margins of osseous destruction are better shown with high-resolution CT. While CT and MRI are mandatory for the purpose of investigation, their findings are not always characteristic of paragangliomas and can be mimicked by benign or malignant nerve sheath tumors. In a review of 236 patients with 297 paragangliomas, Erickson et al. (2001) demonstrated

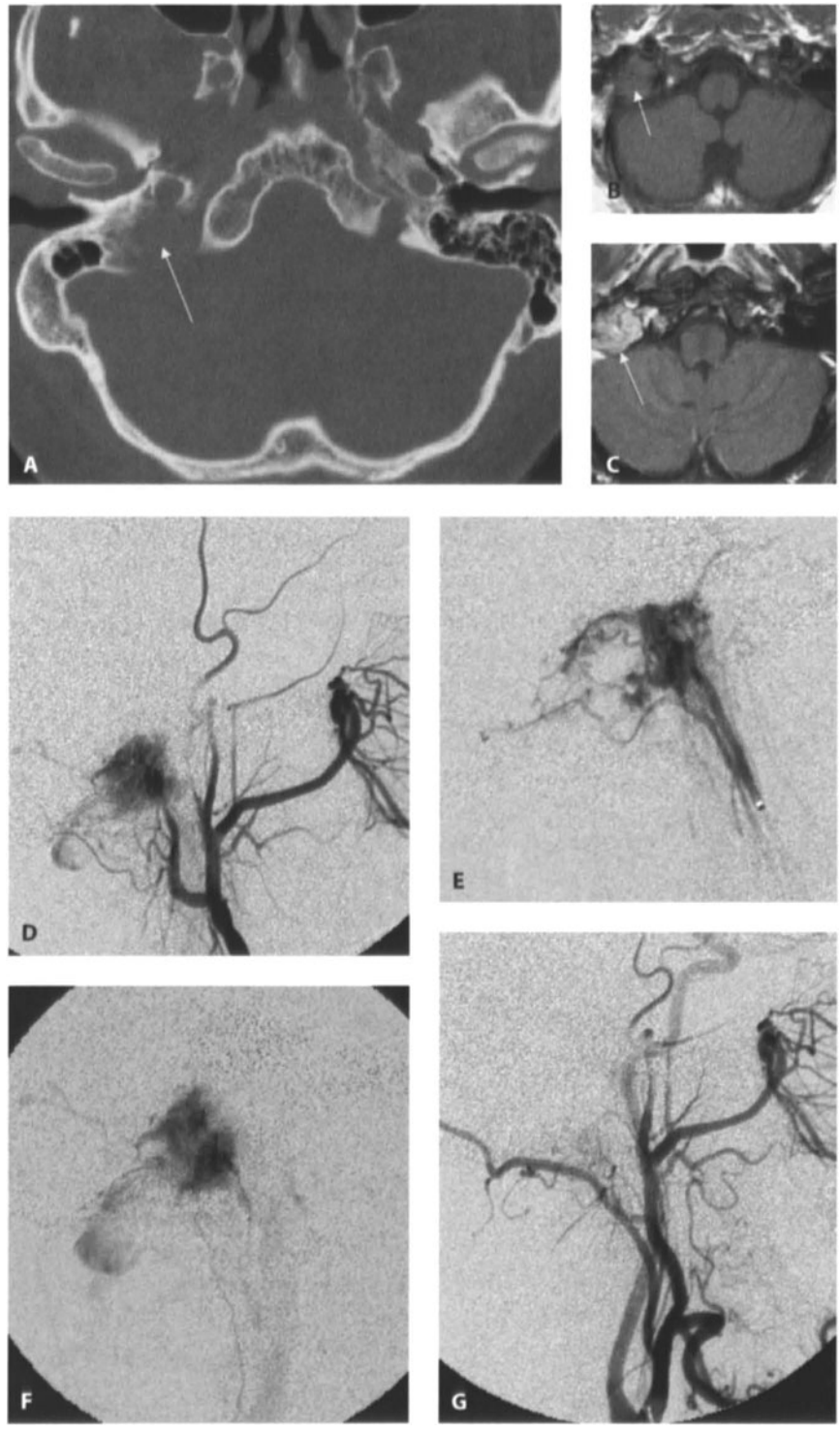

Fig. 4.10A–J. A 42-year-old man presented with a 2-month history of increasing difficulty swallowing. CT (**A**) and T1-weighted MRI, without (**B**) and following contrast enhancement (**C**), showed evidence of an enhancing soft tissue mass lesion associated with bony destruction adjacent to the jugular bulb level (*arrows*). External carotid angiogram in lateral view (**D**) and selective ascending pharyngeal (**E**) and posterior auricular (**F**) injections in lateral views show distinct tumor blush at jugular bulb level. Following selective presurgical embolization with medium-sized particles of polyvinyl alcohol in the individual branches of the external carotid supplying the tumor after embolization, external carotid angiogram in lateral view (**G**) shows complete devascularization of the tumor. **H–J** see p. 252

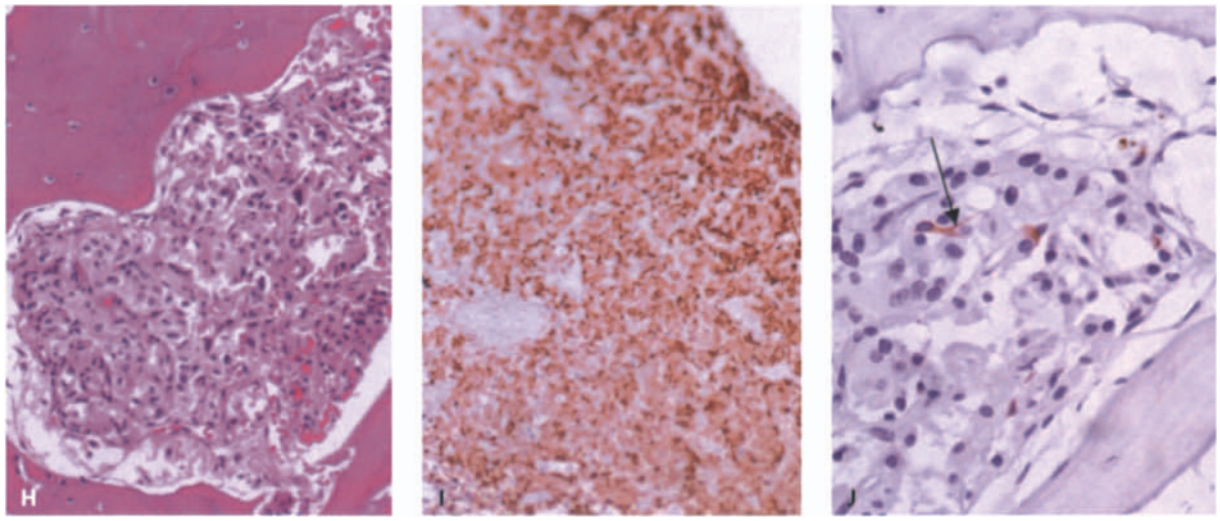

Fig. 4.10 (*continued*). Complete surgical removal was achieved and the pathological examination (**H–J**) demonstrated characteristic bony trabeculae invasion by nests of neoplastic cells, which immunohistochemically stain positive for synaptophysin (**I**) and chromogranin A, while staining for S100 (**J**) demonstrates sustentacular cell (*arrow*) characteristic of paraganglion tissue

that among all the imaging modalities, MRI was the least likely to fail to demonstrate the presence of the tumor.

Superselective angiography remains strongly indicated if a paraganglioma is suspected, and doing it before a biopsy procedure is highly recommended.

4.8.1 Angiographic Protocol

The arterial feeders that should be selectively catheterized can usually be predicted from the topography of the mass demonstrated on the CT examination. Embolization is done at the time of diagnostic angiography.

The typical angiographic features of paragangliomas include moderate enlargement of the feeding arteries, an early, intense parenchymal blush, and rapid venous filling. As previously discussed, some tumors are opacified by a single feeding artery, while others are supplied by several (van den Berg et al. 2002). After all possible arterial supply has been studied, the most effective and safest route for embolization can be selected.

4.8.2 Temporal Paragangliomas: Specific Features

The arteries that should be studied selectively include the ipsilateral vertebral, internal carotid, distal external carotid, posterior auricular, and occipital arteries and the ascending pharyngeal artery bilaterally (ipsilateral neuromeningeal and inferior tympanic branches) (Figs. 4.10, 4.11). The late phase of the dominant vertebral artery injection is also necessary for visualization of the venous flow pattern. Jugular vein occlusion will be

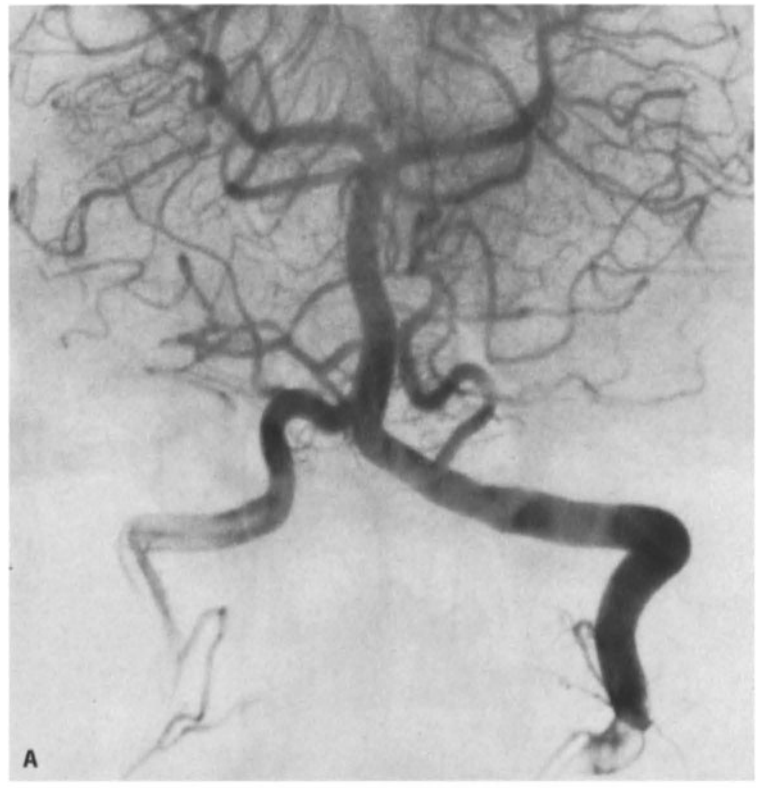

Fig. 4.11A–M. A 40-year-old man presenting with pulsatile bruit in the left ear and ipsilateral lower cranial nerve palsies. **A** Early and **B** late phases of the dominant (left) vertebral artery. Note the absence of the cerebellopontine angle arterial supply, the occlusion of the left jugular foramen (*asterisk*), and the venous collateral circulation via the mastoid foramen (*arrow*). **C–M** see pp. 254–256

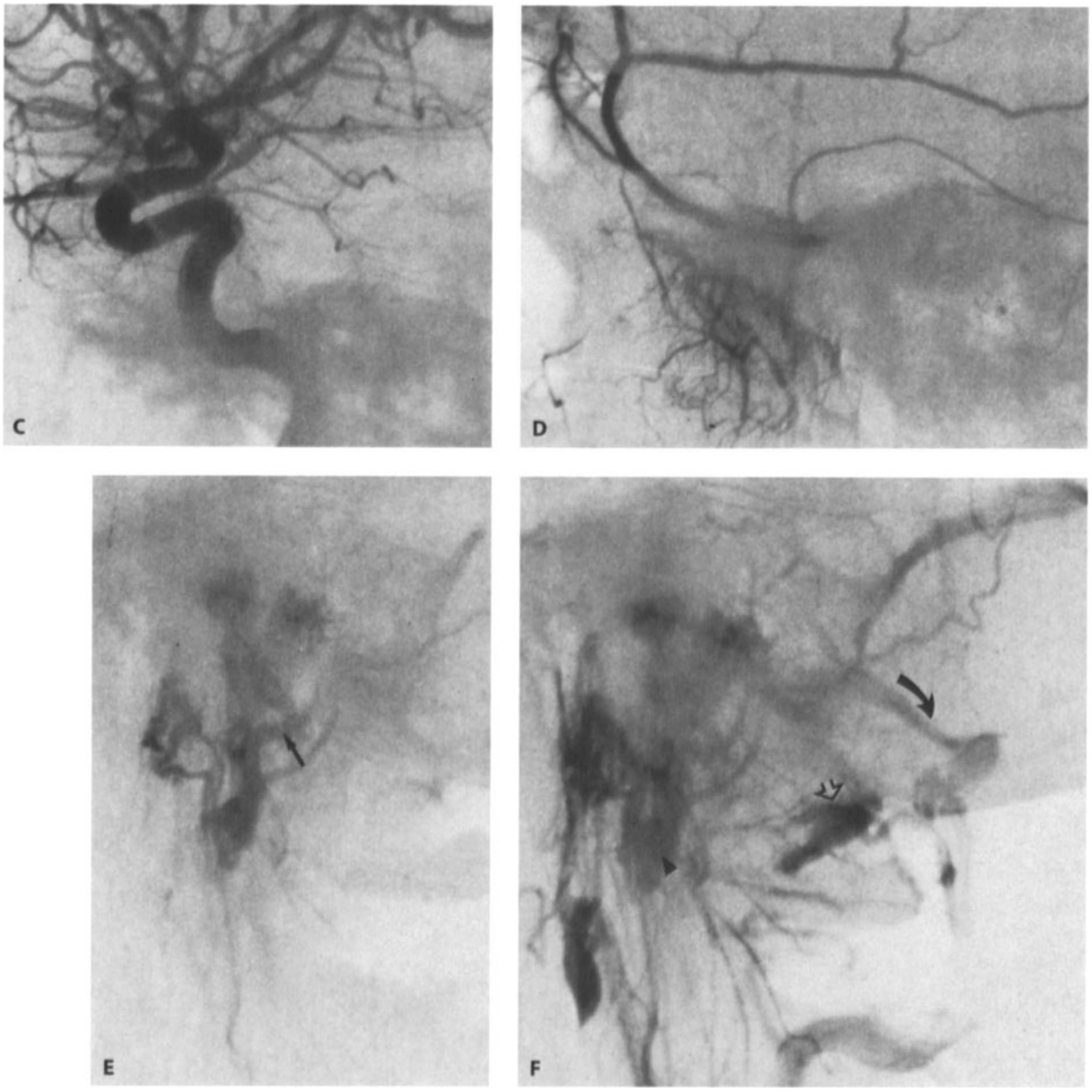

Fig. 4.11 (*continued*). Normal left internal carotid (**C**) and middle meningeal artery (**D**) angiograms. Selective injection in the auricular branch of an occipitoauricular trunk (**E, F**) shows arterial supply to the tumor via the stylomastoid artery (*arrowhead*) and venous drainage via the mastoid (*curved arrow*) and posterior condyloid (*open arrow*) canals. **G–M** see pp. 255, 256

demonstrated and the collateral venous drainage outlined. However, a larger arteriovenous shunt within a tumor draining into the internal jugular vein may produce a wash-out of contrast within this vein and lead to the erroneous diagnosis of venous occlusion. In the presence of true tumor invasion, a discrete intraluminal filling defect will be seen on the venous phase, and selective arterial injections will demonstrate a tumor blush within the vein. In patients whose jugular vein is not clearly seen due to wash-out, its patency should be confirmed by repeat vertebral angiography following embolization (Fig. 4.12).

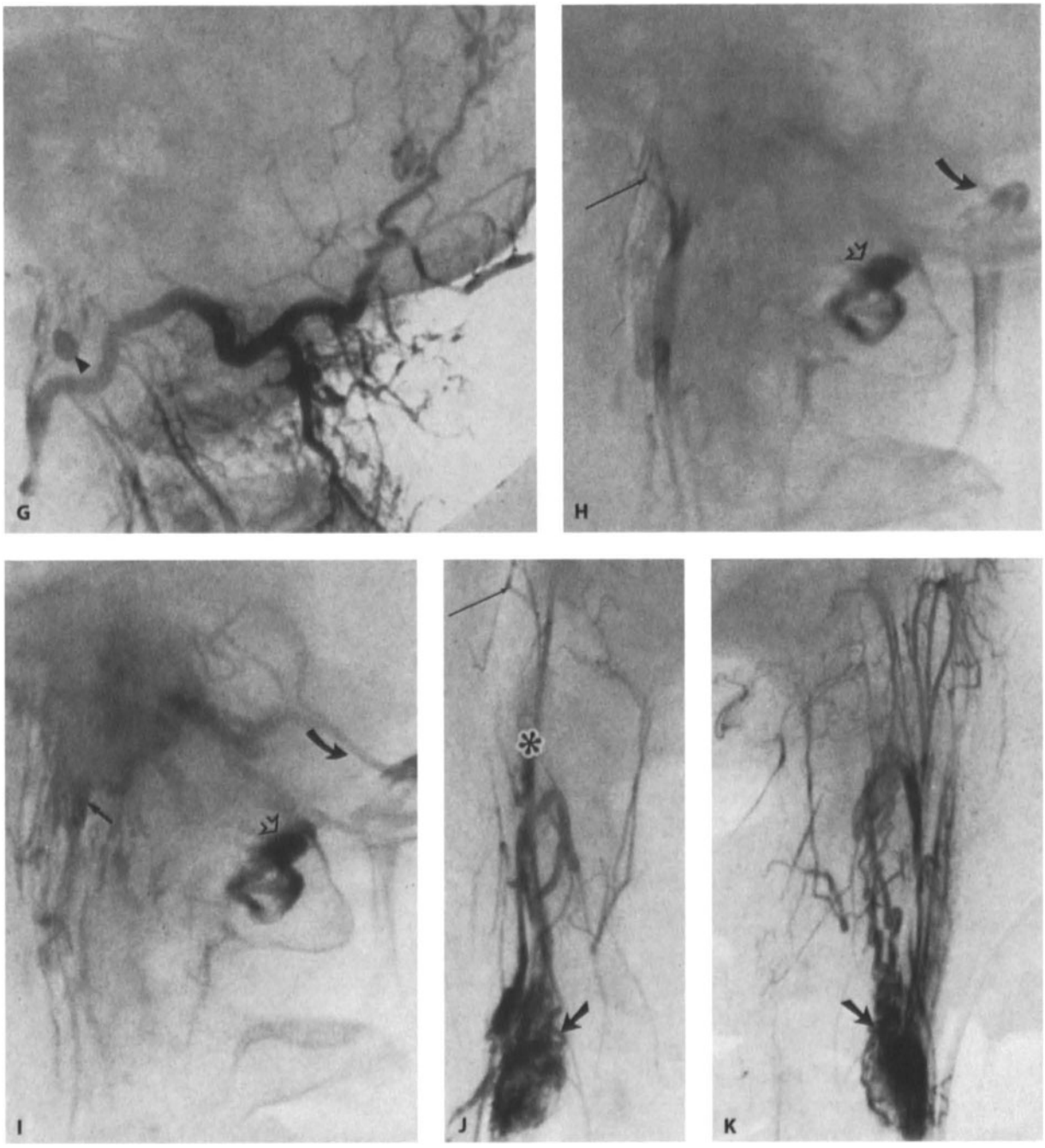

Fig. 4.11 (*continued*). **G** Postembolization injections into the proximal occipitoauricular trunk and (**H**) proximal ascending pharyngeal artery. Note the pharyngeal branch (*arrow*) and the venous drainage of the tumor into the mastoid (*curved arrow*) and the posterior condyloid (*open arrow*) veins. **I** Selective injection of the posterior branch of the ascending pharyngeal artery (*arrow*) demonstrates the venous drainage of the tumor into the mastoid (*curved arrow*) and the posterior condyloid (*open arrow*) veins. **J** Control in the pharyngeal artery after embolization of the posterior branch (*asterisk*). Note the patency of the pharyngeal branch (*arrow*) and the additional tumoral stain proximal on the artery (*solid arrow*). **K** Injection in the ascending pharyngeal artery on the opposite side shows the same type of proximal stain (*solid arrow*). **L, M** see p. 256

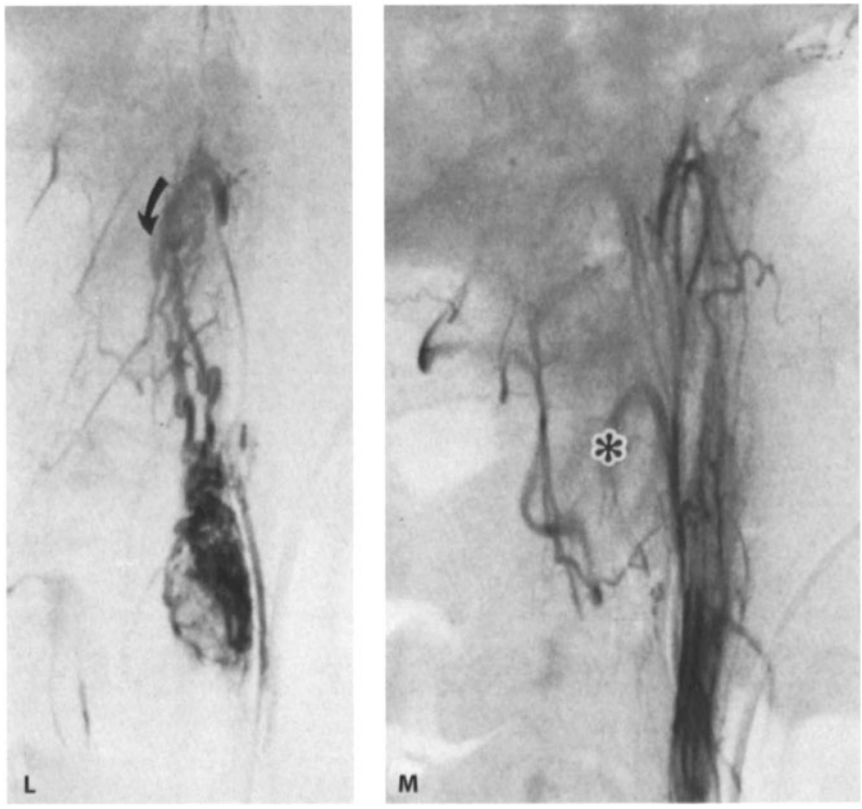

Fig. 4.11 (*continued*). **L** Selective injection of the musculospinal artery (*solid curved arrow*), and the follow-up study of the ascending pharyngeal trunk (**M**) shows satisfactory occlusion of the feeder (*asterisk*). The three lesions were removed in one surgical session. The temporal lesion was a typical tympanojugular paraganglioma, whereas both cervical ones were lymph node metastases

1. Intradural posterior fossa extension (Fig. 4.2) must be carefully distinguished from extradural or extracranial tumor, in order to avoid misinterpretation that could result in avoidance of surgery in potentially resectable lesions. A tumor blush is frequently seen at or caudal to the level of the temporal bone on vertebral angiograms, but in most instances it originates from the extradural branches of the vertebral artery at C1, C2, or C3, and is extradural tumor. True intradural tumor spread is best confirmed or ruled out by careful analysis of the ipsilateral anterior inferior cerebellar artery (AICA) and posterior inferior cerebellar artery (PICA) territories in Townes's projection, as the intradural tumor will be supplied by branches of these arteries. Comparison of the vertebral angiographic findings with those from the ipsilateral selective occipital and ascending pharyngeal injections usually provides an accurate assessment of tumor extent. Misinterpretation of the tumor blush produced by the extradural vertebral artery branches may account for the high incidence (40%) of intracranial extension reported by Farrior et al. (1980).
2. Carotid canal invasion is diagnosed by the detection of soft tissue mass and bone destruction involving the carotid canal on CT or MRI examination, associated with narrowing of the intrapetrous carotid artery at

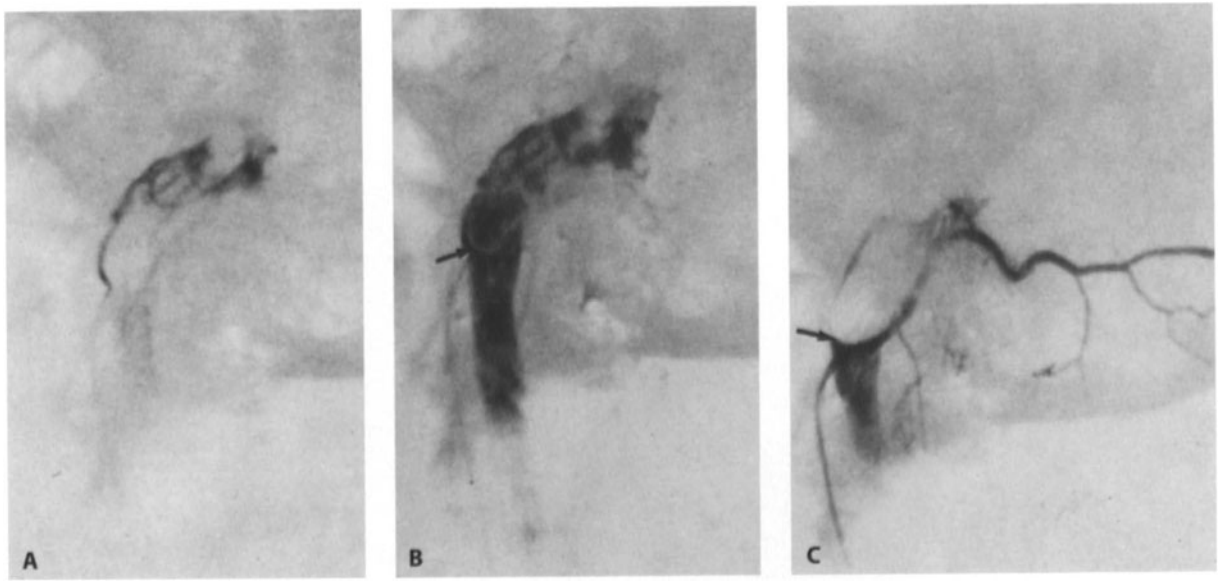

Fig. 4.12A–C. Jugular paraganglioma. **A** Early and **B** late phases of the ascending pharyngeal artery injection. **C** Ipsilateral occipital artery angiogram. Note how the intraluminal jugular vein tumor delineates the lower extension of the lesion. Distal jugular vein injection is obtained through the tumoral arteriovenous shunt, which shadows the inferior convex margin of the paraganglioma (*arrows*)

angiography. Arterial supply to the tumor (e.g., tympanic paraganglioma) by branches of the internal carotid artery does not necessarily signify invasion of the carotid canal. The internal carotid artery constantly has a branch to the tympanic cavity through a small foramen posterior to the petrous angle of the vessel. The Stenvers projection, in which the X-ray beam is perpendicular to the intrapetrous carotid artery, best demonstrates the free bony margin between the vessel and the tumor blush.

3. Angiographic blush in the region of the petrous bone adjacent to the soft tissue mass outlined on CT or MRI examination may correspond to increased vascularity of healthy tissue, probably the result of mucosal congestion.

4.8.3 Cervical Paragangliomas: Specific Features

The arteries that should be selectively injected in the investigation of a suspected cervical paraganglioma include the ipsilateral vertebral, proximal internal carotid, facial, lingual, superior laryngeal, carotid body artery, ascending cervical, inferior laryngeal and bilateral ascending pharyngeal arteries (Figs. 4.13, 4.14).

Cervical paragangliomas frequently compress the internal jugular vein without parietal invasion. Unfortunately, true tumor involvement of the adventitia of the internal carotid artery is not rare. The pattern of vessel displacement is a useful distinguishing feature, as vagal paragangliomas typically displace the internal carotid artery anteriorly and medially,

Fig. 4.13A–F. A 15-year-old female patient presenting with a left cervical mass. **A** Early and **B** late phases of the dominant left vertebral artery injection demonstrates a vagal paraganglioma (*arrow*) and the extrinsic indentation of the jugular vein (*arrowheads*). **C–F** see p. 259

whereas carotid paragangliomas displace the internal carotid artery laterally and posteriorly (Fig. 4.3).

Bilateral disease can be effectively diagnosed or ruled out by selective contrast injection in the contralateral ascending pharyngeal artery, which is generally the first part of our angiographic study. Each of the 95 branchial paragangliomas that we have studied was supplied at least partially by the ascending pharyngeal artery, and 20% of them received their blood supply exclusively from this vessel. Therefore, a normal contralateral ascending pharyngeal arteriogram eliminates the possibility of bilateral cervical paragangliomas. Only laryngeal and orbital lesions are supplied by other vessels (Figs. 4.11, 4.13).

Angiographic features that suggest malignancy include arterial invasion and indistinctness of the tumor margins (after the entire puzzle reconstruction is complete).

Metastases have the same angiographic features as primary paragangliomas so that for those lesions that present in unusual locations in the head and neck, it may be impossible to distinguish between ectopic or metastatic tumors.

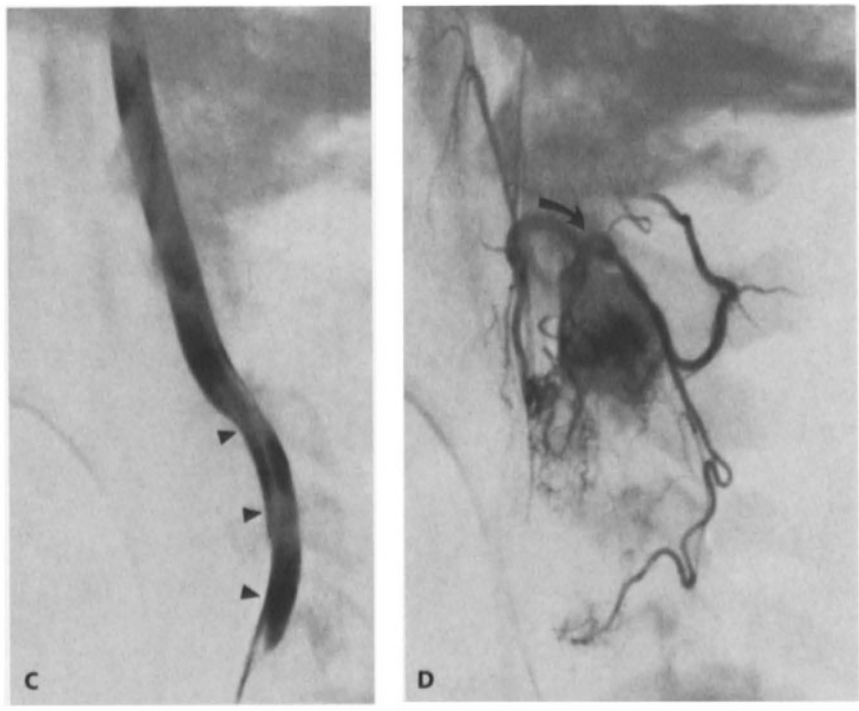

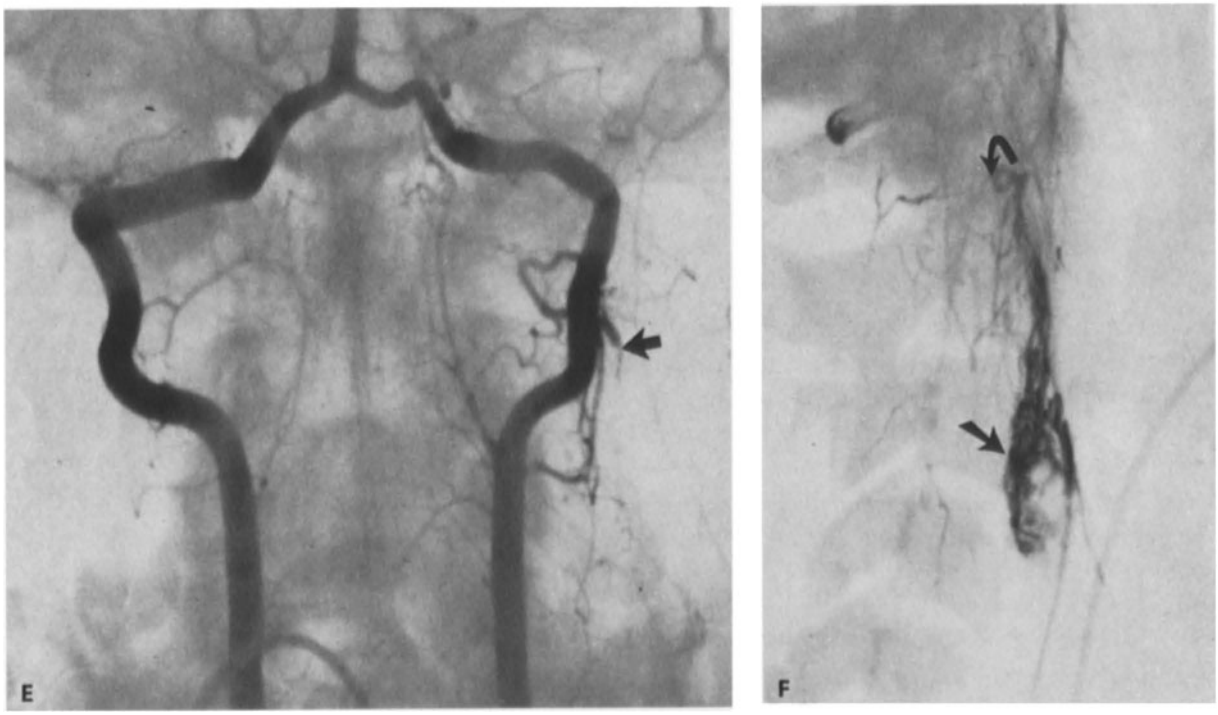

Fig. 4.13 (*continued*). **C** Left internal carotid injection shows posterior displacement by the tumor (*arrowheads*). **D** Selective injection of the pharyngeal artery demonstrates the tumoral supply via the musculospinal artery (*curved arrow*). **E** Vertebral artery angiogram after embolization of the sole supply from the ascending pharyngeal artery fails to demonstrate the tumor blush (*arrow*). **F** Opposite ascending pharyngeal angiogram discloses an additional lesion (*arrow*) fed by the musculospinal artery (*curved arrow*). The tumors were removed in two surgical sessions and were found to be typical bilateral left vagal and right carotid paragangliomas

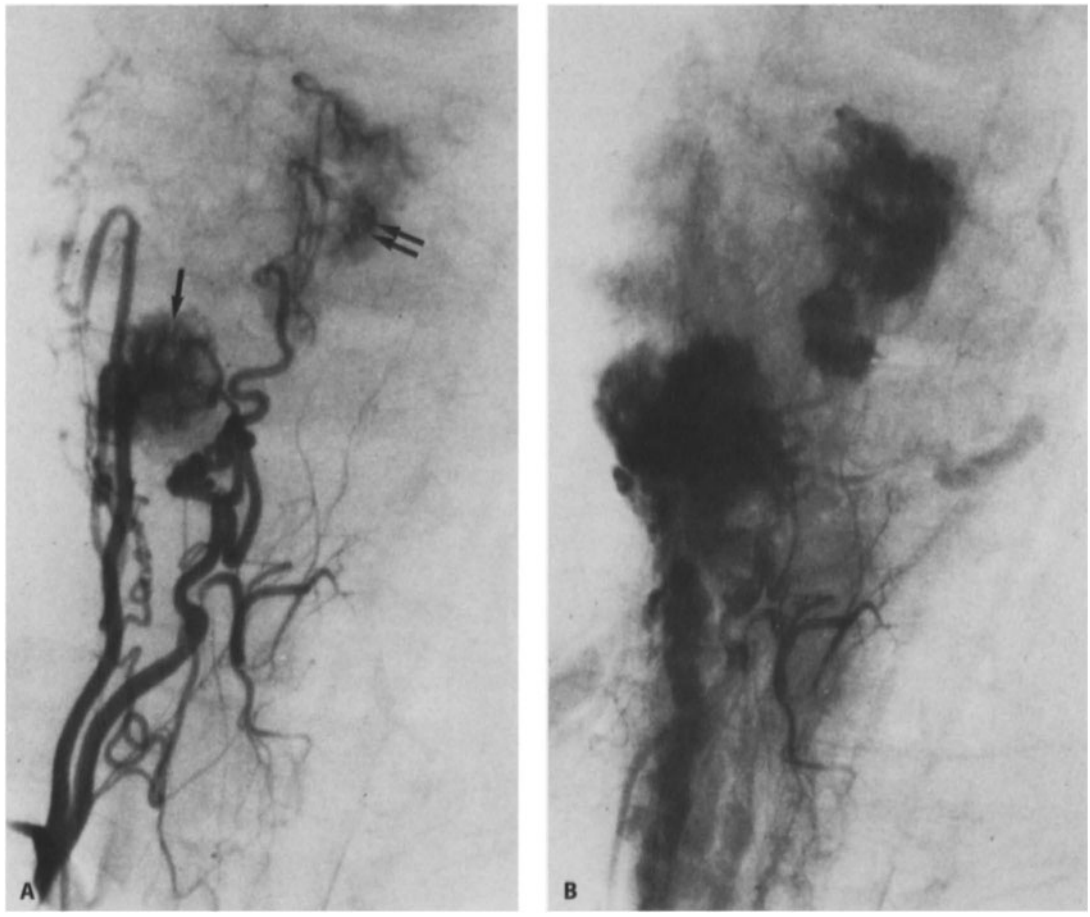

Fig. 4.14A, B. Inferior thyroidal artery injection (right anterior oblique projection). Early **A** and late **B** phases demonstrate large carotid body paraganglioma. Note the laryngeal extension (*double arrow*) and the lymph node invasion (*arrow*)

4.9 Therapeutic Strategies

Like the treatment of other complex lesions of the head and neck area, optimal therapy requires a multidisciplinary approach but will vary between different centers depending upon the skills of the available individuals.

Interpretation of the results of various therapeutic modalities reported in the literature is difficult. In particular, is it often very difficult to distinguish between recurrence, metastasis, and late manifestation of multicentricity.

The efficacy of radiotherapy in the treatment of paragangliomas differs greatly in different series in the literature. Doses of 40 Gy or more have been reported to result in tumor control in over 90% of patients (Cummings et al. 1984), whereas two surgical series found only a 25% cure rate using radiotherapy (Ogura 1978; Spector et al. 1973). Gamma knife radiosurgery in a series of 66 patients with paragangliomas was noted to decrease tumor size in 40%,and no change in tumor volume was noted in 60% on 2-year follow-up after treatment (Liscak et al. 1999). It is recognized that the tumor cells are not radiosensitive, and the predominant ef-

fects of radiation are via induced vascular arteritis and fibrosis. Late complications such as brain necrosis are being recognized more frequently (Sharma 1984).

We feel that the treatment of choice is complete removal of the tumor whenever possible, and this opinion is shared by many others in different centers (House and Glasscock 1974; Spector et al. 1973; Ogura 1978, Fisch 1982). Complete surgical excision was possible in 95% of patients' carotid body tumors with a perioperative morbidity of 2% (Nora et al. 1988).

We believe that embolization is still underutilized in the management of paragangliomas. It is a safe and efficient method to devascularize these tumors (Gruber 2000a) and it can be used as the sole therapy for inoperable tumors, where the objective is the stabilization of growth.

There is electron microscopic evidence (Bosq 1983, unpublished data) that presurgical embolization with particles produces cellular damage, which can be irreversible and related to ischemia. Necrosis and fibrotic transformation of the tumor can also be observed. Therefore, if an active agent can be safely delivered into the tumor bed, one can expect complete control of the lesion with regression of some of the symptoms (Figs. 4.16, 4.17).

Preoperative embolization allows for easier resection of the lesion and may allow resection of a tumor initially felt to be inoperable. Mean blood loss and mean operating time were shown to be significantly reduced when embolization was performed prior to surgical removal of the paraganglioma (Tikkakoski et al. 1997).

4.10 Technical Aspects of Embolization

In most cases, embolization is performed prior to surgical resection, so that polyvinyl alcohol (PVA) particles of 150–250 μm in diameter are sufficient. The capillaries within the tumor measure about 200 μm in diameter. Liquid embolic agents should be used only in the treatment of inoperable tumors and only when optimal flow control can be achieved. As with other tumors, there is no indication for the use of larger particles.

The embolization techniques that we use are similar to those described in the treatment of other benign craniofacial tumors. Individual feeding arteries are selectively catheterized and embolized with PVA particles, and then the same arteries are occluded proximally using strips of Gelfoam. This proximal Gelfoam occlusion helps to promote the distal thrombosis induced by the small particles (Fig. 4.10, 4.15).

Special attention must be paid to the intracranial and orbital anastomoses whenever the middle meningeal or occipital arteries are embolized.

Angiographic series may be necessary during embolization in the ascending pharyngeal artery, if the quality of the fluoroscopic image is not satisfactory to confirm the preferential flow towards the tumor.

The ascending cervical and inferior laryngeal arteries can be safely embolized in most cases of large vagal or carotid lesions, but one must be aware of and avoid the possibility of flow toward the spinal artery and reflux into the vertebral artery.

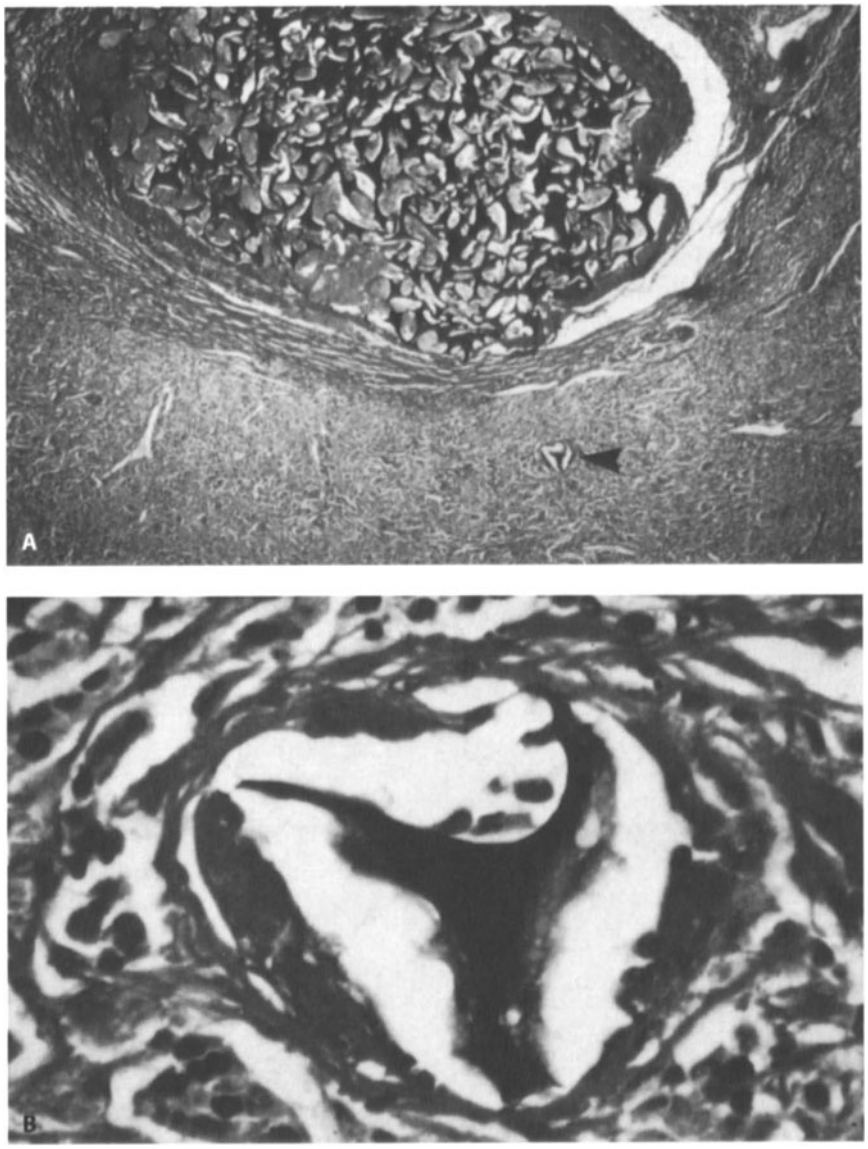

Fig. 4.15. **A** Pathological section of a cervical paraganglioma. Note the large vessel occlusion and the polyvinyl alcohol (PVA) particle in a small artery (*arrowhead*). **B** Pathological section in a case of paraganglioma, intraluminal PVA particle (250 μm)

In specific cases in which a compartment has to be reached more effectively (common compartment with the internal carotid artery or vertebral artery branches) microparticles, fluid material, or cytotoxic agents may be used (Figs. 4.16, 4.17).

However, in Fisch's classification, two specific stages present difficult situations for embolization. The D3 type, in which the AICA or the PICA supply the lesion, are almost never amenable to embolization. The C3 type, with petrous apex involvement, on the other hand, can be controlled by sacrificing the internal carotid artery and proximal embolization.

In exceptional cases, selective catheterization and embolization of the caroticotympanic artery can be performed, but we do not recommend this technique until after first attempting to reach the same territory via the ascending pharyngeal artery, with or without flow control.

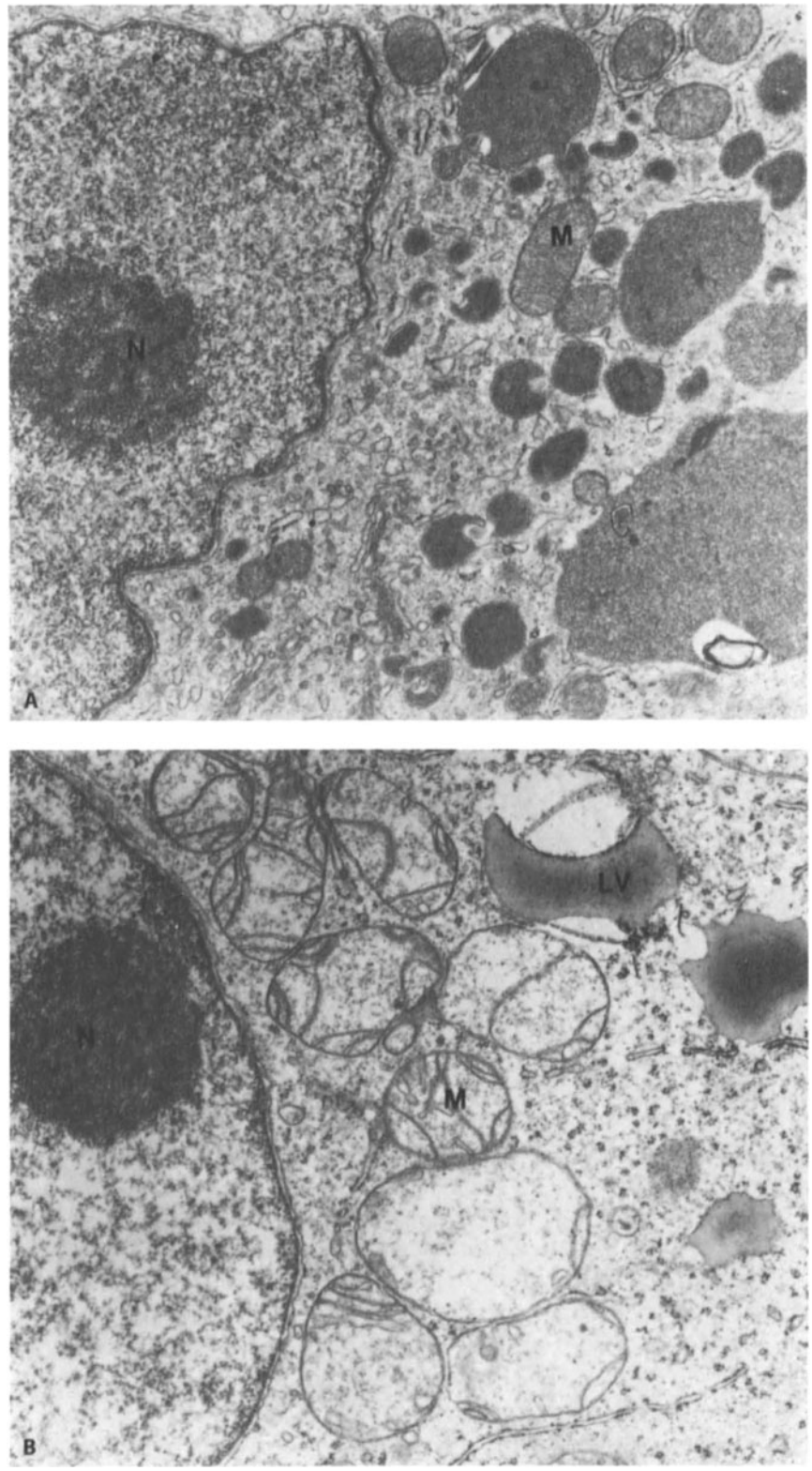

Fig. 4.16A, B. Electron microscopy of two separate paragangliomas. One was not embolized (**A**); the second one after embolization (**B**). Note the swelling of mitochondria (*M*) and lipoid vacuolization of the cytoplasm (*LV*) on the embolized lesion (*N*, nucleus). (Bosq, unpublished data; Institut Gustave Roussy, France)

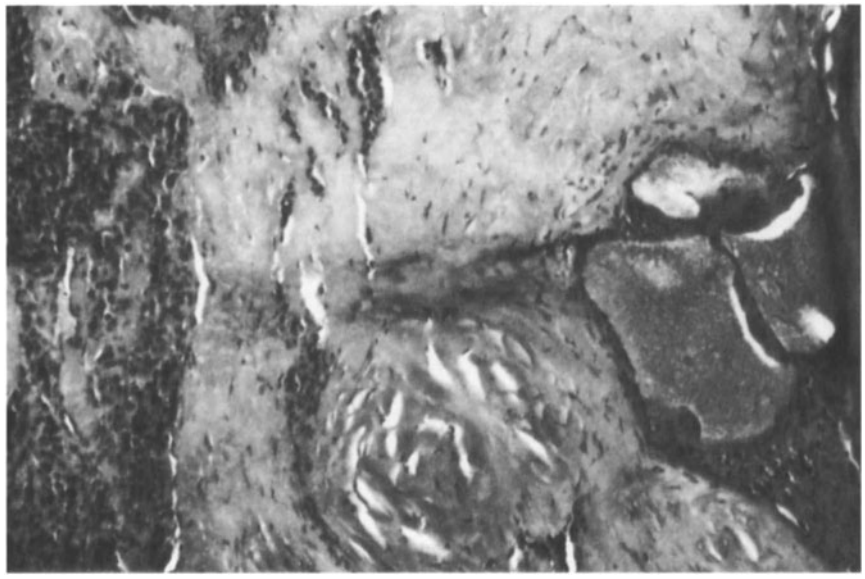

Fig. 4.17. Pathological section of a vagal paraganglioma embolized with polyvinyl alcohol (160-μm particles) 1 year prior to its removal. Note the fibrotic transformation of most of the tumor

4.11 Complications of Embolization of Paragangliomas

In our series reported in 1983, we noted minor complications. In two patients, extravasation of contrast medium below the tumor occurred during embolization and was probably related to the high pressure of injection of embolic material. This problem involved catheterization of the inferior tympanic artery and embolization with particles in both cases, and has not occurred again in the past 20 years.

One patient developed a transient facial nerve palsy following embolization of a large tympanomastoid paraganglioma, which involved the third portion of the facial nerve.

Finally, embolization of the ascending pharyngeal artery with fluid agents may produce lower cranial nerve palsy, regardless of the skill of the angiographer. Therefore, the patient should always be warned in advance of this potential complication.

5 Other Head and Neck Tumors

5.1 Thyrolaryngeal Tumors 265
5.2 Craniofacial Tumors 270

5.1 Thyrolaryngeal Tumors

Most thyrolaryngeal tumors are malignant and although they are usually highly vascular (Zachrisson 1976), surgical resection is generally not limited by intraoperative bleeding, and most of them are not referred for either diagnostic or therapeutic angiography.

We have used embolization to treat patients with the following lesions:

- Soft tissue and bony hemangiomas in adults
- Capillary hemangiomas in children
- Pharyngeal paragangliomas
- Thyroidal paragangliomas (Fig. 5.1)
- Malignant synoviomas
- Parathyroid adenomas (Fig. 5.2)

Pretherapeutic evaluation of thyrolaryngeal tumors (Noyek et al. 1983) includes ultrasound, radionuclide scanning, computed tomography (CT), and magnetic resonance imaging (MRI). It is well recognized that CT is of limited value in the specific diagnosis of these tumors (Laccourreye et al. 1983), particularly in malignant ones.

Thyrolaryngeal lesions illustrate the usefulness of angiographic protocols (Fig. 5.3) and also the hazards related to this specific territory, arterial supply to the laryngeal nerve, tracheal cartilages, etc. To our knowledge, thyroid gland dysfunction has not been reported following embolization.

Highly vascularized tumors of this area usually require embolization of the superior and inferior thyroidal arteries bilaterally.

Paragangliomas of the larynx, thyroid, or ectopic carotid body tumors (Zak and Lawson 1982; Ali et al. 1983; Marks and Brookes 1983) are rare. Their association with neuroendocrine tumors has been discussed in the section on temporal and parapharyngeal lesions (Chap. 4, this volume). Because paragangliomas are uncommon in this location, simultaneous parapharyngeal and thyroid tumors are usually related to thyroid malignancy or metastasis from pharyngeal carcinoma (Fig. 5.4).

Hemangiopericytomas (Pesavento and Ferlito 1982; Hertzanu et al. 1982) and other highly vascularized locally malignant lesions (Geachan et al. 1983) benefit from presurgical embolization.

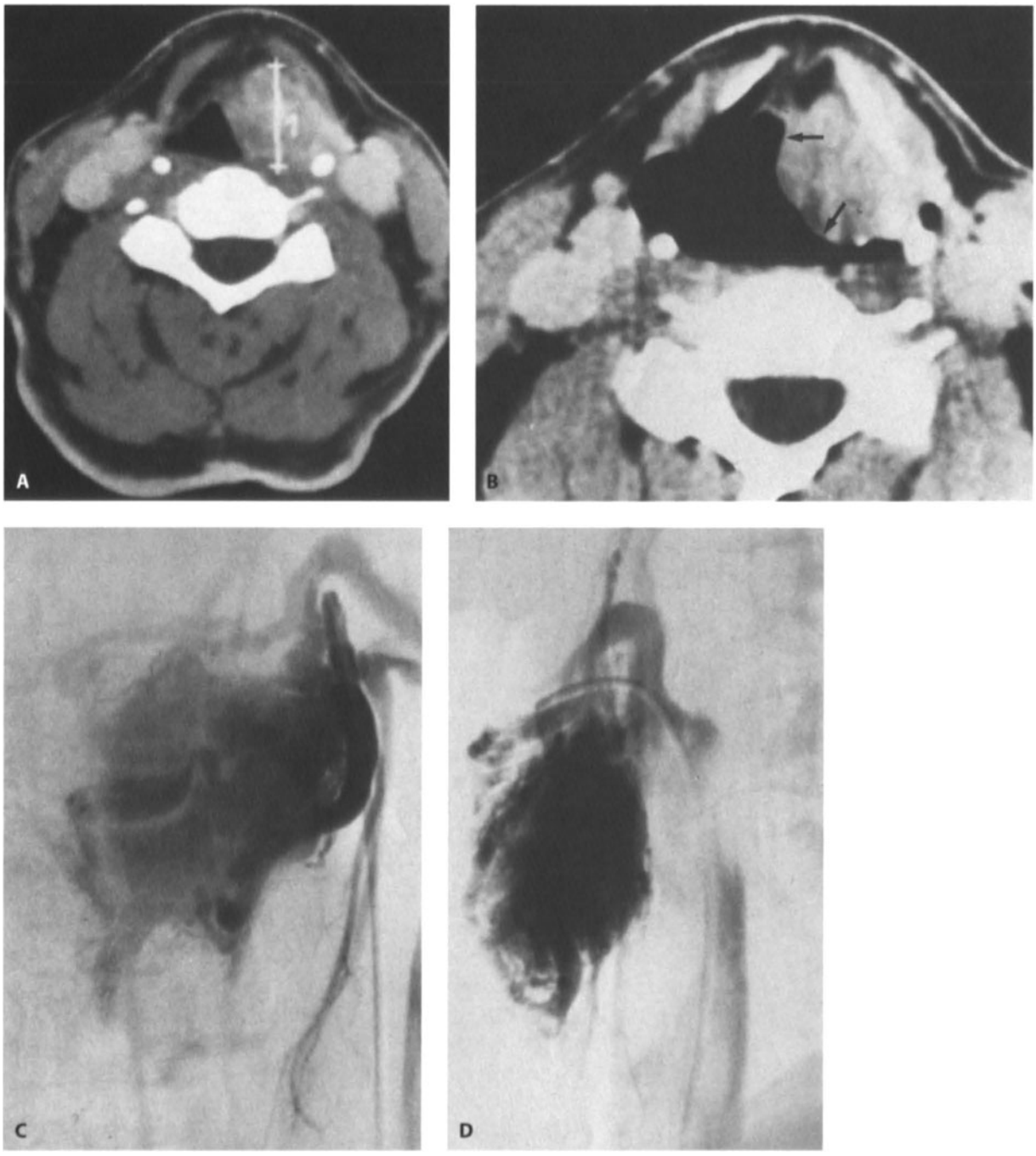

Fig. 5.1A–D. A 55-year-old man presenting with progressive dysphonia. Laryngoscopy shows a tumor mass along the left subglottic pharyngolaryngeal wall. No other lesions (mass or adenopathy) were found at clinical or CT examination (**A, B**). **C** Pretherapeutic evaluation shows a well-demarcated enhancing mass, highly vascularized, fed mainly by the superior laryngeal artery; it also received some supply from the opposite superior laryngeal and ipsilateral inferior laryngeal arteries (not shown). **D** Presurgical embolization with polyvinyl alcohol (160 μm) made total resection of a laryngeal paraganglioma possible. Swallowing was normal 3 weeks after surgery

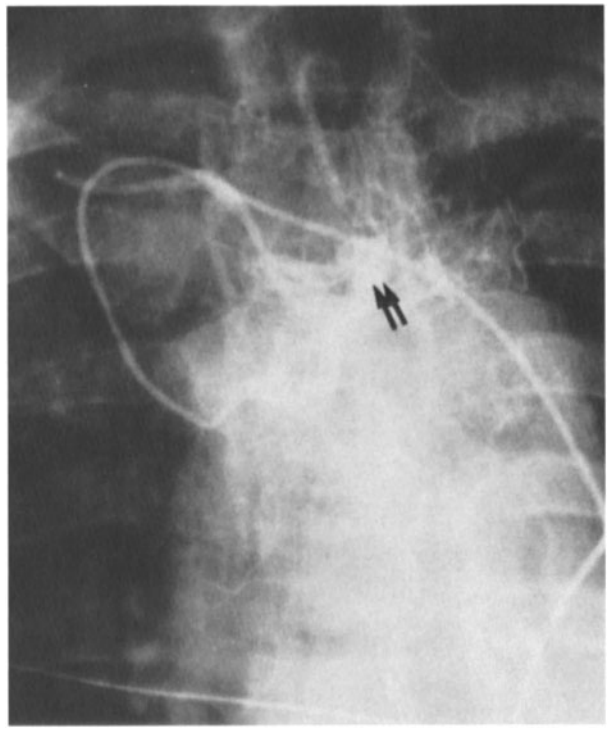

Fig. 5.2. A 26-year-old patient with hypercalcemia. Selective injection of the thymic branch of the right internal mammary artery demonstrates an upper mediastinal adenoma (*double arrow*). Contrast material ablation was selected in this case, with excellent results. After 5 years, the result remained stable. No surgery has been done

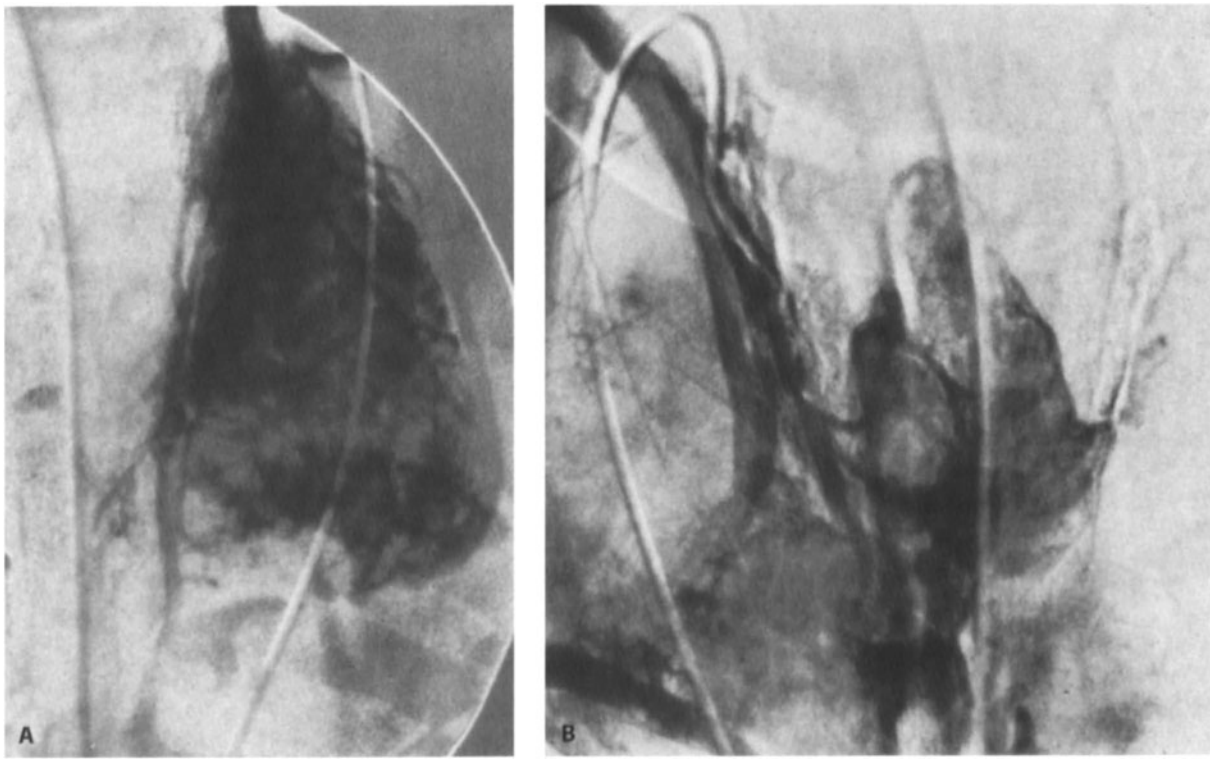

Fig. 5.3A, B. Patient presented with a goiter and thyrotoxicosis. Left (**A**) and right (**B**) superior thyroidal angiograms show hypervascularization of the thyroid tissue and the role played by the marginal arcade in the supply to the pyramid. Early venous filling was observed without evidence of arteriovenous fistulae

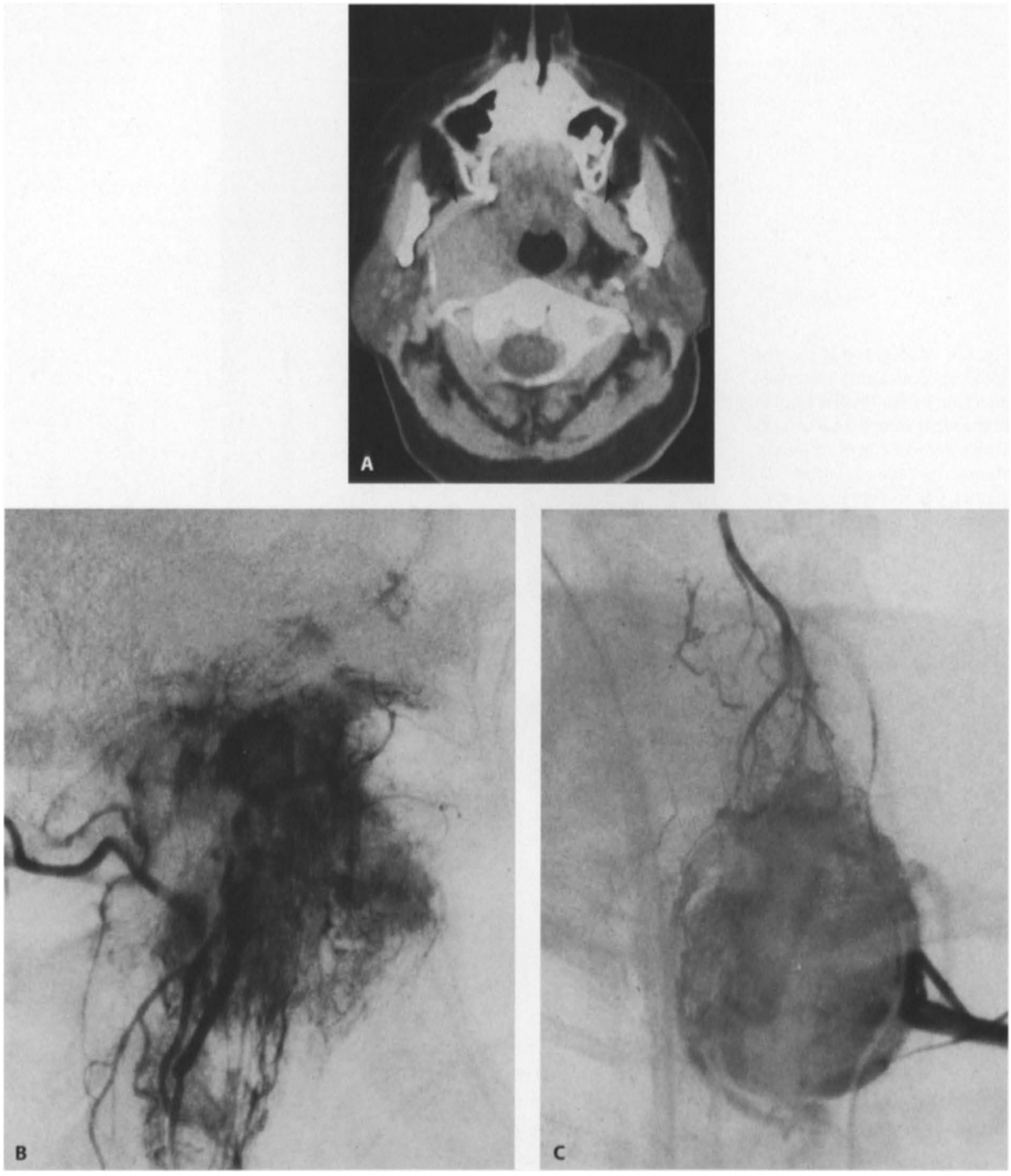

Fig. 5.4A–C. A 50-year-old woman presented with multiple painful subcutaneous nodules, paralysis of the ninth and tenth cranial nerves, and hypersecretion of thyrocalcitonin, without elevated carcinoembryonic antigen levels. A mass was prominent in the parapharyngeal space as shown on CT scan (**A**) and on latral view right ascending pharyngeal angiogram (**B**). No tumor could be palpated in the thyroid area. Histological examination of one of the nodules was consistent with a metastasis from an undifferentiated carcinoma, but certain staining characteristics were suggestive of a neuroendocrine tumor such as paraganglioma. This hypothesis was reinforced by the thyroid scintigram, which showed a nonfunctioning area within the left lobe while frontal view inferior thyroidal angiogram showed dense tumor blush on the left side (**C**). The final diagnosis following further surgery was a typical medullary thyroid carcinoma with cutaneous lymph node and parapharyngeal metastasis

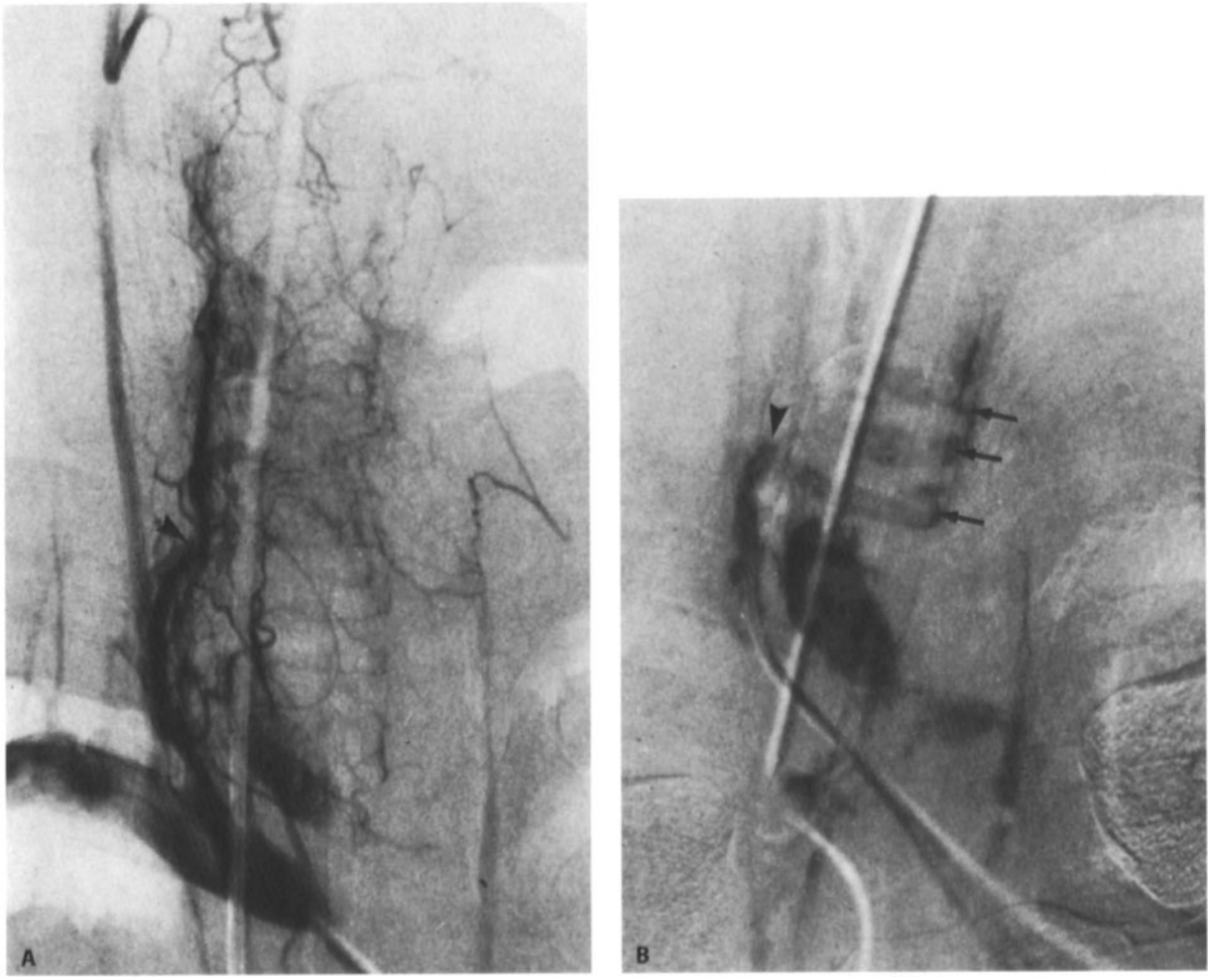

Fig. 5.5. Selective injection of the inferior laryngeal artery in a patient with a parathyroid adenoma before (**A**) and after (**B**) therapeutic angiography. Two surgical procedures in this patient have modified the initial anatomical patterns, since the four thyroid arteries were ligated. Only the right side of the laryngeal arcade persisted, and this permitted retrograde opacification of the ventral branch of the superior laryngeal artery, which originates from the ascending pharyngeal artery. Note that the tracheal rings (*arrows*) are opacified following infusion of the contrast material

Even though primary tumors of the thyrolaryngeal area are rarely treated by embolization, the thyroidal arteries are frequently used in endovascular techniques. They constitute one of the major sources of collateral circulation to the floor of the mouth and the carotid region and therefore may be occluded during the embolization of lesions that arise in those territories.

In presence of previous proximal ligation of the linguofacial system, the thyroidal channels often provide the sole access to the floor of the mouth.

Parathyroid adenomas still represent a diagnostic challenge, with the exception of very large tumors; the available noninvasive techniques can rarely document the location of the hormone-secreting lesion (Wolverson et al. 1981; Obley et al. 1984; Adams et al. 1981; Stock et al. 1981). Since Doppman's (1980b) contribution to the angiographic approach to para-

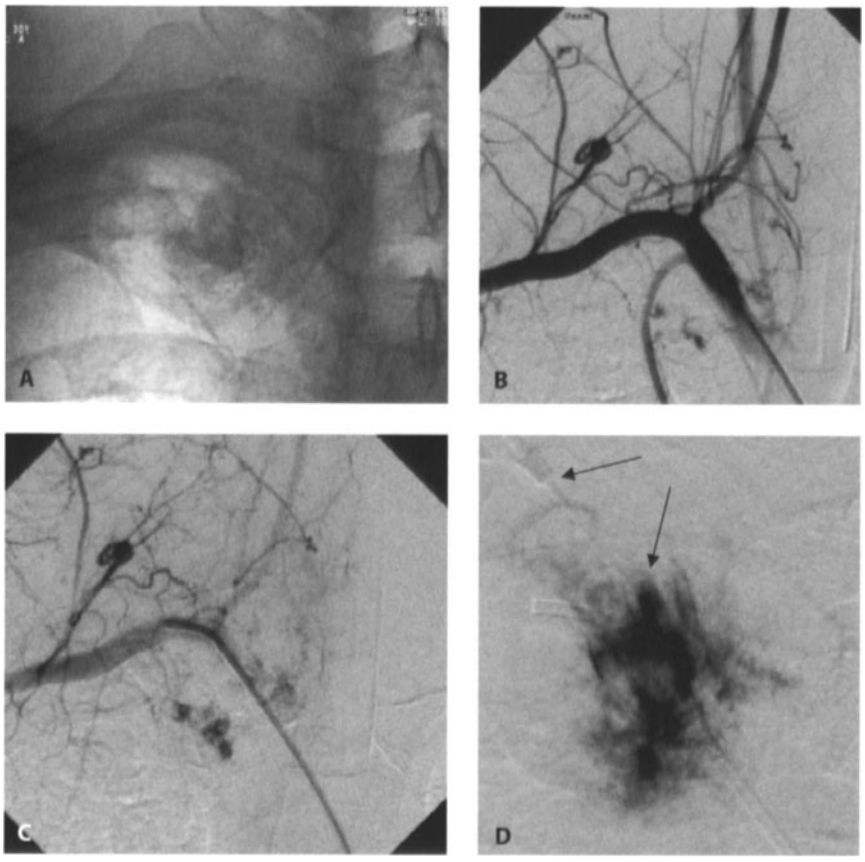

Fig. 5.6A–D. A 34-year-old man presented with enlarging mass lesion over the right clavicular region, associated with progressive pain syndrome. Plain film (**A**) demonstrates expansion of medial aspect of right clavicle with course bony trabeculation. Right subclavian angiogram in early (**B**) and late (**C**) arterial phases demonstrates slight puddling of contrast material in vascular spaces, which are better visualized during percutaneous injection (**D**) directly into the mass lesion (*arrows*). Corresponding direct injection of absolute alcohol into the bony hemangioma resulted in dramatic and persistent relief of pain

thyroid adenomas and the review of venous sampling of Dunlop et al. (1980), little attention has been devoted to angiographic studies in this disease.

Classic embolization of this type of tumor without surgical excision is always potentially incomplete. In our experience as well as in Doppman's (1980b), parathyroid adenomas treated by particle embolization alone usually recur (Fig. 5.5). Tumor infusion with cytotoxic agents such as ethanol is attractive and can be done percutaneously under ultrasound guidance (Fig. 5.6).

5.2 Craniofacial Tumors

Therapeutic angiography for malignant lesions of the head and neck should be discussed for two different groups:

1. Malignant or locally invasive lesions that have recurred following incomplete surgery. Some have already been illustrated or described in the chapters dealing with lesions of the scalp, meninges, nasopharynx, temporal, and laryngeal regions.
2. Primary malignant lesions or metastasis in the head and neck area (Figs. 5.7, 5.8).

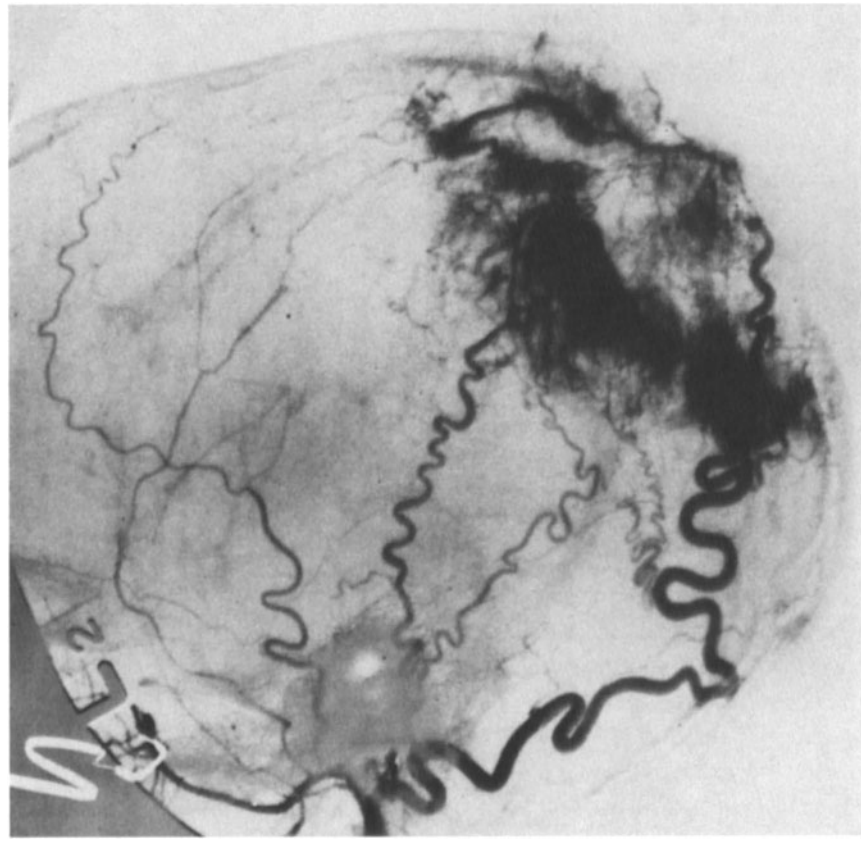

Fig. 5.7. Selective external carotid angiogram in a case of metastatic adrenal carcinoma. Note the highly vascularized aspect of the lesion, which can easily be reached by endovascular approach. The patient was treated with 95% ethanol with good palliation

The latter group does not make up a large part of the present practice of embolization. Ischemic damage is the main impact that endovascular treatment can cause. As a sole treatment, embolization should be reserved for nonsurgical lesions.

Certain techniques may maximize the effect of particle embolization, in particular the rearrangement of the vascular supply to the lesion. In large tumors of the base of the skull and nasal fossa, the goal may be to reach as much of the tumor as possible with minimal side effects. The internal maxillary, ascending pharyngeal, and internal carotid siphon bilaterally are theoretically involved in the supply to the nasopharynx. In our cases, the lesions tended to be slightly lateralized and we then used a technique that increased the role of one feeder to the territory. The contralateral branches of the internal maxillary and ascending pharyngeal arteries are embolized first. The remaining feeder is deliberately left open. A few weeks later, repeat angiography verifies the stability of the results and assesses the territory supplied by the internal maxillary or the ascending pharyngeal artery that has been left open. Catheterization of this branch then makes it possible to use more aggressive agents such as Gelfoam powder, cytotoxic chemotherapy, ethanol, microcapsules, etc. In our limited experience with this technique, patients treated this way showed a spectacular decrease in the size of their mass lesions.

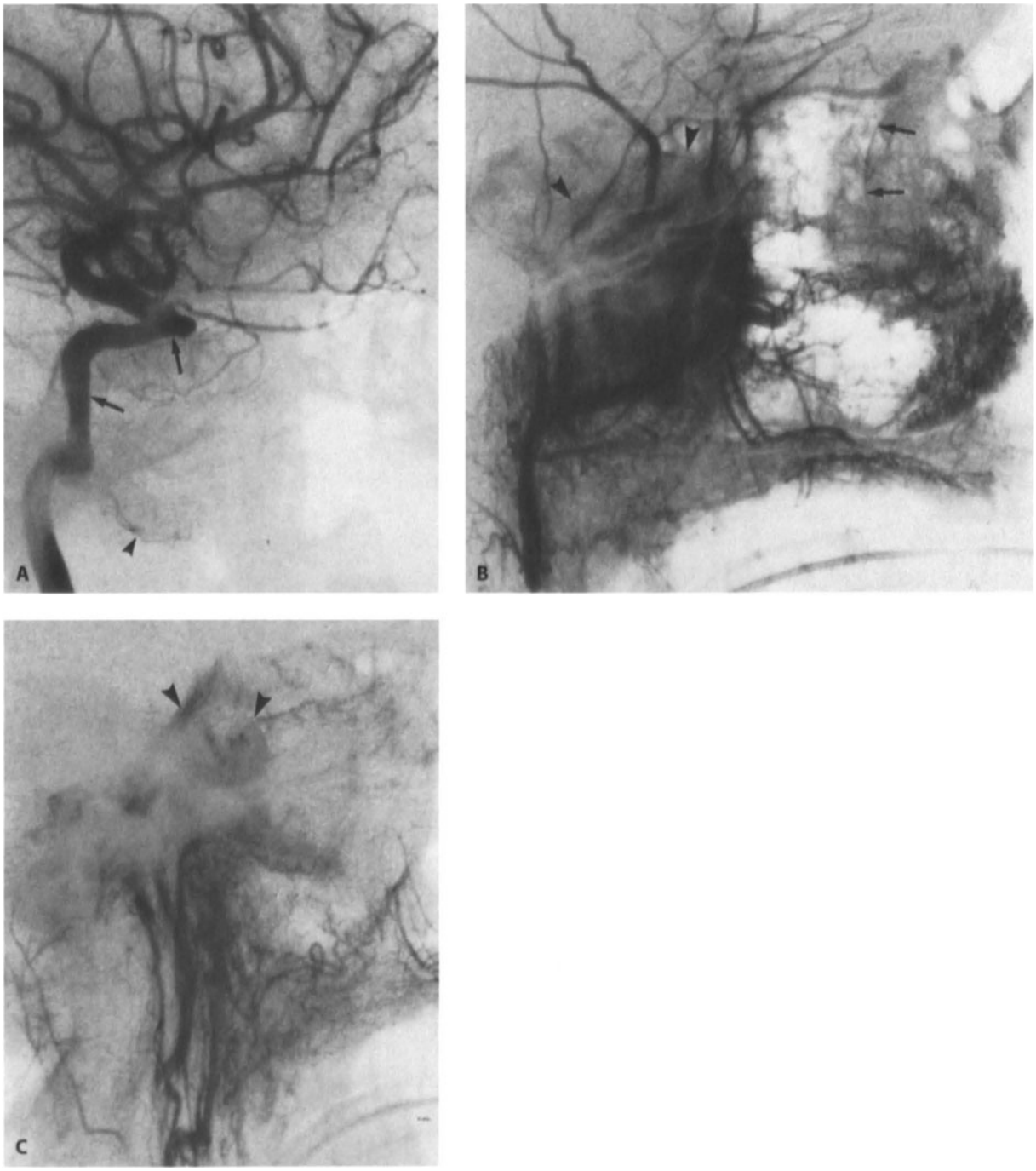

Fig. 5.8A–C. A 46-year-old female patient who had been treated for breast cancer presented with a skull base tumor. An attempt to biopsy led to profuse bleeding. No conclusive pathological diagnosis could be made. Internal carotid injection (**A**) shows a cavernous extension, which is probably extradural (*arrows*) from an extracranial tumor. Note the mandibular remnant (*arrowhead*). Distal external carotid angiogram (**B**) shows a capillary enhancement of the tumor, which occupies the base of the skull and extends to the cavum as well as to the intradural region (*arrowhead*). Note the choroidal crescent visualized through a middle meningeal–ophthalmic artery anastomosis. **C** Selective injection of the ascending pharyngeal artery showing posterior extension of the lesion and inferior part of its nasopharyngeal portion (*arrowheads*). Control of the supply to the area was achieved by particle embolization; the packing was removed and biopsy and surgical resection were achieved later. Pathology concluded breast cancer metastasis

Fig. 5.9A–D. A 64-year-old female patient presented with persistent pain and mass effect from a progressively growing orbital and facial metastasis from thyroid carcinoma. Surgery, radiation therapy, and biological agents were either rejected or ineffective. Polyvinyl alcohol embolization of the left distal external carotid and facial arteries was carried out. The ophthalmic artery also supplied the lesion and the eye was thought to be nonfunctional. No attempt was made to occlude this system, although catheterization of the ophthalmic artery could have been achieved. **A** Lateral and **B** frontal view of the lesion before embolization. **C, D** Four days after the embolization almost 30% of the mass was evacuated through the left nasal fossa without any bleeding. The pain disappeared simultaneously. The patient could see with the left eye although she had diplopia. Three years later this metastasis had not recurred, but the patient died from metastases in other locations

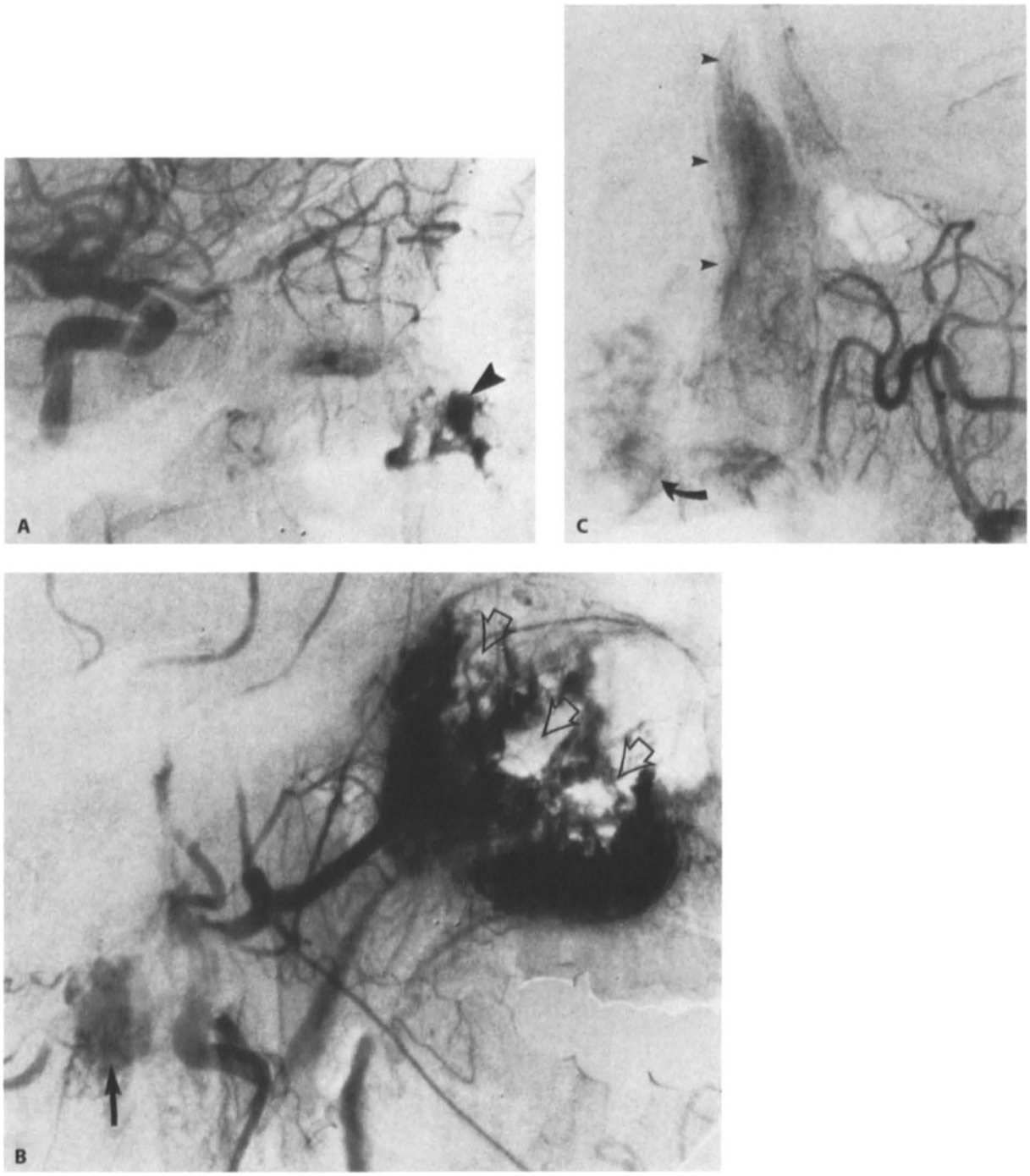

Fig. 5.10. Selective internal carotid artery (**A**), ipsilateral (**B**), and opposite distal external carotid artery (**C**) injections. A 56-year-old man presented with significant spontaneous epistaxis, which required packing and transfusion. Clinical examination showed a tumor to be the source of the nose bleed and biopsy confirmed its metastatic nature. Embolization was performed to stabilize the bleeding and to facilitate the surgical resection. Note the nonheterogeneous appearance of the blush, which was related to intratumoral necrosis and multicompartmental vascular arrangements: ethmoidal (*arrowhead*) and distal internal maxillary arterial (*open arrows*) territories. The absence of supply from the septal branches of the contralateral internal maxillary artery (*small arrowhead*) and of cross-filling of greater palatine artery collaterals (*curved arrows*) from the opposite side is unusual. Note the incidental discovery of an additional metastasis in the mastoid region (*solid arrow*, **B**)

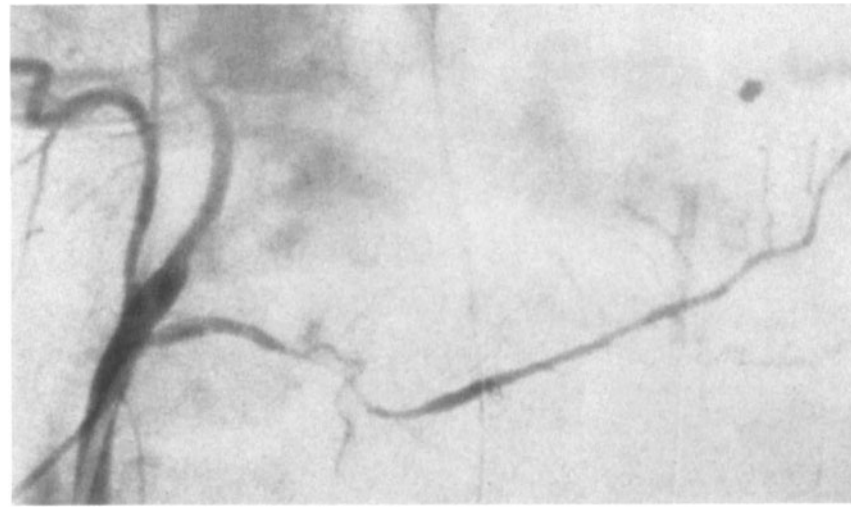

Fig. 5.11. Proximal injection in the external carotid artery in a patient presenting with cancer of the base of the tongue extending to the floor of the mouth. Previous surgery, radiation therapy, and chemotherapy had stabilized this extensive lesion for a short period of time. The patient was referred as an emergency with acute intraoral hemorrhage. Cutaneous changes and postradiation therapy trismus made surgical control and analysis of the bleeding site extremely difficult. Note the changes involving the proximal lingual artery. Embolization successfully controlled the bleeding

In the future, manipulating the vascular supply in this fashion could possibly be combined with embolization of chemotherapeutic agents in the form of long-acting microcapsules, maintaining patency of the arterial route for future multiple courses of treatment.

Embolization is also used in two other situations in patients with malignant lesions:

1. Prior to diagnostic biopsy where hemorrhagic complications are anticipated (particles should be used to preserve tissue diagnosis; Fig. 5.8)
2. To treat complications of the disease or its treatment such as pain, hemorrhage, and mass effect

Malignant lesions always respond dramatically to particle embolization, probably because they are already in a subischemic state, as often seen at pathology. Embolization usually produces significant necrosis and a decrease in the mass effect in a few days (Fig. 5.9).

Hemorrhage due to arterial ulceration may result from either tumor invasion or from postradiation necrosis. In both situations, control of the bleeding depends on accessibility. Arterial changes following radiation may compromise intravascular navigation. Surgical control of these hemorrhages is usually very difficult. In the presence of intraoral bleeding due to lingual ulceration, associated with postradiation trismus, local compression of the involved area may be difficult. Embolization may be useful in controlling acute and chronic bleeding due to neoplastic ulceration (Figs. 5.10, 5.11).

The overall prognosis of the tumor is obviously not significantly modified by embolization; however, the quality of the remaining life is sometimes dramatically improved.

6 Traumatic Arteriovenous Fistulae

6.1 Introduction 277

6.2 Traumatic Carotid Cavernous Fistulae 279
6.2.1 Etiology and Epidemiology 279
6.2.2 Clinical Aspects of Traumatic Carotid Cavernous Fistulae 285
6.2.2.1 Ophthalmological Symptoms 293
6.2.2.2 Corneal Ulcerations and/or Infections and Secondary Glaucoma 293
6.2.2.3 Diplopia 298
6.2.2.4 Cranial Nerve Involvement in Traumatic Carotid Cavernous Fistulae 298
6.2.2.5 Bruit 300
6.2.2.6 Arterial Steal 300
6.2.2.7 Hemispheric Arterial Insufficiency 300
6.2.2.8 Associated Traumatic Lesions 302
6.2.3 Pretherapeutic Evaluation 306
6.2.3.1 Location of the Fistula 308
6.2.3.2 Venous Drainage of the Fistula 314
6.2.4 Therapeutic Objectives and Strategy 321
6.2.4.1 Embolization 321
6.2.4.2 Emergency Treatment 322
6.2.4.3 Surgical Approach to Carotid Cavernous Fistulae 324
6.2.4.4 Conservative Treatment of Traumatic Carotid Cavernous Fistulae 325
6.2.5 Technical Aspects of Embolization 325
6.2.5.1 Balloon Selection 325
6.2.5.2 Manual Compression 332
6.2.5.3 The Use of NBCA in the Management of Carotid Cavernous Fistulae 332
6.2.6 Postembolization Care 333

6.3 Other Traumatic Arteriovenous Fistulae 334
6.3.1 Extracavernous Arteriovenous Fistulae 334
6.3.2 Vertebral Arteriovenous Fistulae 338
6.3.3 Common Carotid Fistulae 342
6.3.4 External Carotid Fistulae 342
6.3.5 Malignant Fistulae 354
6.3.6 Other Epistaxis 354
6.3.6.1 Coagulopathy 357
6.3.6.2 Spontaneous Epistaxis 357
6.3.6.3 Tumoral Epistaxis 357
6.3.6.4 Biopsy 359
6.3.6.5 Traumatic Epistaxis 362

6.1 Introduction

Traumatic arteriovenous fistula (AVF) (Table 6.1) is an abnormal communication between an artery and a vein secondary to vessel injury. Therefore, it may be part of a more complex clinical situation where other structures such as soft tissues, bone, brain, and cranial or peripheral

nerves may also be injured. Fistulae may be part of other vascular abnormalities such as preexisting developmental aneurysms or angiodysplasias, which are discussed in Chap. 7. There are sites where fistulae are likely to occur because the anatomical relationship between an artery and an adjacent or surrounding vein makes it likely for a ruptured or lacerated artery to communicate directly with a vein. The consequences of this acute hemodynamic change can occur at the site of the fistula, distal to the fistula, or be systemic or secondary to venous hypertension.

Locally, secondary to venous dilatation and high flow, a pulsatile mass with a thrill may be apparent and a variable pitch bruit can be heard at the site of the fistula. A bruit can also be heard at other locations, depending on the venous drainage. This is a classic sign to assist in the clinical localization of fistulae, which are deep and impalpable or when bony structures surround the fistula. Fistulae can also be discovered by the patient describing a new onset pulsatile tinnitus.

A sudden deprivation of arterial blood flow in the territories neighboring or distal to the fistula can produce ischemia. If the steal from the arteries supplying the brain is severe enough, then neurological changes may occur that can vary from mild transient insufficiency syndromes, such as dizziness, unsteadiness, or other circulatory insufficiencies, to more severe permanent insults, including stroke. These may be difficult to assess in the presence of severe head trauma with coma or associated cerebral injuries.

Abrupt venous hypertension, which may vary from mild to severe, can produce reversal of flow in the venous system. This in turn may produce symptoms of mass effect or venous congestion, which include secondary glaucoma, hydrocephalus, or engorgement of cortical cerebral veins. The risk of intradural hemorrhages exists when cortical venous drainage is present. These hemorrhagic episodes secondary to cortical venous rerouting in traumatic arteriovenous fistulae (AVFs) are rare (as opposed to those associated with dural arteriovenous shunts), unless the protective effect of the multiplicity of venous outflow opportunities is restricted by traumatic thrombosis. Frequently, a delay between the vascular traumatic insult and the clinical manifestations is seen and relates to the development of a false aneurysm and/or the tamponade effect from the hematoma. Only after rupture of the pseudoaneurysm, or lysis of the hematoma, do the symptoms of the abnormal arteriovenous communication become apparent. Any traumatic fistula implies arterial wall rupture, and the so-called arteriovenous (AV) chamber should be considered as a false aneurysm without arterial wall structure and contained by the surrounding hematoma.

Systemic manifestations of these high-flow fistulae such as high-output failure are unusual and may be seen in fragile debilitated patients with a preexisting insufficiency of the cardiovascular system (Fig. 6.53). Older children or young adults are usually asymptomatic, although some degree of left ventricular hypertrophy and/or cardiomegaly may be detected in chronic traumatic high-flow fistulae.

6.2 Traumatic Carotid Cavernous Fistulae

In the craniofacial area, the most frequent type of AVFs are the traumatic carotid cavernous fistulae (TCCFs). They occur secondary to rupture of the internal carotid artery, or from rupture of one of its intracavernous branches. On occasion, the ruptured internal carotid artery branch will not be seen on the internal carotid artery angiogram and only the external carotid system will visualize the fistula. Spontaneous dural AV shunts of the cavernous sinus constitute a different entity and are discussed in Chap. 8.

6.2.1 Etiology and Epidemiology

TCCFs may be produced by direct or indirect trauma during head injury, with or without skull base fracture (Hamby 1966). Blunt trauma, usually frontal and on the same side as the lesion (Pool and Potts 1965), penetrating orbital injuries associated with optic globe injury, gunshot wounds with laceration of the carotid artery and/or cranial nerves can be encountered. Iatrogenic fistulae have been described secondary to transsphenoidal surgery (Fig. 7.27) (Takahaski 1969; see Chap. 7), internal carotid artery thromboendarterectomy (Baker 1968) (Fig. 6.1), and thermocoagulation or rhizolysis of the gasserian ganglion or vidian nerves. In some patients, there will be no history of trauma or only minor trauma, while in others there will be some mechanical precipitating factor such as vomiting, sneezing, or the occurrence of acute hypertension. The angiographic findings are those of a typical TCCF. In some cases, one may suspect either a traumatic rupture of a preexisting aneurysm (Figs. 6.2, 6.3), an angiodysplasia such as Ehlers-Danlos syndrome (Graf 1965), or pseudoxanthoma elasticum (Koo and Newton 1972). In these instances, the CCFs are usually high flow and often recurrent and bilateral. By far the most frequent trauma is caused by motor vehicle accidents, with associated injuries at multiple levels. Clinical assessment is mandatory to establish the therapeutic priorities (Table 6.3; Figs. 6.4, 6.5).

TCCFs best illustrate the clinical syndromes produced by high-flow traumatic AVFs. The management of these fistulae requires a thorough knowledge of the vascular anatomy of the base of the skull (see Vol. 1).

The cavernous portion of the internal carotid artery (ICA) is anchored to the dura at the base of the skull. It is exposed to shear stresses as well as penetrating injuries. A laceration of the ICA or of one of its branches may produce an AVF and result in the reversal of the venous drainage of the cavernous sinus afferents. Such drainage can be multidirectional depending on the patient's anatomy.

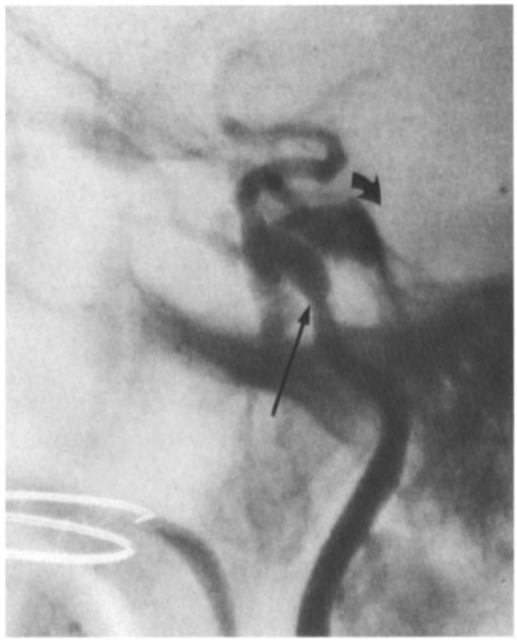

Fig. 6.1. Lateral subtraction angiogram of the left internal carotid artery. Iatrogenic cavernous carotid fistula occurred following surgical thromboendarterectomy using a Fogarty balloon catheter. Note the dilated cavernous carotid artery where the Fogarty balloon was inflated (*arrow*) and filling of the cavernous sinus (*curved arrow*)

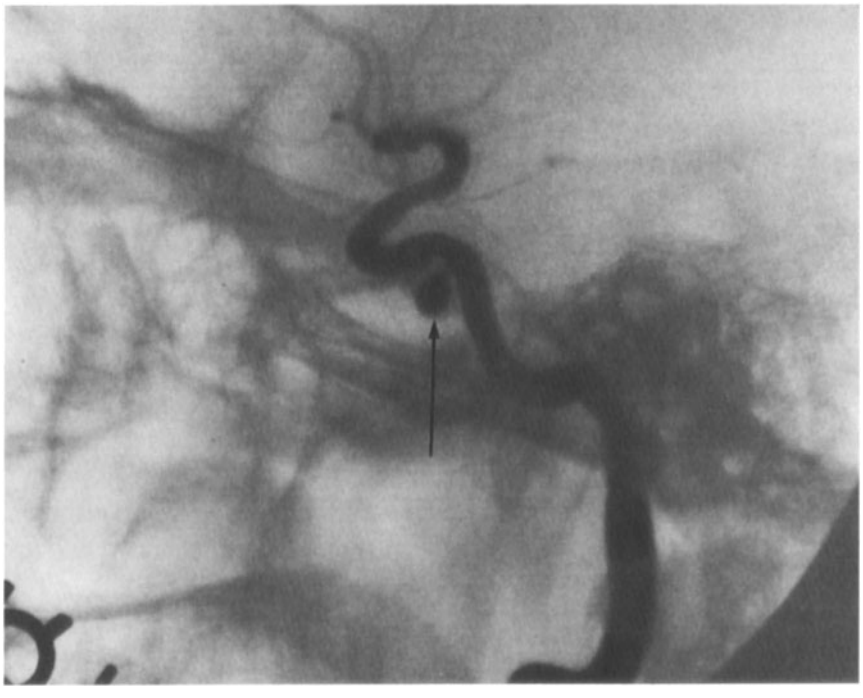

Fig. 6.2. Lateral subtraction angiogram of the right internal carotid artery in early arterial phase. Only minor trauma preceded the onset of symptoms. A narrow neck aneurysm of the cavernous internal carotid artery is noted (*arrow*)

Fig. 6.3. Spontaneous cavernous carotid fistula in a patient with Ehlers-Danlos (ED) type IV disease (**A**). Balloon placement was satisfactory (**B**), but despite cautious detachment, secondary displacement of the balloon occurred (**C**). Gugliemi detachable coils coiling attempt was not satisfactory with a persistent open internal carotid artery (ICA) tear (**D, E**). Sacrifice of the ICA was then undertaken; tolerance to the occlusion was excellent (**F**) ▶

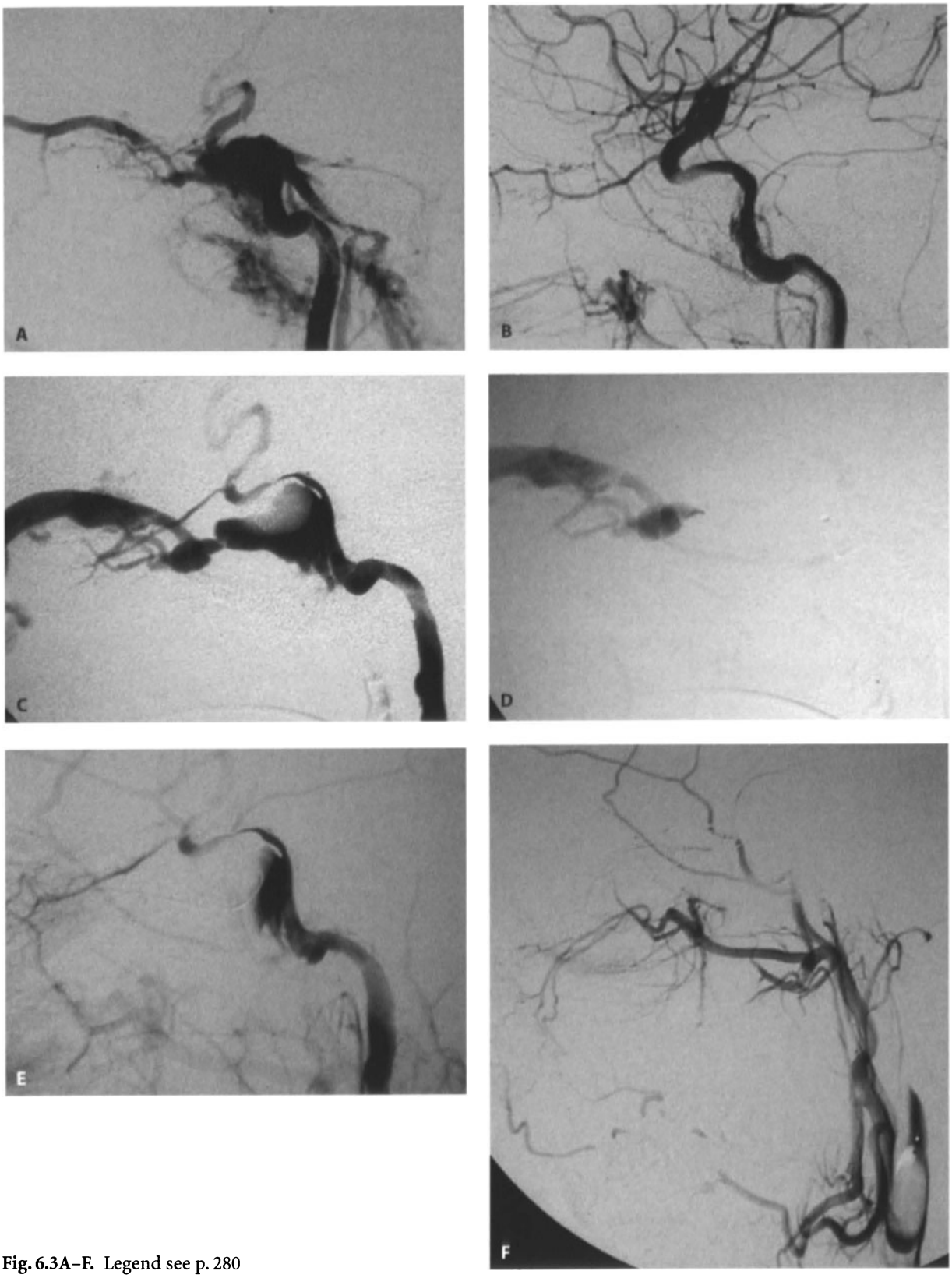

Fig. 6.3A–F. Legend see p. 280

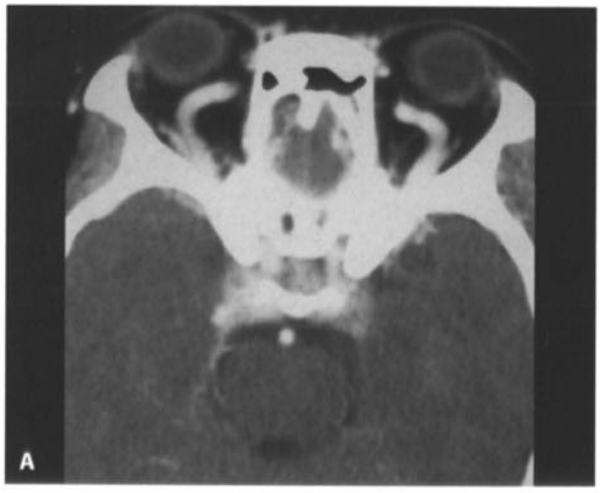

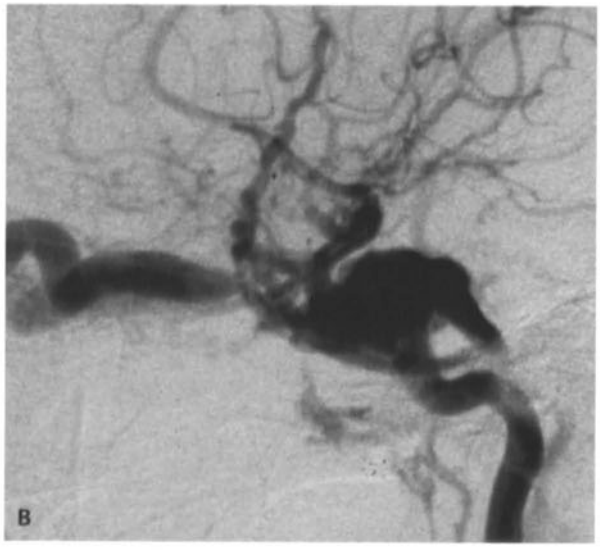

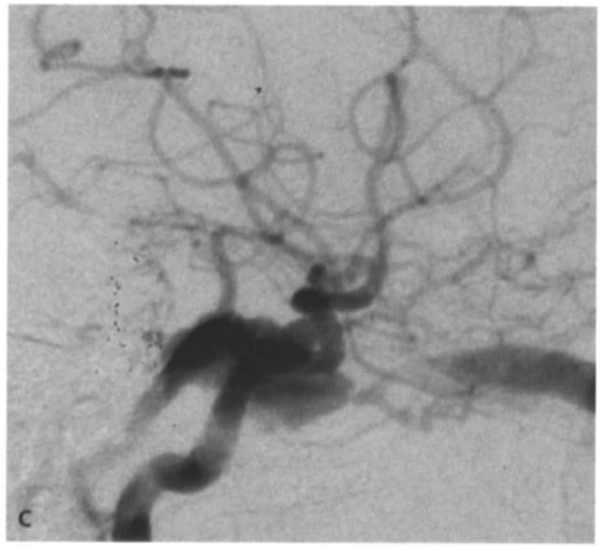

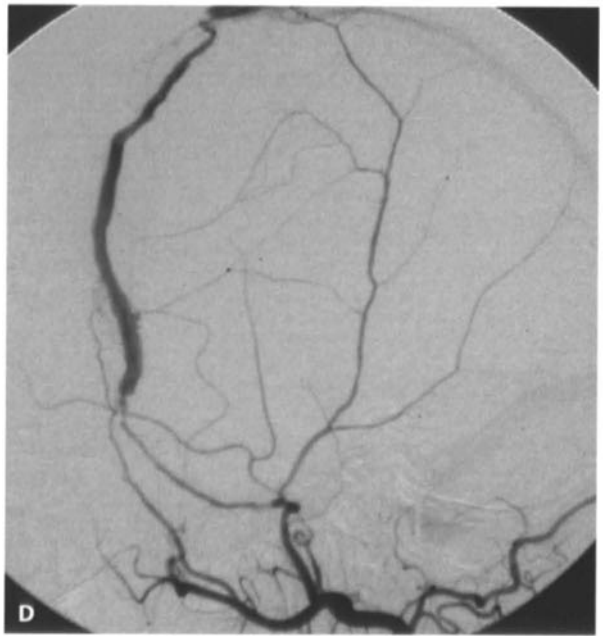

Fig. 6.4A–E. Legend see p. 283

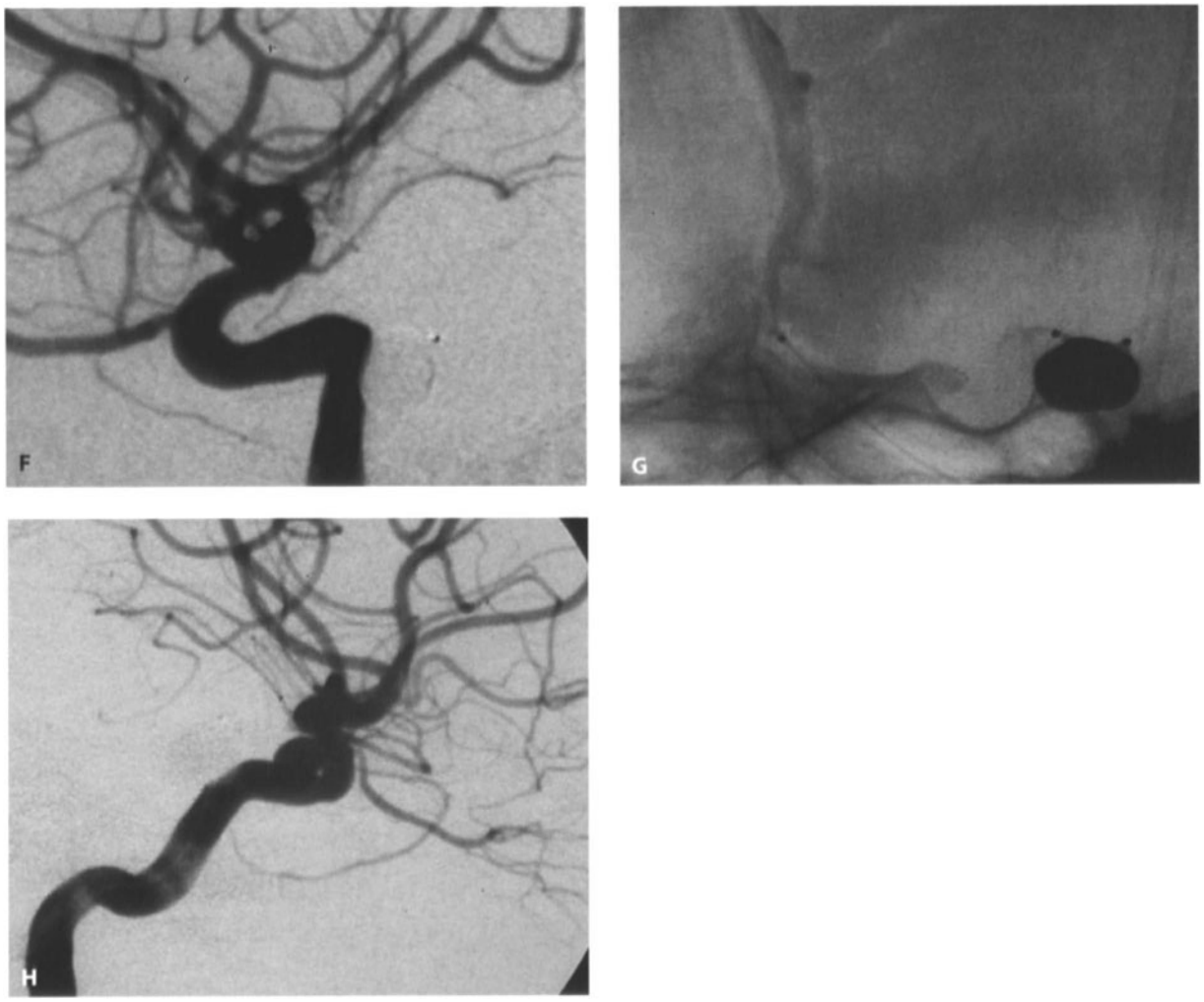

◀ **Fig. 6.4.** A 68-year-old woman was involved in a motor vehicle accident and presented immediately with bilateral proptosis (**A**). Angiography demonstrated bilateral traumatic cavernous carotid fistula (TCCF) (**B, C**). Right intradural internal carotid artery (ICA) traumatic arterial aneurysm and bilateral middle meningeal arteriovenous fistula (AVF) were demonstrated (**D, E**). The Left TCCF was treated first in view of the cortical venous reflux (**F**); the right TCCF was then occluded (**G**) and showed the ICA aneurysm (**H**), which was treated during a second session. Both dural AVFs were then occluded with coils and glue. (Courtesy of S. Pongpech)

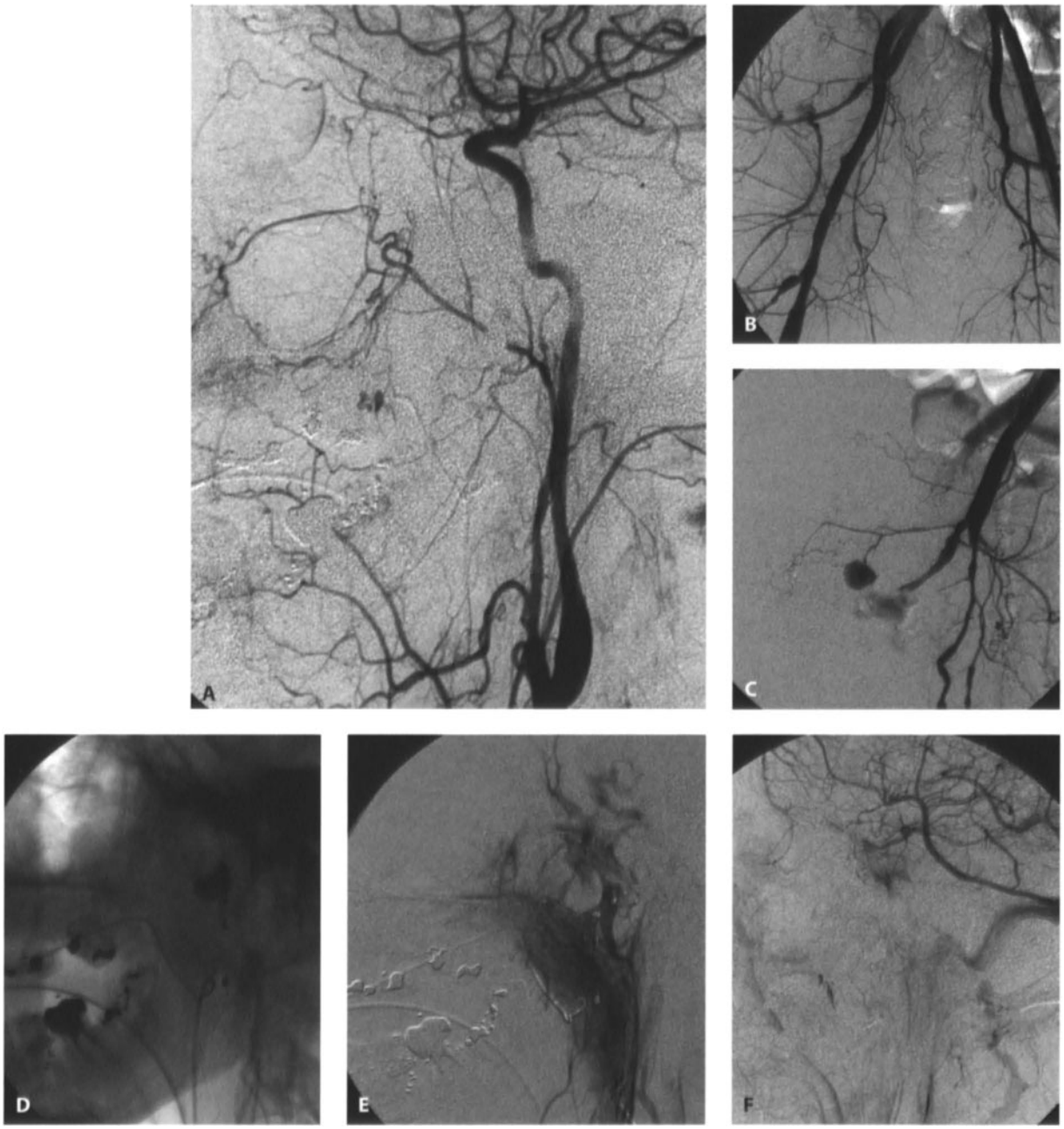

Fig. 6.5. Typical appearance of multiple false aneurysms in a patient who sustained multiple injuries, including maxillary bone fracture with oral hemorrhage (**A**) and pelvic fractures with acute arterial bleeding from the internal iliac branches (**B, C**) requiring emergent embolization. Posttraumatic migrated tooth in the cavum region (**D**) resulted in arteriovenous fistula of the distal branch of the ascending pharyngeal artery (**E**) with reflux toward the cavernous sinus (**F**)

6.2.2 Clinical Aspects of Traumatic Carotid Cavernous Fistulae

Symptomatology will depend on venous drainage. The ophthalmic vein opening into the sinus is a constant disposition, therefore often one of the most important presenting problems are those related to the orbit (Figs. 6.6, 6.7; Table 6.2).

The reversed blood flow in the ophthalmic system will then drain toward the facial venous system and external jugular vein. Drainage to the ophthalmic venous system produces proptosis, chemosis, dilated conjunctiva, lid engorgement, venous retinopathy, disc edema, increased intraocular pressure with secondary glaucoma, and visual loss. Similar symptoms may be present in the absence of anterior drainage if there is sufficient venous hypertension. Associated symptoms related to anterior venous hyperpressure may be congestion of the extraocular musculature and anterior displacement of the eyeball (exophthalmos). Mechanical restrictions to movement of the eye secondary to venous hypertension and orbital congestion (Fig. 6.6A) will occur, but this will resolve after repair of the fistula (Fig. 6.6B); they should be differentiated from cranial nerve impairment. It is possible that TCCFs produce orbital symptoms without evidence of ophthalmic drainage, and in those cases the actual symptoms are related to the venous injury of the cavernous sinus and result from the thrombosis of the cavernous sinus compartment communicating with the orbit (Hasso et al. 1979). The fistula then drains directly into other, patent afferent veins to the sinus. These patients usually present with pulsatile tinnitus and/or some dysfunction of cranial nerves VI, IV, III or V_1 (Fig. 6.8).

Drainage to the sphenoparietal sinus, superficial sylvian, or deep sylvian veins may lead to aneurysmally dilated venous pouches that may even act as a large extradural mass (Fig. 6.9) or even project intradurally.

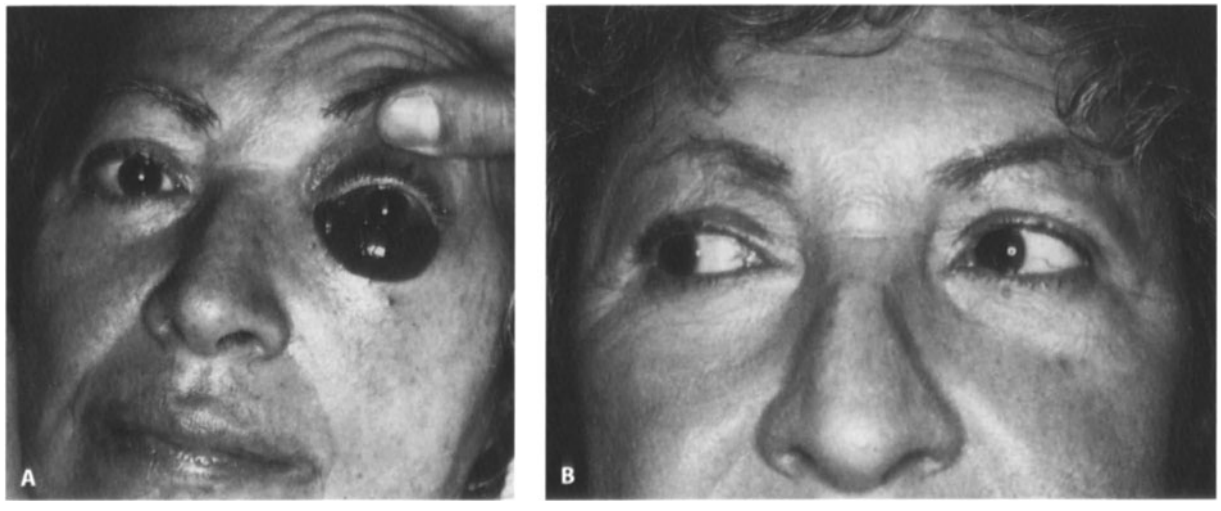

Fig. 6.6A, B. Traumatic cavernous carotid fistula sustained as the result of a motor vehicle accident. **A** Clinical picture 3 weeks after the accident. Note the proptosis and the conjunctival and eye-lid engorgement. Associated secondary glaucoma, ptosis, and muscle entrapment were also present. **B** Photograph of the face 10 days after balloon repair of the fistula. All signs and symptoms had resolved

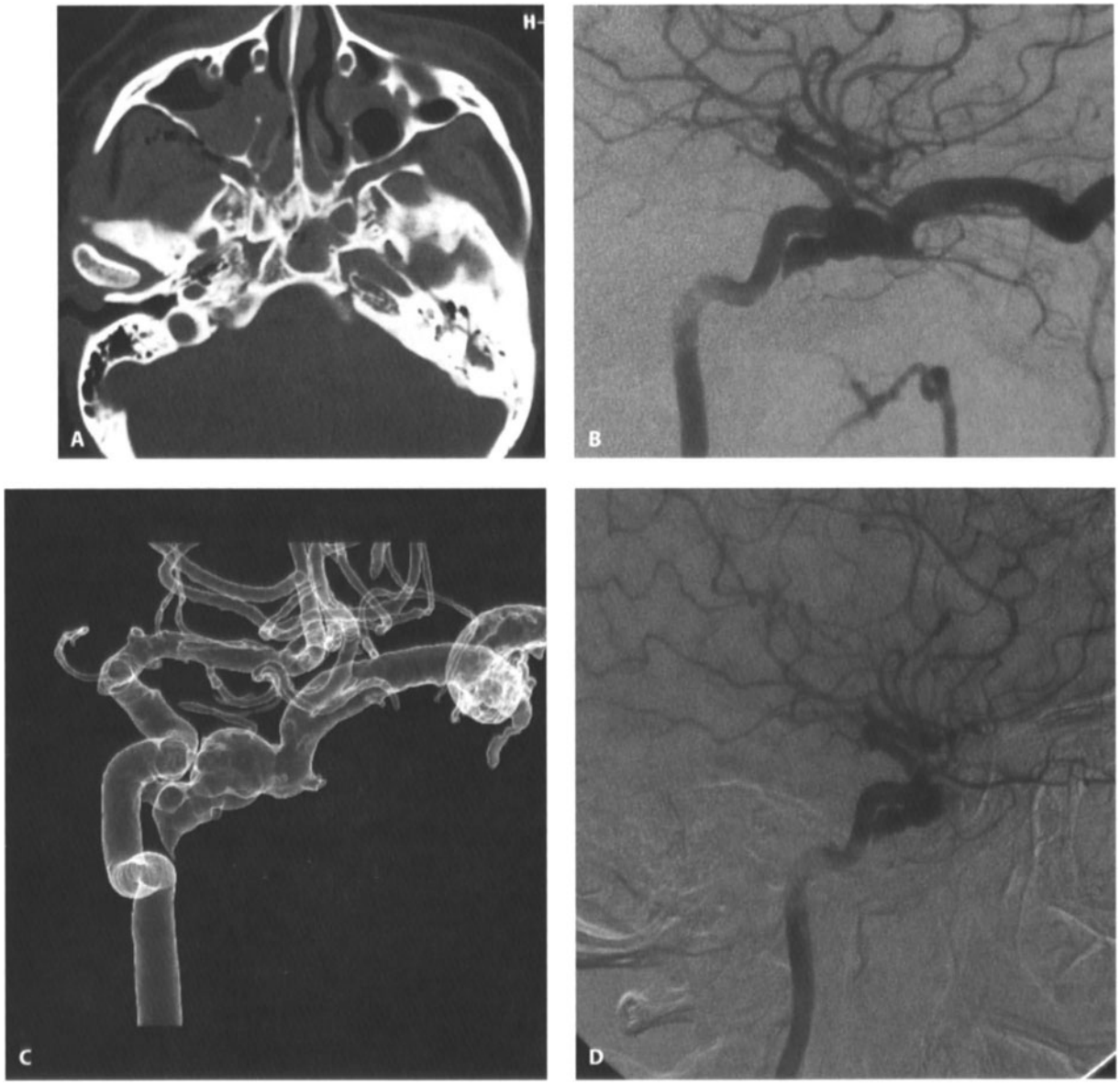

Fig. 6.7A–J. Typical appearance of traumatic cavernous carotid fistula (TCCF) secondary to a motor vehicle accident in a 25-year-old woman, who was receiving anticoagulation treatment for aortic valve surgery. CT (**A**) demonstrates skull base fractures involving the sphenoid bone. Angiography shows the TCCF opacified via an intracavernous branch (**B**). The 3-D image suggests a posterior collateral is involved (**C**). Functional testing with manual compression at the medial canthus demonstrates only ophthalmic venous drainage (**D**). **E–J** see p. 287

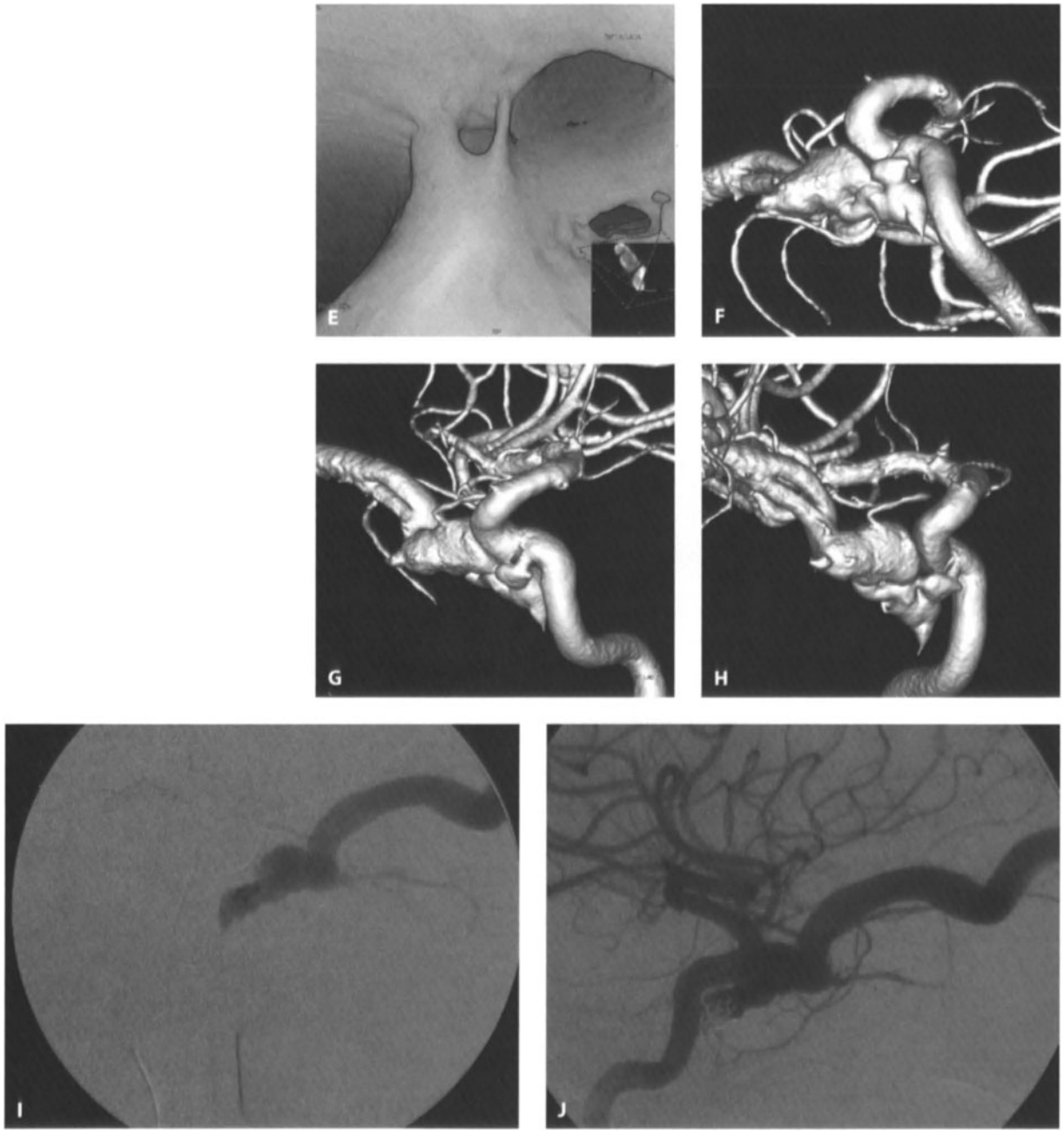

Fig. 6.7 (*continued*). Additional endovascular (**E**) images and inferior (**F**), medial (**G**), and anterior (**H**) views in 3-D demonstrate the medially located lesion draining into a venous pouch inferior to the horizontal portion of the siphon. A microcatheter is advanced inside the venous compartment (**I**) and several coils are deployed (**J**) to promote thrombosis expected after a few days of manual compression

Fig. 6.8. Lateral subtraction angiogram of the left internal carotid artery. Posttraumatic fistula with only posterior drainage (*arrow*) into the inferior petrosal jugular confluence (*open curved arrow*) is noted. (From Manelfe and Berenstein 1980, with permission)

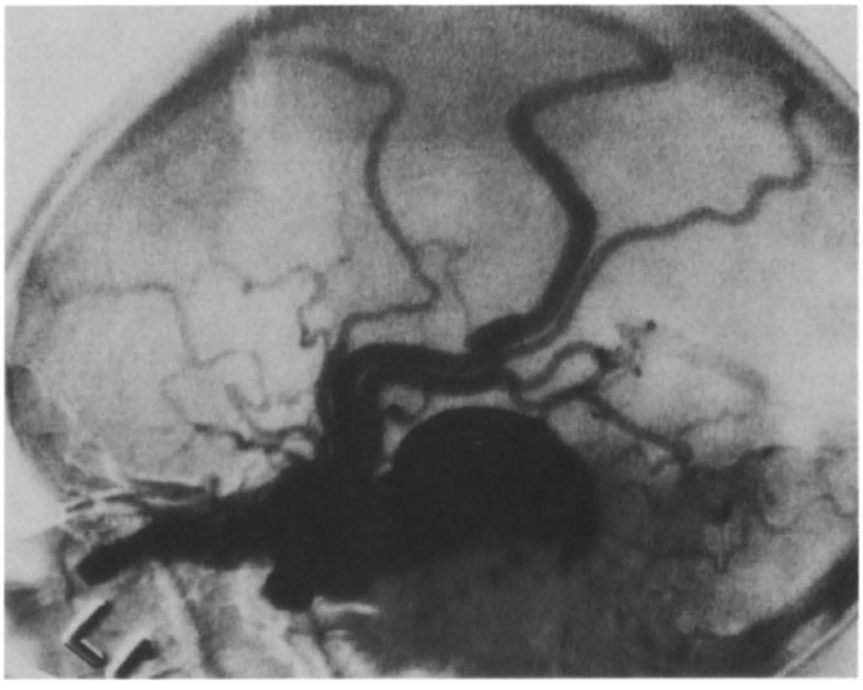

Fig. 6.9. Lateral subtraction angiogram of chronic posttraumatic fistula. Note the aneurysmal dilatation of the cavernous sinus and superior cortical venous drainage through the sphenoparietal sinus. Note the complete angiographic steal with respect to the cerebral arterial system (same patient as Figs. 6.26 and 6.46)

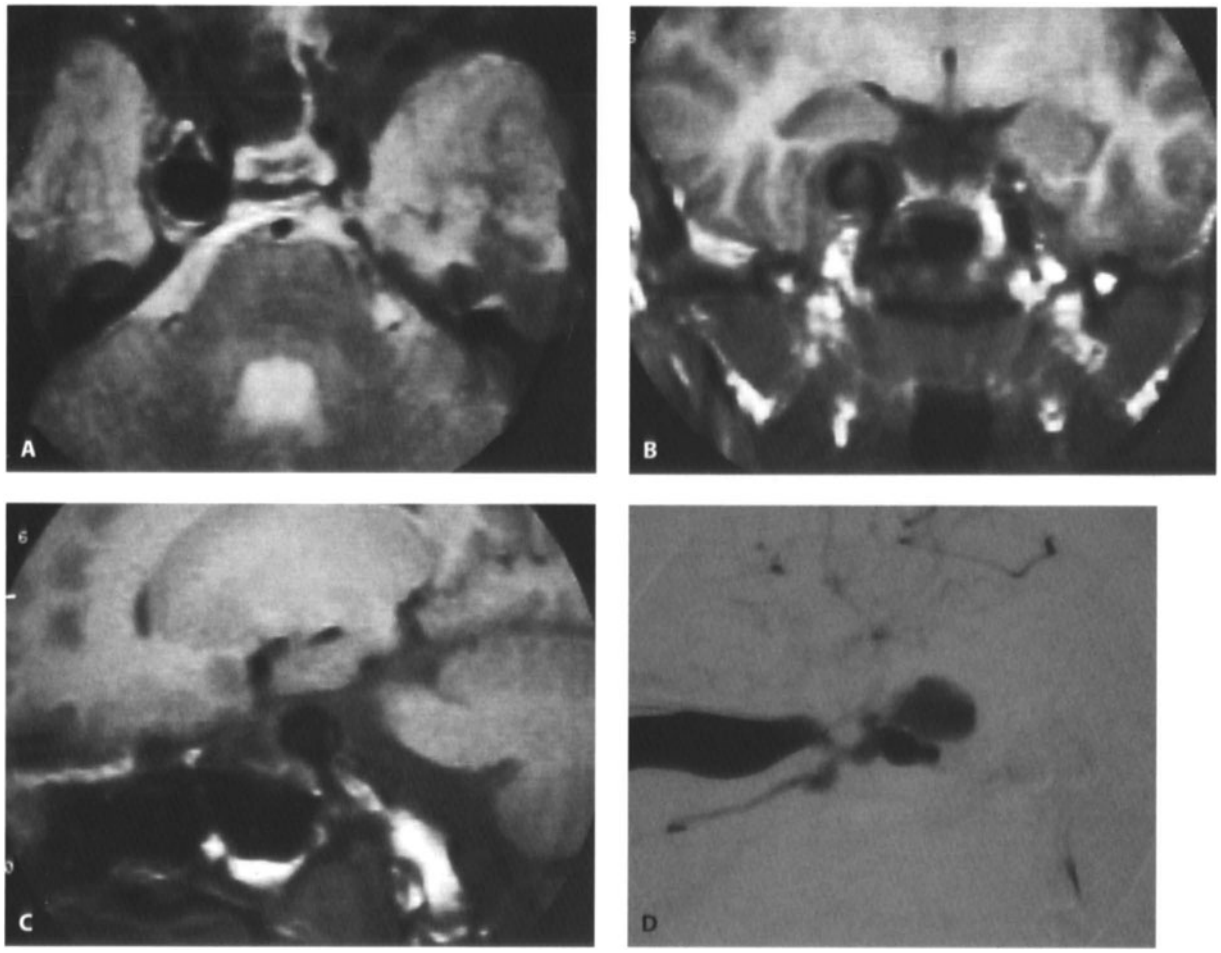

Fig. 6.10. A traumatic cavernous carotid fistula is demonstrated on axial (**A**), frontal (**B**), and sagittal (**C**) MRI projections. Note the intradural venous pouch (**D**)

They may enlarge over several weeks and produce subarachnoid hemorrhage (SAH) (Figs. 6.10, 6.11). These are associated with severe skull base injuries and are often seen in chronic TCCFs, where the risk of late rupture is extremely low. Congested cortical veins can be seen (Fig. 6.12) and carry the potential risk of intracranial hemorrhage at the acute stage. Rerouted cortical venous drainage after suboptimal treatment carries a similar potential risk (Fig. 6.13). A phlebitic appearance of the cortical veins is suggestive of associated restricted venous outlets at the skull base or superior sagittal sinus. After occlusion of the fistula, these cortical veins are seen filling within the normal time frame on the immediate postembolization angiogram (Fig. 6.12). The cortical veins return to normal appearance and drain in the cavernous sinus on follow-up angiograms some months later (despite the presence of a balloon in the cavernous sinus) (Fig. 6.12).

Since the cavernous sinus plexuses are anastomosed in the midline, TCCFs may drain to the opposite side or bilaterally (Figs. 6.14, 6.15). All the clinical signs may be sited opposite the fistula location. Bilateral drainage is frequent, and the orbital signs are of little assistance in pre-

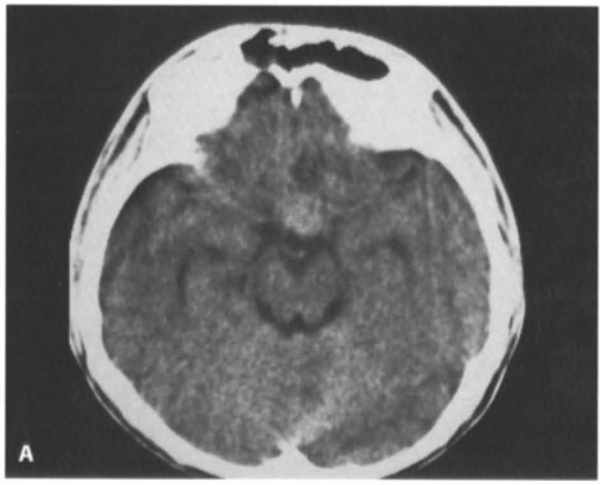

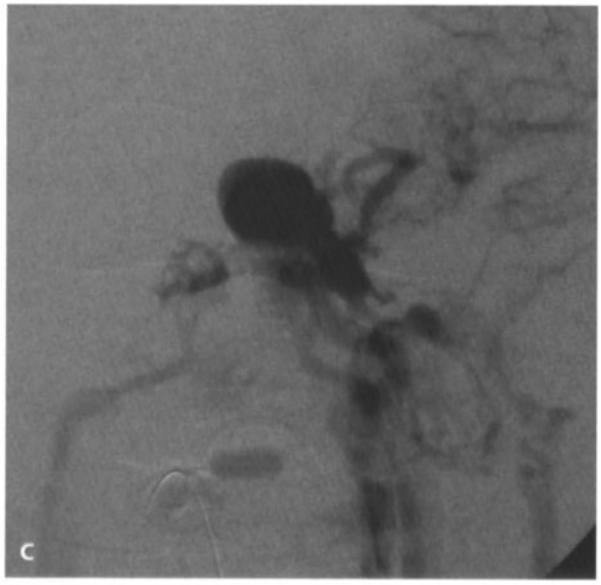

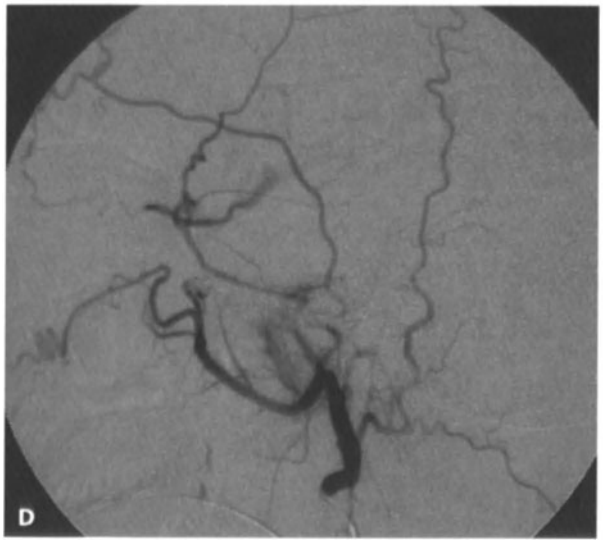

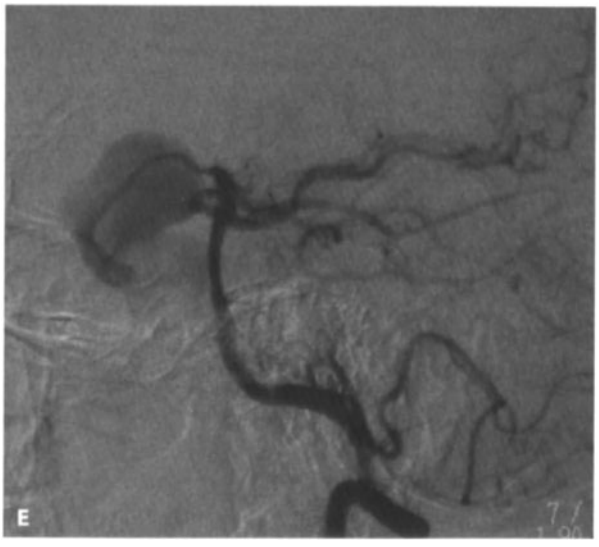

Fig. 6.11A–E. Legend see p. 291

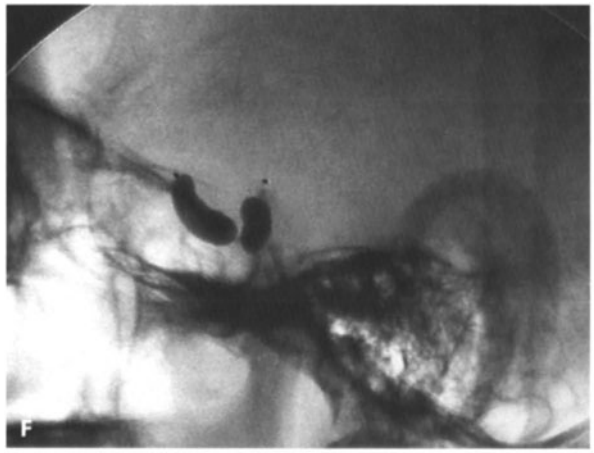

◀ **Fig. 6.11.** A 25-year-old man with a traumatic cavernous carotid fistula (CCF), with a large venous pouch bulging in the optic chiasm cistern, as shown on CT scan (**A**). The angiogram confirmed the CCF and the pouches (**B, C**). The external carotid artery (ECA) and vertebral artery (VA) injections demonstrate the intracavernous location of the orifice (**D, E**). Note the middle meningeal artery-associated trauma. The internal carotid artery siphon is sacrificed with two balloons (**F**). The long-term follow-up angiogram of the ECA and VA confirms total exclusion and shrinkage of the pouches (**G, H**). (Courtesy of S. Suthipongchai)

dicting the side of the TCCF. In addition, the severe head trauma may produce bilateral TCCFs in some cases (Fig. 6.4).

Drainage into the pterygoid plexus usually does not give specific symptoms. Drainage in multiple directions (Figs. 6.9, 6.12) is actually the most frequent situation. On occasion, previous procedures such as surgical ligations or associated occlusion of the venous drainage may alter the usual pattern of drainage.

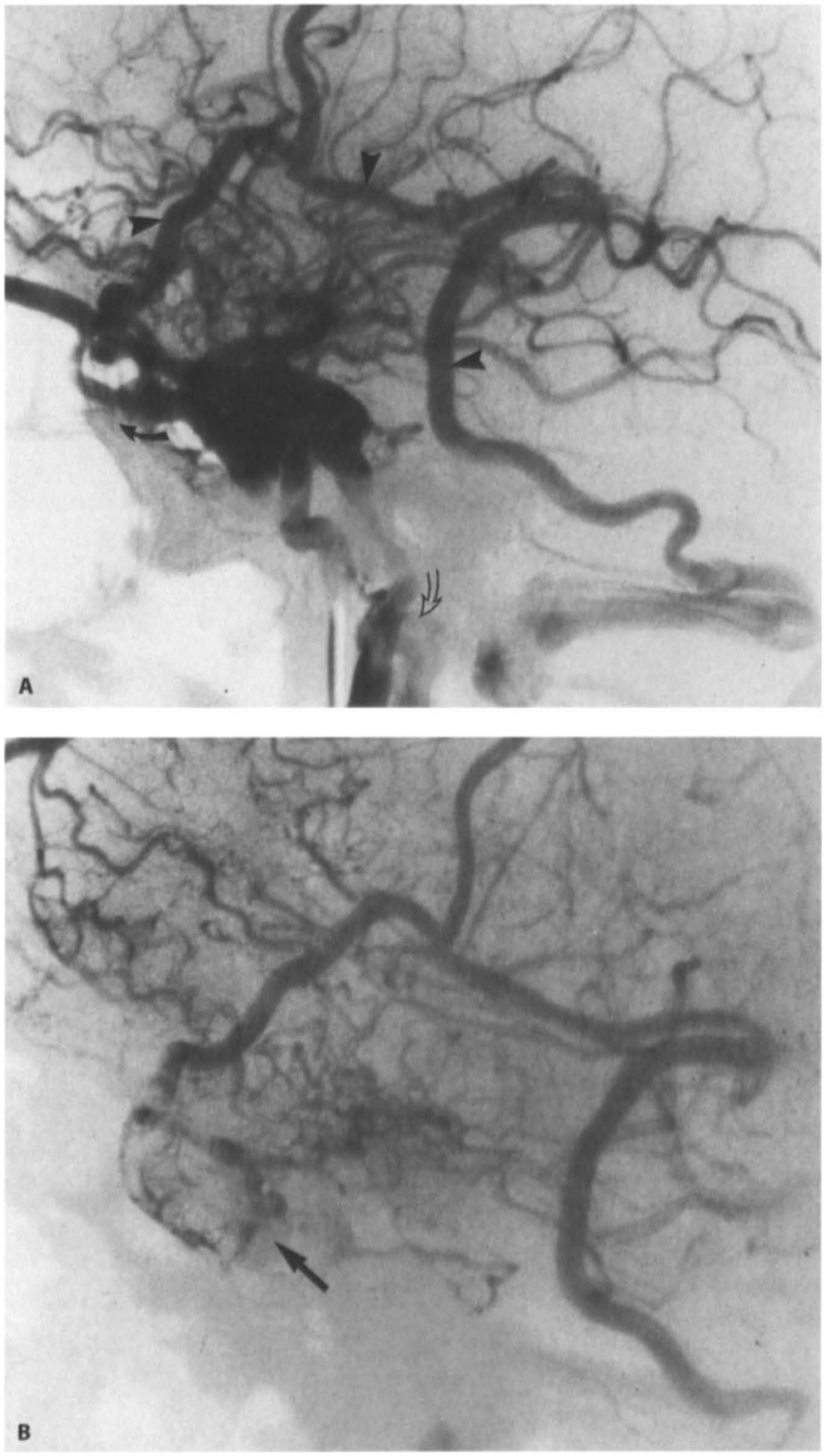

Fig. 6.12A–C. Traumatic cavernous carotid fistula (CCF) with mixed drainage. **A** Lateral subtraction angiogram of the left internal carotid artery demonstrates a CCF with drainage anteriorly toward the ophthalmic venous system (*curved arrow*), posteriorly toward the inferior petrosal sinus, jugular vein (*open curved arrow*) and superiorly toward cortical veins (*arrowheads*). **B** Lateral subtraction angiogram was performed immediately after balloon (*arrow*) repair of the fistula. Note the dilated cortical veins, filling antegrade and in normal sequential time. **C** see p. 293

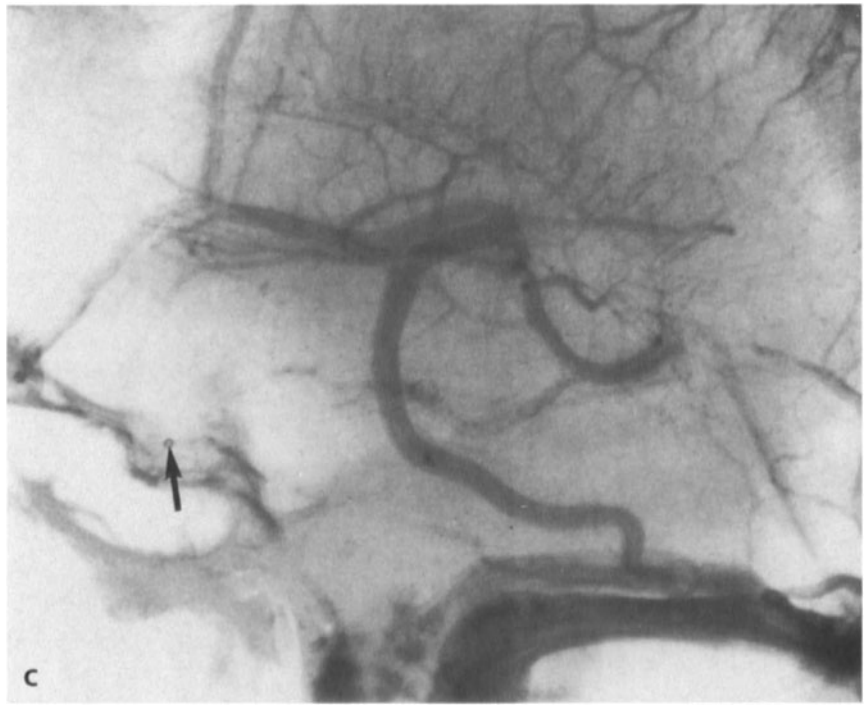

Fig. 6.12 (*continued*). **C** Follow-up angiogram 3 months later in venous phase. Note the return to a normal appearance of the veins. The balloon has deflated (*arrow*). The cavernous sinus is not opacified

6.2.2.1 Ophthalmological Symptoms

Visual loss occurs in approximately 54% of cases (Kupersmith et al. 1986) and progressive visual loss represents one of the main indications for emergency treatment in a TCCF. Progressive visual loss and epistaxis are the two main indications for emergent endovascular treatment (Table 6.4). The significantly better results in recovery of visual loss with endovascular embolization treatment, as compared with Henderson's (1959) or Hamby's (1966) methods, is related to the closure of the fistula and preservation of the ophthalmic artery (Fig. 6.16, p. 297).

6.2.2.2 Corneal Ulcerations and/or Infections and Secondary Glaucoma

Acute and chronic exposure from proptosis can lead to infectious conjunctivitis, keratitis; fifth nerve involvement diminishes corneal sensitivity, leading to noninfectious ulceration of the cornea. These complications require proper protection of the exposed globe with lubricants and/or temporary tarsorrhaphy to prevent ulceration.

Glaucoma secondary to poor aqueous outflow and elevated episcleral venous pressure may be difficult to control medically. The intraocular pressure normalizes in all cases where the shunt is successfully occluded (Table 6.1, p. 297). As long as the fistula remains patent, the patient is not a candidate for any type of intraocular surgery; embolization should be done first.

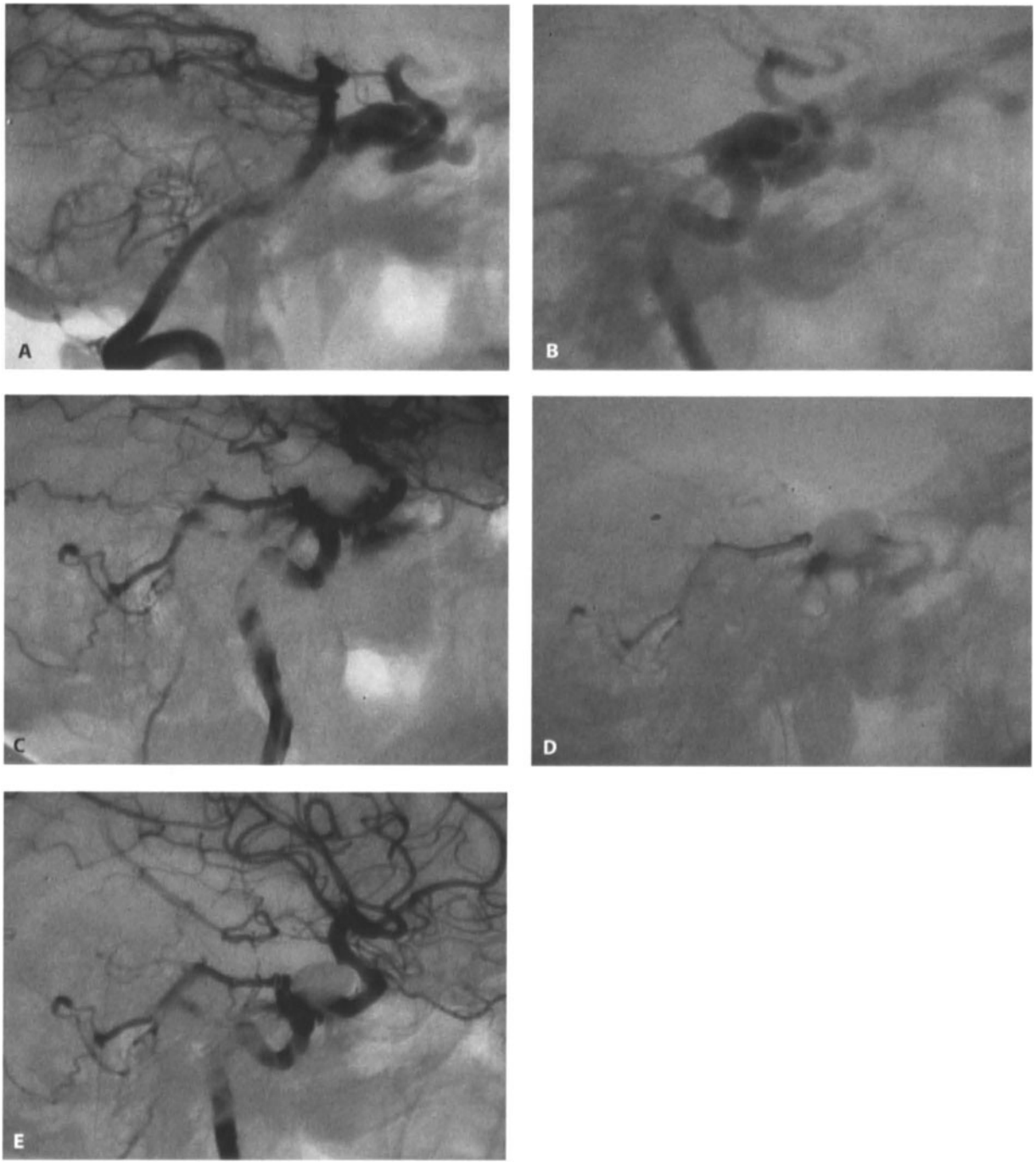

Fig. 6.13. Traumatic cavernous carotid fistula (TCCF; **A, B**) fed by the internal carotid artery. Treatment with detachable balloon excluded the TCCF but following detachment the balloon moved to occlude ophthalmic vein drainage. The drainage was rerouted into the subarachnoid veins of the posterior fossa (**C**). A potential risk of hemorrhage resulted from this drainage. Subsequent catheterization of the posterior branch of the siphon (**D**) was used to place several coils (**E**) to achieve rapid exclusion of the TCCF. **F, G** see p. 295

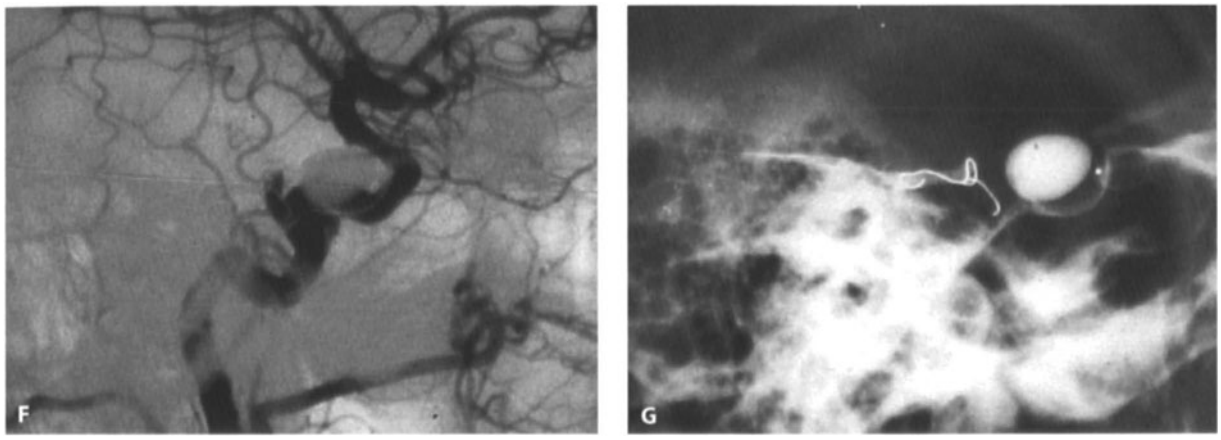

Fig. 6.13 (*continued*). Since the goal of disconnection was not achieved, glue was injected (**F, G**)

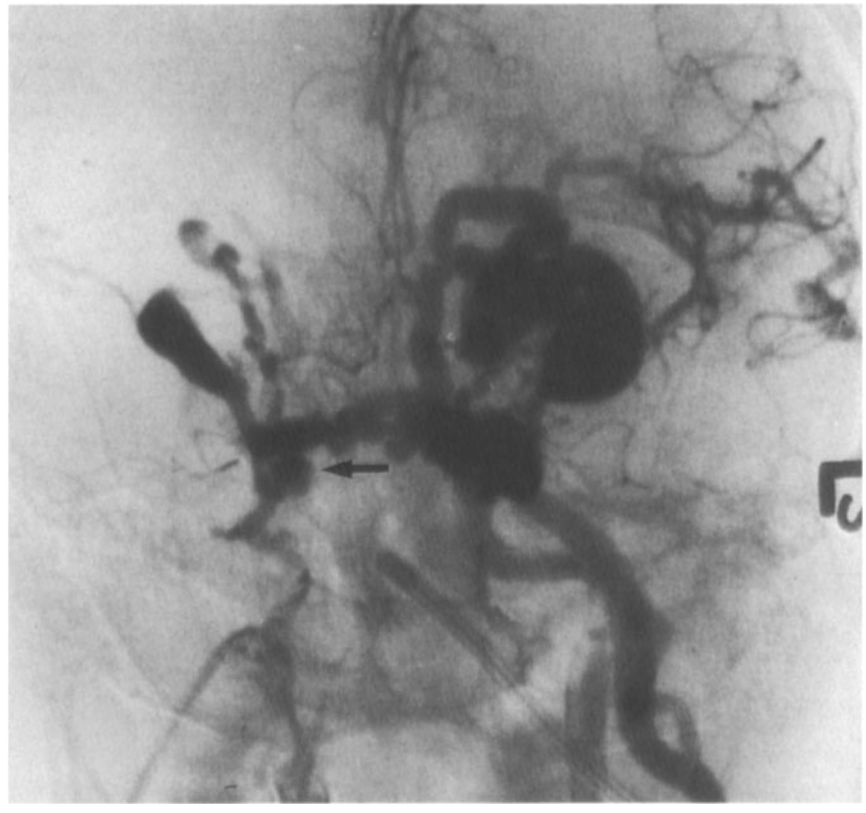

Fig. 6.14. Left traumatic cavernous carotid fistula with bilateral ophthalmic drainage. Frontal subtraction angiogram of the left internal carotid artery in late arterial phase. Note filling of both cavernous sinuses and ophthalmic veins, through the coronary sinuses (*arrow*)

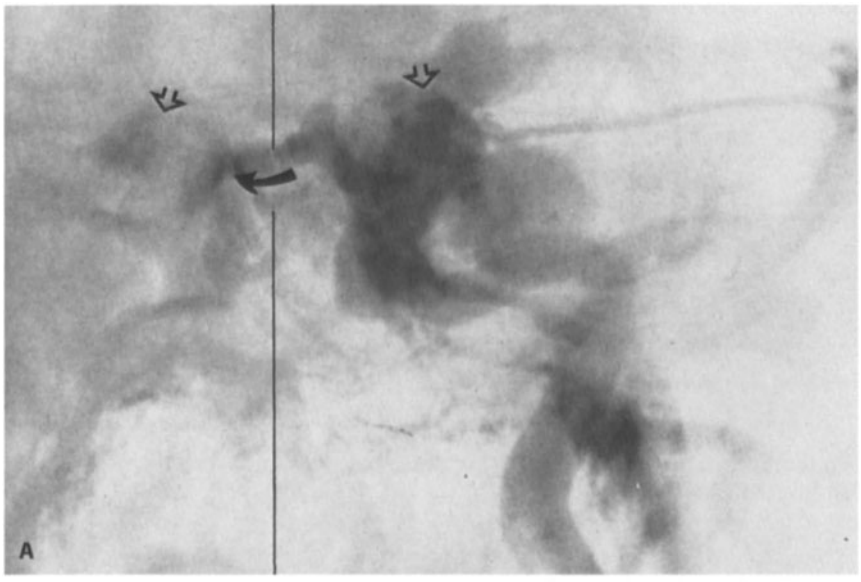

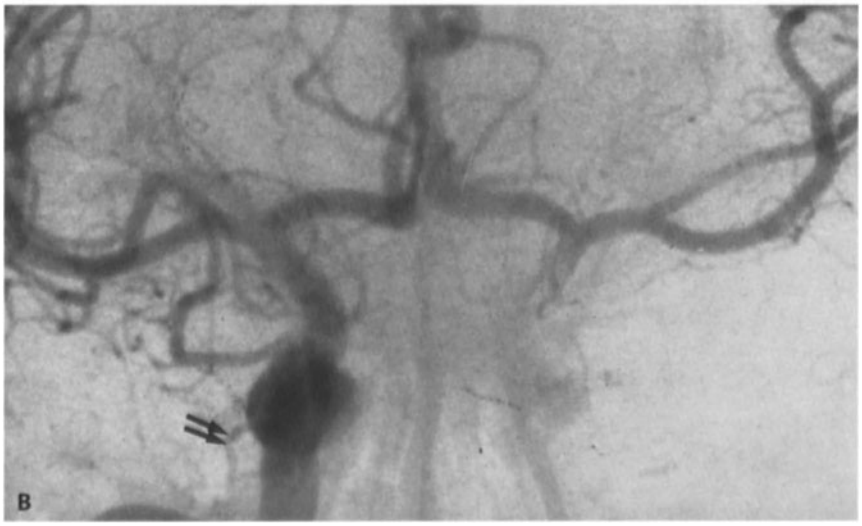

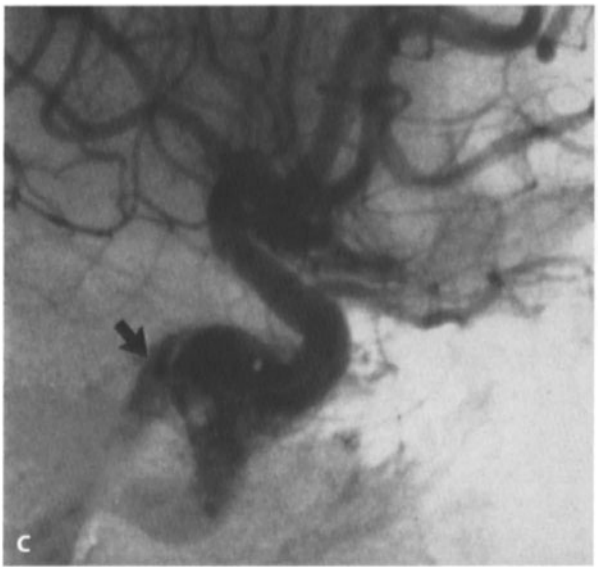

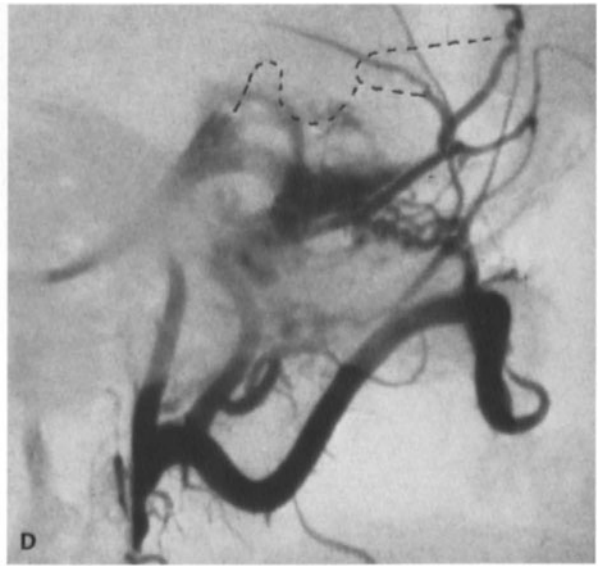

Fig. 6.15A–D.
Legend see p. 297

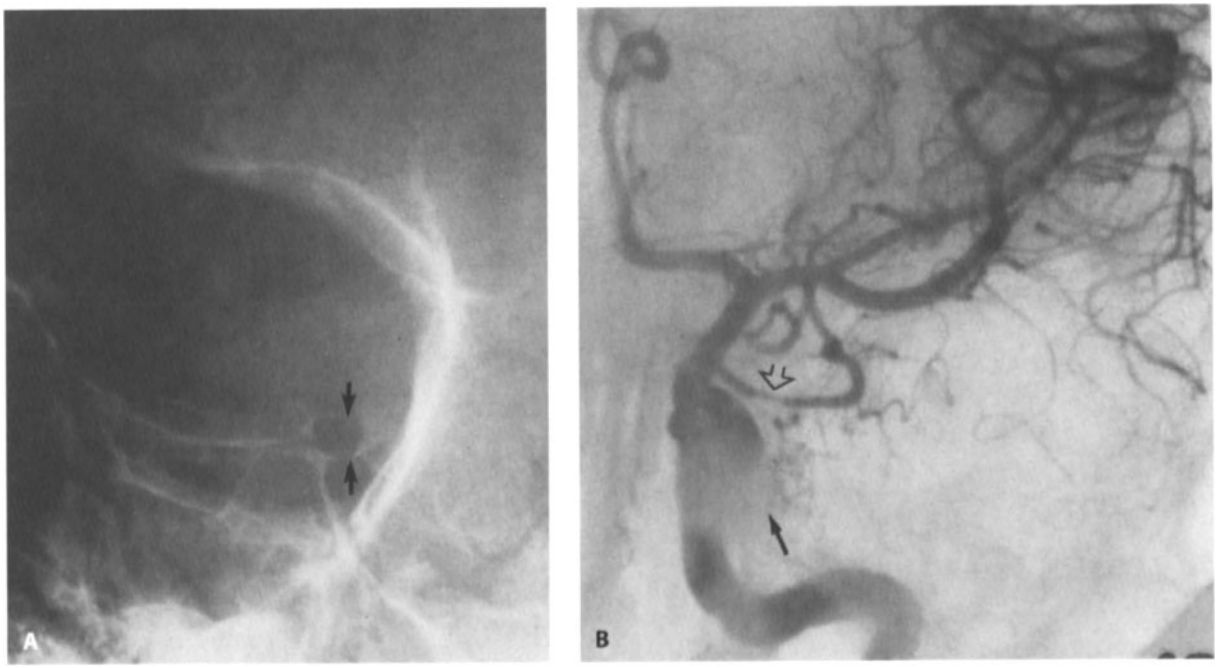

Fig. 6.16. **A** Optic foramen view demonstrates a fracture of the optic canal (*arrows*) that resulted in immediate nonreversible visual loss. **B** Frontal subtraction angiogram of the same patient after balloon (*arrow*) repair of the fistula. Note the focal narrowing of the ophthalmic artery (*open arrow*) at the level of the optic canal

Table 6.1. Arteriovenous fistulas etiologies

I. Traumatic	II. Spontaneous
A. Blunt	A. Congenital
B. Penetrating	B. Acquired
C. Iatrogenic	a) Secondary to a preceding thrombosis?
	b) Secondary to a ruptured aneurysm?
	c) Associated to an angiodysplasia
	1. FMD
	2. Neurofibromatosis
	3. Ehlers-Danlos syndrome
	4. Other dysplasias

◀ **Fig. 6.15.** **A** Left internal carotid angiogram in a patient with a traumatic cavernous carotid fistula (CCF). Note the bilateral venous outflow (*curved arrow*) and opacification of both superior ophthalmic veins (*open arrows*). **B** Opposite internal carotid angiogram. Note the visualization of infero-lateral trunk (ILT; *double arrow*) with no evidence of shunt. **C** Right internal carotid angiogram 3 months after successful embolization of the left CCF. The patient had complained of right-sided pulsatile tinnitus. A spontaneous dural arteriovenous malformation (AVM) is seen at the level of the cavernous sinus (*arrow*). **D** Internal maxillary artery branches also supply the lesion. Note the unique drainage posteriorly

Fig. 6.17. **A** A patient with prominent collateral venous dilatation, following surgical ligation of the internal jugular vein as well as the internal carotid artery (ICA) and the external carotid artery (ECA). Note the prominent angular and upper eyelid veins. **B** Complete regression after surgical exposure of the previously ligated internal carotid artery and successful embolization of the fistula

6.2.2.3 Diplopia

The frequent involvement of cranial nerves in the cavernous sinus often produces diplopia. Although cranial nerve function improves in the great majority of cases, complete normalization of extraocular muscle function is only observed in 32% of cases. Extraocular eye muscle palsies that remain may cause diplopia. Prism therapy (temporary Fresnel) may help in providing binocular vision during the recovery phase. Some cases with permanent cranial neuropathy may benefit from ptosis repair and/or strabismus surgery if no improvement is made within 6 months of the fistula closure (Fig. 6.17).

6.2.2.4 Cranial Nerve Involvement in Traumatic Carotid Cavernous Fistulae

Cranial nerves III, IV, VI, and V_1 can be impaired as they course in the wall of the cavernous sinus (Tables 6.2, 6.4; Fig. 6.9). As mentioned previously, nerve dysfunction may occur at the time of the trauma (as a direct injury to the nerve), or may present later (as a compression of the nerve by the

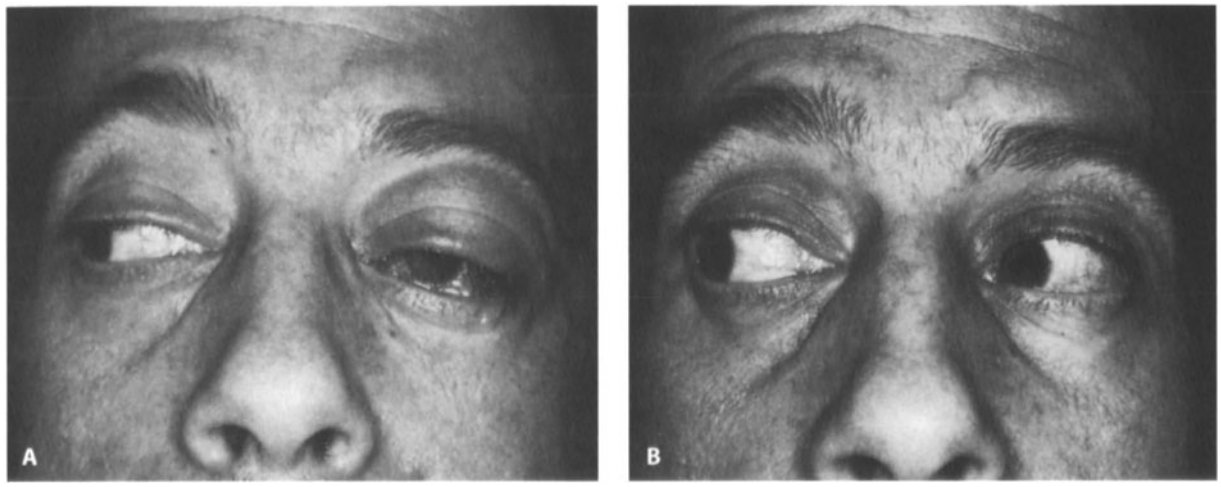

Fig. 6.18A, B. A 31-year-old man with left side ophthalmoplegia, which developed some weeks after trauma. **A** Clinical picture demonstrates the incapacity of medial gaze in the left eye. **B** Two weeks after treatment, there was complete recovery

Table 6.2. Neuro-ophthalmic abnormalities before and after embolization (Kupersmith 1986)

Pre-embolization	Postembolization improvement	Postembolization[a] normal
Ptosis 62%	85%	52%
Third nerve 68% (1b)	69%	35%
Fourth nerve 50%	76%	41%
Sixth nerve 85% (1b)	76%	55%
Pupillary defects III 35%	(III) 8%	8%
Sympathetic 39%	67%	67%
Iris dilated vessels 9% (1b)	33%	33%
Proptosis 88% (1b)	100%	80%
Chemosis 59% (1b)	67%	63%
Dilated conjunctival vessels 100% (4b)	100%	88%
Bruit 85%	100%	100%
Thrill/pulsation of globe 15%	100%	100%
Lid engorgement 47%	100%	94%
Venous retinopathy 38% (2b)	85%	85%
Disc edema 15% (1b)	80%	80%
Visual loss 50% (1b)	35%	24%
Increased intraocular pressure 79% (3b)	96%	96%
Pain[b]	100%	100%

b, bilateral.

[a] 2 weeks to 5 years follow-up.

[b] Pain may start or aggravate following treatment, when the cavernous sinus collapses. It will resolve in 3–5 weeks.

dilated cavernous sinus or secondary ischemia to the cranial nerves), or a combination of these factors. When the nerve is injured at the time of the trauma, there likely will be no recovery after treatment of the fistula. There is a greater chance of improvement or complete recovery after treatment of the fistula when the dysfunction is delayed (Figs. 6.17, 6.18), although it may take several months for complete normalization. When the limitation in ocular motion is due to mechanical factors, resolution will uniformly follow soon after repair of the fistula (Fig. 6.6). Associated facial nerve impairment and deafness are usually secondary to traumatic impairment of the petrous pyramid and involvement of the inner and/or middle ear.

6.2.2.5 Bruit

Bruit is the most constant finding (in association with a hyperemic conjunctiva) in traumatic fistulae and is caused by the high flow of the lesion. It is usually maximal over the ipsilateral eye. The bruit can radiate to the frontal, temporal, jugular, or other areas, depending on the venous outflow of the fistula. Subjective bruits are related to posterior drainage and bone conduction. Thrills and/or pulsations of the globe are infrequent and related to a dominant anterior drainage.

6.2.2.6 Arterial Steal

Arterial steal may affect the ophthalmic artery territory and produce impaired vision. This is infrequently present, unless compression or damage of the ophthalmic artery and nerve in the optic canal (hematoma, contusion, edema, etc.) occurs. The hypoxia of the anterior segment of the eye is manifested by changes in corneal epithelium and the presence of cells in the anterior chamber; ocular dysfunction is further aggravated by increased intraocular pressure. It may even result in occlusion of the central retinal artery (Kupersmith et al. 1986).

6.2.2.7 Hemispheric Arterial Insufficiency

An acute neurological deficit may be the presenting symptom when the fistula is large and a complete hemodynamic steal (Fig. 6.9) occurs on congenitally and/or acquired underdeveloped cerebral collateral circulation, usually at the level of the circle of Willis (Day and Rhoton 1982). However, it is clinically difficult to distinguish the exceptional occurrence of arterial steal from the more common consequences of the venous drainage of the TCCF (Fig. 6.19), the possible associated venous injuries, and cerebral contusion.

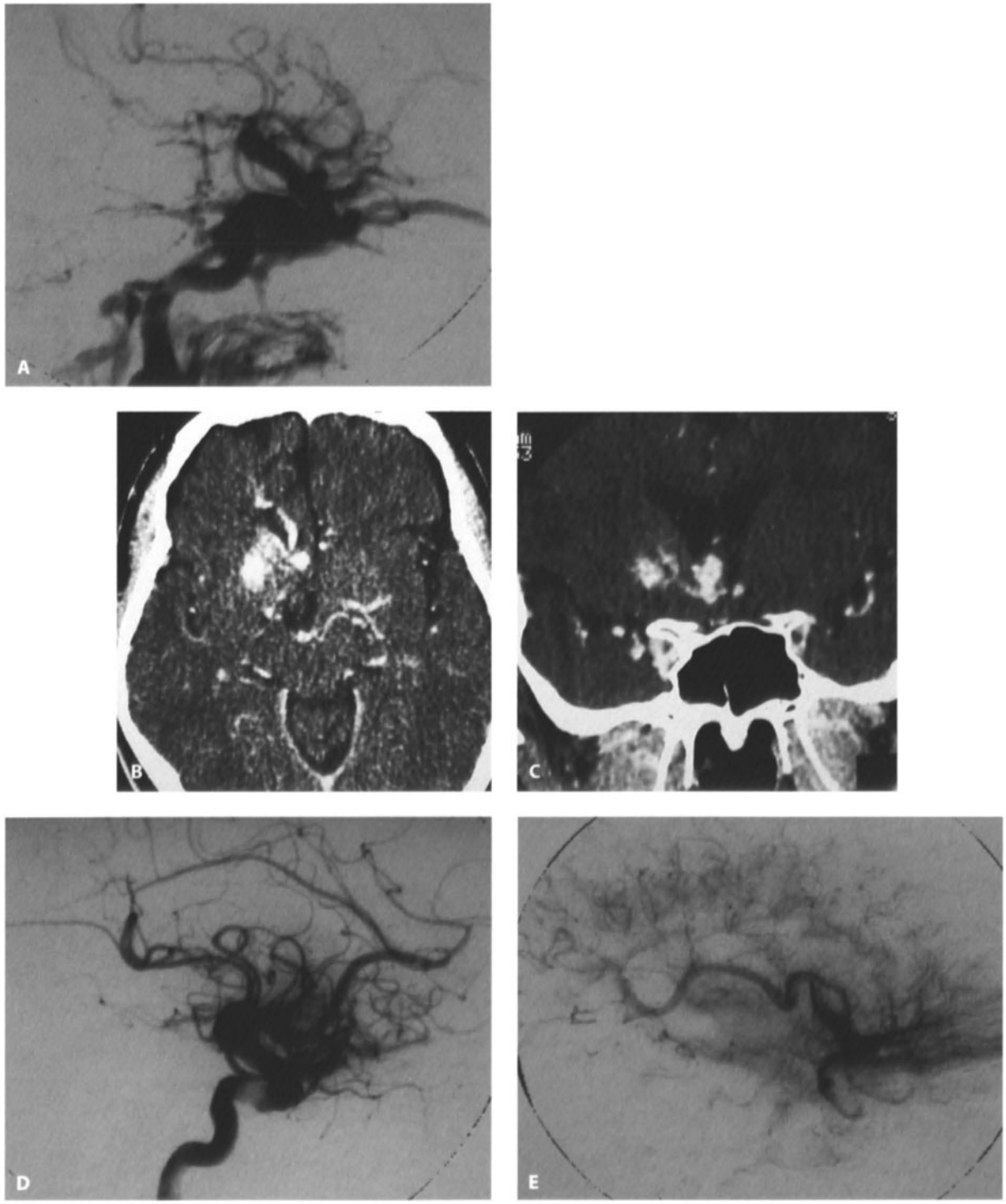

Fig. 6.19. Traumatic cavernous carotid fistula (CCF) (**A**) with abnormal appearance on CT (**B, C**) examination. After balloon exclusion of the CCF, the peculiar CT images proved to be related to a congested, associated developmental venous anomaly (**D, E**). (Courtesy of R. Piske)

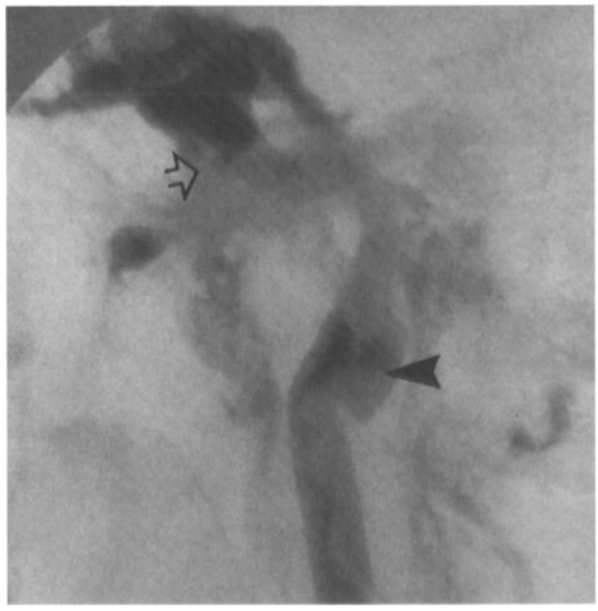

Fig. 6.20. Associated vascular injuries. Lateral subtraction angiogram of the right internal carotid artery, early arterial phase. A traumatic pseudoaneurysm of the petrous carotid (*arrowhead*) is associated with a high-flow cavernous carotid fistula with multiple venous drainages. Note the vein of foramen ovale (*open arrow*) draining toward the pterygomaxillary plexus. (From Berenstein et al. 1980)

6.2.2.8 Associated Traumatic Lesions

Traumatic fistulae are part of a more complex clinical problem where other soft tissue or vascular structures of the head and neck region have also been injured. These may be associated with epidural and/or subdural hematomas, intracerebral hematomas, contusions, depressed fractures, CSF leaks, and traumatic pseudoaneurysms in other segments of the internal carotid artery (Fig. 6.20), or other brachiocephalic vessels, whether arterial or venous (Fig. 6.21; Table 6.3).

The literature on the natural history in most CCF series tends to lump traumatic and spontaneous fistulae together. The risk of untreated lesions as reported by Hamby (1966) includes total loss of vision in 25% of cases and visual impairment in another 20%. Kupersmith et al. (1986) showed visual loss in 54% of cases, of which 23% remained blind; in the other 31%, the visual loss was reversible and returned to normal after treatment (Table 6.4).

Sattler (1920) reported a 3% mortality rate as the result of intracranial or nasal hemorrhage. Patients with nasal hemorrhage are likely those that have an ICA rupture into the sphenoid sinus (Fig. 6.21), whereas those with intracranial hemorrhage have a direct intracranial vascular injury or brain contusion (Figs. 6.22, 6.23).

Spontaneous regression has been reported in 6% by Hamby (1966) and 10% by Dandy (1928); both series combined TCCFs and DAVSs of the cavernous sinus area. Regression is rare in TCCFs (Churojana 2001) (Fig. 6.30). Late progression of TCCFs has been associated with the secondary development of true dural arteriovenous shunts (DAVSs) locally or remote from the trauma site.

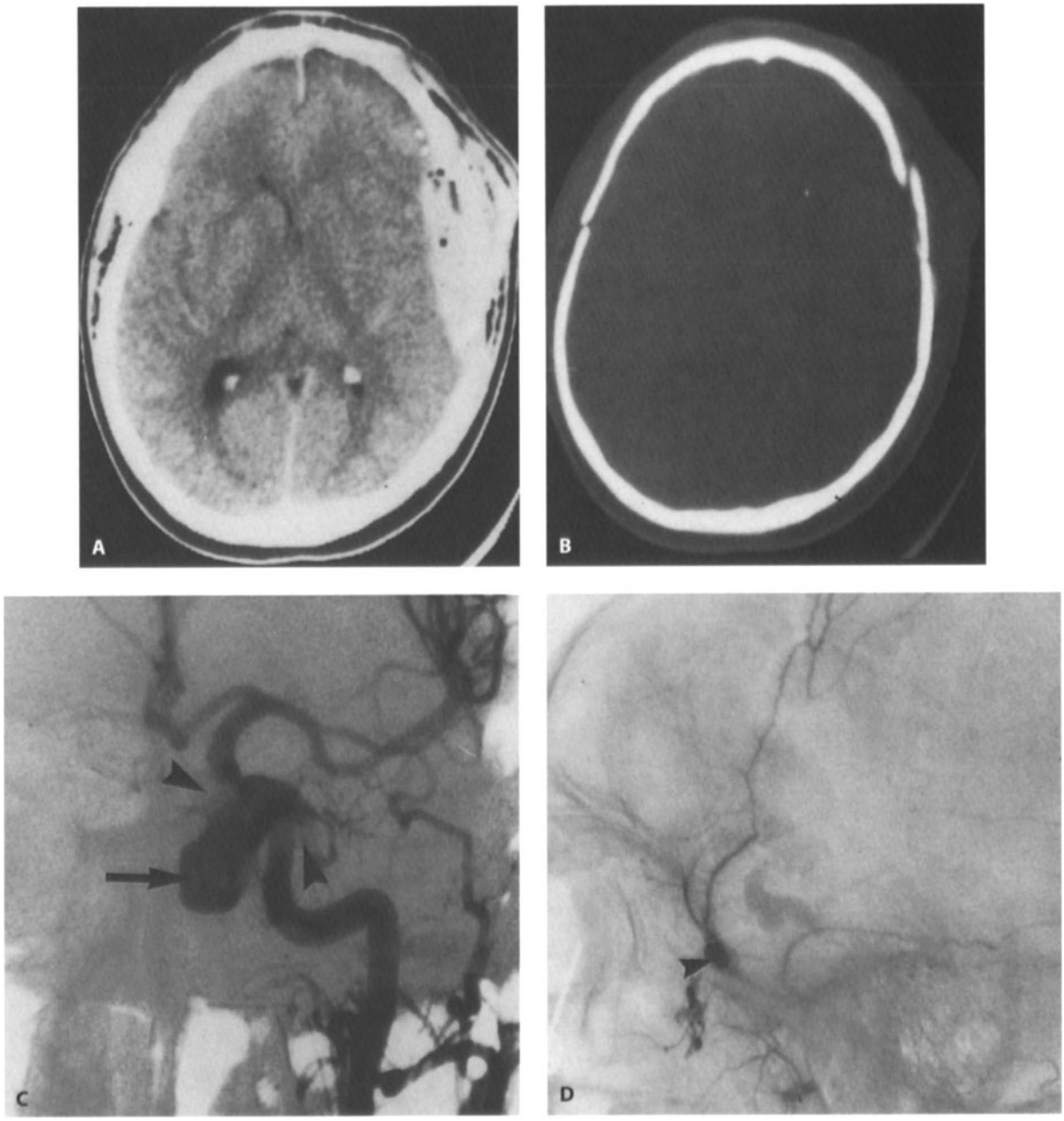

Fig. 6.21A–D. A 26-year-old male patient was referred because of severe and repeated epistaxis that started 1 year after incomplete repair of a traumatic fistula. **A** Enhanced axial CT demonstrates bilateral epidural hematomas and soft tissue injuries. **B** Bony windows demonstrate bilateral skull fractures. **C** Frontal subtraction angiogram of the left common carotid artery. Note the large pseudoaneurysm (*arrow*) projecting into the spheroid sinus. Two silastic balloons are seen in the cavernous sinus (*arrowheads*) from the previous treatment. **D** Lateral subtraction angiogram of the right (contralateral) middle meningeal artery after balloon trapping of the internal carotid artery; note a middle meningeal artery false aneurysm (*arrowhead*)

Table 6.3. Associated traumatic lesions in CCFs

Brain	Contusion Hematoma Subdural hematoma Epidural Hematoma Contre coup
Bone	Frontal fracture Orbit roof fracture Orbit floor fracture with muscle entrapment Medial wall of orbit fracture Petrous bone fracture (± VIIth, VIIIth damage) Sphenoid fracture Optic canal fracture Nasal fracture Craniofacial fracture
Sinuses	Fluid level Intracranial air Contralateral side
Soft tissue	Soft tissue injury
Others	Cervical trauma Other fractures

CCF, carotid cavernous fistula.

Table 6.4. Visual loss in TCCFs (Kupersmith 1986)

Pre-embolization causes of visual loss (54%)	Postembolization
Traumatic optic neuropathy (15%)	No change
Postsurgical optic neuropathy (6%)	No change
Optic globe damage (6%)	No change
Reversible optic neuropathy "steal" (12%)	Normalized
Venous hypoxic retinopathy[a] (9%)	2 normalized
Surgical anophthalmos (3%)	No change
Central retinal artery occlusion secondary to elevated intraocular pressure (3%)	No change

TCCFs, traumatic carotid cavernous fistula.

[a] One patient with venous hypoxic retinopathy represents our only unsuccessful embolization.

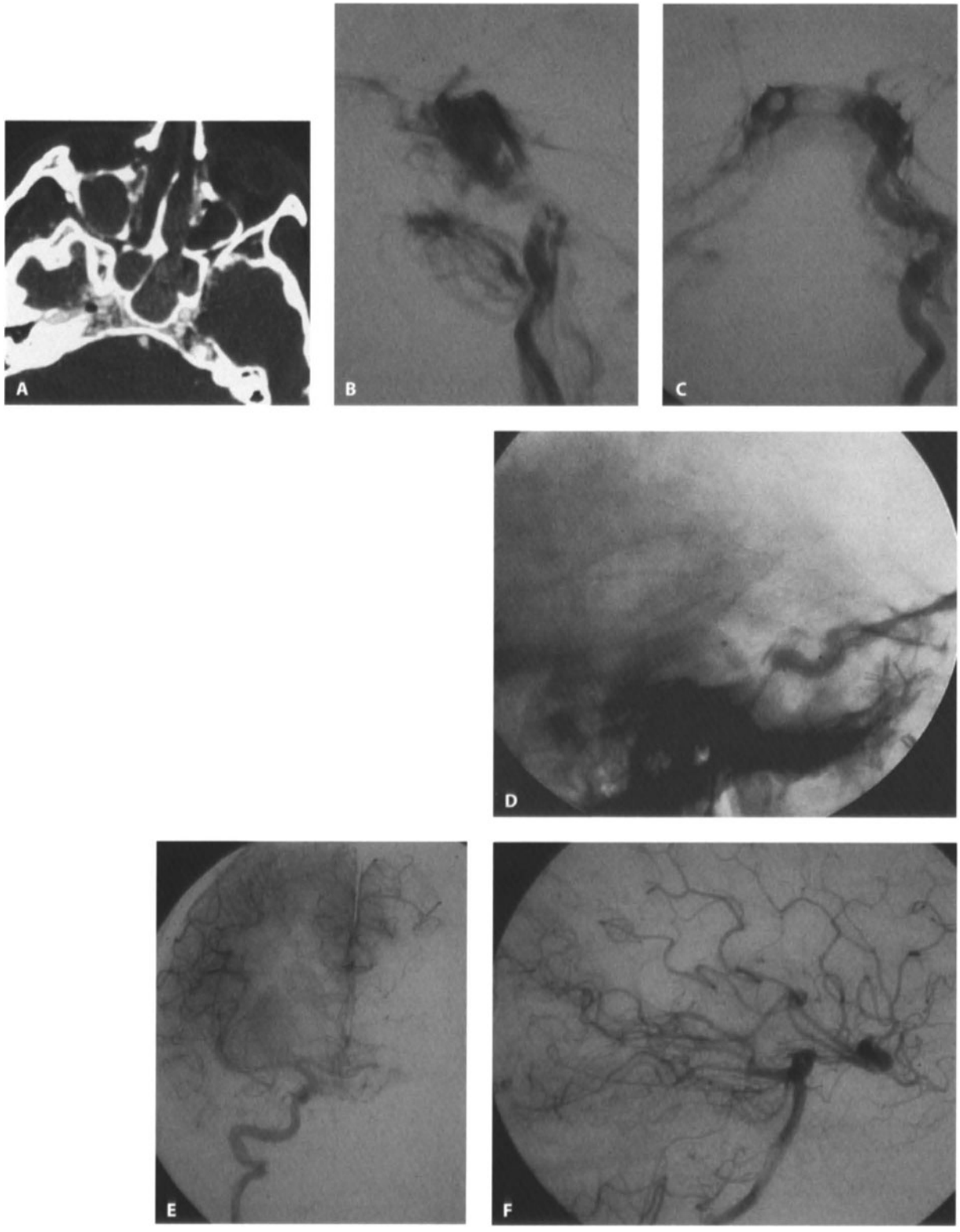

Fig. 6.22A–F. Motor vehicle accident victim with rupture of the internal carotid artery (ICA) into the sphenoid sinus. The CT shows air in the carotid canal (**A**). The emergency angiogram shows a traumatic cavernous carotid fistula without extravasation outside the skull base due to the efficient packing of the maxillofacial-associated lesions (**B, C**). The ICA (**D**) is immediately sacrificed after checking the patency of the circle of Willis (**E, F**)

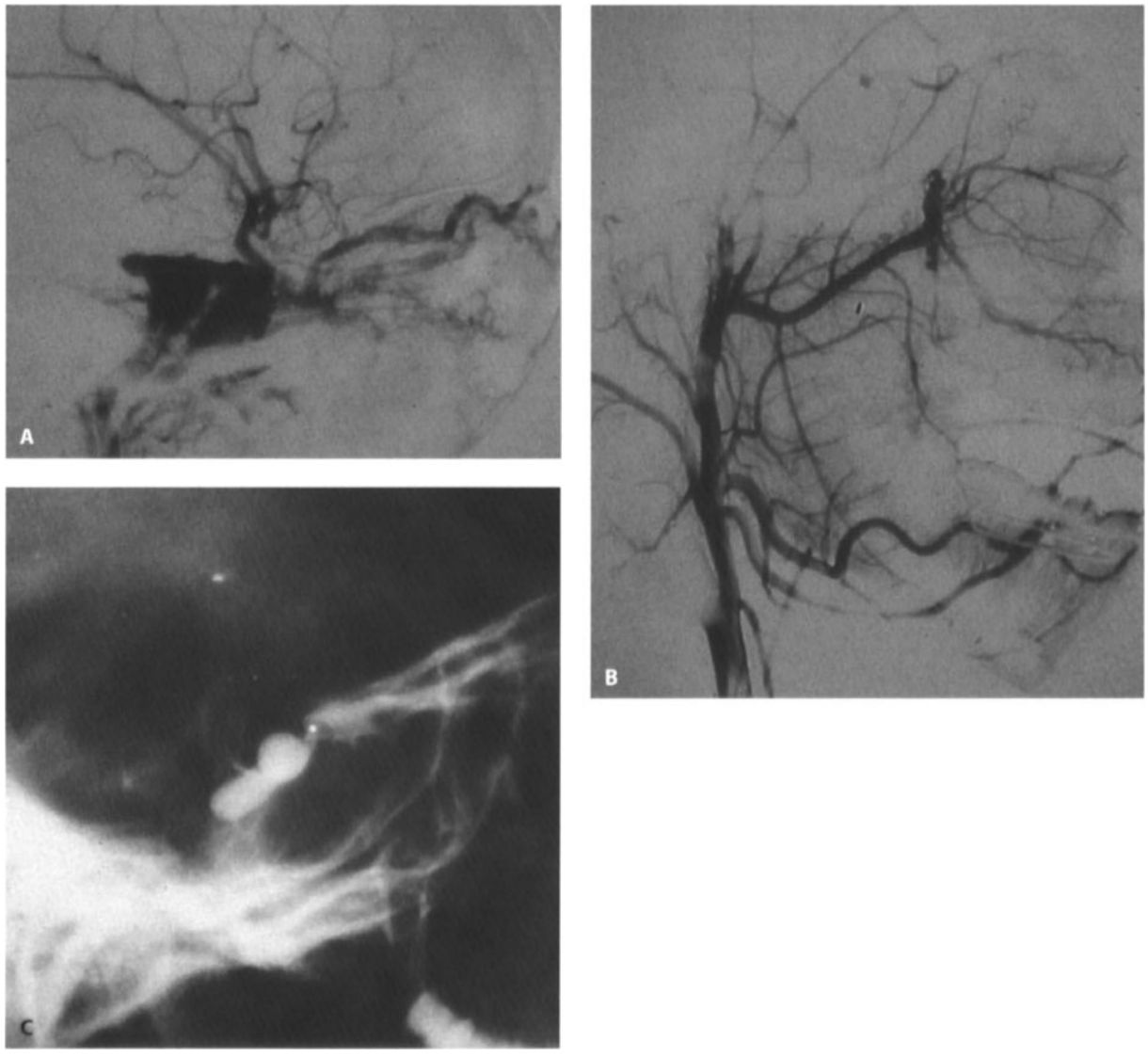

Fig. 6.23A–C. Posttraumatic massive epistaxis with evidence of subarachnoid hemorrhage on CT. Angiogram shows traumatic cavernous carotid fistula (**A**) with extracavernous contrast filling along the tentorium, testifying to the rupture of the internal carotid artery (ICA) and the dural tear. The ICA was immediately sacrificed with detachable balloon (**B, C**)

6.2.3 Pretherapeutic Evaluation

Based on the clinical picture, the diagnosis of TCCF is easy. However, planning the best therapeutic regimen requires consideration of all clinical problems caused by the trauma and not only the vascular injury, which is often not the most dangerous aspect at the acute stage.

Computed tomography (CT) and magnetic resonance imaging (MRI) are the best imaging modalities to assess the extent of cranial injury and the consequences of the trauma in order to anticipate vascular complications (Table 6.3) such as proptosis, prominent ophthalmic veins (Fig. 6.24), extraocular muscle congestion, lateral bulging of the cavernous sinus,

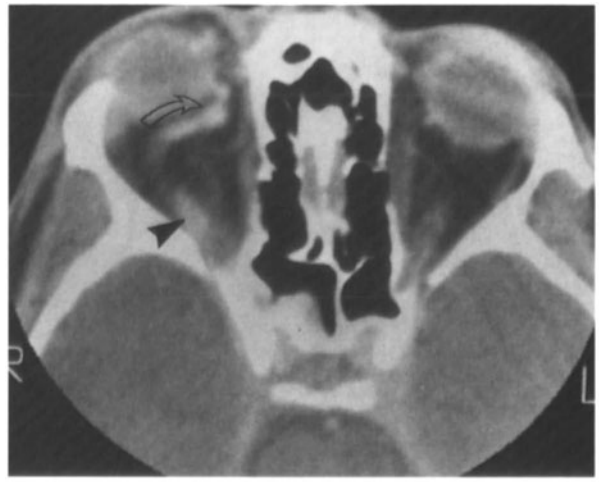

Fig. 6.24. Axial enhanced CT shows the characteristic prominence of the ophthalmic vein (*open curved arrow*) and the engorgement of the superior rectus muscle (*arrowhead*)

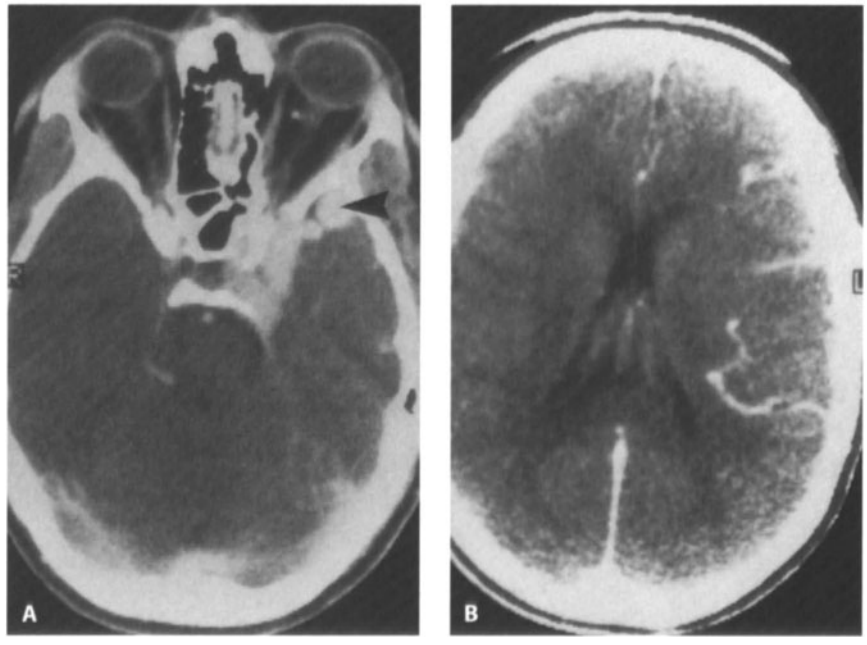

Fig. 6.25. **A** Axial CT. Multiple aneurysmal dilatations of the left cavernous sinus, including the sphenoparietal sinus (*arrowhead*) and mild exophthalmos. **B** Axial CT at the level of the lateral ventricle. Note the prominent cortical veins in the left cerebral hemisphere

dilatation of its tributaries (Fig. 6.25), and compression of the third ventricle (Fig. 6.26) with hydrocephalus. Associated injuries such as bony fractures, soft tissue injuries, intracranial blood collections (Fig. 6.21), paranasal opacification and/or air fluid levels, usually the result of additional trauma, can also be seen (Fig. 6.22). The presence of subarachnoid hemorrhage, with skull base fracture involving the sphenoid sinus or the petrous apex, and the presence of air in the carotid canal are highly suggestive of an ICA rupture outside the cavernous sinus and are an absolute emergency for investigation and therapeutic angiography.

It is important to establish the vascular anatomy systematically, with the aim of answering the following questions (Sects. 6.2.3.1, 6.2.3.2).

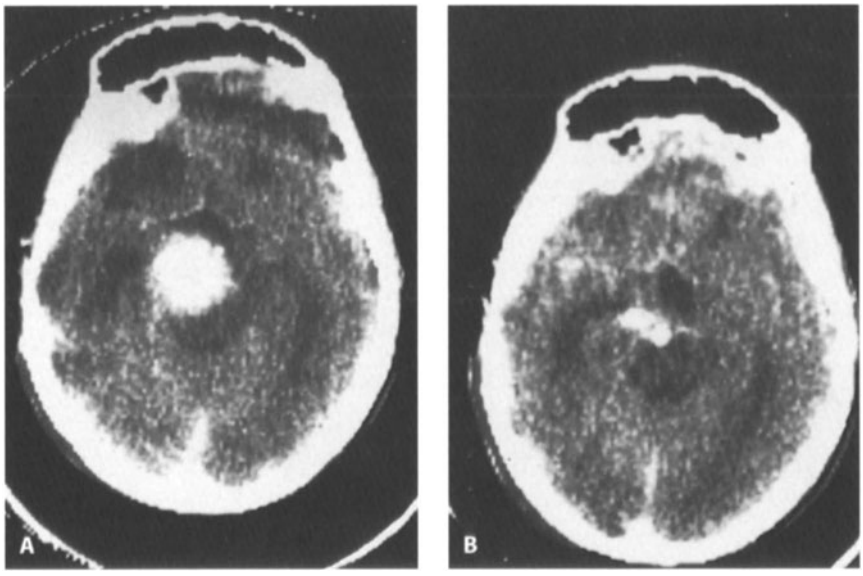

Fig. 6.26A, B. Same patient as Figs. 6.9, 6.46. **A** Pre-embolization enhanced axial CT demonstrates the aneurysmally dilated cavernous sinus compressing the 3rd ventricle. **B** Enhanced CT after embolization. Note collapse of the cavernous sinus (see Fig. 6.50). (Berenstein et al. 1980, with permission)

6.2.3.1 Location of the Fistula

1. Is the fistula in the cavernous sinus? Does it involve the internal carotid siphon wall? And if so, where is it located (Fig. 6.7)?
2. Is it a rupture of an intracavernous branch, and if so, can it be reached from the external carotid side (Figs. 6.27, 6.28)?
3. Is there a complete arterial steal related to the fistula (Fig. 6.9) and what is the circulation to the normal brain?
4. Are there associated vascular lesions?
   - Associated arterial aneurysms or pseudoaneurysms, proximal and/or distal to the fistula (Fig. 6.4) on the internal carotid artery itself, the external carotid artery, or their branches (Figs. 6.20, 6.27).
   - Associated posttraumatic venous thrombosis (Fig. 6.29).
   - Other AVFs (Figs. 6.4, 6.30) on the opposite side or on other brachiocephalic arteries.
   - Presence of a traumatic dissection.
   - Evidence of an underlying arterial disease (atheroma, stenosis, angiodysplasias, etc.; Figs. 6.2, 6.3).

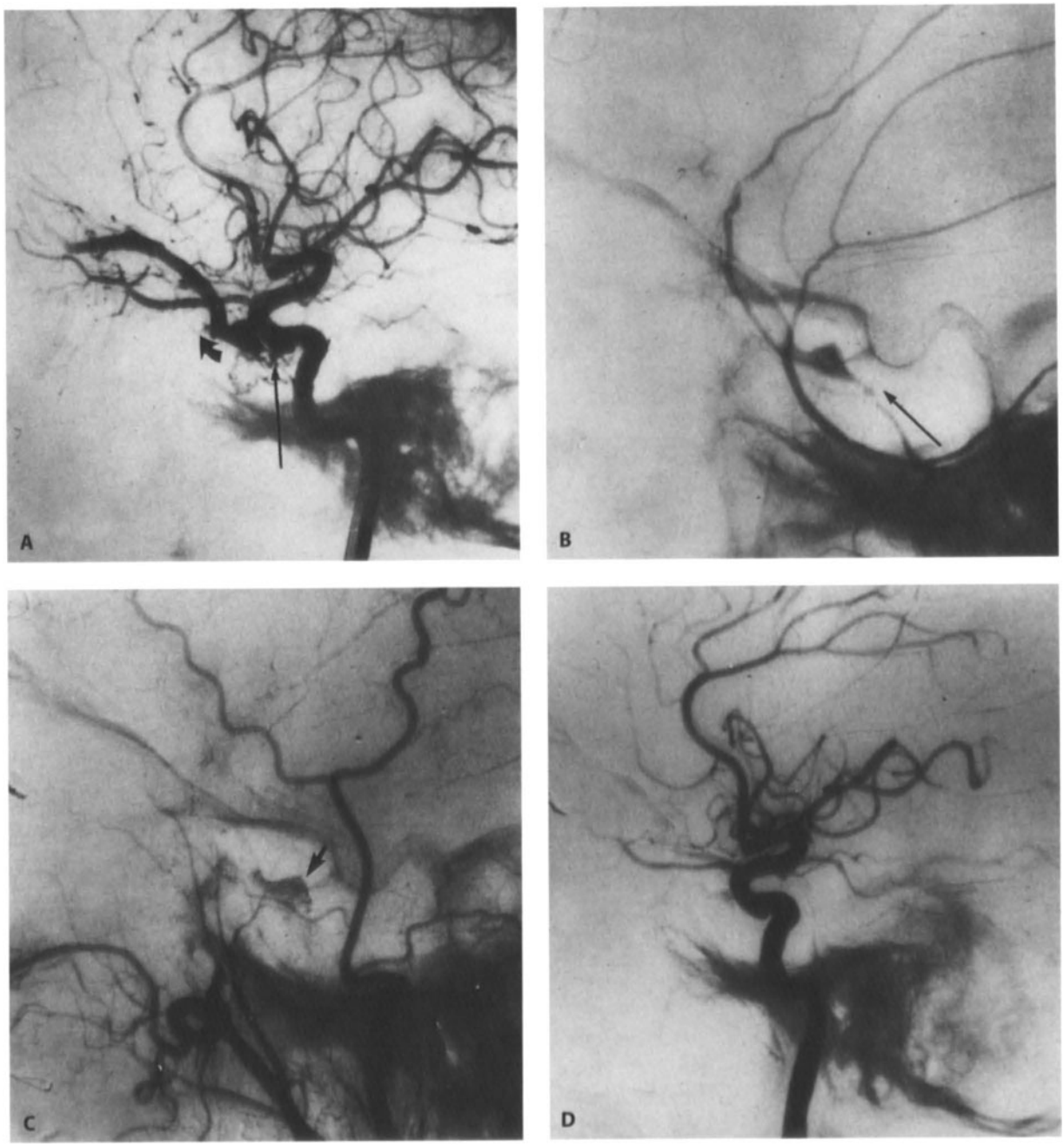

Fig. 6.27. **A** Lateral subtraction angiogram of the left internal carotid artery (arterial phase). There is early filling of the cavernous sinus and ophthalmic venous system (*curved arrow*) with a prominent infero-lateral trunk (ILT; *arrow*). **B** Lateral subtraction angiogram of the ipsilateral middle meningeal artery. The cavernous sinus is also opacified without filling the internal carotid artery, showing laceration of the ILT (*arrow*). **C** Lateral subtraction angiogram of the left external carotid artery after successful isobutyl cyano acrylate (IBCA) embolization of the middle meningeal artery (*arrow*). **D** Left internal carotid artery control: there is no filling of the ILT fistula (the internal carotid artery was not embolized but used to control the result of embolization)

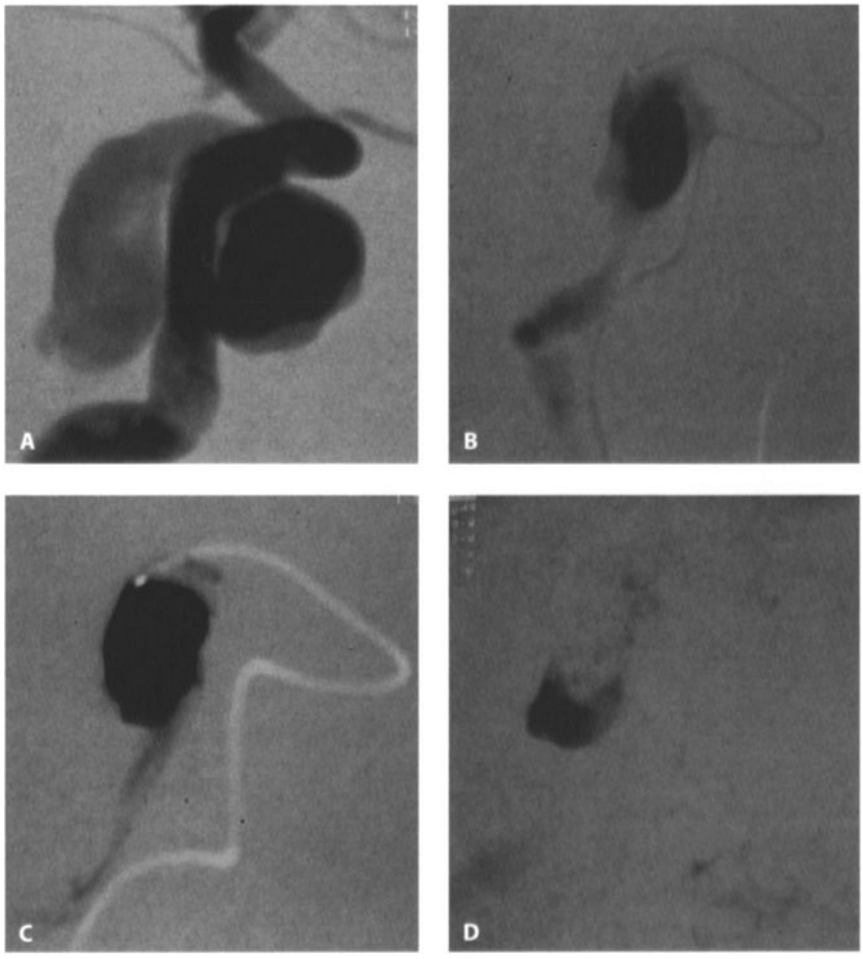

Fig. 6.28A–J. Bilateral traumatic cavernous carotid fistula (CCF); detachable balloons were not available, and fistula was embolized with glue. Right CCF (**A**) was catheterized across the arterial fistula beyond the first venous pouch (**B**); pure glue with tantalum powder was injected (**C**). **D** Stagnation and occlusion was immediately obtained. The left CCF (**E**) was then accessed via its external carotid artery supply (**F**); glue was delivered via the accessory meningeal artery (**G**). **H, I** Follow-up of left-sided CCF. **J** Glue cast. **E–J** see p. 311

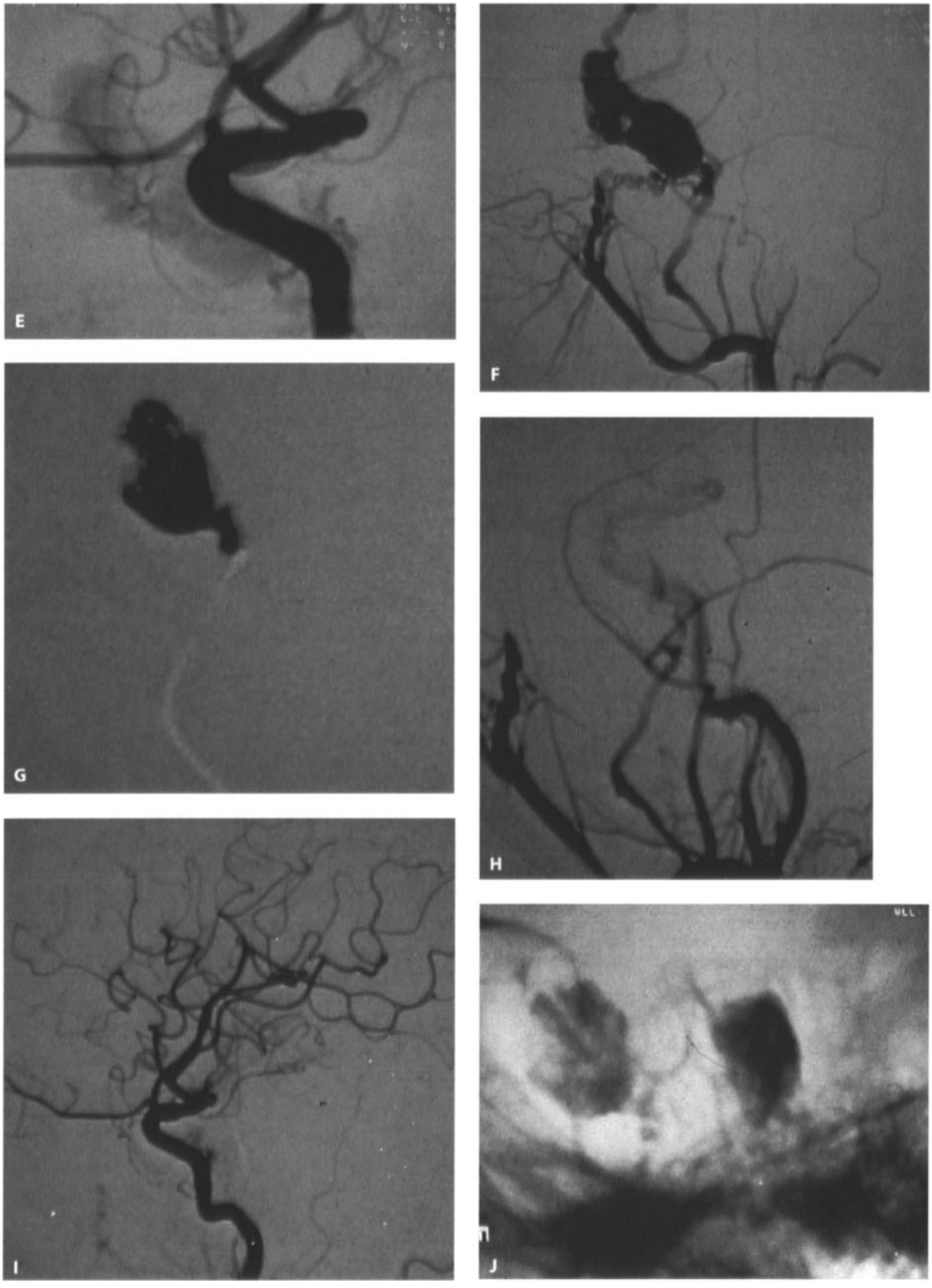

Fig. 6.28E–J. Legend see p. 310

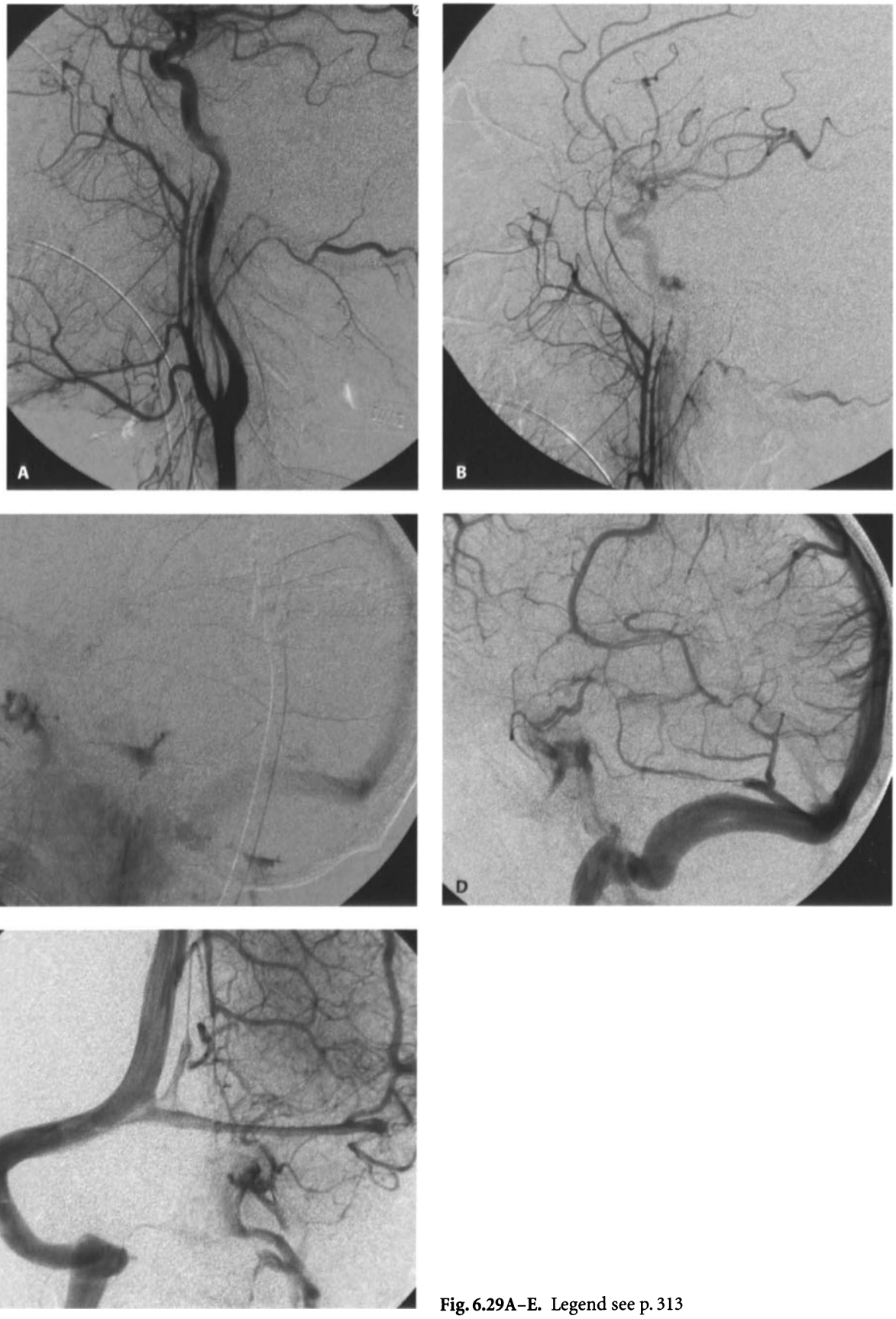

Fig. 6.29A–E. Legend see p. 313

◀ **Fig. 6.29.** Skull base trauma with minimal shunt at the skull base and spastic reaction of the distal external carotid artery (ECA) branches (**A, B**). Careful analysis of the venous phases shows venous damage at the vein of the foramen ovale (**C**, ECA late phase; **D, E**, ICA late phase). The venous lesion is better demonstrated with the arterial mask to the venous phase (**F, G**)

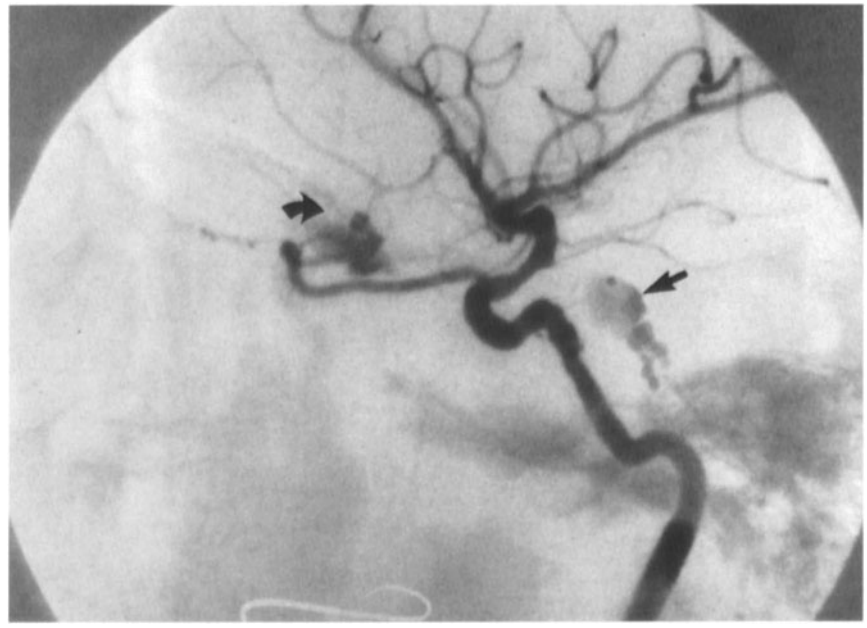

Fig. 6.30. Lateral subtraction angiogram after repair of the internal carotid to cavernous fistula (*arrow*, subtracted balloon). The orbital bruit persisted and follow-up angiogram demonstrates a traumatic fistula of the ophthalmic artery to the superior ophthalmic vein (*curved arrow*). This fistula was not treated, and had disappeared spontaneously on the 3-month follow-up examination

6.2.3.2 Venous Drainage of the Fistula

1. Does venous drainage of the fistula explain the clinical symptoms?
   - Is it draining immediately extracranially into sinuses or is there subarachnoid venous reflux?
2. How is the brain draining?
3. Is there evidence of associated venous plexus or sinus thrombosis?
4. Is there evidence of venous ectasias? Where are they located?
5. Is there cross-filling to the opposite cavernous sinus and its tributaries?

Some unusual vascular arrangements can occur if the fistula or fistulae remain patent after multiple proximal ligations or incomplete embolizations (Figs. 6.31, 6.32).

The ophthalmic artery is often better assessed through the internal maxillary artery, as there is less superimposition of venous structures; retrograde filling of the siphon and the fistula can also be seen better through collateral circulation. When the fistula is in the posteromedial wall of the internal carotid artery (C5), the ascending pharyngeal artery may point precisely to the fistulous point and is a source of collateral circulation. The fistula site can be determined by the use of a double-lumen balloon catheter in the involved internal carotid artery (Berenstein and Kricheff 1979a) (Figs. 6.33, 6.34).

A test for tolerance of internal carotid occlusion (see Sect. 6.2.3, and Chaps. 7 and 14) can be done, but the balloon should never be inflated proximal to the site of the TCCF, as it would produce a true cerebral arterial steal.

Unusual anatomical dispositions should be recognized: trigeminal artery (Fig. 6.35) or persistence of the dorsal ophthalmic artery (Fig. 6.36).

Fig. 6.31A–C. Selective angiography in a case of caroticocavernous fistula (*solid arrow*). Multiple therapeutic attempts – surgical trapping (*asterisks*) and embolization – have developed unusual collateral circulation pathways. **A** Selective injection of the vertebral artery in lateral view. Opacification of an arterial network (*small arrows*) on the internal carotid artery course, via the C2 vertebro-occipital anastomosis (*curved arrow*) and the C2 lateral muscular channel (*double arrow*). **B** Proximal external carotid injection. Note the proximal narrowing (*asterisk*) due to traumatic dissection during previous catheterization. Note the arterial network (*small arrows*) following the intrapetrous portion of the internal carotid artery. **C** Selective injection of the ascending cervical artery in lateral view. Note the C4 collateral anastomosis (*curved arrows*) opacifying the external carotid artery distal to a previous ligation (*asterisk*) and the arterial network (*small arrows*) ▶

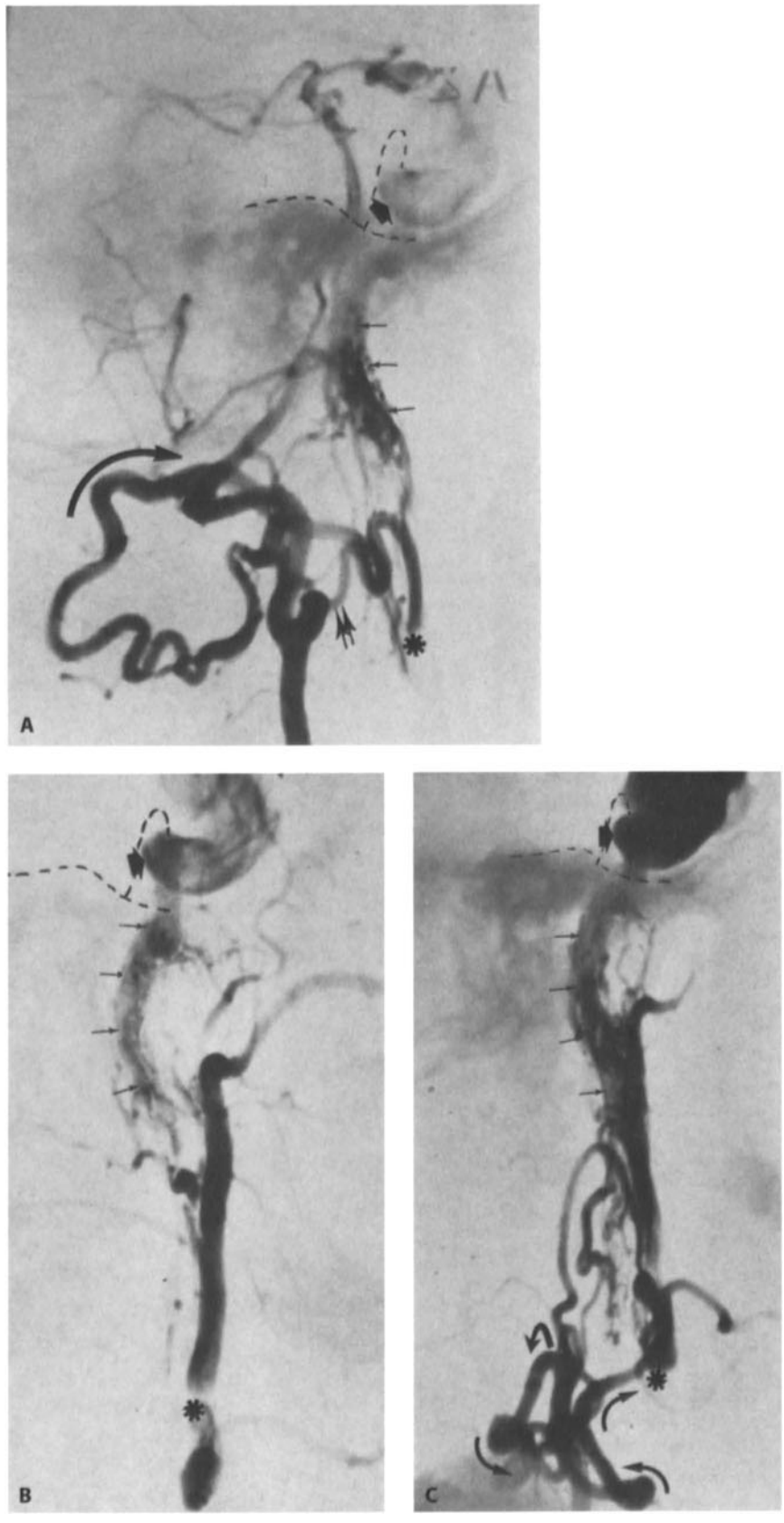

Fig. 6.31A–C.
Legend see p. 314

Fig. 6.32. Lateral views of selective injection of (**A**) deep cervical (right-angled) artery and (**B**) ascending cervical artery (*arrow*). The carotid artery had been ligated several times. The persistence of the cavernous carotid fistula (CCF) symptoms and their rapid worsening motivated the present exploration. During the catheterization, no patent ipsilateral common carotid artery was found. The ipsilateral vertebral artery injection (not shown) demonstrates the CCF, which opacified via the posterior communicating artery and the supracavernous carotid artery. The cervical injections show the site of the ligation (*asterisks*, **A**) the patency of the ipsilateral internal carotid artery (*arrows*, **B**), and its supply to the cavernous sinus fistula (*asterisk*, **B**). It also demonstrates that the external carotid branches do not supply the fistula (**A**).
B–D see pp. 317, 318

Fig. 6.32 (*continued*). **B** The difference in the aspect of these two injections can be explained by the separate origin of the occipital artery and ascending pharyngeal artery from the external carotid trunk. The ascending pharyngeal artery arises from the proximal external carotid artery closer to its origin compared to the occipital artery. Therefore, the injection of the occipital artery above the ligations via the deep cervical artery fills the distal external carotid artery and, poorly, the common carotid stump. However, the ascending pharyngeal artery, opacified via the ascending cervical artery, fills the common carotid stump below the incomplete ligation of the external carotid artery. **C, D** see p. 318

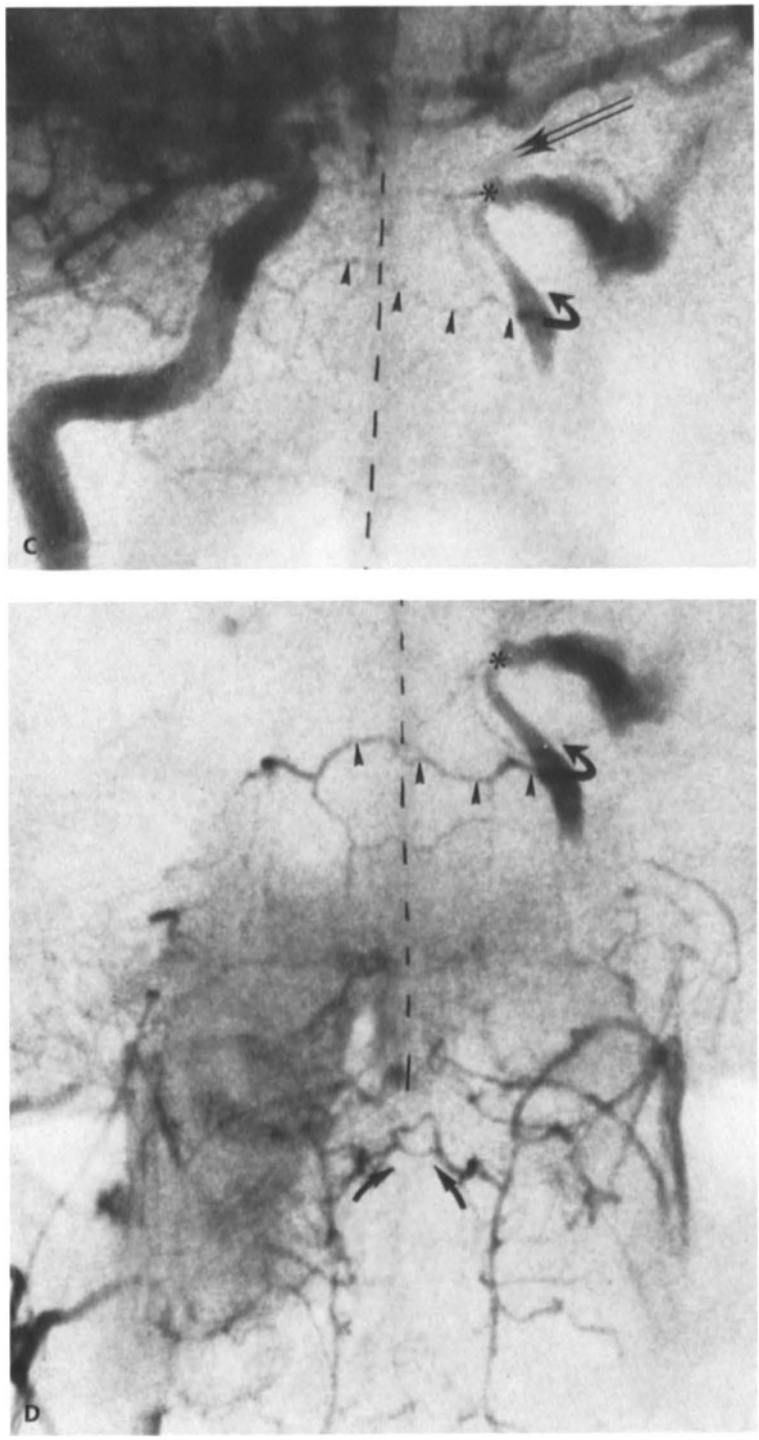

Fig. 6.32 (*continued*). **C** Selective injection of the contralateral internal carotid artery. Note the cross-filling of the ipsilateral C5 internal carotid siphon (*broken arrow*) via the medial clival anastomosis (*arrowheads*); the site of the fistula is clearly demonstrated (*asterisk*) below the clips (*double arrow*). **D** Injection of the contralateral ascending pharyngeal artery fills the same medial clival anastomosis (*arrowheads*) and C5 siphon (*broken arrow*) prior to the visualization of the fistula (*asterisk*). The *two arrows* show the upper limit of the odontoid arterial arch system

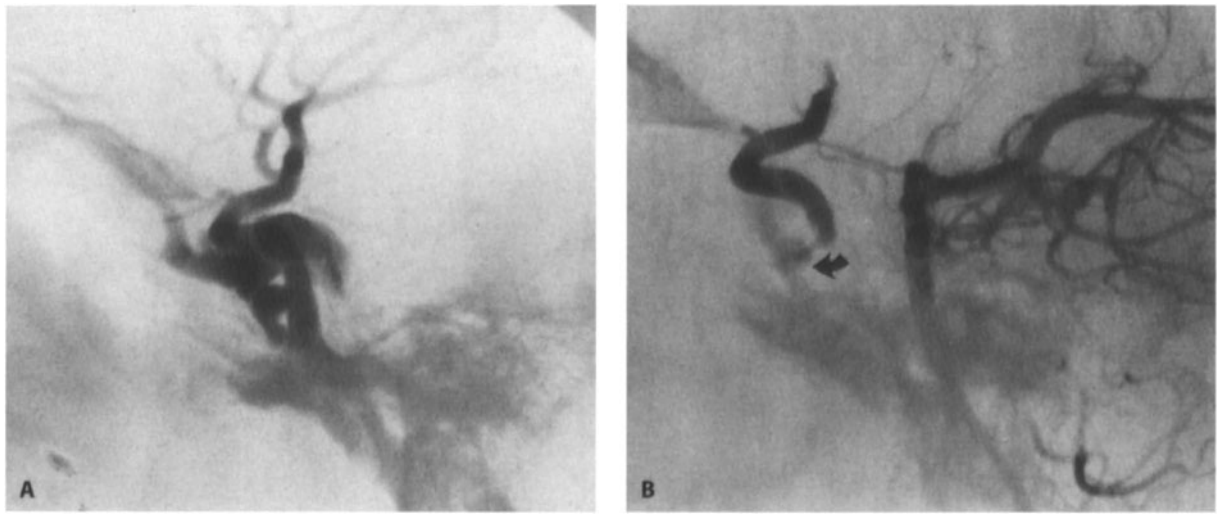

Fig. 6.33. **A** Lateral subtraction angiogram of the right internal carotid artery demonstrates a cavernous carotid fistula. **B** Lateral subtraction angiogram of the left vertebral artery with manual compression of the right internal carotid artery filling the fistula (*curved arrow*)

Fig. 6.34. Frontal subtraction angiogram of the right internal carotid artery. A double lumen balloon catheter (*curved arrow*) is occluding the internal carotid artery. The fistula site is clearly demonstrated (*open arrowhead*). (From Berenstein 1979, with permission)

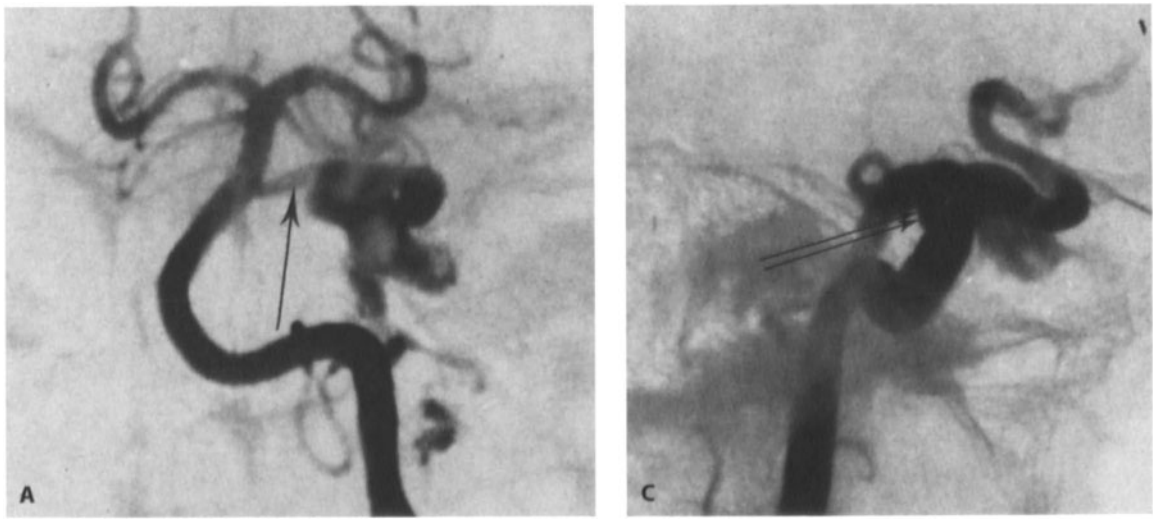

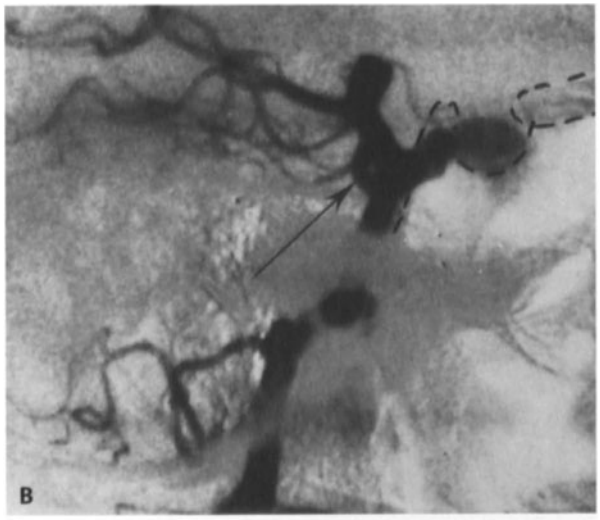

Fig. 6.35. Selective vertebral angiogram in frontal (**A**) and lateral (**B**) views and selective internal carotid artery injection in lateral view (**C**) in a case of traumatic carotid cavernous fistula with persistence of the trigeminal artery. Note the dual filling of the fistula from both vertebral (*arrow*) and carotid (*double arrow*) injection

Fig. 6.36. Selective injection of the internal carotid artery in a patient with carotid cavernous fistula (*asterisk*). Note the C4 origin of the ophthalmic artery (*arrow*)

6.2.4 Therapeutic Objectives and Strategy

After a thorough analysis from a clinical, anatomical, and hemodynamic point of view, the therapeutic objective is planned. As previously stated, there are situations in which therapy should commence immediately on an emergency basis. Most forms of TCCFs do not require urgent treatment but cortical reflux, decreasing vision, or low cerebral perfusion do require rapid therapeutic management.

6.2.4.1 Embolization

The endovascular approach to CCFs is by far the treatment of choice (Tables 6.2, 6.4). Various reported series have confirmed the effectiveness and safety of this technique (Serbinenko 1974; Debrun et al. 1981; Berenstein and Kricheff 1980; Scialfa et al. 1983; Kendall 1983; Kupersmith et al. 1984; Hieshima 1985, 1985; Wu et al. 2000). The most frequently used endovascular approach is via the femoral artery. However, direct cervical carotid puncture can be used when tortuosity at the arch or common carotid ligation prevents femoral catheterization of the internal carotid artery. For traumatic laceration of the internal carotid artery siphon, the use of detachable balloons is the best available method of treatment. The balloon will enter the cavernous sinus and with progressive inflation will occlude the pathological arteriovenous communication and preserve the carotid flow. In the largest reported series, the fistulae were cured in 85%–98% of cases, with a recurrence rate from 1.3% to 9%, which usually responded well to a second transvascular treatment (Wu 2000).

The permanent complication of cerebral infarctions secondary to a stray balloon or thromboemboli has been reported in less than 2% of cases. Permanent cranial nerve deficit that was not present prior to balloon treatment has been reported to occur in 0%–5%. Death related to the embolization occurred in one (1.8%) of Kendall's patients and one (3%) of Scialfa's patients.

Premature balloon detachment (Kendall 1983; Scialfa et al. 1983;), dislodgment of previously detached balloons, and intracranial migration secondary to delayed balloon deflation (Tsai 1983) have been reported in 1%–2.7%, occasionally resulting in cerebral dysfunction. Immediate measures to increase the blood pressure may resolve some of these neurological symptoms and gain time to permit surgical extraction of the dislodged balloon.

Although preservation of the carotid blood flow is one of the main advantages of the technique, most authors in the largest recent series have reported a preservation of carotid flow in more than 70%. Even in those instances where the internal carotid artery was intentionally occluded (Berenstein 1981) or when it is technically impossible to preserve carotid flow, the transvascular approach is preferred, as it closes the carotid artery at the fistula site and therefore prevents collateral filling or recanalization of the pathological arteriovenous communication.

The exception for the use of balloon catheters in the management of these fistulae would be in cases of traumatic lacerations of the C4 or C5

branches of the internal carotid artery, where the lesion can only be reached from the external carotid system (Fig. 6.27). In these instances, balloons may not enter the small cavernous branches, or occlusion of the internal carotid artery will not solve the problem. In these instances, the venous side can usually be reached with a fast polymerization tissue adhesive such as NBCA introduced superselectively from the external carotid side, and the internal carotid artery can be used to check the effectiveness of the treatment (Figs. 6.27, 6.28).

The retrograde transvenous approach can also provide similar good results using fiber coils to occlude the venous compartment of the fistula and is particularly useful in subacute TCCFs with slow flow (Fig. 6.13).

6.2.4.2 Emergency Treatment

1. Progressive visual loss has already been discussed in Sect. 6.2.2 and is an indication for emergent treatment.
2. Epistaxis: nasal bleeding associated with a TCCF is probably the most urgent problem to be dealt with, as it may truly be a life-threatening situation (Figs. 6.21, 6.23, 6.37). However, this should be distinguished from epistaxis in the acute phase of a traumatic incident, which is most often related to maxillofacial injury and can be managed conservatively or by bilateral internal maxillary artery and/or facial embolization.
3. Sphenoid sinus aneurysm. If during pretherapeutic evaluation a soft tissue mass is noted in the sphenoid sinus, which during angiographic evaluation proves to be an aneurysm or pseudoaneurysm of the internal carotid artery (Figs. 6.21–23, 6.37), then treatment should be immediately undertaken, as this lesion has a significant risk of rupture, with a potential for lethal uncontrollable hemorrhage. Parent artery occlusion is recommended at the acute stage. Intrasaccular coiling or stenting can be proposed at the subacute or chronic stage.
4. Comatose patients. In patients with a depressed level of consciousness where intracranial lesions have been excluded, treatment should be instituted. This probably also applies to the unconscious and/or stuporous

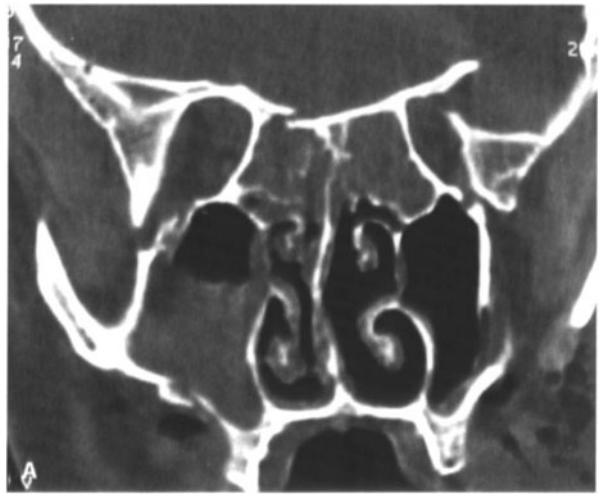

Fig. 6.37A–F. Skull base trauma secondary to motor vehicle accident (MVA) resulted in massive epistaxis with hemorrhagic shock. At CT (**A**) multiple fractures of the anterior and middle cranial base were demonstrated. **B–F** see p. 323

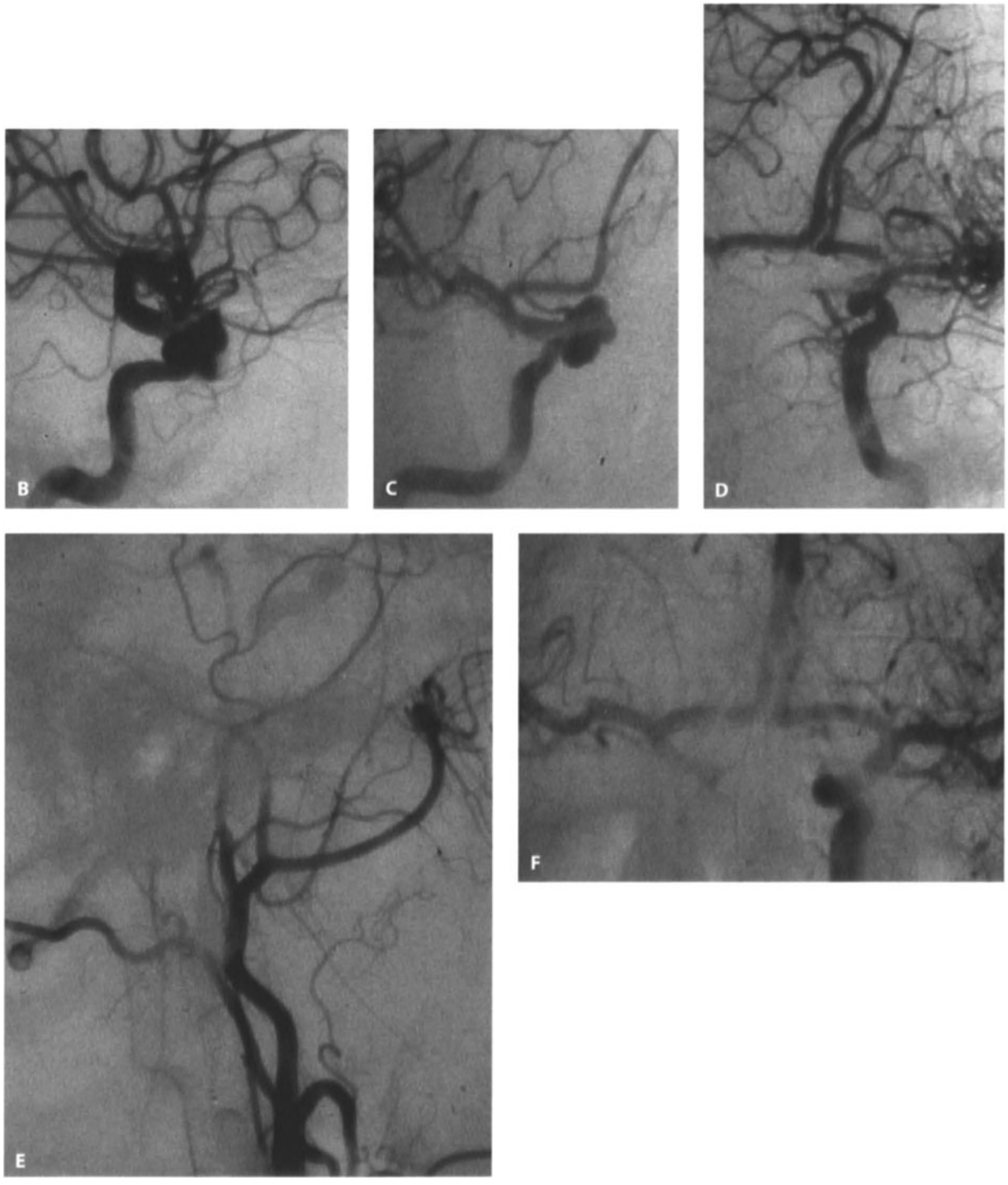

Fig. 6.37 (*continued*). **B, C** Emergency angiography shows a ruptured internal carotid artery (ICA) in the posterior ethmoidal cells and sphenoid sinus with false aneurysm. Circle of Willis assessment shows satisfactory collateral circulation (**D**). **E, F** Embolization with intracavernous occlusion of the ICA was performed immediately

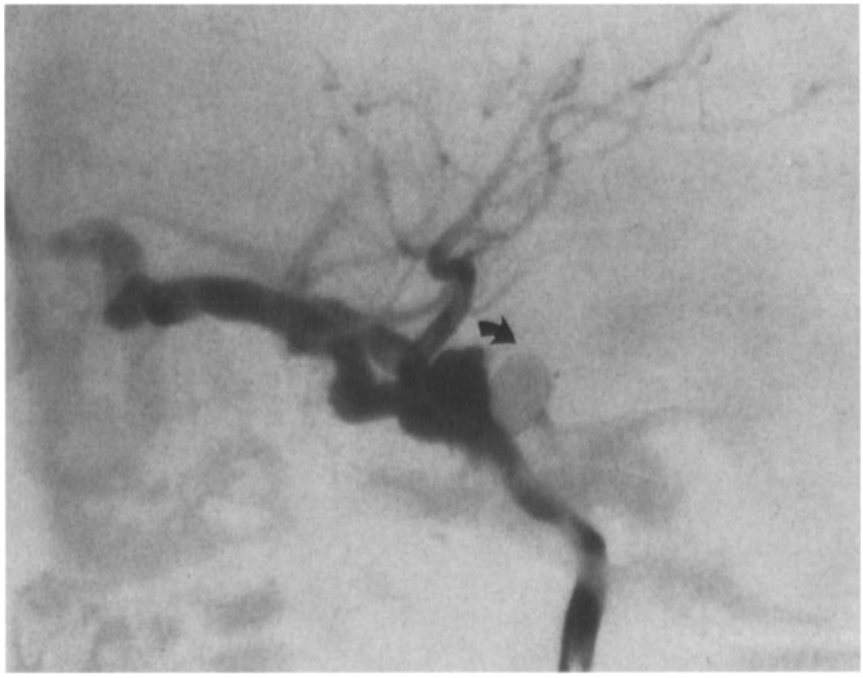

Fig. 6.38. Lateral subtraction angiogram of the internal carotid artery 8 h following satisfactory repair of a traumatic cavernous carotid fistula with preservation of the internal carotid flow (not shown). The balloon (*curved arrow*) had migrated posteriorly as a result of severe vomiting and has blocked the posterior drainage, followed by aggravation of ocular signs and symptoms, with deterioration of visual acuity. The internal carotid artery was sacrificed. The symptoms regressed immediately after the embolization

patient with increased intracranial pressure, even if no cortical venous rerouting is demonstrated.

5. If during the course of treatment a balloon is placed in such a manner that the posterior venous drainage is blocked, or if in the immediate postembolization period the balloon migrates to block the posterior venous drainage following partial balloon deflation or vomiting (Fig. 6.38), rapid aggravation of ophthalmic symptoms may occur. Conversely, if the balloon migrates forward and reroutes the previous ophthalmic drainage toward the subarachnoid venous system, then the risk of intradural complication will occur (SAH, seizure, or deficit). Both situations require urgent management (Figs. 6.3, 6.13).

6.2.4.3 Surgical Approach to Carotid Cavernous Fistulae

There is no indication for any type of nonendovascular (open surgical) approach for carotid cavernous sinus fistulae as the primary form of treatment.

In Isamat's (1970) review of 545 reported cases of surgically treated carotid cavernous fistulae, cervical ligation of the internal carotid or common carotid arteries or both had a cure rate of 31%–40%. Trapping the carotid cavernous fistula in a combined intracranial internal carotid clipping and internal carotid ligation in the neck provided good results in 56.7% of cases. A complete trapping approach would include intracranial occlusion of the internal carotid and ophthalmic arteries followed by cervical ligation of the internal carotid and external carotid arteries. This technique achieved satisfactory results in 78.8% of a group of 76 patients. Morley and Barr (1969) showed that the operative mortality and cerebral

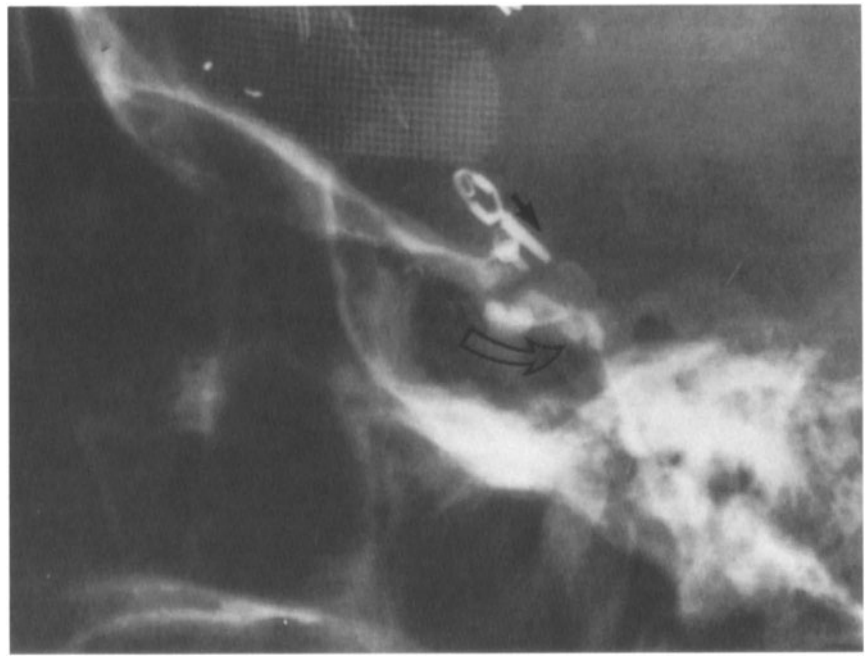

Fig. 6.39. Plain film of the skull in lateral projection after surgical exposure of the supraclinoid carotid artery below the lower surgical clip and following injection of glue. A second clip (*arrow*) was placed in the posterior communicating artery (*arrow*). Note the radiopaque cast of the cavernous carotid artery, the fistula, and the infero-lateral trunk (*open curved arrow*)

morbidity in the surgical approach to CCF has been distressingly high. Parkinson (1973) shows that it is surgically possible to repair these fistulae and preserve the carotid flow; however, this is a complex and major surgical endeavor. In 1975, Hosobuchi reported a venous approach to cavernous sinus electrothrombosis, and although successful, it was apparent that significant technical skill was needed for operation. Mullan et al. (1979) reported 33 fistulae treated by a variety of ingenious approaches to the venous side using the thrombogenic technique with good results.

Surgical reconstruction of cervical vessels or intraoperative embolizations should be discussed when previous procedures (surgical ligations or proximal embolizations) have removed the percutaneous accesses (Fig. 6.39).

6.2.4.4 Conservative Treatment of Traumatic Carotid Cavernous Fistulae

When the symptoms are mild and there is no immediate risk for vision, conservative follow-up should concentrate on verifying the intraocular pressures, visual acuity, and cranial neuropathies.

6.2.5 Technical Aspects of Embolization

6.2.5.1 Balloon Selection

Various detachable balloon systems are available at present. These are discussed in Chap. 14.

A latex balloon filled with contrast material will eventually deflate in weeks or months and even silastic balloons filled with iso-osmolar con-

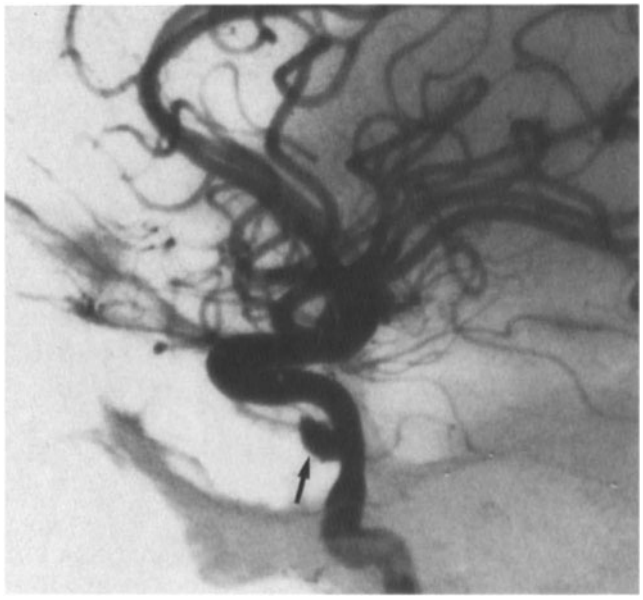

Fig. 6.40. Lateral subtraction angiogram, 6 months after balloon repair of a traumatic cavernous carotid fistula. The patient is asymptomatic. The contrast-filled balloon has deflated. An aneurysmal pouch (*arrow*) has formed at the site of the original balloon repair (same patient as Fig. 6.12)

trast material can or will eventually deflate. This deflation produces venous pouches in a significant number of patients, usually without symptoms (Fig. 6.40). Most reports on traumatic fistulae describe that when only minimal filling of the fistula persists, the lesion tended to thrombose spontaneously. Debrun (1978) makes no mention of the relationship between his symptomatic pouches and persistent minimal shunting. Balloon deflation often leaves a venous pouch at the site of the repair. In our experience, we have not had to treat any patient for a symptomatic pouch. There are many more examples of shrinkage and/or stabilization of these pouches rather than the relatively rare occurrence of them becoming symptomatic.

We have had one carotid stenosis out of four instances where we filled the balloon with silicone. Our only other instance of carotid stenosis was in a patient with a carotid cavernous fistula secondary to a gunshot wound. In one instance, a delayed occlusion of the ICA occurred in a patient with an iatrogenic CCF (following endarterectomy).

A similar experience was reported by Tsai and Hieshima (1983). The development of oculomotor palsies after the repair in Debrun's series (1978) was 36% when the balloon was filled with silicone and 17% when inflated with iodinated contrast material. Debrun makes no mention of the material used to fill the balloon in his patient with a permanent oculomotor palsy. Peeters and Kroger (1979) filled their latex balloons in six (out of seven) patients with silicone, and only one of three patients with oculomotor palsy had recovery of the third nerve but not the sixth nerve. Tsai (1983), who uses nondeflating silicone balloons, has reported a rate of 5.4% permanent ophthalmoplegia after treatment.

Although we do not have a full explanation for the variable progression of the postdeflation pouches, one must realize that these lesions, which in the internal carotid artery usually follow trauma, could lead to either rupture of a developmental arterial aneurysm or a secondary traumatic rupture not previously observed (Fig. 6.41). The overwhelming carotid flow

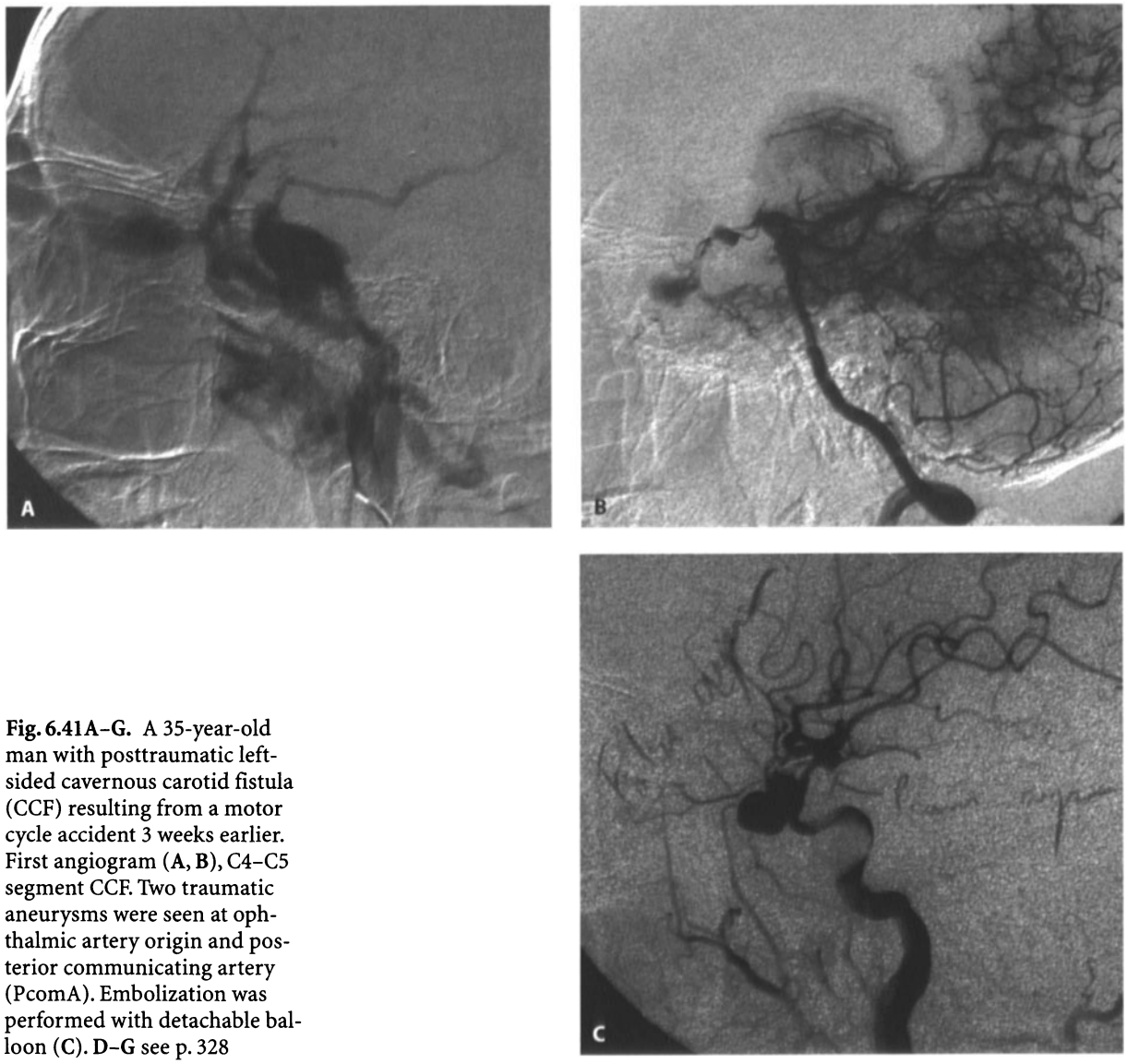

Fig. 6.41A–G. A 35-year-old man with posttraumatic left-sided cavernous carotid fistula (CCF) resulting from a motor cycle accident 3 weeks earlier. First angiogram (**A, B**), C4–C5 segment CCF. Two traumatic aneurysms were seen at ophthalmic artery origin and posterior communicating artery (PcomA). Embolization was performed with detachable balloon (**C**). **D–G** see p. 328

supplying the AVF following repair is then exerted on the weakened or false wall of the preexisting aneurysm. Observation of the venous phase of the postembolization angiogram, paying attention to the patency of the ipsilateral cavernous sinus, in the presence of a venous pouch, may suggest the progression of a small preexisting traumatic or developmental arterial aneurysm; it may be an indication for sequential follow-up angiograms.

The balloon may be superimposed on the carotid lumen in one or two views; oblique projections should be obtained to be certain that the balloon clears the lumen of the carotid artery before detaching it (Fig. 6.42).

Balloons of any type, when entering the cavernous sinus, may take a lobulated configuration as they mold to the septations within the cavernous sinus (Fig. 6.43). One balloon is usually needed to close most fistulae, but on occasion multiple balloons may be needed.

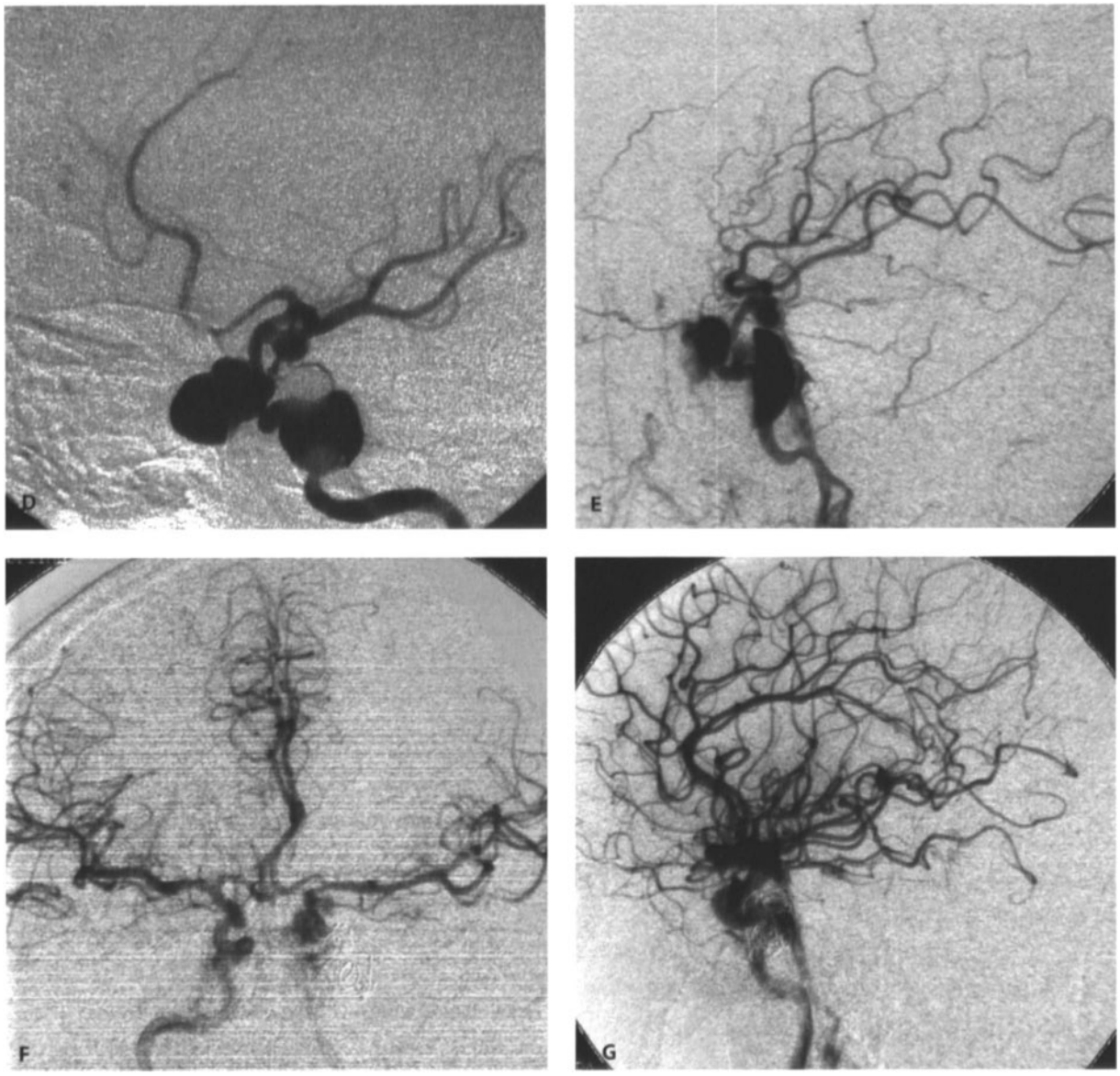

Fig. 6.41 (*continued*). **D, E** Five weeks later, balloon deflated partially and moved. Some opening of the CCF was noted and enlargement of the arterial aneurysms and intracavernous sac. Three weeks later, the patient presented a subarachnoid hemorrhage: the PcomA lesion was considered to be the cause. The patient was referred after recovery with conservative treatment 3 weeks later. Progressive narrowing of the left internal carotid artery (ICA) system was seen and stagnation of contrast in all pouches was noted. Following a failed attempt to cross the two proximal aneurysms to get into the PcomA for coiling, the left ICA was sacrificed after the occlusion test. The occlusion was achieved with the first gold valve balloon (GVB) partly in ophthalmic aneurysm and partly into the ICA, which was further packed with coil to achieve complete exclusion (**F, G**). The patient recovered well and the last follow-up angiogram (6 months later) shows shrinkage of the left PcomA. (Courtesy of S. Pongpech)

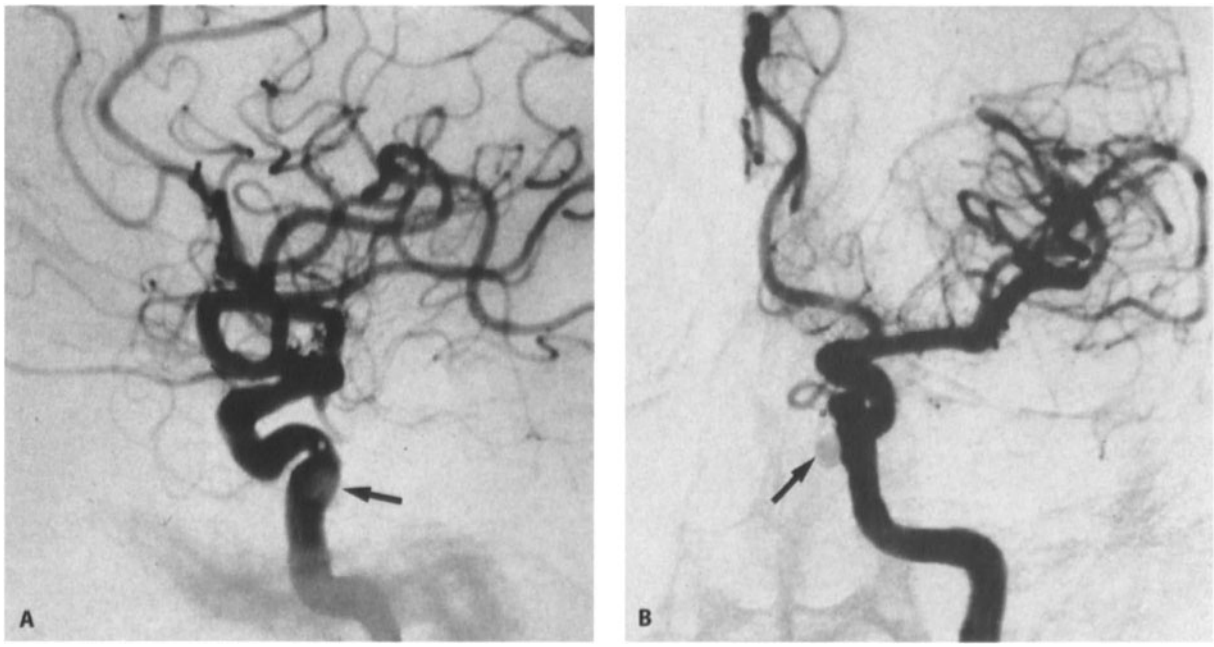

Fig. 6.42. **A** Lateral subtraction angiogram of the left internal carotid artery after balloon occlusion of the traumatic cavernous carotid fistula (*arrow*). **B** Frontal projection. The balloon is outside the carotid artery (*arrow*) and can be safely detached

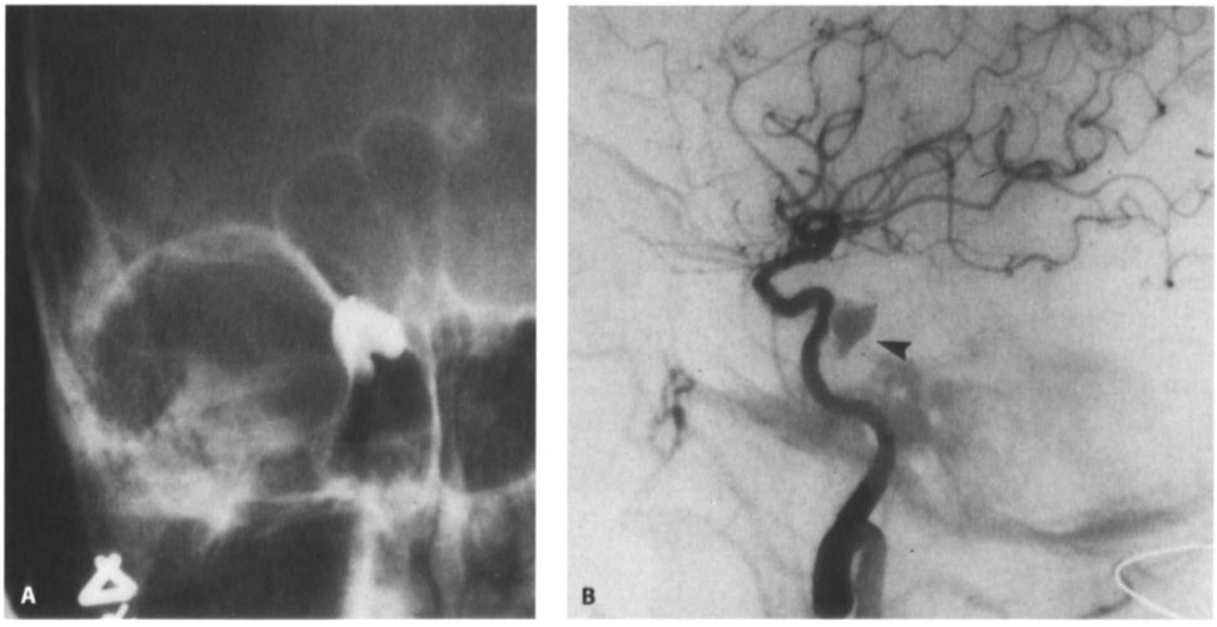

Fig. 6.43. **A** Frontal plain skull film after balloon repair of a traumatic cavernous carotid fistula. Note the lobulated configuration of the balloon. **B** Lateral subtraction angiogram, same patient. The balloon (*arrowhead*) is in the posterior cavernous sinus. The internal carotid artery flow is preserved

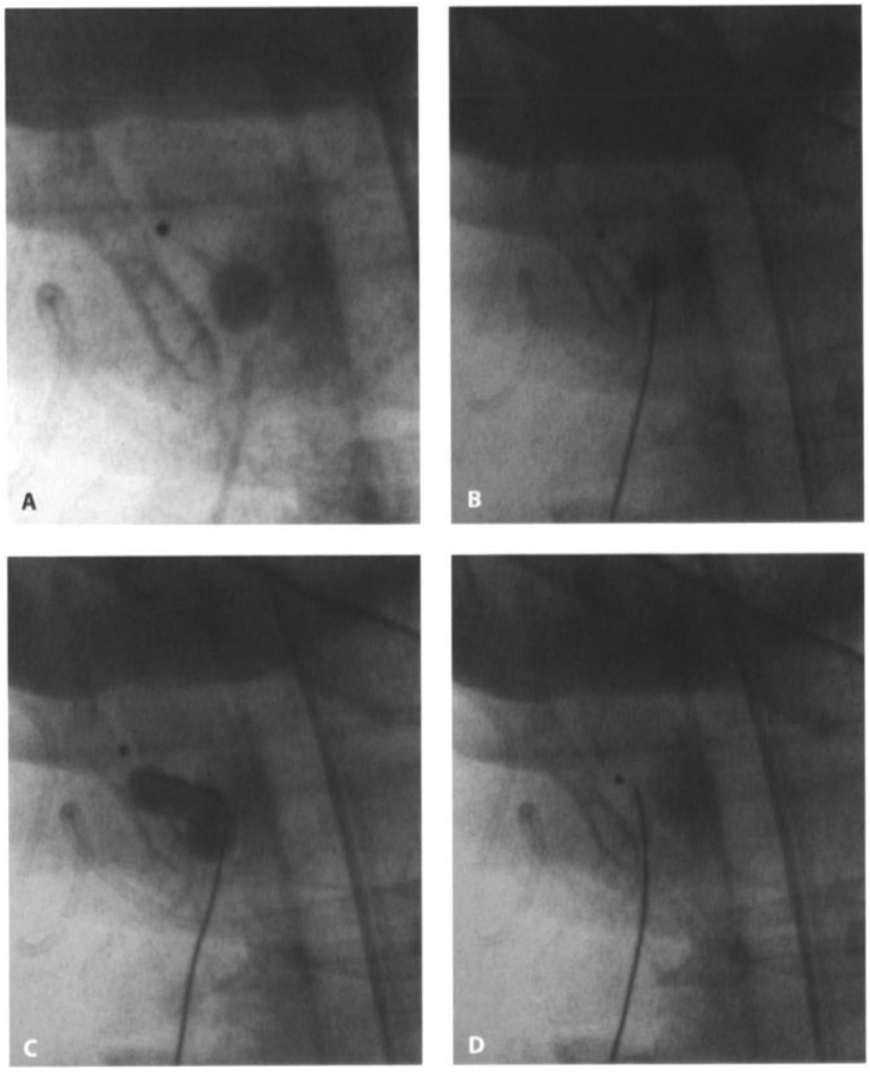

Fig. 6.44. When the detachable latex balloon failed to deflate (**A**), a 0.012-in. (or smaller) microguidewire (**B**) was inserted and the balloon reinflated to push the tip of the guidewire into the distal part of the balloon (**C**). When deflated again, the guidewire will center the nose of the microcatheter in the lumen of the balloon, which can then be completely deflated (**D**). The guidewire can subsequently be withdrawn

When one cannot preserve the carotid artery (by balloon, coils, stenting, or glue), trapping the fistula will be necessary by putting a balloon distal to or at the fistula site and a second balloon proximal to the fistula (Fig. 6.13), as close as possible, to ensure occlusion of the communication.

The use of a microguidewire inside the balloon catheter may be useful to negotiate difficult turns or to deflate a balloon completely prior to repositioning (Fig. 6.44).

Venous Approach

The venous approach is very useful in the subacute or chronic stages, and it is more hazardous in the acute stage when the draining veins have not acquired much wall thickening and strength. Mechanical perforation may occur while catheterizing transvenously (Fig. 6.45).

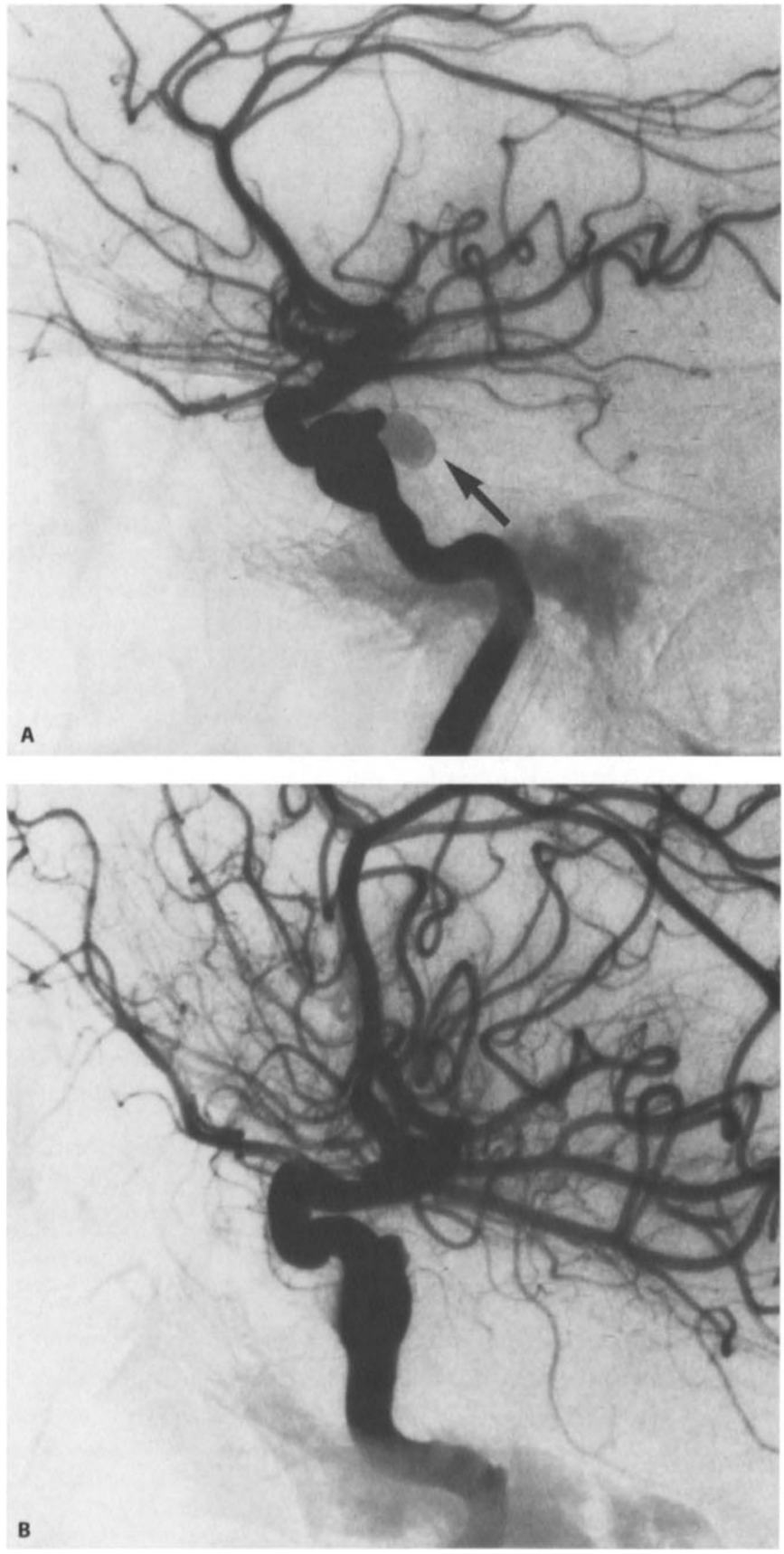

Fig. 6.45A, B. Same patient as Fig. 6.8, venous approach. **A** Lateral subtraction angiogram of the right internal carotid artery after a Fogarty balloon catheter (*arrow*) was inserted retrograde via the jugular inferior petrosal route. Note preservation of the internal carotid artery. A small cavernous aneurysm remains. **B** Lateral subtraction angiogram 3 months later. The balloon has deflated and the cavernous aneurysm has decreased in size. (From Manelfe and Berenstein 1980, with permission)

Inferior Petrosal Approach

If the anatomy of the fistula and its venous drainage are favorable (the fistula being in the posterior superior compartment, draining into the inferior petrosal sinus), then occlusion of the fistula can be accomplished by the retrograde transjugular approach using a microcatheter for coils or even a detachable balloon catheter system. When using this approach, one should be cautious not to convert the posterior drainage into a purely anterior one. It is also often possible to reach the involved cavernous sinus region across the midline via the retroclival anastomosis from the opposite inferior petrosal sinus (Mullan et al. 1979; Manelfe and Berenstein 1980; Debrun et al. 1981; Kendall 1983).

Retrograde Ophthalmic Vein Catheterization

The first three cases reported used detachable balloons or coils (Uflaker 1983). This approach should be considered in cases of previous ligations of the internal carotid artery and where there is no access via the arterial or posterior venous side. In Uflaker's (1983) experience, the procedure was done after cutting down on the frontal division of the vein rather than percutaneously. Furthermore, the safety of the technique is directly related to the age of the fistula. In the chronic group, the thickened wall of the ophthalmic vein provides easy control, whereas in acute fistulae the venous wall is thinned and fragile. Intraoperative transvenous retrograde catheterization of the sylvian venous system towards the cavernous sinus region is yet another option, sometimes necessary to gain access to and obliterate the venous aspect of the fistula.

6.2.5.2 Manual Compression

Manual compression of the medial canthus in CCFs draining exclusively into the ophthalmic system is usually very effective. Testing at the time of the angiographic study may show stagnation of contrast in the cavernous sinus during compression (Fig. 6.7). This maneuver is not recommended in the acute stage.

6.2.5.3 The Use of NBCA in the Management of Carotid Cavernous Fistulae

N-butyl-cyano-acrylate (NBCA) has limited indications in the management of CCF (Fig. 6.28), but it is the agent of choice for lesions of the infero-lateral trunk (ILT) (Figs. 6.7, 6.13, 6.28), where balloons cannot enter the small ruptured vessel. Prior to NBCA injection, one must ensure reliable protection of the cerebral and ophthalmic circulation.

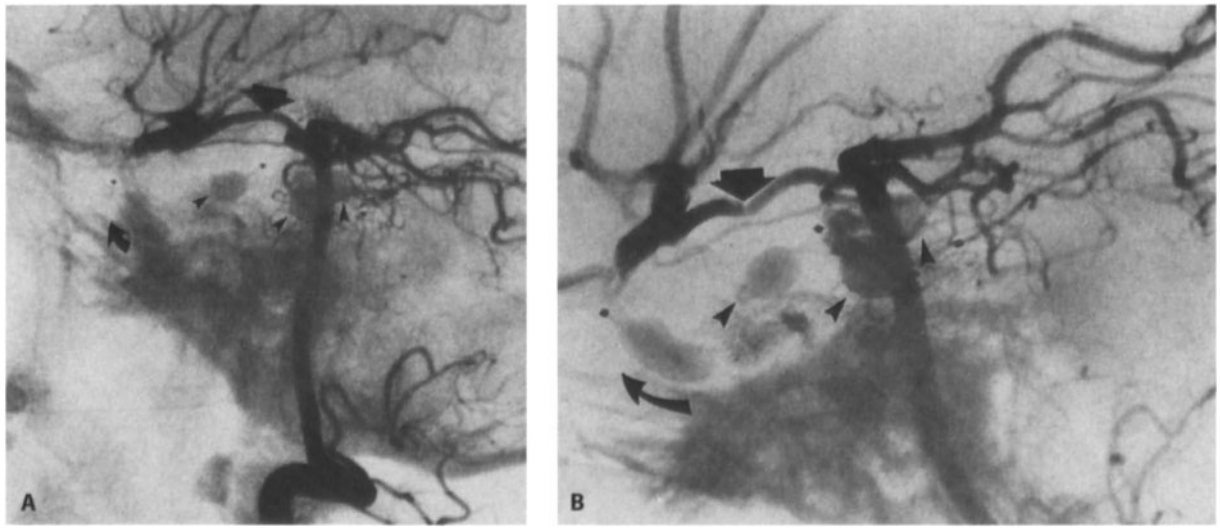

Fig. 6.46A, B. Same patient as Figs. 6.9, 6.26. **A** Lateral subtraction angiogram of the left vertebral artery after three balloons were placed in the aneurysmally dilated cavernous sinus (*small arrowheads*), and a fourth balloon (*curved arrow*) in the internal carotid artery trapping the fistula. Note the elevation of the posterior communicating artery by the distended cavernous sinus (*solid arrow*) (compare with Fig. 6.9). **B** 24 h after embolization, while the patient was ambulant, a severe headache developed, associated with the development of a sixth nerve palsy, which resolved spontaneously in 4 weeks. Note collapse of the dilated cavernous sinus with the corresponding downward displacement of the left posterior communicating artery (*broad arrow*). (From Berenstein et al. 1980, with permission)

6.2.6 Postembolization Care

Postembolization care is primarily related to the early postembolization period and refers to bed rest, control of nausea and vomiting, and other maneuvers to prevent balloon migration (Fig. 6.38); 24–36 h appears sufficient. Analgesics are needed to control the pain that may occur in the first weeks as the cavernous sinus and/or the fistula is thrombosing. On occasion, delayed cranial nerve dysfunction may occur as the distended cavernous sinus collapses (Fig. 6.46) but usually resolves in 2–5 weeks. This is a more frequent event following treatment of cavernous aneurysms.

A frontal and lateral skull X-ray should be obtained immediately after detachment to document the baseline position and size of the balloons. If any clinical problems occur a repeat plain skull film will be of assistance to possibly explain the clinical change or deterioration. If the internal carotid artery had to be sacrificed the postoperative care protocol, as reviewed in Chap. 14, should be followed.

Secondary changes, including balloon deflation or untreated dissecting aneurysms, should be anticipated and followed up carefully (Fig. 6.41). Intradural flow-related aneurysms associated with TCCFs should be analyzed carefully and will not need to be treated in most cases at the subacute or chronic stage. Their regression is expected following exclusion of the TCCF, similar to what is seen in cerebral arteriovenous malformations (Figs. 7.122, 11.123).

6.3 Other Traumatic Arteriovenous Fistulae

6.3.1 Extracavernous Arteriovenous Fistulae

Extracavernous TCCFs can be encountered and correspond to the ICA rupture at the clinoid portion, probably at the level of the carotid cave. The drainage often creates venous ectasias near the chiasm, with a risk of secondary rupture (Figs. 6.47, 6.48). Medial ruptures of the capsular arteries into the pituitary venous plexus also tend to produce large subarachnoid venous pouches (Fig. 6.49). Failure to recognize these fistulous locations outside the cavernous sinus region will often lead to unsuccessful endovascular procedures.

Extracavernous extracranial AVFs with intracranial venous drainage may cause similar symptoms and signs when the drainage involves the cavernous sinus secondarily (Figs. 11.1, 11.3). They may have clinical manifestations similar to any other intracranial AV shunt: headaches, seizures, and intracranial hemorrhage or neuro-ophthalmic symptoms.

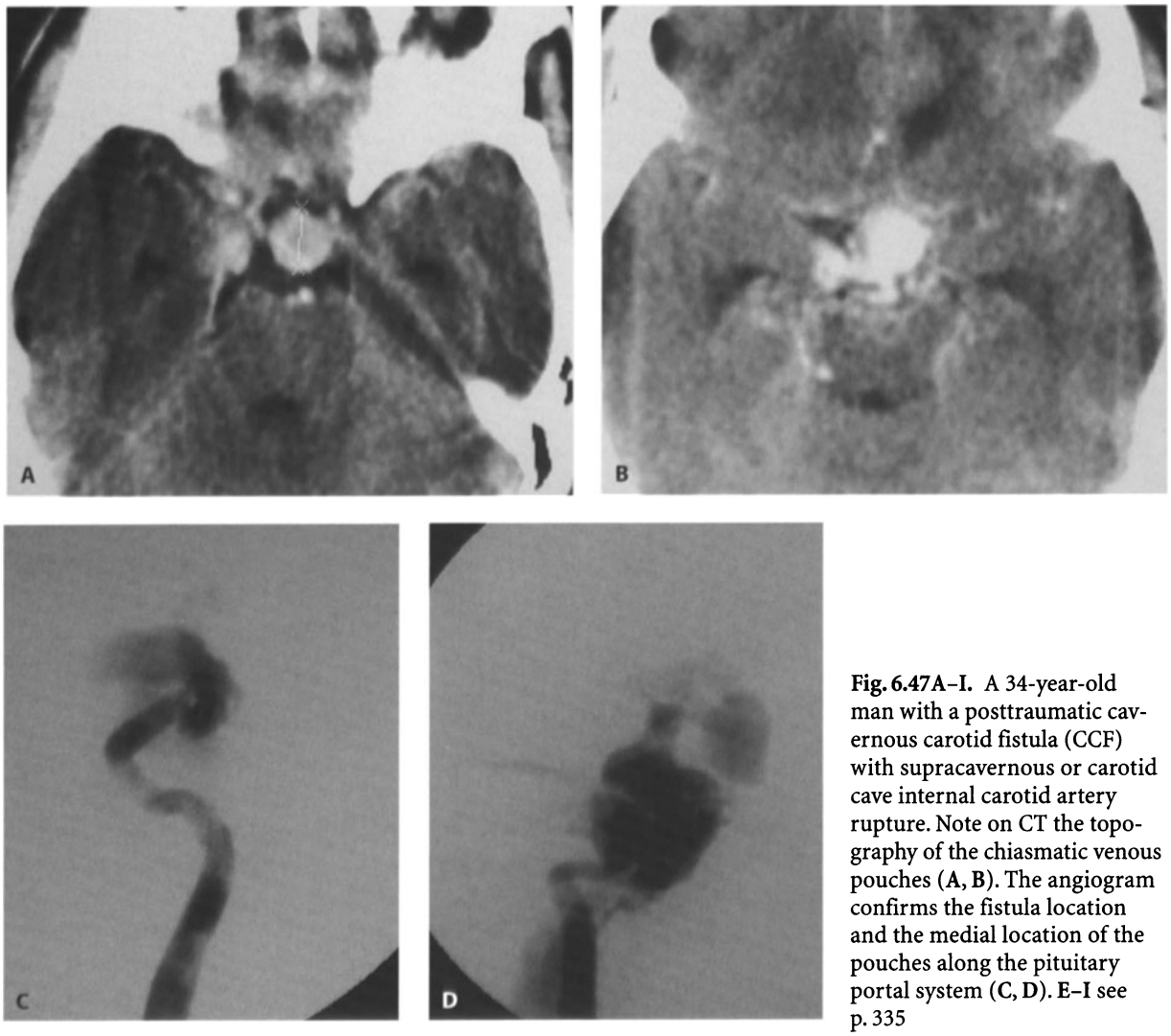

Fig. 6.47A–I. A 34-year-old man with a posttraumatic cavernous carotid fistula (CCF) with supracavernous or carotid cave internal carotid artery rupture. Note on CT the topography of the chiasmatic venous pouches (**A, B**). The angiogram confirms the fistula location and the medial location of the pouches along the pituitary portal system (**C, D**). **E–I** see p. 335

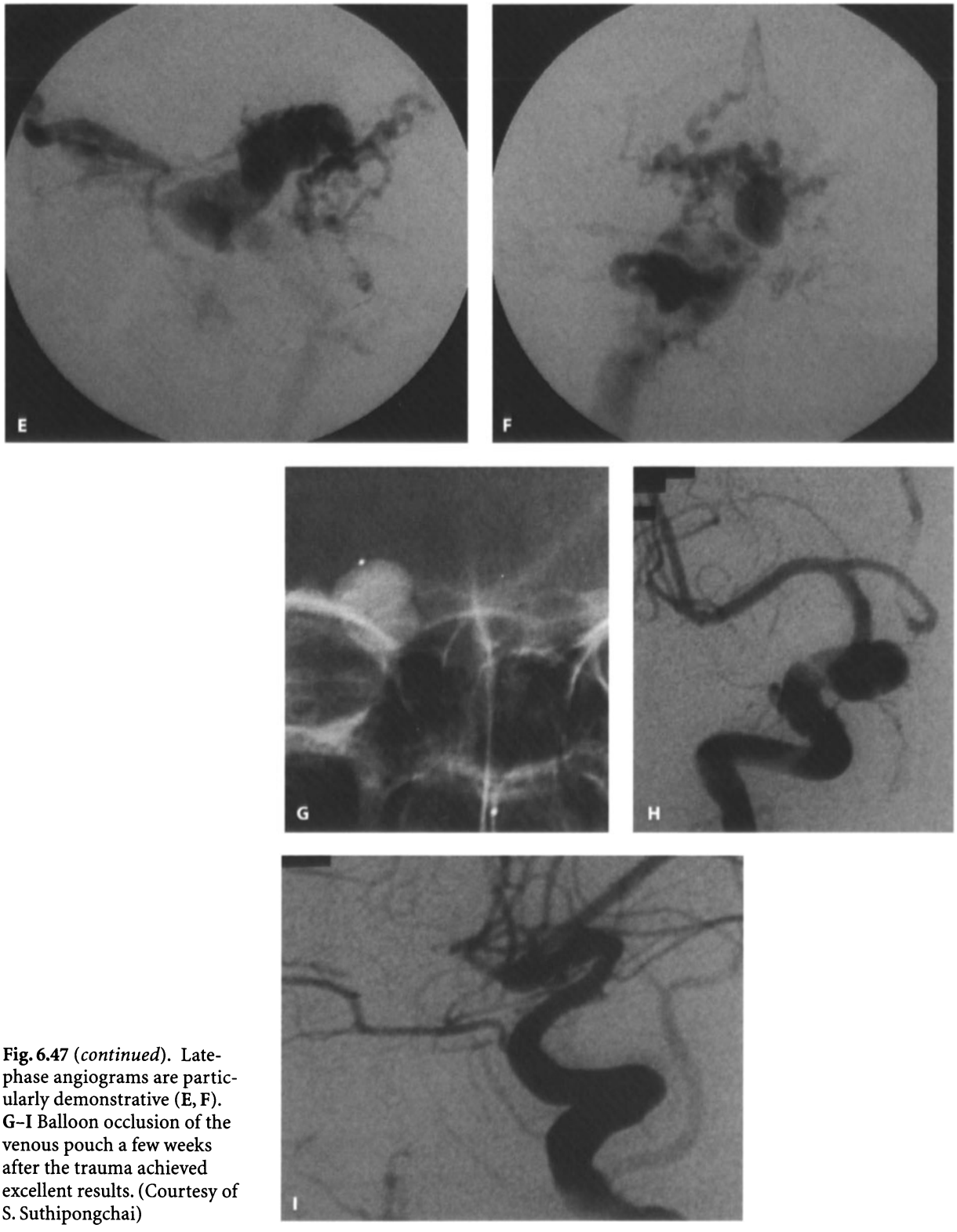

Fig. 6.47 (*continued*). Late-phase angiograms are particularly demonstrative (**E, F**). **G–I** Balloon occlusion of the venous pouch a few weeks after the trauma achieved excellent results. (Courtesy of S. Suthipongchai)

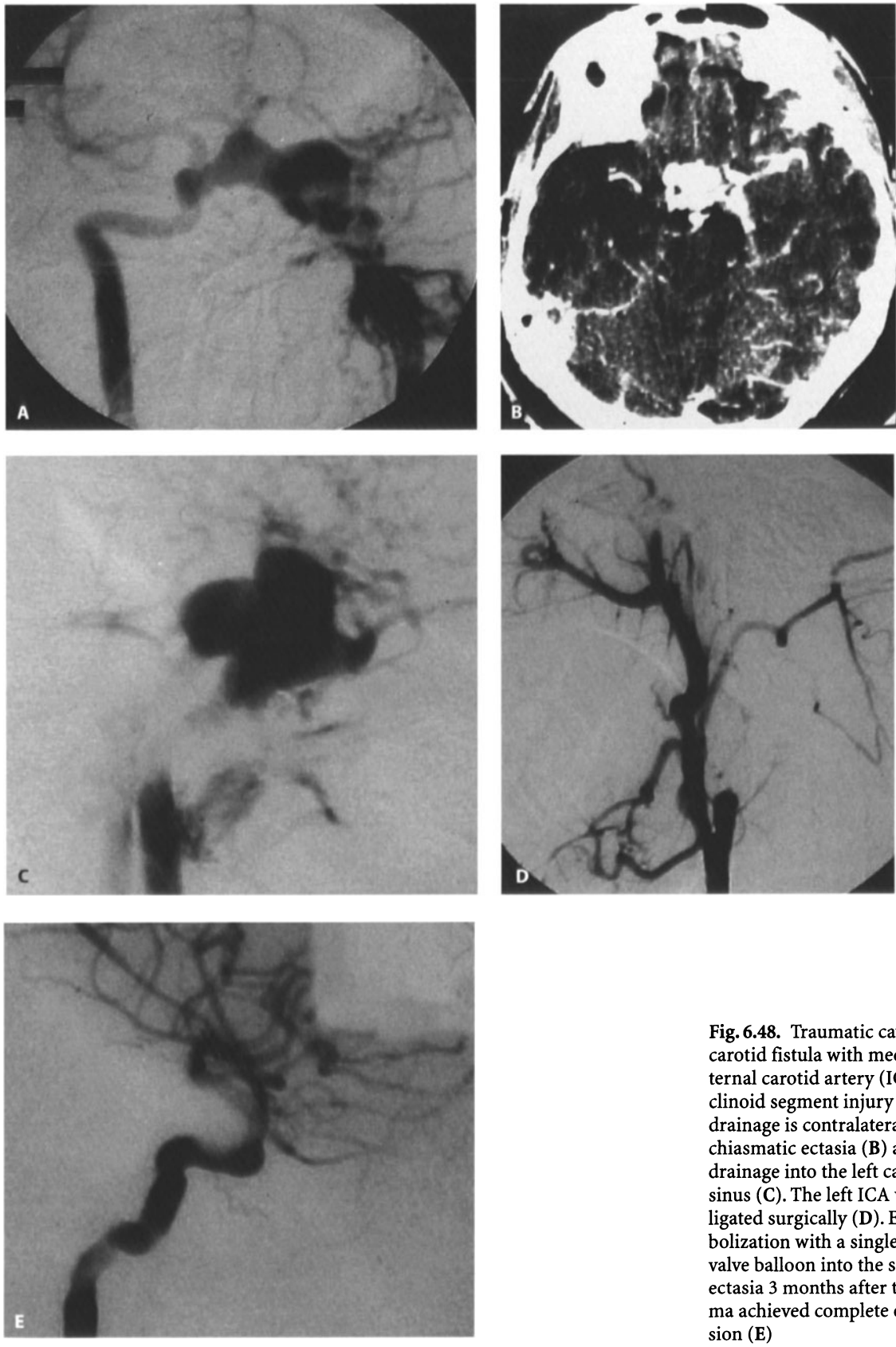

Fig. 6.48. Traumatic cavernous carotid fistula with medial internal carotid artery (ICA) clinoid segment injury (**A**). The drainage is contralateral with chiasmatic ectasia (**B**) and drainage into the left cavernous sinus (**C**). The left ICA was ligated surgically (**D**). Embolization with a single gold valve balloon into the sellar ectasia 3 months after the trauma achieved complete exclusion (**E**)

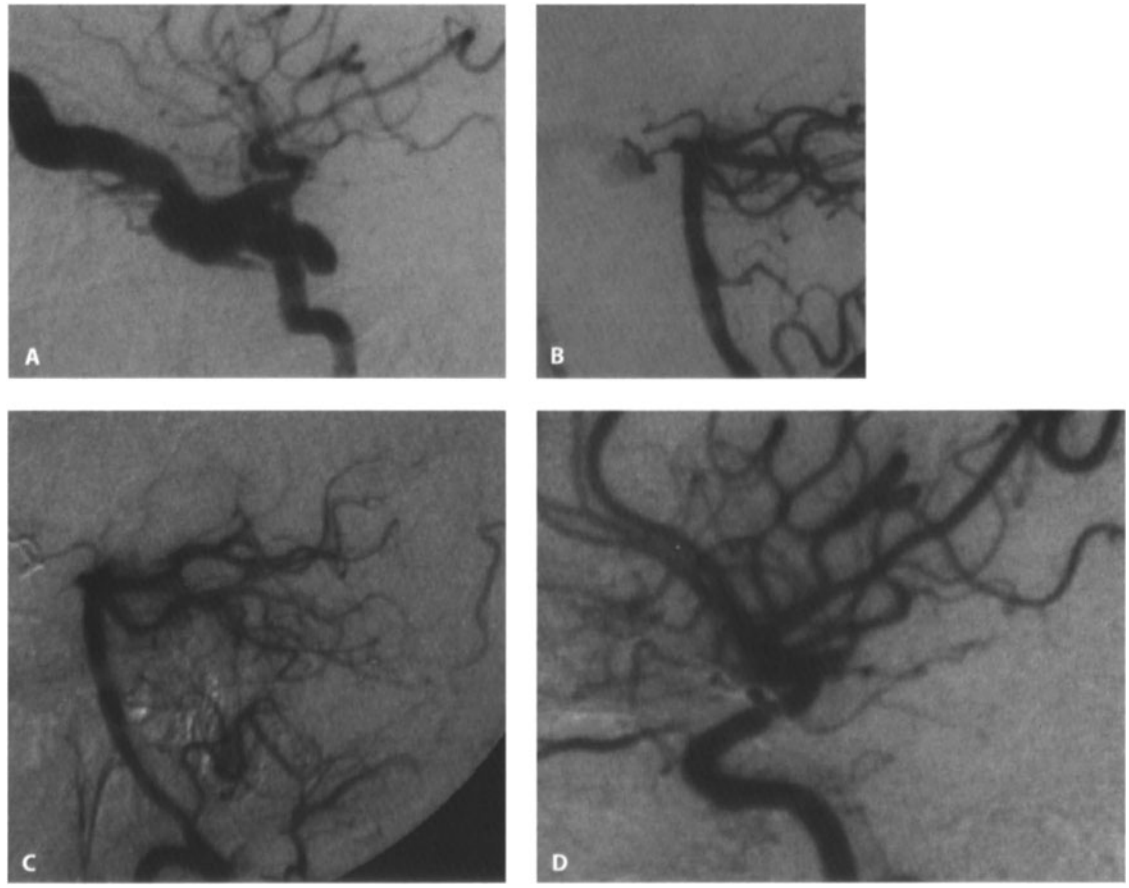

Fig. 6.49. Traumatic cavernous carotid fistula related to an intradural arterial rupture into the hypophyseal portal system (**A, B**). The disposition was only recognized after failure to enter the fistula from the cavernous sinus. The intradural surgical approach was adopted, which allowed successful clipping of the feeder (**C, D**). (Courtesy of S. Suthipongchai)

Similar to TCCFs, the clinical symptoms will not depend on the site of the arteriovenous communication, but on the venous drainage of the AVF.

Scialfa et al. (1979) reported the case of an AVF fed by the external carotid artery and draining into the internal jugular vein. This patient presented with a thrill in the mandibular region and generalized seizures that were related to intracranial cortical venous drainage.

When analyzing the architecture of these lesions, it is mandatory to distinguish those with purely extracranial drainage from those with intracranial venous drainage in order to anticipate future risks – or the natural history – of these diseases. In AVFs with purely extracranial venous drainage, clinical manifestations include facial pain (Halsted 1919) and deformation of the pathological region because of the pulsatile mass associated with a thrill and bruit. Specific symptoms such as cardiac overload in the pediatric population (Kuss et al. 1979; Girevendulis et al. 1980) or epistaxis (Reinhoff 1924) have been described. Spontaneous high-flow AVFs of the extracranial carotid system are extremely rare and only 14 patients with spontaneous AVFs of the extracranial external carotid artery (Sedat et al. 1999 for review) and two patients with spontaneous AVFs of

the cervical internal carotid artery (Fraser 1971) have been reported in the literature. When discovered, one should suspect spontaneous rupture of an abnormal arterial wall related to a collagen disease such as Ehlers-Danlos disease. Other disorders affecting the vascular wall such as fibromuscular dysplasia (Bahar et al. 1984) or neurofibromatosis (Deans et al. 1982) may also be detected. This situation requires careful management of these patients because any vessel manipulation may lead to further vascular damage. Surgery does not cure these difficult lesions because of their nature, location, architecture, and vessel fragility. Treatment must exclude the fistula totally. Simple ligation or proximal embolization of the feeding vessel carries the high risk of recurrence due to the vast collateral network in the head and neck region. Endovascular treatment of these AVFs has now been accepted as the treatment of choice. It offers a very high rate of cure (Scialfa et al. 1979; Berenstein et al. 1986; Reizine et al. 1985) and is associated with low morbidity. The goal of treatment is to occlude specifically the fistulous communication preserving, if possible, the parent artery. Therefore, it is important to analyze the exact location of the fistula, despite its insignificance in the understanding of the symptoms. In some circumstances, sacrifice of the parent vessel cannot be avoided and will have to be tested and balanced against the risk of the present venous drainage. Because they are simple, safe, and cheap, detachable balloons are the most commonly used embolic agents (Halbach et al. 1988a; Wu et al. 2000) in traumatic AVFs. Transarterial approaches are therefore often preferred to transvenous techniques (Halbach 1988).

6.3.2 Vertebral Arteriovenous Fistulae

Fistulous connections of the vertebral artery occur frequently after trauma (Markham 1969). The anatomical location and relationship of the vertebral artery and surrounding veins, as well as the mechanism of formation in traumatic VAFs, are similar to what has been reviewed with traumatic pseudoaneurysms. It appears that AVFs are more frequent than traumatic pseudoaneurysms in the vertebral distribution, which is probably related to the proximity of the vertebral artery and its surrounding venous plexus (Davis and Zimmerman 1983).

Traumatic lesions can occur at any level of the vertebral artery. They may be associated with a large expanding false aneurysm (Fig. 6.50) and/or multiple AV fistulae on other vessels as well as other traumatic vascular injuries such as thrombosis.

They may follow gunshot wound injuries (Fig. 6.51). The most frequent location is high at the C1, C2, or C3 level (Goodman 1975). Proximal VAFs will be seen in some rare iatrogenic cases (Fig. 6.52).

Hematomas in the neck may occur subsequent to the acute injury with tamponade or delayed presentation of the fistula days, weeks, or even years later. They may be secondary to direct injury of the vertebral artery by a fractured bone and therefore careful analysis of associated bony injuries is important.

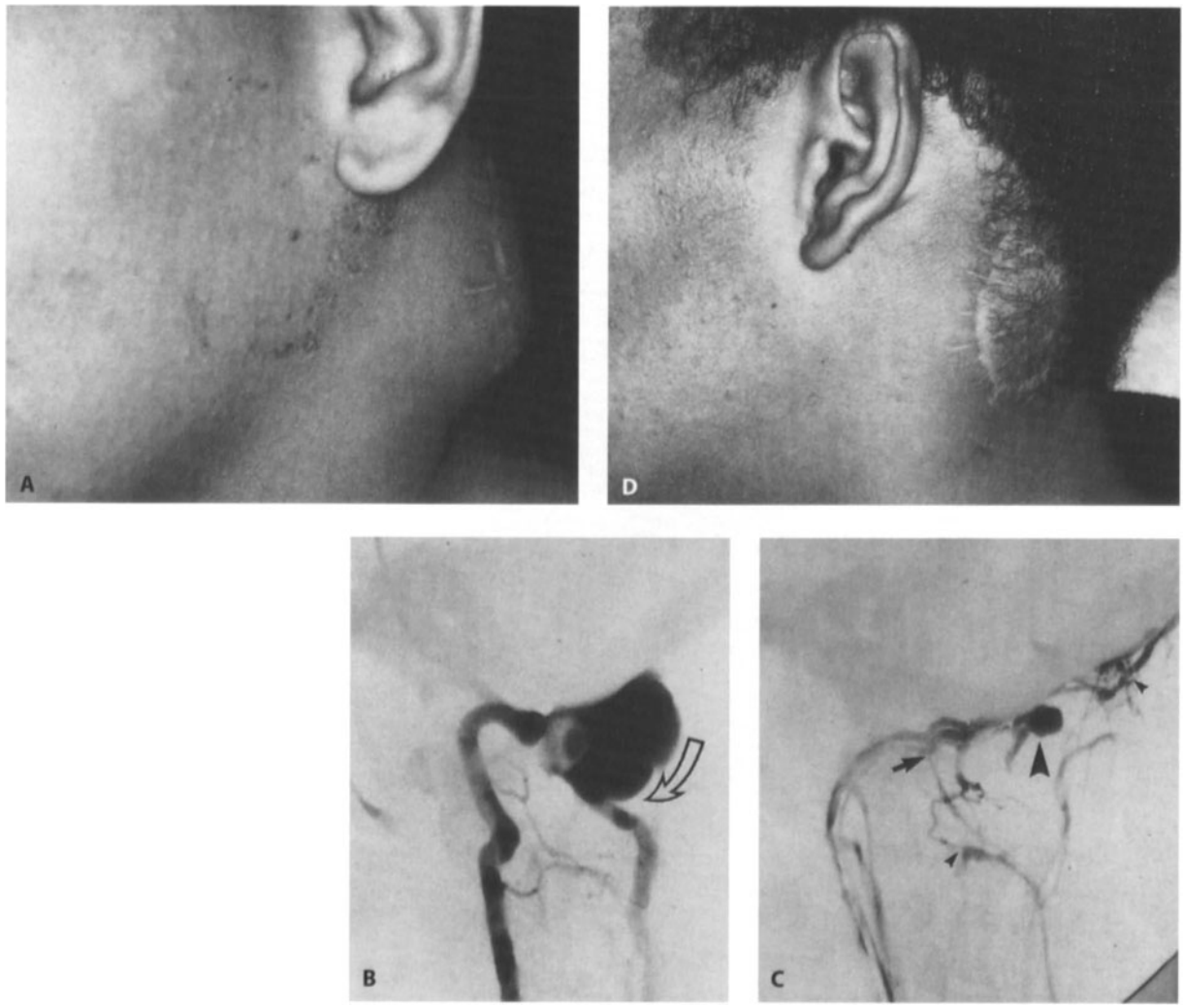

Fig. 6.50. **A** Clinical picture of a 19-year-old male patient demonstrates an old scar from the original injury as well as the pulsatile soft tissue mass in the retroauricular region. **B** Lateral subtraction angiogram of the left vertebral artery demonstrates a fistula at C1 with an aneurysmally dilated venous outflow (*open curved arrow*). **C** Lateral subtraction angiogram in arterial phase of the left occipital artery (*arrow*). Additional fistulae are demonstrated (*arrowheads*). **D** Clinical picture of the same patient 3 weeks after embolization, with complete disappearance of the abnormal pulsations and mass

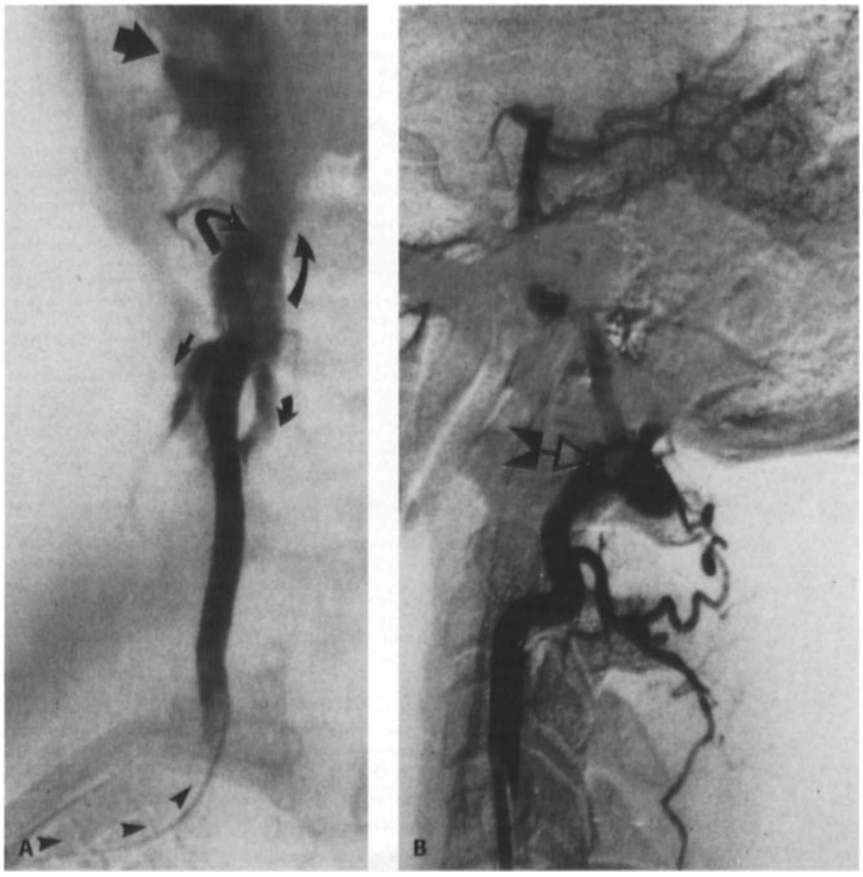

Fig. 6.51. **A** Vertebral angiogram by axillary approach (*arrowheads*) in case of traumatic vertebral arteriovenous fistula following gunshot wound injury. The fistula (*bent arrow*) is at the C2 level. The venous outflow is cranial toward the epidural venous plexus (*curved arrow*) and to the paravertebral venous plexus (*solid arrow*) and caudal to the epidural plexus (*small curved arrow*). Note a vein following the C3 nerve (*arrow*). **B** Lateral subtraction angiogram after embolization; the balloon is (*arrow*) in the venous side and the vertebral artery is patent

Fig. 6.52A, B.
Legend see p. 341
▼

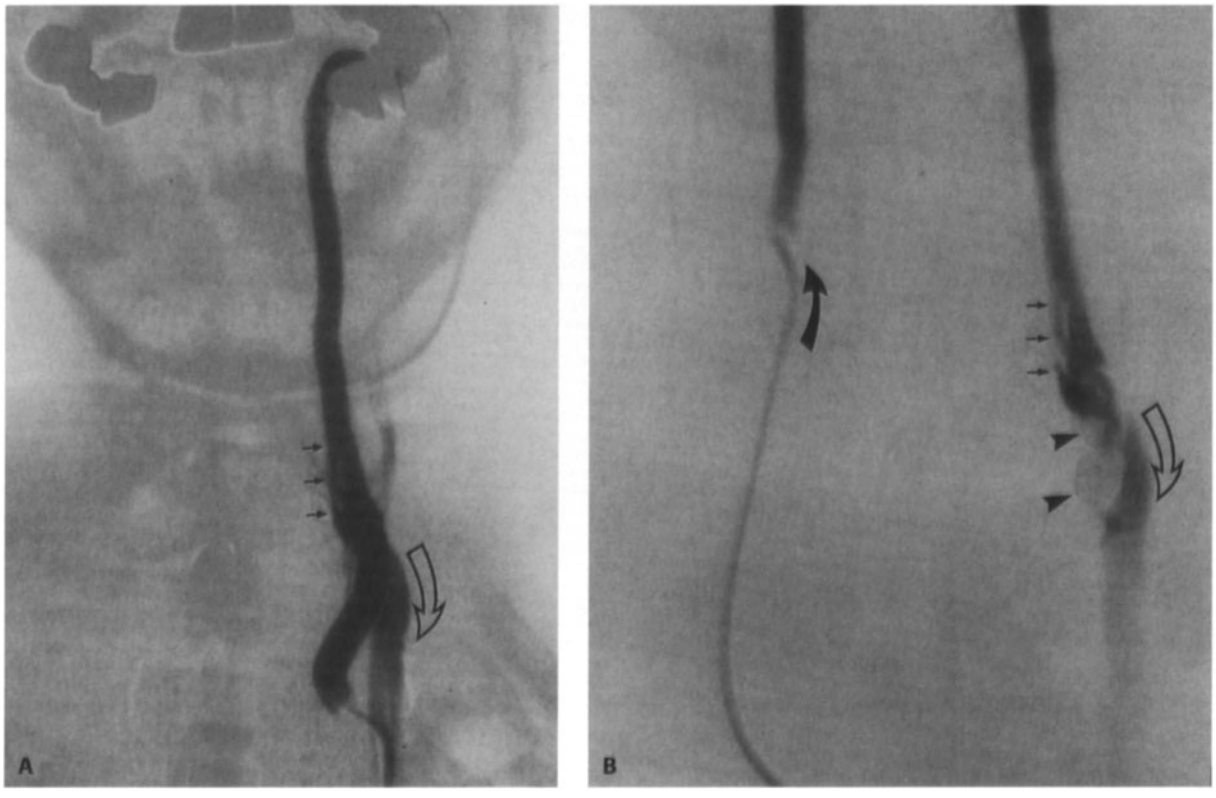

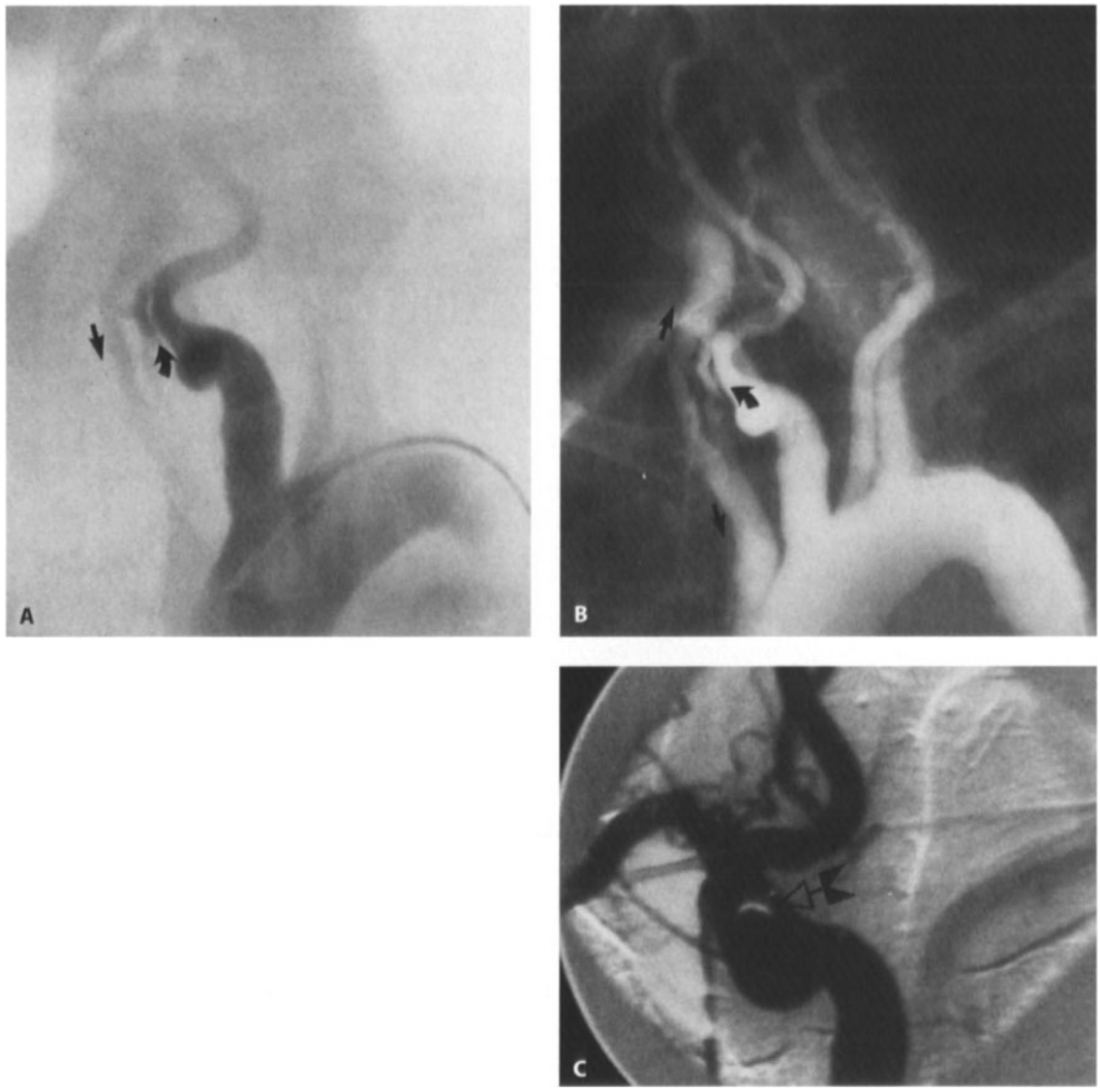

Fig. 6.53A–C. Iatrogenic common carotid fistula following percutaneous placement of a Swan-Ganz catheter in an 80-year-old woman with congestive heart failure (CHF). The fistula further aggravated the cardiac insufficiency. **A** Right anterior oblique subtraction angiogram: small fistula at the proximal segment of the right common carotid artery (*curved arrow*) draining into the jugular vein (*arrow*). **B** Later phase. **C** Innominate artery angiogram after balloon repair of the fistula. The CHF resolved after occlusion of the fistula

◀ **Fig. 6.52.** **A** Frontal subtraction angiogram, early arterial phase, demonstrates an iatrogenic fistula following accidental puncturing of the vertebral artery during angiography. A fistula in the proximal one-third of the vertebral artery associated with subintimal dissection (*small arrows*) is seen to drain primarily downward the innominate vein (*open curved arrow*). **B** Opposite right vertebral injection (*curved arrow*) for verification before balloon detachment; the fistula fills in a retrograde manner. The dissection (*small arrows*) is seen best, as well as downward filling of the innominate vein (*open curved arrow*). Two balloons are seen in the proximal left vertebral artery (*arrowheads*). Complete obliteration of the fistula could be obtained by further inflation of the second balloon

6.3.3 Common Carotid Fistulae

The incidence, natural history, and clinical presentation of these lesions is difficult to assess in view of their rarity. They usually follow trauma related to penetrating injuries (Fig. 6.53, p. 341). Airway compression from large hematomas and associated venous injuries should be investigated. Phrenic nerve and cervical injuries can be associated with lateral injury.

The pretherapeutic evaluation, principles, and techniques of treatment are similar to other fistula situations; detachable balloons are still the agents of choice while the role of covered stents is being explored.

6.3.4 External Carotid Fistulae

The incidence of external carotid fistulae (ECFs) of any kind is very low. ECFs cover 7% of all our head and neck AVFs and 11% of all carotid artery fistulae. The middle meningeal artery (Fig. 6.54) is most frequently involved in traumatic fistulae, followed by the occipital (Fig. 6.50) and superficial temporal arteries (Fig. 6.55). Extracranial fistulae are most frequently of the spontaneous or congenital type (see Chap. 11). The history of trauma, although suggestive of a traumatic AVF, should be taken with caution, and underlying arterial fragility such as in Ehlers-Danlos type IV (ED IV), and neurofibromatosis type 1 (NF1) needs to be considered even in minor trauma with high flow and recurrent or bilateral lesions.

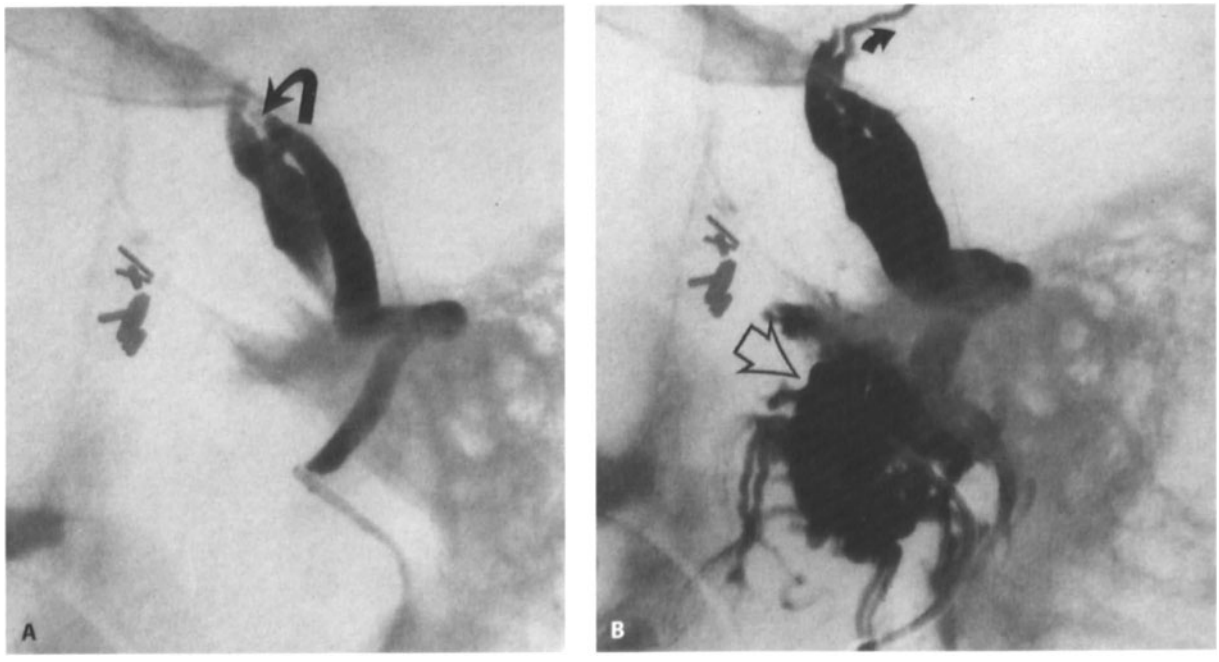

Fig. 6.54. **A** Lateral subtraction angiogram of the middle meningeal artery shows a direct arteriovenous fistula draining into a dural vein (*curved arrow*). **B** Later phase, the lesion is secondarily draining into the pterygoid venous plexus via the vein of the foramen ovale. Note the normal caliber of the middle meningeal artery (*small curved arrow*) distal to the fistula

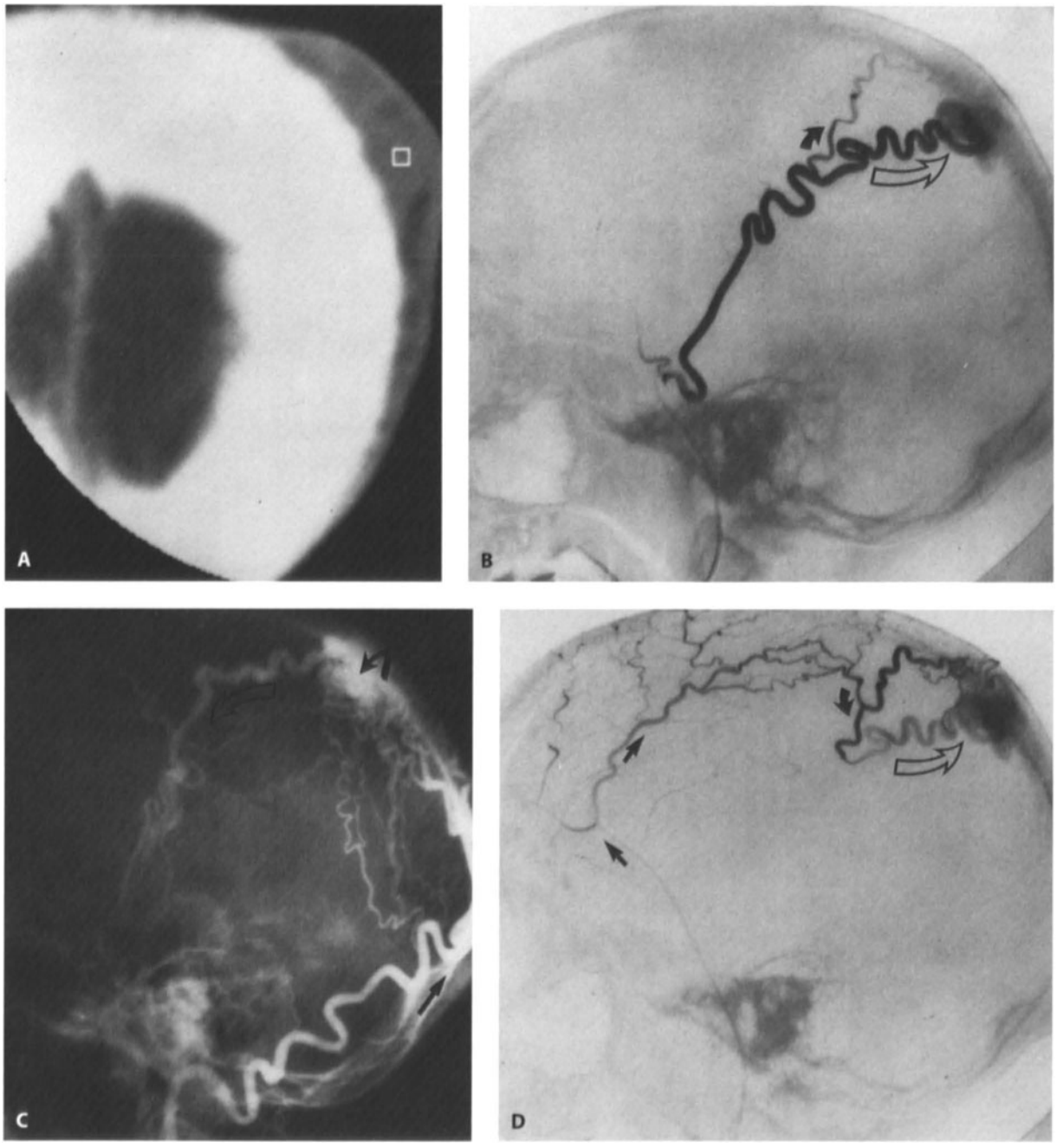

Fig. 6.55A–G. Traumatic scalp fistula in a 13-year-old boy presenting with a pulsatile tumefaction of the left side of the scalp. **A** Enhanced CT scan demonstrates the soft tissue tumefaction. **B** Superselective catheterization of the parietal branch of the superficial temporal artery (*open curved arrow*) demonstrates the fistula (*curved arrow*). Note the smaller branch (*curved arrow*), to be compared with **D** and **F**. **C** Lateral angiographic examination of the occipital artery (*arrow*) demonstrates the fistula (*bent arrow*) and retrograde filling of the parietal branch of the superficial temporal artery (*open curved arrow*). **D** Catheterization of the frontal branch of the superficial temporal artery (*arrow*) fills the same collateral pathway demonstrated in **B** (*small curved arrow*) and the parietal branch of the superficial temporal artery (*open curved arrow*). **E–G** see p. 344

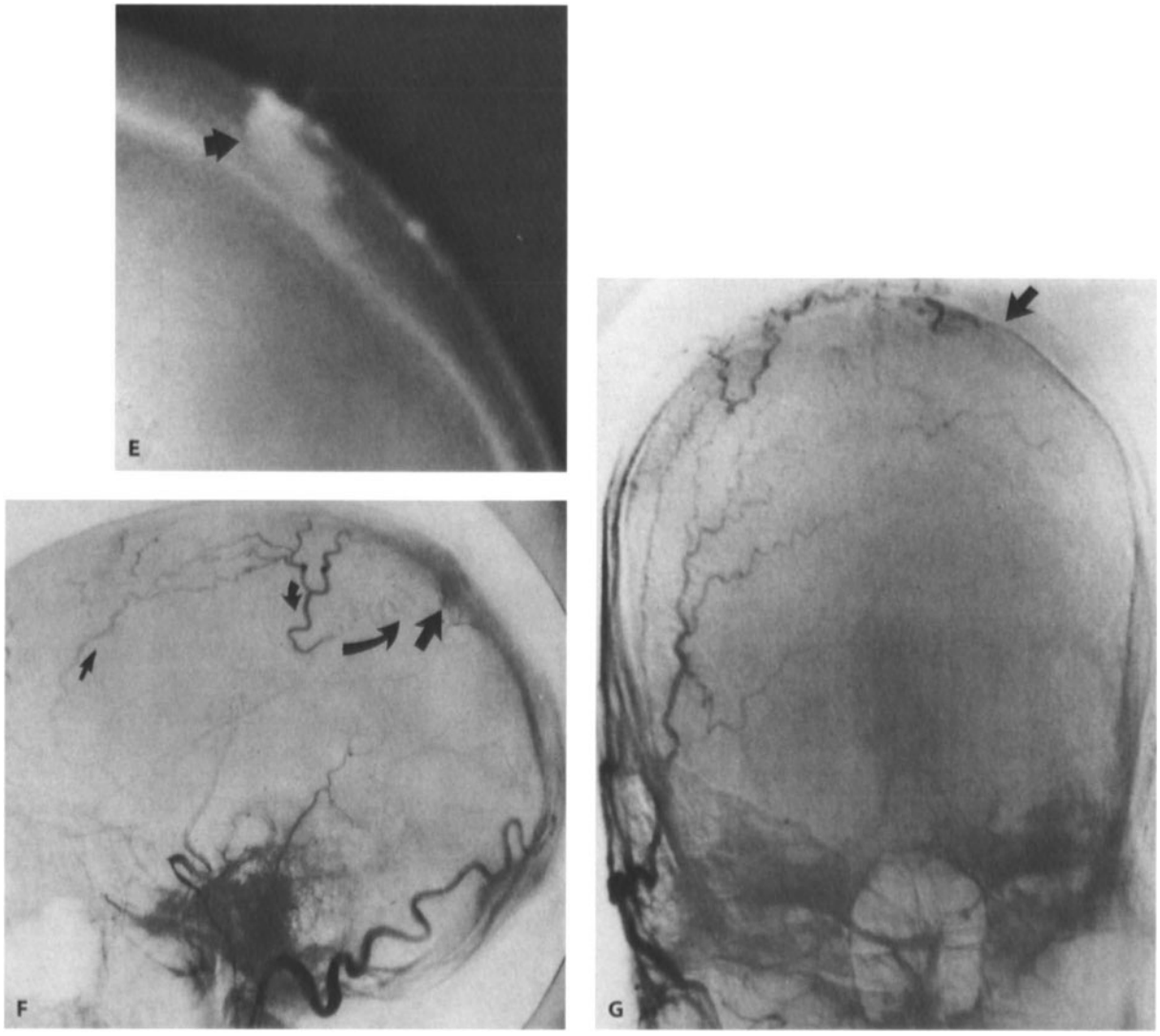

Fig. 6.55 (*continued*). **E** Radiopaque glue. **F** Postembolization follow-up angiogram of the external carotid artery. Note filling of the frontal branch of the superficial temporal artery, the same collateral anastomotic pathway (*small curved arrow*) with no filling of the fistula. IBCA cast (*curved arrow*). IBCA in the fistula is subtracted (*solid arrow*). The occipital artery does not reach the lesion although this vessel was not embolized (compare to **C**). **G** Contralateral superficial temporal follow-up angiogram demonstrates cross-circulation without filling of the fistula

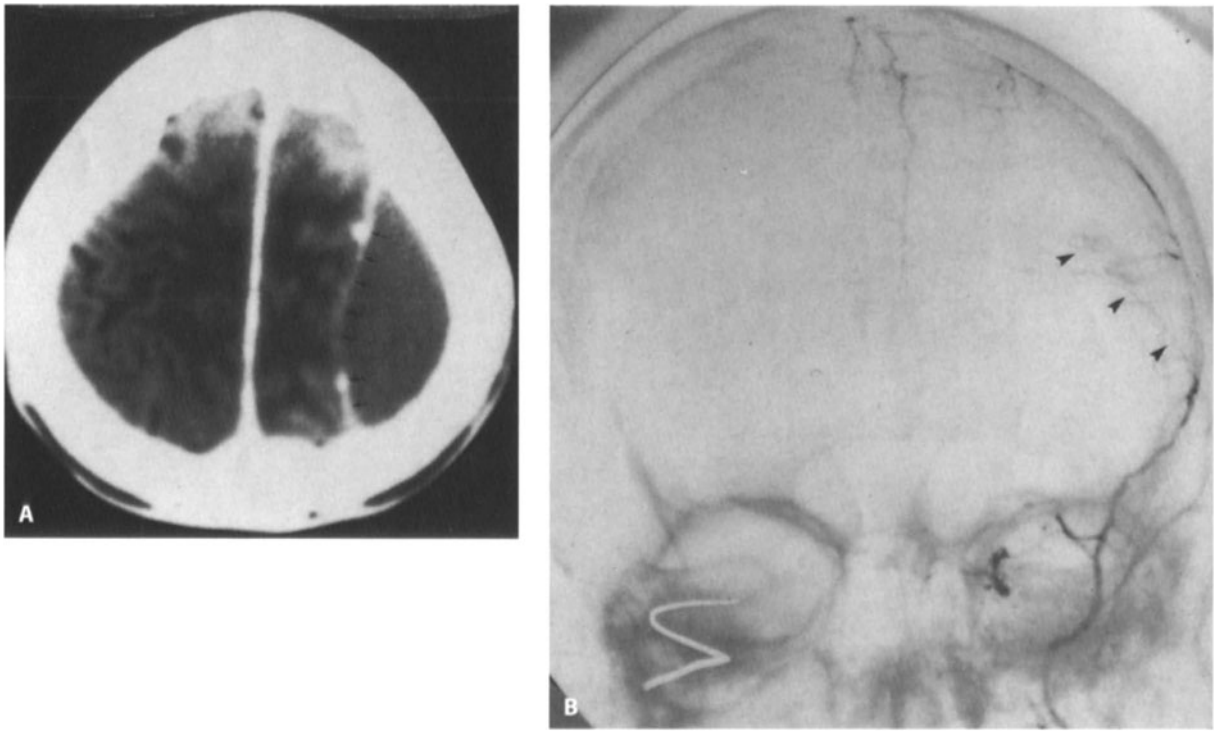

Fig. 6.56. **A** Axial enhanced CT demonstrates a subdural hematoma with enhancing membrane (*small arrows*). **B** Frontal subtraction angiogram of the selective middle meningeal artery demonstrates some extravasation (*arrowheads*). Two years after embolization of the middle meningeal artery with particles and surgical evacuation of the recurrent hematoma, there is no evidence of recurrence

Intracranial fistulae may originate from dural branches of the external carotid artery. Because of their intracranial location, they may present with intracranial hemorrhage that may be an extra-axial collection, either acute or chronic (Fig. 6.56), or they may also present with intracerebral hemorrhages if they have cortical venous drainage.

In traumatic middle meningeal fistulae, there was a frequent association with AVFs and pseudoaneurysms. If a middle meningeal fistula or other intracranial fistula has a purely dural or diploic drainage chances of hemorrhage are low and SAH will be absent. Although associated with cortical venous drainage, they carry a high risk of hemorrhage and in addition they can present with convulsions or neurological deficits (Bitoh et al. 1980). In patients with pure dural drainage, although it involves the cavernous sinus, they may present with neuro-ophthalmological findings similar to those of TCCFs.

Endovascular embolization is the treatment of choice, with a cure rate of over 95%, with low therapeutic risks and significantly less morbidity and hospitalization than any other form of treatment (Berenstein and Kritcheff 1980; Scialfa et al. 1979; Reizine et al. 1985). The choice of embolic agents depends on the location of the fistula and its flow characteristics. AVFs of the main trunk of the external carotid artery can occur secondary to trauma, including complete transection of the external carotid artery, but they may be difficult to demonstrate. Collateral circulation

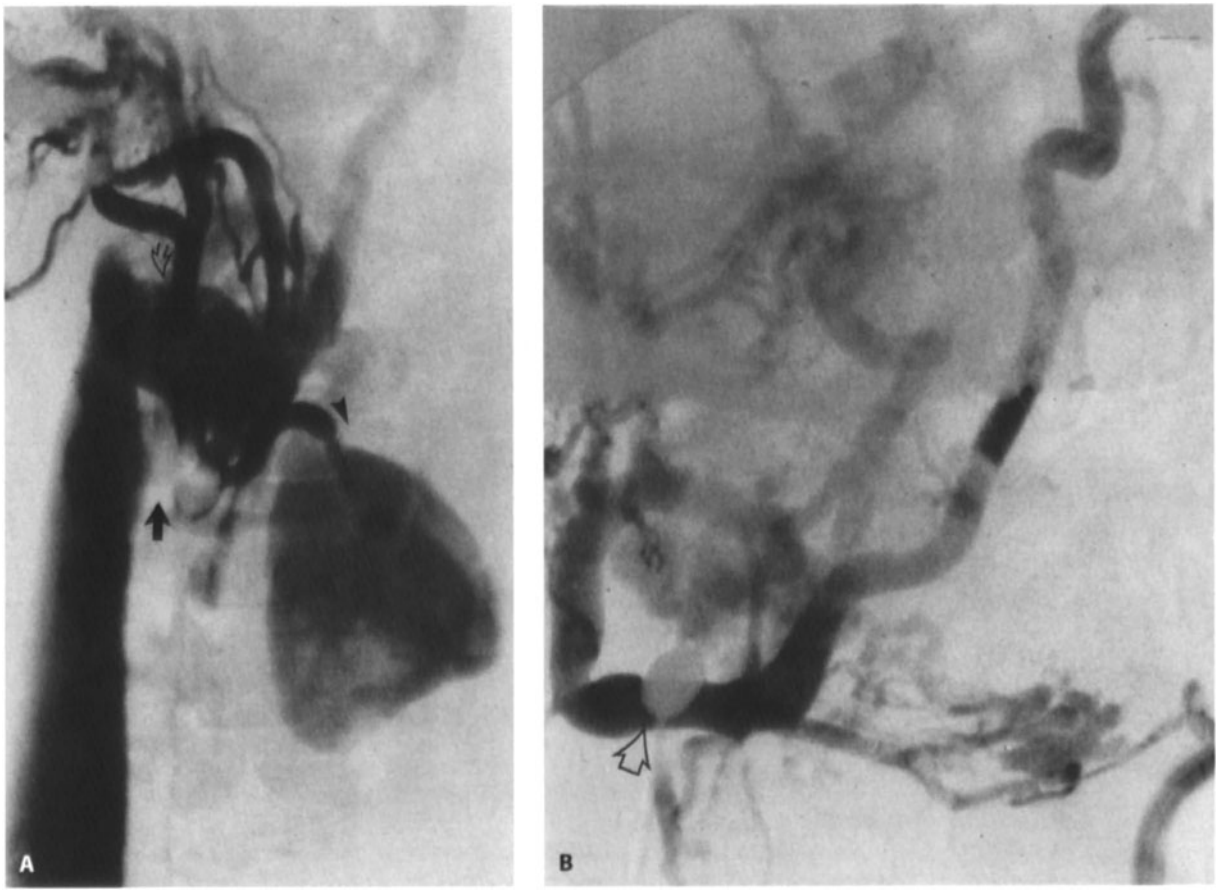

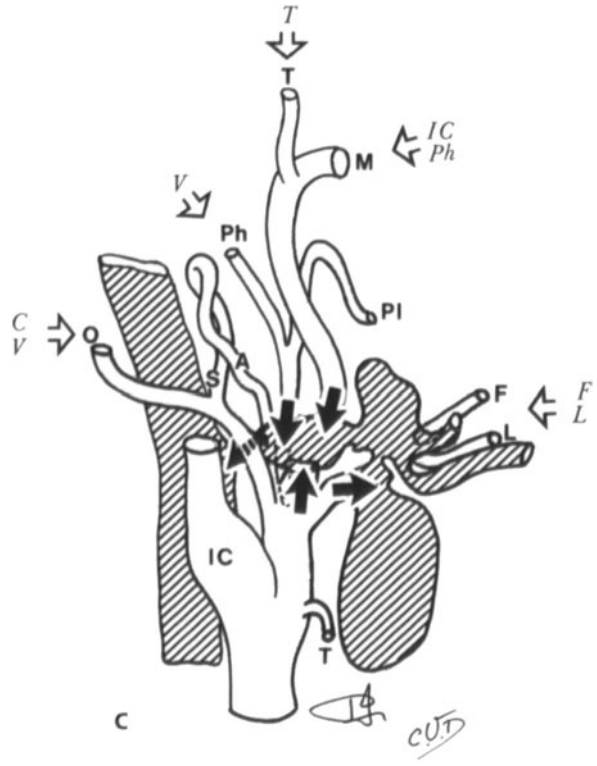

Fig. 6.57A–C.
Legend see p. 347

◀ **Fig. 6.57A–N.** Complete laceration of the external carotid main trunk following penetrating trauma. The upper segment of the fistula is demonstrated via collateral circulation. However, the proximal transected segment was difficult to assess; in addition, due to the high-flow hemodynamic steal toward the fistula, associated vascular injuries could have been missed. **A** Proximal external carotid angiogram with flow arrest using a double-lumen Berenstein occlusive balloon catheter (*arrow*). Note the transection of the external carotid artery (*double arrowhead*), the distal portion of the fistula (*open curved arrowhead*) and the pseudoaneurysm of the facial artery (*arrowhead*). **B** Late phases demonstrate the venous anatomy with dilatation of the facial veins. **C** Diagrammatic representation of this complex lesion. *IC*, internal carotid; *T*, superior thyroidal artery; *F*, facial artery; *L*, lingual artery; *O*, occipital artery; *S*, stylomastoid artery; *A*, posterior auricular artery; *Ph*, ascending pharyngeal artery; *Pl*, ascending palatine artery; *M*, maxillary artery; *T*, superficial temporal artery. Legends in *italic* correspond to contralateral opacification of the arteries listed above. *C*, cervical arteries; *V*, vertebral artery. **D** Vertebral angiogram: *1*, neuromeningeal trunk; *2*, middle pharyngeal branch of the ascending pharyngeal artery (giving rise in this case to the artery of the soft palate); *3*, arterial odontoid arch system; *4*, posterior radicular anastomotic branch of the second cervical space; *5*, proximal occipital artery. **E–N** see pp. 348–351

analysis may be useful to localize the fistula (see Vol. 1, Figs. 4.6, 9.9, 9.15, 9.25, 10.8, 11.3). However, if complete transection of the main trunk occurs the proximal segment may be difficult to visualize. In addition, they may be part of a complex vascular hemodynamic steal and fail to opacify other existing branches. In these circumstances, the use of flow arrest with a double-lumen balloon catheter can be useful to see the fistula better (Fig. 6.57).

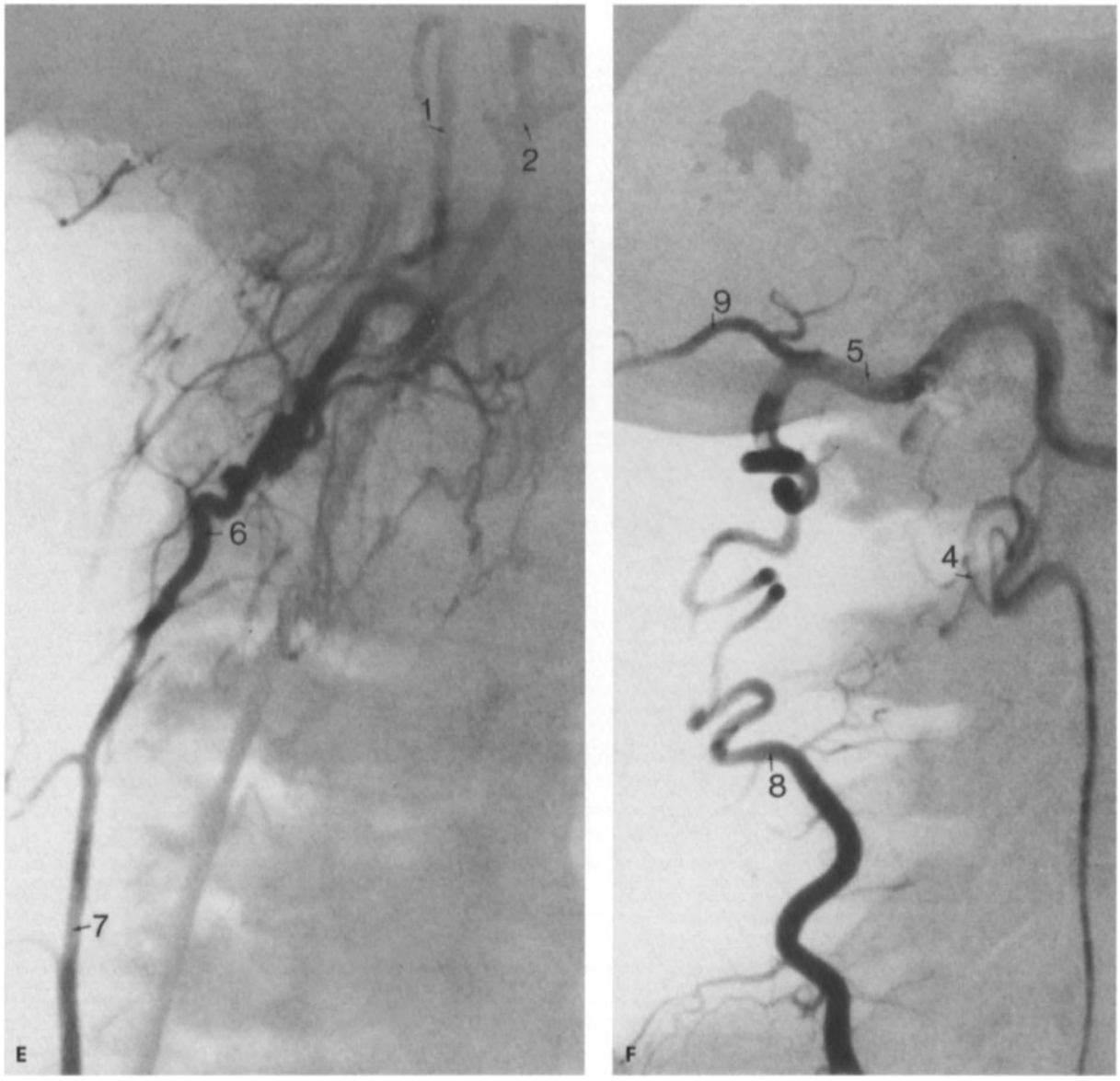

Fig. 6.57 (*continued*). **E** Ascending pharyngeal angiogram, oblique projection. Visualization of the musculospinal artery (*6*) and retrograde filling of the ascending cervical artery (*7*). **F** Deep cervical angiogram: *8*, deep cervical artery showing the distal occipital artery (*9*). Internal carotid injection in lateral view early (**G**) and later (**H**) phase: the cavernous anastomoses (*curved arrow*) are recruited. **G–N** see pp. 349–351

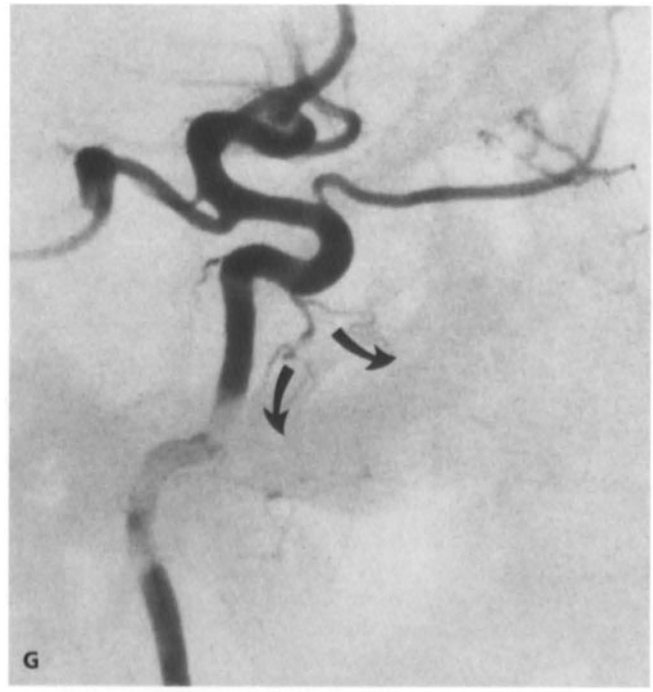

Fig. 6.57G, H.
Legend see p. 348

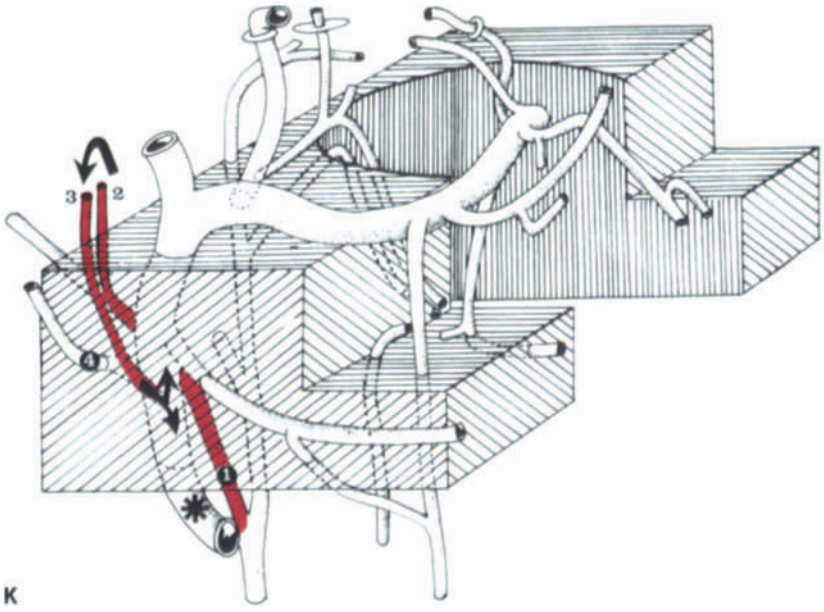

Fig. 6.57 (*continued*). Selective injection of the distal external carotid artery (**I**), distal to the fistula; note the caliber of the stylohyoid artery (*arrow*). **J** Selective catheterization (*small arrows*) and injection of the occipital artery (*asterisk*) distal to the external carotid ligation (*two solid arrows*). Visualization of the fistula through the stylomastoid anastomosis (*curved arrow*) and the posterior auricular artery (*curved arrow*). **K** Schematic representation in lateral view of the distal external carotid artery and its branches. The occipital (*1*), stylomastoid (*2* and *3*) as well as the posterior auricular (*4*) arteries are seen. **L–N** see p. 351

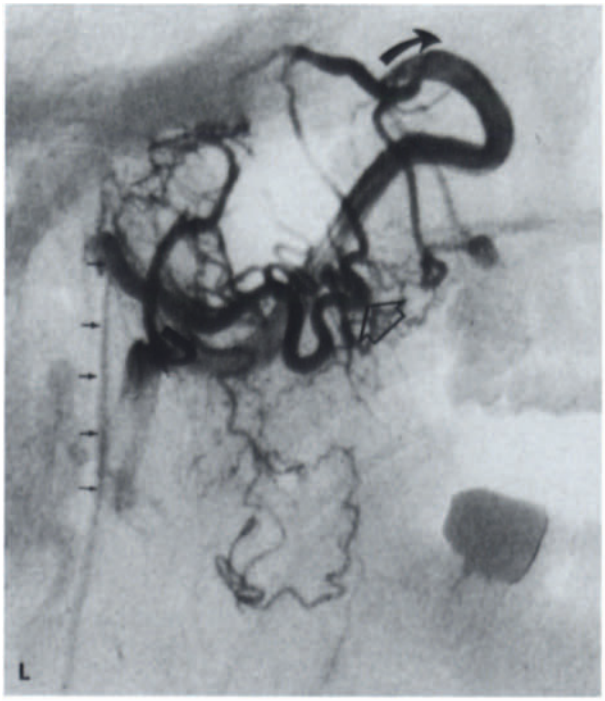

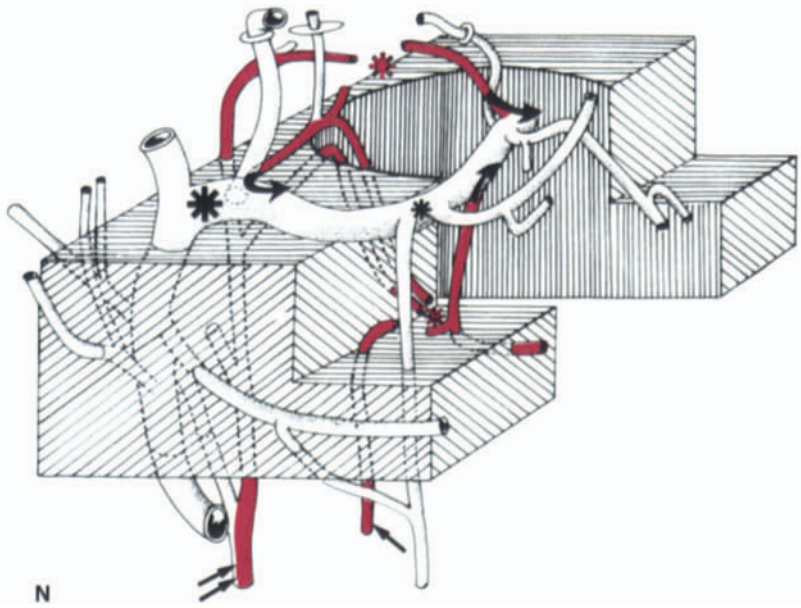

Fig. 6.57 (*continued*). **L–N** Selective injection (*small arrows*) of the distal ascending palatine artery. Lateral view, (**L**) early and (**M**) late phases. Note the soft palate anastomosis (*open arrow*), internal maxillary trunk. **N** Schematic representation of the soft palate anastomotic confluence (*small asterisk*). The *large asterisks* illustrate a theoretical elementary constraint on the internal maxillary trunk. The main channels for resupply are the accessory meningeal (*curved arrow*), greater (*curved arrow*) and ascending palatine (*arrow*) arteries. Note the eustachian tube meatus anastomotic system (*asterisk*) in which the ascending pharyngeal artery (*double arrow*) resupplies the maxillary artery (*curved arrow*) distal to the ligation (*small black asterisk*). (From Lasjaunias 1979, with permission)

Fig. 6.58A–H. A 54-year-old woman with a penetrating trauma (gunshot wound). Two entries were found: one in the submandibular region ending in the vicinity of the jugular foramen on the right side and the second one from the temporal fossa to the orbit on the right side as well. **A** Tongue hemorrhage with extravasation of contrast at the origin of the palatine artery. **B, C** Injury of the middle meningeal artery. **D** Adventitial injury to the right internal carotid artery (ICA). **E–H** see p. 353

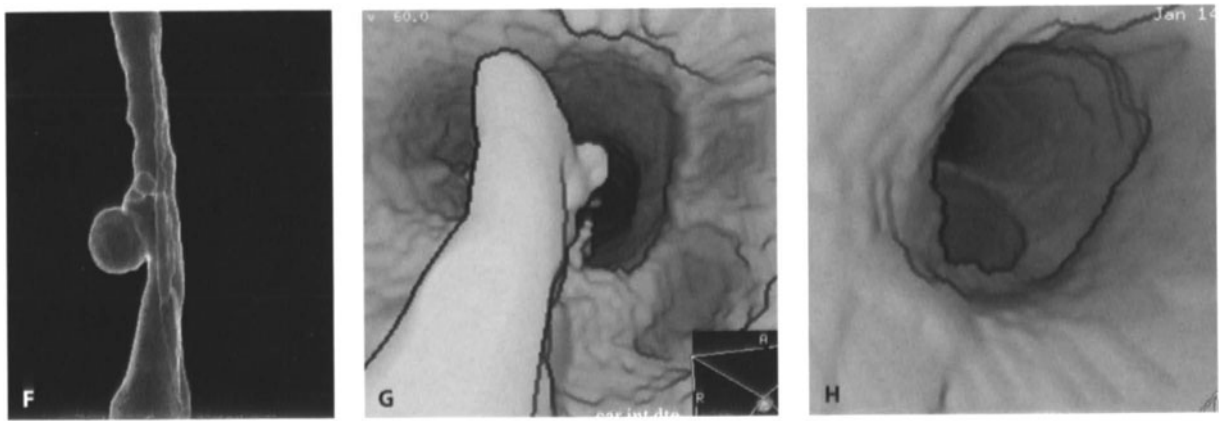

Fig. 6.58 (*continued*). **E–H** With secondary dissection on the left ICA

Detachable balloons are the preferred embolic agent for large AVFs of the external carotid artery trunk and its branches. The high flow helps guide the balloon to the site of the fistula. When using detachable balloons in these high-flow conditions, precise placement of the balloon at the fistula site may be difficult, as the high flow may push the balloon into the venous side with significant sump force. Manual compression of the distal drainage may secure the position of the first balloon before detachment of a second one. The AVF is usually at the site of an abrupt change in caliber between the artery and the vein. Large fiber coils are sometimes used to create a cage allowing the balloon to remain at the fistulous point. Actually these AVFs are seldom of a high flow, as they correspond to penetrating injury with a local hematoma. Only chronic partially treated ones with emergency surgical ligation and hematoma removal may become challenging, with flow similar to the congenital ones (see Chap. 11).

For fistulae that are more distal in location (Fig. 6.55), a liquid embolic agent such as NBCA is often chosen. Coils should be used at the venous opening of the fistulous point.

Associated dissections should be anticipated at the early stage but also later in the progression when the hematomas have reabsorbed or been evacuated, in particular with adventitial injuries (Fig. 6.58). Venous injuries should be sought in order to orientate the ICU central line management when one jugular vein has already been injured by the trauma (Fig. 6.59).

Coils are sometimes used in subacute management of cervical traumatic AVFs (Fig. 6.60).

Fig. 6.59. Penetrating trauma of the neck treated by surgical ligation of the right internal carotid artery and external carotid artery (**A**). Note the occlusion of the jugular vein that was not seen at the time of the surgery (**B, C**). Left jugular central line should be avoided to preserve good intracranial venous drainage

6.3.5 Malignant Fistulae

Vessel erosion by malignant infiltration or following radiation of a malignant lesion may result in a fistula between an eroded artery or arteries and the tumor. These lesions can even communicate with other vessels through the same fistula (Fig. 6.61), which may be a major unexpected danger during embolization. For the most part, malignant invasion of a major artery will manifest itself as a pseudoaneurysm with massive bleeding, requiring immediate management (see Chap. 7). During treatment the fragility of the involved vessels requires particular caution. The principles of management discussed in pseudoaneurysms should be followed (see Chap. 7).

6.3.6 Other Epistaxis

Epistaxis may be the presenting symptom of other diseases and may create specific complications related to the particular conditions of the patient (Fig. 6.62) and following minimal trauma. Hereditary hemorrhagic telangiectasia is one of these conditions, discussed in Vol. 3.

Fig. 6.60. A 22-year-old man suffered a gunshot wound with loss of consciousness, right-sided hemiparesis (**A**) and dysphasia. Four weeks later he was treated for carotid–jugular arteriovenous fistula (**B**) by self-expanding stent graft (**C–E**). Five months later the patient had good recovery with return to independent life. (Courtesy of L. Batista)

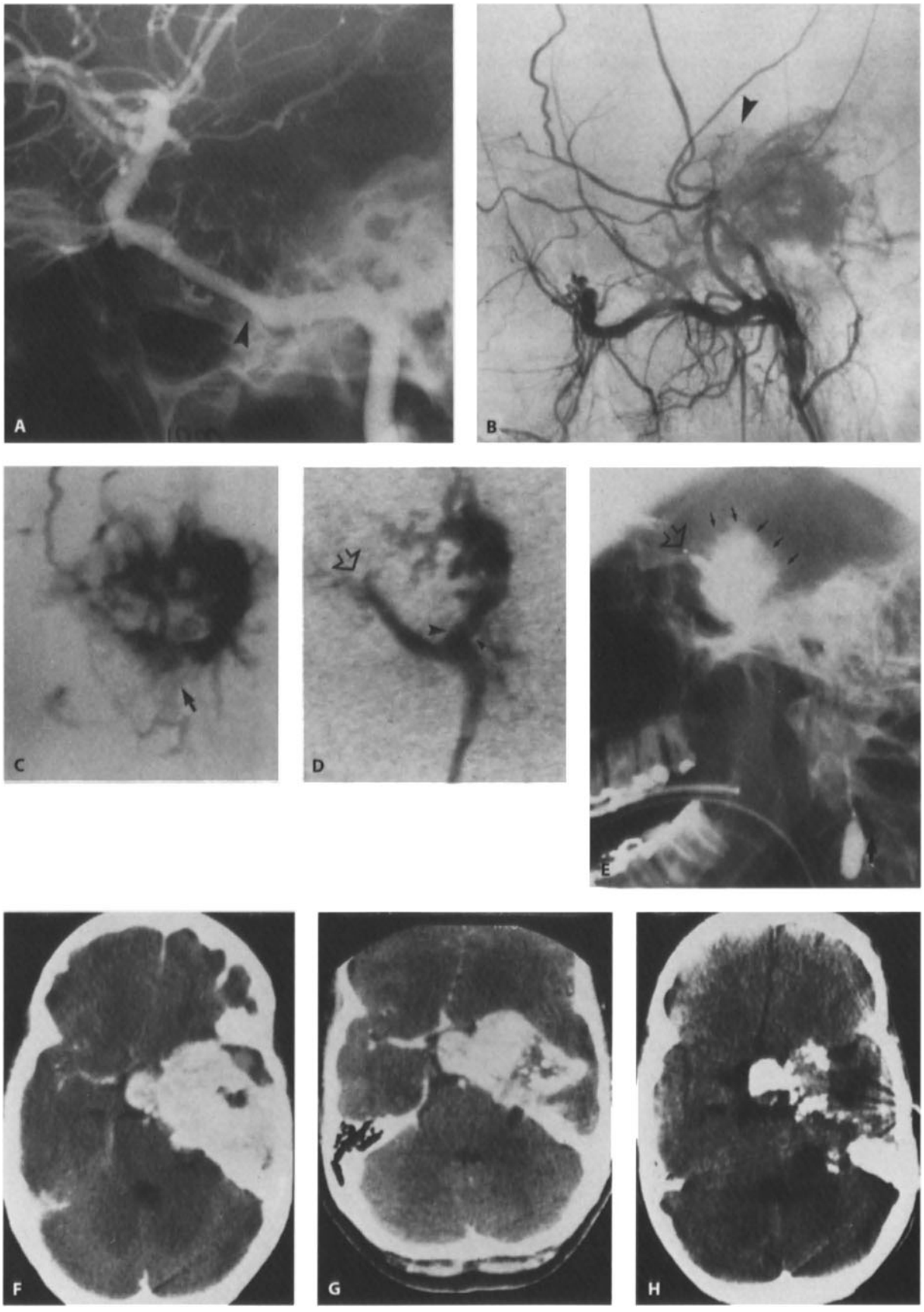

Fig. 6.61A–H. Legend see p. 357

◀ **Fig. 6.61A–H.** A 23-year-old female patient with a mesenchymal chondrosarcoma in the cavernous–petrous area treated with radiation therapy. **A** Lateral carotid angiogram demonstrates narrowing of the internal carotid artery (*arrowhead*). **B** Lateral subtraction angiogram of the distal external carotid artery demonstrates minimal hypervascularity from the petrosal branch of the middle meningeal artery (*arrowhead*). **C** Four years later, the patient was referred because of rapid increase in the size of the tumor. Note the marked change in the tumor hypervascularity, as shown on the lateral subtraction angiogram of the middle meningeal artery (*arrow*). **D** Lateral internal carotid artery angiogram after a balloon (*open arrowhead*) occlusion distal to the cavernous branches. Note the development of a fistula between the petrous segment of the internal carotid artery and the tumor (*arrowheads*). **E** Lateral film of the skull following 95% ethanol infusion of the tumor bed after the distal internal carotid artery was protected by a detachable balloon (*open arrow*). A second balloon was placed more proximally to trap the carotid artery (*arrow*). Tumor bed (*small arrows*). **F** Contrast-enhanced CT prior to ethanol infusion shows tumor filling the temporal fossa, and suprasellar cistern and invading the petrous bone. **G** CT 1 week after the ethanol treatment. Note the significant reduction in size of the infused area. **H** CT follow-up 16 months later (contrast could not be given for technical reasons). The patient underwent partial resection of tumor, which was mostly necrotic and remained stable. There has been subsequent calcification in most of the remaining tumor

6.3.6.1 Coagulopathy

Epistaxis is a frequent complication of coagulopathies in children. If needed, they can be controlled and stabilized by particle embolization in addition to the general treatment of the primary disease. Angiography usually shows a normal appearance of the nasal mucosa. The goal is therefore only local dearterialization with careful avoidance of the orbital anastomoses, which are usually widely patent in children.

6.3.6.2 Spontaneous Epistaxis

Spontaneous epistaxis usually occurs in the fifth decade and may be associated with hypertension or hepatic insufficiency. The epistaxis resolves with packing and usually does not recur. However, in some patients, the intensity or repetition of hemorrhages in a short period of time may be an indication for more invasive treatment. In this situation, embolization is preferred to ligation since it can take into consideration the various anatomical variations and predictably results in hemostasis and allows for removal of the packing in the angiography room. Treatment of the hypertension or the liver disease must obviously be addressed at the same time.

6.3.6.3 Tumoral Epistaxis

Epistaxis may form part of the presenting symptoms with lesions such as juvenile angiofibroma, capillary hemangiomas of the nasal fossa, or malignant tumors. Although embolization may allow removal of the packing, a strategy attempting to treat the primary disease as well as its hemorrhagic complication should be considered simultaneously. Therefore, pa-

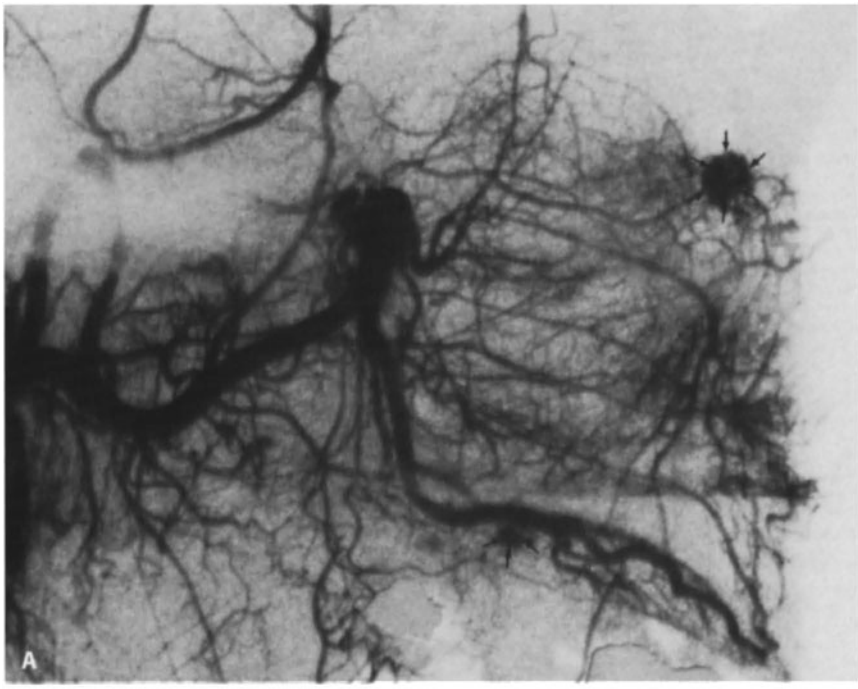

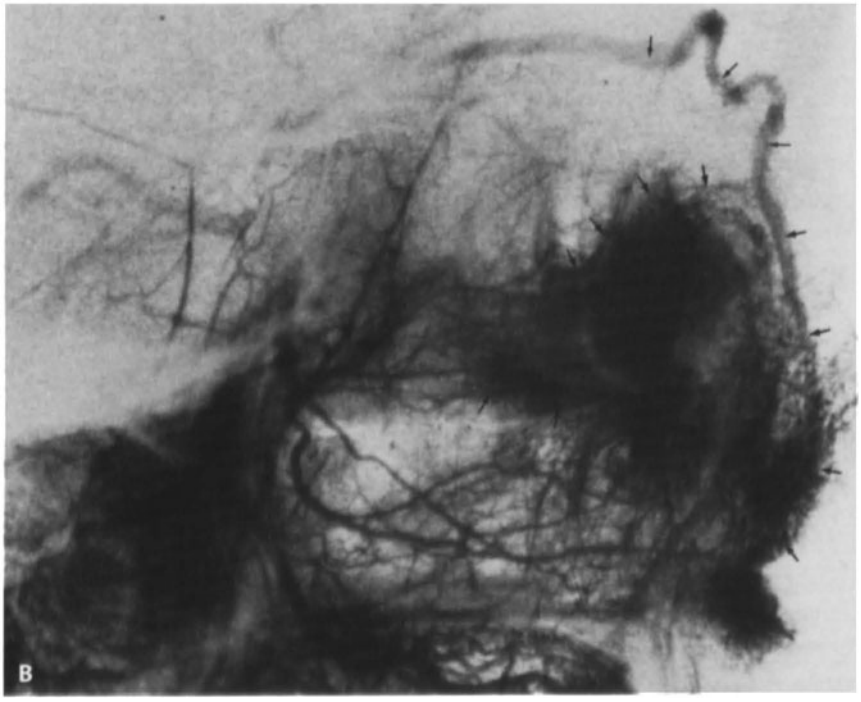

Fig. 6.62A–C. Selective injection of the internal maxillary artery in three different clinical situations (lateral view). **A** Congenital hemorrhagic telangiectasia with major ipsilateral bleeding. Note the small vascular malformations on the palate and the nasal fossa (*small arrows*). **B** Posterior orbital tumor in a 28-year-old female patient who had no history of epistaxis. The angiogram was performed 2 days before her menstrual period. Note the intensity of the nasal blush and its drainage in the superior ophthalmic vein (*small arrows*). **C** see p. 359

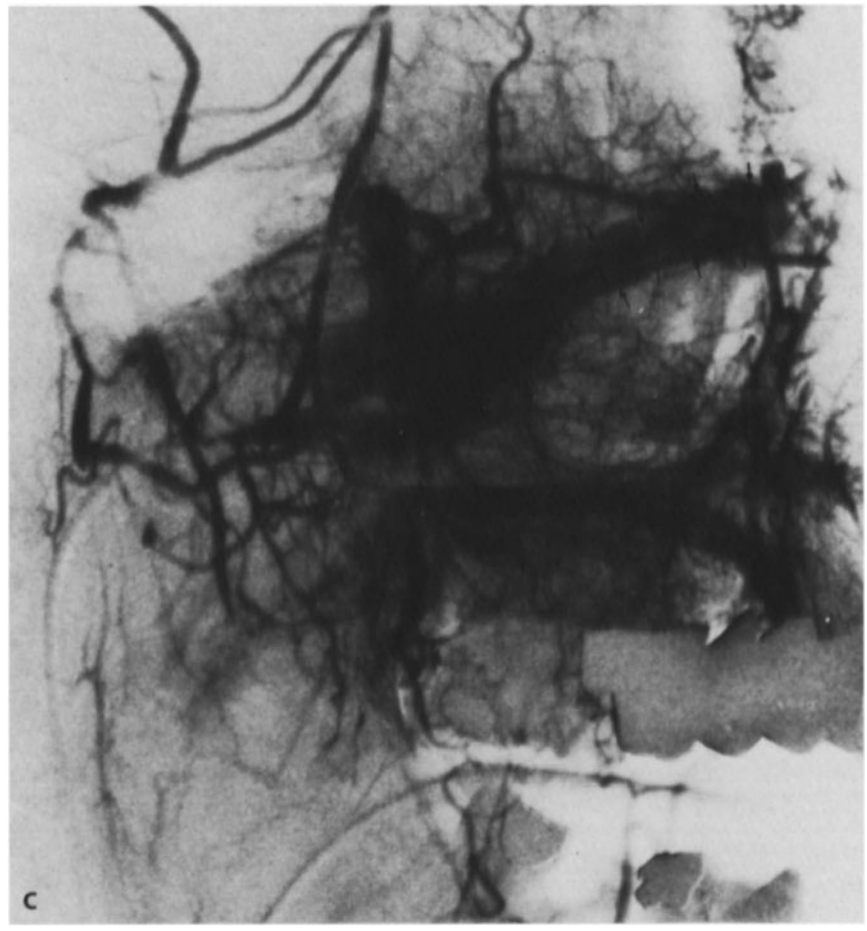

Fig. 6.62 (*continued*). C Spontaneous and massive epistaxis in a premenopausal 52-year-old female patient with neither personal nor familial epistaxis. Note the extravasation of contrast material between the middle and inferior turbinates (*small arrows*)

tients presenting with spontaneous epistaxis in the fifth decade of life should undergo CT examination to rule out possible nasal tumor or a sphenoid lesion.

6.3.6.4 Biopsy

Diffuse epistaxis may follow biopsy of an unexpectedly highly vascular lesion. Embolization can provide hemostasis if this cannot be obtained by conventional packing. Endovascular dearterialization of the base of the skull or the nasal fossa area prior to biopsy in a highly vascularized lesion (Figs. 6.63, 6.64) most often does not alter the pathological diagnosis if the embolization is performed with particles. On the other hand, misinterpretation of the histological findings related to tumor necrosis may occur after aggressive embolization with a liquid embolic agent, and such management should not be used in these circumstances if possible.

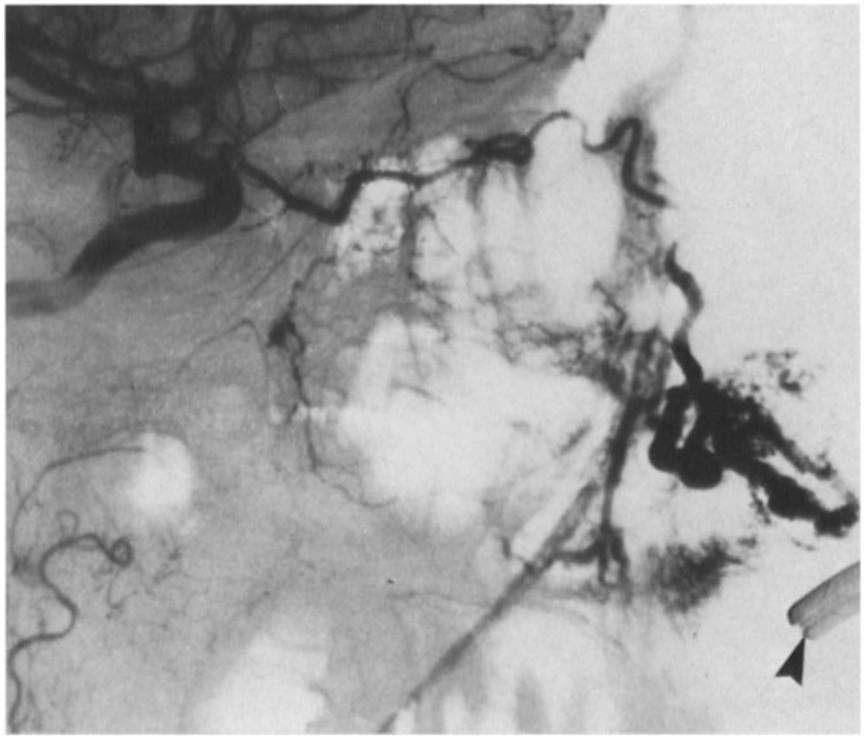

Fig. 6.63. Acute hemorrhage occurring after biopsy in a patient with a vascular malformation of the nasal fossa. Note the forceps (*arrowhead*) necessary to ensure hemostasis. In this case, the nasal branch of the ophthalmic artery is the major supply to the lesion. The other feeders from the maxillary and facial arteries have been embolized. Manual compression on the medial canthus after the external carotid embolization allowed satisfactory control of the bleeding

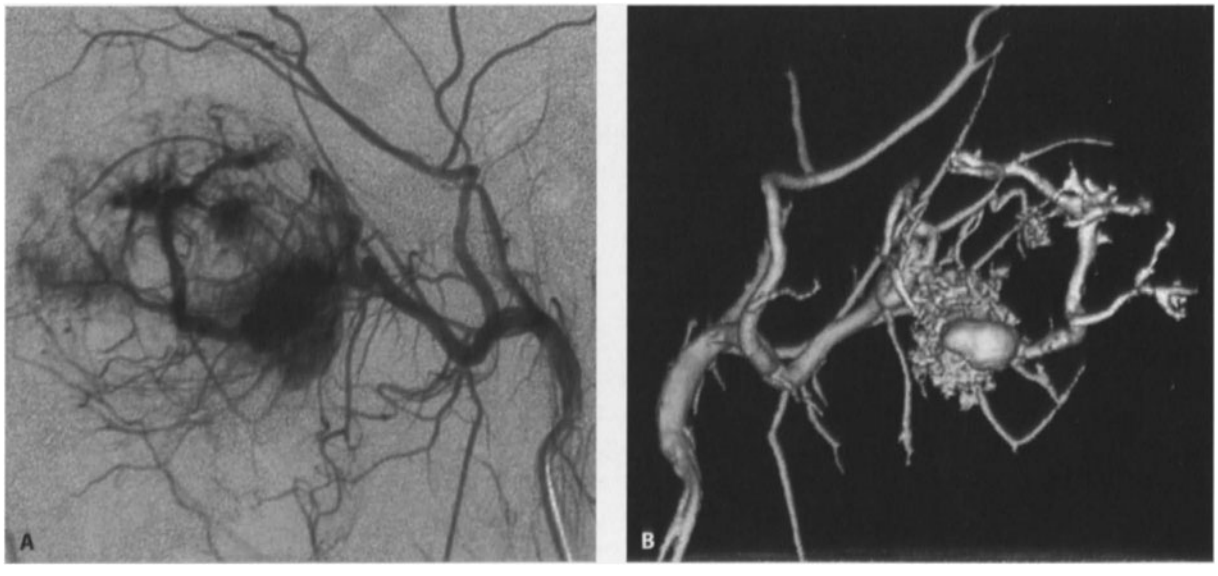

Fig. 6.64A, B. Massive epistaxis following transnasal biopsy of a maxillary tumor. Presence of a small iatrogenic fistula (**A**). 3-D angiogram clearly shows the posttraumatic aneurysm and the draining vein on the medial (nasal) view of the tumor (**B**)

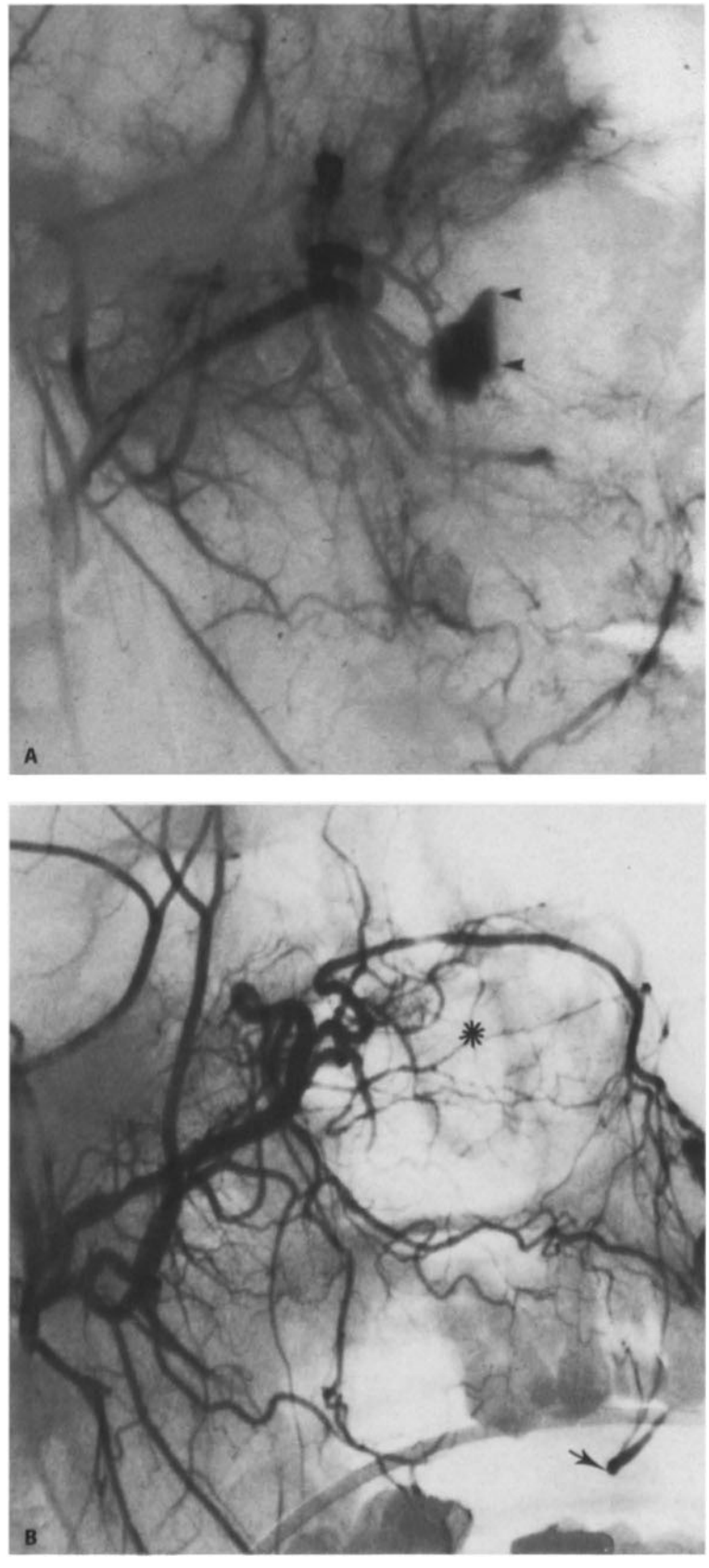

Fig. 6.65. **A** Intrasinus extravasation of contrast material (*arrowheads*) in a patient presenting with difficulty controlling epistaxis following maxillofacial trauma. **B** Complex trauma of the maxillofacial area with massive ipsilateral bleeding. Note the absence of nasal abnormality (*asterisk*) and the posttraumatic facial artery occlusion (*arrow*)

6.3.6.5 Traumatic Epistaxis

Traumatic epistaxis events illustrate the most rewarding aspect of embolization, given the efficiency of endovascular treatment required to help the normal vasculature to produce hemostasis. Internal carotid artery angiography should be carried out first to rule out bleeding from this vessel into the sphenoid sinus. Attention should be paid to the ethmoidal arteries as a possible source of bleeding. Then the protocol of embolization can be carried out and the packing removed at the end of the procedure, prior to withdrawal of the angiographic catheters. In general, embolization is indicated when anterior and posterior packing are not effective, when the epistaxis recurs after removal of the packing, or when septic complications develop in patients with fractures of the paranasal sinuses (Fig. 6.65, p. 361).

As a general principle, we feel that every patient with epistaxis should initially receive traditional treatment with anterior and posterior nasal packing. Embolization, which almost always produces hemostasis, is pre-

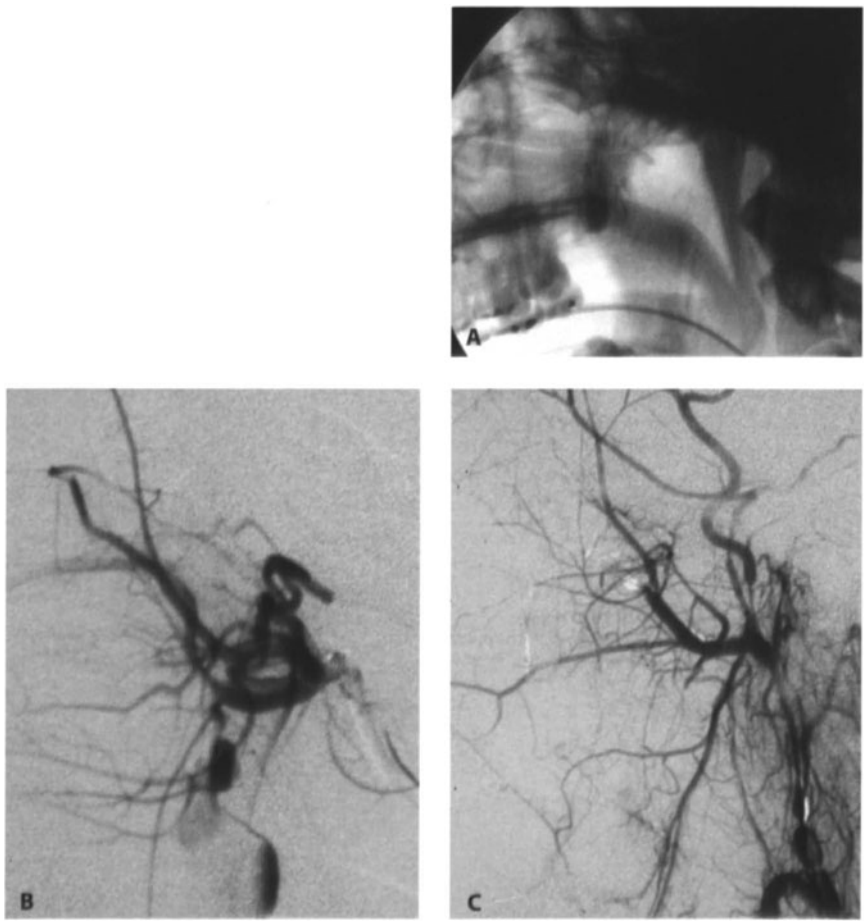

Fig. 6.66A–C. A 23-year-old female patient presented with profuse bleeding immediately after wisdom tooth extraction. CT showed no bone lesion; after spontaneous hemostasis, sudden massive recurrence led to emergent transarterial embolization with glue. Note the extravasated opacified blood at the level of the removed tooth (**A, B**). Immediate embolization with glue successfully obtained hemostasis (**C**)

ferred over vascular ligation. Angiography will not demonstrate extravasation if the packing is effective enough to transiently produce the necessary hemostasis (Fig. 6.65). Immediate embolization should be done when extravasation of contrast is demonstrated, as it points to the arterial leakage (Fig. 6.66). Superselective injection and embolization of the false sac should always be avoided at the acute stage. Surgical clipping of the ethmoidal arteries is indicated when there is direct angiographic evidence of their involvement or when following proper embolization of both internal maxillary and facial arteries, epistaxis continues to occur.

7 Aneurysmal Vasculopathies

7.1 From Aneurysm to Aneurysmal Vasculopathies 366
7.1.1 General Perspectives 366
7.1.1.1 Medical Challenge 367
7.1.1.2 Decision-Making Challenge in Patients with Unruptured Aneurysms 370
7.1.1.3 Ethical Challenge 370
7.1.1.4 Academic and Nosological Challenges 371
7.1.2 Physiopathogenesis and Risks 371
7.1.2.1 Classification 374
7.1.3 Segmental Vulnerability 375
7.1.3.1 Embryological Origin 377
7.1.3.2 Age of Aneurysms 380

7.2 Extradural Aneurysms 382
7.2.1 Introduction 382
7.2.2 Extradural Internal Carotid Artery Aneurysms 382
7.2.2.1 Cervical Internal Carotid Aneurysms 384
7.2.2.2 Acute Spontaneous Dissection of the Carotid Artery 394
7.2.2.3 Petrous Internal Carotid Artery Aneurysms 399
7.2.2.4 Aneurysms of the Cavernous Segment of the Internal Carotid Artery 401
7.2.2.5 Cervical Fibromuscular Dysplasia 415
7.2.3 Internal Carotid Artery Occlusion in Extradural Internal Carotid Artery Aneurysms 417
7.2.3.1 Tolerance to Carotid Occlusion 418
7.2.3.2 Postembolization Care 420
7.2.4 Extradural Vertebral Aneurysms 420
7.2.5 Aneurysms of the External Carotid Artery 425

7.3 Intradural Aneurysms 431
7.3.1 Saccular Arterial Aneurysms and Associated Diseases 431
7.3.1.1 Polycystic Kidney Disease 431
7.3.1.2 Ehlers–Danlos Syndrome 434
7.3.1.3 Neurofibromatosis Type 1 435
7.3.1.4 Bourneville Disease 436
7.3.1.5 Fibromuscular Dysplasia 438
7.3.2 Saccular Arterial Aneurysms Without Diagnosed Associated Diseases 438
7.3.2.1 Nonsyndromic Familial Arterial Aneurysms 438
7.3.2.2 Multiple Saccular Arterial Aneurysms 440
7.3.2.3 Arterial Anatomy, Single, Mirror, and Twin Saccular Arterial Aneurysms 442

7.4 Intradural Artery Dissections 454

7.5 Intradural Giant Saccular and Nonsaccular Arterial Aneurysms 478
7.5.1 General Remarks 478
7.5.2 Giant Intracranial Aneurysms with Thrombosis 486
7.5.3 Nonsaccular Giant Arterial Aneurysms 497
7.5.3.1 Megadolicho Arteries and Serpentine Arterial Aneurysms 498
7.5.4 Multiple Giant Arterial Aneurysms and Mirror Giant Arterial Aneurysms 500

7.6 Infectious, Immune, and Inflammatory Intradural Aneurysms 502
7.6.1 Infectious Arterial Aneurysms 502
7.6.2 Intradural Fusiform Aneurysms in Patients with Immune Deficiencies 509
7.6.3 Inflammatory Diseases and Arterial Aneurysms 513

7.7 Flow-Related Arterial Aneurysms and Other Aneurysmal Vasculopathies 514
7.7.1 Intradural Traumatic Arterial Aneurysms 518
7.7.2 Arterial Aneurysms Associated with Proliferative Diseases 523
7.7.3 Arterial Aneurysms with Congenital Heart Disorders and Coarctation of the Aorta 524

7.8 Therapeutic Management 527
7.8.1 Introduction 527
7.8.2 Method 532
7.8.3 Results of the Endovascular Approach 538
7.8.4 Management of Multiple Arterial Aneurysms 549
7.8.5 Management of Giant Arterial Aneurysms 560

7.1 From Aneurysm to Aneurysmal Vasculopathies

7.1.1 General Perspectives

The prevalence of arterial aneurysms (AAs) in Western populations is 3%–5%, ten times higher than the frequency of arteriovenous malformations (AVMs) in the same population group. Arterial aneurysms are the cause of primary subarachnoid hemorrhage (SAH) in 65%–85% of cases; AVMs account for 5% of cases and the etiology is unknown in 15%–30% of cases. The incidence of aneurysmal SAH is 5–10/100,000 per year and it reaches 20/100,000 in Finland and Japan (Ronkainen et al. 1993). For comparison, the incidence of AVM cases is about 2/100,000 per year. Such statistics led Wiebers (International Study of Unruptured Intracranial Aneurysms 1998) to suggest that "most intracranial aneurysms do not rupture."

The clinical consequences of SAH are such that emphasis should be placed on the understanding of AA as a group of diseases and on the prevention of their rupture.

The incidence of AAs increases with age both in autopsy and in clinical series; the incidence of AAs in children is very low, even in familial AA or associated disease (see Vol. 3). In adults, females are more often affected than males and this observation cannot be explained by the increased proportion of females in the older age group. The female predominance is not seen in children, where a male dominance is noted, nor is it present in the Finnish familial forms of AA, particularly in the anterior communicating artery location (AComA) (Ronkainen et al. 1997).

In 1997, Schievink proposed a relatively simple concept. "Intracranial AAs are acquired lesions, that are most commonly located at the branching points of the major cerebral arteries coursing through the subarachnoid space at the base of the brain." He also stated, "Intracranial arteries have an attenuated tunica media and a lack of external elastica lamina, intracranial AA have a thin tunica media or none, and the internal elastica lamina is either absent or severely fragmented." Although these remarks

are generally acceptable, in order to develop a better understanding of cerebral aneurysms that will eventually lead to improved management strategies, an attempt should be made to recognize different groups (diseases) within the generic denomination of AA. The idea that the arterial blood stream "blows" and then "bursts" an "aneurysmal herniation of the wall" should be abandoned. Several issues will be stressed in this chapter to emphasize the heterogeneity of the various types of AAs.

Even with our current knowledge and understanding, AAs continue to raise a number of questions and challenges.

7.1.1.1 Medical Challenge

The treatment of aneurysms raises complex technical and therapeutic problems, including prevention of their recurrence and management of the complications caused by their rupture. Aneurysmal rupture still carries high morbidity and mortality rates. Published data illustrate this complex technical and therapeutic challenge.

The incidence of SAH has not declined over time.

Ten percent of patients with AA rupture die before reaching the hospital, 13% in Pakarienen's series in 1967, with an overall incidence of AA of 10.3/100,000 per year. The incidence by age was 0.3 in the first decade of life, 0.4 in the second, 3.8 in the third, 9.4 in the fourth, 20.3 in the fifth, 25.3 in the sixth, 16.2 in the seventh, and 13.1 in the eighth decade of life.

The risk of rebleed from a nonsecured AA is 60% at 6 months (3%–4% during the first few days after the rupture, 2% risk per day during the first month) and 10% during the remainder of the first 6 months) and thereafter appears to stabilize at 3% per year. Subsequently, the mortality from bleed or rebleed is 50%. Eight percent of patients will die from the severity of the initial hemorrhagic event, 7% will die despite surgical intervention, and an additional 7% will be left with severe neurological deficit. This implies that overall, one-third of patients presenting with a ruptured AA will have a good outcome. The probability of developing a de novo AA after SAH is about 1%–2% a year (Juvela et al. 1993b; Rinne and Hernesniemi 1993; Porter et al. 2001).

The abruptness of onset and the severity of the symptomatology has led to passionate debates that unfortunately have not helped in the understanding of the underlying disease (or diseases). Although most ruptures are symptomatic, the question as to whether previous subclinical hemorrhages have already occurred should not be ignored. On careful questioning of the patient and their family, a history of previous headache or acute event can frequently be revealed.

Careful grading (review by Mooij 2001, Tables 7.1–7.7) of a hemorrhage on patient admission (according to Hunt and Hess 1968, Fisher et al. 1980, or the World Federation of Neurosurgical Societies scores) should not obscure the fact that we have limited information on how the actual hemorrhage occurred. Indeed, we can assume that some degree of bleeding, perhaps even an early recurrence of hemorrhage, had gone undiscovered, and that some patients may have already bled several times before reaching the hospital.

Table 7.1. Hunt and Hess classification of subarachnoid hemorrhage

Grades	Description
0	Unruptured aneurysm
1	Asymptomatic, or mild h.a./nuchal rigidity
1a	Only fixed neurological deficit
2	Moderate/severe h.a./nuchal rigidity
3	Mild focal deficit, lethargy/confusion
4	Stupor/moderate or severe hemiparesis, early decerebrated hypertony
5	Deep coma, decerebrated rigidity, moribund

Some authors preferred a more personal touch. For example, Yasargil (1984) proposed a grading system based on the revised Botterell system that recognized the importance of focal neurological deficit by adding "b" when present and "a" when absent.

Table 7.2. The grading system used by Yasargil

Yasargil grade	Description
0a	Unruptured aneurysm, no neurological deficit
0b	Unruptured aneurysm, neurological deficit, as in cranial nerve III palsy, chiasma syndrome, or progressive hemisyndrome (in giant arterial aneurysms)
Ia	Asymptomatic following subarachnoid hemorrhage (SAH)
Ib	SAH, alert and orientated, but with focal pronounced neurological deficit such as hemiparesis, paraparesis, aphasia, visual field loss (no simple lesion of cranial nerve II, III, or IV)
IIa	Alert, but with headache and meningism
IIb	Same, with focal neurological deficit
IIIa	Lethargic, confused, disoriented, combative
IIIb	Same, with focal neurological deficit
IV	Semicomatose, response to pain, not to voice; may show extensor posturing; pupils reactive to light
V	Comatose, pupils not reactive to light, extensor posturing or no reaction to pain, failing vital signs

The rationale behind this grading system is again the relationship with outcome: 0a, Ia, and IIa with the best results, followed by Ib and IIb, then by IIIa, 0b, IIIb, IV, and V, respectively.

Table 7.3. The World Federation of Neurosurgical Societies (WFNS) grading scale for subarachnoid hemorrhage

WFNS grade	GCS score	Major focal deficit	Comment
0	–	–	Intact aneurysm
1	15	Absent	Comp. with H&H I and II
2	13–14	Absent	Comp. with H&H III(II)
3	13–14	Present	Comp. with H&H III
4	7–12	Present or absent	= H&H IV (III)
5	3–6	Present or absent	= H&H V

H&H, Hunt and Hess grading scale; GCS, Glasgow Coma Scale.

Table 7.4. GCS-based scales

Tagaki GCS-based scale					
GCS	15	11–14	8–10	4–7	3
GCS-based grade	I	II	III	IV	V
Johns Hopkins GCS-based grading scale in SAH					
GCS	15	12–14	9–11	6–8	3–5
GSC-based scale	I	II	III	IV	V

GCS, Glasgow Coma Scale; SAH, subarachnoid hemorrhage.

Table 7.5. Fisher's grading system of intracranial blood on CT in patients with subarachnoid hemorrhage (SAH)

Fisher grade	Blood on CT (<5 days after SAH)
1	No subarachnoid blood detected
2	Diffuse or vertical layers <1 mm thick
3	Localized clot and/or vertical layer >1 mm
4	Intracerebral or intraventricular clot with diffuse or no SAH

Table 7.6. The Glasgow Outcome Scale

Grade	Neurological status
1	Good recovery; patient can lead a full and independent life with or without minimal neurological deficit
2	Moderately disabled; patient has neurological or intellectual impairment but is independent
3	Severely disabled patient, conscious but totally dependent on others to get through daily activities
4	Vegetative survival
5	Dead

Table 7.7. Karnofsky score

100	Normal. No complaints
90	Normal activity. Minor signs
80	Normal activity with effort
70	Cares for self. Unable to carry on normal activity or do active work
60	Requires occasional assistance
50	Requires considerable assistance and frequent medical care
40	Disabled. Requires special care and assistance
30	Severely disabled. Hospitalization required
20	Very sick. Hospitalization necessary
10	Moribund
00	Dead

It is also possible that multiple episodes of bleeding have occurred at such close intervals that they were not individually recognized, despite our modern imaging techniques. Cisternal filling with blood may result from repeated bleeding from the aneurysm over a short period of time, whether hours or days. In other cases, a single, sudden rupture will flood the cisterns. Quantitative assessment of the amount of cisternal blood cannot answer these questions; therefore, basing the potential for vasospasm simply on the volume of extravasated blood is unsatisfactory. Other etiological factors may play a role, such as single versus repeated hemorrhage, the age of the vascular system, the degree of atherosclerosis, etc.

7.1.1.2 Decision-Making Challenge in Patients with Unruptured Aneurysms

The term "unruptured" does not always mean inactive, but denotes that the aneurysm has not been associated with a clinical hemorrhage. Here the challenge is not acute care management, but rather prevention of future rupture or growth of the aneurysm. Decision making can be improved by a better understanding and recognition of the various types of lesions referred to as aneurysms. The decision needs to focus on the therapeutic objective or objectives to be reached. Once active intervention has been chosen, then the choice of a specific therapeutic technique, whether medical, observational, surgical, or endovascular will need to be considered (Wiebers 1998). Despite the dramatic implication associated with the diagnosis of aneurysms, the decision not to intervene should certainly be considered in the appropriate clinical circumstances. Such a decision may be made even though the very same aneurysm in a different setting may result in a decision to operate or to embolize, with no contradiction in the coherence of the decision. The choice of the treatment should first consider the patient's needs, and second, the quality of the treatment available. The point is to adapt one's decision to one's means.

7.1.1.3 Ethical Challenge

The ethical challenge involves informing the patient of his or her medical condition: what we as physicians know about it and what can be done about it. What are our team results and the complications of the proposed treatment? We must avoid quoting the reported literature that may not reflect the individual physician's experience.

Finally, how does one recognize the subgroups of patients and aneurysms that should be treated? There are undoubtedly indicators of imminent rupture, but at present we do not know how to recognize them. There are probably signs of stability as well, but we do not trust them to be long-lasting. Preventing rupture also has a cost, in terms of public finances and patient impact, creating ethical and moral issues. The former is a choice of society, while the latter relates to the invasiveness of the treatment and personal choice. For these reasons, teams that are ready to treat unruptured aneurysms should document their reasons and their means to achieve their goals, all the while recognizing the different sub-

groups of patients (diseases) that they are treating. Teams should also document and monitor the quality of their results. Permanent self-assessment is not a new idea, but today it has become more relevant than ever in view of the publication of medical data considered as universally applicable and internationally available.

7.1.1.4 Academic and Nosological Challenges

Morphology and disease are two separate facets of the academic and nosological challenge. While aneurysms of different shapes often reflect different pathologies, similar shapes can also reflect different situations. A saccular aneurysm of the basilar trunk that has developed at the origin of the P1 segment may be single, associated with multifocal aneurysms, or familial (Figs. 7.47, 7.64). Similarly, associations with Ehlers–Danlos syndrome, Marfan syndrome, polycystic kidney disease, or an AVM of the occipital lobe may distinguish aneurysms in the same location beyond their appearance and clinical presentation (Fig. 7.48). Therefore, it can be proposed that aneurysms are merely a symptom of a more subtle dysfunction of the blood vessel wall (Table 7.8). Abnormalities of intracellular and regionally contained disorders maintain a delicate interaction between the vessel wall and its neighboring tissues via endoluminal (endothelial) and extravascular signals similar to most other types of vascular malformations.

Therefore, we should shift our focus from aneurysmal vasculopathy to mural vasculopathy (Tables 7.9, 7.10, p. 373) and as a result attempt to change the objectives of our treatment from mechanical to biological.

Recognition of these two distinct entities has not resulted in conducting well-constructed therapeutic research. Instead, it has resulted in investigations that are increasingly diverse and involve different types of specialists. This concept does not reject the current mechanical management of ruptured aneurysms, since the focus has been not so much to analyze the underlying disease but rather to manage the complication represented by the rupture itself and prevent further hemorrhage. However, treatment of the rupture should not be confused with the preventive treatment of the rupture or that of the underlying disorder, which are all entirely different issues.

7.1.2 Physiopathogenesis and Risks

The physiopathogenesis of aneurysms is complex, just as it is for other vascular disorders. This is because we have little knowledge about the life span or the regeneration frequency of arteries, in normal or in pathological circumstances, at their branching or nonbranching portions. In vitro studies only provide a very crude model, as they isolate blood vessels from their perivascular environment, which in our opinion is a key element in the maintenance and renewal of the arterial wall. Are aneurysms simply a result of aging of the arterial wall or are they caused by the progression of a more specific disorder (Table 7.11, p 374)? Is the physiopathogenesis

Table 7.8. Most frequent topographies reported according to the type of arterial aneurysm (AA)

Type of aneurysm		Small	Large	Giant	Fusiform	Cervical ICA	Intracav. ICA	C OPH A ICA term.	PComA	Distal A	AComA	MCA	Mirror	Multifoc.	Multimetamer.	VBA	PICA	B tip	F/M
Genetic	PKD1	+	–	–	+	–	+	–	–	–	++	+	+	+	+	–	–	–	=
	ED IV	–	++	–	+	++	++	+	–	–	+	+	+	–	+	–	+	+	+
	FMD	+	–	–	–	–	–	+	++	–	–	–	++	++	+	+	–	+	++
	Marfan	–	+	–	+	+	+	+	–	–	–	–	–	–	–	–	–	–	=
	Familial I	+	–	–	–	–	–	++	–	–	+	–	++	+	+	–	–	–	+
	Familial II (Finl)	++	–	–	–	–	–	–	–	–	–	++	–	+	+	–	–	–	–
	NF1	–	+	++	+	–	+	–	–	–	–	–	–	–	–	++	–	–	=
Metameric	Unimetameric	+	–	–	–	–	+	++	+	–	+	+	++	++	–	–	–	–	+
	Multimetameric	+	–	–	–	–		++	–	–	+	++	++	++	++	+	+	+	+
Immature	Fusion	–	+	–	–	–			+	–	++	+	–	–	–	++	–	++	+
	Branchial	–	+	+	–	+	++	++	–	–	++	–	–	–	–	–	–	+	+
Growth sprouting	Fusiform/ serpentine	–	–	++	++	–	–	–	–	–	–	+	–	–	–	++	–	++	–
	Giant	–	–	++	+	–	+	–	–	–	–	++	–	–	–	+	–	+	–/+*
Remodeling	High flow	+	+	–	–	–	–	–	+	–	+	+	–	++	–	+	–	+	=
	High pressure	++		–	–	–				+									
Dissecting	Spontaneous	– –	+	–	++	++	–	–	–	–	–	+	–	+	–	++	+	–	–
	Infectious	++			+	–	+	–	–	++	–	–	–	++	–	–	–	–	=
Immune	HIV		+	+	++	–	–	++	+	–	–	+	–	++	–	+	–	+	=
	Candidiosis		+	–	++	–	–	+	+	–	–	–	–	++	–	++	–	++	=

F/M, female/male ratio.
* Cav. Sin AA have exceptionally high female dominance.

Table 7.9. Aneurysmal vasculopathies 1: lumen herniation and lumen repair

Hemodynamic triggers	Flow, velocity, turbulence, pressure, jet effect, valve effect
Mechanical treatment	Balloons, coils, remodeling, stents, liquids, bags
Morphological assessment	3-D images, virtual arterioscopy, vessel lumen models
Future	Telenavigation, telereconstruction
Goal	Selectivity of the delivery system and accuracy of the reconstruction
Specialists involved	Surgeons, neuroradiologists, anatomists, pathologists, engineers

Table 7.10. Aneurysmal vasculopathies 7–10: vessel wall herniation and vessel wall repair

Disorders	Infectious, immune, inflammatory, constitutional remodeling defect, familial or nonfamilial, embryonic or postnatal program defects, proliferative defects
Therapeutic agents	Antibiotics, growth factors, gene therapy, cellular engineering, bioactive therapies
Functional assessment	Endothelial and wall physiology, phenotypic characteristics, mutations, molecular biology
Goal	Selective recognition of the diagnosis and focal effect of the therapeutic agent
Specialists involved	Geneticists, physiologists, pharmacologists, molecular biologists, immunologists

morphological, biological, or clinical? Does the clinical examination provide us with enough information? Is physiopathogenesis an ongoing process? Is it linear and/or reversible? Is it random or predictable? Can it be modeled? Is it created by events or on the contrary, by a lack of events? Can it sustain itself or can it induce a series of events independent of the disease itself?

The history of the disease that we diagnose is always retrospective. As a result, there is a time gap: through physiopathogenesis, we collect and attempt to understand a fragment of the past even though we do not know its beginning. History is always incomplete, because we focus on events rather than on mechanisms. The danger of physiopathogenesis lies in its extrapolation toward the future in an attempt to anticipate possible events, while ignoring whether the underlying mechanisms are still present. A model of the future is the projection of a past time interval, but does not take into account that certain influences may have changed. Answers provided by such models are never completely true, nor will they be entirely wrong. A predictive physiopathological model tends to create a fuzzy atmosphere and the possibly fuzzy management thereof should call for caution. Minute differences at the time of diagnosis may carry with them major differences in subsequent development. Actually, future physiopathogenesis is isomeric; its course most likely changes after a sequence of outside events that shift the real history of the disease from one theo-

Table 7.11. Vascular phenotypic vulnerability: variability over time

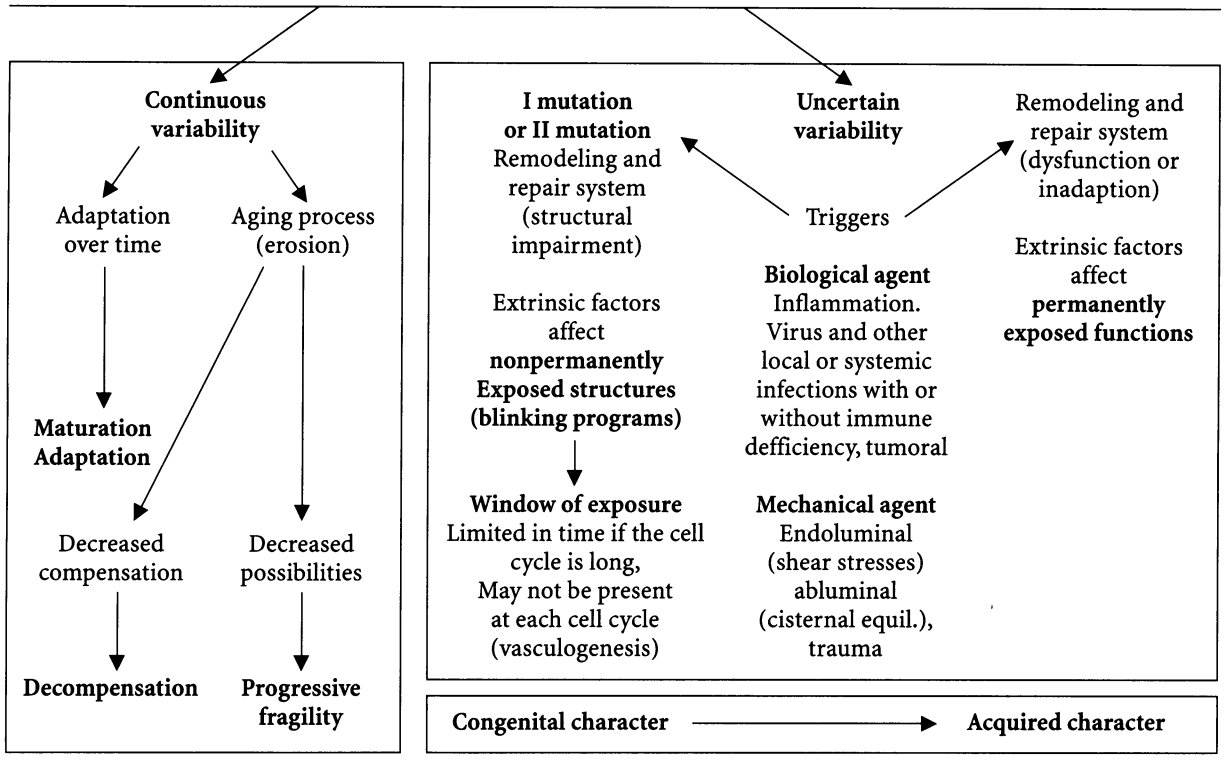
Continuous variability
Adaptation over time
Aging process (erosion)
Maturation Adaptation
Decreased compensation
Decreased possibilities
Decompensation
Progressive fragility
I mutation or II mutation
Remodeling and repair system (structural impairment)
Extrinsic factors affect nonpermanently Exposed structures (blinking programs)
Window of exposure
Limited in time if the cell cycle is long,
May not be present at each cell cycle (vasculogenesis)
Uncertain variability
Triggers
Biological agent
Inflammation. Virus and other local or systemic infections with or without immune defficiency, tumoral
Mechanical agent
Endoluminal (shear stresses) abluminal (cisternal equil.), trauma
Remodeling and repair system (dysfunction or inadaption)
Extrinsic factors affect permanently exposed functions
Congenital character
Acquired character

retical curve to another. One of the major stakes in the preventive treatment of aneurysms is probably to identify factors that stabilize or destabilize the disorder.

Because of its variability, physiopathogenesis is difficult to determine. The concept of individual host response must be introduced prior to making a management decision in a given patient. Indeed, where does the physiopathogenesis of the aneurysm belong: to the patient or the disease? The physiopathogenesis, as established from a heterogeneous population, tends to average out information, decisions, and ultimately the outcome.

7.1.2.1 Classification

Traditionally, aneurysms are classified according to their physiopathology. The diagnosis begins with the discovery of an already-formed aneurysm. Aneurysms, although discovered in similar clinical contexts, may result from entirely different diseases processes, i.e., bacterial or viral infections; traumatic or spontaneous dissections; familial or isolated aneurysms, flow-related in cerebral AVMs; multifocal, unilateral, or mirror aneurysms; multiple, supratentorial, or infratentorial aneurysms, etc. (Table 7.8). Crude as this list of dissimilar disorders may appear, aneurysms are often discussed as if they were of a single type before deciding on a treatment plan. The differences in pathologies are often ignored while presenting results. However, the goal of the treatment cannot be identical for each type of

aneurysm. Physiopathologies may not be pooled and subsequently applied to each case.

Additional issues remain, such as the significance of mirror aneurysms. Why are aneurysms not diagnosed in children with polycystic kidney disease, but only later at adult age, yet some 10 years earlier than in the population without polycystic kidney disease? Other unanswered questions relate to the difference in the location of aneurysms, arterial hypertension, flow-related aneurysms, and isolated saccular aneurysms. Aneurysms are never found in very-high-flow arteriovenous fistulae in children and unruptured AAs are not found in autopsy series in the pediatric population. Saccular aneurysms have not been demonstrated to become giant or fusiform aneurysms. Flow-related aneurysms do not rupture once the AVM has been treated, and subsequently they often regress. There are certain anatomical locations such as the branches of the splenic artery in portal hypertension where aneurysms tend to develop, even enlarge, but seldom rupture. The regression of flow-related aneurysms and occasionally so-called berry AAs (Fig. 7.118) raises speculation on whether the body continuously develops aneurysms but is capable of repairing them before rupture occurs. Therefore, aneurysms could be considered the result of two simultaneous processes: their production and the failure of the vessel wall to repair them.

The higher incidence of intracranial aneurysms in women in the adult population is reversed in the pediatric population, where the male-to-female ratio varies from 3:1 in children up to 8 years of age to a nearly equal ratio of 1.2:1 in the 10- to 20-year-old age group (George 1989; Heiskanen 1981; Meyer et al. 1989; see Vol. 3). The change in sex ratio occurs in the fifth decade (male to female, 0.9:1) and reaches 1:3 in the seventh decade.

All these questions reflect our lack of knowledge and the need for improved understanding. As was the case in genetics, our ability to classify each type of aneurysm in a given disease class requires the in-depth study of the morphological (Campos 1998a, b; Mazighi 2002), clinical, biological, and genetic context in which the aneurysm occurs. As a result, the aneurysm population will need to be more subdivided to facilitate a homogeneous analysis and adjusted therapeutic prevention.

7.1.3 Segmental Vulnerability

Both the construction and the maintenance of blood vessels involve repetitive steps and feedback to the vascular tree. Construction of a vascular structure is the result of complex biological factors and events starting in the embryo, which continue in the fetus, neonate, and small infant. The vascular tree is maintained, repaired, and modified according to metabolic demand, resulting over time in a renewal of the entire structure. This is genetically programmed and controlled. Vascular remodeling is an active and adaptive process of structural alteration. It includes changes in at least four cellular processes: cell growth, cell death, cell migration, and production or degradation of extracellular matrix. Shear stress activates a genetic program that alters the balance of the mediators of remodeling. It activates the transcription of genes for factors such as nitric oxide syn-

thase, platelet-derived growth factor (PDGF), and transforming growth factor $\beta 1$ (TGF$\beta 1$) (Gibbons and Dzau 1994). However, alterations in the program or the cellular logistics to achieve it will result in a different reconstruction (Table 7.11).

Time naturally decreases the capacity of the vessel wall to adapt to variations in the hemodynamic parameters, or to compensate for stressful events. This progressive aging process changes the options of the system and is an acquired vulnerability of the vessel wall, which will be different at different ages of the vascular system, and will differ in males and females.

The remodeling capability of the vasculature emphasizes the possibility of repair of the arterial system. The actual appearance and eventual formation of an AA, through the various cell cycles, indicates the failure of that repair system at a given period in time, or the persistence of the abnormal triggering factors responsible for the failure of the remodeling processes.

Several situations that alter the luminal information given to the vessel wall will subsequently lead to the development of an AA. Thus the AA becomes the expression of normal vasculature abnormally triggered and is the expression of a biological process. The disease is not at the vessel wall level but is caused by various triggering factors that impact the wall; correction of these factors is likely to free the remodeling system to repair.

Three types of AA belong to this group: flow-related AA, nondysplastic dissections, and infectious (nonimmune-related) AA. Each of them impairs the vasculature differently and uses different triggers to produce an AA; however, they can all repair spontaneously or after correction of the causative factors (Figs. 7.110, 7.116–118). The topography of the flow-related AA is not the same as that of the isolated saccular intradural AA (Table 7.36). The distal location on the arterial tree of the middle cerebral artery (MCA) or posterior cerebral artery (PCA) in the infectious AA is highly suggestive of this diagnosis. Dissecting AAs are common proximal to the vertebrobasilar junction in elderly people and in the Asian population or at the intradural internal carotid level and the P1–P2 junction of the PCA in young Western patients. This geotropism expresses yet another structural propriety of the arterial system, which translates into a segmental vulnerability.

Arterial segmental specificities suggest an invisible discontinuity in an apparently anatomical, histological, and hemodynamic continuous system. Many of these regional specificities have been commented on in Vol. 1, such as the extravascular spaces, the wall itself, and the flow conditions, among other factors (Table 7.12) (Fig. 7.1).

In addition to these anatomical and physiological conditions, a less obvious characteristic identifies consecutive arterial segments: their phylogenetic age. The cerebral arteries in humans appeared as the result of various selections and maturation processes over approximately 100 million years. Phylogenetic steps indicate the different generations or ages that coexist in two consecutive arterial segments. The M2 branching tree appeared and developed since the appearance of birds, while the M1 segment had already existed for a few million years in fish. A given triggering factor will recognize such a difference; in other words, the resistance, bio-

Table 7.12. Environment

Epidural venous plexuses
Hemodynamics
Subarachnoid cisterns
Vasa vasorum
Pericytes
Perivascular monocytes
Glial relationships
Innervation

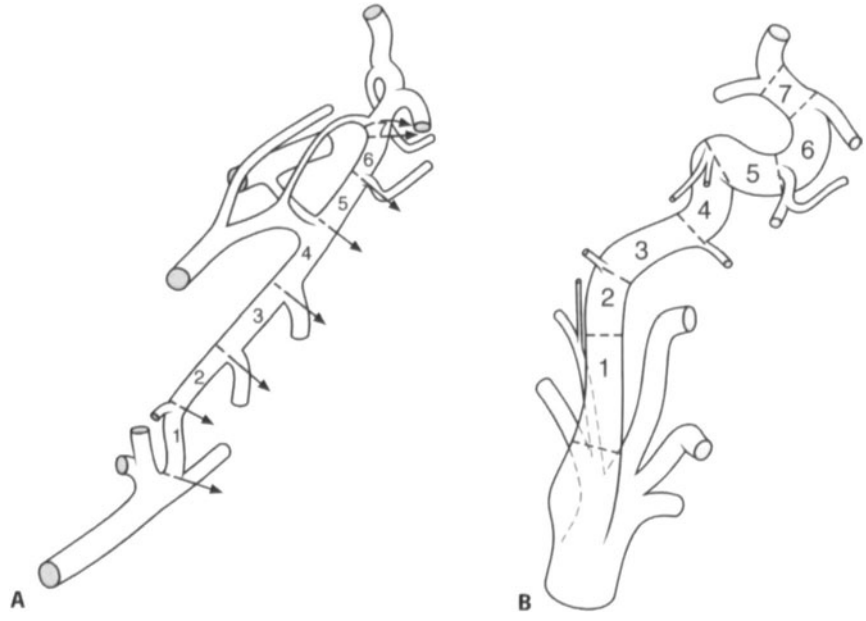

Fig. 7.1A, B. Schematic representation of the internal carotid artery (ICA) segments as they result from embryology. Note the proximal margin of the first segment is distal to the common carotid bifurcation. **A** ICA embryological segments; **B** ICA segments (see Vol. 1)

logical stability, and vulnerability of these consecutive segments are not the same.

The developmental sequence of the various arterial segments explains why certain diseases have an impact on some areas while sparing others. The resulting lesion involving a segment can be either acquired or congenital (Table 7.13):

- A group of normal cells shares a specific characteristic (stabilized during the evolution of the species) that creates a permanent recognizable identity. That identity, be it a strength or a weakness, belongs to the normal development of that segment. Highly specific triggers similar to antibodies can recognize this identity and may focally impair that segment.
- A defect occurs in a mother cell and is subsequently transmitted; that characteristic has a clonal distribution. It is present in topographically regrouped cells. The vulnerability is structural and represents a quiescent weakness, permanently recognizable by a trigger. It can also be episodically exposed (window of exposure), depending on the system involved; the character is secondarily recognized and the lesion revealed by a nonspecific trigger.

7.1.3.1 Embryological Origin

Such an approach to the aneurysmal vasculopathies modifies the way one looks at AAs and facilitates the acceptance of clinical differences among apparently identical lesions from a strictly morphological point of view. The association with anatomical arterial variations raises yet another type of hypothesis for AA development. The stability (degree of variation) of the patterns of arterial supply decreases from the spinal cord (and ex-

Table 7.13. Postulated origin of intracranial aneurysms

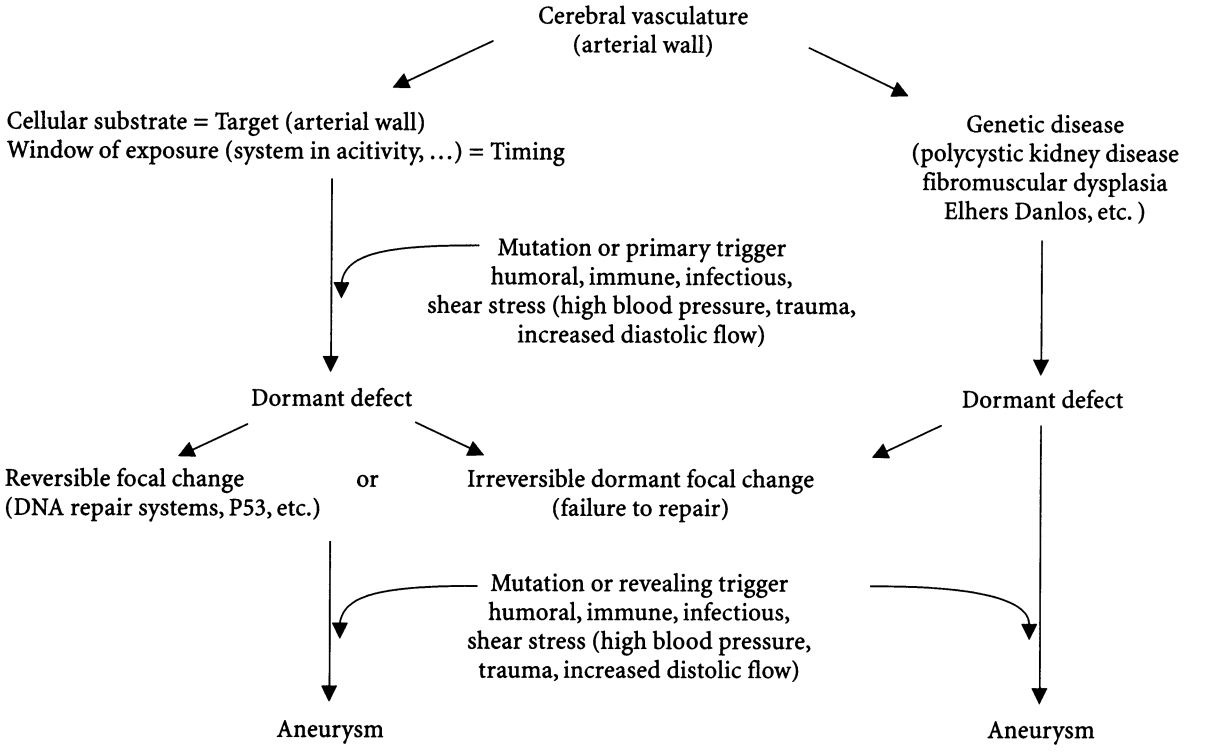

Table 7.14. Angiogenic activity from postnatal to vasculogenesis

Angiogenesis
Angiogenesis (postnatal) (endothelial cells, muscle cells, and matrix) is involved in maintenance, repair, regeneration, adaptation to needs, and response to injury. It includes arterial and venous remodeling and neovascularization
Angiogenesis (in utero) corresponds to longitudinal organization of existing vascular channels (the first vessel to be formed in such a way is the vertebral artery). It is associated with vascular growth (patterning), arterial wall production, and capillary lumen fusion (ectasia). It includes lumen production from capillary budding (neovascularization)
The first remodeling of the earliest network adjusts to flow conditions and maturation from shear stress signals in the recently developed vascular cord networks
Vasculogenesis
The maturation process of the arteries at the base of the brain implies: *fusion* of ventral longitudinal neural arteries (anterior spinal, basilar, azygos artery) and *regression* of embryonic channels (ophthalmic, trigeminal, hypoglossal). Such fusion and regressions suggest cell *selection* (apoptosis). Failed fusion of the ventral longitudinal arteries will result in caudal basilar fusion, fenestrations, or incomplete maturation of branchial arteries. Therefore, persistence of embryonic arteries suggests poor cell selection
During the early stages of vasculogenesis, a capillary network from mesoderm-derived angioblasts (endothelium) and cranial neural crest (media) forms and follows a regional cerebrofacial organization, similar to a cephalic metameric organization (vegf 206) (Couly et al. 1995; Etchevers 2001; Campos et al. 1998b)

ternal carotid artery) to the rostral end of the central nervous system; the latter were transformed dramatically during the last stages of evolution and did not fully stabilize optimal dispositions, therefore retaining some old functions (so-called embryonic persistence). The maturity of the system is expressed by the accomplishment of various construction and regression programs (of the previously used patterns deleted in the most common anatomical arrangements), as established by dissections in normal specimens. Vascular construction and maintenance involve three mechanisms: vasculogenesis, angiogenesis, and remodeling. Remodeling has been addressed above and most of its phases are explained in Vol. 1. It is the response of the vessel wall to external triggers, aimed at preserving the integrity of the vascular structure. Remodeling occurs as the vascular system starts to function and remains as its repair and maintenance (Table 7.14).

Table 7.15. Clonal mutation/clonal phenotype

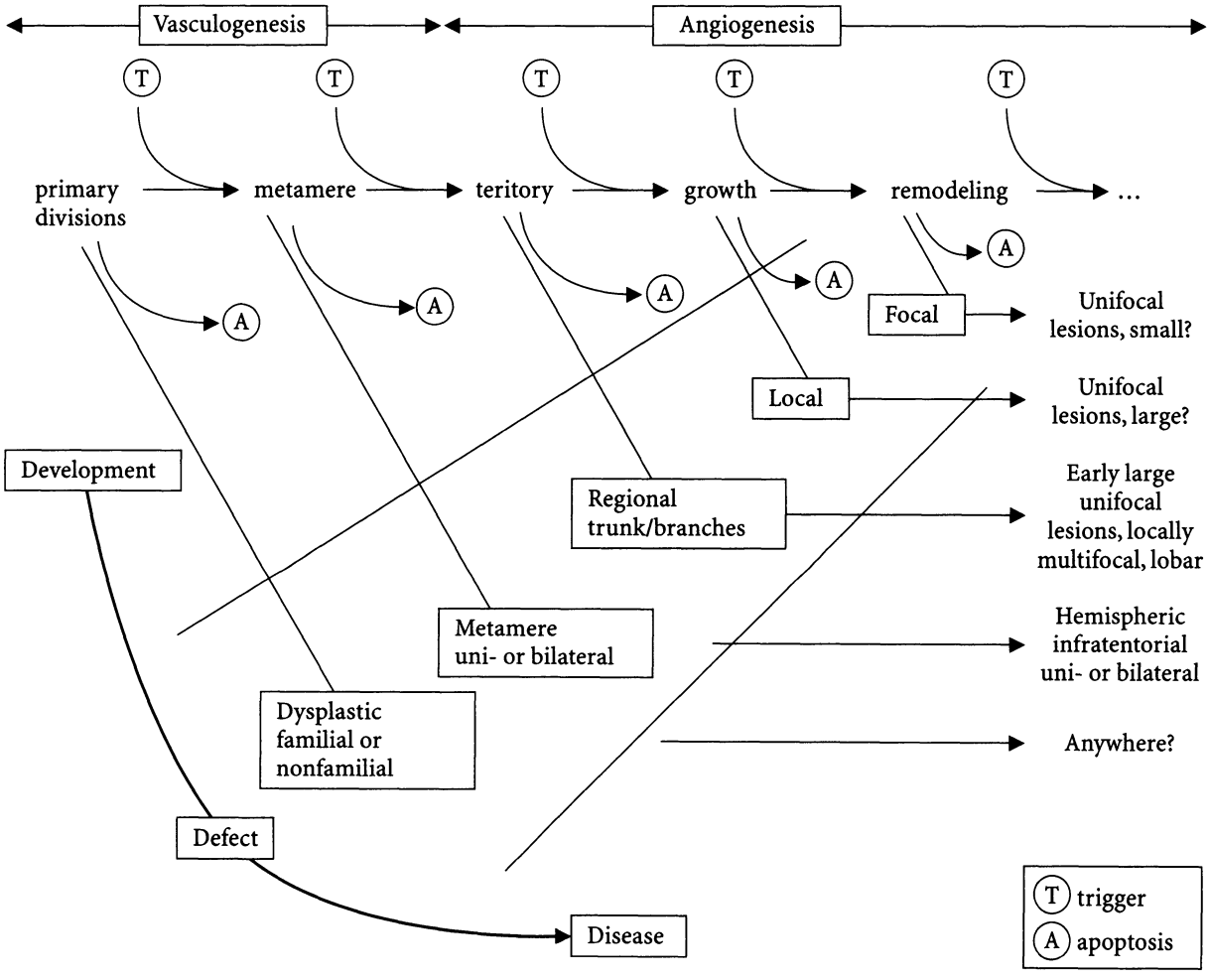

Specificity of the timing (window) and a specific trigger: a mutation involves a clone of cells.
Specificity of the character and recognition by the trigger: a genotype or phenotype shared by a group of cells at a certain moment creates an identity, thus a recognizable group.

While the developmental program is being executed, various events will generate different types of associations with certain aneurysms depending on the timing of the impact of the trigger (Table 7.15, p. 379). The associated arterial anatomical variation then becomes a time marker.

- Germinal mutations or familial diseases randomly affect the arterial system and involve various cephalic metamers.
- Early somatic mutations cause a metameric distribution of lesions, the so-called mirror locations of aneurysm that become twin AAs.
- Late somatic mutations will be associated with abnormal fusion or persisting branchial embryonic arteries.
- Growth factor disorders with or without dissection, resulting in vessel wall proliferative processes leading to fusiform or giant aneurysms.
- Abnormal vascular remodeling due to flow or pressure disorders, occurring later, will alter long-term programs and potentially cause aneurysms that may rupture.
- Vessel wall aggression by unpredictable extrinsic factors such as infectious agents are another cause of aneurysm development.

Each one of these disorders (each contributing to a time-marking process) may lead to clinical, morphological, and topographic phenotypes that currently make up the core of modern classifications. For each of them (Table 7.15), we should be able to trace the physiopathology, with its implications for the natural history of the disease, and compare the proposed treatment with the calculated prospective risk.

7.1.3.2 Age of Aneurysms

Although the acquired aspect of aneurysms has often been emphasized (Schievink 1997), one cannot help but realize that they do not develop haphazardly with time. Determining the real age of the AA is therefore an immediate challenge (Table 7.16). We must accept that aneurysms are the visible part of an iceberg, and that they combine and reflect the following in reverse order:

- A symptomatic clinical stage (due to compression, vascular accident, SAH, etc.). This clinical stage results from the collective effects of decompensating factors affecting the previous stage. Rupture of an aneurysm results from the vascular wall failure to produce the necessary quality or quantity of wall components quickly enough. Rupture is a biological event.
- An asymptomatic clinical stage. This is a morphological phase during which aneurysms slowly develop without disturbing the organism's stability, until triggering factors make them symptomatic. This is also the stage during which prevention of bleeding from unruptured aneurysms is currently being discussed. The identification of triggering factors appears to be a key element to prevent an asymptomatic aneurysm from progressing to the symptomatic phase. The clinically asymptomatic morphological stage (of unknown duration) results from the incapacity of the body to repair the previous biological stage.

Table 7.16. Age of vascular lesions

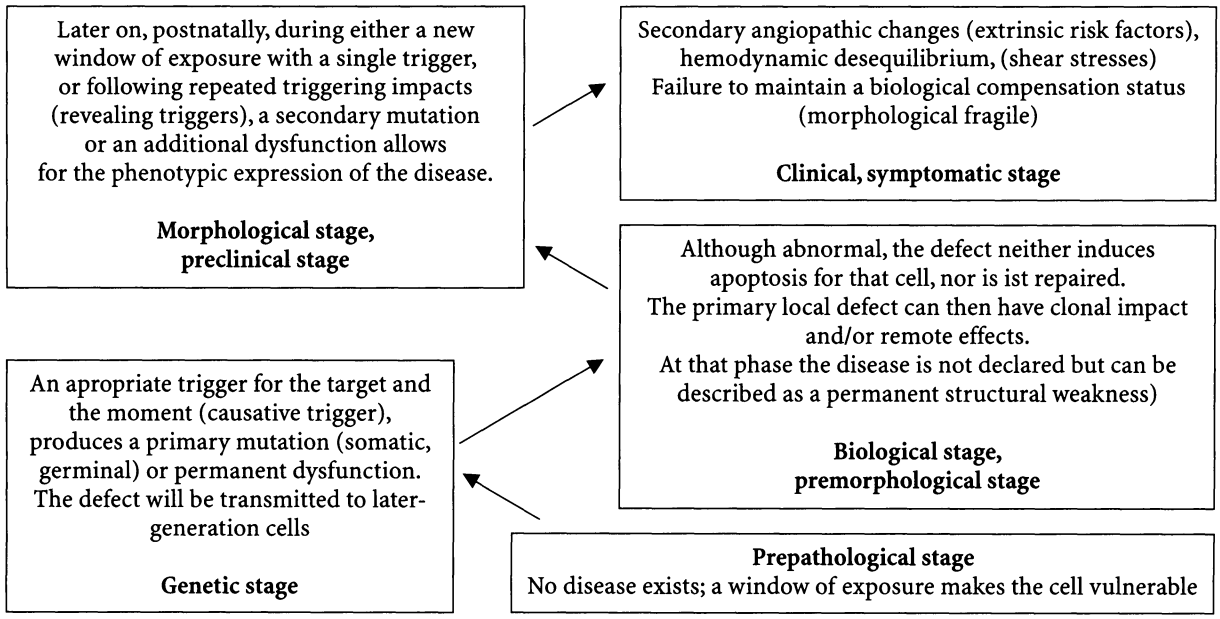
Later on, postnatally, during either a new window of exposure with a single trigger, or following repeated triggering impacts (revealing triggers), a secondary mutation or an additional dysfunction allows for the phenotypic expression of the disease.
Morphological stage, preclinical stage
Secondary angiopathic changes (extrinsic risk factors), hemodynamic desequilibrium, (shear stresses) Failure to maintain a biological compensation status (morphological fragile)
Clinical, symptomatic stage
Although abnormal, the defect neither induces apoptosis for that cell, nor is ist repaired. The primary local defect can then have clonal impact and/or remote effects. At that phase the disease is not declared but can be described as a permanent structural weakness)
Biological stage, premorphological stage
An apropriate trigger for the target and the moment (causative trigger), produces a primary mutation (somatic, germinal) or permanent dysfunction. The defect will be transmitted to later-generation cells
Genetic stage
Prepathological stage
No disease exists; a window of exposure makes the cell vulnerable

- A biological stage. This is the stage during which the disorder becomes ingrained in the cell and is subsequently detectable by triggering factors, (whereas it was dormant before) if biological repair fails to occur. The biological stage varies in duration. It seems to be very long in cases of germinal mutations. Over this long time period, an inversion of the male–female ratio becomes apparent, thought to be due to hemodynamic triggering factors (hypertension, high flow), general stress, smoking, estrogens, etc. Some have suggested that a secondary mutation occurs, to explain that a genetic disorder may lead to a local disease, even though arteries and veins are all carriers of the same defect. The mutation may involve the loss of the normal allele or a mutation impeding the compensation of the initial abnormality (Tables 7.13, 7.15).
- A prepathological stage. This applies to somatic mutations. The time at which they occur determines the risk of contracting a multifocal disorder. The developing endothelium and pericytes (Le et al. 1998; Carmeliet 2000) are exposed to various agents, depending on their degree of vulnerability at a given phase of the development.

Formulating hypotheses and raising questions are stepping stones toward knowledge. The fourth dimension, time, has been introduced over the past few years to explain physiopathological mechanisms, with the extremes being apoptosis and cellular immortality. Situated in between is biological aging. Congenital or acquired arterial wall weakness, triggered by intrinsic or extrinsic agents, may lead to proliferation or apoptosis of the arterial layers. Saccular, berry, single, multiple, mirror, infectious, immune, inflammatory, dissection, giant, fusiform, and flow-related AAs can all be discussed using this simple framework.

The rest of the chapter will be devoted to specific aspects of AA according to what is known, confirmed over time, and part of our clinical experience. The so-called berry AA will be discussed for what it is: a shape, a target, a challenge but not a disease entity. Many diseases can give a berry AA. The simplistic nature of our tools should not mask the complexity of the diseases for which we use them. Extradural AA, familial and multiple AA, dissections and giant AA, infectious and immune AA, and flow-related AA will then be discussed prior to making general recommendations for therapeutic strategies.

7.2 Extradural Aneurysms

7.2.1 Introduction

Aneurysms of the extradural carotid and vertebral arteries are significantly less common than intracranial aneurysms, and their real incidence is not known, (Margolis et al. 1972). They are usually described in relation to the vessel involved, or their etiological origin when it is known. They most frequently involve the internal carotid artery, then the vertebral artery, and rarely the external carotid artery and its branches.

The most likely etiological cause varies depending on the location of the aneurysm, the age of the patient, and the type of population analyzed. In general, lesions may be secondary to arteriosclerosis, structural familial or nonfamilial vessel wall diseases, trauma, infection, radiation, or special flow conditions. In some cases no preexisting or associated abnormality can be found.

7.2.2 Extradural Internal Carotid Artery Aneurysms

Extradural aneurysms most frequently involve the internal carotid artery and the most commonly affected area is the cavernous segment (Table 7.17). Symptomatic cavernous aneurysms are often larger than 2.5 cm and therefore are classically referred to as giant aneurysms. In the literature, they are usually discussed together with the intradural aneurysms. When larger than 25 mm, they account for 5% of the giant AAs reported by Drake (1979) and 39% of those reported by Morley (1969). However, their true incidence in relation to other extradural carotid aneurysms is unknown.

Table 7.17. Extradural internal carotid aneurysms, etiology and location

Location		Congenital developmental	Traumatic	Mycotic	Atherosclerotic
Cervical	6 (91.5%)	2 (33%)	3 (50%)	–	1 (16%)
Petrous	5 (8.7%)	–	5	–	–
Cavernous	46 (80.0%)	40 (87%)	6 (13%)	–	–
Total	57 (100.0%)	42 (73.6%)	14 (24.5%)	–	1 (1.7%)

Fig. 7.2 (*left*). Common carotid artery angiogram in a patient with a large pulsatile neck mass following placement of a central venous line. Note a small dissection at the mouth of the large pseudoaneurysm (*double arrow*). The false aneurysm was surgically resected

Fig. 7.3 (*right*). A 73-year-old male patient with epiglottic cancer who was operated on in 1993 and received chemotherapy and radiation therapy for recurrent tumor in 1995. Post-radiation ruptured common carotid artery false arterial aneurysm. Note also the post-radiation dysplastic changes involving the cervical internal carotid artery

In a previous experiment of 53 internal carotid artery aneurysms (Table 7.17), 83% were in the cavernous segment, 7.5% were in the petrous segment, and 9.5% were located in the cervical internal carotid artery. In this selected population, some cervical and bifurcation aneurysms might not have come to the attention of the interventional neuroradiologist, as these are usually treated surgically.

In our experience, aneurysms of the common carotid artery were most frequently traumatic. In the past, infectious aneurysms were seen more often, but these are now relatively rare (Houser and Baker 1968). False aneurysms (Figs. 7.2, 7.3) have often been reported following attempted placement of a central line.

The most frequent type of aneurysm involving the cervical internal carotid artery is referred to in the literature as congenital or developmental (Fig. 7.4), followed by traumatic, arteriosclerosis, and mycotic pseudoaneurysms.

At the level of the petrous segment of the internal carotid artery, they are most often traumatic in origin (either secondary to blunt trauma or iatrogenic following biopsies of the aberrant position of the internal carotid artery), and they are rarely dysplastic in origin.

At the level of the cavernous carotid artery, 86% of aneurysms have been called congenital in origin, emphasizing that their size and shape cannot be subjectively correlated to any form of flow condition. It is difficult to exclude the possibility that some of these lesions are of arteriosclerotic origin, in particular large AAs that are partially thrombosed.

Specific attention should be paid to the vascular anastomoses along the base of the brain and the possible effect of increased flow in the con-

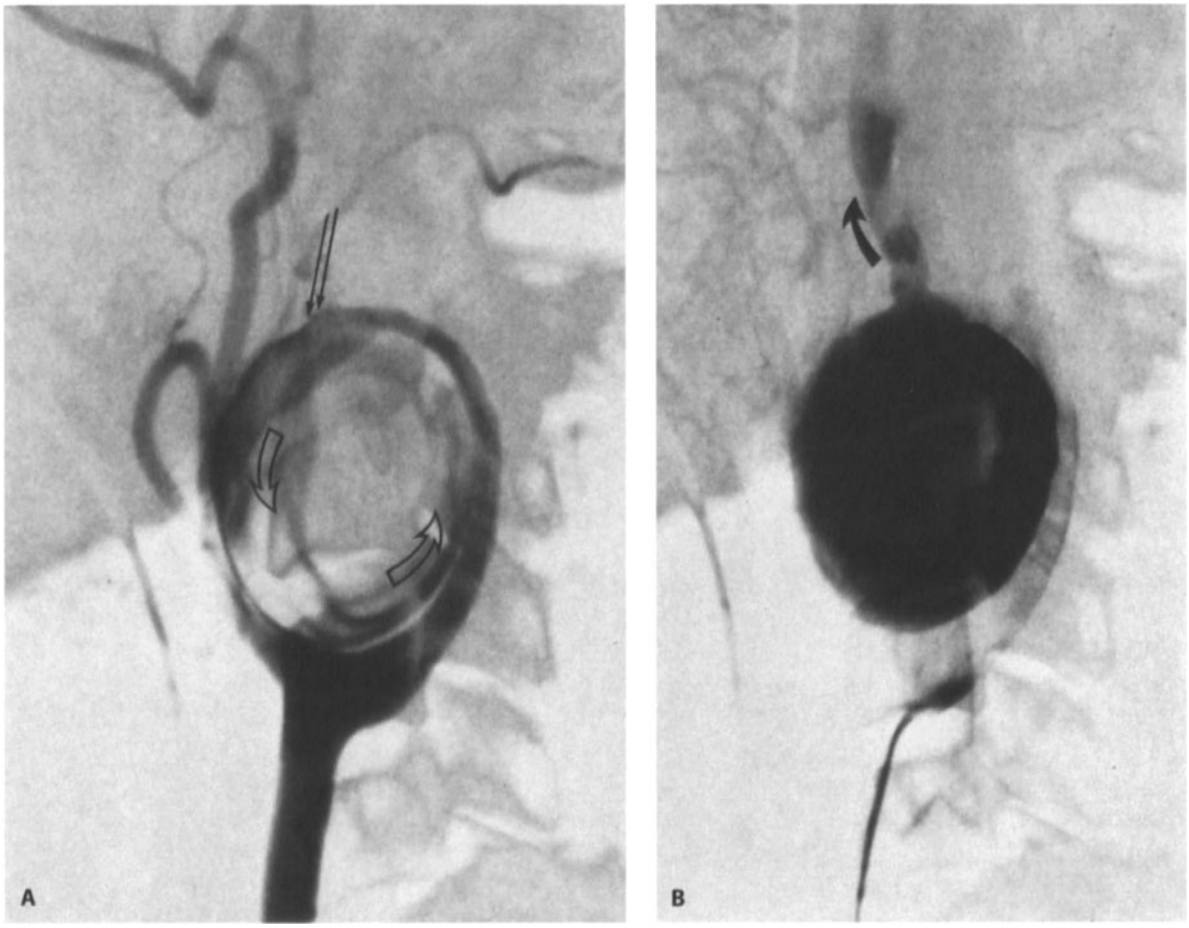

Fig. 7.4A, B. Left common carotid artery angiogram. **A** Early and **B** late phase, from a 32-year-old female patient with a cervical pulsatile mass. Note the turbulent flow (*open curved arrows*) and the entry point (*double arrow*) into the arterial aneurysm. The distal internal carotid artery is well opacified (*curved arrow*)

tralateral ICA if sacrifice of the ipsilateral ICA harboring the AA was contemplated. The study of the posterior circulation is equally important in these circumstances.

7.2.2.1 Cervical Internal Carotid Aneurysms

The most frequent and clinically serious presentation of carotid aneurysms is related to distal embolism, which in our experience occurred in over 60% of cases. Other symptoms vary according to the location of the aneurysms: a pulsatile mass in the oropharynx or neck, murmur, and Horner's syndrome. The aneurysms can be asymptomatic (Wychulis et al. 1964) or may have a long silent period. Often the symptoms are vague or nonspecific (e.g., headaches, tinnitus, or vertigo) (Boatmann and Bradford 1958; Winslow 1926), and are therefore neglected. The patient may then present when the aneurysm has ruptured with interstitial or external hemorrhage. Unruptured aneurysms have been misdiagnosed as pharyn-

geal masses and profuse hemorrhage has been encountered at the time of incision or biopsy. Spontaneous severe epistaxis and bleeding from the ear have also been reported (Harrison 1954; Young 1941), although these events are significantly more common in higher petrous aneurysms (Barrett and Lawrence 1960; Ehni and Barrett 1960) (Fig 7.22). Acute local mass effect can produce airway obstruction (Fig. 7.15). Local neural compression usually involves the lower cranial nerves, producing a retropharyngeal syndrome.

Developmental Aneurysms

The diagnosis of a congenital or developmental aneurysm is often made by exclusion when there is no previous history of trauma, infection, or sign of arteriosclerosis (Alexander et al. 1966; Melot et al. 1966). Margolis (1972), in his review of 20 aneurysms involving the cervical portion of the internal carotid artery, found that developmental aneurysms were the most frequent (35%), similar to our experience (33%). The coexistence of other aneurysms (primarily intracranial aneurysms) is suggestive of congenital aneurysms (Duplay et al. 1957; Houser and Baker 1968; Kramer 1969; Manelfe et al. 1974), polyarteritis nodosa (Rob 1954), or pseudoxanthoma elasticum (Dixon 1954). The congenital nature of the cervical aneurysms can be discussed because of their segmental distribution (see Vol. 1) (Fig. 7.1) or be made at the time of the screening examination of a

Fig. 7.5. **A** Early and **B** late phase of a common carotid angiogram. Fusiform dysplastic segmental arterial aneurysm of the internal carotid artery (ICA) in a child. The first cervical ICA segment is involved and the glomus as usual is preserved (see Fig. 7.1 and Vol. 1). (Courtesy of S. Pongpech)

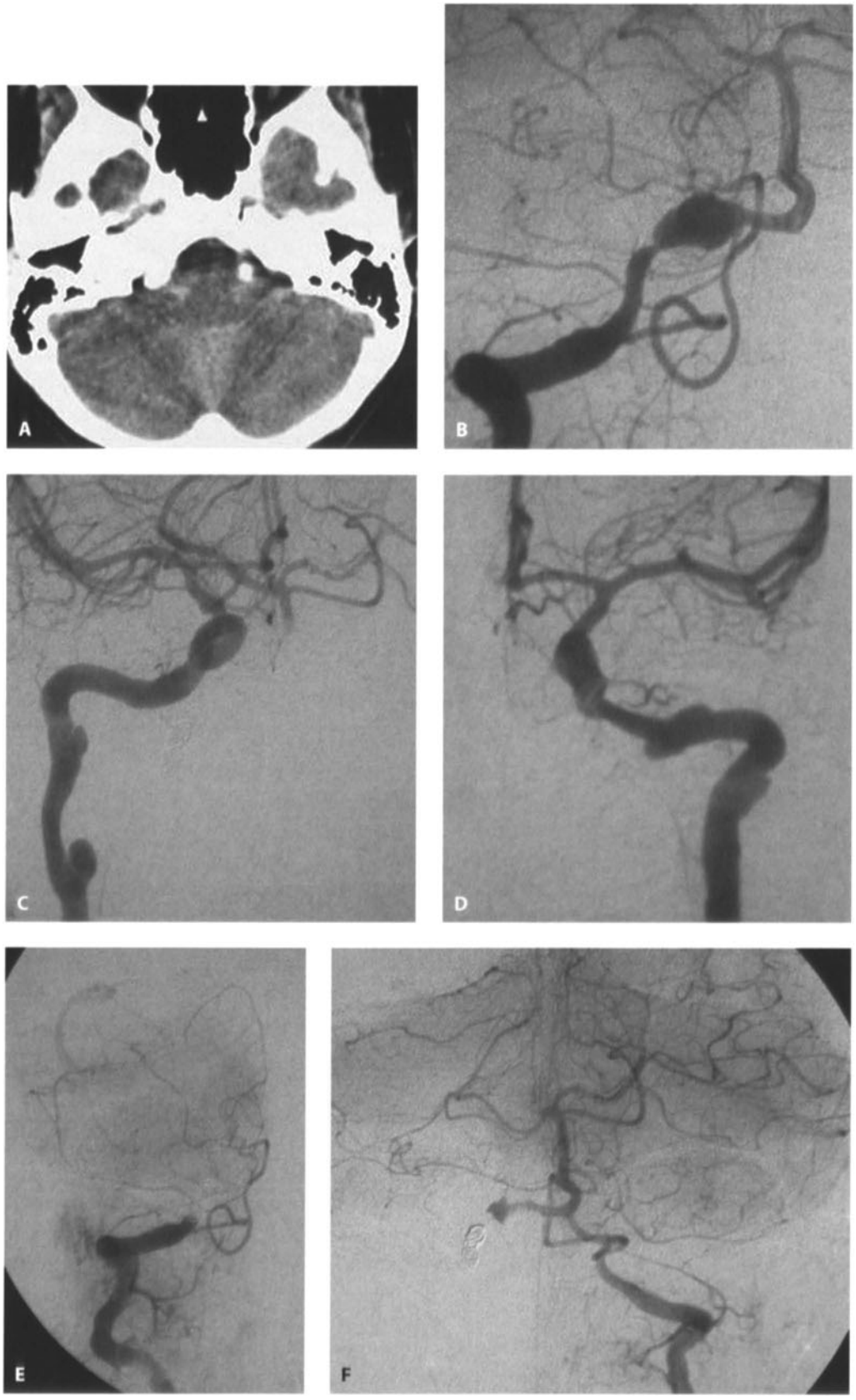

Fig. 7.6A–F. Legend see p. 387

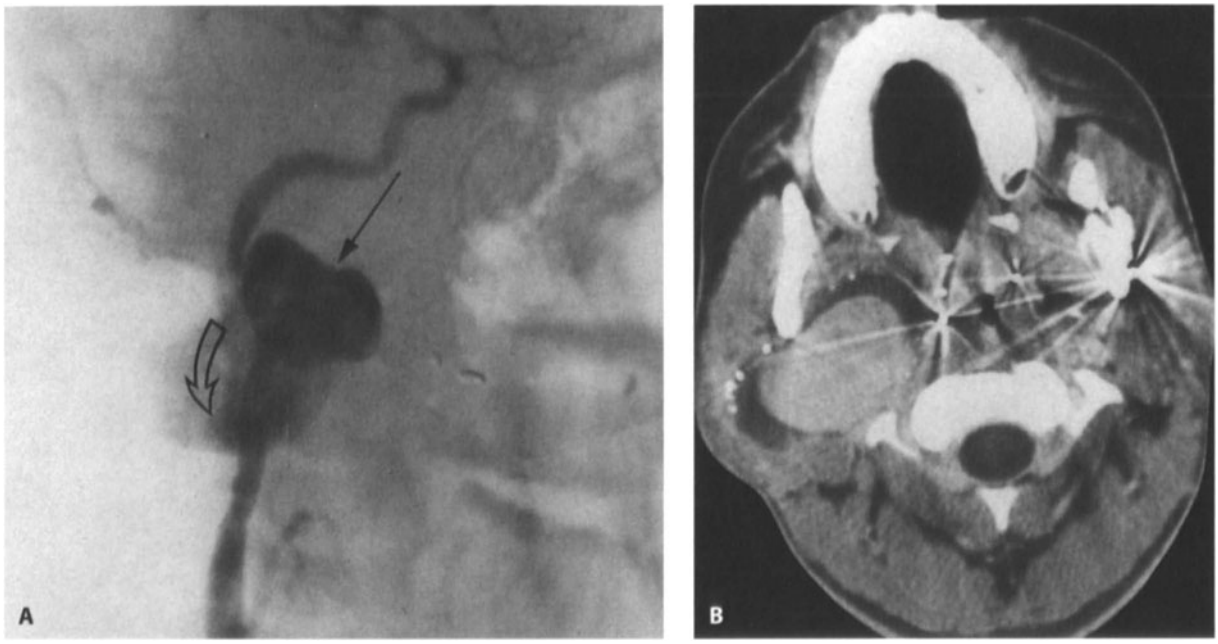

Fig. 7.7. **A** False aneurysm of the cervical internal carotid artery (ICA) following a gunshot wound. Oblique subtraction angiogram of the right common carotid artery. Filling of a pseudoaneurysm (*arrow*) followed by laminar flow into a second pouch (*open curved arrow*). Although the level of the arterial tear is well documented by angiography, the true size of the lesion cannot be fully assessed by the angiographic picture. **B** Same patient: axial CT image after IV administration of contrast material shows the true size of the false aneurysm more clearly. Note the enhancement of the patent lumen, which is surrounded by an area of low attenuation, representing the thrombosed portion of the false aneurysm. Metallic artifacts from fragments of the bullet can be seen in its trajectory

◀ **Fig. 7.6.** A 44-year-old female patient with subarachnoid hemorrhage (**A**) from an intradural dissecting arterial aneurysm distal to an extradural origin of the posterior inferior cerebellar artery (PICA) (**B**). Associated bilateral asymptomatic dissecting type of cervical and petrous internal carotid artery aneurysm (**C, D**). History of neonatal visceral perforation. High suspicion of Ehlers–Danlos type IV (ED IV) disease, despite no definite clinical evidence (two normal pregnancies). **E, F** Treatment included occlusion of the vertebral artery between the PICA origin and the dissection

dysplastic disease (Figs. 7.5, 7.6). These AAs can be associated with a carotid cavernous fistula that occurred after minimal trauma and be highly suggestive of Ehlers–Danlos IV disease. They can also be found at the time of investigation of a neck mass (Fig. 7.4).

Traumatic pseudoaneurysms are second in overall frequency but comprise the most frequent type of aneurysm involving the cervical ICA (50%) (Table 7.17) (Beall et al. 1962).

Penetrating Trauma

Traumatic aneurysms may result from penetrating injuries such as a stabbing accident, a high-velocity gunshot wound (Fig. 7.7), or from iatrogenic trauma (Teal et al. 1972) (Fig. 7.8). These injuries most often result in a false sac or pseudoaneurysm, which is produced by disruption of the arterial wall. An extravascular hematoma communicates with the arterial lumen. The fibrotic reaction produced in the surrounding tissues forms the wall of the false aneurysm (Figs. 7.7, 7.9).

Rich et al. (1970), while analyzing acute arterial injuries in 1,000 patients during the Vietnam war, found that 88% of carotid injuries resulted from shrapnel. However, carotid injuries were relatively infrequent: only 5% of all arterial injuries involved the carotid arteries. In Perry's (1961)

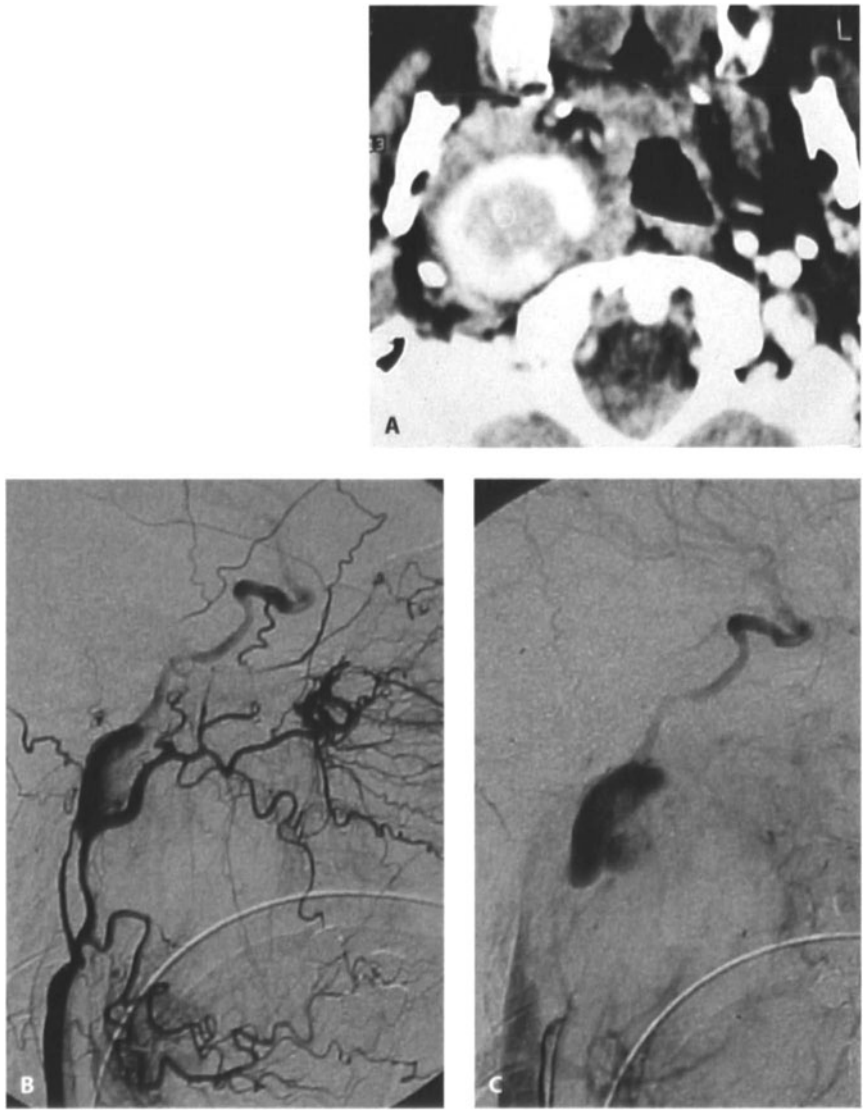

Fig. 7.8A–C. A 73-year-old female patient. Diagnosis of parapharyngeal abscess was mistakenly made on contrast CT (**A**). Direct puncture was performed and produced a severe hemorrhage requiring sedation and artificial ventilation. **B, C** A ruptured cervical internal carotid artery giant aneurysm

review of penetrating arterial injuries in the civilian population, only 7.5% occurred in the carotid arteries. Of these, 4.7% involved the common carotid artery, 1.6% the internal carotid artery, and 1.2% the external carotid artery. In 1962, Beall et al. reported an equal number (17%) of carotid injuries from stab wounds as compared to gunshot wounds.

In the pediatric population, an additional type of carotid injury may occur as a result of intraoral trauma. After a fall onto an object that enters the mouth or a fall with an object already in the mouth, an injury is produced in the tonsillar region. Bickerstaff (1964) reported that these so-called pencil injuries have a mortality rate of about 30%.

False carotid aneurysms may also occur following carotid endarterectomy, infections associated with carotid surgery, or following disintegration of silk sutures (Ehrenfeld and Hays 1972) and may progress to vessel thrombosis (Maddison 1970). Lord (1958) reported carotid injury after tracheostomy and following radical surgery, while Barrett and Lawrence (1960) reported it as a complication of mastoidectomy. Pseudoaneurysm

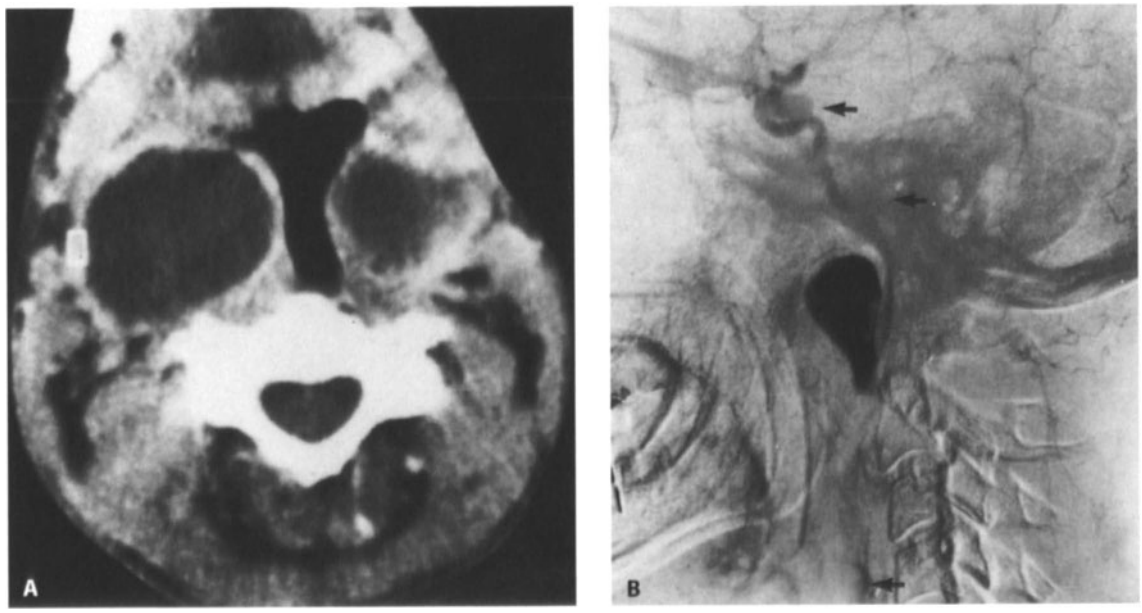

Fig. 7.9A, B. Bilateral false aneurysms following blunt (MVA) trauma. **A** Axial CT scan demonstrates bilateral large thrombosed portions of false internal carotid artery (ICA) aneurysms with encroachment on the airway. **B** Late phase of a lateral subtraction angiogram of the left common carotid artery shows the recanalized lumen of the aneurysm. Subtracted balloons (*arrows*) in the contralateral right cavernous, petrous, and cervical ICA are seen, following trapping of the right-sided false aneurysm. Prior to bilateral carotid trapping, bilateral EC–IC bypass was performed (not shown)

formation of the carotid arteries after direct internal carotid artery puncture for cerebral angiography has also been reported (Miller et al. 1977) and has occurred after radiation therapy (Fig. 7.3).

Blunt Trauma

Other mechanisms of vessel injury, for example, following blunt trauma (Beall et al. 1962), may affect the vessel wall in a manner similar to penetrating injuries. This may occur following the application of force to the angle of the mandible, which is then transmitted to the carotid wall. If the mandible is fractured, a bony fragment may lacerate the internal carotid artery (or the ascending pharyngeal artery), producing a pseudoaneurysm (Beall et al. 1962). Ingested foreign bodies also have been reported to cause pseudoaneurysms of the internal carotid artery (Morris 1969).

Blunt injuries of the cervical internal carotid artery are relatively uncommon (Davis and Zimmerman 1983; Beatty 1977; Nelson and Nahru 1963) (Fig. 7.9). The most frequent lesion resulting from blunt trauma is spasm or thrombosis (Fig. 7.10). These are followed in frequency by pseudoaneurysms, dissections, extraluminal and/or intramural hematomas (Figs. 7.11–7.13, pp. 390–392), which may then become dissecting aneurysms. Rarely will blunt trauma give rise to a complete vascular transsection or arteriovenous fistula (AVF) formation (Jiminez and Goree 1969). One form of blunt trauma involves combined rotatory

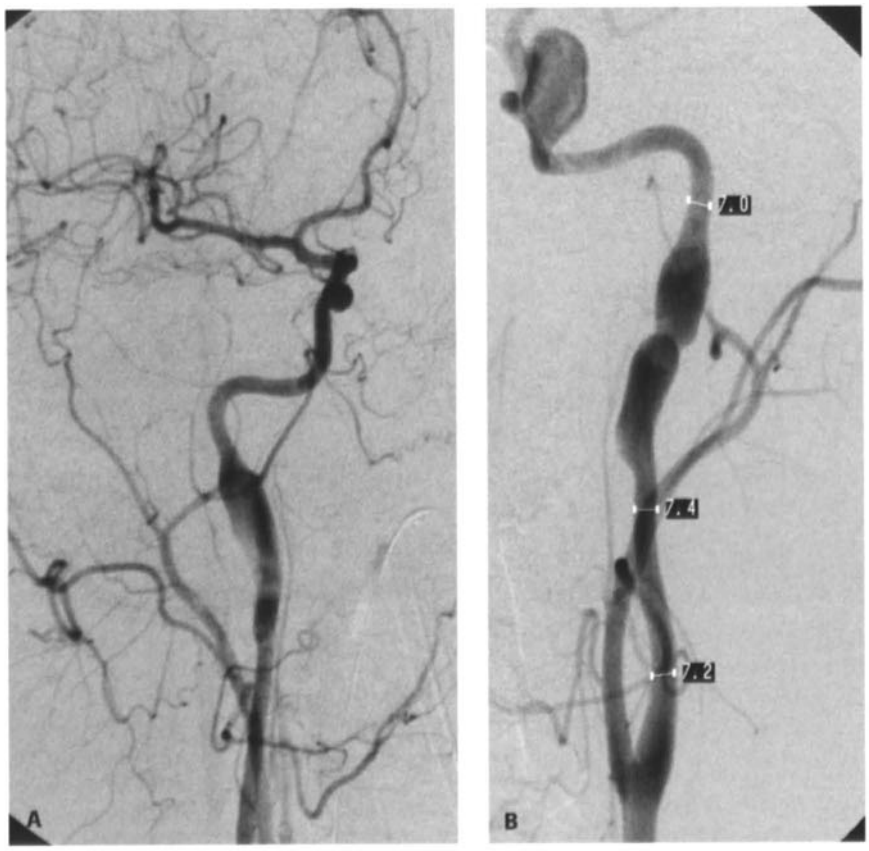

Fig. 7.10A, B. Right and left common carotid angiograms in a 29-year-old male patient. Investigation for headaches following motor vehicle accident revealed on noninvasive imaging and confirmed at angiography evidence of multiple and bilateral internal carotid artery fusiform dissecting aneurysm. Pretherapeutic evaluation before stenting repair (see Fig. 14.92)

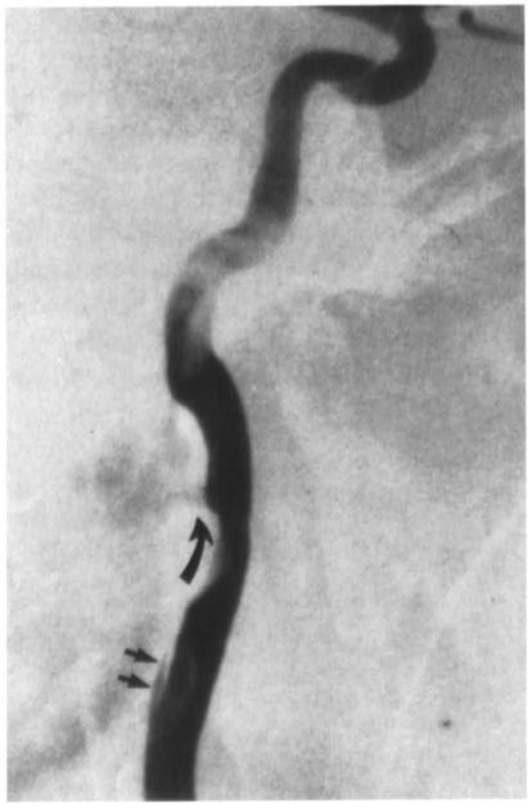

Fig. 7.11. Posttraumatic dissection of the cervical internal carotid artery (*small arrows*) with a smooth extraluminal, subintimal compression (*curved arrow*) due to mural hematoma

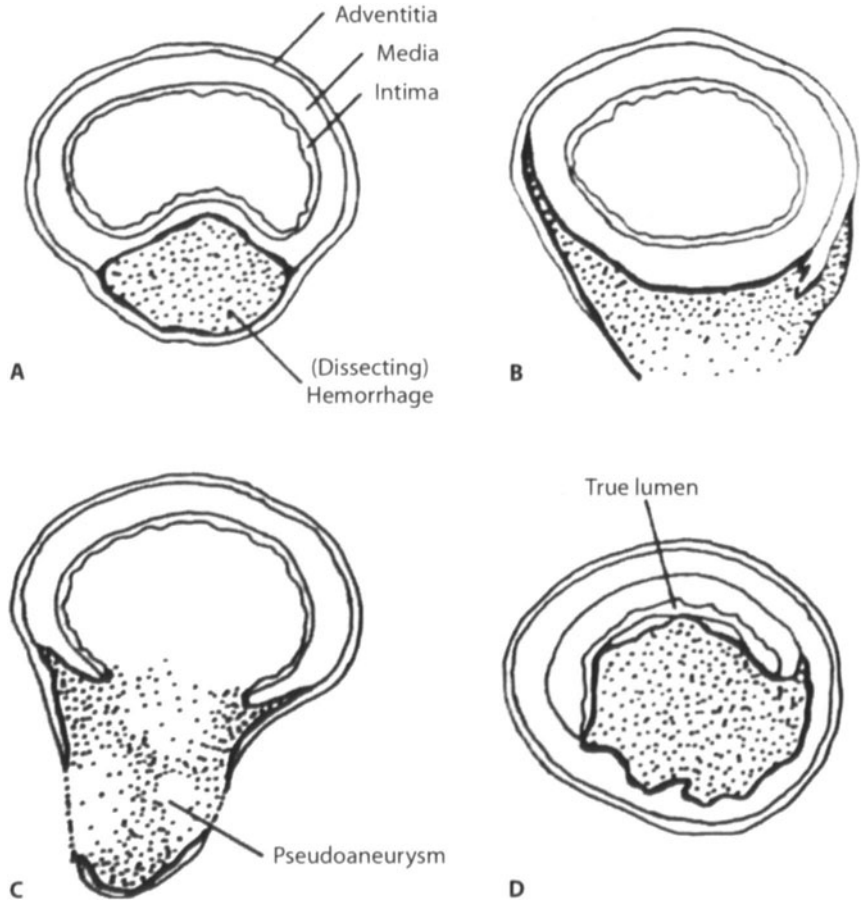

Fig. 7.12A–D. Classic types of vessel wall disruption during subadventitial dissection. (From Endo et al. 1993, with permission)

hyperextension of the neck, which stretches and compresses the internal carotid artery over the lateral mass of the atlas and axis, resulting in damage to the arterial wall. This type of injury occurs more frequently in young patients, as in the elderly loops in the carotid arteries tend to straighten before they become stretched during sudden hyperextension and rotation movements. The internal carotid artery is usually damaged at the level of the atlas (Boldrey et al.1957; New and Momose 1969). A similar injury may occur at the side of fixation of the internal carotid artery at its entry point into the petrous bone, at the level of the carotid canal (Davis and Zimmerman 1983).

The most frequent lesion resulting from cervical blunt trauma is an intimal tear with subsequent intimal dissection and thrombosis (Fig. 7.14, p. 393). Clot propagation is at least partially responsible for the high incidence of neurological complications in this type of circumstance. Soft tissue swelling may displace and compress the carotid arteries, further aggravating the already compromised lumen. In other situations, the trauma involves the adventitial layer, subsequently leading to dissection and progression toward vessel disruption or lumen reduction (Fig. 7.12). In trauma situations involving the carotid arteries, attention should be paid to the veins that are often involved and usually ignored. Emergency removal of the cervical clot may be required. ICA repair is therefore sometimes

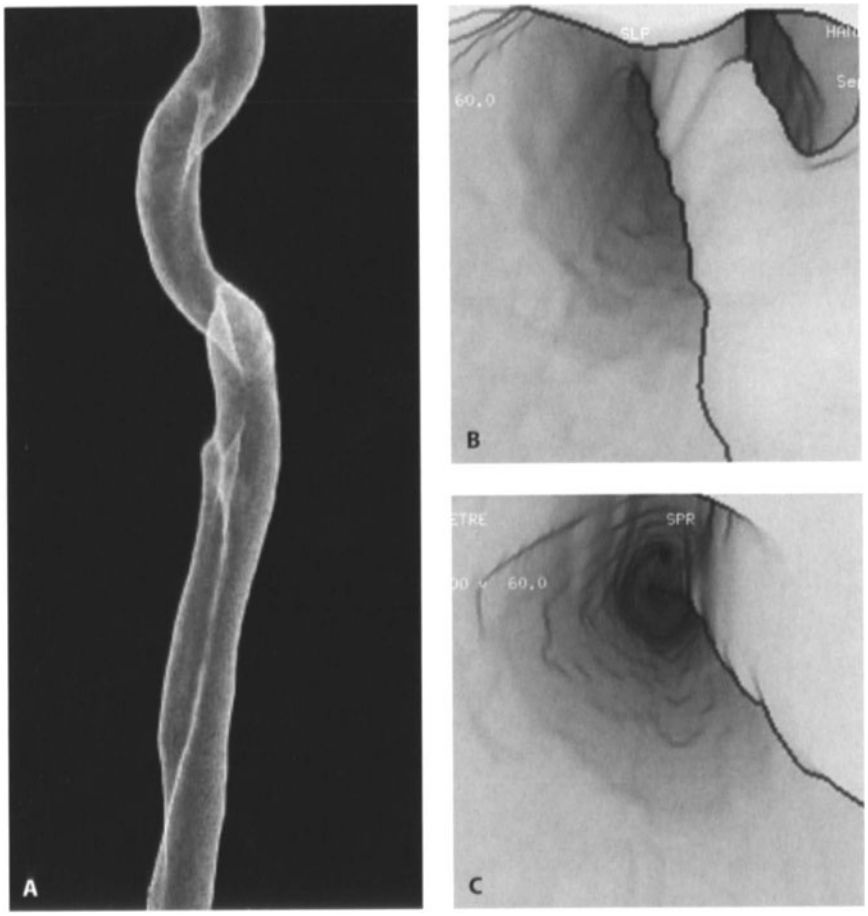

Fig. 7.13. **A** Volume rendering and **B, C** endoluminal views of cervical internal carotid artery subintimal trauma during angiography resulting in mural hematoma and endoluminal clot formation, successfully treated with anticoagulation therapy

discussed at that time as well as angiography for stenting if the patient's clinical condition permits this strategy (Fig. 7.15, p. 394).

In 1967, Yamada et al. reported the clinical significance of posttraumatic arterial thrombosis, which was associated with high mortality and neurological morbidity. The initial symptoms characteristically appear hours or even days after the initial trauma. In addition to the neurological symptoms of carotid occlusion and/or progressive thrombosis, the presence of Horner's syndrome secondary to disruption of the sympathetic fibers in the carotid wall (Yamada et al. 1967) may be an important clinical sign of carotid injury. This may be an important clue, especially when external signs of trauma are absent, as is not infrequently the case following blunt trauma (Davis and Zimmerman 1983).

Frequently, a false aneurysm of the cervical internal carotid artery protruding into the posterior pharyngeal wall is misdiagnosed as a peritonsillar abscess (Fig. 7.8).

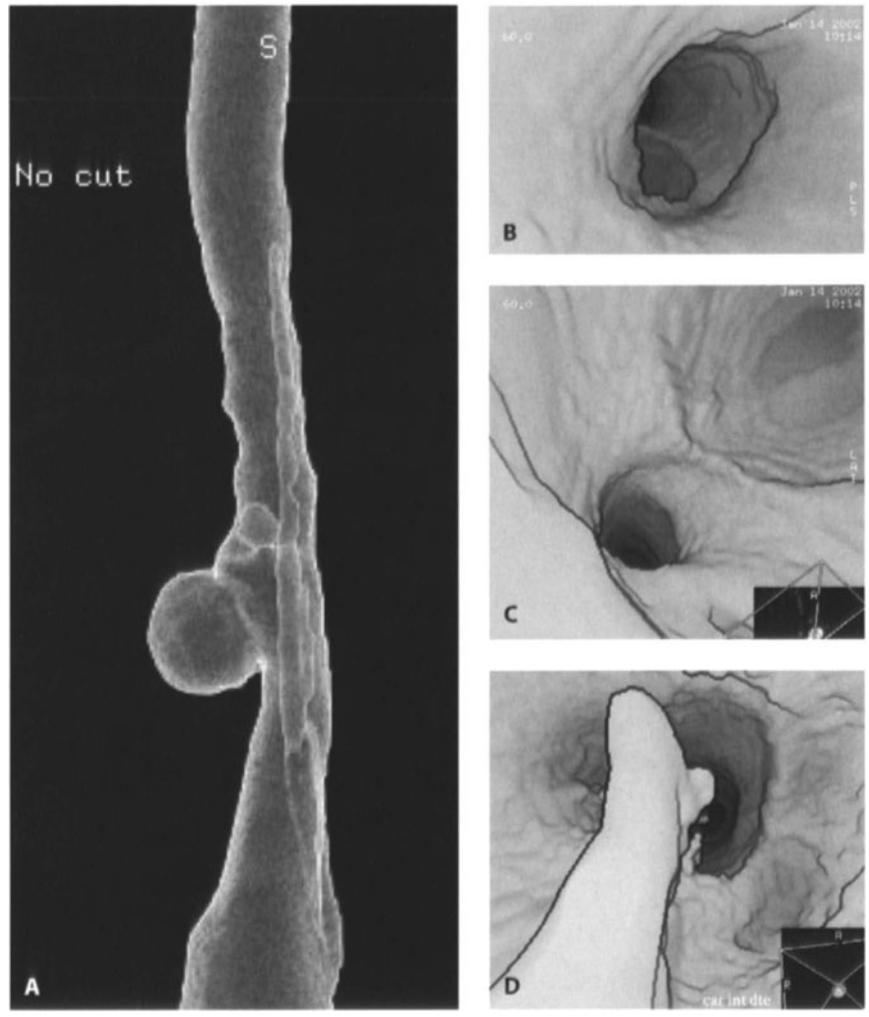

Fig. 7.14. **A** Volume rendering and **B–D** endoluminal views of cervical penetrating trauma resulting in subadventitial internal carotid artery injury. The dissection produced an arterial aneurysm, a double lumen, and endoluminal clot formation, which was managed with anticoagulation therapy

Fig. 7.15A, B. A 25-year-old female patient with a cervical gun shot wound. Large cervical hematoma was increasing rapidly in size and necessitated intubation. False arterial aneurysm on the common carotid artery was demonstrated (**A**). Immediate surgical treatment with evacuation of the hematoma and reconstitution of the internal carotid was preformed (**B**)

7.2.2.2 Acute Spontaneous Dissection of the Carotid Artery

Spontaneous dissection (SD) may occur when an intimal tear permits the extension of blood into the vessel wall with or without the formation of a pseudoaneurysm. In both traumatic (Fig. 7.16) and spontaneous (Fig. 7.17) types, the dissection usually extends cranially and frequently terminates where the internal carotid artery enters the petrous carotid canal. The internal carotid lumen is often narrowed, with intimal irregularities. If the blood dissects into the subadventitial rather than a subintimal space, then a pseudoaneurysm may be formed (Davis and Zimmerman 1983) (Figs. 7.17, 7.18). In contrast to aortic dissecting aneurysms extending toward the carotid arteries, opacification of both the false and true lumen occurs very rarely (Fig. 7.11).

The incidence of spontaneous carotid artery dissection ranges from 2.5 to 3/100,000 per year (Schievink 2001). In comparison, the annual incidence of spontaneous vertebral artery dissection is estimated to be between 1 and 1.5/100,000 per year. SD is the cause of 2% of all ischemic strokes, although they are the cause in 10%–25% of the young and middle-aged patients. Ehlers–Danlos syndrome type IV, Marfan syndrome, polycystic kidney disease, and osteogenesis imperfecta type I can all present with SD.

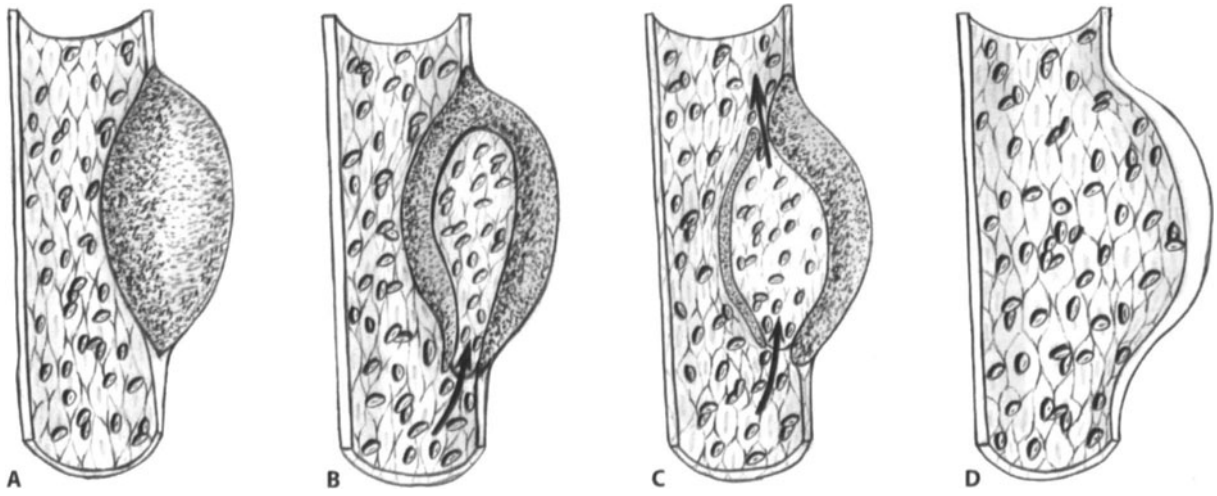

Fig. 7.16A–D. Schematic illustration of the various lesions that can be seen either following an arterial dissection or in the course of a specific one. **A** Mural hematoma, **B** dissecting arterial aneurysm, **C** double lumen with or without clot formation, **D** repair and fusiform scar

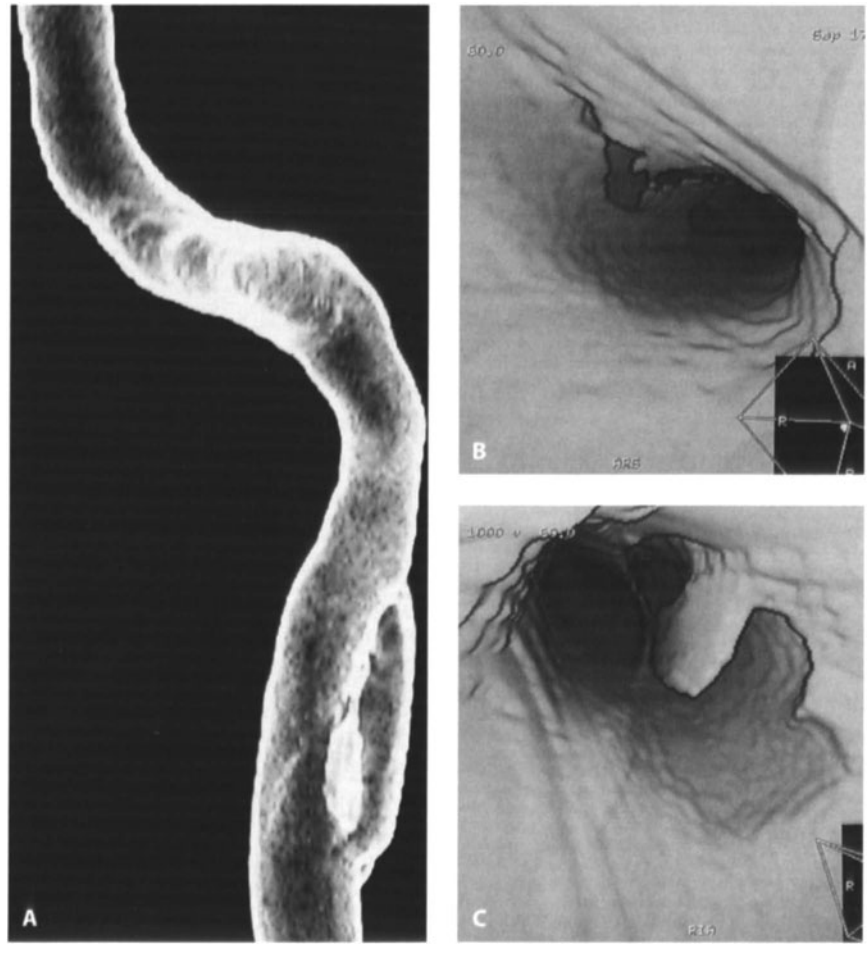

Fig. 7.17. **A** Volume rendering and **B, C** endoluminal views of traumatic cervical internal carotid artery dissection: fusiform arterial aneurysm, intraluminal flap, double lumen

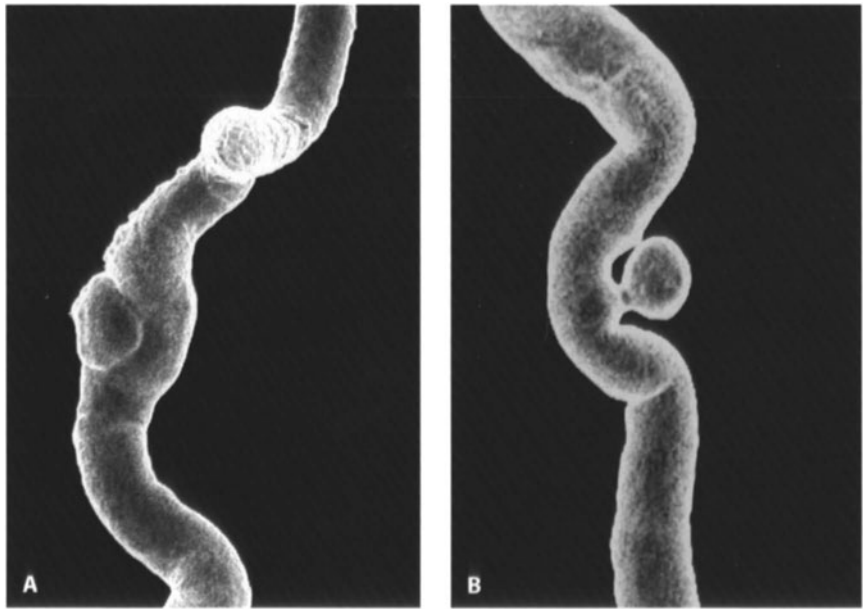

Fig. 7.18A, B. Bilateral spontaneous dissection of both cervical internal carotid arteries, revealed by persistent moderate headaches; no history of trauma

Certain hereditary connective tissue disorders have been identified in 1%–5% of patients with SD of the carotid or vertebral artery, but we suspect up to 20% of patients may have a sporadic but as yet unnamed underlying connective tissue disorder. In our experience, 5% of patients with a SD of the carotid or vertebral artery have at least one family member who has had an SD of the aorta or its main branches, including the carotid and vertebral arteries. Angiographic changes of fibromuscular dysplasia are found in about 15% of patients with an SD of the carotid or vertebral artery. Extensive studies, however, have failed to identify any mutations in the gene for type III procollagen (*COL3A1*), the gene for type V procollagen (*COL5A1*), or the gene for tropoelastin (*ELN*). Staining for antibody against fibrillin-1 has been negative in these patients. Connective tissue disorders have been identified in one-fourth of patients with such dissections. The finding of seasonal variations supports the possibility of an infectious trigger in the incidence of SD of the carotid and vertebral arteries, with a peak incidence in the fall.

Pain on one side of the head, Horner's syndrome, as well as cerebral or retinal ischemia may be presenting symptoms. Unilateral facial or orbital pain is present in about half the patients and may be the only symptom in about 10% of cases. Cranial nerve palsies can be detected in about 12%. Cerebral or retinal ischemic symptoms are reported in 50%–95% of patients with a SD of the carotid artery. Bilateral dissection of the carotid or vertebral arteries occurs in up to 15% of cases and therefore investigation should always include the entire vasculature of the head and neck region (Fig. 7.18).

SD affecting the carotid system is usually located 2–3 cm distal to the carotid bulb and tends not to extend beyond its entry into the petrous portion, where the lumen is abruptly restored, therefore involving only the first ICA segment (Fig. 7.1).

Most stenoses associated with SD, 90% will eventually resolve with conservative medical therapy. About two-thirds of the occlusions following

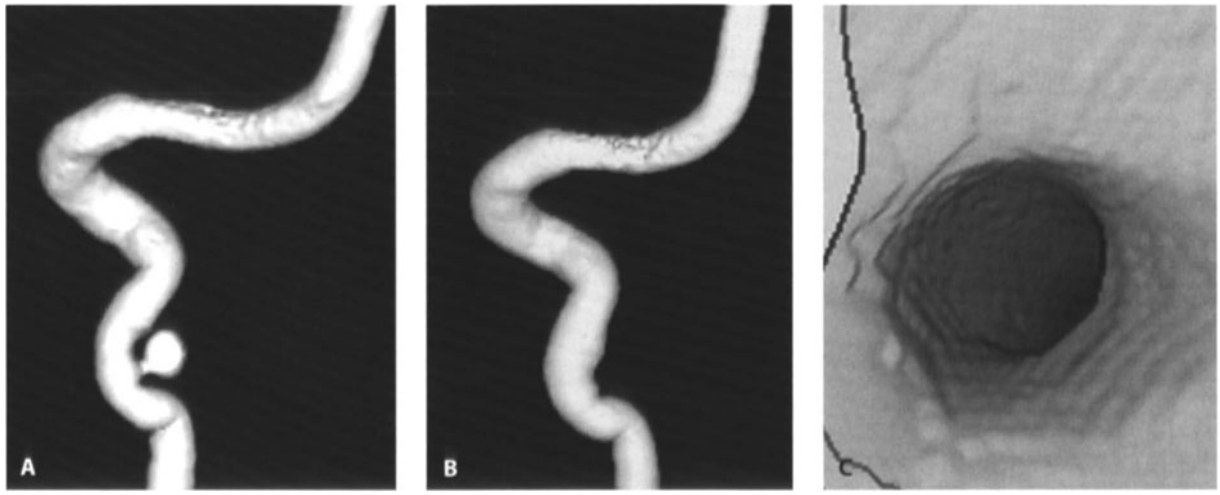

Fig. 7.19. **A, B** Surface rendering and **C** endoluminal view of spontaneous cervical arterial aneurysm (AA) dissection with AA and repair over 6 months with antiplatelet therapy

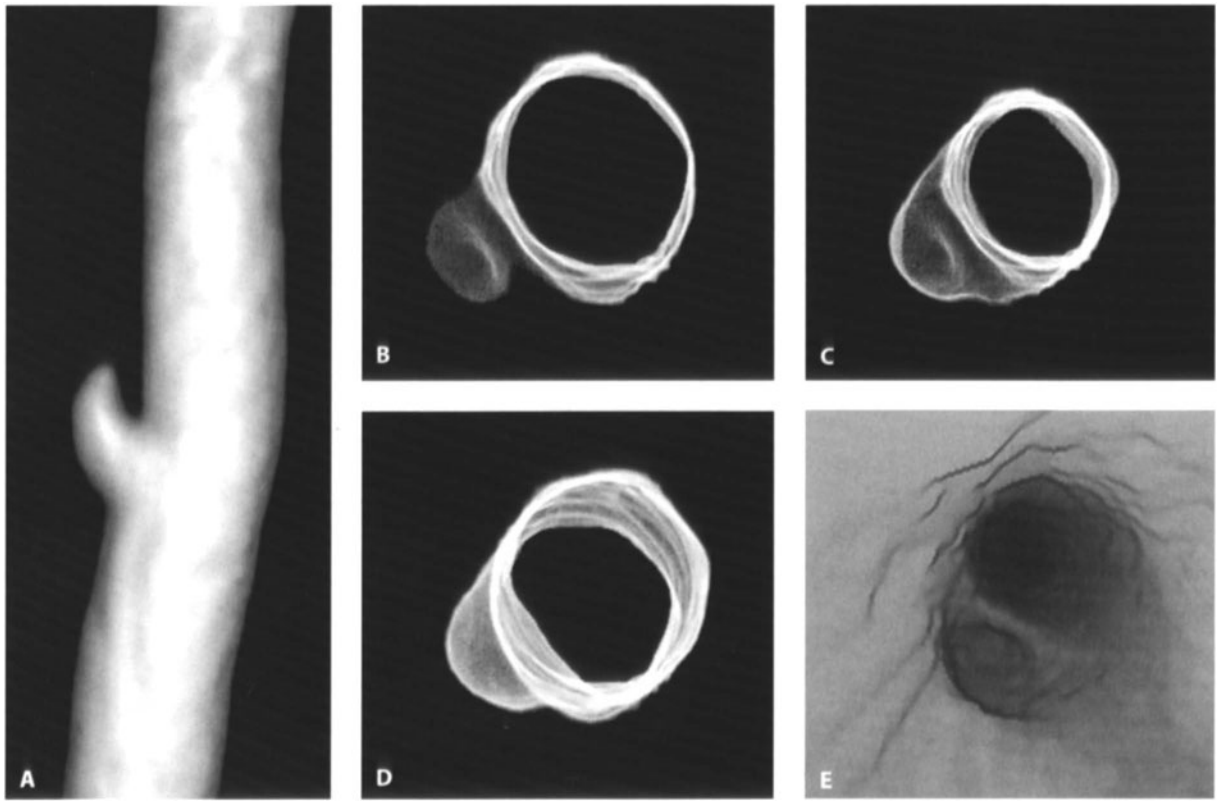

Fig. 7.20. **A** Surface rendering and **B–D** sectional views of volume rendering, **E** endoluminal view of healing of an asymptomatic iatrogenic internal carotid artery dissection (same patient as Fig. 7.17). Spontaneous closure of the double lumen and progressive exclusion of the AA pocket (antiplatelet treatment)

SD will reopen with anticoagulation therapy, while one-third of the associated aneurysms will decrease in size (Figs. 7.19, 7.20). Persistent extracranial aneurysms may cause thromboembolic complications years after the SD, but they tend not to rupture. SD in another artery, which was initially not shown to be affected, may occur in about 2% during the first month but then decreases to a rate of only about 1% per year. Only extremely rarely does SD recur in the same artery.

The recommended medical management for extracranial SD is heparin followed by warfarin 2–3 times the baseline INR for 3–6 months. Some patients are treated with antiplatelet therapy alone, particularly those who have no symptoms of ischemia (Figs. 7.19, 7.20). A distinction between embolic and hemodynamic stroke should be made; in the former situation, anticoagulation is preferred by most teams, whereas antiplatelet coverage is chosen for the latter or for asymptomatic patients. Surgical or endovascular treatment should be reserved for patients who have persistent symptoms of ischemia despite adequate anticoagulation therapy (Fig. 7.10; see Chap. 10, this volume).

Atherosclerotic aneurysms of the extradural internal carotid arteries are usually seen in older patients (Margolis et al. 1972) and typically occur just distal to the common carotid bifurcation in areas of severe atherosclerotic involvement. The mechanism of formation of these aneurysms has been the subject of much debate. Although lipid metabolism may have some impact, local factors play an important initial and perhaps predominant subsequent role. Deposition of fibrin and other blood substances in the intima, accumulation of ground substances, disruption of elastic lamina, and perhaps disturbance of the vasa vasorum circulation (Gore and Dalen 1966; Rob 1954; Wood and Correll 1969) with focal repeated dissections will eventually lead to a large partially thrombosed AA (see Sect. 7.5.2).

Mycotic Aneurysms

Infections of pyogenic or syphilitic origin are a less common cause of cervical carotid aneurysms than in the past. The mechanisms include septic microemboli to the vasa vasorum, septic emboli within the vessel lumen with thrombosis, and perivascular infections (Lansky and Makwell 1975; Sunwanwela 1972).

In the cervical region, the internal carotid artery courses cranially within its sheath. An aneurysm may result from the focal extension into the arterial wall of contiguous pharyngeal infections (Finney and David 1964).

At present, postoperative infections are the most frequent cause of cervical carotid aneurysms. Less commonly, aneurysms may occur after radiation therapy or be the result of vascular erosion secondary to advanced malignancies (Fig. 7.3).

7.2.2.3 Petrous Internal Carotid Artery Aneurysms

Because of the protection provided by the bony structures, the lack of significant branches and the rarity of atheromatous changes involving the petrous segment of the internal carotid artery, the most common type of aneurysms in this location proved to be the false aneurysm subsequent to injury. Less common causes include penetrating injuries, including biopsy of an intratympanic internal carotid artery (Fig. 7.21) and infection (Davis and Zimmerman 1983). Some are associated with the embryonic remnant of the hyoid-stapedial system (see Vol. 1) (Fig. 7.22). Aberrant ICA flow in the tympanic cavity can be associated with true dysplastic AA, for example in PHACE (*P*osterior fossa malformation, *H*emangiomas, *A*rterial anomalies, *C*oarctation of the aorta, *E*ye malformations) syndrome (Fig. 7.23).

The clinical symptoms caused by these aneurysms are primarily related to distal cerebral embolization and local hemorrhage, usually manifested as profuse bleeding from the ear (Ehni and Barrett 1960; Harrison 1954; Young 1941; Wemple and Smith 1966). They also often directly affect the cranial nerves (Harrison 1954; Harrison et al. 1963) and may produce recurrent facial pain, fifth and sixth cranial nerves paresis, deafness, or less frequently facial nerve paralysis (Wemple 1966) (Fig. 7.24). The management of these patients is difficult, because of poor surgical access to the internal carotid artery at the level of the carotid canal. However, in the presence of associated dissection, intraluminal thrombi, or a very broad neck, the internal carotid often needs to be sacrificed.

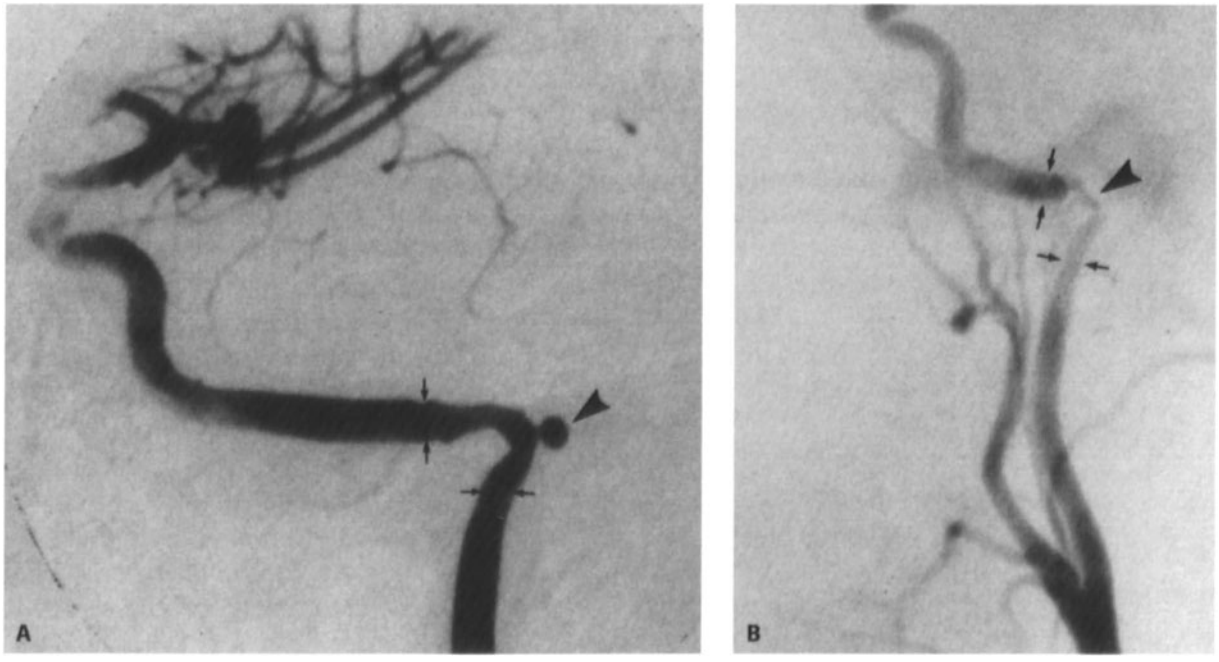

Fig. 7.21A, B. Iatrogenic (penetrating) pseudoaneurysm following biopsy of middle ear mass. **A** Subtraction angiogram, the left internal carotid artery (ICA) in Stenvers view shows a false aneurysm (*arrowhead*) of the aberrant intratympanic (*arrows*) ICA flow. **B** Two weeks later, spontaneous repair of the false aneurysm is demonstrated and secondary arterial narrowing (*arrowhead*)

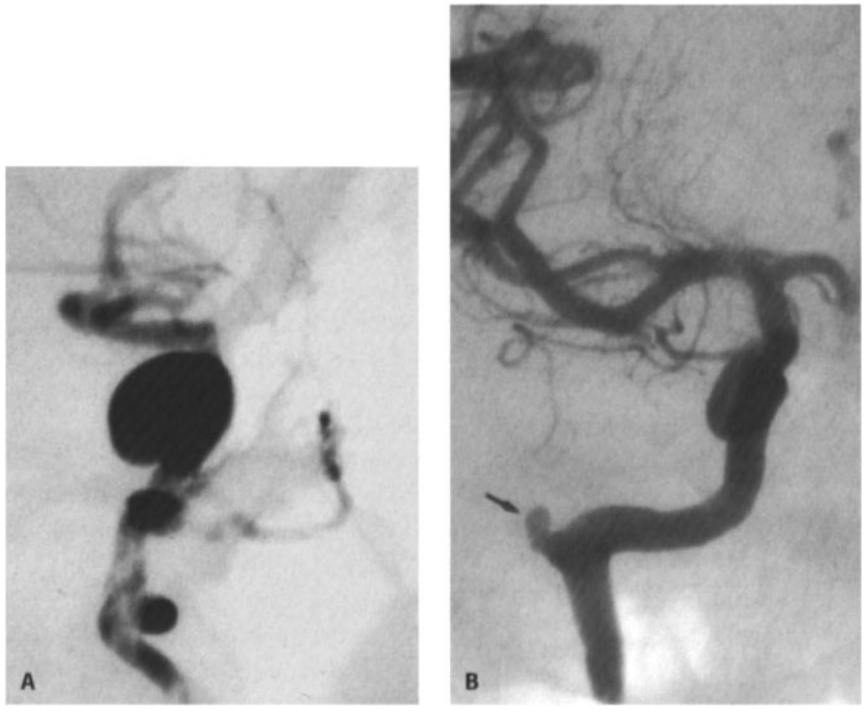

Fig. 7.22. Intrapetrous internal carotid artery aneurysm associated with embryonic hyostapedial artery persistence (**A**) or on its previous site of origin (*arrow*, **B**). The small one (**B**) revealed by epistaxis, corresponds to focal hemorrhage in the auditory tube. (From Willinsky et al. 1987, with permission; see Vol. 1)

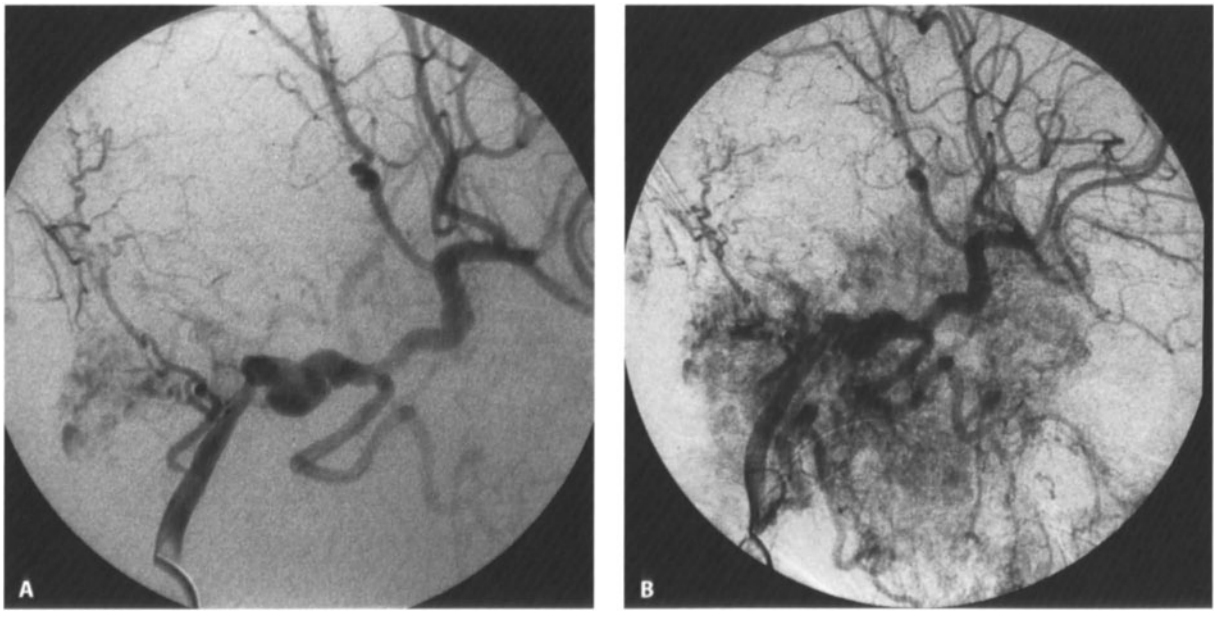

Fig. 7.23. **A** Intratympanic ascending pharyngeal (hyostapedial) fusiform arterial aneurysm in an infant with PHACE syndrome. Note the cervical and petrous internal carotid artery agenesis and the stapedial persistence. **B** On the late phase the supply to the facial hemangioma is clearly seen

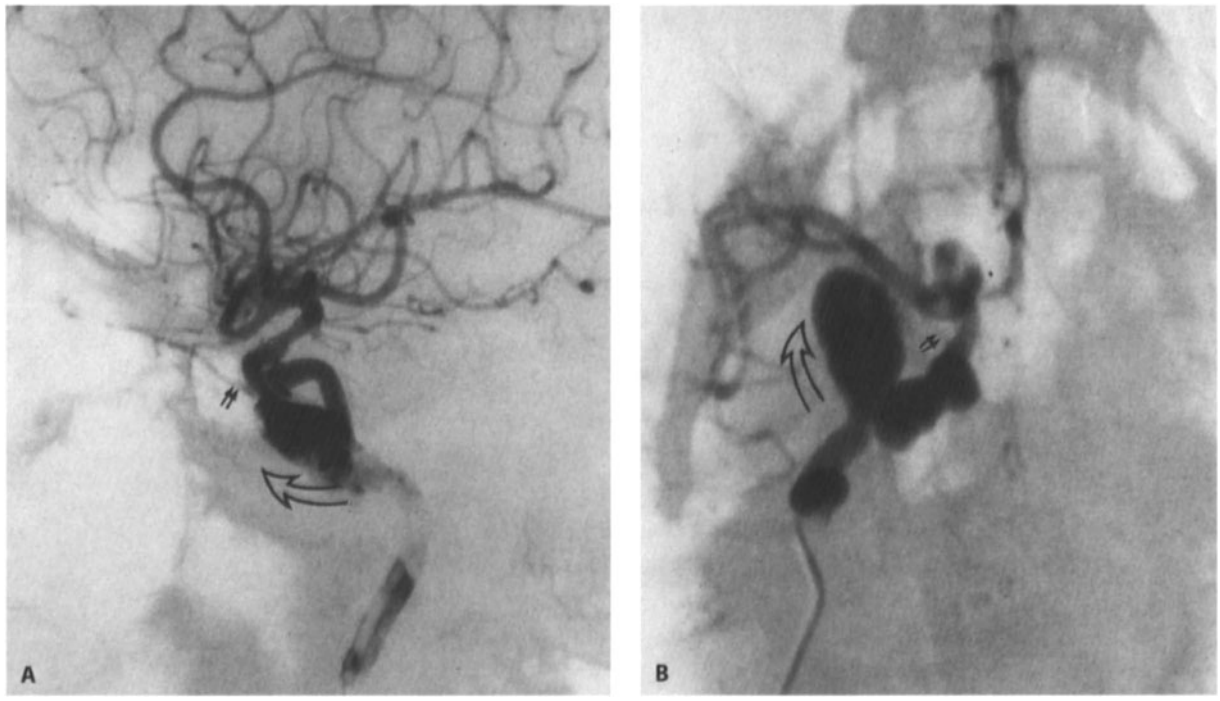

Fig. 7.24. **A** Dysplastic aneurysm of the intrapetrous carotid artery is shown on lateral and **B** axial views. The aneurysm (*open curved arrow*) bulges into the foramen lacerum and vidian canal. Note also the C4 origin of the ophthalmic artery (*double arrow*). This 22-year-old patient presented with excruciating chronic facial pain and Horner's syndrome, which resolved within hours following balloon occlusion of the petrous carotid artery. The patient's vision was preserved

7.2.2.4 Aneurysms of the Cavernous Segment of the Internal Carotid Artery

The most frequent site of extradural internal carotid artery aneurysms is the cavernous segment (Fig. 7.1). It is of interest to note that, in the Kupersmith et al. series (1984), a significantly higher incidence occurred in females (13:1) and of the three males of that series, two had traumatic pseudoaneurysms. Females are particularly sensitive to certain other vascular diseases of that area: rostral to the basioccipital (osteodural AVSs). If one excludes the younger male patients with traumatic lesions, the mean age was 58 years. The youngest patient was a 24-year-old woman in whom symptoms developed after a pregnancy. These AAs have often been considered to be of atherosclerotic origin. However, the clinical pathological study by Barr et al. (1971) clearly showed that these large saccular aneurysms arise as a result of a weakness in the lateral wall of the cavernous segment of the carotid artery at the origin of one of the C4 or C5 branches of the internal carotid artery. Similar to Drake's observations (1979), we have seen these lesions in young patients with no evidence of arteriosclerosis; we have also seen a relatively high incidence of associated coexisting berry aneurysms.

Among 44 cavernous aneurysms, five patients (11%) had aneurysms at other locations (Figs. 7.25, 7.26), a statistically significantly higher incidence than in the general population.

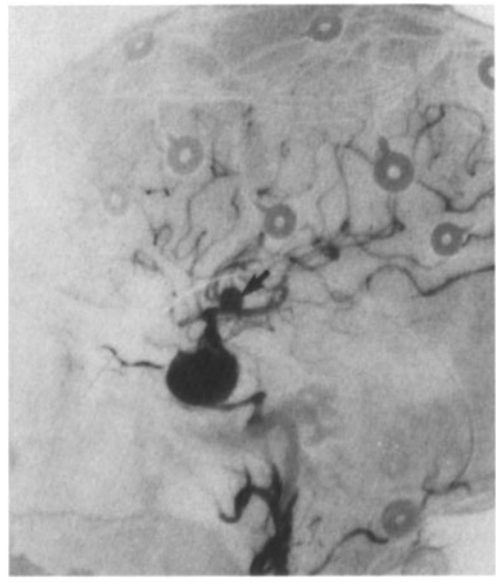

Fig. 7.25. Associated extradural and intradural arterial aneurysms (AAs). The left internal carotid artery (ICA) shows an AA of the cavernous portion with narrowing of the C5 segment due to compression. An associated left middle cerebral artery (MCA) aneurysm (*arrow*) is seen (subtracted artifacts from EEG helmet). The MCA aneurysm was clipped, prior to balloon occlusion of the left ICA aneurysm

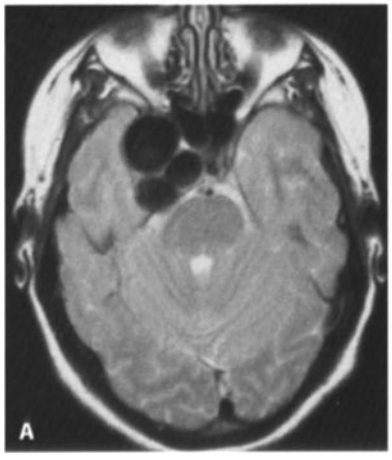

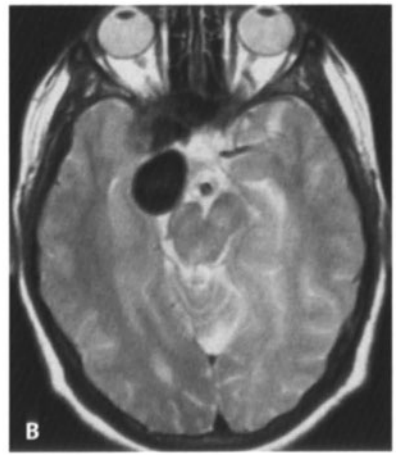

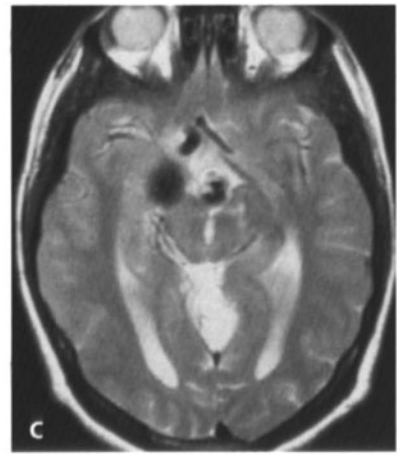

Fig. 7.26A–J. A 30-year-old female patient with a 2-month history of moderate persistent occipital headaches associated with vertigo and with no family history of vascular disease. Neurological examination was normal. **A–C** MRI demonstrates multifocal large, partially thrombosed aneurysms involving the intracavernous internal carotid artery (**D–H**) and basilar termination (**I, J**). **F–J** see p. 403

Mishkin (1965) presented 68 patients with intracavernous aneurysms; three had bilateral aneurysms (4.4%) and nine (13%) had small aneurysms in other locations. Atherosclerotic changes that occur commonly in the cavernous portion of the internal carotid artery may further weaken the arterial wall (Rob 1954) and may be an aggravating factor in the progression of these lesions. Similarly, the higher incidence of hypertension (Table 7.18) in these patients may be an added factor in their pathogenesis (Barr et al. 1971).

Less frequently, traumatic cavernous pseudoaneurysms may result from penetrating injuries, carotid endarterectomy, and transsphenoidal surgery (Fig. 7.27). As with pseudoaneurysms at other levels, the clinical presentation may be delayed. Thrombosis and dissections may also occur in this location, primarily following blunt trauma.

Spontaneous dissection or intramural hematoma may occur in patients with blood dyscrasias or coagulopathies such as disseminated intravascular coagulation (DIC) and often present with acute ophthalmoplegia.

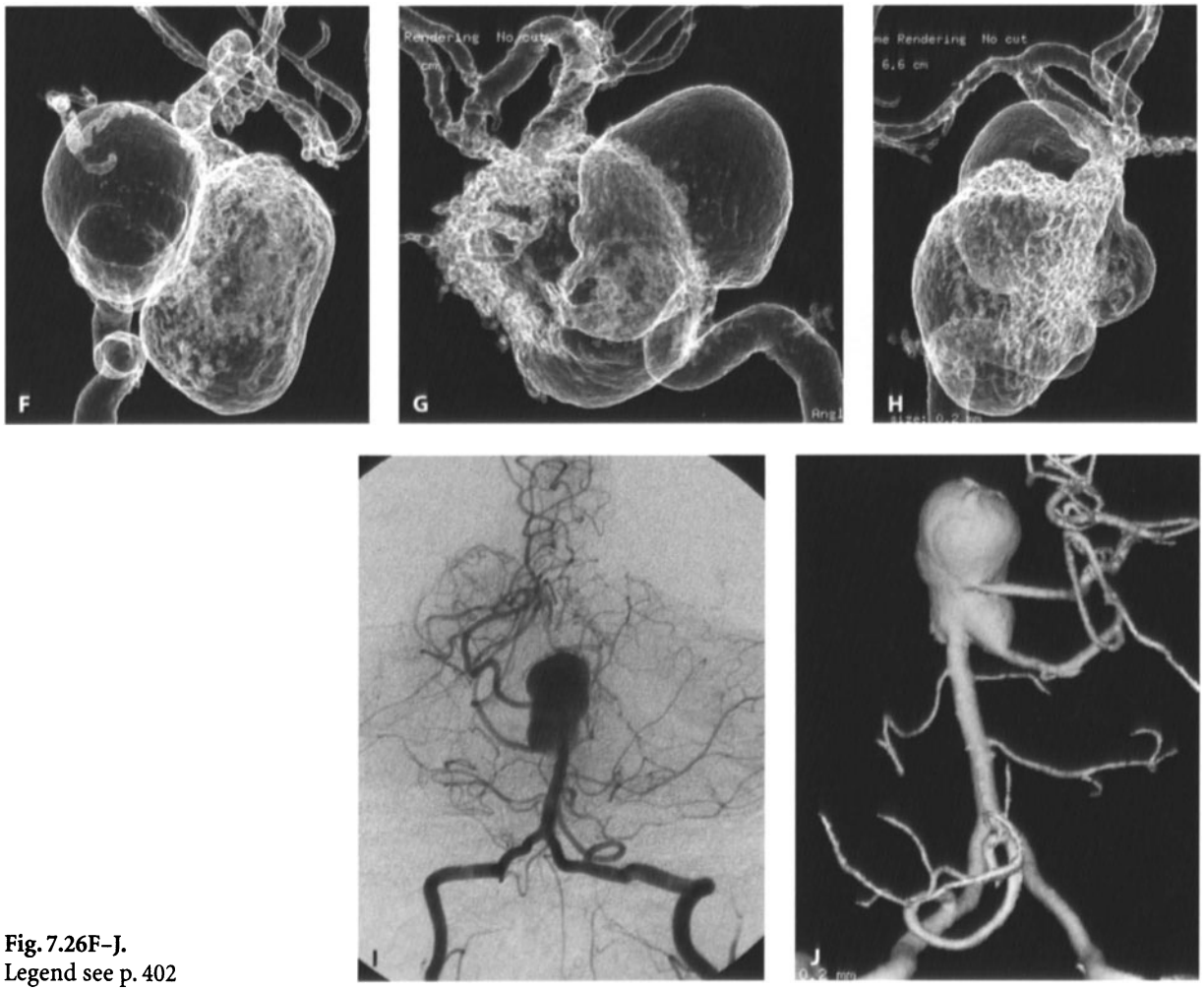

Fig. 7.26F–J.
Legend see p. 402

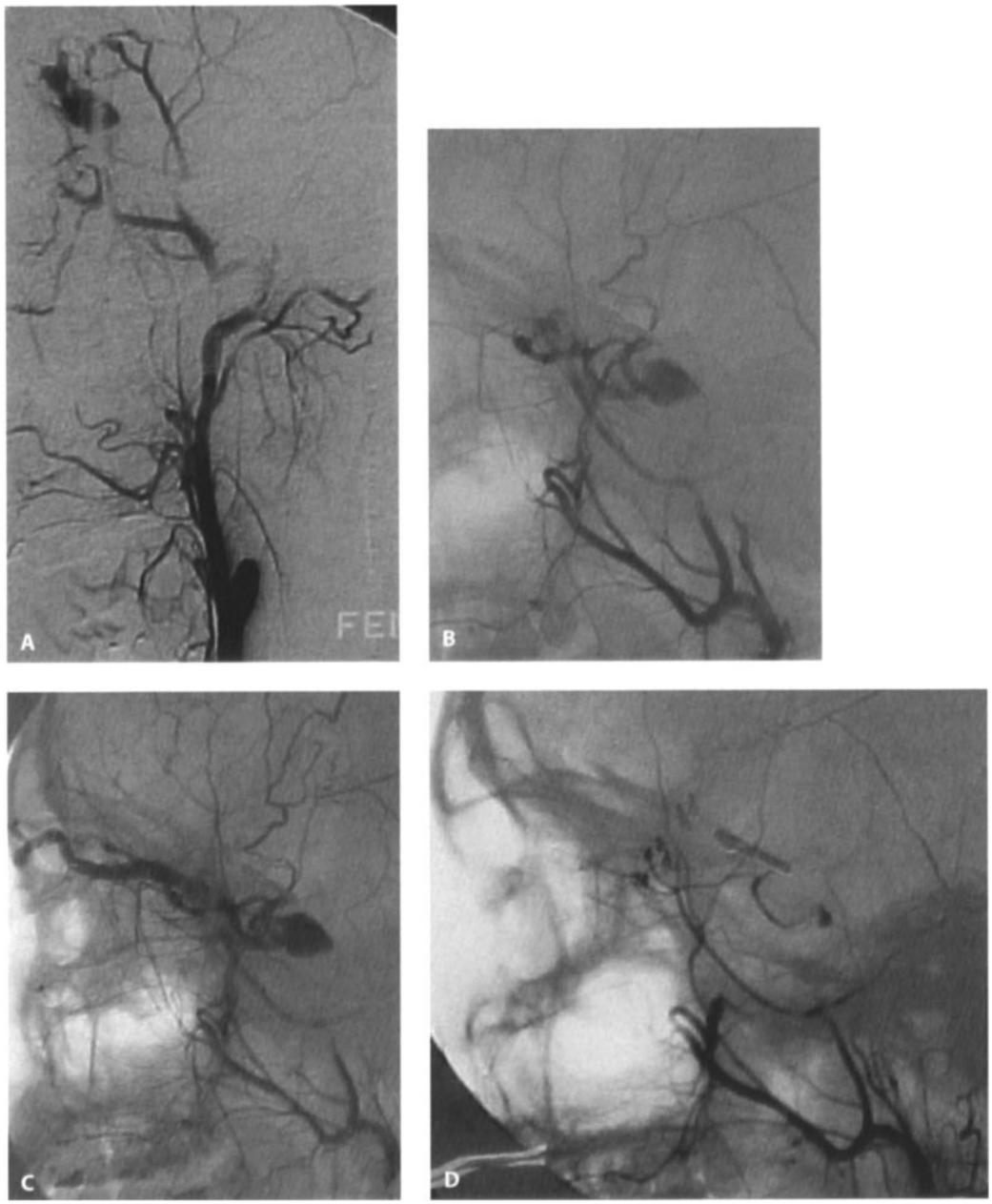

Fig. 7.27A–D. Intraoperative injury of the internal carotid artery (ICA) siphon during transsphenoidal surgery. Immediate supracavernous clipping of the ICA and carotid ligation at the neck were needed to stop the hemorrhage. Immediate postsurgical common carotid angiogram (**A**) and selective external carotid angiograms (**B, C**) demonstrate the clinoid portion of the siphon to be opacified through the maxillary-ophthalmic anastomoses. The risk of visual impairment excludes a transarterial approach to the residual false sac and associated carotid cavernous fistula (CCF). **D** Manual compression at the medial canthus for several weeks was sufficient to induce a complete thrombosis of the CCF and the residual sac, with preservation of vision

Table 7.18. Clinical presentation of carotid cavernous aneurysms

	Initial symptoms (%)	Present (%)
Pain (V1)[a]	64.5	82
Diplopia	23.5	82
Ptosis[b]	12	82
Visual loss[c]	–	29
Proptosis	–	6
Additional aneurysms	1	11
HBP or CVD[d]		

[a] Pain in the distribution of the V2 was seen in 12%.
[b] Complete absence of levator muscle function was seen in 24% and some degree of ptosis was seen in all patients on careful examination.
[c] 1 patient (2.2%) had loos of vision secondary to corneal ulceration.
[d] HBP, high blood pressure; CVD, cardiovascular disease.

Progressive thrombosis and the risk of distal embolization (Fig. 7.28) occur like other secondary dissections. Even after the internal carotid artery has thrombosed, embolic episodes to the ophthalmic and/or intracerebral circulation may continue from the stump of the internal carotid artery through external carotid to internal carotid collaterals. To prevent emboli from either the distal carotid or the stump, balloon trapping and stumpectomy may be required (Fig. 7.29).

Rupture of an intracavernous ICA aneurysm may occur, causing a spontaneous carotid cavernous fistula (CCF), with its typical clinical presentation. Such a presentation should raise two questions: are there any symptoms suggesting collagen disease in this patient and is the bony floor of the sella turcica preserved (Fig. 7.30)?

Intracavernous giant AAs make up a special group among these AAs, as their possible erosion into the sphenoid sinus is a serious risk for severe and often fatal epistaxis. Careful CT analysis of the floor of the sella turcica will show whether or not the lesion needs to be treated. Partial thrombosis of these pouches leads to inflammatory perivascular changes and subsequent cranial nerve impairment. Anti-inflammatory treatment often results in relapse of symptoms. Rupture of such lesions creating a CCF should be treated with ICA reconstruction unless bony erosion is noted to destroy the floor of the sella. In this case, complete and stable exclusion of the pouch needs to be achieved even if this means sacrifice of the ICA after test occlusion. The risk of SAH from intracavernous ICA is extremely low except in AAs that develop superiorly or medially.

Fig. 7.28. A 38-year-old female patient who developed disseminated intravascular coagulation (DIC) syndrome after abdominal surgery and presented with dysarthria, right-sided weakness, and left-sided acute and complete ophthalmoplegia. The left common carotid artery angiogram demonstrates lateral and superior displacement of the cavernous carotid artery with a relatively small irregular aneurysm lumen (*open arrow*), and significant stenosis distal to the aneurysm. The carotid narrowing due to intramural dissection is seen proximally (*double arrowhead*). Three days later, she developed a transient episode of amaurosis fugax. The internal carotid artery (ICA) had thrombosed spontaneously and turbulent flow of the ICA stump was noted. A balloon stumpectomy was performed to prevent further embolic episodes

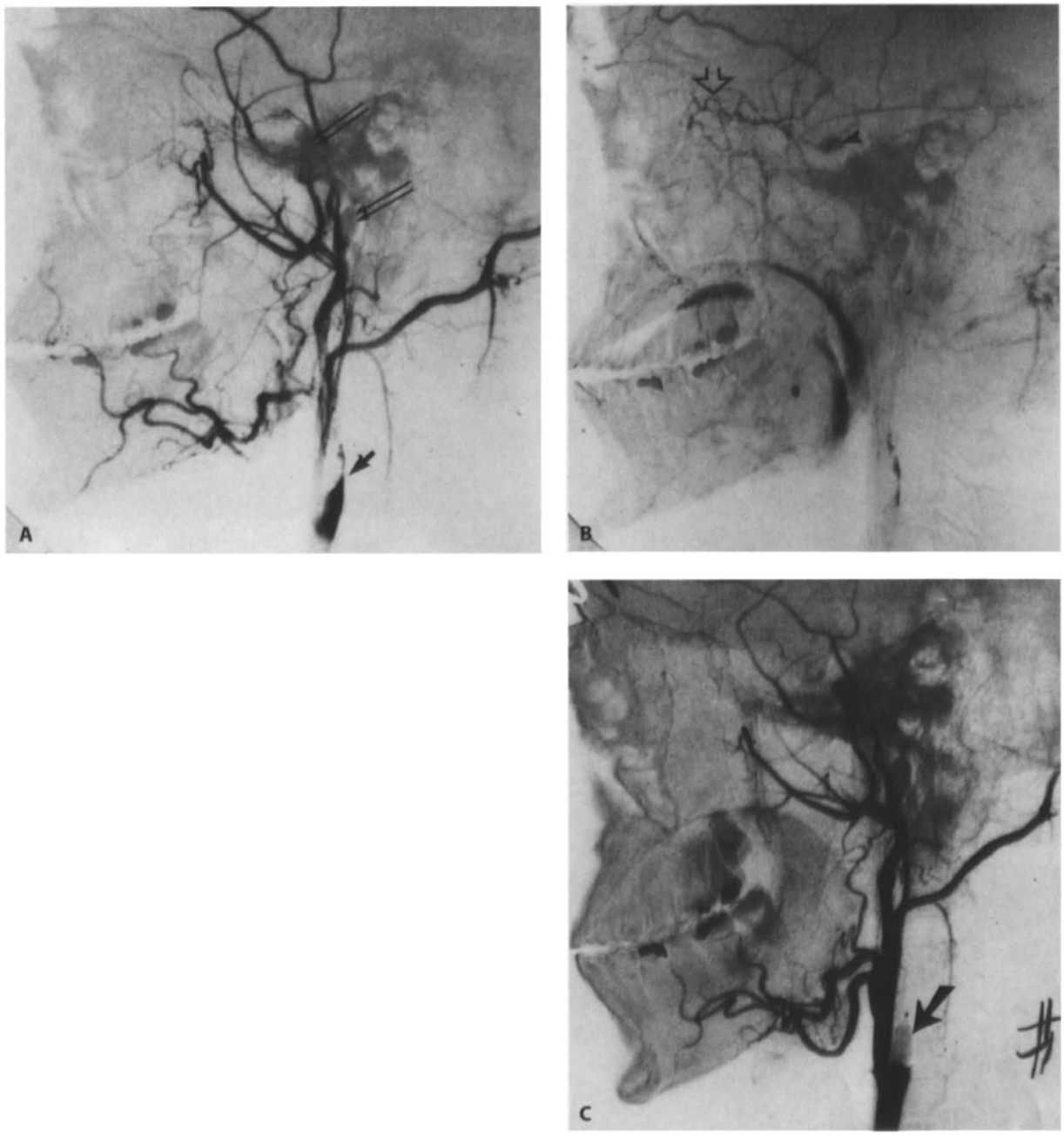

Fig. 7.29A–C. A 39-year-old male patient developed amaurosis fugax 1 week after balloon occlusion of the left internal carotid artery (ICA) for an aneurysm of the cavernous portion. **A** Note the stump of the left ICA with thrombi (*arrow*) and two partially subtracted balloons in the precavernous and high cervical carotid arteries (*double arrows*). **B** Stasis of contrast in the ophthalmic artery (*open arrow*) and in the cavernous carotid artery (*arrowhead*), suggesting an embolic event from the turbulent flow of the ICA stump. **C** Follow-up angiogram after a detached balloon was used for stumpectomy (*arrow*). No further embolic episodes occurred

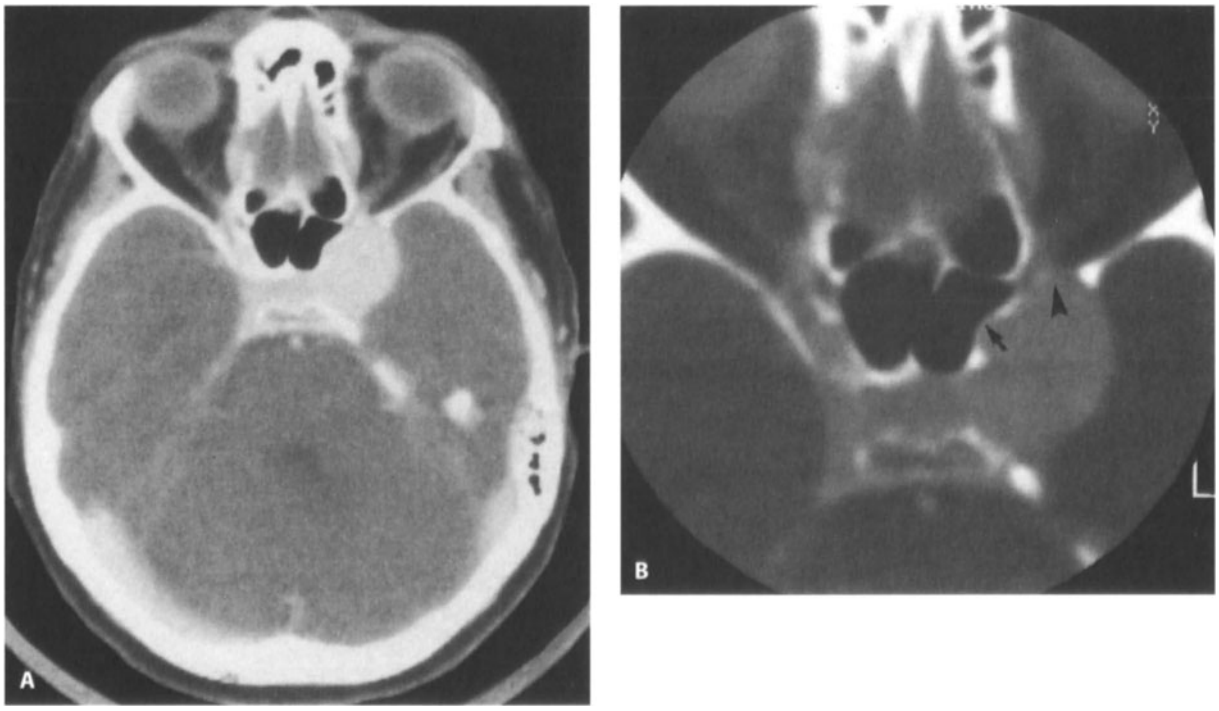

Fig. 7.30A, B. Aneurysm of the cavernous carotid artery. **A** Axial CT image after IV administration of contrast material demonstrates a well-circumscribed parasellar mass with homogeneous enhancement and lateral bulging of the cavernous area (compare with right side). **B** Bony window demonstrates the erosion of the lateral spheroid bone (*arrow*) and widening of the superior orbital fissure (*arrowhead*)

Clinical Presentation

The clinical features and natural history of this condition have been studied by Barr (1971), who described the sequence of clinical events progressing through cranial nerve palsies, visual impairment, and proptosis, correlating with the way the aneurysm tends to grow laterally and compress the cranial nerves, as described by Barr (1971). In the Kupersmith series (1984), the clinical presentation (Table 7.18) and neuro-ophthalmological findings were carefully analyzed (Table 7.19).

Pain in the distribution of the first division of the fifth nerve was the most frequent initial symptom and was eventually present in most cases. Severe debilitating pain occurred in one-third of our patients and was the primary reason for consultation. In the remainder, the pain was either progressive or stable, but never explosive. Partial sensory loss in the distribution of the fifth nerve caused diminishing corneal reflex and decreased light and touch perception in the distribution of the first division of the trigeminal nerve. When severe, the sensory loss may lead to corneal anesthesia and ulceration, with resulting blindness. Diplopia was the initial complaint in less than one-third of the patients, but eventually was present in most. The absence of levator function alone, without internal ophthalmoplegia and with normal pupillary function, was seen in one-third of patients with ptosis and reflected partial third nerve dysfunction. This did not improve in any of our patients following treatment (Beren-

Table 7.19. Neuro-ophthalmological findings in cavernous carotid aneurysms

	Isolated[a] (%)	Impaired (%)
Cranial nerve III (14)	12	82
Cranial nerve IV	–	47
Cranial nerve VI	12	71
All muscles involved	–	35
Complete ophthalmoplegia	–	18
Cranial nerve VI sensory loss[b]	–	24
Parasympathetic	–	53
Sympathetic abnormality	–	35

[a] 29% of patients with oculomotor nerve palsy had no internal ophthalmoplegia.
[b] A profoundly anesthetic cornea in one patient (2.2.%) resulted in corneal ulceration and visual loss.

stein 1984a). Progressive unilateral loss of vision occurred relatively late in the course and was usually due to compression of the optic nerve secondary to anterior expansion of the aneurysm. Second nerve sensory involvement was a less frequent cause of visual loss.

Proptosis rarely occurred in Kupersmith's patients and was mild when present, probably because of the ability to make an early diagnosis on CT scans, as compared with a higher incidence and degree of proptosis in older series (Jefferson 1938).

Varying degrees of ipsilateral ophthalmoplegia were present in 94% of patients but occurred as the initial symptoms in less than one-third of patients, probably reflecting compensation of mild ocular motor changes (Morley 1968). Isolated extraocular nerve compression was unusual and involved only the sixth and third cranial nerves; isolated fourth cranial nerve involvement was not seen. All muscles were involved in 30% and a complete ophthalmoplegia was present in 18%. Contrary to other series (Jefferson 1938; Morley 1968), we found that the third nerve was involved more frequently than the sixth nerve.

Parasympathetic or sympathetic pupillary abnormalities ipsilateral to the aneurysms were observed in most patients. Additional aneurysms were seen in 11% and bilateral cavernous lesions were seen in 3%, comparable to the experience of Drake (19%) (1979) and Mishkin (1965), but less than reported by Barr (1971). There was a high incidence of associated high blood pressure and cerebrovascular disease, and these are probably significant aggravating factors.

Further expansion of the aneurysm will eventually strip the dura from the floor of the middle cranial fossa. Anterior extension is usually a late event and results in erosion of the anterior clinoid process. Eventually, inferolateral extension occurs into the optic foramen and the superior orbital fissure. Nonpulsatile exophthalmos with compression of the optic nerve may result and lead to progressive visual loss and optic atrophy. Posterior expansion, often a late event, can lead to ipsilateral facial nerve palsy and deafness, sometimes followed by rupture and massive hemorrhage (Barr 1971). Medial expansion may erode the lateral aspect of the sella. Severe epistaxis may occur with aneurysm rupture into the sphenoid sinus (Figs. 7.30, 7.31).

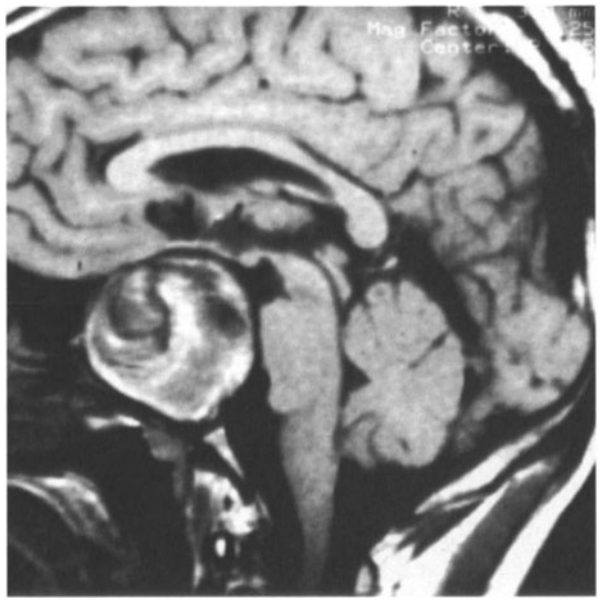

Fig. 7.31. Partially thrombosed intracavernous arterial aneurysm with significant skull base erosion at the level of the sella turcica

Surgical ligation of the parent artery as treatment for these aneurysms has been replaced by endovascular parent artery occlusion with balloons or coils (Fig. 7.32). More recently, parent vessel preservation and aneurysm exclusion has been accomplished using a combination of stent placement across the aneurysm neck and simultaneous endosaccular occlusion of these aneurysms using coils (Figs. 7.33, 7.34) or liquid materials (see Chap. 1, this volume). Technical limitations to the stenting of tortuous vessels in the neck and along the skull base are gradually being overcome, making it the preferred method of treatment for these aneurysms. Advances in covered stent technology will likely make it possible in the future to cross the often wide neck of these aneurysms, preserving the parent artery, without having to deposit material into the aneurysm itself (see Chap. 1, this volume).

Bone erosion is best shown on CT and should be looked for (Figs. 7.31, 7.35) (Mishkin 1965). A negative noncontrast CT is insufficient to rule out aneurysm of the cavernous carotid siphon (ACCS). Following the intravenous administration of contrast material, the patent ACCS shows as a uniformly enhancing lesion with well-circumscribed borders and no edema (Fig. 7.30). In a smaller number of cases, the CT will demonstrate the characteristic appearance of a partially thrombosed aneurysm (Pinto et al. 1979), i.e., an area of ring enhancement with an eccentric enhancing lumen surrounded by irregular low attenuation (representing the thrombus). Similarly, MRI and MRA have been used to clarify these parasellar mass lesions and to demonstrate in detail the relationship between the ACCS and the adjacent soft tissue structures (Figs. 7.32, 7.35). The vascular study chosen, whether invasive or noninvasive, should contribute to making the diagnosis of ACCS and include the evaluations relevant to the therapeutic management. The anatomy of the vessels involved in the AA as well as the anatomy of the rest of the vasculature should be visualized to better understand the potential for collateral supply to the territory. The current challenge in most large AAs, when endovascular stenting is

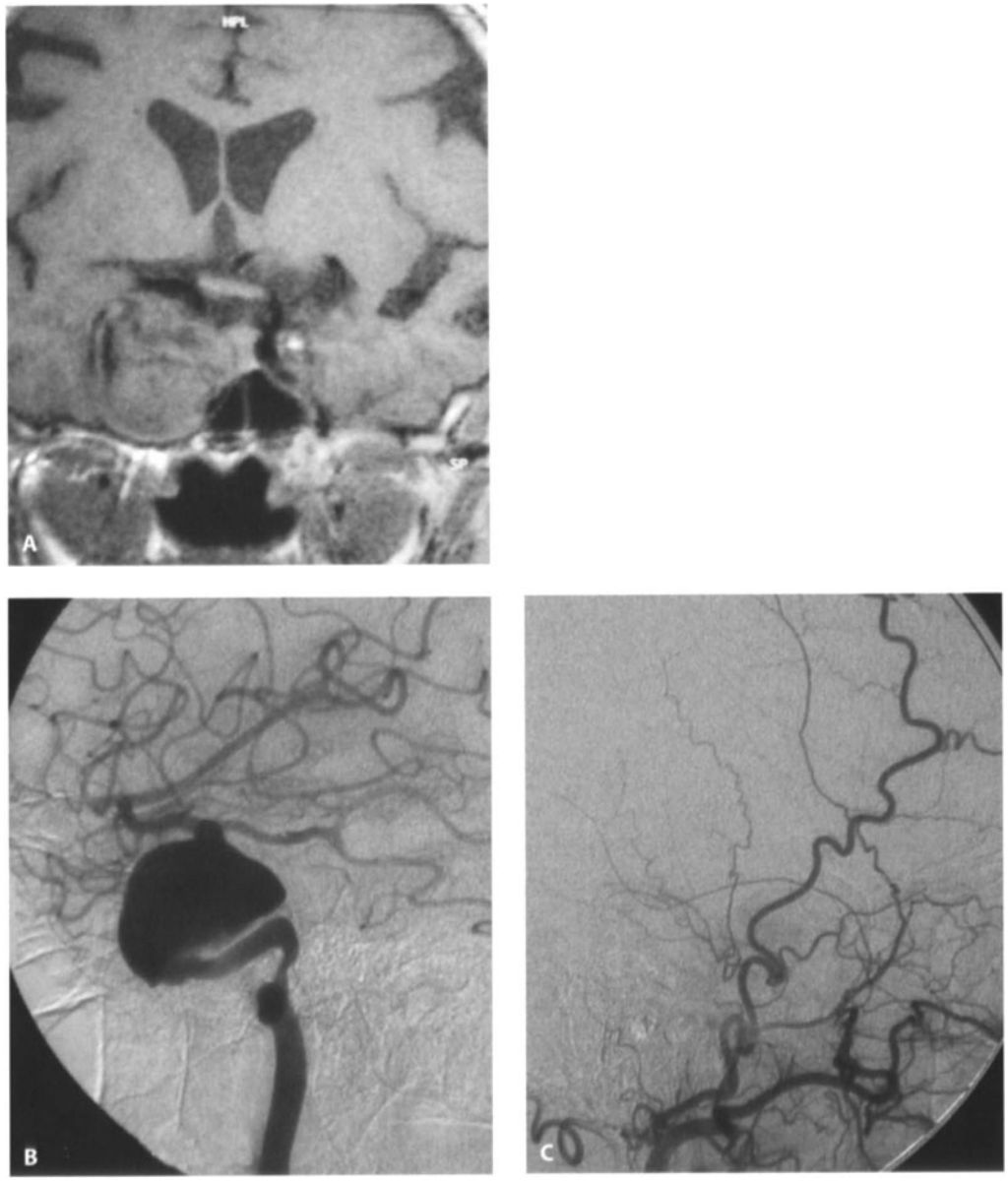

Fig. 7.32A–G. A 78-year-old female patient with sudden ophthalmoplegia and headaches. At admission right-sided ptosis; third and sixth nerve palsies were noted. **A** MRI demonstrates unruptured giant internal carotid artery (ICA) aneurysm. **B, C** Pre-embolization angiograms. Note the stenosed intrapetrous ICA and the superficial temporal artery (STA) appearance, information required if an STA–MCA by-pass was to be proposed. ICA balloon occlusion is performed after the patient passed an occlusion test. Rapid improvement of ophthalmoplegia and headaches occurred. **D–G** see p. 412

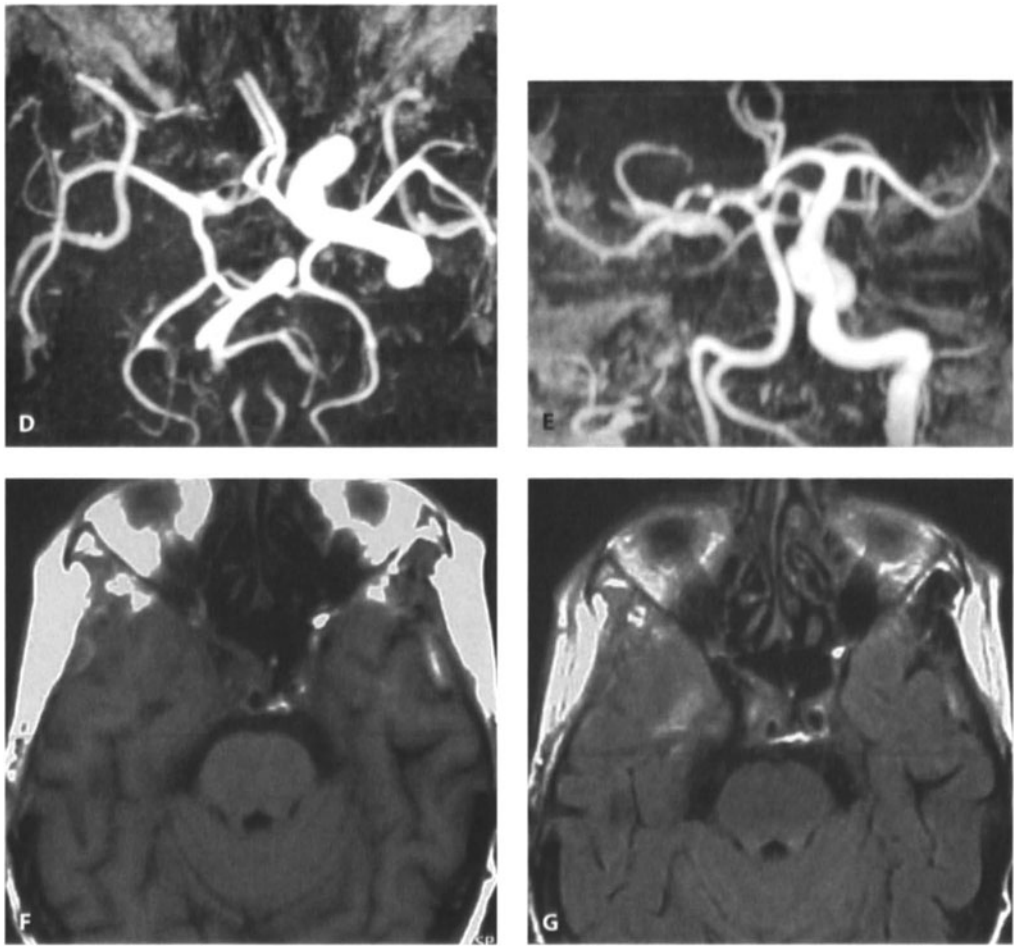

Fig.7.32 (*continued*). **D–G** Follow-up MRA and MRI confirm the complete occlusion of the AA and its shrinkage

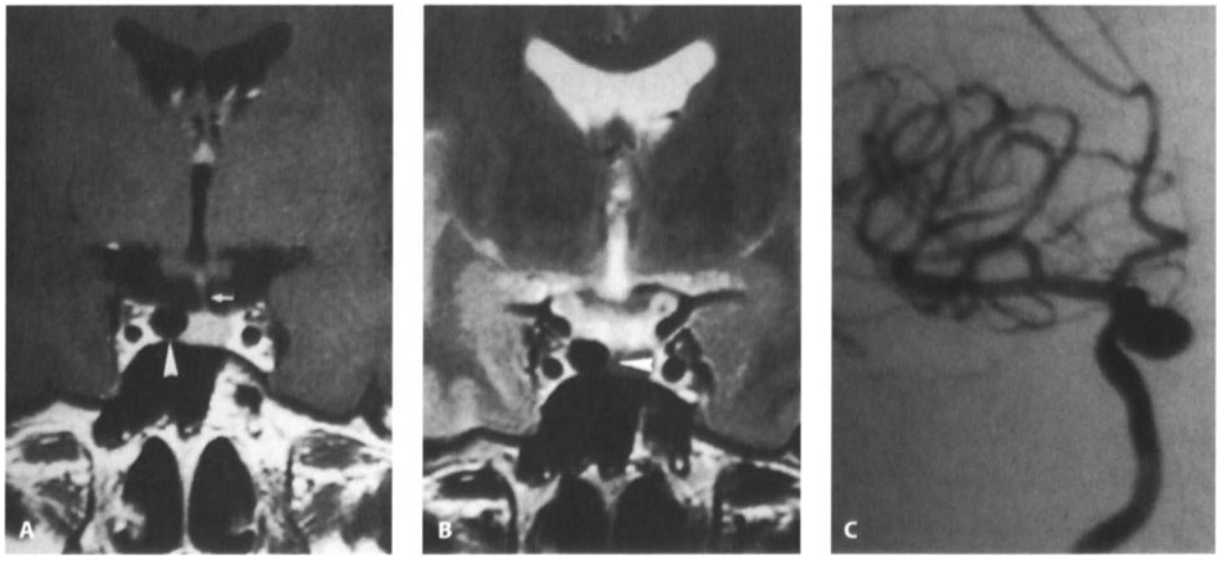

Fig. 7.33A–C. Legend see p. 413

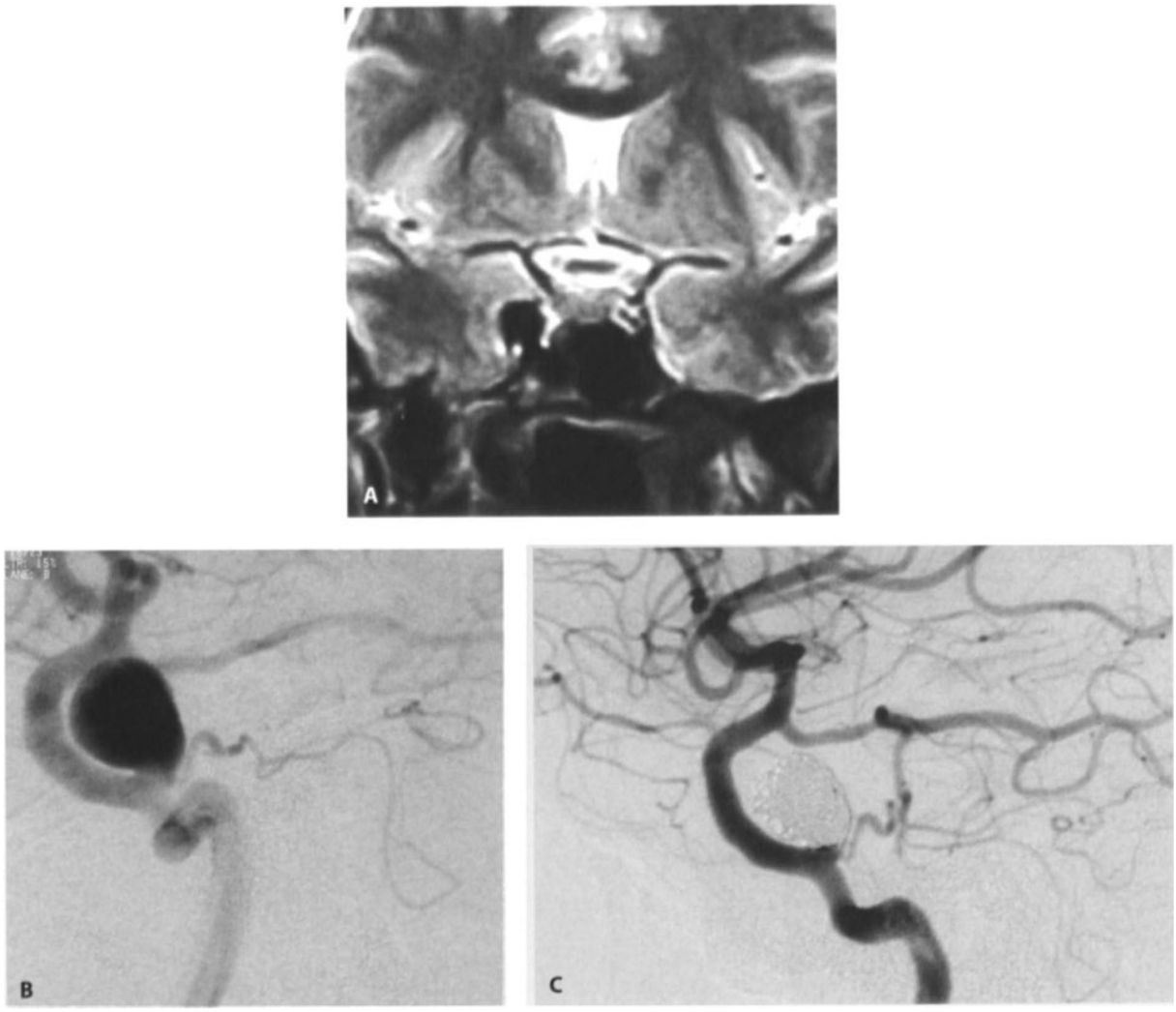

Fig. 7.34A–C. A 60-year-old female patient presenting with facial pain. Intracavernous internal carotid artery (ICA) aneurysm (**A**, MRI), associated with a trigeminal artery variant (ICA origin of AICA). **B** Before and **C** after coiling (see also Fig. 1.66)

◀ **Fig. 7.33. A, B** MRI and **C** internal carotid artery (ICA) angiogram. Intracavernous ICA aneurysm in a patient presenting with hyperprolactinemia and galactorrhea. Normalization of endocrine activity occurred following complete exclusion of the arterial aneurysm with coiling. (From Caldas et al. 1998, with permission)

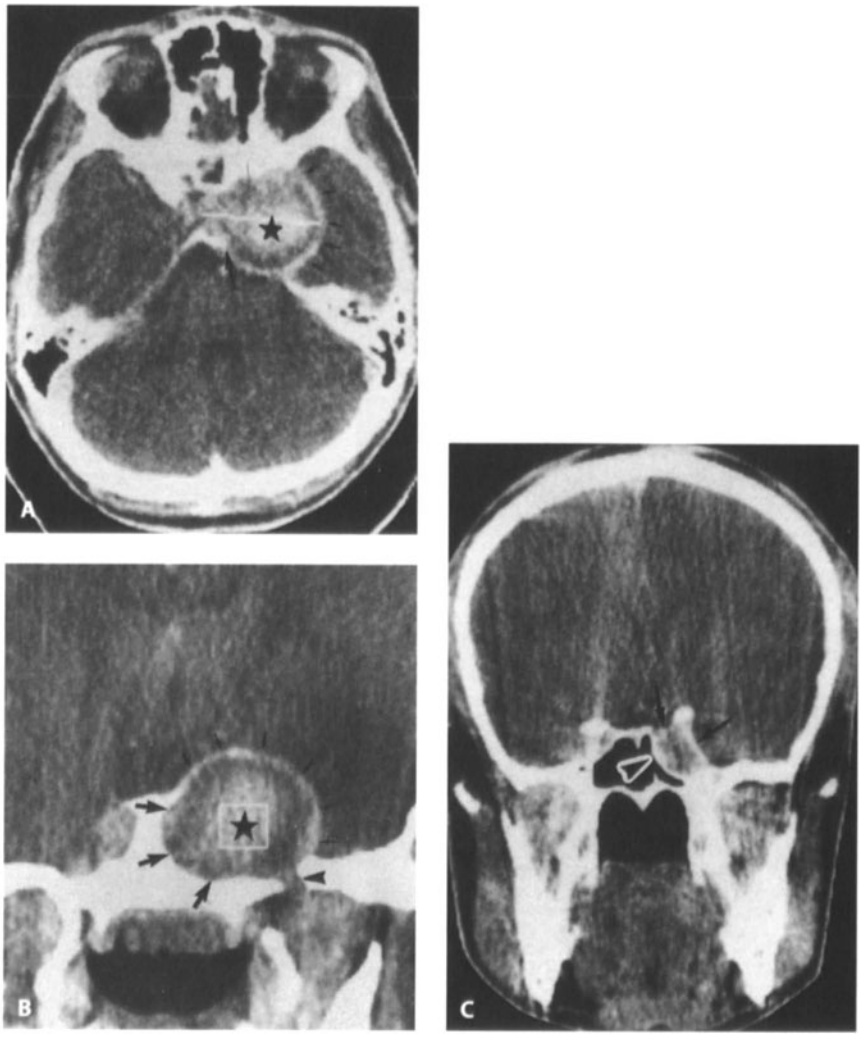

Fig. 7.35A–C. Thrombosed giant cavernous aneurysm with bony erosion. **A** Axial image. **B** Coronal image on the enhanced CT 2 days later, after embolization, shows a thrombosed aneurysm (*star*) with the enhancing wall (*small arrows*). Note the bone destruction involving the posterior clinoid process (**A**) and parasellar (**B**) areas. **C** Eight months after embolization, note the shrinkage of the aneurysm (*arrows*) and the bulging towards the sphenoid sinus (*arrowhead*)

considered to be the optimal treatment, is our capacity to catheterize the artery beyond the AA. Finding the outlet may be difficult without satisfactory 3-D pictures, virtual endoscopic reconstructions, and eventually 3-D fluoroscopy (Fig. 7.26). Obviously, the risks of endovascular manipulation will vary depending on the presence of a patent versus a partially thrombosed lumen of the ACCS.

All of our patients with cavernous carotid artery aneurysms benefited from endovascular treatment (Tables 7.20, 7.21) (Kupersmith 1984). The most constant improvement was the complete resolution of pain in all patients.

Diplopia improved in more than half of the patients and it resolved completely in over 60% of these. Visual loss improved in 20% and stabilized in an additional 40%. Proptosis, although infrequent, resolved in all. For our only patient who presented with SAH, we occluded the internal carotid artery, and this resulted in thrombosis of the aneurysm. During thrombosis of the aneurysm early after embolization, CT will show the typical target appearance (Pinto 1979). We have documented thrombosis and a decrease in mass effect, with collapse of the aneurysm sac

Table 7.20. Clinical results after embolization

	Improved (%)	Resolved (%)	Unchanged (%)	Worsening[a] (%)
Pain	–	100	–	–
Diplopia	62	24	14	14
Ptosis[b]	27	36	36	–
Visual loss	20	–	80[c]	–
Proptosis	–	100	–	–

[a] Transient with eventual improvement as compared to pre-embolization.
[b] Including 66% of patients with complete ptosis prior to embolization.
[c] Stabilized in 40%.

Table 7.21. Neuro-ophthalmological findings after embolization

	Improved (%)	Resolved (%)	Worsened[a] (%)	Unchanged (%)
Cranial nerve III	20	60	6	20
Cranial nerve IV	17	50	–	33
Cranial nerve VI	12.5	50	12.5	37.5
Complete ophthalmoplegia	–	–	–	100
Cranial nerve V_1 sensory loss	44	56	6	–
Sympathetic	–	–	–	100
Parasympathetic	–	–	–	100

[a] Transient with eventual improvement as compared to pre-embolization.

(Figs. 7.32–7.35). The results of treatment on cranial nerve dysfunction are outlined in Table 7.21. Dysfunction in the third, fourth, fifth, and sixth cranial nerves resolved in more than half of the patients and improved in others. The fifth nerve was the only one that showed either full recovery or some improvement in all patients.

No improvement occurred in the sympathetic or parasympathetic dysfunctions.

7.2.2.5 Cervical Fibromuscular Dysplasia

Cervical fibromuscular dysplasia (FMD) is characterized by multifocal dysplasia of the vessel wall of branches of the aorta and is frequently associated with intracranial aneurysms. The lesions (Fig. 7.36) may be stable or progressive. Over 30%–50% of patients have a family history of FMD and a number of other vascular disorders (stroke, high blood pressure, migraine, impaired hearing, cerebral hemorrhage, etc.). It has been suggested that FMD is inherited as a dominant trait, with reduced penetrance in males (Rushton 1980).

The morphological features in affected head and neck arteries are the same as those described in the renal artery and include fibroblast-like transformation of smooth muscle cells. Each of the three layers of the arterial wall may be dysplastic. The spectrum of lesions include the beaded

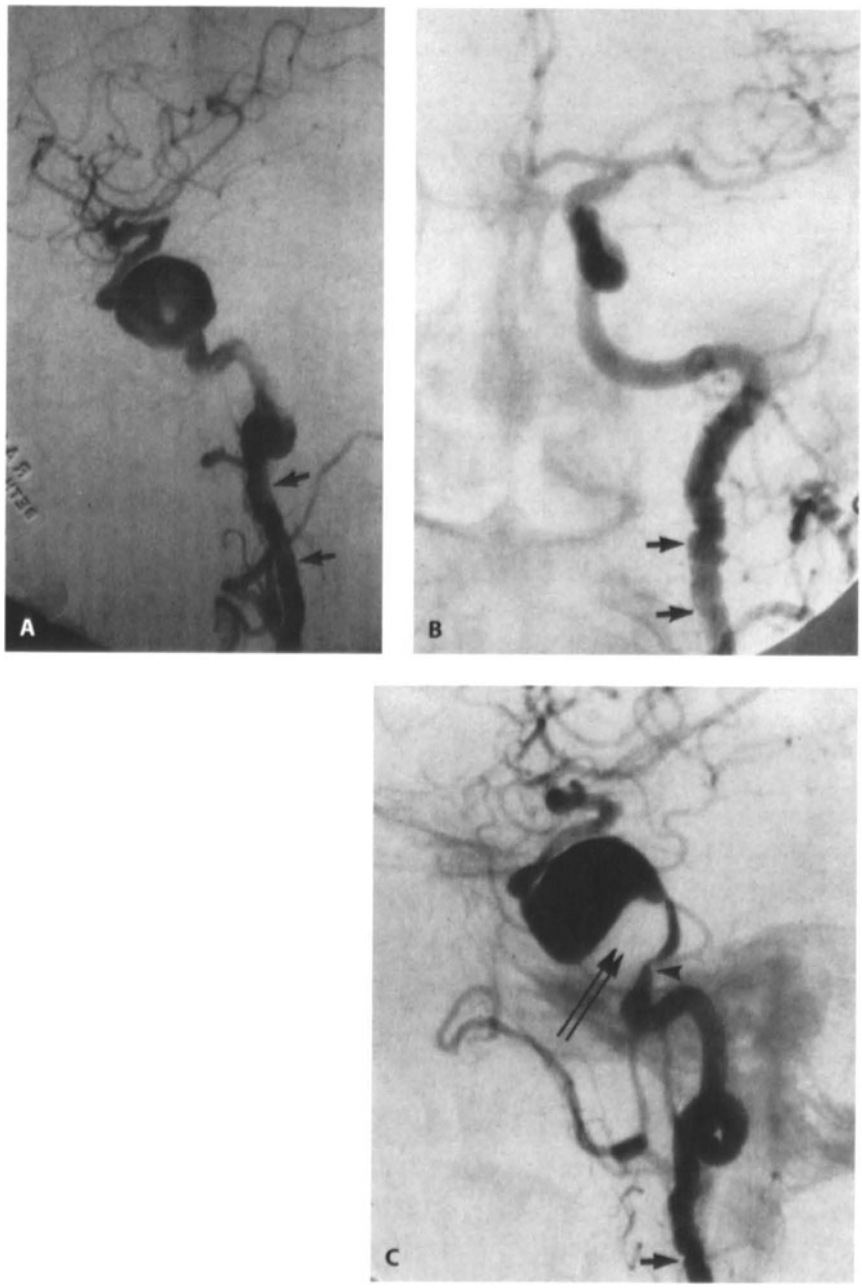

Fig. 7.36A–C. Cavernous aneurysm associated with fibromuscular dysplasia (FMD) of the progressive type. A 39-year-old female patient with high blood pressure, chronic headache, fluctuating ophthalmoplegia, and rapid onset of diplopia and delayed onset of Horner's syndrome. **A** Note the characteristic string-of-beads appearance of FMD (*arrows*). The diplopia resolved spontaneously in 3 weeks. She was placed on an antiplatelet regimen. **B** The left internal carotid artery (ICA) is also involved with FMD (*arrows*). **C** Lateral subtraction angiogram of the right ICA, 1 year later. While still on aspirin therapy, the patient presented with acute onset of Horner's syndrome. Note the progression of the disease, with significant tubular stenosis (*arrowhead*) and partial thrombosis of the aneurysm (*double arrow*)

type, which is generally caused by medial fibroplasia (60%–85%), with alternating ridges (fibroproliferative tissue or collagen disrupting the smooth muscle) and aneurysms in the media (deficient smooth muscle or lamina elastica interna). Tubular stenosis (elongated narrowing of the lumen) and focal ring-shaped or eccentric stenoses may also occur. Macroscopic aneurysmal outpouchings and dissections can be present at angiography and at gross pathological examination and are thought to be complications of FMD.

FMD of the brachiocephalic vessels characteristically occurs distal to the cervical bifurcations and is rarely found in the proximal portions of the common carotid or vertebral arteries (see Sect. 7.3.1.5).

In more than 90% of cases, the clinical presentation of FMD includes frequent headaches, high blood pressure, high incidence of associated ruptured cerebral aneurysms, as well as ischemic cerebral episodes. Associated Horner's syndrome and hearing impairment may occur. These symptoms, when present in a young patient (particularly a Caucasian female) are highly suggestive of FMD (Manelfe et al. 1974; Mettinger 1982). The renal arteries should also be analyzed. Stenotic lesions of the carotid arteries were in the past treated either by surgical resection of the involved segment or by progressive intraoperative dilatation (Ehrenfeld and Wylie 1974). Hasso et al. 1979 was the first to report the use of angioplasty balloons to dilate single symptomatic constrictions with good results, and this treatment is now standard treatment for symptomatic stenotic FMD of the cervical ICA that does not respond to antiplatelet medication. The disease mostly runs a benign course, provided that efficient prevention of embolic stroke can be achieved. The association with intradural AA will be discussed in Sect. 7.3.2.1.

When an extradural aneurysm associated with FMD is deemed to require treatment, parent vessel sacrifice should probably be considered, similar to the treatment of aneurysms in other vascular dysplasias (neurofibromatosis). Parent vessel preservation using angioplasty and stenting may cause the dysplastic wall to fail to support the hemodynamic changes, resulting in distal embolization, particularly in collagen diseases. This issue remains controversial and therefore should be thoroughly assessed in each individual case.

7.2.3 Internal Carotid Artery Occlusion in Extradural Internal Carotid Artery Aneurysms

For a long time the treatment of choice of cervical aneurysms was surgical resection of the aneurysm with reconstitution of the carotid lumen using venous or Dacron grafts, or if possible, with primary anastomosis when there was significant redundancy of the carotid artery (Benvenuto et al. 1961; Buxton et al. 1964; Cifarelli and Sadiq 1971; Halasz and Kennady 1964; Ohara et al. 1968; Raphael et al. 1963; Shea et al. 1955; Wilson and Jordan 1961). Transcatheter treatment has now been developed and benefits largely from the experience gained in cervical arterial occlusive disease stenting. While preservation of the cervical arteries to the brain is the ideal goal to reach, there will still be a significant number of cases in which carotid occlusion is a safe and stable treatment.

Surgical experience seems to favor gradual occlusion with a clamp (Drake 1979b; Gianotta et al. 1979; Oller et al. 1976; Pia 1978). This gradual and reversible occlusion theoretically appears safer than acute ligation, as it can reestablish flow if necessary, but ischemic cerebral symptoms can occur as the occlusion nears completion. Distal embolization may occur after reopening the clamp, or prior to complete clamping from residual antegrade flow through the partially thrombosed aneurysm or from partial thrombosis of the carotid artery proximal to the clamp.

In a cooperative study, Nishioka (1966) reported deficits, thought to be ischemic, that occurred during gradual occlusion of the internal carotid artery and that reversed in 56% of the patients when the clamp was reopened. However, in some patients the deficit worsened after the clamp was opened, and although the term "ischemic" was used, the worsening of the symptoms after increasing carotid flow must reflect an embolic potential. In 62 patients reviewed by Landolt (1970), 38% of patients treated by gradual occlusion developed complications, as opposed to only 24% of those treated by abrupt carotid occlusion. These authors concluded that most of the so-called ischemic deficits encountered during or after therapeutic carotid occlusions are thromboembolic in nature. A similar conclusion was reached by Heros et al. (1983). They recommend the use of detachable balloons or abrupt ligation of the internal carotid artery with the patient awake following angiographic demonstration of good collateral circulation and proper balloon test occlusion.

In patients who have poor collaterals or those who fail provocative testing, an EC–IC bypass may be advisable. We suggest retesting following this bypass and prior to carotid occlusion.

Peerless, in the comment to Heros' article (1983), concurred with this conclusion and suggested that the balloon occlusion just proximal to the aneurysm would leave a shorter stump in the carotid for thrombi to form. He already suggested systemic anticoagulation with a gradual tapering dose of heparin over 7 days and then aspirin for 1 month. Interestingly, in Peerless's group of 15 patients with giant aneurysms treated in this way, no complication occurred. However, in three (20%), after occlusion proximal to the aneurysm, the aneurysms continued to fill and required surgical trapping. Unfortunately, he failed to mention if any of these aneurysms were beyond the cavernous area.

7.2.3.1 Tolerance to Carotid Occlusion

If treatment is contemplated during the angiographic work-up prior to embolization, a test of tolerance to acute carotid occlusion is needed. Various tests have been reported, including xenon cerebral blood flow studies and stump pressures after temporary occlusion (Drake 1979; Gelber and Sundt 1980; Sharbrough et al. 1973; Berenstein 1984b) (see Chap. 1, this volume). In patients in whom an associated intracranial aneurysm is found, primarily in another circulation, and in whom carotid occlusion is contemplated, the incidental aneurysm should be treated first (Fig. 7.25).

Following internal carotid artery occlusion, primarily at the cervical level, delayed (3–5 days) neurological complications may result from em-

bolization through retrograde filling of the aneurysm via recanalized segments of the cavernous carotid at the C4 or C5 levels (Drake 1983) or from the proximal internal carotid stump (Barnett et al. 1978) (Fig. 7.29). To prevent this complication, balloon occlusion of the internal carotid artery has the advantage over cervical (surgical) carotid ligation in that it permits easy percutaneous trapping of the aneurysm in one procedure (Fig. 7.29).

Since we started using balloon stumpectomy, we have seen no episodes of embolism from the external carotid to the ophthalmic or internal carotid arteries. As an additional precaution, the use of platelet aggregation inhibitors such as low doses of aspirin for 1 month has proven useful.

Minor transient aggravation of ocular symptoms or trigeminal pain can occur following embolization, and may be due to a traction phenomena on the nerves in the cavernous sinus during collapse of the thrombosing aneurysm sac (Fig. 7.35), (Strenger 1966).

Drake (1979) has postulated that enlargement of the aneurysm during thrombosis could also be responsible for frequent transient and reversible aggravation of ocular symptoms. On one occasion, emergency surgery to decompress the optic chiasm was needed in Drake's experience. Most probably a combination of both phenomena is responsible for this relatively infrequent transient clinical worsening.

Aneurysm trapping may not be possible in all cases, as the outlet into the distal carotid may be at an unfavorable segment of the aneurysmal sac (Fig. 7.26). In some cases, an elongated Gold Valve 16 latex balloon can be used to reach the distal outlet of the aneurysm. In others, it may be unwise to manipulate a microballoon catheter through an aneurysm if the preliminary angiogram shows a partially thrombosed lesion (Figs. 7.28, 7.32). When there is an ophthalmic artery origin from the cavernous carotid artery (Fig. 7.24), this segment must be preserved, as its occlusion carries a high risk of blindness.

The technique used for test occlusion is different depending on the available tools in various areas of the world; however, the following issues remain essential:

- Careful analysis of the anatomical disposition and transcranial anastomoses in most cases make it possible to anticipate the result of the test.
- The test should be done under systemic heparin protection.
- The occlusive device used for the test should not damage the vessel wall.
- Assessment of the other vessels' contribution during balloon inflation is necessary and requires access by two catheters.
- The simultaneous appearance of the venous phases of the distal territory of the occluded artery and that of the supratentorial and infratentorial brain is a strong indicator of good tolerance.
- Clinical assessment should be simple and rehearsed with the patient before the test.
- The duration of the occlusion can range from 10 to 30 min; usually intolerance is immediate. The blood pressure at which the test is made should be carefully chosen, noted, and monitored during and after the test if the artery is sacrificed.

- If the test is done with a detachable balloon it should be placed at the site of optimal detachment but gently inflated, enough to allow occlusion. If the test is favorable the balloon is not deflated. It will be inflated further if the decision is made to proceed to the sacrifice.
- If the test is done with a nondetachable double-lumen balloon catheter distal heparinized saline dripping should be maintained, as deflation will proceed regardless of the result of the test.
- Finally, we recommend that when a major cerebral vessel is occluded, more than one balloon should be used as a safeguard in case of early deflation. The last balloon should be placed in the cervical internal carotid artery just distal to the bifurcation to obtain an endovascular balloon stumpectomy (Fig. 7.29).

At present, EC–IC bypass is an excellent adjunct prior to balloon occlusion of the internal carotid artery, when one can predict insufficient collateral circulation from the angiographic investigation, or when the patient fails the tolerance test. EC–IC bypass will decrease the potential of ischemic complications, but will not prevent delayed embolic episodes. The value of prophylactic EC–IC bypass is questionable (Heros et al. 1983).

7.2.3.2 Postembolization Care

In addition to routine postembolization care (see Chap. 1, this volume), special considerations must be taken after occlusion of the internal carotid artery. Frequent and careful neurological and cardiovascular assessment is mandatory. Ischemic deficits may result from fluctuations in blood pressure, position, or cardiac output. These patients have a high incidence of high blood pressure and periods of relative hypotension may require aggressive management with volume expanders or vasopressor medication (see Chap. 1, this volume). On occasions when ischemic symptoms develop (early or delayed), a pharmacological increase in cerebral perfusion by medical means may be necessary for up to several days, until the autonomic regulatory system compensates and sufficient collateral flow is established. Strict bed rest is mandatory during the immediate postoperative period. Patients may start ambulation progressively 36 h after embolization, but physical activity should be restricted for approximately 3–4 weeks.

7.2.4 Extradural Vertebral Aneurysms

Extradural vertebral aneurysms are rare. In a review of 125 cases, Killian (1951) reported that 17.5% involved the first or proximal segment, 70% the second portion, and 12.5% the third portion of the vertebral artery. Trauma is the most frequent cause.

After its origin from the subclavian artery, the first segment of the vertebral artery is enclosed by fascia as it traverses the neck to enter the transverse foramen of the sixth cervical vertebral body. At this point, it courses between tendons of the scalenus anterior, longus coli, and

scalenus media muscles. It then ascends through the transverse foramina of the upper cervical vertebra. It is accompanied by a plexus of veins, which communicate with the epidural longitudinal vertebral plexus, the basivertebral veins, and the prevertebral veins, which ultimately drain into the internal jugular vein. The third segment exists from the transverse foramina of the atlas and courses posteriorly and medially around the lateral mass of the atlas to reach a groove on the upper surface of the posterior arch of the atlas. The fourth segment of the vertebral artery penetrates the oblique ligament of the atlas (inferior border of the atlanto-occipital membrane), pierces the dura of the spine and then courses upward through the foramen magnum to unite with the opposite side to form the basilar artery (Davis and Zimmerman 1983).

Most traumatic pseudoaneurysms of the vertebral artery result from penetrating injuries, including osseous fracture fragments. Because of the close proximity between the vertebral artery and the paravertebral venous plexus, arteriovenous fistulae following trauma and direct puncture vertebral angiography are relatively more frequent than pseudoaneurysms (Davis and Zimmerman 1983; Dutton and Ihserwood 1970; Jamieson 1965; Lester 1966; McDowell 1971).

It has been estimated that as many as 1 in 20,000 spinal manipulations will result in a stroke, often involving the vertebral basilar system.

In vertebral artery SDs, neck pain and nuchal rigidity are frequent, even without SAH. Spinal epidural hematomas are unusual manifestations of vertebral artery dissection. Ischemic symptoms occur in more that 90% of patients and affect mostly the brain (Fig. 7.37). Isolated ischemia of the cervical spinal cord is an uncommon but increasingly recognized complication of vertebral artery SD. Ninety percent of infarcts due to SD are thromboembolic rather than hemodynamic. The reported rate of death from SD of the carotid and vertebral arteries is less than 5%, and about 75% of patients who have had a stroke make a good functional recovery (see Chap. 1, this volume). Vertebral artery SDs are most often at the level of the first and second cervical vertebrae, 10% of vertebral artery SDs extend intracranially (Fig. 7.38).

In about 10%–20% of patients, SD is detected in two or more vessels, and these multivessel SDs often appear to have occurred at the same time.

Nontraumatic aneurysms of the vertebral artery are rare (Fig. 7.39).

Among 125 cases reported by Kilian (1951), seven had mycotic aneurysms associated with osteomyelitis of the cervical vertebrae. A primary dissecting aneurysm of the vertebral artery resulting from degeneration of the media was described in a hypertensive 56-year-old female by Bostrom in 1967. Newton and Adams (1968) reported an unusual case of bilateral saccular aneurysms of the vertebral arteries, internal carotid artery, and brachial artery, probably the result of a congenital defect in the media. Enlargement of the adjacent neural foramina indicated that the lesions were long standing.

Some cases are associated with familial vessel wall diseases leading to large AAs, as seen in neurofibromatosis type I (Fig. 7.40). In other situations, the dysplastic arteries will present fusiform alterations in conjunction with stenotic segments. The appearance is that of an abnormal proximal artery, which at a given segment suddenly returns to normal caliber

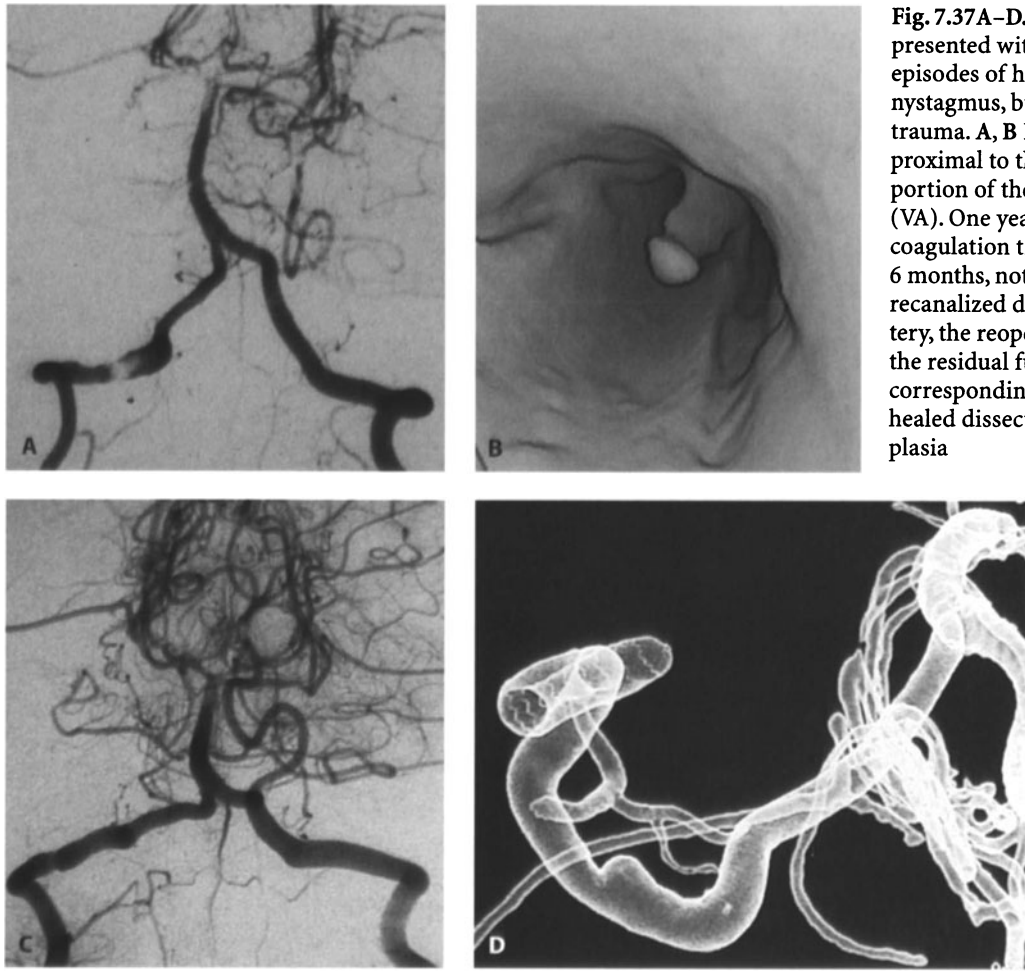

Fig. 7.37A–D. A 7-year-old boy presented with repeated episodes of headaches and nystagmus, but no history of trauma. **A, B** Intraluminal clot proximal to the transdural portion of the vertebral artery (VA). One year later, after anticoagulation treatment for 6 months, note (**C**) the partially recanalized distal basilar artery, the reopened VA, and (**D**) the residual fusiform ectasia corresponding to a possibly healed dissection or focal dysplasia

with a normal distal vascular bed. As seen following rupture of these vessels into the vertebral plexus, repair of these abnormal arteries cannot be achieved and they eventually thrombose.

C1–C2 and C2–C3 dissections with aneurysmal dilatation, endoluminal clot, and distal emboli are often noted on investigation of recurrent posterior fossa stroke in children (Figs. 7.37, 7.38). They are usually nontraumatic, yet no underlying disease is found, and the treatment is medical (see Vol. 3). The angiographic appearance is one of a fusiform dissecting AA; following anticoagulation and aspirin treatment, the lesion heals but the segmental or focal fusiform ectasia (Fig. 7.37) tends to remain, apparently without risk of future rupture (as in the second type reported by Mizutani et al. 1999; see Sects. 7.4 and 7.5.2).

The angiographic work-up of vertebral AA is the same as described for patients with cavernous aneurysms and includes full angiographic analysis to rule out additional lesions, assessment of collateral circulation and tolerance testing. The treatment of choice for surgically inaccessible lesions is trapping of the aneurysm with preservation of supply to the ipsilateral posterior inferior cerebellar artery. The technique and principles are similar to those mentioned in the treatment of carotid artery aneurysms and vertebral artery fistulae. In addition, the arterial supply to

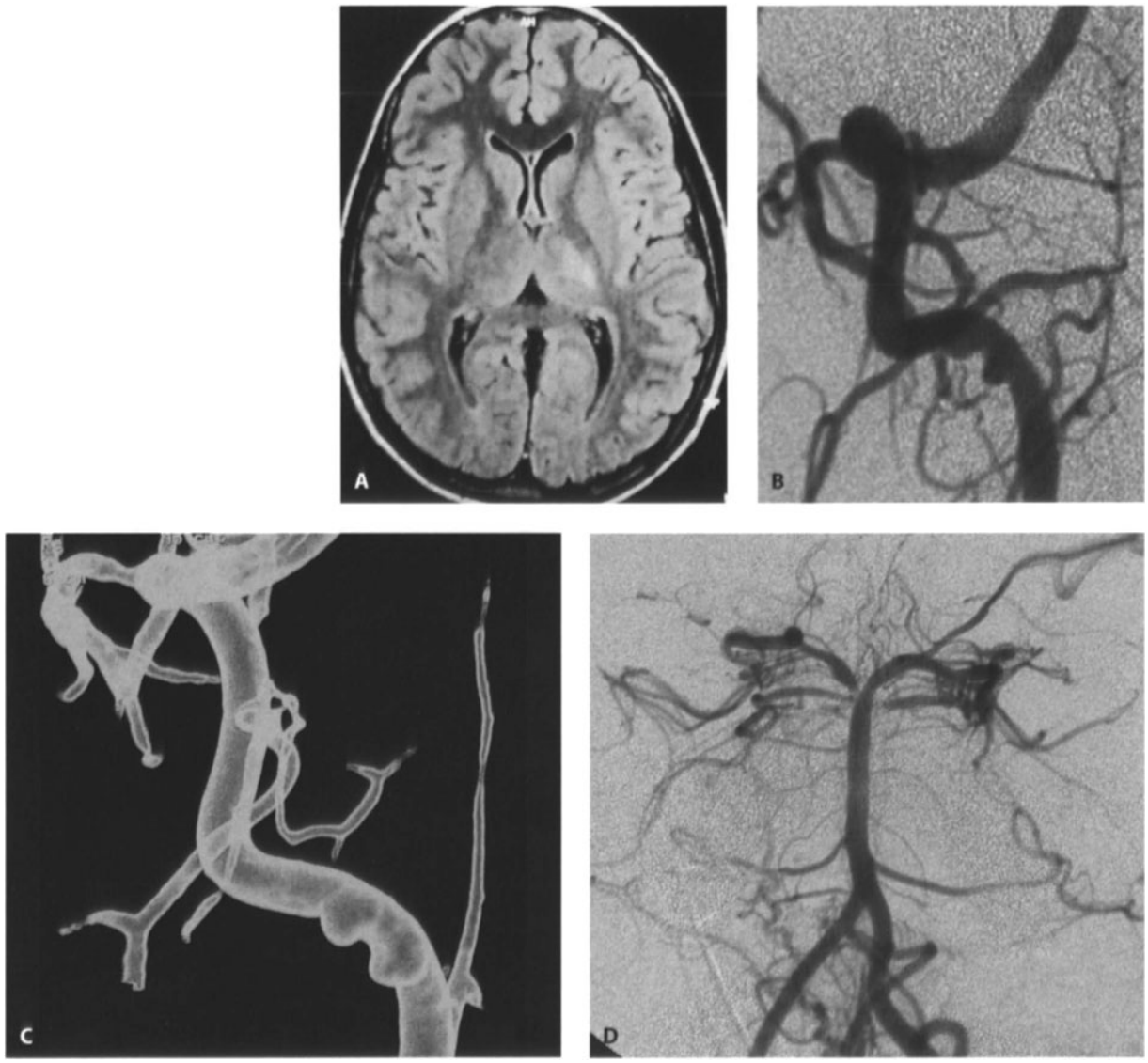

Fig. 7.38A–D. A 3-year-old boy presented with transient episodes of bilateral blindness and right-sided paresthesias involving the upper limb. Repeated accidents over a few weeks. Sudden vertigo, double vision, headaches before right-sided hemiparesis. Normal CT, MRI shows increased signal involving the left thalamus (**A**) and cerebellar hemispheres. C2–C3 dissecting type of AA with no intraluminal clot (**B, C**). Microemboli in posterior fossa circulation (**D**). Good clinical recovery; treatment included 6 months of anticoagulation therapy

the cervical spinal cord should be scrutinized and verified prior to vertebral artery sacrifice. In particular, both its role in the supply to the cord and potential for collateral circulation are important to note (Fig. 7.150). As many of the diseases involved will weaken the arterial wall, high-quality noninvasive vascular imaging such as enhanced MRI is highly recommended prior to selective transarterial catheterization.

Numerous cases of FMD of the cervicocephalic arteries have been published, including a series of 383 cases reported by Mettinger and Ericson in 1982. In contrast, little is known about FMD lesions affecting the verte-

Fig. 7.39. Nontraumatic fusiform aneurysm (*arrow*) of the extradural vertebral artery, likely to be of the dissecting type

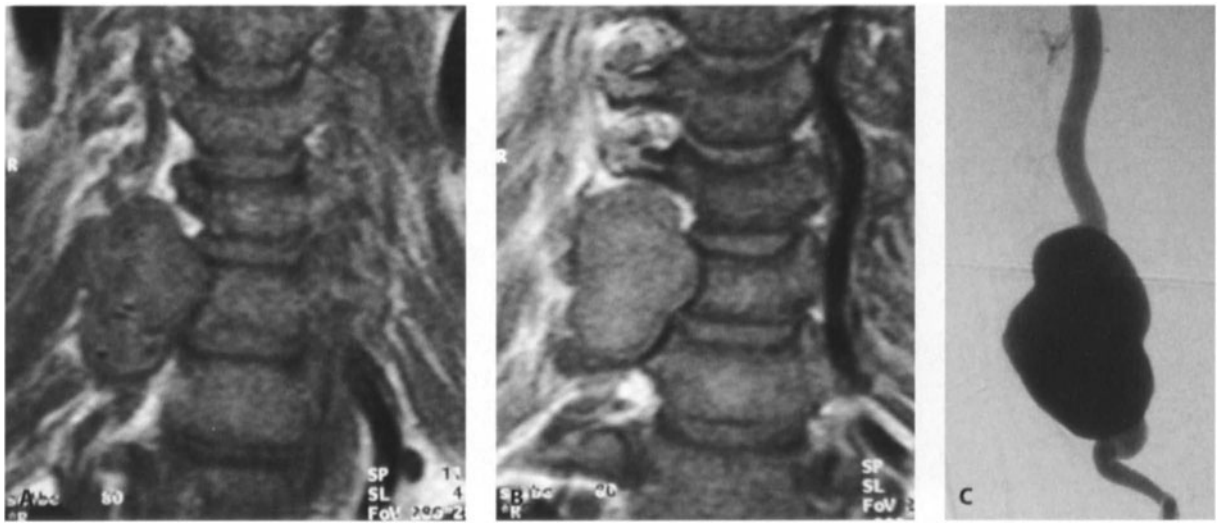

Fig. 7.40A–C. A 21-year-old female patient with neurofibromatosis type 1. She presented with right cervicobrachial pain with no peripheral nerve palsy, suspected to be related to a neurofibroma. **A, B** MRI showed paravertebral soft tissue mass lesion with bony erosion. **C** Angiography demonstrated giant fusiform arterial aneurysm of the V1 segment of the right vertebral artery. Proximal coil occlusion of the vertebral artery was subsequently performed with incomplete resolution of the pain at long-term follow-up

bral artery and a search of the literature yielded a total of only 85 cases (Vega et al. 1985).

The clinical findings were extremely varied. Thirteen percent of the patients had an established or transient ischemic accident in the vertebrobasilar territory and one-third of these presented with a dissection of the vertebral artery; 32% exhibited symptoms (vertigo, cranial nerve paralysis, dizziness) that could be ascribed to vertebrobasilar insufficiency; 13% complained of headache associated with other neurological signs

suggestive of vertebrobasilar insufficiency or ischemic accident. A cervical bruit perceived by the patient was noted in 15%; one-fifth of these patients had a vertebrovertebral AVF.

In 32% of patients, however, FMD of the vertebral artery was discovered by chance, either during an ischemic event in the carotid territory, during evaluation of SAH (2/85 cases), or after a bruit was detected at auscultation.

At angiography, 121 vertebral arteries were found to have FMD lesions. Among the 50 patients who underwent bilateral vertebral arteriography, 72% had bilateral and 28% unilateral FMD involvement.

In 75 of Vega's 95 patients, FMD of the vertebral artery was associated with FMD of the extracranial portion of the internal carotid artery. In 9 of 75, the disease affected not only the internal carotid artery, but also other major vessels, notably the external carotid artery or its branches (five cases), the axillary artery (one case) and the right and left MCA arteries (one case).

In a series of 150 patients with FMD of the cervicocephalic arteries, the disease involved the carotid arteries in 140 cases (93%) and the vertebral arteries in 85 cases (53.5%) (Vega et al. 1985). The greater incidence in the carotid vasculature might be because all patients did not have angiography of the vertebrobasilar vessels.

7.2.5 Aneurysms of the External Carotid Artery

Aneurysms of the external carotid artery are rare. Schechter's review (1979) of all reported cases of cervical carotid aneurysms from 1687 to 1977 revealed that only 2.2% affected the external carotid artery. The great majority of these AAs were posttraumatic and usually secondary to penetrating injuries, as reported by Hite et al. (1966).

Davies (1961) collected 115 patients with superficial temporal aneurysms prior to 1935: 72% were posttraumatic. He also reported two traumatic pseudoaneurysms secondary to penetrating injuries and Wortzman (1963) reported the first angiographically documented pseudoaneurysm. In 1979, De Stephano reported a pseudoaneurysm of the lingual artery. In 1983, Gomori et al. reported the angiographic and CT findings of a lingual pseudoaneurysm confirmed pathologically, although no history of trauma or infection could be obtained.

Pseudoaneurysms of the internal maxillary artery from a penetrating injury (gunshot wound) (Fig. 7.41) and of the facial artery after blunt trauma (fistulous pouch without bone fracture) (Fig. 7.42) are classic findings that were noted during embolization of severe hemorrhagic complications of maxillofacial trauma.

Pseudoaneurysms of the superficial temporal artery (Fig. 7.43) and middle meningeal artery after surgery or in association with other vascular injuries can also be observed. Although the former may have little clinical significance if stable and expansive, the latter carries the potential of producing an extra-axial fluid collection. Extradural hematomas were seen in 70% of patients and subdural collections in 20% of patients reported by Treil et al. (1977). In 80% of cases, the lesion was secondary to skull trauma.

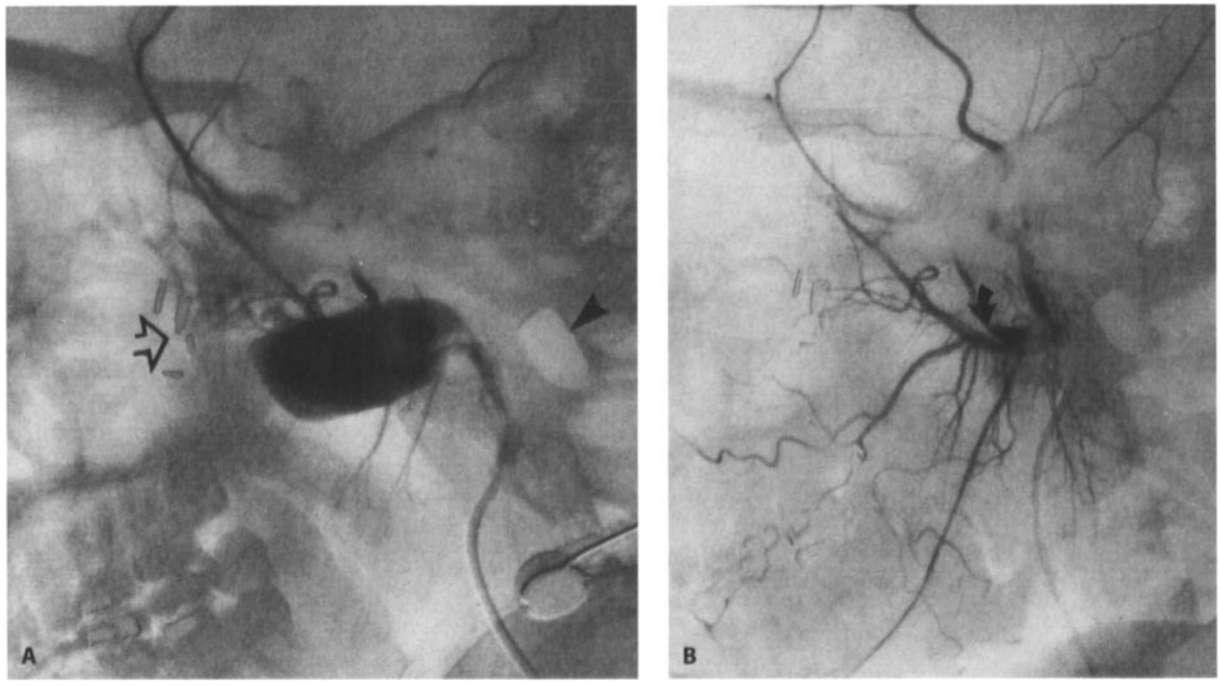

Fig. 7.41A, B. Traumatic false aneurysm of the IMA following a gunshot wound. The patient presented with acute epistaxis, which responded to surgical clipping of distal IMA branches. Delayed recurrence of epistaxis brought the patient to angiography. **A** Maxillary artery angiogram shows a large pseudoaneurysm at the origin of the middle meningeal artery. **B** The aneurysm was occluded (*curved arrow*) with a large piece of Gelfoam. In a previously healthy vascular system, Gelfoam accomplishes an occlusion that lasts long enough for definitive repair

The filling of diploic or dural veins following head trauma with or without epidural hematoma is frequent; it does not necessarily indicate a true AVF, but may be secondary to active extravasation into a closed compartment at high pressure.

With the exception of the intracranial branches, traumatic lesions of the external carotid artery tend not to produce symptoms, probably because of the rich local collateral circulation. In symptomatic patients, the clinical presentation is that of a pulsatile mass in the distribution of one of the external carotid artery branches. Epistaxis may occur in sphenopalatine injuries and can be intermittent. Turbulent flow within the aneurysm may give the false impression of a bruit, suggesting the presence of a fistula. The diagnosis is usually made by enhanced CT and confirmed at angiography. Extravasation of contrast material may be demonstrated during periods of active bleeding (Fig. 7.43). One should be prepared to embolize when performing emergency angiography after trauma, even without evidence of active bleeding at angiography. Special attention should be paid to the missing artery or focal spasm. It is important to conduct a complete study of the arterial and venous circulation at the skull base prior to making a decision based on the interpretation of the angiographic findings and symptoms.

Other causes of pseudoaneurysms in the external carotid distribution include radiation therapy for malignant disease, vessel wall invasion by

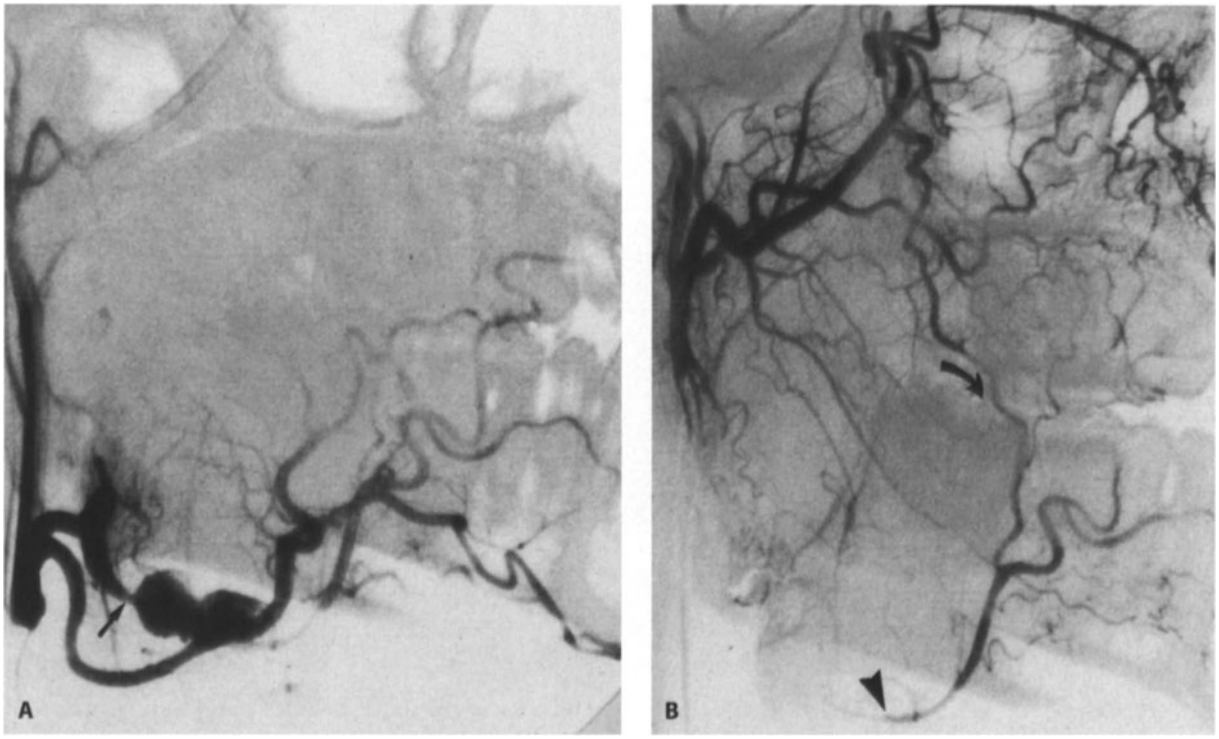

Fig. 7.42A–C. False aneurysm of the facial artery following blunt trauma. **A** Bilobed aneurysm of the facial artery (*arrow*). **B** After embolization, note the collateral circulation distal to the aneurysm (*arrowhead*) via the buccal artery (*curved arrow*). **C** CT without contrast following embolization of the facial artery shows the thrombosed false aneurysm. *Arrows* indicate the intra-arterial glue

tumor (Fig. 7.44), and iatrogenic vessel injury during surgery or percutaneous biopsy. The evaluation of acute bleeding in a patient who may have an external carotid artery pseudoaneurysm is one of the few situations where superselective angiography is *not* indicated, as rerupture and hemorrhage can occur if the catheter is inadvertently wedged during injection.

Nontraumatic aneurysms of the proximal middle meningeal artery can be associated with Paget's disease and in meningiomas. Mujica et al. (1981) reported a 54-year-old female presenting with SAH in whom two aneurysms were found in the meningeal branch of the ascending pharyngeal artery. One sac was at the level of the foramen magnum, immediately lateral to the medulla; the second one was found along the side of the

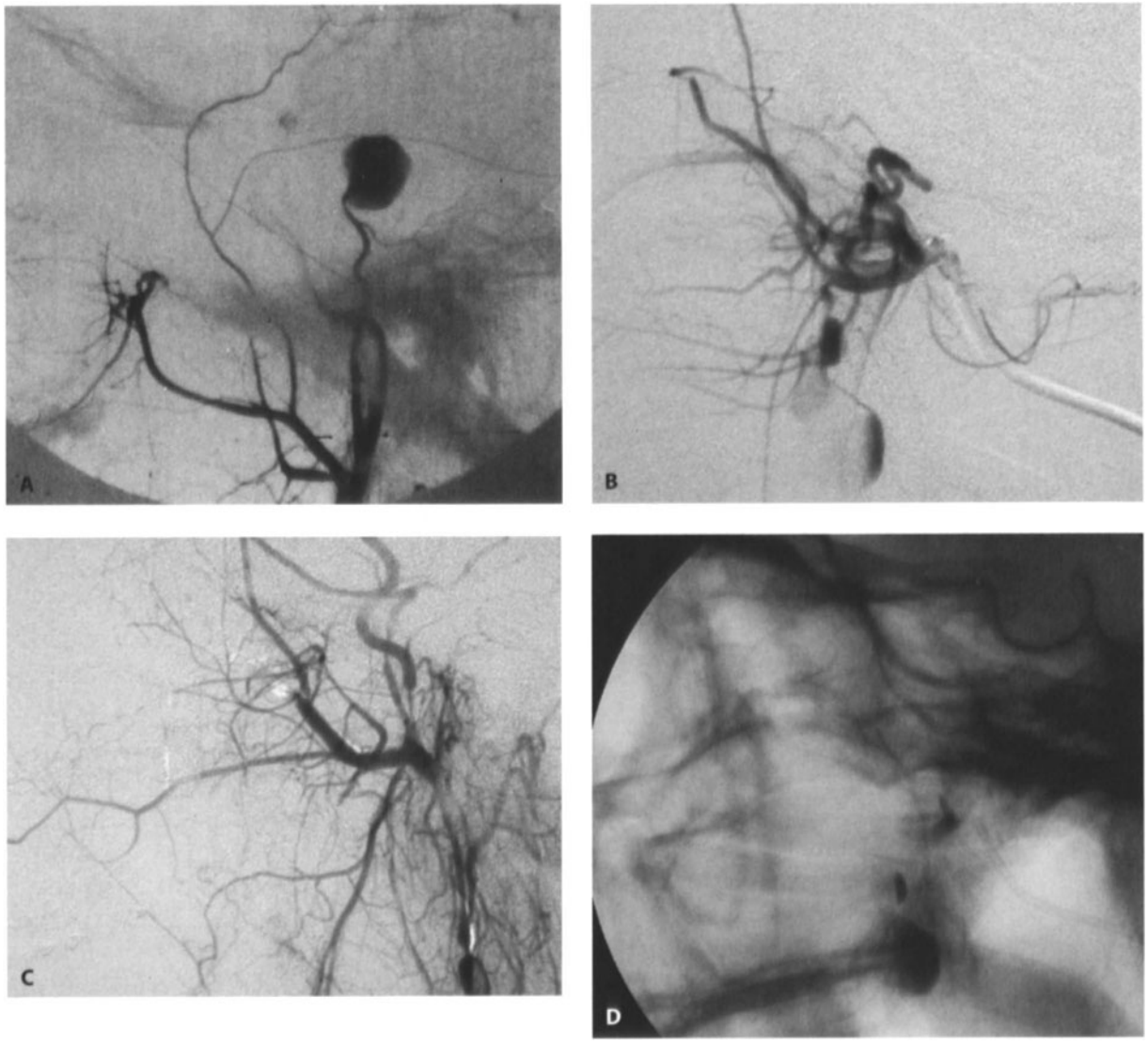

Fig. 7.43. **A** Traumatic pseudoaneurysm of the superficial temporal artery, presenting as a pulsatile mass. **B** A 23-year-old female patient presented sudden intraoral hemorrhage during the postoperative course of an uneventful wisdom tooth removal, in a different patient; false arterial aneurysm of the alveolar artery is shown on selective internal maxillary angiogram (**B**). Angiogram immediately after embolization with glue (**C**) demonstrates exclusion of the bleeding point and fluid level in the pouch on plain film (**D**)

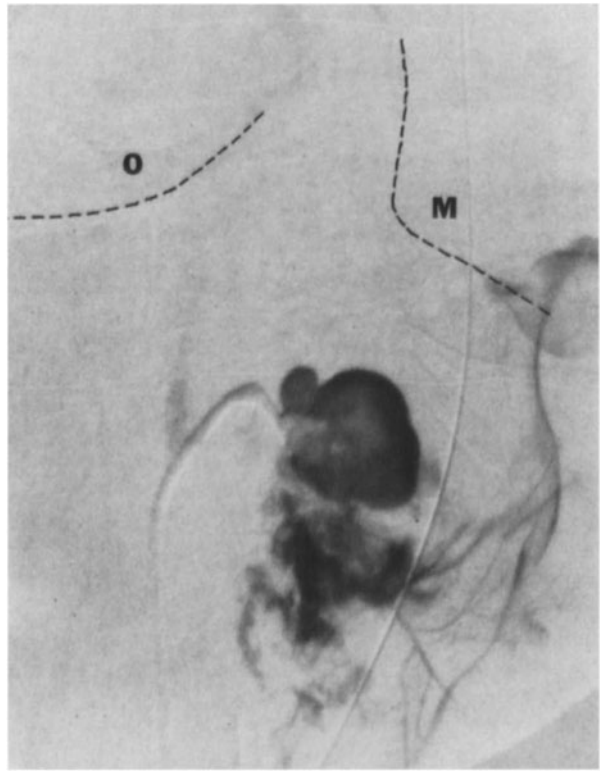

Fig. 7.44. A 48-year-old male patient with nonsurgical laryngeal malignancy treated with irradiation presented with significant oral bleeding from the larynx. Superselective catheterization of the superior thyroidal artery demonstrates a false aneurysm. The pressure injection produced a significant extravasation. *O*, occiput; *M*, mandible

medulla. These were most likely partially thrombosed dural arteriovenous shunts (AVSs) draining in the subarachnoid space.

Flow-related AAs are not seen on the ECA branches supplying high-flow lesions. Hemodynamic changes may account for the few specific situations where AAs are seen: middle meningeal AAs in juvenile-type dural sinus AVSs Fig. 7.117) (see Vol. 3) and in superficial temporal artery (STA) aneurysms after STA-MCA anastomosis. Mycotic aneurysms of the external carotid artery are extremely rare. Dysplastic aneurysms of the external carotid artery are seen in some rare maxillofacial AVMs (Fig. 7.45) and in familial vessel wall diseases. In the latter situation, AAs are associated with multiple changes in arterial caliber of the vessel. In PHACE syndrome, AAs of the fusiform type involve ECA branches; however, these arteries supply the brain in rare anatomical features, preserving embryonic channels (Fig. 7.46).

Aneurysms of the external carotid artery are usually easy to treat by endovascular occlusion, and the success rate is near 100%. Almost any technique that produces a mechanical obstruction of the parent artery at the orifice of the pseudoaneurysm will be effective.

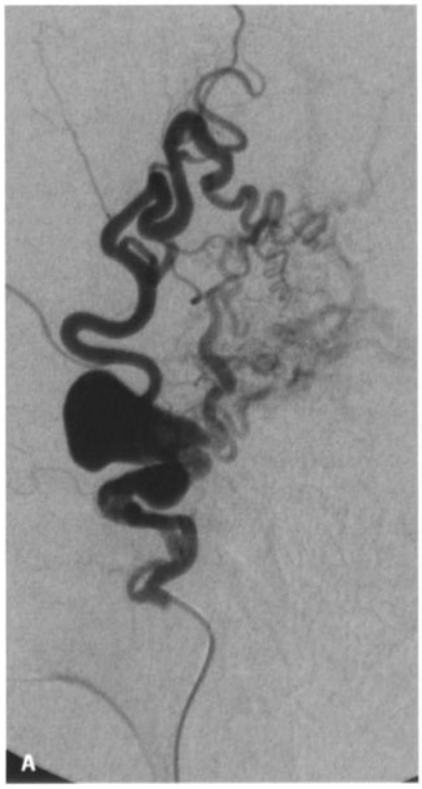

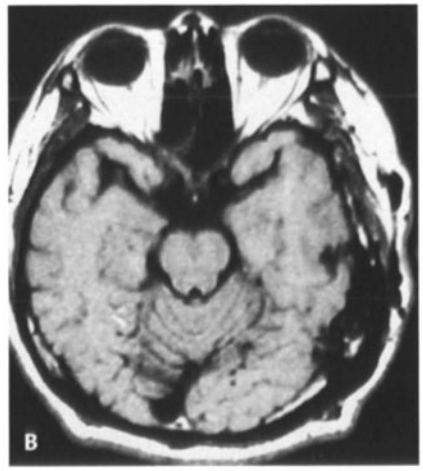

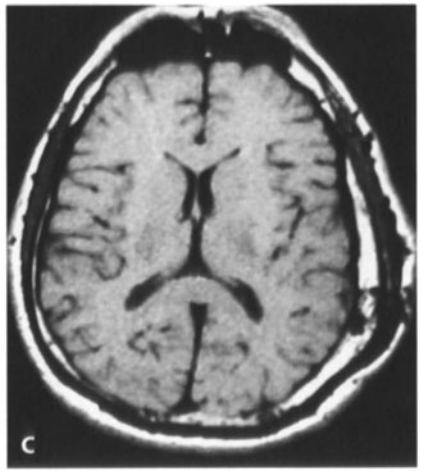

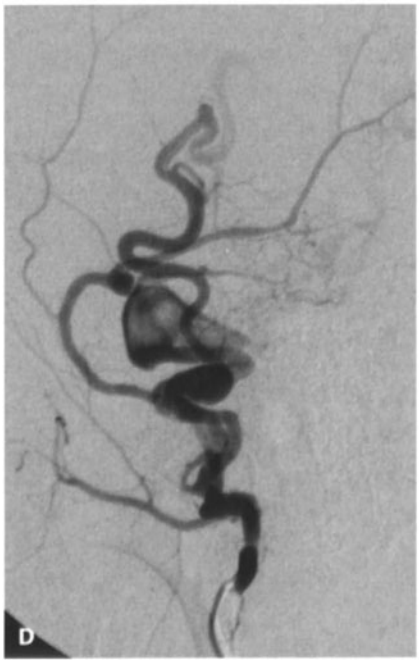

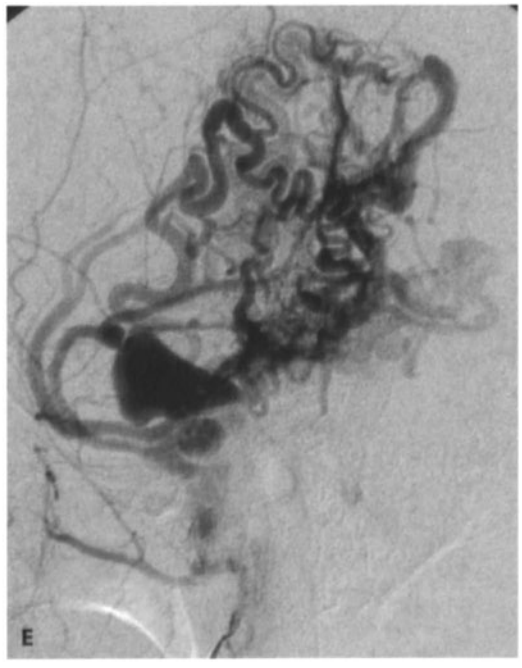

Fig. 7.45. **A** Nontraumatic superficial temporal artery aneurysm in a patient with a subcutaneous arteriovenous malformation invading the parietal bone (**B**, **C**, MRI) and extending into the epidural space, as shown on the middle meningeal supply (**D**, **E**)

Fig. 7.46. **A** Distal maxillary artery aneurysm and **B** facial artery aneurysm in a patient with cerebrofacial arteriovenous metameric syndrome (CAMS 1–2; see Chap. 9). (From Bhattacharya et al. 2001, with permission)

7.3 Intradural Aneurysms

7.3.1 Saccular Arterial Aneurysms and Associated Diseases

7.3.1.1 Polycystic Kidney Disease

The association of autosomal dominant polycystic kidney disease (PKD) and intracranial aneurysms is classic in the adult age group and rare in children, despite its familial character. The recessive form combined with AA is exceptional. The recessive form (infantile form) involves chromosome 4 (De Blasi et al. 1997). Most of the PKD discussion below concerns the autosomal dominant form on chromosome 16 (Fig. 7.47).

PDK1 and *PDK2* are the two recognized genes of PKD. They are located on chromosome 16 (the translocation of 85% of PKD, in the vicinity of Bourneville disease) and on chromosome 4, respectively.

PDK is genetically heterogeneous, with two chromosomal loci accounting for the disease. When the mutation is located on chromosome *16p13.3*, the so-called *PKD1* gene, extrarenal manifestations such as the rupture of the ICA are common. In case of localization on chromosome 4, the *PKD2* gene, the phenotype is mild and only three case reports associated PKD2 with AA (van Dijk et al. 1995).

PDK1 codes a membrane protein, polycystin, with the extracellular domain involved in cell–cell or cell–matrix interaction. *PKD2* codes a transmembrane protein, functioning as a ion channel or a pore. In specimens with AA, aortic dissection, and dolichoectatic arteries from 13 patients with PKD1, Griffin et al. (1997) demonstrated immunostaining for polycystin in arterial smooth muscle cells and myofibroblasts, along with dis-

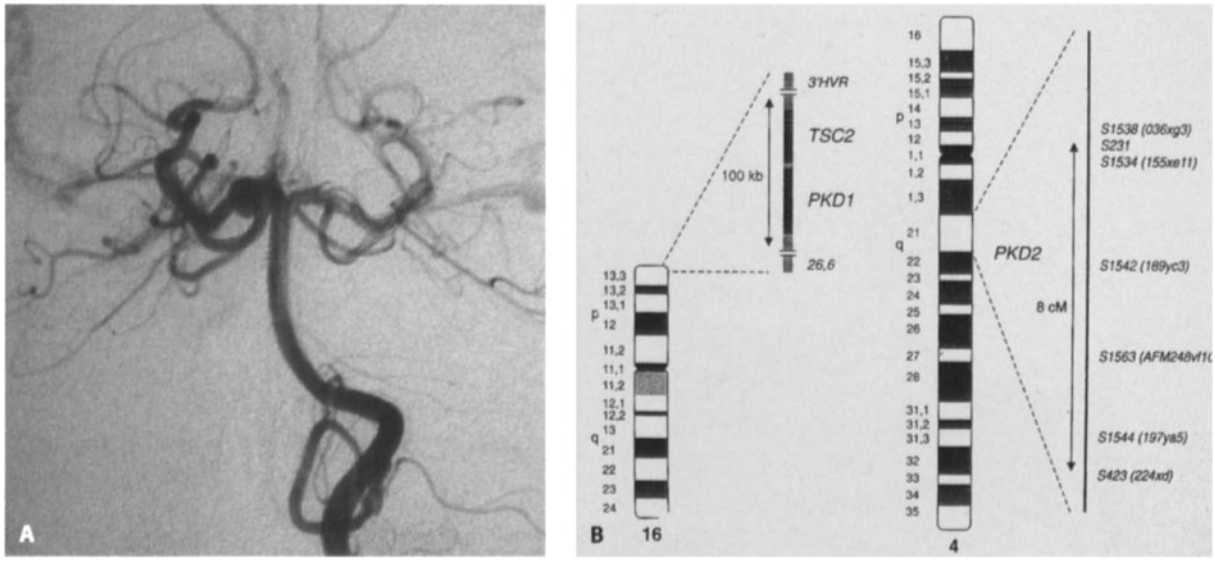

Fig. 7.47. **A** A 13-year-old boy with recessive (chromosome 4) form of polycystic kidney disease (PKD) with liver fibrosis, diagnosed when he was 4 years old, presented with subarachnoid hemorrhage. Angiography showed three intracranial aneurysms: one basilar tip arterial aneurysm (responsible for the bleed) and a bilateral mirror-type aneurysm of middle cerebral artery bifurcation. **B** Genetic disorders of PKD are carried by chromosome 16 or chromosome 4

ruption of the elastic laminae. AA in patients without PKD1 showed a variable degree of similar response in the same location. This suggests the direct role of polycystin in the development of AA in PKD1. The prevalence of the disease is as high as 1/400–1,000.

PKD accounts for 2%–7% of all patients with intracranial AA (IAA), usually of the saccular type.

Using magnetic resonance angiography (MRA) on 263 PKD patients, Houston (1993) and Ruggieri et al. (1994) found IAA prevalence to be 5.9% in patients with a negative family history of IAA. Prevalence increased to 16% when there was a family history of IAA in these PKD patients. In the largest and best-conducted autopsy study, unruptured AAs were found in 25% of PKD patients in whom the cause of death was not a ruptured aneurysm (Schievink et al. 1992). The most frequent location of IAA in PKD is supratentorial (91%), with 50% of these on the middle cerebral artery (MCA).

The frequency of AA rupture in the PKD population is about 1/2,000 persons per year, about five times higher than the general population (Schievink et al. 1992). There is no sex dominance. The mean age of rupture is 41 years, with a mean of 39 years in the series of Lozano and Leblanc (1992) and Chauveau et al. (1994) and 47 years in the Schievink et al. (1992) series. This is close to the value of the familial forms of AA without PKD (43 years), but 10 years earlier than the sporadic forms (Pirson and Chauveau 1996). The age of PKD patients with ruptured IAA at their bleeding episodes ranges from 6 to 69 years (Pirson and Chauveau 1996). The only characteristic clearly associated with AA rupture in PKD is a family history of AA, which is five times more common in patients with

an AA rupture than in a control group without AA rupture. More than 90% of the ruptured AAs are found in the anterior circulation and on the anterior cerebral artery (ACA). About 30% of PKD patients have additional unruptured AAs.

Maintaining euvolemia may be easier with peritoneal dialysis than with intermittent hemodialysis. Another advantage of peritoneal dialysis in this setting is that anticoagulants are not required. Rebleeding is about 5% within 24 h, 20% within 2 weeks and 50% within 6 months after the initial hemorrhage. Mortality from rebleeding is 50%. IAA rupture is the cause of death in about 20% of PKD patients (Schievink et al. 1992).

Rupture of another AA occurred in 10% of patients successfully treated by AA clipping, in two of them within the first 3 months after the operation and in four others 6–14 years later. In three out of the four late recurrences, the second ruptured ICA was not present (detectable) on the four-vessel angiography taken at the time of the first rupture (Pirson et al. 1996).

Fifty-four percent of patients still had normal renal function at the time of rupture. Twenty-six percent had normal blood pressure before rupture (Chauveau et al. 1994; Kaarlainen et al. 1998). Why IAAs are formed in PKD and why they bleed remains unexplained. The reason for the development of anomalies affecting the walls of other arteries is also unclear, such as coronary aneurysms and dissections of the descending aorta (Pirson and Chauveau 1996). A common mechanism leading to formation of renal cysts and cerebral aneurysm should exist, probably linked to the genetic disorder that has its expression in the support tissues, respectively the basal membrane and the elastic lamina (Pirson et al. 1997). No connection has been proven between the level of renal and/or hepatic failure and AA bleeding. The occurrence of bleeding in children raises the issue of earlier diagnosis with noninvasive exploration of intracranial vessels (angio-CT or MRA). AA rupture entails a 35%–55% risk of combined mortality and morbidity (Schievink et al. 1992). Of patients with PKD, 5%–10% harbor an AA, and such figures could be as high as 22% in families with previously demonstrated AA. Thus, before considering eliminating invasive angiographic techniques, the overall risk of overlooking a small AA that may rupture should be balanced against the morbidity of that rupture. In addition, it is unclear whether a demonstrated unruptured IAA carries the same risk as an SAH from an undemonstrated one. It seems that bleeding during follow-up in PKD patients mostly occurs from IAAs that had not been previously demonstrated (Chauveau et al. 1994). Therefore, there is no evidence that screening patients with PKD for AA is beneficial. This is not contradictory with the benefit of screening in familial SAH in first-degree relatives.

PKD is one of the possible predisposing causes for AA. Its target is not the endothelium per se, and the young age of the patients affected demonstrates the limited role played by hemodynamic factors.

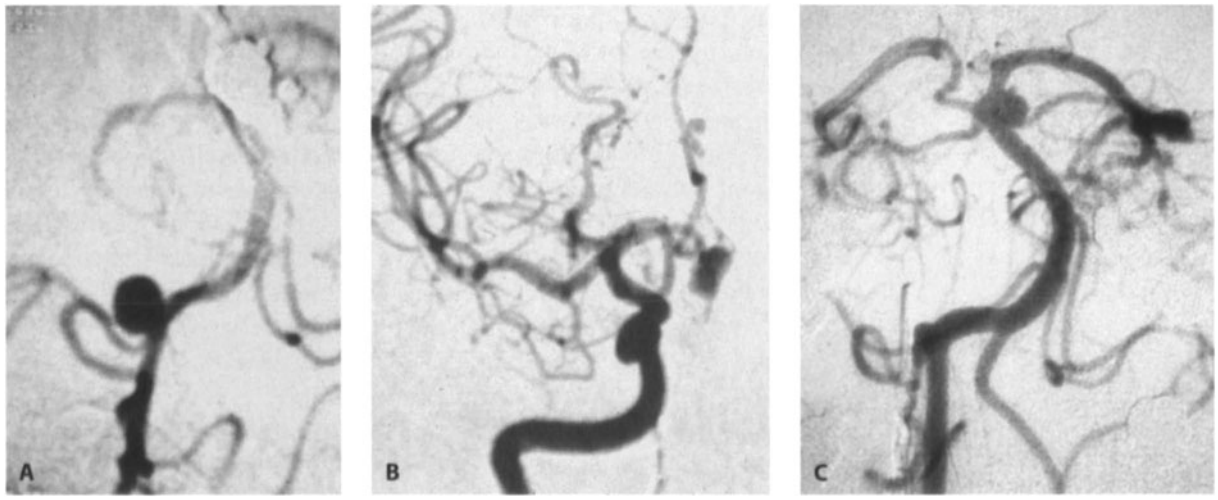

Fig. 7.48. A 30-year-old female patient presented in 1990 with a subarachnoid hemorrhage (SAH) due to rupture of a right PICA aneurysm (**A**). This lesion was clipped; there was no other aneurysm detected at that time. In 1995 she presented with a new SAH from a previously undemonstrated AcomA aneurysm (**B**). An associated right pericallosal arterial aneurysm (AA), as well as an ectasia at the basilar tip, were also detected. The ruptured aneurysm was clipped but postoperative thrombosis of the pericallosal artery occurred. The patient at that time was diagnosed with collagen III, type IV Ehlers–Danlos disease. At follow-up, progressive enlargement of the basilar artery aneurysm was seen (**C**). Preventive embolization was done without complication. (Courtesy of G. Rodesch)

7.3.1.2 Ehlers–Danlos Syndrome

Ehlers–Danlos syndrome (ED) type IV is a disease of the collagen (Fig. 7.48). It classically affects the *COL5A1 and COL5A2* genes. Vascular ED (type IV) was described in 1967; it involves the *COL3A1* gene (Pope 1991). Diagnosis is established on cultured fibroblasts that synthesize abnormal type III collagen. A mutation in the gene for the type III procollagen (*COL3A1*) is the cause for the disease and will be transmitted as an autosomal dominant trait. Multiple mutations are described. However, there is no relation between the nature and location of the mutation on *COL3A1* and the type of complication (phenotype). The prevalence is estimated at 1/50,000 (Schievink et al. 1994). The clinical diagnosis of ED type IV is established on two of four criteria: thin translucent skin; arterial, intestinal, or uterine rupture; easy bruising; and facial appearance.

The classic manifestations include recurrent bilateral spontaneous high-flow CCF because of rupture of the ICA at the cavernous sinus level (see Chap. 6, this volume). Most of the arterial ruptures involve the large vessels, the extradural ICA or vertebral artery (VA). The ECA is not affected. The vessel wall fragility of the arteries is considerable and explains the high mortality of the ruptures and the extreme danger of surgery (out of 69 surgical patients, 28 died during or after surgery) and endovascular manipulations in such patients.

The causes of 103 deaths in ED reviewed by Pepin et al. (2000) were arterial rupture in 78, rupture of the thoracic or abdominal vessels in nine, and the CNS arteries (AA) in 16. The mean age of the first complication

was at 23.5 years and the gastrointestinal rupture occurred before the arterial rupture in most cases (Fig. 7.6). Complications were observed in 272 out of 419 cases; 44 complications involved the CNS in 43 patients at a mean age of 32.8 years, similar to other familial diseases associated with AA. The most frequent complications involving the cephalic region were high-flow spontaneous CCF in ten patients (recurrent), ICA dissection in eight, and arterial aneurysm in seven. As any of the familial type of AA, the lesions are often multiple and spread out along the arterial tree in similar locations as berry aneurysms; they are saccular or fusiform. They are not confined to a single metameric location but can involve all three of them (Fig. 7.48) or be noncontiguous such as the AComA and PICA.

The natural history of these AAs is unknown, but the risk of SAH in unruptured AAs will be high. Cervical locations are frequent and may involve the entire ICA, from a few millimeters beyond the bifurcation up to the ophthalmic artery origin. Segmental dysplastic changes can be observed on the ICA or the VA. In our experience, the rupture is located at the junction of the abnormal and the apparently normal segment cranially. Sacrifice of the ruptured vessel is most often needed at the neck or skull base, despite the risk of recurrence on the opposite side. The danger of intracranial extension of the dissecting process following lengthy and traumatic endovascular maneuvers is high. The rupture is not only a problem as far as hemorrhage is concerned, but it also indicates that the disease has reached a certain stage in its progression. Screening patients in their 30s for intradural AA is recommended, and careful preventive endovascular approaches by highly experienced teams should be offered.

Ehlers–Danlos syndrome type IV, similar to Marfan syndrome, polycystic kidney disease, and osteogenesis imperfecta type I can be diagnosed following SD. But extensive studies have failed to identify any mutations in the gene for type III procollagen (*COL3A1*), the gene for type V procollagen (*COL5A1*), or the gene for tropoelastin (*ELN*) in these cases. The diagnosis is thus suspected on clinical investigation and familial history. Staining for antibody against fibrillin-1 has been negative in these patients (Schievink et al. 2001).

7.3.1.3 Neurofibromatosis Type 1

Neurofibromatosis type I can be associated with AA, single and large or giant, and located extradurally on the cervical petrous ICA or cervical VA. Renal artery stenosis is the most common lesion associated with NF1. AAs are associated with occlusive disease. The diagnosis is often made following rupture secondary to traumatic puncture or SDs similar to Marfan, FMD, and ED type IV. In NF1 there is a female to male dominance of 5:1. The mutation involves the long-arm chromosome 17. The mutation is transmitted as an autosomal dominant trait; in half the cases the disease is caused by a new mutation. The prevalence of NF is around 1/3,000–5,000. The associated clinical diagnosis includes subcutaneous nodules, skin pigmentation, neurofibromatosis, schwannomas, gliomas, hamartomas, neurofibrosarcomas, skeletal abnormalities such as scoliosis, and cystic erosions. The vascular rupture often brings to attention patients

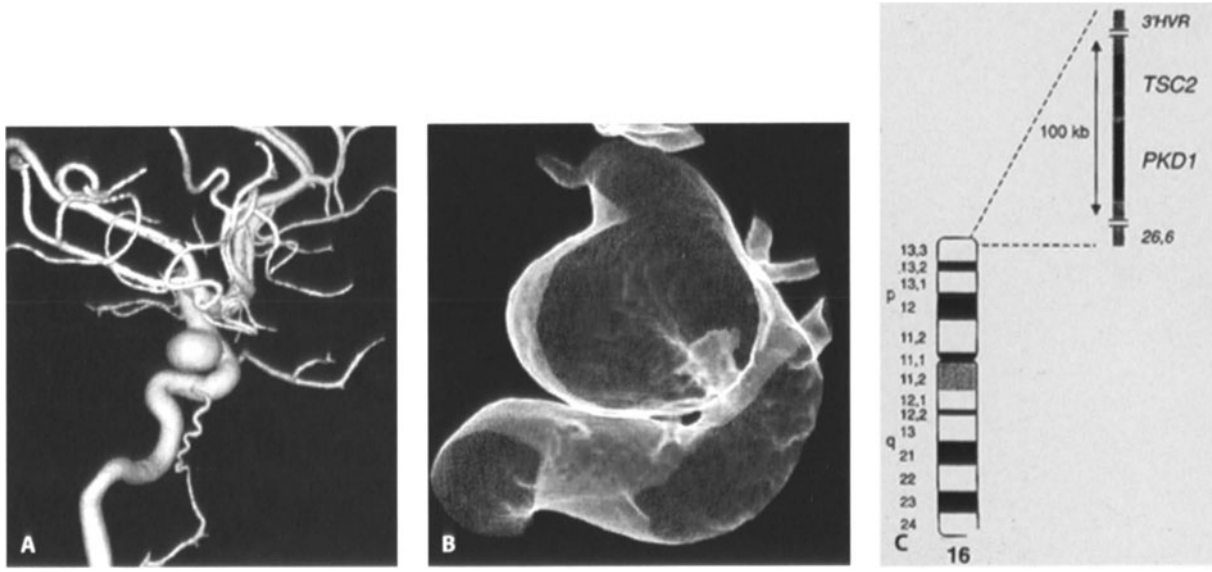

Fig. 7.49. Patient presenting with tuberous sclerosis complex and bilateral renal cysts with an unruptured intracranial internal carotid artery aneurysm (**A, B**). Contiguous gene syndrome TSC2 and polycystic kidney disease PKD1 on chromosome *16p13.3* (**C**). (From Chen et al. 2001, with permission)

with the diagnosis of cervical AVFs (see Chap. 11, this volume). Review of 100 consecutive intracranial AA patients showed one case of NF1 (Schievink 1997).

Neurofibromatosis type II is located on the long arm of chromosome 22. It may be associated with bilateral eighth cranial nerve neurinomas, meningiomas, and meningoceles, but vascular lesions are not part of this disorder.

7.3.1.4 Bourneville Disease

Tuberous sclerosis complex (TSC), or so-called Bourneville disease (Fig. 7.49), was first described by Vogt in 1908 as a triad of clinical features: mental retardation, epilepsy, and adenoma sebaceum. However, the clinical expressions are variable and half of TSC patients will have normal intellect, one-quarter will not have epilepsy, and almost any organ in the body can be affected (O'Callaghan and Osborne 2000). Recent investigation confirmed that TSC is caused by gene mutations that affect the migration and differentiation of neural crest cells in many organs and tissues, mainly involving the brain, skin, kidneys, lung, and heart (O'Callaghan and Osborne 2000; Hyman and Whittemore 2000). The disease is estimated to have a birth incidence of 1 in 6,000, and more than 70% of cases will be new mutations. Of these new mutations, it appears that 75% are caused by *TSC2* mutations (Hyman and Whittemore 2000).

There are two genes causing the TSC clinical phenotypes: *TSC1* is found on the long arm of chromosome 9 and the *TSC2* gene is situated on the short arm of chromosome 16. Brook-Carter et al. 1994 showed the locus

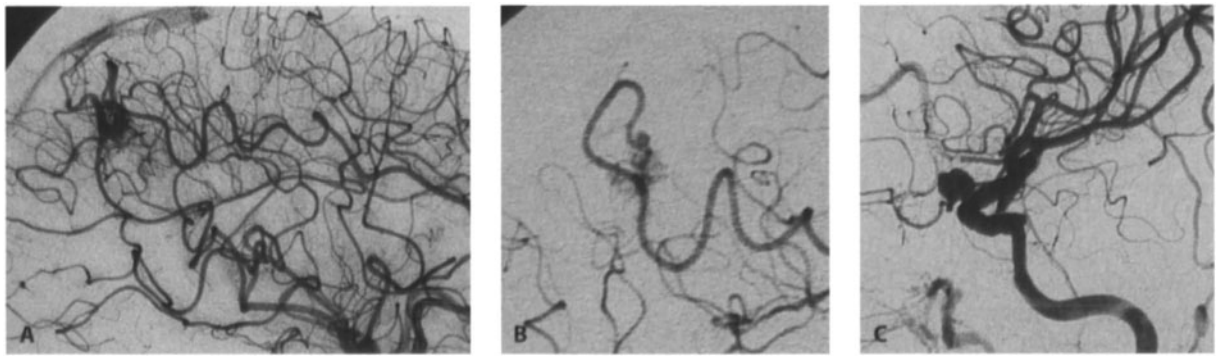

Fig. 7.50A–C. A 57-year-old male patient with known HHT1. The pre-embolization angiogram for pulmonary arteriovenous fistula carotid injection demonstrates multifocal cerebral arteriovenous shunt (**A**) with intranidal aneurysm (**B**), and (**C**) an associated incidental internal carotid artery aneurysm. (Courtesy of A. Boulin and G. Rodesch)

of *TSC2* on the proximal side of the ADPDK type 1 (*PKD1*) gene on chromosome *16p13.3*, only 48 base pairs of DNA from the gene for PKD1 and in a tail-to-tail orientation (Longa 1999). Recently several reports have shown clinical manifestations of PDK occurring in patients with tuberous sclerosis complex such as tuberous sclerosis with ICA aneurysm, multiple renal and liver cysts of variable size, and early onset of end-stage renal disease (Beltramello et al. 1999). *TSC2* and *PKD1* genes share a common location at chromosome *16p13.3*. The occurrence of *TSC2* and *PKD1* gene deletion and the overlapping of the phenotypes of TSC and ADPDK have been demonstrated (Hyman and Whittemore 2000). As a result of advances in molecular genetics, the TSC2/PKD1 continuous gene syndrome has been illustrated in one AA case with Bourneville disease and a renal cyst (Chen et al. 2001) (Fig. 7.49).

Marfan syndrome is a disease involving elastic fiber formation. It produces ocular, skeletal, and cardiovascular abnormalities. The prevalence is 1/10,000. It is transmitted as an autosomal dominant character even if 30% of cases are sporadic. The mutations involve chromosome 15 encoding for fibrillin-1 (*FBN1*) microfibril component involved in the extracellular matrix. The usual cause of death in children is aortic or mitral insufficiency and in young adults aortic dissection. Minor forms can survive to adulthood (see Vol. 3). AAs are usually large or fusiform. IAA as well as extradural AA can be seen.

Pseudoxanthoma elasticum (PXE) and familial tumoral calcinosis may produce both large vessel dysplastic changes involving the cavernous ICA, as well as intradural ICA aneurysm. Adams et al. (1999) suggested an overlap between these two conditions. The disease prevalence is around 1/100,000. It is genetically heterogenous, with autosomal dominant and autosomal recessive types (Pope 1991).

Hereditary hemorrhagic telangiectasia (HHT1) associations with AA appear fortuitous, as the disease impacts the venous system rather than the arterial system (Fig. 7.50). Polymorphism at a genetic variant of endoglin (binding protein for TGFβ1) appears to be involved in these AAs (Takenaka et al. 1999).

7.3.1.5 Fibromuscular Dysplasia

Fibromuscular dysplasia (Fig. 7.36) is characterized by multifocal dysplasia of vessel walls, involving cervical branches of the aorta, and is associated with intracranial aneurysms. Over one-third of patients have a family history of certain vascular disorders (stroke, high blood pressure, migraine, impaired hearing, cerebral hemorrhages, etc.). It has been suggested that FMD is inherited as a dominant trait with reduced penetrance in males.

FMD causes irregular thickening of the vessel wall from proliferation of smooth muscle and fibrous tissue of the media. Angiographic changes of fibromuscular dysplasia are found in about 15% of patients with an SD of the carotid or vertebral artery (Schievink et al. 2001). To a similar extent, AAs, including dissecting AAs, are known to be associated with this disease. In our experience, the importance given to FMD in females with AA and SAH by George et al. (1989) might be an overestimation, although it confirmed several of the observations made by Mettinger and Ericson (1982). There is a female to male dominance of 5.6:1, where the disease is transmitted as a autonomic dominant trait in the familial forms, 30%–50% of all FMD patients. Multiple locations are more frequent than in males with AA at the same age or females without FMD. The prognosis of SAH in this female group with FMD was worse, with a higher degree of vasospasm. Frequent locations were the ICA (AComA) or the VA. Renal artery involvement tends to precede involvement of the carotids.

In Moyamoya disease, most AAs are false and develop on the lenticulostriate collaterals. They are often visualized at the time of a hemorrhagic episode. Some AAs can be seen on the basilar system, likely triggered by the shear stresses related to collateral supply from the vertebrobasilar system.

7.3.2 Saccular Arterial Aneurysms Without Diagnosed Associated Diseases

7.3.2.1 Nonsyndromic Familial Arterial Aneurysms

When reviewing the literature, one encounters a mixture of data that include nonfamilial unruptured AA (FAA) series, nonfamilial SAH series, the familial series of AA, and the familial series of SAH. In the Western world, grossly two groups can be identified in the AA populations: those with a male dominance in Sweden and Finland (Norrgard et al. 1987) and the others with a female dominance (61% in Fox et al. 1982).

In both familial and nonfamilial AA groups, ICA aneurysms are more frequent in females, AComA aneurysms are more frequent in males, and MCA aneurysms are equally distributed. The number of multiple aneurysms is the same in both populations (21%), although one would expect *PComA* As to be more frequent in females, at least because of the possibility of FMD.

The incidence of SAH in Finland is more than twice that in other Western countries.

The incidence of FAA in SAH patients in Finland is 10% (6% of the 91 FAAs reviewed presented PKD), but the prevalence of unruptured AA is 2.2%–3%, similar to other countries. There is a female dominance (54%–70%) in familial SAH, as assessed by the review of 137 families (Ronkainen et al. 1993). The SAH occurs 7–10 years younger in FAA in males than in non-FAA patients. Sibling pairs with AA bleed within the same decade. Females with SAH are 5 years older in both familial and nonfamilial AA groups. MCA topography is the most frequent (50%), preferably on the right side, with very small AA size (<6 mm) at rupture; 80% of the AAs were between 7 and 14 mm in size in FAA (Ronkainen et al. 1993). The vertebrobasilar artery system accounts for 6% of the locations, whether in FAA or in non-FAA. The classic topography in non-FAA is nearly equally shared by the ICA, ACA, and MCA. In 77% of FAA cases, there are two SAH occurrences.

The risk of having an AA is four times higher for close relatives than for someone from the general population. (Ronkainen et al. 1998). First-degree relatives in FAA make up a high-risk group for AA (4.2 relative risk); this group will benefit from screening after the age of 30 and before 65 (ter Berg et al. 1992). Decreasing the risk of screening using MRA versus angiography would increase the benefit only minimally, even with a 100% sensitivity and specificity (Dippel et al. 1992). Conversely, screening in families with only one affected member (relative risk, 1.8) or in the general population is not recommended (Ronkainen et al. 1998).

In their review, Schievink et al. (1994d) found that over 238 FAA siblings were affected in 156 families, and parents or children in 61 families. This observation may focus on the screening procedures but does not tell us how frequently screening should be done, if one remembers that an AA may develop in hours, days, or weeks (Wiebers 1995). No additional benefit could be demonstrated for screening more than once (ter Berg 1992).

In a series of 8,680 participants, Kojima et al. (1998) demonstrated a prevalence of asymptomatic AA in 7% of the overall group, and 10.5% in the group of 380 that had a family history of AA. The prevalence of asymptomatic AA in female participants was 12.3% versus 7.9% in males ($p<0.0001$). AAs were mostly located at the ICA/PComA and MCA. The prevalence of AA in 115 members of the 20 families was 33.9%. Although the members of 14 families with SAH showed a higher prevalence of ruptured and asymptomatic AA (42.1%) than the six families with only asymptomatic AA, the former had very low prevalence of asymptomatic AA; this suggests that in SAH families fewer AAs remain asymptomatic, as the data do not tell whether the asymptomatic AAs are those that will eventually bleed or if the SAH will be caused by new ones.

Schievink (1994d), creating a model based on 73 families, showed that from an AA-affected male, family screening would reveal a 24% risk of AA for brothers and 30% for sisters; from an AA-affected female, family screening would reveal a 10% risk for brothers and 14% for sisters.

The risks and benefits of screening for intracranial aneurysms in first-degree relatives of patients with sporadic subarachnoid hemorrhage have been analyzed (Raaymakers 1999). In a consecutive series of patients with SAH, 626 first-degree relatives were screened and 33 unruptured aneurysms were found in 25 of them (4% incidence, nearly twice the au-

topsy series, with a rate of 2.3%). Surgery in 18 increased life expectancy, at the expense of a decrease in function in 11, which was disabling in one. The average gain in life expectancy per person screened was 0.9 months. To prevent one SAH over the course of a lifetime, 149 relatives would have to be screened.

Implementation of a screening program for the first-degree relatives of patients with sporadic SAH does not seem warranted at this time, since the resulting slight increase in life expectancy does not offset the risk of postoperative sequelae.

The risk of rupture may be higher among persons who have non-first-degree relatives with AA. The rate of SAH is three to seven times higher in first-degree relatives of patients with sporadic SAH as compared to the general population. The frequency of aneurysms in their study was not quite twice that of the general population. This suggestion is supported by a recent finding that asymptomatic aneurysms are more likely to rupture in relatives of patients with SAH than in relatives of patients with unruptured aneurysms.

The multiplicity is not higher in familial AA. Yet the presence of multiple lesions suggests a genetic disorder that is rarely identified. The hereditary connective tissue diseases associated with intracranial AAs are estimated to occur in 5% of cases, including PKD, FMD, Marfan syndrome, Ehlers–Danlos disease, and pseudoxanthoma elasticum (Forbus 1930; George et al. 1989; Lejeune 1997). Fibromuscular dysplasia (FMD) has been suggested in the multifocality observed in females and involving the posterior division of the internal carotid artery (George et al. 1989).

7.3.2.2 Multiple Saccular Arterial Aneurysms

In a review study, Locksley (1966) found that multiple aneurysms seen at autopsy ranged from 18.5% to 22% of aneurysms; in the Yasargil clinical series (1984), multiple aneurysms represented 24% (243 patients) of cases with modern neuroimaging, slightly higher figures were found by Campos et al. (1998b) (Tables 7.22–7.24).

Among 1,088 intracranial saccular lesions, Suzuki and Yoshimoto (1979) found 166 (15.4%) multiple AAs, with a female predominance. In 254 consecutive cases, Wilson et al. (1989) found 44.9% of patients admitted for subarachnoid hemorrhage had multiple AAs. Females accounted for two-thirds of them. The incidence was higher in patients over 40 years of age (52.8%) than under 40 years (26.3%) (Wilson et al. 1989), yet the rate of newly formed AAs may be quite low after the age of 60 (Juvela 1999). Cigarette smoking and female gender appear to be independent risk factors for the presence of multiple AAs, with odds ratios of 1.7 and 2.1, respectively (Qureshi et al. 1998). The presence of multiple AAs does not seem to increase the risk of rupture (Juvela 1999).

Patients with multiple intradural aneurysms present unique clinical challenges, particularly when presenting with SAH. Porter et al. (2001) reviewed a total of 147 patients with multiple intracranial saccular aneurysms from among 557 consecutive aneurysm cases (26.4% multiplicity) in a non-Scandinavian Western population (Table 7.25).

Table 7.22. Multiple aneurysms (from Campos et al. 1998b, with permission)

No. of patients	No. AA/patient	%
74	02	65
27	03	24
09	04	8
03	05	3
Total (113)	280	100

Table 7.23. Type of AA and gender distribution in 398 consecutive cases of intracranial AA (from Campos et al. 1998b, with permission)

Type of AA	No. of patients	%
Single berry	228	57.2
Multiple berry	113	28.3
Giant saccular	38	9.5
Fusiform	08	2
Dissecting	07	2
Mycotic	04	1
Total	398	100
	Multiple AA	Single AA
Male	37 (33%)	93 (41%)
Female	76 (67%)	135 (59%)
Total	113 (100%)	228 (100%)

Table 7.24. Patient age at diagnosis in 341 consecutive cases of intracranial AA (from Campos et al. 1998b, with permission)

Age	Multiple AA		Single AA	
	No. patients	%	No. patients	%
0–9	0	0	04	1.8
10–19	2	1.8	08	3.5
20–29	7	6.2	16	7
30–39	27	24	50	22
40–49	35	31	64	28
50–59	18	16	46	20
60–69	18	16	27	12
70–79	6	5	13	6
Total	113	100	228	100

The mean age at presentation was 46.4 years (range, 12–77 years). There was a female dominance (68.9%). The sex distribution was not significantly different between patients with and without a history of SAH (67.7% of patients with SAH were female, compared to 73.9% with no such history, p=0.55). Past medical history included hypertension in 21 patients (17%), polycystic kidney disease in seven, Ehlers–Danlos syndrome in one, and fibromuscular dysplasia in one. The average maximal diameter of the aneurysms was 5.4 mm (range, 2–20 mm). This was significantly larger for aneurysms that had bled (mean, 7.0 mm) than for unruptured aneurysms (mean, 4.7 mm) (p<0.001). However, the maximal size was less than 1 cm for 64 of the 84 aneurysms (76.2%) responsible for the bleed in the hemorrhagic group. The average neck size, 2.7 mm, was also larger for ruptured aneurysms (mean, 3.1 mm) than for unruptured aneurysms (mean, 2.5 mm) (p=0.001).

In most patients presenting with SAH, the aneurysm responsible for the bleed could be identified with a fair degree of certainty. There was a

Table 7.25. Location of ruptured and unruptured aneurysms: multiple AA in 147 consecutive patients (from Porter et al. 2001, with permission)

Location	Ruptured aneurysms	Unruptured aneurysms	Total no. aneurysms at this location	Percent of all aneurysms[a]	Percent responsible for SAH[b]
Paraophthalmic	7	33	40	13.1	17.5[c]
Posterior communicating	22	28	50	16.4	44.0
Anterior choroidal	0	6	6	2.0	0
Carotid termination	2	15	17	5.6	11.8
Middle cerebral	32	80	112	36.7	28.6
Anterior communicating	17	17	34	11.1	50.0[d]
Pericallosal	2	10	12	3.9	16.7
Posterior inferior cerebellar	8	2	10	3.3	80.0[d]
Anterior inferior cerebellar	0	1	1	0.3	0
Superior cerebellar	2	3	5	1.6	40.0
Basilar termination	7	9	16	5.2	43.8
Posterior cerebral	0	2	2	0.7	0
Total	99	206	305	99.9	32.5[e]

[a] Number of aneurysms at this location divided by total number of aneurysms.
[b] Number of ruptured aneurysms divided by number of unruptured aneurysms at this location.
[c] Significantly less frequently responsible for SAH ($p<0.05$).
[d] Significantly more frequently responsible for SAH ($p<0.05$).
[e] Average percentage of aneurysms responsible for SAH (total ruptured divided by total unruptured).

trend for patients with uncertainty regarding the site of bleeding to have all aneurysms treated, and for cure to be obtained in a shorter time. Surgical and endovascular complication rates and patient outcomes were not dissimilar in the Porter et al. (2001) series from what one would expect for single-aneurysm patients.

Certain aneurysm locations appear under-represented (anterior communicating and posterior communicating arteries) or over-represented (MCA, paraophthalmic artery) relative to the distribution reported for aneurysms overall (Suzuki and Yoshimoto 1979; Mizoi et al. 1989; Fults and Kelly 1984; Wood 1964; Weir and MacDonald 1996). Other reports on multiple aneurysms found similar distributions to what was observed (Mizoi et al. 1989; Rinne et al. 1995; Pierot et al. 1997). This of course raises the question of whether patients with multiple aneurysms are a fundamentally different population, with various genetic or environmental factors predisposing to multiplicity (see Sect. 7.8).

7.3.2.3 Arterial Anatomy, Single, Mirror, and Twin Saccular Arterial Aneurysms

In a series of 305 saccular AAs reviewed by Porter (2001), there was a total of 271 anterior circulation AAs (88.9%) and 34 posterior circulation AAs (11.1%). The most frequent location, the MCA, was more than twice as common as the next most frequent site, the posterior communicating artery (PComA). AAs of the posterior inferior cerebellar artery (PICA) and anterior communicating artery (AComA) were significantly more likely than other sites to be responsible for SAH (p=0.001 and 0.02, re-

spectively), while paraophthalmic lesions had a lesser propensity to account for the SAH (p=0.03). One hundred and twenty-four patients (88%) had associated vascular anomalies.

Some locations are always associated with vascular anomalies: basilar tip and PCA (P1) aneurysms (Figs. 7.51, 7.52) (Table 7.26). On the contrary, MCA aneurysm have one of the highest rates of aneurysm location, with no associated vascular anomaly (Mazighi et al. 2001).

The most frequent findings were 61 cases (43.2%) of asymmetric caudal basilar fusion, 44 cases (31.2%) of AcomA complex variations, 37 cases (26.2%) of symmetric caudal basilar fusion, 22 cases (15.6%) of AICA–PICA, 15 cases (10.6%) of extradural PICA, five cases (3.5%) of dorsal ophthalmic artery (dOPH) (Figs. 7.53–7.57, pp. 444–447; Table 7.26).

These anomalies are actually associated with the AA but not necessarily present on the vessel carrying the AA. The purpose of the collection of such variations is to suggest the presence of an embryonic event for which the variation behaves as a time marker. Campos (1998a) reviewed 55 basilar tip AAs among 580 consecutive AAs.

The analysis of the anatomical disposition of the distal basilar artery in 47 of them showed the prevalence of the caudal fusion in 91% of the cases. A control angiographic group of 46 cases without aneurysm in any location showed 69.6% caudal fusion disposition (26.1% symmetrical, 43.5% asymmetrical, 2.8% with unilateral absence of P1). The neck of the AA is preferentially implanted on the caudal part of the fusion (Fig. 7.51). Full knowledge of the distal basilar artery anatomy makes it possible to predict the origin and extent of the perforating branches arising from the P1 segment in each type of basilar tip disposition (see Vol. 1). The caudal segment supplies unilateral structures, while the cranial segment supplies bilateral territories. The PComA flows caudally in caudal fusions and is likely to supply diencephalic-mesencephalic territories, while cranial fusion expresses a basilar contribution to the supply to the area.

Table 7.26. Incidence of the different vascular anomalies in the AA patient population (from Mazighi et al. 2001, with permission)

Vascular anomaly	No. of patients	%
Asym caudal	61	43.2
AComA complex	44	31.2
Sym caudal	37	26.2
AICA-PICA	22	15.6
Extradural PICA	15	10.6
dOPH	5	3.5
Access MCA	1	0.7
Trigeminal	1	0.7
None	17	12

Asym caudal, asymmetric caudal basilar fusion; AComA complex, variations of the anterior communicating artery complex; Sym caudal, symmetric caudal basilar fusion; AICA-PICA, anterior-inferior cerebellar artery–posterior-inferior cerebellar artery; extradural pica, extradural origin of the PICA; dOPH, cavernous origin of the ophthalmic artery origin or dorsal ophthalmic artery; Access MCA, accessory middle cerebral artery; Trigeminal, persistent trigeminal artery.

Fig. 7.51. **A** Basilar tip anatomy and **B** ruptured basilar tip aneurysm with asymmetrical caudal fusion. (From Campos et al. 1998a, with permission)

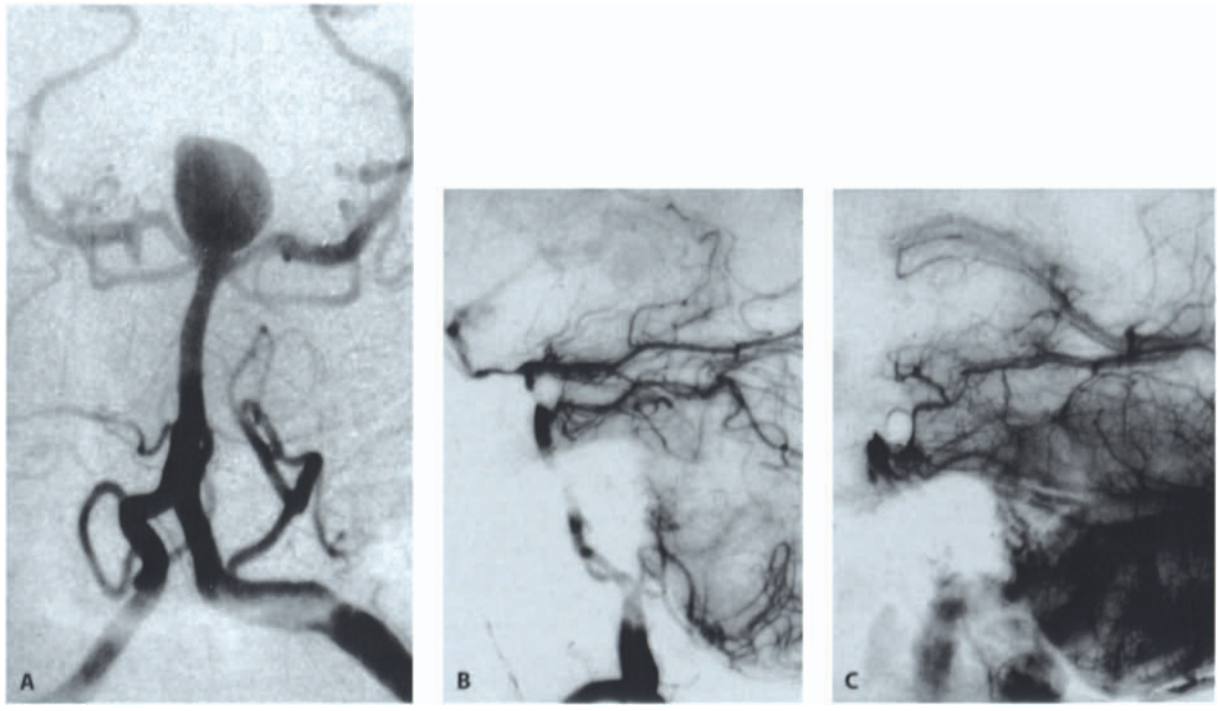

Fig. 7.52. **A** Basilar tip arterial aneurysm (AA) with characteristic symmetrical caudal fusion. **B** Coiled ruptured basilar tip AA, caudal fusion. **C** Note the low (caudal) position of the coils in front of the upper pons on the venous phase

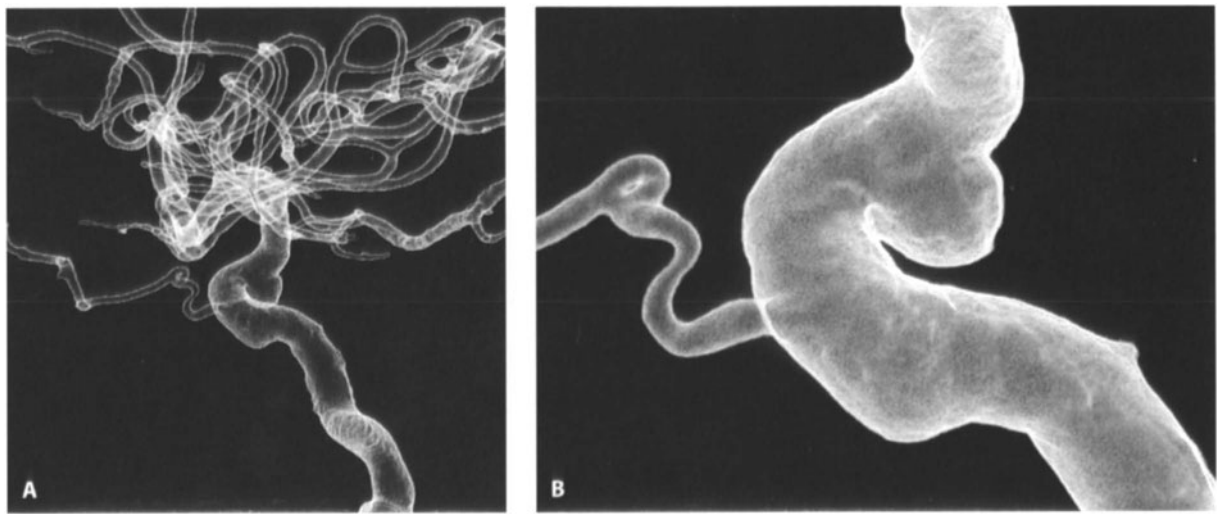

Fig. 7.53A, B. Volume-rendered 3-D digital subtraction angiograms of an internal carotid artery aneurysm associated with migration of the ventral ophthalmic artery (carotid cave origin)

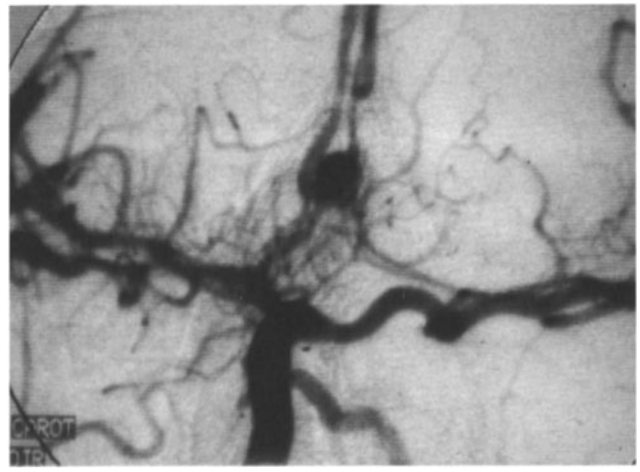

Fig. 7.54. Left internal carotid artery (ICA) agenesis. Ruptured AComA aneurysm with transsellar course of the ICA. (Courtesy of G. Freytas)

In the single aneurysm group with a caudal fusion arrangement, there was a male prevalence (62.5%), whereas in the multiple aneurysm group, also with caudal fusion arrangements, there was a female prevalence (62%).

Structural weakness of intracranial arteries combined with hemodynamic forces is widely believed to be the major underlying cause of AA (Schievink 1997; Yong-Zhong and van Alphen 1990; Sekhar and Heros 1981; Stebhens 1989) and the currently available treatment modalities (surgical and endovascular) are also based on such assumptions. However, hemodynamic shear stresses alone cannot explain the occurrence of AAs at various locations within the intracranial vasculature, especially at locations such as the MCA bifurcation (Fig. 7.58, p. 448), the origin of the posterior inferior cerebellar artery, etc., where such forces would be expected to be small. Moreover, there is no satisfactory explanation for the

Fig. 7.55A–D. Ruptured AComA aneurysm and associated vascular anatomy. **A** Left internal carotid artery (ICA) digital angiogram, AP view. **B** 3-D volume-rendering posterior view. **C** Vertebral artery with asymmetrical caudal fusion. **D** Right ICA, A1 agenesis

development of multiple aneurysms, especially in a mirror-image location based on hemodynamic principles.

Forty-four of the 122 patients (36%) in the Porter et al. series (2001) had aneurysms located in mirror positions, more than half of which (52.3%) were on the MCA (Figs. 7.59–7.61, pp. 449, 450).

A multifactorial origin for intracranial AA has been put forward by some authors (Pia et al. 1979; Oostergard and Voldby 1983; Weir 1987). The segmental identity or vulnerability of arteries to certain diseases is established during development (Lasjaunias 2000b). Secondary mutations or triggers can then act on such a constitutional vasculopathic state and stimulate the overproduction of arterial wall without remodeling, resulting in aneurysm formation. That genetically based diseases express themselves phenotypically or clinically at a specific time during life is an accepted fact (Carmeliet 2000). A good example is autosomal polycystic kidney disease type 1 (PKD1), where the development of intracranial AA usually occurs nearly 10 years earlier than in the sporadic forms of AA (Pirson et al. 1996).

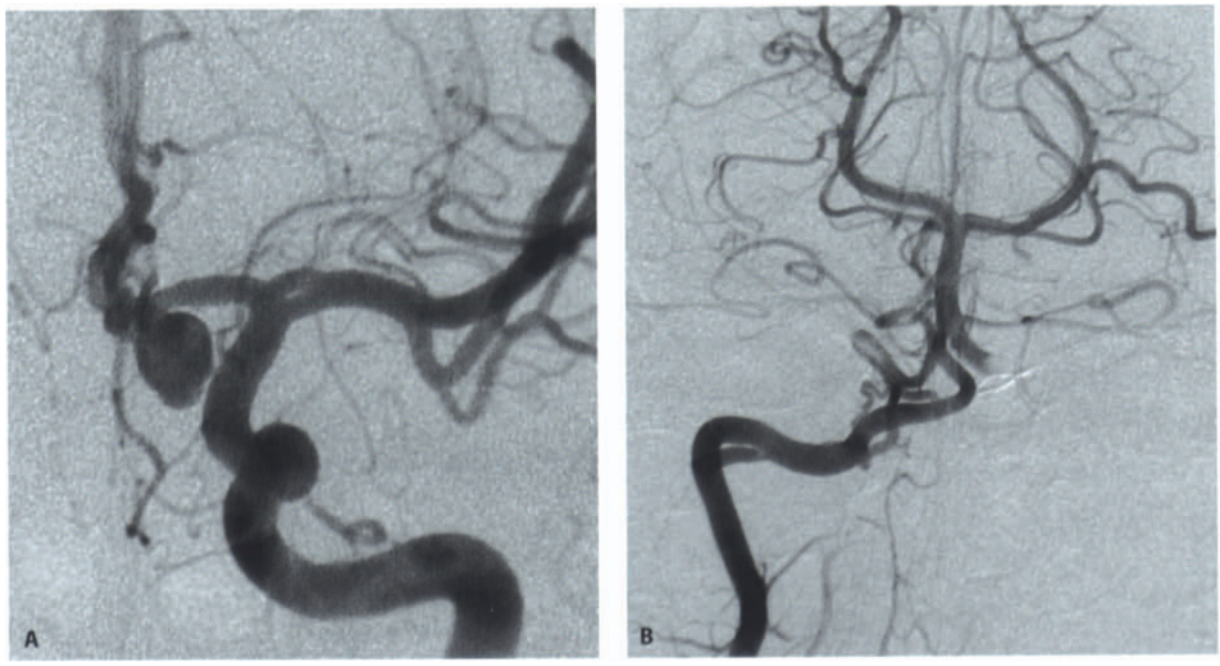

Fig. 7.56. Ruptured AComA aneurysm associated with M1 fenestration (**A**) and duplicated channel at C1 of the vertebral artery (**B**)

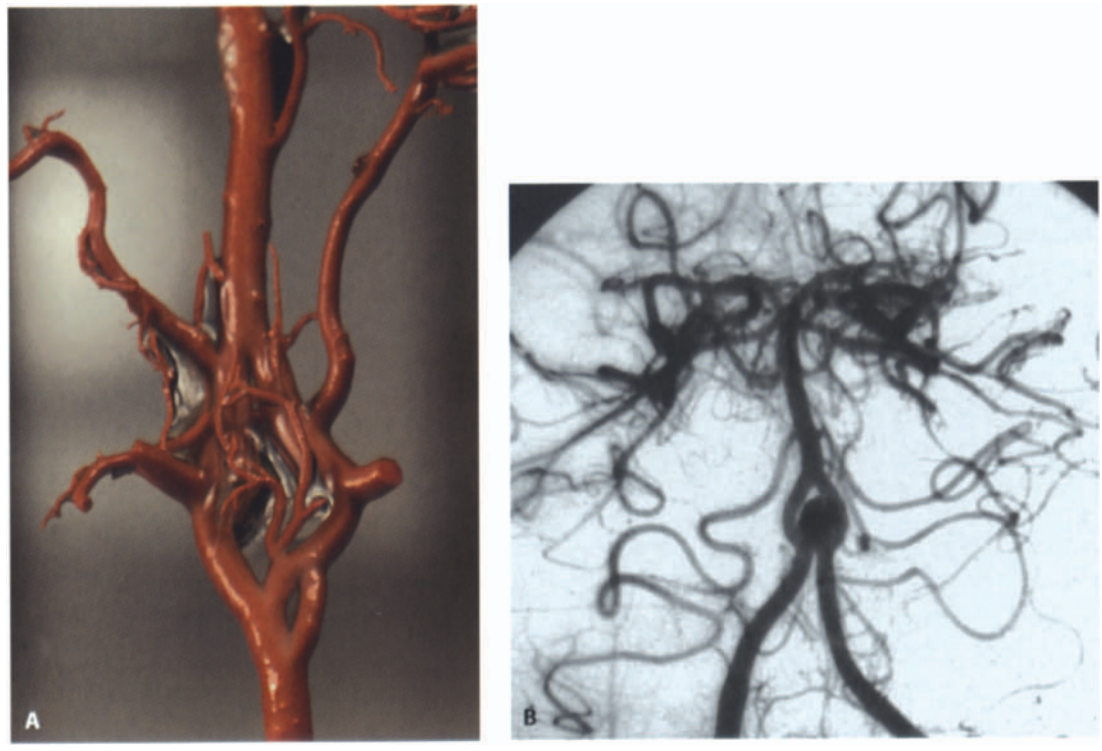

Fig. 7.57. **A** Segmental unfused basilar artery and **B** unruptured basilar aneurysm with unfused segment

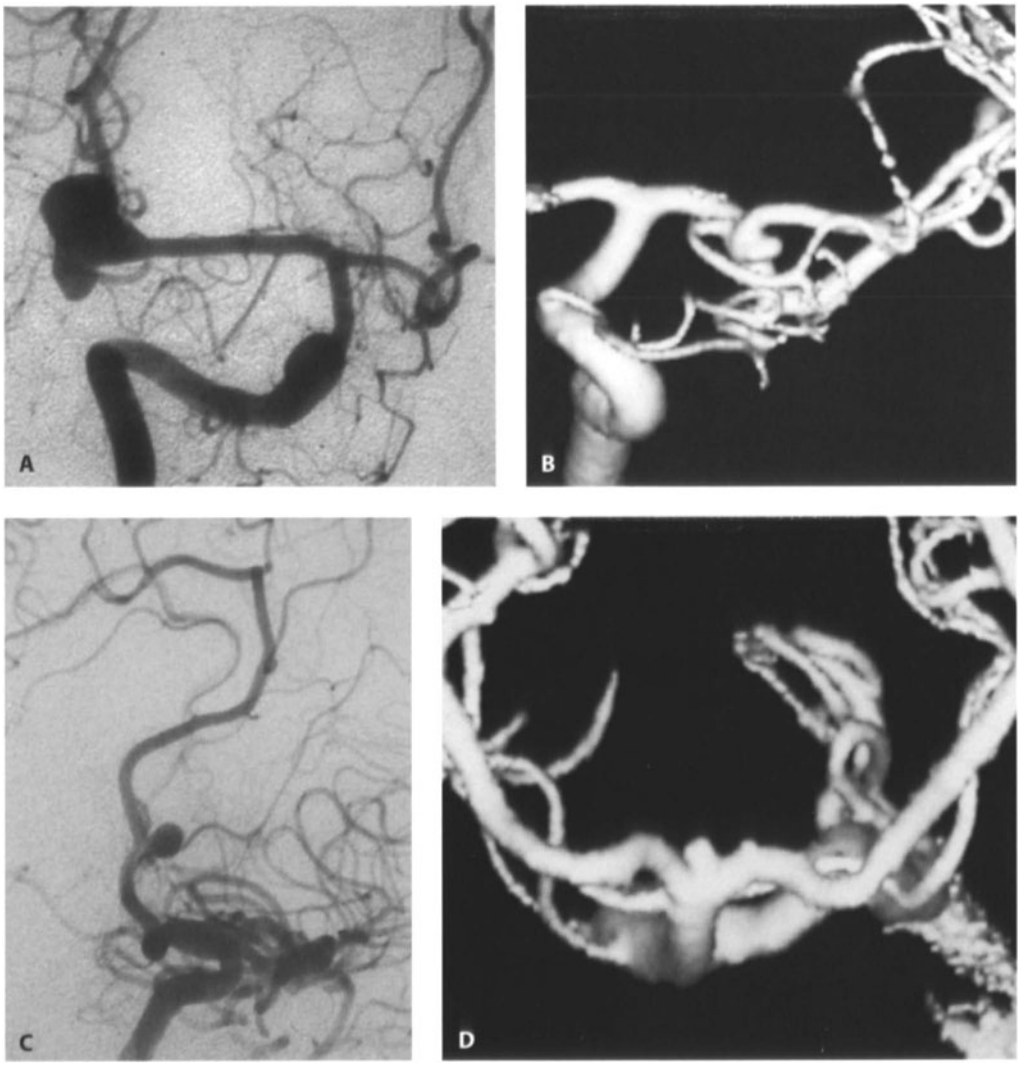

Fig. 7.58. **A** Ruptured right middle cerebral artery (MCA) aneurysm associated with **B** MCA aneurysm in mirror position. **C** Anterior cerebral artery and **D** basilar tip additional aneurysms are demonstrated

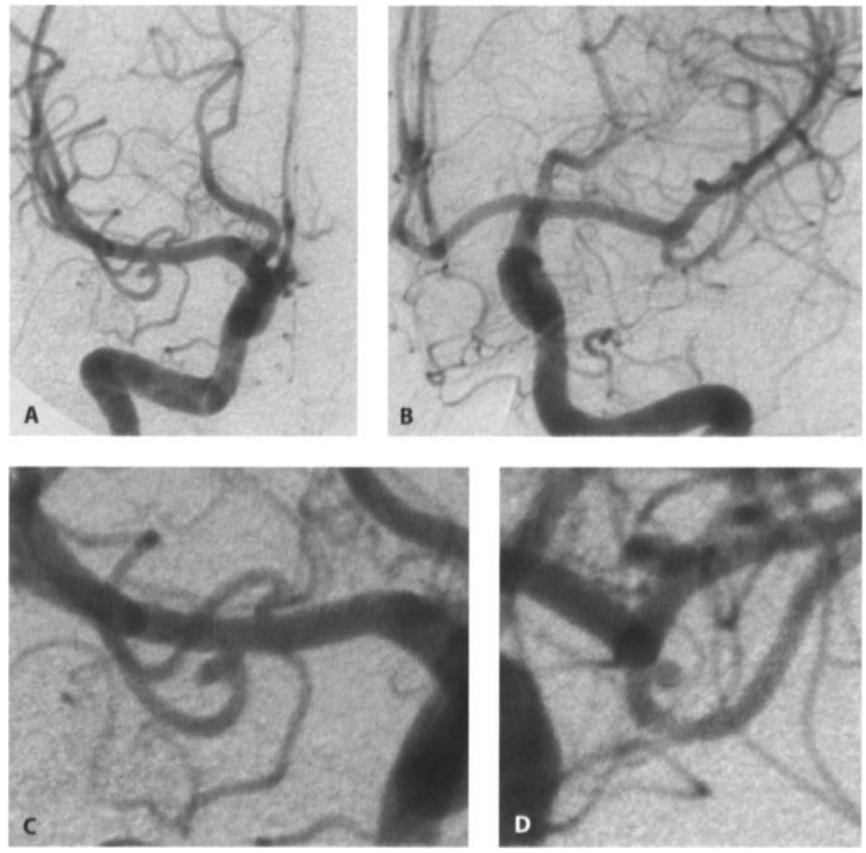

Fig. 7.59A–D. Middle cerebral artery division mirror AA. Note the dramatic symmetry of the location site and size of the AA (**C, D**)

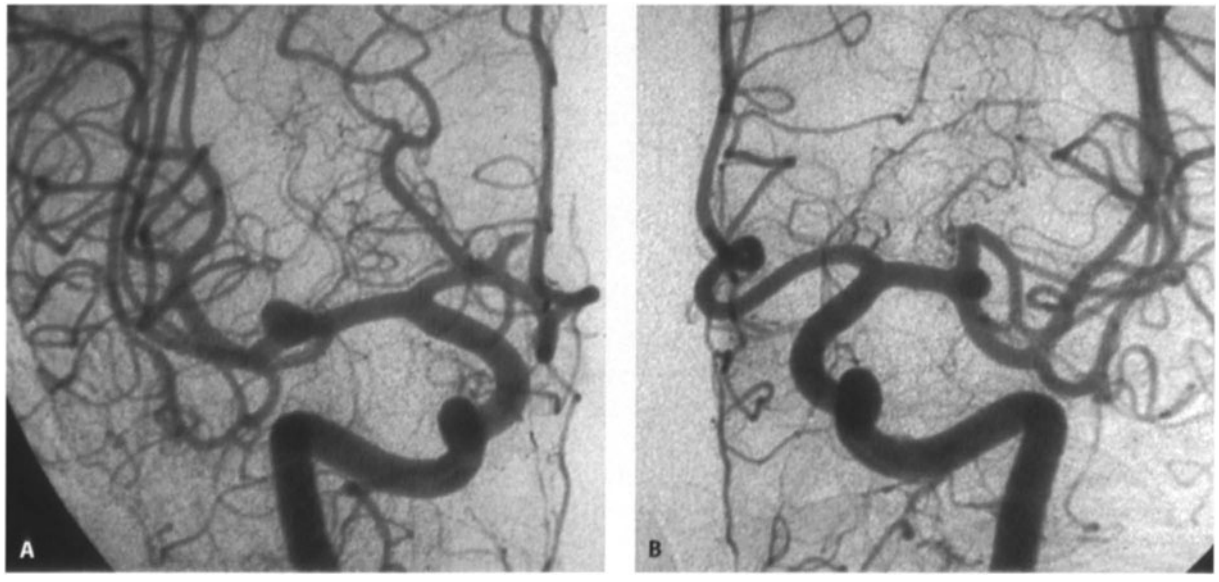

Fig. 7.60. Ruptured right-sided middle cerebral artery (MCA) aneurysm (**A, B**) and a simultaneous typical mirror left MCA division AA

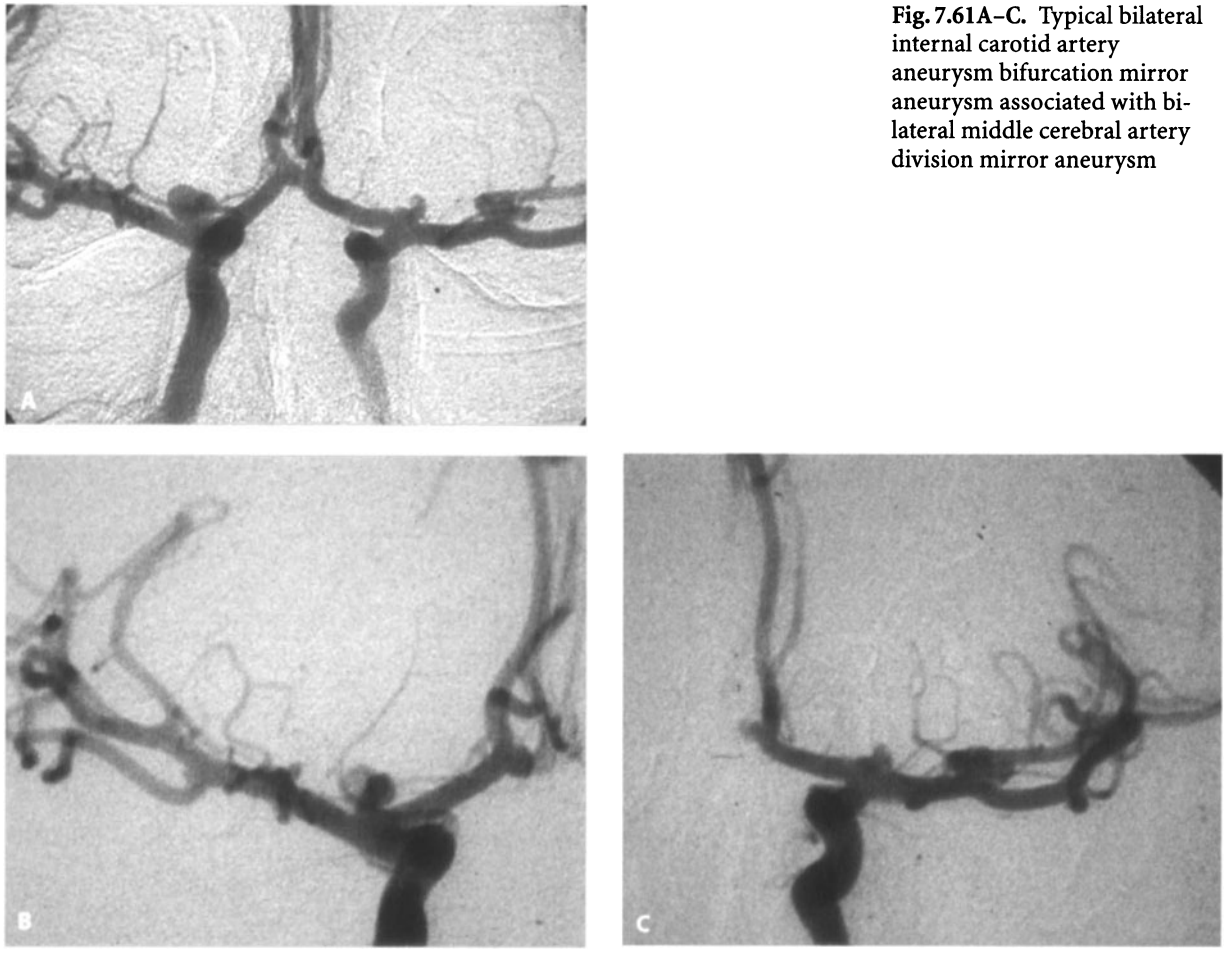

Fig. 7.61A–C. Typical bilateral internal carotid artery aneurysm bifurcation mirror aneurysm associated with bilateral middle cerebral artery division mirror aneurysm

Explanation of why some aneurysms occur in mirror-image locations can be based on the congenital metameric principle, as was postulated by Campos in an analysis of 113 multiple AAs compared with a group of single AAs (228 cases) of the same material (Campos et al. 1998b) (Table 7.27).

Three longitudinal embryological territories giving rise to cranial endothelial cells and media (Couly et al. 1995) were used to regroup the aneurysm sites (Figs. 7.62, 7.63; Tables 7.28–7.30).

- The prosencephalic or rostral region corresponds to the anterior circulation, as it is made up of the internal carotid system and its rostral branches, the posterior communicating artery, and probably the P2 segment of the posterior cerebral artery.
- The mesencephalic or middle region corresponds to the upper basilar complex composed of the P1 segments, the anterior superior cerebellar artery (ASCA), and the basilar tip.
- The rhombencephalic or caudal region corresponds to the caudal posterior circulation (vertebrobasilar junction), comprising the proximal basilar artery, the anterior–inferior cerebellar arteries (AICA), the posterior–inferior cerebellar arteries (PICA), and the intradural portion of the vertebral arteries.

Table 7.27. Incidence of the different aneurysmal locations (from Mazighi et al. 2001, with permission)

Arteries	No. of aneurysms	%
Middle carotid	121	34.2
Posterior communicating	52	14.7
Paraophthalmic	50	14.1
Anterior communicating	40	11.3
Carotid termination	20	5.6
Basilar tip	18	5
Anterior cerebral	14	3.9
Posterior-inferior cerebellar	12	3.3
Cavernous	12	3.3
Anterior-superior cerebellar	7	1.9
Anterior choroidal	6	1.6
Posterior cerebral	4	1.1

Table 7.29. Bleeding rate of the different aneurysm locations (from Mazighi et al. 2001, with permission)

Arteries	No. of ruptured AAs	%
Middle cerebral	26	23.2
Anterior communicating	17	15.1
Posterior communicating	14	12.5
Paraophthalmic	7	6.25
Basilar tip	7	6.25
Posterior-inferior cerebellar	6	5.3
Carotid termination	2	1.7
Anterior-superior cerebellar	2	1.7
Anterior cerebral	1	0.8
Unknown	30	26.7

Table 7.28. Aneurysm location and associated vascular anomalies (%; from Mazighi et al. 2001, with permission)

	Asym Caudal	AComA Complex	Sym caudal	AICA PICA	Extra dural PICA	dOPH	None
Middle cerebral	42.9	28	22.3	14	86.6	1.6	18.1
Anterior communicating	42.5	47.5	25	15	20	2.5	10
Posterior communicating	42.3	21.1	21.1	17.3	60	3.8	7.6
Paraophthalmic	46	22	30	16	13.3	6	12
Basilar tip	44	16.6	44	16.6	33.3	5.5	0
Posterior-inferior cerebellar	58.3	16.6	16.6	25	6.6	0	16.6
Carotid termination	20	40	20	10	33.3	0	6
Anterior-superior cerebellar	85.7	57.1	0	0	0	0	42.8
Posterior cerebral	100	25	0	25	0	0	0

Asym caudal, asymmetric caudal basilar fusion; AComA complex, variations of the anterior communicating artery complex; Sym caudal, symmetric caudal basilar fusion; AICA-PICA, anterior-inferior cerebellar artery–posterior-inferior cerebellar artery; Extradural PICA, extradural origin of the PICA; dOPH, cavernous origin of the ophthalmic artery origin or dorsal ophthalmic artery.

Table 7.30. Vascular anomalies and ruptured aneurysm location (Mazighi 2001)

Vascular anomalies	MCA	PComA	Paraophth	AComA	Car term	Bas tip	PICA	SCA	PCA
Asym caudal	23%	14.7%	5%	10%	0%	1.6%	5%	1.6%	0%
AComA complex	20%	11%	4.5%	25%	4.5%	2.2%	4.5%	0%	0%
Sym caudal	13.5%	10.8%	2.7%	13.5%	0%	8.1%	0%	0%	0%
AICA-PICA	13.6%	9%	13.6%	9%	0%	4.5%	13.6%	0%	0%
Extradural PICA	13.3%	16.6%	0%	6.6%	0%	13.3%	0%	0%	0%
dOPH	0%	0%	20%	20%	0%	0%	0%	0%	0%

MCA, middle cerebral artery; AComA, anterior communicating artery; PComA, posterior communicating artery; Bas tip, basilar tip; Paraophth, paraophthalmic; Car term; carotid termination; PICA, posterior-inferior cerebellar artery; ASCA, anterior-superior cerebellar artery; PCA, posterior cerebral artery; Asym caudal, asymmetric caudal basilar fusion; AComA complex, variations of the anterior communicating artery complex; Sym caudal, symmetric caudal basilar fusion; AICA-PICA, anterior-inferior cerebellar artery–postero-inferior cerebellar artery; Extradural PICA, extradural origin of the PICA; dOPH, cavernous origin of the ophthalmic artery origin or dorsal ophthalmic artery.

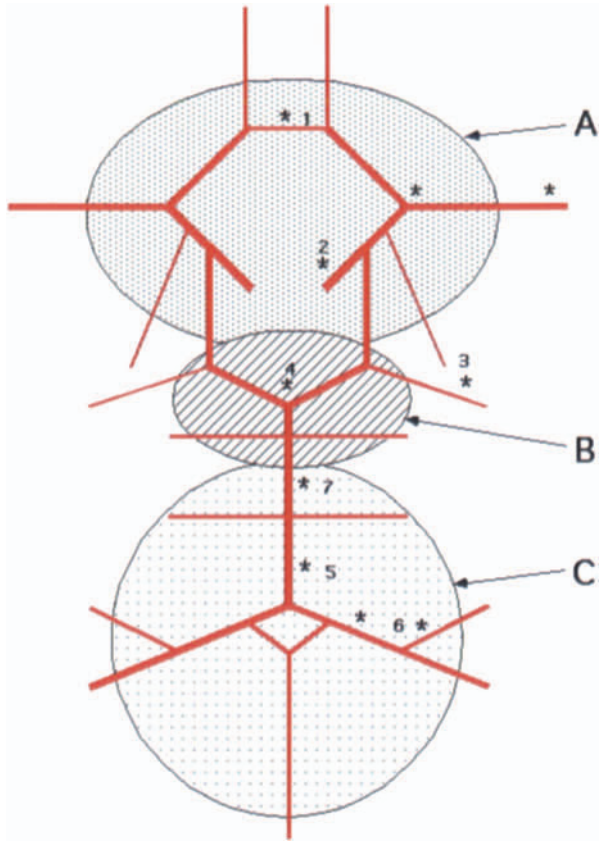

Fig. 7.62. Representation of the three main areas of origin of endothelial cells (*A*, *B*, *C*). The *asterisks* point to the usual locations for arterial aneurysm development and their embryonic significance: *1*, AComA; *2*, ICA ophthalmic (ventral ophthalmic OPH); *3*, AChA-PCA anastomoses; *4*, basilar tip (ICA posterior division fusion); *5*, basilar artery (long neural fusion); *6*, PICA origin (hypoglossal); *7*, upper basilar (trigeminal). (From Campos et al. 1998b, with permission)

Eighty-four cases harbored multiple aneurysms in the rostral region (74%), 20 cases presented with aneurysms involving rostral and middle territories (18%), one case with aneurysms involving the middle and caudal territories (0.9%), five cases with aneurysms in the rostral and caudal territories (4.4%), and three cases with aneurysms involving rostral, medial, and caudal territories at the same time (2.7%). None of the multiple group was located in the middle or caudal territories alone. If several arterial territories were involved they were found to be adjacent in 95.6% (Table 7.28) (Campos et al. 1998a).

Multiple AAs could therefore result from mesodermal/neural crest stem cell or focal endothelial cell defects within one or two (usually consecutive) embryonic segments. Mirror lesions would correspond to the impairment of a group of cells with bilateral distribution. Their symmetrical location therefore reflects their single origin, making them twin AAs rather than mirror AAs. Over time, the weak characteristics shared by the two groups of cells will be triggered and subsequently lead to the development of a grossly identical lesion (Tables 7.31–7.33). A peculiar association of basilar tip AA was recently reported by Porter (2001) in homozygotic twins (Fig. 7.64).

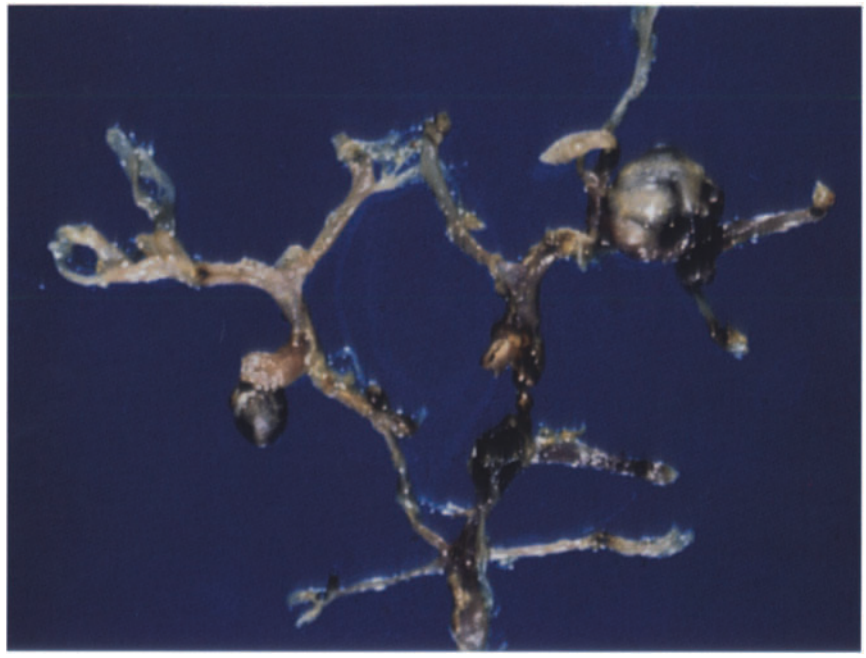

Fig. 7.63. Multiple arterial aneurysms shown in a vascular specimen of a neonate. Note the symmetrical caudal fusion of the basilar artery

Table 7.31. Multiple AA patients (32/113): mirror aneurysm location

	No. of patients	Multiple AAs (%)
MCA	18	16
OPH	06	5.3
Pcom	06	5.3
Carotid siphon	01	0.9
Bifurc ICA	01	0.9
Total	32	28%

MCA, middle cerebral artery; OPH, ophthalmic; Pcom, posterior communicating; Bifurc ICA, bifurcation of internal carotid artery.

Table 7.32. 113 Multiple aneurysm patients: location (from Campos et al. 1998b, with permission)

	No. of patients	Multiple AAs (%)
Rostral region	84	74
Rostral + middle region	20	18
Middle + caudal region	01	0.9
Rostral + caudal region	05	4.4
Rostral + middle + caudal	03	2.7
Total	113	100

Table 7.33. Single saccular AA patients (228): location (from Campos et al. 1998b, with permission)

	No. of patients	Saccular AAs (%)
Rostral region	187	82
Middle region	29	13
Caudal region	12	05
Total	228	100

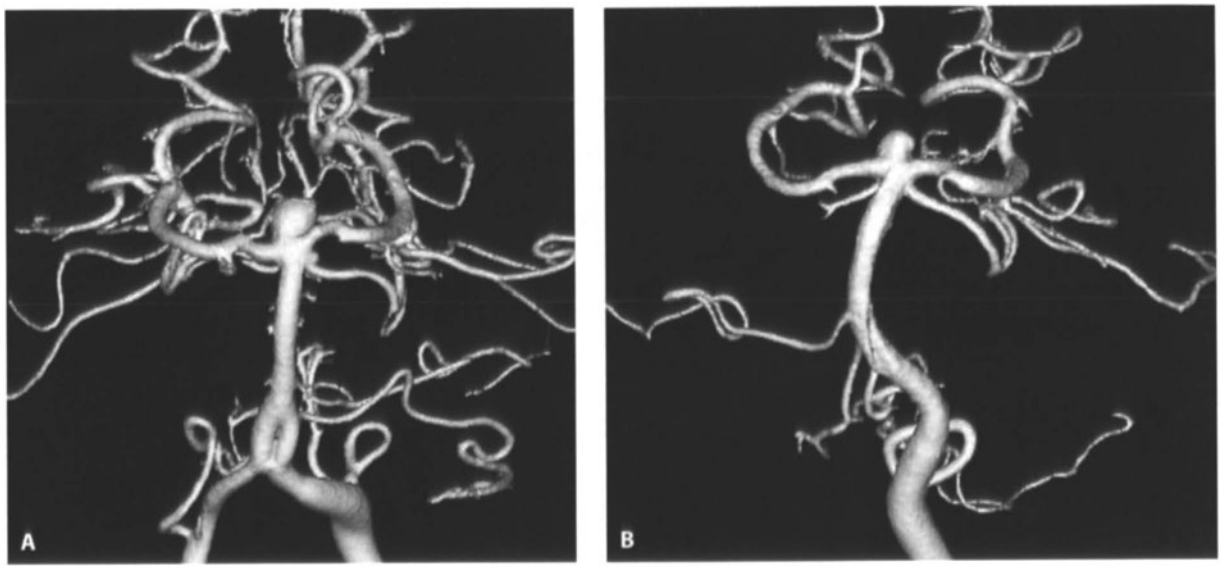

Fig. 7.64A, B. Basilar artery aneurysm demonstrated in homozygotic female twins following subarachnoid hemorrhage in one of them. (From Porter et al. 2001, with permission)

7.4 Intradural Artery Dissections

Intradural spontaneous dissections (SDs) are different from cervical or extradural SDs, although they may be associated with the same underlying diseases (Figs. 7.6, 7.65). Most reports in the literature are Japanese contributions and describe different groups of patients and diseases compared to SDs occurring in Western populations, which, with the exception of children, are mostly extracranial in location (see Vol. 3).

Stehbens (1963), in his review, reported the location of SDs to be in the MCA in 41% of cases, vertebrobasilar artery (VBA) in 23%, internal carotid artery (ICA) in 21%, anterior cerebral artery (ACA) in 13%, and others in 2% of cases. In 82% of cases, the dissection was subintimal. Most of these cases were not associated with subarachnoid hemorrhage (SAH). Trauma (Figs. 7.66, 7.67) and syphilis were among the multiple suspected etiologies, with syphilis suspected of accounting for 60% cases occurring prior to 1950 (Berger and Wilson 1984). Some stroke syndromes associated with intraluminal clot may be caused by focal dysplastic changes or localized dissections, as can be seen in the posterior fossa.

This description illustrates how difficult it is to distinguish which aspect belongs to a repair process, the effects produced by the triggers, the agent if it is morphologically expressed, or the vessel wall disease. Yamaura et al. (1990) emphasized the rarity of the syndrome as well as the underestimation of SAH compared to intracranial SD. The subadventitial hemorrhage from SD, while associated with SAH, showed multiple noncontiguous areas of intramural hemorrhage and new capillaries in and around the arterial wall (Endo et al. 1993) (Fig. 7.12). In all cases that could be examined pathologically, there was a dissection between the media and the adventitia, with a rupture site at the level of the adventitia (Fig. 7.68).

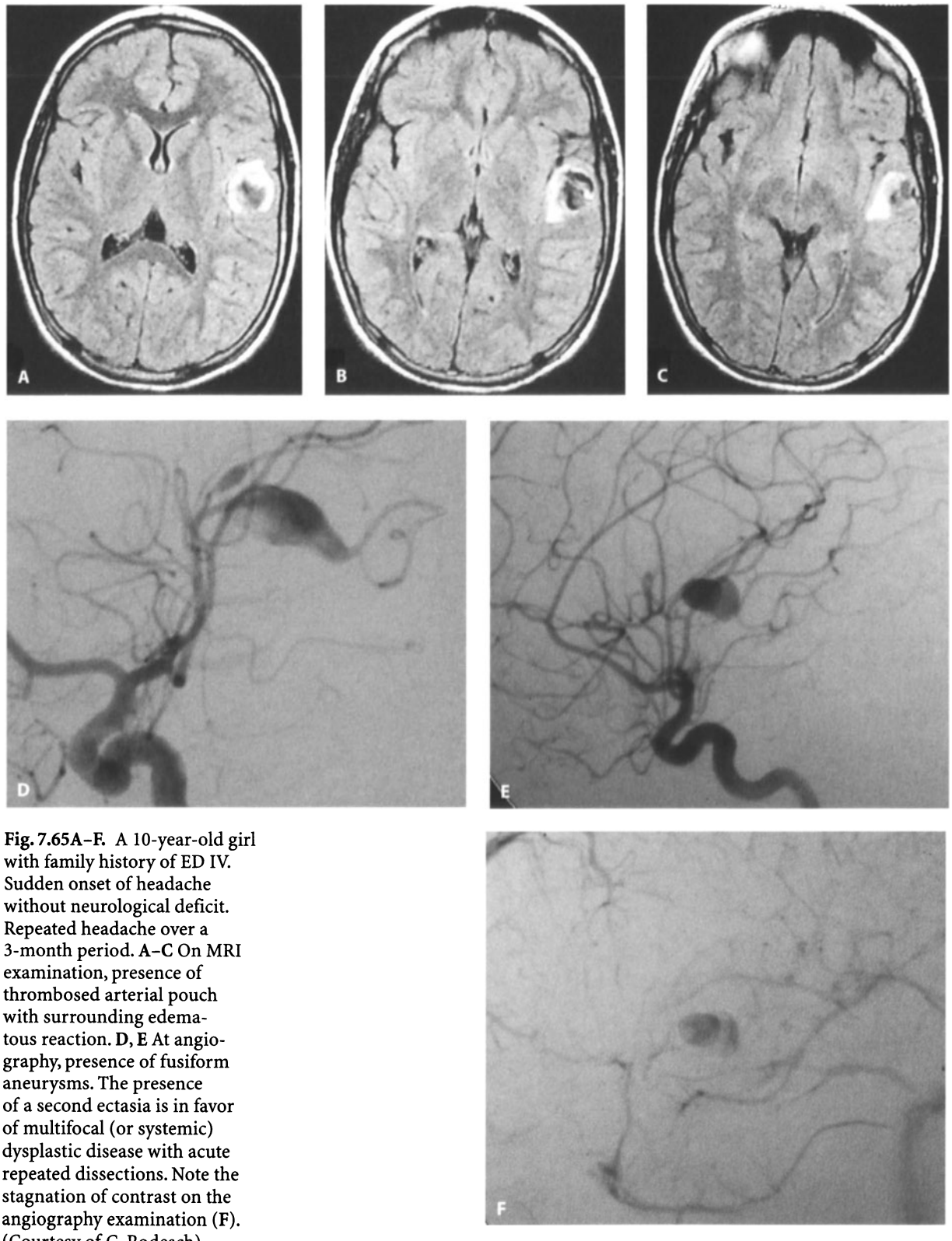

Fig. 7.65A–F. A 10-year-old girl with family history of ED IV. Sudden onset of headache without neurological deficit. Repeated headache over a 3-month period. **A–C** On MRI examination, presence of thrombosed arterial pouch with surrounding edematous reaction. **D, E** At angiography, presence of fusiform aneurysms. The presence of a second ectasia is in favor of multifocal (or systemic) dysplastic disease with acute repeated dissections. Note the stagnation of contrast on the angiography examination (**F**). (Courtesy of G. Rodesch)

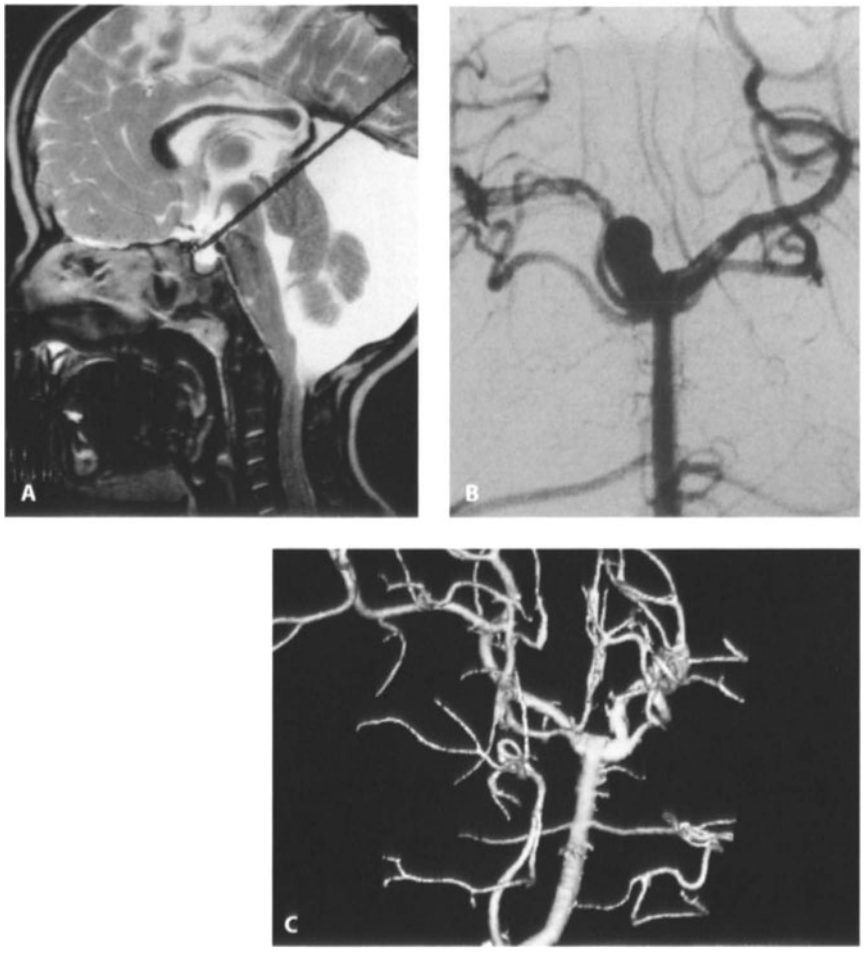

Fig. 7.66. A patient who was referred 2 years after hemorrhagic complication during third ventriculostomy (**A**); a posttraumatic dissecting aneurysm was demonstrated (**B**) and embolized with coils (even though healed dissecting arterial aneurysms usually do not rupture at long-term follow-up). Follow-up angiogram 1 year after uneventful endovascular treatment shows stable exclusion of the aneurysm (**C**)

In one case, the internal elastica lamina (IEL) was disrupted and demonstrated degenerative changes of the media due to atherosclerosis (Fig. 7.69); neovascularization and subadventitial dissecting hemorrhage at the site of rupture of the upper basilar artery was noted. Seventeen cases had a disruption of the entire arterial wall, and in three cases there was no luminal connection apparent. In his second case, a fusiform dissecting AA of the VA distal to the origin of PICA was noted (Figs. 7.70, 7.71, p. 459). There was no double lumen and no evidence of atherosclerosis.

The wall of intracranial arteries is thin compared to similar size arteries elsewhere in the body. The absence of IEL makes the site of the intramural hemorrhages as well as its consequences different. The vertebral arterial wall changes its structure as it pierces the dura. Therefore, intracranial dissections should be separated from cervical and peripheral ones. Intradural dissections of M1 (Fig. 7.69), or the basilar artery may, in addition to being associated with occlusion of perforators, cause ischemia in the territories involved (Figs. 7.72, 7.73, pp. 460–462).

Dissection between the media and adventitia with rupture into the subarachnoid space is a universal finding. The outlet of dissection is thought to be a disrupted site of the adventitia (Fig. 7.68). Sasaki et al. (1991) suggested that the dissection initially occurs between the intima

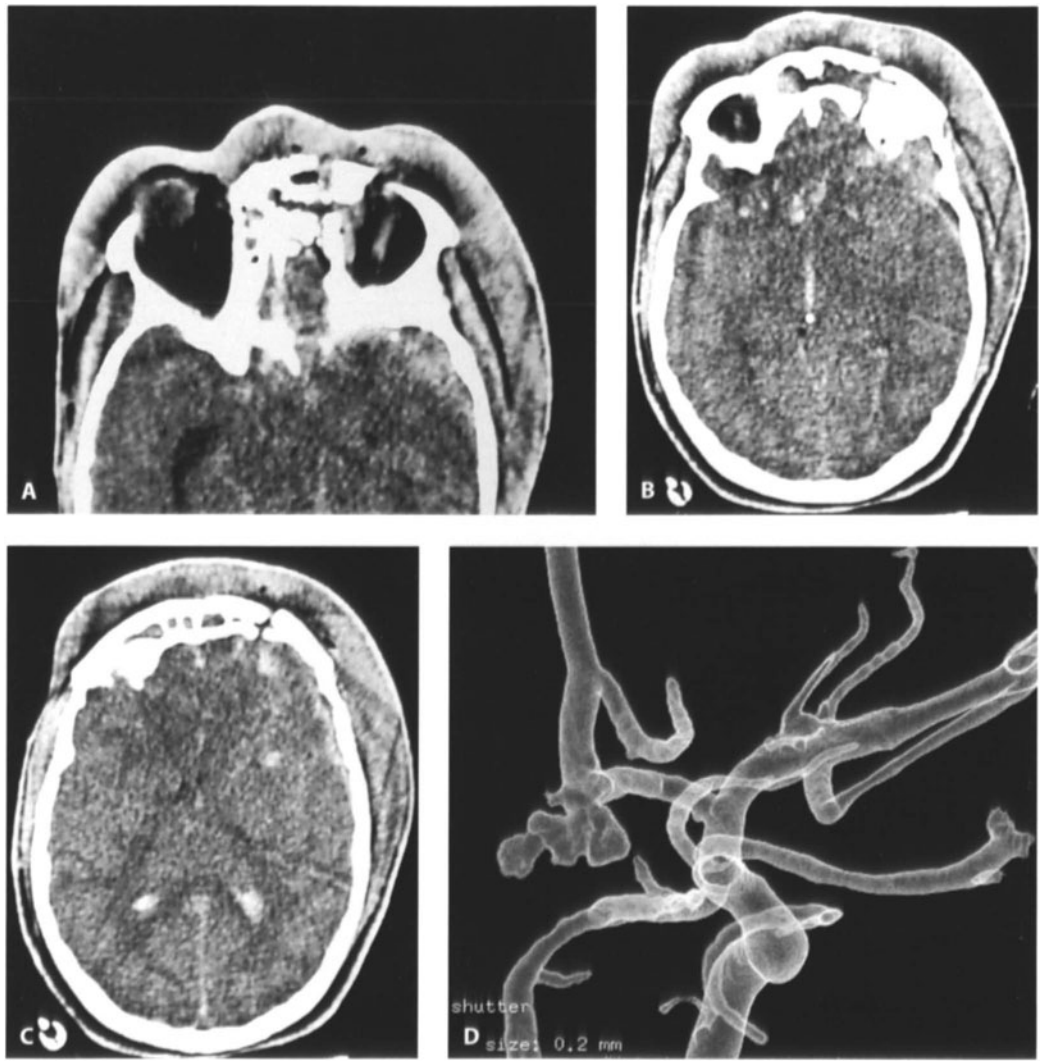

Fig. 7.67A–D. Severe maxillofacial trauma. Multiple hemorrhages in the brain and different meningeal compartments. Complex skull base fracture with direct injury of the AcomA from traumatic dissection

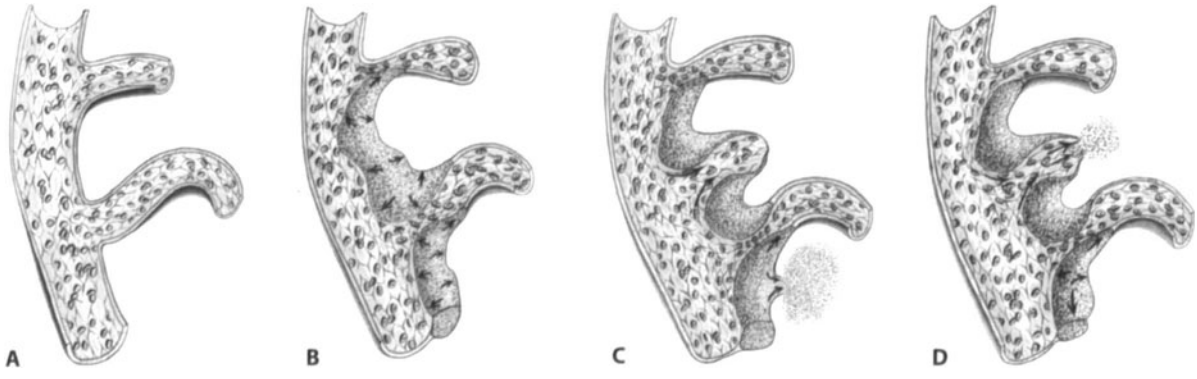

Fig. 7.68A–D. Schematic representation of dissecting processes of the intradural arteries. **A** Normal aspect; **B** mural hematomas, parent artery stenosis, ostial narrowing, and vessel diameter widening with the ruptures; **C** subadventitial rupture and unruptured dissecting aneurysm; **D** vessel wall disruption

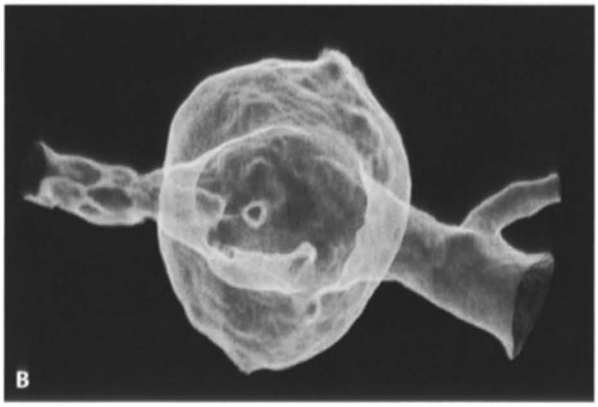

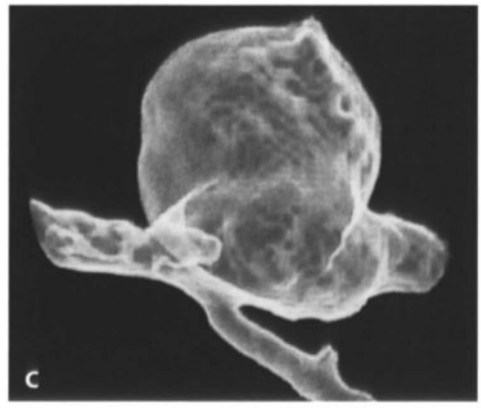

Fig. 7.69. A–C Ruptured middle cerebral artery dissecting aneurysm. Note the fusiform aspect and the narrowed segments adjacent to the aneurysm. **D, E** Endoluminal flap involving the M1 segment and atheromatous disease of the basilar artery and right vertebral artery

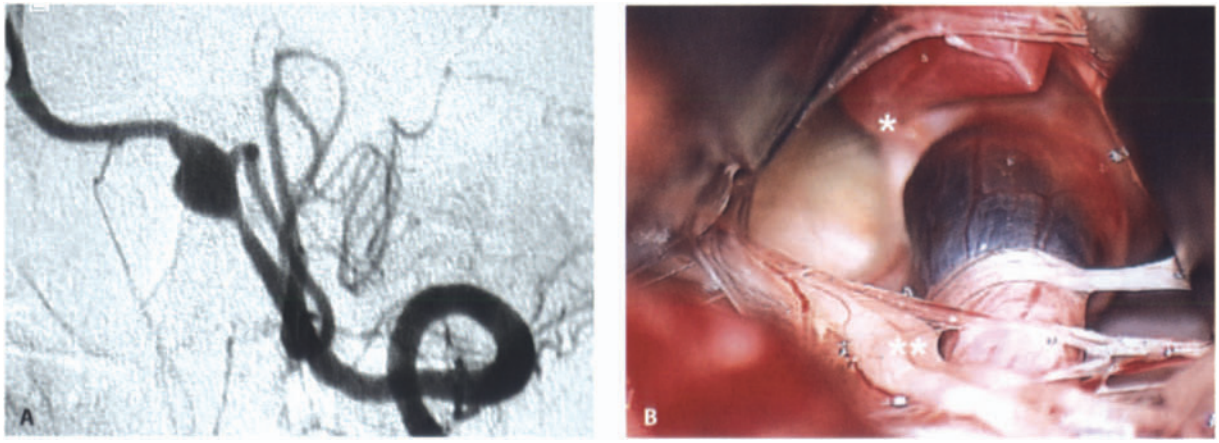

Fig. 7.70A, B. Subarachnoid hemorrhage with ruptured fusiform dissecting intradural vertebral artery (VA) aneurysm; (**A**) angiogram and (**B**) surgical view before wrapping. VA was subsequently occluded at C1, with favorable clinical outcome. (From Reyes 2001, with permission)

Fig. 7.71A–C. Subarachnoid hemorrhage with intradural vertebral artery (VA) dissecting aneurysm. **A, B** Angiographic aspect with extradural origin of the posterior inferior cerebellar artery (PICA). **C** Sacrifice of the intradural VA distal to PICA, proximal to the vertebrobasilar junction. The coils are placed across the dissection; note the loose packing

and the media and subsequently all the arterial wall layers are destroyed and SAH develops. In dissections with SAH and without lumen communication, Yonas et al. (1977) proposed that rupture of vasa vasorum or rupture of new vessels formed in response to medial ischemia and necrosis would be responsible. The vasa vasorum are not present in all intradural arteries but they are found in the vertebrobasilar system and ICA. They are normally absent or rarely observed in the ACA or MCA. Associated atheromatous disease increases the presence of vasa vasorum of the intradural arteries (see Vol. 1) (Fig. 7.69). One can see associated giant partially thrombosed aortic AAs with large partially thrombosed intradural AAs (Fig. 7.87); both are likely to correspond to mural vasa vasorum ruptured in association with atheromatous disease (Fig. 7.74, p. 463).

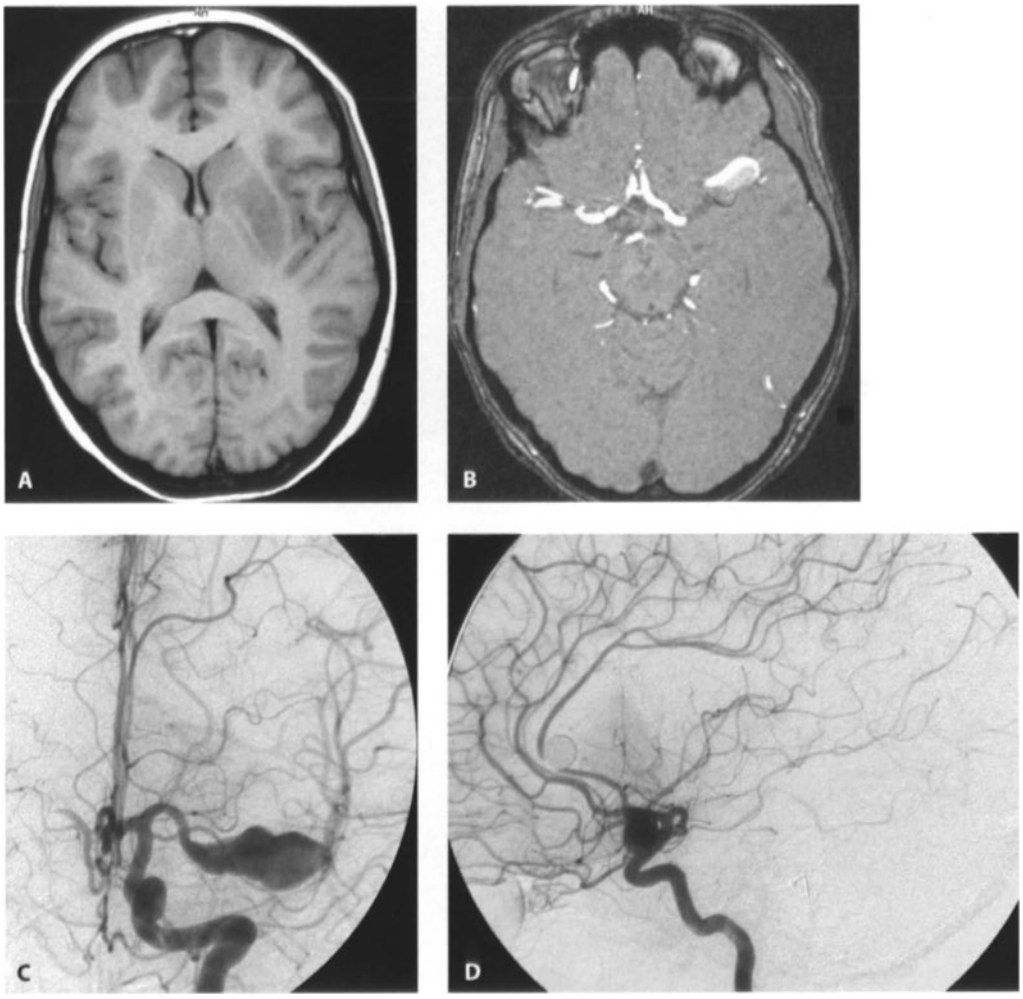

Fig. 7.72A–J. A 16-year-old female patient presented with progressive right-sided deficit without headaches. **A** MRI shows a deep-seated stroke in relation to a fusiform arterial aneurysm (AA), as seen on MRA (**B**) and angiography (**C, D**). Occlusion of cortical arteries and the aspect on endoscopic view (**E, F**) favor the diagnosis of embolic events. Occlusion of cortical arteries and the aspect on 3-D (**E, F**) and endoscopic (**G, H**) views favor the diagnosis of embolic events from a partially thrombosed AA. Dissection is suspected. During the subsequent 3 weeks, she recovered from her stroke while on antiplatelet therapy. She was scheduled 2 weeks later for M1 occlusion with STA–MCA anastomosis, but 1 week before her admission for such treatment, she presented with subarachnoid hemorrhage (**I, J**) and a GCS of 3. The AA was probably an unruptured fusiform AA that continued to dissect initially involving M1 perforators and subsequently extending into the subarachnoid space. **E–J** see p. 461

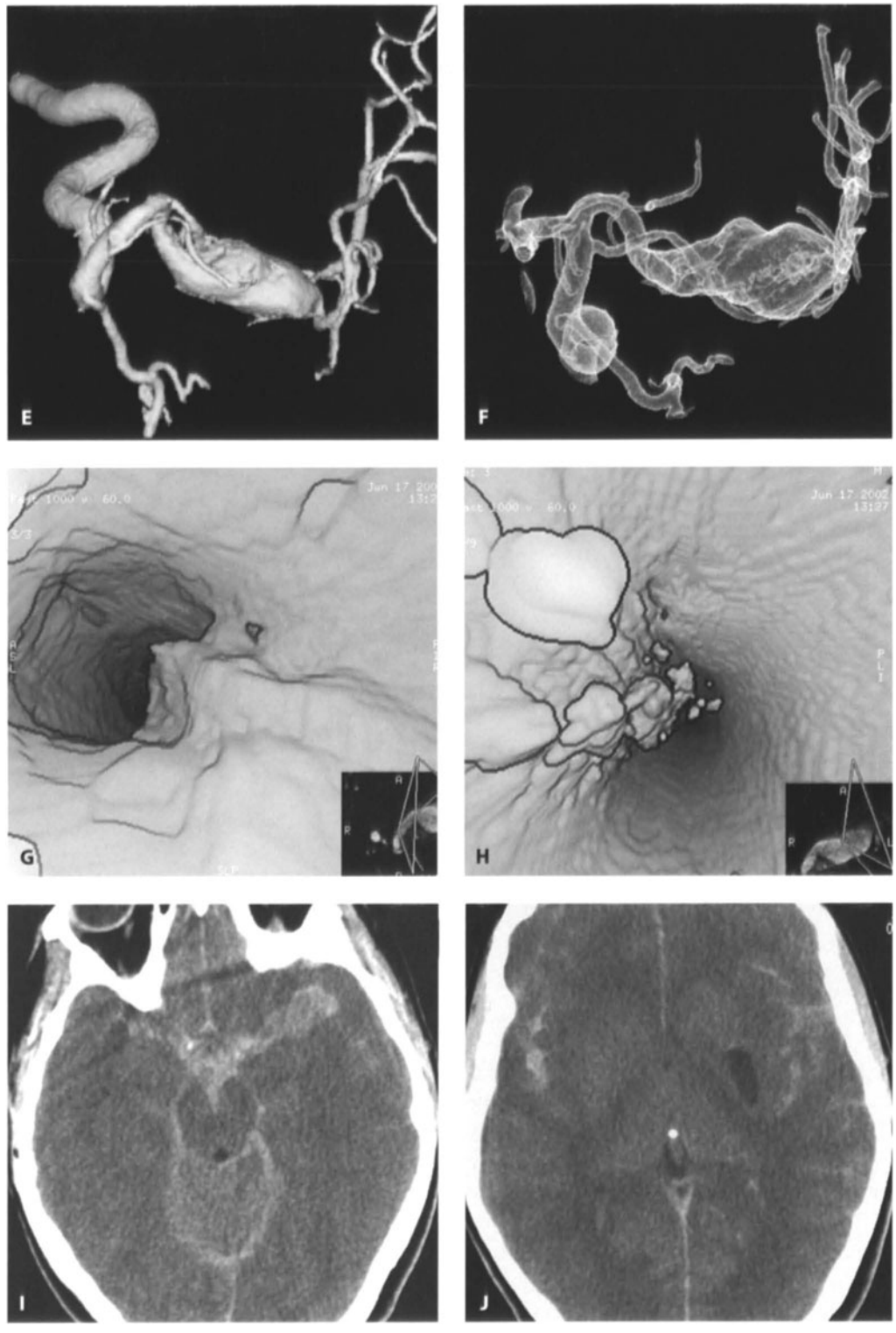

Fig. 7.72E–J. Legend see p. 460

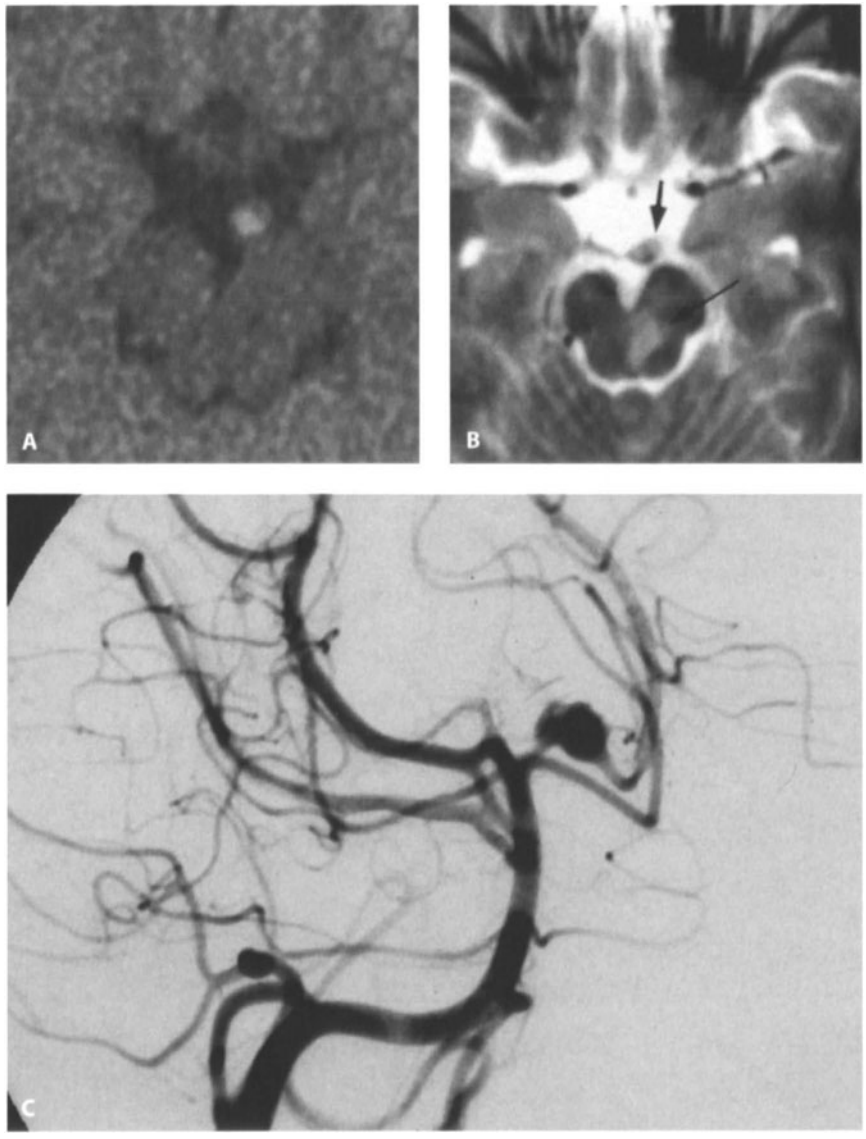

Fig. 7.73A–C. A 16-year-old male patient presented with right-sided weakness and left ophthalmoplegia. **A, B** Midbrain infarct (*arrow*). Evidence of a dissecting P1 posterior cerebral artery aneurysm (*small arrow*) well demonstrated on the vertebral angiogram (**C**). Anticoagulation treatment for 6 months resulted in complete clinical recovery with aneurysm healing

Rupture of the mural hematoma into the lumen of the artery may lead to the typical double lumen that is often seen extradurally but rarely demonstrated intradurally. More often they turn out to be recanalization of a proximally occluded segment (distal ICA or M1 segment in children or young adults) (Fig. 7.75).

The primary cause for the dissection is unknown but includes infection, ischemia, and minimal mechanical constraints. They classically occur in patients in their fifth or sixth decade. A history of hypertension is equally present in the SD with and without SAH and occurs in less than one-quarter of cases.

In Kitana's review (1994) of 24 cases, 16 presented with SAH while eight were diagnosed as intracranial SD without SAH. In the group with SAH, 14 had aneurysmal dilatation in association with proximal or distal narrowing (pearl and string sign), while the remaining two demonstrated AA only. Three dissections involved the PICA, two were proximal to its origin,

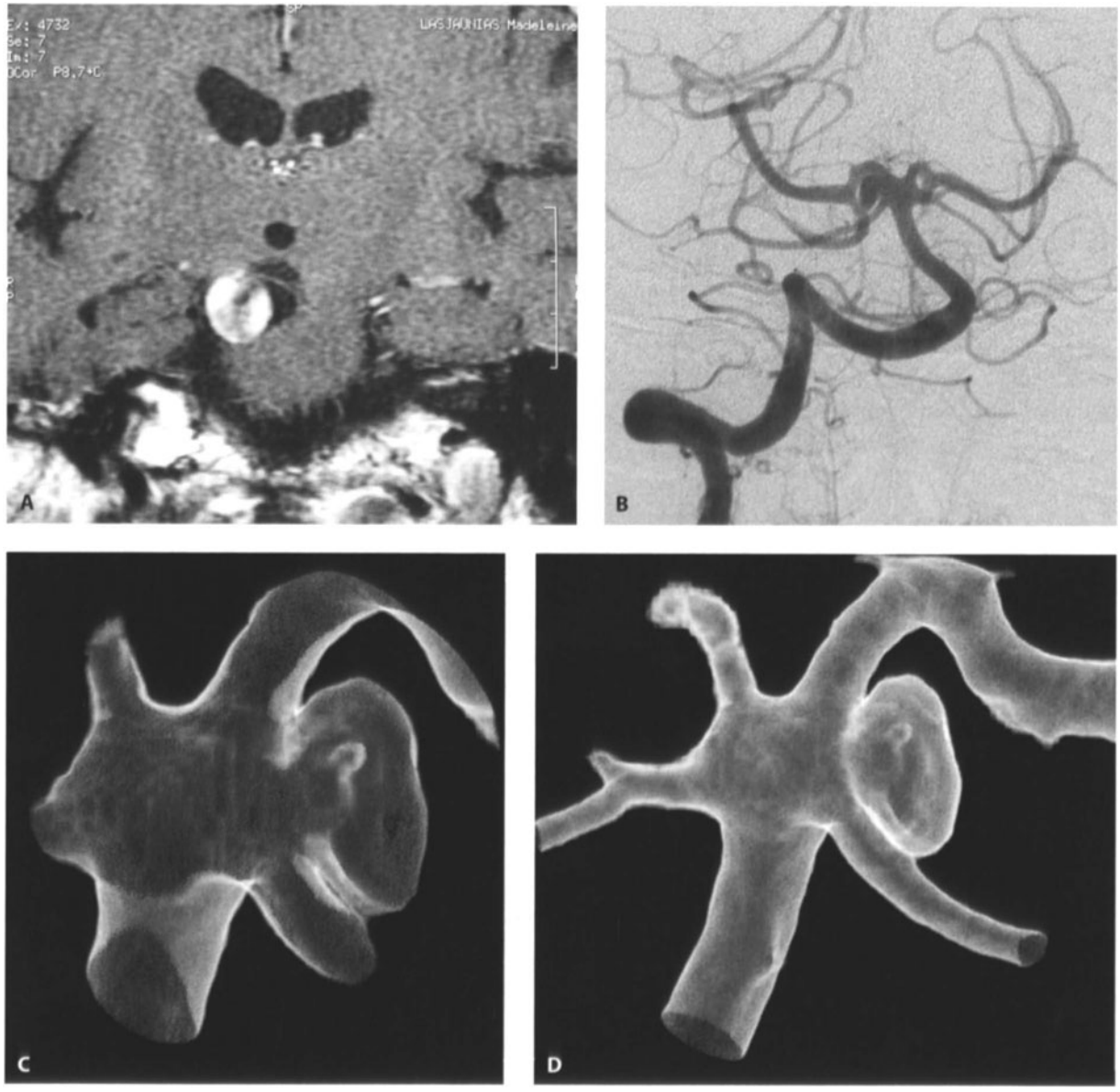

Fig. 7.74A–D. A 72-year-old female patient with progressive ptosis and mild headaches. **A** MRI shows subacute dissecting aneurysm of the upper basilar artery, confirmed on angiography (**B**) located between P1 and the anterior superior cerebellar artery (**C–D**)

16 were distal. Two VA dissections extended to the basilar trunk, whereas the basilar artery (BA) was not involved in any of the SDs with SAH.

The dissection of a PICA without involvement of the VA is rare (Nagahiro et al. 1993). Piske et al. (1998) found nine cases in the literature, four revealed by SAH, while the others suffered ischemic strokes. Shinoda et al. (1998) reported bilateral PICA dissections without VA impairment (Figs. 7.75–7.77) following rehemorrhage in one case, which was confirmed at autopsy. The topography of these lesions indicates the potential multifocal nature of the process (while sparing the VA in some instances). The literature on clinical (Kitana 1994; Nagahiro et al. 1997) and autopsy

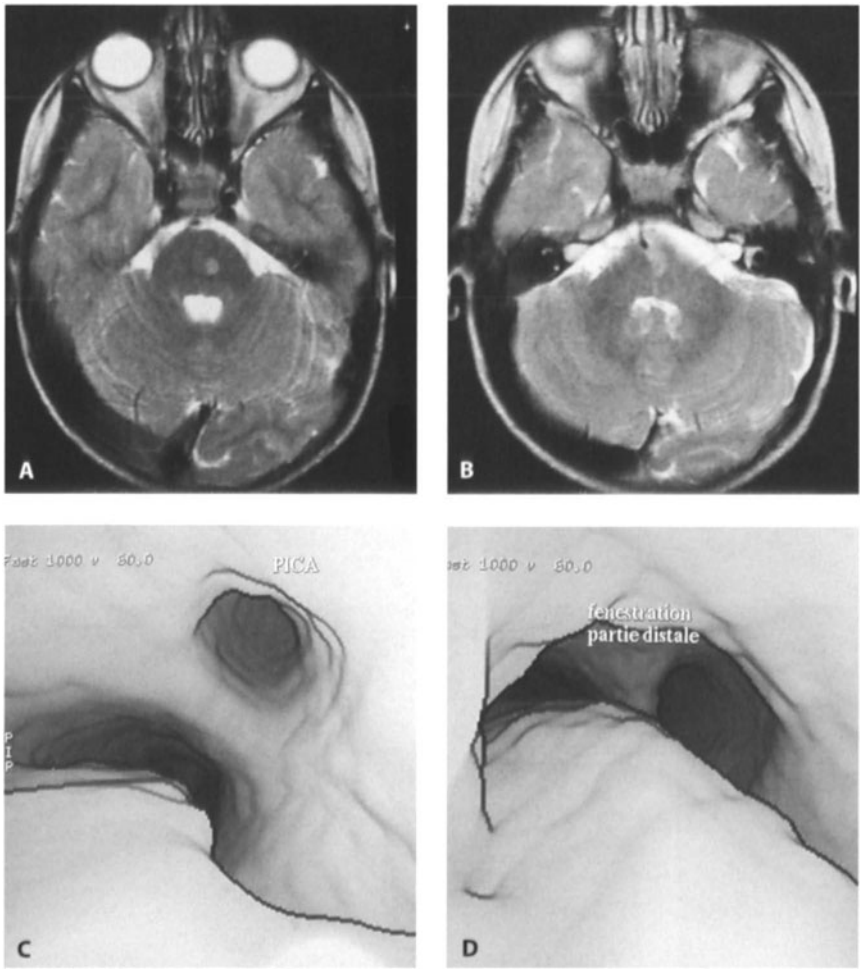

Fig. 7.75A–H. A 5-year-old boy with rapidly progressive paraparetic syndrome. Minor trauma. NF1 in the mother, factor XII deficit in the mother's sister. **A, B** Posterior fossa strokes caused by spontaneous dissection (**C, D**) of a duplicated intradural vertebral artery (**E, F**). **E–H** see p. 465

series (Endo et al. 1993) with SAH report nearly a 3:1 male dominance. Such figures are in contrast with most of the disorders known to be associated with dissections and SAH, where a strong female dominance is usually noted, even autosomal familial disorders such as FMD.

The diagnosis of a true dissection is challenging and has been confirmed at angiography in relatively few cases in comparison to the actual number of cases where it probably occurred. Angiographic criteria for SD are the stagnation of the contrast in the AA pouch (Figs. 7.65, 7.78, 7.79), the presence of stenotic segments proximal and/or distal to the ectasia, and a more fusiform appearance, except when it involves the PICA origin (Fig. 7.79).

MRI can sometimes demonstrate increased signal intensity on T1-weighted images, indicating the intramural hematoma (Fig. 7.74, 7.78–7.80). The images are well known and particularly eloquent in the cervical SD, with or without AA (Sellier et al. 1983; Brugières et al. 1989). On contrast-enhanced MR, most cases show thick ring-like or railroad-

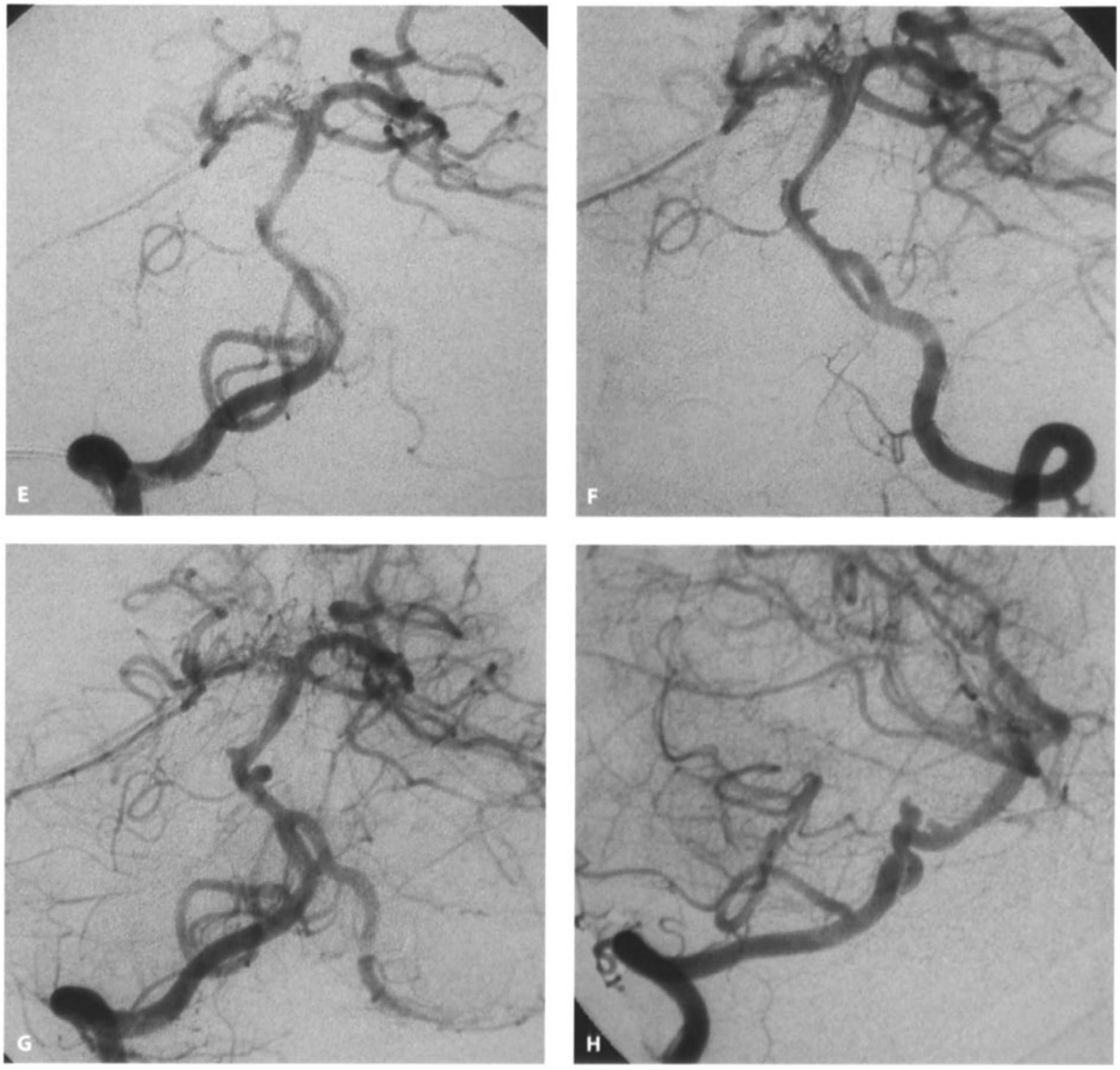

Fig. 7.75 (*continued*). **E, F** Duplicated intradural vertebral artery. **G, H** Six months later, conservative treatment resulted in excellent clinical outcome; however, aneurysmal aspect of the healing process at the lower mid third of the basilar artery was demonstrated

like enhancement that includes the entire vessel wall with a central or eccentric signal flow void. In other instances, the mural bulge enhancement is focal. The enhancement is thought to correspond to increased permeability of contrast material from the dissected false lumen to the vessel wall. The thick and dense enhancement disappears at approximately the same time as the dissecting AA disappears on the angiograms (Nagahiro et al. 1997) (Figs. 7.74, 7.79, 7.81).

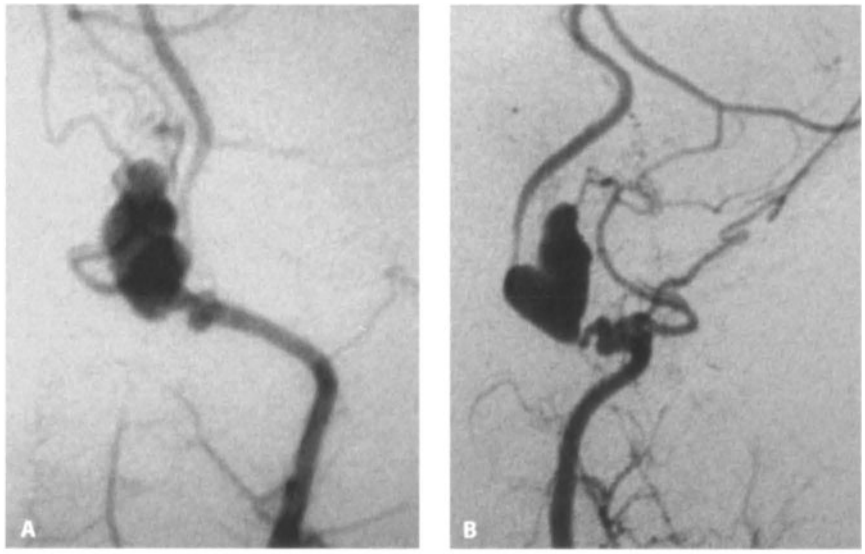

Fig. 7.76. **A** Frontal and **B** lateral vertebral angiogram. Nonhemorrhagic acute medullary syndrome. Angiography demonstrates a dissecting arterial aneurysm (AA) involving a suspected distal vertebral artery dysplasia. Note the arterial narrowing proximal and distal to the neck of the dissecting AA

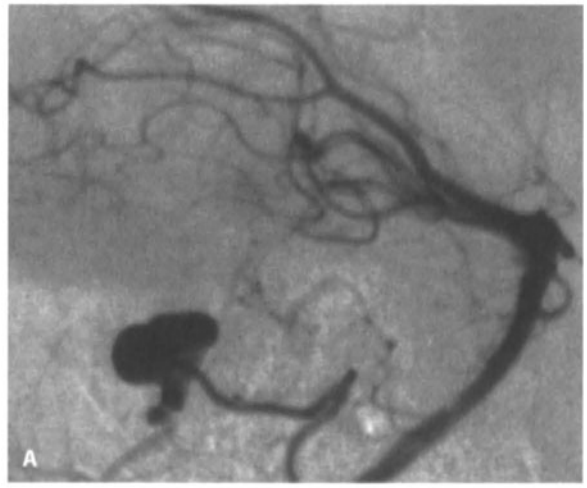

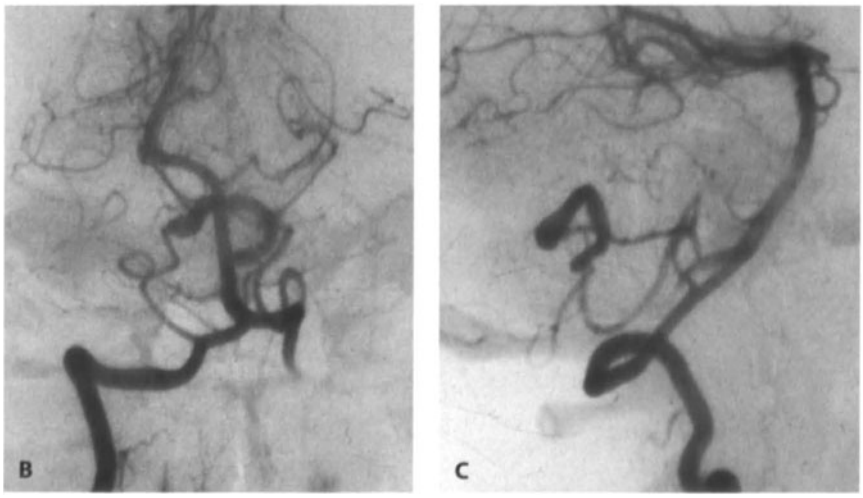

Fig. 7.77A–C. Subarachnoid hemorrhage with distal dissecting posterior inferior cerebellar artery aneurysm. **A** Angiogram at the acute stage. **B, C** Angiograms 3 months later showing partial repair

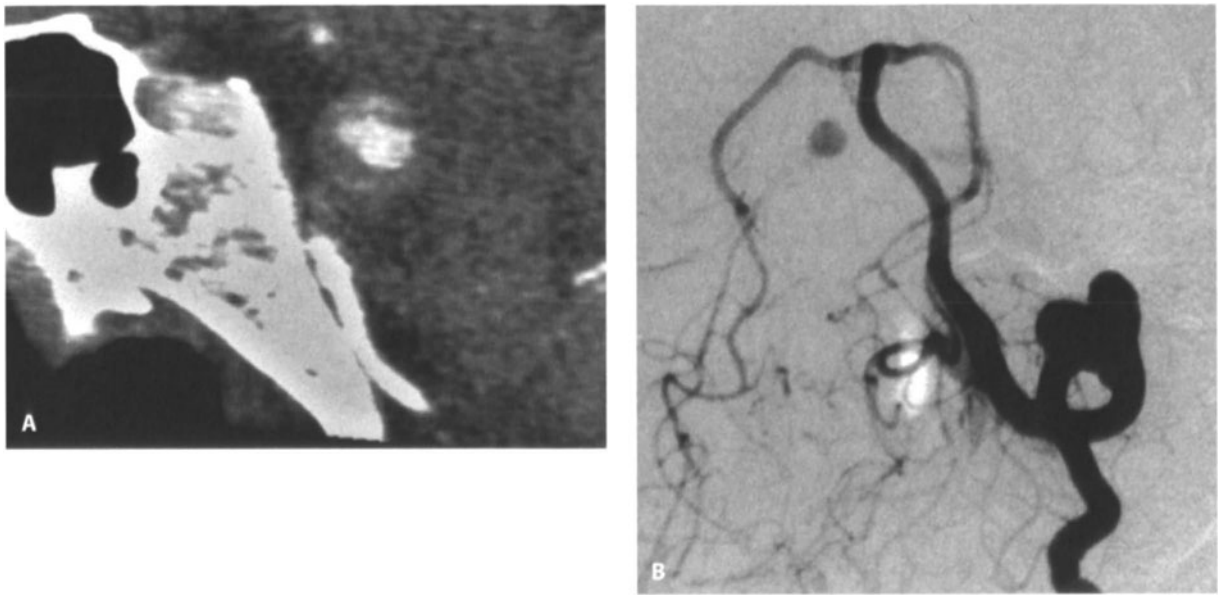

Fig. 7.78. Trigeminal subacute dissecting arterial aneurysm (AA) with enhanced lumen (**A**) and stagnation of contrast within the AA on the angiographic examination (**B**)

Fig. 7.79. **A, B** Parasagittal and frontal MRI sections, **C** lateral internal carotid artery, and **D** lateral vertebral artery angiogram. Fusiform dissecting P2 posterior cerebral artery (PCA) aneurysm with left PCA territory infarction because of insufficient retrograde opacification of the PCA branches from the middle cerebral artery

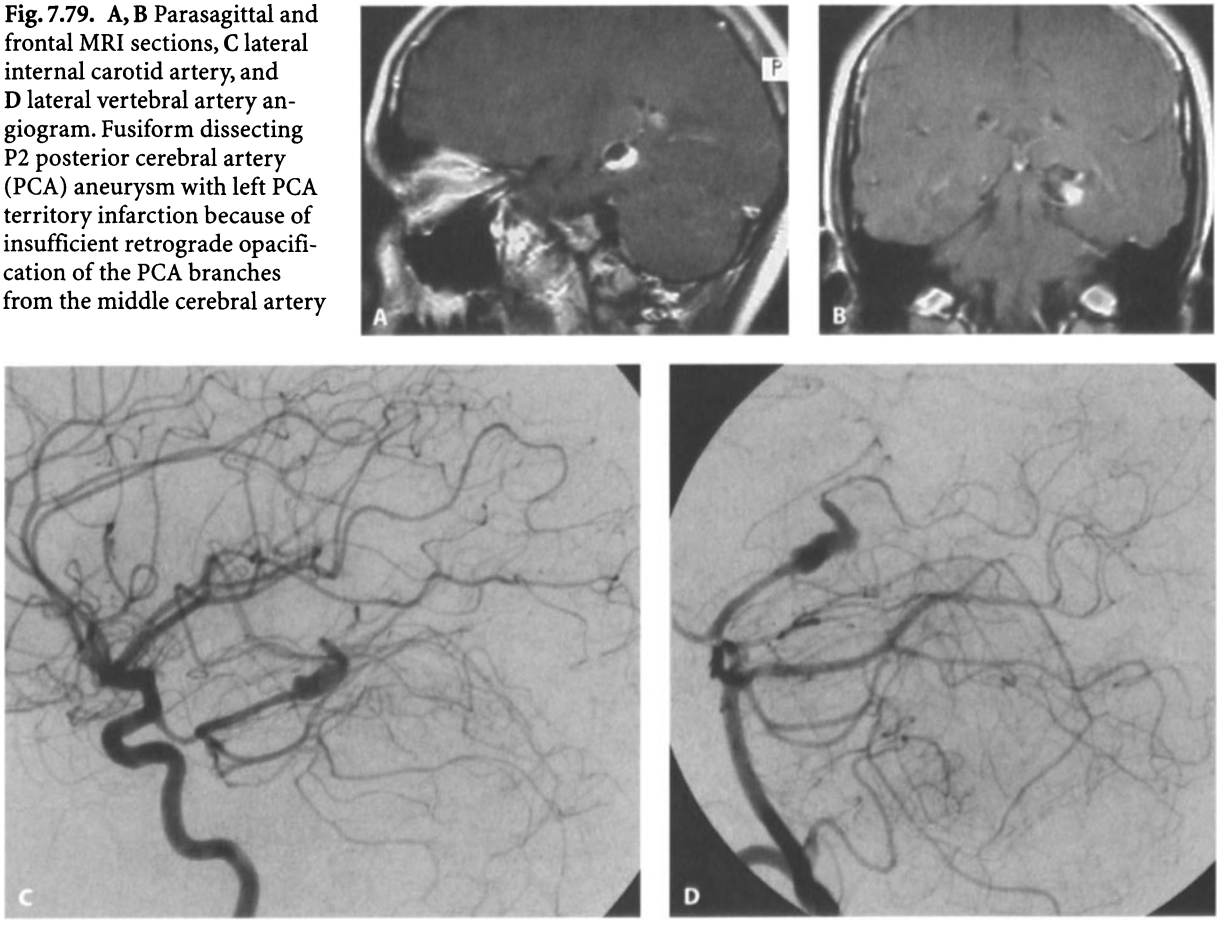

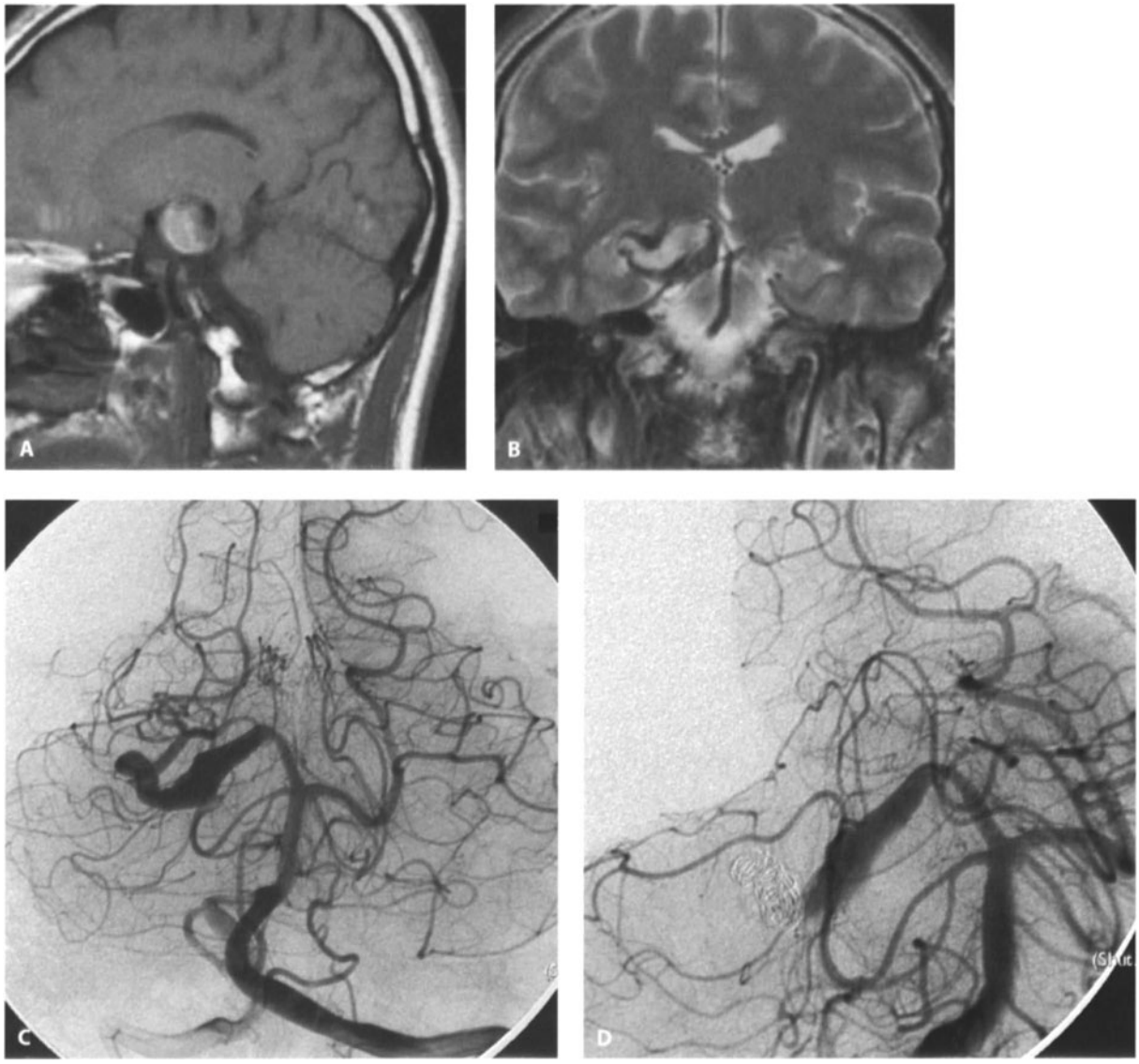

Fig. 7.80A–D. A 31-year-old man presented with headaches and nausea. MRI (**A, B**) demonstrates a fusiform dissecting P2 posterior cerebral artery (PCA) aneurysm confirmed at angiography (**C**). Treatment consisted of distal coil occlusion (**D**); excellent visual tolerance through anterior choroidal–PCA anastomoses and exclusion of the aneurysm on long-term follow-up (not shown)

Repeated episodes of ischemia or hemorrhage (24% in the Yamaura et al. (1990) series within 17 days after the initial ictus) can be observed in the progression of the dissection (Figs. 7.72, 7.75), as well as spontaneous healing (Pozzati et al. 1991; Piske et al. 1998) (Figs. 7.77, 7.82–7.84). Rehemorrhage tends to occur early; otherwise healing will likely occur. Recurrence of clinically symptomatic dissection, months or years after spontaneous healing or following treatment, has not occurred in our experience. Yet over time, repeated subclinical dissections are likely to produce large partially thrombosed mural AAs, eventually becoming giant in size following recurrent dissecting episodes. The exact risk of rupture from these subacute or chronic dissections with moderate to large AAs is unknown

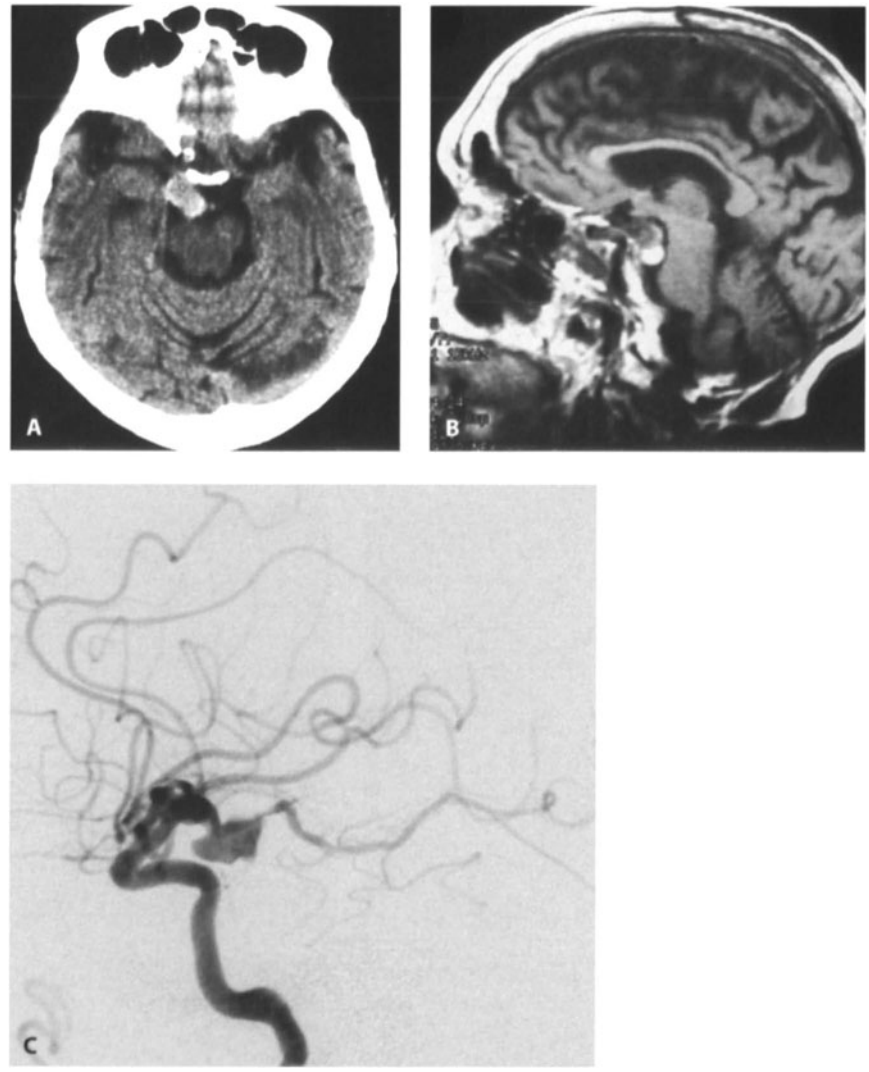

Fig. 7.81. **A, B** MRI and **C** ICA angiogram in an 83-year-old female patient who presented with right facial pain in the trigeminal distribution caused by a P1–P2 junction dissecting arterial aneurysm

(Figs. 7.74, 7.85). They are often included in the group of partially thrombosed AAs less than 25 mm in diameter. Their shape can be either saccular or fusiform.

Simple hemodynamic changes (Aymard et al. 1989) or proximal sacrifice of the VA at the extradural level (if well tolerated during functional testing) is often sufficient to resolve the dissection (Figs. 7.71, 7.80, 7.86). However, in some instances, despite appropriate flow changes, the dissection seems to remain active and may be responsible for early SAH recurrence (Kitana 1994). The SD resulting from a biological phenomenon, which may create communication between the wall hematoma and the vessel lumen, will continue to remain active despite the occlusion of the vessel (with balloon or coil) or the exclusion of the vessel lumen from the dissection (using a stent). The multifocality (including bilateral lesions) of the mural hemorrhages noted by Endo et al. (1993) and the cases reported by Piske et al. (1998) and Kominami et al. (1996) may account for early rebleeding, despite what appears to be appropriate treatment (Müller-Forell and Bohl 1999).

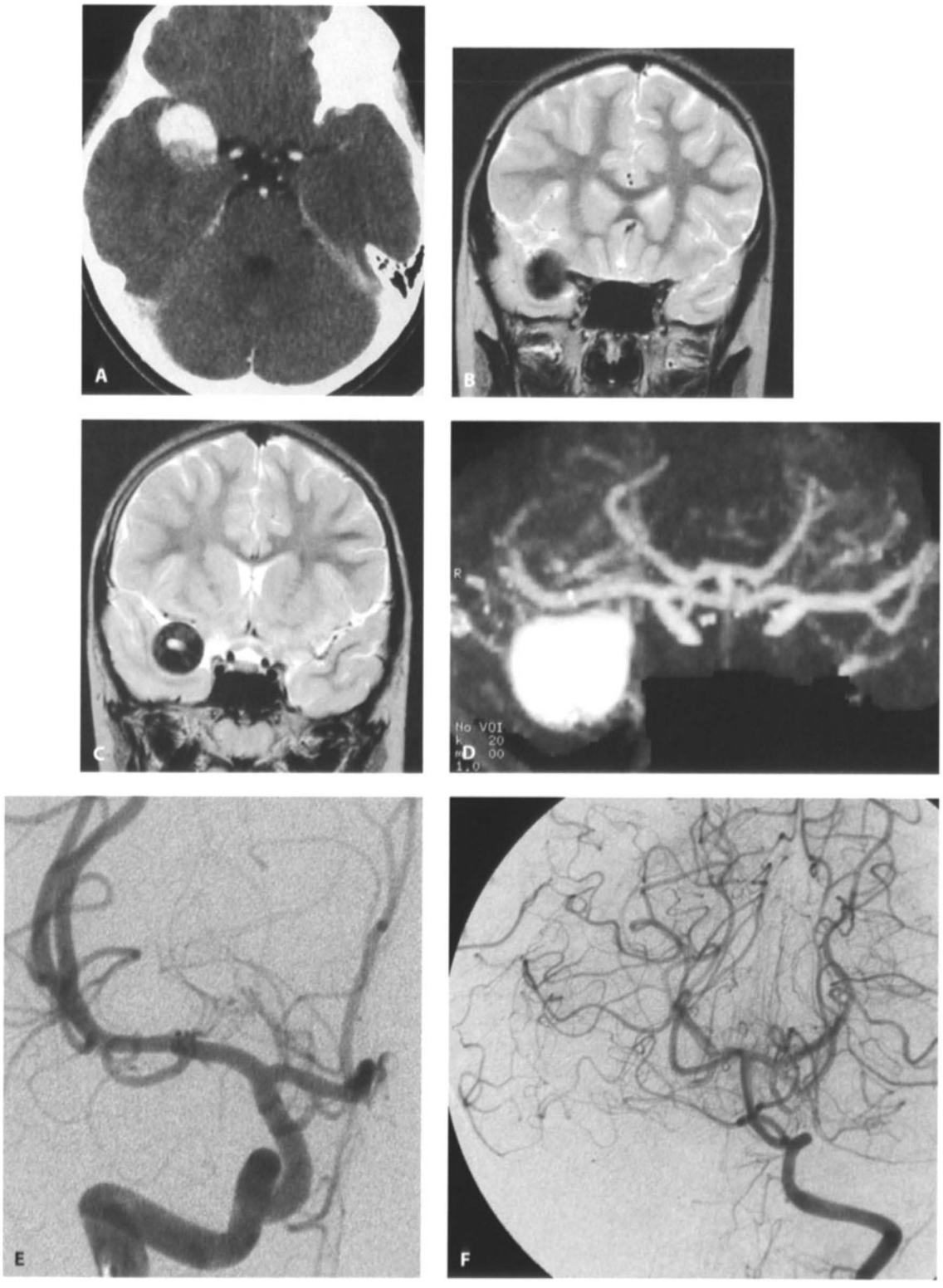

Fig. 7.82A–G. A 7-year-old boy with unremarkable personal and family history presented with headaches and vomiting following head injury. Persistence of the symptoms led to CT (**A**), MRI (**B, C**) and MRA (**D**), which show a partially thrombosed giant middle cerebral artery (MCA) aneurysm without subarachnoid hemorrhage. The lesion was felt to be unrelated to the trauma. Neurological examination was normal. Four days later, angiography (**E, F**) shows complete thrombosis of the aneurysm, which was also confirmed by MRA (**G**). **G** see p. 471

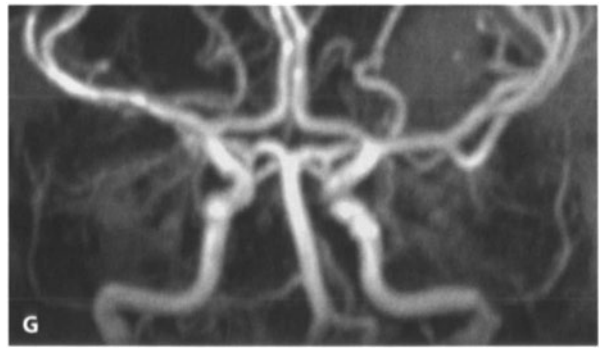

Fig. 7.82 (*continued*). There is evidence of MCA temporal branch occlusion with focal narrowing, as shown from the frontal internal carotid artery projection and the collateral circulation around the temporal lobe on the vertebral injection, suggesting a spontaneously repaired MCA branch dissection

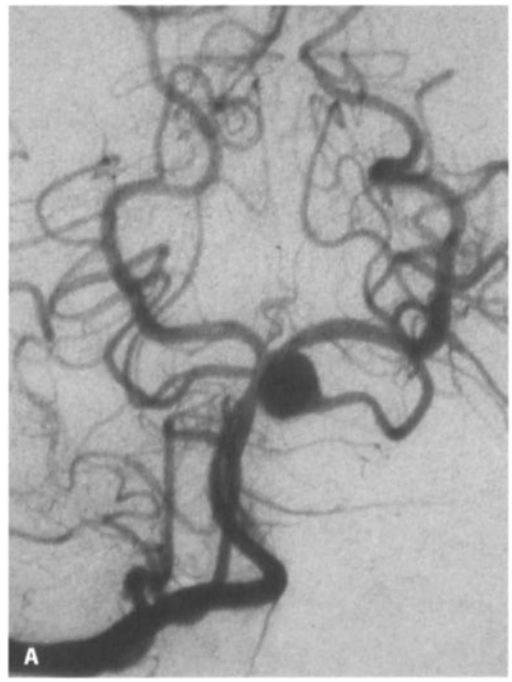

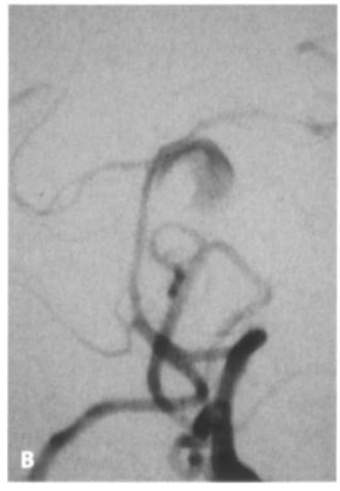

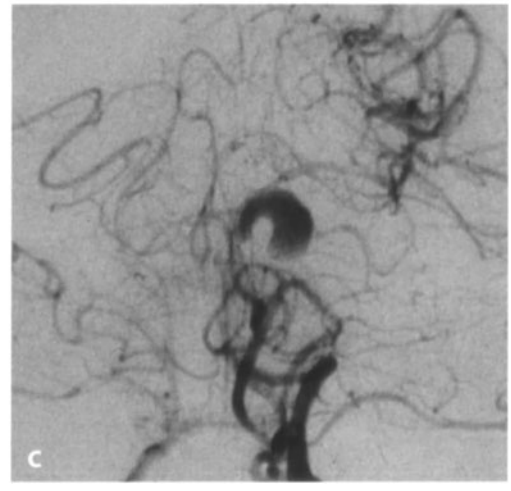

Fig. 7.83A–C. Subarachnoid hemorrhage with distal basilar artery (BA) aneurysm. **A** Angiogram at the acute stage. Focal narrowing on the BA and anterior superior cerebellar artery suggested dissection. **B, C** Partial thrombosis at 1 week

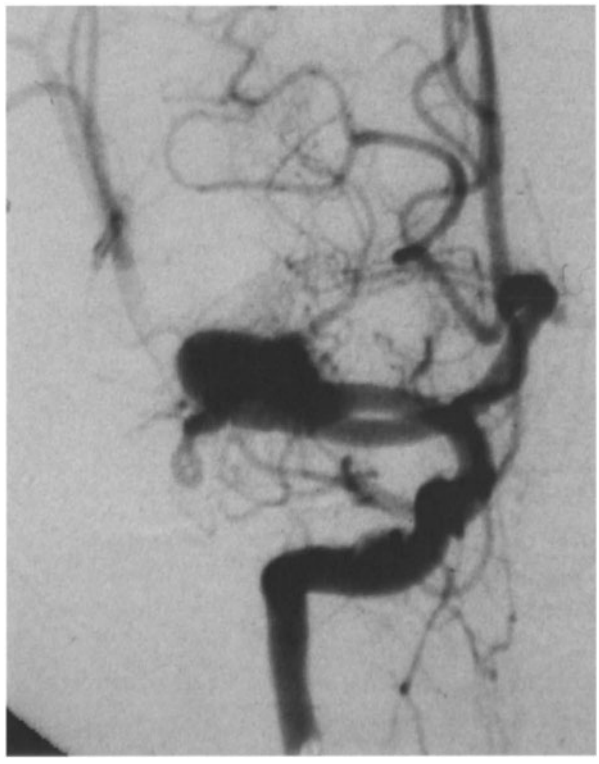

Fig. 7.84. Dissection arterial aneurysm with remodeling of M1. Various aspects of angiogenesis are noted leading to dolicho A1, ectatic arterial segment of M1, occlusion of the M1–M2 junction, and capillarectasia. (Courtesy of R. Piske)

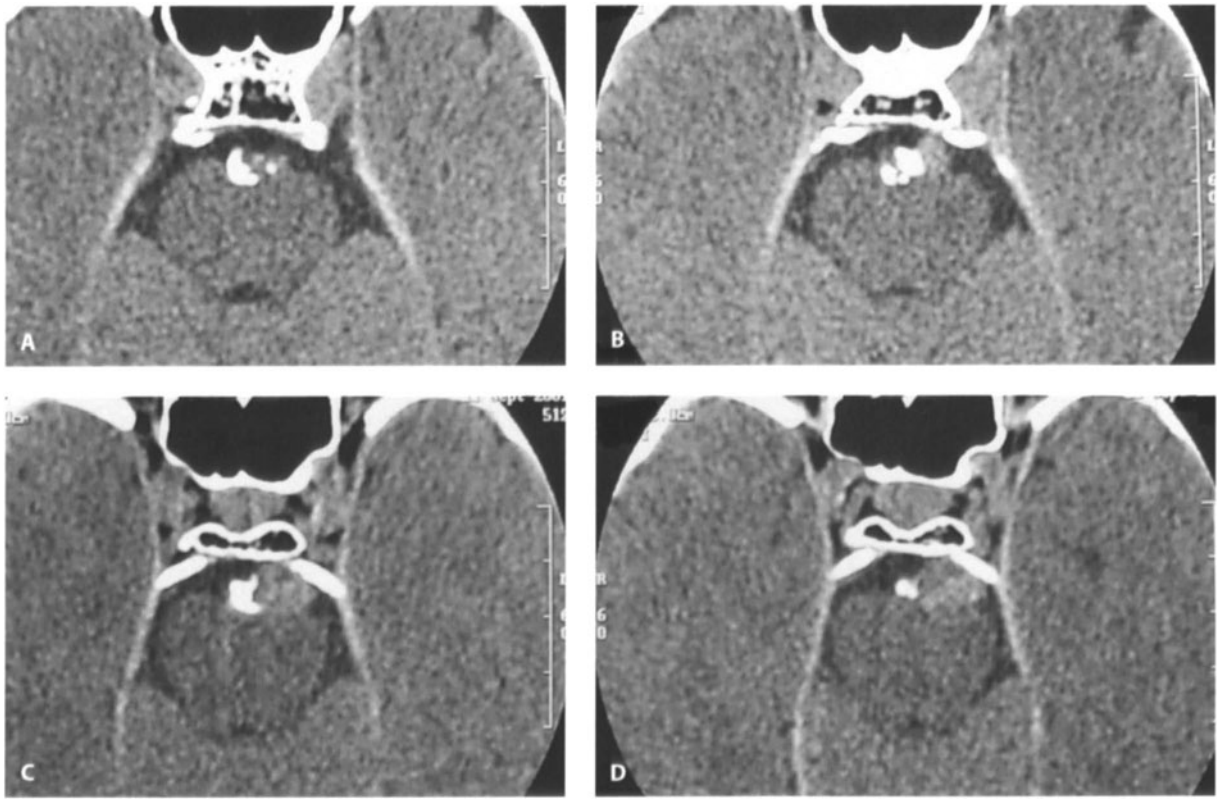

Fig. 7.85A–S. A 57-year-old male patient presented with transient intranuclear ophthalmoplegia. **A–D** CT evidence of subacute dissecting aneurysm of the upper basilar artery (BA) with mural calcifications. **E–S** see pp. 473–475

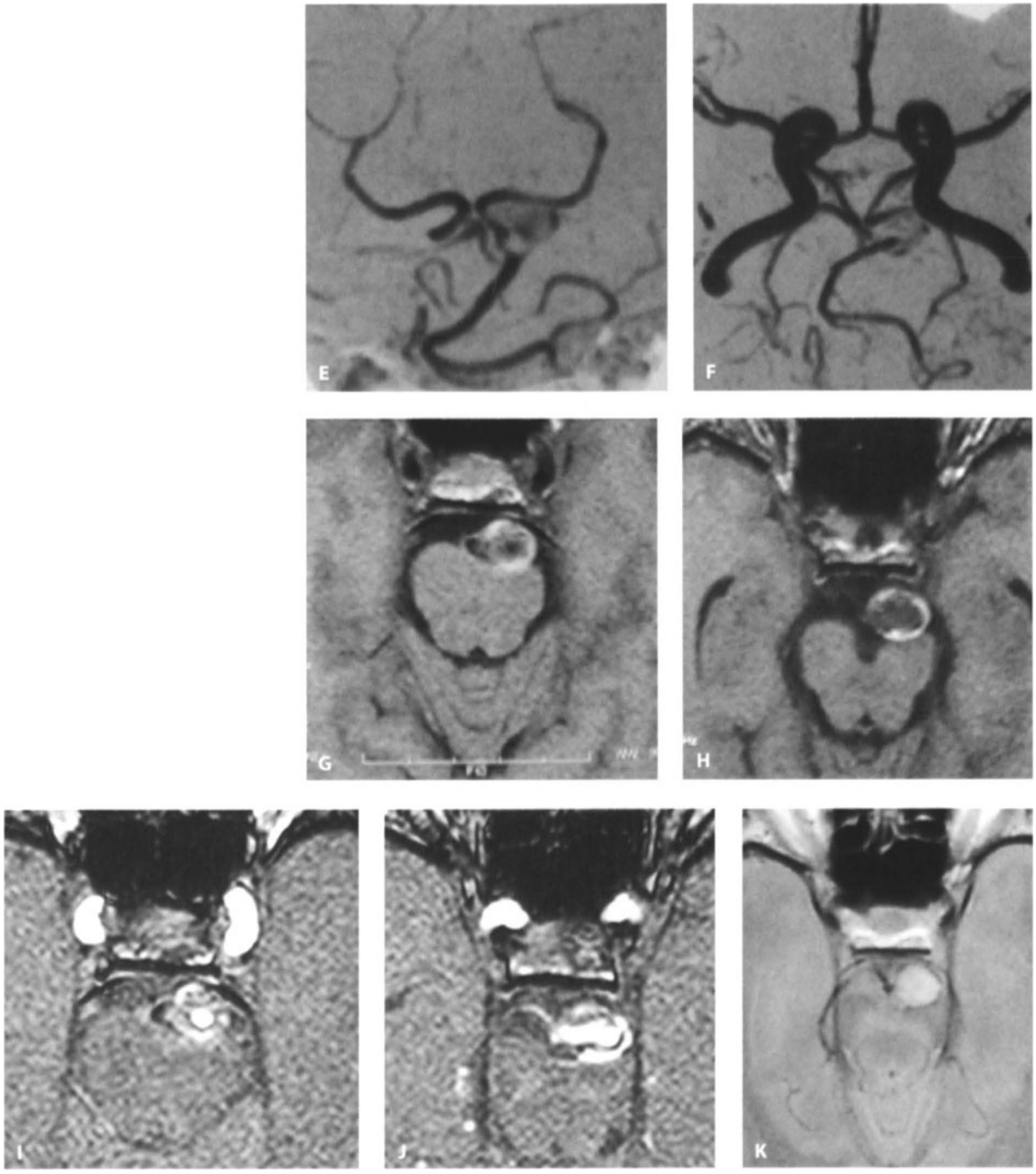

Fig. 7.85 (*continued*). **E–H** MRA and MRI demonstrate subacute dissecting aneurysm of the upper BA. **I–K** Contrast-enhanced MRI shows the persistent lumen. Mesencephalic perforators may have been included in the dissection or the progression of subadventitial dissection and may be responsible for minimal increasing mass effect. **L–S** see pp. 474, 475

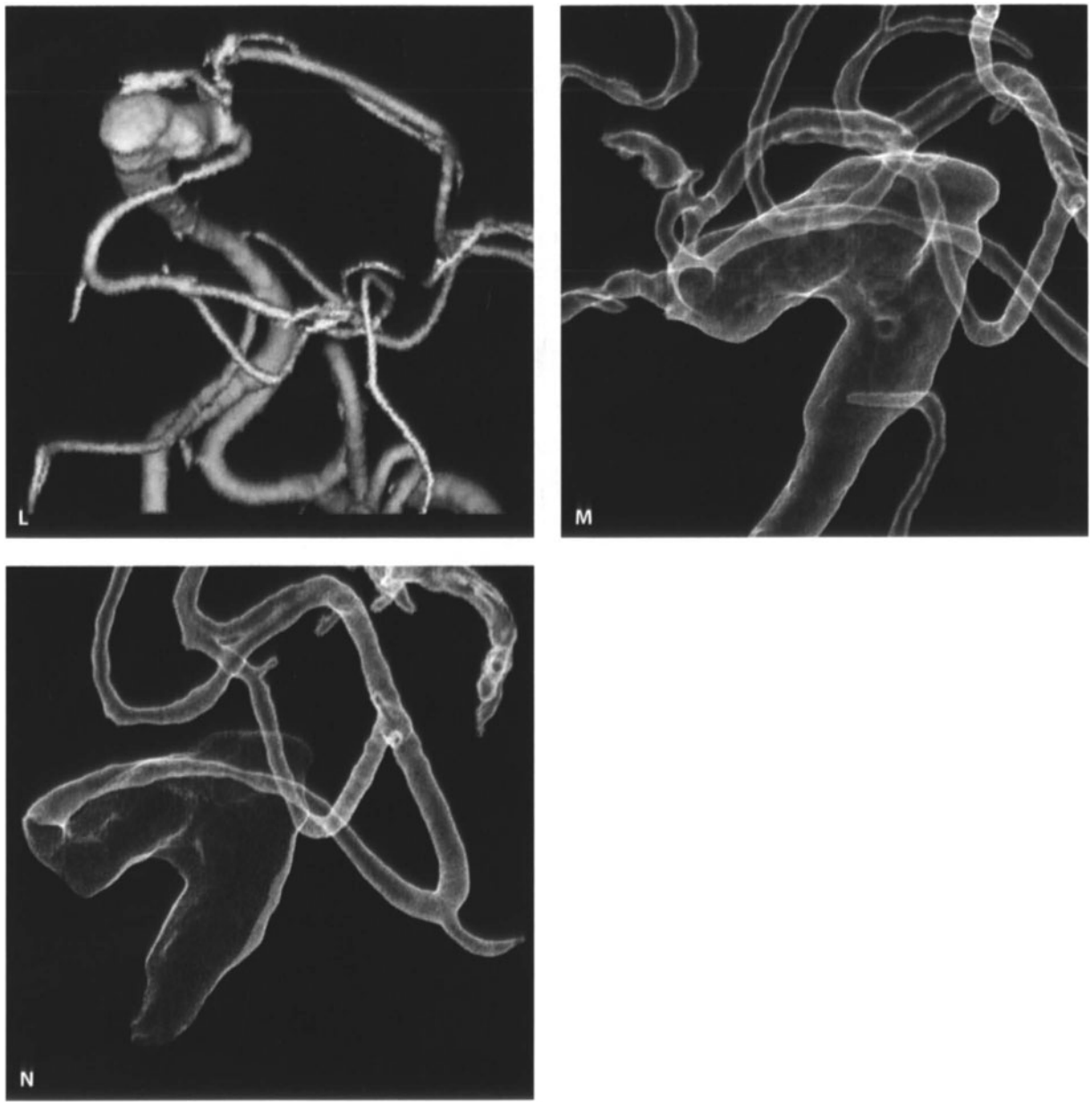

Fig. 7.85 (*continued*). **L–N** Three-dimensional angiography with surface, volume rendering, and electronic dissection shows the involvement of all P1 and anterior superior cerebellar arteries in the remaining cavity. **O–S** see p. 475

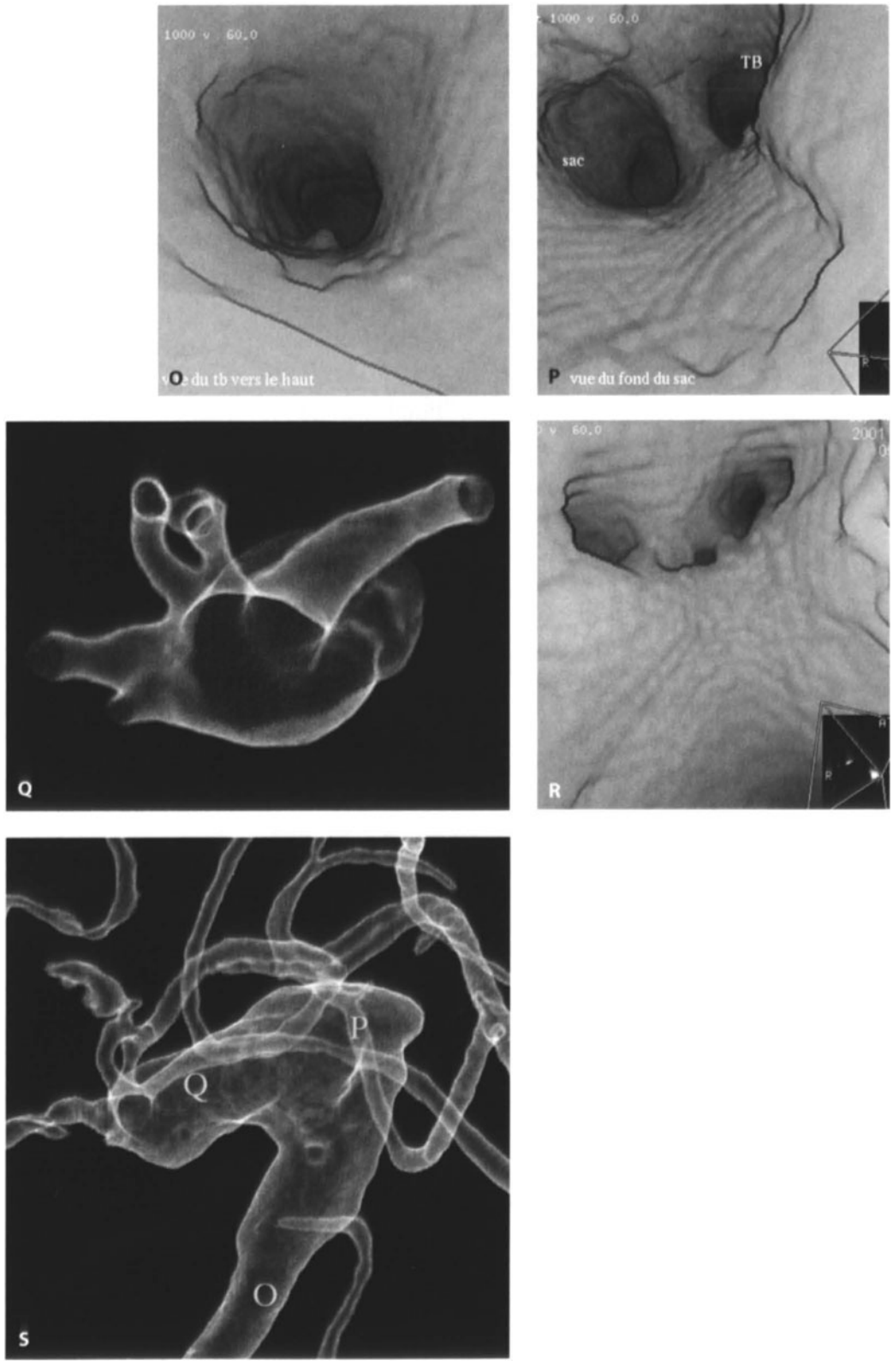

Fig. 7.85 (*continued*). O–S Endoscopic views (see position of endoscopic views on S) confirm the intrasaccular opening of both superior cerebellar and P1 arteries. The patient was placed on antiplatelet treatment and remained stable on follow-up

Fig. 7.86A–C. Subarachnoid hemorrhage with intradural ruptured dissecting arterial aneurysm. **A** Right vertebral artery angiogram. **B** Surface rendering. **C** Balloon sacrifice proximal to the site of dissection. The patient progressed favorably

Multiple treatment approaches have been used: proximal occlusion, trapping, wrapping, and stenting with or without coiling (see Chap. 1, this volume). The most common complication of direct surgery has been lower cranial nerve paralysis involving cranial nerves IX, X, and XI. In addition, medullary syndromes may result, related to the technique used, the specific vascular anatomy involved, or as a result of the extension of the dissection. According to Takenaka (1994), the narrowing distal to the ectasia, regardless of its appearance, is to be considered the very end of the dissected portion. Packing of coils into the dissection AA's false lumen or angioplasty of the narrowed vessel lumen is, in our opinion, very dangerous and should be avoided. Stenting of the dissected segment, sacrifice of the dissected segment using coils, or proximal sacrifice of the vessel with balloons or coils resulting in flow reversal is preferable to the morbidity related to the direct surgical approach. The possibility of multifocal areas of mural hemorrhage, local persistence of the dissecting process or in another location, or the presence of a collagen disease should be considered.

Table 7.34. Mural diseases and dissections

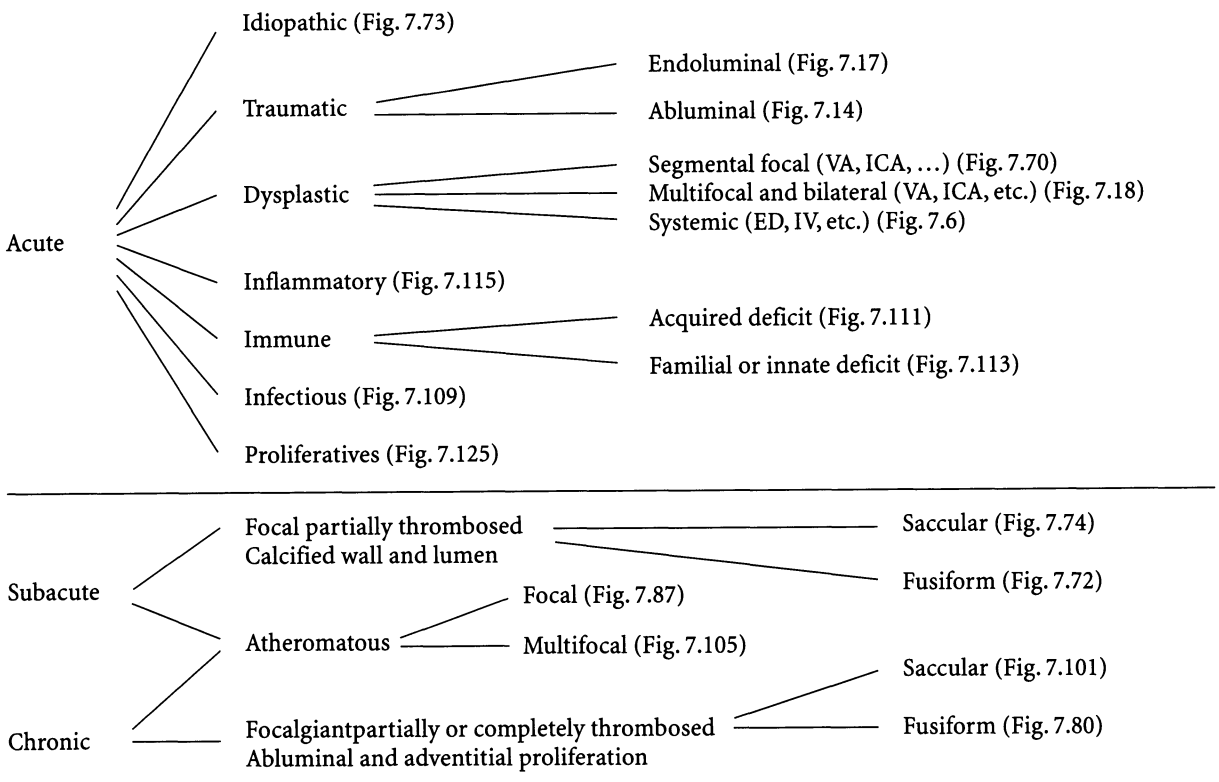

Table 7.35. Arterial dissections: clinical complications

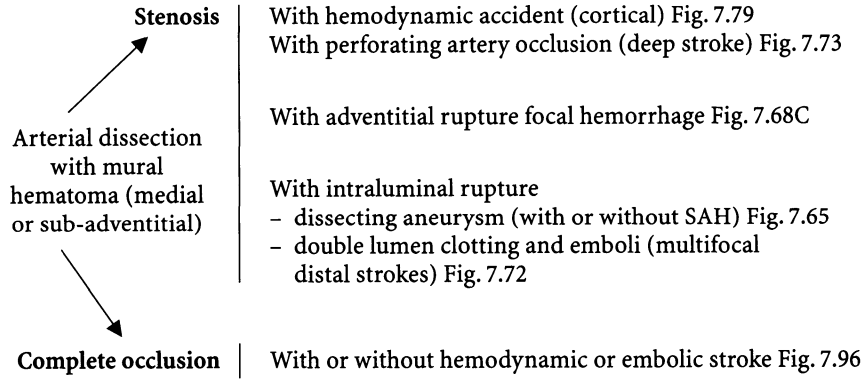
Arterial dissection with mural hematoma (medial or sub-adventitial)
Stenosis
With hemodynamic accident (cortical) Fig. 7.79
With perforating artery occlusion (deep stroke) Fig. 7.73
With adventitial rupture focal hemorrhage Fig. 7.68C
With intraluminal rupture
- dissecting aneurysm (with or without SAH) Fig. 7.65
- double lumen clotting and emboli (multifocal distal strokes) Fig. 7.72
Complete occlusion
With or without hemodynamic or embolic stroke Fig. 7.96

Dissection, as a process, may generate a wide range of intradural AA types, reflecting the variable impact of extrinsic factors (infectious, immune, stress, etc.), the intrinsic structural weakness, and persistent extrinsic triggering factors combined in the vague group of risk factors, microtrauma, etc. (Table 7.34). Depending on the area of involvement, the dissection of the vessel wall will produce various clinical presentations (Table 7.35). A better understanding of their repair capabilities (Table 7.36) will lead to an improved understanding of the natural history of this group of AAs.

Table 7.36. Aneurysms resulting from dissection process; types are related to Mizutani's classification (1999)

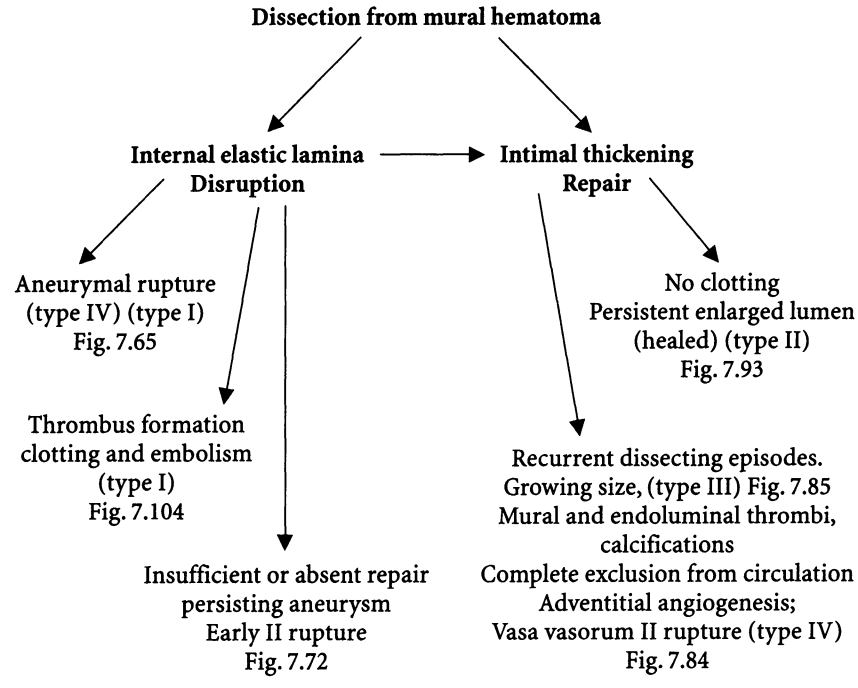
Dissection from mural hematoma
Internal elastic lamina Disruption
Intimal thickening Repair
Aneurymal rupture (type IV) (type I) Fig. 7.65
Thrombus formation clotting and embolism (type I) Fig. 7.104
Insufficient or absent repair persisting aneurysm Early II rupture Fig. 7.72
No clotting Persistent enlarged lumen (healed) (type II) Fig. 7.93
Recurrent dissecting episodes. Growing size, (type III) Fig. 7.85 Mural and endoluminal thrombi, calcifications Complete exclusion from circulation Adventitial angiogenesis; Vasa vasorum II rupture (type IV) Fig. 7.84

7.5 Intradural Giant Saccular and Nonsaccular Arterial Aneurysms

7.5.1 General Remarks

Without histology, the classification of a giant saccular or nonsaccular aneurysm is often speculative. The presentation with symptoms of mass effect, the findings at surgery (calcification), and the clinical progress of the aneurysm suggest either an atheromatous aneurysm (Fig. 7.87) or a dolichoectatic-type giant aneurysm, as classified by Mizutani et al. (1999). Saccular so-called giant aneurysms tend to develop away from arterial branching.

The dolichoectatic-type aneurysms described by the Mizutani et al. classification involved the basilar artery, were fusiform and tortuous, and contained thrombus (Fig. 7.88). There was no evidence of atheromatous change in the aneurysms in their series. In the past, some authors suggested that fusiform aneurysms were atherosclerotic in origin. However, pathogenetic factors unrelated to atherosclerosis have been implicated. The study consisted of 85 patients with nonatherosclerotic cerebral aneurysms, unrelated to the branching zones (Mizutani et al. 1999). The mean age of the 85 patients (50 men and 35 women) at the time of initial diagnosis was 55.4 years. Of the 85 aneurysms, 80 were located in the vertebrobasilar system, and the other five aneurysms were located in the anterior circulation. This male dominance was also observed in serpentine AA (Anshun et al. 2000).

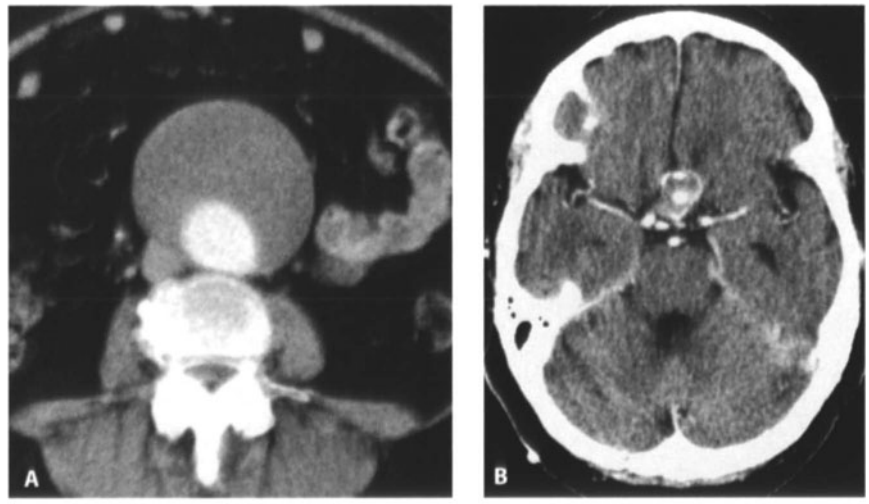

Fig. 7.87. Incidental finding of a partially thrombosed AcomA aneurysm (**B**) in 75-year-old woman with an aortic aneurysm (**A**). This situation can also be described as multifocal subacute or chronic dissecting aneurysm during the course of atheromatous disease. (Courtesy of M. Soderman)

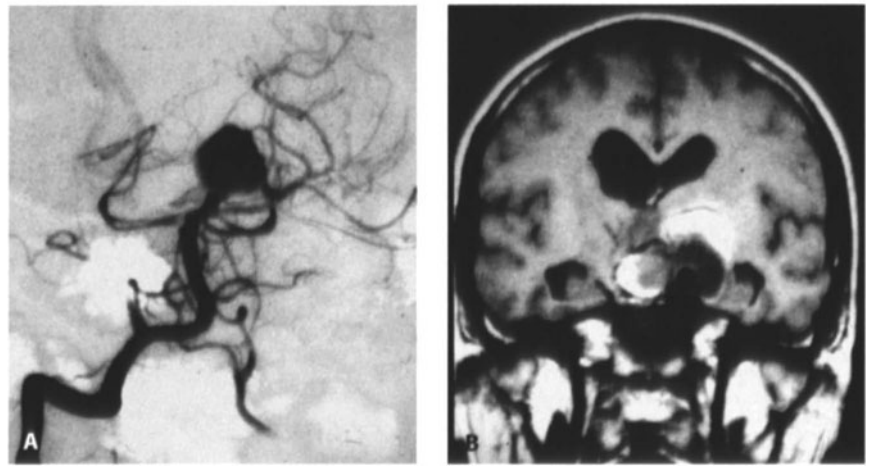

Fig. 7.88A, B. Giant partially thrombosed basilar tip arterial aneurysm

This dolichoectatic type of aneurysm grows by a process of repeated intramural hemorrhages, as observed with the so-called dissecting AA (Fig. 7.89). As expressed 20 years earlier by Schubiger et al. (1980, 1987), Mizutani et al. use the dissecting process to explain the subacute and chronic changes leading to giant AA, as outlined in their classification:

Type 1: Classic dissecting aneurysm (acute)
Classic dissecting aneurysm (Figs. 7.70, 7.72, 7.86, 7.90). Widespread disruption of the internal elastic lamina (IEL) is observed at the mid portion of the aneurysm without intimal thickening and fragile adventitia. Many of the aneurysms have an irregular stenotic portion near the proximal or distal end. Forty-two (64.6%) of the 65 patients experienced bleeding, 19 of them on day 0. Of the 23 deaths reported, 22 were attributed to rebleeding. Fresh thrombus was formed between the media and adventitia near the end of the aneurysm.

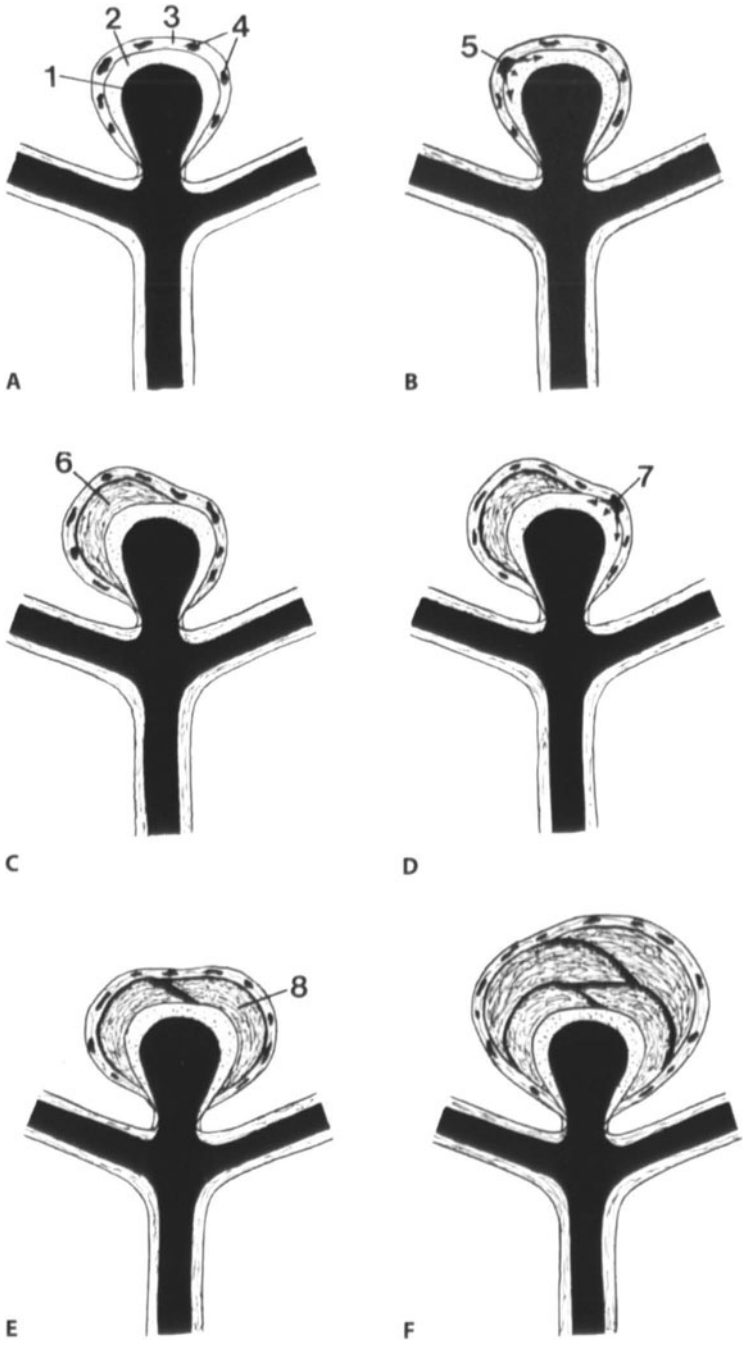

Fig. 7.89A–F. Recurrent subacute arterial dissection leading to partially thrombosed arterial aneurysm of enlarging size. *1*, lumen; *2*, thrombosis; *3*, capsule; *4*, hypervascularization; *5*, neo-vasa vasorum rupture; *6*, fresh clot; *7*, recurrent bleed; *8*, crescent-shaped fresh clot. (From Schubiger et al. 1987, with permission)

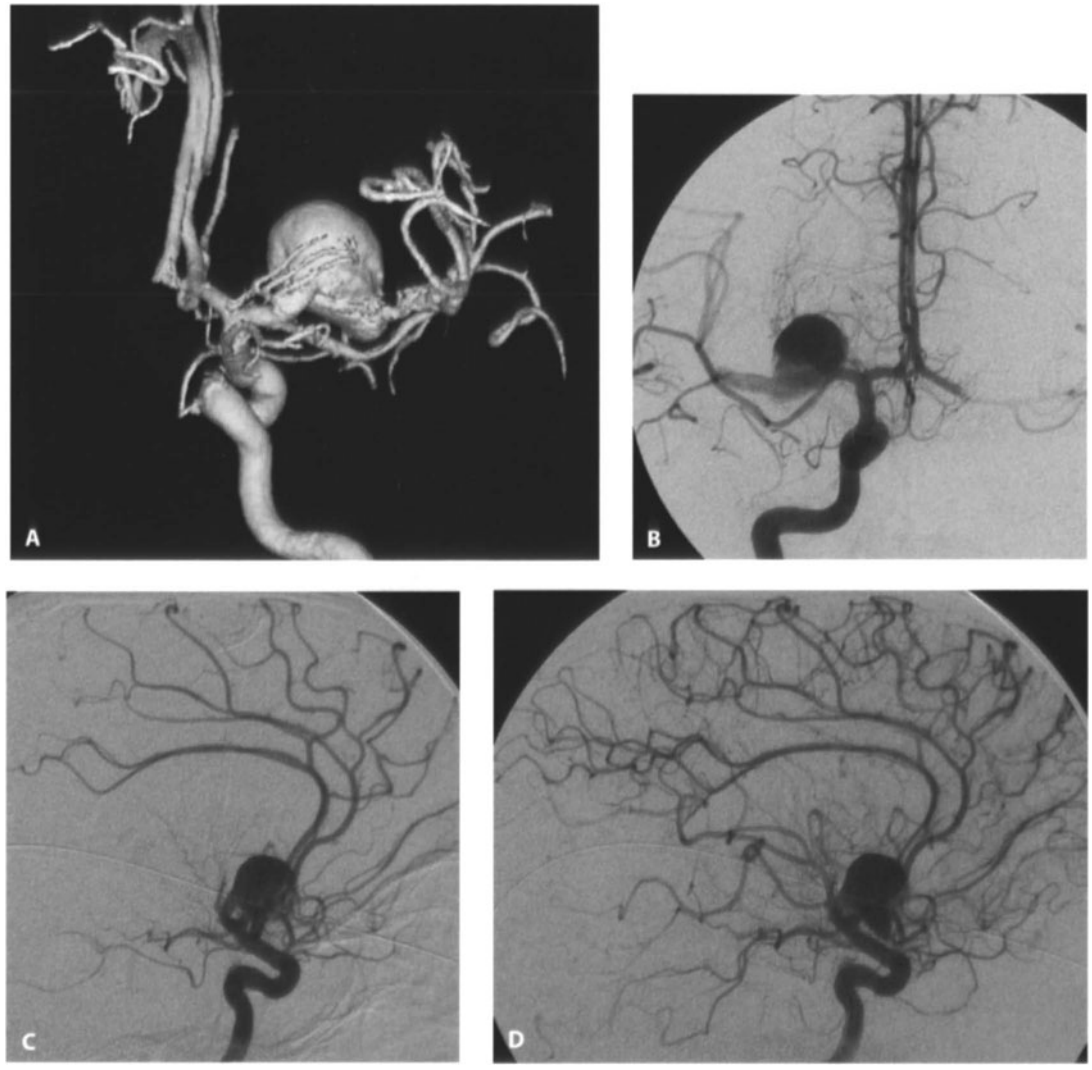

Fig. 7.90A–D. A 23-year-old female patient presented with sudden onset of headaches related to severe subarachnoid hemorrhage (HH4, Glasgow 5). **A** Three-dimensional internal carotid artery angiogram. **B–D** Two-dimensional angiogram in lateral view demonstrates a large acute fusiform dissecting arterial aneurysm involving M2 with delayed opacification of the middle cerebral artery branches

Type 2: Segmental ectasia

All aneurysms of the series were asymptomatic and incidentally discovered (Figs. 7.91–7.94). They were larger in size than the type 1 aneurysms. Most aneurysms were located on the vertebrobasilar tree, and two involved the anterior circulation. Neither angiography nor MRI revealed thrombus formation within the lumen. No significant progression was noted over time. Moderately thickened intima was noted. These AAs likely correspond to a healed subclinical dissection.

Type 3: Dolichoectatic dissecting aneurysm

All aneurysms were located on the basilar artery. Luminal thrombus or development of an intimal flap was seen. All patients had

Fig. 7.91. Segmental basilar dolichodysplasia without ectasia located distal to the origin of the trigeminal artery. (Courtesy of T. Hyogo)

symptoms such as cranial nerve palsy, hydrocephalus, or brainstem dysfunction by mass effect. Three-quarters of the aneurysms progressively enlarged to a giant size. Over one-third of patients died of fatal SAH, and one died of brain stem dysfunction. Multiple dissections of the thickened intima were noted. This appearance suggested a failed yet attempted healing process.

Type 4: Saccular aneurysm (blister) arising from the arterial trunk, with or without fusiform ectasia

Saccular aneurysms away from arterial branching locations and presenting with SAH (Fig. 7.94). They were located on type 2 fusiform aneurysms in the anterior circulation in 75% of cases. One-fourth arose from a left vertebral artery of normal caliber. Three patients died of fatal SAH. Minimally disrupted IEL without adjacent intimal thickening was noted. No pseudolumen or organized thrombus could be detected. These mimic the so-called blebs, or blister-like aneurysms easily demonstrated on 3-D angiography (Fig. 7.135). It has been argued that the aneurysms arising from the dorsal wall of the internal carotid artery may be dissecting aneurysms (Satoh et al. 1993) (Fig. 7.95). Blister-like aneurysms (Ishikawa 1997) might also be included as type 4 aneurysms.

Fig. 7.92. **A, B** Intradural dolichoectatic C7 internal carotid artery segment. **C** Similar disposition in a different patient. (Courtesy of M. Castillo)

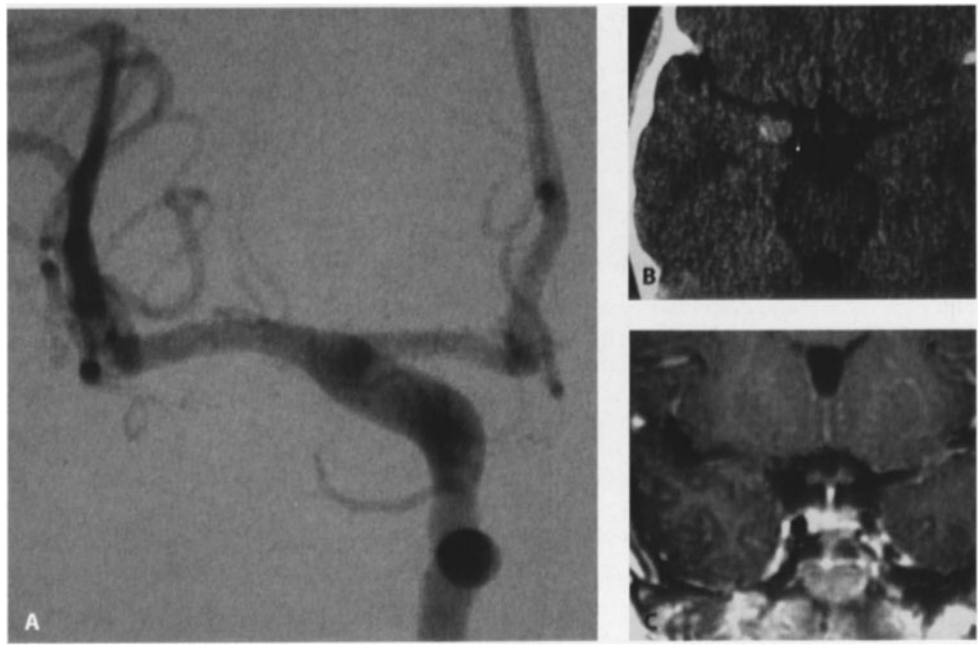

Fig. 7.93. **A** Internal carotid artery (ICA) angiogram; **B, C** MRI. Intradural fusiform segment of the ICA termination compatible with a healed dissection

Fig. 7.94A–C. A 61-year-old female patient operated on for an ethmoidal meningioma 3 years earlier. Incidental discovery of multiple fusiform aneurysms on the supratentorial arteries: **A** ICA; **B**, AcomA; **C** left MCA

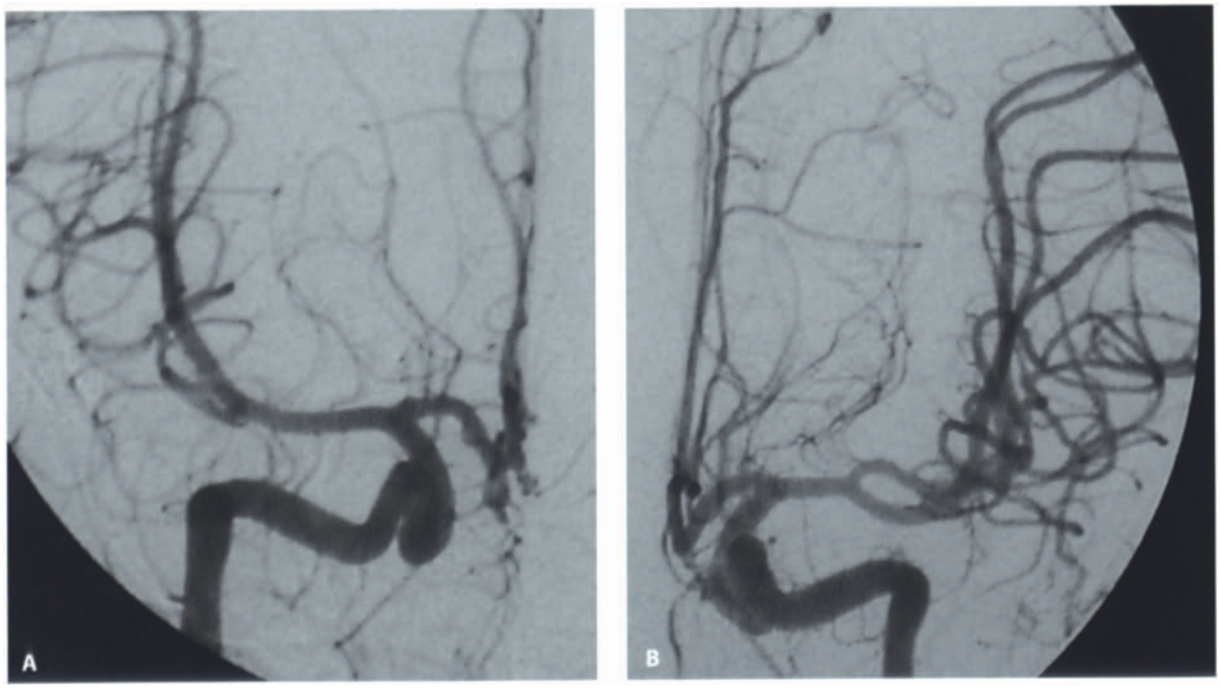

Fig. 7.95. A, B Angiography for subarachnoid hemorrhage. Suspicion of internal carotid artery (ICA) anterior division blebs in mirror position. **C, D** Three-month follow-up angiogram showed significant growth of left ICA aneurysm. The right ICA blebs have remained unchanged. The left ICA aneurysm was successfully coiled. **E–G** Seven months after embolization, angiograms show the stable result for the left ICA aneurysm, but the right ICA blebs have enlarged slightly. The coiling attempted for the right ICA aneurysm during the same session failed ▶

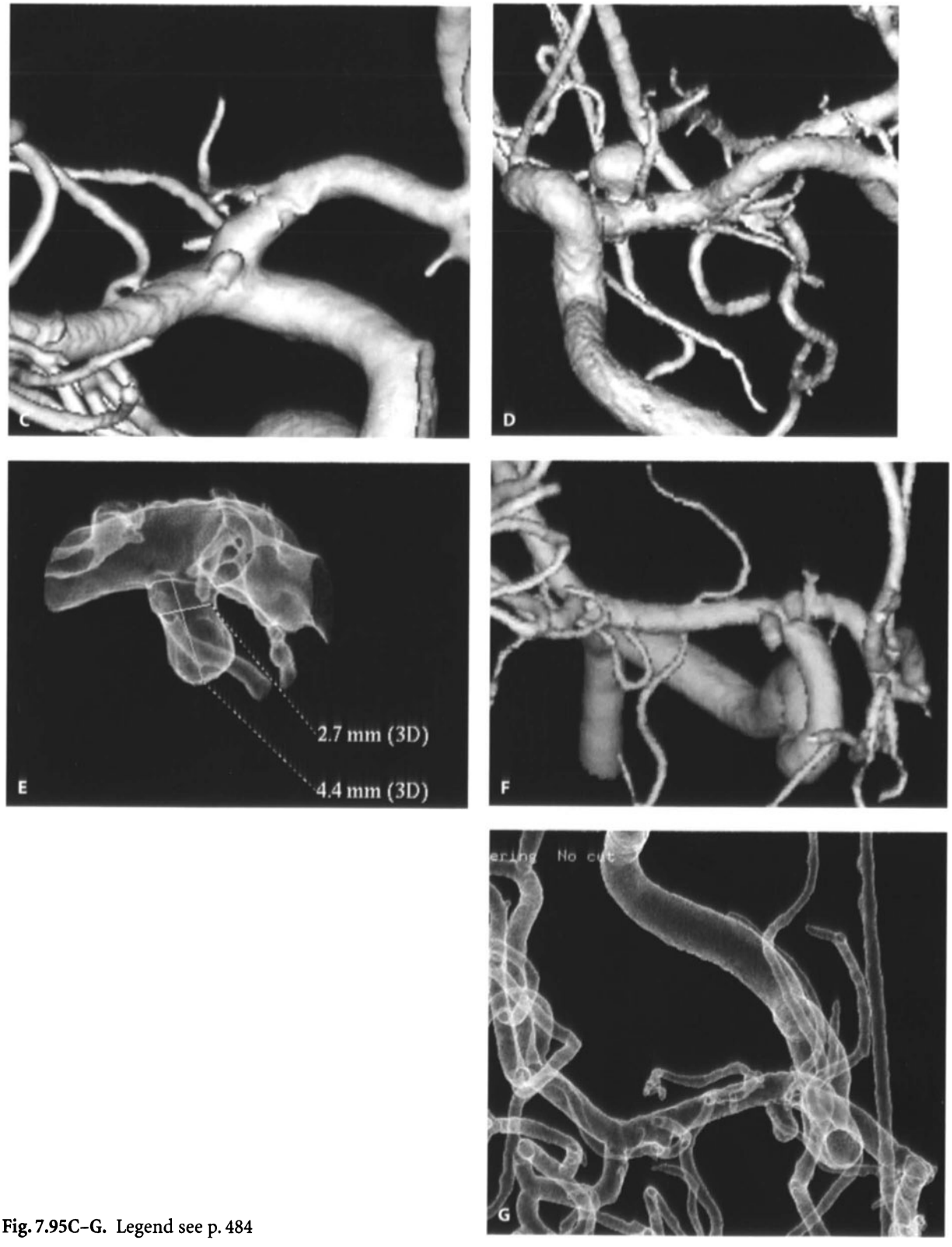

Fig. 7.95C–G. Legend see p. 484

These authors suggest that this adaptive intimal thickening compensates for the weakening of the arterial wall caused by the damaged IEL. Factors that weaken the structure of IEL such as inflammation, infection, trauma, and congenital factors may be associated with the etiology of fusiform aneurysms, dissecting aneurysms, partially thrombosed lesions, or saccular aneurysms unrelated to branching zones (Table 7.34).

7.5.2 Giant Intracranial Aneurysms with Thrombosis

The capacity to distinguish a giant thrombosed aneurysm from a dolichoectatic-type or chronic dissecting-type aneurysm is limited on the basis of imaging data. The term "giant aneurysm" fails to convey any information about the lesion other than an agreed minimum size. The definition of each of these entities is based on their appearance; however, this is not helpful in understanding the clinical course of the lesion or the response of the surrounding tissues (Figs. 7.96, 7.97). In the 1980s, Schubiger (1980, 1987) had already closely linked the giant partially thrombosed saccular AA and the chronic dissection processes suspected in dolichoectatic or fusiform AA (Fig. 7.89).

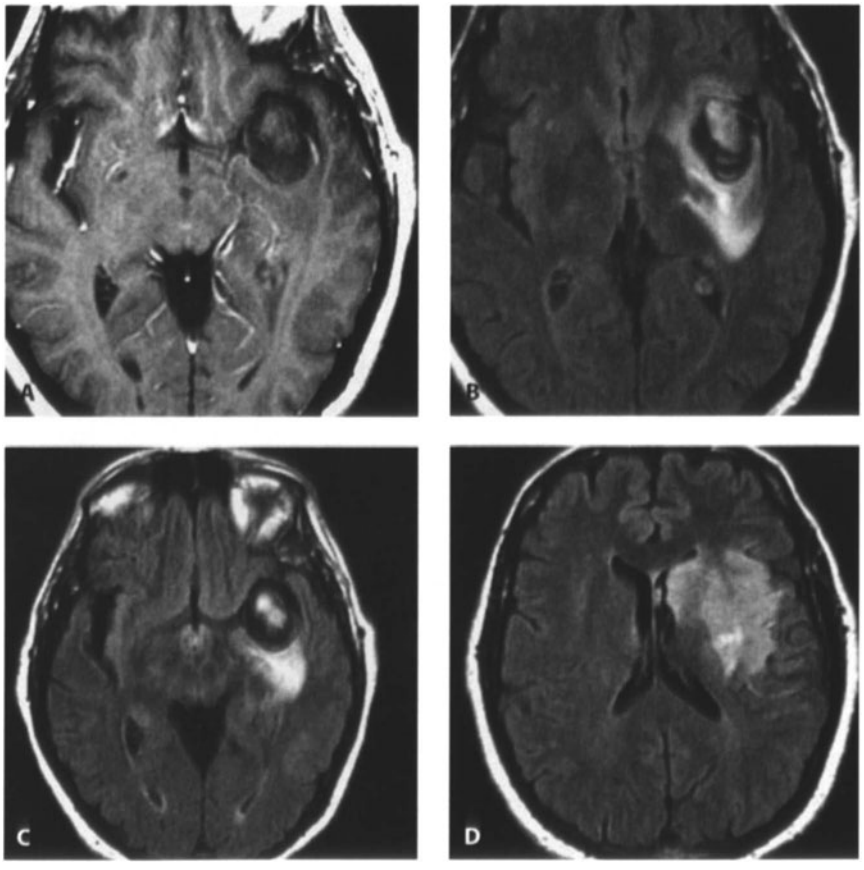

Fig. 7.96A–H. A 42-year-old male patient presented with acute onset of neurological deficit, which continued to worsen over the subsequent 2 weeks. Recently thrombosed giant middle cerebral artery (MCA) aneurysm is noted on MRI (**A–D**), with significant perianeurysmal edematous reaction. **E–H** see p. 487

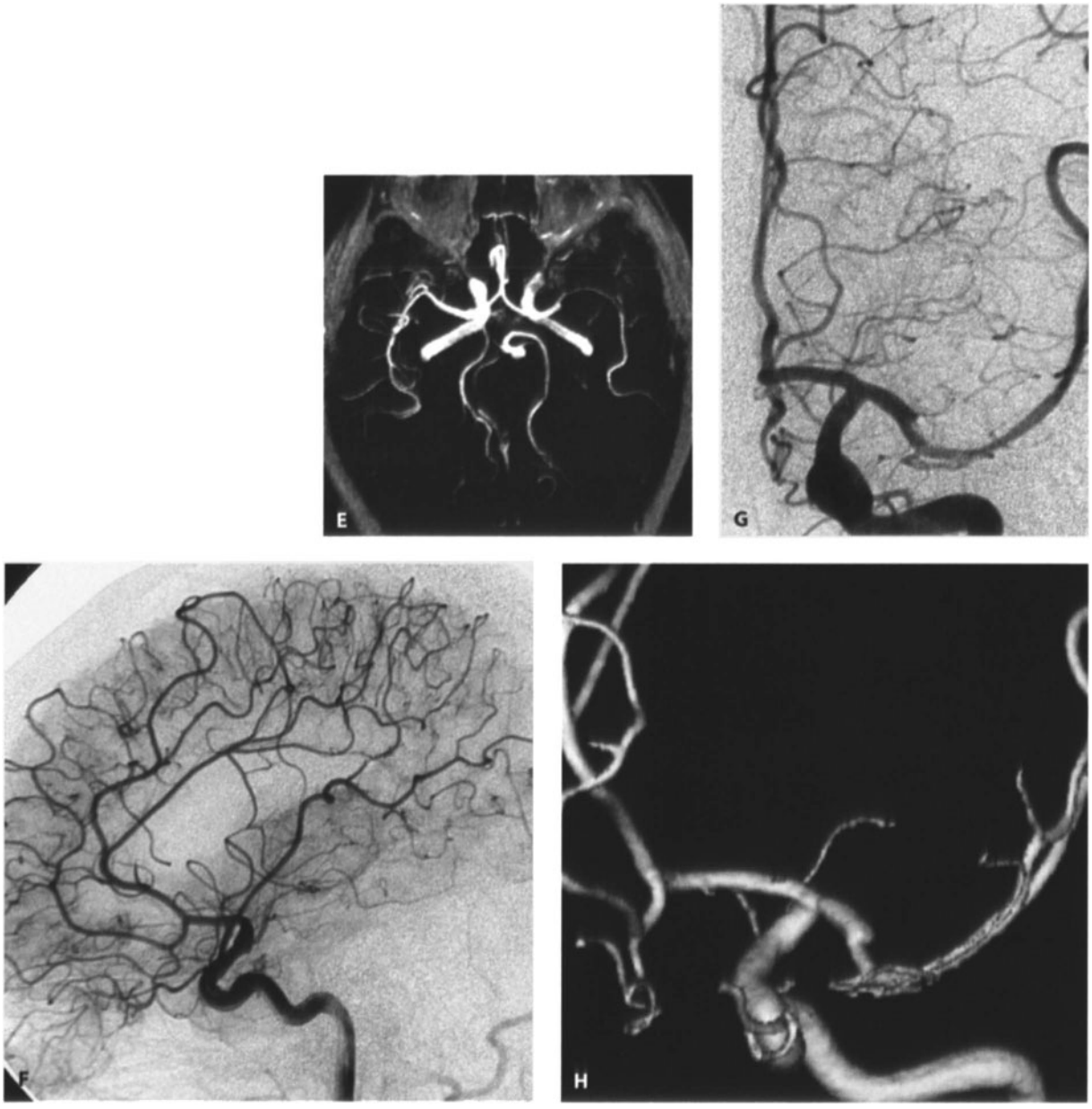

Fig. 7.96 (*continued*). **E** MRA and angiography (**F–H**) confirm the complete exclusion of the aneurysm and the occlusion of a temporal division of the MCA

Giant saccular aneurysms have some degree of permanent intraluminal (or mural) thrombosis and measure over 25 mm in diameter. Giant saccular AAs are therefore different from large or giant berry AAs since they have a fully patent lumen.

The largest berry AA could probably be of the same size as a partially thrombosed smaller giant AA. In the giant AA, there is no relation between hemodynamics and size, whereas in large berry-type saccular AAs, the visualized lumen is the same size as the pouch.

Giant intracranial aneurysms occur most frequently at the carotid bifurcation (59%) and basilar tip (Fig. 7.98). The MCA bifurcation and an-

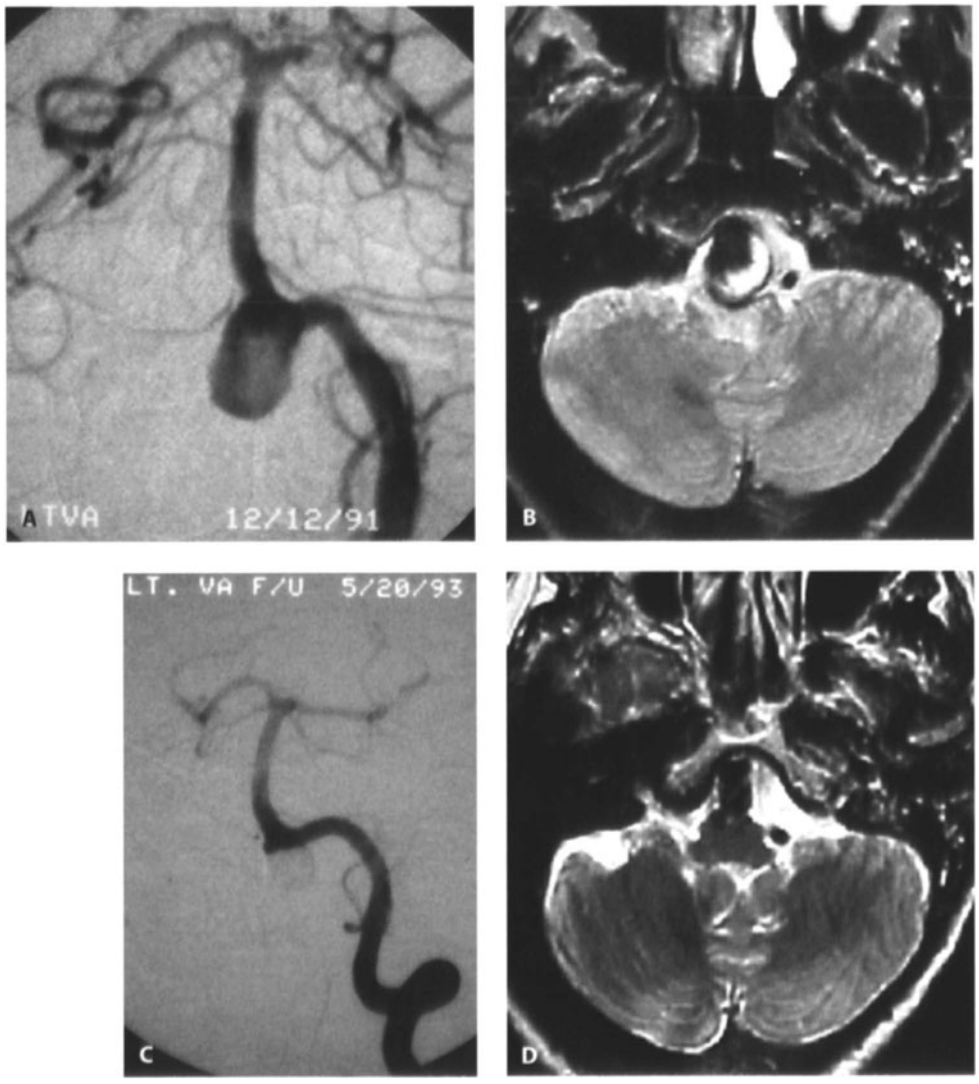

Fig. 7.97. A 70-year-old female patient presented with focal subarachnoid hemorrhage in relation to a ruptured dissecting arterial aneurysm (**A**) treated with coils. MR evidence of mass effect (12/91) (**B**). Follow-up angiogram (**C**) shows stable morphological results. Nine-year follow-up image documented favorable clinical outcome and resolving mass effect (11/99) (**D**)

terior communicating artery are also common sites for giant aneurysms (Weir 1987). Up to 13% of MCA aneurysms are giant and the majority of giant MCA aneurysms occur at the bifurcation (Fukuoka et al. 1984) (Fig. 7.96). A giant aneurysm originating from the M2 segment beyond the bifurcation is rare (Table 7.33).

Analysis of a giant intracranial aneurysm with acute or subacute clinical deterioration can be used to approach the special nature of this group of lesions (Schubiger et al. 1987). In these cases, acute or subacute clinical deterioration will show a hyperdense rim on CT, with a density typical of fresh clot at the periphery of the thrombosed portion of the aneurysm (Fig. 7.96). The clinical deterioration could best be explained by recent aneurysm growth from intramural hemorrhage. Signs of a mild SAH,

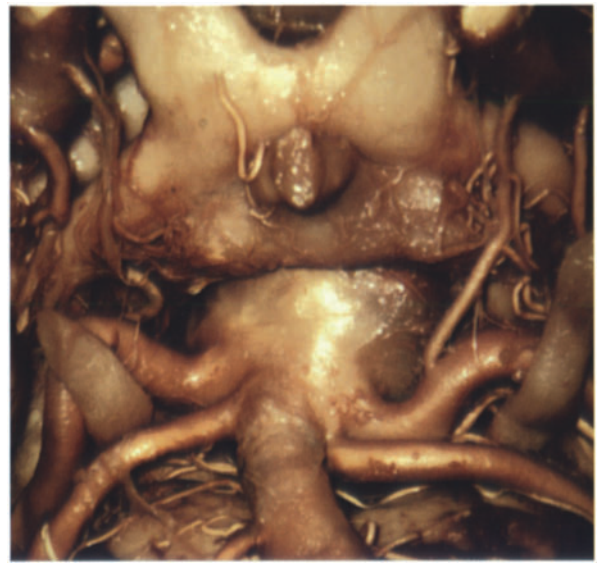

Fig. 7.98. Giant partially thrombosed basilar tip arterial aneurysm. Symmetrical caudal fusion. Note the origin of the perforators from both P1 segments

proved by CT, can be seen (Fig. 7.97). At surgery, the SAH is seen to have originated from the aneurysm wall, with formation of fresh clot both inside and outside the wall. In other cases, the recent hemorrhage occurs at the periphery of the aneurysm and has no communication with lumen (Figs. 7.68, 7.89) (Schubiger et al. 1987).

Patients presenting with acute clinical deterioration can show a sickle-shaped zone of enhancement on CT at the periphery of known, partially thrombosed aneurysm (Yasargil 1984). On pathological examination, this zone proves to be a fresh hematoma. Surgical exploration of giant intracranial aneurysms often reveals a tremendous network of fine vessels covering the aneurysm (Yasargil 1984). In an earlier publication, Schubiger et al. (1980) suggested that these vessels may be the vasa vasorum of the aneurysmal wall and that they may be responsible for the curvilinear enhancement of the aneurysmal wall regularly observed on postcontrast CT.

Three weeks after aneurysmal wall rupture, collagen is found as a protective layer and capillaries begin to proliferate. The formation of a neomembrane over the site of rupture of the aneurysm may be comparable to the formation of neomembranes around chronic subdural hematomas. Blood vessels are a constant feature of neomembranes, whereas the normal dura–arachnoid interface layer is an avascular structure (Friede and Schachenmayr 1978; Sato and Suzuki 1975). A vicious cycle could start in which minimal trauma induces bleeding into the neomembrane and the hemorrhage then induces further proliferation of neomembranes (Friede and Schachenmayr 1978).

The common feature of all reported cases of growing intracerebral hematomas is the presence of collagenous capsule that contains numerous vascular channels (Aoki and Mizuguchi 1984, 1986; Terada et al. 1985). Currently, there is no explanation why most intracerebral hemorrhages heal without formation of a capsule. In the reported cases of growing intracerebral hematomas (Aoki and Mizuguchi 1984, 1986; Terada et al.

1985), these hematomas were all located superficially. It can be speculated that the hematoma in these cases reached the arachnoid membrane, and from there the arachnoid cells initiated the formation of a neomembrane.

If the postulated growth mechanism is correct, then the more peripheral layers will represent the more recent clot and aneurysm growth is by apposition of new layers at the periphery. If the intra-aneurysmal hemodynamics change and turbulent flow occurs, then intraluminal clots may reduce or, in the extreme case, completely obliterate the lumen of the aneurysm and probably do not cause enlargement of the aneurysmal mass (Figs. 7.96, 7.99, 7.100).

It remains unclear why some giant intracranial aneurysms remain unchanged in appearance over many years, while others may disappear completely after occlusion or thrombosis of the aneurysm neck (see Vol. 3). Although the hypothesis that the primary aneurysm corresponds to a common berry-type aneurysm might be appealing, the topography, epidemiology, and multifocality is entirely different for giant aneurysms than for berry aneurysms.

The role of the arachnoid or pial interface is likely a key factor in understanding the chronic progression of the lesion. The time scale from acute to chronic allows for different biological signaling processes and answering cascades, although it still remains insufficient to explain the geotropism of certain lesions.

Giant arterial aneurysm is a proliferative disease of the vessel wall, with growth induced by extravascular activity (angiogenesis), as shown by the enhancing ring shape of these lesions. The resorption of blood clot stimulates perivascular growth factors, some of which may end up stimulating the proliferation of the vessel wall, leading to enlargement of the lesion. Some MCA giant AAs have been shown to continue to enlarge even after sacrifice of the parent vessel and complete exclusion of the lumen.

Meziti et al. 1998 reports a case of a 76-year-old patient with a 12th nerve neurinoma, which worsened clinically and increased in size progressively over 2 years. The mass was enhancing but was not showing any lumen. At surgery it turned out to be a completely thrombosed giant AA of the intradural VA. At pathology the AA was associated with a lipophagic granuloma on an atheromatous giant AA. A more rapid postembolization progression was reported by Blanc et al. (2001). A giant ICA aneurysm increased in size over 8 days, producing a major MCA stroke by mechanical compression. Swelling related to angiogenic activity was one of the hypotheses.

As opposed to the commonly accepted principle that giant AAs are saccular AAs that have grown, we would prefer the concept of uncontrolled proliferation of the wall and mural thrombosis as a chronic triggering factor for its further enlargement with or without mural dissection. The balance between the clotting phenomenon and the angiogenic resorption of the clot would govern the capacity of the giant AA to enlarge or to completely thrombose and eventually remodel. In these circumstances, the surrounding cerebral tissue will show a hyperintense edematous reaction to the thrombosis (Figs. 7.96, 7.101), similar to spontaneous clotting of large pouches in brain AVMs (see Chap. 9, this volume). Rupture of such giant AAs probably includes a dissecting phenomenon insufficiently controlled by the remaining repair systems.

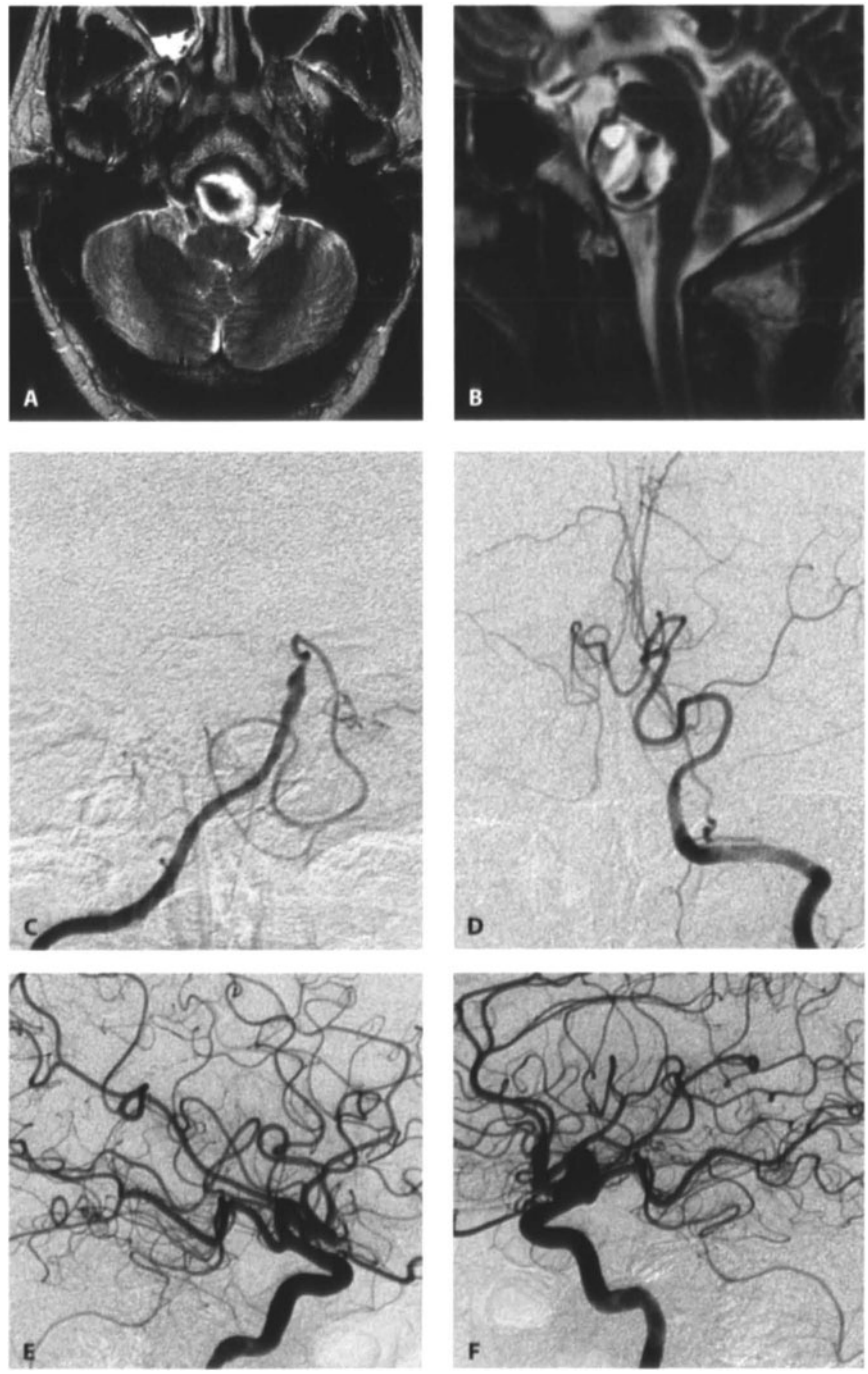

Fig. 7.99A–F. A 43-year-old male patient presented with mild hypoesthesia of both upper extremities. Complete spontaneous thrombosis of giant basilar artery (BA) aneurysm. **A, B** Note the different ages of the thromboses seen on MRI, as well as the absence of perianeurysmal reaction. Angiography (**C–F**) confirms the exclusion of the aneurysm and the collateral circulation to the posterior fossa structures

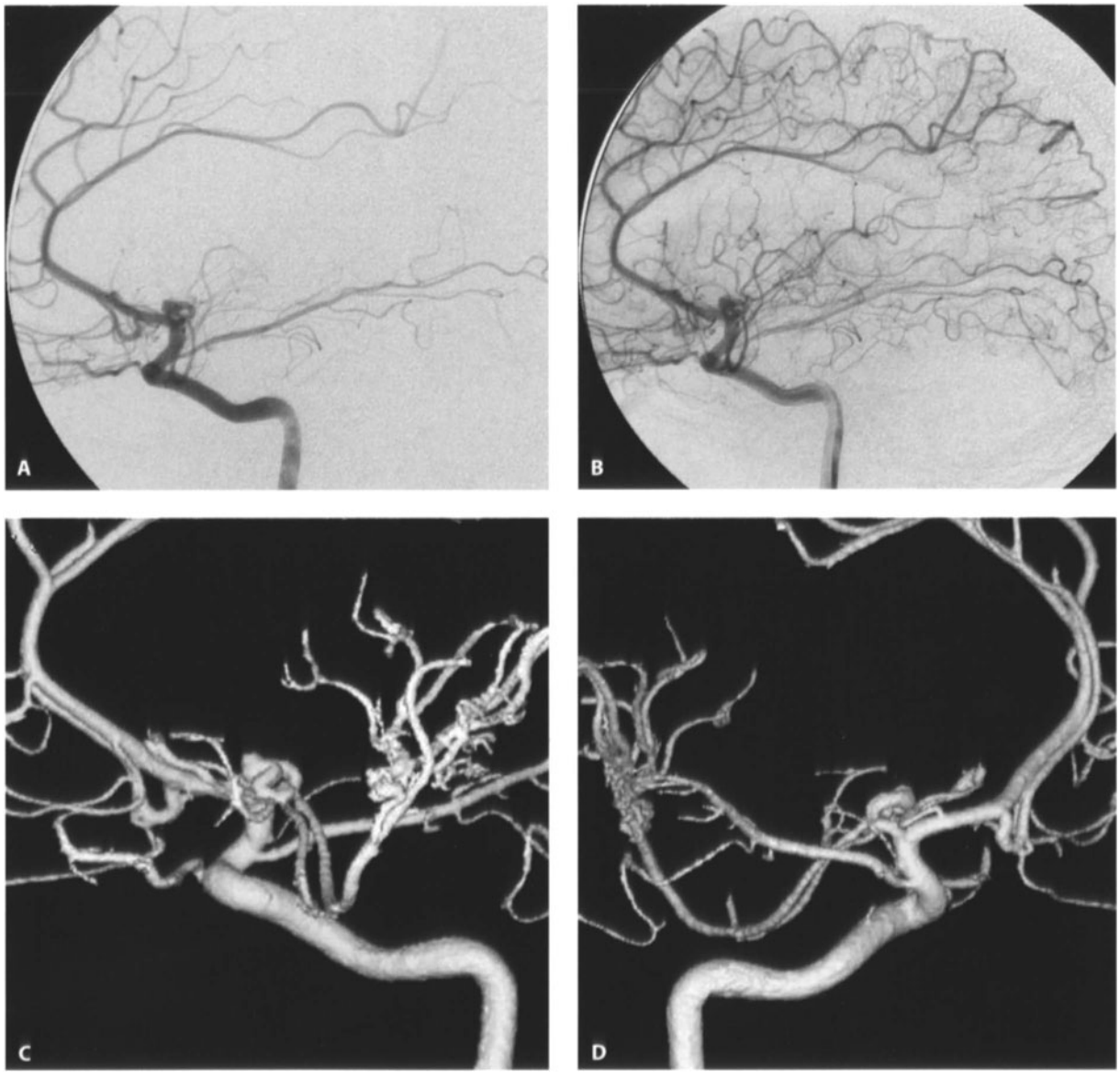

Fig. 7.100A–D. A 35-year-old male patient admitted with a 6-month history of seizure disorder treated with medication. Clinical examination is normal. CT shows calcified mass corresponding to saccular giant middle cerebral artery (MCA) aneurysm. At angiography (**A–D**), thrombosis of the aneurysm was noted with distal occlusion of M1, leptomeningeal anastomoses. Conservative treatment was chosen with antiplatelet therapy and yearly MRI and MRA follow-up

All dissecting processes do not lead to fusiform or giant lesions, since the repair capacities can be preserved in single traumatic lesions, for example. The geotropism for certain locations of giant or fusiform AAs suggests either the repetition of microtrauma (PCA aneurysms) (Figs. 7.73, 7.79, 7.80) or segmental vulnerability involving the remodeling capacities (ICA, MCA, BA). Certain dissections occurring in specific locations such as the ICA in the neck may indicate a transient vulnerability in the repair system with a segmental distribution at the time of the primary insult. Persisting failure favors extension of the dissecting process and its sec-

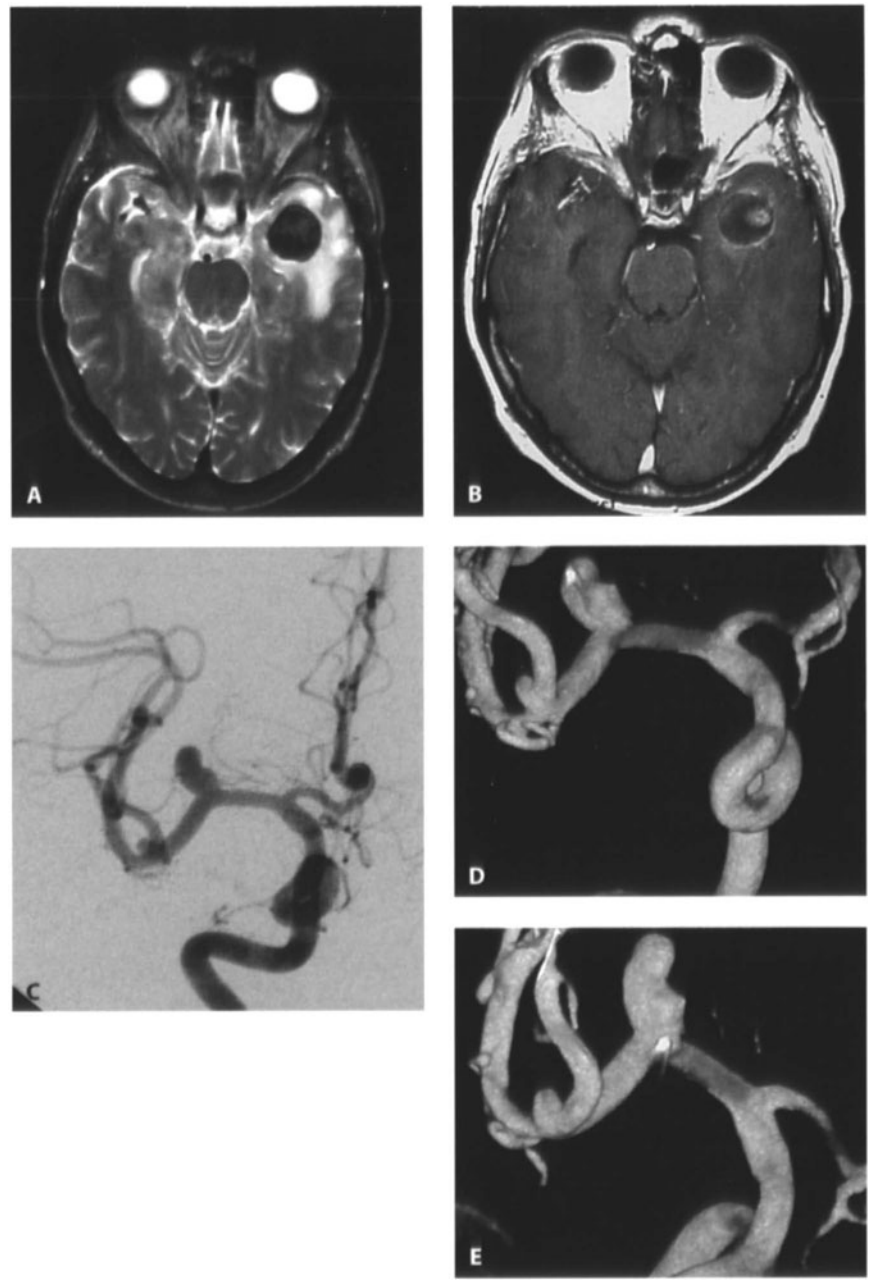

Fig. 7.101. **A, B** Axial MRI; **C** frontal internal carotid artery angiogram; **D, E** 3-D pictures of a 54-year-old male patient with seizure. Partially thrombosed giant aneurysm

ondary complication by producing an all-layer disruption or intraluminal clotting. Medical management, different from passive conservative management, allows the system to recover enough to remodel the damaged vessel wall. Late recurrence being exceptional in the same location exemplifies the efficiency of the healing processes.

Intra-aneurysmal thrombus occurs in approximately 50% of giant aneurysms; however, the factors that determine the balance between thrombogenesis and thrombolysis within giant aneurysms are poorly understood (Whittle 1982). Previous studies have suggested that the size of

the aneurysm is important in determining the risk of in-situ thrombosis (Whittle 1982; Fukuoka et al. 1984; Qureshi et al. 2000a). Factors that are thought to influence the balance between thrombus formation and degradation include the ratio of aneurysm volume to orifice size, endothelial injury due to turbulent blood flow, distortion of the parent artery, SAH, vasospasm, prothrombotic states, and antifibrinolytic agents (Whittle 1982; Fukuoka et al. 1984; Qureshi et al. 2000a). These and other factors that influence aneurysm formation and growth such as perivascular environment (Table 7.12), genetic susceptibility, somatic mutations, growth factor disorders, abnormal vascular remodeling, and arterial segmental vulnerability vary between and within individuals.

The onionskin appearance of a giant aneurysm is a characteristic finding on MRI and is thought to correspond to layers of intraluminal thrombus deposited over time (Figs. 7.88, 7.102). Distinguishing intraluminal from intramural thrombus within a partially thrombosed aneurysm is not possible without histological examination. We prefer that all giant AAs by definition harbor intraluminal or mural thrombosis or calcification.

Complete thrombosis of intracranial aneurysms is uncommon and occurs most frequently following SAH and in fusiform or giant saccular aneurysms (Figs. 7.96, 7.99, 7.100).

Complete aneurysm thrombosis following SAH occurs in 1%–2% of cases and has been reported in up to 55% of giant aneurysms demonstrated on CT scans (Brownlee et al. 1995). Spontaneous thrombosis of the majority of a giant aneurysm has been reported to occur as quickly as 1 month following diagnosis of the lesion (Weir 1987). Parent or distal vessel thrombosis has been reported in association with aneurysmal thrombosis following SAH, during treatment with antifibrinolytic agents, spontaneously in giant aneurysms (Fig. 7.82), and following surgical and endovascular procedures (Figs. 7.97, 7.103). The long-term stability of thrombosed aneurysms is uncertain and recanalization of thrombosed aneurysms is well recognized, both in the acute setting of angiogram-negative SAH and in cases of spontaneously thrombosed aneurysms without SAH (Atkinson et al. 1993). We have not observed such situations. In Atkinson's case of a thrombosed P1–P2 segment aneurysm, the parent vessel remained patent, but MRI 3 months after the ictus demonstrated recanalization of the aneurysm, which was subsequently treated surgically. Growth of completely thrombosed giant aneurysms is also recognized by continued intramural hemorrhage from the vasa vasorum.

Embolic ischemic events have been attributed to both unruptured and ruptured aneurysms of all sizes (Fig. 7.72). Qureshi et al. (2000a) reported a 3.3% incidence of strokes or TIAs from the aneurysm sac in 269 patients with unruptured aneurysms. Of the nine patients identified, four had MCA aneurysms and three had internal carotid aneurysms. In a review of the literature, a further 41 patients presenting with stroke or TIA were identified. Of these patients, 37% had MCA aneurysms. Medical treatment with antiplatelet agents was proposed to reduce platelet aggregation within the aneurysm sac in patients presenting with TIAs. The theoretical disadvantage of impairing platelet-mediated fibroblast migration and scar formation within the wall of the aneurysm potentially inhibiting the healing process (Fig. 7.72) was discussed; however, the authors concluded that

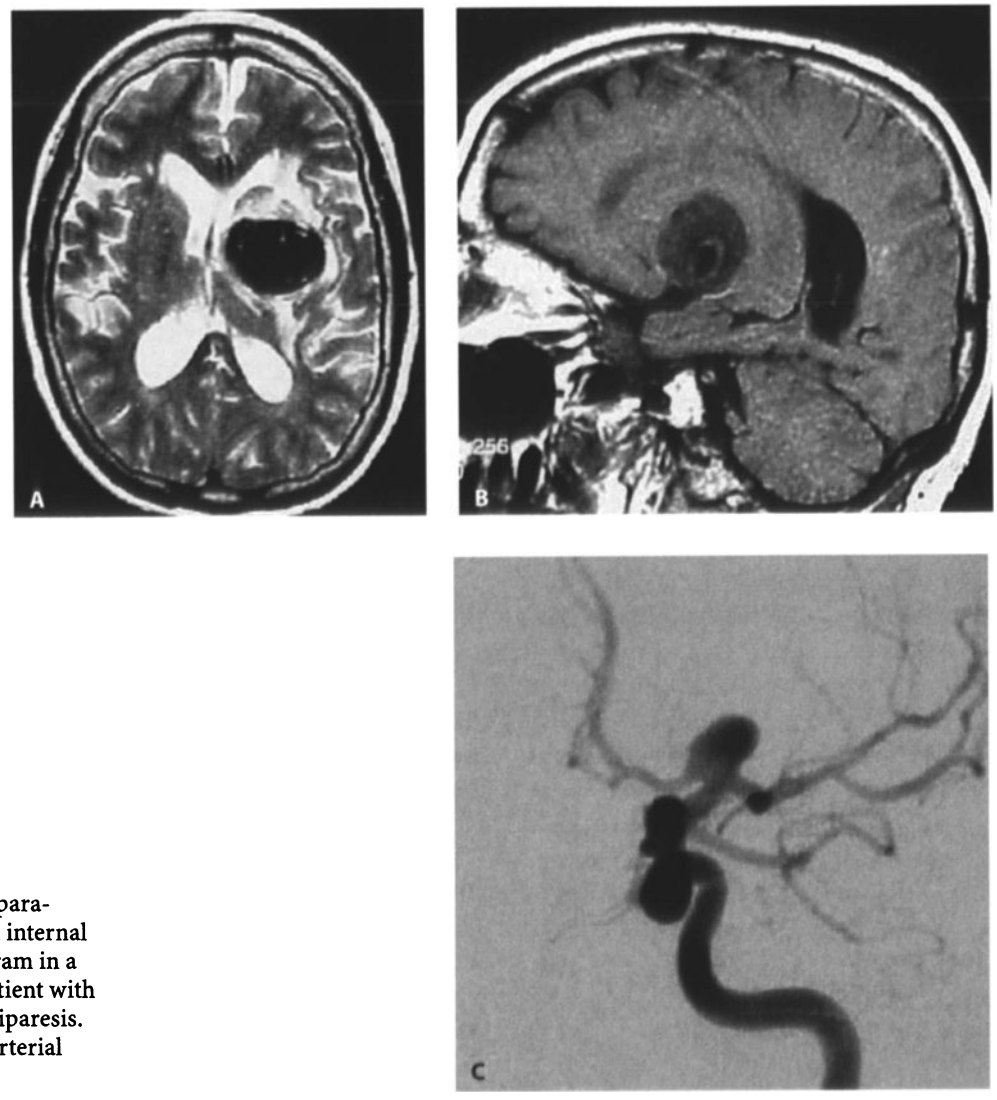

Fig. 7.102. A Axial, B parasagittal MRI, C frontal internal carotid artery angiogram in a 20-year-old female patient with progressive right hemiparesis. MRI discovery of an arterial aneurysm

in patients with a small (<10 mm) aneurysm, aspirin may be used to reduce the risk of TIAs (Qureshi et al. 2000a). It is crucial to evaluate collateral circulation downstream from a giant AA in order to choose the best therapeutic management and discuss the need for functional testing with parent vessel occlusion. It is remarkable that a PCA giant or fusiform partially thrombosed AA can develop rapidly efficient collateral circulation, either through the geniculate body network (P1–P2 AA) or by retrograde leptomeningeal anastomoses (Figs. 7.79, 7.82; see Vol. 1). In occluded arteries associated with giant AA, most of the collateral circulation as seen in the skull base tends to use the oldest arterial channels: lateral geniculate anastomoses between the AchA and PCA, pericallosal arch between the ACA and PCA. Conversely, giant or fusiform partially thrombosed AAs developed along the MCA seldom recruit (or stimulate) efficient leptomeningeal angiectasia. Strokes in giant AA patients are not always related to distal embolic accident from the lumen, but may result from sudden extravascular edema secondary to thrombosis or recurrent mural bleed, from distal hemodynamic insufficiency secondary to complete lu-

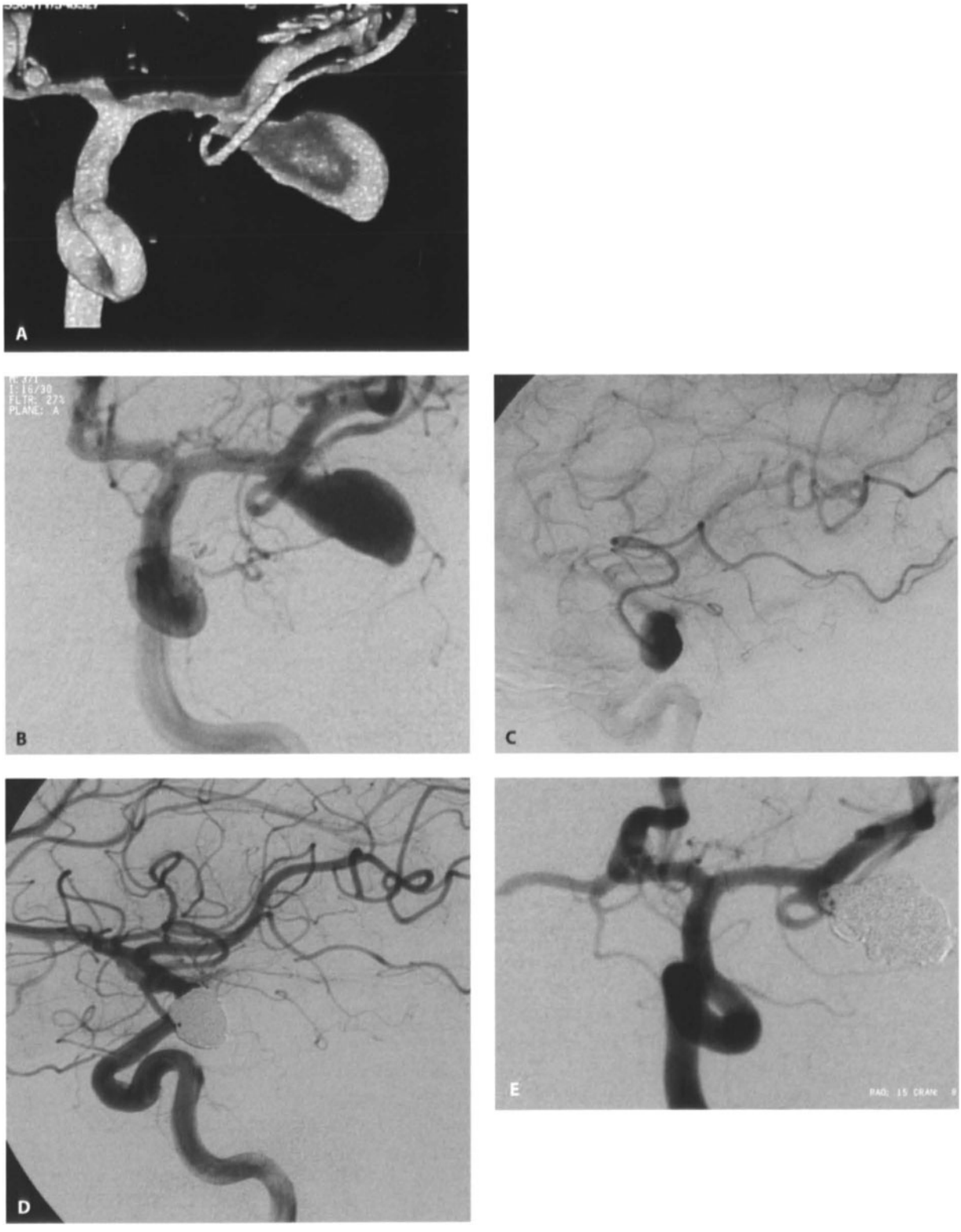

Fig. 7.103. Giant partially thrombosed middle cerebral artery (MCA) aneurysm with a saccular development from temporal artery division (**A–C**). **D, E** Giant partially thrombosed MCA aneurysm treated with coils

men and parent artery thrombosis, or from extension of the recurrent dissecting events involving perforators (Fig. 7.96). In each case, the type of AA and the topography of the stroke will suggest the mechanism most likely involved.

7.5.3 Nonsaccular Giant Arterial Aneurysms

Fusiform AA corresponds to an enlargement of the entire vessel circumference over a segment of the artery (Fig. 7.90). It can be seen in various situations, in particular in dissecting AA associated with connective tissue disease, infectious AA, and inflammatory or immune diseases, where they are often multifocal and large (Figs. 7.91, 7.92). They should be distinguished from dysplastic pseudoaneurysmal segments that are elongated into a dolichodysplastic segment. The giant fusiform aneurysms (0.6% of all AAs) are a peculiar entity characterized by perforators or cortical branches coming from the sac; they are associated with intraluminal thrombosis (Tables 7.37, 7.38). This makes their treatment particularly challenging: the operative mortality was 23% in the Drake and Peerless series (1997), in 120 giant fusiform AAs. They are almost indistinguishable from the giant saccular AAs and they account for 21% of the overall population of giant AAs. On the other hand, they seldom bleed (SAH, 17%) and mostly present with mass effect (50%), regardless of the topography in the anterior or posterior circulation. Almost all embolic complications that were noted occurred in the anteriorly located giant fusiform cases (Drake and Peerless 1997). They are mostly diagnosed in young males (60% before 40 years of age) with no history of hypertension or atherosclerosis. Twenty-five percent are located in the anterior circulation and mostly involve the MCA (50%) (Figs. 7.72, 7.90). In the posterior circulation, half of them involve the vertebrobasilar trunk (VA, VB junction, BA), and 30% the PCA artery at P1 and P2 segments. Proximal occlusion

Table 7.37. Topography of giant and fusiform AAs (from Drake and Peerless 1997, with permission)

Location of AA	Total patients	Patients with fusiform AAs[a]	%
Internal carotid	178	6	3
Middle cerebral	54	12	22
Anterior cerebral	19	5	26
Basilar bifurcation	136	4	3
Anterior-superior cerebellar	55	1	2
Basilar trunk	56	29	52
Vertebral–basilar junction	38	9	24
Vertebral	39	15	38
P1	39	13	33
P2	27	17	63
Total	641	111	NA

NA, not applicable.

[a] Of unknown etiology; excludes six patients with atherosclerosis, three with specific causes, and 82 with petrous and cavernous AA.

Table 7.38. Revealing symptoms in giant intracranial fusiform aneurysms (modified from Drake and Peerless 1997)

Location of giant intracranial fusiform aneurysm	No.	Mass	SAH	Seizure	Embolism	Headache
Anterior division (ICA, MCA, AChA)	25 (20%)	12 (19%)	5 (17%)	1	5	1[a]
Posterior division (basilar bifurcation) P1–P2, ASCA)	37 (30%)	15 (25%)	11 (35%)	1	–	10
Vertebrobasilar (BA/VB junction, VA, PICA)	58 (50%)	34 (56%)	14 (48%)	–	–	10
Total	120 (100%)	61 (100%)	30 (100%)	2	5	21

ICA, internal carotid artery; MCA, middle cerebral artery; AChA, anterior choroidal artery; ASCA, anterior-superior cerebellar artery; BA, basilar artery; VB, vertebrobasilar; VA, vertebral artery; PICA posterior inferior cerebellar artery.
[a] Incidental.

of the parent vessel almost invariably causes complete thrombosis of the AA; the safety of the outcome depends on the collateral circulation in both the deep and superficial territory. Spontaneous occlusion can occur and is usually clinically associated with severe headaches and deficit, often related to an increase in size.

The PCA fusiform AAs deserve a special mention in this group since the clinical tolerance with respect to vision preservation is usually excellent. The collaterals around the lateral geniculate body account for this tolerance (see Vol. 1). In case of giant fusiform partially calcified AA on the same PCA, resolution of the perianeurysmal hypersignal is expected following sacrifice of the parent vessel; the quality of the spontaneously established cortical collateral circulation improves the preoperative visual impairment (Kon et al. 1997). The specific fusiform aspect of P1–P2 AAs, even without thrombosis, makes them unlikely to be of the same etiopathogenesis as the so-called berry or saccular AA. The constant fusiform aspect in this topography suggests the triggering role of microtraumatic insults to the PCA at the tentorium edge and subsequent dissection, explaining the aspect of the aneurysm (Lazinski et al. 2000).

The dissections may have variable clinical presentations, depending on the balance between the triggering trauma and the repair system. Acute dissection would likely lead to SAH or brain stem stroke when they involve perforators. Subacute dissection would be more likely to result in distal microembolic strokes, while chronic dissection would eventually lead to giant fusiform lesions as the result of mural angiogenesis (Table 3.35). The mural clot would in this instance have the same long-term effect in stimulating vessel wall proliferation and AA growth to reach the giant size.

7.5.3.1 Megadolicho Arteries and Serpentine Arterial Aneurysms

In 1977, Segal and McLaurin first introduced the concept of giant serpentine aneurysm (GSA), defined as partially thrombosed giant aneurysms with an irregular vascular channel, a subcategory of intracranial giant aneurysms (Fig. 7.104).

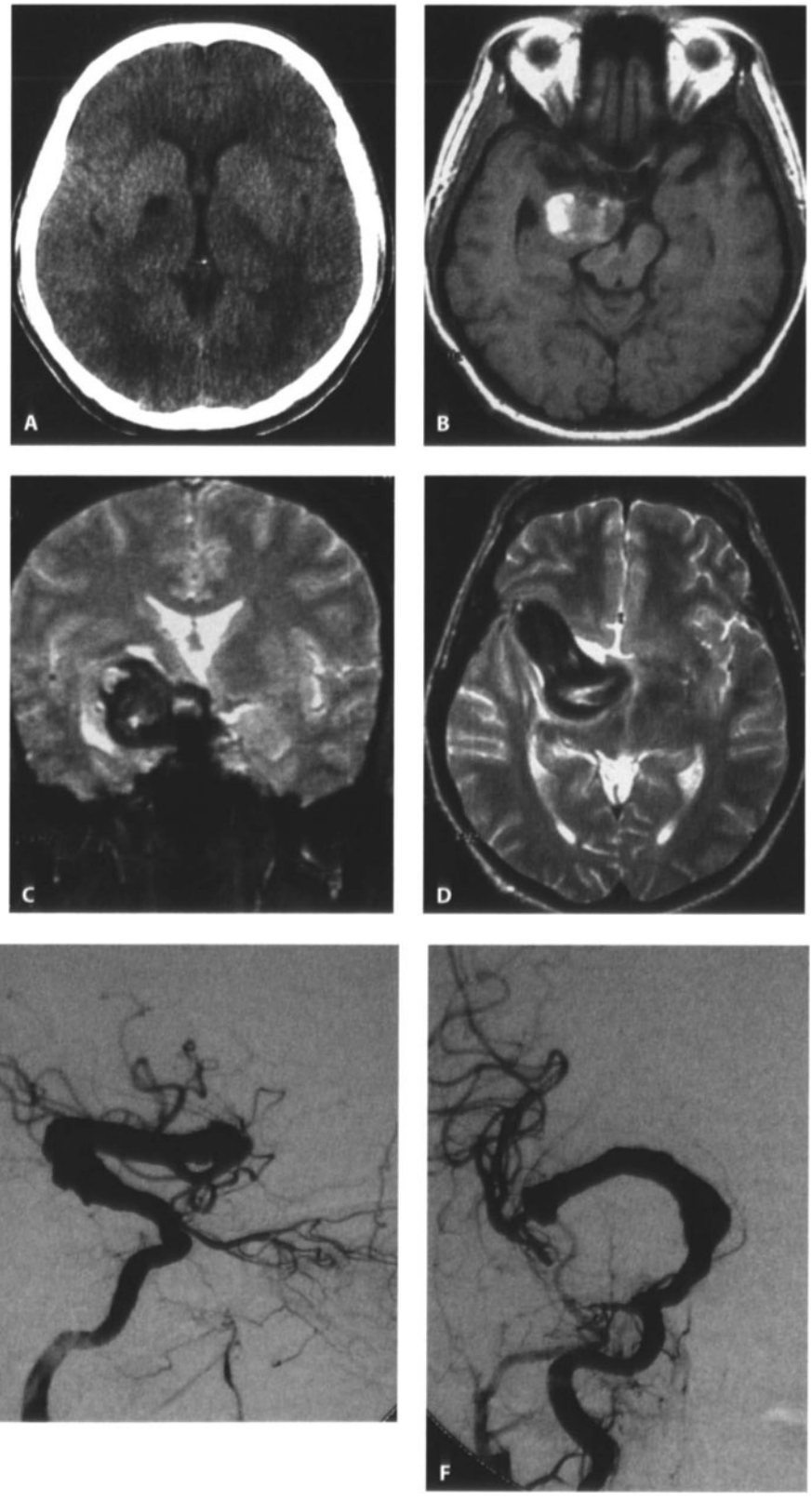

Fig. 7.104A–F. A 31-year-old male patient. CT shows deep-seated infarct on the right side (**A**) 2 months after presentation with left-sided hemiparesis. MRI shows partially thrombosed arterial aneurysm from the midline to the entrance of the right sylvian fissure (**B–D**). **E, F** Angiograms show a serpentine aneurysm of the internal carotid artery termination (7th segment), involving the M1 segment. The right A1 segment is absent. Posterior circulation was normal with asymmetrical caudal fusion of the basilar tip. (Courtesy of S. Pongpech)

Sixty-five cases were reviewed by Anshun et al. (2000), who found that the main clinical presentation of GSAs was mass effect, ischemia, and hemorrhage. SAH occurred in 23.5% (12/51). GSAs occur more frequently in males (41/64). They ranged in age from 5 to 69 years, with a mean age of 41 years. Forty-three percent (28/65) of GSAs are located in the middle cerebral artery territory, 20% (13/65) at the internal carotid artery, 14% (9/65) at the posterior cerebral artery, 6% (4/65) at both the basilar and vertebral arteries, 5% (3/65) at the basilar-vertebral junction, 3% (2/65) at the PICA, and 1.5% (1/65) at both the anterior cerebral artery and the posterior communicating artery.

CT demonstrates calcification in the wall, while MRI clearly shows the AA thrombus at various stages. Postmortem microscopic studies of 18 cases (Segal and McLaurin 1977; Belec et al. 1988; Khan 1990; Li et al. 1988) demonstrated that the aneurysmal wall consisted of fibrous tissue measuring 2–4 mm in thickness, often with calcification, loss or almost complete loss of internal elastic lamina and muscularis, and a number of small vessels within the wall. The sac contains thrombi of various ages, occasionally with calcification and hemorrhage. There is no endothelial lining of tiny channels that end blindly in the thrombus.

Anshun et al. (2000) propose that congenital defects of the arterial wall combined with dissection caused by an acquired injury are the possible underlying causes of GSA formation, because GSAs occur in all age groups and the gross appearance of GSAs is similar to that of intracranial dissection. The findings of GSAs on MRI are also similar to those of intracranial dissection. The majority of GSAs did grow over time, and hemorrhage occurred in 23.5%.

7.5.4 Multiple Giant Arterial Aneurysms and Mirror Giant Arterial Aneurysms

Multiple giant and mirror giant AAs are rare and usually involve the extradural carotid system unilaterally or the ICA and VA intradurally (Fig. 7.26). We have exceptionally encountered mirror giant aneurysms (Fig. 7.105) of the saccular or the fusiform type. Since their cause and natural history is unknown, the therapeutic challenge is great. Such lesions are different from the multiple fusiform AA described in immune deficiencies (Figs. 7.111, 7.113) or the bilateral cavernous sinus ICA mycotic aneurysms. The multifocal character of giant AAs suggests nonhemodynamic triggering factors such as a congenital vessel wall defect associated with or related to growth factor dysfunction. It is striking that most of the genetic or familial diseases known to give single or multiple AAs are not involved in the etiological discussion of single or multiple giant AAs, except for NF1 in the extracranial region (Fig. 7.40). This observation stresses the difference that exists within the AA group and underlines that several causes can be extrapolated to produce similar morphological types. Phenotypes that are similar may be treated the same mechanically to obtain short-term goals. If on the other hand disease-based therapy is to be provided it will be unlikely that similar AA phenotypes (morphologically identical) will benefit from the same therapeutic agent.

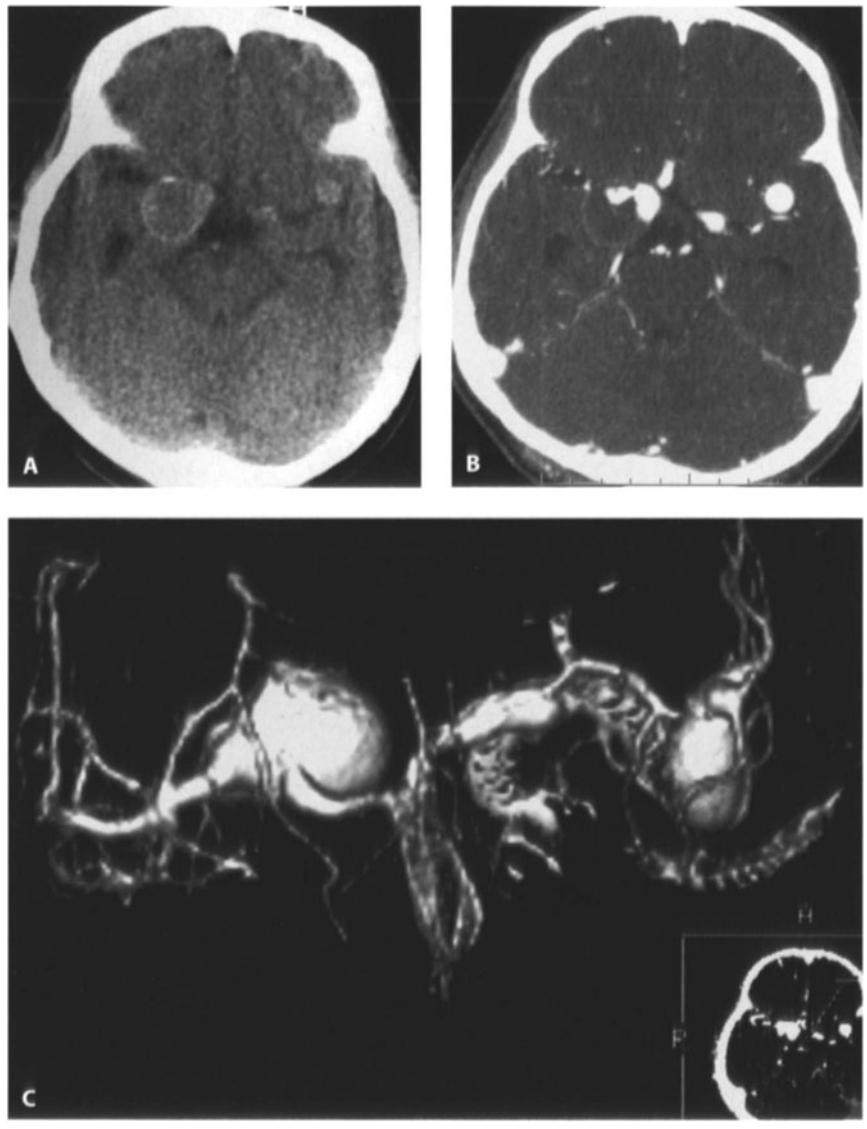

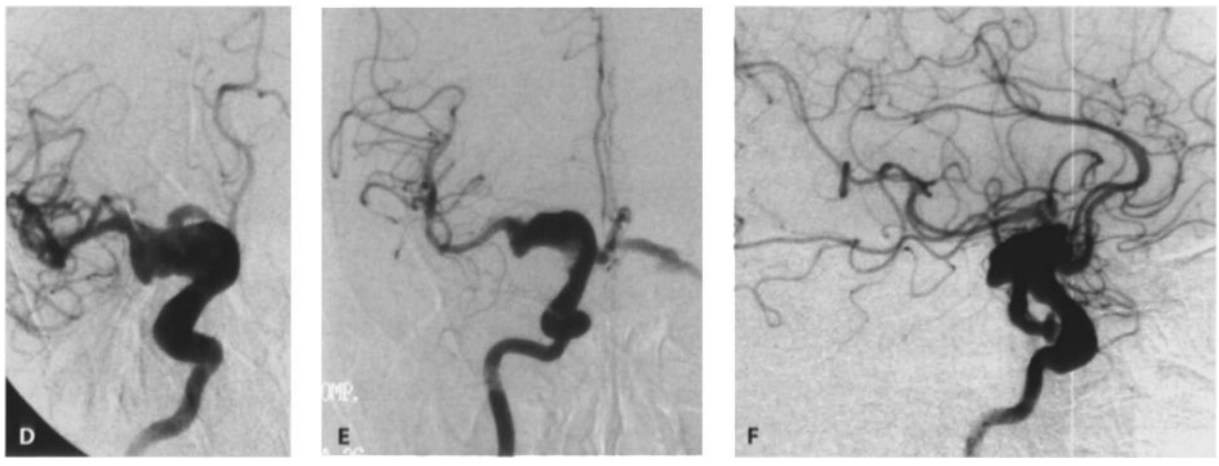

Fig. 7.105A–H. A 63-year-old male patient presented with progressive left hemiparesis for 1 week. At onset mild headaches were noted followed by the deficit without fever. **A–C** CT and angio-CT showed minor white matter ischemic accidents and bilateral calcified aneurysmal masses smaller on the right than on the left. **D–F** Multifocal giant partially thrombosed aneurysms were confirmed on angiograms. The right-sided aneurysm involved the internal carotid artery (ICA) termination (6th and 7th segments) and A1. **G, H** see p. 502

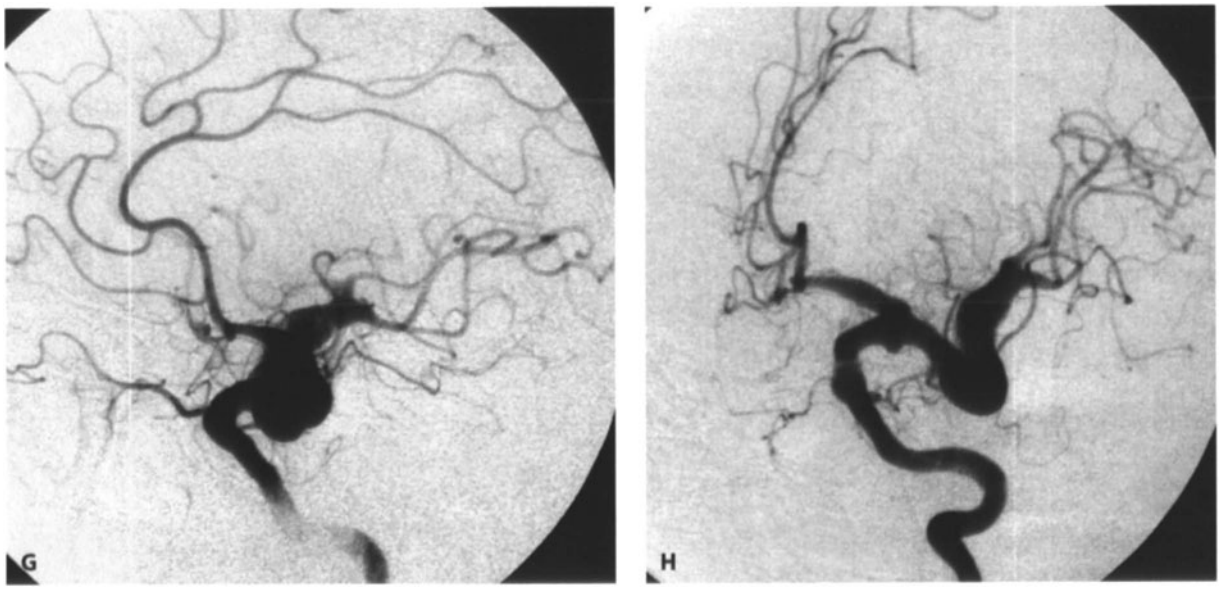

Fig. 7.105 (*continued*). **G, H** On the left side, the ICA termination was involved as well as the A1, M1, and M2 segments. Distal middle cerebral artery territories were normal. ICA posterior divisions were not involved with asymmetrical basilar caudal fusion. (Courtesy of S. Pongpech)

7.6 Infectious, Immune, and Inflammatory Intradural Aneurysms

7.6.1 Infectious Arterial Aneurysms

The term "mycotic arterial aneurysm" was proposed by Osler in 1901 to describe AAs seen during bacterial endocarditis (Fig. 7.106). The designation has been kept to name the AAs associated with an infectious state (Hurst et al. 1992). Today the term "infectious arterial aneurysm" (IAA) seems more appropriate (Micheli et al. 1989). Although they can be caused by fungal infections, they are most often of bacterial origin (Barrow and Prats 1990; Bohmfalk et al. 1978; Horten et al. 1976). They account for 1.5%–9% of all intracranial aneurysms (Clare and Barrow 1992) but less than 1%–2% in an interventional practice. The proportion of such IAAs depends on the local situation: e.g., the presence of a cardiothoracic department for adults or children. Of patients with subacute bacterial endocarditis (SBE), 3%–15% present with an IAA (Fig. 7.107). Other causes include dental and maxillofacial surgery. IAAs are usually small and distally located on the MCA or less frequently in the PCA territories (Fig. 7.108); they rarely involve the ACA or the posterior fossa. They are more proximal in location in 23% of cases.

IAAs may involve the intracavernous ICA by contiguity, following severe sphenoid sinus infections with osteomyelitis and cavernous sinus thrombophlebitis (Suwanela et al. 1972; Marsot-Dupuch et al. 2000). Cavernous IAAs are often bilateral (19%) and caused by staphylococcus infection (50%). They occur more frequently in children (56%) (see Vol. 3).

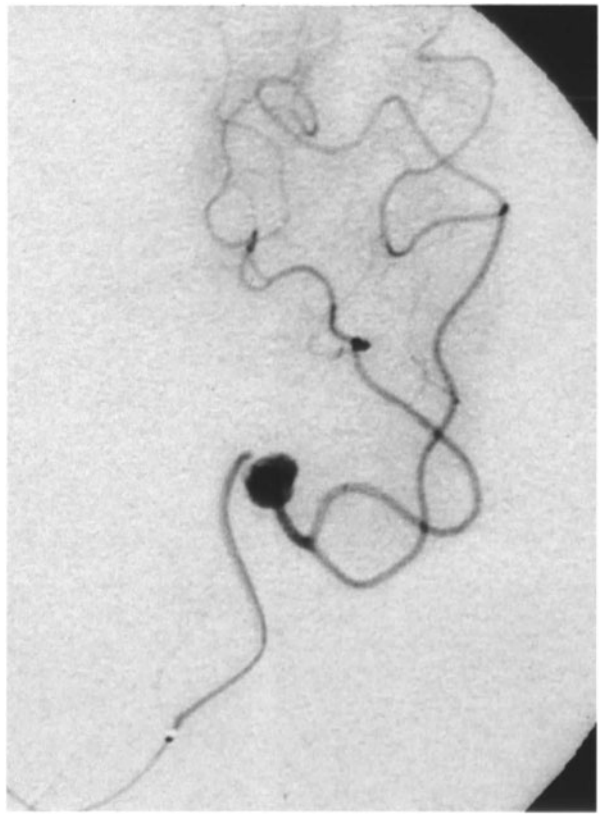

Fig. 7.106. A 13-year-old girl presented with seizure-like episodes. CT showed focal intracranial hemorrhage. Angiography was suggestive of mycotic AA on the distal branch of the middle cerebral artery. Doppler demonstrated cardiac vegetations, which was treated with antibiotics

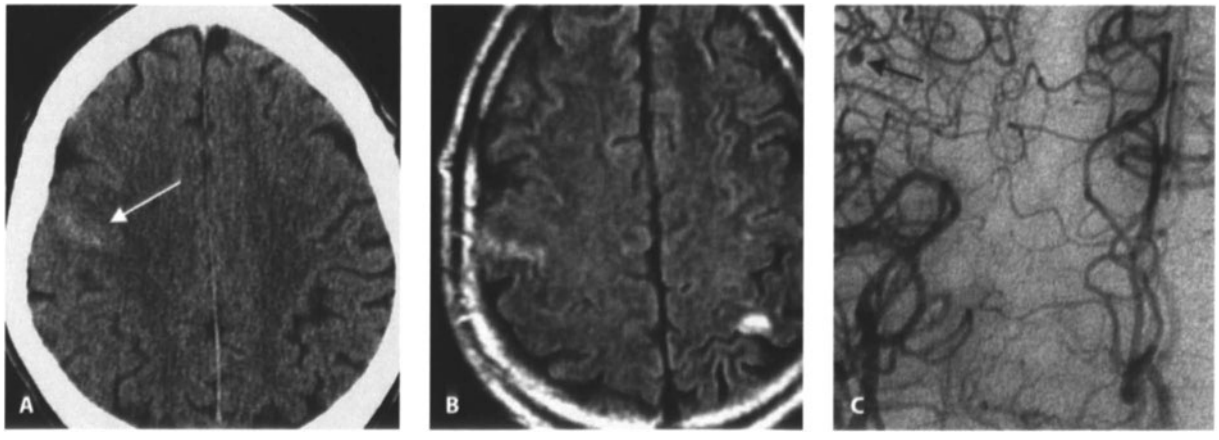

Fig. 7.107. A 52-year-old male patient with subacute bacterial endocarditis of an aortic valve, presented with sudden onset of headaches in relation to focal subarachnoid hemorrhage (*arrow*) shown on CT (**A**). Note the multifocal lesions on MRI (**B**) and the distal mycotic aneurysm on the angiogram (*arrow*, **C**). Treatment comprised aortic valve replacement and antibiotics

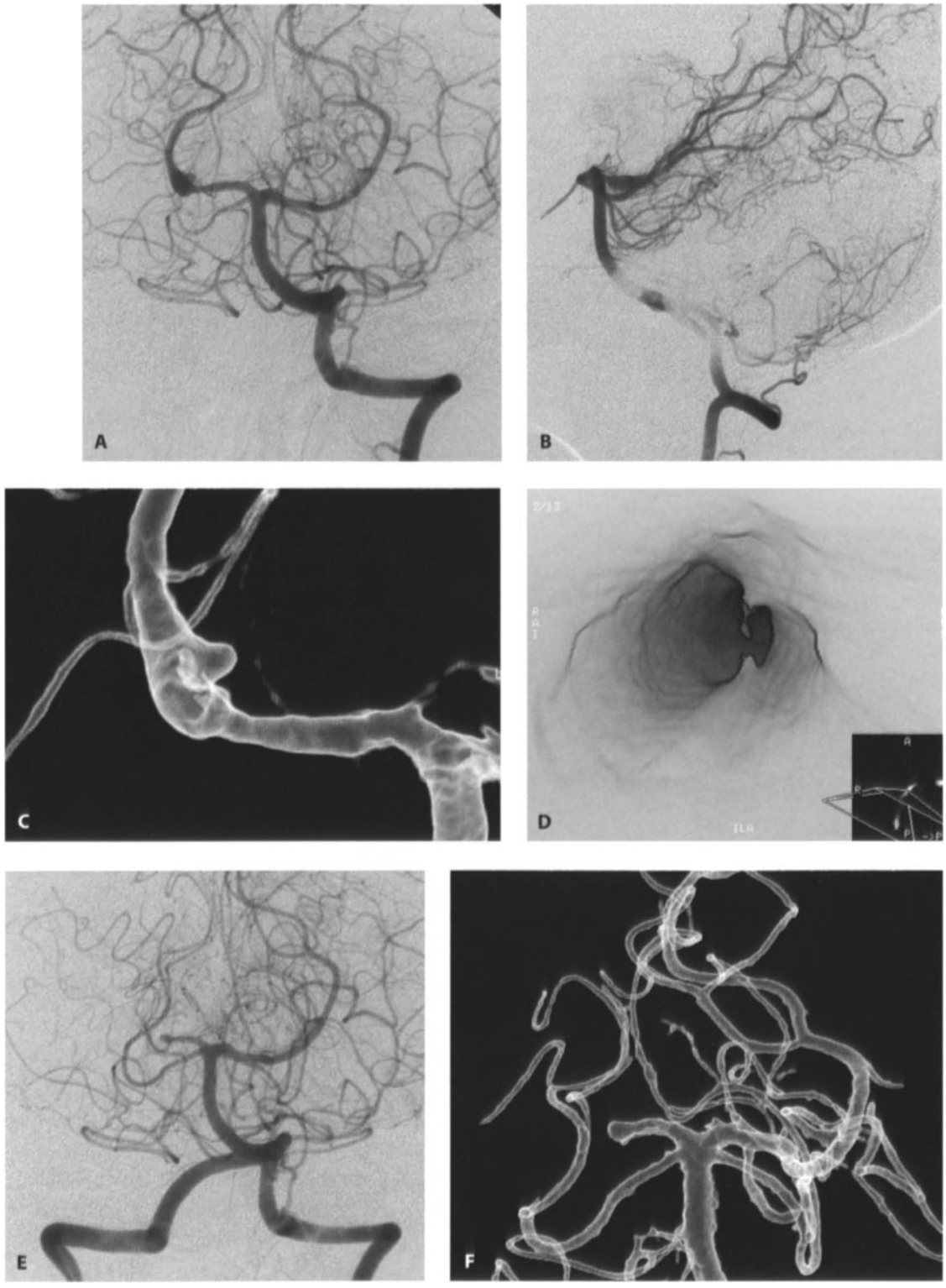

Fig. 7.108A–F. A 42-year-old male patient presented with severe renal insufficiency in relation to HIV with cryptococcus infection. Antibiotics, triple-therapy, and diuretics were used. Admitted in emergency for subarachnoid hemorrhage Glasgow 15, Hunt and Hess II. At angiography, fusiform ectasia of P2 on the right side (**A**, **B**). Three-dimensional (**C**) and endoscopic (**D**) views suggest dissection. Conservative treatment is decided in view of the late stage of the renal failure. **E**, **F** Follow-up angiograms performed 2 months later show spontaneous occlusion of P2 with efficient collateral circulation toward the distal territory

In half of the cases, their size increases on follow-up angiography, but they will disappear in 25% of cases with antibiotic treatment, with occlusion of the ICA in one-quarter of them. Other extravascular causes include meningitis.

In 20% of cases, IAAs are multiple and this frequency increases in immune-deficient patients and with inappropriate use of antibiotics or cytotoxic drugs (Schnee and Flamm 1997). The most frequently involved infectious agents are *Streptococcus viridans* and *Staphylococcus aureus*, mostly in cases of subacute or acute endocarditis (Fig. 7.109). Blood and CSF cultures will classically show the suspected causative agent but in one-third of cases, no infectious agent can be identified. Bacteria were found in the wall of the IAA as early as the nineteenth century. However the etiopathogenic role of septic emboli, septicemia, meningitis, or encephalitis associated with the IAA is unclear.

The time interval between the infectious emboli and IAA development, including rupture, can be as short as 24–48 h (Clare and Barrow 1992). The more aggressive the infectious agent is (such as salmonella), the higher the chance of rupture will be. The direct involvement of the arterial wall (Clare and Barrow 1992) is the mechanism most often advocated. It involves an infectious process progressing from the lumen to the extravascular space. The infectious agent circulates during septicemia, and endothelial impact occurs in vulnerable zones where there is turbulence or at the level of preexisting atheromatous AAs (Patra et al. 1986).

Infection extending from the outside toward the lumen involves infectious emboli originating from the vasa vasorum (Patra et al. 1986; Rice et al. 1997). Such a mechanism is suggested in AAs affecting arteries with high flow and in cases of salmonellosis, tuberculosis, and treponematosis. Adventitial involvement is thus primarily in those circumstances and media, and intima infection occurs secondarily (Foote et al. 1978). Such local diffusion is the result of vascular stasis and occlusion of the vasa vasorum (Patra et al. 1986) in the vicinity of an infected area (abscess, meningitis, or an infectious thrombophlebitis of the cavernous sinus) (Lawson and Reino 1997; Suwanwella et al. 1972). Exceptionally, an immunoallergic mechanism has been proposed to explain some infectious aneurysms during proper therapeutic management of a case of infectious endocarditis (Barrow and Prat 1990).

In nearly 80% of endocarditis patients, the prominent associated location will be the aortic valves. In 35% of patients, embolic episodes have been recorded, 43% of them in the brain. However, 4% of the 442 endocarditis cases did present with a SAH from IAA, and 21% of them had had an embolic episode before (Gates 1951). The peculiar similarities between the aorta and the intracranial arteries (neural crest involvement; Etchevers 2001) suggests that an acute or subacute cardioaortic infection may be the reflection of a general but also a local decrease in the defense ability. A secondary decrease in these abilities at the level of the intradural artery may expose them to any circulating agent that otherwise would not have been capable of producing vessel inflammation and rupture. Most of the so-called IAAs are in fact either dissected or false AAs, the lumen communicating with the endothelialized cavity within the hematoma (Patra et al. 1986; Barker 1953), with peripheral fibrous changes constituting a dense capsule. There is a consistent impairment of the internal elastic lamina.

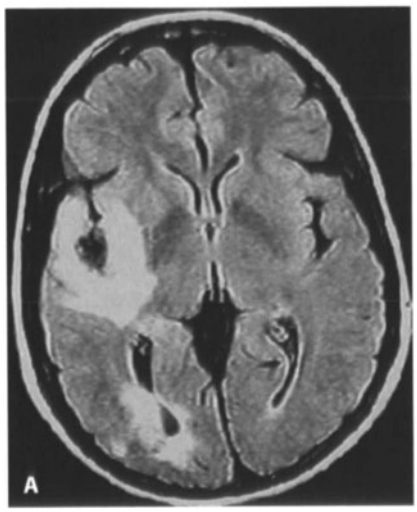

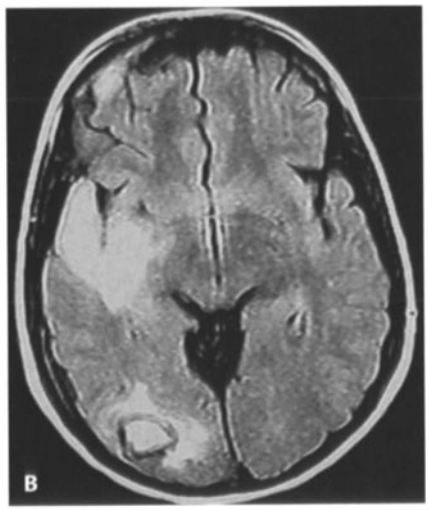

Fig. 7.109A–L. A 26-year-old female patient with mitral valve prolapse presented a sudden onset of left visual field defect. Multiple mycotic aneurysms were demonstrated. **A, B** Initial MRI. **C, D** Angiograms show aneurysms in the occipital and sylvian regions (*arrows*). **E, F** Following 3 weeks of antibiotics, the occipital lesion is healed while the middle cerebral artery lesion does not show significant change. **G–L** see p. 507

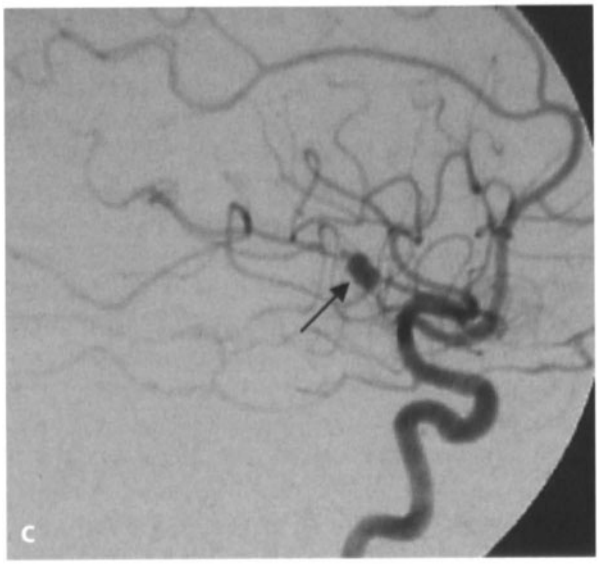

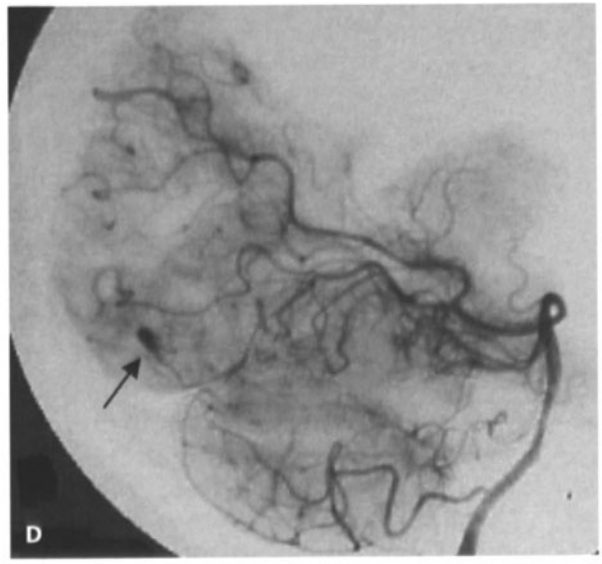

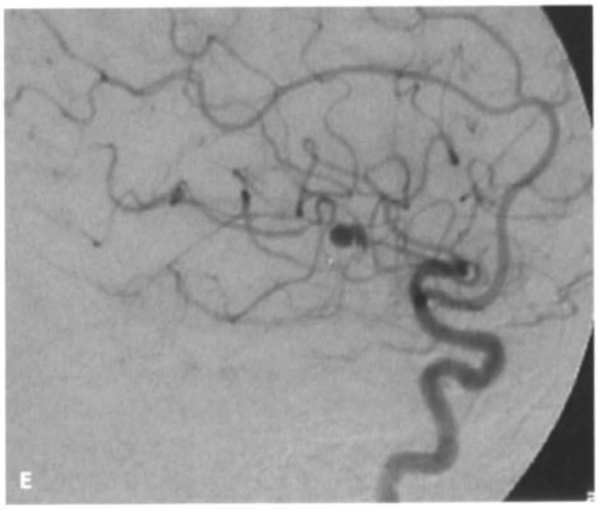

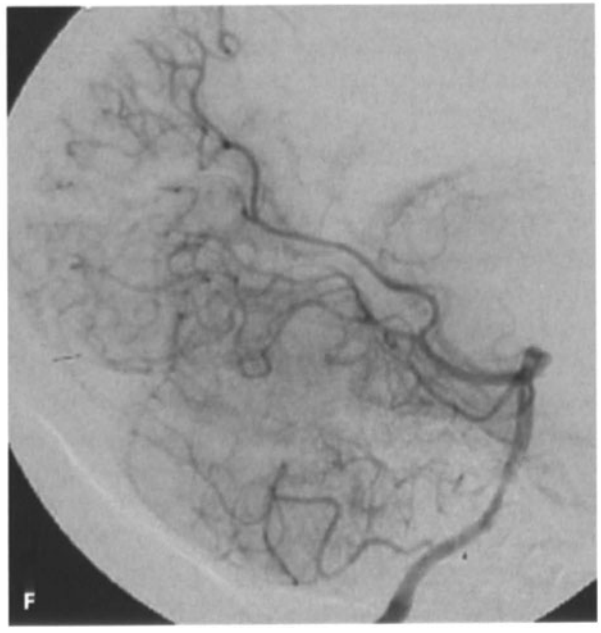

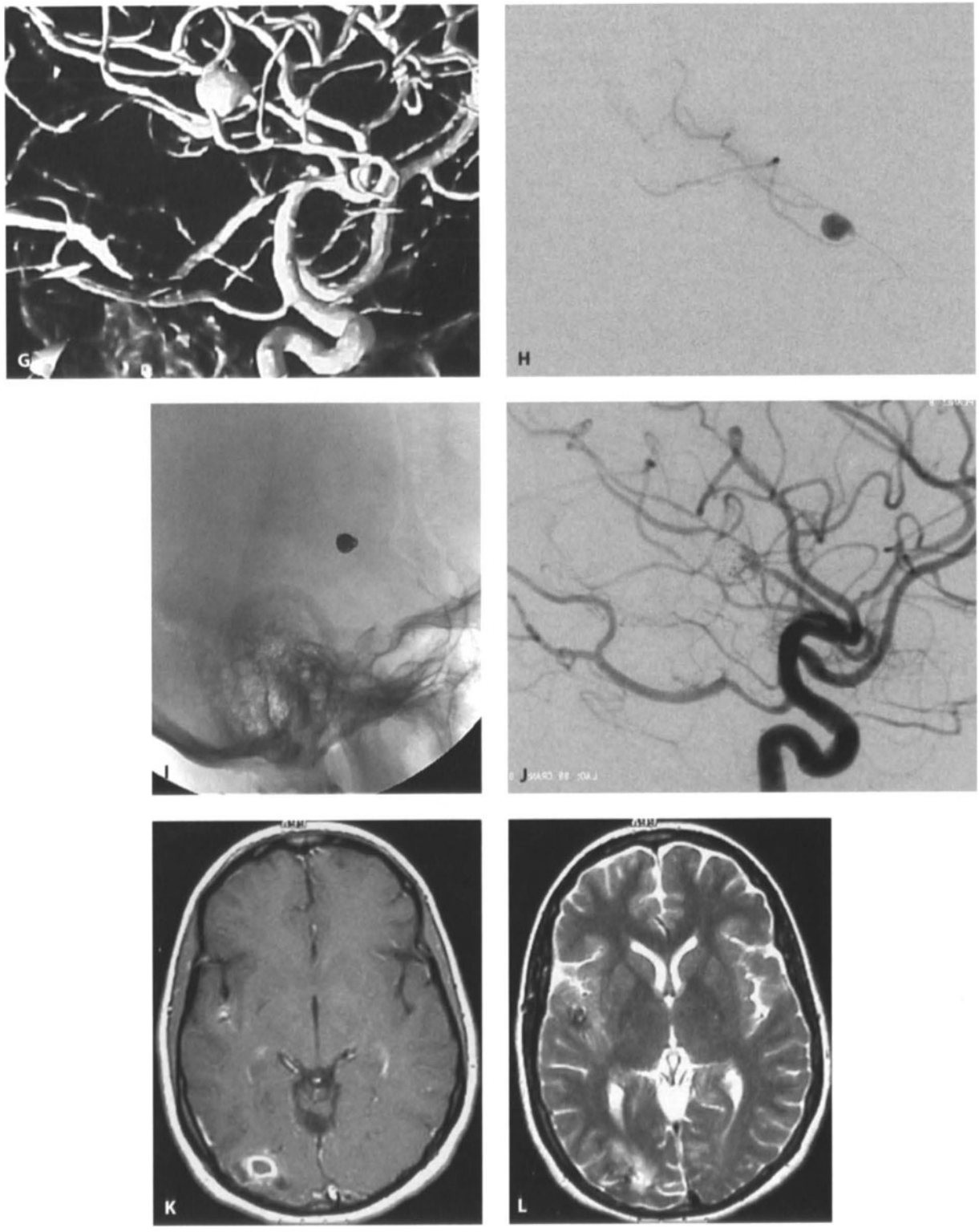

Fig. 7.109 (*continued*). G–J Three-dimensional analysis aided in successful endovascular coiling (H–J). K, L Follow-up MRI after 5 weeks

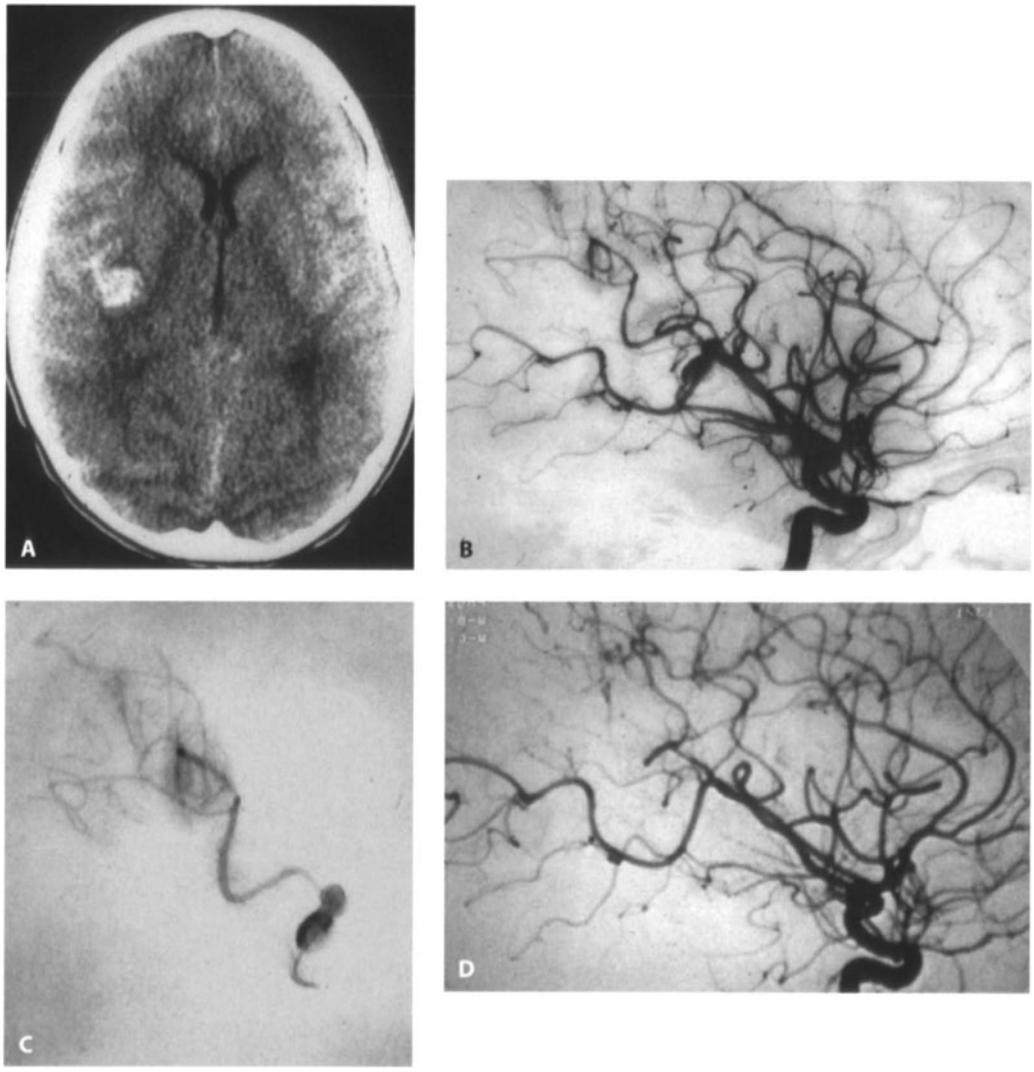

Fig. 7.110. A 10-year-old boy presented with acute subarachnoid hemorrhage and a small intracranial hemorrhage in the right sylvian fissure (**A**). This bleed was caused by the rupture of a bilobed fusiform arterial ectasia located on the parietal branch of the middle cerebral artery (**B, C**). A mycotic aneurysm was suspected despite lack of evidence of an infectious focus. Conservative treatment with antibiotic therapy was chosen because of the eloquence of the territory fed by this vessel and the appearance of the arterial aneurysm. Thrombosis of the lesion was noted on the 6-month follow-up angiogram (**D**)

IAA lesions are mostly distal on the arterial tree and reveal themselves by intracranial hemorrhage (ICH). They are often small, extending into the hematoma (Fig. 7.110), and have a fusiform appearance with no neck, as they involve the full thickness of the vessel wall as a focal dissection. When diagnosed, they require urgent antibiotic treatment for a minimum of 4 and preferably 6 weeks. In rare cases, a focal SAH may be the presenting event (Fig. 7.107). Mortality is reported as high as 80% in the ruptured cases and 30% for the unruptured ones (Bohmfalk et al. 1978). Mortality despite medical treatment is 57%; when surgery and antibiotic therapy are combined (Weir 1987), the mortality drops to 23%. Following

medical treatment, the IAA tends to regress completely (30%) or incompletely (19%), with or without occlusion of the parent vessel. They may persist (15%) or even grow (22%) despite medical treatment, and some will rebleed (Fig. 7.109).

In 15% of cases, new IAAs will appear (Ojeman 1982) and treatment should therefore be discussed carefully in every case following an appropriate course of medical treatment. Early endovascular management is sometimes mandatory for ruptured IAAs responding poorly or not at all to treatment. This may require sacrifice of the involved arterial segment, even in eloquent areas, after assessing the leptomeningeal anastomotic circulation (Scotti 1996; Houdart 1997; Chaloupka 1998), as preservation of the artery is usually not possible. The relevance to treat several locations or unruptured IAAs will need to be discussed case by case, taking into consideration the apparent efficiency of the antibiotics on the infectious disease, the morphological changes under appropriate treatment, and the postulated risk carried by certain locations in case of hemorrhage (sphenoid sinus). The need for anticoagulation in some specific cardiac situations may also prompt intervention. Surgery has little to add in this pathology unless a decompressive operation for ICH needs to be performed. The long-term patency rate of end-to-end anastomosis in these small distal vessels is still a problem.

Of utmost importance is the need for repeated cerebral angiography at short intervals, to detect changes in aneurysm size, configuration, or the development of new lesions. MRI and MRA are not sufficient for this purpose, as they may fail to detect new small distal aneurysms.

7.6.2 Intradural Fusiform Aneurysms in Patients with Immune Deficiencies

Neurovascular manifestations of AIDS in adults usually consist of vascular occlusions associated with distal emboli and complications of thrombocytopenia. In children, cerebrovascular lesions are mostly due to arteritis in combination with arterial sclerosis, vascular occlusions, and formation of intracranial aneurysms (Dubrovsky et al. 1998; Philippet et al. 1994; Shah et al. 1996). These aneurysms are typically multiple, subarachnoid in location, fusiform in shape and involve the proximal arteries of the base of the brain, preferentially the supraclinoid part of the internal cerebral artery (ICA) (Sedat et al. 1999a) (Figs. 7.108, 7.111, 7.112). Although these lesions were initially considered as relatively specific (Park et al. 1990), we observed similar features in chronic mucocutaneous candidosis (CMCC) (Fig. 7.113). CMCC is a rare and familial disorder of unknown etiology, characterized by recurrent infections of the mucous membranes, nails, and skin with *Candida albicans* (Groubi et al. 1998). The very similar neuroradiological aspect of these cases was remarkable and raised several questions regarding the etiology and mechanism of these lesions.

None of the patients had evidence of coagulopathy, collagen vascular disease, or familial hereditary disease, but most of them suffered from severe immunosuppressive disorders or syndromes, with a long history of multiple opportunistic infections preceding the diagnosis of cerebral arteriopathy.

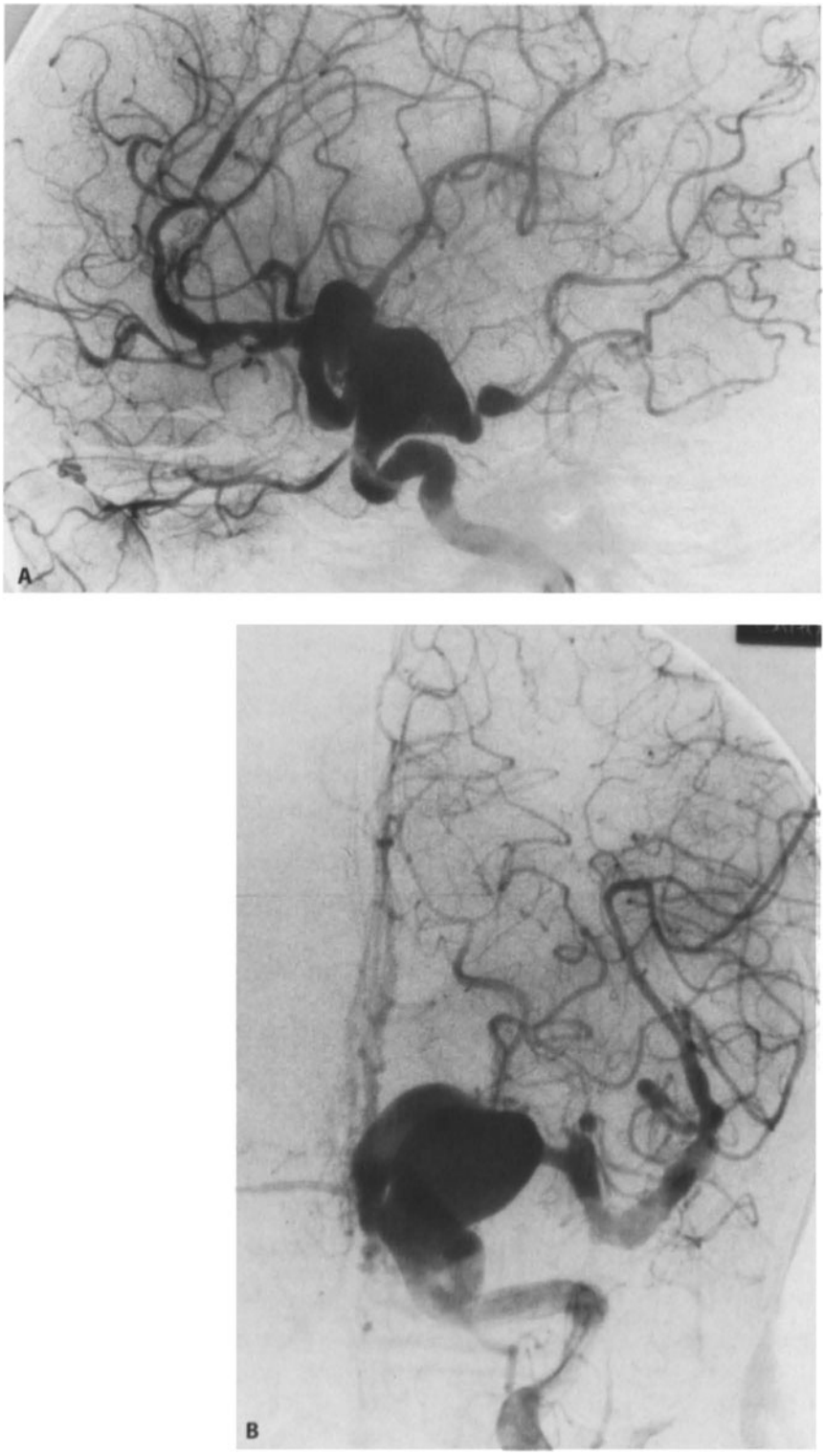

Fig. 7.111A, B. Internal carotid artery angiograms in a patient with HIV. Note the multiple giant and fusiform arterial aneurysms

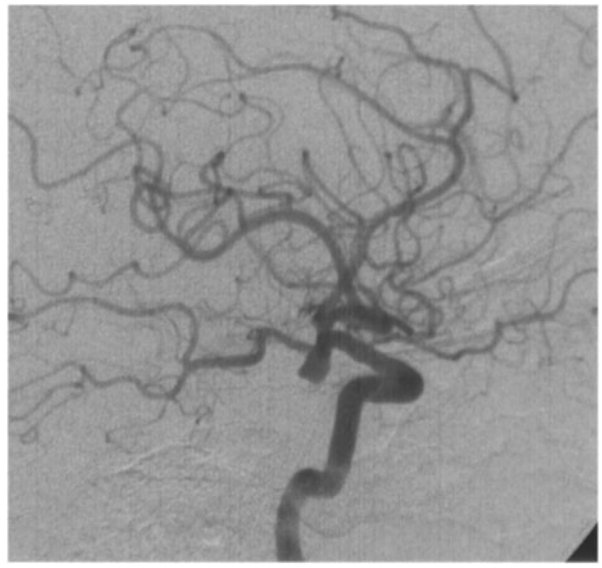

Fig. 7.112. A 45-year-old male patient with HIV for over 10 years and hepatitis B. Currently on anti-K treatment for lower limb phlebitis. He presented sudden loss of consciousness with rapid spontaneous recovery, GCS 14; CT shows subarachnoid hemorrhage; angiogram showed a PComA aneurysm

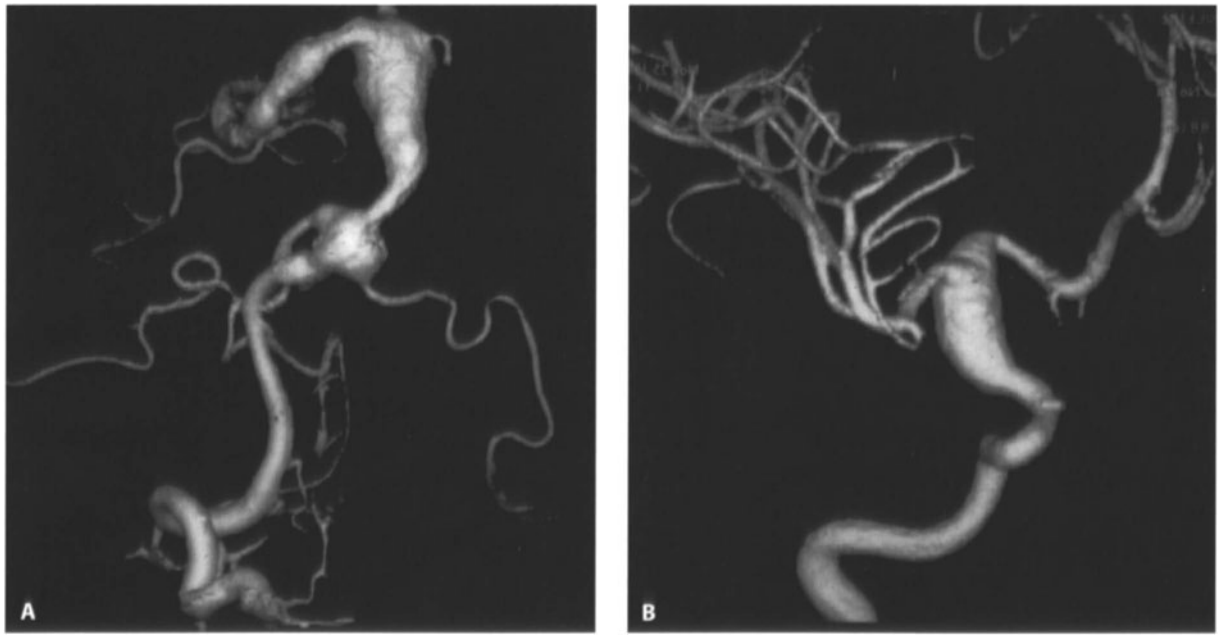

Fig. 7.113A, B. Multiple fusiform arterial aneurysms (AAs) in a 7-year-old child with familial candidiosis. **A** Three-dimensional angiography shows a fusiform AA of the right ICA. **B** Three-dimensional angiography of the left vertebral artery shows a large fusiform basilar artery aneurysm, and another fusiform AA of the distal part of the left vertebral artery at the vertebrobasilar junction. (From Sedat et al. 1999, with permission)

CMCC is a familial disease with primary immunodeficiency disorder that must be distinguished from the opportunistic candidiosis seen in globally immunocompromised patients (steroid therapies, chemotherapies, etc.). The association of CMCC with cerebral vasculitis or aneurysm is very rare, and only four cases have been described: a 19-year-old woman with fusiform aneurysms of the major vessels of the circle of Willis, a 21-year-old man with thromboses and stenoses of the distal territory of the MCA and ACA with no aneurysm (Groubi et al. 1998), a 38-year-old man with a fusiform aneurysm associated with vasculitis, and a child with multifocal fusiform lesions (Sedat et al. 1999a). None of these patients presented with bacterial, fungal, or viral infections at the time of the diagnosis, nor did they present with coagulopathy, metabolic abnormalities, or CNS infection.

The pathogenesis of fusiform aneurysms in HIV-infected patients (Fig. 7.111) remains controversial. Most authors advocated the vasculopathy to be secondary to an infectious cause.

In a review of the literature, Dubrovsky et al. (1998) found two patients with mycobacterium avian intracellular infection, one with cytomegalovirus (CMV) infection, four patients with herpes zoster virus (HZV) infection, and two others with elevated spot-checked HZV antibody titers. Kure et al. (1989) and Park et al. (1990) found one with a major HIV transmembrane glycoprotein (gp41) in the walls of aneurysmal arteries, suggesting a direct cause of the HIV in the formation of the arterial dilatations. Lang et al. (1992) did immunohistochemical studies but failed to detect glycoprotein gp41 in the wall of such lesions.

The mycotic origin (primary affection of the arterial wall by an infectious agent) of these aneurysms is unlikely. Histological and bacteriological analyses of these lesions have rarely been done but, when available, have failed to detect the presence of an infectious agent. Furthermore, none of these patients had a laboratory-confirmed CNS infection at the time of the diagnosis and no time relation was noted between the moment of the diagnosis of the aneurysmal lesions and the infectious episodes. No patient improved despite proper medical treatment.

Shah et al. (1996) suggested that the aneurysmal dilatations were in fact due to lesions of pan arteritis, resulting in the destruction of the lamina elastica with subintimal fibrosis. He postulated that these lesions resulted from ischemia of the arterial wall because of an inflammatory reaction involving adventitia and vasa vasorum (Fig. 7.108). The similarities between cerebral aneurysms in CMCC and in AIDS (multifocality and multiplicity, location, fusiform aspect, association with lesions of vasculitis, and absence of proven infectious cause) are remarkable. Sparing of the distal territories and other vascular systems is also noteworthy.

Such observations suggest a variable topographical susceptibility of the cerebral arterial system where the midline ventral vessels are primarily involved. Intracranial aneurysms in CMCC and AIDS reveal exposed areas of the cerebral vasculature, sharing the same identity or vulnerability (Lasjaunias 2000b). The immune disease exposes these areas to specific or nonspecific triggers. These vascular markings would then correspond to topographic phenotypes. The aneurysms are not present on the distal cerebral vasculature or small vessels, which may reflect the interaction be-

tween the vessel wall and the perivascular space (subarachnoid for the large arteries of the circle of Willis and aneurysms, as opposed to subpial for smaller arteries). Apart from their topography, the vulnerability of these arterial segments appears to be time related: their expression evolves from fusiform ectasias (in the pediatric population) to an occlusive arteritis (in adult patients). Lesions do not regress despite medical therapy (as mycotic aneurysms often do), indicating that these fusiform dilatations are not directly related to a pathogenic agent, but result from an active biological response of the vessel wall to an unknown trigger beyond the classically proposed infectious or hemodynamic triggers.

Additional situations can produce multifocal large or giant fusiform AAs, as in children with X chromosome-linked lymphoproliferative disease (Drake and Peerless 1997).

7.6.3 Inflammatory Diseases and Arterial Aneurysms

Various syndromes are known to be sometimes associated with intradural AAs; however, a fortuitous association cannot always be excluded. There will remain some cases in which the immune deficiency present suggests a similar mechanism of vessel wall impairment through the immune complexes. Sjögren's syndrome (Fig. 7.114) and lupus syndrome (Fig. 7.115) are two of the possible associations to be considered. The lesions are usually distal and of fusiform type. Their incidence and natural history is unknown.

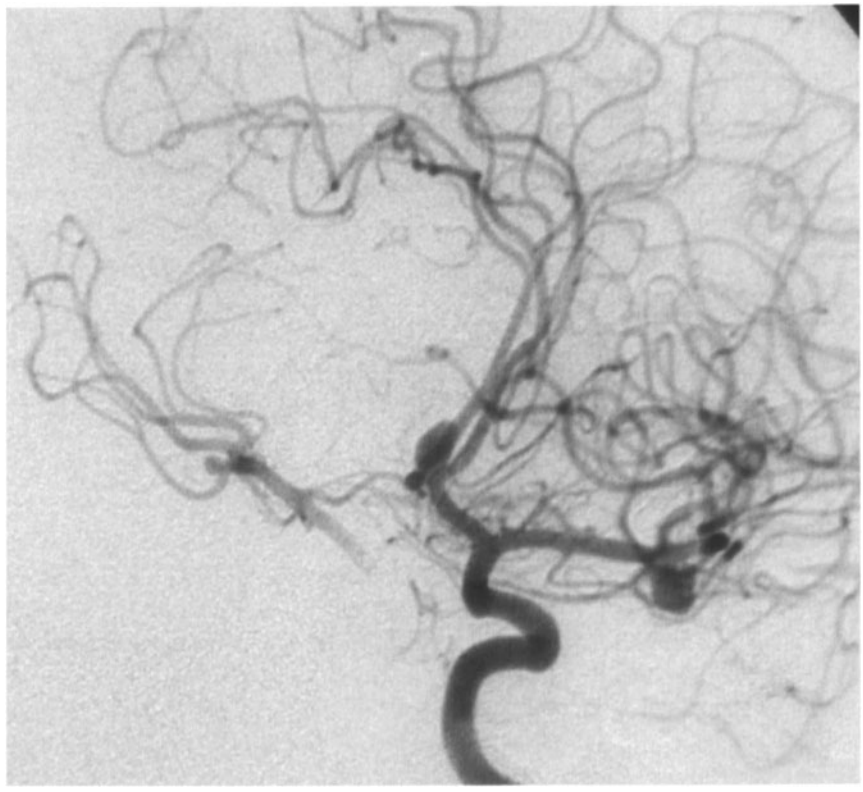

Fig. 7.114. A 51-year-old woman with Sjögren's syndrome and previous pulmonary emboli. Headaches prompted the initial MRI that disclosed one of four aneurysms. There was no evidence of subarachnoid hemorrhage. (Courtesy of G. Edner and M. Söderman)

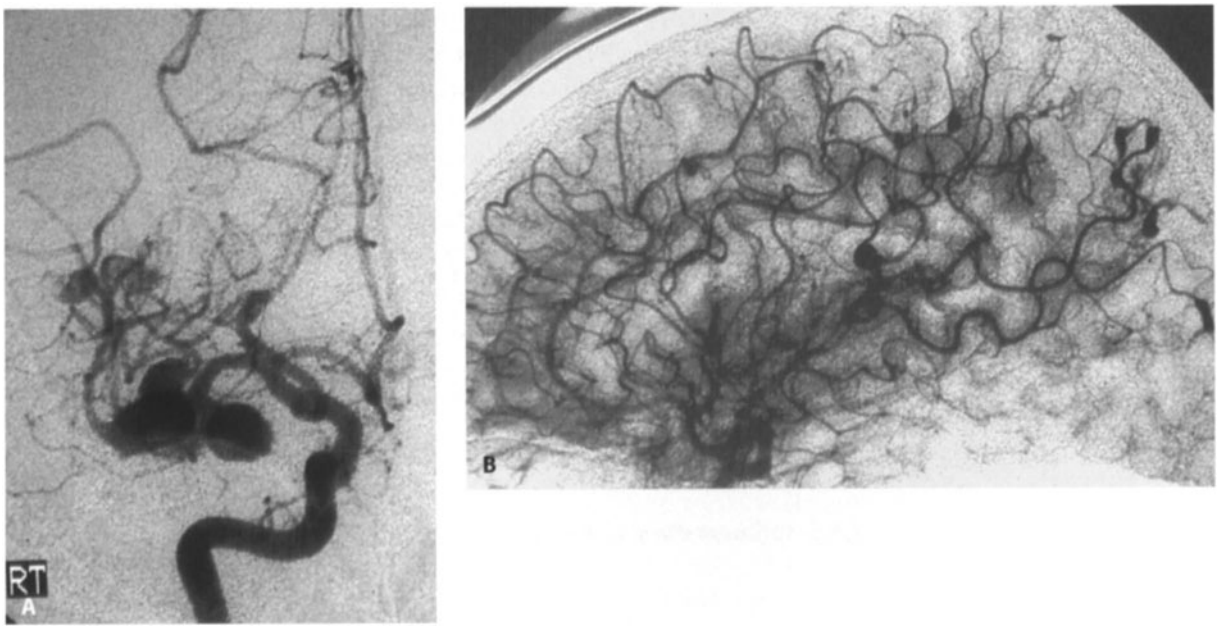

Fig. 7.115. Frontal (**A**) and lateral (**B**) ICA angiograms. Multiple bilateral proximal and distal fusiform arterial aneurysm. Inflammatory etiology related to lupus syndrome

7.7 Flow-Related Arterial Aneurysms and Other Aneurysmal Vasculopathies

The idea that all AAs are generated by hemodynamic or shear stress has been proposed and propagated over the past few decades at scientific meetings, in peer-reviewed journals, and in the practice of those dealing with AAs. In the introduction of this chapter on AAs as vasculopathies, we emphasized the biological factors that relate to and act on the vessel wall as the result of flow conditions. The fact that hemodynamic stress may produce signals that can be detected by the arterial wall and may reveal an underlying defect, whether congenital or postnatal, does not prove it as the etiology for most AAs or the cause of their rupture. Yet some AAs are clearly flow dependent, as abnormal increases in shear stress seem to result in a paralysis of the remodeling process and AA formation. Interestingly, this process can be reversed once these factors have been normalized.

The presence of increased diastolic fraction associated with an intradural or sinusal high-flow arteriovenous shunt (AVS) is likely to trigger the development of so-called flow-related AA (Lasjaunias et al. 1988). This phenomenon has also been encountered in brain AVMs (Fig. 7.116; Tables 7.39–7.41) (see Chap. 9, this volume), in the dural arterial supply of juvenile DAVMs (Fig. 7.117) (see Vol. 3), in the collateral flow that occurs after surgical arterial ligation, after traumatic occlusion of the cervical arterial trunks, on the STA after STA–MCA anastomosis, or potentially on any chronic contribution of the ECA to the ICA circulation. The hallmark of these AAs is their ability to remodel and repair following correction of the

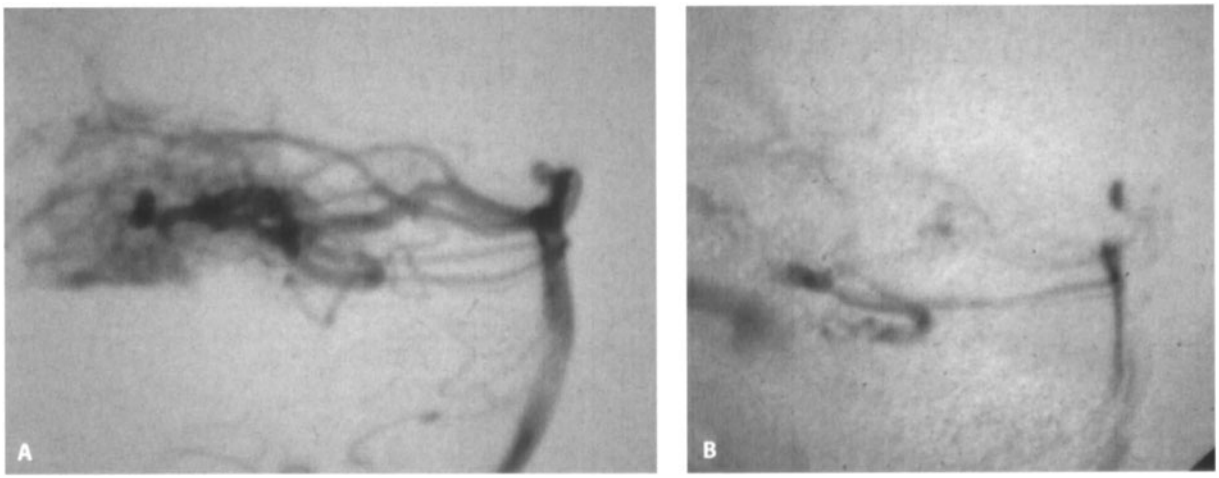

Fig. 7.116A, B. P1 arterial aneurysm (AA) associated with a temporal-occipital brain arteriovenous malformation (AVM). Before (**A**) and immediately after (**B**) the AVM embolization. Note the fluid level in the AA pouch

Table 7.39. 662 consecutive AVM patients (1985–1995): 323 patients with AA (from Meisel et al. 2000, with permission)

Age	Mean age 29.72 years
Gender	42% female 58% male

Table 7.40. Location of proximal AAs (from Meisel et al. 2000, with permission)

Middle cerebral artery	22.6%
Anterior cerebral artery	20.7%
Posterior cerebral artery	18.6%
Internal carotid artery	13.5%
Circle of Willis	11.6%
Basilar artery	5.5%
Posterior-inferior cerebellar artery	3.8%
Anterior-superior cerebellar artery	2.2%
Anterior-inferior cerebellar artery	1.5%

AComA, anterior communicating artery; PComA, posterior communicating artery; Bas tip, basilar tip: Paraophth, paraophthalmic; Car term, carotid termination, PICA, posterior-inferior cerebellar artery; ASCA, anterior-superior cerebellar artery; PCA, posterior cerebral artery.

Table 7.41. Shape of proximal AAs (from Meisel et al. 2000, with permission)

AA with neck	40.6%
Infundibulum	23.7%
AA with wide neck	21%
Fusiform AAs	10.6%

abnormal hemodynamic condition. Such AAs rarely rupture and their management should be based on an approach to normalize the diastolic fraction by restoring distal capillary resistance. These AAs do not rupture after embolization of the AVS that involves the same feeding pedicle. A fluid level can be noted in the sac immediately after the embolization procedure of the AVF (Fig. 7.116), and remodeling may take place up to 6 months afterward and reshape the arterial wall (Fig. 7.118). Of course, flow-related AAs must be distinguished from false or pseudo-AAs, which are communications between the arterial lumen and a hematoma from a previous vessel rupture, as their management is entirely different (see Chap. 9, this volume) (Fig. 7.119). In spinal cord AVMs, these AAs are not rare and justify special management to prevent recurrent hemorrhages (Figs. 7.120, 7.121).

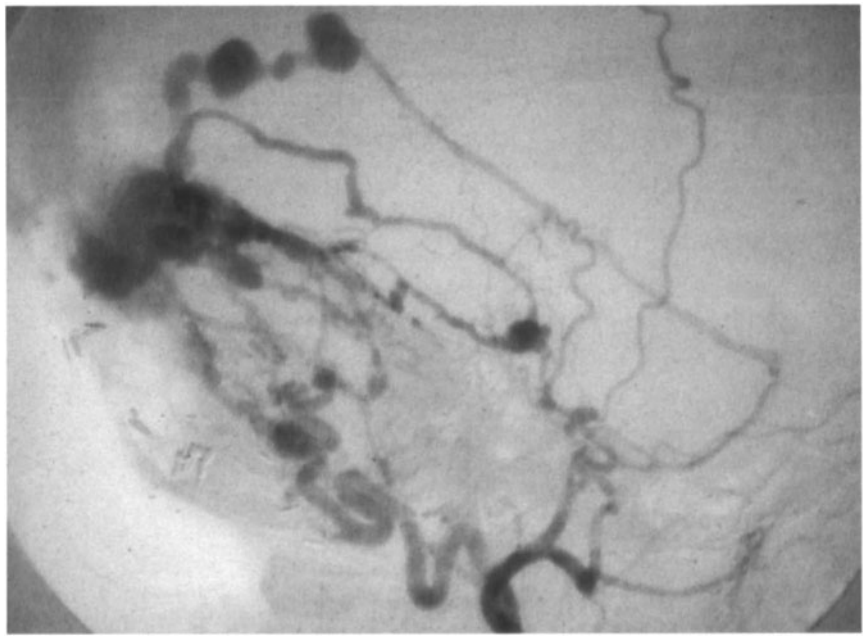

Fig. 7.117. Middle meningeal arterial aneurysm, flow-related, typically seen on the feeders supplying the juvenile type of dural arteriovenous malformation (high flow, high velocity, low pressure)

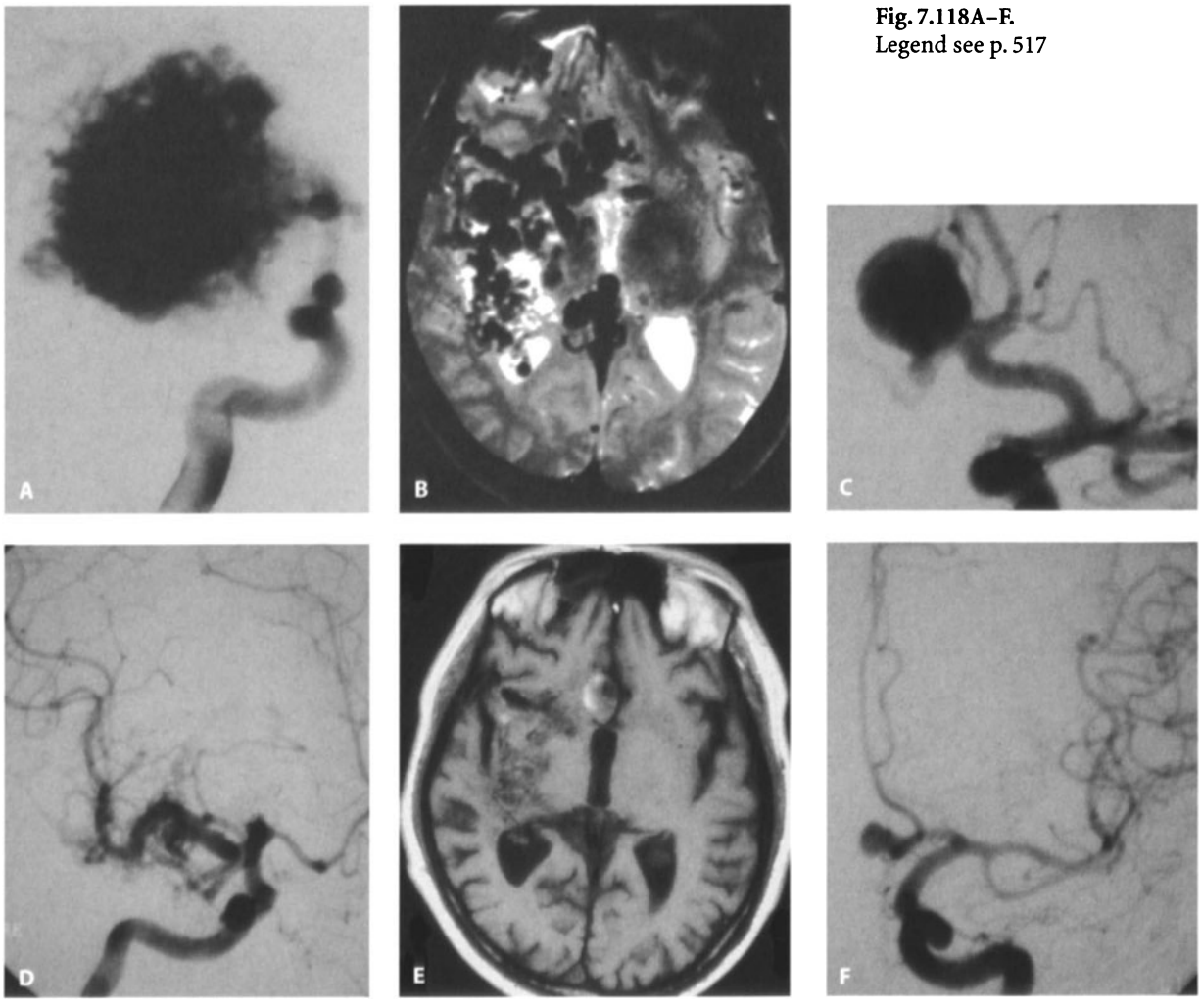

Fig. 7.118A–F.
Legend see p. 517

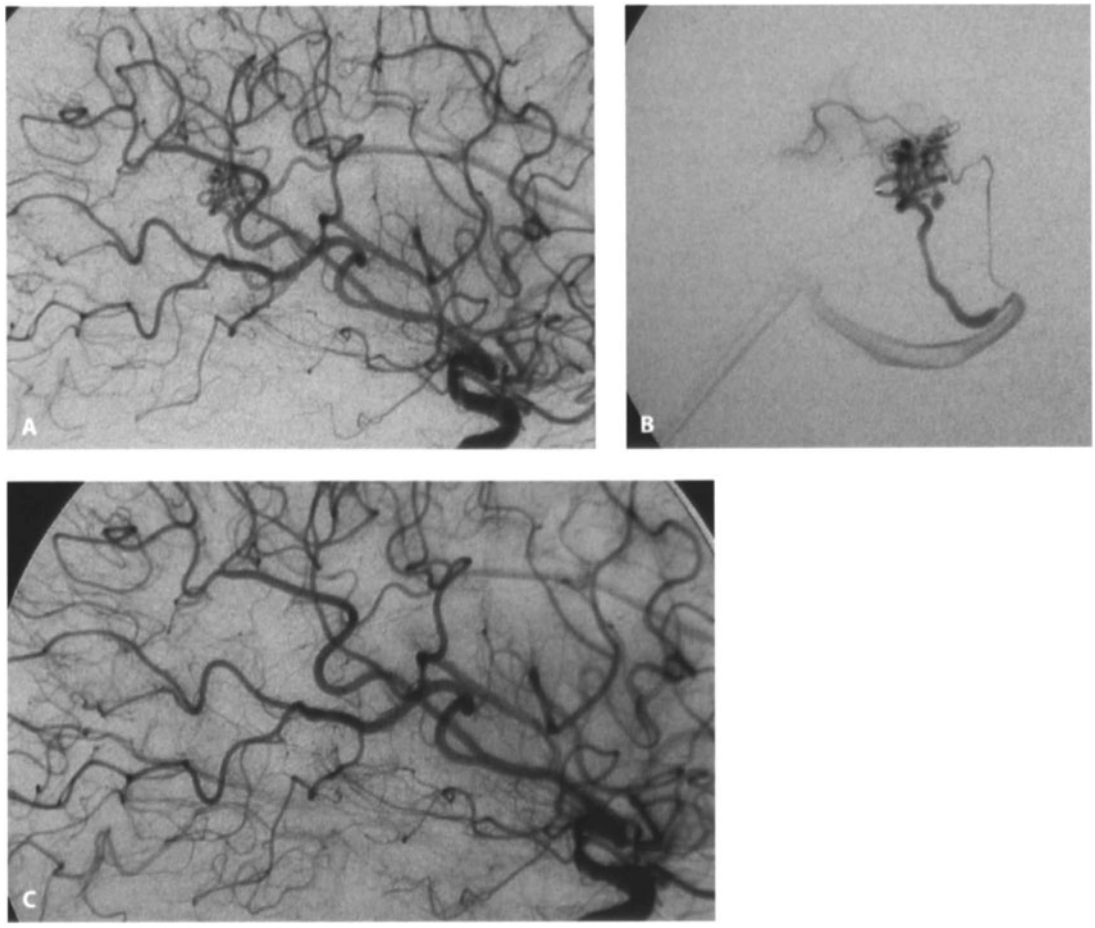

Fig. 7.119. Intracerebral hematoma from a small ruptured arteriovenous malformation (**A**). Selective injection shows a typical false sac (**B**), which was embolized with glue (**C**)

◀ **Fig. 7.118A–F.** Cerebral arteriovenous malformation (AVM) associated with AComA aneurysm. **A** Right internal carotid artery (ICA) injection shows the frontal-insular AVM. **B** Axial T2-weighted MRI. **C** Left ICA shows a large flow-related aneurysm. **D–F** Angiographic and MRI follow-up after partial embolization of the AVM. Note the remodeling of the aneurysm wall in response to the AVM embolization

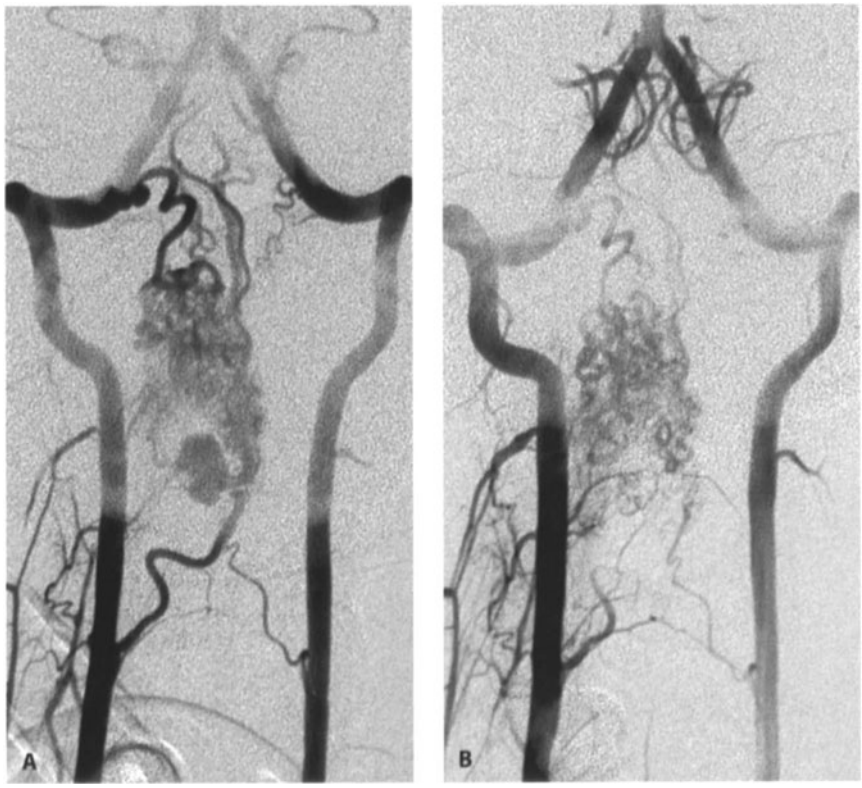

Fig. 7.120. Typical arterial aneurysm associated with a spinal cord arteriovenous malformation (**A**). It is located on the radicular portion of the artery. This is an angioarchitectural feature often seen with repeated subarachnoid hemorrhages, which here has been treated with specific partial targeted embolization (**B**)

7.7.1 Intradural Traumatic Arterial Aneurysms

Intradural traumatic aneurysms are rare and most commonly involve the internal carotid and vertebral arteries at their transdural portions (Figs. 7.122, 7.123). Vascular injury can be a fatal complication of third ventriculostomy. The anatomical changes created by a posterior fossa mass lesion may modify significantly the mesencephalodiencephalic region and predispose these patients to vascular injury at the time of ventriculostomy (Fig. 7.66) (Lenthall et al. 1999).

Two iatrogenic aneurysms in a previous series (Laughlin et al. 1997) were treated with endovascular coils. One of these patients had a basilar aneurysm following third ventriculostomy for hydrocephalus secondary to a cerebellar astrocytoma. Such aneurysms can be treated by endovascular means, with the understanding that they are in fact pseudo-AAs. In Lenthall's case, a trauma related basilar tip aneurysm proved to be asymptomatic and morphologically stable for 2 years. The natural history of such a lesion is unknown and it appears unlikely that this type of residual traumatic aneurysm would disappear with remodeling after 2 years.

Other intradural traumatic AAs include the PCA fusiform AA, in which microtrauma along the tentorium may produce subacute or chronic dissection (Fig. 7.80). Similarly, traumatic AAs have been described as involving the ACA along the falx and the tentorium, either following major head injuries (Fig. 7.67) or as part of the shaken baby syndrome. Minor physical exercise often precedes intracranial ICA dissection associated with stroke in children. Those present in the P2–P3 segment may present later in life as mass effect.

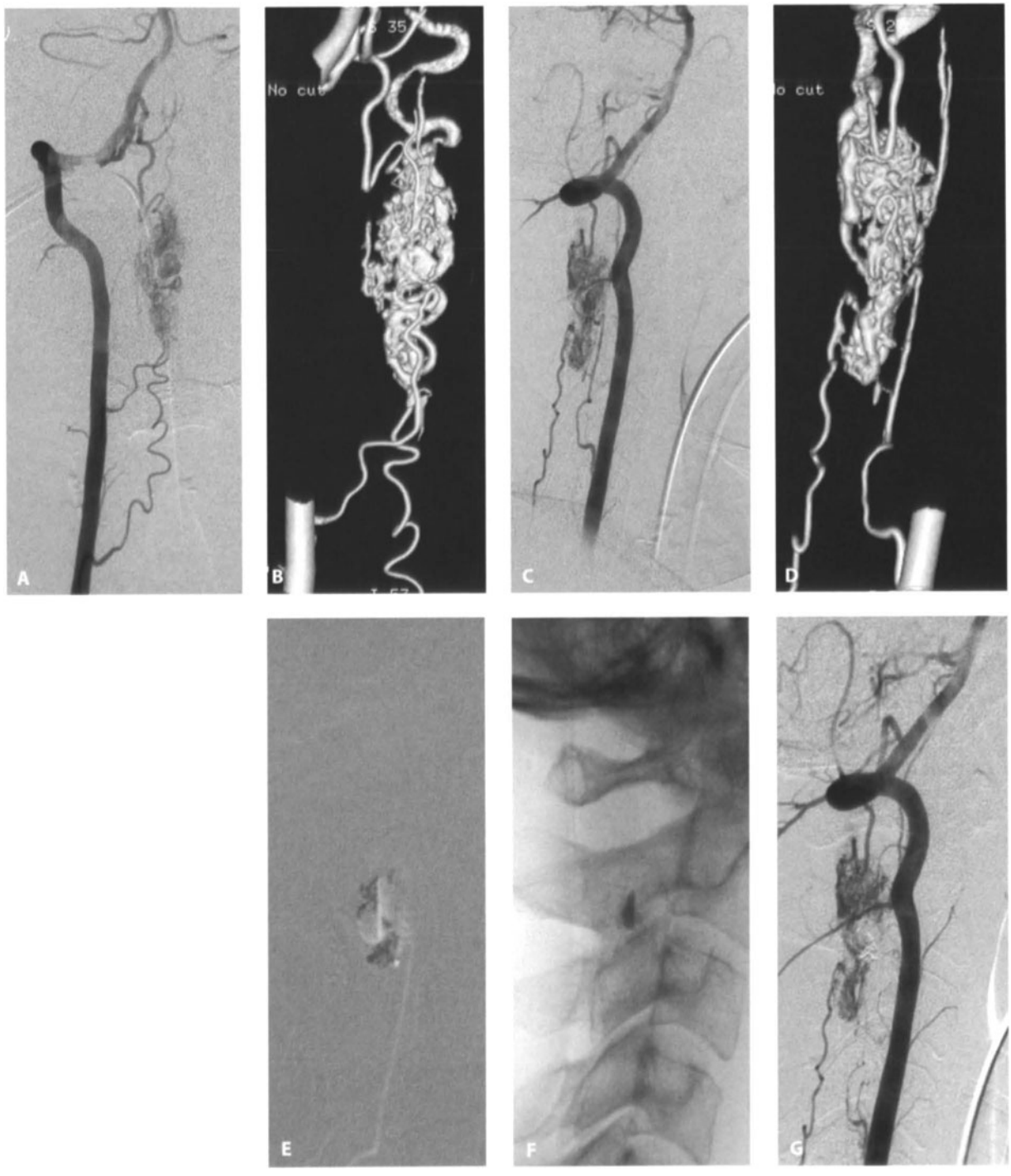

Fig. 7.121A–G. A 23-year-old male patient presented with hematomyelia from a cervical spinal cord arteriovenous malformation. Note on the angiogram and 3-D image the intranidal aneurysm in the depth of the central sulcus. **A, B** Frontal views, anterior and posterior surface reconstructions. **C, D** Angiogram and 3-D digital subtraction angiogram: lateral views, right and left surface reconstructions. **E–G** Lateral views. Targeted glue embolization through a pial branch of the anterior spinal artery selectively excluded the aneurysm pouch. Note the fluid level on the plain film. The patient remained asymptomatic

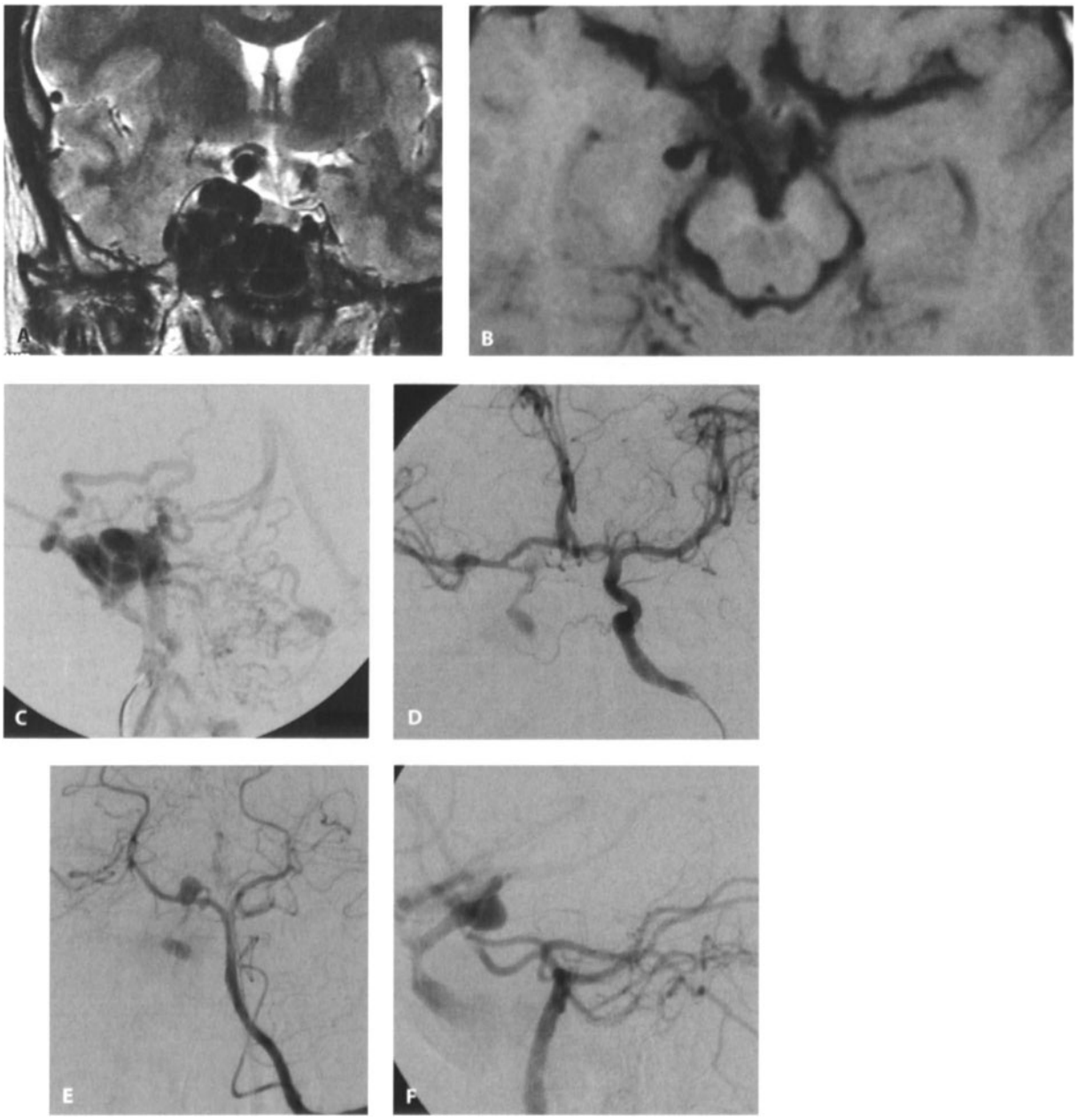

Fig. 7.122. **A, B** MRI of patient with previous history of severe motor vehicle accident (MVA). Evidence of carotid cavernous fistula (CCF) with intradural chronic flow-related aneurysm, or healed traumatic dissecting aneurysm. **C–F** Pre-embolization angiograms. **G–L** see p. 521

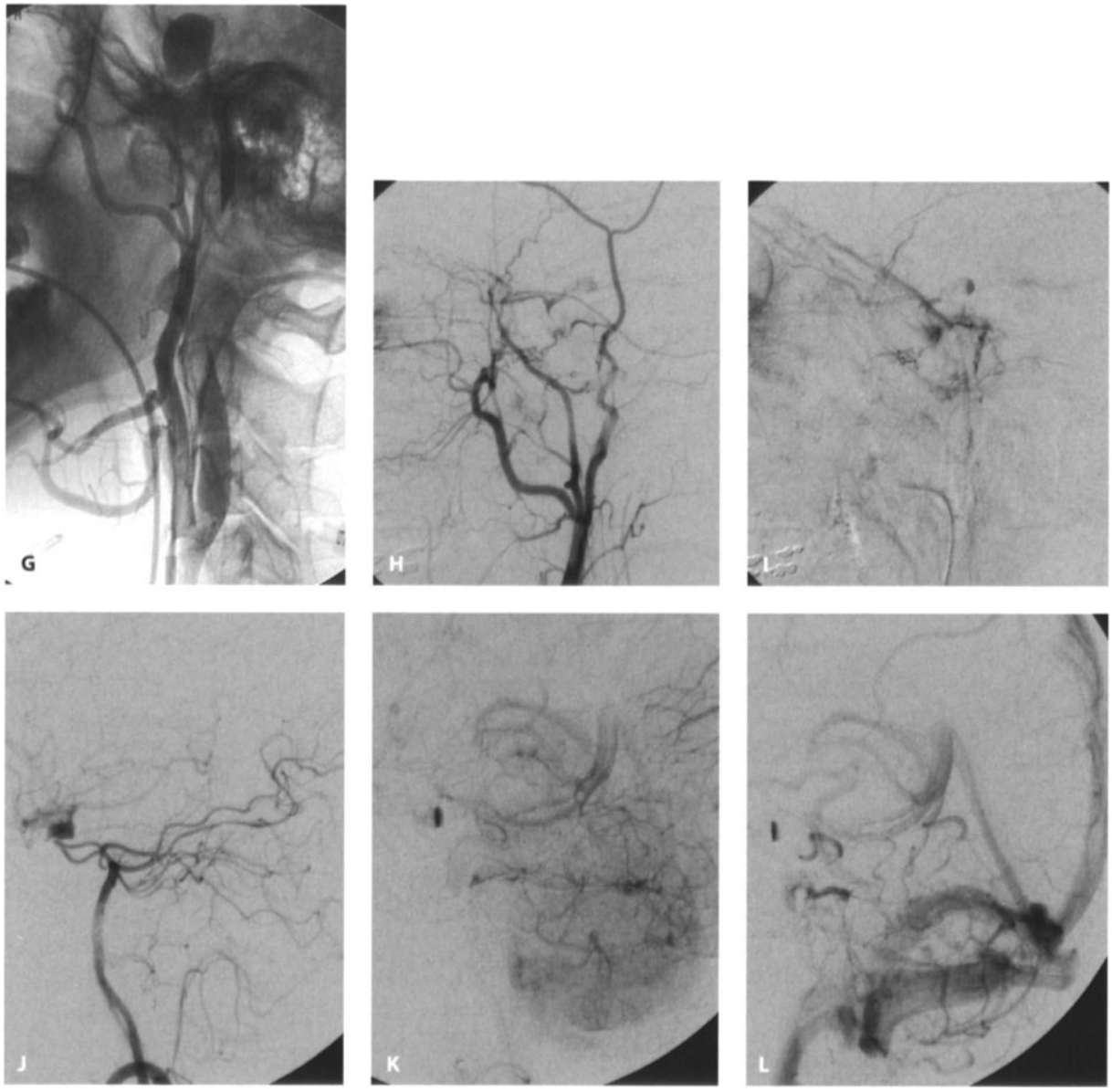

Fig. 7.122 (*continued*). **G–I** Postembolization angiograms in the common carotid. The internal carotid artery was sacrificed with detachable balloons, including stumpectomy. Note the stagnation in the aneurysm as soon as the CCF was treated. **J–L** Postembolization vertebral artery angiograms. Note the stagnation in the arterial pocket also demonstrated via the PComA. (Courtesy of S. Pongpech)

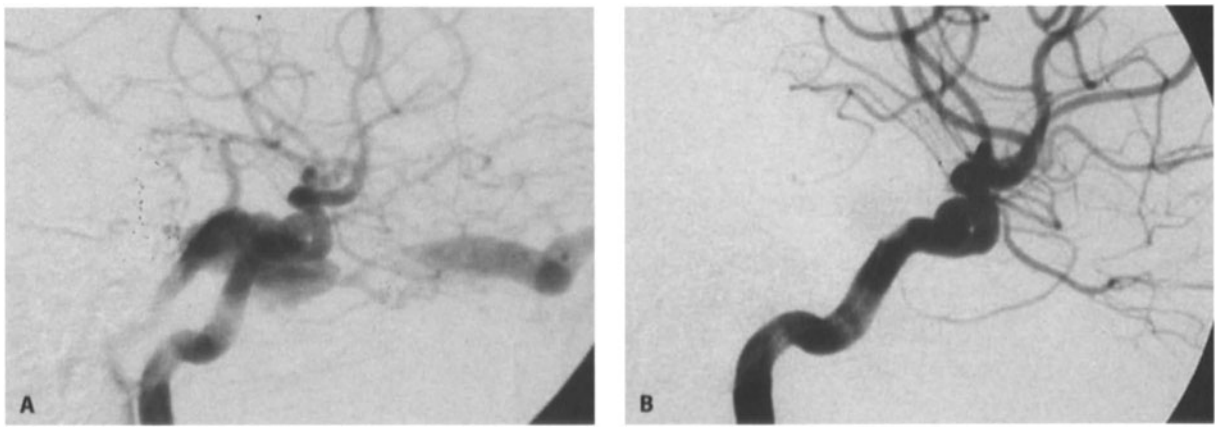

Fig. 7.123. Traumatic carotid cavernous fistula (CCF) associated with an intradural internal carotid artery aneurysm at the acute stage (**A**). The lesion is clearly seen after the CCF embolization (**B**). (Courtesy of S. Pongpech)

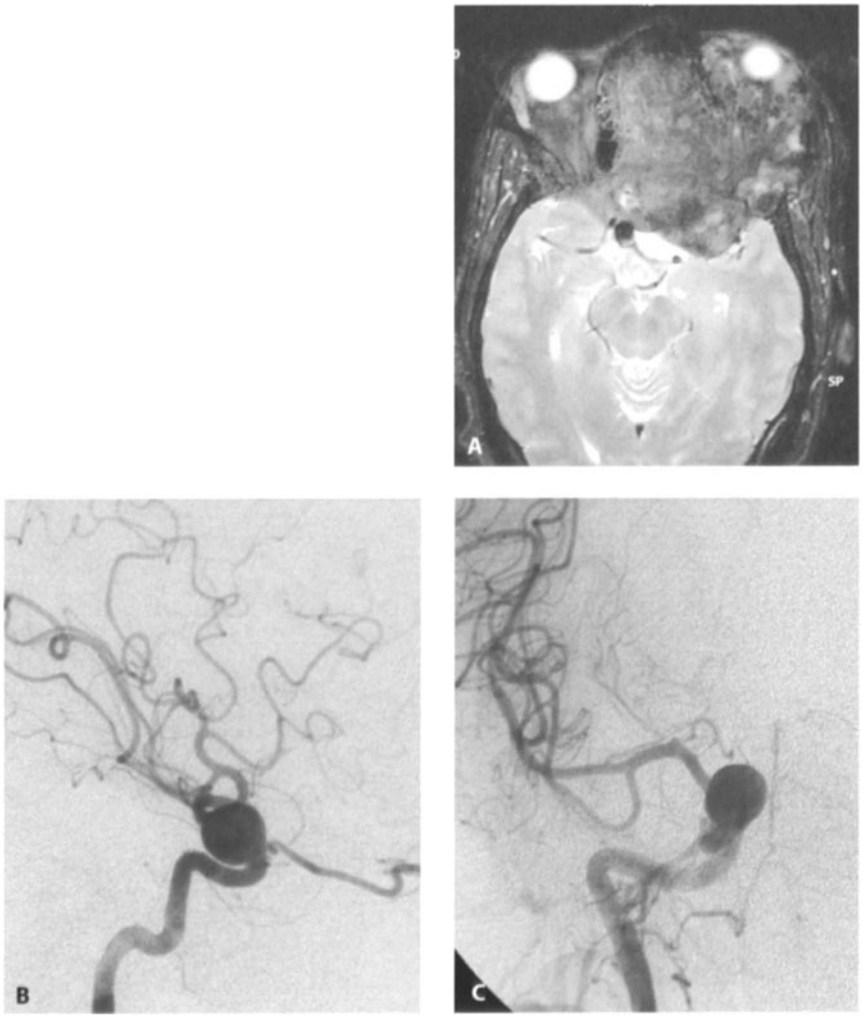

Fig. 7.124A–C. McCune Albright syndrome. A 50-year-old male patient with heterozygotic α thalassemia, frontal fibrous dysplasia. Surgery was performed at the age of 30, 40, and 45 years. Left-sided blindness, acromegalia, and hypertension by renal artery stenosis. Incidental discovery of an internal carotid artery aneurysm during pituitary screening

7.7.2 Arterial Aneurysms Associated with Proliferative Diseases

The simultaneous occurrence of a cerebral AA and a brain tumor is rare (Gibbon and Brookes 1967; Edner and Feuerberg 1984; Weir 1987). With few exceptions, the coexistence of an AA in a patient with a brain tumor appears random (Fig. 7.124). This may complicate the approach to both lesions. Children with neurofibromatosis carry a 12% risk of harboring a brain tumor: an optic glioma is the most common. Edner and Feuerberg (1984) reported the case of a 23-year-old man with neurofibromatosis combined with an optic glioma and a ruptured aneurysm. AAs and hemangiomas are encountered in the PHACE syndrome. They usually involve embryonic arteries of the ECA system (Figs. 7.23, 7.127).

Atrial myxomas are neoplasms thought to be derived from pluripotential subendocardial mesenchymal cells (Fig. 7.125). They are more common in women and have no familial preponderance (Tazelear et al. 1992). Emboli composed of tumor, blood clot, or both lodge in cerebral vessels and cause cerebral infarction. Stoane et al. (1996) demonstrated arterial filling defects and focal dilatations at cerebral angiography in two patients with atrial myxomas, and showed an increase in the size of the aneurysms

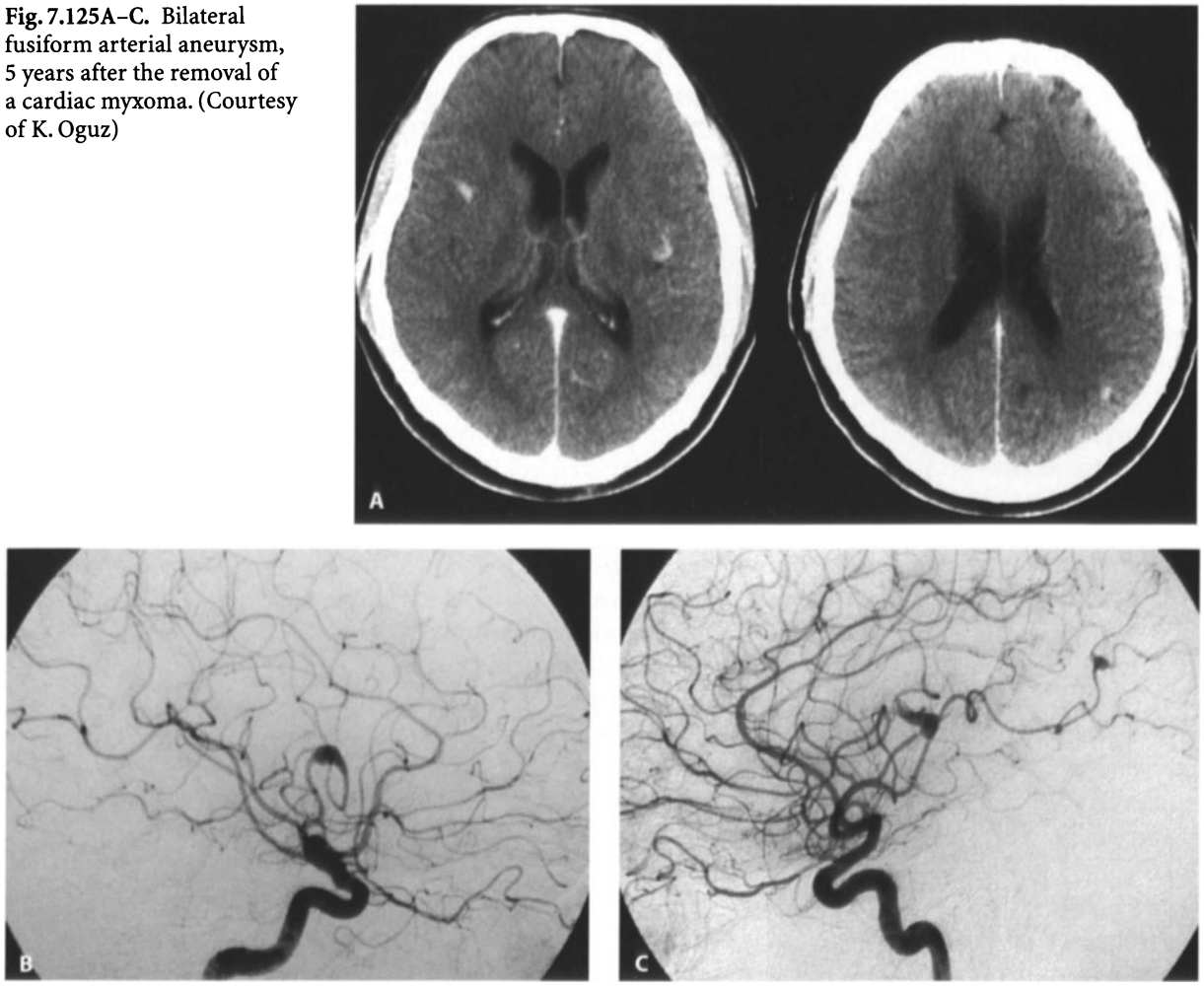

Fig. 7.125A–C. Bilateral fusiform arterial aneurysm, 5 years after the removal of a cardiac myxoma. (Courtesy of K. Oguz)

2 months after the removal of the cardiac tumor in one patient (Fig. 7.125). Burton and Johnston (1970) showed invasion and proliferation of the myxomatous tissue replacing the vessel wall of a dilated artery. According to Price et al. (1970), aneurysms are the result of tumor material that lodges and grows in situ, invading the intima and media of the vessel wall. Aneurysm growth may continue up to 5 years after removal of the atrial myxoma (Oguz et al. 2001).

Metastatic disease from different primary locations has been seen associated with AAs, but this is rare. Metastatic tumoral colonization of the cerebral vessel wall is often implicated but remains mostly unproven.

AAs are not infrequently seen following radiation treatment of patients treated for head and neck cancers. Superficial uncovering of the ICA and life-threatening hemorrhages may occur and require emergent endovascular management.

7.7.3 Arterial Aneurysms with Congenital Heart Disorders and Coarctation of the Aorta

Intracranial aneurysms and cervicocephalic arterial dissections in pediatric and adult patients can be associated with a variety of congenital heart disorders.

The mean age at the time of diagnosis of the cerebrovascular abnormality was 32 years (range, 13–58 years). Congenital heart disease may consist of complex cardiac anomalies in 20% (truncus arteriosus, transposition of the great arteries, and tricuspid atresia in one patient each), pulmonic valve or arterial stenosis (12%), aortic coarctation (23%), and bicuspid aortic valves (30%).

In 80% of cases, the diagnosis of congenital heart disease preceded the diagnosis of intracranial aneurysm or arterial dissection. None of the intracranial aneurysms were located in the distal vasculature. Half of the aneurysms were saccular and unremarkable in configuration (Schievink et al. 1996).

Coarctation of the aorta (CoA) is a rare disorder; cerebral AAs occur in 3% of patients with CoA. Conversely, CoA is encountered in 1.2% of all AA patients (Fox 1983). Ten percent of CoA patients die from SAH, a high mortality rate from this aspect of the disease, compared to the mortality rate for cardioaortic problems; 74% of patients die before age 40. The AAs are located at the same sites as common saccular AAs and they are often multiple (30%). The incidence of all forms of aneurysm formation in aortic coarctation markedly increases with age, up to 42% in patients over the age of 40. Feng and Yu-Hai report a case of aortic arch interruption with myelopathy and multiple aneurysms of the radicular arteries and the distal vertebral artery (Feng and Yu-Hai 1994) presenting with acute SAH. Ruptured aneurysms at the circle of Willis are seen in 10% of patients with coarctation of aorta (Baysal et al. 2000), whereas associated spinal artery aneurysms were sparsely reported (Damon et al. 1996; Rengachary and Derek 1993).

Aneurysmal SAH has occurred many years after successful surgical repair of the coarctation, and a generalized structural abnormality of

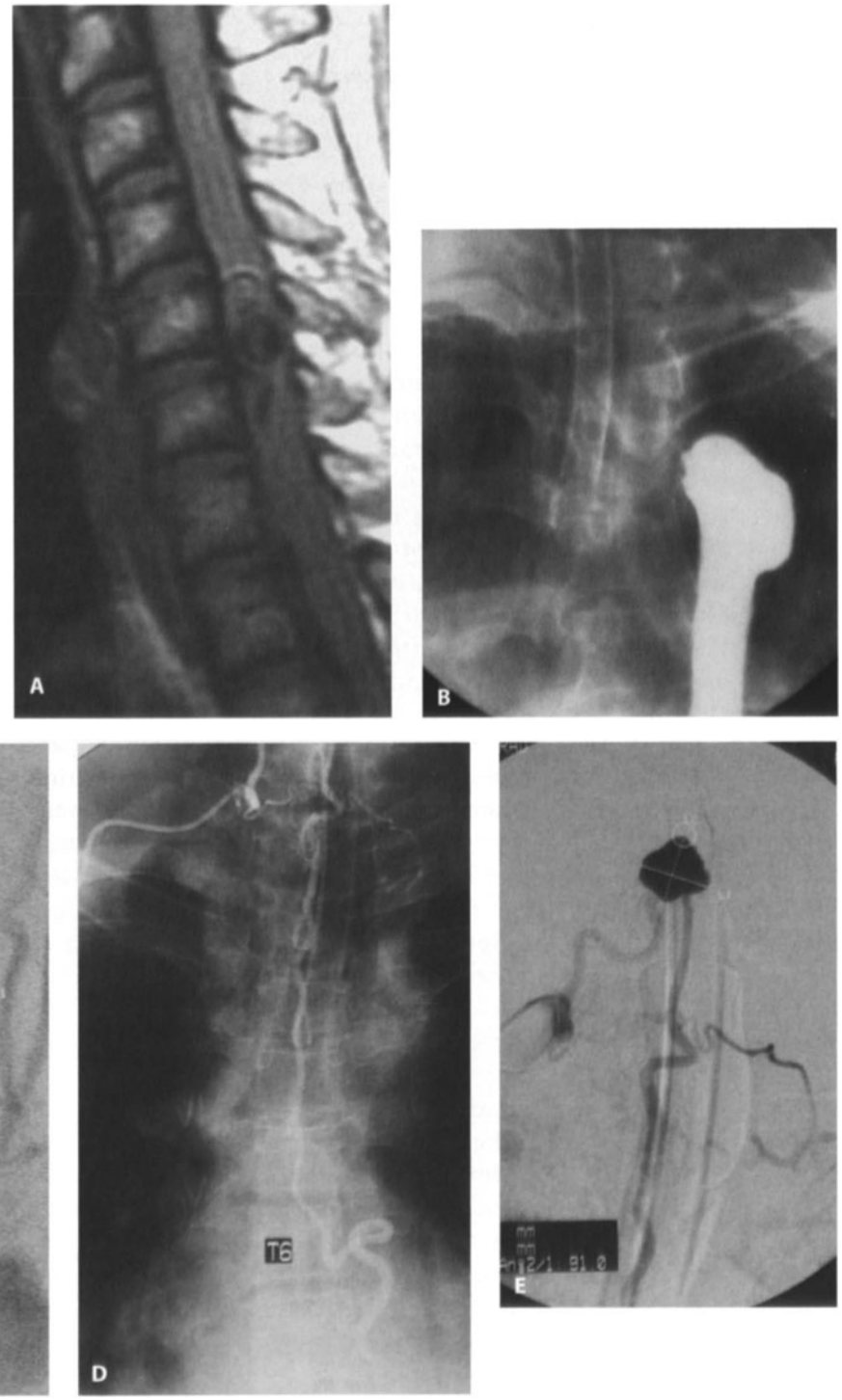

Fig. 7.126A–E. A 39-year-old male presented with acute headache and neck pain, followed by quadriparesis and quadriparesthesia. **A** Lumbar puncture showed subarachnoid hemorrhage. **B** Angiogram by right axillary approach revealed severe coarctation of the aorta between the left common carotid artery and left subclavian artery. **C–E** Multiple collateral including an enlarged anterior spinal arterial axis were noted to bridge the stenotic arch to the abdominal aorta. A small lobulated aneurysm was seen on the radiculomedullary anterior spinal artery junction with the right ascending cervical artery. The patient underwent successful surgical clipping of the aneurysm. (Jiarakongmun et al. 2002)

the arterial system has been implicated in these patients (Gardiner et al. 1994).

The coexistence of aortic coarctation and intracranial aneurysms associated with hypertension is impressive and some researchers have argued that hypertension alone might be responsible for this association (Stehbens 1989). The association of aortic coarctation and intracranial aneurysms

suggests an abnormality of the neural crest as a possible common embryological pathogenic factor (Schievink et al. 1996; Lasjaunias 2000a).

The neural crest contributes to both the left and right cardiac ventricular outflow tracts, and the neural crest has been implicated in the development of bicuspid aortic valve and coarctation of the aorta as well as in pulmonic valve stenosis (Kappetein et al. 1991) and pulmonary artery stenosis. Its impact in the PHACE syndrome is also highly probable (Hino et al. 1989).

Caroscio et al. (1980), in a review of the literature up to 1980, found that there were 12 patients with arterial dilatation of the spinal arteries associated with coarctation of the aorta (Fig. 7.126); there were only three isolated aneurysms out of all 30 aneurysm cases. Intercostal aneurysms have also been reported in up to 10% of patients with aortic coarctation; subclavian aneurysms are another rare associated finding.

Pathogenesis of the spinal AA associated with coarctation of the aorta appears as a result of hemodynamic stress from high blood flow for collateral circulation through the anterior spinal axis rather than segmental arterial disease or angiodysplastic disease. Multiple collaterals contribute flow to the contralateral subclavian artery and descending aorta below the coarctation, including the intercostal artery, the internal mammary artery, the bronchial artery, the internal carotid artery, and the vertebrobasilar system via the circle of Willis and uncommonly the spinal arterial axis. In fact, there are also some case reports of AAs along the other collateral pathways of a different embryological origin such as the intercostal artery, subclavian artery, and the circle of Willis, as mentioned above. Kawamura et al. (1999) reported a case of spinal AA associated with bilateral vertebral arterial occlusion, whereas the vertebrobasilar system was supplied by the enlarged anterior spinal axis. These reports support the argument that spinal artery aneurysms along the collateral pathways for arterial occlusion belong to the flow-related group of aneurysms (Jiarakongmun et al. 2002) (Fig. 7.126).

A special mention should be made of the PHACE_syndrome. Even though cerebral AAs are not part of the acronym, they are often present. In this syndrome, the malformation seems to involve the apoptotic system with a lack of arterial regression, arterial wall proliferation, and unsuppressed angiogenesis. The combination of lesions resulting from malformations and proliferative activity makes PHACE syndrome a singular entity within the group of vascular diseases (see Vol. 3) (Fig. 7.127).

Aortitis syndrome is a systemic vasculitis of unknown etiology that mainly affects the aorta, its major branches, and the pulmonary artery. The syndrome occurs predominantly in relatively young Asian women. To date, only 16 cases of aortitis syndrome associated with intracranial AA have been reported, with a total of 25 aneurysms. Cerebral angiography was not performed because of the bilateral absence of arterial pulsation in the groin regions (Asaoka et al. 1998). Encephalopathy associated with the aortitis syndrome usually presents as cerebrovascular insufficiency caused by stenosis or occlusion of the major branches of the aorta and a hypersensitive carotid sinus reflex. Patients aged 40–60 years made up 81.3% of this group.

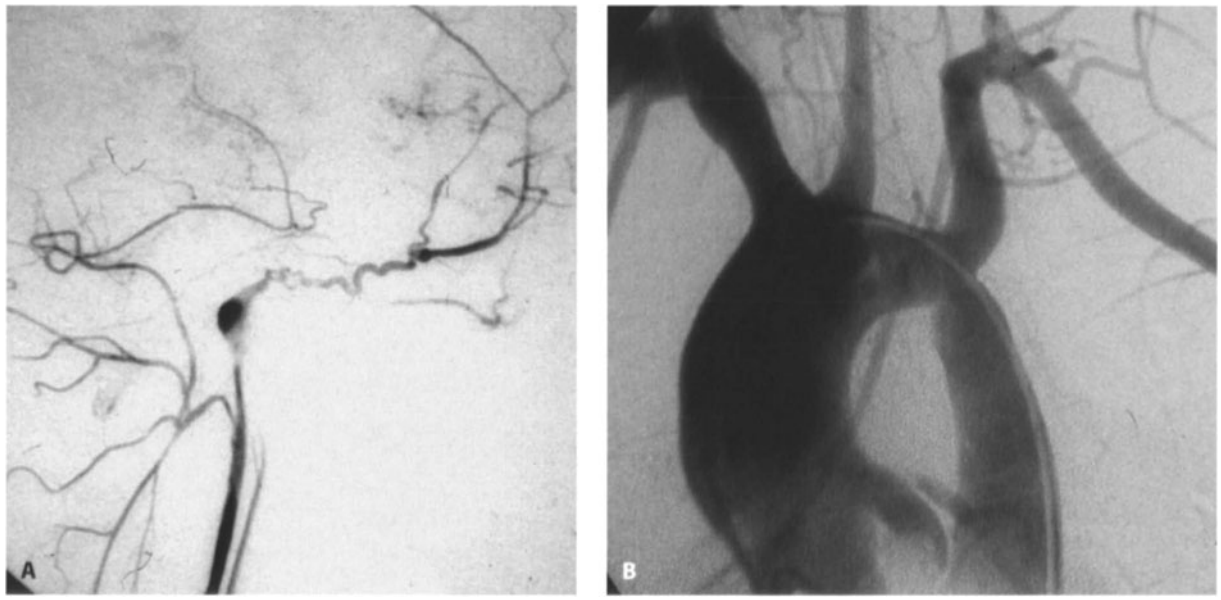

Fig. 7.127. **A** Intratympanic ascending pharyngeal artery aneurysm (aberrant ICA flow) associated with aortic coarctation (**B**) in a child with PHACE syndrome

There is an almost 30-year gap between the manifestation of aortitis syndrome (with the peak age in the 20s) and the development of cerebral aneurysms. Woman represented 93.8% (15/16) of all cases in this series. The vertebral artery is less often affected than the common carotid artery in this syndrome and functions as collateral flow to compensate for decreased cerebral blood flow. Of the patients diagnosed as having cerebral aneurysms after presenting with SAH, 43.8% exhibited multiple aneurysms. In 81.3%, the real incidence of AA in aortitis syndrome is not known (Asaoka et al. 1998).

7.8 Therapeutic Management

7.8.1 Introduction

Treatment of AAs is based on preventing hemorrhage or rebleeding, with preservation of the cerebral arterial supply. This goal may imply various techniques and approaches that will not include the treatment of SAH, ICH, or ventricular drainage, all beyond the scope of this book. AA exclusion, parent vessel occlusion, flow correction, or the use of biologically active substances make up the currently available tools (see Chap. 1, this volume). Their indications and mastery require experience and training. All AAs are not the same and while the overall desire is the prevention of rebleeding, the risks involved in the treatment must be balanced against the risk of each situation, if this can be predicted.

Mycotic AAs, giant lesions, dissecting AAs in ED type IV, traumatic dissection with emboli, unruptured berry AAs, multiple AAs with SAH, distal false AAs, AAs associated with BAVM are all situations that will require

special care in order to achieve the goal at the lowest acceptable risk. However good the intention may be, a therapeutic risk higher than the anticipated natural history of the specific lesion is unacceptable. Yet many diseases are being discovered within the generic name of intradural AA; therefore, further adjustments are to be expected in the future to more accurately tailor the figures pertaining the acceptable level of therapeutic risk.

Various therapeutic techniques apply to AA treatment and will be discussed in Chap. 14:

1. Exclusion of the AA with parent artery preservation is obtained with endovascular coils (Fig. 7.52), surgical clips (Fig. 7.144), endoluminal stent (Fig. 14.92), and liquid agents (Fig. 7.42).
2. Parent vessel occlusion is obtained with a balloon (Fig. 7.9), coils, glue, or a clip (Fig. 7.71).
3. Hemodynamic correction is stimulated by remote balloon occlusion (Fig. 7.123), with or without by-pass (Fig. 7.32), ligation, AVS, or glue occlusion in associated AVMs, and AAs (Fig. 7.118).
4. Pharmacological support can be offered with heparin in clot formation or antibiotics.
5. Coated devices (see Chap. 14, this volume).
6. Combinations of these tools (see Chap. 14, this volume).

As illustrated in the analysis of the AA vasculopathies, the mechanical approach to AA is still simplistic, albeit the best one available at the present time. Since the morphological goal is derived from this, the overall approach should therefore not be considered satisfactory nor definitive. As an acceptable approximation before being more accurate in the treatment it should be realized that the clinical outcome should guide the treatment decision strategies.

During the first year of Gugliemi detachable coils (GDCs), indications for use were restricted to nonsurgical AAs. Since then, all intradural AAs felt to be both surgical and embolizable have been embolized. From the authors' accumulated experience, it is clear that GDC coiling of properly selected AAs, with the help of remodeling in a few rare cases (less than 5% of cases in our experience) (see Chap. 14, this volume), offers a better outcome for both ruptured and unruptured AAs than classic surgery, in terms of operative morbidity, mortality, as well as bleeding protection. This has been confirmed by Molyneux (2002) and recommended by Johnston et al. (2002). Both clinical and morphological follow-up confirmed the protection for future hemorrhage and the stability of the results obtained beyond 5 years (Tables 7.42–7.45) (Batista et al. 2002).

For AAs where complete occlusion was achieved at immediate angiogram, long-term stability was obtained if stable at the 1-year follow-up angiogram; further angiogram follow-ups do not seem justified in this group. In AAs with immediate subtotal occlusion where complete occlusion was achieved after secondary spontaneous thrombosis at 1-year angiogram follow-up (27.6% in our series), long-term stability was always obtained and confirmed; further follow-up angiograms also do not seem justified in this group. AAs that showed loss of morphology at 3 months or 1 year, had to be re-embolized and followed up according to the date of

Table 7.42. Morphological changes: 10/53 AAs in 45 patients. Immediate completely occluded AA (from Batista 2002, with permission)

Occluded on follow-up (%)	100%	99–90%	89–80%	<80%
Immediate occlusion	10	–	–	–
1 year	8	1	1 r	
3 years	8+1	1 r	–	–
5 years	8+2	–	–	–
Total	10			

r, Re-embolized AA; underlined AA, stability over 3 consecutive years of follow-up.

Table 7.43. Morphological changes: 35/53 AAs in 45 patients. Immediate subtotally occluded AA (from Batista 2002, with permission)

Occluded on follow-up (%)	100%	99–90%	89–80%	<80%
Immediate occlusion	–	35	–	–
1 year	18	3	11 r	3 r
3 years	18+4	2+4	4+1 r	2 r
5 years	18+5	2+3	4+1	2[a,b]
Total	23	5	5	2

r, Re-embolized AA; underlined AA, stability over 3 consecutive years of follow-up.
[a] Recommended re-embolization refused by patient.
[b] Patient referred to surgery with good results.

Table 7.44. Morphological changes: 8/53 AAs in 45 patients. Immediate partially occluded AA (from Batista et al. 2002, with permission)

Occluded on follow-up (%)	100%	99–90%	89–80%	<80%
Immediate occlusion	–	–	8	–
1 year	2	1	4	1 r
3 years	2	1+1	2	2 r
5 years	2	1+1	2+1	1
Total	2	2	3	1

r, Re-embolized AA; underlined AA, stability over 3 consecutive years of follow-up.

the second intervention. If immediate occlusion is less than 80%, a second intervention is required.

These observations and protocols in the Batista et al. series (2002) are valid when there are multiple AAs (37.2% in their series). In this series, no bleed or rebleed was observed during the follow-up period.

This was observed in a population of patients whose saccular intradural AAs were in the great majority less than 10 mm in size, with a neck smaller than 4 mm. AA topography and Hunt and Hess grading for the ruptured AAs were similar to most surgical series; none of these AAs were suggestive of giant, inflammatory, fusiform, or dissecting AAs, nor were they flow related.

There is clearly little benefit in comparing the interventional teams' "immediate 100% rate of exclusion" before comparing the therapeutic risks involved and the populations concerned without 3 years of follow-up.

Table 7.45. Selected literature review of endovascular treatment for intracranial aneurysm

Authors	*n*	SucEmb	Rupt	Location	%Btip	Mb (P/T)	Mt	100%E	Angiographic follow-up		Clinical follow-up		Bleed or rebleed
									Mean duration	Recan	Mean duration	GOSm <1–2	
Lempert et al. (2000)	112	97% (109/112)	100%	P	49%	2.8/7.3	0	54%	7.2 months	1.8% (overall, 22.4%)	13.1 mo.	83%	0.9% (1/109)
Debrun et al. (1998)	144	86.1% (124/144)	38.2%	A+P	19.7%	1.6/5.6 (perf, 2.4%)	0	72.6%	Up to 2 years	4% (overall, NA)	Up to 2 years	90%	1.8% (1/55)
Fuse et al. (2000)	203	88.7% (180/203)	66%	A+P	20%	3/11.6 (perf, 1.9%)	0	61%	>1 year	NA	>1 year	85.6%	0.6% (1/180)[a]
Raymond et al. (1997)	75	96% (72/75)	100%	A+P	32%	4/14.7 (perf, 4.0%)	4.0	40%	>6 mo	NA (overall, 16%)	6 months	76.0%	5.3% (4/75)
Cognard et al. (1998)	208	86% (182/208)	72.1%	A+P	N/A VB, 16%	4/8 (perf, 2.9%)	2.2	57%	Up to 41 months	9.1% (overall, 14%)	19 months	76.6%	0.5% (1/182)
Byrne and Molyneux (1999)	317	100%	100%	A+P	24%	NA	NA	63.7%	6–12 months	13.9%	22.3 months	81.5%	1.2% (4/317)
Malisch et al. (1997)	100	100%	53%	A+P	28.8%	NA	NA	NA	NA	NA	3.5 years	78%	5.8%§ (1.2%)[d]
Kuether et al. (1998)	74	100%	40%	A+P	29%	NA (TE, 6.5%, perf, 2.1%	6.4	40%	1.4 years	36.8%	2.2 years	80%	2.9%§ (2/70)

Table 7.45 (*continued*)

Authors	*n*	SucEmb	Rupt	Location	%Btip	Mb (P/T)	Mt	100%E	Angiographic follow-up		Clinical follow-up		Bleed or rebleed
									Mean duration	Recan	Mean duration	GOSm <1–2	
Vinuela et al. (1997)	403	94.3%	100%	A+P	31.5%	9.18/NA (perf:2.7%, TE, 2.5%)	1.74	49.9%	6 months	NA	6–36 months	NA	2.2% (9/403)
Gruber et al. (1999)	21	100%	52.4%	P	100%	9.5/NA	0	66% (>95%)[c]	>6 months	NA (80% in <90% occl)	26 months	90.5%	0
Raymond et al. (1997)	32	96.9% (31/32)	74%	P	100%	3/22.6 (perf, 6.5%)	3	42%	>6 months	NA (29% in wide neck)	16.8 months	83%	0
Eskridge et al. (1998)	159	94.3% (150/159)	55.3%	P	100%	NA (TE, 22.6%)	NA	75% (≥90%)[c]	6 months	NA	13.7 months	78.2%	4.7% (4/84)[b]

SucEmb, successful embolization; Rupt, percentage of ruptured aneurysm; An, aneurysm; Mb, % procedure related morbidity; P/T, permanent/transient; perf, perforation during the procedure; TE, thromboembolic complication; Mt, % procedure-related mortality; 100%E, complete obliteration on discharge; Recan, percentage of recanalization in completely obliterated aneurysm; GOSm, score of (modified) Glasgow Outcome Scale; Rebleed, overall + percentage of rebleeding from ruptured aneurysm; PC, posterior circulation; AC, anterior circulation; %Btip, percentage of basilar tip aneurysm; NA, not available, VB, vertebral artery; occl, occlusion.

[a] Ruptured AA recurrent after two embolizations, scheduled for surgery; patient refused treatment and bled.

[b] Three of four were giant AAs.

[c] 100% occlusion rate is not available but occlusion rate over certain percentage is available.

[d] Rebleeding rate after exclusion of giant aneurysm.

[e] Described as a subarachnoid hemorrhage after Gugliemi detachable coils (GDC), no rebleeding.

Compaction rates, regrowth, and de novo lesions need to be documented to avoid emotional consideration and rapid judgment (Figs. 7.138, 7.139, 7.149). Operator-dependent factors should not be forgotten, nor economical issues that will further modify the therapeutic management in a given situation. One should also realize and document decisions that certain untreated AAs could possibly be treated elsewhere, by another technique or by somebody else.

7.8.2 Method

Among the criteria used to choose embolization over a surgical approach or even conservative treatment were appropriate vascular characteristics for a safe endovascular approach, a clear working projection for optimal visualization of the AA neck, appropriate AA size-to-neck ratio (Fig. 7.128), and AA size-to-parent-artery-diameter ratio. For ruptured AAs, the lesions should be treated as rapidly as possible after the diagnosis of SAH has been made. Whenever possible, the treatment should take place at the same time as the diagnostic angiography, as a continuation of the same procedure. Ruptured aneurysms are considered appropriate for embolization according to morphological criteria, irrespective of the grade on admission. Surgery is performed if the patient is considered a poor candidate for embolization, or if the attempted endovascular procedure fails. Size (Figs. 7.128, 7.129), shape, multifocality, distribution within a possible surgical field, neurological status, and family history are taken into consideration in the indications for unruptured aneurysms. Giant, traumatic, mycotic, or dissecting AAs are not considered for primary endovascular treatment if exclusion of the lesion cannot be obtained with preservation of the parent artery.

Since the late 1990s, 3-D angiography has been used by the authors (Siemens or GE Advantix LCN+, SUN workstation) to evaluate all aneurysms. This includes volume and surface rendering as well as virtual endoscopic views (Fig. 7.130, p. 534); it provides a very precise delineation of the AA and optimal analysis of its neck and characteristics (Fig. 7.95). Detailed analysis of the rest of the arterial tree is crucial both to disclose other AAs and to understand the general vascular anatomy involved. Angio-CT and MRA (Figs. 7.105, 7.131, p. 535) remain insufficient to fully appreciate the lesion, the associated AA, the position, etc. Architecture of the ruptured AA is analyzed to find the precise rupture point of the AA, indicated by a false or pseudoaneurysm, or suggested by multilobulation (see Sect. 7.8.4; Fig. 7.132, p. 536).

All procedures are carried out under general anesthesia. After femoral puncture, a 5- to 6-F guiding catheter is positioned in the main arterial trunk harboring the aneurysm (internal carotid or vertebral artery) and the patient is given a bolus of intravenous heparin (50 IU/kg) followed by an infusion to maintain full heparinization (500–1,000 IU/h). For ruptured AAs treated at the acute stage, heparin is preferentially started after deployment of the first coil into the AA cavity.

The lesion is approached under fluoroscopy and road mapping. All ruptured cases are embolized with GDC-10 coils. GDC-18 coils are used

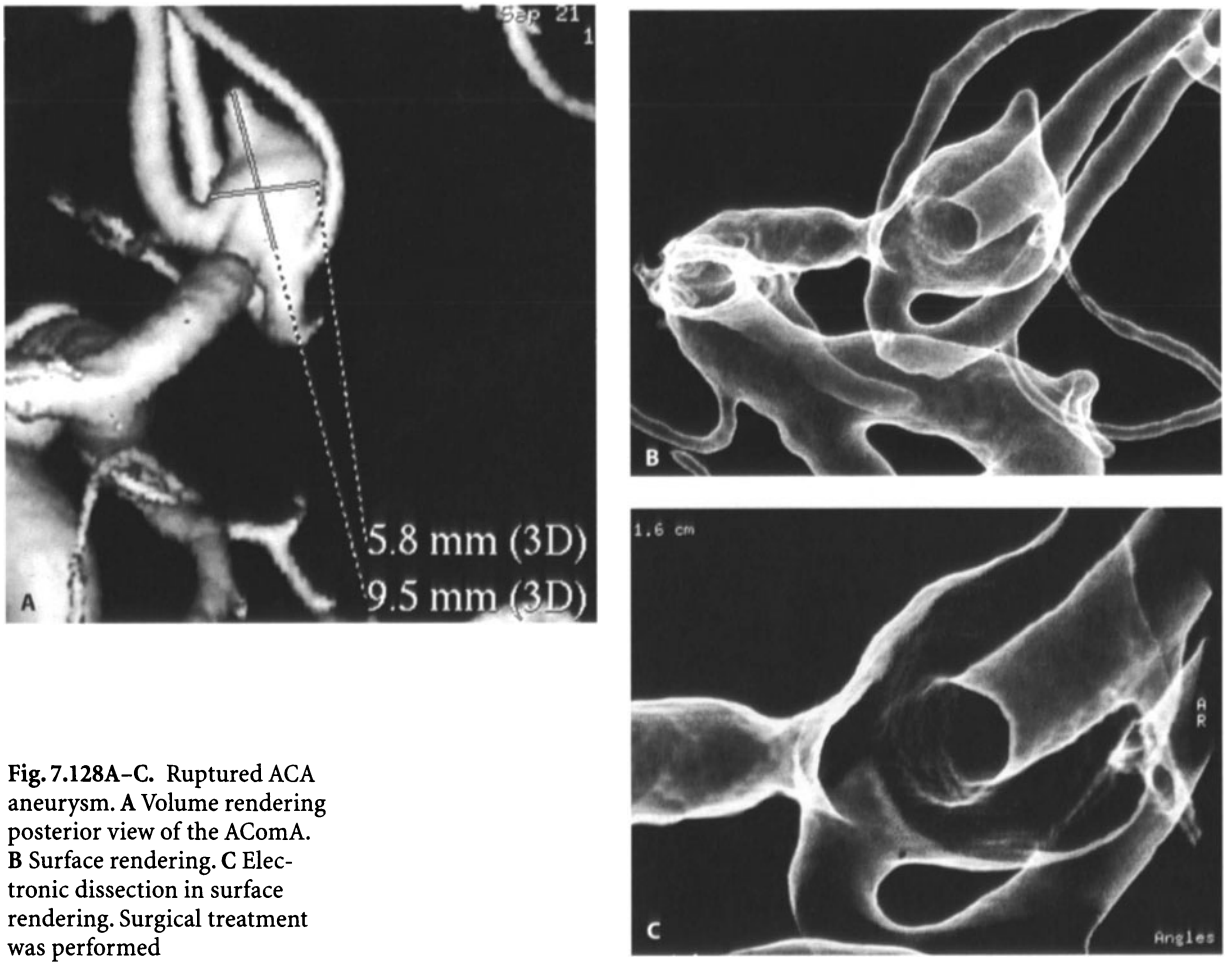

Fig. 7.128A–C. Ruptured ACA aneurysm. **A** Volume rendering posterior view of the AComA. **B** Surface rendering. **C** Electronic dissection in surface rendering. Surgical treatment was performed

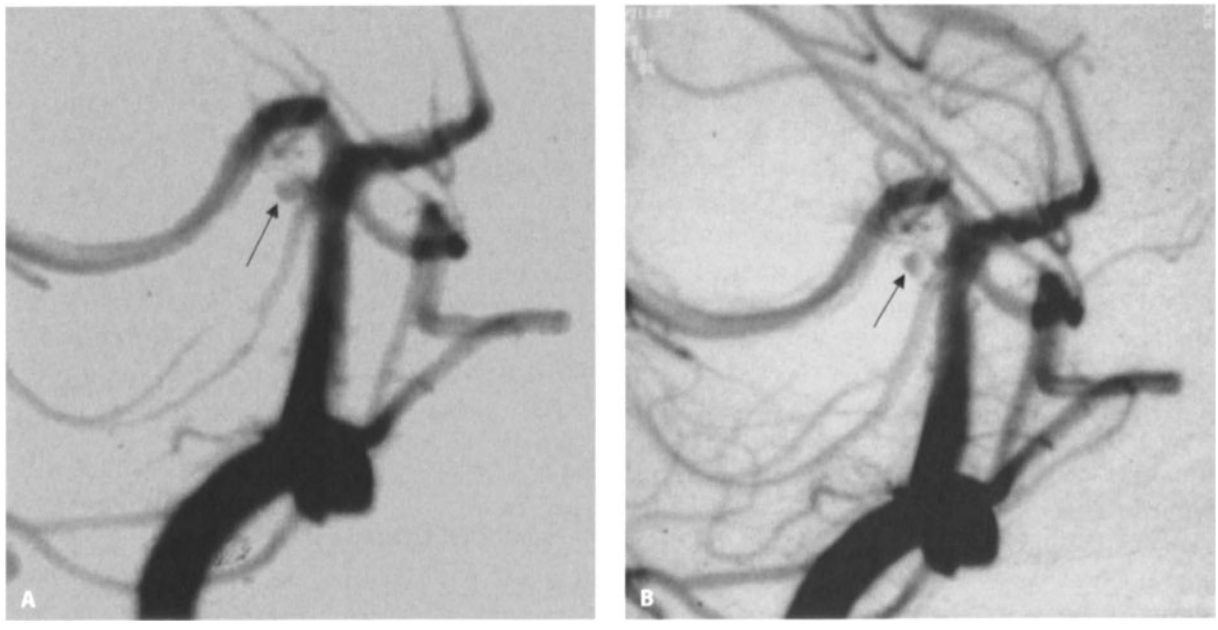

Fig. 7.129A, B. Ruptured superior cerebellar micro-AA. **A** False sac (*arrow*); **B** with fluid level (*arrow*)

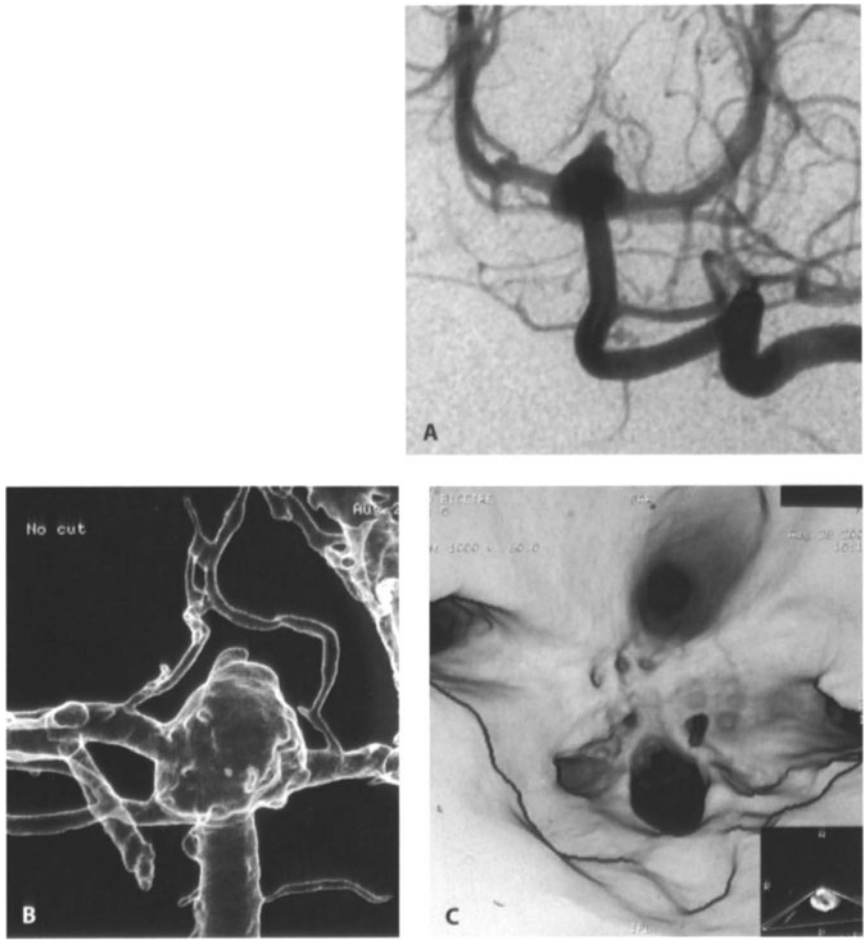

Fig. 7.130A–C. Ruptured basilar tip arterial aneurysm. **A** Conventional angiogram. **B** Surface rendering. **C** Virtual endoscopy

for unruptured AAs larger than 8 mm; if smaller, continuous coaxial saline solution flushing (without heparin) into the guiding catheter and microcatheter is used; the anticoagulation management aims to achieve an ACT greater than 300. Dense packing is attempted in every case. We avoid overpacking a ruptured AA, as it is clearly associated with intraoperative rupture and secondary migration of coils into the false sac (Fig. 7.133, p. 537). In addition, it is our experience that secondary induced thrombosis occurs even without overpacking (Fig. 1.137). We prefer not to use the remodeling technique in the ruptured AA at the acute stage (see Chap. 14).

We assess the rate of occlusion as follows: complete angiographic exclusion of the sac is considered a 100% occlusion, a persistent orifice demonstrated on one or two projections is equivalent to 90%–99% and 80%–89% occlusion, respectively, while partial opacification of the sac is demonstrated.

For 24 h, full heparinization is maintained, with the activated clotted time at a level twice as high as normal in order to avoid clotting complications in the parent artery. In general, the introducer sheath is left in place during this period and removed after the discontinuation of heparinization and normalization of the clotting time. All patients with rup-

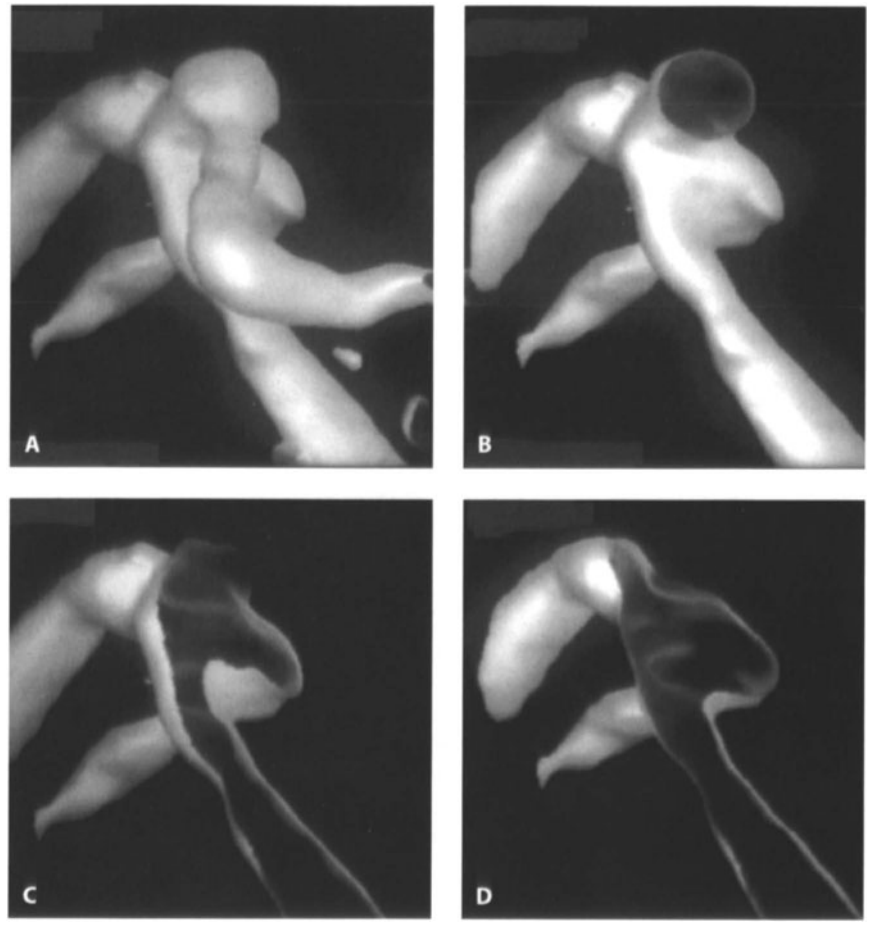

Fig. 7.131A–D. MRA aspect in **A** volume, **B** surface rendering, and **C, D** electronic dissection of a basilar tip arterial aneurysm. (From Bontozoglou et al. 1994, with permission)

tured aneurysms are treated in the acute phase with calcium channel blockers.

At day 1, plain X-ray films of the skull are obtained to document the position and stability of the coils. After heparin has been stopped, antiplatelet therapy (aspirin 250 mg/day) is initiated and can be continued until the first angiographic follow-up study. Follow-up with plain skull X-rays is a good way of anticipating changes in the immediate postoperative results; however, the follow-up angiogram provides a more precise assessment of the AA disease, in particular with the cases that harbor multiple AAs.

Follow-up includes general and neurological examination. Clinical evaluation is recommended using the Glasgow Outcome Scale (GOS) and the Karnofsky score (Tables 7.1–7.7). The latter, although designed initially for patients suffering from brain tumors, seems useful since it provides more precise evaluation of quality of life in patients with a good GOS. Plain X-ray films of the skull can be taken at regular intervals to anticipate AA changes, either from packing or regrowth. In the New York experience, such easy control was reliable in predicting AA changes and in indicating more precise morphological evaluation (Hwang et al. 2000).

Follow-up angiography is performed in all cases (at 3 months, depending on the immediate result obtained) 1 year after the initial procedure.

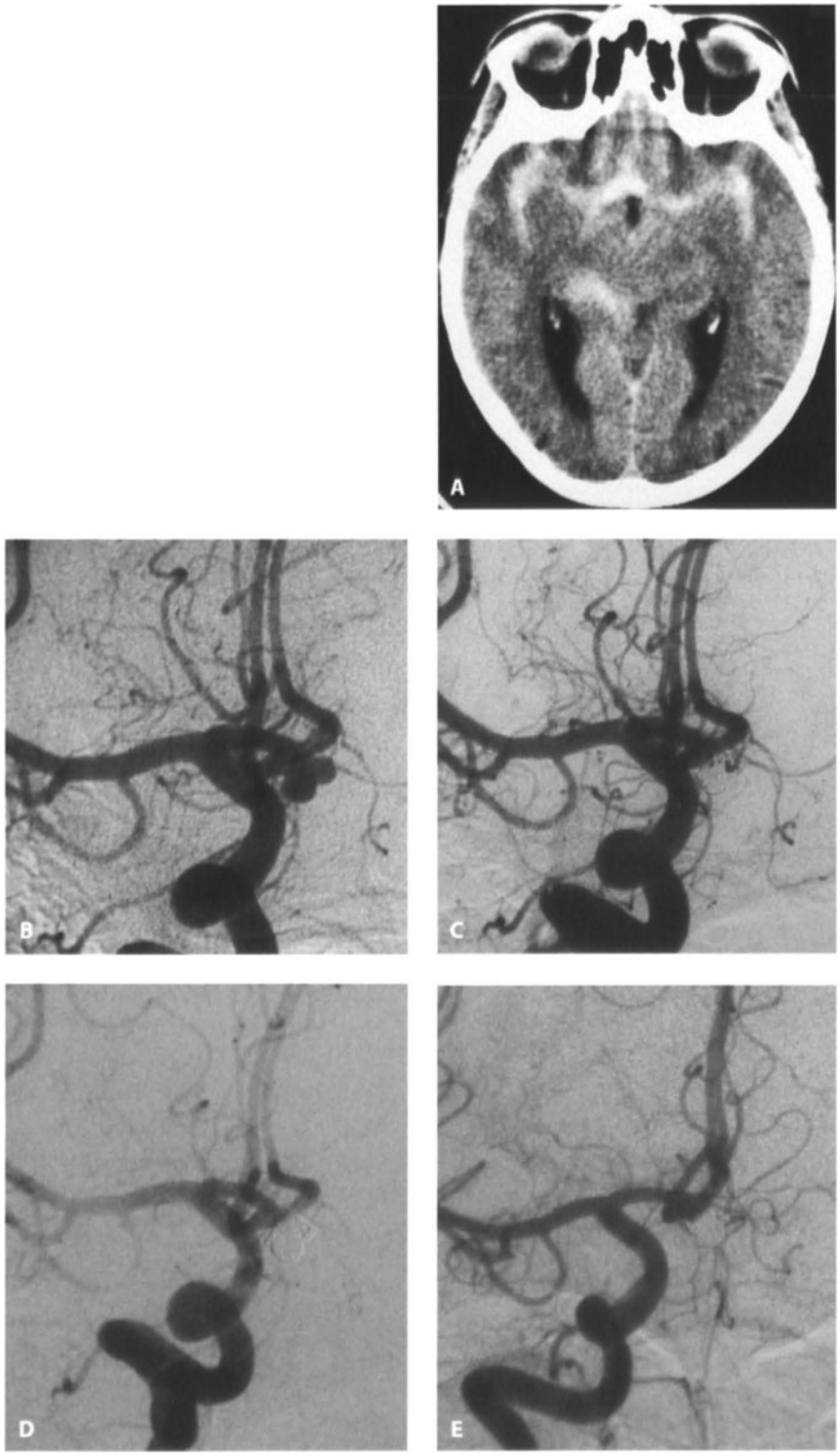

Fig. 7.132. Subarachnoid hemorrhage (**A**) from AComA arterial aneurysm (**B**); 95% coiling at the acute stage (**C**). Follow-up at 6 months shows completion exclusion of the arterial aneurysm (**D**). At 5 years, the result was stable (**E**)

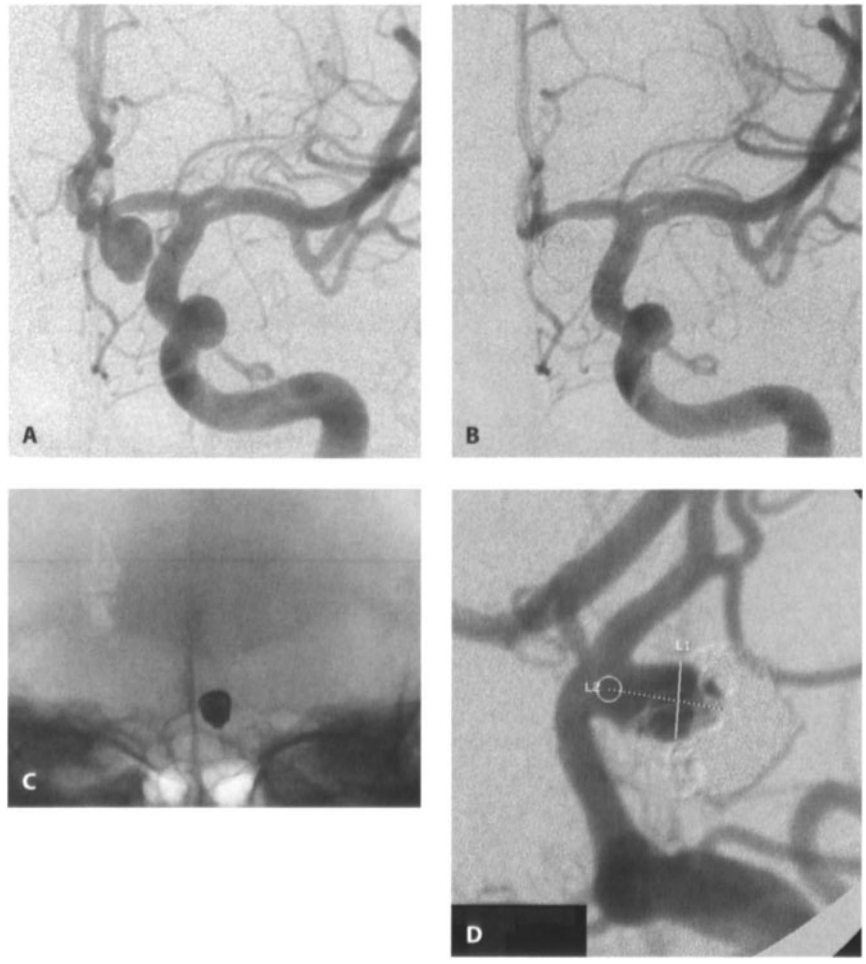

Fig. 7.133. **A, B** Frontal internal carotid artery angiogram before and after coiling; **C** immediate plain skull X-ray film; **D** oblique ICA angiogram at 3-month follow-up. Typical compaction, at 3-month follow-up, of a coiled ruptured arterial aneurysm (AA); no AA growth. Repeat embolization was the elected treatment

When the AA is considered totally excluded, follow-up tests are done at 3 years. Intermediate follow-up examinations at 6 and 18 months may be proposed in cases of partial occlusion of the AA and/or if recanalization or regrowth of the lesion are demonstrated. If needed, the AA is again embolized with GDCs during one of these sessions (Fig. 7.133). The role of contrast-enhanced MRI in the follow-up of coiled AAs appears to be encouraging.

Between 1993 and 1998, 225 AAs seen in 203 patients were reviewed by Fuse et al. (2000). Of these lesions, 201 (in 180 patients) were treated. A female dominance was noted (64.5%) with a mean patient age of 44.3 years. They treated 65.6% of the patients in at the acute phase after intracranial hemorrhage, 72% of them being Hunt and Hess grade 1 or 2. Most of these AAs (73.6%) were located in the anterior circulation. In 86.1% of cases, the AA was smaller than 10 mm; 85.6% of the AAs needed only one session of endovascular therapy. None of the unruptured AA patients died. Overall management mortality was 11% in ruptured AAs (3.5% in HH1–2, 30.3% in HH3–5). Technical or transient complications occurred in 11.6% of cases, but permanent morbidity was seen in 3.1% of cases. Follow-up angiograms were done 3 months and 1 year after therapy. In doubtful cases, a follow-up angiogram at 6 months was also done. A 100% occlusion rate

was noted in 60.8% of cases; 22.8% of AAs were occluded between 90%–99%, and 13.3% between 80%–90%. Only 3.1% of AAs had an occlusion rate of less than 80%. The ruptured basilar tip AA of one patient that was partially coiled (<90%) regrew and rebled 3 months later. The patient declined the recommended complementary surgery. None of the others rebled.

7.8.3 Results of the Endovascular Approach

The review of the literature is particularly disappointing. The management of ruptured and unruptured AAs is clearly not the same from one region to another (Europe, USA and Canada).

- Different AAs are coiled depending on the region, with large (>15 mm) to giant AAs (>25 mm) making up over 10% and reaching as many as 50% of the lesions treated in the North American series (Malisch et al. 1997; Vinuela et al. 1997; Lempert et al. 2000; Eskridge et al. 1998), compared to only 5% in European series (Cognard et al. 1998; Fuse et al. 2000; Byrne and Molyneux 1999).
- Results may include parent artery occlusion (in 25% of cases of Lempert et al. 2000).
- The number of ruptured AA patients with low (4 or 5) Hunt and Hess grades at admission is also consistently different (under 11% of patients in European series and over 25% in the American series).
- Assessment of AA multiplicity is often unclear and the quality of morphological screening variable, leading to diagnosis of multiple lesions ranging from less than 10% to more than 30%.
- In series with both ruptured and unruptured AAs, the clinical outcome (GOS) per Hunt and Hess grade sometimes includes unruptured AAs.
- Morbidity related to the procedure is extensively commented but the results of other teams are not mentioned, even with similar patient groups. The so-called self-learning curve is apparently accepted already published pertinent patient series.
- Mortality is often difficult to assess since the mortality related to the SAH is part of the results in patients treated by coiling. It is sometimes extremely low in comparison to the high grades at admission when the paper focuses solely on the aneurysm treatment, thus considering technical complications only.
- Long-term follow-up results are difficult to obtain since authors are reluctant to analyze the results of coiling in a more homogenous subgroup of patients. The clinical capacity of neuroradiologists to organize and plan morphological and clinical follow-up, particularly in ruptured AAs, also varies from center to center and from region to region.
- Some series have included AAs associated with BAVMs or dissecting AAs.
- In different institutions, the priority given to the endovascular approach versus surgery for saccular AAs less than 15 mm varies from 25% embolized to over 85%. The selection of patients appears to depend greatly on the role played by the neurosurgical team in the decision-making process.

The volume of cases that has been amassed argues that coiling is successful at providing acute protection from recurrent hemorrhage (Leber et al. 1998; Lempert et al. 2000; Byrne and Molyneux 1999; Lemme-Plaghos 1999; Cognard et al. 1998; Malisch et al. 1997; Vinuela et al. 1997; Fuse et al. 2000; Molyneux, ISAT 2002). The emphasis is thus shifted to the long-term outlook, largely because of the proven track record for surgery in this respect. Surgical success has been documented not so much by formal, quality studies as by a volume of collective experience over many years. Clinicians and patients continue to worry about coil compaction, aneurysm regrowth, and residual body or neck filling, while the significance of these findings remains uncertain. On the other hand, if clinical follow-up is the appropriate method, then one may decide to ignore small neck remnants or changes in coil mass appearance as long as the patient does not suffer from a rebleed. The duration required for clinical follow-up would necessarily be longer, requiring a certain number of patient-years to reassure us that the risk is below some arbitrary, acceptable limit. To accumulate enough experience, one must bear in mind the difference between following many patients for a short duration versus fewer patients for a long time. Although both may yield the same number of patient-years, long-term follow-up is essential, since recurrent bleeding is not a random event. The protection may be good for several years until the vessel has been remodeled in an adverse way, at which time there is a renewed risk of SAH.

During a 5-year period, 317 patients presenting with aneurysmal SAH were successfully treated by coil embolization within 30 days of hemorrhage (Byrne and Molyneux 1999). Patients were followed for 6–65 months (median, 22.3 months) by clinical review, angiography done 6 months after treatment, and annual questionnaires. Stable angiographic occlusion was evident in 86.4% of small and 85.2% of large aneurysms, with recurrent filling in 38 (14.7%) of 259 aneurysms. Rebleeding was caused by aneurysm recurrence in four patients. The annual rebleeding rates were 0.8% in the first year, 0.6% in the second year, and 2.4% in the third year after aneurysm embolization, with no rebleeding in the subsequent year. Rebleeding occurred in three (7.9%) of 38 recurrent aneurysms and in one (0.4%) of 221 aneurysms that appeared stable on angiography.

A total of 2,069 patients were treated in California for unruptured aneurysm (Feinberg et al. 2001). Adverse outcomes were more frequent in the 1,699 patients treated with surgery (25%) than in those treated with endovascular therapy (10%, $p<0.001$). The difference persisted after multivariable adjustment (surgery vs. endovascular therapy: odds ratio for adverse outcomes, 3.1; 95% CI, 2.5–4.0; $p<0.001$). Adverse outcomes declined from 1991 to 1998 in patients treated with endovascular therapy ($p<0.005$) but not for surgery. In-hospital deaths occurred in 3.5% of surgical cases and 0.5% of endovascularly treated cases (CI, 3.5–11.4; $p>0.001$). Total length of stay and hospital charges were greater in surgical cases ($p>0.001$). Results were similar in a confirmatory analysis focusing on treatment differences between institutions. Institutional treatment volume was also associated with outcome but did not account for the differences between surgery and endovascular therapy.

In a large cohort of patients with unruptured intracranial aneurysms treated at 60 university hospitals in North America between 1994 and 1997, in-hospital mortality was 2.3% and adverse events were observed in an additional 18.5% of patients. Similarly, Yamashita and co-workers (2000) reported on a large cohort of patients with unruptured intracranial aneurysms treated aggressively with prophylactic surgery at different neurosurgical centers in the Yamaguchi prefecture in Japan. Surgical intervention in these patients was accompanied by a combined morbidity and mortality rate as high as 20%.

The degree of packing required for optimal clinical results is as yet unresolved; terms such as "sufficient" and "overpacking" are emerging to describe the beliefs of each therapeutic team regarding the ideal morphological end point results.

In a prospective study, Acevedo et al. (1997) showed over 267 surgically treated ruptured AAs in 217 patients, 17 (6.3%) had an incompletely clipped AAs (4.1% neck residue, 2.2% AA sac remnant). Some locations gave a higher rate of postoperative remnants AchA + OPH-ICA (5/22 cases), while others had a lower rate (MCA, 1/75).

It is clear that incomplete packing beyond a certain point will often lead to recanalization and/or compaction, and thus an ongoing risk of hemorrhage (Cognard et al. 1998; Gurian et al. 1995; Horowitz et al. 1999; Martin et al. 1996; Murayama et al. 1999; Vinuela et al. 1997; Yoichi et al. 1999). However, there is a difference of opinion on whether very tight packing to the absolute limit of feasibility (failing to deploy the final attempted coil or doing so with significant friction and repositioning of the microcatheter within the aneurysm) is necessary. One may imagine that more coils are always better, but this strategy comes at a cost (including financial), but more importantly at a cost of potential intra- and postoperative risk to the patient. There is, for every aneurysm, a certain stage at which the change in flow within the aneurysm due to a given mass of foreign material will lead to a favorable clinical course with thrombosis and exclusion of the aneurysm from the circulation. Any coil added after this stage incurs additional risk and cost without achieving further benefit. The stage at which this happens may be influenced by a number of factors, including aneurysm size, direction of flow vis-à-vis the aneurysm neck, neck width, and so on. The degree of packing required to achieve this success is one of the many factors that can vary among teams, and about which a given group may feel very strongly, yet which has not been systematically studied to determine the best protocol to follow (Porter's comment on Fuse et al. 2000).

Batista et al. (2002) reviewed a series of coiled AA patients with 5 years follow-up and showed no bleed from previously treated AAs, even if there was a small remnant at the neck. In addition, nearly 35% of 90 excluded ruptured AAs by coiling completed their obliteration within the first year. No further morphological change was seen if the result was stable at the 3-year follow-up examination. This could correspond to the classic 3-year cycle for complete remodeling of the vasculature advanced by Folkmann (1995). Interpretation of the results obtained varies with the quality of initial assessment and follow-up. In particular, the use of 3-D pictures helps demonstrate previously unseen associated locations, for the most part at

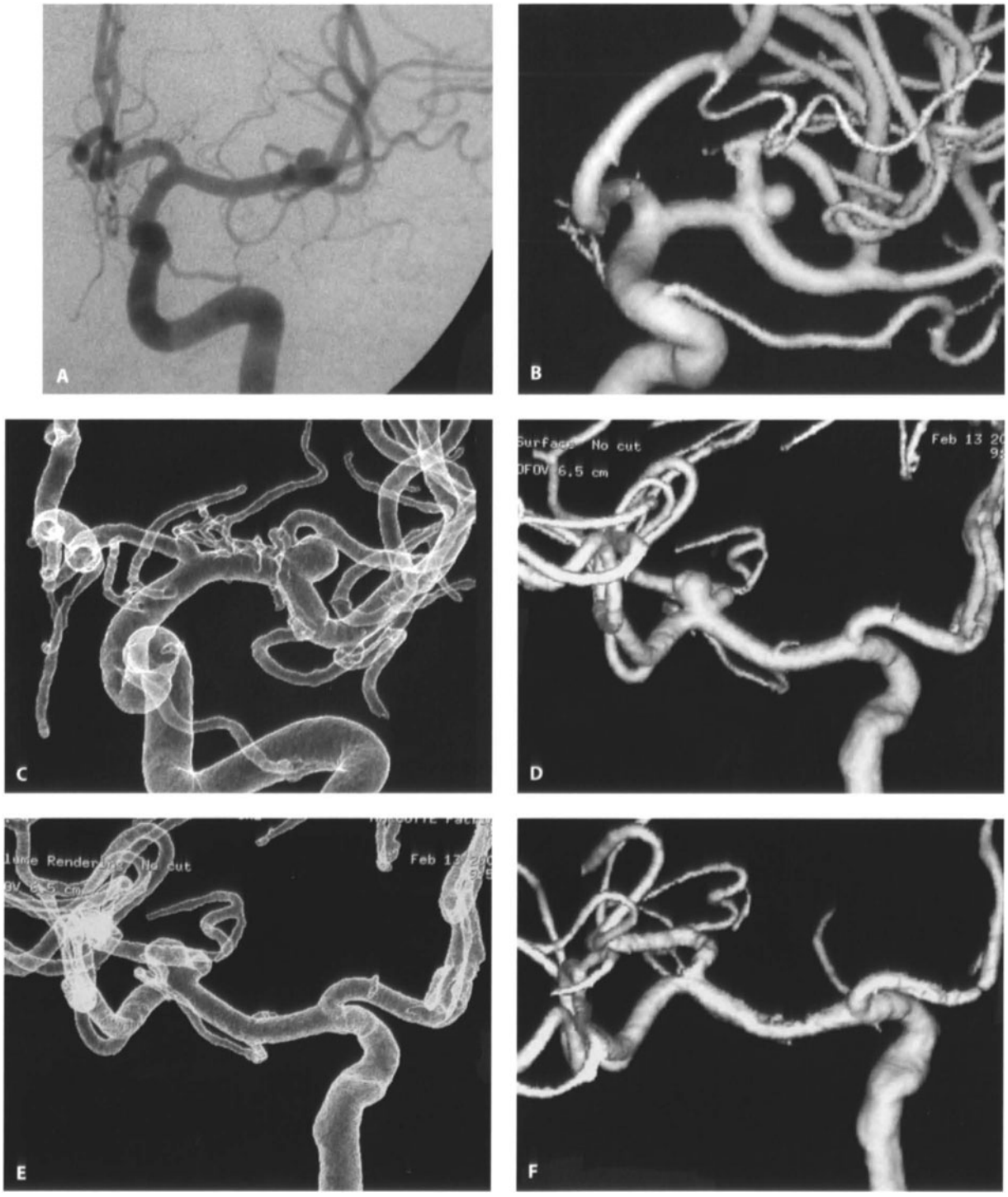

Fig. 7.134. Ruptured left MCA division aneurysm on conventional (**A**), volume rendering (**B**), and (**C**) surface rendering images. Follow-up after coiling (**D–F**). Analysis of the posterior surface of the left MCA aneurysm before and after coiling shows no abnormality. **G–I** see p. 542

Fig. 7.134 (*continued*). Follow-up after coiling (**G–I**). Analysis of the posterior surface of the right MCA aneurysm shows abnormal blebs. The patient was subsequently operated on a few days after the coiling procedure

the posterior aspect of the ICA, MCA, or basilar tip divisions (Figs. 7.95, 7.134). Coiling of unruptured AAs probably requires different attention, since an incompletely coiled lesion (90%–99%) usually remains unchanged, as if the ruptured AA contributed to the healing process induced by the coils. The degree of change depends on the size of the AA: the bigger the pouch the more likely the chances of compaction or regrowth.

The most classic intra- and postoperative complications related to the coil treatment and independent of the complication resulting from the SAH (in ruptured cases) are the following:

- Mechanical rupture of the AA
- Parent artery clot formation (Fig. 7.135) or dissection
- Distal emboli
- Coil prolapse (Fig. 7.136)
- Secondary thrombosis or induced spasm (Fig. 7.137)

Fig. 7.136A–E. Ruptured 2.5 mm internal carotid artery (ICA) termination aneurysm (**A, B**). Insufficient packing because of fear of rerupturing the adjacent false sac was associated with prolapse of two loops of the endosaccular coil without clinical sequel. The patient was kept on heparin and remained asymptomatic, although follow-up 2 weeks later showed vasospasm of the distal ICA and proximal M1 segment (**C**). **D, E** Follow-up angiograms at 3 months and 4 years show progressive coverage of the prolapsed coil and resulting projection outside the vessel wall ▶

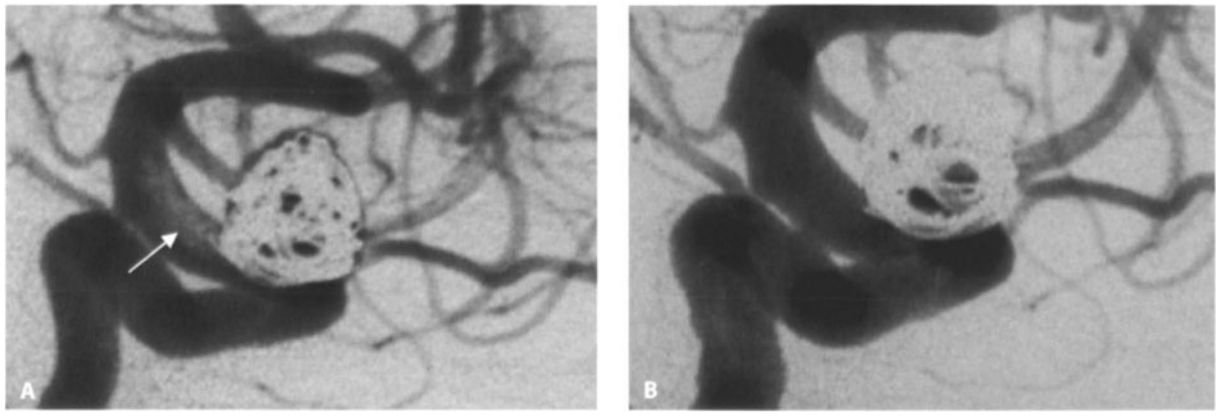

Fig. 7.135A, B. Immediate follow-up angiogram after coiling of a ruptured ICA-OPH aneurysm. Evidence of an intraluminal clot (*arrow*) (**A**). The patient was asymptomatic and was treated for 1 week with heparin, and thereafter with aspirin, until the next follow-up angiogram 3 months later, which showed the complete disappearance of the clot (**B**)

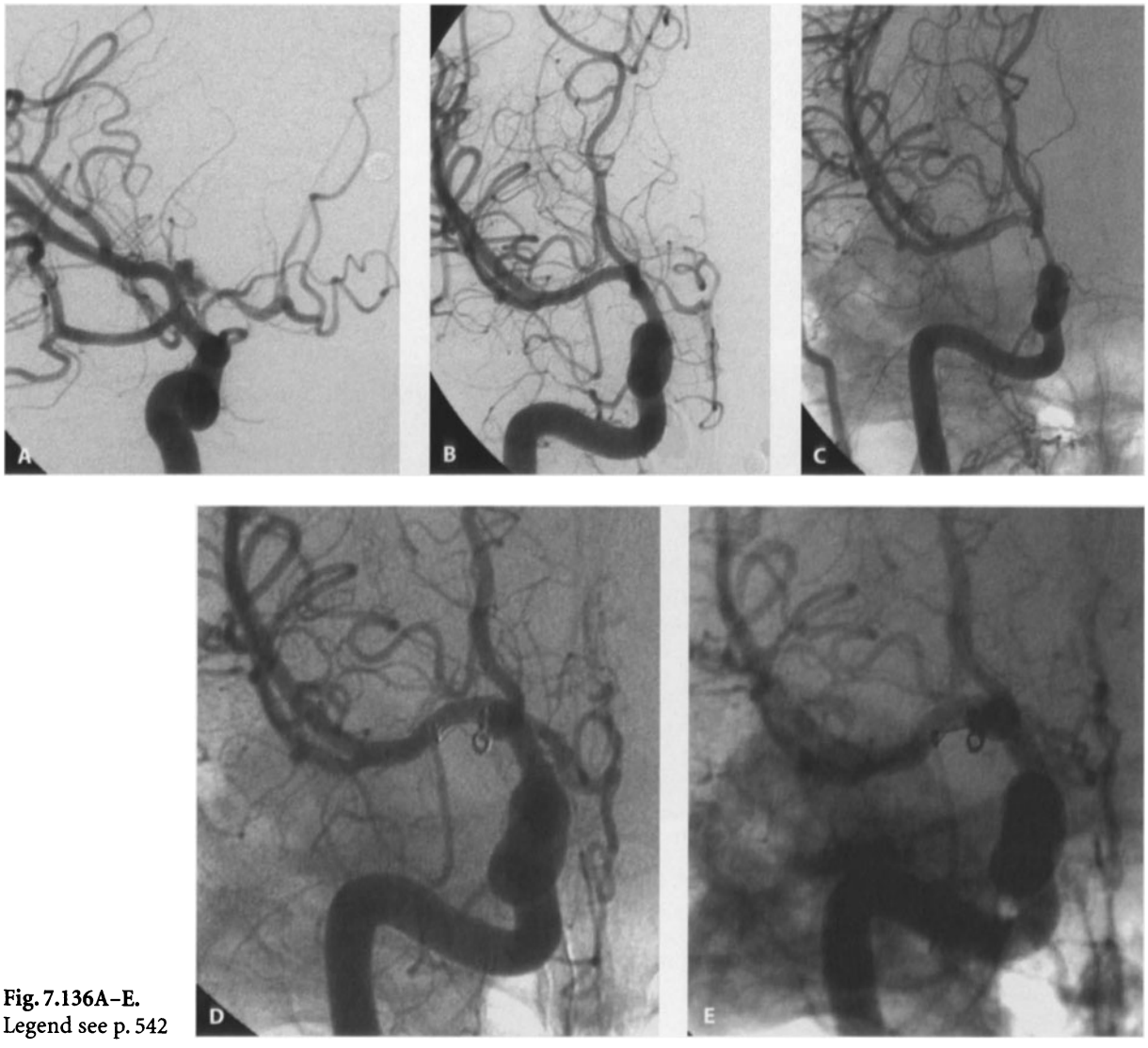

Fig. 7.136A–E.
Legend see p. 542

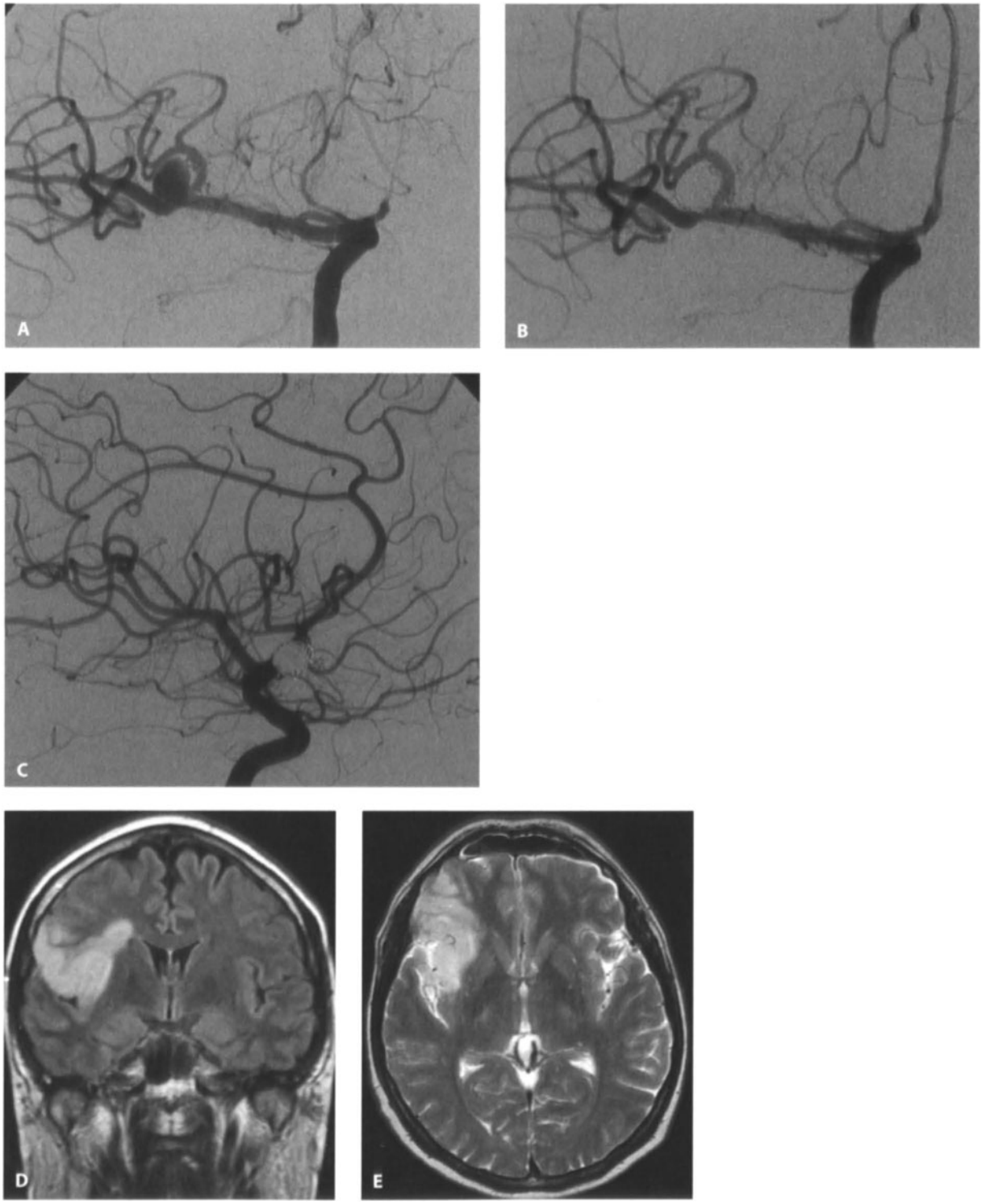

Fig. 7.137. A 50-year-old male patient with incidentally discovered middle cerebral artery aneurysm (**A**) was treated with coiling (**B, C**). While on heparin therapy and neurologically intact, 24 h later vague symptoms stimulated an MRI, which showed opercular ischemia (**D, E**). He was kept on heparin for 2 weeks. Some loss of cognitive abilities occurred but he made a complete recovery and returned to work in 6 months

Many of these will be managed without neurological consequences and often medically.

Rebleed in previously coiled patients (for ruptured or unruptured AA) will need careful investigation before making definitive statements and require very precise imaging examinations. In our experience, bleed or rebleed in such population groups was only once caused by AA regrowth and the patient refusing to undergo recommended surgery (Fuse et al. 2000). All the other cases involved de novo AAs in the area of a previously demonstrated AA (Fig. 7.138) or remote from the former operative field (Fig. 7.139).

Jayakrishnan (2001) reported a case of multiple intracranial aneurysms in which mirror aneurysms at the middle cerebral artery bifurcation were found initially during the screening of the ruptured left-sided aneurysm. Six years later, the patient had subarachnoid hemorrhage on the right side. Three-dimensional angiography showed that the rupture came from a de novo aneurysm that had developed separately from but adjacent to the unruptured aneurysm already demonstrated 6 years earlier, which was actually unchanged.

Intracranial aneurysms may develop over a short period of time and either rupture immediately or remain stable without rupturing (International Study of Unruptured Intracranial Aneurysms 1998). If Jayakrishnan's patient had had treatment for her incidental aneurysm it might not have protected her from future SAH, and moreover, if she had undergone endovascular treatment, it would have been considered a failure of therapy at the time of the second SAH. The concept of single AA and results obtained over a lifetime needs serious review in order to realistically take into account the reality of multiple lesions and de novo locations in aneurysmal vasculopathies now being recognized (see below in this section).

However, how good these results are depends not on comparison to other groups, but rather on comparison to the best alternative treatment and ultimately to the natural history of the disease (which is particularly pertinent for unruptured aneurysms). To be excellent or even the best at delivering a given therapy is not sufficient to warrant adoption if that management strategy still does not produce better outcomes than the disease if untreated. The true natural history is often difficult to determine, since almost all series incorporate some degree of selection bias when determining which patients make up the untreated group. However, the publication on unruptured aneurysms (International Study of Unruptured Intracranial Aneurysms 1998), although potentially biased toward a benign natural history, suggests that our therapy may have to carry extremely low risks in order to justify treatment. The spontaneous risk of hemorrhage is considered as low as 0.05%/year for AAs less than 10 mm with no history of previous SAH, and about 11 times higher in patients who had a history of SAH from a different aneurysm that was repaired successfully.

If one considers that the incidence of AA is 3%–5% in Western populations and the incidence of SAH is 10/100,000 in the same population group, Wieber's statement that most intracranial aneurysms do not rupture is probably valid (International Study of Unruptured Intracranial Aneurysms 1998).

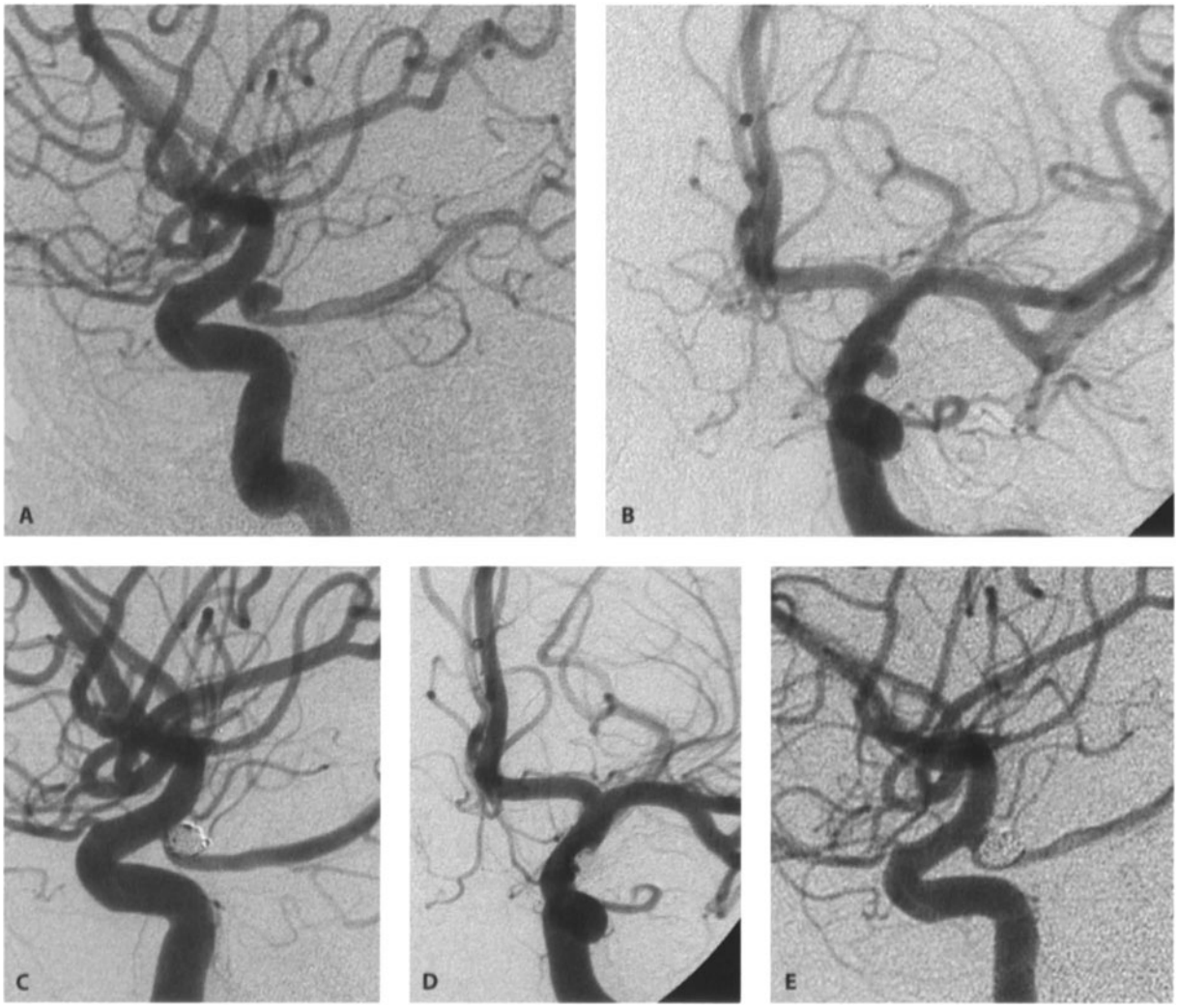

Fig. 7.138. **A, B** A 27-year-old male patient with previous medical history of subarachnoid hemorrhage in 1995 due to rupture of the left posterior communicating artery aneurysm. **C–E** The aneurysm was treated at that time by embolization with Gugliemi detachable coils (GDCs) and satisfactory occlusion was obtained, confirmed on several follow-up angiographic images between 1995 and 1998. The patient was then lost to follow-up. **F–I** see p. 547

A total of 2,621 patients at 53 participating centers in the United States, Canada, and Europe were enrolled in Wieber's study, which had retrospective and prospective components.

In the retrospective component, the natural history of unruptured intracranial aneurysms in 1,449 patients with 1,937 such aneurysms was assessed.

Group 1: 722 with SAH from another AA
Group 2: 727 with no history of any sort of SAH

In group 1, the cumulative rate of rupture of aneurysms less than 10 mm in diameter at diagnosis was less than 0.05% per year (less than one-tenth that of group 1). The rupture rate of aneurysms that were 10 mm or more

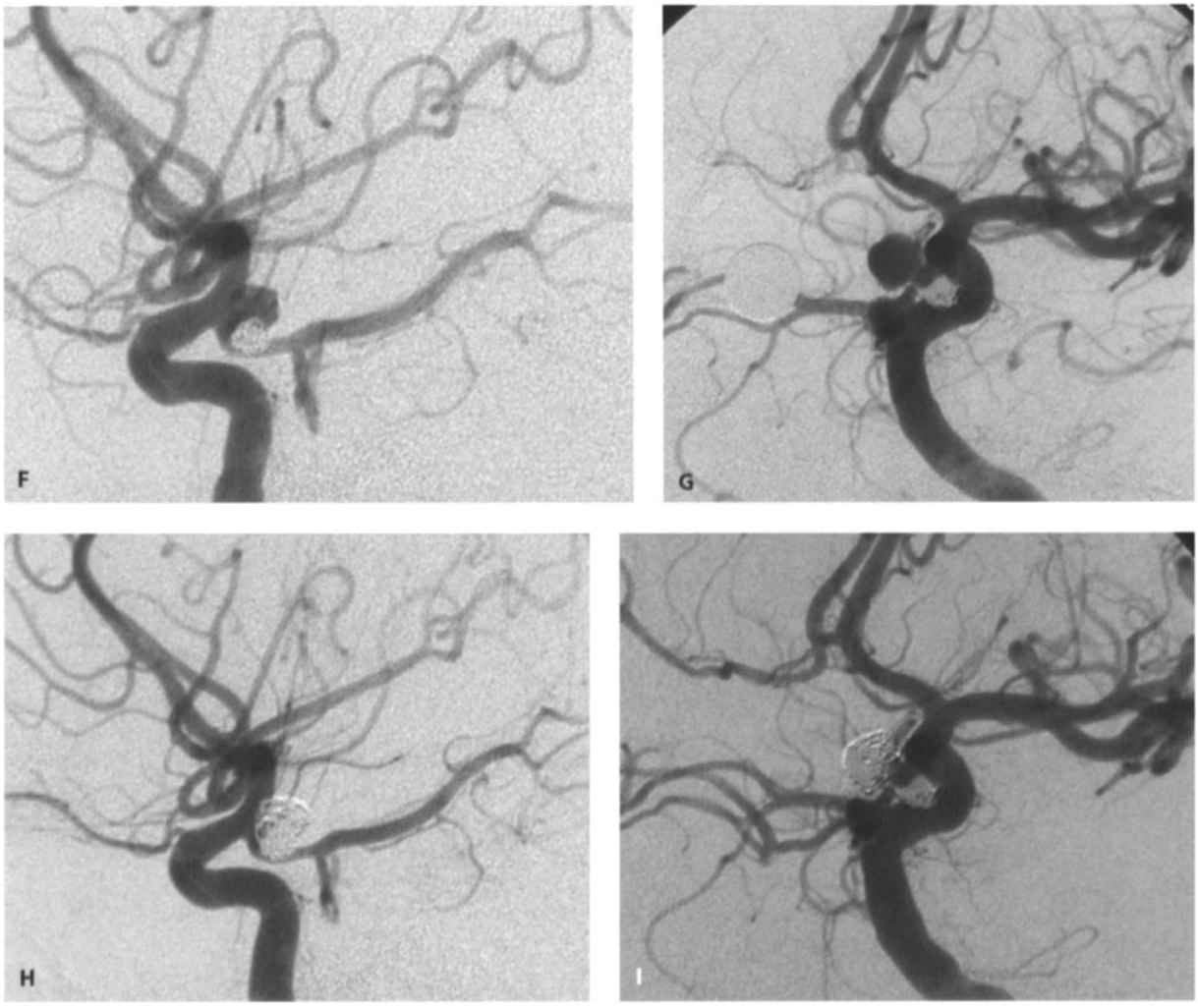

Fig. 7.138 (*continued*). **F, G** Six years later, he was readmitted in emergency for recurrent acute headache. CT showed a new subarachnoid hemorrhage near the PCom region. Angiography confirms stable result of the previously embolized aneurysm and demonstrates a de novo aneurysm 8 mm in diameter of the PComA itself. **H, I** This second aneurysm was also successfully treated by embolization

in diameter was less than 1% per year in both groups, but in group 1, the rate was 6% the first year for giant aneurysms (>25 mm in diameter). The size and location of the aneurysm were independent predictors of rupture.

In the prospective component, the treatment-related morbidity and mortality in 1,172 patients with newly diagnosed unruptured intracranial aneurysms was assessed for the period 1991–1995.

- Mortality (at 30 days): 2%
- Morbidity (at 30 days): 15%
- Mortality (at 1 year): 4%
- Morbidity (at 1 year): 12%

The overall rate of surgery-related morbidity and mortality was 15.7% and 13.1%, respectively, at 1 year. Age independently predicted surgical outcome.

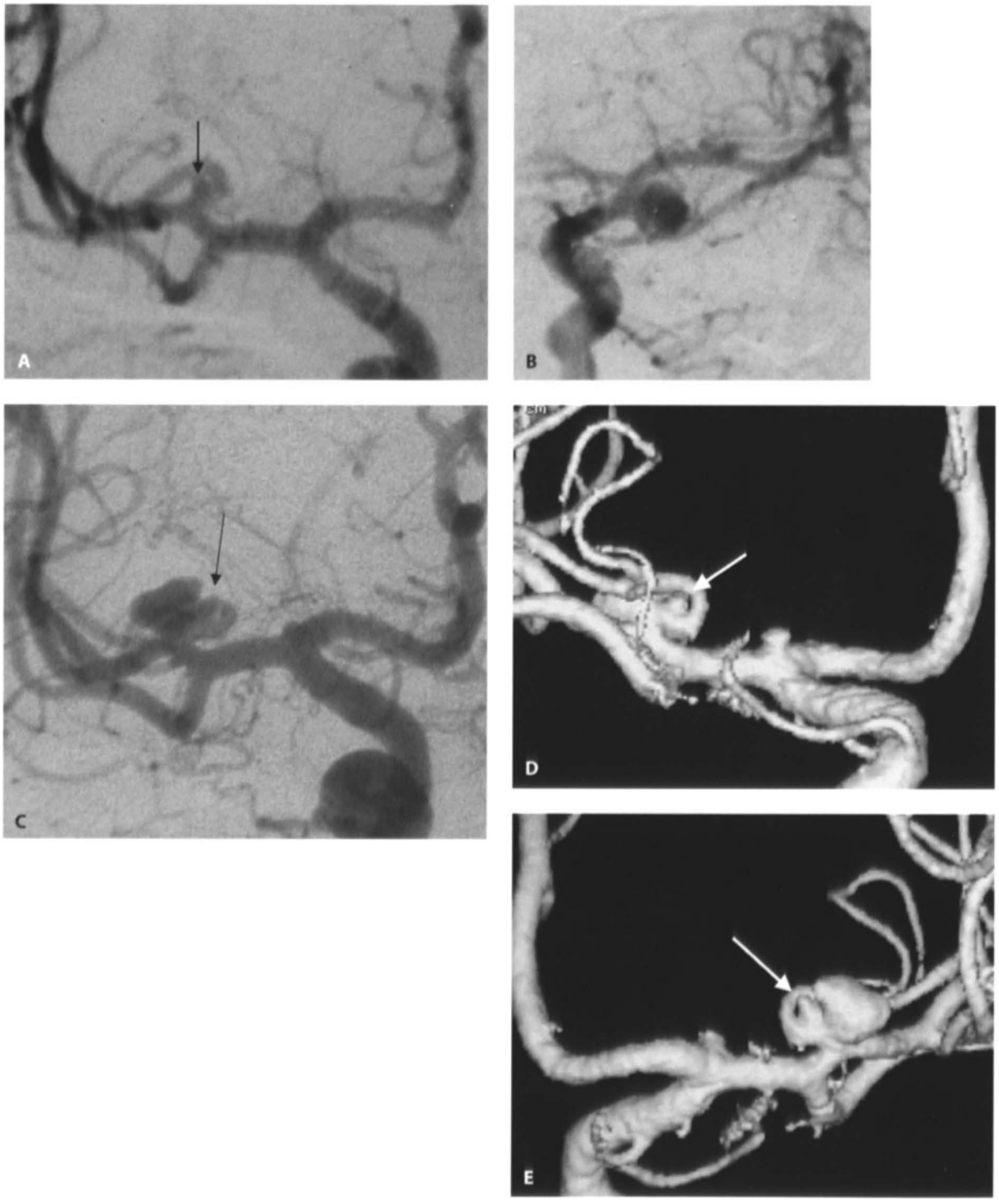

Fig. 7.139A–E. Mirror middle cerebral artery (MCA) aneurysm found initially with rupture of the left-sided lesion. **A** Right carotid angiogram shows a 2-mm aneurysm (*arrow*) at MCA division. **B** Left carotid angiogram shows the ruptured saccular aneurysm at MCA bifurcation. Six years later, the patient had a new subarachnoid hemorrhage on the right side. **C–E** Right carotid angiogram shows a lobulated saccular aneurysm; 3-D angiograms, viewed from behind, show the previous small aneurysm (*arrows*) separate from a new one believed to be responsible for the new subarachnoid hemorrhage. This de novo aneurysm had developed separately from but adjacent to the already present aneurysm on the right side. (Jayakrishnan et al. 2001, with permission)

In conclusion, the risk of morbidity and mortality related to surgery greatly exceeded the 7.5-year risk of rupture among patients in group 1 with unruptured intracranial aneurysms less than 10 mm in diameter.

Within any group of patients there will always be heterogeneity. Patients are frequently categorized according to clinical grade, age, aneurysm size, etc., in order to gauge and compare outcomes while in some way accounting, at least qualitatively, for baseline differences in patient populations. However, the traditionally used variables may be insufficient, since a saccular aneurysm in isolation may carry a significantly different natural history or therapeutic risk than a saccular aneurysm in a patient with multiple aneurysms, mirror aneurysms, or a positive family history, as these may reflect very different diseases. This is analogous to the situation in brain AVMs, where the morphological distinctions are recognized but the significance of subgroups may still not be fully appreciated (Lasjaunias 1997b).

The following conclusions can be derived from our combined experience with over 1,000 AAs coiled in our centers over the past 10 years, considering that the technique we used was similar and stable, despite various referral differences (see above in this section and Chap. 14, this volume).

- In randomly referred ruptured AA cases, embolization is always considered first unless a life-threatening hematoma needs evacuation.
- With this strategy, two-thirds of ruptured AAs are primarily embolized.
- AAs of the MCA make up less than 10% of embolized cases.
- Since the advent of 3-D angiography, we have diagnosed multiple AAs in 30% of patients.
- Embolization is successful in over 90% of cases.
- Transient procedure-related neurological complications are seen in 5%–6% of cases.
- Permanent procedure-related neurological complications are seen in 2%–3% of cases.
- Mortality related to the procedure is seen in 2% of patients.
- When 3 years of morphological stability is obtained, no further change occurs.
- No bleeding was observed in follow-up of this group of coiled ruptured AAs.
- In unruptured saccular AAs that are less than 15 mm treated by coils, no rupture from the treated AAs occurred at follow-up.

7.8.4 Management of Multiple Arterial Aneurysms

When managing an AA patient with or without SAH, one must always bear in mind the high incidence of aneurysm multiplicity and scrutinize the original angiogram for potential multiplicity and particularly for mirror locations (Figs. 7.95, 7.135, 7.139). In addition, AAs are seldom a focal problem, particularly if one of the therapeutic goals of treatment is the prevention of bleeding or rebleeding.

Porter et al. (2001) reviewed 122 consecutive patients, with a total of 305 aneurysms, managed between 1993 and 1999. The patient population had

a rate of intradural aneurysm multiplicity (26.4%) within the range of previous studies, which have been reported to be between 7.7% and 44.9% (Qureshi et al. 1998; Rinne et al. 1994; Wilson et al. 1989; Juvela et al. 2000).

The probability that an aneurysm at a given site could be responsible for hemorrhage is potentially useful information in cases of uncertainty regarding which aneurysm has bled. Previous information implies that anterior communicating, posterior inferior cerebellar, and basilar locations have a high probability of rupture, and MCA a low risk (Nehls et al. 1985). In Porter's series (2001), posterior inferior cerebellar and anterior communicating locations were significantly more frequently responsible for SAH, while paraophthalmic aneurysms were less frequently responsible. Clearly, other criteria are required to determine which among several aneurysms visualized was the source of bleeding. In the past, a large number of criteria have been used to make this judgment, including clinical signs (e.g., focal neurological findings), electroencephalography, a localized pattern of bleeding on CT or MRI, and angiographic criteria, including focal mass effect or vasospasm, intra-aneurysmal clot, proximity along a vessel, and aneurysm size or irregularity (lobulation, false sac) (Figs. 7.128, 7.134, 7.136) (Almaani and Richardson 1978; Hackney et al. 1986; Nehls et al. 1985); many of the criteria used previously continue to add useful information, but in isolation are often not definitive.

For example, the CT scan added useful information in the majority of cases (69%), yet Lee et al. (1996) pointed to the risk of false localization. This is a risk in patients who lost consciousness at the time of the stroke: they may collect blood by gravity in the opposite cistern to the actual hemorrhagic site. Others may have arachnoid scarring from previous hemorrhage or surgery, which could make the spread of subarachnoid blood atypical. Four decades ago, Wood (1964) reported the tendency for the largest aneurysm to be responsible for the bleed. This was the case in 85.7% of patients in Porter's (1991) study. Greatest neck width was almost equally correlated, since the aneurysm with the largest neck had bled 81% of the time. Aneurysm irregularity, and in particular the presence of a false sac, remained the most important and definitive piece of information for determining which aneurysm had bled. The term "false sac" is a radiological one, and should not be confused with the traditional pathologically defined "false aneurysm." The two terms may or may not refer to the same entity, and thus in the absence of a radiological–pathological correlation, they should be considered as separate. Using all of the above criteria, the choice of the culprit aneurysm is obvious in more than half of the cases (54.7%). Even assuming that all cases classified as "probable" were correct, there were still 14.3% of patients for whom there was significant uncertainty about which aneurysm had ruptured.

Older studies have reported numbers as low as 48% for determining the causal lesion, while more recent reports state the ability to identify the aneurysm that bled in 97.5% of cases. Regardless of the precise percentage, in most cases we can be fairly confident of which aneurysm bled, but we must ensure that we never misjudge, and as a result fail to treat a ruptured aneurysm. The degree of uncertainty may have implications for the type of therapy used for a given patient.

Surgery has often been recommended in the past because of the ability to treat many aneurysms during the same surgical exposure or the same surgical session with bilateral craniotomies (Edner 1991). In fact, it has previously been estimated that as high as 63% (Rinne et al. 1995) and 74% (Ulrich et al. 1997) of multiple aneurysm patients could have all aneurysms treated with a single craniotomy. In Porter's (1991) series, this estimate was only 46.4%, similar to the 53% reported by Hino et al. (2000). Endovascular therapy alone is a very good option, for example if multiple craniotomies would be required for treatment, but only if all aneurysms that are potentially responsible for the hemorrhage have appropriate morphology to be treated in this manner. When this is not the case, the direct surgical approach (if they are all in one territory) or combined surgery and coiling is preferable. Although coiling of several aneurysms (Van Rooij and Tijssen 1999; Solander et al. 1999) has been performed in a single session, (Figs. 7.140, 7.141), we have concerns that working for a prolonged time in one or more vessels will put multiple vascular territories at risk for thromboembolic complications simultaneously and increase treatment-related risk. We would therefore only recommend such interventions in ruptured AAs and for treating the AA in the same circulation, starting with the vessel that is likely to have bled, and if it is not known, starting with the most distal one. Currently, endovascular and surgical approaches are often combined in a variety of situations: with bypass (in stroke or a fusiform AA), to treat an AA regrowth after clipping or to operate on a regrown noncoilable AA, and to coil a broad-base AA after surgical reduction in its neck in mirror locations with unruptured AA below 2 mm (Figs. 7.142–7.146).

One may also indirectly validate the criteria used for choosing which aneurysm has bled at clinical follow-up, by demonstrating the absence of rebleeding. If the wrong aneurysm was selected for treatment the observed rebleed rate should follow the natural history of a ruptured, untreated aneurysm.

This is initially very high (4% in the first 24 h), reaches a cumulative value of 50% at 6 months, and thereafter is approximately 3% per year. Taking the total patient follow-up time among hemorrhagic patients, from the time of treatment of the first aneurysm until death or the treatment of other aneurysms, and using the above figures, one would expect to see a significant number of rebleeds [26 in Porter's (1991) series] if the wrong aneurysm was consistently being treated. Thus, the absence of any rebleed observed in these patients following SAH argues that the criteria used for determining which aneurysm has bled are reliable, although we could still be wrong some of the time and be fortunate enough to not have the patient suffer a rebleed during the observation period.

Failure to recognize all aneurysms on the initial study still remains a significant source of error. Clearly, the implications of missing an aneurysm in the acute phase after SAH are even greater, since it may become the source of bleeding and thus missing it would place the patient at risk of recurrent hemorrhage.

Other authors have reported similar problems in the past (Hino et al. 2000; Rinne et al. 1995; Yasui et al. 1996). Yasui et al. report that seven out of 25 patients presenting with hemorrhage from previously unruptured aneurysms had the aneurysms missed on original studies.

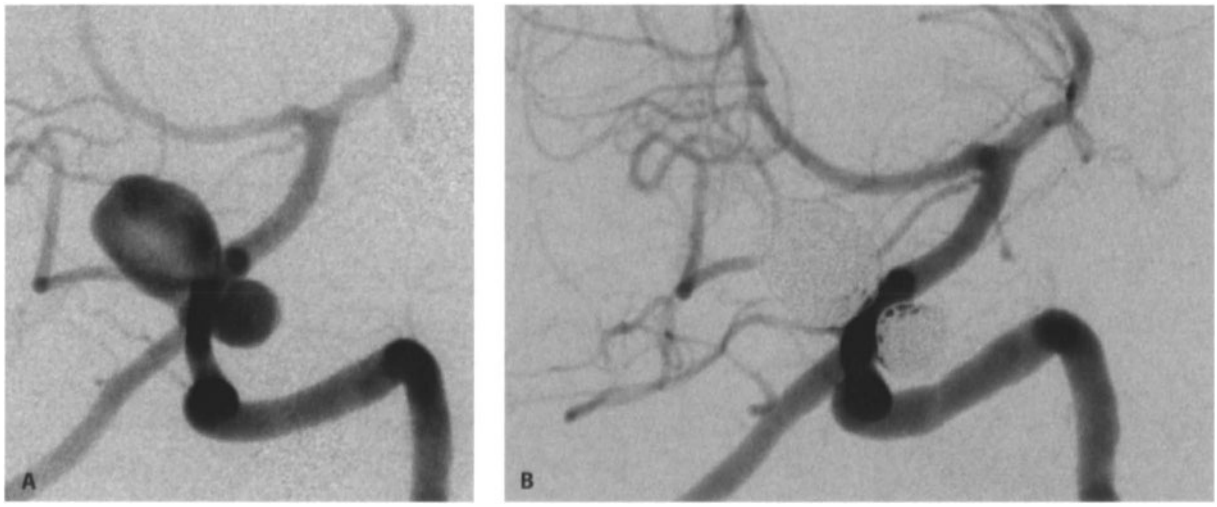

Fig. 7.140A, B. A 57-year-old female patient, who had had a subarachnoid hemorrhage 30 years before. Consultation for dizziness and discovery of two vertebrobasilar junction AAs on vertebral artery angiogram (**A**). Both were treated in the same session with coils (**B**)

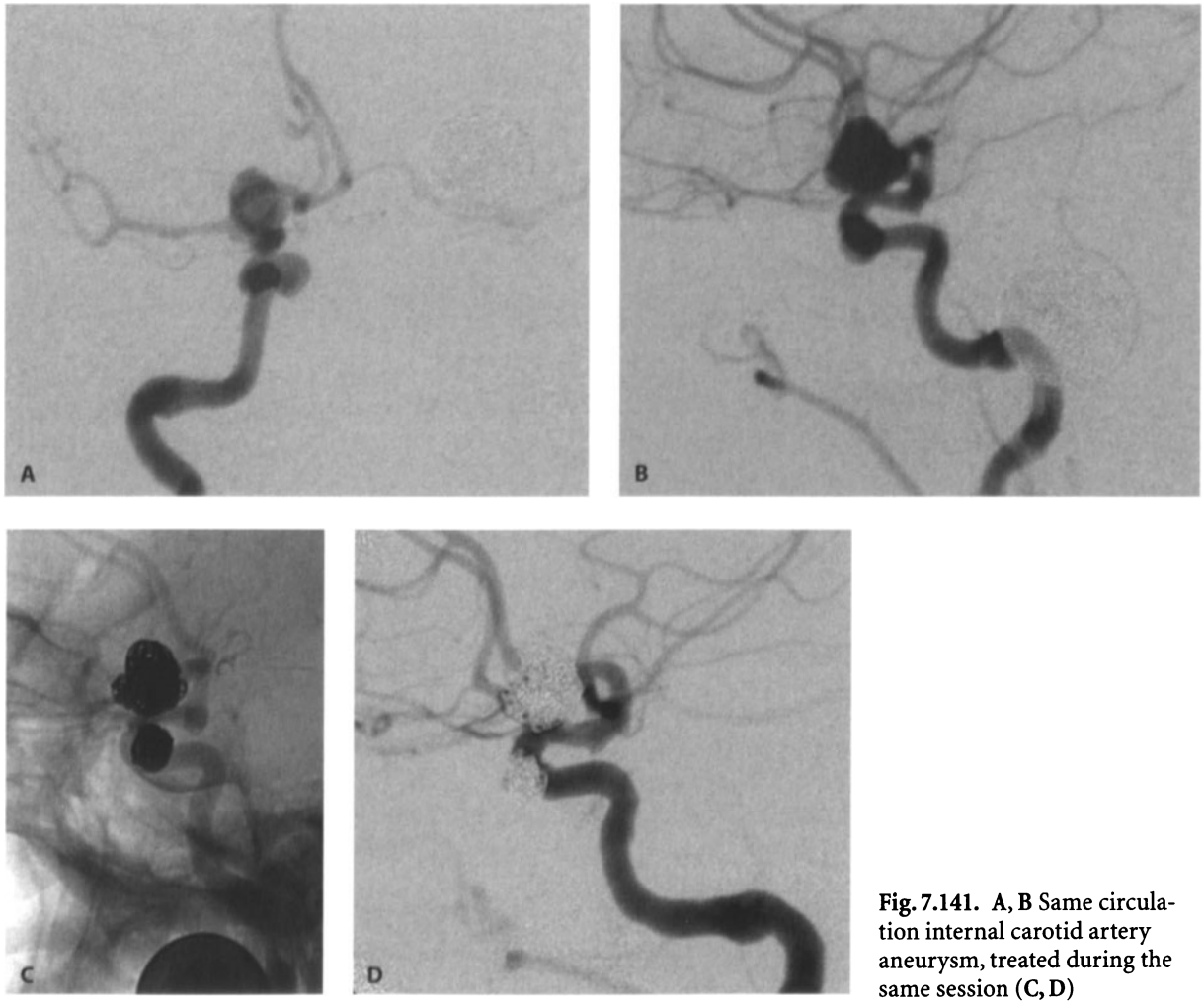

Fig. 7.141. **A, B** Same circulation internal carotid artery aneurysm, treated during the same session (**C, D**)

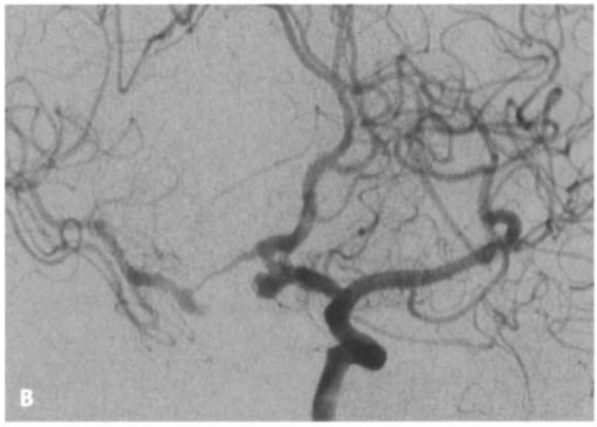

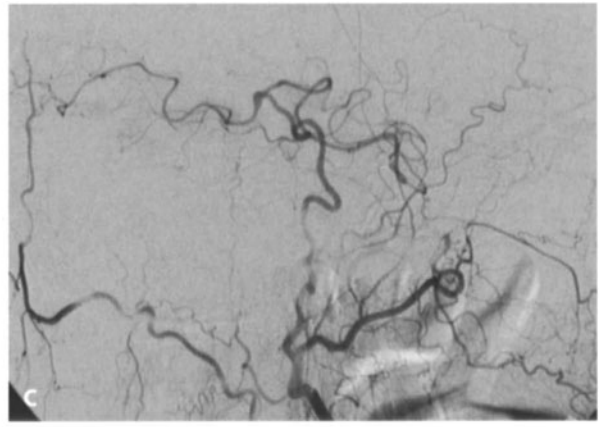

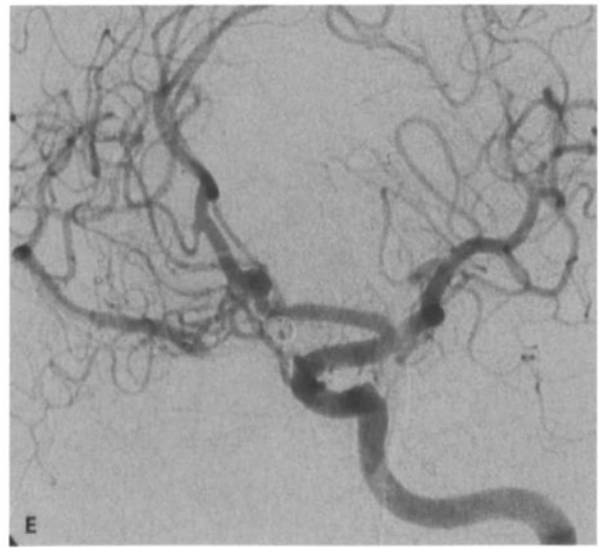

Fig. 7.142. A 59-year-old male patient presented with right-sided cerebral stroke due to internal carotid artery occlusion (**A**). Incidental discovery of an unruptured aneurysm of the AComA (**B**). The patient had no residual neurological deficit from the stroke. Extracranial– intracranial by-pass was performed (**C**). **D, E** A few days after the STA-MCA anastomosis preventive exclusion of the AcomA aneurysm by endovascular approach is performed

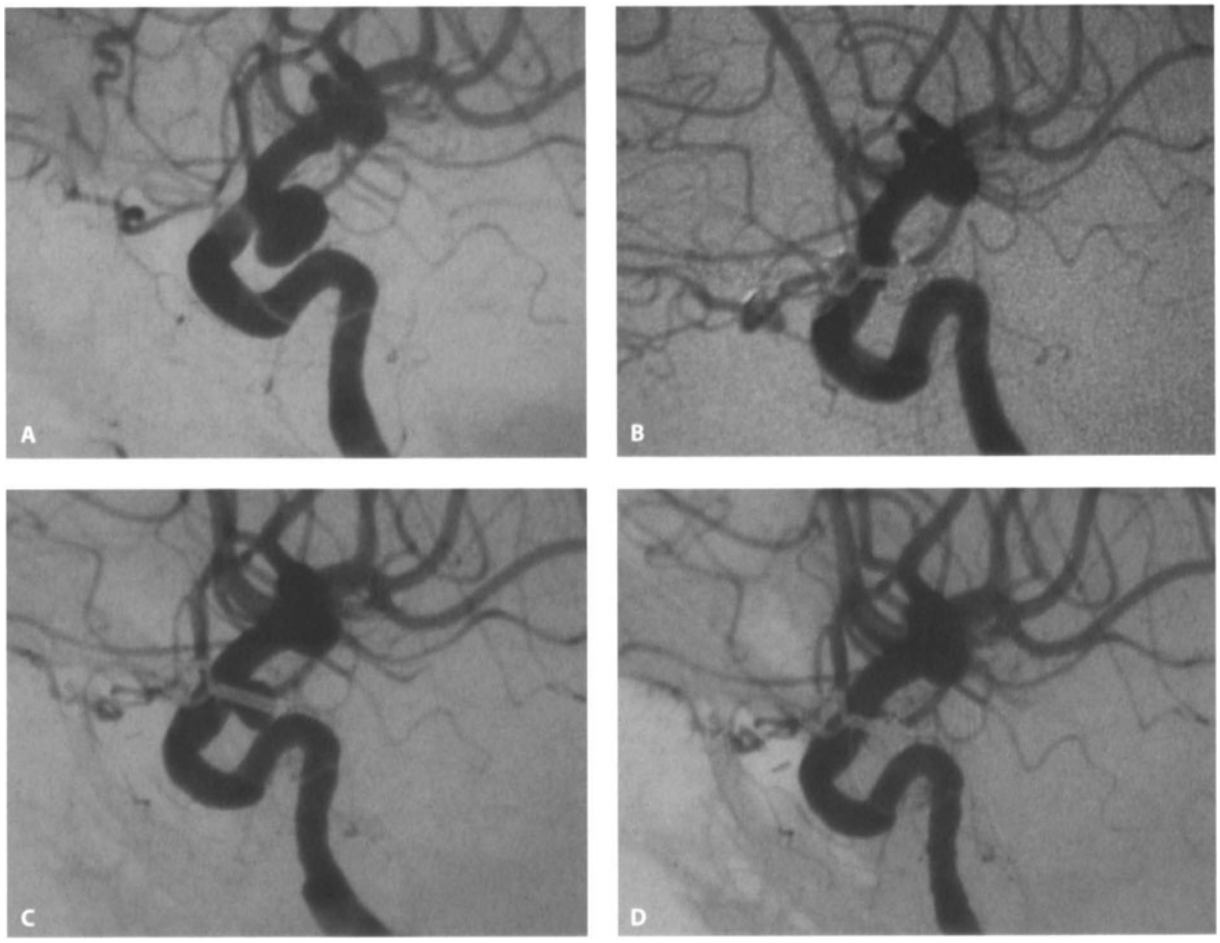

Fig. 7.143. Investigation for tinnitus lead to the discovery of an internal carotid artery (ICA) aneurysm (**A**) for which surgery was performed. Follow-up angiogram 10 years later showed regrowth of the aneurysm (**B**). Coiling was performed and follow-up angiograms 1 year (**C**) and 8 years later showed stable result (**D**)

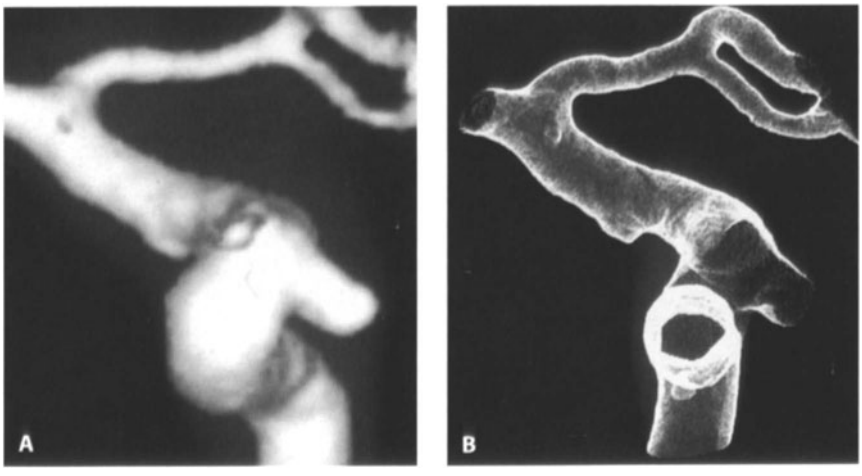

Fig. 7.144A, B. Legend see p. 555

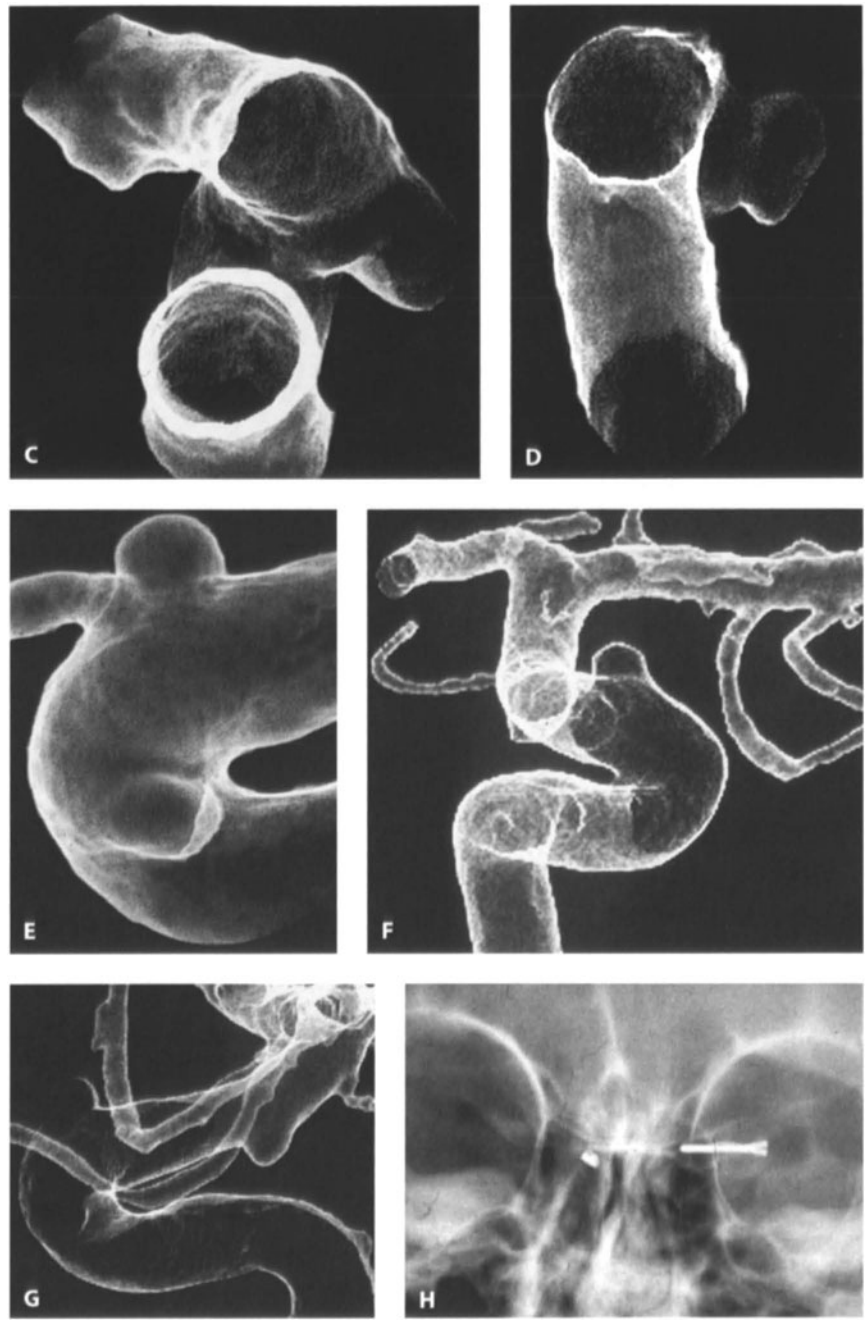

◄ **Fig. 7.144A–H.** Mirror internal carotid artery ophthalmic aneurysm. **A–D** On the right side, volume and surface rendering images provided information which helped coil the aneurysm without remodeling. **E–G** On the left side, surface rendering images provided information leading to the decision to clip this aneurysm. **H** Follow-up after both treatments

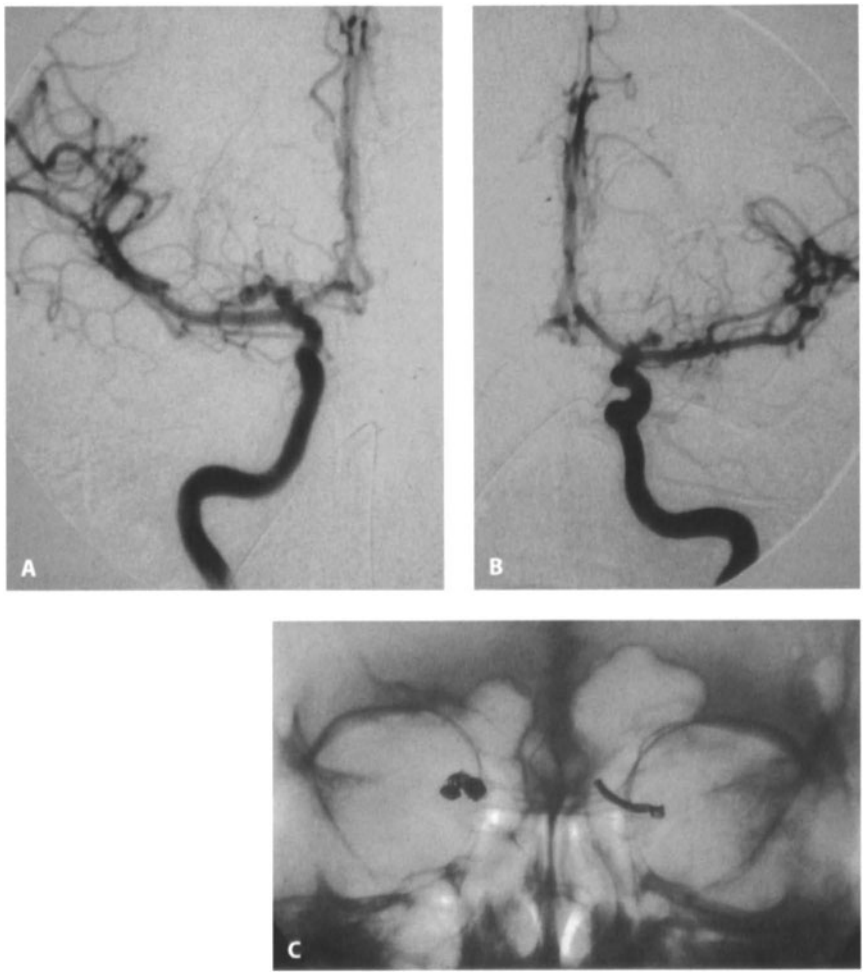

Fig. 7.145. **A** Ruptured right internal carotid artery aneurysm with false sac, **B** associated with mirror aneurysm. **C** Plain skull film after treatment

Kato et al. (1997), discussing 16 of 1,524 fully grown AAs, pointed to the period before recurrence is noted. AAs that recurred within 1 year after clipping had become larger 18.5 days on average after clipping; those that recurred 1 year or more after clipping became larger 7.3 years on average after clipping. Two patients had new AAs at other sites, three others developed AAs near the previously treated one, yet with no continuity (Fig. 7.147); two more had small bud-like AAs located on a distal branch of the MCA.

Hino et al. (2000) found that among patients with multiple aneurysms presenting with SAH, in five out of six cases where the aneurysm responsible for the bleed was not correctly diagnosed preoperatively, it was a problem of the aneurysm being missed on the original angiogram. Autopsy data have confirmed angiographic misses, with 12% of patients thought to have a single aneurysm actually harboring more than one, and 8% of patients with recognized multiple aneurysms on angiography having more than expected (McKissock et al. 1964). The use of rotational angiography (with or without 3-D reconstruction) and close scrutiny of the angiogram by one or more individuals may help to reduce these numbers (Figs. 7.95, 7.138, 7.139).

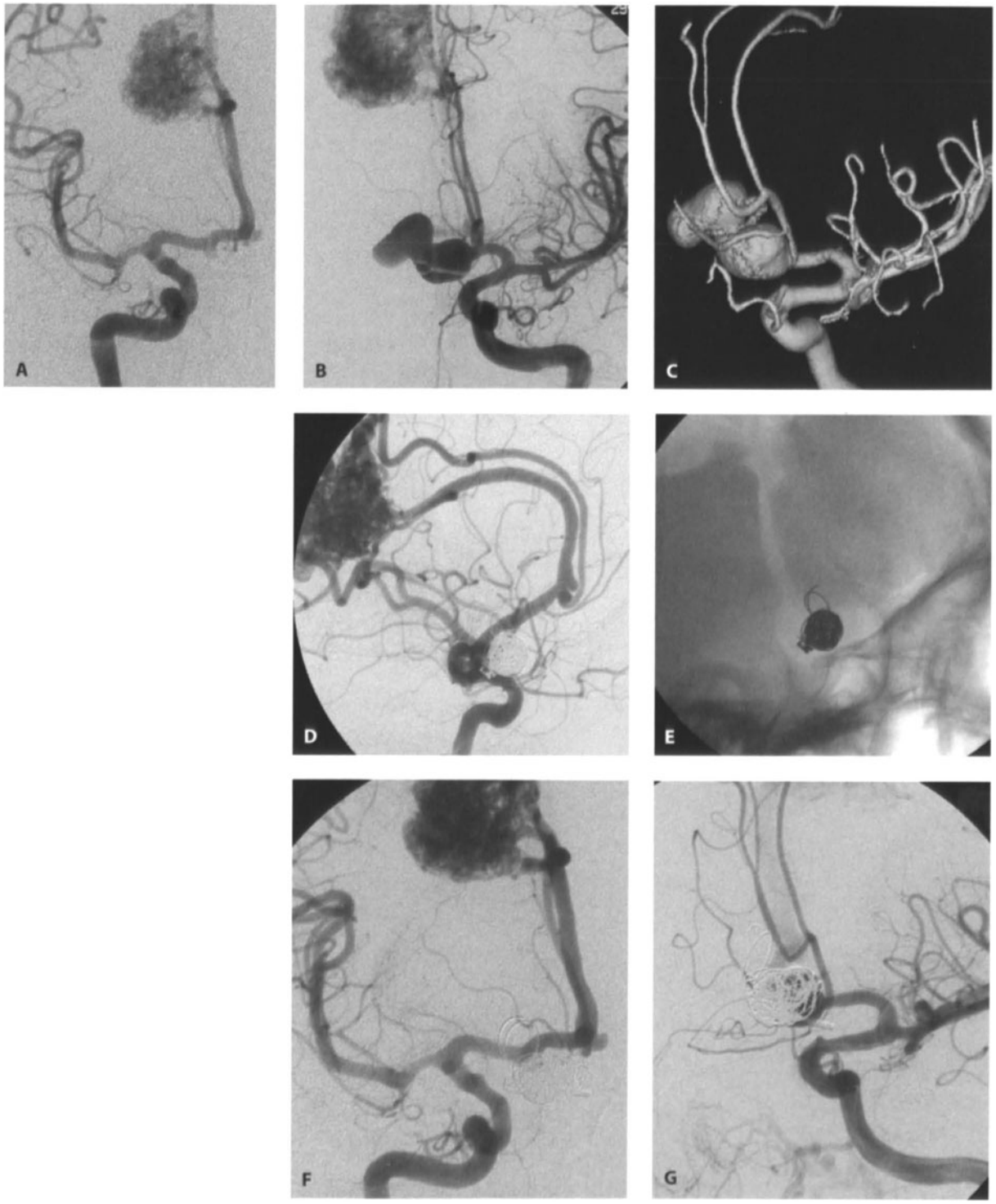

Fig. 7.146A–G. This 46-year-old male patient had presented with several hemorrhagic episodes during the past 20 years and a giant AComA had been previously clipped but demonstrated recurrence. A3 ACA aneurysm associated with a medium-sized frontal arteriovenous malformation(AVM) was also noted (**A–C**). **D–G** The proximal aspect of the multilobulated recurrent AComA aneurysm was preventively coiled prior to embolization of the AVM

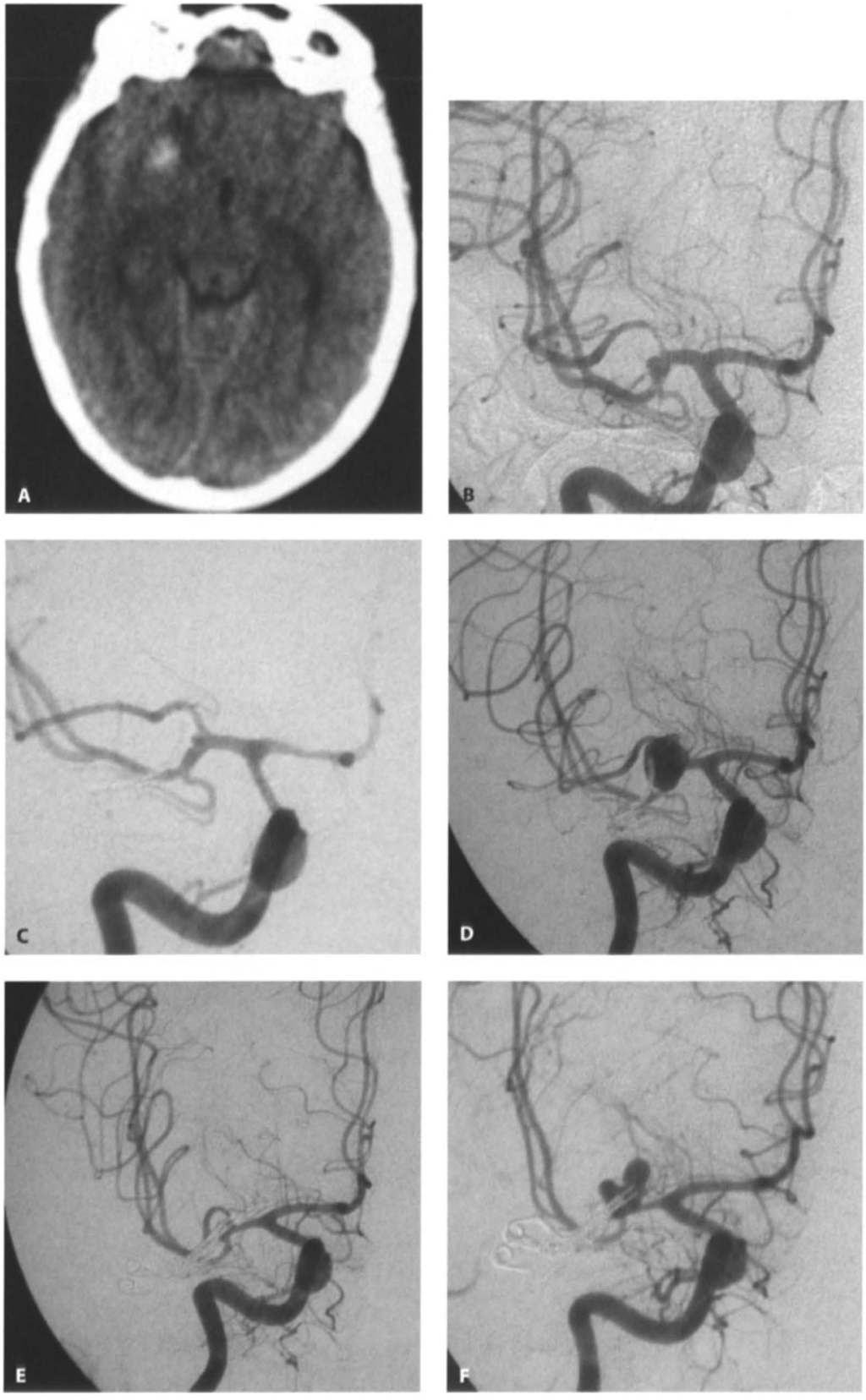

Fig. 7.147A–F. Legend see p. 559

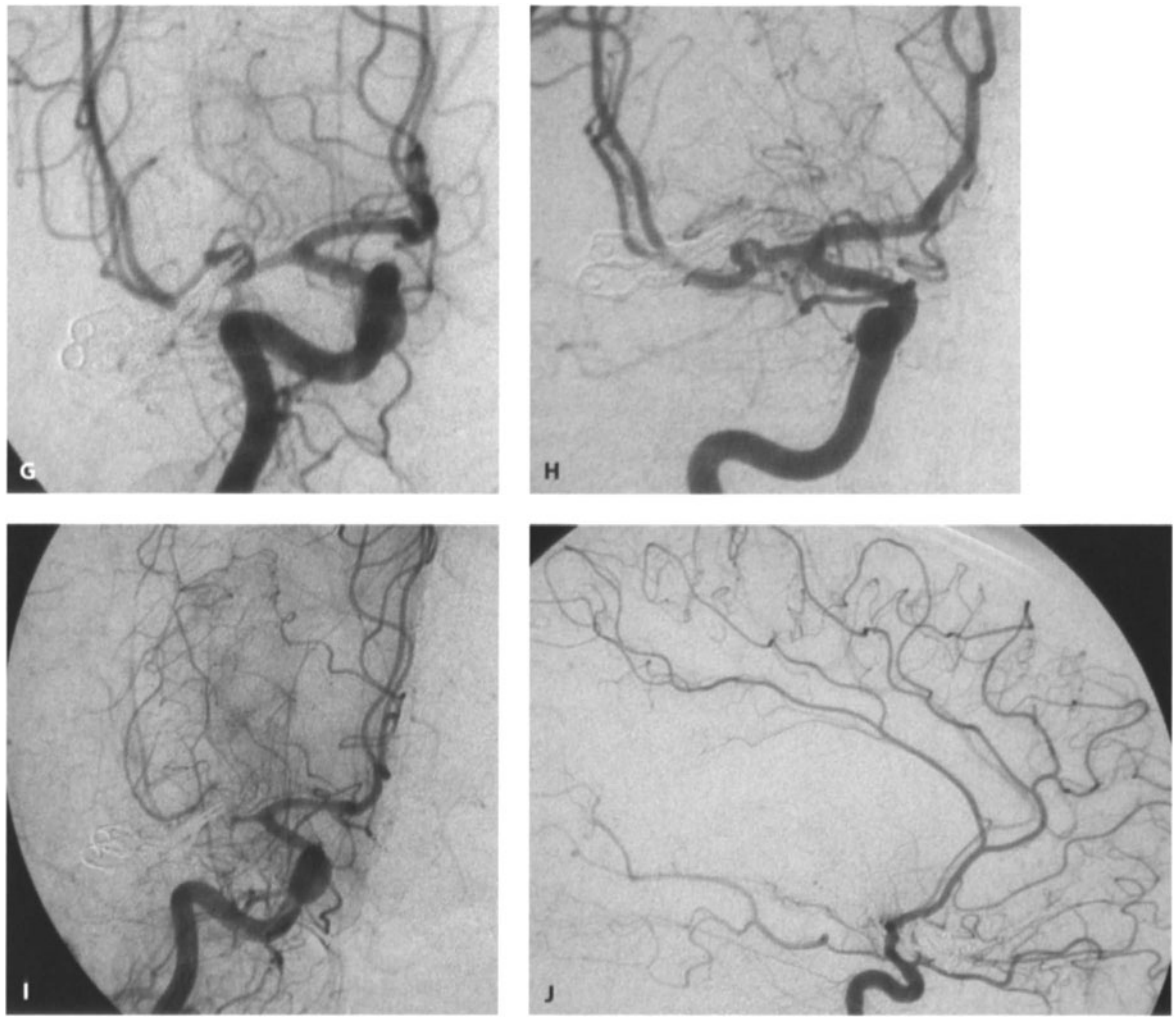

◀ **Fig. 7.147.** December 1999: non-contrast CT demonstrated hematoma in right temporal lobe with subarachnoid hemorrhage in right sylvian fissure (**A**). **B** Subsequent cerebral angiogram revealed an aneurysm at the right middle cerebral artery (MCA) bifurcation with small neck remnant of the aneurysm on the postoperative angiogram (**C**). April 2000. Patient was asymptomatic but regrowth of the aneurysm in the subsequent cerebral angiogram was noted (**C**). Small neck remnant persisted after second surgical clipping (**D**). Frontal internal carotid artery angiogram revealed partial thrombosis and decreasing size of the aneurysm after the failed STA–MCA by-pass surgery (**F**). September 2000. The neck of the aneurysm enlarged further to become a bilobed aneurysm 5 months after the second clipping (**E**). One week after the surgical attempt, transient (2 days) left-sided upper limb weakness occurred. The aneurysm became smaller with a clot within the sac of the aneurysm (**G**). Flow to the distal MCA branches was decreased and the caliber of the MCA branches was diminished. October 2000. Frontal (**H**) and lateral (**I**) cerebral angiogram show complete obliteration of the aneurysm and the right MCA at its bifurcation. **J** Thrombosed right MCA extended to the first insular branch. Clinically, mild weakness of the right hand persisted but slowly recovered with physiotherapy. (From Tan et al. 2001, with permission)

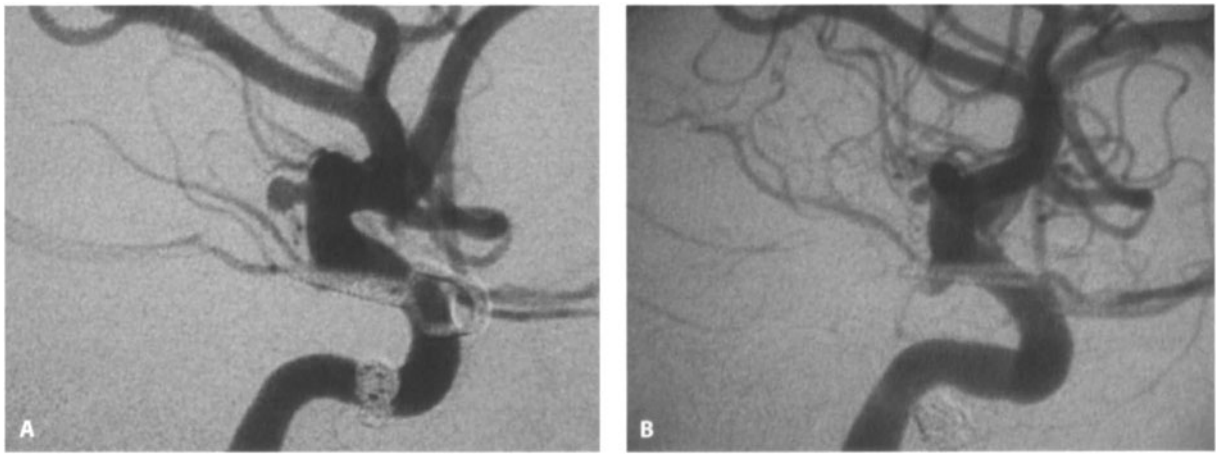

Fig. 7.148. Patient had presented with subarachnoid hemorrhage and three arterial aneurysms (AAs) were demonstrated: one was coiled, one was operated on, and the third was left untreated (*arrow*) (**A**). Three-year follow-up angiogram (**B**) showed significant shrinkage of the untreated AA (*arrow*)

Thus, a major problem in patients with multiple aneurysms is recognizing all the aneurysms, not only choosing the correct one responsible for the hemorrhage. Follow-up of these cases is crucial, as it may demonstrate spontaneous increase (Fig. 7.147) or shrinkage of untreated AAs (Figs. 7.148, 7.149). In other situations, recurrent SAH is wrongly attributed to the previously coiled or clipped or untreated AA, where in fact it was caused by a new lesion either close to or remote from the operative site.

Consequently, one must always be cautious when referring to a newly discovered aneurysm as de novo, as opposed to one that is simply recognized at subsequent angiography (Figs. 7.138, 7.139). Prior studies have estimated rates of de novo formation to be approximately 2% per year, with a suggestion that the risk may be increased in patients with multiple aneurysms (David et al. 1999; Juvela et al. 1993b). Porter's (2001) data are within that range (0.76% of patients per year). Patients may have a clear underlying predisposition, Ehlers–Danlos syndrome, PKD1, FMD, or hypertension (Sakaki et al. 1993).

Although some studies (Vajda 1992; Rinne et al. 1995; Mizoi et al. 1989; Pierot et al. 1997; Solander et al. 1999) have suggested poorer outcomes in patients with multiple aneurysms, our surgical and endovascular complication rates and patient outcomes were not dissimilar from what one would expect for single-aneurysm patients.

7.8.5 Management of Giant Arterial Aneurysms

Giant AAs have to be discussed nearly on a case-by-case basis, as the features vary from one individual to the next. Most of the classic papers dealing with giant AAs discussed them almost individually (Drake and Peerless 1997; Yasargil 1984; Pia et al. 1979; Suzuki and Yoshimoto 1979; Kupersmith 1993; Kim and Choi 2000). The therapeutic morbidity and

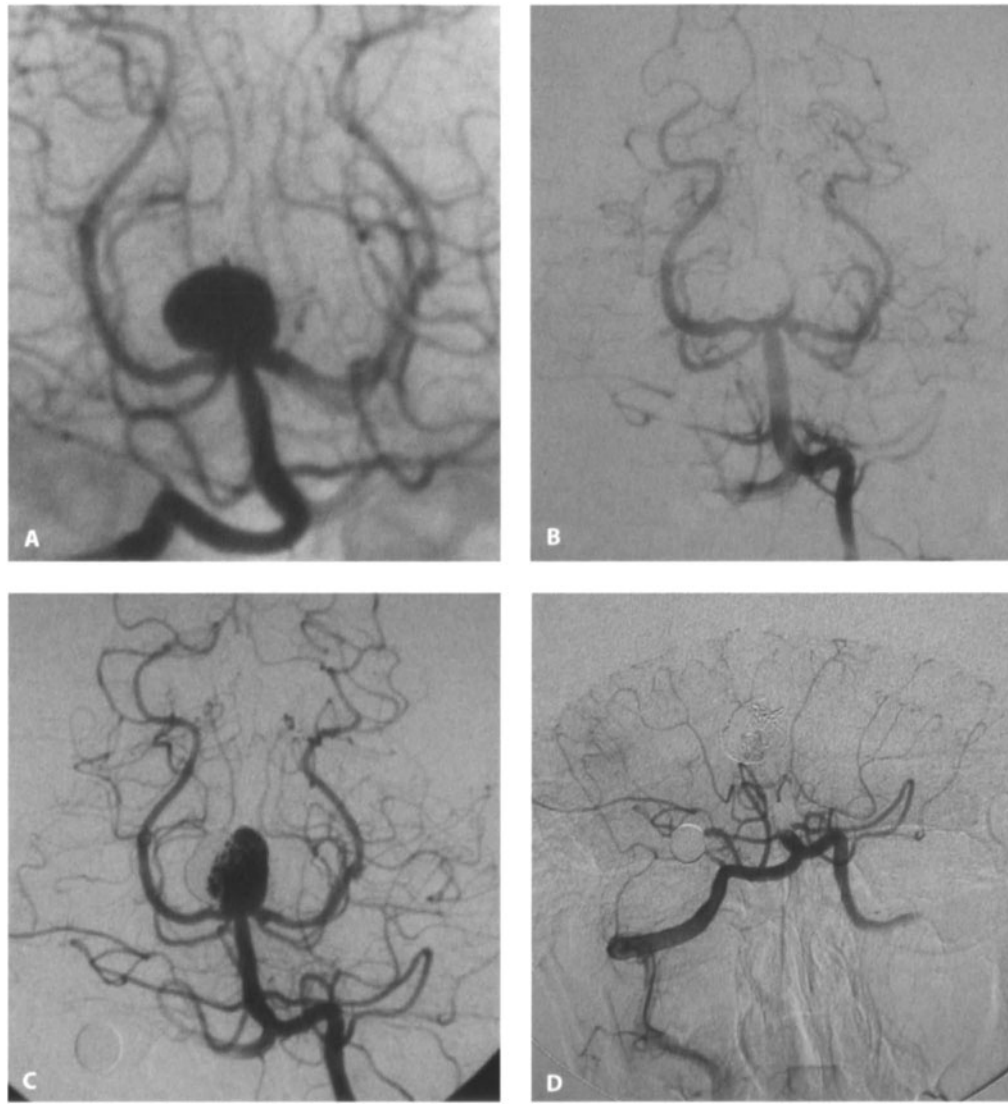

Fig. 7.149. **A** Subarachnoid hemorrhage with large basilar tip arterial aneurysm (AA). **B** Incomplete coiling as shown on immediate postembolization angiogram. Follow-up angiogram shows both compaction and regrowth of the AA (**C**). Test occlusion at the level of the mid-basilar trunk (**D**) was well tolerated clinically but significant stagnation is seen in the AA. Fearing a major delayed stroke, we elected to occlude both vertebral arteries (VAs) in two sessions. Following the second sacrifice, the patient was placed on heparin therapy for a few weeks. At discontinuation, the patient developed mild diencephalic stroke with thalamic dysphasia from which he recovered almost completely. **E–J** see pp. 562, 563

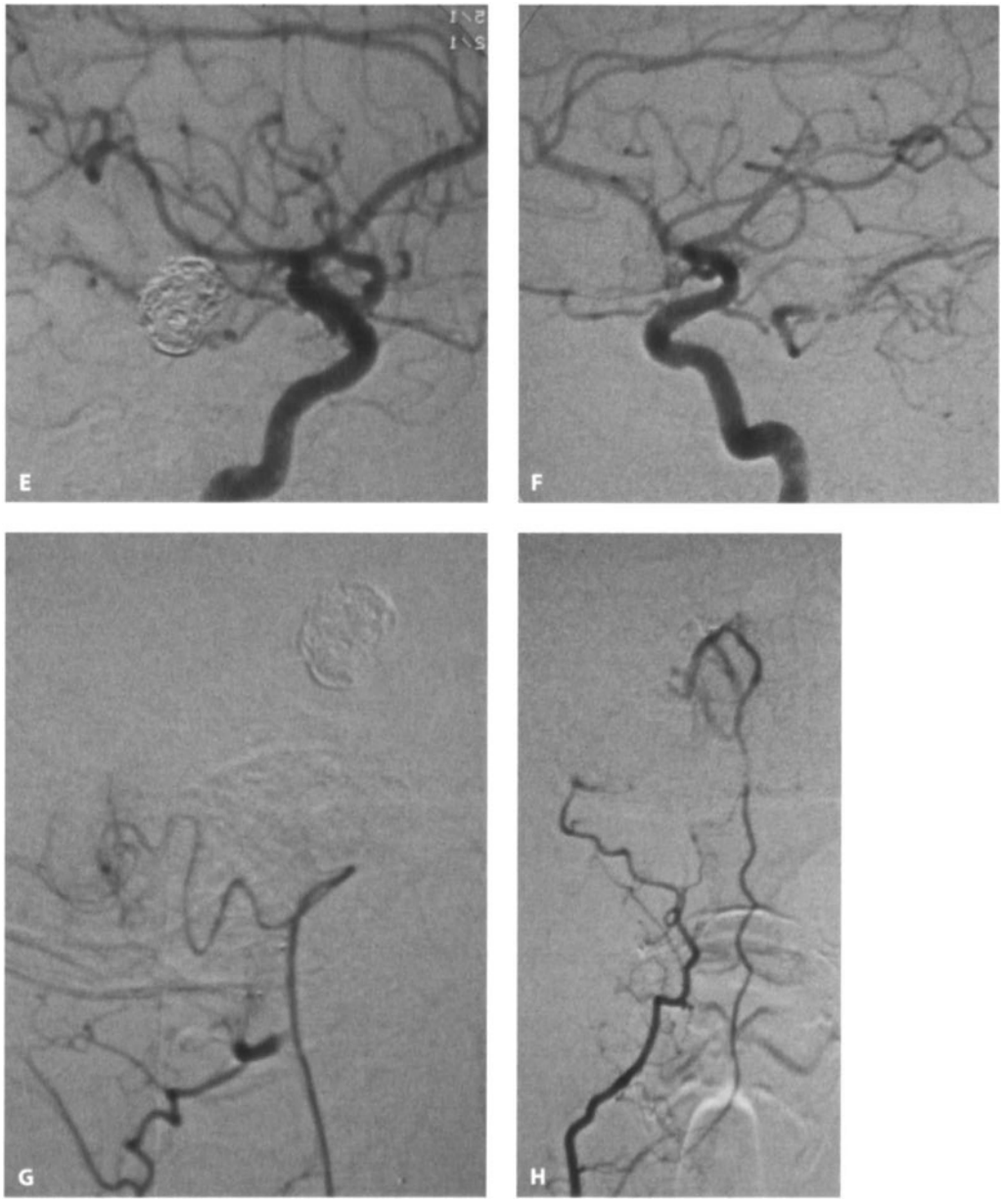

Fig. 7.149 (*continued*). Follow-up angiogram 10 years later shows excellent remodeling of the upper basilar system (**E, F**) and ASA collateral circulation to the right PICA (**G, H**), and cervical to C1 VA on the left. **I, J** see p. 563 ►

mortality is often high. The preventive treatment is based on assumptions that may not apply to every type (biological). As seen previously, some AAs will shrink after completion of their partial thrombosis while others may (although rarely) grow unpredictably. The risk of hemorrhage of giant AAs is unclear and cannot be balanced against the therapeutic risk unless one is dealing with a dissecting giant AA at the acute stage (Fig. 7.72). As discussed above, giant lesions cannot be considered to include ICA cavernous, VA, BA, and MCA aneurysms in the same nosological fashion, even if the challenge of the parent artery posttherapeutic patency and ex-

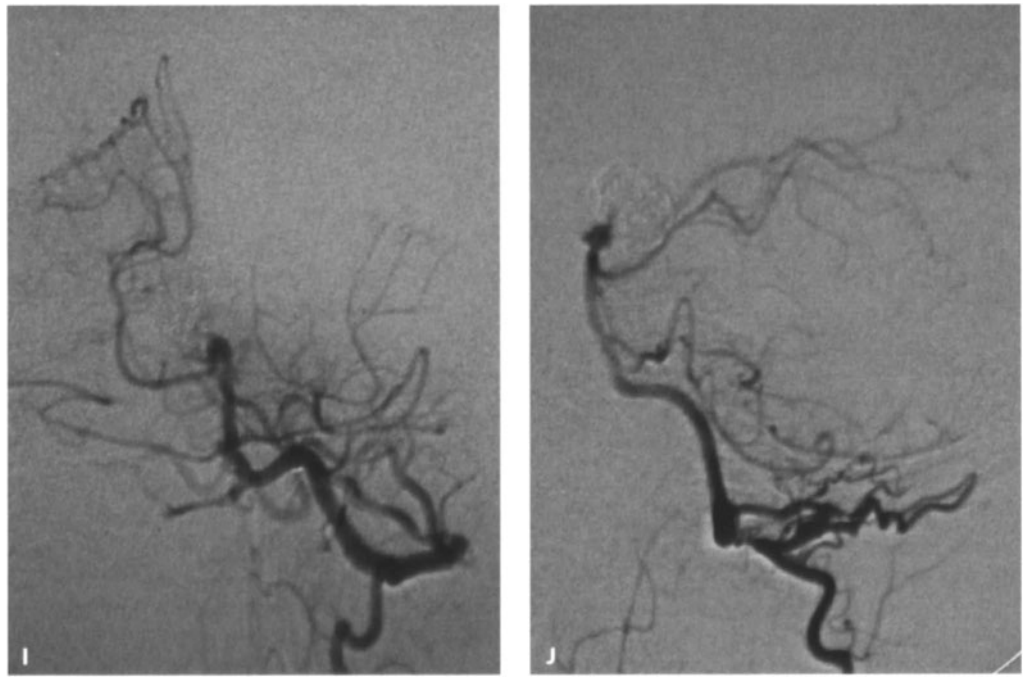

Fig. 7.149 I, F. Legend see p. 562

clusion of the AA lumen are a common concern for all of them. Careful collection of high-quality pictures of the lesion, arterial layout, sources of actual and potential collateral circulation must be thoroughly documented, including external carotid branches, the leptomeningeal network, and the spinal cord (Fig. 7.150), depending on the treatment planned. Given that giant AAs are primarily an uncontrolled or repeatedly stimulated proliferative situation, assessment of growth factor activity and angiogenic potentials will contribute to the future decision and treatment of such targets. At present various techniques can be used:

- Sacrifice of the parent artery with the risk of distal ischemia.
- Intraluminal coiling with the risk of emboli and secondary compaction.
- Liquid filling is still under evaluation, with significant technical skills required and no significant follow-up available at the present time.
- Stenting in some favorable extradural situation will also represent a direction for future management of intradural wide-neck and giant AAs.
- Surgical approaches and reconstructions or by-passes.

The goal of treatment has to clearly express correction or prevention of mass effect, hemodynamic strokes, risk of hemorrhage, embolic strokes, recurrent dissecting process, vasa vasorum rupture, and growth.

Most of the treated lesions do not recur after parent artery occlusion; some do in the immediate postoperative course (Blanc et al. 2001) or after spontaneous thrombosis as a peculiar natural course (Meziti et al. 1998). The more patent the lumen, the more likely that the shrinkage will be obtained after complete exclusion of the AA. Early experience of coiling in partially thrombosed giant or large AAs was disappointing, with a high rate of migration of the coils inside the clotted portion.

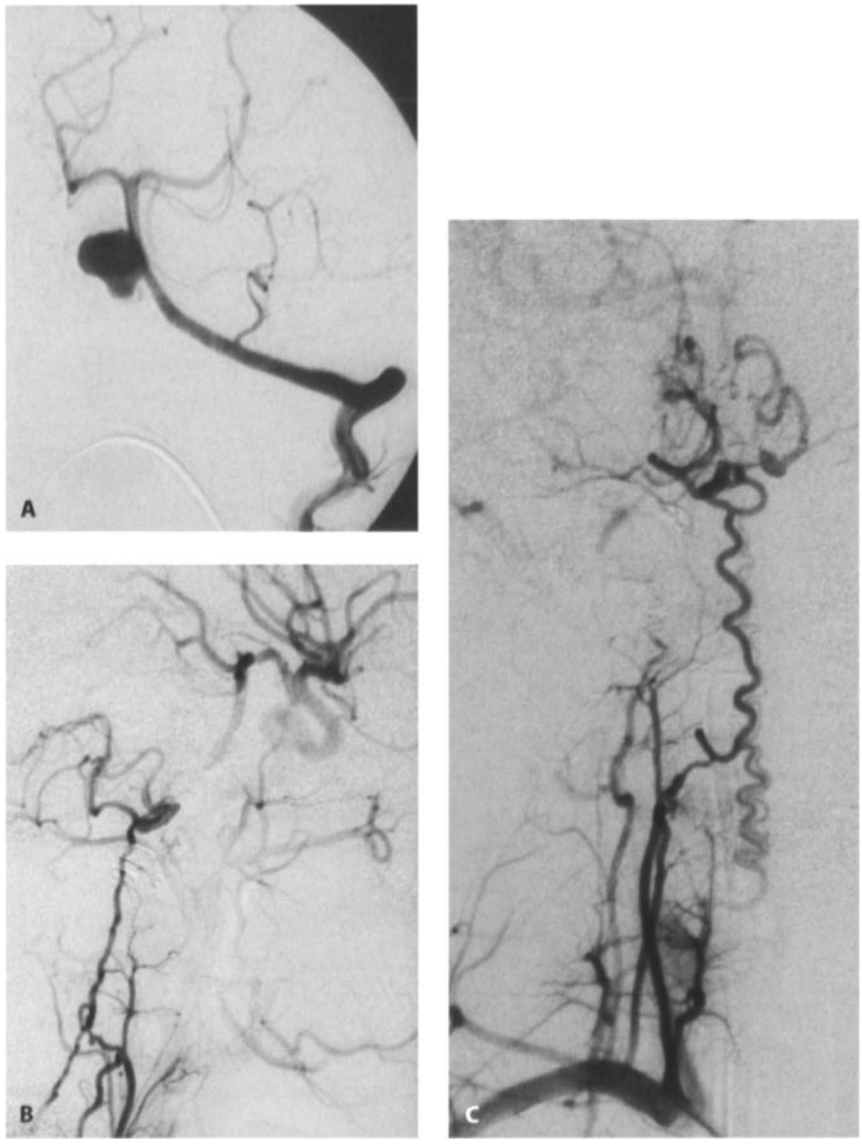

Fig. 7.150. A 7-year-old boy presented with subarachnoid hemorrhage from a mid-basilar arterial aneurysm (**A**). Vertebral arteries were occluded bilaterally. At follow-up 3 years later, there were good collaterals to the PICA from the upper basilar and ventral spinal arteries (**B, C**). Nevertheless, the aneurysm was partially filled. It was then excluded by upper basilar retrograde catheterization with no clinical complications. (Courtesy of J. Bakke)

In cases with sudden worsening, the inflammatory component of the symptoms may require steroid management for a few weeks; this is often sufficient to obtain relief of symptoms and conservative management. Acute manifestations do not always represent SAH or potential risk of SAH by AA rupture. Some of these lesions are chronic (recurrent) or subacute dissection in the subadventitial space and can probably cause bleeding focally with a different morbidity and mortality than saccular AA. The new dissecting event may also include a perforator and be responsible for a nonmechanical symptom (mass effect) instead of being ischemic, which would require medical treatment. The capacity of remodeling after complete AA exclusion is sometimes amazing, in particular in children (see Vol. 3).

Subject Index for Volumes 2.1 and 2.2

A
abciximab 36, 38
acetylcholine 13
acrylate 973, 977, 991, 993, 1059, 1059–1074
- carciogenesis 1063
- catheter withdrawal 1069
- continuous column 1069
- cyanoacrylate 1025
- flow-control 1069
- HEMA (hydroxy-methylmethacrylate) 1144
- histoacryl 1060
- histotoxicity 1060–1063
- IBCA (isobutyl homologue isobutyl-2-cyanoacrylate) 1059
- in situ injection 1069
- injection 1063–1066
- mutagenecity 1063
- NBCA (N-butyl-cyanoacrylate) 332, 946, 1059, 1063, 1140
- octacyanoacrylate 1055, 1059
ACT (activation coagulation time) 923
activated clotting time 38
activated coagulation monitoring 924, 925
Aculynker 1175
adenoma, parathyroid 269
adenosine 14
adenosine diphosphate 14
adenosine receptor antagonists 35
adrenal carcinoma 271
Agility, guidewire 965
AIDS 509
amaurosis fugax 74, 406, 407
amines 12
amobarbital 925–929, 1125
amytal 1125
anastomosis
- intrinsic venous 795
- protection 1101
anastomotic system, intrinsic longitudinal 777
anatomy, venous MRI 141
anesthesia 919–929
- general 919, 920
- input and output monitoring 921
- local 920
- neuroleptic 920
aneurysm
- age 380–382
- anatomy, single/mirror/twin saccular arterial aneurysm 442–453
- arteriovenous malformation 708–715
- - spinal cord 786–794
- associated post-traumatic 59
- associated with proliferative diseases 523, 524
- atherosclerotic 398
- bleeding rate 451
- blister 482–486
- classification 374, 375
- clonal mutation/clonal phenotype 379
- coarctation of the aorta 524–527
- congenital 377
- congenital heart disorders 524–527
- de novo 547, 548
- dissecting (*see also* dissection) 60, 333, 454–477, 1027, 1046
- dolichoectatic type 479, 481–483
- dysplastic 401, 653, 789
- embryological origin 377–380
- extradural 382–430, 1020
- - external carotid artery 425–431
- - - facial artery, false 427
- - - internal maxillary artery 425
- - - superficial temporal 425
- - internal carotid artery 382–384
- - - blunt trauma 389–393
- - - cavernous segment 401–407
- - - cervical 384, 385
- - - clinical presentation 408–415
- - - developmental 385–387
- - - dissection, spontaneous 394–398
- - - mycotic 398, 421
- - - occlusion 417–420
- - - penetrating trauma 387–389
- - - petrous 399–401
- - vertebral 420–425
- familial forms 366
- - nonsyndromic familial 438–440
- false 135, 278, 550, 790, 799, 1109
- fenestration 1016
- flow-related 333, 376, 429, 514–517, 646–653, 787
- fusiform 478, 484, 497
- hypophysial 998
- incidence 366
- intercostal 526
- intradural 431–453
- - giant saccular 478–486
- - - with thrombosis 486–497
- - giant nonsaccular 478–486, 497, 498
- - immunological 509–513
- - infectious 502–509
- - inflammatory diseases 513
- - traumatic 518–522
- location 451, 515
- male-to-female ratio 375
- megadolicho artery 498–500
- mesencephalic region 450
- mid-basilar 1049
- middle cerebral artery 135
- mirror 448, 449, 453, 555, 556
- - giant 500
- morbidity 367, 538, 547
- mortality 367, 538, 547
- multiple 453
- - giant 500
- mycotic 398, 421, 502–509
- origin 378
- phylogenetic age 376
- physiopathogenesis 371–374
- preexisting 279
- prevalence 366
- prosencephalic region 450
- proximal, shape 515
- pseudoaneurysm 347, 389, 421, 653, 662, 776
- regrowth 554, 559
- rhombencephalic region 450
- risk 371–374
- rupture 1141, 1142
- saccular

aneurysm
- saccular multiple 440–442, 442
- - single 453
- segmental vulnerability 375–377
- serpentine arterial 498–500
- shrinkage 560
- sphenoid sinus 322
- thrombosis 470
- topography 372
- traumatic 283, 360, 973, 1046
- treatment 527–563
- - balloon remodeling 1031–1037
- - coil 1030
- - combined endovascular treatment 1147, 1148
- - deconstructive operation 1020–1028
- - endovascular treatment
- - - literature review 530, 531
- - - results 538–549
- - EVAL 1083–1089
- - giant arterial aneurysm 560–564
- - method 532–538
- - multiple arterial aneurysms 549–560
- - postembolization care 1128, 1129
- - reconstructive operation 1030
- - sclerotherapy 1074–1083
- - second intervention 529
- - *Trispan* 1039–1043
- - two-microcatheter technique 1039, 1040
- unrupted 380, 545
- - natural history 546
- venous 790
- wide-neck 1031
angiofibroma, juvenile
- angiography 211–214
- clinical findings 210
- CT examination 211
- development, global hypothesis 207–210
- embolization 214
- - technical aspects 221–223
- epidemiology 205
- extension
- - intracranial, false 213
- - intracranial, true 211–213
- - pattern 202
- invasion, pattern 203
- macroscopic pathology 201–204
- microscopic pathology 204, 205
- MRI examination 211
- nasal mucosa 206
- natural history 211
- pathophysiology 206–210
- radiation therapy 221
- sex hormons 206
- therapeutic findings 214–221
- tumor recurrence 223
angiogenesis 378, 756
angiography, angiographic evaluation 41–44
- carotid 84
- catheter, 3-D selective 85
- cerebral 100–103
- computer tomographic (CTA) 78–80, 99, 100
- follow-up angiography 535
- MRA (magnetic resonance angiography) 80–83, 100, 535
angiopathy, high-flow 786
angioplasty 53, 90–98, 116–135
- balloon (*see there*)
- techniques 1152–1181
- - intervention 1154–1163
- - postdeployment 1173
- - predilatation 1164
- - premedication 1153, 1154
- - vasoactive medication 1154
- and stenting (CAS) 92
angioseal 933
angiotensin II 14
anterior horn syndrome 839
antibiotics 505
anticoagulation 104, 804, 845, 1132, 1133
anticonvulsants 918, 919
antiedema 1134, 1135
antiphospholipid antibody syndrome 141
antiplatelets 34, 398, 475, 919, 1128, 1132
α_1-antitrypsin deficiency 58
aorta
- abdominal 23
- coarctation 786
aortic arch study 41, 42
aortitis syndrome 526
apoptosis 378
Aquaphor 1130
arterial stenosis 524
arteriopathy, idiopathic regressing 57, 58
arteriotomy sites 929–933
- closure device 932, 933
- introducer sheath 930
arteritis, *Takayasu* 115, 116
aspirin 34, 35, 39, 419, 495, 1153
astrocyte 3
atheroma, aortic arch 99
atherosclerosis 23–29, 73
- accelerated 97
- atherogenesis, mechanisms 24–27
- carotid 29
- epidemiology 23
- introduction 23
- middle cerebral artery 44
- pathogenesis 24
ATP 8
atropine 917, 1152, 1154
Attracter 18 1052
austenite phase 1170
autoregulation, cerebral 5–7, 22, 40
- breakthrough 6
Avatine 1077
azygos vein 739

B
balloon angioplasty 36, 53, 57, 62, 68, 80, 95
- guidewire through balloon technique 123, 124
- *Higashida* balloon catheter 119
- latex balloon 122–124
- over-the-guidewire balloon tip catheter 125
- over-the-guidewire *Dotter* technique 125
- silicone balloon 119–121
- vasospasm, indications and results 128–133
barbiturates 1135
baroreceptor 1152
Barthel Index 150–152
basilar artery
- thrombosis 110–114
- unfused 447
BAVM (*see* malformation, arteriovenous)
Berenstein
- double lumen occlusive balloon catheter 944
- liquid coil (BLC) 993, 995
- variable stiffness 934
bicuspid aortic valve 524
bifemoral approach 1030
biopsy, epistaxis 359
biorheological factors 1133, 1134
blebs 482, 484, 542
blindness, transient monocular 74
blister 482–486
blood flow, cerebral (*see* CBF)
blood pressure 433
blood-brain barrier 3, 4, 10
blunt trauma 389–393
bone
- cyst, aneurysmal 890–892
- erosion 410, 414, 755
brachial nerve, deficit 805
brachiocephalic vessel 106
- totally occluded 1176–1178
brachytherapy, endovascular 1019
bradykinin 13
breast carcinoma 155, 272

bruit
- carotid 73
- dural arteriovenous shunt 581, 582
- traumatic arteriovenous fistula 299, 300
- vertebro-vertebral arteriovenous fistula 751
bypass 102, 105, 1020, 1027, 1029

C
Ca^{2+} channel blocker 918, 921
calcification 1163
- arteriovenous malformation 676, 677
- mural 472, 500
calcitonin gene-related peptide 13
calcium channel antagonist 21, 1135
calibrated leak technique 119–127, 130, 959, 961
candida albicans 509
candidosis, chronic mucocutaneous 509
capilarectasia 472
capilary 3
CAPTURE 38
carbon dioxide reactivity 9
carbon monoxide 14
cardiac overload 739
carotid artery 931
- extracranial, stenosis
- - asymptomatic 86–89
- - imaging 75–84
- - natural history 73–75
- - symptomatic 86
- - treatment 84, 85
- internal
- - aneurysm, extradural (*see there*)
- - dissection 57–67
- - ligation 418
- - occlusion 48, 52–57, 417, 418
- - - intravenous thrombolysis 56
- - - revascularization 55
- - - tolerance test occlusion 418–420
- - stenosis, above carotid bulb 68, 69
- petrous 103
- physiology 1096
carotid bulb 1153
carotid trapping 389
catheter, balloon 53
- angioplasty 958–961
- balloon-tip 1031
- *Berenstein* variable stiffness 934
- detachable 955–958, 1006
- double-lumen 924, 943–949
- - *Berenstein* 944
- - *Comodor* 125, 950
- - modified 950
- *Envoy 5-F* 935
- flow control 942, 943
- *Fogarty* 280
- *Flowrider* 1091
- guiding catheter 933, 935
- *Headway* catheter 935
- *Hieshima Apollo* 958, 959
- *Higashida* balloon catheter 119, 953
- *Lasjaunias 4-F* catheter 986
- latex balloon 122–124, 325, 957, 958
- - *Debrun* 957, 958, 960, 1144
- - gold valve balloon 957
- - *O'Reilly* 958
- microcatheter (*see there*)
- *Mini-Torquer* 936, 942, 943
- silastic 958
- silicone balloon 119–121, 326
- single-lumen 950–955
- - *Endeavor* 952
- - *Equinox* 125, 956, 959, 1034, 1085
- - *Hyperglide* 956
- - *Sentry* 125, 955, 958, 1034
- - *Stealth* 125, 950, 952, 958
- stent delivery 962–964
- tolerance testing 314, 942, 943, 1020, 1029, 1030
- withdrawal 1069, 1111
catheterization, distal 1106, 1107
caudal fusion 444
CAVATAS 93
cavernoma 587, 687–690
- classification 687
- de novo 688
- familial 688
- multiple 689
CBF (cerebral blood flow) 4, 5, 27
- metabolism 8
- regional (rCBF) 10
CBV (cerebral blood volume) 7
cerebral arteriovenous malformation (*see also* shunt)
- angioarchitecture 631–634
- aneurysms (*see there*)
- arteries 634
- brain function 678, 679
- calcifications 676, 677
- cavernoma 687–690
- choroid plexus 629–631
- classification 614, 615
- - principles 612–614
- cryptic 690
- CSF changes 676
- DAVS (*see* arteriovenous shunt, dural)
- deep-seated 629
- dural supply 642–644
- fistula (*see there*)
- headache 681–683, 704, 707
- hemangioma, cavernous 686, 687
- hemorrhage 677, 678, 703, 704
- incidence 609–612
- lesions, reach the cortex 626
- management/treatment 695–735
- - age 700, 701
- - combined endovascular treatment 1147, 1150
- - embolization
- - - contraindications 732–734
- - - curative 720–727
- - - emergency 732
- - - intraoperative 729
- - - palliative 720
- - - partial (targeted) 716–720
- - - postembolization care 1128
- - - presurgical 728, 729
- - - prior to radiosurgery 729–731
- - - results 734, 735
- - - staging 732
- - indications 696–699
- - lifestyle/occupation 701
- - location/size 708
- - sex 701
- - strategy 715, 716
- - symptoms 703–708
- maxillofacial 1083
- microarteriovenous 655, 656, 940
- multiple 618–625
- natural history 677
- neurological deficit 708
- nidus 794–801
- - angioarchitecture 654, 655
- - intranidal ectasias 659–664
- - size change 656–659
- occult 690
- paravertebral 862
- pregnancy 683, 684
- rupture 1137–1141
- seizures 679, 680, 704
- stenotic changes 638–642
- thrombosis 669
- topographic analysis 625, 626
- unclassified 624, 625
- variations, arterial 644–646
- vasospasm 642
- veins 668
- - developmental anomalies 685
- - variations 668–675, 684
cerebral artery, middle (MCA)
- hyperdense sign 60
- stroke 44, 45
cerebral-facial syndromes 621–624
chemoembolization 877–880, 1094

chemotherapy 1093, 1094
- intra-arterial infusion 1093, 1094
chiasmatic ectasia 336
Chlamydia pneumoniae 24
chromosome
- chromosome 4 431, 432
- chromosome 9 436
- chromosome 16 431, 436
- chromosome 17 435
cigarette smoking 440
cisplatinum 1094
clipping 131
clival artery, lateral 569
clopidogrel 35
closed-cell design 1164
closure device 923, 1129
CMV (cytomegalovirus) 512
coagulation profile 99
coagulopathy 357
coarctation, aorta, aneurysm 524–527
coaxial assembly system 1155
Cobb syndrome 755, 773
coil
- *Cordis 3-D* 1000, 1012, 1013
- 3-D shape memory 1000
- detachable 981, 1030
- - *Cook* 1012, 1013
- - *Guglielmi* 528, 998–1002
- - radioactive 1019
- fiber 746, 980
- fixation 1053
- GDC, bioabsorbable polymeric 1012, 1016
- *Gianturco* coils 980
- glue, combination 991
- *Hilal* coil 987
- hydrocoil 1012, 1014
- liquid 980, 981, 1066
- - *Berenstein* 993, 995, 1118, 1119
- microcoils 986, 1025
- *Micrus* 1010, 1011
- pusher 987
- retrieval 1051
- stretch-resistant 1000–1002
- stretching 1045
- ultrasoft 1000
COL5A1/COL5A2 gene 434
collagen disease 739
collateral circulation 101, 314
combined endovascular treatment
- aneurysm therapy 1147
- brain arteriovenous malformation 1147
- occlusive/hemorrhagic vascular disease 1147
Comodor double-lumen balloon-tip catheter 125, 950
compaction 537, 562, 1035, 1039, 1049, 1090
complications, embolization 1129–1146
connective tissue disorder 396
contiguous gene syndrome 436, 437
contraceptives, oral 136
contrast material, extravasation 359, 361, 1136, 1139
conus medularis 839
Cook detachable coil 1012, 1013
Cordis 3-D coil 1000, 1012, 1013
Corinthian stent 1171
cortical artery, occlusion 54
corticosteroids 918, 1096, 1129
costocervical artery 747
coumadin 39
cranial nerve
- deficit 1129
- dysfunction 285, 298–300
- paralysis 476
- symptoms 580, 581
cranial sinus 739
craniofacial tumor 270–275
CREST (carotid revascularization endarterectomy versus stenting trial) 93
CT (computed tomography) 30
CTA (computer tomographic angiography) 78–80, 99, 100
cutaneous discoloration 756
cyanoacrylate 1025
cyst
- liver 437
- renal 433
cytokinase 10
cytotoxics 1059

D
DAVS (dural arteriovenous shunt) 565–607
- associated conditions 590–593
- cavernous sinus 603, 996
- classification 570, 575–579
- cranial fossa, anterior 589, 602
- cranial nerve symptoms 580, 581
- clinical presentation 579–593
- neurological deficits
- - focal 582–585
- - global 585–587
- foramen magnum 583, 589, 603
- historical review 566–569
- hormonal influence 587, 588
- intracranial hemorrhage 587
- multiplicity 590–593
- natural history 594–596
- pathophysiology 570, 571
- pretherapeutic evaluation 598
- sagital sinus, superior 602
- symptoms, progression 596–598
- tentorium 602
- therapy
- - embolization 983
- - - complications 606
- - - results 606
- - - timing 605, 606
- - indications/strategy 598–602
- - surgery 607
- - technical aspects 605
- - topographic considerations 602–605
- tinnitus and objective bruits 581, 582
- torcular 583
- transverse sinus 582, 603
Debrun catheter 957, 958, 960, 1144
deconstructive operation 1002, 1020–1028
- middle cerebral artery aneurysm 1023
- vertebrobasilar junction aneurysm 1020
degeneration, neuronal 20
- anterograde 21
- axon (*Wallerian*) 21
- retrograde 21
delta sign 138
dextran 1133
dialysis, peritoneal 433
diastolic fraction 514
DIC (dissemianted intravascular coagulation) 406
diplopia 298, 405
diseases (*see* syndromes)
dissection 106
- carotid 57–67, 1159
- - iatrogenic 65
- - spontaneous 394
- catheter 1159
- complications 477
- fusiform 456, 467, 468
- healing, spontaneous 468
- intracranial iatrogenic 1179
- intradural artery 454–477
- multifocality 469
- mural diseases 477
- process 478
- subacute 472
- subadventitial 391
- subintimal 454
- vertebral artery 83
DMSO (dimethyl sulfoxide solvent) 1083
dopamine 12, 1154
Doppler
- color-flow 76
- transcranial 76, 99
double lumen 393, 395
drainage
- bilateral 289
- external ventricular (EVD) 1141

- venous, thrombosed 793
drug treatment 97
dual therapy 34
duplex scan 76
duplex ultrasonography, carotid 74
dural venous plexus 572, 573
DWI (diffusion-weighted imaging) 70–72, 81, 100

E
echocardiography, transesophageal 99
ECST 86, 87
ectasia, segmental 481
edema, brain 1134
edematous reaction 490
EEG 918
Ehlers-Danlos syndrome 57, 279, 280, 297, 387, 434, 435, 743
eicosanoids 13
elastica lamina, internal (IEL) 456, 479
electrical current 998
electrolysis 998, 1039
embolic agents
- absorbable materials 970–973
- coils (*see there*)
- liquid 977
- nonabsorbable particulate materials 974–979
- particulate agents 969, 970
embolism
- cardiogenic 99
- pulmonary 138
embolization
- fluid 1050
- - liquids 1055
- - nonabsorbables 1059–1089
- - silicone fluid 947, 1059
- partial targeted 788, 792
- palliative 835
embospheres 977–979
endarterectomy, carotid (CEA) 86–89, 92, 105, 1153
- restenosis 89, 93–97
Endeavor catheter 952
endocarditis, subacute bacterial 503
endoluminal clot 392, 422, 423, 490, 543
endoscopy, virtual 534
endothelial cells 26, 51
- origin 452
endothelial dysfunction 24
endothelin 14
endothelium 10, 25, 94
Envoy 5-F 935
ephedrine 923
EPIC 97
epidural lake 751
epidural venous plexus, transvenous occlusion 749
epistaxis 303, 306, 354–359, 409, 426, 674
- biopsy 359
- coagulopathy 357
- emergency treatment 322
- spontaneous 357
- traumatic 362, 363
- tumoral 357–359
EPISTENT 37
eptifibatide 36
Equinox catheter 125, 956, 959, 1034, 1085
equipment, angiographic 917
esthesioneuroblastoma 199, 200
esthesioneuroepithelioma 224
ethanol 977
Ethiodol 1063, 1077, 1093
- ethanol-*Ethiodol* mixture 1079
ethmoidal artery, anterior/posterior 567
ethyl cellulose 1094
ethylic alcohol 1074–1083
- arterial system, injection 1075, 1076
- arteriovenous malformation, injection 1080–1083
- ethanol-*Ethiodol* mixture 1079
- venous malformation, injection 1076–1080
EVAL (ethylene-vinyl alcohol copolymer) 1059, 1083, 1084
EVOH (*see Onyx*)
Ewing's sarcoma 875
Excelsior 10 microcatheter 938
exophthalmos 285, 409
extravasation, contrast material 359, 361, 1136, 1139

F
facial nerve, monitoring 925, 926
Fahraeus-Lindqvist effect 8
false sac 517
female gender 440
FGF (fibroblast growth factor) 25
fibrinogen 35
fibrinolysis 67
fibromuscular dysplasia (FMD) 57, 338, 438, 743
- cervical 415–417
fibrous cap 26
filum terminale lesion 767, 789
Fisher's grading 369
fistula, arteriovenous
- carotid cavernous 520
- filum 774, 802
- high-flow 337, 778, 791, 991, 1066, 1119, 1124
- - congenital 945
- iatrogenic 341
- microarteriovenous 801
- parachordal
- - ascending pharyngeal-internal jugular (hypoglossal) 743
- - clinical manifestation 739
- - direct 784
- - general remarks 738–740
- - maxilla artery-to-vein (stapedial) 743
- - paraspinal 752–758
- - throacolumbar paraspinal 755
- - vertebro-vertebral (proatlantal and intersegmental, VVAVF) 743–752
- spinal dural (*see* SDAVF)
- tentorial dural 761
- traumatic 277–363
- - carotid cavernous 522
- - common carotid 342
- - external carotid 342–353
- - extracavernous 334–338
- - malignant 354
- - middle meningeal 345
- - scalp 343
- - traumatic carotid cavernous fistula (*see* TCCF)
- - vertebral 338–341
flow
- arrest 946, 1111
- bidirectional, *figure* 1100
- control 1097–1128
- - cerebral circulation 1104, 1105
- - cortical level 1110
- - craniofacial area 1097
- - distal catheterization 1106, 1107
- - dural surface 1104
- - intralesional 1101, 1102
- - surgical 1104
- modifications 954
- reversal 948, 1064, 1099, 1101, 1108–1110
- - occlusive balloon 1102–1104
flow-directed navigation 937
Flowrider 1091
flushing solutions 1095, 1096
Fogarty balloon 280
follow-up 1146
foramen lacerum 401
foramen rotundum, artery 569
fracture
- optic canal 297
- pelvis 284
- skull base 279
functional
- evaluation 925
- investigation 946
fusiform ectasia 422

G
galactorrhea 413
gastrointestinal rupture 435
GDC coil 528, 998–1002
- bioabsorbable polymeric Matrix 1012, 1016
Gelfoam 839
- gelatin sponge 970, 971
- particles 973
- powder 948, 971–973, 1077, 1098, 1102
geniculate body network 495
Gerolakos and Nicolaides classification 78
GFX II 1171–1173
giant cell tumors 893–895
Gianturco coils 980
Glasgow Coma Scale 369
Glasgow Outcome Scale 147, 369, 535
glaucoma 285
- secondary 293
glial cells 19
glossopharyngeal nerve 1152
glucose 8, 18
glue 758
glycoprotein IIb/IIIa receptor 27
- antagonists 35–39, 1055
- safety 38, 39
gold valve balloon 957
guanylyl cyclase 9
Guard-Wire system 1175
Guglielmi detachable coils (GDC) 528, 998–1002
- bioabsorbable polymeric matrix 1012, 1016
- *Vortex* 1002, 1004
guidewires 965–969, 1158–1163
- microguidewires 965–969
- monorail 967
gunshot wound 279, 338, 387, 426

H
head injury 470
headache 681–683, 704, 707, 1129
Headway
- catheter 935
- valve 1031, 1095
heart disease 75
- congenital, aneurysm 524–527
hemangioblastoma, spinal cord 898–900
hemangioendothelioma 1073
hemangioma
- bony 265
- cavernous 686, 687
- vertebral 883–890
- - associated lesions 888
- - embolization 889, 890
- - MRI 884
- - pretherapeutic evaluation 888, 889
- - spinal angiography 884
hemangiopericytoma 165, 166, 1099
hematocrit 1133
hematoma
- extradural 425
- fresh 489
- mural 392, 457
- spinal epidural 421
- subdural 832
hematomyelia 519, 805, 826, 828, 829, 1120
- morbidity 828
hemodilution 1133
hemodynamic
- insufficiency 112
- stress 514
hemorrhage 973
- aneurysm (*see* subarachnoid)
- arteriovenous malformation 677, 678, 703, 704
- epidural 832
- generalities 1135–1137
- intracranial 587
- intradural 278
- intraventricular 740
- postembolization 1138
- recurrent 841
- spinal 778, 825–828
- subadventitial 454
- subarachnoid (SAH) 116, 289, 740, 752, 826
- tongue 352
hemorrhagic conversion 111, 114, 139
hemorrhagic vascular disease, combined endovascular treatment 1147
heparin 398, 843, 1153
- adjunctive 37, 38
- low-molecular-weight (LMWH) 143
heparinization 534, 923, 924, 1128
hepatic failure 433
hepatitis B 511
herpes virus 24
HHT1 (hereditary hemorrhagic teleangiectasias) 618–621, 794, 812, 822
Hieshima Apollo catheter 958, 959
Higashida balloon catheter 119, 953
Hilal coil 987
histamine 12
histoacryl 1060
HITS (high-intensity transient signals) 77
HIV 504, 510, 512
HMCAS (hyperdense middle cerebral artery sign) 47
homocysteine 24
Horner's syndrome 396, 401, 417
Hunt and Hess Classification 148, 368
hydrophilic coating 939
5-hydroxytryptamine (5-HT) 12
hypercapnia 9
hypercholesterolemia 23
Hyperglide catheter 956
hypernephroma, metastatic 881
hyperplasia, intimal 89, 93–97, 1170
hyperprolactinemia 413
hypertension 58
- venous 804
hypocapnia 9
hypophyseal portal system 337
hypotension 921, 922
- systemic 1111
hypotube 1174
HZV (herpes zoster virus) 512

I
IBCA (isobutyl homologue isobutyl-2-cyanoacrylate) 1059
ICP (intracranial pressure) 5
immunoallergic mechanism 505
In Time 1052, 1053
infarction
- atheroembolic 30
- embolic 83
- incomplet 18
inferolateral trunk 567
integrin uperfamily 35
intimal tear 391
iodized oil 1093
iophendylate 1093
ischemia, cerebral 51
- cell change 19
- depolarization 19
- focal 18
- global 18
- hemodynamic effects 21
- necrosis 19
- neuronal metabolism 17
- nitrous oxide 21, 22
ischemic stroke, arterial
- acute 31
- age 15
- angiographic evaluation 41–44
- causes 16
- cryptogenic 99
- definition 14–16
- incidence 15
- middle cerebral artery 44, 45, 51
- neuroimaging 30, 31
- neuronal metabolism 17, 18
- neuronal vulnerability, selective 18–21

- North America 15
- posterior circulation 98–109
- presentation 74
- race 15
- risk factors 16, 74
- treatment 31–73
- - medical therapy 1130, 1131
ischemic syndrome, crescendo 51
isovolemia 1133

J
J-curve 966, 1036
jugular puncture 930

K
Karnofsky score 369, 535, 829
Kassel Bach syndrome 1073
kinking, carotid 942
Klippel-Trénaunay syndrome 766, 767, 771, 820

L
laceration, external carotid 347
laryngeal malignancy 429
Lasjaunias 4-F catheter 986
LDL (low-density lipoprotein) 24
leak, calibrated 952, 953
lenticulostriate artery 51, 54
lesion, intermediate 25
leukotriene 13
LIAT (local intra-arterial thrombolytic therapie) 45–52, 110, 1131
ligation
- endovascular 1105, 1110
- intradural 843
- proximal 314
lipid mediators 13
Lipiodol 1063, 1093
liver
- cyst 436
- fibrosis 432
locked-in state 112
lupus syndrome 513
lymphoproliferative disease, X-chromosome-linked 513

M
macrophage 25
magnesium 41
malformation
- arteriovenous
- - cerebral (*see there*)
- - spinal cord (*see there*)
- venous 1081
Mani 1155
Marfan syndrome 57, 435, 437
Marlin 1052
martensite phase 1170
matrix coil (polyglycolic/poly-L-lactid acid copolymer) 1012
maxillary trauma 425
maxillofacial trauma 457
McCune Albright syndrome 522
medullary syndrome 466
menigiomatosis, menigeal 166
meningioangiomatosis 166
meningioma 427
- angiographic investigation 184–186
- angioplastic 165, 166
- association with other tumors 155
- cavernous sinus, involving 178
- children 156
- chromosomal patterns 156
- clinical presentation 166–169
- CT-scanning 181, 182
- differential diagnosis 187
- embolization, technical aspects 189–192
- - complications 196–198
- - pre- and postembolization medical management 194
- epidural 177
- etiology 157, 158
- extracranial 224
- familial occurrence 157
- gelfoam powder 972
- growth and spread 162
- incidence 154, 155
- intracranial vascular involvement 179, 180
- malignant 162–164
- MRI-Scanning 182–184
- oncogenic viruses 158–161
- operation, time 196
- orbit 177, 178
- origin 154
- pathology 161, 162
- peritumoral edema 181
- pial supply 194
- pretherapeutic evaluation 181
- recurrent 192–194
- sex hormone receptors 156
- sites 169–177
- spinal cord 910
- therapeutic strategy and clinical objectives 187–189
- tumor extension, extracranial 192
- unusual sites 179
menstruation 831, 832
MEP (motor-evoked potential) 925, 928, 1032, 1124
metalloproteinase 14, 28
metamere 379
metameric artery 738
metameric syndrome, spinal arteriovenous (*see* SAMS) 764, 766, 770, 813–821
metaraminol 1154
metastases, vertebral 895
metastatic disease 524
methylene blue 929
metrizamide powder 1077
microcapsules, time-released 1094
microcatheter 934, 936
- calibrated leak 119–127, 130, 959, 961
- *Excelsior* 10 938
- flow-guided 937, 939
- over-the guidewire 937
- *Rebar* 938, 1085
- two-microcatheter technique 1039, 1040
- variable-stiffness 936, 937
- wire-braided 938
microcirculation agents 1132
microcoils 986, 1025
microemboli 77
microseal adapter 1174
microtrauma, tentorium 518
Micrus coil 1010, 1011
Mini-Torquer 936, 942, 943
miscellaneous 1094–1096
mitochondria 19
Mönckeberg disease 23
monorail 1164
Moret's technique 1032
MRI (magnetic resonance imaging) 30
- angiography (MRA) 80–83, 100, 535
- diffusion-weighted (DWI)/perfusion-weighted (PWI) 70–72, 81
MRV (magnetic resonance venography) 142
muscle atrophy 832
mutation 374
- germinal 380
- somatic 380
mycobacterium 512
myelomere 767
- topography, *figure* 778
myelopathy 760
- cervical 761
myoamoya phenomenon 638
myxoma, atrial 523

N
naloxone 1132
nasal mucosa, physiology 206, 207
NASCET 84, 86–88
NBCA (N-butyl-cyanoacrylate) 332, 946, 1059, 1063, 1140
- *Trufil* 1060

neck
- bridging 1039
- protection 1030, 1031
necrosis, ischemic 19, 971, 972
- coagulative 20
- focal 26
- generalized neuronal 20
- skin 1130
nerve root compression 751
neurinoma 199
neuroblastoma 224
neurofibromatosis 57, 297, 338, 739, 743, 748
- type I 421, 424, 435, 436
- type II 436
Neuroform, stent 963, 1171
neurological deficits 708, 1129
- focal 582–585
- global 585–587
neuronal vulnerability, selective 18–21
neuro-ophtalmic abnormalities 299
neuropeptide Y 14
neuroprotective agents 39, 40
- binding properties 41
- pharmacological properties 40, 41
neutrophil 23
nidus 794–801
- angioarchitecture 654, 655
- intramedullary 763
- intranidal ectasias 659–664
- size change 656–659
NIH Stroke Scale 148–150
nitinol 962, 963, 1168–1170
nitric oxide synthase (NOS) 9
- isoforms 10
nitroglycerin 133–135, 921, 1031, 1032, 1089, 1146
nitroprusside drip 921
nitrous oxide (NO_2) 21, 22, 920
- cerebral circulation 9, 10
NMDA (*N*-methyl-D-aspartate) 18
norepinephrine 12
notochord 738
nucleus tractus solitarius 1152
NYU introducer 974

O
O'Reilly catheter 958
occipital artery 567
occlusion
- deconstructive 1005
- test 328, 1029
octacyanoacrylate 1055, 1059
OER (oxygen extraction ratio) 17
Ohm's law 4
Onyx (EVOH) 946, 1055, 1059, 1084–1091, 1149
- aneurysm treatment 1084–1089
- arteriovenous malformation treatment 1089–1091
opacifying agents 1092, 1093
open-cell design 1164
ophtalmoplegia 409
- acute 403
optic atrophy 409
orbit, menigioma 177, 178
orbital injury 279
osteoblastoma 878
osteodural-venous complex 571, 572
osteomyelitis 421
oxygen 8
- reactivity 9

P
pacemaker 1154
packing 540
PAF (platelet-activating factor) 13
pain
- dorsal 819
- facial 751
Palmaz, stent 1153
Pantopaque 1093
papaverine 131, 133, 135, 1160
paraganglioma 224, 227, 228
- angiographic protocol 252
- associated lesions 246
- cervical 238–243, 257–260
- classification 235, 237
- differential diagnosis 246–250
- embolization 261
- - complications 264
- - technical aspects 261–263
- embryology 228–230
- epidemiology 230–232
- familial distribution 231
- jugular 238
- laryngeal 244
- malignant 231
- multicentric 231
- natural history 235, 236
- orbital 245
- pathology 232, 233
- pharyngeal 265
- pretherapeutic evaluation 250–259
- radiotherapy 260, 261
- secretory 245, 246
- spinal cord 909–911
- temporal 252–257
- thyroidal 265
- tympanic 236–238
- vagal 241
- vascular architecture 233–235
Parkes-Weber syndrome 766, 820, 821
partial repair 466
patient preparation 917–919
patterning 378
PDGF (platelet derived growth factor) 25, 376
PDK1/PDK2 431
pentoxifylline 1134
penumbra, ischemic 17
peptide 13
perclose 932
perfusion
- misery 22
- reserve 17
pericallosal arch 495
pericytes 3, 376
peritoneal dialysis 433
PET (positron emission tomography) 30, 31
petrous lesion 68
pH 8, 9
PHACE syndrome 399, 400
phagocytosis 4
pharyngeal artery, ascending
- carotid branch 567
- neuromenigeal division 569
physiology, cerebrovascular 3–14
pial network 797
PICA (posterior inferior cerebellar artery), dissection 463
plaque
- complicated 28, 29
- fatty 28
- fibrous 28
- morphology 77
- - *Gerolakos and Nicolaides* classification 78
- ulceration 75
plasma 1133
plasmocytoma 875, 880
platelets 26, 27
Plavix 1153
Poiseuille, equation 5, 8
polyarteriitis nodosa 385
polycystic kidney disease 431–433, 436
- children 375
polycystin 431
polyglycolic/poly-L-lactid acid copolymer 1012
polyvinyl alcohol foam (PVA) 839, 974–977, 1063, 1123
- ethanol combination 977
postembolization care
- cerebral arteriovenous malformation 1128
- head and neck 1128
- intradural aneurysm 1128, 1129
- spinal arteriovenous malformation 1129
pouch, venous 755

pregnancy 136, 787, 831
preoperative medication 917, 918
pressure
- arterial, mean 5
- cerebral perfusion pressure 5
- intracranial (ICP) 5
- venous 5
prism therapy 298
PROACT II (prolyse in acute cerebral thromboembolism trial II) 46, 47
proatlantal artery 740
probucol 97
procollagen
- type III 396, 434
- type V 396
proptosis 299
prostacyclin (PGI_2) 13
prostaglandines 12, 13
protamine sulfate 923
protection/protecting
- agents 1134
- distal cerebral 1173–1175
- mechanical 1099
protein C 136
protein S 136
provocative testing, cranial nerve 1129
pseudoaneurysm 347, 389, 653, 662, 776
pseudonidus 813
pseudoxanthoma elasticum (PXE) 385, 437
PT (prothrombin time) 38, 923
PTT (partial thromboplastin time) 38, 923
puerperium 136
pulmonic valve stenosis 524
pupillary abnormality 409
purine nucleotide 14
Purkinje cells 19
PVA (polyvinyl alcohol foam) suspension 839, 974–977, 1063, 1123
PWI (perfusion-weighted imaging) 70–72, 81

R
radiation 97
- beta radiation 1019
radical, free 41
radicular vein 739
radiosensitizer 916
Radius, stent 964
Rankin Scale, modified 148
reanastomosis 930
Rebar microcatheter 938, 1085
rebleed 539
recanalization 45, 494, 975, 977, 979, 1063, 1119, 1131, 1132
reconstructive operation 1030
remodeling 25, 374, 376, 955, 1031–1037
- *Moret's* technique 1032
- technique 534
renal artery stenosis 435
renal function 433
Rendu-Osler-Weber disease 739, 766
ReoPro 36
reperfusion, cerebral 19
- injury 22, 23, 39, 41
resistance, vascular 6
- segmental 6
restenosis 89, 93–97
retinal artery, central, occlusion 67, 68
Retriever 1052
revascularisation 42, 52, 55, 62, 105–109, 923, 931, 1143, 1144, 1162
- complications 1178, 1179
- emergency 65
- mechanical 1176
Robin Hood effect 1132
r-TPA (recombined tissue plasminogen activator) 31–33, 67, 144, 1131
r-UK (recombined urokinase) 46, 60, 144, 961, 1131
rupture, vessel 1137

S
sacral artery, lateral 752
salmonella 505
SAMS (spinal arteriovenous metameric syndrome) 764, 766, 770, 813–821
SCAVM (spinal cord arteriovenous malformation) 760–773
- aggravating factors 831, 832
- angioarchitecture 775, 829, 830
- angiography 809810
- arterial aneurysm 786–794
- arterial features 775–784
- associated malformations 822–825
- bifocal 763
- classification 767–773
- clinical aspects 825–832
- clinical assessment 808
- CSF pulsation artifact 809
- CT 808
- embolization 1116, 1117
- hemodynamics 810, 811
- incidence 769, 814
- intradural fistula 811, 812
- MRI 808
- multifocal 815
- myelography 808
- natural history 760, 825
- nidus (*see there*)
- postembolization care 1129
- prognosis 830
- retromedullary 806
- thrombosis, spontaneous 843, 844, 847
- treatment
- - complications 840–842
- - indications 833–839
- - medical therapy 843–847
- - radiotherapy 843
- - results 839, 840
- - surgery 842, 843
- veins 802–807
- - thrombosis 803
sclerosis, medial
- calcified 23
- cystic 57
sclerotherapy 1074–1083
SDAVF (spinal dural arteriovenous fistula) 849–872
- age distribution 849
- clinical presentation 858, 859
- embolization 1125–1128
- - indication 867
- - results 871
- - technique 867–869
- imaging 859–867
- location 863
- macro 812, 813
- macroscopic apearance 851–853
- micro 812
- microscopic apearance 853, 854
- pathology 850, 851
- pathophysiology 854–858
- sacrum 778
- surgery 871, 872
security point 928
segmental vulnerability 492
seizure 918
- outcome 919
sella turcica 410
Sentry catheter 125, 955, 958, 1034
SEP (somatosensory-evoked potential) 809, 840, 925, 928, 1124
Serbinenko 955
serotonin 12
sex hormons 206, 207
shear stress 514
shunt, arteriovenous (*see also* malformation)
- dural (*see* DAVS)
- epidural 861
- filum terminale 797
- general appearance 615–618
- radicular 766
silicone
- fluid 947, 1059
- spheres 977
Silvadene 1130

Silverspeed, guidewire 965
size-to-neck ratio 532
size-to-parent-artery-diameter ratio 532
Sjögren's syndrome 513
skin
- discoloration 817, 1092
- vascular malformation 814
SMART 1165
smoking 440
smooth muscle 26, 27
- proliferation 97
snare, microvena 1051, 1052
Sorcerer, guidewire 965
sphenoid
- bone 408
- sinus 305, 509
spinal artery, anterior, pial branches 798, 799
spinal cord
- aneurysmal bone cyst 890–892
- angiographic protocol 875, 876
- angiography 874, 875
- arteriovenous malformation (*see* SCAVM)
- catheterization, distal 1116
- collateral circulation 1114
- embolization 876–883
- - arteriovenous malformation 1116, 1117
- - cervical tumors 877
- - chemoembolization 877–880
- - flow control 1117–1120
- - intralesional 880
- - thoracic/lumbar/sacral tumors 877
- endovascular treatment, technical aspects 1113, 1114
- giant cell tumors 893–895
- hemangioblastoma 898–900
- - pretherapeutic evaluation 904–906
- - treatment 906–909
- hemangioma, vertebral 883–890
- malignant tumors 895–897
- - embolization 897
- meningioma 910
- metastases 895
- monitoring 1124, 1125
- paraganglioma 909–911
- pathological changes 854
- vascular lesion 758–760
- *von Hippel-Lindau* disease 900–904
steal
- arterial 300, 754
- intracerebral 9
- subclavian 105, 1176
Stealth catheter 125, 950, 952, 958
stenosis, arterial 1143–1146
- carotid 16, 99
stent 36, 57, 62, 69
- balloon-expandable 59, 106, 962, 1161, 1164, 1165, 1171, 1180, 1181
- coating 97
- collapsed 1178
- construction design 1164
- covered 962
- delivery catheter 962–965
- metal alloys 1164
- nitinol 962, 963, 1168–1170
- protection 1045
- retrieval 1179–1181
- selection 1164–1168
- self-expandable 59, 962, 1160, 1164, 1169, 1170
stenting 90–98, 104
- hemodynamic disturbances 1152, 1153
- techniques 1152–1181
- - intervention 1154–1163
- - premedication 1153, 1154
- - vasoactive medication 1154
stopcocks 1095
streaks, fatty 23, 24, 27, 28
streptokinase 33
stroke 421, 495, 1129
- children 422
- deep-seated 460
- embolic 477
- ischemic (*see there*)
stroke center 71
stroke emergency team 70, 71
Sturge-Weber syndrome 691–694, 812
subclavian artery 105
- revascularisation 42
subclavian steal syndrome 105, 1179
subintimal trauma 392
substance P 12, 13
sump effect 747
superelasticity 1170
surface
- abluminal 4
- rendering 532, 533, 541
swelling
- postembolization 1060
- postoperative 1130
Symbiot, stent 964
Symphony 1165
syndromes/diseases (names only)
- *Bourneville* disease 436, 437
- *Cobb* syndrome 755, 773
- *Ehlers-Danlos* syndrome 57, 279, 280, 297, 387, 434, 435, 743
- *Horner's* syndrome 396, 401, 417
- *Kassel Bach* syndrome 1073
- *Klippel-Trénaunay* syndrome 766, 767, 771, 820
- *Marfan* syndrome 57, 435, 437
- *McCune Albright* syndrome 522
- *Mönckeberg* disease 23
- Moyamoya disease 438
- *Paget's* disease 427
- *Parkes-Weber* syndrome 766, 820, 821
- *Rendu-Osler-Weber* disease 739, 766
- *Sjögren's* syndrome 513
- *Sturge-Weber* syndrome 691–694, 814
- *von Hippel-Lindau* disease 900–904
- *von Willebrand's* disease 750
syphillis 454
syringes 1094

T
Takayasu's arteritis 115, 116
tandem lesion 68, 69
tantalum powder 947, 1063, 1084, 1092, 1093
TCCF (traumatic carotid cavernous fistula)
- clinical aspects 285–306
- - associated traumatic lesions 302–305
- - ophtalmological symptoms 293–298
- etiology/epidemiology 279–284, 297
- location 308–313
- pretherapeutic evaluation 306–320
- therapy
- - embolization 321, 322
- - - balloon selection 325–330
- - - inferior petrosal approach 332
- - - postembolization care 333
- - - retrograde ophthalmic vein catheterization 332
- - - venous approach 330
- - emergency treatment 322–324
- - manual compression 332
- - NBCA 332
- - surgical approach 324, 325
- venous drainage 314
teleangiectasias, hereditary hemorrhagic (HHT1) 618–621, 794, 812, 822
tentorium, microtrauma 518
Terumo, guidewire 965
TGFβ1 (tissue growth factor β1) 376
thalassemia, heterozygotic α 522
thrombin 36
thrombocytopenia 38, 144

thromboembolism 110
thromboendarterectomy 54
thrombolysis/thrombolytic therapy 32, 33, 39, 53, 144
- local intra-arterial thrombolytic therapie (LIAT) 110, 1131
- - anterior circulation 45–52
thrombolytics 1055
thrombosis
- aneurysm 470
- arteriovenous malformation 669
- basilar artery 110–114
- cerebral venous (*see* venous occlusive disease)
- cortical vein 139
- spontaneous 791
- superior sagital sinus 138, 140, 147
- traumatic 278
- venous 752
thromboxane A_2 (TXA_2) 13, 27, 34, 35
thrombus 479, 494
thyroid carcinoma 273
thyrolaryngeal tumors 265–270
TIA (transient ischemic attack) 14, 44, 73, 74
- posterior circulation 99
ticlopidine hydrochloride 35, 37, 1153
TIMI (thrombolysis in myocardial infarction) 46, 47
tinnitus 581, 582
- pulsatile 285
tirilazad 41
tirofiban 36
tissue plasminogen activator, recombined (r-TPA) 31–33, 67, 144, 1131
tolerance test 314, 942, 943, 1020, 1029, 1030
tongue hemorrhage 352
torticollis, painfull 751
tracheostomy 920
transdural veins 573–575
Transent platinum, guidewire 966
transitory deficits 840
transmedullary
- supply 795
- vein 796
transphenoidal surgery 279, 403, 404
transposition, great arteries 524
transvenous approach 756
tray container 1095
tricuspid atresia 524
trigeminal artery 103
trigger 374
Trispan 1039–1043
tropoelastin 396, 435
Trufil 1060
truncus arteriosus 524
tuberous sclerosis 436, 437
tubular design 1164
Tuohy-Borst 1095
- Y-adapter 944, 960
twin, homocygotic 452
two-arteriotomy-site 1178

U
ultrasound, carotid 75–78, 98
- double enhanced 77
- hemodynamic assessment 77
urokinase, recombined (r-UK) 46, 60, 144, 961, 1131

V
VA (veterans Administration) 87
Valsalva maneuver 814, 831, 920, 922
vasa vasorum 94, 96, 376, 398, 459, 489, 494
vascular insufficiency, cerebral
- management 104–109
- pretherapeutic evaluation 99–103
vascular lesion
- limb 820
- pelvic 821
vascular phenotypic vulnerability, variability 374
vascular system, sex hormons 207
vasculitis 83
vasculogenesis 23
vasculopathy, mural 371
vasoactive substances 11
vasopressin 14
vasoseal 932
vasospasm 117–135, 952, 959, 1031, 1146
- angioplasty, indications and results 128–133
- arteriovenous malformation 642
- chemical treatment 133–135
VCAM-1 (vascular endothelial molecule) 26
venography, magnetic resonance (MRV) 142
venous nerve, perispinal network 807
venous occlusive disease
- clinical presentation 137, 138
- combined endovascular treatment 1147
- etiology 135, 136
- imaging 138–143
- incidence 136, 137
- natural history 137, 138
- risk factors 136
- treatment 143–147
ventriculostomy 456
vertebral artery
- dissection 83
- duplicated 447
- fenestration 447
- occlusion 107
vertebrobasilar insufficiency 98, 425, 751
vertebroplasty, percutaneous 897
vessel wall, proliferative disease 490
vidian canal 401
viscosity, blood 8, 1133
vision loss 66
visual loss 299, 302, 304, 405
vitamin E 41
Vitek 1155
volume rendering 532, 533, 541
volume, cerebral blood (CBV) 7
von Hippel-Lindau disease 900–904
von Willebrand's disease 750
vulnerability, segmental 492
VVAVF (vertebro-vertebral arteriovenous fistula, proatlantal and intersegmental) 743–751
- clinical findings 751, 752

W
Wada test 928
Wallerian degeneration 21
Wallstent 1046, 1165, 1167, 1169
warfarin 398
WFNS gerading scale 368
Willis, circle 1108, 1109
wisdom tooth extraction 362
Wyburn-Mason 758

X
xylocaine 927, 929, 1125

Y
Y hemostatic valve 1031, 1095
Yasargil, grading system 368

Z
Zubkov's technique 117, 118

Manufacturers

AVE/Medtronic
Minneapolis, MN 55432, USA

Beiersdorf Inc.
187 Danbury Road, Wilton, CT 06897, USA

Biosphere Medical
1050 Hingham Street, Rockland, MA 02370, USA

Boston Scientific
One SciMed Place, Maple Grove, MN 55311-1566, USA

Cook Inc.
PO Box 489, Bloomington, IN 47402, USA

Cordis Endovascular
14000 NW 57th Court, Miami Lakes, FL 33014, USA

Ethicon Inc.
Somerville, NJ 08876, USA

Lilly Research Laboratories
Lilly Corporate Center, Indianapolis, IN 46285, USA

Medtronic
3576 Unocal Place, Santa Rosa, CA 95403, USA

Microtherapeutics Inc.
2 Goodyear, Irvine, CA 92618, USA

Microvena
1861 Buerkle Road, White Bear Lake, MN 55110-5246, USA

Microvention
72 Argonaut, Aliso Viejo, CA 92656, USA

Micrus Corporation
495 Clyde Avenue, Mountain View, CA 94043, USA

Monarch Pharmaceuticals
335 Beecham Street, Bristol, TN 37620, USA

Savage Labs
Melville, NY 11747, USA

Provasis Therapeutics Inc.
9275 Sky Park Ct., Ste. 125, San Diego, CA 92123, USA

Springer
Berlin
Heidelberg
New York
Hong Kong
London
Milan
Paris
Tokyo

The complete three-volume set consists of

Volume 1
Clinical Vascular Anatomy and Variations

Volume 2
Clinical and Endovascular Treatment Aspects in Adults

Volume 3
Clinical and Interventional Aspects in Children

A. Berenstein
P. Lasjaunias
K.G. ter Brugge

Surgical Neuroangiography

2.2 Clinical and Endovascular Treatment Aspects in Adults

- Cerebral Arteriovenous Shunts
- Spinal Arteriovenous Shunts
- Spinal Vascular Tumors
- Technical Aspects of Endovascular Neurosurgery

Second Edition
with 734 Figures in 2926 Separate Illustrations,
Some in Color and 155 Tables

Springer

Alejandro Berenstein, M.D.
Professor of Radiology and Neurosurgery
Albert Einstein School of Medicine, NY
Director of the Hyman-Newman Institute of Neurology and Neurosurgery,
and of The Center for Endovascular Surgery
Beth Israel Medical Center New York
170 East End Avenue at 87th Street, New York, NY 10128, USA

Pierre Lasjaunias M.D., Ph.D.
Professeur des Universités en Anatomie
Chef de Service de Neuroradiologie Diagnostique et Thérapeutique
Centre Hospitalier Universitaire de Bicêtre
78, rue du Général Leclerc, 94275 Le Kremlin Bicêtre, France

Karel G. ter Brugge, M.D.
Professor of Radiology and Neurosurgery
Head, Division of Neuroradiology University of Toronto /
University Health Network
Department of Medical Imaging, Toronto Western Hospital, FP3-210
399 Bathurst Street, Toronto, ON M5T 2S8, Canada

The second volume of the second edition of *Surgical Neuroangiography* combines the previous volumes 2, 4 and 5 in a two part volume.

ISBN 3-540-41668-4 Springer-Verlag Berlin Heidelberg New York

Cataloging-in-Publication Data applied for

Bibliographic information published by Die Deutsche Bibliothek
Die Deutsche Bibliothek lists this publication in the Deutsche Nationalbibliografie; detailed bibliographic data is available in the Internet at <http://dnb.ddb.de>.

This work is subject to copyright. All rights are reserved, whether the whole or part of the material is concerned, specifically the rights of translation, reprinting, reuse of illustrations, recitation, broadcasting, reproduction on microfilm or in any other ways, and storage in data banks. Duplication of this publication or parts thereof is only permitted under the provisions of the German Copyright Law of September 9, 1965, in its current version, and permission for use must always be obtained from Springer-Verlag. Violations are liable for prosecution under the German Copyright Law.

Springer-Verlag is a part of Springer Science+Business Media

springeronline.com

© Springer-Verlag Berlin Heidelberg 1987/1992, 2004

The use of general descriptive names, registered names, trademarks, etc. in this publication does not imply, even in the absence of a specific statement, that such names are exempt from the relevant protective laws and regulations and therefore free for general use.

Product liability: The publishers cannot guarantee the accuracy of any information about the application of operative techniques and medications contained in this book. In every individual case the user must check such information by consulting the relevant literature.

Cover design: E. Kirchner, Heidelberg, Germany
Typesetting: Fotosatz-Service Köhler GmbH, Würzburg, Germany

Printed on acid-free paper 21/3150/ih 5 4 3 2 1 0

Preface

Anatomy is a language and mastery of this language is in our opinion essential for physicians involved in the management of patients with vascular diseases of the central nervous system, head and neck, and spine and spinal cord. Understanding the clinicopathological aspects of vascular disease, its natural history, and the various therapeutic options is mandatory for optimal patient management.

Functional endovascular therapeutic strategies continue to expand and those that are currently available are discussed within the realm of the authors' combined experience. Our approach goes beyond today's technological advances and involves a new understanding of how vascular pathology is expressed, its impact on the structure of the vascular systems, and the possible repair mechanisms of the vascular system in various environments. The latest techniques that improve such therapeutic goals are illustrated in the individual chapters on the diseases and highlighted in the chapter on techniques.

The important field of occlusive vascular disease and our ability to reopen stenotic or even occluded vessels are revolutionizing Endovascular Neurosurgery. An in-depth study of occlusive vascular disease is a major addition to this second edition of *Surgical Neuroangiography (Vol. 2)*. Functional anatomical strategies and protocols are illustrated with the latest technological devices. As the rapid technological evolution continues, our approach and understanding will help guide us to the safest and most effective revascularization strategy.

Our new concepts with respect to aneurysms as a group of diseases of different etiologies and pathophysiologies alter the therapeutic indications for their management and therefore the role of specific treatment techniques.

Our experience in the management of patients with vascular disorders now extends over many decades and forms the basis for an approach to cerebral and dural vascular malformations that is both at the leading edge and well balanced. Management decisions based on a thorough understanding of these vascular pathologies, their natural history, as well as the risks associated with their treatment have been outlined in the text. This work is a reflection of the authors' ongoing commitment to balancing the exciting technological advances of the tools that have become available with thorough knowledge of vascular anatomy and an exhaustive understanding of vascular pathologies. It is this unique approach that facilitates ongoing progress in the safe management of patients with vascular disorders affecting the brain, the spine, and the head and neck.

December 2003 A. Berenstein, P. Lasjaunias, K.G. ter Brugge

Contents of Volumes 2.1 and 2.2

1	**Occlusive Vascular Disease**	1
1.1	***Introduction***	2
1.2	***Arterial Occlusive Disease***	3
1.2.1	Cerebrovascular Physiology	3
1.2.1.1	The Blood–Brain Barrier	3
1.2.1.2	Cerebral Blood Flow	4
1.2.1.3	Cerebral Autoregulation	5
1.2.1.4	Cerebral Blood Volume	7
1.2.1.5	Blood Viscosity	8
1.2.1.6	Metabolism in Cerebral Blood Flow	8
1.2.1.7	Carbon Dioxide Reactivity	9
1.2.1.8	Oxygen Reactivity	9
1.2.1.9	Nitrous Oxide in Cerebral Circulation	9
1.2.1.10	Other Factors	10
1.2.2	Arterial Ischemic Stroke	14
1.2.2.1	Definition	14
1.2.2.2	Neuronal Metabolism and Cerebral Ischemia	17
1.2.2.3	Selective Neuronal Vulnerability	18
1.2.2.4	Hemodynamic Effects of Ischemia	21
1.2.2.5	Nitrous Oxide and Cerebral Ischemia	21
1.2.2.6	Window of Opportunity	22
1.2.2.7	Neutrophil	23
1.2.3	Atherosclerosis	23
1.2.3.1	Introduction	23
1.2.3.2	Epidemiology	23
1.2.3.3	Pathogenesis	24
1.2.3.4	Mechanisms of Atherogenesis	24
1.2.3.5	Fatty Streak	27
1.2.3.6	Fibrous Plaque	28
1.2.3.7	Unstable Fibrous Plaques	28
1.2.3.8	Complicated Plaque	28
1.2.3.9	Carotid Atherosclerosis	29
1.2.3.10	Conclusion	29
1.2.3.11	Neuroimaging of Ischemic Stroke	30
1.2.4	Ischemic Stroke Treatment	31
1.2.4.1	Medical Treatment of Acute Stroke	31
1.2.4.2	Thrombolytic Therapy: Introduction	32
1.2.4.3	Thrombolytics (IV)	32
1.2.4.4	Recombined Tissue Plasminogen Activator	32

1.2.4.5 Streptokinase 33
1.2.4.6 Antiplatelets 34
1.2.4.7 Coumadin Versus Aspirin 39
1.2.4.8 Neuroprotective Agents 39
1.2.4.9 Pharmacological Properties of Neuroprotective Drugs . 40
1.2.4.10 Binding Properties 41
1.2.4.11 Angiographic Evaluation 41
1.2.4.12 Middle Cerebral Artery Stroke: Natural History 44
1.2.4.13 Local Intra-arterial Thrombolysis in the Anterior Circulation 45
1.2.4.14 Internal Carotid Artery Occlusion 52
1.2.4.15 Carotid Dissection 57
1.2.4.16 Central Retinal Artery Occlusion 67
1.2.4.17 Internal Carotid Artery Stenosis Above the Carotid Bulb 68
1.2.4.18 General Organization of a Stroke Emergency Team . . . 70
1.2.4.19 Evolving Treatment Strategies 72
1.2.5 Extracranial Carotid Artery Stenosis 73
1.2.5.1 Introduction 73
1.2.5.2 Natural History 73
1.2.5.3 Carotid Bruit 75
1.2.5.4 Imaging 75
1.2.5.5 Treatment 84
1.2.5.6 Symptomatic Carotid Stenosis 86
1.2.5.7 Asymptomatic Carotid Stenosis 86
1.2.5.8 Restenosis After Carotid Endarterectomy 89
1.2.6 Carotid Angioplasty and Stenting 90
1.2.6.1 Introduction 90
1.2.6.2 Techniques of Carotid Angioplasty and Stenting 93
1.2.6.3 Intimal Hyperplasia and Restenosis 93
1.2.6.4 Follow-up Monitoring 98
1.2.7 Posterior Circulation Stroke (Stroke Prevention) 98
1.2.7.1 Introduction 98
1.2.7.2 Clinical Presentation 98
1.2.7.3 Pretherapeutic Evaluation in Cerebral Vascular Insufficiency 99
1.2.7.4 Management of Posterior Circulation Insufficiency . . . 104
1.2.7.5 Basilar Thrombosis 110
1.2.7.6 Takayasu's Arteritis 115
1.2.8 Cerebral Angioplasty 116
1.2.8.1 Vasospasm 117

1.3 Venous Occlusive Disease 135
1.3.1 Etiology 135
1.3.2 Incidence 136
1.3.3 Clinical Presentation and Natural History 137
1.3.4 Imaging 138
1.3.5 Treatment 143
Appendix 147

2 Dural and Bony Tumors 153

2.1 Introduction 154

2.2 Meningiomas 154
2.2.1 Epidemiology 154
2.2.1.1 Origin 154
2.2.1.2 Incidence 154
2.2.1.3 Association of Meningiomas with Other Tumors 155
2.2.1.4 Sex Hormone Receptors in Meningiomas 156
2.2.1.5 Chromosomal Patterns in Meningiomas 156
2.2.1.6 Meningiomas in Children 156
2.2.1.7 Familial Occurrence 157
2.2.1.8 Meningioma Incidence, Prevalence, and Mortality 157
2.2.1.9 Etiology of Human Meningiomas 157
2.2.1.10 Oncogenic Viruses 158
2.2.2 Pathology 161
2.2.2.1 Growth and Spread 162
2.2.2.2 Malignant Meningioma 162
2.2.2.3 Angioblastic Meningioma and/or Hemangiopericytoma 165
2.2.2.4 Meningioangiomatosis 166
2.2.2.5 Meningeal Meningiomatosis 166
2.2.3 Clinical Presentation 166
2.2.3.1 Sites 169
2.2.3.2 Epidural Meningiomas 177
2.2.3.3 Meningiomas of the Orbit 177
2.2.3.4 Meningiomas Involving the Cavernous Sinus 178
2.2.3.5 Meningiomas in Other Unusual Sites 179
2.2.3.6 Intracranial Vascular Involvement 179
2.2.3.7 Peritumoral Edema in Meningiomas 181
2.2.4 Pretherapeutic Evaluation 181
2.2.4.1 CT Scanning in Meningiomas 181
2.2.4.2 MRI Scanning 182
2.2.4.3 Angiographic Investigation 184
2.2.4.4 Differential Diagnosis 187
2.2.5 Therapeutic Strategy and Clinical Objectives 187
2.2.6 Technical Aspects of Embolization 189
2.2.7 Special Considerations in Meningioma Embolization . . 192
2.2.7.1 Extracranial Tumor Extension 192
2.2.7.2 Recurrent Meningiomas 192
2.2.7.3 Internal Carotid Supply to Recurrent or Malignant Meningiomas After Radiation Therapy Has Failed 194
2.2.7.4 Pial Supply 194
2.2.7.5 Pre- and Postembolization Medical Management 194
2.2.7.6 Time of Operation 196
2.2.7.7 Complications of Embolization 196

2.3 Other Bony and Dural Tumors 198
2.3.1 Cerebral Tumors 198
2.3.2 Neurinomas 199
2.3.3 Esthesioneuroblastomas 199

3 Nasopharyngeal Tumors 201
3.1 Juvenile Angiofibromas 201
3.1.1 Macroscopic Pathology 201
3.1.2 Microscopic Pathology 204
3.1.3 Epidemiology 205
3.1.4 Pathophysiology 206
3.1.4.1 Juvenile Angiofibromas and Sex Hormones 206
3.1.4.2 Physiology and the Nasal Mucosa 206
3.1.4.3 Hormones and the Vascular System 207
3.1.4.4 Global Hypothesis for the Development of Juvenile Angiofibromas 207
3.1.5 Clinical Findings 210
3.1.6 Natural History 211
3.1.7 Pretherapeutic Evaluation 211
3.1.7.1 Computed Tomography 211
3.1.7.2 Magnetic Resonance Imaging 211
3.1.7.3 Angiography 211
3.1.8 Therapeutic Goals 214
3.1.8.1 Radiation Therapy 221
3.1.9 Technical Aspects of Embolization 221
3.1.10 Tumor Recurrence 223
3.2 Other Nasopharyngeal Tumors 224
3.3 Conclusion 226

4 Paragangliomas 227
4.1 Introduction 227
4.2 Embryology 228
4.3 Epidemiology 230
4.4 Pathology 232
4.4.1 Vascular Architecture 233
4.5 Natural History 235
4.6 Clinical Aspects 236
4.6.1 Tympanic Paragangliomas 236
4.6.2 Jugular Paragangliomas 238
4.6.3 Cervical Paragangliomas 238
4.6.4 Paragangliomas in Other Locations 244
4.6.5 Secretory Paragangliomas 245
4.6.6 Associated Lesions 246
4.7 Differential Diagnosis 246
4.8 Pretherapeutic Evaluation 250
4.8.1 Angiographic Protocol 252
4.8.2 Temporal Paragangliomas: Specific Features 252
4.8.3 Cervical Paragangliomas: Specific Features 257
4.9 Therapeutic Strategies 260
4.10 Technical Aspects of Embolization 261
4.11 Complications of Embolization of Paragangliomas . . . 264

5 Other Head and Neck Tumors 265

5.1 Thyrolaryngeal Tumors 265
5.2 Craniofacial Tumors 270

6 Traumatic Arteriovenous Fistulae 277

6.1 Introduction 277

6.2 Traumatic Carotid Cavernous Fistulae 279
6.2.1 Etiology and Epidemiology 279
6.2.2 Clinical Aspects of Traumatic Carotid Cavernous Fistulae 285
6.2.2.1 Ophthalmological Symptoms 293
6.2.2.2 Corneal Ulcerations and/or Infections and Secondary Glaucoma 293
6.2.2.3 Diplopia 298
6.2.2.4 Cranial Nerve Involvement in Traumatic Carotid Cavernous Fistulae 298
6.2.2.5 Bruit 300
6.2.2.6 Arterial Steal 300
6.2.2.7 Hemispheric Arterial Insufficiency 300
6.2.2.8 Associated Traumatic Lesions 302
6.2.3 Pretherapeutic Evaluation 306
6.2.3.1 Location of the Fistula 308
6.2.3.2 Venous Drainage of the Fistula 314
6.2.4 Therapeutic Objectives and Strategy 321
6.2.4.1 Embolization 321
6.2.4.2 Emergency Treatment 322
6.2.4.3 Surgical Approach to Carotid Cavernous Fistulae 324
6.2.4.4 Conservative Treatment of Traumatic Carotid Cavernous Fistulae 325
6.2.5 Technical Aspects of Embolization 325
6.2.5.1 Balloon Selection 325
6.2.5.2 Manual Compression 332
6.2.5.3 The Use of NBCA in the Management of Carotid Cavernous Fistulae 332
6.2.6 Postembolization Care 333

6.3 Other Traumatic Arteriovenous Fistulae 334
6.3.1 Extracavernous Arteriovenous Fistulae 334
6.3.2 Vertebral Arteriovenous Fistulae 338
6.3.3 Common Carotid Fistulae 342
6.3.4 External Carotid Fistulae 342
6.3.5 Malignant Fistulae 354
6.3.6 Other Epistaxis 354
6.3.6.1 Coagulopathy 357
6.3.6.2 Spontaneous Epistaxis 357
6.3.6.3 Tumoral Epistaxis 357
6.3.6.4 Biopsy 359
6.3.6.5 Traumatic Epistaxis 362

7	**Aneurysmal Vasculopathies**	365
7.1	***From Aneurysm to Aneurysmal Vasculopathies***	366
7.1.1	General Perspectives	366
7.1.1.1	Medical Challenge	367
7.1.1.2	Decision-Making Challenge in Patients with Unruptured Aneurysms	370
7.1.1.3	Ethical Challenge	370
7.1.1.4	Academic and Nosological Challenges	371
7.1.2	Physiopathogenesis and Risks	371
7.1.2.1	Classification	374
7.1.3	Segmental Vulnerability	375
7.1.3.1	Embryological Origin	377
7.1.3.2	Age of Aneurysms	380
7.2	***Extradural Aneurysms***	382
7.2.1	Introduction	382
7.2.2	Extradural Internal Carotid Artery Aneurysms	382
7.2.2.1	Cervical Internal Carotid Aneurysms	384
7.2.2.2	Acute Spontaneous Dissection of the Carotid Artery	394
7.2.2.3	Petrous Internal Carotid Artery Aneurysms	399
7.2.2.4	Aneurysms of the Cavernous Segment of the Internal Carotid Artery	401
7.2.2.5	Cervical Fibromuscular Dysplasia	415
7.2.3	Internal Carotid Artery Occlusion in Extradural Internal Carotid Artery Aneurysms	417
7.2.3.1	Tolerance to Carotid Occlusion	418
7.2.3.2	Postembolization Care	420
7.2.4	Extradural Vertebral Aneurysms	420
7.2.5	Aneurysms of the External Carotid Artery	425
7.3	***Intradural Aneurysms***	431
7.3.1	Saccular Arterial Aneurysms and Associated Diseases	431
7.3.1.1	Polycystic Kidney Disease	431
7.3.1.2	Ehlers–Danlos Syndrome	434
7.3.1.3	Neurofibromatosis Type 1	435
7.3.1.4	Bourneville Disease	436
7.3.1.5	Fibromuscular Dysplasia	438
7.3.2	Saccular Arterial Aneurysms Without Diagnosed Associated Diseases	438
7.3.2.1	Nonsyndromic Familial Arterial Aneurysms	438
7.3.2.2	Multiple Saccular Arterial Aneurysms	440
7.3.2.3	Arterial Anatomy, Single, Mirror, and Twin Saccular Arterial Aneurysms	442
7.4	***Intradural Artery Dissections***	454
7.5	***Intradural Giant Saccular and Nonsaccular Arterial Aneurysms***	478
7.5.1	General Remarks	478
7.5.2	Giant Intracranial Aneurysms with Thrombosis	486
7.5.3	Nonsaccular Giant Arterial Aneurysms	497
7.5.3.1	Megadolicho Arteries and Serpentine Arterial Aneurysms	498

7.5.4 Multiple Giant Arterial Aneurysms and Mirror Giant Arterial Aneurysms 500

7.6 Infectious, Immune, and Inflammatory Intradural Aneurysms 502
7.6.1 Infectious Arterial Aneurysms 502
7.6.2 Intradural Fusiform Aneurysms in Patients with Immune Deficiencies 509
7.6.3 Inflammatory Diseases and Arterial Aneurysms 513

7.7 Flow-Related Arterial Aneurysms and Other Aneurysmal Vasculopathies 514
7.7.1 Intradural Traumatic Arterial Aneurysms 518
7.7.2 Arterial Aneurysms Associated with Proliferative Diseases 523
7.7.3 Arterial Aneurysms with Congenital Heart Disorders and Coarctation of the Aorta 524

7.8 Therapeutic Management 527
7.8.1 Introduction 527
7.8.2 Method 532
7.8.3 Results of the Endovascular Approach 538
7.8.4 Management of Multiple Arterial Aneurysms 549
7.8.5 Management of Giant Arterial Aneurysms 560

8 Dural Arteriovenous Shunts 565

8.1 Historical Review 566
8.2 Pathophysiology 570

8.3 The Osteodural–Venous Complex 571
8.3.1 Dural Venous Plexus 572
8.3.2 Transdural Veins 573

8.4 Classification 575

8.5 Clinical Presentation of Dural Arteriovenous Shunts . . 579
8.5.1 Cranial Nerve Symptoms 580
8.5.2 Tinnitus and Objective Bruits 581
8.5.3 Focal Neurological Deficits 582
8.5.4 Global Neurological Deficits 585
8.5.5 Intracranial Hemorrhage 587
8.5.6 Hormonal Influences 587
8.5.7 Associated Conditions and Multiplicity 590

8.6 Natural History 594
8.7 Progression of Symptoms 596
8.8 Pretherapeutic Evaluation 598

8.9 Therapeutic Aspects 598
8.9.1 Indications and Strategy 598
8.9.2 Topographic Considerations 602
8.9.3 Technical Aspects 605
8.9.4 Timing of Embolization 605
8.9.5 Results of Embolization 606

8.9.6 Complications of Embolization 606
8.9.7 Surgery 607

9 Cerebral Vascular Malformations: Incidence, Classification, Angioarchitecture, and Symptomatology of Brain Arteriovenous and Venous Malformations 609

9.1 Incidence of Cerebral Vascular Malformations 609
9.2 Principles of Classification 612

9.3 Classification of Cerebral Vascular Malformations . . . 614
9.3.1 Brain Arteriovenous Shunts 615
9.3.1.1 General Appearance of Arteriovenous Shunts 615
9.3.1.2 Multiple Brain Arteriovenous Malformations 618
9.3.1.3 Topographic Analysis of Brain Arteriovenous Malformations 625
9.3.1.4 Angioarchitecture of Brain Arteriovenous Malformations 631
9.3.1.5 Clinical–Angioarchitectural Correlation in Brain Arteriovenous Malformations 677
9.3.2 Venous Variations, Malformations, and Mixed Lesions . . 684
9.3.2.1 Developmental Venous Anomalies 685
9.3.2.2 Cavernous Hemangiomas 686
9.3.2.3 Cerebral Cavernous Malformations 687
9.3.2.4 Occult and Cryptic Malformations 690
9.3.2.5 Sturge–Weber Syndrome 691

10 Goals and Objectives in the Management of Brain Arteriovenous Malformations 695

10.1 Introduction 695

10.2 Indications for Treatment of Brain Arteriovenous Malformations 696
10.2.1 Age 700
10.2.2 Sex 701
10.2.3 Lifestyle and Occupation 701
10.2.4 Presenting Symptoms 703
10.2.4.1 Hemorrhage 703
10.2.4.2 Seizures 704
10.2.4.3 Headaches 704
10.2.4.4 Neurological Deficits 708
10.2.5 Location, Size, and Deep Venous Drainage 708
10.2.6 Brain Arteriovenous Malformations and Arterial Aneurysms 708

10.3 Therapeutic Management Strategy 715

10.4 Embolization 716
10.4.1 Partial (Targeted) Embolization 716
10.4.2 Partial (Palliative) Embolization 720

10.4.3 Curative Embolization 720
10.4.4 Preoperative Embolization 728
10.4.5 Intraoperative Embolization Therapy 729
10.4.6 Embolization Prior to Radiosurgery 729
10.4.6.1 Size Reduction 729
10.4.6.2 Targeted Embolization Prior to Stereotactic Radiosurgery 731
10.4.7 Staging of Embolization 732
10.4.8 Emergency Embolization 732
10.4.9 Contraindications for Endovascular Treatment 732
10.4.10 Embolization Results 734

11 Spinal Arteriovenous Malformations 737

11.1 Parachordal Arteriovenous Fistulae (Extracranial, Vertebro-Vertebral, Paraspinal, Extradural, and Extraspinal Arteriovenous Fistulae) 738
11.1.1 General Remarks 738
11.1.2 Cranial (Branchial) Arteriovenous Shunts 740
11.1.2.1 Maxillary Artery-to-Vein Arteriovenous Fistulae (Stapedial) 743
11.1.2.2 Ascending Pharyngeal-Internal Jugular Arteriovenous Fistulae (Hypoglossal) 743
11.1.3 Vertebro-Vertebral Arteriovenous Fistulae (Proatlantal and Intersegmental) 743
11.1.3.1 Vertebro-Vertebral Arteriovenous Fistulae 743
11.1.3.2 Clinical Findings 751
11.1.4 Paraspinal Arteriovenous Fistulae 752

11.2 Spinal Cord Vascular Lesions 758

11.3 Spinal Cord Arteriovenous Malformations 760
11.3.1 Classification of Spinal Cord Arteriovenous Malformations 767
11.3.2 Angioarchitecture 775
11.3.2.1 Arterial Features 775
11.3.2.2 Direct Arteriovenous Fistulae 784
11.3.2.3 High-Flow Angiopathy 786
11.3.2.4 Arterial Aneurysms in Spinal Cord Arteriovenous Malformations 786
11.3.2.5 Dural Supply 794
11.3.2.6 Nidus 794
11.3.2.7 Veins 802
11.3.3 Pretherapeutic Evaluation 808
11.3.3.1 Clinical Assessment 808
11.3.3.2 Noninvasive Imaging Modalities 808
11.3.3.3 Angiography 809

11.4 Spinal Cord Hemodynamics 810
11.4.1 Particular Forms of Spinal Cord Arteriovenous Malformations 811
11.4.1.1 Spinal Cord Intradural Arteriovenous Fistulae 811
11.4.1.2 Spinal Arteriovenous Metameric Syndromes 813

11.4.1.3 Associated Cerebral and Spinal Arteriovenous Malformations 822
11.4.2 Clinical Aspects 825
11.4.2.1 Natural History and Clinical Presentation 825
11.4.2.2 Prognosis 830
11.4.2.3 Aggravating Factors 831

11.5 Treatment of Vascular Lesions 833
11.5.1 Indications 833
11.5.2 Results of Spinal Cord Arteriovenous Malformation Embolization 839
11.5.3 Complications of Embolization 840
11.5.4 Surgery in the Treatment of Spinal Cord Arteriovenous Malformations 842
11.5.5 Radiotherapy of Spinal Cord Arteriovenous Malformations 843
11.5.6 Medical Therapy 843

12 Spinal Dural Arteriovenous Fistulae 849

12.1 Pathology 850
12.1.1 Macroscopic Appearance 851
12.1.2 Microscopic Appearance 853
12.1.3 Pathological Changes in the Spinal Cord 854

12.2 Pathophysiology 854
12.3 Clinical Presentation of Spinal Dural Arteriovenous Fistulae 858
12.4 Imaging of Spinal Dural Arteriovenous Fistulae 859

12.5 Treatment of Spinal Dural Arteriovenous Fistulae . . . 867
12.5.1 Indications 867
12.5.2 Embolization of Spinal Dural Arteriovenous Fistulae: Techniques 867
12.5.3 Results of Spinal Dural Arteriovenous Fistula Embolization 869
12.5.4 Surgery for Spinal Dural Arteriovenous Fistulae 871
12.5.5 Postoperative Follow-up 872

13 Tumors of the Spinal Column and Spinal Cord . . 873

13.1 Introduction 874
13.2 Spinal Angiography 874
13.3 Angiographic Protocol 875

13.4 Embolization 876
13.4.1 Cervical Tumors 877
13.4.2 Thoracic, Lumbar, and Sacral Tumors 877
13.4.3 Chemoembolization 877
13.4.4 Intralesional Embolization 880

13.5 Benign Tumors 883
13.5.1 Vertebral Hemangiomas 883
13.5.1.1 Associated Lesions 888

13.5.1.2 Pretherapeutic Evaluation . . . 888
13.5.1.3 Treatment . . . 889
13.5.1.4 Embolization . . . 889
13.5.2 Aneurysmal Bone Cysts . . . 890
13.5.2.1 Clinical Presentation . . . 890
13.5.2.2 Pretherapeutic Evaluation . . . 891
13.5.2.3 Angiography . . . 891
13.5.2.4 Differential Diagnosis . . . 891
13.5.2.5 Pathogenesis . . . 892
13.5.3 Other Benign Vascular Tumors . . . 893
13.5.4 Giant Cell Tumors . . . 893
13.5.4.1 Pathology . . . 893
13.5.4.2 Clinical Presentation . . . 893
13.5.4.3 Radiographic Findings . . . 893
13.5.4.4 Embolization . . . 895

13.6 Malignant Tumors . . . 895
13.6.1 Pretherapeutic Evaluation . . . 897
13.6.2 Embolization . . . 897

13.7 Spinal Cord Tumors . . . 898
13.7.1 Hemangioblastomas . . . 898
13.7.1.1 Histopathology . . . 898
13.7.1.2 von Hippel-Lindau Disease . . . 900
13.7.2 Pretherapeutic Evaluation of Hemangioblastomas . . . 904
13.7.2.1 Computerized Tomography . . . 904
13.7.2.2 Magnetic Resonance Imaging . . . 904
13.7.2.3 Angiography . . . 905
13.7.3 Feeding Arteries . . . 906
13.7.4 Draining Veins . . . 906
13.7.5 Treatment and Embolization . . . 906

13.8 Other Intradural Vascular Tumors and Spinal Hemorrhage 909

14 Technical Aspects of Surgical Neuroangiography . . . 913

14.1 Introduction . . . 915

14.2 Patient Preparation . . . 917
14.2.1 Angiographic Equipment . . . 917
14.2.2 Preoperative Medications . . . 917
14.2.2.1 Corticosteroids . . . 918
14.2.2.2 Anticonvulsants . . . 918
14.2.2.3 Antiplatelets . . . 919

14.3 Anesthesia . . . 919
14.3.1 General Anesthesia . . . 919
14.3.2 Neuroleptic Analgesia . . . 920
14.3.3 Tracheostomy . . . 920
14.3.4 Local Anesthesia . . . 920
14.3.5 Input and Output Monitoring . . . 921
14.3.6 Arterial Line and Venous Line . . . 921
14.3.7 Heparinization . . . 923

14.3.8 Activated Coagulation Time Monitoring 924
14.3.9 Functional Evaluation 925
14.3.9.1 Somatosensory- and Motor-Evoked Potentials 925
14.3.9.2 Facial Nerve Monitoring 925
14.3.10 Pharmacological Testing 926
14.3.10.1 Amobarbital 926
14.3.10.2 Xylocaine 929
14.3.10.3 Mucocutaneous Territories 929

14.4 Arteriotomy Sites 929
14.4.1 Introducer Sheath 930
14.4.2 Closure Devices 932
14.4.2.1 Hemostasis of the Arteriotomy Site Closure 932
14.4.2.2 Internal Closure Devices 932

14.5 Catheters and Delivery Systems 933
14.5.1 Guiding Catheters 933
14.5.2 Microcatheters 934
14.5.3 Balloon Catheters 942
14.5.3.1 Tolerance Testing and Flow Control 942
14.5.3.2 Detachable Balloons 955
14.5.3.3 Angioplasty Balloon Catheters 958
14.5.3.4 Balloon-Mounted Stents 962
14.5.3.5 Stent Delivery Catheters 962

14.6 Guidewires 965
14.6.1 Microguidewires 965

14.7 Embolic Agents 969
14.7.1 Particulate Agents 969
14.7.1.1 Absorbable Materials 970
14.7.1.2 Nonabsorbable Particulate Materials 974
14.7.1.3 Flow-Directed Particle Embolization 980
14.7.1.4 General Principles in Aneurysm Treatment 1020
14.7.1.5 General Principles of Coil Treatment of Aneurysms . . . 1030
14.7.2 Nonabsorbable Liquid Agents 1059
14.7.2.1 Introduction 1059
14.7.2.2 Acrylates 1059
14.7.2.3 Sclerotherapy 1074
14.7.2.4 Ethylene-Vinyl Alcohol Copolymer 1083
14.7.3 EVOH in Brain Arteriovenous Malformation Treatment 1089

14.8 Opacifying Agents 1092
14.8.1 Tantalum Powder 1092
14.8.2 Iophendylate (Pantopaque) 1093
14.8.3 Iodized Oil 1093
14.8.4 Ethiodol 1093

14.9 Chemotherapy 1093
14.9.1 Intra-arterial Infusions 1093
14.9.2 Time-Released Microcapsules (Chemoembolization) . . 1094

14.10 Miscellaneous 1094
14.10.1 Syringes 1094

14.10.2 Stopcocks and Y-Adapters . . . 1095
14.10.3 Tray Containers . . . 1095
14.10.4 Flushing Solutions . . . 1095
14.10.5 Corticosteroids . . . 1096
14.10.6 Normal Physiology of the External Carotid Arteries . . . 1096

14.11 Flow Control . . . 1097
14.11.1 Introduction . . . 1097
14.11.2 Flow Control in the Craniofacial Area . . . 1097
14.11.2.1 Protection of an Endangered Anastomosis . . . 1101
14.11.2.2 Intralesional Flow Control . . . 1101
14.11.2.3 Occlusive Balloon Flow Reversal . . . 1102
14.11.2.4 Functional Rearrangement of the Supply to a Territory . 1104
14.11.2.5 Surgical Flow Control . . . 1104
14.11.3 Flow Control in the Meningeal Arcade and Dural Surfaces 1104
14.11.4 Flow Control in the Cerebral Circulation . . . 1104
14.11.4.1 Distal Catheterization . . . 1106
14.11.4.2 Flow Reversal . . . 1108
14.11.4.3 Flow Arrest . . . 1111
14.11.4.4 Systemic Hypotension . . . 1111
14.11.4.5 Catheter Withdrawal . . . 1111
14.11.5 Spine and Spinal Cord . . . 1113
14.11.5.1 Technical Aspects of Endovascular Treatment in the Spine and Spinal Cord . . . 1113

14.12 Postembolization Care . . . 1128
14.12.1 Head and Neck . . . 1128
14.12.2 Cerebral Arteriovenous Malformations . . . 1128
14.12.3 Intradural Aneurysms . . . 1128
14.12.4 Spinal Arteriovenous Malformations . . . 1129

14.13 Complications of Embolization . . . 1129
14.13.1 Complications of Head and Neck Embolization . . . 1129
14.13.1.1 Neurological Deficit . . . 1129
14.13.1.2 Cranial Nerve Deficit . . . 1129
14.13.1.3 Postoperative Swelling . . . 1130
14.13.1.4 Skin Necrosis . . . 1130
14.13.2 Complications of Cerebral Embolization . . . 1130
14.13.2.1 Medical Therapy for Acute Ischemic Stroke . . . 1130
14.13.2.2 Recanalization . . . 1131
14.13.2.3 Microcirculation Agents . . . 1132
14.13.2.4 Antiplatelets . . . 1132
14.13.2.5 Anticoagulation . . . 1132
14.13.2.6 Biorheological Factors . . . 1133
14.13.2.7 Antiedema and Pharmacological Protection Agents . . . 1134
14.13.2.8 Additional Measures . . . 1135
14.13.3 Hemorrhage . . . 1135
14.13.3.1 Generalities . . . 1135
14.13.3.2 Brain Arteriovenous Malformation Rupture . . . 1137
14.13.3.3 Aneurysm Rupture . . . 1141
14.13.3.4 Arterial Stenosis . . . 1143
14.13.3.5 Vasospasm . . . 1146

14.14 Follow-up 1146

14.15 Combined Endovascular Treatments 1146
14.15.1 Combined Endovascular Treatment in Aneurysm Therapy 1147
14.15.2 Combined Endovascular Treatment in Brain Arteriovenous Malformation Therapy 1147
14.15.3 Combined Endovascular Treatment in Occlusive and Hemorrhagic Vascular Disease 1147

14.16 Techniques of Carotid Angioplasty and Stenting 1152
14.16.1 Introduction 1152
14.16.2 Hemodynamic Disturbances During Stenting 1152
14.16.3 Premedication 1153
14.16.4 Vasoactive Medications 1154
14.16.5 Intervention 1154
14.16.6 Predilatation Angioplasty 1164
14.16.7 Stent Selection 1164
14.16.7.1 Self-Expandable Stents 1169
14.16.7.2 Nitinol 1169
14.16.7.3 Balloon-Expandable Stents 1171
14.16.7.4 Low-Profile Balloon-Expandable Stents 1171
14.16.7.5 GFX II 1171
14.16.8 Postdilatation Angioplasty 1173
14.16.8.1 Distal Cerebral Protection 1173
14.16.9 Mechanical Revascularization of Totally Occluded Brachiocephalic Vessels 1176
14.16.10 Complications of Mechanical Revascularization 1178
14.16.11 Stent Retrieval 1179

References 1183

Subject Index for Volumes 2.1 and 2.2 1259

Manufacturers 1271

Abbreviations

AA	Arterial aneurysm
ACAS	Asymptomatic Carotid Atherosclerosis Study
Ach	Acetylcholine
ACA	Anterior cerebral artery
AcomA	Anterior communicating artery
ACT	Activated coagulation time
ADC	Apparent diffusion coefficient
ADP	Adenosine diphosphate
AICA	Anterior inferior cerebellar artery
ASCA	Anterior superior cerebellar artery
ASD	Atrial septal defect
ATII	Angiotensin II
AVF	Arteriovenous fistula
AVM	Arteriovenous malformation
AVS	Arteriovenous shunt
BAVF	Brain arteriovenous fistula
BAVM	Brain arteriovenous malformation
BBB	Blood-brain barrier
BLC	Berenstein liquid coil
BP	Blood pressure
CAMS (1-3)	Cerebrofacial arteriovenous metameric syndrome
CAS	Carotid angioplasty and stenting
CBF	Cerebral blood flow
CBV	Cerebral blood volume
CCA	Common carotid artery
CCF	Carotid cavernous fistula
CEA	Carotid endarterectomy
CGRP	Calcitonin gene-related peptide
CMCC	Chronic macrocutaneous candidosis
CSF	Cerebrospinal fluid
CT	Computed tomography
CTA	Computer tomographic angiography
CVA	Cerebral vascular accidents
CVM	Cerebral vascular malformation
CVMS (1-3)	Cerebrofacial venous metameric syndrome
CVT	Cerebrovenous thrombosis

DAVF	Dural arteriovenous fistula
DAVS	Dural arteriovenous shunt
DBLC	Double lumen balloon catheters
DC	Direct current
DIC	Disseminated intravascular coagulation
DLBC	Double-lumen balloon tip catheters
DMSO	Dimetyl sulfoxide solvent
DSA	Digital subtraction angiography
DVA	Developmental venous anomaly
DWI	Diffusion-weighted imaging
EAA	Excitatory amino acid
ECASS	European Cooperative Acute Stroke Study
EC/IC	Extracranial to intracranial
ECST	European Carotid Surgery Trial
ED IV	Ehlers-Danlos syndrome type IV
EDRF	Endothelial-dependent relaxing factor
EDV	End diastolic velocity
ET-1	Endotheliin-1
EVAL	Ethylene-vinyl alcohol copolymer
EVOH	Ethylene-vinyl alcohol copolymer Onyx
F	French size
FGF	Fibroblast growth factor
FMD	Fibromuscular dysplasia
GDC	Guglielmi detachable coil
GPA	Glycoprotein GP IIb/IIIa receptor antagonists
GSA	Giant serpentine aneurysm
GVB	Gold valve balloon
HHT	Hereditary hemorrhagic telangiectasia
HITS	High-intensity transient signals
HMCAS	Hyperdense middle cerebral artery sign
HR	Heart rate
5-HT	Serotonin (5-hydroxytryptanine)
IBCA	Isobutyl-2-cyanoacrylate
ICA	Internal carotid artery
ICH	Intracranial hemorrhage
ICP	Intracranial pressure
ID	Inner diameter
IEL	Internal elastica lamina
ILT	Inferior lateral trunk
LIAT	Local intra-arterial thrombolysis
LDL	Low-density lipoprotein
LEI	Lamina elastica interna
LIAT	Local intra-arterial thrombolysis
LTICA	Left internal carotid artery
LTS	Cysteinyl leukotrienes

LTSA	Left subclavian artery
LTVA	Left vertebral artery
MAP	Mean arterial blood pressure
MCA	Middle cerebral artery
MCAO	Middle cerebral artery occlusion
MEPs	Motor evoked potentials
MRA	Magnetic resonance angiography
MRI	Magnetic resonance imaging
MSAS	Middle cerebral artery stenosis
NBCA	*N*-butyl-2-cyanoacrylate
NASCET	North American Symptomatic Carotid Endarterectomy Trial
NE	Norepinephrine
NF	Neurofibromatosis
NI	Neurological improvement
NIHSS	National Institutes of Health Stroke Scale
NK-1	Neurokenin-1 (NK-2, NK-3)
NMDA	*N*-methyl-D-aspartate
NO	Nitrous oxide
NOS	Nitric oxide synthase
NPY	Neuropeptide Y
OD	Outer diameter
OER	Oxygen extraction ratio
OVD	Occlusive vascular disease
PACAP	Pituitary adenylate cyclase-activating peptide
PAF	Platelet activation factors
PCA	Posterior cerebral artery
PcomA	Posterior communicating artery
PDGF	Platelet derived growth factor
PET	Positron emission tomography
PGs: PGD_2, PEG_2, PGF_{2a}	Prostaglandins
PGI_2	Prostacyclin
PHACE	Syndrome with posterior fossa malformations hemangiomas arterial anomalies coarctation of the aorta eye malformations
PHI	Peptide histidine isoleucine
PICA	Posterior inferior cerebellar artery
PKD	Polycystic kidney disease
PROCT II	Prolyse in Acute Cerebral Thromboembolism Trial II
PSAVMs	Paraspinal arteriovenous malformations
PSV	Maximal systolic velocity peak
PTT	Partial thromboplastin time
PVA	Polyvinyl alcohol
PWI	Perfusion-weighted imaging
PTA	Percutaneous transluminal angioplasty

rCBF	Regional cerebral blood flow
ROW	Rendu-Osler-Weber syndrome
RTCCA	Right common carotid artery
RTICA	Right internal carotid artery
RTSA	Right subclavian artery
RTVA	Right vertebral artery
r-TPA	Recombined tissue plasminogen activated
rUK	Recombined urokinase
SAH	Subarachnoid hemorrhage
SAMS (1-31)	Spinal arteriovenous metameric syndrome
SBE	Subacute bacterial endocarditis
SCA	Superior cerebellar artery
SD	Spontaneous dissections
SEPs	Somatosensory evoked potentials
SCAVMs	Spinal cord arteriovascular malformations
SP	Substance P
TIA	Transient ischemic attack
TIMI	Thrombolysis in myocardial infarction
TXA_2	Thromboxane A_2
UK	Urokinase
VBA	Vertebrobasilar artery
VCAM-1	Vascular endothelial addition molecule (vasodilator peptides)
VGAMs	Vein of Galen aneurysmal malformations
VHL	Von Hippel-Lindau disease
VIP	Vasoactive intestinal peptides
VP	Vasopressin
VVM	Venous vascular malformation
VVJ	Vertebrobasilar junction

8 Dural Arteriovenous Shunts

8.1 Historical Review 566

8.2 Pathophysiology 570

8.3 The Osteodural–Venous Complex 571
8.3.1 Dural Venous Plexus 572
8.3.2 Transdural Veins 573

8.4 Classification 575

8.5 Clinical Presentation of Dural Arteriovenous Shunts 579
8.5.1 Cranial Nerve Symptoms 580
8.5.2 Tinnitus and Objective Bruits 581
8.5.3 Focal Neurological Deficits 582
8.5.4 Global Neurological Deficits 585
8.5.5 Intracranial Hemorrhage 587
8.5.6 Hormonal Influences 587
8.5.7 Associated Conditions and Multiplicity 590

8.6 Natural History 594

8.7 Progression of Symptoms 596

8.8 Pretherapeutic Evaluation 598

8.9 Therapeutic Aspects 598
8.9.1 Indications and Strategy 598
8.9.2 Topographic Considerations 602
8.9.3 Technical Aspects 605
8.9.4 Timing of Embolization 605
8.9.5 Results of Embolization 606
8.9.6 Complications of Embolization 606
8.9.7 Surgery 607

Dural arteriovenous shunts (DAVSs) are abnormal shunts within the dura. Theoretically, they can occur at any site within the dura, but most frequently they develop near the venous sinuses. Venous drainage may occur into the dural sinuses, into osteodural veins, retrogradely via leptomeningeal veins toward the cortical cerebral, cerebellar, or perimedullary veins, or any combination thereof. Arterial supply is usually from adjacent branches of the dural arteries, less frequently from osseous branches, while pial supply is rare.

The term "malformation" was used in the past for all types of DAVSs, pediatric and adult, but we have found this to be inappropriate, as it implies a developmental origin in all of them. DAVSs have been demonstrated in utero and may be clinically present at neonatal age. Their association with a malformation of the dural sinuses attests to their developmental origin. On

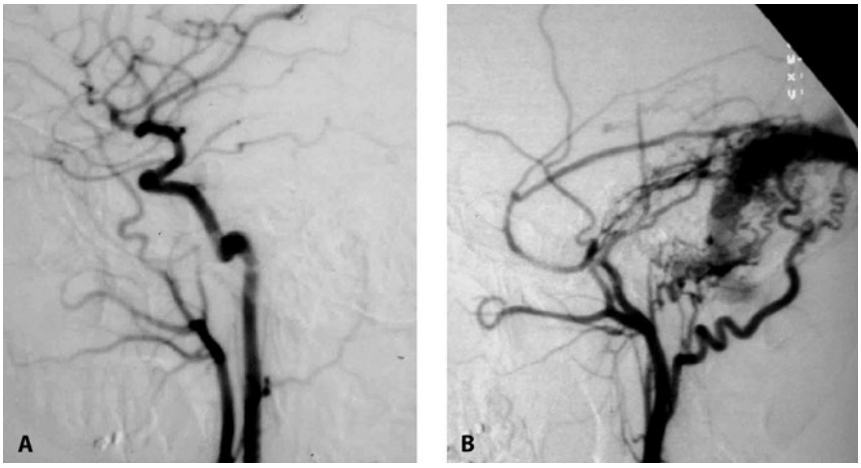

Fig. 8.1. A 20-year-old male patient investigated for mild head injury associated with left-sided subdural hematoma showed no abnormality at presentation on left common carotid angiogram in lateral view (**A**). Eight months later, following an 8-week history of bruit, the left external carotid angiogram in lateral view (**B**) demonstrates transverse sinus dural arteriovenous shunt

the other hand, there is good evidence that these shunts in adults are an acquired disease (Fig. 8.1). As vein of Galen malformations cannot be grouped together with brain arteriovenous malformations, we suggest separating the neonatal and infantile DAVSs from the adult type. The terms "dural arteriovenous shunt" (DAVS) and "dural arteriovenous fistula" (DAVF) should be used in the adult population to indicate their acquired nature.

8.1 Historical Review

Historically, these lesions have attracted considerable interest. Dural arteriovenous malformations (DAVMs) were first described by Tonnis in 1936 and subsequently by Tonnis in 1936 and referred to by Aminoff in 1973. Verbiest (1951) and Fincher (1951) were the first to introduce the concept of the so-called spontaneous dural fistulae. The early case reports described low-flow lesions, but in 1964 van de Werf presented the first case of a congenital high-flow DAVM in a 3-year-old child.

The 1960s were marked by emphasis on the topography of individual cases (Hayes 1963; Laine et al. 1963; Pecker et al. 1965). It was Hans Newton at the University of California at San Francisco, in the late 1960s (Newton and Cronqvist 1969; Newton and Hoyt 1970; Newton et al. 1968), who routinely started to explore all intracranial vascular disorders, including DAVSs, with external carotid injections at angiography. In Europe, René Djindjian used superselectivity at angiography in the mid-1970s to establish the first angioarchitectural classification of DAVSs (Table 8.1).

Table 8.1. Djindjian classification of dural arteriovenous shunts by venous drainage (from Djindjian and Merland 1978, with permission)

Type I	Drainage into a sinus
Type II	Sinus drainage with reflux into cerebral veins
Type III	Drainage solely into cortical veins
Type IV	With supra- or infratentorial venous lake

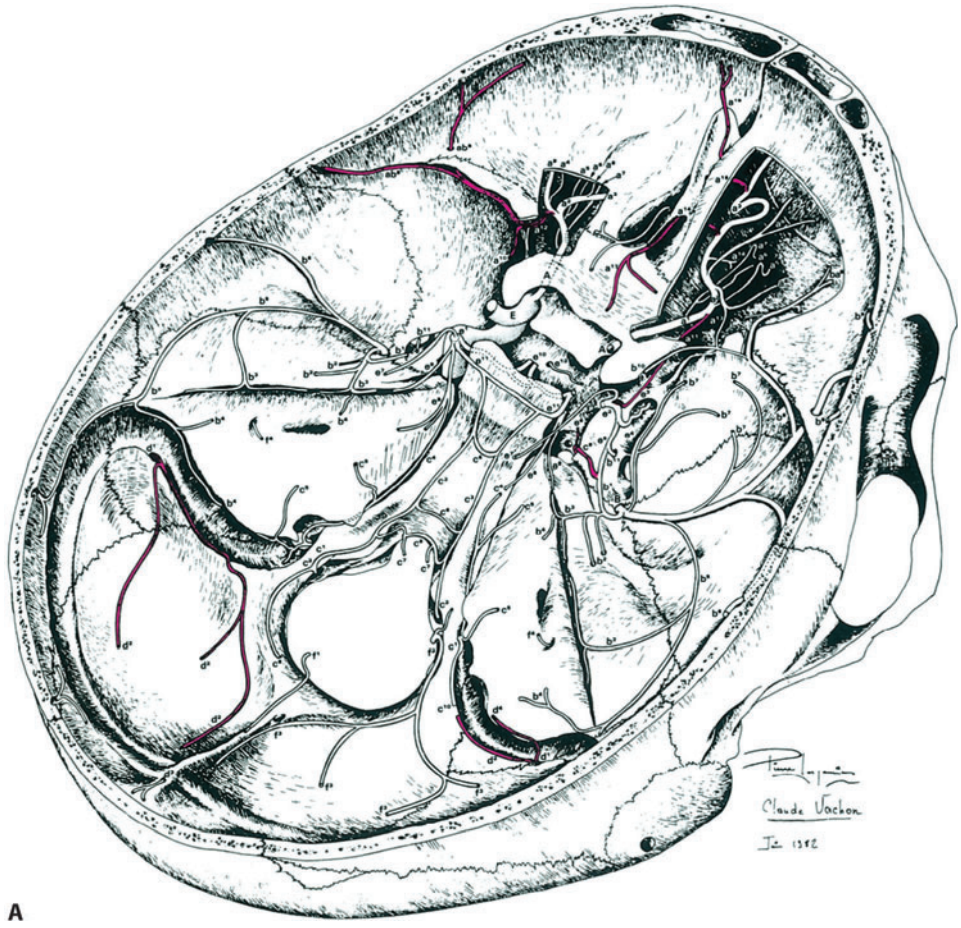

A

Fig. 8.2A–C. Illustrations showing the meningeal arteries at the base of the skull (right posterolateral view). All of the dural meningeal envelopes and the right carotid siphon have been removed. The roof of the right orbit and optic canal, and posterior part of the left orbital roof have been opened to show the branches of the ophthalmic artery. **A** The anatomical disposition on the right side of the meningeal branches of the anterior and posterior ethmoidal arteries and the anastomotic branch between the ophthalmic artery and the inferolateral trunk of the carotid siphon (passing through the superior orbital fissure). The carotid branch of the ascending pharyngeal artery passes trough the foramen lacerum while a collateral of the occipital artery can be seen to run to the sigmoid sinus. The left half of the base of the skull shows the ophthalmic origin of the frontal and parietal branches of the middle meningeal artery, as well as a mastoid branch of the occipital artery supplying all of the posterior fossa on the left side. Note also the transosseous artery at the level of the sinusal confluence. **B, C** see p. 568

Additional European and North American contributions further established the entity of spontaneous DAVMs (Houser 1972; Aminoff 1973; Obrador et al. 1975; Chaudhary et al. 1982). The early 1980s were marked by a great number of individual case reports, indicating the significant potential for hemorrhagic complications with DAVMs of the anterior cranial fossa and the tentorium (Ito et al. 1983; Terada et al. 1984; Grisoli et al. 1984). In 1983, Albright et al. outlined the characteristic features of DAVMs in the pediatric population. Detailed descriptions of the vascularization of the intracranial dura by Lasjaunias et al. (1986a) helped further under-

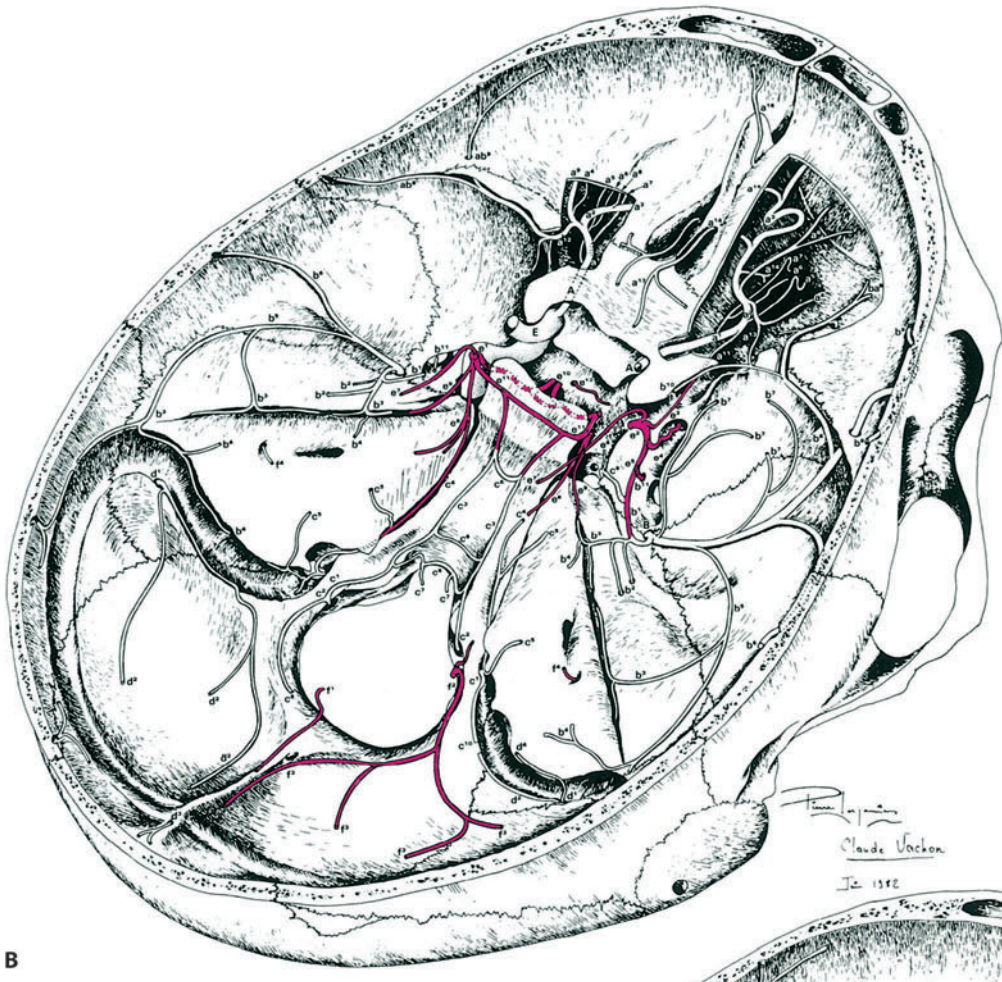

B

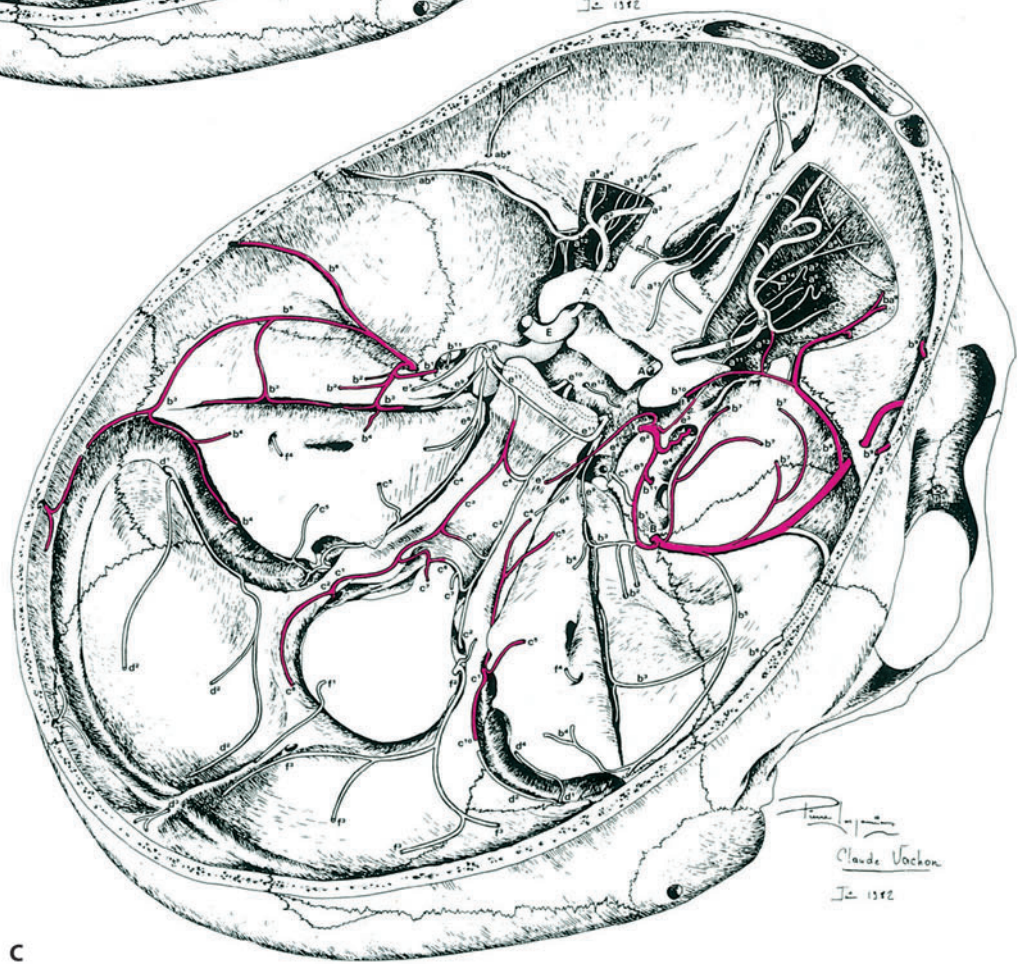

C

◄ **Fig. 8.2** (*continued*). **B** The branches of the carotid siphon. On the *left*, these branches arise from a common trunk originating from the posterior vertical portion of the carotid siphon, while on the *right*, the branches to the petrosal apex and dorsum sella arise separately. Note also on the *right* the lateral clival arteries which (when present) originate from the horizontal part of the carotid siphon. The following branches of the vertebral artery are also shown: a meningeal artery supplying the right posterior cerebellar fossa; an artery supplying the falx cerebelli arising from the posterior inferior cerebellar artery (not shown); the subarcuate arteries, both of which are located behind the internal auditory canal. **C** The branches of the internal maxillary and ascending pharyngeal arteries. On the *left*, only the occipital and squamous divisions of the middle meningeal artery are shown, since on this side the frontal and parietal branches can be seen to arise from the ophthalmic artery. The arcade along the superior petrosal sinus is clearly visible, as is the contribution of the middle meningeal artery to the vascularization of the wall of the transverse sinus. Also visible on the *left* is the meningeal territory of the hypoglossal branch of the neuromeningeal division of the ascending pharyngeal artery. Note in particular the contribution of the hypoglossal branch to the dural vascularization of the foramen magnum and its anastomoses with the ipsilateral medial clival artery. On the *right* side, the branches of the accessory meningeal artery are shown to be passing through the Vesalius foramen, medial and slightly anterior to the foramen ovale. The artery of the foramen rotundum and the branches running along the sphenoid ridge on the right side are also clearly shown. The territories of the jugular branch of the neuromeningeal division of the ascending pharyngeal artery are also illustrated, i.e., the inferior petrosal sinus, sigmoid sinus, and lower part of the cerebellopontine angle

stand the potential for endovascular access to DAVSs and the risks for complications at the time of endovascular management (Fig. 8.2).

One of the most significant advances in the understanding of the physiopathology of the DAVS came from the school of La Salpétrière (Paris), which emphasized the role of the cortical venous drainage of these dural shunts. Henceforth, the role of the subarachnoid and subpial venous drainage could be correlated with the type of neurological manifestation and the natural history of dural shunts. This represented a turning point in the understanding of this disease.

Later on, various therapeutic approaches were developed, with increasing emphasis on the role of endovascular techniques.

The accumulation of cases led to additional classifications being proposed by Borden et al. (1995) and Cognard et al. (1995). These classifications of DAVMs (Tables 8.2, 8.3), while important for the purpose of communication, tend to underestimate the dynamic aspect and changes over time that can occur in these disorders.

The recent contributions from the Toronto school completed this quest from the technical challenges to patient selection and therapeutic goals to be reached. Davies et al. (1997a, b), Satomi et al. (2002), van Dijk (2002a, b) identified morphological subgroups with different natural histories and added a prospective dimension to the basic angioarchitectural analysis.

While our ability to diagnose and manage DAVSs has greatly improved over the past 30 years, our understanding of the disease has not advanced to the same extent, as attention has mainly been focused on the various mechanical approaches that could be used for their treatment.

Table 8.2. Borden classification of dural arteriovenous shunts (from Borden et al. 1995, with permission)

1	Venous drainage directly into dural venous sinus or meningeal vein
2	Venous drainage into dural venous sinus with cortical venous reflux (CVR)
3	Venous drainage directly into subarachnoid veins (CVR only)

CVR, cortical venous reflux.

Table 8.3. Cognard classification of dural arteriovenous shunts (from Cognard et al. 1995)

I	Venous drainage into dural venous sinus with antegrade flow
IIa	Venous drainage into dural venous sinus with retrograde flow
IIb	Venous drainage into dural venous sinus with antegrade flow and CVR
IIa+b	Venous drainage into dural venous sinus with retrograde flow and CVR
III	Venous drainage directly into subarachnoid veins (CVR only)
IV	Type III with venous ectasias of the draining subarachnoid veins

CVR, cortical venous reflux.

8.2 Pathophysiology

The association with venous thrombosis was first noted by Djindjian and Merland (1978) and subsequently by Chaudhary et al. (1982). DAVFs were reported to occur following intracranial surgery (Watanabe et al. 1984; Bitoh 1980; Aminoff 1973). In 1978, Djindjian and Merland reported the development of DAVFs following surgery in remote parts of the body (e.g., hysterectomy, varices) as well as in the postpartum period. However, tumor invasion of major sinuses resulting in dural sinus thrombosis is infrequently associated with DAVFs. Trauma, infections, dehydration, hormonal disorders, and coagulopathies can all be associated with intracranial dural venous sinus thrombosis but are infrequently followed by the development of DAVFs (Table 8.4).

The wide variety of these possible etiological factors demonstrates the spectrum of events that can lead to the same result, i.e., the creation of a shunt inside the dura. These factors by themselves should therefore not be considered as the direct cause of DAVSs, but rather they make up an environment that may be conducive to the development of a DAVF, depending on the individual host response to their presence. For instance, not all patients presenting with a sinus thrombosis will develop a shunt, and in fact the majority of DAVSs do not reveal any evidence of pre- or coexisting thrombosis.

We propose that DAVFs in adults are triggered by a factor (or factors) that stimulates angiogenesis. New venular channels will then connect the regional periosteal, dural, or even adjacent leptomeningeal veins to the regional osteodural arteries, and rarely to the pial leptomeningeal arterial systems. Shunting will subsequently occur, with the extent, as well as other factors, related to the topography of the venous outlet(s). If this angiogenic process is simultaneously associated with a loss of some of the venular surface properties, then venous thrombosis is likely to occur. The

Table 8.4. Most common types of drainage of intracranial dural arteriovenous malformations in adults

Location	Sinusal venous drainage	Cortical venous drainage
Cavernous sinus	Frequent	Infrequent
Sigmoid sinus	Constant	Rare
Superior sagittal	Depending on type	Depending on type
Transverse sinus	Depending on type	Depending on type
Torcular	Depending on type	Depending on type
Anterior cranial	Not described	Constant fossa
Tentorium	Rare	Almost constant

effects of the angiogenesis and the associated thromboses will depend on the location and the remaining venous outlet(s). It has been noted that angiogenic growth factors such as basic fibroblast growth factor (bFGF) and vascular endothelial growth factor (VGEF) are expressed in the DAVFs (Uranishi et al. 1999). The absence or presence of thrombosis in association with nonsprouting angiogenesis will determine the clinical presentation and natural history of the DAVS.

In order to avoid confusion in terminology, it is important to understand that DAVFs are to be distinguished from other AVSs that can involve the intracranial dural sinuses and are caused by a variety of distinct pathologies:

- Traumatic lesions of the skull base vessels producing AVSs are clearly different entities, which occur in otherwise normal vasculature (e.g., carotid cavernous fistulae).
- Rupture of a preexisting arterial aneurysm of the internal carotid siphon or a dysplastic internal carotid artery into adjacent venous structures, as may occur in Ehlers–Danlos syndrome, is a preexisting arterial disease and is unrelated to factors involving the dura.
- Other conditions such as transdural supply to pial arteriovenous lesion or proliferative angiopathy are the reflection of an active dural angiogenic process that occurs following ischemic triggers or growth factors from the cortical vessels.

8.3 The Osteodural–Venous Complex

The dural sinuses will vary physiologically and morphologically with age. At birth, the total cerebral venous drainage is directed towards the posterior sinuses, i.e., a true sinusal system. The cavernous venous plexuses are the unique venous drainage channels for the nasal fossa, the orbital cavities and the midline bony structures at the base of the skull. It is a few months after birth that the so-called cavernous capture of the sylvian vein will occur and offer the infant brain an alternate drainage via the cavernous plexus toward the orbit or the pterygoid plexuses and into the external jugular venous system. The jugular bulb continues to mature after birth and subsequent to the regression of the medial occipital and mar-

ginal sinuses. The hydrodynamic role played by each of these venous drainage directions at various developmental stages, including the impact of closure of the fontanels, will create distinguishing features among the various venous plexuses and sinuses.

The dura mater along the convexity of the cranial vault has a different origin than the dura along the base of the skull (membranous vs. cartilaginous bone). The consequence of this difference is morphologically not detectable but may have a biological expression. The cartilaginous bone of the notochord derivatives draining into the epidural venous plexuses also emphasizes the different relationships that may exist between various types of bone versus the periosteum, the dura, and the venous system.

Anatomical differences related to the dural and venous structures in various locations will in turn have a specific impact on the nidal angioarchitecture of a DAVF and consequently on their natural history.

Dural sinuses are large venous channels between two layers of dura mater. They only occur in certain intracranial locations: along the attachment of the margins of the tentorium cerebelli and the falx cerebri, the straight sinus, the confluence of sinuses (torcular), the transverse sinus, the sigmoid sinus, the superior and the inferior longitudinal sinuses, and the superior and the inferior petrosal sinuses. Certain embryonic or fetal venous structures can persist and be assimilated into the sinuses such as the marginal, medial occipital, and tentorial sinuses.

The transverse sinus extends from the confluence of sinuses to the opening of the superior petrosal sinus. It continues as the sigmoid sinus, which extends down to the jugular bulb. The combination of the transverse and the sigmoid sinus forms the lateral sinus.

Classifications in which the term "transverse sinus" describes lesions located on the confluence of sinuses as well as near the jugular bulb are actually combining sinusal locations, which always have venous cranial afferents (transverse sinus) with portions that never receive any cerebral veins (sigmoid sinus). The potential for an AVS in these locations evolving toward leptomeningeal venous drainage is therefore not the same.

Septations may occur within the dural sinuses and result in separate venous channels, which may run parallel to each other. One of these channels may be used for the brain to drain while the other is sometimes exclusively used for drainage of the DAVF and may be a specific target for treatment (Fig. 8.27).

8.3.1 Dural Venous Plexus

There are no dural sinuses in the midline at the skull base; nor do they occur at the spinal levels. In these locations, venous plexiform channels will be present in the epidural space, between periosteum and dura. These venous plexiform channels are the cavernous plexus (improperly called sinus), the retroclival venous plexus, the venous plexus along the anterior margin of the foramen magnum, and the spinal venous plexus. DAVSs have been described in these areas, but they do not drain primarily into dural venous sinuses.

The cervical (vertebral) transverse canal cannot be included in the epidural space. To equate the venous plexus around the vertebral artery to a dural sinus will mistakenly mix paraspinal venous structures with epidural ones. Also, for embryonic reasons, arteriovenous fistulae of the maxillary, vertebral, intercostal, or lumbar arteries should all be classified into paraspinal or parachordal AVSs, as their respective clinical history differs from that of DAVSs.

8.3.2 Transdural Veins

Other structures combine both the dural sinus and venous channel, yet differently from the two previous types described. They are the transdural portions of the cerebral veins intracranially, before they join a sinus, or an epidural collector. Of variable length, they are found near the longitudinal sinus, the lateral sinus close to the tentorium cerebelli, and the middle cranial fossa, near the lamina cribriform. DAVSs that develop in these locations are what Piske and Lasjaunias (1988) have referred to as "extrasinosal dural lesions."

The spinal radicular veins opening at the spinal levels belong to this latter group. Unlike the radicular arteries, there is no metameric link between the radiculomedullary veins and the spinal nerves. Radiculomedullary veins perforate the dura mater to open into venous lakes located between periosteum and dura, sometimes between two consecutive (adjacent) dural arterial territories. Hence, some of the spinal DAVSs may be supplied by arteries from two metameric levels, reflecting the location of the venous communication with or between the nerve roots.

Finally, there is a venous network paralleling the dural arteries at the convexity outlining the grooves seen on the skull. However, this system virtually never develops DAVSs, unless arterial disease or direct trauma of

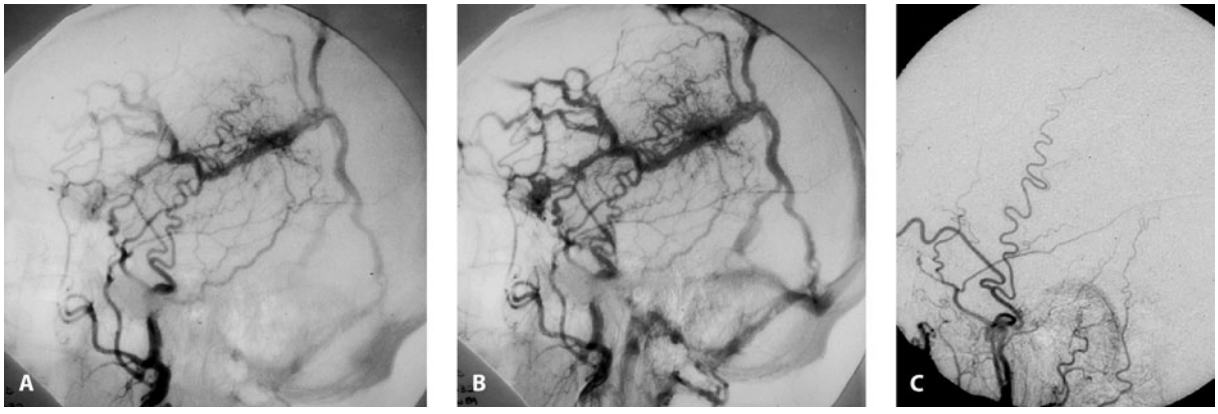

Fig. 8.3A–C. A 45-year-old man presented with a 3-month history of bruit. The left external carotid angiogram in lateral view (**A**, **B**) showed evidence of a convexity osteodural arteriovenous shunt (AVS) with drainage towards the osseous venous system. Six months later, symptoms disappeared (no treatment given), and a follow-up left external carotid angiogram in lateral projection (**C**) 11 years later showed spontaneous closure of the AVS

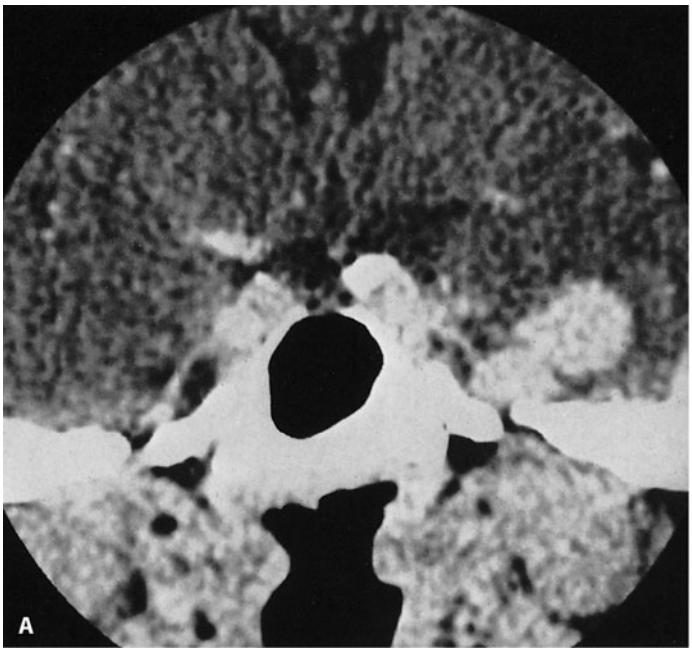

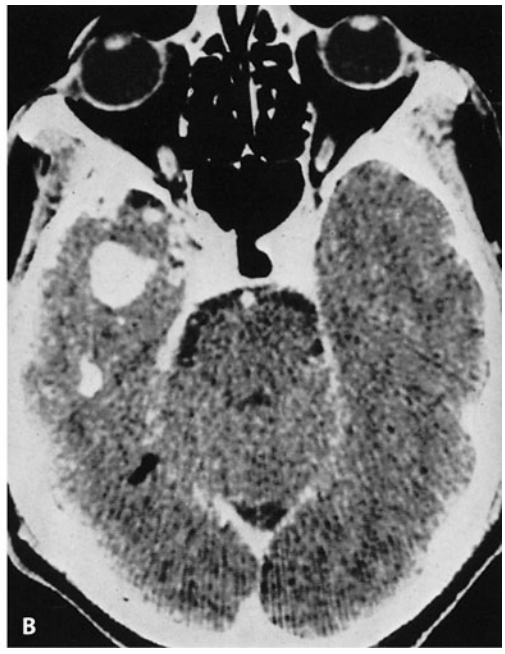

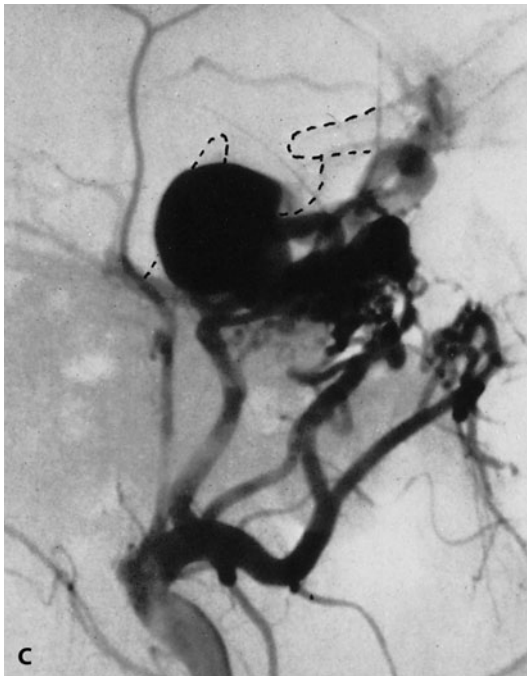

Fig. 8.4A–E. Osteodural arteriovenous malformation of the middle cranial fossa in a 57-year-old man, who presented with temporal lobe seizures. Note the venous ectasia on the CT section in axial (**A**) and coronal (**B**) views. The supply to the nidus is seen on distal external carotid injection (**C**). **D, E** see p. 575

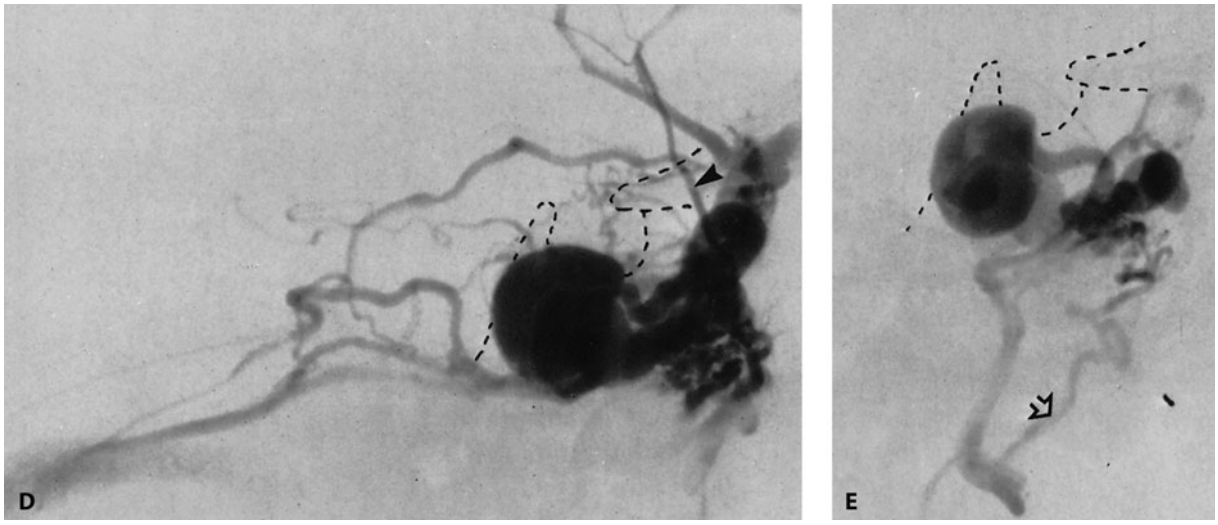

Fig. 8.4 (*continued*). However, selective catheterization of the middle deep temporal artery (**D**) and middle meningeal system (**E**) provided even better visualization and safer embolization. *Arrowhead*, distal temporal branches; *open arrow*, accessory meningeal artery

the middle meningeal artery is responsible for an arterial rupture into the adjacent venous network.

A peculiar group of lesions are the intracranial arteriovenous shunts fed by the dural arteries (that also supply the bone), which are located within bony structures along the convexity (Fig. 8.3) or at the base of the skull (Figs. 8.4, 8.5): the so-called osteodural AVSs. Particularly at the base of the skull, they are often mistaken for dural shunts. They are located within the sphenoid or occipital bones and the adjacent epidural space. They show a strong male dominance caudally, similar to the spinal DAVS, and a female dominance cranially, signifying the hormonal sensitivity of the sphenoid bones at that end of the notochord. In addition, they may be associated with giant epidural and bony lakes and cause significant bone remodeling (Fig. 8.5).

8.4 Classification

Although a topographical classification of DAVSs according to location is useful in planning the therapeutic approach, from a clinical point of view it is more appropriate to classify these lesions according to their venous drainage pattern (Table 8.2).

Subsequent to Djindjian and Merland's classification (1978), a number of other DAVS classifications have been proposed (Cognard et al. 1995; Borden et al. 1995). They all emphasize the venous outflow characteristics of DAVSs and their relationship to presentation (Tables 8.3, 8.4). Validation of these classifications with respect to clinical presentation was subsequently carried out by Davies et al. (1996). DAVS classification schemes tend to be rigid, ignore changes occurring over time, and fail to recognize anatomical predispositions (Lasjaunias 1997). We therefore recommend

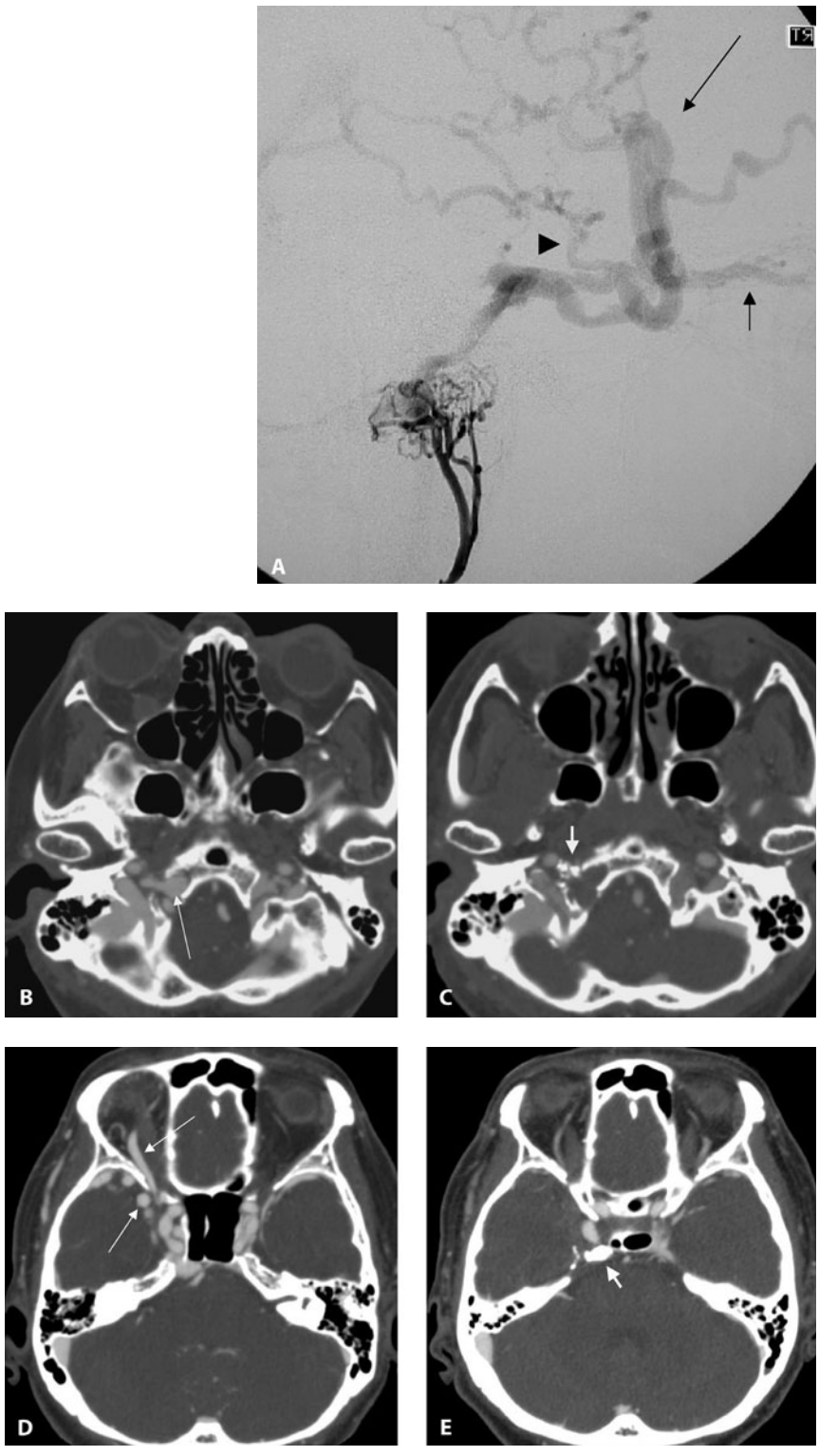

Fig. 8.5A–E.
Legend see p. 577

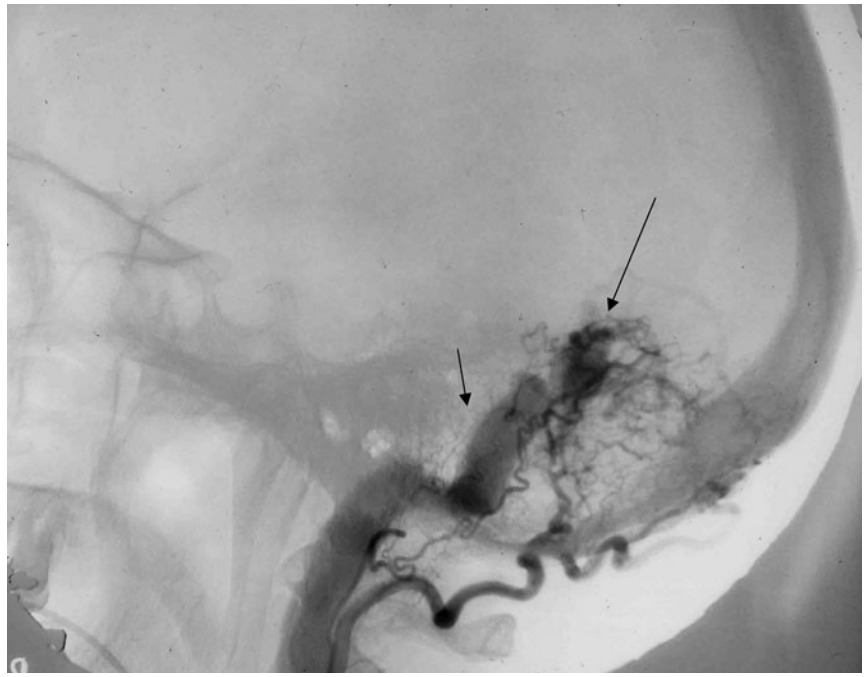

Fig. 8.6. A 38-year-old female patient presented with a 3-month history of progressive left-sided bruit. Left occipital angiogram in lateral view shows dural arteriovenous shunt along the transverse sinus (*long arrow*) with antegrade sinusal drainage (*short arrow*)

◄ **Fig. 8.5A–E.** A 62-year-old female patient presented with progressive right ophthalmoplegia and bruit with a 3-month history. Selective right ascending pharyngeal angiograms in lateral view (**A**) demonstrate osteodural arteriovenous shunt along posterior inferior aspect of the clivus, with drainage upward to the cavernous plexus and then forward to the orbital venous system (*small arrow*) and also with reflux toward the sylvian cortical venous system (*long arrow*) and deep venous system (*arrowhead*). Angio-CT at lower clivus level, before (**B**) and after arterial (ascending pharyngeal) embolization with glue (**C**) demonstrates bony erosion involving the clivus opacified with contrast (*long arrow*) prior to embolization but not afterwards. Angio-CT at cavernous sinus level before (**D**) and after embolization (**E**) demonstrates prominent draining veins towards the orbital and sylvian venous systems (*long arrows*) prior to embolization but not afterwards. Note glue at the entrance to the clival venous pouch (*short arrow*, **C**) and at the entrance to the cavernous plexus (*short arrow*, **E**). The patient's symptoms dramatically improved in 5 days. (Courtesy of Dr. T. Marotta)

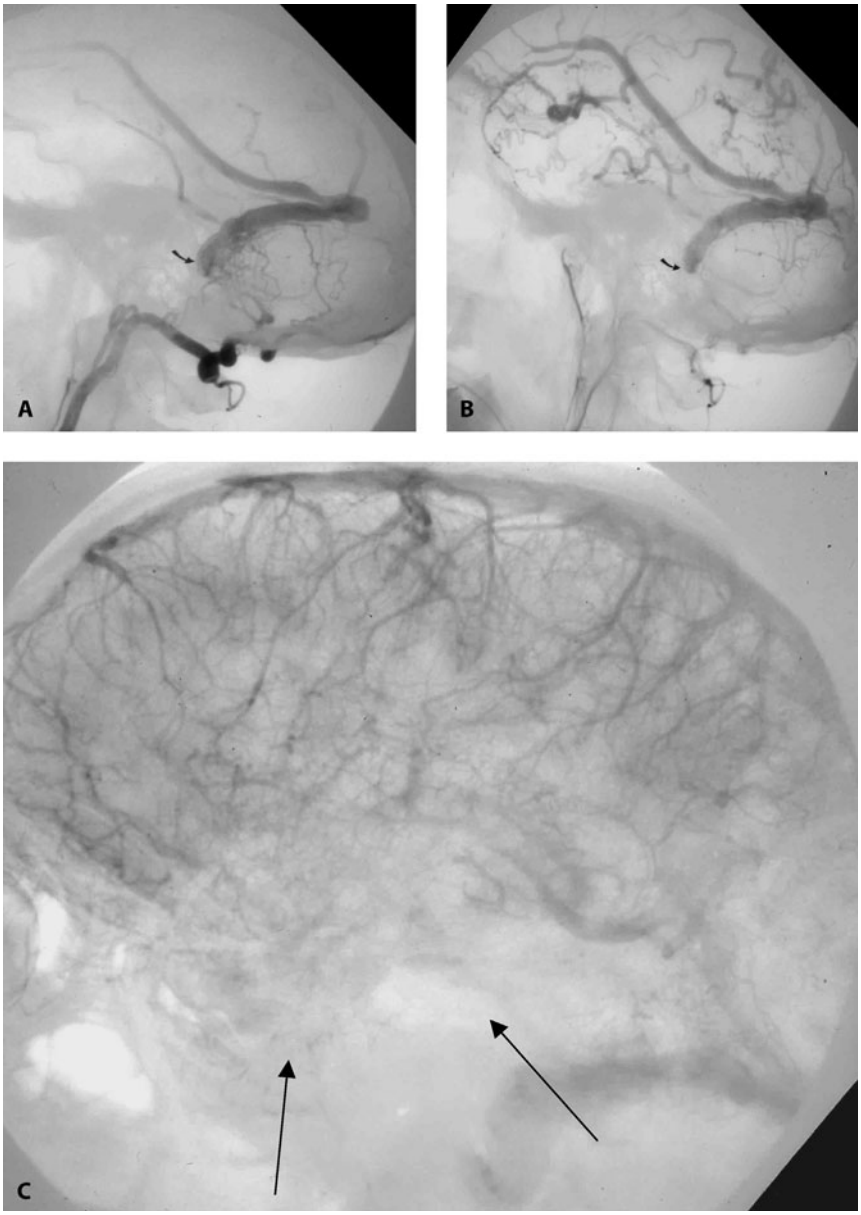

Fig. 8.7A–C. A 60-year-old male patient presented with intermittent aphasia. Left occipital (**A**) and left ascending pharyngeal angiogram (**B**) in lateral views shows evidence of dural arteriovenous shunt (DAVS) along transverse sinus with retrograde leptomeningeal reflux toward the temporal lobe cortical venous system associated with proximal and distal thrombosis of the dural sinus (*curved arrow*). Left internal carotid angiogram in lateral view (**C**) demonstrates delayed opacification of the temporal lobe venous system (*arrows*) because of venous hypertension caused by the cortical venous reflux from the DAVS

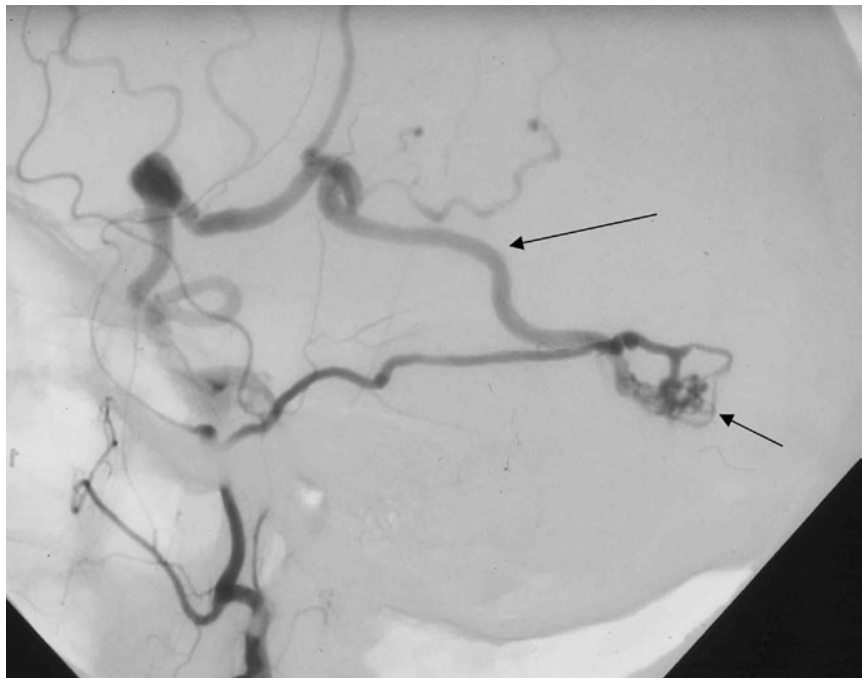

Fig. 8.8. A 42-year-old man presented with a single temporal lobe seizure. External carotid angiogram in lateral view shows evidence of dural arteriovenous shunt (*short arrow*) adjacent to transverse dural sinus but directly draining towards the cortical temporal lobe venous system (*long arrow*)

assessing each case individually, with a strong emphasis on the venous angioarchitecture. DAVSs may drain solely into osteodural veins or directly into the dural sinus with antegrade flow in the sinus (Fig. 8.6, p. 577). They may also drain into a dural sinus, but because of distal dural sinus thrombosis flow, will reverse in the sinus and be directed upstream. Flow may then also occur retrogradely into the leptomeningeal veins, with reflux toward the cortical cerebral veins (Fig. 8.7). The location of a DAVS may be adjacent to a dural sinus, but venous drainage can be directed immediately into a cortical cerebral or cerebellar vein (Fig. 8.8). While certain DAVS locations tend to be associated with predictable venous drainage patterns (Table 8.4), anatomical variations and acquired host response differences may result in variable venous outlets. It is of paramount importance to distinguish between those lesions with and those without retrograde leptomeningeal venous drainage. Irrespective of the location of the shunt, the natural history of these two groups of dural shunts is different and therefore they require a different type of management strategy (Davies et al. 1996; van Dijk et al. 2002b).

8.5 Clinical Presentation of Dural Arteriovenous Shunts

The symptomatology of DAVSs is variable, depending on the location of the shunt, the type of venous drainage, and the flow characteristics (Lasjaunias et al. 1986). They include exophthalmos, bruit, cranial nerve deficits, focal and global neurological deficits, increased intracranial pressure, papilledema, and CSF reabsorption abnormalities, resulting in ventricular enlargement. Most symptoms can be directly related to angioarchitecture of the DAVS. The analysis of DAVSs should include imaging

information obtaining dynamic and morphological data related to the venous drainage of the brain versus that of the DAVS and a search for vascular and parenchymal changes that have occurred as the result of these interactions. The mechanism of the symptoms will be evaluated and clinical objectives and morphological goals established.

The clinical expression of arteriovenous dural lesions is indeed conditioned by the topography of the shunt, but not exclusively: a lesion of the sigmoid sinus cannot itself give rise to retrograde flow in the leptomeningeal veins unless a regional modification of the jugular bulb and the transverse sinus creates, at a distance from the shunt, retrograde leptomeningeal reflux from the lateral sinus to the cortical veins. Conversely, a lesion of the cribriform plate bone will always have leptomeningeal venous drainage; no regional drainage modification is needed or could change this.

8.5.1 Cranial Nerve Symptoms

The cranial nerves are supplied by the meningeal arteries and ischemia due to an arterial steal phenomenon may contribute to some of the cranial nerve palsies encountered in these lesions (Lasjaunias et al. 1984, 1986). The fact that cranial nerve symptoms may be relieved following selective arterial embolization supports the concept of an arterial steal phenomenon (Fig. 8.9). We have never seen, even in high-flow DAVFs, angiographic evidence of an arterial steal affecting the CNS, and therefore CNS symptoms are always related to the venous side of the shunt.

Mechanical phenomena may also be responsible for pseudoextraocular motor nerve palsies in patients with cavernous sinus DAVSs draining into the orbital venous system; diplopia and restricted ocular motor function may be secondary to the proptosis and altered muscle tension and edema

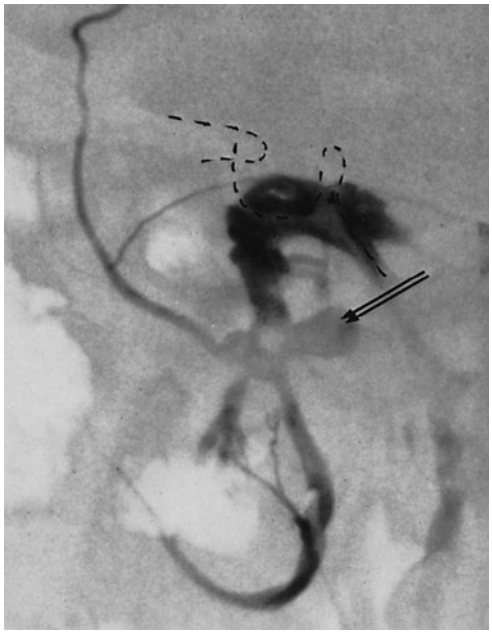

Fig. 8.9. A 35-year-old woman who presented during the last trimester of her first pregnancy with a spontaneously regressive left facial nerve palsy. Three months postpartum she developed a pulsatile bruit on the left side. She was blind in the right eye due to a congenital cataract. The middle meningeal angiogram demonstrates a dural arteriovenous malformation at the level of the foramen spinosum fed by the petrous artery. Note the arterial ectasia (*double arrow*) and the posterior venous drainage

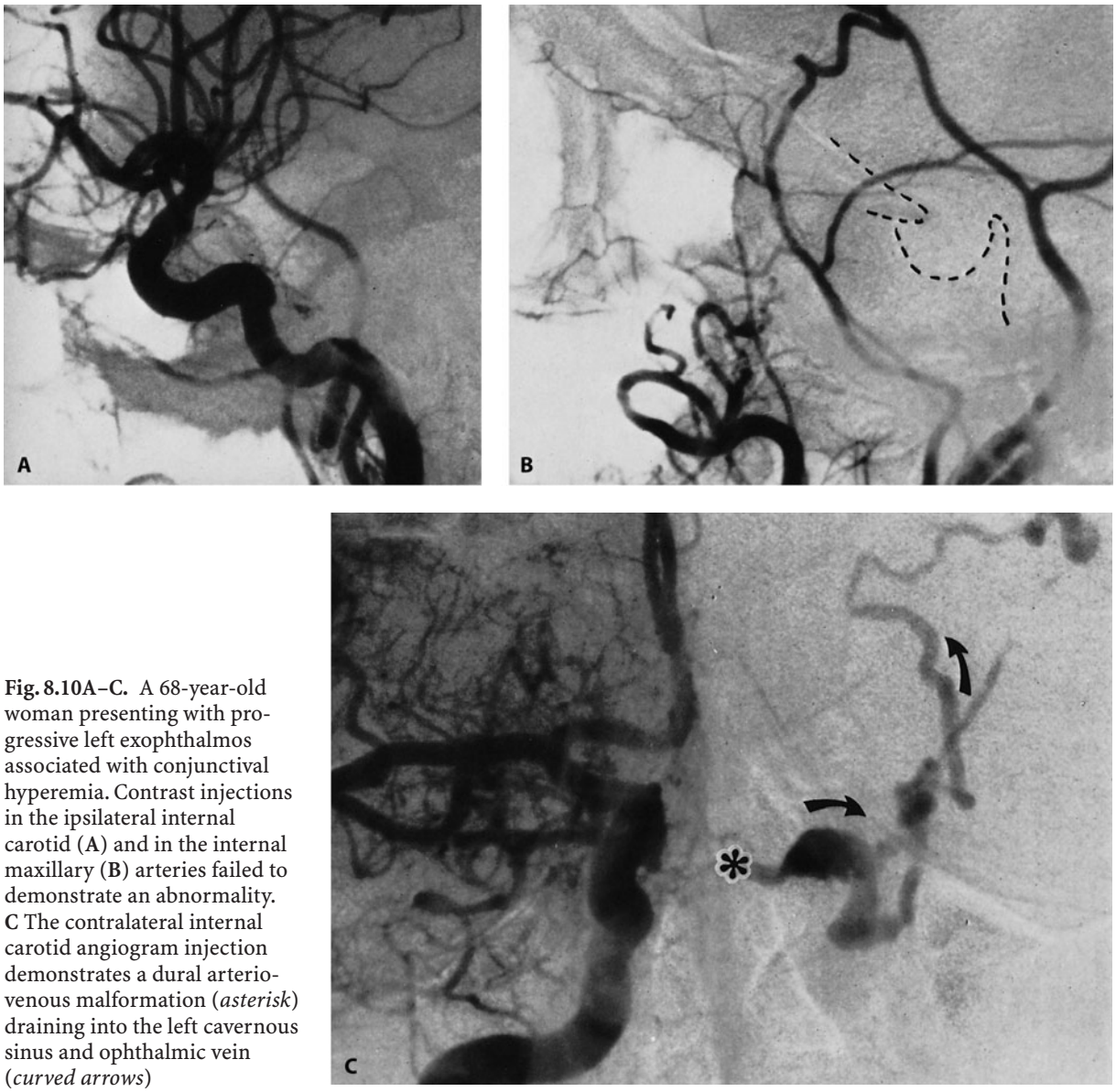

Fig. 8.10A–C. A 68-year-old woman presenting with progressive left exophthalmos associated with conjunctival hyperemia. Contrast injections in the ipsilateral internal carotid (**A**) and in the internal maxillary (**B**) arteries failed to demonstrate an abnormality. **C** The contralateral internal carotid angiogram injection demonstrates a dural arteriovenous malformation (*asterisk*) draining into the left cavernous sinus and ophthalmic vein (*curved arrows*)

rather than nerve dysfunction (Kupersmith 1993). An interesting feature of cavernous sinus DAVSs is the occurrence of paradoxical symptoms, when ipsilateral cavernous sinus thrombosis causes rerouting of venous drainage to the contralateral orbital veins (Fig. 8.10).

8.5.2 Tinnitus and Objective Bruits

Pulsatile tinnitus is produced by turbulent flow in the nidus and the adjacent draining veins. DAVMs in certain locations are more likely to be associated with this symptom than with others. Tinnitus is most frequently perceived when the drainage involves a venous sinus, which is in direct contact with the petrous bone. The higher the flow in the nidus, the more intense the tinnitus will be. About 40% of patients with pulsatile tinnitus

will have objective bruits (Lasjaunias et al. 1986a). The disappearance of the bruit in time is important clinical information that will need to be taken into consideration with respect to the need for reinvestigation.

8.5.3 Focal Neurological Deficits

Focal neurological deficits in adults occur in the presence of retrograde leptomeningeal drainage and reflux into cortical cerebral, cerebellar, or perimedullary veins (Castaigne et al. 1976; Lasjaunias et al. 1986b) (Figs. 8.11–8.14). The symptomatology depends on the location of the DAVS and the direction of the venous drainage, as it will cause regional venous congestion. These symptoms are ischemic in nature and are related

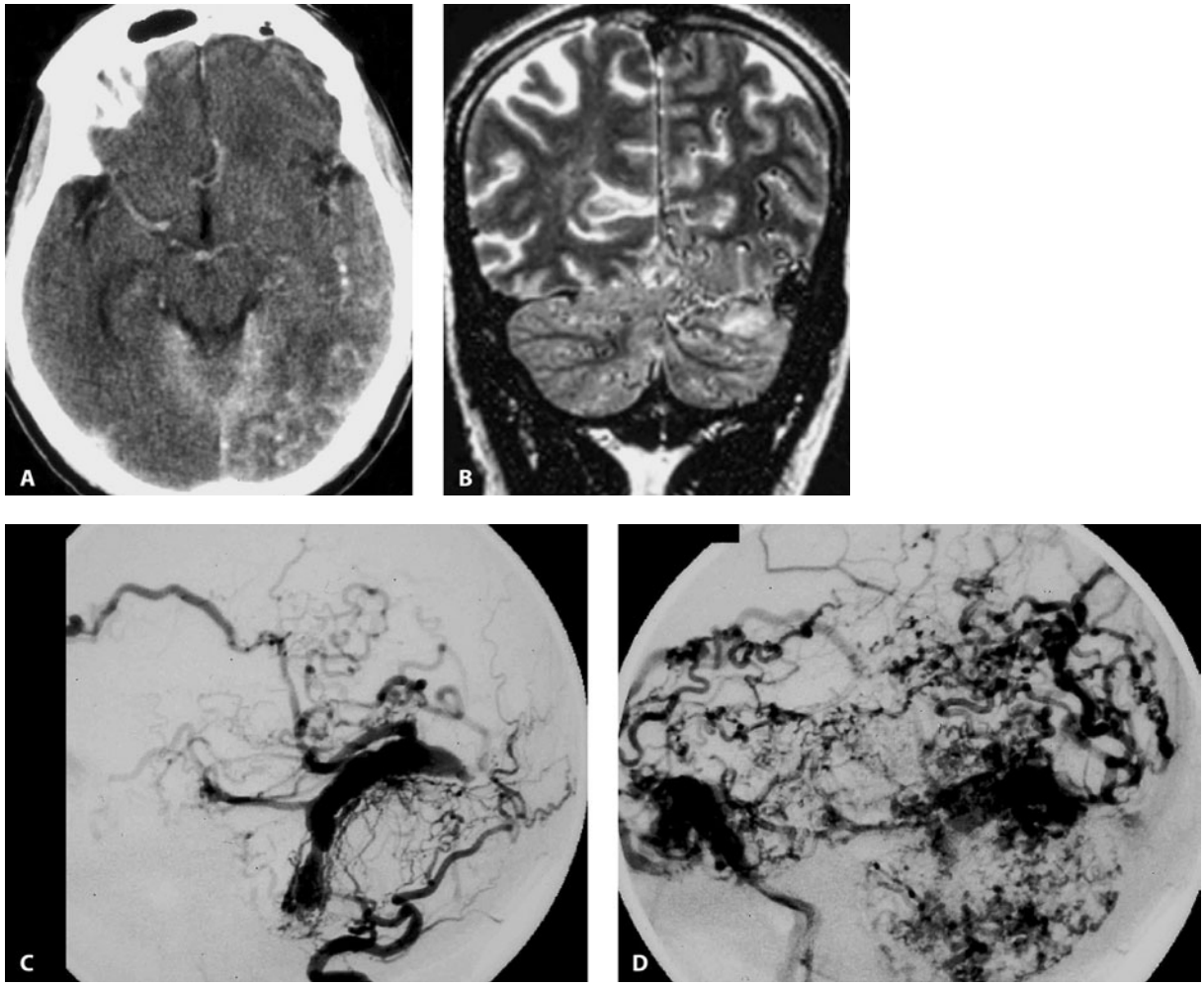

Fig. 8.11A–D. A 45-year-old man presented with new onset seizures and headaches. The enhanced CT scan (**A**) and coronal view T2-weighted MRI (**B**) show prominent vasculature along the surface of the posterior temporal lobe and adjacent cerebellum as well as parenchymal edema. Left occipital angiogram in lateral view (**C, D**) demonstrates DAVS along transverse sinus with drainage into the sinus and subsequent leptomeningeal reflux towards the cerebral and cerebellar cortical venous system in association with proximal and distal thrombosis of the transverse sinus

Fig. 8.12A, B. A 57-year-old man presenting with progressive cerebellar neurological deficit. Unenhanced CT scan (**A**) shows evidence of a nonspecific edema pattern affecting the right cerebellar hemisphere; the right vertebral angiography in AP view (**B**) demonstrates the cause to be a torcular dural arteriovenous shunt (*long arrow*) with direct drainage into the cerebellar cortical venous system (*short arrow*)

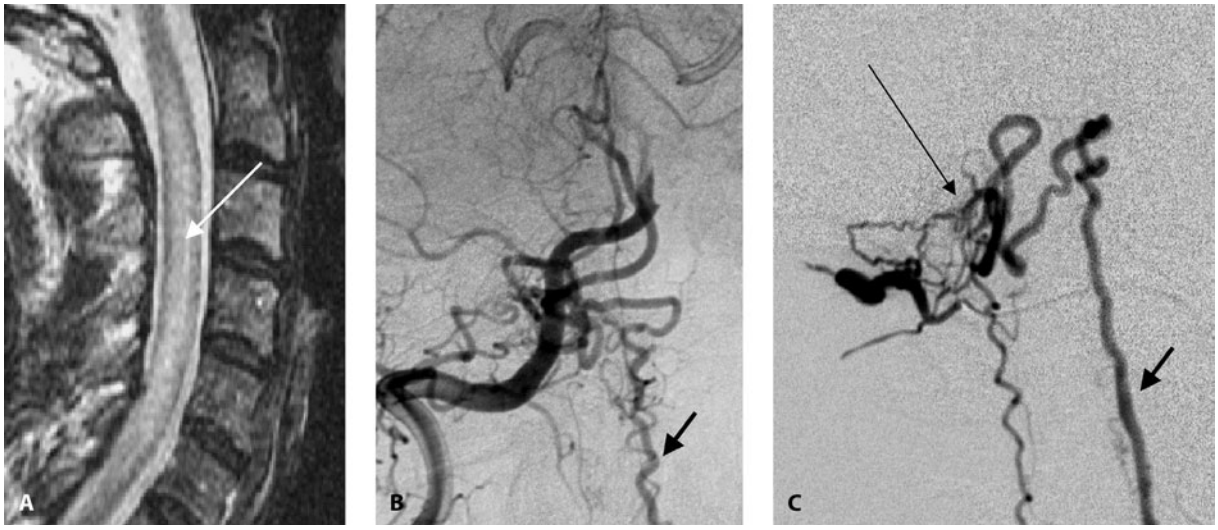

Fig. 8.13A–C. A 55-year-old man presenting with slowly progressive cervical myelopathy. T2-weighted MRI (**A**) shows evidence of edema within the cord (*arrow*) but no abnormal vascularity. Right vertebral angiogram in AP view (**B**) and selective transosseous branch of the occipital artery angiogram in lateral view (**C**) demonstrates the cause to be a dural arteriovenous shunt at the lateral border of the foramen magnum (*long arrows*), with venous drainage towards the cervical ventral (*short arrows*) and dorsal perimedullary venous system

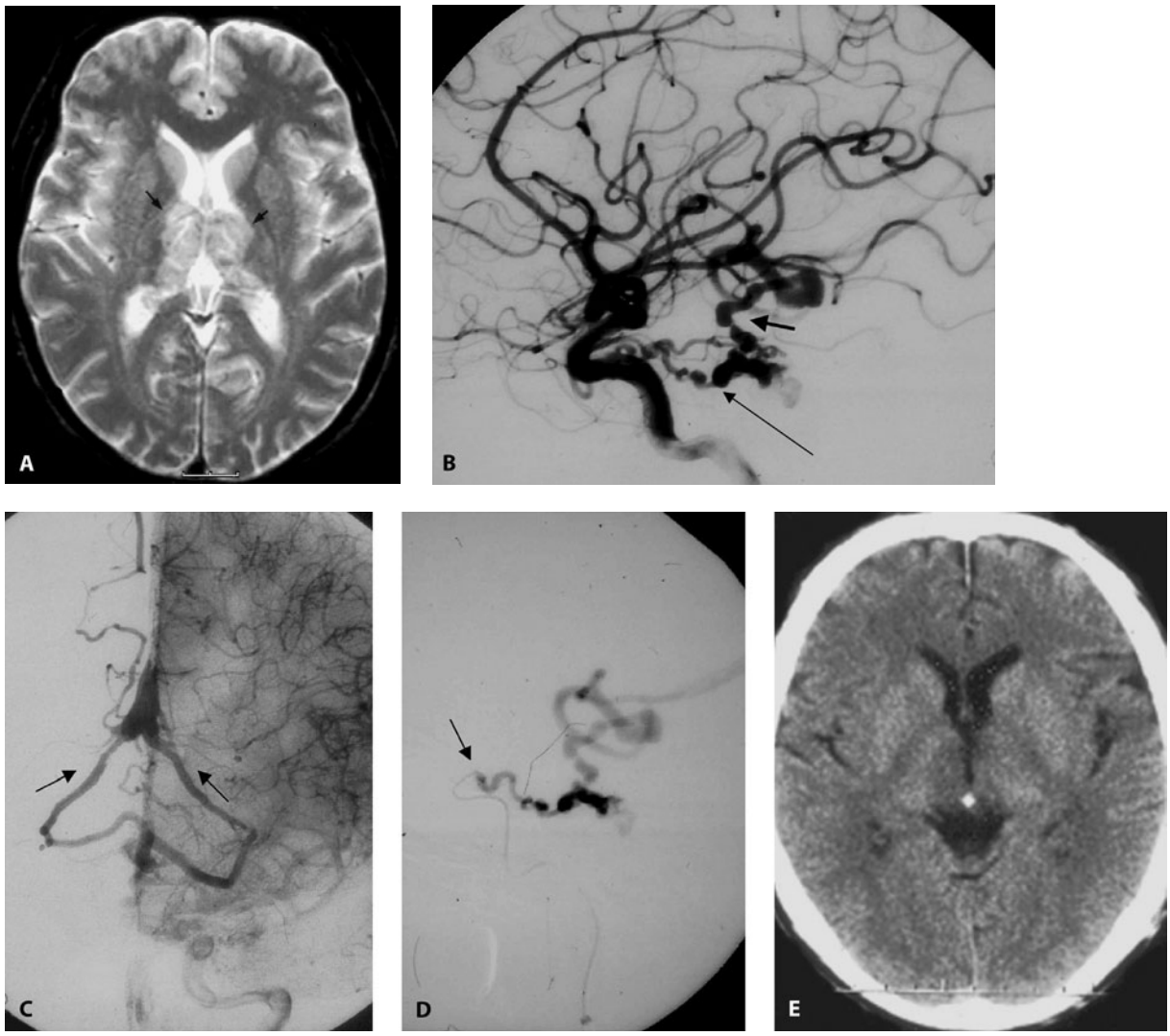

Fig. 8.14A–E. A 48-year-old male patient presenting with progressive thalamic syndrome. T2-weighted MRI (**A**) shows evidence of bilateral thalamic edema (*small arrows*), which at left internal carotid angiography in lateral view (**B**) proved to be caused by a dural arteriovenous shunt (DAVS) (*long arrow*) along the inferior margin of the tentorium, with venous drainage towards the perimesencephalic venous system (*short arrows*), also shown on the carotid angiogram AP view (**C**). Selective angiogram in lateral view (**D**) of the dural supply from the internal carotid artery and embolization of this branch (*arrow*) with glue resulted in immediate obliteration of the AVS with reversal of symptoms and normalization of the unenhanced CT scan 1 week later (**E**)

to chronic increased pressure in the veins, which drain both the DAVS and the underlying normal brain (Kosnick et al. 1974). This phenomenon can be demonstrated at angiography (Fig. 8.7). Prior to treatment, the venous phase of the cerebral angiogram shows absence of opacification of the cortical veins that drain the DAVS and rerouting of drainage to adjacent territories, demonstrating a pseudophlebitic pattern (Willinsky et al. 1999) (Fig. 8.16). Following successful treatment, cerebral angiography typically shows a return of the drainage of the involved brain into the veins previ-

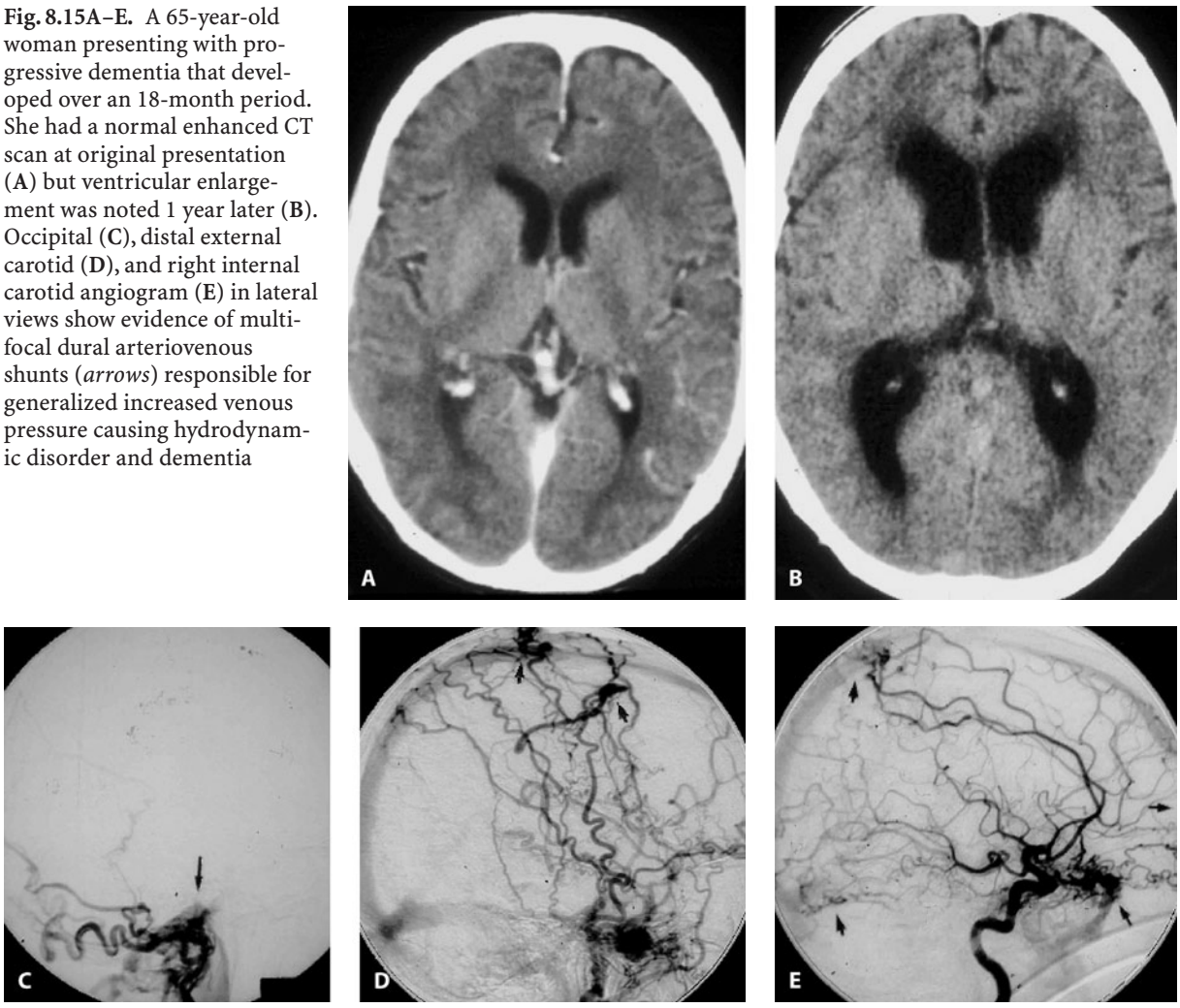

Fig. 8.15A–E. A 65-year-old woman presenting with progressive dementia that developed over an 18-month period. She had a normal enhanced CT scan at original presentation (**A**) but ventricular enlargement was noted 1 year later (**B**). Occipital (**C**), distal external carotid (**D**), and right internal carotid angiogram (**E**) in lateral views show evidence of multifocal dural arteriovenous shunts (*arrows*) responsible for generalized increased venous pressure causing hydrodynamic disorder and dementia

ously opacified by the DAVS. Subsequently, the focal cerebral symptoms may reverse themselves. Willinsky et al. (1994) described the MRI equivalent of this phenomenon. Parenchymal compression by venous lakes draining the DAVSs in adults does not produce clinical symptoms, although it does in the pediatric population.

8.5.4 Global Neurological Deficits

Moderate- and high-flow DAVSs in adults may produce global neurological deficits such as dementia, in particular when associated with stenosis or occlusion (thrombosis) of the major dural venous sinuses (Figs. 8.15, 8.16) (Lasjaunias et al. 1986b; Hurst et al. 1998). Reversal of flow may occur and be directed upstream towards the superior sagittal and straight sinuses. Papilledema and increased intracranial pressure will occur as well as CSF hydrodynamic disorders and ventricular enlargement. These effects are due to chronic impairment of CSF absorption caused by venous sinus hypertension (Lamas et al. 1977). In our experience, this clinical

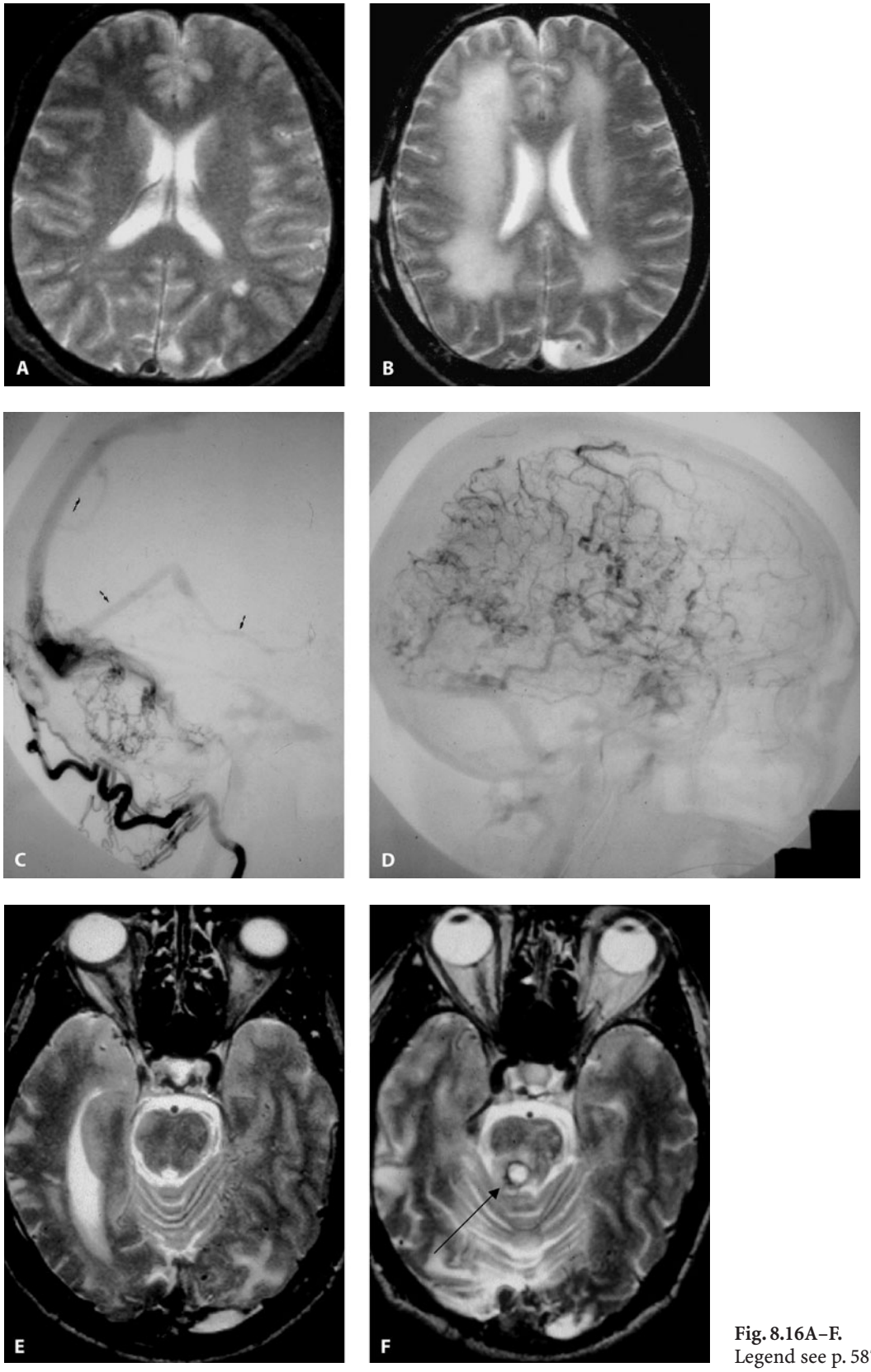

Fig. 8.16A–F.
Legend see p. 587

◀ **Fig. 8.16A–F.** A 49-year-old man underwent uneventful surgical removal of a right-sided acoustic neuroma. CT scan at that time (**A**) showed a normal supratentorial appearance. The follow-up CT scan (**B**) 1 year later aimed to investigate progressive neurological decline demonstrates edema pattern involving both hemispheres. Right occipital angiogram in lateral view (**C**) demonstrates dural arteriovenous shunt along right transverse sinus, with retrograde venous drainage toward the deep venous system and superior sagittal sinus (*arrows*) associated with distal thrombosis of the ipsilateral transverse sinus. Venous phase of the left internal carotid angiogram in lateral view (**D**) shows delayed and impaired venous drainage of the left hemisphere, with pseudophlebitic pattern evidence of the venous hypertension responsible for the hydrodynamic disorder. Symptomatic midbrain cavernoma (proven at surgery) developed in this patient. MRI at the time of original presentation (**E**) and 5 years later (**F**) demonstrates de novo cavernoma (*arrow*)

presentation is more frequent with DAVSs located along the transverse sinus and torcular region.

8.5.5 Intracranial Hemorrhage

Intracranial hemorrhage (ICH) is a specific complication of DAVSs with retrograde leptomeningeal drainage towards the cerebral and/or cerebellar cortical veins. Because these veins traverse the various compartments from the dura to the brain parenchyma, their rupture may create subdural, subarachnoid, or intracerebral hemorrhage. A focal ectasia of the abnormal draining venous system can sometimes be seen at the site of rupture (Fig. 8.17).

The incidence of ICH has been reported between 35% and 42% (Castaigne et al. 1976; Cognard et al. 1995; Davies et al. 1997b). ICH occurred more frequently if the retrograde leptomeningeal drainage was directly from the shunt into this vein as opposed to this type of reflux via a dural sinus, 48% versus 11% (Davies et al. 1997b). The hemorrhage may rarely flow into the subdural or subarachnoid space (Fig. 8.17), but more frequently the hemorrhage is intraparenchymal in location (Figs. 8.18, 8.19). All intracranial locations of DAVSs have been associated with leptomeningeal venous reflux and can therefore present with ICH. However, because of their regional venous anatomy, certain DAVS locations will be more likely (tentorial) or necessarily be associated with retrograde leptomeningeal venous drainage (anterior cranial fossa). Hemorrhagic presentation in those locations has been reported to occur in 75%–95% of cases (Awad et al. 1990; Cognard et al. 1995).

8.5.6 Hormonal Influences

The onset of DAVS-related symptoms during pregnancy has been reported several times (Doyon and Metzger 1973; Toya et al. 1981; Lasjaunias et al. 1984). We have noted premenstrual worsening of symptoms in some females. We have not observed distinguishing features in the angioarchitecture of the DAVS in such patients. The exact target of the hormonal action in patients with DAVSs is unknown. However, these cases do illustrate

Fig. 8.17A–D. A 42-year-old female patient presented with sudden onset of headache. Enhanced CT scan (**A**) shows evidence of small subdural hematoma (*white arrow*) as well as parenchymal hemorrhage with adjacent enhancement (*black arrow*) of a structure that on MRI (**B**) demonstrates a flow void (*arrow*) also seen on the source images of the MRI in coronal view (**C**) and proven to be a venous pseudoaneurysm (*short arrow*) associated with dural arteriovenous shunt (DAVS), with direct cortical venous reflux towards the subtemporal and deep venous system (*long arrow*), shown on the superselective angiogram of the left middle meningeal artery in lateral view (**D**) a venous pseudoaneurysm (*short arrow*) associated with DAVS, with direct cortical venous reflux towards the subtemporal and deep venous system (*long arrow*)

a definite relationship between hormonal changes and clinical symptoms in some patients, and this subgroup may benefit from a trial of estrogen therapy prior to more aggressive treatment. Sphenoid osteodural lesions and cavernous plexus DAVSs have shown a strong female dominance and sensitivity to hormonal changes.

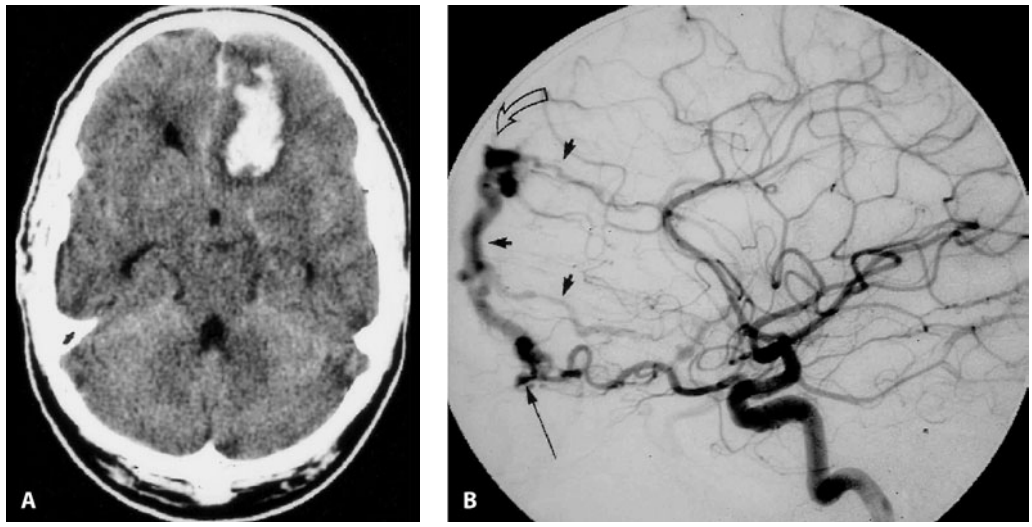

Fig. 8.18A, B. A 58-year-old man presented with sudden onset of severe headache. CT scan (**A**) shows evidence of left frontal lobe hemorrhage, which on left internal carotid angiogram in lateral view (**B**) was demonstrated to be caused by an anterior cranial fossa dural arteriovenous shunt (*long arrow*) supplied by ethmoidal branches of the ophthalmic artery with direct reflux towards cortical cerebral veins and transcerebral veins (*short arrows*) associated with apparent thrombosis at the entrance into the superior sagittal sinus (*open curved arrow*)

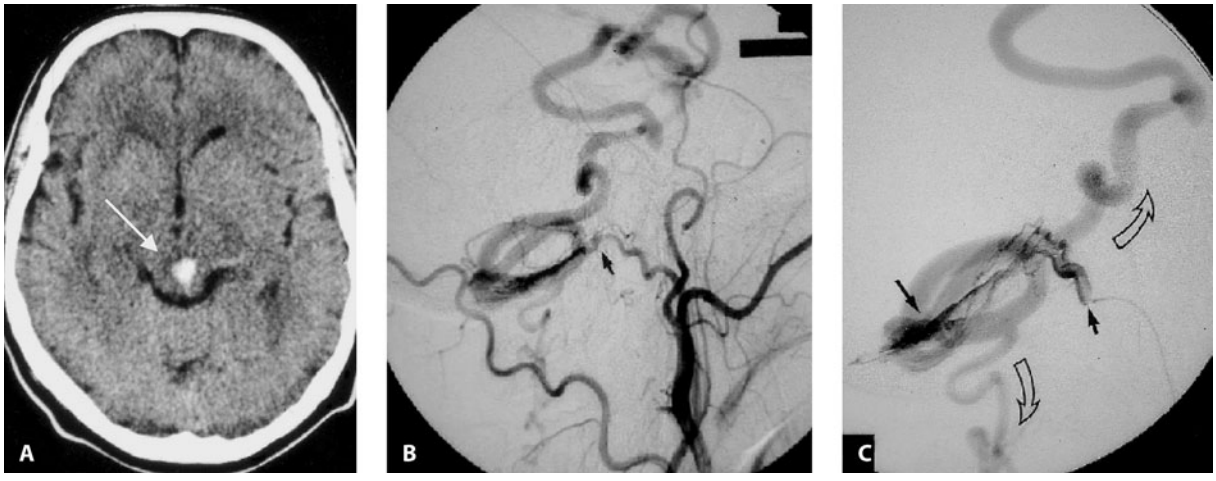

Fig. 8.19. A 55-year-old man presented with acute onset of headache and midbrain neurological deficit, which the unenhanced CT scan (**A**) shows to be caused by a small midbrain hemorrhage (*arrow*). Right external carotid (**B**) and selective ascending pharyngeal angiograms (**C**) in lateral view and catheter tip in the neuromeningeal branch (*short arrow*) demonstrate the cause to be a foramen magnum dural arteriovenous shunt (*long arrow*) with direct reflux towards the perimedullary and perimesencephalic venous systems (*open curved arrows*) and rupture at the midbrain level

8.5.7 Associated Conditions and Multiplicity

DAVSs in adulthood are an acquired disease, and there is no relationship to hereditary or developmental disorders. On the other hand, we have seen brain AVMs as well as cavernomas occur in patients with DAVSs (Figs. 8.16, 8.20) (Table 8.5). Treatment priorities should take into consideration the natural history of the various coexisting disorders. In exceptional circumstances similar to those in high-flow multifocal DAVFs in children, we have seen the apparent induction of pial AVSs upstream from a DAVS. These pial shunts tend to regress after treatment of the DAVS.

Table 8.5. Vascular diseases associated with dural arteriovenous shunts

Cerebral AVM
Maxillofacial AVM
Hereditary hemorrhagic telangiectasia (HHT) or Rendu-Osler-Weber syndrome (ROW)
Bone AVM (local extension or metameric expression)
Cavernomas
Intra- or extradural arterial aneurysms

AVM, arteriovenous malformations.

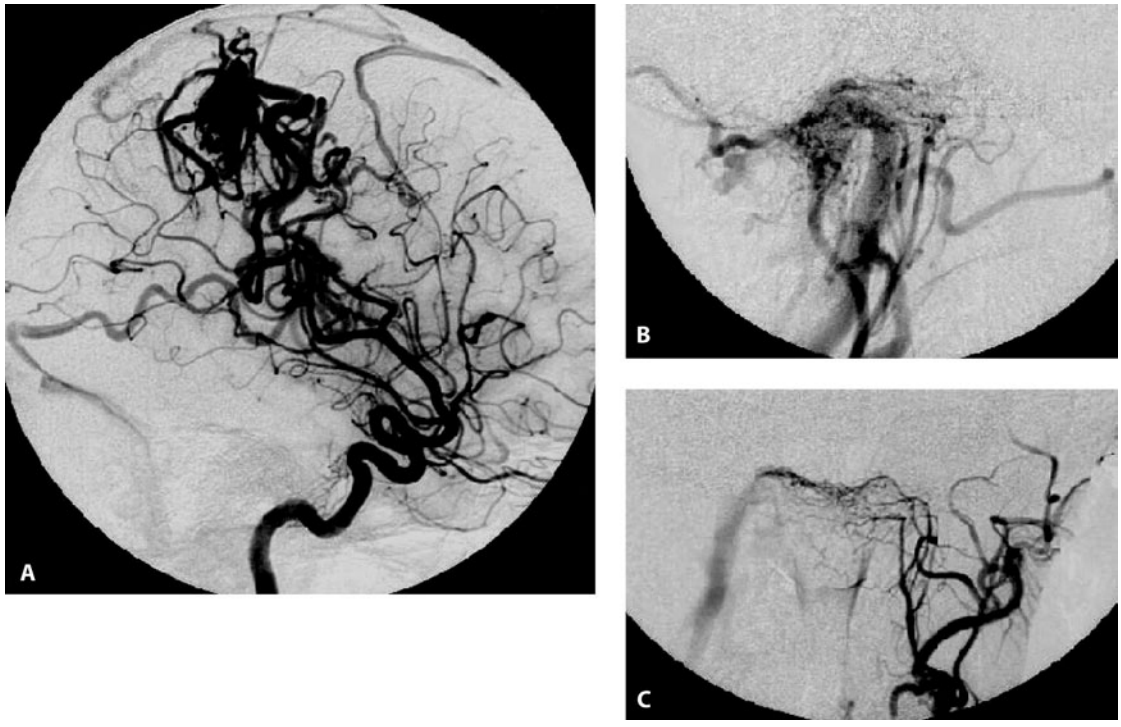

Fig. 8.20A–C. A 45-year-old woman with a 3-month history of right-sided bruit. Right internal carotid angiogram in lateral view (**A**) shows a moderate size parietal lobe brain arteriovenous malformation, while right external carotid angiogram (**B**) in lateral view and left ascending pharyngeal angiogram (**C**) in AP view demonstrate a right-sided retroclival dural arteriovenous shunt with antegrade venous drainage toward the jugular venous system

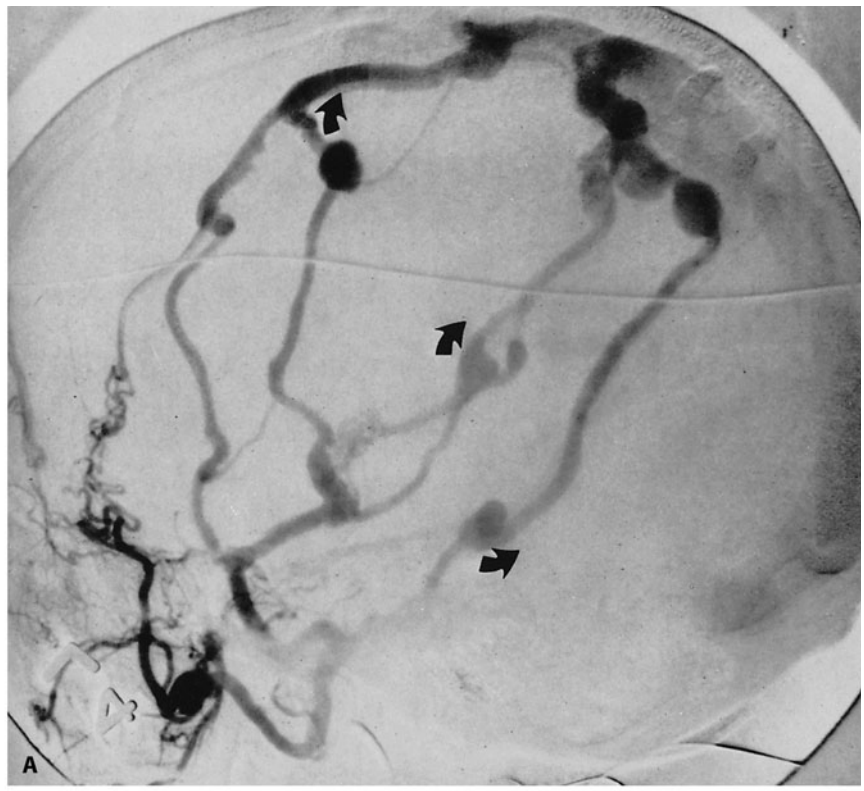

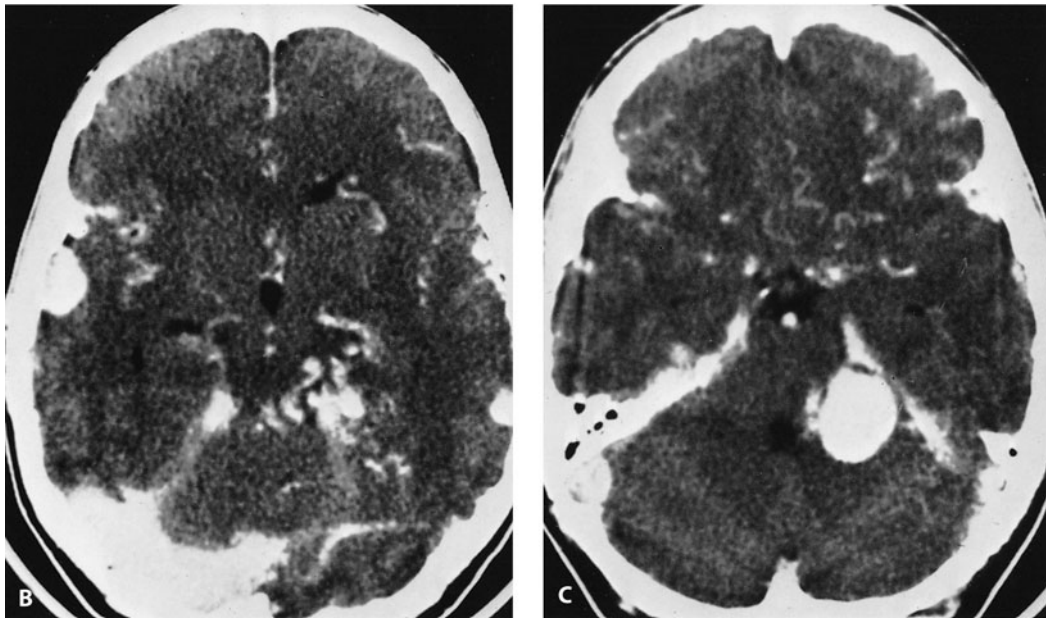

Fig. 8.21A–C. A 28-year-old patient with a family history of Ehlers–Danlos syndrome presented with multiple episodes of subarachnoid hemorrhage. Angiography (**A**) demonstrates DAVM with cortical venous drainage. Enhanced CT study shows the venous ectasias, both supra- (**B**) and infratentorial (**C**)

Aneurysms are occasionally associated with DAVSs and may be on the feeding vessels, either extradural or subarachnoid in location. They are slightly more common in the pediatric DAVSs and are rarely symptomatic.

The appearance of a DAVS may be modified in the presence of an underlying vessel wall disorder such as Ehlers–Danlos syndrome (Fig. 8.21).

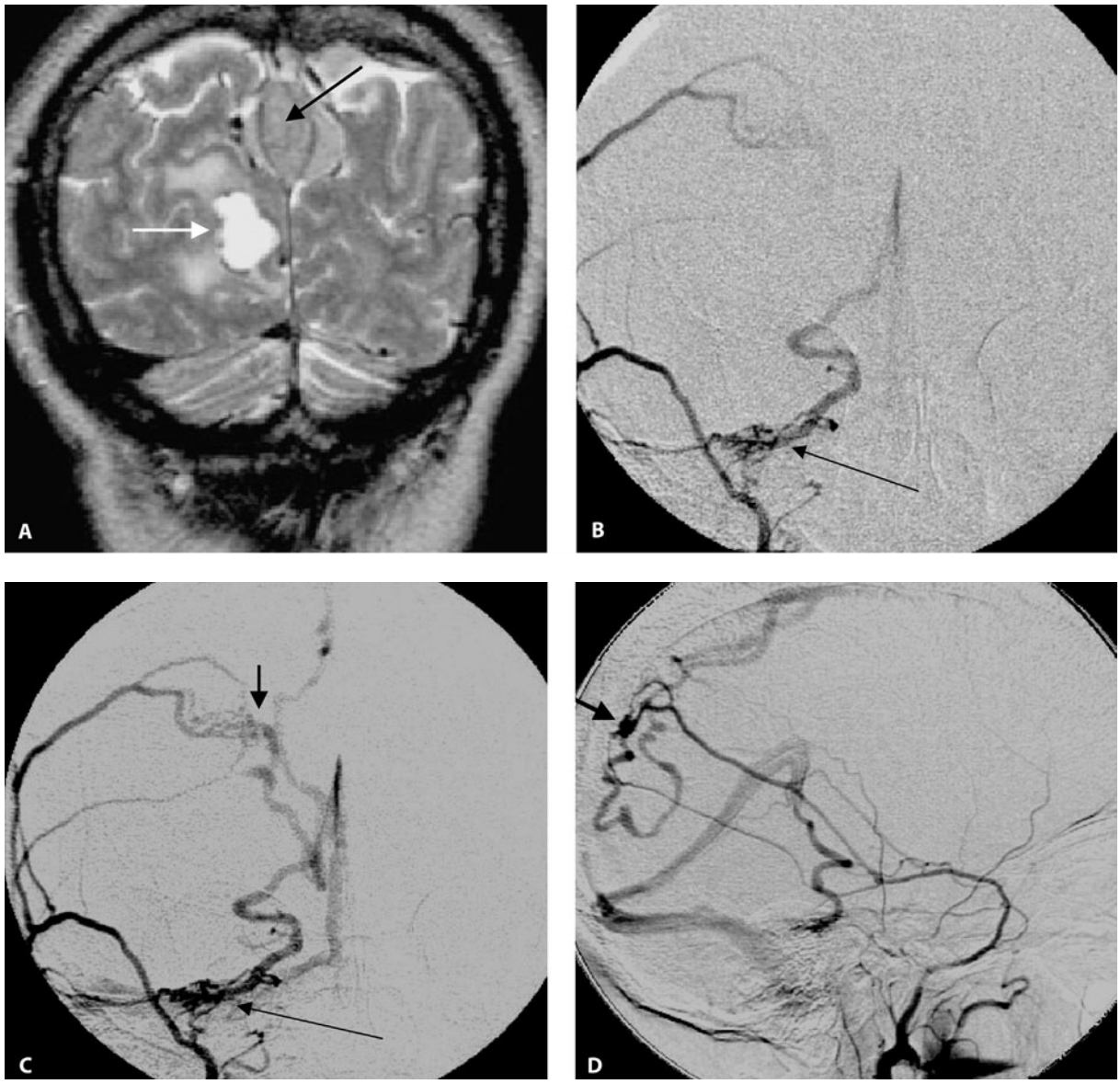

Fig. 8.22A–D. A 54-year-old male patient presented with sudden onset headache. T2-weighted MRI (**A**) shows evidence of small parenchymal hemorrhage (*white arrow*) as well as posterior falx meningioma (*black arrow*). Distal right external carotid angiogram in AP (**B, C**) and lateral views (**D**) demonstrate evidence of a dural arteriovenous shunt (DAVS) along petrous ridge (*long arrows*), supplied mostly by the squamosal branch of the middle meningeal artery and with deep venous drainage as well as a second DAVS located along the parietal convexity (*short arrows*) draining directly into cortical veins and responsible for the hemorrhage

Multiple DAVSs in clearly separate anatomical locations in the same patient were demonstrated in 8.1% of the Toronto series (van Dijk et al. 2002a) (Fig. 8.22). In this series, multiplicity was associated with a twofold increase in the incidence of cortical venous reflux.

The development of additional DAVSs over time is very rare but emphasizes the need to continue to follow patients with DAVFs and to reinvestigate them when new symptoms or signs occur (Fig. 8.23).

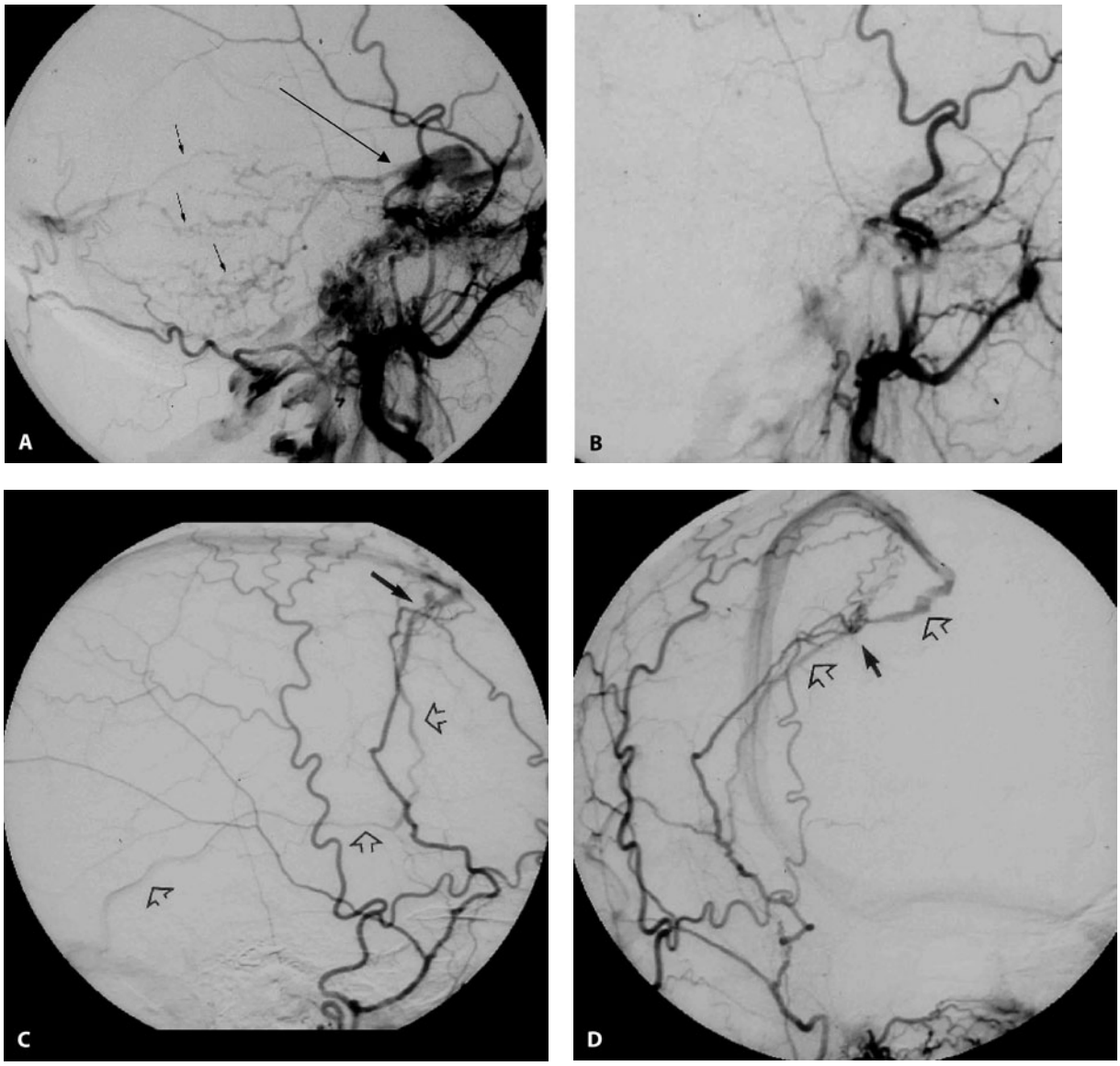

Fig. 8.23A–D. A 70-year-old woman presented with a 2-month history of red eye. At right external carotid angiogram in lateral view (**A**), she was shown to have a cavernous plexus dural arteriovenous shunt (DAVS, *long arrow*) with orbital drainage as well as cortical reflux toward the cerebellar venous system (*short arrows*). Combined transarterial embolization and surgical disconnection resulted in complete obliteration of this DAVS shown on posttreatment distal external carotid angiogram in lateral view (**B**). Follow-up distal external carotid angiogram in lateral view (**C**) and right anterior oblique view (**D**) confirms closure of the cavernous plexus DAVS but demonstrates a newly developed DAVS along the right frontal convexity (*arrow*), with direct drainage into the adjacent cerebral cortical venous system (*open arrows*)

In a small number of our patients, we have documented the coexistence of benign intracranial neoplasms, mostly meningiomas, some of which were noted to involve the dural sinuses (Figs. 8.22, 8.24) (Vilela et al. 2001). The coexistence of these diseases may or may not be fortuitous, and treatment should first be directed toward the symptomatic lesion.

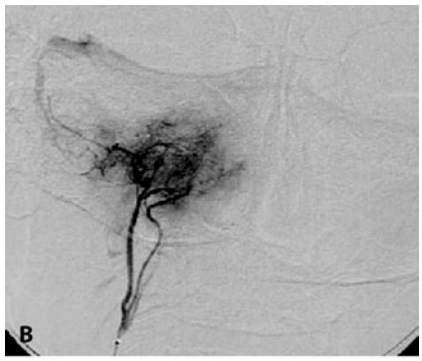

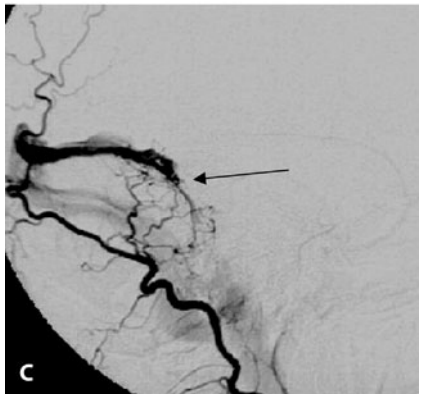

Fig. 8.24A–C. A 38-year-old female patient presented with tinnitus and multiple cranial nerve palsies. Enhanced T1-weighted MRI (**A**) shows evidence of a meningioma (*arrow*) involving the skull base, mostly supplied by the ascending pharyngeal artery, AP view (**B**), and shown to be associated with a dural arteriovenous shunt along the ipsilateral transverse sinus with transosseous supply from the occipital artery, lateral view (**C**), and retrograde flow in the dural sinus because of distal thrombosis (*arrow*)

8.6 Natural History

The natural history of DAVSs was until recently poorly documented and mostly reviewed retrospectively (Fernand et al. 1987; Awad et al. 1990; Cognard et al. 1995). Davies et al. reported the first large prospectively collected series of patients with DAVSs in 1997 (Davies et al. 1997a, b). In this Toronto series, 102 patients with intracranial DAVSs were followed for an average of 33 months, with complete follow-up in 91%. Of the 55 patients who had a DAVS without leptomeningeal and cortical venous reflux, 32 received no treatment. Symptom improvement or resolution occurred in 81% of these patients as compared to 86% of the treated patients with the same angioarchitecture. In the same series, there were 46 patients who had a DAVS with leptomeningeal and/or cortical venous reflux and 14 of these declined further treatment. At follow-up, this group had an 11% nonhemorrhagic neurological deficit rate per year and a 20% ICH rate per year. During the follow-up there was no transition in the venous drainage pattern from sinusal to leptomeningeal/cortical in any of the patients. All patients who had unsuccessful treatment and persistence of the leptomeningeal reflux developed ICH or neurological deficits on follow-up (Davies et al. 1997a, b).

In an updated review of 118 patients with DAVSs and leptomeningeal reflux, the Toronto team demonstrated an annual risk for nonhemorrhagic neurological deficit of 6.9% and 8.1% for hemorrhage, with an annual mortality rate of 10.4% (van Dijk et al. 2002b). In a group of patients that had originally presented with hemorrhage, Duffau et al. (1999) demon-

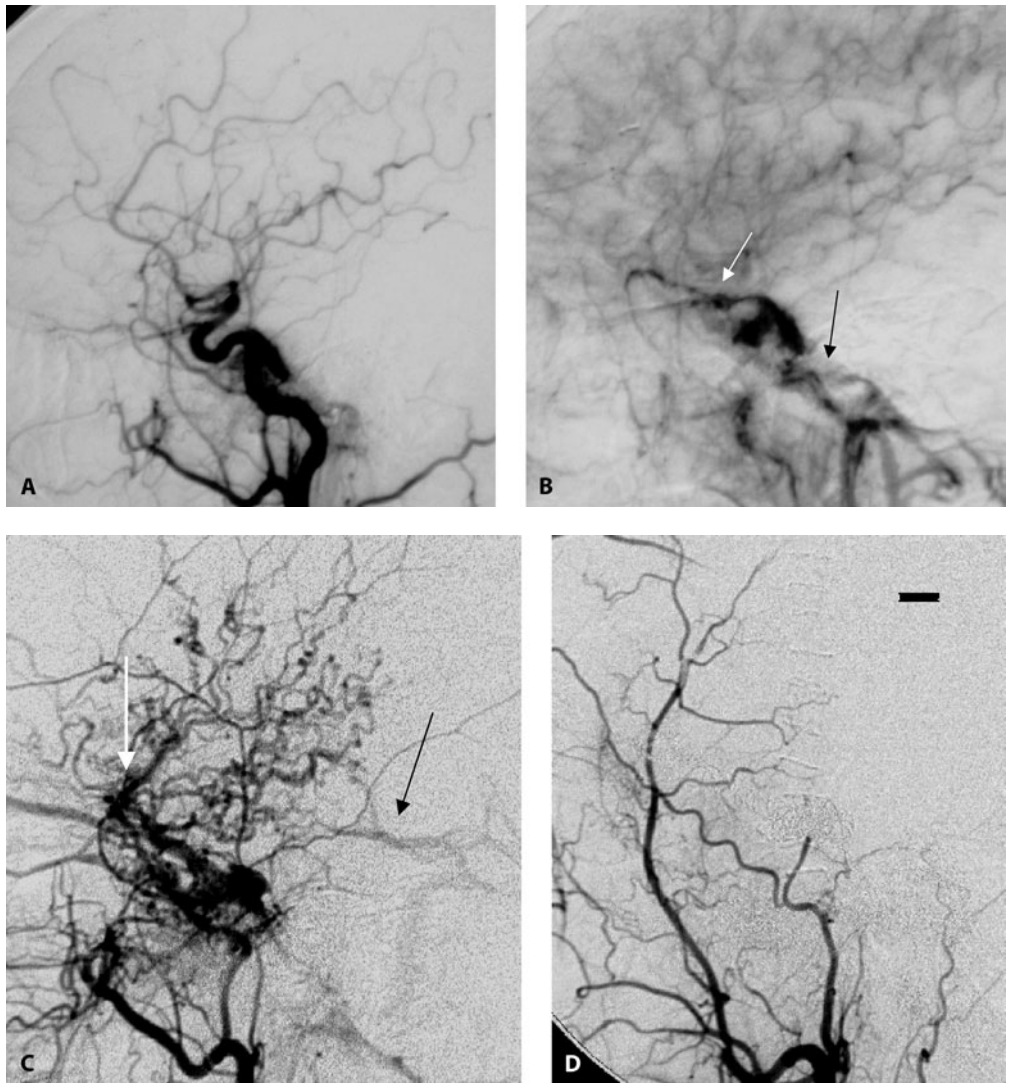

Fig. 8.25A–D. A 45-year-old female patient presented with 3-month history of tinnitus and left red eye. Left common carotid angiogram in lateral view in early (**A**) and late arterial phase (**B**) showed evidence of slow flow cavernous plexus dural arteriovenous shunt (DAVS) with drainage towards the superior ophthalmic (*white arrow*) and inferior petrosal venous system (*black arrow*). No treatment was given and reinvestigation 6 months later, when the bruit had disappeared, demonstrated on left external carotid angiogram in lateral view (**C**), that there was no longer venous drainage towards the petrosal sinus but instead extensive cortical venous reflux had developed towards the sylvian (*white arrow*) and deep venous system (*black arrow*), which was treated with transarterial embolization and intraoperative (via the sylvian vein) retrograde venous coil deposition into the cavernous plexus. Obliteration of the DAVS was confirmed on the posttreatment external carotid angiogram in lateral view (**D**)

strated a 35% risk for rebleed within the first 2 weeks after presentation. These data support the need for active and curative treatment of the DAVS when associated with leptomeningeal and/or cortical venous reflux and very conservative management of those DAVSs that have no such venous drainage.

From a practical point of view, there is no obvious clinical difference between a lesion of the cribriform plate and a lesion of the sigmoid sinus associated with proximal and distal sinus thrombosis and leptomeningeal retrograde flow. However, we suspect that before the thrombosis occurred on both sides, it probably occurred on one side, with the sinus probably patent before this time. However, we postulate here that the DAVS preexisted the thrombosis, a hypothesis that may not always be confirmed. Thus, the natural history may not only be that of the lesion itself but also that of the changes in the adjacent venous outlets.

In our experience and in the literature (Cognard et al. 1997; Satomi et al. 2002), there are isolated cases of DAVS in which transformation of the venous drainage pattern from sinusal to retrograde leptomeningeal/cortical has occurred. Almost all of them developed after previous endovascular or surgical treatment and rarely occurred spontaneously (Fig. 8.25). In our experience, this type of progression has occurred in less than 1% of cases.

8.7 Progression of Symptoms

Additional thrombosis of the venous outlet of a DAVS may result in rerouting or exaggeration of drainage into cortical veins, leading to potential focal CNS symptoms and/or hemorrhagic complications. A change in the clinical symptomatology (the disappearance of pulsatile tinnitus, etc.) may imply a change in the venous drainage pattern and should lead to renewed investigation (Castaigne et al. 1976). Thrombosis may also lead to a so-called spontaneous cure of the DAVS, but probably only if the thrombosis extends into the nidus. Spontaneous regression has been reported following hemorrhage (Katoaka and Taneda 1984; Olutola et al. 1983). Spontaneous thrombosis of DAVSs without leptomeningeal reflux managed conservatively occurs infrequently and is in our experience most frequently associated with the slow flow cavernous plexus localization of the DAVS. Secondary glaucoma and worsening of orbital symptoms may be the result of progressive thrombosis of the posterior or superior venous drainage and should lead to renewed investigations and close clinical monitoring. Visual impairment related primarily to congestive venous ischemia of the optic nerve may progress acutely following venous thrombosis and may require aggressive medical therapy with anticoagulation and steroid medication.

Changes in symptomatology appear, therefore, to be caused by the associated thrombosis and are rarely caused by a worsening of the flow through the shunt itself.

The exception appears to be the high-flow juvenile-type DAVFs persisting into adulthood and the multifocal DAVSs extending along the transverse sinus regions, bilaterally causing a physiological obstruction to

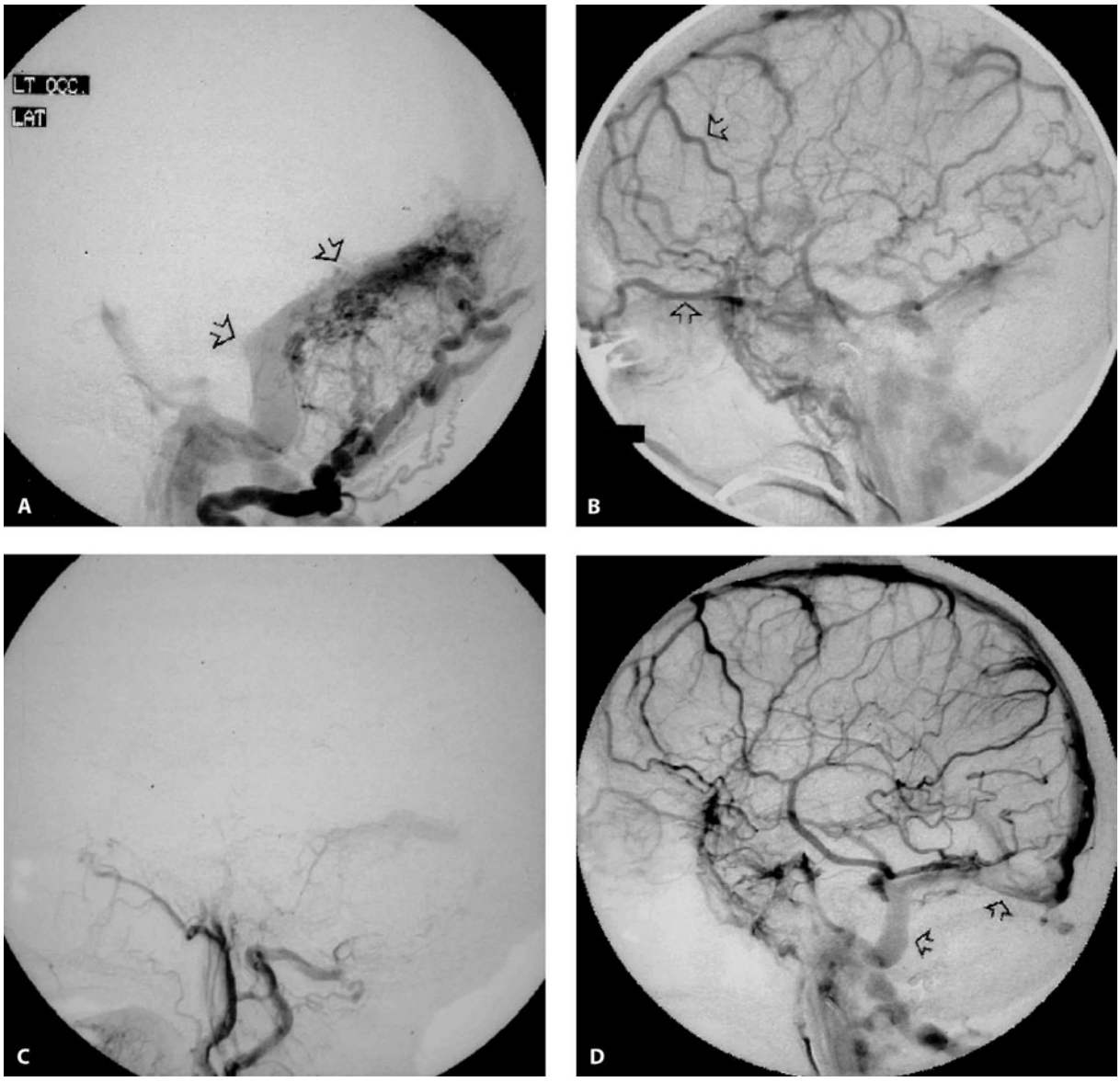

Fig. 8.26A–D. A 53-year-old man presented with a 9-month history of mental decline, ataxia, and increasing bilateral bruits. Left occipital angiogram in lateral view (**A**) shows evidence of high-flow transverse sinus dural arteriovenous shunt (DAVS, *open arrows*). Similar appearance was noted on the opposite side, indicating bilateral high-flow DAVSs with antegrade drainage on both sides. Left internal carotid angiogram in lateral view, venous phase (**B**), shows evidence of hemispheric rerouting of the venous blood towards the convexity cortical venous system, the cavernous sinus and superior ophthalmic venous system (*open arrows*) to bypass the hyperpressure in the transverse sinuses. Aggressive transarterial embolization of the external carotid arterial supply to the DAVS, as shown on the postembolization external carotid angiogram in lateral view (**C**), resulted in return toward normal antegrade flow in the dural sinuses (*open arrows*), as shown on the internal carotid angiogram in lateral view, venous phase (**D**)

the venous return of the brain (Figs. 8.15, 8.26). Depending on the potential for rerouting the venous return of the brain, focal and global CNS symptoms may occur and worsen over time.

8.8 Pretherapeutic Evaluation

In the evaluation of patients presenting with acute symptoms, CT examination should be performed to document the presence of intracranial hemorrhage. The ICH appearance on CT may raise the suspicion but rarely demonstrates the presence of an underlying DAVS. In addition to the presence of ICH, good-quality MRI examination will demonstrate abnormally prominent vessels along the surface of the brain or cerebellum, raising the possibility of a DAVS with cortical venous reflux as the possible cause for patients presenting with acute neurological deficits. We have found MRA to be of limited value in providing information pertaining to the angioarchitecture of the DAVF sufficiently conclusive for decision-making purposes. Cerebral angiography is then carried out to confirm the diagnosis, identify the dural origin of the nidus, and outline its arterial supply and venous drainage as well as its relationship to the venous drainage of the brain. A venous ectasia or pseudoaneurysm (opacified portion of the hematoma communicating with the ruptured vein), may be demonstrated at angiography and attest to the venous cause of the ICH (Fig. 8.17).

The evaluation of patients presenting with subacute and chronic symptoms will most likely include CT and MRI examinations done with contrast enhancement. Both modalities are capable of demonstrating engorged cortical veins over the surface of the brain as well as evidence of venous congestion (Willinsky et al. 1994). When small in size, the nidus is rarely localized, even with MRA, and the diagnosis of intracranial DAVS is not excluded with negative CT and MRI examinations. If clinically suspicious, cerebral angiography will be required to demonstrate the presence or absence of a DAVS.

8.9 Therapeutic Aspects

8.9.1 Indications and Strategy

As a general principle, the therapeutic strategy will be based on the pattern of venous drainage of the lesion, since it determines the natural history of the DAVS.

The indications for treatment of DAVSs that drain directly into a dural venous sinus with normal antegrade flow in the sinus are limited. The natural history of this type of DAVS is now known to be benign and the chances of stability or spontaneous symptom resolution are high. Treatment, from a medical point of view, is therefore rarely indicated. In addition, if treatment is contemplated, the associated risk of such treatment will have to be extremely low and less than the natural history-related risk of the disease itself.

Only in exceptional circumstances will a high-flow DAVS create a physiological obstruction to the drainage of the normal brain, which in turn may produce clinical symptoms and require active treatment (Figs. 8.15, 8.26). In these circumstances, treatment should always be directed toward the arterial side of the lesion in order to preserve the dural sinus and bring the venous pressure in the dural sinus toward normal, enabling the brain to use this sinus again for its drainage.

Double vision and subjective bruits are sometimes not well tolerated by the patient and may require elective intervention. Once again, the treatment-associated risk will then have to be weighed against the very low risk of the disease itself.

With improved understanding of the dural sinus vascular anatomy and improved imaging techniques, it has become possible to selectively transvenously identify and occlude a dural sinus compartment that is exclusively involved in the drainage of the AVS, with preservation of the main dural sinus channel for drainage of the healthy brain (Fig. 8.27).

Because of distal venous obstruction, DAVSs draining into the transverse sinus may be associated with retrograde flow towards the opposite site and reflux upstream to the superior sagittal sinus or the straight sinus and deep venous system. Treatment of such DAVSs is indicated but can be challenging. Reestablishment of flow through the obstructed sinus by means of angioplasty and stenting has so far been problematic. Arterial embolization followed by transvenous disconnection of the involved dural sinus has proven to be the most efficient treatment method.

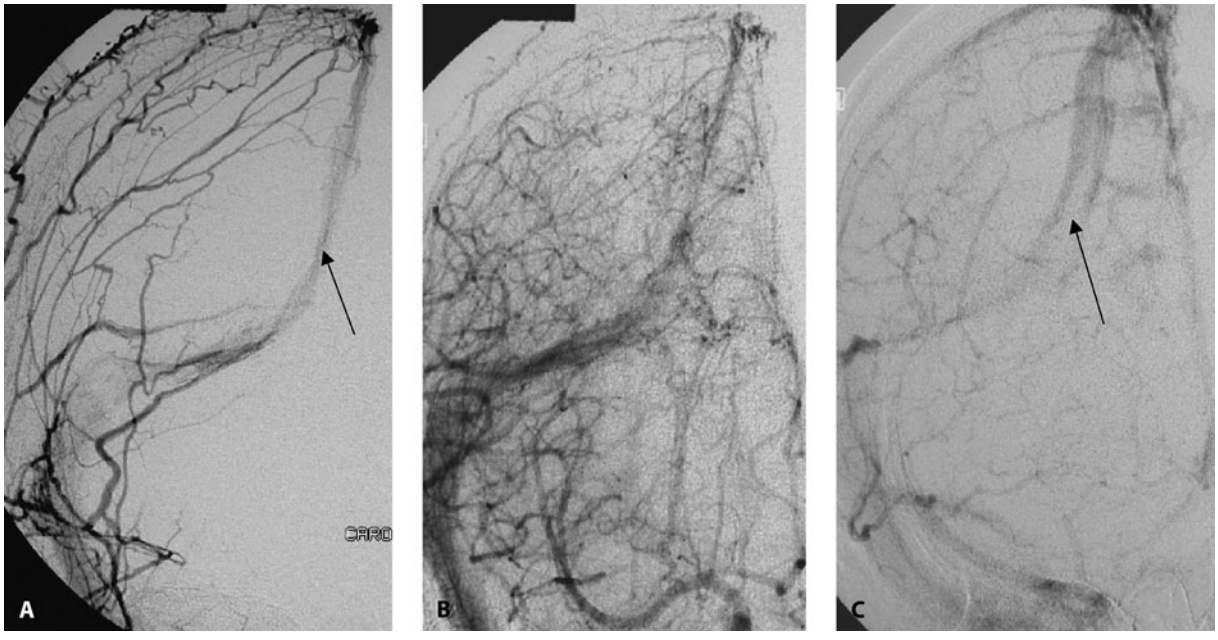

Fig. 8.27A–G. A 66-year-old female patient. Right external carotid angiogram in AP view (**A**) showed evidence of dural arteriovenous shunt (DAVS) along (within) the superior sagittal sinus with antegrade drainage (*arrow*). Right common carotid angiogram in AP view, early arterial phase (**B**) and venous phase (**C**) demonstrate separate venous drainage channels from the brain versus the AVS (*arrow*). **D–G** see p. 600

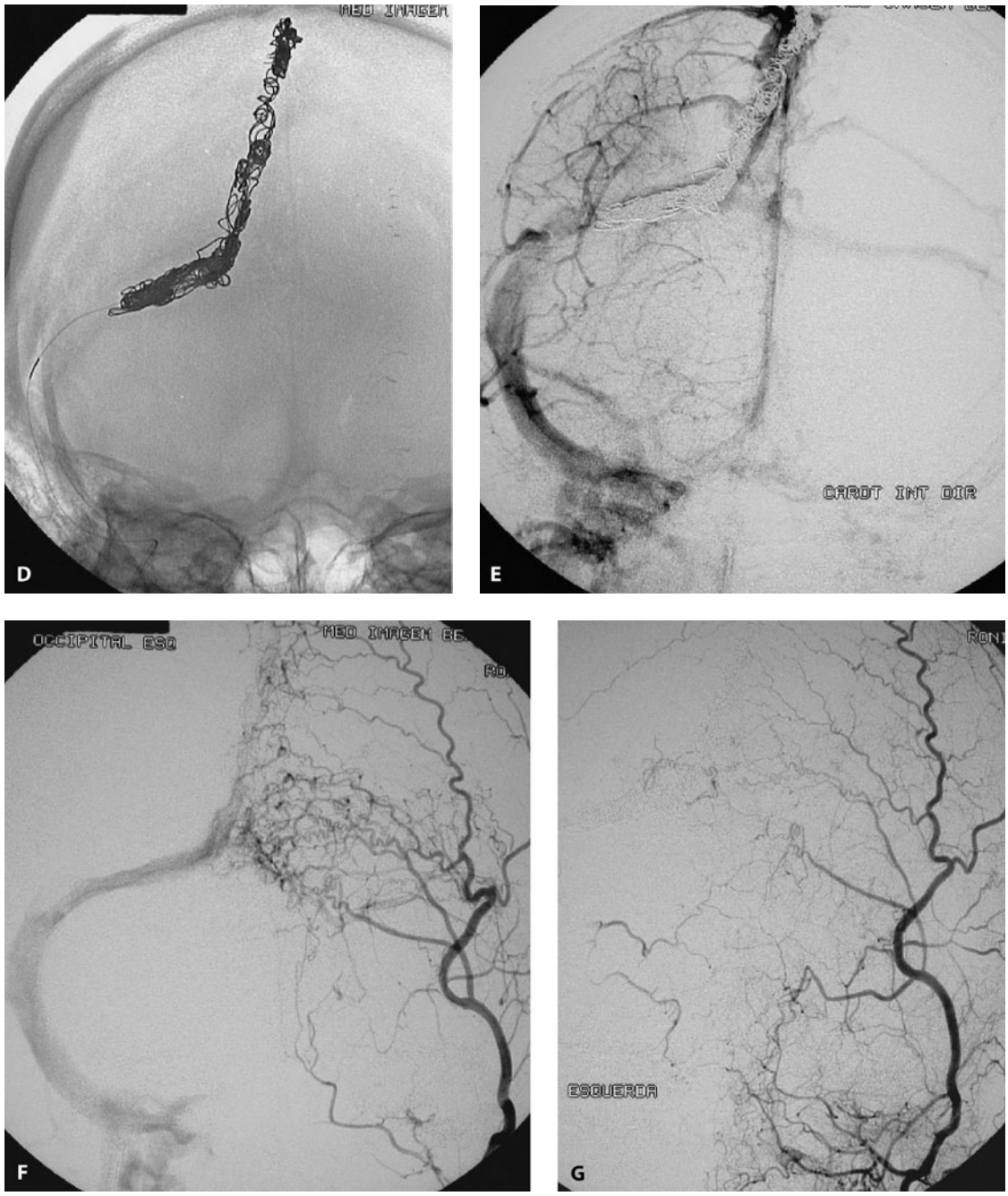

Fig. 8.27 (*continued*). Selective retrograde transvenous obliteration of the compartment draining the AVS was achieved with coils (**D**) and right internal carotid angiogram in AP view (**E**) demonstrates preservation of the compartment of the superior sagittal sinus draining the brain. Left occipital angiogram in AP view before (**F**) and after coiling of the compartment within the dural sinus draining the AVS (**G**) demonstrates obliteration of the AVS. (Courtesy of Dr. R. Piske)

Fig. 8.28A–G. A 48-year-old man presented with sudden onset of headache. CT scan (**A**) shows evidence of left posterior temporal lobe hemorrhage. Left occipital angiogram in lateral view, early arterial phase (**B**), demonstrates evidence of DAVS (*arrow*) adjacent to the transverse sinus, with drainage toward a temporal lobe cortical vein. Late arterial phase (**C**) shows this cortical vein (*curved open arrow*) to reach the transverse sinus beyond an area of thrombosis (*open arrow*). Retrograde transvenous approach (**D**) via the suboccipital venous plexus toward the cortical vein proved feasible (*arrows*) and coils (*arrow*) were deposited at the junction between the dural sinus and the cortical vein, as shown on lateral skull film (**D**). **E–G** see p. 602

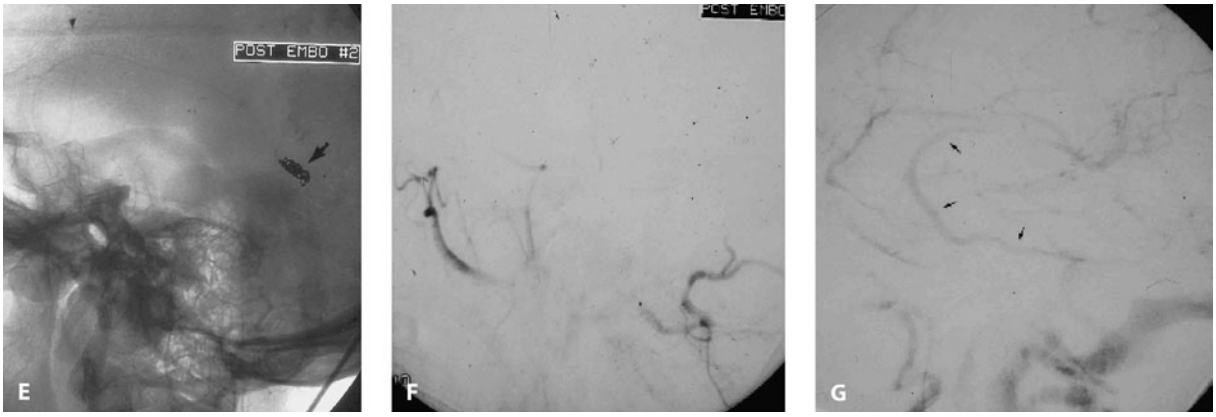

Fig. 8.28 (*continued*). Postembolization external carotid angiogram in lateral view (**E**). Postembolization external carotid angiogram in lateral view (**F**) demonstrates that there is no longer opacification of the DAVS, and the internal carotid angiogram in lateral view, venous phase (**G**), shows preservation of the cortical vein (*arrows*), which is being utilized again by the brain circulation

Careful analysis of the cerebral and cerebellar venous drainage patterns is mandatory to verify the impact and safety of the planned dural sinus sacrifice.

Indications for treatment of these DAVSs, which have direct retrograde leptomeningeal venous drainage, are now well established, and a cure must be obtained in order to prevent future ICH or neurological deficits (Davies et al. 1997b). Arterial or venous approaches can be proposed but must result in a disconnection of the leptomeningeal reflux (Fig. 8.28). There is no role for partial treatment under these circumstances.

8.9.2 Topographic Considerations

Once the indications and the goal of treatment have been established, a choice will need to be made as to how best to approach a DAVS in a given location. Certain specific anatomical features make some locations more difficult to approach than others.

DAVSs along the floor of the anterior cranial fossa can only rarely be reached from the arterial side through the ophthalmic and ethmoidal arterial systems and are usually much more easily and safely treated by surgery.

DAVSs of the superior sagittal sinus (SSS) are technically challenging to treat definitively from the arterial side because of the distal location of the nidus with respect to the achievable position of the tip of the microcatheter in the external carotid artery branches. In selected cases, this approach has proven to be curative. Retrograde venous approaches can be proposed to disconnect cortical venous reflux but sacrifice of the SSS sinus itself is usually not a good choice unless limited to the anterior third of the sinus. Surgical skeletonization of the sinus is often the only choice if a cure has to be achieved. DAVSs along the tentorium can sometimes be cured from the arterial side but this requires a perfect embolization of the

nidus to avoid collateral circulation from other sources and more often surgery will be required to obliterate these shunts.

DAVSs at the cavernous sinus level can be treated in many different ways, depending on the goal to be achieved. For palliative symptom relief, the arterial approach using particle embolization may be sufficient. In a selected group of patients, manual compression may be proposed. It is imperative to confirm that there is no significant disease at the carotid bifurcation and that the patient understands the instructions of compression, i.e., that the contralateral hand is used for compression, to avoid embolic or ischemic complications.

To attain a cure for retrograde leptomeningeal or cortical reflux, the venous approach is most likely to succeed (Fig. 8.29), unless access to the sinus is restricted because of coexisting thrombosis (Fig. 8.25). Even when the inferior petrosal sinus was not opacified, we were frequently able to access the cavernous sinus through this apparently occluded channel. If this fails the retrograde transvenous approach through the superior ophthalmic vein should be considered. This can be done through a direct surgical approach or via the femoral vein approach, retrogradely through the external jugular vein (EJV) toward the facial vein, the supratrochlear vein, the ophthalmic vein, and finally the cavernous sinus. Transvenous disconnection of the refluxing vein (cavernous sinus to sylvian) can also be performed by intraoperatively accessing the sylvian vein and advancing a microcatheter retrogradely toward the cavernous sinus and depositing coils into the sinus (to achieve a cure) or into the proximal aspect of the sylvian vein (to protect from future hemorrhage and neurological deficit) (Fig. 8.25).

Disconnection of the cortical venous reflux in the absence of obliteration of the DAVF may result in redirection of the venous flow toward another outlet or worsen the flow toward an existing venous outlet and thus worsen clinical symptoms (blindness, etc).

DAVSs located along the petrous bones and at the foramen magnum level are often fed by arteries, which are hazardous to embolize because of patent anastomoses with the posterior circulation and spinal cord arteries (i.e., occipital or pharyngovertebral anastomoses, the lateral spinal artery), or their supply to the transcranial nerves. Since these DAVFs frequently demonstrate retrograde leptomeningeal reflux towards the cerebellar and perimedullary venous systems, a cure must be achieved. This can sometimes be accomplished by careful arterial embolization using flow control and a liquid embolic agent (Fig. 8.5) or by the retrograde venous approach. If incomplete, microsurgical disconnection will be needed.

DAVSs located along the transverse sinus region can be treated in many different ways, depending on the goal to be achieved. For palliative symptom relief, we recommend arterial embolization. To treat retrograde leptomeningeal and cortical reflux, the venous approach will more likely result in a predictable cure. Superselective disconnection of the refluxing vein is preferred over sacrifice of the dural sinus although this is often necessary to achieve a cure. Attention should be paid to the drainage pattern of the brain and the cerebellum in order to assess the risk of treatment-related venous infarction. Proximal or distal thrombosis involving

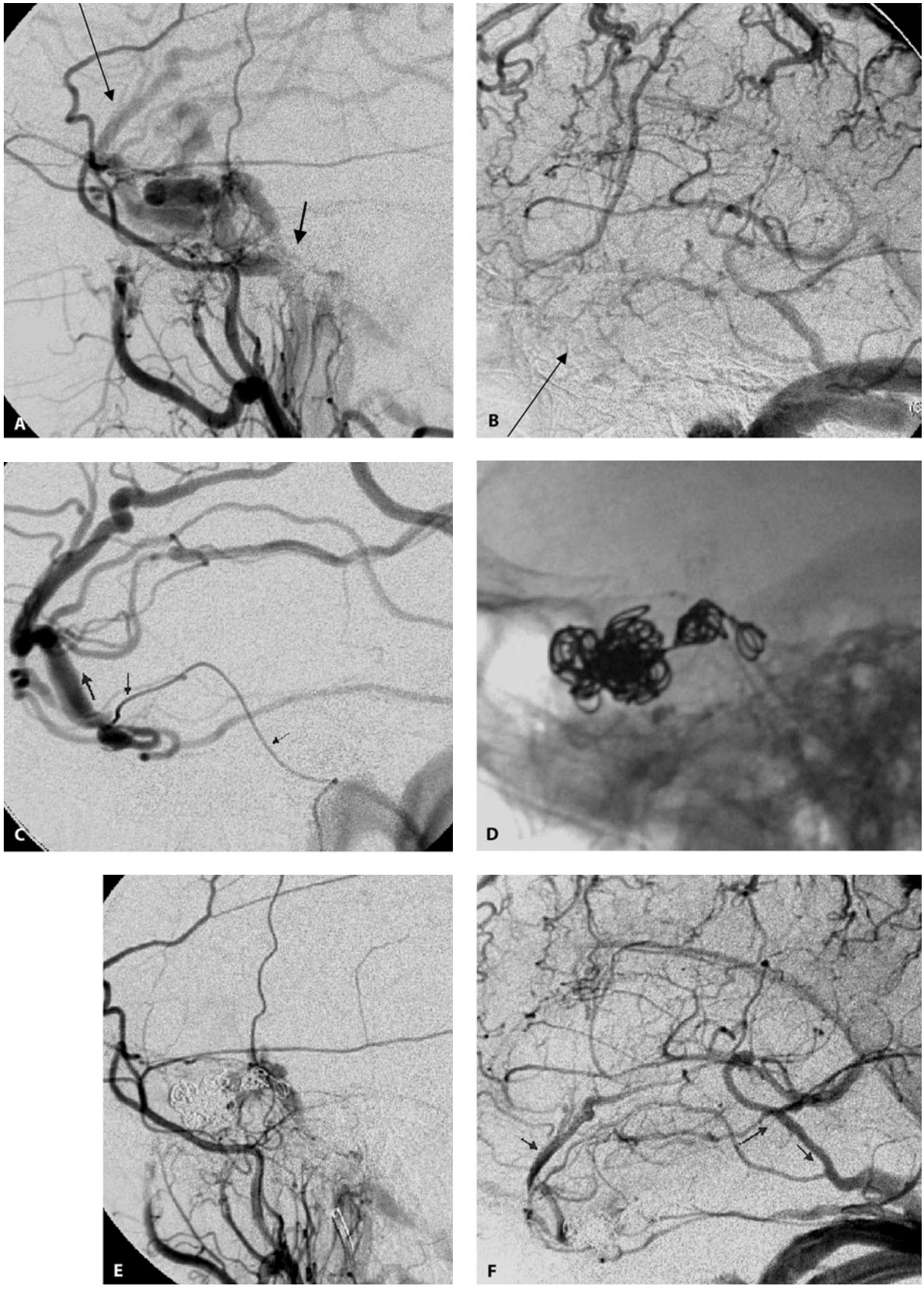

Fig. 8.29A–F. Legend see p. 605

◀ **Fig. 8.29A–F.** A 77-year-old female patient presented with a 3-month history of left eye chemosis. Left external carotid angiogram in lateral view (**A**) shows evidence of dural arteriovenous shunt (DAVS) at cavernous plexus region with reflux towards the sylvian cortical venous system (*long arrow*) and the inferior petrosal vein (*short arrow*). Left internal carotid angiogram in lateral view, venous phase (**B**) shows no opacification of the sylvian venous system (*arrow*), indicating venous congestion caused by cortical venous reflux from the DAVS. Venogram (**C**) in lateral view following retrograde transvenous approach via the inferior petrosal sinus to the junction between the cavernous plexus and the sylvian vein was achieved (*arrows*) and shows opacification of the sylvian cortical venous system. Coils were placed at this junction as well as into part of the cavernous plexus, as shown on plain film in lateral view (**D**). Left external carotid angiogram in lateral view (**E**) demonstrates that there is no longer opacification of the sylvian cortical venous system, which was opacified (*small arrows*) on the venous phase of the internal carotid angiogram in lateral view (**F**)

the dural sinus may interfere with retrograde venous access and surgery may be the only alternative.

8.9.3 Technical Aspects

The various techniques of embolization are discussed in Chap. 14 of this volume.

As discussed in the preceding section, the type of embolization (arterial vs. venous) will depend on the goal to be achieved and the access available.

If palliative treatment is the goal arterial embolization with polyvinyl alcohol (PVA) particles or tissue-adhesive liquid embolic agent is our preferred strategy.

If, on the other hand, treatment is expected to be curative then such arterial embolizations may not be sufficient and may have to be carried out in combination with a retrograde transvenous approach. The embolic materials to be used for leptomeningeal/cortical vein disconnection as well as dural venous sinus sacrifice are most likely various types of coils alone or in combination with liquids (see techniques).

8.9.4 Timing of Embolization

Treatment carried out for the purpose of symptom palliation can be performed electively after selective angiography and cortical venous reflux has been excluded. Sometimes treatment has to be carried out in stages, in particular when dealing with extensive and multifocal DAVSs.

DAVSs of the cavernous sinus presenting with rapid visual deterioration should be treated urgently, as they require aggressive therapy to preserve vision. This may include topical ophthalmic medications, Diamox to inhibit and decrease aqueous production, or even systemic diuretics such as Mannitol or Lasix. Steroid medication as well as anticoagulation should be seriously considered when venous thrombosis is perceived to be the cause of the clinical deterioration.

Treatment for patients who presented with ICH or neurological deficit and who at diagnostic angiography were found to have a DAVS with retrograde leptomeningeal reflux should be managed aggressively. If the ICH is well tolerated endovascular treatment should be scheduled within the next few weeks. There is evidence that rebleed may occur early (Duffau et al. 1999) and we recommend treatment be carried out soon after the diagnosis has been made in view of the known poor risk associated with the natural history. Endovascular treatment, which in these circumstances may require several stages, must be curative, and if leptomeningeal and/or cortical reflux continues to exist after embolization surgical disconnection or skeletonization will be needed.

8.9.5 Results of Embolization

The results of any type of treatment (manual compression, endovascular treatment, etc.) with DAVSs draining forward into the dural sinuses will have to be weighed against the favorable spontaneous symptom resolution that occurs in these patients as part of their natural history. According to Davies et al. (1997a), 86% of such patients experienced symptom relief after arterial embolization versus a similar clinical result in 81% of patients who did not undergo any specific treatment.

The results of endovascular treatment (arterial or venous) of DAVSs that have retrograde leptomeningeal and/or cortical venous reflux have been reported in single case reports and a few larger series (Urtasun et al. 1996; Roy and Raymond 1997; Davies et al. 1997b; Goyal et al. 1999). Since the goal of such treatment is to obliterate the venous reflux, the outcome of the embolization must be an anatomical cure and not just symptom relief. An anatomical cure was achieved in 70%–88% of patients treated by arterial and/or venous or combined endovascular approaches (Urtasun et al. 1996; Roy and Raymond 1997; Davies et al. 1997b).

We favor starting with the arterial approach, using a permanent embolic agent such as NBCA. If this approach is not curative, then the retrograde transvenous approach should be used immediately afterwards in order to achieve an anatomical cure. We prefer to disconnect the leptomeningeal or cortical reflux by the venous approach as a primary objective, and only as a secondary choice do we sacrifice the affected dural sinus.

8.9.6 Complications of Embolization

The potential hazards of arterial embolization of DAVSs are related to the neurological territories of these feeders, their potential anastomoses to the intracranial circulation, and their blood supply to the transcranial nerves. Such complications should be avoidable with thorough knowledge of the vascular anatomy and their variations described in Vol. 1 of this series. The position of the tip of the microcatheter and the type of embolic material chosen should be selected with this risk in mind. There is, in our opinion, no benefit from provocative injection of certain drugs (Xylocaine, etc.) if the above guidelines are followed.

The risks associated with the retrograde transvenous approach are, other than vessel perforation, mostly related to the underestimated effect that the dural sinus sacrifice might have on the venous drainage of the cerebral and cerebellar circulations. Transient neurological deficits have been reported between 4% and 33%, permanent neurological deficits in 4%–5%, and mortality in 0%–4% (Urtasun et al. 1996; Roy and Raymond 1997).

Reports describing the retrograde superior ophthalmic vein approach to DAVSs of the cavernous sinus region have noted complications to be mostly related to vascular access and vessel perforation (Teng et al. 1988; Monsein et al. 1991; Goldberg et al. 1996).

8.9.7 Surgery

Surgery should be considered whenever a complete cure is indicated and endovascular techniques have failed to be curative or were considered unfeasible. Possible surgical approaches include direct intraoperative meningeal arterial or venous embolization, resection of the abnormal dura, or sinus endoluminal packing. More recently, surgical disconnection of the retrograde leptomeningeal venous drainage has been proposed (Grisoli et al. 1984; Davies et al. 1997b), a technique similar to that used for spinal dural fistulae. Skeletonization of the dural sinus can be performed to treat extensive multifocal DAVSs, with preservation of the sinus and cortical venous entrances while disconnecting the dural arterial supply. Presurgical arterial embolization is still recommended in these circumstances.

The risk associated with surgical management of DAVSs has gradually improved over the past two decades, with better understanding of the goals to be achieved and the realization that it should only be done if embolization failed (Malik et al. 1984; Sundt and Pipegras 1983; Borden et al. 1995; Lucas et al 1997; Davies et al. 1997b; Collice et al. 2000).

More recently stereotactic radiosurgery has been proposed for treatment of deep-seated DAVSs, which could not be treated by endovascular or microsurgical techniques. The results are preliminary but appear to be encouraging for this particular indication (Guo et al. 1998).

With a natural history risk of up to 15% per year for ICH or neurological deficit, DAVSs associated with leptomeningeal or cortical reflux should be cured as soon as possible with the lowest possible risk, which is in our opinion embolization followed by surgery if embolization is incomplete.

9 Cerebral Vascular Malformations: Incidence, Classification, Angioarchitecture, and Symptomatology of Brain Arteriovenous and Venous Malformations

9.1 Incidence of Cerebral Vascular Malformations 609

9.2 Principles of Classification 612

9.3 Classification of Cerebral Vascular Malformations 614
9.3.1 Brain Arteriovenous Shunts 615
9.3.1.1 General Appearance of Arteriovenous Shunts 615
9.3.1.2 Multiple Brain Arteriovenous Malformations 618
9.3.1.3 Topographic Analysis of Brain Arteriovenous Malformations 625
9.3.1.4 Angioarchitecture of Brain Arteriovenous Malformations 631
9.3.1.5 Clinical–Angioarchitectural Correlation in Brain Arteriovenous Malformations 677
9.3.2 Venous Variations, Malformations, and Mixed Lesions 684
9.3.2.1 Developmental Venous Anomalies 685
9.3.2.2 Cavernous Hemangiomas 686
9.3.2.3 Cerebral Cavernous Malformations 687
9.3.2.4 Occult and Cryptic Malformations 690
9.3.2.5 Sturge–Weber Syndrome 691

9.1 Incidence of Cerebral Vascular Malformations

The prevalence of brain arteriovenous malformations (BAVMs) in a given population is difficult to estimate. It is believed that between 0.14% and 0.8% of the population may present with a BAVM in a given year (Garretson 1985; Jellinger 1986). These varying figures result from studies of disparate populations, ranging from the residents in a small community (Mohr 1984) to autopsy series (Jellinger 1986). Overall, however, the incidence of symptomatic BAVMs in adults appears to represent about one-tenth the frequency of intracranial arterial aneurysms. Various neurosurgical series comparing the relative incidence of symptomatic BAVMs to that of brain tumors also show considerable variability, with figures ranging from 0.59% to 7.9% (Yasargil 1987). This reflects different referral patterns and the introduction of more sensitive diagnostic tools.

Table 9.1 shows the incidence of each type of cerebral vascular malformation (CVM) in a review of a general autopsy series. Jellinger (1986) reviewed the various published autopsy series from 1945 (Courville) to 1985 (the Linz Hospital experience).

When comparing the overall incidence of CVM in the general autopsy series to the incidence of CVM in autopsies performed specifically for cerebral hemorrhage associated with a lethal bleeding episode, one should be able to ascertain the bleeding potential for each type of CVM.

The accuracy of the reported incidence and number of telangiectasias in relation to other CVMs in any autopsy series is questionable, since

Table 9.1. Incidence of cerebral vascular malformations (from Jellinger 1986, with permission)

	General autopsy series (n=45,464)	Autopsy series for cerebral hemorrhage (n=1,529)
Cerebral vascular malformations	6%	7%
Arteriovenous malformations	0.15%	3% (×20)
Cavernomas	0.05%	0.5% (×10)
Venous angiomas	0.25%	0.8% (×3)
Telangiectasias	0.15%	2.7% (×18)

telangiectasias that have not previously bled are usually not identified at autopsy.

Despite this caveat, arteriovenous malformations (AVMs) and telangiectasias are encountered 18–20 times more frequently in autopsies for cerebral hemorrhage. Cavernomas show a tenfold higher incidence in autopsies performed for cerebral hemorrhage. Developmental venous anomalies (DVAs; venous angiomas) showed a threefold increased incidence in the presence of cerebral hemorrhage, which is not statistically significant and supports the view that the incidental discovery of most such lesions is a normal variant in their venous system. The associated hemorrhages are in fact almost always related to an associated cavernoma, as was clarified when MRI came into practice. BAVMs and telangiectasias are equally present in both the general population (0.15%) and in autopsies of patients with cerebral hemorrhage (3%). This suggests the overall fatal outcome of both types of lesions; however, there is some discrepancy between autopsy findings (Table 9.2) and their discovery in clinical series (Table 9.3).

In clinical series, the percentage of supratentorial CVMs is higher than in autopsy series (9% vs. 20%). The opposite is true in infratentorial CVMs, where the percentage in autopsy series is two to five times higher than in clinical series. Telangiectasias, however, are significantly more frequent in the posterior fossa (60%–70%) and occur mainly in the brainstem (Table 9.4). They have not been described in children below 5 years of age. In addition, they are usually silent until they bleed. This difference in preferential location, favoring the brainstem, combined with infratentorial hemorrhages generally being more lethal than supratentorial bleeding, explains the discrepancy between clinical and autopsy results.

Attempts to understand the incidence of CVM from reviewing the literature are often disappointing and misleading. Various names are given to the same lesions, and different lesions are collected under the same labels. The lack of recognition that DVAs are vascular anomalies and not malformations further alters the reliability of the numbers given.

Pathological classifications of CVMs can be limited, due to the origin of the material: some are based on autopsy specimens, while in others only a portion of the lesion is reviewed. Frequently, the specimen was not imaged in vivo, missing the often critical hemodynamic factors of a vascular lesion. Therefore, the true clinical significance of the lesion and its actual

Table 9.2. Overall distribution of cerebral vascular malformations regardless of type, autopsy findings[a] (from McCormick and Rosenfield 1973; Jellinger et al. 1968)

Cerebral vascular malformation	Distribution (%)
Cerebral hemisphere and corpus callosum	64.8–70
Intraparenchymatous and deep-seated	8.5–9
Brainstem	13–16.1
Cerebellum	11.8–17

[a] Autopsy series, *n*=1,019.

Table 9.3. Overall distribution of cerebral vascular malformations regardless of type, discovery in clinical series[a] (from Morello and Borghi 1973; Krayenbuhl 1972; Berry 1966; Perret and Nishioka 1966)

Cerebral vascular malformations	Distribution(%)
Cerebral hemisphere and corpus callosum	76.6–90
Intraparenchymatous and deep-seated	2–8
Brainstem	2.6–7
Cerebellum	5–9.6

[a] Clinical series, *n*=1,320.

Table 9.4. Topographic distribution by type of cerebral vascular malformation[a] (from McCormick and Rosenfield 1973; Jellinger 1986)

	Supratentorial (%)	Infratentorial (%)
Arteriovenous malformations	70–76	24–30
Cavernomas	61–74	26–39
Venous angiomas	57–60	40–43
Telangiectasias	30–37	63–70

[a] Autopsy series, *n*=854.

biological behavior is often unclear (Tables 9.4, 9.5). Topographic and morphological descriptions are hindered by poor anatomical analysis, incomplete angiographic studies, and failure to understand or to recognize unusual vascular variations or dispositions, thereby making the description and interpretation of many lesions inaccurate.

Surgical classifications are technically oriented (Drake 1979; Forster et al. 1972; Luessenhop and Gennarelli 1977; Wilson et al. 1979; Parkinson and Bachers 1980; Shi and Chen 1986; Spetzler and Martin 1986) and are mostly geared toward surgical decision making. They are technique oriented and do not assist in the understanding of the pathophysiology of the disease and its epidemiology. They often assume that the behavior of the vascular tree is identical from one patient to another and remains unchanged throughout life. Surgical series tend to overlook potentially important features such as arterial aneurysms, venous pouches, and anatomical variations that were demonstrated in 30% of Yasargil's patients (1987)

Table 9.5. Distribution by type of cerebral vascular malformations[a] (from McCormick 1968; Jellinger 1986)

Cerebral vascular malformation	Distribution (%)
Arteriovenous malformations	13–57
Cavernomas	9–16
Venous angiomas	15.4–59.3
Telangiectasias	12–20.6
Varix	1.2–2.3
Multiple lesions	2–3.5

[a] Autopsy series, n=1,019.

and 24%–32% in Willinsky's series (1990). Spetzler and Martin (1986), in their classification, did not take into consideration the possible displacement of functional (eloquent) territories in response to the presence of the AVM. Their grading system does incorporate the size of the AVM, the pattern of venous drainage, and the neurological eloquence of brain regions adjacent to the AVM. The objective of the Spetzler classification was to anticipate the surgical risk when confronted with an AVM while presuming that surgical skills are equal among neurosurgeons. However, the Spetzler grading system has also been used as a reference to the assumed natural history of all AVMs as a group. We believe this to be wrong since this classification does not recognize the individual characteristics of an AVM in a given patient (associated aneurysms, etc.); nor does it recognize that a surgical high-grade AVM is not necessarily a dangerous one for the patient.

9.2 Principles of Classification

Several CVM classifications have been proposed. The various schemes listed below reflect our evolving knowledge and techniques available to study or treat these lesions:

1. Pathological classifications (macroscopic and microscopic) relate to the era of visual description.
2. Demographic classifications enhance subpopulations or specific groups (pediatric, adult, neurological, neurosurgical, etc.).
3. Topographic classifications and the concept of eloquent areas refer to modern imaging and open surgery.
4. Hemodynamic and morphological classifications express the interests of modern surgery and neuroanesthesia in hemodynamically challenging situations (the perfusion breakthrough phenomenon).
5. Anatomical–clinical and radiological classifications introduce the biological behavior of the normal and abnormal vascular system.

While realizing that all classifications have their limitations, some type of reference is needed that allows for discussion and comparison. We will attempt to set forth a classification that meets a number of goals. Such a classification should aid in the comparison of clinical series, first by

establishing common terminology to better communicate features of CVMs, and secondly by considering known mechanisms of evolution and symptom production to clarify pathophysiological features. The goals of a useful classification should also include the enhancement of significant differences between apparently identical lesions or patients, prediction of clinical outcome, and prediction of the natural history of CVMs prior to treatment planning. Our contribution to the understanding of CVMs is based on a fundamental principle: *both the vascular system and the vascular malformation are evolving entities in time* and exhibit change with aging. Thus, when assessing a vascular malformation, one must take into consideration the possible impact of two dynamic situations: (1) the congenital defect expressing itself as the malformation and (2) the individual host response to the presence of the malformation.

The congenital defect depends on the embryonic stage at which the disorder has occurred. In that sense, the embryological classification of vascular malformations could be universal. Despite certain restrictions in the lack of specificity in the development of brain vessels, certain broad categories of vascular malformations remain: arterial, arteriovenous, capillary, and venous. Fundamentally, all correspond to a defect or a dysfunction of the embryonic capillary maturation process. Pathological studies have helped in characterizing these different broad categories of CVM. Confusion and contradictions occurred when the pathology of the secondary effects (representing the vascular system's response to the lesion) was overemphasized for the purposes of precision and completeness. We will preserve the basic part of the pathological classification (primary classification) and separate these points from the specific response of the system representing the secondary changes.

The effects on the surrounding vessels are acquired and correspond to the reaction and adaptation of the vascular tree to the congenital defect and to the hemodynamic alterations that it produces. These acquired effects will influence the differences in clinical presentations and outcome. As is often seen in clinical practice, an apparently similar lesion can produce major symptoms in one patient and none in another. Conversely, some vascular malformations with vastly different architecture may create the same clinical problems. This further emphasizes the importance of the individual host response. Similar lesions can present in different ways in different patients at different ages, with different preexisting vascular systems, which will have an individual natural history that may lead to completely opposite therapeutic decisions.

The reaction of the vascular tree may start immediately, i.e., in utero, after the flow abnormalities (anatomical adaptation) have become established, or occur after birth. The reaction persists or evolves with age (development of thrombosis, steal, kinking, vessel wall defects, collateral circulation, etc.) and may respond to acute events (rupture of the malformation, surgery, radiation therapy, embolization, etc.). Many of these acquired features are potentially reversible. Some express a weakness in the system (high-flow angiopathy), while others indicate compensatory capabilities (spontaneous thrombosis, anatomical dispositions, collateral circulation, etc.). Appreciation of the weaknesses and the adaptability of the system may help us to predict the biological effect of a malformation in a

specific host and not merely a statistically probable event in a given population. The concept of response and/or adaptation of the host (carried out by the vascular system) has mostly been ignored and is therefore not considered in the natural history of the specific lesion.

The topographic location of a malformation is best assessed by MRI or CT. Angiography, however, provides anatomical identification of the arterial feeders, the angioarchitecture of the nidus, the draining veins, and the hemodynamic aspects of the shunt. These features confirm and accurately delineate the presence of other associated vascular lesions as well as significant arterial and venous variations, and will also define the vascular anatomy and physiology of the normal cerebral vasculature. MRI or MRA alone, as well as poor angiographic studies, will not be able to identify this type of vascular anatomy and will make a comparison between series impossible and/or unreliable. Such inadequate information will have only limited value for the predictability of the natural history of the malformation being examined.

9.3 Classification of Cerebral Vascular Malformations

Four major types of primary defects or malformations of the vascular systems can be identified (Table 9.6): arterial, arteriovenous, capillary, and

Table 9.6. Classification of cerebral vascular malformations

Arteriovenous
Malformations
Fistulae
Capillary
Telangiectasias
Venous
Cavernous malformations (cavernomas)
Mixed types
Capillary venous

Table 9.7. Primary classifications of the cerebral arteriovenous vascular lesions

Arteriovenous shunts
Single
Micro-AV shunts (mAVM or mAVF)
Macro-AV shunt (compartmented nidus or mAVF)
Multiple (nonfamilial)
Metameric (Wyburn–Mason, cerebral–facial)
Nonmetameric (multiple separate nidi or separate compartments within one nidus
Multiple (familial)
Systemic (Rendu–Osler–Weber or hereditary hemorrhagic telangiectasia)
Nonsystemic (multiple separate nidi, with or without AVF)

AV, arteriovenous; mAVM, microarteriovenous malformation; mAVF, microarteriovenous fistula; AVF, arteriovenous fistula.

venous. For each of them, different effects on the remaining vascular system can be encountered (Table 9.7).

We will consider the arteriovenous and venous malformations separately. The DVAs (Saito and Kobayashi 1981; Yasargil 1987; Valavanis et al. 1983; Lasjaunias et al. 1986a) can be seen alone or associated with cavernomas, capillary telangiectasias, or AVMs.

9.3.1 Brain Arteriovenous Shunts

Arteriovenous shunts correspond to an abnormal capillary bed with a shortened arteriovenous transit time. The exact location of the shunt has been somewhat controversial; whether they are located within the pia or subpially depends on the theory that one accepts for the relationships between pia mater and cortical vessels. We favor the description that places all BAVMs subpially and consequently does not differentiate (as far as the relationship to the meningeal space is concerned) between purely cortical and intraparenchymatous malformations (Hutchings and Weller 1986). All arteriovenous lesions can therefore be viewed as subpial in location, including those involving the spinal cord. This contradicts the microsurgical concept that all BAVMs can be regarded as being primarily extraparenchymatous, even though they may be buried in the depth of the neural tissue (Yasargil 1987).

9.3.1.1 General Appearance of Arteriovenous Shunts

Schematically, two broad categories of arteriovenous shunts can be recognized: the arteriovenous malformations (AVMs) and the arteriovenous fistulae (AVFs). The AVMs are characterized by a network of abnormal channels (nidi) between the arterial feeder(s) and the draining vein(s). They may be small (micro-AVMs) with normal-sized arteries and draining veins and a nidus smaller than 1 cm in diameter (Fig. 9.1). Macro-AVMs, in contrast, have arteries and veins that are usually larger than normal; the size of the nidus is larger than 1 cm in diameter (Fig. 9.2).

Compartments can be observed within the lesions either during angiography or at surgery. AVFs may be of the micro (Fig. 9.3) or macro type (Fig. 9.4).

AVMs and AVFs are the two basic forms of arteriovenous shunts that can be encountered throughout the CNS. Theoretically, all combinations of types, sizes, flow patterns, and topographies can be seen, but micro- or macro-AVFs have only been encountered on the surface of the brain or the spinal cord. AVFs appear to be more frequent in children and are relatively rare in adults. They were seen in only 2% of our patients (Berenstein et al. 1990).

The association of different types of CVMs (AVM and cavernomas, AVM and DVAs, AVM and capillary telangiectasias) is rare, but can be seen. Their coexistence should induce a discussion with regard to the perceived natural history under such circumstances, as well as the indications and risks of their treatment. Treatment of a BAVM draining into a DVA

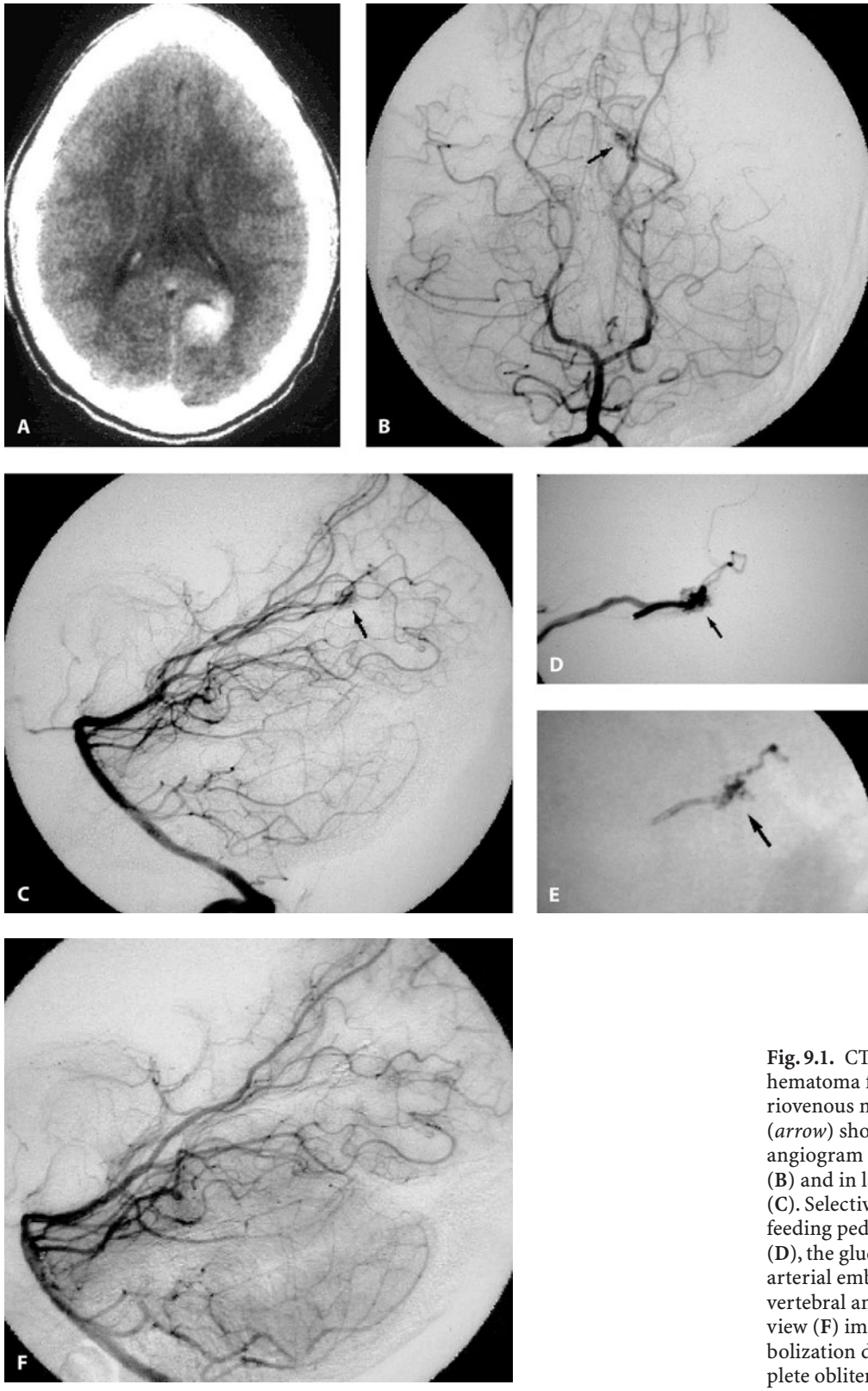

Fig. 9.1. CT (**A**) shows lobar hematoma from microarteriovenous malformation (*arrow*) shown on vertebral angiogram frontal projection (**B**) and in lateral projection (**C**). Selective angiogram of the feeding pedicle in lateral view (**D**), the glue cast following arterial embolization (**E**) and vertebral angiogram in lateral view (**F**) immediately after embolization demonstrates complete obliteration of the nidus

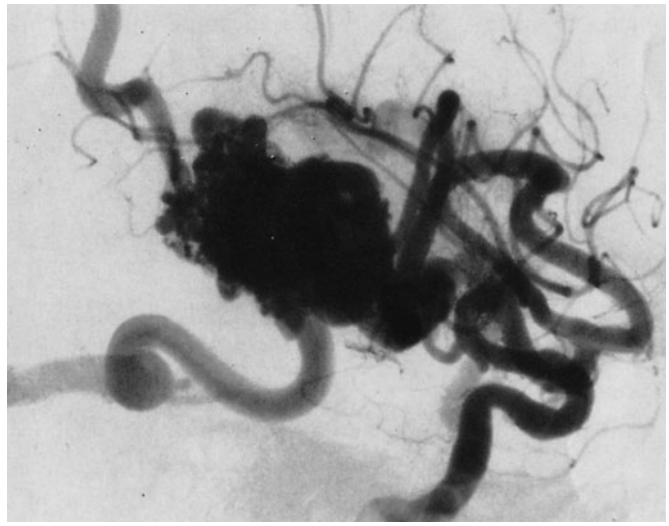

Fig. 9.2. Right internal carotid injection, lateral view. Temporal (T-2) arteriovenous malformation draining into cortical veins

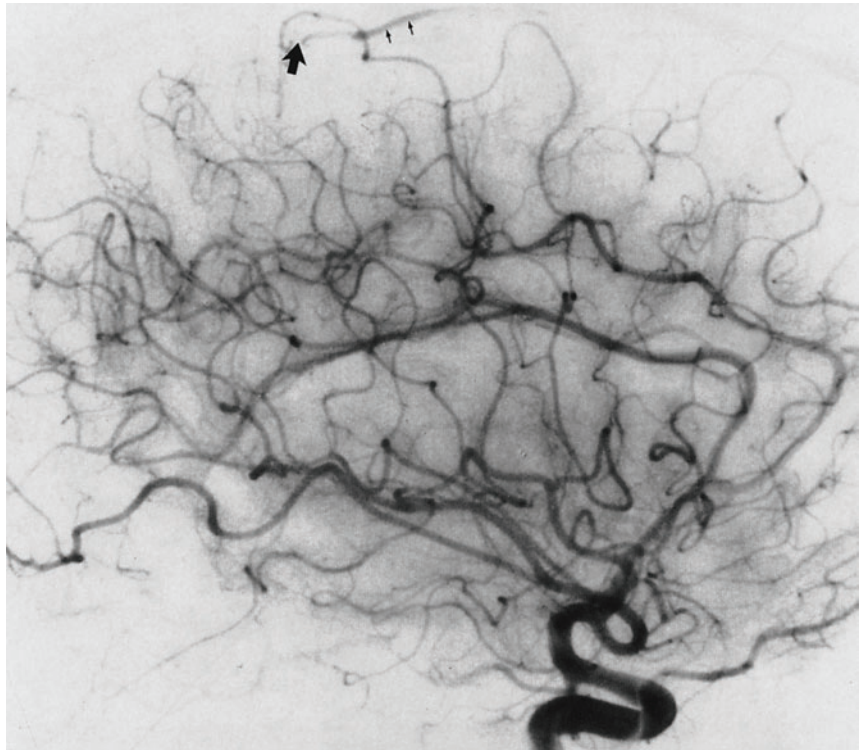

Fig. 9.3. Right internal carotid injection in lateral view. Micro-arteriovenous fistula of the upper frontal convexity (*arrow*). Note the normal size draining vein (*small arrows*)

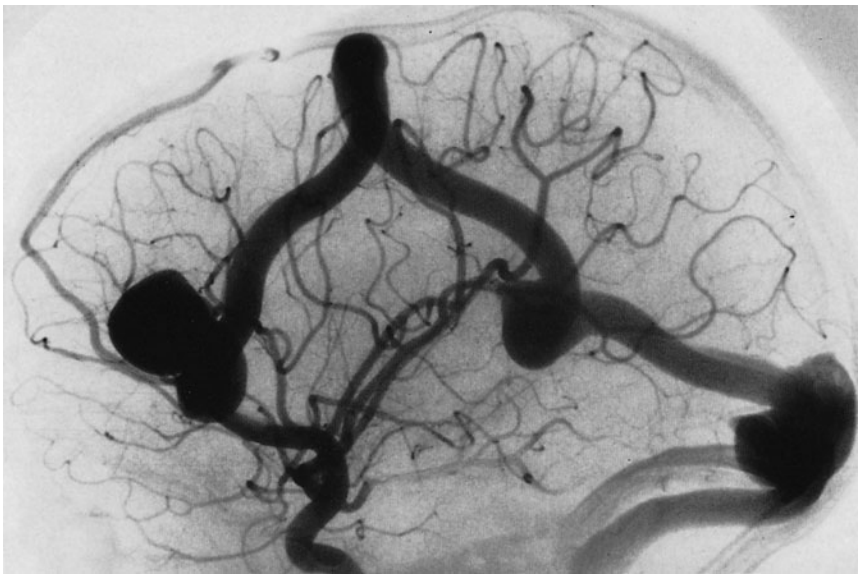

Fig. 9.4. Left internal carotid injection in lateral view. Single-hole pial arteriovenous fistula draining into a medial hemispheric vein and the straight sinus

(worse natural history) will require preservation of the DVA, as this also contributes to the venous drainage of the surrounding brain and in turn this carries an increased risk during treatment.

9.3.1.2 Multiple Brain Arteriovenous Malformations

Multiple BAVMs are rare and were noted in 3% of 500 patients in Yasargil's 1987 series. Multiplicity of BAVMs was reported to be 2.2% in the Toronto series (Matsubara et al. 2000), while Willinsky et al. (1990a) found a 10% incidence of multiple AVMs in the Bicêtre series and an even higher incidence in children. These differences may be related to referral patterns, population differences, better angiography, more awareness of these associations, or a combination of factors.

In this heterogeneous group with multifocal BAVMs, three types of patients were identified (Table 9.7): (a) those with hereditary hemorrhagic telangiectasia (HHT), also called Rendu-Osler-Weber disease (ROW), (b) those with metameric cerebral and cerebral–facial syndromes, and (c) those with unclassified multiple lesions.

Hereditary Hemorrhagic Telangiectasias

HHT has been identified as an autosomal dominant disorder characterized by a multisystemic vascular dysplasia and recurrent hemorrhage (Guttmacher et al. 1995). Two gene mutations have been identified: on chromosome 9 (endoglin; HHT-1) (McAllister et al. 1994) and on chromosome 12 (activin receptor-like kinase, ALK-1; HHT-2), and a third mutation is suspected to exist. An endoglin knockout mouse model has shown the development of what appears to be AVM nidus (Fig. 9.5). HHT accounted for 25% of the multifocal AVMs in the Bicêtre series and 50% in the Toronto series. Most of our patients were young (half of them less

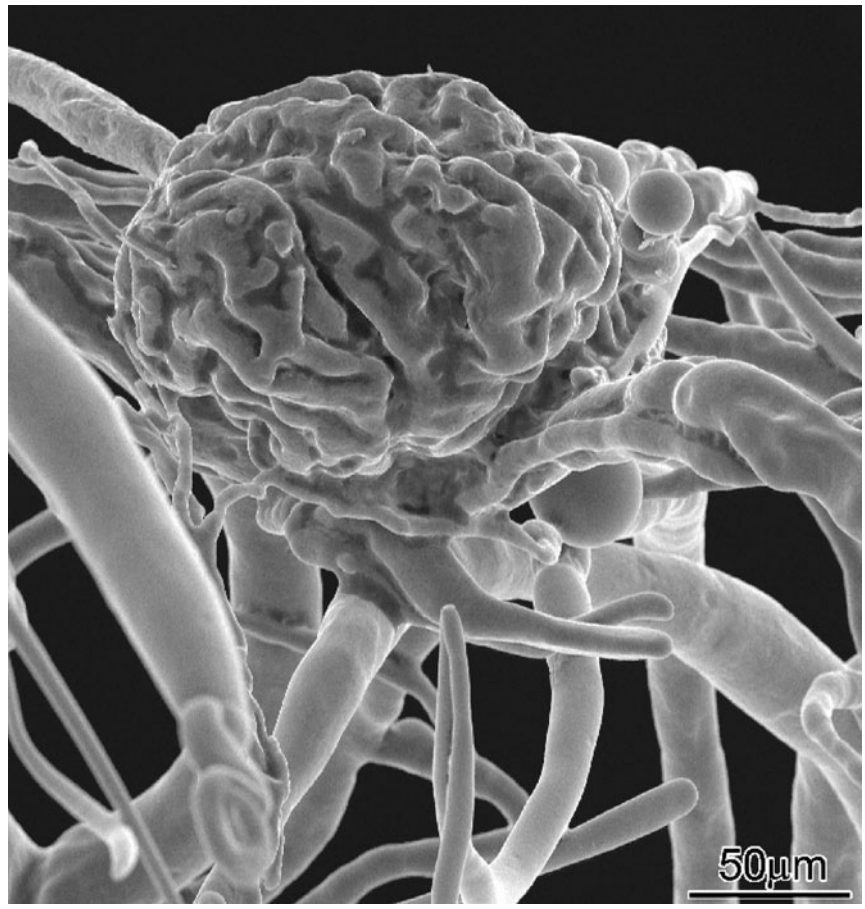

Fig. 9.5. Endoglin knock-out murine model showing evidence of micronidus development at scanning electron microscopy of mouse brain vasculature. (Courtesy of M. Letarte)

than 16 years of age), presenting with CNS symptoms related to a brain arteriovenous shunt and a family history of HHT. Roman et al. (1978) found that 28% of HHT patients had cerebral AVMs, whereas 8% had spinal cord lesions.

Angiography of the CNS lesions may show multiple areas of arteriovenous shunting that is nearly always cortical in location, either supra- or infratentorial (Figs. 9.6, 9.7). In the Toronto series, the nidus was in 42% of cases less than 1 cm in diameter (micro-AVM). AVFs of the high-flow type with venous ectasias were noted in 29% (Fig. 9.6). The presentation of HHT patients with small BAVMs and AVFs included hemorrhage in 21% and seizures in 42% of patients, while all the micro-AVMs were asymptomatic on presentation and on follow-up. This appears to contradict the experience with isolated micro-AVMs in the non-HHT population, patients who often present with hemorrhage, and it raises questions with respect to their different natural history and the need for treatment in the HHT population. The natural history of BAVSs associated with HHT may therefore not be the same as for the sporadic type of AVSs (Matsubara et al. 2000; Maher et al. 2001).

HHT patients presenting with systemic complaints were more likely to develop acute CNS symptoms related to their pulmonary AVFs (brain abscess, embolic stroke) than to the presence of a BAVM (Putman et al. 1996).

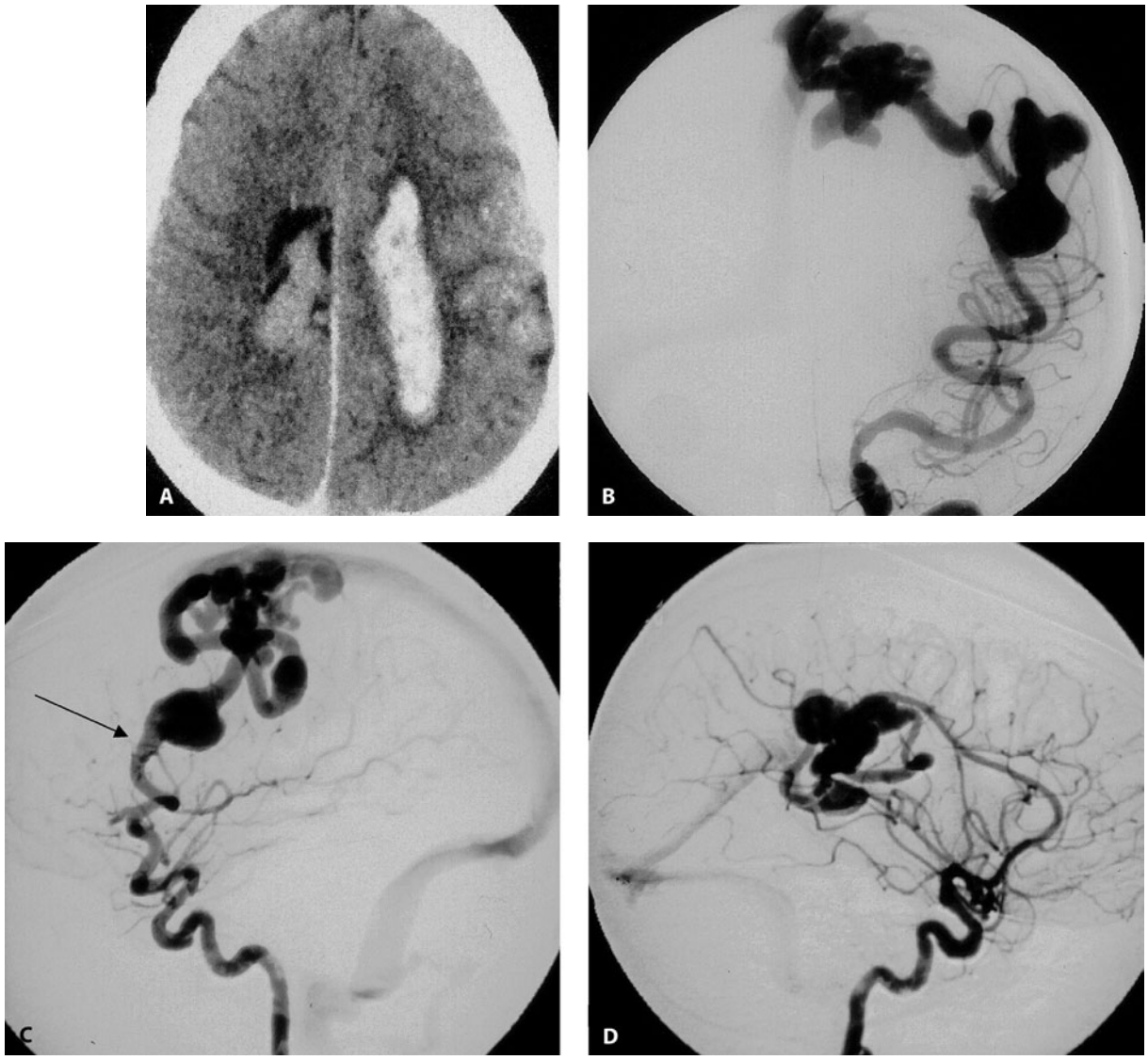

Fig. 9.6. Multiple arteriovenous fistulae (AVFs) in a patient with a family history of hemorrhagic telangiectasia presenting with intracerebral hemorrhage shown on CT (**A**) from left middle cerebral artery AVF (*arrow*) demonstrated on left internal carotid angiogram in frontal view (**B**) and lateral view (**C**). Second AVF was shown to be fed from right pericallosal artery, as shown on right internal carotid angiogram in lateral view (**D**)

While the clinical diagnosis of HHT is based on the combination of family history and cutaneous and mucous membrane manifestations, the angiographic findings of multiple cerebral micro-AVMs or multiple AVFs is highly suggestive of HHT.

The exact relationship between CNS AVMs and telangiectatic disease is not clear. While new telangiectasias may form along the nasal and gastrointestinal tract mucosa, we have never seen such developments in the CNS, nor has the development of new AVMs in the CNS been reported.

While MRI examination of the brain has been recommended as part of the screening protocol for patients with known systemic manifestations

Fig. 9.7. Vertebral artery injection in lateral view in a patient presenting with a family history of hereditary hemorrhagic telangiectasia. Note two micro- and one macro-nidus (*arrows*). Previous surgical clips indicate direct surgical approach to cerebral abscess related to septic emboli from an associated pulmonary arteriovenous shunt

of HHT or for their family members clinically suspected of HHT, the ability to demonstrate CNS involvement and in particular the presence of a micro-AVM is limited (Putman et al. 1996; Matsubara et al. 2000). High-quality angiography is therefore still the modality of choice to exclude CNS manifestation of HHT or to demonstrate multiplicity of lesions when MRI has demonstrated a single AVM.

Metameric Cerebral and Cerebral–Facial Syndromes

A number of syndromes such as Wyburn-Mason (1943a), Bonnet et al. (1937) and cerebral–facial AVM, or CAMS (Bhattacharya et al. 2001), have associated ipsilateral AVMs with vascular malformations of the retina and facial regions (Figs. 9.8, 9.9). Their metameric expression reflects the common background of the tissues involved in vasculogenesis and their differences in extension expresses their different origin in time when the trigger occurred. The metameric patterns of involvement suggest the origin of these syndromes to be a disorder of the neural crest or adjacent cephalic mesoderm (Bhattacharya et al. 2001).

Theron et al. (1974) reviewed 25 patients with Wyburn-Mason syndrome and referred to this entity as a unilateral retinocephalic vascular

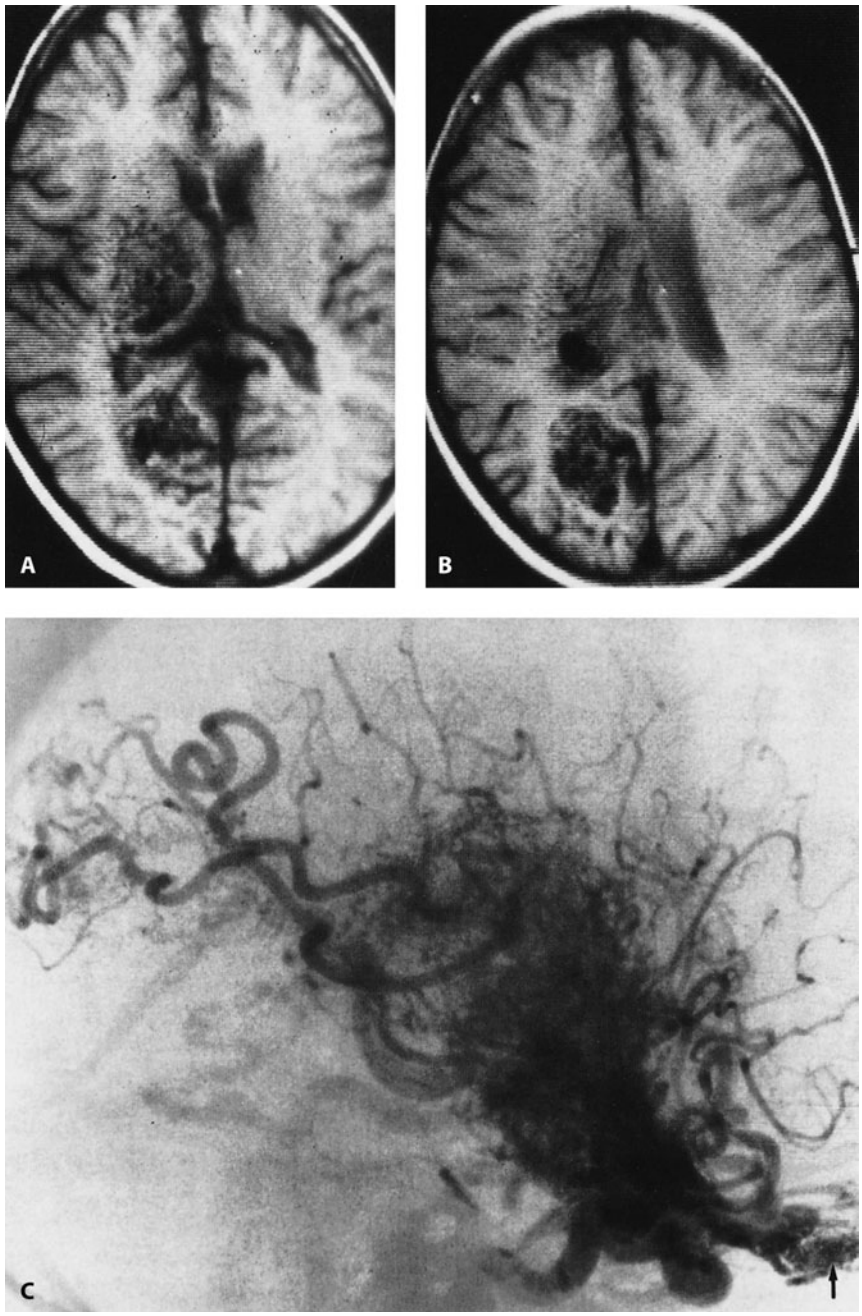

Fig. 9.8A–E. Arteriovenous malformation in a patient with Wyburn–Mason syndrome. **A**, **B** T1-weighted MRI, axial cuts, demonstrating the apparent discontinuity between the diencephalic and occipital location of the lesion. **C** Right internal carotid injection in early and **D** late phases. Note the extensive aspect of the diencephalic nidus, the optic nerve location (*arrow*, **C**), and the separate precuneus nidus. **E** Vertebral injection in lateral view. Note the separate supply of the thalamic and occipital lesions ►

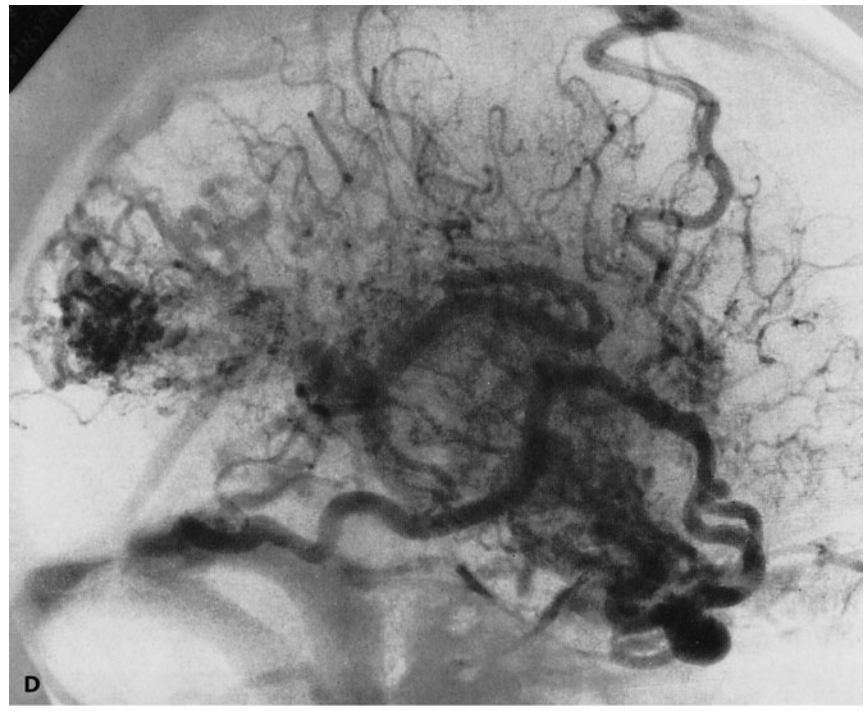

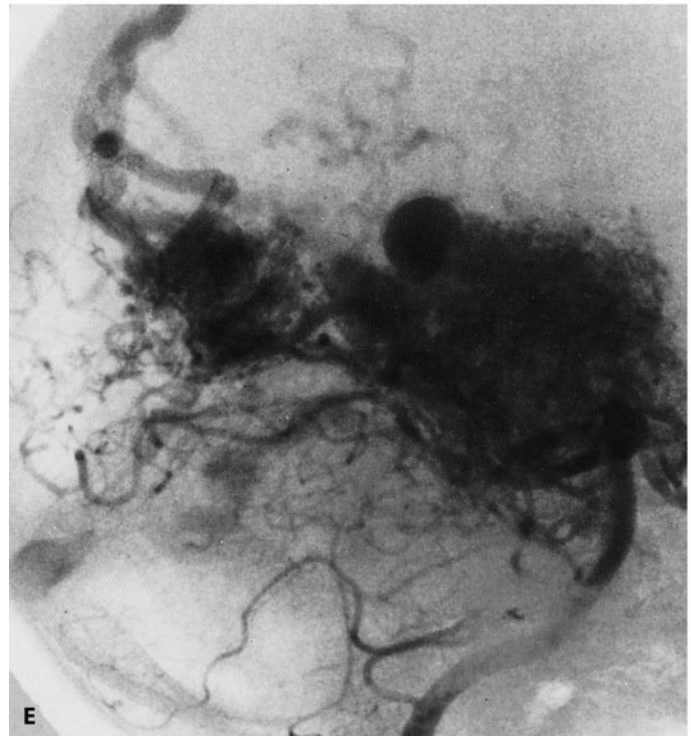

Fig. 9.8D, E. Legend see p. 622

Fig. 9.9A–C. Associated facial and cerebral arteriovenous malformation (AVM). **A** Right facial artery injection. **B, C** see p. 625

malformation. The lesion in all but three of his patients involved the optic nerve. The AVM closely follows the visual pathways and extends to the thalamus and hypothalamus. The nidus may be compact or separated by noninvolved normal brain, constituting multifocal AVMs along the optic pathways (Fig. 9.8). Treatment is particularly challenging (Morgan et al. 1985) and should target the symptomatic portion or lesion.

Other multifocal AVMs that combine facial and cerebral AVMs in a less specific fashion (Hanieh et al. 1981; Smith and Donat 1981) are probably a transitional form between HHT and WMS (polymorphic involvement in the vascular system and multifocality in the craniocerebral region). In rare instances, associations with extracranial AVMs can be seen, where the extracranial lesion is the symptomatic one.

Unclassified Multiple Arteriovenous Malformations

Several case reports have described so-called recurrent BAVMs in separate locations. Unfortunately, the angiographic analysis prior to surgery

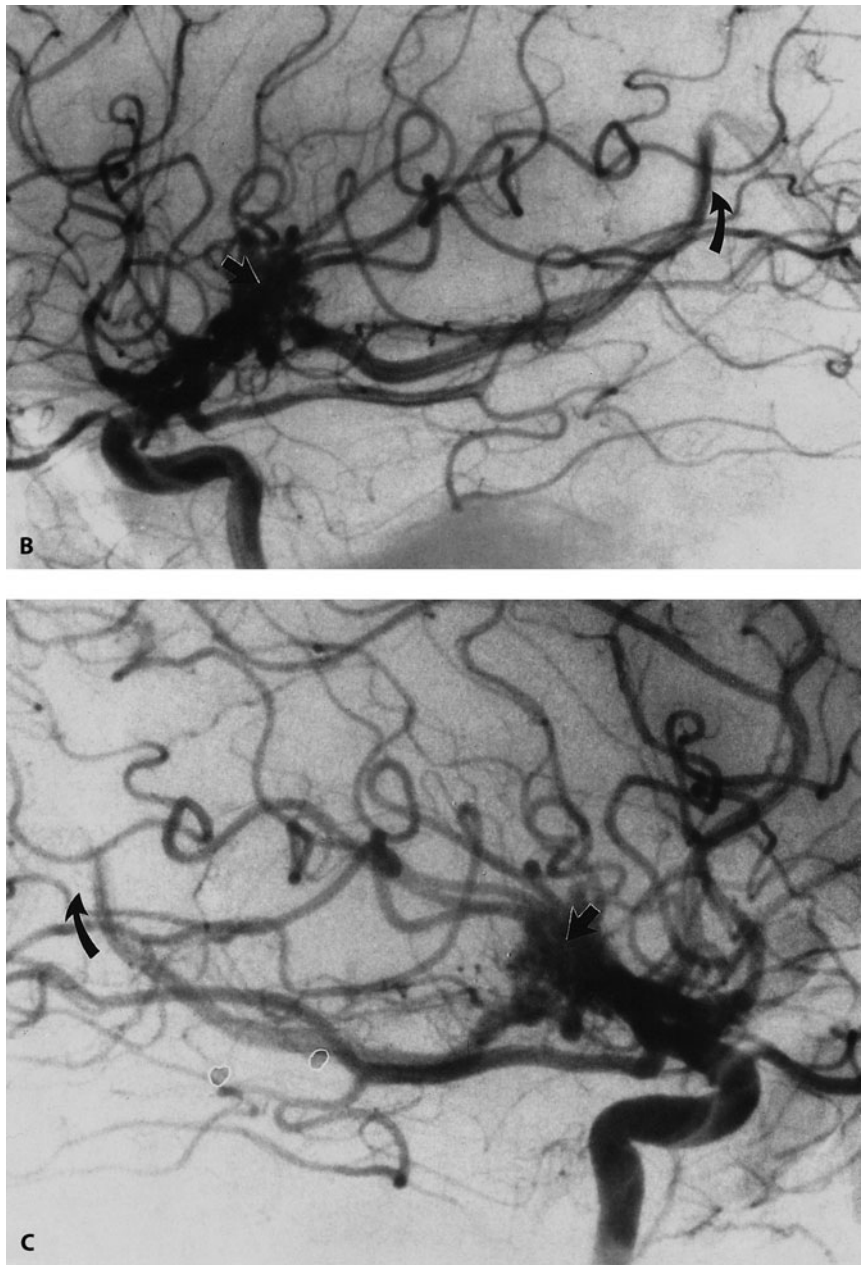

Fig. 9.9 (*continued*). **B** Left and **C** right internal carotid artery angiograms in lateral view. The hypothalamic AVM (*arrows*) drains into the basal vein (*curved arrows*)

was often incomplete and one may postulate that most cases involved either misdiagnosed multiple AVMs or incompletely removed AVMs.

9.3.1.3 Topographic Analysis of Brain Arteriovenous Malformations

Topographic location of an AVM (Table 9.8) is best assessed by combining the MRI and the angiographic information. Lesions in most locations recruit predictable arterial feeders and specific draining veins. One assumes that the primary defect is at the capillary level. Thus, both the arterial tree from which the feeders originate and the venous system that drains the le-

Table 9.8. Topography of intracranial arteriovenous lesions and gross vascular territories

	Cortical arteries	Perforating arteries	Choroidal veins	Deep veins	Superficial veins
Cortical	+	–	–	–	+
Corticosubcortical	+	–	–	–[b]	+
Corticoventricular	+	+[a]	+[a]	+	+
Corticocallosal	+	–	+[a]	+	+
Deep-seated	+[c]	+	–	+	+[b]
Choroid plexus	–	+[a]	+	+	+[b]

+, involved; –, noninvolved.
[a] Subependymal arterial anastomosis or branches can be seen.
[b] Can be recruited via transcerebral veins.
[c] Insular and cerebellar.

sion are, a priori, assumed to be normal. The analysis of arterial feeders and venous drainage can therefore accurately delineate the topography of the various compartments or nidi involved. Several general types of lesion can be differentiated based on localization. Of importance is the differentiation when venous thrombosis creates alternate patterns of drainage.

Lesions That Reach the Cortex

1. Cortical arteriovenous lesions reach the cortex and are exclusively fed by cortical arteries and drain into superficial veins. These lesions (Fig. 9.10) are the sulcal AVMs, as described by Valavanis and Yasargil (1998).
2. Cortical-subcortical lesions recruit cortical arteries and drain into superficial veins but may also drain into the deep venous system if the transcerebral venous system is patent. These represent the gyral type of AVMs, as described by Valavanis and Yasargil (1998).
   In both cortical and cortical-subcortical lesions, some regions of the cortex drain to deeply located veins that should not be considered as truly part of the deep venous system. Such vessels include the medial veins of the temporal lobe and the basal vein of Rosenthal, the veins of the cerebellar vermis, and the precentral cerebellar veins (Fig. 9.11).
3. Corticoventricular arteriovenous lesions correspond to the classic pyramid-shaped malformation, reaching the ventricular wall at their apex. Feeding arteries are both perforating and cortical. Draining veins are also deeply and superficially located (Fig. 9.12).
4. Corticocallosal lesions belong to the corticoventricular group, as they present the same venous characteristics but do not recruit perforating arteries. They drain into the subependymal veins and later into the deep venous system (Fig. 9.13). The arterial supply to the corpus callosum is linked to the cortical arterial network, even though it may simulate perforating arterial channels in the supraoptic region, and to choroidal arteries at the splenium.

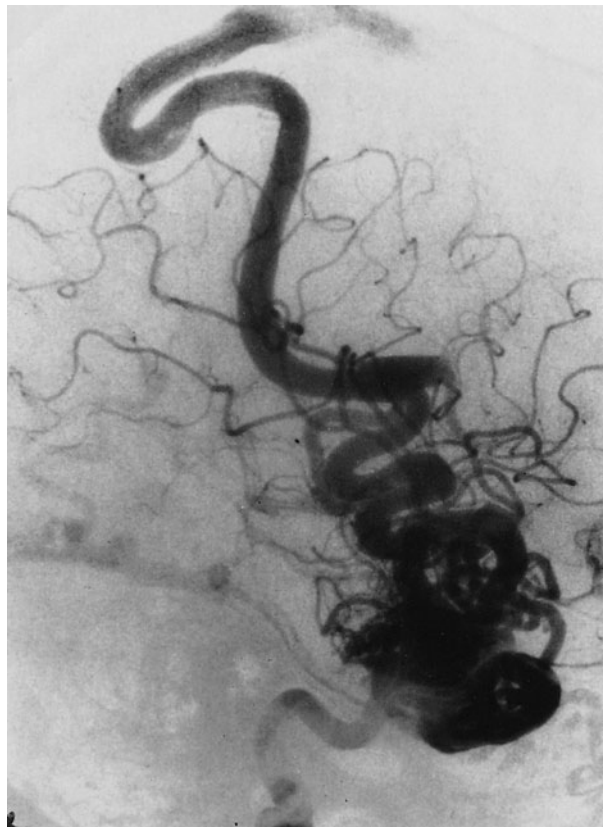

Fig. 9.10. Right internal carotid artery injection in lateral view in a patient with a temporopolar arteriovenous malformation draining into cortical veins

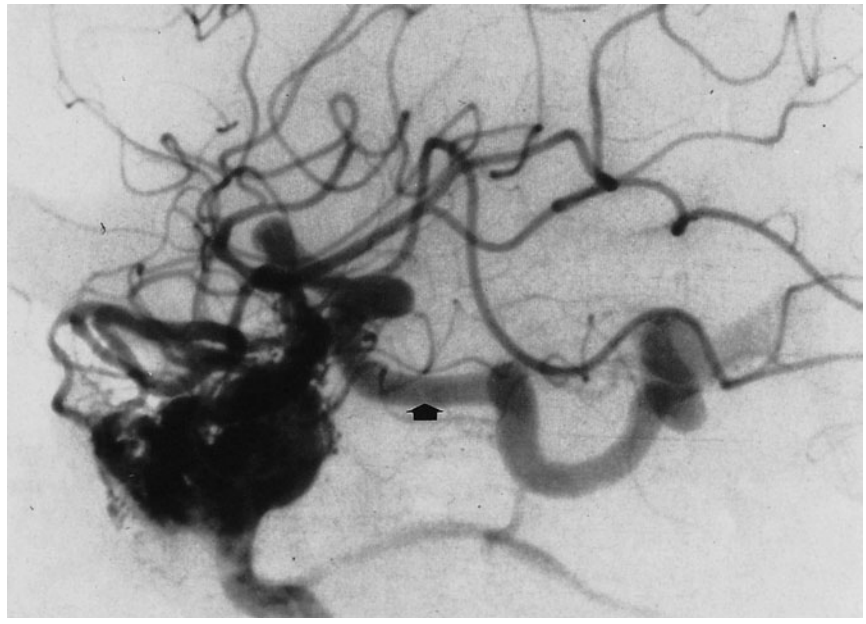

Fig. 9.11. Left internal carotid injection in lateral view in a patient with a cortical temporomedial lesion draining into the basal vein (*arrow*)

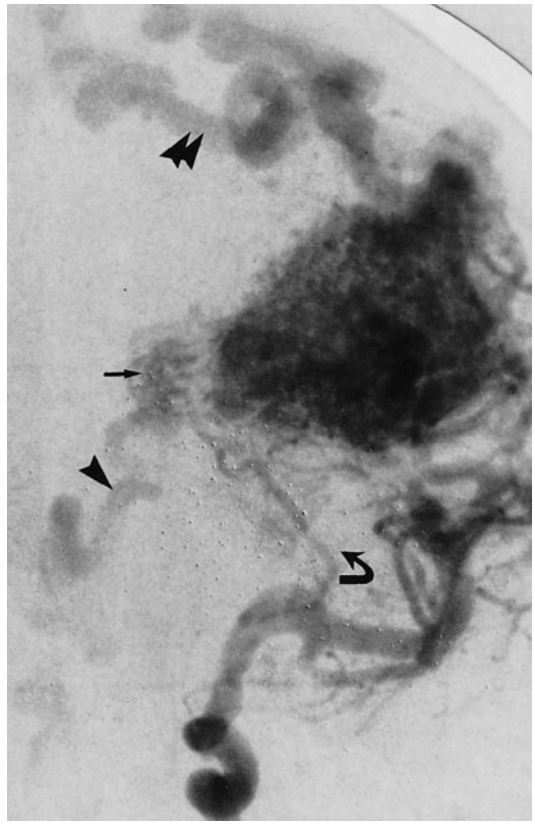

Fig. 9.12. Corticoventricular arteriovenous malformation. Left internal carotid injection in frontal view. Note the ventricular extension (*arrow*). The lesion is fed by cortical and lenticulostriate arteries (*curved arrow*) and drains into both cortical (*double arrowhead*) and subependymal veins as well as the ventricular veins (*arrowhead*)

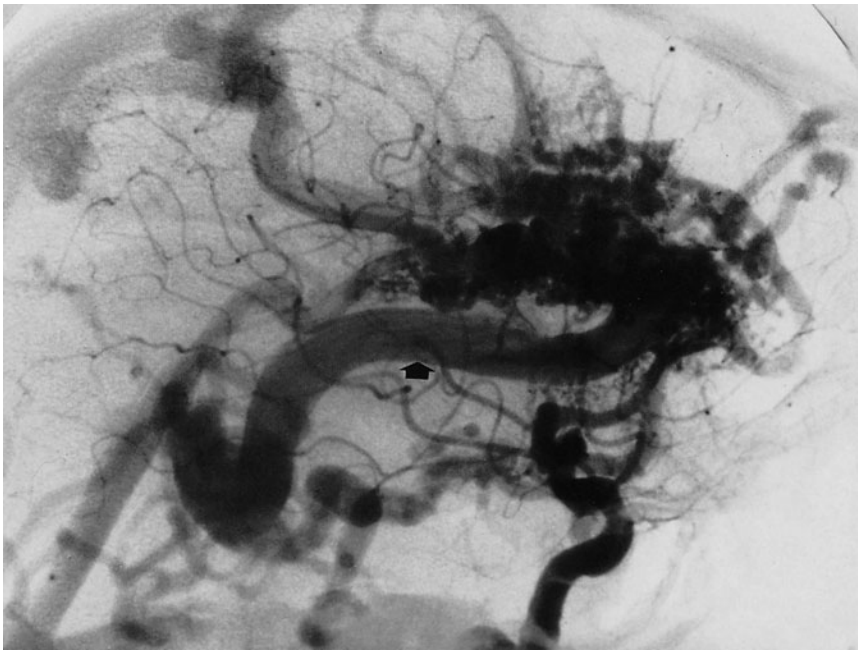

Fig. 9.13. Right internal carotid injection in lateral projection. Corpus callosum arteriovenous malformation draining into medial cortical vein and septal and internal cerebral veins (*arrow*)

Deep-Seated Arteriovenous Lesions

Deep-seated lesions can be located supra- or infratentorially in the depth of the telencephalon, diencephalon, brainstem, or cerebellum (Fig. 9.14). Their nidus involves the deep nuclei and the long fiber tracts with their arterial and venous connections. They recruit exclusively perforating arteries and drain into the deep venous system. They may use transcerebral veins if patent, either as a direct venous outlet (Fig. 9.15) or as a collateral pathway. Transcortical arteries from the insular branches of the middle cerebral artery and the hemispheric collaterals of the cerebellar arteries can be involved in lenticulostriate nucleus and in dentate nucleus arteriovenous lesions, respectively (Fig. 9.16). MRI and angiography will be able to distinguish these deep-seated lesions from cortical-subcortical lesions, particularly since the dominant supply of the intracerebrally located deep lesions arises from the perforators.

Choroid Plexus Arteriovenous Lesions

Choroid plexus AVMs are difficult but important to recognize due to their extracerebral nature and their surgical and endovascular accessibility. They are fed primarily by choroidal arteries and subependymal arterial feeders arising from the circle of Willis. They include arteries arising from the basilar tip that course through the walls of the third ventricle to reach its roof and the adjacent choroid fissure (Fig. 9.17, p. 632). Cortical arterial supply is excluded in this type of lesion. Drainage is via ventricular

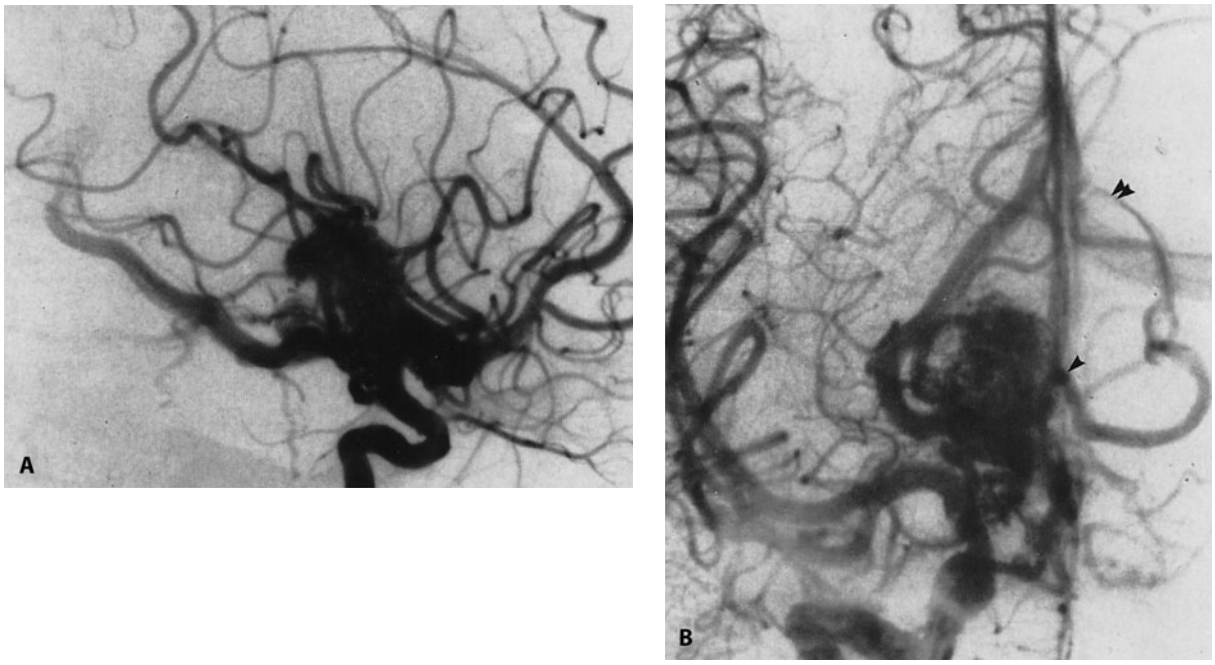

Fig. 9.14A, B. Ventral thalamic and hypothalamic arteriovenous malformation (AVM). **A** Lateral and **B** frontal projections of the right internal carotid artery. The AVM is draining into the basal vein on the right side, and on the left side via the anterior communicating vein (*arrowhead*). Note the tentorial sinus on the left side (*double arrowhead*). Also see Fig. 9.10

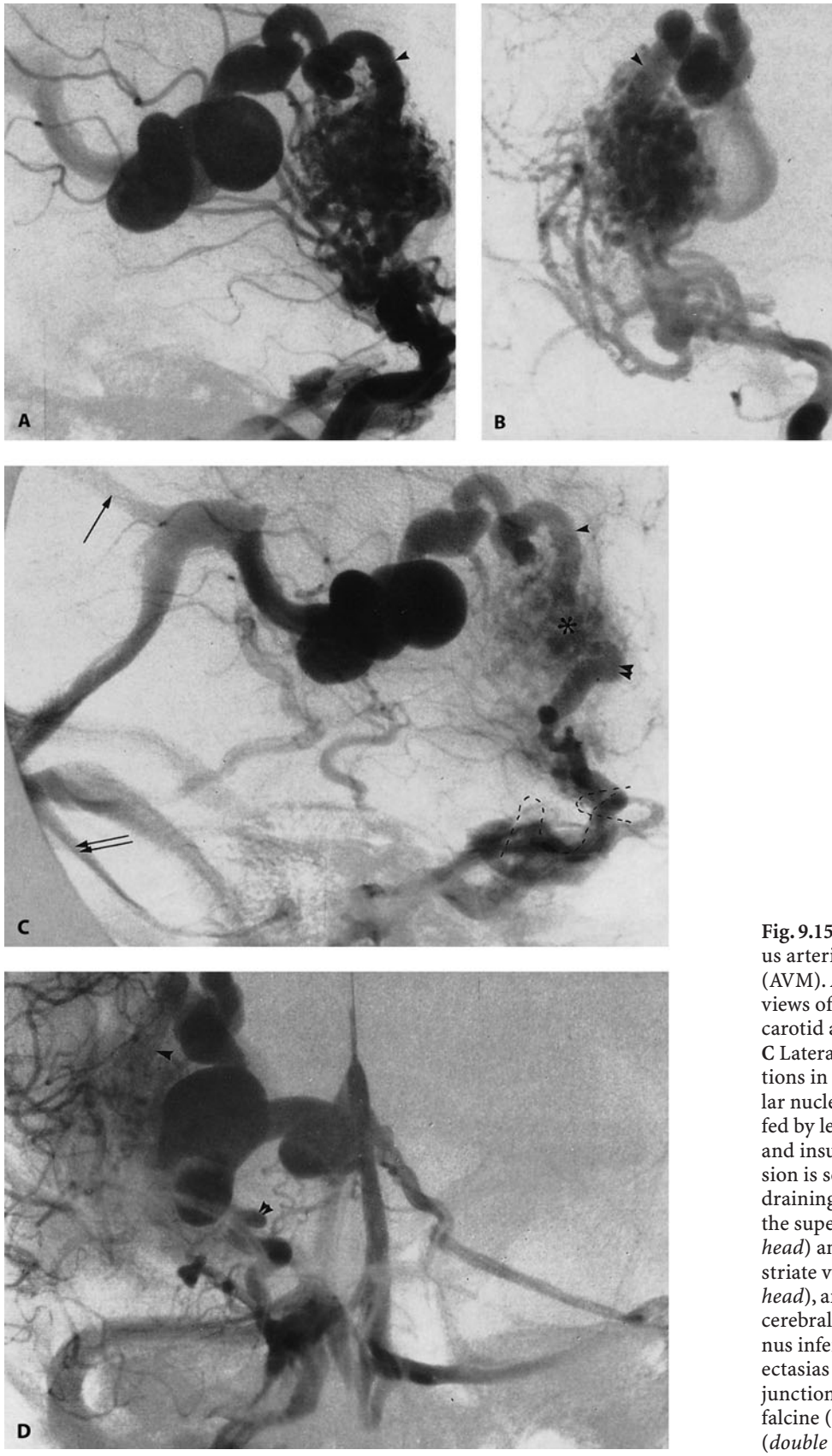

Fig. 9.15A–D. Lenticular nucleus arteriovenous malformation (AVM). **A** Lateral and **B** frontal views of the right internal carotid artery in early phase. **C** Lateral and **D** frontal projections in venous phase. Lenticular nucleus AVM (*asterisk*, **C**) fed by lenticulostriate arteries and insular perforators. The lesion is seated on the interstriate draining system. It drains into the superior striate (*arrowhead*) and atrial veins, inferior striate vein (*double arrowhead*), and into the deep middle cerebral vein and cavernous sinus inferiorly. Note the venous ectasias at the subependymal junction and the persistence of falcine (*arrow*) and occipital (*double arrows*) sinuses

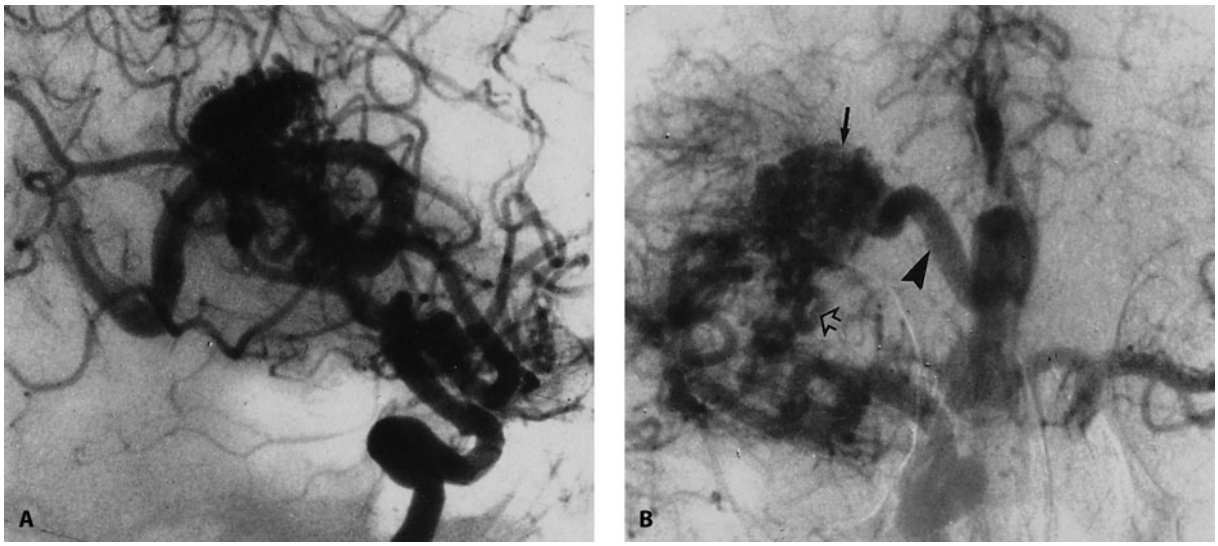

Fig. 9.16A, B. Deep-seated arteriovenous malformation (AVM). **A** Lateral and **B** frontal views of the right internal carotid artery injection. Deep-seated AVM (*arrow*) supplied by lenticulostriate arteries (*open arrow*) and draining exclusively into thalamostriate and internal cerebral veins (*arrowhead*)

veins, with occasional recruitment of transcerebral veins. Similarly, these extra-axial lesions can be distinguished from intra-axially located AVMs using angiographic criteria (Fig. 9.18).

9.3.1.4 Angioarchitecture of Brain Arteriovenous Malformations

Analysis of the angioarchitecture (Table 9.9, p. 633) of BAVMs should include the study of the various components of the lesion (arteries, nidus, and veins) as well as how these components affect the rest of the circulation. It should be able to separate the primary abnormality (AVM) from the host response to the presence of chronic shunting (arterial stenosis or aneurysms, venous stenosis and ectasias). The differentiation between the original disposition, the primary defect, and the acquired features will demonstrate the additional vascular arrangements of the lesion and the remaining vascular system (host) in response to the chronic shunting. Some of the vascular patterns are due to associated anatomical variations that provoke a predictable change while others are acquired and related either to the high-flow character of the lesion (kinking, plications, arterial aneurysms, etc.) or to the development of secondary obstacles (stenosis, venous ectasias) (Fig. 9.15) or both (Fig. 9.22). The high-flow hemodynamics or decreased tissue perfusion associated with AVM shunting can stimulate nonsprouting angiogenesis (Folkman 1986) and development of collateral supply, which may be reversible after elimination or significant partial treatment of the shunt. Temporary or permanent changes may occur following hemorrhagic or ischemic sequelae associated with the AVM (Figs. 9.42, 9.50, 9.52). Thrombosis of a draining vein, development of transdural supply, or intralesional ectasias may occur (Fig. 9.47).

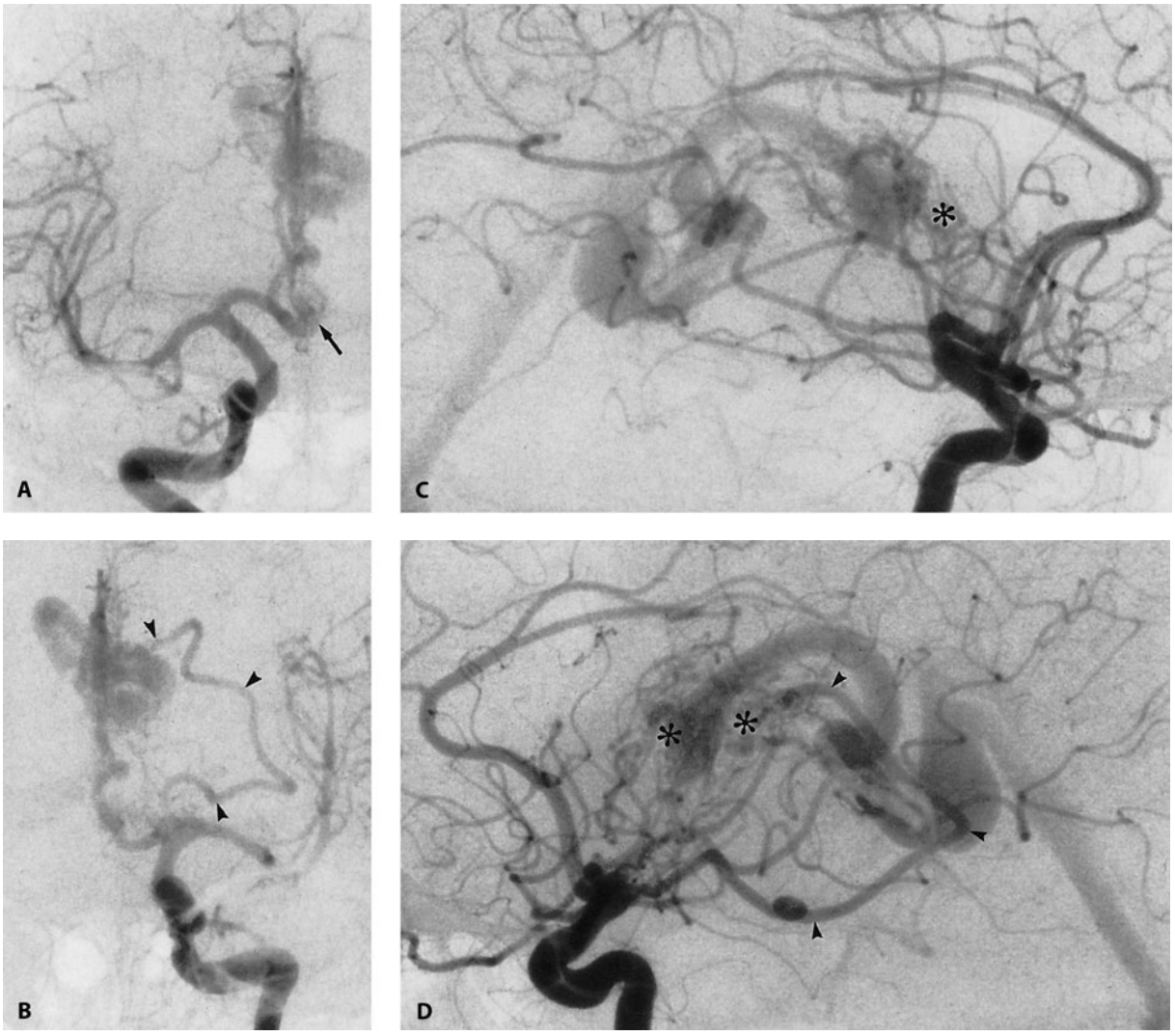

Fig. 9.17A–E. Third ventricle choroid plexus arteriovenous malformation (AVM). **A** Frontal and **B** lateral views of the right internal carotid artery. **C** Frontal and **D** lateral projections of the left internal carotid artery. **E** Vertebral artery injection in lateral view. Third ventricle choroid plexus AVM (*asterisks*, **D**) draining into the choroidal vein and vein of Galen. All choroidal arteries participate in the supply to this lesion, including subependymal perforators arising from the circle of Willis, anterior communicating hypothalamic perforators (*arrow*, **A**), and the anterior choroidal artery (*arrowheads*, **B**, **D**)

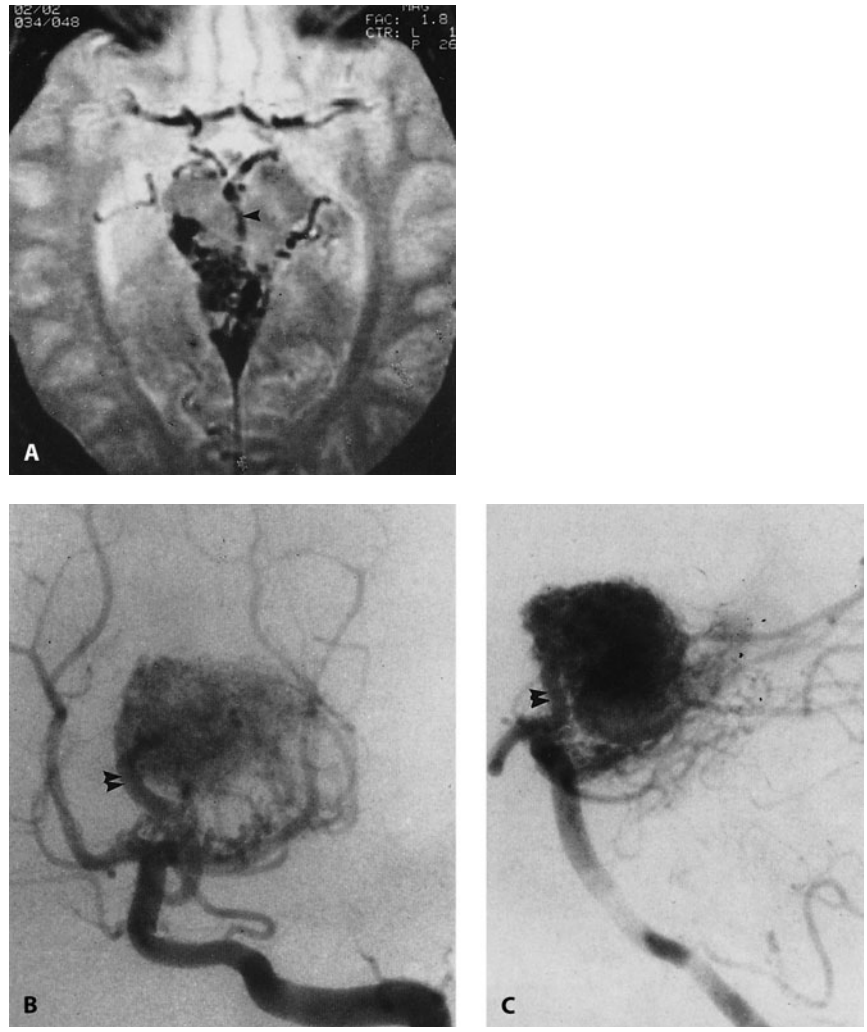

Fig. 9.18A–C. Transmesencephalic supply in a tectal arteriovenous malformation (AVM). **A** Axial MRI study demonstrates the transmesencephalic supply (*arrowhead*) to a tectal AVM. **B** Frontal and **C** lateral views of the left vertebral artery injection in a different patient, demonstrating a thalamoperforating artery supplying a thalamic AVM and projecting above the mesencephalic region (*double arrowhead*)

Table 9.9. Cerebral arteriovenous malformations: elements of angioarchitecture

Arteries	Nidus veins
Direct feeder	Size
Variations	
Indirect feeder	Arteriovenous shunting, ectasias
Leptomeningeal anastomoses	Aneurysm, pseudoaneurysm
Stenotic segments	Pseudoaneurysm, stenosis
Ectatic segments	Thrombosis
Focal (aneurysms)	Flow-related
Dysplastic (remote)	
Pseudoaneurysm	
Generalized	
Dural supply	
Flow-related	

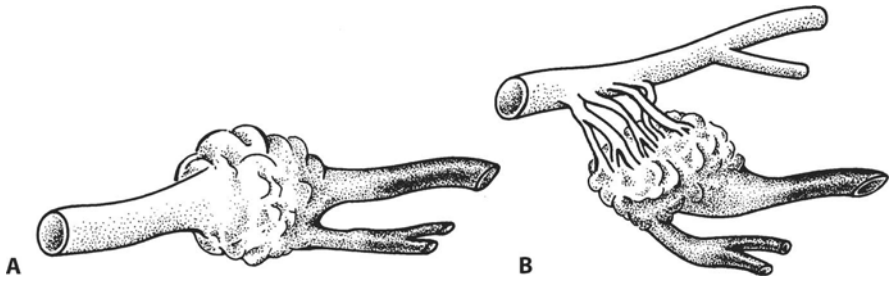

Fig. 9.19A, B. Two types of arterial supply to an arteriovenous malformation nidus: **A** direct and **B** en passage

Knowledge of the potential impact that angiogenic reactions, recanalization of thrombosed channels, and organization of hematomas may have on the AVM and the adjacent circulation is necessary for complete assessment of the lesion (Fig. 9.50). Ignoring these factors may result in misinterpretation of the size of the malformation and its topography.

Arteries

Arterial feeders in arteriovenous shunts can be of different types: (a) direct feeders supply the shunting area as a terminal branch; (b) indirect feeders supply the shunting area *en passage*, i.e., they predominantly supply normal territories and only secondarily the shunt (Fig. 9.19). Indirect feeders may arise from the chronic sump effect of the lesion. As the sump effect increases, indirect feeders can become more involved in the AVM supply (nonsprouting angiogenesis), reestablishing flow into a direct feeder. They will then be responsible for the displacement of watershed areas. Both direct and indirect feeders may develop stenotic segments, which further increases collateral circulation around the AVM. Indirect feeders may also become more prominent following ligation or proximal embolization of direct feeders if the nidus is not completely eliminated.

The various phenomena that increase rheological demands are fundamentally angioectatic. However, the same phenomena can become angiogenic as soon as they produce ischemia. Stenosis of AVM feeders will further decrease tissue perfusion and produce or aggravate existing hypoxia in the surrounding parenchyma and may stimulate further angiogenesis.

Angioectatic and angiogenic responses may develop to such an extent that they can mimic the presence or the development of an additional AVM or the apparent enlargement of the primary lesion. Differentiation of these conditions may be difficult. Angiogenesis (nonsprouting) is observed in ischemic regions at pathology and is also a normal feature of an organizing thrombus (sprouting) (Fig. 9.45). Yasargil (1987) observed such perilesional angiogenesis. Dobbelaere et al. (1979) and Laine et al. (1981) noted that both evolving and recurrent AVMs often present with the same architectural aspect, "a dense capillary bed with no special venous character." Although the changes seem related to neovascularization, there is no in vitro growth of specimens derived from these lesions.

Arterial Enlargement. Arterial enlargement is a purely hemodynamic phenomenon that stimulates natural (anatomically preexisting) channels to supply both the lesion itself and adjacent territories (Figs. 9.20–9.23).

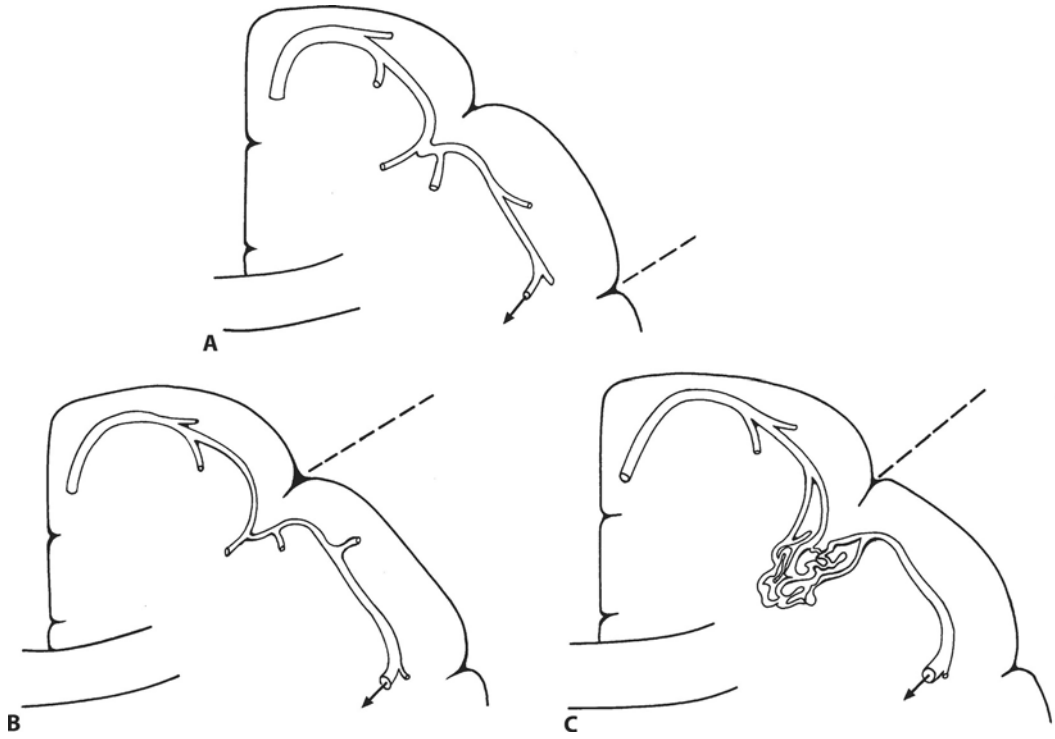

▲ **Fig. 9.20A–C.** Watershed transfer in brain arteriovenous malformations (BAVMs). The three stages in the transfer of the watershed (*dashed line*) in cerebral BAVMs. **A** Congenital transfer of the watershed, as demonstrated by the harmonious decrease in the caliber of the cortical arteries (see Fig. 9.21). **B** Secondary transfer of the watershed demonstrated by the decrease and increase in cortical artery caliber (see Fig. 9.22). **C** Secondary transfer of the watershed zone with postischemic nonsprouting angiogenesis (see Fig. 9.23) at the watershed level

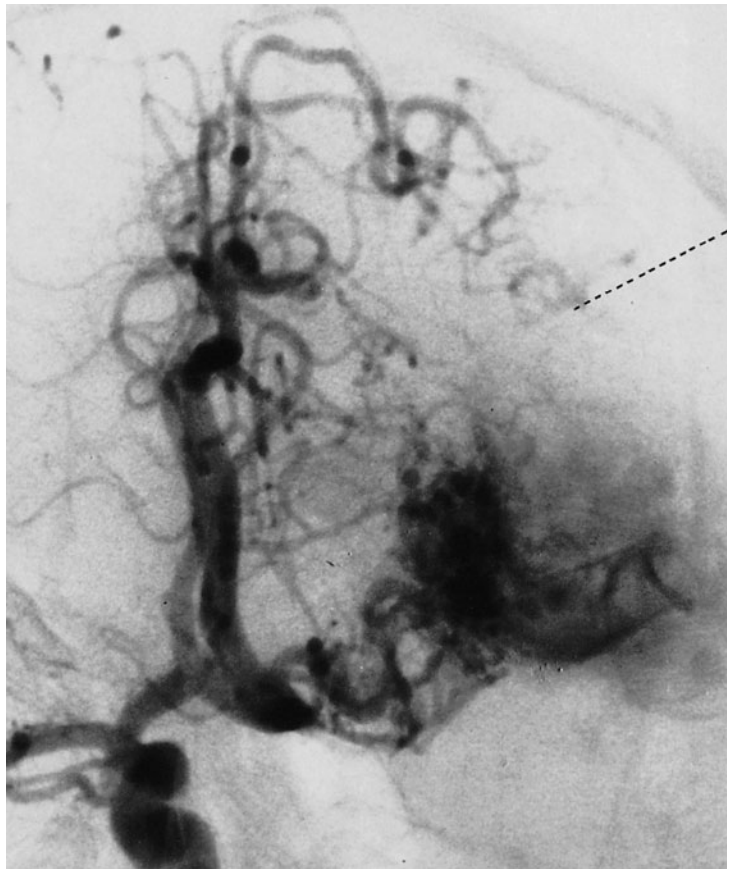

▶ **Fig. 9.21.** Right internal carotid artery injection in frontal view. High-flow left frontal arteriovenous malformation demonstrating congenital transfer of the watershed area of the anterior–middle cerebral artery territories (*dashed line*)

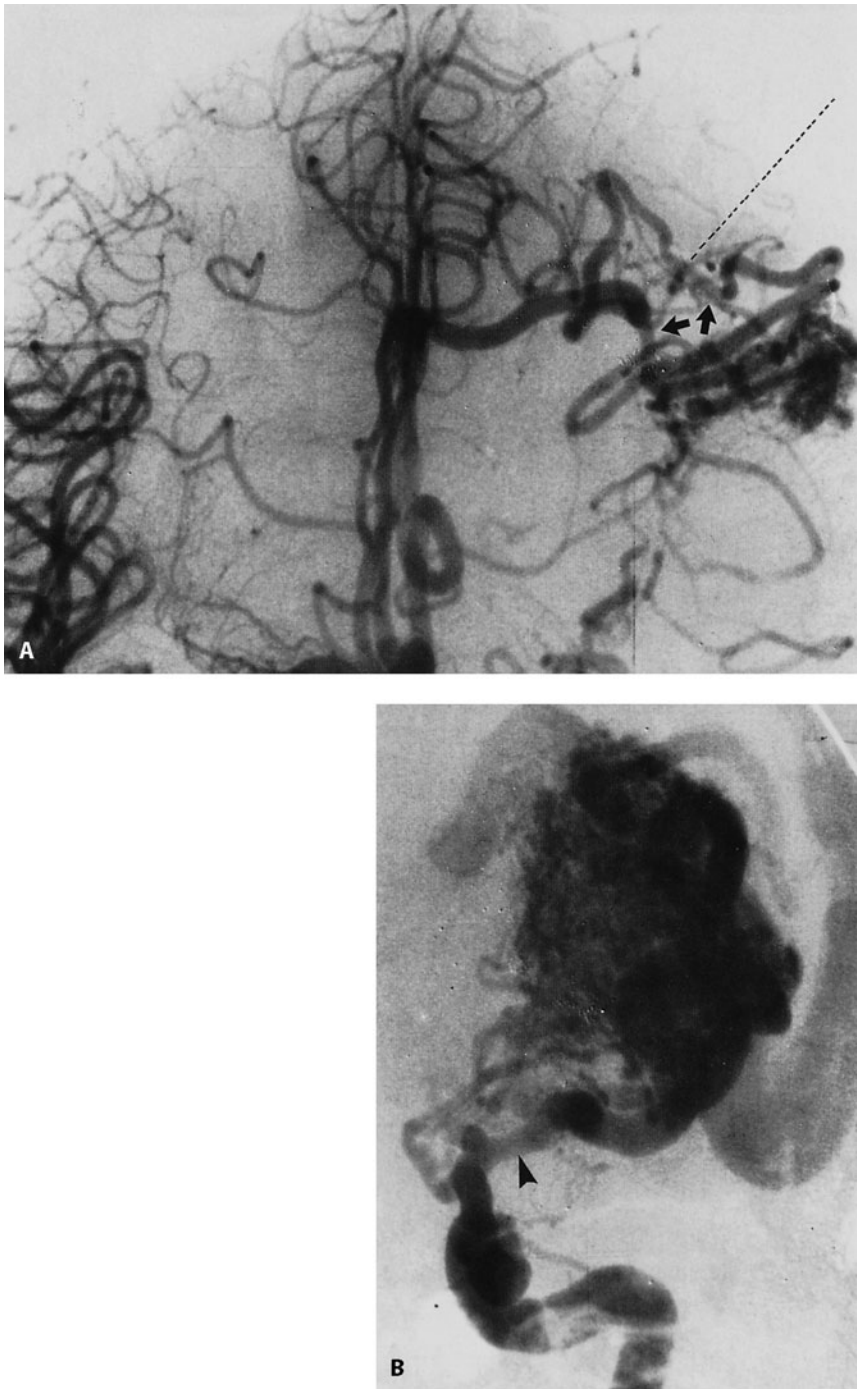

Fig. 9.22. **A** Right and **B** left internal carotid injection in frontal views in a patient presenting with a high-flow frontal arteriovenous malformation (AVM). Note the secondary transfer (*arrows*) of the watershed area between the anterior-middle cerebral artery territories (*dashed line*). Also note the middle cerebral arterial stenosis (*arrowhead*) proximal to the lesion (**B**) secondary to the high-flow angiopathy, therefore testifying to the secondary transfer of the watershed junction distal to the AVM

Within the CNS, such enlargement corresponds to recruitment of leptomeningeal and subependymal anastomoses. Depending on the period when the shunt forms and on the hemodynamic demands of the lesion on the circulation, interference with the usual development of the arterial supply to the normal brain can occur. Such changes may result in the persistence of embryonic vascular arrangements, as seen in vein of Galen aneurysmal malformations.

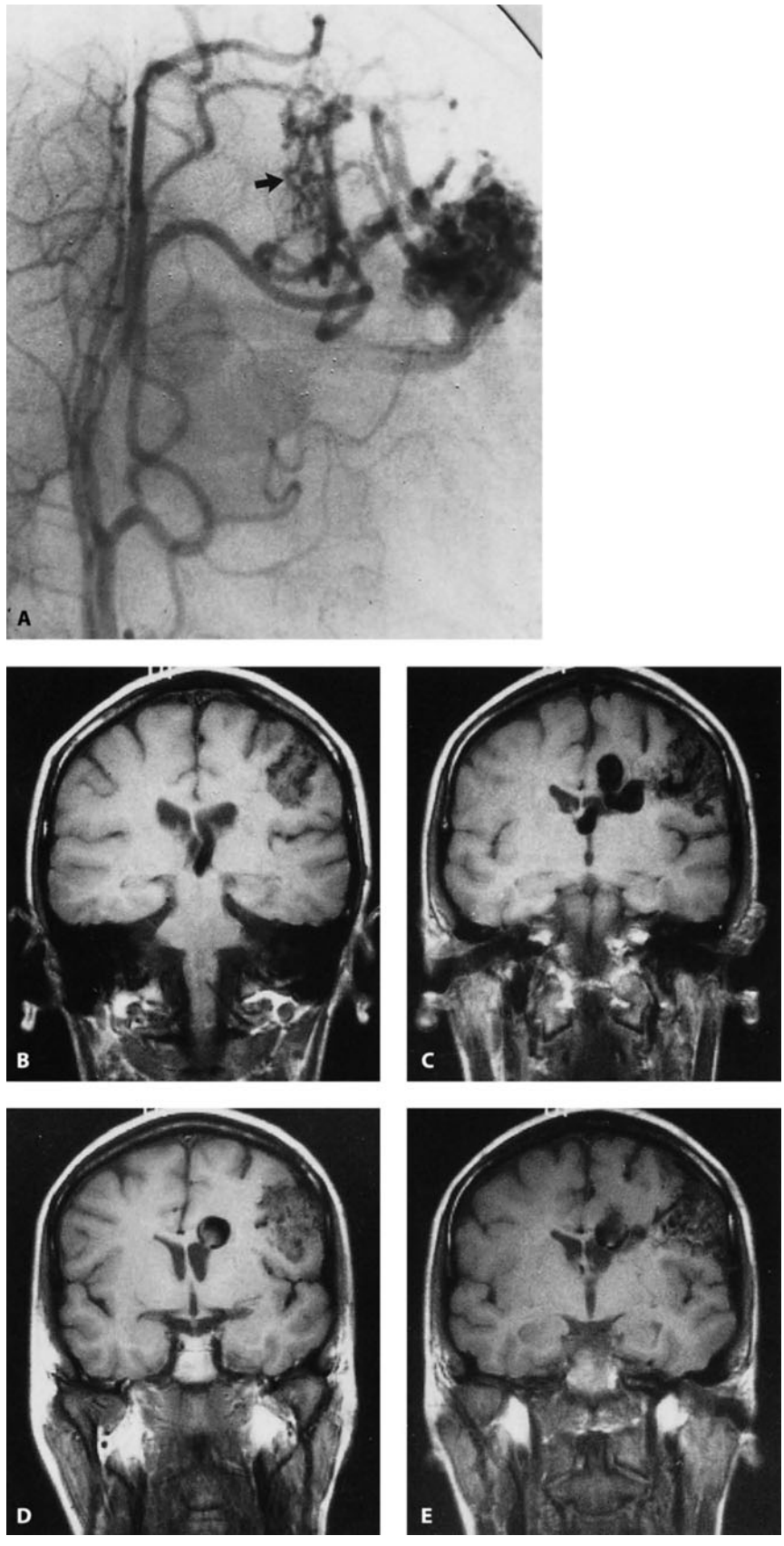

Fig. 9.23. Frontal internal carotid angiogram (**A**). Sulcal arteriovenous malformation with secondary transfer of the anterior-middle cerebral watershed area, representing leptomeningeal nonsprouting angiogenesis (*arrow*). **B–E** Coronal MRI confirms the absence of a true malformed nidus in that region. Note the absence of venous drainage at the level of the secondary angiogenesis

Table 9.10. High-flow angiopathy in the rabbit (from Pile-Spellman et al. 1986)

Luminal protrusion of the endothelial cells with desquamation
Smooth-muscle vacuolization
Mesenchymal cell proliferation
Corrugation and destruction of the internal elastic lamina
Capillary proliferation in the adventitia
Fenestrated and leaky endothelial junctions

Capillary proliferation is part of the constellation of findings constituting the high-flow angiopathy (Pile-Spellman et al. 1986) (Table 9.10). Some of these features of induced angiogenesis can regress following occlusion of the dominant shunt. However, this outcome is not predictable and failure to completely occlude a dominant shunt will often transform such accessory supply into a more prominent one.

Stenotic Changes. Stenosis of feeders to vascular malformations is also seen as part of the high-flow angiopathy disorder (Table 9.10). Intraluminal protrusion of the endothelial cells and mesenchymal cell proliferation may result in intraluminal stenosis (Fig. 9.29).

A so-called moyamoya phenomenon is infrequently associated with BAVMs (Mawad et al.1984; Kayama et al.1986; Montanera et al. 1990).

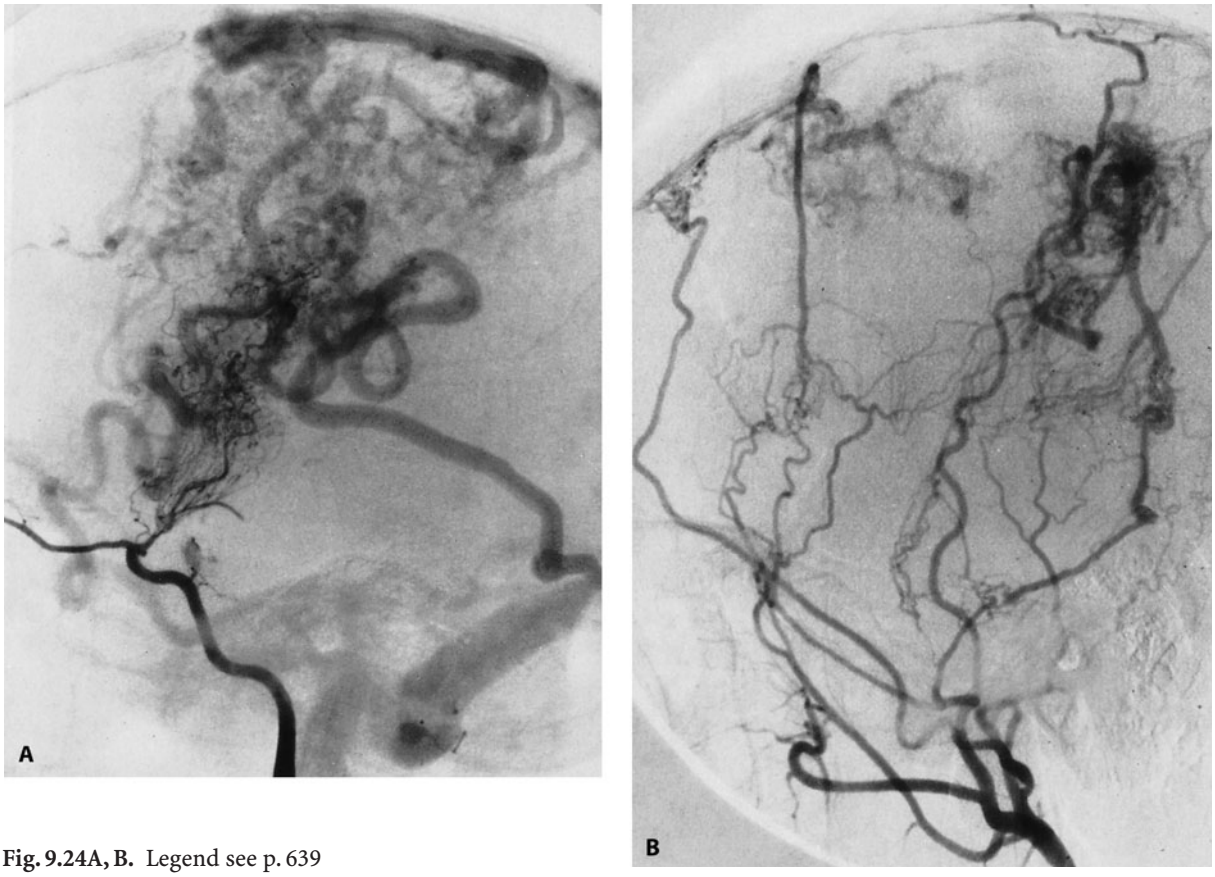

Fig. 9.24A, B. Legend see p. 639

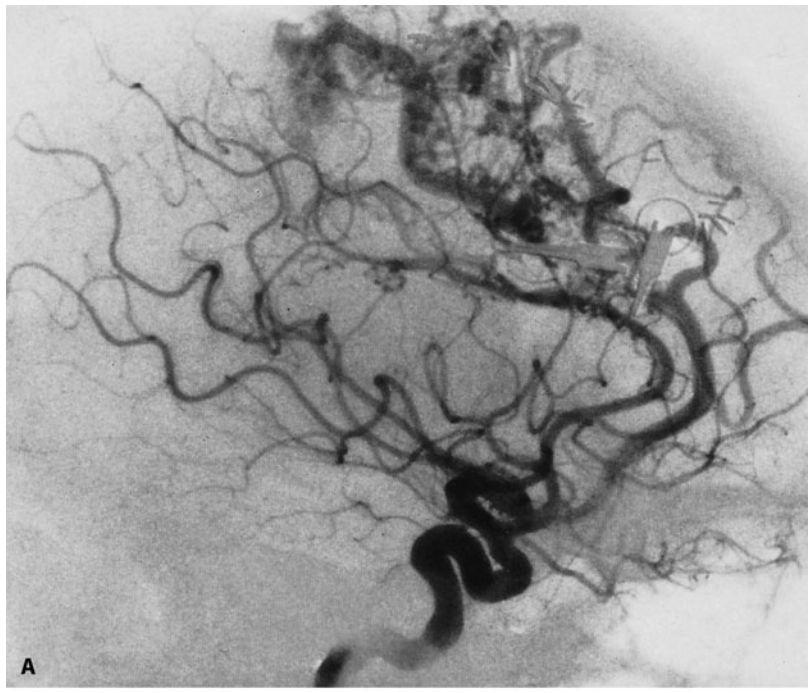

◀ **Fig. 9.24A, B.** Moyamoya type of supply to a brain arteriovenous malformation (BAVM). **A** Left internal carotid and **B** internal maxillary injections in lateral view. Moyamoya-type supply to a frontal AVM, interpreted as the final evolution of the high-flow angiopathy. Note the transdural supply into what was considered to be normal cortical territories (**B**)

Fig. 9.25. **A** Right internal carotid and **B** vertebral artery injections in lateral view. In a medial frontal arteriovenous malformation (AVM), note the early nonsprouting angiogenesis (*arrowheads*, **B**) around what appears to be remaining AVM, following attempted surgical removal of the lesion. These changes illustrate the early stages of the vascular response to the persistent shunt and to the previous ligations at surgery

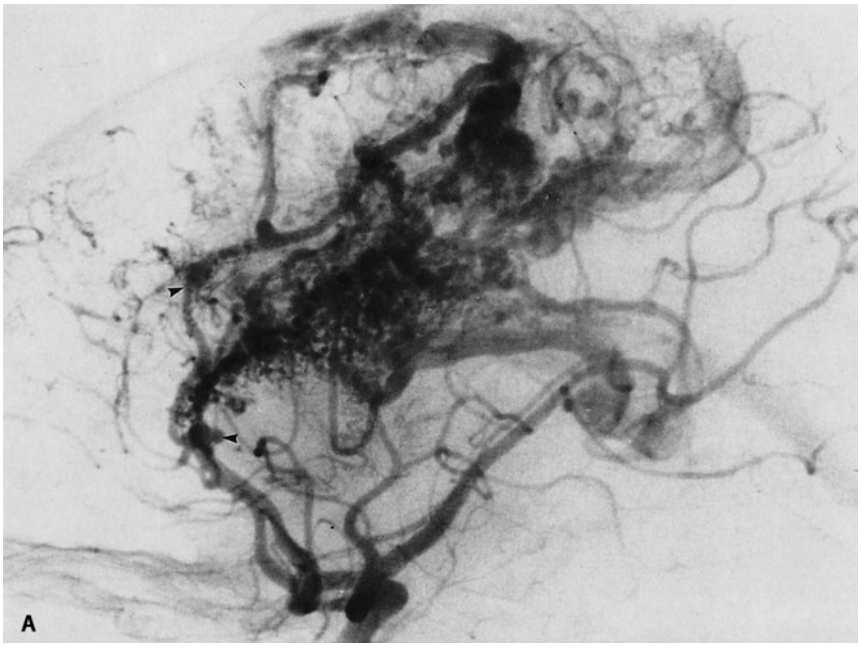

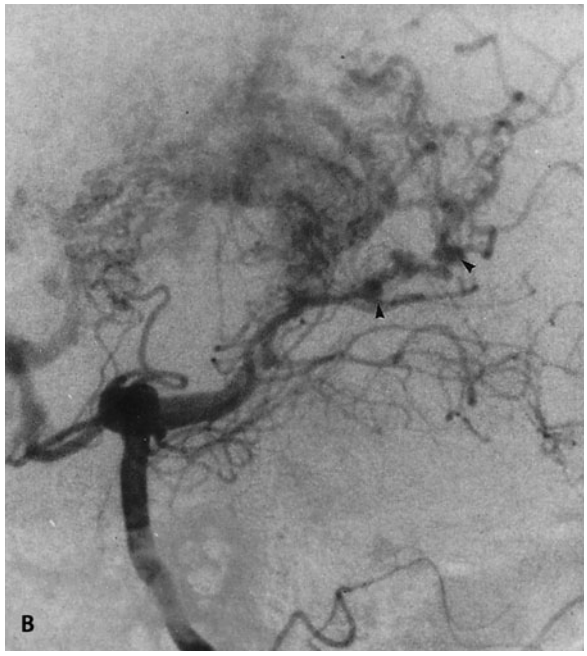

Fig. 9.26. **A** Right internal carotid and **B** left vertebral artery injections in lateral view of a corticocallosal arteriovenous malformation. The high-flow angiopathy has modified the aspect of the lesion, with multiple arterial stenoses and ectasias (*arrowheads*). The nonsprouting angiogenesis makes the limits of the nidus difficult to recognize. This stage is considered as a pre-moyamoya situation

Suzuki reports a 3% incidence while Yasargil (1987) noted only a 0.3% incidence in his experience (Fig. 9.24, p. 638). Mawad et al. (1984) and Montanera et al. (1990) hypothesized that high flow through the feeding vessels to the AVM led to intimal proliferation, stenosis, and eventually occlusion of these vessels as an individual host response to the presence of the AVM. The ischemic brain as well as the low resistance of the AVM nidus distal to the arterial stenosis or occlusion stimulate vascular channels (nonsprouting angiogenesis) (Fig. 9.25, p. 638). This process does not appear to be reversible. It is not known whether this phenomenon has a

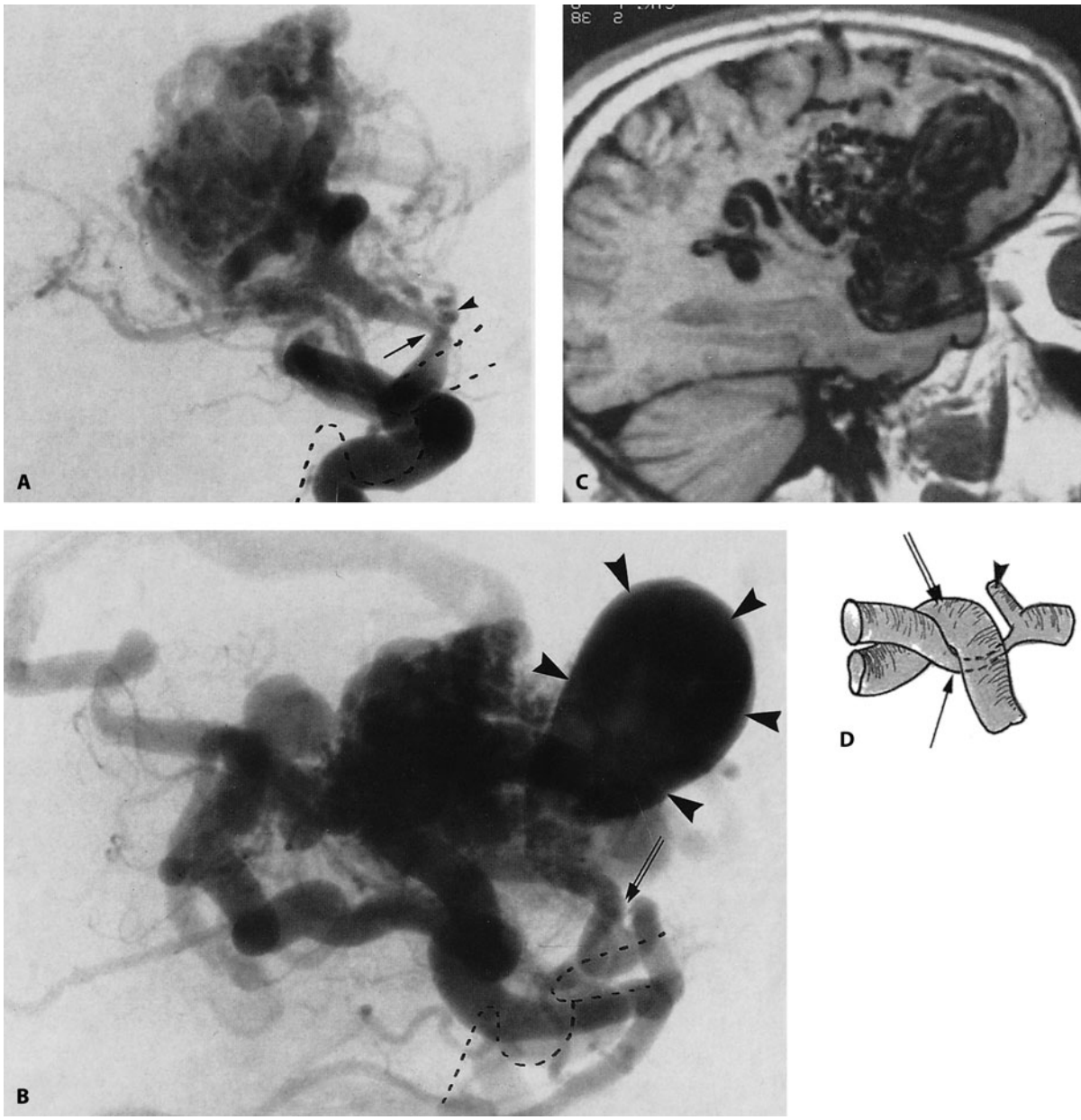

Fig. 9.27. Early (**A**) and late phase (**B**) of the right internal carotid injection in lateral view. Sagittal MRI study (**C**). Deep frontal arteriovenous malformation fed by stenotic frontal branches from the ipsilateral middle cerebral artery (*arrow*). Note the presence of a large, deep-seated, venous ectasia (*arrowheads*, **B**), which, in conjunction with the remaining nidus and congested medullary vein, is producing a mass effect on the stenosed arterial feeder. Note the apparent strangulation of the feeder around the vein (*double arrow*) and the mass effect on the sphenoid ridge (*single arrowhead*, **A**). The changes associated with the high-flow angiopathy can also explain this stenotic aspect. **D** The mechanism of arterial stenosis produced by venous dilatation

protective effect with respect to future hemorrhage from the AVM or a worsening effect related to the fragility of the moyamoya vascular network, similar to that observed in moyamoya disease (Suzuki 1986).

The extreme of this process leads to upstream arterial narrowing, extensive leptomeningeal and transdural collateral flow to an area of arteriovenous shunting that hardly resembles a typical BAVM. The authors in fact question whether this process, called proliferative angiopathy, is a variation in the spectrum of BAVMs or indeed is a condition which mimics such lesions and should be considered a false AVM (Fig. 9.26). Recognizing proliferative angiopathy is important as management will differ from that of a characteristic type of BAVM.

Rarely, arterial stenosis is extrinsic (bony or dural compression, venous compression, etc.) and such stenosis can be reversible if the external mechanical constraint is relieved. Extrinsic narrowing is usually encountered in high-flow lesions with mass effect (Fig. 9.27).

Other caliber irregularities can be seen following embolization (Fig. 9.28), surgical excision of the AVM, or during the progression of a stenotic process. The apparent increased diameter of the opacified lumen, however, actually remains within the size of the direct feeder in its original state.

Vasospasm. Vasospasm is very rare after hemorrhage from a BAVM. Parkinson and Bachers (1980), for example, reported only a 1% incidence of vasospasm following hemorrhage from BAVMs. This is reasonable, as it is believed that all CNS AVMs are located subpially. This is the compartment into which hemorrhage will most likely occur, and subpial hemorrhage would not be expected to produce the same effect as aneurysm rupture into the subarachnoid space. When present, vasospasm should therefore raise the suspicion of an associated ruptured aneurysm as the symptomatic cause of the hemorrhage (Fig. 10.8).

Dural Supply. Dural supply to cerebral arteriovenous shunts also attests to the hemodynamic and angiogenic effects of the BAVM. Two types of dural supply can be described: (a) direct supply to the BAVM through dural leptomeningeal anastomosis (Newton and Cronqvist 1969) (Fig. 9.29) and (b) indirect supply via anastomosis to normal cortical feeding arteries on the way to the BAVM (Russell and Berenstein 1981). Dural supply was noted in 27% of Newton's (1969) series and in 32% of the Bicêtre series (Willinsky et al. 1988b).

Both types of dural blood vessel involvement can be induced by surgery, when adhesions occur between dural layers. Meningeal supply has also been noted to develop following partial embolization, probably the response to ischemia that induced (nonsprouting) angiogenesis. Subarachnoid hemorrhage is an additional factor that may induce dural supply. In Faria and Fleischer's (1980) series, six of the seven patients who presented with dural supply had bled. Although no definite correlation has been established between dural supply to a lesion and the clinical history of hemorrhage, one should keep in mind that at surgery there is frequently evidence of previous subclinical bleeding. In our experience, there appears to be a positive correlation between headaches and the presence of dural supply to a BAVM.

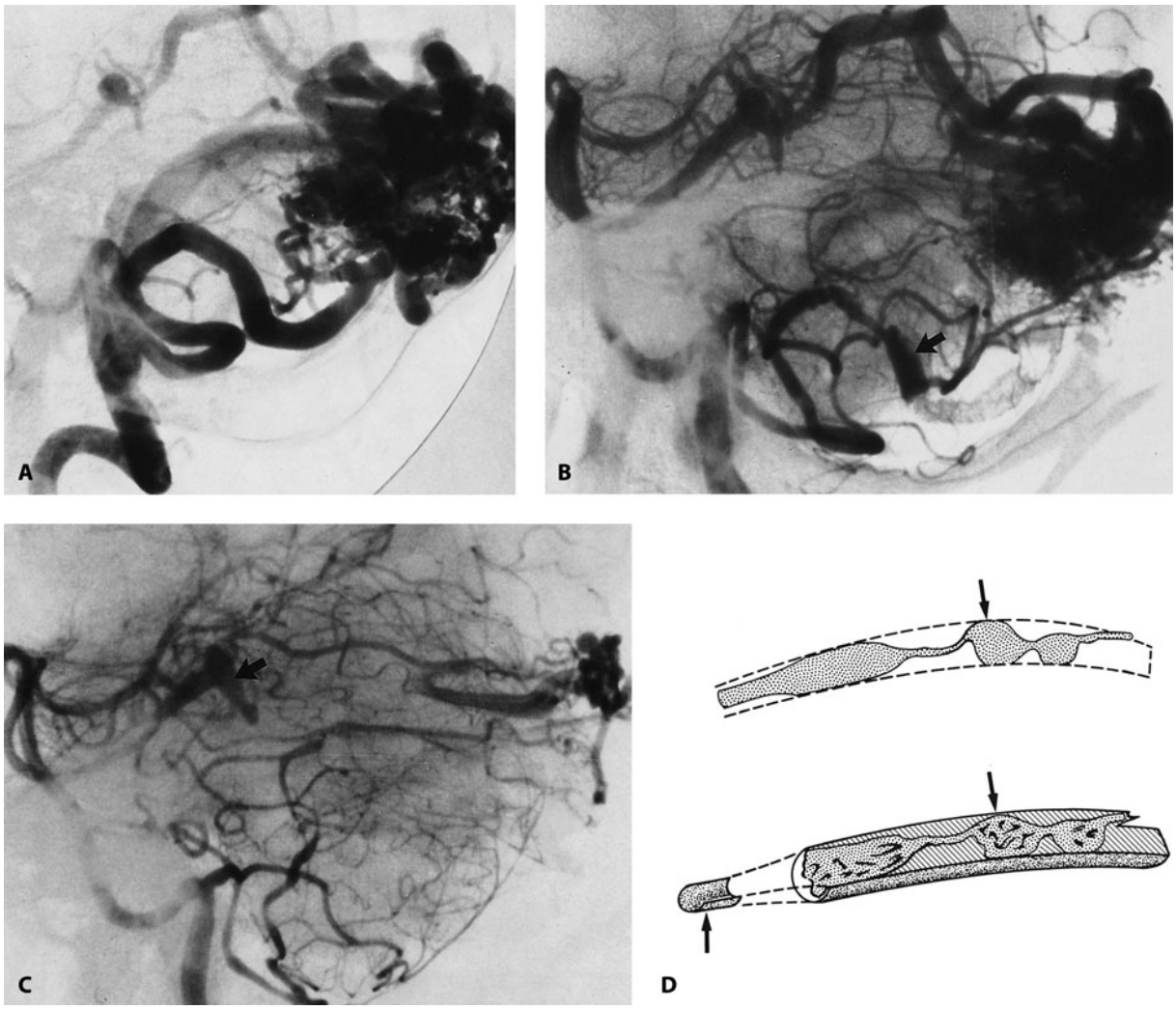

Fig. 9.28. **A** Left vertebral artery injection in lateral view, prior to embolization and after partial treatment (**B**) in a patient who presented with a cerebellar and vermian arteriovenous malformation. Three months after the first session of embolization of the posterior inferior cerebellar artery, note the caliber changes in the proximal aspect of the vessel mimicking an aneurysm (*arrow*). **C** After additional embolization of the anterosuperior cerebellar artery contribution to the lesion, note similar changes onto the artery embolized. The remaining nidus was removed surgically. **D** The progressive and irregular changes in vessel caliber that may occur proximal to the occlusion. The regression of the increased caliber may occur with or without associated acrylic deposition and proximal intraluminal clot resorption. Additional regression will bring the feeding artery into an almost normal aspect, as demonstrated on the last vertebral control angiogram (**C**). These irregularities do not carry any risk of rupture, despite their pseudoaneurysmal aspect

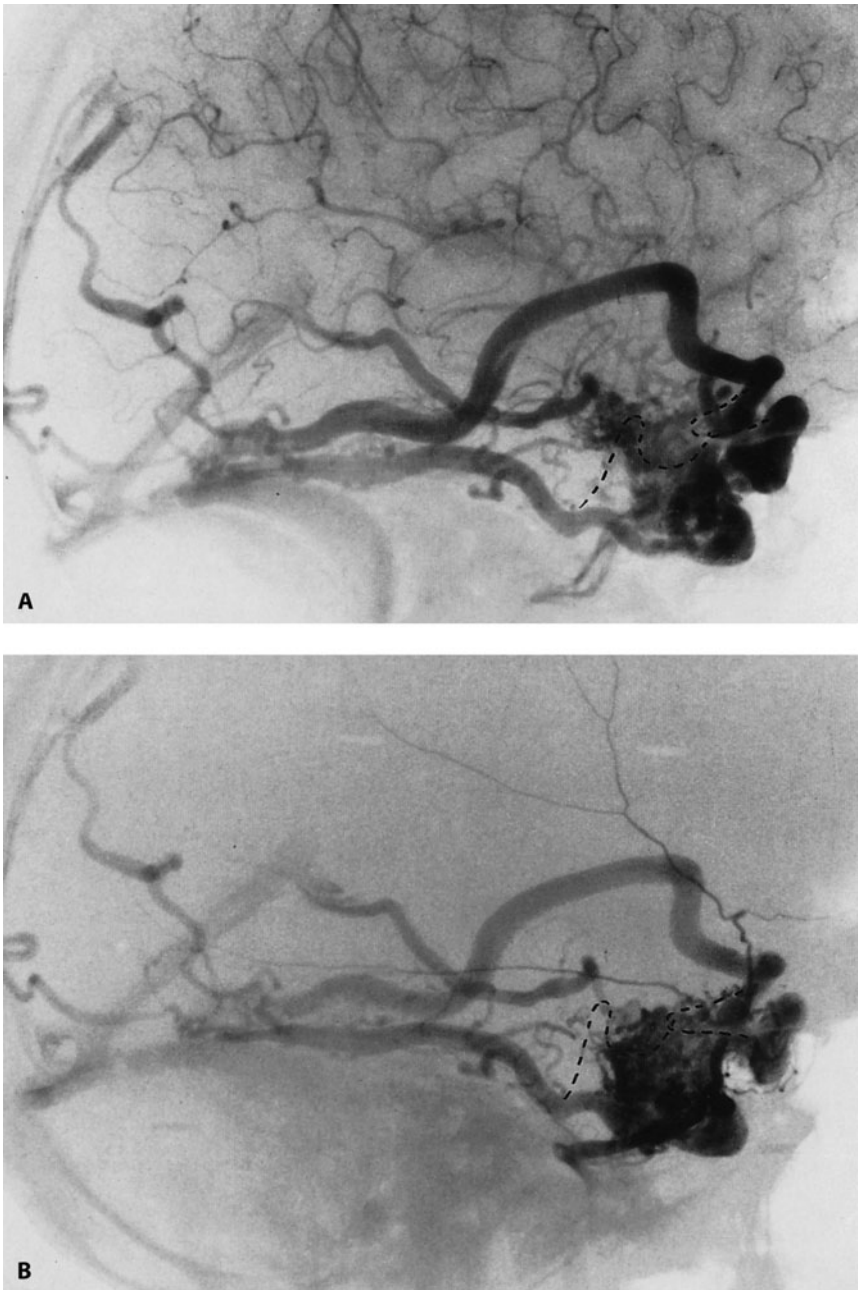

Fig. 9.29. **A** Right internal carotid artery in mid-arterial phase and **B** ipsilateral middle meningeal artery injections in lateral projection. Temporal pole arteriovenous malformation in which the transdural supply opacifies the entire nidus and all the draining venous system

In rare instances, dural supply can be seen in the presence of a separate dural sinus arteriovenous shunt in the area of the BAVM (Fig. 9.30). The etiological relationship between these two conditions is most of the time not easy to establish, but in some cases we have seen high-flow dural AVFs that apparently were able to induce pial arteriovenous shunting. Acquired BAVFs can be reversed following successful treatment of the dural AVF.

Arterial Variations. Arterial variations seem to be more frequent in patients with BAVM (24%, Willinsky 1988) than in patients evaluated for occlusive disease or in autopsy series. They are known to be associated

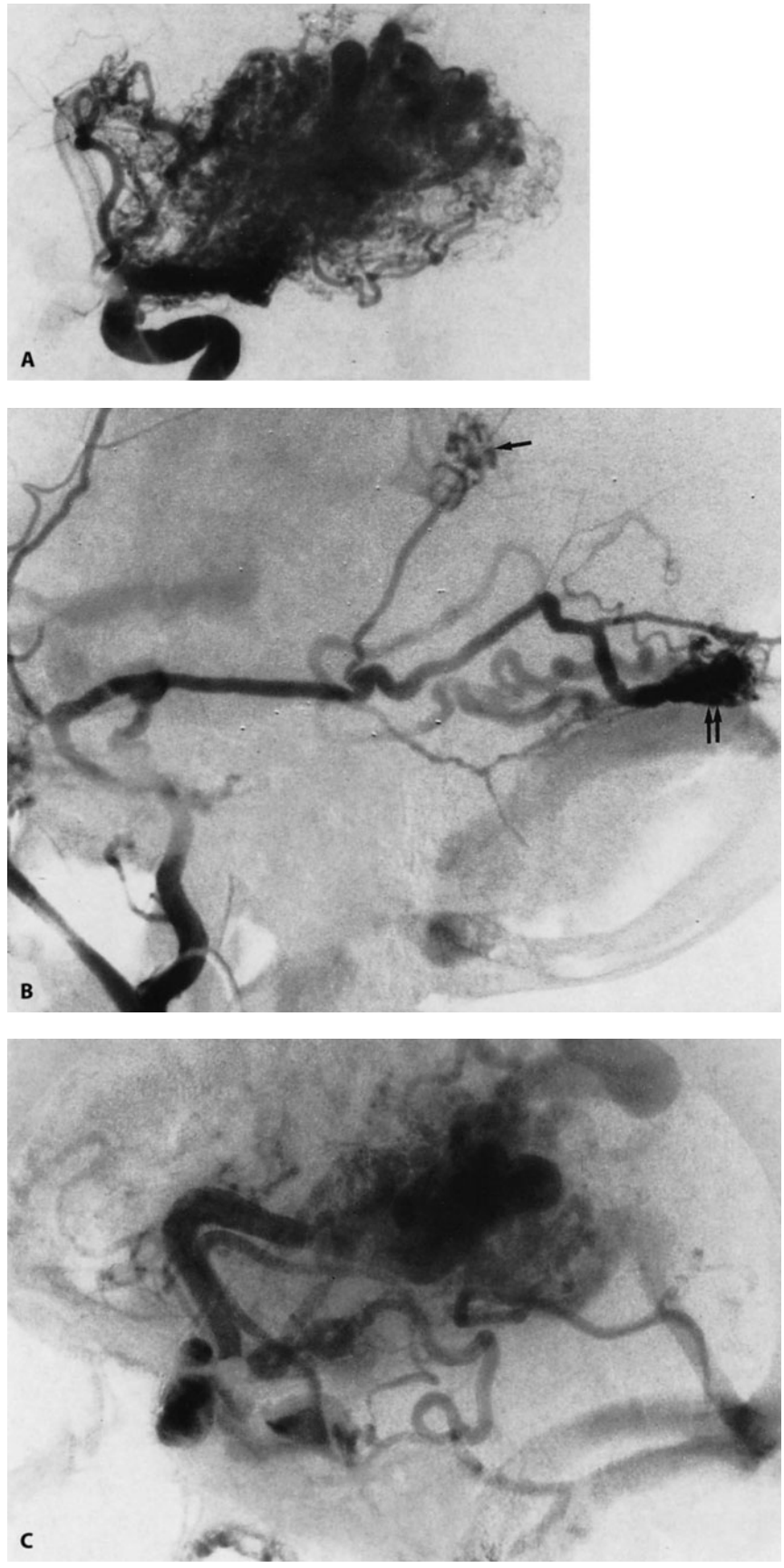

Fig. 9.30. **A** Left internal carotid and **B** internal maxillary artery injections in lateral view. Large temporal arteriovenous malformation. Note the transdural supply to the lesion (*arrow*) and the associated arteriovenous shunt separate from the pial nidus (*double arrow*). **C** Late venous phase of the internal carotid angiogram confirms the absence of a connection between the dural and the pial nidi

with arterial aneurysms, but the prevalence in these circumstances has not been systematically analyzed. Their presence is often underestimated because most investigators do not recognize them as such. Variations at the level of the larger vessels (carotid, vertebral), with persistence of embryonic dispositions (trigeminal, hypoglossal, etc.), seem only moderately increased in BAVM patients as compared to their slightly increased incidence in patients with aneurysms. Conversely, variations of the posterior and anterior portions of the circle of Willis are not infrequent in the BAVM group. These variations are noted mainly when the area of shunting is located at the watershed zone. When the lesion develops within the dominant area of supply, only the distal branching pattern of anastomotic arteries shows anatomical variations. Many of these variations remain remote from the area of actual arteriovenous shunting and probably are incidental occurrences. Only VGAM (vein of Galen malformation) seems to be frequently associated with a primitive disposition, such as the limbic arterial ring (Vols. 1 and 3), as if the early presence of the shunt prevented normal maturation of the vasculature in the region. Correction of the shunt allows this maturation to occur secondarily with disappearance of the primitive disposition (Vol. 3). It is therefore important to know the arterial territories of these variants, in order to predict potential risks of endovascular treatment. These are in the distribution of the artery of the corpus callosum, accessory middle cerebral artery, duplicated posterior communicating artery, etc. In addition, these anatomical arrangements may represent locations that favor the development of flow-related aneurysms.

Arterial Aneurysms. The reported association between arterial aneurysms (AAs) and cerebral AVMs varies from 2.7% (Paterson and McKissock 1956) to 16.7% (Miyasaka et al. 1982). The difficulties in understanding the link between BAVM and arterial aneurysm are due in part to the underestimation of their association. In the series reported by Graf et al. (1983) and Perret and Nishioka (1966), only 6%–7% of patients presented with aneurysms. These numbers are low compared to reports of series benefiting from complete, high-quality, diagnostic, and superselective angiography (Lasjaunias 1988a; Turjman et al. 1994; Redekop et al. 1998; Meisel et al. 2000). In the Toronto and the Bicêtre series, the incidence of associated aneurysms with BAVMs was 15% and 46%, respectively, and the number of associated aneurysms increased with the size of the AVM.

The presence of arterial aneurysms has been thought to constitute a marker for increased risk for future hemorrhage that needs to be taken into consideration in the management strategy. Brown et al. (1990) demonstrated a twofold (7% vs. 3.5%) increased risk for future hemorrhage in patients with BAVM and aneurysms who had not previously bled. There are three types of arterial aneurysms associated with BAVMs: (a) flow-related aneurysms, (b) intranidal aneurysms, and (c) dysplastic or remote aneurysms (Fig. 9.31)

Flow-Related Aneurysms. Flow-related aneurysms develop on the pedicle supplying the BAVM. Two types can be recognized: those that are upstream and some distance away from the AVM nidus (proximal arte-

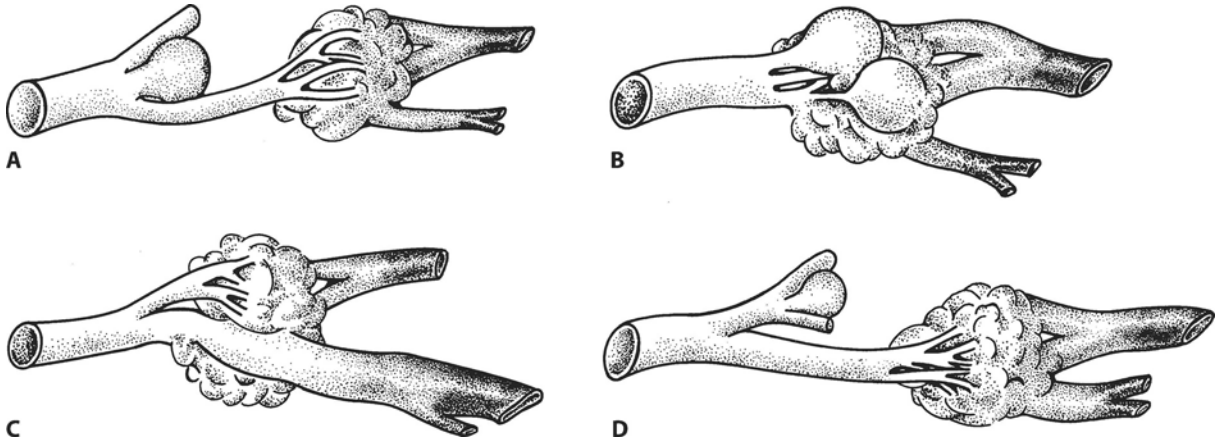

Fig. 9.31. Schematic drawing of flow-related aneurysm (**A**), intralesional arterial ectasias (**B**), intralesional direct arteriovenous fistulae (**C**) and dysplastic (remote) aneurysm (**D**) in brain arteriovenous malformations

Fig. 9.32. Vertebral artery injection in frontal view demonstrates P1 (*arrow*) and posterior communicating (*double arrows*) flow-related aneurysms in a frontoparietal arteriovenous malformation

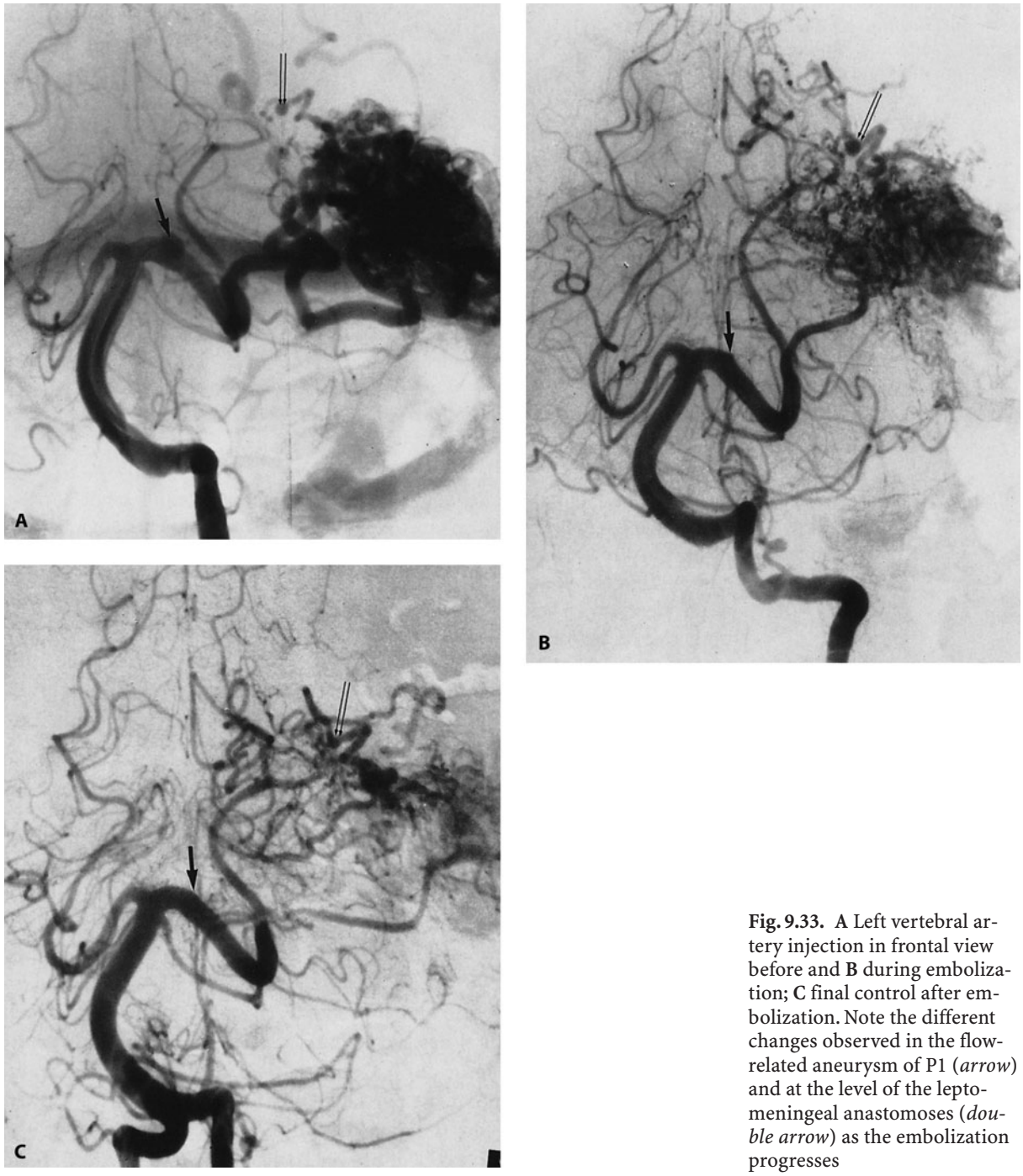

Fig. 9.33. **A** Left vertebral artery injection in frontal view before and **B** during embolization; **C** final control after embolization. Note the different changes observed in the flow-related aneurysm of P1 (*arrow*) and at the level of the leptomeningeal anastomoses (*double arrow*) as the embolization progresses

rial aneurysms) (Fig. 9.32) and others that are located farther downstream on the feeding pedicle closer to the nidus (distal arterial or prenidal aneurysms) (Fig. 9.33–9.35). It is believed that 37%–82% of arterial aneurysms are flow related (Batjer et al. 1986; Lasjaunias et al. 1988a; Meisel et al. 2000). This includes ectasias and infundibula greater 3 mm in size (Hayashi et al. 1981; Miyasaka et al. 1982; Batjer et al. 1986).

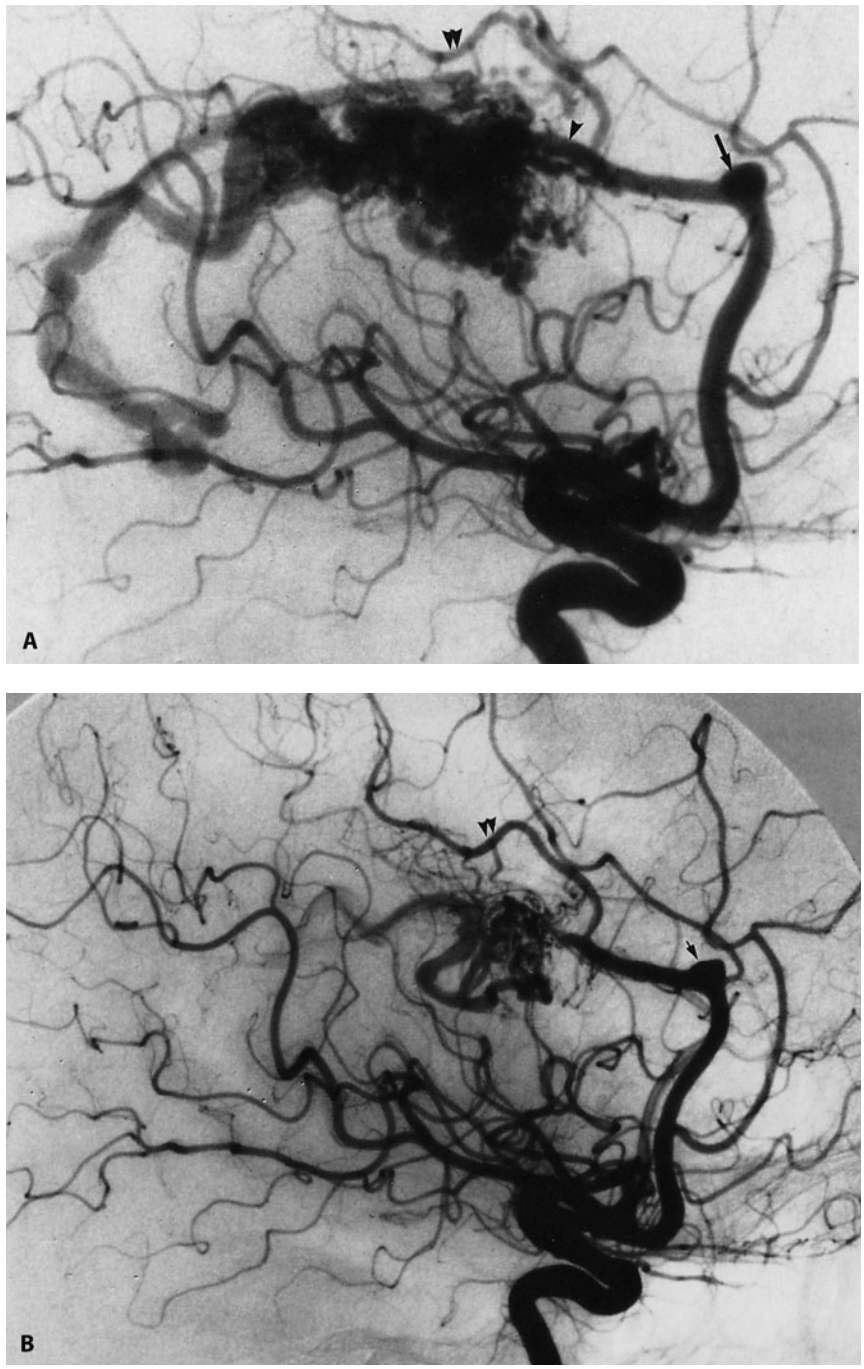

Fig. 9.34. Left internal carotid injection before (**A**) and after (**B**) partial embolization with glue. Note the preexisting direct (*arrowhead*) and indirect (*double arrowhead*) supply, and the proximal, flow-related, arterial aneurysm (*arrow*). Following embolization, the nidus is partially excluded. The en passage supply is well demonstrated. Further embolization will later exclude the lesion entirely. The aneurysm will not be treated and will disappear completely

In the literature, the relationship between the development of arterial aneurysm and the flow of the AVM is mentioned in such diverse ways that a clear-cut approach to the problem cannot be found. However, Okamoto et al. (1984) and Hayashi et al. (1981) demonstrated that patterns of aneurysm distribution in patients with BAVMs were significantly different than in patients without BAVMs. Hayashi's review of 112 aneurysms in 74 patients with BAVMs showed a high incidence of aneurysms in areas where aneurysms usually do not occur, i.e., peripheral, lenticulostriate,

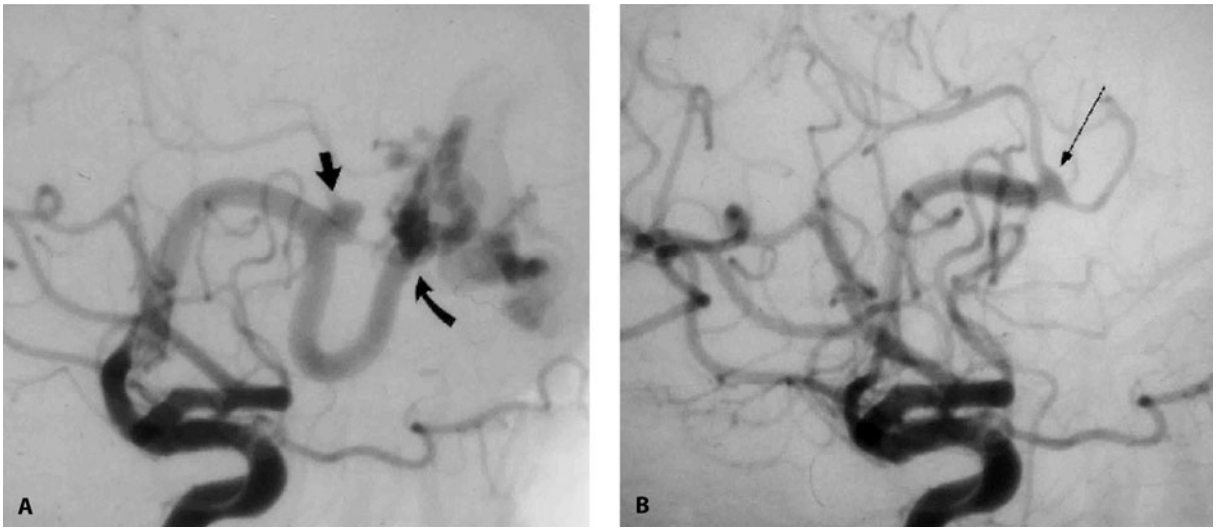

Fig. 9.35A, B. Right internal carotid angiogram in lateral view (**A**) demonstrates aneurysm (*arrowhead*) on feeding pedicle toward frontal lobe arteriovenous malformation (AVM, *curved arrow*). Two months following arterial embolization of the AVM with glue, the right internal carotid angiogram in lateral view (**B**) demonstrated complete regression of the aneurysm (*arrow*)

anterior choroidal, etc. In AVM patients, the great majority of aneurysms were noted on the feeding arteries of the AVMs, irrespective of the circulation. This finding was confirmed in our analysis (Lasjaunias et al. 1988a; Meisel et al. 2000). It is therefore apparent that the presence of a BAVM predisposes one to the formation of aneurysms on the feeding vessels. The exact pathogenesis of the BAVM and the aneurysm are, however, probably not related to the same developmental abnormality.

The link between BAVM-associated aneurysms and increased flow to the malformation has long been suspected (Anderson and Blackwood 1959). Arterial aneurysms have been observed to develop on the internal carotid artery years after a surgical occlusion of the contralateral internal carotid artery (Somach and Shenkin 1966). They also developed on the superficial temporal artery after a surgical anastomosis of this vessel to a sylvian branch (Lantos et al. 1984). Experimentally, in high-flow angiopathy (Pile-Spellman et al. 1986), vessel changes proximal to the shunt involving the internal elastic lamina have been demonstrated (Table 9.10). These changes may predispose one to the development of an arterial aneurysm. Further progression these induced changes could lead to specific clinical manifestations and complications (ischemic symptoms or rupture of an aneurysm). Therefore, when present, an arterial aneurysm worsens the prognosis of the AVM.

While the risk for future hemorrhage was shown to be increased in patients with BAVM and AA (Brown et al. 1988), several important questions remain. Does this risk vary according to the location of the AA in relationship to the AVM nidus and should one anticipate the AA as responsible for the future hemorrhage or is the presence of an AA merely a marker of a more fragile vascular tree (including the AVM) (Figs. 9.36, 9.37). Redekop et al. (1998) demonstrated a clear difference in the hemor-

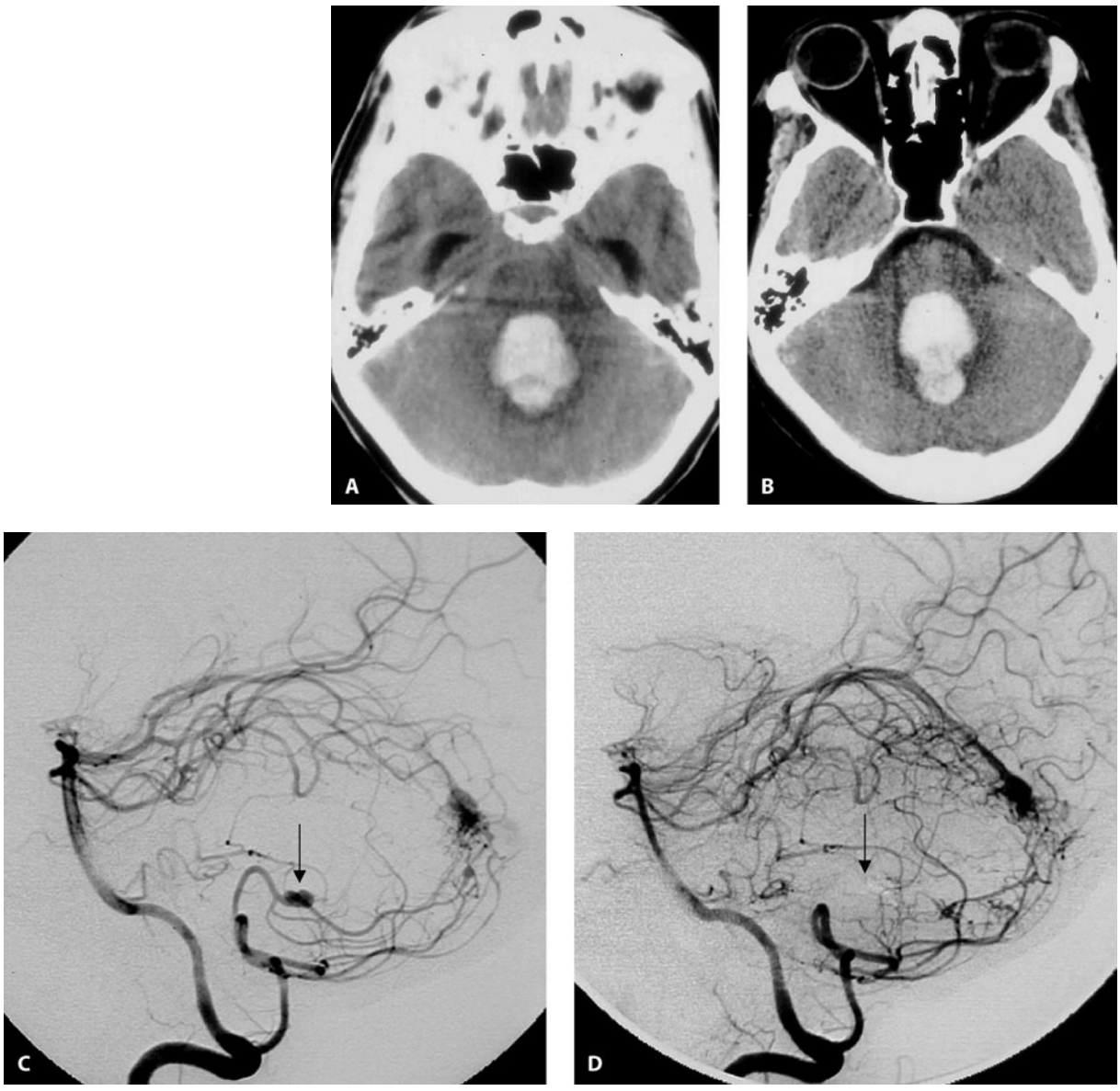

Fig. 9.36. Patient presented in poor clinical grade and showed on CT (**A**) evidence of intraventricular and parenchymal hemorrhage adjacent to the 4th ventricle. Repeat CT (**B**) 5 days later showed additional hemorrhage, which on angiography at presentation (not shown) was demonstrated to be caused by an aneurysm on the feeding pedicle (PICA) toward a vermian arteriovenous malformation (AVM). Repeat vertebral angiogram in lateral view (**C**) after second hemorrhage demonstrated enlargement of the proximal (pseudo-) aneurysm (*arrow*). Treatment was carried out toward the symptomatic aneurysm and the feeding pedicle, which were embolized with glue (*arrow*) and shown to be obliterated on the immediate as well as the 2-month postembolization vertebral angiogram in lateral view (**D**) prior to surgical resection of the residual AVM nidus

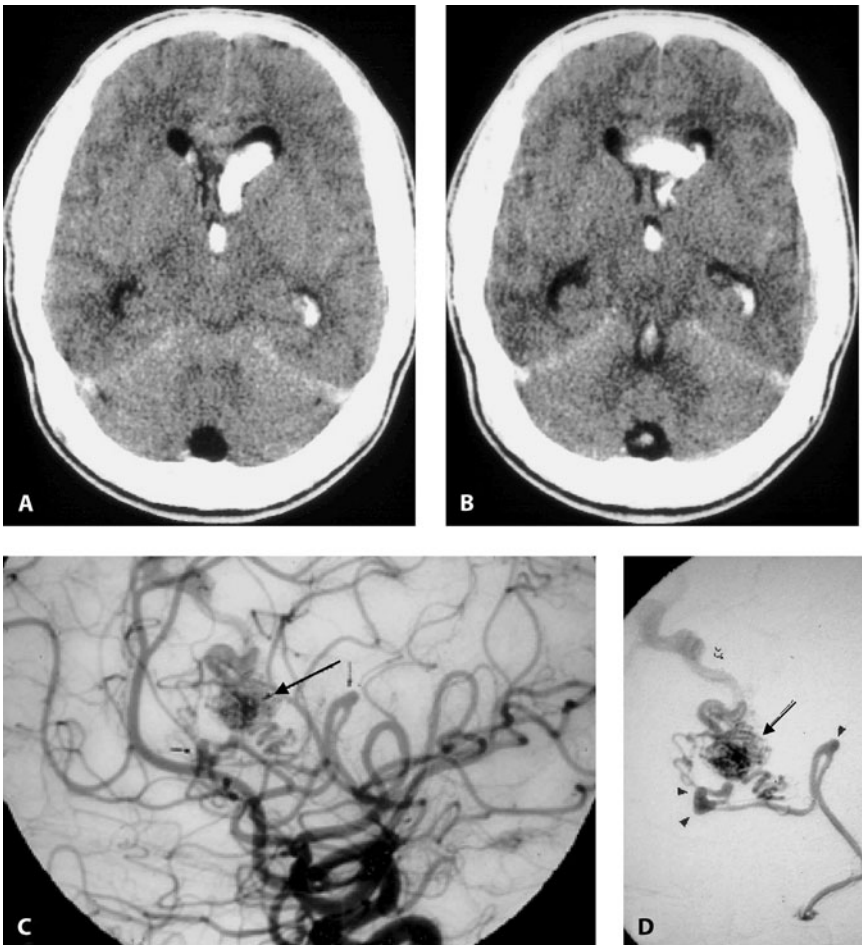

Fig. 9.37. CT at initial presentation (**A**) and 3 months later (**B**) shows repeated bleeding (IVH, intraventricular and intracerebral hemorrhage), which was demonstrated on left internal carotid angiogram in lateral view (**C**) and selective angiogram (**D**) to be caused by small size deep-seated frontal lobe arteriovenous malformation (*long arrows*) associated with prenidal aneurysms (*arrowheads*)

rhagic rate at presentation between BAVMs with flow-related aneurysms and those with intranidal aneurysms (40% vs. 72%). Remote or dysplastic AAs, although capable of bleeding, do not appear to significantly increase the overall risk for future hemorrhage in patients with BAVM. On the other hand, the presence of intranidal AAs does significantly increase the risk of future hemorrhage in our experience (Meisel et al. 2000). This has, of course, significant management implications. In the acute situation, in order to target the treatment, a decision needs to be made to identify the symptomatic lesion (Fig. 9.36), which can be difficult and prone to error (Deruty et al. 1990). In our experience, the farther the AA is located from the nidus, the less likely it is the cause of the hemorrhage and the more likely the hemorrhage was caused by the AVM, even when the hemorrhage is mostly subarachnoid in location.

If we accept that the aneurysm is induced by the AVM then one should anticipate that removal of this trigger (AVM obliteration) might result in aneurysm regression (Figs. 9.33, Fig. 9.35). Contrary to the treatment strategy reported in the literature (Batjer et al. 1986; Thompson et al. 1998), it has been our practice when electively managing patients with BAVM and associated AAs to start with the treatment of the AVM. The feeding pedicle is embolized toward the nidus that contains the upstream

AA first. Numerous embolizations of this sort have never led to AA rupture, even though the feeding pedicle arterial pressure was affected by the downstream embolization (Kondziolka et al. 1988; Redekop et al. 1998; Meisel et al. 2000). It was also noted that 80% of the distally located AAs regressed subsequent to complete obliteration of the AVM by embolization, while 67% of the distally located AA regressed after 50% or more of the AVM had been obliterated (Redekop et al. 1998). Eight percent of proximal AAs regressed and occluded when embolization of the AVM resulted in 100% obliteration (Meisel et al. 2000). It therefore appears that the farther the AA is located from the AVM nidus, the less likely it will regress following AVM treatment, as it is probably an independent arterial wall abnormality.

The authors treat proximal feeding pedicle AA and remote dysplastic AAs only when they can be definitively identified as the source of bleeding in the acute situation (Fig. 9.36) or if they have failed to regress after treatment of the AVM in the elective situation.

Dysplastic Aneurysms. Dysplastic aneurysms develop on an arterial branch independent from the AVM (Batjer et al. 1986; Perret and Nishioka 1966) and are therefore not considered to be flow related.

In most reported series (Batjer et al. 1986; Miyasaka et al. 1982), there is no overall sex predominance in aneurysms associated with BAVMs. In our series of BAVMs, dysplastic aneurysms had a female predominance of 5:1 and are discovered in patients who are 11–55 years of age. Flow-related arterial aneurysms showed a male predominance of 2:1 and are more likely to occur in older patients (Hayashi et al. 1981; Lasjaunias et al. 1988). The association of BAVM and arterial aneurysm in our series showed a distinct increase with age: 8% of the patients with AVMs had associated arterial aneurysms prior to age 25; 24% of patients were between 25 and 49 years of age, while 37% of patients were older than 50. The fourfold increase in the frequency of BAVM and associated arterial aneurysm in patients in the sixth versus those in the first decade of life reinforces the roles played by long-standing high flow and the aging of the vascular system.

In our patients with BAVM and associated aneurysm, multiplicity of the AA was noted in 67% (Meisel et al. 2000) (Figs. 9.32, 9.33). In these patients, there was no personal or family history of vascular disease. Interestingly, in patients with multiple BAVMs (9% of our series of adults with BAVMs), multiple aneurysms were not demonstrated.

With regard to topography, arterial aneurysms were found predominantly in association with corticoventricular AVMs (66%), followed by cortical AVMs (30%). In deep-seated lesions, the association with an arterial aneurysm was rare (4%). On the other hand, the association of hemorrhage in deep-seated AVMs with a distal aneurysm is very high, and these aneurysms are frequently distal pseudoaneurysms (Figs. 9.36, 9.37). A review of our cases showed a similar percentage of BAVM plus aneurysm in patients with cerebellar AVMs compared to those with supratentorial AVMs (Garcia-Monaco 1990).

Nidus Angioarchitecture

The nidus arrangement of BAVMs can be approached in different ways. A single-hole fistula is the simplest type of arteriovenous shunting.

Dobbelaere (1979) suggested that the transition of a nidus AVM to a nidus AVF is a common occurrence, "the passage from one [AVM] to the other [AVF] is certain." He proposed that all arteriovenous shunts change from one type to the other with "evolution or involution." These findings contradict our observations, since the lesions that we have followed have not gone through such a predetermined evolution or involution. In the past, the nidus of an AVM has been classified, primarily for surgical interventions, either by topography, size, or intrinsic morphological or hemodynamic patterns. A description of compartments, as disclosed angiographically, has also been used for classification. AVMs in which a specific and separate venous drainage is seen after each feeder is injected are considered AVMs with multiple compartments. These lesions, in which a single or the same venous outlet is opacified after every feeder is injected, are considered AVMs with a single or converging compartment (Yasargil 1987) (Table 9.11). Most of the multiple compartment lesions are arranged on a radius (cortical and paraventricular nidi in corticoventricular lesions) or a meridian (cerebellar AVMs). Yasargil (1987) made several additional observations on the arrangement of these lesions, emphasizing their compact or diffuse appearance (Table 9.11).

We have observed similar patterns in which diffuse lesions show less dominant but more numerous feeders. In many cases, these numerous feeders may indicate the host response to the development of arterial stenotic segments (pre-moyamoya phenomena) and angiogenic stimulation. The veins draining such diffuse AVMs are surprisingly almost normal in caliber; the transit time in the shunt is often moderate. They are mostly cortical-subcortical lesions and can be seen both supra- and infratentorially.

Table 9.11. Nidus (epicenter) (from Yasargil 1987, with permission)

Compact
Single
Without fistula
With arteriovenous fistulae
Only arteriovenous fistulae
Multifocal (multicentric or polycentric) compact (subdivided into same types as above)
Unilateral
Bilateral
Supra- and infratentorial
Orbital and cerebral
Cutaneous, dural and cerebral
Diffuse (no visible nidus, scattered pathological arteries and veins without recognizable connections angiographically or at operation)
Small areas
Large areas
Entire hemispheres
Both hemispheres
Supra-and infratentorial

Table 9.12. Type and size of arteriovenous malformations

Cryptic Not seen at angiography, not found at surgery, and not demonstrated pathologically
Occult Not seen at angiography, not found at surgery, may be recognized by histological examination
Micro (<1 cm)
Small (<2.5 cm)
Moderate (2.5–5 cm)
Large (>5 cm)

Most AVMs are composed of several types of arteriovenous communications, including both nidi and fistulae. However, both compact and diffuse types as part of the nidus of a genuine AVM do not occur. A diffuse appearance may indicate secondarily acquired perilesional angiogenesis, at least in some of the diffuse types of lesions reported by Yasargil. The significance of the size of the nidi lies primarily in their surgical or radiosurgical accessibility (Table 9.12). Most authors have grouped BAVMs according to the size of the nidus and considered small BAVMs as those less than 3 cm. Small BAVMs had a tenfold increased likelihood to present with hemorrhage as compared to larger AVMs (Crawford et al. 1986; Graf et al. 1983; Parkinson and Bachers 1980; Shi and Chen 1986; Spetzler and Martin 1986; Waltimo 1973). In contrast, patients with smaller lesions rarely present with seizures, neurological deficits, or headaches (Hashima et al. 1985). The Toronto experience showed a slightly increased risk for future hemorrhage in the larger size AVMs in deep locations, irrespective of their mode of presentation.

Microarteriovenous Malformations. Micro-AVMs and micro-AVFs consist of a small nidus (<1 cm) or a fistula fed by a normal-sized artery and draining into a normal-sized vein (Figs. 9.1, 9.3, 9.7).

Micro-AVMs cover 7% of all AVMs and 21% of the AVMs that were diagnosed following hemorrhagic presentation (Willinsky et al. 1988a). In the series of Papatheodorou et al. (1961) as well as ours (Willinsky et al. 1988a), 53% of patients had no history of symptoms prior to the discovery of their lesions; the ages ranged from 8 to 52 years, without sex predominance. All patients presented with intracerebral hematoma, with minimal or no subarachnoid blood. Conventional magnification angiography with subtraction demonstrated the micro-AVM in 85% of patients; however, in 18% of these, the AVM could be seen only after resolution of the hematoma, during a second angiographic study 3 months later (Fig. 9.65). In the remaining 15% of patients, the lesions were angiographically occult but were seen at surgery during removal of the hematoma. All the lesions were superficial: 77% were cortical supratentorial, 15% were infratentorial, and 3% were at the base of the brain. No dural supply or associated arterial aneurysms were demonstrated. Some 82% of patients were operated on (13% of patients refused surgery), and the remaining 5% were re-

ferred for radiation therapy. All of the lesions in patients who were operated on showed the usual aspects of cerebral AVMs at pathology. At both angiography and surgery, the intracerebral hematoma helped to localize the lesion, as the micro-AVM could be seen at the edge of the hematoma. There were no postoperative complications. Follow-up angiograms showed that the lesion had disappeared, and no recurrences were noted. Interestingly, none of the nonoperated patients rebled at follow-up 1–5 years later, although 7% had apparently bled in the same site within 10 years prior to diagnosis and surgery. The incidence of rebleeding from a micro-AVM, i.e., the natural history, is not well known since most lesions are surgically removed at the time of presentation. Micro-AVMs have been suspected to be the cause of many intracerebral hematomas in young healthy individuals in whom no obvious lesion is found (Krayenbuhl and Siebenmann 1965; Margolis et al. 1961; Tanaka et al. 1986).

To explain how venous outflow obstacles of an arteriovenous shunt can be considered as one significant cause of rupture, one should recall the normal disposition of cortical veins (Duvernoy et al. 1981). Small bridging arteries anchor the cortical veins onto the parenchyma and narrow them in the depth of the sulci. These potential anatomical restrictions on increased venous flow may lead to upstream venous hyperpressure and secondary rupture. In fact, when we described a normal-sized draining vein, the most proximal venous outlet from the micro-AVM actually corresponds to an enlarged subpial cortical vein, which is usually not visible angiographically. Micro-AVMs are frequent (43%) in the HHT (ROW) population, and in these patients they are nearly always asymptomatic at presentation and on follow-up (Matsubara et al. 2000). This raises questions with respect to the need for treatment of micro-AVMs in that particular group of patients, as they appear to have a different natural history compared to the sporadic micro-AVMs.

The differential diagnosis of nontraumatic intracerebral hematoma should include AVMs, aneurysms, blood dyscrasias or a bleeding diathesis, amyloid angiopathy, drug abuse, sympathomimetic drugs, or tumors (Lipton et al. 1987). Vascular malformations have accounted for 10%–40% of lobar hematomas. No identifiable etiology can be seen in up to 41% of patients with intracerebral hematomas. In autopsy series, no etiology was found in 15%.

Nidus Size Changes. The literature contains conflicting data as to the growth of BAVMs, with some reports of size increase in cerebral malformations (Hook and Johanson 1988; Krayenbuhl 1977; Spetzler and Wilson 1975; Stein 1979; Waltimo 1973; Minakawa et al. 1989) and other reports of decreases in BAVM size or even complete thrombosis (Eisenmann et al. 1972; Kushner and Alexander 1970; Levine et al. 1973; Omojola et al. 1985; Sukoff et al. 1972; Pascual-Castroviejo et al. 1977; Minakawa et al. 1989; Lee et al. 2002a) (Fig. 9.59). Overall, a review of 63 vascular malformations with size changes concluded that in 25% there was an increase in size. It is of interest that the patients in whom the AVMs had enlarged were mostly children at the time of first presentation and diagnosis. In contrast, AVMs that decreased in size or thrombosed without associated hematoma occurred more often in the older age

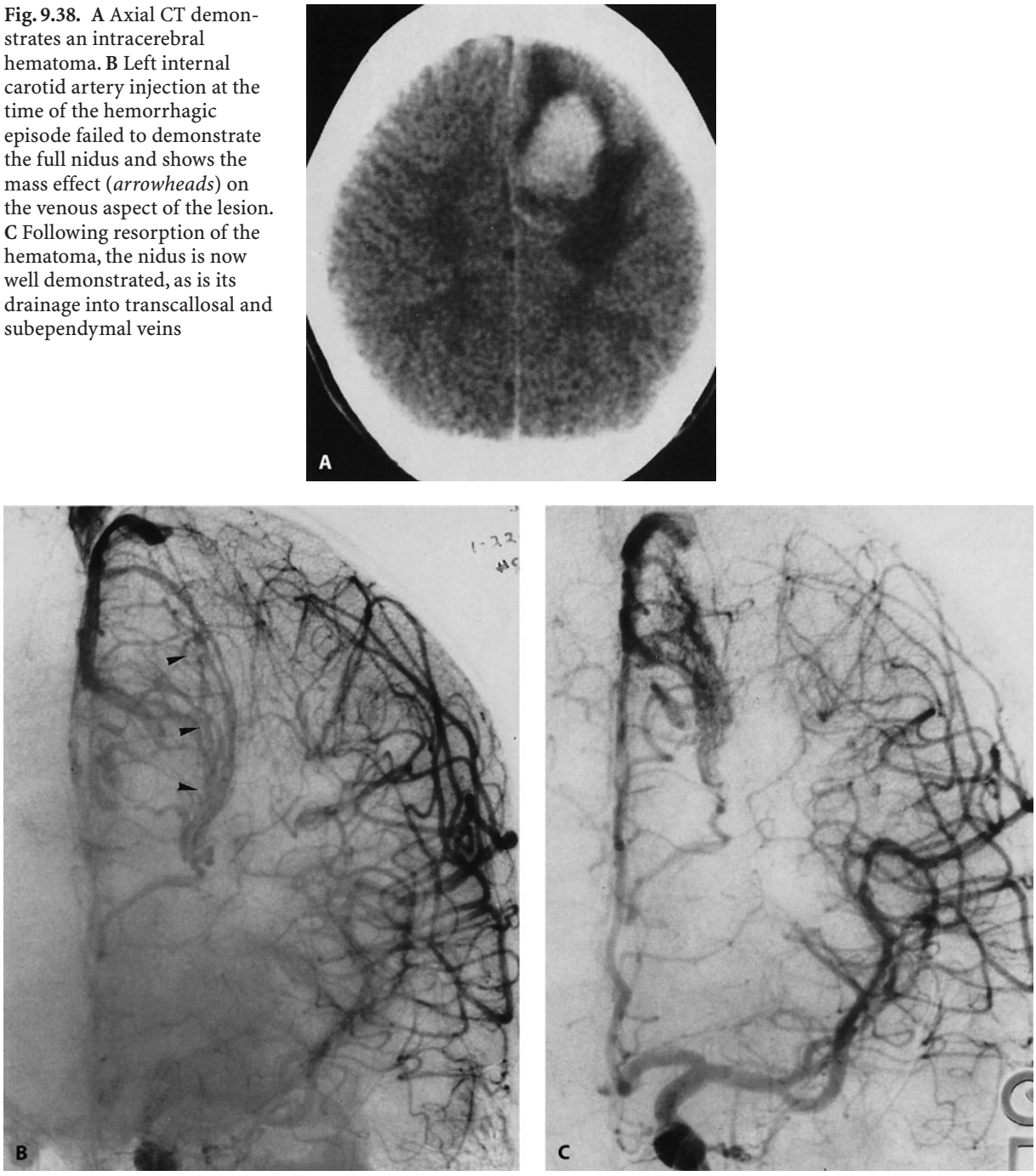

Fig. 9.38. **A** Axial CT demonstrates an intracerebral hematoma. **B** Left internal carotid artery injection at the time of the hemorrhagic episode failed to demonstrate the full nidus and shows the mass effect (*arrowheads*) on the venous aspect of the lesion. **C** Following resorption of the hematoma, the nidus is now well demonstrated, as is its drainage into transcallosal and subependymal veins

group. Whether the enlargement of an AVM is real or apparent remains controversial but angiogenic factors almost certainly play a role in the changing appearance of a BAVM over time.

Apparent changes in nidal size are a well-recognized phenomenon associated with hemorrhagic presentation of BAVMs. The hematoma may temporarily compress the nidus and be angiographically occult at that time but will be revealed on follow-up angiography in 2–3 months

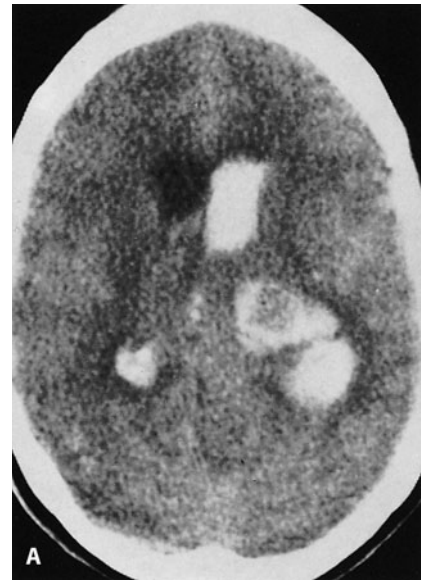

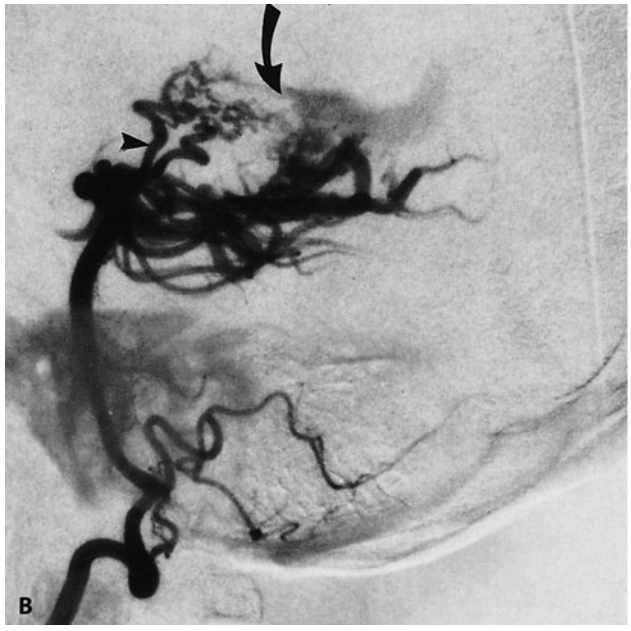

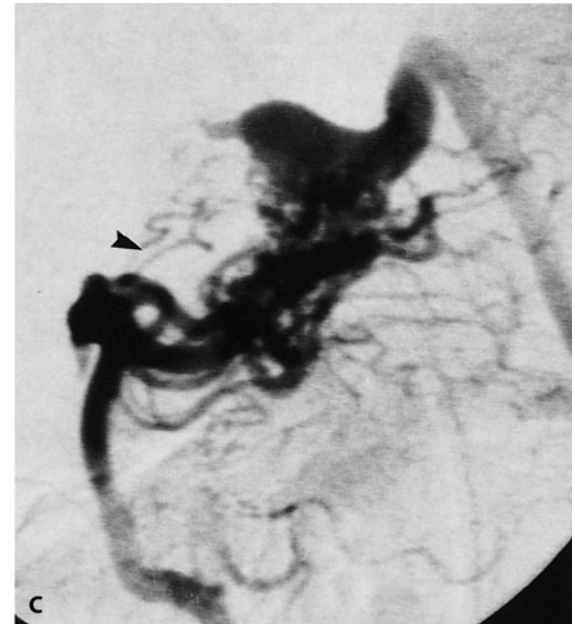

Fig. 9.39. **A** Axial CT in a patient who presented with an intracerebral hemorrhage with ventricular extension. **B** Left vertebral artery injection in lateral projection at the time of the bleed demonstrates a thalamic arteriovenous malformation, and its venous drainage, compressed by the hematoma (*curved arrow*). Note the size of the thalamoperforators (*arrowhead*). **C** Left vertebral angiogram in lateral view. Following ventricular shunting and resorption of the hematoma, there is better opacification of the malformation and its venous drainage. Note the compensatory decreased caliber of the thalamoperforator feeders (*arrowhead*)

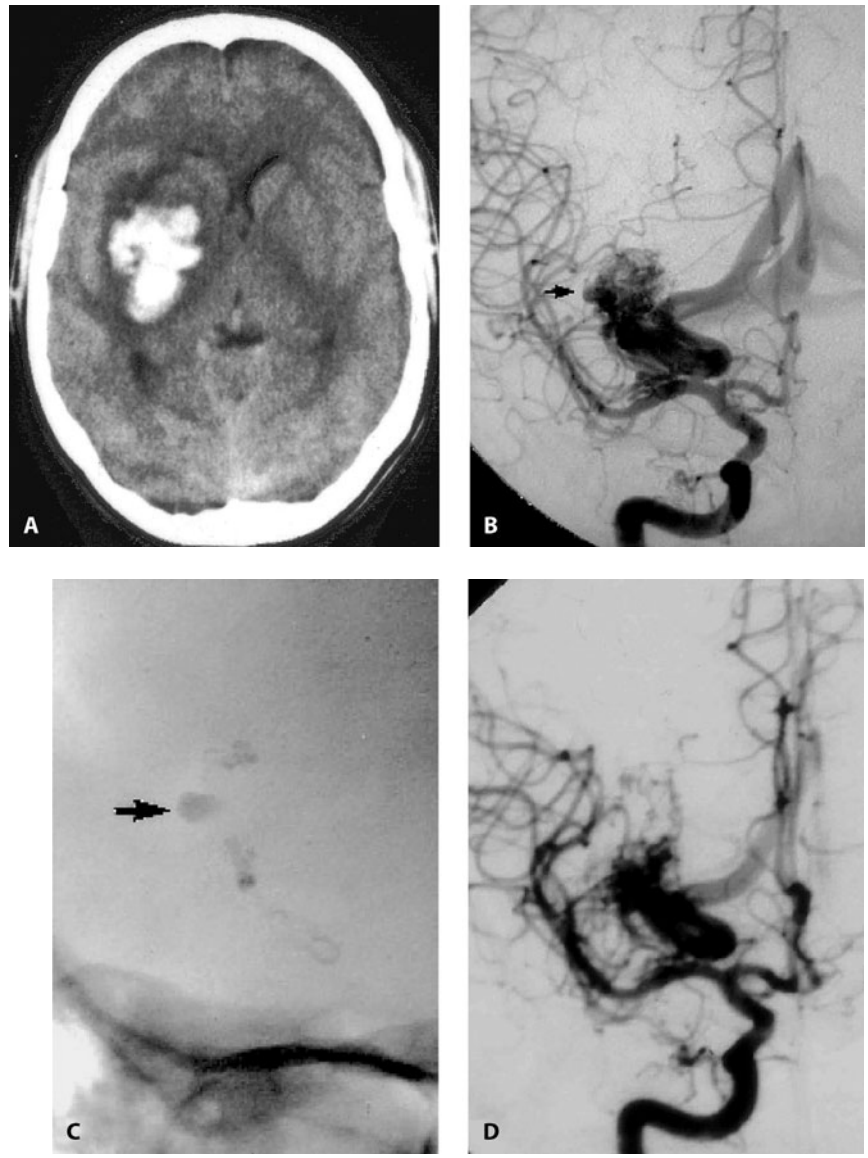

Fig. 9.40. CT scan (**A**) demonstrates hemorrhage shown on carotid angiogram in AP view (**B**) to be caused by deep-seated arteriovenous malformation associated with an intranidal aneurysm (*arrow*), which was selectively obliterated with glue (*arrow*, **C**). The residual nidus as shown on postembolization carotid angiogram in AP view (**D**) was subsequently treated with stereotactic radiosurgery

(Fig. 9.65). The hemorrhage may also partially compress the nidus at the acute stage and make the nidus appear smaller (Fig. 9.38) or have an impact on the appearance of the prenidal arterial system (Fig. 9.39).

Intranidal Ectasias. Ectasias or pouches within the AVM nidus can be either arterial or venous. The former may belong to the group of distal arterial aneurysms adjacent to or within the nidus and may be difficult to see on global injections (Figs. 9.39–9.41). They are a small portion of the nidus and were proven to be associated with an increased risk for future hemorrhage in the Bicêtre series (Meisel et al. 2000). Thrombosis and regression of intranidal aneurysms is extremely rare (Fig. 9.42). These aneurysms may be difficult to distinguish from pseudoaneurysms, which are spaces within the unclotted portion of the hematoma (Fig. 9.43).

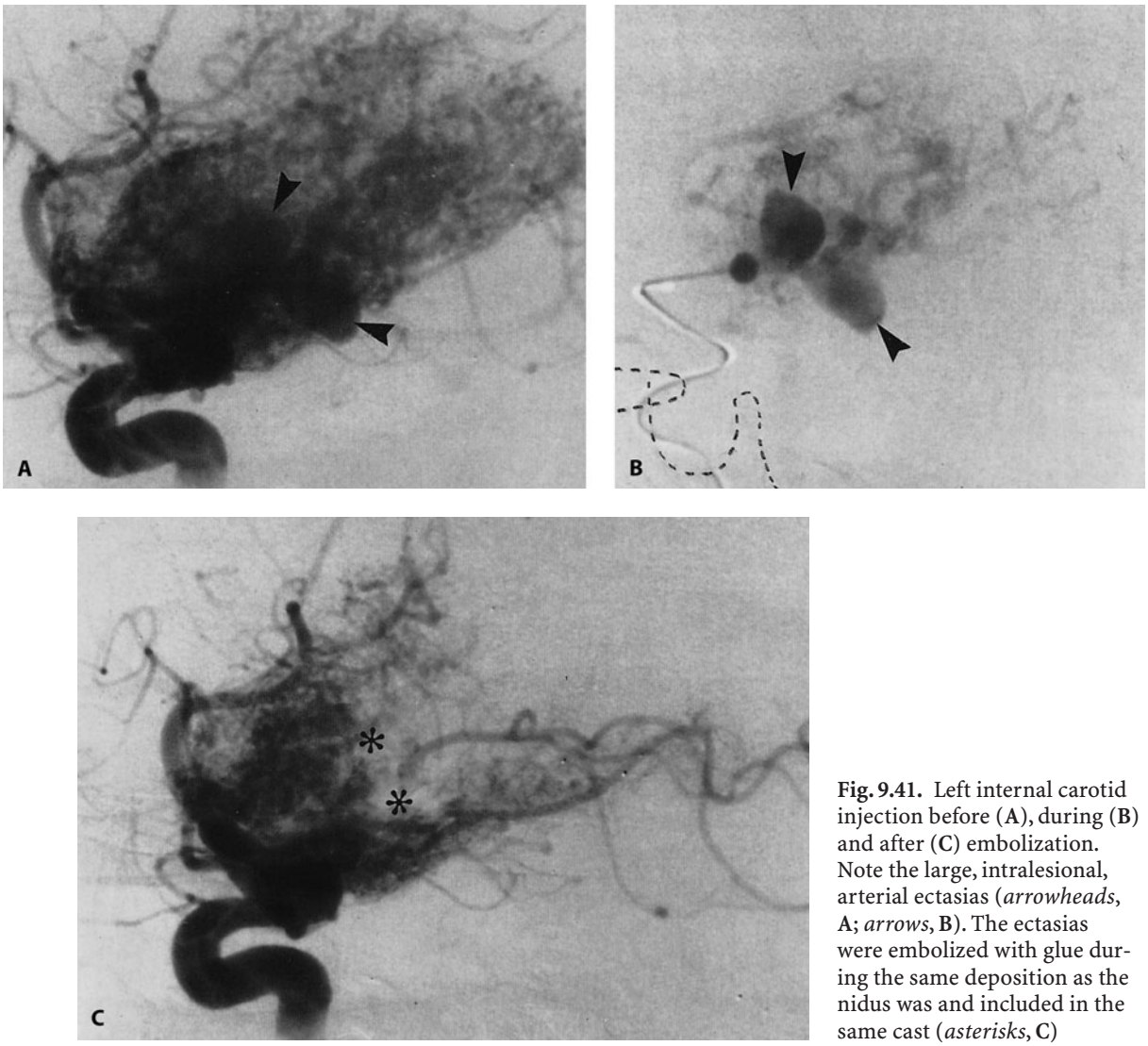

Fig. 9.41. Left internal carotid injection before (**A**), during (**B**) and after (**C**) embolization. Note the large, intralesional, arterial ectasias (*arrowheads*, **A**; *arrows*, **B**). The ectasias were embolized with glue during the same deposition as the nidus was and included in the same cast (*asterisks*, **C**)

Fig. 9. 42. Right internal carotid angiogram in AP projection (**A**) and left internal carotid angiogram in lateral projection (**B**) at the time of presentation, with a venous hemorrhage from an arteriovenous malformation demonstrated two intranidal aneurysms (*arrows*). Two months later and without specific treatment, follow-up right internal carotid angiogram in AP projection (**C**) and left internal carotid angiogram in lateral projection (**D**) demonstrated spontaneous thrombosis of the two intranidal aneurysms (*arrows*). MRI at presentation (**E**) and 2 months later (**F**) confirmed thrombosis of the aneurysms (*arrows*) ▶

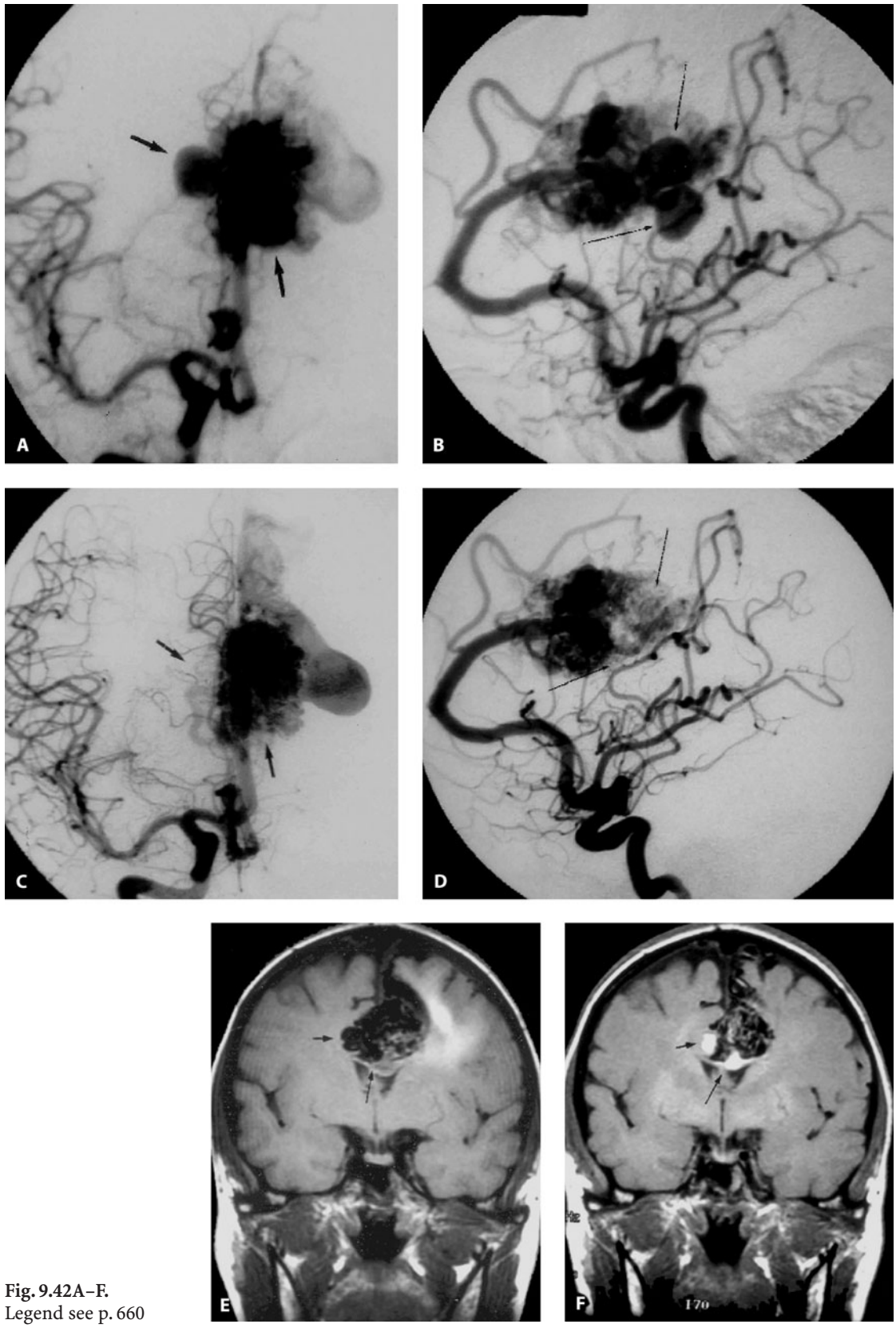

Fig. 9.42A–F.
Legend see p. 660

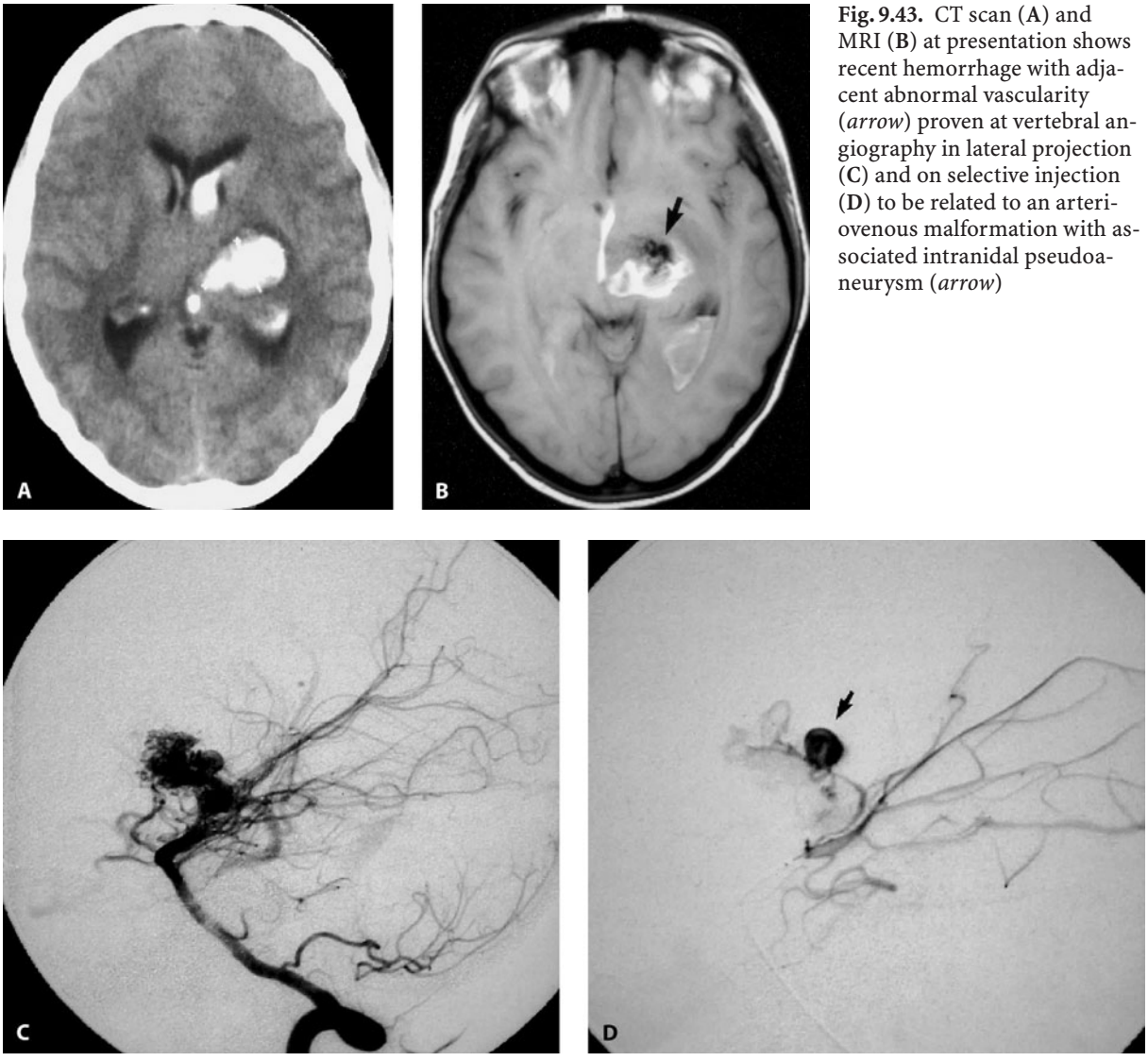

Fig. 9.43. CT scan (**A**) and MRI (**B**) at presentation shows recent hemorrhage with adjacent abnormal vascularity (*arrow*) proven at vertebral angiography in lateral projection (**C**) and on selective injection (**D**) to be related to an arteriovenous malformation with associated intranidal pseudoaneurysm (*arrow*)

Up to 8% of AVMs presenting with hemorrhage may reveal evidence of pseudoaneurysms (Garcia-Monaco et al. 1993). These aneurysms are usually small in size but may enlarge to produce early rerupture. An enlarging pseudoaneurysm constitutes one of the few indications for emergency endovascular or surgical treatment. Partial embolization targeting the enlarging pseudoaneurysm will remove the risk of early rerupture and appears to reduce the chance of future hemorrhage if stereotactic radiosurgery is chosen to treat the residual nidus, in the event that it could not be completely obliterated by embolization or removed surgically.

Arterial pseudoaneurysms are usually encountered during the acute stage of an intracerebral hematoma of arterial origin (Figs. 9.43, 9.44). They can be targeted for early endovascular treatment, or if this is not technically feasible are an indication for early surgery. Fusion of 3-D digital subtraction angiography (DSA) and MRI is helpful to locate these aneurysms prior to surgery (Fig. 9.44). The aneurysms are usually small

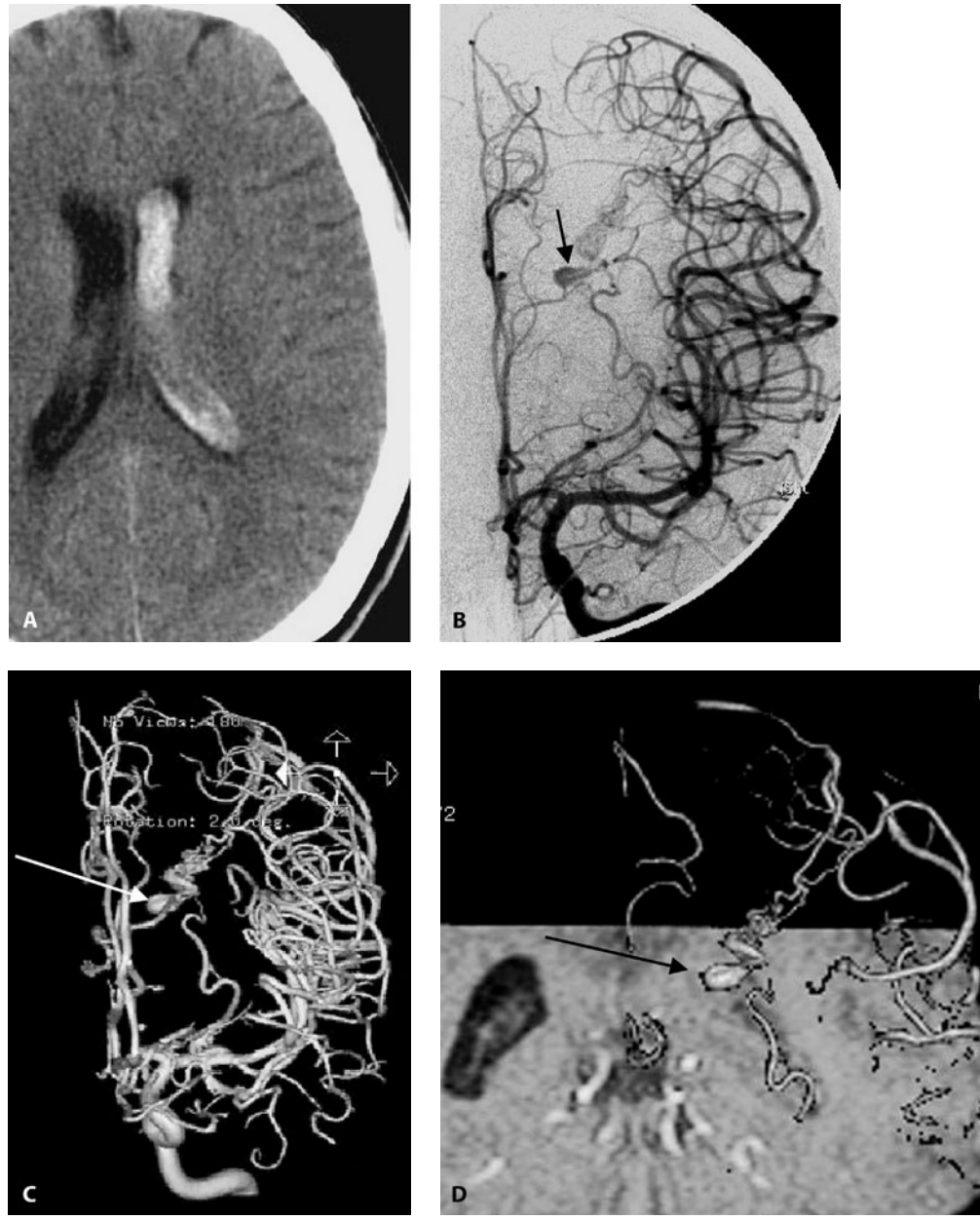

Fig. 9.44. CT scan (**A**) demonstrates IVH (intraventricular hemorrhage) caused by a choroidal type arteriovenous malformation associated with pseudoaneurysm (*arrow*) shown on carotid injection AP view (**B**) and on 3-D digital subtraction angiography (DSA, **C**). Fusion of 3-D DSA and MRI demonstrates the exact location of the pseudo aneurysm (*arrow*) in the coronal plane (**D**) and axial planes (**E, F**). **E, F** see p. 664

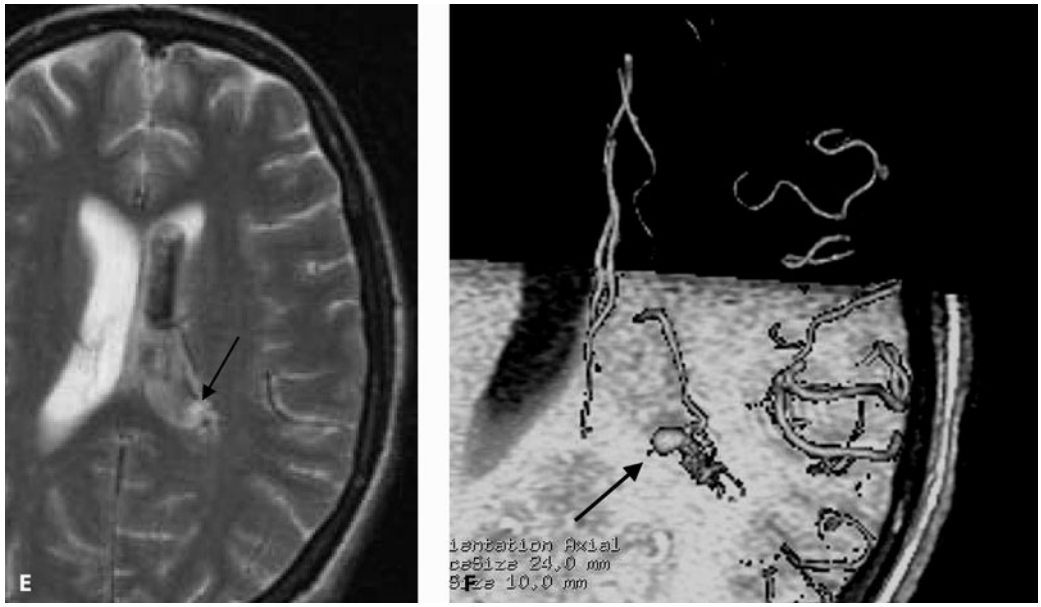

Fig. 9.44E, F. Legend see p. 663

in size but may enlarge to produce an early rerupture. In some instances, pseudoaneurysms will evolve favorably with thrombosis of the ruptured vessel but this can hardly be predicted.

Intralesional venous ectasias are usually opacified as part of the distal nidal vascular network. The appearance can be similar to a venous pseudoaneurysm in which the hematoma cavity is recanalized and incorporated into the venous outlet (Figs. 9.45–9.47). The venous origin of a pseudoaneurysm is difficult to prove. As a sequence of events, however, most of these intralesional pouches do correlate with a recent history of hemorrhage. They appear to be more frequent in deep AVMs and should be searched for adjacent to or as part of the hematoma area (Fig. 9.48). Their acquired nature exemplifies the angioarchitectural changes that BAVMs may undergo over time.

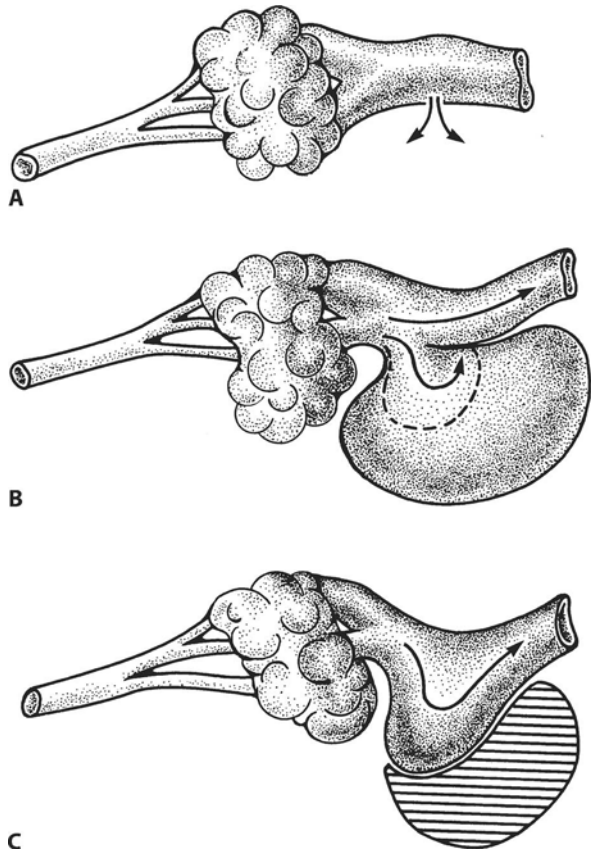

Fig. 9.45A–C. Evolution of a venous pseudoaneurysm with partial incorporation of the recanalized hematoma into the venous outlet. See text

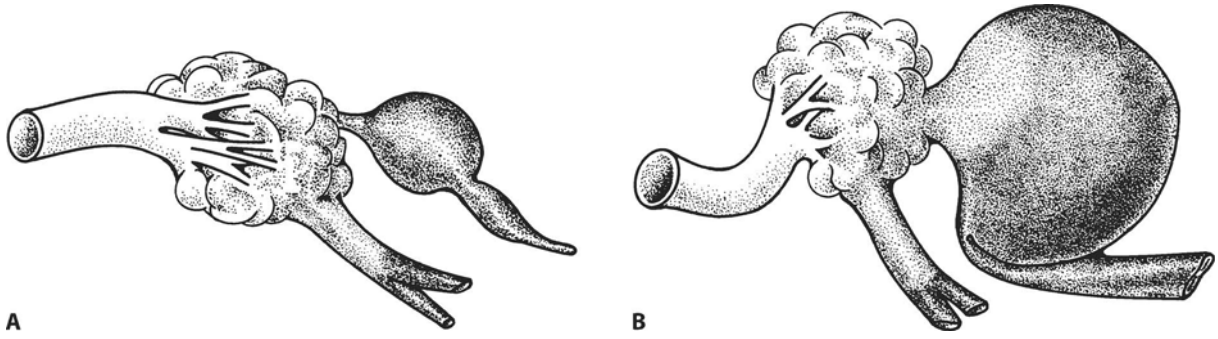

Fig. 9.46. Venous ectasia **A** proximal to a venous thrombosis and **B** proximal to venous kinking. See text

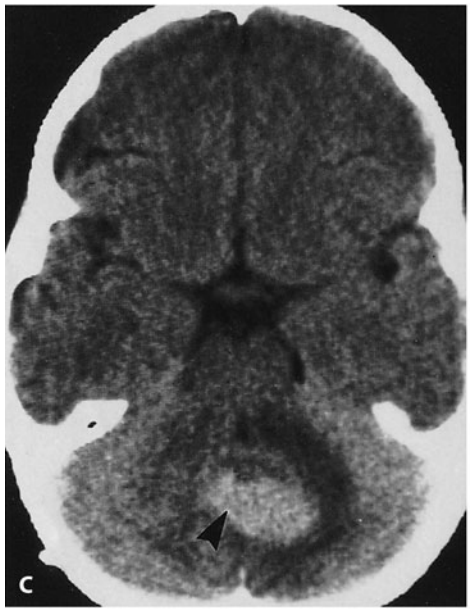

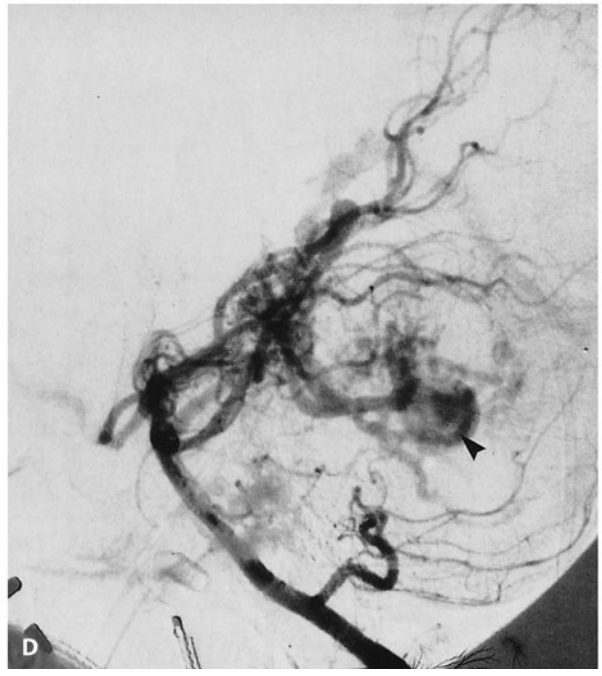

Fig. 9.47A–D.
Legend see p. 667

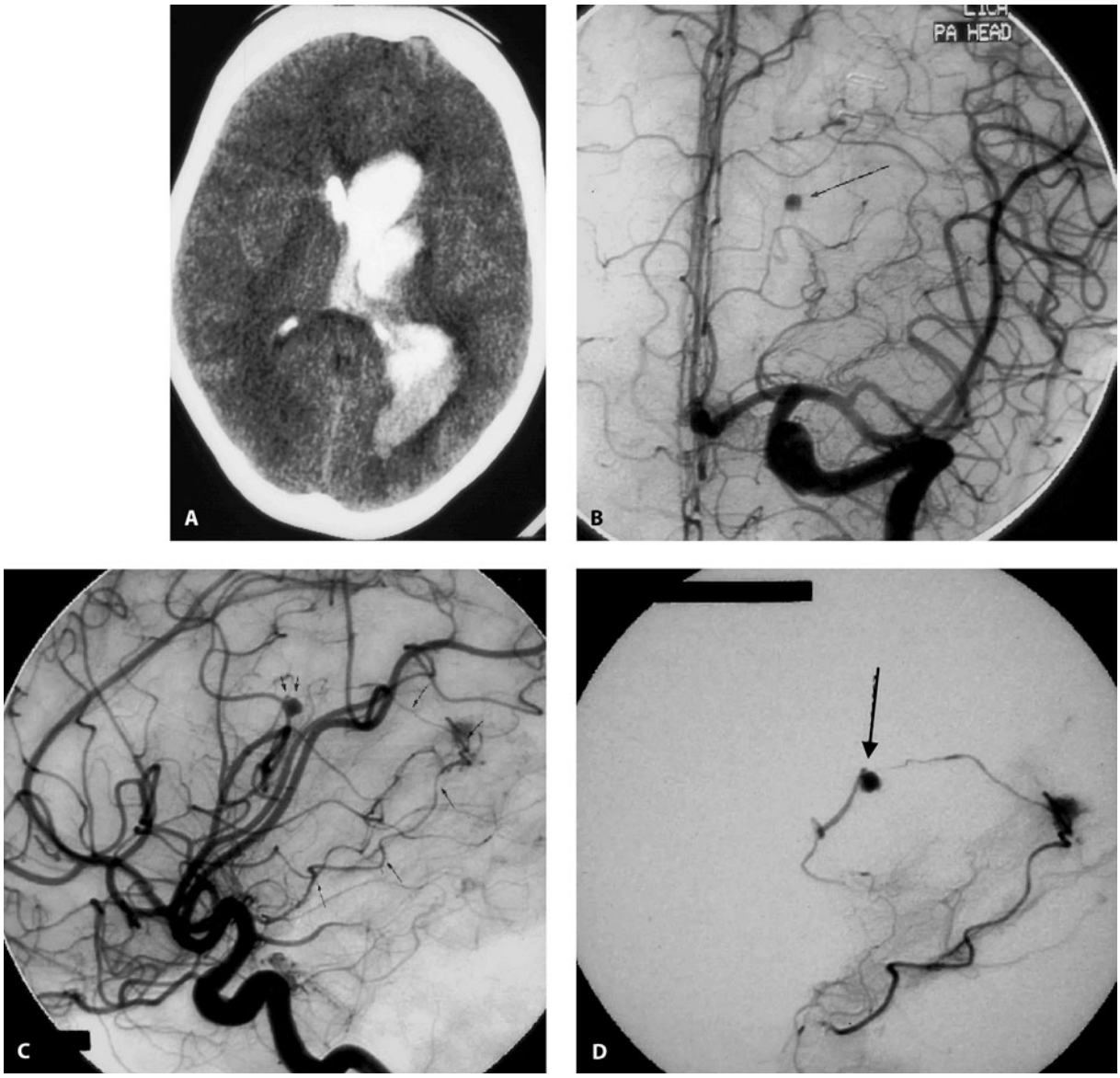

Fig. 9.48. CT scan (**A**) demonstrates intracerebral and intraventricular hemorrhage and IVH shown at carotid angiography AP view (**B**) to be caused by microarteriovenous malformation (micro-AVM) with pseudovenous aneurysm (*arrow*). Carotid angiogram lateral view (**C**) and selective injection of anterior choroidal artery (**D**) shows supply to the micro-AVM and postnidal venous pseudoaneurysm (*arrow*)

◄ **Fig. 9.47.** **A** Axial noncontrast CT and **B** left vertebral angiogram in lateral projection at the time of a hemorrhagic episode demonstrate a localized vermis arteriovenous malformation with a venous pseudoaneurysm (*arrowhead*, **B**), corresponding to the larger area of hematoma seen in **A** (*arrowhead*). **C** Noncontrast axial CT and **D** left vertebral angiogram at the time of increased symptomatology, with enlargement of the intracerebral hematoma. Note the increased size of the pseudoaneurysm (*arrowhead*) within the vermis

Veins

The venous drainage of AVMs can be very difficult to study due to the vast number of outlets that can be superimposed. Nevertheless, drainage of a shunt should always be analyzed for its own characteristics but also assessed in relationship to the regional venous drainage pattern of the brain. In general, the developmental nature of the shunt alters the normal course of the development of the venous system similar to its impact on the arteries.

Venous Variations. Venous variations were noted in 30% of Yasargil's (1987) patients and in 32% of our patients (Willinsky et al. 1988b). Variations may involve cerebral veins, dural sinuses, or both. Careful attention is required to recognize these variations (Fig. 9.14), since they may be in the venous channel draining either the lesion or normal brain parenchyma. Drainage of the lesion is usually predictable from the location of the nidus (Fig. 9.12). In some cases, however, thrombosis may reroute the drainage to additional channels, which may be ipsilateral, contralateral, or transcerebral.

These venous variations must be distinguished from collateral circulation that expresses a secondary response to the presence and the chronicity of the shunt. Analysis of the possible influences of the AVM venous drainage and the brain drainage on each other may assist in the understanding of some of the symptoms, and possibly predict the natural history, and will aid in recognition of therapeutic pitfalls (Laine et al. 1981). Such analysis must include the effects of reflux, due to both venous hyperpressure and collateral circulation. Yasargil (1987) suggests that most hemorrhages occur as the result of venous or vein–nidus junction rupture. Embryonic veins have been described morphologically and histologically to persist in BAVM (Vidyasagar 1979; Deshpande and Vidyasagar 1980) (Table 9.13).

Venous variations can create patterns that make up an artificial group of lesions, such as in vein of Galen and dural malformations (Vols. 1 and 3). Schematically:

1. The immediate or developmental venous adaptation tends to compensate for the initial hemodynamic disturbance. It alters the rest of the venous system in an attempt to bypass the higher pressure lesion and is a morphological reaction, creating anatomical variations or allowing the persistence of embryonic venous structures.
2. The collateral venous circulation is a secondary adaptation. It tends to preserve the equilibrium of both shunt-related and normal parenchymal drainages. It absorbs the increased pressure that exists in the venous outlet of the AVM into normal channels, a pure hemodynamic response. Its failure to compensate will result in neurological or hemorrhagic complications.

Venous collateral circulation creates evolving patterns that continuously adapt to the changes created by the changes in the AVM environment (chronicity of the high-flow conditions, dystrophic changes of the veins, aging of the vascular tree).

Table 9.13. Embryonic veins in brain arteriovenous malformations (from Vidyasagar 1979, with permission)

Irregular thickness (fibrocollagenous or fibromuscular)
No elastic tissue
No prominent endothelial cells
Fenestrated endothelium

Table 9.14. Areas of venous obstacle

Foramen of Monro
Ventricular–choroid fissure junction
Deep sylvian fissure
Tentorial edge
Inferior vermian–dural junction
Vein of Galen-Falx-tentorial junction

Thrombosis and kinking of the veins are two obstacles to flow that can occur in the venous system draining either the AVM or the brain (Figs. 9.24, 9.46). Mechanical interference (Table 9.14) by the sphenoid ridge or tentorial edge is frequent and may account for the high incidence of hemorrhagic episodes in lesions located along the incisura or in the medial temporal lobe (Willinsky et al. 1988b). Some areas of venous narrowing without upstream ectasia can be seen, which may be caused by the indentation of bridging arteries in their subpial location. In other instances, without clinical evidence to suggest a previous event, thrombosis has occurred, producing a secondary rerouting of the BAVM drainage (Figs. 9.54, 9.55). In these cases, thrombosis must be distinguished from venous agenesis. The etiological difference highlights the basic distinction between anatomical variation (congenital disposition) and collateral circulation (acquired condition).

Spontaneous partial thrombosis of one of the venous outlets can occur and tends to be associated with new or worsening clinical symptomatology such as headaches, seizures, or neurological deficit (Fig. 9.58).

Complete thrombosis of BAVMs was reviewed by Nehls and Pittman (1982) and revealed that in 48% of patients, a preceding hemorrhagic episode could be identified. The mean age was 39 years and there was no sex difference. Lee et al. (2002a) noted similar findings (Fig. 9.52).

On the other hand, in Eisenman's (1972) review, all spontaneous thromboses occurred following hemorrhage. The compression of a hematoma may thrombose an AVM or alternatively may compress only a portion of the AVM, which will appear smaller during the acute episode and then reexpand after the hematoma has resolved. Even the caliber of some feeders may be altered by compression of the nidus or the draining veins. Repeat angiography, after the hematoma has reabsorbed, is therefore indicated prior to treatment.

The limitations in assessing spontaneous thrombosis are illustrated in Becker's review of 18 histologically verified occult CVMs (Becker et al. 1979). He reported that 50% were found to be "thrombosed arteriovenous malformations." The criterion he used to call them AVMs was the ability of the small arterial structures within the malformation to be stained using elastic van Gieson preparation. This criterion, however, fails to differentiate AVM from cavernoma, and most so-called thrombosed AVMs are probably cavernomas. There was also a significant female predominance in his series. The diagnosis of thrombosed AVM does not seem to have any prognostic significance. It has been suggested that if surgically accessible, the lesion should be removed, to decrease the propensity for rebleed and seizures. Evidence to support this approach is lacking, and we recommend

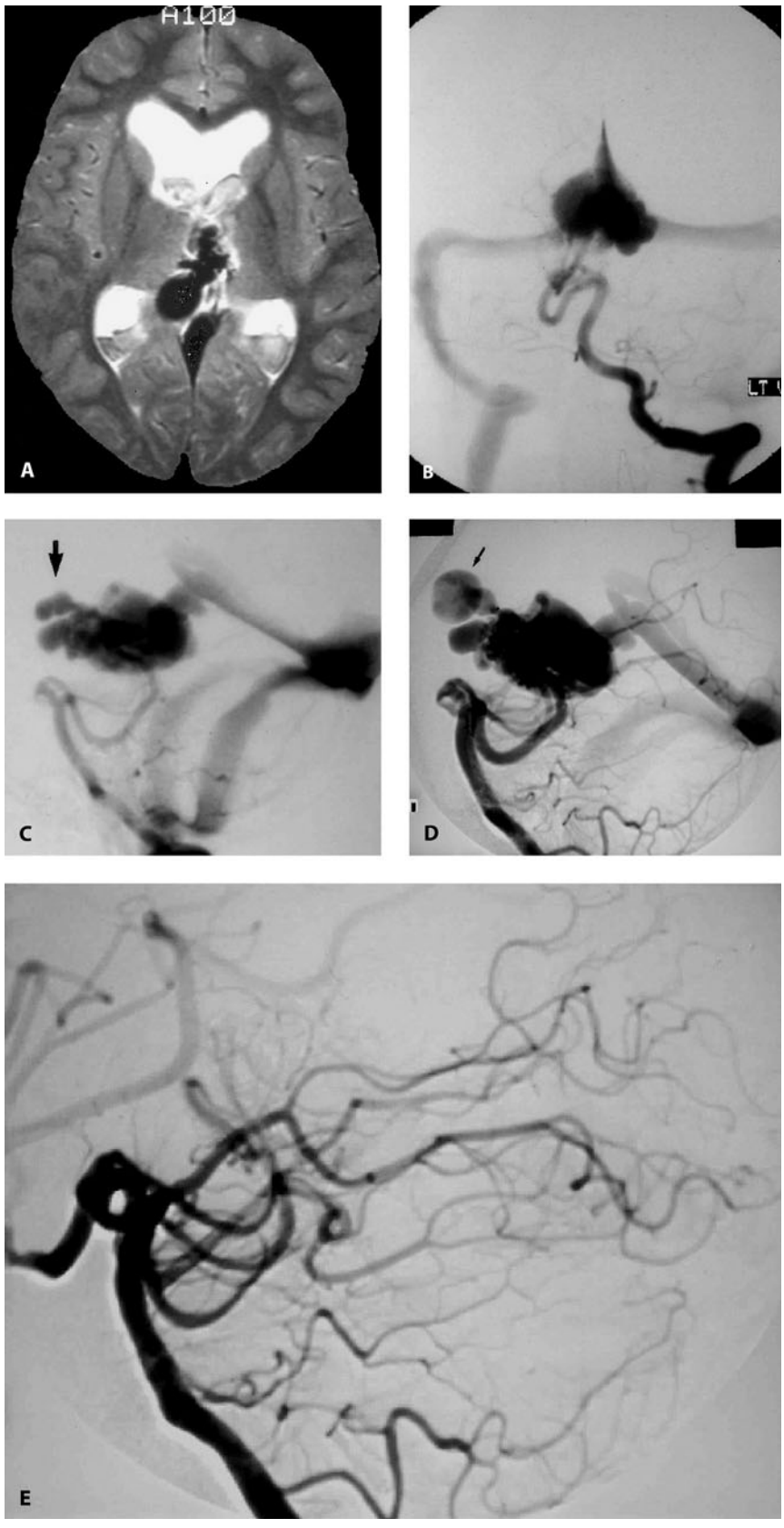

Fig. 9.49. MRI (**A**) demonstrates recent intraventricular hemorrhage, which on vertebral angiography AP view (**B**) proved to be caused by a midline choroidal arteriovenous malformation (AVM). The immediate (**C**) and 2-month follow-up vertebral angiogram lateral view (**D**) demonstrates significant enlargement of a venous pouch (*arrows*) projecting into the 3rd ventricle. Complete obliteration of the AVM following embolization with glue was demonstrated on vertebral angiogram in lateral view (**E**)

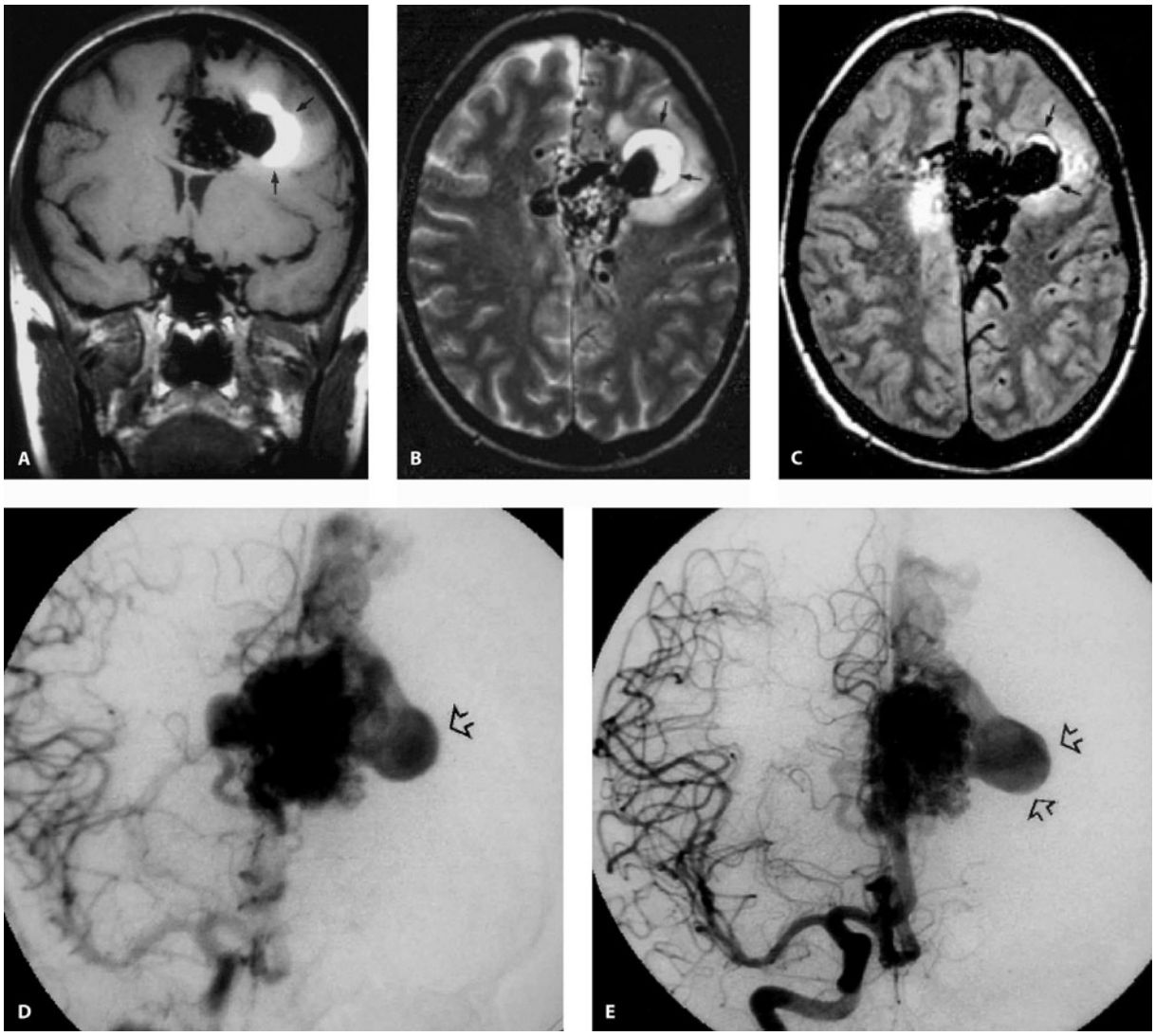

Fig. 9.50. MRI coronal view (**A**) and axial view (**B**) 1 week after intracranial hemorrhage (ICH) demonstrates recent hemorrhage (ICH) outside as well as a blood clot within a vascular channel (vein), both of which showed resolution on follow-up MRI axial view 2 months later (**C**). Carotid angiogram AP view at presentation (**D**) and 2 months later (**E**) showed apparent enlargement of the venous pouch (*open arrows*), which was in fact caused by thrombus resolution within the vein that had ruptured

a follow-up angiogram in 6–12 months. If the AVM persists in not filling, it should be permanently occluded; no further intervention is needed.

Finally, the spontaneous thrombotic process that may occur in BAVMs seems more frequent in children than in adults (9.6% incidence of spontaneously thrombosed VGAM in our series) and may be more prominent in adult females than in males. Of interest is that 25.8% of BAVMs in children are multiple, whereas only 6.8% in adults are. Could it be that a certain percentage of the multiple AVMs in children thrombose before the remaining ones become symptomatic in adulthood? On the other hand, spontaneous occlusion of AVMs is often symptomatic (Fig. 9.59), resulting in investigation and diagnosis at that time.

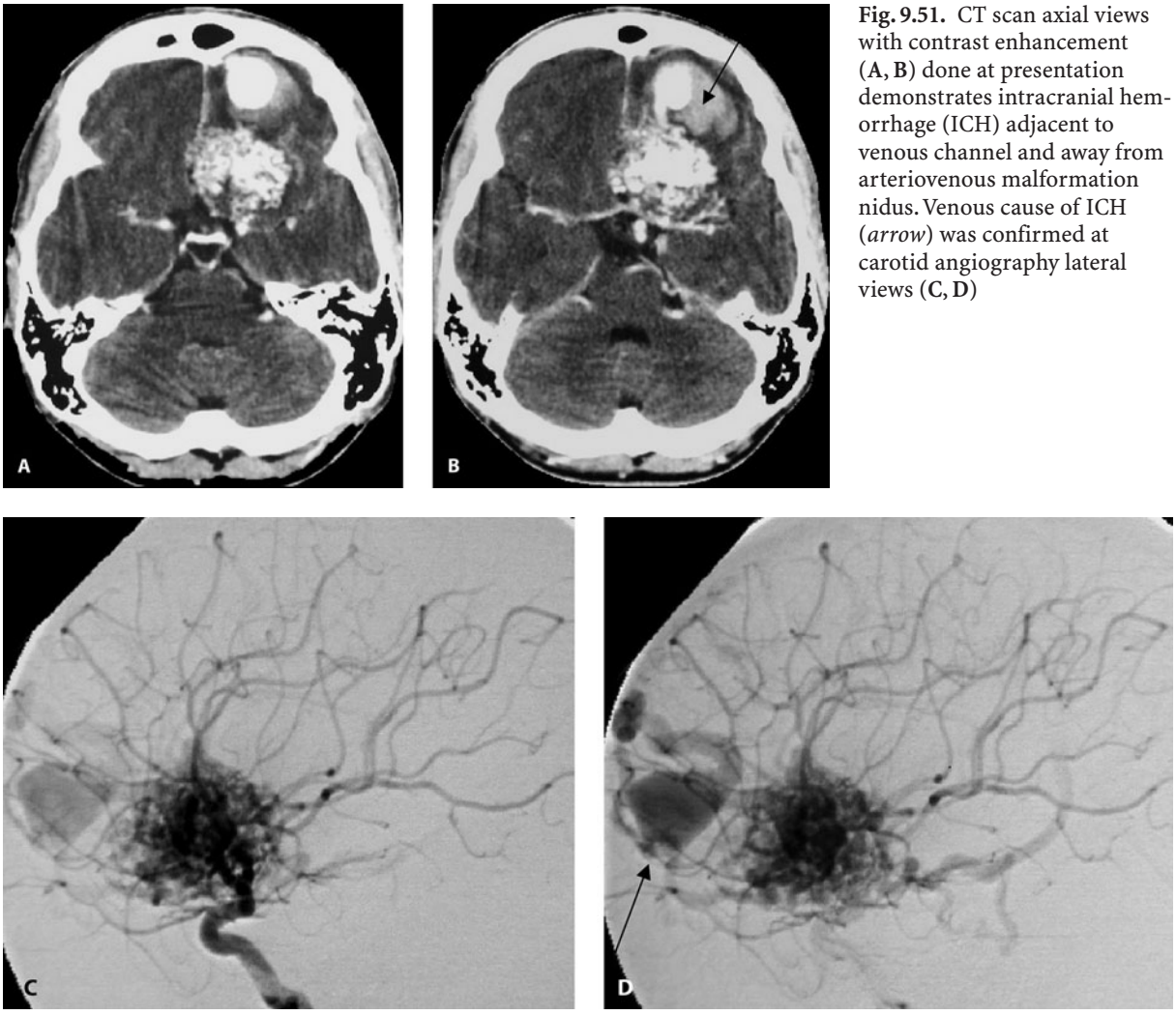

Fig. 9.51. CT scan axial views with contrast enhancement (**A**, **B**) done at presentation demonstrates intracranial hemorrhage (ICH) adjacent to venous channel and away from arteriovenous malformation nidus. Venous cause of ICH (*arrow*) was confirmed at carotid angiography lateral views (**C**, **D**)

One may suggest the effect of chronic activation of the coagulation system in a lesion that is known to trap platelets (Sutherland et al. 1988). Association with a true or dominant coagulation (C or S protein, antithrombin III) deficiency can be suspected in some patients (Dusser 1988). A peculiar pattern of anti-factor VIII secretion has been noted in the endothelium of some venous malformations of the face (Berenstein and Choi 1988) and in some patients with Von Willebrand disease.

Venous ectasias are the continuous response of the venous wall to restricted outflow, resulting in turbulence and vascular venous remodeling. The aneurysmal dilatation of the vein of Galen illustrates this situation in an extreme fashion. Venous ectasias or pouches tend to occur when the flow through an enlarged vein encounters an obstacle, which then narrows it or induces kinking (Table 9.14). The venous dilatation results from a failure to find an efficient exit to relieve the increased pressure and may be responsible for hemorrhage (Figs. 9.49–9.51). Converging systems (deep venous, posterior portion of the basal vein, and deep sylvian vein) have a greater chance of developing ectasias than diverging venous sys-

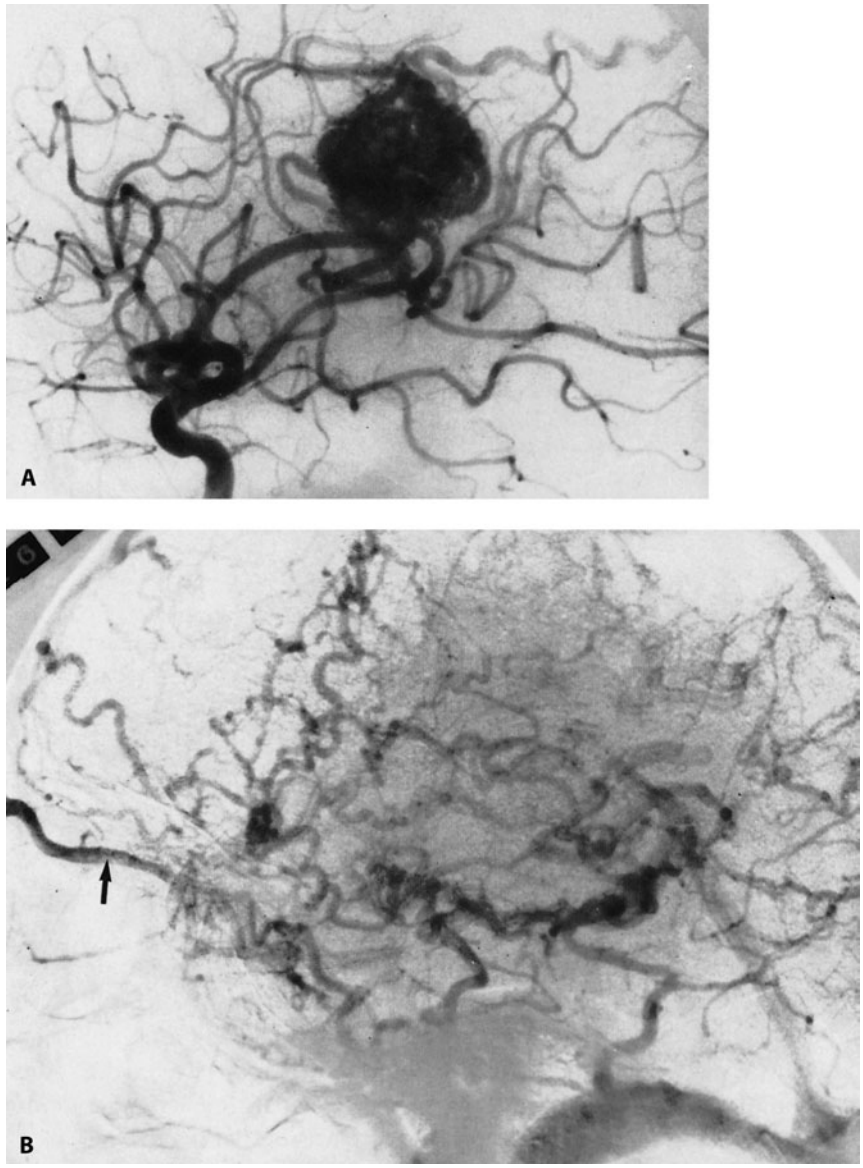

Fig. 9.52. **A** Early and **B** late phases of the left internal carotid injection in lateral view. Rolandic arteriovenous malformation in a patient presenting with conjunctival congestion of the left eye. Note the pseudophlebitic aspect of the cortical venous drainage into the ophthalmic vein (*arrow*, **B**) responsible for the ophthalmic symptomatology

tems (cortical veins). The impact of the increased venous pressure related to the AVM will depend on the individual anatomical situation. Separation of the venous drainage of the AVM from that of the brain would protect the brain from retrograde venous hypertension. This would be facilitated by efficient alternate outlets allowing for transosseous, transorbital, and contralateral drainage (Figs. 9.52, 9.53). It may also be responsible for rare extracranial manifestations of a BAVM such as epistaxis (Fig. 9.54). Partial treatment of the AVM may improve the venous drainage capabilities of the brain. The closer the AVM is located to a dural sinus that drains its venous outflow, the less likely it will interfere with the brain venous drainage in the region. The farther the AVM is located from the sinus, the higher the chance for it to reflux into cerebral veins and create retrograde venous congestive sequelae such as decreased tissue perfusion and seizures (Figs. 9.55, 9.56).

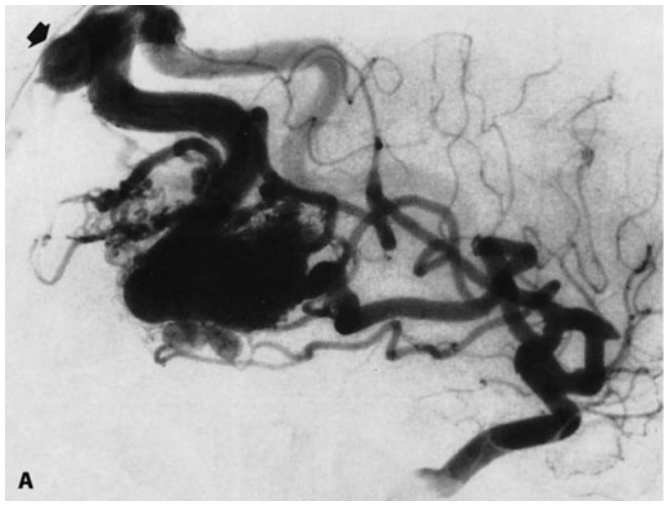

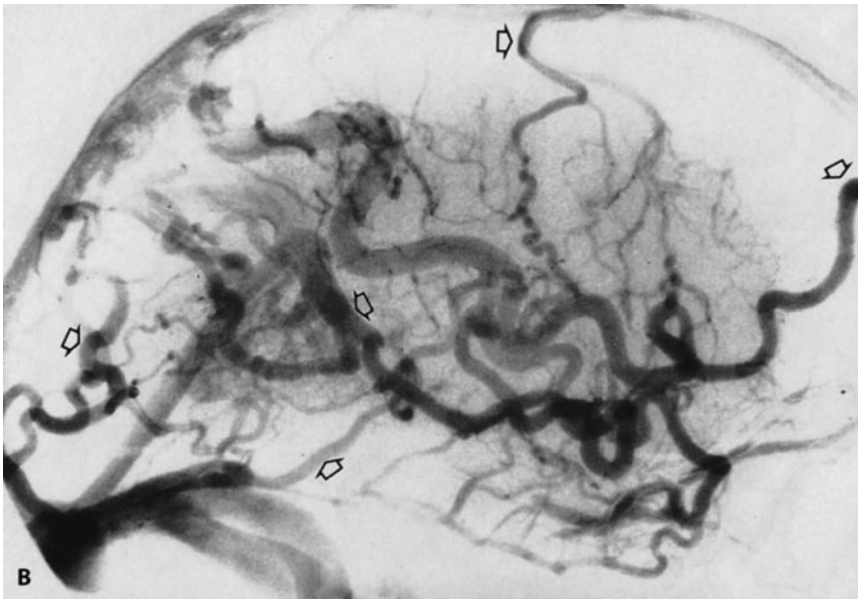

Fig. 9.53. **A** Early and **B** venous phases of the right internal carotid injection in lateral view. Posterior temporal arteriovenous malformation draining into a large temporoparietal vein joining the superior sagittal sinus without opening into it (*solid arrow*, **A**). Note the reflux into a parietofrontal venous system leading to congestion of the entire hemisphere (*open arrows*, **B**)

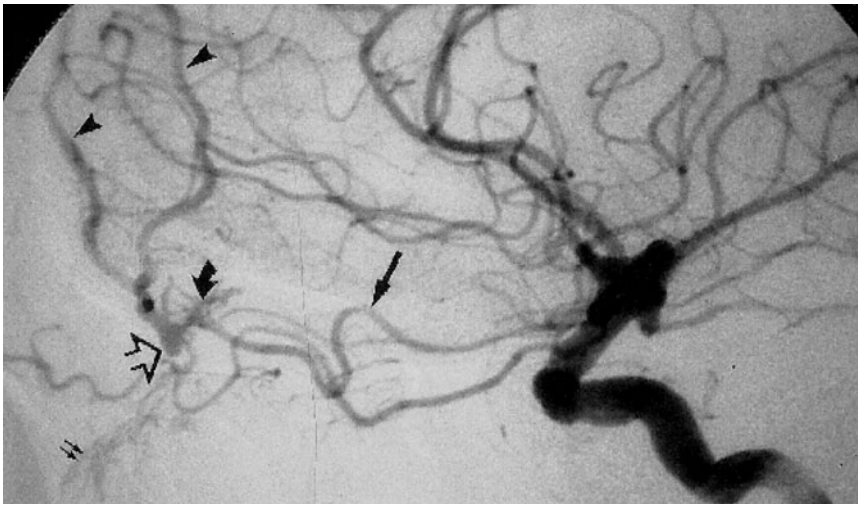

Fig. 9.54. In a patient who presented with epistaxis, the carotid angiogram lateral view demonstrates a small frontal polar brain arteriovenous malformation (*curved arrow*) fed by a frontal polar anterior cerebral artery branch (*long arrow*) and draining into cortical cerebral veins (*arrowheads*) as well as toward the nasal fossa venous system (*open arrowhead*) through the cribriform plate

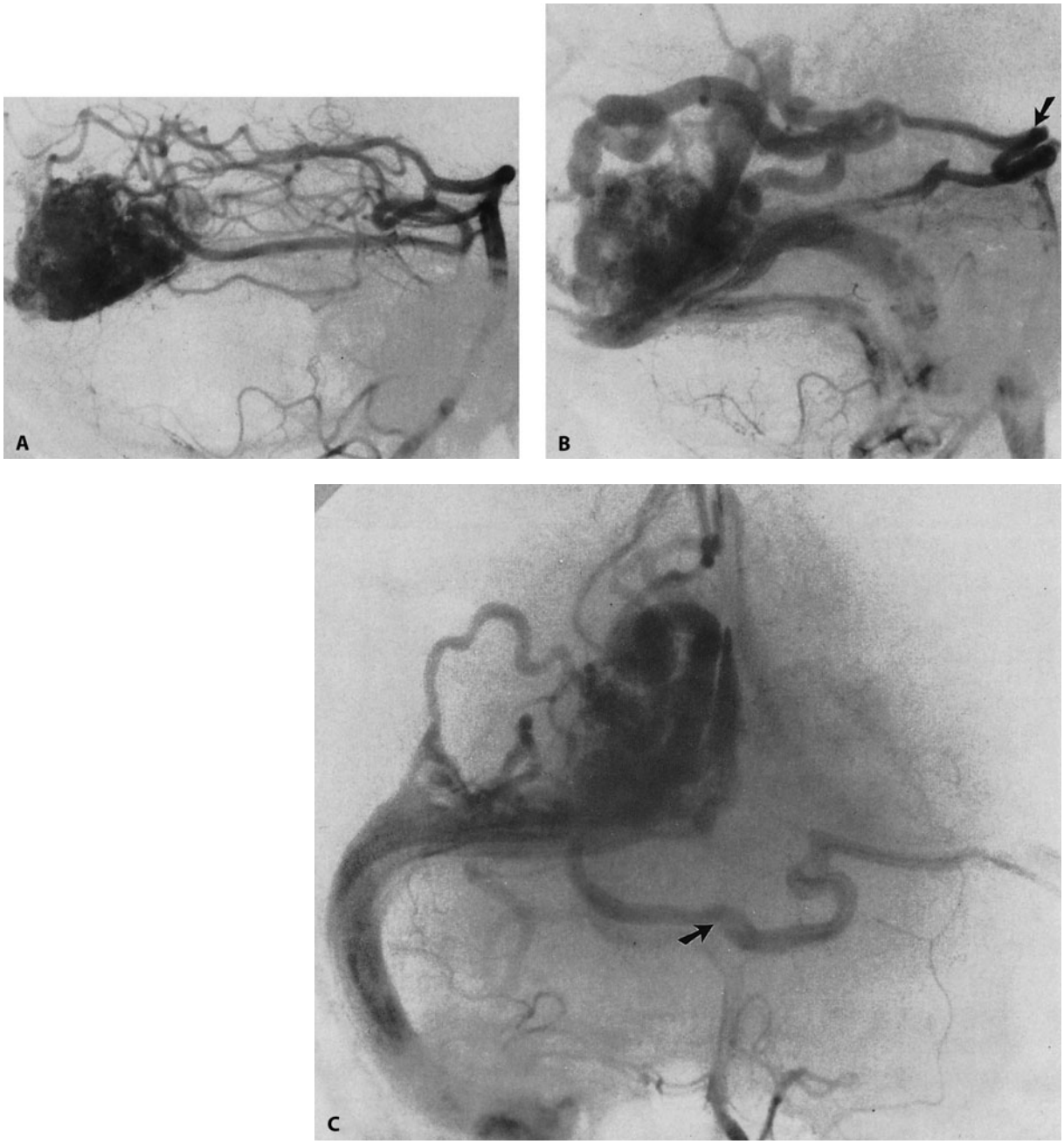

Fig. 9.55. **A** Early and **B** late phases of the left vertebral artery angiogram in lateral and **C** frontal views. Occipital pole arteriovenous malformation fed by the posterior temporal branch of the right posterior cerebral artery. Note the congested venous drainage that crosses the midline to open into the opposite medial, temporal venous system via the posterior communicating vein (*arrow*)

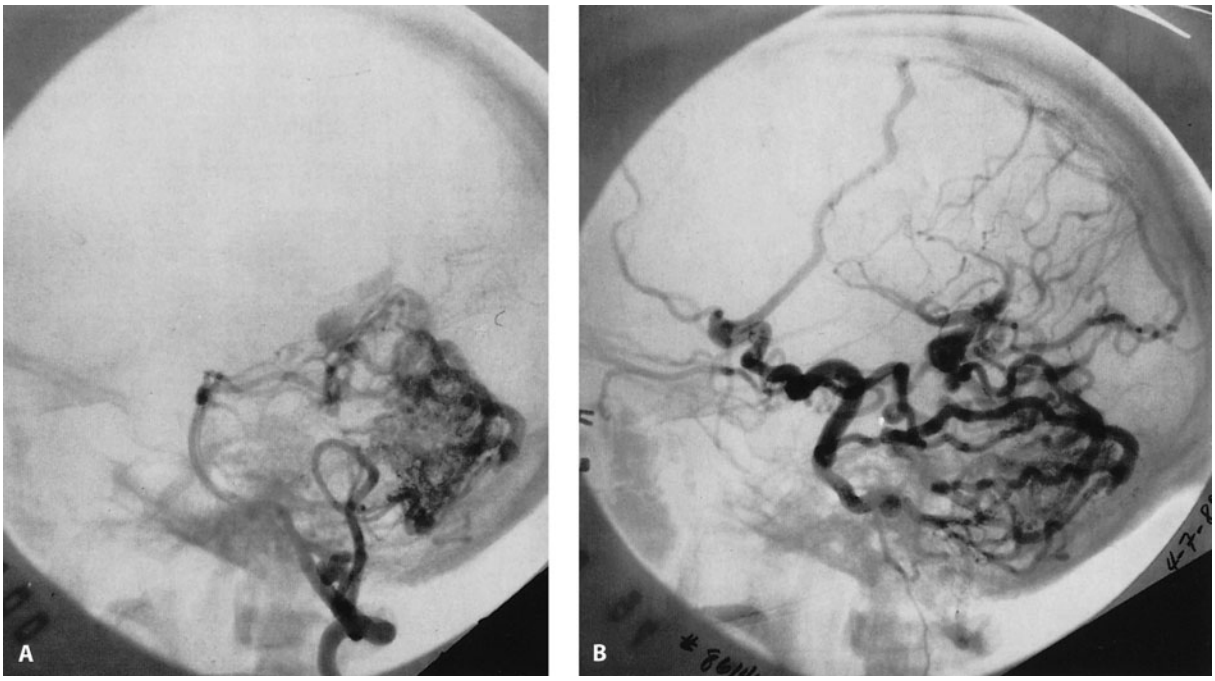

Fig. 9.56. **A** Early and **B** late phase of the left vertebral artery injection in lateral view. Posterior fossa arteriovenous malformation revealed by temporal seizures. Note on the late phase (**B**) the congested supratentorial venous system, opacified through the lateral mesencephalic venous connections

CSF Changes

Alterations in CSF circulation and absorption may be caused by increased venous pressure related to the AVM drainage or due to thrombosis within the superior sagittal sinus. Reflux into the superior sagittal sinus and stagnation in its posterior segment may, in some AVMs, induce segmental thrombosis that finally separates the shunt drainage from that of normal brain parenchyma. Transosseous and orbitofacial venous collateral circulation may occur and if efficient, such drainage may allow the abnormal venous reflux to remain asymptomatic. Many CSF disorders associated with BAVM remain unexplained, and less well-known phenomena such as transcerebral vein dysfunction and lack of cerebral compliance are just two examples of mechanisms that may result in significant modification of the extravascular intracerebral water compartment (see Vol. 3) (Zerah et al. 1992).

Calcifications

Calcifications in BAVMs are usually located in the venous walls. In children, calcifications may occur at a distance from the shunt, in normal veins, probably secondary to hypoxia at the venous watershed zones or at the subpial cortical venous level (Sturge 1879; Weber 1922) (Fig. 9.66). They can appear with age but once present they do not disappear. Calcifications are rarely parenchymatous and usually correspond to a calcified cerebral hematoma. Sutherland et al. (1988) were able to demonstrate

platelet aggregation within the malformation in two patients with calcified BAVMs.

9.3.1.5 Clinical–Angioarchitectural Correlation in Brain Arteriovenous Malformations

The natural history of brain arteriovenous malformations (BAVMs) has been related to every conceivable facet of the lesion, including size and topography (Shi and Chen 1986; Spetzler and Martin 1986), the age and sex of the patients, the location of the lesion (Crawford et al. 1986; Forster et al. 1972; Jomin et al. 1985), the presence and type of venous obstruction (Laine et al. 1981; Lasjaunias et al. 1986a), and associated arterial aneurysms (Miyasaka et al. 1982; Batjer et al. 1986; Lasjaunias et al. 1988). Most natural history studies have been retrospective reports (Graf et al. 1983; Crawford et al. 1986; Brown et al. 1988). The best available prospective studies are those of Ondra et al. (1990) and Mast et al. (1997). A prospective correlation between the angioarchitecture of the AVM and its clinical implications has, however, not yet been made.

Hemorrhage and Angioarchitecture

Hemorrhage in a patient with a BAVM is a significant change in the compliance of the vascular system. Similarly, the onset of seizures or neurological deficits in an AVM patient is an imbalance in the compliance of brain function in relation to the AVM.

It has been postulated that sudden headaches, with or without seizures, and other acute symptoms (often transient) can be considered as expressions of minor local hemorrhage. Evidence of such small hemorrhages has been noted at surgery (Stein and Wolpert 1980; Yamada 1982). If this correlation is correct, then these minor bleeding events increase the true incidence of hemorrhage in BAVMs, but by the same token, it would decrease the real morbidity and mortality risks of a BAVM.

There is evidence that bleeding can result from rupture of the AVM nidus, arterial aneurysm rupture, or from venous rupture, which may occur close to or remote from the AVM.

Analysis of Crawford's patients who bled reveals that arterial aneurysms were significantly more frequent in the hemorrhage group (41%) than in the overall population of those with AVMs without aneurysms. Redekop (1998) noted in the Toronto series that the occurrence of hemorrhagic presentation increased from 40% to 72% if the location of the AA was intranidal versus being on the feeding pedicle to the AVM and resulted in an expected future annual risk of hemorrhage of 10%. In the Bicêtre series, it was noted that the presence of intranidal AAs significantly worsened the natural history for future hemorrhage (Meisel et al. 2000).

It is also relevant that the incidence of both associated aneurysms and hemorrhage increases with age. Therefore, it becomes evident that, in any given AVM patient, the overall 3%–4% risk of hemorrhage per year may not apply.

In addition, each individual will react differently to the presence of a malformation. Consequently, although acquired features are linked to the

AVM, they also express the host's capacity to compensate for the presence of an AVM. The increased chance (89%) of rebleed in an AVM patient diagnosed after the age of 60 (Crawford et al. 1986) may testify to the acquired rigidity of the vascular system with aging and its vulnerability to the presence of the AVM.

Deep venous drainage and deep location of the AVM were also noted to be associated with a higher risk for hemorrhage at presentation in the series of Langer et al. (1998) and Porter et al. (2000a). However, in the subsequent natural history after presentation, only deep location and increased size were risk factors for future hemorrhage (Porter et al. 2000; Stefani et al. 2002).

Hemorrhages located at a distance from the nidus are usually related to venous bleeding (Figs. 9.48–9.51). Yasargil (1987) found the venous pressure in ruptured AVMs to be higher than in unruptured ones (as measured during open surgery).

In conclusion, a hemorrhagic episode accounts for the failure of the host vascular system to compensate for the morphological alterations that have been induced by the AVM upon the arterial and venous systems or that have occurred within the nidus of the AVM itself. This may also explain why the risk factors for hemorrhage at presentation are not necessarily the same as the factors for future risk of hemorrhage after presentation (natural history). While these factors in the various retrospective and prospective series are not always identified as the same (reflecting referral and management biases) (Hofmeister et al. 2000), the fact remains that a relationship between angioarchitecture and hemorrhage can almost always be identified.

Cerebral Function and Angioarchitecture of Brain Arteriovenous Malformations

The interaction between cerebral AVMs and brain function represents the most challenging aspect of analysis of these lesions. The goal of the analysis of the AVM angioarchitecture is to appreciate specific patterns that have or will create symptoms. Such analysis tends to be mostly retrospective, but their interpretations may help us to identify the vascular arrangements responsible for future clinical problems.

Neurological deficits and seizures may be caused by the AVM through several mechanisms: (a) ischemia, either arterial or venous, and (b) direct or indirect mechanical compression. Arterial ischemia may arise from two types of mechanisms: (a) a steal phenomenon or (b) occlusive changes. In our experience, evidence of the steal phenomenon has never been conclusively demonstrated, except by angiographic studies.

The concept of steal in angiography is based on the nonvisualization of vessels in a normal area of the brain that should have been visualized at the time of injection. However, careful angiographic evaluation will always demonstrate the nonvisualized branches through leptomeningeal anastomosis from adjacent territories, thus expressing the capability of the brain circulation to adapt. Most of the territories that presumably were "stolen" from, were not symptomatic even when the flow within the AVM was high enough to steal all the contrast material from the ipsilater-

al hemisphere. Although there is doubt with regard to the symptomatic aspect of this phenomenon, the finding itself cannot be denied.

Arterial stenosis and occlusion proximal to the AVM may range from a single vessel narrowing to a moyamoya pattern but will always testify to the acquired response of the upstream arterial tree. Such changes are usually slowly progressive, allowing for a stepwise compensation, which accounts for their clinically silent development. These changes may eventually lead to progressive symptoms such as headaches, neurological deficits, and seizures. In our experience patients with occlusive changes may have fewer hemorrhagic complications than those patients without such changes.

The concept of venous ischemia is accepted by most authors involved in the management of cerebral arteriovenous lesions but is rarely acknowledged for its significance. Laine et al. (1981) pointed out the key role played by the veins in understanding the symptoms from dural and BAVMs. The absence of any arterial steal or contribution from pial arteries to the supply of dural AVMs, while often presenting with identical neurological manifestations as BAVMs, points to the predominant role of the venous drainage in producing symptoms.

It is also important to remember that 60%–80% of the cerebral blood volume is located in the venules of the cerebral venous system. They have all the necessary characteristics for active exchange with the surrounding tissue, testifying to their role in nutrient exchange. Flow in venules in the white matter is bidirectional, allowing them to fulfill their nutrient role even in a retrograde fashion. Most of these nutrient functions involve catabolic reabsorption (Auer and McKenzie 1984). The progressive nature of the deficits and their fluctuation in severity reflect the attempts of the collateral circulation to overcome the increased pressure in the venous outlet of the shunt. Decreased tissue perfusion secondary to venous ischemia may produce virtually any type of neurological symptom (motor or sensory deficits, neuropsychological alteration, seizures, etc.). The greater the distance between the shunt site and its venous exit into the dural sinus the higher its chances of interfering with the normal brain circulation.

The impact of the BAVM on the surrounding brain circulation and function is starting to be evaluated with high field strength (3T) MRI examination. While these investigations are still preliminary, they appear to confirm our beliefs with respect to the dynamic interrelationship between the BAVM and the individual host and consequently the potential for altering this impact with selected targeted endovascular therapy.

Seizures and Angioarchitecture of Brain Arteriovenous Malformations

Seizure is the second most frequent presenting symptom in all BAVM patients and will occur in up to 53% of cases. The most frequent AVM locations associated with seizure production are the motor-sensory strip and the temporal areas, representing close to 70% of patients with seizures (Crawford et al. 1986). In patients without an obvious hematoma or subarachnoid hemorrhage, the cause of seizures has been controversial. It has been said that this symptom is frequently associated with small hemor-

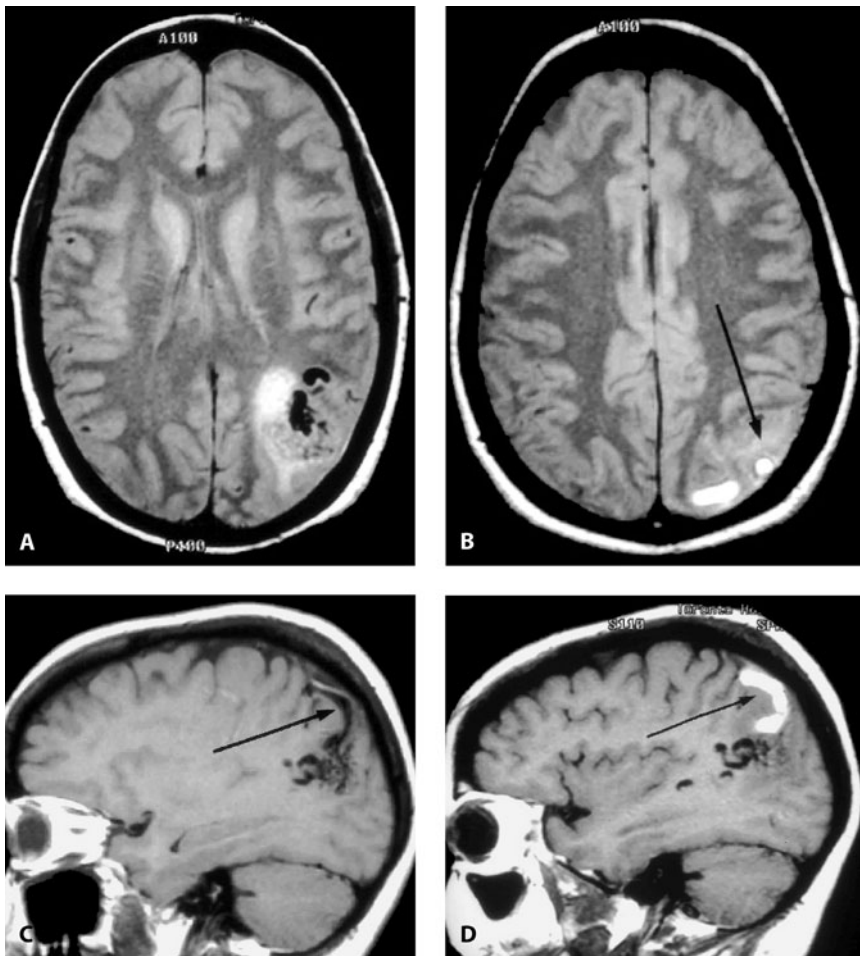

Fig. 9.57A–D. Patient with new onset of acute headaches and focal seizure. MRI axial views show increased signal in the brain adjacent to an arteriovenous malformation (AVM, **A**) as well as increased signal (*arrow*) in superficial vascular channel (**B**). The sagittal MRI performed 1 year earlier (**C**) had shown flow void (*arrow*) in one of the veins draining the AVM. The new MRI 1 year later (**D**) demonstrates recent thrombosis of this vein (*arrow*), producing new onset of seizures and headaches

rhages, discovered only at the time of surgery (Stein 1985). However, only 6.5% of Yasargil's surgery patients who presented with a seizure had evidence of bleeding at the time of surgery. Some of the discoloration noted at this time may have represented old areas of previously thrombosed malformation or veins. The onset of seizures in a previously healthy individual must reflect an acute or abrupt change in hemodynamics, which may be due to rerouting of drainage from the malformation through a vein that previously drained normal brain.

The increase in pressure produces secondary neurological dysfunction of the affected brain and seizures may result. A patient with a posterior fossa vascular malformation developed venous drainage that was rerouted toward the temporal lobe and subsequently presented with temporal lobe seizure (Fig. 9.56). Headaches and new onset seizures can also occur when venous thrombosis develops in association with a BAVM (Fig. 9.57). It may lead to its complete obliteration when such thrombosis involves the only venous outlet of the AVM, (Fig. 9.58).

Mass effect associated with unruptured BAVM has been observed for a long time (ter Brugge et al. 1977) and has been demonstrated by CT and MRI in up to 18% of patients. In unruptured AVMs, the size of the venous component is often the dominant factor responsible for mass effect.

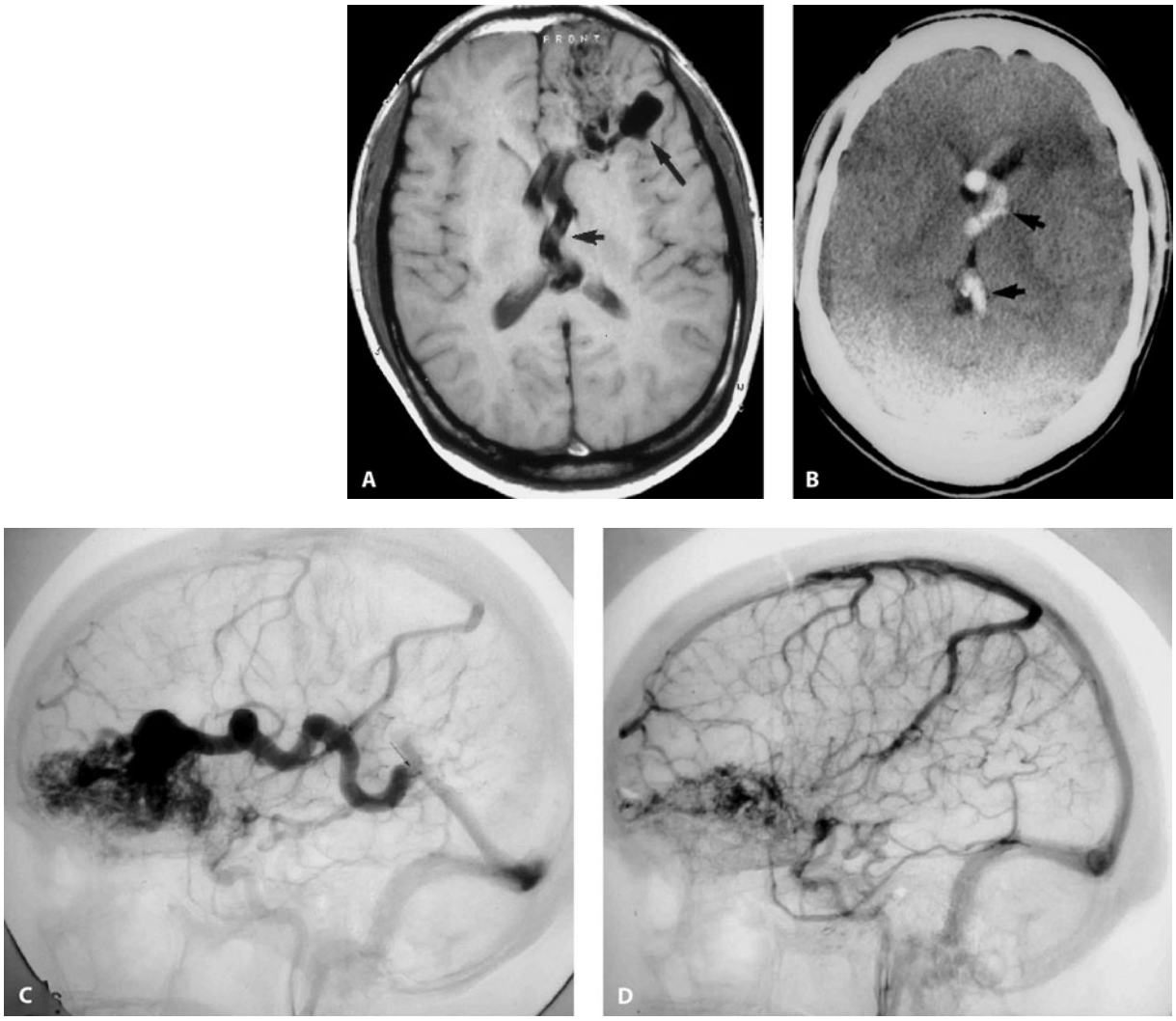

Fig. 9.58. MRI (**A**) performed at the time of the original investigation for seizure disorder had shown frontal arteriovenous malformation (AVM, *long arrow*) with prominent internal cerebral venous drainage (*short arrow*). Nonenhanced CT scan (**B**) done 1 year later after new onset of sudden headaches demonstrates thrombosis of internal cerebral vein (*short arrows*). Carotid angiograms lateral view at the time of the original investigation (**C**) and 1 year later (**D**) after acute onset of headaches demonstrates that there is no longer opacification of the AVM and the internal cerebral vein

Headaches and Angioarchitecture of Brain Arteriovenous Malformations

Headaches are subjective and difficult to quantify and to study. In patients with BAVMs, headaches can be divided into those that accompany an episode of a subarachnoid or intracerebral hemorrhage versus those that are more subacute or chronic in nature.

The acute headaches associated with hemorrhage are those typically related to an acute event, presenting abruptly and usually severe in nature, associated with photophobia, nausea, vomiting, convulsion, and loss of consciousness. While the headaches may signify the hemorrhage, the im-

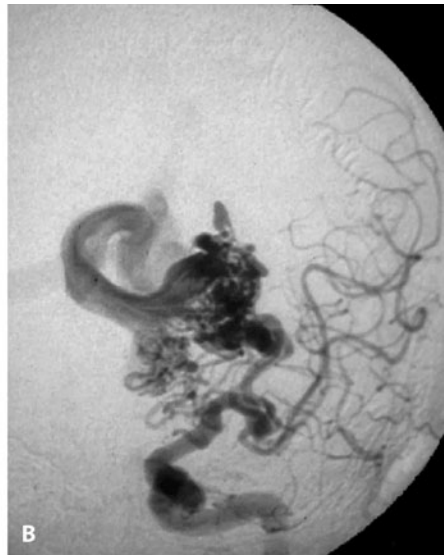

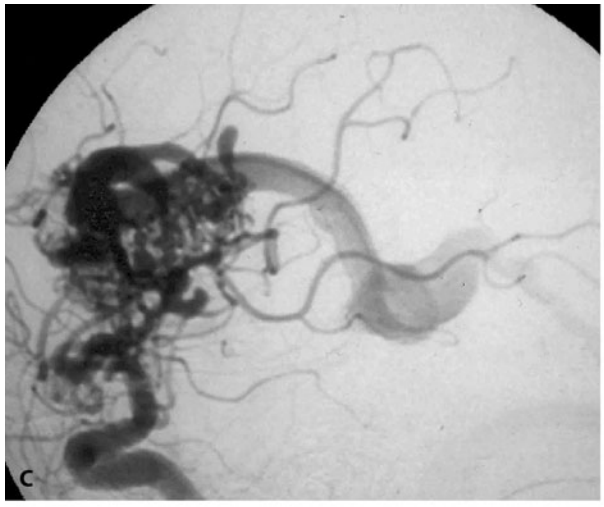

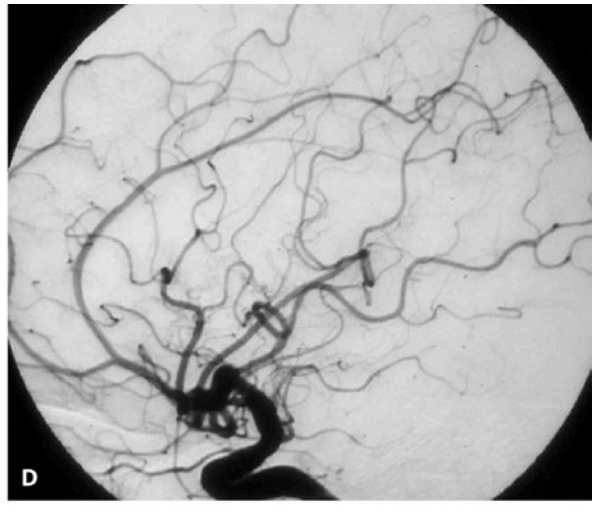

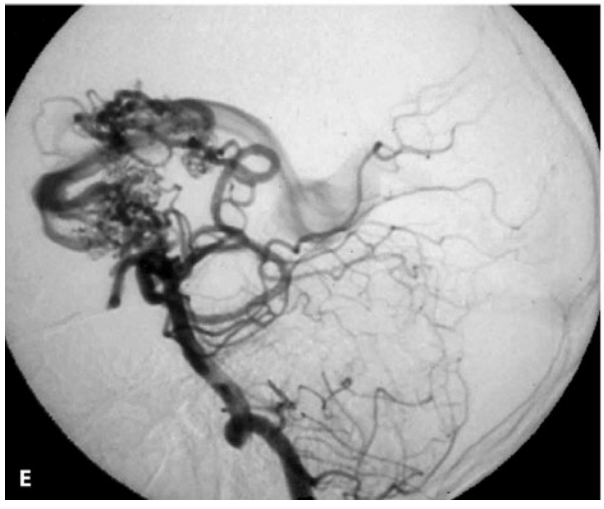

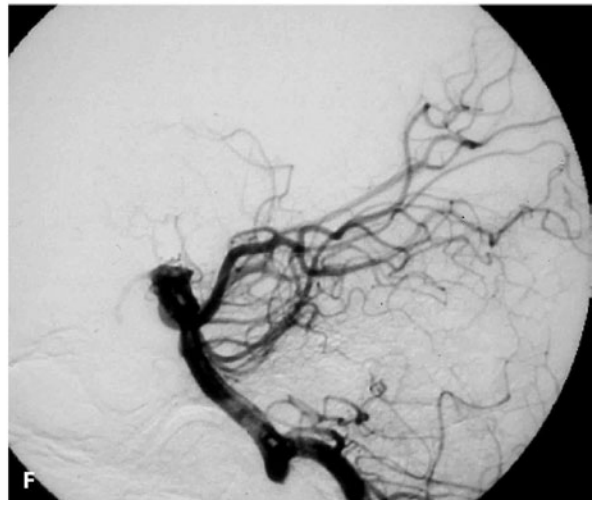

Fig. 9.59. CT scan (**A**) at presentation demonstrates intracerebral and intraventricular hemorrhage and IVH from a basal ganglia arteriovenous malformation (AVM) shown on carotid angiogram AP view (**B**). Carotid angiogram lateral views at presentation (**C**) and 3 months later (**D**), as well as vertebral angiograms lateral views at presentation (**E**) and 3 months later (**F**), demonstrate that there is no longer opacification of the AVM. No treatment was given in the interval

pact of the hemorrhage on the angioarchitecture may in fact be positive and in exceptional circumstances lead to obliteration of the AVM (Fig. 9.59). Depending on the extend of the hemorrhage, the patient may deteriorate acutely with generalized cerebral dysfunction and may progress to respiratory and/or cardiac arrest.

Constant headaches or episodes of throbbing (migraine-like) headaches can occur in the same patient. The headaches are often localized to the same side as the AVM. Headache is the first symptom in approximately 60% of patients and was present in over 20%–30% of our patients. The headaches associated with various vascular distributions are those that relate specifically to the dural supply and/or external carotid participation in a vascular malformation. These types of headaches may have a precise distribution. They are usually throbbing in nature and often are associated with some eye symptoms. Patients with significant or predominant posterior cerebral artery supply to a BAVM may have associated headaches, most often localized to the same side as the malformation. These may also be associated with various types of visual prodromes and/or intermittent episodes of field defects.

Patients with arterial stenotic lesions in association with an AVM frequently appear to have chronic headaches that are not responsive to treatment.

The management of the headaches will vary depending on their perceived cause. Embolization, in general, may relieve headaches of vascular nature. When the dural participation to an AVM is properly embolized, associated headaches usually resolve or diminish. On occasion, the visual prodrome may persist, but the headaches will not reappear. In patients with BAVMs with posterior cerebral artery participation, the headaches may actually be exacerbated for a short period of time, usually days, after embolization of this supply and then improve or disappear. Conversely, in patients with middle or anterior cerebral artery contribution in the presence of posterior cerebral artery supply, the headaches may worsen after embolization of the middle and anterior cerebral artery supply and again improve following subsequent embolization of the posterior cerebral supply.

Arteriovenous Malformations and Pregnancy

While there appears to be an increased rate of presentation at the time of pregnancy, much controversy continues on the possible increased risk of neurological complications, primarily hemorrhage, during pregnancy. Neither in our experience nor that of Yasargil (1987) was there any evidence of an increased bleeding rate associated with the BAVM during pregnancy. Controversy also exists as to the increased risk of hemorrhage during delivery. It is known that the venous pressure will be increased during Valsalva maneuvers at the time of delivery and also that a number of patients with AVMs have had acute symptoms or aggravation of preexisting symptoms during the third trimester of pregnancy or during delivery. On the other hand, a significant number of patients have gone through multiple pregnancies and deliveries without manifestations of their disease (Dias and Sekhar 1990). It appears prudent that if a vaginal delivery

is contemplated the procedure should be done with an epidural block and nausea-producing drugs be avoided.

In our opinion the presence of a BAVM is not a contraindication to becoming pregnant.

9.3.2 Venous Variations, Malformations, and Mixed Lesions

Over the years venous lesions of the CNS have generated a large number of publications (Nishizaki et al. 1986; Koussa et al. 1985; Tagle et al. 1986). Among the most controversial venous lesions are the so-called cavernous type, which were called venous angiomas or cavernous hemangiomas. Some of these lesions have been regrouped under the generic name of venous hamartomas (Crawford and Russell 1956). Hamartomas, however, are spontaneous proliferations of elements derived from the regional tissues in which they develop (Rubinstein 1972, 1981). Such proliferation and growth produces a large number of cells that eventually reach maturation and become self-limiting. The resulting mass appears as an exaggeration of a physiological process. These lesions do present some tumor-like characteristics and they should not be considered as malformations. While capillary hemangiomas of infants correspond to this definition, none of the cerebral venous anomalies or abnormalities can be accurately described as hemangiomas (Table 9.15).

As some of the venous vascular malformations (capillary telangiectasias, cavernomas) are not readily visible at angiography, improved noninvasive imaging (MRI) has assisted us in the documentation of these CVMs.

The coexistence and possible interrelationships between various vascular malformations have recently become better documented (Awad et al. 1993; Chang et al. 1997; Nussbaum et al. 1998). This is particularly important in order to have a better understanding of their individual or combined natural history, and in turn this may lead to more appropriate management strategies.

Table 9.15. Classification of venous lesions (from Lasjaunias et al. 1989)

Traditional classification	New classification
Cerebral venous angiomas	Developmental venous anomaly (anatomical variation)
Cavernous hemangiomas (cerebral or spinal cord)	Cavernomas (cavernous malformations)
Cavernous hemangiomas (dural or epidural)	Cavernous hemangiomas (tumors)

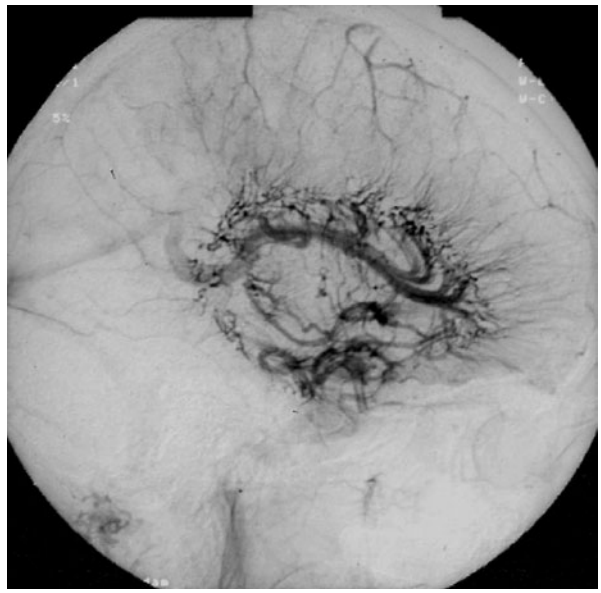

Fig. 9.60. Carotid angiogram lateral view demonstrates hemispheric developmental venous anomaly with poorly developed superficial cortical venous system and most of the hemisphere draining into the deep venous system (DVA)

9.3.2.1 Developmental Venous Anomalies

Saito and Kobayashi (1981) were the first to question the malformation basis of venous angiomas. Subsequently, they were named developmental venous anomalies (DVAs) (Lasjaunias 1986) on the basis of their distribution along transmedullary venous anastomoses, where cortical differentiation has occurred (see Vol. 1) (Fig. 9.60). We also expressed doubts regarding the role these lesions have in most of the clinical events when they were demonstrated, thus questioning the need for therapeutic intervention (Lasjaunias et al. 1989; Jimenez 1989). They are not encountered elsewhere in the CNS, as opposed to other vascular malformations. Their frequent incidental appearance on CT and MRI has become well recognized (Fig. 9.61) and emphasizes their benign nature. Failure to efficiently drain cerebral tissue would explain their possible role in ischemic or hemorrhagic events, independent of their association with true pathologies (cavernoma, AVM, etc.) (Nussbaum et al. 1998). Furthermore, the not infrequent association of DVAs with true vascular malformations, mostly of the capillary or venous type (Fig. 9.62), has raised speculation regarding their causative interrelationships. Nevertheless, clinical symptomatology is rarely directly related to the presence of the DVA, and therefore management should be directed toward the preservation of the DVA, as it represents the key to good clinical outcome.

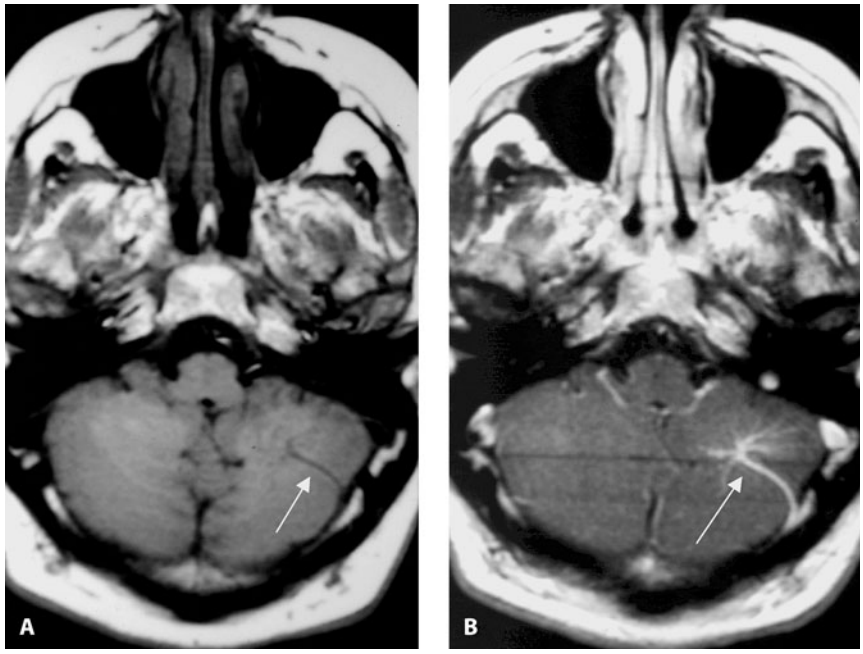

Fig. 9.61. T1-weighted MRI (**A**) and T1-weighted postcontrast enhancement (**B**) demonstrates typical appearance of superficial deep venous anomaly (*arrows*) draining most of the deep left cerebellar hemisphere

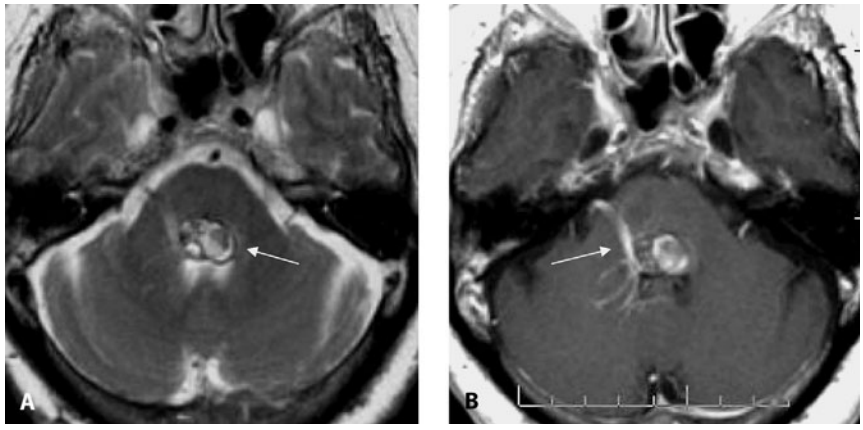

Fig. 9.62. T2-weighted MRI (**A**) demonstrates characteristic popcorn appearance of a cavernoma (*arrow*) along the floor of the 4th ventricle, while enhanced T1-weighted MRI (**B**) shows the associated developmental venous anomaly (*arrow*) draining the adjacent brainstem as well as the deep right cerebellar hemisphere

9.3.2.2 Cavernous Hemangiomas

In vitro studies presently make it possible to differentiate a proliferative lesion (tumor) from a nonproliferative one (malformation). The clinical and therapeutic consequences of this distinction are obviously very important. Confusion results from the fact that both lesions have always been presented under the same name.

Cavernous hemangiomas, benign neoplasms of blood vessel origin, are typical tumors. They can occur in the intracranial or intraspinal epidural space (Simard et al. 1986; Buonaguidi 1984) and exceptionally occur in the CNS itself. They may also develop in the peripheral nervous system (Fehlings and Tucker 1988). Angiography usually shows a faint homogeneous capillary stain, suggesting the preoperative diagnosis of meningioma (Numaguchi 1979). Cavernous hemangiomas are best demonstrat-

ed on contrast-enhanced MRI; angiography is seldom required to make the diagnosis. Cavernous hemangiomas are more frequent in females in whom a progressive mass effect may expand the lesion acutely during menstruation or pregnancy (Kobayashi et al. 1984).

These lesions are mostly treated surgically (Padovani et al. 1982), although certain authors have suggested the possibility of radiation therapy (Yamasaki et al. 1984), but this method has not proven to be consistently effective and may be associated with significant morbidity. These lesions seldom bleed and there have been no incidental recordings at autopsy. They were nosologically believed to be close to the lingual or orbital hemangiomas (Harris and Jzkobiec 1979).

More recently Biondi et al. (2002) have cast doubt on this concept of their tumoral origin and in an extensive review of the literature combined with their own experience, they propose that extra-axial cavernous hemangiomas are not of tumoral origin. In their opinion, no evidence exists as to their proliferative nature and in fact histopathological examination of available specimens suggested a strong resemblance to intracerebral cavernomas. Their different imaging characteristics (increased T2 signal on MRI, enhancement with contrast, and opacification at angiography) are merely a reflection of their location, with access to the function of the subarachnoid space such as the wash-out of blood products (Biondi et al. 2002).

9.3.2.3 Cerebral Cavernous Malformations

Cerebral cavernous malformations (cavernomas) are the only true venous malformation of the CNS (Table 9.16) (Stein 1985). Their incidence is 0.5% (Otten et al. 1989), and they can be encountered anywhere in the cerebral or spinal cord tissue (Fontaine et al. 1988; Cosgrove et al. 1988; Iplikcioglu et al. 1986; Wang et al. 1988; Lejeune et al. 1989). Cavernous malformations are usually angiographically occult. Their association with DVAs (Fig. 9.62) or confusion with true cavernous hemangiomas (see pre-

Table 9.16. Classification of cerebral venous malformations

Single cavernoma (cavernous malformation)
Multiple cavernomas (cavernous malformations)
Familial
Nonfamilial
Associated cerebral vascular lesions
Capillary malformations
Arteriovenous malformations
Developmental venous anomalies
Associated extracerebral vascular lesions
Venous or venolymphatic extracranial malformations
Associated systemic venous malformations
Sturge–Weber
Cobb and Klippel–Trenaunay
Blue rubber bled nevi

ceding section) accounts for most of the reports of so-called positive angiography (Simard et al. 1986). Only 4.5% of cavernous malformations are symptomatic (Otten et al. 1989; Steiger et al. 1989).

Fundamentally stable, these lesions can expand by confluence of the vascular spaces and further achieve cystic forms through secondary confluence of intralesional spontaneous hematomas (Belloti et al. 1985). There is no cerebral tissue interspersed between the vascular lumens and no evidence of cellular proliferation, capsule formation, or a relationship between the age of the patient and the size of the lesion (Steiger et al. 1989). Numerous cavernous malformations have been reported in newborns and children (El Gohary et al. 1987; Yamasaki et al. 1984; Iwasa et al. 1983; Hubert et al. 1989; Mazza et al. 1989).

Cavernomas can develop de novo particularly following previous radiation therapy (Pozzati et al. 1996; Detwiler et al. 1997; Larson et al. 1998; Maeder et al. 1998). The proliferative capacity of their endothelial cells has been reported in some cavernomas and may explain the growth and the de novo appearance of these lesions (Rutka et al. 1988; Notelet et al. 1997). We have also seen the de novo appearance of cavernomas in patients with extensive dural AVFs with and without deep venous reflux (Fig. 9.63).

Familial cavernomas have been found to be particularly prevalent among the Hispanic population of Mexican descent, with over 50% of affected patients having one or more relatives with cavernomas. Multiple cavernomas (Fig. 9.64) invariably denote familial disease (Bicknell et al. 1978; Clark 1970; Giombini and Morello 1978; Hayman et al. 1982), and intracranial (cerebral) as well as intraspinal (medullary) cavernous malformations can be present in the same individual. The transmission, like all inherited CVMs, is autosomal dominant. Genetic analysis has localized a gene causing cavernomas to a segment of the long arm of human chromosome 7 (7q), although additional gene mutations are suspected (Dubovsky et al. 1995; Marchuk et al. 1995; Gunel et al. 1996). Even though intralesional hemorrhage is consistently found at pathology, few of these hemorrhages are clinically apparent. Patients with cavernous malformations rarely present with subarachnoid hemorrhage, including those in spinal cord locations (Ueda et al. 1987).

Whether the natural history for all types of cavernomas (single, multiple, familial, de novo), is the same remains speculative, and we anticipate differences between these groups to become recognized in the future. Recent natural history studies that did not separate out these potential differences have shown an overall annual event (hemorrhage) rate between 3% and 4% (Porter et al. 1997; Moriarty et al. 1999). However, cavernomas in lobar locations had an annual event rate of less than 1%, while those in deep locations (basal ganglia, thalamus, and brain stem) had an annual event rate of up to 10%. The neurological deficit caused by acute events from cavernomas in deep locations resulted in less than 40% of patients in complete resolution of their symptoms (Porter et al. 1997b), indicating an apparently worse natural history for cavernomas in deep locations.

Cavernomas can be associated with telangiectasias as well as DVAs (Izukawa et al. 1987; Awad et al. 1993). It has become apparent in the literature (McLaughlin et al. 1998; Abdulrauf et al. 1999) as well as in our own experience that patients presenting with a clinical event (hemorrhage)

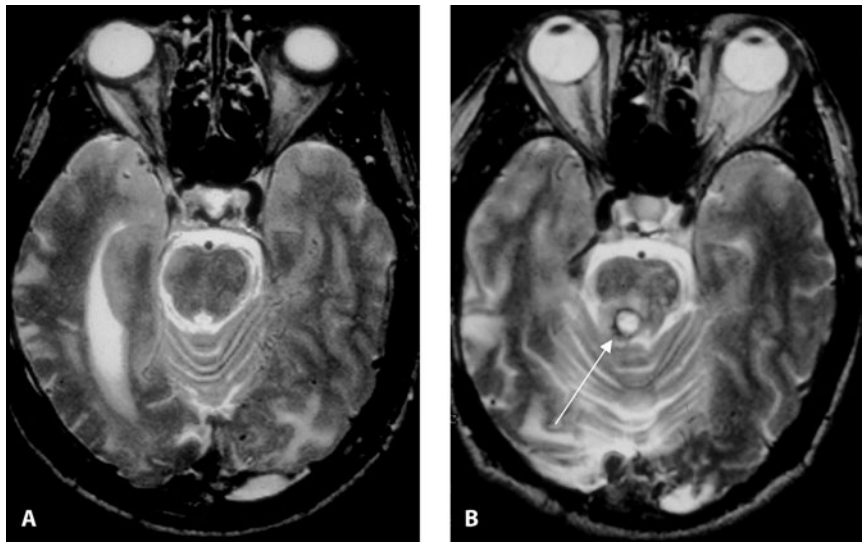

Fig. 9.63A, B. Symptomatic midbrain cavernoma (proven at surgery) developed in patient with transverse sinus dural arteriovenous fistula associated with deep venous reflux. MRI at original presentation (**A**) and 5 years later (**B**) demonstrates de novo cavernoma (*arrow*)

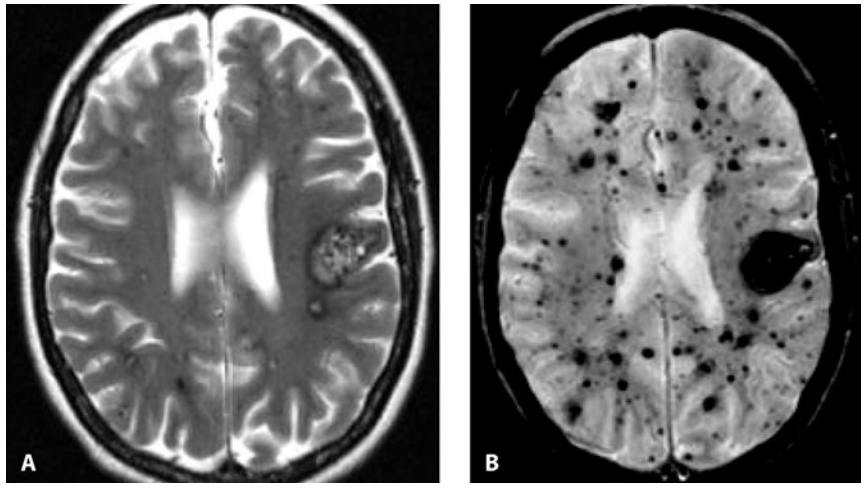

Fig. 9.64. T2-weighted MRI (**A**) and with gradient echo sequences (**B**) demonstrate multiple cavernomas involving both cerebral hemispheres in patient with family history of cavernomas

and imaging studies that reveal the coexistence of a cavernoma and a DVA or a telangiectasia, the cause of the clinical symptoms invariably is the cavernoma.

Whether the DVA could be responsible for the development of a regional cavernoma remains speculative. However, since the DVA drains normal brain tissue it should always be preserved while the indication for treatment of the cavernoma depends on its clinical stability versus its surgical accessibility.

The interrelationship between cavernomas and capillary telangiectasias does not appear to be etiologically or clinically significant.

From a patient management point of view, we recommend that, following CT demonstration of an acute intracerebral hematoma and a negative angiogram, or an angiogram demonstrating a DVA in the region of the hematoma, a MRI should be obtained with grading echo sequences to identify the presence of hemosiderin, reflecting previous hemorrhagic

events or other lesions, and to differentiate cavernoma from neoplasm. If inconclusive and the hematoma is clinically well tolerated, then a repeat MRI examination should be performed in 2–3 months' time. If the hematoma reabsorbs to a cleft an angiogram should be performed to exclude a micro-AVM but if the hematoma mass persists to a significant extent a cavernoma is strongly suspected and a baseline for follow-up is established. Further enlargement of the hematoma mass would of course raise a strong suspicion of neoplastic disease.

9.3.2.4 Occult and Cryptic Malformations

Angiographically occult lesions refer to a multifactorial situation in which the quality of the examinations performed is important. At present no single imaging modality has the ability to diagnose all of the so-called occult vascular lesions. A lesion that would be occult to all modalities including pathology is cryptic. By definition, cryptic lesions are mysterious and hidden, whereas occult lesions are difficult to diagnose. This does not mean that occult lesions are invisible to all modalities since their existence is not questioned (Table 9.17). When Crawford introduced the concept of cryptic AVM in 1956 (Crawford and Russell 1956), examples of intracerebral hemorrhages with AVMs were cited. These cryptic lesions were encountered in 4.5% of patients with intracerebral hemorrhage (Russell 1954). Following many additional publications, the term "cryptic" has been accepted but has been applied to a heterogeneous group of malformations.

Intralesional thrombosis or compression of an AVM by an intracerebral hematoma may account for the nonvisualization of an otherwise visible lesion at angiography (Fig. 9.65). Only cavernomas and telangiectasias are truly angiographically occult. The appearance of cavernomas and their relationship to clinical events at MRI are now well established (Willinsky et al. 1996), while telangiectasias are becoming more recognized at MRI (Lee and Libby 1997) and are of course recognizable at pathology.

Cryptic lesions represent neither a specific clinical or anatomical entity. They correspond to the remaining causes for hemorrhagic episodes when other lesions have been excluded. Their incidence reflects our lack of understanding and knowledge, and by itself has no epidemiological value since it represents a postulated disease or group of diseases.

Occult lesions represent our failure to demonstrate with a given imaging tool a heterogeneous group of pathologies. Similar to cryptic lesions but for different reasons, the incidence of occult malformations has no epidemiological value but is mainly of technological interest.

Table 9.17. Angiographically occult cerebral vascular malformations

Permanently angiographically occult
Cavernomas
Capillary malformations
Thrombosed arteriovenous malformations
Transiently occult
Small arteriovenous malformations (compressed by recent hemorrhage)

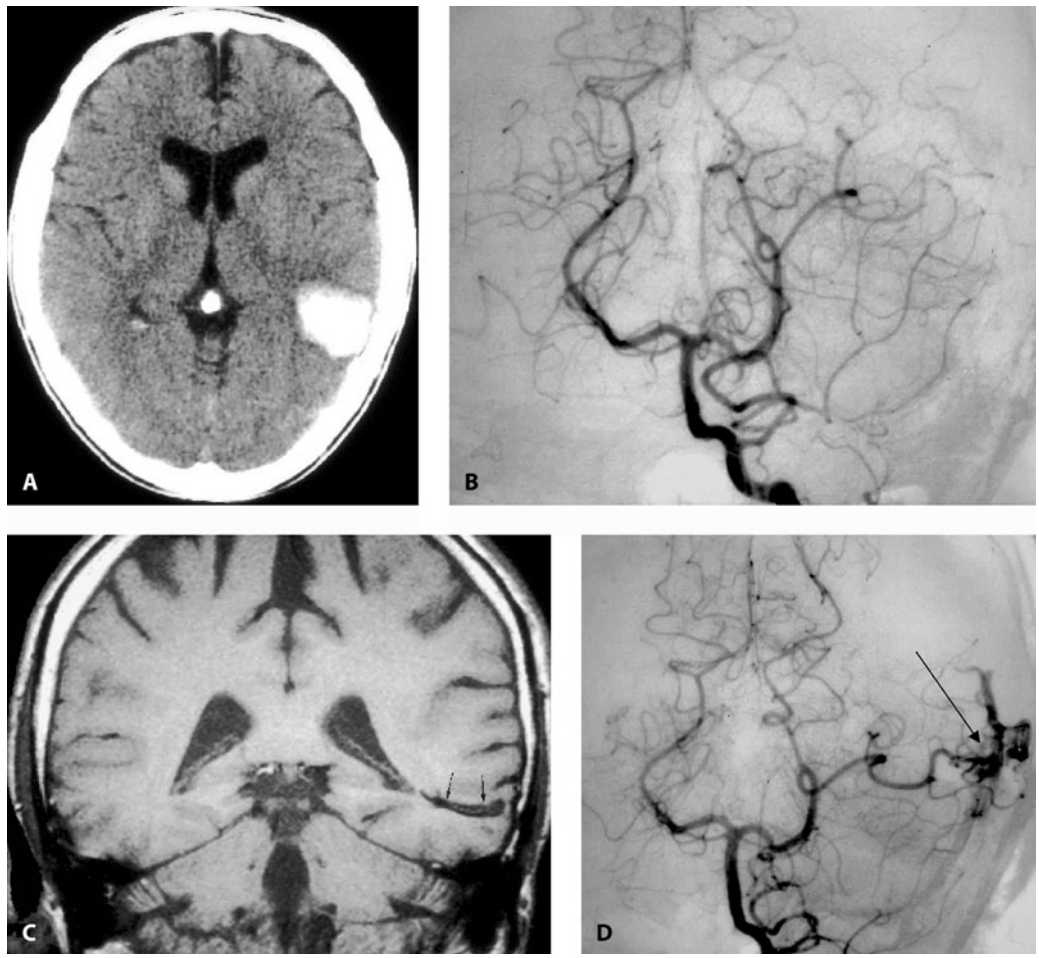

Fig. 9.65. CT scan at presentation (**A**) shows small recent lobar intracranial hemorrhage with no vascular cause apparent on immediate vertebral angiogram AP view (**B**). MRI coronal view (**C**) obtained 6 weeks later shows resolution of the hemorrhage into a cleft (*arrows*) and no cause to be apparent. Vertebral angiogram AP view (**D**) repeated at that time does now demonstrate a small arteriovenous malformation (*arrow*) to be responsible for the bleed (angio-occult at presentation)

9.3.2.5 Sturge–Weber Syndrome

Two types of Sturge–Weber syndrome can be distinguished angiographically, depending on the patency of the deep venous system and its capacity to collect the drainage of the hemispheres (Fig. 9.66) (Bentson et al. 1971).

Although traditionally described as a pial vascular malformation, this does not reflect our current understanding of the clinical and radiological findings in these patients. The developmental defect (malformation) is probably only manifested by the venular, lymphatic, or mixed malformation seen on the face. The relationship of the facial lesion to the trigeminal nerve root topography is only of historical interest. Any port wine stain of the face will, by definition, involve some or all of the trigeminal root territory without causative relationship. Its topography does not allow any reliable prediction concerning the status of cerebral involvement.

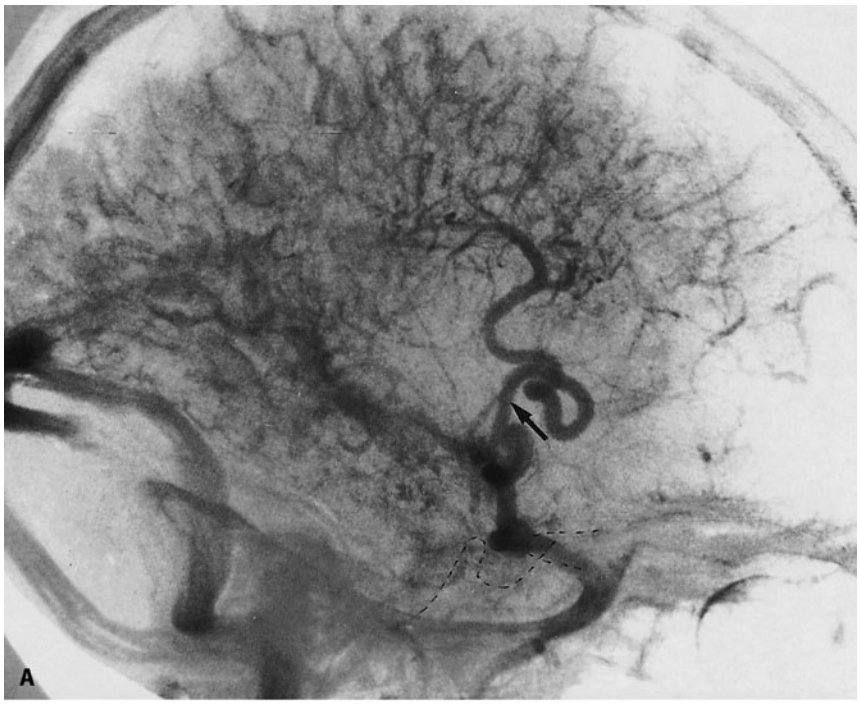

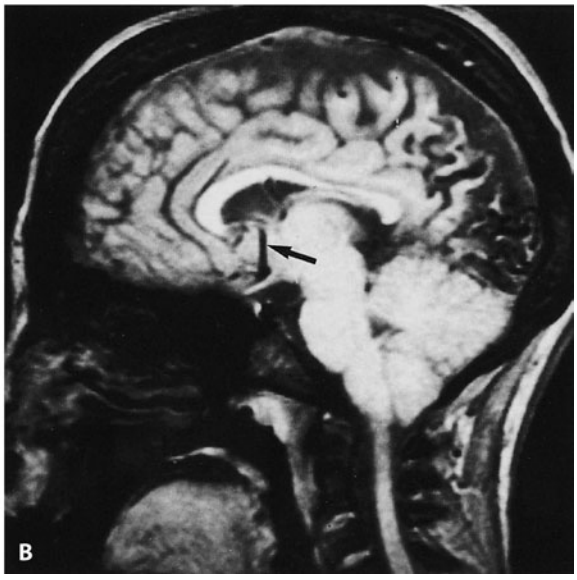

Fig. 9.66. **A** Late phase of a right carotid angiogram in lateral projection in a patient with Sturge–Weber syndrome. The only draining vein to the hemisphere is a deep-seated vein that connects the superior striate to the inferior striate system (*arrow*). **B** Sagittal MRI confirms this venous anastomosis. No cortical vein is demonstrated in the parieto-temporo-occipital region

The cortical lesion may arise from an early (in utero) thrombosis of the medullary veins on either side of their opening (deep or superficial), leading to the unusual venous pattern described in the disease. Secondary postischemic (venous) atrophy and, eventually, calcification create the traditionally reported appearance. The thrombosis could be related to an unknown (or undetected) coagulation problem associated with the venular malformation or to the response of the coagulation system to the presence of anti-factor VIII, as encountered in some venous malformations. Therefore, cerebral anomalies without facial port wine stain (Ambrosetto et al. 1983), enlargement of the choroid plexus (Stimac et al. 1986), pro-

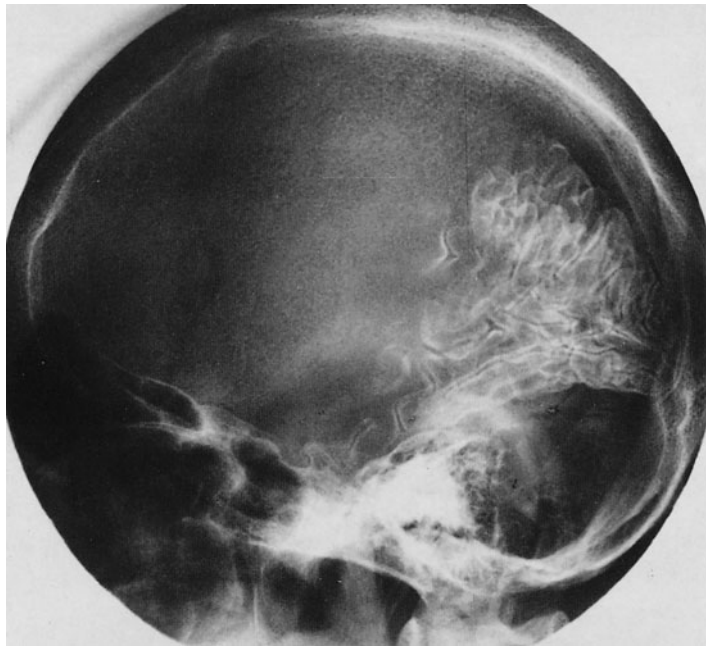

Fig. 9.67. Sturge–Weber syndrome. Plain skull X-ray demonstrates typical aspect of the subcortical calcification

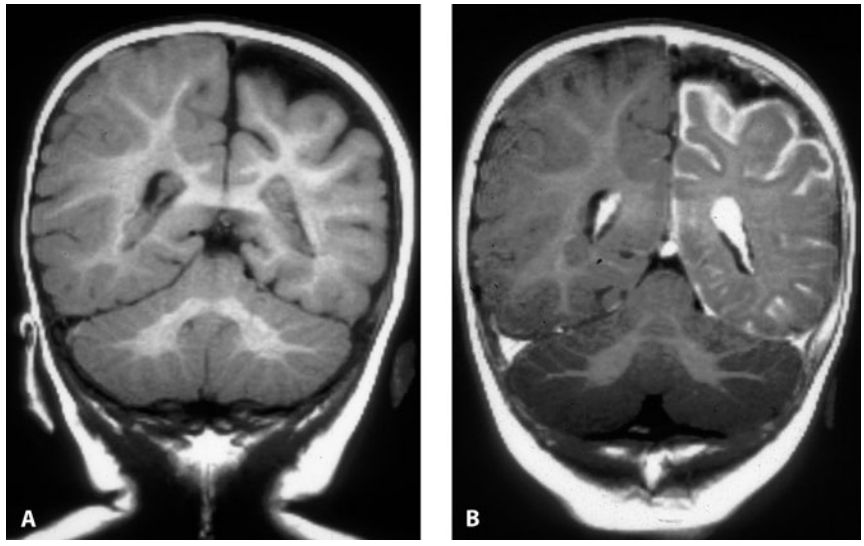

Fig. 9.68. MRI coronal views T1-weighted without (**A**) and with contrast enhancement (**B**) in a patient with Sturge–Weber disease demonstrates cortical atrophy involving left parietal lobe and enhancement along its surface as well as prominent ipsilateral choroid plexus. (Courtesy of S. Laughlin)

gression of the disease (Probst 1980; Garcia et al. 1981), localization of the calcifications and atrophy in the hemisphere opposite the port wine stain (Chaudary 1987; Cersoli et al. 1989), and posterior fossa locations characterize the heterogeneity and the spectrum of the disease. Thus, Sturge–Weber syndrome can be summarized as follows:

1. Facial venular malformation (port wine stain), sometimes capillary venular or venolymphatic, with facial bone (maxillary and malar) hypertrophy.
2. Cerebral venular thrombosis, due to an associated coagulopathy or local hemodynamic disorder (but eventually isolated).

There is no direct relationship between the facial and cerebral topographies. The skin manifestation of the port wine stain is stable and the trigeminal distribution is fortuitous. The cerebral venular disease is active as long as triggering factors continue to produce ischemia in the venules leading to focal decreased circulation through the affected cerebral hemisphere. Calcifications and atrophy may occur (Figs. 9.67, 9.68) and neurological deficits and seizures may develop.

10 Goals and Objectives in the Management of Brain Arteriovenous Malformations

10.1 Introduction 695

10.2 Indications for Treatment of Brain Arteriovenous Malformations 696
10.2.1 Age 700
10.2.2 Sex 701
10.2.3 Lifestyle and Occupation 701
10.2.4 Presenting Symptoms 703
10.2.4.1 Hemorrhage 703
10.2.4.2 Seizures 704
10.2.4.3 Headaches 704
10.2.4.4 Neurological Deficits 708
10.2.5 Location, Size, and Deep Venous Drainage 708
10.2.6 Brain Arteriovenous Malformations and Arterial Aneurysms 708

10.3 Therapeutic Management Strategy 715

10.4 Embolization 716
10.4.1 Partial (Targeted) Embolization 716
10.4.2 Partial (Palliative) Embolization 720
10.4.3 Curative Embolization 720
10.4.4 Preoperative Embolization 728
10.4.5 Intraoperative Embolization Therapy 729
10.4.6 Embolization Prior to Radiosurgery 729
10.4.6.1 Size Reduction 729
10.4.6.2 Targeted Embolization Prior to Stereotactic Radiosurgery 731
10.4.7 Staging of Embolization 732
10.4.8 Emergency Embolization 732
10.4.9 Contraindications for Endovascular Treatment 732
10.4.10 Embolization Results 734

10.1 Introduction

Decisions pertaining endovascular treatment of brain arteriovenous malformations (BAVMs) require complete information with respect to the clinical circumstances and the imaging characteristics, including the angioarchitecture of the AVM as well as the brain. With these factors in mind, a clinical-morphological analysis can be made to formulate the best plan for therapy, which might include embolization as well as other modalities. The angioarchitecture of the AVM will determine both the approach to the lesion and the expected chances of reaching the therapeutic goal. The various treatment modalities and treatment skills available may change in time, whereas the original objective, as determined by clinical and angioarchitectural features, will likely remain the same.

10.2 Indications for Treatment of Brain Arteriovenous Malformations

The discovery of a BAVM in a patient is not necessarily an automatic indication for treatment. Various attempts have been made to devise decision analysis programs to determine the risks of conservative versus active treatment of BAVMs such as those introduced by Fisher (1989) and Steinmeier et al. (1989). All are based on the ability to deal with the lesion from a purely surgical viewpoint. They did not consider the role of embolization as a preoperative adjunct, a sole mode of treatment (when complete obliteration of the malformation is obtained with a permanent agent), or as part of a combination of treatments. While some surgical investigators have started to realize that not all BAVMs carry the same risk for future hemorrhage, the recommendation for management has continued to be the same. Obliterate (remove) the AVM and use a method that has the highest chance of accomplishing obliteration in one setting: surgery, the limiting factors being surgical accessibility (AVM size, location, etc.) and therefore anticipated surgical morbidity and mortality associated with the treatment. Such a strategy fails to act upon growing evidence in both surgical and endovascular literature that all BAVMs are not the same and do not carry a similar risk for future symptoms (Hofmeister et al. 2000) and therefore the risk of treatment should be less than the natural history of that particular lesion. Targeted embolization is a viable, safe, and effective means of therapy in appropriate circumstances (Meisel et al. 2001). At the same time, when building a rationale for management strategy based upon data from the literature, one must realize that many of the reports are necessarily biased because of referral patterns. Although such data (hemorrhagic presentation rate, natural history, etc.) may very well support their recommendations for the treatment strategy of their referred group of patients, it may not apply for a different (population-based or other) referred group of BAVM patients (Hofmeister et al. 2000). In addition, when a treatment strategy is to be considered, it should take into account the local expertise available (endovascular, neurosurgical, and radiosurgery) as well as their treatment record with BAVM patients. Their treatment data should be known and compared to standards published and from time to time be reassessed. An incidentally (during screening) discovered cortical micro-BAVM in an older patient with hereditary hemorrhagic telangiectasia (HHT) disorder does not have the same prognosis as a large thalamic AVM in a young patient presenting with progressive neurological deficit, and therefore their management should be different. Yet the former can easily be cured with low morbidity and no mortality while the latter can only be partially embolized. The treatment strategy should not be based on our capacity of achieving cure but rather on the posttherapeutic clinical benefit expected over time and its related price in terms of risks.

We therefore recommend that in addition to gathering clinical information, great care be given to analyzing the imaging studies and in particular the angioarchitecture. The angiogram is performed with the aim of obtaining a complete study of the vascular system: the supply to the AVM, the angioarchitecture of the malformation, its venous drainage, as-

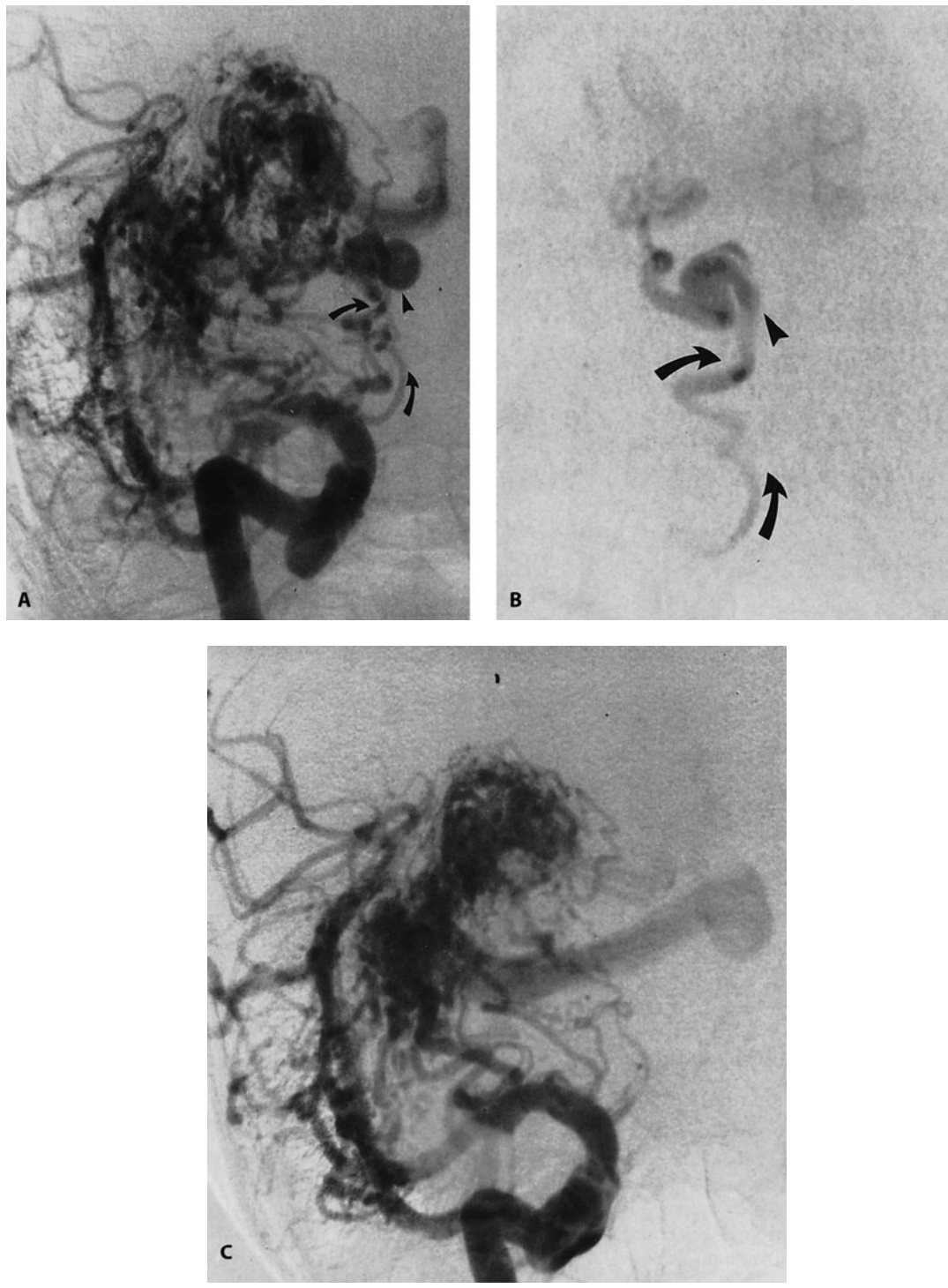

Fig. 10.1A–C. Thalamic malformation with an intralesional aneurysm. **A** Frontal view of the right internal carotid artery demonstrates a basal ganglionic malformation supplied by the lenticulostriate arteries. Note the intralesional aneurysm (*arrowhead*) from a prominent lenticulostriate artery (*curved arrows*). **B** Superselective catheterization of the lenticulostriate artery (*curved arrows*) demonstrating partial filling of the dysplastic aneurysm (*arrowhead*). **C** Postembolization angiogram of the right internal carotid artery in the frontal projection. The lesional aneurysm does not fill

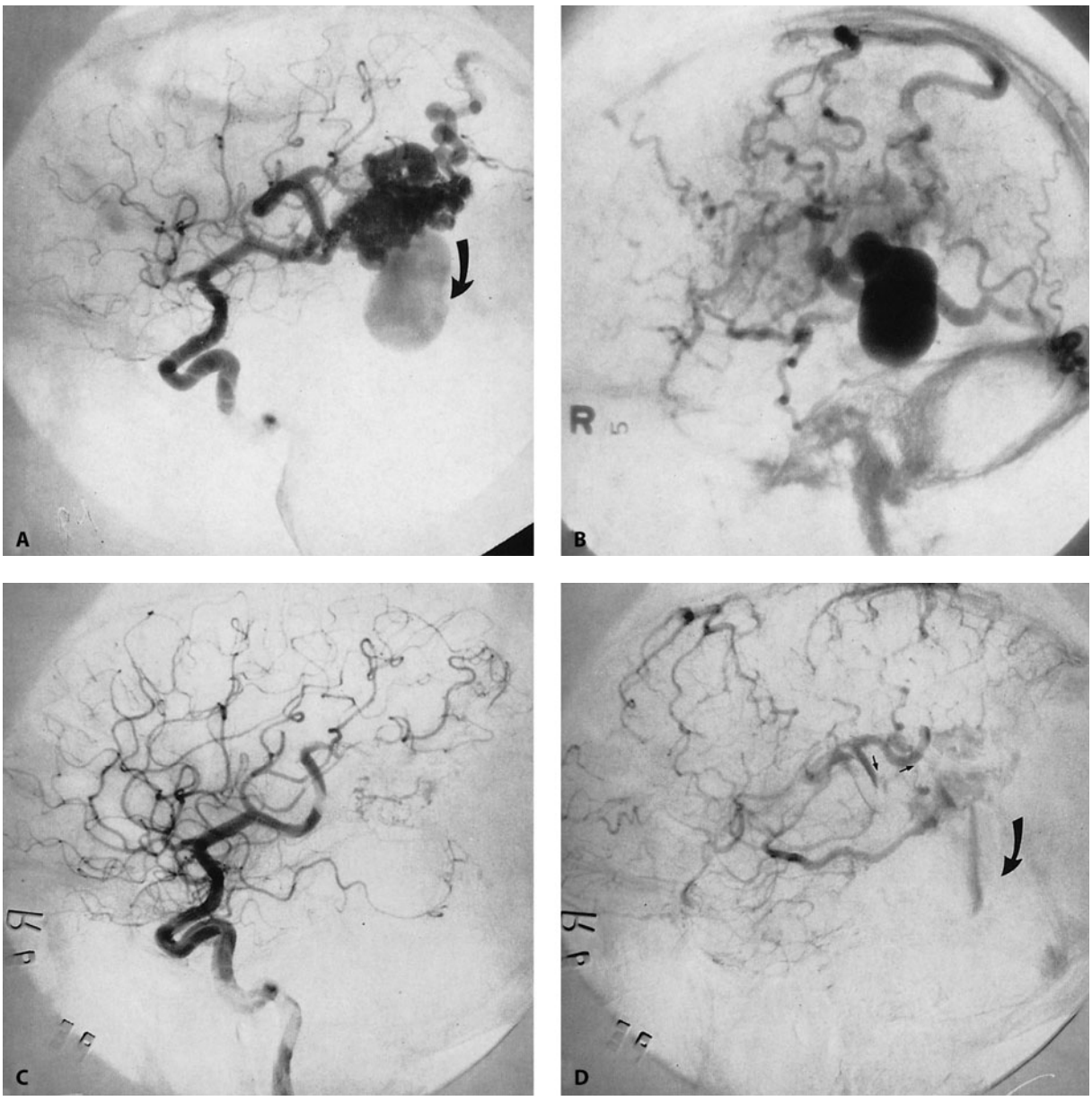

Fig. 10.2A–F. Large venous pouch, preoperative embolization. **A** Lateral view of the right internal carotid artery in mid-arterial phase demonstrates a posterior temporal vascular malformation draining into a large aneurysmal pouch (*curved arrow*) **B** Later phase of the same injection demonstrates the giant aneurysmal sac and the venous drainage of the malformation. **C** Lateral mid-arterial phase and **D** late venous phase after embolization demonstrate almost complete obliteration of the malformation, with stagnation in the venous pouch that is partially subtracted from previous stagnant contrast material (*curved arrow*) and stagnation proximally in the embolized feeding pedicles of the middle cerebral artery (*small arrows*). **E, F** see p. 699

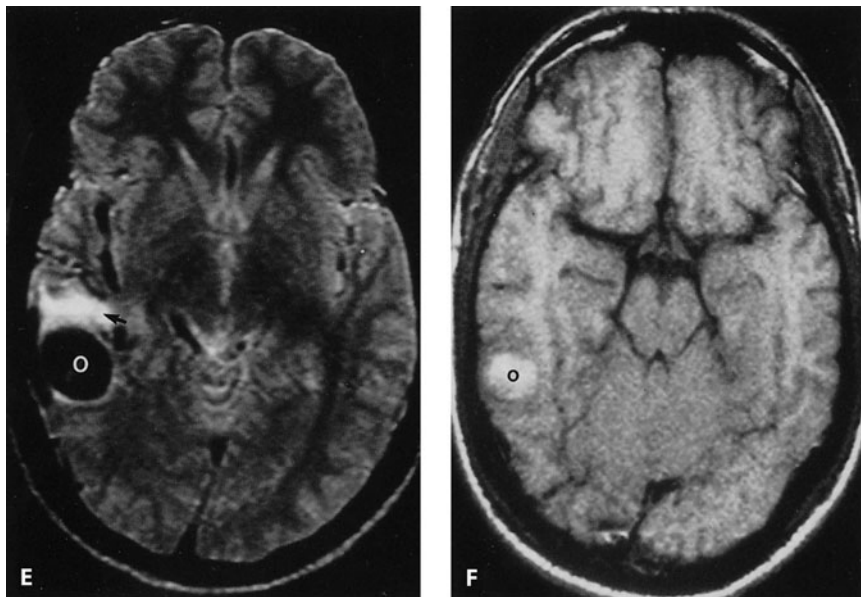

Fig. 10.2 (*continued*). **E** Axial MRI prior to treatment shows the large venous pouch (*O*) as a signal void and the increased signal changes anterior to the venous dilatation (*arrow*). **F** MRI after embolization. Note the complete thrombosis of the venous pouch (*O*)

sociated or additional vascular lesions, the status of the collateral circulation, and the venous drainage of the normal brain.

The information obtained from the angiographic investigation will play a key role in deciding on the need for treatment. The latter will be based on the evidence of weakness in the angioarchitecture, which may point to a potential instability. This information is then analyzed in conjunction with other factors such as the age of the patient and the location of the lesion.

The presence of an associated arterial aneurysm or pseudoaneurysm on the feeding pedicle, in the nidus (Fig. 10.1), venous thrombosis, or outflow restriction, venous hyperpressure, venous pouches or dilatations (Figs. 10.2, 10.3) will all be factors favoring active intervention. But when the risk of total elimination of the malformation (by embolization, microsurgery, or combination of therapies) is prohibitive, then a different management strategy will need to be considered such as partial targeted embolization.

An important part of the management of incidentally discovered BAVMs is educating the patient. It is important to provide him with information regarding the natural history, as it may apply to his particular situation, as well as the treatment options and associated risks that are known to exist in the local treatment environment. If no significant weaknesses are demonstrated in the angioarchitecture a treatment strategy of not treating the patient at this time can be proposed, while reassuring the patient that she is expected to lead a normal productive life without restrictions. Yet progression is not linear and biological events may produce unexpected changes that may long remain subclinical. Follow-up is therefore crucial in all the patients, including those for whom a decision not to treat was chosen.

Follow-up is usually clinical and with imaging (MRI), but if clinical or imaging changes are noted repeat angiography may be indicated.

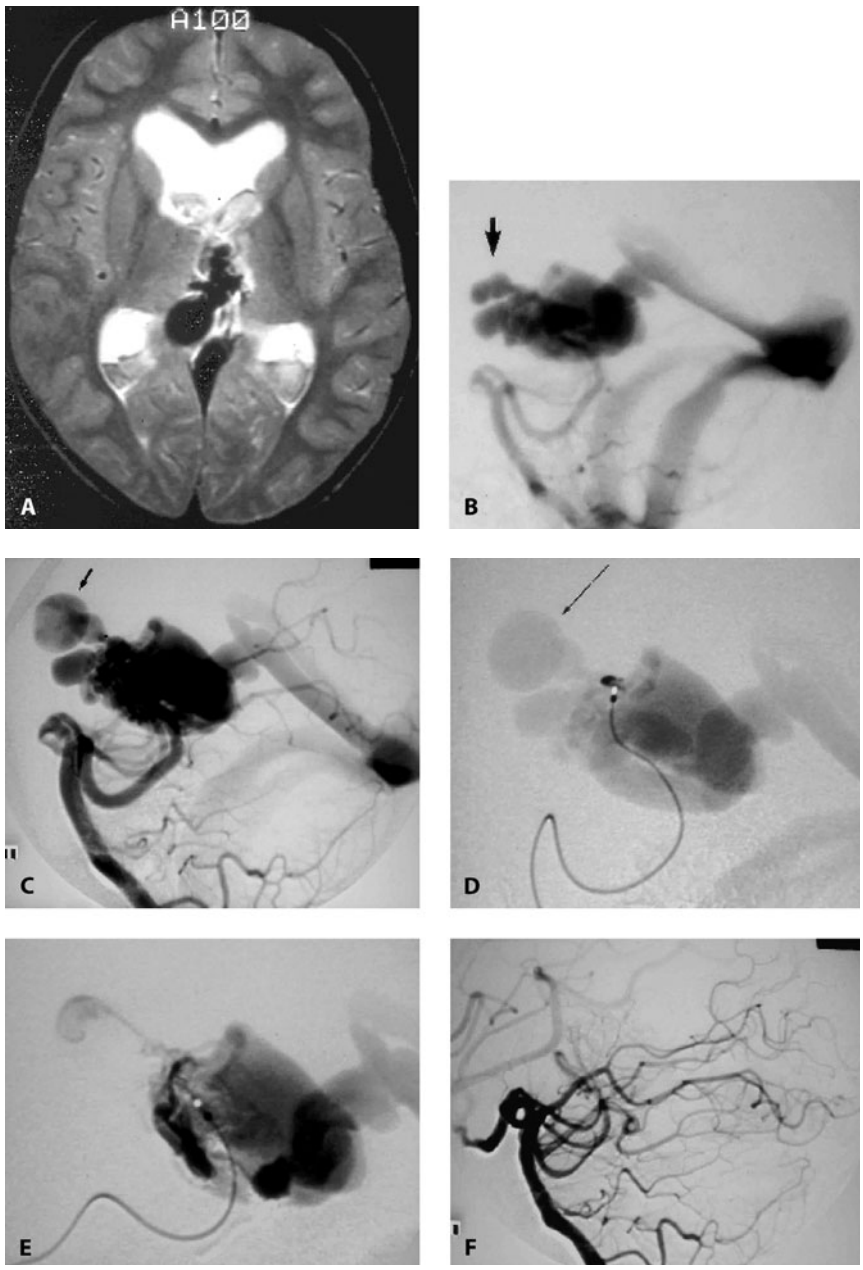

Fig. 10.3. MRI (**A**) demonstrates recent intraventricular hemorrhage, which on vertebral angiography lateral view (**B**) proved to be caused by a midline choroidal arteriovenous malformation (AVM). The immediate (**B**) and 2-month follow-up vertebral angiogram lateral view (**C**) demonstrate significant enlargement of a venous pouch (*arrows*) projecting into the 3rd ventricle. Selective injection of the feeding pedicle prior to (**D**) and following targeted intra-arterial embolization with glue (**E**) resulted in complete obliteration of the AVM, as shown on the follow-up vertebral angiogram in lateral view (**F**)

10.2.1 Age

The younger the patient is at the time of presentation, the more likely treatment should be considered. Presentation at an early age reflects an early imbalance between the lesion and the host. Newborns presenting with congestive heart failure are the most dramatic example of such an imbalance. Hydrocephalus may also occur following CSF absorption abnormalities and may result in irreversible developmental delay if endovascular treatment is not undertaken. Crawford et al. (1986) showed that patients older than 60 years of age at presentation were at a higher

risk of bleeding, up to 89% by 9 years, compared to a 15% risk in the same period for patients aged 20–29. Additionally, in older patients, the outcome of bleeding has a very high morbidity and mortality, as the older brain has less plasticity to recover. This may influence the management strategy toward partial targeted therapy to restore the equilibrium between host and AVM.

10.2.2 Sex

In the general discussion of the management of BAVMs, the sex of the patient does not play a major role, with the exception of females at childbearing age or even younger women in whom symptoms are already present prior to having children. There is some controversy as to the increased risk of hemorrhage or other symptoms during pregnancy. It is not infrequent that women with BAVMs have had one or more normal pregnancies and deliveries without being aware of the malformation, whereas other women present with an acute syndrome related to the malformation for the first time during pregnancy. In his series, Crawford found no statistical difference in the incidence of affected males versus females; however, one in four women between 20 and 29 years of age presented with a hemorrhage while pregnant, compared with the one out of four women in the same age group who became pregnant and did not have an AVM.

Yasargil's (1987) results suggested that pregnancy had no particular effect on the incidence or severity of bleeding from AVMs. In our patients, pregnancy did not increase either the risk of hemorrhage or the risk of progression of neurological symptoms. If a patient presents during pregnancy with an intracranial hemorrhage this should be managed according to the clinical status of the patient. If imaging showed the cause of the hemorrhage to be a BAVM without evidence of associated aneurysms the pregnancy is allowed to come to term and vaginal delivery is carried out at a high-risk facility. There is no evidence that the rebleed risk is increased under such circumstances. Subsequently, a treatment strategy can be proposed that will allow for safe obliteration of the malformation in time (Fig. 10.4)

10.2.3 Lifestyle and Occupation

The lifestyle of an individual with a BAVM may play some role in the indications for treatment or in the selection of the best form of treatment.

If the symptoms produced by the lesion interfere with the patient's activity, intervention is favored. Conversely, if the potential deficit that may occur following treatment would significantly curtail activity, intervention may be discouraged.

For example, in a pilot or professional truck driver harboring a medial occipital AVM, any treatment that will likely result in a homonymous hemianopsia will not be acceptable. Conversely, the discovery of a lesion that has the potential of producing a seizure or a hemorrhage in the same individual may force the patient to change his/her occupation.

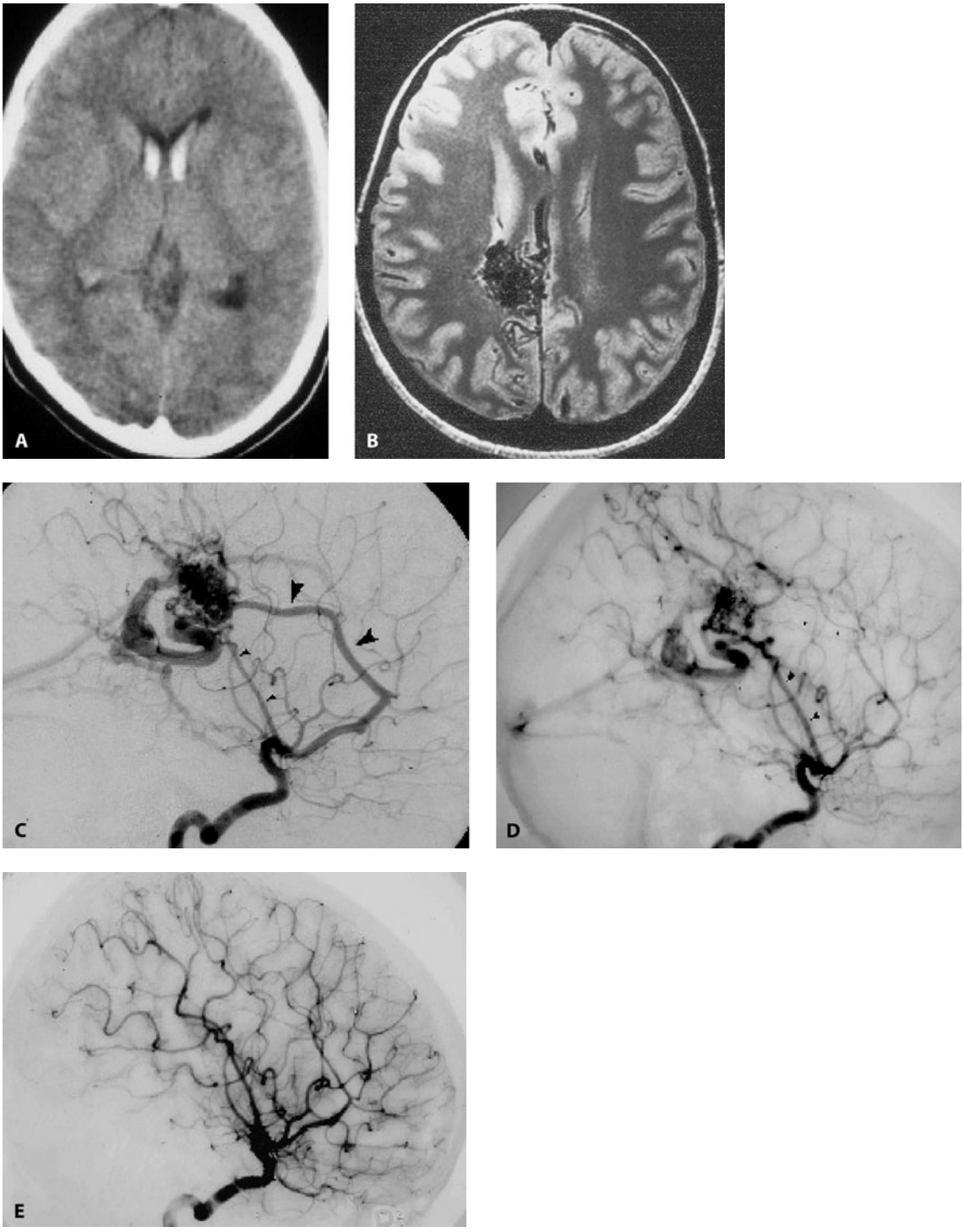

Fig. 10.4. CT scan (**A**) demonstrates intraventricular hemorrhage that was clinically well tolerated in 28-year-old woman who was 32 weeks pregnant. MRI (**B**) and carotid angiography in lateral view (**C**) at that time shows the cause to be a brain arteriovenous malformation (BAVM). Patient was managed conservatively and delivered at term. Two months after uneventful delivery, partial arterial embolization with glue was performed (**D**) and the residual AVM was treated with stereotactic radiosurgery 2 months later, resulting in complete obliteration of the AVM, shown on 2-year follow-up carotid angiogram lateral view (**E**)

10.2.4 Presenting Symptoms

The presenting symptoms and the demonstrated angioarchitectural changes will play a significant role in the indications and choice of treatment.

10.2.4.1 Hemorrhage

The treatment strategy following presentation with hemorrhage depends on how well the hemorrhage is tolerated. When surgical intervention is required to remove the intracerebral hematoma it will sometimes allow for excision of the malformation to be accomplished at the same time. Angiographic follow-up under these circumstances is mandatory, as some aspects of the AVM may not have been identified and removed at surgery.

The great majority of hemorrhages are well tolerated and no immediate AVM treatment is usually necessary. While there is some controversy regarding the expected rebleed rate the first year after hemorrhagic presentation (Ondra et al. 1990; Mast et al. 1997), such incidence is generally believed to be similar to or just above the natural history risk of 3%–4% per year but may vary in different referral centers and be as high as 6% (Meisel et al. 2001).

There is seldom a need for urgent treatment after BAVM hemorrhage and a treatment strategy can be planned accordingly. Careful analysis of the angioarchitecture is clearly mandatory and if it shows features that are highly suspicious of being responsible for the hemorrhage (pre- or intranidal aneurysm, pseudoaneurysm) this is an indication for early treatment targeted toward obliteration of the weakness (partial targeted embolization) (Figs. 9.36, 9.40).

If exceptionally repeated hemorrhages do occur the angioarchitecture of the AVM should again be scrutinized for possible weaknesses (aneurysm, etc.), and a targeted embolization or–if not possible or successful–a surgical removal should be considered (Fig. 9.37). In these circumstances, the chance of permanent neurological deficit and death increases with each recurrence of the hemorrhage (Graf et al. 1983; Crawford et al. 1986).

While hemorrhage associated with a BAVM is recognized as undesirable, it should also be noted that its associated morbidity and mortality is not the same in every referral center, with moderate and severe disability reported as low as 13% (Hartman et al. 1998).

Although the type of treatment may vary from center to center and depend on local strengths and capabilities, the overall goal should be the same. A standard of care should be provided that will reduce or eliminate the patient's expected natural history risk of morbidity from future hemorrhage. A benefit for the patient will only occur if the risk of morbidity and mortality associated with the treatment provided by the managing team is less than that associated with the expected natural history of the disease.

This means that treatment provided cannot be carried out at any cost (risk to the patient) and a role for partial treatment (endovascular but not surgery or radiotherapy) exists provided that its perceived goal can be reached at an acceptably low associated treatment risk.

Partial treatment for patients presenting with hemorrhage does not improve their expected natural history when treatment included all treatment modalities (Porter et al. 1998). On the other hand, partial targeted embolization did reduce the risk of future hemorrhage Lasjaunias's series (Meisel et al. 2002), and as a general principle we favor a targeted endovascular approach.

10.2.4.2 Seizures

Seizures occur at presentation in 10%–53% of patients with BAVMs, the majority being partial or partial complex seizures. Subsequent seizure control with antiepileptic medication is achieved in the great majority of patients and rarely does seizure control by itself become an indication for intervention. Refractory status epilepticus may be an indication for endovascular treatment, and such management has been successful in our experience in bringing seizure management under control (Fig. 10.5).

Subclinical hemorrhage in patients presenting with seizures occurs and was demonstrated in 6.5% of Yasargil's surgical AVM patients presenting with seizures.

Seizures as the mode of presentation do not appear to influence the natural history, according to Ondra (1990), and the long-term disability and mortality was similar to all symptomatic patients harboring a BAVM.

Treatment can therefore be proposed according to the previously outlined principles. The impact on seizure type and frequency of the various treatment modalities (embolization, surgery, and radiosurgery) has generally been favorable (Fournier et al. 1991b; Piepgras et al. 1993; Kurita et al. 2000), and worsening or new onset of seizures after treatment is rare.

10.2.4.3 Headaches

Headaches not associated with hemorrhage are a subjective nonspecific symptom that is often difficult to assess. While in most cases the exact cause of the headache remains unclear, a number of patients with BAVMs may have a possible relationship between angioarchitectural features and

Fig. 10.5A–F Venous hypertension producing grand mal seizure, which, despite proper levels of anticonvulsants, progressed toward status epilepticus and required general anesthesia for control. **A** Lateral view of the left internal carotid artery demonstrates a relatively slow-flow brain arteriovenous malformation. Note filling of the vein of Labbé (*curved arrow*). **B** Later arterial phase of the same injection and **C** late venous phase; additional venous drainage superiorly toward the cortical venous system (*curved arrowheads*), toward the medial and lateral aspect of the temporal lobe, and toward the cavernous sinus (*curved arrow*) producing congestion of the main venous outflow of the entire hemisphere. **D** Postembolization angiogram demonstrates a small remaining shunt toward the vein of Labbé (*open curved arrow*). **E** Late phase shows the remaining drainage but significant reduction in the arterial outflow. **F** Normal venous transit time of the same cortical veins draining primarily normal cerebral parenchyma. The patient has been seizure-free 3 years on anticonvulsants ►

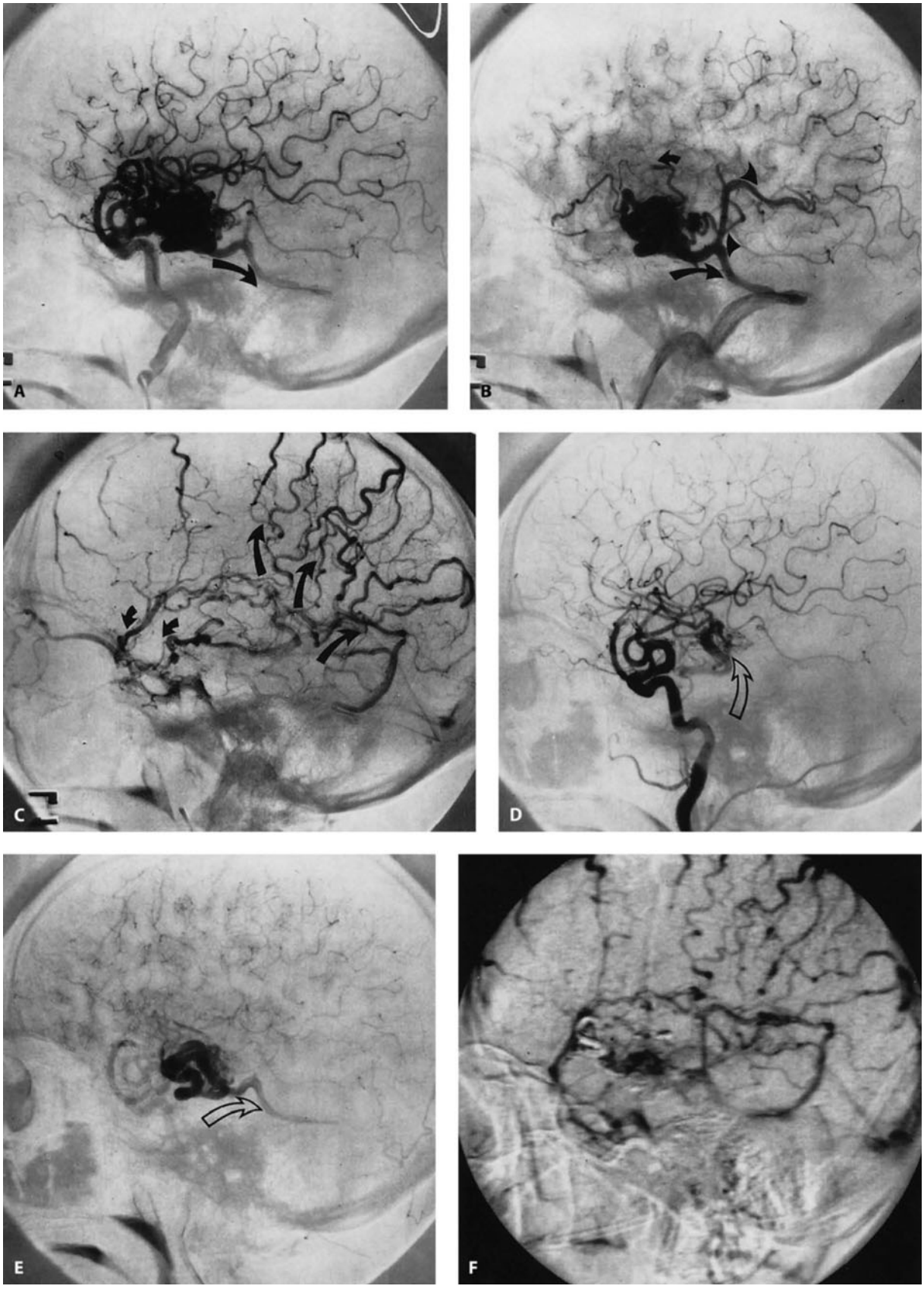

Fig. 10.5A–F. Legend see p. 704

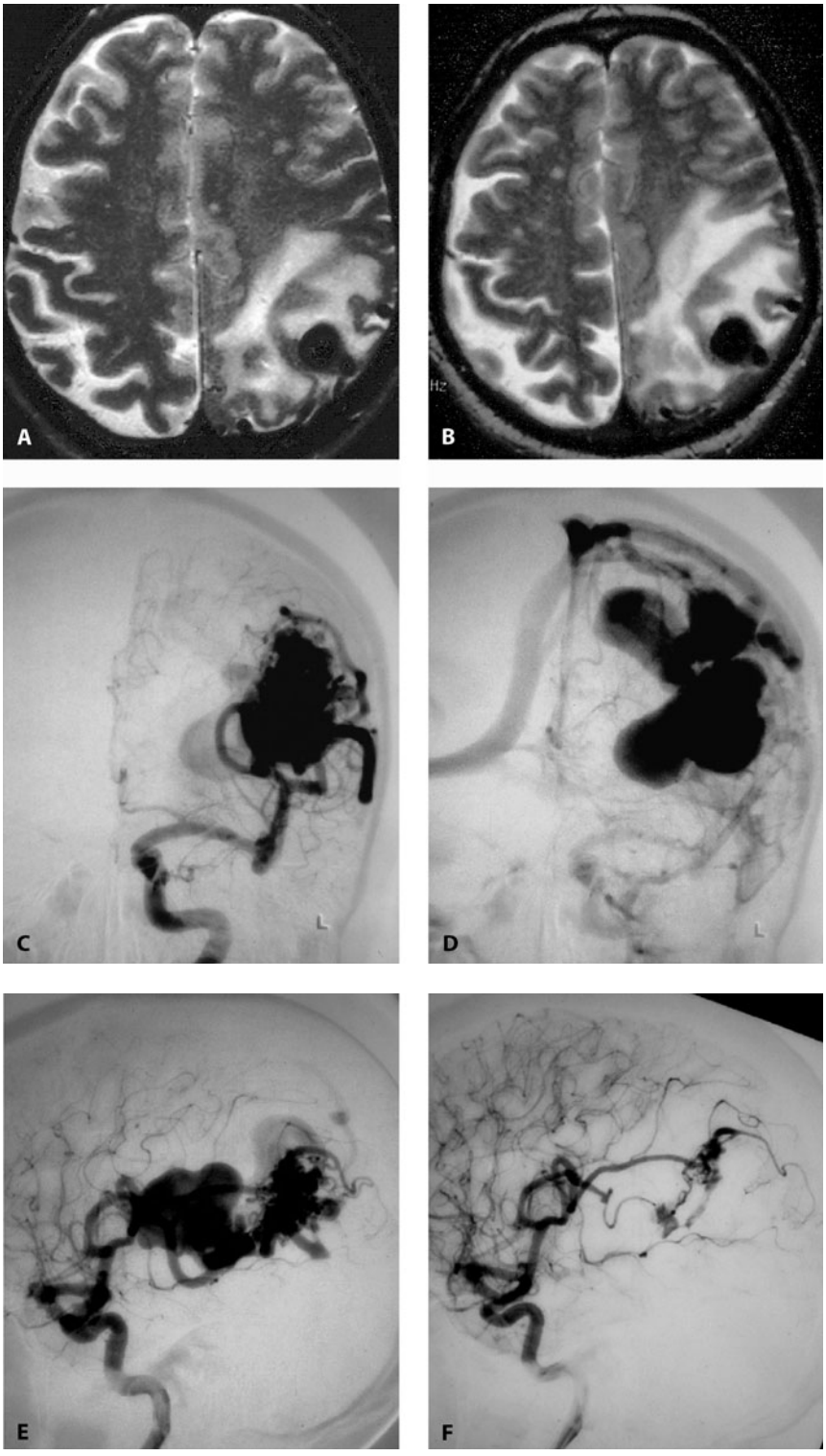

Fig. 10.6A–J. Progressive neurological deficit in 64-year-old male patient showed increasing mass effect and surrounding edema on MRI at presentation (**A**) and 3-month follow-up (**B**). Carotid angiogram demonstrated on AP view in addition to proximal aneurysm to the arteriovenous malformation (AVM), slow flow in markedly enlarged venous draining veins (**C, D**). Carotid angiogram in lateral view prior to (**E**) and 2 months after embolization of the feeding pedicle harboring the aneurysm showed partial obliteration of the AVM (**F**). **G–J** see p. 707

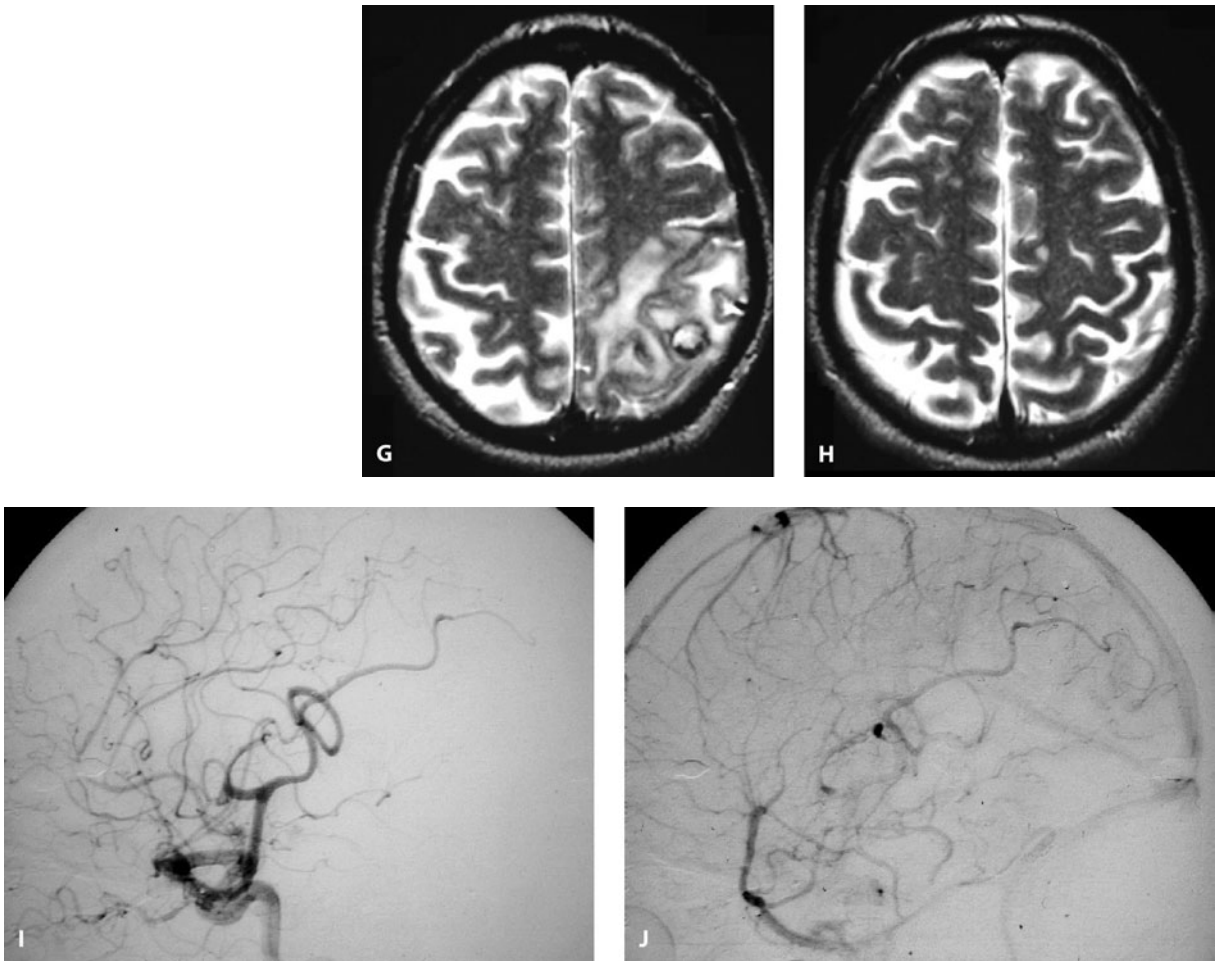

Fig. 10.6 (*continued*). Reversal of the neurological deficit occurred over a 12-month period and MRI showed diminishing edema pattern at 4 months (**G**) and 1 year (**H**). Complete thrombosis of the AVM was demonstrated on 1-year follow-up carotid angiogram on lateral views (**I, J**). Neurological deficit cleared completely

their headaches. Dural as well as posterior cerebral artery supply to a BAVM is known to be potentially responsible for headaches, which tend to disappear after embolization therapy, in our experience. Conversely, embolization of middle and anterior cerebral artery supply to a parietal lobe AVM may worsen the headaches if the posterior cerebral artery supply is increased following such embolization.

Although headaches by themselves are not an indication for treatment in patients with BAVMs, partial targeted embolization has its place when headaches are disabling and significant dural and/or posterior cerebral artery supply to the AVM is demonstrated.

10.2.4.4 Neurological Deficits

Neurological deficit at presentation and not associated with hemorrhage is a somewhat infrequent BAVM presentation, occurring in only 8% of patients over a 10-year period (Crawford et al. 1986). In 1,289 consecutive BAVM patients, Hofmeister et al. (2000) identified 7% presenting with a stable and 5% presenting with a progressive neurological deficit. Although arterial steal and mass effect have been implemented as possible causes for these deficits (Carter and Gumerlock 1995; Miyasaka et al. 1997), it is our opinion that venous congestion and venous ischemia are more likely to be responsible for these symptoms. The development of perilesional edema and partial thrombosis in the draining veins from the AVM, as shown on MRI, may confirm that the venous drainage patterns of the adjacent brain are involved. In our experience, these changes have been reversible in lobar AVMs presenting with progressive neurological deficit when treated with partial embolization (Fig. 10.6, pp. 706, 707).

Similarly, partial embolization of thalamic and basal ganglia AVMs has resulted in stabilization in 27% or reversal of the progressive neurological deficits in 64% of our patients treated for that reason (Al-Yamany et al. 2000).

10.2.5 Location, Size, and Deep Venous Drainage

Location of a malformation, size, and deep venous drainage are the most important factors in determining the risks of surgical therapy (Spetzler and Martin 1986). These features are of only minor concern for the endovascular approach to BAVMs, as the need for meticulous technique and sparing of all normal noncontributing arteries is essential, regardless of the location of the malformation. We concur with Yasargil's belief that any normal parenchyma has some function; therefore, the endovascular approach is for the most part the same whether the location involves ineloquent cortex or a lesion is located in the motor, speech, or an other eloquent area of the brain. Technically, morbidity associated with embolization is related to the capacity to reach the lesion and to remain strictly within the AVM nidus; therefore lesions located in the brainstem, thalamus, or basal ganglia, although obviously more risky to treat, can be obliterated by careful embolization (Fig. 10.7).

10.2.6 Brain Arteriovenous Malformations and Arterial Aneurysms

As was discussed in Chap. 9 of this volume, aneurysms associated with AVMs can be flow related (on the way to the AVM), intranidal, or remote and apparently unrelated. Their presence is an individual host response to the AVM, indicating a weakness in the vascular system. This weakness is a marker for future hemorrhage and worsens that natural history risk from 3% to 7% (Brown et al. 1988).

Remote, non-flow-related aneurysms may occur in patients with BAVMs, but their presence may not alter the natural history of these patients. How-

Fig. 10.7A–C. Basal ganglia vascular malformation. **A** Frontal subtraction angiogram of the left internal carotid artery demonstrates a basal ganglia malformation supplied by lenticulostriate arteries (*curved arrows*) and transinsular supply from the middle cerebral artery (*arrow*). **B** Frontal plain radiogram shows the radiopaque cast of the malformation after embolization. **C** Frontal subtraction angiograms after embolization, in mid-arterial phase, show complete obliteration of the malformation

ever, the presence of flow-related and in particular intranidal aneurysms are markers for hemorrhagic presentation (Redekop et al. 1998), and this once again indicates a weakened vascular system (Meisel et al. 2000).

In the presence of subarachnoid hemorrhage (SAH), it is often exceedingly difficult to know whether the AVM itself has bled or stems from a proximal flow-related arterial aneurysm (AA). With few exceptions, it is most often the AVM itself (± intranidal aneurysms) or an AA adjacent to the AVM that has caused the SAH.

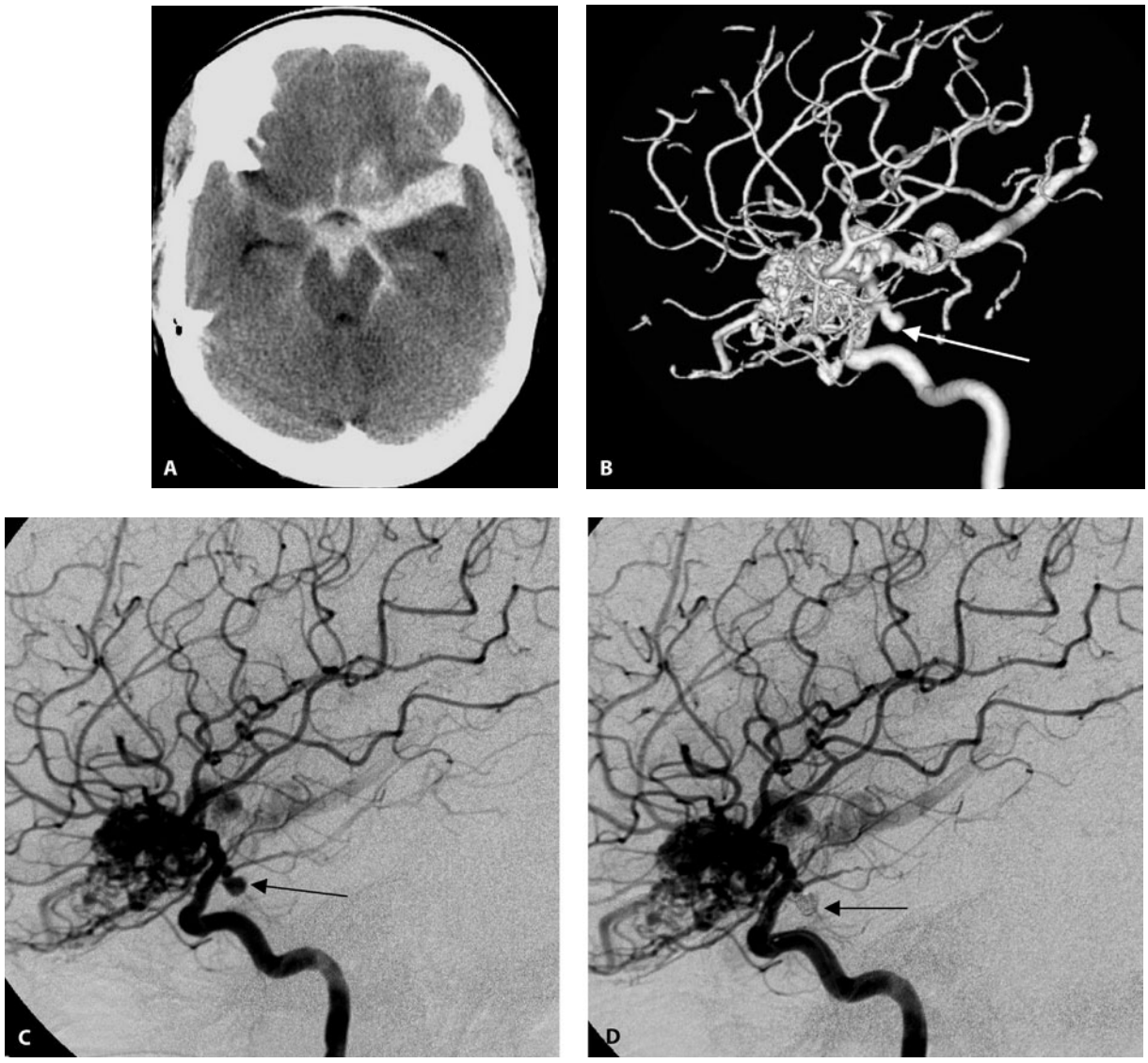

Fig. 10.8. A 47-year-old female patient presented with grade III subarachnoid hemorrhage (SAH), shown on CT (**A**) and at left internal carotid angiogram, lateral view (**B**) to be caused by a posterior communicating aneurysm (*arrow*) associated with a left inferior frontal lobe arteriovenous malformation. The aneurysm was perceived to be responsible for the SAH, and endovascular coiling was performed in the acute phase. Angiography prior to (**C**) and immediately after coiling (**D**) showed obliteration of the symptomatic aneurysm (*arrows*). **E, F** see p. 711

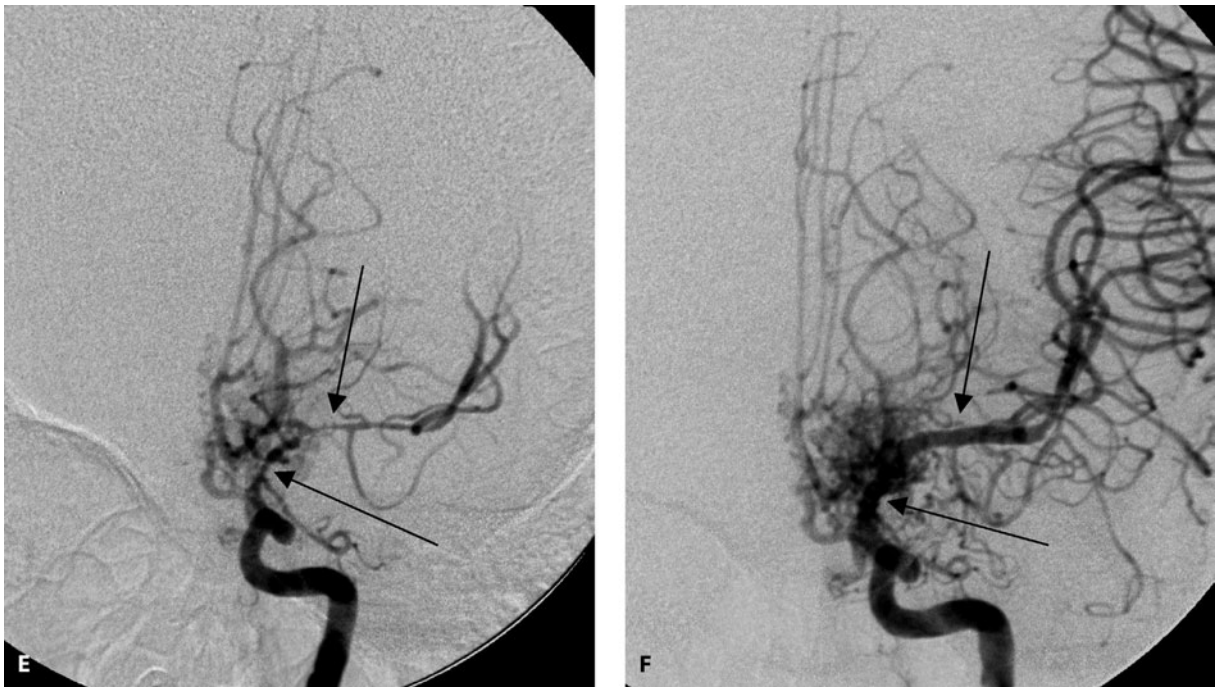

Fig. 10.8 (*continued*). Several days later, symptomatic vasospasm of the supraclinoid internal carotid artery and the M1 segment of the middle cerebral artery occurred, as shown on the left internal carotid angiogram in frontal projection (**E**), and balloon angioplasty of these vessels was performed (**F**), resulting in lasting clinical improvement

Patients presenting with SAH and or intracranial hemorrhage (ICH) and in whom angiography demonstrates the presence of a BAVM with an associated AA, should have their treatment directed toward the lesion that is suspected as symptomatic (Fig. 10.8). Most of the time, this will mean that treatment will be directed toward the AVM (+ adjacent and intranidal AA) (Figs. 10.9, 10.10). Special attention should be given to enlarging pseudoaneurysms, as they often produce an unstable situation.

In our experience, it has been rare to have to treat a proximal AA as symptomatic and responsible for the hemorrhage (SAH or ICH) in patients with BAVM.

We have also not seen rupture of a proximal flow-related aneurysm during or following endovascular treatment of the AVM when the AVM distal to the AA was targeted. Regression of the proximal flow-related aneurysm may occur following complete or more than 50% obliteration of the AVM by endovascular means and is more likely to occur the closer the AA is to the nidus of the AVM (Redekop et al. 1998; Meisel et al. 2000) (Figs. 10.11, 10.12).

If no regression of the associated AA occurs on follow-up angiography in 6–12 months active treatment of the AA should be considered. As its natural history (when the AVM is not treated) is not well known, the treatment-associated morbidity will therefore need to be low (similar to the management of incidentally discovered AA).

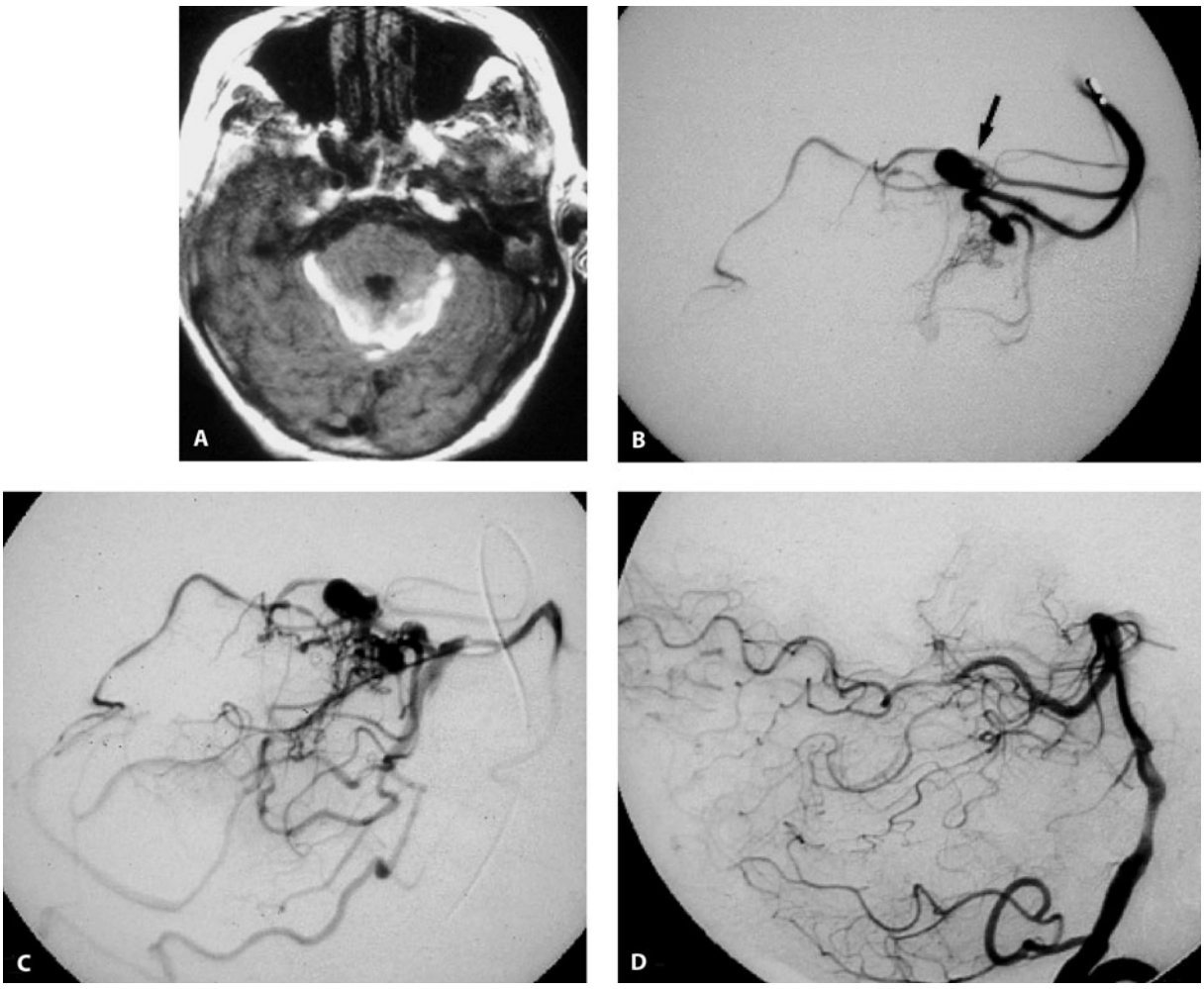

Fig. 10.9. Grade II subarachnoid hemorrhage shown on MRI (**A**) and at selective superior cerebellar artery angiogram in lateral view (**B**, **C**) caused by small arteriovenous malformation (AVM) with associated intranidal (pseudo)aneurysm (*arrow*). Embolization with glue was performed in the acute phase to obliterate both the aneurysm and the AVM. This objective was achieved and confirmed on the immediate postembolization vertebral angiogram in lateral view (**D**)

Fig. 10.10A–D. A 67-year-old male patient originally presenting with a grand mal seizure. **A** Frontal view of the right common carotid artery injection at the time of the original seizure demonstrates an arteriovenous malformation on the parietal region supplied by the middle cerebral artery. **B** Six months later, the patient has an intracerebral hemorrhage. At this time, angiography examination demonstrates an intralesional aneurysm (*arrowhead*) not present before. **C**, **D** Postembolization follow-up angiogram of the right common carotid artery demonstrates remaining malformation but no filling of the intralesional aneurysm (*curved open arrow*). The remaining malformation was treated with radiosurgery ►

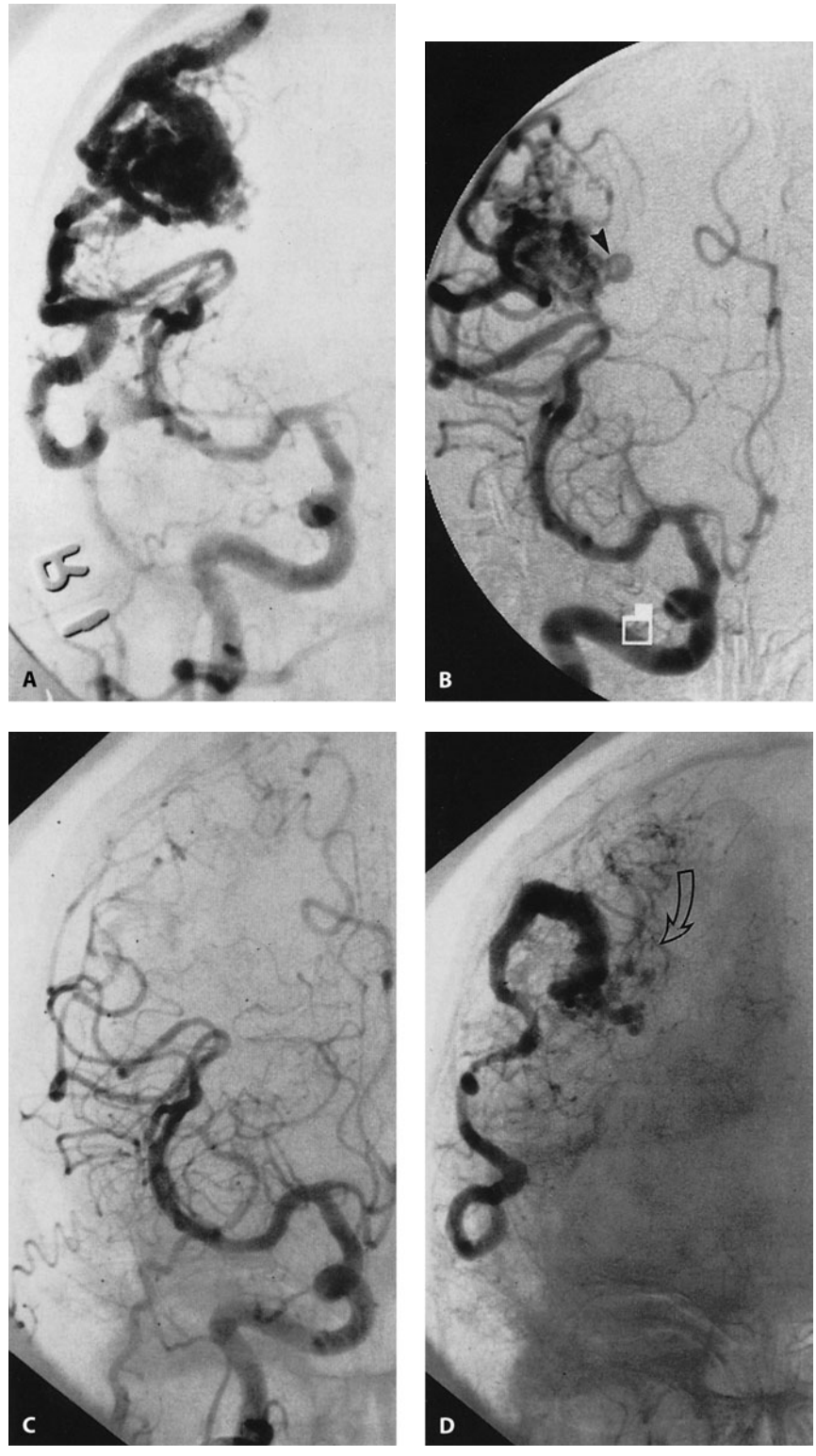

Fig. 10.10A–D. Legend see p. 712

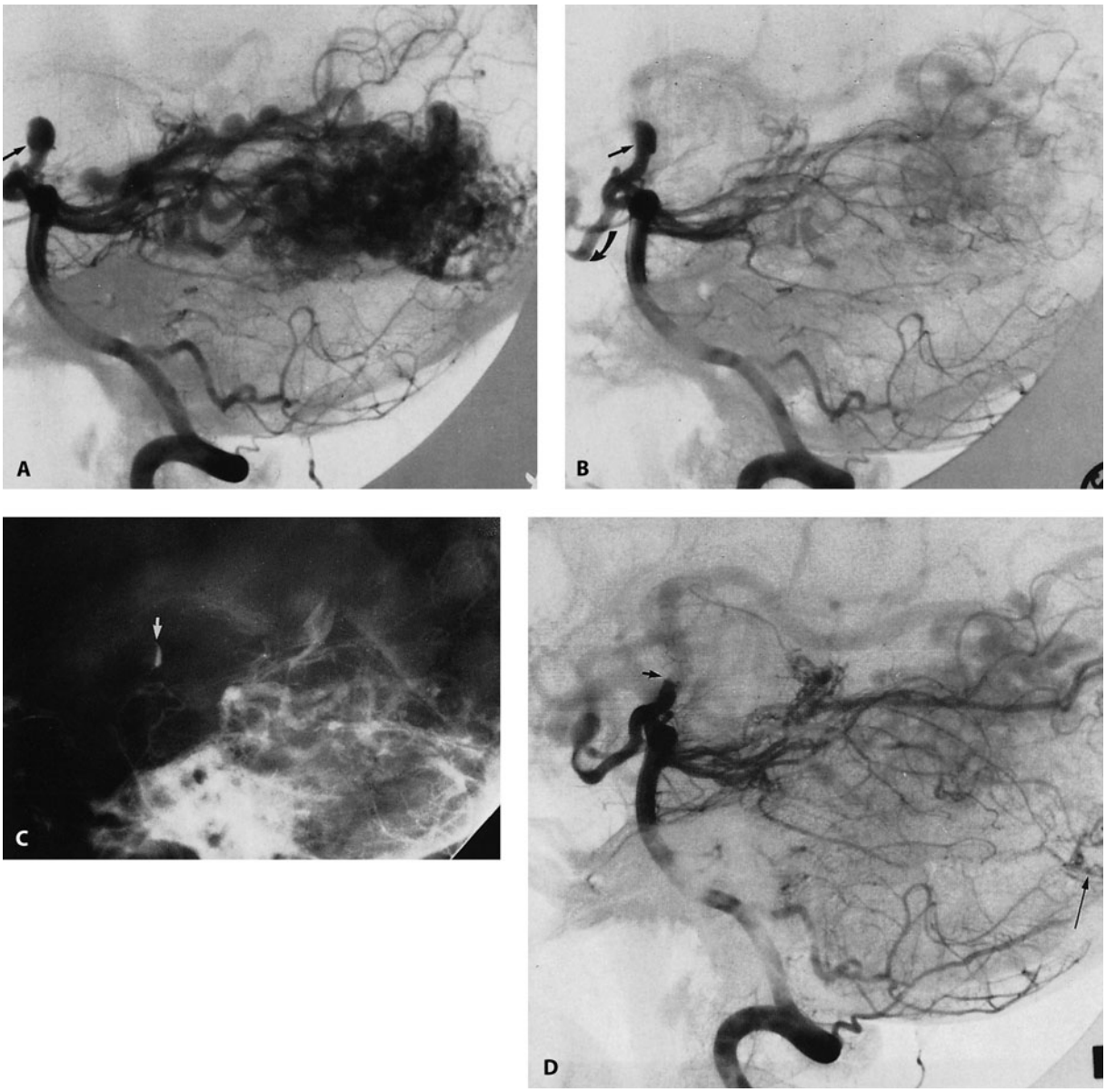

Fig. 10.11A–D. Flow-related aneurysm. **A** Lateral view of the left vertebral artery shows a flow-related basilar aneurysm (*arrow*). Note the dysplastic appearance of this aneurysm. The aneurysm is proximal to a high-flow occipital malformation. **B** Immediate postembolization angiogram of the left vertebral artery in lateral view. There is a significant decrease in the supply to the malformation and a slightly decreased filling of the aneurysm. Note the compensatory filling of the posterior communicating artery (*curved arrow*). **C** Lateral view of the same injection in late venous phase. Note the fluid level stagnation at the dome of the aneurysm (*white arrow*). **D** Three-month follow-up angiogram demonstrates partial thrombosis of the upper dome of the aneurysm (*arrow*). Note also the development of collateral circulation of the nonsprouting type in the occipital region (*long arrow*)

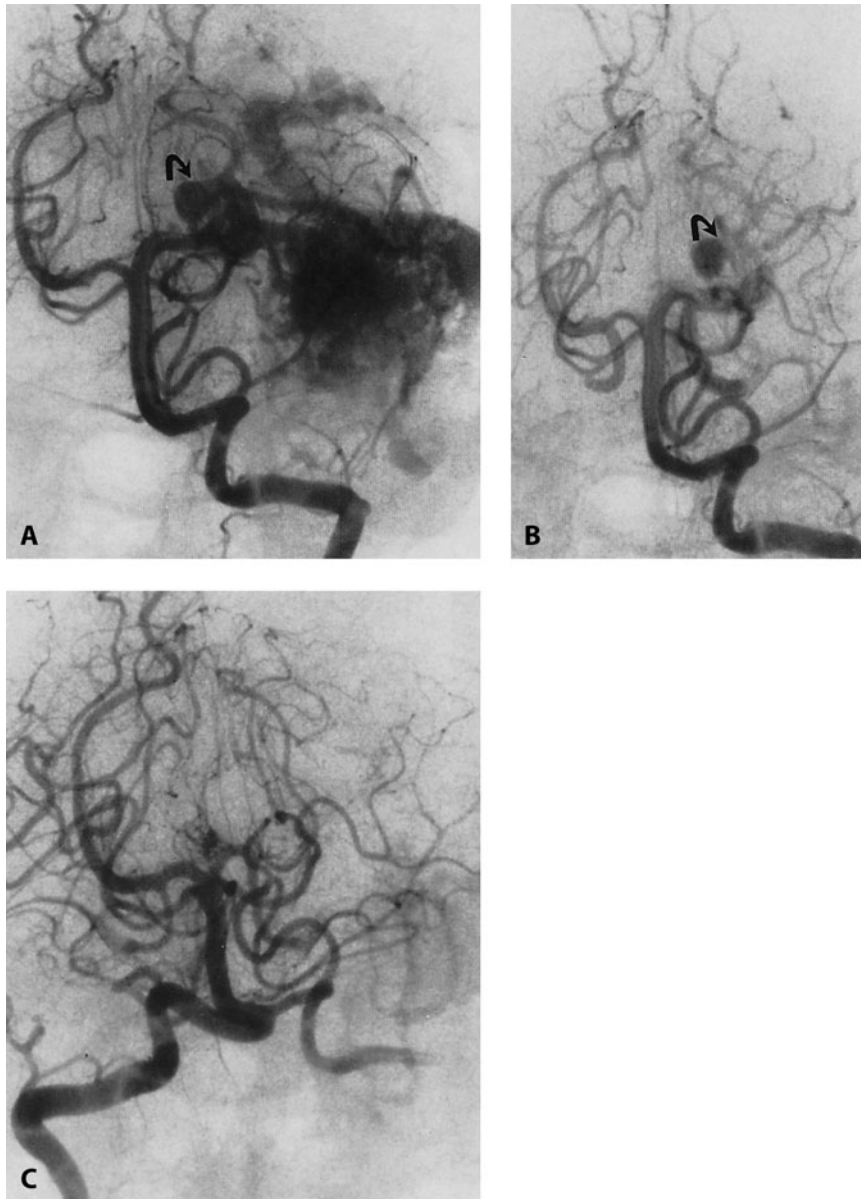

Fig. 10.12A–C. Flow-related aneurysm. **A** Frontal subtraction angiogram of the left vertebral artery supplying a temporal arteriovenous malformation (AVM) also fills a large aneurysm at the posterior communicating level (*curved arrow*). **B** Immediate post-embolization follow-up study shows stagnation in the aneurysm and no filling of the AVM. **C** At 3-month follow-up, no filling of the aneurysm. The distal posterior cerebral artery is filled by the carotid circulation, without filling of the aneurysm (not shown)

10.3 Therapeutic Management Strategy

The decision to treat can be made by a single individual who is competent in managing patients with BAVMs. Whether that decision is the right choice for the patient depends on a multitude of factors, often determined and limited because of local circumstances. The formation of multidisciplinary teams with a special interest in neurovascular diseases with representation of interventional neuroradiology, vascular neurosurgery, and stereotactic neurosurgery has been encouraged (Gentili et al. 1992; Deruty et al. 1990). Such a team would offer the patient a balanced approach to the management of their AVM, presuming that all members of the team were equally capable. Data collection, quality control, and follow-up would be facilitated as well as research and teaching in neurovascular diseases.

The results of treatment using various treatment modalities may differ because of different referral patterns or the unique strengths and weaknesses in individual centers, and therefore reported results may not be applicable to a given local center. The same applies to the reported treatment-associated morbidity and mortality, which, although nonhomogeneous in the literature, will give a reasonable indication to the local center of the standard of practice around the world.

As a basic rule, a patient should be treated if an improvement over the expected natural history (relevant to that patient because of clinical symptoms, age, angioarchitecture, etc.) will result. Therefore, treatment-associated risk pertinent to the local team will be a significant factor to be considered in the management discussions, as will as the patient's acceptance of these up-front treatment-related risks.

In such circumstances, a complete cure may neither be desirable (unknown benefit vs. risk taken) nor necessary (partial treatment may restore the AVM–host equilibrium).

Currently, five major methods of management exist in the treatment of BAVM patients: medical, embolization, surgery, stereotactic radiosurgery, and combined therapies. Each method can be used alone or in combination with the other modalities.

Combination treatments may facilitate obliteration of an AVM that might not have been curable by a single modality but of course at an increased risk to the patient (combined risk of several treatments).

It is therefore imperative that the goal of the treatment be established and the potential benefit and risk of the treatment modalities (alone or combined) be understood by both the physician and the patient.

As this text focuses on endovascular therapies, we will not discuss the indications and results of surgery or radiation therapy in detail but rather highlight the role of embolization in the management strategy of BAVM patients.

10.4 Embolization

Embolization can be carried out as a unique treatment, the intended goal being partial and targeted, palliative, curative, or in combination with surgery or stereotactic radiosurgery. It may be given as elective treatment or in emergent fashion, depending on the indication and circumstances.

10.4.1 Partial (Targeted) Embolization

The rationale for partial embolization is derived from the concept that the patient (host) will be asymptomatic as long as there is equilibrium between the host and the AVM. Treatment should be carried out once the patient becomes symptomatic to reestablish this equilibrium. To accomplish this goal, curative treatment may not be necessary and partial targeted embolization may be sufficient.

The possible relationship between clinical symptoms and angioarchitecture has been described in previous chapters. Accurate assessment of

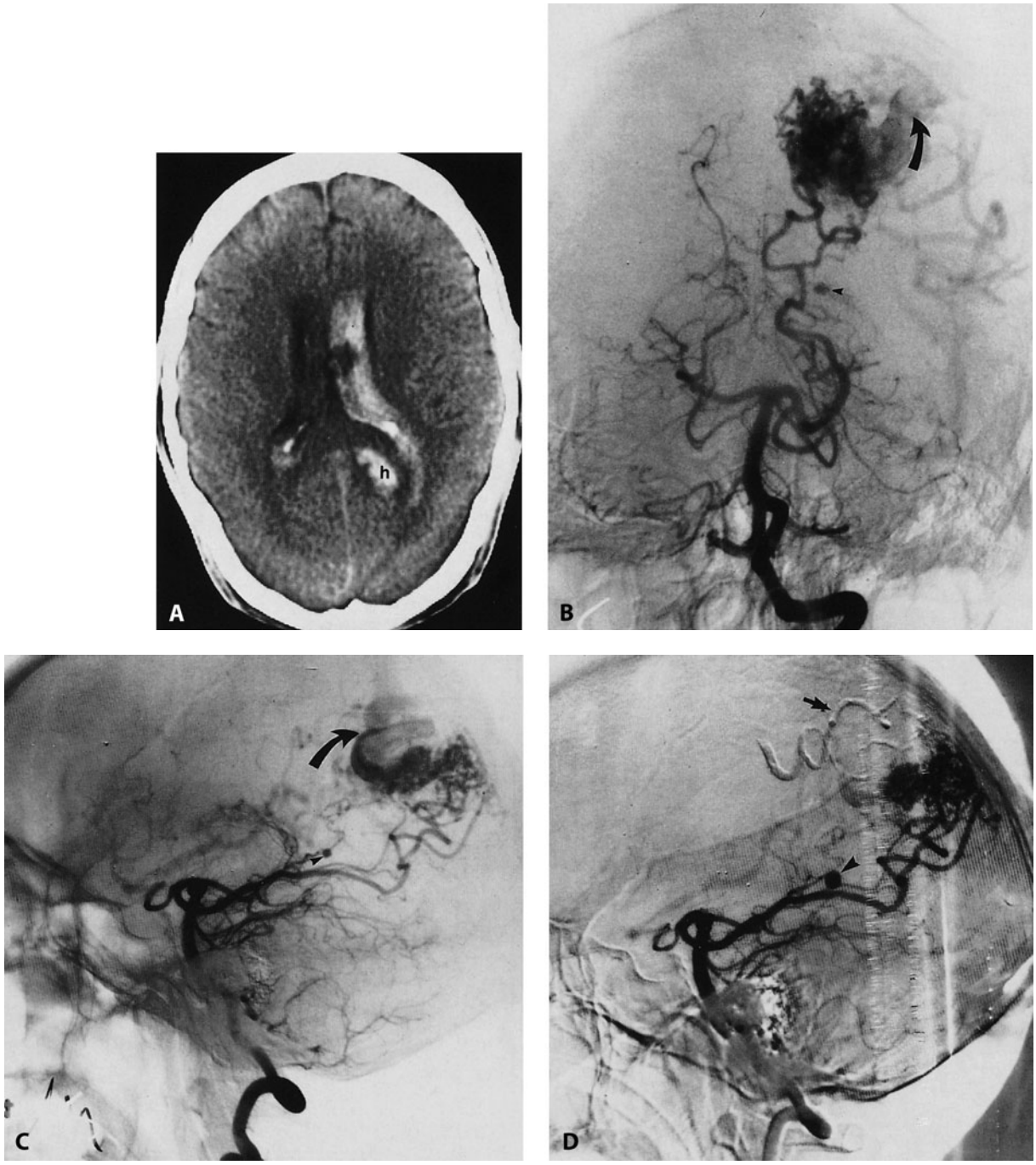

Fig. 10.13A–D. Sequence of staged embolization. **A** Axial CT scan demonstrates an intraparenchymal hemorrhage (*h*) with ventricular extension. **B** Frontal and **C** lateral views of the left vertebral artery injection demonstrate a small arterial aneurysm (*arrowhead*) from a posterior choroidal artery, corresponding to the location of the hemorrhage. There is a distal malformation in the parietal area with cortical venous drainage (*curved arrow*). **D** Follow-up angiogram of the left vertebral artery 2 days after middle cerebral artery embolization (*arrow*) shows the aneurysm to have increased in size (*arrowhead*), with increased flow toward the malformation. The posterior cerebral artery at the level of the choroidal artery was closed at that time. The initial embolization of the pedicle that did not harbor the aneurysm diverted the flow toward the aneurysm, increasing its size and the risk for rebleed

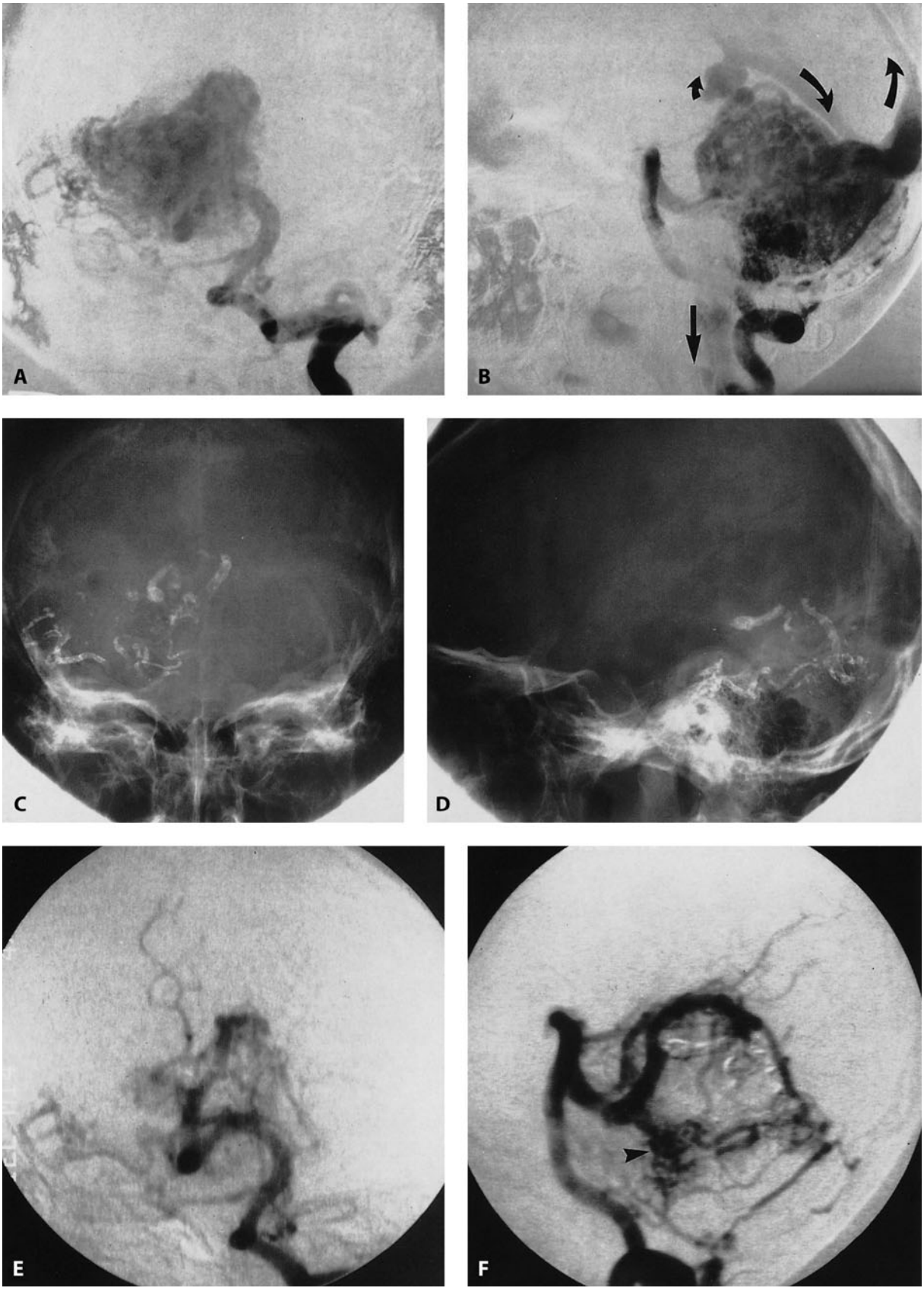

Fig. 10.14A–F. Legend see p. 719

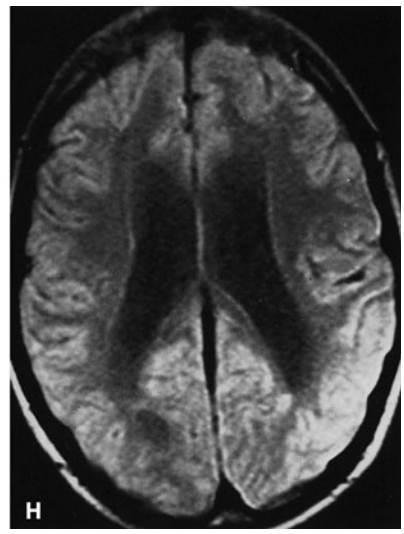

◄ **Fig. 10.14A–H.** Posterior fossa malformation in a patient presenting with headaches and ventricular dilatation. **A** Frontal and **B** lateral angiograms of the left vertebral artery in mid-arterial phase demonstrate an extensive cerebellar vascular malformation draining to the precentral cerebellar vein and toward the vein of Galen (*small curved arrow*) and straight sinus, with reflux into the superior sagittal sinus (*large curved arrows*) and downward toward the jugular vein (*arrow*). **C** Frontal and **D** lateral plain radiograms after partial embolization demonstrate the radiopaque cast. **E** Frontal and **F** lateral digital subtraction angiography in mid-arterial phase after embolization demonstrates significant reduction in the amount of malformation, with the remaining supply coming from the marginal branch of the superior cerebellar artery (*arrowhead*, **F**) and preservation of the normal posterior inferior cerebellar and superior cerebellar arteries, with significant relief of the venous hypertension. **G**. Axial MRI, T2-weighted, prior to treatment. Note the ventricular dilatation. **H** After the partial embolization, there was a decrease in the size of the ventricular system and relief of the headaches

these findings is important, as incorrect interpretation may lead to embolization of the wrong part of the AVM, destabilizing the equilibrium further, making the patient more symptomatic and even increasing the risk of future hemorrhage (Fig. 10.13).

Partial, targeted, endovascular treatment, when carried out with a complete understanding of the clinical–angioarchitecture relationships, will result in improved natural history (Meisel et al. 2002) (Fig. 10.14).

Once partial treatment has been given, both clinical and imaging follow-up will need to be carried out to verify the achieved result.

If the indications for partial treatment were the elimination of angioarchitectural changes noted following a recent hemorrhage follow-up angiography should be done within days of the embolization procedure, if there was a concern that the goal was in fact not achieved or an unstable situation was created during the treatment. If the goal of the partial treatment was achieved follow-up angiography should be carried out in 2–3 months as needed.

This management strategy should be clearly defined by the team and discussed with the patient before beginning treatment, as it will facilitate compliance and follow-up. It will also allow the follow-up strategy to be

modified if clinical or imaging data that require a change in the treatment strategy become available.

10.4.2 Partial (Palliative) Embolization

Partial embolization can be performed for patients whose clinical follow-up examination demonstrates objective evidence of progressive neurological deficit and whose BAVM cannot be cured by current technology. The majority of these AVMs are large in size and in deep locations (Al Yamany et al. 2000). Certain lobar locations have shown perilesional edema that may center on the venous outflow channels, suggesting venous congestion or even occlusion as the possible mechanism for the progressive neurological deficits in these patients. As we are currently unable to target the venous component of the angioarchitecture directly, we tend to focus embolizations on occlusion of the largest shunts within the nidus, thereby decreasing the venous hyperpressure (Fig. 10.15). Stabilization or reversal of the neurological deficit may occur even after limited partial treatment and postembolization clinical monitoring to verify objectively the clinical status of the patient (Al Yamany et al. 2000). Clinical and MRI assessments at 3- to 6-month intervals are appropriate to confirm that the goal has been achieved or to assess whether additional partial treatment should be recommended.

10.4.3 Curative Embolization

Curative embolization refers to complete anatomical obliteration of the malformation by the endovascular route. If embolization is to be curative, a permanent nonbiodegradable agent must be used to form a cast of the pathological angioarchitecture. We believe that there is no place for particulate or reabsorbable agents in this instance, with the possible exception of direct brain arteriovenous fistulae, in which one or more detachable balloons or coils may accomplish a cure (Vinuela et al. 1982; Halbach et al. 1989a; Berenstein et al. 1990).

Cure by the endovascular route, as demonstrated by the immediate postembolization angiogram, must be confirmed by a follow-up at least 6 months later, preferably 1 or 2 years later, to confirm the stability of the result (Fig. 10.16). Immediate postembolization studies are not sufficient, as small remnants may not be apparent immediately, or the mixture of embolic material (even if radiopaque) with nonopaque autologous blood may recanalize at a later time (Fournier et al. 1990; Gruber et al. 1996). Of importance is the potential recruitment of arterial collaterals, probably via a mechanism of nonsprouting angiogenesis, because the embolization achieved proximal occlusion of the feeding vessels without sufficient penetration toward the nidal–venous junction. Delayed thrombosis may still occur in these circumstances but needs to be confirmed on long-term angiographic follow-up. Once the venous outlets of the AVM have thrombosed, no new veins can be recruited and a cure will have been achieved (Figs. 10.17, 10.18).

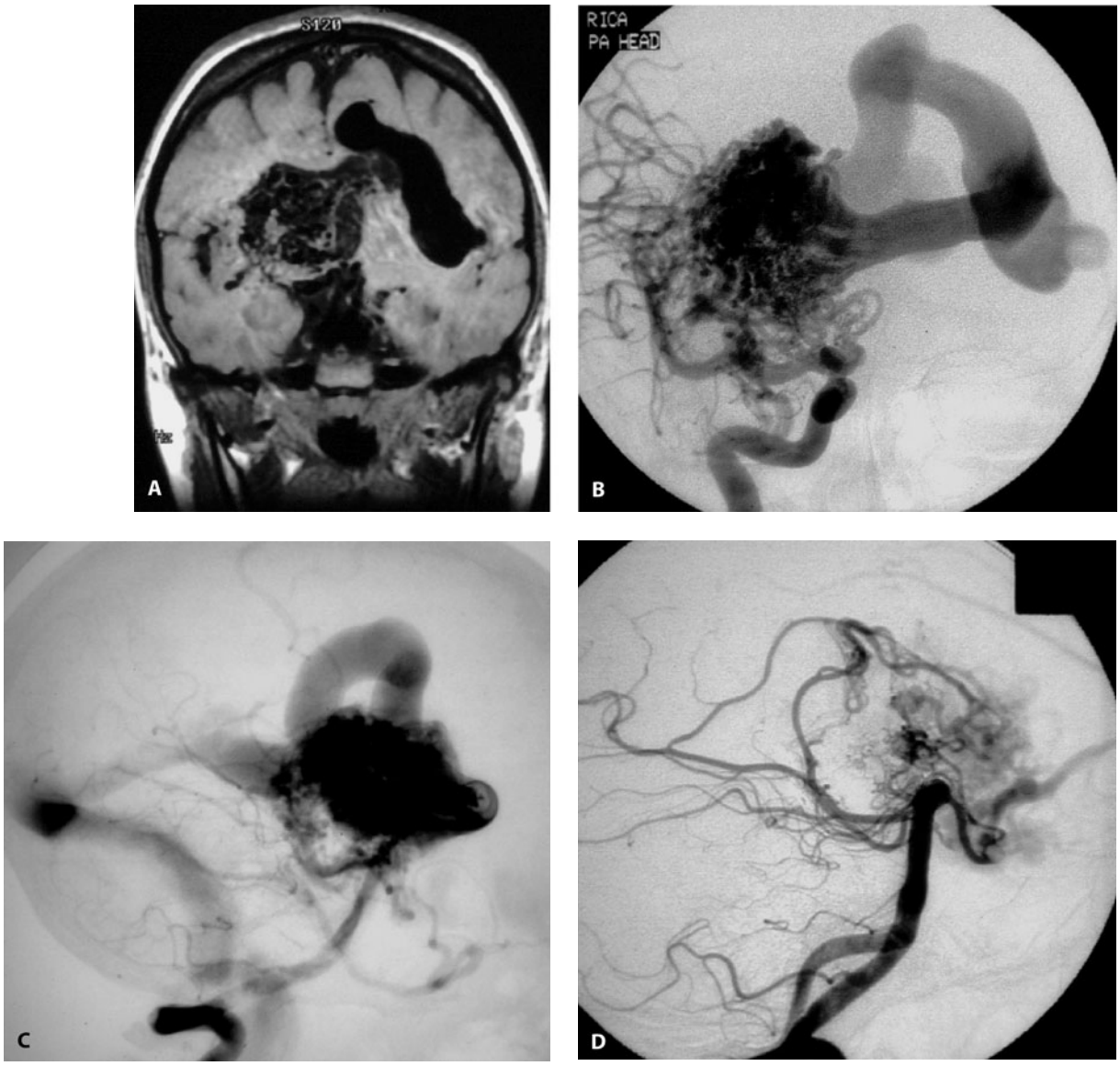

Fig. 10.15. Coronal MRI (**A**) shows large basal ganglia and thalamic arteriovenous malformation (AVM) in a 22-year-old female patient presenting with motor and sensory neurological deficit that had continued to worsen over several years. Carotid angiogram in AP view (**B**) and vertebral angiogram in lateral view prior to embolization (**C**) and immediately after partial embolization with glue (**D**) demonstrate a residual AVM. The clinical progression stabilized over the next few weeks, and improvement with partial recovery of neurological function occurred over the subsequent months

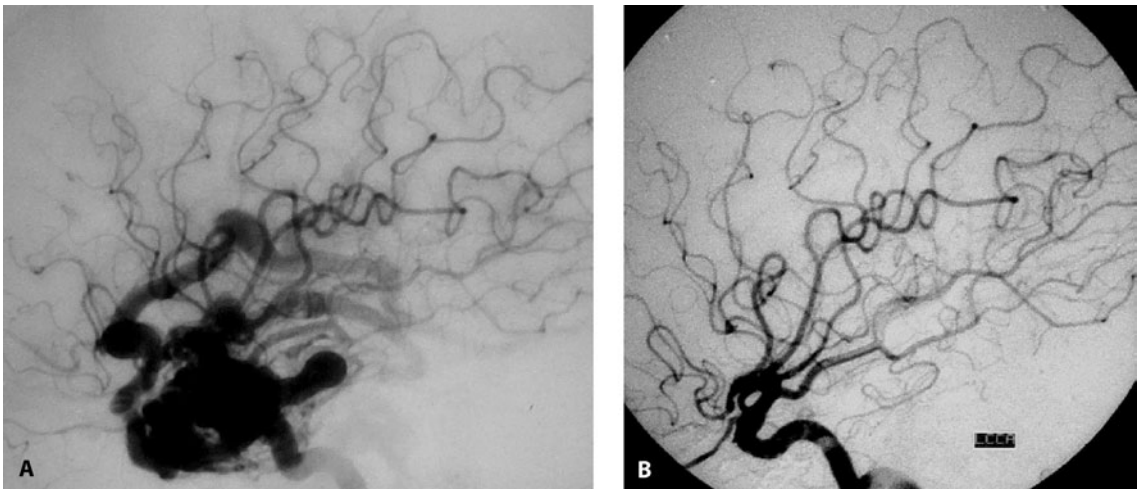

Fig. 10.16. Carotid angiogram in lateral view (**A**) prior to embolization with glue of a small temporal lobe arteriovenous malformation and 2-year follow-up carotid angiogram in lateral view (**B**) demonstrating long-term stability of the achieved endovascular obliteration

In general, if embolization results in complete obliteration of the malformation, with no residual opacification of the malformation, no arteriovenous shunting, and without stasis in the nidus, recanalization does not occur (Fig. 10.19).

Complete obliteration of BAVMs by embolization alone has been reported to be possible in 10%–40% of AVMs (Fournier et al. 1991b; Wikholm 1995; Valavanis et al. 1998; Willinsky et al. 2001). Valavanis et al. (1998) noted that in addition to the small size and limited number of arterial feeders, certain topographical locations (sulcal, deep extrinsic) favored complete obliteration outcome with embolization alone. On the other hand, there is currently limited data regarding the ability to achieve a complete cure when the up-front goal of the treatment is to achieve complete obliteration by embolization alone, but in such circumstances, the obliteration rate may be as high as 70% (Willinsky et al. 2001).

The results of embolization of small BAVMs (<3 cm) compared favorably to surgery or stereotactic radiosurgery with respect to procedure-related morbidity and mortality (Willinsky et al. 2001; Schaller and Schramm 1997; Pollock et al. 1996) (Fig. 10.20). However, similar to surgical resection, complete obliteration with embolization provides immediate protection for future hemorrhage, which is not the case for radiosurgery.

We recommend that before starting the treatment, the role and goal of the embolization therapy be identified and records be kept by the local treatment team as part of the overall quality-control management so that these can be compared with reference standards of care in the literature.

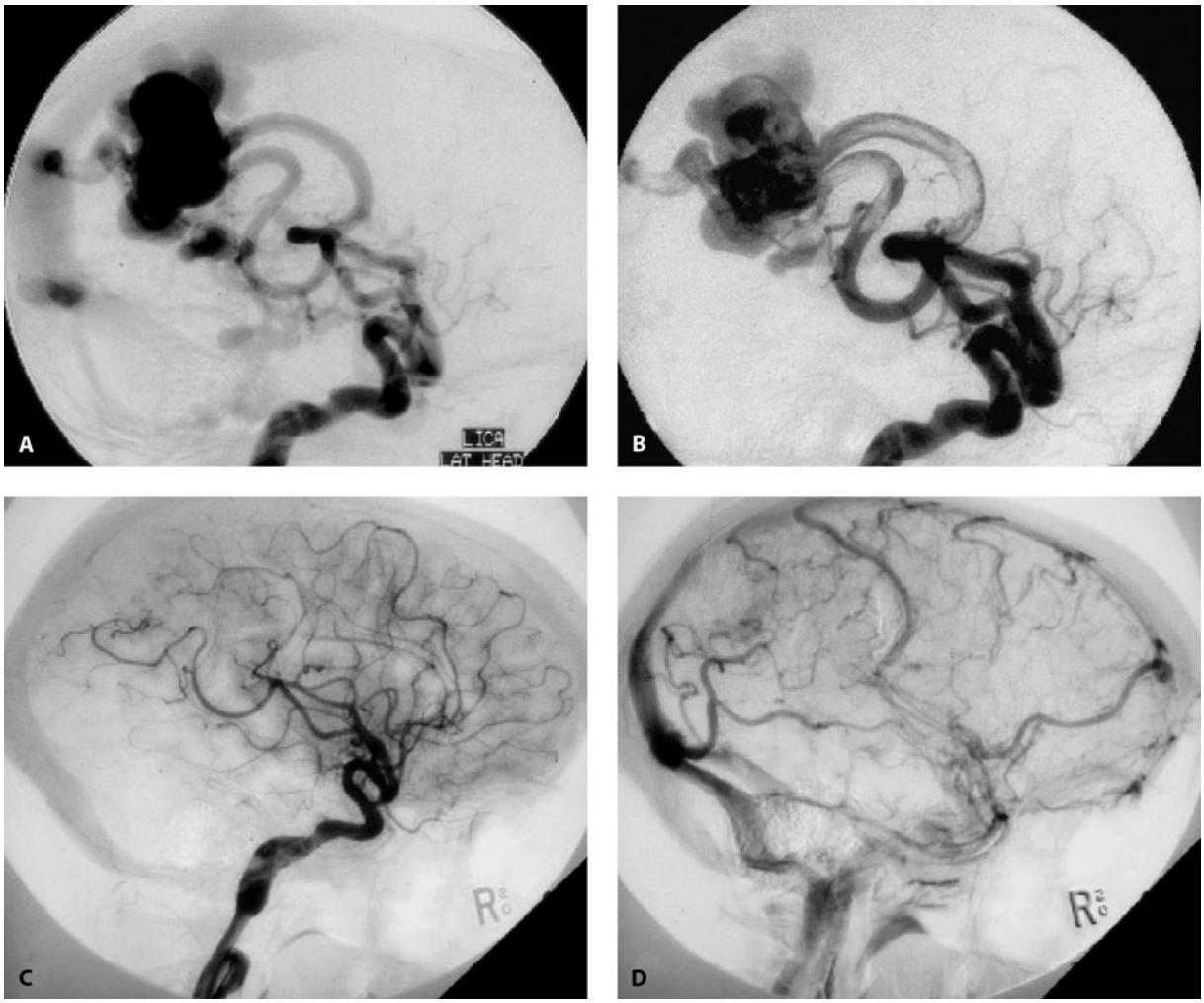

Fig. 10.17. Carotid angiogram in lateral view (**A**) of a 20-year-old female patient presenting with a seizure. The carotid angiogram in lateral view immediately following embolization with glue of the parietal lobe multiple fistula arteriovenous malformation (AVM) demonstrates residual flow through the AVM (**B**). Two-year follow-up carotid angiogram in lateral view, arterial phase (**C**), and venous phase (**D**) demonstrates subsequent complete thrombosis of the AVM and long-term stability of the embolization

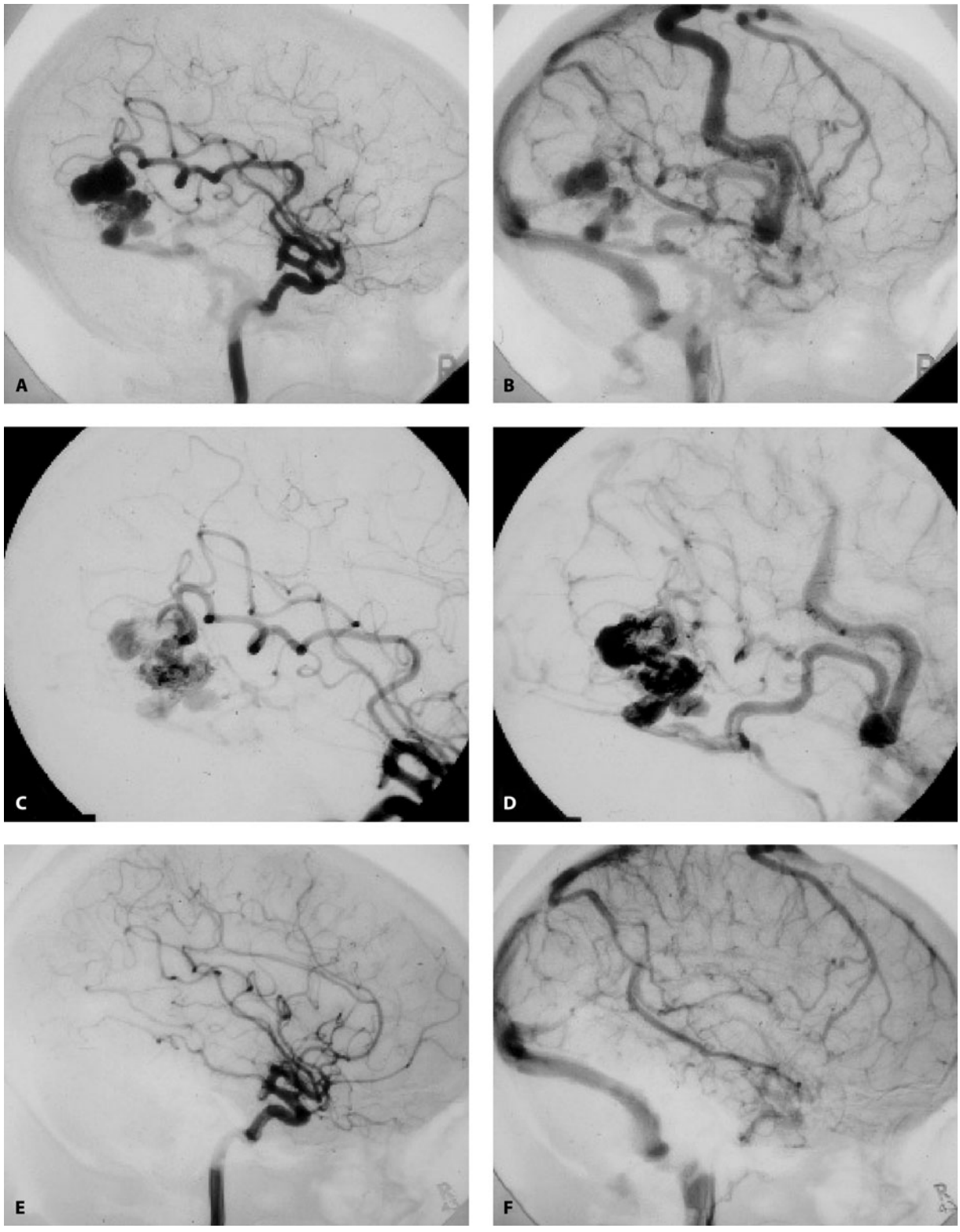

Fig. 10.18A–F. Legend see p. 725

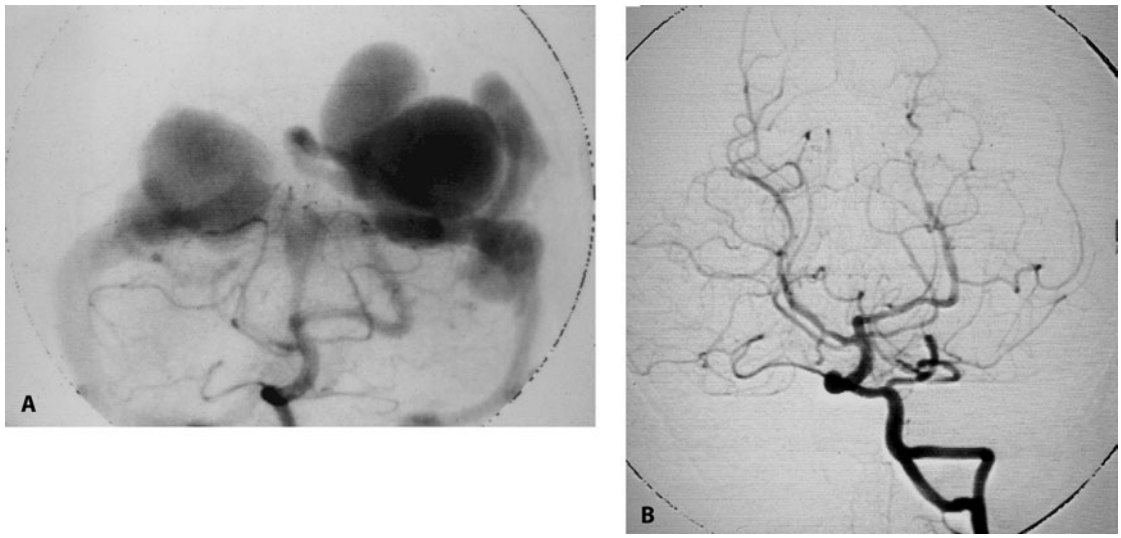

Fig. 10.19. Vertebral angiogram in AP view prior to (**A**) and 10 years following transarterial embolization with glue of bilateral occipital lobe arteriovenous fistulae (**B**) demonstrates long-term stability after embolization

◄ **Fig. 10.18.** Carotid angiogram in lateral view arterial (**A**) and venous phase (**B**) of a 34-year-old female patient presenting with complex seizure disorder prior to embolization with glue. Immediate postembolization carotid angiogram in lateral view early arterial phase (**C**) and late arterial phase (**D**) shows partial obliteration of posterior temporal lobe arteriovenous malformation (AVM). Subsequently, the seizure disorder became easily manageable and 2-year follow-up carotid angiogram in lateral view arterial phase (**E**) and venous phase (**F**) demonstrates subsequent complete thrombosis of the AVM with long-term stability after embolization. Note the remodeling of the arterial and venous vascular system

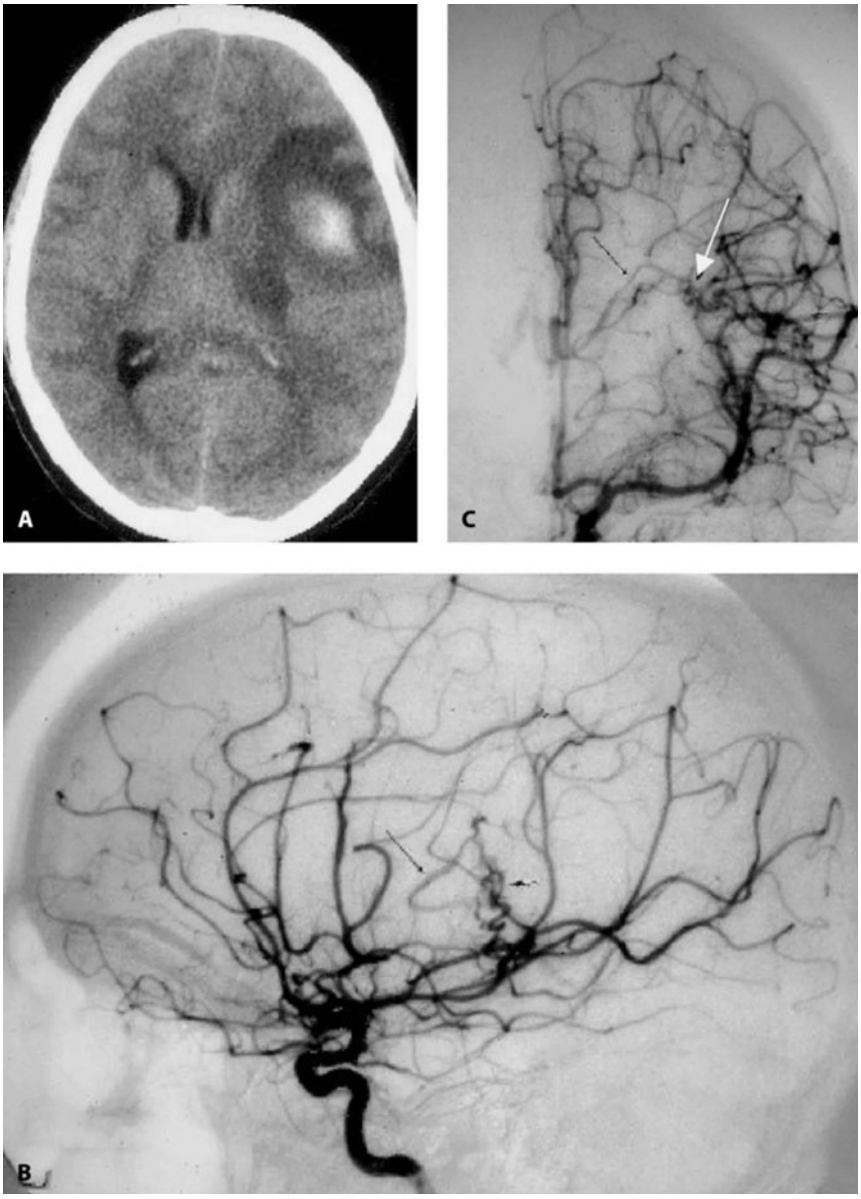

Fig. 10.20. CT scan (**A**) obtained 1 week after sudden onset of neurological deficit in 18-year-old female patient showed recent intracranial hemorrhage with surrounding edema. Surgical removal of microarteriovenous malformation (micro-AVM, *arrows*) involving the left insular cortex as shown on carotid angiogram in lateral view (**B**) and AP view (**C**) was attempted but unsuccessful and associated with worsening neurological deficit. While referred for radiosurgery, embolization was offered to achieve more immediate protection. **D–H** see p. 727

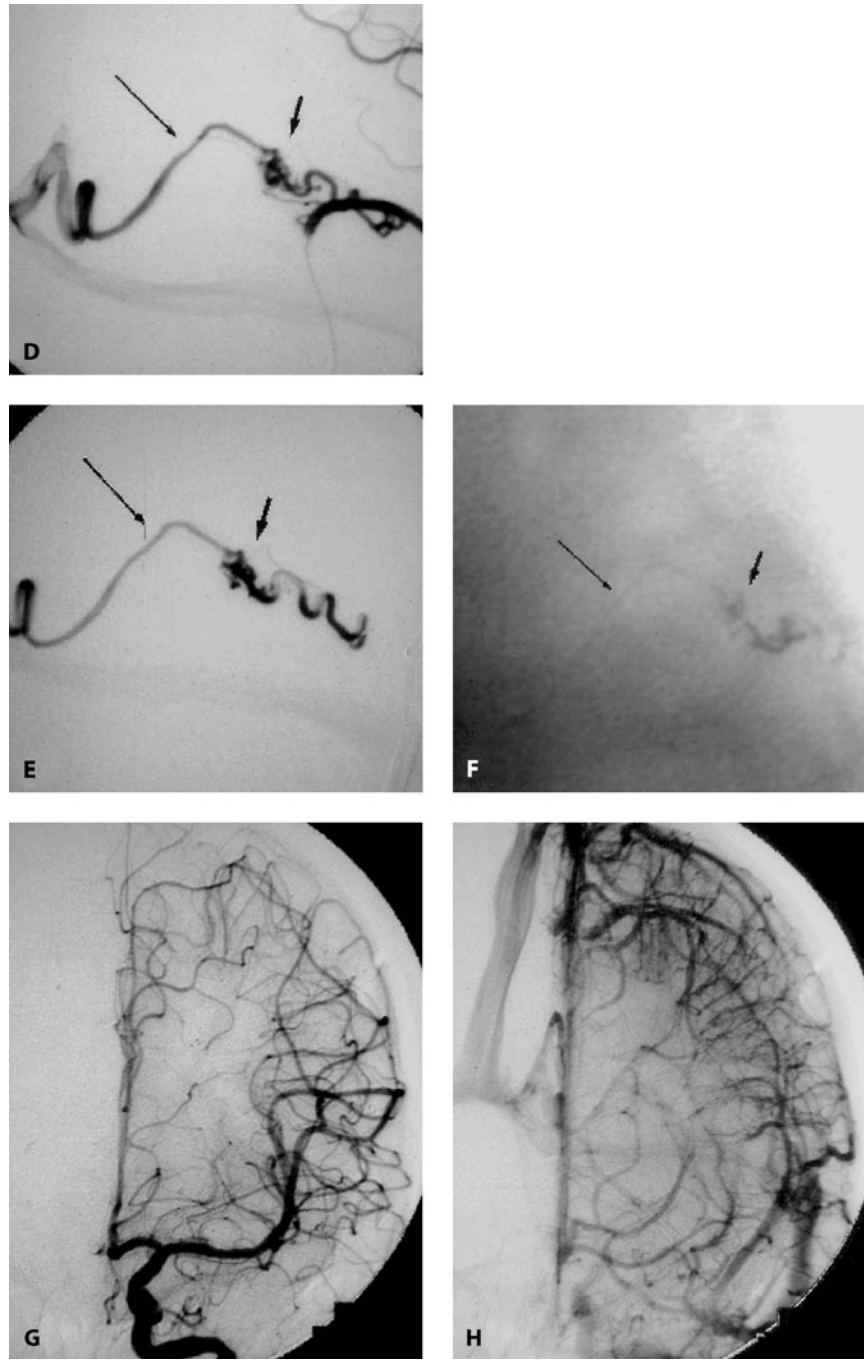

Fig. 10.20 (*continued*). Selective middle cerebral artery angiogram in AP view (**D**) and superselective injection of the feeding pedicle toward the nidus (*short arrow*) and draining vein (*long arrow*) in AP view (**E**); glue cast of the nidus and draining vein (**F**) following uneventful embolization of the micro-AVM, which resulted in immediate complete obliteration of the AVM, as shown on the carotid injection in AP view arterial phase (**G**) and venous phase (**H**)

10.4.4 Preoperative Embolization

Presurgical embolization of BAVM is a well-accepted and frequent application of endovascular therapy. Its role has become firmly established over the past 20 years (Vinuela et al. 1991; Jafar et al. 1993; Wallace et al. 1995).

The goal of therapy in these circumstances is to facilitate surgical removal of the AVM. The specific goals of such embolization should therefore be discussed with the vascular neurosurgeon to provide the best possible benefit at surgery at the lowest combined (endovascular + surgery) risk for treatment-associated complications to the patient.

The embolization goals in these circumstances are often elimination of deep feeding arterial supply, occlusion of intranidal arteriovenous fistulae, and overall size and flow reduction through the nidus (Fig. 10.21).

A variety of materials have been used for the purpose of presurgical embolization, starting in the early 1960s with silicone spheres (Luessenhop et al. 1962; Kricheff et al. 1972; Wolpert et al. 1975; Hilal and Michael-

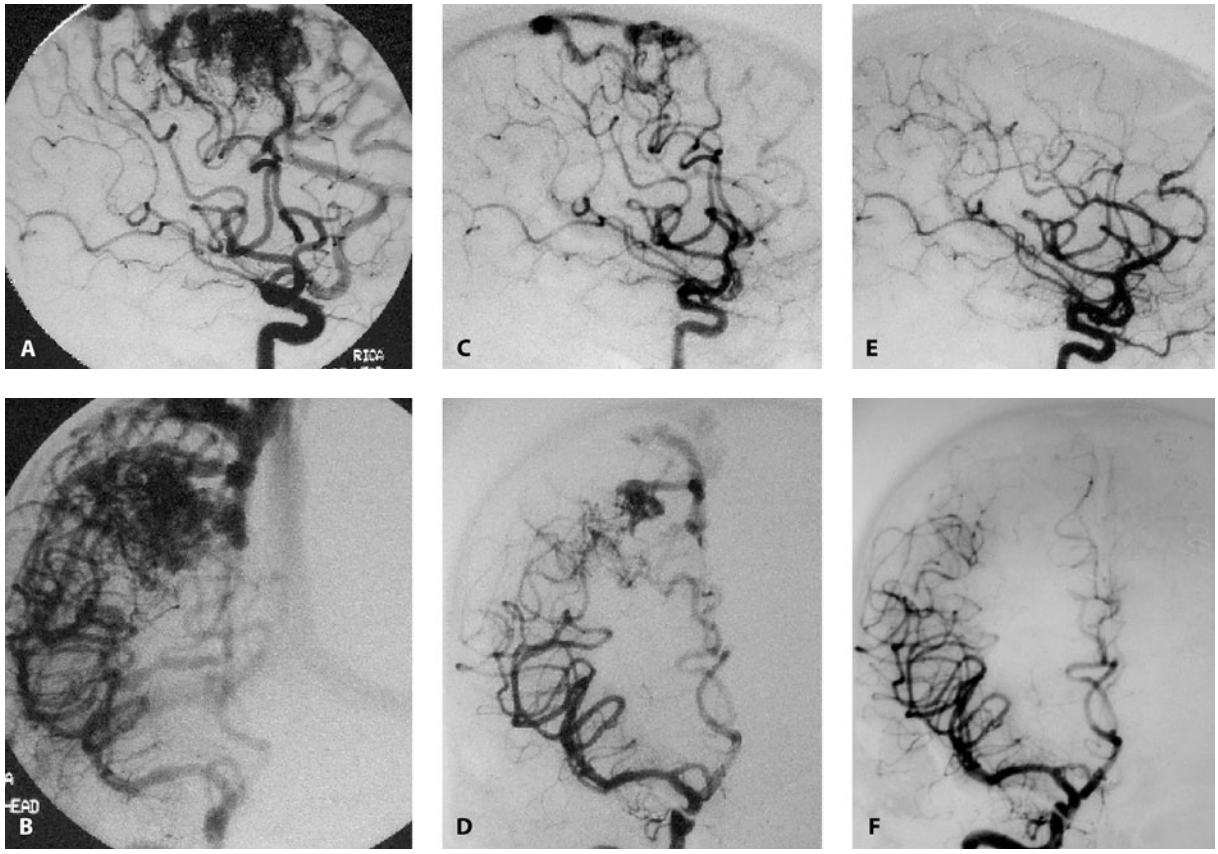

Fig. 10.21A–F. Presurgical embolization. Carotid angiogram in lateral (**A**) and frontal view (**B**) prior to embolization demonstrates right-sided frontal–parietal arteriovenous malformation (AVM). Presurgical embolization with glue of the anterior cerebral artery supply to the AVM was performed; follow-up carotid angiogram in lateral view (**C**) and frontal view (**D**) demonstrates partial obliteration of the nidus. Surgical resection was facilitated and confirmed on postoperative carotid angiogram in lateral view (**E**) and frontal view (**F**)

son 1975). Subsequently, silk or polyethylene threads (Benati 1987) were used, as well as polyvinyl alcohol (PVA) particles (Latchaw and Gold 1979). Liquid tissue adhesives such as isobutyl-cyanoacrylate (IBCA) and subsequently *N*-butyl-cyanoacrylate (NBCA) have been used since 1980 (Cromwell and Kerber 1980; Cromwell and Harris 1980). Both PVA and NBCA have been used extensively for the purpose of presurgical embolization in various centers around the world, and their safety and efficiency have been established (Vinuela et al. 1991; Jafar et al. 1993; Wallace et al. 1995; DeMeritt et al. 1995; Jordan et al. 1996). When clinical outcomes were assessed and complications related to embolization and surgery were combined, the use of NBCA was felt to be clearly better than that of PVA for the purpose of presurgical embolization (Wallace et al. 1995). Surgical removal of the AVM is not significantly impeded by the use of NBCA (Jafar et al. 1993), although mobilization of the AVM at the time of resection can be somewhat more difficult.

In order for local and regional hemodynamic changes to stabilize and to take full advantage of progressive thrombosis that may occur following presurgical embolization, we recommend that surgery take place 1–3 weeks after embolization.

In our experience, the risk associated with presurgical embolization using NBCA is exceptionally low, with less then 1% procedure-related morbidity and no mortality.

10.4.5 Intraoperative Embolization Therapy

Following the initial experience reported by Drake et al. (1979), certain modifications were proposed by Cromwell and Harris (1980) and Spetzler et al. (1987). However, with the improvement of percutaneous endovascular catheter technology, the role of intraoperative embolization of BAVM has been almost eliminated and it is nowadays rarely needed.

10.4.6 Embolization Prior to Radiosurgery

The purpose of embolization prior to stereotactic radiosurgery can be twofold: overall size reduction and targeted embolization toward specific angioarchitectural abnormalities.

10.4.6.1 Size Reduction

Embolization can be used to decrease the size of the malformation to a volume, which can then be radiated, with a reasonable chance of accomplishing a cure (Fig. 10.22) (Gobin et al. 1996). The size of the AVM and the dose given, in particular to the margins of the AVM, are the most important indicators for success of stereotactic radiosurgery, irrespective of the type of device used (Bragg peak proton beam, gamma knife or linear accelerator), as reported by Steinberg et al. (1990), Karlsson et al. (1997), Pollock et al. (1998), and Schlienger et al. (2000).

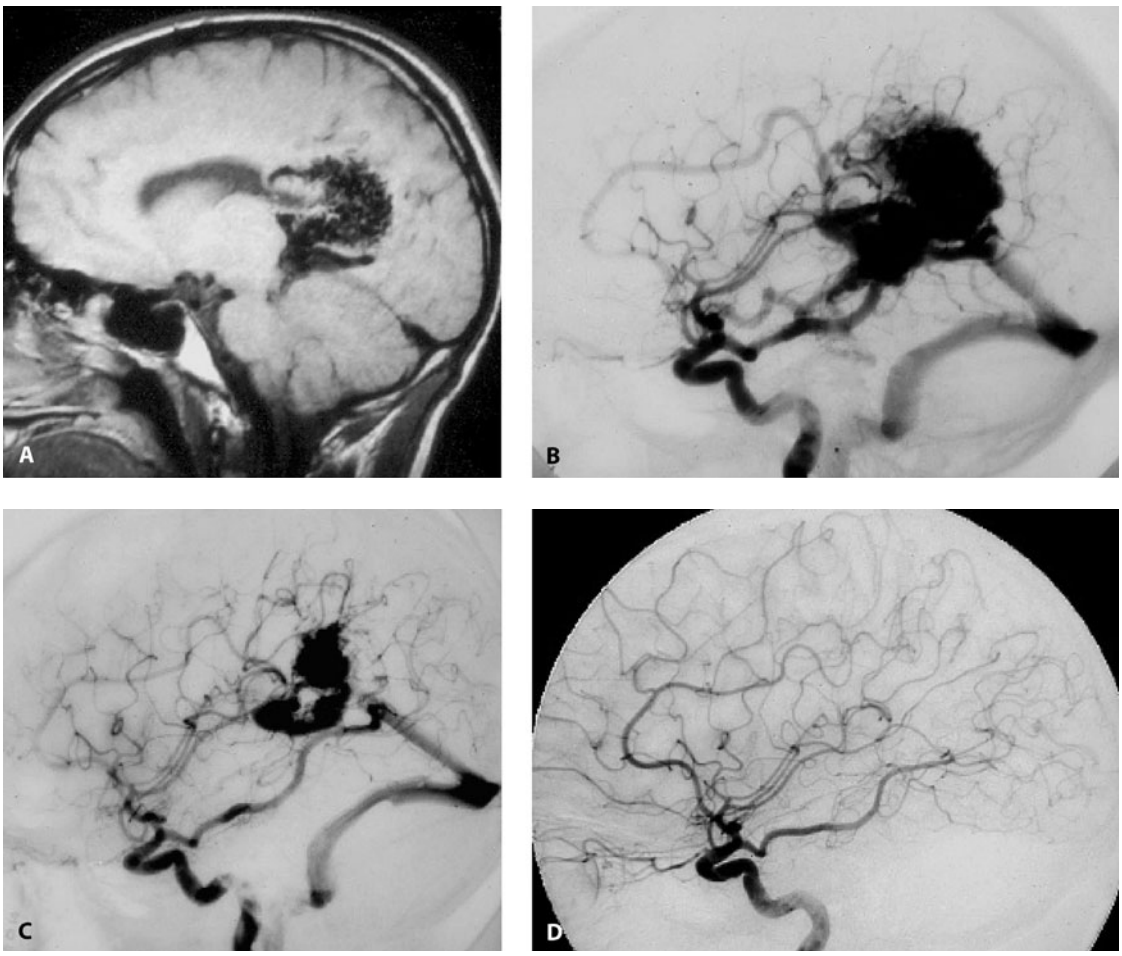

Fig. 10.22A–D. Embolization prior to radiosurgery. **A** MRI, T1-weighted in sagittal projection, demonstrates parietal arteriovenous malformation (AVM) too large for efficient radiosurgery. Carotid angiogram in lateral projection prior to (**B**) and 2 months after partial embolization with glue (**C**) demonstrates nidus size reduction. Stereotactic radiosurgery was performed and 2-year follow-up carotid angiogram in lateral view (**D**) demonstrates complete obliteration of the AVM

Unfortunately, size reduction of large-volume AVMs is not always possible and is more difficult to achieve when arterial supply is derived from multiple territories (anterior, middle, and posterior cerebral artery supply) and in certain locations with rich potential for collateral supply (occipital lobe). In such circumstances, intranidal deposition of embolic material is mandatory to avoid the induction of collateral supply. Although limited data is available on the success rate of embolization for size reduction (Gobin et al. 1996), it is often the only method available that can reduce the size of the AVM to bring it within reach of radiosurgery (Fig. 10.23). On the other hand, although intended to be done prior to radiosurgery, embolization resulted by itself in obliteration of the AVM in about 10% of patients, obviating the need for radiosurgery.

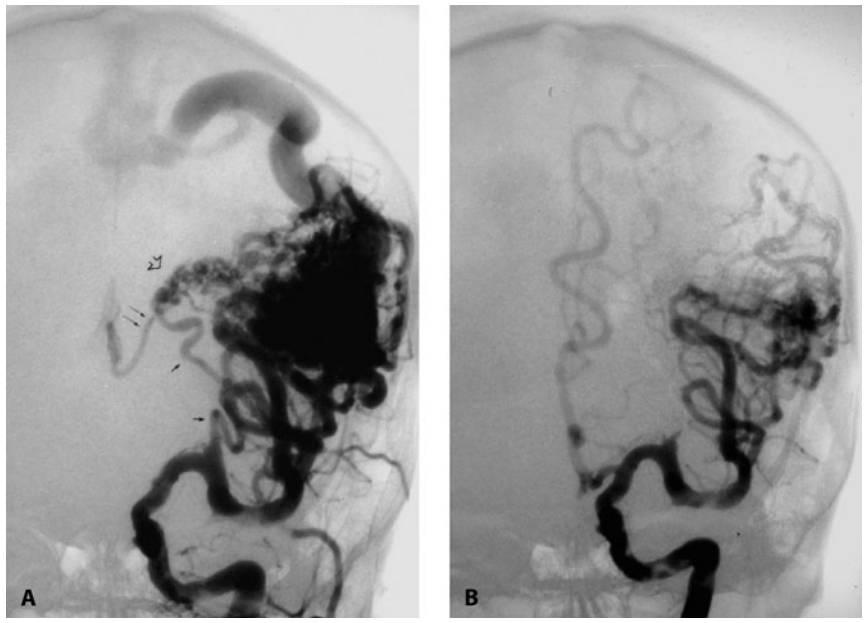

Fig. 10.23A, B. A 23-year-old female patient presented with history of seizures. Carotid angiogram AP view (**A**) shows evidence of large cortical-ventricular arteriovenous malformation (AVM), which was treated with partial targeted embolization toward deep extension of the AVM (*arrows*) with glue, as shown on post-embolization angiogram (**B**), facilitating size reduction for subsequent radiosurgery

10.4.6.2 Targeted Embolization Prior to Stereotactic Radiosurgery

Embolization can be performed prior to radiation therapy in patients with demonstrated angioarchitectural changes that might be responsible for previous clinical symptoms or might be markers for possible future hemorrhagic events (aneurysm, etc.). This can be done irrespective of the size of the AVM; we have experienced a slight decrease in the hemorrhagic event rate on follow-up of patients who had undergone embolization prior to radiosurgery as compared to the group with radiosurgery alone, irrespective of the mode of initial presentation.

When planning the embolization prior to radiosurgery either to reduce the size or to eliminate angioarchitectural weaknesses, it is imperative that a permanent embolic agent such as NBCA be used. There is no role for embolization with particulate matter (PVA) or coils in preparation for radiosurgery, as it will not lead to permanent obliteration of the nidus. Similarly, feeder occlusions inadvertently performed with NBCA may also lead to induction of collateral supply and destabilization of the lesion (Fournier et al. 1990; Gruber et al. 1996).

We recommend at least a 2-month waiting period between the embolization procedure and stereotactic radiosurgery and angiography confirmation of the stability of the embolization results achieved.

As the embolization prior to stereotactic radiosurgery must result in permanent obliteration of the targeted component of the AVM, its complication rate will be similar to that of embolization as a sole treatment. The dual modality cumulative risk to the patient (embolization + radiation) versus the benefit must therefore be taken into account.

10.4.7 Staging of Embolization

Embolizations are usually staged in large malformations, or a small feeder is allowed to enlarge in order to facilitate future catheterization. There is no apparent increased risk in leaving part of a malformation patent, even if a large or high-flow portion is occluded. Therefore staging in large malformations may be advantageous from a technical and hemodynamic viewpoint.

Staging is of utmost importance and value in the very young patient with a delicate cardiovascular state, in whom careful monitoring of fluids and contrast material is imperative (see Vol. 3).

Staging is also advisable in patients in whom a deficit or other complications occur. The embolization is then resumed when the deficit has cleared. There is no need for staging if none of the above circumstances exist and if the lesion can be completely obliterated in one session.

10.4.8 Emergency Embolization

There are few indications for emergency embolization in adults. Urgent need for embolization may arise when the angiographic study at the time of presentation demonstrates the presence of an arterial (or intranidal) pseudoaneurysm or an enlarging aneurysm on one of the feeding arteries, demonstrated on a previous examination (Fig. 9.36). Embolization should probably also be done early if a venous pseudoaneurysm is shown at the time of hemorrhagic presentation. The natural history of pseudoaneurysm is not fully known (Garcia-Monaco et al. 1993), but in our opinion they are a significant feature of instability that warrants active intervention.

Other instances requiring emergency intervention relate to preoperative embolization in the presence of an acute hematoma in a sick patient in whom embolization may permit evacuation of the clot without the risk of rebleed from the AVM at the time of surgery. However, surgical evacuation of the clot remains the priority and only if expeditious embolization can be done will it be warranted. In general, early rebleeding is such an exceptional situation that it rarely warrants early endovascular intervention. Recovery from the hemorrhagic insult may, in fact, be compromised by aggressive, early, endovascular intervention.

10.4.9 Contraindications for Endovascular Treatment

In general, the contraindication for endovascular treatment of a BAVM is the absence of an indication for treatment. More specific contraindications pertain to cases in which the goal of treatment cannot be achieved: no cure in an asymptomatic patient or the inability to catheterize the pedicle harboring an arterial aneurysm.

When there is a technical failure, either to reach the desired pedicle or to achieve distal catheterization, it may be prudent to stop and make a second attempt later, when that goal can often be achieved.

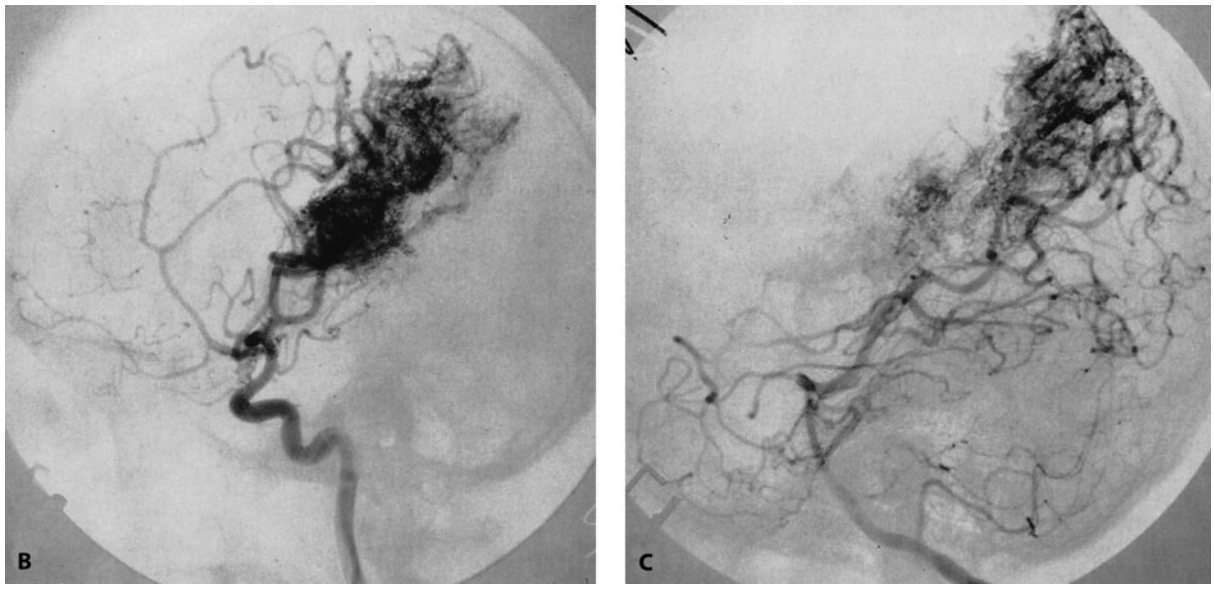

Fig. 10.24A–C. Ill-defined vascular malformation without distinctive weakness in the angioarchitecture. There are no good pedicles for embolization, and the amount of collateral circulation versus nidus is difficult to distinguish. **A** Frontal and **B** lateral subtraction angiograms of the left internal carotid artery and **C** lateral view of the left vertebral artery. Note the amount of vascularization, which is difficult to distinguish from true malformation. There is relatively slow filling of the venous part of the malformation. This case reflects a technical limitation of embolization

With present technology, treatment is possible in the great majority of patients. Current limitations for treatment still include ill-defined vasculature where it may be impossible to distinguish between malformation and nonsprouting angiogenesis or collateral formation (Fig. 10.24). Anatomical limits may prevent adequate treatment of certain portions of a malformation (Fig. 10.25).

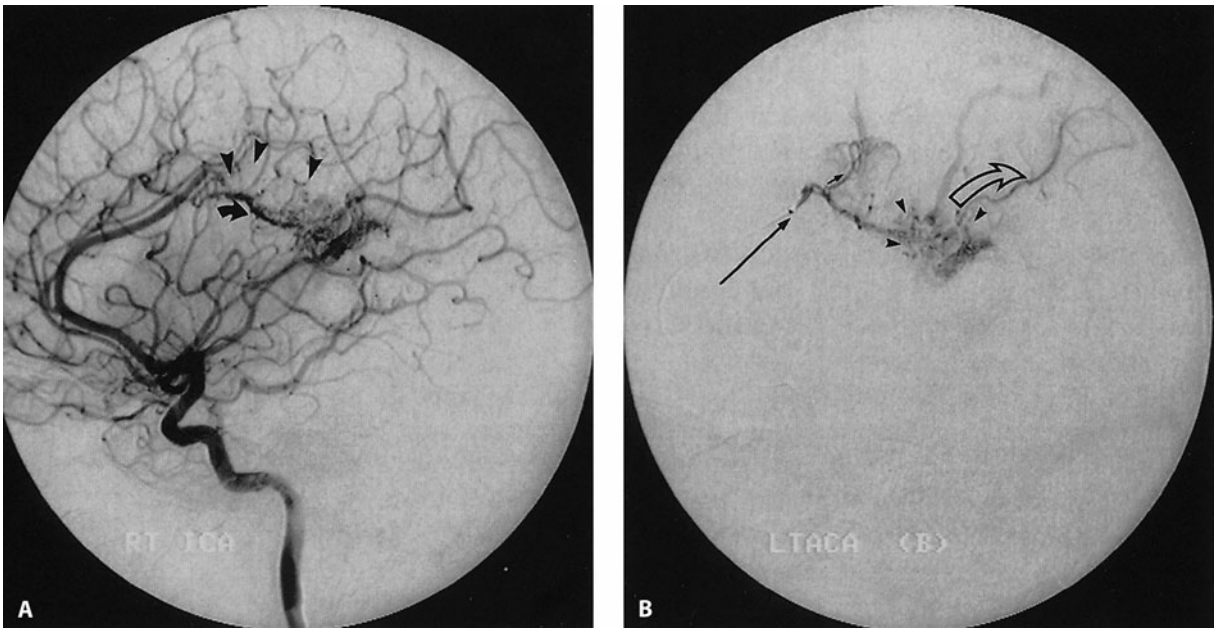

Fig. 10.25A, B. Anatomical limitation. **A** Lateral digital subtraction angiogram of the right internal carotid artery after embolization of a midline malformation. The pericallosal supply has been embolized and is subtracted (*arrowheads*). Note remaining malformation supplied by a small pericallosal branch (*curved arrow*). **B** Superselective injection of the anterior cerebral artery. Note the anatomical limitation for embolization. There is a normal branch to the singular gyri (*small arrow*). There is supply to the malformation in vessels *en passage* (*arrowheads*) and supply to normal brain distally (*open curved arrow*). Embolization of this pedicle would result in occlusion of normal cerebral arteries

10.4.10 Embolization Results

Our results of embolization of BAVMs have been previously published (Fournier et al. 1991b; Jafar et al. 1993; Al-Yamany et al. 2000; Willinsky et al. 2001; Meisel et al. 2002) and now reflect a combined experience of over 2,500 adult patients embolized. Our results of embolization of BAVMs have proven to be stable over time. The authors have exclusively used glue as the primary embolic material of choice, with results thus based on a standardized experience extending now over more than 17 years.

Our ability to reach the nidus of a given AVM and inject the acrylic material safely has obviously benefited from improved delivery systems that have become available over time, also facilitating the so-called intranidal deposition of the embolic material.

The specific goal of the embolization will be different in each patient and should always be related to providing the patient with a benefit at a risk which should outweigh the natural history.

Our experience has shown that the ability to reach the predetermined goal is predictable, confirmed by our results. The ability to obliterate a BAVM is clearly angioarchitecture-dependent and will be as high as 100% in the fistulous types. The authors' recommended strategy in the management of BAVM patients is not necessarily an obliterated AVM (although desirable) but rather a stable patient functioning at optimal level.

During this risk management process, it becomes obvious that the complications related to endovascular treatment (and similarly for surgery and radiation therapy) will have to be within a certain range in order to provide a positive risk–benefit ratio to the patient.

Our combined experience (>2,500 patients with BAVM embolized) has shown that procedure-related nonpermanent neurological deficit was below 6%, permanent neurological deficit occurred in less then 2.5%, and mortality was below 1.5%.

These numbers pertain to our overall experience, i.e., all embolizations performed. The complications associated with embolization of certain subgroups of patients (presurgical BAVMs and small BAVMs) approach levels compatible with the risk of diagnostic angiography.

This indicates once again that each BAVM patient should be managed according to a number of guiding principles: the anticipated natural history, the anticipated positive impact of treatment, and the established treatment record of the physicians involved. Only when the ratio is positive can we expect the patient to accept our treatment recommendation.

11 Spinal Arteriovenous Malformations

11.1 Parachordal Arteriovenous Fistulae (Extracranial, Vertebro-Vertebral, Paraspinal, Extradural, and Extraspinal Arteriovenous Fistulae) 738
11.1.1 General Remarks 738
11.1.2 Cranial (Branchial) Arteriovenous Shunts 740
11.1.2.1 Maxillary Artery-to-Vein Arteriovenous Fistulae (Stapedial) 743
11.1.2.2 Ascending Pharyngeal-Internal Jugular Arteriovenous Fistulae (Hypoglossal) 743
11.1.3 Vertebro-Vertebral Arteriovenous Fistulae (Proatlantal and Intersegmental) 743
11.1.3.1 Vertebro-Vertebral Arteriovenous Fistulae 743
11.1.3.2 Clinical Findings 751
11.1.4 Paraspinal Arteriovenous Fistulae 752

11.2 Spinal Cord Vascular Lesions 758

11.3 Spinal Cord Arteriovenous Malformations 760
11.3.1 Classification of Spinal Cord Arteriovenous Malformations 767
11.3.2 Angioarchitecture 775
11.3.2.1 Arterial Features 775
11.3.2.2 Direct Arteriovenous Fistulae 784
11.3.2.3 High-Flow Angiopathy 786
11.3.2.4 Arterial Aneurysms in Spinal Cord Arteriovenous Malformations 786
11.3.2.5 Dural Supply 794
11.3.2.6 Nidus 794
11.3.2.7 Veins 802
11.3.3 Pretherapeutic Evaluation 808
11.3.3.1 Clinical Assessment 808
11.3.3.2 Noninvasive Imaging Modalities 808
11.3.3.3 Angiography 809

11.4 Spinal Cord Hemodynamics 810
11.4.1 Particular Forms of Spinal Cord Arteriovenous Malformations 811
11.4.1.1 Spinal Cord Intradural Arteriovenous Fistulae 811
11.4.1.2 Spinal Arteriovenous Metameric Syndromes 813
11.4.1.3 Associated Cerebral and Spinal Arteriovenous Malformations 822
11.4.2 Clinical Aspects 825
11.4.2.1 Natural History and Clinical Presentation 825
11.4.2.2 Prognosis 830
11.4.2.3 Aggravating Factors 831

11.5 Treatment of Vascular Lesions 833
11.5.1 Indications 833
11.5.2 Results of Spinal Cord Arteriovenous Malformation Embolization 839
11.5.3 Complications of Embolization 840
11.5.4 Surgery in the Treatment of Spinal Cord Arteriovenous Malformations 842
11.5.5 Radiotherapy of Spinal Cord Arteriovenous Malformations 843
11.5.6 Medical Therapy 843

11.1 Parachordal Arteriovenous Fistulae (Extracranial, Vertebro-Vertebral, Paraspinal, Extradural and Extraspinal Arteriovenous Fistulae)

11.1.1 General Remarks

Because of the role of the neural crest and the mesoderm in the development of the segmental vascularization, extracranial branchial and paraspinal arteriovenous fistulae (AVFs) are similar in nature. Although they are located in different anatomical areas, the fistulae are fed by arteries supplying the craniocervical junction (the maxillary, the ascending pharyngeal artery, the occipital artery and the thyro- and costocervical arteries). The internal carotid artery (ICA) in its first cervical segment can also be included in this group, as it corresponds to the third aortic arch. The vertebral arteries are intersegmental channels that bridge and link three to eight cervical segmental arteries (Vol. 1). The arteriovenous shunts (AVSs) supplied by the vertebral arteries should also be considered as segmental. We can therefore include vertebral artery-to-vertebral vein fistulae or vertebro-vertebral AVFs (VVAVFs) in the group of extracranial and paraspinal AVFs (parachordal, following the notochord).

The embryonic core of these malformations is the notochord. It ends at the basisphenoid level, where it marks the junction between the somitic and the prebranchial somitic portion of the branchial region. In vascular terms, the rostral limit of the notochord is the cavernous venous plexus with the arterial supply to the region from the maxillary artery branches; it also includes the extradural ICA, and therefore the most appropriate name for this group of lesions is parachordal AVFs (Table 11.1).

No nontraumatic AVFs in the cranial region, other than those fed by the metameric arteries (ICA, maxillary, ascending pharyngeal, laryngeal, occipital and vertebral arteries) are fed by the thyrolingual-facial arteries. At the thoracic, lumbar, or sacral levels, the extraspinal paraspinal AVFs are supplied by their respective segmental arteries and located according to the appropriate site of the shunt, either on the main trunk or on its branches. Analysis of the similarities and differences in the anatomy of

Table 11.1. Parachordal arteriovenous fistulae

Region	
Cephalic	Maxillary, EJV Ascending pharyngeal, IJV Occipital, C1 vertebral or PJV Occipital, C2 vertebral or PJV
Somitic	Thyro-cervical-vertebral or PJV Costo-cervical-vertebral or PJV Cervico-vertebral vein Segmental (intercostal, lumbar, sacral), azygos vein

EJV, external jugular vein; IJV, internal jugular vein; PJV, posterior jugular vein.

the venous drainage is equally enlightening, as it is the key factor in understanding and predicting the clinical manifestations of parachordal AVFs (Rodesch et al. 1996) (Table 11.2).

The role played by the internal jugular vein and the azygos veins as low-resistance outlets may facilitate cardiac overload in some rare pediatric cases (see Vol. 3). Conversely, the high resistance of the posterior external jugular veins, the vertebral veins, and the epidural venous plexuses explains the absence of cardiac symptoms as the clinical presentation of AVF draining primarily into these systems (Table 11.3). If we consider only the AVFs that are located ventral to the notochord (extracranial and paraspinal), drainage of the AVF in most cases is centrifugal and seldom epidural and almost never intradural (Goyal et al. 1999).

From a purely academic point of view, epidural AVSs of the spine and the cavernous plexus could be linked together, since both are osteoepidural in location. When looking at the differences in the venous structures of the spine and cranial region, the absence of a dural venous sinus in the former is immediately apparent. Intracranial venous sinuses are vascular pathways within the dural sheet and cannot be considered as venous channels located within the epidural space. There are no venous

Table 11.2. Modalities of venous drainage in parachordal arteriovenous fistulae

Type of drainage	Veins involved
Centrofugal drainage	Jugular vein (external, posterior, internal) Vertebral vein Azygos vein
Epidural drainage	Cranial sinuses Venous plexuses
Centropetal drainage	Cerebropial drainage Radicular vein

Table 11.3. Clinical manifestations in parachordal arteriovenous fistulae

Manifestation	Mechanisms involved
Congestive cardiac failure	Internal jugular vein drainage Azygos vein drainage
Neurological deficits	Pial venous congestion by epidural hyperpressure Pial venous congestion by pial reflux Compression from epidural venous ectasia Radiculomedullary arterial shunt Associated myelomeric arteriovenous shunt (Cobb syndrome)
Hemorrhage	Pial reflux Venous infarction
Symptoms related to associated tumors or vascular sites in specific pathologies	Neurofibromatosis type 1 Collagen diseases Rendu–Olser–Weber disease, etc.

dural sinuses at the spinal level, the spinal epidural venous plexuses have the same appearance all along the notochord, from the sacrum to the basisphenoid. These epidural venous channels have mainly axial and longitudinal anastomoses.

For the most part, there will be no central nervous system consequences of extraspinal or extracranial fistulae, unless they have radicular venous drainage and subsequent pial reflux or if their epidural venous drainage creates expansion, mass effect, and cord compression. Special locations or anatomical dispositions of the cerebral venous outlets or radicular veins at the level of the shunt may account for the pial venous opacification that is occasionally seen. The usual venous impairment of the brain or cord seen with intradural or dural AVSs is rarely encountered in parachordal AVFs (Sedat et al. 1999). The chronic effect of the AVF is mainly expressed on the venous side of the lesion. There is no high-flow arterial angiopathy in the branches supplying the shunt, as the hemodynamic conditions of these segmental arteries differ from those of the central nervous system (cerebral or cervical cord) (Figs. 11.1, 11.3). The effects of epidural venous congestion on the pial venous system can be seen in rare cases. If the AVF is part of an underlying vascular dysplasia, the shunt may not become apparent until adulthood. Some of these extracranial or spinal AVFs can be part of a cerebral–facial or spinal arteriovenous metameric syndrome (CAMS, SAMS), therefore associated with true intradural arteriovenous lesions (Bhattacharya et al. 2001).

11.1.2 Cranial (Branchial) Arteriovenous Shunts

Branchial arteriovenous shunt (AVS) is the name given to those AVFs that are fed by branchial arteries (cervical ICA; Fig. 11.1), proatlantal, hypoglossal, and stapedial). These vessels (an exception is made for the ICA) constitute the arterial supply to the cranial nerves, and the hazards of embolization of these vessels are inherently related to this anatomical coincidence. Two types of AVSs can be encountered: maxillary and pharyngeal AVFs (often called external carotid-to-jugular vein fistulae). The proatlantal artery is involved in the construction of the vertebral artery at the C1 and C2 levels and the AVFs developed from them are included in the VVAVFs. Most often, these lesions are incidentally discovered in children (Hui et al. 1994; see Vol. 3). All these branchial AVFs can successfully be treated by endovascular occlusion.

Fig. 11.1A–E. A 36-year-old hypertensive male patient presented with sudden headaches and loss of conscience. At admission he had a score of 3 on the GOS with bilateral myosis and right-sided hemiplegia. Evidence of subarachnoid hemorrhage and intraventricular hemorrhage was seen on CT (**A**, **B**). Extracranial rupture of the ICA in the jugular bulb (**C**, **D**) was treated in emergency with three gold valve latex balloons and internal carotid artery sacrifice (**E**), for fear of a possible persisting dissecting process from an undiagnosed collagen disease. Favorable clinical evolution ►

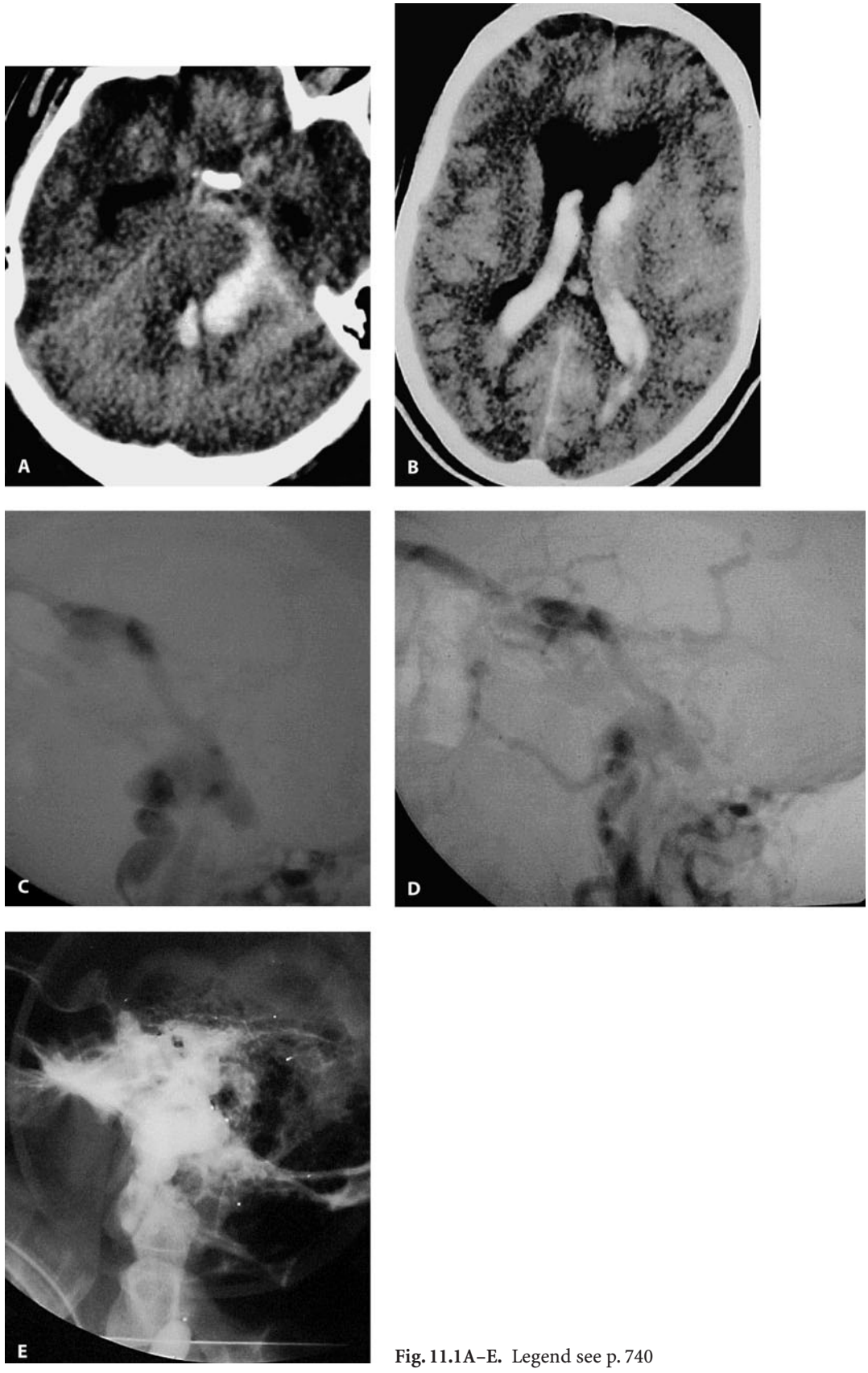

Fig. 11.1A–E. Legend see p. 740

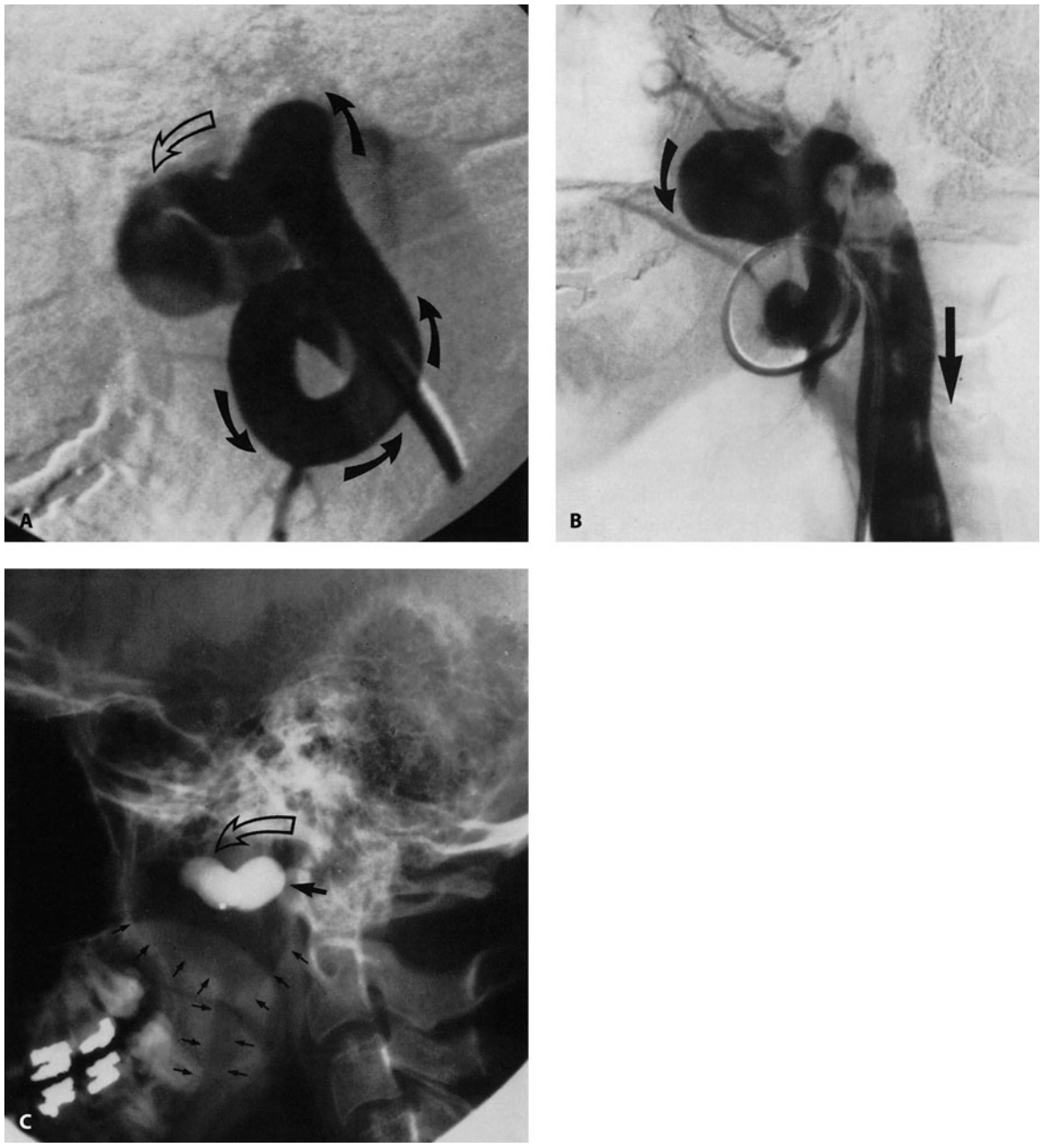

Fig. 11.2A–C. A 23-year-old female patient with left facial asymmetry and a pulsatile tumefaction on the left side of the face. No previous history of trauma was found. **A** Lateral digital subtraction angiography (DSA) of the distal external carotid artery on the left side. Note marked tortuosity of the distal external carotid artery and internal maxillary artery (*curved arrows*) as well as abrupt transitional caliber at the side of the fistula (*open curved arrow*). **B** Later phase demonstrates the large venous dilatation (*curved arrow*) and drainage into the jugular venous system (*arrow*). **C** Plain film following balloon embolization. The most distal balloon shows an hourglass appearance as part of the balloon at the fistula site (*open curved arrow*). A second balloon is placed in tandem to prevent distal displacement of the balloon. Note the well-circumscribed bony expansion in the pterygoid region and inferior alveolar canal (*small arrows*)

11.1.2.1 Maxillary Artery-to-Vein Arteriovenous Fistulae (Stapedial)

Maxillary artery-to-vein AVFs are often discovered by the mother of a child when she hears a noise while kissing or hugging the child (Berenstein et al. 1984b) (Fig. 11.2). In most instances, the fistula is located at the origin of the middle meningeal or accessory meningeal artery and rarely on the maxillary artery itself, where the maxillomandibular branch of the stapedial artery is annexed by the external carotid system (see Vol. 1). The flow is usually high, and the exact location of the fistulous point is often better assessed by selective injection of the adjacent arteries in the region, using the collateral circulation. Retrograde opacification of the cavernous venous plexus with drainage toward the ophthalmic vein or superior petrosal sinus with pial venous reflux is rarely seen, but might result in cerebral venous congestion. In such instances, the risk of intracranial hemorrhage and neurological deficit should then be anticipated and therapeutic indication discussed accordingly.

11.1.2.2 Ascending Pharyngeal-Internal Jugular Arteriovenous Fistulae (Hypoglossal)

Ascending pharyngeal-internal jugular AVFs are seen in young adults (Figs. 11.3, 11.4). Symptoms may include bruit and cranial nerve impairment (IX–XII). In adults, the mechanism of the impairment is unclear, but probably related to arterial or venous ischemia rather than mechanical compression or retrograde intracranial drainage. These fistulae are rare.

11.1.3 Vertebro-Vertebral Arteriovenous Fistulae (Proatlantal and Intersegmental)

11.1.3.1 Vertebro-Vertebral Arteriovenous Fistulae

"Vertebro-vertebral arteriovenous fistulae" (VVAVF) is a generic term covering various types of diseases that involve the vertebral arteries and veins. A clear distinction should be made between these AVFs and the traumatic arteriovenous communications that cover the majority of cases listed in the literature (see Chap. 6, this volume). A separate group is made up of dysplastic vessels, which rupture spontaneously or following minimal injury. Spontaneous vertebral arteriovenous fistulae can be associated with fibromuscular dysplasia (FMD) (Bahar et al. 1984), neurofibromatosis (Deans et al. 1982), and in young adults with collagen type III diseases (Elhers-Danlos IV). In this case, the disease is rather arterial and the fistula microtraumatic.

Since Rubi's (1945) original report, there has been an increased awareness of the vascular lesions associated with neurofibromatosis, which include stenosis, aneurysms (Itzchak et al. 1974), and AVFs. Deans et al. (1982) reported two cases of such fistulae in patients with neurofibromatosis; one had a spontaneous fistula of the left internal maxillary artery that presented with spontaneous hemorrhage.

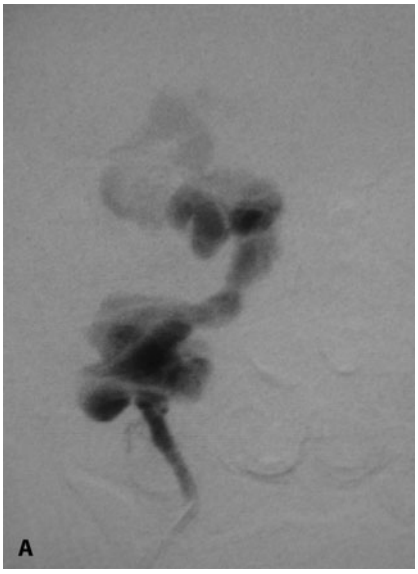

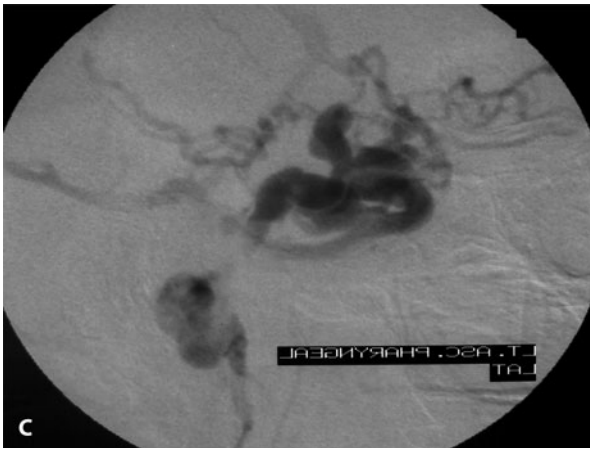

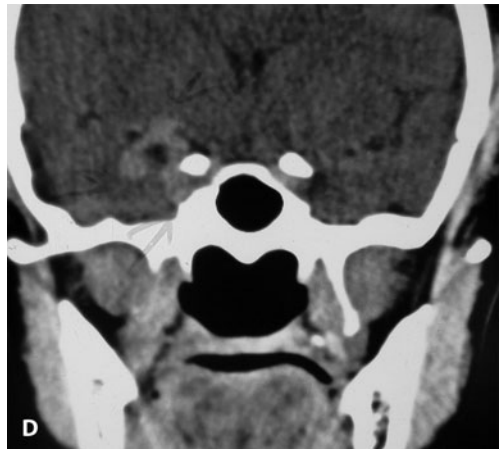

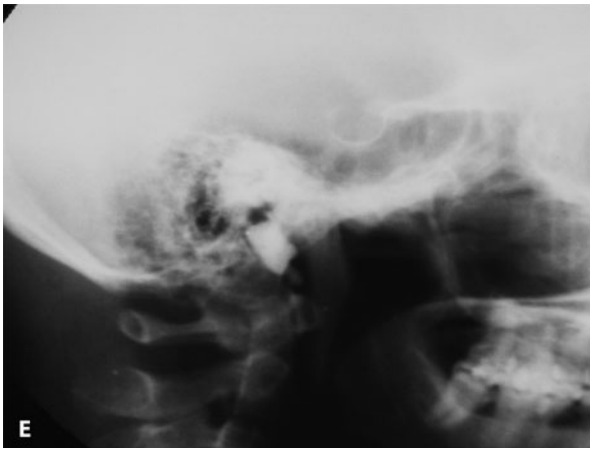

Fig. 11.3. A 44-year-old female patient presented with nontraumatic exophthalmos and tinnitus from a spontaneous ascending pharyngeal-inferior petrosal sinus arteriovenous fistula (**A**, **B**). No evidence of collagen disease. Treated with latex balloon, resulting in complete resolution of symptoms (**C**–**E**). 12th postoperative cranial nerve paralysis was noted. (Courtesy of P. Chewit)

Fig. 11.4A–F. A 35-year-old male patient presented with tinnitus caused by a spontaneous (nontraumatic) occipital-pharyngeal-jugular bulb arteriovenous fistula. No evidence of collagen disease. Internal carotid artery (**A**), occipital (**B**), ascending pharyngeal (**C, D**) angiograms. **E, F** see p. 746

Fig. 11.4 (*continued*). Treatment was achieved by transvenous embolization (**E, F**) with fiber coils and complete resolution of symptoms. (Courtesy of S. Pongpech)

The histological analysis of some of these patients with neurofibromatosis showed proliferation of Schwann cells in the adventitia of the arterial wall, as well as intimal fibrosis and fragmentation of the elastica and thinning of the smooth muscle with aneurysm formation; nodular masses of spindle-shaped cells are also seen between the media and adventitia in the involved artery (Deans et al. 1982). In 1974, Saylor and Saylor actually found such lesions in almost 50% of neurofibromatosis patients studied at autopsy, even if they did not have fistulae. Green et al. (1974), in his study of aneurysmal and nodular lesions in patients with neurofibromatosis, found no evidence of Schwann cell proliferation, and the electron microscopy (EM) characteristics of the spindle cells in these lesions were those of smooth muscle. They suggested that some of the vascular changes in these patients result from a primary dysplasia of the arterial wall. Either dysplasia of the arterial wall or neurofibromatosis proliferation in the arterial wall, or a combination of both, can lead to aneurysm formation and eventual rupture into an adjacent vein, which then produces a pathological AVF.

An upper- and a lower-cervical group can be distinguished within the VVAVF group. The upper-cervical group is seen in the pediatric population (see Vol. 3) and is seldom associated with dysplastic disease, whereas the lower-cervical group is likely to correspond to an older population carrying systemic diseases.

– Upper VVAVFs are shunts that have developed at the C1–C2 level from the proatlantal system. The role of the occipital artery in the supply to the AVF depends on the anatomical balance between the occipital and vertebral sources (Moret et al. 1979). Pure VVAVFs or pure occipitover-

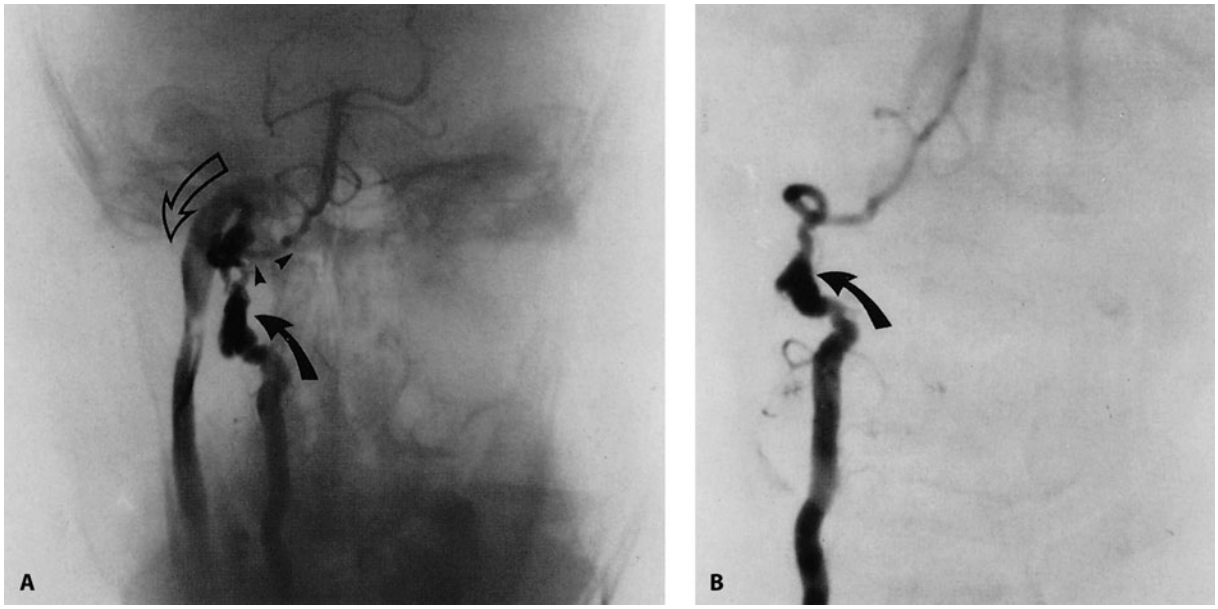

Fig. 11.5A, B. Spontaneous fistula in a 48-year-old woman who presented with a sudden onset of a swishing noise on the right side. The patient demonstrated evidence of fibromuscular dysplasia at multiple brachiocephalic vessels (not shown). **A** Frontal subtraction angiogram of the right vascular artery. Note the dysplastic segment of the vertebral artery (*curved arrow*), filling of the internal jugular vein (*open curved arrow*), and a dysplastic distal vertebral artery (*arrowheads*). **B** Frontal subtraction angiogram of the right vertebral artery following spontaneous closure of the fistula while attempting balloon embolization. The dysplastic vertebral artery affected by fibromuscular dysplasia is seen better (*curved arrow*)

tebral vein AVFs are seen, in addition to intermediate stages. If the shunt is located at the C2 level the same rules apply. Venous drainage of the AVF uses the suboccipital and vertebral network (Fig. 11.5). Understanding the clinical correlation depends on the anatomical knowledge of the operator, as does the capacity to predict the natural history. The exact location of the AVF on the segmental part of the artery or its intersegmental course may impact the potential to preserve the patency of the vertebral artery.

- Intersegmental VVAVFs constitute a rupture of the vertebral continuity, and the vertebral axis may not be preserved unless the hole is small and the embolic agent can be placed on the venous site only. In contrast, a segmental VVAVF is the rupture of the continuity in a vertebral artery branch, and in this situation the vertebral axis can more easily be preserved, even in the presence of large venous pouches. A sump effect, affecting the regional segmental arteries, will opacify the shunt without representing true direct supply. The ascending pharyngeal and costocervical arteries are most frequently involved in this process. They are also alternative pathways to the VVAVF or occipitovertebral AVFs if the shunt is improperly treated.
- Lower-cervical VVAVFs are very different from upper VVAVFs. They involve the cervical arteries, are less frequent, and are usually of the slow-flow type. They are often associated with an underlying vessel wall

Fig. 11.6A, B. Spontaneous fistula in a 52-year-old woman who presented with a sudden onset of a swishing noise on the right side. The patient had cutaneous signs and a family history of neurofibromatosis. **A** Right vertebral injection demonstrates the C3–C4 arteriovenous fistula. **B** After balloon occlusion of the fistula (*arrow*), the proximal dysplastic segment demonstrated significant stagnation for which the vertebral artery was completely obliterated. Note the dysplastic appearance of the vertebral artery, proximal to the fistula

Fig. 11.7A, B.
Legend see p. 749
▼

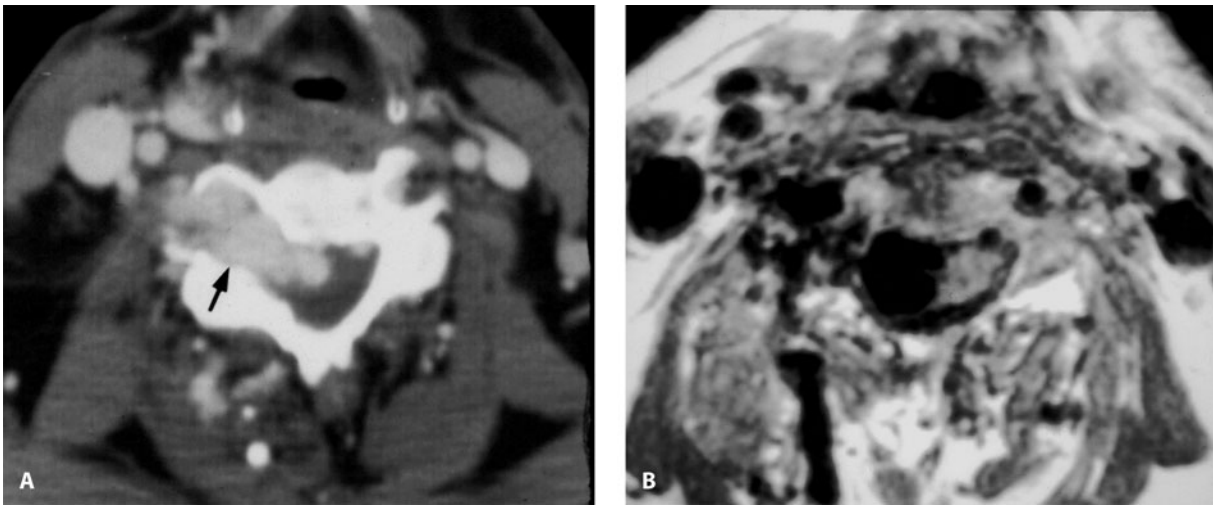

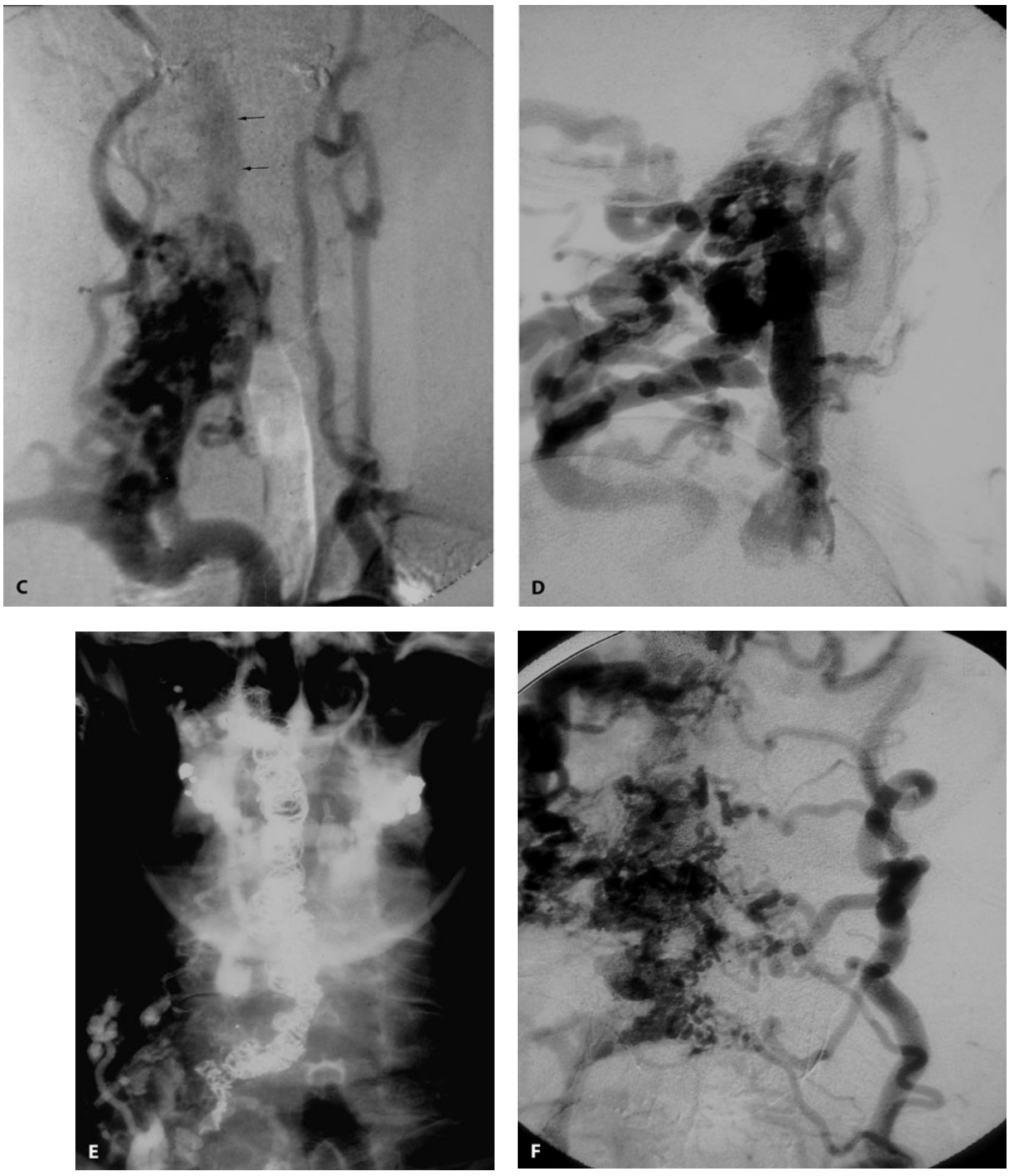

◄ **Fig. 11.7.** A 72-year-old male patient presenting with slowly progressive radicular and cord compression symptoms seen on CT (**A**) and MRI (**B**). Pre- and postarterial embolizations of the paravertebral arteriovenous malformation resulted in transient clinical improvement, while retrograde transvenous occlusion of the epidural venous plexus produced permanent neurological recovery (**C–F**)

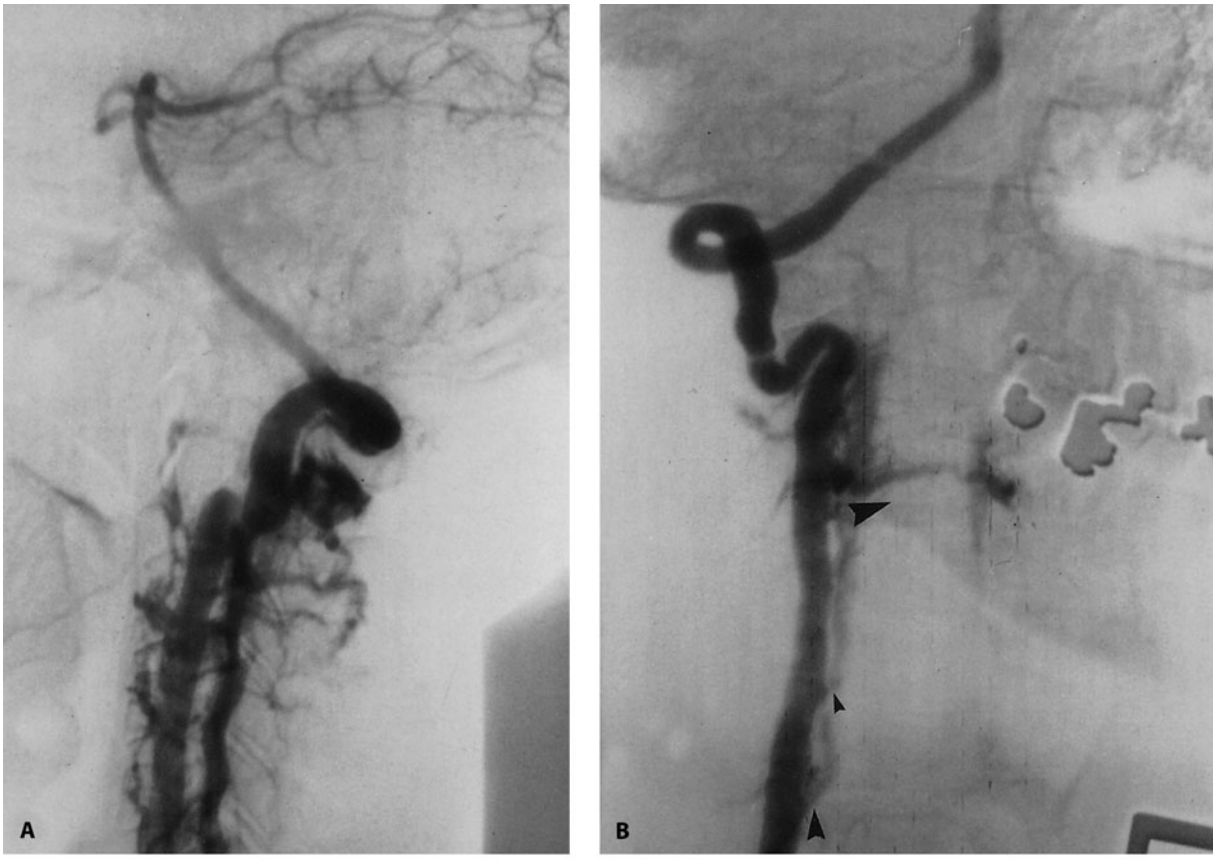

Fig. 11.8. **A** Lateral subtraction angiogram in a patient with von Willebrand's disease and factor VIII deficiency. The multiplicity of fistulae or exact fistula site could not be accurately demonstrated. **B** Oblique subtraction angiogram demonstrates separate arteriovenous fistulae (*arrowheads*). The largest fistula at C3 drains anteriorly toward the contralateral epidural venous plexus. **C** Lateral plain film of the cervical region demonstrates multiple balloons in tandem from C2 to C5. As balloons were placed in the most superior portion of the vertebral artery, additional fistulae were seen. All signs and symptoms were relieved after the embolization

disease (Fig. 11.6, p. 748). The enlarged dural lakes may create spinal cord symptoms. Arterial steal to the cord is unlikely considering the amount of segmental supply to the cervical spinal cord at this level; however, this mechanism has been proposed to explain central nervous system manifestations in VVAVF. These fistulae are most often located at the level of the vertebral canal and in contrast to their upper cervical counterparts, they drain into the epidural space, where they can produce large epidural lakes bulging into the spinal canal and can compress the cord (Fig. 11.7, p. 749) (Willinsky et al. 1990c; 1993; Goyal et al. 1999).

Spontaneous fistulae may be present simultaneously at multiple levels and may not be caught on the initial study (Fig. 11.8). They will be demonstrated in oblique projections or become apparent after occluding the most distal one. Multiple occlusion sites will be identified and treated to trap all the fistulae. In the case illustrated in Fig. 11.8, an associated blood dyscrasia (von Willebrand's disease), with deficiency of factor VIII down to 12.5% (normal is more than 40%), and low pro-coagulant assay were also found (Fig. 11.8).

11.1.3.2 Clinical Findings

The clinical manifestation of VVAVFs is related to the arterial deprivation in the territory distal to the fistula, which may result in vertebrobasilar insufficiency (Reivich et al. 1961) or spinal cord ischemia (Nagashima et al. 1996). Inadvertent occlusion of the ipsilateral vertebral artery proximal to the shunt in these circumstances will immediately produce major neurological symptoms. Venous hypertension and/or congestion is the second mechanism by which VVAFs produce signs and symptoms of spinal cord ischemia and/or nerve root compression (Deans et al. 1982). These symptoms include spasticity, spastic quadriparesis, painful torticollis, blurring of vision, and facial pain. The high arteriovenous shunting may manifest itself by a prominent paraspinal bruit that usually does not change with manual compression of the carotid arteries, but may be associated with a decrease in distal pulses in the ipsilateral upper extremity. They present as a bruit or swishing noise of acute onset occurring after a sudden neck movement, straining, or sneezing (Bartal and Levy 1972). These fistulae may also occur after a previous thrombosis or rupture of a preexisting aneurysm, although this will be difficult to prove. Mechanical compressions at the intervertebral foramen level can present with radiculopathy.

The clinical response to transarterial embolization can be immediate and spectacular, but if the shunt is not completely obliterated clinical improvement will be temporary. In such circumstances, if transarterial control cannot be obtained, then a transvenous approach can be proposed (Fig. 11.7) (Willinsky et al. 1990c, 1993).

Local opening into a radicular vein may produce medullary venous reflux and the possibility of neurological manifestations, hemorrhage (Kominami et al. 1996), ischemia, or atrophic changes (Berenstein and Lasjaunias 1992). Large venous lakes may compress the cord and provoke progressive myelopathy (Goyal et al. 1999). These compressive lakes have been seen in children intradurally with spinal cord vein reflux (see Vol. 3)

and epidurally in adults without evidence of spinal cord vein reflux. The anatomy and pathophysiology of symptoms in this location are the same as those in the paraspinal AVF (Table 11.3).

Doppman and Di Chiro reported a 39-year-old male patient who presented with a subarachnoid hemorrhage at the age of 19. At age 35, he had a documented cervical arteriovenous malformation (AVM), which was significantly larger at myelography than at angiography. In the single frontal study, the lesion appears as a slow-flow lesion. Some 5 years later, while the symptom course was progressive, the lesion appeared smaller by both myelography and angiography. At surgical exploration, a large thrombosed AVM overlying the dural surface of the cervical spinal cord was found. The progression of venous thrombosis in this condition can result in an ascending myelopathy with a fatal outcome.

The natural history of these fistulae depends on the venous angioarchitecture. However, once symptomatic (neural compression and/or remote venous insufficiency), they are usually progressive.

All previous discussions as to the advisability for or against treatment have been based on the difficulty of open surgery where complete eradication is needed and not merely ligation of a few feeders. At present, the recommended treatment is the percutaneous endovascular closure of these VVAVFs.

11.1.4 Paraspinal Arteriovenous Fistulae

When looking at the anatomy of the spinal cord arteries and their segmented sources of supply, all the possible paraspinal AVF locations can be anticipated. Para-axial longitudinal intersegmental extraspinal arterial anastomoses, similar to the vertebral artery (supreme intercostal, thoracic, or lumbar multimetameric, lateral sacral arteries; see Vol. 1) may also be the site of the fistula. The amount of apparent supply to the shunt depends on the type of artery involved and the individual anatomy. In general, indirect opacification of the AVF will be noted following injection of the adjacent segmental arteries. The options for drainage follow the same general rules as in the other sites. However, epidural reflux and some spinal cord vein involvement appear more frequent. The direct opening of the ventrally located fistulae into the azygos vein or its affluent may cause cardiac overload in children (see Vol. 3). The supply to the cord prior to occlusion of the fistula must be carefully established. The prominent flow into the shunt may preclude the appropriate opacification of a radicu-

Fig. 11.9A–E. Extraspinal malformation. Purely extraspinal arteriovenous malformation (AVM) presenting as an enlarging pulsatile mass. **A, B** Axial MRI showing the multiple signal voids within the soft tissue mass on the left side. **C** Coronal MRI examination shows multiple signal voids in the extraspinal space (*arrowheads*). **D** CT scan after multiple embolization demonstrates marked reduction in the mass effect with relief of the pain and discomfort. The patient underwent successful surgical excision of the obliterated malformation. **E** Representative film of the extraspinal tissues demonstrating the multicompartment AVM supplied by T8 (*curved arrows*) ►

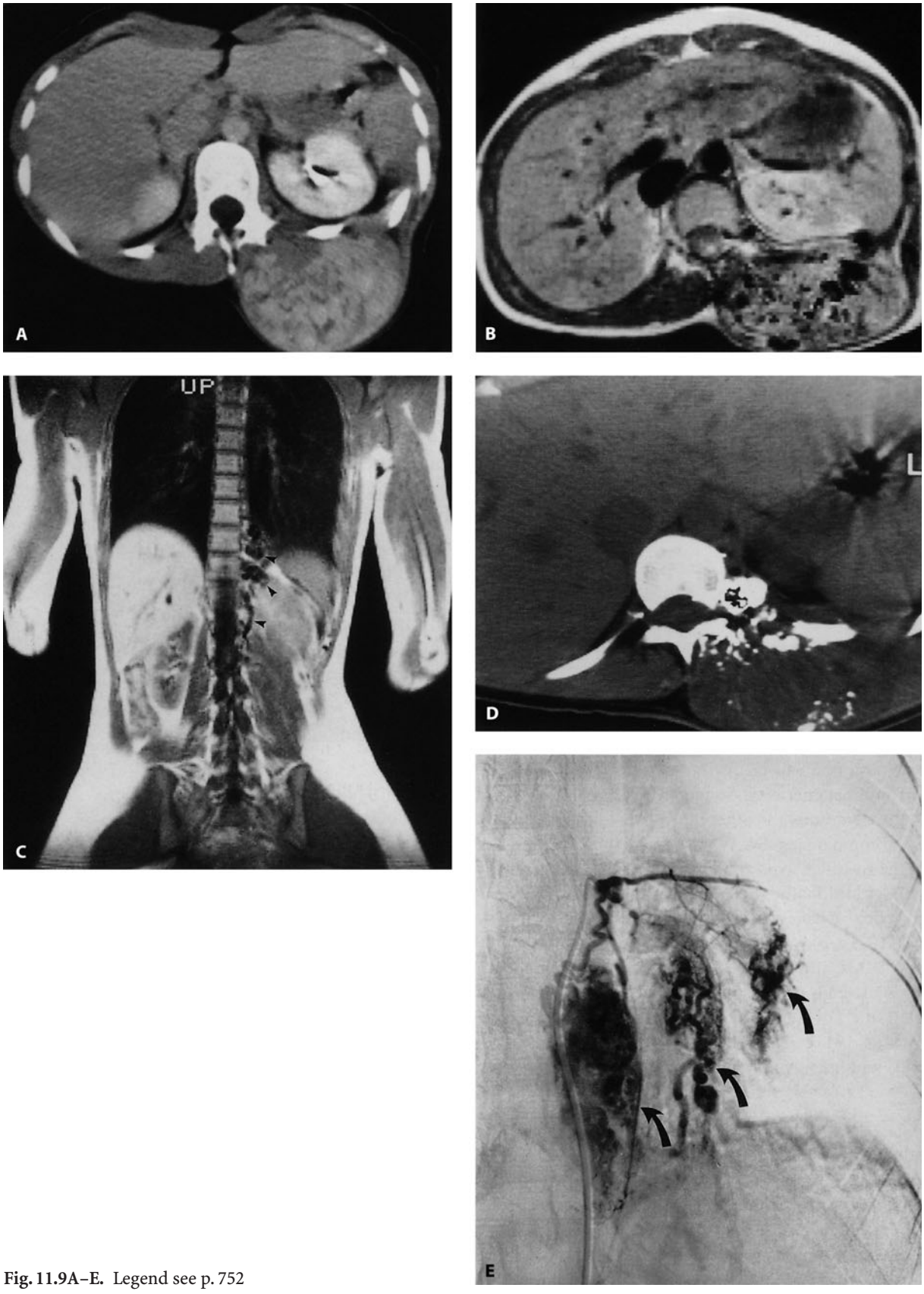

Fig. 11.9A–E. Legend see p. 752

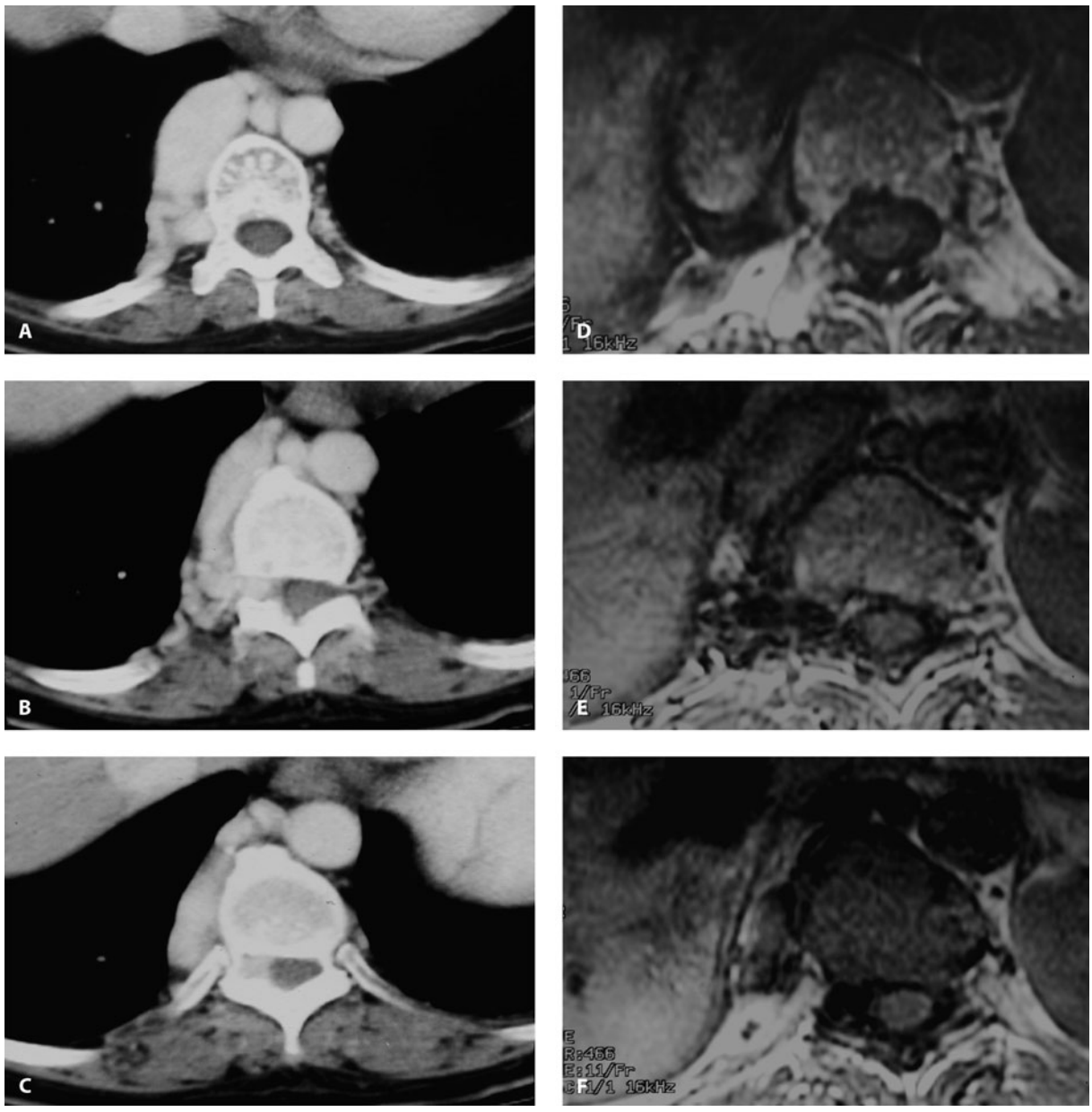

Fig. 11.10A–F. A 47-year-old female patient presented with localized back pain and known multiple limb arteriovenous malformations and Hermitt Duclos syndrome. Contrast-enhanced CT (**A–C**) and axial T1 MRI (**D–F**)

lomedullary artery originating at the same level, and inadvertent embolization in this case would carry the risk of major spinal cord arterial complication, in particular when a liquid embolic agent is used (Fig. 11.9).

In a young adult, we have seen another contributor to the ventral arterial axis of the cord opacify the AVF several metameres above the paraspinal lesion, via the cord, suggesting a possible arterial steal. The clinical significance of this finding was difficult to establish, as epidural lakes were also present and might have been responsible for the cord symptoms.

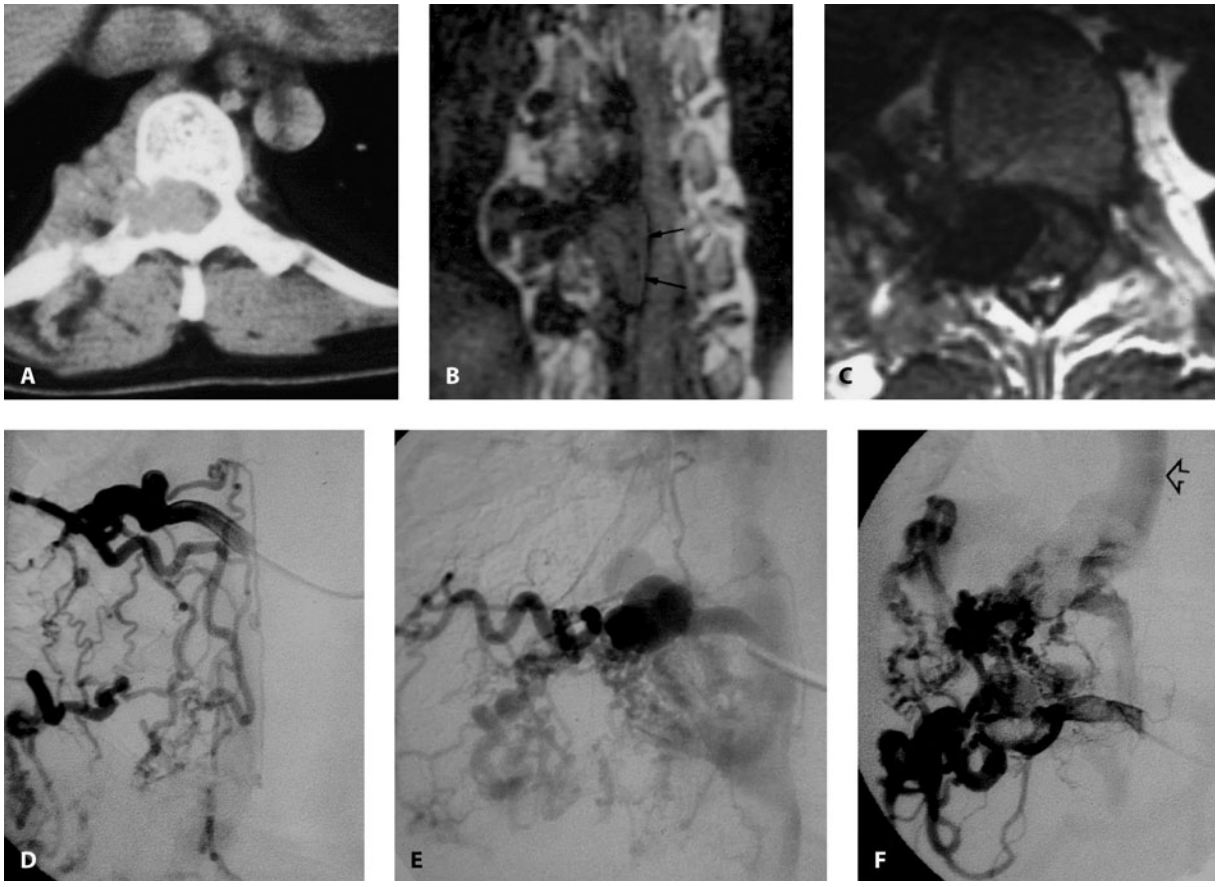

Fig. 11.11. A 32-year-old man presented with slowly progressive radicular pain and cord compression symptoms in relation to an intraspinal extradural bulging dilated epidural vein, as seen on CT (**A**) and MRI (**B**, **C**). Extensive intersegmental arterial collateral network supplying the arteriovenous malformation was seen on angiograms (**D–F**). **G–J** see p. 756

Pure thoracolumbar paraspinal AVFs are even rarer than the more rostral branchial locations in both adults and in the pediatric population. Symptoms are often minimal, related to the cutaneous and muscle involvement of the lesion or its drainage (Fig. 11.10). The clinical symptoms appear to occur later than the probable onset of the fistulae.

Progressive medullary symptoms can be noted in relation to bone erosion or large venous pouches (Fig. 11.11) bulging in the spinal canal and compressing the cord (Rodesch et al. 1996; Goyal et al. 1999) (Fig. 11.12). The MRI features of paravertebral AVMs depend primarily on the location of the nidus and the venous drainage pattern. Hyperintense signal within the spinal cord on T2-weighted images and an increase in perimedullary flow voids is seen in cases with intradural venous reflux. Prominent vascular channels in the vertebra or paraspinal tissues can be seen and are consistent with the paravertebral location of the arteriovenous malformation. Careful scrutiny may be required to detect these abnormal vessels. Coexistent intramedullary lesions as in Cobb syndrome should be sought. MRI examination should include the entire spine. The parasagittal

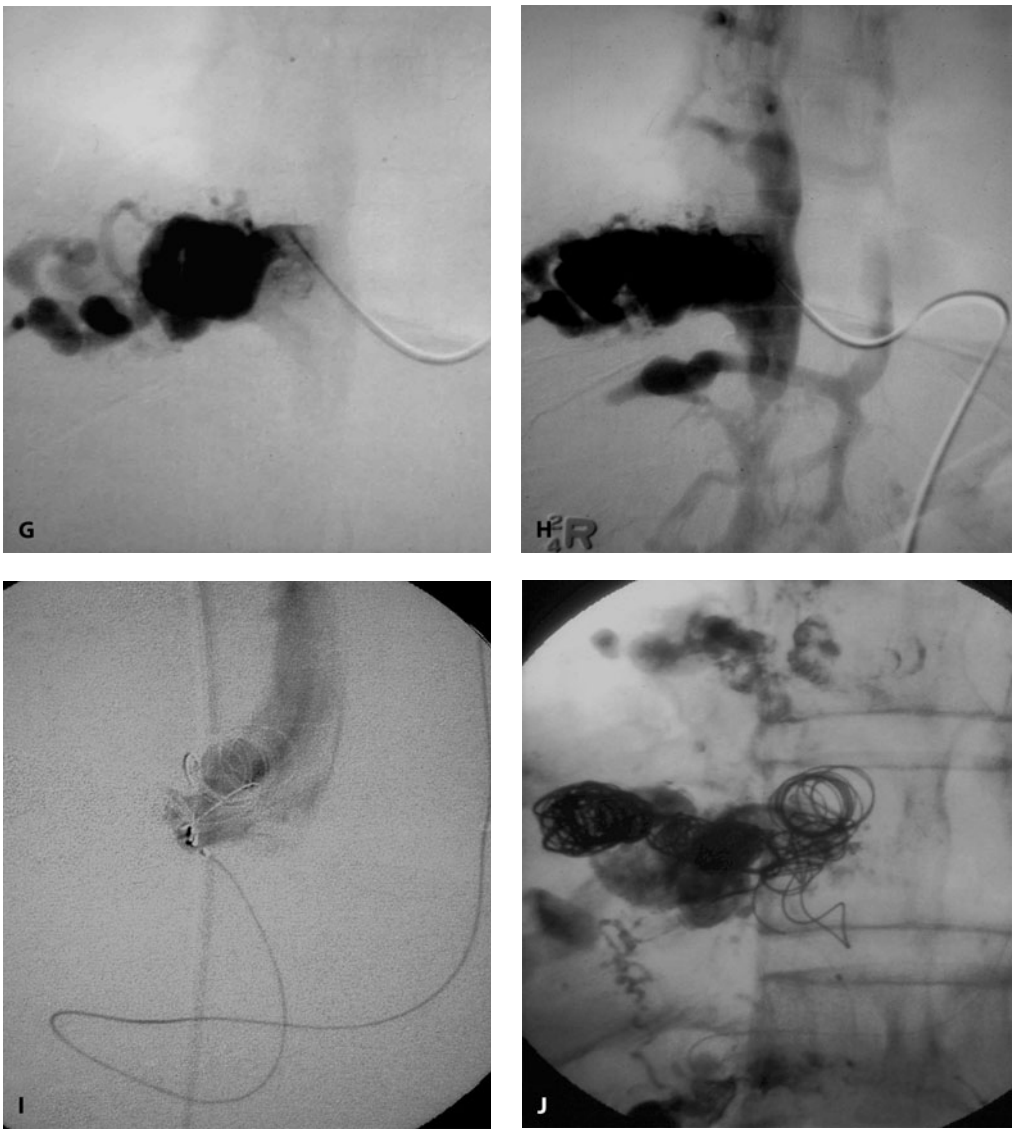

Fig. 11.11 (*continued*). Retrograde transvenous approach after repeated arterial embolizations resulted in improvement of clinical symptoms (**G–J**)

plane is useful to evaluate the paraspinal region. Axial and/or coronal images should be taken of suspicious areas (Goyal et al. 1999) (Fig. 11.12).

Several vascular features may result in symptoms from the thoracolumbar AVFs (Table 11.3). Some rare slow-flow epidural lesions drain into the epidural venous plexus and then reflux upstream toward the pial veins; their physiopathological interference with the cord circulation is similar to that of spinal dural arteriovenous shunt (SDAVS). Finally, vascular angiogenesis in the epidural space may mimic vascular malformations (Fig. 11.13).

In all cases of paraspinal AVF, an associated spinal cord arteriovenous malformation (SCAVM), bone involvement, and cutaneous discoloration should be sought to rule out a spinal arteriovenous metameric syndrome (SAMS); this association is more common than previously thought.

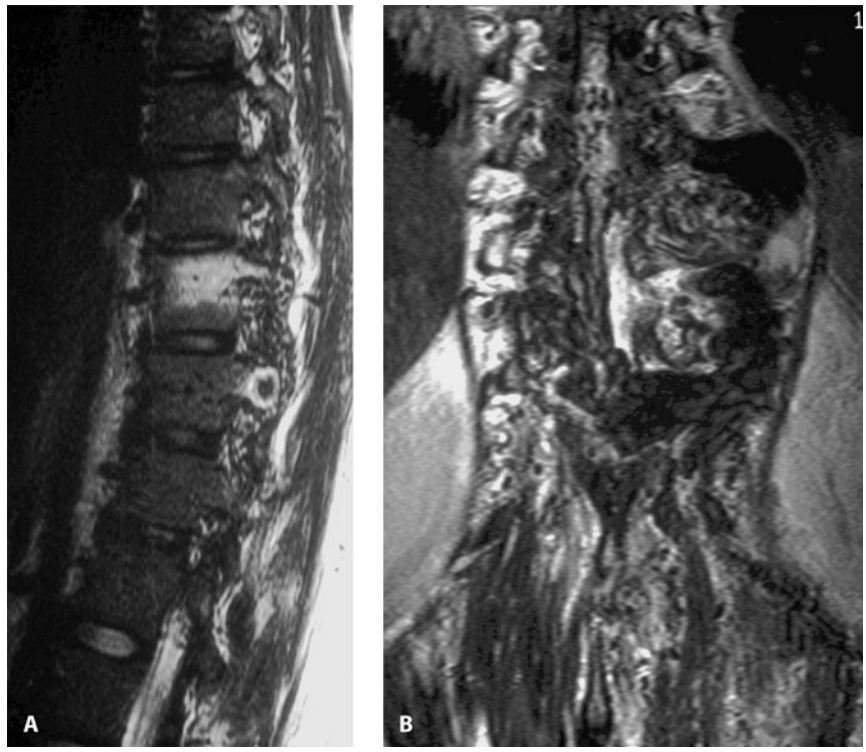

Fig. 11.12A, B. Extensive paravertebral arteriovenous malformation with epidural venous drainage is noted on sagittal and coronal MRI

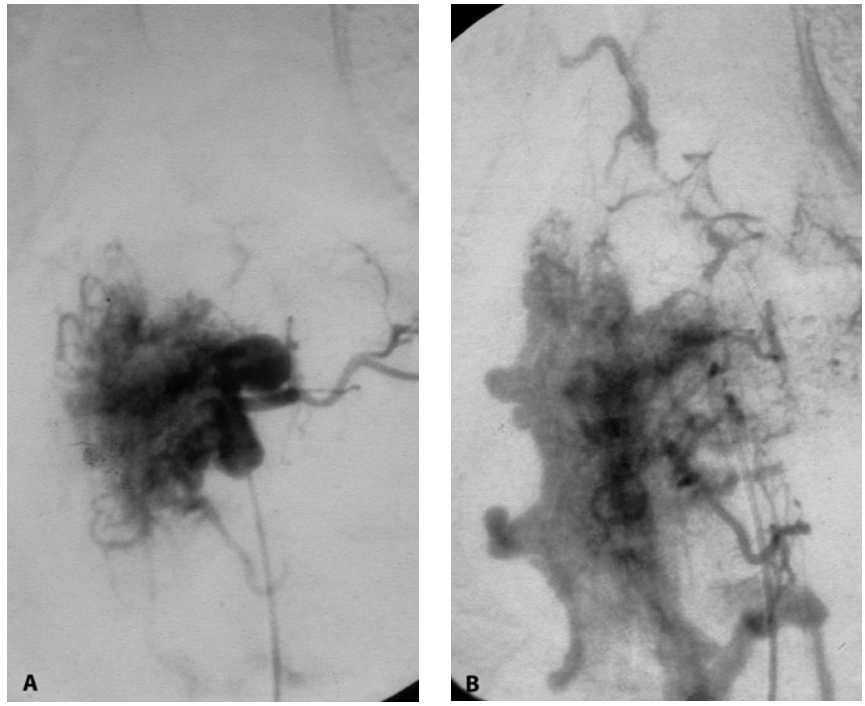

Fig. 11.13A, B. Epidural proliferation with venous plexus congestion. Absence of pial venous reflux (**A**, **B**)

The objective of treatment of parachordal AVFs is the occlusion of the AVS, with preservation of the parent artery as well as the arterial supply to the neural structures. In our experience, this can be achieved with glue (Fig. 11.9), balloons (Figs. 11.1–11.3, 11.8), coils (Fig. 11.4) and in some cases a combination of embolic agents (Figs. 11.7, 11.11; see Chap. 14, this volume).

11.2 Spinal Cord Vascular Lesions

Since the early days of the classic interpretation of the various events that can occur with SCAVMs, we have progressed to a better understanding of the morphological information obtained so as to use it and transform it into therapeutic strategies such as targeted embolization. Since 1980, the authors have managed and followed up a total of 320 SCAVM patients. This experience has been published in various papers and was also documented in the first edition of Vol. 5, the largest series and source of information on this disease accumulated to date.

A portion of the chapter on SCAVMs from our first edition has been retained to highlight the difficulties in obtaining valid information from the literature and to demonstrate our progressive understanding with respect to SCAVMs.

Credit for first recognizing that spinal vascular malformations can cause subarachnoid hemorrhage must be given to Hebold (1985) and Gaupp (1988), who referred to these lesions as hemorrhoids of the pia mater. Since then, multiple eponyms and classifications have been used for the various types of vascular malformations of the spine and spinal cord. Based on microscopic appearance and structure, topographic relationship, and pathological nature, the various classifications that emerged have become a source of confusion. The complexity of the nomenclature makes it more difficult to understand and compare the various lesions considered to be vascular malformations of the spinal cord. Historically, Wyburn-Mason's classic monograph recognized two main types of spinal vascular lesions:

1. The venous type, consisting of an abnormal mass of sinuous, turgid, blue, pial veins, is usually located posteriorly and below the mid-thoracic region of the cord. Wyburn-Mason described the microscopic findings as thick-walled pial vessels with abnormal structures and marked "proliferation of intramedullary capillaries, precapillaries and venules."
2. The arteriovenous type, consisting of a fistulous capillary bed, is preferentially located in the cervical enlargement anteriorly or at the lumbar enlargement. Distended veins appear macroscopically. Microscopic examination showed the presence of numerous vessels of different sizes and structures, some resembling arteries, others veins. In arteriovenous-type lesions, symptoms often presented early in life, in contrast to patients with the venous type of vascular anomalies, in whom symptoms tended to present later on. Wyburn-Mason thus understood the duality between true medullary AVMs and what we know today are spinal dural fistulae.

In the late 1960s and early 1970s, following the introduction of selective spinal angiography and the study of large series of patients (Houdart et al. 1966; Di Chiro et al. 1967; Baker et al. 1967; Djindjian et al. 1969a, 1970a), one type of abnormality was recognized as common, irrespective of the gross appearance. This lesion consisted essentially of an abnormal communication between the arterial and venous systems without intervening capillaries. The variations in individual lesions were related to the volume of shunting and the number of feeding vessels. Aminoff, in 1974 and 1976, extensively reviewed the pathophysiology, clinical presentation, and prognosis of vascular malformations of the spinal cord. In his 1976 monograph, he stated that "since venous and arteriovenous angiomas could not be distinguished satisfactorily, either angiographically or pathologically, they will be grouped together." He did, however, recognize that lesions with large shunts corresponded to Wyburn-Mason's arteriovenous form, while lesions with a shunt of small volume probably corresponded to the venous type. Aminoff also noted the early presentation and high incidence of hemorrhage in the high-flow shunts. Similarly, Djindjian (1978) and Hurth et al. (1978) noted differences in the cervical lesions compared with those in the thoracic and lumbar areas. In his chapter on angiography of spinal cord angiomas, Djindjian states, "one cannot avoid being struck by the fact that malformations having a direct contribution from the artery of Adamkiewicz corresponded to those cases which present early (average 33 years), compared with age 51 for those cases which are exclusively posterior" (Djindjian 1978). Confusion remained, however, in attempts to classify spinal AVMs based on the relationship of the lesion to the various compartments of the spinal canal (intradural, extradural, intramedullary, extramedullary, paramedullary, vertebral, etc.).

In 1977, Kendall and Logue reported on ten patients with spinal dural AVMs, and Merland in 1980 review 13 patients, referring to their lesions as "intraspinal extramedullary arteriovenous fistulae draining into medullary veins." Only with the recognition of the true pathological nature of these spinal dural arteriovenous fistulae (SDAVFs) or meningeal fistulae has much of the confusion relating to spinal cord AVMs been resolved. More than 20 years later, the classifications remain and even the latest one persists in confusing dural AVS with spinal cord AVS.

Vascular malformations of the spine and spinal cord are considered uncommon lesions. Their incidence, expressed as a percentage of the total number of the various types of spinal space-occupying lesions, ranges from 3% (Wyburn-Mason 1943b; Newman 1959) to 16% (Pia and Vogelsang 1965). The discrepancy is explained by the introduction of better diagnostic modalities. Even so, the true incidence of spine and spinal cord vascular malformations may still be underestimated. The introduction of spinal angiography, by Djindjian in 1962, and spinal subtraction angiography, by Doppman in 1965, were important advances in the radiological visualization of vascular malformations. However, only when selective spinal angiography was reported by Djindjian in 1966 and di Chiro et al. in 1967 did a better understanding of this group of conditions become possible.

The incidence of spinal AVMs (SAVMs) in relation to brain AVMs (BAVMs) is reported at 1:4 (Lombardi and Migliavacca 1959); 1:6 (Jellinger

1966, 1978), or 1:8 (Bergstrand 1963). Although cerebral vascular malformations are more common than spinal ones, the comparative incidence in relation to brain versus spinal tumors is very similar, ranging from 2% to 4% (Olivecrona 1957; Krenshel 1961). This suggests that the frequency of spinal cord AVMs (SCAVMs) compared to BAVMs correlates with the mass or volume ratio between spinal cord and brain tissue. The prevalence of incidental or asymptomatic spinal vascular malformations is difficult to ascertain, as the spinal cord is usually not inspected on routine autopsy series.

Brion et al. (1952), in an autopsy series of 31 patients who died with unclassified myelopathies, found AVMs in nine (29%). Doppman (1968a), in his classic monograph, quotes Porter's experience based on 50 autopsies of patients with posttraumatic cord injuries in which two (4%) patients had underlying AVMs. Now, however, it is generally accepted that all of the so-called retromedullary thoracolumbar lesions of slow flow, supplied by a single pedicle and occurring in patients after the fourth decade of life, reported prior to 1980 were most likely SDAVFs.

In Symon's 1984 series, there are 55 patients with well-documented SDAVFs and only five with SCAVMs. Unfortunately, whether any of the lesions were spinal arteriovenous fistulae or metameric lesions was not mentioned. In an NIH series of 81 patients (Rosenblum 1987a), there were 27 patients (33%) with dural arteriovenous fistulae and 43 (53%) with intramedullary SCAVMs in various locations. There were 11 patients (13.5%) who had direct arteriovenous fistulae involving the anterior spinal, posterior spinal, or both medullary arteries. In three patients, there were lesions with cutaneous manifestations assumed to be metameric (6%). In 1987, Guegen et al. reported on 11 patients with arteriovenous fistulae fed by medullary arteries seen over a 14-year period. Some of these were part of the previous experience reported in Djindjian (1976).

In attempting to establish the natural history of SCAVMs, careful analysis of the various series reported prior to the recognition of SDAVFs as a separate entity gives only limited information. The series of Di Chiro and Doppman (1968a), Aminoff (1976), Pia and Vogelsang (1965) as well as others were based on different classifications, and the investigators often did not distinguish between the various entities. In the series of Djindjian, Hurth, and Houdart (1969a), the different lesion types were also not separated. However, after careful review of the 150 patients reported by Djindjian (1976), information available regarding 130 of them was sufficient to separate SDAVFs from SCAVMs and metameric lesions (Table 11.5).

11.3 Spinal Cord Arteriovenous Malformations

This group of arteriovenous shunt includes lesions developed intradurally, supplied by radicular arteries (radiculomedullary and radiculopial), the anterior spinal artery, the pial network, their perforators, or any combination of them. The lesion may be located along the surface of the cord, be intramedullary, or both. In this group, we also include AVMs that are located along the intradural portion of the spinal nerves and on the filum

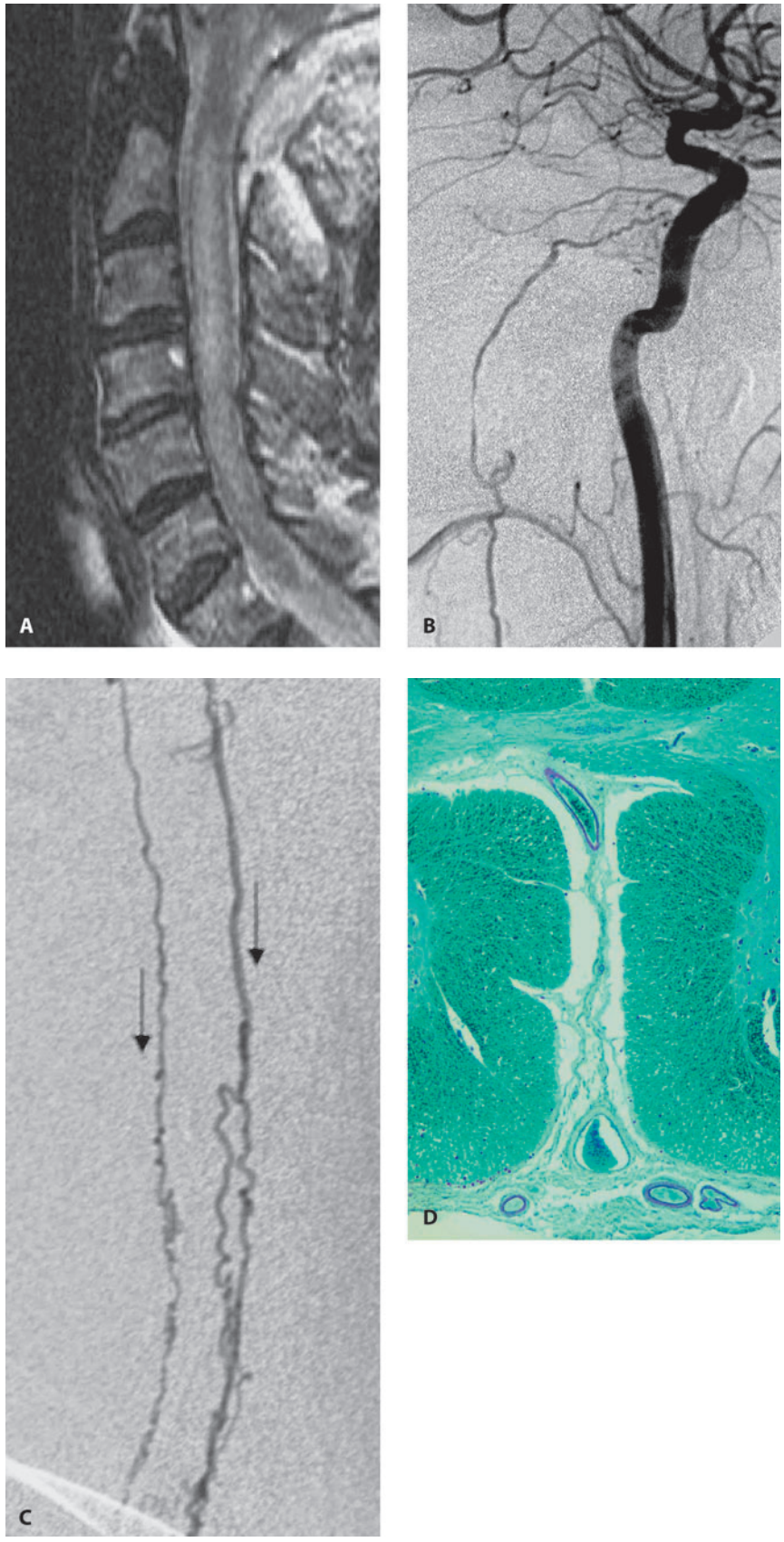

Fig. 11.14. Patient presenting with cervical myelopathy demonstrated increased signal in the cord (**A**) but no MRI evidence of spinal cord veins draining a tentorial dural arteriovenous fistula (**B, C**). The veins are ventrally located within the ventral subpial space (**D**)

Fig. 11.15. MR occult (**A**) symptomatic spinal cord arteriovenous malformation (**B**). Ventrally located drainage (*arrowheads*) within the ventral subpial space in a patient with MRI evidence of venous congestion (*arrow*)

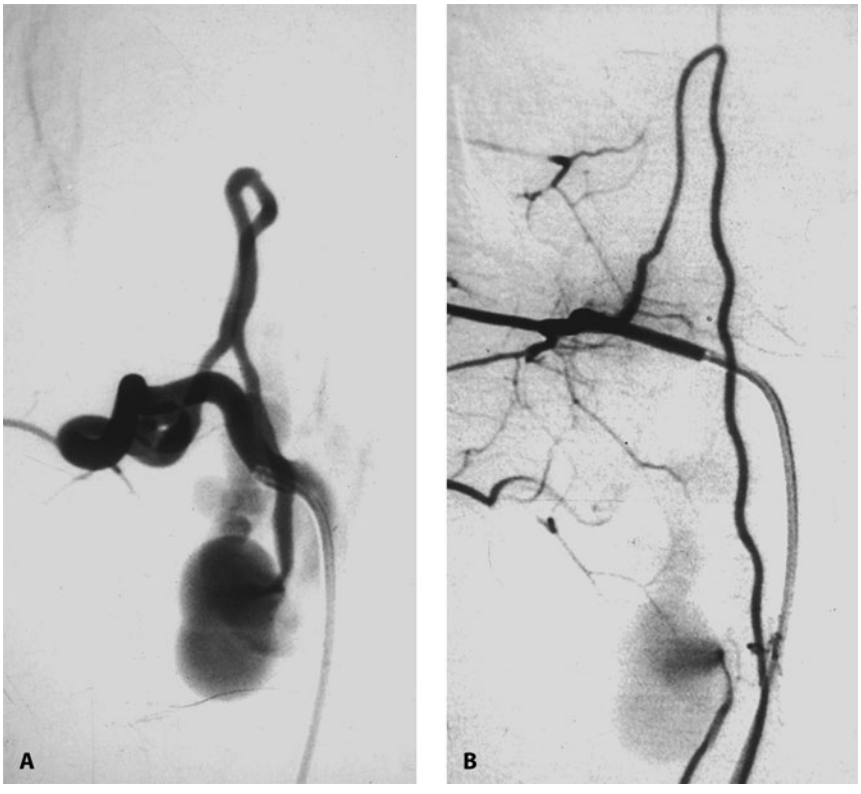

Fig. 11.16. Typical appearance of spinal cord arteriovenous fistula (**A**) in a young adult with family history of HHT1. Note the role played by the basket arteries (**B**) in the opacification of the fistulous point located on the dorsolateral portion of the pial network

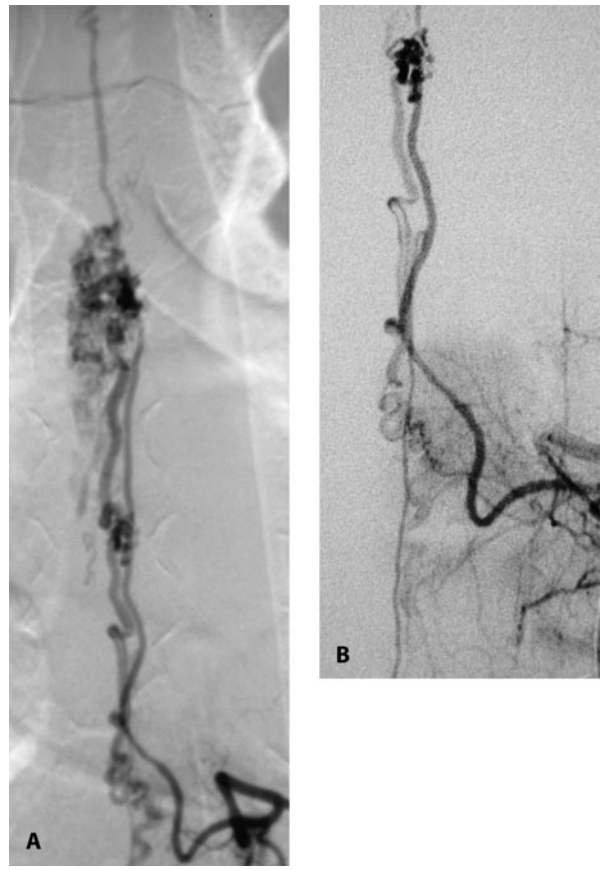

Fig. 11.17A, B. Bifocal spinal cord arteriovenous malformations: intramedullary for the upper one, and in the ventral sulcus for the caudal one. Note the converging draining vein. (From Meisel et al. 2000)

terminale. They are likely to be both subarachnoid and subpial since the pial veins of the cord are subarachnoid. Different from the cephalic region, the subpial space is consistently present at the level of the ventral sulcus. Imaging the subarachnoid space (myelography, T2, or other similar MRI sequence) will demonstrate the dilated veins, except for the minimally dilated ventral spinal vein, which is buried in the depth of the ventral sulcus (see Vol. 1; Figs. 11.14, 11.15). For that reason, nearly all spinal cord arteriovenous shunts (AVS) will be detected on MRI, but some may be MRI occult (Lasjaunias 2001).

All, however, are supplied by pial and perforating arteries; they will drain through the intrinsic or pial veins. As will be discussed in Sect. 11.3.2.6, they may have a nidus, have single or multiple direct fistulae (high-flow), or may be a combination of the two. They may also be associated with arterial aneurysms or venous pouches and be associated with various changes induced by the constraints they produce.

Among all our spinal cord arteriovenous shunts (SCAVSs), 20% were AVFs (one-fourth macrofistulae, MAVFs; Fig. 11.16), three-fourths microfistulae (mAVF; Fig. 11.14). All fistulae were localized on the surface of the cord. Of these SCAVMs, 80% had an at least partially intramedullary nidus; 80% of SCAVS were single lesions.

Multiple shunts were found in 20%. In this latter group, over half harbored true multiple intradural shunts corresponding to either separate spinal cord nidi distributed over different myelomere levels (Fig. 11.17)

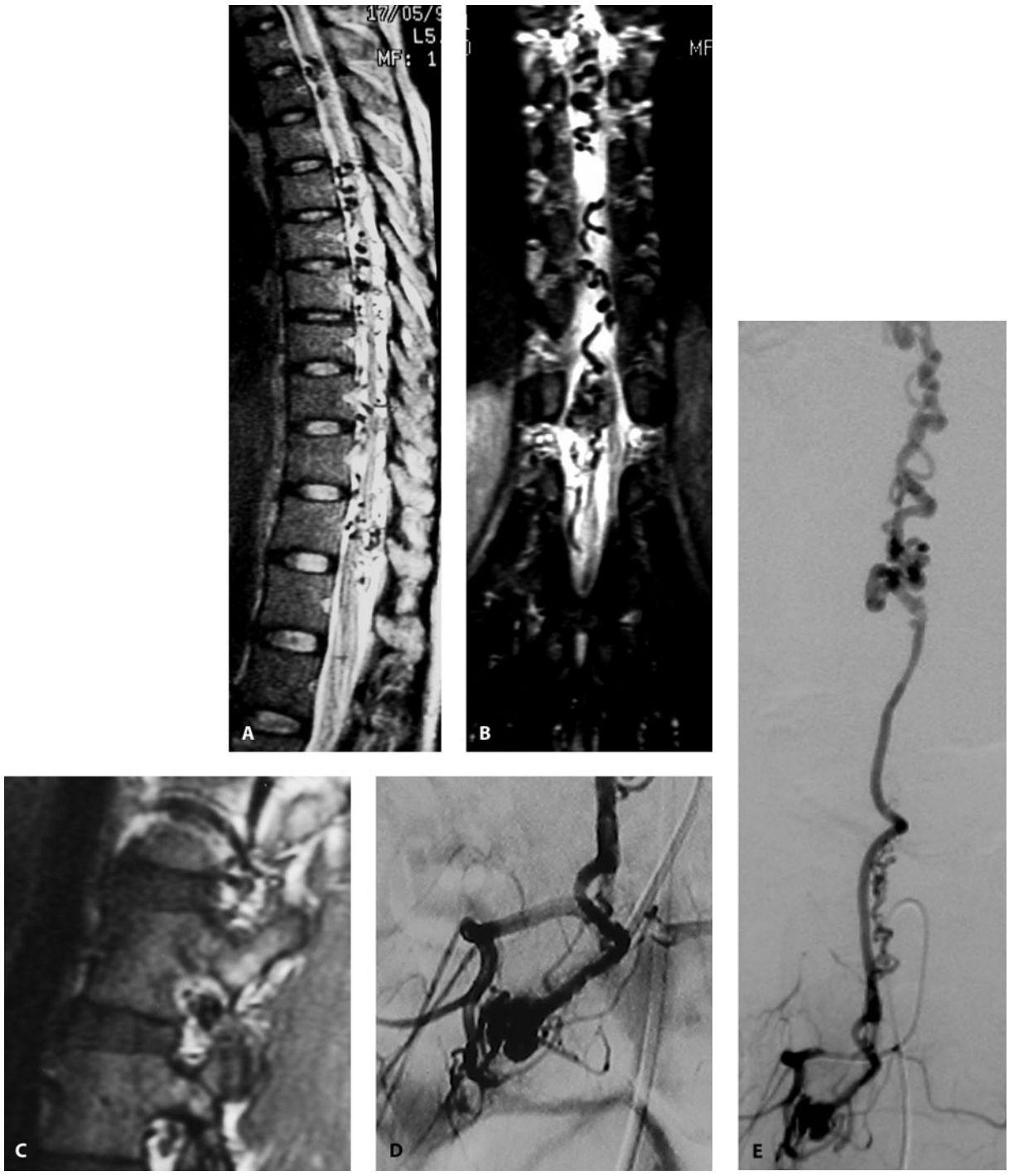

Fig. 11.18A–K. Spinal arteriovenous metameric syndrome (SAMS) 22/23 in a 32-year-old female patient presenting for low back pain and right leg numbness lasting 1 year. MRI, multiple signal voids around the cord down to conus level (**A**, **B**). Involvement of L2 lumbar nerve root (**C–E**) and corresponding spinal cord (**F**, **G**). Both lesions were embolized in two separate sessions. Glue cast of the SCAVM (**H**). **I–K** One-year postembolization follow-up of both radicular and SCAVM locations. (Courtesy of S. Pongpech)

►

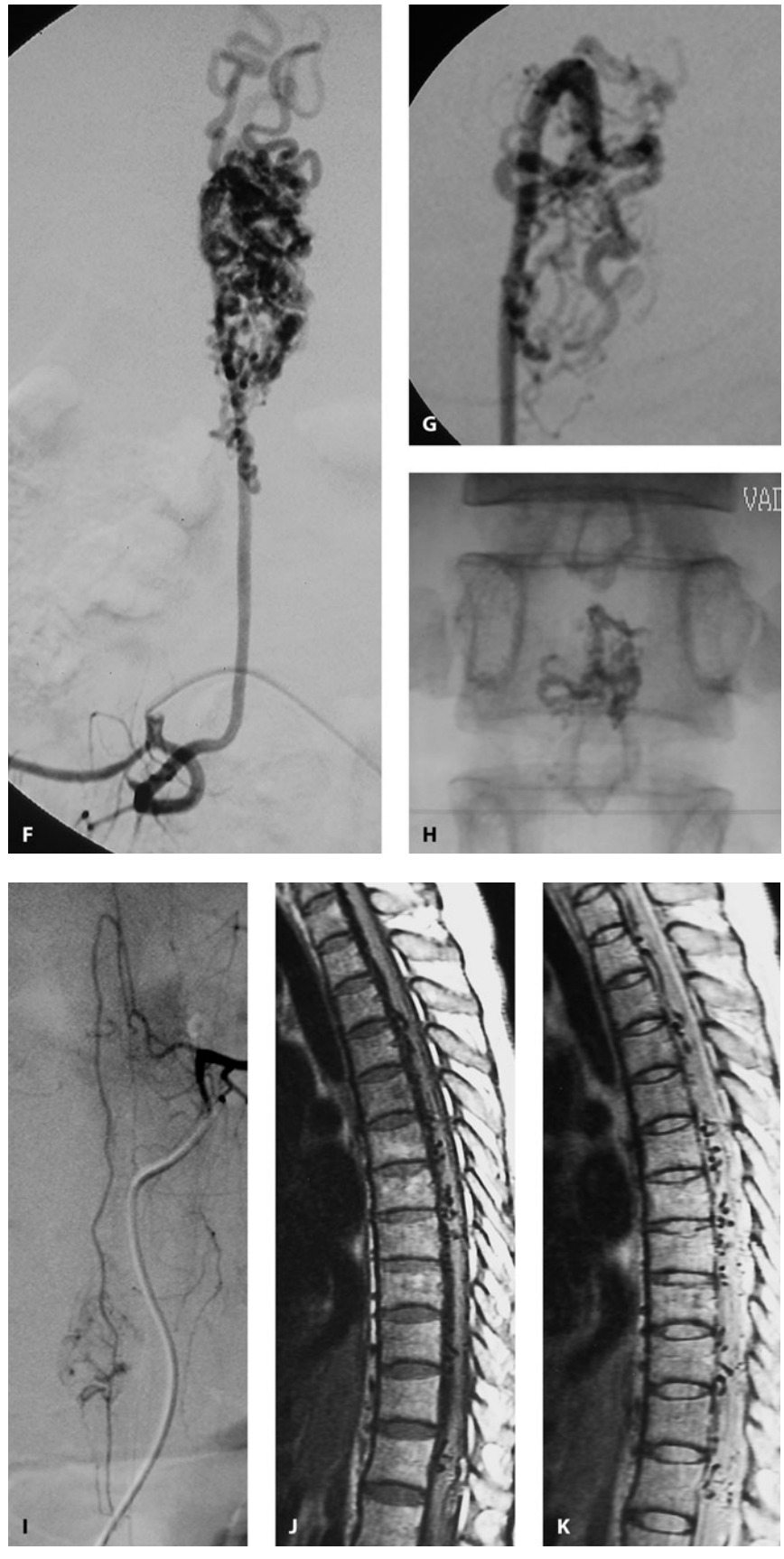

Fig. 11.18F–K.
Legend see p. 764

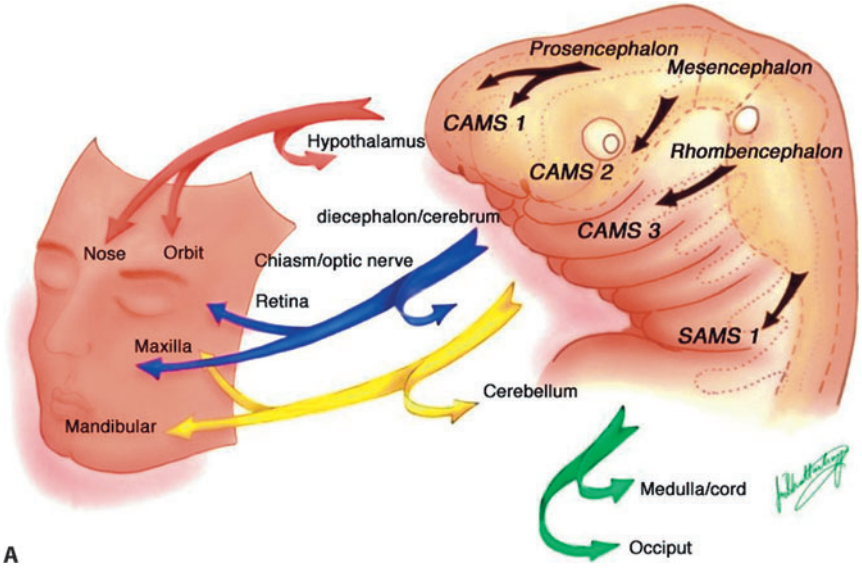

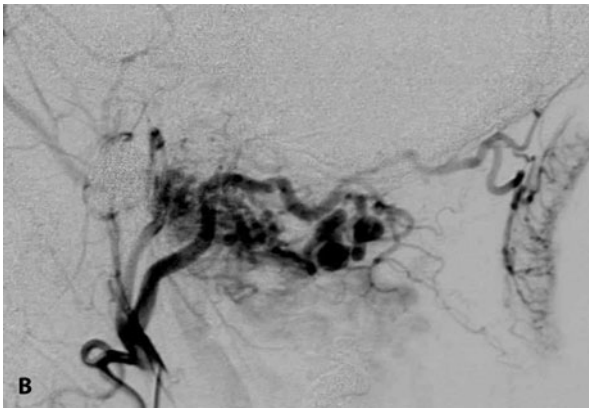

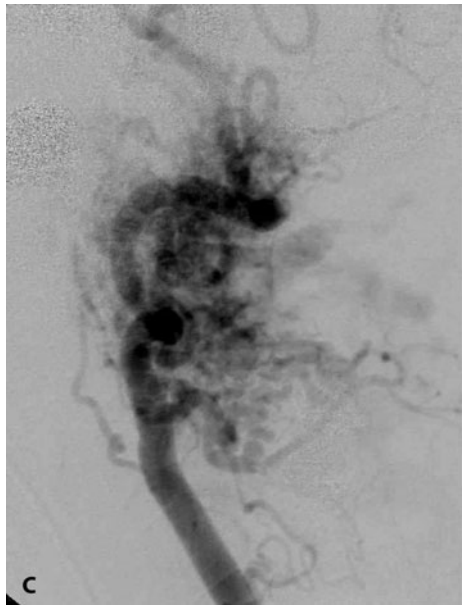

Fig. 11.19. Spinal arteriovenous metameric syndrome 1/2 (**A**) involvement of C1–C2 superficial tissues (**B**) and corresponding spinal cord (**C**). (Courtesy of R. Kwok)

and/or to SCAVMs associated with intradural radicular arteriovenous shunts (Fig. 11.18). Other intra- and extradural localizations included typical spinal arteriovenous metameric syndromes (SAMS) (Fig. 11.19) for two-thirds of them, and Klippel–Trénaunay syndrome (Fig. 11.20) or Parkes–Weber syndrome (Fig. 11.21, p. 768) in which associated SCAVMs could be suspected to follow a segmental disposition. No SCAVFs were detected in these latter associations. Patients with hereditary hemorrhagic telangiectasia (HHT or Rendu–Osler–Weber disease, ROW) all presented with MAVFs (Fig. 11.16). None had multifocal spinal cord lesions, which are mostly diagnosed in children (see Vol. 3).

Fig. 11.20. Typical Klippel–Trénaunay aspect of the lower limb

11.3.1 Classification of Spinal Cord Arteriovenous Malformations

Several classifications have been proposed (Marsh 1999; Heros et al. 1986; Bao and Ling 1997; Merland et al. 1992; Grote and Voigt 1999; Anson and Spetzler 1992; Malis 1982a; Spetzler et al. 2002; Feng et al. 1999). These authors divide SCAVSs into subgroups based on descriptive morphological data; however, their descriptions tend to pigeonhole the SCAVSs into static entities.

The files of 155 consecutive patients (adult and children) with SCAVS shunts were analyzed retrospectively (Rodesch et al. 2002). Only intradural vascular malformations (spinal cord, radicular, or filum terminale lesions) were taken into consideration. SCAVSs were examined according to their number (single or multiple), their gross aspect (arteriovenous fistulae, arteriovenous malformations, or nidus type) (Table 11.4), their link to possibly associated metameric disorders (involvement of the spinal cord, bone, paraspinal, subcutaneous, and skin tissues in the same spinal segment), and their myelomere location. During embryogenesis, each spinal nerve receives a radicular artery that nourishes both anterior and posterior nerve roots. The central end of the artery will supply the corresponding neural tube segment (myelomere) to which the nerve roots are connected. The level at which the radicular artery joins the cord points to the origin of the nerve root and to the myelomere origin; the junction between the radicular segment and the cord segment indicates the myelom-

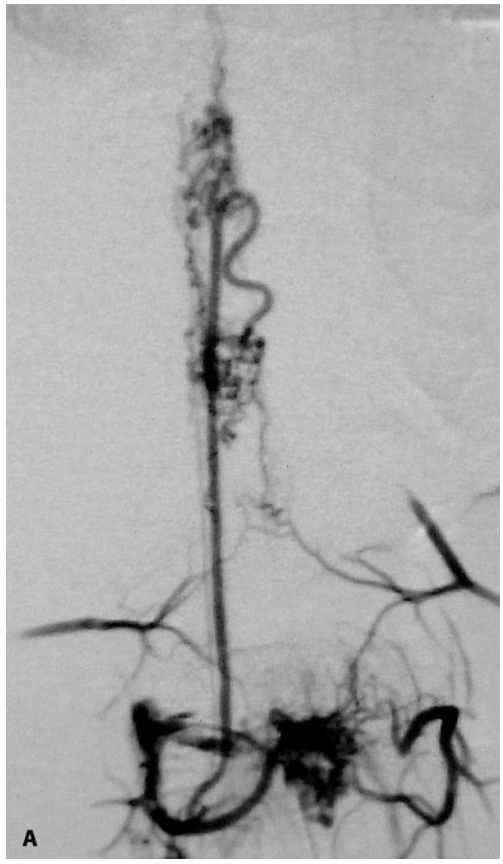

Fig. 11.21A–D. Spinal arteriovenous metameric syndrome 21/23. Thigh arteriovenous malformation (AVM) noted at the age of 21. Four years later the patient developed spinal claudication. At the age of 17, weakness of lower limbs and difficulties in urination and spastic paraparesis at presentation lasting 2 months, which had worsened over the preceding 24 h. Severe paraplegia was noted with fixed sensory level at T10–T11. CT arteriogram shows two separate lesions at L1 and L3 (**A**). SCAVM with spinal lesion at L1; limb angiogram shows AVM of the thigh in the territory of L3 (**B–D**). No evidence of hematomyelia. Anticoagulation was given and the patient remains severely handicapped. (Courtesy of J. Meisel)

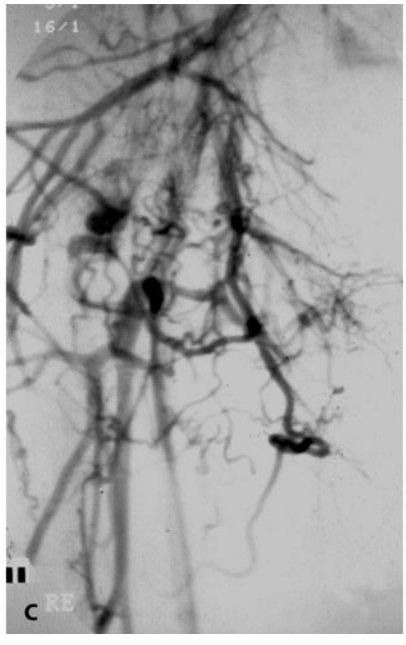

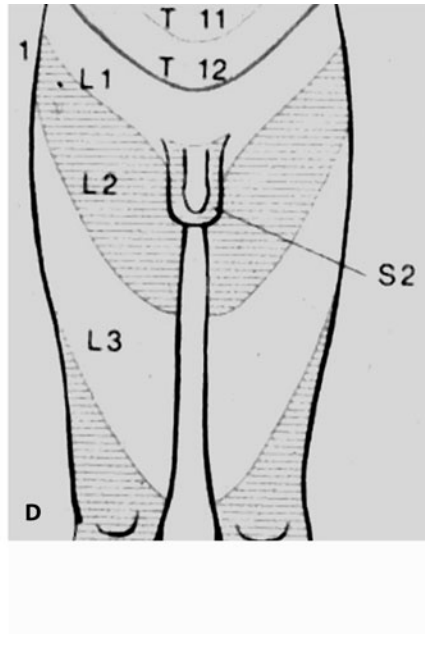

Table 11.4. Incidence of SCAVMs versus SCAVFs in 97 patients (from Rosenblum et al. 1987b; Berenstein and Lasjaunias 1992)

	n	%
SCAVMs	79	81
SCAVFs	18	19
Total	97	100

SCAVM, spinal cord arteriovenous malformation; SCAVF, spinal cord arteriovenous fistula.

ere cord level (Matsumaru et al. 1999; Vol. 1, Chap. 1). The classification is derived from this framework.

The classification that we support separates SCAVSs into three groups:

1. The first group encompasses single shunts caused by a genetic hereditary disorder. In these circumstances, the vascular cells are affected by the disease at the germinal stage. The main syndrome in which genetic links can be recognized is hereditary hemorrhagic telangiectasia (HHT), or Rendu–Osler–Weber disease (ROW). It is an autosomal dominant disease where to date two genotypes have been recognized (HHT1, HHT2). The impact of the disorder on the venous endothelial cells outlines the role played by the veins as the primary target in the development of AVMs (Lasjaunias 1997a).
   SCAVSs associated with ROW are almost always single MAVFs, (Fig. 11.16), in particular in the pediatric population. Multiple SCAVSs were never related to ROW in the Rodesch et al. (2002) series. Indeed, the telangiectasias classically described in ROW appear at later ages and MAVFs may be the first expression of the disease in children. The discovery of a MAVF should therefore always raise the possibility of this underlying genetic hereditary disease (Mandzia et al. 1999; Garcia Monaco et al. 1995; Coubes et al. 1996).
2. The second group involves multiple SCAVSs; they are not related to a hereditary disorder but may potentially share metameric links (genetic somatic). These metameric links have been described in detail in previous papers (Benhaiem Sigaux et al. 1985; Matsumaru et al. 1999; Nimii et al. 1998). The detailed analysis of the vascular anatomy will confirm the potential relationship between the lesions. Any disorder that affects mother cells very early in their biological and/or embryonic life can affect the organs to which these cells migrate, even after they have acquired their phenotypic specificity. Any secondary trigger may then bring these abnormal cells from a quiescent to a more active state, where they will express the disorder (Vol. 1). Thus, the type of lesion will not predict the date of its creation nor the date of its appearance. Two types can be observed:
   – Multiple shunts with a clear metameric disposition (Fig. 11.22). They involve several myelomeres of the cord (multimyelomere AVMs), both on the cord and intradural nervous roots (either AVFs or AVMs). The association of SCAVSs and radicular AVSs is metameric if

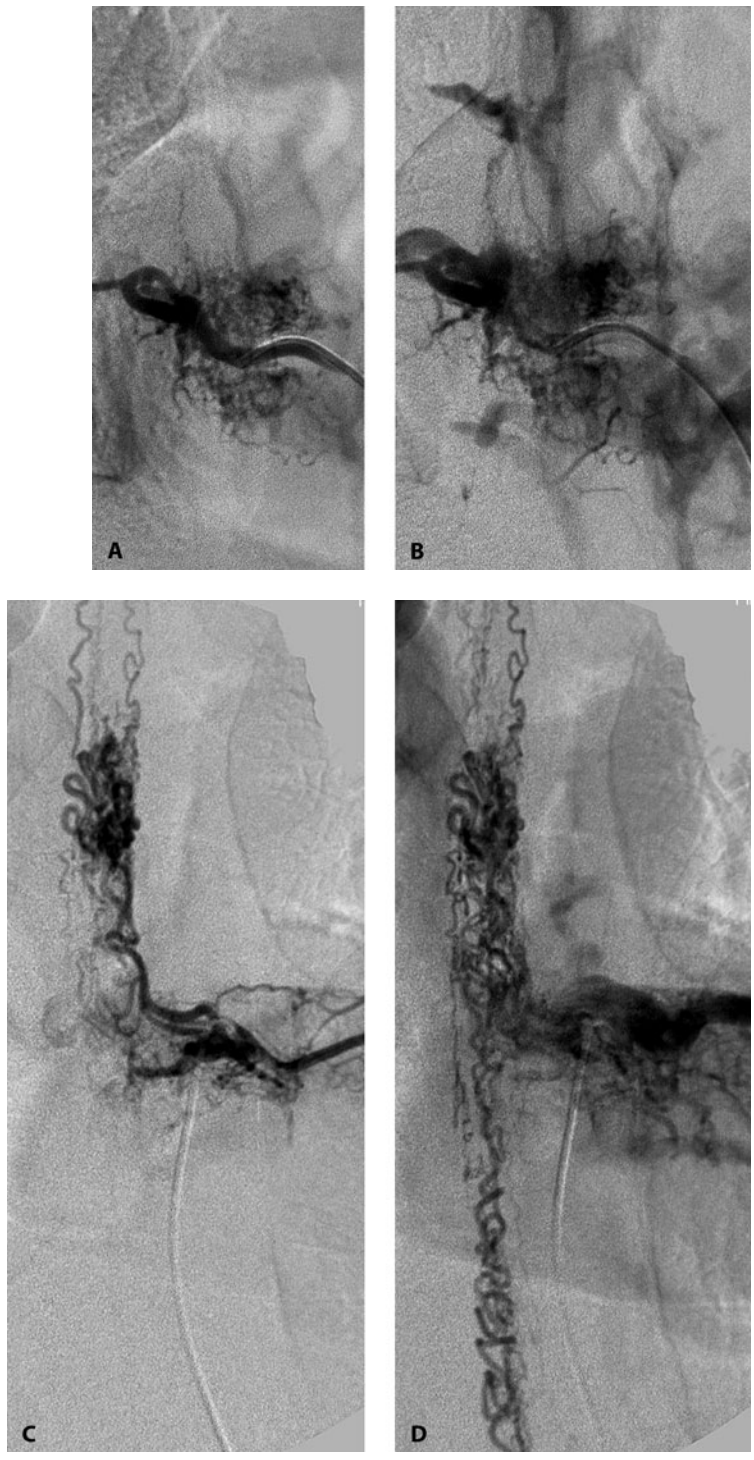

Fig. 11.22A–D. Spinal arteriovenous metameric syndrome 17/18. T10 injections bilaterally with involvement of the T10 vertebra (**A**, **B**) and corresponding spinal cord (**C**, **D**)

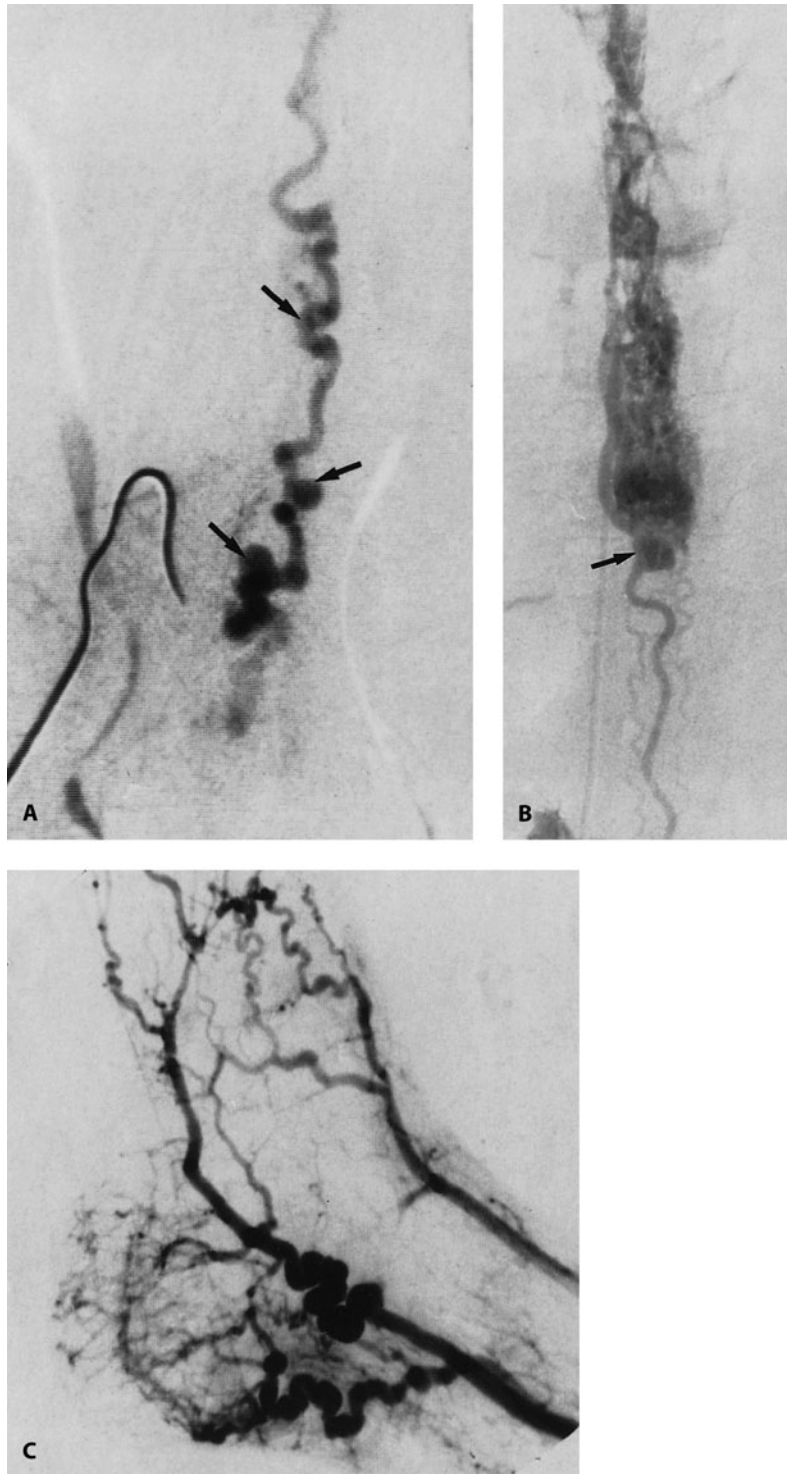

Fig. 11.23A–C. Klippel–Trénaunay syndrome. **A** Injection of the right internal iliac artery shows multiple dysplastic aneurysms on the radiculomedullary artery (*arrows*). **B** Injection of T10 shows the anterior spinal artery supplying an extensive vascular malformation with evidence of a dysplastic aneurysm in the distal anterior spinal artery (*arrow*). **C** Angiographic examination of the foot in the same patient shows multiple dysplasia but no arteriovenous fistula. (Courtesy of R. Piske)

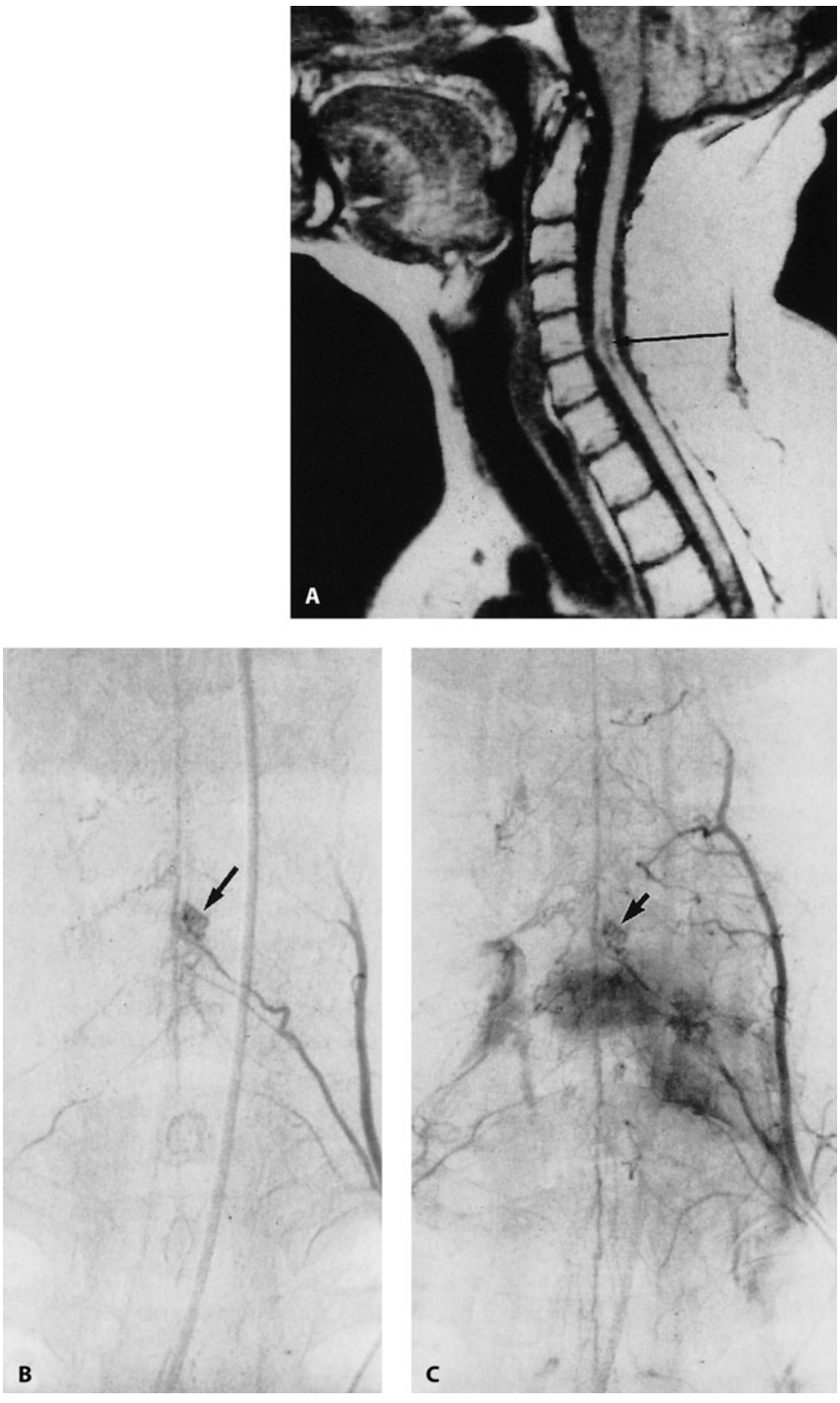

Fig. 11.24A–C. MRI of a microvascular malformation that shows evidence of a previous event, namely, a cavity in the mid-cervical region. **A** Sagittal MRI demonstrates a signal void in a longitudinal aspect representing an intramedullary cavity (*arrows*). **B** Early and **C** later phases (frontal view) of the ascending cervical injection, which demonstrates a small vascular malformation (*arrow*)

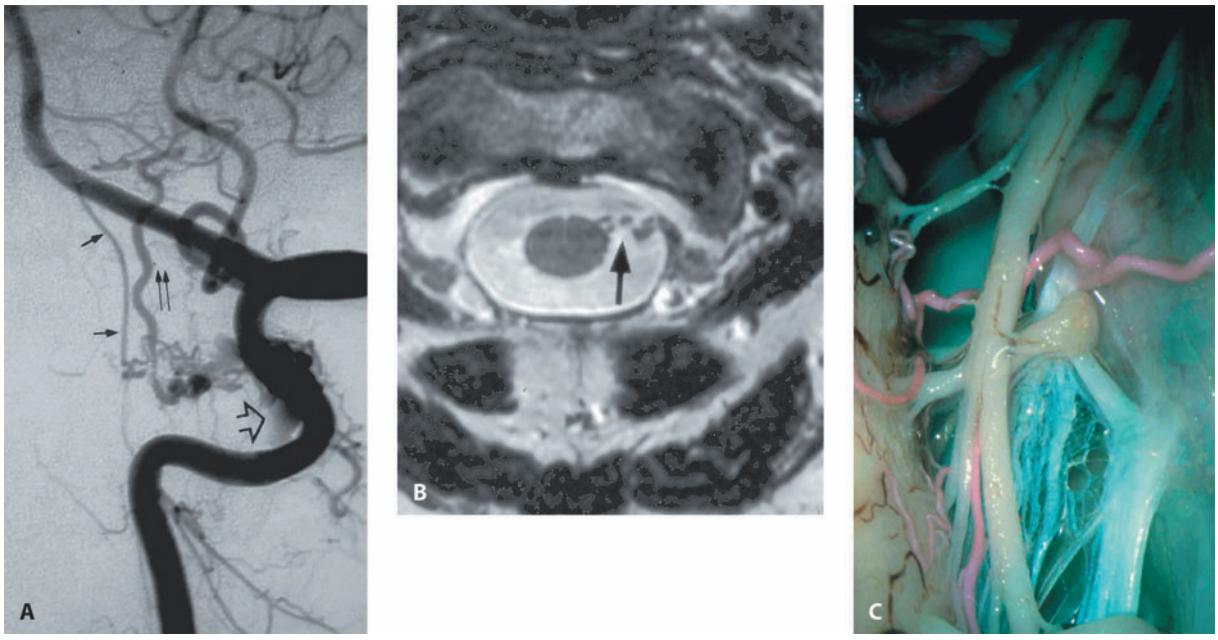

Fig. 11.25. **A**, **B** Radicular nerve arteriovenous malformation developed on the left C2 nerve. **C** Anatomical preparation at the same level. (Courtesy of B. Vallee)

the myelomere involved with the SCAVS corresponds to that of the nerve involved. Cobb syndrome belongs to this metameric category and corresponds to the spinal arteriovenous metameric syndromes (SAMS). Depending on its location and involvement at the vertebral and metameric levels, it can be numbered from 1 to 31 (Figs. 11.19, 11.21, 11.23, p. 771).

- Multiple shunts where the metameric disposition cannot be definitively demonstrated but is strongly suspected. In these cases, the SCAVSs are associated with a limb vascular malformation (Figs. 11.21, 11.23). In the overall population of SCAVMs, more than 20% of patients have associated other vascular malformations or dysplasias (Berenstein et al. 1990; Rodesch et al. 2002; Nimii et al. 1998) and up to 16% had clear metamerically related multiple lesions (Matsumaru et al. 1999).

– The third group concerns single lesions, either AVMs or mAVFs. This group may perhaps reflect the incomplete expression of one of the previously described situations. The lesions are located in the intradural compartment, on either one of the intradural nervous structures, cord (Fig. 11.24), root (Fig. 11.25), and filum (Fig. 11.26).

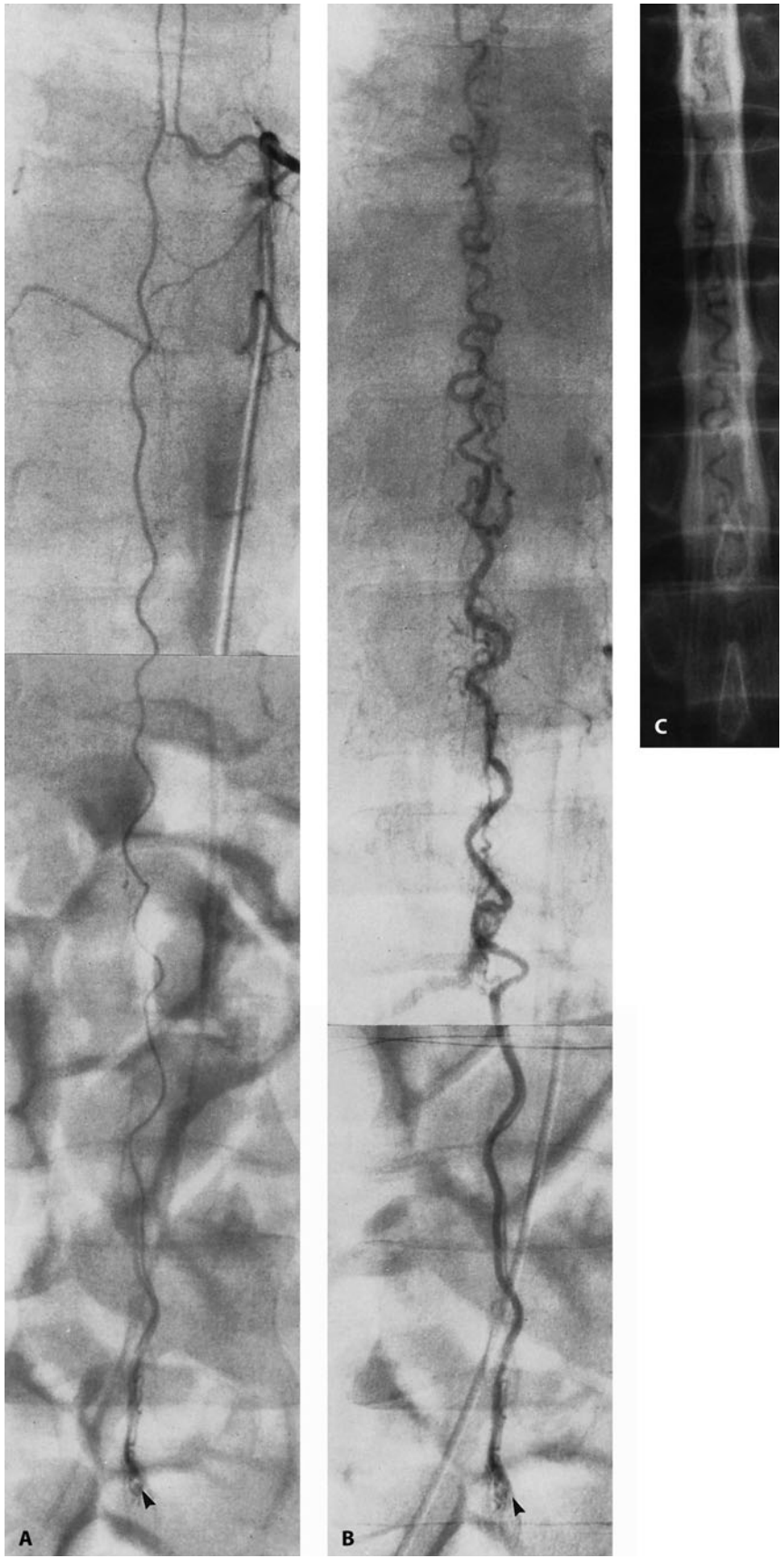

Fig. 11.26A–C. Arteriovenous fistula of the filum. **A** Selective injection of the left T7 fills the radiculomedullary artery, which shows the arteriovenous fistula at the level of the filum terminale (*arrowhead*). **B** Later phase of the same injection shows the level of the fistula (*arrowhead*) and the ascending venous drainage, similar to those seen with spinal dural arteriovenous fistulae. **C** Myelogram in the same patient

11.3.2 Angioarchitecture

As in cerebral AVMs, proper analysis of SCAVMs is necessary to differentiate the primary malformation from other features, which reflect the arterial or venous host response over time. Although there is substantial information available on the anatomical, surgical, and angiographic aspects of cerebral AVMs, the incidence of SCAVMs is low and these lesions are rarely surgically accessible, with potentially hidden compartments in intramedullary and ventrally located lesions. Due to these limitations, most SCAVMs are poorly described in the available literature. The concentration of large numbers of patients with SCAVMs in a few neuroradiological centers has facilitated more homogeneous data collection.

The angioarchitecture presented here describes elementary features that can be recognized at the time of selective angiography in almost all central venous system (CNS) vascular malformations. These features include both the primary AVM arrangement as well as their acute and chronic impact on the adjacent feeding and draining vessels and the spinal cord parenchyma.

11.3.2.1 Arterial Features

The peri- and intramedullary anastomoses of the arteries of the spinal cord make it possible for SCAVM to be angiographically visualized via different sources. Lateral views are often of poor quality and frequently do not provide more information than high-quality frontal projections when properly interpreted. Arterial variants are not as easily identified as in the brain and they occur less frequently. Phrenospinal, bronchospinal, and sacrospinal common trunks can be found, but they are within the usual anatomical variability of the system far from the spinal cord (see Vol. 1). Special radicular contributions to the cord supply and unfused segments of the ventral spinal artery are the most frequent type of variants encountered. An intrinsic longitudinal spinal cord arterial network is sometimes opacified in SCAVMs (Fig. 11.27).

The anatomical characteristics of a feeding artery may help in identifying the myelomere location of the lesion (Fig. 11.28, p. 778). However, the presence of axial and longitudinal, intrinsic and extrinsic, arterial anastomosis (see Vol. 1) can make the angiographic diagnosis of intra- versus extramedullary location sometimes confusing. MRI studies have brought some complementary information to more accurately localize the SCAVMs in relation to the cord tissue and the meningeal spaces.

Arterial steal in SCAVMs, although theoretically possible, can only be discussed in correlation with the anatomical disposition of the individual arterial territories. Today's capability for early diagnosis of SCAVM, particularly in children, has demonstrated that many high-flow lesions were discovered before they actually bled. In contrast, patients with slow-flow lesions, such as the filum terminale lesions, tend to present with progressive ischemic syndromes secondary to venous hypertension, similar to SDAVS (see Chap. 12, this volume).

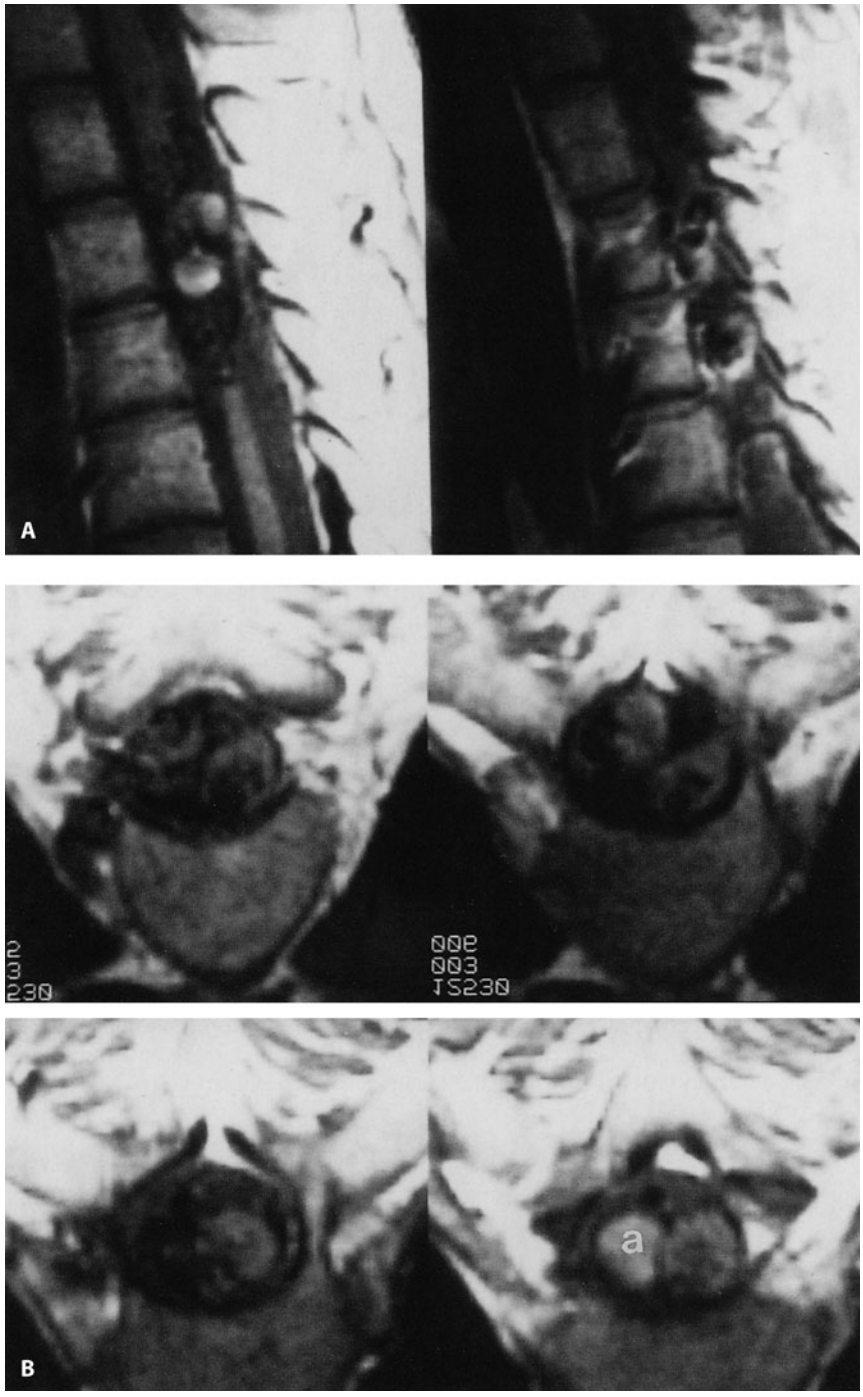

Fig. 11.27A–F. Pseudoaneurysm with hemorrhage. **A** Sagittal MRI T1-weighted image shows bilobed increased signal in the region of the pseudoaneurysm. **B** Axial view at the same level demonstrates that the spinal cord is displaced to the left by the pseudoaneurysm (*a*). **C–F** see pp. 777, 778

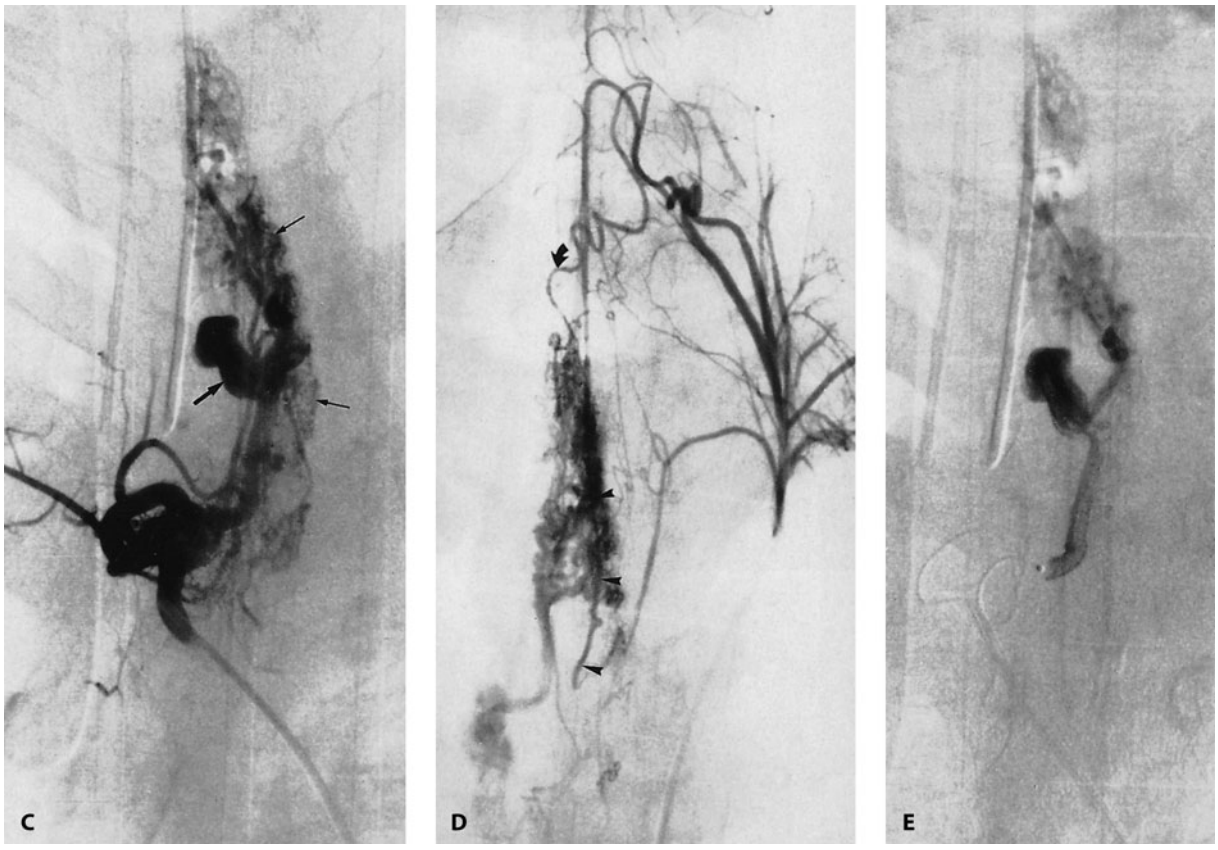

Fig. 11.27 (*continued*). **C** Injection of the right supreme intercostal artery demonstrates displacement of the spinal cord from right to left with a bilobed irregular aneurysm (*arrow*). Also note the intrinsic longitudinal anastomotic system (*small arrows*). **D** Injection of the contralateral artery of the cervical enlargement showing the radiculomedullary artery displacement and contribution and the left dorsal radiculopial artery (*curved arrow*) supplying the right posterolateral aspect of the malformation. Note the displacement of the distal anterior spinal artery (*arrowheads*). **E** Superselective catheterization of the radiculomedullary artery feeding both the pseudoaneurysm and the malformation. **F** see p. 778

Direct versus indirect supply is difficult to differentiate at the spinal cord level. In fact, one often associates direct supply with the larger branch entering the AVM at each division of the arterial tree. Indirect supply represents AVM feeders whose caliber is smaller and which also feed normal adjacent territories (Fig. 11.29, pp. 779, 780; Fig. 14.130, p. 781). This feature is important since indirect supply probably relates to a secondary phenomenon, i.e., an adjacent sump effect and subsequent local collateral circulation recruitment. As seen in other territories, these secondary phenomena could be reversible following embolization of direct feeders as long as the arteriovenous shunt itself is occluded (Fig. 11.30). Otherwise, the indirect feeders become the only source of residual supply to the lesion. In some instances, an indirect supply may allow easier or safer navigation to reach the nidus than a highly tortuous one arising from a difficult radicular artery. In most publications, AVM feeders are confused with sources of AVM opacification.

Fig. 11.27 (*continued*). **F** Follow-up after embolization (IBCA) in which the aneurysm was occluded. Intrinsic network in a spinal cord arteriovenous malformation. Frontal subtraction angiogram of the supreme intercostal artery on the right side fills the spinomedullary artery with hypertrophy of the intrinsic network (*arrows*)

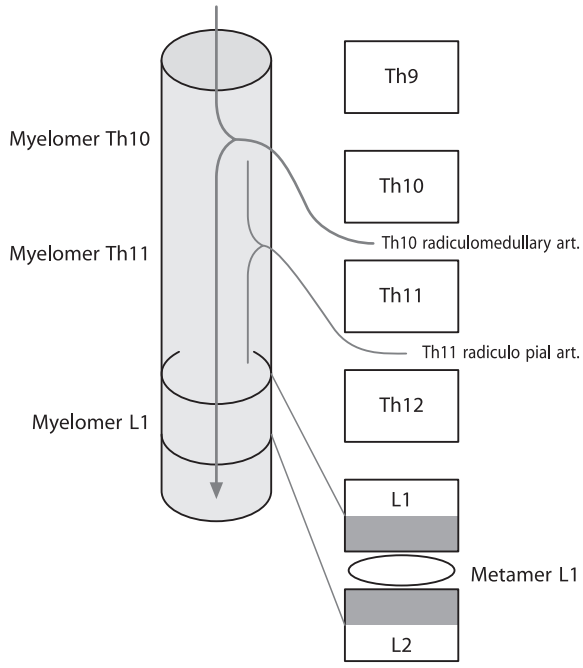

Fig. 11.28. Myelomere topography and metameric spinal cord arteriovenous malformations. (Matsumaru et al. 1999)

Fig. 11.29A–H. High-flow dorsolateral spinal arteriovenous fistula (AVF) of the conus in a 25-year-old female patient who presented with spinal hemorrhage. She was partially treated through the right dorsal radiculopial feeder (**A**), returned 2 years later with a progressive myelopathy characteristic of a spinal dural AVF (SDAVF), and showed a SDAVF of the sacrum draining cephalad and into the anterior spinal vein, which also drained the remaining malformation (**E, F**). **A** Selective injection of the T12 intercostal artery feeding the right dorsal radiculopial artery, which supplies the lesion at the posterior lateral aspect of the conus (*arrowhead*). Note filling of the anterior spinal artery (ASA) via retrocorporeal anastomoses of the opposite side; the *curved arrow* points to the anastomosis with the ascending anterior spinal axis. **B** Injection of the right T9 intercostal artery, which supplies a dorsal radiculopial artery (*small arrow*) and contributes to the anterior spinal axis (*large arrow*). Note the change in vessel caliber at the lower anastomosis (*curved arrow*) and filling of the dorsolateral fistula (*arrowhead*). **C** Left T12 injection after embolization of the right dorsal radiculopial spinal artery with IBCA. Note better filling of the remaining fistula (*arrowhead*) compared to **B**. **D** Two-year follow-up angiogram after the patient presented with progressive myelopathy. Injection of the right T9 intercostal artery shows the anterior spinal axis. Note the significant decrease in caliber of the lower ASA segment (*curved arrow*). There has been regression of the remaining fistula with a slow-flow shunt (*arrowhead*). **E–H** p. 780

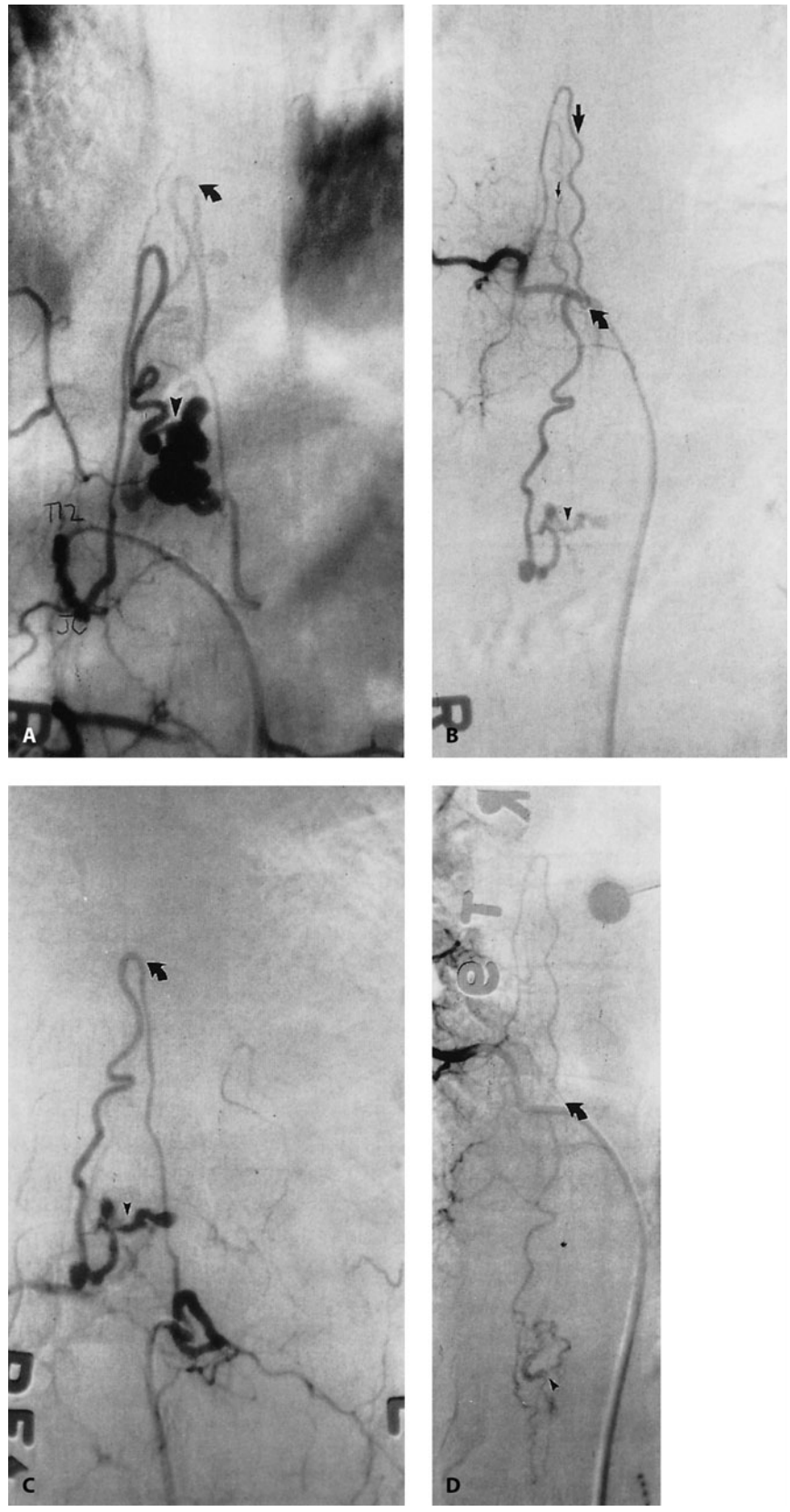

Fig. 11.29A–D.
Legend see p. 778

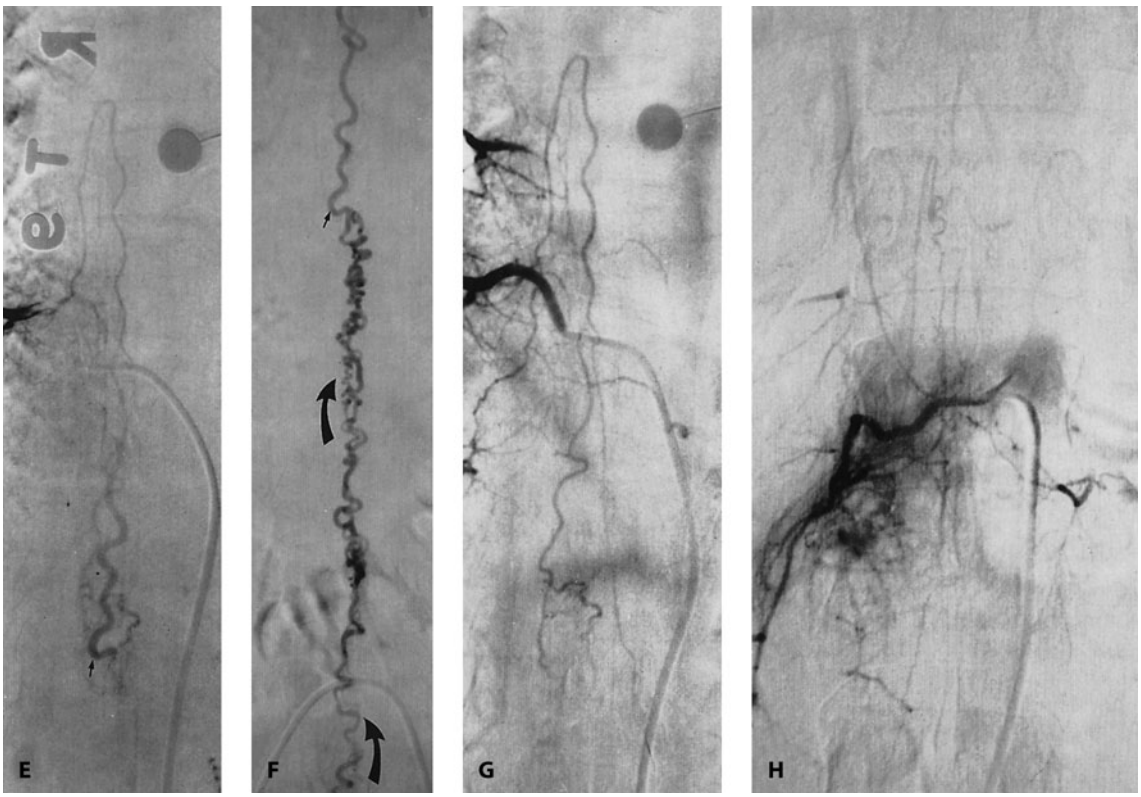

Fig. 11.29 (*continued*). **E** Later phase of the same injection as **D** shows the ascending anterior spinal vein (*arrow*). **F** Late phase of the left internal iliac injection where a SDAVF is now present (not present before). Note the ascending venous drainage (*curved arrow*) and the venous anastomosis to the same site of fistulization demonstrated in **D** (*arrowhead*) and **E** (*arrow*). **G** Follow-up angiogram of the right T9 intercostal artery and **H** of the T12 intercostal artery on the right after embolization of the SDAVF on the left lateral sacral artery. Note disappearance of the shunt (compare to **D**) and retrograde filling of the radiculomedullary contribution to the ASA

Fig. 11.30A–D. Direct versus indirect supply in an arteriovenous malformation of the spinal arteries. **A** Mid-arterial phase of the selective injection of the left L1 lumbar artery demonstrates the dorsal radiculopial artery on the left (*long arrow*). Note partial filling of the right dorsal radiculopial artery (*double arrow*). **B** Selective injection of the right L1 lumbar artery shows filling of the right dorsal radiculopial artery (*double arrow*), which also fills the malformation. Note filling of the left dorsal radiculopial artery (*arrow*) via retrocorporeal anastomosis. **C** Superselective injection of the left dorsal radiculopial artery shows the direct supply to the malformation and was used for embolization. **D** Follow-up postembolization (IBCA) angiogram of the right side shows preservation of the right side dorsal radiculopial artery and the pial anastomosis to the left side, representing indirect supply to the malformation ▶

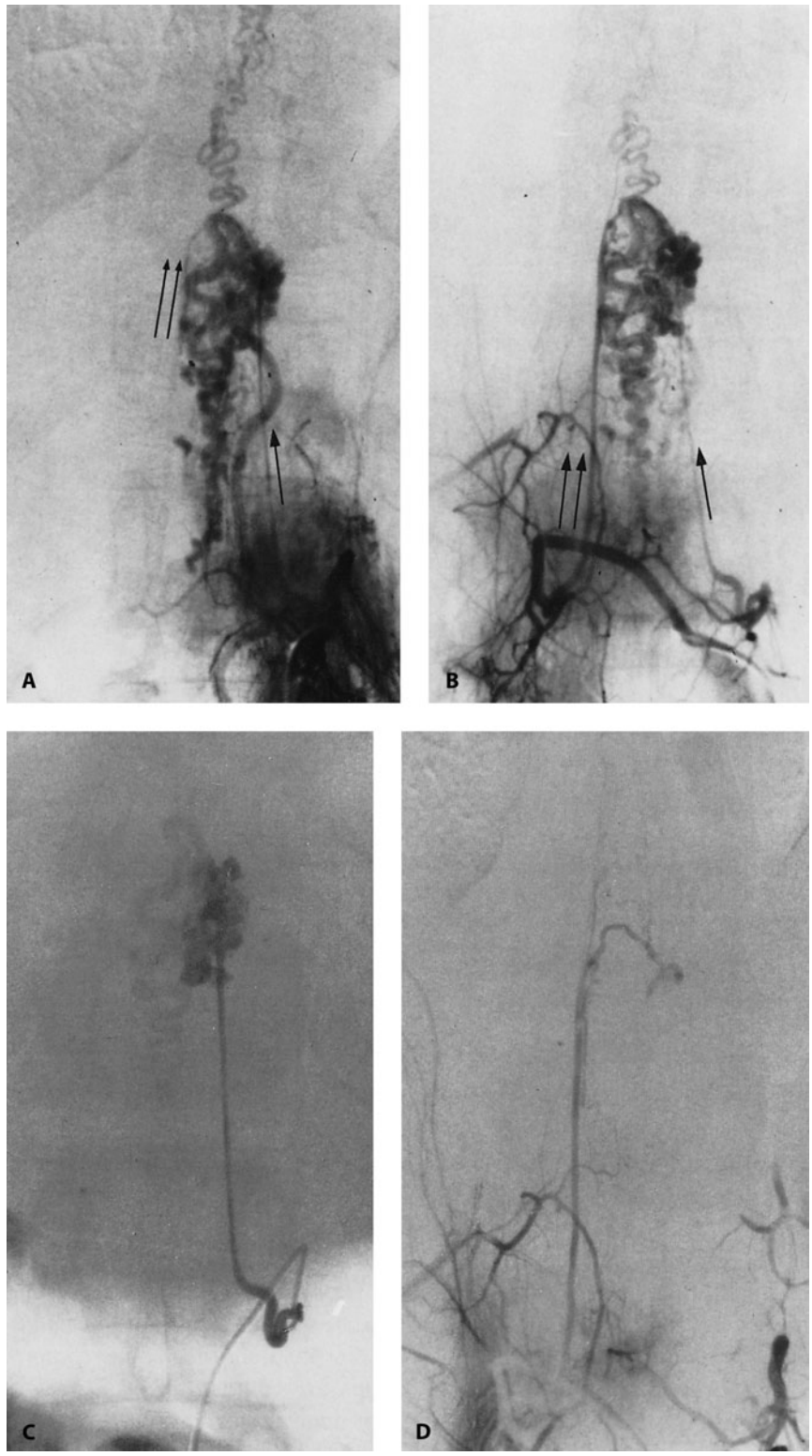

Fig. 11.30A–D.
Legend see p. 780

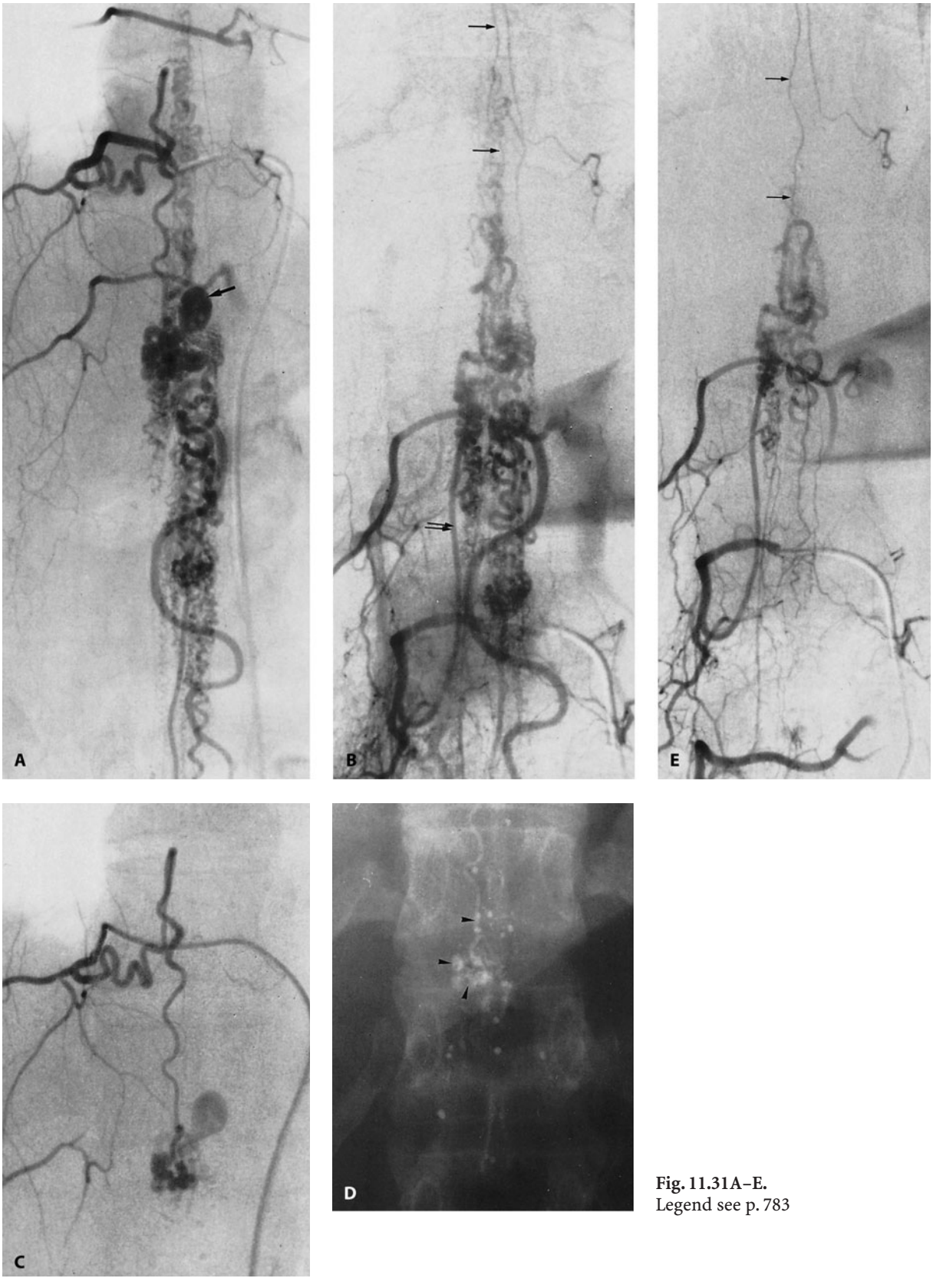

Fig. 11.31A–E.
Legend see p. 783

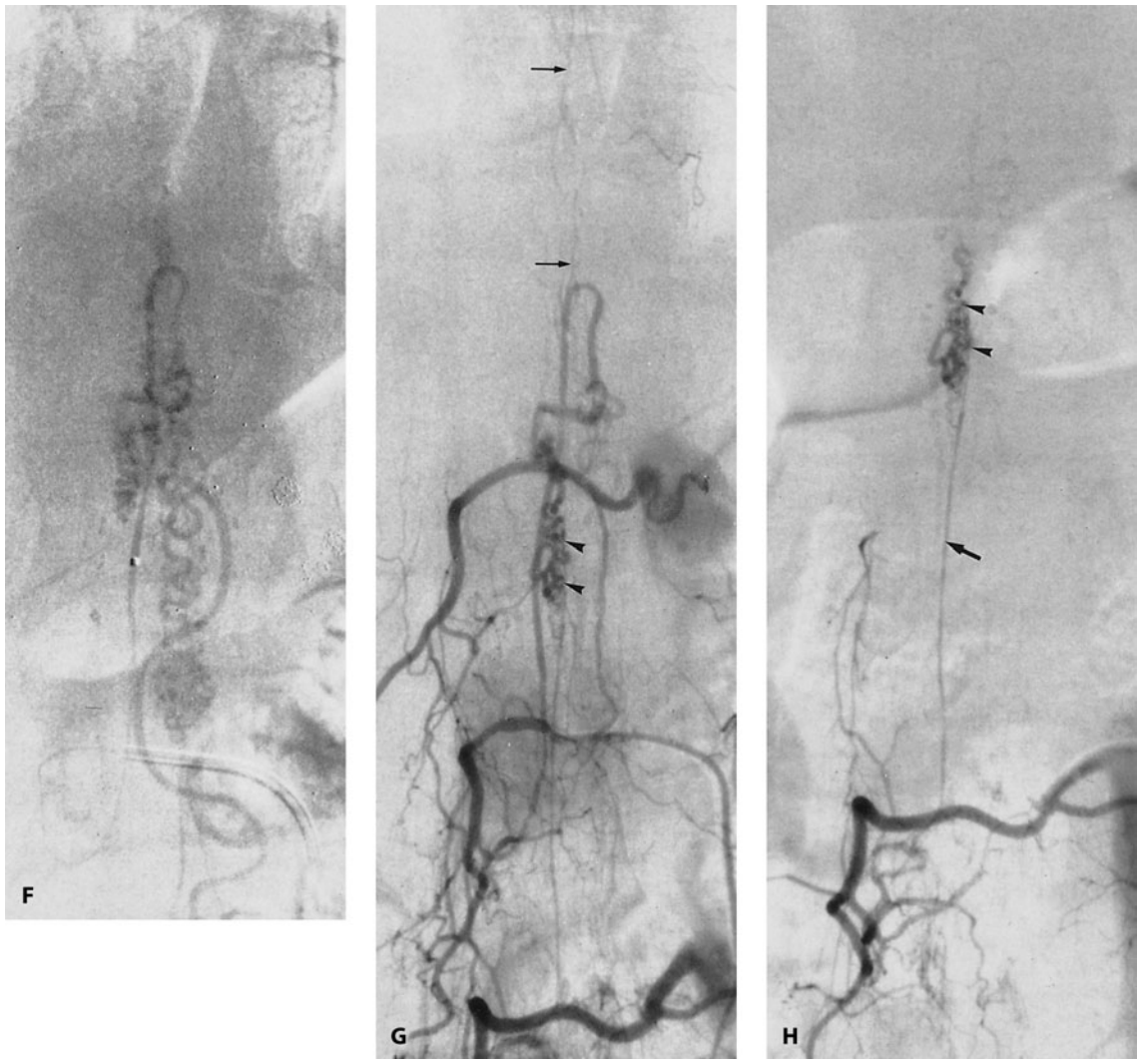

◄ **Fig. 11.31.** **A** Selective injection of the right T9 intercostal artery shows the radiculopial artery filling a high-flow vascular malformation with a large venous aneurysm (*arrow*). **B** Selective injection of the right radiculopial artery (*double arrow*) supplying the lower portion of the malformation. There is no filling of the aneurysm, but there is similar venous drainage. Also note filling of the normal anterior spinal axis (*small arrows*). **C** More selective injection of the T9 dorsal radiculopial contribution clearly defines the arteriovenous fistulization and direct filling of the venous aneurysm. **D** Radiopaque cast of the IBCA (*arrowheads*) obtained from this embolization (and lipiodol droplets from previous myelographic examination). **E** Follow-up of right L1 demonstrates the remaining multifocal malformation. There is no filling of the venous aneurysm. Note the better opacification of the anterior spinal artery (*small arrows*). **F** Superselective catheterization of the ventral radiculopial (and radiculomedullary) artery *on the right* shows nidus and its venous drainage. **G** Follow-up angiogram after the pial portion was embolized demonstrates the remaining nidus (*arrowheads)* from a lower contribution and preservation of the anterior spinal axis (*arrows*). **H** Selective injection of the level below better demonstrates the remaining malformation supplied by a ventral radiculopial artery (*arrow*)

Although injection of many radicular arteries reaching the pial network around the cord may visualize a SCAVM, this does not necessarily mean either direct or indirect supply to the lesion (Fig. 11.31). This arrangement is analogous to the injection of the vertebral and the carotid arteries, both demonstrating opacification of an arteriovenous fistula of the posterior cerebral artery in a patient with a complete functional circle of Willis. For this reason we advocate describing AVSs according to their myelomere level because symptoms are easier to characterize and they can be better related to the available venous outlets (see SAMS; Fig. 11.28).

11.3.2.2 Direct Arteriovenous Fistulae

Direct arteriovenous fistulae are the simplest type of SCAVM. They are located on the surface of the cord and present in younger individuals (Figs. 11.32, 11.33). Multiple SCAVFs can occur. In most instances, the multifocal character of arteriovenous fistulae within a lesion can only be recognized after occlusion of one of them (see Sect. 11.5).

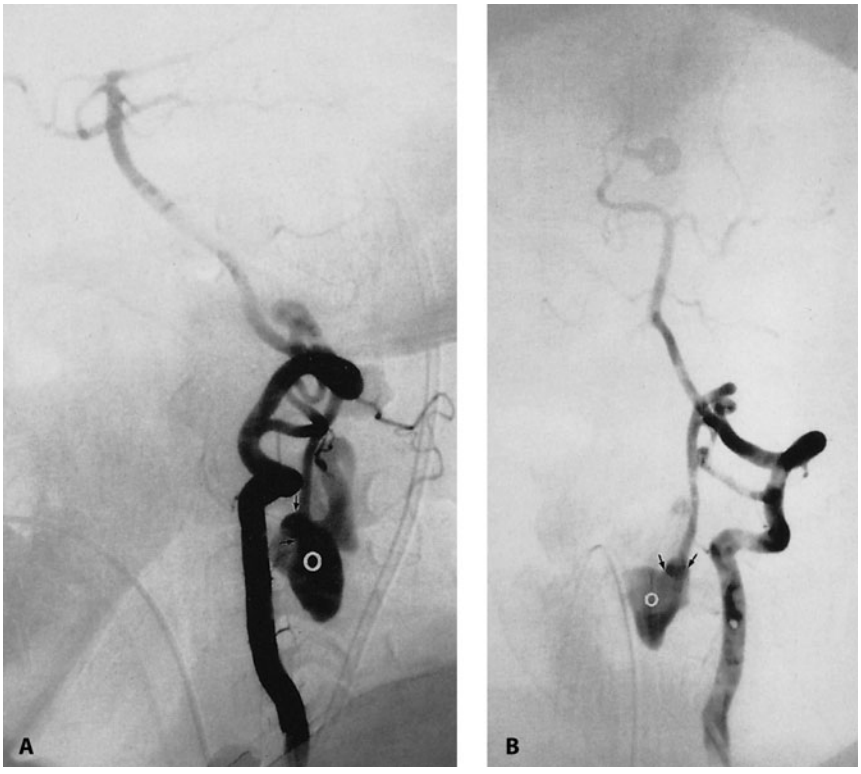

Fig. 11.32A, B. Single-hole arteriovenous fistula of the lateral spinal artery (*arrows*). **A** Lateral and **B** frontal early phase. Note the large venous ectasias (*white circle*) and the origin of the posterior inferior cerebellar artery (PICA) from C2

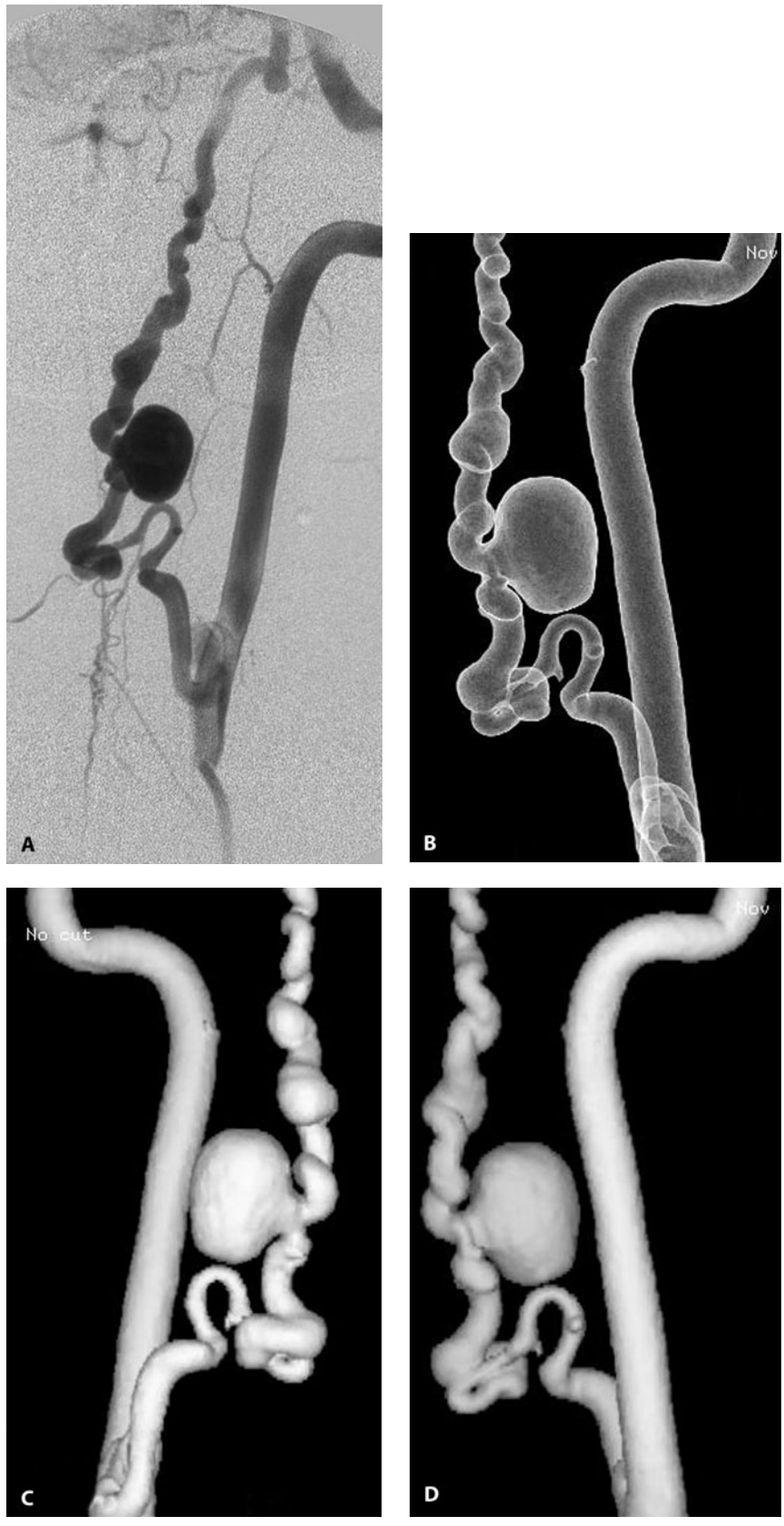

Fig. 11.33A–G. Ventral arteriovenous fistula revealed by progressive peripheral neurological deficit in a 24-year-old female patient. Arterial supply from ventral pial artery (**A–D**). **E–G** see p. 786

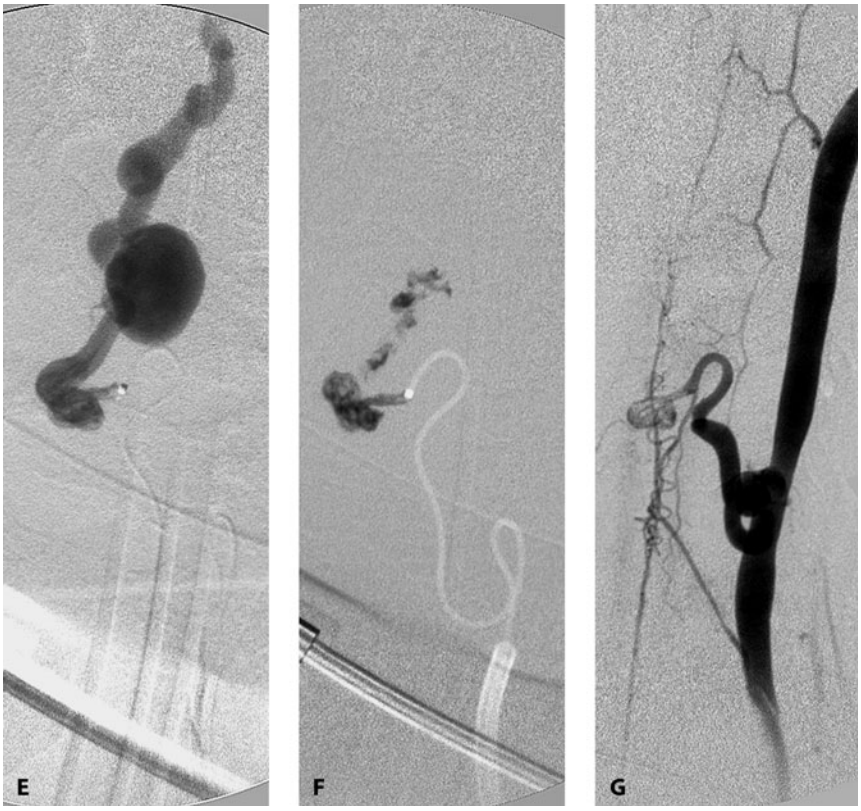

Fig. 11.33 (*continued*). Selective injection (**E**), NBCA embolization (**F**), and postembolization angiogram (**G**)

11.3.2.3 High-Flow Angiopathy

High-flow angiopathy is less frequently observed in high-flow angiopathy SCAVMs than in BAVMs. Occasionally, narrowed portions of enlarged anterior spinal radicular arteries to an AVM or draining veins may be seen, often in their transdural portion. Pseudonarrowing can be seen to involve the anterior spinal artery supplying a SCAVM. This appearance is caused by the unopacified flow from merging radicular arteries as they enter the main arterial trunk to the lesion (Fig. 11.29) or as they penetrate the subpial space. A careful search for additional sources of supply in such cases usually reveals the responsible afferent radicular artery.

11.3.2.4 Arterial Aneurysms in Spinal Cord Arteriovenous Malformations

The incidence of arterial aneurysms in spinal cord AVMs is difficult to assess from the literature. In a review of the literature up to 1980, Caroscio et al. (1980) found that of 30 reported patients, only three isolated aneurysms of the spinal arteries were seen. One additional patient was reported by Yonas et al. in 1980. In over 3,000 spinal angiograms reviewed by Djindjian (1976), only one isolated aneurysm was found. Caroscio et al. (1980) found 12 patients with arterial dilatation of the spinal arteries associated with coarctation of the aorta (see Chap. 7 and Fig. 7.126, this volume). In their review of the literature, 14 patients, plus one of his own, had an

aneurysm that was associated with an AVM (Fig. 11.35). In seven instances, the AVM occurred in the cervical region, in five in the thoracic area, and in two at the lumbar level. Of these patients, 50% presented with subarachnoid hemorrhage, an incidence similar to the overall incidence of SCAVMs without demonstrable aneurysm. A complete block was found at myelography in an additional five patients. All but two patients were under 40 years of age; there was no gender difference. Miyamato et al. (1983) reported on two patients who had an arterial aneurysm associated with a SCAVM. Both patients presented with subarachnoid hemorrhage, and in both the arterial aneurysm disappeared after embolization. In 1973, Di Chiro and Wener noted the almost constant presence of subarachnoid hemorrhage in the association of SCAVMs and arterial aneurysms. Our experience is more in line with that of Djindjian and Merland (1978), who found aneurysmal dilatation in 18 patients (20%). Eight of the diagnoses were confirmed histologically and ten were documented by angiography.

In fact, if one wants to compare flow-related arterial aneurysms in SCAVMs with aneurysms seen in BAVMs, one should expect to find these aneurysms on branches of the anterior or posterior axis (perforators, coronary system, etc.). In our series, such aneurysms were found most frequently in high-flow lesions, mainly located at the cervical level, or in patients with a previous history of spinal hemorrhage. Aneurysms encountered on the radicular arteries (proximal aneurysms) are associated with repeated subarachnoid hemorrhage episodes (Figs. 7.120, 11.34). Some of these can be flow related or dysplastic (Fig. 11.35) when associated with Klippel–Trénaunay syndrome, as observed in patients who presented with subarachnoid hemorrhage (Fig. 11.23) or SAMS syndromes. As in the brain, flow-related arterial aneurysms can disappear following occlusion of the AVM. The differences in the hemodynamic conditions between the brain and the cord likely account for the rarity of flow-related arterial aneurysm in SCAVMs.

Rupture of an arterial aneurysm can sometimes be documented as a pseudoaneurysm (Fig. 11.36, p. 790). Occasionally there may be more than one arterial aneurysm (Fig. 11.37, p. 790; Fig. 11.38, p. 791). The pseudoaneurysm may change in size and shape, although early recurrent hemorrhage in SCAVM is extremely rare. Such changes demonstrate an unstable situation requiring treatment. In other instances, hemorrhage may lead to thrombosis of the lesion (Fig. 11.39, p. 791). Arterial aneurysm can be seen as an irregular dilatation proximal to the AVM; it can be suspected on the preliminary angiogram and/or MRI and documented by selective angiography. Aneurysms can be thrombosed directly, through collateral circulation or can thrombose after embolization of the AVM.

Garcia et al. (1979) reported an isolated aneurysm in the anterior spinal artery of a pregnant woman; Vincent (1981) also reported on a pregnant woman with subarachnoid hemorrhage secondary to an anterior spinal artery aneurysm. Patients such as these likely had an acute thrombosis of the vein draining an arteriovenous fistula, leaving behind a residual pouch. The thrombosis results from hemorrhage on the venous side. When these patients are seen subsequently, the final diagnosis of rupture of an arterial aneurysm is mistakenly made (see also Fig. 7.126).

Fig. 11.34A–I. A 15-year-old female patient. Cervical spinal cord arteriovenous malformation (SCAVM) at C2–C3 revealed by subarachnoid hemorrhage and extramedullary hematoma misinterpreted as hematomyelia. Right-sided hemiparesis with sphincter and respiratory problems. Typical subarachnoid aneurysm on the ventral nerve root (**A**). Two vessels were embolized via the anterior spinal artery (ASA) using the radiculomedullary access from below and above the SCAVM (same case as Fig. 7.120). **B, C** Eight-month follow-up after partial targeted embolization. No evidence of residual angiographic risk factors and significant decrease in the shunt. **E–I** see p. 789

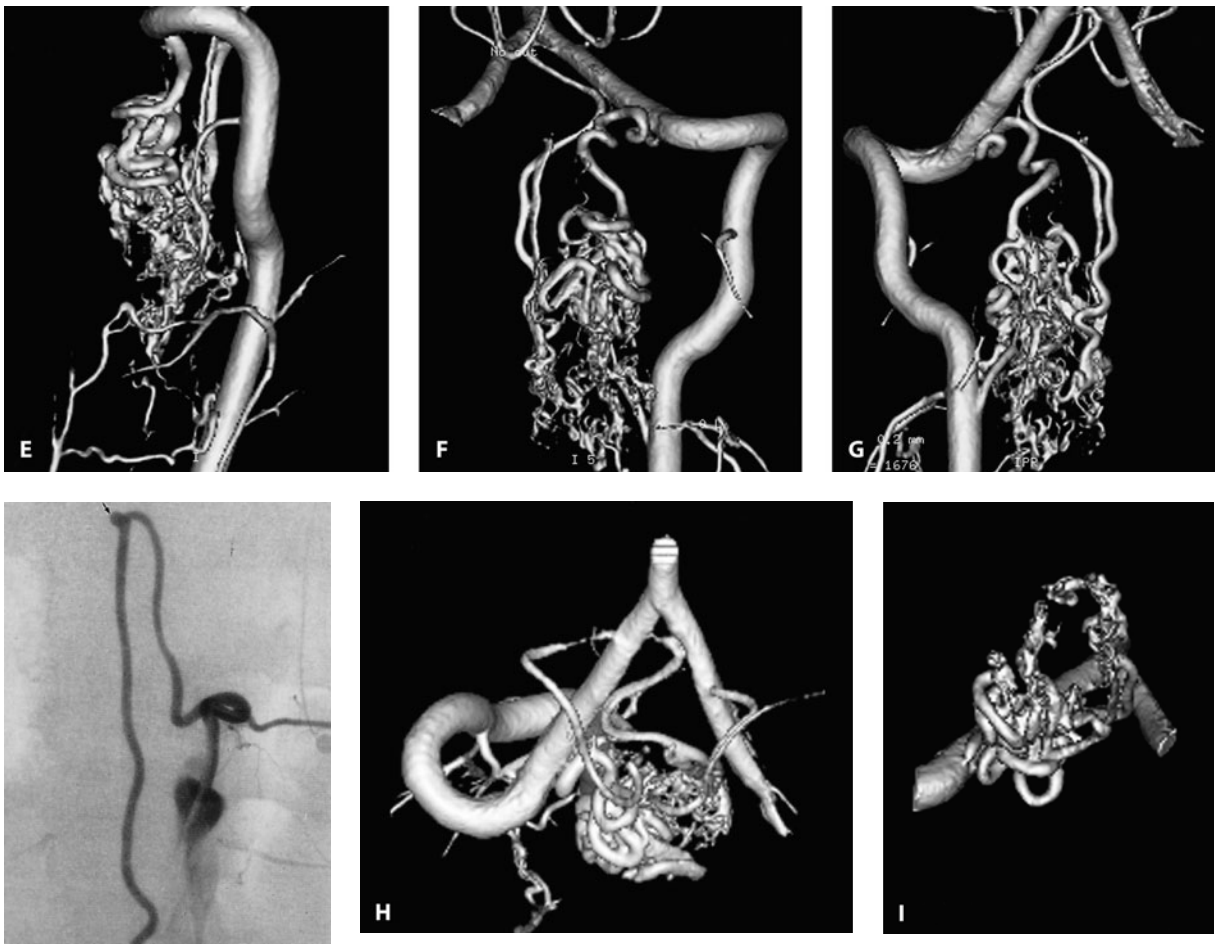

Fig. 11.34 (*continued*). **D–I** 3-D angiography demonstrates the nidus, mostly superficial and dorsal to the cord. Incomplete clinical recovery

◀

Fig. 11.35. Selective injection of the left T8 intercostal artery shows hypertrophy of the anterior spinal axis with multiple dysplastic aneurysms (*arrows*) and filling of a fistula of the filum terminale (*arrowhead*)

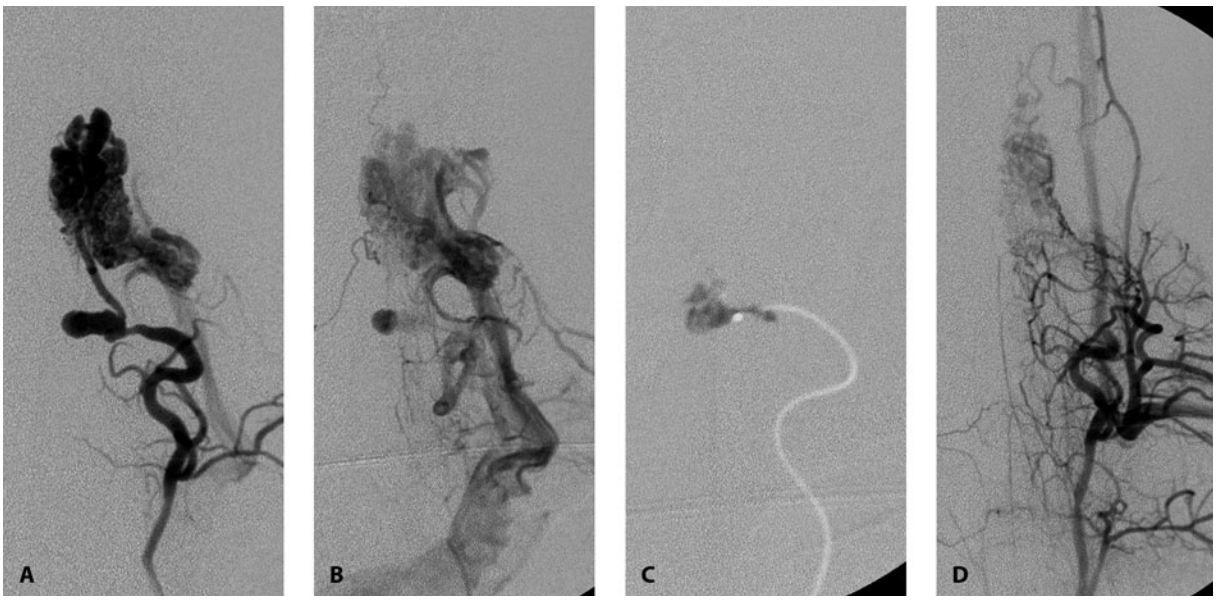

Fig. 11.36A–D. A 22-year-old male patient with recurrent episodes of subarachnoid hemorrhage from a spinal cord arteriovenous malformation with prominent radiculopial false aneurysm bulging into the subarachnoid space (**A**, **B**). Partial targeted embolization with NBCA was performed (**C**, **D**)

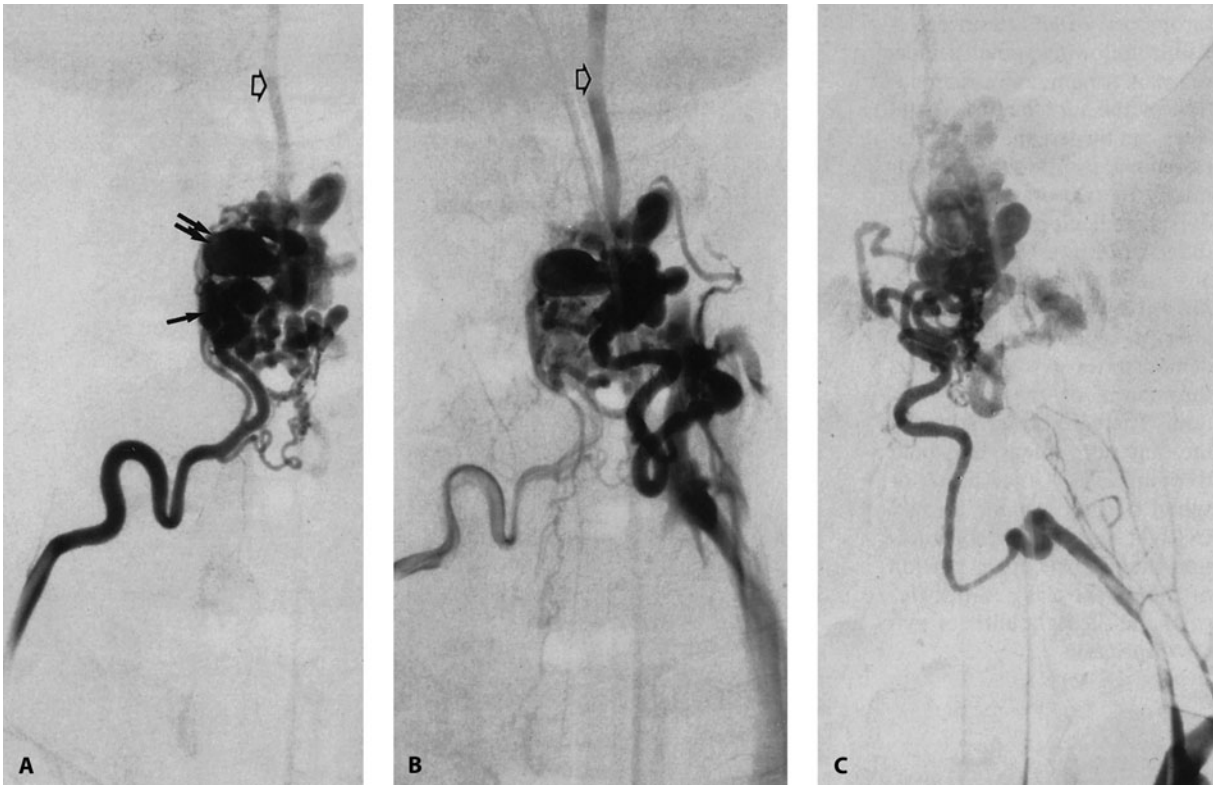

Fig. 11.37. **A** Ascending cervical injection shows multiple aneurysms in the vicinity and within the nidus. **B** Lateral phase shows the extraspinal drainage and the venous aneurysms. **C** Left thyrocervical injection showing the contralateral radiculomedullary contribution to the malformation with similar venous drainage

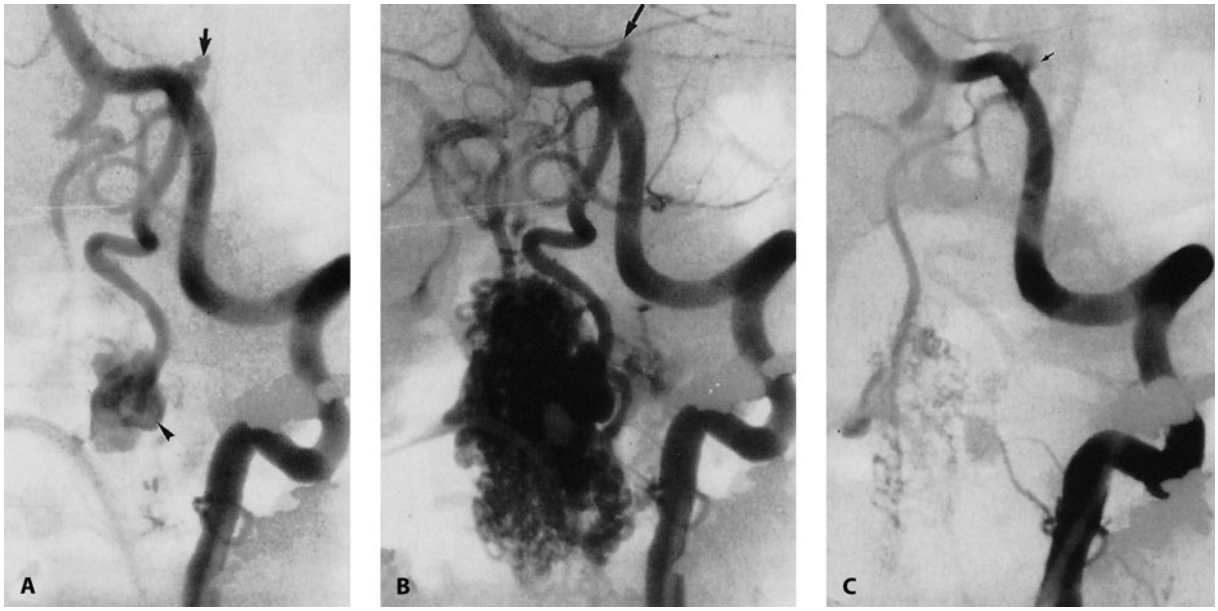

Fig. 11.38. **A** Left vertebral artery injection in early arterial phase demonstrates the lateral spinal artery supplying an arteriovenous malformation with a high-flow fistula (*arrowhead*) in the cervical region. Note the flow-related arterial aneurysm (*arrow*). **B** Later phase showing the extensive nidus. **C** Follow-up angiogram after embolization. The subtracted IBCA cast of the lateral spinal artery (*arrow*) and the remaining anterior spinal artery venous drainage

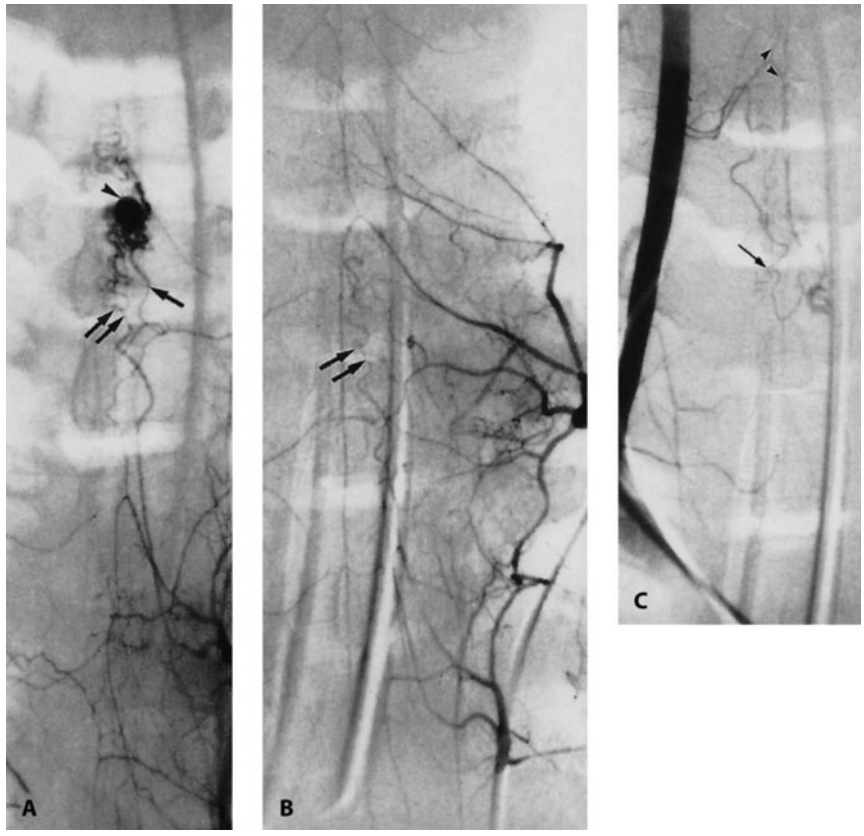

Fig. 11.39. **A** Angiographic examination of the supreme intercostal artery on the left shows an arteriovenous fistula supplied primarily by two branches of the dorsal radiculopial artery (*arrow*). Note filling of a pseudoaneurysm (*arrowhead*). **B** Follow-up angiogram after a repeated hemorrhage demonstrates spontaneous thrombosis of the malformation. There is preservation of the anterior spinal axis and thrombosis of the posterior spinal portion (*double arrow*). **C** Right vertebral artery injection shows the upper portion of the dorsal pial network (*arrow*) and the right anterior axis (*arrowheads*)

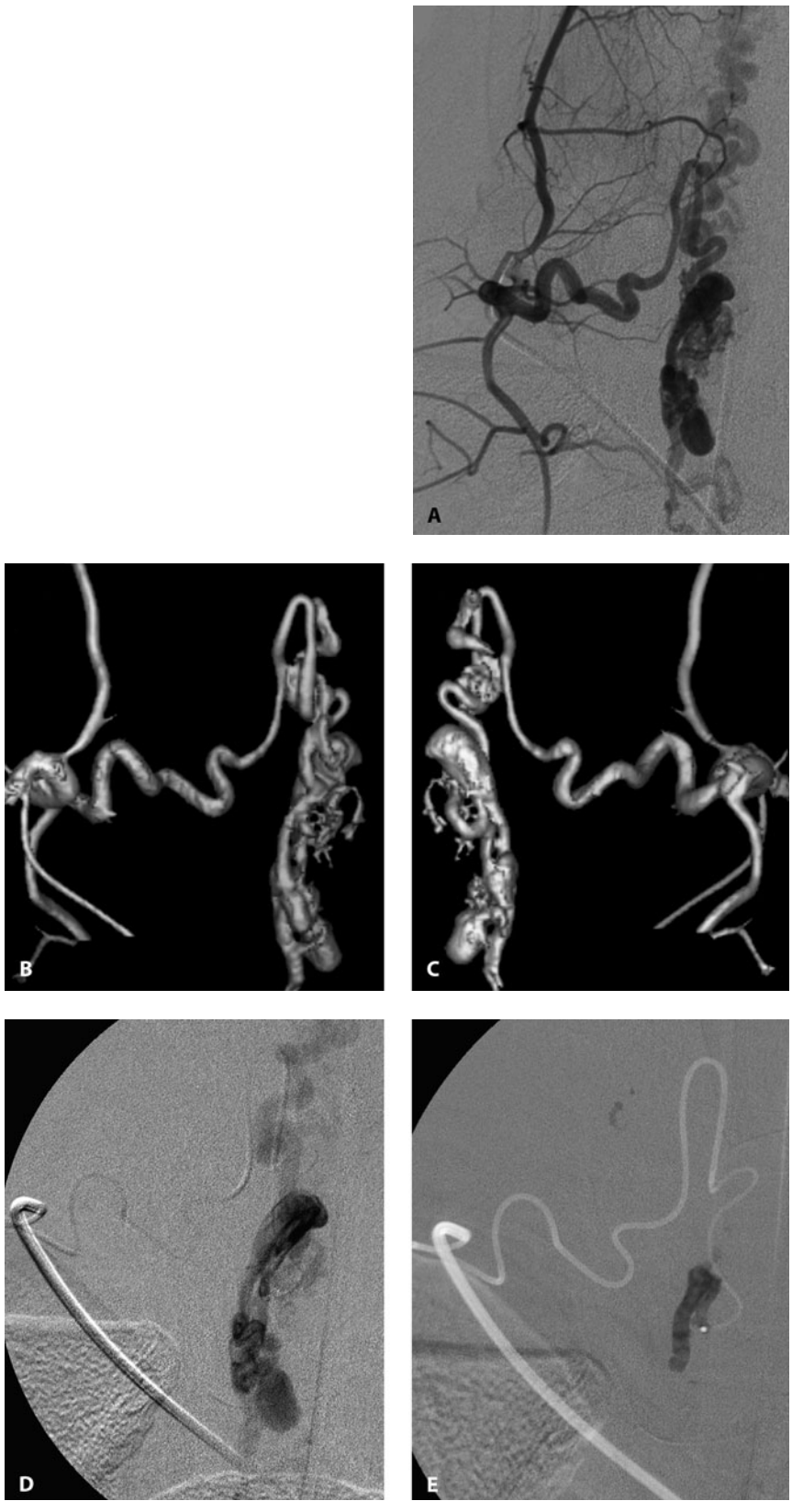

Fig. 11.40. A 16-year-old female patient with subarachnoid hemorrhage and subsequent sensory motor paraplegia as well as sphincter problems from thoracic spinal cord arteriovenous malformation (**A–C**). The false aneurysm seems to have developed from the retromedullary pial network. Partial targeted embolization was performed (**D**, **E**) with complete exclusion of the sac (**F**, **G**). Almost complete recovery occurred with no recurrence; Karnofsky score, 90 ►

Fig. 11.40F, G.
Legend see p. 792

Thrombosed venous drainage in single-hole arteriovenous fistulae has been previously interpreted as an anterior spinal artery aneurysm on the basis of the angiographic ectasia and stagnation involving both the anterior spinal artery and the pouch (Djindjian et al. 1975). At surgery, however, resection of the thrombosed venous outlet will allow proper diagnosis. Shortly after a hemorrhage, a partially filled pseudoaneurysm may also mimic a spinal artery aneurysm. Again, careful analysis of the angiographic series should aim at disclosing venous filling of the remaining portion of the SCAVM. The features of these aneurysms are comparable to those presenting in the brain.

Distal arterial aneurysms (AAs) are often seen at the time of an intramedullary hemorrhagic complication and should be considered as false AAs. They must be differentiated from venous pouches seen at or downstream from the arteriovenous junction (Fig. 11.37). The junction is usually easy to recognize and is marked by a clear increase in the caliber of the abnormal vessel (Fig. 7.121). This caliber change is particularly well demonstrated in single-hole arteriovenous fistulae, where it is often associated with venous ectasias. Dilatation in the vein draining SCAVMs is

infrequently seen (Fig. 11.40) and appears to be less common than in BAVMs, except in HHT1 patients. The relative absence of venous dilatation can be explained by the lack of anatomical barriers interfering with the spinal venous outflow in the subarachnoid space. Venous ectasias are, however, nearly constant in SCAVF in HHT1 patients or children with a similar arteriovenous architecture.

11.3.2.5 Dural Supply

Dural supply in SCAVMs is difficult to demonstrate angiographically, but may be similar to that seen in BAVMs, particularly in the rare instances of spinal dural adhesions following repeated hemorrhages or surgical intervention. Dural recruitment will occur at the level of the adhesions, whereas the supply to the SCAVM will always follow the rules of radicular supply to the myelomere involved (see Vol. 1). The dural contribution may be apparently dominant at the dural and extradural region in SAMS, in relation with the radicular foramen corresponding to the myelomere involved.

11.3.2.6 Nidus

The nidus arrangement proper is difficult to appreciate at the cord level. This difficulty is related to the axial, transmedullary (Fig. 11.41), arterioarterial and venovenous anastomoses (Fig. 11.42, p. 796) and to the complex intrinsic and extrinsic longitudinal anastomoses (Fig. 11.43, p. 797). Anastomoses between the coronary-arranged pial arterial network (Fig. 11.44, p. 798; Fig. 11.45, p. 799) and the sulcal perforators create further obstacles to nidus visualization. For practical purposes, we have chosen to discuss only direct arteriovenous fistulae and nidus-associated lesions.

Direct SCAVFs correspond to an anterior spinal or pial posterior spinal artery opening into a dominant anterior spinal or pial spinal cord vein. Arteriovenous fistulae supplied by the anterior spinal artery are often of the high-flow type and correspond to macroarteriovenous fistulae (MAVF), except when located on the filum. Microarteriovenous fistulae (mAVF) (Fig. 11.46, p. 800), when their flow is moderate or slow, are often misinterpreted as large arterial spinal arteries. The ventral (anterior) spinal cord vein is dorsal to the artery, thus deeply located within the ventral fissure (Fig. 11.14), which makes some mAVF MRIs occult (Lasjaunias et al. 2001). Drainage into the anterior spinal vein is rapid, but high flow can involve the pial and radicular veins. Dorsal arteriovenous fistulae are usually of the slow-flow type. When located off the midline, they can be mistaken for SDAVFs, which also may present with congestive venous symptomatology (Fig. 11.47, p. 801). The dogma that lesions supplied by the anterior spinal artery are intramedullary is no longer valid: pial branches of the artery supply the surface of the cord ventrally, and transmedullary perforating anastomoses (see Vol. 1) may in fact supply extramedullary or retroextramedullary lesions (Fig. 11.41).

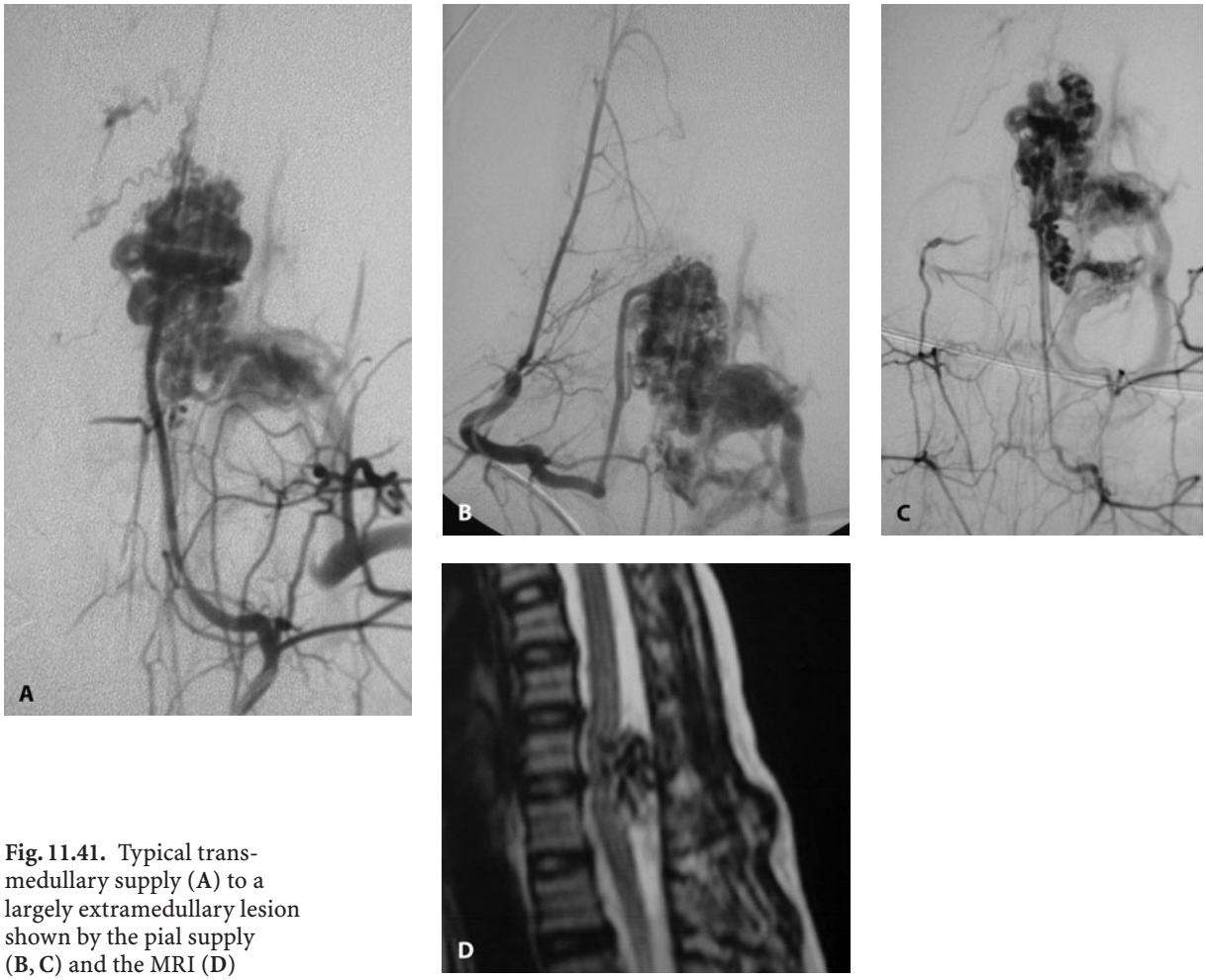

Fig. 11.41. Typical transmedullary supply (**A**) to a largely extramedullary lesion shown by the pial supply (**B**, **C**) and the MRI (**D**)

Nidus-arranged lesions may reproduce the compartmentalized aspect (Figs. 11.31, 11.44, 11.45), as described in tumors such as paragangliomas or cerebral AVMs. However, most SCAVMs seem to be single-compartment lesions: even if each feeder fills a different portion of the network, the venous outlet remains the same. In fact, we do not know if the convergence of communication or unrecognized compartments occurs at the nidus level or as part of the intrinsic venous anastomoses. Analysis of the venous drainage may help with the diagnoses of cervical (Figs. 11.34, 14.134) or low thoracolumbar AVMs (Fig. 11.17), where transmedullary anastomoses are less frequent.

In all regions, single anterior or posterior venous drainage corresponds to lesions involving the ventral and dorsal aspect of the cord, respectively. However, isolated posterior drainage may be seen in centrally located lesions since the dorsal perforating veins drain the gray matter (see Vol. 1).

Drainage involving both anterior and posterior veins of the cord can still be consistent with a limited and even superficial SCAVM. In this situation, the AVM drains rapidly into a patent, transmedullary, venous anastomosis (Fig. 11.41).

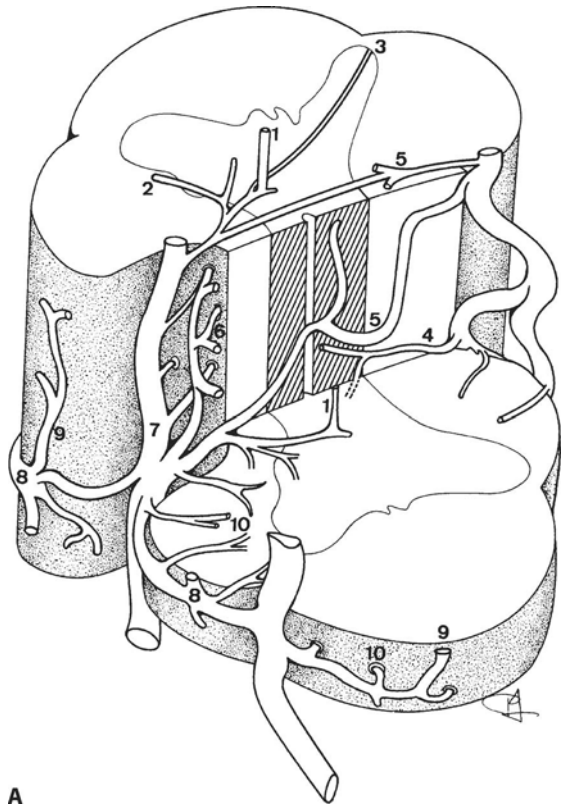

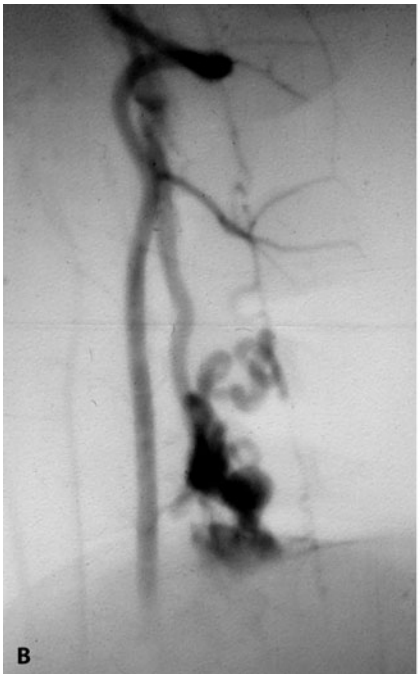

Fig. 11.42. Transmedullary veins (**A**) in a case of a ventrally located spinal cord arteriovenous malformation, as shown on lateral view vertebral angiogram (**B**) and sagittal MRI (**C**)

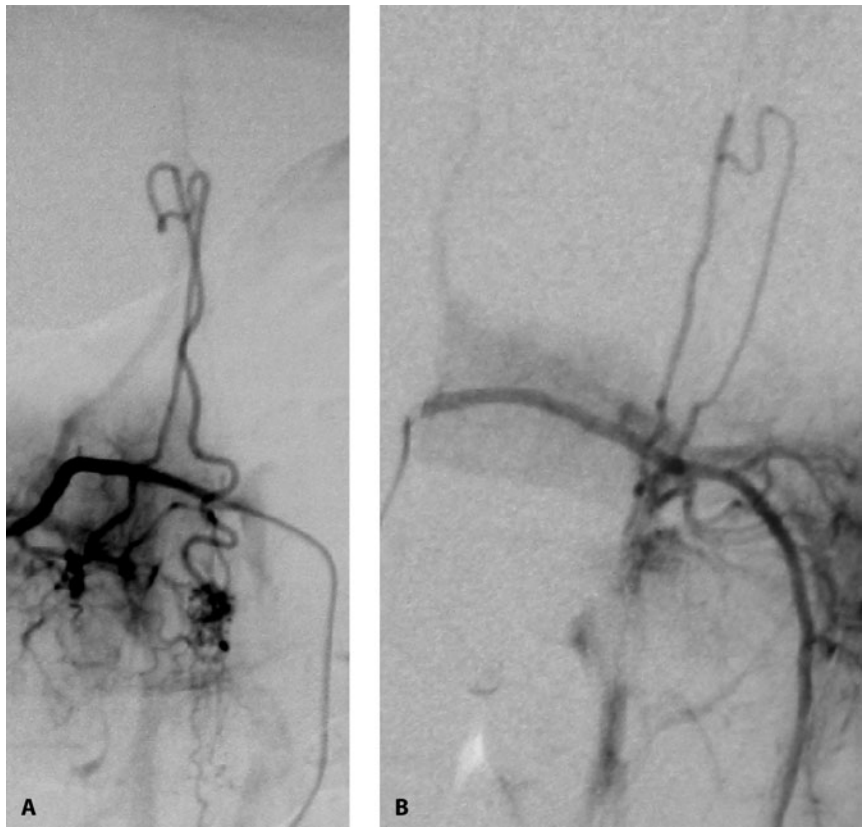

Fig. 11.43A, B. Pial network around the cord opacifies the ventral artery and the dorsal system. (Courtesy of R. Piske)

Therefore, thrombosis of one of the venous outlets of a SCAVM can be suspected on the basis of a patent arterial supply to a compartment draining in another venous system (i.e., dorsal pial arterial supply and ventral venous drainage).

Coexisting arteriovenous fistula and nidus within a single SCAVM is possible. The advent of superselectivity and embolization within the spinal cord artery branches will help in delineating these intrinsic features. Some of the associated arteriovenous fistulae and nidi may appear separate and can be dealt with separately (Figs. 11.31, 11.45). Many of them belong to the group of multifocal spinal cord lesions and the remaining ones to the multicompartment AVMs, in particular those with single or multimetamere involvement of the nidus (Fig. 11.21).

Filum terminale arteriovenous shunts are usually of the mAVF type (Fig. 11.26, 11.48, p. 802; Fig. 11.49, p. 803); they are exclusively supplied by the anterior spinal artery and they cannot receive supply from the radicular arteries since the filum is not subsegmented and does not give rise to spinal nerves. Only through its attachment at S1–S2 can dural supply be seen coming from the midline and from the middle sacral artery in filum AVMs (Hsu et al. 2002). Any caudal SCAVM receiving contribution from the lateral sacral artery is either radicular in location or at the cauda equina level. Lesions of the conus or those that involve a nerve root will recruit from the radicular and pial or anterior spinal artery supply. Filum lesions can be managed by surgery, while the others are usually best treated with the endovascular technique.

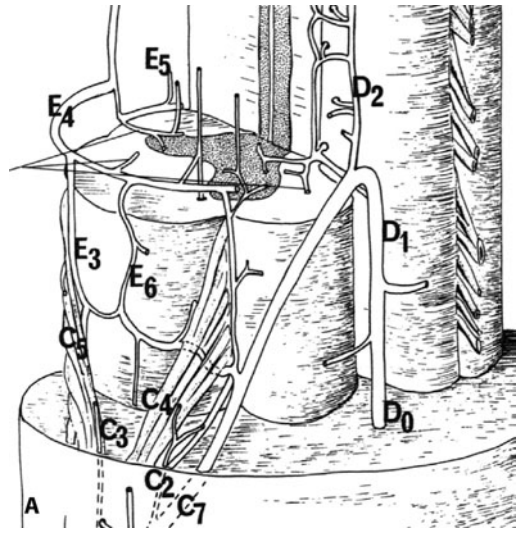

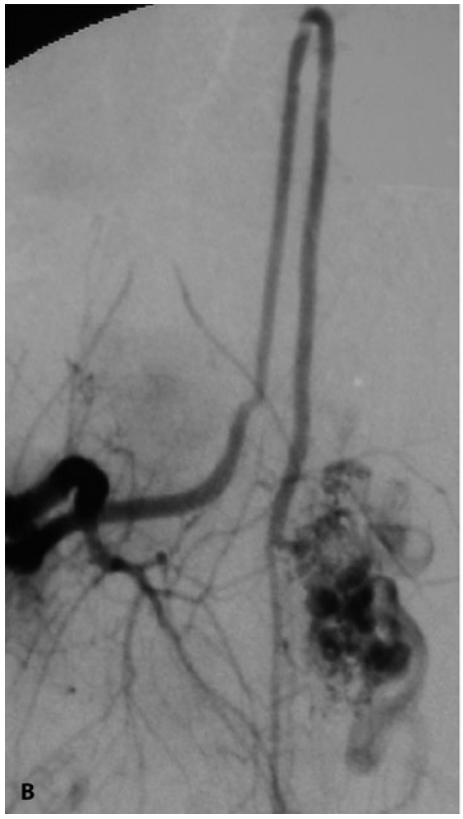

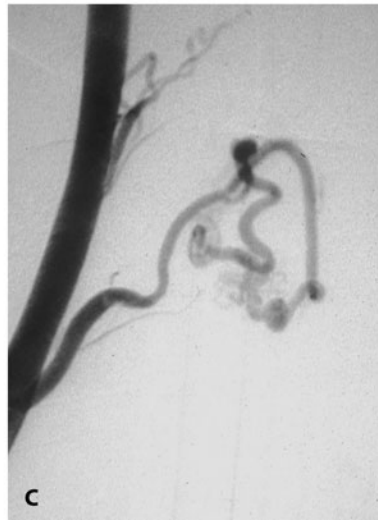

Fig. 11.44. Pial branches of the anterior spinal artery supplying the ventral funiculus (**A**), can (in two different patients) opacify a single (**B**) or two separate arteriovenous shunts (**C**)

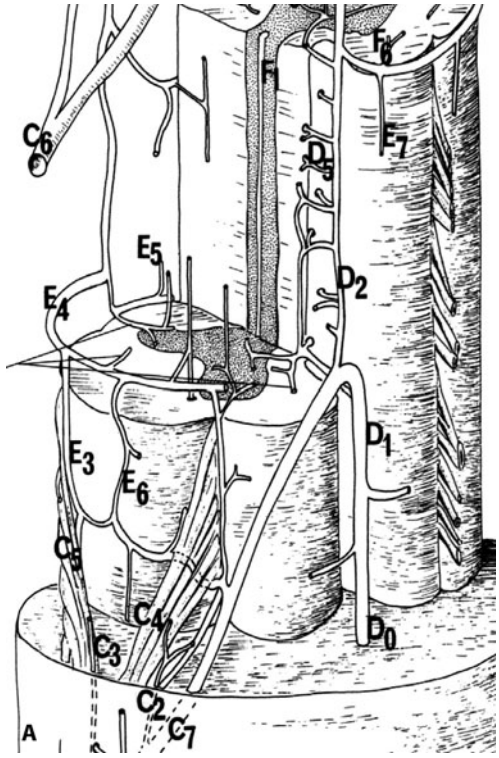

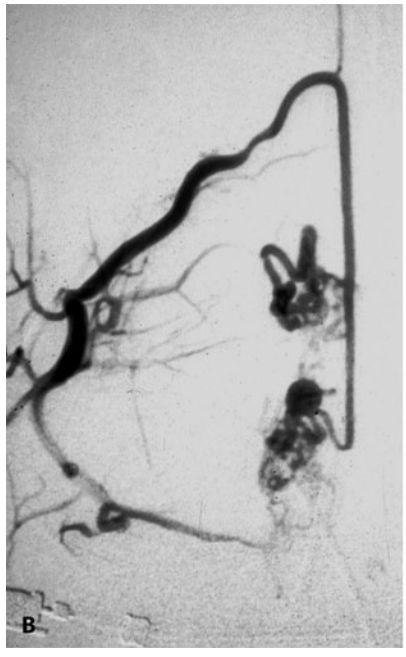

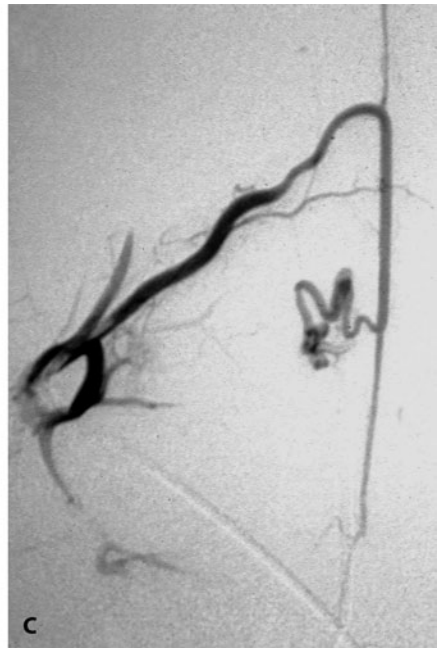

Fig. 11.45. Pial branches of the anterior spinal artery (**A**) supplying the ventral funiculus and two separate spinal cord arteriovenous malformations with acute rupture and false aneurysm (**B**). Follow-up angiogram after partial targeted NBCA embolization (**C**)

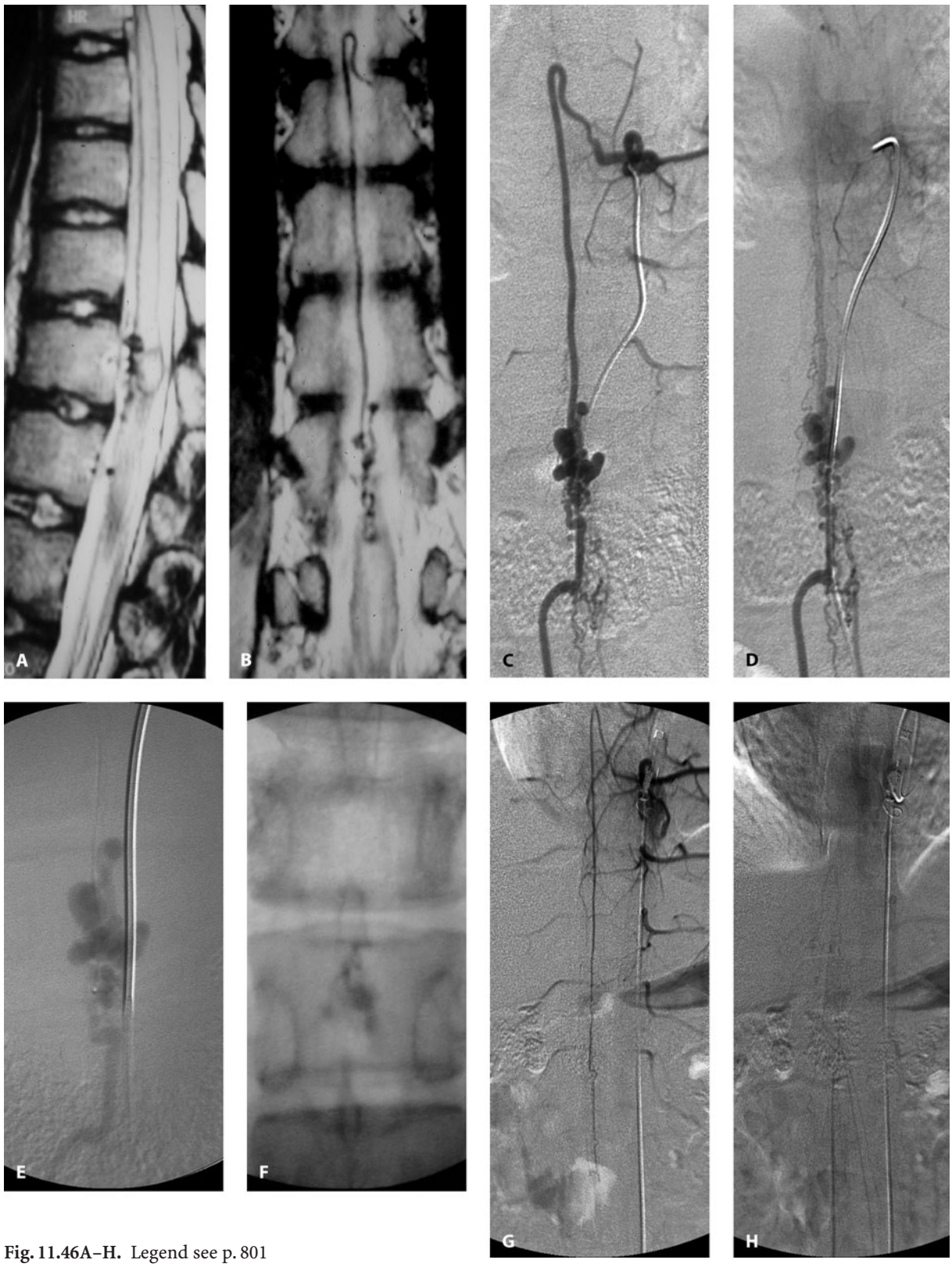

Fig. 11.46A–H. Legend see p. 801

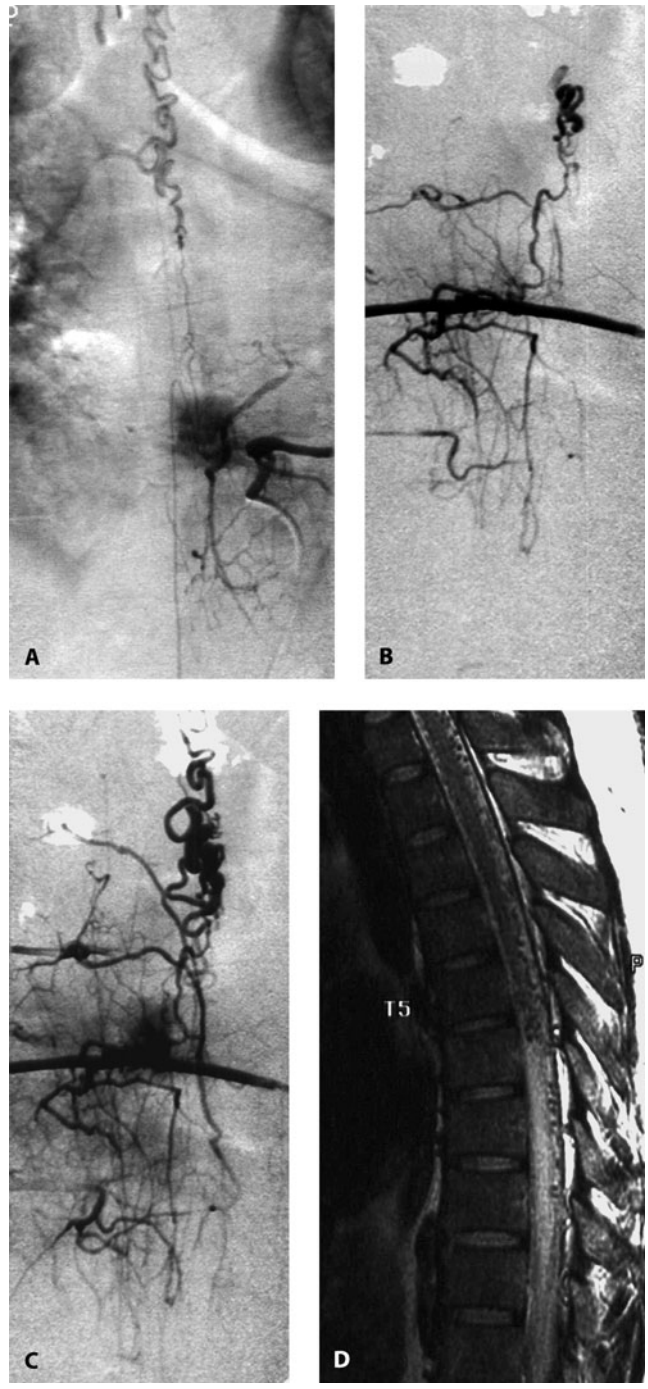

Fig. 11.47A–D. Dorsal superficial microarteriovenous fistulae with clinical and MRI findings simulating a spinal cord arteriovenous fistula

◄ **Fig. 11.46A–H.** Acute paraplegia with sensory level and sphincter dysfunction in a 15-year-old girl. MRI findings (**A, B**) could correspond to either a thrombosed pouch or hematomyelia. At angiography (**C, D**), a microarteriovenous fistula of the ventral spinal artery was demonstrated. Embolization was performed via the ventral spinal artery (**E, F**). Six-month follow-up angiogram (**G, H**) after NBCA embolization shows remodeling of the vessels. Complete clinical recovery occurred

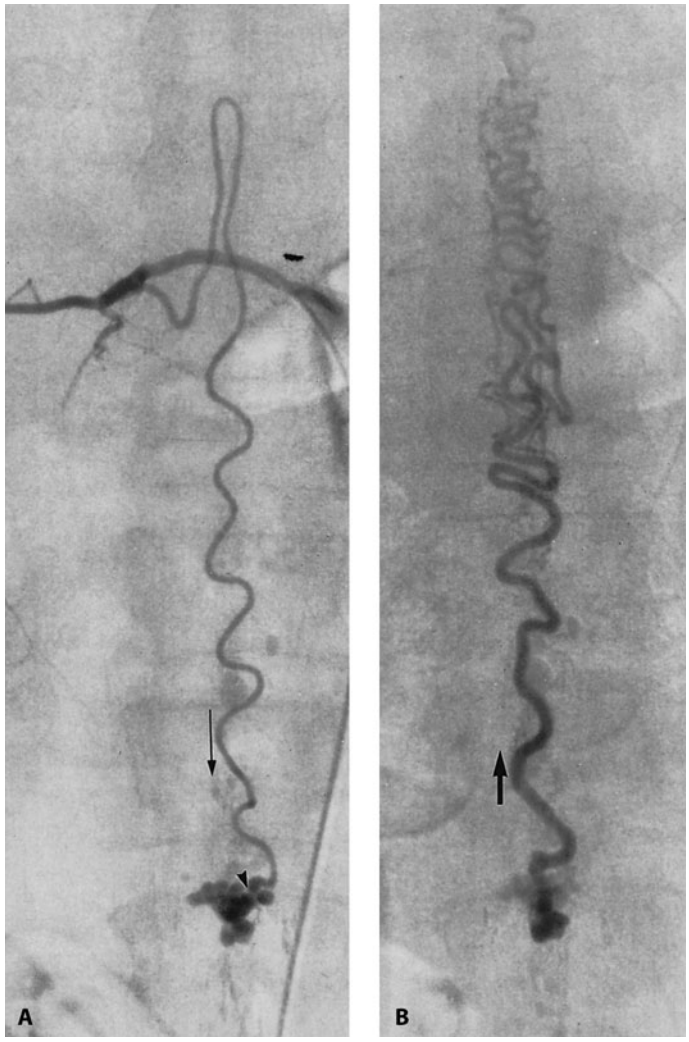

Fig. 11.48A, B. Arteriovenous fistula of the filum terminale supplied by the anterior spinal artery (*thin arrow*). **A** Arterial phase showing the site of fistulization (*arrowhead*). **B** Late phase shows the ascending venous drainage (*arrow*)

11.3.2.7 Veins

Various aspects of the venous drainage of SCAVMs have been mentioned previously. The relatively slow flow and the unique intrinsic venous network of the spinal cord make any attempt to fully explain and understand the pathophysiology of these lesions based on venous patterns alone unreliable. Congenital variations of the venodural junction and their tributaries are poorly understood and such variants are rarely described in the neuroradiological literature. The available radioanatomical data do not allow for an accurate correlation between the anatomy of the extraspinal venous system and the pathophysiology of certain spinal cord syndromes.

The venous drainage of some vascular malformations toward the intracranial circulation may be sufficient to produce signs and symptoms of a space-occupying lesion (Di Chiro and Doppman 1970) or result in signs and symptoms of intracranial pathology (Djinjian 1970b). This further supports the role of venous hypertension in the production of remote neurological symptoms or hemorrhage. Seen primarily in association

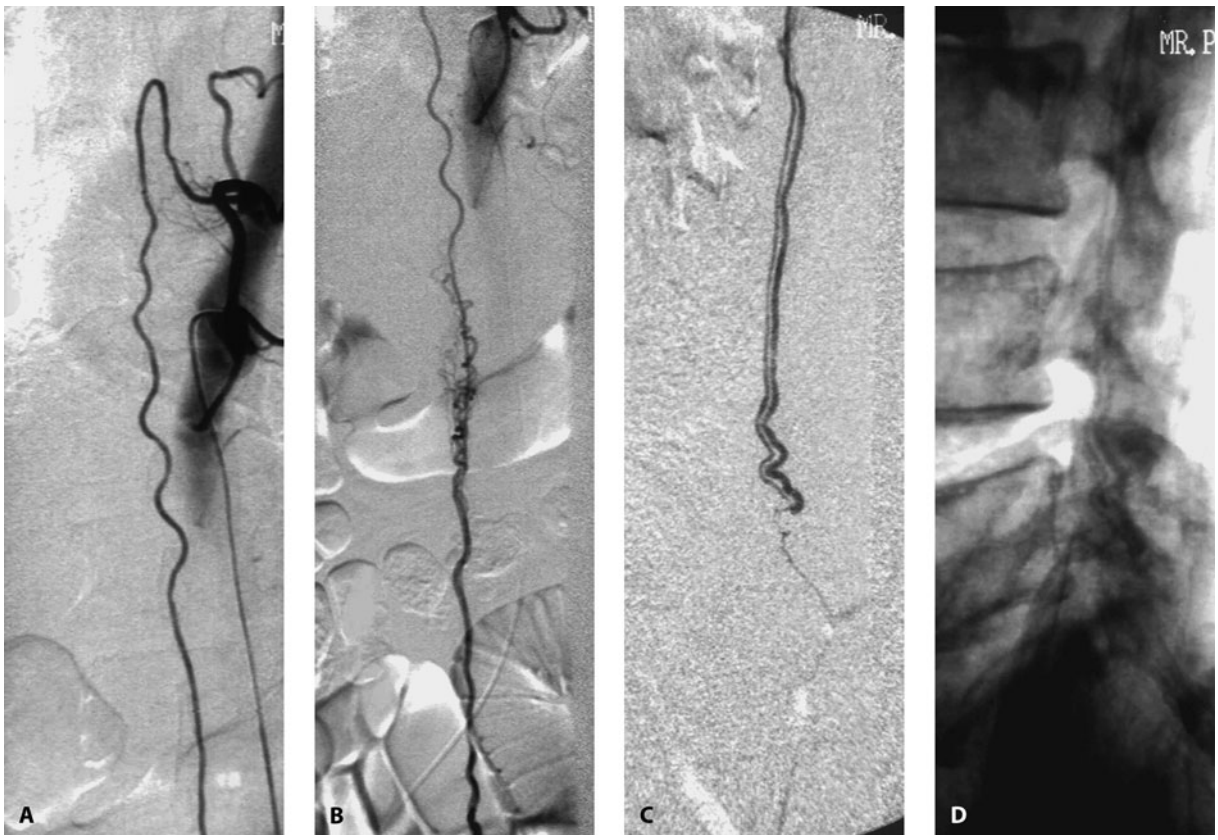

Fig. 11.49A–D. Typical filum terminale arteriovenous malformation with direct arteriovenous fistula. (Courtesy of S. Pongpech)

with cervical AVMs, such symptoms may include intracranial subarachnoid hemorrhage secondary to rupture of an intracranial vein at the level of the anatomical restriction or hemorrhagic venous infarction; they mostly occur in children (see Vol. 3).

The hemodynamics of SCAVMs evolve with time. The flow within the malformation, for example, can affect the drainage from adjacent areas of the CNS. Subsequent changes may be rheological in nature but may also produce structural changes in the vessel wall. Depending on the venous adaptations to such changes, thrombosis of the draining vein and/or venous ectasia may result. These changes may manifest themselves as hemorrhage, an acute thrombotic episode simulating an intraspinal hemorrhage, or may occur more chronically, mimicking a tumor. The diagnosis of such thrombotic changes was formerly made only during direct surgical intervention. CCT and/or MRI can show this occurrence for a preoperative diagnosis (Figs. 11.15, 11.46, 1.47, 11.50).

Occasionally patients benefit from the surgical removal of a large thrombosed sac (Cogen and Stein 1983). This applies mainly to high-flow fistulae in HHT1 patients and children (see Vol. 3).

Progressive thrombosis of the spinal cord veins mimicking SDAVFs can also be seen in true SCAVMs; however, spontaneous thrombosis of a SCAVM rarely occurs and is usually associated with transient worsening

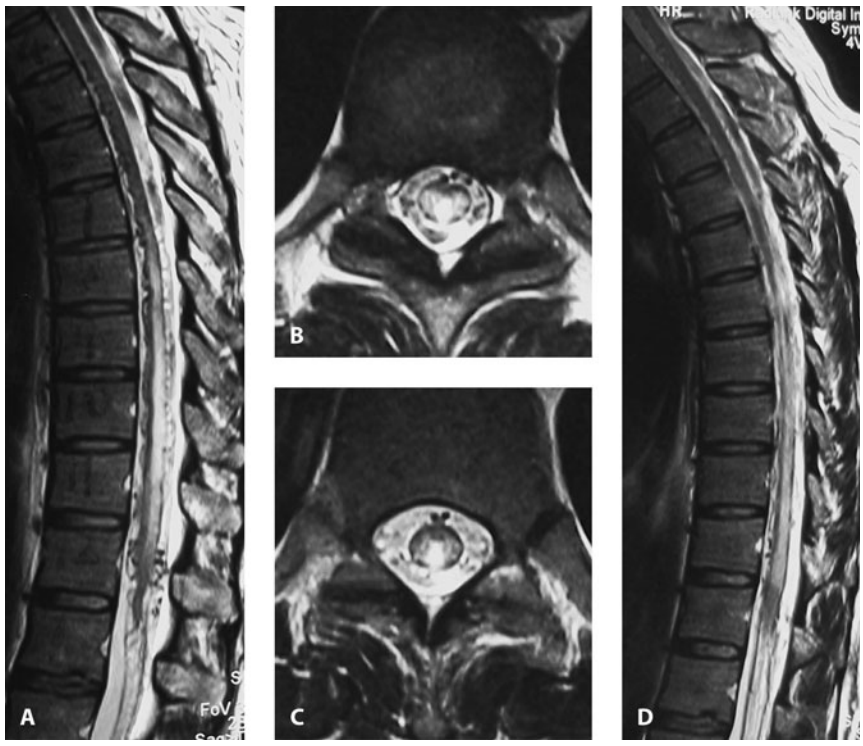

Fig. 11.50A–D. A 35-year-old male patient with rapidly progressive sensory-motor deficit of the lower limbs. Dorsal spinal cord increased signal in relation to a superficial retromedullary spinal cord arteriovenous malformation (SCAVM) located at the level of the conus medullaris (**A–D**). Symptoms and MR examinations are similar to those encountered in spinal dural arteriovenous shunt (SDAVS), yet the vascular flow void signals are much less apparent in this case of SCAVM than when associated with a SDAVS

of symptoms (Figs. 11.47, 11.50). Anticoagulation can be given to limit the extent of the thrombosis and favor remodeling.

One of our patients had progressive thrombosis of the spinal cord veins presenting 15 days after an initially successful embolization of a lumbar dorsal spinal cord arteriovenous fistula. The patient developed a progressive ascending myelopathy; repeat angiography was negative and the patient died several months later. In retrospect, this course of events might have been avoided by systemic heparinization following deterioration of a treated lesion with compromised venous return (Fig. 11.51).

Intraspinal hemorrhage as the cause of symptom aggravation must obviously be ruled out before starting anticoagulation therapy. It is also important to differentiate an AVM producing venous hypertension from the presence of progressive thrombosis, as the former will benefit from arteriovenous shunt occlusion but the latter will not. Prominent, descending, venous drainage in cervical or upper thoracic lesions, associated with scarce or absent opacification of the radicular venous exits, suggests the presence of significant venous outflow restriction and is an indication for postoperative use of systemic heparinization. Yet it is unlikely that venous infarction would lead to hemorrhagic conversion at the cord level (at least below the cervical spine) as it often does in the brain. The absence of hemorrhagic events with SDAVS testifies to this peculiar difference. Atrophy of the cord seems to be the result of chronic venous ischemia in adults, which it seldom produces in the adult brain.

Venous pouches, ectasias, and kinking are commonly observed in SCAVMs (Figs. 11.31, 11.38, 11.51).

Considering the little space available in the spinal canal, venous dilatation might be expected to mechanically compromise the cord (Kaufman

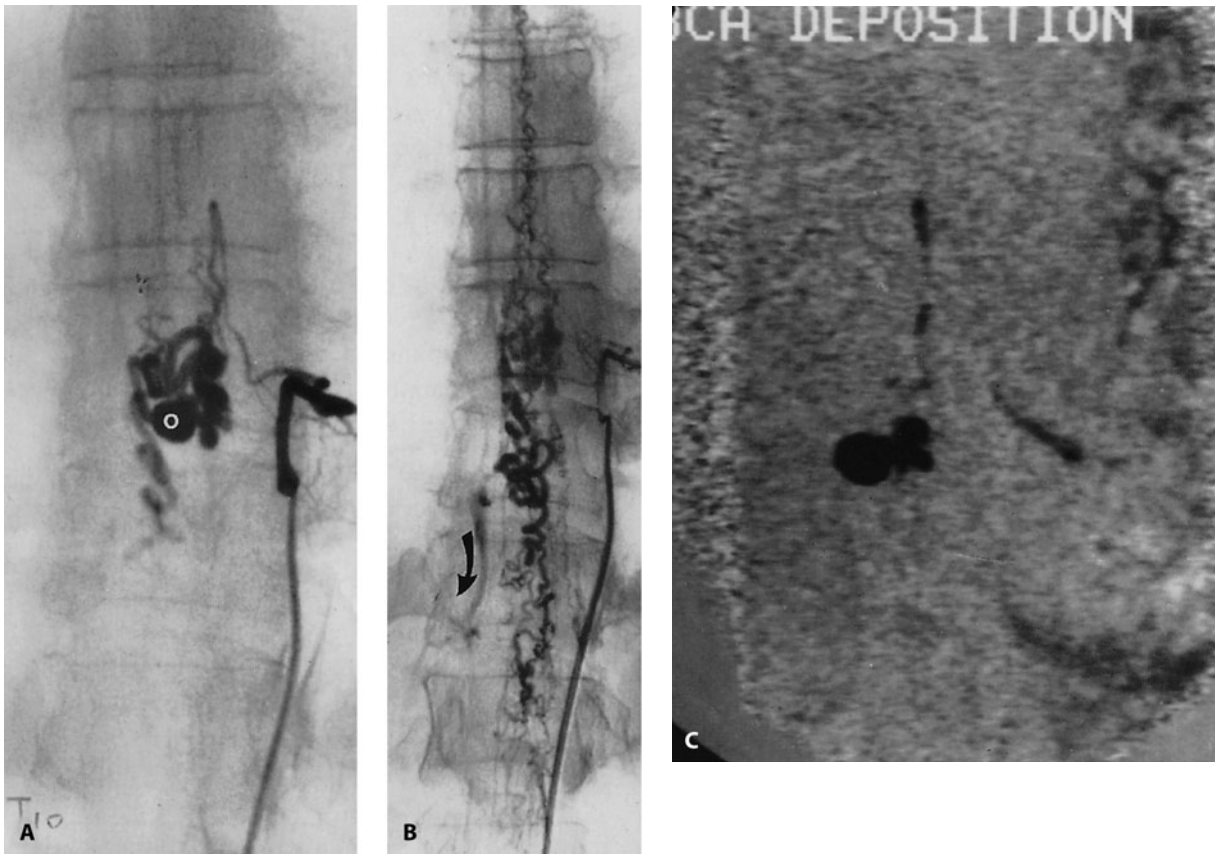

Fig. 11.51A–C. Posterolateral spinal arteriovenous fistula with venous outflow restriction. **A** Selective injection of the left T10 intercostal artery shows the dorsal radiculopial artery *on the right* feeding a fistula. There is aneurysmal dilatation of the veins (*white circle*). **B** Late phase of the same injection shows the marked venous congestion. Note the filling of the pial venous system with only one venous exit at T12 (*curved arrow*). **C** Digital subtraction angiography image of the IBCA injection with occlusion of the fistula and the venous aneurysm

et al. 1970). In our experience, there was seldom a direct anatomical relationship between these dilatations (usually in high-flow lesions) and the level at which the symptoms occur. In fact, dilatation appears to indicate increased flow while obstacles to drainage suggest the presence of retrograde congestion. Some of these ectasias may thrombose and mimic evidence of hematomyelia clinically and on MRI. Careful interpretation of all the available data, including angiography, will show the true intravascular nature of the clot. Most of these events will show abnormal MRI findings on T1, T2 and FLAIR sequences and are often best shown on coronal imaging of the spinal cord (Fig. 11.52).

Congestion of radicular veins is often seen at the low cervical level and accounts for most of the brachial nerve deficits encountered in this location (Figs. 11.41, 11.53). Radicular veins are usually patent in comparison to SDAVS, where occlusion of the radicular veins is part and may be the cause of the disease (see Chap. 12, this volume). However, fibrotic changes of these veins with age may decrease their capacity to absorb the arteriovenous flow.

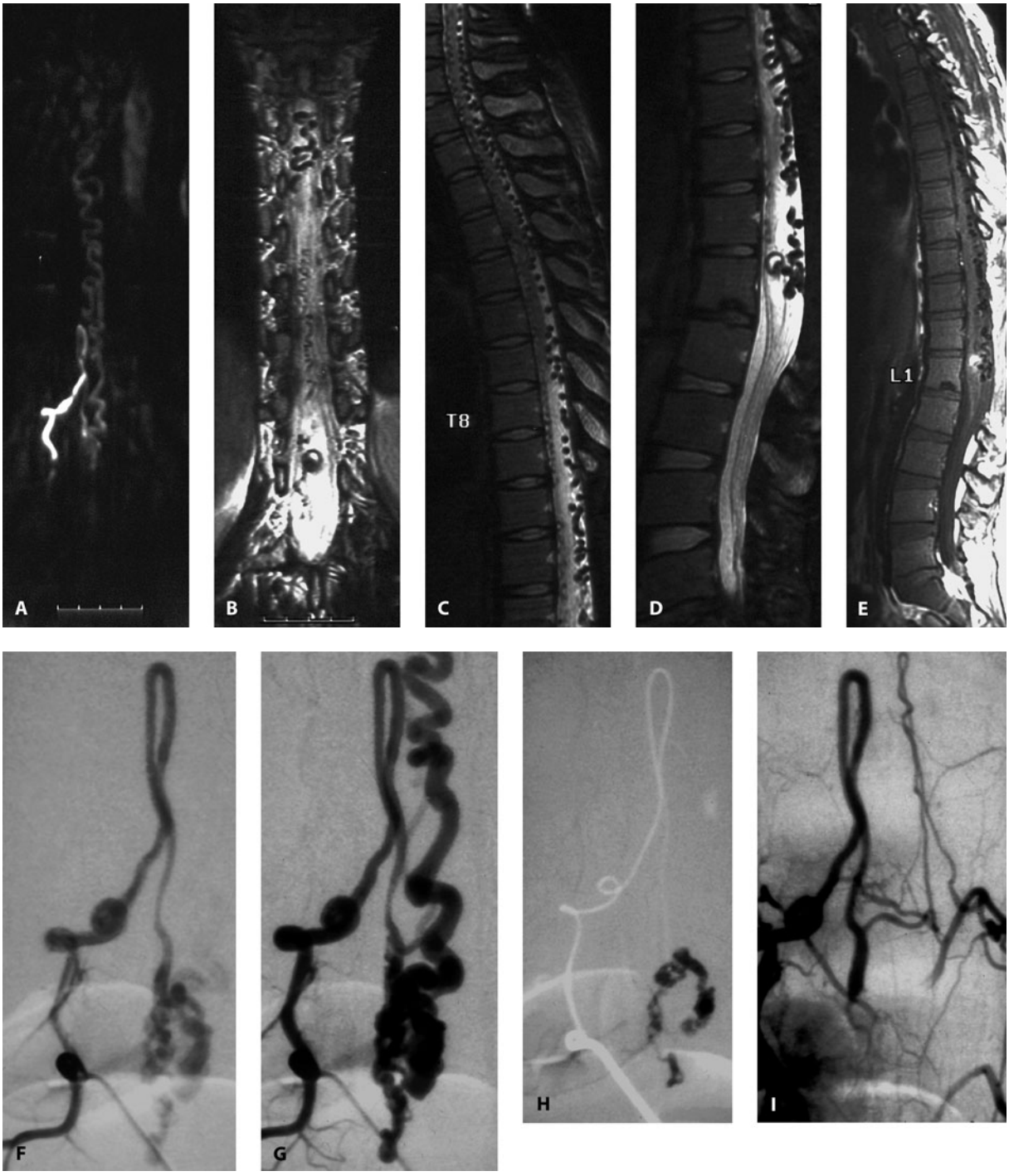

Fig. 11.52A–I. Acute onset of paraparesis in a 27-year-old female patient. Retromedullary spinal cord arteriovenous malformation located at the level of the conus. MRI/MRA shows a partly thrombosed venous pouch (**A–E**). Curative embolization with NBCA was achieved with subsequent complete clinical recovery (**F–I**). (Courtesy of S. Pongpech)

Fig. 11.53A–F. Progressive sensory motor deficit in a 32-year-old female patient. Pseudomultifocal lesions in relation to perispinal nerve venous network before (**A**, **B**) and 1 year after embolization (**C**–**F**), absence of venous congestion and normal venous phase to the cord. Complete clinical recovery. (Courtesy of S. Pongpech)

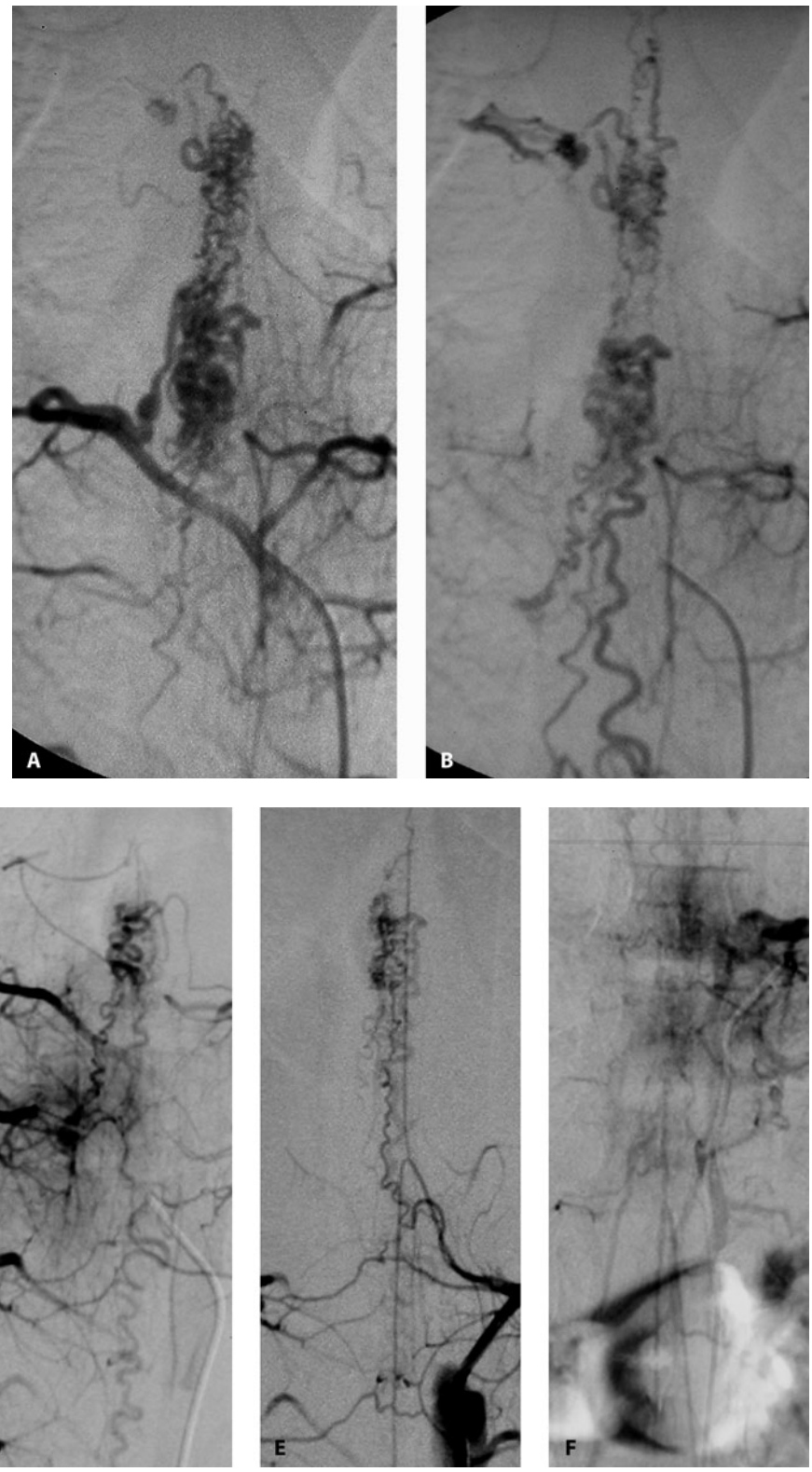

11.3.3 Pretherapeutic Evaluation

In the assessment of patients with SCAVM, pretherapeutic evaluation is divided into clinical assessment, noninvasive imaging modalities, and spinal angiography.

11.3.3.1 Clinical Assessment

A complete clinical history and physical examination is essential in the assessment of patients with suspected vascular disorders of the spinal cord. The neurological status needs to be accurately determined and will often need to be repeated in time to objectively establish stability or worsening of the neurological status.

Pretherapeutic evaluation is then carried out and is indicated in all patients, even those with incidentally discovered vascular malformations or those with permanent neurological deficits. Complete evaluation includes both noninvasive imaging techniques and angiographic examinations.

11.3.3.2 Noninvasive Imaging Modalities

CT scanning and myelography no longer have a significant role in the initial screening of suspected SCAVM, and plain films are usually of very limited interest. Plain CT with bone windows may demonstrate vertebral body erosion and assist in determining whether the lesion originates from the spinal canal or from the vertebral body (Figs. 11.7, 11.10, 11.11). Foramen enlargement may also suggest the presence of dilated venous structures compressing exiting nerve roots in patients with symptoms of radiculopathy.

The great majority of patients referred for investigation of vascular pathology of the spinal cord require an MRI scan. Since the early reports by Doppman et al. (1987) and Dormont et al. (1987), MRI has become the modality of choice in the preliminary assessment of patients harboring SCAVMs or SCAVFs. T2-weighted images may be more useful for smaller slow-flow lesions (Figs. 11.47, 11.50). Axial cuts show areas of low signal intensity in the center of the cord, which in a more T2-weighted study become high signal. These findings can be seen at multiple levels associated with cord atrophy.

In patients with SCAVMs, MRI may be of great assistance in delineating intramedullary pathologies such as bleeding within the spinal cord, intravascular thrombosis, intramedullary cavities, or atrophy (Figs. 11.27, 11.52). MRI can also assist in demonstrating extraspinal extension of the SAMS (Fig. 11.9). Changes at a distance from the malformation may be present (Fig. 11.27) and may explain otherwise confusing neurological symptoms. MRI can supplement information obtained by other modalities but has significant limitations. It still remains limited in its ability to accurately locate the site of arteriovenous communication (Fig. 11.18), the nidus of a lesion, its intramedullary relationship, or its venous drainage (Figs. 11.46, 11.50, 11.52).

It is important to understand the pitfalls of this technique in the assessment of patients with vascular lesions of the spinal cord. These primarily relate to CSF pulsation artifacts that may produce images highly suggestive of spinal cord vascular lesions (Levy et al. 1988). This is of particular importance in pediatric patients in whom such artifacts may lead to unnecessary angiographic exploration. On the other hand, if the study is negative or inconclusive and if the diagnosis is compatible with venous congestion from a small AVS draining into the ventral spinal cord vein angiography should be done (Lasjaunias et al. 2001). For treatment planning, spinal angiography still remains the study of choice.

11.3.3.3 Angiography

Angiography remains the gold standard in the diagnosis and treatment planning of vascular lesions of the spine and spinal cord. Spinal angiography is done under general anesthesia with controlled respiration. Neuroleptic drugs are used only if SEP monitoring is done (Berenstein et al. 1984b). An indwelling catheter in the urinary bladder is important for patient comfort, accurate fluid monitoring, and to obtain adequate vessel visualization, primarily when studying the sacral and lumbar areas. Three-dimensional pictures have been used in this pathology and may be of assistance in determining the relationship of the AVS to the bony and dural structures in SDAVFs (see Chap. 12, this volume) or in SCAVMs in demonstrating their location on the surface or within the spinal cord (Figs. 7.120, 7.121, 11.33, 11.34, 11.40). Spinal angiography is performed using different protocols at different institutions and may be guided by MRI. However, as in any other vascular study, a territorial approach must be undertaken. As a rule, the angiographic investigation must show both the pathology and the surrounding normal tissue (impact of the pathology on the environment) to insure that the entire disease process has been properly studied.

Catheterization of the various lumbar, intercostal, and/or brachiocephalic pedicles is done in an orderly fashion. Preliminary radiographic examinations may be done with radiopaque markers placed in the skin of the back for identification of levels. Digital subtraction angiography (DSA) is performed to provide the best possible spatial resolution when a radiculopial or radiculomedullary artery is seen at fluoroscopy. Spinal angiography requires the visualization of vessels in the 150–700 μm range. Furthermore, proper spinal cord angiography requires the visualization of spinal cord veins. Therefore, in contrast to global injections, only selective injections will meet these criteria for proper vessel visualization. A variety of catheter configurations have been suggested for spinal angiography: probably the most important technical recommendation is to become familiar with one type of catheter in order to ensure consistency (see Chap. 14, this volume). In screening SCAVMs, the catheterization of the segmental artery (intercostal, lumbar, or sacral) should be achieved as close as possible of the origin of the dorsospinal division to avoid bony opacification and superposition or reflux in the aorta. On some occasions, catheterization of the ostia may be very difficult via the femoral route, and

an axillary approach may be necessary. This is an important consideration if very distal catheterization is needed for endovascular treatment in the older population, especially if the anatomy is tortuous and difficult. For subselective catheterization, primarily for endovascular treatment or provocative testing, the use of coaxial systems with variable stiffness microcatheter assembly systems is necessary. In high-flow vascular lesions, if the malformation involves the spinal cord or extramedullary space, supply is usually from medullary arteries. Therefore, the potential supply to the SCAVM must be studied based on the information derived from the MRI. Exhaustive study of all 62 potential sources of supply to the cord are most of the time unnecessary.

As in all other anatomical areas, the angiographic examination must outline the normal vasculature around the vascular pathology to ensure that the full extent of the lesion is visualized and the effect of the lesion on the remainder of the spinal cord is understood, and in order to properly plan and monitor treatment. We strongly recommend selective angiography for this approach. In spinal angiography, the frontal view should be performed first. In most instances, this will suffice to determine the nature of a feeding vessel and to discern whether it belongs to the anterior or posterior spinal complex (see Vol. 1). The mass effect that displaces the spinal arteries may give a false impression of a midline or paramedian location. A lateral projection may be very useful in case of doubt or a complex mass effect with cord rotation from the lesion. Three-dimensional reconstructions at the cervical level may give eloquent pictures that can help with difficult anatomical situations (Fig. 11.34). In SCAVMs in general and in SCAVFs in particular, one can often reflux the contrast material through the lesion to opacify the various contributions from above or below the level of injection (Fig. 14.130). This may be important information to plan both the best route to reach the lesion and an alternative route to either maximize the effect, redistribute blood flow, or control the result of embolization. Visualization of the various contributions to the anterior and pial spinal axes can also be evaluated with superselective studies (Figs. 11.29, 11.31) (Berenstein et al. 1984b; Theron et al. 1986). The complications of spinal angiography are primarily related to ischemic insults affecting the spinal cord. Such events may be related to either the accidental introduction of air or blood clot.

11.4 Spinal Cord Hemodynamics

Palleske cited by Jellinger (1972) compared blood flow in the brain with that of the spinal cord. He demonstrated that in both physiological and pathological conditions, the spinal and cerebral circulations react in a similar way. Most vasoactive substances, when used in physiological conditions, caused only brief changes in the circulation or had no effect whatsoever. The same was true of anesthetics. Papaverine and its derivatives were found to cause a considerable increase in both cerebral and spinal cord blood flow.

Epinephrine consistently caused a reduction in blood flow. These findings suggest that the reaction of the spinal cord and brain vasculature to

vasoactive substances is the same. In physiological conditions, compensation for induced circulation alterations is rapidly achieved by autoregulatory mechanisms similar in both brain and spinal cord. In pathological conditions, for example, experimental cord edema or spinal cord compression, the autoregulation of spinal cord hemodynamics fails, is disturbed, or even abolished. As autoregulation fails, blood flow depends mainly on the systemic circulation rate, blood pressure, and changes in tissue pressure. Crawford et al. (1980) demonstrated that the response of feline pial arterioles to norepinephrine confirmed the presence of noradrenergic receptors on smooth muscle. He noted that sympathetic control of blood flow in the brain applied also to the spinal cord and could be blocked by phentolamine. Hickey et al. (1986) demonstrated the similarities between brain and spinal cord vascular dynamics in the rat. Autoregulation curves for brain and spinal cord were identical, with an autoregulatory range of 60–112 mmHg perfusion pressure. The use of vasoactive drugs, in an attempt to influence blood flow in the spinal cord, appears unlikely to be successful. Hypocapnia and epinephrine induce a certain increase in circulation in the damaged tissue secondary to a rise in vascular resistance in the healthy tissue, while vascular resistance in the damaged tissue remains unchanged.

Disturbances in venous drainage may also significantly decrease tissue perfusion, as is the case in SDAVFs. Decreased venous pressure is also noted during compression of the spinal cord by space-occupying lesions that produce regulatory disturbances in the venous system. Slow progressive compression can impair the venous circulation, causing decreased tissue perfusion. The experimental data suggest that, to improve spinal cord circulation, one needs to influence the total circulation of the cord and its surrounding vascular territories by removing the initiating mechanism of compression or edema in any pathological condition.

Apnea or increased intrathoracic pressure will impair venous drainage of the large epidural venous plexus system, resulting in a reduction in the difference in the arteriovenous gradient within the spinal cord. The venous portion of the vascular system is hemodynamically of greater significance for the spinal cord than for the cerebral circulation. This can be explained by the contra-gravity venous drainage of the spinal cord (below the heart level) as compared to that of the cerebral circulation.

11.4.1 Particular Forms of Spinal Cord Arteriovenous Malformations

11.4.1.1 Spinal Cord Intradural Arteriovenous Fistulae

Within the group of lesions recognized as SCAVMs, there is a specific group of direct arteriovenous fistulae (AVFs), which are supplied by the ventral spinal artery and/or dorsal spinal arteries without an intervening nidus. Although these lesions have been reported to be in the cord itself, in our experience they are subpial when ventral and directly fed by the anterior spinal artery, and they are subarachnoid in location when they are fed by pial (posterior spinal) arteries (Heros 1986; Gueguen et al. 1987). These SCAVFs make up close to 20% of all SCAVMs (Table 11.4). There is

no gross gender difference. The age at onset of symptoms ranges from birth to 24 years of age, with a predominance in the second decade of life (Gueguen et al. 1987). SCAVFs were later classified and subclassified into different groups according to their own architecture (Merland et al. 1992; Mourier et al. 1993; Barrow 1994; Marsh 1999; Spetzler et al. 2002).

Ectasia of the vein usually marks the transition point between artery and vein (Figs. 11.33, 11.40). The presentation of SCAVFs is most frequent in children and characterized by an acute onset, devastating neurological deficits, and poor prognosis if untreated, similar to what is seen in patients with SCAVMs (see Vol. 3). When a SCAVF presents in childhood there is a high association with HHT1. However, none of our adult SCAVF patients had HHT and none of our HHT cases had multifocal lesions involving the cord.

In the SCAVF population, two groups could be distinguished. The largest group of lesions (75%) corresponded to what can be described as micro-AVFs (mAVFs) with one (or more) slightly enlarged arteries feeding a shunt draining directly into congested pial veins. The other group of lesions are giant or macro-AVFs (MAVFs). One-third of the SCAVFs are diagnosed in the pediatric population (almost all MAVFs) and two-thirds occur in adults.

Micro-AVFs

Micro-AVFs (mAVFs) account for 90% of all adult SCAVFs. Of these, 10% were located in the cervical cord, 50% were found along the thoracic cord, and 40% in the lumbar region (two-thirds at the filum terminale).

The cervical lesions present with progressive sensory deficits. Thoracic mAVFs are revealed mostly by hemorrhage (54%), two-thirds of these with hematomyelia and one-third with subarachnoid hemorrhage. Progressive myelopathy was described in the other cases (46%). Conus mAVFs all manifested by progressive myelopathy. None of the filum terminale mAVFs bled: 80% presented with progressive symptoms and 20% with acute nonhemorrhagic paraplegia.

Macro-AVFs

Macro-AVFs (MAVFs) account for 10% of all SCAVFs. They are located either at the cervical or the lumber level. They presented with progressive motor and sensory disorders (including pain), but not hemorrhage as the initial symptom. Overall hemorrhage during the course of the disease is seen in 27% of the adults (Nimii et al. 2000; Rodesch et al. 2002).

In both series, transarterial embolization was the preferred treatment method, and in none of the MAVFs was the surgical option felt to be appropriate. In these series, 88% were actually embolized MAVFs and 71% were cured, while in the 29% the lesion was obliterated by more than 75%. None of these treated patients worsened after endovascular therapy. All improved significantly and 71% became neurologically normal.

We have not observed a mAVF increase in size to become a MAVF, nor have we seen a MAVF spontaneously thrombosed or regressed to become a mAVF unless it had been embolized. It is likely that both types of lesions

are different entities and behave differently in adults and children. Some lesions initially considered as intramedullary-type AVMs are simple mAVFs that reflux deeply into the ventral spinal or intrinsic veins and create a pseudonidus appearance. Postischemic, posthemorrhagic, or postthrombotic angiogenesis may complicate the architecture of the shunt further. Targeted embolization toward the AVS transition area leads to complete exclusion of the lesion, with relief of the venous congestion and clinical improvement.

The surgical experience in spinal cord vascular lesions, in particular in SCAVFs, has shown that finding the fistula site embedded between congested veins was particularly challenging, and that surgical eradication of the shunt was therefore associated with high morbidity (Mourier et al. 1993; Touho et al. 1995). Surgery should be considered each time embolization appears to be associated with higher risk or is deemed to be technically unfeasible because of small feeders or tortuous long arteries far from the shunt such as in filum terminale lesions.

Among the mAVFS, 46% were embolized during the first procedure. In 22% transient complications occurred but resolved spontaneously in a short time. None of the embolized patients permanently worsened and none of them bled or rebled after embolization. The follow-up period between the first consultation and the last consultation, or information after treatment obtained, ranges between 1 and 13 years (mean, 64 months). Because of anticipated technical difficulties with the endovascular approach, 40% of mAVFs were operated on (100% of filum terminale lesions). No deaths occurred in either group (Nimii and Berenstein 1999; Rodesch et al. 2002).

To obtain lasting effects, embolization must be performed with a stable embolic agent: glue is the most appropriate material. Previous reports using other embolic materials such as balloons (Riche et al. 1983; Ricolfi et al. 1997) or particles (Biondi et al. 1990; Hida 1999; Touho et al. 1995; Mourier et al. 1993) are less appropriate, with a higher rate of clinical complications or recanalization. Particles can sometimes be used in small slow-flow AVMs in order to complete the thrombosis (Nimii et al. 2000) and detachable coils may be useful in selected AVF cases (see Chap. 14, this volume).

Retrograde thrombosis of spinal cord arteries has been reported after surgery (Heros 1986), and most of the time heparin was not needed. Anticoagulation has been used in a few cases of mAVF that were associated with severe congestion of the pial venous plexuses along the cord, with no evidence of radicular venous outlets. Patients are usually managed by elevating the head of the bed to allow gravity to assist in decreasing the intradural venous pressure. Heparin was never required after embolization of MAVFs.

11.4.1.2 Spinal Arteriovenous Metameric Syndromes

The term "spinal arteriovenous metameric syndromes" (SAMS) is reserved for vascular malformations that extend beyond the ectodermal tissues and can involve the spinal cord, bony structures, paraspinal muscu-

lature, subcutaneous tissues, and skin in the same segment. SAMS lesions involve structures derived from two or more embryonic layers. One can describe 31 pairs of SAMSs depending on the segment involved. The name derives from the cerebral-facial arteriovenous metameric syndromes (CAMS) described by Bhattacharya et al. (2001). SAMSs are a spectrum that theoretically can affect all derivatives of a single segment. Most often it is incompletely expressed. The anatomical variations derived from the various embryological origins of each segment do not always clearly define the exact boundaries, similar to what is seen in cerebral-facial venous metameric syndromes (SVMS) when pertaining the Sturge–Weber syndrome. SAMSs correspond in part to what was previously described as Cobb syndrome. The term "Cobb syndrome" comes from the triad of skin, bone, and spinal cord involvement, also called cutaneous vertebral medullary angiomatosis (Djindjian et al. 1971a, b; Pia 1978; Serze et al. 1966; Kissel and Dureux 1972).

The presence of a skin vascular malformation, although suggestive of spinal cord myelomere involvement, may also be a separate dysplastic skin lesion (Djindjian 1976, 1969; Rosenblum et al. 1987; Doppman et al. 1968a). Involvement of all layers was seen in two patients with metameric lesions in Djindjian's series, constituting 2% of all his SCAVM patients or 17% of the 12 with metameric lesions. In Doppman's original 28 patients, in addition to the six (21%) with metameric cutaneous lesions, five patients (18%) had cutaneous vascular malformations that were not metameric, and two had vascular malformations at other locations (Table 11.6). Some cutaneous vascular lesions may be prominent venous drainage of a larger deep malformation. Such lesions often change in appearance with changes in intra-abdominal pressure such as those caused by the Valsalva maneuver (Doppman et al. 1968a, b), which, when performed, may assist in recognition.

SAMS lesions may be clinically apparent from the cutaneous vascular malformation. This usually is of the capillary or arterial type and frequently has fistulization and high-flow characteristics; therefore a bruit is often present.

The frequency of multiple lesions was found to be as high as 19% of SCAVMs in Matsumaru's series (Tables 11.4, 11.5), which included adults

Table 11.5. Incidence of SDAVFs, SCAVMs[a], and metameric AVMs in 296 patients (1990)

Series	SDAVFs	SCAVMs[a]	Metameric AVMs	Total
Djindjian (1978)	46	74	10	130
Rosenblum et al. (1987b)	27	51	3	81
Berenstein and Lasjaunias (1992)	31	50	4	85
Total	104 (35%)	175 (59%)	17 (6%)	296 (100%)

SDAVF, spinal dural arteriovenous fistula; SCAVM, spinal cord arteriovenous malformation; SCAVF, spinal cord arteriovenous fistula; AVM, arteriovenous malformation.

[a] Includes SCAVMs and SCAVFs.

and children. The age at referral ranged from 11 months to 44 years, with a mean age of 21 years. There was a 2:1 male-to-female ratio. Lesions were equally located in the cervical, thoracic, and lumbar or conus medullaris regions.

The associated lesions included vertebral vascular malformations (Fig. 11.54), cutaneous (Fig. 11.55), limbs (Fig. 11.22), radicular AVMs (Figs. 11.18, 11.25, 11.56), bifocal SCAVMs (Fig. 11.7), and bifocal metameric cord lesion associated with vertebral and limb localization (Fig. 11.21). Various "syndrome associations" are noted as Klippel–Trénaunay (Fig. 11.22) and Parkes–Weber (Fig. 11.21).

In our recent SCAVMs series, the incidence of multiple vascular lesions was higher than a few years ago, in particular the multifocal intradural ones (Meisel 1995). Metameric distribution was the most frequent type of multiplicity. Identification of the myelomere level involved in SCAVM makes it possible to discuss segmental links between various lesions.

Multifocal SCAVMs are exceptional compared to multifocal cerebral AVMs (see Chap. 9, this volume). Willinsky (1990) reported that 18 (9%) patients among 203 cases of cerebral vascular lesions could be included in the multiple BAVM category. The number of multifocal intradural SCAVMs that do not correspond to multimyelomere lesions (multi-SAMS) is extremely low. Theoretically, HHT1 could be one of the disorders to be suspected; however, none of our patients with multifocal SCAVM presented with other findings of HHT or a family history favoring the diagnosis of HHT1. In the pediatric population, Iizuka et al. reported that 20% of SCAVMs to be multiple. In our series, 25% of patients were under the age of 15.

Benhaiem-Sigaux et al. (1985) explained the association of the Klippel–Trénaunay syndrome and the SCAVM on a developmental basis. In fact, the segmented mesodermic origin of the endothelial cells establishes the topographic link between these segmentally related targets.

The association of SCAVM and radicular AVMs is rare and potentially metameric if the myelomere involved with the SCAVM corresponds to that of the nerve involved. In this situation, the radiculomedullary or radiculopial arteries supply the SCAVMs directly (as soon as they reach the cord surface), nourishing the radicular AVM (Fig. 11.57, p. 818; Fig. 11.58, p. 819). In other situations, the SCAVM nidus extends over several myelomere levels, allowing for different sources of supply for each lesion (Fig. 11.18).

In cases with cervical spinal cord and cervical nerve involvement, the role played by the vertebral and cervical arteries has to be carefully analyzed (Figs. 11.25, 11.56, 11.59, p. 820) to identify the associated lesions. False multifocal lesions can be diagnosed when an intradural radicular venous rete is seen in the vicinity of their transdural course (Fig. 11.41, 11.53). However, MRI often fails to demonstrate the myelomere level, the associated radicular lesions, or the SCAVM multifocality. The absence of dural involvement is remarkable and must be related to the absence of dural sinuses at the spinal level.

It is of particular importance to properly delineate the arterial supply and extent of the extraspinal and cutaneous lesions in relation to the SCAVM. Such anatomical information is essential for localization and, more importantly, for planning treatment.

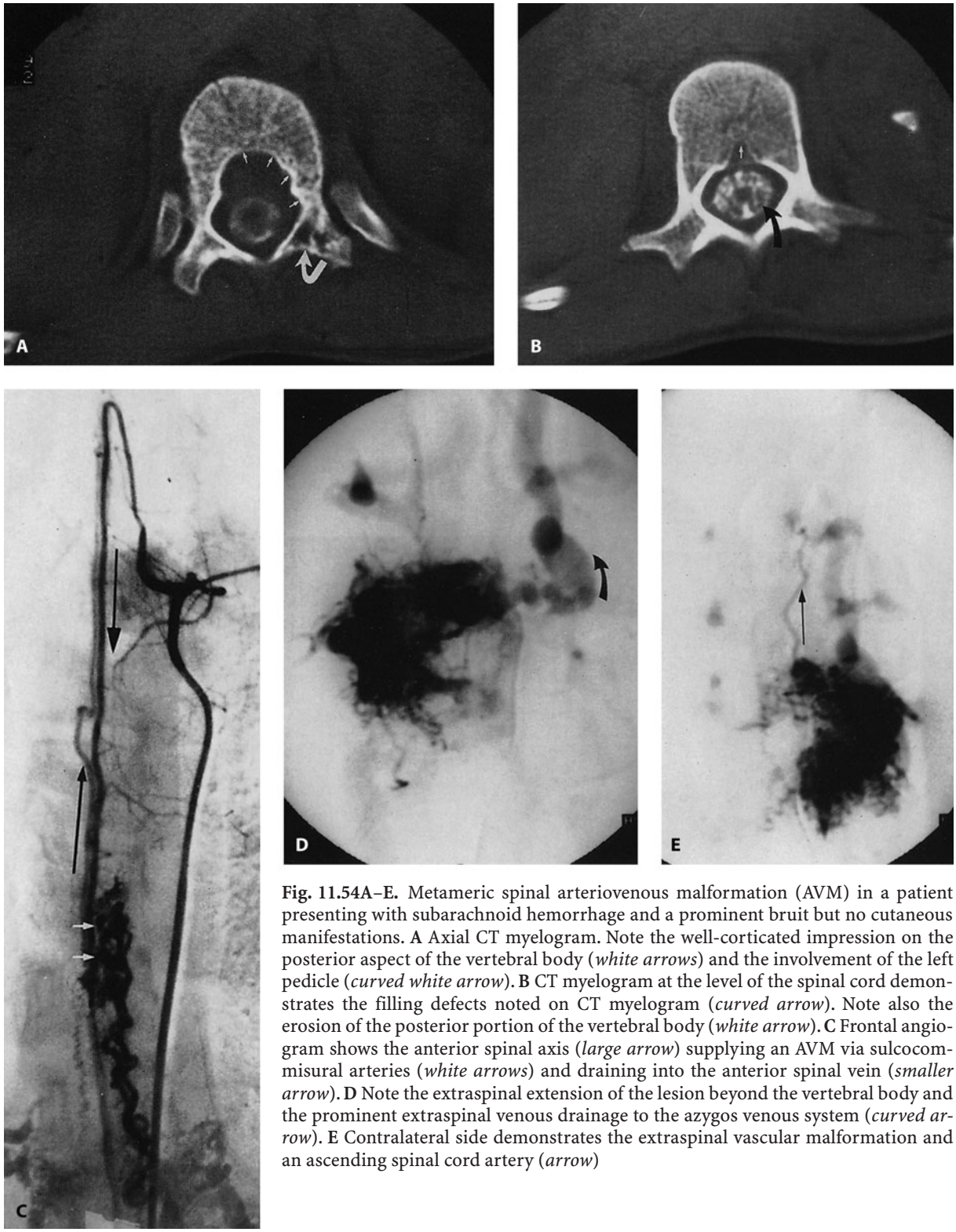

Fig. 11.54A–E. Metameric spinal arteriovenous malformation (AVM) in a patient presenting with subarachnoid hemorrhage and a prominent bruit but no cutaneous manifestations. **A** Axial CT myelogram. Note the well-corticated impression on the posterior aspect of the vertebral body (*white arrows*) and the involvement of the left pedicle (*curved white arrow*). **B** CT myelogram at the level of the spinal cord demonstrates the filling defects noted on CT myelogram (*curved arrow*). Note also the erosion of the posterior portion of the vertebral body (*white arrow*). **C** Frontal angiogram shows the anterior spinal axis (*large arrow*) supplying an AVM via sulcocommisural arteries (*white arrows*) and draining into the anterior spinal vein (*smaller arrow*). **D** Note the extraspinal extension of the lesion beyond the vertebral body and the prominent extraspinal venous drainage to the azygos venous system (*curved arrow*). **E** Contralateral side demonstrates the extraspinal vascular malformation and an ascending spinal cord artery (*arrow*)

Fig. 11.55. Skin discoloration in a case of thoracic spinal metameric arteriovenous syndrome

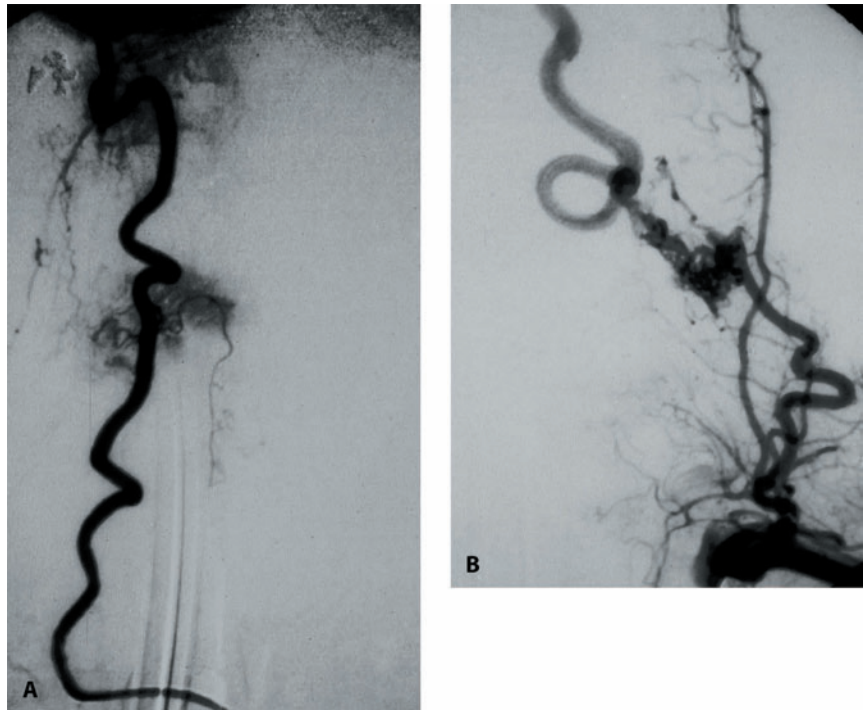

Fig. 11.56A, B. Spinal arteriovenous metameric syndrome 5/6. **A** Involvement of the C5 vertebra and C6 nerve root (**B**). (Courtesy of R. Piske)

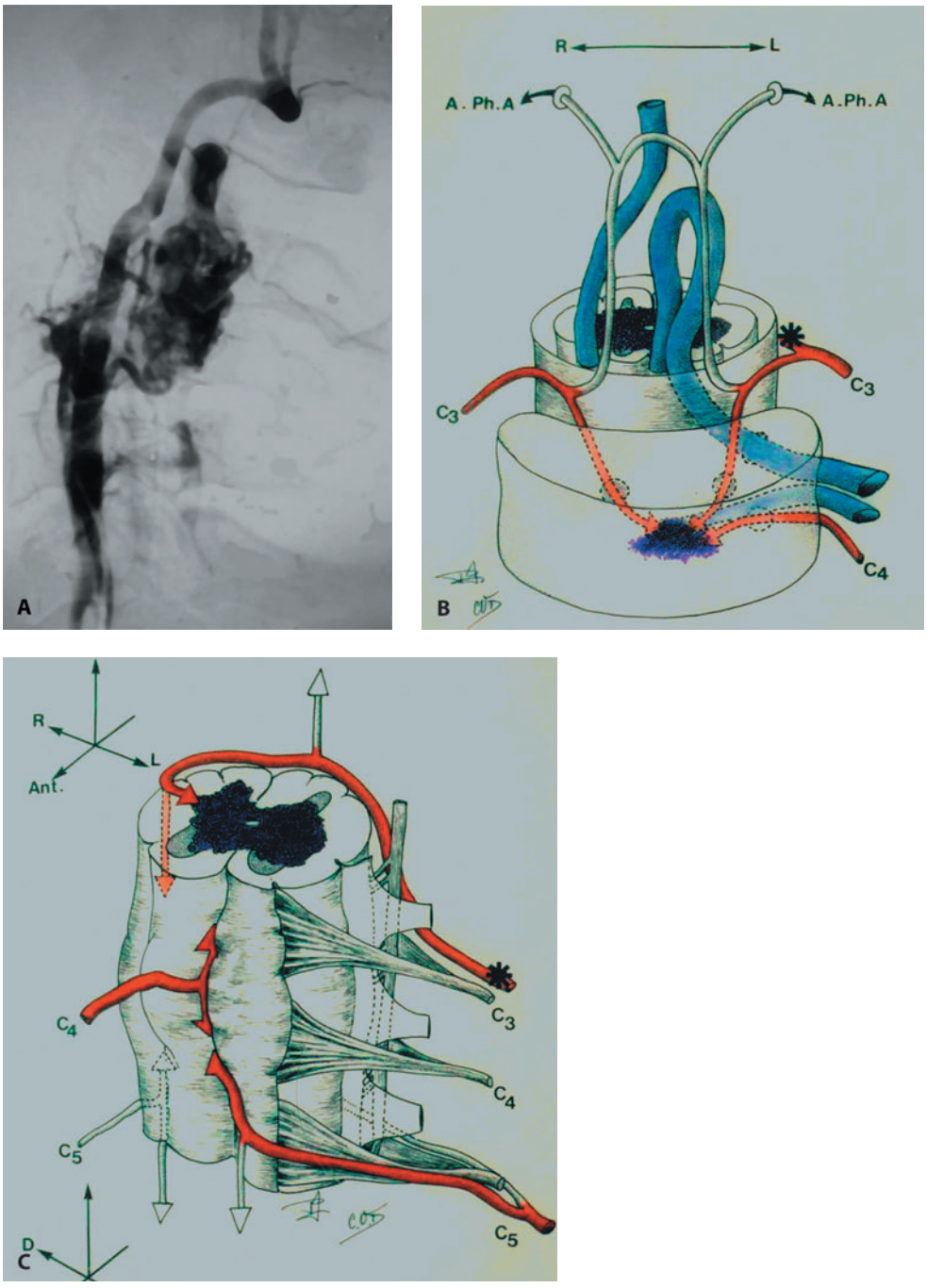

Fig. 11.57A–C. Spinal arteriovenous metameric syndrome 3/4. **A** Involvement of the C3 vertebra (**B**) and corresponding spinal cord (**C**)

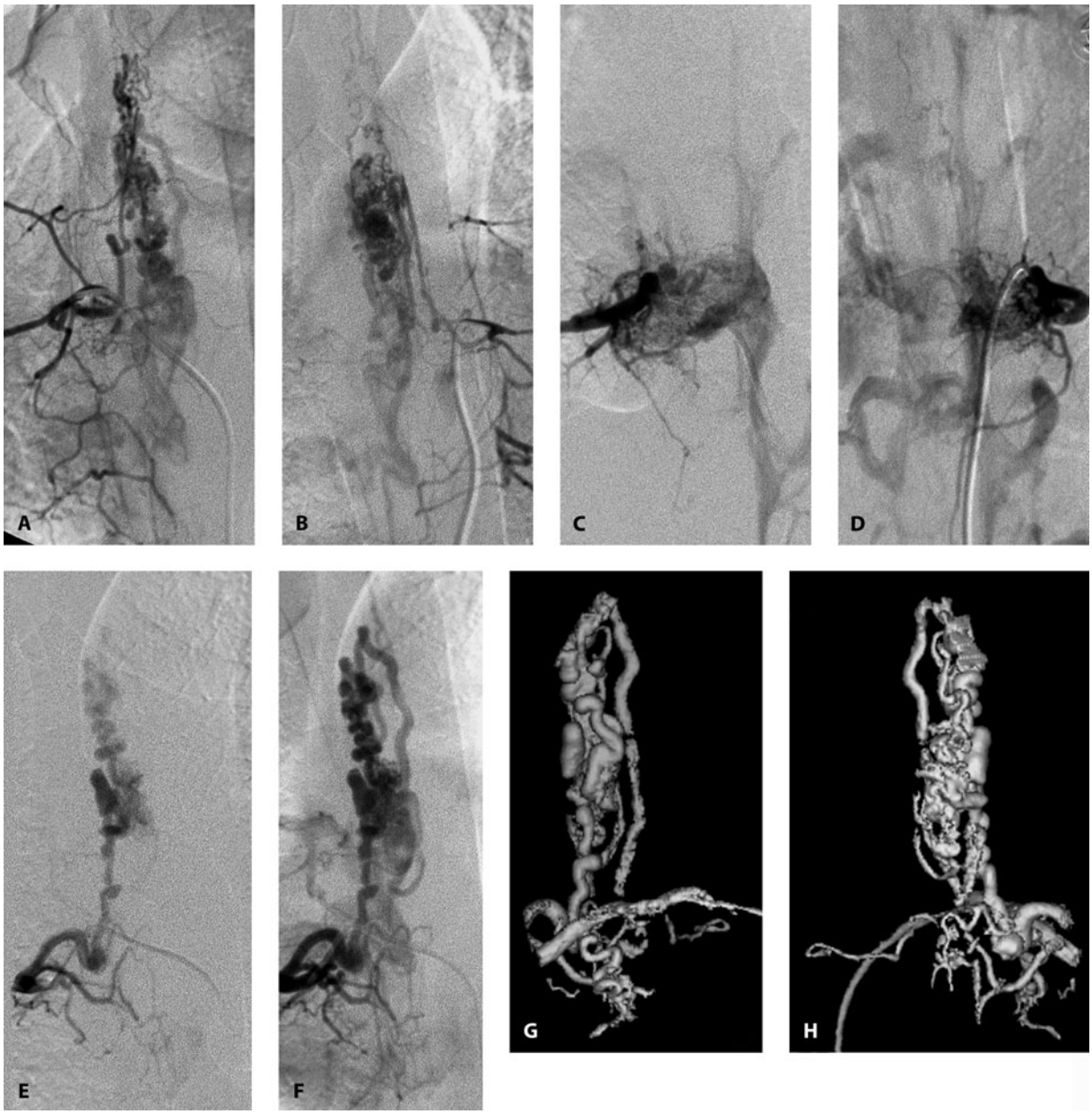

Fig. 11.58A–H. Spinal arteriovenous metameric syndrome 16/17. Involvement of the T9 vertebra and corresponding spinal cord at the myelomere T8–9 in a 20-year-old female patient presenting with acute onset of dorsal pain and moderate lower limb deficit. No evidence of hemorrhage. Injections of T7 (**A**, **B**) and T9 bilaterally (**C**, **D**). Injections of T8 (**E**, **F**), anterior and posterior 3-D views (**G**, **H**)

Fig. 11.59A–C. Spinal arteriovenous metameric syndrome 6/7. MRI shows soft tissue and cord involvement. Left metameric spinal arteriovenous malformation at C6 in a 33-year-old woman with a 7-year history of back pain, numbness of the left leg aggravated during pregnancy that improved after delivery, 1 month of numbness of the left hand, pain in the left scapular area, weakness of intrinsic muscle of the left hand. (Courtesy of S. Pongpech)

Patients with SAMS who present with spinal cord symptoms are dealt with in the same way as those with other SCAVMs. It is the spinal cord involvement that carries the greatest clinical and prognostic significance (Figs. 11.18, 11.21, 11.54). Treatment is therefore geared toward the SCAVM.

In patients with symptoms related to the extraspinal AVM, treatment is directed specifically to that malformation. In other situations, the presence of a high-flow muscular AVF fed by a segmental (intercostal or lumbar artery) giving rise to the radiculomedullary artery may be the cause of cord symptoms (Rodesch et al. 1996). These are likely to be related to a steal syndrome, particularly when no SCAVM is present or when there is no pial venous retrograde congestion. The treatment of the muscle lesion alone will improve the symptoms. In some patients, the SAMS is incomplete; the only expressed malformations are paraspinal and cutaneous without cord involvement (Figs. 11.7, 11.9, 11.11). With these vascular malformations that do not have spinal cord symptoms in relation to an associated SCAVM, one must identify the supply to the normal spinal cord in order to best plan treatment and avoid accidental occlusion or ligation.

Limb vascular lesions also require careful analysis. Klippel–Trénaunay and Parkes–Weber syndromes with, respectively, associated venous or arteriovenous malformations of the extremities are rare but justify spinal MRI screening to rule out associated SCAVM.

In Djindjian's series (1976), two patients had vertebral body hemangiomas at the same or other levels, three had Klippel–Trénaunay–Weber syndrome, two had a second AVM at another site, and one had associated

Table 11.6. Incidence of metameric and associated dysplasias in 192 patients with SCAVMs

Series	No. of patients	Metameric lesions (%)	ROW (%)	Other dysplasias or conditions (%)	Associated lesions (%)
Djindjian (1978)	84	12[a] (14)	7 (8)	11[b] (13)	30 (36)
Rosenblum et al. (1987b)	54	4 (7)	1 (2)	9[c] (17)	14 (26)
Berenstein and Lasjaunias (1992)	54	4 (7)	2 (4)	4[d] (7)	10 (19)
Total[e]	192	20 (10)	10 (5)	24 (13)	54 (28)

SCAVM, spinal cord arteriovenous malformation; ROW, Rendu–Osler–Weber syndrome.

[a] Two patients with Cobb syndrome.

[b] Two patients had vertebral body hemangiomas at the same or different levels, two had Klippel–Trénaunay–Weber syndrome, two had a second arteriovenous malformation at another site, and one each had associated neurofibromatosis, von Willebrand's disease, and Parkes–Weber syndrome. One patient had two metameric lesions and one patient had a facial vascular malformation.

[c] Two patients had cerebral aneurysms, three patients had other arteriovenous malformations, two had vessel agenesis or hypoplasia, and one had Klippel–Trénaunay–Weber syndrome.

[d] One patient had a facial arteriovenous malformation, two had associated vertebral body hemangiomas, and one had neurofibromatosis.

[e] In addition, in Doppman's series of 28 patients, 6 (21%) had associated metameric, cutaneous, vascular malformations; 18 (5%) had cutaneous vascular malformations that were unrelated and nonmetameric, and 2 (7%) had arteriovenous malformations at other locations, one in the right lung and the other in the liver and right kidney.

neurofibromatosis, another von Willebrand's disease, and a last one had Parkes–Weber syndrome. One patient had two metameric lesions, one had an associated facial vascular malformation, and two had Cobb syndrome. In Rosenblum's series (1987b), two patients had cerebral aneurysms, three had other AVMs, three had vessel agenesis or hypoplasia, and one had Klippel–Trénaunay–Weber syndrome. In our earliest series, associated lesions included facial AVM, vertebral body hemangiomas, Klippel–Trénaunay syndrome, neurofibromatosis, cutaneous angiomas of nonmetameric types, and AVMs at other locations (lung, liver, and kidney).

Some of the pelvic and limb vascular lesions correspond to the expression of the SAMS 23–31. Vertebral anomalies accompanying SCAVMs can include kyphosis or kyphoscoliosis, giving the so-called syndrome of vertebromedullary angiomatosis (Newman 1959). Additionally, there have been reports of association with other mesenchymal dysplasias, including some of the lymphatic system (Djindjian 1971a, b). The association of SCAVMs with various tumors has also been reported. These include hemangioblastomas of the spinal cord or cerebellum (Djindjian 1971b; Guidetti and Fortuna 1967; Guillian et al. 1932; Jellinger et al. 1968; Wyburn-Mason 1943b; Dilenge et al. 1973), retinocerebellar angiomatosis (Di Chiro 1957), and ependymomas (Krieger 1972) (Table 11.6).

11.4.1.3 Associated Cerebral and Spinal Arteriovenous Malformations

The coexistence of brain AVM (BAVM) with spinal cord AVM (SCAVM) is extremely rare (Figs. 11.60, 11.61) (Hash et al. 1975; Hoffman et al. 1976; Mizutani et al. 1992; Parkinson and West 1977; Tsurushima et al. 1995). A high incidence of multifocal AVMs of the central nervous system has been reported in patients with HHT disorder, and yet their association simultaneously affecting the cord and the brain is exceptional (Hasegawa et al. 1999; Moss et al. 1989). Mazighi et al. (2000) reported two cases of BAVM associated with SCAVM to illustrate the clinical situations and the therapeutic challenges encountered in one infant and one adult (Fig. 11.60; see Vol. 3).

In this situation, HHT disorder should be suspected although arteriovenous shunts in the patient population associated with HHT are more often high-flow macrofistulae with giant venous ectasias. Furthermore, multiple lesions seen in HHT involve various metameric territories. If one estimates the SCAVM/BAVM ratio to be 10%, then the incidence of multiple BAVM–SCAVM would be 1% in our SCAVM series and 0.1% in BAVMs.

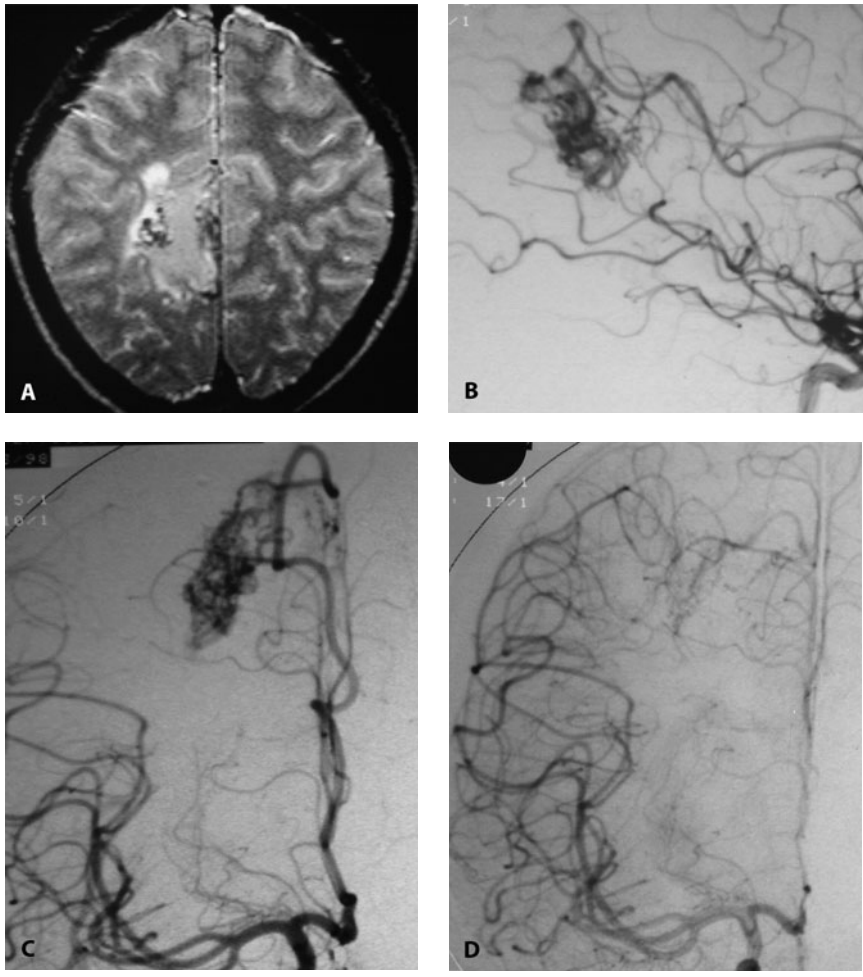

Fig. 11.60A–J. This female patient was 19 years old when referred to our institution. A complete embolization of the brain arteriovenous malformation with glue was performed in two sessions (**A–D**). **E–J**
see p. 823

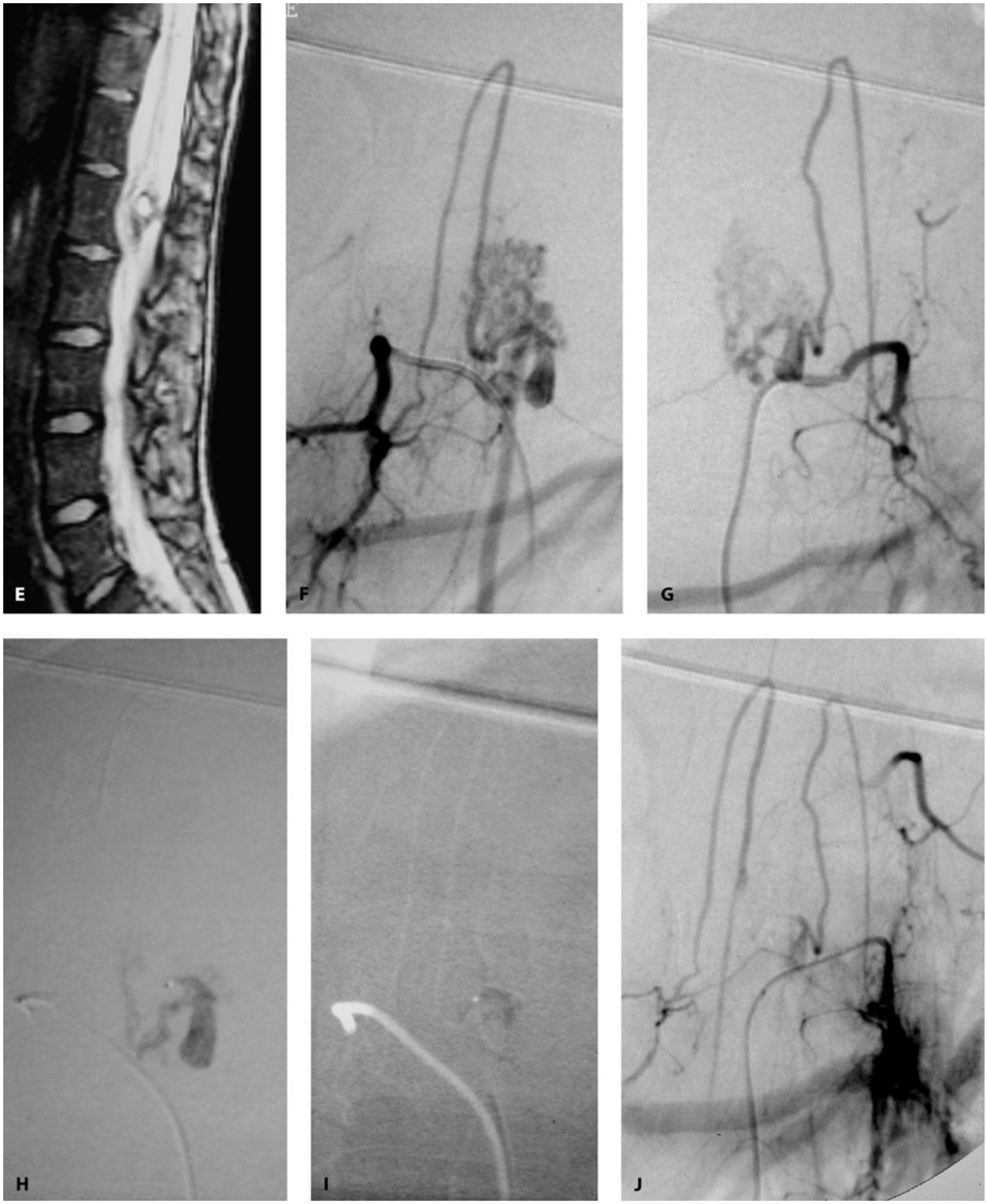

Fig. 11.60 (*continued*). The spinal cord arteriovenous malformation (**E–G**) was secondarily totally embolized (**H–J**). The clinical outcome was excellent with no new symptoms

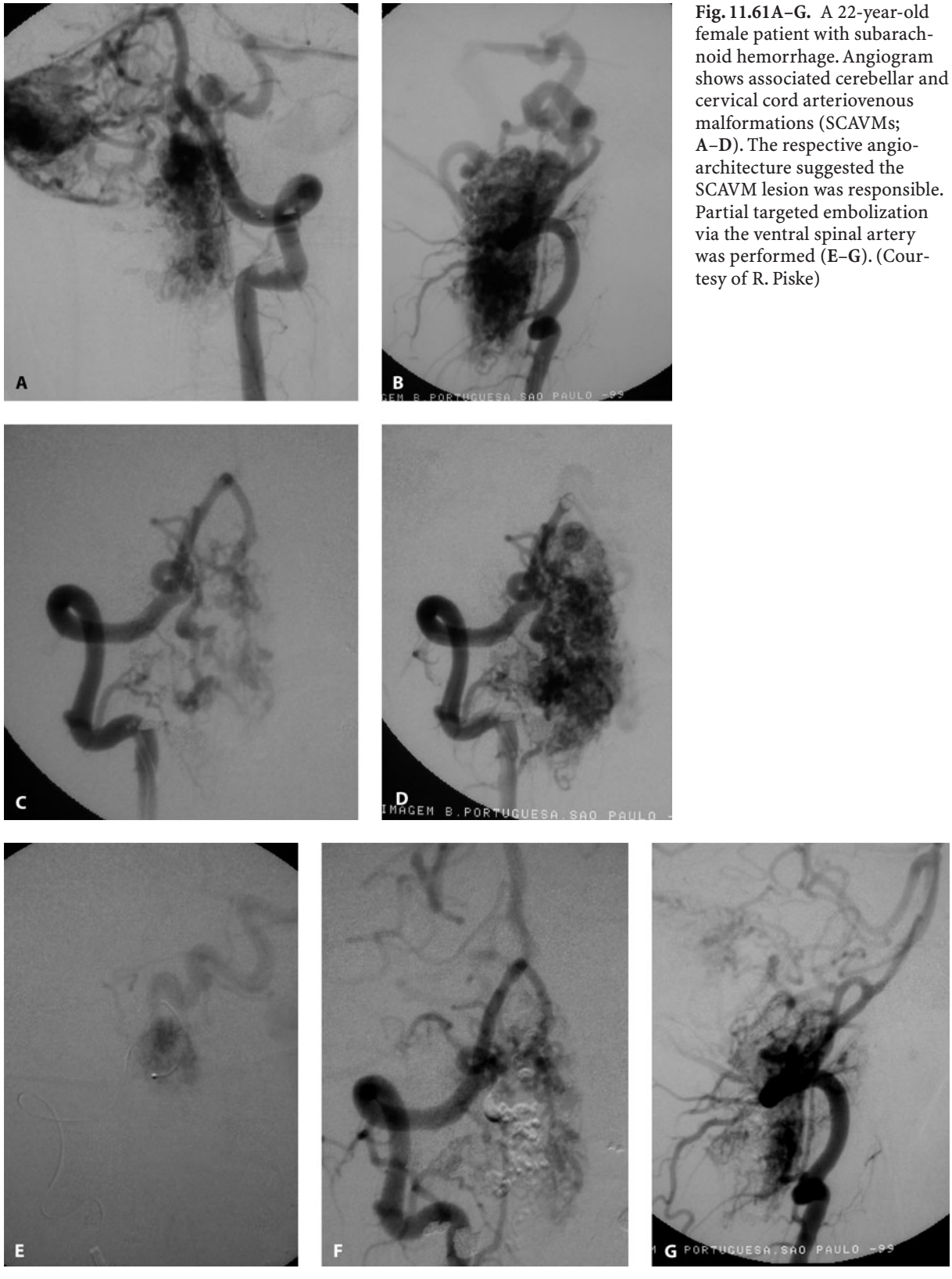

Fig. 11.61A–G. A 22-year-old female patient with subarachnoid hemorrhage. Angiogram shows associated cerebellar and cervical cord arteriovenous malformations (SCAVMs; **A–D**). The respective angioarchitecture suggested the SCAVM lesion was responsible. Partial targeted embolization via the ventral spinal artery was performed (**E–G**). (Courtesy of R. Piske)

Table 11.7. Sex distribution of SCAVMs in 192 patients[a]

Series	Male (%)	Female (%)
Djindjian (1977)	93	45
Rosenblum et al. (1987b)	70	30
Lasjaunias and Berenstein (1992)	53	45

SCAVM, spinal cord arteriovenous malformation.
[a] Includes spinal cord arteriovenous fistulae and metameric lesions.

Table 11.8. Age distribution in SDAVF and SCAVM patients at the time of diagnosis (n=352)

Series	No. of patients	SDAVFs	Mean	SCAVMs	Mean
Djindjian (1977)	130	34–73	52	3–57	26
Rosenblum et al. (1987b)	81	25–72	49	4–58	27
Berenstein and Lasjaunias (1992)	81	35–87	56	2–42	22
Symon et al. (1984)	60	29–75	57	14–40	31

SDAVF, spinal dural arteriovenous fistula; SCAVM, spinal cord arteriovenous malformation.

11.4.2 Clinical Aspects

11.4.2.1 Natural History and Clinical Presentation

SCAVM series that include adults and children have a slight male to female predominance (Table 11.7); the mean age of presentation is in the mid-20s (Table 11.8), but in close to 20% of cases, the lesion is diagnosed in children under 16 years of age (Yasargil 1984). However, the initial symptoms are present in over 50% of patients prior to the age of 16. In the series of Rodesch et al. (2002) there was a male predominance in the pediatric group (80% boys and 20% girls), 20% of the overall population reviewed. No statistically significant sex predominance is found in the adult population (52% males and 48% females).

Spinal Hemorrhage

The most striking symptom in the clinical presentation of SCAVMs is the high incidence of hemorrhage, which may be either subarachnoid or within the spinal cord itself (hematomyelia) and occurs in 50% of all SCAVM patients. The frequency of this clinical picture as the presenting symptom is likely to decrease with the increased availability of MRI examination. Hemorrhage, and in particular hematomyelia, is associated with the onset of new, significant, and often devastating neurological deficits or with aggravating preexisting deficits. Hemorrhage is seen frequently in cervical lesions (Table 11.9) (Djindjian 1978; Yasargil et al. 1984; Rosenblum et al. 1987b; Berenstein 1980). The differential diagnosis of

Table 11.9. Incidence of hemorrhage in 192 patients with SCAVMs

Series	No. of patients	Cervical (%)	Thoracic and lumbar (%)
Djindjian (1977)	130	57	36
Berenstein and Lasjaunias (1992)	54	78	37
Yasargil et al. (1984)	41	58	20

SCAVM, spinal cord arteriovenous malformation.

Table 11.10. Causes of spontaneous spinal subarachnoid hemorrhage and hematomyelia (modified from Aminoff 1976)

Spinal vascular malformations
Cavernous malformations
Tumors, e.g., ependymoma, neurofibroma, astrocytoma, meningeal sarcoma, hemangioblastoma
Coarctation of the aorta
Mycotic and other spinal artery aneurysms
Polyarteritis nodosa
Toxic infective states, e.g., typhoid fever, smallpox, anthrax, septicemia
Blood dyscrasias
Anticoagulant drugs

spinal subarachnoid hemorrhage or hematomyelia is shown in Table 11.10. SCAVMs are the most frequent cause of spinal hemorrhage, while up to 25% of patients with SCAVFs may also present with or subsequently suffer from hemorrhage. Similar results were observed in the NIH series (Rosenblum 1987a).

Aminoff (1976) reported on 53 patients with SCAVMs who presented with bleeding and analyzed their subsequent course. Although he did not separate patients with SDAVFs from those with SCAVMs, we can roughly postulate that these 53 patients indeed had true SCAVMs. SDAVFs only bleed at the cervical level and they may still be included in the Aminoff series (see Chap. 12, this volume). In this specific group of SCAVM patients, the age of presentation at the time of the first hemorrhage was less than 20 years in 52% of patients. This is similar to Djindjian's findings (1976). Interestingly enough, there was a significant and important delay between the hemorrhagic episode and the establishment of the diagnosis, a frequent occurrence in all publications.

Of SCAVM patients who presented with hemorrhage, 75% had bleeding as the very first symptom and in the remaining 25%, there was a history of preexisting disturbance of the spinal cord or nerve root.

The typical syndrome of spinal hemorrhage gives rise to severe pain, which frequently starts in the back (between the scapulae), and/or at the site of the rupture and then rapidly spreads to the rest of the back, the nuchal area, and to the legs. When hemorrhage is profuse or, in cervical lesions, when blood passes toward the intracranial cavity, there may be headaches and disturbance of consciousness. In severe cases, head retrac-

Table 11.11. Incidence of hemorrhage and subsequent death in 53 patients with spinal cord arteriovenous malformations (from Aminoff 1976)

	Total patients (*n*)	Patients with hemorrhage	
		n	%
First hemorrhage	53	31	58
Death		3	6
Second hemorrhage	41[a]	22	54
Death		4	18
More than two hemorrhages	37[b]	9	24
Death		1	11

[a] Five patients lost to follow-up after hemorrhage, three died from first hemorrhage and four were operated on, leaving patients with a risk of a second hemorrhage.

[b] There were four deaths from second hemorrhage, leaving 37 patients with risk of more than two bleeds. The overall mortality from hemorrhage is 8/44 patients (18%, excluding the four patients who underwent surgery and in whom the risk of rebleed was eliminated, and the five patients who were lost to follow-up).

tion and even opisthotonos in association with papilledema, cranial nerve palsies, and convulsions may be seen. The signs and symptoms can be so severe and rapid in their onset that they may be mistaken for intracranial subarachnoid hemorrhage. In other cases, limb weakness, sensory loss, and disorders of micturition or defecation may follow bleeding within the cord itself (hematomyelia) or may result from compression of the cord by a blood clot. We have also seen a patient with severe high cord dysfunction, which caused respiratory muscle paralysis.

Aminoff and Logue (1974, 1976) analyzed the outcome of first hemorrhage, recurrence rate, and severity. However, they noted the difficulty of properly analyzing a small group of patients, including those who might have died from initial or subsequent hemorrhage without a SCAVM being recognized (Table 11.11). Out of 53 patients, three (6%) died within a few days of the initial bleed. In five of the remaining patients, no further details were available. If, in addition, we exclude the four patients who were operated on at or within 1 month of their hemorrhage and in whom rebleeding risk was eliminated, 41 patients remained with a risk of rebleeding. Of these, 22 (54%) had a second subarachnoid hemorrhage and four (18%) of these 22 died (9% of 41). Of the 18 patients surviving the second hemorrhage, nine had at least one additional hemorrhage. Another patient (11%) died with more than two hemorrhages.

Second hemorrhages occurred from within 24 h after the first episode to well over 5 years after the initial bleed. There was considerable variation in the intervals between successive episodes in the same patient. Aminoff further analyzed the data and showed that the recurrence rate within the first month was nearly 10% and within 1 year 40%, which is significantly higher than the rebleed rate in BAVMs.

The total mortality from subarachnoid hemorrhage resulting from SCAVM is difficult to assess accurately and can be estimated to be at least 18%. Additional morbidity and mortality occur from hematomyelia (Table 11.12)

Table 11.12. Death from intraspinal hemorrhage secondary to spinal cord arteriovenous malformations

	Subarachnoid hemorrhage %	Hematomyelia %	Total %
Aminoff (1976)	18	2.4	20.5
Gregarious[a] and Weingarten (1970)	11	19	30

[a] Autopsy series of 27 patients. In an additional 40% of autopsied patients, the cause of death was due too complications from neurological deficits (decubitis indirect ulcers, septicemia, urinary tract infections, etc.

Hematomyelia

The incidence of hematomyelia is difficult to ascertain. It is estimated to be close to 5%. The related mortality is historically estimated between 5% and 19%. However, these numbers do not reflect the currently available early diagnosis and treatment options.

Aminoff (1976) reported on 13 patients (3%) with hematomyelia or cord compression among 421 patients with spinal angiomas. If we agree that 36% of these 421 patients had SDAVFs that did not bleed (see Table 11.12), the remaining 270 patients were those with true SCAVMs (a 4.8% incidence of hematomyelia). In more than half of the patients, hematomyelia was documented only at autopsy. This suggests an additional 2.4% overall mortality from hematomyelia, thus raising the total mortality from spinal hemorrhage in SCAVMs to at least 20.5%. Gregarius (1970), in an autopsy series of 27 patients with lethal untreated SCAVMs, found an 11% mortality from subarachnoid hemorrhage and 19% from hematomyelia, corresponding to an overall mortality of 30% from intraspinal hemorrhage (Table 11.12). An additional 40% of his series died from indirect complications resulting from neurological deficits such as sepsis from decubitus ulcers and urinary tract infections. Most patients presented between ages 25 and 45, and at the time of death the most common age group was 41–51 years. From the analysis of Djindjian's series (1978), of 21 patients with cervical AVMs who were followed for up to 20 years, three died (14% mortality); the incidence of hemorrhage was 57% for patients with cervical malformations and 36% for those with thoracic and lumbar malformations. These results are similar to Aminoff's (1976). Bailey (1969) reviewed the cases of 54 patients with SCAVMs of the cervical region and reported that, of 29 patients with onset of symptoms prior to age 30, 14 (48%) died of neurological complications. Only three of these 14 lived more than 15 years after presentation.

The morbidity or permanent disability related to hemorrhage is also difficult to assess from the literature. For Djindjian (1978), Rosenblum (1987a), and Aminoff (1976), over 80% of patients had some disability at the time of diagnosis.

Bailey (1969) reported disability in 88% of his patients with cervical AVMs. In Djindjian's (1978) series, of the 97 patients who had SCAVMs (21 cervical and 76 thoracic and lumbar) at the time of diagnosis, 6% had

complete cord transsection, 34% were completely disabled, 27% had a grade III disability (they had gross handicaps but were able to ambulate with two canes and to take care of themselves), 15% had functional problems but were able to work, 13% had minor disabilities, and only 3% were normal.

In our adult population, 45% of lesions presented with hemorrhage. The frequency of hemorrhagic presentation varied according to the loction of the SCAVSs. Overall SCAVSs were located in the cervical cord (38%), in the thoracic cord (45%), and in the lumbar region (17%). Of these, 62% of the cervical and 45% of the thoracic malformations bled, where only (9%) of the lumbar malformations did so. Hematomyelia was diagnosed in 36% of cases and subarachnoid hemorrhage in the remaining 64% of cases. The neurological manifestations were most severe in hematomyelia. No deaths were seen after hemorrhage.

Recovery was observed in most cases. Posthemorrhagic follow-up showed that 71% had a Karnofsky score of 80 of higher after several months.

Symptoms and Related Angioarchitecture in the Adult Population

In our adult population, 84% of SCAVM lesions were nidus-type AVMs, 15% mAVFs, and 1% MAVF. No personal or family history of HHT1 disorder was found. Multiple lesions were seen in 13% (one-third were multifocal AVMs). An important difference in hemorrhages between the pediatric and the adult population must be noted: bleeds are more frequent (p=0.02), and the rates of hematomyelia are higher in children than in adults. The same ratios are found in other studies dealing with pediatric SCAVSs (Scarff and Reigel 1979; Rodesch et al. 1995; see Vol. 3).

A predictable correlation between the hemorrhages and false arterial aneurysm (AA; as an actual hemorrhagic site) was found in adults. Pial venous congestion, distal AA, associated AVFs, and venous ectasias are the dominant architectural features.

If distal AAs are more frequently seen in adults than in children, then flow factors alone cannot be responsible for their appearance. No AAs associated with high-flow MAVFs were noted in our series.

The association of AA with SCAVSs has been considered as a hemorrhagic risk factor (Konan et al. 1999). However, 47% of patients with AA bled versus 51% of patients without AA (p 0.64). As in BAVMs (see Chaps. 9 and 10, this volume), having both an AA (false AA excluded) and a SCAVS is not a significant risk for a hemorrhagic episode. Associated AAs are considered priority targets for partial embolization, but there is no evidence that eliminating them protects patients from future bleeds. However, the impact of such a strategy is probably positive, just as it has been proven to be beneficial in BAVMs (Meisel et al. 2000, 2002).

Pial venous congestion is a common finding in SCAVSs because of the dense and rich anastomotic vascular intrinsic and extrinsic network. Spinal cord veins are all located in the subarachnoid space, except for the anterior spinal vein, which is situated in the subpial space (Maillot 1996; Lasjaunias et al. 2001). Given this anatomical disposition, it could be postulated that rupture of the subarachnoid veins might also be responsible for subarachnoid hemorrhage.

There is no significant difference between the percentage of hemorrhage among patients with and without venous ectasia (VE) (p=0.89). These particular data are also observed empirically since MAVFs, characterized by giant VE, rarely bleed and mostly present with symptoms caused by venous congestion and pulsatile mass effect on the cord. AVFs within nidi or in isolation produce venous congestion and ectasias more rapidly, yet there is no significant difference between the percentage of hemorrhage among patients with AVF and without AVF.

Rehemorrhage prior to our consultation occurred in 18% of patients: two-thirds had cervical SCAVSs and one-third thoracic AVMs. Only two patients (3.6%) rebled within the 12 months that followed the first hemorrhage; in all the other cases the recurrent hemorrhagic episode occurred over a period of 4–31 years (mean, 11.6 years).

Nonhemorrhagic Manifestations

Among the nonhemorrhagic group, 1% were asymptomatic (incidental discovery), 9% were revealed by acute nonhemorrhagic neurological symptoms, and the remaining 90% had progressive neurological impairment either in a continuous or stepwise (acute) fashion. The overall progression between the beginning of the symptoms and the first consultation extended over 1–43 years (mean, 7 years).

Root or back pain as the initial symptom was seen in 15%–20% of patients. Weakness was present in one-third of patients as the initial symptom but will eventually develop in over 90% of patients. Sensory changes are present in an additional 70%. Impotence is present in almost half of the patients, while bowel and bladder dysfunction can be seen in almost all. The presence of a bruit is a relatively uncommon finding and has been reported in only 8% of patients. If present, however, a bruit is strongly suggestive of a high-flow lesion. It is also conceivable that a bruit could be present in a larger number of patients, as it is often not specifically sought.

11.4.2.2 Prognosis

At least 40% of SCAVM patients undergo neurological deterioration in a stepwise fashion following intraspinal hemorrhage accidents (Houdart 1978). Relapse is a frequent event occurring in over 80% of patients. The causes for deterioration are multiple. Among the well-accepted causes are intraspinal hemorrhage, thrombosis within the AVM, arachnoiditis, and increased venous pressure (Malis 1982b). Other causes to be considered are arterial or venous ischemia or mechanical cord changes (secondary to compression, pulsatile effect of dilated vessels). Deterioration can be followed by actual improvement or stabilization of symptoms (Ommaya 1985; Ommaya et al. 1969; Hurth et al. 1976; Malis 1982a).

11.4.2.3 Aggravating Factors

Maneuvers that result in increased intra-abdominal or intrathoracic pressure, such as the Valsalva maneuver and bending, often aggravate intramedullary venous pressure. The intramedullary effects are secondary to the elevation in venous pressure of the intraspinal (osseous) or inferior vena cava circulation into which the SCAVM empties. Such pressure increases may precipitate an intraspinal hemorrhage with all of its consequences.

Pregnancy may also aggravate the symptomatology of SCAVMs by various mechanisms, including (a) increases in intra-abdominal pressure, (b) increased intravascular volume, (c) hormonal changes, and (d) the added stress on the venous circulation during delivery.

Trauma as a causative factor for the symptoms of SCAVMs has been controversial. It is known that approximately 5% of patients in the general medical and surgical population are able to recall an injury sustained within 3 months of the onset of their disease. Therefore, the validity of such an association may have important medicolegal implications. At present, it is difficult to ascertain a direct effect of trauma as an aggravating factor. However, the temporal relationship of symptoms to injury has been noted by many authors and was reviewed by Aminoff and Logue (1974). Trauma may alter the hemodynamics within a vascular malformation by secondary thrombosis or rupture and therefore cause symptoms. This appears to be the case in a patient reported and reviewed by Aminoff (1976).

Pain can be related to posture by many patients with SCAVMs. The symptoms can be rapidly relieved by changing to a different position, suggesting that compression of a nerve root by a congested vascular structure may be responsible.

Weakness or other neurological deficit may present or be aggravated during bowel movements. This was first noted by Therkelsen in 1958, and we have seen it in two patients with SDAVFs but not SCAVMs.

Aminoff reported that, out of 60 patients in whom the information was available, 19 had symptoms that were precipitated or aggravated by exercise and relieved by rest. Pain was the most commonly produced symptom. When leg weakness was the presenting symptom, it was usually radicular in distribution but, like pain due to peripheral vascular disease, it bore a direct relationship to exercise and was relieved with rest. In some patients, the symptoms progressed as exercise was continued. The amount of exercise necessary to produce symptoms varied. In almost all of the patients, symptoms remitted after no more than a few minutes rest only to recur after variable periods when exercise was resumed.

Other Aggravating Factors

Menstruation (Tobin 1976), infections, increased body temperature, and corticotrophin therapy (Aminoff 1976) have also been reported to be aggravating factors in patients with SCAVMs.

Lee and Kobrine (1983) reported the acute presentation of neurogenic pulmonary edema following the rupture of an SCAVM. The mechanism

was presumed dysfunction of paraganglionic sympathetic fibers of the spinal cord, and should be suspected when all other causes of such pulmonary edema having been excluded.

Subdural Hematomas

Subdural hematomas are a rare finding in patients with intraspinal hemorrhage from SCAVMs. If seen, one must suspect an extradural component to the malformation, which would most likely occur in lesions with metameric or paraspinal muscle involvement; the present authors have not seen such a patient.

Epidural Hemorrhage

Epidural hemorrhage is a clinically important cause of paraplegia affecting all age groups and with a preference for men in a ratio of 2:1. In the majority of cases of epidural spinal hemorrhage, no cause is demonstrated (Aminoff 1976). Etiologies of spinal epidural hemorrhage include anticoagulant therapy, hemorrhagic diathesis, spinal vascular malformations, spinal tumors, and trauma (Table 11.10). The clinical picture is similar to that of other extradural processes; however, the course is usually dramatic and severe. The onset may be characterized by radicular pain, followed within hours by rapidly progressing paraparesis of tetraplegia. Among patients with vascular malformations, the most frequently encountered lesions responsible for spinal epidural hemorrhage are extradural AVMs and extraspinal lesions draining into the epidural venous plexus. Early radiological diagnosis and urgent surgical decompression with removal of the hematoma are recommended to prevent permanent damage to the spinal cord. This condition is seen more often in association with tumors such as bone hemangiomas (see Chap. 13, this volume).

Other Clinical Findings

Muscle atrophy and sensory disturbances that may result in multiple injuries can be observed in patients with SCAVMs. Spinal deformities such as kyphosis and scoliosis are also seen. In addition, presentation may be with complications common to other types of spinal cord dysfunction such as urinary tract infections, respiratory infections, and decubitus ulcerations, which must be taken into consideration in determining the morbidity and final outcome of these patients.

Varicose leg veins developing at an unusually early age or of marked degree can be seen in some patients with high-flow lesions draining to the inferior vena cave (IVC) and/or azygos venous system. In cases associated with Klippel–Trénaunay syndrome, additional bony abnormalities exist (Figs. 11.20, 11.23).

11.5 Treatment of Vascular Lesions

The final outcome of patients with vascular lesions of the spine and spinal cord is directly related to the prompt diagnosis and treatment of the abnormality.

The primary objective of any therapeutic modality should be to obtain a neurologically normal patient, free of future risks in relation to the SCAVM. Cure of these lesions is seldom obtained without morbidity. In patients in whom a complete cure is not possible at an acceptable level of risk, partial targeted treatment can be proposed with the aim to arrest or improve the clinical situation or to favorably modify the natural history of the disease. Such partial targeted embolizations will obliterate weak portions of the angioarchitecture (e.g., arterial aneurysm and nidus aneurysm), reduce the nidus, or slow down the flow through the malformation to decongest the venous drainage. These maneuvers improve the venous drainage of the normal spinal cord, often with beneficial effect.

Factors that will modify the objectives in a particular patient include (a) the age of the patient; (b) the clinical presentation (hemorrhage, more than one hemorrhage, etc.); (c) the morphological appearance of the lesion (the presence of an aneurysm, venous varix, etc.); (d) impaired flow or venous drainage of the spinal cord (stagnation in the anterior spinal artery circulation, nonvisualization of the medullary veins).

11.5.1 Indications

The indications for treatment in SCAVMs include all patients with symptomatic lesions that can be cured. If total anatomical cure is deemed impossible the factors mentioned in the previous section must be considered in detail to best determine treatment strategy. In the young symptomatic patient, treatment should be pursued aggressively. If complete obliteration appears unfeasible, an anatomical goal or objective is defined, looking for the morphological high-risk portion of the lesion (Figs. 11.27, 11.29). The presence of an associated aneurysm is an indication for targeted treatment. They are especially dangerous if they are pseudoaneurysms resulting from previous hemorrhage (Figs. 11.34, 11.36). The occlusion of an arteriovenous fistula within the malformation, or of that portion of the malformation that drains into a territory with outflow restriction as manifested by a venous pouch, varix, or ectasia, can result in a favorable long-term outcome.

In the acute stage following a spinal hemorrhage, the neurological deficit may be very severe, including total loss of function. Although rebleeding is a risk, the great majority of patients will improve significantly over the next several weeks or months. Therefore, one should not interfere with the natural recovery. Spinal angiography may be done early to exclude a pseudoaneurysm or other potentially risky angioarchitectural feature that may justify early targeted embolization, mostly if more than one hemorrhage has occurred. However, it is not acceptable to intervene aggressively early and to not consider complications in a totally paralyzed patient who has the chance of natural recovery (Figs. 11.45, 11.46, 11.62).

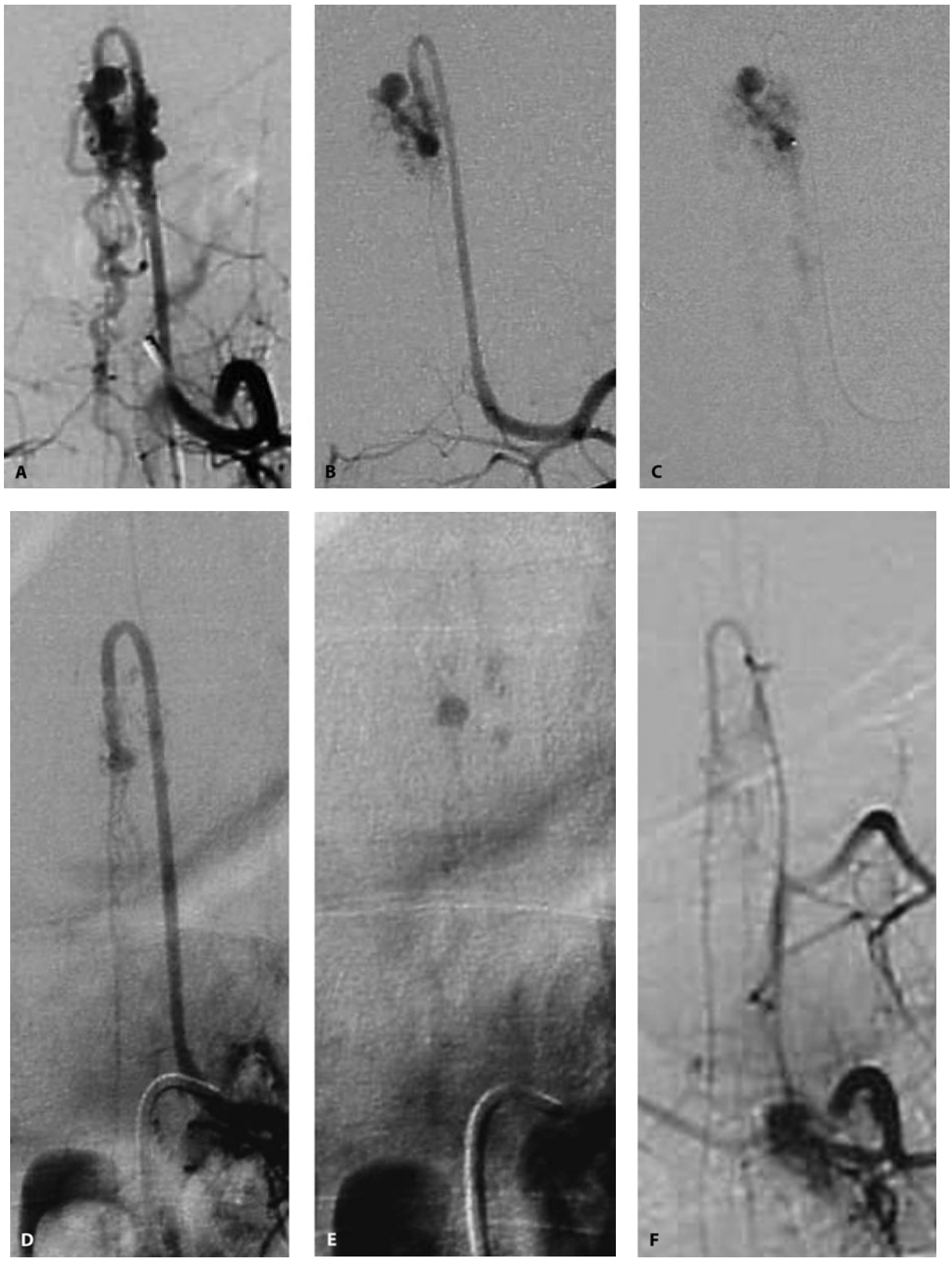

Fig. 11.62A–F. Typical false aneurysm buried in the depth of the ventral sulcus. Frontal view (**A**) is suboptimal for working projection. Oblique views show the embolization possibilities (**B, C**). Following embolization with glue (**D, E**), remodeling is seen on the follow-up angiogram (**F**)

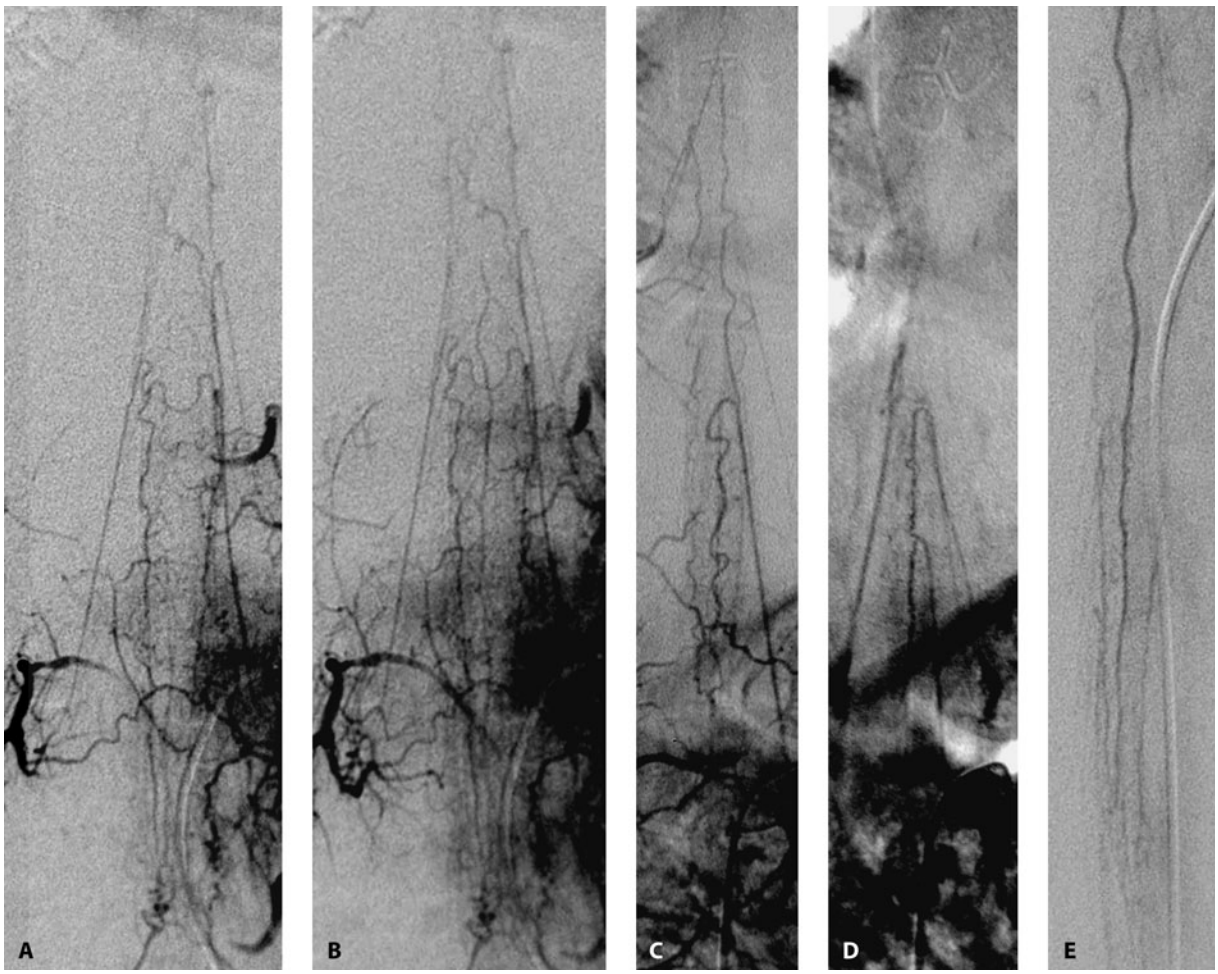

Fig. 11.63A–E. Conus medullaris arterial connections. Filum terminale (**A**, **B**) pial network opacifies the basket and the entire supply to the caudal region of the cord. **C**, **D** Radiculomedullary artery injection shows ventral arteries and veins and filum supply (**E**)

With respect to the indications for treatment in a patient with a fixed deficit or clinical cord transsection, in which it is unlikely that treatment will be of functional benefit, such treatment is nonetheless indicated, as repeated life-threatening spinal hemorrhage can be avoided by proper closure of the malformation and/or aneurysm. Complete obliteration is also easier as it will not aggravate a fixed deficit or a complete transsection. In some patients with sufficient pain and spasm, palliative embolization may be necessary and beneficial and may avoid extensive decompressive laminectomy or other procedures.

Occlusion should be performed aggressively in patients with high thoracic or cervical lesions in whom progression of the lesion or repeated hemorrhages can affect upper extremity function, sphincter control, respiratory muscles, etc. In such patients, spinal hemorrhage can extend intracranially and produce higher-level impairment with severe or even lethal consequences.

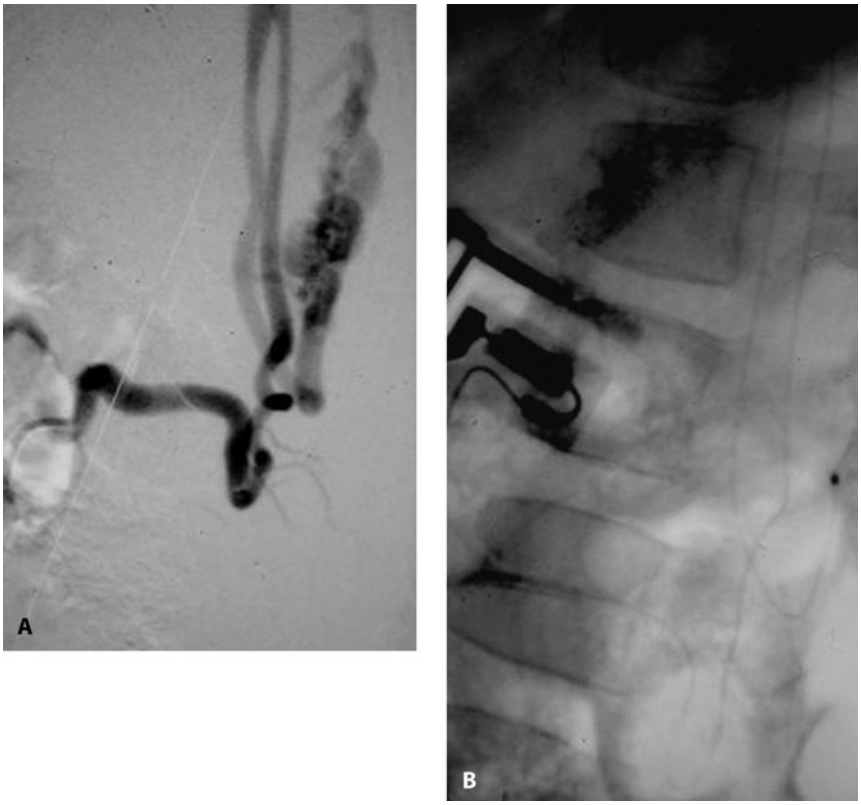

Fig. 11.64. Retromedullary spinal cord arteriovenous malformation fed by a pial branch opacified via the ventral spinal artery and the basket anastomosis (**A**). The microcatheter is advanced to the nidus using the same route (**B**)

In patients with lower thoracic or lumbar AVMs that have a fixed deficit and in whom no clinical improvement is possible, repeated spinal hemorrhages may not be life threatening and the indications for aggressive treatment may be less obvious. If sphincter control and/or sexual functions are spared, aggressive intervention may result in loss of such important remaining functions. Treatment may be appropriate, however, in those patients in whom complete obliteration of the malformation can result in preservation of those functions or if repeated hemorrhage occurs.

The indications for treatment are the same for the various types of SCAVMs and SCAVFs. In metameric lesions, the spinal cord lesion is treated as any other SCAVM. The extraspinal component may not require treatment or may be dealt with as a separate AVM and treated if symptomatic (i.e., pain, deformity) (Figs. 11.7, 11.9, 11.11) or managed preoperatively.

The anterior spinal artery (ASA) is often considered as an unsafe artery for endovascular therapy. Comparable to other similar vessels (anterior choroidal artery, ophthalmic artery), the anatomy of the ASA indicates the exact territory supplied by the system and makes it possible to predict its resources in case of occlusion (see Vol. 1).

The ASA is made up of the descending and ascending branches of the radiculomedullary arteries lying within the ventral sulcus in the subpial space (Maillot 1996; Nicholas and Weller 1988). It forms a continuous axis from the vertebrobasilar junction to the filum terminale. The ASA may supply some pial arteries that vascularize the ventral funiculi, and, at each

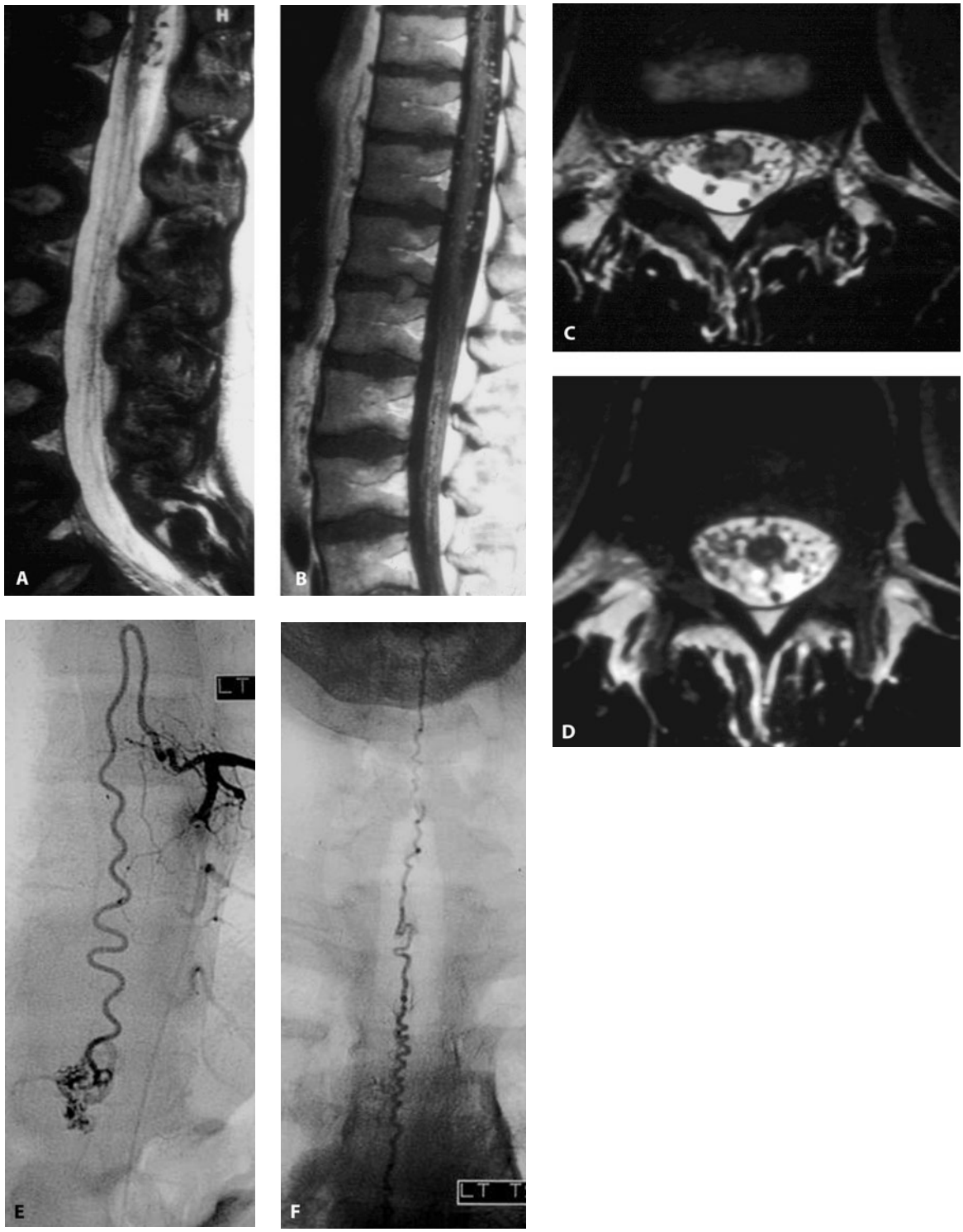

Fig. 11.65A–K. A 19-year-old male patient presented with subacute onset of progressive weakness of both legs over a 3-month period. MRI demonstrates increased signal within the conus and multiple flow voids along the spinal cord, which were enhanced with contrast (**A–D**). Ventral spinal artery supply was demonstrated toward a spinal cord arteriovenous malformation (SCAVM) located along the posterior aspect of the conus with venous drainage directed upward to the thoracocervical level (**E, F**). **G–K** see p. 838

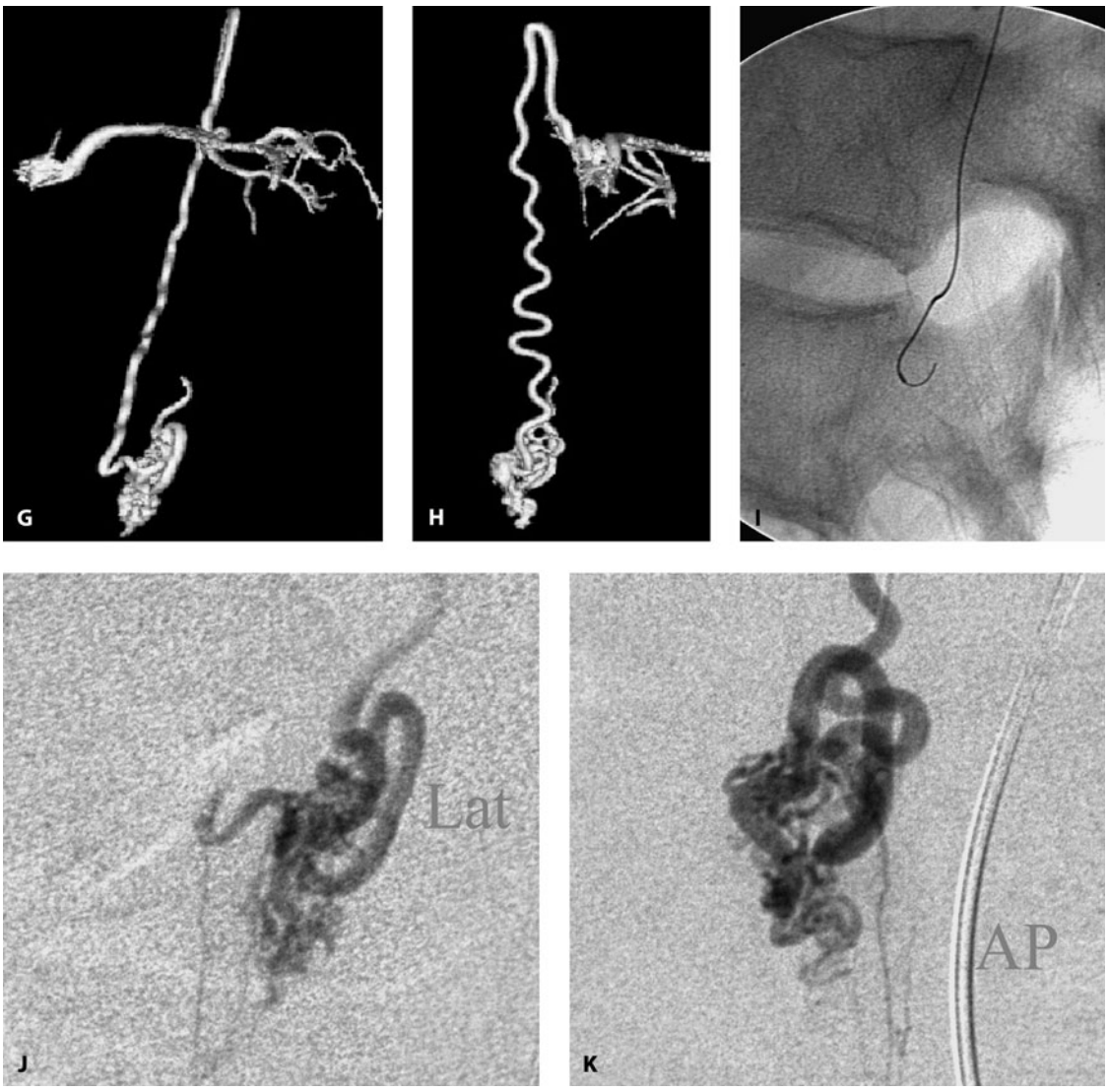

Fig. 11.65 (*continued*). 3-D angiogram (**G**, **H**). **I–K** Catheterization of the anterior spinal axis was achieved followed by selective catheterization of the sulcocommisural branch leading toward the SCAVM, thereby facilitating embolization of the nidus with preservation of the anterior spinal axis

myelomere level, sulcal arteries (similar to perforating arteries) to vascularize the gray matter. Each sulcal artery supplies one half of the cord (right or left). When duplicated, each ASA supplies sulcal arteries to the ipsilateral hemicord. Before penetrating into the cord, the perforators may anastomose within the subpial space, with adjacent sulcal arteries. After penetrating the cord, the sulcal arteries constitute a dense intrinsic network axially and longitudinally anastomosing with the radial arteries arising from the radiculopial arteries.

Embolization of a SCAVM vascularized by individual ASA branches will need to be a selective endovascular occlusion of these branches. Precise deposition of glue in the pathological network will not lead to any neurological deficit, as it will respect the cord (Figs. 14.134, 11.29, 11.45,

11.46). Reflux in the ASA itself carries the risk of paraplegia; reflux in a normal sulcal artery would create an anterior horn syndrome (ventral radiculopial artery running to the ventral funiculus without contributing to the anterior spinal axis). The use of the basket anastomoses (Fig. 11.63) may help approaching extramedullary pial SCAVM of the conus medullaris (Figs. 11.64, 11.65).

11.5.2 Results of Spinal Cord Arteriovenous Malformation Embolization

Since the first reports of endovascular embolization of SCAVMs using 1.5- to 3-mm stainless steel pellets (Doppman et al. 1968b) or lead pellets and small fragments of muscle (Newton and Adams 1968), it became obvious that the endovascular approach to SCAVMs was feasible. In both instances, no harm was done and the treatment was successful in improving both patients' condition.

By 1971, Doppman (1971a) reported the successful occlusion of the lesions of five out of seven patients following embolization with a combination of metallic pellets, gelatin sponge and muscle fragments. Embolization was used as an alternative to ligation of the feeding artery to the malformation. Doppman (1968b) took advantage of the narrowing of the spinal/radicular arteries and/or spinal pial arteries as they cross the dura to accomplish intradural occlusions, reproducing the surgical technique of the time. No deterioration of cord function was noted in any of his patients. Since 1966, Sano et al. have been working with a liquid plastic for the purpose of obtaining an endovascular cast of cerebral AVMs. In 1968, Shiromura et al. were assessing ischemic damage to the cervical cord using liquid plastic made radiopaque with tantalum powder. In France, Djindjian (1971a, b) reported preliminary results of muscle embolization in an intramedullary SCAVM. By 1973 Djindjian et al. had encouraging results in ten patients, although he used Gelfoam as the main embolic agent and obviously encountered recanalization of the lesions. At that time, he concluded that, while this treatment was initially efficient, it was without lasting success. He recognized that future advancements in embolic material development, including the use of liquid acrylics, would improve the final outcome (Djindjian et al. 1975).

In 1977, Kerber mentioned the successful use of iso-butyl-cyano-acrylate (IBCA) in two patients with spinal cord vascular lesions (Kerber et al. 1978). Silicone fluid as an embolic agent was originally reported by Doppman (Doppman 1971; Doppman et al. 1976). In 1978, Hilal et al. succeeded in occluding the lesions of 9 out of 11 patients using a modification of silicone fluid embolization. In the early 1980s, we used acrylic material as the embolic agent of choice in certain types of SCAVMs and in the anterior spinal artery branches. At that time, polyvinyl alcohol (PVA) was playing a role in treating certain intramedullary cervical SCAVMs (Berenstein et al. 1984b). Theron et al. reported on five patients whose lesions involved the anterior spinal artery. The lesions were embolized with PVA with complete occlusion and without complications (Theron et al. 1986). In two of Theron's patients, the follow-up angiogram showed continuous occlusion, but in three there was recanalization. Biondi et al. (1990) showed very fre-

quent recanalization in 70 patients with SCAVMs who were then retreated with particles. He reported overall favorable results and no rebleeding, except for patients who did not receive repeat treatment.

In the assessment of patients with SCAVMs, there may be some difficulty in assigning improvement that can be credited to the procedure versus the natural improvement that can follow an acute insult to the spinal cord. Our approaches, techniques, and results are comparable, although one of us uses SEPs and chemical monitoring and the others do not.

In our assessment of the outcome, we consider the results to be excellent in patients who after treatment were normal and whose AVM was obliterated. Good results were concluded when neurological status after embolization in the available follow-up was better than or at baseline, with at least 90% obliteration. Fair results were ascribed to patients who had not improved or in those with mild (functionally of little importance) aggravation of the baseline neurological status. The results were judged to be poor if the patient's outcome was worse than baseline or if there was a permanent complication.

In our previous series, 49% (23 of 47) of patients had an excellent outcome and 28% (13 of 47) the outcome was good; thus, endovascular embolization in SCAVMs had a favorable result in 36 out of 47 patients (77%), significantly better than the natural history described in the beginning of this chapter. In those patients with a preexisting fixed deficit, treatment did not result in a return to normal. In an additional three patients (6%), the procedure was technically not successful but no harm was done. In one initially successful patient who went from paraplegia to normal in 3 days, there was a delayed aggravation 15 days later, in which an ascending myelopathy related to venous thrombosis occurred. The patient continued to deteriorate and died 19 months later. At autopsy, a necrotizing thrombophlebitis of the spinal cord was found (Fig. 11.51).

Complete obliteration of the malformation, as determined during the immediate postembolization study, can be accomplished in almost half of the patients by embolization alone. The remaining group of patients benefits from partial targeted embolization or combined approaches associating embolization and surgery.

Our embolic agent of choice is liquid acrylic *N*-butyl cyano-acrylate (NBCA), which is used in the majority of patients. Only when superselectivity was not achieved, if partial changes in flow within the lesion or a collector were needed, or if embolization at a distance from the nidus was performed, was particulate embolic material (such as PVA) used (Fig. 11.66).

11.5.3 Complications of Embolization

In our series, permanent worsening directly related to the procedure occurred in 11% of the cases: 4% were serious, 4% moderate, and 3% mild. Transient complications occurred in another 11%.

In the Rodesch et al. series (2002), transitory deficits were seen in ten patients (14%): all resolved rapidly either spontaneously or with corticosteroid treatment (where the quantity of glue was felt to be associated with

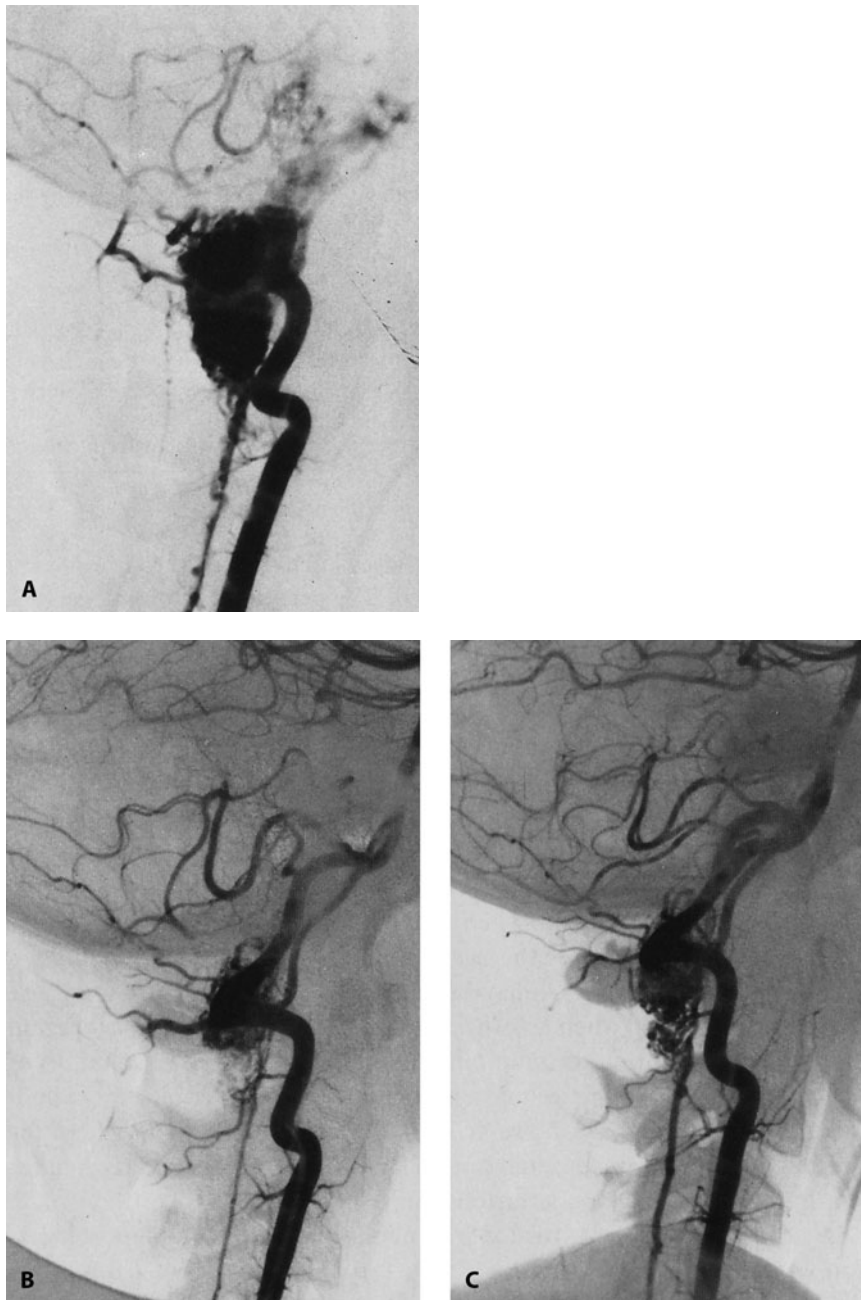

Fig. 11.66. **A** Lateral view of the right vertebral artery shows a large malformation of the upper cervical cord. **B** Postembolization angiogram after the use of polyvinyl alcohol (PVA) particles in three different sessions shows a marked reduction in the size of the malformation. **C** Follow-up angiogram 2 years later shows recanalization of the lower portion as compared to the final postembolization study shown in **B**

a local inflammatory reaction) or anticoagulation (when the venous congestion and the slow character of the flow after the embolization was felt to be worsened). Permanent complications occurred in 4% patients with the Karnofsky score at 70. All occurred after embolization performed through the anterior spinal artery. In 9% of patients, a mild deficit occurred after endovascular therapy with a Karnofsky score of 80. All these patients had 50% of their SCAVS controlled and none have rebled since then.

Recurrent hemorrhage occurred in 4% patients, all with cervical nidus intramedullary AVMs. Treatment was not completed at the time of their

recurrent bleeding episode; all of them were waiting for complementary embolization session. One patient refused further embolization, but she is stable at 4 years of follow-up. None of the remaining embolizations rebled (follow-up of 1–8 years), although none is anatomically cured.

No mortality related to endovascular therapy was noted in our series.

In a patient with a cervical lesion, after the second embolization procedure and after approximately two-thirds occlusion of the AVM with IBCA, a Brown-Sequard syndrome resulted, which persisted 4 years later. In one patient with a cervical lesion, a mild complication following embolization of a radiculomedullary artery in an unfused anterior spinal artery resulted in an anterior horn syndrome. In the lumbar area, after IBCA occlusion of a conus AVM in a patient who presented with subarachnoid hemorrhage and acute paraplegia, a 12-h delayed paraplegia with sphincter disturbances and impotence occurred. The paraplegia resolved, the lower extremity function has completely recovered, but the sphincter deficits and impotence remain.

Analysis of our results shows that the technique is reliable, reproducible, and safe using liquid embolic agents. Although it has been said that particles such as PVA are safer, the results are only temporary (Hall et al. 1989). We have seen a similar result with PVA (Fig. 11.66), not only in SCAVMs, but also in other locations. The recanalization mechanism is clearly explained in Chap. 14. This type of recanalization does not occur when using IBCA or NBCA in intranidal occlusion.

In highly specific instances, PVA may be acceptable as an agent that can give temporary protection when no other option exists. None of our patients treated by embolization with complete obliteration experienced a second hemorrhage.

In our historical series, two of the 47 embolized patients (4%) had a second hemorrhage; both patients had incomplete occlusions. The mean follow-up was 7.5 years. In our series, prior to treatment of three patients with cervical lesions, two had bled four times in less than 1 year and one had bled six times in less than 1 year. All three patients were treated with IBCA. No repeat hemorrhage has occurred after 4 years follow-up for one patient, after 6 years for the second, and after 5 years for the third. Although this is a relatively short time, it compares favorably to the natural history of SCAVMs, in which a second hemorrhage occurs within 1 month in 10% of patients and by 1 year in 40%.

11.5.4 Surgery in the Treatment of Spinal Cord Arteriovenous Malformations

In our neurovascular units, when assessing patients with SCAVMs, the options including surgical therapy are evaluated after MRI and angiography and prior to embolization.

In 41 patients reported by Yasargil et al. (1984), the AVM was completely removed as judged by surgery; in 73% of patients, no early or delayed angiographic confirmation was available and in 48% improvement was noted, although no mention was made as to how many were normal. These results compare favorably with those in our excellent and good groups, in which we achieved either a 77% normal condition or an improved condi-

tion in patients following embolization. Eight (19.5%) of Yasargil's patients were worse after total or partial AVM removal as compared to 17% in our series. In both groups, two recurrent hemorrhages occurred. There was one death directly related to surgery in Yasargil's experience; there were none in ours. Late death secondary to infection occurred in one in the surgery group, and a delayed ascending venous thrombosis resulted in death in one of our patients (Fig. 11.51). Three patients treated by surgery developed chronic postoperative pain, no new pain developed in the embolized group. Two patients with severe chronic pain and spasm did not benefit from embolization, whereas 10 of 13 patients of Yasargil's series did not show improvement in their pain.

What is important in some of the surgically treated patients is that surgical intervention with intradural ligation of feeding vessels (Ommaya et al. 1969) seems to favorably affect the natural history of the disease, but we do not think that such an approach should be discussed at the time of the endovascular decision, but rather only if that fails and if the patient needs immediate partial treatment.

In some rare instances where embolization is not possible or may carry high risk, surgery can be discussed. If the lesion is deemed embolizable and surgically accessible, endovascular surgery will be attempted first. The patient is followed up with repeat angiography. If obliteration is not complete or satisfactory, embolization is repeated.

Two patients in the Rodesch et al. series (2002) were operated on after embolization: one cervical SCAVS with multiple hemorrhagic episodes and an intranidal false aneurysm that could not be safely embolized. Subsequent surgical clipping of a radiculopial artery at the nidus was performed in order to change the flow into the lesion; it failed to produce secondary thrombosis of the arterial ectasia. A new embolization session through the anterior spinal successfully achieved exclusion of the patient's intranidal arterial aneurysm. The other patient had a thoracic SCAVM, where proximal arterial clipping was performed hoping to improve pain. This treatment failed and the patient was further managed medically. No other patients were proposed secondary surgery.

11.5.5 Radiotherapy of Spinal Cord Arteriovenous Malformations

Radiotherapy has currently no role in the management of SCAVMs.

11.5.6 Medical Therapy

Medical treatment for the various complications of spinal vascular lesions is an important part of patient management and should be provided. Physical therapy, nursing, pain control management, and psychotherapy all play an important role in treating patients with SCAVMs. A properly trained team is essential to obtain the best overall results. Heparin should be discussed when complete occlusion of a slow-flow SCAVM leaves a highly congested pial venous network at follow-up. Spontaneous thrombosis of SCAVMs is a rare situation; it is associated with worsening symptoms and may require heparin support for few weeks (Figs. 11.67, 11.68).

Fig. 11.67A–J. A 32-year-old female patient with a history of neurological events involving the lower limbs during childhood, for which no diagnosis was established, but resulted in mild spasticity involving the left lower leg. She remained stable for 25 years until subacute onset of rapidly progressive motor weakness and sensory disturbance occurred involving both legs. MRI at that time shows increased signal within the spinal cord with multiple flow voids along the level of the conus (**A–C**). Rapid neurological deterioration occurred over the next 4 days and repeat MRI demonstrates signal changes within the previous signal voids suggestive of acute thrombosis within several of the enlarged vascular channels (**D**, **E**). **F–J** see p. 845

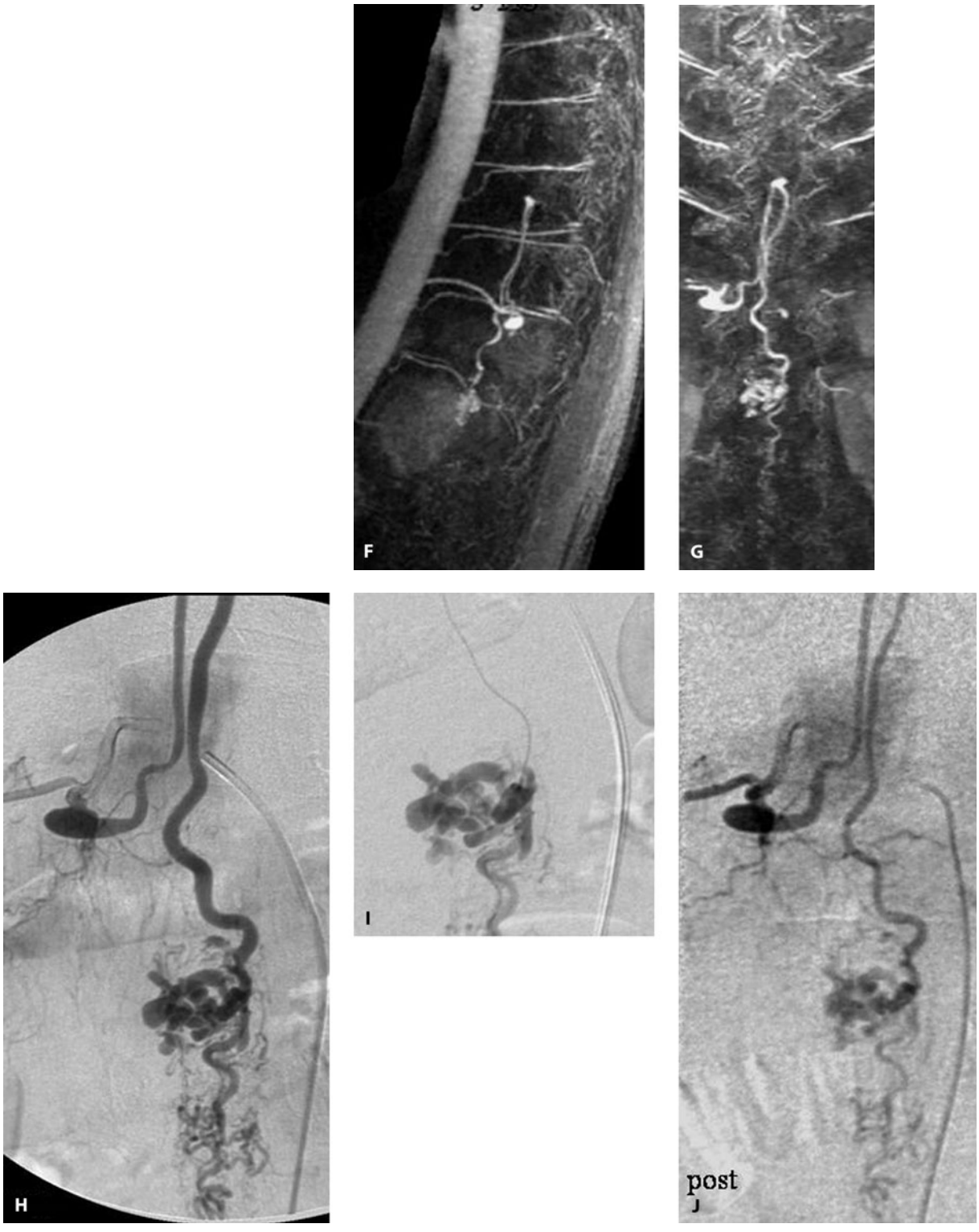

Fig. 11.67 (*continued*). MRA demonstrates spinal cord arteriovenous malformation (SCAVM) at the conus level (**F, G**). As venous thrombosis was thought to be the cause of the neurological worsening, the patient was started on anticoagulation therapy. Progressive worsening prompted partial endovascular treatment (**H–J**) to diminish the flow through the SCAVM in order to relieve the venous congestion associated the partial venous outlet thrombosis of the SCAVM and resulted in stabilization and subsequent improvement of neurological function

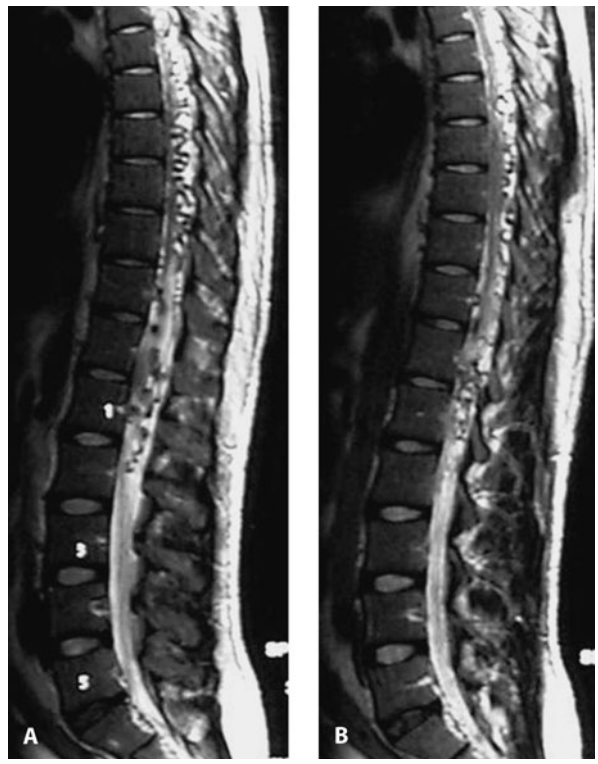

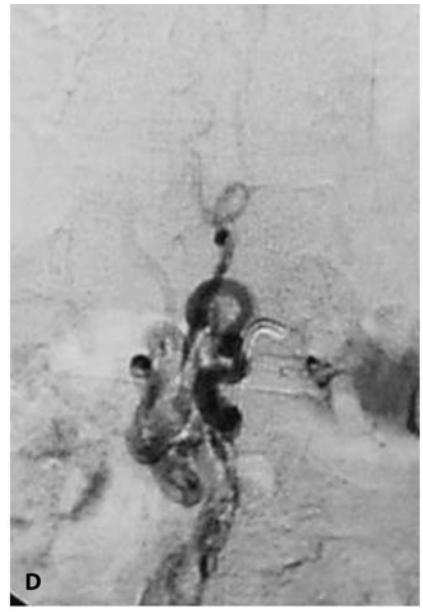

Fig. 11.68A–J. A 30-year-old male patient presented with progressive neurological deficit. **A**, **B**, MRI. **C–E** Angiography at that time shows slow-flow spinal cord arteriovenous malformation. **F–J** see p. 847

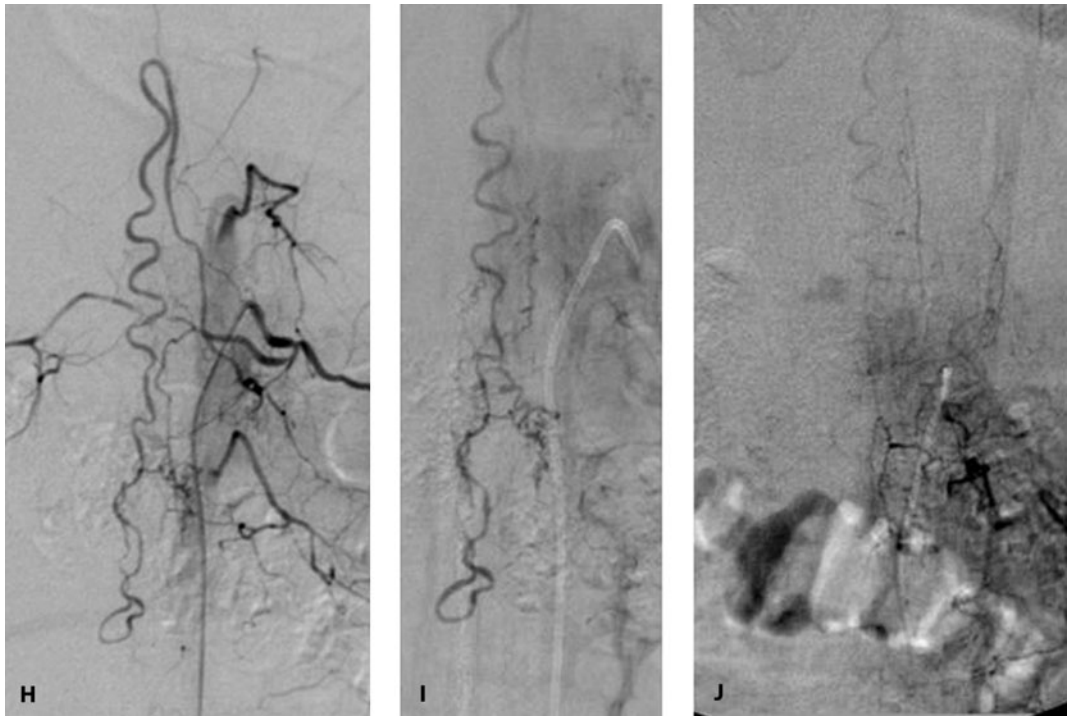

Fig. 11.68 (*continued*). **F, G** Worsening of the symptoms occurred and MRI follow-up 14 months later shows almost complete disappearance of vascular channels around the cord. **H–J** Follow-up angiogram at T11 and T12 confirms the complete thrombosis of the shunt with incomplete remodeling of the ventral spinal cord artery. The patient was placed on anticoagulant and steroid therapy for a few days, which resulted in early clinical recovery. (Courtesy of W. Lim)

12 Spinal Dural Arteriovenous Fistulae

12.1 Pathology 850
12.1.1 Macroscopic Appearance 851
12.1.2 Microscopic Appearance 853
12.1.3 Pathological Changes in the Spinal Cord 854
12.2 Pathophysiology 854
12.3 Clinical Presentation of Spinal Dural Arteriovenous Fistulae 858
12.4 Imaging of Spinal Dural Arteriovenous Fistulae 859
12.5 Treatment of Spinal Dural Arteriovenous Fistulae 867
12.5.1 Indications 867
12.5.2 Embolization of Spinal Dural Arteriovenous Fistulae: Techniques 867
12.5.3 Results of Spinal Dural Arteriovenous Fistula Embolization 869
12.5.4 Surgery for Spinal Dural Arteriovenous Fistulae 871
12.5.5 Postoperative Follow-up 872

As opposed to the so-called congenital arteriovenous malformations (AVMs) involving cord and paraspinal structures, spinal dural arteriovenous fistulae (SDAVFs) are acquired shunts located within or adjacent to dura along the spinal canal. They are by far the most frequent arteriovenous shunt (AVS) that occurs in older adults. They usually present after the fourth or fifth decade of life, with an 85% (5:1) male predominance (Tables 12.1, 12.2). The reason for this male predominance at the spinal level is not known, and this dominance is reversed in dural and osteodural AVSs at the skull base and sphenoid level, where there is a female predominance. The location of the fistula has been reported throughout the spinal canal, from the sacrum to the level of the foramen magnum. The venous drainage may be very extensive and reach the intracranial dural sinuses even if the shunt is at the sacral level (Fig. 12.1) or conversely reach the thoracic perimedullary venous plexus level from an intracranial shunt.

Table 12.1. Age distribution in 352 SDAVF and SCAVM patients at time of diagnosis

	n	SDAVFs	Mean	SCAMVs	Mean
Djindjian et al. 1977	130	34–73	52	3–57	26
Rosenblum et al. 1987a	81	25–72	49	4–58	27
Berenstein and Lasjaunias 1992	81	35–87	56	2–42	22
Symon et al. 1984	60	29–75	57	14–40	31

SDAVF, spinal dural arteriovenous fistula; SCAVM, spinal cord arteriovenous malformation.

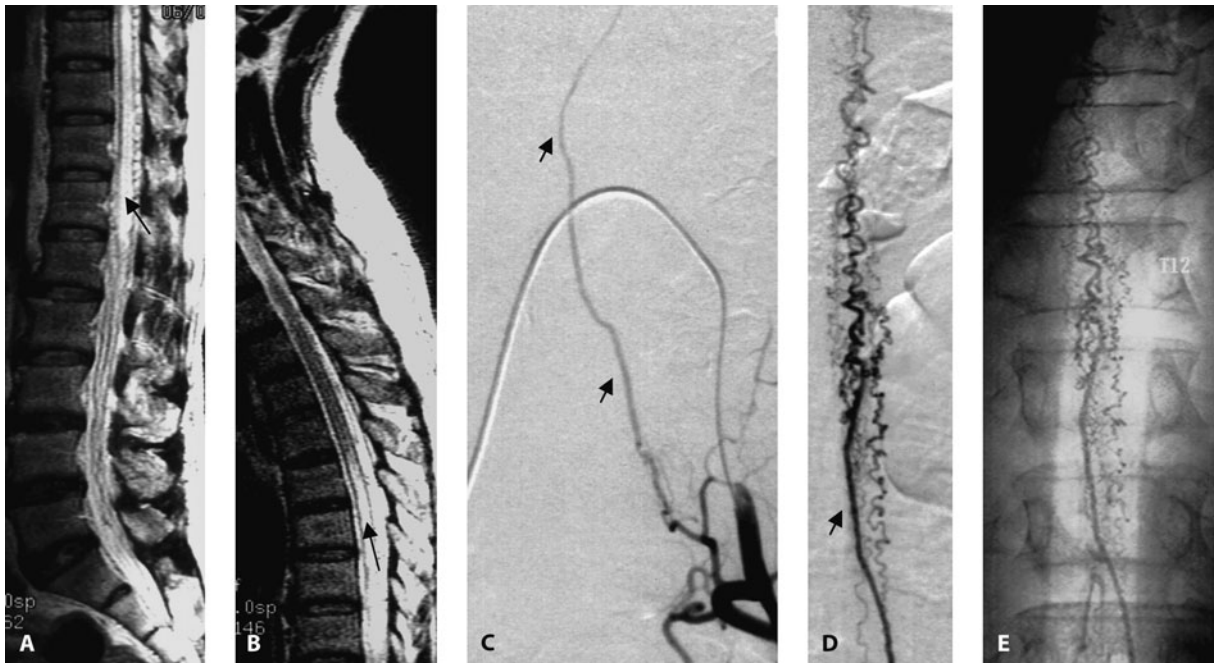

Fig. 12.1A–E. Progressive thoracic myelopathy. MRI investigation (**A**, **B**) shows evidence of increased signal changes in the cord extending up to the mid-thoracic level (*arrows*) and prominent flow voids, in particular along the dorsal aspect of the spinal cord. Angiography shows this was caused by a spinal dural arteriovenous fistula fed by the lateral sacral artery (**C**), with retrograde venous drainage via the sacral radicular vein (*arrows*) toward the dorsal perimedullary venous plexus at the conus level (**D**, **E**)

Table 12.2. Sex and age distribution in 172 patients with SDAVF

	(Patients) *n*	Male	Female	Mean age
Djindjian et al. 1977	46	38	6	52
Merland et al. 1980a	13	10	3	59
Symon et al. 1984[a]	55	49	6	57
Rosenblum et al. 1987a	27	23	4	49
Berenstein and Lasjaunias 1992	31	25	5	56
Total	172	145 (85%)	25 (15%)	55

SDAVF, spinal dural arteriovenous fistula.
[a] Includes Kendall's first ten patients.

12.1 Pathology

An SDAVF is an abnormal arteriovenous shunt in the dura, most commonly at the level of the intervertebral foramen (Kendall and Logue 1977; Merland et al. 1980b; Symon et al. 1984; Rosenblum et al. 1987a). The arterial supply mostly arises from a dural (radicular) branch of the dorsospinal artery (see Vol. 1) in the region of the intervertebral foramen. The spinal cord veins (in contrast to the arteries) can pierce the dura quite far from a nerve root. In this venous disposition, a potential bimetamere

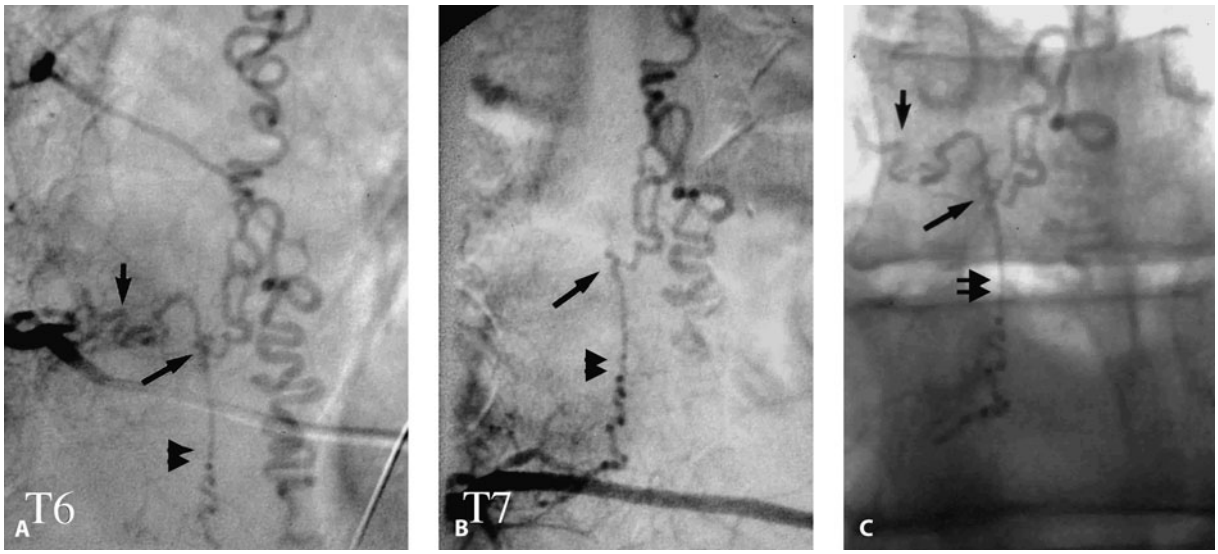

Fig. 12.2A–C. Spinal dural arteriovenous fistula supplied by intersegmental dural anastomosis. Angiography of intercostal artery at *T6* (**A**) demonstrates radicular supply (*short arrow*) towards SDAVF (*long arrow*) with reflux down the intersegmental anastomosis (*double arrows*). Angiography of intercostal artery *T7* (**B**) shows radicular supply to the SDAVF via the same intersegmental anastomosis (*double arrows*). Injection of liquid glue via T6 (**C**) shows deposition of embolic material down the intersegmental anastomosis as well as across the arteriovenous fistula toward the perimedullary venous plexus of the spinal cord, resulting in permanent obliteration of the shunt and good clinical outcome

arterial supply to the dural arteriovenous fistula (DAVF) can be demonstrated (Figs. 12.2, 12.3). However, in the great majority of patients, there is a single extradural arterial pedicle that gives rise to a small (sometimes microscopic) shunt that is within the dura itself. From this shunt, a highly tortuous, single draining vein emerges. This vein pierces the dura several millimeters from the accompanying nerve root (either above or below it) to reach the perimedullary venous system (Benhaim et al. 1983) and then produces venous hypertension of the medullary veins (see Sect. 12.2).

12.1.1 Macroscopic Appearance

The nidus of the DAVF can be located anywhere along the dura but is most commonly situated near the nerve root exit. The abnormal arteriovenous shunt is usually not readily visible using an extradural surgical approach (Benhaim et al. 1983).

The spinal radicular veins enter the dura close to the nerve root in 60% of patients and away from the nerve root in 40%. Shunting of arterialized blood from the DAVF into the radicular vein causes reversal of flow in this vessel, resulting in enlargement of the radicular vein in the intradural space. The ascending vein is usually a single, dilated, tortuous channel that reaches the perimedullary venous network most frequently on the dorsal surface of the spinal cord. Patients with both posterior and anterior medullary drainage tend to have more severe symptoms than those

Fig. 12.3A–D. A 48-year-old female patient presented with slowly progressive thoracic myelopathy and MRI compatible with venous congestion from spinal dural arteriovenous fistula (SDAVF). Spinal angiography demonstrates dual supply from *T8* (**A**) and *T7* (**B**) toward the intersegmental dural anastomosis (*small arrows*), which in turn supplied the DAVF (*arrowhead*). Selective catheterization of the radicular artery at the *T8* level (**C**) and embolization with glue resulted in deposition of the embolic material just proximal to the fistulous communication (*arrowhead*). Immediate follow-up angiogram at the *T7* level shows the continued opacification of the fistula (*arrowhead*) from the radicular artery at that level (**D**), indicating the lack of venous penetration of the embolic material. Surgical disconnection was achieved 2 days later by dividing the radicular vein intradurally, resulting in good clinical recovery

with exclusively posterior drainage. The subsequent direction of the perimedullary venous drainage is most often upward toward the thoracic and cervical levels.

12.1.2 Microscopic Appearance

The dural (feeding) arteries originating at the sacrolumbar or thoracic levels often divide into small branches and then merge into a single artery before entering the shunt. These small arteries show no structural abnormalities.

The large draining radicular vein is always single, intradural, and usually very dilated and tortuous, with irregular partial thickening and variable luminal narrowing. The normal dorsal medullary vein is rarely single at the thoracolumbar level (see Vol. 1) but normally divides into three channels of a smaller caliber at the lower mid-thoracic level. Due to this normal disposition of venous architecture with limited venous outflow capacity, recruitment of additional venous drainage often involves the vasa corona and dorsolateral spinal venous channels. Wall thickening of these venous channels, whether circumferential and/or limited to a cushion-like plaque, is nearly always present. Such thickening frequently involves the intima and/or the media. Atherosclerotic changes and calcifications can sometimes be found in the veins. Stenosis to near complete occlusion is also found in some segments.

Various stages of thrombosis can be seen, which may range from occlusion to full recanalization. Similar changes have been described as a frequent incidental finding at autopsy.

In general, the arteriovenous communication is microscopic and therefore may be difficult to identify at surgery. Benhaim et al. (1983) were able to obtain two specimens of the fistula itself. Examination revealed the vascular lesion to be situated within the dura mater. The structure of these fistulous vessels was not that of normal veins or arteries. Some of the vessel wall will appear similar to that of arteries, with a lamina elastica interna (LEI), prominent smooth muscle cells, poor connective tissue, and a thick and rigid wall. The LEI frequently divides into two or more layers of elastin; muscular atrophy and increased connective tissue were present in the media. Other vessels looked more like veins without evidence of anomalous changes in the media. Still others looked like veins with no LEI, much more connective tissue, and a rather thin and flexible wall, with modifications such as irregular thickening due to collagen and/or elastin fibrosis and hypertrophy of smooth muscle cells. Interestingly, Benhaim et al. (1983) found no calcifications or thromboses in the arteriovenous fistula and in both specimens they were able to describe a free communication between vessels of different structure. The arteriovenous shunt could be seen in serial sections, demonstrating two arterial structures anastomosing and merging with a small-caliber vein through a short, narrow channel.

The histological description, and in particular the appearance of the draining vein, would suggest evidence of a dystrophic aspect rather than a dysplastic lesion, with changes secondary to local venous hypertension

resulting from the arteriovenous shunt. The histological changes seen in these veins are very similar to those seen in saphenous veins used for coronary bypass grafts. The atherosclerotic and calcific changes in the veins are also quite compatible with an acquired lesion.

12.1.3 Pathological Changes in the Spinal Cord

Extensive pathological changes may be present within the cord itself, even though the primary structural abnormality is entirely extramedullary. In advanced lesions, histological abnormalities are evident throughout the cord. The changes particularly involve the lateral corticospinal tract and appear to spread gradually into adjacent portions of the white matter of the lateral funiculus. More advanced changes progressively involve the anterior gray matter and the posterior columns. Gillilian (1970) pointed out consistent sparing of the anterior median segment. A typical feature in long-standing advanced lesions is the appearance of neocapillaries within the cord itself. This particular change has been confused with the presence of an arteriovenous nidus. Our current understanding of the venous anatomy and the pathophysiology of the disease has taught us that these neocapillaries are primarily the congested intrinsic venous network of the spinal cord. This is different from secondary neovascularization, which will result from chronic and extensive hypoxia secondary to long-standing venous congestion (sprouting angiogenesis from venules) (Folkman 1975). The end stage of this venous congestion, venous ischemia and its impact on the spinal cord, will be similar to the syndrome described by Foix and Alajouanine (1926).

12.2 Pathophysiology

In 1972, Manelfe et al. described a glomerulus-like structure that he called *peloton vasculaire*, or vascular balls (Fig. 12.4). These are normal vascular structures, usually situated between two layers of the dura mater. In his specimen, usually two or more afferent arterioles converged into this vascular ball and drained through a single vein located intradurally. Unfortunately, in Manelfe's specimen the dura mater was transected and the vein could not be followed. These normally present structures, which we will call the glomerulus of Manelfe, can routinely be found in the upper lumbar or dorsal regions but are absent at the cervical level. The striking resemblance between the glomerulus of Manelfe and the SDAVF was noted by Merland et al. (1980a). The former structures are believed to have the function of preserving constant venous pressure in the spinal cord, regardless of changes in intra-abdominal or intrathoracic pressure. Therefore, it appears that SDAVFs may result from a loss of the normal physiological control of this system.

However, if this were the sole mechanism responsible for SDAVFs one would expect the condition to occur far more frequently. Therefore, additional factors must also contribute to the development of these fistulae.

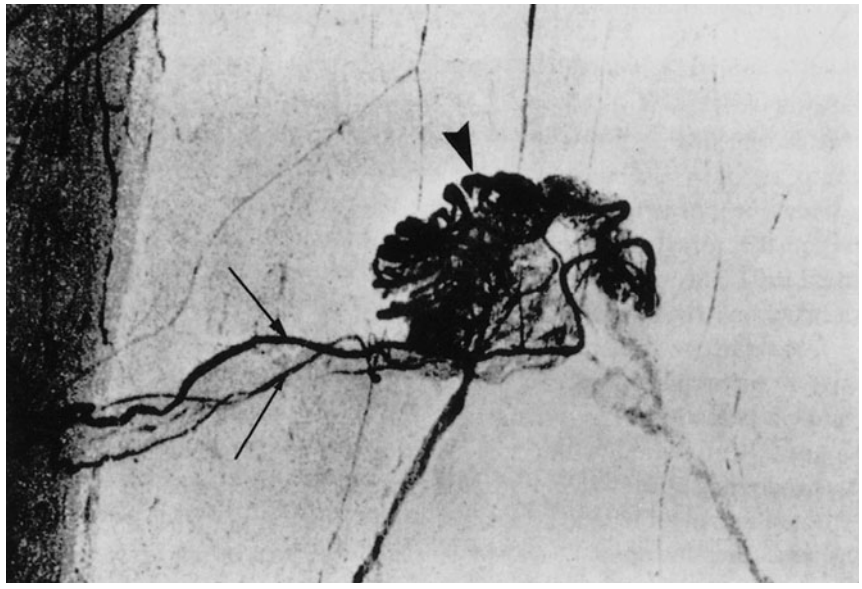

Fig. 12.4. Glomerulus of Manelfe specimen removed from a normal dura of the spinal cord, after injection with a radiopaque material, demonstrates a glomerulus-like structure (*arrowhead*) situated between two layers of the dura mater. Note the two afferent arterioles (*arrows*) reaching into this vascular ball, with a single draining vein that has been cut. (Courtesy of Prof. C. Manelfe)

Tadie et al. (1985), in their study of the morphological functional anatomy of the spinal cord veins, demonstrated that the lumbar and lower thoracic portions of the spinal cord normally drain cephalad into the radiculospinal veins , which are small in caliber (see Vol. 1). This makes drainage from the lumbar and thoracic cord somewhat tenuous and sensitive to hemodynamic alterations. At the cervical level, symptomatic SDAVFs are extremely rare, since the venous drainage is divergent and therefore favorable, in contrast to the convergent lumbothoracic venous drainage (Moss et al. 1989).

During normal physiological changes of intra-abdominal and/or intrathoracic pressure (Valsalva, defecation, respiration, etc.), the pressure in the spinal cord veins remains constant. Furthermore, Tadie claimed that it is impossible to inject the spinal veins from the periphery. To explain this, various investigators have postulated the presence of valves in the spinal venous system (Lazorthes 1978), although no anatomical proof can be provided.

Tadie, in his histological sections, was also unable to find actual valves in the spinal veins. He did, however, demonstrate an important narrowing of the radiculospinal veins at the point where they cross the dura mater. At this point, the vein loses its own wall, which is replaced by an arachnoid cuff and by the dura itself. In addition, as the vein enters and exits the dura, it does so in a zigzag fashion. Tadie postulated that, under normal physiological conditions, the narrowing and zigzagging opposes any blood flow from the periphery into the intradural space, so that blood flow is only permitted in the physiological direction. Such a configuration is a consistent disposition at the normal sinodural junction. If the venous pressure were to increase abnormally, then the arachnoid cuff would become engorged and obstruct the vein. In addition, a glomerulus-like structure (similar to the glomerulus of Manelfe) was demonstrated at the point where the normal draining vein crosses the dura mater. These observations have led to the term "the protective anti-back flow system."

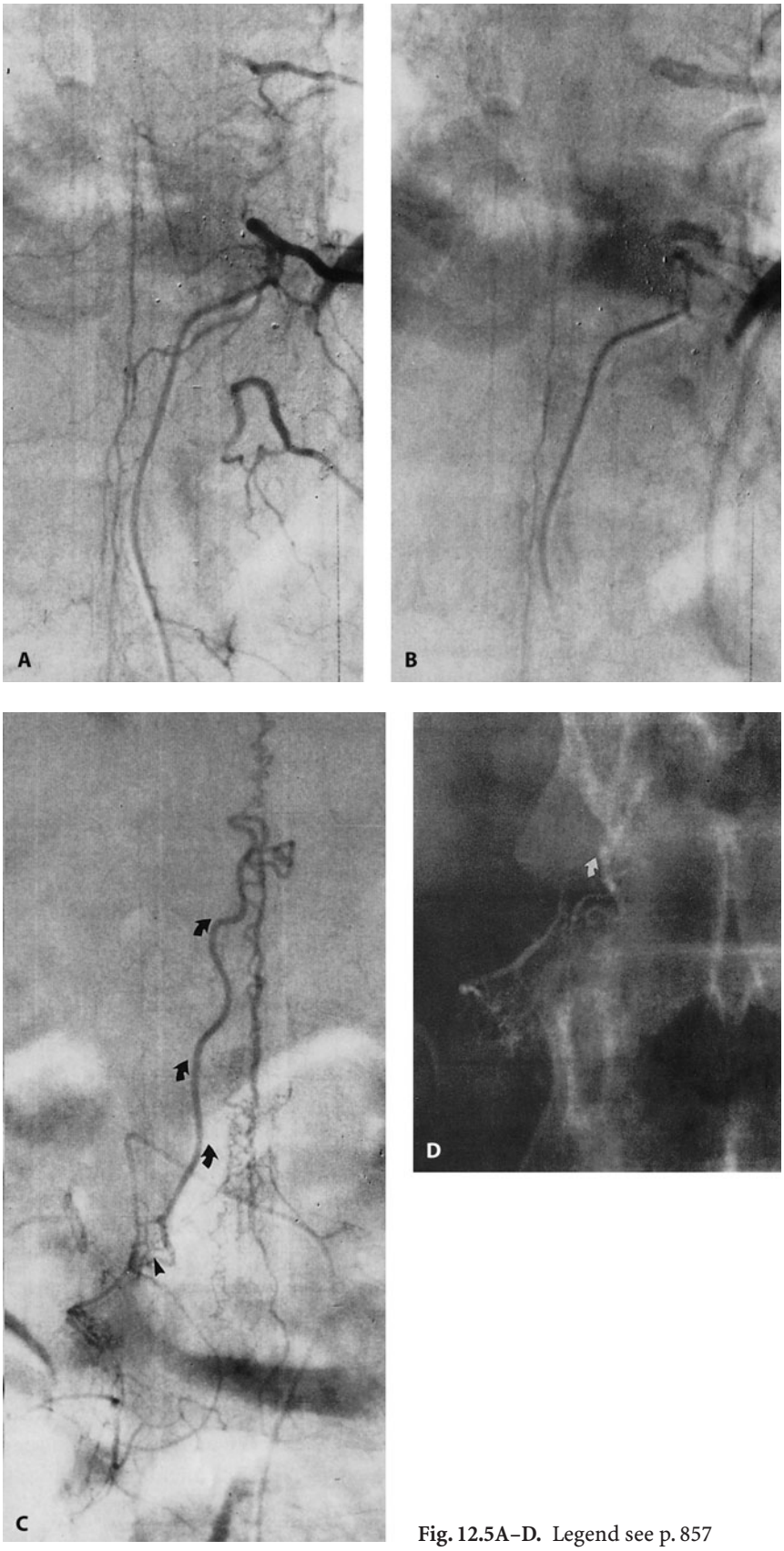

Fig. 12.5A–D. Legend see p. 857

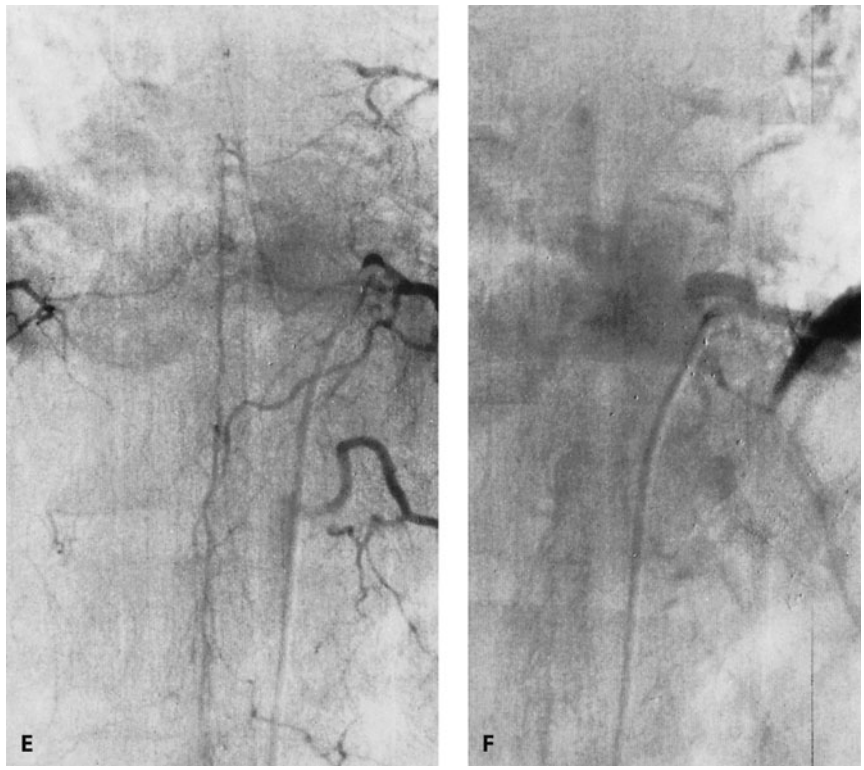

◄ **Fig. 12.5A–F.** Spinal dural arteriovenous fistula (SDAVF): anterior spinal artery and vein circulation. **A** Mid-arterial phase. **B** Late phase of the left T10 intercostal artery, which gives rise to the spinomedullary artery; this phase failed to demonstrate the radiculospinal vein. **C** Superselective injection of the right L2 lumbar artery demonstrates the SDAVF (*arrowhead*), the single ascending draining vein (*curved arrows*), and the ascending venous drainage. **D** Plain film shows the radiopaque acrylic deposition with occlusion of the dural lesion and the first centimeter of the ascending draining vein (*white curved arrow*). **E, F** Postembolization follow-up angiogram of the anterior spinal axis shows normal arterial (**E**) and venous (**F**) circulation time after treatment, with opacification of the radiculomedullary vein (compare to **A** and **B**)

During selective spinal angiography, following the injection of the anterior spinal artery, one can routinely demonstrate the drainage of the spinal cord into the radiculospinal veins. In SDAVFs, such spinal cord drainage is delayed (Fig. 12.5) and the venous return of the DAVS usually takes an ascending course toward the cervical and/or intracranial regions. Furthermore, maneuvers that change intra-abdominal or intrathoracic pressure can aggravate symptoms in this condition. Tadie has proven that in SDAVFs one can reflux into the spinal veins from extraspinal injections, testifying to an impaired venous protective system.

In one of our patients, an abnormal shunt at the epidural level was noted as causing root pain at that time. Some 4 years later, with venous drainage towards the medullary veins, the patient developed a myelopathy.

An additional factor to consider is the requirement that a preexisting restriction of the venous drainage of the spinal cord and/or meninges may be present to make the acquired SDAVF symptomatic. The presence of thrombosis and recanalization seen pathologically is consistent with the pathophysiology of intracranial dural AVMs.

Thiebot et al. (1986) reported the case of a 24-year-old female patient with multiple SDAVFs draining into spinal veins without venous restrictions or flow impairment. The patient had exhibited minimal nonprogressive symptoms since childhood and was followed for an additional 5 years. The angiographic studies in this patient showed multiple SDAVFs with vascular structures similar to the glomerulus of Manelfe. Clear arteriovenous shunting was noted in the angiograms but no associated outflow restrictions were seen. The lesions drained through spinoradicular veins. This finding is highly suggestive of a congenital anomaly of the normal anti-back flow mechanism described by Tadie et al. (1985). In contrast to the acquired (symptomatic) type of SDAVF, this lesion was in a very young patient, the arteriovenous fistulae were multiple (and only in the thoracolumbar area), the paraspinal venous drainage had a normal appearance, and an unimpaired, normal-to-increased medullary transit time was present without stagnation.

The usual clinical findings of the slowly progressive mixed motor and sensory myelopathy are reversible if properly treated in its early stage, although its effects may become irreversible in later stages when it is associated with a necrotizing myelopathy. This myelopathy can be explained by chronic venous hypertension (Aminoff et al. 1974b; Merland et al. 1980a; Symon et al. 1984).

The arteriovenous shunting into the coronary venous plexus of the spinal cord may extend to the dorsal and/or ventral surface of the cord. Extension may also occur upward to the cervical or intracranial dural sinuses. One will not see the radicular spinal veins at the lumbar or thoracic area draining these lesions or the spinal cord itself. As the pressure in the venous system increases, it is progressively transmitted toward the intrinsic veins of the spinal cord, mainly those of the posterolateral white matter and lateral corticospinal tract, and subsequently affects the lateral funiculus, posterior column, and anterior gray. The relative sparing of the anterior median segment of the spinal cord is probably related to the anatomical organization, which preserves the central veins and of the anterior median spinal vein (Symon et al. 1984).

Venous hypertension reduces the arteriovenous pressure gradient and decreases tissue perfusion, resulting in progressive hypoxia to the spinal cord. The raised venous pressure further decreases blood flow by producing progressive intramedullary vasodilatation, with possible progressive exhaustion of autoregulation in the affected areas. Progressive vascular dilatation in this uncontrolled fashion reaching the capillaries results in the transmission of undamped pulsations to the cord, decreased tissue perfusion with edema formation, and progressive loss of cord tissue function.

12.3 Clinical Presentation of Spinal Dural Arteriovenous Fistulae

The clinical presentation of DAVFs has been documented in various series in the literature (Kendall and Logue 1977; Merland et al. 1980a; Djindjian 1978; Symon et al. 1984; Rosenblum et al. 1987a) and was documented

Table 12.3. Symptoms of spinal dural arteriovenous fistulae[a]

Symptoms	Initial symptoms (%)	Symptoms at diagnosis (%)
Back and/or root pain	28	37
Paresis	40	88
Impotence	3	43
Bowel disturbance	4	75
Bladder disturbance	5	85
Hemorrhage	0	0

[a] Total number of patients, 172. Based on Djindjian et al. 1977; Merland et al. 1980a; Symon et al. 1984; Rosenblum et al. 1987a; Berenstein and Lasjaunias 1992.

in the first edition of this book (Vol. 5, Chap. 1) (Tables 12.1–12.3). Subsequently, additional series and case reports have been published (Brunerau et al. 1996; Hurst et al. 1995; van Dijk et al. 2002).

There is a 5:1 male-to-female ratio in SDAVFs and age ranges from 25 to 78 years. The vast majority of the patients, however, were older than 50 years of age at the time of presentation, and the average age at presentation was 68 in the van Dijk series (2002).

In van Dijk's series the clinical history showed that the first signs of DAVFs were spastic gait in 55%, paresthesias in 47%, and pain in 33%. The time interval between initial symptoms and diagnosis was on average 10.5 months.

At the time of presentation for medical consultation, leg weakness or paraparesis was documented in 96%, sensory numbness or paresthesia occurred in 90%, urinary incontinence or retention in 82%, bowel problems in 65%, and pain in 55% of patients. Sexual dysfunction is a frequent presenting symptom but often not discussed and poorly recorded. Intradural hemorrhage, as a rule, does not occur with SDAVFs but has been reported in exceptional circumstances (Do et al. 1999).

12.4 Imaging of Spinal Dural Arteriovenous Fistulae

Advances in noninvasive imaging have greatly contributed to our ability to establish the timely diagnosis of spinal DAVFs. The role of plain films, myelography, and computed tomography has been taken over by MRI, which reliably demonstrates the presence of signal changes within the cord, signifying the imaging equivalent of the clinical symptomatology. The absence of significant mass effect and the nonspecific slight enhancement following intravenous contrast administration all favor the nonneoplastic or nondemyelinating cause of these MRI findings (Masaryk et al. 1987; Gilbertson et al. 1995). In addition, abnormal flow voids can be seen, representing the prominent perimedullary venous system associated with the retrograde venous reflux from the DAVF. These findings on MRI are nonspecific for the actual location of the dural fistula (Figs. 12.1, 12.6) but are highly specific for their impact. Epidural, dural, and perimedullary AVSs may all produce similar MRI findings, and therefore their clinical symptoms may also be similar (Figs. 12.7–12.9). Spinal

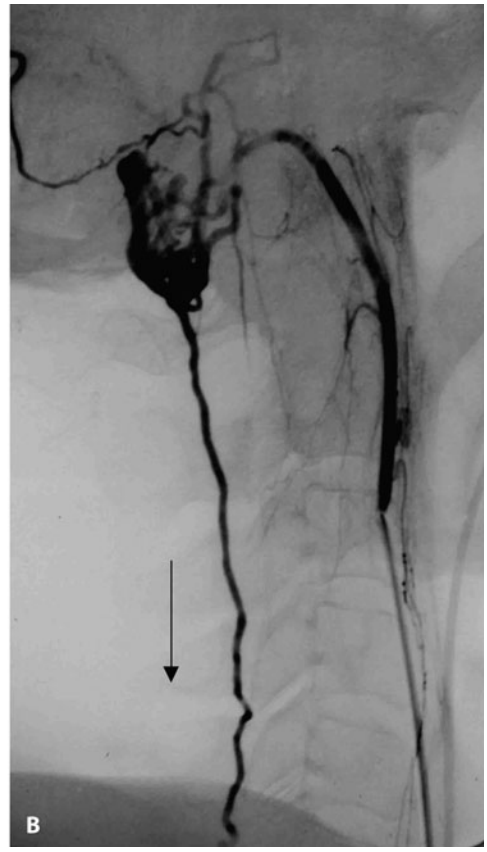

Fig. 12.6A, B. A 52-year-old man presented with a 5-month history of progressive thoracic myelopathy. MRI (**A**) shows increased signal changes within the thoracic spinal cord (*arrows*) and possible flow voids along posterior aspect of the cord. Spinal angiogram with verification of the anterior spinal axis at the thoracic level showed delayed venous phase, requiring a search for a dural arteriovenous fistula, which, at the time of a second angiogram (**B**) was shown to be located at the foramen magnum and fed by the ascending pharyngeal artery and to be draining downward toward the cervical and thoracic levels (*arrow*)

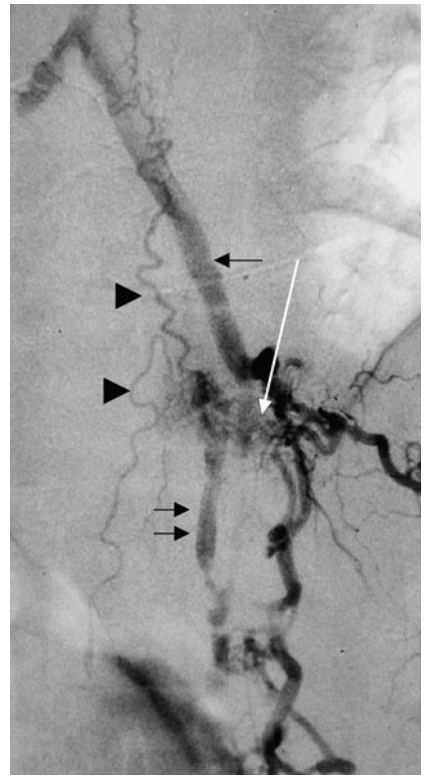

Fig. 12.7. Epidural arteriovenous shunt at the low thoracic level (*long arrow*) with drainage outward toward the hemiazygos system (*short arrow*) as well as toward the epidural venous plexus within the spinal canal (*double arrows*) and associated with retrograde pial spinal cord venous drainage (*arrowheads*)

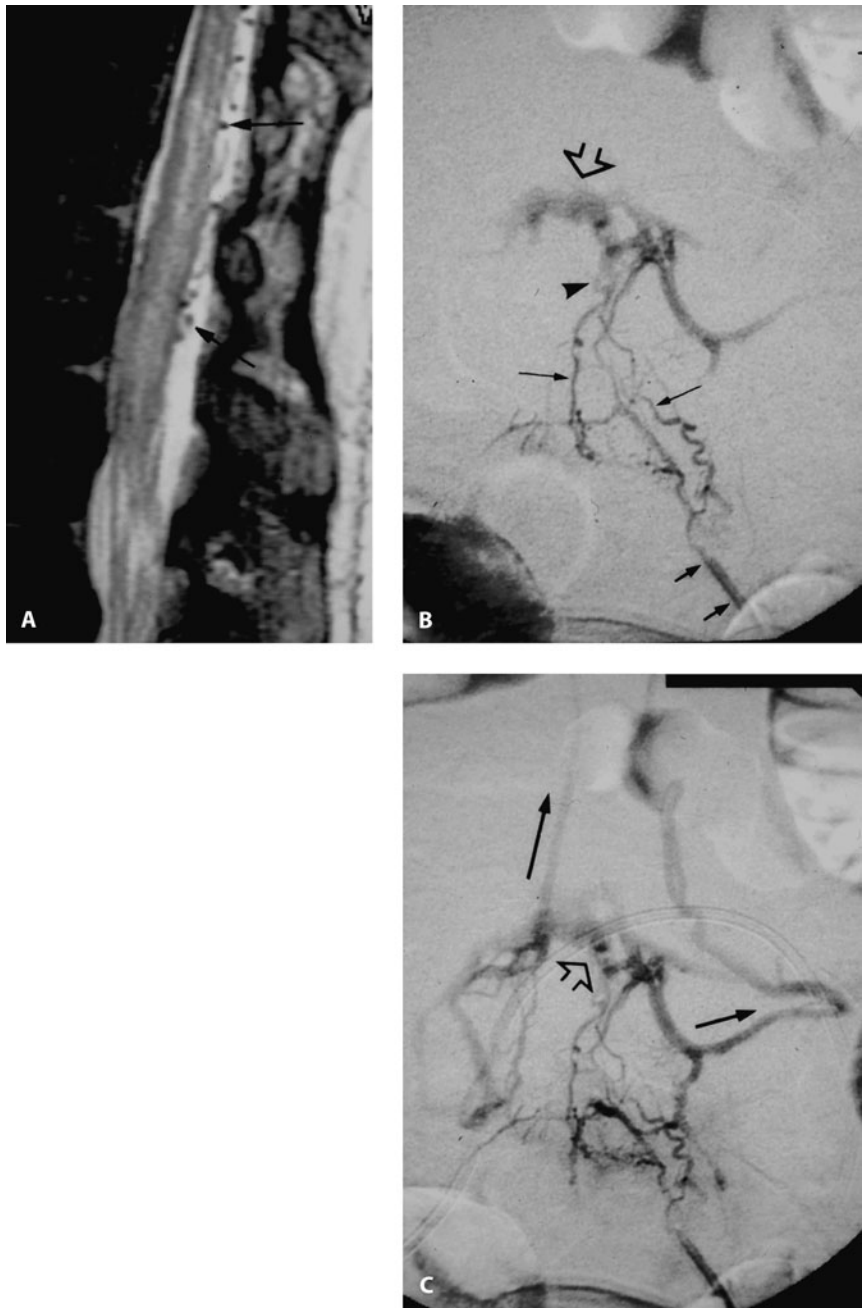

Fig. 12.8A–C. A 72-year-old man presented with a 2-month history of progressive myelopathy. MRI (**A**) demonstrates evidence of prominent flow voids (*arrows*) along posterior aspect of the cord and increased signal at the conus level. Selective angiography into the lateral sacral artery (*double arrows*, **B**) shows arterial supply (*short arrows*) converging toward an epidural sacral arteriovenous shunt (*arrowhead*) draining toward the epidural venous plexus (*open arrowhead*). **C** Drainage toward the ascending lumbar venous system was noted as well as reflux toward the sacral radicular vein, which drained cranially toward the conus along the R S1 nerve root (*long arrow*)

angiography will be needed to separate out these different etiologies and establish the exact nidus location of the AVS. Improvements in MRI technique (Farb et al. 2001, 2002) have resulted in our ability to noninvasively demonstrate the actual location of the AVF along the dura, which, when present, will help focus the spinal angiogram on a specific segmental level (Figs. 12.10, 12.11).

Spinal angiography is done when MRI has demonstrated evidence compatible with a venous congestive myelopathy as the explanation for the clinical symptomatology. While in the past the angiogram was done as part of the investigative process, nowadays it is done with the diagnosis of

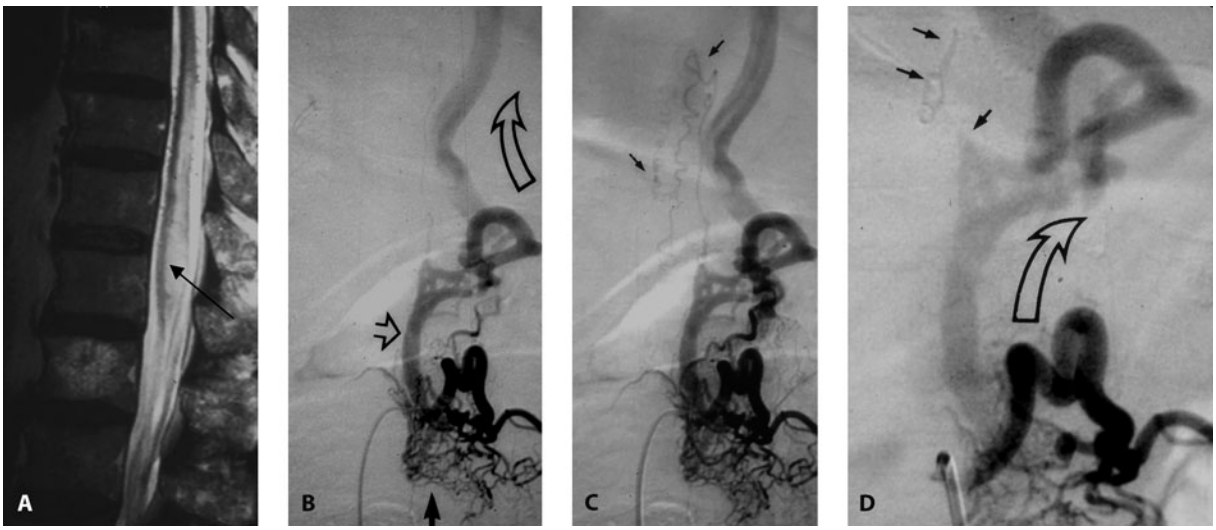

Fig. 12.9. Paravertebral, epidural arteriovenous malformation presenting with myelopathy, which on MRI (**A**) shows evidence of increased signal changes within the spinal cord (*arrow*). At selective angiography (**B**, **C**), this proved to be related to retrograde radicular venous drainage from the epidural venous plexus (*open straight arrow*) to the perimedullary veins of the cord (*arrows*). The draining vein was surgically clipped (*arrows*, **D**) to disconnect the epidural venous system from that of the spinal cord, leaving the epidural arteriovenous shunt to continue to drain toward the paravertebral hemiazygos venous system (*open curved arrow*)

DAVF already strongly suspected or even confirmed by MRI. It can therefore be more efficient and focused on the potential for endovascular treatment. It remains important to assess the blood supply to the spinal cord and in particular the origin of the main supply to the anterior spinal artery (radicular-medullary arterial supply). This will allow for assessment of the circulation time within the spinal cord, which should be delayed if the myelopathy is caused by venous congestion (Fig. 12.5) (Launay 1979; Merland et al. 1980; Merland and Reizine 1987; Willinsky 1990b). It has been our routine to inject nonionic contrast material at 1 cc/s for 10 s into the intercostal or lumbar artery that supplies the anterior spinal axis (radicular-medullary arterial system). Delayed opacification of the venous phase (perimedullary and radicular-venous systems) of the region (supplied by the anterior spinal artery) beyond 20 s confirms the probable venous cause of the myelopathy. If the myelopathy is at the cervical level the cervical anterior spinal axis should be examined rather then the radicular-medullary arterial system at the thoracolumbar level.

Another important reason to examine and to establish the origin of the anterior spinal artery is that it can be located at the same level as the radicular supply to the dural fistula. This information may preclude safe endovascular treatment of the DAVF (Figs. 12.12, 12.13) (Agarwal et al. 1992).

While the majority of the DAVFs are located in the dura adjacent to the nerve root, occasionally the location is along the dura between two adjacent nerve roots (intersegmental). This will invariably result in dual arterial supply to these types of DAVSs and make it imperative at the time of treatment to reach the venous outlet of the shunt, as otherwise the shunt will continue to be fed by the untreated arterial pedicle.

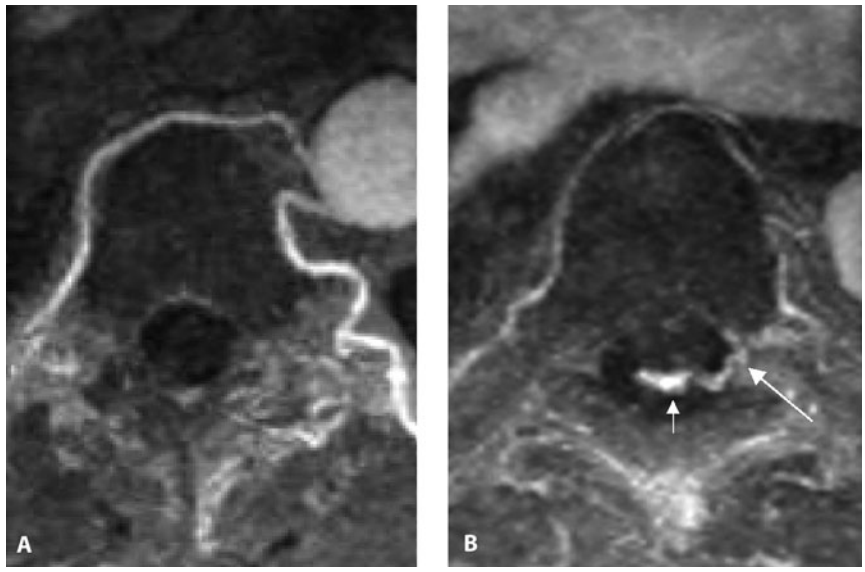

Fig. 12.10. Example of contrast-enhanced MRI axial view, at the level of the intercostal arteries, demonstrating normal vascular appearance (**A**) and findings in a case of spinal dural arteriovenous fistula (SDAVF, **B**). A prominent vascular channel enters the spinal canal at the foraminal level (*long arrow*) and runs toward the posterior aspect of the spinal cord, showing the draining radicular vein from an SDAVF at the foramen level refluxing toward the dorsal perimedullary venous plexus of the spinal cord (*short arrow*)

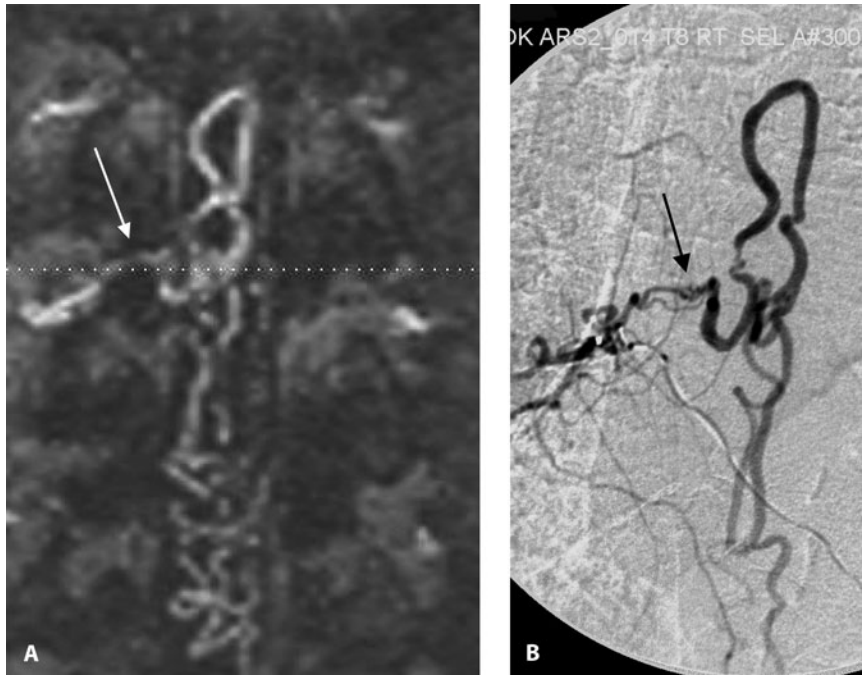

Fig. 12.11A, B. Example of contrast-enhanced MRI (coronal view, **A**) in a patient investigated for possible spinal dural arteriovenous fistula (SDAVF), demonstrating prominent vascular channel (*arrow*) entering intervertebral foramen as well as tortuous prominent channels within the spinal canal. Selective angiography of the radicular artery at that same level demonstrates excellent correlation with the MRI findings, confirming the presence of SDAVF (*arrow*) and the refluxing radicular vein towards the perimedullary venous plexus of the spinal cord

While the location of the DAVF can be anywhere along the dura, a cervical localization is extremely uncommon. In the Toronto series (van Dijk et al. 2002), the most frequent location was mid-thoracic and 70% of DAVFs were located on the left side. It is also accepted that the location of the dural shunt may be at the level of the foramen magnum or even intracranial (Figs. 12.6, 12.14) and yet present with spinal cord myelopathy due to the rerouting of the venous drainage of the shunt toward the perimedullary venous system of the spinal cord (Willinsky et al. 1990c; Mahagne et al. 1992; Bret et al. 1994). Part of the angiographic protocol

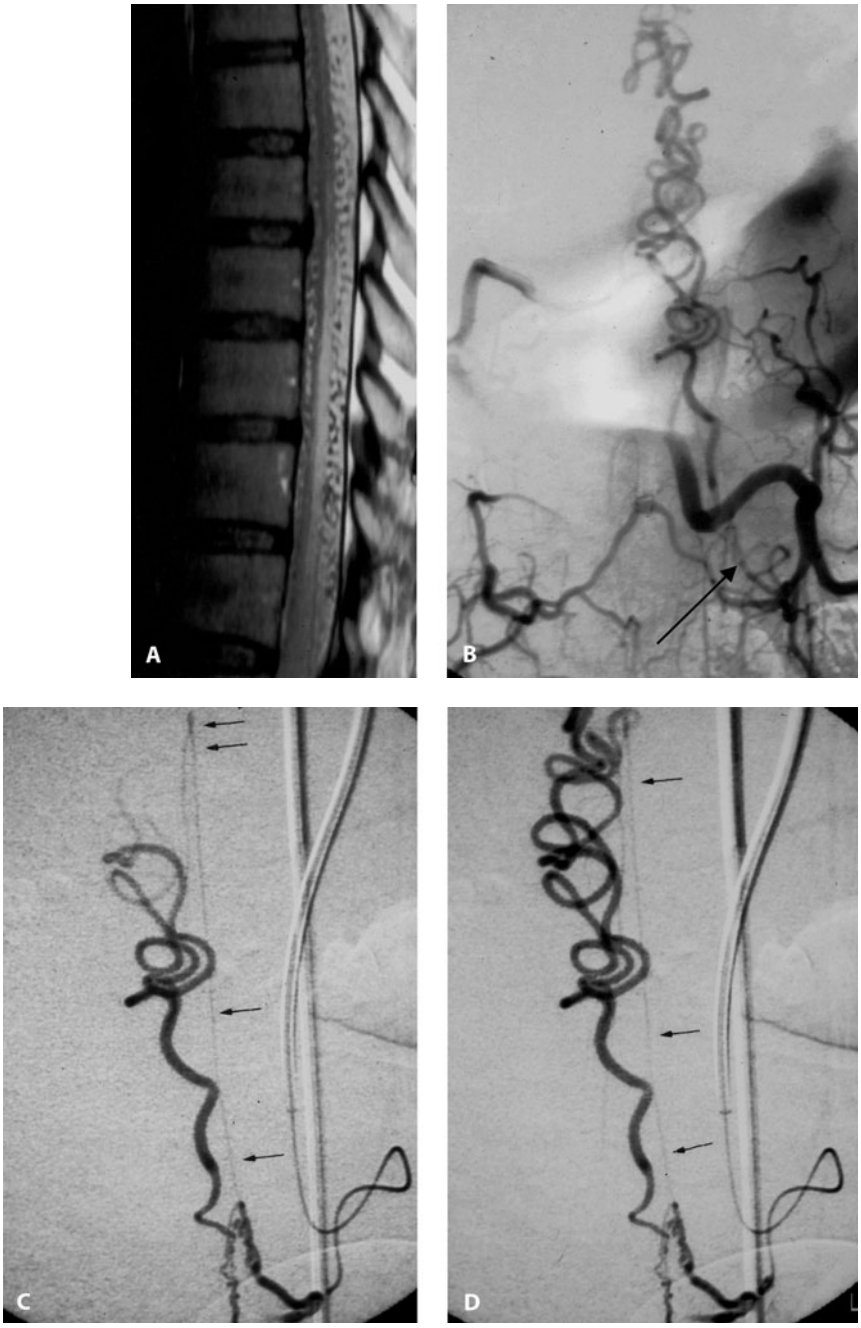

Fig. 12.12A–D. A 48-year-old woman presented with progressive myelopathy of several months duration. MRI (**A**) shows evidence of increased signal changes within the spinal cord and prominent flow voids along the dorsal and ventral aspect of the cord. Angiogram at L2 (**B**) shows evidence of opacification of spinal dural arteriovenous fistula (SDAVF) on the left side (*arrow*). Selective catheterization of the radicular branch of the L2 lumbar artery (**C, D**) shows that the same radicular artery supplies the AVF and the spinal cord (radiculospinal artery, *arrows*), a contraindication for endovascular treatment

Fig. 12.14A, B. Intracranial dural arteriovenous malformation at the level of the left petrous bone and drainage into the anterior and posterior spinal medullary veins. The patient presented with progressive myelopathy involving the lower extremities and sphincter dysfunction. **A** Cervical myelographic examination demonstrates prominent vascular structures (*arrows*). **B** Lateral subtraction angiogram of the superselective injection of the stylomastoid artery (*small arrow*). The site of fistulization is at the basal tentorial edge of the cerebellopontine angle (*arrowhead*), draining into the petrosal vein (*curved arrows*) and reaching the anterior and posterior medullary veins (*long arrows*). There is also reflux into cerebellar vermian veins and drainage into the straight sinus (*curved arrows*). Note filling of the middle meningeal artery via its tentorial branches

►

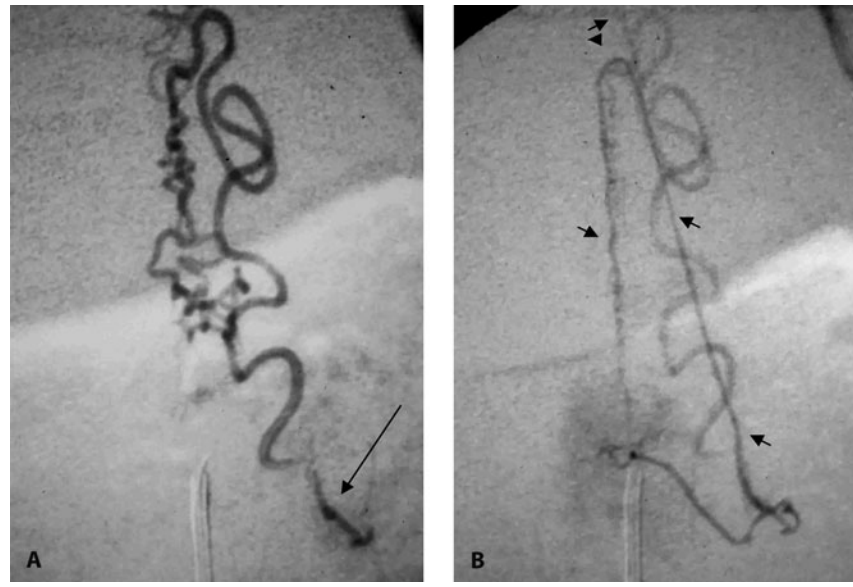

Fig. 12.13A, B. Selective angiography into the radicular branch of the L2 lumbar artery demonstrates supply to both a spinal dural arteriovenous fistula (*long arrow*, **A**) and the anterior spinal axis (radiculomedullary spinal artery, *short arrows*, **B**), a contraindication to endovascular treatment

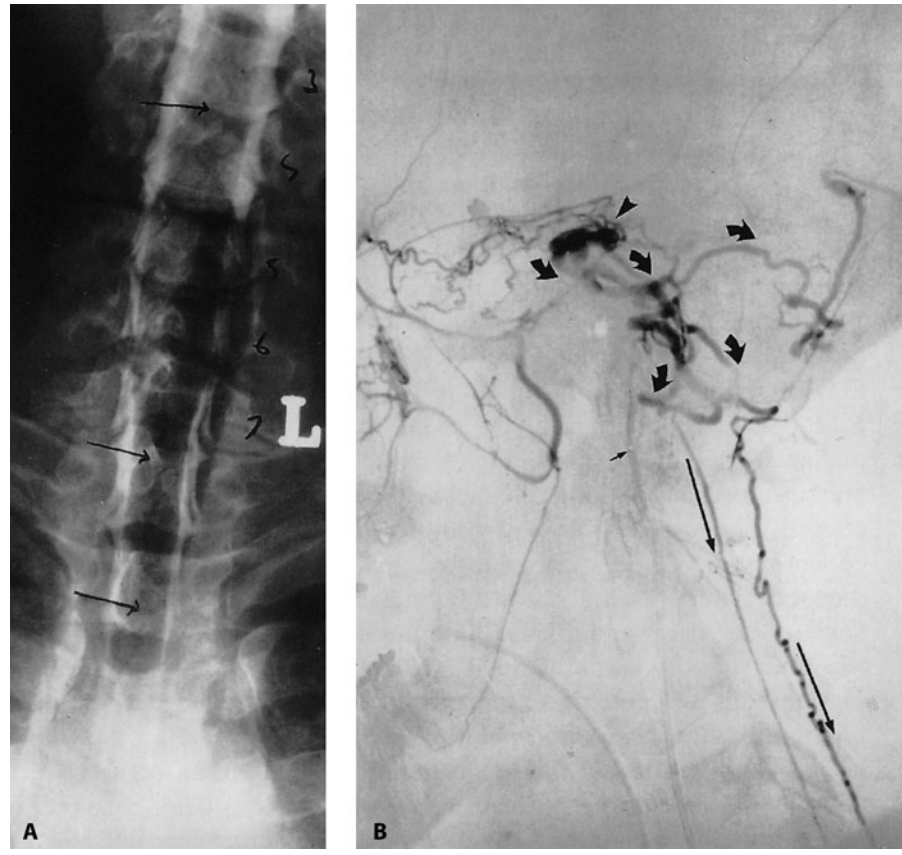

Fig. 12.14A, B. Legend see p. 864

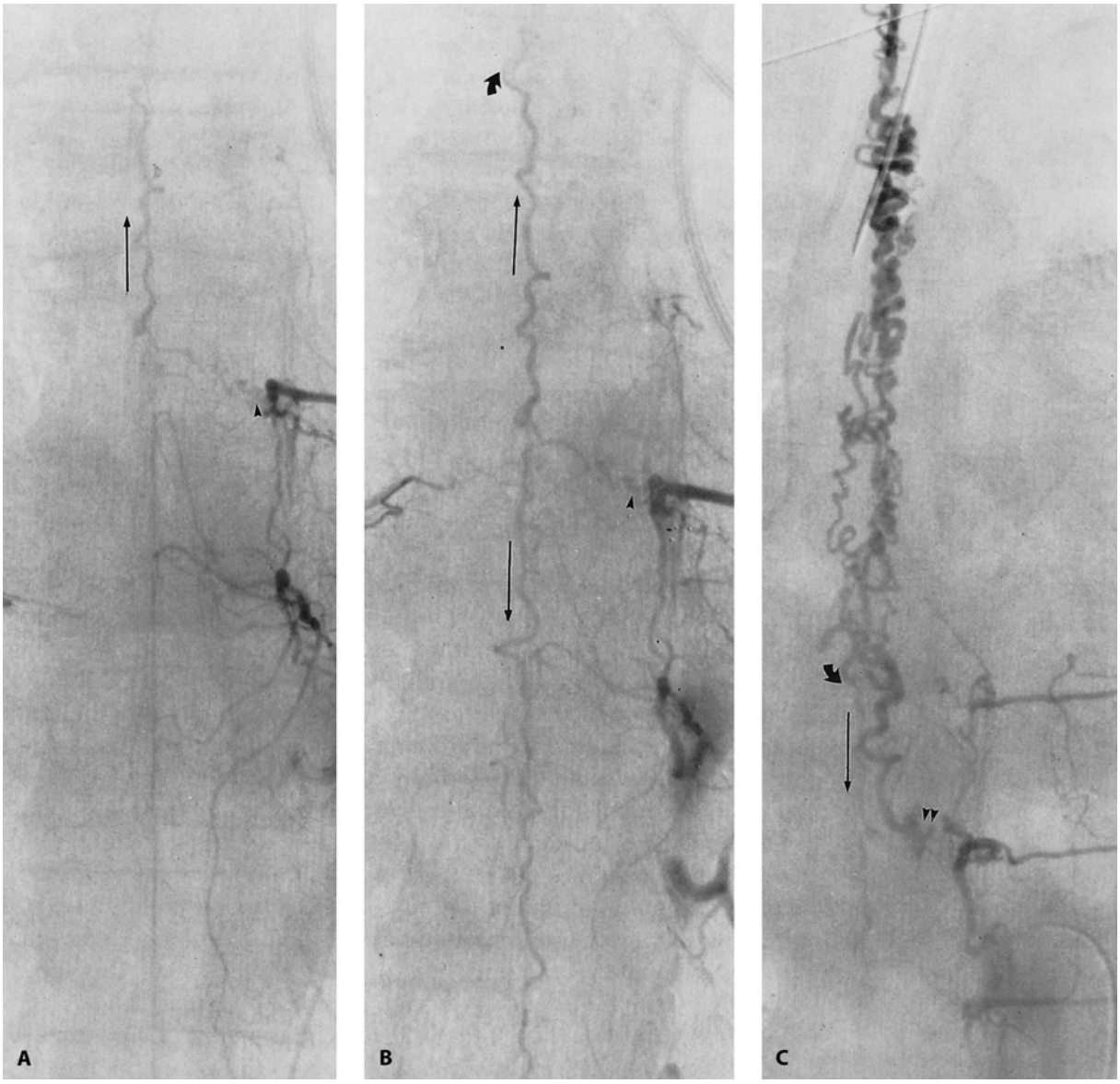

Fig. 12.15A–C. Multifocal spinal dural arteriovenous fistula (SDAVF). **A** Selective injection of the left T10 fills the radiculomedullary artery and an SDAVF on the level above the *arrowhead*, draining into the anterior spinal vein (*arrow*). **B** Late phase of the same injection. Note the descending and ascending drainage (*arrows*) and the dilution at the highest level (*curved arrow*). **C** Injection of T7 shows a second dural lesion (*double arrowhead*) draining cephalad. Note downward drainage to the same vein that drains the T10 lesion (*long arrow*) and the exact site of venous anastomosis (*curved arrow*)

while investigating patients suspected of harboring a DAVF is to assess the intra- and extracranial circulation, in particular when no shunt can be identified at the thoracic, lumbar, or sacral levels.

Multiple DAVFs in the same patient at the same time or occurring over time are exceptional (Fig. 12.15) (Pierot et al. 1993; Chaloupka et al. 1995) and they occur much less often than in intracranial DAVFs.

Spontaneous closure of an SDAVF without treatment is extremely rare (Meder et al. 1995).

12.5 Treatment of Spinal Dural Arteriovenous Fistulae

12.5.1 Indications

The presence of an SDAVF is an excellent indication for treatment in all patients, as the risk of endovascular or surgical treatment is minimal and the possible benefits are significant. This applies even to patients presenting with what appear to be fixed neurological deficits.

12.5.2 Embolization of Spinal Dural Arteriovenous Fistulae: Techniques

The main objective of SDAVF treatment is to occlude the draining radicular vein as it exits from the arteriovenous shunt, thereby insuring disconnection of the microfistula from the spinal cord venous system. It is occluded (at the time of embolization) within the first millimeters of the exiting vein (Figs. 12.16, 12.17) or (at the time of surgery) prior to its opening into the pial network (Fig. 12.9). In sacral lesions, the long draining vein can be occluded over several centimeters, as it only reaches the medullary veins at the conus level. The only significant contraindication to endovascular treatment of SDAVF occurs in those patients in whom the anterior or posterior spinal artery originates from the same pedicle as the SDAVF (Figs. 12.12, 12.13) (Merland et al. 1980a, b; Agarwal et al. 1992). In the great majority of patients, embolization can close the lesion in a very safe manner.

In view of the small size of the afferent arteries and the fistula itself (in the 40–60 μm range), only a low-viscosity liquid agent will reach the nidus and the proximal vein. Particulate agents, such as polyvinyl alcohol (PVA) or dura mater, will not be effective or may only give temporary good results. Almost invariably their use results in recanalization and recurrence (Hall et al. 1989; Morgan and Marsh 1989). Particles will not penetrate effectively to obtain complete cure and we consider them contraindicated in the endovascular management of SDAVFs.

Closure of SDAVFs using a liquid embolic agent is best accomplished with a mixture that will have a long polymerization time, such as $^{1}/_{3}$ N-butyl-cyanoacrylate (NBCA) with $^{2}/_{3}$ iophendylate (lipiodol). The injection can be done with a simple superselective catheter or with a coaxial assembly system. The acrylic-iophendylate mixture can be injected in a continuous column or using a so-called sandwich or push technique. The technical goal of therapy is occlusion of both the nidus and the proximal portion of the afferent vein.

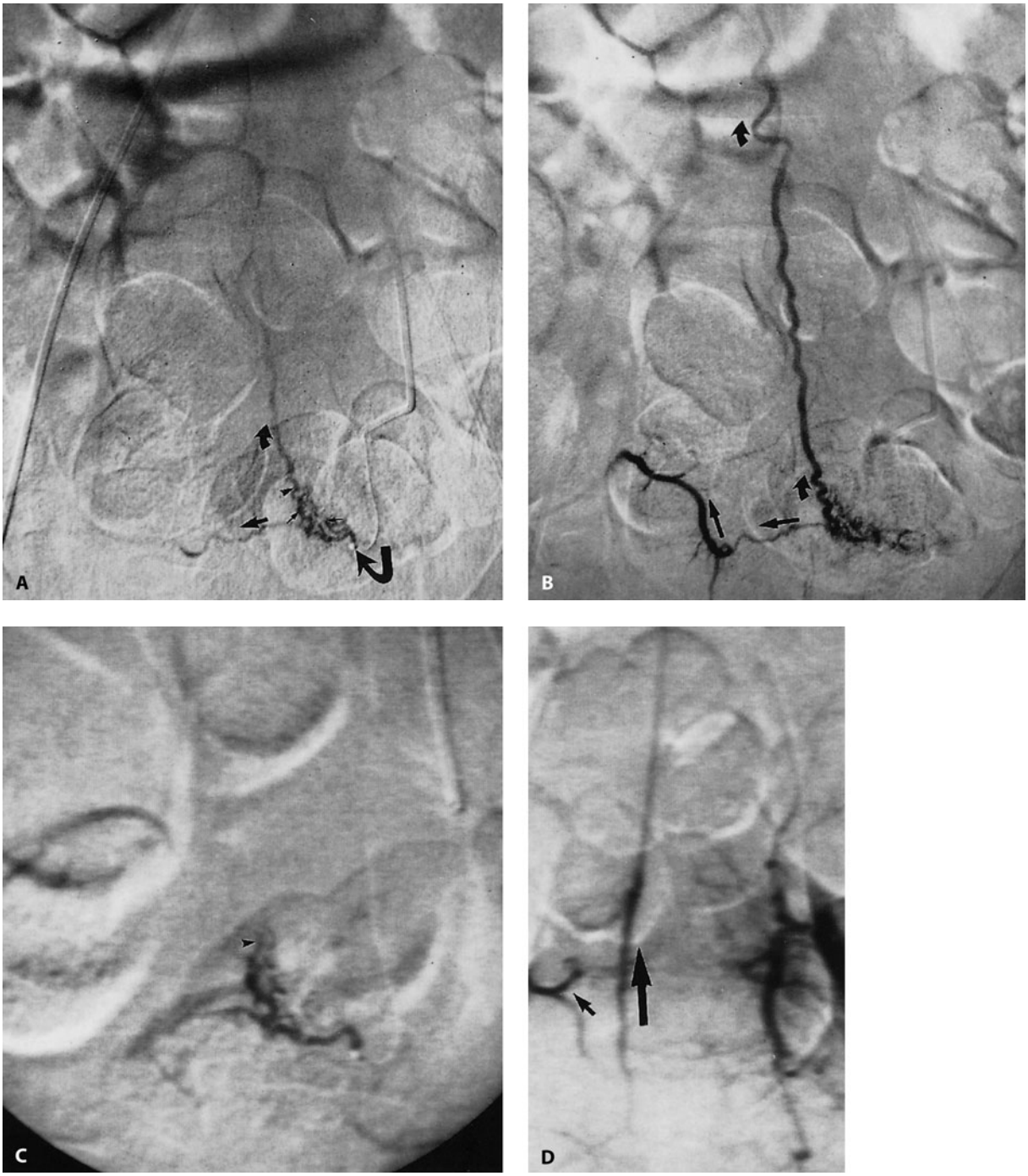

Fig. 12.16A–D. Spinal dural arteriovenous fistula (SDAVF) of the sacrum. **A** Angiography using a coaxial system with a variable stiffness microcatheter (*arrow*) demonstrates the arterial component (*small arrows*) and the site of shunting (*arrowhead*) with its ascending venous drainage (*curved arrow*). Note the retrograde filling of the contralateral dural supply to the sacrum (*arrow*). **B** Later phase of the same injection with better filling of the right lateral sacral artery (*large arrows*). **C** Digital subtraction angiography image of the acrylic deposition at the time of embolization shows the cast of the SDAVF as well as the proximal aspect of the radicular vein (*arrowhead*) and the distal segment of the right lateral sacral contribution. **D** Follow-up left internal iliac injection. There is no filling of the SDAVF and good opacification of both the right lateral sacral artery (*arrow*) and the medial sacral artery (*large arrow*). This confirms that there is no filling of the lesion

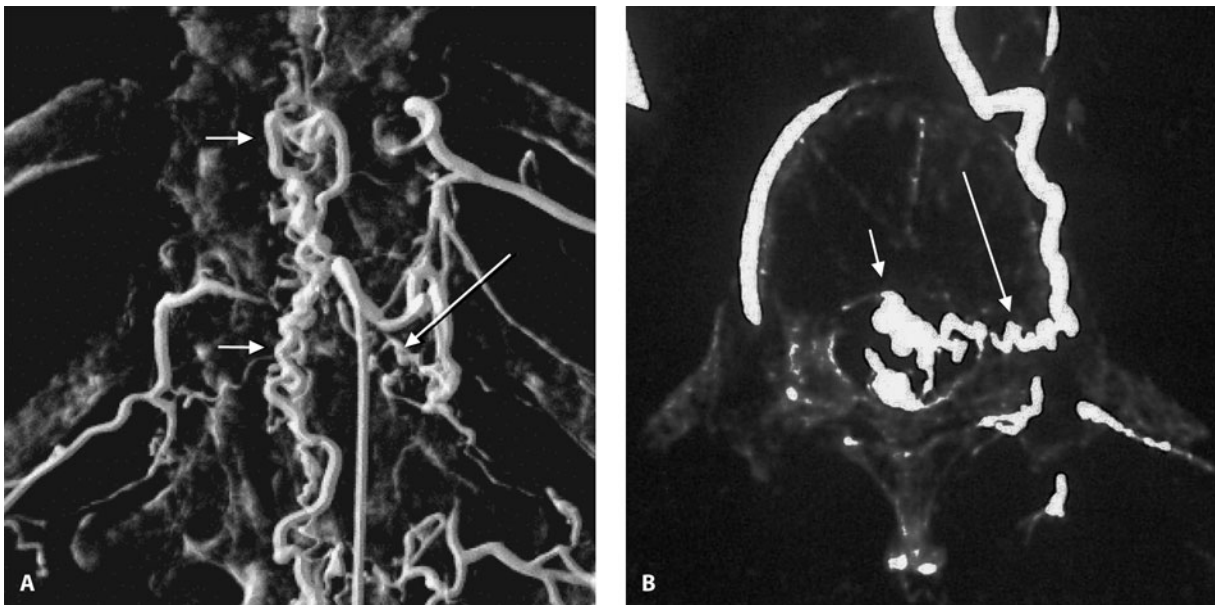

Fig. 12.17. Spinal dural arteriovenous fistula (SDAVF) shown at 3-D digital subtraction angiogram on frontal view (**A**) and axial view (**B**) to be located at T12 (left side) and supplied by the radicular artery (*long arrows*) and to be draining first toward the ventral medullary venous plexus (*short arrows*). **C–G** see p. 870

As in other anatomical locations, the collateral circulation of the dura of the involved region must be examined for the presence of natural arterial collaterals: ipsilateral above and below the level of the fistula as well contralateral at the same level of the DAVF and repeated on the immediate postembolization studies (Fig. 12.3).

The absence of radicular vein opacification at the thoracic level, during the ascending venous drainage phase of a thoracolumbar or lumbosacral SDAVF might favor the use of heparin following embolization. Similarly, patients with descending venous drainage in a thoracic SDAVF may benefit from postembolization anticoagulation therapy for at least several days.

As opposed to the treatment of spinal epidural AVFs, there is no role for the venous endovascular approach to SDAVFs (Willinsky et al. 1993).

12.5.3 Results of Spinal Dural Arteriovenous Fistula Embolization

Nimii et al. (1997) (49 cases), Song et al. (2001a) (27 cases), Westphal and Koch (1999) (47 cases) and van Dijk et al. (2002) (49 cases) reported the initial success rate of endovascular treatment with liquid adhesive embolic materials to vary between 25% and 90% of all cases. Nimii et al. (1997) considered penetration of the liquid adhesive into the fistula without penetration into the proximal vein as adequate, which is reflected in their high recurrence rate of 23%. Song et al. (2001a) reported a failure rate of 25%, but follow-up angiography was done in only 65% of the patients.

Up to 80% of patients will show clinical benefit from this form of treatment, ranging from clinical improvement of various degrees to stabiliza-

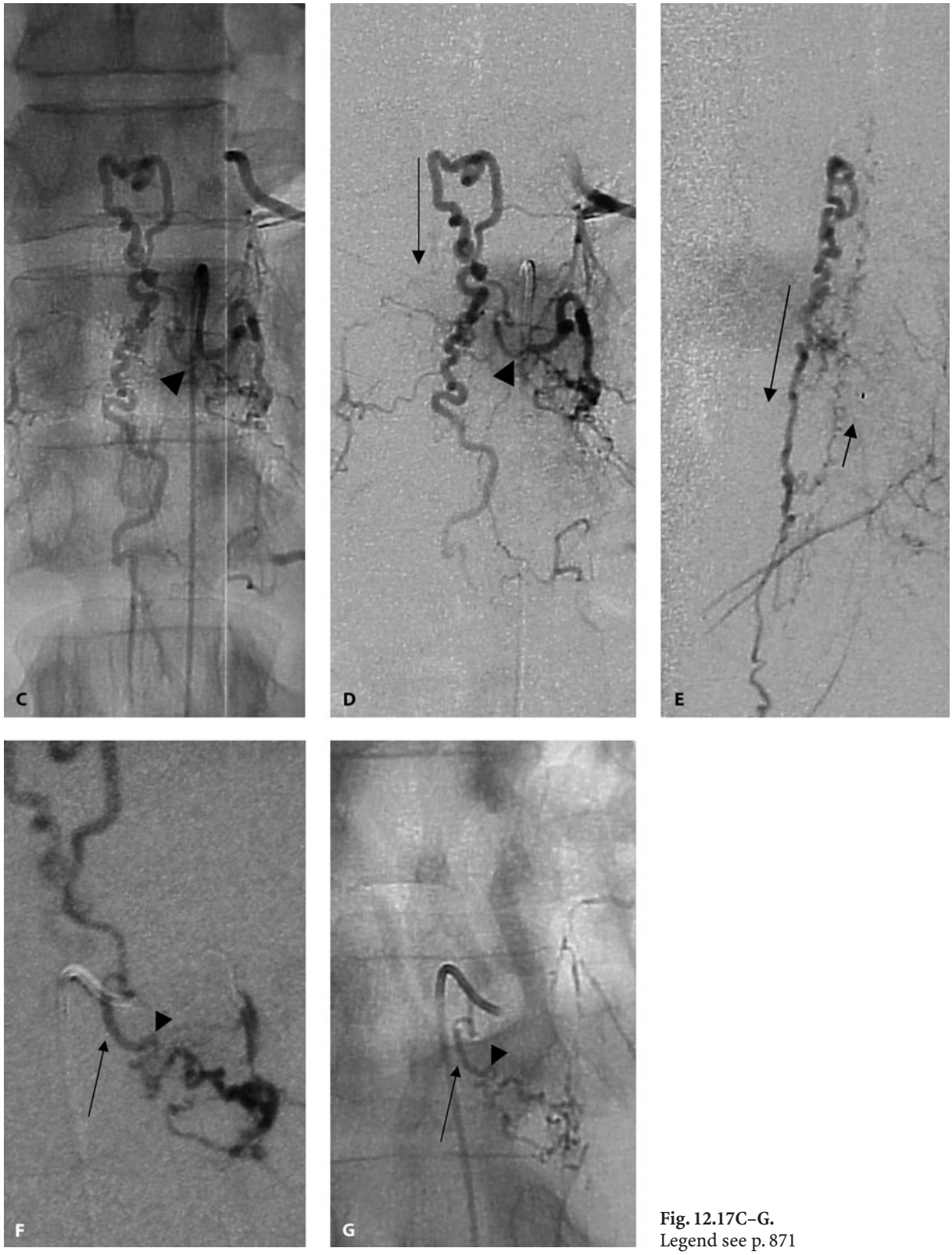

Fig. 12.17C–G.
Legend see p. 871

tion. Merland and Reizine (1987) reported on 63 patients treated at Lariboisiere Hospital (27 operated on and 36 embolized). In 50% of patients, there was a significant improvement of symptoms, in 20% only minor improvement occurred, in 16% the progressive myelopathy stabilized, and in 4% there was an aggravation or continued deterioration. Clinical improvement was noted in days, weeks, or within 3 months. The best results were seen in patients with the shortest time between onset of symptoms and treatment. Clinical improvement occurred primarily in motor function, deep sensory function, and strength. Superficial sensation and sphincter improvement was noted later and was less satisfactory. These results are similar to those reported by Merland and Reizine (1987), Barth et al. (1984), and more recently by Song et al. (2001b). Significant improvement in motor and bladder function was also demonstrated by van Dijk et al. (2002), with a mean follow-up of 32.3 months. Song et al. (2001b) demonstrated that if the patient was treated within 13 months of symptom onset, improvement in gait and to a lesser extend bladder function could be anticipated.

Complications associated with endovascular treatment could be related to the failure to recognize that the same radicular artery supplying the AVF is also contributing to the supply of the anterior or posterior spinal arterial systems with inadvertent embolization of this supply. Another potential cause for complication is the inadvertent deposition of the embolic material beyond the nidal-venous junction and into the perimedullary venous system of the spinal cord, causing thrombosis of the spinal cord venous system. Both these potentially devastating complications are avoidable with proper analysis of the anatomical situation and choice and method of injection of the embolic material. Recent experience by well-trained teams has shown the complication rate associated with endovascular treatment to be extremely low or even absent (van Dijk et al. 2002).

12.5.4 Surgery for Spinal Dural Arteriovenous Fistulae

If endovascular therapy is unsuccessful, surgery should be performed during the same hospital stay. As indicated above, the goal of surgical treatment will be the same: disconnection (transection, division) of the radicular vein as it runs intradurally from the dura toward the spinal cord perimedullary venous plexus (Fig. 12.13).

◄ **Fig. 12.17** (*continued*). Selective angiography in to the intercostal artery (**C–E**) showed radicular branches to be converging toward a DAVF, with retrograde drainage into the radicular vein and subsequently to the ventral perimedullary venous plexus (*long arrow*) and then downward around the conus and upward to the dorsal venous plexus (*short arrow*). Selective injection into the radicular artery (**F**) showed converging branches towards the DAVF (*arrowhead*) draining into the ascending radicular vein (*long arrow*). Embolization with a liquid mixture of glue (**G**) demonstrates that the embolic material has reached the proximal portion of the radicular vein (*long arrow*), resulting in permanent obliteration and cure

In the past, excision of the dura at the site of fistula was proposed (Hurth et al. 1978; David 1982; Oldfield 1989; Symon et al. 1984; Morgan and Marsh 1989); however, this approach has for the most part been abandoned (Afshar et al. 1995). The results of surgery are very much the same as glue embolization. Of 55 patients reported on by Symon et al. (1984) (50 with SDAVFs), 7 (13%) deteriorated after surgery. Symon ascribed this deterioration to excision of some of the coronary venous plexus of the spinal cord in association with division of the radicular vein emptying into the medullary venous system. Stripping the vein on the dorsal surface of the spinal cord must therefore be discouraged at all costs, as it is the wrong type of operation and may lead to clinical worsening. In Symon's series, in 65% of the 31 severely disabled patients and in 80% of 15 moderately disabled patients, there was appreciable improvement of gait and sphincter control. Similarly good results were noted in five out of six patients reported on by Oldfield (1989) and in seven of eight operated on by Morgan and Marsh (1989) (one patient was not operated on by the author). A good surgical response was also more recently noted by Westphal et al. (1999) and van Dijk et al. (2002). In patients with intracranial shunts draining downward toward the spinal cord veins, interruption of the vein draining the fistula will give similar good results.

12.5.5 Postoperative Follow-up

In the great majority of patients with SDAVFs who have undergone endovascular or open surgery, some improvement or arrest in progression follows. In those with no improvement within 4–6 weeks after treatment, repeat MRI and angiographic investigation should be considered. MRI may be able to show evidence of progressive venous thrombosis as an extremely rare unfavorable progression of previously successful treatment. MRI at 4–8 weeks after treatment rarely shows improvement in signal changes within the spinal cord, even in patients who respond favorably to treatment (Willinsky et al. 1995). Therefore, the absence of improvement as shown on MRI does not necessarily reflect residual or recurrent DAVF, as the MRI findings tend to lag behind the clinical findings. On the other hand, if MRI clearly shows the persistence of flow voids along the spinal cord in a patient who did not respond to therapy, then repeat angiography is indicated (Mascalchi et al. 2001). The repeat angiographic work-up should start with the injection of the anterior spinal artery to verify the circulation time again. If prolonged, the ipsilateral and contralateral arterial pedicles at the level of the DAVF as well as those above and below that level should be reevaluated. If no residual fistula is demonstrated a search should be made to exclude the occurrence of a second fistula. Similarly, in those patients showing initial improvement but subsequent cessation of improvement or deterioration, reevaluation is mandatory, as recanalization or development of a second fistula, although extremely rare, may be found.

13 Tumors of the Spinal Column and Spinal Cord

13.1 Introduction 874

13.2 Spinal Angiography 874

13.3 Angiographic Protocol 875

13.4 Embolization 876
13.4.1 Cervical Tumors 877
13.4.2 Thoracic, Lumbar, and Sacral Tumors 877
13.4.3 Chemoembolization 877
13.4.4 Intralesional Embolization 880

13.5 Benign Tumors 883
13.5.1 Vertebral Hemangiomas 883
13.5.1.1 Associated Lesions 888
13.5.1.2 Pretherapeutic Evaluation 888
13.5.1.3 Treatment 889
13.5.1.4 Embolization 889
13.5.2 Aneurysmal Bone Cysts 890
13.5.2.1 Clinical Presentation 891
13.5.2.2 Pretherapeutic Evaluation 891
13.5.2.3 Angiography 891
13.5.2.4 Differential Diagnosis 891
13.5.2.5 Pathogenesis 892
13.5.3 Other Benign Vascular Tumors 893
13.5.4 Giant Cell Tumors 893
13.5.4.1 Pathology 893
13.5.4.2 Clinical Presentation 893
13.5.4.3 Radiographic Findings 893
13.5.4.4 Embolization 895

13.6 Malignant Tumors 895
13.6.1 Pretherapeutic Evaluation 897
13.6.2 Embolization 897

13.7 Spinal Cord Tumors 898
13.7.1 Hemangioblastomas 898
13.7.1.1 Histopathology 898
13.7.1.2 von Hippel-Lindau Disease 900
13.7.2 Pretherapeutic Evaluation of Hemangioblastomas 904
13.7.2.1 Computerized Tomography 904
13.7.2.2 Magnetic Resonance Imaging 904
13.7.2.3 Angiography 905
13.7.3 Feeding Arteries 906
13.7.4 Draining Veins 906
13.7.5 Treatment and Embolization 906

13.8 Other Intradural Vascular Tumors and Spinal Hemorrhage 909

Table 13.1. Vascular tumors of the spinal column

Benign
Hemangiomas
Aneurysmal bone cyst
Osteochondroma
Osteoid osteoma
Osteoblastoma
Chondromas
Malignant
Giant cell tumors
Osteogenic sarcoma
Chondrosarcoma
Malignant tumors of hematopoietic origin, e.g., lymphomas
Multiple myelomas
Hemangiopericytoma
Chordoma
Plasmacytoma
Metastatic tumors of the kidney, thyroid, etc.

13.1 Introduction

The indications for spinal angiography and endovascular embolization of spinal tumors are mostly related to the evaluation prior to percutaneous biopsy or surgical intervention. Less frequently, embolization may be performed following an unsuccessful attempted resection, because of excessive bleeding, or to palliate inoperable tumors.

Angiography may be indicated prior to biopsy or surgery of tumors, which have shown prominent enhancement on contrast-enhanced CT or MRI examinations. Tumors that present with areas on MRI suggestive of high flow or hypervascularity (signal void on T1- and T2-weighted) are also candidates for angiography.

Highly vascular tumors such as known metastatic disease from kidney or thyroid tumors are lesions in which endovascular treatment may be performed preoperatively or as a palliative measure for either pain, spinal cord compression, or when intra-arterial chemotherapy is considered.

Angiography is also of value to localize the origin of spinal cord arteries prior to transthoracic operative approaches or other extensive spinal instrumentation procedures. Table 13.1 lists the most frequent vascular tumors of the spinal column, including those for which angiography or endovascular intervention may be requested.

13.2 Spinal Angiography

The angiographic findings of spinal and bony tumors are not specific, except for some benign lesions such as vertebral body hemangiomas and osteoid osteomas. Other imaging studies such as plain film, CT, and MRI will contribute more toward the histological diagnosis. Malignant spine and paraspinal tumors, although histologically different, may in fact have similar angiographic patterns, plasmacytoma versus Ewing's sarcoma, as

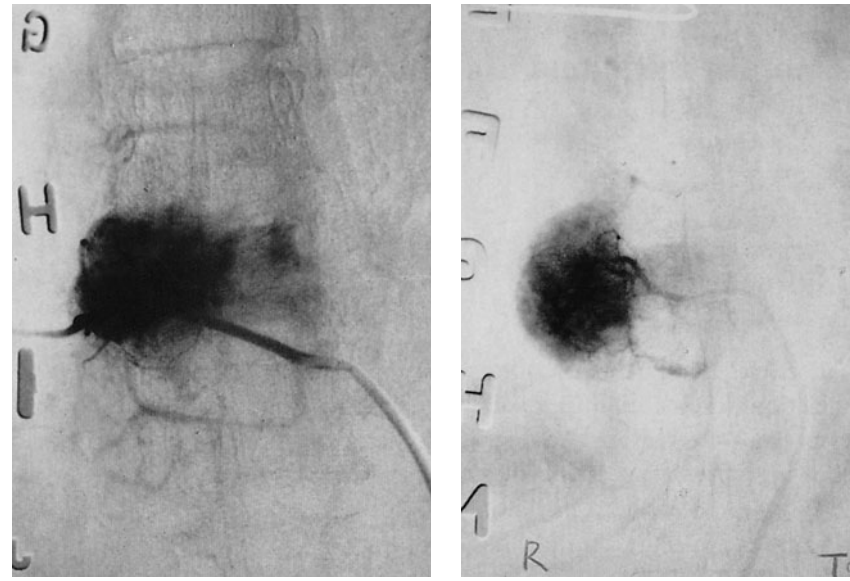

Fig. 13.1 (*left*). Plasmacytoma. Selective injection of the T10 intercostal artery demonstrates a tumor blush. Note the extension of the blush beyond the confines of the partially collapsed vertebral body. There is no evidence of arteriovenous shunting

Fig. 13.2 (*right*). Ewing's sarcoma. Selective injection of the right T9 intercostal artery shows a tumor extending beyond the vertebral body with a well-circumscribed, convex, outward margin, showing a paraspinal extension. There are no angiographic findings to differentiate this tumor from that shown in Fig. 13.1

illustrated in Figs. 13.1 and 13.2. The definitive histological diagnosis of spinal vascular mass lesions is therefore made by percutaneous image-guided biopsy. Depending on this information as well as the patient's clinical status, a treatment plan is made that may include presurgical spinal angiography and embolization.

13.3 Angiographic Protocol

When investigating tumors of the spine and paraspinal structures, regardless of their etiology, an angiographic protocol should be followed that varies according to the level that the tumor involves the spine or spinal cord. Irrespective of the indication for angiography (presurgical identification of spinal cord supply, embolization of metastatic tumor, etc.), the same protocol for angiographic evaluation will apply.

In general, different levels of the spinal column will have different vascular arrangements. For practical purposes, we have divided the spinal column into five territories (Table 13.2). Since the spinal column is a midline structure, blood supply to lesions involving the spinal column may be derived from the right or the left side. Therefore, both sides should be studied systematically.

Most of the symptomatic spinal tumors are not confined to the spine itself but may have an extension into the spinal canal or have a paraspinal

Table 13.2. Arteries to be studied angiographically in patients with spinal tumors

Upper cervical regions (C1–C4)
Vertebral arteries
Occipital arteries
Ascending pharyngeal arteries
Thyrocervical (anterior) trunks
Costocervical (dorsal) trunks
Midcervical region (C5–C7)
Vertebral arteries
Thyrocervical trunks
Costocervical trunks
Supreme intercostal arteries
Ascending pharyngeal arteries
Upper thoracic region (T1–T4)
Supreme intercostal arteries
Thyrocervical trunks
Thoracic and upper lumbar regions (T5–L3)
Intercostal lumbar artery of the involved level
Intercostal arteries of two levels above and below the tumor site
Lower lumbar and sacral region (L4 sacrum)
Lower lumbar arteries (L3–L4)
Iliolumbar arteries
Lateral sacral arteries
Medial sacral arteries

component, which is best demonstrated on CT or MRI. As the tumor grows into the adjacent vertebral foramen or when it extends into the paraspinal soft tissues, additional vascular supply will be recruited.

13.4 Embolization

Since the introduction of selective spinal angiography and the development of selective endovascular embolization (Djindjian and Faure 1965; Di Chiro and Doppman 1969), many reports have been published on the value of embolization of vascular tumors of the spine (Benati et al. 1974a, b; Djindjian et al. 1981; Lum and ter Brugge 2002).

Embolization is not a curative treatment for spinal tumors. It can, in certain circumstances, reduce mass effect and palliate immediate symptoms such as pain, relieve spinal cord compression, and possibly slow tumor growth. When surgical intervention is to be performed, preoperative embolization will facilitate more complete tumor removal. Moreover, tumors previously considered unresectable may become resectable after embolization (Choi and Berenstein 1988a). Over the past 20 years, embolization has become an accepted and valuable adjunct mode of treatment for certain benign and malignant vascular tumors of the spine (Sundaresen et al. 1985, 1986).

13.4.1 Cervical Tumors

In spinal tumors of the cervical region, consideration must be given to specific vascular anatomical details. This includes the bilateral supply from the vertebral arteries and the bilateral supply from the occipital, the dorsal, and/or ascending cervical and/or ascending pharyngeal arteries. The competence of the circle of Willis and the dominance of the vertebral arteries is to be assessed in case one vertebral artery needs to be sacrificed. Versatility of interventional materials and techniques may be needed when superselective catheterization of the branches of the vertebral artery cannot be accomplished and the distal (cerebral) territory needs to be protected. In these circumstances a balloon can be placed distally in the vertebral artery in order to protect the cerebral circulation. With the aid of such temporary balloon occlusion, good devascularization can be obtained, often facilitating removal of extensive and very vascular lesions (Fig. 13.3).

13.4.2 Thoracic, Lumbar, and Sacral Tumors

In the thoracic and lumbar regions, the level of involvement is studied bilaterally as well as the two levels above and below the involved area (Figs. 13.1, 13.4, p. 880). If significant paraspinal disease is present, then more levels may need to be studied and possibly treated. In sacral tumors, the internal iliac arteries, including the lateral sacral arteries as well as the middle sacral artery, must be evaluated.

Preoperative embolization of benign tumors is performed with polyvinyl alcohol (PVA), alone or mixed with 20%–40% ethanol, and sometimes with *N*-butyl-cyanoacrylate (NBCA) or with a combination of agents. The circulation may be rerouted by closing collaterals or less direct feeders, often with Gelfoam or coils, or by devascularizing one side. This will leave the tumor fed by a single or dominant pedicle, which will facilitate the delivery of more aggressive embolic materials. This pedicle is not occluded proximally, leaving access for retreatment if necessary. Coils or other forms of occlusion may also be used to protect normal territory or anastomoses to adjacent levels that supply a spinal cord artery in order to best direct the embolic or cytotoxic agent to the target (Fig. 13.5, pp. 881, 882).

13.4.3 Chemoembolization

Kato first introduced the term "chemoembolization" in 1978. In order to increase the local release of a chemotherapeutic agent into a tumor, mitomycin C microcapsules, with particle sizes of 224.6±45.9 mm, were prepared and injected through an angiographic catheter toward the target. The microcapsules produced local ischemia. The sustained release of mitomycin C from the capsules increased the duration of contact between the drug and target cells.

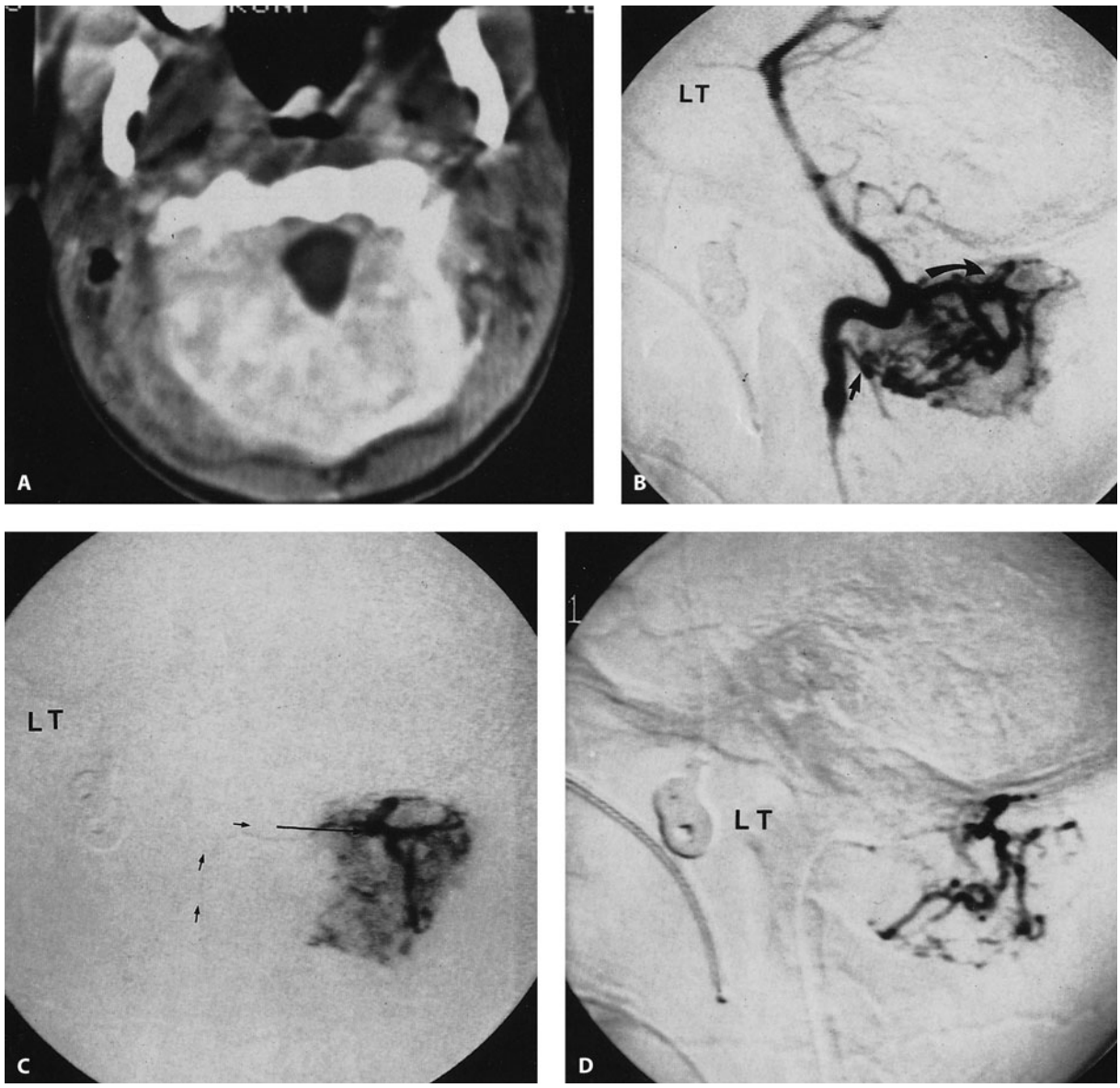

Fig. 13.3A–H. Osteoblastoma at C1. **A** Axial CT at C1 after intravenous administration of contrast material demonstrates marked enhancement in an aneurysmally dilated C2. **B** Left vertebral artery injection in lateral projection demonstrates a hypervascular tumor supplied by C1 (*curved arrow*) and C2 (*arrow*). **C** Superselective catheterization of the distal C1 (*long arrow*) with the variable stiffness microcatheter (*small arrows*). Note the hypervascularity of the tumor but no arteriovenous shunting. **D** Lateral digital subtraction angiography, last image hold, from a radiopaque (low viscosity) liquid acrylic embolization. Note the excellent catheterization obtained and the very distal penetration. **E–H** see p. 879

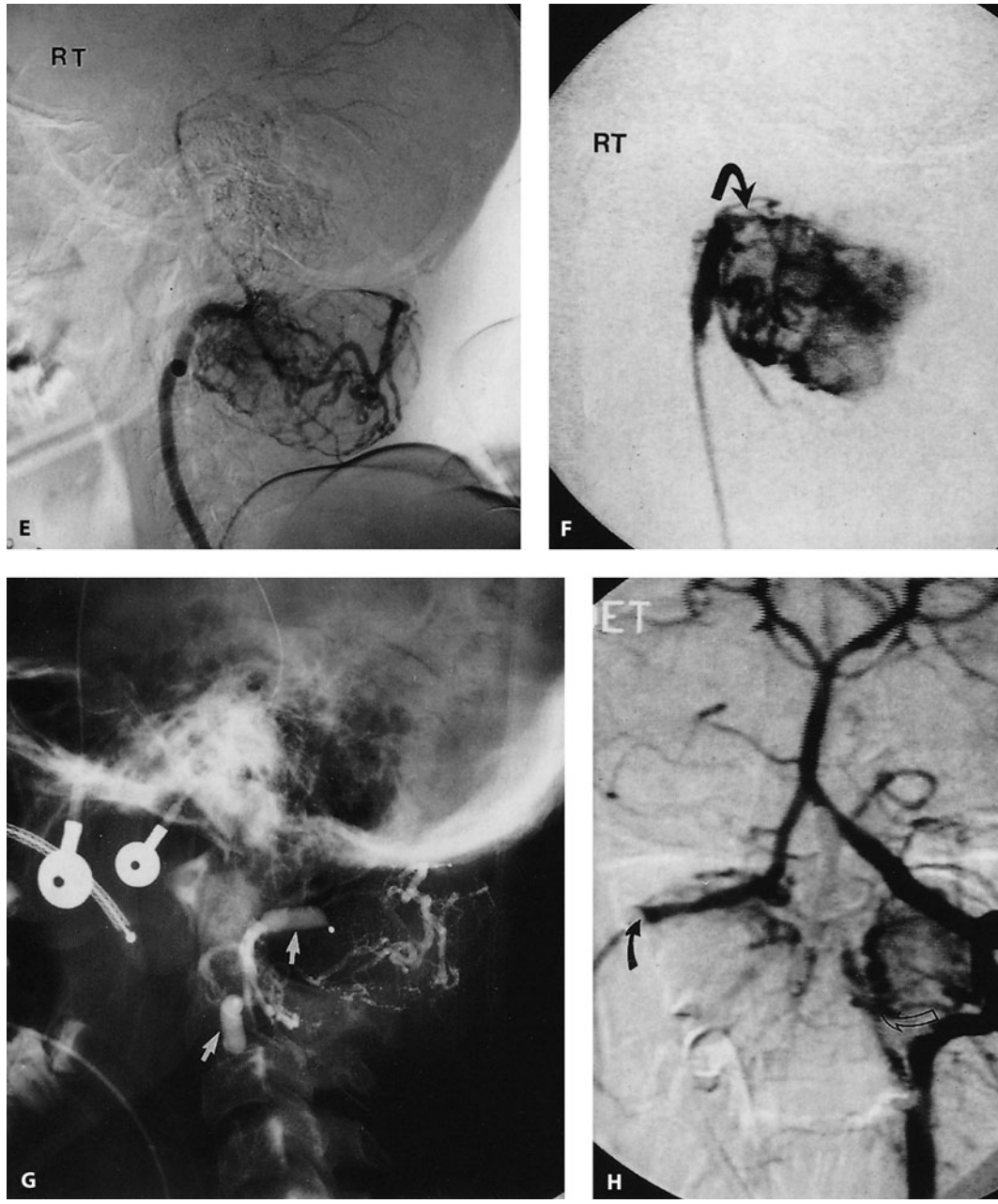

Fig. 13.3 (*continued*). **E** Right vertebral artery injection shows the right side contribution. Multiple small pedicles originated from the right vertebral artery (best seen in **F**). **F** Balloon occlusion of the vertebral artery distal to the small feeding vessels (*curved arrow*). **G** Plain film after embolization on both sides demonstrates the radiopaque cast of the embolized tumor and the position of the two detachable balloons (*arrow*). Note the excellent penetration into the interstices of the tumor. **H** Follow-up postembolization angiogram of the left vertebral artery, which has been preserved, showing the small remaining vessel (*open curved arrow*) and the retrograde filling of the right vertebral artery up to the level of the detached balloon (*curved arrow*)

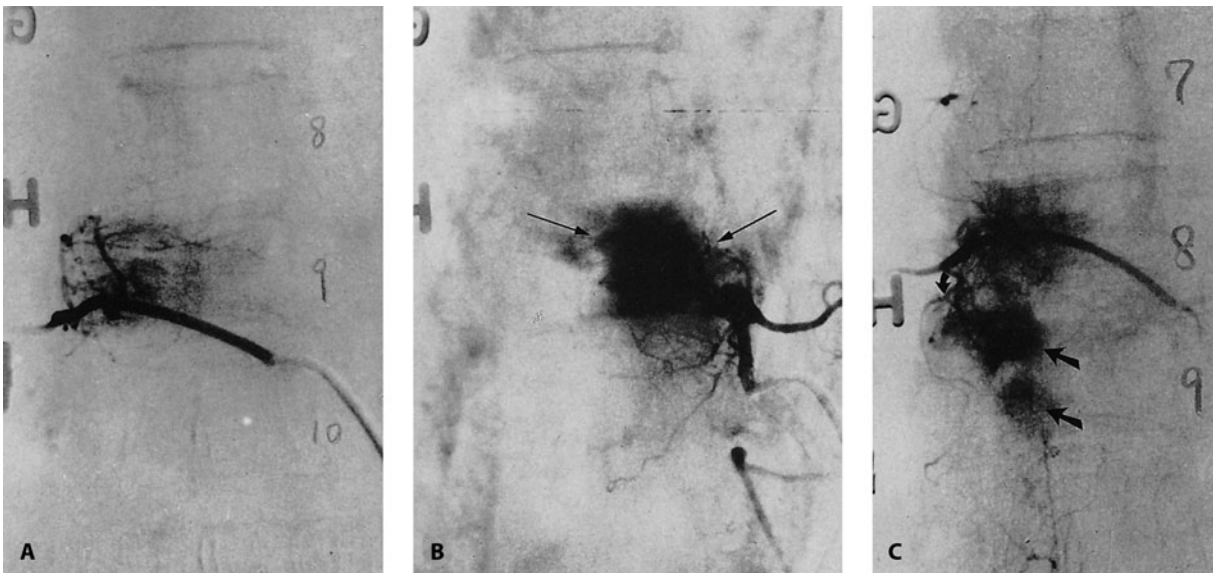

Fig. 13.4A–C. Thoracic plasmacytoma (same patient as in Fig. 13.1). **A** Right T9 intercostal injection early phase. Note the tumor vascularity and displacement. **B** Late phase of the left T9 shows the extension of tumor above the partially collapsed vertebral body (*arrows*). **C** Injection one level above T8 on the right. Note the parasitic supply to the posterior elements (*arrows*) from the extraspinal longitudinal anastomotic system (*curved arrow*)

Courtheoux et al. (1985) reported on chemoembolization of spine metastases using mitomycin C microcapsules or doxorubicin (adriamycin) mixed with dura mater. Improvement of clinical symptoms such as pain and neurological deficits was noted during a 58-month follow-up period.

Early results of chemoembolization suggested that this technique was an excellent palliative treatment for unresectable metastases. Nonetheless, further clinical and pharmacological studies are needed in conjunction with comparative studies with other cytotoxic embolic agents such as ethyl alcohol, which in our experience has been encouraging.

13.4.4 Intralesional Embolization

Direct intralesional embolization was reported on by Nicola and Lins in 1987, who injected methyl methacrylate into a hemangioma of a vertebral body. Transarterial embolization with particles was followed by laminectomy, and methyl methacrylate was injected through a cannula positioned in the pedicles during surgery. Since that time, the experience with percutaneous image-guided injection of methyl-methacrylate has grown considerably and is now widely used around the world. The polymerized acrylate supports the weakened vertebral body so that no further stabilization is necessary, and dramatic relief of pain occurs with excellent long-term effect (Galibert et al. 1987; Chiras et al. 1997; Jensen et al. 1997).

Profuse bleeding is rarely a significant problem during percutaneous biopsy procedures of spinal lesions, but can be managed by direct injection of an embolic agent such as Gelatin (Gelfoam) powder, microcollagen (Avatine) slurry, or acrylic material (Fig. 13.6).

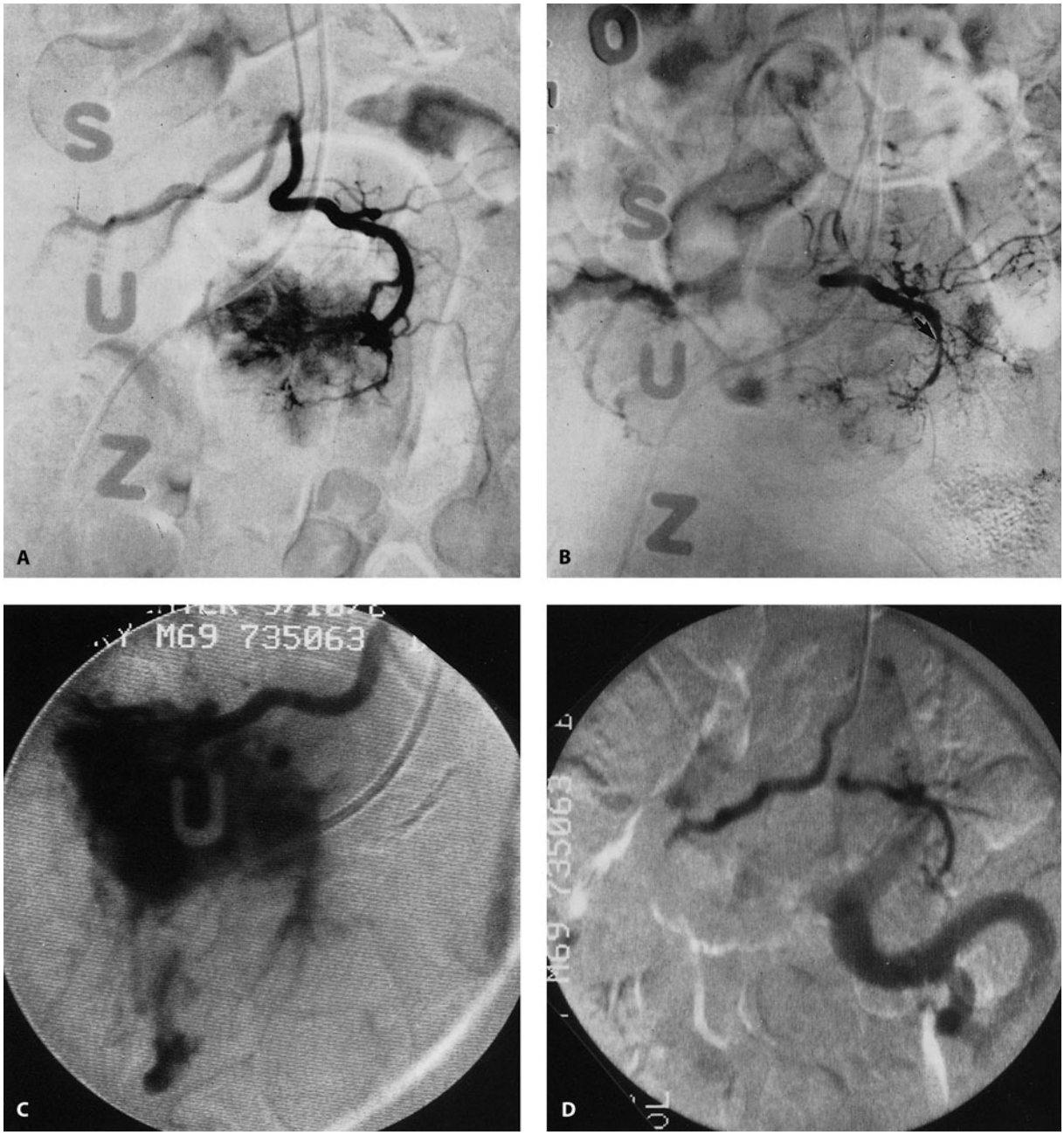

Fig. 13.5A–G. Metastatic hypernephroma of L5. **A** Selective injection of L4 shows the left side supply to the tumor at L5. **B** Follow-up angiogram after embolization of polyvinyl alcohol (PVA) microparticles in 30% ethanol. Note the distal spasm from the ethanol (*arrow*). **C** Digital subtraction angiogram of the right-side contribution. **D** Follow-up angiogram at the ostia of L4 and following chemoinfusion of the right side with 95% ethanol, leaving the pedicle opened for future treatments. Note reflux to the left iliac artery. **E–G** see p. 882

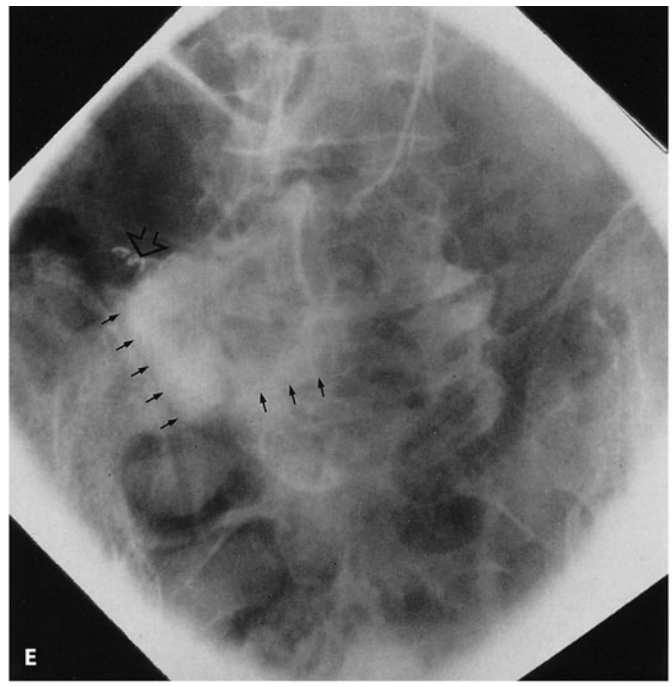

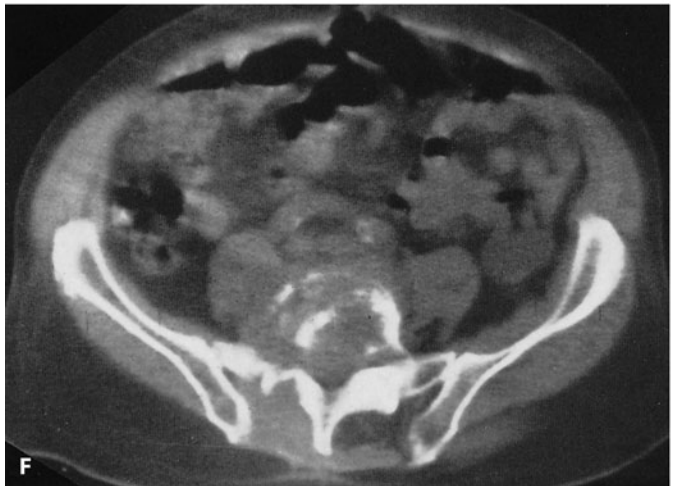

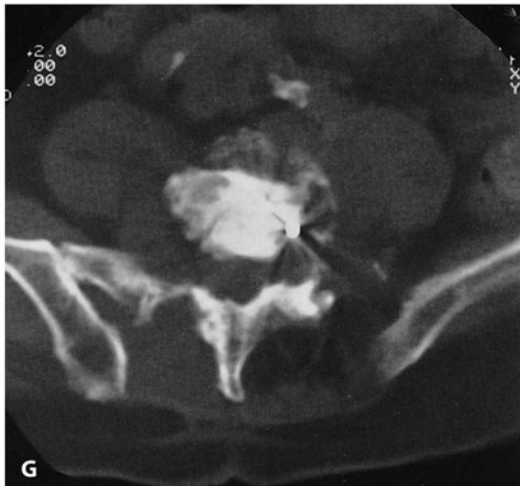

Fig. 13.5 (*continued*). Plain film after the chemoembolization (**E**). Note the radiopaque 95% ethanol mixed with metrizamide (Amipaque) in the interstices of the tumor (*arrows*). Gianturco coils were used prior to chemoinfusion to protect normal branches. **F** Axial CT scan at the level of L5 prior to treatment shows the destructive lesion of the vertebral body with extraspinal extension. **G** Follow-up axial CT at the same level 6 months later demonstrates ossification of part of the lesion. There was significant relief of pain

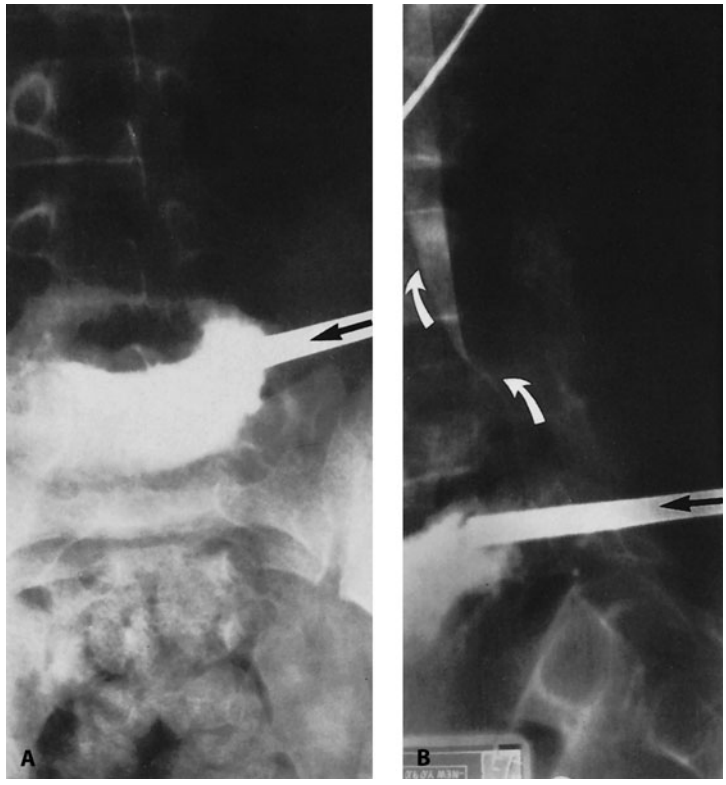

Fig. 13.6A, B. Direct intralesional embolization. **A** Frontal and **B** lateral views of the lumbar spine during a percutaneous biopsy. Massive bleeding was encountered. Injection of contrast material demonstrates a hypervascular lesion with arteriovenous shunting into the inferior vena cava (*curved white arrows*). To stop the bleeding, direct embolization through the cannula with microcollagen (Avatine) suspension was accomplished. Pathological diagnosis was intraosseous vascular malformation

13.5 Benign Tumors

13.5.1 Vertebral Hemangiomas

Vertebral hemangiomas are a common incidental finding at autopsy and their overall incidence has been estimated at 11% (Schmorl and Junghanne 1971). In the great majority of patients, these lesions are asymptomatic. The incidence increases with age (McAllister et al. 1975). The thoracic spine is most frequently affected, but any part of the spine may be involved, including the sacrum and cervical vertebrae (McAllister et al. 1975; Djindjian et al. 1981). Multiple lesions may be present in the same individual. There is a slight female predominance; in Djindjian's series of 20 symptomatic patients (Djindjian et al. 1981), the mean age at time of presentation was 37 years. This is similar to our experience with a series of 29 patients with symptomatic lesions. Presentation in childhood is rare but has been reported (Hoefnagel and Wegner 1961; Paige and Hemmati 1977).

Symptoms, when present, depend on the degree of bony involvement. Local pain, tenderness, and back pain were seen in lesions confined to the vertebral body in close to 50% of patients in Djindjian's series. The true incidence of symptoms, however, is probably higher, as few patients are referred exclusively for pain. Slow, progressive spinal cord or root compression may occur when extension of the lesion occurs beyond the confines of vertebral body. Cord compression may result in a progressive myelopathy, with symptoms ranging from paraparesis to paraplegia.

McAllister referred to the epidural extension of a soft tissue mass without bony collapse (McAllister et al. 1975). Cord compression may also result from compression fracture (Graham and Yang 1984) or epidural hemorrhage; the presentation of symptoms in such patients will be acute (Kosary et al. 1977).

Histopathologically, the lesions have been described as consisting of thin-walled blood-filled vessels and sinuses lined by endothelium and interspaced among the longitudinally oriented bony trabeculae. The dilated vascular channels are set in a substrate of fatty marrow (Murray and Jacobson 1977).

Plain radiographic findings are often characteristic, consisting of either parallel linear streaks or a course trabecular pattern in a vertebral body of overall decreased radiodensity. CT scan will demonstrate prominent vertical trabeculae with intervening regions of low (<90 HU) attenuation within the vertebral body, giving a characteristic honeycomb appearance (Price and Batznitzky 1985). On contrast-enhanced CT, one may see the enhancement of epidural and/or paraspinal soft tissue extension of the lesion.

MRI of vertebral hemangiomas produces a characteristic appearance (Ross et al. 1987). T1-weighted images show areas of increased signal intensity within the involved vertebral body, while on T2-weighted images, they appear as areas of moderately to markedly increased signal intensity compared to the remainder of the involved vertebral body (Figs. 13.7, 13.8). At times these bright areas may be intermixed with areas of decreased signal intensity, giving a mottled appearance, and rarely do they show decreased signal on T1-weighted images (Fig. 13.9). It is noteworthy that the appearance of the extraosseous component, which shows an intermediate soft tissue signal on T1-weighted images and increased signal intensity on T2-weighted images (Fig. 13.7). Chemical shift images show an increased lipid component in the osseous portion of the lesion, which correlates well with histopathological findings. In contrast, the extraosseous component contains little, if any, adipose tissue, which explains the lack of a high-intensity signal on T1-weighted images. Contrast enhancement will best show the full extent of the lesion (Fig. 13.7).

At the time of spinal angiography of hemangiomas, certain basic principles, which govern the vascularization of the spinal column at the thoracic level, will need to be kept in mind. The posterior portion of the vertebral body is best filled from a left-side injection (Fig. 13.10), whereas the anterior portion of the vertebral body is often opacified after injection of

Fig. 13.7A–D. MRI of a hemangioma. **A** Sagittal MRI T1-weighted image demonstrates the decreased signal of the T4 vertebral body with evidence of soft tissue mass extending toward the spinal canal (*arrows*). **B** Gadolinium-enhanced sagittal MRI clearly demonstrates the tumor enhancement of T4 extending into the spinal canal. Note the epidural extension cephalad (*arrow*) and the bright signal in the spinal cord (*curved arrow*). **C** Frontal digital subtraction angiogram of the T6 intercostal artery on the right demonstrates the tumor vascularity without evidence of arteriovenous shunting. **D** Superselective catheterization of the feeding pedicle (*arrow*). Note the tumor vascularity without evidence of arteriovenous shunting. Variable stiffness microcatheters make this distal catheterization possible, preserving the bronchial and distal anastomoses ►

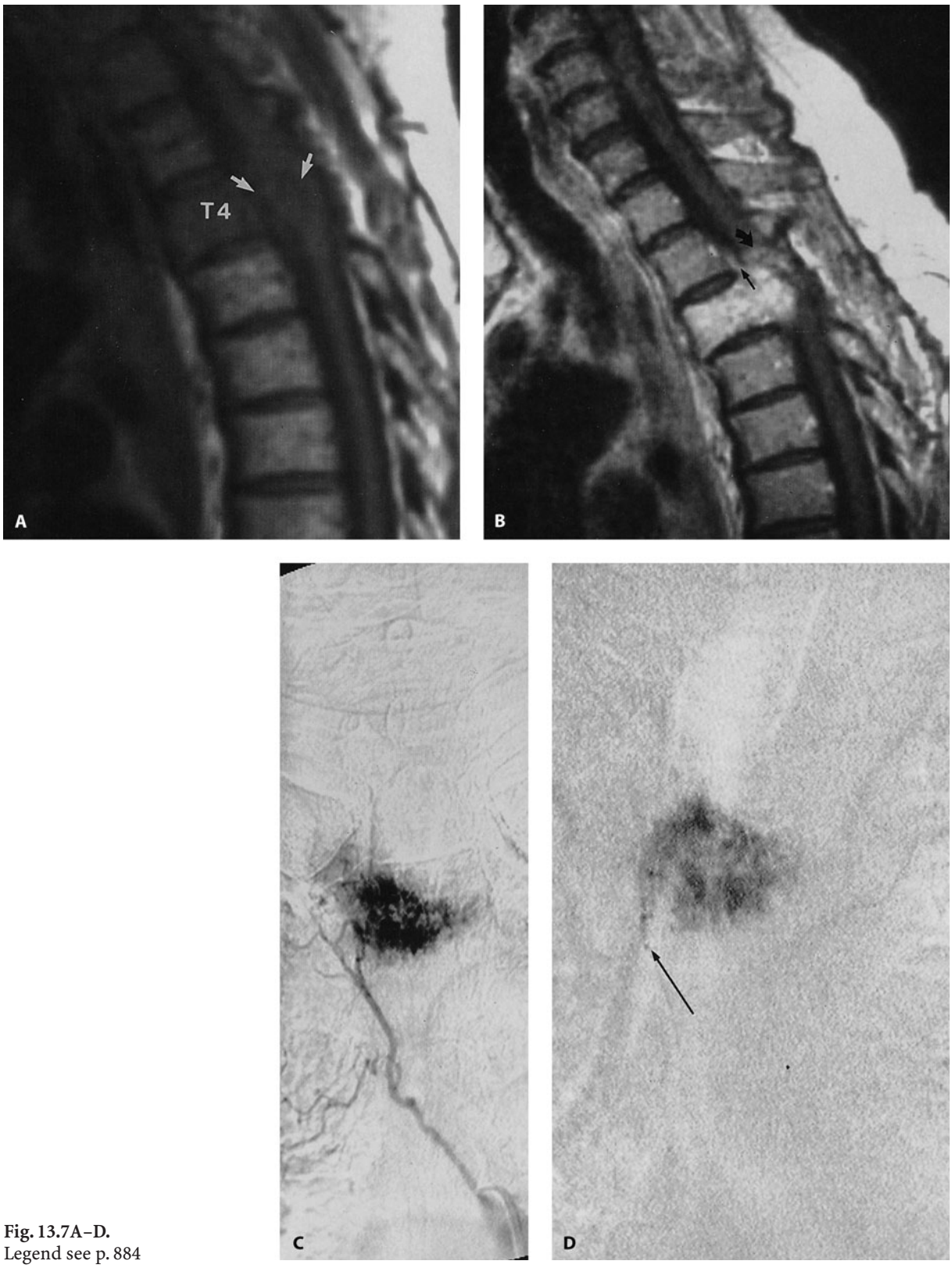

Fig. 13.7A–D.
Legend see p. 884

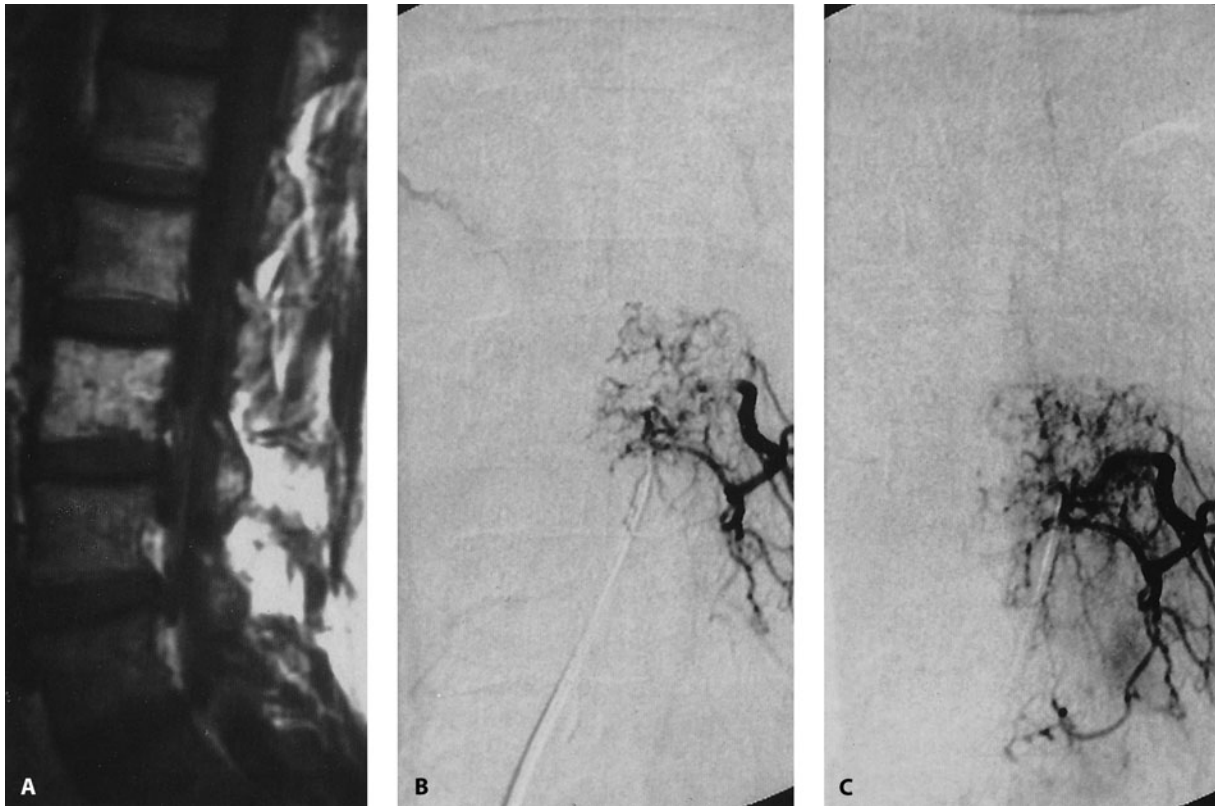

Fig. 13.8A–C. Type B hemangioma. **A** T2-weighted image after gadolinium enhancement. Note the inhomogeneous enhancement of L3 without extension beyond the confines of the vertebral body. **B** Early and **C** late phase of the left L3 injection demonstrates multiple hemangiomatous vessels and a vascular pattern compatible with the MRI findings

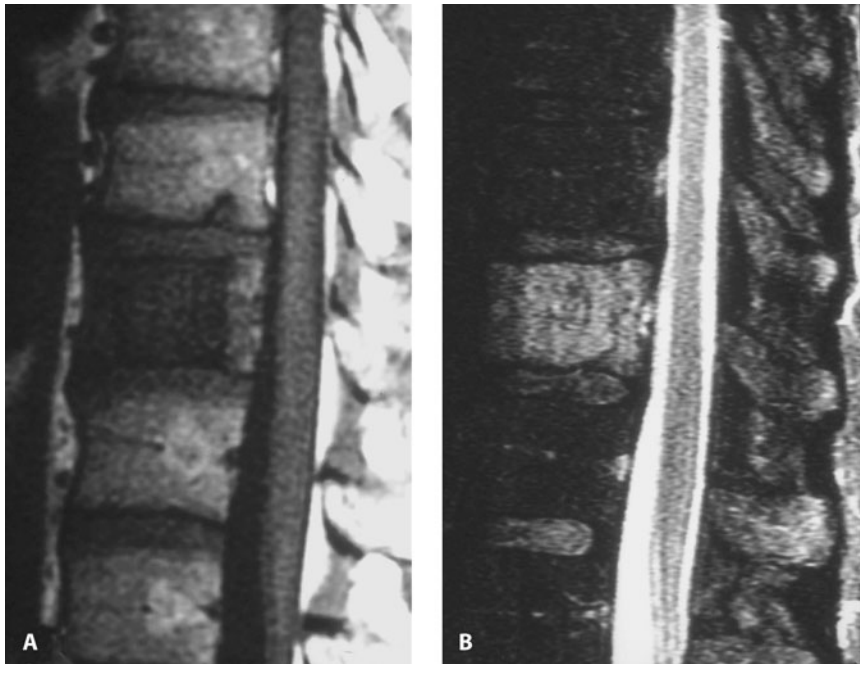

Fig. 13.9A, B. A 28-year-old female patient presented with a 3-month history of localized back pain. T1-weighted MRI (**A**) shows evidence of increased signal intensity within the T11 vertebral body, with increased signal on the fat-suppressed T2-weighted MRI (**B**), a rare MRI appearance of vertebral hemangioma

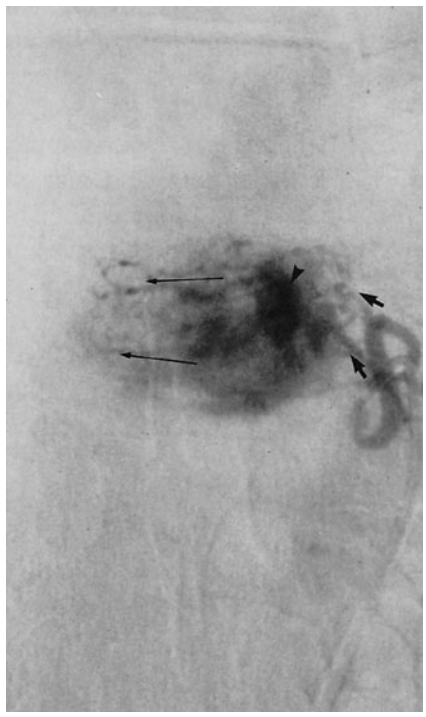

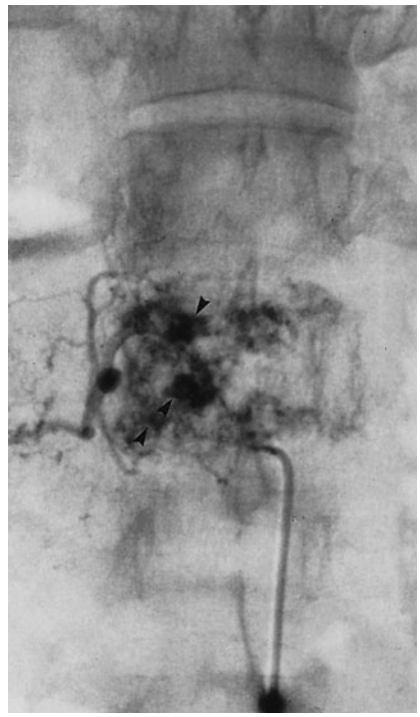

Fig. 13.10 (*left*). Type A vertebral body hemangioma. Selective injection of left T11 intercostal artery in early arterial phase shows the hypervascular tumor with dilated osseous branches (*arrows*). A hypervascular dense blush (*arrowhead*) and filling of the posterior portion of the vertebral body (*long arrows*) on the left side are present

Fig. 13.11 (*right*). Type B hemangioma. Selective injection of the right, L1 late phase shows small irregularly distributed pools of contrast material (*arrowhead*), which remain in the late phase

the right intercostal artery (Fig. 13.11) (Djindjian et al. 1981). In the mid-arterial phase, densely stained pools of various sizes fill progressively and persist far into the venous phase (Figs. 13.7, 13.10). The injection of the intercostal arteries of the appropriate level will show both the osseous and the epidural and paraspinal extensions of the lesion (Lum and ter Brugge 2002).

The angiographic appearance of the affected vertebral bodies may vary. Djindjian divided them into three groups and correlated the angiographic appearance with the clinical presentation. Group A consisted of patients with extravertebral extension of their lesions that presented with signs and symptoms of long-standing and progressive spinal cord compression. On angiography, the lesions of the group A patients appeared to be dense, with heterogeneous opacification of the total vertebral body via dilated osseous branches. No arteriovenous shunting was present (Fig. 13.7).

In the group B patients, the lesions appeared angiographically as small irregularly distributed pools of contrast material, with similar anterior and posterior distribution on the vertebra (Figs. 13.8, 13.11). These tumors did not have an extravertebral extension. The symptoms correlated well with the angiographic appearance and consisted of back pain and local tenderness, while some patients were asymptomatic.

Group C consisted of asymptomatic patients with the radiographic diagnosis of hemangioma of the vertebral body, in which no pathological opacification was noted during angiography. Voigt and Lumper (1976) were able to opacify such vertebral hemangiomas by percutaneous transosseous injections of contrast material.

The term "hemangioma" has been frequently used to describe the group of vascular lesions involving osseous elements of the spinal canal and its surroundings. However, as seen in the above description of the clinical and histopathological characteristics of these lesions, they are not true hemangiomas. Specifically, they have rarely been described in children (Hoefnagel and Wegner 1961; Paige and Hemmati 1977), and their incidence increases with age (McAllister et al. 1975). They do not behave as true hemangiomas in that they do not go through a period of rapid cellular growth or proliferation, nor do they go through a period of regression or involution. No mast cells can be seen pathologically, and no stroma is found, as seen in hemangiomas involving craniofacial or other soft tissues. Therefore, when purely intraosseous, these benign lesions appear and behave more as vascular malformations within bone and marrow. When extraosseous, they become symptomatic by local compression. This is not infrequently related to the degrees of bony fracture, with extraosseous extrusion of vascular elements.

The angiographic appearance of lesions found in the group A patients, with various-sized pools and referred to by Djindjian et al. (1981) as being in a more advanced stage, probably signifies rupture or fragmentation of the trabeculae and communication of vascular elements to marrow spaces, but without frank arteriovenous shunting.

13.5.1.1 Associated Lesions

Involvement of more than one vertebral body can often be seen and corresponds to additional independent lesions.

The association of vertebral body hemangiomas and vascular malformations involving the spinal cord and/or skin (spinal arteriovenous metameric syndrome, or Cobb's syndrome) probably is a separate entity, a true segmental arteriovenous malformation (AVM) with bony involvement (Bhattacharya et al. 2001). The feeding vessels are hypertrophied and there is a high-flow condition with arteriovenous fistulization. The vertebral body involvement is different from that seen in isolated hemangiomas of bone. The plain film examination may show changes caused by pressure erosion, which are greater than those with intraosseous hemangioma. Incidental hemangioma of bone may be seen in a patient harboring a spinal cord arteriovenous malformation (SCAVM), as it can be found in the general population.

13.5.1.2 Pretherapeutic Evaluation

Incidental lesions that are asymptomatic should not be treated. In symptomatic lesions, CT and/or MRI may provide additional information rele-

vant to the diagnosis and extension of the lesion, while angiography is reserved for patients who will undergo subsequent surgical treatment.

13.5.1.3 Treatment

In patients with localized pain, treatment will depend on the ability of more conservative measures to control the symptoms. If conservative measures are successful and there is no evidence of spinal cord compression, sequential noninvasive imaging (CT/MRT) can be used to follow patients conservatively. Although radiation therapy has been reported as useful, even in the presence of cord compression (Ferber and Lampe 1942; McAllister et al. 1975), we reserve its use for patients who do not respond to embolization and surgery.

13.5.1.4 Embolization

In symptomatic lesions without cord compression, transarterial embolization may relieve pain, although frequently this relief is only temporary. Transarterial embolization with liquid embolic material may provide a longer-lasting effect (Fig. 13.12).

If embolization is to be the sole form of treatment, and in the absence of cord compression, percutaneous image-guided intralesional injection of polymethyl methacrylate has become the treatment of choice (Fig. 13.13). Nicola and Lins were the first to describe this technique (Nicola and Lins 1987) and since that time, numerous investigators have confirmed its benefit in the treatment of symptomatic spinal hemangiomas (Galibert et al. 1987; Chiras et al. 1997; Jensen et al. 1997).

Fig. 13.12. Plain film after liquid acrylic embolization of a hemangioma. Same patient as in Fig. 13.10. Note the excellent cast obtained. Liquid acrylic is more effective and has a longer-lasting effect than particles

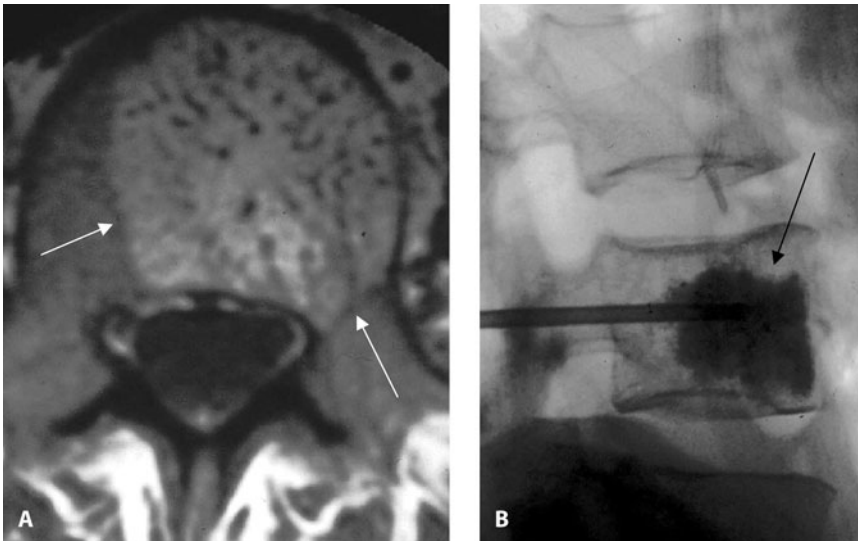

Fig. 13.13A, B. A 32-year-old female patient with progressive back pain localized to the L4 vertebral body. MRI T1-weighted image shows (**A**) characteristic appearance of hemangioma (*arrow*) involving most of the vertebral body. Percutaneous transpedicular injection of methyl methacrylate (*arrow*, **B**) resulted in dramatic total pain relief

Its role presently does not include treatment of patients presenting with cord compression, as they need urgent surgical decompression preceded by spinal angiography and transarterial embolization with small particles of PVA. Percutaneous intralesional treatment in these circumstances may in fact worsen the clinical symptomatology.

In patients with Cobb's syndrome, the treatment is usually geared toward the SCAVM. In extraspinal AVMs with secondary involvement of bone, the best treatment appears to be an aggressive endovascular embolization followed, if possible, by surgical excision.

13.5.2 Aneurysmal Bone Cysts

Lichtenstein (1950) first introduced the term "aneurysmal bone cyst" in 1942. In 1950, Lichtenstein differentiated aneurysmal bony cysts from giant cell tumors and established criteria for the differential diagnosis between giant cell tumors, hemangiomas, and osteogenic sarcomas.

Pathologically, the lesion consists of unclotted venous blood under pressure; the walls of the spaces are lined by an indistinct epithelium made of a brownish fibro-osseous patchwork with a few giant cells. Extravasated blood, hemosiderin-laden phagocytes, and fields of osteoid and new bone formation are seen (Lichtenstein 1950). Communicating bone spaces causing expansion and ballooning of the periosteal shell of bone is the typical radiographic appearance.

13.5.2.1 Clinical Presentation

Aneurysmal bone cyst is a disease that primarily affects young people: 80% of patients present before the age of 20 (Tillman et al. 1968), and both sexes are equally involved. The lesions can grow rapidly, with the duration of symptoms averaging 4 months. There can be acute exacerbation of

symptoms that may result in permanent spinal cord or nerve root damage secondary to compression. However, patients may also be asymptomatic or symptoms may even regress. These tumors may occur at any location, although 90% of them involve the spine (Hay et al. 1978; Ameli et al. 1985). Most involve the posterior elements of the vertebra, but the ventral portion may also be involved. In about 15%–20% of patients, aneurysmal bone cysts may involve adjacent vertebral bodies. Clough and Price (1973) stated that aneurysmal bone cyst is the only benign tumor that involves two adjacent vertebrae, but hemangiomas may also involve more than one vertebral body (Djindjian et al. 1981).

The main symptom of aneurysmal bone cysts of the spine is pain. The involved area is tender to palpation, and/or symptoms secondary to spinal cord or nerve root compression may be present.

13.5.2.2 Pretherapeutic Evaluation

Plain radiographs, CT, and MRI are of great value in establishing the diagnosis. Radiographic findings include a destructive expansile lesion associated with aneurysmal ballooning of the surrounding bone and surrounding by a thin shell of bone. This finding may be best appreciated on plain films or CT. MRI is the method of choice to show the soft tissue extent of the lesion and its relationship to the adjacent dural sac, spinal cord, and nerve roots. Visualization of the abnormal bone cysts by percutaneous injection of radiopaque contrast material directly into the lesion has been reported by MacPherson (1980). Percutaneous needle biopsy can be done but carries the risk of producing an extradural hematoma (Hay et al. 1978).

13.5.2.3 Angiography

Selective spinal angiographic findings may vary from a faint or slightly dense vascularity, consisting of irregular, mostly dilated tortuous arteries and only partial filling of the lesion, to a rich vascular network of dilated, tortuous vessels and a dense heterogeneous tumor stain with enlarged feeding vessels. On occasion, arteriovenous shunting may be seen (Djindjian et al. 1981). Additional angiographic features of some aneurysmal bone cysts include patchy areas of contrast material collection within the cyst, with late disappearance during the venous phase (Lindborn et al. 1961), or a densely vascularized cyst (Pouyanne et al. 1951).

The apparent discrepancy in the vascular patterns seen in aneurysmal bone cysts may be successive stages of development of the lesion itself.

13.5.2.4 Differential Diagnosis

Aneurysmal bone cysts of the spine must be differentiated from giant cell tumors, hemangiomas, cysts, fibrous dysplasias, osteosarcoma, osteoblastoma, and metastatic lesions. Giant cell tumors are rarely seen in patients

younger than 20 years of age and occur most commonly in the sacrum. There is no ballooning of the bone and no cavernous vascular spaces (Gruszkiewicz et al. 1982). Vertebral hemangioma can be differentiated by its characteristic radiographic appearance (see Sect. 13.5.1), although there is a cavernous type, which affects the vertebral body. However, this lesion does not show aneurysmal expansion and does not involve neighboring vertebrae (Poolos and White 1980). Simple bone cysts can be easily differentiated by lack of enhancement on either contrast-enhanced CT or MRI. Fibrous dysplasia affects the same age group but usually involves more than one vertebra and may involve bones at a distance such as the pelvis or skull. These lesions are painless and proportional; they grow slowly with skeletal growth and stop growing when skeletal growth stops. Osteosarcoma and metastatic lesions tend to produce more significant pain and are generally present in an older age group; they fail to show any ballooning or expansion of bone.

13.5.2.5 Pathogenesis

There are several theories on the pathogenesis of aneurysmal bone cyst. Lichtenstein (1972) believed that the condition is the result of local hemodynamic alterations within the bone circulation and could result from intraosseous shunts. Biesecker et al. (1970) measured the pressure with the cavities of aneurysmal bony cysts and found an increased pressure within the vascular spaces. It is interesting to note that Bonakdarpour et al. (1978) found that in approximately one-third of 75 patients presenting with aneurysmal bone cyst, the lesions were associated with other pathologies such as fibrous dysplasia, osteoblastoma, or chondrosarcoma. Other aneurysmal bone cysts were noted to be associated with trauma (Ameli et al. 1985).

Ameli et al. (1985) suggest that the bone cyst may be due to the hemodynamic imbalance in a bone with a preexisting congenital vascular anomaly. The triggering factor (associated lesion, trauma, etc.) can interfere with the venous drainage of the area. Therefore, the rate of growth of the lesion will be adversely affected by venous congestion. They suggest that this hypothesis can explain the presence of communicating spaces containing unclotted venous blood under pressure. This in turn will produce expansion of the affected bone and a sclerotic rim. Furthermore, the hypothesis can also explain why some of these lesions may be arrested or cured following biopsy or curettage. Recurrence of the lesion following curettage may then be related to isolated cavities not being opened during the original operation. Therefore, radiation therapy or endovascular embolization may suffice in controlling this condition by occluding the feeding arteries and thereby decreasing intraosseous pressure. It is presently not known whether these mechanical factors alone or growth factors and intercellular signaling are more likely to be responsible for the peculiar progression of these lesions.

13.5.3 Other Benign Vascular Tumors

Spinal angiography for other benign tumors is rarely performed since plain radiographs, CT, and MRI are more useful for specific diagnosis.

Osteoblastomas are usually diagnosed by clinical findings and conventional radiography. Osteoid osteoma, osteochondroma, chondroma, or osteoblastoma may frequently show a hypervascular tumor stain without arteriovenous shunting or dilated feeding arteries. We have experience with two unusual large osteoblastomas, one involving C2 (Fig. 13.3) and a second one involving T9. There were dilated feeding arteries entering the tumor and branching, with a dense irregular tumor stain. Several areas of contrast pooling were observed with prominent venous drainage. The preoperative management is the same as for other bony tumors.

13.5.4 Giant Cell Tumors

Giant cell tumors can be considered as malignant. Although they are most commonly present in the epiphysis of long bones, they can also involve the spine. Of 218 lesions reported on by Goldenberg et al. (1970), 11 affected the sacrum, 2 were in the lumbar spine, and 1 affected the cervical region.

13.5.4.1 Pathology

Histopathologically, the lesions have small loculi that are divided by thin septae containing abundant hemosiderin. The malignant characteristics of giant cell tumors can be graded on a 1–10 scale depending on the appearance of the cellular elements, with the less malignant type containing a higher ratio of giant cells than the more malignant type, which contains a higher number of atypical, mitotic mononuclear cells and few giant cells (Jaffee et al. 1940).

13.5.4.2 Clinical Presentation

The clinical presentation may be insidious or acute, depending on the biological behavior of the tumor and local compression of the spinal cord or nerve roots.

13.5.4.3 Radiographic Findings

On plain film radiography and CT, the affected vertebral body usually demonstrates a lytic lesion. The vertebral body may be expanded with cortical disruption and extension of tumor into the paravertebral and epidural spaces, causing spinal cord or nerve root compression. MRI will show these features to the best advantage (Fig. 13.14).

A variety of angiographic patterns have been described including (a) a homogeneous well-circumscribed stain, with a network of long narrow

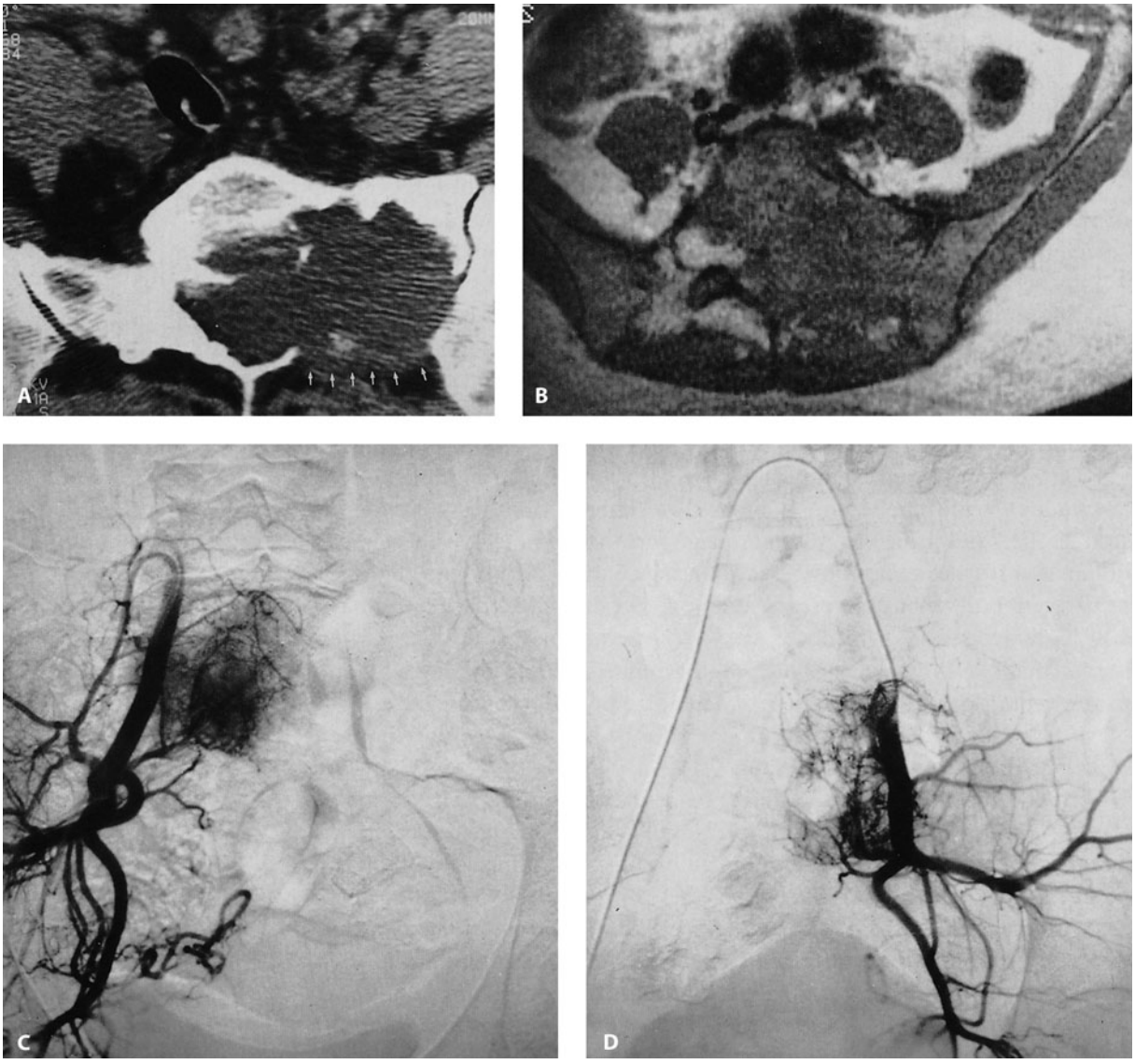

Fig. 13.14A–D. Giant cell tumor. **A** Axial CT scan demonstrates a destructive lesion of the sacrum with extraspinal extension (*white arrows*). **B** MRI T2-weighted image of the same patient. **C** Right and **D** left internal iliac artery injections demonstrate the rich tumor vascularity without arteriovenous shunting

arteries producing a faint capillary opacification (Fig. 13.14), (b) a highly vascular tumor extending beyond the vertebral body that may affect the adjacent rib or soft tissues, and (c) a dense heterogeneous opacification, with pools and venous stagnation but without early arteriovenous shunting (Djindjian 1976; Djindjian et al. 1970b). Djindjian described what he felt were characteristic vascular patterns of giant cell tumors consisting of (a) dilated arteries and veins that branch near the cortex of the tumor with fine corkscrew-shaped vessels running in a parallel fashion, (b) prominent arteriovenous shunting, and (c) an absence of blood pools. Based on the mixed reports and the rarity of the tumor, no characteristic angiographic pattern has so far been identified.

It may therefore not be possible to differentiate giant cell from other malignant tumors or even some benign tumors by angiography alone (Table 2.1).

13.5.4.4 Embolization

Angiography and embolization for giant cell tumors are indicated as preoperative or prebiopsy measures. This will apply to all other vascular tumors, primarily those of malignant nature. The possibility of developing protocols for endovascular infusions of chemotherapeutic agents or ethanol will be discussed under metastatic disease.

13.6 Malignant Tumors

Various imaging techniques will be used at the time of investigation and treatment planning of patients presenting with spinal malignant neoplastic disease. Plain radiographs, CT, nuclear bone scanning and most importantly MRI, all have a role to play in the demonstration of bone and soft tissue involvement by neoplastic disease and reveal, in certain cases, tumor type-specific characteristics.

Since differentiation between different malignant tumors by angiography is difficult and impractical, only typical angiographic findings of malignancy will be discussed.

The most frequent malignant tumor referred for preoperative or palliative embolization is metastatic disease and among them, those from renal cell carcinomas and thyroid carcinomas are the most frequent.

In general, the feeding arteries in malignant lesions are dilated. Small osseous branches are recognizable, in contrast to the homogeneous stain of normal vertebral bodies in which no distinct branches can be seen. The usual distribution of a hemivertebral stain is lost. The pathological blush can extend beyond the confines of the bone. The vascularity may vary from lesion to lesion. The tumor vessels are irregular in caliber and have a distorted course with abrupt angulations within the tumor. Compared to benign lesions, the tumor stain occurs earlier and irregular vascular lakes are often noted. The venous drainage frequently shows arteriovenous shunting. Early filling of the epidural or paravertebral venous plexuses is common (Fig. 13.15). The draining veins may or may not be dilated.

Malignant lesions often extend to the adjacent vertebral bodies and paravertebral spaces, recruiting new vascular supply. To recognize the extent of the lesion, the boundary of the tumor must be identified by studying the collateral circulation.

Vertebral metastases are the most frequent spinal tumors. In Torma's (1957) series; of 250 patients with spinal malignancies, 170 had metastatic disease. Schmorl and Junghanne (1971), reviewing a series of autopsy findings, found metastatic lesions of the thyroid represented 33% of all lesions in females, whereas in men 34% were metastatic lesions of the kidney. The thoracic and lumbar areas were the most frequently affected

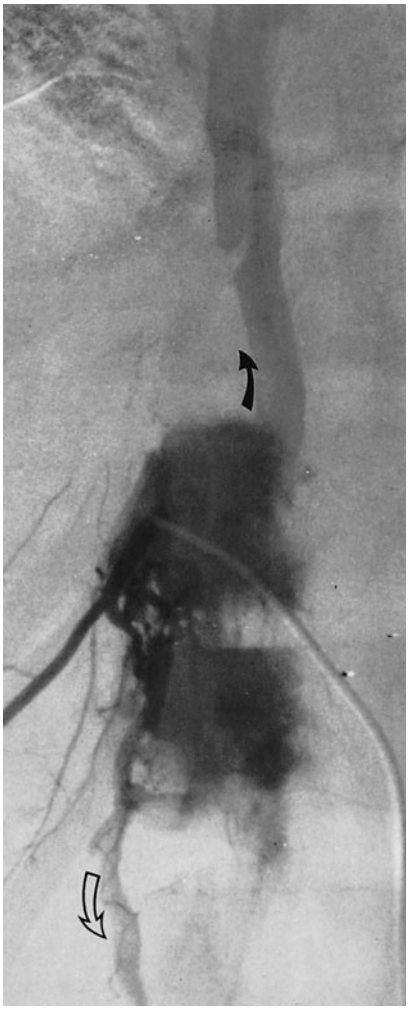

Fig. 13.15 (*left*). Malignant metastatic paraganglioma involving two adjacent vertebral bodies with preservation of the intervertebral disc space, with arteriovenous shunting. Note the intraspinal venous drainage (*curved arrow*) and the extraspinal, longitudinal, venous drainage (*open curved arrow*)

Fig. 13.16 (*right*). Metastatic lesions of L2 and L3 (*arrowheads*) receive their blood supply from the same pedicle that supplies the spinomedullary (ASA) artery. This is a contraindication for embolization

(Barron et al. 1959). Any part of the vertebral body may be affected with the pedicles being most frequently involved.

The most common clinical presentations are spinal cord compression or pain caused by bony collapse or extradural extension of tumor.

Besides kidney and thyroid, epidermoid epithelioma, epithelial carcinoma, and undifferentiated carcinomas can all produce similar angiographic patterns (Djindjian et al. 1981).

13.6.1 Pretherapeutic Evaluation

The pretherapeutic evaluation includes CT and/or MRI for diagnosis of the primary tumor and evaluation of the metastatic extension. Spinal angiography and embolization are then performed focusing on the symptomatic lesion prior to spinal instrumentation. Success with an aggressive surgical approach to malignant tumors of the spine, including metastatic disease, has been established over the past two decades (Sundaresen 1985, 1986). This type of surgical approach often requires preoperative embolization to reduce intraoperative blood loss (Choi and Berenstein 1988a, b). In some patients, endovascular treatment alone may also be done as palliation for spinal cord compression or pain unresponsive to other forms of therapy.

13.6.2 Embolization

The endovascular treatment of malignant lesions will consist of a pretherapeutic assessment of the intercostal, lumbar, or cervical pedicles involved (Figs. 13.4, 13.5). High-quality, digital subtraction angiography is performed under general anesthesia to exclude the presence of a radiculomedullary artery at the same level as the tumor (Fig. 13.16). The more selective the catheterization can be, the more easily one can identify the possible coexisting supply to the spinal cord at the same level as the tumor, as less selective injections may fail to show such supply due to the superimposed tumor blush. In the absence of a radiculomedullary or radiculopial contribution, endovascular treatment is performed by injection of small particles of PVA until flow stagnates. Surgery can be performed within days after the embolization procedure.

In selected cases, such as recurrent malignant tumors, tumor palliation with the intra-arterial infusion of a cytotoxic agent such as 95% ethanol can be proposed. Progressive infusion of 95% ethanol made radiopaque with metrizamide powder is done to progressively devascularize the lesion. This is then followed by PVA microparticles suspended in ethanol. The main pedicle is preserved, if necessary, for additional treatment. We recommend caution, as in the immediate postembolization course, a temporary disseminated intravascular coagulation syndrome can occur, probably secondary to the release of intracellular elements, particularly following aggressive ethanol infusion in metastatic hypernephroma. Therefore, appropriate blood coagulation studies are recommended prior to surgical resection. If endovascular treatment is the only modality of treatment patients are left on strict bed rest for the first 48 h to prevent vertebral body collapse.

Percutaneous vertebroplasty has also been used successfully to stabilize and treat pain associated with vertebral body collapse from malignancies such as multiple myeloma. Similar to such treatment for hemangioma, it should only be performed when there is no evidence of cord compression. The symptomatic level should be treated first, but if adjacent levels are involved multiple levels can be treated at the same time (Fig. 13.17).

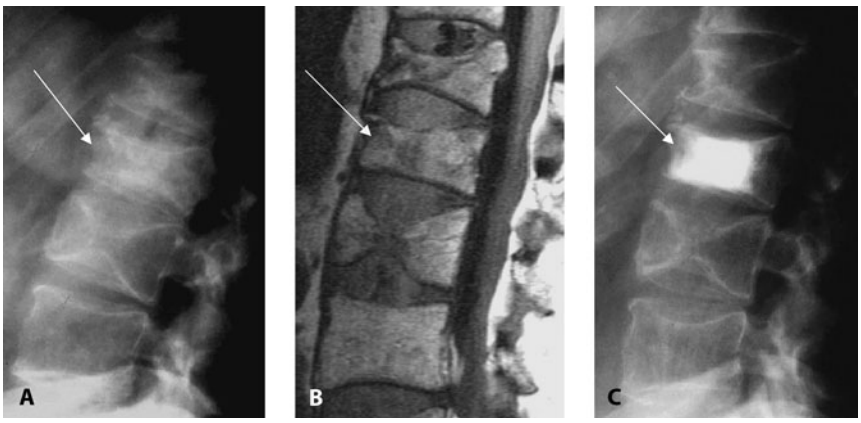

Fig. 13.17A–C. A 67-year-old man with a known history of multiple myeloma presented with severe recent onset of back pain localized to the L2 vertebral body. Lateral view lumbar spine on plain film (**A**) and MRI T1-weighted image (**B**) demonstrates partial compression and anterior wedging of L2 body (*arrow*). Clinical symptoms were immediately relieved after percutaneous injection of methyl-methacrylate (*arrow*, **C**)

13.7 Spinal Cord Tumors

Angiography and embolization of spinal cord tumors is limited to hemangioblastomas, as they represent the only clinically significant vascular tumor of the spinal cord.

13.7.1 Hemangioblastomas

A variety of synonyms have come into practice for the term "hemangioblastoma", including capillary hemangioblastoma, capillary hemangioendothelioma, hemangioendothelioma, and angioreticuloma.

The incidence of hemangioblastomas among tumors of the spinal cord and cauda equina varies from 4%–5% (Jellinger 1978) to 10%–12% according to Hurth (1975a, b), which most likely reflects individual surgical referral bias. They may be multiple, even without full expression of von Hippel-Lindau disease. Hemangioblastomas may be found anywhere in the spinal cord, but there is a preponderance in the cervical and thoracic regions (85%). Simultaneous posterior fossa and spinal lesions are quite common. Yasargil (1978) found an incidence of 34% in 65 patients that he reviewed from the literature and of 67% in his 12 patients. In addition, five (56%) out of nine patients autopsied in his review had simultaneous lesions.

13.7.1.1 Histopathology

These tumors are composed of vascular spaces forming endothelial elements that are separated by large cells, termed "stromal cells," whose origin and nature are obscure. Histologically, they resemble angioblastic

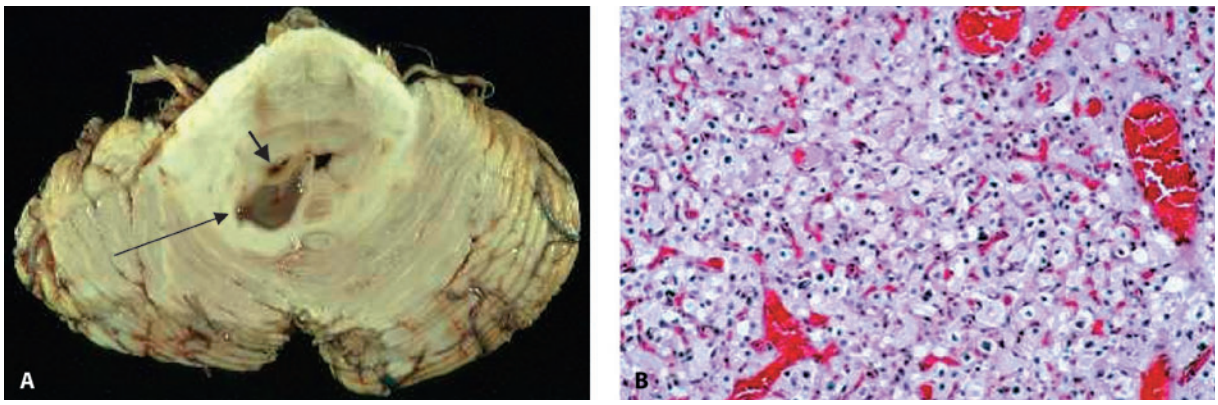

Fig. 13.18. Autopsy specimen (**A**) demonstrates small hemangioblastoma at cerebellar brainstem junction with tumor nodule (*small arrow*) and associated gelatinous cystic component (*long arrow*). Histopathological examination (**B**) shows large numbers of thin-walled fairly closely packed blood vessels lined by plump endothelial cells and separated by large pale cells, with either central or extrinsic nuclei (stromal cells)

meningiomas or clear cell carcinomas of the kidney (Rubinstein 1972). Russell and Rubinstein (1971) felt that many hemangioblastomas originated from the pia and therefore constituted a variant of meningeal neoplasms. This, however, has been a controversial issue. Much of the problem hinges on the difficulty of determining the nature of the stroma cell and on whether it or the endothelial elements constitute the primary neoplastic cell in these tumors.

Gross pathological examination almost always shows a well-circumscribed tumor, which may be either solid or partially cystic (Rubinstein 1972) (Fig. 13.18). Some 40% are solid and about 60% are cystic with a mural nodule. Although they are well circumscribed they do not have a discrete capsule. The cut surface of a hemangioblastoma is spongy, and the smaller cystic areas consistently disclose dilated blood spaces. Another characteristic feature is the presence of opaque, golden yellow foci due to large amounts of lipids (Rubinstein 1972). Sometimes there are regions in which a rusty brown color is found due to old hemorrhage.

Microscopically, the most striking feature is the presence of large numbers of thin-walled fairly closely packed blood vessels lined by plump endothelial cells and separated by large pale cells with either central or extrinsic nuclei (Fig. 13.18). An abundant network of reticular fibers that intersect the tumor cells and clear delineation of the outlets of the vascular architecture can be noted. The cytological features of both endothelial and the stroma cells are usually benign. The exact nature of the stroma cells is unclear. They resemble the xanthomatous cells found in meningiomas. Pericytes may be found in the so-called angioblastic meningioma.

Spence and Rubinstein (1975) studied the histogenesis of capillary hemangioblastomas by tissue culture and electron microscopy. These studies demonstrated three cell types: endothelial cells, pericytes, and stromal cells, all of which were neoplastic. Capillary hemangioblastomas were thus suggested to originate from vessel-formative elements, sharing vari-

able, angiogenic, differentiation features, to form capillary walls. The stromal cells are now felt to be an aberrant cell type of an angiogenic mesenchymal lineage, which do not convert into endothelial cells.

13.7.1.2 von Hippel-Lindau Disease

von Hippel-Lindau disease (VHL) is a hereditary familial disease transmitted by an autosomal dominant gene and although the age of onset and the severity of the condition may vary, penetrance is virtually 100% (Gough et al. 1984). VHL is characterized by tumors of the CNS and abdominal viscera, including cerebellar hemangioblastoma (36%–60% of patients), retinal angiomatosis (more than 50%), renal cell carcinoma (25%–38%), pheochromocytomas (10%), and medullary and spinal cord hemangioblastomas (less than 5%) (Fig. 13.19). Other frequent but less devastating lesions include adenomas, angiomas, and cysts of the kidney, pancreas, liver, and epididymis.

The association of hemangioblastoma with VHL varies from 10% to 20%. The existence of incomplete forms is more frequent. Houdart and Djindjian (1974) suggested that the term "von Hippel-Lindau disease" should be used to refer to all forms of hemangioblastomas, single or multiple, with or without visual lesions, in which a familial character can be demonstrated. Kendall and Russell (1966) suggested that the association of spinal and cerebellar hemangiomas is sufficient to establish the diagnosis. Additional associated lesions present in VHL include pheochromocytomas of the adrenals; cysts and tumors of the pancreas, lung, liver, kidney; and cystadenomata of the ovaries. Vascular skin nevi and anomalies of the diploic vessels, with enlargement and tortuosities of the veins of the mesentery and stomach wall, are also seen (Djindjian et al. 1981). The presence of hypertension suggests the possibility of associated pheochromocytomas (Nibbelink et al. 1969).

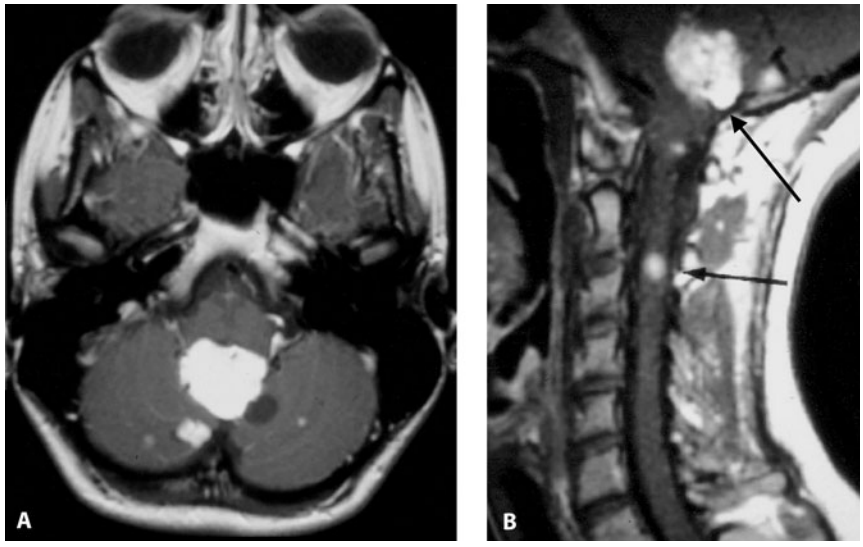

Fig. 13.19A, B. A 38-year-old female patient with a known family history of von Hippel-Lindau disease presented with progressive ataxia. Contrast-enhanced T1-weighted MRI axial plane at the posterior fossa level (**A**) and sagittal plane at the cervical level (**B**) demonstrate multiple enhancing nodules (*arrows*) characteristic of hemangioblastomas involving both the spinal cord and the cerebellum

Waldmann et al. (1961) reported the association of polycythemia with cerebellar hemangioblastoma and postulated the production of an erythropoietic stimulating factor by the tumor. After resection of the tumor, the hematocrit often returns to normal but polycythemia characteristically reappears with recurrence of the tumor (Hoff and Ray 1968). Waldmann (1961) was able to isolate an erythropoietic substance from the tumor cyst fluid of one patient. It is interesting to note that this polycythemia has been reported with cerebellar tumors and was actually noted in 1943 by Carpenter et al. Cramer and Kinsey (1952) estimated it to be present in 9% of 53 patients they reviewed. No report of polycythemia associated with a spinal lesion is available, although Yasargil (1976) speculated that spinal tumors might also be associated with polycythemia.

Growth and Spread

Although grossly they are well-defined tumors, hemangioblastomas have no capsule. Frequently the capillaries appear to sprout in a slightly irregular fashion into the adjacent brain tissue. Incomplete removal will therefore lead to recurrence. Distant metastasis from the hemangioblastoma does not occur.

Presentation and Natural History

The natural history of spinal cord hemangioblastoma is that of a typical intramedullary tumor producing pain and progressive sensorimotor deficits, progressing to paraplegia or tetraplegia (Herrmann 1999). The course is usually slow, with an average duration of 3 years (Yasargil 1978). Symptoms of cord compression are more prominent and more rapidly progressive with extradural hemangioblastomas than with the intramedullary lesions. Hemangioblastomas are located primarily in the posterior aspect of the spinal cord (Kinney and Filzgerald 1947). With simultaneous posterior fossa and spinal lesions, the initial symptoms are usually those of increased intracranial pressure.

Hemorrhage is rarely the presenting symptom of hemangioblastoma. Djindjian (1962) reported this to occur in 1 out of 22 patients. Yasargil (1978) stated that hemangioblastomas do not present with bleeding but may do so following surgical intervention. Subarachnoid hemorrhage presentation is extremely rare (Yasargil 1976, 1978).

A syrinx is present in approximately 70% of patients with spinal lesions (Fig. 13.20), root involvement in about 15%, and associated visual retinal lesions in about 30%. The latter are usually asymptomatic. Hurth et al. (1975a, b) reported on the largest series, consisting of 138 patients with 180 tumors. Some 91% of tumors were intradural. Of these, 76% were intramedullary, 7% were extramedullary, 17% were radicular, and 12% were epidural. Some 29% of tumors occurred at the cervical region, 61% in the thoracic, and 9% in the lumbar area (Table 13.3). The intramedullary hemangioblastomas were usually situated in the posterior half of the cord. The intradural extramedullary lesions were separate from the cord and nerve roots. They were usually located posterolateral to the cord. Radicular hemangioblastomas arise from the nerve roots alongside the spinal

Table 13.3. Location of intraspinal hemangioblastomas (180 tumors in 138 patients; modified from Hurth et al. 1975a)

Location	*n* (%)
C1	23 (13%)
C4	30 (17%)
T7	67 (37%)
T10	44 (24%)
L2	16 (9%)

Thus 29% of all tumors were cervical, 61% were thoracic, and 9% were lumbar.

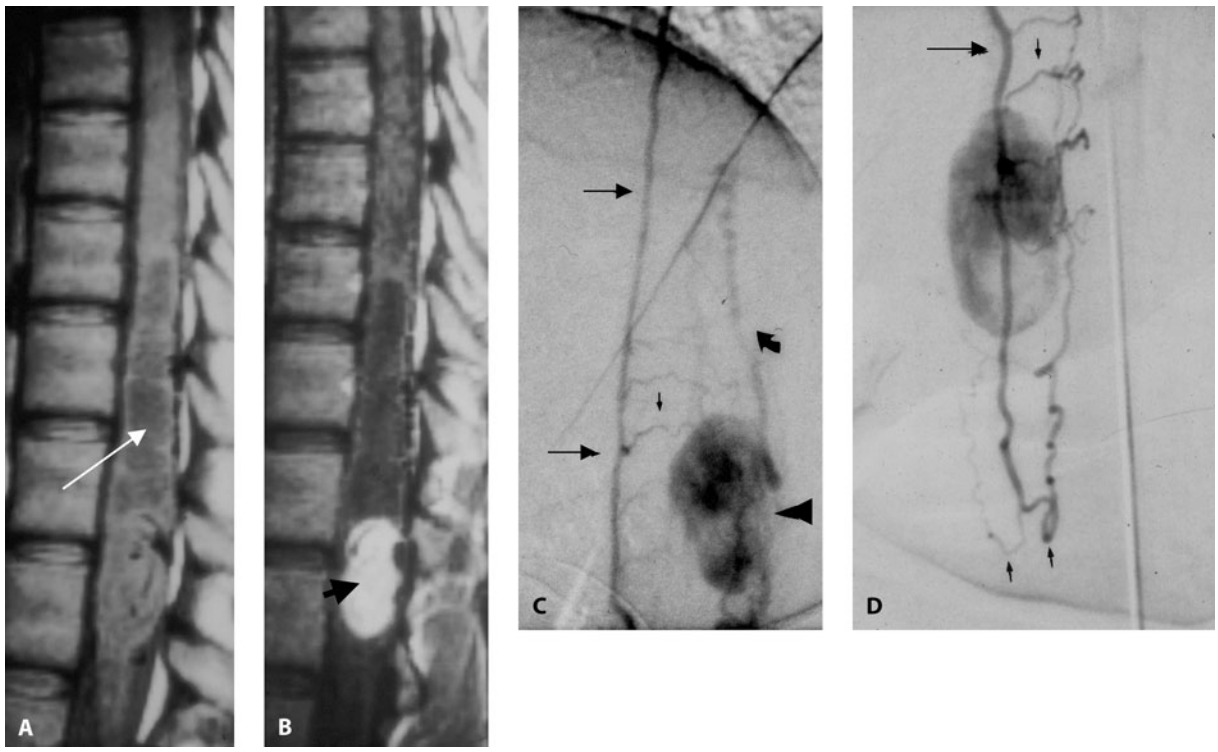

Fig. 13.20A–D. A 41-year-old female patient presented with progressive myelopathy. MRI PDI (**A**) showed evidence of syrinx (*arrow*) within the lower thoracic cord. Contrast-enhanced T1-weighted MRI sagittal plane (**B**) demonstrates enhancing nodule (*arrowhead*) along dorsal aspect of the conus medullaris. Injection of the radiculomedullary artery in lateral (**C**) and AP view (**D**) shows the anterior spinal artery (*long arrows*) to be the dominant supply to the hemangioblastoma (*arrowhead*) via circumferential anastomosis to the posterior spinal network as well as via the collateral anastomosis around the basket (*small arrows*). Venous drainage along the dorsal aspect of the spinal cord is noted (*curved arrow*)

Fig. 13.21A–G. A 33-year-old female patient with known von Hippel-Lindau disease presented with new onset of progressive myelopathy over a 4-month period. MRI examination T1-weighted (**A**), proton density imaging (PDI) (**B**), and T1-weighted (**C**) showed evidence of increased signal within the lower thoracic cord (*long arrow*) and flow voids along the surface of the cord (*short arrow*). Enhanced MRI TWI showed numerous enhancing nodules (*arrows*) within the thoracic and lumbar spinal canal. Selective spinal angiography demonstrated delayed opacification of the anterior spinal axis (not shown) and multiple posterior spinal arteries supplying numerous hemangioblastomas (*arrows*; only two shown), with extensive opacification of the dorsal venous network, presumably responsible for venous congestion and clinical symptoms ►

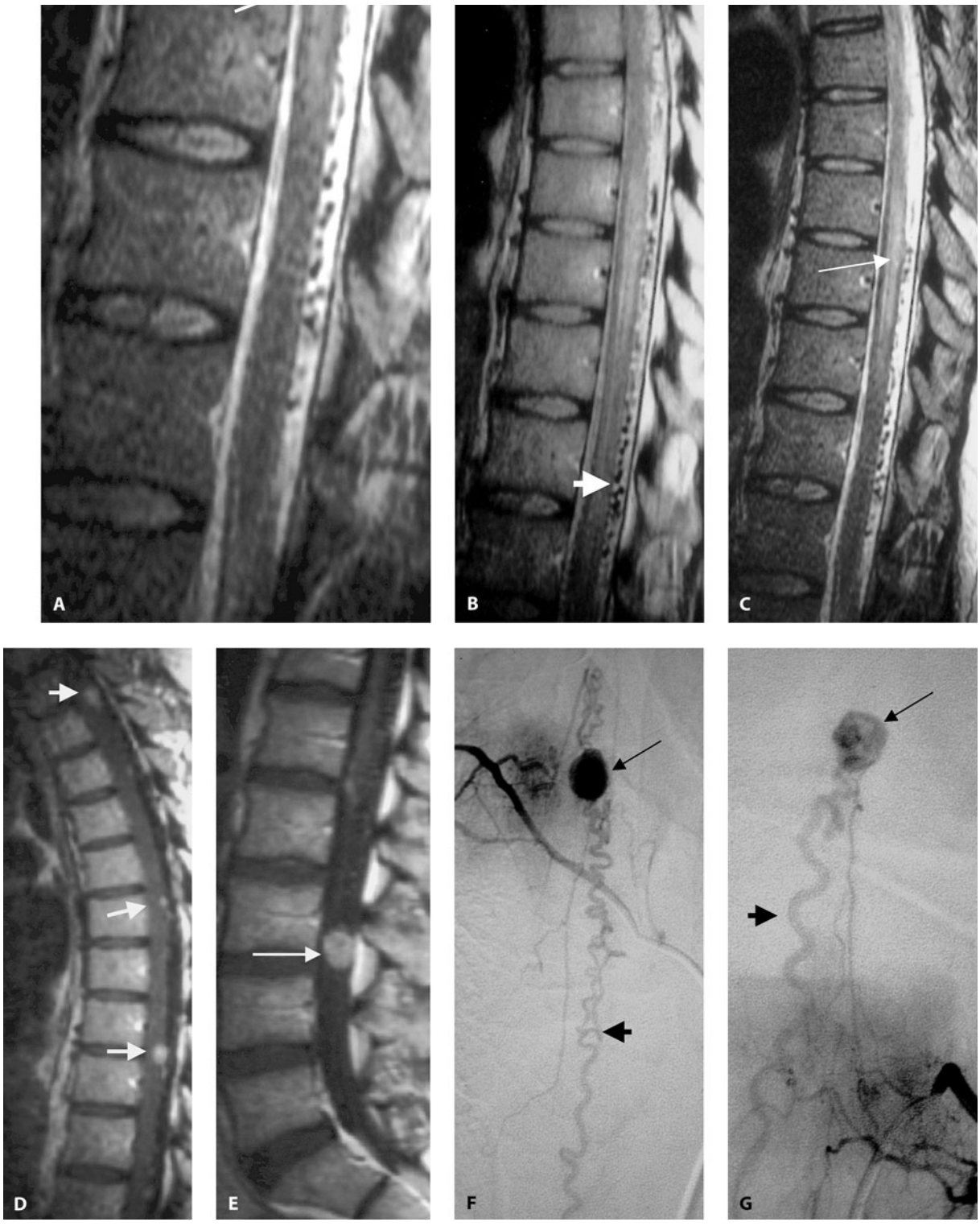

Fig. 13.21A–G. Legend see p. 902

cord. The posterior root is involved in 36% of radicular tumors, the anterior root in 7%, and the cauda equina in 57%. At the cauda equina level they attain quite a large size. When the tumors originate from a radicular location they will frequently have an hourglass appearance. The occurrence of epidural lesions is controversial (Djindjian et al. 1981). Cysts within or close to the tumor are present in about 50% of patients. There is associated syringomyelia in 67% of intramedullary tumors (Browne et al. 1976).

Progressive myelopathy is a rare clinical presentation of patients with hemangioblastomas (Fig. 13.21) but can occur in the presence of multiple lesions and poor venous drainage from the spinal cord venous system, creating a venous congestion type of phenomenon similar to patients with dural spinal arteriovenous fistulae.

Retinal lesions are typically peripheral, with tortuous, dilated arterial and venous structures. They are present in approximately 50% of patients with spinal hemangioblastomas and are often bilateral (Craig et al. 1941; Hardwig and Robertson 1984). Retinal symptoms usually precede spinal symptoms and are generally the earliest manifestation of the disease. Due to the common association of spinal, posterior fossa, and retinal tumors, careful ophthalmological examination is mandatory once a hemangioblastoma has been diagnosed. Direct ophthalmoscopic examination is the best way to detect retinal lesions (Hardwig and Robertson 1984); radiological imaging plays only a minor role in the diagnosis of ophthalmic lesions. Photocoagulation is effective in treating the majority of early retinal lesions, whereas the untreated lesions progress to blindness of the affected eye (Yasargil 1978).

In view of the genetic character of the disease, once a diagnosis of VHL has been made, screening and long-term follow-up of the patient's relatives is mandatory. Sato et al. (1988) demonstrated the important role of MRI in the diagnosis and follow-up of patients with VHL.

While there have been various reports of cerebellar hemangioblastomas becoming symptomatic during pregnancy (Robinson 1965; Ferrante et al. 1984; Rand 1957; Kasarskis et al. 1988), such progression has not been demonstrated with the spinal cord localization of the hemangioblastoma.

13.7.2 Pretherapeutic Evaluation of Hemangioblastomas

13.7.2.1 Computerized Tomography

Contrast-enhanced CT scanning is of limited use in establishing the diagnosis of spinal hemangioblastoma, as it is less accurate and less practical than MRI.

13.7.2.2 Magnetic Resonance Imaging

At present, MRI with gadolinium is the procedure of choice in the investigation of patients with possible spinal cord hemangioblastomas.

MRI with contrast enhancement has the great advantage of showing:

- Tumor nodules associated with serpentine tubular structures representing prominent draining veins
- The cystic portion of the lesion
- Associated edema
- The presence and extent of syringomyelia
- The status of the spinal cord (Figs. 13.19, 13.20)

MRI is also an excellent way to follow up patients with multiple hemangioblastomas and to establish coexisting intracranial localizations (Sato et al. 1988). Signal changes within the spinal cord may mimic those with progressive myelopathy associated with spinal dural arteriovenous fistulae, but contrast enhancement will demonstrate the tumor nodules (Fig. 13.21)

The pretherapeutic evaluation usually starts with investigation of the symptomatic location. Once the diagnosis is suspected or confirmed, a more extensive investigation is indicated to explore more than one tumor, the family history, and other organ involvement. The availability of CT and MRI justifies a complete CNS and abdominal diagnostic work-up.

13.7.2.3 Angiography

The characteristic angiographic appearance is that of a hypervascular mass, which is opacified early and persists as a dense homogeneous stain, usually well delineated (Figs. 13.20–22). No arteriovenous shunting is present. The angiographic appearance of hemangioblastomas in all locations is the same (Di Chiro et al. 1967; Djindjian et al. 1981). The absence of arteriovenous shunting is an important point in the angiographic differentiation between hemangioblastoma and AVM. In AVMs, individual

Fig. 13.22. Vertebral angiogram in lateral view (**A**) and frontal view (**B**) demonstrates characteristic dorsal location of hemangioblastoma (*open arrow*) at the upper cervical cord level, with arterial supply from the posterior–lateral spinal artery (*arrows*) arising directly from the vertebral artery and venous drainage toward the midline dorsal venous system (*double arrows*)

vessels, although superimposed, are seen through the angiogram. If multiple nodules in the spine or posterior fossa are seen, then the diagnosis will be obvious.

13.7.3 Feeding Arteries

In the spinal cord, screening requires demonstration of the entire anterior spinal artery axis and pial network since all tumors receive their blood supply from spinal cord vessels.

In the spinal cord, the most frequent supply is from the posterior spinal artery or arteries, as the tumors are most frequently located on the dorsal surface of the cord. At the upper cervical levels, this means supply from the posterior-lateral spinal artery should be expected (Fig. 13.22). At the level of the cervical or lumbar enlargement or in deep intramedullary tumors, sulcocommissural arteries from the anterior spinal artery are dilated when supplying the lesion (Fig. 13.20).

Hemangioblastomas for the most part receive their blood supply from a single pedicle. In tumors in which more than one pedicle is demonstrated, the possibility of more than one nodule must be considered. When a large tumor recruits more than one territory, a multicompartmental arrangement is seen, in which the various compartments fill only from one pedicle.

13.7.4 Draining Veins

There is no arteriovenous shunting in these hypervascular tumors; the draining vein(s) are primarily retromedullary and may be large, usually proportional to the size of tumor they drain, and should not be mistaken for SCAVMs.

13.7.5 Treatment and Embolization

Surgical excision using microsurgical techniques is the treatment of choice for symptomatic lesions.

In tumors with posterior spinal artery supply, the posterior spinal artery can be superselectively catheterized and embolized prior to surgical

Fig. 13.23A–D. Embolization of a hemangioblastoma. **A** Frontal subtraction angiogram of the right ascending cervical artery, which gives a radiculomedullary artery (*arrow*) and a radiculopial supply (*arrowheads*). Due to the spinomedullary supply, embolization of this vessel carries the risk of damaging the spinal cord. **B** Left ascending cervical artery injection demonstrates good access to the left portion of the tumor via the spinopial supply from the left (*curved arrow*). Note that the portion of the tumor supplied by the contralateral (*right*) side is not opacified, representing a second compartment or tumor nodule. **C** Superselective catheterization of the left radiculopial artery (*curved arrow*). **D** After gelatin sponge (Gelfoam) powder embolization, there is complete stagnation of radiopaque microemboli within the tumor (*white arrows*) ►

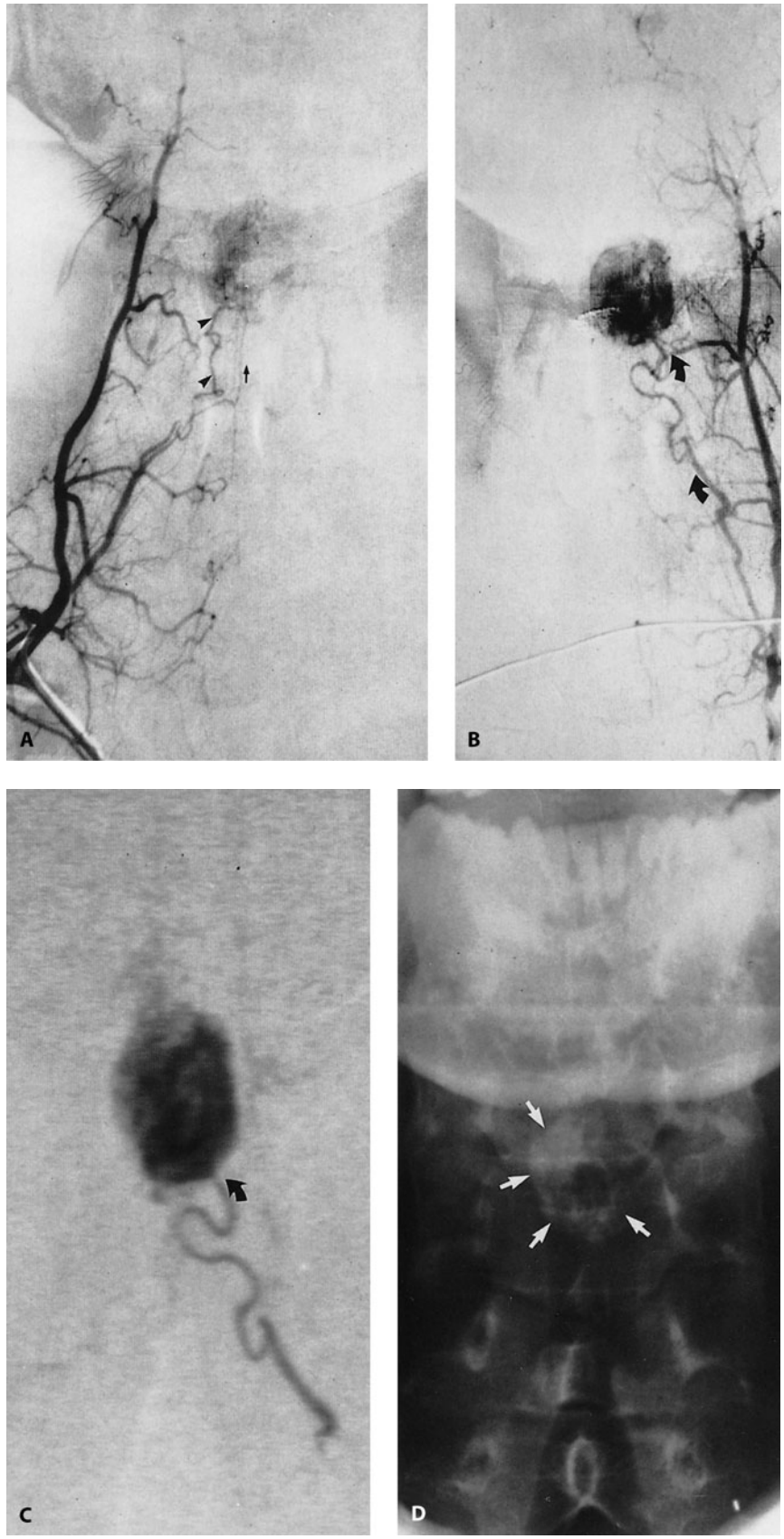

Fig. 13.23A–D.
Legend see p. 906

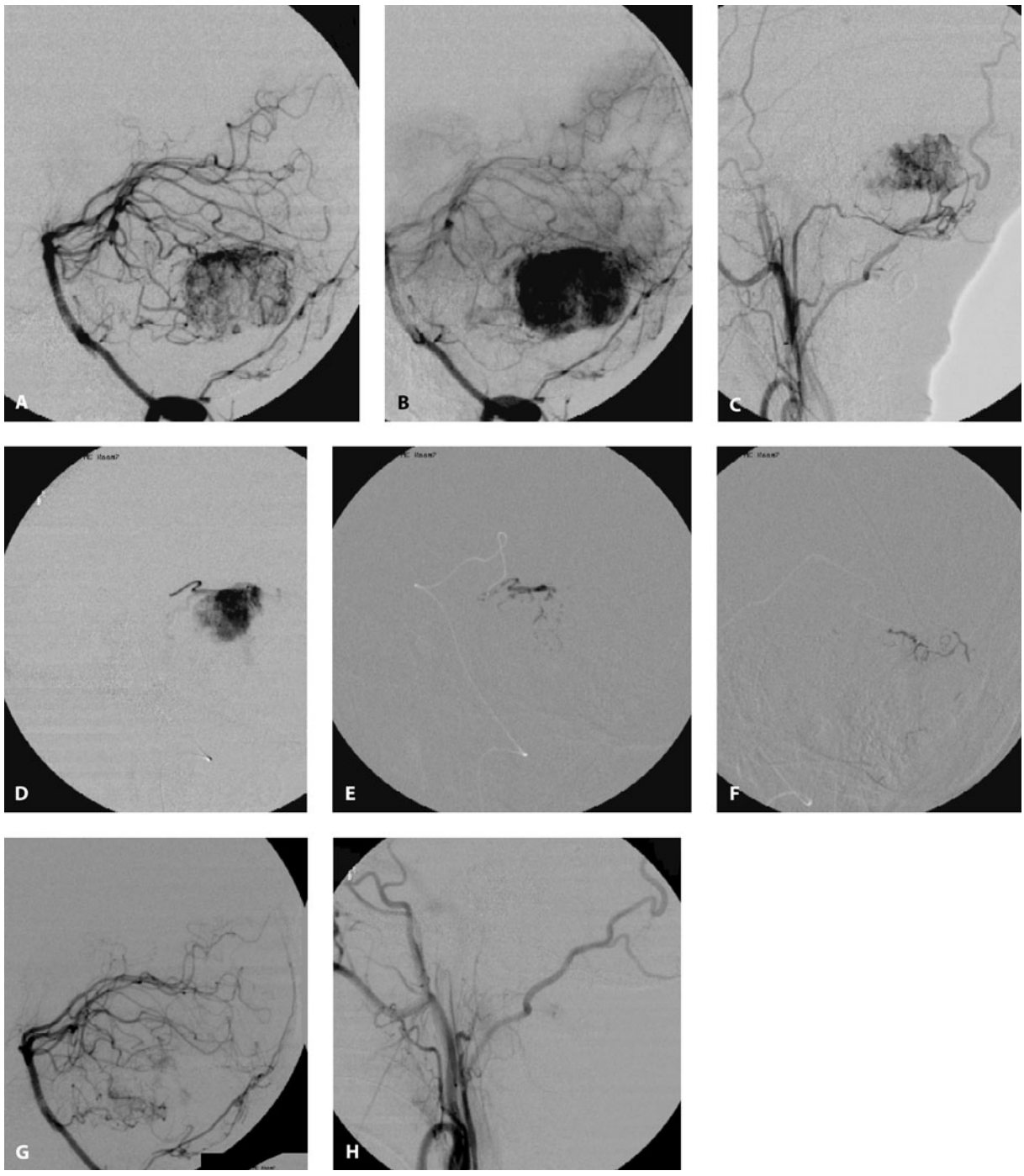

Fig. 13.24A–H. A 33-year-old female patient with symptomatic cerebellar hemangioblastoma was preoperatively treated with transarterial injection of glue. Vertebral angiogram in lateral view, early (**A**) and late arterial phase (**B**), shows dense tumor blush without venous shunting. Dural supply from the ascending pharyngeal artery is noted on the lateral view of the external carotid angiogram (**C**). Superselective injection of the superior cerebellar artery supply to the hemangioblastoma with contrast (**D**) and with liquid glue (**E**) as well as a second branch with glue (F) resulted in significant devascularization of the hemangioblastoma, as shown on postembolization vertebral (**G**) and external carotid angiogram (**H**)

removal (Fig. 13.23). The obvious contraindication is the presence of an anterior spinal artery contribution from the same pedicle.

Lesions in the cervicomedullary junction can receive supply from the lateral spinal artery from both sides; these vessels can be safely embolized (Tampieri et al. 1993).

For superselective catheterization, the variable stiffness microcatheters (0.10–0.14 F) are used, which will allow distal catheterization and gentle flow-controlled embolization with small particles of PVA (Fig. 13.23). Embolization of healthy territories and reflux of embolic material should be avoided, and as a general rule underembolization is recommended over a perfect postembolization picture. Embolization with the tip of the microcatheter in a wedged position should be avoided, as it may result in intratumoral hemorrhage. The role of transarterial embolization of liquid embolic material is currently being explored (Fig. 13.24).

13.8 Other Intradural Vascular Tumors and Spinal Hemorrhage

Other intradural vascular neoplasms such as paragangliomas are extremely rare (Figs. 13.25, 13.26) (Steel et al. 1994). Meningiomas can be intra- or extradural in location but their presurgical embolization is rarely necessary.

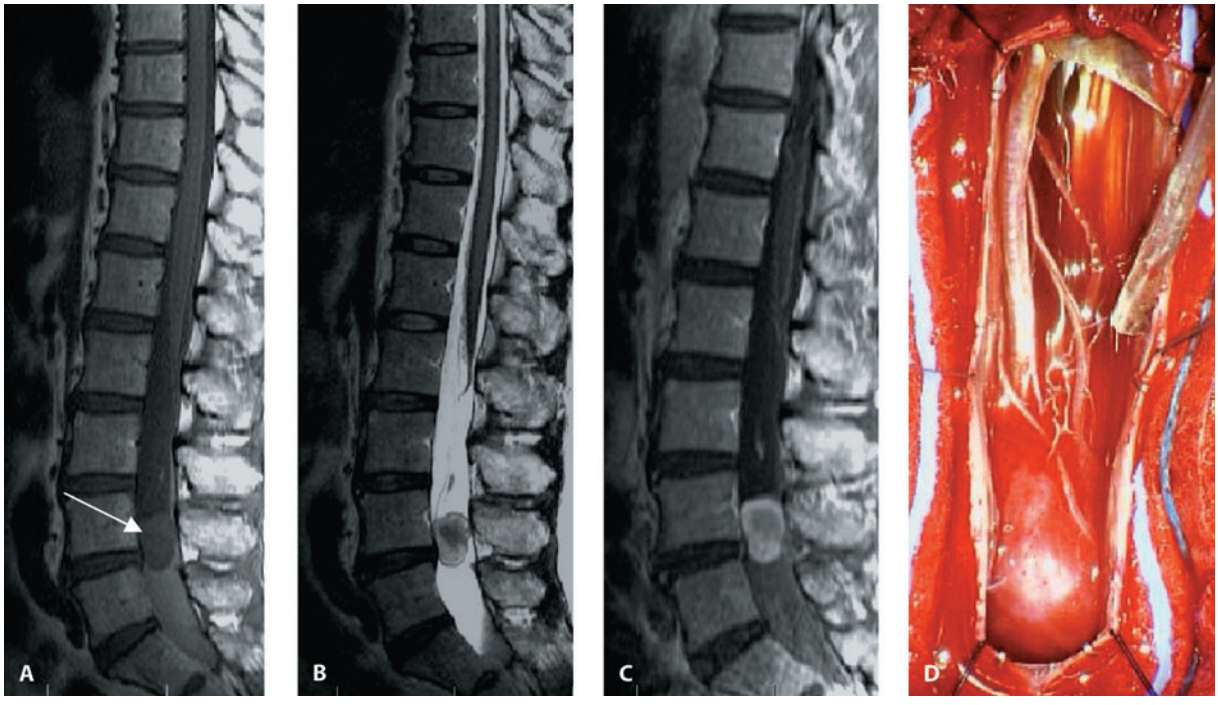

Fig. 13.25A–D. A 38-year-old female patient with progressive cauda equina syndrome over a 6-week period. T1-weighted MRI (**A**) shows evidence of intradural mass lesion (*arrow*) with different densities of CSF above and below the neoplasm. T2-weighted MRI (**B**) shows the relationship of the tumor to the adjacent nerve roots and nonhomogeneous enhancement on MRI following contrast enhancement (**C**) and at surgical exposure (**D**) prior to removal of what proved to be a paraganglioma

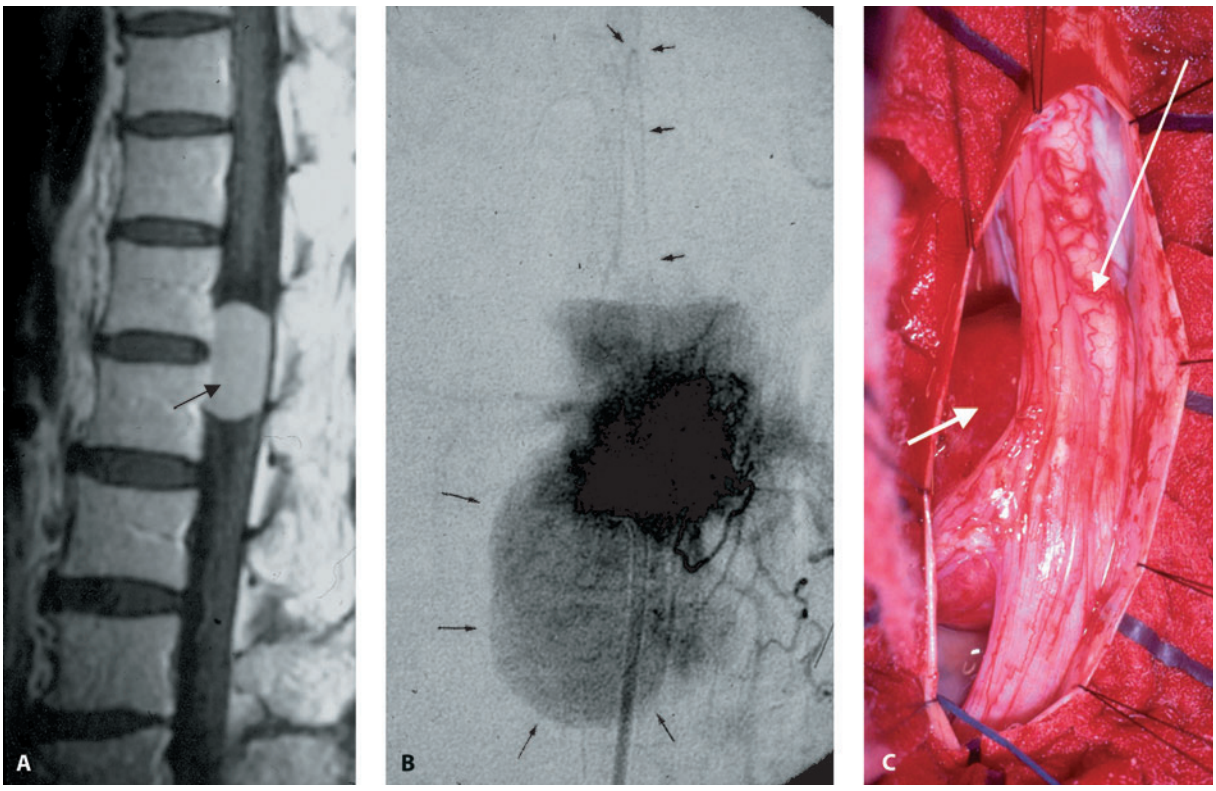

Fig. 13.26A–C. A 33-year-old female patient presented with progressive cauda equina syndrome. Contrast-enhanced T1-weighted MRI in sagittal view (**A**) shows homogeneous enhancing intradural mass lesion (*long arrows*) which at angiography AP view (**B**) was noted to be supplied by the same segmental radicular branch as the medullary arterial system (*short arrows*). Surgical exposure (**C**) demonstrated the cauda equina (*long arrow*) to be compressed and draped over an intradural meningioma (*short arrow*)

Subarachnoid hemorrhage caused by spinal tumors is a well-recognized entity (Djindjian et al. 1981). The most common tumors that can produce subarachnoid hemorrhage are ependymomas, which are found in more than 60% of patients, followed by neurinomas, astrocytomas, and other tumors. The type of hemorrhage reported from these tumors in most cases is subarachnoid. There is a higher incidence of subarachnoid hemorrhage associated with tumors located in the cauda equina (Table 13.4).

Table 13.4. Spinal hemorrhage due to tumor in 50 patients (modified from Djindjian et al. 1981)

Type of tumor	%	Location	%
Ependymoma	64	Cauda equina	88
Neuroma	18	Thoracolumbar	6
Astrocytoma	10	Thoracic	2
Meningioma	5	Cervical	4
Hemangioblastoma	2		
Meningeal sarcoma	2		

The clinical picture is that of sudden onset of back pain not infrequently preceded by headache. This may or may not be associated with nerve root involvement; absent reflexes, primarily of the lower extremities; and transient, lumbar, radicular dysfunction. This is the classic clinical presentation of spinal subarachnoid hemorrhage. When signs of meningeal irritation are dominant in a confused patient and an adequate history is not obtained, the diagnosis of subarachnoid hemorrhage from a cerebral origin is usually first suspected and investigated. Usually only after cerebral angiography is negative will the spinal cause of the hemorrhage be suspected and investigated.

14 Technical Aspects of Surgical Neuroangiography

14.1 Introduction 915

14.2 Patient Preparation 917
14.2.1 Angiographic Equipment 917
14.2.2 Preoperative Medications 917
14.2.2.1 Corticosteroids 918
14.2.2.2 Anticonvulsants 918
14.2.2.3 Antiplatelets 919

14.3 Anesthesia 919
14.3.1 General Anesthesia 919
14.3.2 Neuroleptic Analgesia 920
14.3.3 Tracheostomy 920
14.3.4 Local Anesthesia 920
14.3.5 Input and Output Monitoring 921
14.3.6 Arterial Line and Venous Line 921
14.3.7 Heparinization 923
14.3.8 Activated Coagulation Time Monitoring 924
14.3.9 Functional Evaluation 925
14.3.9.1 Somatosensory- and Motor-Evoked Potentials 925
14.3.9.2 Facial Nerve Monitoring 925
14.3.10 Pharmacological Testing 926
14.3.10.1 Amobarbital 926
14.3.10.2 Xylocaine 929
14.3.10.3 Mucocutaneous Territories 929

14.4 Arteriotomy Sites 929
14.4.1 Introducer Sheath 930
14.4.2 Closure Devices 932
14.4.2.1 Hemostasis of the Arteriotomy Site Closure 932
14.4.2.2 Internal Closure Devices 932

14.5 Catheters and Delivery Systems 933
14.5.1 Guiding Catheters 933
14.5.2 Microcatheters 934
14.5.3 Balloon Catheters 942
14.5.3.1 Tolerance Testing and Flow Control 942
14.5.3.2 Detachable Balloons 955
14.5.3.3 Angioplasty Balloon Catheters 958
14.5.3.4 Balloon-Mounted Stents 962
14.5.3.5 Stent Delivery Catheters 962

14.6 Guidewires 965
14.6.1 Microguidewires 965

14.7 Embolic Agents 969
14.7.1 Particulate Agents 969
14.7.1.1 Absorbable Materials 970
14.7.1.2 Nonabsorbable Particulate Materials 974
14.7.1.3 Flow-Directed Particle Embolization 980

14.7.1.4 General Principles in Aneurysm Treatment 1020
14.7.1.5 General Principles of Coil Treatment of Aneurysms 1030
14.7.2 Nonabsorbable Liquid Agents 1059
14.7.2.1 Introduction 1059
14.7.2.2 Acrylates 1059
14.7.2.3 Sclerotherapy 1074
14.7.2.4 Ethylene-Vinyl Alcohol Copolymer 1083
14.7.3 EVOH in Brain Arteriovenous Malformation Treatment 1089

14.8 Opacifying Agents 1092
14.8.1 Tantalum Powder 1092
14.8.2 Iophendylate (Pantopaque) 1093
14.8.3 Iodized Oil 1093
14.8.4 Ethiodol 1093

14.9 Chemotherapy 1093
14.9.1 Intra-arterial Infusions 1093
14.9.2 Time-Released Microcapsules (Chemoembolization) 1094

14.10 Miscellaneous 1094
14.10.1 Syringes 1094
14.10.2 Stopcocks and Y-Adapters 1095
14.10.3 Tray Containers 1095
14.10.4 Flushing Solutions 1095
14.10.5 Corticosteroids 1096
14.10.6 Normal Physiology of the External Carotid Arteries 1096

14.11 Flow Control 1097
14.11.1 Introduction 1097
14.11.2 Flow Control in the Craniofacial Area 1097
14.11.2.1 Protection of an Endangered Anastomosis 1101
14.11.2.2 Intralesional Flow Control 1101
14.11.2.3 Occlusive Balloon Flow Reversal 1102
14.11.2.4 Functional Rearrangement of the Supply to a Territory 1104
14.11.2.5 Surgical Flow Control 1104
14.11.3 Flow Control in the Meningeal Arcade and Dural Surfaces 1104
14.11.4 Flow Control in the Cerebral Circulation 1104
14.11.4.1 Distal Catheterization 1106
14.11.4.2 Flow Reversal 1108
14.11.4.3 Flow Arrest 1111
14.11.4.4 Systemic Hypotension 1111
14.11.4.5 Catheter Withdrawal 1111
14.11.5 Spine and Spinal Cord 1113
14.11.5.1 Technical Aspects of Endovascular Treatment in the Spine and Spinal Cord 1113

14.12 Postembolization Care 1128
14.12.1 Head and Neck 1128
14.12.2 Cerebral Arteriovenous Malformations 1128
14.12.3 Intradural Aneurysms 1128
14.12.4 Spinal Arteriovenous Malformations 1129

14.13 Complications of Embolization 1129
14.13.1 Complications of Head and Neck Embolization 1129
14.13.1.1 Neurological Deficit 1129
14.13.1.2 Cranial Nerve Deficit 1129
14.13.1.3 Postoperative Swelling 1130
14.13.1.4 Skin Necrosis 1130
14.13.2 Complications of Cerebral Embolization 1130
14.13.2.1 Medical Therapy for Acute Ischemic Stroke 1130
14.13.2.2 Recanalization 1131
14.13.2.3 Microcirculation Agents 1132
14.13.2.4 Antiplatelets 1132

14.13.2.5 Anticoagulation 1132
14.13.2.6 Biorheological Factors 1133
14.13.2.7 Antiedema and Pharmacological Protection Agents 1134
14.13.2.8 Additional Measures 1135
14.13.3 Hemorrhage 1135
14.13.3.1 Generalities 1135
14.13.3.2 Brain Arteriovenous Malformation Rupture 1137
14.13.3.3 Aneurysm Rupture 1141
14.13.3.4 Arterial Stenosis 1143
14.13.3.5 Vasospasm 1146

14.14 Follow-Up 1146

14.15 Combined Endovascular Treatments 1146
14.15.1 Combined Endovascular Treatment in Aneurysm Therapy 1147
14.15.2 Combined Endovascular Treatment in Brain Arteriovenous Malformation Therapy 1147
14.15.3 Combined Endovascular Treatment in Occlusive and Hemorrhagic Vascular Disease 1147

14.16 Techniques of Carotid Angioplasty and Stenting 1152
14.16.1 Introduction 1152
14.16.2 Hemodynamic Disturbances During Stenting 1152
14.16.3 Premedication 1153
14.16.4 Vasoactive Medications 1154
14.16.5 Intervention 1154
14.16.6 Predilatation Angioplasty 1164
14.16.7 Stent Selection 1164
14.16.7.1 Self-Expandable Stents 1169
14.16.7.2 Nitinol 1169
14.16.7.3 Balloon-Expandable Stents 1171
14.16.7.4 Low-Profile Balloon-Expandable Stents 1171
14.16.7.5 GFX II 1171
14.16.8 Postdeployment Angioplasty 1173
14.16.8.1 Distal Cerebral Protection 1173
14.16.9 Mechanical Revascularization of Totally Occluded Brachiocephalic Vessels 1176
14.16.10 Complications of Mechanical Revascularization 1178
14.16.11 Stent Retrieval 1179

14.1 Introduction

Surgical neuroangiography refers to image-guided procedures that use the endovascular route to reach the target. This therapeutic modality is used for the devascularization of a territory or abnormality, i.e., embolization, or to reestablish flow, i.e., revascularization or repermeation of an occluded vessel or vascular territory.

The understanding of the cerebral vasculature, its variations, and the technical capabilities that have been developed to navigate through the spine, spinal cord, brachiocephalic, and brain circulations (arterial and venous) provide significant opportunities for both diagnosis and therapy of a variety of pathological entities affecting the CNS and maxillofacial areas. In addition, these advances show the potential for expanding our field into yet unforeseen areas.

At present, surgical neuroangiography is at the forefront in the management of aneurysms and the various vascular malformations. This includes

endovascular obliteration of aneurysms and the management of the devastating sequelae of cerebral vasospasm by mechanical and/or chemical vasodilatation, with significant improvement in the final outcome of patients suffering from aneurysmal subarachnoid hemorrhage (SAH). In vascular malformations, embolization is used as the sole form of treatment, preoperative devascularization, and as a palliative treatment.

The potential therapeutic modalities of thrombolysis and vascular recanalization may be one of the most challenging but rewarding contributions in advancing the treatment of occlusive cerebrovascular disease.

Our abilities to navigate in the venous system makes the treatment of difficult arteriovenous shunts possible, even in occluded venous structures, and may play an important role in the retroperfusion of ischemic areas or chemotherapy of neoplasms.

The superselective infusion of pharmacological agents such as amobarbital promises to advance our understanding of CNS function and may become an important adjunct to functional magnetic resonance imaging (FMRI) in the planning of functional neurosurgical operations such as the treatment of epilepsy.

Our ability to reach distal vascular territories may make the use of otherwise toxic chemotherapeutic drugs possible in the treatment of malignant lesions. The addition of agents that can cross the blood–brain barrier or radiosensitizers may further enhance these capabilities.

Our approach to these interventions is based on solid principles of functional vascular anatomy, collateral circulation, blood supply to eloquent structures, and hemodynamic balances between the various areas in the circulation to be analyzed and/or treated. These principles will allow us to understand the individual variations in a specific patient, plan treatment in the most efficient and safe manner, and assess the results of such treatments.

Embolizations or infusions accomplish devascularization; revascularization is mechanical with a variety of catheters, guidewires, angioplasty balloons, and stents, or pharmacological agents. Rapid technical advances are facilitating and improving our results, and will continue to do so at an accelerated pace. We believe that no single device or technique fulfills all needs in every case and that various approaches using different tools may achieve the same clinical goal.

The purpose of this section is to regroup and comment on the tools we currently use to reach our objectives and best fulfill our needs in the management of our patients.

We would like to emphasize that the tools available cannot replace proper training, nor will technical solutions replace proper knowledge of the vascular anatomy, including collateral circulation and anastomotic pathways between the various territories or between the extracerebral and intracerebral circulations. Proper understanding of functional vascular anatomy may allow the endovascular surgeon to compensate for any or all of the limitations of our present technology. Finally, the clinical goal is the primary objective to compare outcomes and techniques, as some tools or manipulations carry higher risks than the natural history of the disease.

14.2 Patient Preparation

As our specialty evolves, the complexity of the patients and diseases that we deal with are expanding, and our responsibility in the management of our patients is increasing.

Discussing the details of the procedure with the patient and his or her family is vitally important, including the risks and goals involved, as well as alternative modes of treatment. The objective of the procedure and the possibility of additional treatment (multiple stages, shunting, postembolization surgical resection, radiation, etc.) must be planned and discussed in advance.

14.2.1 Angiographic Equipment

Head and neck embolization can be performed with almost any conventional fluoroscopic unit; however, with available technology, the minimum equipment necessary for proper, safe, and accurate surgical neuroangiography is optimal fluoroscopy with the largest possible field size, a C arm, or biplane-type fluoroscopic capabilities. Digital subtraction angiography with immediate life subtraction and road map capabilities is a major advancement. All the optimal tube, small focal spot, film screen combinations are all important, but their description is beyond the scope of this book. However, the angiographic suite should be serviced as a conventional operating room.

The use of rotational angiography with three-dimensional (3-D) reconstruction has become a great advantage, mostly in the treatment of aneurysms, and provides an additional perspective. As we are learning this new way to display vascular anatomy, searching for added information will continue, from surface rendering to virtual endoscopic explorations. Three-dimensional imaging is an interpreted way of imaging vasculature.

14.2.2 Preoperative Medications

In general, no specific preoperative medications or measures are required prior to endovascular embolization of the head and neck or of cerebral and spinal lesions, with the exception of those related to anesthesia, such as 6-h fasting, mild sedation, and atropine in case emergency endotracheal intubation is required.

In patients undergoing elective revascularization procedures, 2–3 days of preoperative antiplatelet medications, in addition to their regular medications, is needed to avoid thromboembolic complications. Patients on Coumadin must be converted to heparin or low-molecular-weight heparin; both must be stopped prior to the procedure, and heparin is restarted once the puncture site is secured.

Preoperative clinical assessment includes a detailed neurological examination and neuropsychological testing for fine cortical functions in appropriate cases, which not infrequently are impaired in patients other-

wise thought of as neurologically intact. Preliminary EEG testing is not needed for the procedure but may be important as part of a complete neurological evaluation in diseases prone to seizures. The prophylactic use of Ca^{2+} channel blockers, to prevent cerebral vasospasm, has been advocated by some investigators (Merland and Reizine 1987; Picard 1988, unpublished data). However, vasospasm during cerebral navigation has not been a problem in our experience, and we do not routinely use Ca^{2+} channel blockers for that purpose. In selected cases, primarily in females, prophylactic Ca^{2+} channel blockers may be of help in preventing spasm during catheterization at the cervical internal carotid artery (ICA). Ca^{2+} channel blockers are started 24 h before the procedure and can be supplemented during the procedure. It is important to be aware that Ca^{2+} channel blockers will produce some hypotension. Prophylactic steroids prior to the procedure are not routinely used (see Sect. 14.2.2.1).

In patients with known allergies to iodinated contrast material, premedication with corticosteroids and antihistamine drugs is used.

14.2.2.1 Corticosteroids

In general, corticosteroids are not used as a prophylactic measure but may be used in long procedures if there is a possibility of swelling or after a complication. Steroids may be of more value in posterior fossa and spinal cord lesions than in supratentorial malformations. The use of corticosteroids as part of the management of acute stroke is very controversial. It may, however, be of assistance in the edema that follows a hemorrhagic complication (mass effect).

Postoperative corticosteroids are used in most cases as an antiedematous agent. Dexamethasone (Decadron, 8 mg IV is given) during the procedure as soon as the embolization is started and is repeated every 8 h for 3 days (it is given p.o. as soon as tolerated), followed by tapering off over 3 days. Appropriate prophylactic antacids are used to prevent gastrointestinal complications.

Corticosteroids are used by two of the authors (K.T.B., A.B.) in high doses if the treatment is sclerotherapy, for example, ethanol sclerotherapy in maxillofacial lesions.

One of the present authors (P.L.) uses corticosteroids started during the procedure when a large quantity of glue is used, to avoid pain secondary to inflammatory foreign-body reaction.

14.2.2.2 Anticonvulsants

Endovascular embolization neither produces seizures nor increases their frequency (Table 14.1). Therefore, anticonvulsant medications are used only in patients who have had previous seizures, an intracerebral hematoma, or SAH, or in those already on an anticonvulsant or with EEG evidence of possible epileptogenic activity. In such patients, we maintain the anticonvulsant doses, but no additional doses are given for the procedure. If complete obliteration of the malformation is obtained and confirmed in

Table 14.1. Seizure outcome in 257 patients (from Berenstein et al. 1989a, with permission)

Present prior to embolization (*n*)	Seizure free (*n*)	New seizures (*n*)
134	91	8

a patient with seizures, the patient is clinically followed for 1 year. If no seizure activity occurs in the intervening year, a repeat EEG is done. If potential epileptogenic activity is not present, the anticonvulsant medication is tapered off and eventually discontinued.

14.2.2.3 Antiplatelets

In patients undergoing revascularization procedures as an elective intervention, in addition to the individual needs of the patient, the single most important preoperative medications are antiplatelet agents, which must be started 2–3 days before the procedure. Plavix (75 mg) started 2–3 days before the procedure is preferred. If Plavix is contraindicated, ticlopidine (250 mg) or aspirin (325 mg) is used. In high-risk instances such as severe posterior circulation revascularization, in very selected cases the prophylactic use of glycoprotein IIb/IIIa receptor antagonist (GPA) has been recommended (Connors and Wojak 1999a, b). We do not use them prophylactically, but have only used GPA in extreme situations, where thrombolytics failed to dissolve clot, with excellent results. Specific preoperative and perioperative measures are discussed in their appropriate section.

Just as in the management of unruptured aneurysms, we have had instances where coil protrusion has been the nidus for clot formation, in which IV abciximab (ReoPro) reabsorbed the clot (Fig. 14.101).

14.3 Anesthesia

Various types of anesthesia can be used during interventional neuroradiological procedures in the brain, head, neck, and spine. The role of anesthesia includes the overall monitoring of the patient's physiological and metabolic status. This includes not only the level of consciousness but also all other physiological functions, including input and output, blood pressure control, degree of anticoagulation, and when needed, reversal of anticoagulation. A close cooperation and familiarity with the procedure by anesthesia personnel is required for optimal results.

14.3.1 General Anesthesia

We routinely use general anesthesia except when carotid or vertebral occlusion will be done, or where general anesthesia is contraindicated. In

cases of revascularization, anesthesia is used unless the patient's medical condition makes anesthesia a high risk.

The type of anesthesia used is primarily a decision of the anesthesiologist and may be modified in individual situations when specific monitoring is to be used. If using somatosensory-evoked potential monitoring for spinal cord, brainstem, auditory, or visual cortex function (Berenstein et al. 1984b), neuroleptic drugs are used, as most of the anesthetic gases alter the evoked potentials.

Nitrous oxide (NO_2) is *not* used during general anesthesia in view of its risk of air expansion. If an air bubble is accidentally introduced into the circulation, nitrous oxide will expand the bubble with the risk of occluding an important vessel.

Apnea is frequently used during angiographic acquisitions to decrease motion artifacts. It is of greatest importance when small vessels are studied, such as in the spinal cord. Valsalva maneuvers can be used in venous lesions to enhance their filling, or used to increase venous pressure, and should probably be avoided in patients who present with intracranial hemorrhage (ICH), or infants with CSF absorption problems.

14.3.2 Neuroleptic Analgesia

Neuroleptic analgesia is most useful for surgical neuroangiographic procedures. It allows easy neurological monitoring throughout the procedure and at the same time gives both analgesia and sedation. It is used even in young patients and carries less risk than general anesthesia in the older or medically compromised patient. The neuroleptic combination to be used is the choice of the anesthesiologist.

In patients with lesions near the airway, where the risk of swelling can produce obstruction, endotracheal intubation and general anesthesia are preferred. A nasogastric tube is placed in lesions that may compromise the alimentary pathway when direct ethanol embolization is used, or in very sick patients as needed. The use of laryngeal mask airway (LMA) is of great help.

14.3.3 Tracheostomy

Prophylactic tracheostomy may be required where lesions at or near the airway are treated, especially if multiple procedures or surgery is foreseen. Swelling of the tongue or pharyngeal venous malformations may obstruct the airway.

14.3.4 Local Anesthesia

When neuroleptic anesthesia is used, a long-lasting local anesthetic such as Marcaine (bupivacaine hydrochloride) 0.25% is recommended to avoid the need for reinfiltration during the procedure. On occasion, the femoral nerve can be anesthetized, and this will produce a motor and sensory monoplegia that will clear completely in 12–15 h and should not be mistaken for a PNS complication.

14.3.5 Input and Output Monitoring

A Foley catheter will permit accurate monitoring of urinary output in patients who are not under general anesthesia and will prevent patient discomfort and restlessness during the latter part of the procedure when the critical part of the embolization is being performed. In addition, narcotics for neuroleptic analgesia can cause bladder distention and retention.

In case of emergency treatment or if surgery will follow, an indwelling catheter is already in place. If no Foley catheter is used, bladder evacuation is accomplished at the end of the procedure, prior to compression of the groin and after reversal of heparinization.

14.3.6 Arterial Line and Venous Line

An arterial line is used in most cases by one of the authors (A.B.), selectively used by the second (K.T.B.), and almost never used by the third (P.L.), and is related to the group's anesthesiologists and their requirements. It is helpful in accurately monitoring the arterial pressure, mostly in patients with very-high-flow fistulae (neonates and infants), where an increase in the total blood volume exists. When hypotension is needed, such as in cases of brain arteriovenous malformations (BAVMs), where blood pressure modifications can be of help to obtain better penetration and to decrease the chances of venous migration of embolic agents. In older, sicker patients with cardiac problems, it may also be of assistance for proper patient monitoring. In cerebral aneurysms, where full heparinization is usually employed, an arterial line is convenient for repeated blood sampling. The line is accessed prior to heparinization. A central venous line is not needed unless a major cerebral artery will be occluded because fluids and/or volume expanders and/or hypertensive drugs may be needed to maintain proper cerebral perfusion.

A central venous line or access may be used in revascularization of the carotid bulb in unstable patients who may require emergent passing.

If medical management of blood pressure is needed both arterial and central venous lines will be kept in the postembolization period until the patient is stable. If no medical management of blood pressure is needed the arterial line is removed at the end of the procedure but the central line is kept in for 24 h.

Controlled hypotension is usually done with a nitroprusside drip, nitroglycerin, or a combination of narcotics and hypotensive drugs. In very young children, the blood pressure can be easily and expeditiously lowered with high-dose inhalation agents. Blood pressure control may be of value in the immediate postocclusion period (especially if an aneurysm is proximal to the embolized territory or if a very-high-flow pedicle has been occluded). The systolic blood pressure is not allowed to rise above the baseline and preferably is kept 10–20 mmHg below the baseline. Alternatively, blood pressure may be lowered with Ca^{2+} channel blockers such as nicardipine. This is given as a loading dose of 1 mg IV bolus and repeated up to 2–4 mg/h, aiming for a 20%–30% reduction in the baseline blood pressure.

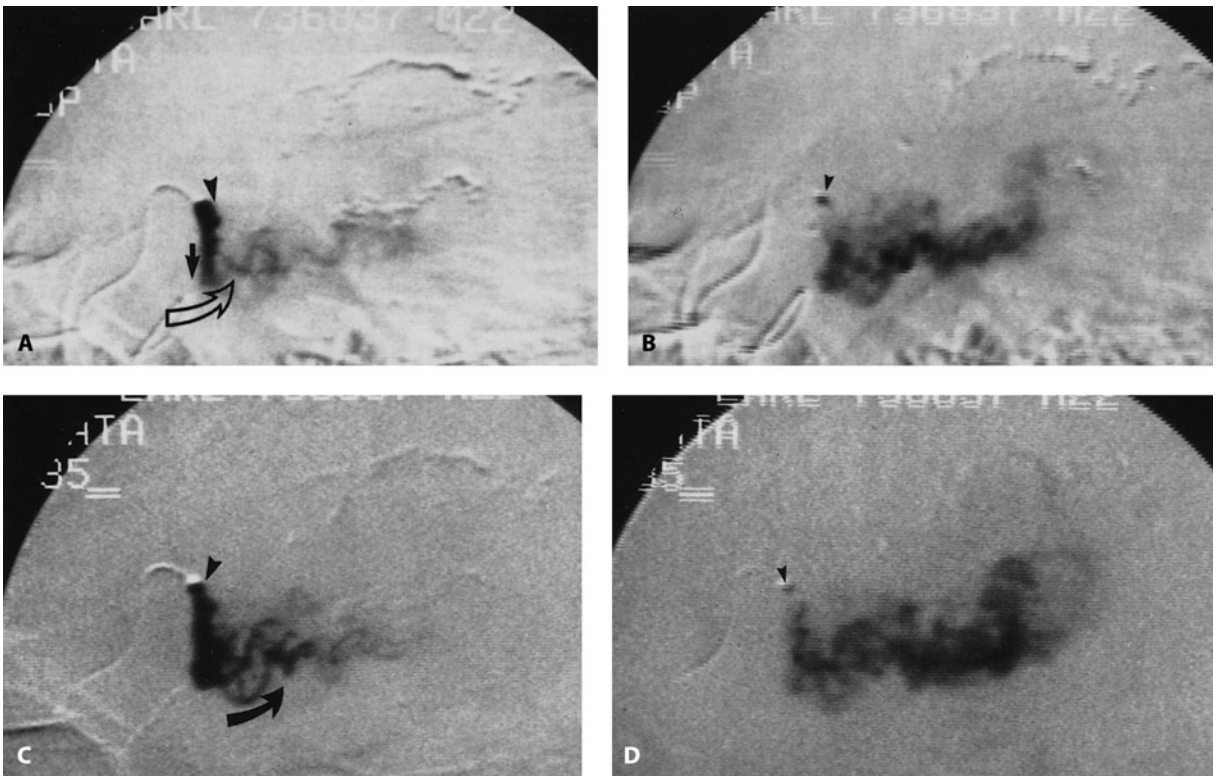

Fig. 14.1A–D. Use of hypotension in brain arteriovenous malformations. **A**, **B** Under normotensive conditions (135/95 mmHg), injection of a middle cerebral artery demonstrates poor flow control. **A** Lateral digital subtraction angiogram with the balloon (*arrowhead*) inflated produces only limited flow arrest (*arrow*), with dilution (*open curved arrow*) from another pedicle. The balloon has been deflated (*arrowhead*), with rapid washout of the contrast material, best appreciated fluoroscopically. **C**, **D** In hypotensive conditions (BP 70/35 mmHg). **C** With balloon inflation (*arrowhead*), note the significantly better opacification of the malformation without dilution (*curved arrow*). **D** Following balloon deflation, there is slow emptying of the malformation with significantly better opacification of the malformation. An appreciable difference in circulation time is noted with fluoroscopy

Lowering the systemic blood pressure may provide better penetration into the nidus of the arteriovenous malformation (AVM), as flow through the AVM is dependent on the systemic blood pressure (Fig. 14.1)

An arterial line may also be advantageous in young children or infants for easy accessibility in repeated blood gas measurements. In addition, a central venous line may be necessary if hypotensive medication will be given for a long period of time or if significant amounts of fluid will be used. Central venous pressure monitoring is especially useful in the infant with cardiac problems or in the older patient.

One of the authors (P.L.) seldom uses blood pressure control during the actual occlusion or in the immediate postocclusion period. In such cases, the use of Valsalva and deeper general anesthesia is used to reduce flow. We all agree that the most important aspect of blood pressure monitoring is to prevent abrupt systolic blood pressure elevation at the time of embolization or immediately after occlusion when the mean pressure

in the occluded feeder increases (Duckwiler et al. 1990; Jungreis and Horton 1989).

Intentional elevation of the baseline blood pressure may be useful in children when the femoral pulse is not optimally palpated. Any decrease in blood pressure in this situation is usually secondary to the anesthesia itself. Permitting the patient to become lighter will usually be sufficient to raise the blood pressure and increase perception of the pulse. Rarely, a small dose of ephedrine may be needed to improve the pulse perception. The use of Doppler guidance may also facilitate puncture in small children.

In theory at least, short increases in blood pressure may assist in flow-guided distal catheterization and may be attempted on rare occasions, although this is less important with the newer variable-stiffness microcatheters and those with hydrophilic coatings.

14.3.7 Heparinization

Systemic heparinization is recommended when using coaxial catheter assembly systems or when using balloons and during revascularization procedures. Heparinization in these circumstances is to prevent fibrin clot aggregation between catheters and/or balloons. Preliminary prothrombin time (PT), partial thromboplastin time (PTT), and, if available, activation coagulation time (ACT) (Scott et al. 1986) are obtained and used as guidelines and to calculate protamine sulfate dosage when heparinization is to be reversed.

Two techniques of heparinization can be used:

1. A bolus loading dose of 50 IU/kg, with a continuous maintenance IV infusion of up to 500 IU/kg over 24 h. When using this technique, there is no need for additional heparin in the liquids used for continuous perfusion between coaxial catheters or in the sheath at the arteriotomy site.
2. If heparin is used in the flushing solution, in the various perfusion lines between coaxial catheters, and at the sheath site (2,000 USP/1,000 ml of 2.5% D/W in children, and 4,000 USP/1,000 ml of 5% D/W in adults) a loading dose is usually not necessary unless cerebral navigation is immediately started, in which case a loading dose of 1,000–1,500 USP is given as a bolus. No heparin is used in children or neonates if non-coaxial systems are employed or if treating a postoperative or postictal emergency.

In unruptured aneurysm treatment and in revascularization procedures, we do start with a bolus dose, once the femoral puncture is secured.

At the end of the procedure, protamine sulfate can be used to reverse heparinization if indicated. In most aneurysm treatments and in revascularization procedures, we do not reverse the heparin; patients will either be continued on heparin or we let its effect wear off. When heparinization is maintained, a closure device is used or the sheath is left in place until heparin is stopped. If hemorrhage occurs during the procedure, immediate reversal is done. In such patients, the dose is determined by calculat-

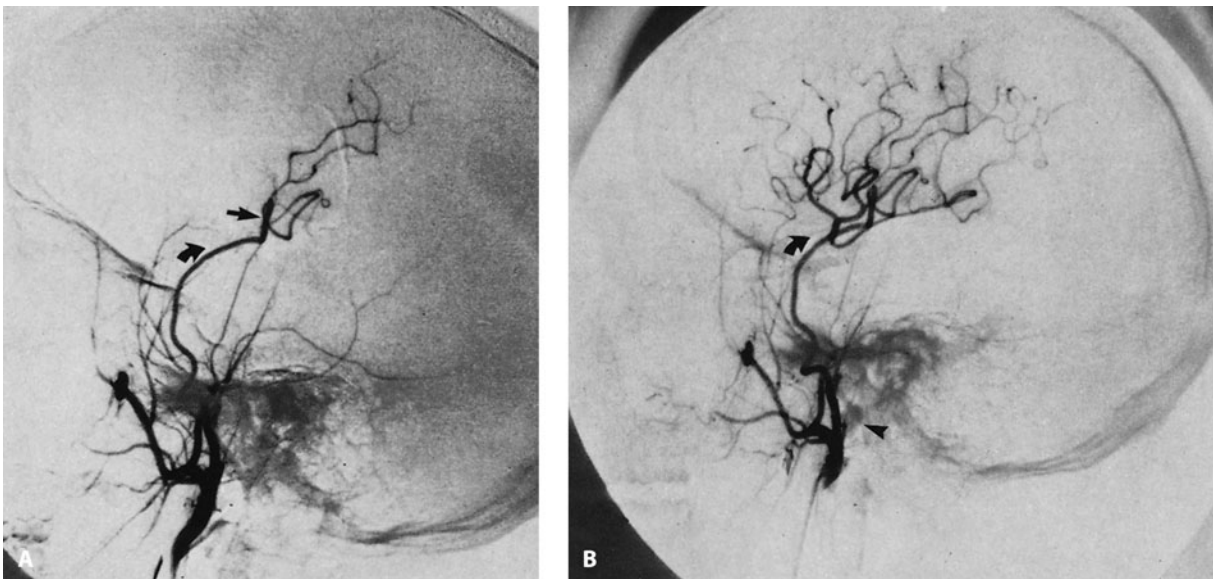

Fig. 14.2A, B. Double-lumen balloon catheters for functional investigation. **A** Lateral subtraction angiogram of the distal left external carotid artery, which demonstrates a superficial temporal artery (*curved arrow*) to middle cerebral artery by-pass (*arrow*). Note filling of one middle cerebral artery opercular branch. **B** Lateral subtraction angiogram of the left distal external carotid artery after a double lumen occlusive balloon catheter (*arrowhead*) has been placed in the left internal carotid under systemic heparinization to test for tolerance. Note the superficial temporal (*curved arrow*) increased perfusion to the middle cerebral artery territory (same amount of contrast material was injected). Note the preferential flow toward the brain, with poor filling of internal maxillary branches

ing the amount of heparin given per unit of time, per coagulation time, or simply by the ACT value.

When performing a tolerance test occlusion (Fig. 14.2), systemic heparinization is routinely used. In a 70-kg adult, 5,000 IU of heparin sulfate is given as an IV push. Prior to balloon occlusion of the parent vessel, an ACT test is obtained to confirm proper heparinization. At the end of the tolerance test and/or the procedure, reversal is done based on the information of the ACT sample (Scott 1987).

14.3.8 Activated Coagulation Time Monitoring

One of the authors (A.B.) routinely uses an ACT measurement during the interventional procedures (Scott 1987), using a hemochrome (International Technidyne Corp., Edison, NJ, USA) for the monitoring. A baseline ACT sample is obtained immediately after gaining access to the arterial system. A 2-ml blood sample is drawn via the side arm of the catheter introducer sheath. At the end of the procedure, prior to removal of the sheath and/or catheter, a repeat ACT is measured. Protamine sulfate is then administered intravenously if one wants to reverse the heparin and normalize the ACT prior to the removal of the sheath or catheter. In some indications such as aneurysm treatments and revascularization proce-

dures, we do not reverse heparin. We give 20–35 mg of protamine (depending on the patient's age) over 10 min if the postprocedure ACT is greater than twice the baseline ACT; 10–20 mg is administered if the postprocedure ACT is less than twice the baseline. A repeat ACT is then measured 5–10 min after the administration of protamine and the necessity for a second dose is evaluated. Once the normal ACT value is obtained, the sheath of the catheter is removed and manual compression is applied to the femoral puncture site for 15–20 min.

14.3.9 Functional Evaluation

A variety of tools are presently available for functional evaluation before, during, and after endovascular procedures (Berenstein et al. 1984b; Hacke et al. 1983).

Clinical assessment of the patient is the most reliable monitoring during occlusive balloon testing of major cerebral arteries such as the ICA. Except for somatosensory- and motor-evoked potential monitoring used by one of the authors (A.B.), other testing is employed in very selected situations.

14.3.9.1 Somatosensory- and Motor-Evoked Potentials

Somatosensory-evoked potential (SEP) monitoring in cerebral embolization has significant limitations and may even be confusing. It may have limited applications in patients in whom the procedure is done under general anesthesia. SEP monitoring can be helpful in patients who have a lesion in the thalamus, perirolandic area, or brainstem. The role of SEPs or brainstem-evoked potentials may expand in intracranial procedures as more experience accumulates (Berenstein et al. 1984b; Hacke et al. 1983; John et al. 1989).

In spine and spinal cord lesions, SEPs and motor-evoked potentials (MEPs) are routinely used by one of the authors (A.B.) and are felt to be very sensitive in detecting potential dangers. The addition of pharmacological testing, with the intra-arterial injection of amobarbital and xylocaine, adds further reliability and safety (Berenstein et al. 1989b; John et al. 1989).

14.3.9.2 Facial Nerve Monitoring

In maxillofacial vascular malformations treated percutaneously and with ethanol, the major risks are facial nerve palsies and skin necrosis. For the past year, we have been monitoring facial nerve function using evoked potentials, with impressive correlation and safety. The facial nerve course is first mapped with the patient under general anesthesia; thresholds needed for stimulation are assessed and act as controls (Fig. 14.3). As the embolization progresses, changes in threshold can be easily monitored, and if progressive, the injection is stopped and resumed either in a different location (Fig. 14.3C) or at a different session. The intravascular injection

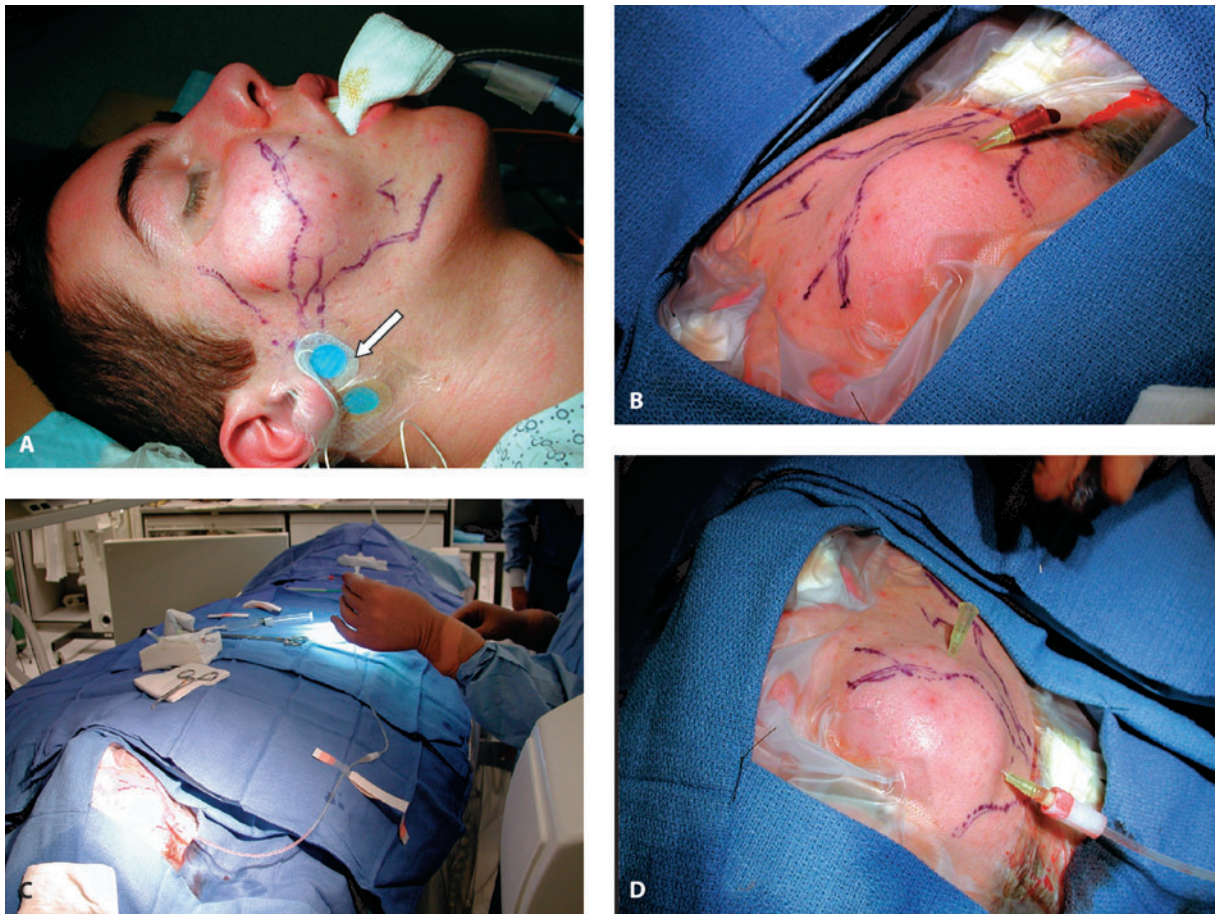

Fig. 14.3A–D. Facial nerve monitoring during sclerotherapy. **A** Following general anesthesia, the facial nerve is mapped by stimulation and painted over the skin (*arrow* points to stimulation-monitoring electrodes). **B** Direct percutaneous puncture is done with a fine angiocatheter or butterfly between the facial nerve branches until blood return is established. **C** The puncture site is connected to a venotube, and pressures are obtained. At the beginning of the procedure, venous pressure is at heart level. **D** Two areas of puncture between facial nerve mapping

of the sclerosing agent is mandatory to prevent damage to any normal structure and is of greater importance than the monitoring. During fluoroscopy and preferably with road mapping following contrast material injection, the tip of the needle must be free of contrast material, as it layers into the dependent position (Fig. 14.4).

14.3.10 Pharmacological Testing

14.3.10.1 Amobarbital

During cerebral and spinal cord embolization, a major risk is the occlusion of functionally important tissue. This complication is best avoided by a solid knowledge of functional anatomy, careful analysis of the preliminary selective and superselective angiograms, very distal catheterization

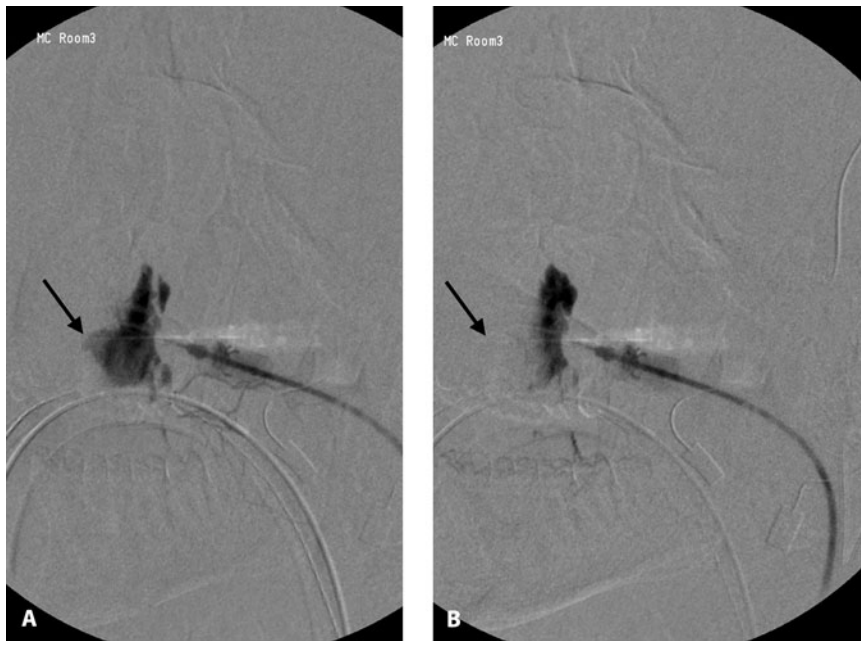

Fig. 14.4A, B. Direct percutaneous puncture of venous vascular malformation, same patient as Fig. 14.3. **A** Lateral road map of the direct puncture shows contrast material within the venous compartment. The *arrow* points to the tip of the needle. **B** Same projection, later phase. Note the layering of the contrast material away from the tip of the needle (*arrow*), which confirms that the contrast material is in a vascular compartment

(as close as possible to the nidus), and meticulous technique to avoid reflux. In some cases, the ideal point of catheterization may not be achievable, and one must identify the most proximal point of catheterization where safe occlusion can be performed. This must be done with the knowledge that the ideal morphological result may be more difficult to obtain from the more proximal position. Between these two locations lies the embolization security area (Fig. 14.5).

When a normal branch is visualized or when in doubt as to the functional significance of a pedicle, a provocative functional test can be done. Amobarbital (Amytal), 50–75 mg injected superselectively to test neuronal function, or 40 mg of Xylocaine is injected to test axonal function, or both. It may clarify the importance of the tissue irrigated by that specific artery (Wada and Rasmussen 1972; Berenstein et al. 1984b; Horton and Dawson 1988). Development of neurological deficit is a contraindication for embolization at that position. In this case, either more distal catheterization, preferably beyond normal branches, is achieved or an alternative route is chosen. If no normal vessels are visualized, provocative testing may give a false sense of security. Hemodynamics in high-flow lesions may give an inaccurate picture. As the contrast materials or amobarbital is injected, it may travel only to the high-flow channels of the AVM, bypassing adjacent normal tissue. The dynamics that occur during the injection of the embolic liquid agent are different; the first portion of the column of acrylic will polymerize, rerouting the additional, still liquid embolic agent to other areas not opacified by the contrast material or infused by the amobarbital. Thus, the injection of amobarbital and/or Xylocaine in this circumstance is potentially misleading. In addition, multiple injections of amobarbital can result in a sleepy uncooperative patient, making monitoring more difficult. Although testing may be used in very

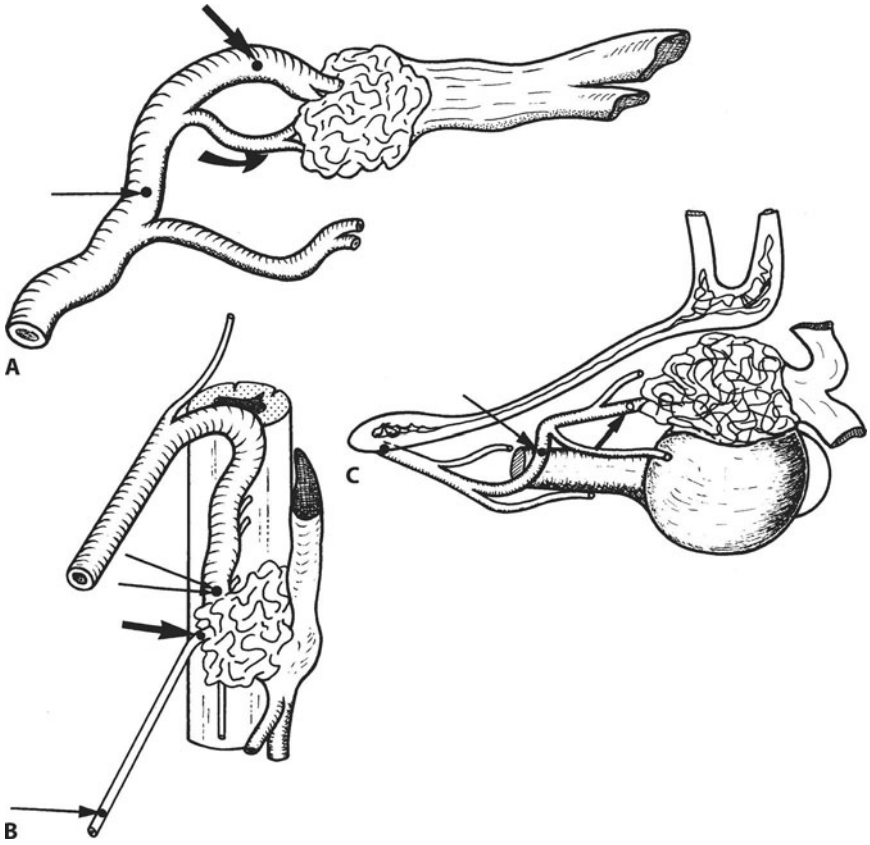

Fig. 14.5A–C. Security point in brain, spinal, or ophthalmic embolization. **A** Pedicle feeding an arteriovenous malformation (AVM) demonstrates a dominant pedicle to the malformation (*broad arrow*) and a secondary feeder (*curved arrow*). The ideal point of embolization (*broad arrow*) would be in the major feeder and a similar point in the secondary feeder. However, the security point is at the origin of the common trunk (*long arrow*). **B** A spinal cord AVM supplied by a radiculomedullary artery. The ideal point of embolization is shown by the *broad arrow*; the security point is at a more proximal position (*long arrow*). Also note that the ideal and security points in the venous system in the spinal cord are the same (*double long arrows*). **C** The ideal point (*broad arrow*) and security point (*long arrow*) in an ophthalmic artery embolization

selective instances, its limitations and the nearly universal use of general anesthesia mean that testing is seldom used.

Despite these constraints, in spine and spinal cord embolization, in which perforating vessels may be smaller than the ability of the X-ray equipment to resolve them, intra-arterial amobarbital (Amytal), alternated with Xylocaine combined with SEP and MEP monitoring, often adds further reliability and safety (Berenstein et al. 1984b).

As part of the preoperative (embolization, surgery) investigation, the need may arise to determine hemispheric dominance for speech (left-handed individual, speech difficulties in a right-sided AVM, etc.). In these patients, a Wada test may be an important part of assessing the risks of treatment of the AVM. When an intracarotid amobarbital test is done in a patient harboring an AVM, the amobarbital should be first injected into the hemisphere not harboring the high-flow lesion. This is designed to

prevent a falsely negative test as the amobarbital (100–400 mg) may be sumped selectively through the malformation, thereby bypassing normal ipsilateral speech areas.

Electrophysiological and pharmacological tests do not guarantee safety or better results and are not a replacement for anatomical knowledge and recognition of normal territories. One of the present authors (P.L.) has used neither since 1986, without added morbidity or mortality.

It may even be an added danger to rely exclusively on monitoring in an attempt to compensate for lack of anatomical knowledge, particularly in the spinal cord.

14.3.10.2 Xylocaine

Xylocaine 40 mg injected superselectively has been used for functional testing of peripheral nervous tissue supplied by the external carotid artery. In CNS patients, Takahashi (personal communication) has used it to test axonal function. Only cardiac Xylocaine can be used intra-arterially and in the CNS, and we only use it in spinal cord work.

We have noted that in spinal cord monitoring, Xylocaine is more reliable than Amytal.

14.3.10.3 Mucocutaneous Territories

The safety of embolization in musculocutaneous territories is primarily determined by anatomy. Discoloration or compromising of skin can be predicted. Following the superselective injection of a 60% concentration contrast material in a pedicle, one can see blanching of the skin supplied by that vessel, which is a good predictor of potential skin compromise. Djindjian (1978) reported the use of low-concentration methylene blue injected superselectively to predict skin vascularization.

14.4 Arteriotomy Sites

The conventional Seldinger technique is used in all of our procedures including infants and newborns. Distal pulses in the popliteal and foot area are marked prior to puncture for further reference, primarily in children. If the pulse is lost during the procedure, one may inject intra-arterial vasodilators such as 40 mg of cardiac Xylocaine (without preservatives or epinephrine) through the side arm of the introducer sheath. At present, the availability of ultrasound guidance makes catheterization possible in practically all cases.

Transfemoral catheterization of the external carotid artery may not be possible after a previous ligation and surgical exposure, or preferably end-to-side reanastomosis by an experienced vascular surgeon may be needed (Fig. 14.6). A period of 3 weeks is recommended for healing of the anastomosis. The advantage of reconstructive reanastomosis is that the femoral approach can be used and repeated (Fig. 14.6). We have experi-

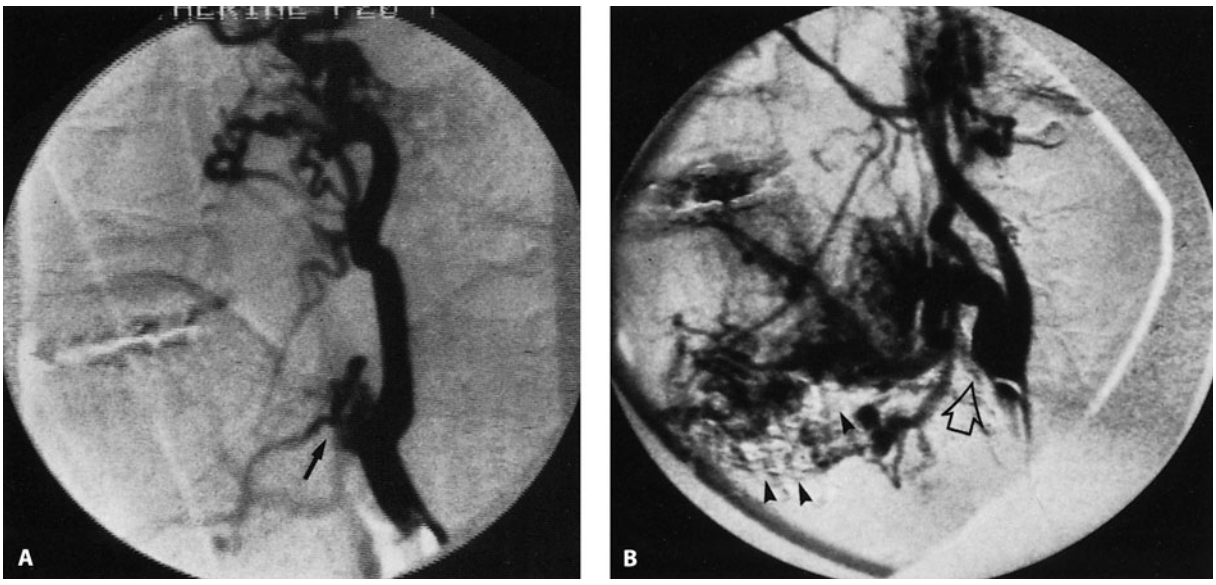

Fig. 14.6A, B. Surgical reanastomosis. **A** Common carotid artery digital subtraction angiography (DSA) demonstrates ligation of the external carotid artery distal to the superior thyroidal artery (*arrow*). **B** Lateral DSA after the external carotid artery was reanastomosed to the common carotid artery (*open arrowhead*) and after the first stage microembolization of the submental region (*arrowheads*). In general, embolization should be delayed 3–4 weeks after reanastomosis, to permit proper healing of the suture lines

enced the need to revascularize a failed surgical reanastomosis by dilating and deploying a stent to establish access (Fig. 14.7).

In high-flow lesions, e.g., BAVMs, brain arteriovenous fistulae (BAVFs), and vein of Galen aneurysmal malformations (VGAMs), if the venous approach is to be used, direct jugular puncture is *contraindicated*. Direct puncture of the jugular vein presents a higher risk and may compromise the venous drainage. The femoral venous approach is safe and easy, as are punctures of dilated veins of the scalp or alternative access sites such as the umbilical area (see Vol. 3 for techniques in the pediatric population).

14.4.1 Introducer Sheath

Various types of introducer sheaths are commercially available and there are few differences between them, making their choice an individual decision. In general, the purposes of introducer sheaths include:

1. Easy exchange in catheters of the same or smaller diameters
2. Use of smaller catheters without retrograde bleeding, thanks to their hemostatic valve
3. Exchange in an occluded catheter without losing access to the vascular system
4. Significantly less trauma to the artery at the puncture site while manipulating the catheter
5. Finer manipulation of the catheter

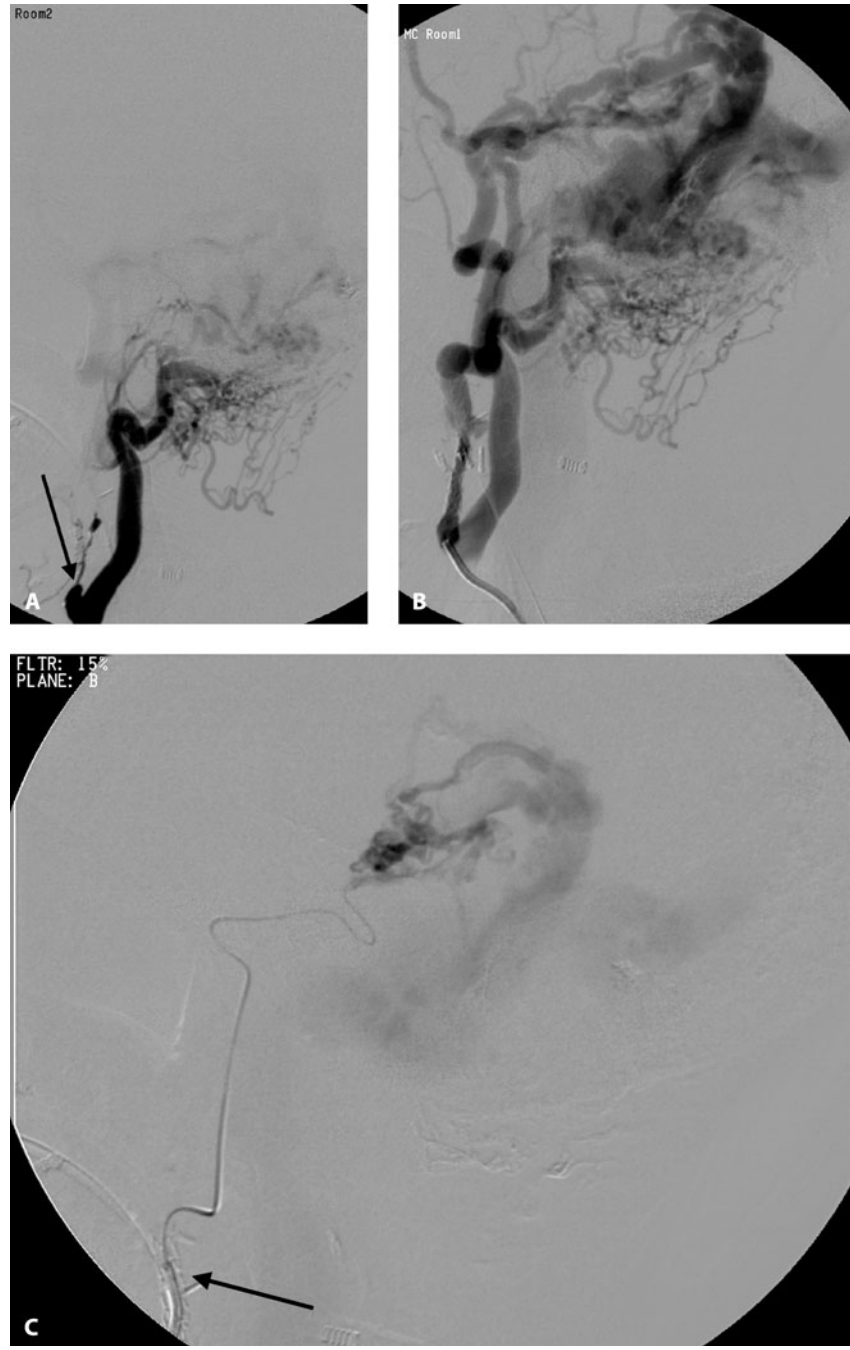

Fig. 14.7A–C. Endovascular revascularization of a spontaneously thrombosed reanastomosis of the external carotid artery. **A** Lateral digital subtraction angiogram (DSA), after failure of a venous graft anastomosis between the external carotid artery and the common carotid artery (*arrow*). **B** Lateral DSA after a stent was placed and the external carotid artery graft revascularized. Note filling of the distal external carotid artery and middle meningeal artery supplying a vascular malformation. **C** Coaxial catheterization of the petrosal distal branch of the middle meningeal artery through the stent that had previously been revascularized (*arrow*)

Introducer sheaths used are from 4- to 9-French in size (most manufacturers will make other sizes on request). They come with a short guidewire and a leading dilator. They are usually made of thin-walled Teflon to maintain a large inner diameter (ID), with a relatively small outer diameter (OD). Long sheaths 70–90 cm are used in patients with tortuous anatomy. Some type of fixation of the sheath to the skin is needed to prevent accidental removal of the sheath, either with a stitch or sterile tape.

14.4.2 Closure Devices

14.4.2.1 Hemostasis of the Arteriotomy Site Closure

Various devices have been introduced for percutaneous closure of the arteriotomy site following interventional procedures. A variety of techniques have been introduced and continue to be developed. Most of them were introduced following interventional endovascular procedures in the field of cardiology. We will briefly review the more frequently employed. As developments of newer devices is occurring rapidly, a detailed description is beyond the scope of this volume.

External compression devices are used primarily as support following conventional manual compression. Most frequently we use the Femostop device (Radi Medical Systems AB, Uppsala, Sweden). This device uses a pneumatic ball with a transparent window for monitoring. It has the ability to gauge the level of compression, so that once hemostasis has been achieved, it can be left in place at lower pressures for patient comfort.

14.4.2.2 Internal Closure Devices

1. Perclose (Abbott Laboratories Company, Redwood City, CA, USA). This device comes in three sizes: a two-needle version for the 6-F arteriotomy puncture size, a four-needle for the 8-F arteriotomy size, and a larger device for the 10-F. The device is inserted into the arteriotomy, which may be done at the beginning of the procedure if a larger introducer sheath is to be used, or at the end of the procedure for the appropriate size. The device is advanced over a 0.038-in. (1-mm) wire and may be used in fully heparinized patients. The device has needles that are plunged with two suture threads through the arteriotomy wall, forming the basis for the grip of the threads on the arterial wall. A special stitch is required for proper hemostasis. The potential for delayed infection must be taken into account. To avoid this complication, we now routinely reprepare the arteriotomy site, and change gloves and scalpel prior to deployment. In addition, an IV single-dose broad-spectrum antibiotic is used. The device is usually very reliable, although there is a small failure rate. Patients are instructed to remain in bed for 2 h following deployment of the Perclose device.
2. Vasoseal ES (Datascope Corp., Montvale, NJ, USA). This device consists of a coagulant plug of collagen.

3. Angioseal (Sherwood Davis & Gleck, St. Louis, MO, USA). This device consists of a polyglycolic acid seal plug. These last two devices can be of help when large sheaths and anticoagulation with antiplatelet medications have been used. However, they have the potential of distal embolization (Morris and Branden 1999).

When using these various devices, a single wall puncture is recommended.

14.5 Catheters and Delivery Systems

As the field is expanding, multitudes of catheter and delivery systems have been introduced at a fast pace, and more are being developed (Table 14.2).

Table 14.2. Catheters and delivery systems

1. Guiding catheters
2. Microcatheters
3. Balloon catheters
4. Detachable balloon catheters
5. Stent-delivery catheters

In general we can divide delivery systems into broad categories:

1. Guiding catheters
2. Microcatheters
3. Balloon catheters
4. Detachable balloon catheters
5. Stent-delivery catheters

14.5.1 Guiding Catheters

A variety of guiding catheters of various diameters are presently available. When planning the procedure, it is important to select a series of assemblies that are compatible with one another in length and diameter. A careful choice of sheath, guiding catheter, and coaxial assembly must be compatible (microcatheter, balloons, balloon-tip catheters, stents, etc.; Figs. 14.8, 14.9).

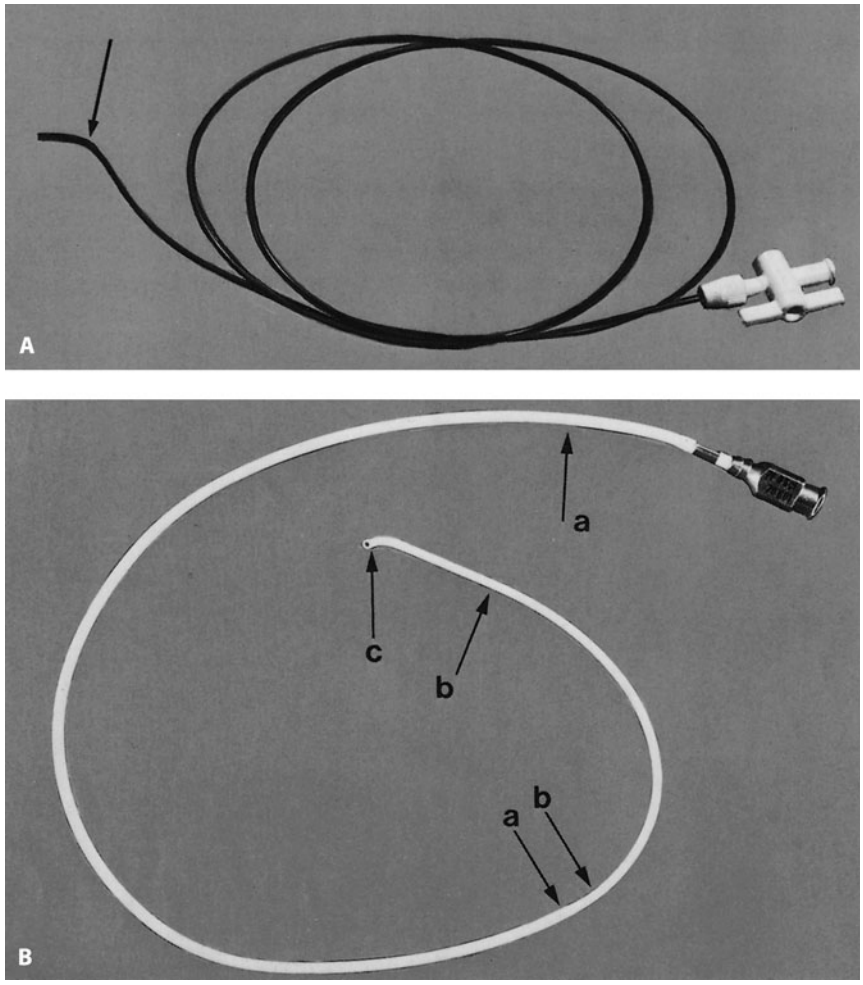

Fig. 14.8A, B. Conventional catheters. **A** Lasjaunias 4-French catheter with a tapered tip and a 125° distal curve (*arrow*). **B** Berenstein catheter, 7-F wire-braided polyethylene shaft (*a*) in the proximal 100 cm. It then tapers in its outer diameter to a 5-F nonwire-braided polyethylene tubing (*b*) in its distal 10 cm, maintaining a constant internal diameter. The last 1 cm has a 105° hockey stick-type curve and is not tapered (*c*)

14.5.2 Microcatheters

Two types of microcatheters are presently available: over-the-guidewire and flow-guided microcatheters. Most catheters and microcatheters currently used are variable-stiffness shafts. The concept of variable-stiffness and variable-size selective and superselective catheters was introduced earlier (Berenstein et al. 1983). These early-model catheters could reach only distal branches of the external carotid artery (ECA) but could not be introduced into the brain (Fig. 14.8). The development of 1- to 3-F variable-stiffness microcatheters (Kikuchi et al. 1987) opened a new horizon in selective catheterization of the brain and spinal cord (Figs. 14.10–14.12). These catheters permit cerebral navigation without having to use cumbersome systems. They can be used with steerable microguidewire.

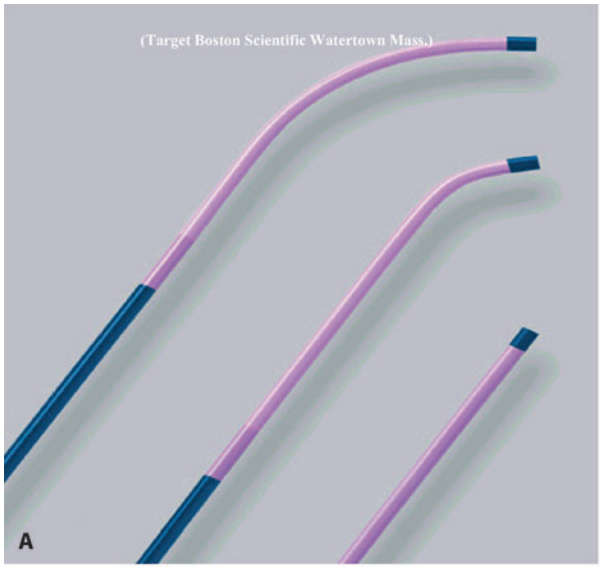

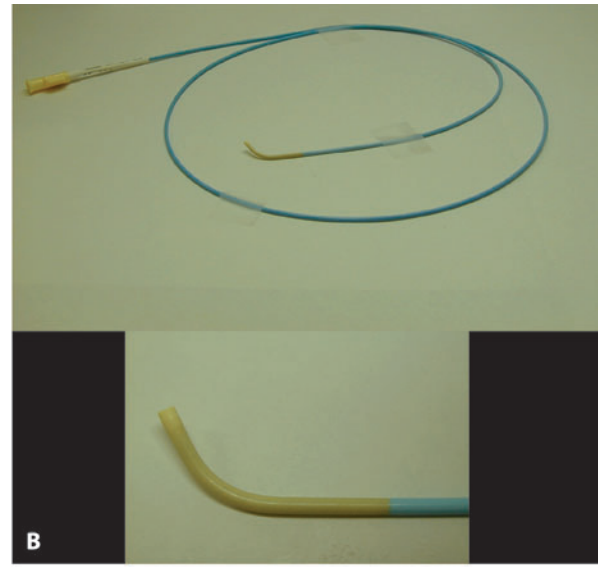

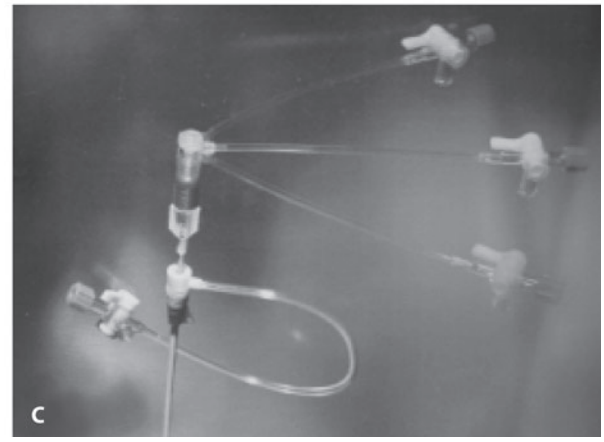

Fig. 14.9A–C. Guiding catheters. **A** Variable distal curves on a Guider 5-F delivery catheter (Target, Boston Scientific, Watertown, MA, USA). **B** Envoy 5-F Cordis Endovascular (Johnson and Johnson, NJ, USA). Note the flexible distal tip and thin wall on both catheters for a maximum internal diameter. **C** Headway catheter assembly (CathNet-Science SA, Paris, France), with an integrated hemostatic valve, rotating hub, and side arm with three-way tap connections

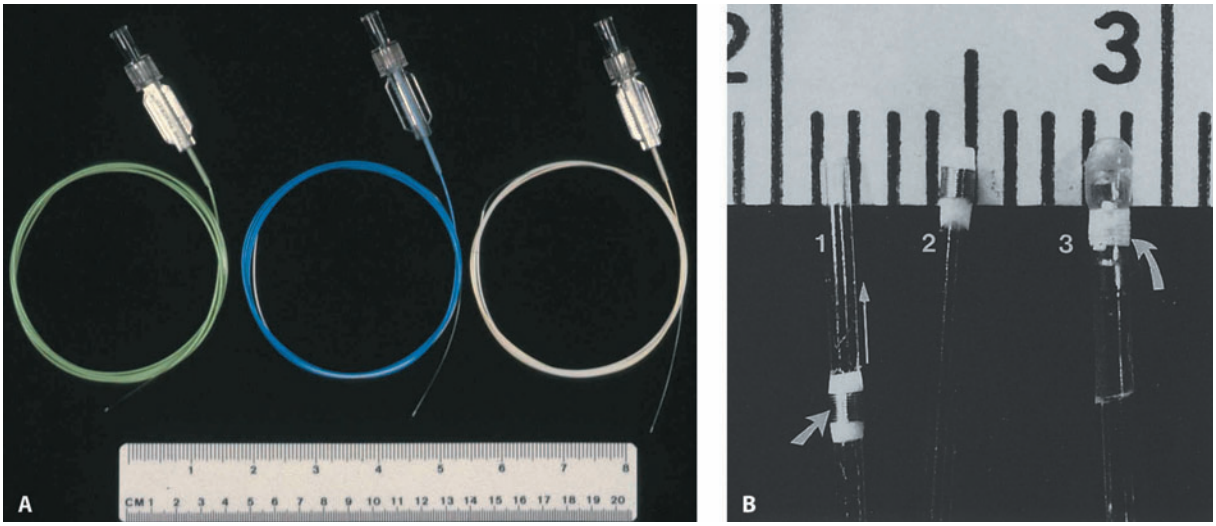

Fig. 14.10A, B. Variable-stiffness microcatheters. **A** Various-sized Tracker microcatheters are available. **B** *1*, Tracker 10 with an internal diameter (ID) at the tip of 0.014 in. (0.35 mm) and an outer diameter (OD) at the tip of 0.027 in. (0.69 mm). *2*, Tracker 18 with an ID at the tip of 0.020 in. (0.51 mm) and an OD at the tip of 0.036 in. (0.92 mm). *3*, Tracker 25 with an ID at the tip of 0.027 in. (0.69 mm) and an OD at the tip of 0.049 in. (1.25 mm)

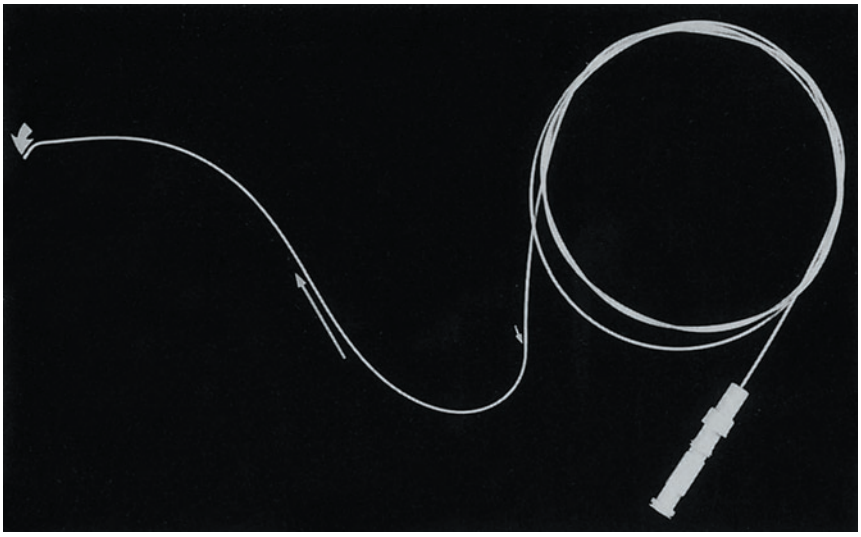

Fig. 14.11. Variable-stiffness Mini-Torquer. This microcatheter is used with a stylus for introduction. The transition from the rigid catheter (*arrow*) to the very soft portion (*long arrow*) is usually 20 cm long. A gentle curve (*curved arrow*) is usually best for cerebral navigation and is formed with steam

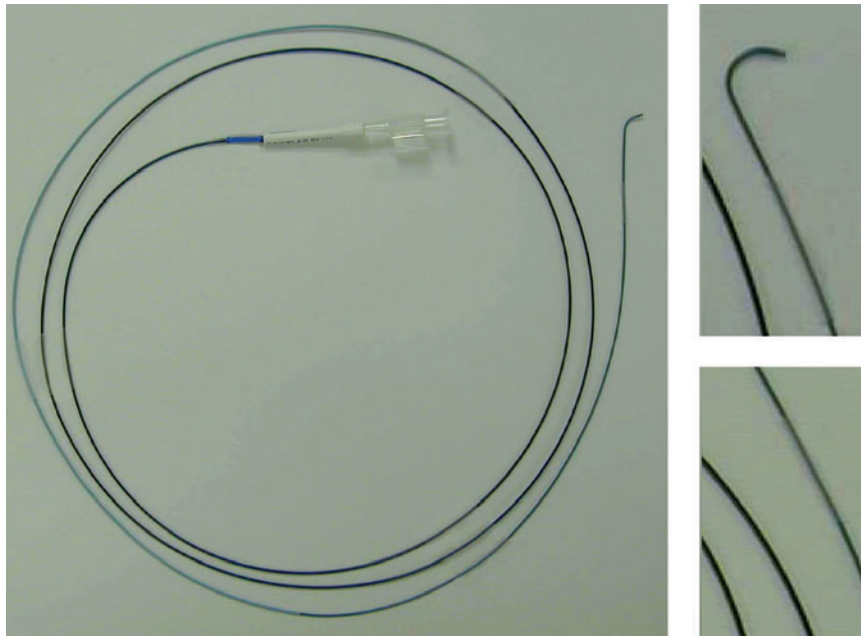

Fig. 14.12. Variable-stiffness microcatheters with wire-braided shaft and preshaped curve from Cordis Endovascular

In the past several years, currently available catheters and microcatheters have incorporated various technologies that make them superior to those in the past, including special coatings of the outer surface of the catheter's usually hydrophilic technology, which makes them more lubricious and therefore easier to advance. Catheter shafts are presently made of variable stiffnesses, with the more proximal portion of the catheter stiffer, and the more distal segment more pliable and softer (Berenstein 1983). Most over-the-guidewire microcatheters are presently constructed with braided shafts (wire or other polymers) (Fig. 14.13), which gives them added torque and pushability, and prevents the inner diameter (ID) of the lumen from collapsing or kinking. Maintaining integrity of the catheter lumen throughout is essential for the easy and safe delivery of the various devices used (Fig. 14.14).

For cerebral catheterization, the distal 7–30 cm are very supple, permitting flow-directed navigation, which allows them to negotiate distal, tortuous anatomy. Flow-guided microcatheters come in various sizes and distal configurations (Fig. 14.15). We prefer flow-guided microcatheters for cerebral catheterization. They are less traumatic, and with present microguidewires can reach very distal and small vessels, even if they are not high-flow vessels (Fig. 14.16, pp. 940, 941). Over-the-guidewire microcatheters can also be used for cerebral navigation (Fig. 14.17) and are primarily used for ECA, spinal artery, and spinal cord catheterization, as well as for aneurysm treatments or revascularization.

When tortuosity and loops are encountered, such as in the cervical or cavernous carotid arteries, the vessel loop can be straightened by pulling back on the catheter (Fig. 14.17, p. 942). In adults, loops can be corrected with the combination of the microcatheter and the guiding catheter (Fig. 14.18, p. 943) (Garcia-Monaco et al. 1990b).

Fig. 14.13. Wire-braided microcatheter shaft with a DMSO-compatible inner lining Rebar microcatheter (MicroTherapeutics, Inc. Irvine, CA, USA)

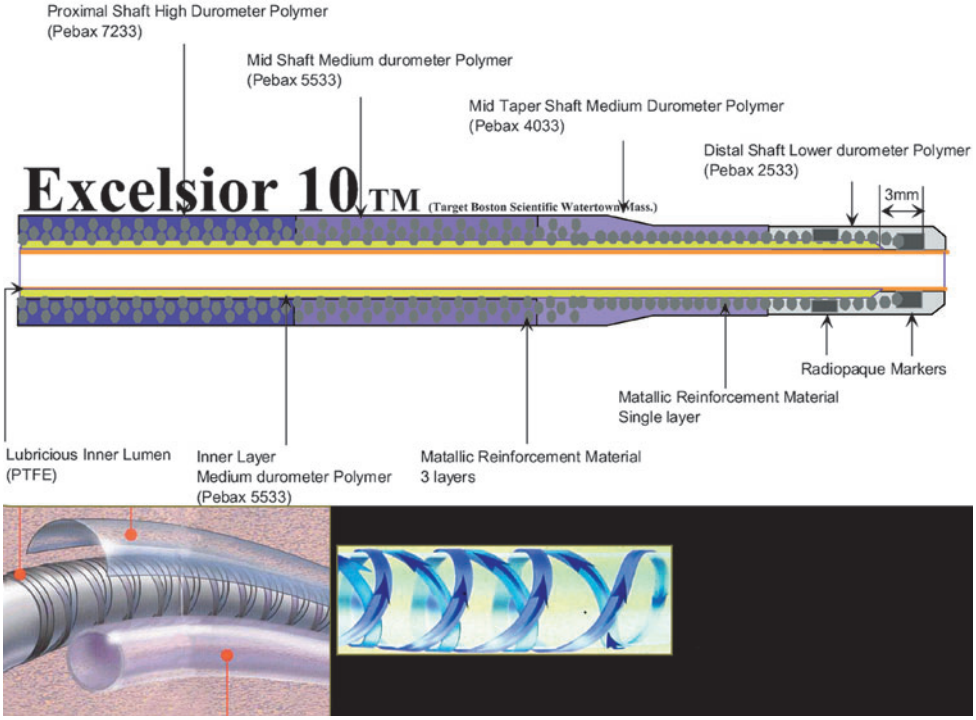

Fig. 14.14. Excelsior 10 microcatheter. Note the variable construction at the different parts of the shaft. Currently available microcatheters use a variety of materials in combination to obtain better characteristics: flexibility, kink resistance, hydrophilic qualities, variable stiffnesses, etc.

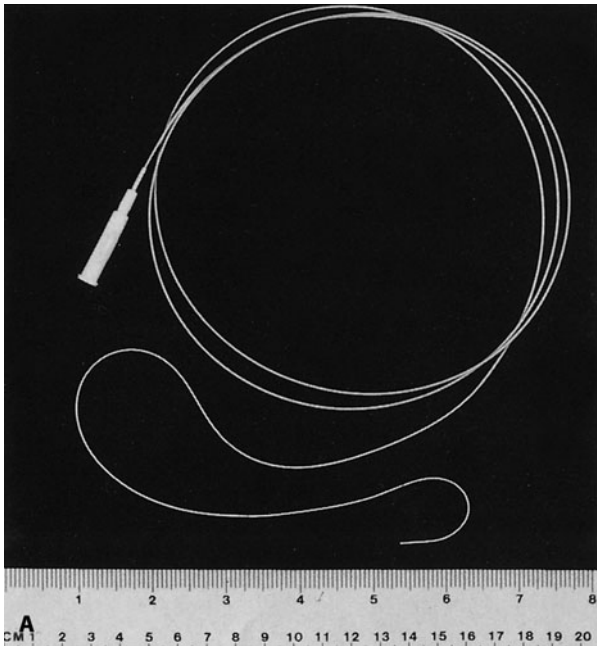

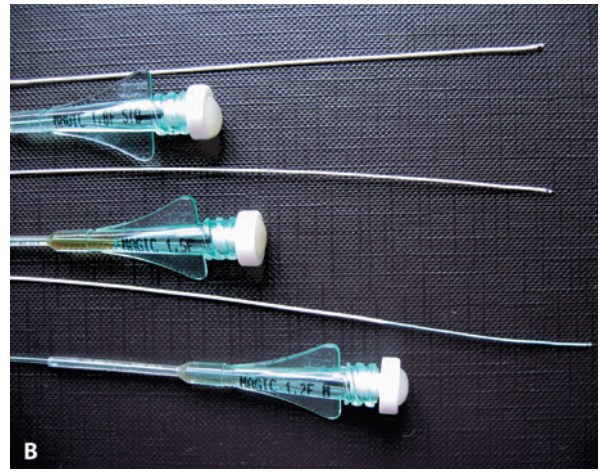

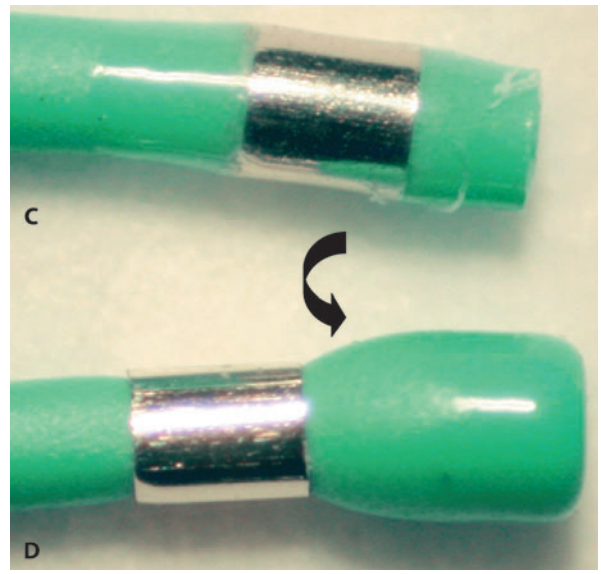

Fig. 14.15A–D. Flow-guided microcatheters. **A** Magic (Balt, Paris, France) variable-stiffness microcatheter. This microcatheter has a very supple distal end. **B** Hydrophilic coated shaft, in three different diameter sizes. **C** At the distal end, they have a radiopaque marker, with conventional tip, or **D** olive design (*curved arrow*), with a larger distal size, for flow navigation and easier wedging for flow control

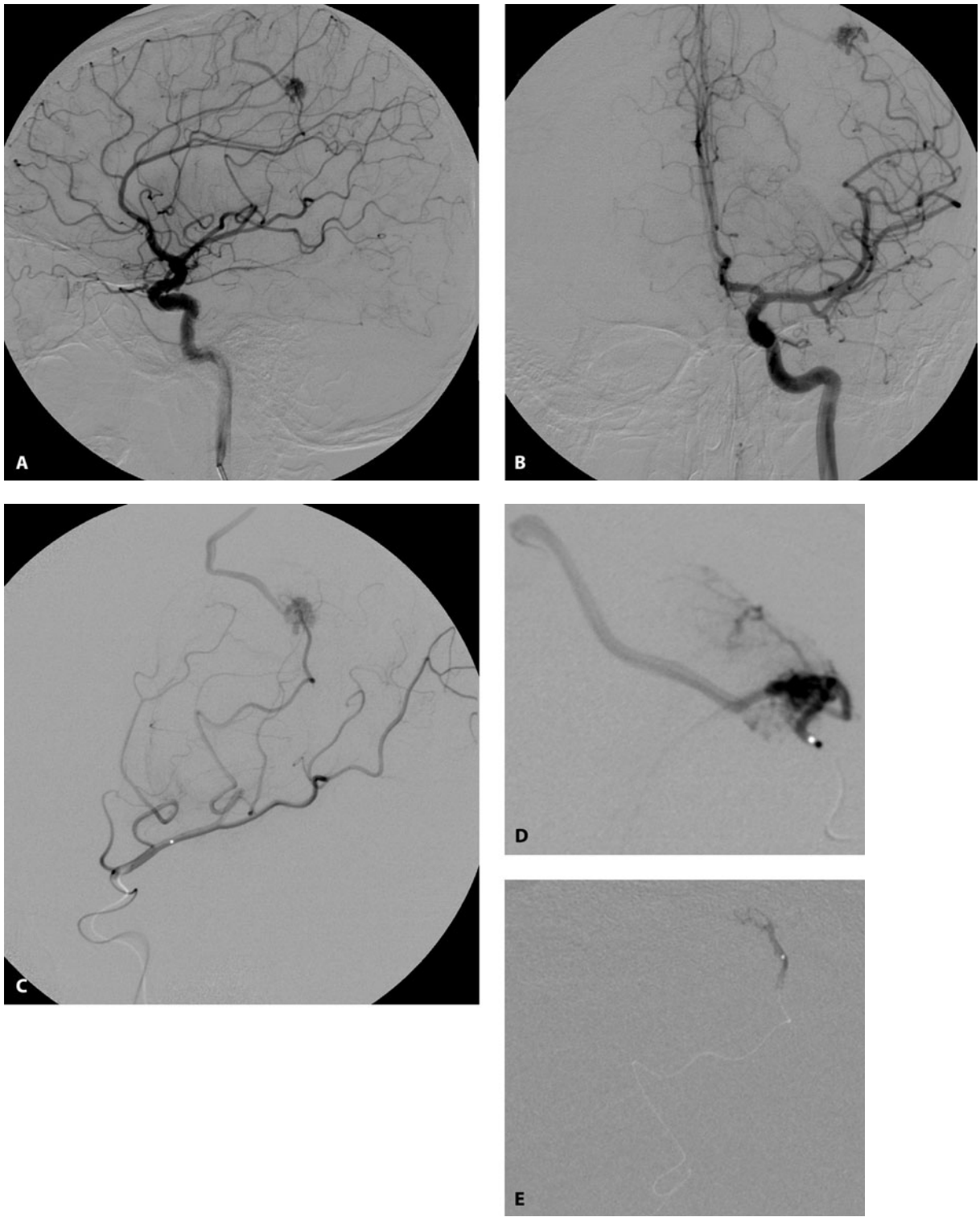

Fig. 14.16A–I. Microarteriovenous malformation (micro-AVM) distal cerebral catheterization. **A** Lateral and **B** frontal digital subtraction angiograms (DSA) demonstrate a distal small single-feeder arteriovenous malformation. **C** Selective catheterization of the angular branch of the middle cerebral artery. Note the small-caliber single-pedicle feeder of similar caliber to the other branches. **D** Distal superselective catheter position. **E** DSA of the acrylic injection. **F–I** see p. 941

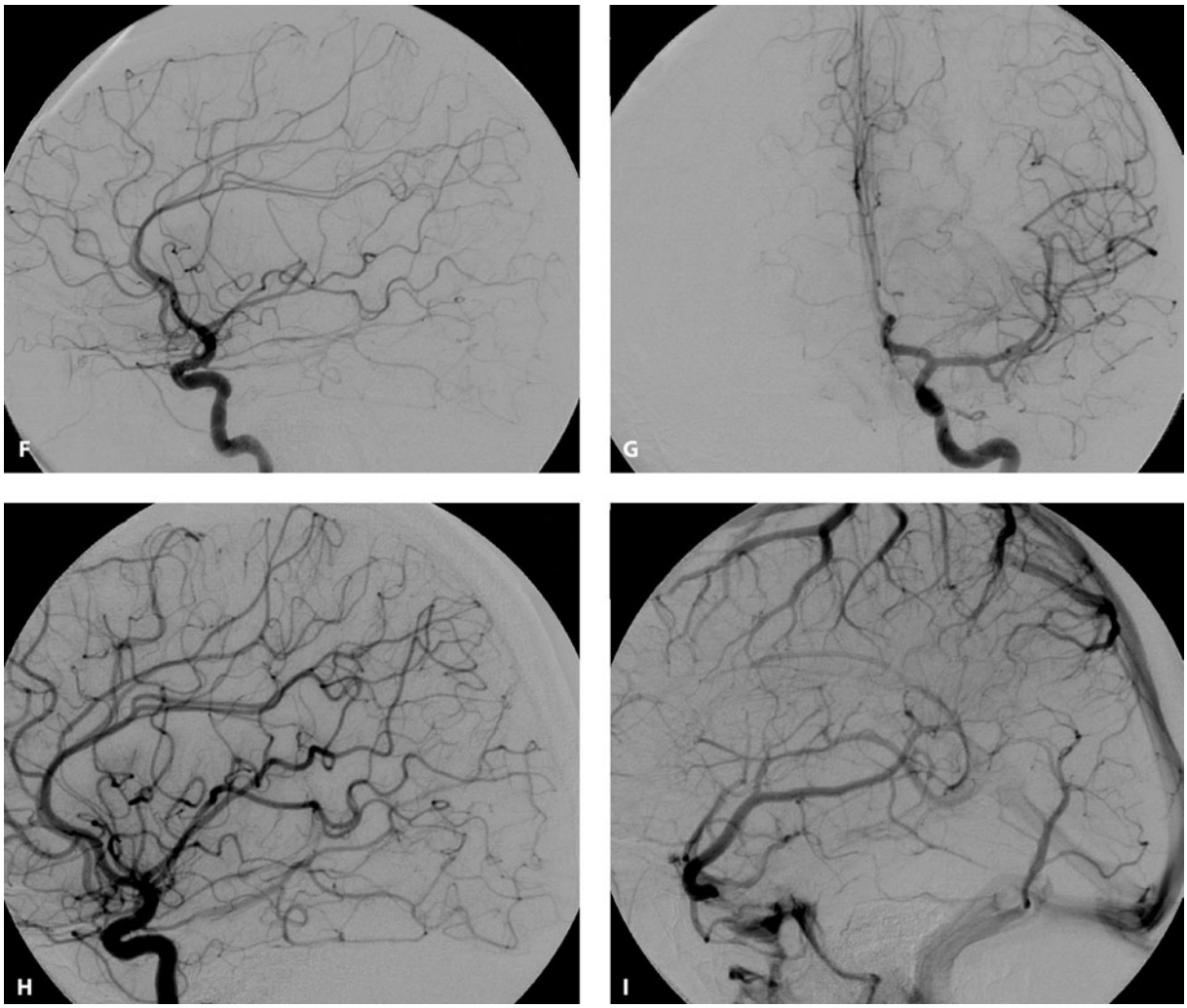

Fig. 14.16 (*continued*). **F** Lateral and **G** frontal DSA angiogram after embolization showed the total obliteration of the AVM. **H** Lateral DSA on 6-month follow-up angiogram demonstrates persistence of the occlusion **H** arterial phase, **I** late venous phase. Note the persistence of the obliteration of the malformation

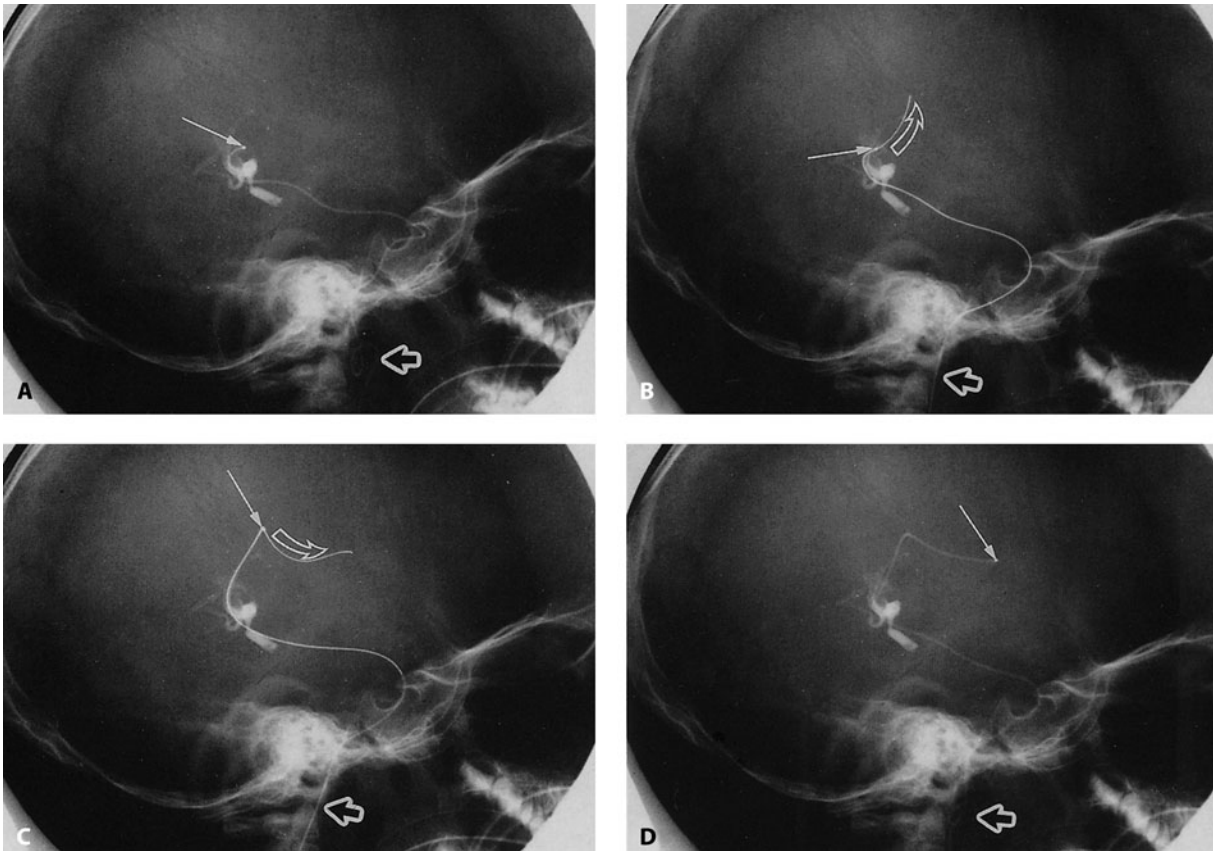

Fig. 14.17A–D. Progressive catheterization with a Mini-Torquer system and guidewire in a patient with a choroidal type vein of Galen aneurysmal malformation. Note the disappearance of the carotid kinking (*arrow*) during manipulation of the devices. By gently pulling back on the catheter, the carotid curves can be straightened (*broad arrow*), subsequently permitting more distal advancement of the guidewire (*curved open arrow*); the microcatheter tip (*small arrow*) is then advanced. Prior to acrylic deposition, excess catheter should be avoided

14.5.3 Balloon Catheters

We divide balloon catheters into those that are used primarily for control of the blood flow or for tolerance testing, those used as the embolic agents themselves, balloon-tip catheters for angioplasty and neck bridges during aneurysm treatment, and those used for stent deployment.

14.5.3.1 Tolerance Testing and Flow Control

When performing a balloon occlusion tolerance test in a major brachiocephalic artery, the following principles must be observed:

– Careful analysis of the anatomical position of the primary and collateral circulations, including the circle of Willis and the transcranial anastomosis, in most cases makes it possible to anticipate the result of the test.

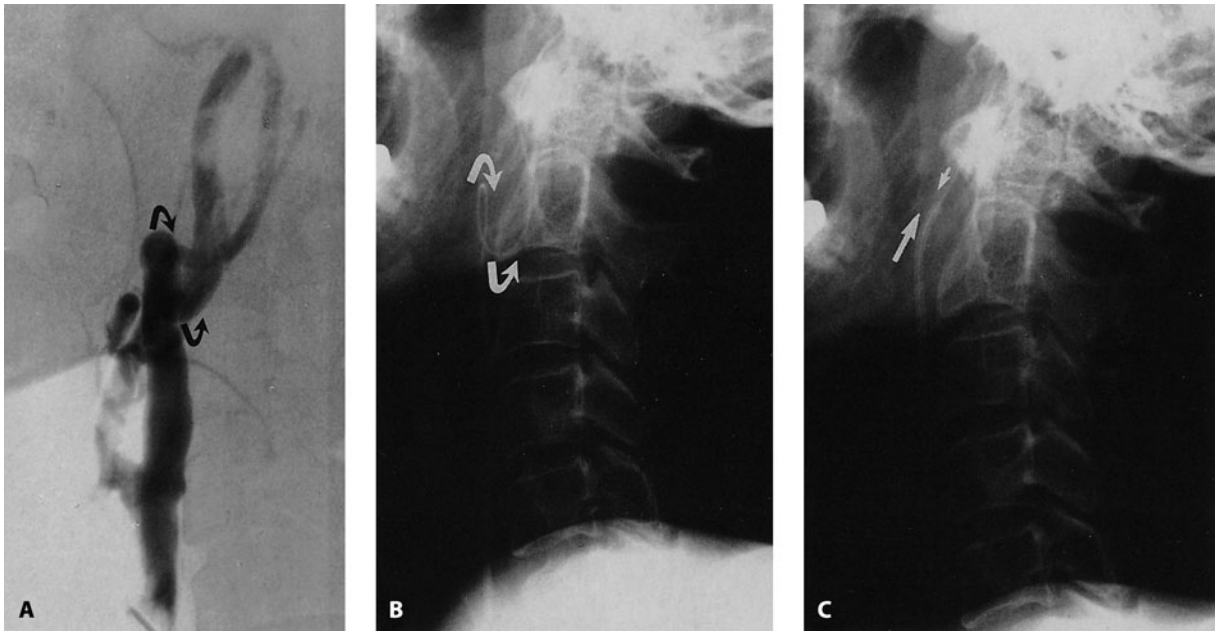

Fig. 14.18A–C. Adult patient with an arteriovenous malformation and marked tortuosity. The ability to straighten out the curve with a coaxial assembly maneuver is shown. **A** Lateral view of the common carotid artery demonstrates the marked tortuosity of the internal carotid artery (*curved arrows*). **B** Mini-Torquer passing through the tortuous carotid (*curved arrows*). **C** By retracting the Mini-Torquer (*small arrow*) and advancing the 5-French introducer (*large arrow*), the tortuous loop is straightened

- The test should be done with systemic heparin protection.
- The occlusive device used for the test should not damage the vessel wall.
- Assessment of the other vessels' contribution during balloon inflation is necessary and requires access by two catheters, unless a double-lumen balloon technique is used.
- Simultaneous appearance of the venous phases of the distal territory of the occluded artery and that of the supra- and infratentorial brain is a strong indicator of good tolerance.
- Clinical assessment should be simple and rehearsed with the patient before the test.

Double-Lumen Balloon-Tip Catheters

Conventional double-lumen balloon catheters (DLBC) come in 4- to10-F diameters. Nearly all balloons in these catheters are made of latex and have a limited shelf life (Fig. 14.19). The proximal lumen is used for balloon inflation, whereas the distal lumen is for distal injection. To free the balloons of air, a low-viscosity solution such as low-concentration (30%) iodinated contrast material is used to make the balloon radiopaque, while retaining easy inflation or deflation. They are used for flow arrest during embolization in very high-flow conditions, mostly in very young patients (Fig. 14.20), during the injection of nonadhesive liquids such as silicon

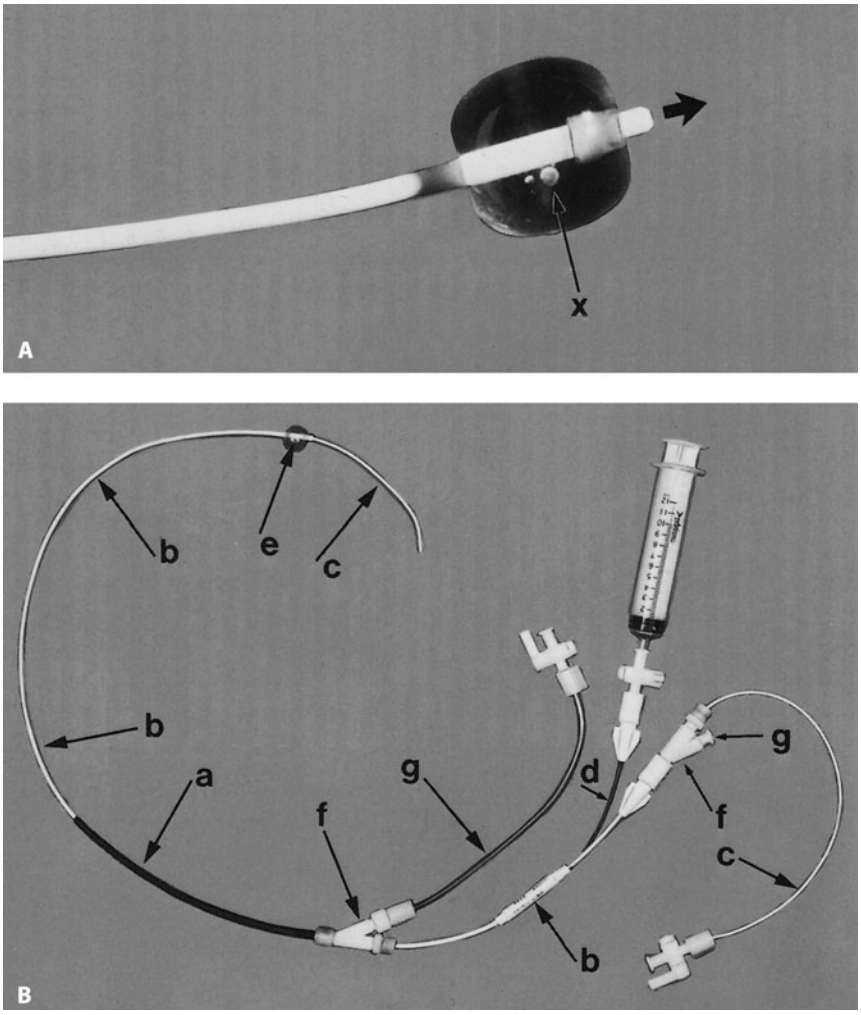

Fig. 14.19A, B. Double-lumen balloon catheters. **A** Conventional double-balloon catheter. The proximal lumen is used for balloon inflation whereas the distal lumen (*arrow*) is used for distal injection of contrast material, embolic agents, or infusions (*arrow*). Bubbles of air (*x*) should be purged prior to balloon insertion into the circulation. **B** Modified Berenstein double-lumen occlusive balloon catheter and its assembly system. An introducer sheath (*a*) of 2-F size larger than the modified occlusive balloon catheter (*b*) is used. A smaller (2- to 3-F) catheter (*c*) can be used coaxially. The proximal lumen of the modified double-lumen balloon catheter (*d*) is used for balloon (*e*) inflation. The Tuohy-Borst Y-adapter (*f*) with a side arm (*g*) for continuous perfusion between the sheath (*a*) and the balloon catheter (*b*) is used to prevent clot formation between coaxial assembly systems. Similarly, a Tuohy-Borst Y-adapter is used between the proximal occlusive balloon catheter (*b*) and the small 2-F (*c*) coaxial catheter. (From Berenstein and Kricheff 1979a, with permission)

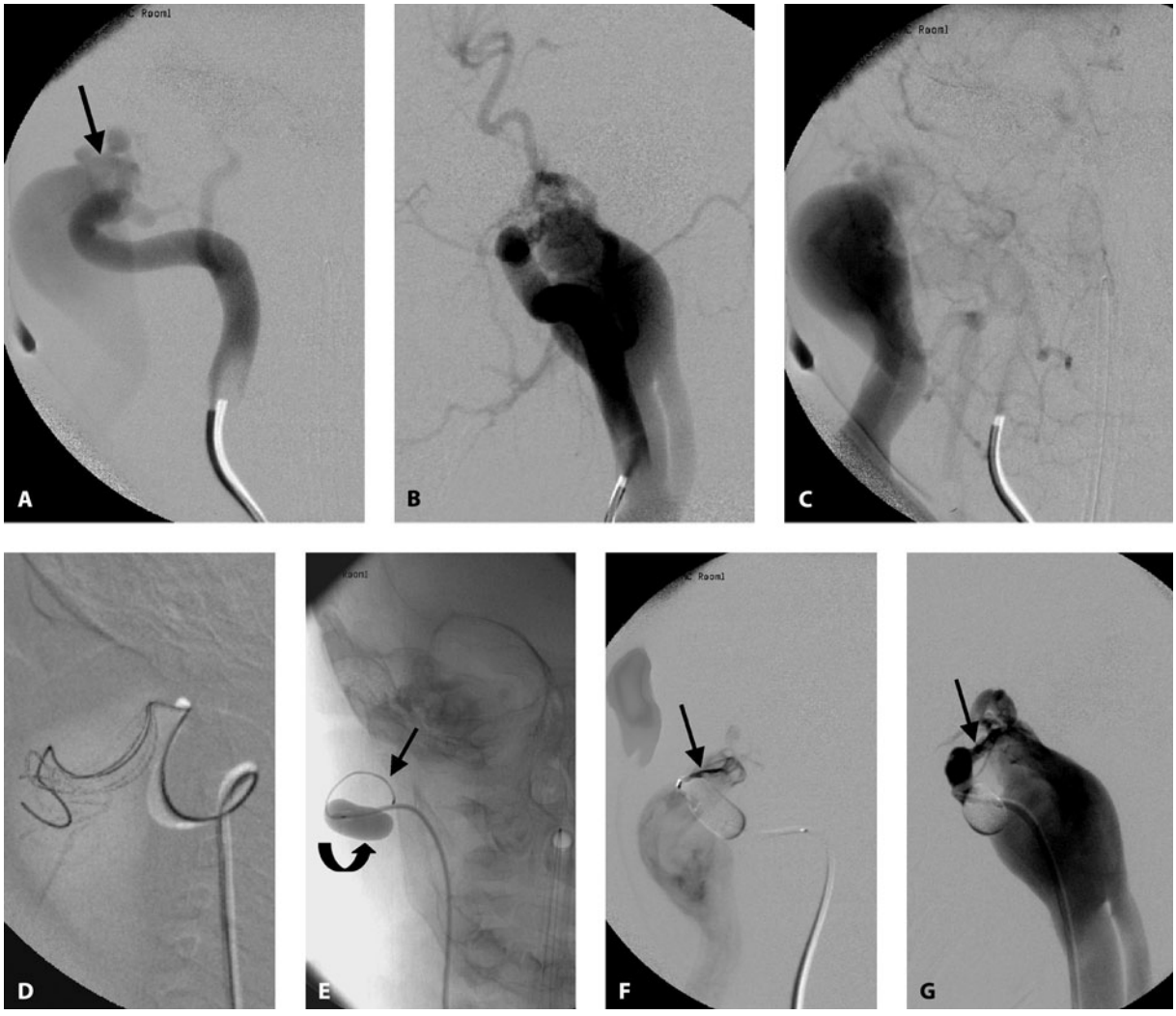

Fig. 14.20A–L. Double-lumen balloon catheters can be used for liquid embolization in high-flow conditions under flow control. A 2-year-old infant, with a very high-flow congenital arteriovenous fistula (AVF). **A** Frontal and **B** lateral early and mid arterial phases and **C** frontal late phase right common carotid artery angiogram demonstrate a high-flow AVF (*arrow*, **A**). Note the ballooning of the draining vein, which prevents proper anchoring of a coil (**D**) or a balloon. **E** Frontal plain films show the balloon (*curved arrow*) and the distal coaxial microcatheter (*arrow*). **F** Frontal and **G** lateral early and later phase injection under flow control demonstrate the fistula (*arrow*). **H–L** see p. 946

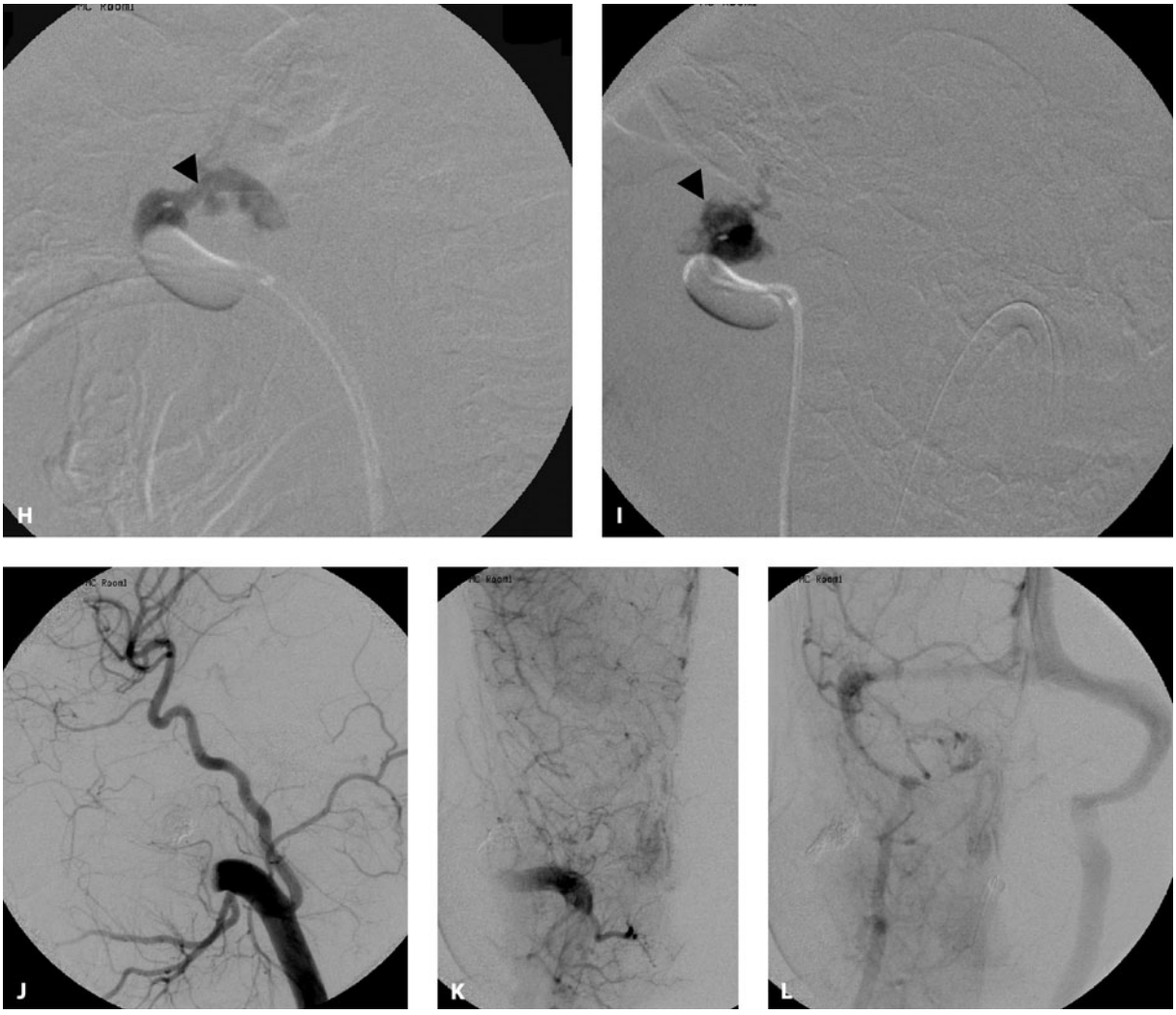

Fig. 14.20 (*continued*). **H** Lateral and **I** frontal last image hold of the *N*-butyl-cyanoacrylate (NBCA) cast of the fistula (*arrowhead*). **J** Lateral and **K, L** frontal digital subtraction angiogram demonstrating total obliteration of the AVF

fluid or Onyx (MicroTherapeutics, Inc. Irvine, CA, USA) (Fig. 1.21) or to permit reversal of flow (Fig. 14.22).

We also utilize these balloon catheters for functional investigation of tolerance to major vessel occlusion (Fig. 14.2) (Berenstein and Kricheff 1978) or for flow arrest angiography for the investigation of the point of fistulization (Berenstein Kricheff 1979b) (Fig. 14.20), when rapid sequential angiography fails to do so. In general, balloon inflation is easier with a small (1–3 ml) Luer-Lok syringe; however, if rapid deflation is needed, the larger the syringe the more negative pressure can be applied and the faster the balloon will deflate.

In general when using conventional DLBCs, one should use an introducer sheath to prevent balloon damage during the insertion or while withdrawing the catheter.

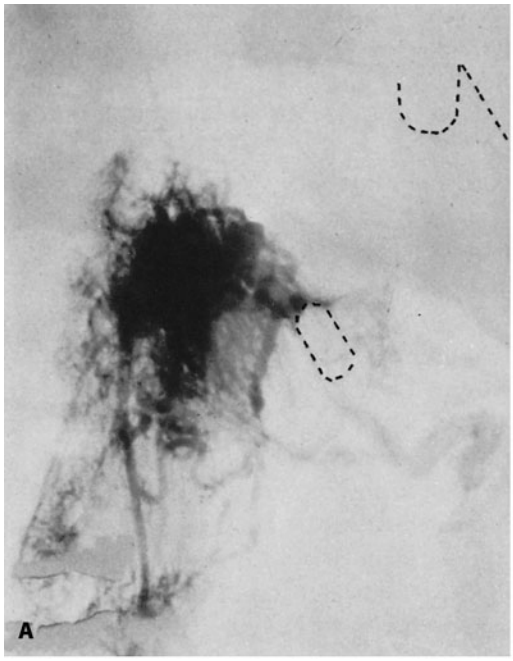

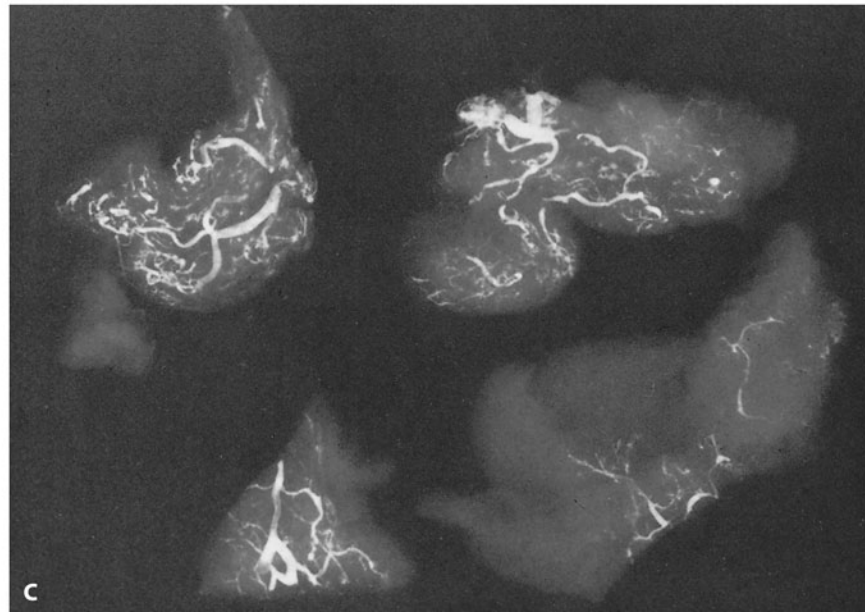

Fig. 14.21A–C. Silicone fluid embolization with flow arrest. **A** Lateral subtraction angiogram of the distal internal maxillary artery with flow arrest using a double-lumen occlusive balloon catheter (*dotted lines*). **B** Lateral plain radiogram demonstrates the excellent radiopaque cast obtained with the liquid silicone and tantalum mixture. Note some silicone in the draining vein (*open curved arrow*). **C** Radiogram of the fragmented specimen demonstrating the deep penetration of the liquid radiopaque silicone mixture. Same patient as Fig. 10.14

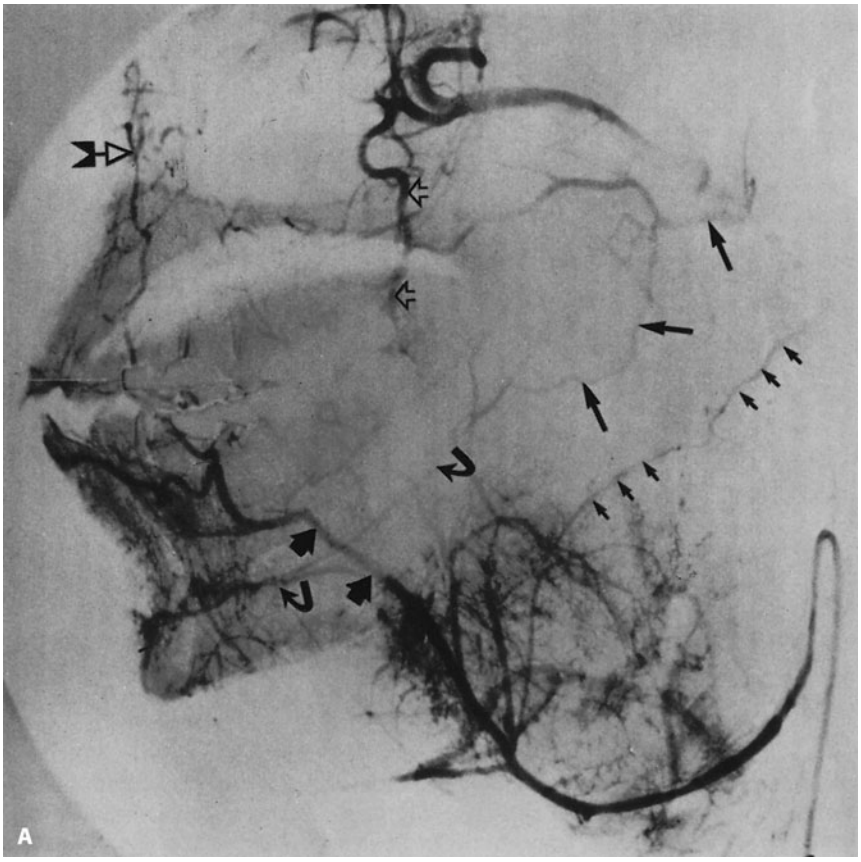

Fig. 14.22A–C. Balloon flow reversal in a capillary-venous vascular malformation. **A** Selective right facial injection demonstrates filling of the collateral circulation with filling of the inferior to superior masseteric arteries (*small arrows*), transverse facial (*arrows*) and distal facial arteries (*broad arrows*), mid-mental to inferior dental (*broken arrows*), buccal to internal maxillary artery (*open arrowheads*), and the infra-orbital point (*flagged arrow*), with only modest opacification of a capillary venous vascular malformation of the submental area. **B** Using a double-lumen occlusive balloon catheter in the proximal facial artery (*flagged arrows*), one can fill the capillary venous vascular malformation to best advantage. Note the superior ascending palatine circumferential artery (*open curved arrow*) and only very modest opacification of the distal facial artery. Using fluoroscopic monitoring, the reversal of the flow through the collateral anastomotic pathways toward the lesion can be seen. **C** This provided an excellent microembolization with 40 μm of Gelfoam powder (*arrowheads*), preserving the collateral circulation ►

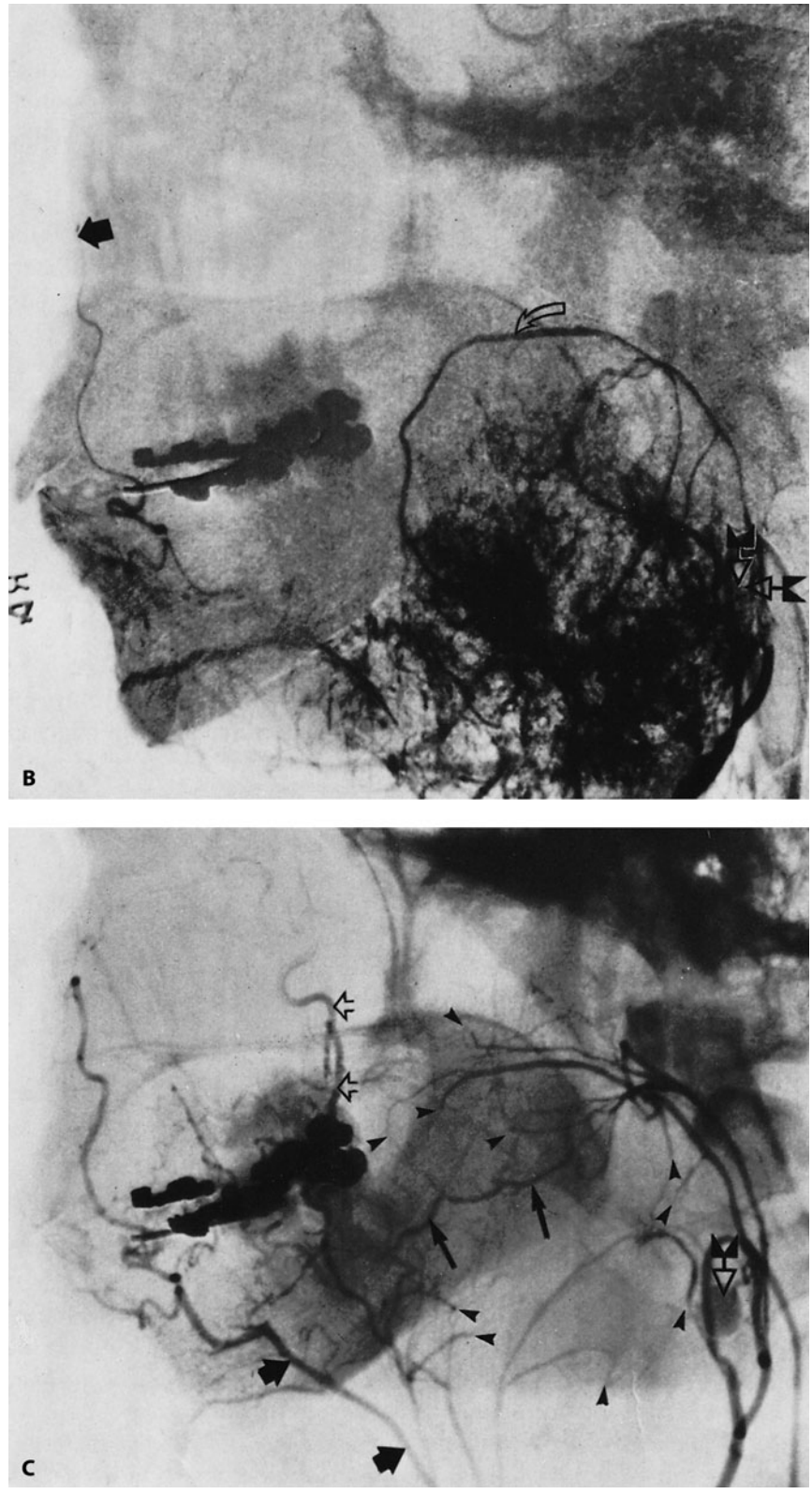

Fig. 14.22B, C. Legend see p. 948

Modified Double-Lumen Balloon Catheters (Berenstein Double-Lumen Balloon Catheter)

The purpose of this modified double-lumen balloon catheter is to maintain a large ID of the injection lumen to permit the injection of larger particles, more viscous fluids, or coaxially smaller catheters (Fig. 14.19B). These catheters increase the ID by approximately 30% depending on the catheter size, without changing the OD of the shaft. The OD of the nontapered tip at the site of the balloon attachment is not a problem when introducer sheaths are used. In general, sheaths that are 2 F larger than the catheter are needed.

More recently a small-profile double-lumen balloon-tip catheter has been introduced, the Comodor (Cordis Endovascular, Warren, NJ, USA) (Fig. 14.23), which may play a role in intracranial endovascular procedures such as flow arrest embolizations, remodeling, or angioplasties.

Single-Lumen Balloon Catheters

Single-lumen calibrated-leak microballoon catheters are no longer used; they were used to inject liquid embolics (IBCA, NBCA) and are only used by one of the authors (A.B.) for angioplasty.

Currently available single-lumen balloon-tip catheters such as the Stealth catheter are used for distal angioplasty (Fig. 14.24) and are used

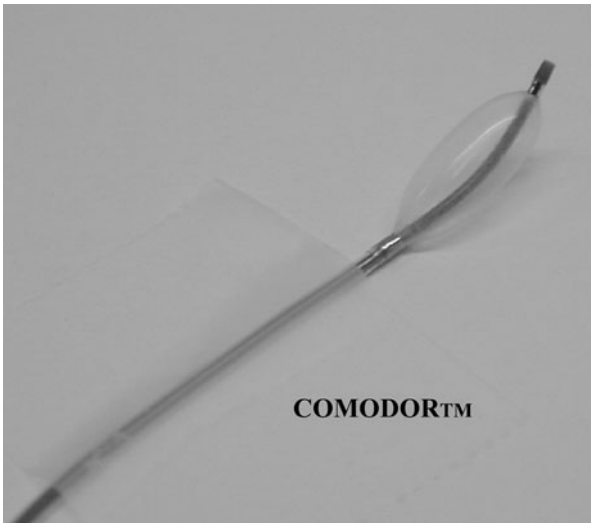

Fig. 14.23. Comodor (Cordis Endovascular) double-lumen balloon catheter with a very low-profile 3-F caliber

Fig. 14.24A–C. Stealth angioplasty microballoon catheter (Target, Boston Scientific, San Jose, CA, USA). Variable-stiffness catheter assembly system with similar low-profile Tracker catheter technology, with a distal angioplasty balloon. The catheter is single lumen and uses a valve wire mechanism. **A** Valve wire engaged position to inflate the balloon (*1*) and valve wire disengaged position for deflation of the balloon (*2*). **B** Three different sizes of balloons in the deflated stage with the valve wire disengaged. **C** With the valve wire engaged, the balloon can be inflated. This catheter has been most useful for larger-diameter vessels (see Fig. 3.21) and for atherosclerotic-type stenosis. The low profile of these catheters provides very distal catheterization with a relatively strong angioplasty balloon ►

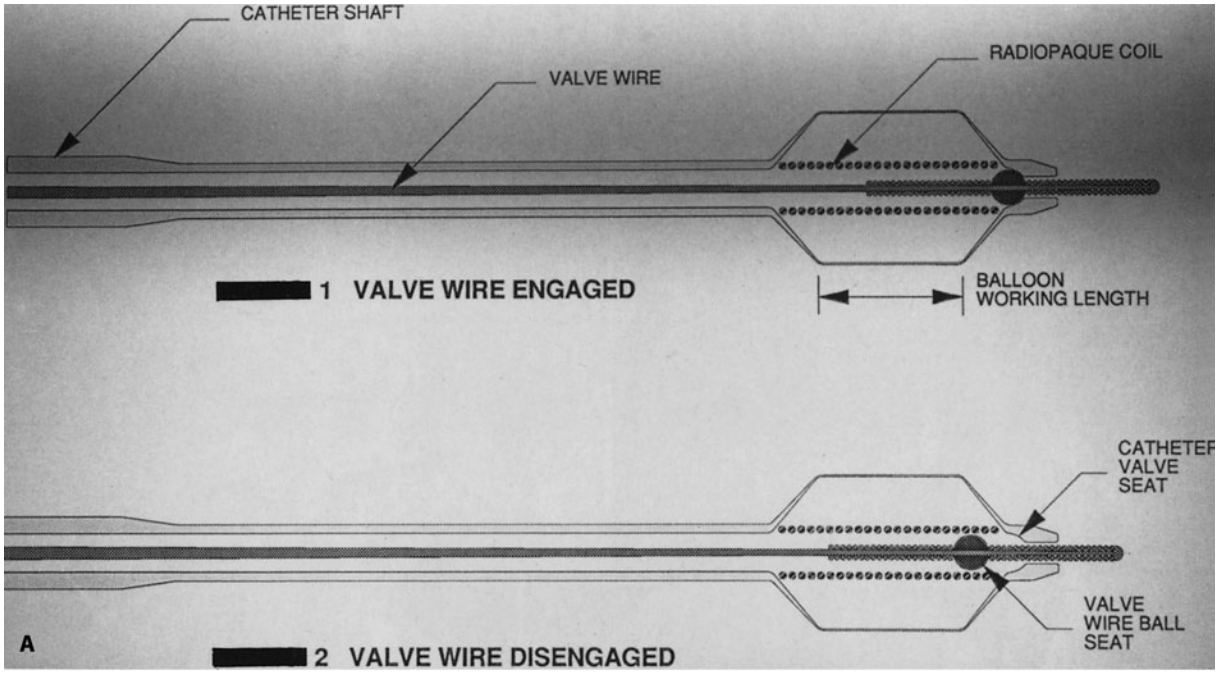

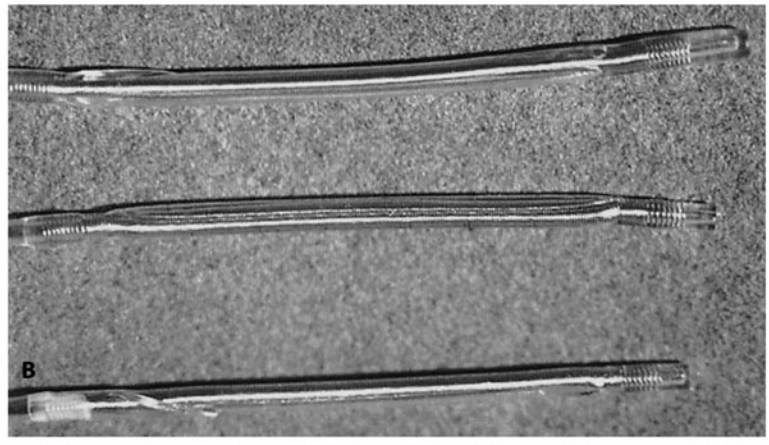

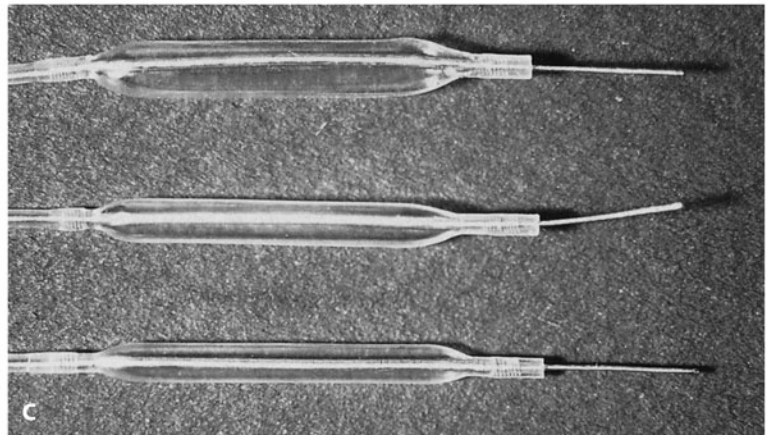

Fig. 14.24A–C.
Legend see p. 950

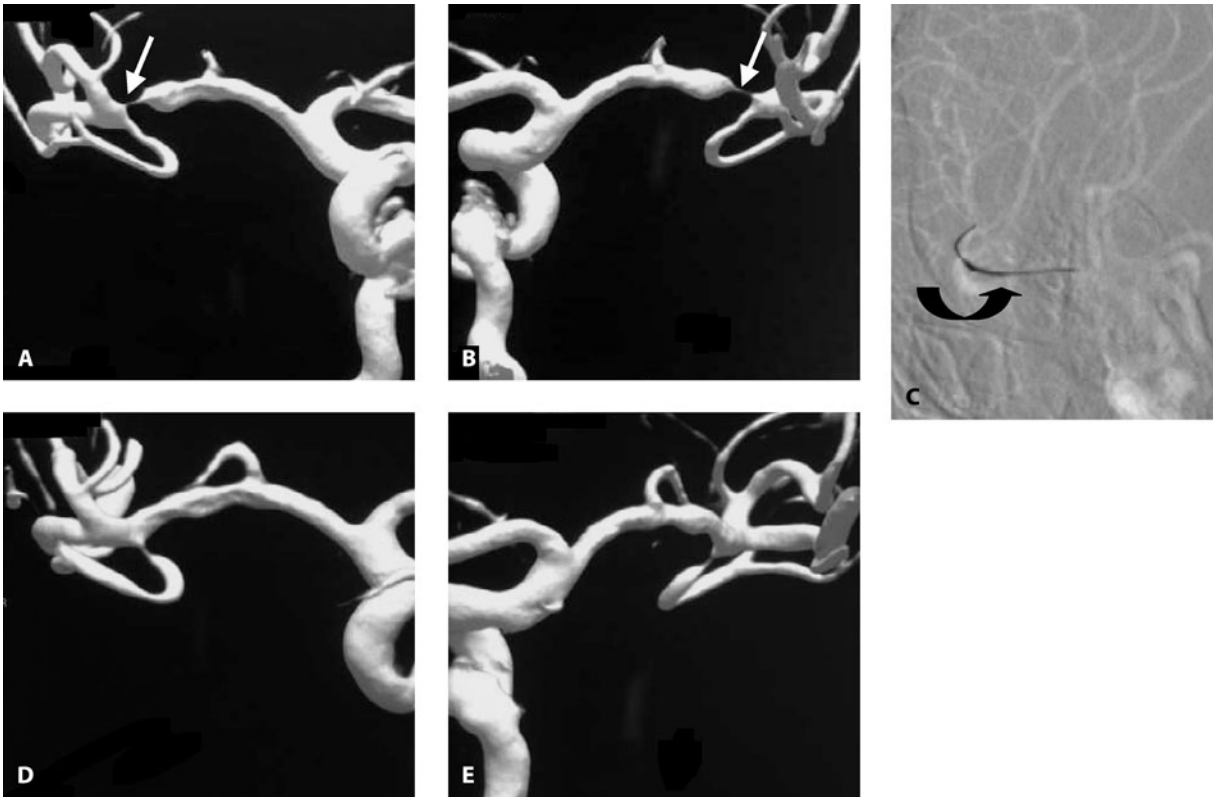

Fig. 14.25A–E. Balloon angioplasty of the right middle cerebral artery with a Stealth balloon tip catheter (Target, Boston Scientific). **A** Three-dimensional angiogram of the right internal carotid artery (ICA) seen from front and **B** from back, demonstrate a short severe stenosis of the M1 segment (*arrow*). **C** Road map image of the Stealth balloon tip catheter (*curved arrow*). **D** Frontal and **E** posterior views of the right ICA after angioplasty

mainly for atherosclerotic lesions (Fig. 14.25) or vasospasm (Eskridge et al. 1994). The Endeavor (Higashida 1989), a single-lumen silastic balloon, is used primarily for angioplasty of vasospasm (Fig. 14.26A), or a calibrated leak can easily be made with a 25-gauge needle for safer vasodilatation (Fig. 14.26B, C). The Endeavor balloon-tip catheter can also be used to temporarily act as a support for detaching a detachable balloon (Fig. 14.27), temporary balloon occlusion for flow assessment, or for better penetration in competing flows (Fig. 14.28). Various single-lumen balloon-tip catheters have been recently introduced for distal angioplasty and have been used for the remodeling the orifice of an aneurysm (Moret et al. 1997) to prevent embolic agent protruding into the vessel lumen see "Balloon Remodeling") (Figs. 14.29, 14.30, 14.84, 14.85).

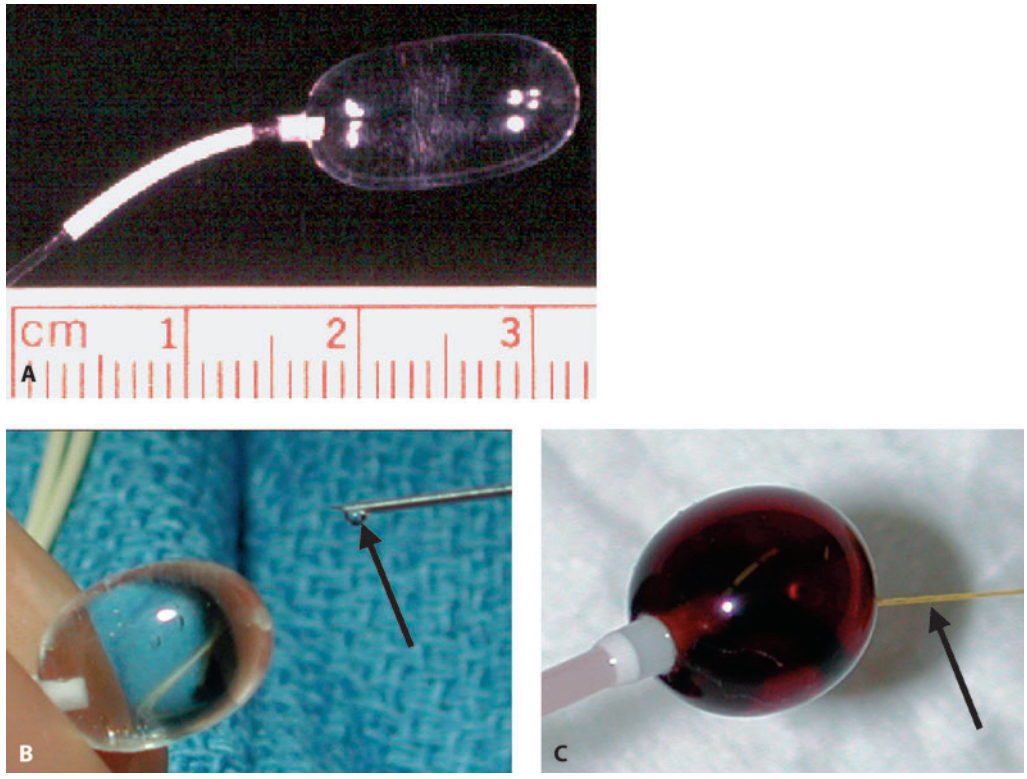

Fig. 14.26. **A** Higashida angioplasty balloon: the Endeavor (Target, Boston Scientific). This is a blind-ended soft silicone balloon that inflates along a longitudinal axis and is attached to a variable-stiffness microcatheter. **B** A calibrated leak is made with a 25-gauge or similar needle (*arrow*). C Thanks to leak control, injection of liquids is possible while still dilating the balloon for infusion of vasoactive substances, thrombolytics or angioplasty (*arrow*)

Fig. 14.27. Double-balloon technique. Two-balloon catheter systems are used to enter a posterior communicating level aneurysm. A nondetachable balloon is placed distal to the origin of the posterior communicating artery aneurysm (*double arrowhead*). The detachable balloon assembly system with a preshaped gentle curve in the catheter shaft enters through the neck of the aneurysm (*curved arrow*)

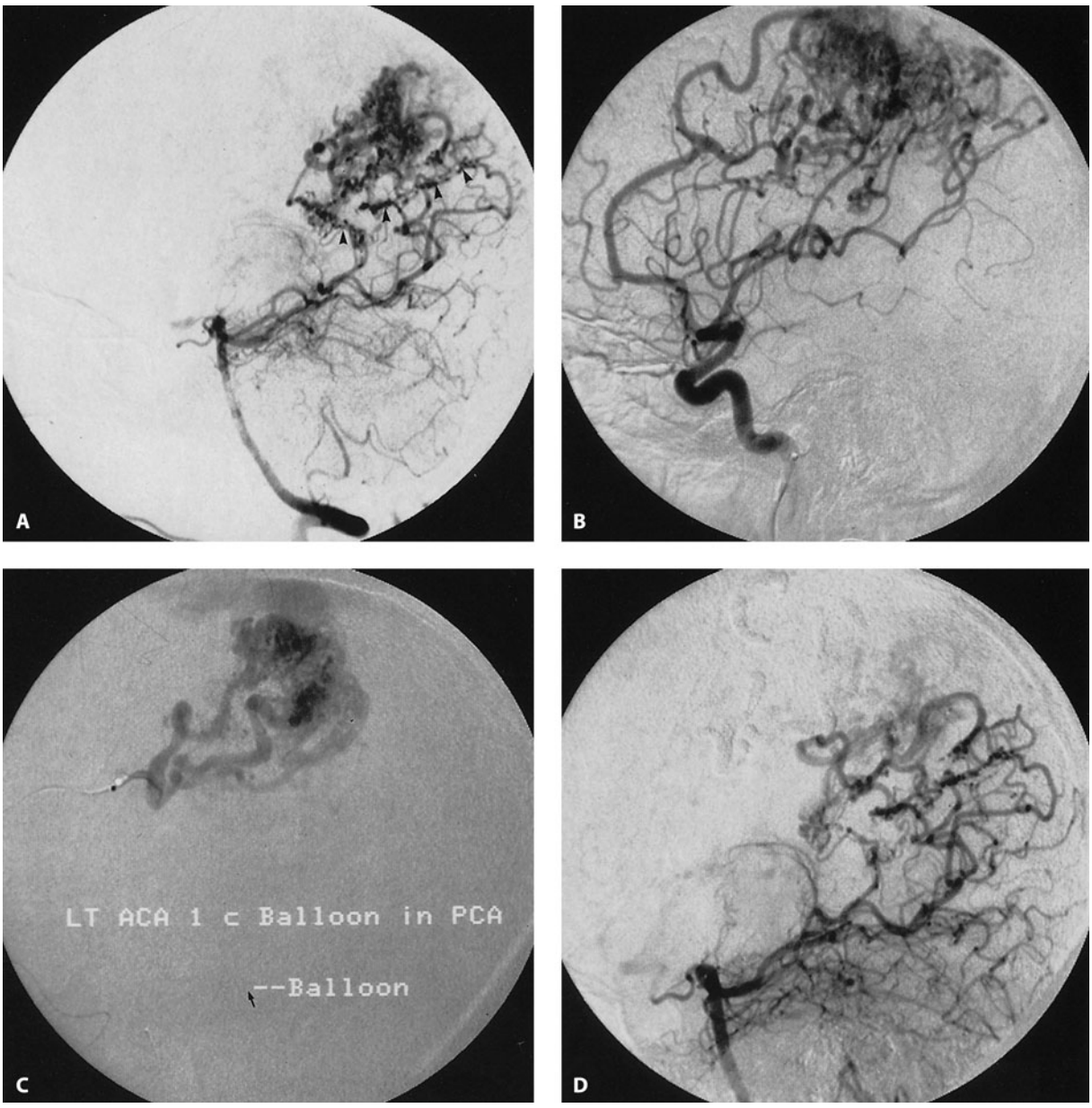

Fig. 14.28A–D. Two variable-stiffness systems to produce flow modifications. **A** Lateral subtraction angiogram (DSA) of the left vertebral artery. There is indirect filling of the arteriovenous malformation (AVM) from the posterior cerebral artery (PCA) via leptomeningeal collaterals (*arrowheads*). **B** DSA of the left internal carotid artery. **C** Lateral DSA of the left anterior cerebral artery (ACA) injection with temporary balloon occlusion of the posterior cerebral artery (*arrow*). **D** Left vertebral artery injection after embolization via the ACA. The posterior cerebral artery was temporarily occluded while the acrylic was injected into the AVM via the ACA. Note the significant decrease in nidus field by the PCA (compare to **A**)

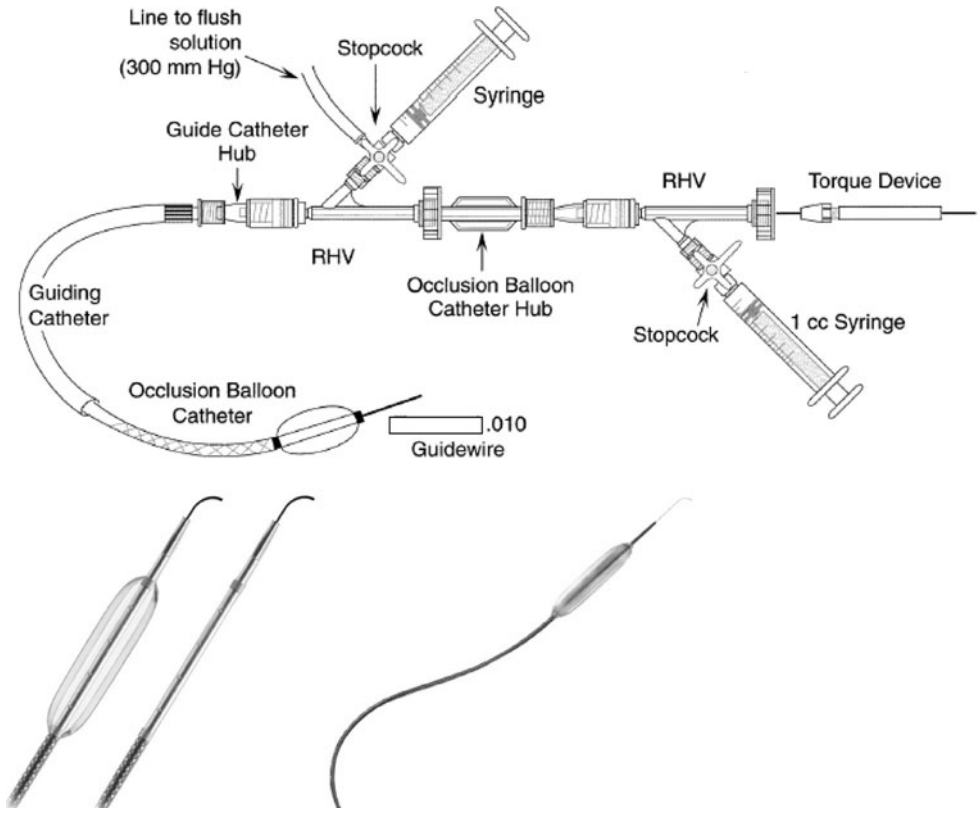

Fig. 14.29. Sentry single-lumen balloon tip catheter used for remodeling technique or dilatation of cerebrovascular spasm. (Target, Boston Scientific). Similar to other single-lumen balloon-tip catheters, a 0.010-in. microguidewire is used to inflate the balloon. The balloon may also be used with a 1-ml Luer-Lok syringe as a calibrated leak balloon catheter

14.5.3.2 Detachable Balloons

Detachable balloons were originally designed by Serbinenko in Russia (1974) and introduced in the Western world by Debrun (1975a). Detachable balloons (Fig. 14.31) are still the embolic agent of choice for single-hole fistulae of the traumatic or congenital type and are very effective when a major artery is to be occluded. The major advantages of detachable balloons when compared to other types of embolic agents (particles, coils, liquids, etc.) are the following:

1. A vessel and/or abnormality can be closed at a precise location.
2. Distal and/or tortuous locations can be reached by flow navigation.
3. As they can be inflated, a vessel of larger diameter (up to 3 cm) can be occluded with a relatively small percutaneous arteriotomy.
4. They can be removed and changed if the position or size of the balloon is incorrect.
5. They can be passed into the venous side for occlusion of a pathological arteriovenous fistula with preservation of the parent artery.

At one time they were used for aneurysm treatment, to exclude the aneurysm from the circulation. They are no longer used for this purpose.

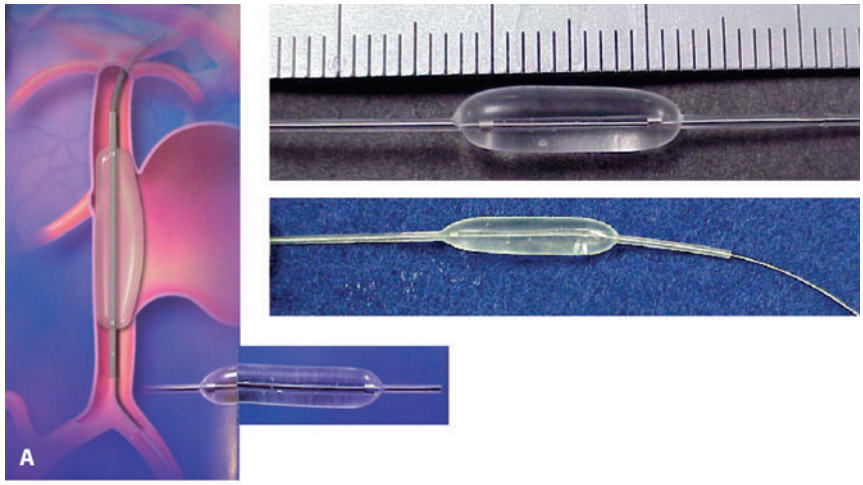

Fig. 14.30A, B. Single-lumen balloon-tip catheters (MTI, San Clemente, CA, USA). **A** Equinox (MTI). Single-lumen pliable balloon tip catheter used for remodeling technique or dilatation of cerebrovascular spasm. The tip of the catheter is sealed off by the 0.010-in. guidewire. The balloon may also be used with a 1-ml Luer-Lok syringe as a calibrated leak balloon catheter. **B** Hyperglide (MTI). A more pliable balloon permits better molding to different anatomy such as the basilar apex

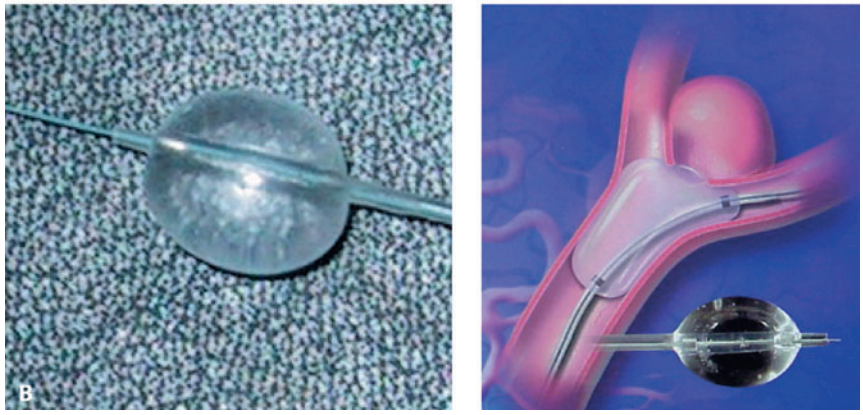

Fig. 14.31.
Legend see p. 957
▼

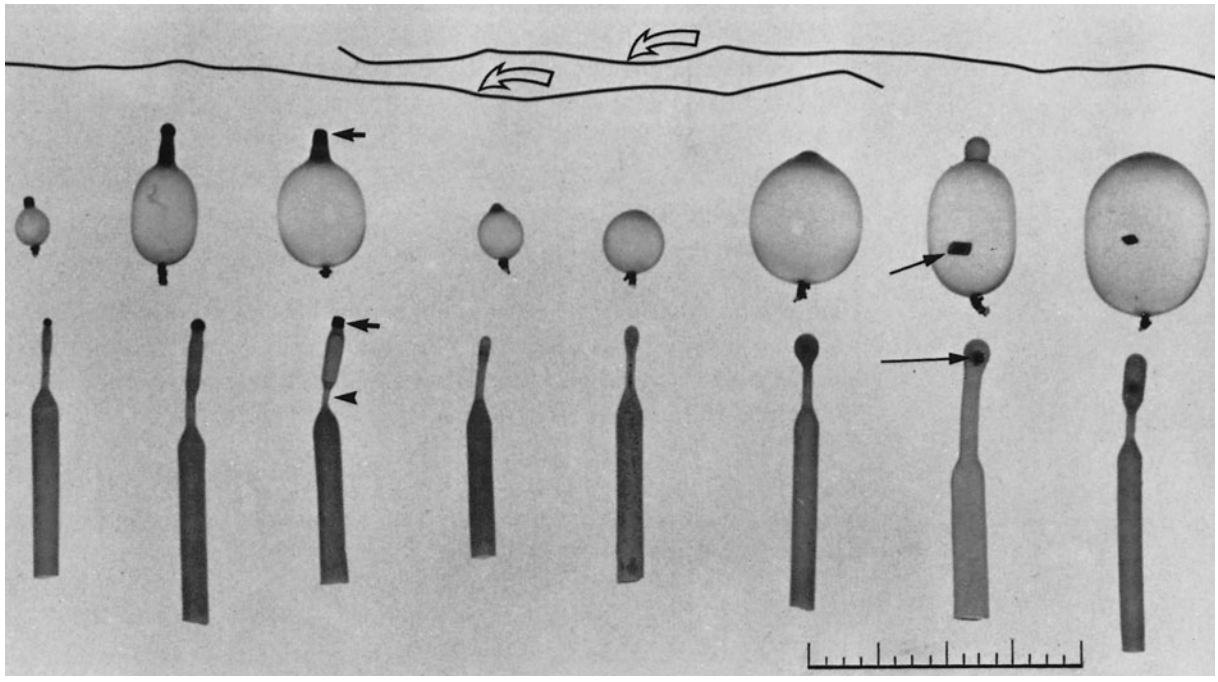

Table 14.3. Detachable balloons

Characteristics	Latex[a]	BD Silicone[b]	Silicone[c]
Distensibility	1:7	1:4	1:6
Hysteresis	–	++	+
Deflation	2–4 weeks	> 24 weeks	> 24 weeks
Shapes	Multiple	Elongated	Round
Inflation diameter (mm)	5–30	4–8	4–35

[a] Debrun Ingenor.
[b] Becton-Dickinson.
[c] Hieshima.

Detachable balloons are made of either latex (Debrun's type, O'Reilly gold valve), or silastic (Hieshima type) (Table 14.3).

Latex Balloons

The commercial version of the balloon designed by O'Reilly et al. (1984) is available and is known as the gold valve balloon (Nycomed, Paris, France). It consists of a small balloon within a larger balloon. The smaller inner balloon has a distal hole through which the microcatheter is introduced. After detachment, the smaller balloon acts as the valve, preventing deflation (Fig. 14.32). While the main advantage of this balloon is its easy assembly, it can also be tested prior to introduction into the circulation and is therefore more reliable.

Latex balloons are frequently used by the authors. The main advantages are the following:

1. Multiplicity of sizes and shapes
2. Easy assembly with the gold valve model
3. Latex distensibility
4. Good memory or hysteresis, even after the balloon has been inflated and deflated on multiple occasions

The balloons come with a radiopaque marker, usually a small silver clip so they can be seen when introduced into the circulation prior to balloon inflation.

The main disadvantages are the following:

1. Relatively short shelf life. Latex is light sensitive (Abele 1978) and should be stored with some type of cover.
2. At present, regardless of the way they are attached to the catheter, they will eventually deflate.

◀ **Fig. 14.31.** Debrun latex balloons come in multiple sizes and shapes. Unmounted balloons have a narrow collar (*arrowhead*) where they are mounted. A radiopaque silver marker is placed in the distal part of the balloon (*arrow*) or in the balloon itself (*long arrow*). Note the distensibility of latex from the deflated to the inflated size. Latex threads (*open curved arrow*) are used for mounting the balloons (see Fig. 14.36)

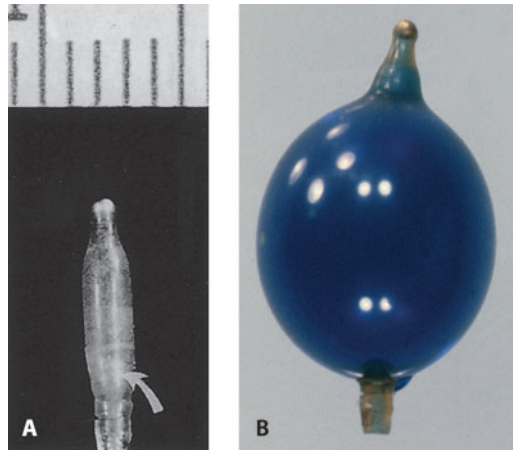

Fig. 14.32A, B. O'Reilly (gold valve) balloon. **A** Deflated and **B** inflated, detachable balloons. They can also be mounted on a Debrun assembly system (Fig. 14.31) or on an extended-tip Tracker variable-stiffness microcatheter. The valve is made of a smaller inner balloon with a calibrated leak (*curved arrow*)

At time of detachment, careful fluoroscopic monitoring to ensure that there is no change in the balloon position is essential to preventing backward migration of the balloon. One can see the proximal neck of the balloon stretching as this maneuver is being performed, with immediate return of the balloon neck to its original position once detachment occurs, which is felt as a subtle give in wire tension.

Silastic Balloons

The Hieshima Apollo detachable balloon (Target, Boston Scientific, San Jose, CA, USA) comes in various sizes (Fig. 14.33), and uses a miter valve for sealing (Fig. 14.34). It has 1:16 distensibility. It is attached to a 2-F polyethylene or Teflon catheter. Like the Debrun (latex) assembly system, detachment can be by coaxial detachment (Figs. 14.35, 14.36), or by gentle long pulling until detachment occurs. Apollo balloons can be easily mounted, tested, and detached in vitro for inspection and reattached to the catheter shaft. It will maintain its distended size if inflated with an isosmolar contrast agent. They come in three detachment strengths, depending on the intended indication, with the low and medium detachment force used in parent vessel occlusion, whereas the high detachment force balloons are used for high-flow fistulae.

14.5.3.3 Angioplasty Balloon Catheters

A great variety of angioplasty balloon catheters are currently available, with various lengths, sizes, and balloon compliances. The devices have been designed for peripheral and cardiac indications. They may be noncompliant or semi-compliant and can reach over 12 atm pressure. In the brachiocephalic and cervical arteries, these catheters are very useful. For intracranial angioplasty, we do not require such high pressures. The single-lumen Stealth or the hydrophilic-coated version, the FastStealth (Fig. 14.24) catheter, is our preferred device for atherosclerotic lesions (Fig. 14.25), whereas the compliance balloons such as the Sentry (Fig. 14.29)

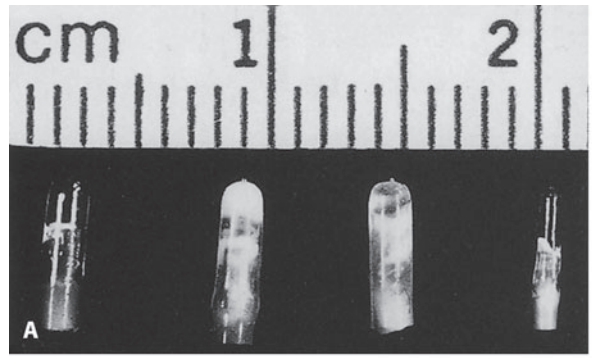

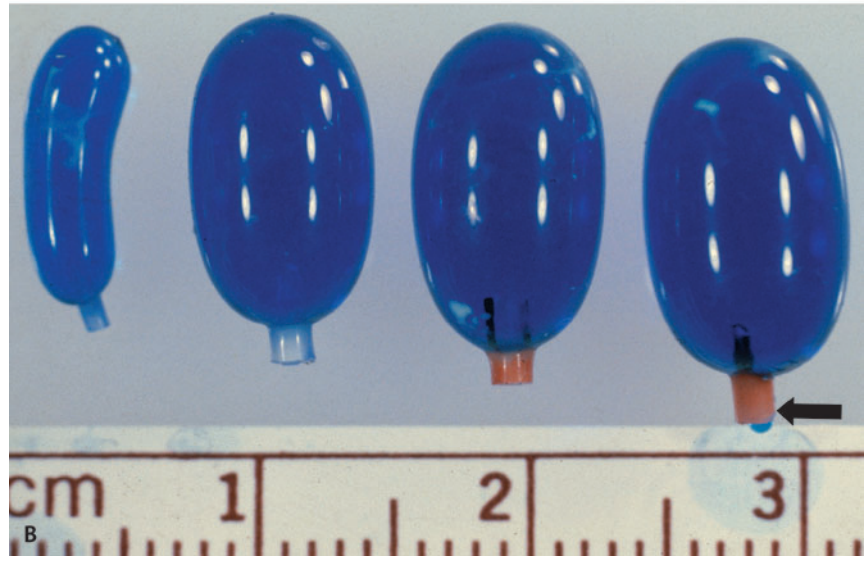

Fig. 14.33A, B. Hieshima Apollo (Target, Boston Scientific) detachable balloons with a miter valve comes in various sizes and detachment strengths. **A** Uninflated balloons. **B** Inflated balloons. The valve reliability can be checked in vitro. If it leaks (*arrow*) the balloon is not used

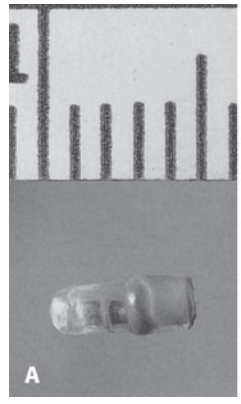

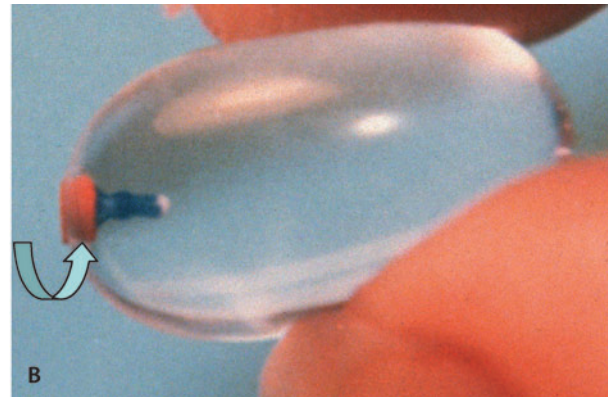

Fig. 14.34A, B. Hieshima Apollo (Target, Boston Scientific) colorless balloon. Note the invaginated self-sealing valve; no collar is present (*arrow*). **A** An uninflated balloon and **B** an inflated balloon

and the Equinox (Fig. 14.30), a calibrated-leak balloon made out of latex (Fig. 14.37), or the Target silicon angioplasty Endeavor balloon-tip catheter (Fig. 14.26B, C) are used for the treatment of vasospasm.

Angioplasty of cerebral arteries requires special care, as the vessel wall is more prone to mechanical damage and dissections, for which underdilatation will result in clinical improvement without the risk of vessel injury (Figs. 14.25, 14.38).

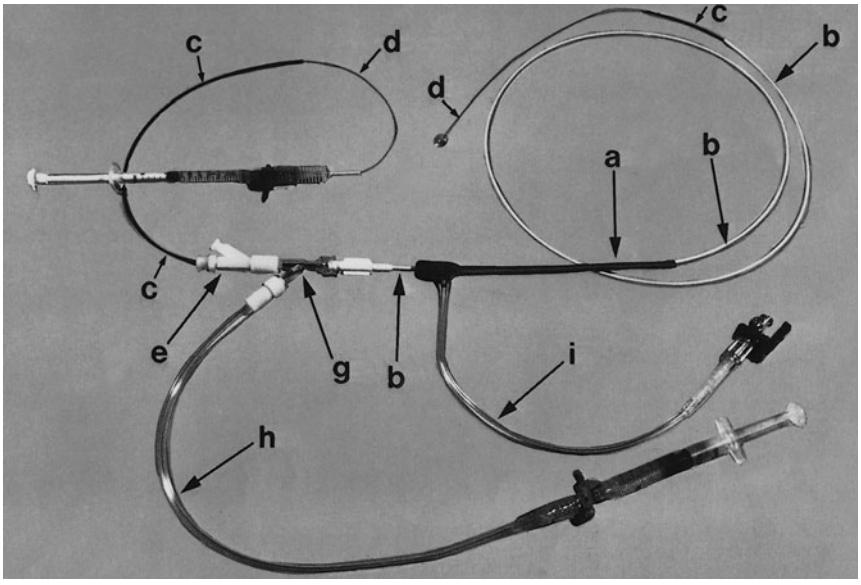

Fig. 14.35. Debrun detachable balloon coaxial system. A sheath (*a*) is placed at the arteriotomy site. A thin-walled introducer (6–9 F) (*b*) is placed in the internal carotid and/or desired vessel using conventional angiographic techniques. The coaxial 3-F (*c*) and 2-F Teflon balloon catheters (*d*) are introduced into the circulation via the thin-walled introducer (*b*) using a Tuohy-Borst "Y"-adapter (*e*) connected to flush solution through its second limb (*h*). A second clear Y-adapter without valves (*g*) is used, through which contrast angiography can be performed via its sidearm. Prior to contrast injection *e* and *h* must be closed. Continuous perfusion through the sheath side arm (*i*) is needed to avoid clot formation

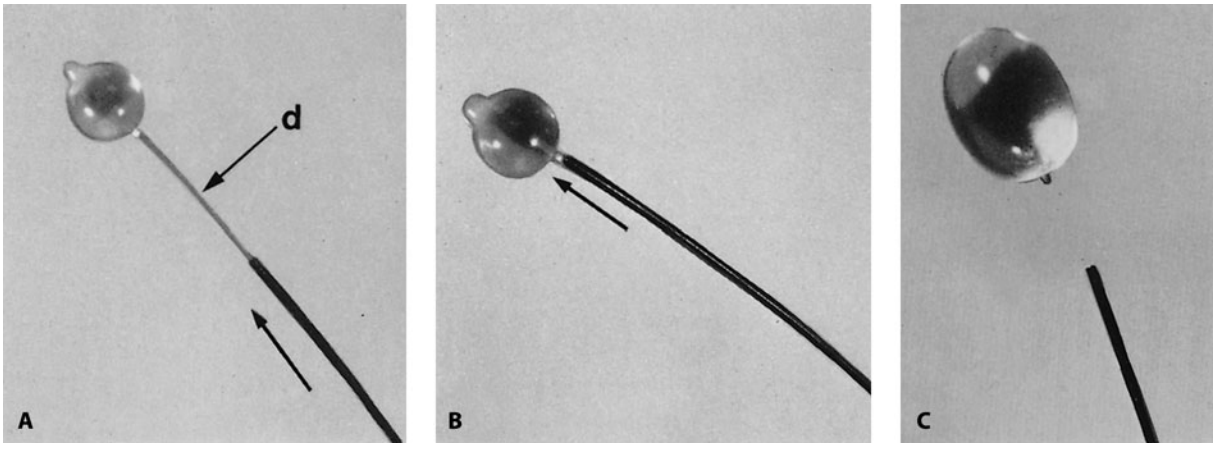

Fig. 14.36A–C. Balloon detachment. Debrun detachable balloon catheter; traction is needed for detachment. **A** Once the balloon is in the inflated and desired position, the outer 3-F catheter is advanced into the circulation (*arrow*) while monitoring the balloon position. **B** Once the 3-F tubing has reached the latex ligature and fixes the balloon, gentle traction is applied to the 2-F Teflon catheter (*d*) (**A**). **C** As the balloon detaches, a gentle give is felt. This maneuver must be carefully monitored fluoroscopically

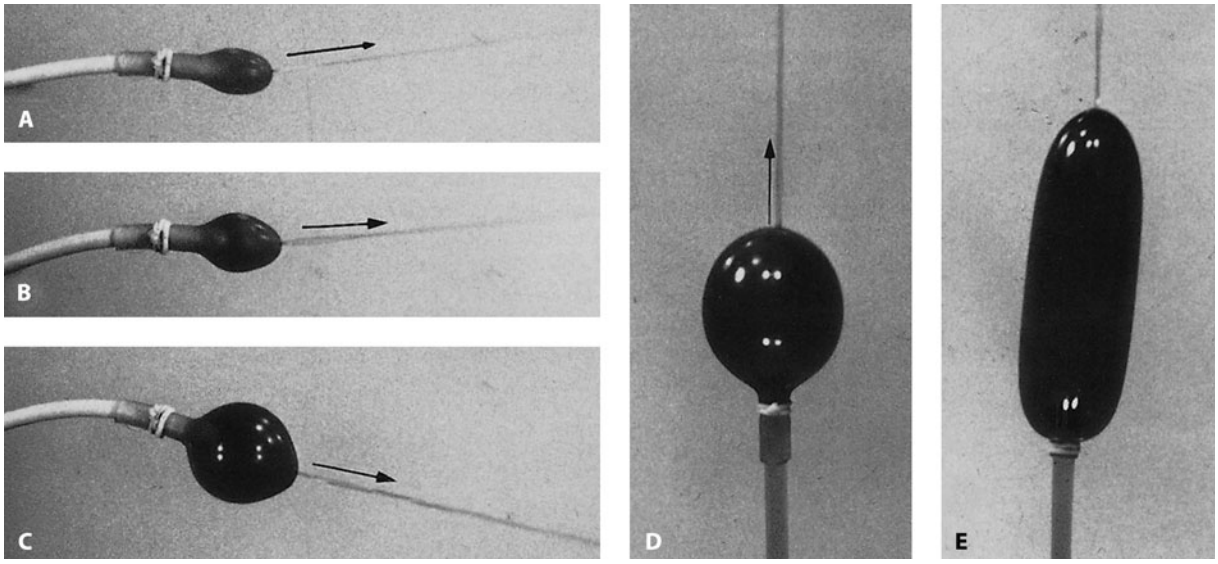

Fig. 14.37A–E. Calibrated leak microballoon. **A** At the beginning of injection, the leak should be large enough to permit infusion (*arrow*) without balloon inflation. **B** Increased pressure increases the flow rate of injection and starts the balloon inflation (*arrow*). **C** Further injection pressure permits infusion with balloon inflation (*arrow*). **D** Larger oval balloons are in a Tracker microcatheter. *Arrow* shows the calibrated leak. **E** Colibri longitudinal balloon. The balloons shown in **D** and **E** also used for angioplasty

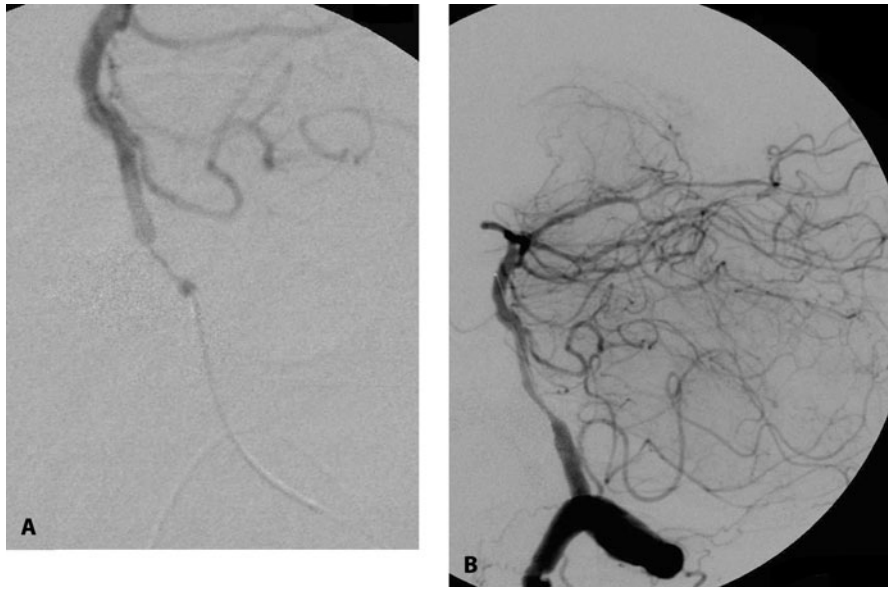

Fig. 14.38A, B. Balloon angioplasty of the basilar artery. **A** Superselective injection of the distal basilar artery showing a severe focal stenosis (*arrow*) after initial 250,000 UI of urokinase (UK), without change. **B** Lateral digital subtraction angiogram of the right vertebral artery after 250 IU of UK and balloon angioplasty, improving the lumen and avoiding damage to the vessel wall

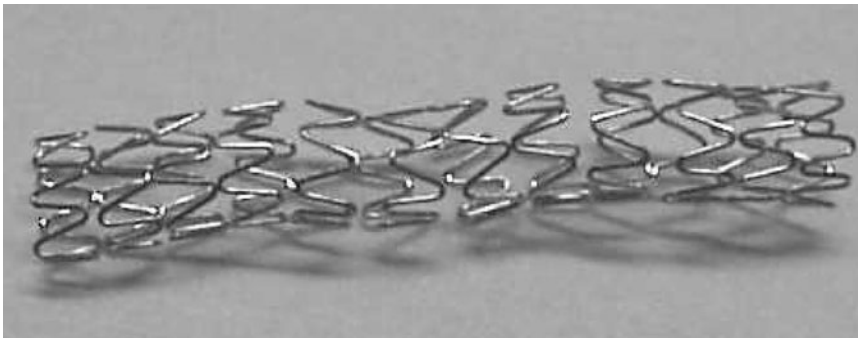

Fig. 14.39. Balloon expanded AVE (AVE/Medtronic, Minneapolis, MN, USA). Stent with open-cell design made out of stainless steel with added flexibility

14.5.3.4 Balloon-Mounted Stents

As stents are improving, with ever lower profile and increased flexibility, balloon-assisted stenting is being used more frequently; if the cardiac and peripheral experience holds in neuroangiography, stenting will soon replace angioplasty.

Currently available devices for distal revascularization are primarily balloon expandable stents. Most have been used off label, as they have been designed for cardiac use, but can frequently be used in the distal carotid arteries, vertebral artery, basilar artery, and even the M1 segment (Fig. 14.39).

Of interest has been the lack of embolization or occlusion of small perforators and side branches, probably related to the very fine struts of the various stents, and the universal use of antiplatelet medications. The most appropriate strut design metal for intracranial applications or even the differences that may be particular to one area versus another (basilar artery vs. MCA) are not presently known.

Several self-expandable nitinol microstents are being developed. They have the advantage of being lower profile and more trackable; however, they may be limited in their radial force, but can be dilated after deployment (Fig. 14.40).

14.5.3.5 Stent Delivery Catheters

Stents are deployed either by balloon inflation (Figs. 14.39, 14.41) or they may be self-expanded, in which case they are introduced in the collapsed state within a sleeve. Various mechanisms have been designed to retrieve the sleeve and allow the stent to expand (Figs. 14.42, 14.154). There are various designs of self-expanding stents (see Sect. 14.6).

Due to their relatively large profile, care as to ID–OD compatibility is imperative; lower-profile self-expanding stents require smaller delivery catheters.

Covered stents are now becoming available and have some advantages in specific cases, although they are still more rigid and of larger profile (Fig. 14.43).

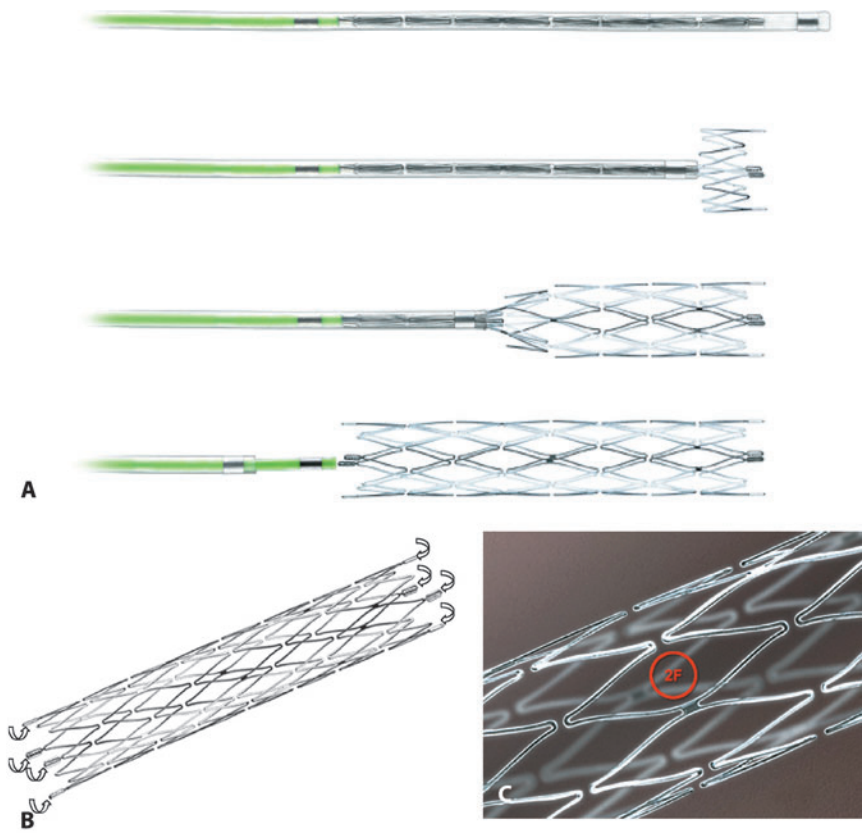

Fig. 14.40A–C. Neuroform (Target, Boston Scientific), a self-expandable nitinol low-profile microstent. **A** The stent comes in a 3-F delivery system and is self-expandable, as the covering sheath is pulled. **B** The fully expanded stent. Note the four radiopaque markers in each end of the stent (*open curved arrows*). **C** Close-up view of the open-cell configuration 2-F stent

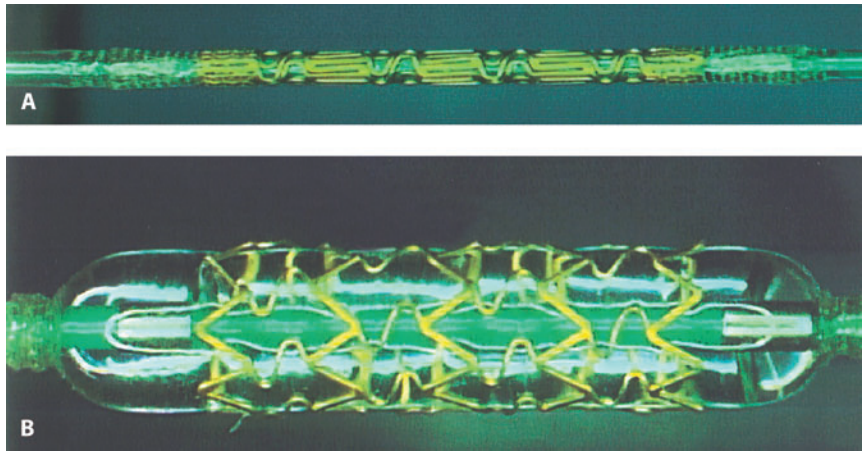

Fig. 14.41A, B. Balloon-expandable stainless steal stent for intracranial navigation. (Target, Boston Scientific), example of a balloon-expandable intracranial stent. **A** Stent mounted over balloon. **B** After balloon inflation there is expansion of the stent. Balloon-expandable stents can be made of different constructions (see text)

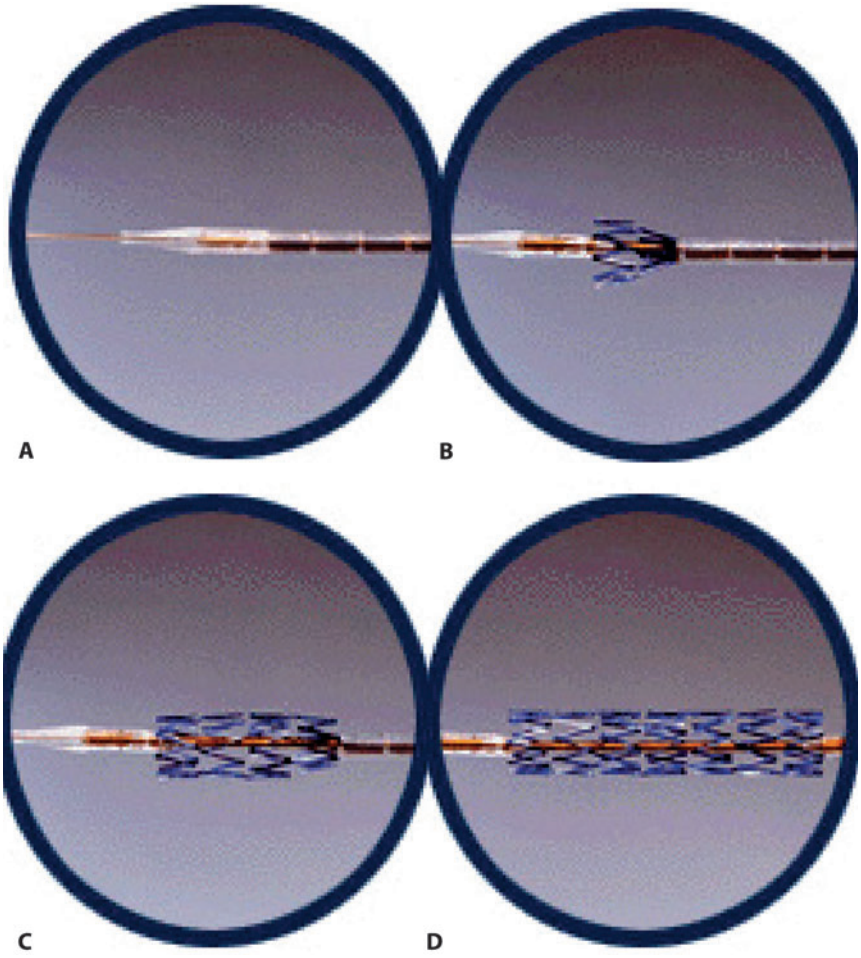

Fig. 14.42A–D. Radius (Target, Boston Scientific) Self-expandable mesh construction stent made out of nitinol. **A** Stent within the delivery catheter. **B** As the introducer sheath is withdrawn, the self-expandable stent begins to expand in its distal portion. **C** Mid-expansion and **D** fully expanded stent

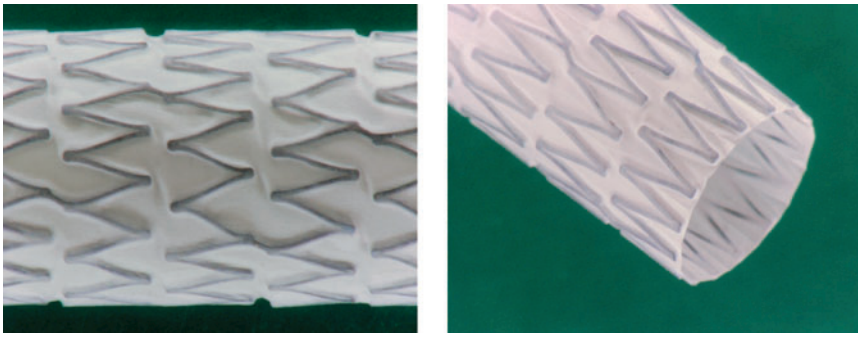

Fig. 14.43. Covered stent. Symbiot (Target, Boston Scientific). This stent is a self-expanding nitinol stent covered with flexible EPTFE covering

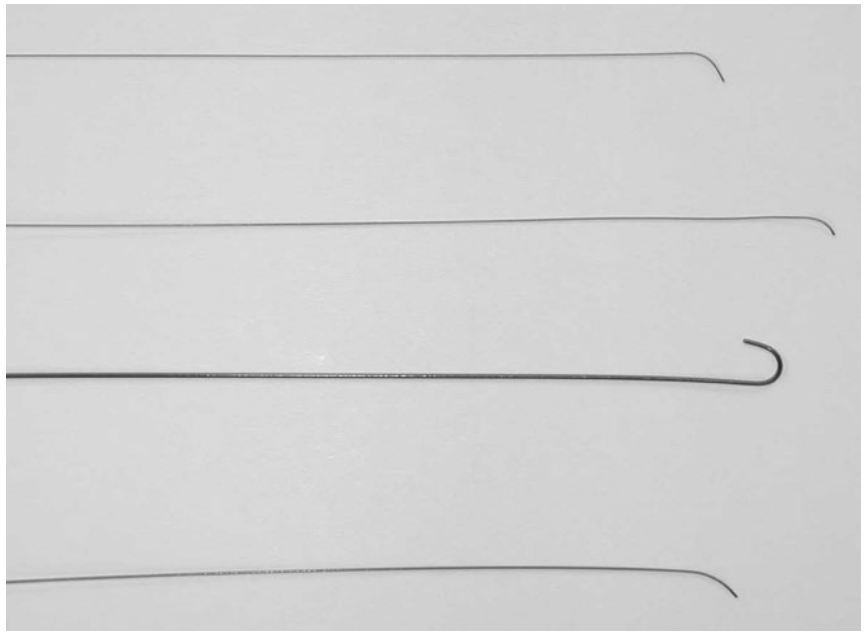

Fig. 14.44. Terumo guidewires. Various sizes of nitinol microguidewires used in cerebral navigation (Terumo, Tokyo, Japan; distributed by Boston Scientific, Maple Grove, MN)

14.6 Guidewires

In general, we employ the Terumo 0.035-in. or 0.038-in. soft or conventional guidewires (depending on the guiding catheter ID). They all have hydrophilic coating and have very good torque control (Fig. 14.44).

14.6.1 Microguidewires

One of the greatest advantages of variable-stiffness microcatheters is the ability to use microguidewire assistance, in addition to torque control and flow-assisted navigation, in distal intracranial locations. Most presently available microguidewires have hydrophilic coatings.

For distal navigation, a variety of microguidewires exist. Our preferred microguidewires include the Terumo 0.012-in. (Terumo, Tokyo, Japan), which has very good torque control, is more kink-resistant, comes with preshaped curves (45°, or 90°), but cannot be reshaped. The Silverspeed 0.08-in. and 0.014-in. (MicroTherapeutics, Inc., San Clemente, CA, USA), with the smaller 0.08-in. are the preferred guidewires with flow-guided microcatheters. The Agility 0.010-in. and 0.014-in. (Cordis Endovascular), the Sorcerer 0.007-in. and 0.009-in. (Balt, Paris, France) are excellent wires for distal catheterization, primarily used in distal cerebral catheterization, spinal cord, and the ECA. The major disadvantage of these types of wire is their softness, and when used in tortuous anatomy, they must be changed frequently, with the obvious increase in cost. An advantage of these types of wire is the ability to shape their distal end; their softness also helps in probing as they are advanced. The very soft microguidewire can be used with a straight or a simple curve in its distal end (Fig. 14.45). The wires can be easily steered with 1:1 torque control. The guidewire curve will permit

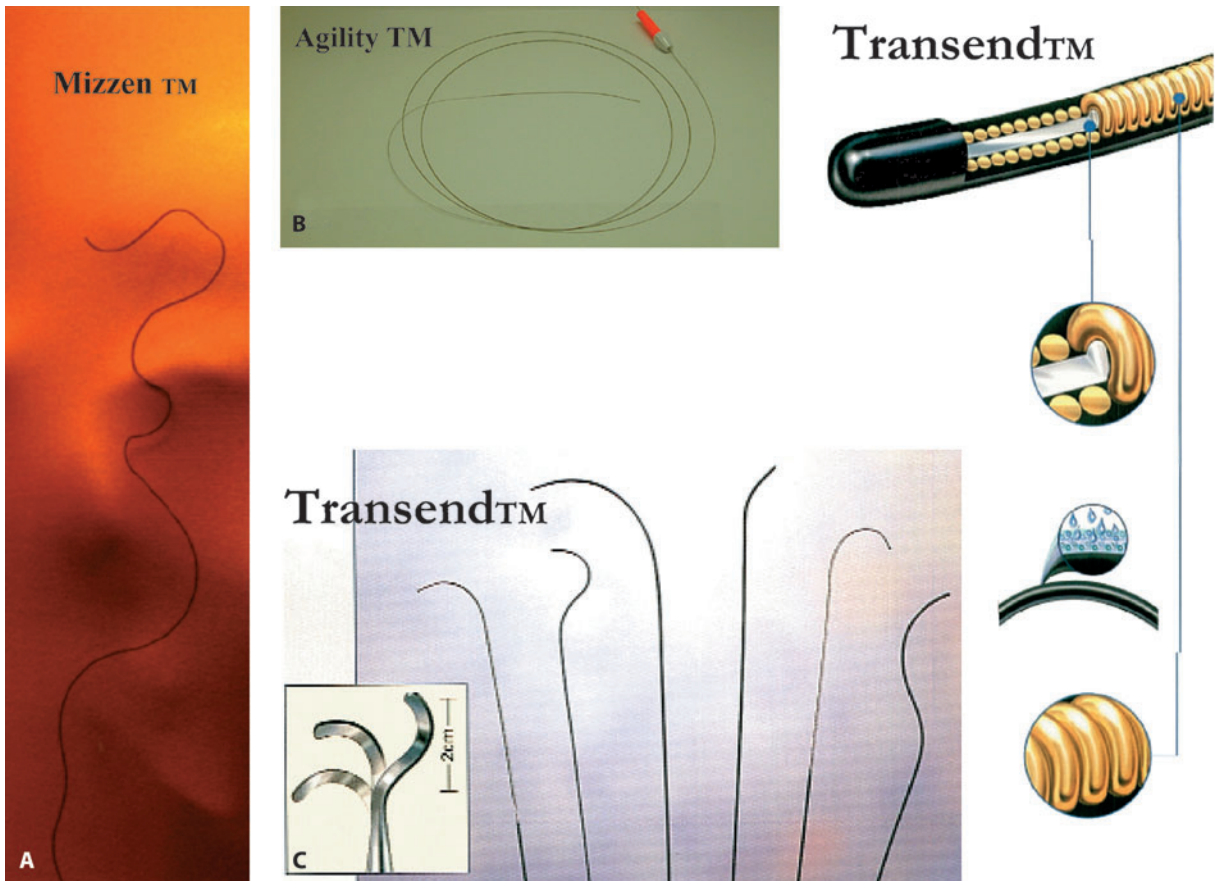

Fig. 14.45A–C. Microguidewire use in cerebral navigation. Current microguidewires come in a variety of constructions and designs, with numerous support characteristics. Ever-improving hydrophilic coatings. **A**, **C** Target products (Boston Scientific). **B** Agility from Cordis Endovascular

engagement of difficult curves such as the choroidal arteries (Fig. 14.46), the anterior cerebral artery, and, once engaged, the proximal stiffness assists in advancing while the soft distal tip prevents vessel damage. If the tip buckles, the guidewire is slightly withdrawn and rotated to prevent reentering the undesired branch.

When using soft microguidewires, advancement is best with a J-curve, to prevent entering more proximal small vessels (ophthalmic, C1, posterior inferior cerebellar artery, basilar tip, etc.) (Fig. 14.47). In addition, a J-curve can be used in a sidewinder fashion. In this technique, the curved wire is initially passed beyond the vessel to be catheterized and then, by withdrawing the system, the desired artery is engaged.

For the smaller microcatheters such as the 1.5-F, or 1.2-F Magic (Balt), the Mirage 0.008-in. (MicroTherapeutics, Inc.) (Fig. 1.41), or the Sorcerer 009-in. and 007-in. by Balt are extensively used.

In aneurysm treatment, the Terumo (Terumo) 0.012-in. guidewire (Fig. 14.44) or Transent platinum 0.014-in. (Target, Boston Scientific) (Fig. 1.45), with its very radiopaque distal segment, are usually able to reach the desired position.

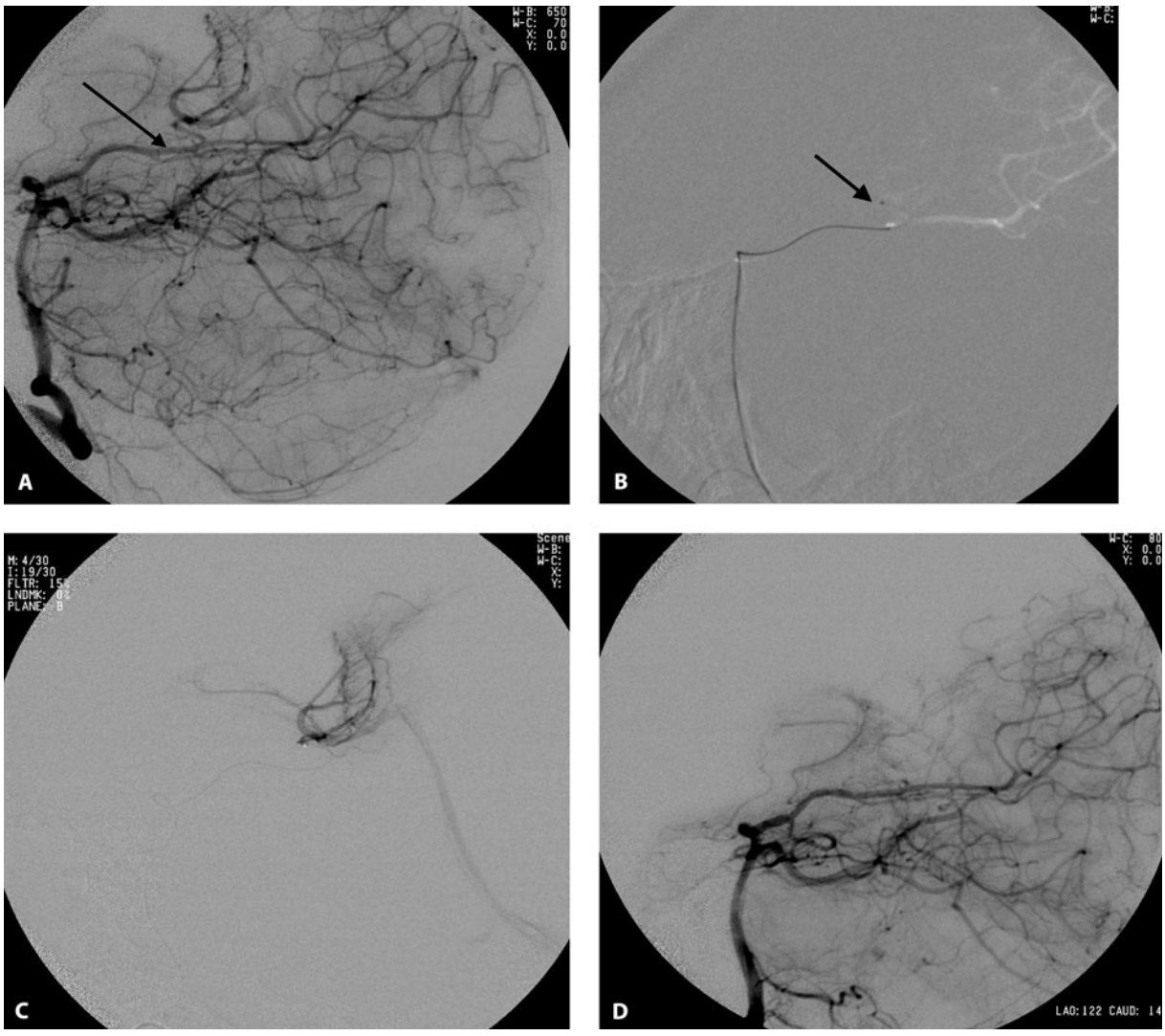

Fig. 14.46A–D. Microguidewire use in cerebral navigation. Small arteriovenous malformation of the lateral ventricle. **A** Lateral oblique subtraction angiogram of the left vertebral artery shows the posterior medial choroidal (*arrow*) supplying a small arteriovenous shunt. **B** Road map view after guidewire catheterization of the sharp curve of the posterior medial choroidal showing the tip of the microcatheter (*arrow*). **C** Superselective injection of the choroidal artery showing the shunt. **D** Postembolization angiogram shows occlusion of the malformation and preservation of all normal arteries

In revascularization procedures, more support is needed for the advancement of angioplasty balloon tip catheters and stent deployment; stiffer 0.018-in. or 0.014-in. microguidewires are necessary. Long exchange sizes of 300 cm or longer are needed, unless compatible monorail systems are used. A great variety exists from the coronary angiography experience and technology. We believe that the operators should familiarize themselves with two or three microguidewires, from moderate stiffness to stiffer wires, for greater flexibility. As will be detailed later (see Sect. 14.16.9), the guidewire is probably the single most important tool in revascularizа-

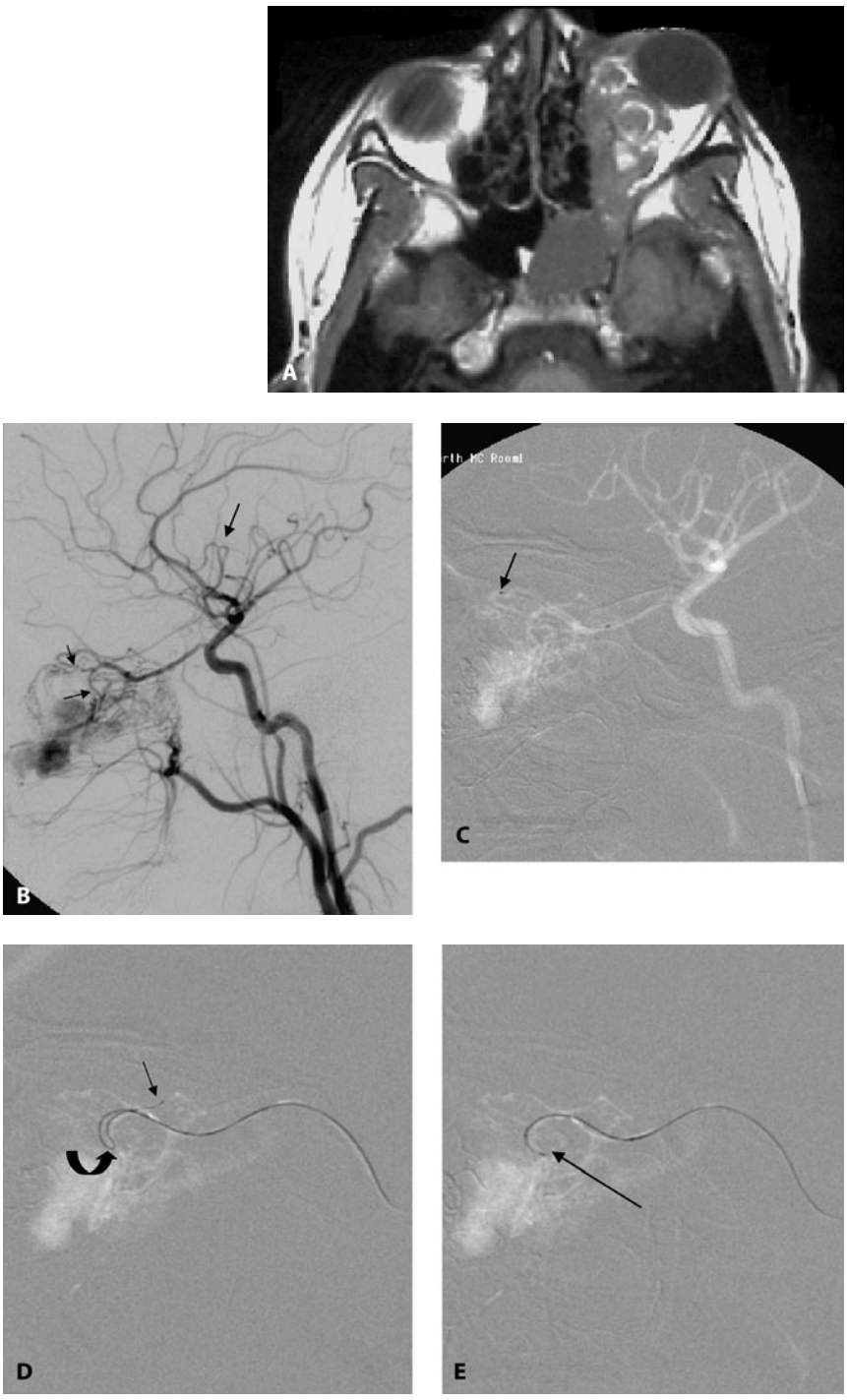

Fig. 14.47A–H. Technique for "J" guidewire advancement. Axial MRI of an intraorbital, extraconal vascular malformation **B** Lateral digital subtraction angiogram (DSA) of the right common carotid artery demonstrates the external carotid artery and ophthalmic contribution to the AVM. Note the two main vessels supplying the lesion (*arrows*). **C** Microcatheter tip in the more distal feeder (*arrow*). **D** The J on the wire is made to catheterize the more proximal feeder by engaging the wire tip in a small branch (*arrow*) and gently advancing the wire to create the J loop (*curved arrow*), for a less traumatic advancement, despite tortuousities, or sharp angulations of the catheter tip (*arrow*, **E**). **F–H** see p. 969

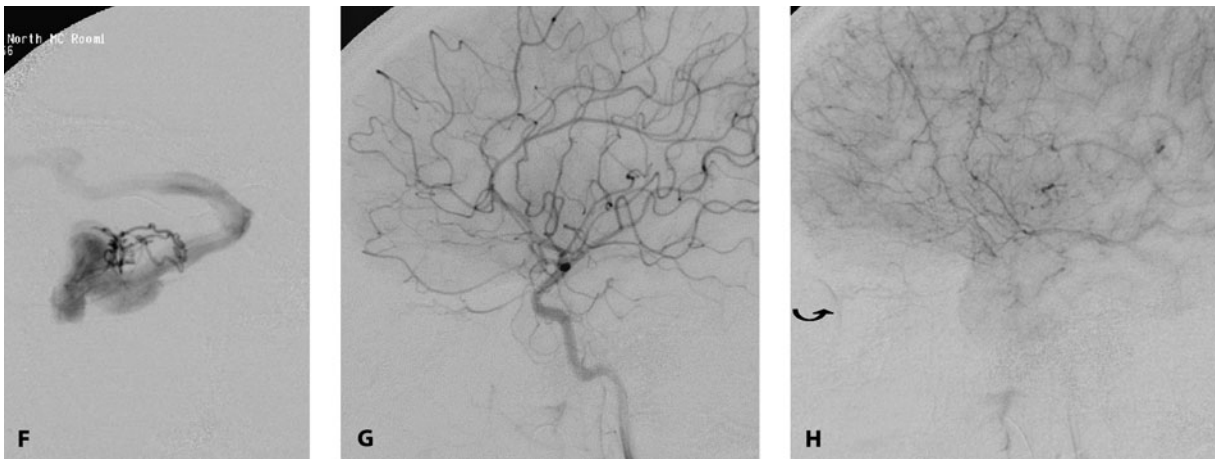

Fig. 14.47 (*continued*). **F** superselective angiogram prior to embolization. Lateral DSA follow-up 6 months after embolization. **G** Early arterial phase and **H** later phase images show no malformation. Note the retinal blush (*curved arrow*)

tion procedures. While the wire is in the appropriate location, most problems can be solved. If the wire position is lost, the complications will be more difficult to resolve (Fig. 14.149).

14.7 Embolic Agents

The choice of embolic agents will depend on the goal of the procedure, the selectivity accomplished, and the vascular anatomy of the angioarchitecture of the pathological territory (Table 14.4).

Embolic agents can be divided into solid particles or liquid agents by their physical characteristics, and into absorbable, nonabsorbable, or cytotoxic types by their biological behavior.

14.7.1 Particulate Agents

Particle embolization refers to a mechanical blockage of a vascular territory utilizing particles that may be of uniform or variable sizes and shapes. Their ability to occlude is related to their size, shape, and friction coefficient. Particulate emboli used during surgical neuroangiographic procedures are of various types: absorbable materials, nonabsorbable materials, and time-releasable microparticles. Particulate agents in general are not able to distally penetrate the nidus of the malformation, resulting in proximal vessel occlusion. In our experience, the long-term results of such proximal occlusions show no improvement over the natural course of BAVMs in terms of rebleeding rate. In some centers, particulate agents are used as the main embolic agent in preoperative devascularization (Hilal and Michaelson 1975; Wolpert and Stein 1975; Hieshima and Higashida 1987) or during intraoperative embolization (Drake 1979a; Spetzler et al. 1987b).

Table 14.4. Embolic agents used by authors

I. Absorbable (biodegradable)
   a. Gelfoam powder (40–60 μm)
   b. Gelfoam particles (any size)
   c. Avatine (collagen powder)

II. Nonabsorbable particulate
   a. Polyvinyl alcohol foam (PVA) microemboli 40–1,000 μm
   b. Embospheres
   c. Detachable balloons
   d. Coils
   e. Fiber coils
   f. Detachable coils
      1. Guglielmi detachable coils (GDC)
      2. Micro coils
      3. Cook coils
      4. Cordis coils
      5. Hydrocoils
      6. Bioabsorbable polymeric GDC Coils (BPM/GDC).
   g. Berenstein liquid coils (BLC)

III. Nonabsorbable Liquids
   a. Adhesive
      1. *N*-butyl-cyanoacrylate (NBCA)
         Hystoacryl
         TruFil
      2. Octa-cyanoacrylate (Neuroacryl)
   b. Nonadhesive
      1. Ethylene-vinyl alcohol copolymer (EVOH) (Onyx)

IV. Cytotoxics
   a. Ethanol (98%)
   b. Chemotherapeutic agents
   c. Time-released microcapsules

In the spine and spinal cord, particulate agents, including reabsorbable particles or coils, can be used to protect normal territories or to redirect flow when superselectivity is not possible.

14.7.1.1 Absorbable Materials

Emboli such as autologous clot, Avatine, or Gelfoam can be used (Djindjian et al. 1973). We have found Gelfoam to be the best for our purpose and do not use any of the others.

Gelatin Sponge Gelfoam

Gelatin sponge Gelfoam (Upjohn, Fort Lee, NJ, USA) was first used to control hemorrhage during surgical procedures by White in 1945. The first report of the intravascular use of Gelfoam was by Speakman in 1964. He tried it for occlusion of a traumatic carotid cavernous fistula via the internal carotid artery. In 1973, Djindjian et al. reported 60 cases treated with the aid of percutaneous catheter embolization using Gelfoam as the occluding agent. Since that time, it has been noted that although Gelfoam

Fig. 14.48. Gelfoam emboli. *1*, Gelfoam particles of different sizes (*A, B*), which can be compressed then soaked in contrast material and cut in various size particles (*C*). Swelling will occur following contrast moistening of the gelatin sponge. *2*, It also comes as a powder with particles 40–60 μg in size

is readily available and easy to use, the vascular occlusion thus accomplished is temporary and recanalization occurs 7–21 days after embolization (Gold and Grace 1975; Barth et al. 1977). It is available as powder (40–60 μm in size), as a sheet, or as cubes from which pieces of varying sizes can easily be cut, placed in contrast material, and injected through small-lumen catheters (Fig. 14.48). Gelfoam comes in sterile, single-use packages.

Gelfoam Powder. We use Gelfoam powder for occlusion of vascular neoplasms prior to surgical removal, or capillary-venular malformations (Berenstein 1981) (Figs. 14.122, 14.125). In these cases, the embolic occlusion occurs at the capillary or precapillary level. The tumor bed is deeply penetrated, allowing no possibility of subsequent collateralization. Perivascular tumor necrosis may be observed pathologically (Fig. 14.49). The particles are injected after mixing the powder in 60% iodinated contrast material until a homogeneous suspension is obtained. Injection is accomplished under fluoroscopic monitoring using a 1- to 3-ml Luer-Lok syringe held in a horizontal position. Depending on the size of the lesion, small amounts (0.3–0.5 ml) of the suspension are injected during systole (in the external carotid) and the contrast material washout is fluoroscopically monitored to follow the progressive obliteration of the tumor microcirculation. If changes in vascular resistance are noted, the catheter is purged backward and rinsed thoroughly. Contrast material is injected at a low pressure, with fluoroscopic monitoring to evaluate the distal territory remaining after the embolization. In general, Gelfoam powder should be carefully used in the external carotid due to the multiple anastomosis

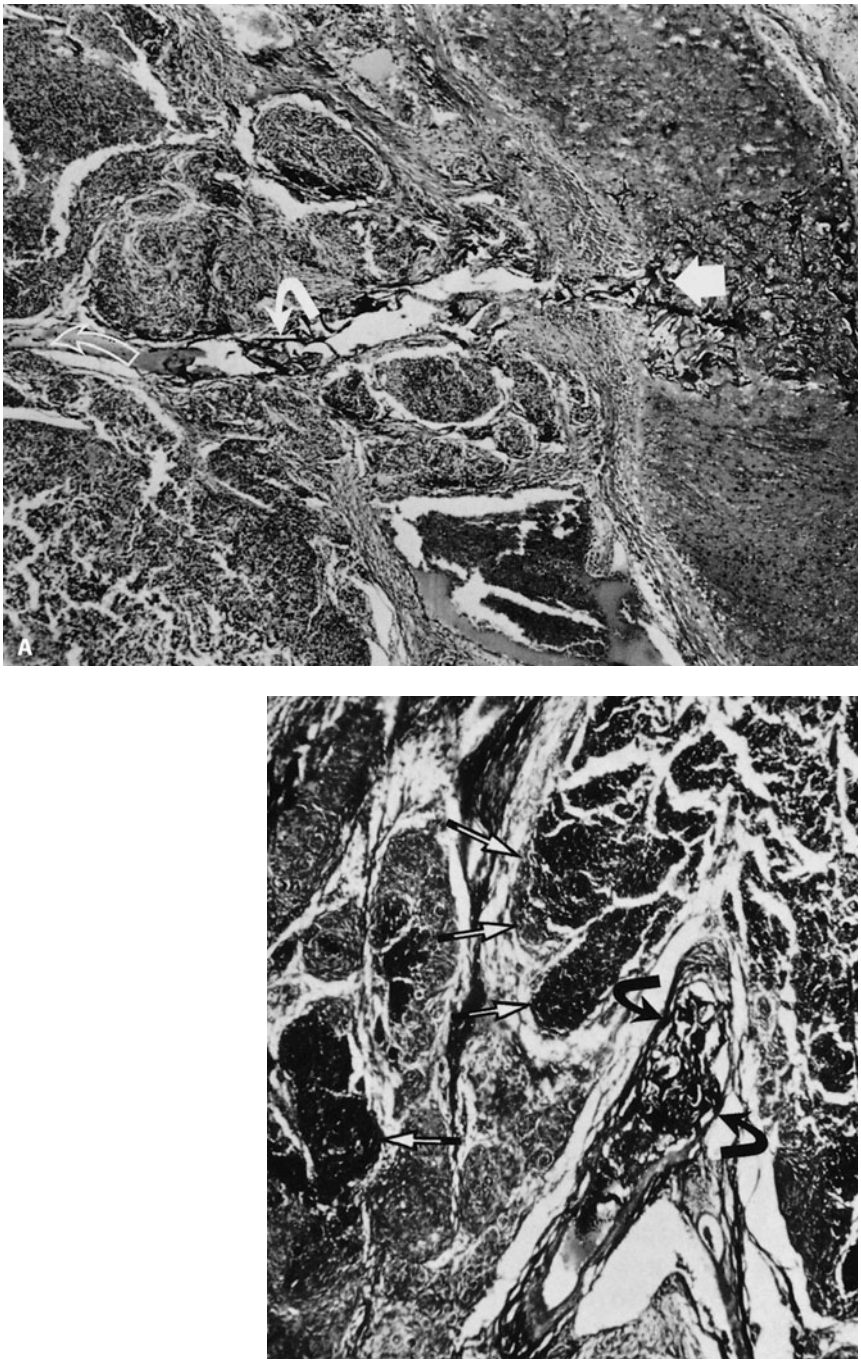

Fig. 14.49. **A** Pathological specimen after Gelfoam powder embolization of a meningioma. HE stain at low-magnification power demonstrates aggregated Gelfoam particles (*solid arrow*) as they enter a small capillary distally occluded (*broken arrow*). Note thrombosis of the vessel distal to the microparticle (*open curved arrow*). **B** Azocarmine stain at larger magnification demonstrates the foreign body Gelfoam (*broken arrows*) as well as darker areas of perivascular early necrosis (*white arrows*). (From Berenstein and Kricheff 1981b, with permission)

between the external carotid system and the intracerebral circulation. As the embolized territory is progressively occluded, one may opt for a slower rate of injection and if necessary, larger particles to prevent passage of the microemboli through the anastomotic pathways.

In the middle meningeal territory, in addition to the collateral circulation to the carotid and ophthalmic systems, Gelfoam powder (or liquids and cytotoxic agents) should be avoided. The proximal 11- to 15-mm segment of the middle meningeal artery beyond the foramen spinosum, where the petrosal branch of the middle meningeal artery arises, supplies the peripheral seventh cranial nerve. The proximal middle meningeal artery can then be closed with a Gelfoam strip to maximize preoperative thrombosis. The same applies to all branches supplying eloquent territories and in particular the cranial nerves. One of the authors (A.B.) has been using a combination of Gelfoam powder, 95% ethanol, and metrizamide in the management of malignant lesions at the base of the skull, or in selected maxillofacial capillary malformations.

Gelfoam Particles. These larger particles have been used for preoperative hemostasis; however, they do not enter the tumor, and necrosis is not observed pathologically. At present, we do not use Gelfoam in particles for occlusion of abnormal vessels, even as a preoperative measure. We use a permanent particulate agent such as polyvinyl alcohol foam or liquid agents, primarily acrylates (Berenstein 1980b).

The use of Gelfoam particles to devascularize a vascular lesion prior to surgical removal carries an immediate risk similar to that encountered with any permanent agent. If an intracranial vessel is occluded with any agent (absorbable or not) this complication is the same.

When superselectivity cannot be accomplished and a permanent agent must be used, a Gelfoam particle, 1×2 or 1×3 mm, or even larger in size, may be injected to occlude and protect normal vessels partially or completely. The occlusion needs to be sufficient to change the hemodynamics of the involved territory so that at the time of injection of the permanent agent, only pathological vessels will be filled. Theoretically, Gelfoam absorption, when used in this manner, is an added advantage, as late recanalization should result in restoration of flow to the normal vessels that were temporarily occluded.

In cases of traumatic arterial hemorrhage or traumatic aneurysms, Gelfoam particles are probably still the best choice as they are easy to inject and produce the desired hemostasis in the majority of cases. A possible exception is when the vessel is larger in diameter than the particles. In these instances, expansile polyvinyl alcohol foam, detachable balloons, or liquid acrylics will easily occlude a large vessel.

For the most part we do not use particle embolization in trauma, particularly in emergency situations, when anastomoses are present. Glue is often the agent of choice with a false arterial aneurysm (AA); superselectivity is done at the time of embolization. The injection of multiple volumes of particles carries the risk of rerupturing the false sac.

14.7.1.2 Nonabsorbable Particulate Materials

Multiple materials of the nonabsorbable particulate type have been introduced (Table 14.4). The oldest of these, silastic spheres, was originally introduced by Luessenhop and Valesquez (1964). This agent has primarily been used for embolization of cerebrovascular malformations. For head and neck embolization, the authors feel that the nonabsorbable particles of polyvinyl alcohol foam are probably best suited. The new hydrogels such as embospheres are another option.

Polyvinyl Alcohol Foam

Polyvinyl alcohol foam (PVA), has improperly been referred to as Ivalon (Fig. 14.50) (Cathnet, Paris, France; Cook Inc., Bloomington, IN; Cordis Endovascular, Miami, FL; Target Boston Scientific). The sponge is a water-insoluble material made by the reaction of polyvinyl alcohol foam with formaldehyde. It is resilient when wet but semirigid when dry. The wet volume is about 20% greater than the dry volume. It is a nonabsorbable, biocompatible sponge. It has been used in the repair of patent ductus arteriosis (Bentson and Crandall 1972), skin grafts (Hogemann et al. 1961), colon surgery (Boutsis 1974), and as an embolic agent (Tadavarthy 1979). In the dry compressed form, only gas sterilization should be used. The sponge expands 10–15 times in length (depending on its original thickness) approximately 30 s after contact with moisture (Fig. 14.50C). Dry compressed PVA is useful for occluding a medium- to large-sized vessel for it expands to occlude an artery larger in diameter than the internal diameter of the catheter. This material is difficult to handle in the dry, compressed state. However, if small discs are made from the original sheet by catheter hand punchers, or the NYU introducer catheter is used (Kricheff and Berenstein 1979), the injection of compressed PVA is facilitated. PVA can be made radiopaque with 60% barium sulfate; however, the addition of tantalum powder may add further radiopacity to small particles. In general, at present, the dry compressed PVA is seldom used.

PVA Suspension. PVA suspension material is supplied in dry particles 100–1,000 μm in diameter. Present preparations are ready to use (Cordis Endovascular, Boston Scientific, Cathnet) (Fig. 14.50).

Immediately before use, the sterile water is decanted and the particles are resuspended in full-strength iodinated contrast material (even with digital subtraction angiography). This results in a homogeneous uniform suspension, which can easily be injected.

The microparticles of PVA can be injected in various ways depending on the objectives. These particles (as others with irregular margins) may or may not enter the abnormal angioarchitecture of a vascular lesion. Factors that will affect the final position include superselectivity, force of injection, concentration of particles per milliliter of contrast material, and the presence or size of a capillary barrier.

Quisling et al. (1984) showed that the irregular surface of precut PVA has a high coefficient of friction, which allows the particles to stop against the vessel wall without completely occluding it.

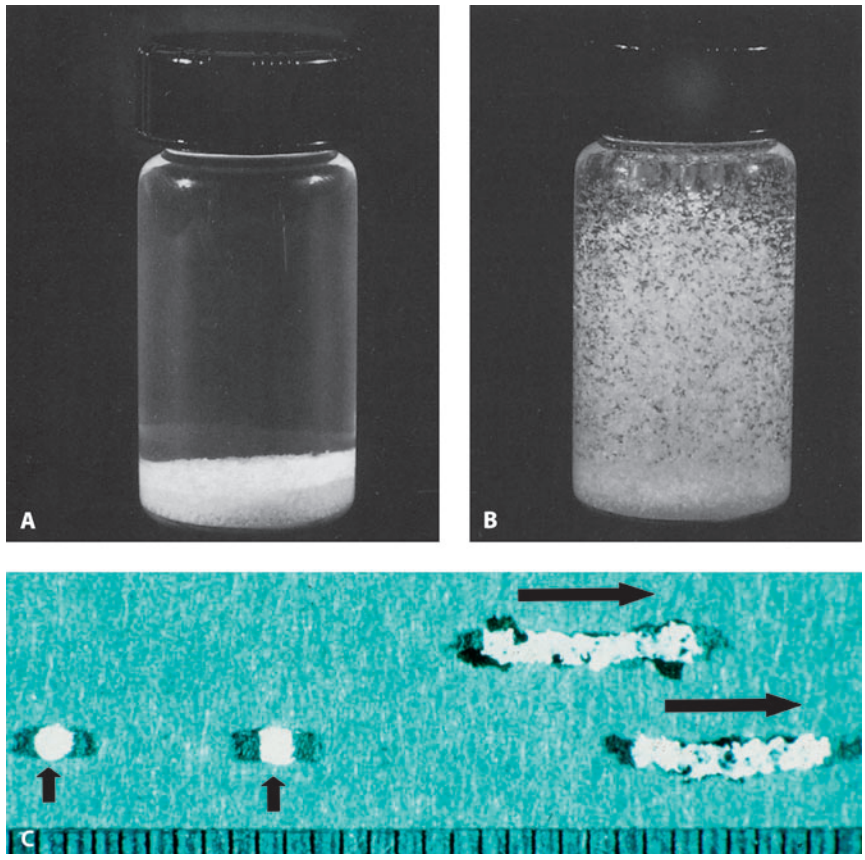

Fig. 14.50A–C. PVA suspension. **A** PVA microparticles layered in the bottom of the bottle after blending, filtration, resuspension, and sterilization. **B** After decanting the sterile water, the microparticles are resuspended in contrast material. After a moment's shaking, a relatively homogeneous suspension is obtained. (From Berenstein and Graeb 1982, with permission). **C** Dry compressed PVA discs (*small arrows*) can be seen to expand after rewetting (*large arrows*). (From Berenstein and Kricheff 1979c, with permission)

This irregular partial occlusion may stagnate blood, producing a combination of PVA and autologous clot that will eventually recanalize (Fig. 14.51), producing re-endothelialization of the unabsorbed PVA. The dilute concentrations of PVA microparticles are useful with small ID catheters and are best in the embolization of lesions with an arteriocapillary barrier (Berenstein 1980a). We start the embolization with a relatively low concentration of microparticles for a deeper penetration. As the smaller vessels are occluded, we change to a more concentrated suspension or a larger size to pack the larger vessels with embolic material. One must be familiar with the capacity of the delivery system to avoid clogging the catheter. If the lumen of the delivery device is occluded, one uses a 1-ml syringe with nonopaque material (normal saline) and gently pushes the aggregated particles producing the plug. As a general rule, if one is unable to easily and smoothly unplug the delivery system, it is best to exchange it. The guidewire should not be used to attempt to unplug the lumen, as it usually worsens the problem by impacting the emboli even further.

Although PVA particles are not reabsorbed (Tadavarthy 1977; Latchaw and Gold 1979), in follow-up of some of our patients, where an apparently excellent embolization was achieved, they sometimes later resulted in complete irregular recanalization (Fig. 14.51). Therefore, we feel that the best indication for PVA is for preoperative devascularization of tumors, epistaxis, few vascular malformations, and flow rerouting, in preparation

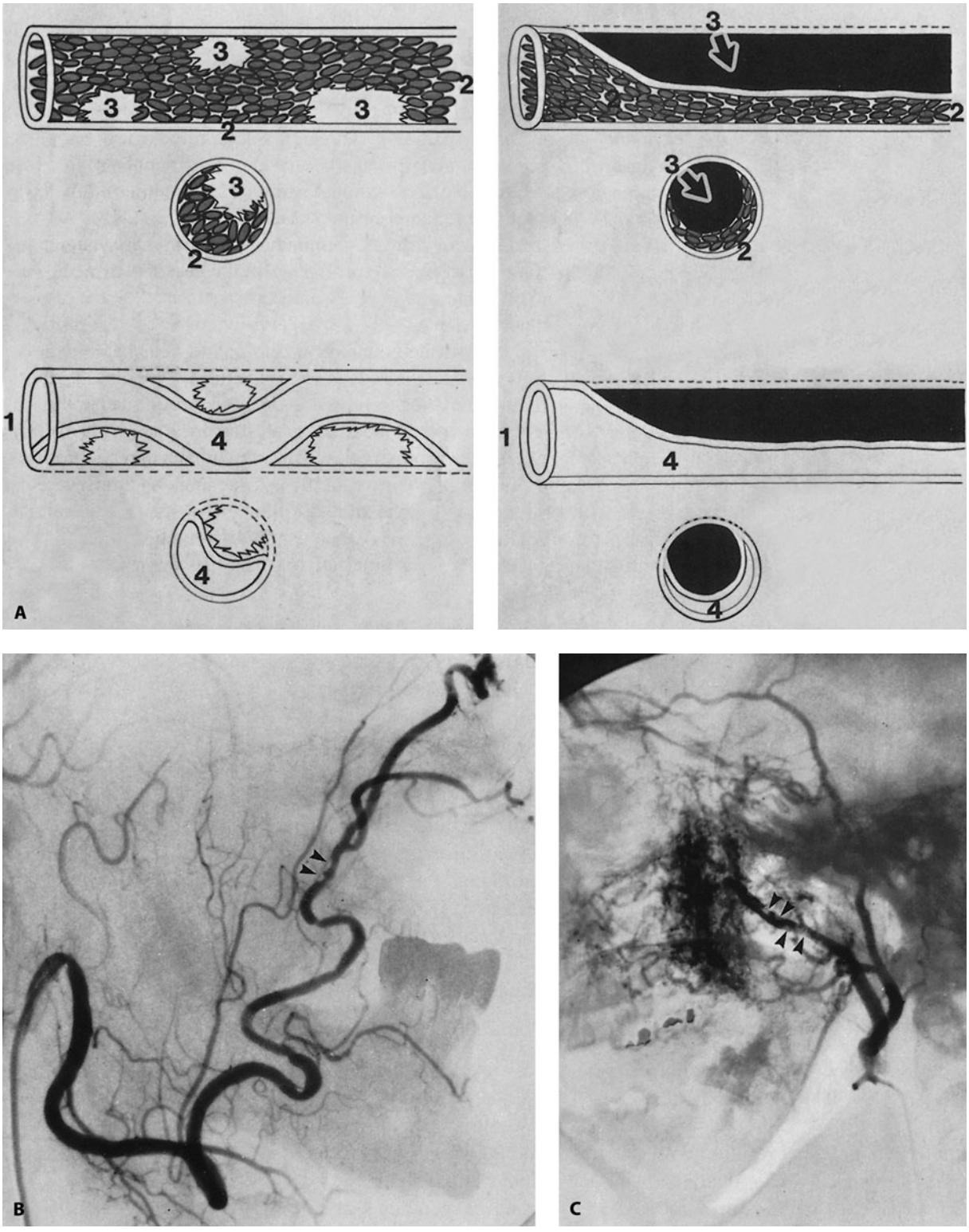

Fig. 14.51A–C. Legend see p. 977

◀ **Fig. 14.51A–C.** Recanalization of nonbiodegradable embolic agents. **A** Diagrammatic representation of the various embolic agents (*3*) and the recanalization (*4*) of the autologous clot (*2*) with re-endothelial lining of the embolic agents. Although the material is not biodegradable, the vessel and territory are revascularized (*1*) vessel wall. **B** Lateral subtraction angiogram of the facial artery which has recanalized after PVA embolization. Note the filling defects of the endothelial-covered PVA particles (*arrowheads*). **C** Lateral subtraction angiogram in a 24-year-old patient with a capillary vascular malformation that was previously embolized with silicone spheres in the internal maxillary and transverse facial arteries. Note the contrast material surrounding the subtracted radiopaque spheres (*arrowheads*). See Fig. 14.52

for liquid embolics or ethanol injection. In our experience, even after dense packing, PVA may recanalyzed. We infer from these observations that a similar recanalization can occur with any other particles. Interestingly, hydrogel-based spheres are of uniform size with smooth borders and are not adhesive or reactive. The recanalization that we have observed in silicon sphere embolization suggests a similar phenomenon where the endothelial lining covering the spheres and the vessel are being opened above and below (Fig. 14.51). Recanalization has been seen with the detachable balloon, deflated prematurely (Fig. 14.52) and silicon spheres (Fig. 14.51B). We have observed similar occurrences in acrylic embolization of BAVMs.

Polyvinyl Alcohol Foam and Ethanol Combination. The combination of PVA and ethanol is used as an enhancement to the mechanical occlusion properties of the irregular PVA particles and the cytotoxic effects of high-concentration ethanol. The dry PVA particles are suspended in 95%–98% ethanol, after mixing and removing the air in the PVA particle interstices, so that the PVA acts as a sponge, retaining a higher concentration of alcohol, to enhance its effect when in contact with the vessel wall.

The PVA–ethanol suspension is then diluted in 60% iodinated contrast material prior to injection. Note that as time passes, some or all the particles will dissolve, resulting in a liquid with a relatively high viscosity, a very effective embolic mixture, which must be used in small volumes at any one time.

Embospheres

Embospheres are beads of cross-linked acrylic impregnated with gelatin, producing spheres with elastic shape and a hydrophilic surface, which prevent aggregation within the catheter (Fig. 14.53). The resulting vessel occlusion and penetration is more predictable and uniform. The material is inert, it remains unchanged over time, and in a 6-year follow-up study, the occlusions were permanent (Biosphere Medical, Rockland, MA, USA).

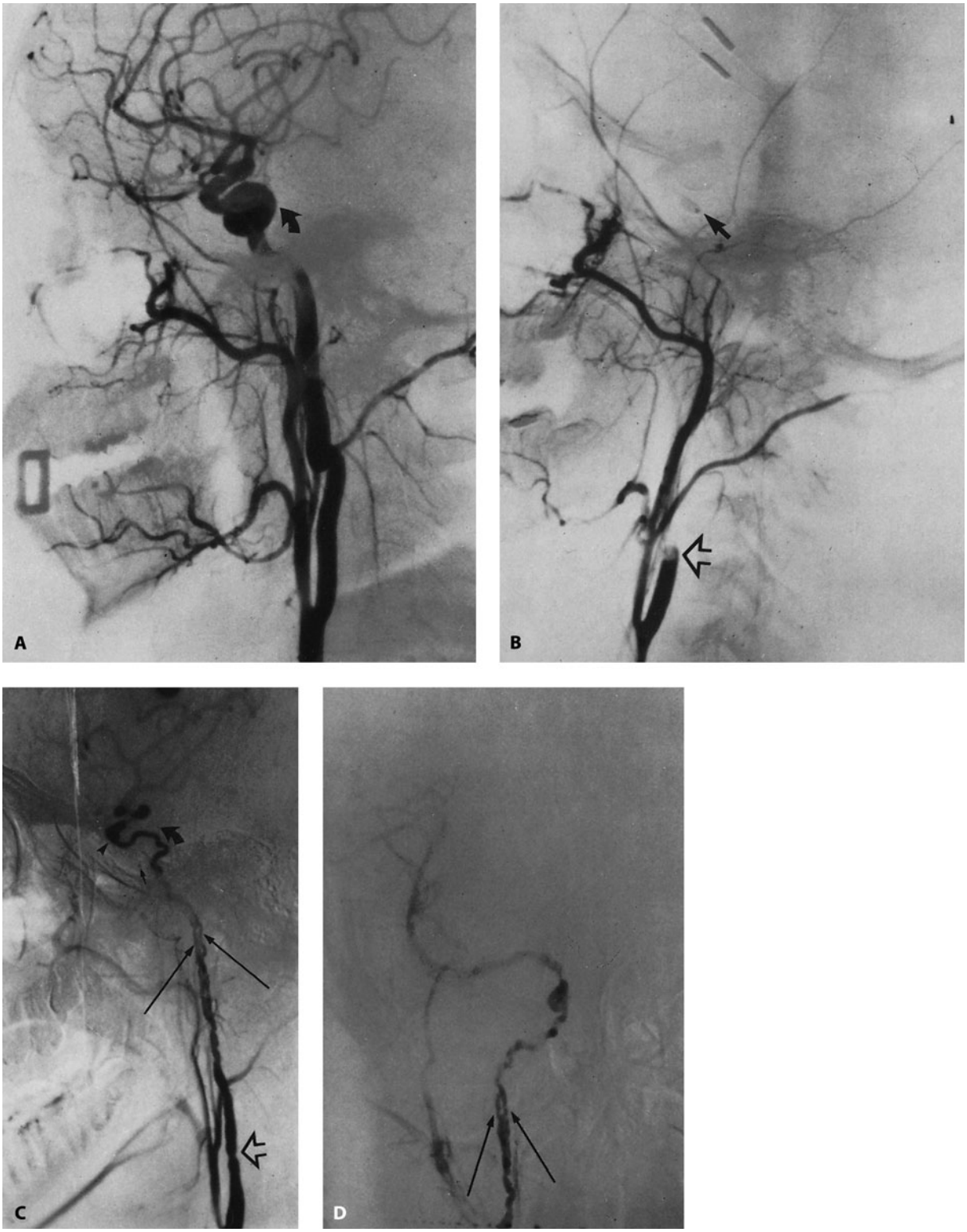

Fig. 14.52A–D. Legend see p. 979

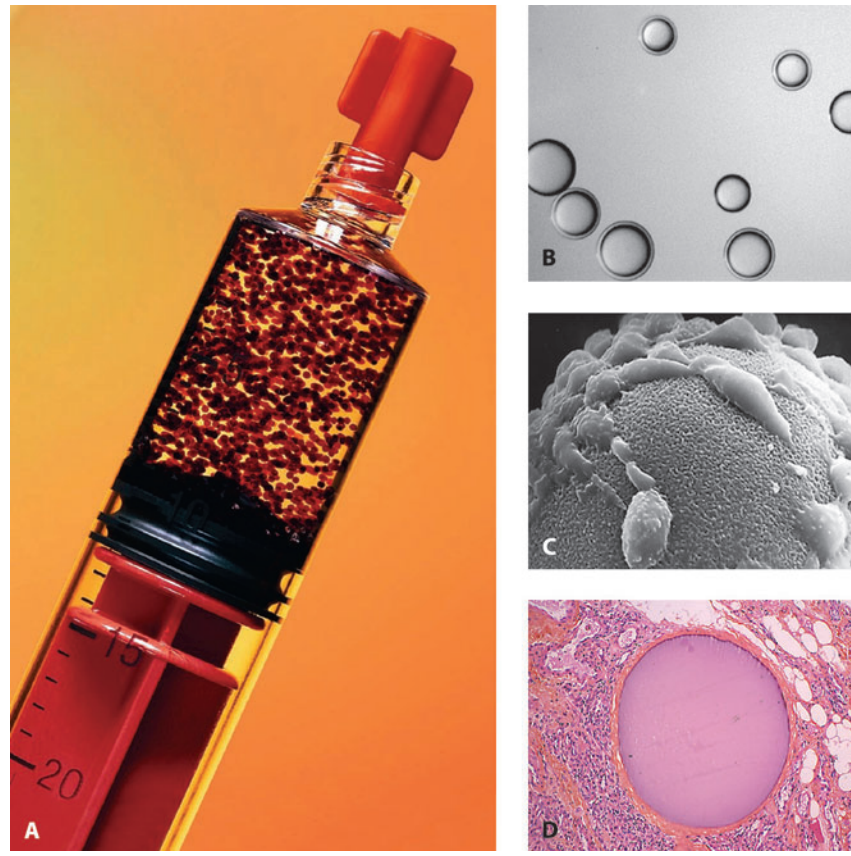

Fig. 14.53A–D. Embospheres (Biosphere Medical, Rockland, MA, USA). **A** Embospheres suspended in a 20-ml syringe. **B** Microscopic view of the uniform embospheres of various sizes. **C** Electromicroscopy of the surface of an embosphere. **D** Six-year follow-up histological examination shows complete mechanical occlusion of this inert material, with no inflammatory response. The material remains unchanged over time

◄ **Fig. 14.52A–D.** Recanalization from a prematurely deflated balloon. **A** Lateral subtraction angiogram of the common carotid artery demonstrates an internal carotid artery (ICA) cavernous sinus aneurysm (*curved arrow*). **B** Immediate postembolization common carotid artery study demonstrates a detached balloon approximately 2 cm distal to the origin of the ICA (*open arrowhead*); a second balloon is in the cavernous segment of the ICA (*arrow*). **C** Lateral and **D** frontal subtraction angiograms 3 months later demonstrate an area of narrowing where the previous proximal balloon was placed (*open arrowhead*). Two separate channels had recanalized (*arrows*). In the cavernous ICA, the recanalized lumen corresponds to the angiographic dome of the aneurysm (*curved arrow*). The ICA then acquires its normal caliber at the level of the ophthalmic artery (*arrowhead*)

14.7.1.3 Flow-Directed Particle Embolization

Coils

Gianturco Coils. Gianturco coils (Cock, Indianapolis, IN, USA) were the first coils introduced as embolic clips. Embolic coils are small pieces of guidewire with the inner core removed; a foreign body such as cotton or Dacron is added to promote thrombosis. They have very little use in head and neck embolization and may even be contraindicated if used as the main agent to obtain devascularization. In our experience, coils frequently do not produce thrombosis and become an obstacle to reaching the pathological territory with other agents. Their main uses are to protect a normal vessel or anastomosis (see Sect. 14.11; Fig. 14.123). They are easily introduced with the assistance of a conventional guidewire or a coil pusher (Cordis Endovascular; Target, Boston Scientific; Cook, Inc.) (Graves et al. 1989; Hilal et al. 1988) and can be made at various gauges and lengths. In our experience in the head and neck, very small coils, no more than 1 cm in length with a 0.90-mm diameter or smaller, are usually best.

Smaller sizes are used for microcatheters (0.010-in. and 0.016-in.) and come in multiple sizes, are straight, curved, or elliptical, and come in complex shapes, for closing vessels larger than the ID of the catheter. Fiber threads may be incorporated into the coil, to promote thrombogenicity (Figs. 14.54, 14.71).

Additional indications for coil embolizations involve the transvenous approach, for example, in dural AVMs (Halbach et al. 1989) (Fig. 14.55). We have used them in combination with transarterial acrylic embolization (Fig. 14.56, pp. 986–991), although we rarely use them in this indication. Coils may be useful as a mechanical buffer to retain more thrombogenic agents such as acrylic and reduce the chances of distal migration (Berenstein et al. 1990) (Fig. 14.57, pp. 991, 992).

Fiber Coils. Fiber threads may be incorporated in to the coil to promote thrombogenicity (Fig. 14.54B). In addition, fewer fiber coils would be needed to achieve vessel occlusion, as compared with bare platinum coils. When pushed, the fibers increase friction slightly [also see Vortex, a fiber coil with a Guglielmi detachable coil (GDC) electric detachment (Target, Boston Scientific)].

Liquid Coils. So-called liquid coils are very supple injectable coils that will conform better to the container. They will therefore pack denser at the desired location. Liquid coils can easily injected through conventional microcatheters and can also be injected through flow-guided microcatheters. They come in two diameters: 0.016 in. for 0.018-in. microcatheters and 0.08 in. for 0.014-in. and 0.010-in. microcatheters. The 10 coil is recommended in all flow-guided microcatheters down to the 1.5-F (Fig. 14.58, p. 993).

They can be used for various needs: to act as a buffer during the closure of a high-flow fistula or to prevent other embolics from migrating to the venous side (Fig. 14.59, pp. 993). They can be used to redistribute flow in a territory, to protect a normal area from being permeated by other embolic materials such as acrylic, and prevent distal embolization with potential tissue damage (Fig. 14.60, pp. 994, 995). Liquid coils can be used to

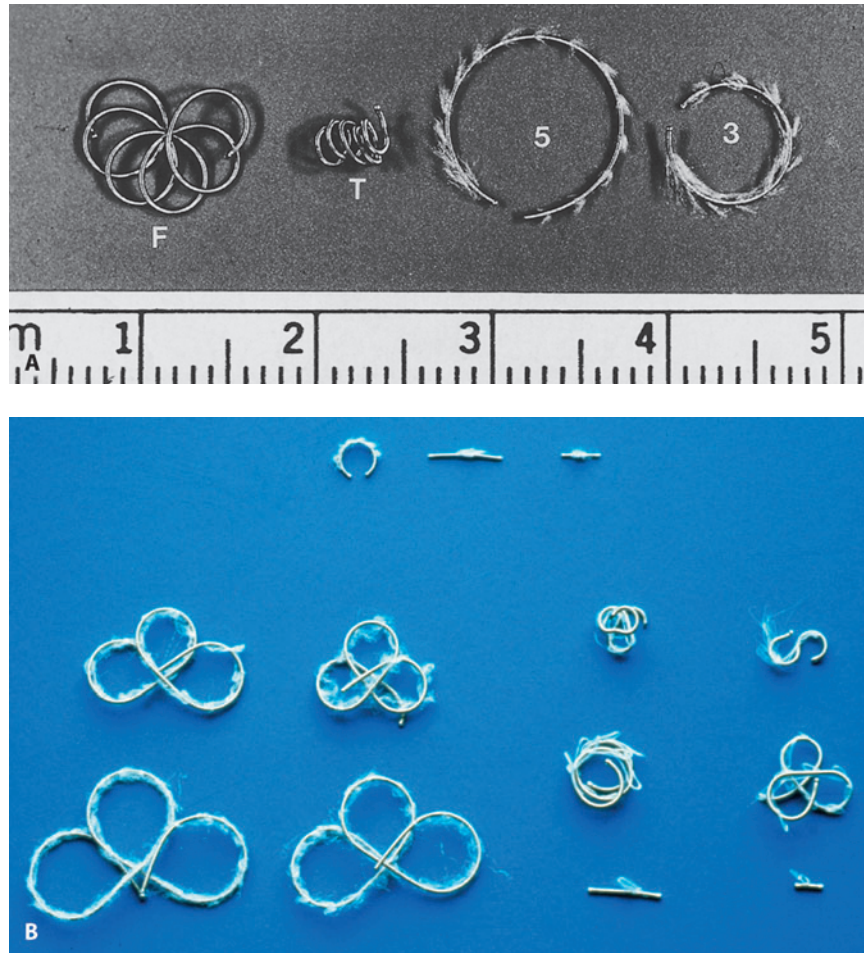

Fig. 14.54A, B. Microcoils for cerebral embolization at present are made of a very soft platinum wire and come in 0.015-in. (0.36-mm) and 0.010-in. (0.25-mm) gauges and in a multitude of lengths. **A** Various coils: *F*, flower; *T*, Target coil; *5*, Hilal 5-mm fiber coil; *3*, Hilal 3-mm fiber coil. **B** Target Therapeutics platinum fiber coils of various configurations, elliptical to straight. (also see Fig. 14.63, GDC; Fig. 14.71, Vortex; Fig. 14.73, Microus; Fig. 14.74, Cook; Fig. 14.75, Cordis; Fig. 14.76, Microvention)

supplement the packing and enhance thrombogenicity of larger vascular compartments, for example, in the obliteration of a vein or sinus in dural arteriovenous shunt (DAVS) (Fig. 14.61, pp. 996, 997).

Detachable Coils. Coils that can be detached at will and can be repositioned, retrieved, or changed, a great advantage if the coil is not at the desired position or not of the optimal size prior to detachment. These devices address many of the mechanical problems of treating aneurysms via an endovascular route and at present are the treatment of choice in a great majority of patients with various types of aneurysms, certain AVFs, vessel occlusion, and in the transvenous approach to some DAVSs.

The original detachable coil design requires a ratio between the neck and the dome of the aneurysm that will allow the coil to remain in the sac of the aneurysm. Proper coil size is one that is large enough and long enough to allow the coil to brake and remain stable within the aneurysm, creating a scaffold or frame for additional coiling (Fig. 14.62, p. 998).

For aneurysms with a broad neck or with a poor neck-to-dome ratio, the addition of two-dimensional (2-D) and three-dimensional (3-D) coil configurations (Target, Boston Scientific; Cordis Endovascular, Micrus Corporation, Mountain View, CA, USA), balloon remodeling, and neck bridges are useful.

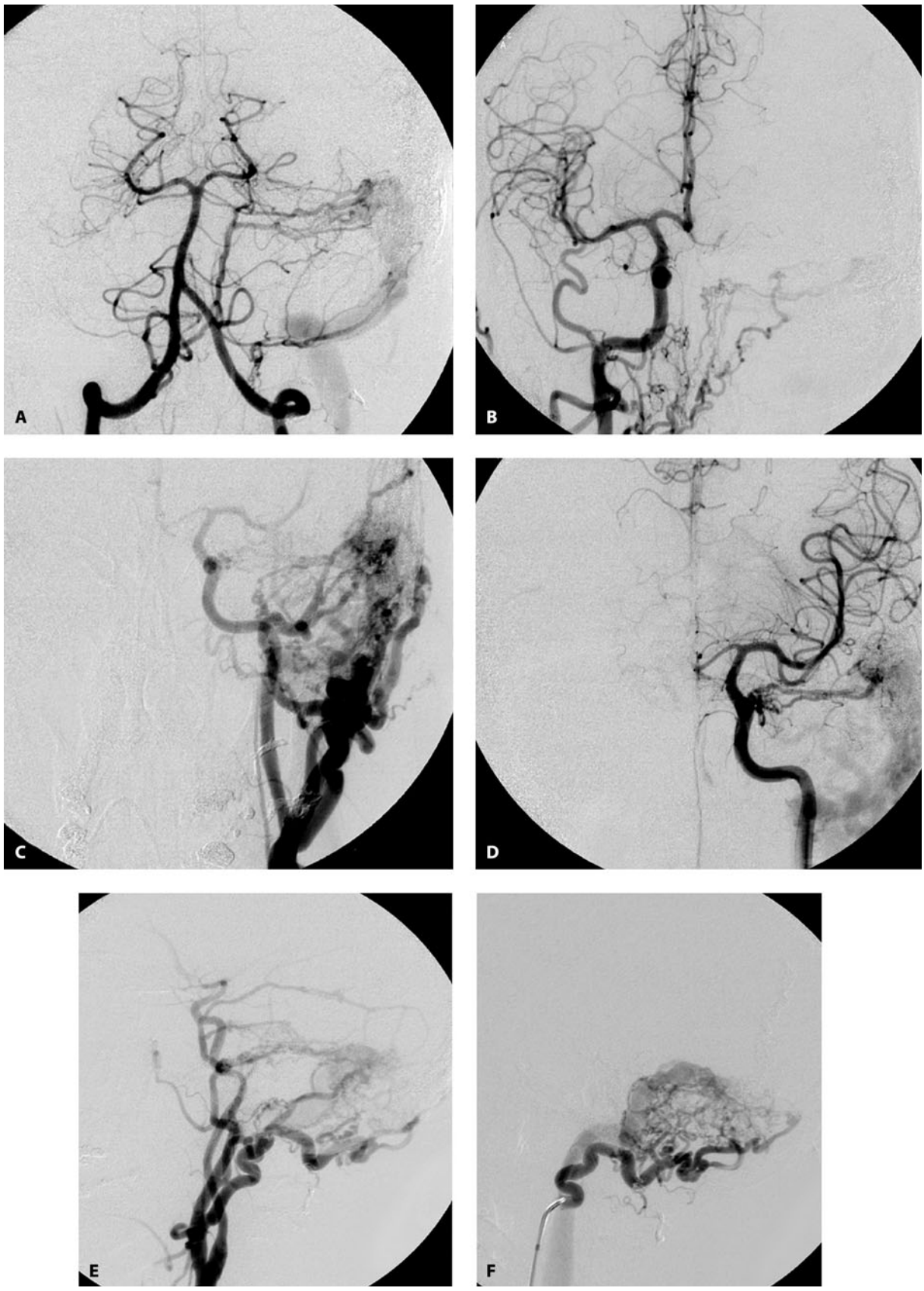

Fig. 14.55A–F. Legend see p. 983

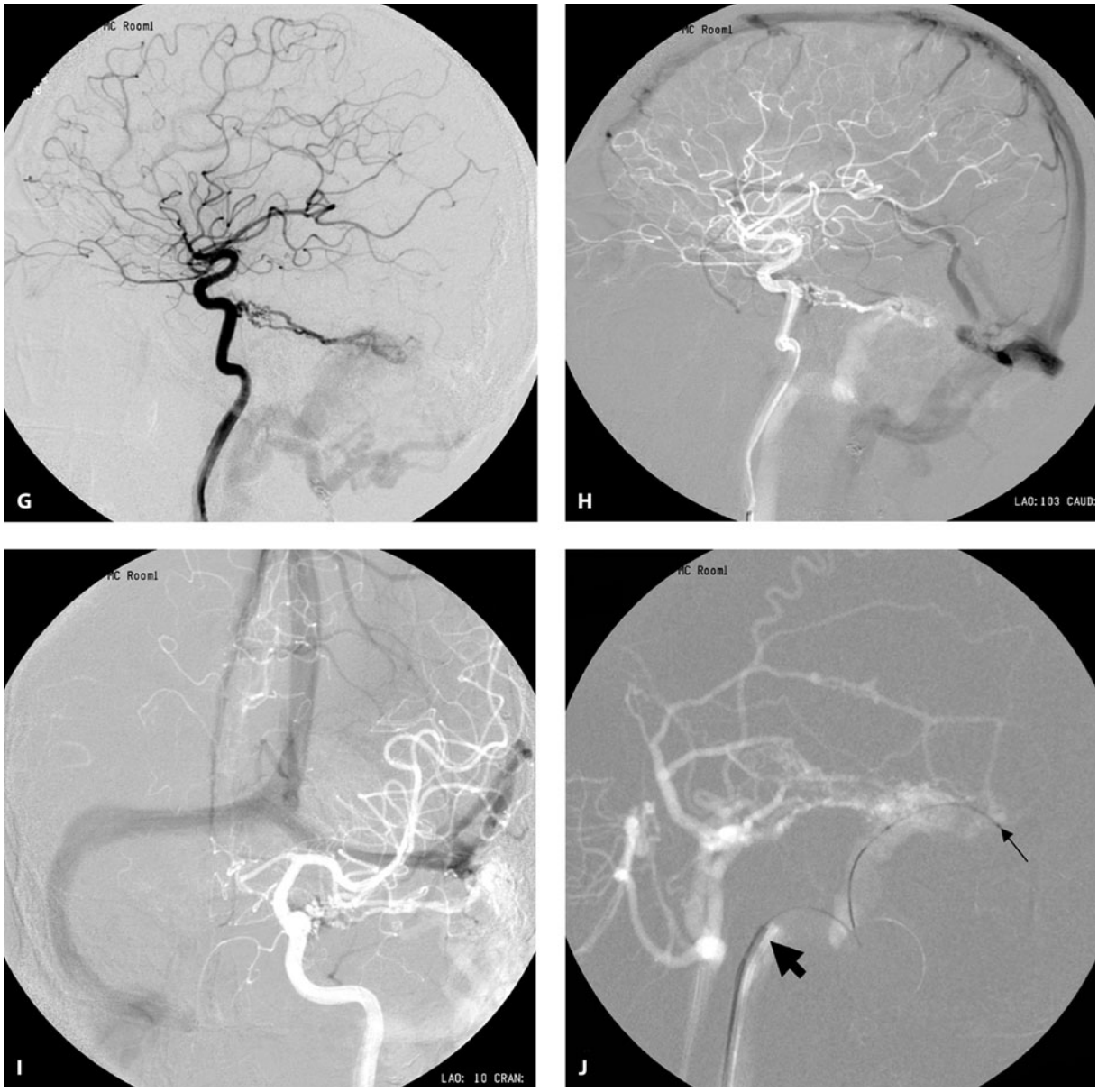

◄ **Fig. 14.55A–S.** Dural arteriovenous malformation treated with coils by a transvenous approach. **A** Frontal digital subtraction angiogram (DSA) of the right vertebral artery demonstrates the supply thorough the cerebellar falcine artery and C3 meningeal branches supplying the left dural vascular malformation of the junction between transverse and sigmoid sinus. **B** Frontal DSA of the left common carotid artery shows the supply across the midline from the external carotid artery via the occipital and ascending pharyngeal arteries. **C** Frontal DSA of the left common carotid artery. **D** Frontal DSA of the left internal carotid artery showing the basal tentorial C5 supply. **E** Lateral DSA of the left common carotid artery early phase. **F** Lateral DSA of the occipital artery injection, early phase. **G** Lateral DSA of the left internal carotid artery showing the C5 basal tentorial supply. The areas of fistulization are in the transverse-sigmoid junction. **H** Lateral and **I** frontal road map images of the left internal carotid artery demonstrating the C5 entrance to the fistula site and the entrance of the vein of Labbe. **J** Lateral road map image showing the tip of the microcatheter (*small arrow*) at the fistula site and the coaxial catheter at the jugular vein (*large arrow*). **K–S** see pp. 984, 985

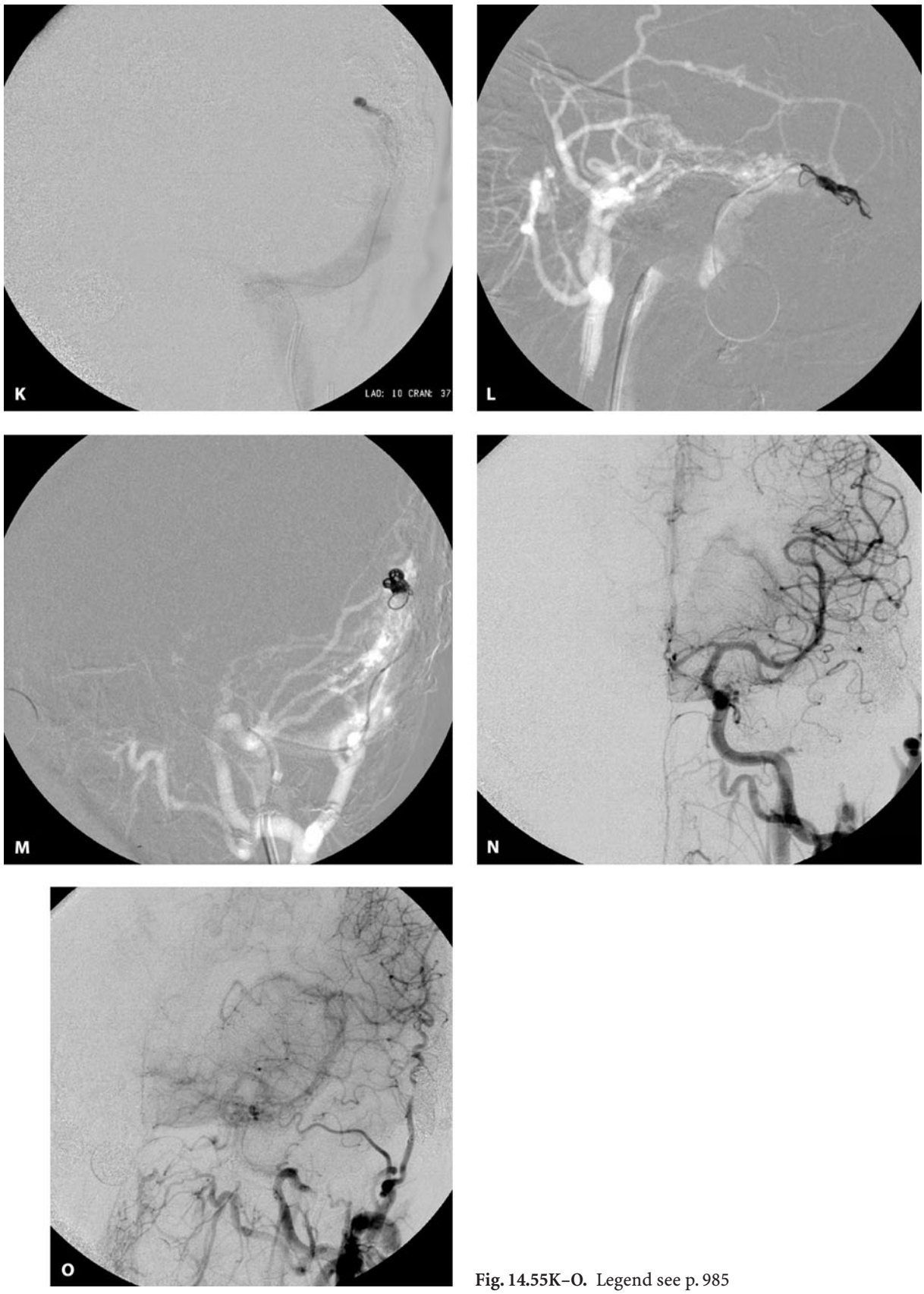

Fig. 14.55K–O. Legend see p. 985

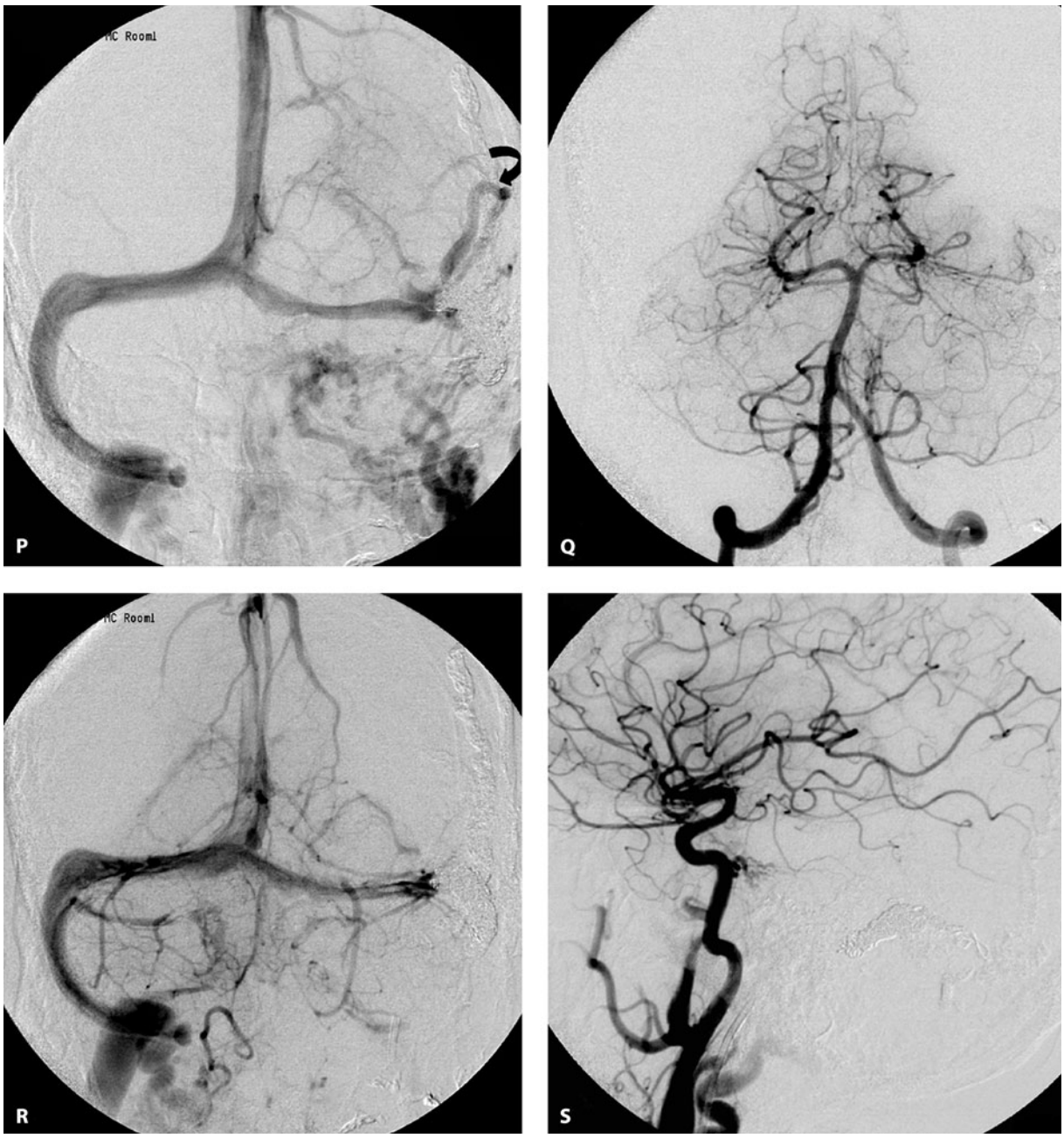

◄ **Fig. 14.55** (*continued*). **K** Frontal DSA showing contrast injection at the fistula site. **L** Lateral and **M** frontal road map images showing the placement of the coils at the fistula site. **N** Frontal DSA of the left common carotid artery after treatment shows no filling of the malformation. **O** Frontal DSA of the left external carotid artery shows no supply to the malformation. **P** Frontal DSA of the left common carotid artery, late phase, shows the venous drainage of the brain and exclusion of the segment of the left transverse sigmoid sinus on the left and preservation of the vein of Labbe; compare with **I** (*curved arrow*). **Q** Frontal DSA of the right vertebral artery in early and **R** late phase confirmed the total regression of the supply to the dural shunt and the total occlusion. **S** Lateral DSA of the left common carotid artery after treatment shows the regression of all the external carotid artery supply, confirming the total obliteration

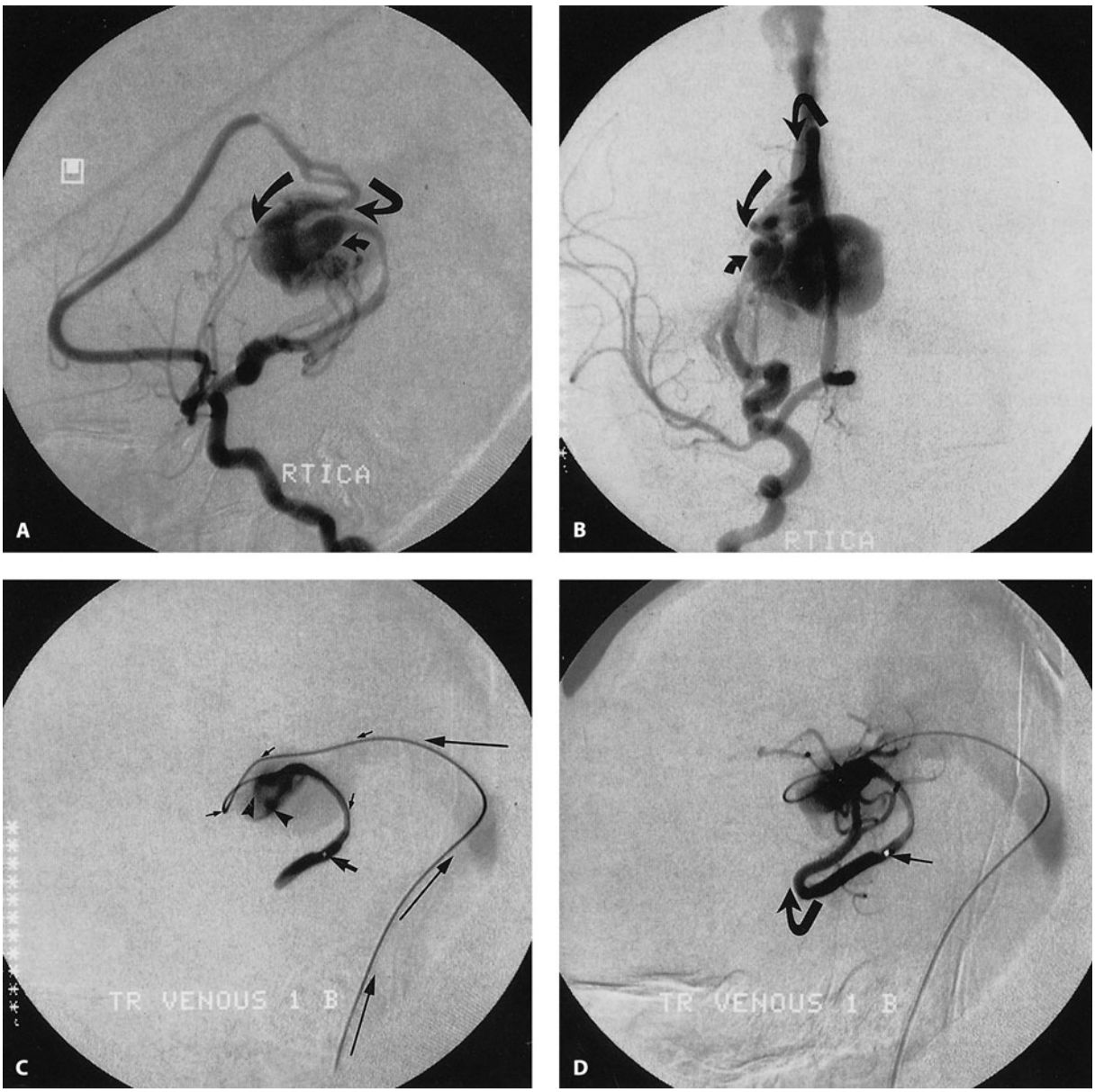

Fig. 14.56A–U. Microcoils used in the management of a vein of Galen aneurysmal malformation by the transvenous and transarterial approach in combination with NBCA. **A** Lateral and **B** frontal digital subtraction angiogram (DSA) examinations of the right internal carotid artery demonstrate the choroidal branch of the anterior cerebral artery (*curved arrows*) entering a choroidal fissure vein (*large curved arrows*). Additional supply is seen from a posterior medial choroidal artery entering another fistulization (*small curved arrow*). **C** Lasjaunias 4-F catheter (nontapered tip) introduced through the femoral vein up to the falcine sinus (*large arrows*) and coaxial introduction of a Tracker 18 (*small arrows*), obtaining superselective catheterization of the posterior medial choroidal artery on the right (*arrow*). Contrast material injection demonstrates in a retrograde manner two sites of fistulization (*arrowheads*). Compare with **A**. **D** Later phase of the same injection. The tip of the microcatheter (*arrow*) shows retrograde flow to a second choroidal artery (*curved arrow*) filling multiple normal branches. **E–U** see pp. 987–991

Fig. 14.56 (*continued*). **E** DSA image of the progressive deposition of a 3-mm Hilal coil (*arrowhead*), which exits the tip of the microcatheter (*arrow*). **F** A second coil (*double arrowheads*) is still within the catheter shaft. The coils can be advanced with a coil pusher (Target Therapeutics) or more progressive injections of saline can be used, whichever is more stable. **G** Four 5-mm and two 3-mm coils have been extruded (*arrowheads*). Contrast material injection demonstrates considerable slowing of flow and two additional fistulizations (*arrows*) entering a fissure vein (*curved arrow*). **H** Retrograde injection of NBCA to seal off this fistulization (*small arrows*) around the microcoils (*arrowheads*). **I–U** see pp. 988–991

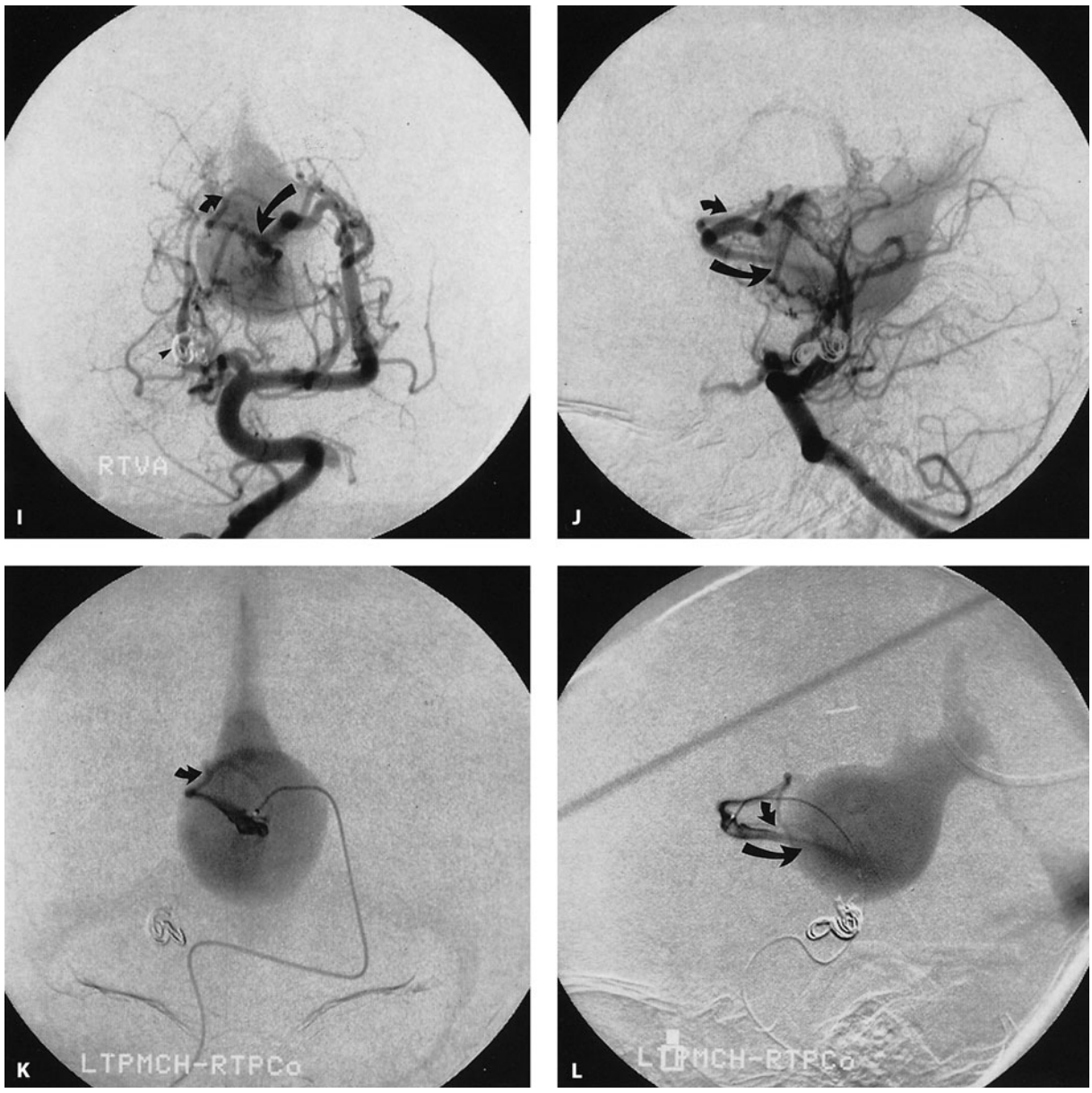

Fig. 14.56 (*continued*). **I** Frontal and **J** lateral DSA examinations of the right vertebral artery after embolization by the venous approach, demonstrating a right-side medial choroidal artery supply with two pedicles (*large curved* and *small curved arrow*). Note the previous coils on the right side (*arrowhead*). **K** Frontal and **L** lateral DSA examinations of the superselective injection of the left posterior medial choroidal artery (compare with **I** and **J**). Note the larger (*large curved arrow*) and smaller (*small curved arrow*) fistulizations with significant flow. **M–U** see pp. 989–991

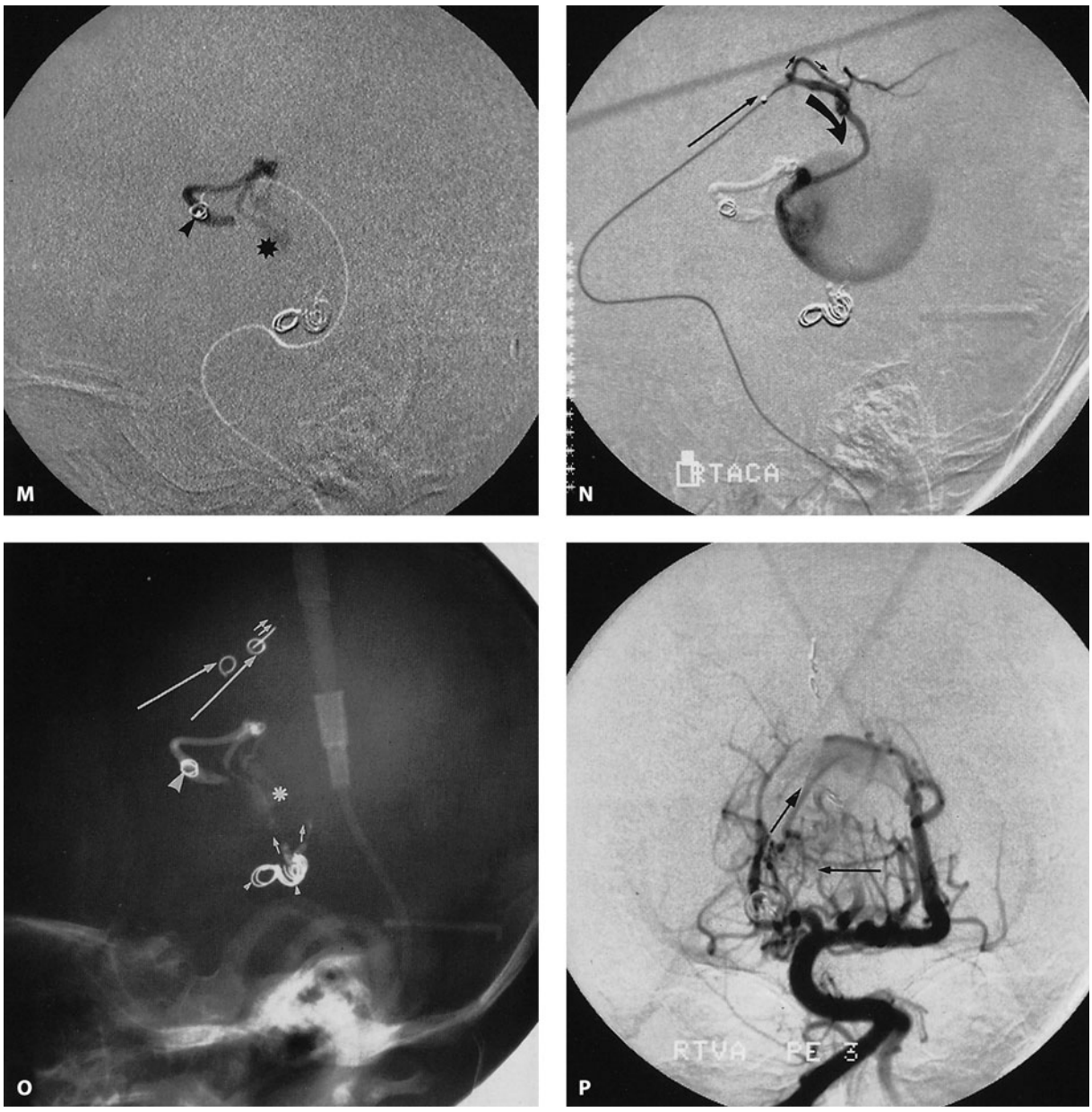

Fig. 14.56 (*continued*). **M** DSA image of the NBCA cast obtained after a transarterial coil (*arrowhead*) was extruded to slow down the flow prior to the NBCA injection. Note the NBCA deposition into the two fistulizations and entering the aneurysmal vein (*). **N** Lateral DSA of the superselective injection of the anterior cerebral artery in the same patient demonstrates the choroidal branch of the anterior cerebral artery reaching the fistula (*curved arrow*) and a normal branch to the singular gyrus (*small arrows*). The microcatheter tip (*long arrow*) could not negotiate the curve toward the choroidal branch. **O** Plain film of the skull, which demonstrates a straight Hilal microcoil in the proximal aspect of the normal anterior cerebral artery branch for protection (*double small arrows*). Two 3-mm curved coils are sealing the pericallosal supply (no acrylic was used because the coils produced proximal occlusion). Note the coils on the right choroidal side (*small arrowheads*), with the acrylic (*small arrows* and compare to **H**) and the embolization of the medial choroidal artery on the left (compare to **L** and **M**). There is acrylic on the venous side (*). **P** Frontal DSA of the right vertebral artery after embolization demonstrates almost complete obliteration of the malformation. There is minimal supply from a medial choroidal artery on the left (*long small arrow*) as it enters the fistulization (*long arrow*). **Q–U** see p. 990, 991

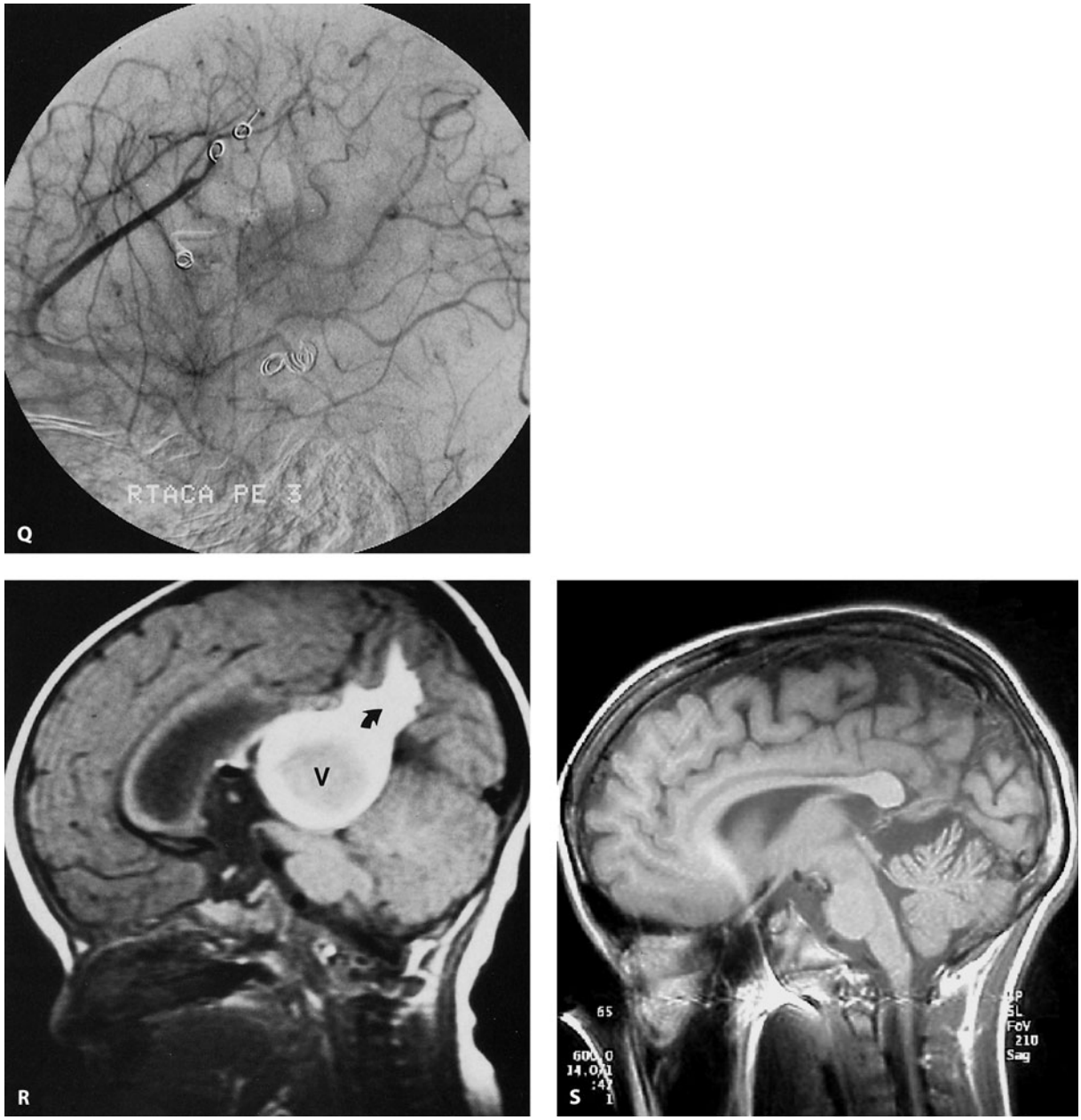

Fig. 14.56 (*continued*). **Q** Lateral DSA of the right internal carotid artery in late phase after embolization. Note the occlusion of the pericallosal artery supply and no filling of the malformation. **R** Follow-up MRI 3 weeks later shows complete thrombosis of the aneurysmal vein (*V*) and falcine sinus (*curved arrow*). The thrombosed vein disappeared, as shown on a 1-year follow up MRI (**S**). **T–U** see p. 991

Fig. 14.56 (*continued*). The child was normal at 5 years of age (**T**)and at 12 years of age (**U**)

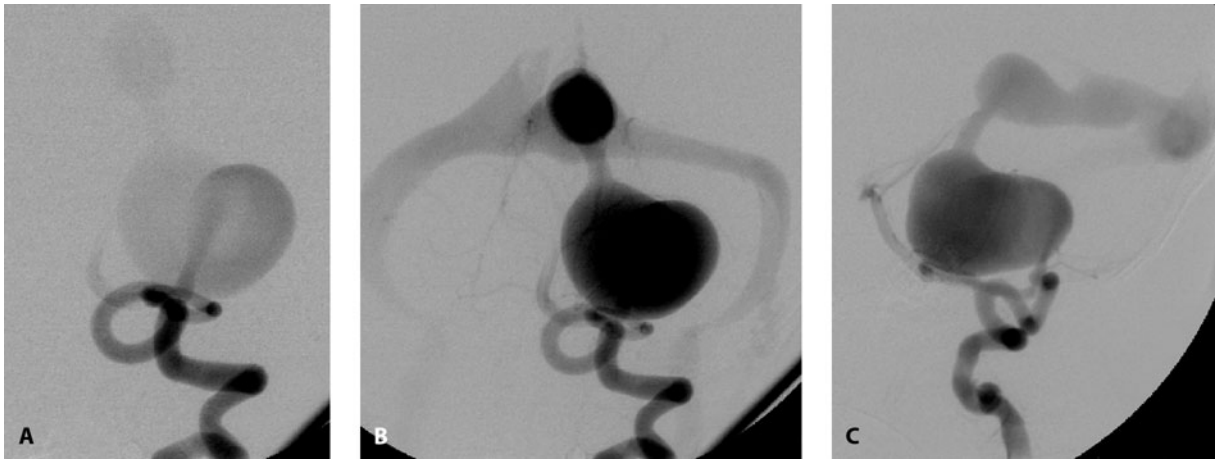

Fig. 14.57A–I. Coils and glue combination. High-flow fistula from the posterior inferior cerebellar artery toward an aneurysmally dilated lateral pontomesencephalic venous system. **A** Frontal early phase. **B** Later phase, frontal view. **C** Lateral view, mid-arterial phase demonstrates a high-flow fistula from the posterior inferior cerebellar artery to an aneurysmally dilated lateral pontomesencephalic vein that then drained through the tentorium (anatomical restriction) into the deep venous system. **D** Lateral road map with the first coil frame placed within the aneurysmal sac. **E** Intermediate angiogram after several coils had been placed as a buffer prior to glue embolization, which decreases the chances for distal migration of the acrylic. **F** Last image hold after NBCA deposition as the radiopaque material is trapped within the dense coil mesh (*arrows*). **G** Frontal, **H** lateral arterial phase, and **I** late phase of the same injection after embolization angiogram shows the total obliteration of the lesion. **D–I** see p. 992

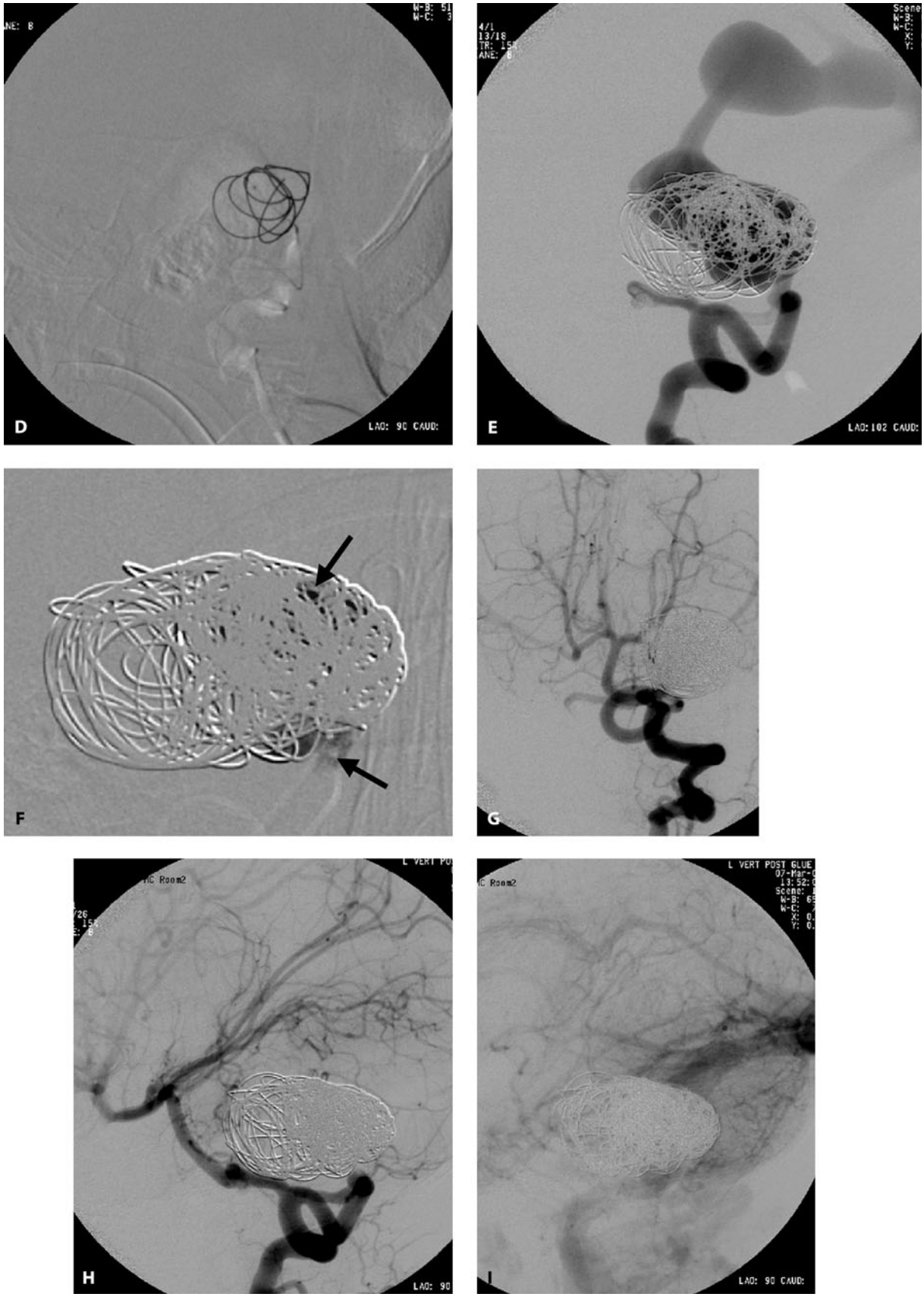

Fig. 14.57D–I. Legend see p. 991

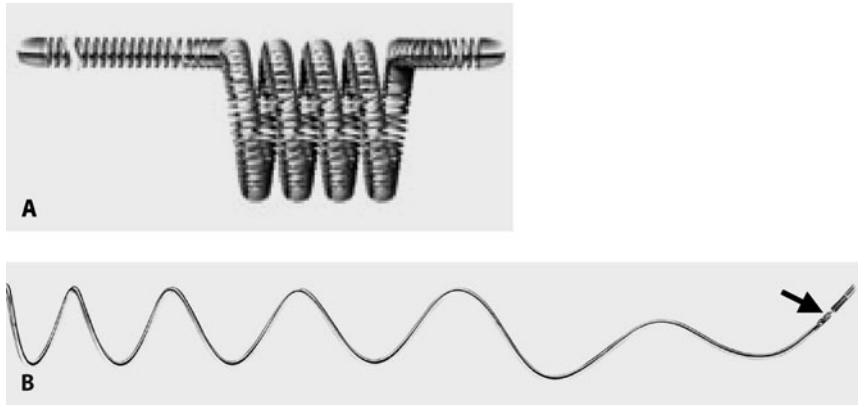

Fig. 14.58A, B. Berenstein liquid coil (BLC; Target, Boston Scientific) **A** Close-up view of the distal segment of the liquid coil. This shape prevents distal migration of the coil. **B** Detachable variation (ultrasoft) with a GDC segment (*arrow*)

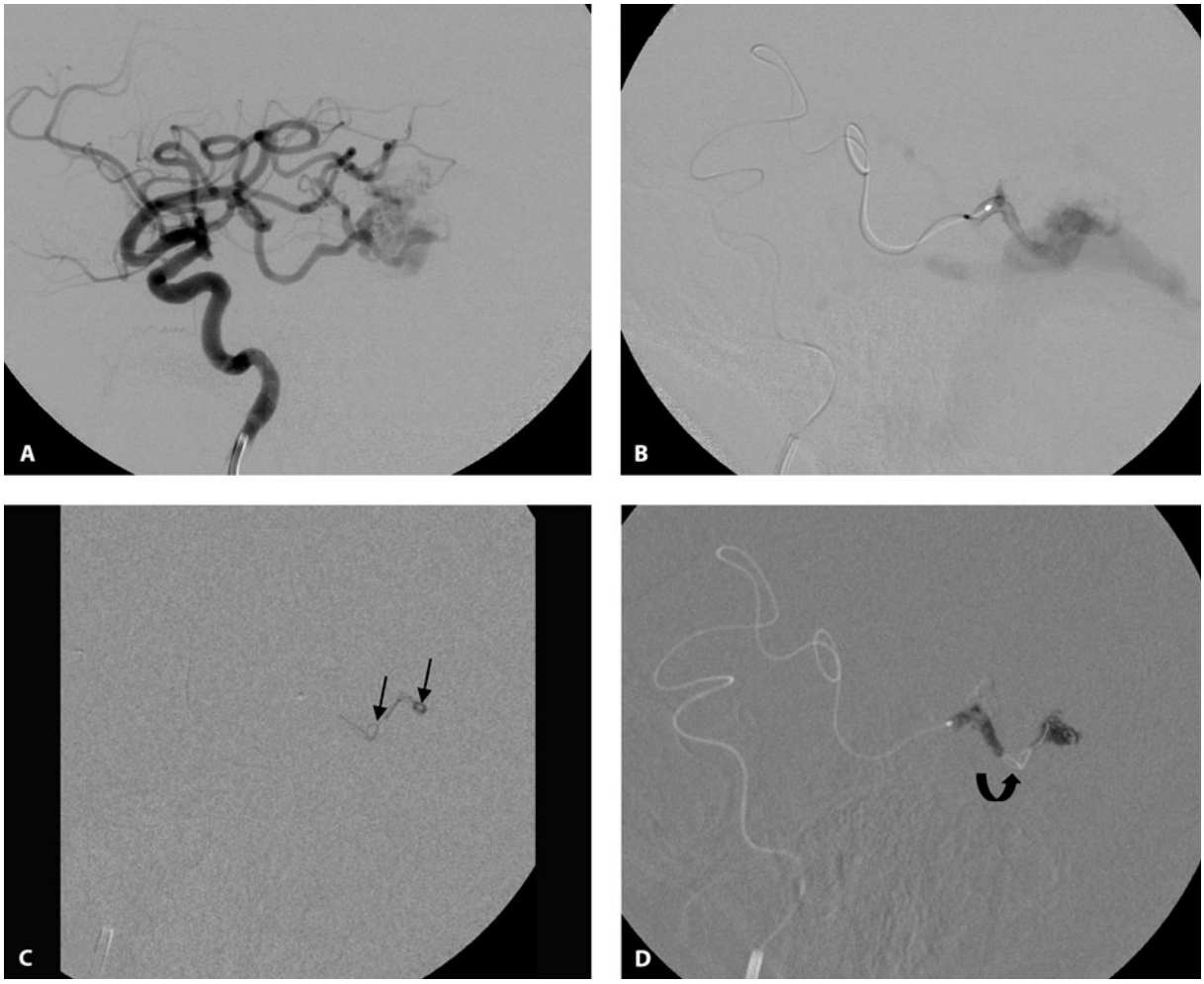

Fig. 14.59A–D. Berenstein liquid coil prior to acrylic embolization of a high-flow fistula within the nidus of a brain arteriovenous malformation (AVM). **A** Lateral digital subtraction angiogram of the left internal carotid artery in a posterior temporal arteriovenous malformation. **B** Superselective injection of the main pedicle supplying the malformation in a fistula fashion. **C** Last image hold from a road map demonstrating two liquid coils at the entrance of the fistula (*arrows*). **D** Last image hold after NBCA deposition. Note the ability of the coils to trap the glue, preventing distal migration. Also note movement of the lower coil by the glue cast (*curved arrow*)

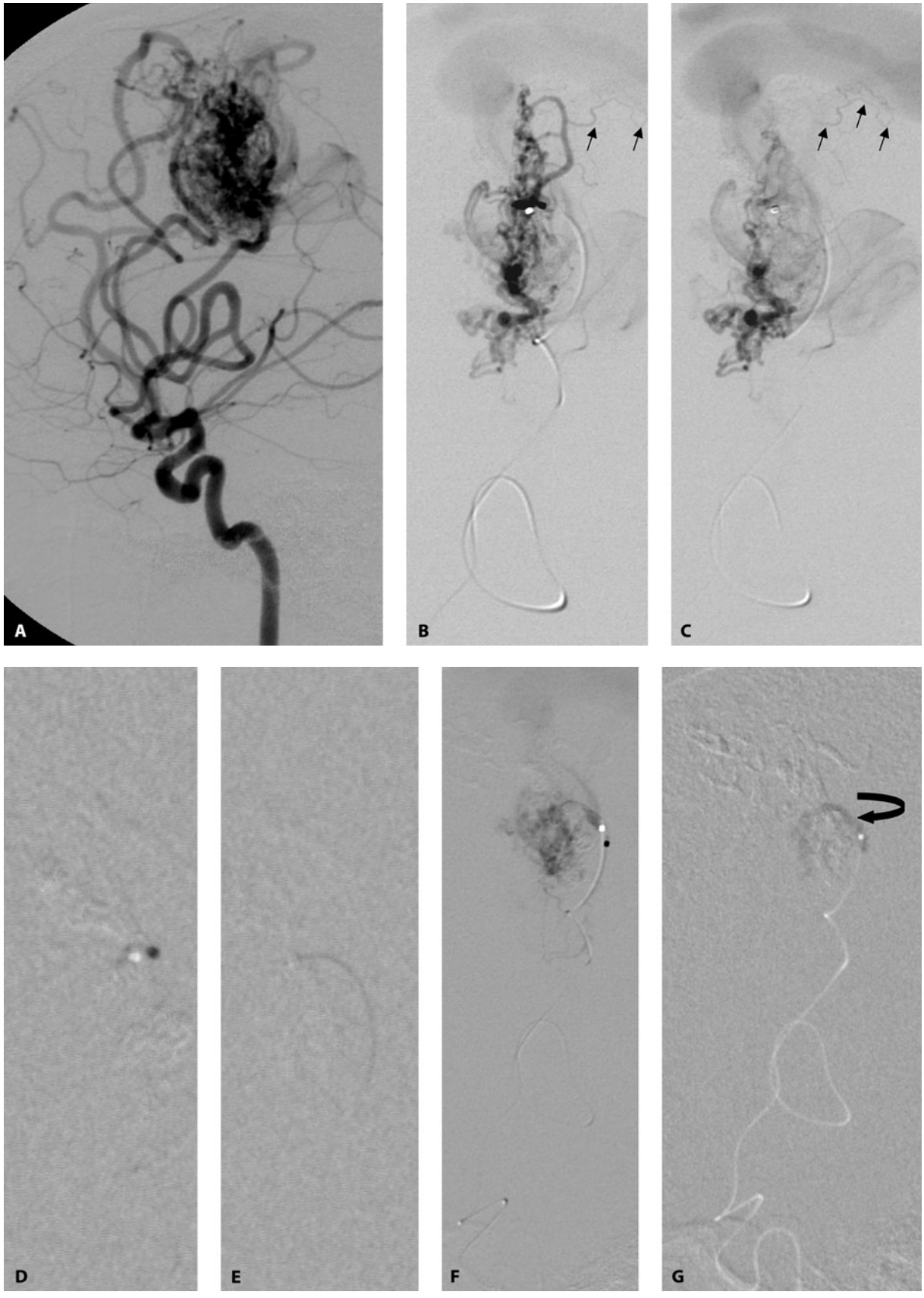

Fig. 14.60A–G. Legend see p. 995

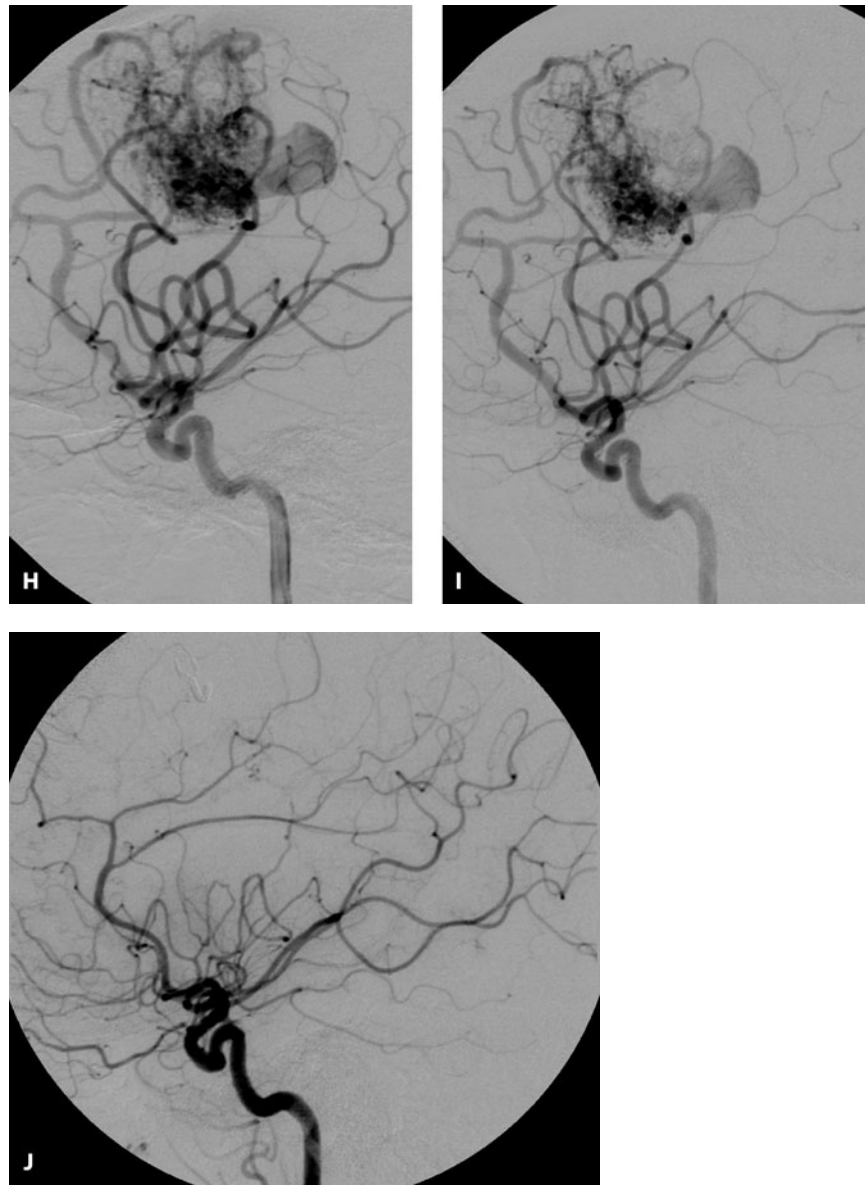

◄ **Fig. 14.60A–J.** Use of Berenstein liquid coils (BLC) in distal cerebral embolization at the cortex level. There must be collateral circulation at the distal territory to prevent complications. **A** Lateral digital subtraction angiogram (DSA) of the right internal carotid artery demonstrates an arteriovenous malformation close to the motor area. **B, C** Mid and late DSA studies of the superselective injection in the posterior branch supplying the malformation in an indirect fashion with supply *en passage* anteriorly. Note the gyral anastomosis through a long anastomotic artery of Duvernua (*small arrows*), which anastomosed to the normal territory. **D, E** Cone-down views of the injection of two liquid coils to protect the distal normal territory. **F** Superselective injection following the two BLC deployments demonstrates the filling of the malformation, with no filling of the more distal normal territory. **G** Last image hold from the road map demonstrating the cast of the injection of NBCA (*curved arrow*). **H** Intermediate lateral DSA run demonstrating devascularization of the upper portion of the malformation (compare to **A**). **I** After additional NBCA injection note the preservation of the normal arterial system and devascularization of nidus (compare to **A**). **J** Lateral DSA after surgical excision of the residual malformation

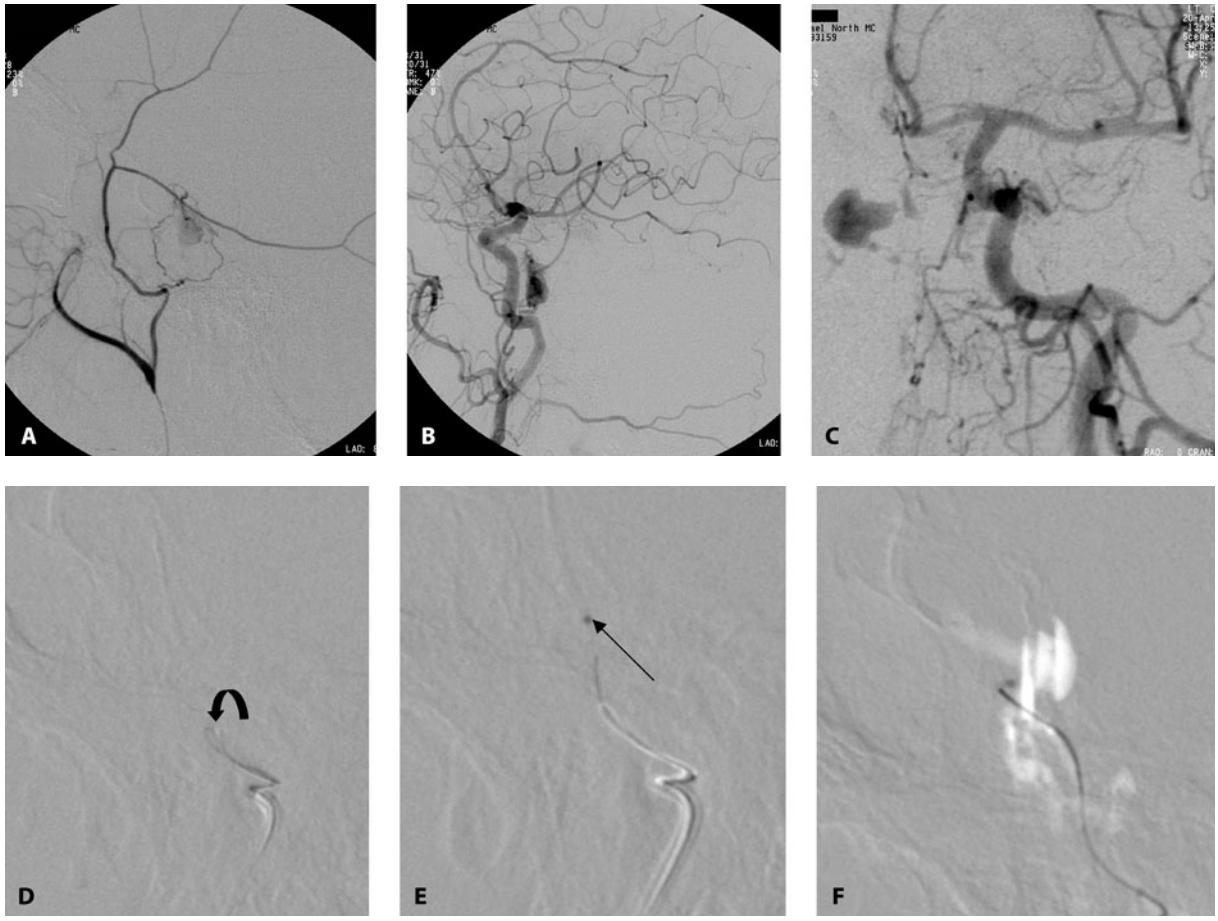

Fig. 14.61A–J. Dural arteriovenous malformation of the cavernous sinus treated by transvenous approach. **A** Lateral digital subtraction angiogram (DSA) of the distal right external carotid artery lateral view demonstrates the petrosal branch of the middle meningeal artery reaching the dural shunt. **B** Lateral DSA of the left common carotid artery in lateral view and **C** in frontal view demonstrates the transclival supply to the dural shunt in the right cavernous sinus region. Note the outflow restriction and impaired drainage of the shunt. **D–G** Sequential road map images of the transvenous approach. Note the progressive ability to mechanically recanalize the nonopacified inferior petrosal sinus using a catheter-guidewire technique (*arrow* in **D** points to the J wire as the leader in reanalyzing the occluded sinus). **E** The tip of the microcatheter reaches the posterior cavernous sinus (*arrow*). **F** Road map injection of the left internal carotid artery showing the stagnation of contrast in the posterior cavernous sinus and the microcatheter reaching that location. **G–J** see p. 997

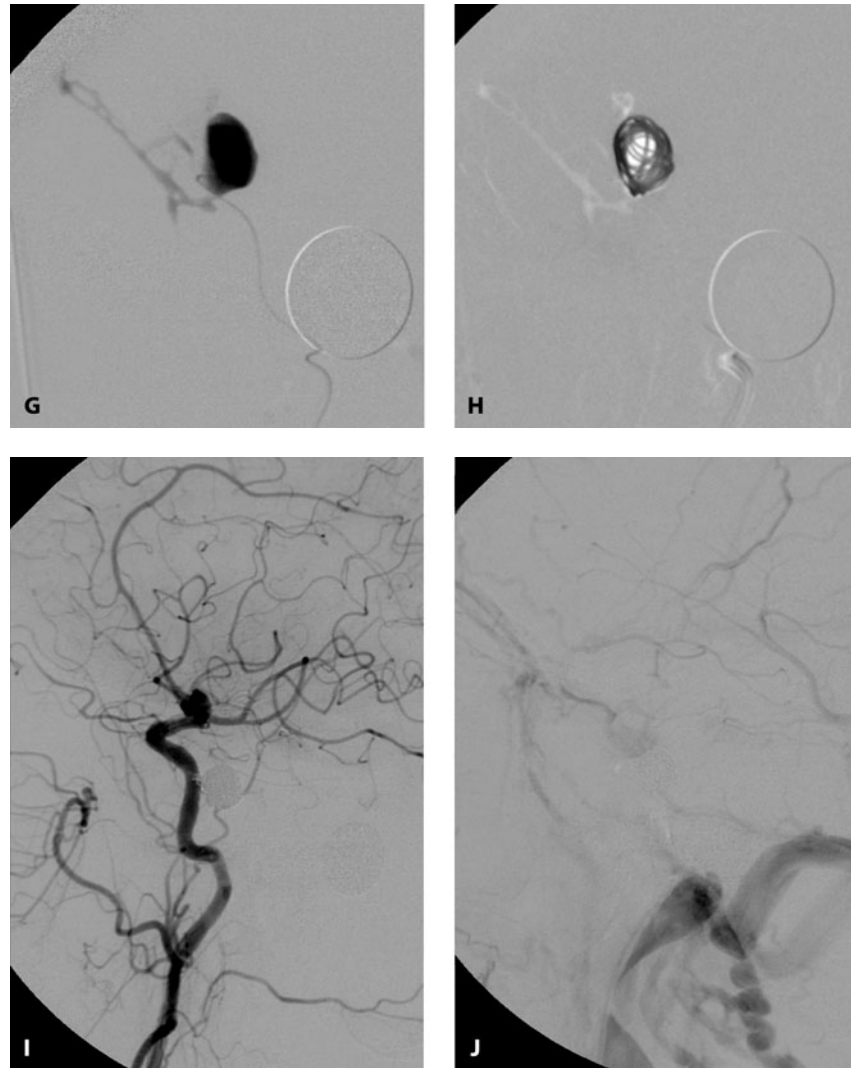

Fig. 14.61 (*continued*). **G** Contrast material injection through the microcatheter, confirming its location in the venous sac. **H** First coil framing the cavernous sinus compartment. **I** DSA lateral view of the common carotid artery in mid-arterial phase and **J** late venous phase after embolization show total obliteration of the shunt

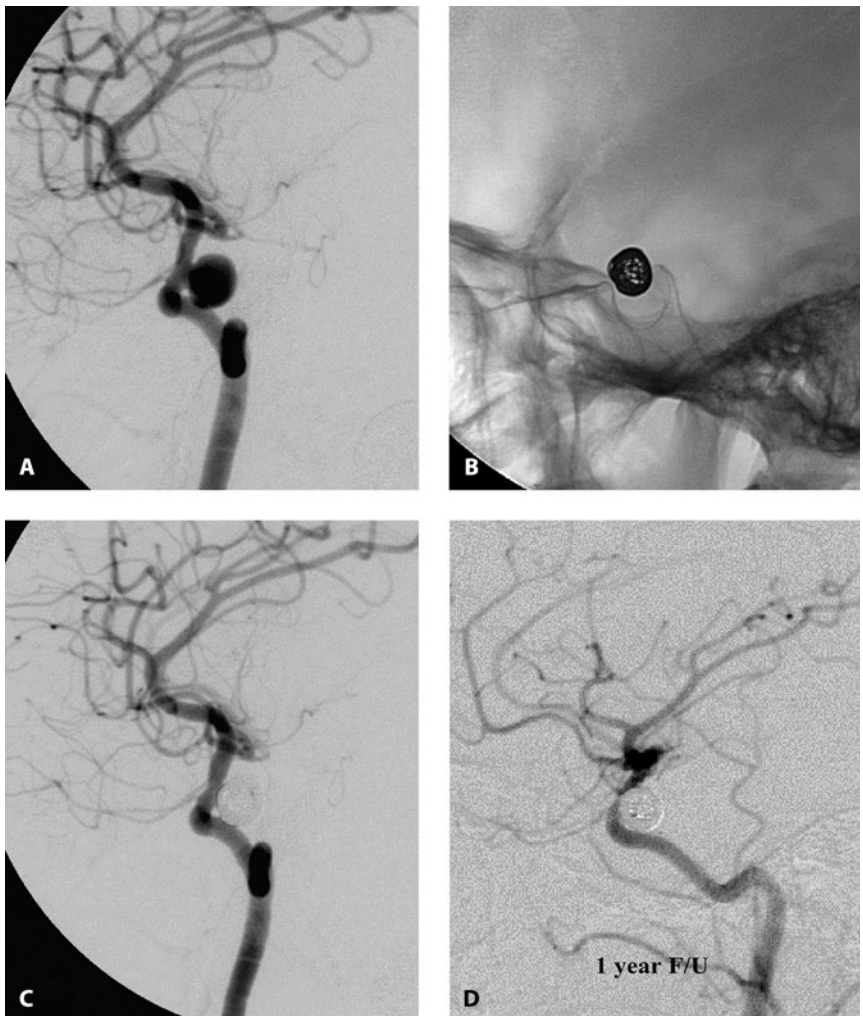

Fig. 14.62A–D. Hypophysial aneurysm. **A** Right internal carotid artery injection in the working projection demonstrates a superior hypophyseal-level aneurysm in the right internal carotid artery. **B** Plain film of the skull shows the coil break or frame of the first coil. **C** Postembolization angiogram shows total obliteration of the aneurysm. **D** One-year follow-up shows the persistence of the total obliteration. Good neck-to-aneurysm ratios are ideal for Guglielmi detachable coils (GDC), where the small neck allows healing with long-term efficacy

Guglielmi Detachable Electrolytic Coils

Guglielmi (1991) introduced a platinum detachable coil: the Guglielmi detachable coil (GDC; Target, Boston Scientific) (Figs. 14.62 and 14.63). Monopolar electrical current activates detachment. At a current of 1 mV, electrolysis occurs at the junction between the platinum coil and the stainless steel mandrill of the guidewire, thereby detaching the coil, usually in less than 1 min (Fig. 14.64) (Synergy, Boston Scientific).

The distal tip of the coil becomes positively charged, in contrast to the cellular elements of blood and the vascular endothelium, which are negatively charged. As the coil is activated, there is a mild attraction of the negatively charged cellular elements.

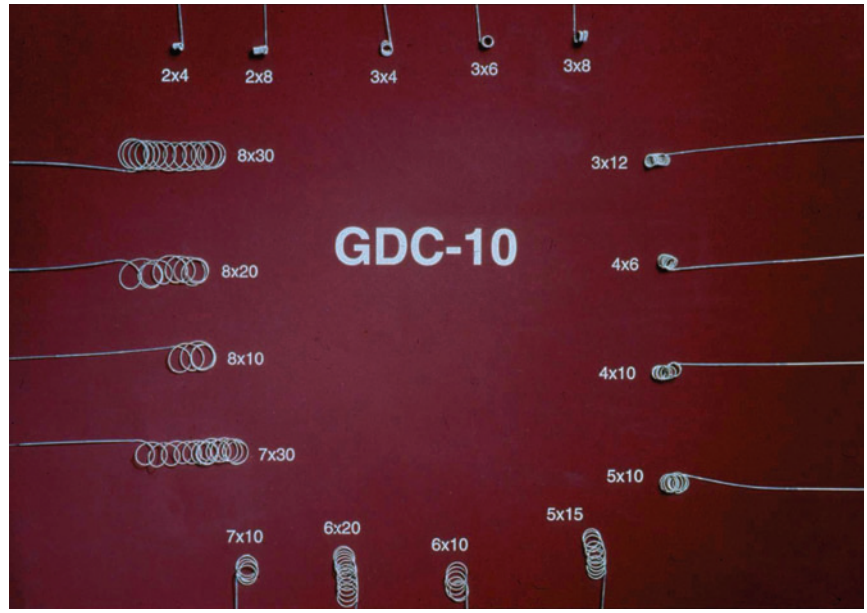

Fig. 14.63. Guglielmi detachable coil (GDC). Example of the multiple sizes and lengths of the helical 0.010-in. coils. There are also multiple sizes and lengths in the larger gauge 0.018-in. GDCs (not shown)

Fig. 14.64A–C. GDC detachment mechanism. **A** Power box. **B** Helical coil. The detachment zone is the transition between the stainless steel delivery mandril and the platinum coil. **C** Close-up of the detachment zone

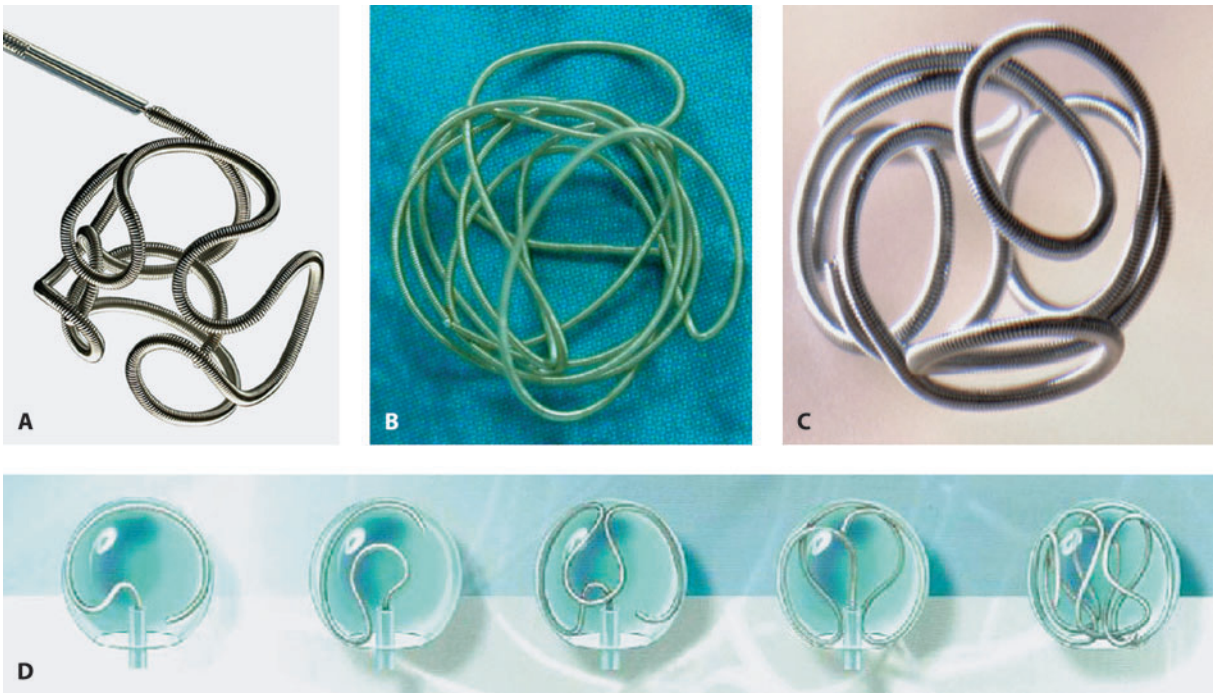

Fig. 14.65A–D. Three-dimensional coils. **A** GDC (Target, Boston Scientific). This design has an omega configuration, with one loop larger, followed by a smaller loop of coil. **B** Cordis 3-D endovascular coil. **C** Micros (Micrus Corporation) coil. **D** Glass model illustrating 3-D framing of a glass model aneurysm with the omega design (Target, Boston)

They come in a variety of sizes, lengths (Fig. 14.63), and shape memories (Figs. 14.65, 1.68).

For the most part, we start with the 3-D shape memory coil, as the framing or scaffold (Fig. 14.66). We usually take the maximum diameter of the aneurysm as the guideline, or we may even oversize it by 1 mm, mostly in unruptured cases, whereas in the acute phase following SAH, we may undersize the first coil, mostly if there is a good neck-to-dome ratio. In general, in acute cases we have preferred the 0.010-in. coils, which are softer and less traumatic. It is important to try to match the delivery microcatheter ID to the coil gauge; unraveling or stretching is more likely if the ID is to large. Most currently available 14-F catheters are able to deliver 0.016-in. (18 coils) and 0.010-in. coils. We also favor the stretch resistance regular, soft, and ultrasoft 10 coils (Fig. 14.67) (Target, Boston Scientific).

Stretch-resistant coils incorporate a monofilament polypropylene suture material, which prevents coil unraveling (Fig. 14. 67).

In some cases of wide neck aneurysms, the 3-D lead coil continues to protrude outwards. A 2-D coil (Fig. 14.68, p. 1003) may stay more reliably in the aneurysm, as the small size of the first revolution makes it remain inside the aneurysm sac until the coil breaks and becomes stable, fixed within the aneurysm to best frame the aneurysm sac.

In large lesions, we would favor the use of an 18 catheter or a 14 microcatheter that accepts 18 coils (0.016-in. true diameter), and start with 18

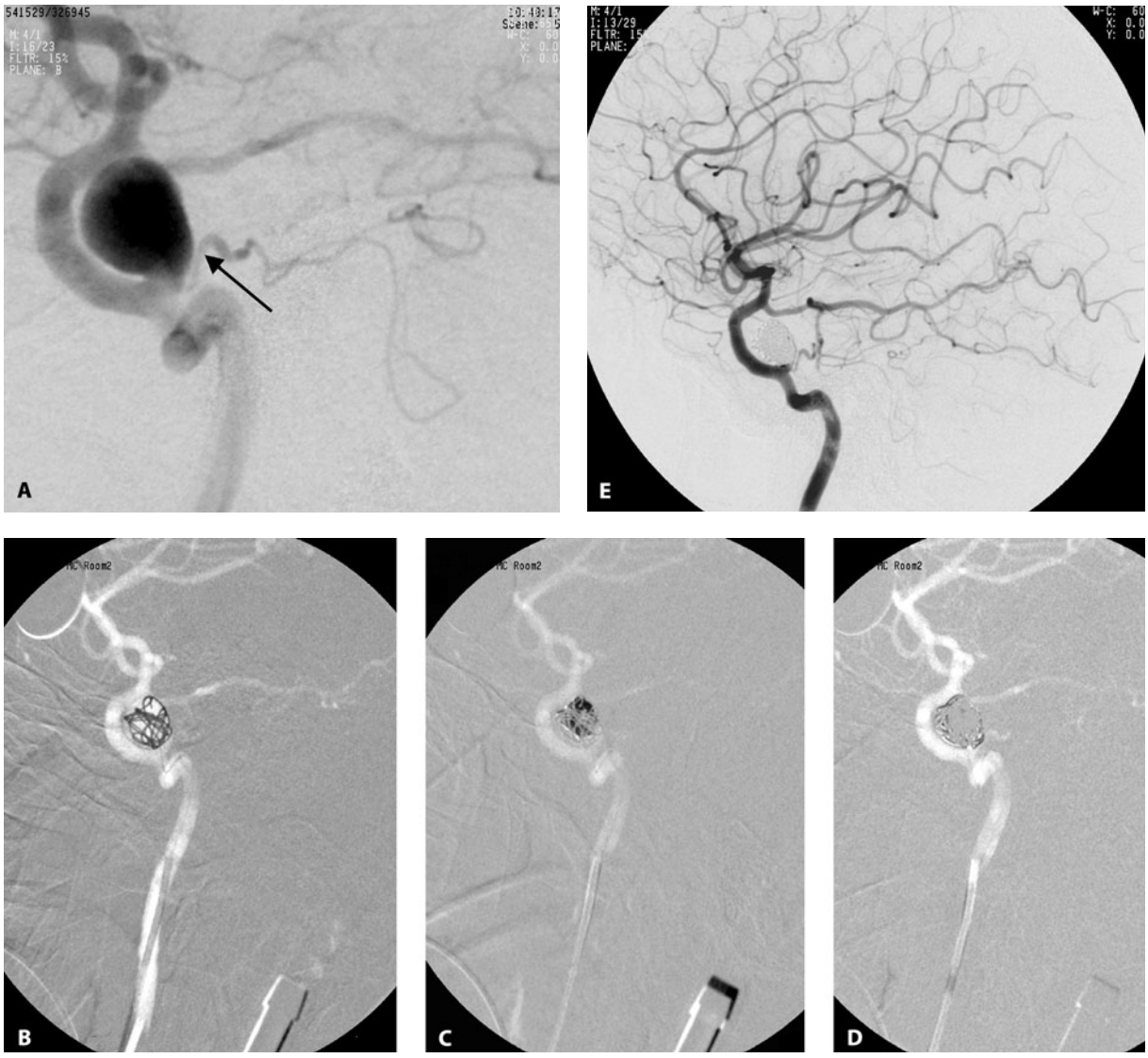

Fig. 14.66A–E. Three-dimensional coil to frame an aneurysm. **A** Lateral digital subtraction angiogram (DSA) of the right internal carotid artery showing an aneurysm at the level of the trigeminal artery with the posterior inferior cerebellar artery coming at the base of the aneurysm (*arrow*). **B–D** Progressive obliteration of the aneurysm. **B** The first 3-D GDC coil formed an excellent frame of the sac of the aneurysm, preserving the origin of the trigeminal artery. **C, D** Filling of the interstices of the 3-D coil. **E** Final angiogram after total endovascular obliteration of the aneurysm. Note the excellent framing and packing of the sac of the aneurysm with a combination of 3-D coils, soft coils, and ultrasoft coils

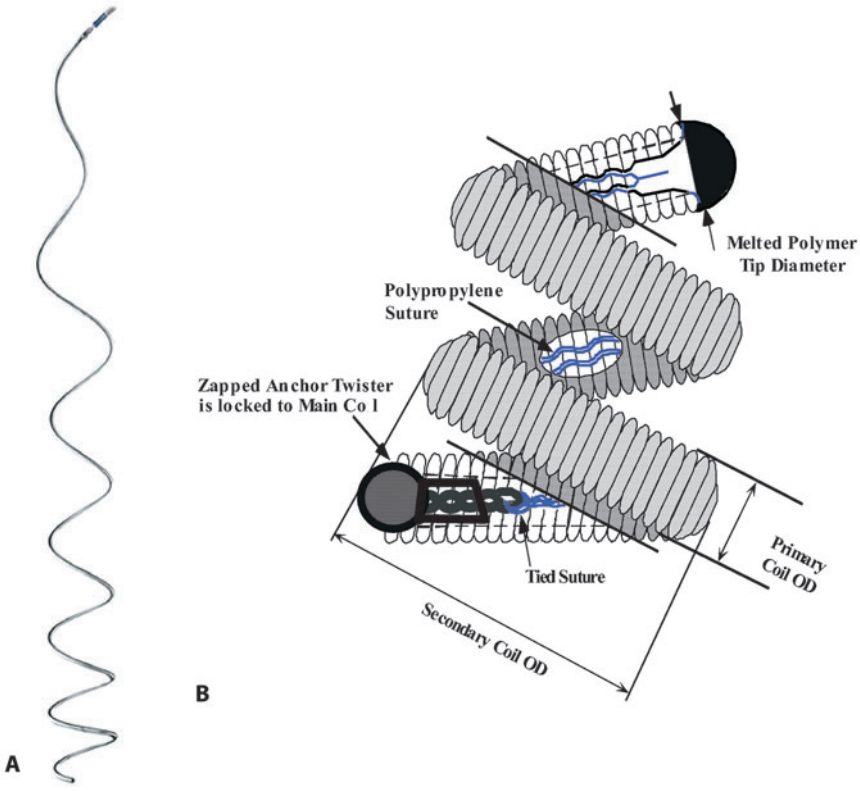

Fig. 14.67A, B. Stretch-resistant GDC 10 ultrasoft coil (Target, Boston Scientific). **A** Ultrasoft coil. **B** Diagram of the coil with the polypropylene suture to prevent coil unraveling

coil in cases of unruptured AAs larger than 8 mm, to constitute a primary net, secondarily completed if necessary with 18 soft, 10, stretch-resistant soft, or ultrasoft, or a combination of the above, depending on the individual set of circumstances (size, space available, catheter tip position, etc.). We may use more than one 3-D coil, but in most cases this is not needed. The packing then can be done with a variety of coils, continuing with the regular coils, and then switching to the softer coils such as the soft and more recently the ultrasoft coil (Fig. 14.69) platinum alloy. The softer coils make it possible to improve the coil density. Soft and ultrasoft coils have also been very helpful toward the end of coiling, to not only increase packing, but also to close small neck remnants (Fig. 14.70). It is the author's experience that we should aim for packing as dense as possible; however, overpacking increases the risk of the procedure and has not proven to be better (see Chap. 7, this volume).

When the GDC system is used for vessel occlusion, AVF closure, or venous occlusion, the Vortex GDC (Target, Boston Scientific) is a very useful coil (Fig. 14.71). One should be aware that there is more friction in its advancement through the catheter.

The ultrasoft stretch-resistant coils can also be used toward the end of a deconstructive procedure, where the occlusion must be very precise, and one must avoid proximal herniation of the occlusive device (Fig. 14.72, pp. 1005–1010).

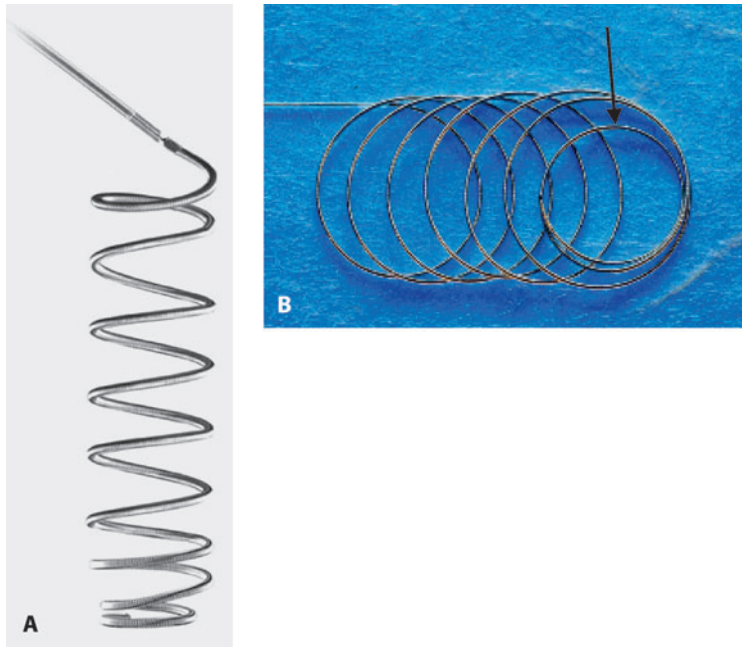

Fig. 14.68. Two-dimensional GDC. **A** Two-dimensional coil. **B** Note the first loop that is of a smaller diameter (*arrow*)

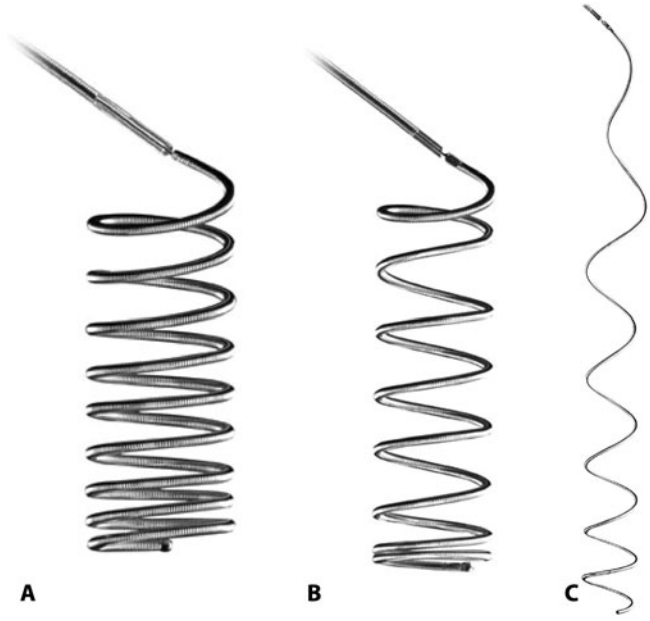

Fig. 14.69A–C. Variable-softness coils in the GDC family. **A** Regular 18 coil. **B** Soft 18 coil. **C** Ultrasoft 10. Note the increased softness of the different coils

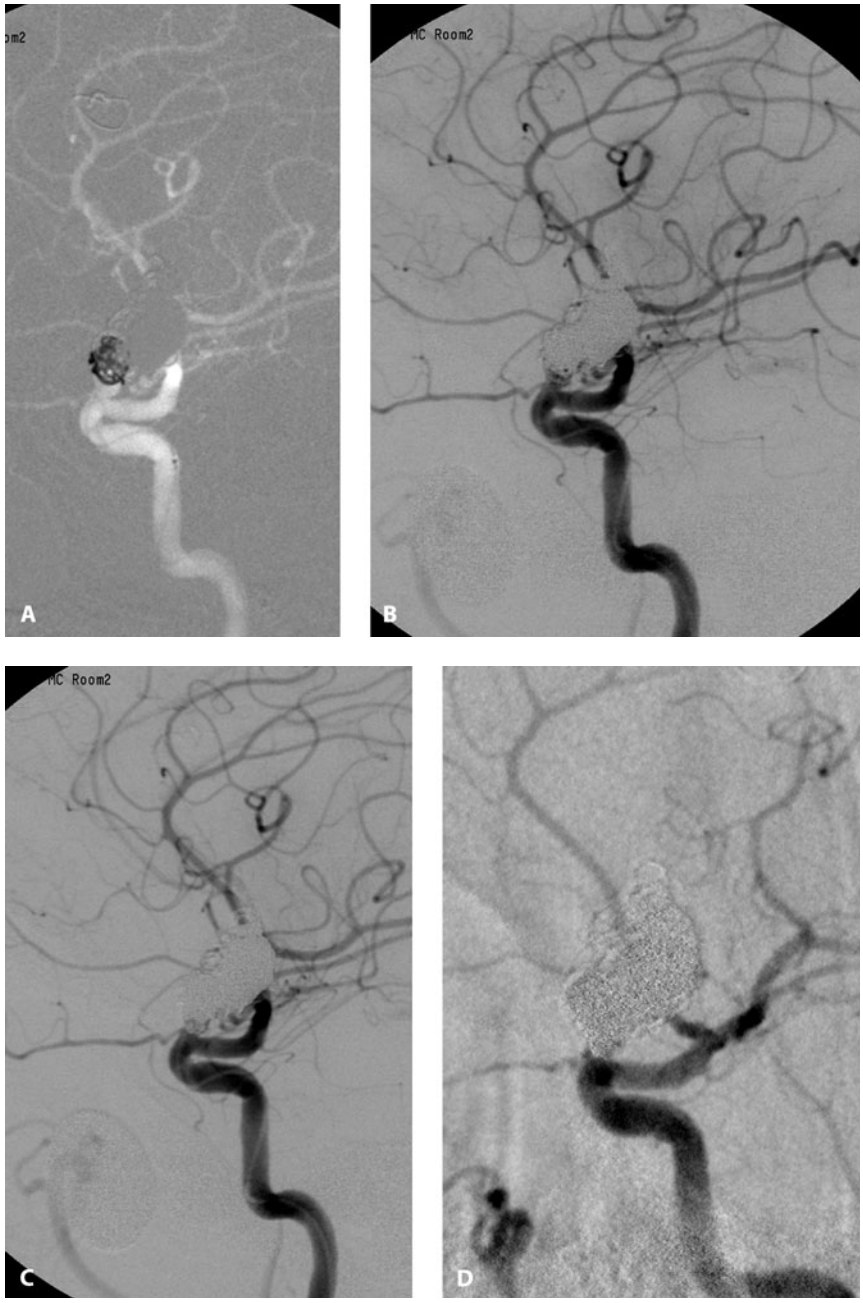

Fig. 14.70A–D. Recurrent paraophthalmic aneurysm. **A** Recurrent paraophthalmic aneurysm after compaction. **B, C** Note the ability of the ultrasoft coils to deal with the neck by filling the neck from a distal to a proximal position with the final angiogram (**D**) showing a near total obliteration

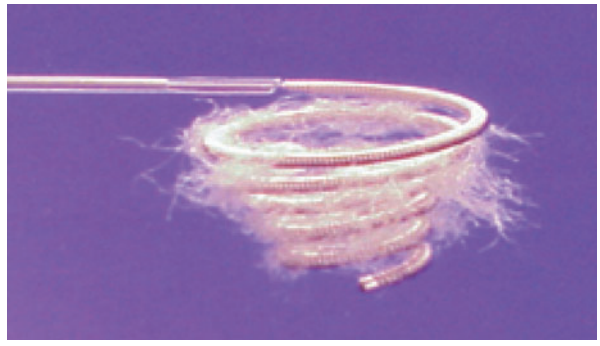

Fig. 14.71. GDC Vortex (Target, Boston Scientific). Close-up view of a detachable GDC to which fiber coils have been added to increase thrombogenicity

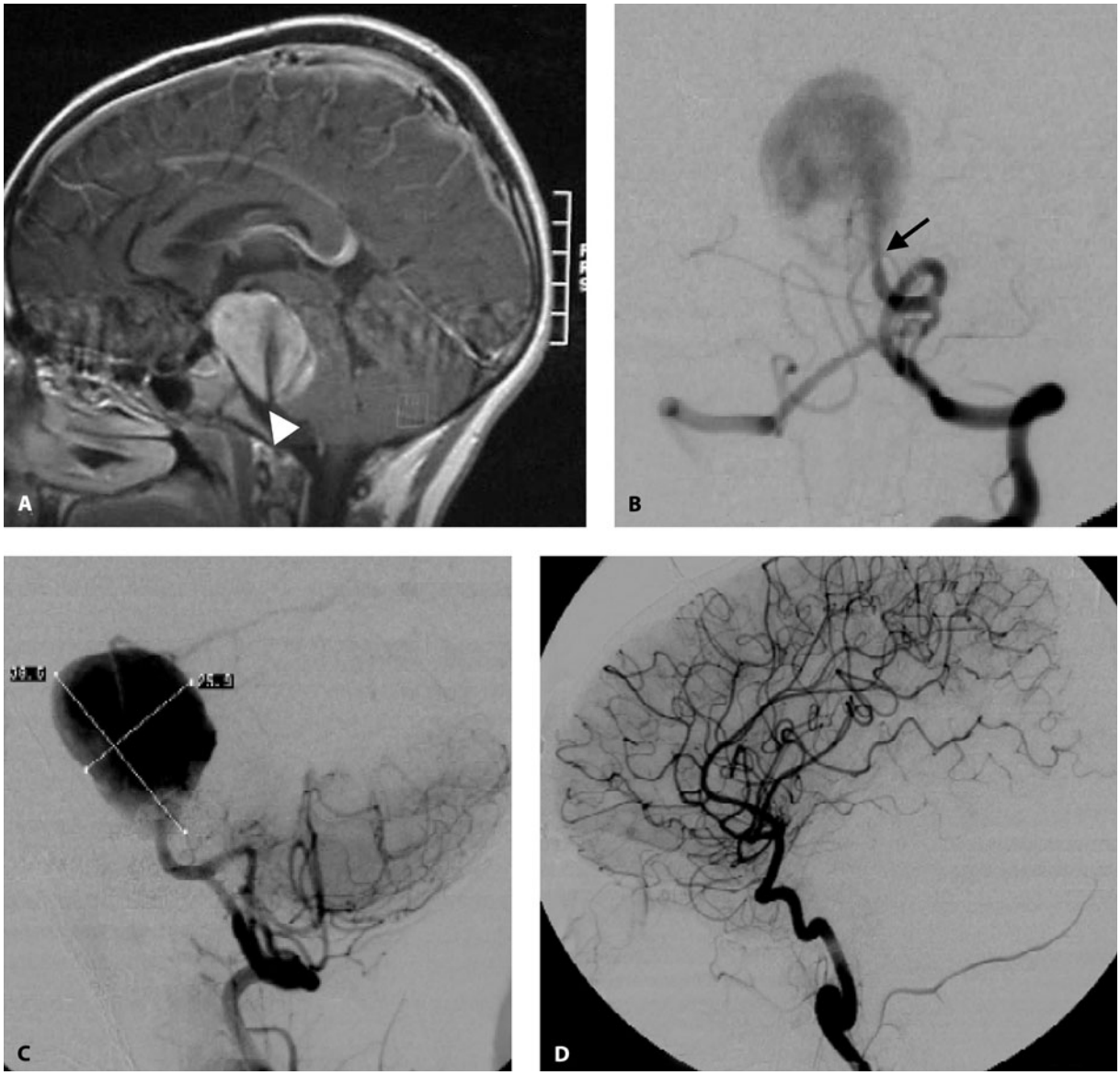

Fig. 14.72A–W. Combination coil in the deconstructive occlusion and functional investigation of the lower basilar artery. **A** Sagittal MRI demonstrates a giant basilar aneurysm. Note the flow disturbance of the lesion (*white arrowhead*). **B** Frontal digital subtraction angiogram (DSA), early phase. The lesion starts distal to the anterior inferior cerebellar artery (AICA, *arrow*). **C** Lateral DSA of the left vertebral artery. **D** Lateral DSA of the right internal carotid artery (ICA). There is no filling of the posterior communicating artery. **E–W** see pp. 1006–1010

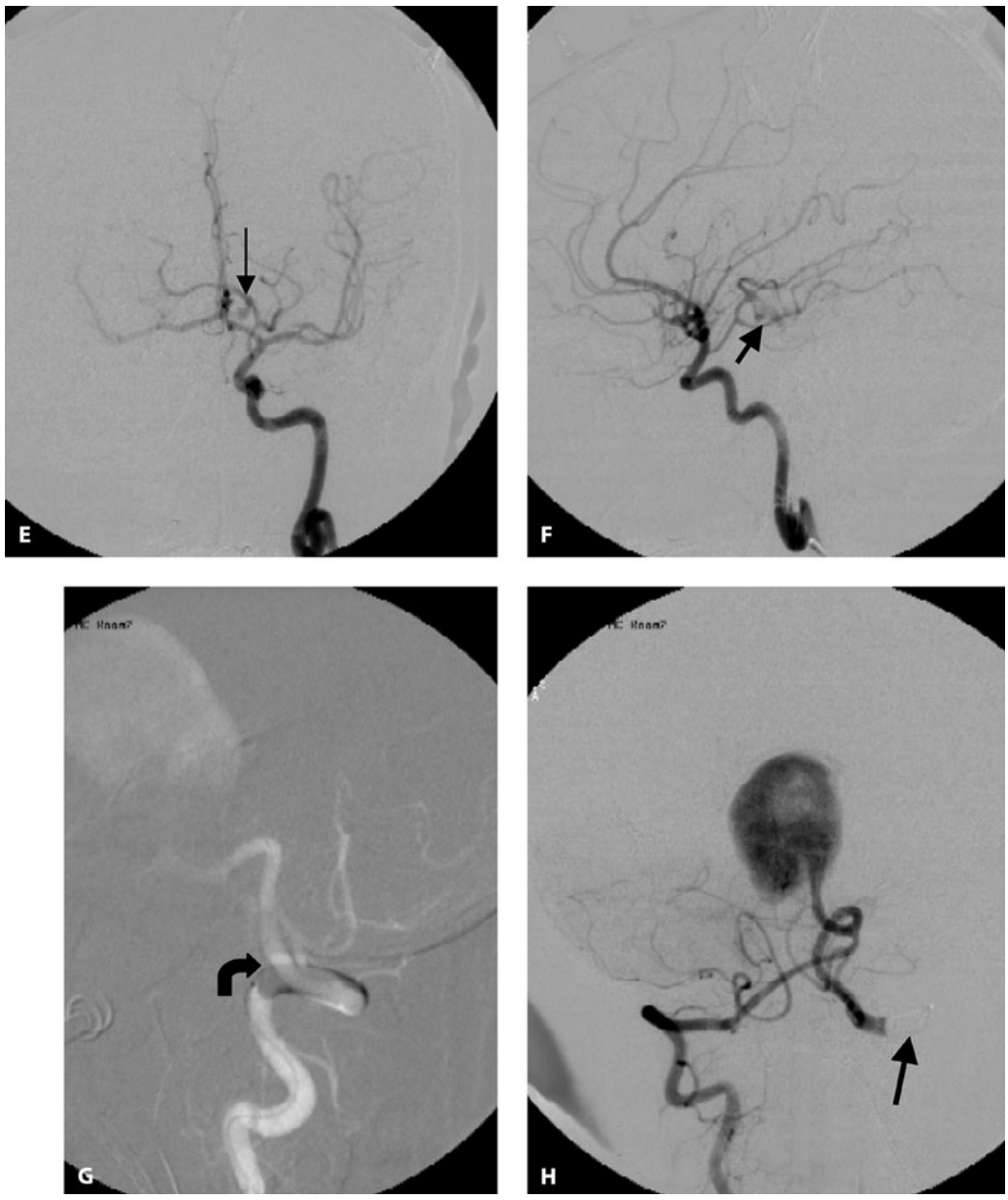

Fig. 14.72 (*continued*). **E** Frontal and **F** lateral DSA of the left ICA. There is a good posterior communicating artery that fills the distal portion of the aneurysm (*arrow*). Note that the lesion extends up to the basilar artery proximal to the superior cerebellar arteries (SCA). **G** Road map image of the left vertebral artery (LTVA) lateral projection with the position of a detachable balloon (*curved arrow*). **H** Right vertebral artery (RTVA) injection prior to detachment. **I–W** see pp. 1007–1010

Fig. 14.72 (*continued*). **I** Left common carotid artery (CCA) DSA with balloon occlusion of the LTVA. There is minimal filling of the aneurysm. **J** Road map image of the RTVA to show the position of a temporary balloon occluding of the RTVA (*arrow*). The LTVA has been permanently occluded. **K** Lateral mid-arterial phase of the left CCA while the RTVA is temporarily occluded and after permanent occlusion of the LTVA. Note the significant filling of the aneurysm (*open curved arrow*). **L–W** see pp. 1008–1010

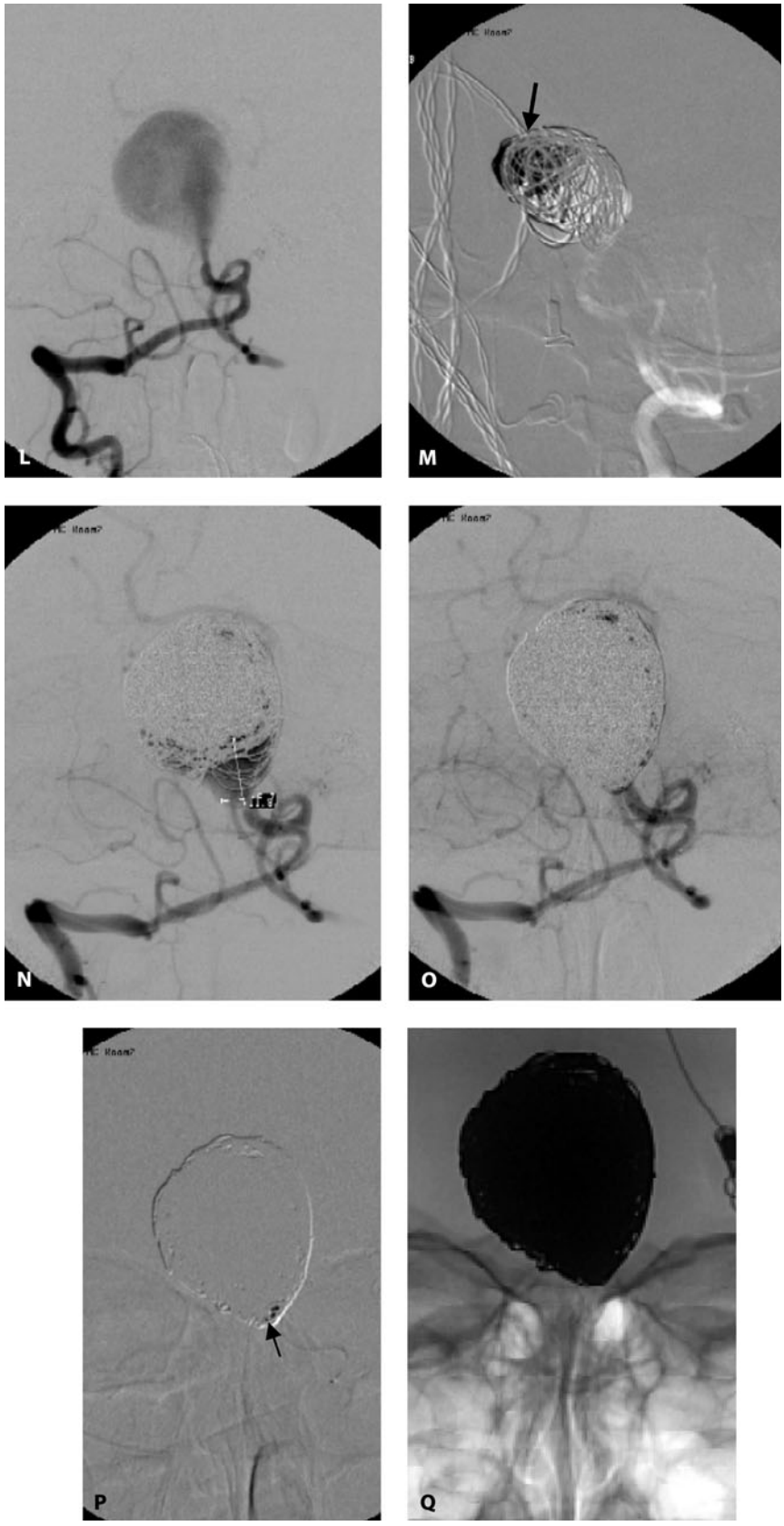

Fig. 14.72L–Q.
Legend see p. 1009

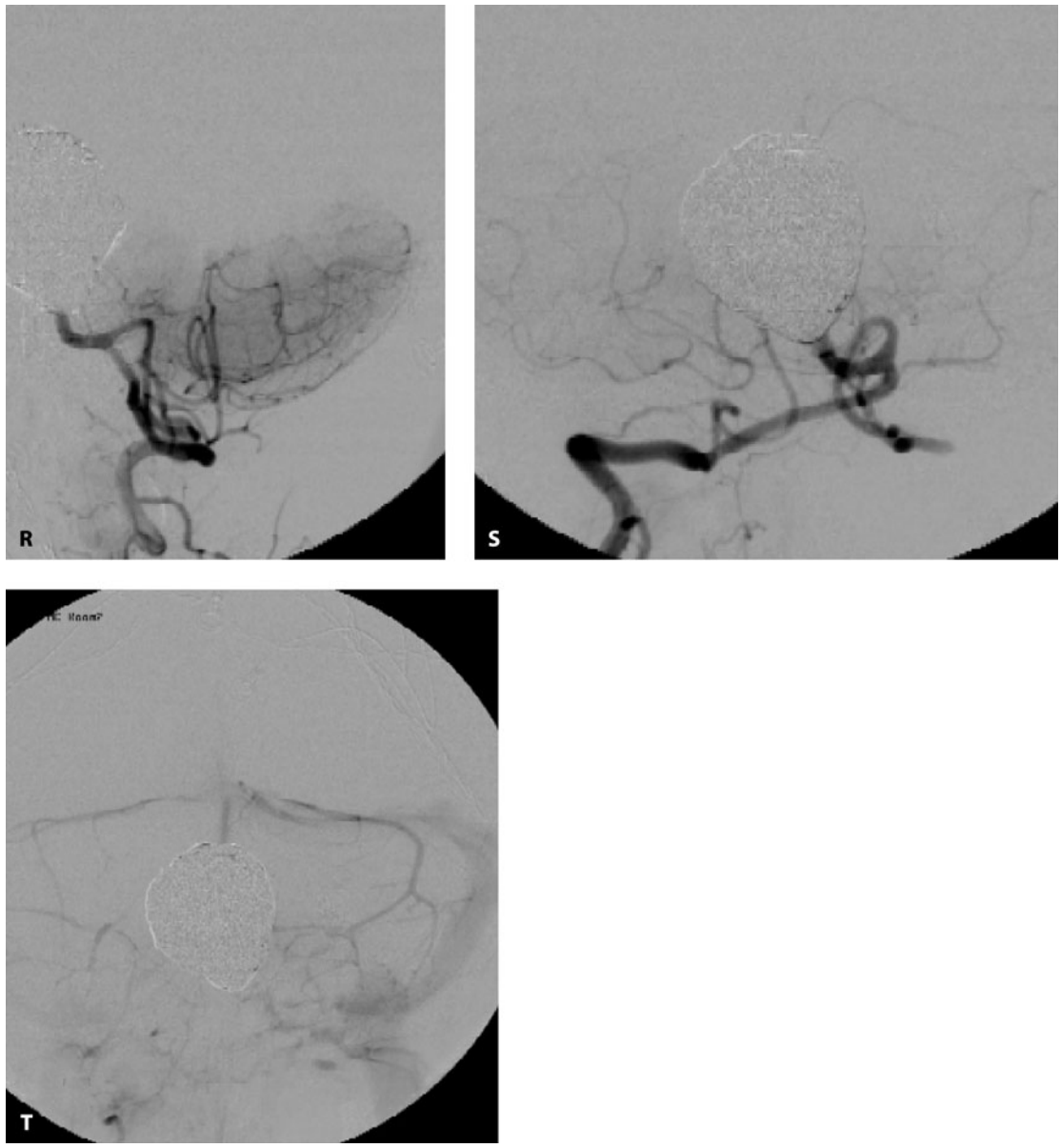

◄ **Fig. 14.72** (*continued*). **L** RTVA 3 weeks later; the aneurysm had increased in size. **M** Coiling of the lesion. Because of its large size, first the distal outflow is coiled. **N**, **O** RTVA angiogram. There is still filling of the distal basilar artery (**O**). Note the remaining interstices filled with contrast material. **P** Filling of the interstices with ultrasoft coils (*arrow*) avoids displacing the microcatheter backward. **Q** Coil mass at the end. Final angiograms. **R** Lateral and **S**, **T** frontal DSA of the RTVA fills up to the AICAs and both PICAs, with no filling of the aneurysm. **U–W** see p. 1010

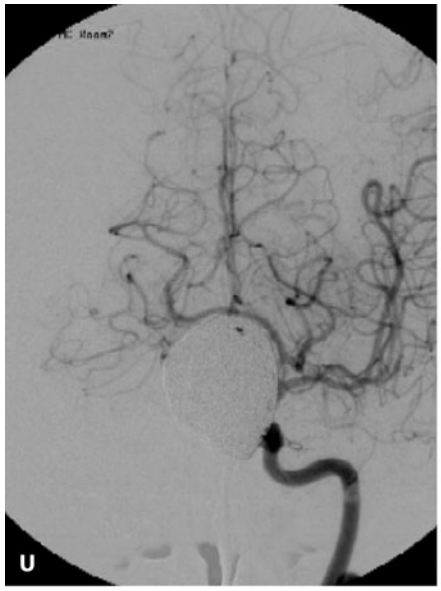

Fig. 14.72 (*continued*).
U–W The left ICA fills the upper basilar artery, with no filling of the aneurysm

Micrus Coils

Micrus coils (Micrus Corporation, Mountain View, CA, USA) are also made of platinum alloy, similar to the GDCs. They differ in the detachment mechanism, which is immediate; detachment is accomplished by electric melting of the junction between the guiding mandrill and the platinum coil. Their 3-D model has more of a box or square shape memory (Fig. 14.65C), which can have certain advantages in broad neck aneurysms (Fig. 14.73).

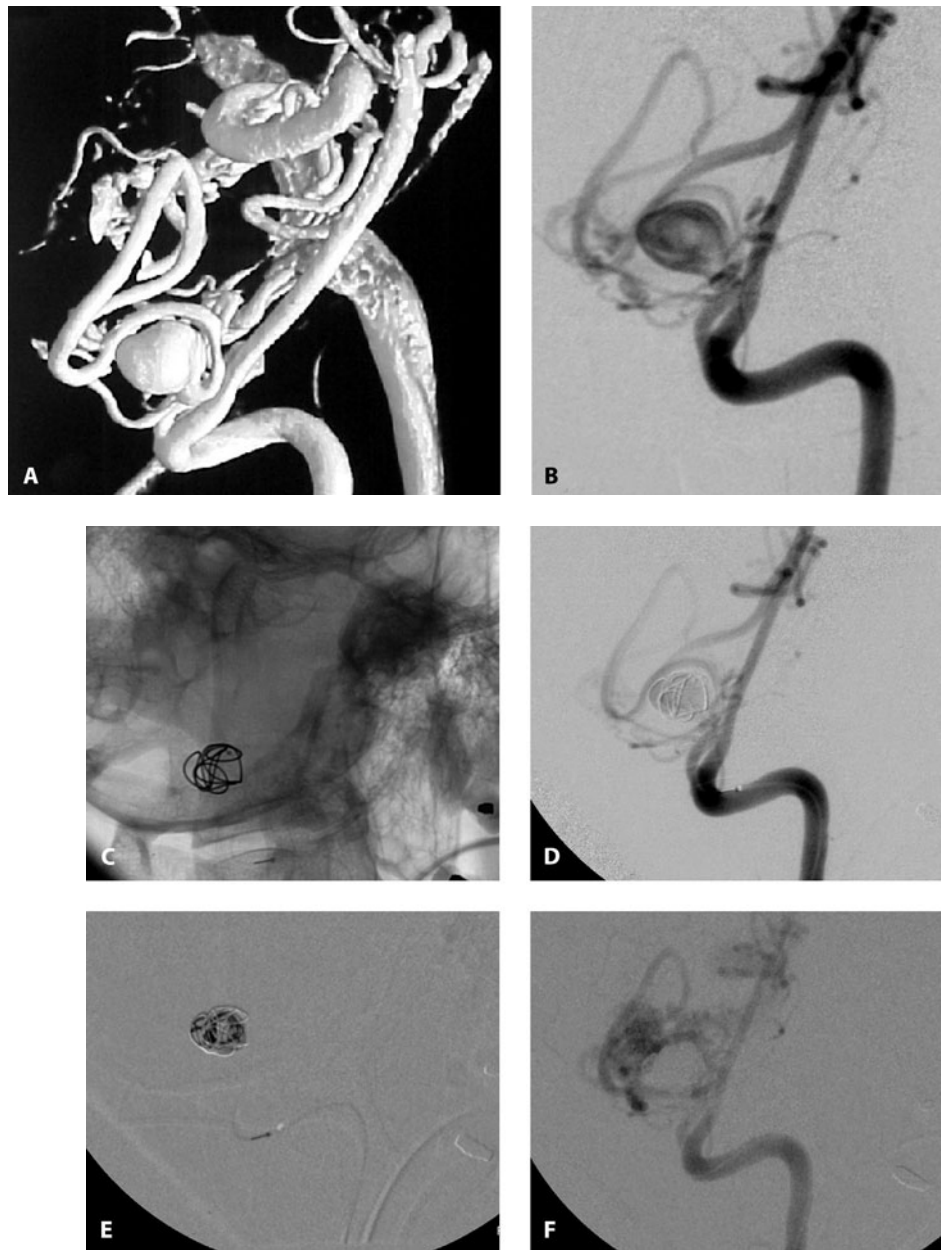

Fig. 14.73A–F. Micros (Micrus Corporation) 3-D coil in a broad neck aneurysm. Posterior inferior cerebellar artery aneurysm (PICA) in the proximal segment of the vessel feeding a high-flow arteriovenous malformation. Note the broad neck of the aneurysm. **A** Three-dimensional image of the right vertebral artery (RTVA). **B** Digital subtraction angiogram (DSA) of the RTVA, early phase. **C** Three-dimensional Micros coil frame. **D** Angiogram after the first coil frame. **E** Filling of the interstices with conventional GDCs. **F** Following the occlusion of the aneurysm prior to catheterization of the distal PICA

Cook Detachable Coils

Cook detachable coils, also made of platinum, are very similar to the others, except for the detachment mechanism, which is mechanical, requiring a counterclockwise rotation movement (Fig. 14.74) (Cook, Inc., Bloomington, IN, USA).

Cordis Coils

Cordis coils are also made out of platinum and are similar, except for the detachment mechanism, which uses hydraulic pressure (Figs. 14.65B, 14.75).

Hydrocoil

Microvention (Aliso Viejo, CA) has introduced an innovative concept of incorporating expandable hydrophilic hydrogel into a platinum coil (Fig. 14.76). A preliminary frame or scaffold of the aneurysm is achieved with a Microplex coil (Fig. 14.76I, K). This platinum coil design is used as the first coil to act as a scaffold at the neck of the aneurysm to prevent the hydrogel from protruding into the parent vessel lumen. The coil loops are positioned in the periphery of the aneurysm in all planes (Fig. 14.76K).

Microplex coils come in a single-diameter loop complex best suited for wide-neck aneurysms and a double-diameter loop complex for small-neck aneurysms. The hydrogel is incorporated into the platinum coil, with a core (0.008-in. diameter) or with gel coating (0.009-in. diameter.) The Overcoil design (0.00125-in. platinum wire diameter) results in a 0.014-in. outer diameter profile device. The hydrogel polymer expands in the presence of blood to a diameter of 0.027 in. Early experience suggest a very good 6 month occlusion rate (personal experience).

Bioabsorbable Polymeric GDC Coils

Bioabsorbable polymeric GDC coils (BPM/GDC; Target, Boston Scientific) were introduced by Murayama, Vinuela, and co-workers in 2001 (Fig. 14.77), and the first patients were enrolled in the summer of 2002. Clinical experience is therefore limited, but promising (Fig. 14.77F–K).

The goal of these new-generation devices is to obtain a more rapid and controlled wound healing or scar at the site of repair, both at the aneurysm neck and in its interstices and dome. To achieve this tissue engineering, they introduced polyglycolic/poly-L-lactic acid copolymer to form the bioabsorbable polymeric material (BPM). The copolymer is heated and affixed to the core platinum frame. The percentage of BPM is one of the more interesting aspects of this emerging technology, as it may have various expressions of inflammation. It is the reabsorption of the suture that results in scarring. The obvious advantage of such tissue response is that it will result in a more stable treatment, overcoming the current shortcomings of all platinum coils, namely compaction and recanalization of the aneurysm. In addition, the improved healing may increase safety, as dense coil packing may not be needed, at least on side-wall lesions. In higher shear stress conditions such as terminal or bifurcation aneurysms, more support may be needed before the healing effect can be fully expressed (Bavinzski et al. 1998a).

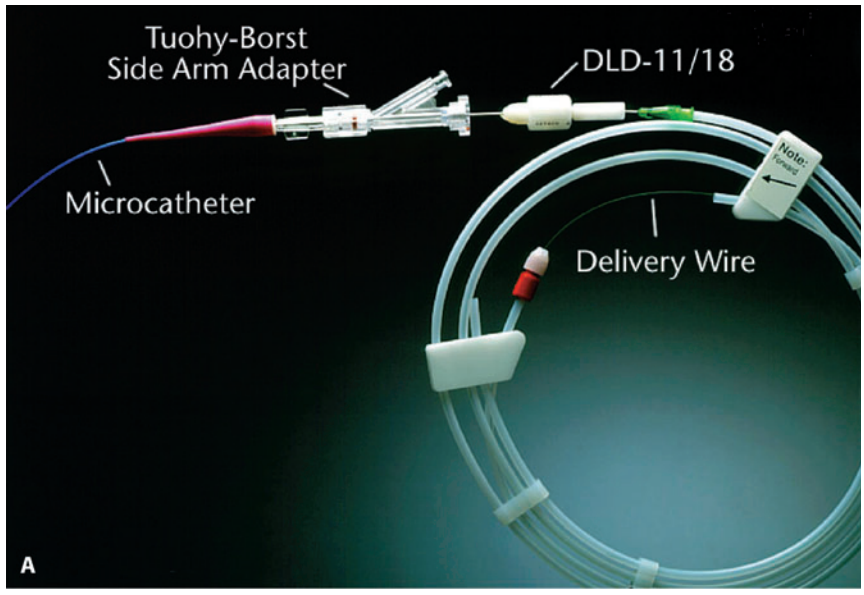

Fig. 14.74A, B. Cook coils (Cook, Inc., Bloomington, IN). **A** Assembly system with the detachment mechanism (DLD) that requires 11–18 counter-clockwise turns of the adapter to detach the coil. **B** J tip and helical Cook platinum coils

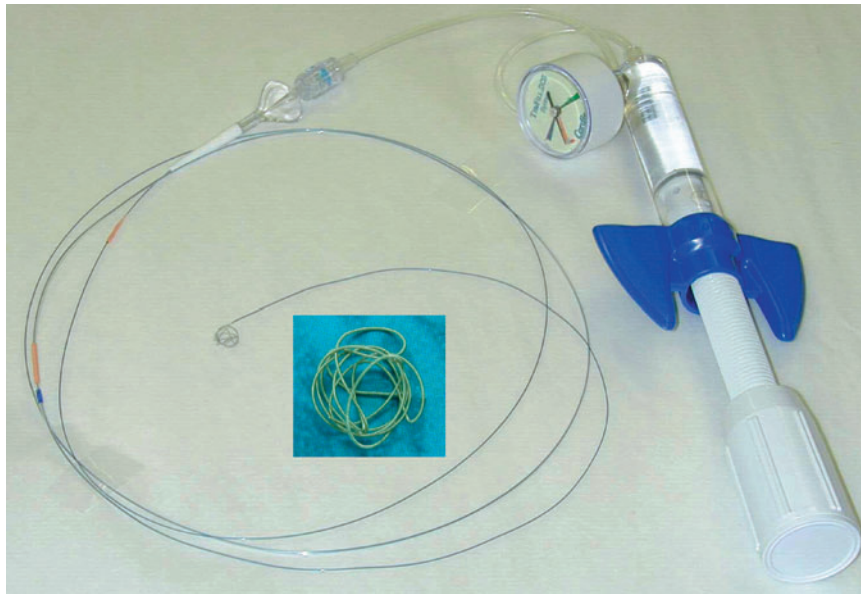

Fig. 14.75. Cordis Endovascular detachable coil. Hydraulic detachable assembly. The coil is detached by hydraulic pressure with the saline-filled syringe

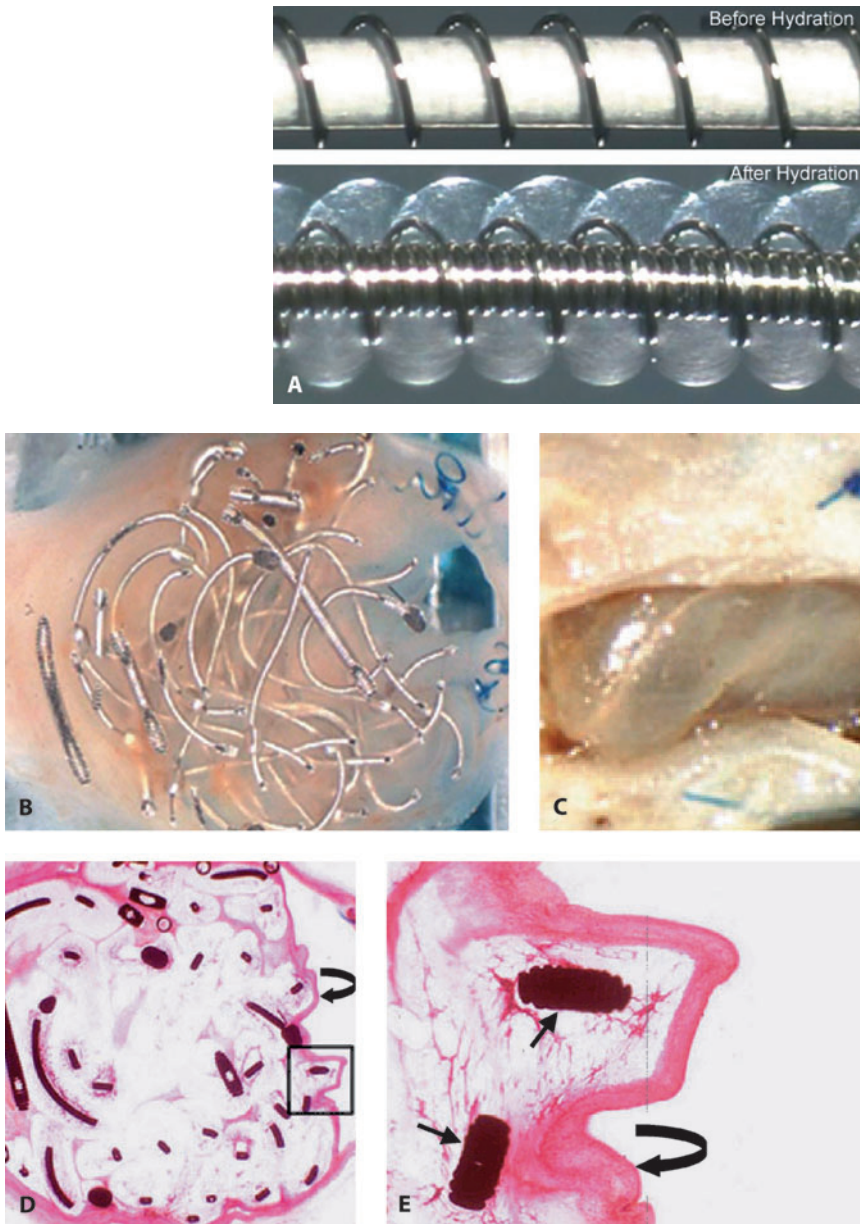

Fig. 14.76A–M. Hydrocoil (Microvention Aliso, Viejo, CA). **A** The hydrogel is incorporated into the platinum coil. Platinum coil core (0.008-in. diameter) with gel coating (0.009-in. diameter). The Overcoil design (0.00125-in. platinum wire diameter) results in a 0.014-in. outer diameter profile device. The Hydrogel polymer expands in the presence of blood to a diameter of 0.027 in. (0.069 mm). **B** Gross specimen of an experimental sidewall canine aneurysm model treated with Hydrocoil. Note the ratio of hydrated gel to platinum. **C** Macroscopic view of the aneurysm neck. **D** Microscopic specimen. There is re-endothelialization with organized healing at the lumen site (*curved arrow*). **E** Higher magnification of **D**, the *arrows* point to the coils. **F–M** see pp. 1015, 1016

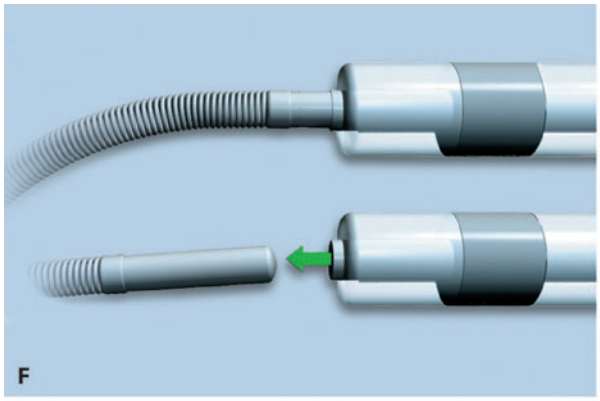

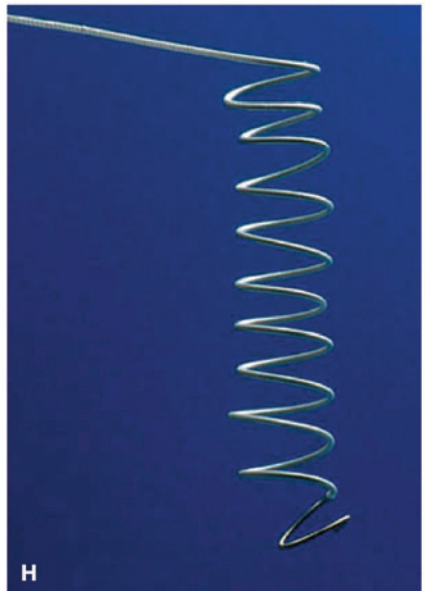

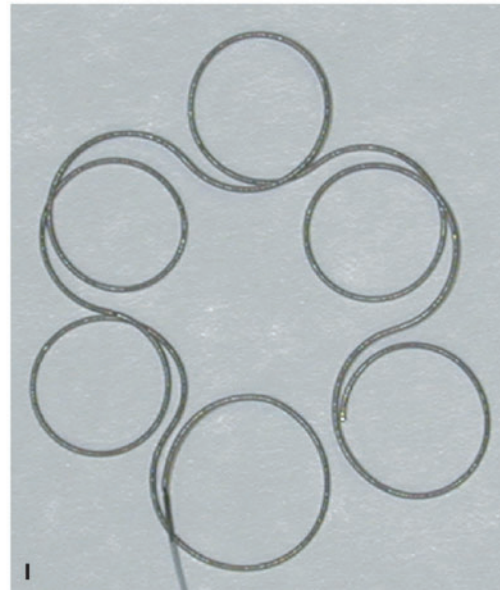

Fig. 14.76 (*continued*). **F** Hydrolink detachment mechanism. **G** Flushing 1-ml (*blue*) syringe and 0.25-ml detaching syringe utilizes hydraulic force to detach the coil. **H** Conventional helical platinum coil. **I** Microplex coil. This platinum coil design is used as the first coil to act as a scaffold at the neck of the aneurysm, to prevent hydrogel from protruding into the parent vessel lumen. The coil loops are positioned in the periphery of the aneurysm in all planes. Microplex coils come in a one-diameter loop complex, best suited for wide-neck aneurysms, or a two-diameter loop complex for small-neck aneurysms. **J–M** see p. 1016

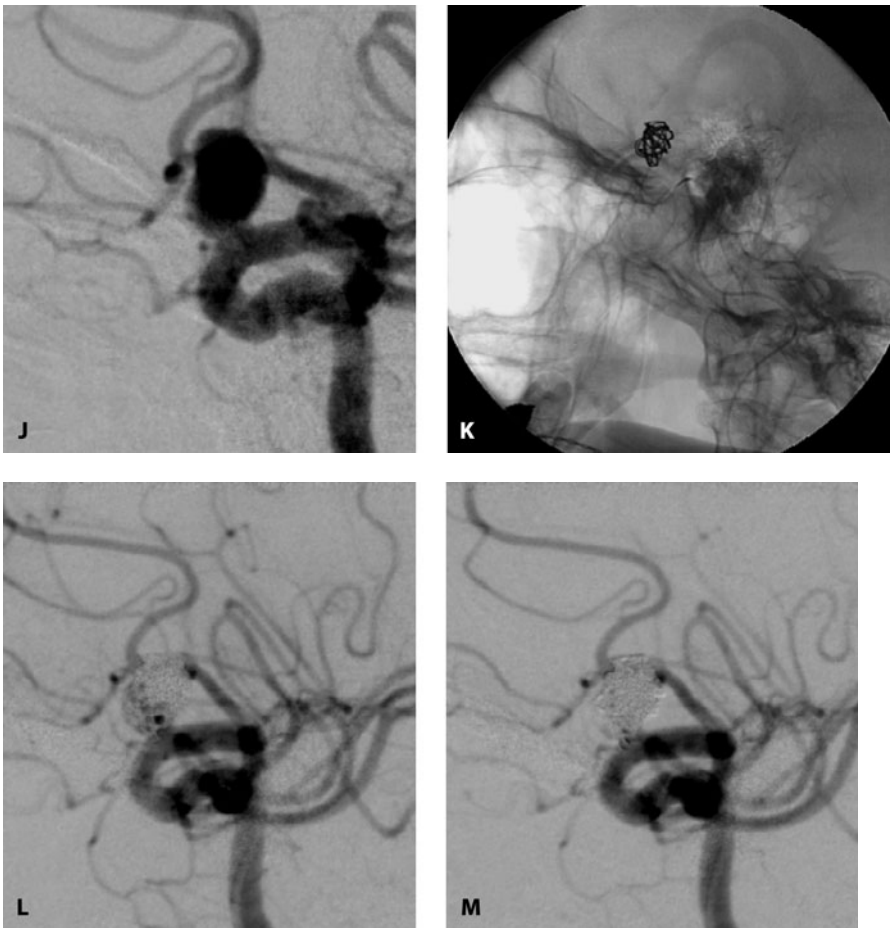

Fig. 14.76 (*continued*). **J** Lateral DSA of a paraophthalmic aneurysm. **K** Plain film showing the Microplex frame. **L** After five additional Hydrocoils, there is still some filling at the lower portion of the aneurysm. **M** After 20 min, as the hydrogel has expanded, there is further obliteration of the aneurysm

Fig. 14.77A–K. Bioabsorbable Polymeric GDC Coils (BPM/GDC). Matrix (Target, Boston Scientific). Canine sidewall aneurysm model comparing **A** bare platinum coils, partial neointima formation at the neck. Note a thin proteinaceous material makes it possible to see the platinum coils. **B** Matrix coil. **C** Gross specimen after Matrix demonstrates a thicker scarring. **D** Histological examination after bare platinum only demonstrates a thin tissue cover over the coils. **E** Histological examination after Matrix embolization shows a thick layer of organized connective tissue covering the neck of the aneurysm (*arrow*). (Courtesy of Y. Murayama and F. Vinuela). **F–H** Basilar artery fenestration aneurysm. **I–K** see p. 1018

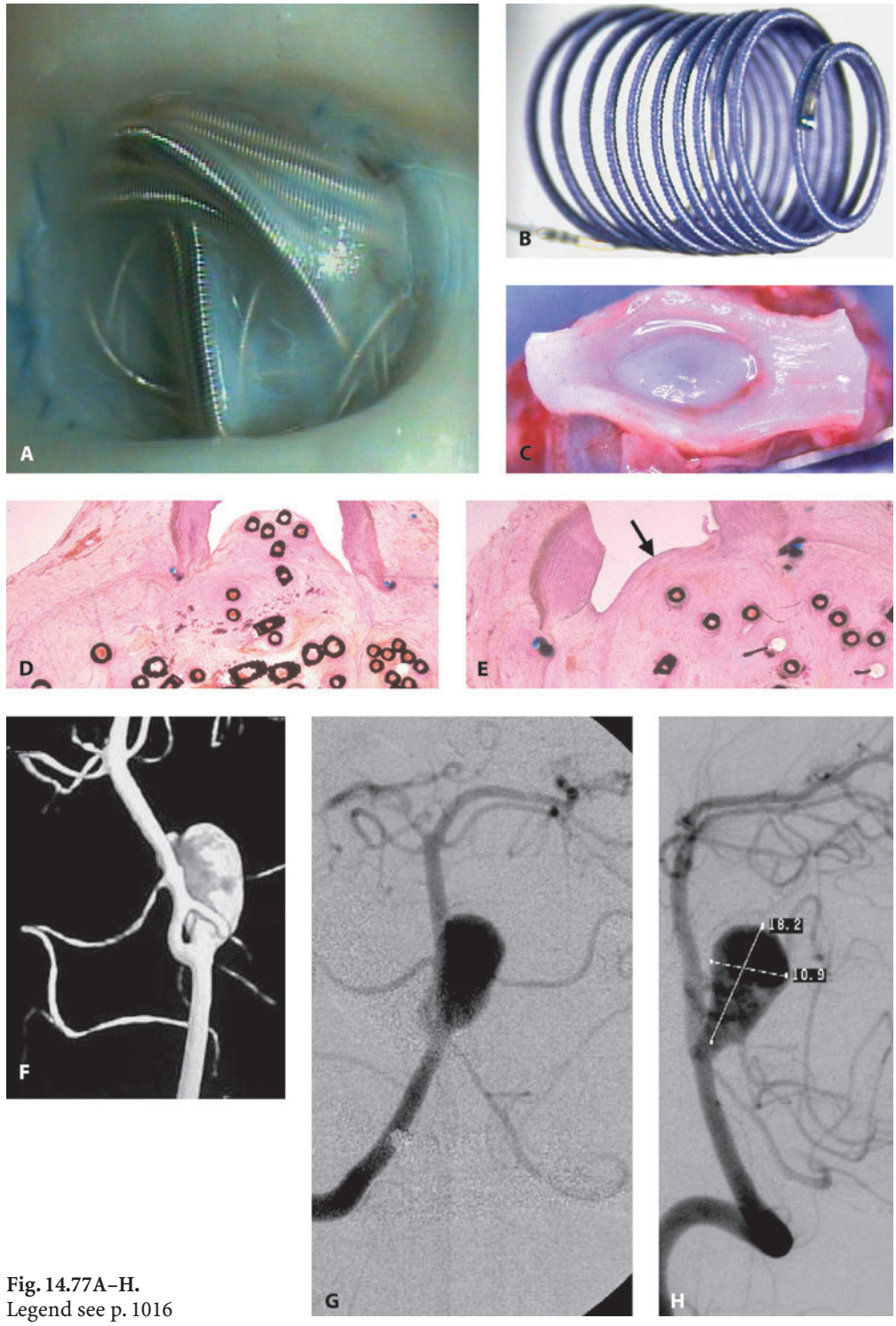

Fig. 14.77A–H.
Legend see p. 1016

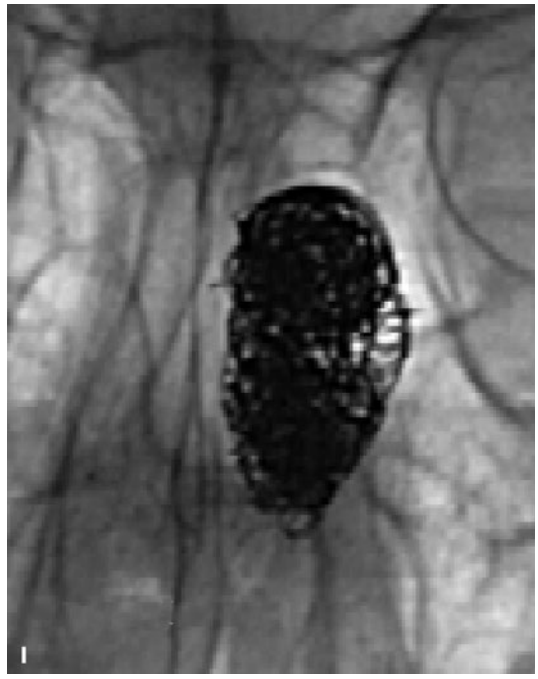

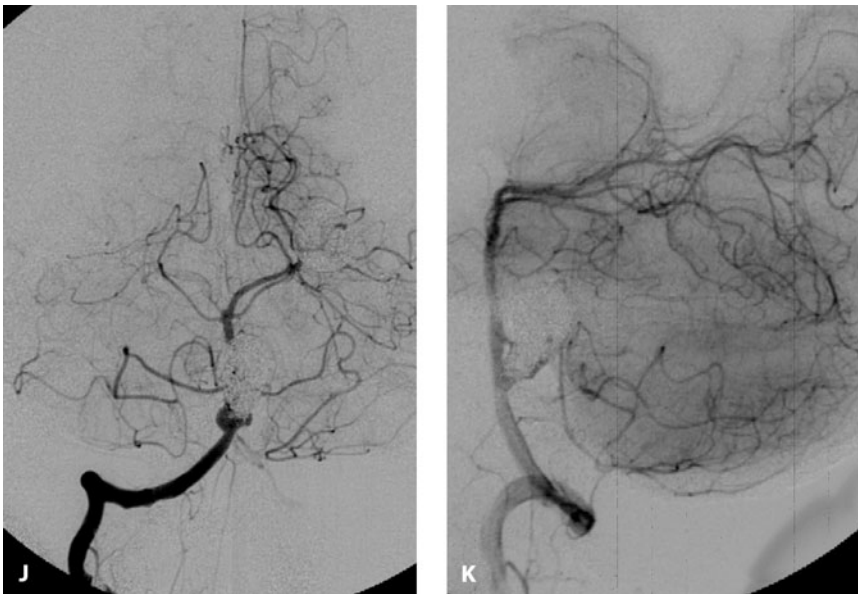

Fig. 14.77 (*continued*). **I** Coil cast. Note a relatively low-density platinum, with some of the interstices filled with the copolymer. **J** Frontal and **K** lateral postembolization digital subtraction angiograms show a small dog ear, but no filling of the aneurysm. Note that some of the nonopaque interstices are filled with the copolymer

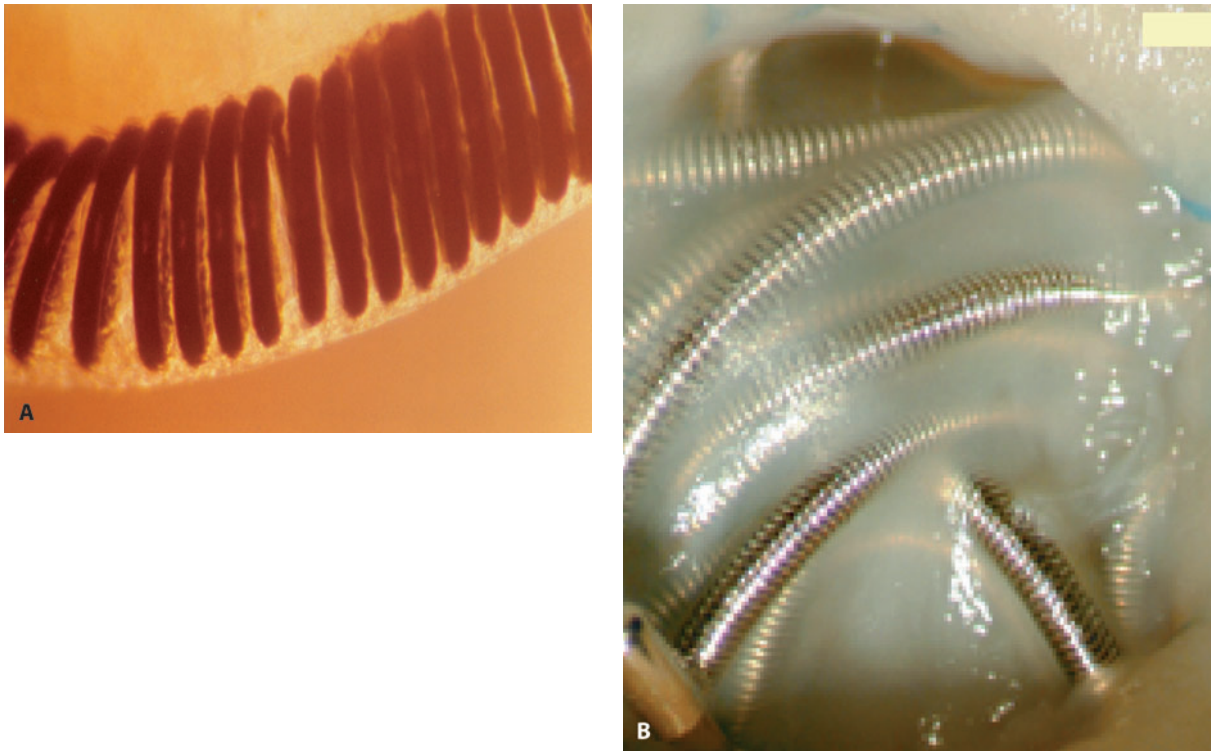

Fig. 14.78A, B. Radioactive detachable coil. **A** Close-up of the coil implanted with 0.13 μCi/cm of ^{32}P. **B** Macroscopic specimen of a canine bifurcation aneurysm embolized with radioactive coils. There is a thick tissue lining the coil, representing fibrosis. (From Raymond et al. 2002, with permission)

Radioactive Detachable Coils

Local beta radiation emitted from ^{32}P ion-implanted platinum coils is a new and promising attempt to add a biological effect to the bare platinum coils. In a canine bifurcation aneurysm model, Raymond and co-workers (2001) demonstrated that endovascular brachytherapy inhibited recanalization that was routinely found 2–12 weeks after bare platinum coil occlusion of arteries in the same canine model. The efficacy of inhibition of recanalization was dependent on coil activities, reaching more than 85% when coils were implanted with 0.13 μCi/cm or more ^{32}P. In further experimental studies, using various combinations of coils implanted with various linear activities, recanalization could be reliably inhibited as long as activities per volume of target arteries were 0.018 μCi/mm^3 or more. Experimental bifurcation aneurysms embolized with radioactive coils did not recanalize, while aneurysms treated with control coils showed recanalization and recurrences at 12 weeks (Fig. 14.78).

Their pilot study on 42 aneurysms in 39 patients has shown that it was feasible to reach target activities in 85% of patients. There was no complication related to radiation after a mean follow-up period of 6 months.

A randomized study comparing radioactive and nonradioactive embolization of aneurysms to assess if beta radiation can improve long-term results of endovascular treatment of aneurysms is now underway.

14.7.1.4 General Principles in Aneurysm Treatment

With the various techniques currently available for endovascular aneurysm obliteration, two possibilities exist: (1) a deconstructive operation, in which the parent vessel is scarified and (2) a reconstructive operation, in which the parent vessel is preserved and the aneurysm is obliterated (Romodanov and Shchegelov 1982).

Deconstructive Operation

The deconstructive operation has been extensively used in the management of extradural aneurysms of the internal carotid and vertebral arteries. It may be done by proximal parent vessel occlusion or preferably by endovascular trapping (Berenstein et al. 1984a; Fox and Drake 1987).

In intradural aneurysms, deconstructive procedures can be very effective in the management of large lesions that do not have a neck. In the major vessels, such as the vertebrobasilar junction (VVJ) (Fig. 14.79), dysplastic aneurysms of the basilar trunk (Fig. 14.72) or serpentine, partially thrombosed lesions in the middle cerebral artery occur (Fig. 14.80, pp. 1023–1026). For selected cases of dissecting aneurysms with poor leptomeningeal anastomosis, where endovascular trapping carries a high risk of distal ischemia, the trapping is preceded with a by-pass to the territory distal to the occlusion is done prior to trapping (Fig. 14.81, pp. 1027, 1028). Prior to sacrificing such vessels, a functional investigation consisting of a proper study of the potential collateral circulation (Fig. 14.72, 14.79) and leptomeningeal collaterals (Fig. 14.80), and when possible a tolerance test, are recommended. Tolerance tests in distal cerebral arteries may not be possible if the vessel to be tested is very small, in anatomical situations where an occlusive balloon may incorporate important branches or perforators. In these cases, the test occlusion must be at the precise anatomical point of the intended occlusion.

Fig. 14.79A–I. Deconstructive operation and functional investigation for vertebrobasilar (VB) junction aneurysm. **A** Frontal view of the right vertebral artery demonstrates a VB junction aneurysm. **B** Lateral view of the left vertebral artery injection shows a hypoplastic vertebral artery. **C** Lateral view of the right vertebral artery at time of diagnosis following a subarachnoid hemorrhage. **D** Angiographic examination of the right vertebral artery in lateral projection 3 weeks after the hemorrhage demonstrates a small posterior dome in the aneurysm (*arrowhead*) not present before (see **C**). **E** Selective injection of the occipital artery on the right side (*curved arrows*), while the vertebral artery is occluded at C4. Note filling of the vertebral artery through the C2 anastomotic pathway, which reconstitutes the vertebral artery and fills the aneurysm (*open arrowheads*). **F** Right internal carotid artery injection in lateral projection. A balloon has been placed to occlude the vertebral artery at C2 (*double arrow*). A second balloon is in the distal vertebral artery proximal to the origin of the posterior cerebellar artery (*arrow*). Note filling of the posterior communicating artery (*curved arrow*) and downward filling of the basilar artery (*large curved arrow*), with poor filling of the aneurysm but good opacification of the posterior inferior cerebellar arteries (*arrowhead*). **G–I** see p. 1022

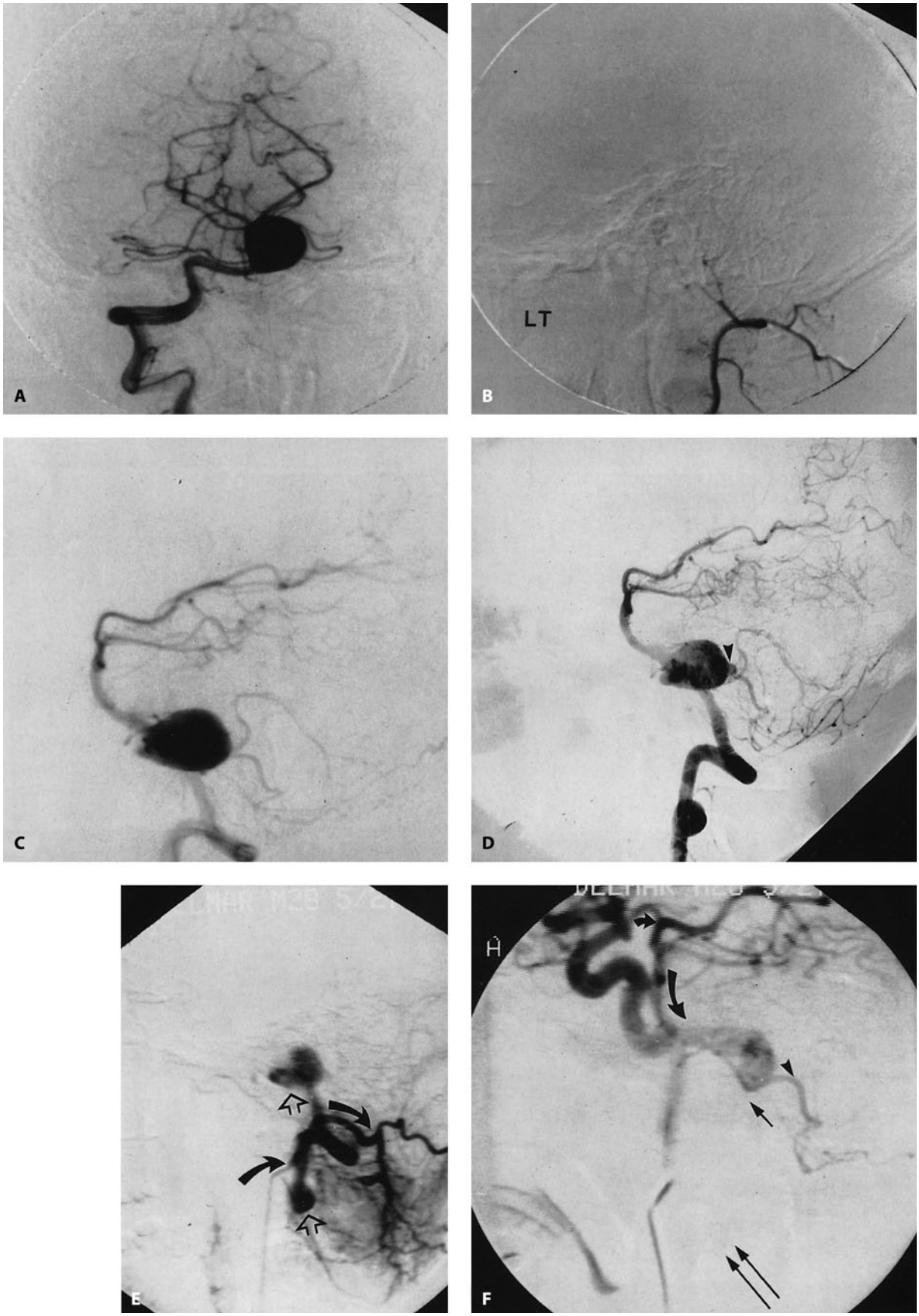
A
LT
B
C
D
E
F

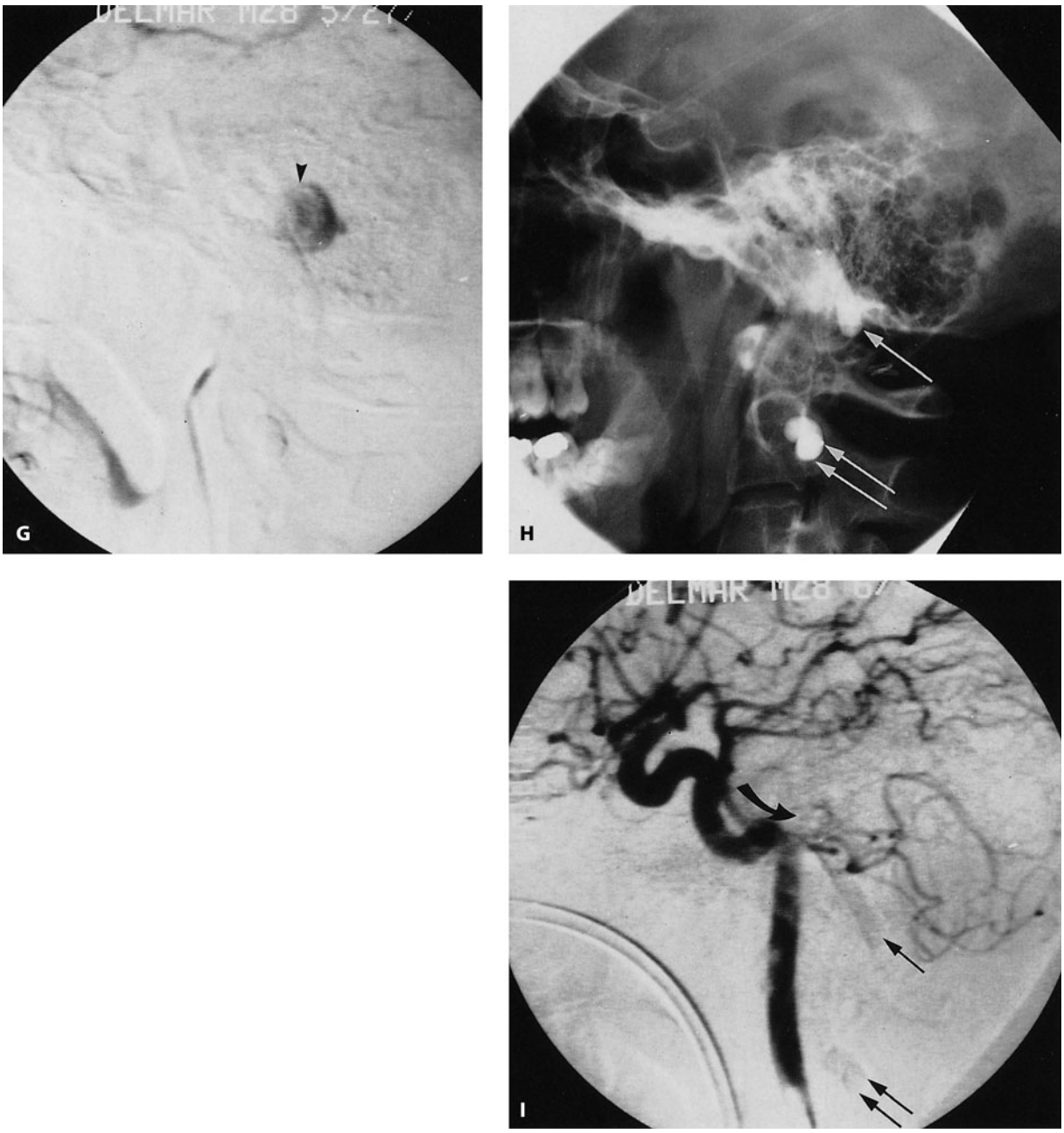

Fig. 14.79 (*continued*). **G** Later phase, same injection as in **F.** Note stagnation in the aneurysm (*arrowhead*). **H** Plain film after detachment, demonstrating the proximal balloon at the level of C2 distal to the occipital anastomosis (*double arrow*) and a second balloon in the distal vertebral artery on the right (*arrow*). **I** One month follow-up angiogram demonstrates the two balloons and filling of the basilar artery in a retrograde manner (*curved arrow*), with excellent filling of the PICA and no filling of the aneurysm

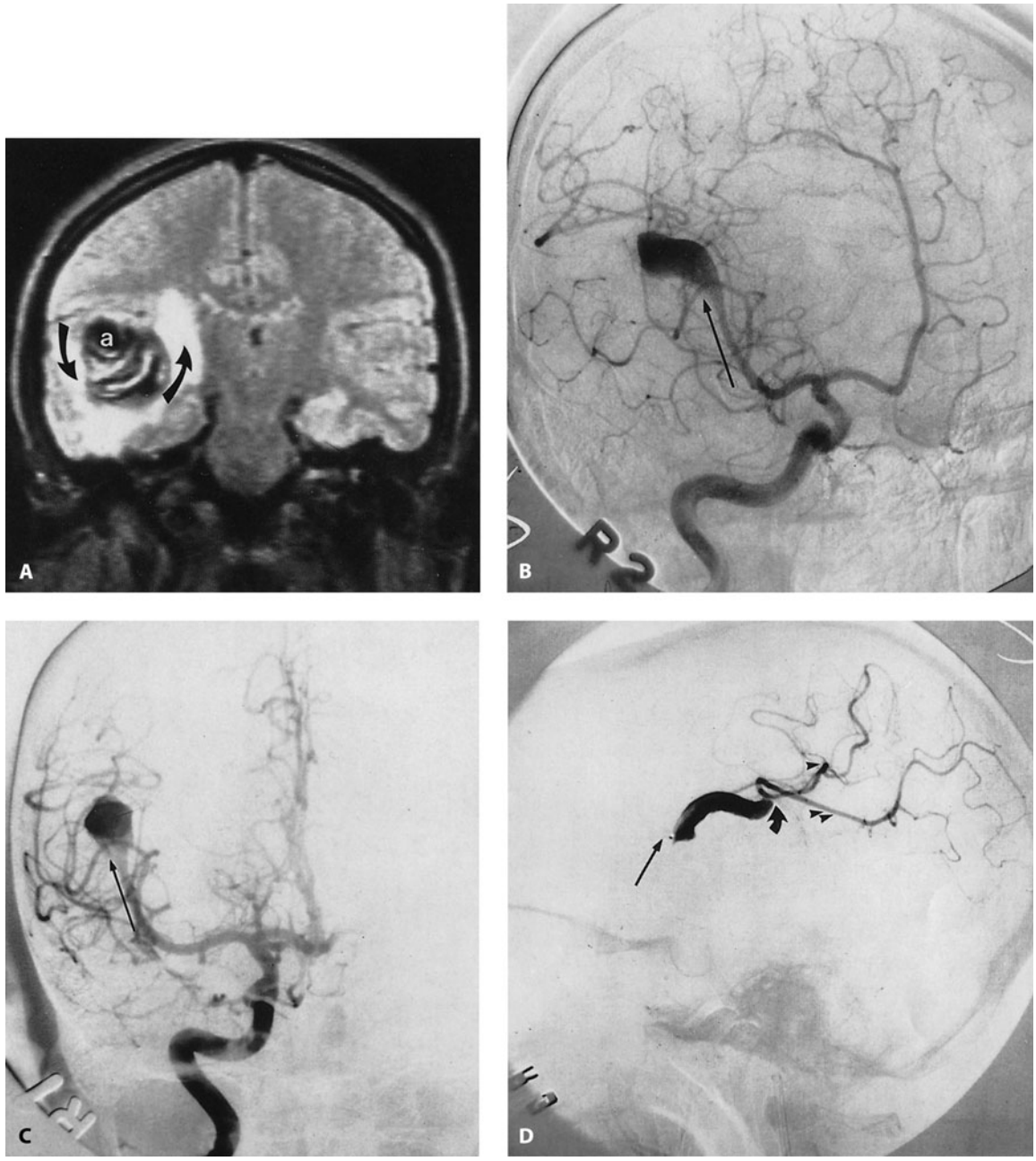

Fig. 14.80A–O. Deconstructive operation in a patient with a middle cerebral artery giant aneurysm, functional investigation. **A** Coronal MRI demonstrates a giant aneurysm in the distribution of the middle cerebral artery with the patent lumen (*a*), a significant thrombosed area with clot formations at various stages, and a significantly increased signal in the white matter (*curved arrows*). The patient was a 21-year-old female, presenting with progressively more refractory seizures. **B** Oblique and **C** frontal views of the right internal carotid artery demonstrate the luminal portion of the giant aneurysm filled by a main middle cerebral artery trunk (*arrow*). **D** Lateral view of a superselective injection at the level of the aneurysm (*arrow*) demonstrates the luminal portion of the aneurysm and the two parietal branches of the middle cerebral artery (*arrowheads*) exiting at the distal end of the aneurysm (*curved arrow*). **E–O** see pp. 1024–1026

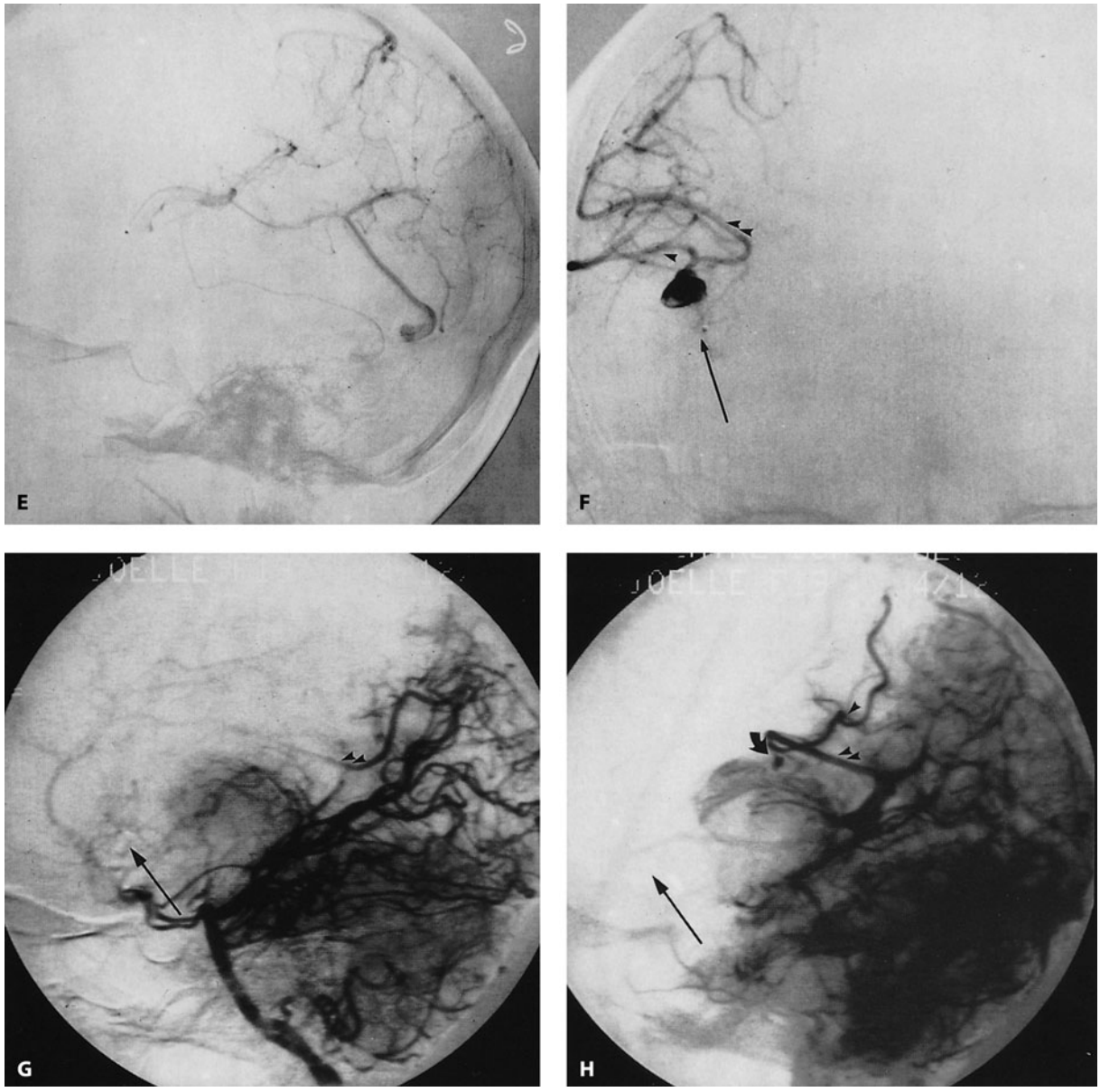

Fig. 14.80 (*continued*). **E** Late phase of the same injection showing the venous phase of the corresponding segment of the right hemisphere. **F** Frontal view of the superselective injection demonstrates the two branches of the middle cerebral artery exiting the distal portion of the dome (*arrowheads*). The *long arrow* points to the position of the microcatheter. **G** Mid-arterial phase and **H** late phase of the left vertebral artery injection while the middle cerebral artery trunk feeding the aneurysm is temporarily occluded with a Hieshima nondetachable balloon (*long arrow*). Note filling of the two parietal branches of the middle cerebral artery through leptomeningeal collaterals of the posterior cerebral circulation (*arrowheads*), corresponding to the same branches as shown in **D**. Note filling of the distal portion of the aneurysm (*curved arrow*, **H**). **I–O** see pp. 1025, 1026

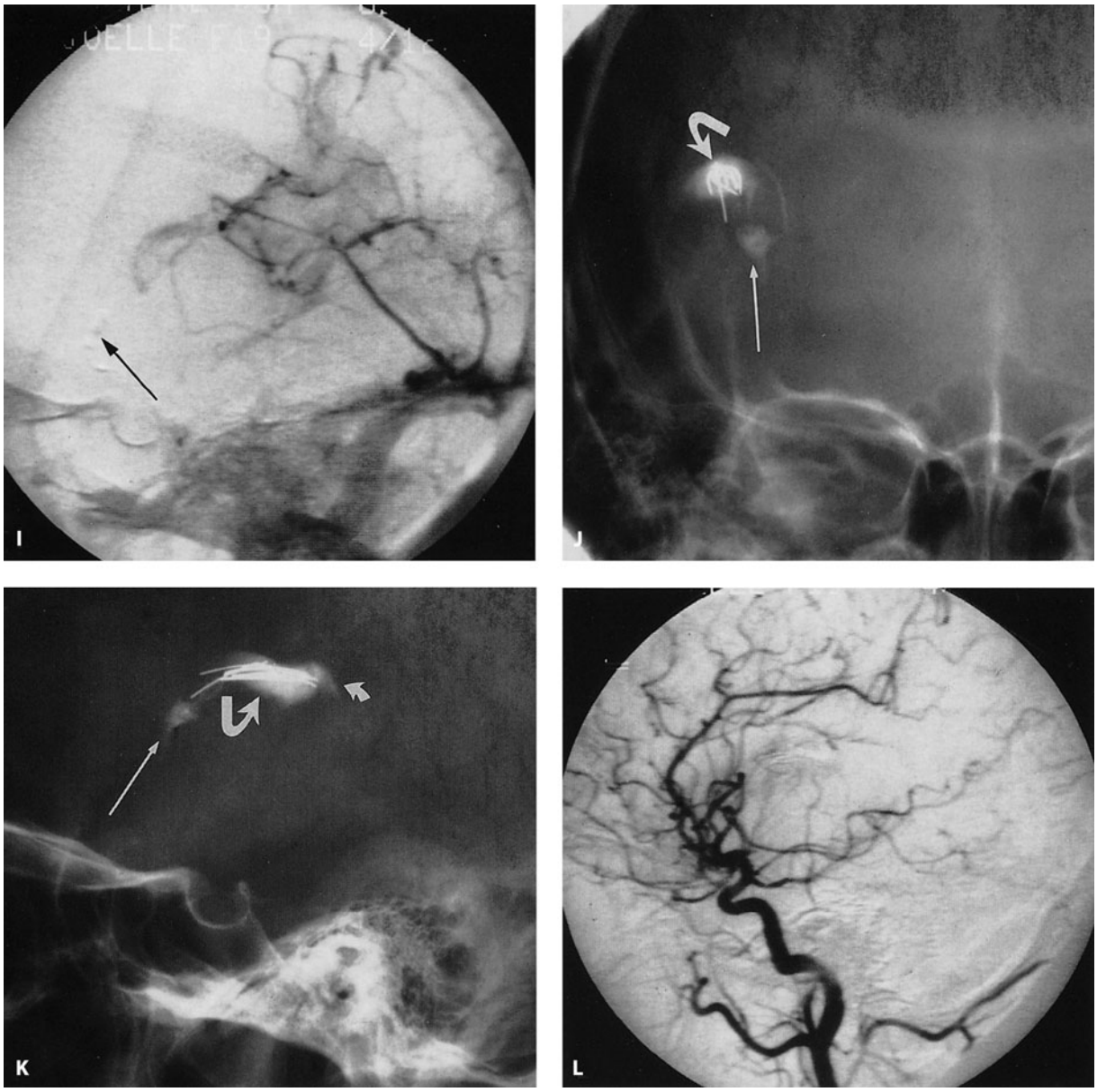

Fig. 14.80 (*continued*). **I** Late venous phase of the same vertebral artery injection demonstrates the venous drainage of the same territory in the parieto-occipital region (compare with **E**). **J** Frontal and **K** lateral views after multiple straight microcoils were placed in the aneurysm to seal off its outflow and act as a buffer for the cyanoacrylate. Note the radiopaque acrylic from the entrance of the aneurysm (*long arrow*) to the dome (*curved arrow*). **L** Lateral view of the common carotid artery on the right demonstrates no filling of the aneurysm and the large mass effect. **M–O** see p. 1026

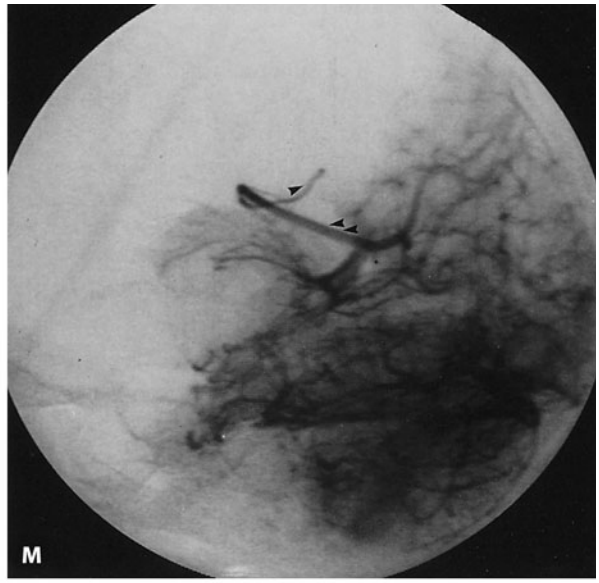

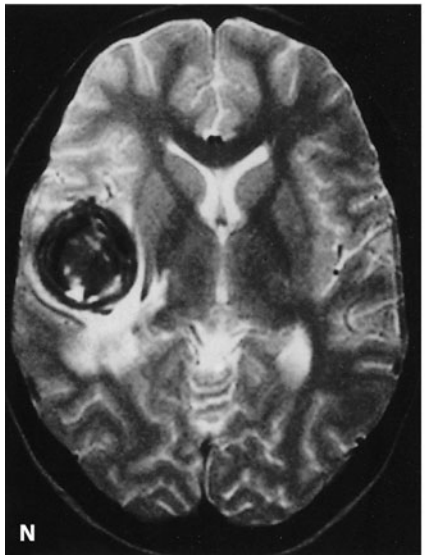

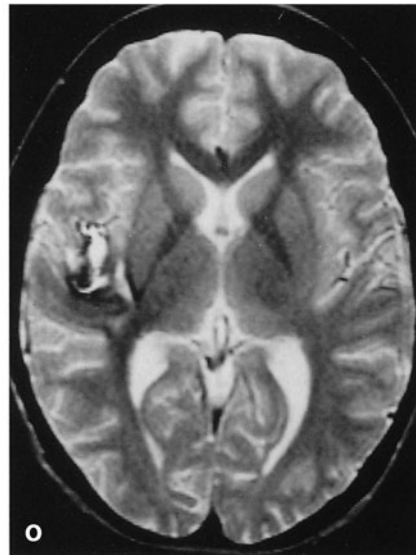

Fig. 14.80 (*continued*). **M** Late phase of the postembolization vertebral artery injection demonstrates the retrograde filling of the two middle cerebral artery branches (*arrowheads*) and no filling of the aneurysm. **N** T1-weighted MRI prior to embolization. **O** Eight-month follow-up MRI at the same level shows the marked reduction in the mass of the thrombosed aneurysm and disappearance of the bright signal in the white matter (compare to **A** and **N**) that correlated with control of the patient's seizures

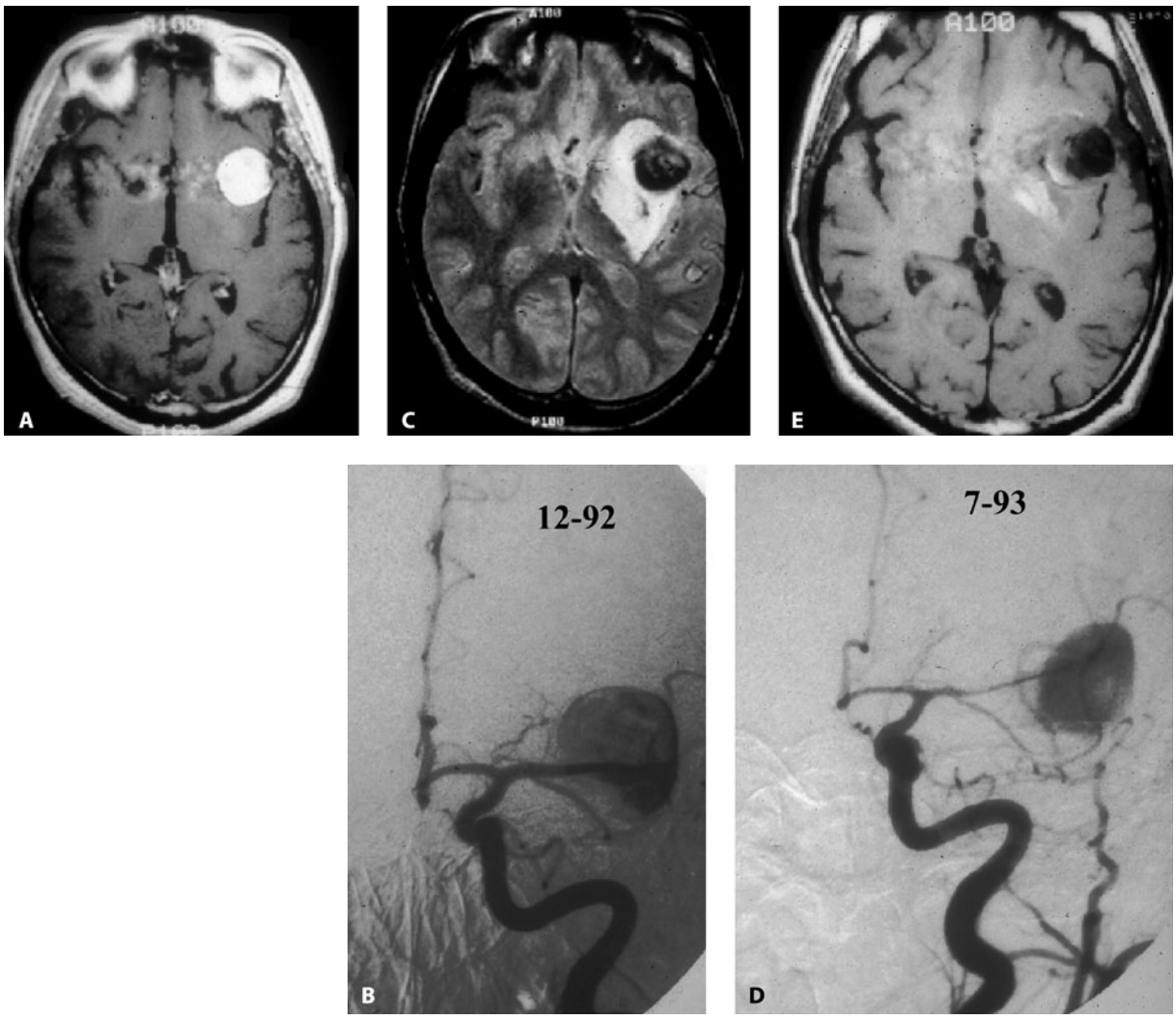

Fig. 14.81A–K. Dissecting aneurysm. A 42-year-old man presented with severe headaches in 1992. **A** Axial MRI after intravenous contrast enhancement shows enlarged 2-cm aneurysm in the left middle cerebral artery distribution. **B** Frontal subtraction angiogram of the left internal carotid artery at that time demonstrates a middle cerebral artery aneurysm. Note the caliber of the M1 segment. **C** Axial T2-weighted MRI in July 1993 following an acute event, which manifested itself by right-side hemiplegia and aphasia. MRI demonstrates significant edema. No evidence of hemorrhage, suggesting an ischemic etiology of the neurological deficits. **D** Frontal subtraction angiogram at the same time demonstrates a long segment of decreased caliber of the accessory middle cerebral artery compatible with a dissection involving the lenticulostriate arterial territory. **E** T1-weighted MRI 2 months later shows resolution of the edema, which correlated with clinical improvement. Note the residual from the ischemic event and thrombi layering in the aneurysm lumen. **F** Early arterial digital subtraction angiogram (DSA) and **G** later arterial DSA at that time demonstrate the dysplastic conversion of this dissecting aneurysm, which incorporates the distal middle cerebral artery. **H** Lateral DSA of the left external carotid artery following a superficial temporal to middle cerebral artery by-pass procedure with two branches anastomosed. **I** Frontal and **J** lateral DSA angiogram of the left internal carotid artery after endovascular trapping of the horizontal middle cerebral artery segment. Note the disappearance of the aneurysm. **K** Lateral DSA of the left external carotid artery late phase shows the by-pass filling the majority of the middle cerebral artery territory with no filling of the aneurysm. **F–K** see p. 1028

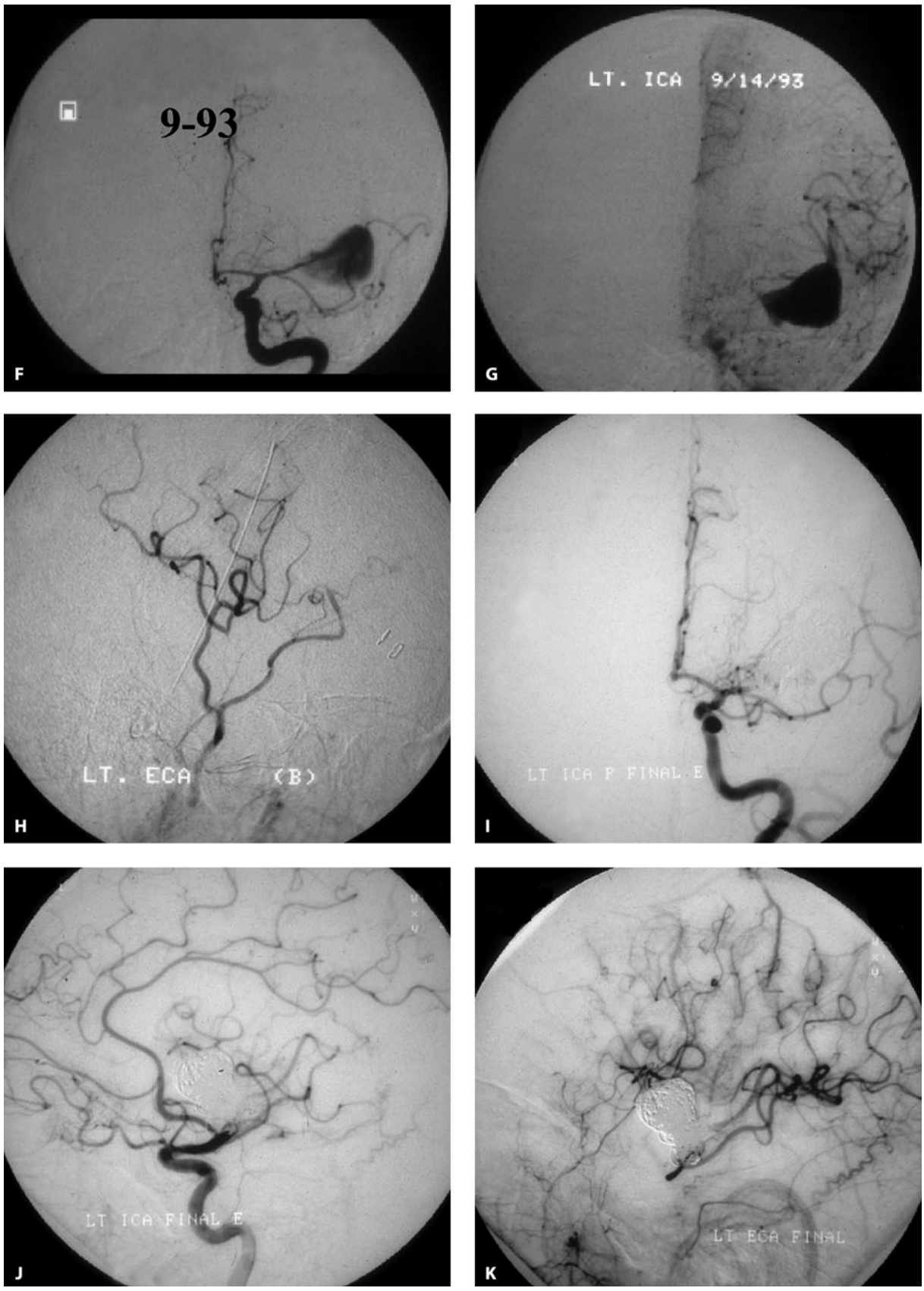

Fig. 14.81F–K. Legend see p. 1027

Tolerance Test Prior to Arterial Occlusion

Various test protocols have been reported, including xenon cerebral blood flow studies and stump pressures after temporary occlusion (Drake 1979b; Gelber and Sundt 1980; Sharbrough et al. 1973); induced hypotensive challenge to the occlusion was proposed by Pile-Spellman et al. (1986). We have used the anatomical assessment supplemented by an intraluminal balloon occlusion test to assess tolerance to acute internal carotid artery occlusion using local anesthesia and systemic heparinization (Berenstein et al. 1984a).

If occlusion of the internal carotid and/or vertebral arteries is not tolerated, the balloon should be deflated immediately. As a point of caution, one should clinically assess the function of both hemispheres.

In patients with an incompetent circle of Willis, bilateral carotid disease, or signs of ischemia during the tolerance test, an EC–IC by-pass should be done (Fein and Flamm 1979) prior to embolization or if the test occlusion is done prior to tumor surgery, where the artery is to be sacrificed. Even patients who have already had an EC–IC by-pass receive a tolerance test (Fig. 14.2).

In patients in whom an associated intracranial aneurysm is found, primarily in another circulation, and in whom carotid occlusion is contemplated, the incidental aneurysm should be treated first.

Theron added an important safety assessment by injecting the ICA that will be preserved and/or the vertebral artery (VA), while the ICA to be sacrificed is temporarily occluded, preferably at the level of the actual occlusion. It is also necessary to look at the circle of Willis and at the symmetry of the venous phase in both hemispheres; if symmetrical, it is a good predictor of tolerance to occlusion.

In the vertebral artery, occlusion tolerance testing is probably less critical, unless there is only one vertebral artery (Fig. 14.79) or if it is the second procedure and the contralateral vertebral artery has already been occluded. It is imperative that the temporary occlusion is done at the exact location of the planned permanent occlusion. For the most part, a good anatomy is a good predictor in the vertebral arteries, as is also true of the basilar trunk (Fig. 14.72).

Determining tolerance prior to sacrificing the basilar artery or a middle cerebral artery is similar to other vessels and is done under systemic heparinization. Contrary to tests in the internal carotid artery or vertebral artery, the test occlusion must be at the exact level of the planned permanent occlusion to avoid closing perforators that may arise millimeters above or below (Hieshima and Higashida 1987) (transverse pontine, lenticulostriate, etc.).

In addition to clinical monitoring, follow-up angiography of the natural collaterals will confirm the ability to fill the territory downstream from the occlusion (Fig. 14.80).

In small subarachnoid aneurysms that have a neck, a deconstructive operation may not be tolerated or, if tolerated, will frequently not exclude the aneurysm from the circulation unless occlusion is at the neck of the lesion. A trapping procedure may be needed, but the presence of important branches at the aneurysm level or close to it may not permit such a procedure. We believe that in most saccular aneurysms in which the par-

ent vessel cannot be preserved, embolization should not be done since currently available microneurosurgical techniques carry low morbidity and excellent results in such patients.

Occlusion can be achieved by detaching the balloon immediately if the test is passed favorably.

We do not believe that occlusion tests can reliably be achieved with coils prior to detachment; however, if the preexisting anatomy and collateral circulation is adequate large and small vessels can be occluded with detachable coils in combination with large fiber coils (Fig. 14.72). During the deployment of the coils, measures to avoid distal embolization should be taken, from systemic heparinization to proximal balloon occlusion flow arrest, or a combination of these.

Reconstructive Operation

The ideal goal is to exclude the aneurysm with preservation of the parent artery (Romodanov and Shchegelov 1979). This goal is presently accomplished in the great majority of saccular aneurysms with currently available coils and liquid embolics.

14.7.1.5 General Principles of Coil Treatment of Aneurysms

Although the vast experience in detachable coil treatments lies with the GDC system, a number of principles apply to all detachable platinum coils, including coil framing, advancement, manipulation, and avoidance of complications; if complications occur, various principles apply to how to deal with them.

Follow-up angiography is recommended prior to coil detachment, either as a full run or as a road map hand injection in the working position, to confirm integrity of the parent vessel and to check distal branches and overall flow, searching for spasm or sluggish flow.

A variety of techniques are available to avoid compromising the parent vessel, prevent clot formation, and to deal with such events.

Neck Protection

As the coil treatment of cerebral aneurysms evolves, and more difficult lesions are treated, the main dangers are compromising the parent vessel, with the potential of vessel occlusion or additional distal embolization by clot or the coils themselves. Therefore, several techniques and devices have been introduced to protect the orifice of the aneurysm.

For many of these techniques, there is a need for more than one catheter assembly system. Several techniques can be used, which will depend on the size and tortuosity of the main brachiocephalic vessel to be catheterized. Whenever possible we use a 7-F catheter of sufficient ID to accept both the balloon tip catheter and the microcatheter, using a three-port hemostatic valve (Fig. 14.82) or two parallel "Y" hemostatic valve. If the ICA or vertebral artery are of small caliber or if one of the catheters to be used is to be placed in another brachiocephalic trunk, a bifemoral ap-

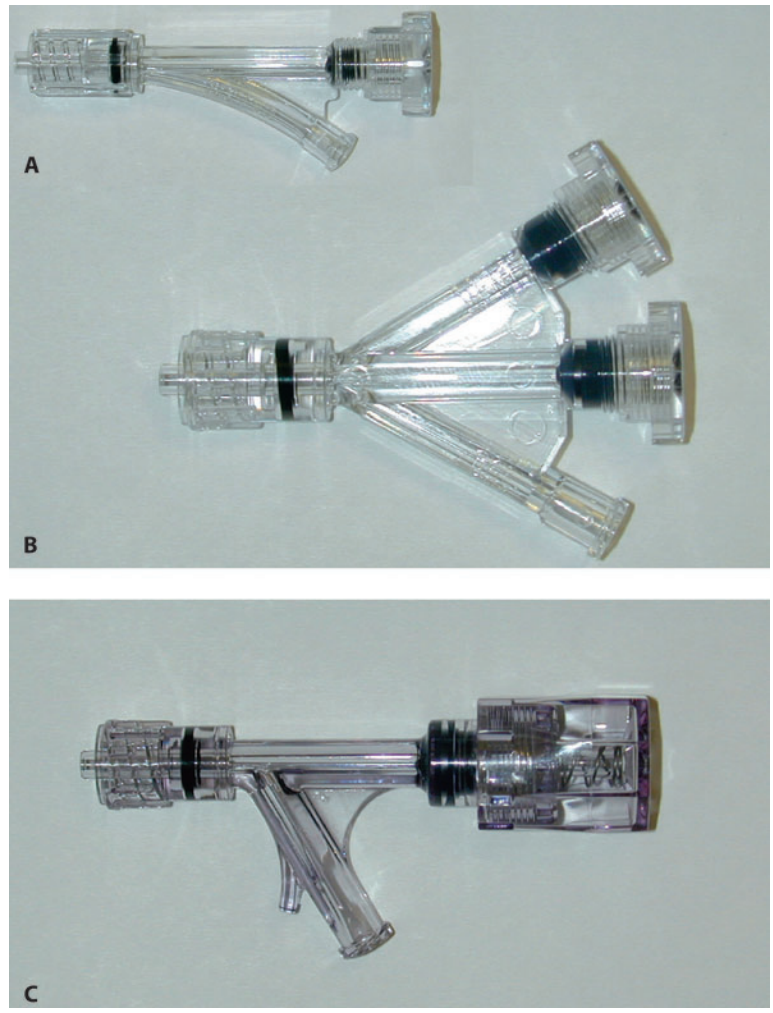

Fig. 14.82A–C. "Y" hemostatic valve adapters. **A** Two-port adapter. **B** Three-port adapter. **C** Headway (Cathnet-Science) valve prevents retrograde backflow

proach can be used. Usually a 5-F guiding catheter is used for the balloon on one side and a 5- or 6-F guiding catheter in the other side for easy, repeated guidance angiography.

When large-caliber guiding catheters are used, or when using multiple catheters in the brachiocephalic, maxillofacial, or spinal arteries, spasm may occur. A very effective way to deal with such spasm is the intra-arterial injection of 50–100 μg of nitroglycerin (Figs. 14.83, 1.48).

Balloon Remodeling. Moret et al. (1997) described a technique to deal with wide-neck aneurysms, or aneurysms with poorly defined necks, to prevent the coils from compromising the parent vessel lumen. The technique consists of a balloon-assisted protection of the native vessel lumen with a balloon-tip catheter, while a second microcatheter delivers the coils (Fig. 14.84A–D). The inflated balloon forces the coils to take a concave configuration, literally remodeling the coil mass and anchoring it within the aneurysm sac. Unless the anatomy of the aneurysm is obviously unsuited for conventional GDC coiling, we will first try to place a 3-D or 2-D frame; if this is not possible we will switch to Moret's remodeling technique.

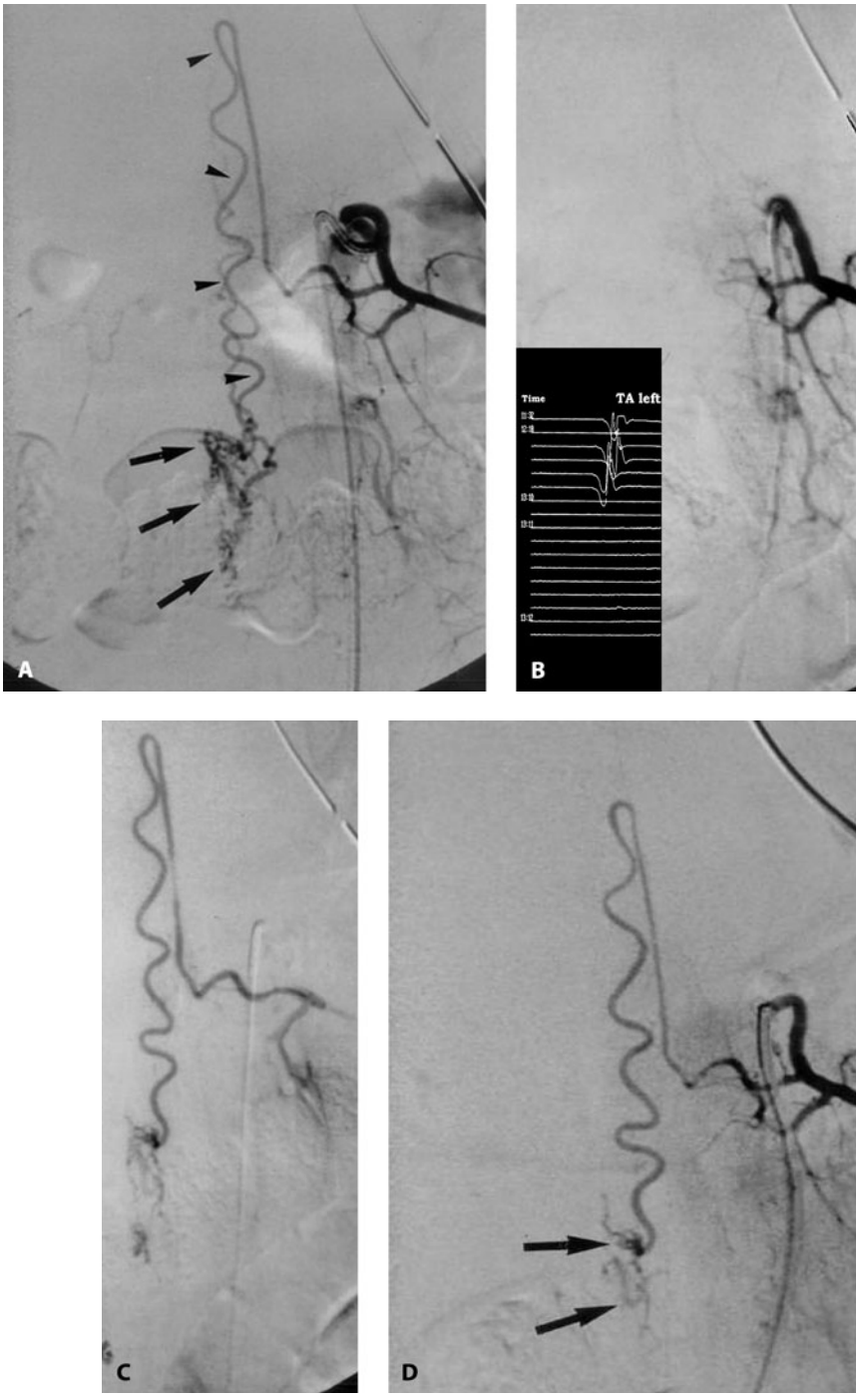

Fig. 14.83A–D. Clinical treatment of vasospasm (also see Fig. 1.48). **A** Spinal cord arteriovenous malformation (AVM, *arrows*) supplied by the ASA (*arrowheads*). The motor-evoked potentials (MEPs) flatten during catheterization. **B** The ASA is not opacified. **C** After 75 µg nitroglycerin the spasm is released, small residual spasm in the ascending limb of the ASA. **D** After particle embolization of the AVM, there is a small residual spasm (*arrows*)

Fig. 14.84A–J. Remodeling balloon technique. **A–D** Diagrammatic representation of Moret's remodeling technique. **A** Broad-base aneurysms, the coils protrude into the parent vessel. **B** Balloon inflation assists by protection of the native vessel lumen, while a second microcatheter is delivering the coils. **C** The coils will be remodeled and **D** will maintain their position after balloon deflation. **E** Three-dimensional angiogram of a hypophyseal aneurysm with a poor neck-to-dome ratio. **F** Road map demonstrating the leading loop of a 3-D coil extruding into the internal carotid artery (*arrow*), which also occurred with a 2-D coil. **G, H** Frontal oblique views show the balloon (*curved arrows*) protecting the coils from protruding into the parent artery. **I–J** see p. 1034

►

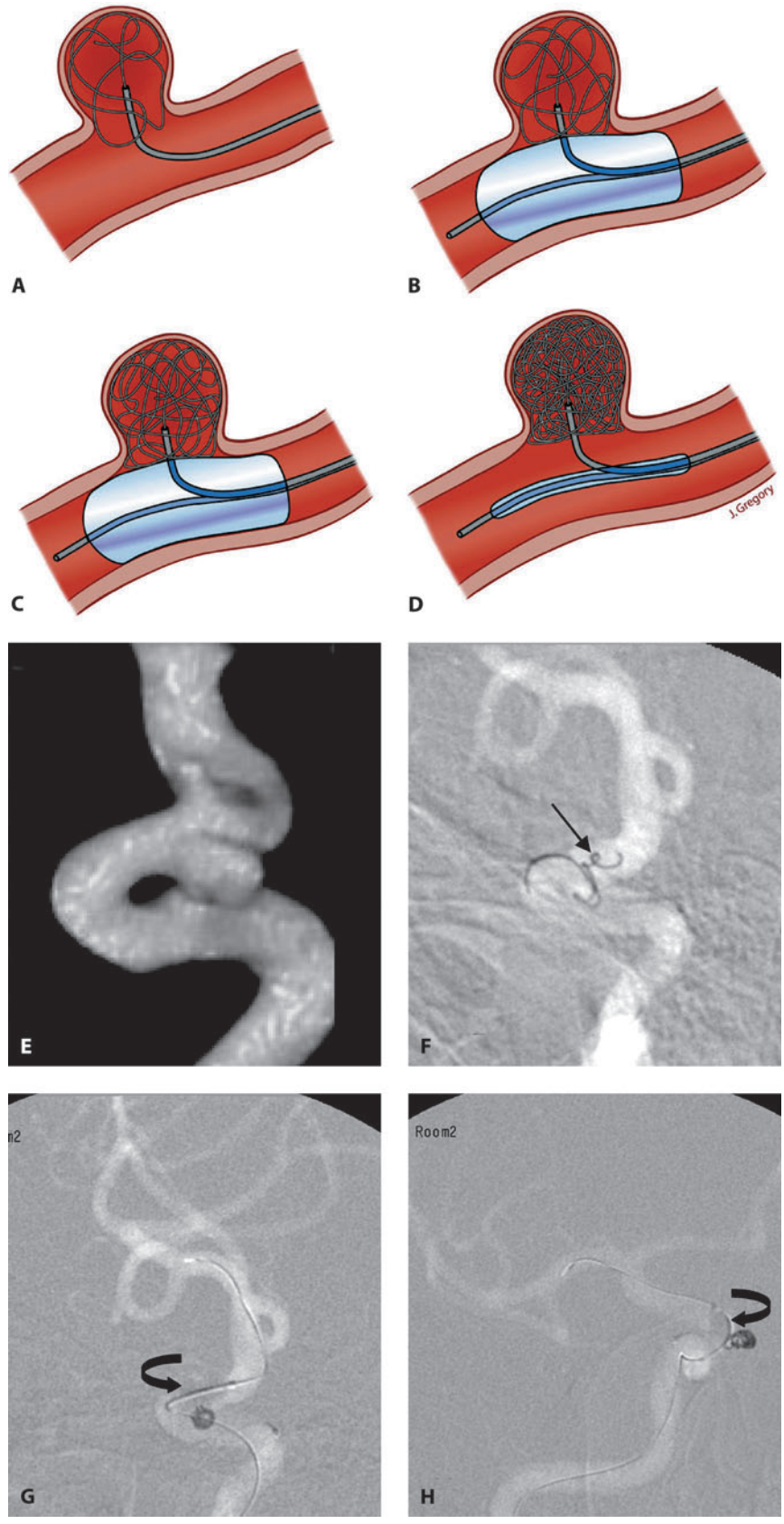

Fig. 14.84A–H.
Legend see p. 1032

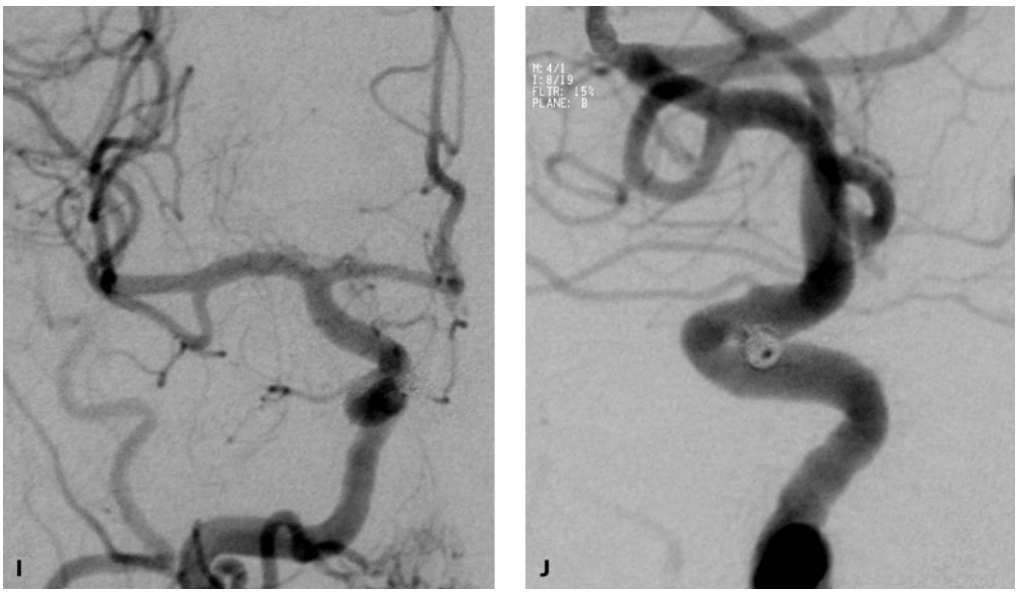

Fig. 14.84 (*continued*). **I** Frontal and **J** oblique lateral projection demonstrate the coils within the aneurysmal sac

This remodeling technique is more difficult and technically more demanding than the single-catheter technique: it is more prone to spasm of the carotid or vertebral arteries, there are more lines to watch, and more hardware in the patient; adherence to meticulous technique is even more imperative with experience, it increases safty in wide neck aneurysms.

Although denser packing can be achieved with this remodeling technique, no long-term advantages have been proven as yet, and we reserve it for difficult cases and not necessarily for denser packing.

Various balloon-tip catheters are presently available for this purpose, including the Sentry from Target (Boston Scientific) (Fig. 14.29), or the Equinox from MTI (San Jose, CA, USA) (Fig. 14.30). Both use a similar design. They are single-lumen low-profile microcatheters with hydrophilic coating. Various distal tip segments and balloon sizes are available. A 0.010-in. microguidewire is used for navigation, to seal the distal end of the catheter, and permit inflation of the balloon (Figs. 14.29, 14.30). The microguidewire will also prevent back flow of blood. The wire is inserted with a Y-adapter with a hemostatic ring (Fig. 14.29); the side arm of the Y-adapter is connected to a 1-ml Luer-Lok syringe with 0.1–0.4 ml for balloon inflation, depending on the balloon size.

The technique can be useful to protect a proximal segment of a vessel that may be partially incorporated in the aneurysm neck (Fig. 14.85).

The guidewire tip is positioned distally into a major branch such as the middle cerebral artery for better support and stability. Whenever possible, we try to have a J shape at the distal wire to prevent accidental entrance in to a small normal vessel. Balloon occlusion should be as short as possible; if the circle of Willis is competent, occlusion times are better tolerated. If the circle of Willis is incompetent short occlusions of probably less than 2–3 min should be attempted, with periods of at least 5 min between inflations, to avoid repeated cumulative periods of ischemia.

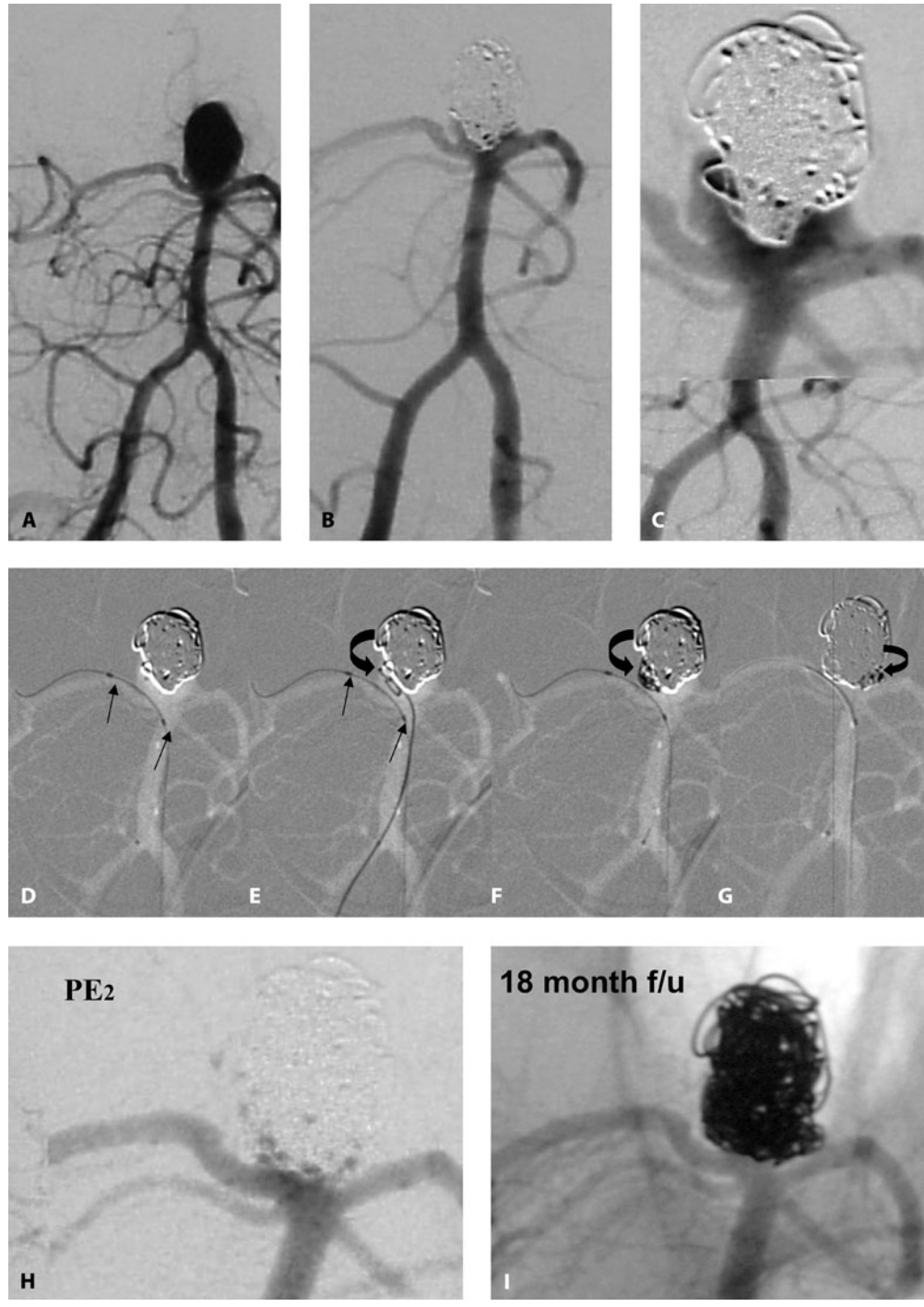

Fig. 14.85A–I. Remodeling technique in the basilar system. **A** Frontal digital subtraction angiogram (DSA) of a large basilar apex aneurysm. **B** Immediate after the first embolization. Note the incorporation of both posterior cerebral arteries (PCAs) into the neck with the right more so than the left. **C** Follow-up DSA 12 months later demonstrates compaction on both sides of the aneurysm. **D** Road map frontal view with the balloon for remodeling protecting the right PCA, (*arrows* point to the two radiopaque markers that indicate the length of the balloon). **E** Placement of the first coil (*curved arrow*). **F** Additional coils are placed with balloon protection (*curved arrow*). **G** After the right-side coiling, it was easy to pack the corner on the left side with ultrasoft coils (*curved arrow*). **H** Immediately after the second procedure, an excellent remodeling of the right PCA was obtained. **I** Eighteen months follow-up in frontal projection

In general we place the balloon-tip catheter first, usually beyond the orifice of the aneurysm (Fig. 14.86D), the microcatheter is then inserted, and the aneurysm is catheterized; the balloon is then positioned across the orifice of the aneurysm with road mapping. There is usually a lag time with these systems, so one should be careful and patient to fine-tune the balloon position (Fig. 14.86C–E).

The balloon is first inflated across the orifice of the aneurysm, the coil is then deployed but not detached, the balloon is then slowly deflated, usually using a new road map acquisition, and the coil or coil mass observed for 1–2 min; if there is no movement of the coil, the coil is detached (Fig. 14.86). For the most part, guidance angiography to check the parent artery and distal branches is frequently done between coils and prior to detachment. The same procedure is followed after each coil deployment and before detachment.

At the end of the procedure, prior to withdrawing the microcatheter, a guidewire is advanced through the microcatheter as a safety measure, which can be used if a coil is seen to come back; the balloon may be partially or fully inflated as an additional precaution.

In cases where the exact location of the parent artery is not clear, or in cases of more than one aneurysm, where the coils in one lesion may overlap the second aneurysm, the balloon is invaluable to know where the vessel lumen is at all times and make it very easy and safe (Fig. 14.87).

Fig. 14.86A–I. Remodeling technique. **A** Lateral digital subtraction angiogram (DSA) of the left internal carotid artery. There is a previously treated aneurysm on the right. The coils are subtracted (*arrow*). The left side aneurysm has a broad neck. **B** Road map of the cervical carotid artery demonstrates the tortuous course of the internal carotid artery. Note there are two microcatheters. We tend to use a "J" curve on the wire as a guiding lead for less traumatic advancement. **C** Frontal oblique projection demonstrates the balloon-tip catheter, which is the first catheter introduced and then advanced beyond the aneurysm. The "J" in the wire (*arrow*) leads. **D** The balloon (*two small arrows*) is beyond the aneurysm and placed first. The tip of the microcatheter to deliver the coils (*arrowhead*) is at the entrance of the aneurysm. **E** The microcatheter has entered the aneurysm (*arrowhead*). The balloon is then brought back across the neck of the aneurysm. **F** First coil delivery. The balloon (*curved arrow*) is inflated to prevent the coils from protruding into the carotid artery. **G** Additional coils have been advanced. The balloon is inflated every time an additional coil is introduced. Note the coil is abutting against the balloon and is remodeled. **H** Using the road-mapping technique, a new mask is obtained. Prior to detachment of the coil, the balloon is deflated (*open curved arrow*), and the coil mass is observed. If there is no motion the coil is then detached. **I** Lateral DSA angiogram after embolization. Note the near total obliteration. There is a small residual aneurysm at the distal portion of the neck ►

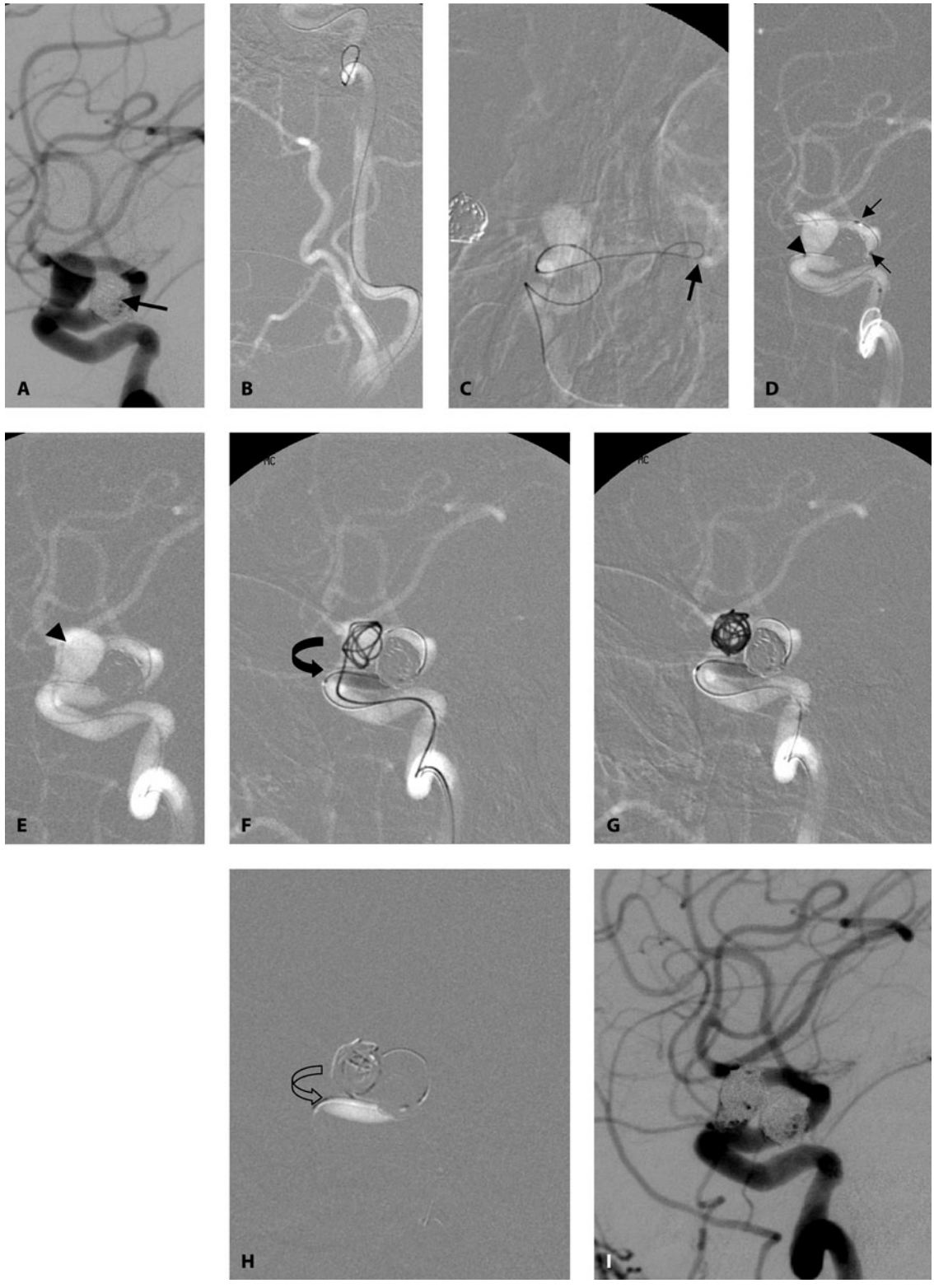

Fig. 14.86A–I. Legend see p. 1036

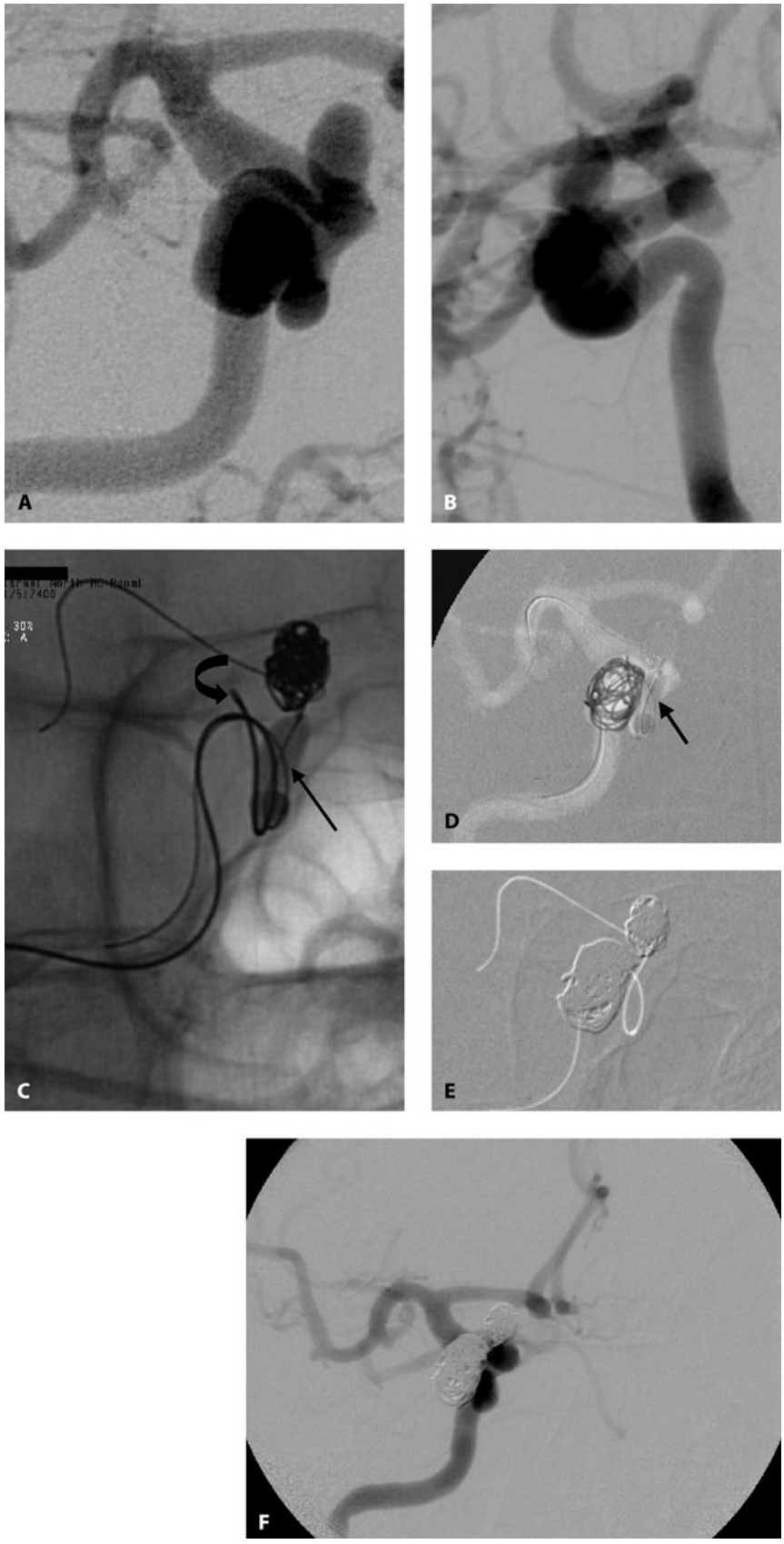

Fig. 14.87A–F.
Legend see p. 1039

Two-Microcatheter Technique. There are specific instances where balloons cannot be properly placed across the neck of an aneurysm, but the aneurysm configuration may permit the use of two microcatheters simultaneously, using one coil to secure the other prior to detachment (Fig. 14.88). It is important that stability of both coils is secured before detachment. A period of observation is recommended; if there is no movement of the coils, detachment is then started. If simultaneous detachment is desired, both proximal markers are advanced to the detachment position. If one would prefer to detach one coil at a time, the coil to be detached is detached, while the proximal marker of the coil that will not be detached is kept proximal to the detachment marker. Note that even if only one detachment box is used, if both markers are in the exposed (detachment) position, electrolysis can occur on both coils.

Trispan. In broad-neck aneurysms, the main problem is to prevent the coil or coils from protruding into the parent vessel (Figs 14.89, 14.90). A multileaf (3–6) or multiloop nitinol ring configuration device, with an outer core platinum radiopaque marker at each loop has been developed (Figs. 14.89, 14.91): the Trispan (Target, Boston Scientific). The device can de detached by electrolysis, like the regular GDC coil. There is a radiopaque marker at the inner and outer portion of the detachment zone, soldered to a pushing mandrill or wire, with an electrolytic detachment zone (Fig. 14.90). The device can be very helpful in aneurysms with a broad neck, broad-based terminal aneurysms such as basilar artery aneurysms, or when a vessel is incorporated at the neck of the aneurysm (Fig. 14.91). There is still limited experience with this technique, and coil compaction continues to be a problem (Fig. 14.91H, I). Interestingly, one can recoil through a previously deployed Trispan, and despite the compaction of the collaterals mass, the Trispan remains in position (Fig. 14.91J–O). The Trispan device is the first attempt to add neck bridging devices to our armamentarium, some placed in to the aneurysm lumen and others in the parent vessel lumen, including stents designed for aneurysm therapy.

◄ **Fig. 14.87A–F.** Remodeling technique in multiple aneurysms. Paraophthalmic and anterior ring aneurysms. The balloon makes it very safe to preserve the internal carotid artery. **A**, **B** Preoperative working position. There are two aneurysms; the exact relation between the carotid artery and the aneurysms is not clear. **C** Plain film after the paraophthalmic aneurysm has been coiled. The balloon (*arrow*) is protecting the carotid artery, and the microcatheter is in the second lesion (*curved arrow*). **D** Monitored by road mapping, the balloon is inflated (*arrow*) and the coils are delivered. **E** At the end, the catheter assembly is removed with a new mask to monitor the stability of the coils. **F** Final angiogram shows an excellent result

Fig. 14.88A–H. Two-microcatheter technique. **A** Frontal digital subtraction angiogram (DSA) of the right internal carotid artery shows a bilobed aneurysm of the right middle cerebral artery bifurcation. **B** Frontal road map with the first coil being delivered. Note the leading portion of the coil protruding toward the middle cerebral artery main trunk (*arrow*). **C** The 3-D coil is delivered within the aneurysmal sac; however, it is unstable in its most distal portion (*arrow*). **D** Prior to detachment of the first coil, a second microcatheter guidewire assembly (*arrow*) is navigated into the aneurysm. **E** The microcatheter tip (*arrow*) is in the second distal dome. **F** A second coil is deposited to anchor the first coil. Note the tip of both microcatheters. **G–H** see p. 1041

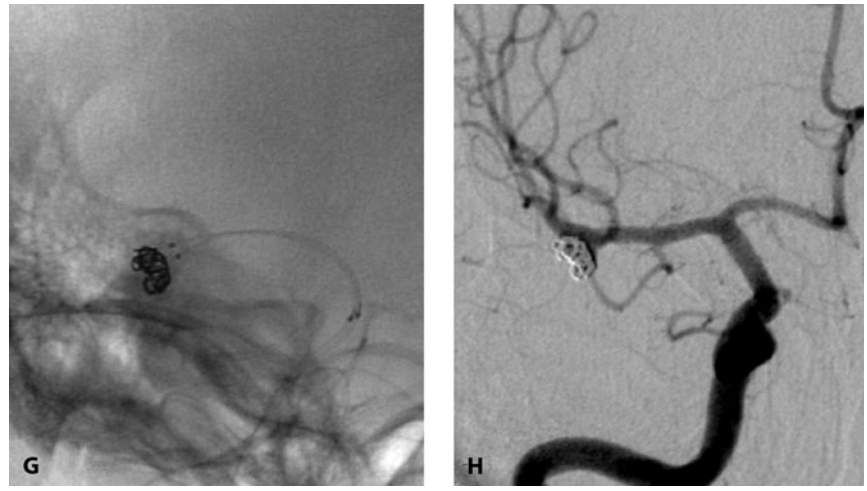

Fig. 14.88 (*continued*). **G** Plain film of the skull demonstrating the tandem use of the two microcatheters with the two microcoils, after a second pair of microcoils have been delivered. **H** Final postembolization angiogram with obliteration of the aneurysm

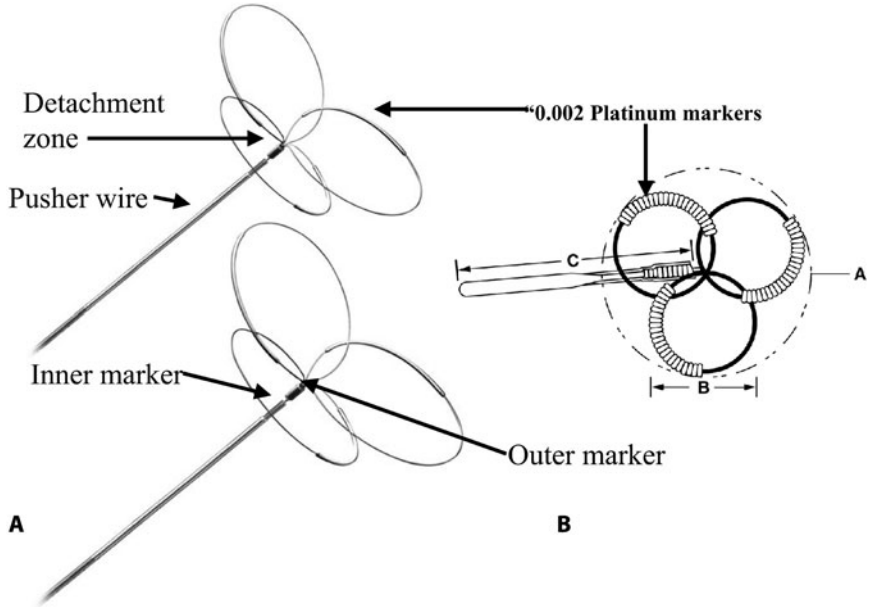

Fig. 14.89A, B. Trispan (Target, Boston Scientific). **A** Device in the open position. Multileaf nitinol loops with platinum radiopaque markers in each leaf, has an electrolytic detachment zone, pusher wire, and inner and outer markers, as the GDC has. **B** Cross-section of the device

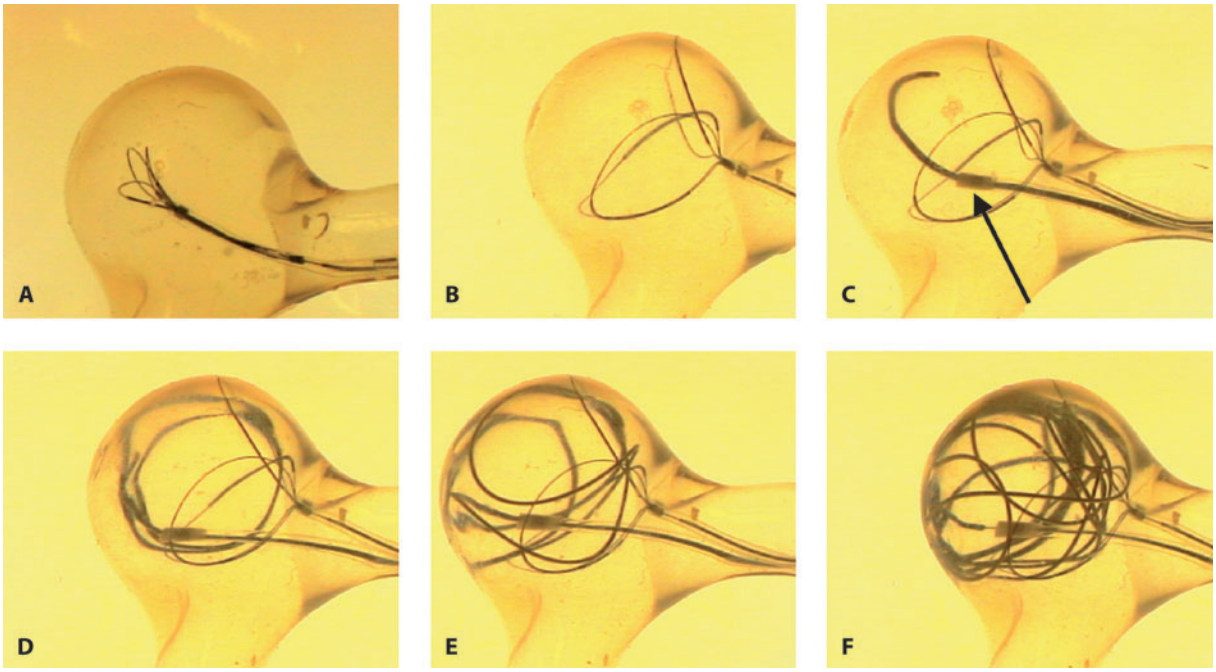

Fig. 14.90A–F. Glass model representing a broad-base aneurysm. **A** First the introduction of the Trispan prior to opening. **B** The Trispan is expanded against the walls of the aneurysmal sac. **C** A microcatheter is then advanced with a guidewire to enter the dome of the aneurysm (*arrow*). **D** As the Trispan is expanded, the first coil, usually a 3-D coil, is then delivered with the Trispan folding the leaves of the coil and preventing it from protruding into the parent vessel. **E** Additional coils are delivered. **F** The coil is within the confines of the Trispan

Fig. 14.91A–N. Giant aneurysm with thrombi and a broad neck. **A** Coronal T1-weighted MRI shows the very large aneurysm with significant thrombi within it. The small luminal portion correlates with the angiogram. **B** Frontal oblique projection of the left internal carotid artery shows the poor neck-to-dome ratio with this broad-base aneurysm incorporating the A1 segment. **C** Working position with a 3-D coil within the aneurysmal sac. Assurance as to stability and protrusion into the parent artery could not be secured and the procedure was aborted. **D** Plain film of the skull shows the radiopaque platinum in the expanded leaves of the Trispan, the proximal and distal markers. **E** Working projection frontal view after coiling demonstrates the dense coil mass within the Trispan confines. The proximal detachment of the Trispan is seen (*arrow*). **F** Postoperative angiogram demonstrates the excellent obliteration of the aneurysm, with preservation of the A1 segment. **G–N** see p. 1044

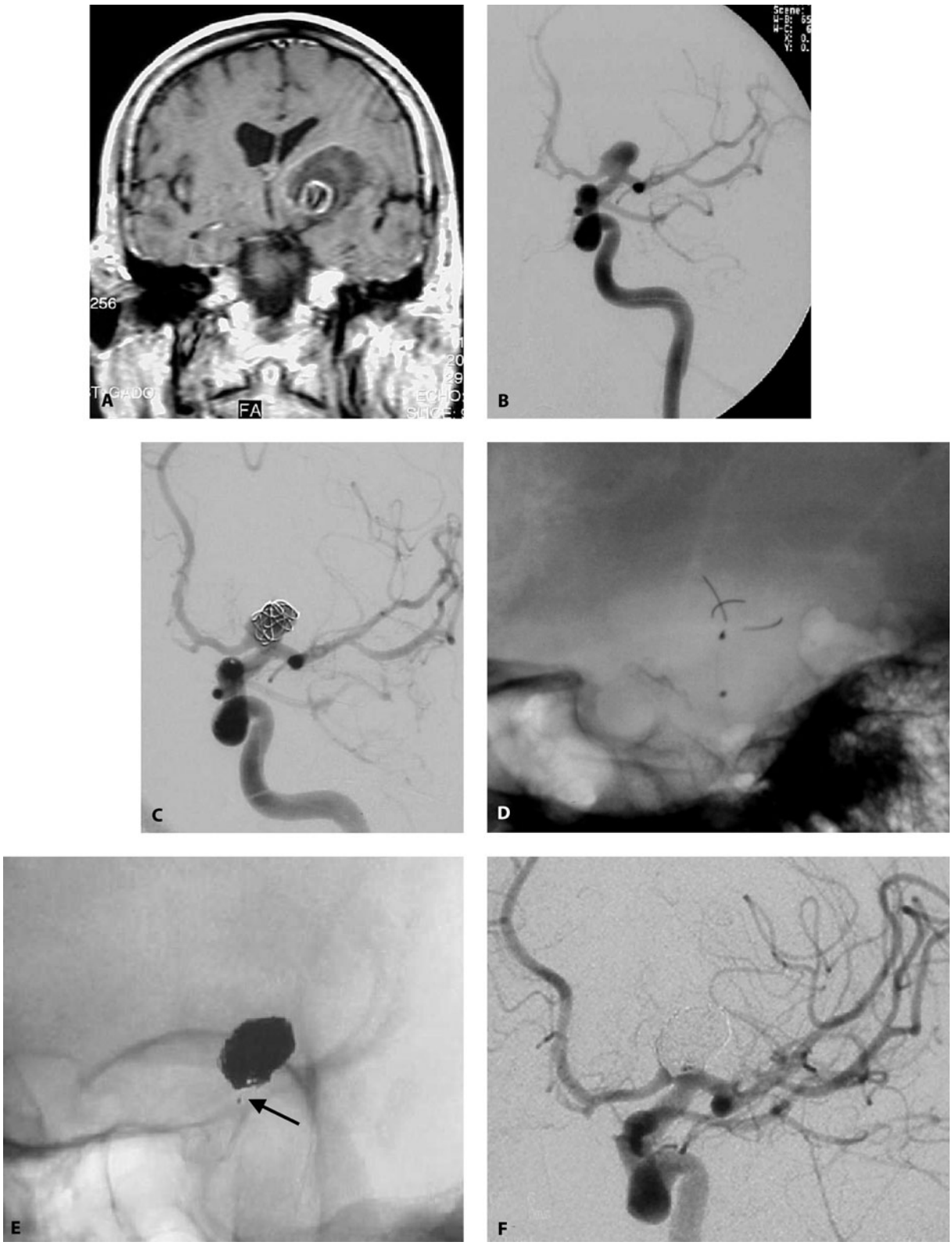

Fig. 14.91A–F. Legend see p. 1042

Fig. 14.91G–N.
Legend see p. 1045

Stent Protection. As stent technology continues to improve, with ever decreasing stent profiles and increased stent flexibility, stents can be used to bridge the neck of an aneurysm. Once the stent has been deployed, coils are detached by passing a second microcatheter through the stent cells or on the outside of the stent. This technique can be used in the carotid artery (Fig. 14.92) or in the basilar artery (Fig. 14.93). Although effective, the long-term outcome of this combination is not yet well established, and we have seen recurrences (Fig. 14.93H–O). Preoperative and postoperative measures must be taken, with a rigorous antiplatelet protocol (see Sect. 14.16). A very promising technique is the combination of balloons, stents, and liquid embolics (Skizora et al. 1996; Mawad et al. 2002). The stent is first deployed, leaving the angioplasty balloon deflated but in place. Prior to the liquid embolic injection, the balloon is inflated, blood flow is stopped, and the liquid is injected. The stent cells will act as a scaffold, allowing the liquid embolic agent to seal the aneurysm and deliver the liquid embolic agent between the vessel wall and the stent (Fig. 14.94).

Coil Stretching

Coil stretching or unraveling refers to the unintentional elongation of the coil while attempting to bring back or reposition the coil. It is more likely to occur in the smaller 10-gauge coils. It is better to avoid stretching than to deal with it when it occurs. To prevent stretching of a coil when bringing it back or repositioning it, careful alignment of the catheter tip to the coil is important. If the coil does not respond with one-to-one responsiveness, slight withdrawal of the microcatheter, and, if needed, the coil and catheter as a unit will prevent the problem. It is imperative to ensure that other coils or the entire coil mass do not move; if this is a possibility, it may be safer to leave the stretched coil in the vessel than risk worsening the situation, and placing the patient on anticoagulants and antiplatelets.

Stretching is also more likely to occur if there is friction during the advancement of the coil through tortuous anatomy, with an attempt to bring back the coil, multiple repositioning, or trying to rotate the device, which should be avoided. The addition of the soft and ultrasoft stretch-resistant GDCs has for the most part resolved this problem (Fig. 14.67).

◄ **Fig. 14.91** (*continued*). **G** Lateral and **H** frontal angiograms following recurrence of the aneurysm. There is recanalization in the anterior inferior portion of the aneurysm. Note the Trispan was unchanged and the radiopaque proximal detachment point. **I, J** Road map images following the advancement of a microcatheter through the Trispan leaves and placement of additional coils in the open portion of the aneurysm. **K** Oblique projection of a superselective injection of the catheter within the aneurysm, demonstrating the relation of the residual dome to the A1 segment. At this point, it was felt that it was unsafe to continue coiling. **L** Frontal and **M** lateral plain film of the skull showing the new coil Trispan appearance. **N** Postoperative angiogram demonstrating the small residual portion in the A1 (*curved arrow*)

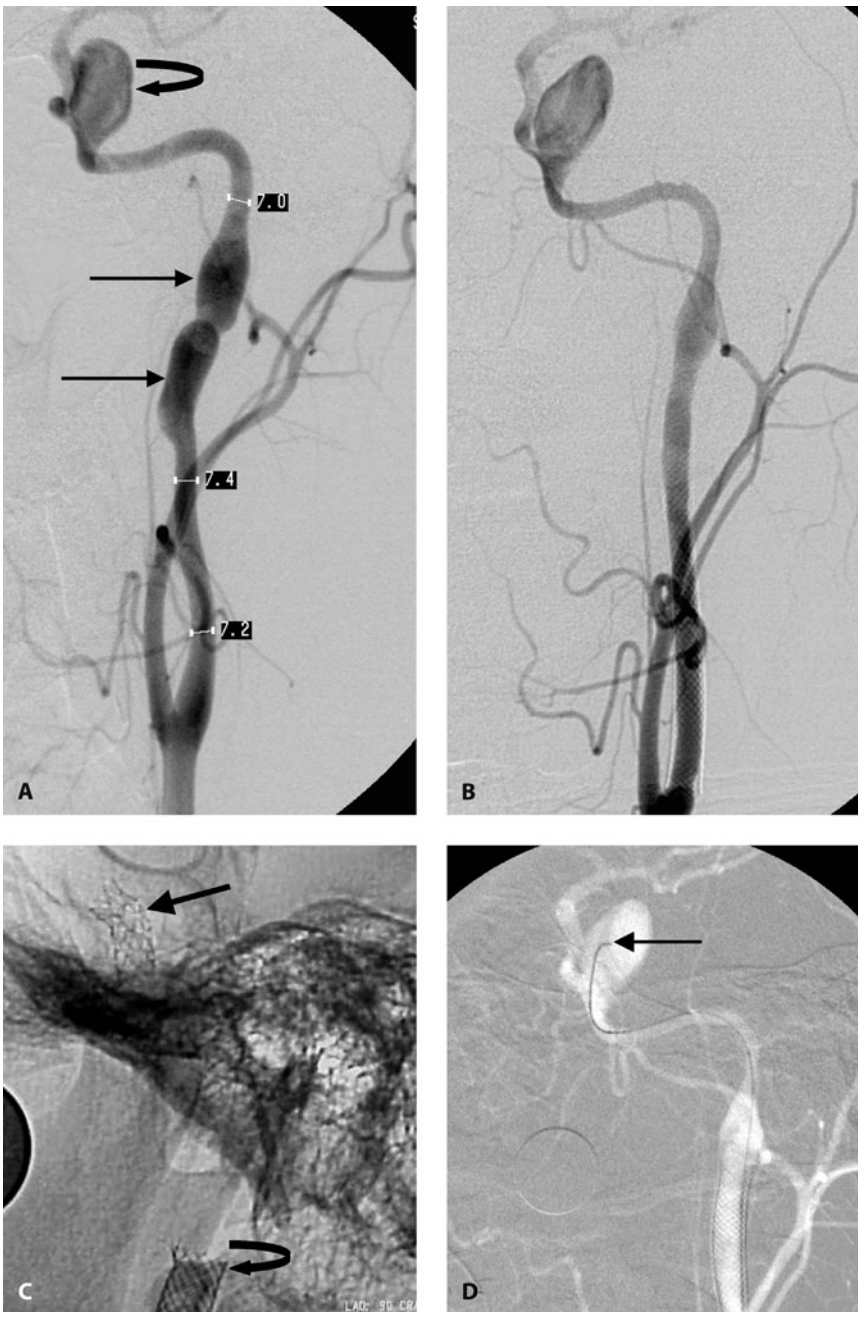

Fig. 14.92A–G. Dissecting aneurysms of the cervical internal carotid artery and traumatic aneurysm of the precavernous internal carotid artery. **A** Frontal oblique projection of the left common carotid artery shows the dissecting aneurysm of the cervical internal carotid artery (*arrows*) and the broad-neck traumatic aneurysm of the precavernous petrous carotid artery (*curved arrow*). **B** Follow-up angiogram 3 months after the placement of a self-expanding Wallstent (Boston Scientific, Watertown, MA, USA) in the cervical internal carotid artery, with near total remodeling of the carotid artery. **C** Cone-down view after a balloon expandable AVE stent (AVE/Medtronic Minneapolis, MN, USA) has been placed across the neck of the petrous aneurysm (*arrow*). Note the distal end of the Wallstent (*curved arrow*). **D** Road map after expansion of the stent at the level of the aneurysm entrance and placement of a microcatheter through the cells of the stent and into the aneurysm (*arrow*). **E–G** see p. 1047

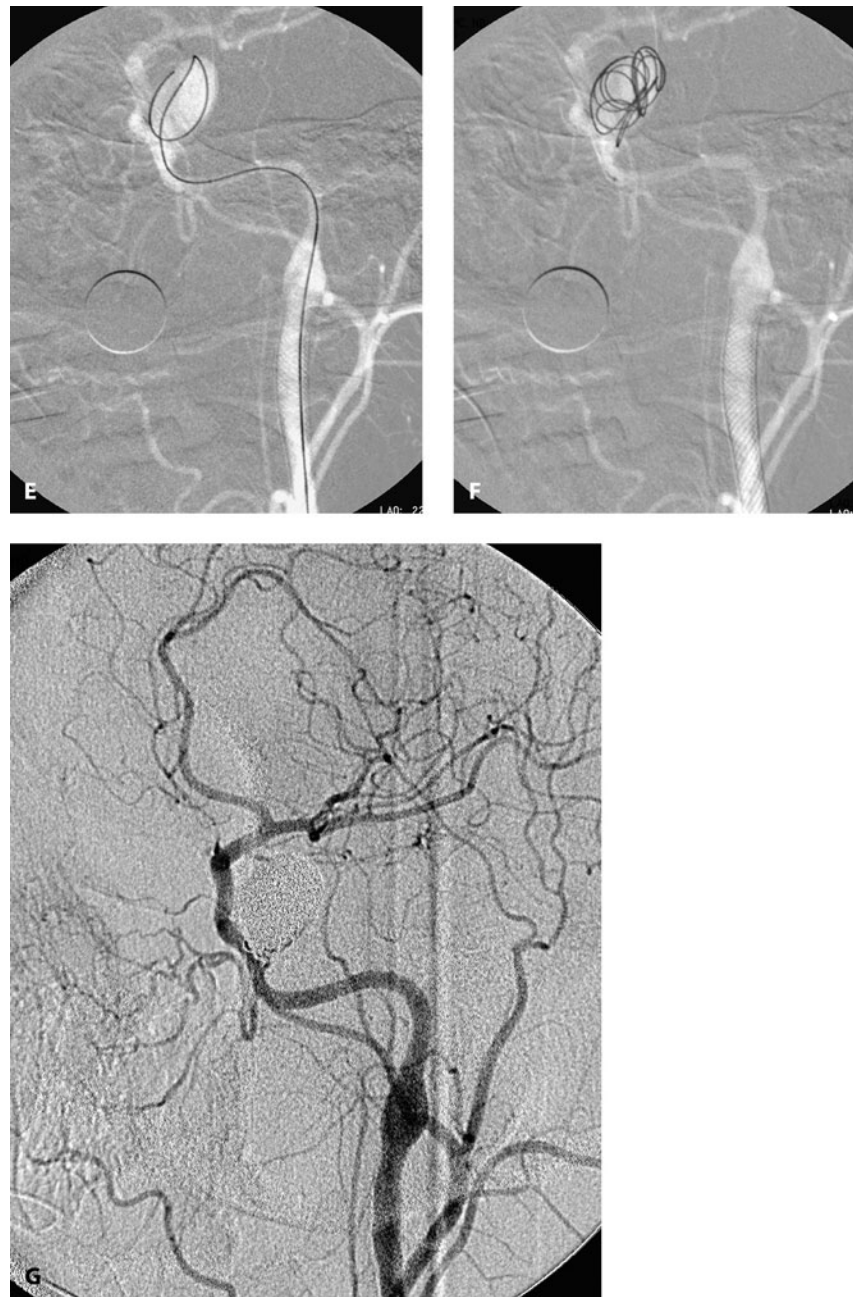

Fig. 14.92 (*continued*). **E, F** Progressive coiling of the aneurysm with the stent protecting the carotid artery lumen. **G** Angiogram of the left common carotid artery after coil placement within the broad-based aneurysm protected by the balloon-expandable stent, with an excellent clinical and angiographic result

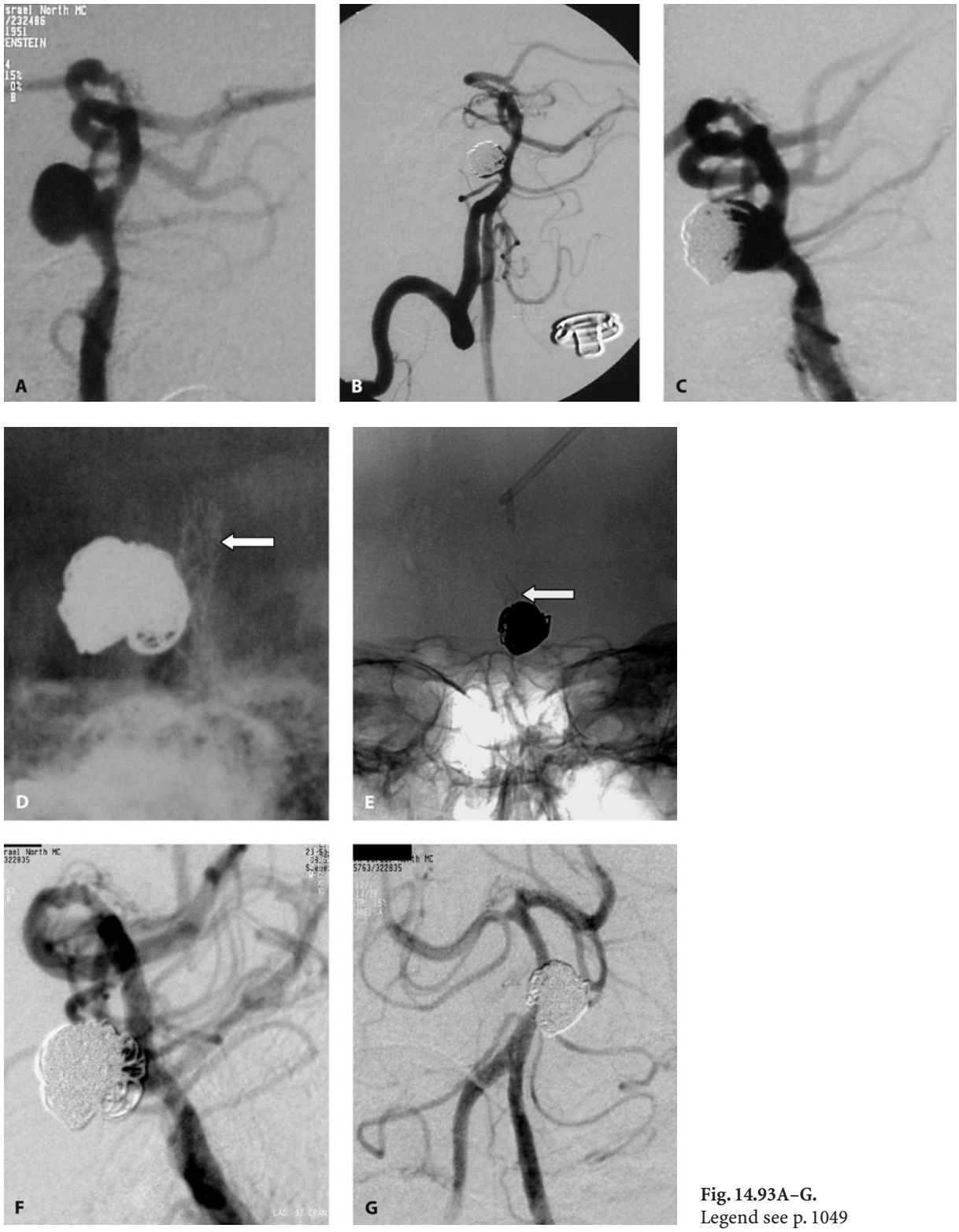

Fig. 14.93A–G.
Legend see p. 1049

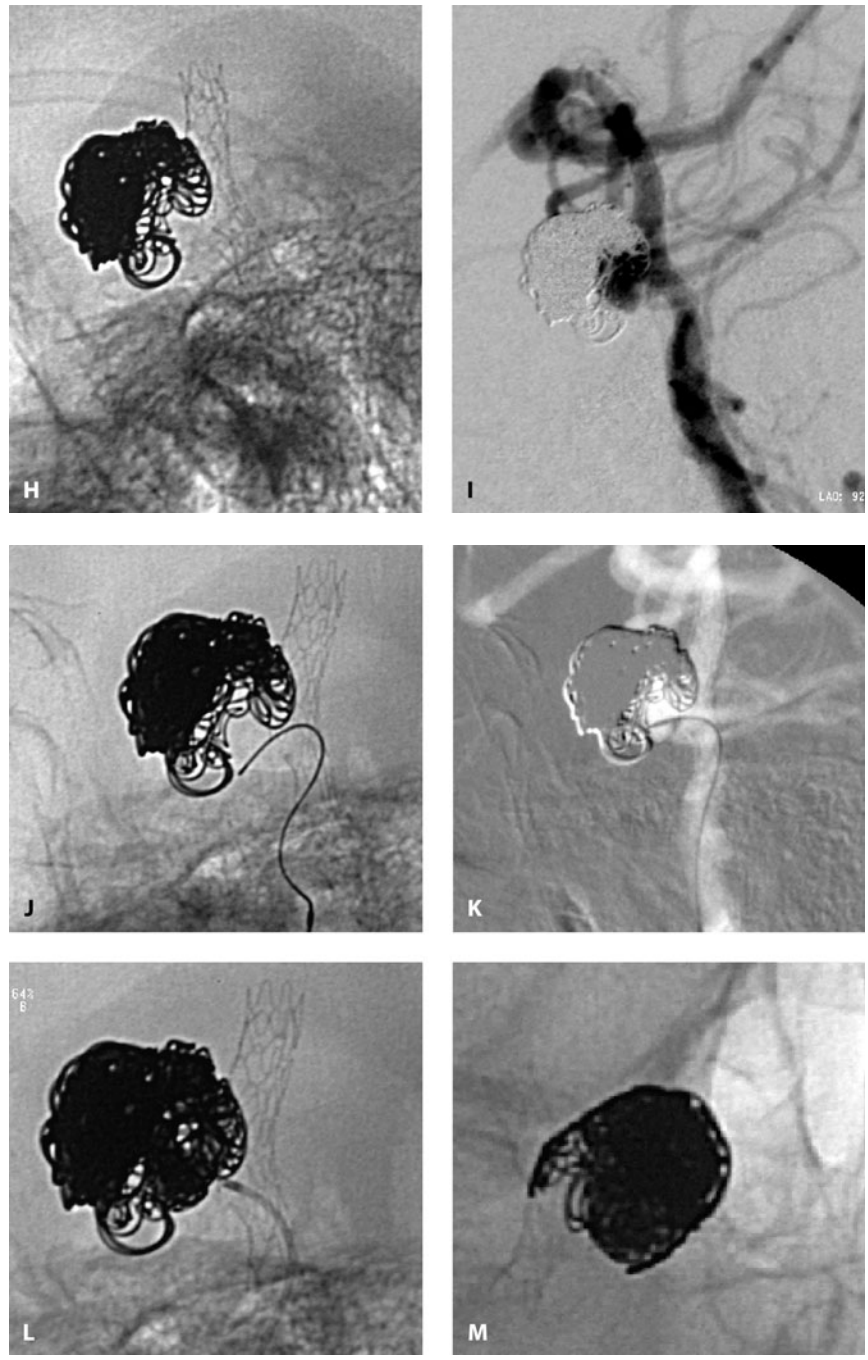

◄ **Fig. 14.93A–O.** Recurrent broad based mid-basilar aneurysm. **A** Lateral view of the left vertebral artery injection shows a broad-based anteriorly pointing mid-basilar aneurysm with a broad neck and atheromatous changes in the vertebrobasilar system. **B** Immediate result after coiling in the acute phase after subarachnoid hemorrhage. **C** Six-month follow-up. There is compaction of the coils with recurrence of the aneurysm. **D** Lateral and **E** frontal plain film of the skull showing a stent (*white arrow*) through which coils were placed to close the recurrence. **F** Lateral and **G** frontal views of the left vertebral artery injection after stenting and coiling demonstrates the coils to be around the basilar artery, and the basilar lumen protected by the stent. **H, I** One year later, there is compaction of the coils. Note the angulation of the mid portion of the stent, where the compaction occurred. **J, K** the lumen of the aneurysm is catheterized, and **L** and **M** after the third time coiling, the stent preserved the basilar artery. **N–O** see p. 1050

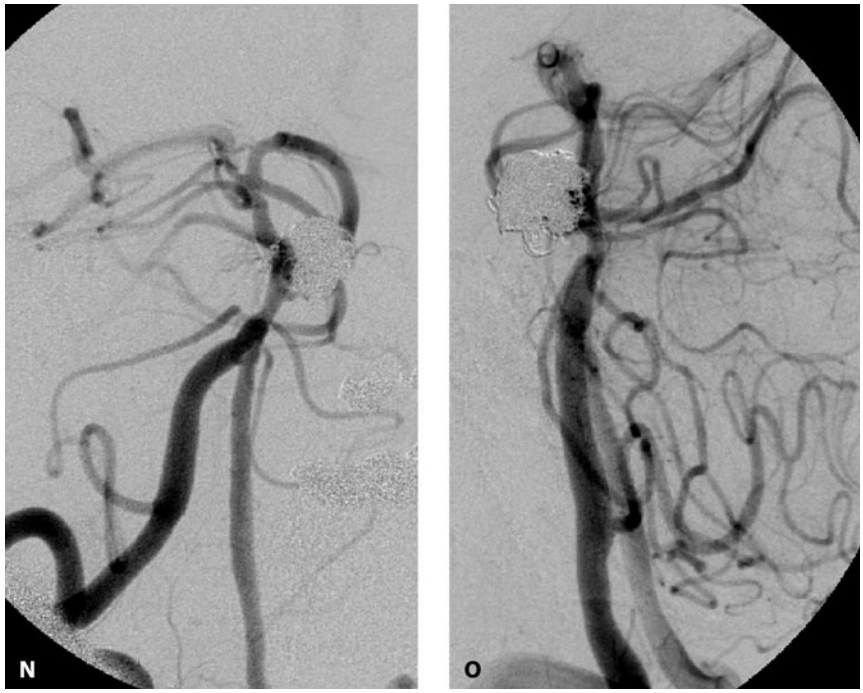

Fig. 14.93 (*continued*). **N, O** Final angiograms

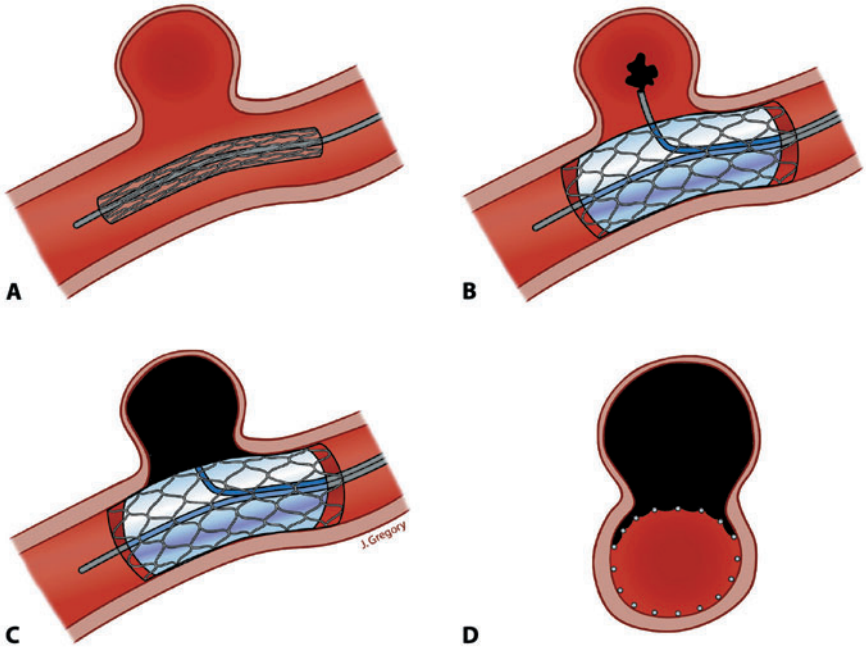

Fig. 14.94A–D. Diagrammatic representation of a stent and balloon protection prior to liquid embolization of a broad-neck aneurysm. **A** The stent must be longer than the neck. **B** The stent is balloon expanded, a microcatheter within the aneurysm delivers the liquid embolic agent with flow arrest by the temporarily inflated balloon. **C** The balloon will retain and model the hardening liquid embolic agent. **D** Cross-section after the treatment. There is a true reinforcement of the vessel wall, with the liquid embolic agent sandwiched by the stent

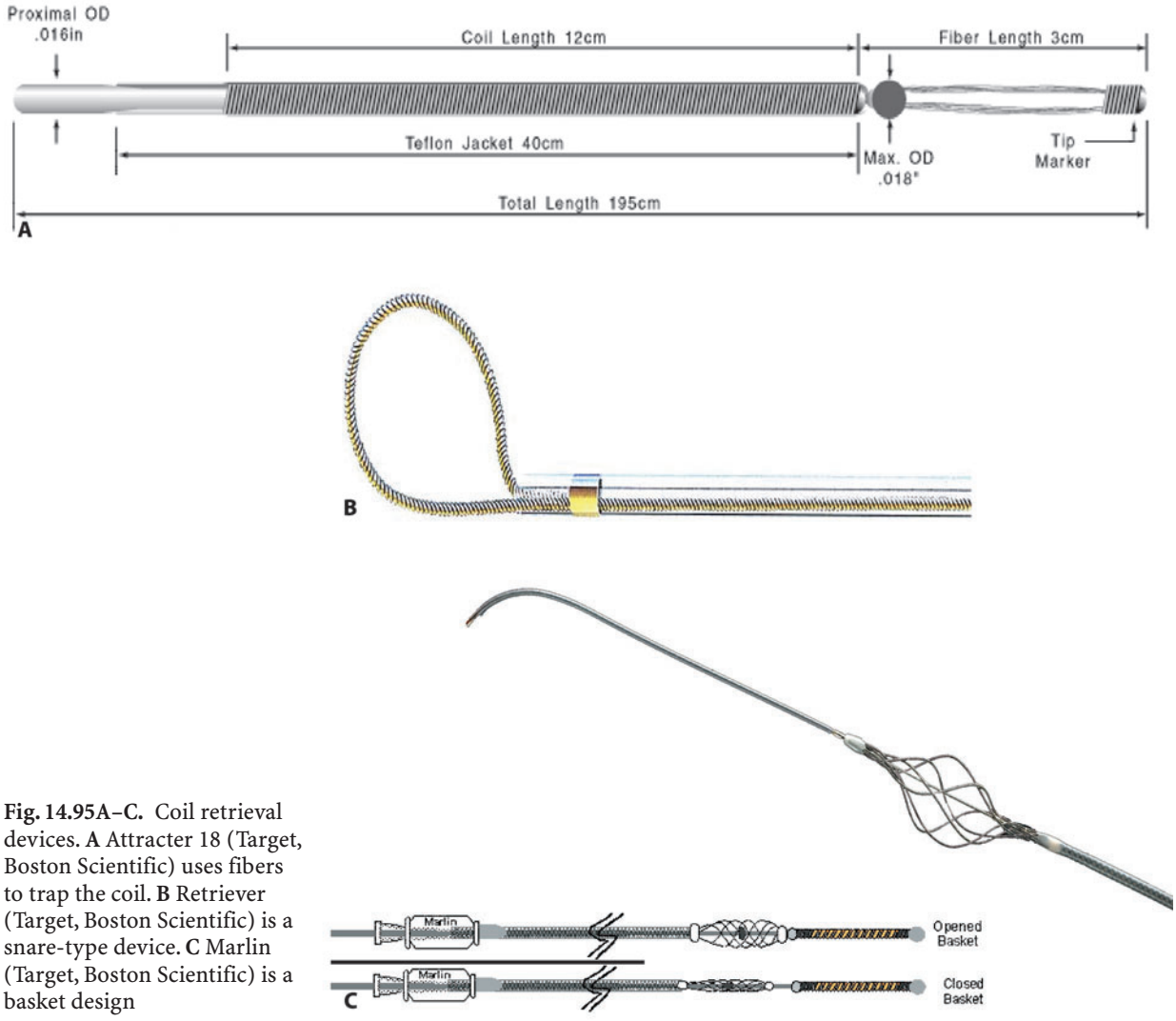

Fig. 14.95A–C. Coil retrieval devices. **A** Attracter 18 (Target, Boston Scientific) uses fibers to trap the coil. **B** Retriever (Target, Boston Scientific) is a snare-type device. **C** Marlin (Target, Boston Scientific) is a basket design

Coil Retrieval

If a coil is accidentally detached or lost in an unwanted location, an attempt should be made to retrieve it, although proper assessment as to the risk versus the benefit of leaving it alone should be considered.

Several devices have been designed for this purpose.

Microvena Snare. The Microvena snare (Microvena, White Bear Lake, MN, USA) is made of a nitinol shaft guidewire with a gold circular ring snare that can be advanced through a microcatheter. Two sizes are available: a 2-mm and a 4-mm ring (Figs. 14.95, 14.96). As the snare exits the catheter, it has a preshaped ring or loop that can turn at right angles to the tip of the catheter and vessel lumen, making it possible to engage the lose end of the coil or another segment of the coil. By then advancing the microcatheter while holding the ring steady until the snare and coil enter the microcatheter, the gold ring then collapses and traps the coil. As the coil is withdrawn, careful fluoroscopic monitoring is mandatory so that the problem

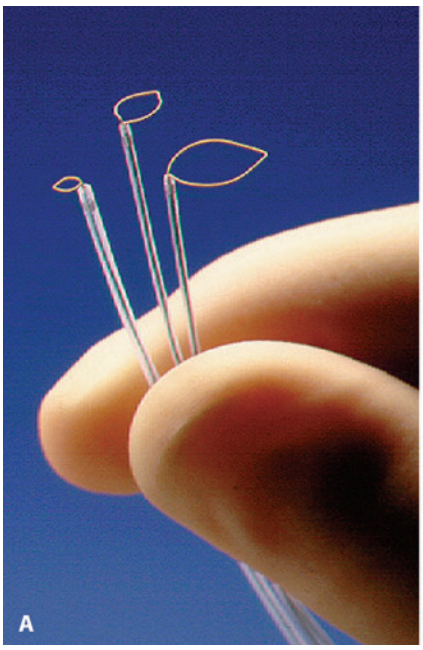

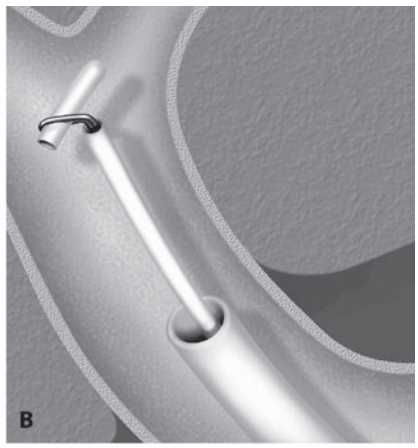

Fig. 14.96A, B. Microvena snare (Microvena, White Bear Lake, MN, USA). We have a limited experience in coil retrieval. The few times we needed to retrieve a coil, this device was used. It comes in various sizes, is made of nitinol (shaft) and gold (ring). **B** Foreign body retrieval (see Fig. 14.167)

is not made worse. Withdrawal is done with the proximal end of the snare firmly fixed, removing the catheter–snare–coil complex as one unit. We have limited experience in coil retrieval, and this is the device we have used in the few instances we have had to retrieve a coil. It can also be used for other foreign body retrieval, including stents (Fig. 14.167).

The Attracter 18. The Attracter 18 (Fig. 14.95A) (Target, Boston Scientific) consists of a 0.016-in. mandrill with a Teflon jacket; the last 3 cm have a fiber complex with a radiopaque marker at its distal end. Turning the wire will trap the loose coil by the fibers.

The Retriever. The Retriever (Fig. 14.95C) (Target, Boston Scientific) is a snare design similar to the Microvena snare.

The Marlin. The Marlin (Target, Boston Scientific) (Fig. 14.95D) is a single-basket unit. It incorporates a nitinol inner guidewire for memory and durability and is wrapped with 4–6 platinum strands for radiopacity. It is Teflon-coated to aid in tracking the device and has hydrophilic coating in the delivery catheter. The basket can be manually opened and closed. Basket expansion is limited to prevent overexpansion, and the basket opens and closes by lateral motion of the inner nitinol guidewire. We have limited experience in coil retrieval, as we believe that it is best to prevent losing a device and have had better results with the 2-mm Microvena device; however, the Marlin retrieval device from Target, Boston Scientific (Fig. 14.95C) is softer and may track better, and the loop size can be varied.

In Time. The In Time device (Fig. 14.97) (Target, Boston Scientific) is made of a nitinol construction, is basket-shaped, and comes in 4- or 6-

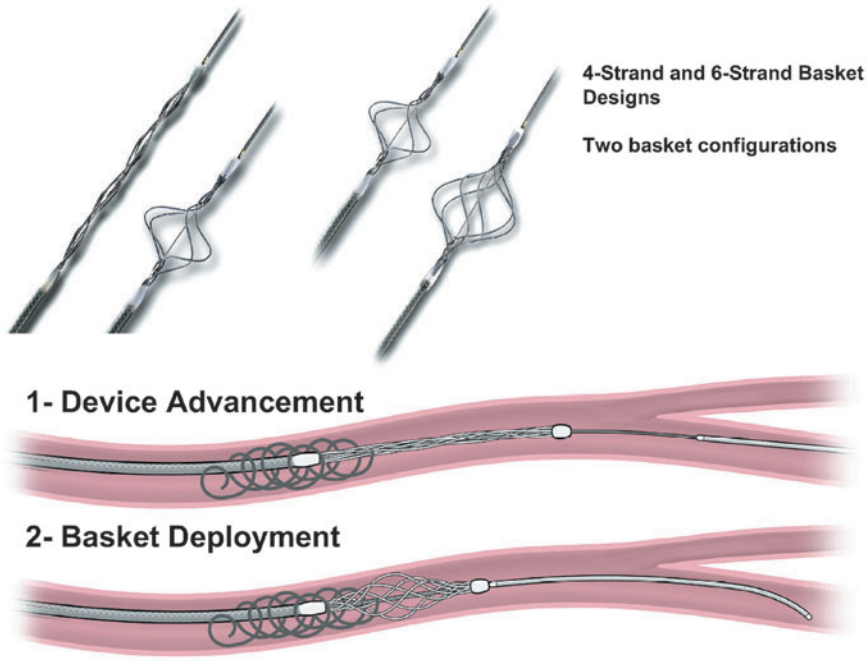

Fig. 14.97. In Time (Target, Boston Scientific) retrieval device. Nitinol construction, basket shape, comes in 4- or 6-strand basket design. First the device is passed beyond the coil (clot or other), the basket is then expanded, the coil trapped and secured with the microcatheter

strand basket design. First, the device is passed beyond the coil (clot or other occlusion), the basket is then expanded, and the coil, clot, or other undesired body is trapped and secured with the microcatheter.

Coil Fixation

In case a loop of coil is protruding into the parent artery, there is a risk of the coil acting as a source of embolus, or it may be unstable and continue to extrude the coil mass pushed by the antegrade flow of blood. Although rare if basic technical principles are respected, it can occur.

Several alternatives exist. Fessler et al. (2000) reported attaching the protruding coil loop with a stent, with a good outcome. In our experience, prolapsed loops will not produce embolic complication if anticoagulant and antiplatelet drugs are used; the stent may even increase the amount of metal exposed to the blood flow (Fig. 14.98). This maneuver should therefore be reserved for extreme instances where there is significant compromise in the parent vessel lumen, or when there is clot formation despite proper anticoagulation.

It is probably wise to first observe the stability of the coil. If stable and no associated clot is formed, a long course of antiplatelets is very effective, and we do not add more exposed metal to the blood flow by adding a stent. We have had two such instances (Fig. 14.98). In one patient a single TIA occurred several weeks after the coiling, which responded to antiplatelet medication.

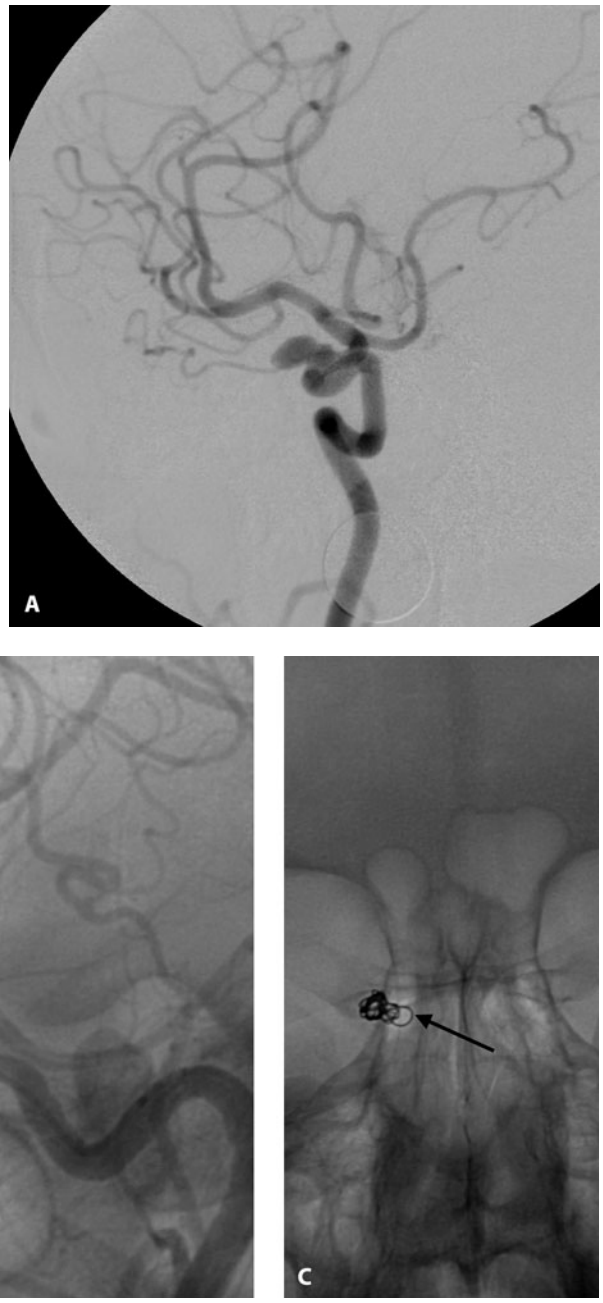

Fig. 14.98A–C. Coil loop protrusion. **A** Digital subtraction angiogram of the right internal carotid artery working position shows a paraophthalmic aneurysm with a broad neck. **B** Lateral oblique projection of the right internal carotid artery following partial coiling of the aneurysm. Note a loop protruding in the parent vessel lumen (*arrow*). **C** AP view with the loop in the carotid lumen (*arrow*). Patient treated with anticoagulation and antiplatelet medication with no complications and long-term follow-up. Placement of a stent in this case would have more metal exposed to the blood flow, and coil retrieval could result in protrusion of the other coils, creating a potentially more difficult situation

Liquid Embolics in Aneurysm Treatment

Kerber et al. (1985) treated a patient with a facial artery pseudoaneurysm with isobytil-2-cyanoacrylate (IBCA). They were unable to preserve the parent artery, although in the facial territory such arterial occlusion is of no significance; in other territories such occlusions would not be tolerated.

We have tried the combination of coils and NBCA. The coils are used as a buffer to retain the acrylic within the aneurysm. To safely accomplish such occlusion, proper functional anatomical investigation is needed (Fig. 14.80). With currently available detachable coils, the same result can be achieved in a safer manner.

The use of Onyx (ethylene-vinyl alcohol copolymer, EVOH) and octacyanoacrylate (C.W. Kerber, personal communication) is expanding the applications of endovascular treatment of cerebral aneurysms; however, no reliable data are available on these technique.

Thrombolytics During Aneurysm Treatment

In the treatment of aneurysms, thromboembolic complications remain the most frequent problem. Such complications are usually avoided with aggressive anticoagulation with heparin during the procedure. However, anticoagulation is not used in the early part of acute aneurysm treatment, until the aneurysm is at least partially protected with the first coil.

Thrombolytics. If embolus is noted during the procedure, most often when the aneurysm has previously ruptured, immediate coiling is done first. If embolus is found early in the procedure in ruptured aneurysms or if heparinization has not been started, heparinization is immediately initiated or augmented if it has already been started, to prevent additional emboli from forming. Once the aneurysm is protected, one then proceeds to revascularizing the occluded branch or branches, usually with superselective thrombolytics (i.e., urokinase or r-TPA) (Fig. 14.99).

If an occluded vessel is seen during the procedure, increased heparinization and observation frequently result in spontaneous reopening of the vessel. If after several minutes of no change, one proceeds to local intra-arterial thrombolysis (LIAT) with urokinase, if available, or r-TPA (Fig. 14.100).

Glycoprotein IIb/IIIa Receptor Antagonist. If toward the end of the procedure, as more coil mass is exposed to the parent artery, clot formation occurs despite proper anticoagulation, in most cases persistent or progressive, with an ACT of more than 300, the use of an IV glycoprotein IIb/IIIa receptor antagonist (GPA) such as ReoPro (Lilly Research Laboratories, Indianapolis, IN) is a very effective way to reabsorb the already formed thrombus and prevent further clot formation. An IV bolus of 10 mg is immediately started and continued for 18–24 h (Fig. 14.101). Before starting GPA or thrombolysis in general, it is important to ensure that the aneurysm is protected and to avoid their use in cases of recent surgery, recent arterial puncture at a different site, recent ventriculostomy, or other situations that may result in bleeding.

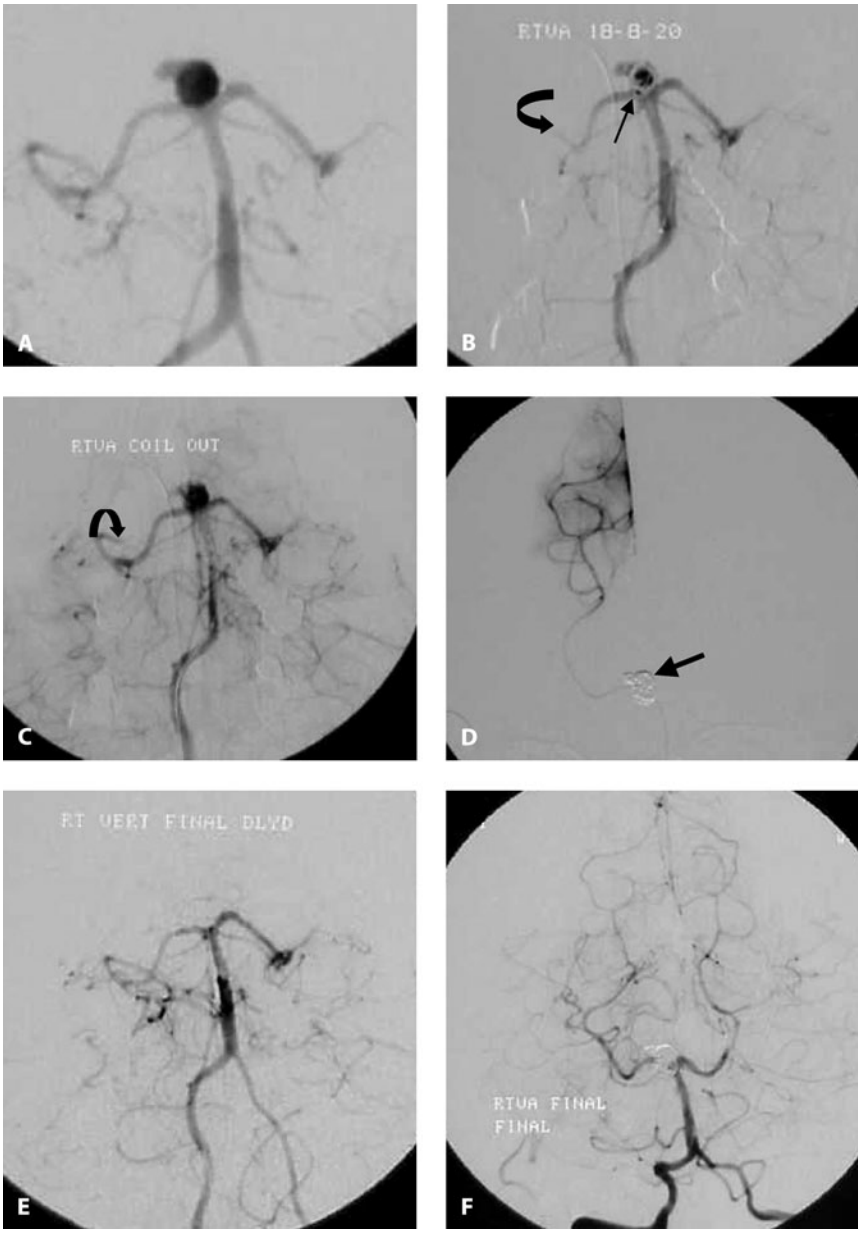

Fig. 14.99A–F. Thrombolytics in aneurysm therapy. **A** Submental-vertex view of the right vertebral artery injection in a grade 3 subarachnoid hemorrhage. There is a basilar artery apex aneurysm with a nipple. **B** After placing the first coil, angiogram demonstrates a distal occlusion of the right posterior cerebral artery (PCA; *curved arrow*). Note the protrusion of one loop into P1 (*arrow*). **C** The coil is removed, the PCA remains occluded (*curved arrow*). Given that the patient had recently bleed, no heparin was used. As the occlusion was recognized and the coil was removed, immediate coiling of the aneurysm proceeded. Once the first coil was in, heparin was started. As soon as the aneurysm was coiled, we proceeded to revascularize the PCA. **D** The aneurysm is coiled (*arrow*), a microcatheter is in the distal PCA that is being recanalized. **E, F** Final angiograms after treatment

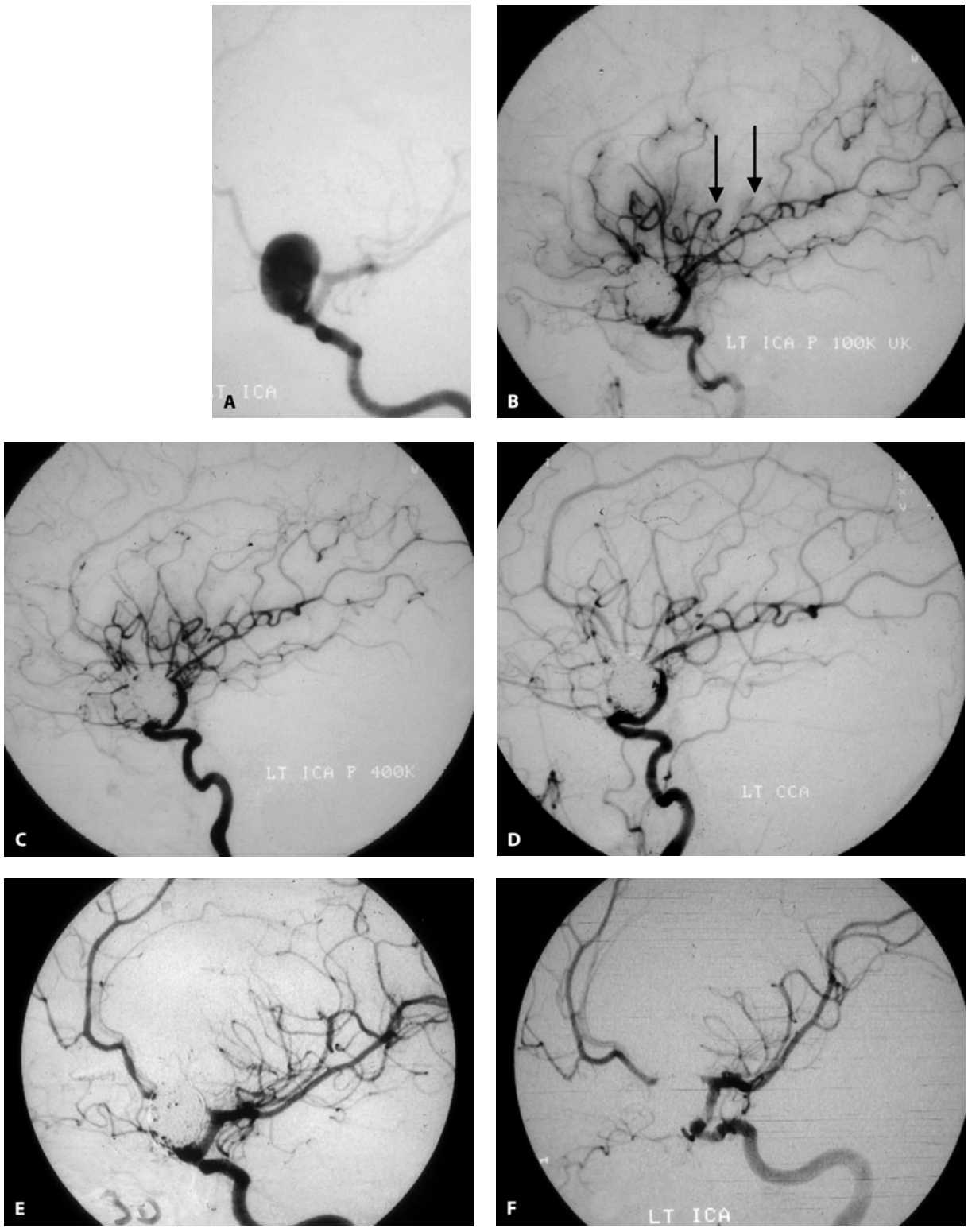

Fig. 14.100A–F. Thrombolytics in aneurysm therapy. **A** Grade 0 ophthalmic aneurysm. **B** Toward the end of coiling, two middle cerebral artery branches are seen occluded (*arrows*). Despite full heparinization, the occlusion persisted. **C** After superselective thrombolysis with 400,000 IU of UK, the vessels were open. **D** Delayed angiogram, the vessels remain open. **E** Three-day follow-up angiogram and **F** 7-month follow-up show persistence in the aneurysm occlusion

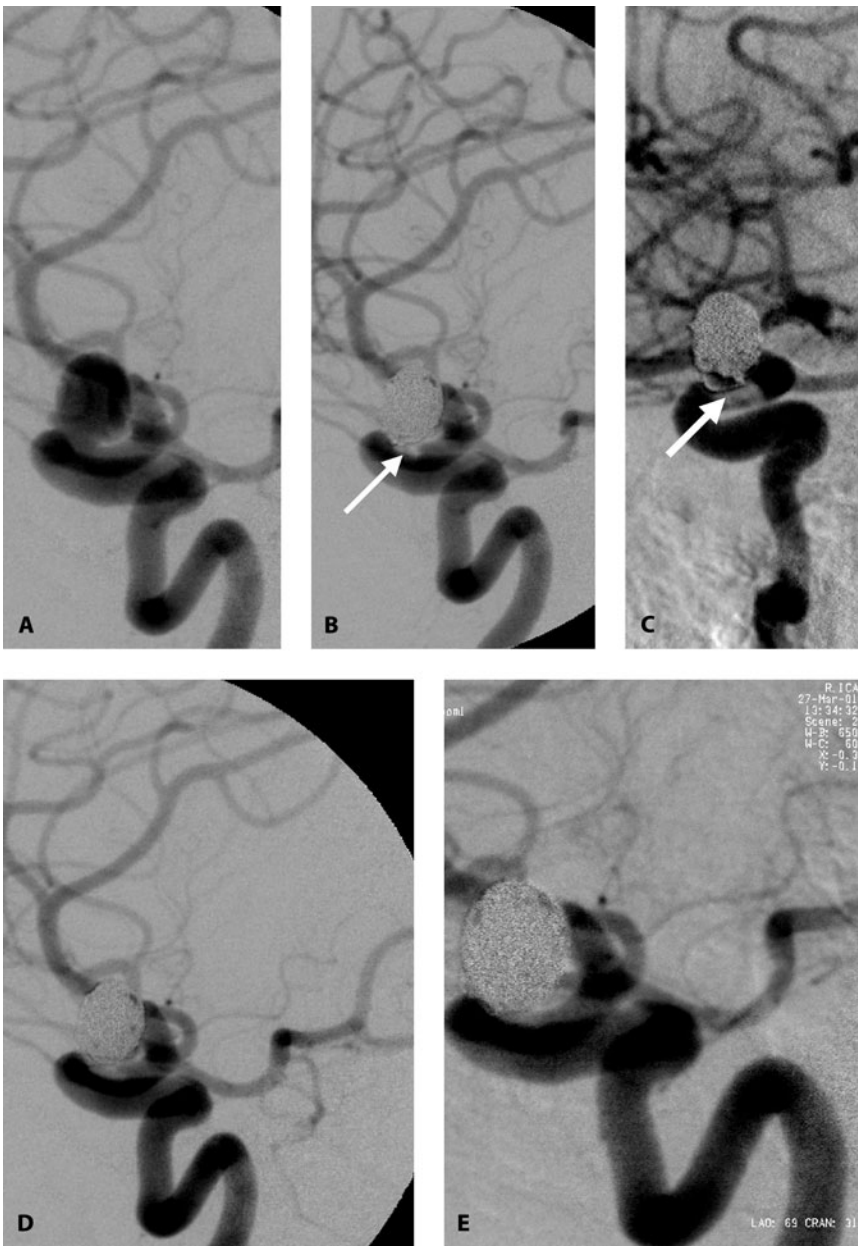

Fig. 14.101A–E. Use of glycoprotein IIb-IIIa receptor antagonists (GPA). **A** Digital subtraction angiogram of the right internal carotid artery paraophthalmic aneurysm, preoperative lateral projection. **B** Shortly after coiling, there was a small lucency in the carotid artery at the aneurysm orifice (*white arrow*). **C** Approximately 10 min later, there was further thrombi formation, probably due to coil protrusion (*white arrow*). **D** Lateral view of the right internal carotid artery 30 min after the IV injection bolus of ReoPro. Note the immediate lysis of the blood clot. **E** Follow-up angiogram the day after showing complete obliteration of the aneurysm and preservation of the carotid flow. No evidence of thrombi was seen. There were no clinical sequelae

14.7.2 Nonabsorbable Liquid Agents

14.7.2.1 Introduction

Liquid embolic agents are nonabsorbable. They must be liquid at the time of injection and should solidify when they have reached the pathological angioarchitecture, producing an endovascular cast of the area without passing to the venous circulation or distal arterial territory. The ideal liquid embolic agent would be one that could be dissolved (with nontoxic byproducts) if injected into an undesirable location. These agents are not yet available. We have used various types of liquid agents such as liquid silicone, acrylates, cytotoxics such as 98% ethanol, and some transarterial chemotherapy trials. Newer liquid agents are being introduced, including newer acrylates such as the octa-cyanoacrylate Neuroacryl (Prohol, San Diego, CA, USA) (C.W. Kerber, personal communication), which will soon undergo clinical trials for cerebral embolization. Another liquid embolic ethylene-vinyl alcohol copolymer (EVAL) was first introduced in Japan by Taki (1984). A similar agent has recently come out: Onyx (MicroTherapeutics, Inc.) (Jahan et al. 2001). This agent is approved in the European Union and is under evaluation for AVM treatment and aneurysm therapy in the United States (see Sect. 14.7.3). This material has been used in spinal cord AVMs (Molyneux and Coley 2000) and in the peripheral circulation (Canstademir et al. 2002).

When using liquid agents in or near skin surfaces, its excellent penetration can produce significant tissue damage, which will manifest itself as marked swelling (Fig. 14.102A), which will then progress to necrosis (Fig. 14.102B). Therefore, when using liquid agents of this type, proper planning is important. The following must be considered:

1. Is the lesion going to be removed after embolization?
2. What tissue or skin can be sacrificed?
3. What tissue or skin has to be preserved?

In deep lesions not involving the skin or mucous membranes, necrosis is usually not a problem, as it will be incorporated by fibrous tissue. However, in skin or mucous membrane, necrosis (mostly if of significant size) can be a problem unless it will be part of the planned resection (Fig. 14.102C). When using aggressive agents and swelling occurs, surgery should be delayed until full demarcation occurs. The necrotic area is not painful and proper local care is advisable to prevent infection.

14.7.2.2 Acrylates

At present the acrylates remain the most frequently employed agent, and of these the *N*-butyl-2-cyanoacrylate (NBCA), remains the most frequently used by the authors.

The isobutyl homologue isobutyl-2-cyanoacrylate (IBCA) was the first available (Zanetti and Sherman 1972; Kerber 1976; Berenstein and Kricheff 1979a, c) and is the one with which we have the longest follow-up.

Fig. 14.102A–C. Postembolization swelling and necrosis following embolization near skin surface. **A** Five days after silicone embolization of the infraorbital and facial systems with radiopaque silicone. **B** Three weeks later, there was a significant shrinkage of the lesion, with an area of well-circumscribed necrosis. Note the white silicone rubber (*arrow*). **C** After resection of the lesion, with removal of the excess skin. The patient has had further reconstruction of the lower eyelid with excellent results

Two commercial versions of NBCA exist. Histoacryl (Braun, Frankfurt, Germany) was intended for neural anastomosis and skin closure. It is the NBCA preparation currently used throughout the world (with the exception of the United States) for endovascular embolizations. Trufil (Cordis Endovascular) is the NBCA available in the United States.

Acrylic Histotoxicity

In the various toxicity studies conducted by Lehman and Hayes (1966, 1967) and Gottlieb (1967), IBCA and NBCA appear to be the most suitable agents for endovascular applications. This opinion is shared by Vinters (1985) in his review of the histotoxicity of cyanoacrylates. Lehman demonstrated that the shorter alkyl substitute compounds are less toxic. Cultures performed on this agent demonstrate that this material fails to

produce any bacterial growth when tested in dog cerebral cortex and monkey chiasm. There was no evidence of neurological deficit when applied in the cortex. The histotoxicity of the octa-cyanoacrylate Neuroacryl (Prohol) appears similar (C.W. Kerber, personal communication).

In Lehman and Hayes's (1967) experience, the IBCA was present 9 months in the dog and 14 months in the chimpanzee. It had disappeared in none of the animals. In his long-term studies of IBCA in chimpanzees, there was no suggestion of tumor formation. Zanetti and Sherman (1972) were the first to use this material for endovascular occlusion of aneurysms and renal arteries in dogs. They noted that when injected, IBCA rapidly polymerized to form a sponge-like mass that increased in size. The dose of the adhesive required was approximately 75% of the original measured aneurysm volume, with the apparent discrepancy being explained by the tendency of the adhesive to trap fluids within its clefts.

Manelfe (unpublished data, 1979) confirmed the increased volume obtained by the IBCA–blood mixture.

The entrapped red blood cells would not hemolyze after 24 h, but faint fibrillar structures suggesting fibrin were seen at pathology (Zanetti and Sherman 1972). White cells composed of about equal numbers of neutrophilic granulocytes and mononuclear cells tended to concentrate adjacent to the polymer at 3 h. By 24 h, these cells had not increased in number and many were degenerating. At 1 week, very few erythrocytes remained in the entrapped blood, which had taken on a uniform, dark eosinophilic stain. A few fibroblasts were disseminated in it while focal groups of macrophages and granulocytes were scattered in the periphery. By 2 months, the IBCA itself showed little change. However, the interstices were densely fibrotic and a few scattered foreign-body giant cells lay adjacent to the polymer (Fig. 14.103); most surfaces of the matrix were found to be covered directly by fibrous tissue. The reaction of the internal surface and endovascular wall was of particular interest to the authors because of its relation to the problem of adhesion and toxicity. The polymer was in direct contact with only about 15% of the endothelial surface and entrapped blood occupied the remainder. After 3 h at points of contact with the wall of the artery, the polymer seems to be touching the internal elastic lamina, rarely with a degenerating endothelial cell interposed. Often the internal elastic lamina seems to be dented slightly outward. The media was altered only by shrinkage and hyperchromatism of a few nuclei adjacent to the internal elastic lamina with no changes in the adventitia. There was no progression of degeneration at 24 h or at 3 months. In their pathological studies, White et al. (1977) noted that the IBCA found in arteries and arterioles manifested as a nonstaining, slightly retractile network surrounded by a large number of foreign-body giant cells and organized thrombosis. There were varying degrees of chronic inflammation manifested by lymphocytes and plasma cells in the thrombosed and surrounding vascular tissue. The vascular outlines were retained, although the internal elastic lamina was often focally disrupted, as noted by Zanetti and Sherman (1972). In many cases, the arteries appear to be dilated by their contents. IBCA and associated giant cells were found in very small arterioles within the submucosa in a gastric ulcer and within fibrous areas of splenic and hepatic infarcts. Zanetti injected IBCA into surgically

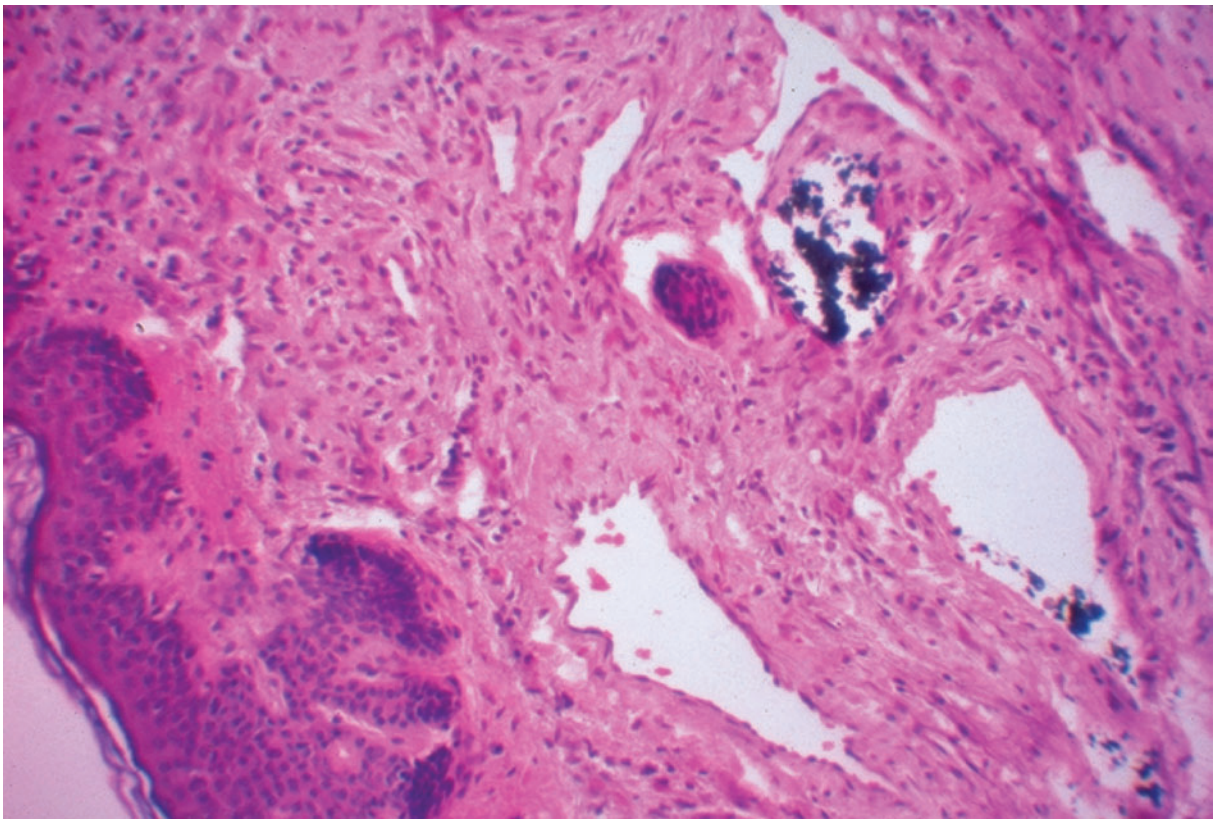

Fig. 14.103. Photomicrogram after IBCA embolization. The IBCA and tantalum mixture is seen in black. Note the inflammatory reaction with foreign-body giant-cell infiltration

constructed aneurysms and 1 week after injection the thrombi did not intrude into the lumen. Fibrous tissue had replaced the blood entrapped in the spongy matrix near the wall of the aneurysm and had not yet reached the central portion. The smooth muscle wall of the aneurysm had degenerated, with fibrous tissue running through it. A fibrous capsule about 1 mm thick surrounded the aneurysm. Specimens at 1, 2, and 3 months had endothelial-lined fibrous walls at the mouth of the aneurysm. The interstices of the IBCA mass were sealed with fibrous tissue containing a few scattered foreign-body giant cells. The walls of the aneurysms were fibrous but did not extend beyond the original venous graft. In 1981, Vinters et al. reviewed the pathology of two arteriovenous malformations previously embolized with IBCA, one 42 days after embolization and the other 1 year after embolization. Their findings were consistent with those reported by Lehman and Hayes (1966), Zanetti and Sherman (1972), and White et al. (1977).

Interestingly enough, Vinters et al. (1981) found that many, although not all, vascular channels were thrombosed and contained a particular black substance: the IBCA tantalum mixture. The lack of filling of some of the branches is probably related to the form of IBCA injection in vivo. In some sections, IBCA was seen within the walls of the embolized vascular malformation channels and in some it was seen extending into the sur-

rounding gliotic brain parenchyma. Vinters (1981, 1985) did not consider the possibility that the extravascular IBCA seen might be artifactual. In the parenchyma, no foreign-body giant cell or particulate material was observed. In the 1985 review by Vinters et al., an additional seven patients were studied pathologically after IBCA embolization with similar pathological findings; one patient had the IBCA for 16 months. The IBCA persisted and could be demonstrated by the black tantalum powder or using a modified oil red O stain. In this publication, Vinters and co-workers did a more detailed histological analysis of the IBCA-embolized AVMs. In addition to the previously mentioned histological findings, they found patchy transmural necrosis of portions of some vessels within days or weeks of IBCA embolotherapy. Some vessels containing IBCA thrombus had undergone recanalization; in others, the IBCA thrombus was lined with endothelium and with time there was actually smooth muscle cell hyperplasia between the endothelial lining and the IBCA. These findings correlate with Quisling's histological findings with PVA, supporting our theory that it is the autologous clot mixed with any type of nonbiodegradable embolic agent that results in recanalization. A tissue covers the nonabsorbable embolic agent with endothelium and virtually makes it extravascular (Fig. 14.51).

As to the question of potential carcinogenesis of the alkyl cyanoacrylates in general and the isobutyl monomer in particular, the preponderance of histotoxicity results seems to point to a purely inflammatory reaction rather than a neoplastic tissue reaction. No reports of neoplasms in man have been made in the more than 38 years that the agent has been used in humans.

An absolute statement denying carcinogenicity, however, cannot be made. Marck (1982), who studied the mutagenicity of NBCA and IBCA using the Ames test in bacteria, where a positive result implies that the product under study is mutagenic for man, found a weak mutagenicity of IBCA. Although the extrapolation of this study to human neoplasms is not absolute, particularly with the small doses used during embolotherapy, the material should be used with care and discrimination, and it is our duty to keep good long-term follow-up records on our patients.

Acrylic Injection

The widest experience in acrylic embolization has been with NBCA. Although the following recommendations are primarily for IBCA and NBCA, they apply for currently available acrylics. Polymerization of acrylates will occur when the material comes in contact with any ionic solution such as contrast material, blood vessel intima, or a basic pH solution. Therefore, prior to any injection of acrylics through any delivery system, the catheter must be rinsed with a nonionic solution such as a 5% dextrose solution to prevent the plastic from hardening within the catheter.

Radiopacity is achieved by mixing the acrylic with tantalum powder (Kenna Metal, Latrobe, PA, USA), or by mixing the acrylic with an oily contrast material such as lipiodol (Guerbet, Aulnay-sous-Bois, France) or Ethiodol (Savage Labs, Melville, NY, USA). Tantalum powder, for the most part, is used if the acrylic is to be injected alone in a high-flow fistula, such

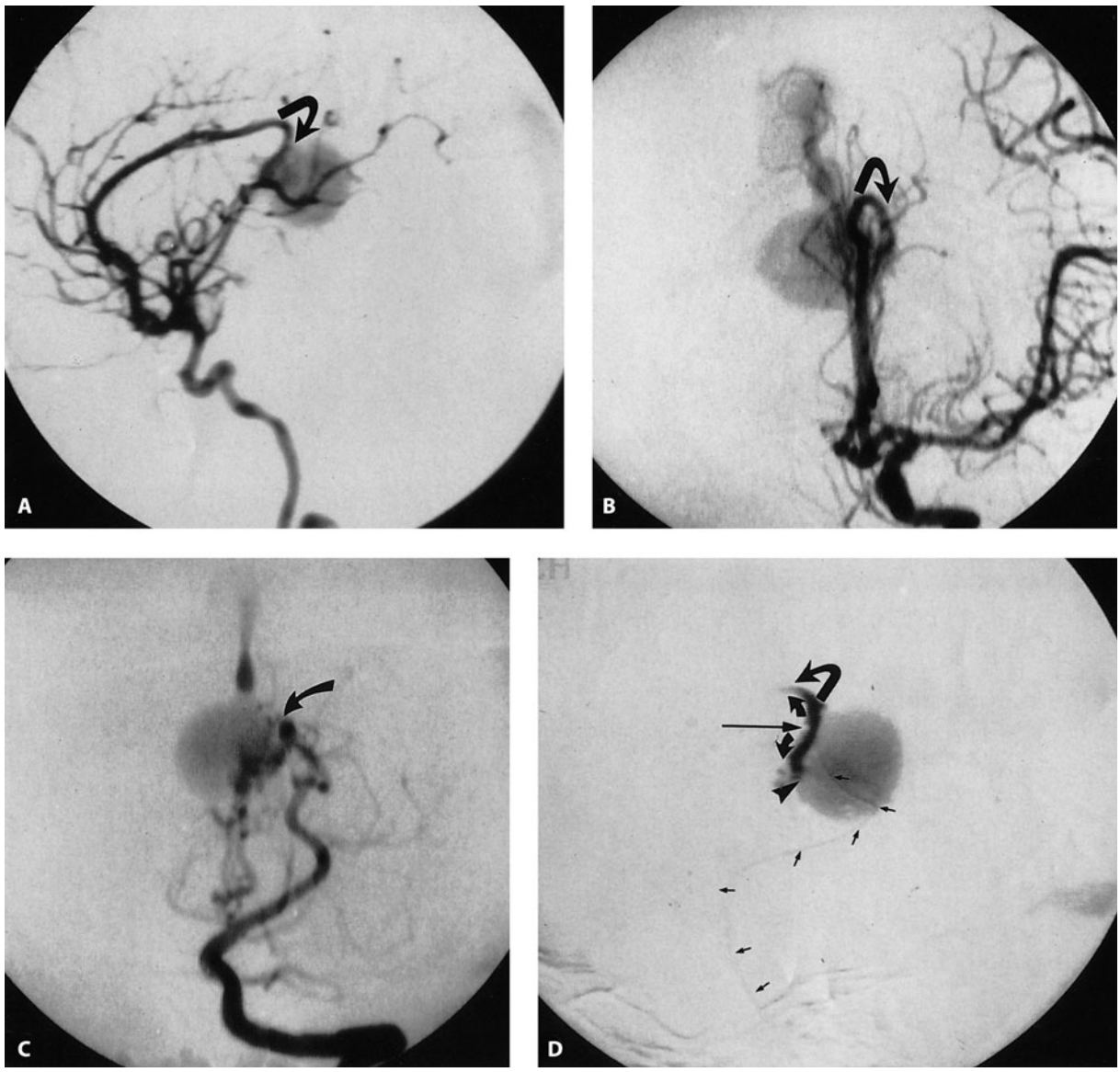

Fig. 14.104A–G. Flow reversal in a mural fistula of the vein of Galen without balloon. **A** Lateral and **B** frontal digital subtraction angiogram (DSA) of the right internal carotid artery demonstrating the choroidal branch of the anterior cerebral artery (*curved arrow*) supplying a mural fistula. **C** Frontal view of the left vertebral artery injection demonstrates the posterior medial choroidal supply to the same fistula (*curved arrow*). **D** Lateral DSA of the superselective catheterization of the posterior medial choroidal artery on the left with a Tracker microcatheter (*small arrows*) without balloon. With sufficient injection pressure at the tip of the catheter (*long arrow*), there is antegrade flow toward the fistula (*curved arrow*) and retrograde flow into the anterior cerebral artery (*bent arrow*). **E–G** see p. 1065

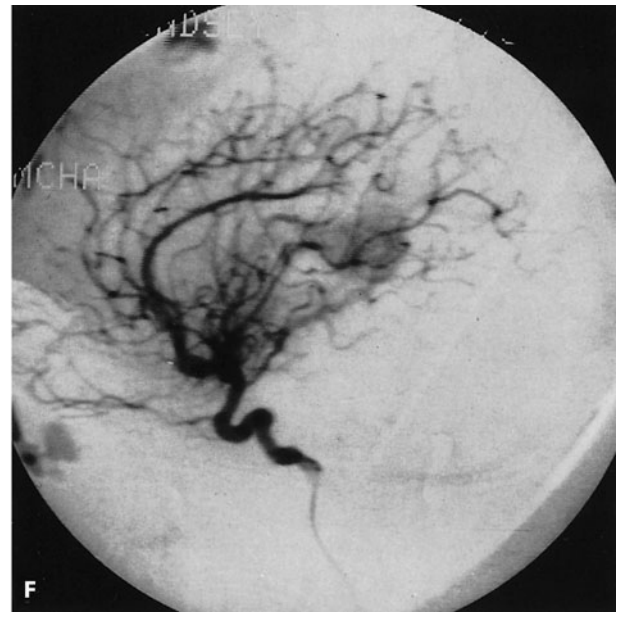

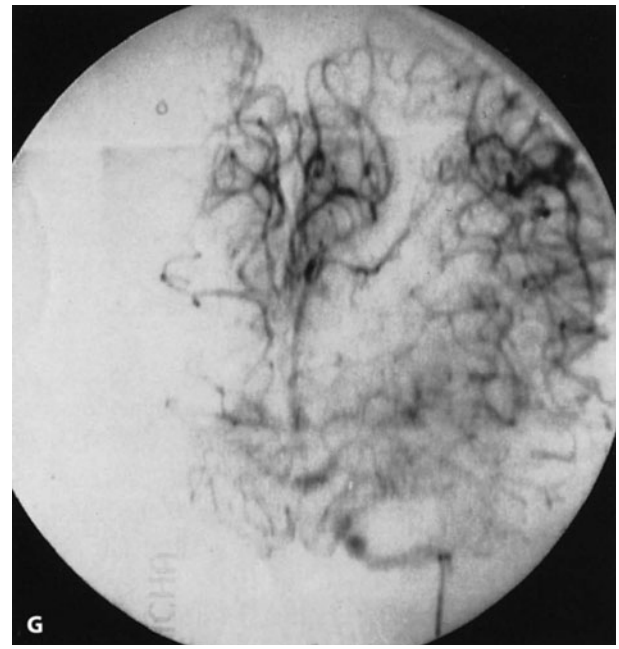

Fig. 14.104 (*continued*). **E** Lateral cone-down plain film demonstrates the occlusion of the fistula (*arrowhead*) with some acrylic in the vein (*arrow*). Note the retrograde occlusion of the choroidal branch of the anterior cerebral artery (*curved arrow*). Additional embolization in a second choroidal artery is also seen (*open curved arrow*). **F** Lateral and **G** frontal DSAs in late arterial phase of the left internal carotid artery after the embolization via the posterior route; there is not filling of the fistula. The anterior cerebral artery was never catheterized or embolized directly

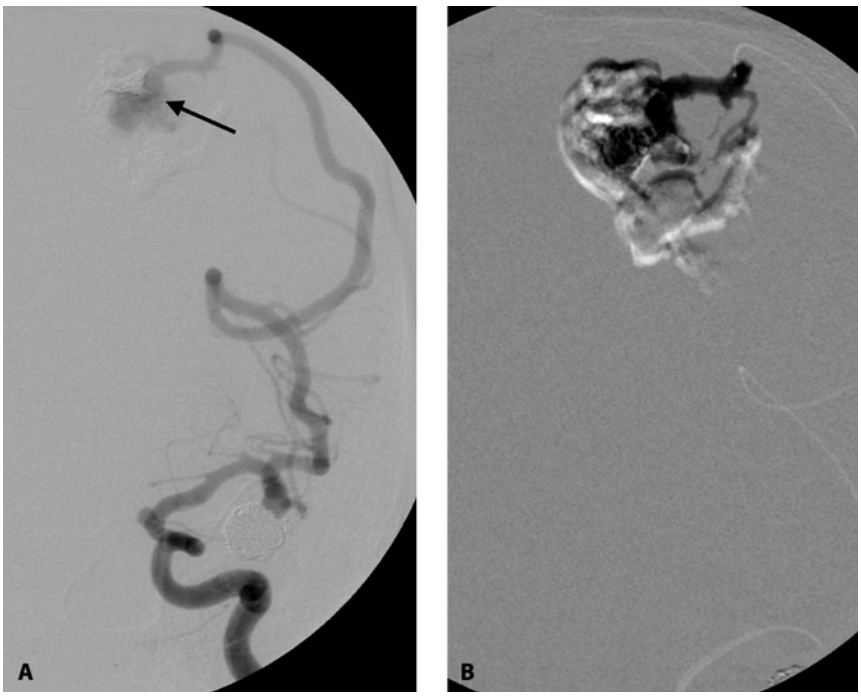

Fig. 14.105A, B. High-flow arteriovenous fistula. High-flow fistula as part of an arteriovenous malformation of the posterior frontal region. **A** Left internal carotid artery shows the high-flow fistula (*arrow*). **B** Last image hold of the NBCA injection. This fistula was treated with 70% NBCA, 30% Ethiodol

as Galenic malformations, or other high-flow fistulae (Fig. 14.104). With NBCA as an alternative, tantalum may be omitted, if the flow conditions allow 50%–80% iophendylate mixed with 50%–80% NBCA (Fig. 14.105).

In general, a complete acrylic cast of the desired vascular tree is needed, as recanalization will occur if the blood clot is left within or around the acrylic cast (Fig. 14.106). Therefore, if contrast material is seen to surround the acrylic on postembolization injection, additional acrylic is deposited in the same pedicle (Fig. 14.107).

Cases of recanalization because of glue disappearance (Rao et al. 1989) result from fragmentation of the acrylic column with intermixture of a large portion of blood clot and small amounts of acrylic (0.1–0.3 ml push). Continuous column injections are preferred. Small push volumes are only used to reach distal small-caliber territory, such as in SDAVFs. Recanalization has been seen in less than 2% of our patients, and most incidents may actually represent collateral circulation (sprouting or nonsprouting angiogenesis), when the shunt is not eliminated. These processes are most prone to occur if the shunt is not completely closed. The late reopening of previously embolized vessels is seen more frequently in the occipital and temporal lobes or other areas rich in leptomeningeal collaterals. With the more diluted mixtures, follow-up examinations s may show disappearance of the radiopaque cast; however, no recanalization has been noted of the embolized territory. For more controlled acrylic injections, it is advantageous to position the tip of the catheter against the wall of the vessel and not in the center of the feeder. This will minimize distal migration of the embolic agent through high-flow fistulae, taking advantage of the slower flow in the periphery of vessels. The use of coils, mostly liquid coils, can be of assistance to prevent distal migration of the acrylic (Fig. 14.59).

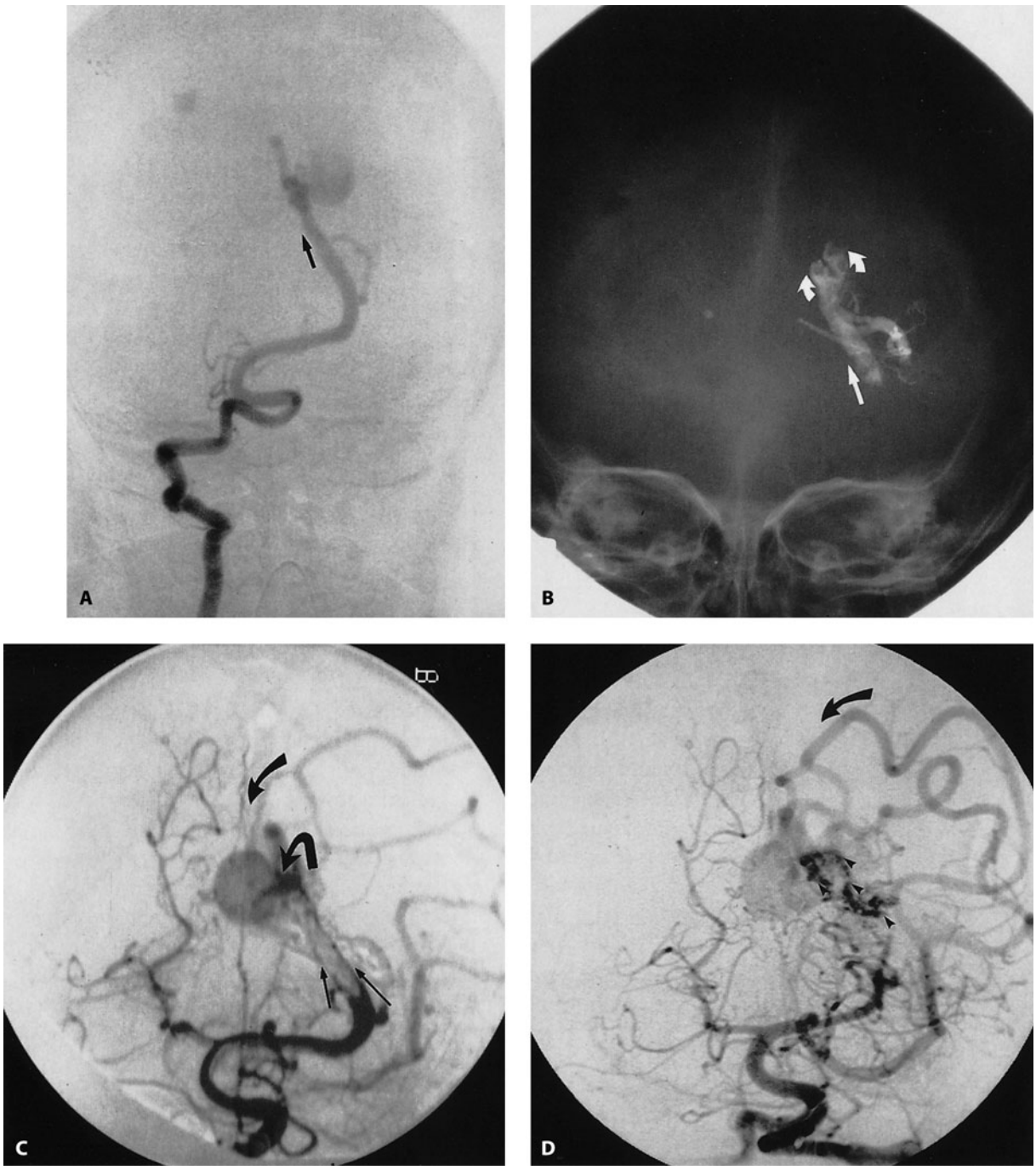

Fig. 14.106A–D. Recanalization of cyanoacrylate. **A** Frontal view of the left vertebral artery, early phase, shows a prominent posterior artery (*arrow*) supplying two separate fistulae. **B** Frontal plain radiogram showing the cast of the posterior cerebral artery filling the beginning of both pedicles going toward the fistulae (*curved arrows*). **C** Immediate postembolization left vertebral angiogram demonstrates contrast material still passing around the cyanoacrylate cast (*long arrows*). The fistula is still filling (*bent arrow*). Note the additional middle cerebral artery contribution (*curved arrow*). **D** Three-year follow-up angiogram demonstrates irregular recanalization around the cyanoacrylate cast (*arrowheads*). Note increased diameter of the middle cerebral artery (*curved arrow*) and decreased diameter of the posterior cerebral artery (compare to **C**)

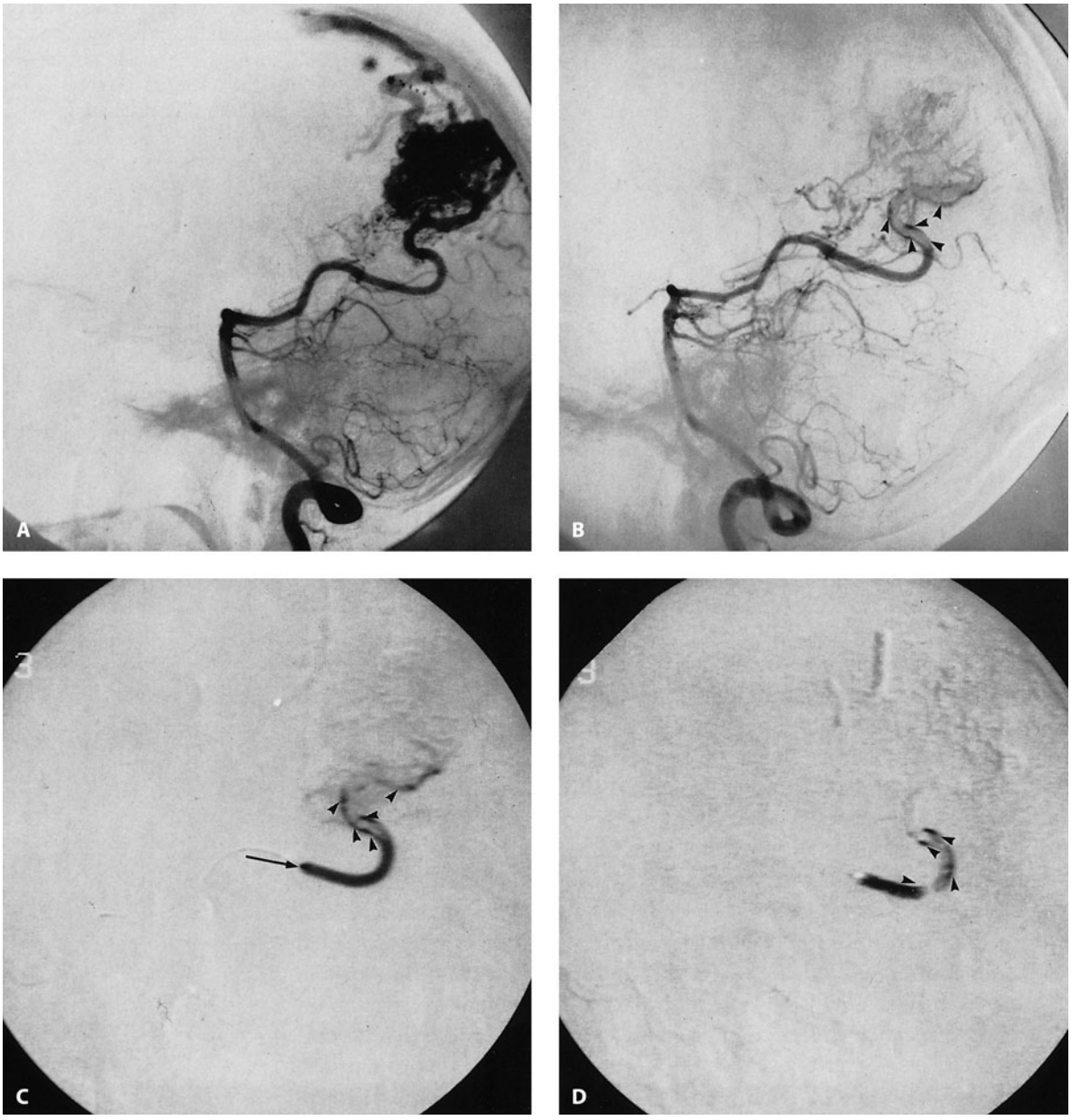

Fig. 14.107A–E. Additional acrylic injection to prevent recanalization. **A** Lateral view of the left vertebral artery demonstrates the parietal branch of the posterior cerebral artery supplying the most posterior medial aspect of a left-side malformation. **B** Immediate postembolization angiogram of the left vertebral artery demonstrates contrast material passing around the acrylic cast (*arrowheads*). **C** Recatheterization of the posterior cerebral artery (*arrow*). Note the injection of contrast material around the acrylic cast (*arrowheads*). Although delayed thrombosis of this vessel with autologous clot is likely, there is also the possibility of recanalization, as seen in Fig. 14.106. **D** Digital subtraction angiogram of the NBCA deposition using a low-viscosity mixture. Note the penetration of the acrylic material (*arrowheads*). **E** see p. 1069

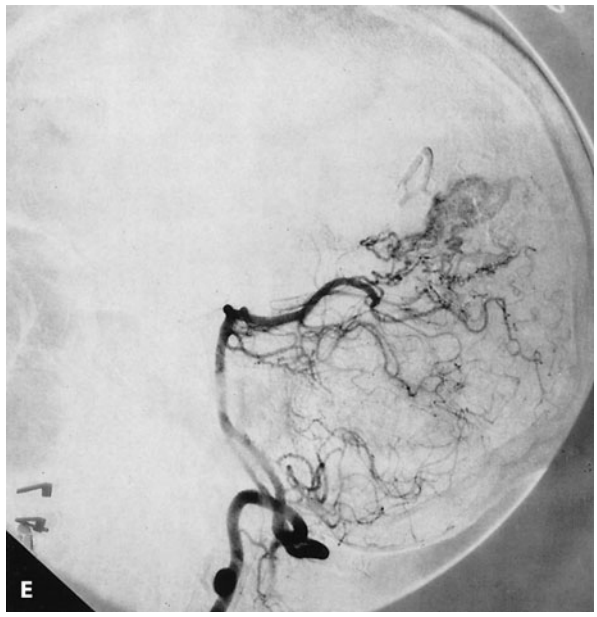

Fig. 14.107 (*continued*). **E** Final postembolization angiogram. Note the retrograde thrombosis of the posterior cerebral artery up to the first branching

Acrylic embolic material can be injected as a continuous column or pushed between a nonionic solution as a sandwich or push technique.

Continuous Column. If superselectivity is accomplished and no normal or endangered vessels are present, one can inject acrylic as a continuous column to produce an intravascular cast. In general, the amount of acrylic needed to reproduce the same filling as the contrast material estimated is 50%–75% of the original test.

Flow-Control Acrylic Embolization. If the microcatheter can be wedged into a feeder, flow arrest in that pedicle permits the nonionic flush of 5% D/W solution to also arrest flow; therefore the acrylic column will not polymerize, permitting long continuous injection of acrylic, without gluing the catheter. Excellent penetration can then be achieved. A nidus may be cast through one feeder, reaching territory that receives more than that pedicle (Fig. 14.108).

In Situ Injection. Acrylics may be injected directly into the nidus of a vascular lesion or tumor in selected instances, if flow control can be achieved. Direct percutaneous injections of various embolic agents has increased in recent years in difficult lesions with compromised access (Fig. 14.109).

Catheter Withdrawal. Catheter withdrawal has been markedly improved with the development of hydrophilic coatings in all currently available microcatheters and is no longer a problem.

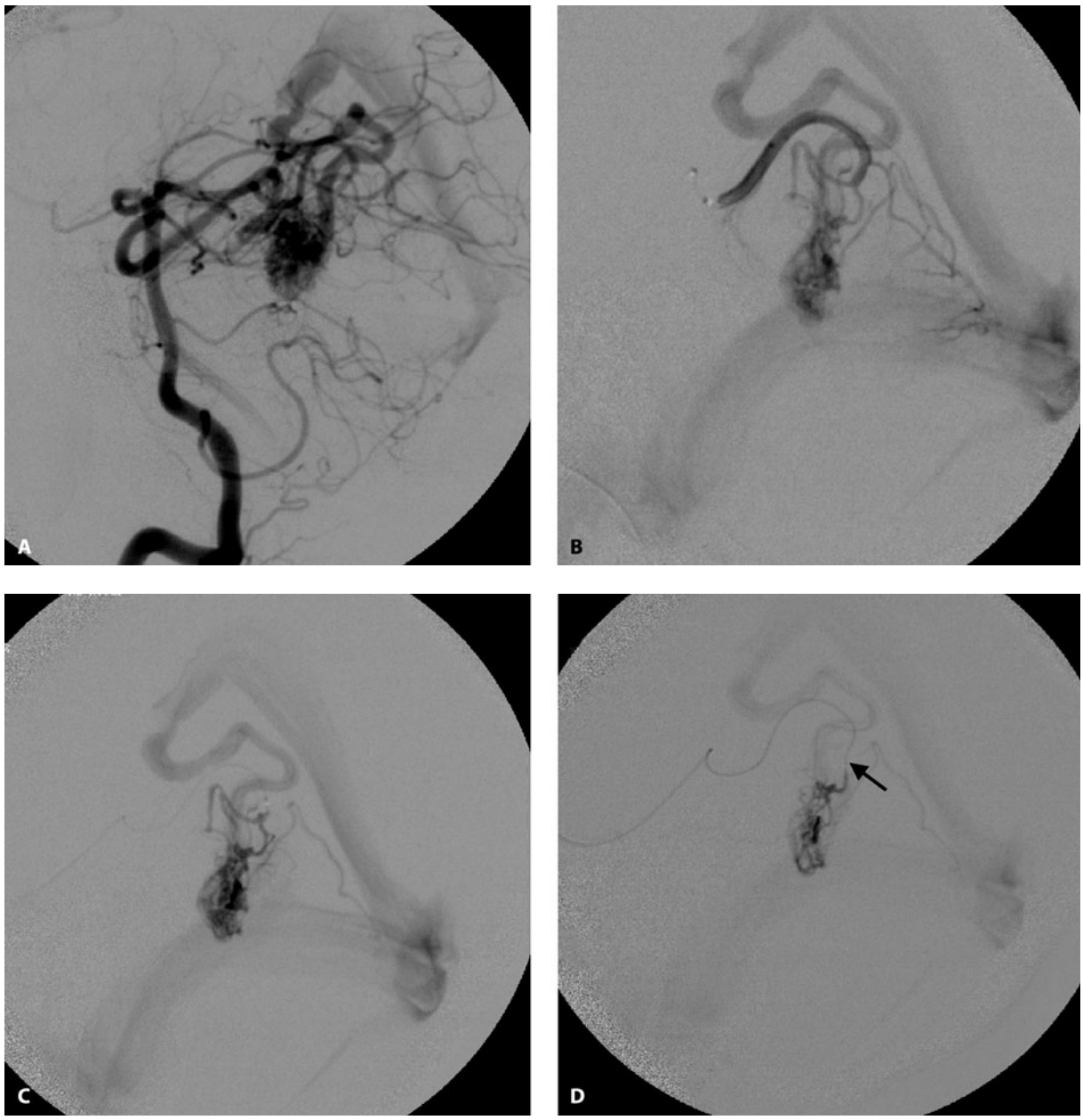

Fig. 14.108A–I. Flow-control cerebral embolization with NBCA. **A** Lateral view of the right vertebral artery showing a vermian vascular malformation. **B** Selective injection of the distal superior cerebellar artery shows the two feeding pedicles to the malformation as well as the superior vermian normal artery. **C** Distal catheterization of the superior vermian artery, proximal to both pedicles. **D** More distal catheterization producing flow arrest. Note the tip of the catheter (*arrow*). **E** Later phase of the same injection shows the contrast arrest due to the flow control over that pedicle (*open curved arrow*). **F** Last image hold from the road map of the NBCA injection. Note the penetration into the nidus of the malformation and filling of the most anterior superior branch. The microcatheter has been removed. **G** Lateral arterial phase. **H** Lateral digital subtraction angiogram late phase. Note total obliteration of the malformation. The precentral cerebellar and superior vermian veins that used to drain the malformation filled in the normal sequential time, confirming the occlusion of the malformation (compare to **A**). **I** Frontal views, late arterial phase show no filling of the malformation

►

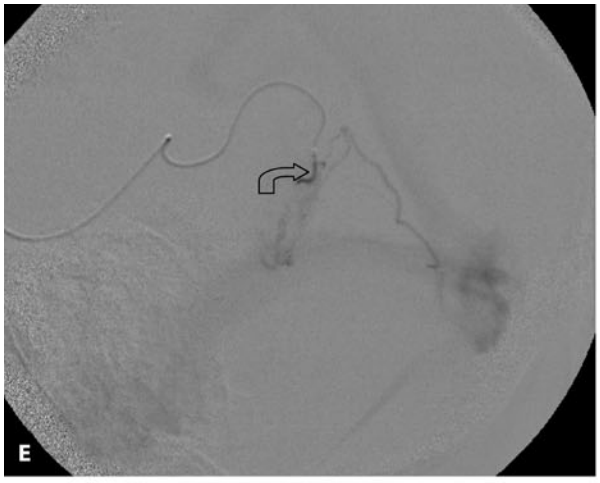

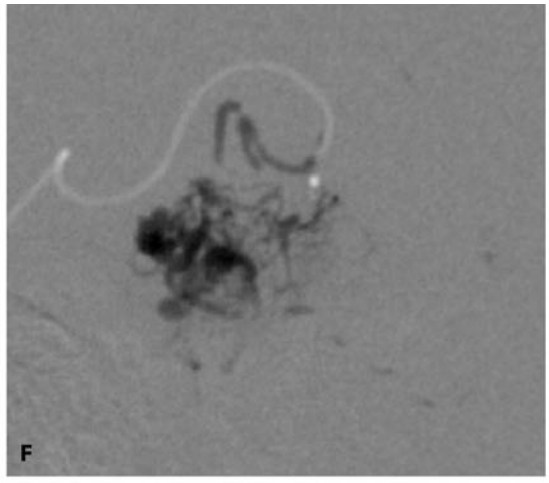

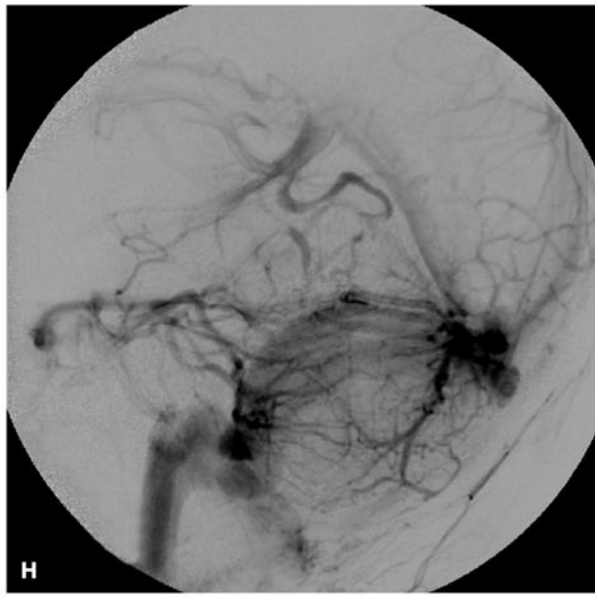

Fig. 14.108E–I. Legend see p. 1070

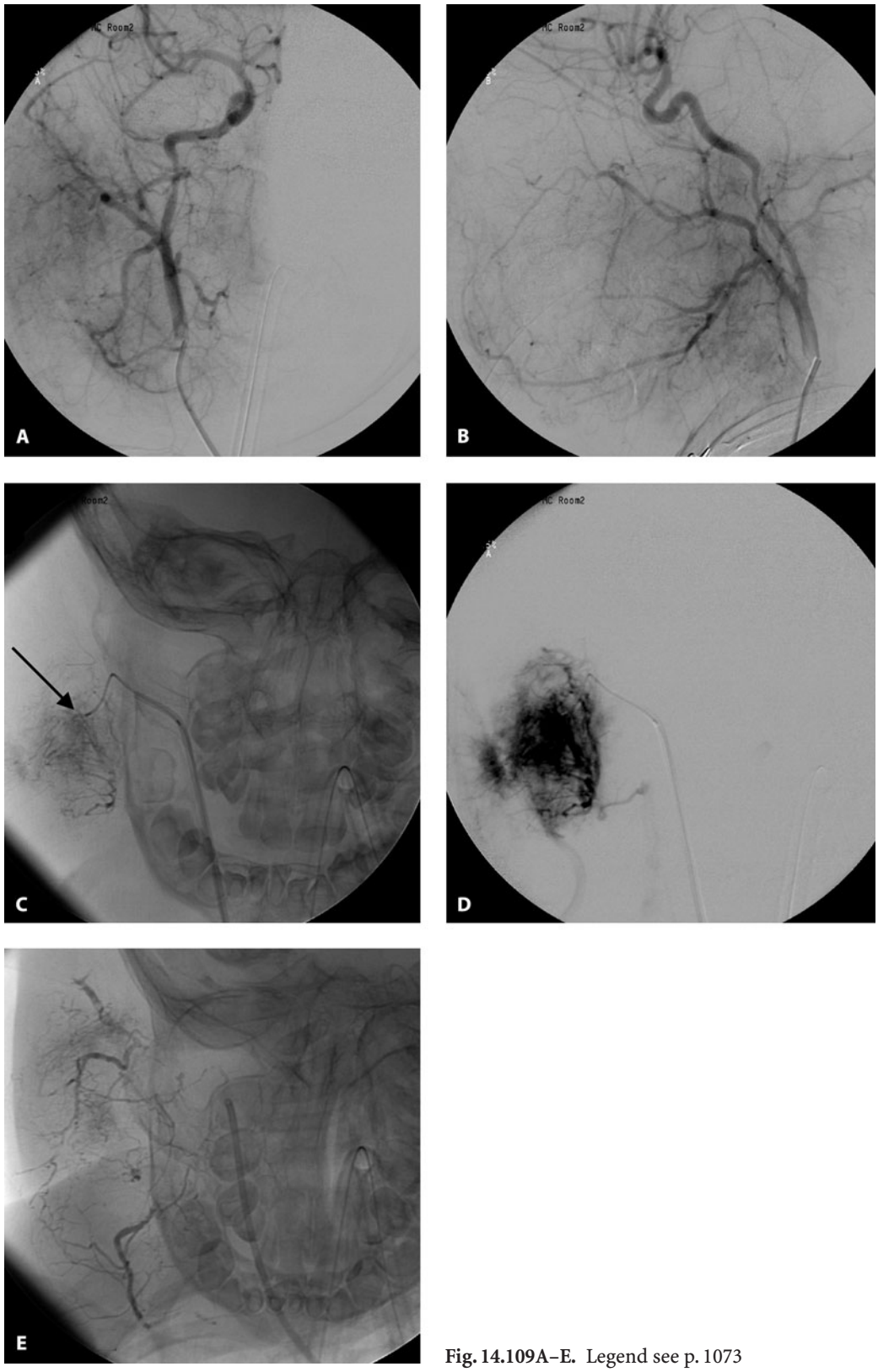

Fig. 14.109A–E. Legend see p. 1073

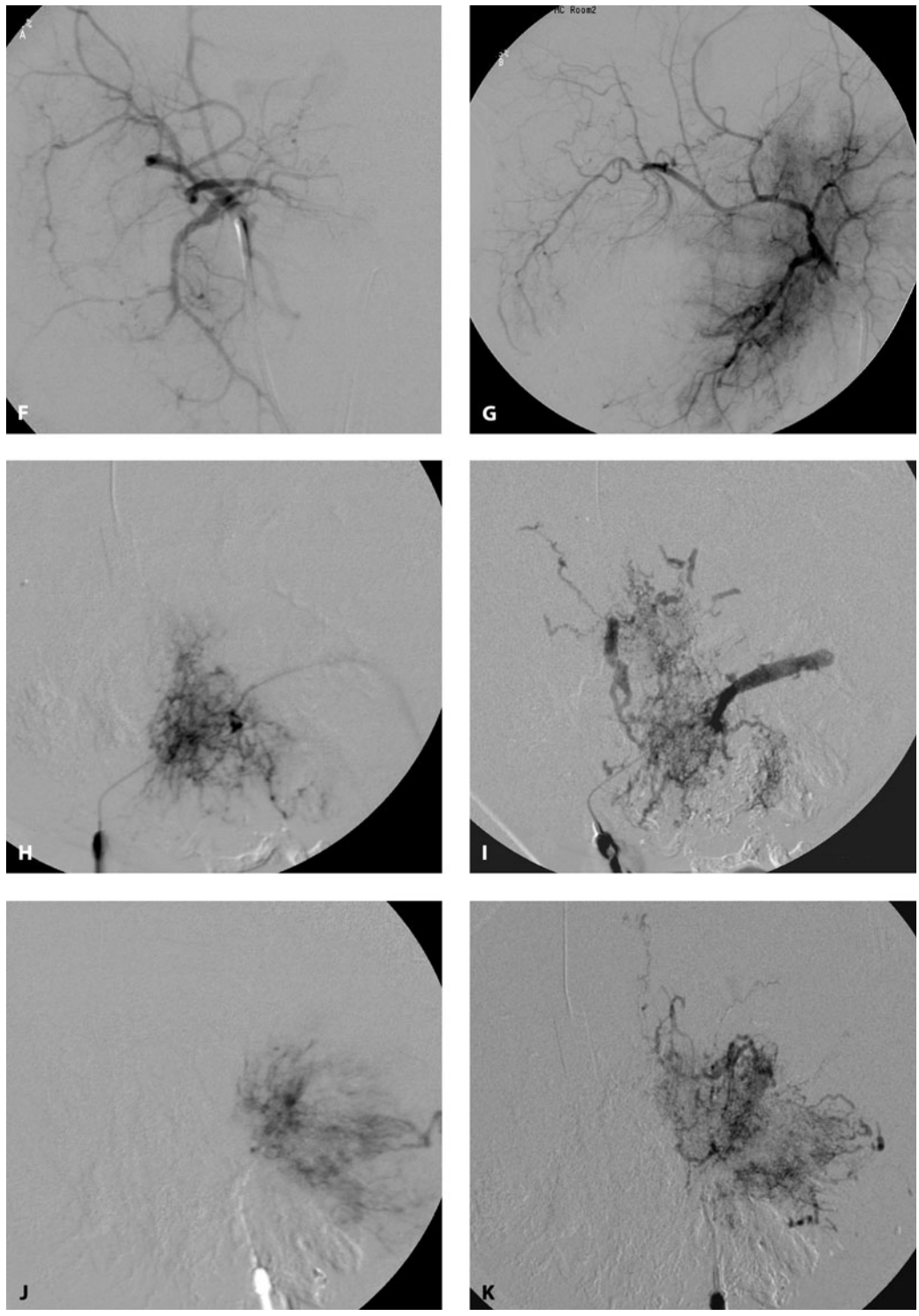

◄ **Fig. 14.109A–O.** Hemangioendothelioma presenting with a consumption coagulopathy (Kassel Bach syndrome). **A** Frontal and **B** lateral digital subtraction angiograms (DSAs) of the right external carotid artery demonstrate a fine tumor hypervascularity. **C** Transarterial catheterization of a masseteric branch (*arrow*). **D** DSA of the same injection. The tumor vascularity is seen better here, as compared to the global injection. **E** NBCA cast after the first transarterial embolization. **F** Frontal and **G** lateral DSA angiograms after embolization. The platelet count temporarily improved. **H** Direct puncture 1 (DP1), **I** acrylic cast, **J** DP2, **K** second cast. **L–O** see p. 1074

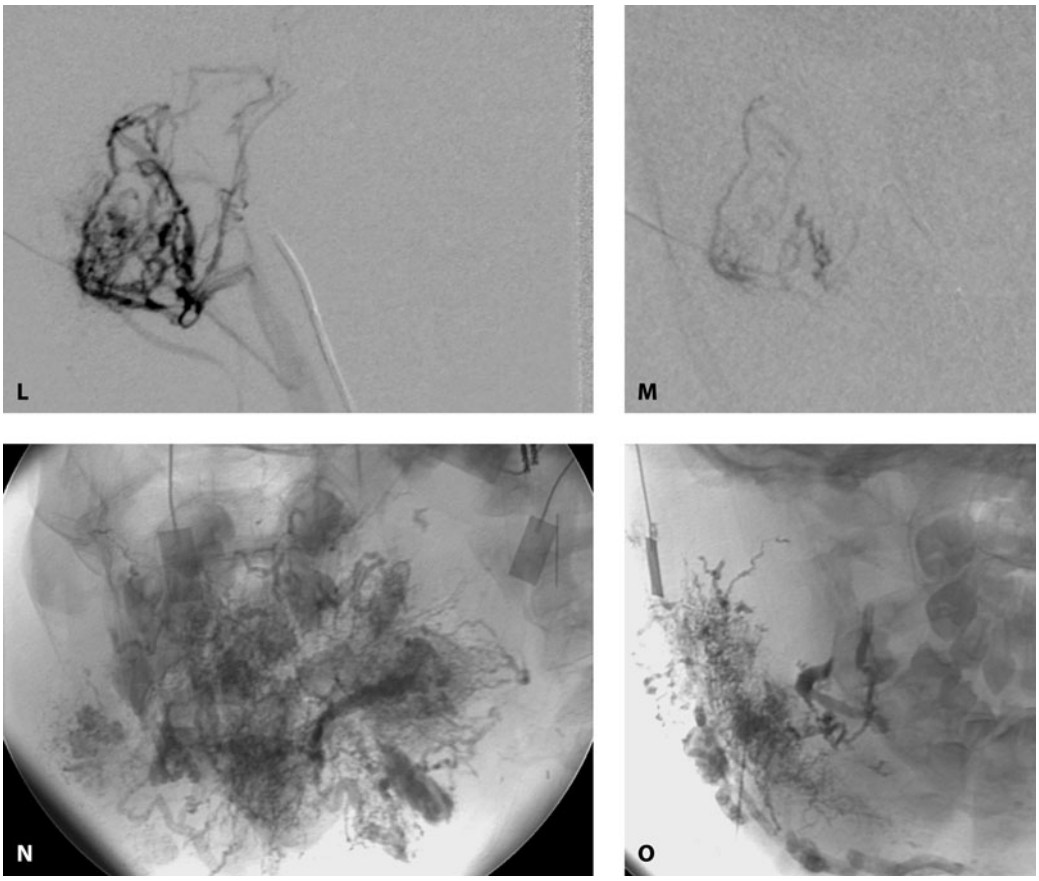

Fig. 14.109 (*continued*). **L** DP3 and **M** cast. **N** Lateral and **O** frontal plain images show the final cast obtained. Note the improved opacification of the vasculature and the penetration of the acrylic into the lesion's angioarchitecture

14.7.2.3 Sclerotherapy

Sclerotherapy refers to the use of agents that produce a severe inflammatory reaction in the tissues in contact with the insult; it is the reaction and enhanced healing response that scars, or scleroses, the vessel that has been in contact with the sclerosing agent. In general, the insult and its triggered response are severe enough so that if in contact with normal tissue, severe damage may persist. Avoidance of such agents in eloquent tissue, skin surfaces, and cranial nerves is important, as the consequences are serious.

A multitude of sclerosing agents have been used in medicine for centuries. For endovascular treatments, ethyl alcohol is the most frequently used by the authors and is the one to be discussed in this section.

Ethyl Alcohol

Ethyl alcohol (98% ethanol) is gaining popularity as an effective and aggressive embolic and cytotoxic agent (Ellman 1979; Buchta et al. 1982). It is available in any hospital in a 95%–98% concentration. It can be easily injected through any delivery system currently available. It produces no

immediate mechanical blockage, only secondary blockage, due to its cytotoxicity on blood cellular elements and endothelium as well as adjacent tissues. It then produces an ischemic or anoxic insult and cytotoxic damage. The local effects of ethanol are related to its potent denaturant and hydrophobic property in high concentrations. In our measurements of systemic concentrations of ethanol in blood using Widmark's factor during endovascular treatment and using up to 60 ml of ethanol (in venous vascular malformations of an adult) at any one treatment, blood levels of alcohol have been well below systemic toxic levels. When the ethanol reaches collateral circulation or the venous outflow, it becomes diluted and nontoxic.

In various experiments and in pathological specimens, Ellman et al. (1981, 1984) and Buchta et al. (1982) demonstrated the effects of ethanol. However, the head and neck and cerebral vasculature were not studied.

In the renal vasculature, Buchta et al. (1982) showed vascular pruning and spasm in the distal circulation, with stasis in the segmental and main renal arteries, and an absence of a nephrogram in the immediate angiogram following slow infusion of 95% ethanol.

Pathologically, changes were noted as early as 2 min later, consisting of protein precipitation and fibrinoid necrosis at the tissue level; the blood vessels were congested but not thrombosed. Electron microscopy studies demonstrated severe cellular changes at various levels, with necrosis of endothelial, epithelial, and mesenchymal cells and distortions of all intracellular elements. In the intravascular space, erythrocytes were congested, lysed, or agglutinated. In 1984, Ellman et al. showed the difference in damage produced by rapid (2 ml/s) versus slow (less than 0.5 ml/s) injection of intra-arterial ethanol. Rapid infusion produced more tissue damage and less blood cellular element aggregation, whereas slow infusions permitted a higher contact of blood cellular elements with the alcohol, producing damage to the cells, aggregation, and thrombosis.

They demonstrated no gross differences between the rapid intra-arterial injection and those produced following balloon occlusion for evaluation of the cytotoxic damage in the absence of blood cellular elements in the renal circulation.

The conclusions of the Ellman et al. (1984) and Buchta et al. (1982) studies suggest that a better way to produce tissue damage may be to produce flow arrest to permit a long contact between the ethanol and the endothelium, in the absence of blood cellular elements.

Ethanol Injection in the Arterial System. In view of its cytotoxic effect, ethanol seems to be a suitable agent when necrosis and not only devascularization is the main objective, such as in malignant or aggressive tumors (Choi 1985). Alcohol is not indicated in very high-flow conditions to meet the objective of mechanical blockage, where detachable balloons or acrylics may be best.

In very hypervascular (but not high-flow) lesions, one may use a combination of ethanol and particulate agents such as PVA (Wallace 1984), Gelfoam powder, and collagen. This has the advantage of producing alcohol stagnation.

When using ethanol, the final result will not be apparent immediately. One may opt for injecting a strip of Gelfoam at the end of the infusion to maximize its effects. The end point of alcohol infusion is difficult to judge, as vessel spasm may give a false picture. Furthermore, spasm may occur at the tip of the catheter where the highest concentration of the ethanol is in contact with the vessel wall; caution must be taken to prevent reflux. If spasm occurs it may be advisable to work on another pedicle and return to the first one at a later time. When ethanol is injected in the arterial system, it must be done with utmost selectivity, particularly in skin and mucous membrane areas.

To avoid spasm, prior to ethanol injection, intra-arterial Xylocaine can be used and is very effective in preventing spasm.

Ethanol Injection in Venous Malformations. Patients are prepared for the procedures with general anesthesia using endotracheal intubation. Tracheostomy and nasogastric intubation is indicated if the clinical evaluation and preliminary CT scan already demonstrate the lesion near the airway or alimentary passages. The puncture site is chosen at a normal area near the lesions in most instances. The skin is prepared in the usual antiseptic manner. We employ an 18- to 24-gauge angiocatheter connected to a venotube (Fig. 14.3), or a 21- to 25-gauge butterfly needle. In general, the angiocatheter is placed in a dependent orientation to facilitate back bleeding, which confirms the intravascular position of the angiocatheter, and to prevent air embolism. Following needle placement and venous sampling with fluoroscopic (road mapping) monitoring, contrast material is then injected to obtain a gross assessment of flow within the lesion, and an estimation of volume capacity of the compartment being treated. Depending on the lesion size or compartment, contrast material is progressively injected and monitored fluoroscopically, to determine the volume of the lesion or a specific compartment of the lesion. Multiple septations can be seen as contrast material enters the pouches and starts unfolding the venous spaces. As the compartments are filled, the walls will bulge outward or will follow anatomical landmarks such as bone (Fig. 14.110). The venous drainage is important, not only to assess potential dangers such as drainage toward the cavernous sinus, epidural venous plexus, or intracranially (Fig. 14.111), but it is important to determine the dominant drainage when there is a need to perform external compression to slow the flow. Contrast injection is also used to differentiate between a monocompartmental and a multicompartmental lesion. Stagnation or very slow flow of the contrast agent is usually observed. To ensure the intravascular position of the tip of the needle, one can observe as the contrast material layers to the dependent position; the clearance of the contrast material from the tip of the angiocatheter should also be observed. If the contrast material is seen as a globe that does not move or forms layers, extravasation is occurring. In case there is a question as to the position of the delivery needle or angiocatheter, back flow is a good confirmation of an intravascular position. As blood returns after being exposed to the ethanol, cell precipitation is seen (Fig. 14.3).

On occasion, the transition from an abnormal-looking vein to a more normal appearing one can be seen. Depending on the pre-estimated vol-

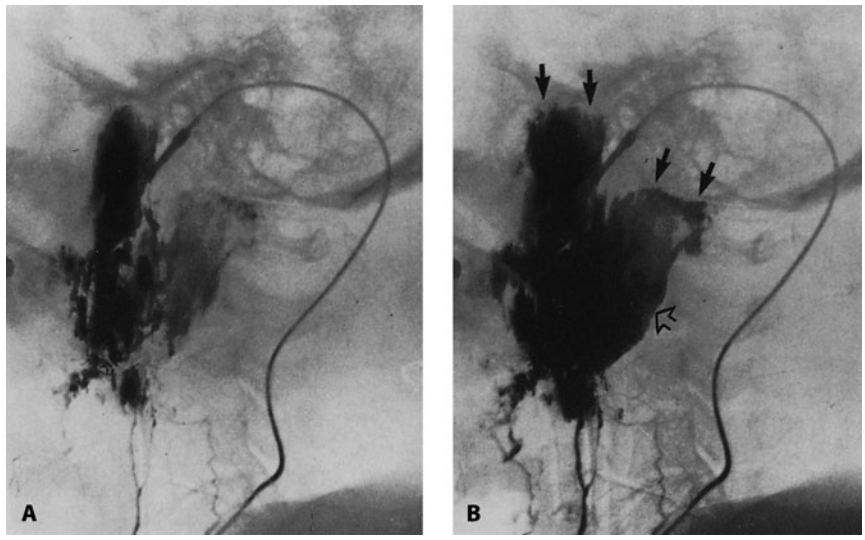

Fig. 14.110A, B. Venous vascular malformation of the parotid area. **A** Following injection of 5 ml of radiopaque ethanol. **B** After 25 ml. Note the upper body limits of the pouch (*arrows*) and the convex aspect of its posterior margins on the styloid muscles (*open arrow*). Note the very poor venous outflow

ume of a lesion or compartment, 98% ethanol is injected. In the past, ethanol could be made radiopaque with metrizamide powder; at present metrizamide powder is no longer available. Instead we inject the ethanol and frequently check the flow returned, and monitor the progression of the occlusion by checking the column of blood return pressure above the heart level. Alternatively, radiopacity can be obtained by combining one-third Ethiodol to two-thirds 98% ethanol (Borrows, personal communication). The combination can be observed as droplets of the oily mixture (Fig. 14.111H). The effect of this mixture clinically appears more effective and durable than with metrizamide, but this was early in our experience. We do not usually inject contrast material following alcohol infusion in the same compartment, to prevent displacing the alcohol beyond the lesion. One must check back bleeding each time or if no blood returns, antegrade flow is checked by gravity by elevating the venotube above the heart level.

If there is no spontaneous back flow or if antegrade flow is not obtained, no alcohol is injected and a new puncture is done. Usually, we inject up to one-third the estimated contrast volume at any one lesion or compartment, with the maximum alcohol injected at any one time at 60 ml.

In tongue localization, one must establish the venous outflow, and ethanol should be injected from a more distal to a more proximal position, to prevent thrombosis of the already compromised venous outflow.

At the end of the alcohol injection, hemostasis is easily achieved using a suspension of hemostatic agents such as Avatine (Microfibrillar Collagen Hemostat Ethicon, Inc., Somerville, NJ, USA). Gelfoam powder mixed with normal saline or a large strip of Gelfoam injected as the angiocatheter is withdrawn to seal off the tract.

Following ethanol infusions, the area becomes swollen, indurated, noncompressible, but it is not tender. This process starts within the first minutes and reaches its maximum in approximately 3–7 days. Resolution occurs in 1–5 weeks.

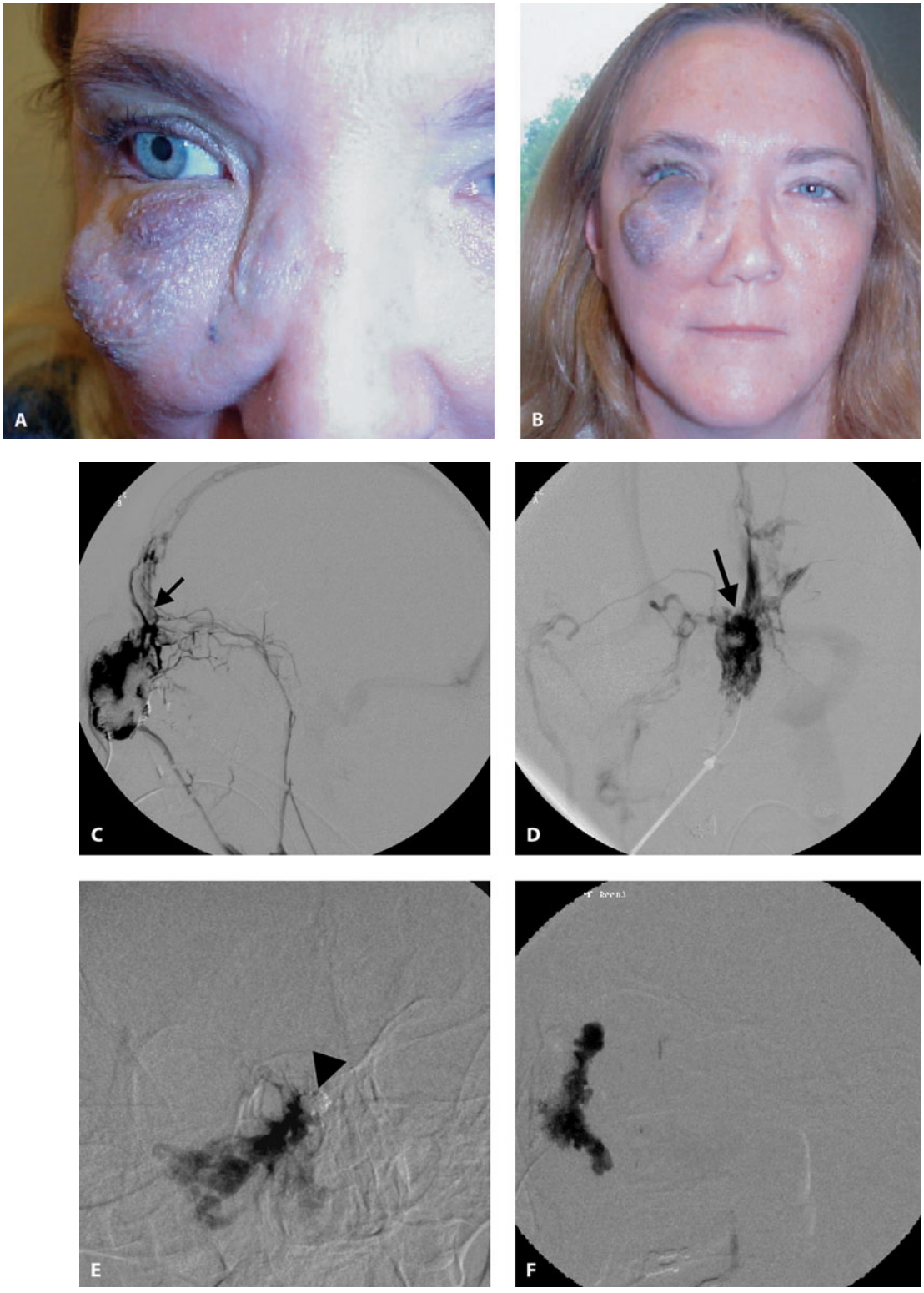

Fig. 14.111A–F. Legend see p. 1079

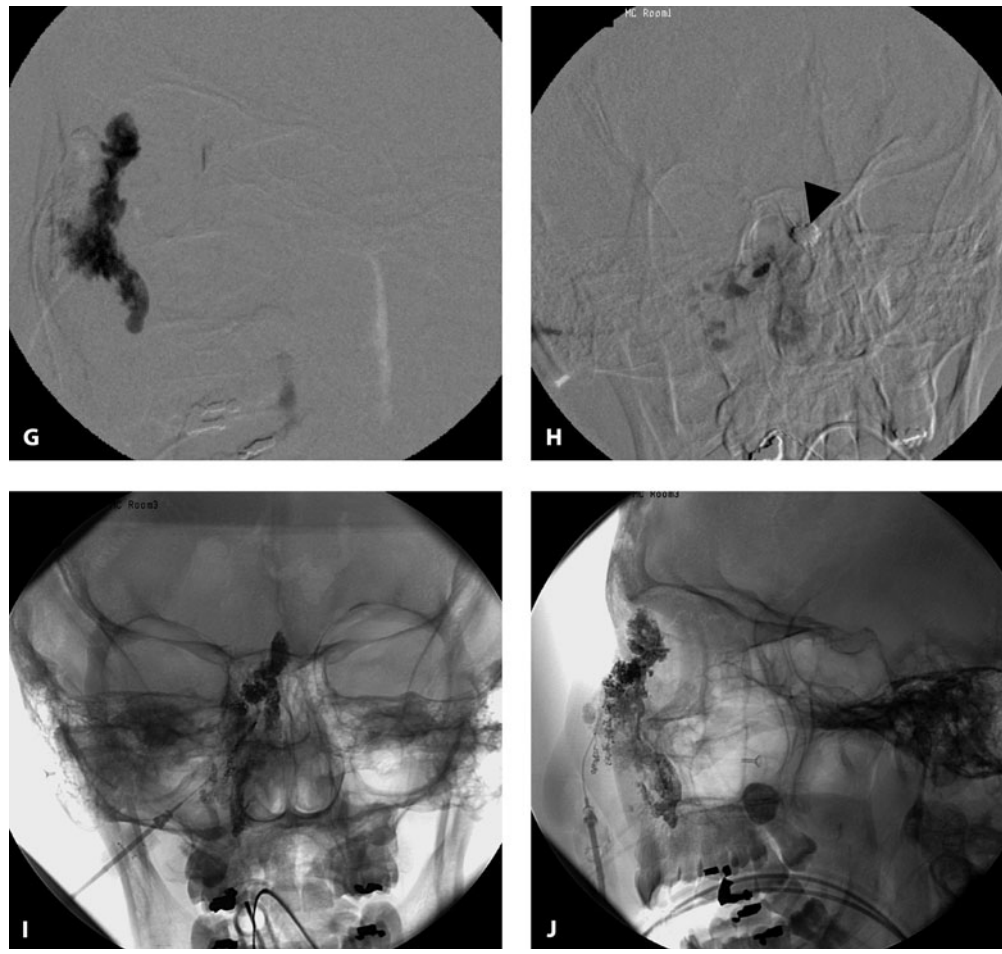

◄ **Fig. 14.111A–N.** A 32-year-old woman with a venous vascular malformation involving the infraorbital and nasal regions with intradural drainage to the superior sagittal sinus. **A**, **B** Clinical images prior to treatment. Note the soft tissue mass, which changes with Valsalva maneuvers. There is bluish discoloration of the skin. This is a nonpulsatile lesion with extension toward the nose. **C** Lateral digital subtraction angiogram (DSA) after direct puncture (DP) and injections of the venous compartment in lateral and **D** frontal views show the intracranial drainage through the cribriform plate into the superior sagittal sinus (*arrows*). **E** Frontal view after liquid coils and coils have been placed at the cribriform plate to block the intracranial venous drainage (*arrowhead*). Note the injection of contrast material with stagnation and no drainage intracranially. **F**, **G** Lateral DSA projections of the radiopaque ethanol stagnant within the venous compartment and no intracranial drainage. **H** Frontal view at a later date with ethanol mixed with Ethiodol, which can be seen as droplets of contrast as the material is in suspension. Again note the lack of filling to the intracranial venous drainage, protected by the coils (*arrowhead*). **I**, **J** Plain films demonstrating the stagnant ethanol–Ethiodol mixture. **K** Clinical pictures taken on the day after the direct ethanol injection. **K–N** see p. 1080

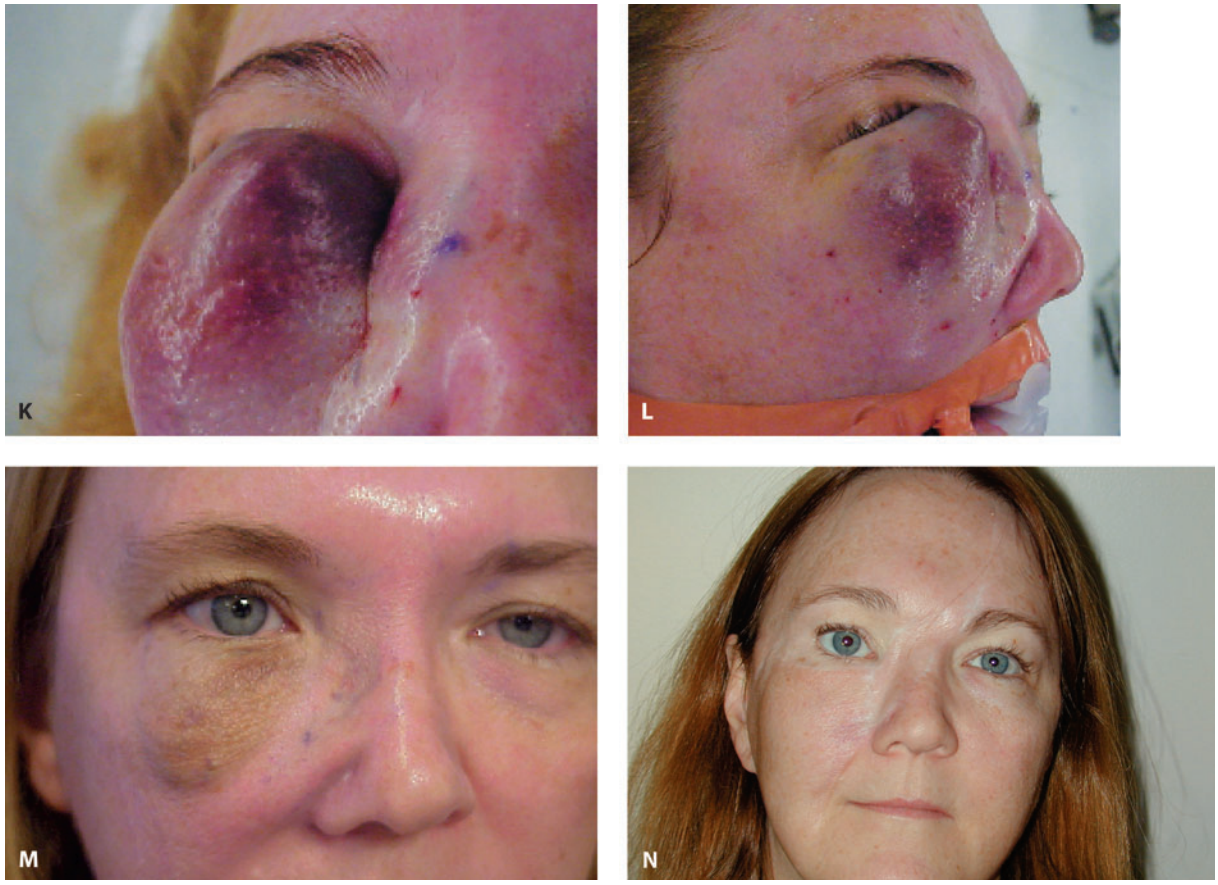

Fig. 14.111 (*continued*). **K, L** Note the significant swelling produced associated with induration as the thrombosis and the sclerosis are acting. **M** Clinical picture after the third treatment: the swelling has resolved. Note the marked involution of the lesion with the overhanging tissue-expanded skin. There was no filling after Valsalva straining, prior to surgical excision. **N** One week postoperative picture

One can then evaluate refilling of portions of the lesion and additional treatment can then be planned. Limited necrosis is sometimes observed, which usually heals spontaneously by granulation (Fig. 14.112).

Ethanol in Arteriovenous Malformations. Yakes et al. (1997) reported the use of 98% ethanol in the treatment of BAVMs, with a high number of total obliterations above those reported with acrylics; however, the reported complication rate of 47%, although mostly transient complications, still led to a permanent complication rate of 17%, in our opinion an unacceptable incidence.

Ethanol is also very effective in the intranidal embolization of maxillofacial AVMs, following superselective nidal catheterization, for better and safer penetration can be achieved following direct percutaneous nidal catheterization (Fig. 14.113).

Fig. 14.112A–F. Venous vascular malformation (VVM) of the neck. **A** Original presentation of the lesion. It has a superficial extension and enlarges with Valsalva maneuvers. **B** Radiopaque alcohol in the multilobulated lesion. **C** Five days after surgery there was development of blistering. **D** Three weeks later there was healing by granulation. **E** Five months later, and **F** 1 year after the original blister. There was only minimal filling on Valsalva

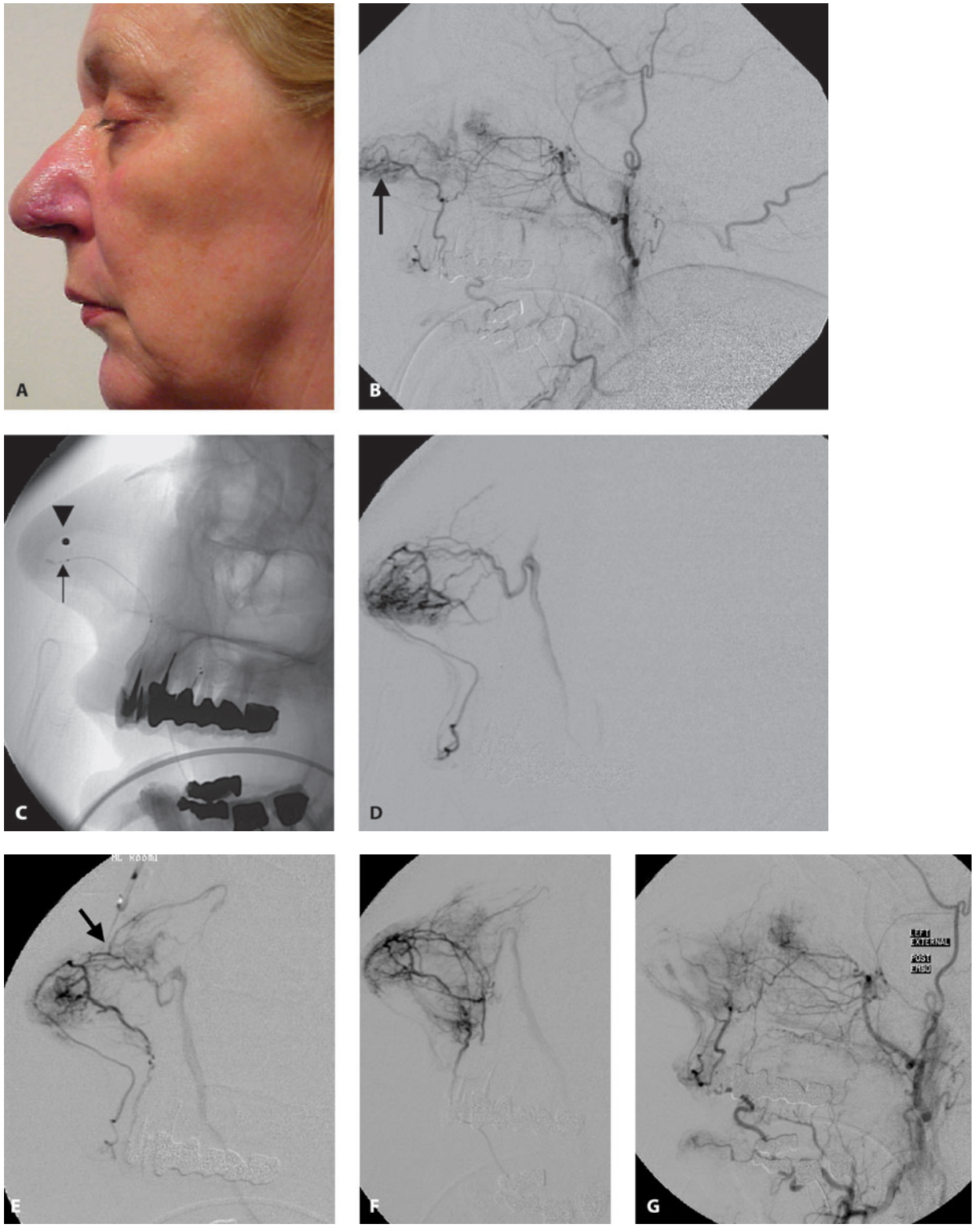

Fig. 14.113A–G. Legend see p. 1083

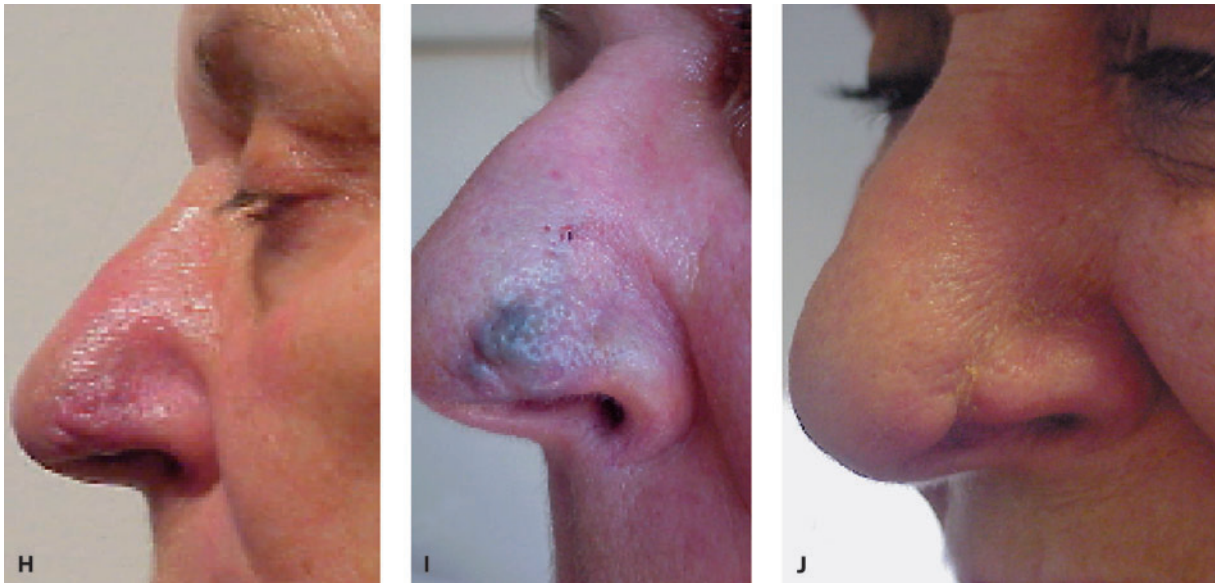

◄ **Fig. 14.113A–J.** Maxillofacial arteriovenous malformation treated by direct percutaneous sclerotherapy. **A** Clinical picture of the lesion on the left side of the nose. **B** Lateral digital subtraction angiogram (DSA) of the external carotid artery, late phase, shows the capillary vascular malformation (*arrow*). **C** Plain film soft tissue technique with a radiopaque marker at the lesion site (*arrowhead*). Note the tip of the microcatheter from the arterial route (*arrow*). **D** Superselective injection from that position shows the capillary vascular malformation with vessels *en passage*. **E** Direct percutaneous puncture of the vascular malformation at the nidus of the lesion (*arrow*) points to the angiocatheter placed directly into the nidus. **F** Superselective arterial injection after sclerotherapy with 98% ethanol injected into the nidus shows the capillary network gone, with preservation of the normal vessels. **G** Lateral DSA of the common external carotid artery after the direct percutaneous sclerotherapy into this capillary vascular malformation shows no filling of the lesion and preservation of the normal vessels. **H** Baseline lateral view of the lesion. **I** Image immediately after treatment within the first week shows the bluish discoloration of the treated area, as the lesion is thrombosed. **J** Four weeks after treatment there is near total disappearance of the lesion. A small area of ulceration was healing at this time. There was no residual malformation

14.7.2.4 Ethylene-Vinyl Alcohol Copolymer

Ethylene-Vinyl Alcohol Copolymer Properties

Ethylene-vinyl alcohol copolymer (EVAL) was first introduced in Japan by Taki et al. (1990). More recently, a similar agent has been introduced Onyx (EVOH) (MicroTherapeutics, Inc.). Both are solved in dimethyl sulfoxide solvent (DMSO) and are dependent on diffusion of the DMSO for the agent to precipitate and solidify. Onyx, however, uses the anhydrous DMSO. In Taki's experience with EVAL, as well as the experience reported by Sadato and Taki (1994) for the treatment of BAVMs, recanalization was a problem, as was angionecrosis seen at the time of surgical excision of the lesion, suggesting a significant toxic reaction believed to be caused by the DMSO. Taki used a 2-ml dose to rinse the catheter, and the rates of injection are dose dependent. Chaloupka (1999a) and Murayama et al. (1998,

2000) demonstrated that if the dose is kept to the dead space of the catheter, and the injection rate is above 60 s, there is no toxicity or spasm. We add the preliminary injection of 50 mg of Xylocaine and thus avoid spasm.

Onyx is available in various viscosities, dependent on the intended use, with the lower viscosity used in AVM embolization (6%–8%) and a higher viscosity preparation for aneurysm treatment (in the 30% range). Modifications of these preparations are expected, as experience is increasing with their use. The agent can be made radiopaque with micronized tantalum powder, which must be well mixed to enter in suspension. Mechanically shaking and warming the Onyx to 70°C facilitates this mixture (Cekirge, personal communication).

As EVOH is exposed to blood and exits the catheter, it undergoes instant polymerization, as the solvent DMSO diffuses away. A liner, or skin, of solidified material forms, with the central material still in liquid form, similar to lava that solidifies from the outside in, with the liquid center able to continue to flow with additional injections. This property allows slow gentle injections of Onyx and therefore observation of its behavior. If Onyx starts entering an unwanted portion of the lesion being treated, the injection is stopped, allowing the DMSO to diffuse and the agent to harden, and then restarting the injection, as the agent finds the remaining unfilled spaces. The column of Onyx is very cohesive, with no fragmentation, providing a true cast of the angioarchitecture of the lesion to be treated. Onyx solidifies as a spongy, polymeric cast (Fig. 14.114).

Because of the DMSO, the entire catheter assembly system, including the stopcock valve, must be DMSO compatible, and in the higher viscosity preparation for aneurysm treatment, the catheter must be able to resist high injection-pressure buildup.

Prior to Onyx injection, the catheter dead space (ID) must be rinsed with DMSO to avoid polymerization of the agent in the catheter lumen. Because of DMSO toxicity, if the DMSO in the dead space of the catheter is injected rapidly, it can produce spasm and even necrosis of the vessel wall (Chalupka et al. 1999). Once the desired catheterization has been achieved, and Onyx injection should be started, except that the catheter ID (0.02–0.025 ml) is first filled with pure DMSO. Onyx injection is then started with a very slow clearance of the catheter ID (filled with DMSO) over a 40- to 60-s injection, to prevent spasm or vessel damage.

At present this agent is also undergoing randomized clinical trials for AVM treatment and aneurysm therapy in the United States.

EVOH in Aneurysm Treatment

As Onyx is being introduced as a treatment for cerebral aneurysms, it is imperative that the risk of this or any embolic agent or technique remain below the risk of other techniques and of the natural history of the disease. Onyx is undergoing a clinical trial in Europe and a randomized trial with GDCs in the United States.

For safe aneurysm treatment, flow control is mandatory. The technique requires two catheter assembly systems, similar to the remodeling technique (see “Balloon Remodeling”). However, all systems must be DMSO

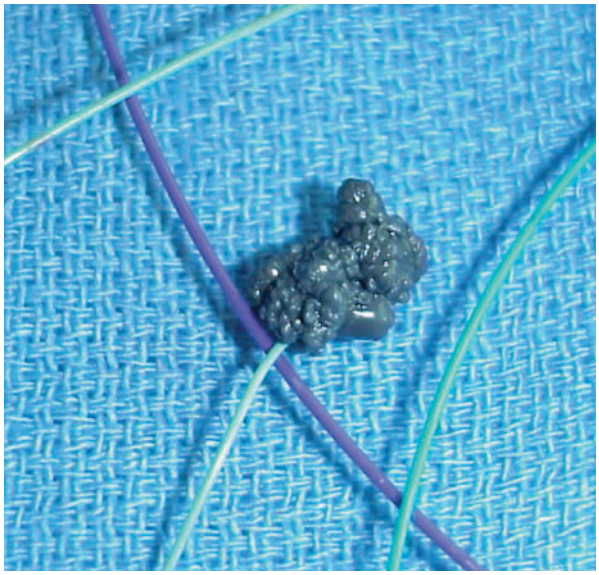

Fig. 14.114 (*left*). Ethylene-vinyl alcohol copolymer (EVOH; Onyx, Microtherapeutics, Sacramento, CA, USA). EVOH will precipitate and immediately solidify when in contact with blood once the DMSO diffuses from the EVOH as a solvent. This produces a shell, or skin, which solidifies from the outside in. The center remains in liquid form and permits additional injections of the material, even after a period of waiting. The final sponge-like polymeric cast of the vascular pathology is created

Fig. 14.115 (*right*). The 1-ml syringes for Onyx delivery. The syringes can do one revolution at a time. They come in different colors to differentiate the various components of the Onyx formula, with yellow used for the injection of DMSO and the other colors for the different concentrations of the material

compatible. For balloon protection, we use the Equinox occlusion balloon-tip catheter (Figs. 14.27, 14.30), a single-lumen balloon catheter that requires a 0.010-in. guidewire for navigation and sealing the distal end of the catheter to inflate the balloon. Balloon sizes come in 10- to 20-mm lengths and can inflate from 3–4 mm in diameter; the volume of injection will depend on the balloon size.

For Onyx delivery, we use the Rebar catheter (Fig. 14.13), a wire-threaded DMSO-compatible catheter with a reinforced shaft that tolerates the high pressures needed to inject the more viscous preparation required for aneurysm casting.

Onyx is injected and the balloon is inflated with specially designed 1-ml syringes that make it possible to carefully control injection and inflation. Injection is accomplished by turning the handle of the syringe, instead of actually pushing as is done with conventional syringes. Each turn of the handle represents an injection of 0.01 ml. They come in different colors to differentiate the different components of the Onyx formula, with yellow used for the injection of DMSO and the other colors for the different concentrations of the material, and purple to inflate the balloon (Fig. 14.115).

Fig. 14.116A–F. Legend see p. 1087

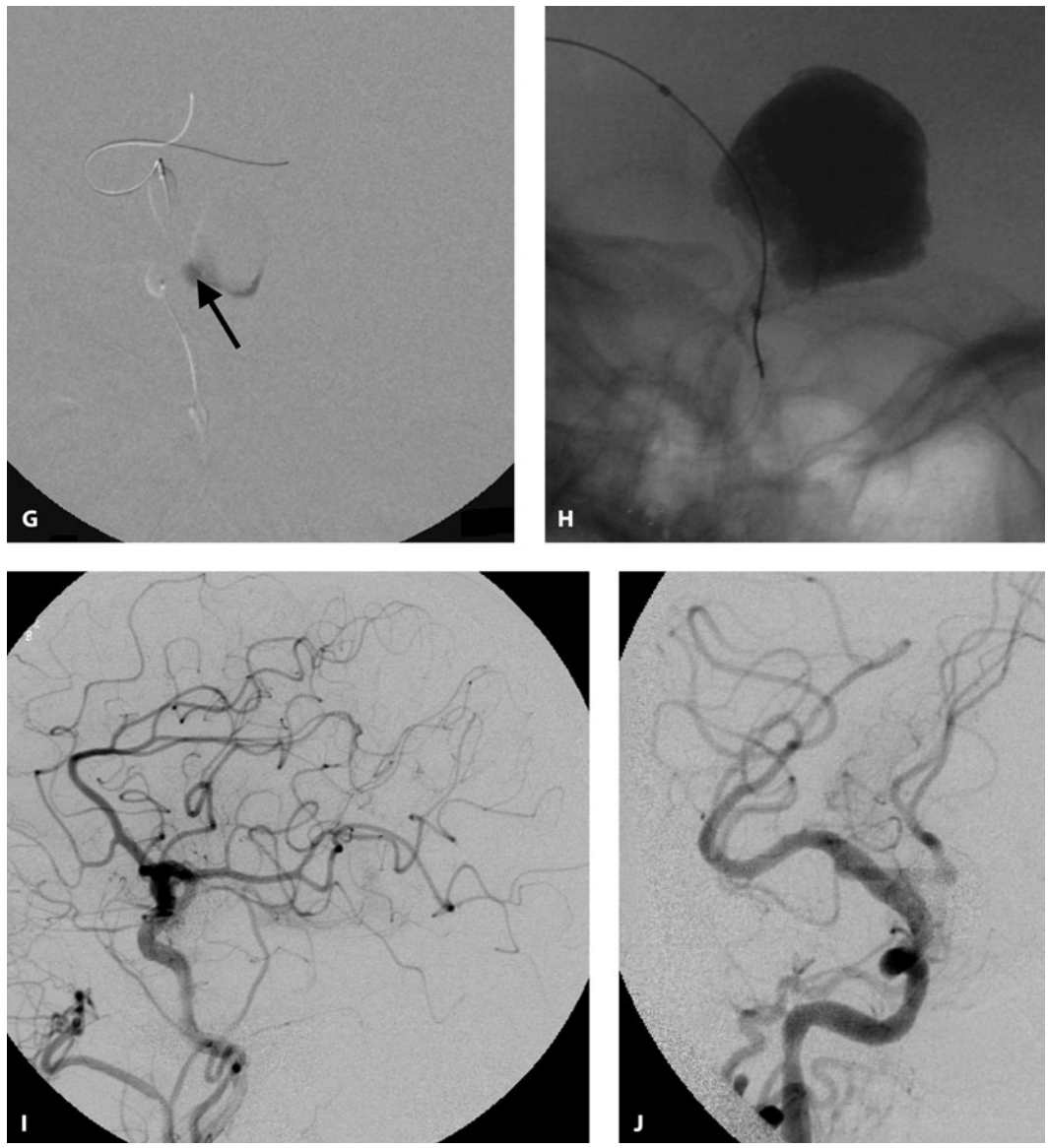

◄ **Fig. 14.116A–L.** Use of Onyx in the treatment of a cerebral aneurysm. **A** Lateral digital subtraction angiogram (DSA) of the right internal carotid artery shows a large broad-neck aneurysm. **B** Lateral road map of the catheterization. The balloon catheter was first advanced beyond the neck of the aneurysm, the microcatheter was then placed within the dome of the aneurysm (*arrow*), and the balloon tip catheter with the J wire was brought back across the neck of the aneurysm (*open curved arrow*, original position; *curved arrow*, more proximal position, with the balloon across the neck of the aneurysm). **C** Lateral road map of the occlusion test. The balloon is inflated while a small amount of contrast material is injected at the catheter tip in the dome and it is observed. If there is total flow control Onyx can then be injected. **D** Road map image of the first Onyx injection with flow control with a balloon inflated, while the Onyx is being injected at the dome of the aneurysm (*arrow*). **E** Intermediate cast of Onyx; the balloon is deflated. **F** Angiogram shows the posterior portion of the aneurysm filled with Onyx. **G** Road map image toward the end of the procedure with additional Onyx injected as it approaches the balloon and entrance of the aneurysm (*arrow*). The balloon is inflated. **H** Plain film in the working position, with the deflated balloon and guidewire still in place demonstrates the Onyx cast with a concave appearance at the place where the balloon was inflated. **I** Lateral and **J** frontal DSA angiograms after Onyx treatment show an excellent anatomical result. **K, L** see p. 1088

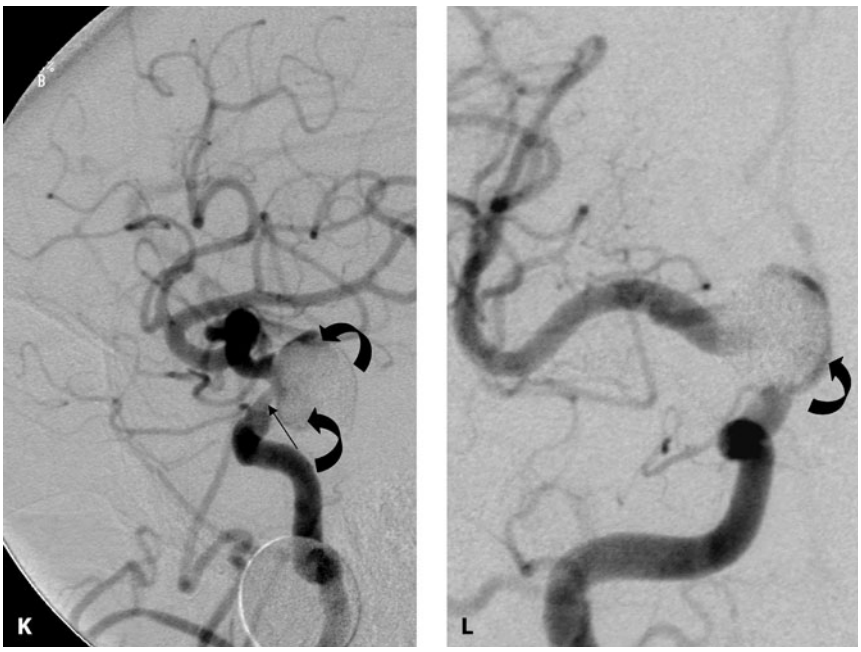

Fig. 14.116 (*continued*). **K** Oblique and **L** frontal angiogram 6 months later, the patient had TIAs that stopped with antiplatelet medication. Note the stenosis at the level of the repair (*arrow*) as well as partial recanalization at the inferior and upper dome of the aneurysm (*curved arrows*). Compare with **I** and **K**

To determine flow arrest prior to initiating Onyx injection, under flow arrest with the Equinox balloon tip catheter, inflated across the aneurysm neck, and with the Rebar catheter position deep in the aneurysm, contrast material is gently injected,. If flow arrest is confirmed, the balloon is then deflated, and Onyx injection is prepared. Prior to Onyx injection, the balloon is reinflated (Fig. 14.116). If the contrast material escapes the balloon may have to be repositioned or inflation increased to close the parent artery; in general the balloon is a pliable, soft balloon that will conform to the vessel shape, although one should avoid overinflation. The balloon is deflated with the same syringe, back to the exact starting point, to ensure full deflation. If road mapping is available, a new mask is obtained before balloon deflation, which will make it possible to reinflate the balloon to match the mask (Fig. 14.116).

At the start of the Onyx injection, pressure must be built up to permit the forward advancement of the Onyx column; consequently there is a time lag between the first revolutions and the arrival of the Onyx from the catheter. Once the injection is started, there is more of a one-to-one response; however, when the injection is stopped, there is still some material that continues to extrude from the catheter; therefore all injections are done slowly. In general, small injections of 0.2–1 ml are done at any one time, over a 2- to 3-min period.

The balloon inflations are restricted to no more than 5 min at any one time, i.e., a 2-min injection followed by a 2-min period for the DMSO to diffuse and the Onyx to solidify. It is important to determine the status of the circle of Willis: if poor or incompetent, total inflation time is de-

creased. After deflation, a period of 3–5 min with the parent vessel open allowing antegrade flow between injections is provided.

As the aneurysm is filling, and the Onyx reaches the inflated balloon, one must stop the injection and allow the Onyx to solidify. Toward the end, a concave modeling of the Onyx can be seen as the balloon protects the parent vessel (Fig. 14.116H). Preventing leakage of Onyx into the parent vessel is important.

At the end of the treatment and before withdrawing the microcatheter, negative pressure is created by reverse drawing with the Onyx syringe, waiting 30–60 s, and pulling the microcatheter with the balloon inflated.

An additional technique is improving the use of Onyx in aneurysm treatment: the combination of a balloon-expanding stent placed across the neck of the aneurysm, assisted with balloon protection. The stent acts as a scaffold so that a seal can be formed at the aneurysm neck, with a layer of concave Onyx between the vessel wall and the stent cells (Fig. 14.94).

It is important to place patients on antiplatelets postoperatively, to prevent delayed distal embolization. Although the early experience in Onyx treatment has been met with great enthusiasm, the lack of sufficient radiopacity can cause leakage of the agent into the parent vessel, with resulting stenosis or even late occlusion (Fig. 14.116K). The lack of adhesiveness has also been a limitation, as we have seen filling around the Onyx cast (Fig. 14.116L).

At this stage, it appears that one of the better indications for Onyx is the recurrence after coil compaction (Fig. 14.117). A contraindication for Onyx, or any other liquid embolic, is the presence of an artery at the aneurysm neck. If it flows into the neck, there is a danger that the Onyx will enter such a vessel with undesirable consequences. For example, in paraophthalmic aneurysm the origin of the ophthalmic artery must be clearly defined.

If spasm is noted in the parent vessel during catheterization the injection of 50–100 μg of nitroglycerin is a very effective way to stop the spasm (Fig. 1.48, 14.83).

14.7.3 EVOH in Brain Arteriovenous Malformation Treatment

Onyx is gaining popularity as an alternative to acrylics in the treatment of BAVMs. It is important that the risk of such treatments remain comparable to that of acrylics, under the natural history of the disease. BAVM treatment is targeted to the angioarchitectural weaknesses of the lesion, and although total obliteration is ideal, the goal of treatment should be clinical at the lowest possible risk (see Chap. 9).

When EVAL was first used in Japan to treat BAVMs (Taki et al. 1990), recanalization was a problem, as well as vessel necrosis seen at the time of surgical excision of the lesions, suggesting a significant toxic reaction, believed to be caused by DMSO.

Onyx has the theoretical advantages of long controlled injections through one pedicle and reaching the nidus supplied by another pedicle (Fig. 14.118). Catheter gluing in situ is much less likely. The technique requires flow-guided DMSO-compatible microcatheters such as the Flow-

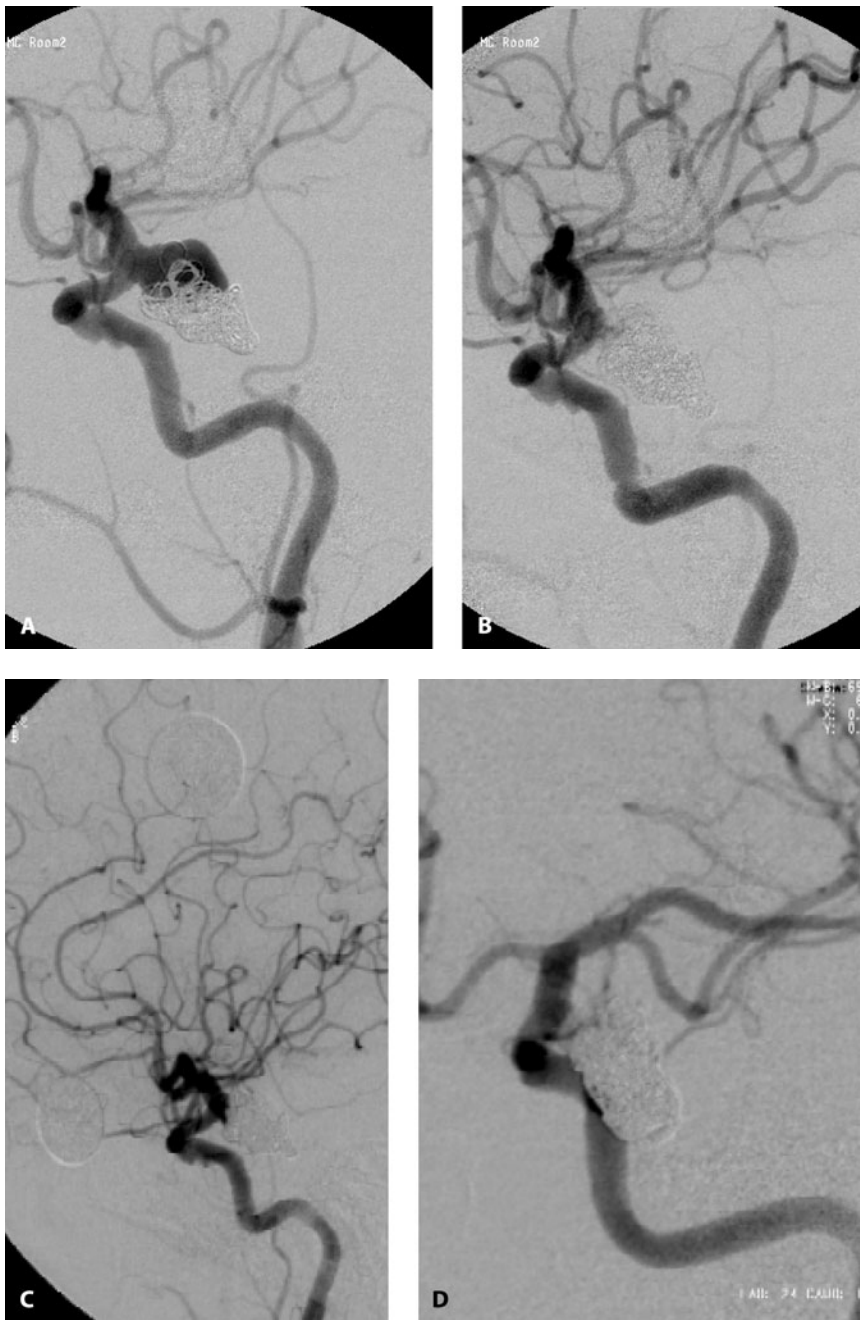

Fig. 14.117. **A** Lateral digital subtraction angiogram of the left internal carotid artery demonstrates compaction following coil treatment, with significant refilling of the aneurysm. **B** After Onyx embolization, note the total obliteration of the aneurysm and preservation of the carotid artery. **C, D** One-year follow-up demonstrates stability in the treatment

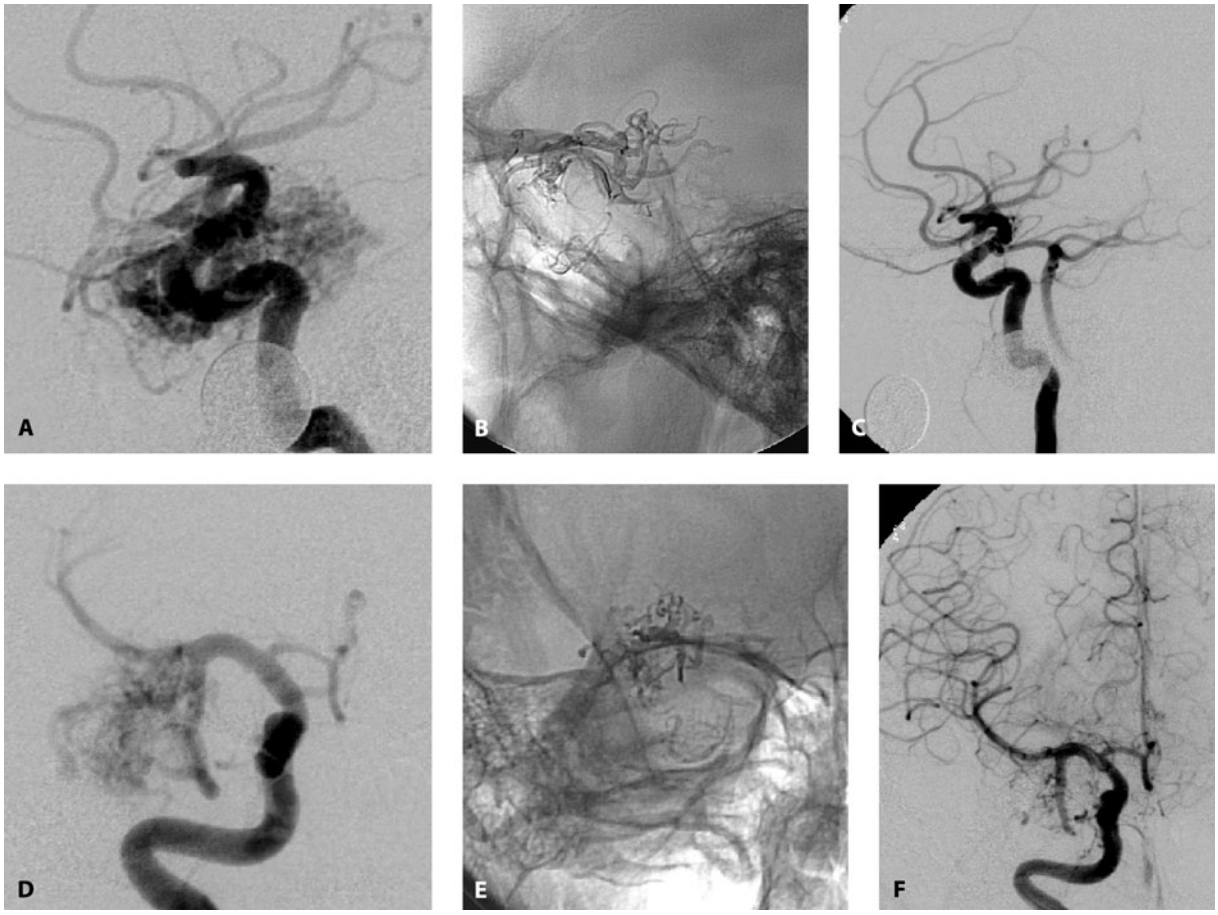

Fig. 14.118A–F. Onyx in brain arteriovenous malformation (AVM). **A** Lateral digital subtraction angiogram (DSA) in early arterial phase of a right temporal arteriovenous malformation. **B** Frontal DSA in early arterial phase. **C** Lateral plain film. **D** Frontal plain film of the skull showing the radiopaque cast of Onyx. Note the relatively low radiopacity of Onyx. **E** Lateral and **F** frontal DSAs after embolization, with near total obliteration of the AVM. This patient underwent a follow-up angiogram, which showed residual malformation and then underwent successful surgical excision

rider or easy Flowrider (MicroTherapeutics, Inc.). The Onyx preparation used for BAVM management has 6% lower viscosity than that used in other interventions. If the catheter can be wedged and flow control can be obtained, Onyx injection is facilitated. If no flow control can be obtained, a small amount of the material is exposed to blood and allowed to solidify. Small amounts are then injected, with the purpose of surrounding the distal tip of the catheter so as to form a curl or plug of Onyx that will act an a flow restrictor. Once some flow reduction is achieved, progressive injections of Onyx follow; as the material reaches an area to be avoided, the injection is stopped, the agent is allowed to solidify, and then the injection is restarted.

Catheter adherence to Onyx has occurred; however, as the technique is evolving, better catheters are being designed. Care should be taken not to surround the catheter with Onyx. Using more than one pedicle in large lesions will also avoid a number of problems.

14.8 Opacifying Agents

14.8.1 Tantalum Powder

Tantalum powder is an inert biocompatible metal first reported by Burke in 1940. He placed it in the fractured and unfractured tibia and femur of dogs and rabbits. Burke could find no detectable microscopic or radiographic evidence of bone or soft tissue irritation. In 1942, Pudense and Ottman showed that strips of tantalum implanted over the surface of the brain caused little reaction. Additional uses of tantalum in man have included tantalum plates for cranioplasty (Tindall et al. 1966), with no adverse tissue reaction even when the tantalum is in contact with nervous tissue. Bailey et al. (1952) studied the reaction to powdered tantalum introduced into various areas of the nervous system of cats and monkeys. The response to tantalum was minimal in all areas except the basilar system.

Tantalum dust (Kenna Metal, Latrobe, PA, USA) came in two preparations, tantalum powder, a black powder, and tantalum oxide, a white powder (Kerber 1980). The powder came in various sizes, the 1- to 2-μm particles are best for embolization (Table 14.5).

This product does not alter the chemical characteristics of the embolic agents, but will increase the viscosity of the mixture. It is important to remember that the black tantalum powder may produce skin discoloration in white patients (Fig. 14.119), whereas the white powder will not, even in black patients. The main disadvantage of tantalum oxide is that it is of lesser weight; therefore, more material is needed for similar radiopacity, further increasing the viscosity of the mixture. This product no longer exists.

Fig. 14.119A, B. Skin discoloration due to black tantalum powder. **A** 7-year-old girl treated with liquid silicone and tantalum powder for the management of an extensive vascular malformation of the maxillofacial area. Embolization was the only treatment. Note the ash discoloration of the cheek. **B** Ten years later, skin discoloration is faint but remains. The patient is free of disease and the problem has been well controlled for over 20 years with liquid silicone exclusively. She has had menstrual cycles without changes in her clinical condition. White tantalum oxide would avoid this problem

Table 14.5. Opacifying agents and retardants

Tantalum powder (1–2 μm), black powder
Tantalum oxide powder (1–2 μm), white powder
Ethiodol or Pantopaque (with acrylics for radiopacity and as a retardant of polymerization)
Ethiodol as a emulsion with ethanol in a 1/3 Ethiodol to 2/3 98% ethanol
Acetic acid retardant for acrylics

14.8.2 Iophendylate (Pantopaque)

Iophendylate (Pantopaque) acts primarily to retard polymerization of the acrylics but also adds radiopacity. If decreased viscosity is required because of small vessels, distal territory, or tumor embolization, a 75% iophendylate–25% NBCA mixture gives sufficient radiopacity.

14.8.3 Iodized Oil

Iodized oil (lipiodol) chemically acts like iophendylate but has a lower viscosity, which can provide a better distal penetration of small vessels.

14.8.4 Ethiodol

In the United States, Ethiodol (Savage Labs, Melville, NY, USA) is the only available oil-based iodinated contrast material. It is used in a similar manner as Pantopaque in combination with acrylics.

Ethiodol has recently been used with ethanol (Barrows, personal communication). When used in this manner, it adds radiopacity, and in addition increases the viscosity of the mixture and enhances contact with the vessel wall. It may be more effective in this manner than metrizamide powder, which is no longer available.

14.9 Chemotherapy

14.9.1 Intra-arterial Infusions

There is renewing interest in intra-arterial chemotherapy infusions for head and neck tumors, combined with radiation therapy, as an effective and simple treatment (Kerber et al. 1998). The technique consists of selecting lesions in anatomically isolated areas such as the tongue. Selective catheterization of, for example, the lingual artery is done, progressively increased quantities of contrast material are injected, until the capacity of the territory to be infused is determined, by observing reflux of contrast material. Once this has been determined, the total dose of the chemotherapy medication is delivered at that flow rate, to flood the desired territo-

ry, achieving very high concentrations of chemotherapy in the tissues. Although this therapy is still in its beginnings, we have observed tumor shrinkage, as reported by Kerber. If indeed these therapeutic strategies results are effective, it could be expanded to other areas.

At present, cisplatinum is the agent used, but in the future other agents may be used. In cerebral pathology, these treatments remain limited because of logistical problems, the need for repeated treatments, and risk of ophthalmic and embolic complications, with long and repeated implanted devices in the carotid artery. We have used chemotherapy drugs on a few occasions with promising results. Functional vascular embolization should maximize the efficacy of this approach, make higher concentrations possible, and decrease toxicity, and they should be encouraged.

14.9.2 Time-Released Microcapsules (Chemoembolization)

Time-released microcapsules have created a significant amount of interest outside the interventional field for many years. Only recently has attention been paid to the synergetic application of these two modalities. It is quite attractive to use the arterial route to deposit microcapsules that can very selectively release high concentrations of cytotoxic agents and add to the insult the effects of ischemia. It would obviate the need for long, tedious, and repeated catheterization and infusions. Unfortunately, there has been slow progress in developing reliable time-released microparticles that are easy to manufacture and use. The principle of microencapsulated agents has been applied to ethyl cellulose (Kato and Nimoto 1978) or carnauba wax (Madoule 1981). Although still not in general use, this has a very promising role in our pursuit of an endovascular approach to various pathological entities and this includes not only currently treated hypervascular conditions, but also hypovascular problems that may be even more sensitive to ischemic insults.

14.10 Miscellaneous

14.10.1 Syringes

We believe that all syringes should be of the Luer-Lok type. As a matter of precaution, syringes used for flushing or contrast injection should be of different size and/or marked differently than those used to inject embolic materials. When learning or testing the flow characteristics in an individual situation, the same type of syringe used to do the testing should be used to inject the embolic material or provocative drugs (e.g., Xylocaine, Amytal).

For the injection of Onyx, special syringes that are DMSO compatible and are able to inject very accurately at high pressures are needed (see sect. 14.7.3).

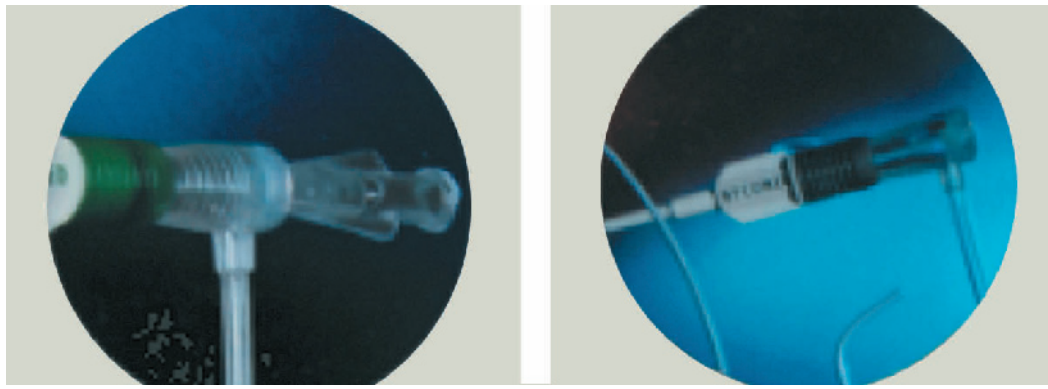

Fig. 14.120. Headway self-sealing valves (CathNet-Science SA) that prevent back-bleeding and accept 5-F to 9-F catheters

14.10.2 Stopcocks and Y-Adapters

One-way Luer-Lok stopcocks are recommended for ideal fitting. Transparent plastic stopcocks are best to detect any air bubbles prior to injection. However, in superselective work, back flow may not be present; in this case, a fluid meniscus is needed to avoid air emboli.

With the newer embolics, compatibility is important: for example, DMSO-compatible connections and the various acrylics.

When using a coaxial system, Y-adapters, which have a side arm for continuous perfusion between the two catheters and can accommodate monitoring angiography, are very useful. In addition, a Tuohy-Borst fitting will make it possible to use catheters or guidewires of a variety of sizes without back leakage (Fig. 14.82).

When using detachable balloons, no proximal washers or Tuohy-Borst adapters are used, so as to prevent accidental balloon detachment when withdrawing or changing the balloon catheters, or when using the self-sealing Headway system (Cathnet-Science, Paris, France) (Fig. 14.120).

With the increased use of two simultaneous catheter delivery assemblies, the use of a triple Tuohy-Borst adapter is very convenient (Fig. 14.82B).

14.10.3 Tray Containers

As with the syringes, different containers should be used for contrast or embolus material to prevent accidentally mistaking one for the other.

14.10.4 Flushing Solutions

Flushing solutions may or may not contain heparin.

One of the authors (P.L.) uses normal saline without the addition of heparin and gives a bolus loading dose, followed by a continuous infusion, depending on the ACT. The others (A.B., K.T.B.), however, use 4,000 IU of heparin sulfate for each 1,000 ml of flushing solution. In adults, 0.9% nor-

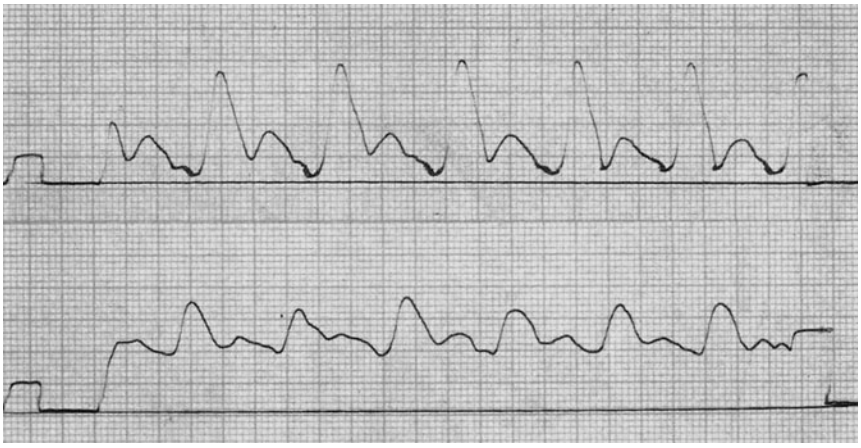

Fig. 14.121. Doppler ultrasound of a normal external carotid artery. Note the elevation during systole, whereas there is no flow during diastole

mal saline is used, whereas in children a solution of 0.35% normal saline and 2.5% dextrose with 2,000 IU of heparin per 1,000 ml of solution is used.

The results and experience are similar with both regimens.

14.10.5 Corticosteroids

The use of prophylactic steroids may be of benefit to reduce postembolization pain and swelling. We routinely administer 4 mg of Decadron t.i.d. 3 days after the procedure and tapered over the next 3 days.

14.10.6 Normal Physiology of the External Carotid Arteries

To best understand flow control as it relates to embolization, a brief analysis of normal physiology of the external carotid artery is necessary.

The normal hemodynamic characteristics of the external carotid artery are the absence of diastolic flow as demonstrated by Doppler ultrasonography (Fig. 14.121). Therefore, embolus injection during diastole carries a higher risk of reflux. As a general principle, particulate emboli are injected in small intermittent injections during systole.

Du Boulay and Darling (1975) demonstrated, in the baboon, the arterial autoregulation response down to a blood pressure of 60 mmHg.

This autoregulatory mechanism is noted to be more effective in the internal maxillary and pharyngeal–occipital system, whereas in the facial artery no real autoregulatory mechanisms were noted. Vasoconstriction in response to hypertension is a function of large and medium-sized arteries, while true autoregulation is seen in more distal branches.

14.11 Flow Control

14.11.1 Introduction

Flow control refers to our ability to alter the flow characteristics in abnormal or normal territories. It may represent a deliberate increase, decrease, or arrest of flow, using proximal and/or distal collateral circulation, with the aim of reaching a target, sparing normal noninvolved territories. It may be accomplished using a variety of techniques, including changes in systemic blood pressure, the use of a wedge catheter or microcatheters, calibrated-leak balloons, occlusive, double-lumen balloon catheters, manual compression, rate of injection, etc. All share the aim of reaching a target and sparing normal tissue. Flow control can be achieved at the larger, more proximal circulation (Fig. 14.122) or at more distal smaller anastomosis (Fig. 14.123) at the circle of Willis, or leptomeningeal collaterals (see "Flow Control in the Cerebral Area").

We originally introduced this concept in the embolization of the lenticulostriate arteries (Berenstein 1981), the maxillofacial region (Berenstein et al. 1983), and then extended the concept to the rest of the craniofacial area using the craniofacial and cervical collateral circulation (Lasjaunias 1986; see Vol. 1).

In the cerebral and spinal cord circulations, the complexity and small size of the vasculature, the vitality of the tissue being supplied, and the distal location within the vascular system require modification of some of the techniques used in the craniofacial area. Permanent mechanical rerouting of flow, for example, even temporary, may not be tolerated in the CNS due to the sensitivity of CNS tissue to hypoxia.

Flow manipulations in the cerebral circulation and spine and spinal cord will follow.

14.11.2 Flow Control in the Craniofacial Area

In our analysis of the functional anatomy of the head and neck, we have illustrated the various anastomoses between the neighboring territories. Some involve greater risk than others, as the anastomoses supply more vital territories: the visual system, brain, peripheral nervous system, and the mucosal and musculocutaneous territories (Fig. 14.124). Anastomoses must be respected; their presence, however, is not a contraindication to embolization, but some type of control in the direction of their flow is mandatory for safe and proper embolization (Fig. 14.122).

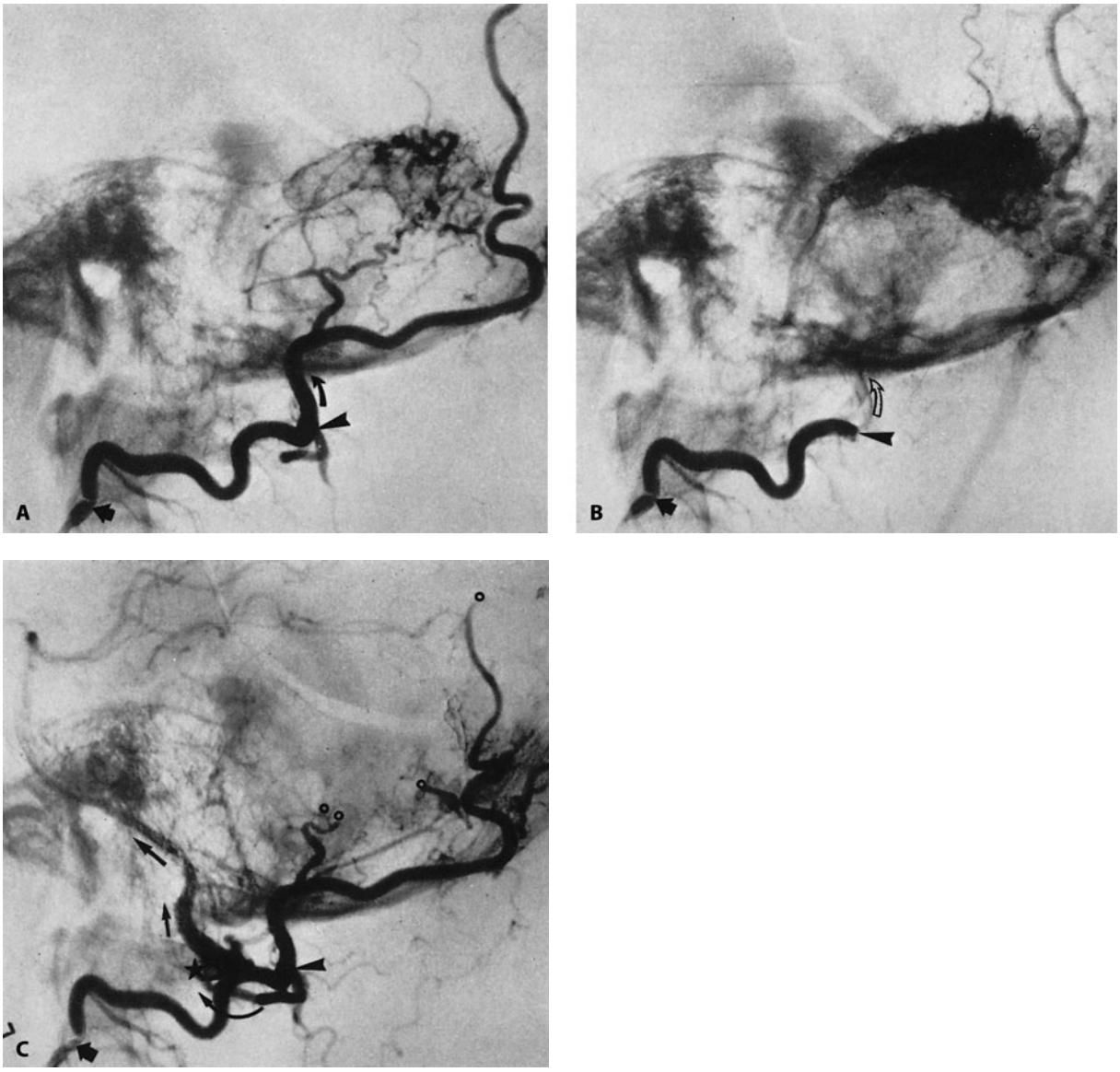

Fig. 14.122A–C. Reversal of flow in an endangered anastomosis. **A** Lateral subtraction angiogram of the left occipital artery supplying a meningiosarcoma invading the sigmoid sinus. The catheter is wedged in the occipital artery (*arrowhead*), obtaining flow control of the proximal segment of the occipital artery from the tip of the catheter to the C2 anastomosis (*arrowhead*). The increased pressure of injection forces contrast material toward the distal occipital artery (*curved arrow*). **B** The injection is stopped, arrested contrast material is seen from the wedged catheter (*solid arrow*) until the C2 anastomosis (*arrowhead*). The nonopacified flow from the vertebral artery is reversed at C2 and washes out of the distal occipital artery (*open curved arrow*). The reversed flow on C2 can therefore be used to push the emboli into the tumor. **C** Postembolization monitoring of the occipital artery. The tumor has been embolized with 40 μm Gelfoam powder (*o*) while the anastomosis has been preserved. Note that at this rate of injection, the C2 collateral has reserved its flow and now fills the vertebral artery (*star*) and basilar system (*arrows*)

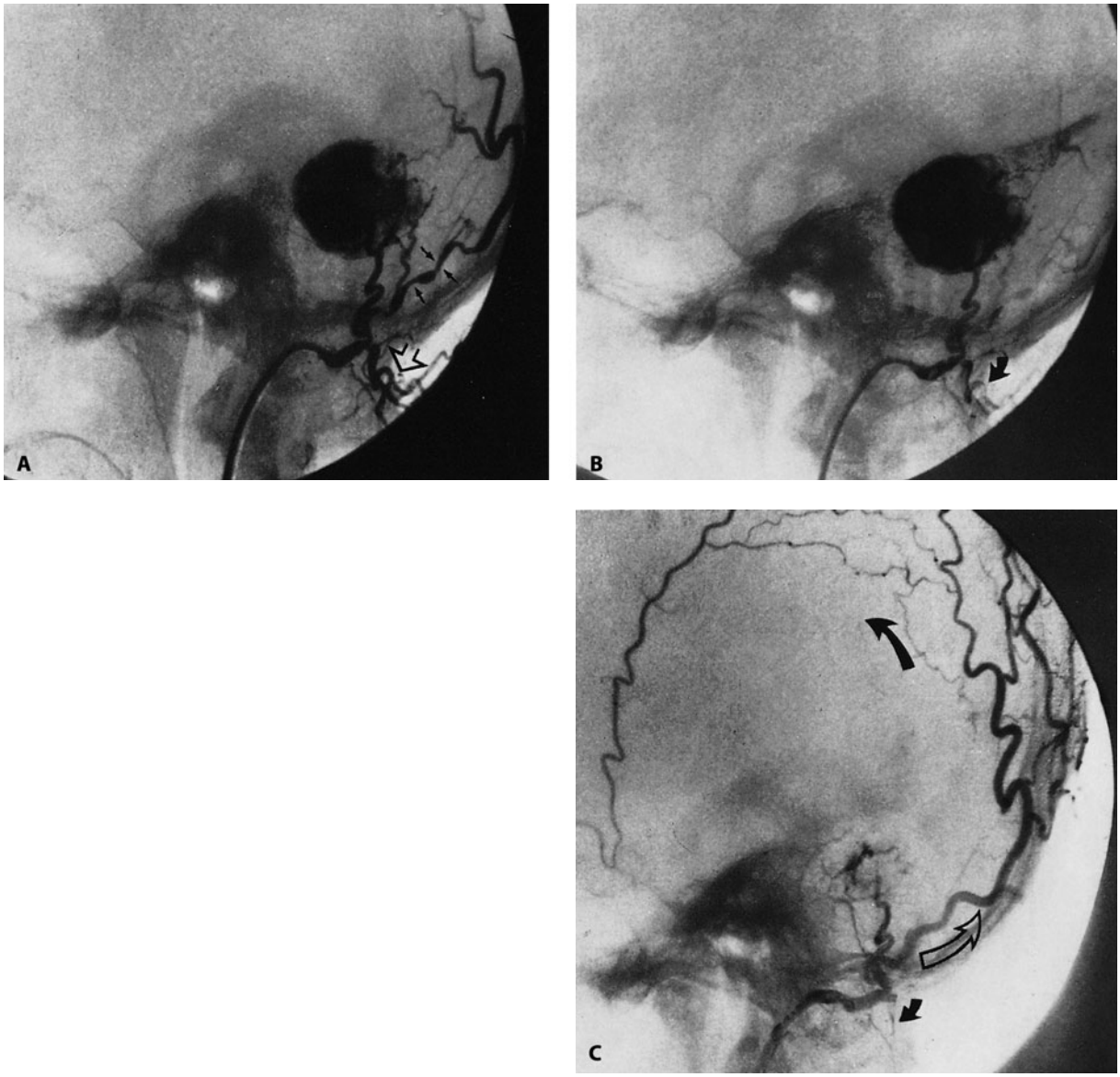

Fig. 14.123A–C. Mechanical protection of an endangered anastomosis with a pushable coil. Hemangiopericytoma (also see Fig. 2.4). **A** Subtracted angiogram of the left occipital artery. Catheterization distal to the C2 anastomosis (*open arrow*) could not be accomplished (1979). While attempting distal catheterization, spasm in the occipital artery at and distal to the transmastoid branches was produced (*small arrows*). **B** A minicoil (0.038 in.) was used to block the endangered anastomosis (*curved arrow*). Note the preferential flow toward the tumor with no filling of the normal distal occipital artery. Complete flow control exists and is dependent on the rate of injection. **C** Toward the end of the embolization, the endangered anastomosis is still protected (*curved arrow*), the tumor has been embolized with 40 μm Gelfoam powder. At this pressure of injection, flow is antegrade to the distal occipital artery (*open curved arrow*). Although powder has been used, thanks to the reversal of flow all the distal microanastomosis between the occipital and superficial temporal arteries (*curved arrow*) have been preserved thanks to the reversal of flow

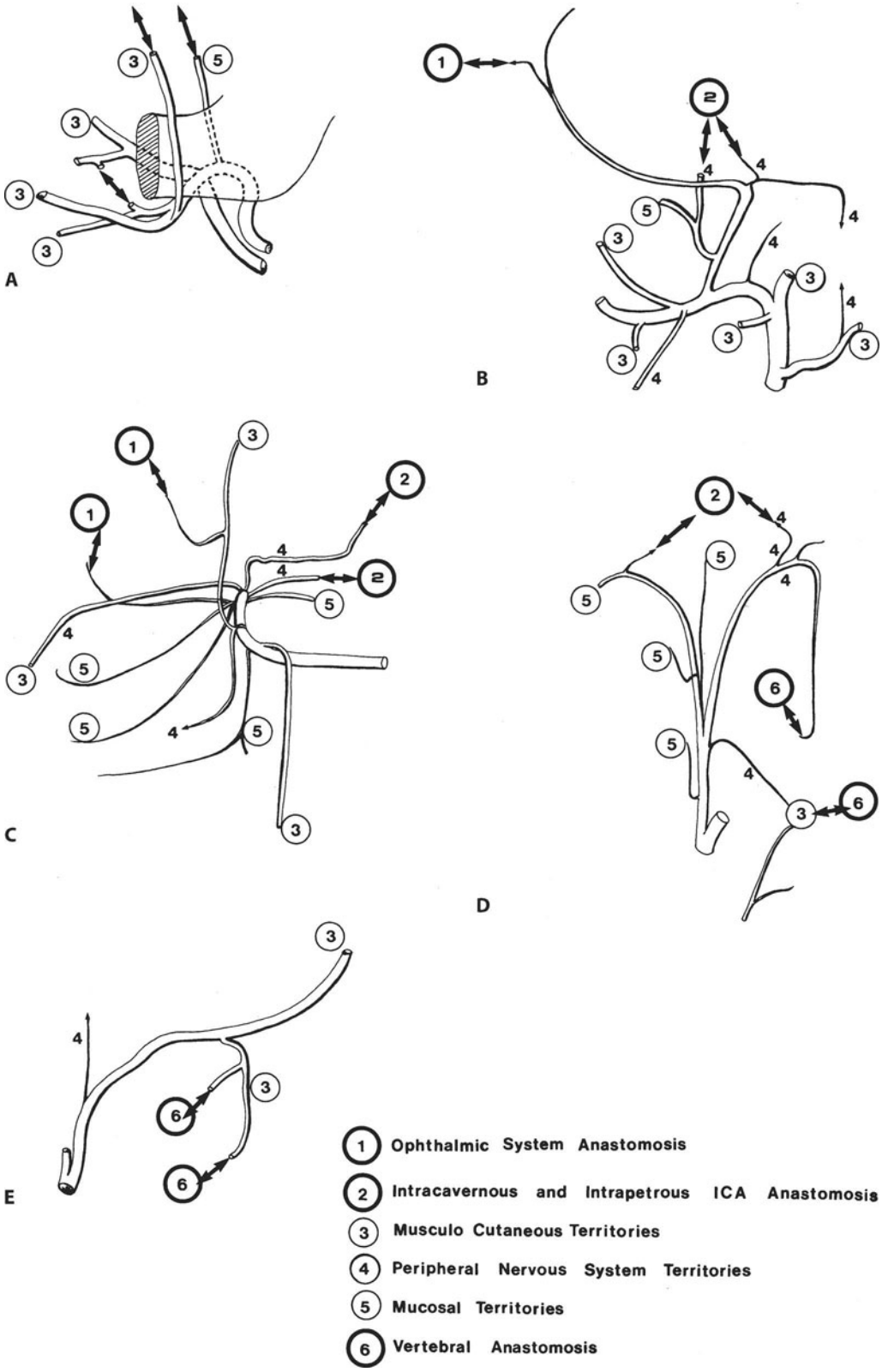

Fig. 14.124A–E. Diagrammatic representation of the various territories and the bidirectional flow through the collateral circulation. **A** Lingual and facial arteries. **B** Proximal internal maxillary artery. **C** Distal internal maxillary artery. **D** Ascending pharyngeal and cervical arteries. **E** Occipital artery

14.11.2.1 Protection of an Endangered Anastomosis

Mechanical Blockage

The simplest and most obvious way to protect an endangered anastomosis is to mechanically block it. This can be done with pushable coils, injectable liquid coils, detachable coils, or a particulate agent. After this anastomosis is blocked, embolization can be done with microparticles, liquid agents, or other embolic agents (Fig. 14.123).

Reversal of Flow in an Endangered Anastomosis

Flow can be reversed with an occlusive balloon catheter proximal to the anastomosis or with a wedged catheter. The aim is to impose the flow through the endangered anastomosis away from the endangered territory (the vertebral artery, for example) and redirect the flow towards the nondistal target or lesion (Fig. 14.122A). This reversed flow will assist, or push, the emboli toward the abnormality. Prior to embolus injection, various test hand injections are done to determine the tolerance and/or pressure needed not to fill the anastomosis. When one sees contrast material flowing toward the anastomosis, one stops or decreases the rate of injection; fluoroscopy will show that the contrast material is reversed and is washed out by nonopacified blood toward the abnormal territory (Fig. 14.122B). As the embolization begins, the contrast and embolus mixture is gently injected and monitored as the nonopacified reversed blood flow away from the vertebral artery washes the emboli distally toward the desired territory. As the embolization is progressing, it can be noted that the washout is slowing and more careful injections are required. When the flow is significantly slowed, the embolization is stopped (Fig. 14.122C).

This maneuver can be done at any level, from larger vessels such as the occipital to vertebral anastomosis (Fig. 14.122), or at a more distal location.

Protection of an Endangered Anastomosis by Distal Catheterization

An obvious safety feature is the catheterization beyond the endangered point. With today's microcatheters and microguidewires, this is virtually always possible.

14.11.2.2 Intralesional Flow Control

Monocompartmental vascular lesions such as some vascular malformations, some paragangliomas, and some intratumoral AVFs may allow us to reach the nidus within the lesion through a feeding pedicle. This will make it possible to use the less critical or endangered pedicle, sparing the more vital one. To determine if this is possible prior to embolization, a relatively high-pressure, high-volume injection is done with the aim of overcoming the intralesional pressure to reflux into the others.

Multiple test injections with contrast material are done to determine the rate of injection and to estimate the volume of embolic agent needed

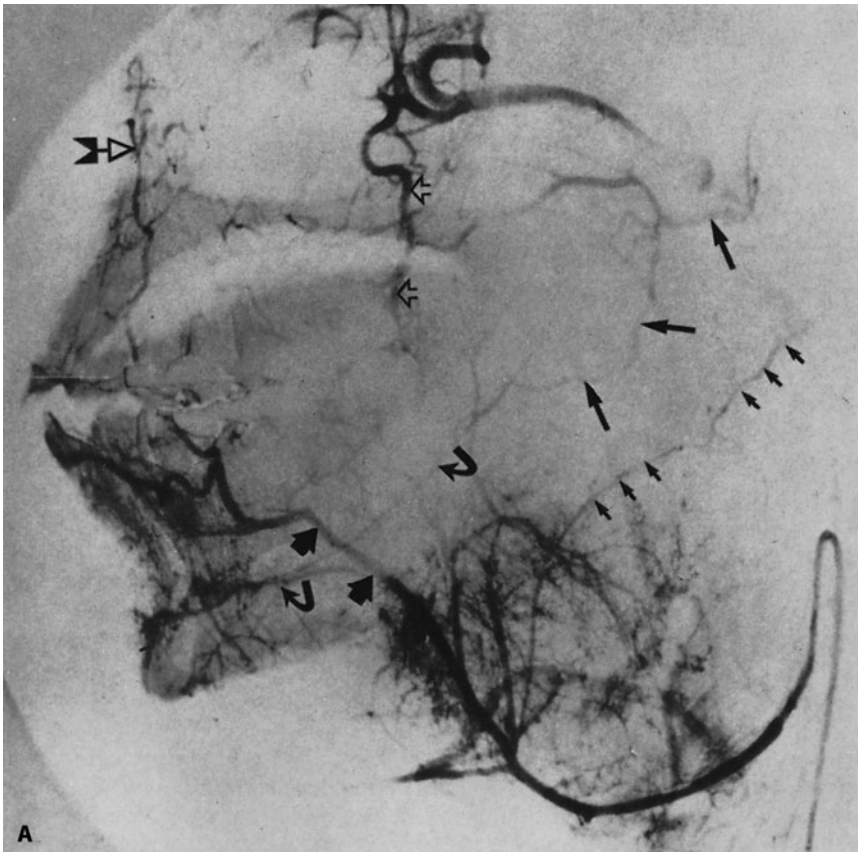

Fig. 14.125A–C. Balloon flow reversal in a capillary-venous vascular malformation. **A** Selective right facial injection demonstrates filling of the collateral circulation with filling of the inferior to superior masseteric arteries (*small arrows*), transverse facial (*arrows*), and distal facial arteries (*broad arrows*), mid mental to inferior dental (*broken arrows*), buccal to internal maxillary artery (*open arrowheads*), and the infraorbital point (*flagged arrow*), with only modest opacification of a capillary venous vascular malformation of the submental area. **B** Using a double-lumen occlusive balloon catheter in the proximal facial artery (*flagged arrows*), one can fill the capillary venous vascular malformation to best advantage. Note, the superior ascending palatine circumferential artery (*open curved arrow*) and only very modest opacification of the distal facial artery. Under fluoroscopic monitoring, the reversal of the flow through the collateral anastomotic pathways towards the lesion could be seen. **C** This permitted an excellent microembolization with 40 μm Gelfoam powder (*arrowheads*) preserving the collateral circulation. **B, C** see p. 1103

to occlude the nidus without reflux into the endangered vessels. This technique is best accomplished with liquid emboli such as acrylics. We must emphasize that a good understanding of all the factors involved is mandatory to accomplish this result safely.

14.11.2.3 Occlusive Balloon Flow Reversal

In hypervascular lesions that do not have a sump effect or when there is no preferential flow, injection of emboli into a feeding pedicle may not reach the lesion and/or only partially occlude it. Many of the emboli will

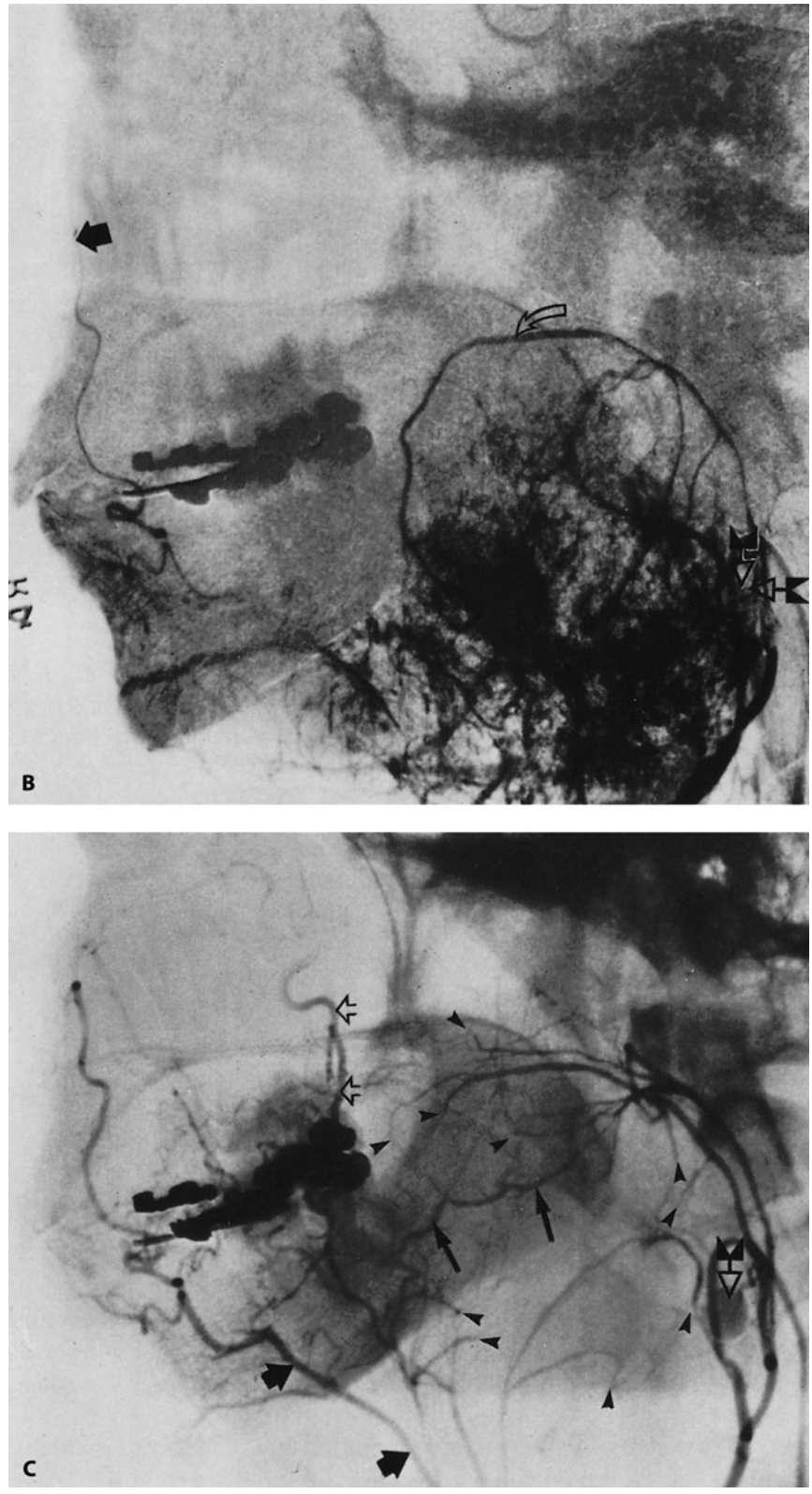

Fig. 14.125B, C. Legend see p. 1102

therefore enter normal territories. Since the collateral anastomosis can carry flow in either direction, a double-lumen balloon catheter placed proximally at the origin of an artery can be used, for example, with the facial artery (Fig. 14.125). This will then force a reversal of flow though the collaterals from the maxillary, transverse facial, or opposite side to supply the facial territory (and therefore a lesion in its territory). One must have absolute control in the proximal facial trunk. If contrast material is progressively injected, one can observe nonopacified blood pushing the contrast material into the lesion. If the right pressure of injection is used all of the contrast will then enter the abnormality, sparing the normal territory (Fig. 14.125). The same maneuver is then repeated with the appropriate size of microparticles until the lesion is devascularized.

14.11.2.4 Functional Rearrangement of the Supply to a Territory

Functional rearrangement of the supply to a territory is primarily used for rearrangement in malignant lesions prior to infusion chemotherapy when an entire territory needs to be infused through a single pedicle or a lesion with bilateral supply must be disconnected and converted into a unilateral one.

14.11.2.5 Surgical Flow Control

Surgical ligation of the anterior ethmoidal arteries or nasal branches of the ophthalmic artery is a very useful adjunct to lesion with dual supply; this will convert the lesion to a purely external carotid artery lesion. It is also used to control epistaxis in some cases.

14.11.3 Flow Control in the Meningeal Arcade and Dural Surfaces

The blood supply to the dural surfaces is rich and involves the maxillofacial, craniocervical, orbital, and cerebral circulations. These arcades supply blood to the cranial nerves and anastomosis in this area is a potential danger, while understanding its dynamics offers great opportunities to safely treat lesions in these territories. The functional anatomy of these territories is essential to the understanding and planning of treatment in a variety of diseases, including dural-based tumors and dural vascular malformations or shunts. They play an important role in occlusive vascular disease as potential collaterals and sources of emboli, as well as in the proper assessment of lesions involving the base of the skull, craniocervical, and convexity linings (see Volume 1).

14.11.4 Flow Control in the Cerebral Circulation

In the cerebral circulation, the complexity and small size of the vasculature, the vitality of the tissue being supplied, and the distal location with-

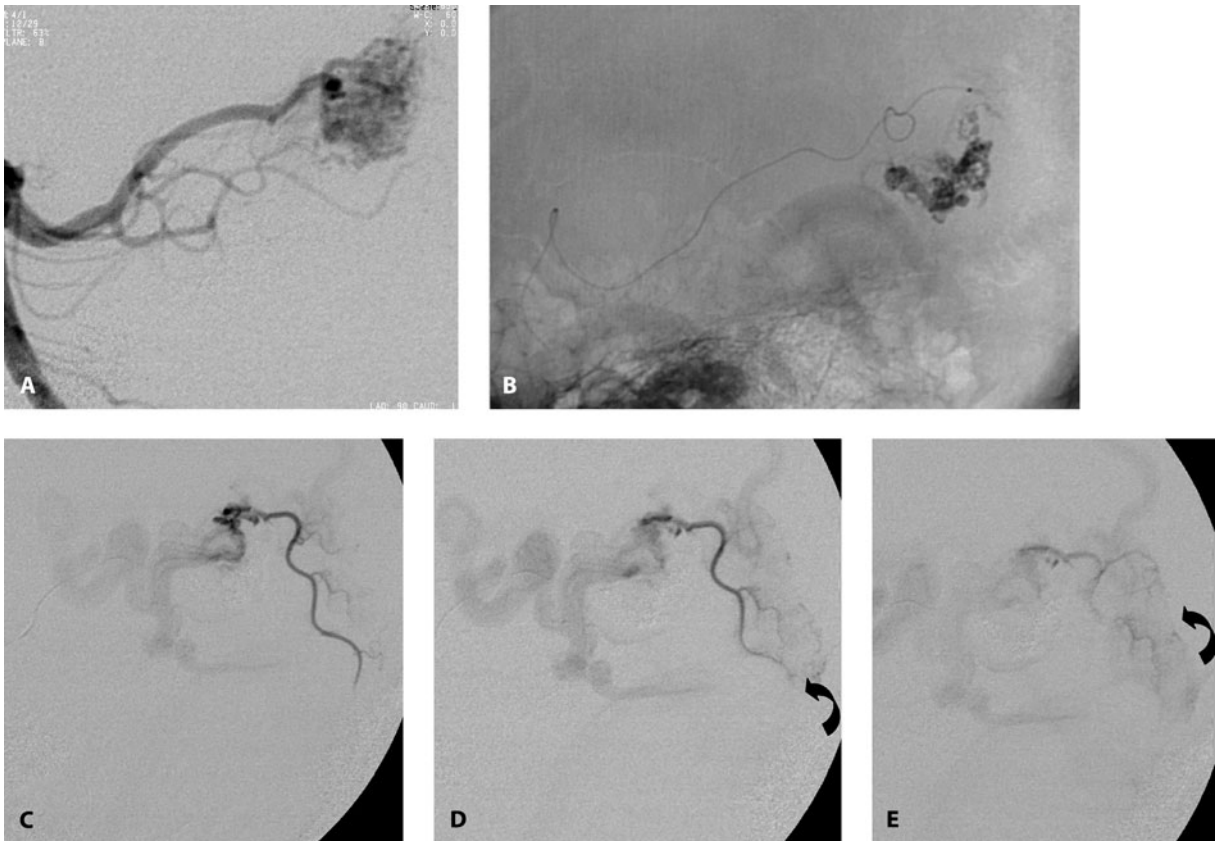

Fig. 14.126A–I. Flow reversal at the level of a gyrus. **A** Left vertebral artery injection shows a vascular malformation. **B** Plain film after embolization of the inferior portion. The microcatheter is in the most superior part of the malformation. **C–E** Superselective injection at that level, with the catheter wedge obtaining flow arrest in this position, demonstrating a normal calcarine artery distal to the malformation. With the wedge catheter, flow reversal can be demonstrated by first injecting contrast material (**C**), filling the more distal territory, and by stopping the injection with the catheter still in the wedge position. See the washout of the contrast material in a reverse fashion (**D**, **E**, *curved arrows*). **F–I** see p. 1106

in the vascular system require modification of some of the techniques described in the craniofacial area. Permanent mechanical rerouting of flow, for example, even if temporary, may not be tolerated in the CNS due to the sensitivity of CNS tissue to hypoxia.

Flow manipulations in the cerebral vasculature can be used for more distal catheterization (induced systemic hypertension), to reverse flow in the circle of Willis in an attempt to cross the anterior or posterior communicating arteries (contralateral manual compression in the neck). As in previously discussed territories, a wedged microcatheter can be used to reverse flow at the level of a gyrus (Fig. 14.126) or through leptomeningeal collaterals, to determine the safety of focal endovascular ligations (Fig. 14.126) and prevent liquid agents from permeating unwanted territory. Despite such helpful techniques, there is no replacement for anatomical knowledge.

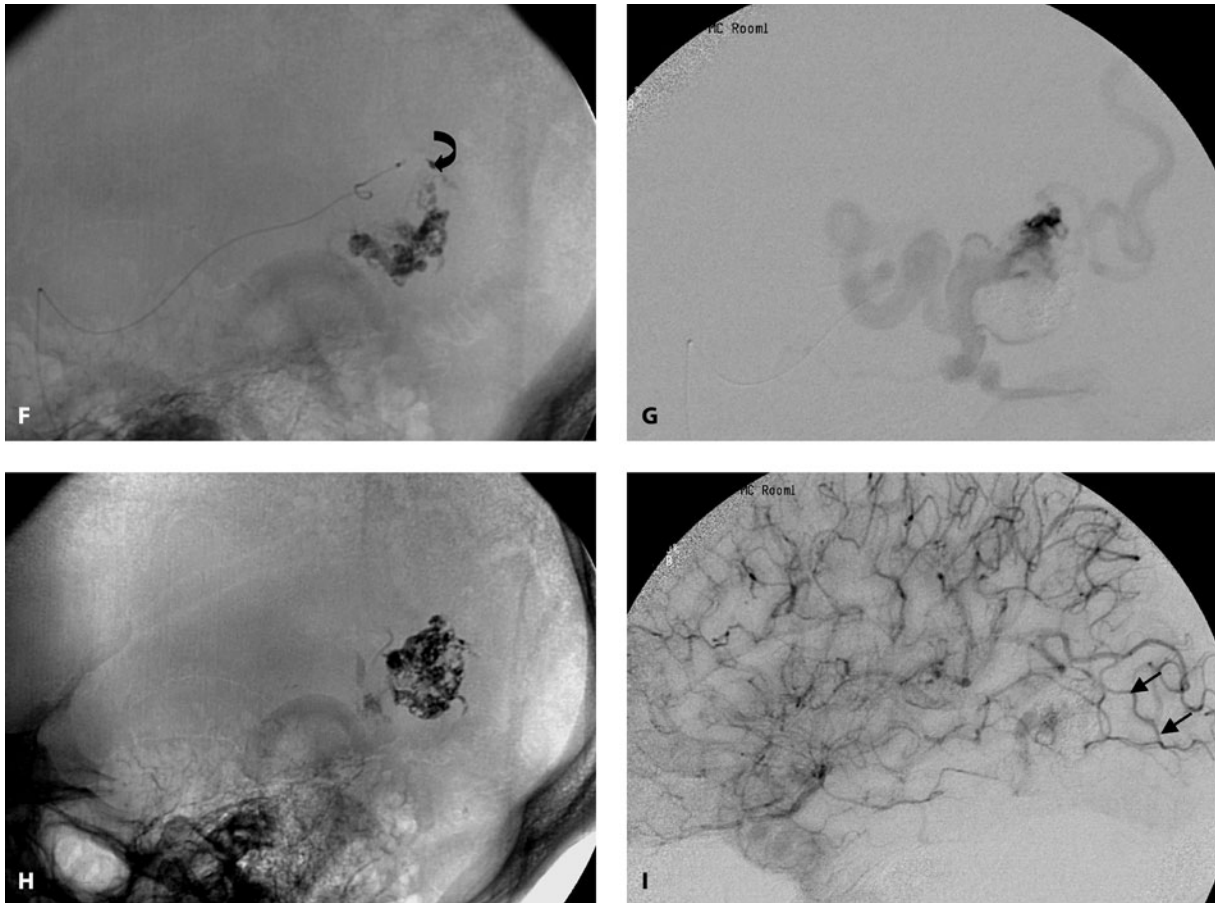

Fig. 14.126 (*continued*). **F** Plain film shows the deposition of a 1.2 × 1-cm liquid coil (BLC; *curved arrow*) to protect the normal artery and prevent the NBCA from permeating that territory. **G** Superselective injection after the BLC deployment demonstrates filling exclusively of the malformation. **H** Plain film of the skull demonstrates the radiopaque embolic acrylic in the nidus of the malformation, preserving the normal artery. **I** Angiogram of the internal carotid artery after embolization demonstrates the same branch filling through leptomeningeal collaterals (*small arrows*). Compare to **C**

14.11.4.1 Distal Catheterization

In some situations, distal catheterization is not possible, either because of the size of a vessel or its tortuosity. Flow in such cases can be augmented by raising the systemic blood pressure (Fig. 14.127) or by temporarily occluding a neighbor or contributing artery, thereby producing temporary compensatory vasodilatation. The resultant flow increases in turn facilitate more distal navigation. Although valuable, such techniques are seldom needed with the availability of the smaller microcatheters and microguidewires (Fig. 14.128). Staged embolization may allow a remaining channel to enlarge for future catheterization.

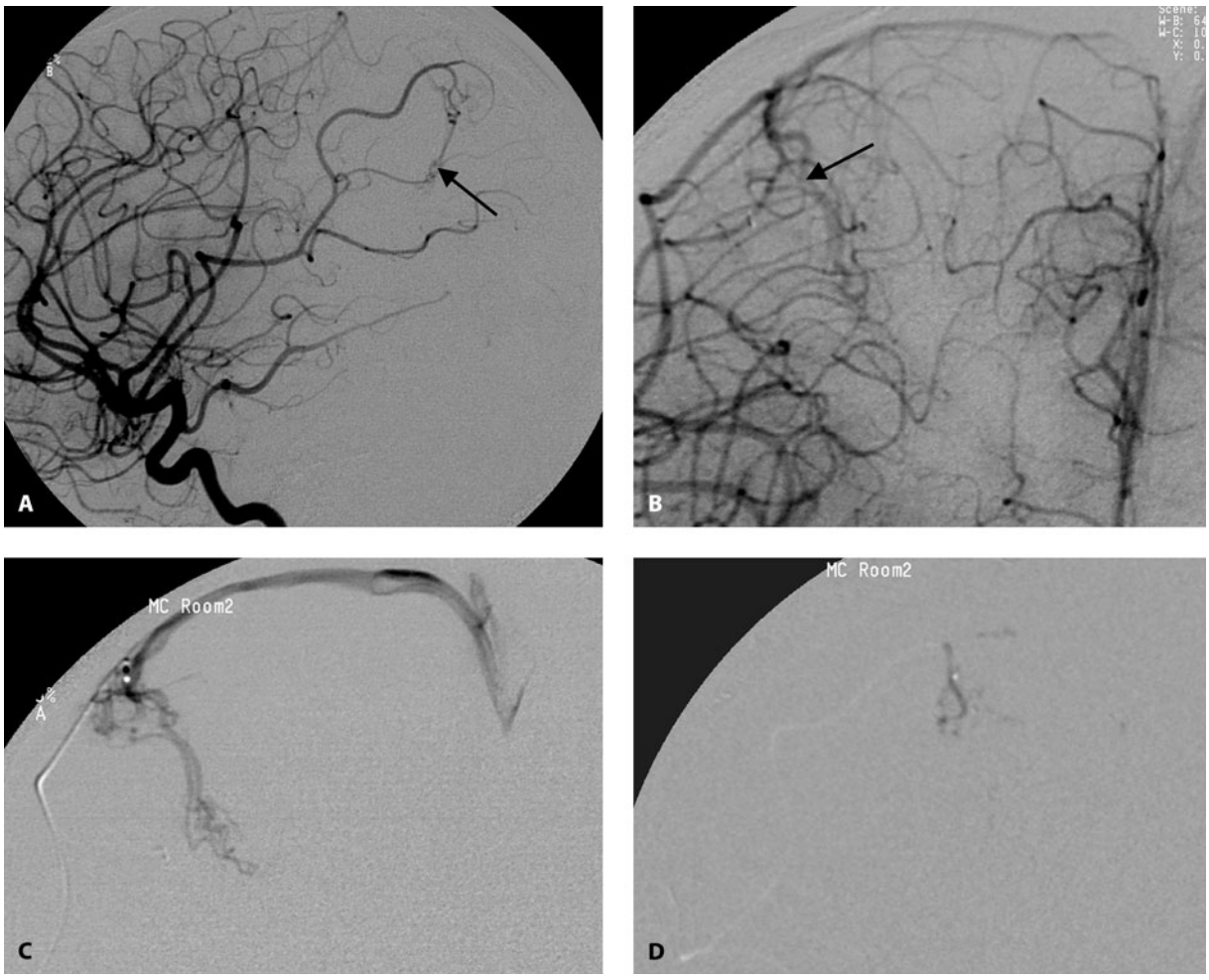

Fig. 14.127A–G. Distal superselective catheterization. **A** Lateral and **B** frontal digital subtraction angiograms (DSAs) of the right internal carotid artery show a distal small-vessel vascular shunt (*arrow*). **C** Frontal superselective views of the microcatheter in the very small distal vessel. **D** Last image hold after NBCA injection demonstrating the acrylic cast. **E–G** see p. 1108

Fig. 14.127 (*continued*). **E–G** Postembolization angiograms demonstrate preservation of normal arteries and drainage of the vein that used to drain the arteriovenous shunt in normal sequential fashion

14.11.4.2 Flow Reversal

Since the arterial system and its collaterals and anastomosis can carry flow in either direction, the flow can be artificially modified. Flow modification or reversal is possible and may be used at different levels of the cerebral circulation.

Modification at the Circle of Willis

Temporary occlusion at the level of the cervical internal carotid arteries is a simple and very useful technique to redirect flow across the anterior communicating artery, to enter the anterior cerebral artery, or when attempting catheterization of a medially originating perforator (Berenstein 1981). The reversal of flow can be accomplished by simple manual compression of the contralateral internal carotid artery at the neck. Occlusion

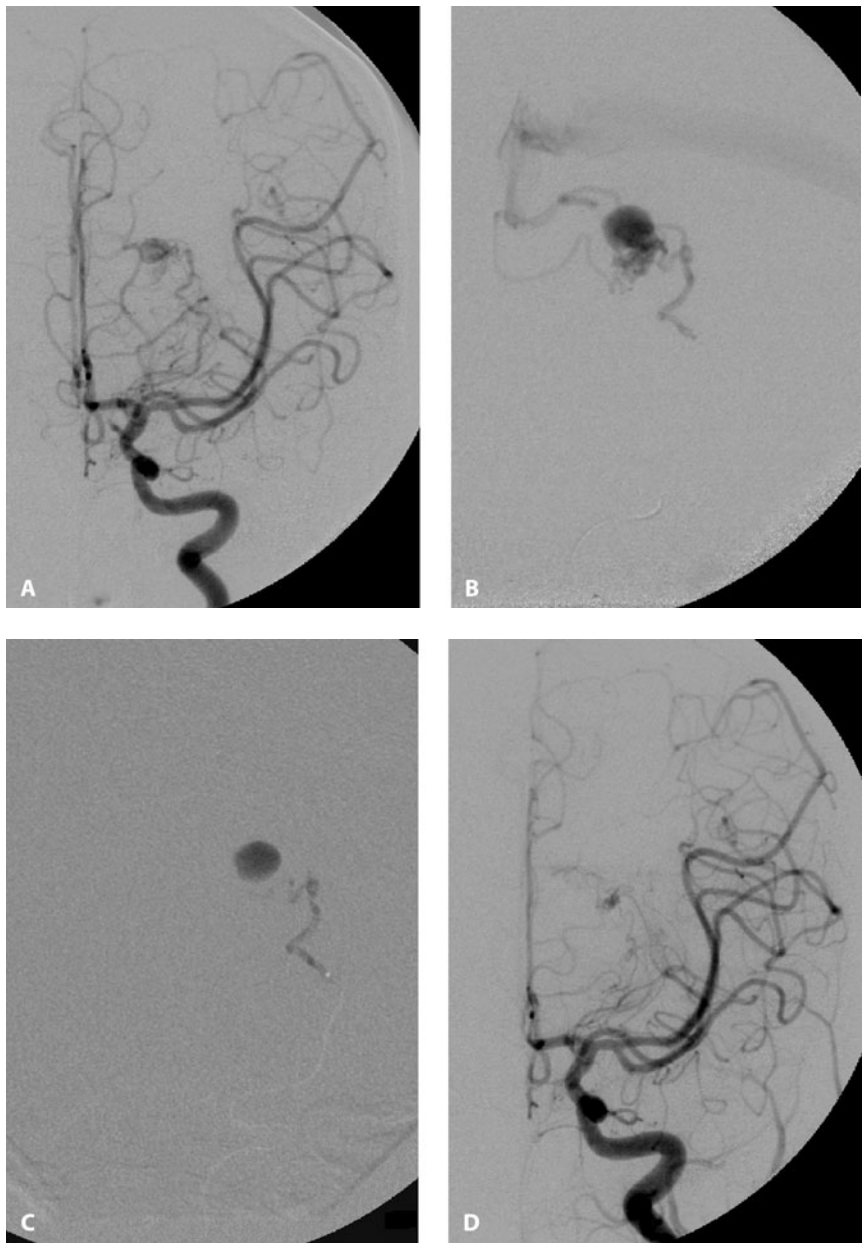

Fig. 14.128A–D. Superselective catheterization with a 1.2-F Magic MP hydrophilic catheter (Balt, Paris, France). **A** Frontal digital subtraction angiogram (DSA) demonstrates a small arteriovenous malformation supplied by the lenticulostriate arteries, with a false aneurysm of the venous side. **B** DSA of 1.2-F Magic microcatheter. **C** NBCA cast. **D** Postembolization angiogram showing small residual shunt

of the contralateral internal carotid artery can alternatively be accomplished either by manual compression or with a single- or double-lumen balloon catheter placed in the cervical internal carotid artery (Berenstein 1981). The technique is also applied to the cervical vertebral artery or arteries when attempting to enter the posterior communicating artery or one of its branches via catheterization of the internal carotid artery. With currently available microcatheters and microguidewires, these maneuvers are seldom needed.

Modification at the Cortical Level

Flow control with a wedged microcatheter can be used to reverse the flow, to protect a normal territory distal to the abnormality. Acrylic is delivered selectively into the nidus without the liquid embolic reaching the undesirable territory, with preservation of the distal (normal) artery.

Modifications can be achieved at the gyral, leptomeningeal, and/or watershed level (Fig. 14.126).

When superselectivity cannot clear a normal branch and the feeder to be embolized is *en passage*, the microcatheter is advanced into the normal artery. With the catheter in a wedged position, contrast material is injected, the distal territory is opacified; when the injection is stopped, flow control remains over a segment of the artery, up to the first branches that have reversed their flow by collateral circulation, confirming alternative supply to that territory. If this can be confirmed, it is safe to gently inject a short liquid 0.010-in. coil, which will act as a focal endovascular ligature and as a buffer, preventing the liquid embolic agent from entering the normal territory. Once this is accomplished, distal penetration into the lesion can be safely achieved (Fig. 14.126). The demonstration of such viable collateral flow is of major significance. It provides indirect evidence that if the particular pedicle is blocked proximally, there will be no ischemic consequences. However, it also illustrates a potential source for revascularization of a territory if proximal occlusion occurs.

The necessary force and rate of injection to accomplish flow reversal is mastered by the repeated injections of contrast material under fluoroscopic monitoring prior to liquid embolization, which is done in a similar manner (Fig. 14.126). One must nonetheless be aware that once the first acrylic column polymerizes, the flow characteristics change immediately, unlike contrast material.

A fistula supplied by two anastomotic sources can be occluded in a similar manner without the need for a balloon (Fig. 14.104). It is important to note is that contrast material will travel and wash out, whereas acrylic will eventually polymerize, stop, and then be redirected; however, the technique is simple and can be easily monitored fluoroscopically. If proper control cannot be accomplished the acrylic can be injected in two movements, first by injecting a small amount of embolic agent, observing it as it enters the proximal part of the normal vessel, and waiting for several seconds to allow polymerization. Additional embolic liquid can then travel only toward the desired territory.

A variation in this technique is useful when, in addition to attempting to preserve the distal normal runoff, one must preserve the proximal segment of the pedicle through which the injection is being made. In this case, a push or sandwich technique to deposit acrylic can be used. In the push technique, a small volume of embolic material (0.05–0.2 ml, less than the catheter dead space, and depending on the territory to be occluded) is placed in the microcatheter and a controlled bolus injection of 5% distilled water is done to push the acrylic into the lesion. We rarely use this push technique in brain embolization but it may be used in the spinal cord.

14.11.4.3 Flow Arrest

Flow arrest using a wedged catheter (Moret, unpublished data) may be of assistance to permit longer injections of liquids, which will result in better filling of the nidus (Fig. 14.109).

14.11.4.4 Systemic Hypotension

Manipulation of the systemic blood pressure is another means to alter the flow in the malformation and surrounding brain. Better filling of the nidus is thus possible, as the malformation is directly dependent on the systemic blood pressure, whereas normal brain is dependent on autoregulation. Controlled lowering of the systemic blood pressure will produce vasodilatation of the normal brain, while diverting flow away from the malformation and slowing flow through the nidus. The slowing of flow in the nidus is clearly seen on fluoroscopy with better opacification of the AVM (Fig. 14.1). If hypotension is used, the catheter should be close to the malformation, with no normal vessels between the catheter tip and the nidus. In such cases, the security point (Fig. 14.5) is brought forward, and, if a normal vessel exists within the location, it will dilate and can be easily penetrated by the liquid emboli.

14.11.4.5 Catheter Withdrawal

Prior to the injection of embolic agents, one must check that no proximal leaks exist in the system. The microcatheter and introducer are then checked and all excess catheter removed before embolization to ensure proper response when withdrawing the microcatheter and/or introducer. Before withdrawing the microcatheter, suction is applied to the catheter at the end of injection.

Prior to embolization, one must determine the security point of venous occlusion, defined as the point in the venous system past which no embolic material should penetrate. In general, this point is proximal to the opening of the first normal vein. The best example is in VGAM, in which the outflow to the fistula is specifically occluded to trap the fistula (Fig. 14.129).

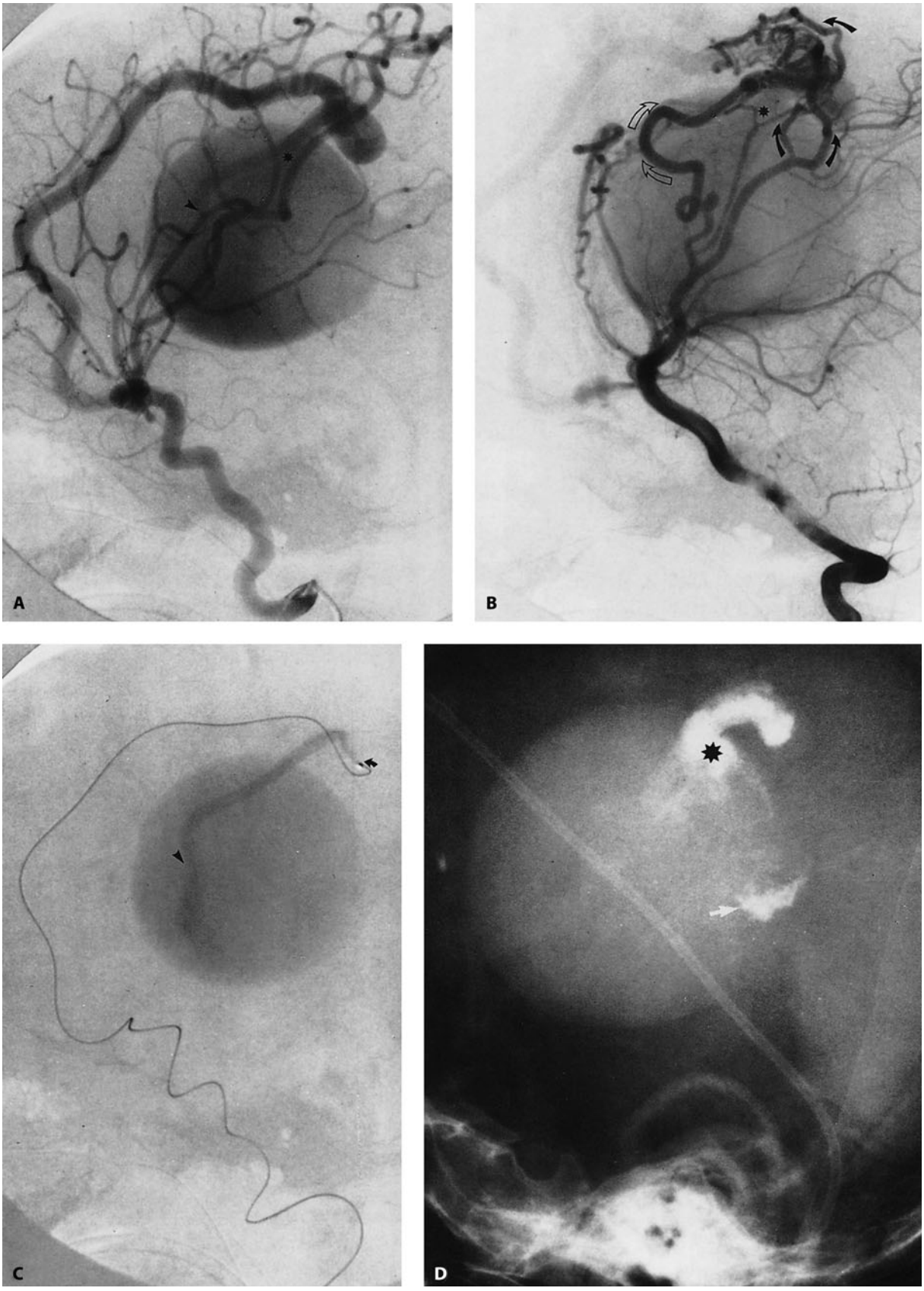

Fig. 14.129A–D. Legend see p. 1113

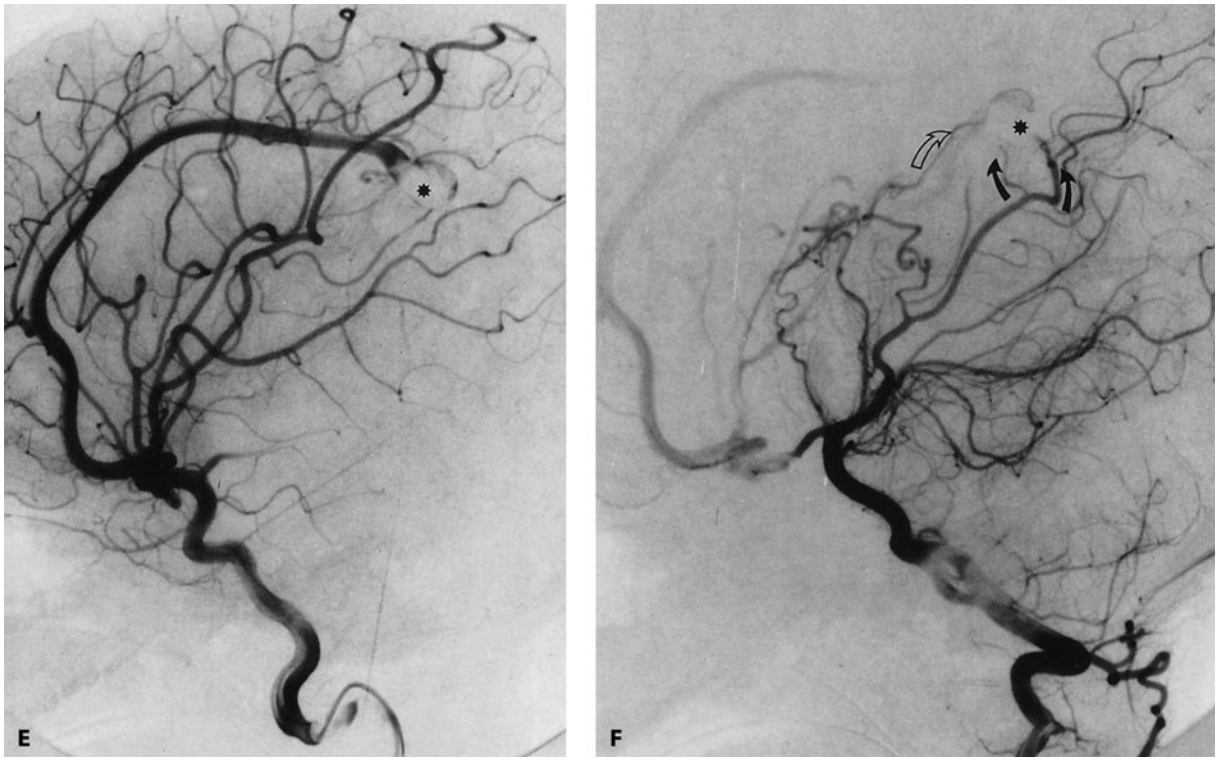

◄ **Fig. 14.129A–F.** Mini-Torquer (Nicomed, Paris, France) used without guiding catheter. This is best in newborns or young infants. **A** Lateral view of the right internal carotid artery demonstrates hypertrophy of the anterior cerebral artery supplying two mural fistulae (*asterisk* and *arrowhead*). **B** Lateral view of the left vertebral artery demonstrates hypertrophy of choroidal arteries (*curved arrows*) with indirect filling of the malformation. **C** Lateral view of superselective catheterization, using the Mini-Torquer, of the choroidal branch of the anterior cerebral artery (*curved arrow*). Note the sump effect with opacification of only one fistula (*arrowhead*). **D** Plain film of the radiopaque cast primarily in the more proximal fistula (*) and in the narrow outflow of the venous obstacle (*arrow*). **E** Postembolization angiogram of the right internal carotid artery shows occlusion of the fistula (*). **F** Monitoring of vertebral artery injection confirms the obliteration of the fistula and regression of the collateral circulation without the need to treat these vessels. The same arrows correspond to the same branches as seen in **B**. Note that even the subependymal supply has regressed

14.11.5 Spine and Spinal Cord

14.11.5.1 Technical Aspects of Endovascular Treatment in the Spine and Spinal Cord

Although the principles of endovascular treatments in the spine and spinal cord are homogeneous with the other territories (Fig. 14.5), the relation between the spinal canal, spinal dural cover, and the spinal cord is unique in its arrangement (Figs. 2.12, 2.13, Vol. 1). Within the blood supply of the spinal cord, the various connections and anastomoses provide an understanding of an individual arrangement and make it possible to select the best and safest route to reach the lesion, as well as assess the result of the intervention (Fig. 14.130A–C).

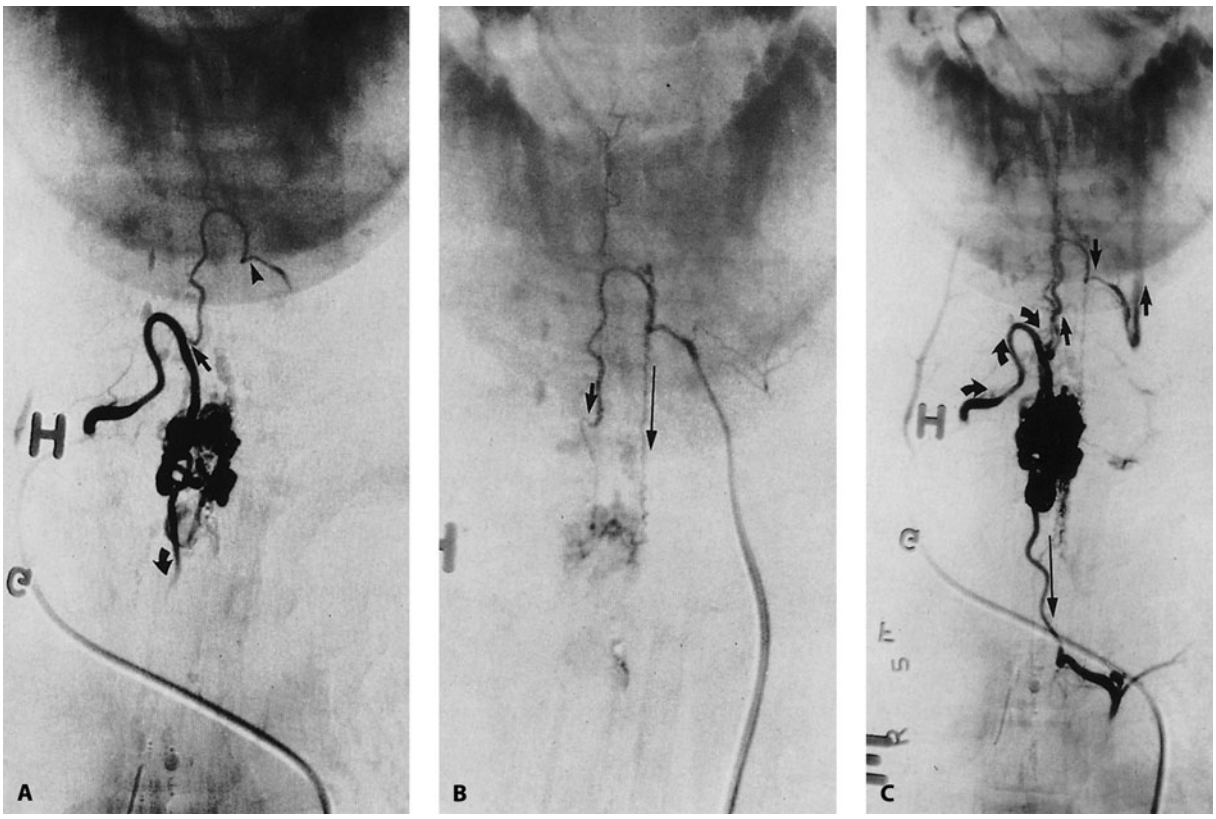

Fig. 14.130. **A** Frontal subtraction angiogram of a selective injection of the radiculomedullary artery of the cervical enlargement feeding a cervical arteriovenous malformation. Note the anastomosis (*arrow*) to the radiculomedullary contribution from the left vertebral artery (*arrowhead*) to the contribution from the contralateral artery of the cervical enlargement (*arrow*). Also note the descending portion of the anterior spinal axis (*curved arrow*), which can also originate from the left supreme intercostal artery. All three arteries supply the same compartment; the left-side contribution is indirectly supplying the shunt. **B** Selective injection of the artery of the cervical enlargement on the left showing the same anastomosis (*arrow*) and the indirect collateral on the ventrolateral aspect of the cord (*long arrow*). **C** Selective injection of the artery of the cervical enlargement on the right (*curved arrows*) shows filling of the malformation and reflux into the various supplying pedicles, including the artery of the cervical enlargement, from the left vertebral artery (*arrows*) and the supreme intercostal contribution to the anterior spinal axis (*long arrow*). (Same patient as in Fig. 14.134)

The embolization of spinal lesions is discussed in Chap. 13 of this volume, including the angiographic protocols and the embolization in the individual spinal canal segments.

In the spinal cord, understanding the collateral circulation in the spinal cord arterial system is necessary to safely treat the majority of cases, following our principle of targeted embolization into the weakness of the angioarchitecture and how it relates to the clinical picture, discussed in Chaps. 11 and 12 of this volume.

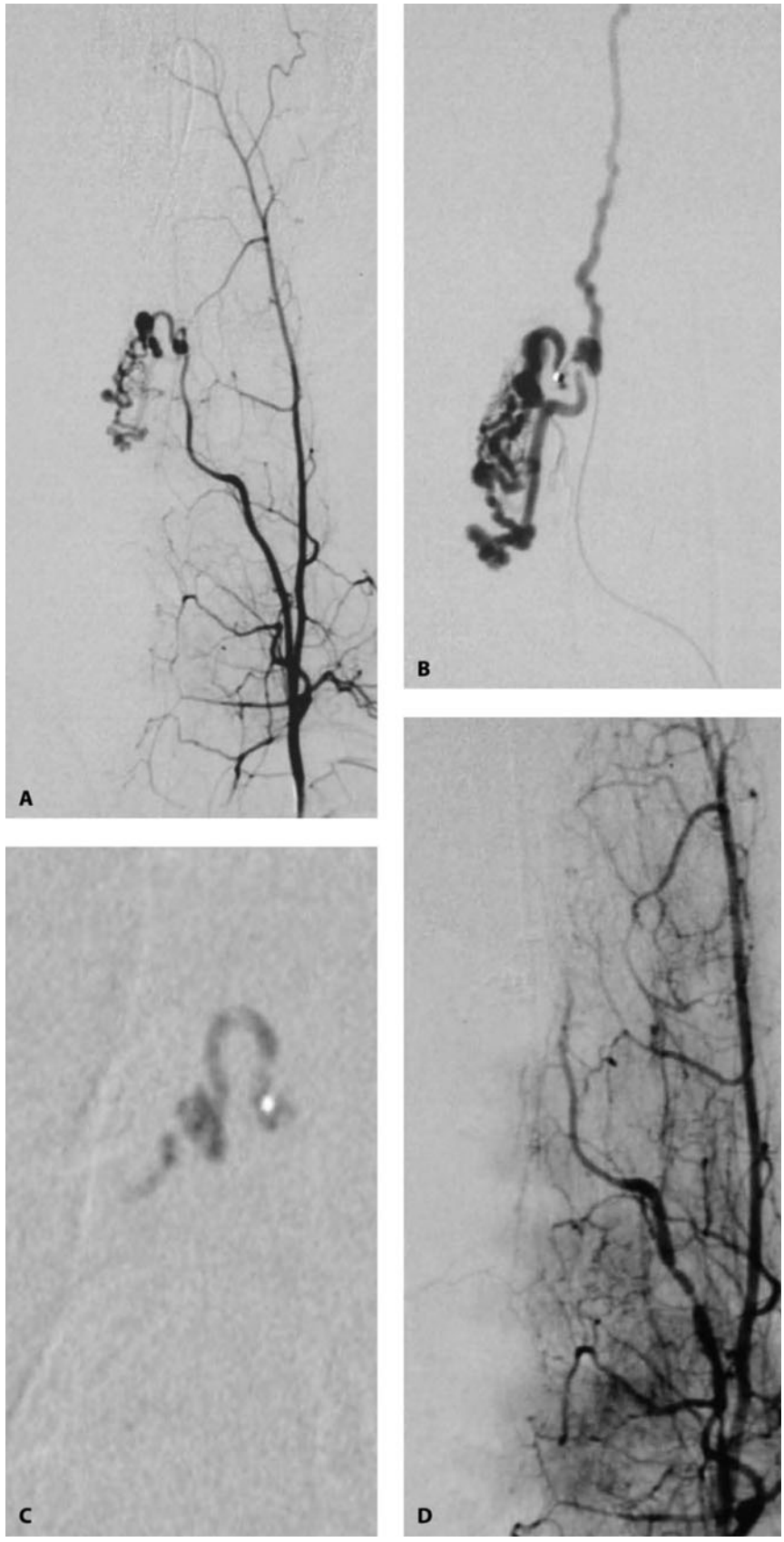

Fig. 14.131A–D. Distal catheterization in the lower cervical ASA. **A** AP of the ascending cervical artery supplying an arteriovenous malformation of the surface of the spinal cord. **B** Superselective catheterization of a pial artery. **C** Acrylic cast. Note the arterial and venous safety points (see Fig. 14.5**B**). **D** Postembolization angiogram, with preservation of the ASA

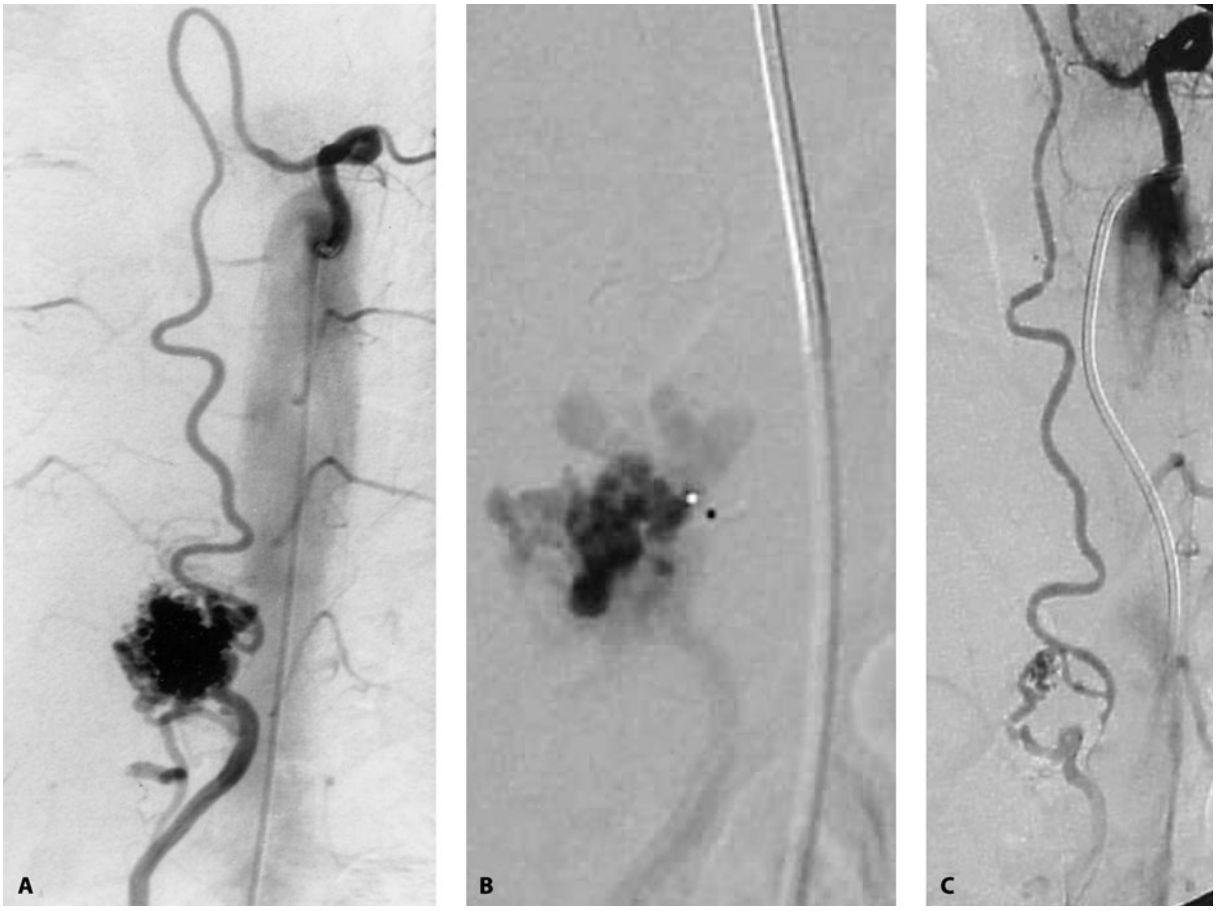

Fig. 14.132A–I. Distal catheterization in the spinal cord and anatomical rearrangement. **A** Left T9 injection shows a surface arteriovenous malformation (AVM) nidus. **B** distal catheterization into the pial artery **C** Angiogram after NBCA. A small pial branch remains; the vein is persevered. **D–I** see pp. 1117, 1118

Embolization of Spinal Cord Arteriovenous Malformations

Spinal cord arteriovenous malformations (SCAVMs) should be treated a priori by endovascular techniques alone or as the first part of a combined approach.

The techniques of endovascular treatment of SCAVMs will depend on the anatomical and hemodynamic characteristics of the lesion and on the ability of superselective catheterization. In general, whenever possible, injection of liquid acrylic is preferred, since it is best for obtaining permanent results, and can be accomplished by redistribution of flow or by superselective catheterization very close to the nidus of the malformation. On occasion, the use of particulate embolic material may be dictated by safety considerations.

Presently available catheterization techniques have significantly advanced the technical capabilities of superselectivity. These techniques provide the potential of reaching the nidus in a very high proportion of patients and make it possible to preserve normal vessels, even in the territory of the anterior spinal artery (Fig. 14.131, p. 1115; Fig. 14.132). In our

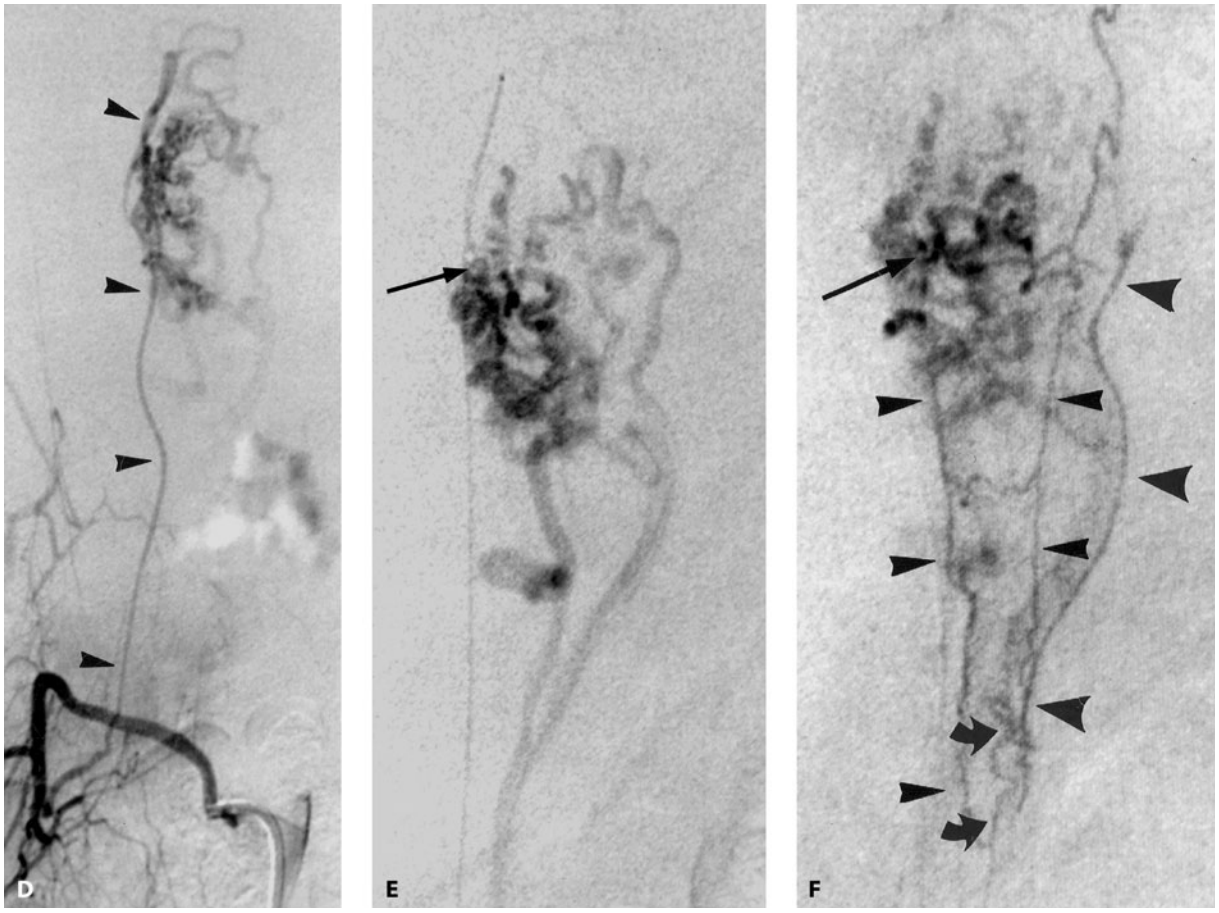

Fig. 14.132 (*continued*). **D** Monitoring study from the PSA (*arrowheads*) shows the true residual AVM. **E** Superselective catheter position (*arrow*). A flattening of the MEPs occurred after a 40-mg Xylocaine injection. **F** Advancement of the microcatheter (*arrow*) demonstrates the distal PSA, the basket (*arrowheads*), including the ASA (*curved arrows*). **G–I** see p. 1118

experience, the use of liquid embolic agents such as IBCA and/or NBCA are best for obtaining a lasting result. In general, small amounts of acrylic material (0.3–0.6 ml) are usually sufficient to reach the goal. Reflux of acrylic (even in minuscule amounts) in the spinal circulation carries a higher risk of permanent damage than in the craniofacial or brain areas (Fig. 14.131). Therefore, even if complete obliteration is not achieved, penetration into the nidus is the goal (Fig. 14.132). We believe that the chance of reflux from one deposition of liquid acrylic is less than that of multiple injections of particles.

Flow-Control Embolization in the Spinal Cord

The sequence of pedicles to be embolized in the anterior spinal artery territory varies. In general, the closest pedicle to the nidus is embolized first. At times the circulation may have to be manipulated to reach the target or protect a territory (Fig. 14.132G).

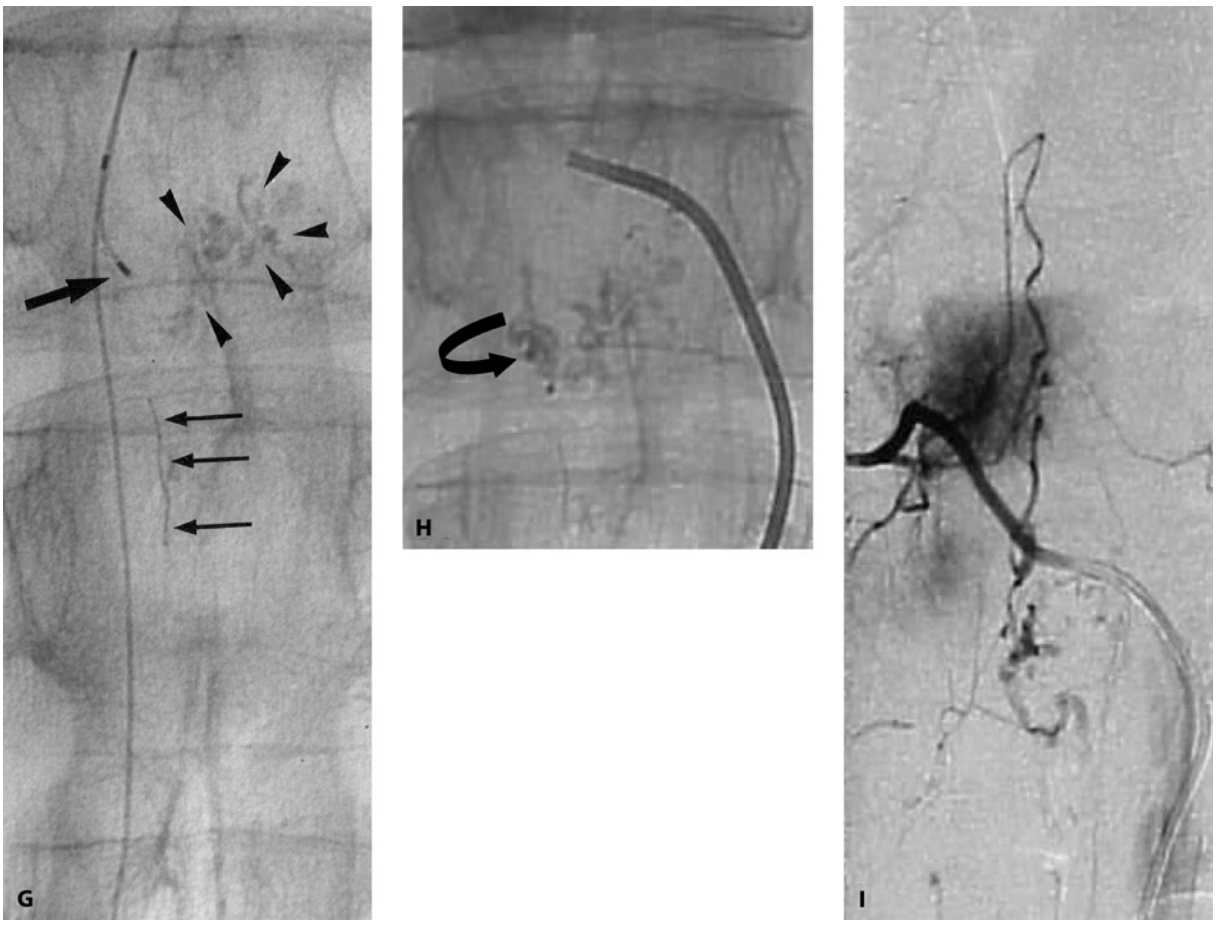

Fig. 14.132 (*continued*). **G** A BLC liquid coil (*arrows*) is injected to prevent liquid embolic material from permeating the territory. Tip of the microcatheter (*large arrow*) Previous glue cast from the ASA (*arrowheads*). **H** New NBCA (*curved arrow*). **I** Final image of the right PSA shows the true small residual shunt

The principles of flow reversal flow control and redistribution of flow, illustrated in the head and neck, also apply in the spinal cord. However, the longitudinal axis of the spinal cord and the segmental contributions to the anterior and posterior axes, their bidirectional flow, circumferential anastomosis, and the critical neurological tissue they supply all combine to imply specific points of both caution and opportunity.

Flow control and flow reversal can be obtained with a wedged catheter (Fig. 14.133), or by balloon catheters (although balloons are not frequently used in the spinal cord). With fluoroscopic monitoring, one can estimate the rate of injection to permit the antegrade washout of embolic material toward the lesion. If the catheter tip is at a distance from the nidus, one can use particles (Fig. 14.134).

In the anterior spinal artery, flow control can be accomplished by various means. If the contribution is from two or more pedicles, the pressure of injection can be altered to recognize and control the balance of supply. In superselective or wedged injections at a low pressure, one can see dilution from reversed nonopacified blood; at higher pressure, the flow is re-

versed toward the major pedicle feeding the nidus, producing the dilution, which can then be seen. This information can subsequently be translated to the flow, and pressure at which to inject embolic material (Fig. 14.133C–E) or the anatomy may be rearranged with a liquid coil (BLC) (Fig. 14.132).

Flow control and flow reversal or protection can also be achieved with more than one catheter. In such cases, one catheter is used to deliver the embolic material while the other is used in a wedged position for protection of the normal territory (Fig. 14.33E, G).

If a pedicle is too small for catheterization, it may be left for the end of the procedure. If the nidus is not completely occluded, the small feeder may enlarge secondarily and catheterization may then be possible to reach the nidus (Fig. 14.133A, J).

Whenever possible, the radiculopial arteries are used first to embolize the lesion, leaving the anterior spinal artery or posterior spinal artery collaterals as the means to control the results of embolization (Fig. 14.132). On occasion, a particulate embolic agent such as PVA is injected into the radiculomedullary artery to reduce flow or to prepare the territory for definitive acrylic embolization via the radiculopial arteries.

In lesions supplied exclusively by the anterior spinal axis via multiple perforators of the sulcocommissural arteries, liquid embolic agents may not be usable and particulate agents may be used as free-floating emboli to permit the progressive obliteration of the nidus with preservation of the anterior spinal axis (Fig. 14.134). Theron et al. (1986) reported on five patients in whom the anterior spinal artery supply was embolized with PVA, with apparently good results. In two patients, follow-up angiograms failed to demonstrate revascularization of the lesion. We have also seen two such patients (Fig. 14.134). As a palliative measure, PVA is useful. Even if some recanalization is seen, repeated embolizations can then be done. Merland and Reizine (1987) has observed clinical stabilization of patients with deteriorating neurological function or even clinical improvement with a very low rebleeding rate. If no alternative exists, particulate embolization may allow us to gain time as new technologies arise.

Particles are also used if at a distance from the target (Fig. 14.134) and may be effective, as determined by the absence of recanalization in follow-up angiograms, which should be done even if the patient is asymptomatic, especially if embolization is performed with particles. The size of the anterior spinal artery can be seen to regress if the nidus is occluded.

Particles should be used with caution, however, as it is possible for recanalization of the nidus but not the feeder to occur, making future embolization impossible.

In spinal cord high-flow fistulae, the principle of occlusion is the same. The goal is to reach the fistula and occlude the venous site, preserving the anterior spinal artery axis (Fig. 14.135).

In metameric lesions or extraspinal malformations, coaxial techniques are advantageous, as the lesions are usually high-flow with tortuous feeders. In such patients, care must be taken not to damage spinal cord vasculature, which may not be well visualized in a high-flow pedicle. When the spinal cord is involved, attention is focused on treating the spinal cord with the same principles used in treating other SCAVMs (see Chap. 11).

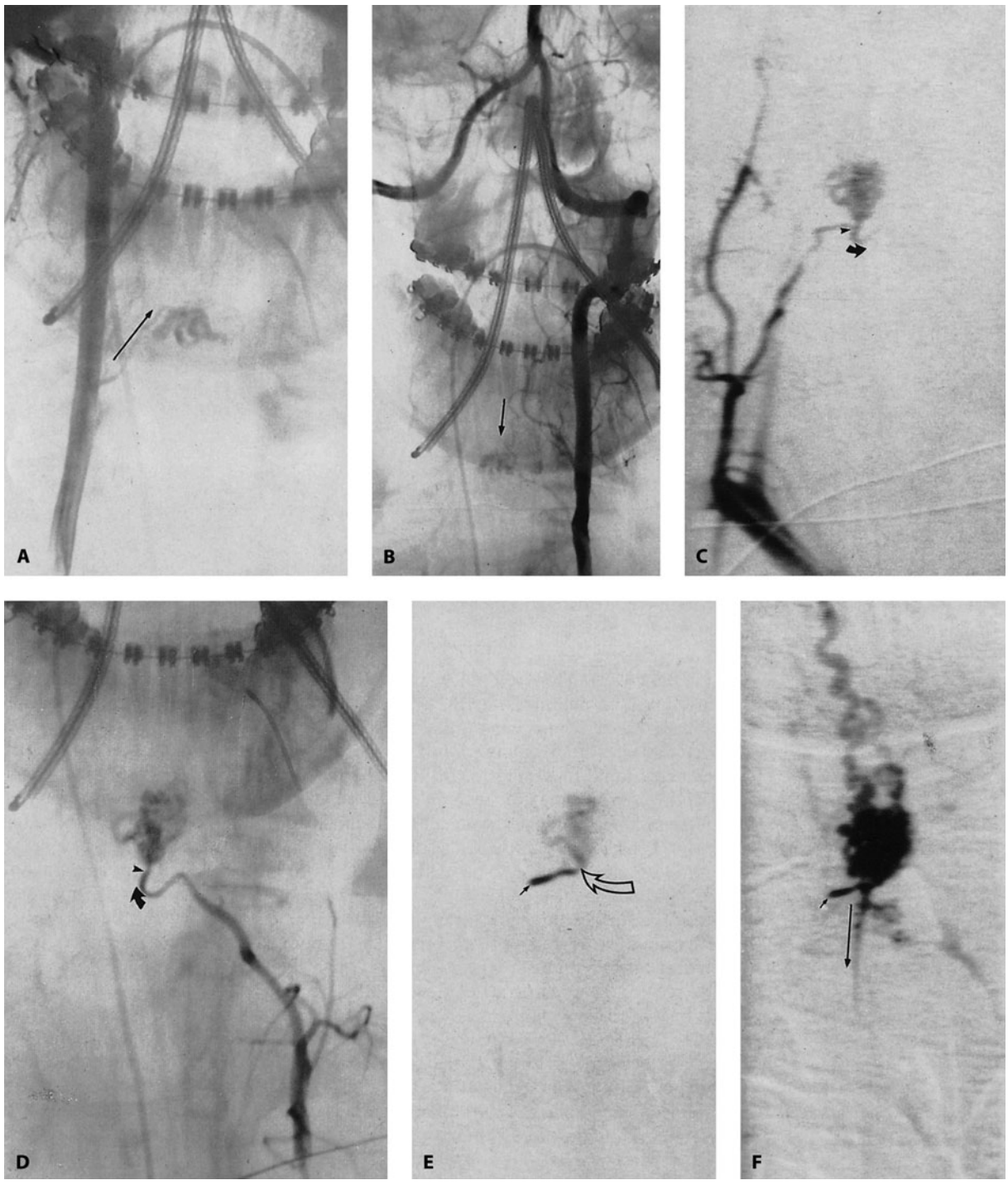

Fig. 14.133A–P. Flow control and flow reversal for protection in a cervical spinal cord arteriovenous malformation (SCAVM) in a patient who presented with two episodes of hematomyelia. **A** Right vertebral artery injection demonstrates a small contribution at the cervical enlargement from the right vertebral artery (*arrow*). **B** Left vertebral artery injection shows indirect contribution from the anterior spinal artery at the cervical enlargement (*arrow*). **C** Right ascending cervical and **D** left ascending cervical injections demonstrating the bidirectional flow in the anterior spinal axis. The point of anastomosis is clearly seen (*arrowhead*). On the right-side injection (**C**), there is antegrade flow toward the left-side contribution (*curved arrow*). Continued on p. 1121

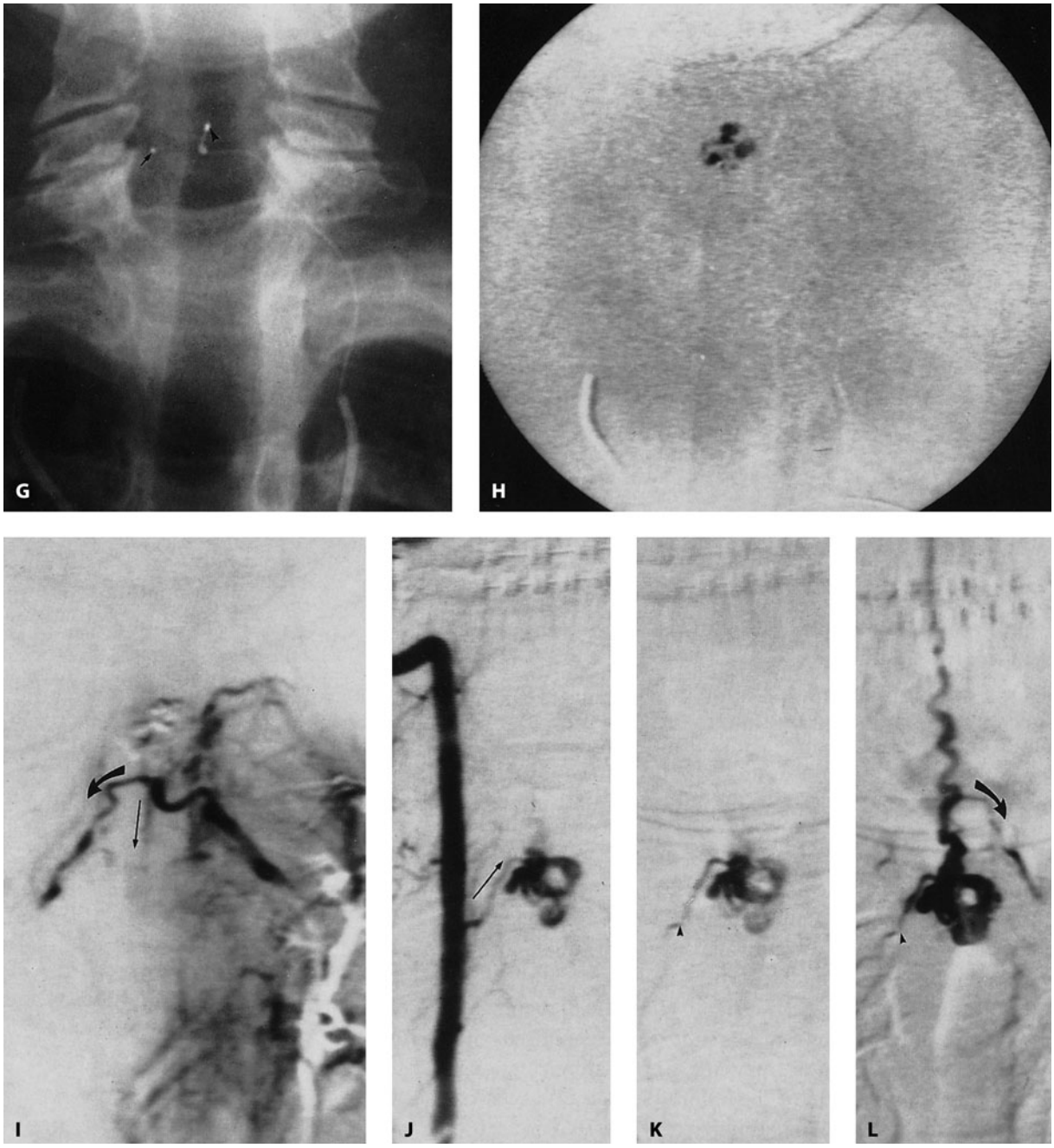

Fig. 14.133 (*continued*). On the left-side injection (**D**), the flow is reversed toward the anterior spinal artery perforator. **E** Superselective injection from the right side. Note flow control over the right-side radicular contribution (*arrow*) until it becomes dilated from the left side (*open curved arrow*). **F** At a higher pressure of injection (*short arrow*), there is downward filling of the anterior spinal axis (*long arrow*). **G** A second microcatheter is advanced through the left side for catheterization of the sulcocommissural artery (*arrowhead*). The right side catheter is producing flow arrest from the right side contribution (*arrow*). **H** Digital subtraction angiogram. Last image hold of the acrylic deposition showing the radiopaque acrylic in the nidus of the malformation. **I** Postembolization angiogram of the left ascending cervical contribution. Note preservation of the anastomosis to the right side (*curved arrow*) and toward the descending portion of the anterior spinal artery (*arrow*). Continued on p. 1122

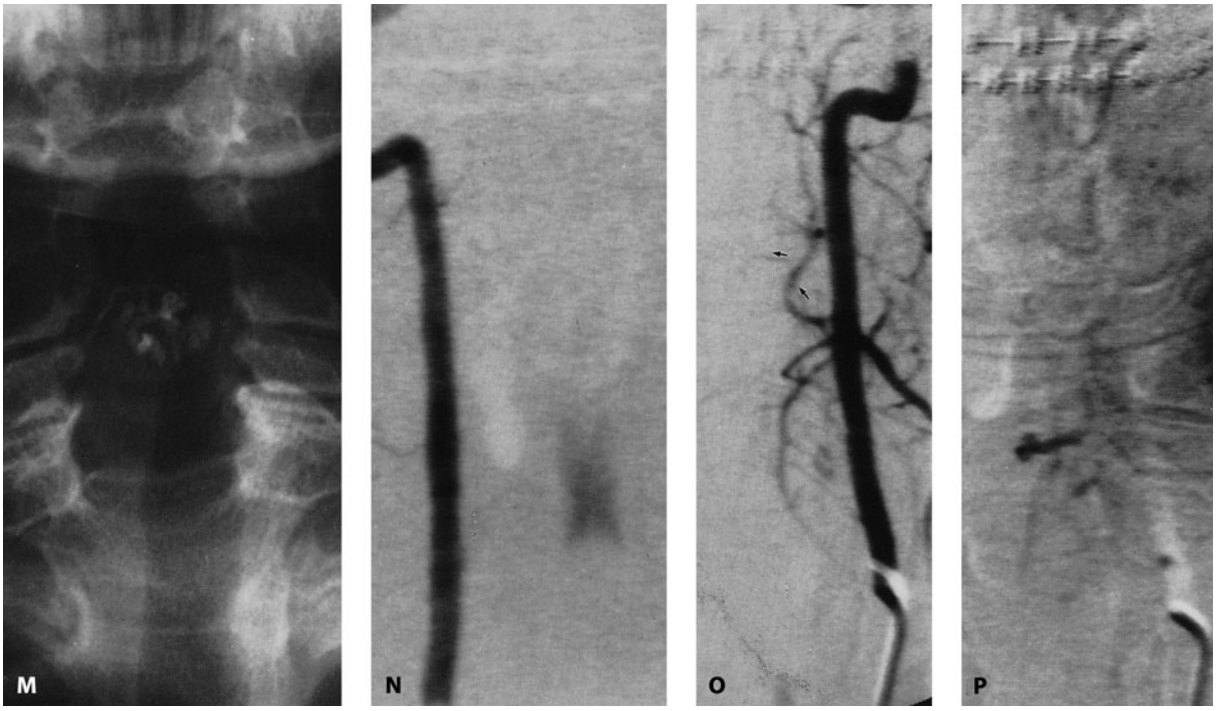

Fig. 14.133 (*continued*). **J** Postembolization angiogram of the right vertebral artery, ascending cervical component. Note enlargement of the radicular contribution as compared to pre-embolization (**A**). Superselective catheterization of the pedicle of the right vertebral artery in early (**K**) and later (**L**) phases. Note the position of the microcatheter (*arrowhead*). This vessel could not be catheterized prior to its secondary enlargement after the embolization (**L**). A pressure injection shows retrograde filling of the anterior spinal contribution of the left vertebral artery (*curved arrow*). **M** Postembolization plain film demonstrating the radiopaque cast of the malformation. **N** Right vertebral postembolization image. **O** Left vertebral artery angiogram with no filling of the malformation. **P** Very late phase of the same injection shows some stagnant contrast material in the region of the nidus and no drainage

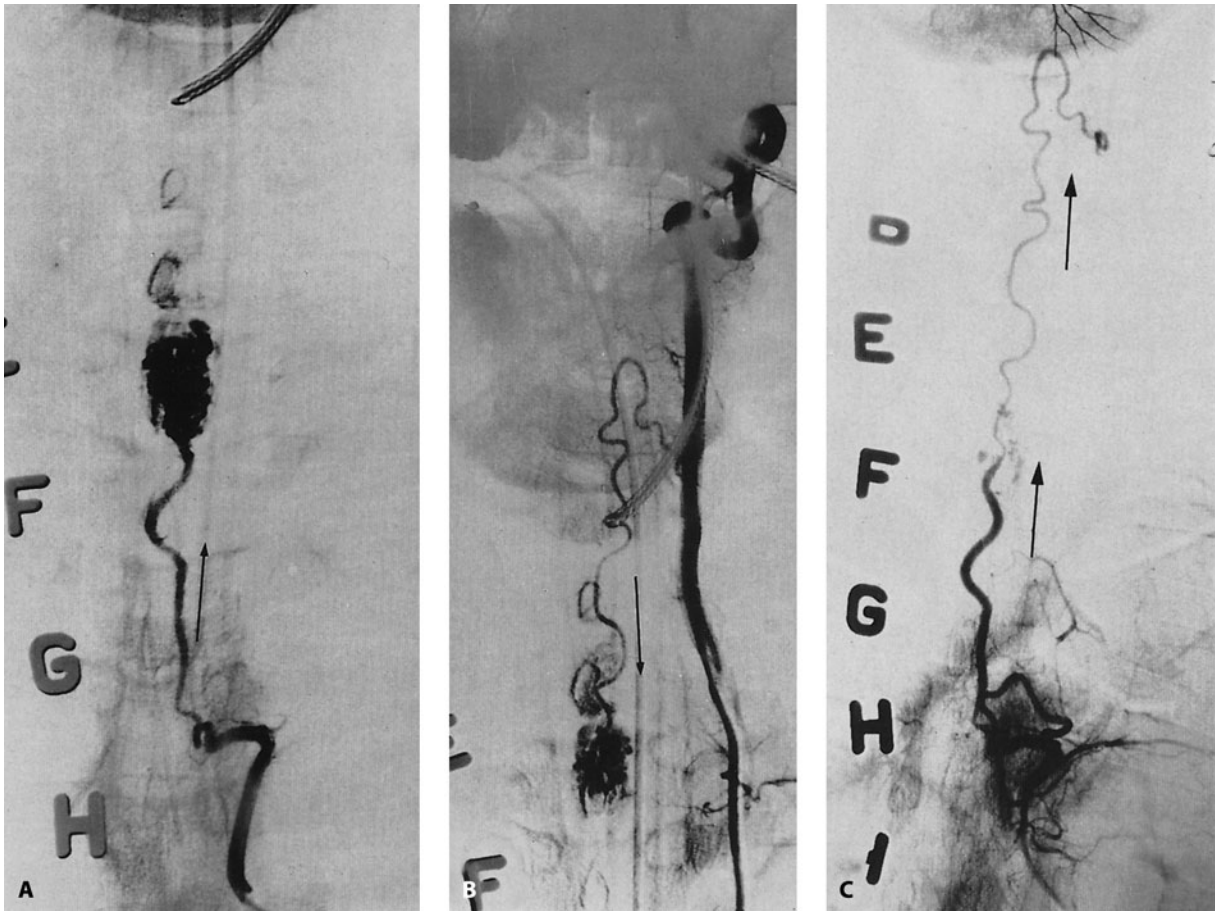

Fig. 14.134A–C. Embolization of a sulcocommissural artery using PVA (same patient as in Fig. 14.130). **A** Left supreme intercostal injection demonstrates the lower portion of the anterior spinal artery axis supplying the lower portion of the spinal cord arteriovenous malformation. **B** Left vertebral artery injection demonstrates the artery of the cervical enlargement and the upper portion of the anterior spinal artery axis supplying the upper portion of the malformation. **C** Postembolization of the supreme intercostal artery with preservation of the anterior spinal axis and no filling of the malformation. Note the anterograde flow toward the artery of the cervical enlargement and its origin in the vertebral artery (*long arrows*). There is complete stagnation in the region of the original nidus (20-year follow-up)

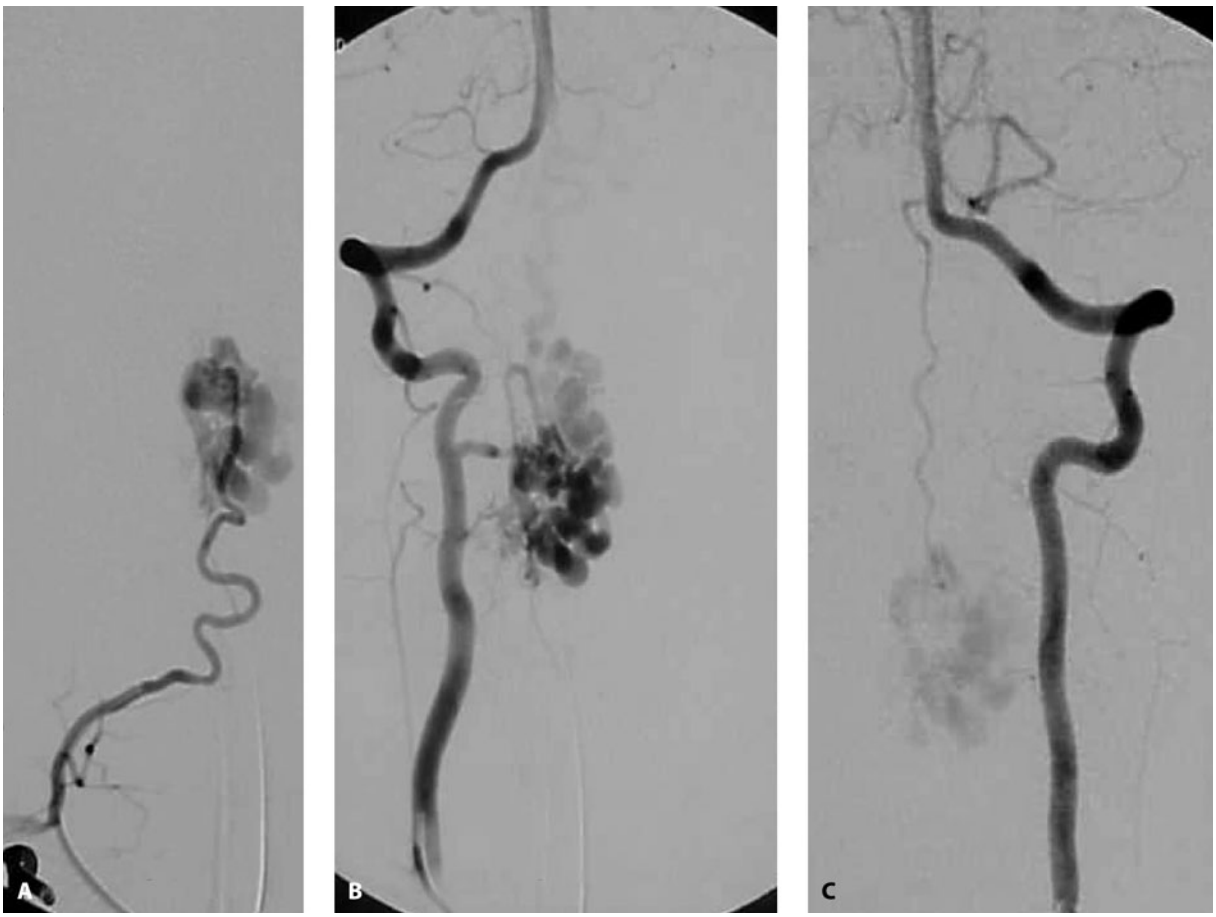

Fig. 14.135A–F. High-flow ASA arteriovenous fistula (AVF). **A** Digital subtraction angiogram of thyrocervical contribution to an AVF of the ASA. **B** Right vertebral artery and **C** left vertebral artery show monocompartmental venous drainage, evidence of an AVF in a 4-year-old child. **D–F** see p. 1125

Spinal Cord Monitoring

Spinal cord monitoring may be of assistance during spinal cord angiography and embolizations. One of the authors (A.B.) uses monitoring routinely, the other two do not, with no difference in outcome and complications. Nonetheless, we all agree that monitoring cannot substitute for a proper understanding of the potential hazards or benefits of a specific vessel or collector and its relationship to the perforators or suppliers to the spinal cord (see Vol. 1, Chap. 2).

Monitoring may be divided into: (a) electrophysiological, (b) chemical (using inhibitors of neurological function), or (c) a combination of both, which may add safety and reliability.

Electrophysiological Monitoring. In the spinal cord, electrophysiological monitoring is best accomplished by the use of somatosensory-evoked potentials (SEPs) (Berenstein et al. 1984b; Young and Berenstein 1984, 1985; Hacke et al. 1983) and more recently with motor-evoked potentials (MEPs).

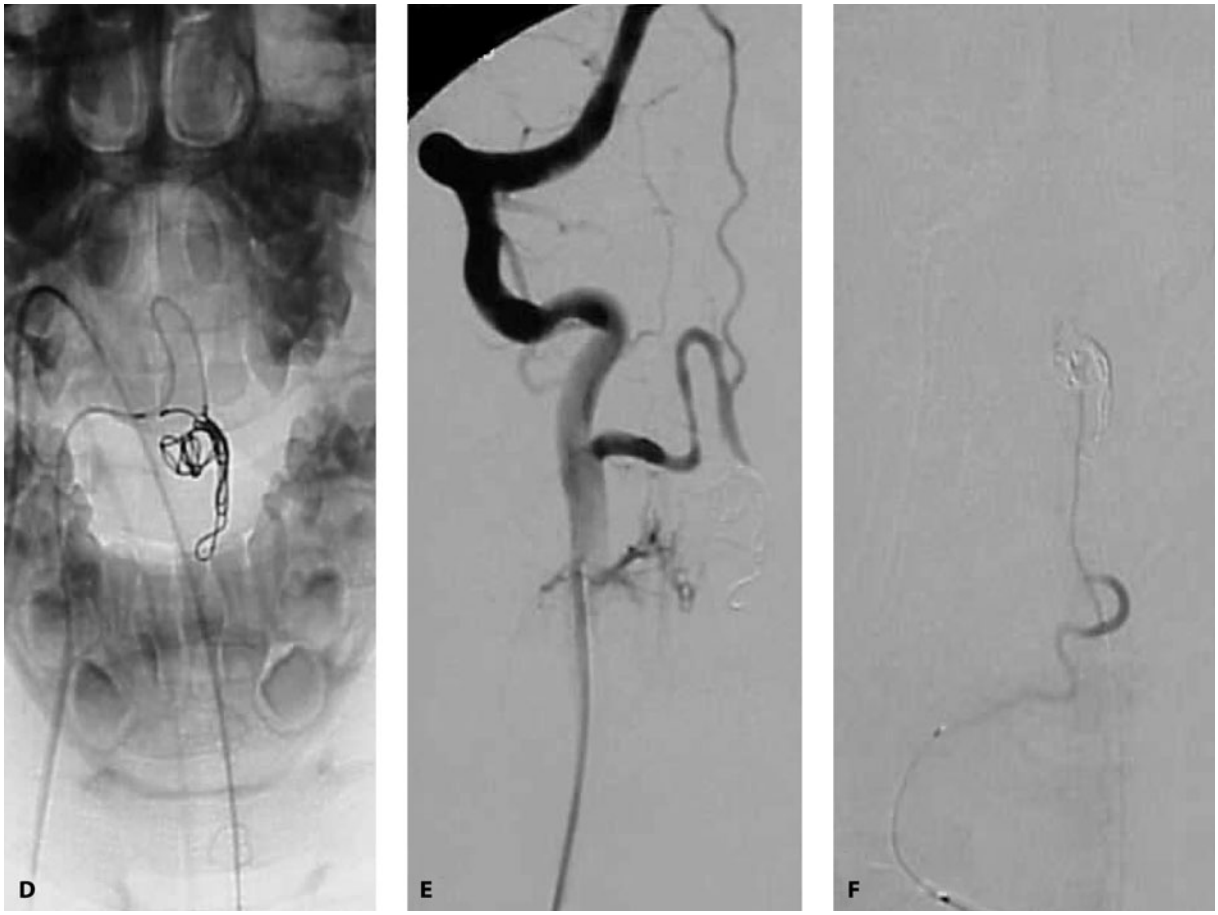

Fig. 14.135 (*continued*). **D** A single GDC in the venous side of the fistula resulted in total occlusion of the lesion (**E**). **F** Thyrocervical angiogram confirms the occlusion; this vessel was only used for monitoring

Angiographic examinations and embolizations are performed under general anesthesia. If electrophysiological monitoring is used neuroleptic agents such as opiates are used; inhalation agents cannot be used.

Chemical Monitoring. Provocative testing in conjunction with electrophysiological monitoring is done with the injection of a depressant of neurological function (Wada 1960). We use 50–75 mg of amobarbital superselectively injected at the site of future acrylic injection (Berenstein et al. 1984b), supplemented with 40 mg of Xylocaine to test the axonal function. Interestingly, Xylocaine appears more sensitive than Amytal.

Embolization of Spinal Dural Arteriovenous Fistulae

The presence of a spinal dural arteriovenous fistula (SDAVF) is an indication for treatment in all patients, as the risks of endovascular or open surgery are minimal and the possible benefits are multiple. This applies even to patients with apparently fixed neurological deficits.

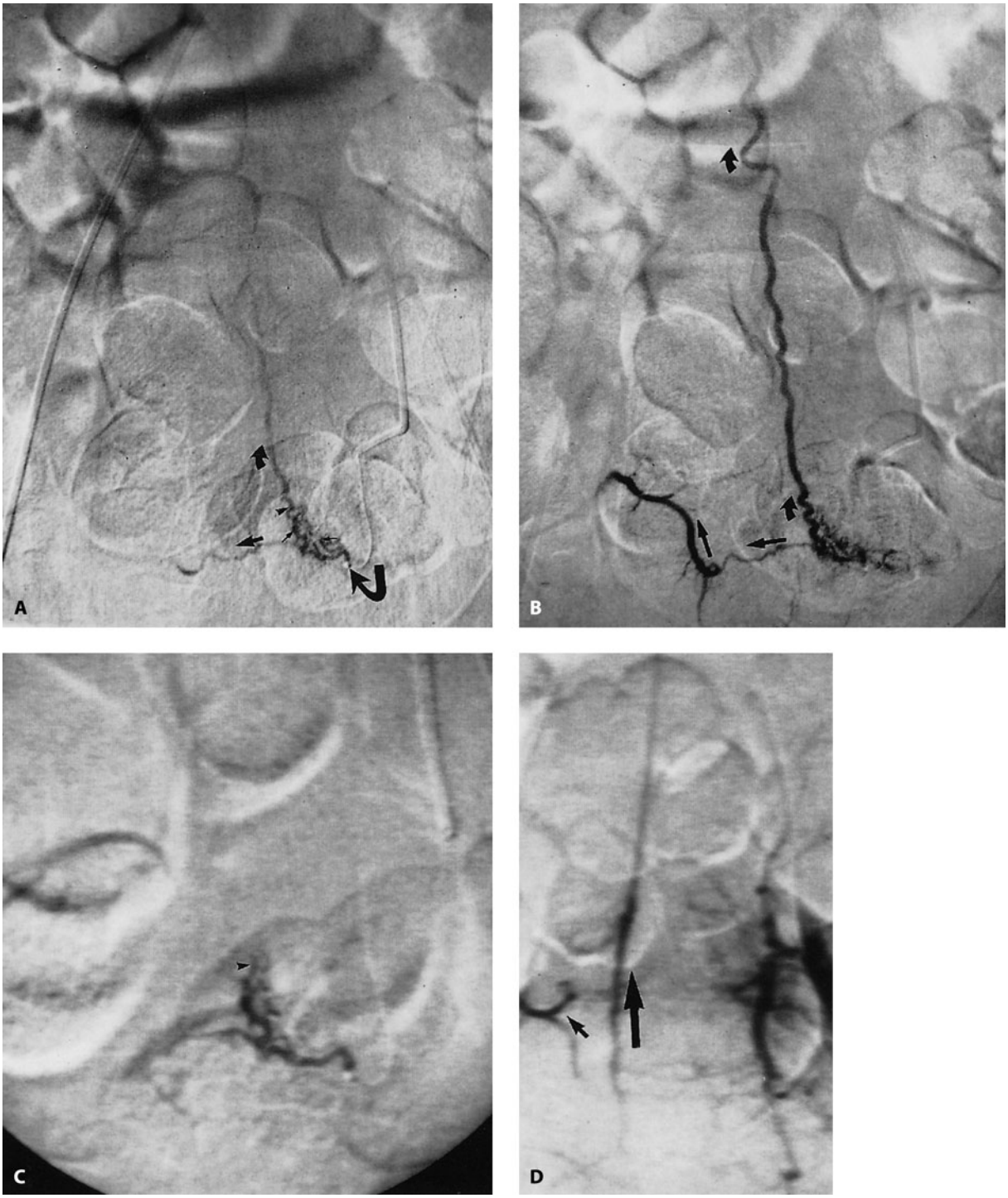

Fig. 14.136A–D. Legend see p. 1127

The main objective of treatment of SDAVFs is to occlude proximally the draining vein as it exits the arteriovenous shunt, thereby ensuring occlusion of the microfistulae. The occlusion is done within the first millimeters of the vein (Figs. 1.136) or before its opening into the pial network. In sacral lesions, the long draining vein can be occluded over several centimeters, as it only reaches the medullary veins at the conus level (see Chap. 12, this volume). In our experience, this occlusion is possible in 81% of patients. Clinical improvement can be seen in the majority and in the remaining patients progression of the congestive myelopathy is usually arrested.

The only significant contraindication to endovascular treatment of SDAVF occurs in patients in whom the anterior spinal artery originates from the same pedicle as the SDAVF (Fig. 14.46) (Merland et al. 1980a, b). Patients in whom proper selective catheterization is technically not possible or in whom the extraspinal longitudinal anastomosis cannot be safely cleared to prevent accidental embolization to the anterior spinal artery (Fig. 14.5) are also not candidates for endovascular treatment.

When embolization can be done, the lesion can be closed in the great majority of patients in a very safe manner. If endovascular therapy is unsuccessful, surgery (duraplasty) can then be performed. Transvascular embolization with a liquid agent (such as cyanoacrylates) should therefore be the first mode of treatment in patients with SDAVFs. Only when it is contraindicated (see above) or fails (20% of our patients) should surgery be done.

As we pointed out at the beginning of this section, the goal of treatment is occlusion of both the fistula and the proximal vein. In view of the small size of the afferent arteries and the fistula itself (in the 40–60 μm range), only a low-viscosity liquid agent, such as IBCA (isobutyl-2-cyanoacrylate) or NBCA (*N*-butyl-cyanoacrylate) can reach the nidus and proximal vein. Particulate agents, such as polyvinyl alcohol (PVA) or dura mater will not be effective or may only give temporary good results. Almost invariably their use results in recanalization and recurrence (Hall et al. 1989; Morgan and Marsh 1989). Particles will not penetrate effectively to obtain complete cure and we consider them contraindicated in the endovascular management of SDAVFs.

Closure of SDAVFs using an acrylic agent is best accomplished with a mixture that will have a long polymerization time, such as 40% IBCA or

◀ **Fig. 14.136A–D.** Spinal dural arteriovenous fistula (SDAVF) of the sacrum. **A** Coaxial system with a variable-stiffness microcatheter (*curved arrow*) showing the arterial component (*small arrows*) and the shunting site (*arrowhead*), with its ascending venous drainage (*small curved arrow*). Note the retrograde filling of the contralateral dural supply to the sacrum (*arrow*). **B** Later phase of the same injection with better filling of the right lateral sacral artery (*large arrows*); *curved arrows* demonstrate the ascending venous drainage. **C** Digital subtraction angiogram of the acrylic deposition at the time of embolization shows the cast of the SDAVF and occlusion of the distal segment of the right lateral sacral contribution, and the beginning of the draining vein (*arrowhead*). **D** Verification of left internal iliac injection; there is no filling of the SDAVF and good opacification of both the right lateral sacral artery (*arrow*) and the medial sacral artery (*large arrow*). This confirms that there is no filling of the lesion

NBCA and 60% iophendylate. It can be injected with a simple superselective catheter or with a coaxial assembly system. The acrylic-iophendylate mixture can be injected in a continuous column (Fig. 14.136) or using a sandwich or push technique. In any case, the technical goal of therapy is occlusion of both the nidus and the proximal portion of the afferent vein. The use of sufficient tantalum powder insures good monitoring and aids in preventing the distal migration of acrylic into the medullary veins.

As in other anatomical locations, the collateral circulation of the meninges of the spinal area must be reached for both occlusion of the natural collaterals and follow-up postembolization studies (Fig. 14.136).

14.12 Postembolization Care

14.12.1 Head and Neck

In routine head and neck embolizations, the usual precautions following a percutaneous femoral stick are followed. Unless a percutaneous closure device is used, bed rest is indicated for 5 h. In situations where detachable balloons are used or major cerebral arteries are occluded, bed rest for 24–48 h is warranted as well as standing orders for antiemetics, as severe vomiting can potentially dislodge a balloon. Analgesics for the most part are given on a p.r.n. basis, as pain is usually not a problem. In the management of some patients with giant aneurysms or with carotid cavernous fistula (CCF), severe headache will occur as the lesion is thrombosing.

These types of headaches will require heavier analgesia, including narcotics. In general, headache lasts 3–5 weeks before subsiding. Following VAF repair, a soft neck collar is advisable for better stabilization.

14.12.2 Cerebral Arteriovenous Malformations

The postoperative care of patients with cerebral vascular malformations after embolization by the endovascular route is minimal. The principles previously discussed as to blood pressure monitoring, fluid restriction, anticonvulsants, corticosteroids, etc., have been reviewed. In general, it is best to avoid abrupt rises in systolic blood pressure in the postoperative period, bed rest is primarily related to the puncture site, and ambulating is resumed the following day.

14.12.3 Intradural Aneurysms

The care of patients with intradural aneurysms is evolving. At present, various protocols can be followed, depending on the operator's use of percutaneous closure devices.

In the majority of patients, we use systemic heparinization for 24–36 h. depending on the neck size, and exposure of coils to the parent vessel, in an ICU setup. In selected cases we may opt for longer-term antiplatelet medication, which is individualized to the patient.

If no percutaneous closure devices are used, or cannot be used, the introducer sheath is left in place while the heparinization is maintained. Connecting the side arm of the sheath to a continuous pressure monitoring device will prevent complications at the puncture site in a fully heparinized patient, which if unattended may even be fatal.

If a percutaneous closure device is used the patient's medical condition and presentation in an ICU setup primarily dictate the management.

14.12.4 Spinal Arteriovenous Malformations

After spinal cord AVM embolization, bed rest for the first 24 h is followed by progressive elevation of the head in patients with cervical lesions. In those with thoracolumbar malformations, the legs should be above the heart level to assist in drainage. In patients with spinal dural AVMs with stagnant flow, a period of postoperative heparinization may be warranted.

14.13 Complications of Embolization

14.13.1 Complications of Head and Neck Embolization

14.13.1.1 Neurological Deficit

In head and neck embolization, cerebral and/or ophthalmic complications can occur in 0.25%–1% of cases. This warrants close cooperation with clinicians familiar with the management of stroke. Although in general there is little that can be done, the use of volume expanders, hypertensive medications, or EC–IC by-pass (Fig. 14.2) should be considered in the individual situations.

The use of a recovery room and/or ICU with strict bed rest is advisable, with patients undergoing occlusion of a major cerebral vessel (e.g., the internal carotid and vertebral artery).

14.13.1.2 Cranial Nerve Deficit

Cranial nerve deficits are directly related to the blood supply to those nerves. The vascular anatomy is described in Vol. 1. We do not do provocative testing, as most of our patients are under general anesthesia. With familiarity with the vascular anatomy, complications are rare.

Cranial nerve deficits can be secondary to compression by mass effect, as can direct percutaneous ethanol sclerotherapy for maxillofacial malformations. Large-dose corticosteroids given preoperatively and facial monitoring can avoid the majority of such complications.

14.13.1.3 Postoperative Swelling

In most arterial embolizations, swelling is not a problem; if it occurs it starts within 24 h. Usually it reflects embolization of normal territory (similar to trismus), resolves spontaneously in a few days, and responds to corticosteroids when needed. On the other hand, painless swelling after direct alcohol injections for venous lesions (Fig. 14.111) is the rule. No treatment is generally needed; however, if there is a problem with closure of an eye or airway impairment, IV diuretics and postural drainage is indicated.

14.13.1.4 Skin Necrosis

If skin necrosis occurs in skin that is going to be part of the resection, no special care other than hygiene is needed (Figs. 14.102, 1.114). If necrosis develops in normal skin, it will heal spontaneously by granulation (Fig. 14.112). Only when a previously compromised territory is embolized, or if too large, will grafting be needed. In the authors' experience, only on one occasion was grafting needed. Local care with antibiotic ointment, or Silvadene or Aquaphor, which decrease bacteria, is used until granulation is ensured (Fig. 14.112).

14.13.2 Complications of Cerebral Embolization

Major complications of cerebral embolization include ischemic episodes, which may be either temporary or permanent. Distal migration of embolic material into normal territory (stroke), embolization of the venous side or pulmonary circulation, and hemorrhage (subarachnoid and/or intracerebral) are also possible and may present either during the procedure or in the immediate postoperative period. Gluing of a microcatheter is less common but still possible. In the treatment of patients with aneurysms, stenosis, or occlusions of the parent vessel, embolic complications and vasospasm (usually secondary to previous subarachnoid hemorrhage) may occur.

14.13.2.1 Medical Therapy for Acute Ischemic Stroke

One of the most important complications that can occur during endovascular procedures in the CNS is acute ischemia and stroke (see Chap. 1, this volume). Potential etiologies are multiple. Ischemia may follow an embolic complication from autologous clot secondary to endovascular manipulation (Figs. 14.100, 14.101), result from traumatic dissection of a major cerebral artery or from the iatrogenic introduction of an air bubble or other foreign material. Perhaps the gravest complication is that of the injection of embolic agent into an undesired location. Therapy for this complication is limited, due to the high sensitivity to hypoxia and ischemia of the CNS. Therefore, immediate aggressive therapy is pursued in the hope

of salvaging areas of partial ischemia or a penumbra prior to the development of tissue death. The aim of therapy in such instances is preserving maximal brain tissue viability to maximize neurological recovery. It is a fact that infarcted brain tissue cannot be revived, but it is also recognized that functionally impaired brain tissue with critically reduced blood flow may not undergo irreversible ischemic damage if sufficient blood flow is maintained or rapidly restored. Therefore, the main goal of therapy is to preserve as much as possible of the ischemic penumbra area, which represents tissue that is dysfunctional from ischemia but not irreversibly damaged.

The clinical management of stroke is based on a presumed pathophysiology of arterial occlusion; little experimental data exists on venous infarctions. In the complications that follow BAVM embolization, a significant, if not the most frequent, cause of postoperative symptoms is probably related to venous dysfunction. The following discussion, although based on experimental and clinical work relating to arterial occlusion, applies to improving the microcirculation at the venular level as well.

Acute ischemic stroke therapy is geared toward seven major elements of potential therapeutic intervention:

1. Immediate recanalization
2. Microcirculation
3. Antiplatelets
4. Anticoagulation
5. Biorheological factors
6. Antiedema agents
7. Pharmacological protection (Yatsu et al. 1987)

14.13.2.2 Recanalization

If autologous blood clot occludes a normal artery during the procedure, resulting in a neurological deficit, reperfusion can usually be accomplished by the direct local intra-arterial thrombolysis (LIAT), with the superselective injection of urokinase (UK) or tissue plasminogen activator (r-TPA) into the clot itself. Urokinase, if available, is very effective in acute clot lysis secondary to endovascular procedures (Fig. 14.101). A starting bolus of 30,000–50,000 IU is required, followed by infusion of up to 1,500,000 IU over 2–3 h. At present, r-TPA is the only available drug for intra-arterial thrombolysis and appears as effective as UK (see Sect. 1.2.4.14, Chap. 1, this volume). Caution is needed in postoperative patients, those with a previous and recent hemorrhage, and those in whom the lesion is still patent. In the acute treatment of subarachnoid hemorrhage (SAH) secondary to a rupture aneurysm, if a thromboembolic complication occurs at the beginning or during the coiling, the lesion *must* first be secure, i.e., coiled first, and then very local and selective clot lysis will follow (Fig. 14.99). In addition, close observation at the arteriotomy site is mandatory.

In BAVM treatment, distal embolization is very rare, but can occur. Early recognition should be followed by immediate revascularization. In such occurrences, further embolization of the lesion is deferred to a later time.

The recent introduction of GPA IIb/IIIa is a major addition to our armamentarium in a rapidly progressive cascade of events, and given IV or IA, can impressively lyse otherwise unresponsive clot formation or propagation (Fig. 14.101; see Sects. 1.2.4.6, 1.2.4.7, Chap. 1, this volume).

In addition to thromboembolic complications, mechanical devices such as coils, balloons, etc. can be the cause of complications, and it may be necessary to remove them, either transvascularly or surgically (Chalif 1987); reocclusion will result and a dilatation may be needed (see Figs. 14.150, 14.165).

14.13.2.3 Microcirculation Agents

No clear-cut agent is effective in the protection of the microcirculation; however, naloxone, an opiate antagonist, is potentially useful. Although no solid evidence confirms its value, some investigators feel justified in using naloxone because it is harmless and inexpensive. Furthermore, a report by Hosobuchi in 1982 suggested a beneficial effect. The recommended dose of naloxone is 0.4–1.2 mg IV and is given in the acute period (Yatsu 1987).

Vasopressor agents may carry the risk of causing intracerebral hemorrhage; they may be used occasionally to carefully elevate the diastolic pressure and initiate improvement. Vasodilators such as prostacyclins show no clear benefit. They may, in fact, produce an intracerebral reversal of flow, or the so-called Robin Hood effect, by stealing blood from the poor or ischemic tissue and diverting blood toward normal brain.

14.13.2.4 Antiplatelets

Platelet hyperaggregability may occur within ischemic tissue immediately after the acute ischemic event; therefore, the use of an antiplatelet agent in the acute stages may be beneficial to prevent propagation or augmentation of thrombosis. Aspirin or dipyridamole can reduce the recurrence of infarctions seen in patients with transient ischemic attacks. Their exact value in treating acute ischemic complications due to interventional endovascular procedures or their ability to prevent propagation of venous occlusion is unknown. Antiplatelet drugs can thus be reserved for patients in whom there is evidence of repeat and/or propagation of ischemic or embolic phenomena secondary to a foreign body, stagnation in a major vessel, or the unwanted remnant of a device in the vascular system. In our experience, this has only been a theoretical possibility, as in clinical practice. Even when endovascular catheters have been left glued in a major cerebral artery, there has been no delayed thromboembolic complication.

14.13.2.5 Anticoagulation

An anticoagulation agent such as heparin is used to prevent propagation of clot. It may be the first line of response when a distal embolus is identified; a period of 10–20 min under full heparinization is warranted, and

may result in revascularization without further, potentially more dangerous interventions.

14.13.2.6 Biorheological Factors

Biorheological manipulations to reduce blood viscosity may be one of the most valuable measures in the treatment of stroke. Blood viscosity is primarily related to the hematocrit, fibrinogen concentration, and erythrocyte flexibility; these are the various factors to be considered in improving regional blood flow in the areas of ischemic penumbra (Wood 1987). Sufficient evidence exists to recommend biorheological manipulation in the management of some acute complications of iatrogenic embolization.

The understanding of hemorheology may be important in the management of the acute complications of endovascular occlusion of normal territories. In regions of focal cerebral ischemia, blood flow slows distal to a narrow or occluded cerebral artery segment. This slowing results in a vicious circle wherein elevation of blood viscosity further compromises perfusion and ischemia deepens. Reversibility of the neuronal insult depends on the severity of ischemia and on the ability to provide sufficient collateral circulation to maintain viability.

Animal studies have demonstrated significant elevation of regional cerebral blood flow in focally ischemic brain following hypervolemic infusion of autologous plasma or low-molecular-weight dextran (Wood and Fleischer 1982). Wood's group has also demonstrated that the volume of hemispheric infarction could be decreased by as much as 60% in animals, which received two serial infusions of low-molecular-weight dextran, each equal to 20% of the total blood volume. The effect of hypervolemic hemodilution on brain perfusion is greater in regions of low blood flow and may be related to infusion-induced alterations in blood viscosity.

Although reduction in hematocrit results in a decrease in blood oxygen content, an actual increase in oxygen delivery to tissue occurs as the hematocrit is lowered to approximately 30%. In clinical practice Wood and co-workers (1987) evaluated low-molecular-weight dextran or 5% serum albumin solutions in patients with ischemic stroke; an improvement in regional cerebral blood flow and in electroencephalographic changes occurred. In addition, the induced augmentation of regional cerebral perfusion correlated inversely with hematocrit. Strand (Strand et al. 1984), in Sweden, confirmed the beneficial effect of hemodilution but suggested that isovolemia may decrease the possibility of edema or fluid overload. An acute reduction in hematocrit using phlebotomy and the use of low-molecular-weight dextran infusions to produce an isovolemic hemodilution were recommended. In patients with acute cerebral ischemia lasting less than 48 h, an improvement in neurological scoring in the first 10 days occurred in 85% of those treated with isovolemic hemodilution, whereas only 64% of the control group showed improvement. At the 3-month follow-up, both groups had similar mortality rates. In the surviving group of hemodiluted patients, however, the final outcome was significantly better. There were three times more patients able to walk than in

the surviving control group. Thus, hemodilution therapy improved the overall clinical outcome of these patients.

Our own experience supports the beneficial use of isovolemic hemodilution in the treatment of acute complications of vessel occlusion during endovascular procedures. In four instances, dramatic reversal of the neurological deficits occurred within less than 48 h in all patients treated with isovolemic hemodilution immediately after appearance of symptoms.

Possibilities for the future may include the use of pentoxifylline, an inhibitor of fibrinogen synthesis, with a significant decrease in blood viscosity and plasma fibrinogen concentration. In addition, improved antiplatelets and erythrocyte filterability improved in patients with cerebral vascular disease, as reported by Ott in 1983. He treated patients for 6 weeks with pentoxifylline, claiming that these patients experienced significantly fewer ischemic episodes than did control patients. Similar regimens may also be used in patients with severe stenosis and ischemic manifestations.

Wood also noted the type of patient in whom hemorheological manipulation will not be beneficial. These include patients with intracerebral hemorrhage and increased intracranial pressure and patients with brainstem lacunar infarction.

It appears that the best regimen is the one recommended by Strand et al. (1984), i.e., isovolemic hemodilution by phlebotomy and simultaneous infusion of an osmotically active agent. This regimen resulted in a reduced mean hematocrit, from 43% to 30%–37%. Treatment should be administered in an intensive care unit, using a central venous line for monitoring volume status and blood osmolality to prevent complications, including acute tubular necrosis. More caution must be exerted in older patients. Properly monitored, this regime is safe and offers a rational means to immediately improve blood flow in the area of ischemic penumbra. The duration of therapy will vary from a minimum of 72 h to a maximum that depends on the ability to taper the infusion while maintaining the level of improvement obtained during the course of treatment.

Other regimens of hemodilution involve continuous infusion of mannitol (Jafar et al. 1986). This has been used in patients with vasospasm secondary to SAH. Mannitol is a diuretic and therefore a large volume of replacement fluid is needed to prevent nephrotoxicity (acute tubular necrosis). The use of pentoxifylline or perfluorocarbons to accomplish viscosity reduction remains to be proven.

14.13.2.7 Antiedema and Pharmacological Protection Agents

Brain edema due to ischemia or infarction may compromise autoregulation, produce mass effect, and further decrease tissue perfusion. The various antiedema agents include mannitol or furosemide, and may be of use as temporary measures to avert herniation syndromes. As noted in the preceding section, continuous infusion of mannitol has been used in some patients with vasospasm, with apparently promising results (Jafar et al. 1986), primarily as a biorheological agent. Steroids, which can reduce vasogenic edema, seen primarily in tumors, have no effect on the cyto-

toxic edema customarily accompanying stroke and are therefore of no value in the management of stroke.

The brain has an exquisite vulnerability to ischemia or anoxia due to its high demands for metabolic substrate. The reduction in these metabolic demands will theoretically avert or minimize brain injury but this tenet is still unproved. The use of barbiturates has not proven to be of benefit for ischemic tissue, although they may be used to obtain a decrease in internal cerebral pressure. Ca^{2+} channel blockers offer a potential means of averting the reversible ischemic damage triggered by cellular influx of Ca^{2+}. In addition, Ca^{2+} channel blockers may produce vasodilatation in the microcirculation. At present there is no good evidence supporting their effectiveness but they may be useful prophylactically.

14.13.2.8 Additional Measures

The obvious measures of general medical care to maintain proper cardiovascular competence and other medical needs in the acute stage of stroke must be considered.

Revascularization may be useful in very specific instances in which an intracranial approach to by-pass or reopening of an iatrogenically occluded vessel may be warranted. This has been true for patients with prematurely detached balloons in whom immediate surgical intervention and removal of the foreign body may be life saving (Chalif 1987).

14.13.3 Hemorrhage

14.13.3.1 Generalities

Hemorrhagic complications of endovascular embolizations include both subarachnoid and intracerebral hemorrhage. Differentiation is important because the treatment may differ significantly. Angiography may be helpful in differentiation, but an immediate CT is of more value in planning surgical treatment, as it will clearly determine if a hematoma is present, its size, location, effect on the surrounding brain, and whether there is extension into the ventricular system, etc.

The availability of a properly trained and multidisciplinary team that is familiar with the acute care of patients with these types of emergencies and the need for endotracheal intubation and other types of resuscitation measures can be the key factor in the final outcome.

The hemorrhagic complications of embolization can be divided into those that occur during the procedure and those that occur after the procedure.

Bleeding that occurs during the procedure may be related to rupture of a cerebral artery during catheterization (Berenstein 1980c; Khangure and Apsimon 1989), rupture of an aneurysm, or to rupture of the AVM itself. In the first instance, the most common cause is balloon overdistension and occurs mainly with the older-model balloons such as the silicone Kerber calibrated-leak balloons. With the smaller, softer, latex balloons, with

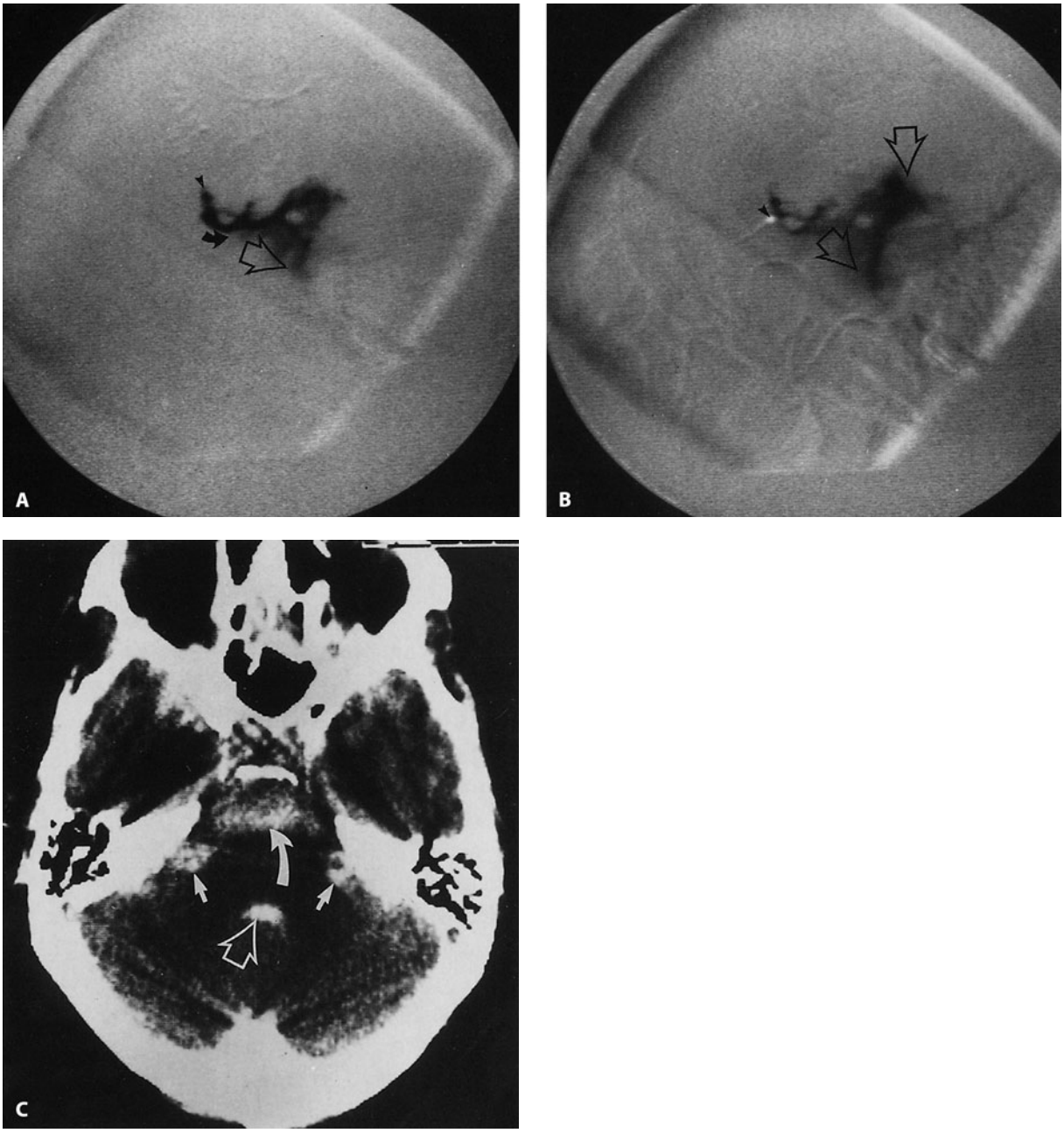

Fig. 14.137A–C. Extravasation of contrast material. **A** Early and **B** later phases of the superselective injection in a posterior thalamoperforating artery with a small, occlusive, calibrated-leak balloon (*arrowhead*); oblique view. Note the vessel filling (*curved arrow*) and the extravasation into the prepontine cistern (*open arrowhead*). **B** The microcatheter was removed (*arrowhead*) and there is further extravasation (*open arrowheads*). Note the appearance of the contrast material delineating the prepontine cistern. **C** Axial CT demonstrates extravasation into the fourth ventricle (*open arrowhead*), prepontine cistern (*curved arrow*), and cerebellopontine cisterns (*arrows*)

a large enough leak and good memory, vessel rupture is less likely. At present rupture may follow guidewire trauma and is very rare, or occur in acute aneurysms.

There may be a short delay between the occurrence of the hemorrhage and its clinical manifestation. Thus, immediate recognition of extravasation fluoroscopically can be life saving. Fluoroscopically, various findings should alert one to the possibility that a vessel has been damaged. When using a balloon for angioplasty, the balloon shape changes if no washout of the contrast material is seen. If contrast appearance does not conform to the expected vessel shape, or if frank extravasation is seen (i.e., contrast material taking the appearance of a sulcus or cistern) (Fig. 14.137), one must be ready to immediately seal off the vessel (Berenstein 1980c). The catheter is left in place as the fastest means to accomplish hemostasis. The microcatheter itself may be tamponading the leak, and if withdrawn further bleeding can occur, as the vessel may not be able to retract. Catheter flushing is stopped to avoid additional extravasation.

Immediately after stabilization, a control low-volume angiogram is done as well as a CT, which will further guide management. The CT appearance of SAH cannot differentiate blood from extravasated contrast material. The purpose of CT is to determine if a surgical lesion exists (Fig. 14.138). If using an over-the-wire or similar microcatheter and extravasation is noted, a coil, preferably of the detachable type, can be used to seal the hole; as the coil is advanced, the microcatheter is withdrawn (V. Halbach 1990, unpublished data). If using a flow-guided microcatheter, immediate injection of a small amount of acrylic may be needed.

14.13.3.2 Brain Arteriovenous Malformation Rupture

An additional cause of intraoperative hemorrhage is a small remnant of malformation or a very small branch that remains at or near the embolized pedicle (Fig. 14.139) after occlusion. This situation can be avoided by completely sealing the pedicle at time of acrylic deposition.

Intraoperative hemorrhage is also caused by occlusion of the venous outflow, without occluding the inflow. Embolic material reaching the venous side of an AVM is not an infrequent occurrence. It is usually of no consequence and may even be advantageous, as it may promote complete thrombosis of the lesion, provided the nidus and afferent pedicle are also occluded.

Venous migration manifests itself fluoroscopically as the column flow is changed in diameter or the diameter of the acrylic (or other liquid embolic agent) column abruptly increases (Fig. 1.134D). This change in column diameter indicates filling of the fistulization site, with flow from other sources washing or spreading the polymerizing acrylic column into the periphery of the vein (Fig. 14.139). When radiopaque acrylic is seen to enter the venous side, the injection of additional NBCA should not be discontinued but should actually be speeded up to seal off the shunt and prevent further migration of glue (see Vol. 3, "Vein of Galen Aneurysmal Malformation"). Alternatively, the injection is resumed 1–2 s later to permit polymerization of the portion that has reached the fistula.

Fig. 14.138A–G. Postembolization hemorrhage. **A** Lateral view of the left internal carotid artery, mid-arterial phase, demonstrates the remaining middle cerebral supply (*curved arrow*) to a temporal vascular malformation in the mid-temporal gyrus. **B** Last vessel to be embolized (*curved arrow*) shows small distal vessels going toward the malformation *en passage* (*arrowheads*). **C** Catheterization of the remaining supply (*arrows*). There is no normal vessel filling. **D** Digital subtraction angiogram from the acrylic deposition, which is radiopaque. The tip of the catheter has been removed (*arrow*). **E–G** see p. 1139

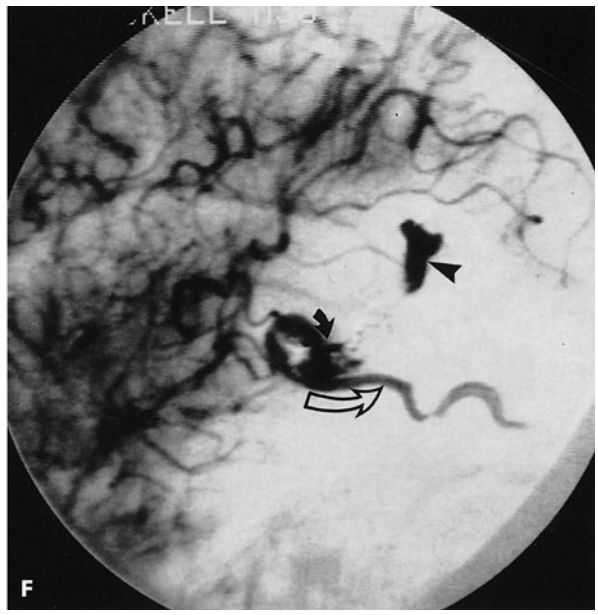

Fig. 14.138 (*continued*). **E** Immediate postembolization angiogram demonstrates extravasation at the site of occlusion (*arrowheads*). A small contribution to the malformation remains (*arrows*). **F** Mid phase of the same injection shows additional extravasation (*arrowhead*), associated with an increase in mass effect and a small amount of filling of the malformation (*curved arrow*) and draining vein (*open curved arrow*). **G** Immediate CT scan demonstrates the large mass effect, with hemorrhage extending into the ventricular system

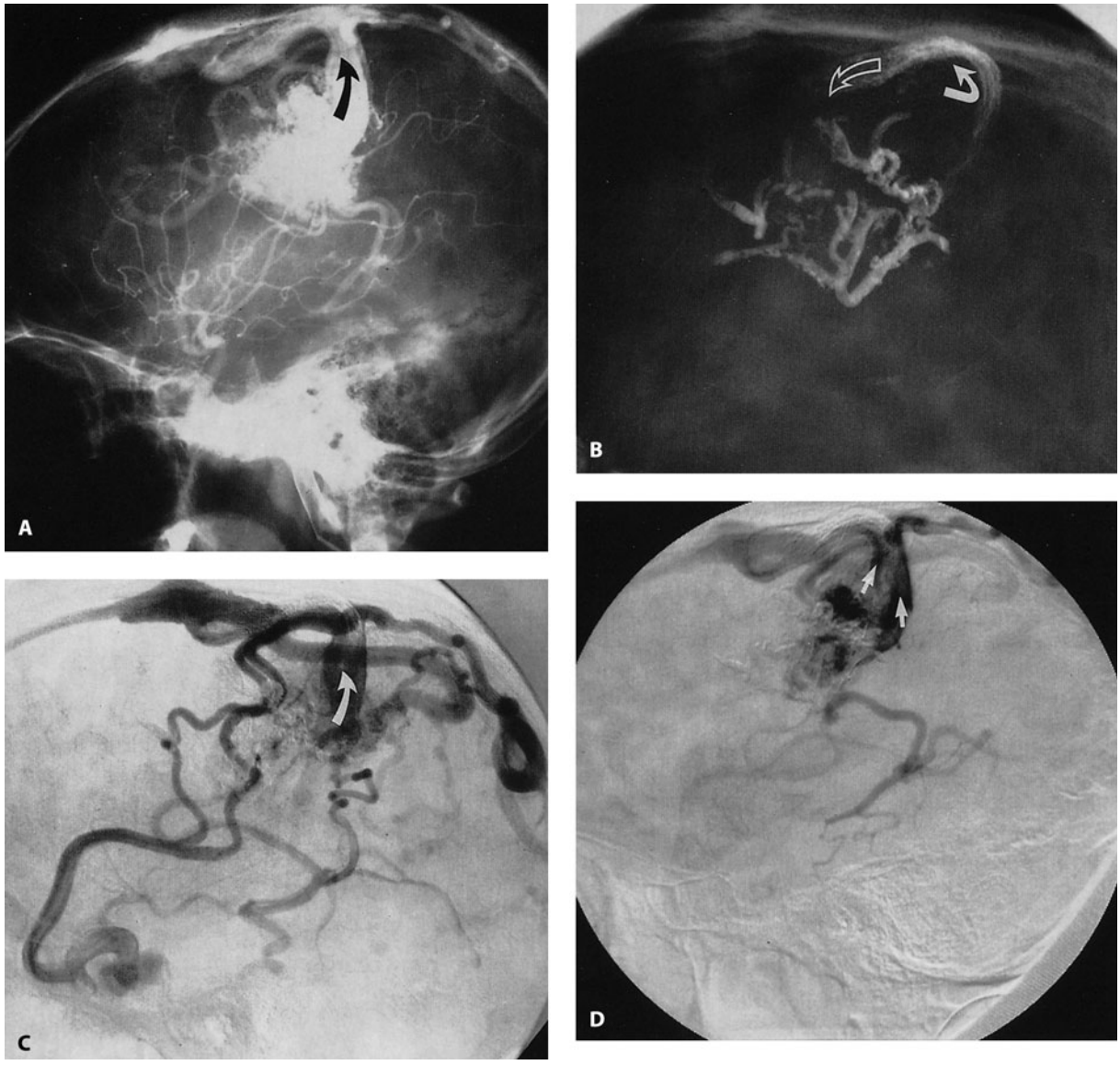

Fig. 14.139A–D. Low thrombogenicity of the cyanoacrylate. **A** Late phase of the left internal carotid artery demonstrates an arteriovenous malformation with drainage through a hypertrophied cortical parietal vein (*curved arrow*). **B** Plain film of the skull after NBCA embolization. Note the migration of the radiopaque acrylic through the vein (*open white arrow*) and the dilution of the cyanoacrylate layering against the vessel wall by nonopaque blood. **C** Immediate postembolization angiogram in the late phase demonstrates contrast material passing around the cyanoacrylate (*white curved arrow*). **D** A 6-month follow-up angiogram demonstrates patency of the same vein. There is no delay thrombosis to the intraluminal cyanoacrylate

Migration of embolic material into a major sinus structure such as the straight sinus is potentially dangerous. In most cases, however, as the unpolymerized acrylic reaches a large venous structure, it will either fragment or layer against one of the vessel walls without occluding it, either acutely or later (Fig. 14.139D). This lack of occlusion testifies to the mechanical nature of cyanoacrylate occlusion with no or minimal delayed

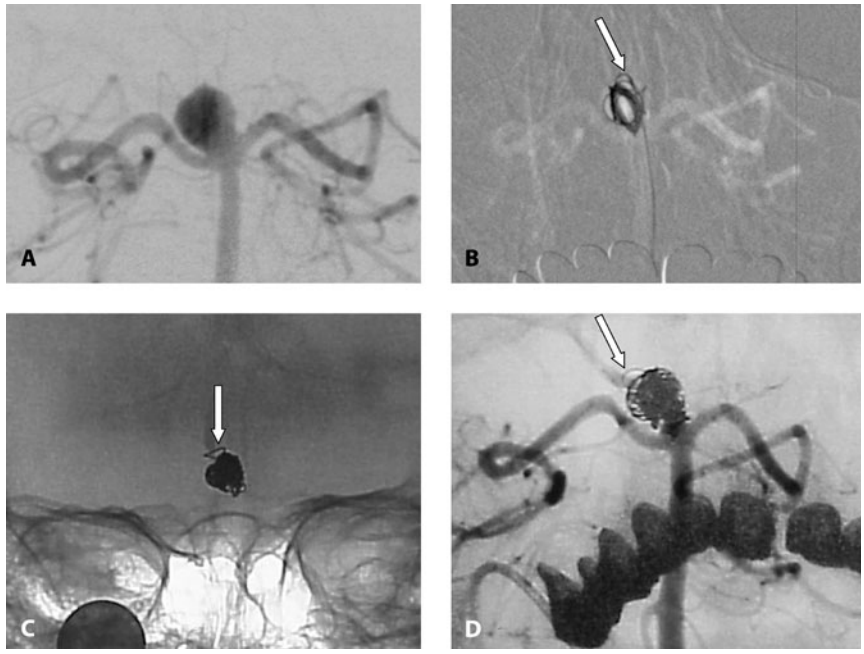

Fig. 14.140A–D. Intraoperative aneurysm rupture. **A** Basilar aneurysm. **B** Frontal road map image. The coil is projecting beyond the aneurysm dome and was associated with an abrupt rise in blood pressure. **C** Plain film and **D** follow-up angiogram show the coils at the end of the procedure. Note the extravascular coil (*arrow*) and a good coiling of the aneurysm. Simultaneous additional coiling and a ventriculostomy were placed

thrombosis. Migration of embolic material into the pulmonary circulation is usually asymptomatic, even with relatively large amounts in adults (Capan et al. 1983). However, in newborns or infants with a compromised cardiopulmonary system, even small amounts of embolic material escaping into the lungs can result in death (Berenstein 1980c).

On rare occasions, a hemorrhage has occurred some hours after embolization (2–24 h). The cause is usually difficult to establish and its management is that of other causes of hemorrhage.

De novo seizures following embolization should be considered as a sign of hemorrhage until CT proves different.

14.13.3.3 Aneurysm Rupture

The acute rupture of an aneurysm during endovascular treatment is an emergency that requires simultaneous immediate and expeditious response by the team. First is the obvious need to recognize that a rupture has occurred. Acute systemic blood pressure elevation is an important indicator that ICP has sharply risen. Medical management is imperative, usually administrated by the anesthesiologist. Recognizing that a coil, for example, is beyond the confines of the aneurysm even if no other clinical or radiographic change occurs should be handled as a perforation (Fig. 14.140).

Contrast material extravasation into the subarachnoid space, intraventricular space, or into the parenchyma is a grave situation (Fig. 14.141).

If rupture has occurred, or it is suspected, in addition to the obvious support measures (ensuring airway, reversing anticoagulation, etc.), immediate and expeditious continuation of the aneurysm occlusion must proceed. At the same time or immediately after placing an external ventricular drainage (EVD) is a life-saving maneuver.

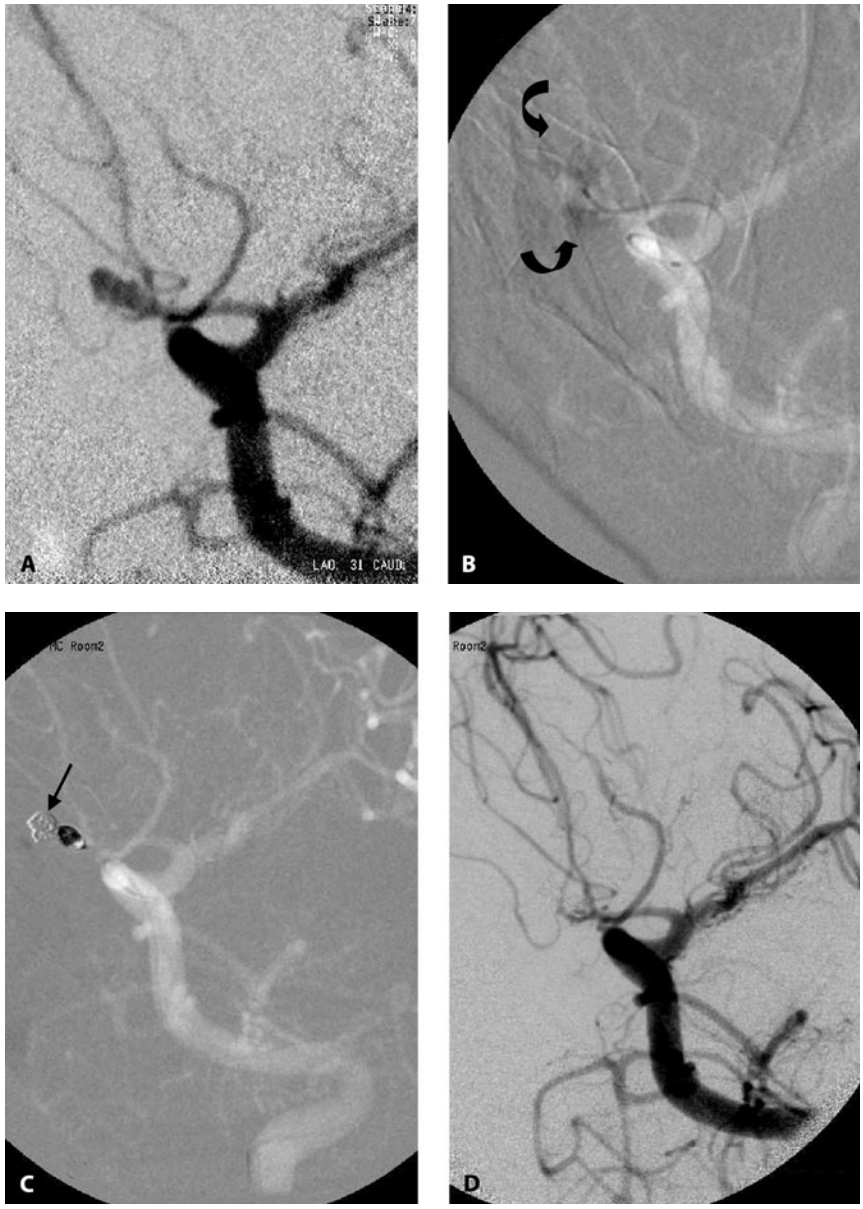

Fig. 14.141A, B. Intraoperative rupture. Grade IV subarachnoid hemorrhage. **A** Anterior communicating aneurysm. **B** Road map image shows the extravasation (*curved arrows*). **C** The perforation is sealed with coils (*arrow*). The last coil is placed in the aneurysm. **D** Postembolization digital subtraction angiogram. The bleeding was stopped, the patient did not recover

In more than 1,000 aneurysm treated by the three authors of this volume, rupture has occurred in 1% of cases. All except one occurred in patients with recently ruptured aneurysms. Recovery can usually happen in good-grade patients, whereas in poor-grade patients, although the hemorrhage was stopped, the patients never recovered (Fig. 14.141).

The best way to deal with a rupture is to prevent it from occurring. In the acute phase following SAH, in the presence of an obvious nipple, i.e., very small aneurysms, dense packing should not be forced, especially if there is a small neck, as the lesion will most likely thrombose on follow-up (Fig. 14.142). Even in larger neck lesions, with some residual aneurysm, protection against bleeding should be provided. If later there is recurrence or residual aneurysm, recoiling can be done later more safely.

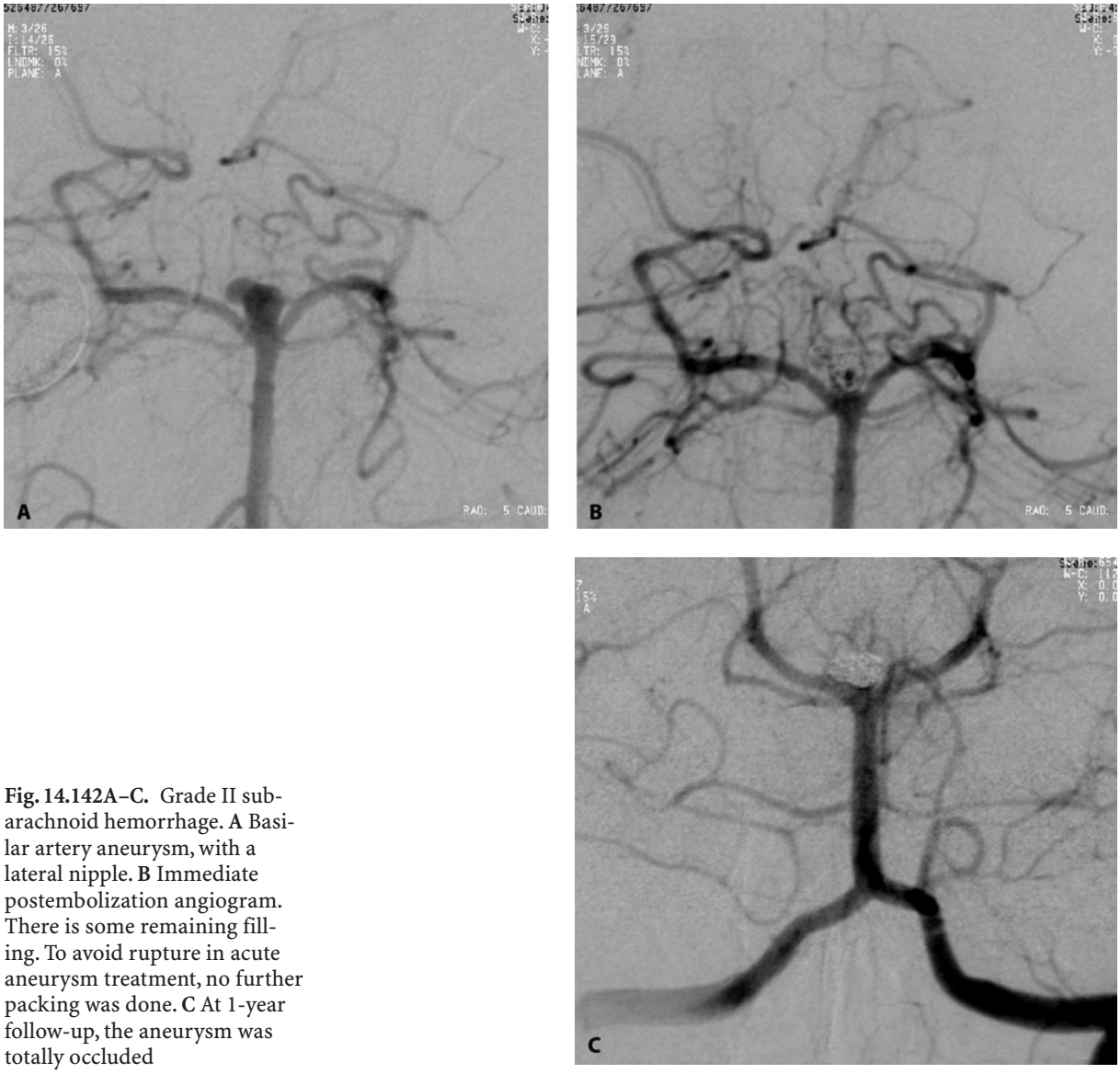

Fig. 14.142A–C. Grade II subarachnoid hemorrhage. **A** Basilar artery aneurysm, with a lateral nipple. **B** Immediate postembolization angiogram. There is some remaining filling. To avoid rupture in acute aneurysm treatment, no further packing was done. **C** At 1-year follow-up, the aneurysm was totally occluded

14.13.3.4 Arterial Stenosis

Stenosis of a cerebral artery can follow balloon detachment or may be caused by the neck of the balloon (Fig. 14.143). Angioplasty of the stenotic segment at the level of the balloon is usually possible using a second nondetachable balloon. Arterial stenosis or impeachment may follow aneurysm treatment with coils or liquids; if no stagnation or clot formation, it can be observed in the procedure room with sequential angiograms. Only if it is progressive or if emboli are forming is intervention indicated. The use of antiplatelet medication, GPA IIb/IIIa, may suffice in controlling the problem (Fig. 14.101). If medical therapy is not sufficient revascularization by mechanical means is usually effective. Balloon angioplasty may be effective in balloon stenosis; however, in coil protrusion, the coils return to their original location after balloon angioplasty. A more effective

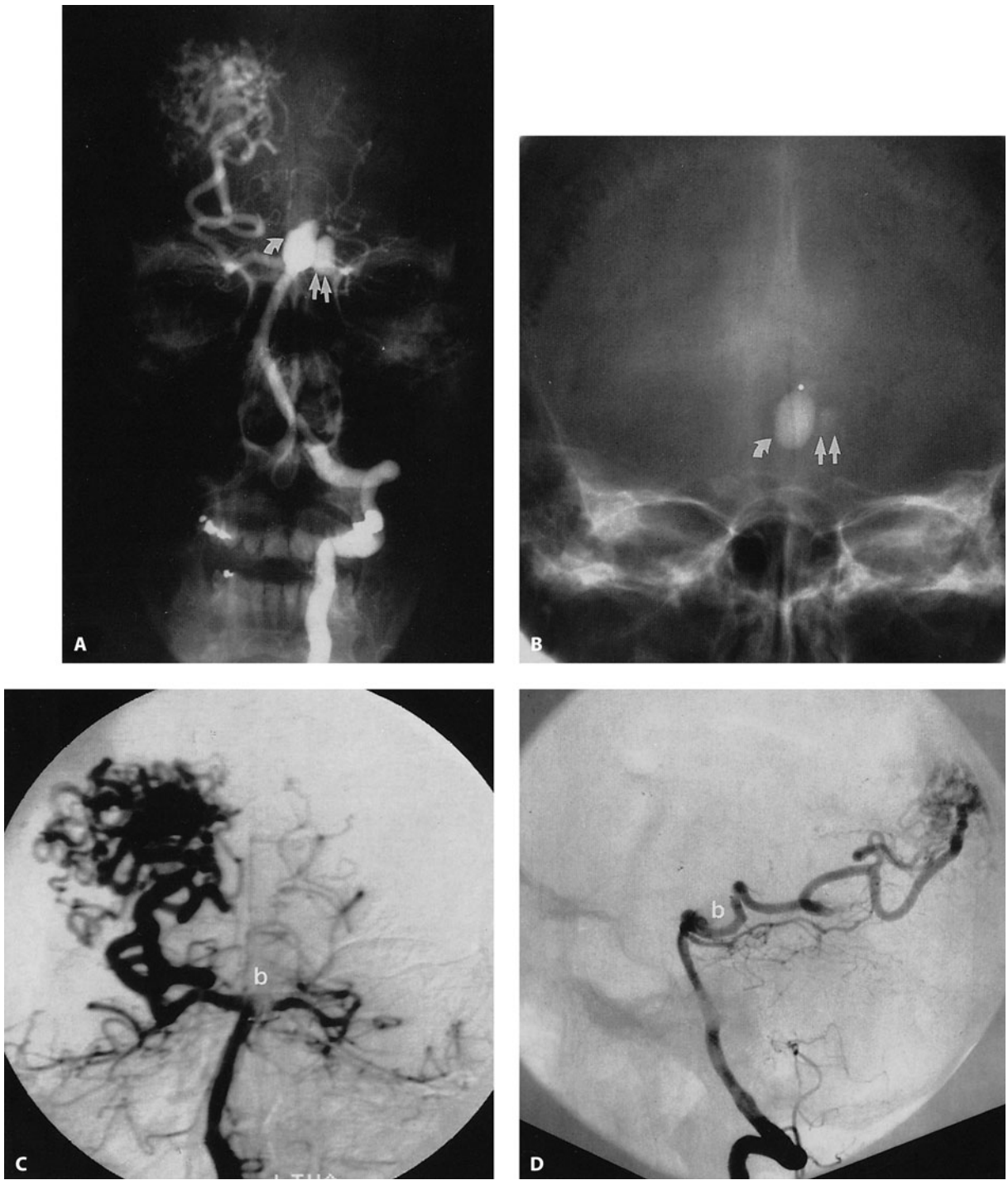

Fig. 14.143A–H. Recanalization and angioplasty. **A** Frontal view of the left vertebral artery injection shows a basilar aneurysm (*curved arrow*) with a second dome (*double arrow*) proximal to an arteriovenous malformation (AVM). The patient presented with compression of the left pons by the aneurysm. **B** A no. 9 Debrun balloon filled with HEMA (hydroxy-methylmethacrylate) was detached in the proximal dome (*curved arrow*). Note the stagnation of contrast material on the second dome (*double arrow*). **C** Frontal and **D** lateral angiograms of the left vertebral artery after balloon (*b*) detachment. There is complete exclusion of the aneurysm and preservation of all normal branches. **E–H** see p. 1145

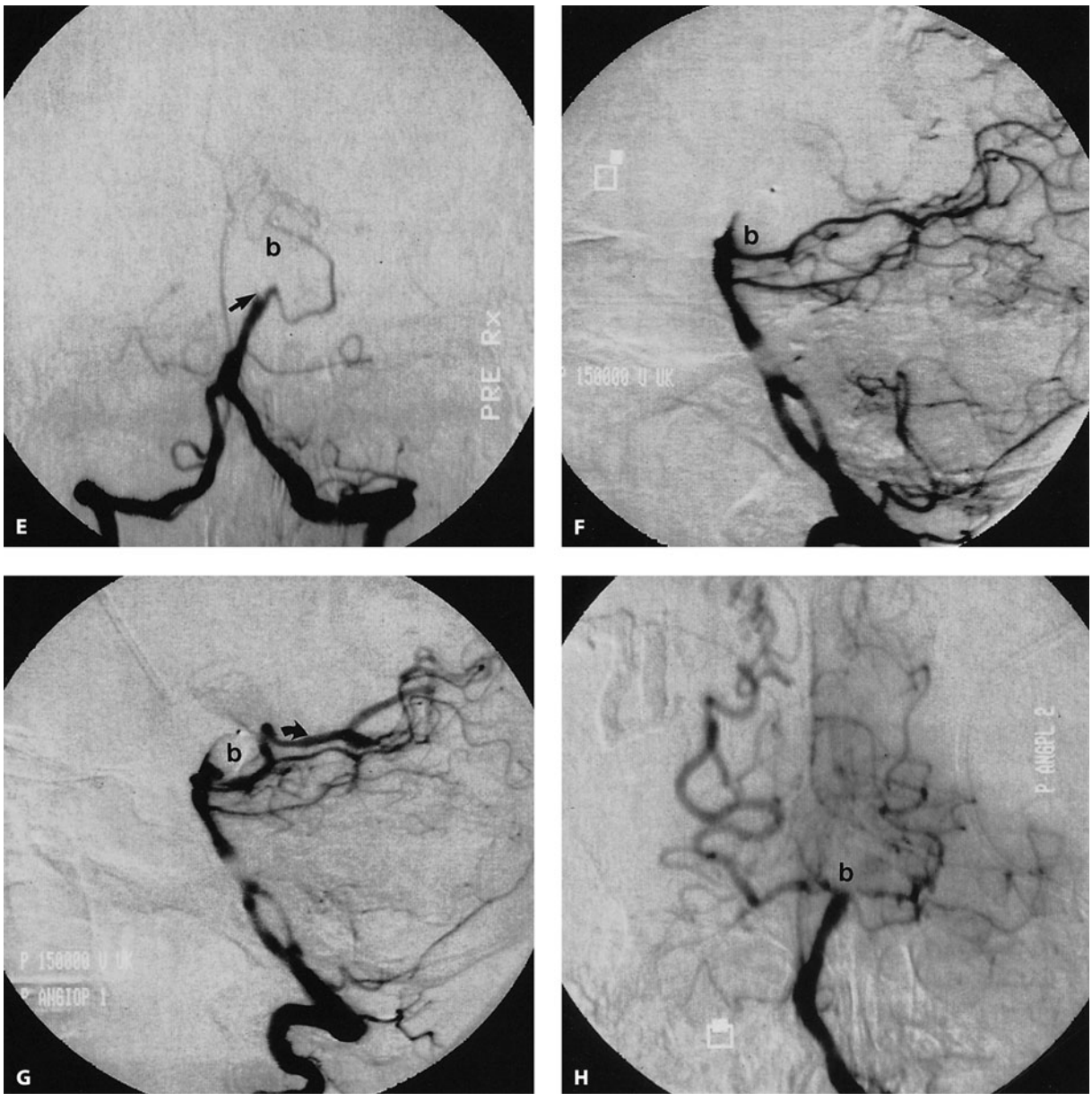

Fig. 14.143 (*continued*). **E** Some 36 h later, the patient became comatose. Frontal digital subtraction angiogram of the left vertebral artery 30 min later demonstrates occlusion of the distal basilar artery (*arrow*) with clot. The balloon (*b*) has come down slightly. **F** After immediate intra-arterial infusion of 150,000 UI of urokinase (intermittent bolus injections of 5,000–20,000 UI at a time), the basilar tip was repermeated. However, there was no filling of the right posterior cerebral artery occluded by the balloon. **G** After angioplasty to reposition the balloon, the posterior cerebral artery on the right (*curved arrow*) was repermeated. **H** After a second angioplasty, there was filling of both posterior cerebral arteries; *b*, balloon. A significant portion of the AVM was also embolized, the patient recovered

measure may be, if possible, to place a stent to keep the coil away from the vessel lumen (Fessler 2000). We have never needed to do such a maneuver.

14.13.3.5 Vasospasm

Cerebral vasospasm during navigation is infrequent. We have seen it almost exclusively when treating patients in the acute stage after hemorrhage. Therefore, embolization of cerebral AVMs is usually delayed 6–8 weeks after hemorrhage, as the risk of rebleed from the AVM in this period is minimal. The use of Ca^{2+} channel blockers has been advocated as a prophylactic measure to prevent vasospasm during cerebral navigation (Merland, unpublished data) and should be given 24 h prior to the procedure. We use it primarily in young females as a prophylaxis measure, and it is usually effective. Spasm can occur at the level of the internal carotid artery when the introducer catheter is wedged, is at a sharp curve, or is frequently moved. For the most part, slight proximal withdrawal of the introducer will be sufficient to relieve the spasm. In the few patients with hyperreactive vessels, preoperative Ca^{2+} channel blockers may be useful. If severe spasm is a problem the procedure can be stopped and repeated after Ca^{2+} channel blockers have been given. It is important to recognize this spasm to avoid inadvertent steal from the opposite side or from the posterior circulation (see Chap. 6, this volume).

When large-caliber guiding catheters are used, when using multiple catheters in the brachiocephalic arteries, or in the spinal vasculature catheterization, spasm may occur. A very effective way to deal with such spasm is the intra-arterial injection of 50–100 μg of nitroglycerin (Figs. 14.83, 1.48).

14.14 Follow-Up

It is the responsibility of the surgical neuroangiographer to monitor the benefits or lack of benefits in his or her patients. Therefore periodic clinical monitoring is advisable. The use of follow-up angiography will depend on the primary problem (such as aneurysms or fistulae), as well as individual and cultural environments. Particular cases and individual problems are discussed in each chapter.

Data base analysis and individual risk measurements are essential for the purpose of patient information and decision making.

14.15 Combined Endovascular Treatments

As endovascular techniques and devices are rapidly evolving, our ability to deal with more complex vascular pathologies is expanding. It is possible today to combine techniques and strategies to treat cerebrovascular lesions that could not be treated previously with endovascular means and that may have needed combination endovascular and surgical treatments.

14.15.1 Combined Endovascular Treatment in Aneurysm Therapy

At the early stages of endovascular treatment of aneurysms, the first indications included parent vessel occlusion for large or giant nonsurgical lesions. At present, although parent vessel occlusion remains an effective and safe treatment in the appropriate setting, every effort is made to preserve the parent vessel.

Figure 14.144 illustrates the case of a young female who was involved in a motor vehicle accident, resulting in blindness in the right eye associated with a posttraumatic right ICA CCF, treated with a detachable Debrun latex balloon 5 years earlier. At that time, an additional posttraumatic dissecting aneurysm of the contralateral left ICA was left untreated, to avoid sacrificing the left ICA. On follow-up, the patient developed a large expanding false aneurysm at the site of the CCF, secondary to deflation of the balloon. With the introduction of detachable coils, endovascular stents and liquid embolics, we were able to reconstruct and preserve both carotid arteries (Fig. 14.144).

14.15.2 Combined Endovascular Treatment in Brain Arteriovenous Malformation Therapy

In a similar manner, brain AVMs associated with other vascular lesions can be addressed endovascularly (Fig. 14.145). In addition to combining endovascular techniques, understanding the concept of flow-related lesions will make it possible to properly select those that can be left untreated and those that can be treated (see Chap. 9, this volume).

14.15.3 Combined Endovascular Treatment in Occlusive and Hemorrhagic Vascular Disease

As patients with occlusive vascular disease are being referred for endovascular treatment, associated lesions are being discovered. Endovascular therapy is uniquely positioned to deal with such circumstances and to address such potentially complex situations. There are different ideas on how to deal with a patient with severe carotid artery stenosis associated with a cerebral aneurysm, with some suggestions that opening the stenosis may increase the risk of the aneurysm to rupture. We prefer to treat them in two separate sessions to permit some re-endothelialization of the stented CA (Fig. 14.146), but it is possible to treat both lesions in the same session.

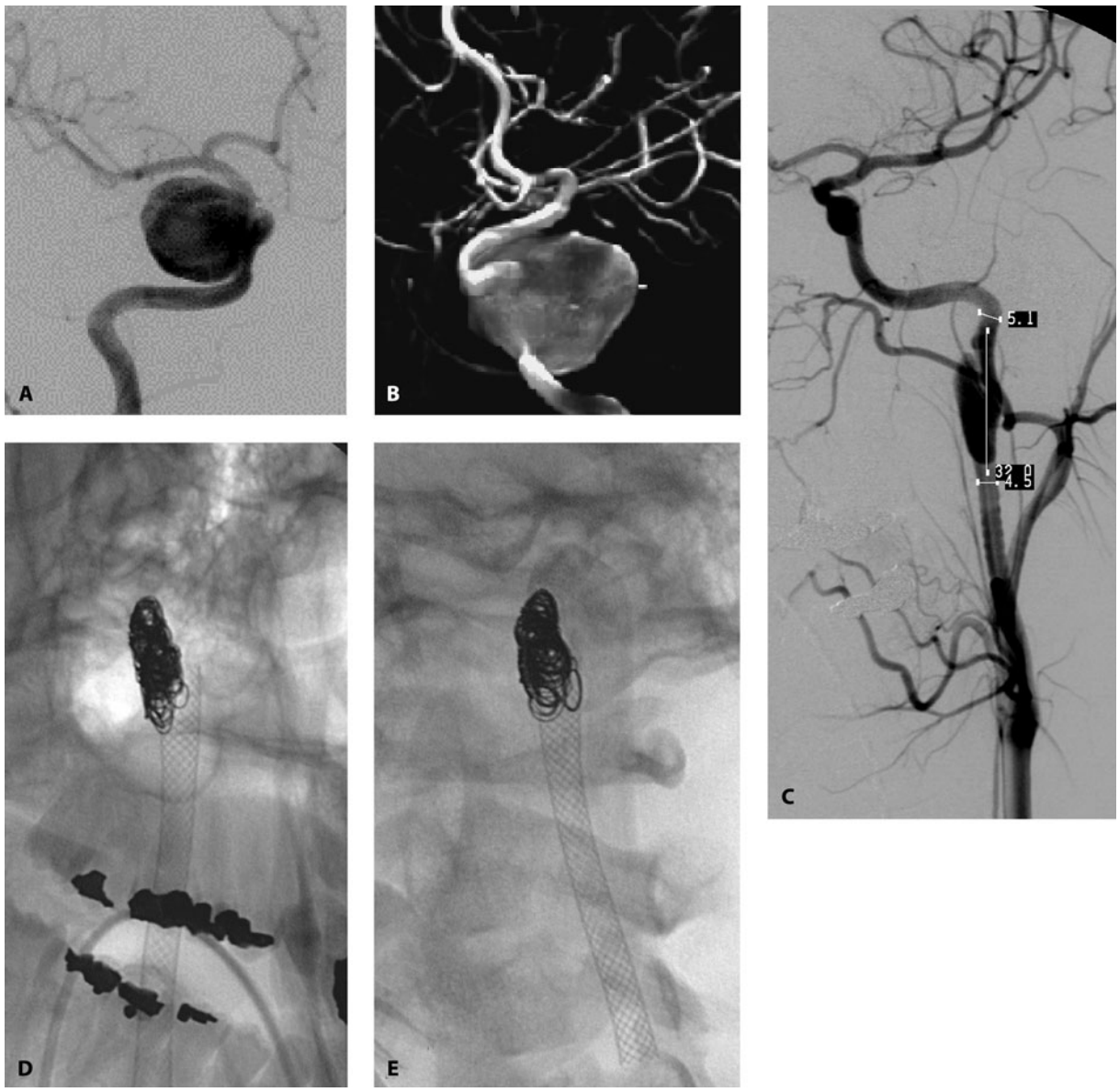

Fig. 14.144A–J. Combined treatments for cerebral aneurysms. A 26-year-old female patient, who 5 years earlier was involved in a motor vehicle accident resulting in a right carotid cavernous fistula on the right internal carotid artery, associated with blindness in the right eye. In addition, she presented with a posttraumatic dissecting aneurysm of the left cervical-petrous carotid artery. She underwent balloon occlusion of the fistula with preservation of the right carotid artery in 1986. The left side was not treated. **A** Frontal digital subtraction angiogram of the common carotid artery on the right demonstrates a posttraumatic aneurysm at the site of fistula repair following deflation of the balloon. **B** Lateral 3-D reconstructed image demonstrates the aneurysm with no discrete neck, the entrance of the carotid artery at one point of the aneurysm, and the exit at a different point. **C** Frontal oblique projection of the left common carotid artery demonstrates the dissecting aneurysm of the cervical carotid artery as it enters the petrous bone. **D**, **E** Two separate plain film projections after stenting of the dissected segment, demonstrating the stent placed across the dissection with coils through the stent. Note how the coils are able to go around the stent in this broad-based aneurysm. **F–J** see p. 1149

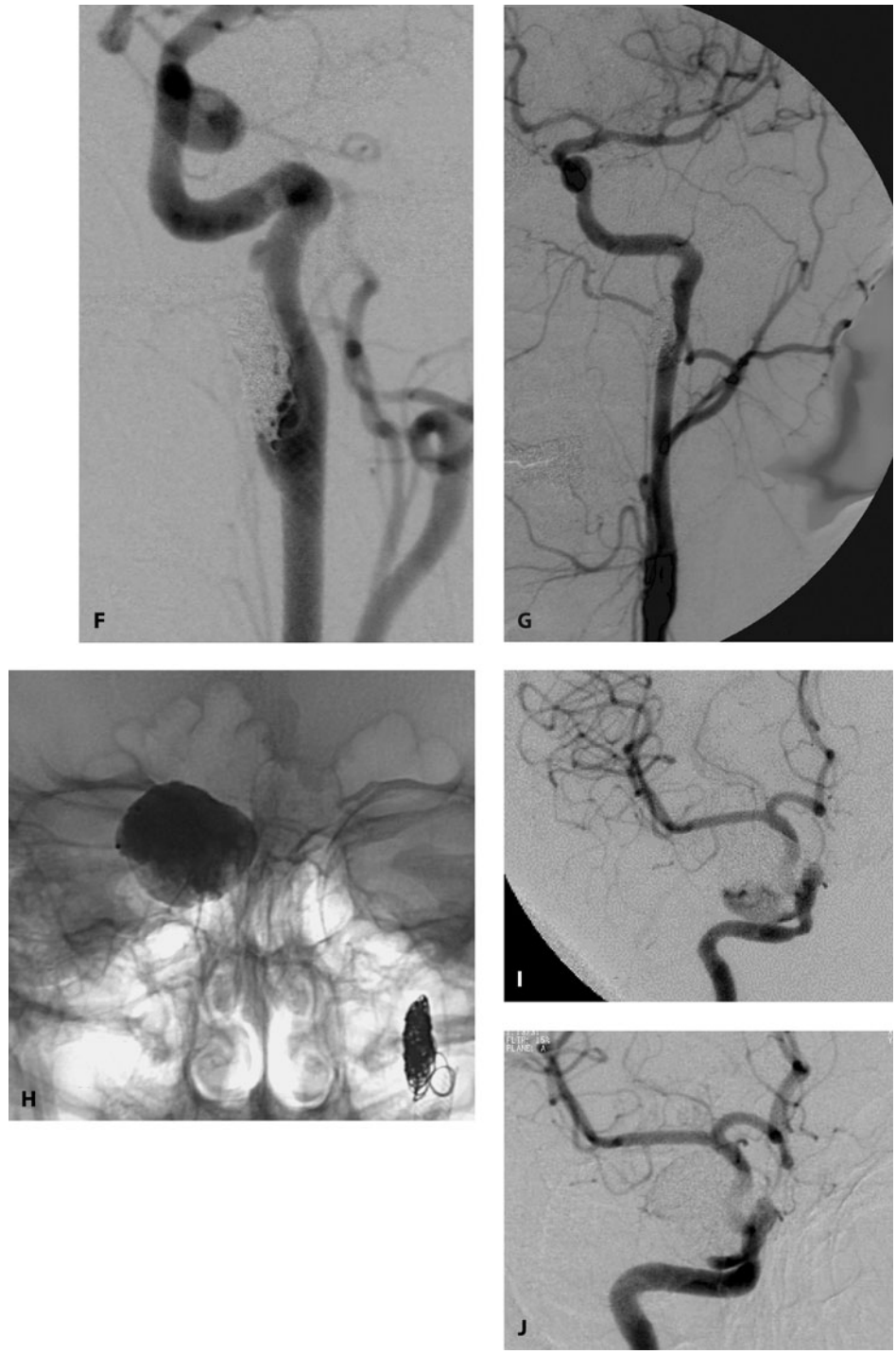

Fig. 14.144 (*continued*). **F** Immediately after treatment of the left side. **G** At 6-month follow-up, there is better remodeling of the aneurysm. **H** Plain film of the skull demonstrating the Onyx cast in the right cavernous aneurysm and the stents and coils on the left. **I** Immediately after Onyx treatment of the right-side cavernous aneurysm. The upper portion of the aneurysm is well covered. The lower portion still shows some filling. **J** Follow-up 6 months after Onyx treatment of the right cavernous aneurysm demonstrates minimal residual in the inferior portion of the aneurysm. There is good preservation of the carotid artery

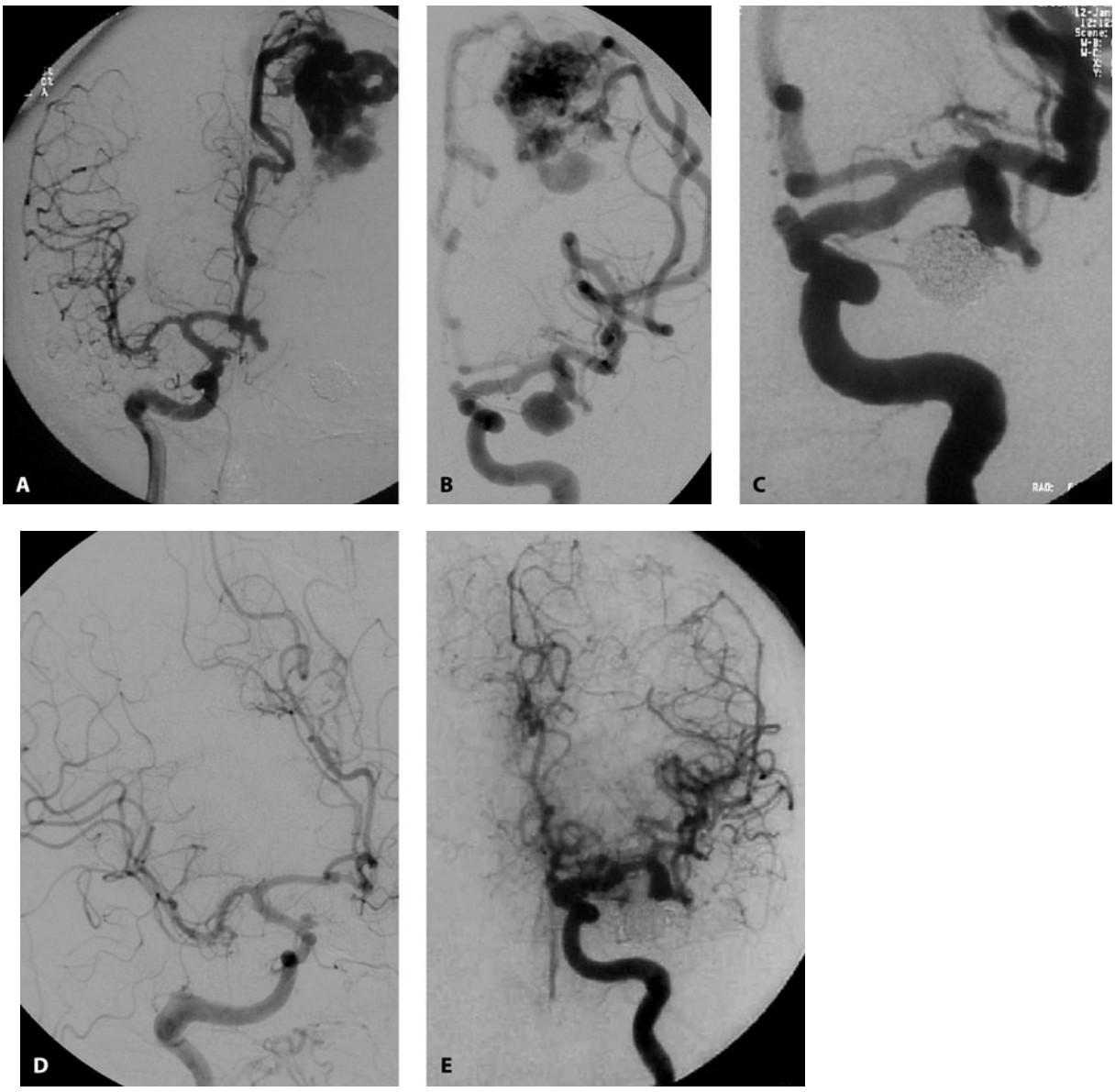

Fig. 14.145A–E. Combined endovascular treatments for brain arteriovenous malformation (AVM) with multiple aneurysms. **A** Frontal digital subtraction angiogram (DSA) of the right internal carotid artery (ICA). Note the presence of right ophthalmic and anterior communicating artery aneurysms and the supply to the AVM by the anterior cerebral artery. **B** Frontal DSA of the left internal carotid artery shows an additional ophthalmic artery aneurysm of the left, a large middle cerebral artery (MCA) aneurysm, and the AVM. **C** Cone-down view after endovascular coiling of the large MCA aneurysm. This was done prior to embolization of the AVM. **D** Right ICA and **E** left ICA follow-up angiograms after three-stage embolizations. Note the disappearance of the AVM, the regression of the anterior communicating artery aneurysm, and no change in the paraophthalmic aneurysm on the right. The left paraophthalmic aneurysm is still present and has reduced in size. The MCA aneurysm remains occluded

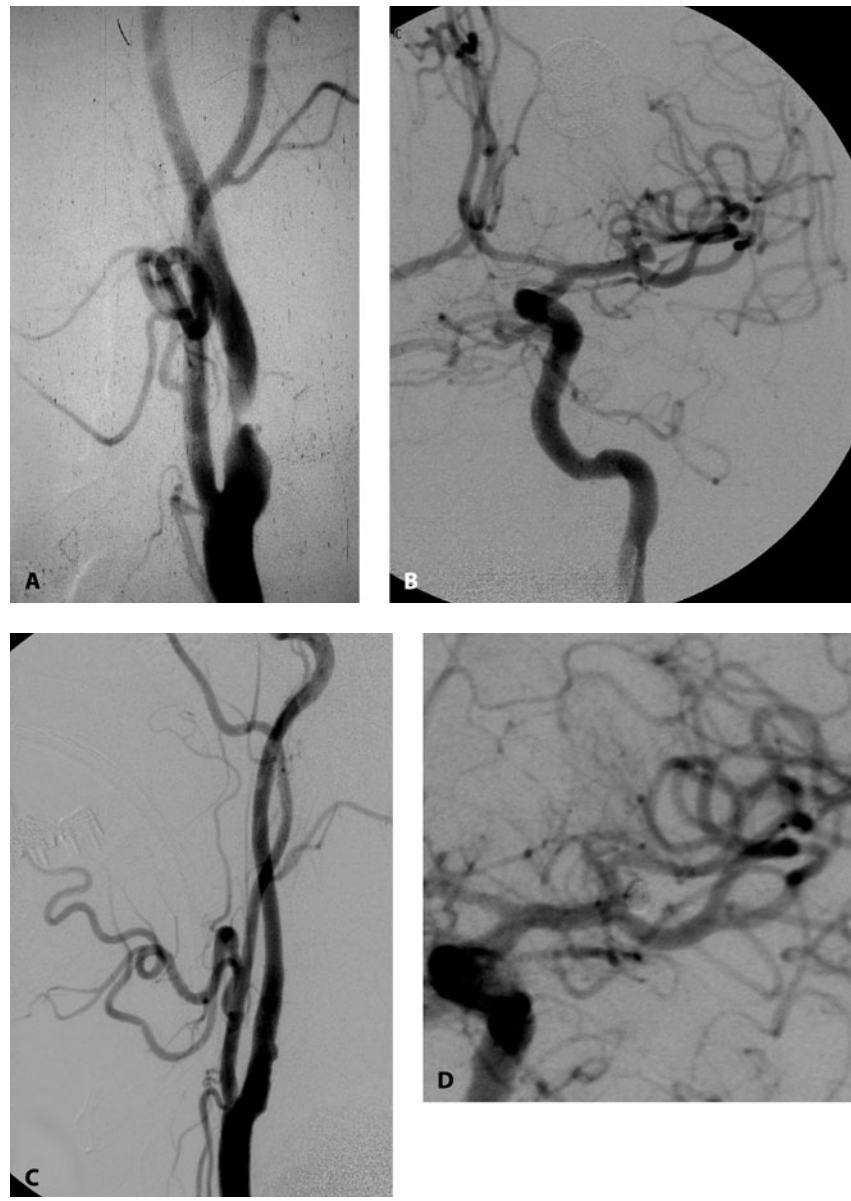

Fig. 14.146A–D. Combined treatments. **A** Lateral angiogram of the left common carotid artery with a severe stenosis on the internal carotid artery (ICA). **B** There was an associated aneurysm of the left middle cerebral artery. **C** Three weeks after stenting of the ICA, there was very good flow in the ICA. **D** The aneurysm was coiled successfully

14.16 Techniques of Carotid Angioplasty and Stenting

14.16.1 Introduction

The techniques and materials used for carotid angioplasty and stenting (CAS) are rapidly evolving, and we propose to establish certain parameters and principles that will make these treatments safe, effective, and less dependent on technological changes.

In general, the essential technical elements for safe and effective vascular revascularization include:

1. Preparing the patient with antiplatelet medication
2. Delineating the extent of disease
3. Crossing the lesion
4. Maintaining the guidewire in the true vessel lumen beyond the lesion (probably the most crucial aspect of vascular revascularization)
5. Stabilizing the guidewire to avoid spasm
6. Avoiding or decreasing the chances for distal migration of debris during predilatation or postdilatation, by slowly inflating or deflating the balloon to accurately deploy the stent, and by ensuring distal protection

14.16.2 Hemodynamic Disturbances During Stenting

Acute hemodynamic disturbances during stenting in the carotid sinus region as measured by changes in heart rate (HR) and blood pressure (BP), and adverse neurological and cardiac outcomes were reviewed by Mendelsohn and co-workers (1998). They describe some degree of bradycardia or hypotension in 68% of carotid stent procedures, but administration of vasoactive medications was necessary in only 37% of patients with more persistent hemodynamic disturbances. Hypotension requiring continuous vasopressor therapy was significantly more common during the postdilatation period (32%) than during the predilatation period (5%) (p=0.02), probably reflecting the smaller balloon used during predilatation. In the Qureshi et al. report (1999), in only one patient was hypotension noted to last more than 24 h. Bradycardia can be reduced by prophylactic atropine. In one of Mendelsohn's patients, the hemodynamic response to stenting may have contributed to an adverse neurological and cardiac outcome. These hemodynamic changes presumably result from baroreceptor stimulation triggered by balloon dilatation and/or stent delivery in the region of the carotid sinus. These maneuvers may distend the carotid sinus, thereby activating stretch-sensitive baroreceptors at the adventitia, which then send electrical impulses through the sinus and glossopharyngeal nerves to the nucleus tractus solitarius in the caudal medulla. From there, enhanced parasympathetic stimulation of the heart may produce bradycardia and diminished sympathetic outflow to the peripheral blood vessels, leading to hypotension (O'Mahony 1995; Eckberg et al. 1975). In our experience, and supported by the report by Qureshi et al. (1999), HR or BP changes are seen primarily after balloon inflation and are mild and infrequent, if balloon dilatation is done gently, over relative-

ly long periods of time: 20–60 s. Using prophylactic atropine can usually prevent HR and BP changes if the lesion is at the level of the carotid bulb. In cases where HR or BP changes occur, immediate deflation of the balloon resolves the hemodynamic change without the need for medication in the great majority of cases. It is interesting to note that in patients with previous carotid endarterectomy (CEA), head and neck radiation, or with lesions above the carotid bulb, these hemodynamic changes are usually not seen.

Hemodynamic alterations associated with carotid endarterectomy such as bradycardia are a frequent but benign perioperative finding (Margulies et al. 1993; Wong et al. 1997). However, Wong et al. (1997) reported on the hemodynamic instability after CEA in a study of 290 consecutive patients undergoing CEA. He found postoperative hypertension in 9%, hypotension in 12%, and bradycardia in 55% of patients. However, only hypertension was significantly associated with stroke or death (p=0.04) as well as cardiac complications (p=0.07). Hypertension has not been reported as a problem during CAS. Wong et al. did not find a correlation between hypotension or bradycardia and adverse outcome. Mendelsohn et al. (1998), however, reported that hypotension associated with carotid endarterectomy increased the rate of stroke and myocardial infarction. Compared with bradycardia, hypotension may be less well tolerated by patients undergoing carotid intervention (Bove et al. 1979; Riles et al. 1979; Qureshi et al. 1999; Ranson et al. 1969).

In patients who became hypotensive, blood pressure returned to baseline 2–15 min after predilatation or stent delivery. Hypotension was more directly linked to postdilatation of the stent. The hemodynamic changes reported during the early experience of stenting appear to be associated with balloon-expanded stents, such as the Palmaz (Cordis Endovascular) stent that was first used at the carotid bifurcation. Hypotension after the stent delivery was observed more often than during the postdilatation. We have not observed such hemodynamic fluctuations with the self-expandable stents and with gentle slow postdilatation angioplasty. Slow inflation permits the vessel to stretch rather than to crack.

14.16.3 Premedication

In general, based on the cardiac and peripheral stenting experience, antiplatelet premedication of elective patients undergoing CAS is mandatory.

The use of aspirin has, for the most part, been replaced with Plavix (75–150 mg) started 2–3 days before the procedure. If Plavix is contraindicated, Ticlopidine (250 mg), or aspirin (325 mg) may be used. In emergency cases, a 325-mg aspirin rectal suppository or IV aspirin can be used (IV aspirin is not available in the United States). Some investigators have used a two-drug regimen, adding 81–325 mg of aspirin to any of the two other drugs, although there is no study that favors one strategy over the other. However, it is agreed by all that some type of premedication with antiplatelets is mandatory. After vascular access is secured, full anticoagulation with heparin is started. A bolus of 3,000–5,000 IU is then followed by a continuous heparin infusion, to maintain an activated coagulation time (ACT) of at least double the baseline.

Most centers perform CAS under local or stand-by anesthesia. One of the authors (A.B.), however, believes that unless there is a high anesthesia risk, general anesthesia is less stressful to both the patient and the doctors.

14.16.4 Vasoactive Medications

Atropine (0.5 mg) can be used before initial balloon inflation. Prophylactic atropine effectively increased HR during the predilatation period by 7.5±8.0 beats/min compared to no prophylactic atropine, which resulted in a decrease in HR by 10.1±15.9 beats/min. Prophylactic atropine, however, does not reduce the incidence of bradycardia during any period. We only premedicate with atropine if the narrowest portion of the lesion is at the level of the carotid bulb or in patients with known cardiovascular instability. After the initial balloon inflation, atropine or metaraminol can be used to treat a HR below 50 beats/min. In patients with high lesions, previous surgery, or radiation, the baroreceptors are not functional, and therefore no premedication is required.

Dopamine infusion is started if systolic BP is under 80 mmHg and the period of hypotension lasts longer than 3 min, despite intravenous administration of a 500-ml bolus of normal saline solution. In the treatment of hypotension, patients started on dopamine usually require its continuation beyond the conclusion of the procedure. The maximum dopamine dose in these patients averaged 7.8±2.9 μg/kg per minute. Patients with a history of severe underlying coronary artery disease tend to have a greater incidence of hemodynamic fluctuations.

There appears to be a statistically significant association between the insertion of large stents (more than 10 mm in diameter and 40 mm in length) and the need for dopamine. Dopamine was used in 38% of carotid procedures in which large stents were deployed. No dopamine was used with smaller stents ($p<0.05$). No patient in whom the stent was both less than 10 mm in diameter and less than 40 mm in length required a vasopressor (Mendelsohn et al. 1998).

We routinely use a stent 8 mm in diameter and 20–40 mm in length. Hemodynamic changes have not occurred in our patients. Hemodynamic changes usually do not occur in the postoperative period if the patient leaves the angiographic suite in stable condition.

14.16.5 Intervention

During the early experience with CAS, most operators noted periods of hypotension, bradycardia, and even asystole, for which a femoral venous line is placed at the beginning of the procedure in case a temporary transvenous pacemaker was needed. Currently, in most centers, a venous line is placed only in patients with a cardiac history or as a precaution when the operator is still at the beginning of his/her experience in CAS.

For current self-expandable stents, a 7- to 9-F delivery catheter, or a long, 5- to 7-F sheath is needed to deploy a stent of sufficient caliber to

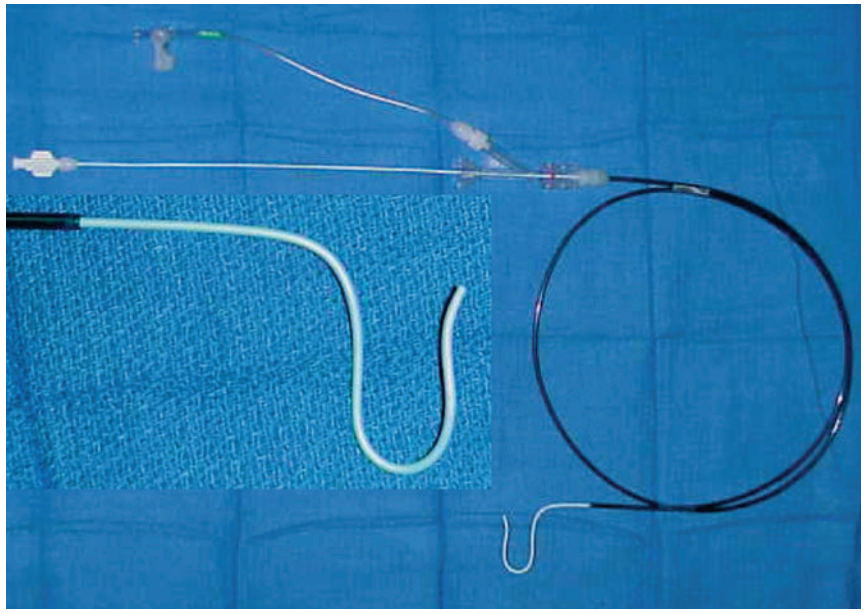

Fig. 14.147. Coaxial assembly system including a 9-F coaxial catheter with a leading Vitek-Manny type curve (*inset*)

cover a common carotid artery (CCA) 7–10 mm in diameter. The stent profiles are decreasing and smaller delivery systems are being used. If a delivery catheter is used, we prefer to have an introducer sheath at the arteriotomy site.

The CCA is catheterized in the usual fashion. Several points of caution should be noted. To avoid distal embolization, do not cross the stenosis with a large guidewire or catheter. To safely place the large-bore catheter in the CCA, a coaxial catheter assembly system works best. A preshaped inner catheter such as the Vitek (Cook) or Mani (Cook) curve is used inside an 8- to 9-F delivery catheter (Fig. 14.147) to engage the ostium of the desired CCA (Fig. 14.148C). Contrast material injection permits assessment of the vessel's status and a control angiogram is done. With the catheter at the CCA ostium, a road map of the bifurcation is obtained to facilitate guidewire placement (Fig. 14.148).

The guidewire used in this part of the procedure should be able to torque and should be stiff enough to permit advancement of the large-caliber outer catheter. The inner (5-F) catheter–guidewire combination is a good support for this maneuver. In addition, we suggest a long exchange-type guidewire (260–300 cm). We favor the long 0.038-in. Terumo hydrophilic wire, but on occasion, in difficult tortuous vessels, stiffer guidewires such as the Amplatz long exchange guidewire may be needed. In general, the guidewire is placed in the ECA for safety (Fig. 14.148D, E).

Once the delivery catheter is placed in the CCA, the area of stenosis is crossed with a small-gauge, long exchange cardiac-type microguidewire, 0.014 in. or preferably 0.018 in., which must be compatible with the various balloons and stent delivery systems. As in other procedures, a review of compatibility with the various materials is planned prior to the procedure.

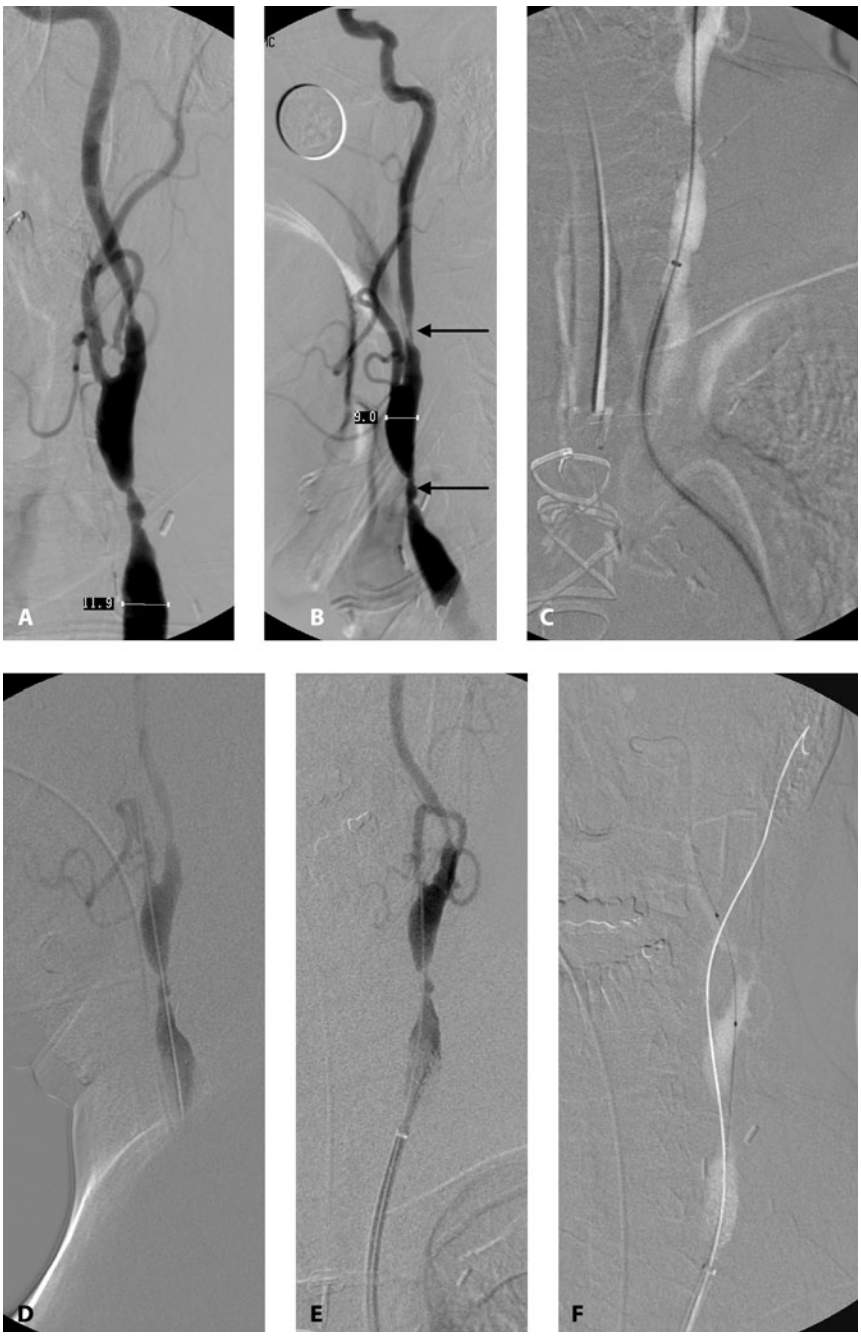

Fig. 14.148A–N. Carotid bifurcation stenting technique. **A, B** Digital subtraction angiogram (DSA) of the common carotid artery in a patient with previous endarterectomy with restenosis on both the proximal and the distal anastomotic sites. The proximal common carotid artery measures 11.9 mm. The distal common carotid artery (CCA) measures 9 mm. Note the two stenotic lesions at the site of surgical anastomosis (*arrows*). **C** Road map of the aortic arch was obtained with the white mask image from the Vitek (Cook, Inc.). The guidewire was placed in the external carotid artery (**D** lateral and **E** frontal images). With that support, the 9-F catheter is advanced using the guidewire and the coaxial catheter for support. The catheter delivery system was placed in the CCA proximal to the lesion. **F** Road map of the CCA. The *white line* shows the original position of the guidewire in the external carotid artery. Note now the predilatation balloon catheter of 2x4 mm in size crossing the most distal stenosis at the distal anastomotic site. Prior dilatation of the more proximal stenosis was done on the way up. **G–N** see p. 1157, 1158

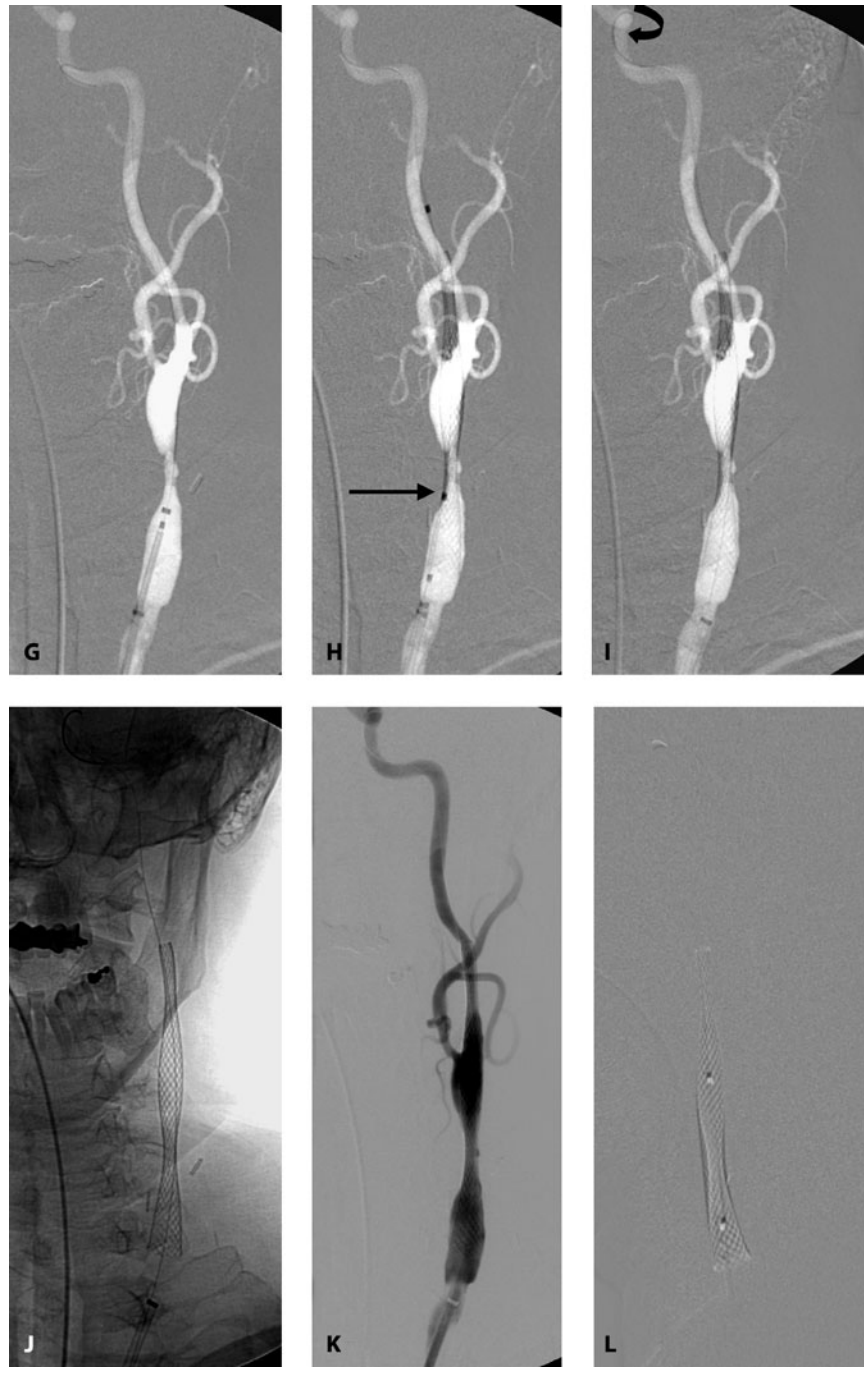

Fig. 14.148 (*continued*). **G–I** The deployment of the self-expandable Wallstent. **G** The stent prior to exiting the introducer catheter. **H** The expanded stent with the most distal marker. Note the shortening of the stent. There is a marker at the midportion of the stent (*arrow*) that indicates that the stent could be re-sheathed. Once crossed, it is no longer possible to retrieve the stent. The proximal marker points to the most proximal location of the stent. **I** The stent has been fully deployed, and the introducer delivery system has been withdrawn, maintaining the guidewire in position (*curved arrow*). **J** Plain film demonstrating the stent with a waist at the proximal stenosis. **K** DSA shows the good dilatation of the distal stenosis, but persistent narrowing of the proximal stenosis. **L** Road map image following balloon dilatation of the stent. The new stent dimensions are seen in black. **M, N** see p. 1158

Fig. 14.148 (*continued*). **M** Plain film showing the dilated proximal stent. **N** Angiographic examination after proximal dilatation shows the excellent restoration of the caliber and the good apposition of the stent against the vessel wall, despite the caliber differences from the CCA to the internal carotid artery

Guidewire manipulation is kept to a minimum to avoid distal embolization, vasospasm, or dissection. If crossing the lesion proves difficult or if there is difficult anatomy the lesion is best crossed with a soft, neuromicroguidewire followed by a neuromicrocatheter (Fig. 14.149). The microcatheter is advanced to cross the stenosis, and then the neuromicroguidewire is replaced for a stiffer, long exchange microguidewire. If there is any question of intraluminal lucencies or ulcerations, the neuromicrocatheter can be used to infuse a small amount of thrombolytics prior to crossing the lesion.

The exchange guidewire is now beyond the lesion and we suggest a high position in the petrous-cavernous carotid level, but keeping the distal segment of the guidewire within the field of view at all times. Visualization of the guidewire throughout the various exchanges permits stabilization of its position, which helps avoid spasm or injury to the vessel wall. The guidewire distal segment should have a long radiopaque segment.

The importance of the guidewire throughout the procedure must be emphasized. As long as the guidewire is in the vessel lumen, beyond the lesion, the procedure is under full control. Even if a complication occurs, such as dissection or occlusion, one can usually resolve the problem, while keeping the guidewire distal to the lesion. The use of road mapping is

helpful to monitor stability of the guidewire. If the proper position of the guidewire is lost spasm or vessel occlusion may occur (Fig. 14.149E). If this happens and the lumen is to be recrossed, a softer system with neuromicrocatheters and microguidewires can solve the problem. If the guidewire position is lost and there is no distal flow there is a possibility of spasm; an infusion of papaverine or nitroglycerin may be of great assistance to find the true lumen (Fig. 14.149G). Once back flow can be reestablished, and contrast material confirms the intraluminal position of the microcatheter, the soft microguidewire is exchanged for a heavier supporting guidewire, and a low profile balloon-expandable stent is deployed, covering the most distal area of narrowing (Fig. 14.145H–J).

It is important to recognize dissection by the catheter as evidenced by contrast material beyond the expected lumen, stagnation, and noncircumferential lining of contrast material (Fig. 14.150). As mentioned previously, maintaining the guidewire in the true lumen will make it possible to solve the problem in nearly all instances. With the guidewire in place, a balloon-expandable stent is deployed, opposing the dissection toward the vessel wall. It is important to determine the full extension of the dissection and cover its full length. If after deploying the stent one realizes that the full extent of the lesion has not been covered, an additional overlapping stent should be deployed (Fig. 14.150F, G).

Fig. 14.149A–L. Techniques of guidewire–stent placement. Severe stenosis secondary to a chronic dissection of the left internal carotid artery (ICA). **A** Lateral digital subtraction angiogram (DSA) of the left common carotid artery shows severe stenosis approximately 1 cm distal to the carotid bulb and extending to the precavernous carotid artery. **B** The lesion is very tight. Crossing the lesion with a Prowler 10 (Cordis Endovascular) microcatheter produced total flow arrest in the carotid artery. **C–L** see pp. 1160, 1161

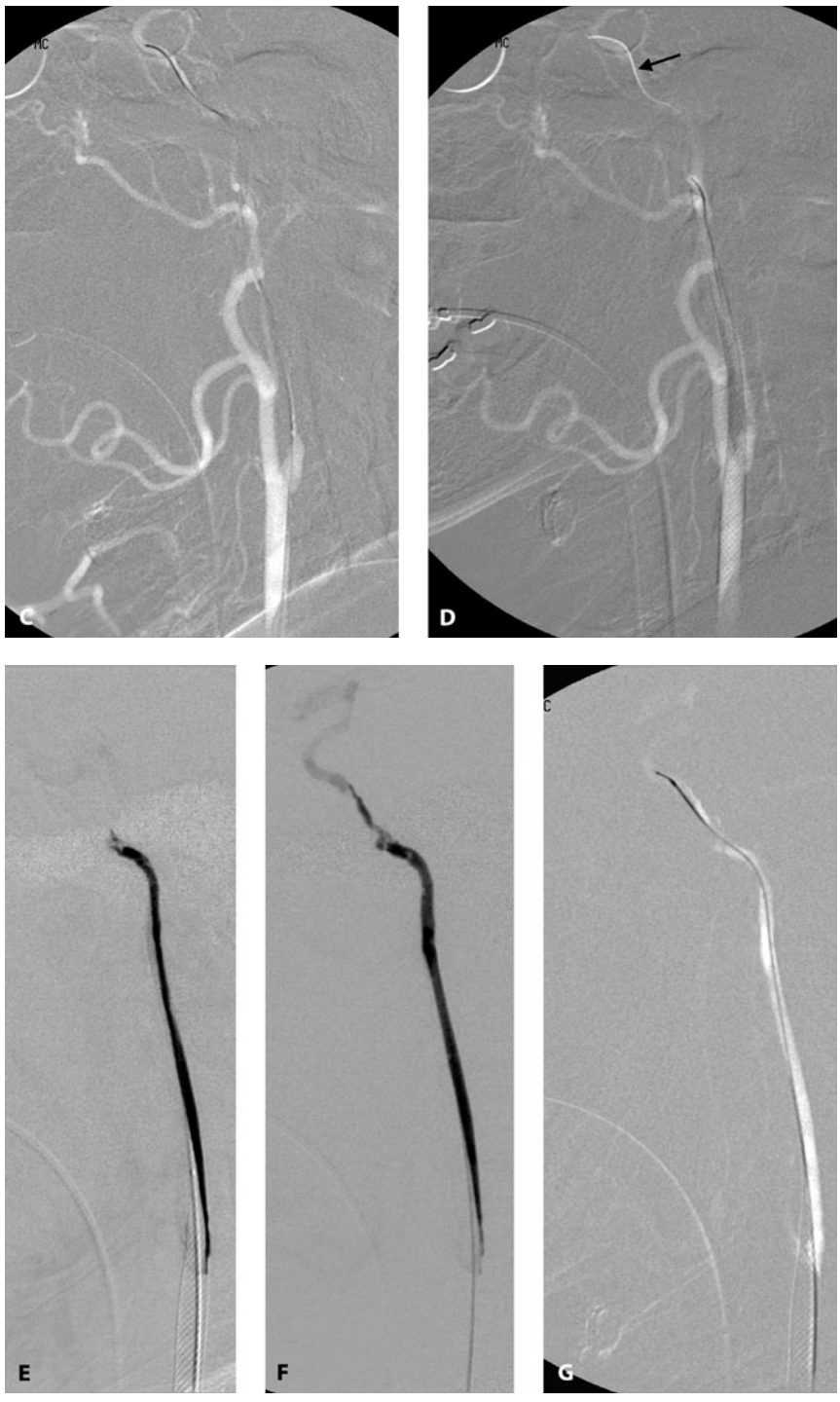

Fig. 14.149 (*continued*). **C** A soft microguidewire is advanced into the normal cavernous segment of the internal carotid artery, with the microcatheter beyond the diseased ICA. **D** After exchanging the guidewire for a stiffer wire with more support, a self-expandable stent was deployed in the cervical carotid artery. Following stent deployment, the position of the microguidewire was unintentionally lost. Note the *white line* from the original position (*arrow*). **E** Total immediate occlusion of the carotid artery occurred. **F** Progressive revascularization. Using papaverine first, the antispasmodic opens the carotid artery, which was in severe spasm. Note the severe disease in the precavernous carotid, which may mean guidewire dissection. **G** The true lumen is found using a soft microcatheter/microguidewire technique, to recross the long lesion. **H–L** see p. 1161

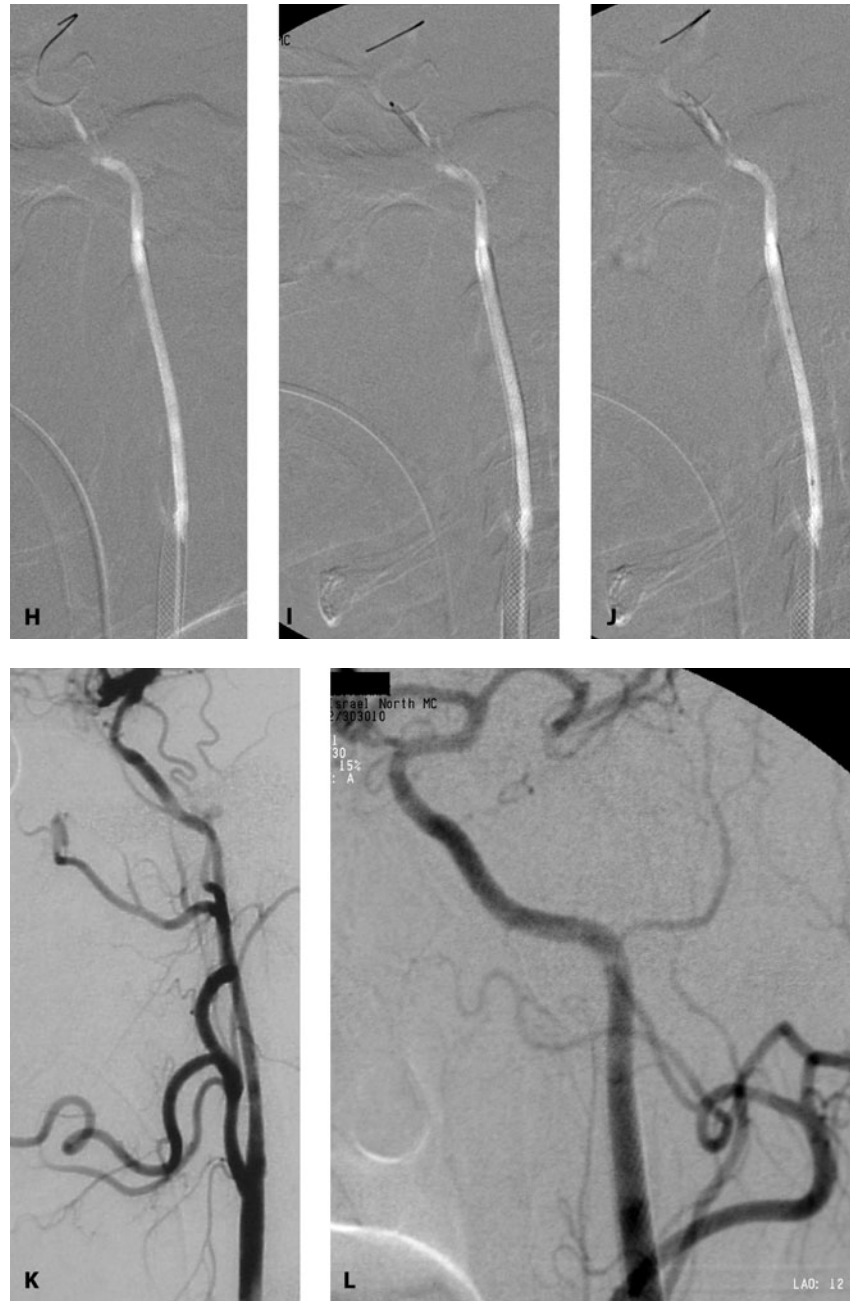

Fig. 14.149 (*continued*). **H** The neuromicroguidewire was then exchanged for a better support: a 300-cm-long exchange guidewire. **I, J** An AVE GFX (Medtronic, Santa Rosa, CA, USA) flexible balloon-expandable stent was deployed to revascularize the ICA. **I** The balloon-mounted stent crossed the stenotic segment, **J** the balloon was inflated to 6 atm of pressure and the stent was expanded and deployed. **K, L** DSA of the common carotid artery after revascularization. Note the excellent reestablishment of carotid lumen

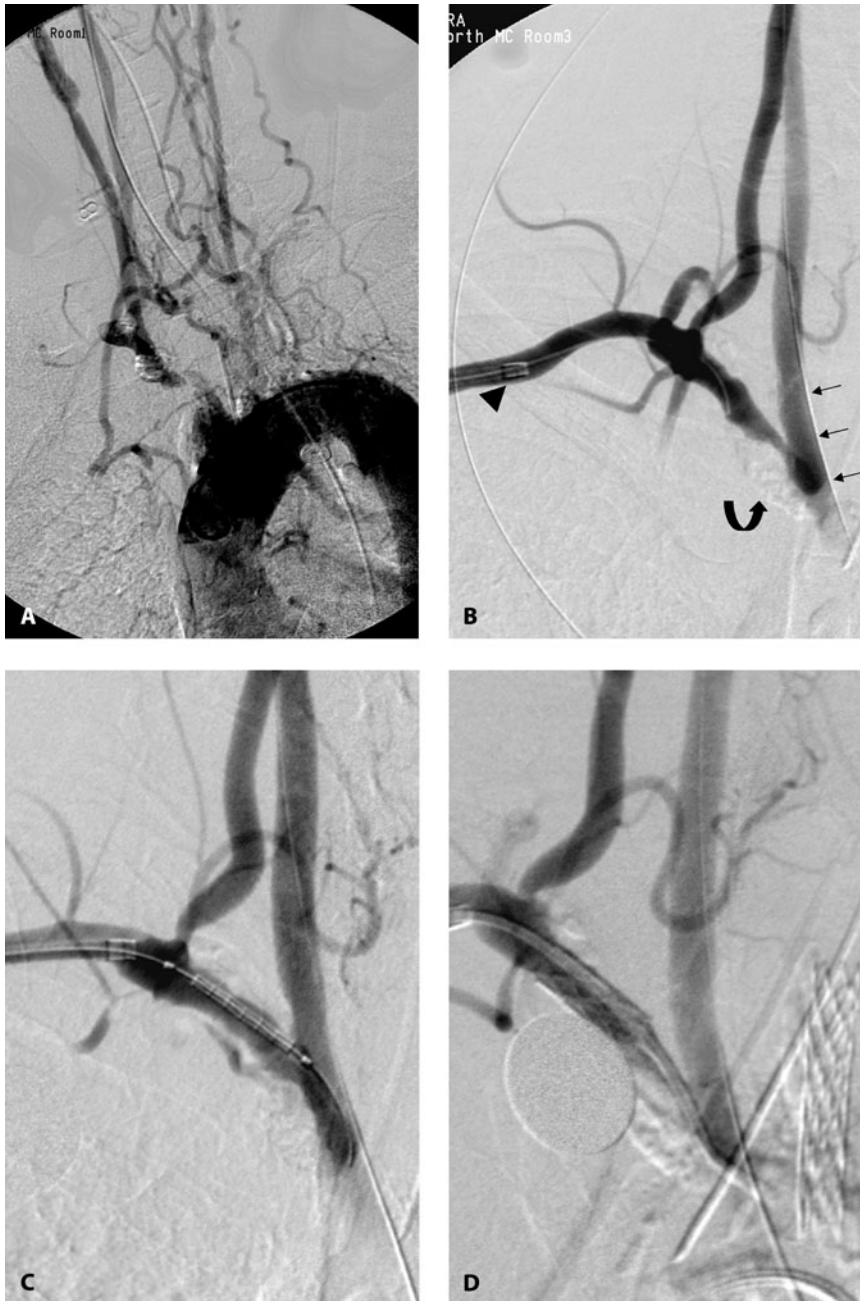

Fig. 14.150A–I. Techniques of revascularization. A 76-year-old female patient with severely disabling global cerebral ischemia and severe vascular disease. **A** Aortic arch study, late arterial phase, demonstrates severe disease involving all brachiocephalic vessels at their origin. There is total occlusion of the left subclavian artery, severe stenosis at the origin of the left common carotid, severe disease at the innominate, and at the origin of the right common carotid artery (CCA) there is atheromatous disease with severe calcifications. The subclavian artery on the right reconstitutes through the supreme intercostal to the internal mammary artery. There is additional disease at the origin of the distal right CCA. Collateral circulation is being taxed to the maximum. **B** Following a retrograde brachial approach on the right side (*arrowhead* points to the introducer catheter), flow in the proximal RTSA was established.
Continued on p. 1163

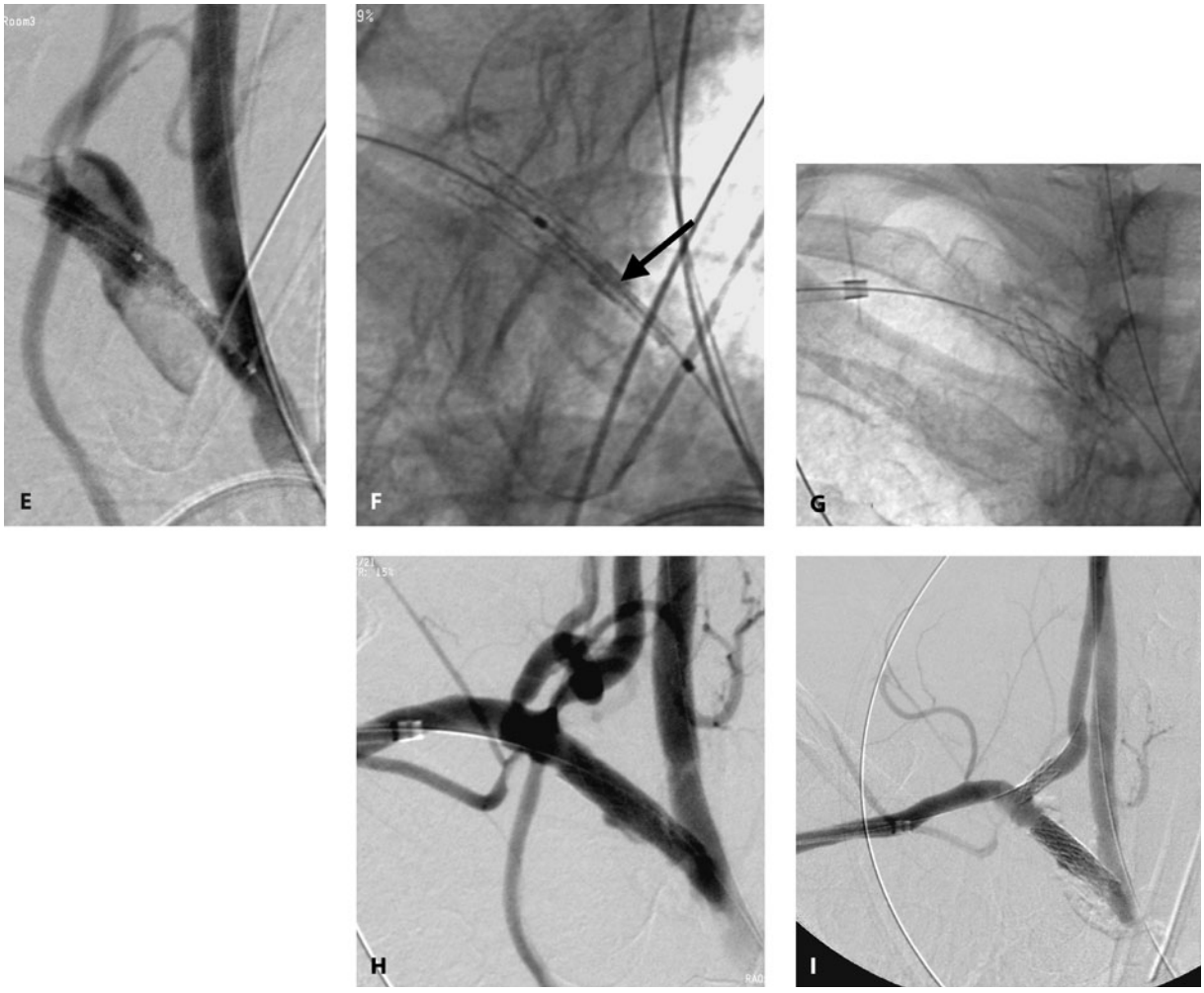

Fig. 14.150 (*continued*). In view of the very severe calcifications of innominate and CCA origin (*curved arrow*), prior to the catheterization of the subclavian artery a guidewire is placed in to the common carotid artery (*small arrows*) from a femoral approach, as a precaution, while the right subclavian-CCA origin is opened. **C** Digital subtraction angiogram (DSA) after the lesion was crossed with a support guidewire and a balloon-mounted stent was placed at the level of the lesion. **D** DSA of the expanded stent with the guidewire distally. The expanded stent is short and a portion of the stenosis is uncovered. **E** Monitoring angiogram demonstrates extravasation in the wall of the subclavian artery, showing a dissection, with the two guidewires still in place. **F** Cone-down view of a second unexpanded balloon-mounted stent placed in tandem passing through the first stent and covering the dissection (*arrow*) and the full extent of the lesion. **G** Cone-down view after the second stent was expanded. **H** DSA after the dissection was repaired. Note a small amount of contrast material at the lower portion. **I** Following angioplasty and stenting at the origin of the right vertebral artery, with excellent reestablishment of flow

14.16.6 Predilatation Angioplasty

Before inserting a self-expandable stent, predilatation is routinely performed with a noncompliance dilatation balloon, 4 mm in diameter by 40 mm in length. The length of the balloon-tipped catheter must be at least 120 cm. The catheter should accept at least a 0.014-in. guidewire. The predilatation angioplasty is a critical part of the procedure, as it is one of the times where distal embolization can occur. To decrease the chances of embolization, slow progressive dilatation to 6–8 atm is probably safest, over a relatively long period of time, 20–40 s, or with the use of a distal protection device. The predilatation is done to permit the larger stent to cross the lesion in a less traumatic fashion. In lesions at the carotid bulb, bradycardia or hypotension can develop during predilation.

Many varieties of such balloons are commercially available and are mostly comparable, with the operator's individual preference the main consideration. At present, monorail models that facilitate guidewire exchange are available and are gaining popularity. Monorail balloons have the advantage of using conventional-length guidewire, and a lower friction coefficient between the catheter and the guidewire over several centimeters, in comparison with coaxial balloons where the friction coefficient extends over more than 135 cm.

Following the predilatation, the guidewire is left in position and is used to deploy the stent.

14.16.7 Stent Selection

From Dotter's original conception of a vascular stent in 1969 to the present, revascularization techniques in general, and stent technology in particular, have advanced rapidly. Newer stents are being introduced and will likely further revolutionize the field of vascular revascularization. The important parameters that will help us in understanding some of their differences include:

1. Mechanism of deployment. There are two mechanisms of deployment: balloon-expandable stents and self-expandable stents.
2. Metal alloys. Stents are being made primarily from different combinations of corrosion-resistant steel alloys: nitinol alloys and platinum alloys.
3. Construction design. There are multiple design types. The cell-type construction relates to flexibility. A closed-cell design (Fig. 14.151A–C) has more radial force but also less flexibility. An open-cell design (Fig. 14.151D) has more flexibility but less radial force. The stent itself can be tubular, spring, coil, ring, or woven mesh, or combinations thereof. Each design has advantages and disadvantages. Present stents still do not fulfill the ideal characteristic for endovascular neurosurgical applications, as they have been developed for cardiac and peripheral applications (Table 14.6).

   Tubular design. The common feature in this design of stents is that they are laser cut from a continuous cylinder of stainless steel or nitinol. The tubular design covers the lesion better and has good resistance to ex-

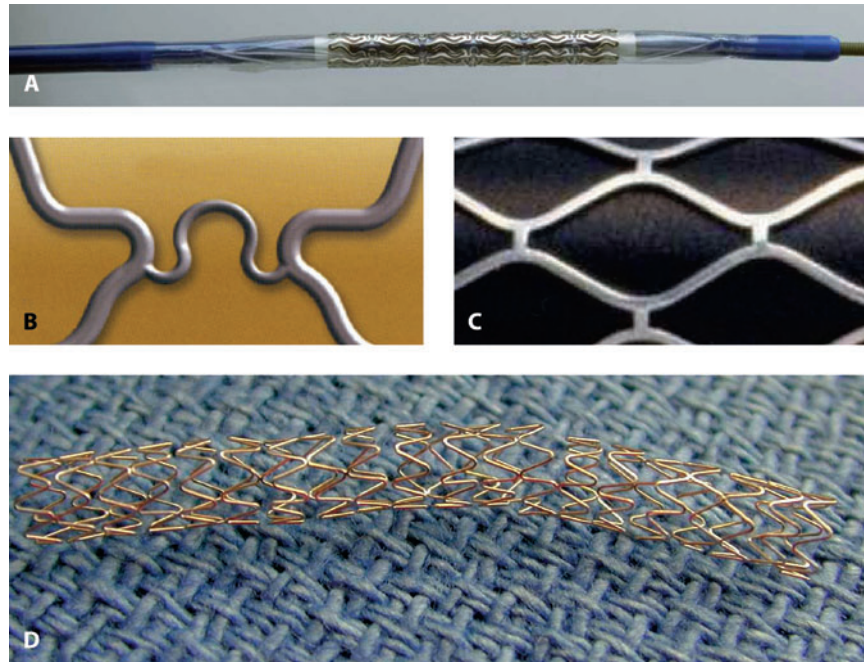

Fig. 14.151A–D. Balloon expandable stents. **A** Closed-cell tubular design Palmaz Corinthia (Cordis Endovascular). Tubular construction is an example of a balloon-expandable stainless steel stent using sophisticated Nesting balloon technology (Cordis Endovascular) to prevent premature deployment of the stent prior to expansion and deployment. Two different closed-cell types and different cell lengths are available. **B** Omega and **C** elliptical construction. **D** Open-cell balloon-expandable S60 (AVE/Medtronic)

Table 14.6. Stent selection

Deployment	Balloon-expandable	Self-expandable			
Metal alloy	Steel (corrosion resistant)	Nitinol	Platinum		
Construction	Tubular	Spring	Coil	Ring woven mesh	Combinations

ternal radial forces, but is relatively inflexible in the closed-cell design (Figs. 14.151A–C, 14.152).

Coil stents are manufactured from a single strand of metal wire woven into a particular pattern.

Ring devices are repeated nodules of short coils. Both these designs have better flexibility, but with an uneven expansion (Fig. 14.153).

Woven mesh designs are self-expanding, they are made of a steel, cobalt, and platinum mixture, or nitinol. Their main disadvantage is the often unpredictable shortening (less so with nitinol), and the delivery system is rigid, preventing placement in tortuous anatomy (Fig. 14.154). They can cover a long segment with a single stent (Fig. 14.155).

At present, most stents used in the cervical carotid artery are self-expanding, rather than balloon-expanding stents, and are made of a platinum and cobalt alloy (Wallstent, Magic Wallstent), or nitinol (SMART stent, Symphony, Guidance). Their performance appears similar, although no comparative studies are available. The longest experience at present is with the Wallstent, followed by the SMART stent (Fig. 14.156).

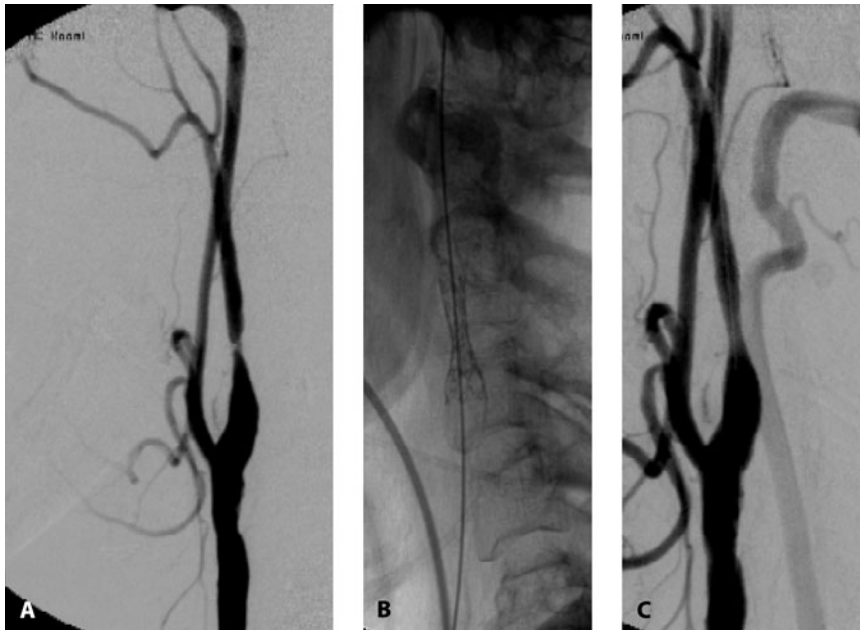

Fig. 14.152A–C. Tubular balloon-expandable stent. In the cervical carotid artery, self-expandable stents are preferable. In very short segments with significant caliber differences, balloon-expandable stents can be very useful, using the balloon to assist proper opposition of the stent to the vessel wall. **A** Before stenting. **B** Note the difference in distal and proximal stent expansion. **C** After treatment

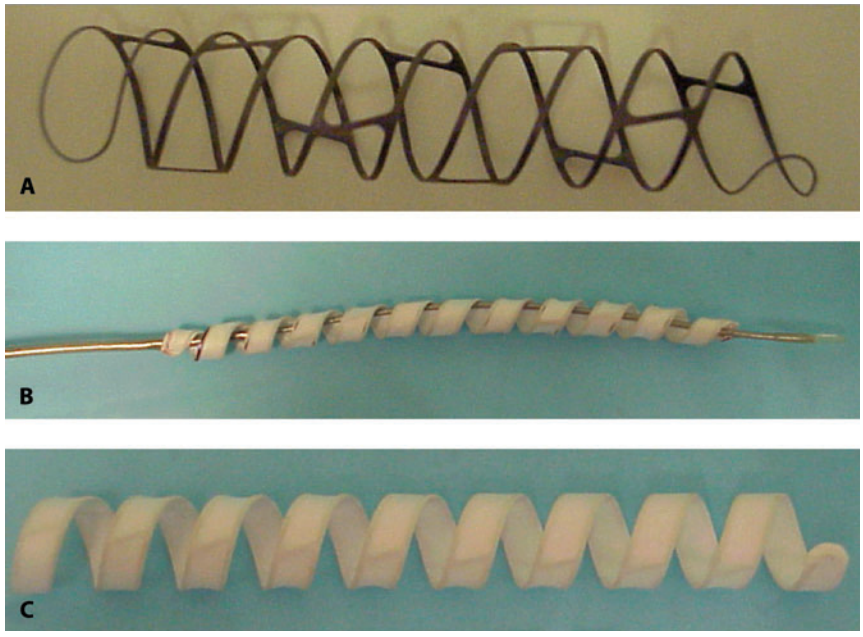

Fig. 14.153A–C. Coil design nitinol stent. Variations in coil design, with a self-expandable covering that can be modified

Nitinol stents appear to have lesser foreshortening than stents made of other materials (Fig. 14.157).

When possible, we prefer to use a single stent (Fig. 14.155). The stent diameter is important, and we usually select a stent 1–2 mm wider than the CCA, with a sufficient length to cover the lesions and obtain good apposition of the stent to the vessel wall. In addition, the cells within the stent will be closer, and act as a filter that will decrease the amount of debris that can migrate distally (Figs. 14.148–14.155).

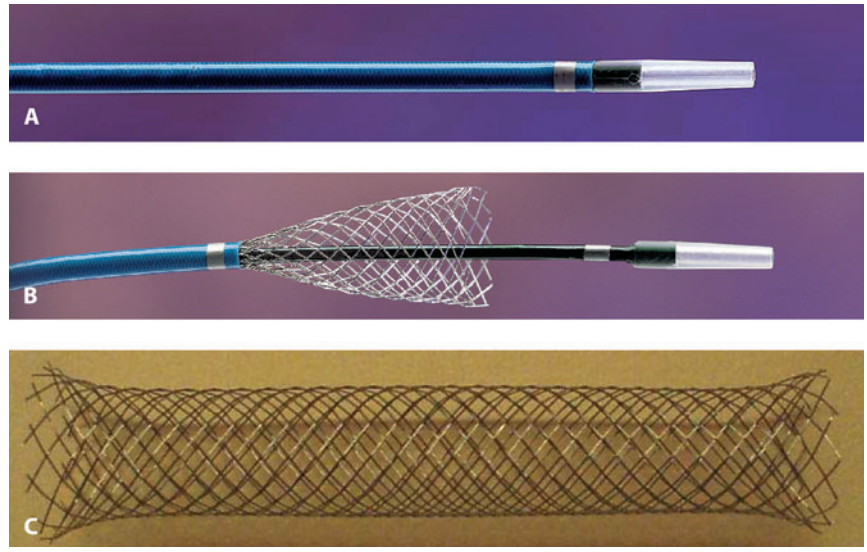

Fig. 14.154A–C. Mesh design, self-expandable stent. **A** The Wallstent (Target, Boston Scientific) is made of a platinum and cobalt alloy mesh. It is self-expandable. **B** Undeployed delivery catheter assembly system. It has significant rigidity and can reach vessels in the horizontal segment of the brachiocephalic arteries up to the petrous carotid artery. **C** Fully expanded stent. With the newer model of Magic Wallstent, half of the stent length can be deployed up to the mid level marker and can be resheathed back (see Fig. 14.143**H**)

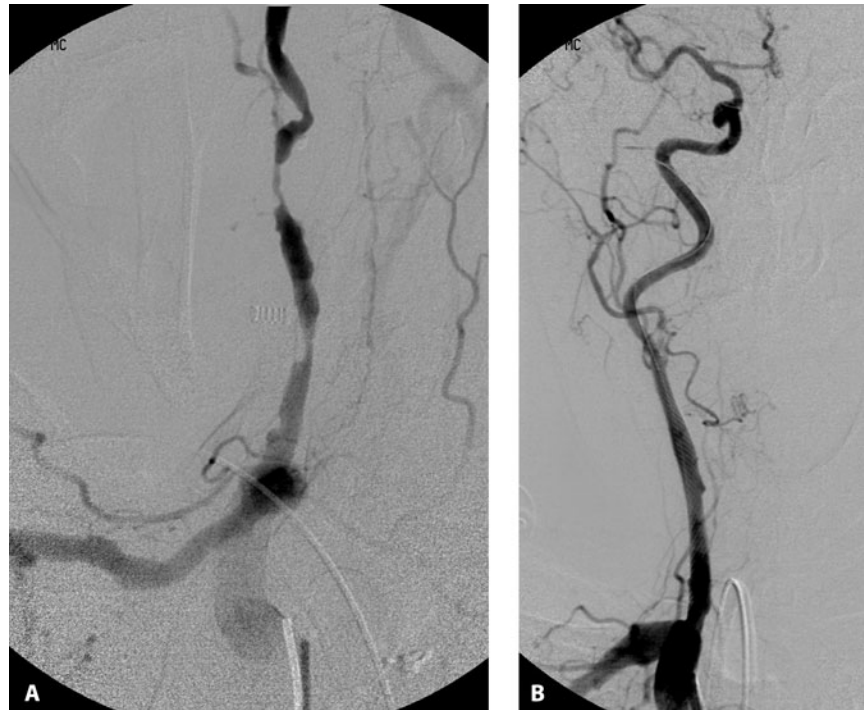

Fig. 14.155A, B. Long segment of involvement. **A** Postradiation severe atheromatous disease. Note the long segment of involvement. **B** Following the stent deposition, note the ability of a single stent to cover the entire pathology, despite various caliber vessels. The guidewire is still in place

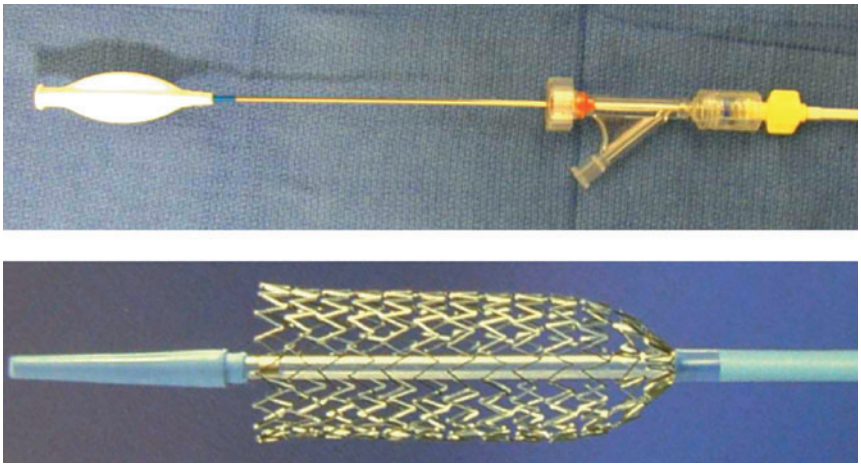

Fig. 14.156. Nitinol self-expanding stent. The SMART stent (Shape Memory Alloy Recoverable Technology, SMART; Cordis Endovascular). Self-expandable tubular design nitinol stent with similar limitations as the other self-expandable stents

Fig. 14.157A, B. Nitinol self-expanding SMART (Cordis Endovascular). **A** Lateral view shows a discrete severe stenosis at the origin of the internal carotid artery as well as some involvement of the posterior wall of the common carotid artery. Note the discrepancy between the bulb-size proximal and distal carotid arteries. **B** Digital subtraction angiogram demonstrates the remodeling of the carotid artery bifurcation with preservation of the external carotid artery despite crossing of the stent at the ostium of the external carotid artery. There is narrowing at the origin of the external carotid artery

14.16.7.1 Self-Expandable Stents

The Wallstent (Fig. 14.154) has been used in the largest number of patients, with excellent short- and mid-term results. It is a self-expanding inner-core platinum and outer-layer cobalt-based alloy mesh construction stent, restrained within a protective sheath. The platinum gives it good radiopacity, and it is MRI compatible. The Wallstent possesses a braided geometry in a tubular mesh configuration. The braided wires are wrapped the entire length of the stent. The braided construction predisposes the stent to adopting a linear rather than curvilinear configuration, resulting in vessel straightening. Its self-expandable construction allows it to conform to the arterial wall to optimize endothelialization. Dynamic radial force maximizes laminar flow and minimizes elastic recoil. Mesh construction flexes with neck movements, preventing crushing. Wallstent comes in many diameters and lengths, which makes it possible to use a single stent most times for a good fit, and to cover long segments, even if confronted with variable lumen size (Fig. 14.155). Halo technology improves its radiopacity. Its major disadvantage is unpredictable shortening, which is dependent on a number of factors such as the ratio between the vessel variable size and the stent size. For the most part, the distal end of the stent can be accurately deployed, but the proximal end is not predictable. The length is usually oversized to cover the ECA, which carries no consequences. The diameter should be 1 or 2 mm larger than the CCA for best vessel apposition. Wallstents are easy to recross after implantation, with excellent scaffolding. They are relatively flexible, which allows them to taper and adapt within the changing caliber of a vessel (Fig. 14.148). They will straighten vessel loops and bends, displacing them toward the edges of the stent, and may result in undesirable restriction in flow, the loop stops at the petrous carotid level.

The Magic Wallstent is a self-expandable wire mesh constrained by a retractable outer sheath. It is made of an inner core of platinum, with an outer layer of cobalt-based alloy. The platinum gives it good radiopacity, it is MRI compatible, although it has a 15%–20% shortening on expansion. It has three radiopaque markers, with the middle marker being at the half-deployment level (Fig. 14.148G). It is fully repositionable up to its half release, which is at the middle marker. Like the Wallstent, it is easy to recross after implantation, with excellent scaffolding. It is relatively flexible, which allows it to taper within the changing caliber of a vessel, and it will straighten vessel loops and bends. It is 1-F larger in diameter than the original Wallstent, and only the 10-mm stent cannot be introduced through a 9-F guiding catheter or a 7-F sheath. At present, it is our preferred stent.

14.16.7.2 Nitinol

The newer nitinol devices are promising. The term “nitinol” is derived from (ni)ckel, (ti)tanium, and (N)aval (O)rdinance (L)aboratories of the United States Government, where nitinol was first developed during the 1960s. Nitinol, a nickel-titanium alloy, is the most elastic metal presently

available (superelasticity), it has the property of shape memory. Nitinol will assume a predetermined shape when heated above a preset transition temperature. In stent manufacturing, the preset transition temperature is set at 26°–32°C. Heating induces a phase transformation in the alloy. The atomic arrangement changes from a martensite phase, in which the material is very malleable, to an austenite phase, in which the material exhibits a high degree of strength and superelasticity, which gives nitinol a high degree of flexibility, as well as kink and fatigue resistance. Uncovering the stent in the circulation exposes the stent to body temperature, whereon it immediately assumes its memorized shape (Figs. 14.156, 14.157). Nitinol stents have a spring-like behavior of crush recoverability if an external force deforms or compresses the stent; its shape memory and superelasticity will immediately reassume its expanded shape after removal of the external stress. This is a major advantage in the soft tissues of the neck and with the movements of the neck, making it very suitable for the cervical carotid artery.

Nitinol stents appear to have better conformability, permitting better adaptation to the vessel's contour, reducing the straightening of the anatomy. With the stainless steal mesh construction, the lack of conformability tends to relocate the arterial loops and redundancies to the proximal and distal ends of the stent, which may result in kinking of the artery at the stent margins. With the Wallstent, this problem is more frequent. However, we have seen no flow restriction problems (nor have any been reported), and the loop seems to stop at the petrous carotid level. On the other hand, with nitinol stents, if placed at a vessel bend the stent may not conform sufficiently to the anatomy and may protrude into the vessel wall, requiring a second device. In addition, the segmented-hoop geometry may make recrossing the stent more difficult, as reported by Phatouros et al. (2000). With a stainless steal mesh construction, the vessel straightens and this problem is avoided.

As with other self-expandable stents and probably more so with nitinol, the stents will exert a chronic outward radial force on the arterial wall. The long-term effect of the shape memory stents is not known at present and its compensatory effect to diminish the consequence of intimal hyperplasia is a potential advantage to all self-expandable stents. Mathias (personal communication), has observed improvement of vessel diameter in the follow-up of patients treated with the Wallstent, so that the effects of intimal hyperplasia is compensated by the chronic outward radial force on the arterial wall. The difference between the different self-expandable stents is not known at present.

The Smart stent has a more accurate deployment, is made of a more elastic metal alloy, with minimal shortening, and is probably best for tortuous anatomy and ostial lesions. The stent will comply best to vessels with changing caliber such as the carotid bulb (Fig. 14.157). The foreshortening is less than 8% at its hub end. The stent has segmented-hoop geometry with very short individual segments (Fig. 14.156).

Guidant has introduced a tapering carotid stent (Guidant Corporation, Menlo Park, CA, USA) (Fig. 14.158) that will be part of a randomized study. Our experience is limited to the research laboratory.

Fig. 14.158. Guidant's tapering carotid stent (Guidant Corporation, Menlo Park, CA, USA)

14.16.7.3 Balloon-Expandable Stents

Balloon-expandable stents are generally tubular, with various designs in their cell configuration, and its articulations give them a gamut of profiles, flexibilities, and resistance to vessel recoiling. The first balloon-expandable stent used in the cervical carotid bifurcation was the Palmaz balloon-expandable stent.

The balloon-expandable Palmaz stent and the articulated slotted tube Palmaz-Schatz stent are no longer used in the cervical carotid arteries, because of their potential for crushing.

Palmaz stents are made of a tubular 316L stainless steel construction, with a slotted tube articulated design. They may be useful in ostial lesions such as the origin of the CCA, subclavian, or vertebral arteries, or if a very accurate deposition without shortening is needed. They are balloon expandable and made of 316L stainless steel, with moderate radiopacity, are MRI compatible, with a diamond-shaped strut design (Fig. 14.46). Shortening on expansion varies from 2.5% to 5.3%. It comes premounted or bare. Two radiopaque markers at the ends assist in deployment. It can easily be recrossed after deployment. The articulated omega design of the Corinthian stent (Cordis Endovascular) has more flexibility than the original Palmaz stent, comes premounted, with added security in its fixation to the balloon (nesting technology), to prevent accidentally losing the stent prior to balloon expansion. They come in various sizes and are very useful for accurate deployment at the origin of the brachiocephalic vessels (Fig. 14.159).

14.16.7.4 Low-Profile Balloon-Expandable Stents

The third- and fourth-generation coronary stent technology has introduced lower-profile stents with improved flexibility, using an open-cell design (Fig. 14.151D). Some of these stents are being used in neuroendovascular applications with good results, and several corporations have active programs to develop derivatives of these stents for neurological applications.

Of the currently available models, the Medtronic AVE Micro Stent II, the GFX, and the GFX II, S670 (Fig. 14.160) are the more suitable for distal tortuous anatomy.

More recently the Neuroform (Target, Boston Scientific), a highly flexible open-cell self-expandable nitinol-construction stent, has been a major breakthrough and will improve the neck protection (Fig. 14.40). It has been used in the brachiocephalic and intracranial circulations.

14.16.7.5 GFX II

The GFX II (Fig. 14.39) is a sinusoidal ring-design balloon-expandable stent with a low profile, made of stainless steel individual 2-, 3- or 4-mm crown segments welded together using laser fusion technology. The welding is either at all junctions (fully connected), or at half of the junctions

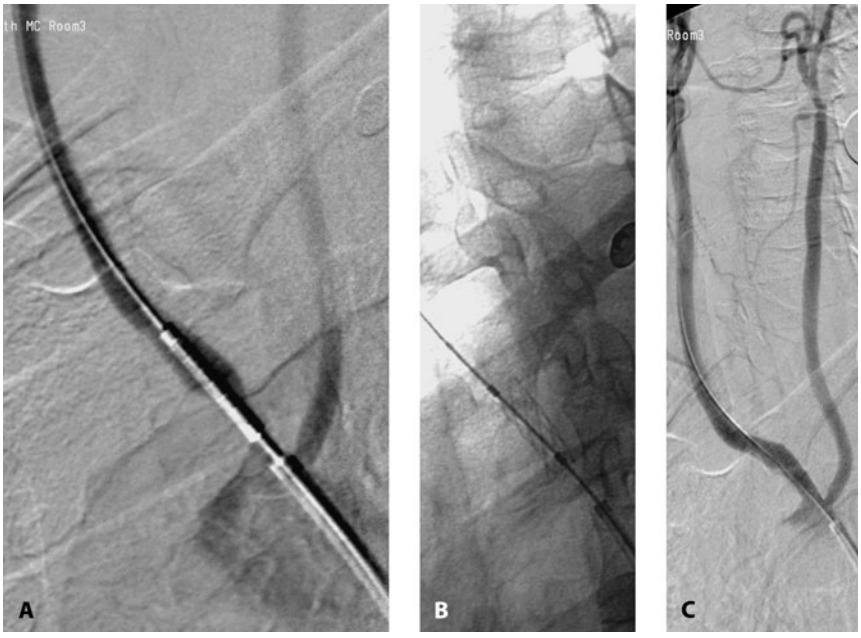

Fig. 14.159A–C. Balloon-expandable stent deployment in the origin of the right common carotid artery. **A** Oblique view of the aortic arch and the introduction of a Corinthian (Johnson & Johnson, New Brunswick, NJ, USA) stent at the ostium of the common carotid artery. **B** Stent after expansion. There is moderate radiopacity to the stent. Bony landmarks are used in anatomical areas with inherent movement. **C** Angiogram demonstrates an accurate revascularization with preservation of the origin of the common carotid artery on the left

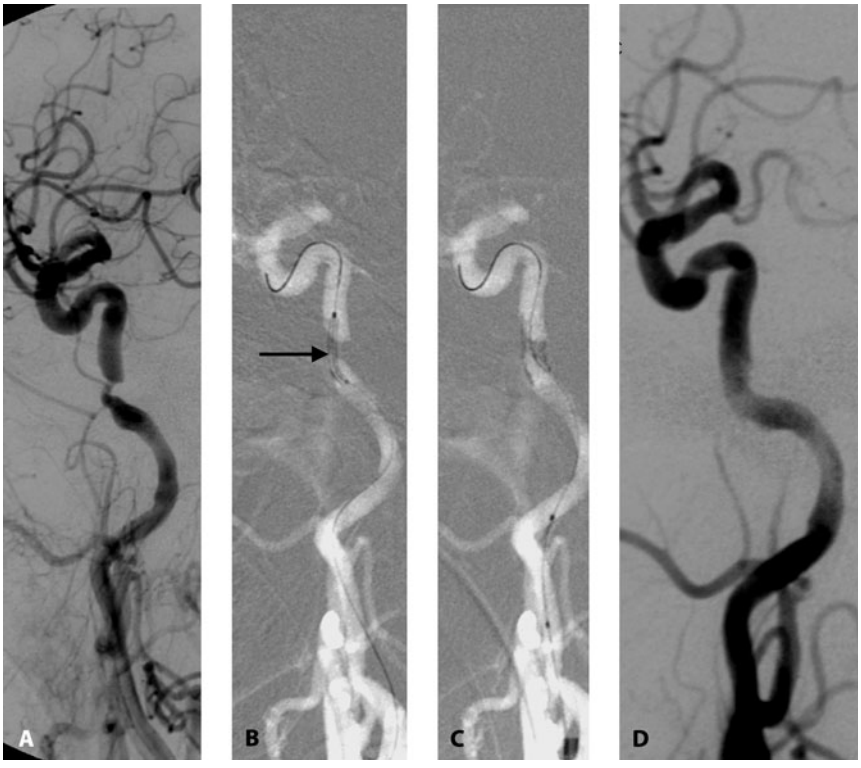

Fig. 14.160A–D. Flexible balloon expandable stainless steel stent. AVE GFX stent. **A** Lateral digital subtraction angiogram (DSA) of the left internal carotid artery showing a severe stenosis at the petrous segment. **B, C** Crossing the lesion with the balloon-mounted stent (*arrow*) as it goes through tortuous anatomy and crosses the lesion, with balloon inflation and deployment of the stent (**C**). **D** Lateral DSA examination after balloon-expanded stent placement, with excellent reconstitution of the normal caliber of the carotid artery

(half connected). The length of the stent depends on how many segments are welded together. The half-connected segments give an exceptional degree of longitudinal flexibility, and their low profile allows them to pass through 6-F guiding catheters. The fully connected GFX II has the radial strength of a tubular design and the flexibility of a coil.

These stents are very useful in lesions at the distal ICA (Fig. 14.160), as scaffolds, or for coil embolization in wide-neck aneurysms (Figs. 14.92, 14.93).

14.16.8 Postdeployment Angioplasty

Following stent deployment, if a waist is seen at the area of stenosis, (Fig. 14.148L), or if the stent is not well opposed to the vessel wall, a postdeployment balloon angioplasty is performed. The balloon diameter is sized to the internal carotid artery, usually 5–6 mm in diameter and 2 cm in length. The postdilatation angioplasty is the more risky part of the procedure, where distal embolization is more likely to occur, as debris is squished through the porous portion of the stent (Ohki et al. 1998; Ohki and Veith 2001). It is at this point, where distal protection should be of most value, as the lumen has all ready been improved; therefore there is less chance for the protection device (balloon or other) to embolize as it crosses the area of stenosis.

14.16.8.1 Distal Cerebral Protection

To enhance safety and avoid distal migration of debris from the site to be dilated and stented, various devices are being proposed. Balloon-tip devices or parachute-like filtering devices placed distal to the lesion are in evaluation, and others are being tested (Figs. 14.161–14.163).

Theron (1990) originally reported the use of a triaxial system, which uses a latex balloon that occludes the ICA beyond the stenosis. The balloon is inflated prior to the various maneuvers obtaining cerebral protection, thus avoiding distal embolism. After each balloon dilatation, the debris is aspirated, and/or flushed or washed into the ECA.

Prior to flow arrest in the ICA, one must study the status of the circle of Willis, and the status of the extracranial-to-intracranial anastomosis, prior to flushing emboli in to the ECA, to avoid unwanted cerebral embolization.

The recent introduction of more sophisticated distal protective devices is likely to make the procedure even safer.

The GuardWire device (Figs. 14.161, 14.162; PercuSurg Inc., Sunnyvale, CA, USA), consists of the GuardWire, a 0.014-in. steerable angioplasty guidewire made of a hollow nitinol hypotube, with an elastomeric inflatable balloon incorporated at the tip of the wire. The proximal hypotube wire incorporates a Microseal, which allows inflation and deflation of the balloon. The GuardWire is advanced through the introducer catheter previously placed in the CCA proximal to the stenosis. The deflated low-profile GuardWire is placed distal to the stenosis, and placed at the petrous

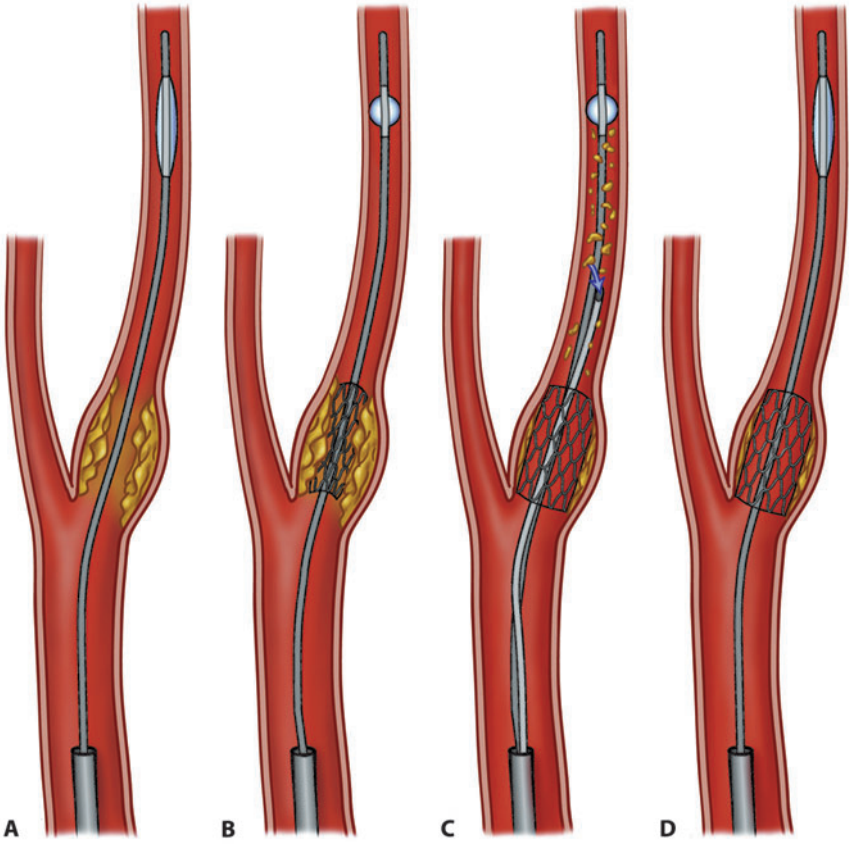

Fig. 14.161A–D. Schematic illustration of the GuardWire (PercuSurg Inc., Sunnyvale, CA, USA) balloon protection technique. **A** The deflated low-profile balloon is passed distal to the lesion where the stent is to be deployed. **B, C** The stent is deployed with the balloon inflated so that the debris can be trapped. If necessary, a postdeployment angioplasty is also done with the balloon inflated. The debris is suctioned back through the 5-F catheter, the balloon is then deflated (**D**)

carotid or in a straight portion of the carotid artery. A Microseal adapter is attached to the hypotube, and the balloon is slowly inflated with a fixed volume of half-strength contrast material to close the carotid artery. The Microseal adapter is then detached and the balloon will remain inflated. Angioplasty and stenting is then done. The debris is aspirated by a special aspiration catheter, which is advanced over the guidewire, and manual suction is applied. The Microseal adapter is then reattached to deflate the balloon and blood flow reestablished.

A modification of the PercuSurg device has been introduced: the Medicorp Henry, Amor, Frid, and Rufenacht device (HAFR), it adds a radiopaque marker at the protective compliant balloon for localization, and any steerable guidewire can be used. We have no experience with this device.

Roubin is introducing a parachute-like filter device, and Yaved a different model, a filtering device that permits blood to flow, but debris to be stopped. Another similar filter has been developed by Guidant (Fig. 14.163). The advantage of such protective devices is that they do not arrest flow distally, and they prevent vasospasm. All these devices are at various stages of development or evaluation, and therefore not yet in clinical use, but it is obvious that some type of distal protection will become the norm. Until they become easy touse and reliable, we have not seen more than 1% clinical deficits without any distal protection.

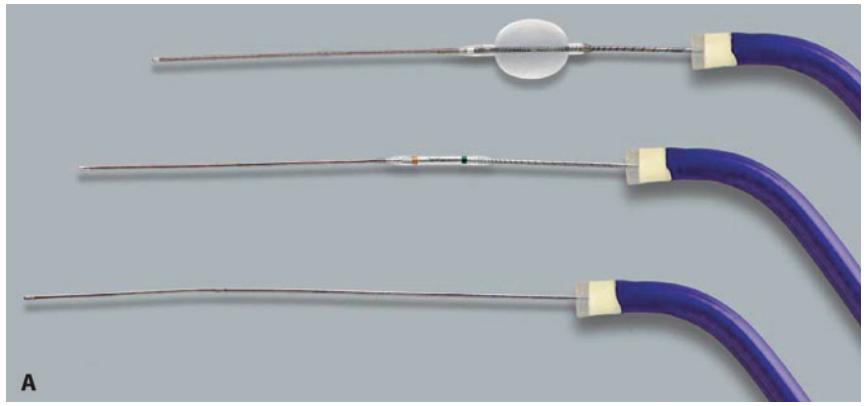

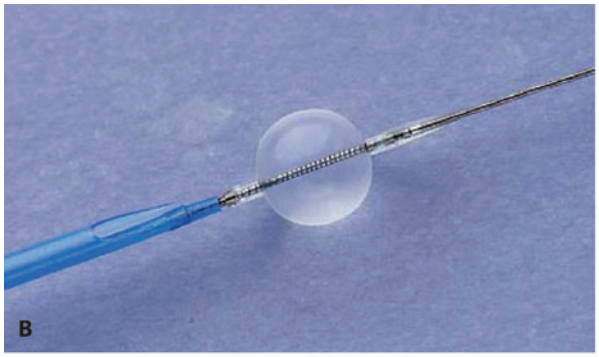

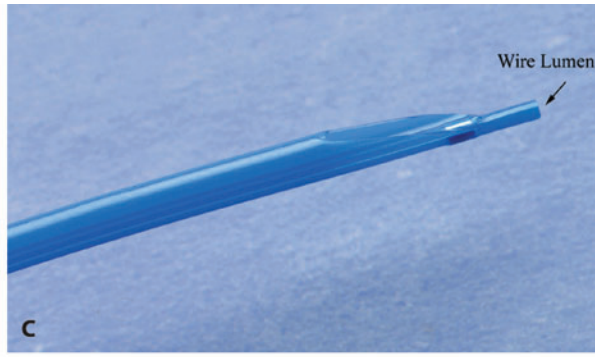

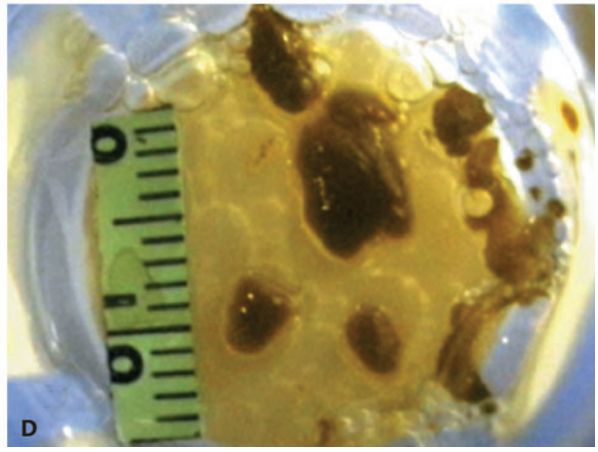

Fig. 14.162A–D. The GuardWire system has a low crossing profile. **A** A 0.14-in. guidewire crosses the lesion followed by the 0.036-in. (0.92-mm) crossing profile of the deflated balloon. The balloon then inflates in the petrous carotid artery to arrest flow. **B** Balloon inflated with a proximal large board out fish mouth 5-F catheter (**C**), which permits backwashing of the embolic debris. **D.** Close-up view of some material obtained during suction

Fig. 14.163A, B. Aculynker (Guidant Corporation). This design uses an open basket or parachute placed beyond the lesion, to trap the debris. **A** The open device. **B** The closed device

14.16.9 Mechanical Revascularization of Totally Occluded Brachiocephalic Vessels

Although experience in mechanical revascularization is increasing, the indications for opening totally occluded vessels have remained limited, but as seen in the peripheral circulation, it is possible. In the brachiocephalic arteries, the fear of distal embolization has inhibited its aggressive use. However, there are territories such as the subclavian artery, when a hemodynamic steal exists, where revascularization is less likely to embolize (Fig. 14.164).

Regarding the age of the occlusion, it appears intuitively that the fresher the occlusion, the more likely that mechanical (similarly to chemical) recanalization will be possible, although the risk of distal embolization is probably more.

In our limited experience, it is relatively easy to mechanically open main brachiocephalic vessels (Figs. 14.149, 14.164; also see Sect. 1.2.7.4, Chap. 1, this volume).

One additional technique of revascularization in cases of stent collapse or difficult access may require a two-arteriotomy-site approach (Fig. 14.165). Access is first obtained trough one entry site, for example the brachial artery, and a second entry site through a femoral artery. A heavy support guidewire is pulled with a snare from one arteriotomy to the other, providing access to then deliver a stent and repermeate the occluded segment or repair the collapsed stent (Fig. 14.165).

Fig. 14.164. Subclavian steal on the left side (**A** and **B**). **C–G** see p. 1177

Fig. 14.164 (*continued*). **C** A road map is obtained from injection into the right vertebral artery (VA), and the origin of the left VA can be obtained and used as the map; the larger delivery catheter and wire are placed at the ostium of the occluded VA, and a lumen is created. This is gently probed until the true lumen on the other side is reached (**C**). **D** The larger catheter is passed beyond the occlusion, and the stent is deployed (**E**, **F**). Balloon-expandable stents are more accurate in these locations (**G**)

Fig. 14.165A–F. Repair of a collapsed stent, using a two-arteriotomy-site approach. **A** Aortic arch study demonstrates severe stenosis of the innominate artery, where previously placed stents had collapsed (*curved arrow*). There was also total occlusion of the right common carotid artery (CCA), the left CCA, a stent in the left SA, and bilateral axillary to CCA by-passes, and bilateral endarterectomies on both CAs. **B** Plain film of the chest demonstrates the collapsed proximal stent (*curved arrow*). **C** Digital subtraction angiogram (DSA) shows the severe stenosis (*curved arrow*). **D** Balloon angioplasty from the brachial approach failed to properly expand the collapsed stent. From the femoral site, a heavy support guidewire was snared from below (*arrow*) and used to deploy a stent within the collapsed stent. **E, F** see p. 1179

14.16.10 Complications of Mechanical Revascularization

The main complication from mechanical revascularization relates to distal embolization, vessel dissection (Figs. 14.149, 14.150), occlusion, or rupture. The main caution to be taken to avoid the majority of complications

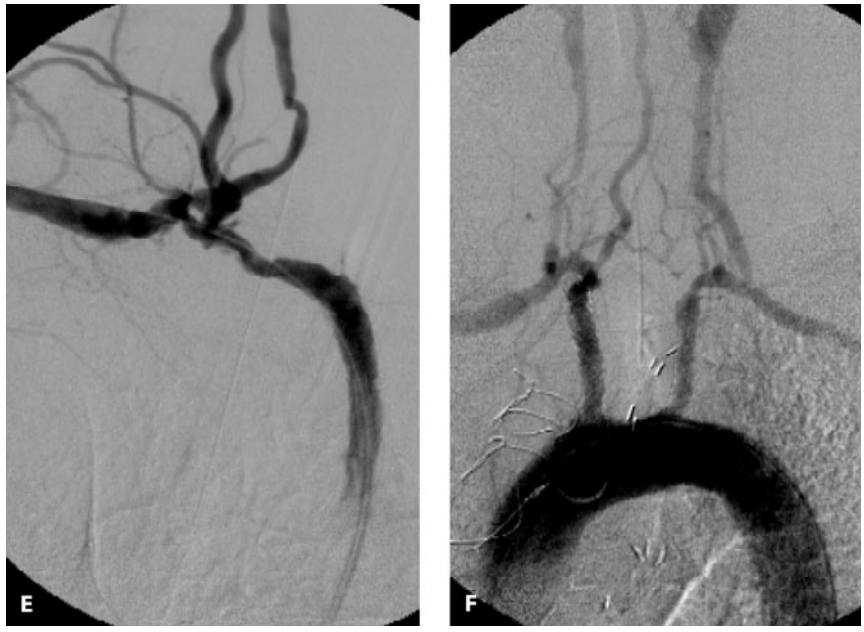

Fig. 14.165 (*continued*). **E** DSA after revascularization. **F** Aortic arch study after stenting of the right SA

is *not* to lose the guidewire. If this happens, vessel occlusion is possibly related to spasm, so that papaverine or nitroglycerin should be tried first to find the true lumen. Then the integrity of that vessel segment should be addressed, followed by a decision as to whether it is necessary to repair that segment with a stent (Fig. 14.149).

In intracranial iatrogenic dissections, a relatively easy maneuver can be the use of a microcatheter to flatten the dissection, permitting the antegrade flow to clip the flap opposed to the vessel wall (Fig. 14.166).

14.16.11 Stent Retrieval

Our experience in stent retrieval is limited, but being prepared for such an event and knowing what to do may be very beneficial. The best recommendation is to prevent this from happening by proper selection and meticulous technique.

A technique described in the peripheral and cardiac experience is illustrated in Figs. 14.166 and 14.167. If there has been partial deployment of the stent, one can anchor and trap a partially deployed stent within the guiding catheter with the assistance of the balloon, by jamming the balloon to fix the stent. If necessary, the balloon may be slightly inflated and the stent brought into a peripheral vessel; there it is deployed (Fig. 14.166). As an alternative, or when the stent has been fully deployed or has prematurely become loose, one may use a snare (Figs. 14.96, 14.168A). In this case, the guidewire is left in the lumen of the stent, a second guidewire is introduced and placed on the outer aspect of the stent, between the stent and the delivery catheter wall. A snare device (Fig. 14.168B) is then used to trap and retrieve the stent. The two-guidewire technique is safer, as it prevents the stent from recoiling or kinking (Fig. 14.168B).

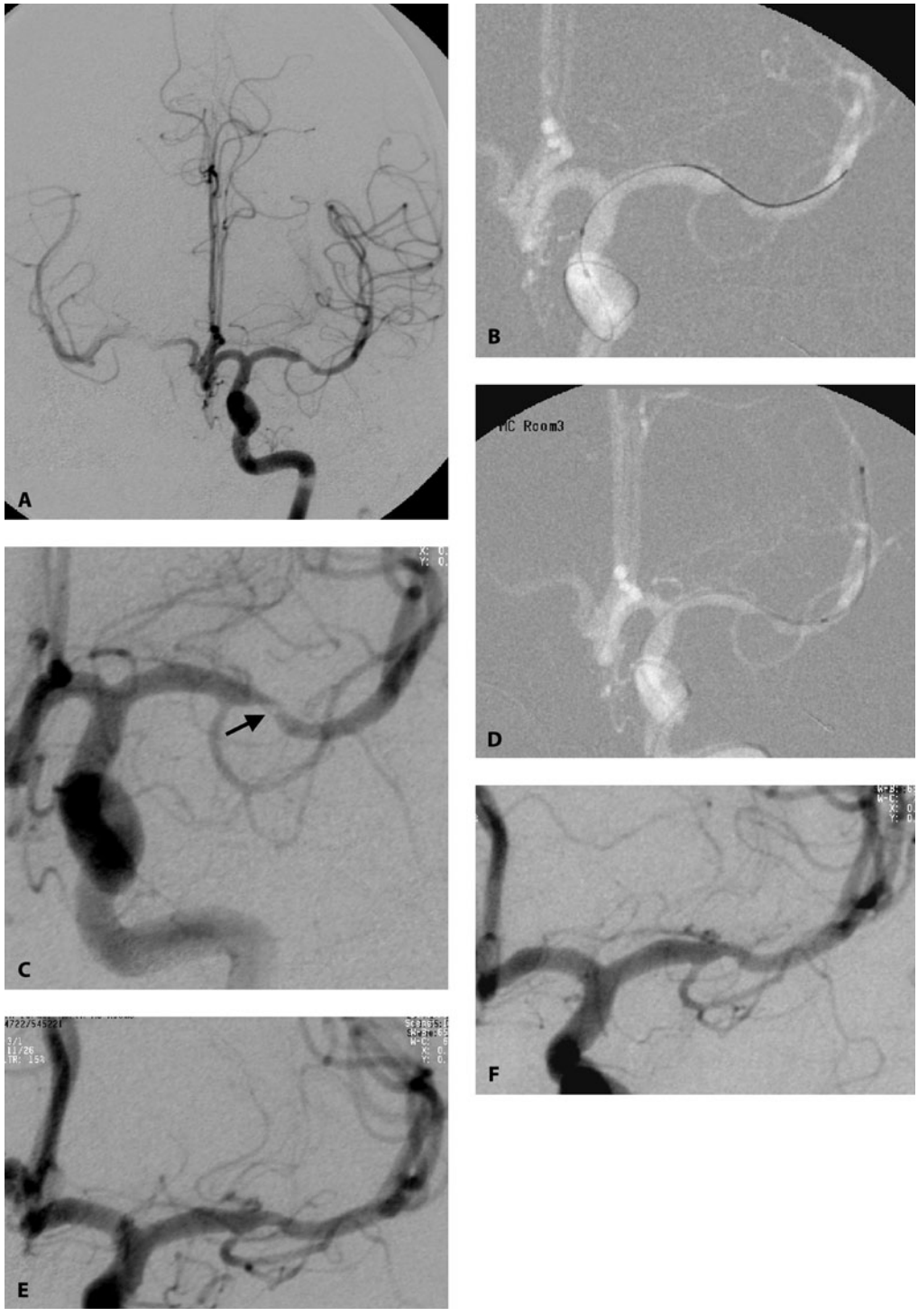

Fig. 14.166A–F. Middle cerebral stenosis and iatrogenic dissection. **A** Digital subtraction angiogram (DSA) AP of the left internal carotid artery with a symptomatic stenosis of the M1 segment, not responding to medical therapy. **B** A balloon-expandable stent is being advanced into the middle cerebral artery for dilatation and stenting. Due to siphon tortuosity, the stenosis could not be reached. **C** There is a flap in the M1 (*arrow*). A balloon-tip catheter also could not reach the flap. An over-the-guidewire microcatheter was then passed beyond the flap (**D**), which resulted in a good immediate outcome (**E**) confirmed 1 week later (**F**)

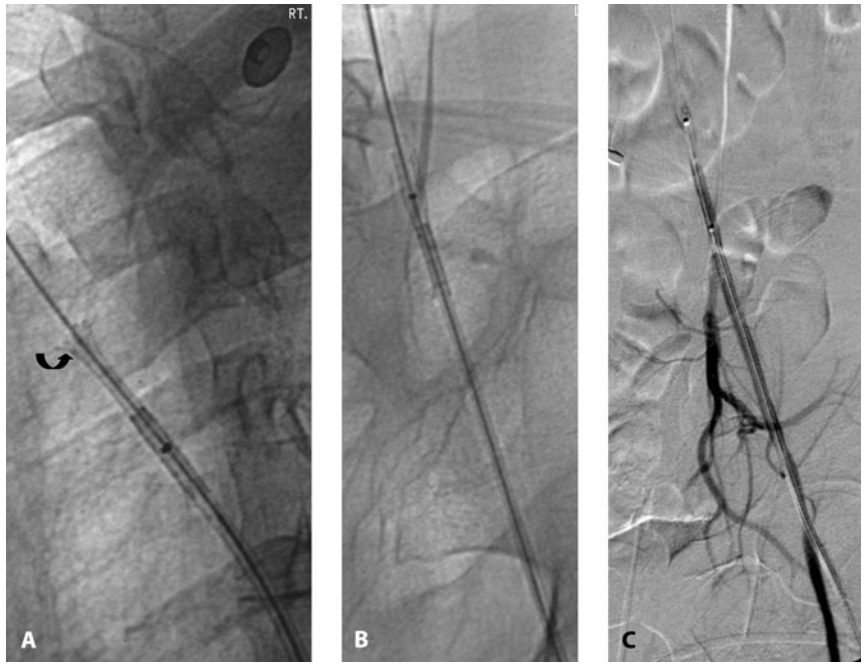

Fig. 14.167A–C. A balloon-expandable stent needs to be removed. **A** If the stent is not fully deployed (*curved arrow*) and the guidewire is distal, the delivery catheter is advanced to trap and fix the stent. Partial balloon inflation can assist in fixing the stent. **B** The assembly is retrieved and is fully deployed in the iliac artery (**C**)

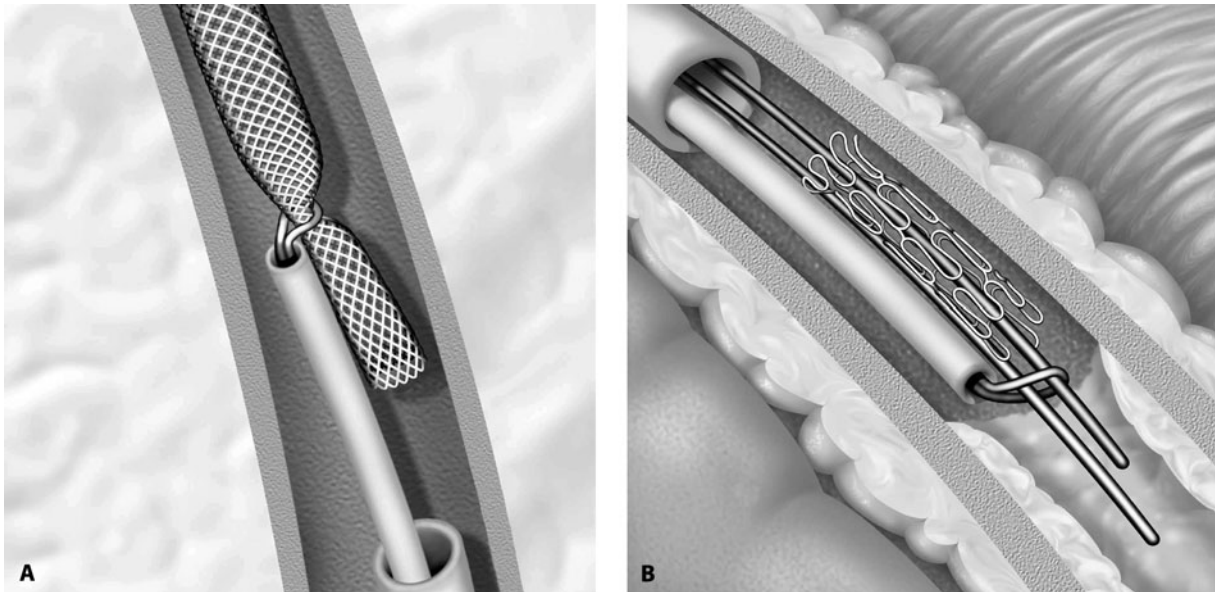

Fig. 14.168. **A** Stent retrieval. **B** Two-guidewire retrieval technique. One wire is passed through the inner lumen of the stent, and the second wire is on the outer part of the stent. This maneuver will prevent the stent from traumatizing the vessel wall, by trapping the stent between both wires

References

Abboud F (1981) Special characteristics of the cerebral circulation. Fed Proc 40:2296–2300

Abdulrauf S, Kaynar M, Awad I (1999) A comparison of the clinical profile of cavernous malformations with and without associated venous malformations. Neurosurgery 44:41–47

Abele J (1978) Balloon catheters: what is available, how they are made and how they are used. MediTech Division

Abercrombie J (1828) Pathological and practical researches of the brain and spinal cord. John Carfrae and Son, Edinburgh

ACAS (1994) Clinical advisory: carotid endarterectomy for patients with asymptomatic internal carotid artery stenosis. Stroke 25:2523–2524

Acevedo JC, Turjman F, Sindou M (1997) L'artériographie post-opératoire dans la chirurgie des anévrysmes intra craniens. Neurochirurgie 43:275–284

Ackerman R, Lev M, Mackay B, Katz P, Babikian V (1989) PET studies in acute stroke: findings and relevance to therapy. J Cereb Flow Metab 1989:S359

Adams H, Brott T, Furlan A et al (1996) Guidelines for thrombolytic therapy for acute stroke: a supplement to the guidelines for the management of patients with acute ischemic stroke. Circulation 94:1167–1174

Adams J (1967) Patterns of cerebral infarction: some comments on their topography and pathogenesis. Scott Med J 12:339–348

Adams JE, Dams PH, Mamtora H, Isherwood I (1981) Computed tomography and the localisation of parathyroid tumors. Clin Radiol 32:251–254

Adams WM, Laitt RD, Davies M, Donavan GO (1999) Familial tumoral calcinosis: association with cerebral and peripheral aneurysm formation. Neuroradiology 41:351–355

Adamson J, Humphries SE, Ostergaard JR, Voldby B, Richards P, Powell JT (1994) Are cerebral aneurysms atherosclerotic? Stroke 25:963–966

Afshar JK, Doppman JL, Oldfield EH (1995) Surgical interruption of intradural draining vein as curative treatment of spinal dural arteriovenous fistulas. J Neurosurg 82:196–200

Agarwal MK, Gupia OP, Smamant HO, Gupia S (1980) Neurilemmoma of the maxillary sinus. J Oral Surg 38:698–699

Agarwal S, Willinsky RW, Montanera W, Ter Brugge K, Wallace MC (1992) Superselective angiography of a spinal dural arteriovenous fistula having a common segmental origin with the artery of Adamkiewicz. Neuroradiology 34: 352–354

Agnoli AL (1982) Vascular anomalies and subarachnoid haemorrhage associated with persisting embryonic vessels. Acta Neurochir (Wien) 60:183–199

Aguirre F, Topol E, Ferguson J et al (1995) Bleeding complications with the chimeric antibody to platelet glycoprotein IIb/IIIa integrin in patients undergoing percutaneous coronary intervention. Circulation 91:2882–2890

Al-Yamany M, TerBrugge KG, Willinsky R, Montanera W, Tymianski M, Wallace MC (2000) Palliative embolisation of brain arteriovenous malformations presenting with progressive neurological deficit. Intervent Neuroradiol 6:177–183

Albores-Saavedra J, Espino-Duran M (1968) Thyroid carcinoma and chemodectoma. Am J Surgery 116:887–890

Albrecht R (1959) Die Wasenchentumoren und ihre Behandlung. Arch Ohr 8: 175:1–68

Albright AL, Latchaw RE, Price RA (1983) Posterior dural arteriovenous malformation in the infancy. Neurosurgery 13:129–135

Aletich VA, Debrun GM, Monsein LH et al (1995) Giant serpentine aneurysms: a review and presentation of five cases. Am J Neuroradiol 16:1061–1072
Alexander E, Wigser SM, Savis SM, Davis CH (1966) Bilateral extracranial aneurysms of the internal carotid artery. Case report. J Neurosurg 25:437–442
Alexandrov A, Norris J (1997) Cervical ultrasound. In: Welch K, Caplan L, Reis D, Siesjo B, Weir B (eds) Primer on cerebrovascular diseases. Academic Press, San Diego, pp 614–620
Alford BR, Guilford FR (1962) A comprehensive study of tumors of the glomus jugulare. Laryngoscope 72:765–805
Ali S, Jones WI (1982) Clinical records: extranasopharyngeal angiofibromas (sex incidence and age distribution). J Laryng Otol 96:559–565
Ali S, Aird W, Bihari J (1983) Pain inducing laryngeal paragangliomas (nonchromaffin). J Laryng Otol 97:181–188
Alleyne CH Jr, Krisht A, Yoo FK, Silverstein A, Colohan AR (1997) Bilateral persistent trigeminal arteries associated with cerebral aneurysms and aortic arch vessel anomaly. South Med J 90:434–438
Almaani WS, Richardson AE (1978) Multiple intracranial aneurysms: identifying the ruptured lesion. Surg Neurol 9:303–305
Alpers B, Berry R (1963) Circle of Willis in cerebral vascular disorders. The anatomical structure. Arch Neurol 8:398–402
Ambrosetto P, Albrosetto G, Michelucci R, Bacci A (1983) Sturge-Weber syndrome without port-wine facial nevus. Report of 2 cases studied by CT. Childs Brain 10:387–392
Ameli NO, Abbassioun K, Saleh H, Eslamdossi A (1985) Aneurysmal bone cysts of the spine: report of 17 cases. J Neurosurg 63:685–690
Aminoff MJ (1973) Vascular anomalies in the intracranial dura mater. Brain 96:601–612
Aminoff MJ (1976) Spinal angiomas. Blackwell, Oxford
Aminoff MJ, Kendall BE (1973) Asymptomatic dural vascular anomalies. Br J Radiol 46:662–667
Aminoff MJ, Logue V (1974) The prognosis of patients with spinal vascular malformations. Brain 97:197–210
Aminoff MJ, Barnard RO, Logue V (1974) The pathophysiology of spinal vascular malformations. J Neurol Sci 23:255–263
Ancri D, Pertuiset B (1985) Instantaneous measurements of flow velocity in internal carotid arteries by pulsed Doppler in cerebral arteriovenous malformations. Neurochirurgie 31:1–6
Anderson RM, Blackwood W (1959) The association of arteriovenous angioma and saccular aneurysm of the arteries of the brain. J Pathol Bacteriol 77:101–110
Andeweg J (1996) The anatomy of venous collateral flow from the brain and its value in aetiological interpretation of intracranial pathology. Neuroradiology 38:621–628
Andoh T, Shirakami S, Nakashima T, Nishimura Y, Sakai N, Yamada H, Tanabe Y, Funakoshi T (1992) Clinical analysis of a series of vertebral aneurysm cases. Neurosurgery 31:987–993
Andrews RJ, Spiegel PK (1979) Intracranial aneurysms. Age, sex, blood pressure, and multiplicity in an unselected series of patients. J Neurosurg 51:27–32
Anon V, Aymard A, Gobin Y et al (1991) Balloon occlusion of the internal carotid artery in 40 cases of giant intracavernous aneurysm: technical aspects, cerebral monitoring, and results. Neuroradiology 34:245–251
Anonymous (1988) Editorial: cerebral aneurysms: clip or coil? Surg Neurol 50:395–402
Anonymous (1994) Use of a monoclonal antibody directed against the platelet glycoprotein IIb/IIIa receptor in high-risk coronary angioplasty. N Engl J Med 330: 956–961
Anonymous (1996) Practice advisory: thrombolytic therapy for acute ischemic stroke-summary statement. Report of the Quality Standards Subcommittee of the American Academy of Neurology. Neurology 47:835–839
Anonymous (1997) Randomised placebo-controlled trial of abciximab before and during coronary intervention in refractory angina: the CAPTURE study. Lancet 349:1429–1435

Anshun W, Feng L, Dawing W (2000) Giant serpentine aneurysms: multidisciplinary management. Report of four cases and review of the literature. Intervent Neuroradiol 6:41–52
Anson J, Spetzler R (1993) Endarterectomy of the intradural vertebral artery via the far lateral approach. Neurosurgery 33:804–811
Anson JA, Spetzler RF (1992) Classification of spinal arteriovenous malformations and implications for treatment. BNI Quarterly 8:2
Antiplatelet Trialists' Collaboration (1988) Secondary prevention of vascular disease by prolonged antiplatelet treatment. BMJ 296:320–331
Antman E, Guigliano R, McCabe C et al (1998) Abciximab (ReoPro) potentiates thrombolysis in ST segment elevation myocardial infarction: results of TIMI 14 trial (abstract). J Am Coll Cardiol 31:191
Aoki N, Mizuguchi K (1984) Chronic encapsulated intracerebral hematoma in infancy: case report. Neurosurgery 14:594–597
Aoki N, Mizuguchi K (1986) Expanding intracerebellar hematoma: a possible clinicopathological entity. Neurosurgery 18:594–597
Apostol JV, Frazell EL (1965) Juvenile nasopharyngeal angiofibroma: a clinical study. Cancer 18:869–878
Archer C, Horenstein S (1977) Basilar artery occlusion. Stroke 8:383–390
Arnaud O, Bille F, Pouget J, Serratrice G, Salamon G (1994) Epidural arteriovenous fistula with perimedullary venous drainage: case report. Neuroradiology 36:490–491
Asaoka K, Houkin K, Fujimoto S, Ishikawa T, Abe H (1998) Intracranial aneurysms associated with aortitis syndrome: case report and review of the literature. Neurosurgery 39:157–160
Astrup J, Siesjo B, Symon L (1981) Thresholds in cerebral ischemia – the ischemic penumbra. Stroke 12:723–725
Atkinson JLD, Lane JI, Colbassani HJ et al (1993) Spontaneous thrombosis of posterior cerebral artery aneurysm with angiographic reappearance. J Neurosurg 79:434–437
Aubin A (1933) Récidive de polype nasopharyngien: extirpation totale par voie palatine. Ann Oto-laryngol 8:974–976
Auer LM, McKenzie ET (1984) Physiology of the cerebral venous system. In: Kapp JP, Schimdek HH (eds) The cerebral venous system and its disorders. Grune & Stratton, New York
Aufdemorte TB (1981) Hemangiopericytoma-like tumor of the nasal cavity. Arch Otolaryngol 107:172–174
Ausman J, Diaz F, Pearce J, de los Reyes R (1982) Endarterectomy of the vertebral artery from C2 to posterior inferior cerebellar artery intracranially. Surg Neurol 18:400–404
Austin G, Schievink W, Williams R (1989) Controlled pressure-volume factors in the enlargement of intracranial aneurysms. Neurosurgery 24:722–730
Autret A, Pourcelot L, Saudeau D et al (1987) Stroke risk in patients with carotid stenosis. Lancet 1:888–890
Awad I, Little J, Akrawi WP, Ahl J (1990) Intracranial dural arteriovenous malformations: factors predisposing to an aggressive neurological course. J Neurosurg 72: 839–850
Awad I, Robinson J, Mohanty S, Estes M (1993) Mixed vascular malformations of the brain: clinical and pathogenic considerations. Neurosurgery 33:179–188
Aymard A, Marciano S, Garcia Cervignon E, Reizine D, Merland JJ (1989) Aneurysm of the posterior inferior cerebellar artery: nonselective endovascular treatment. J Neuroradiol 16:75–79
Back T (1998) Pathophysiology of the ischemic penumbra–revision of a concept. Cell Mol Neurobiol 18:621–638
Badimon J, Meyer B, Feigen L (1997) Thrombosis triggered by severe arterial lesions is inhibited by oral administration of a glycoprotein IIb/IIIa antagonist. Eur J Clin Invest 27:568–74
Bahar F, Chiras JP et al (1984) Spontaneous vertebral–arteriovenous fistula associated with fibromuscular dysplasia. Neuroradiology 26:45–49
Bailey OT, Ingraham FD, Weadon PS et al (1952) Tissue reactions to powdered tantalum in the central nervous system. J Neurosurg 9:83–92

Bailey WL, Speri MP (1969) Angiomas of the cervical spinal cord. J Neurosurg 30:560–568
Baker C, Fiore A, Connolly E, Baker K, Solomon R (1995) Serum elastase and alpha-1-antitrypsin levels in patients with ruptured and unruptured cerebral aneurysms. Neurosurgery 37:56–62
Baker HL, Love JG, Layton DD (1967) Angiographic surgical aspects of spinal cord vascular anomalies. Radiology 88:1078–1085
Bandhyopadhyay S, Sheth RD (1999) Acute spinal cord infarction: vascular steal in arteriovenous malformation J Child Neurol 14:685–687
Bao YH, Ling F (1997) Classification and therapeutic modalities of spinal vascular malformations in 80 patients. Neurosurgery 40:75–81
Barbour P, Castaldo J, Rae-Grant A et al (1994) Internal carotid artery redundancy is significantly associated with dissection. Stroke 25:1201–1206
Barker WF (1953) Mycotic aneurysms. Ann Surg 139:84–89
Barnett GH, Little JR, Ebrahim ZY, Jones SC, Friel HT (1987) Cerebral circulation during arteriovenous malformation operation. Neurosurgery 20:836–842
Barnett H, Kaste M, Meldrum H, Eliasziw M (1996) Aspirin dose in stroke prevention: beautiful hypotheses slain by ugly facts. Stroke 27:588–592
Barnett HJM, Peerless SJ, Kaufmann JCE (1978) "Stump" of internal carotid artery: a source of further cerebral embolic ischemia. Stroke 9:448–456
Barnwell S, Randall T, Higashida R, Halbach V, Dowd C, Hieshima G (1991) Direct endovascular thrombolytic therapy for dural sinus thrombosis. Neurosurgery 28: 135–142
Barnwell S, Clark W, Nguyen T, O'Neill O, Wynn M, Coull B (1994) Safety and efficacy of delayed intraarterial urokinase therapy with mechanical clot disruption for thromboembolic stroke. Am J Neuroradiol 15:1817–1822
Baron J, Bousser M, Comar D, Soussaline F, Castaigne P (1981) Noninvasive tomographic study of cerebral blood flow and oxygen metabolism in vivo: potentials, limitations, and clinical applications in cerebral ischemic disorders. Eur Neurol 20:273–284
Baron J, Bousser M, Comar D, Rougemont D (1983) Apport de la tomographie par émission de positrons dans l'étude physiopathologique de l'ischémie cérébrale chez l'homme. Presse Med 12:3066–3072
Barr HWK, Blackwood W, Meadows SZ (1971) Intracavernous carotid aneurysm: a clinical pathological report. Brain 94:607–622
Barrett JH, Lawrence VL (1960) Aneurysm of internal carotid artery as complication of mastoidectomy. AMA Arch Otolaryng 72:366–368
Barron KD, Hirano A, Araki S, Terry RD (1959) Experiences with metastatic neoplasms involving the spinal cord. Neurology (Minn) 9:91
Barrow DL, Prats A (1990) Infectious intracranial aneurysms: comparison of groups with and without endocarditis. Nerosurgery 27:562–573
Bartal AD, Levy M (1972) Excision of congenital suboccipital vertebral arteriovenous fistula. J Neurosurg 37:452–456
Barth KH, Strandemberg JD, White RI (1977) Long-term follow-up of transcatheter emboli with autologous clot, oxysele and gelfoam in domestic swine. Invest Radiol 12:273–280
Barth MO, Chiras J, Rose M, Molina JV, Bories J (1984) Résultat de l'embolisation des fistules artério-veineuses durales rachidiennes à drainage veineux perimédullaire. Neurochirurgie 30:381–386
Bashir O, Thornton J, Alp S, Debrun GM, Aletich VA, Charbel F, Ausman JI, Polet H (1974b) Carotid-cavernous fistula associated with Ehlers-Danlos syndrome type IV A case report and review of literature. Intervent Neuroradiol 5: 313–320
Batista LL, Mahadevan J, Sachet M, Alvarez H, Rodesch G, Lasjaunias P (2002) 5-year angiographic and clinical follow-up of coil-embolised intradural saccular aneurysms: a single centre experience. Interv Neuroradiol 4
Batjer H, Suss RA, Samson D (1986) Intracranial arteriovenous malformations associated with aneurysms. Neurosurgery 18:29–35
Batjer H, Mickey B, Samson D (1987) Enlargement and rupture of distal basilar artery aneurysm after iatrogenic carotid occlusion. Neurosurgery 20:624–629

Batjer HH, Devoius MD, Meyer YJ, Purdy PD et al (1988a) Cerebrovascular hemodynamics in arteriovenous malformation complicated by normal perfusion pressure breakthrough. Neurosurgery 22:503–509
Batnitzky S, Muller J (1978) Infantile and juvenile cerebral aneurysms. Neuroradiology 16:61–64
Batsakis JG (1979) Tumor of the head and neck, clinical and pathological considerations. Williams & Wilkins, 2nd edn. pp 296–301
Batsakis JG, Jacobs JB, Templeton AC (1983) Hemangiopericytoma of the nasal cavity: electron-optic study and clinical correlations. J Laryng Otol 97:361–368
Batzdorf V, Bentson J, Marchleder H (1979) Blunt trauma to the high cervical carotid artery. Neurosurgery 5:195–210
Bavinzski G, al-Schameri A, Killer M, Schwendenwein I, Gruber A, Saringer W, Losert U, Richling B (1998a) Experimental bifurcation aneurysm: a model for in vivo evaluation of endovascular techniques. Minim Invasive Neurosurg 41:129–132
Bavinzski G, Killer M, Ferraz-Leite H et al (1998b) Endovascular therapy of idiopathic cavernous aneurysms over 11 years. AJNR Am J Neuroradiol 19:559–565
Baysal T, Kutlu R, Sarac K (2000) Ruptured intracranial aneurysm associated with isolated aortic arch interruption. Neuroradiology 42:842–844
Beall AJ, Crawford E, Cooley S, DeBakey M (1962) Extracranial aneurysms of carotid artery: report of 7 cases. Postgrad Med 32:102–104
Beatty R (1977) Dissecting hematoma of the internal carotid artery following chiropractic manipulations. J Trauma 17:248–249
Becker DH, Townsend JJ, Kramer RA, Newton TH (1979) Occult cerebrovascular malformations. A series of 18 histologically verified cases with negative angiography. Brain 102:249–287
Bednar M, Gross C (1999) Antiplatelet therapy in acute cerebral ischemia. Stroke 30:887–893
Belec L, Cesaro P, Brugiere P, Gray F (1988) Tumour-simulating giant serpentine aneurysm of the posterior cerebral artery. Surg Neurol 29:210–215
Belloti C, Medina M, Oliveri G, Barrale S, Ettore F (1985) Cystic cavernous angiomas of the posterior fossa. J Neurosurg 63:797–799
Beltramello A, Puppini G, Bricolo A et al (1999) Does the tuberous sclerosis complex include intracranial aneurysms? A case report with a review of the literature. Pediatr Radiol 29:206–211
Benati A, da Pian R, Mazza C, Maschio A, Perini SG, Bricolo A, Dalle Ore G (1974a) Preoperative embolization of a vertebral hemangioma compressing the spinal cord. Neuroradiology 7:181–183
Benati A, Dalle Ore G, DaPian R, Briccolo A, Maschio A, Perini S (1974b) Transfemoral selective embolization in the treatment of some cranial and vertebrospinal vascular malformations and tumors. Preliminary results. J Neurol Sci 18: 233–238
Benati A, Beltramello A, Maschio A, Perini S, Rosta L, Piovan E (1987) Combined embolization of intracranial AVMs with multi-purpose mobile-wing microcatheter system; indications and results in 71 cases. AJNR 8:938
Benedict WF, Porter IH, Brown CD et al (1970) Cytogenetic diagnosis of malignancy in recurrent meningiomas. Lancet 1:971–973
Benhaim N, Piorier J, Hurth M (1983) Arteriovenous fistulae of the meninges draining into the spinal veins. A histological study of 28 cases. Acta Neuropathol (Berl) 62:103–111
Benhaiem-Sigaux N, Zerah M Gherardi R et al (1985) A retromedullary arteriovenous fistula associated with the Klippel-Trenaunay-Weber syndrome. Acta Neuropathol (Berl) 66:318–324
Benjamin Le Hemo I, Keshet E (1998) A plasticity window for blood vessel remodelling is defined by pericyte coverage of the performed endothelial network and is regulated by PDGF-B and VEGF. Development 125(9):1591–1598
Bentson JR, Crandall PH (1972) Use of the Fogarty catheter in arteriovenous malformations of the spinal cord. Radiology 105:65–68
Bentson JR, Wilson GH, Newton TH (1971) Cerebral venous drainage pattern of the Sturge-Weber syndrome. Radiology 101:111–118

Benvenuto R, Despres JP, Pribram HFW, Callaghan JC (1961) Excision of extracranial aneurysm of internal carotid artery employing hypothermia. J Cardiovasc Surg 2:165–167
Berenstein A (1980a) Flow-controlled silicone fluid embolization. AJNR Am J Neuroradiol 1:61–77
Berenstein A (1980b) Transvascular fracture and repair of a cerebral artery (a). AJNR Am J Neuroradiol 1:358
Berenstein A (1981) Technique for catheterization and embolization of the lenticulostriate arteries. J Neurosurg 54:783–789
Berenstein A (1983) Brachiocephalic vessel: selective and superselective catheterization. Radiology 148:437–441
Berenstein A, Choi IS (1988) Surgical neuroangiography of intracranial lesions. Imaging in neuroradiology, part II. Radiol Clin North Am 26:1143–1151
Berenstein A, Epstein F (1982) Vein of Galen malformations. Combined neurosurgical and neuroradiological intervention. In: McLaurin R, Schut L, Venes J (eds) Pediatric neurosurgery. Grune & Stratton, New York, pp 637–647
Berenstein A, Graeb D (1982) Convenient preparation of ready-to-use polyvinyl alcohol foam suspension for embolization. Radiology 145:846–850
Berenstein A, Kricheff II (1976) Catheter and material selection for transarterial embolization: technical considerations. I Catheters. Radiology 132:619–630
Berenstein A, Kricheff II (1978) Therapeutic vascular occlusion. J Dermatol Surg Oncol 4:874–880
Berenstein A, Kricheff II (1979a) A new balloon catheter for coaxial embolization. Neuroradiology 18:239–241
Berenstein A, Kricheff II (1979b) Balloon catheters of the investigating of carotid cavernous fistulas. Radiology 132:762–764
Berenstein A, Kricheff II (1979c) Catheter and material selection for transarterial embolization: technical considerations. II Materials. Radiology 132:631–639
Berenstein A, Kricheff II (1980) Treatment of vascular abnormalities of the cerebral artery with detachable balloons (a). AJNR Am J Neuroradiol 1:358
Berenstein A, Kricheff II (1981a) Neuroradiologic interventional procedures. Semin Roentgenol 16:79–94
Berenstein A, Kricheff II (1981b) Microembolization techniques of vascular occlusion: radiologic, pathologic and clinical correlation. AJNR Am J Neuroradiol 2:261–267
Berenstein A, Lasjaunias P (1992) Surgical neuroangiography. Springer, Berlin Heidelberg New York, pp 197–251
Berenstein A, Kerber C, Edwards JH, Bank WO, Kricheff II, Cromwell L (1980) Complications of therapeutic transarterial embolization: cooperative study. AJNR Am J Neuroradiol 1:128
Berenstein A, Lasjaunias P, Kricheff II (1983) Functional anatomy of facial vasculature in pathologic conditions and its therapeutic application. AJNR Am J Neuroradiol 4:149
Berenstein A, Ransohoff J, Kupersmith M et al (1984a) Transvascular treatment of giant aneurysms of the cavernous carotid and vertebral arteries. Functional investigation and embolization. Surg Neurol 21:3–12
Berenstein A, Young W, Ransohoff J, Benjamin V, Merkin H (1984b) Somatosensory-evoked potentials during spinal angiography and therapeutic transvascular embolization. J Neurosurg 60:777–785
Berenstein A, Scott J, Choi IS, Persky M (1986) Percutaneous embolization of the arteriovenous fistulas of the external carotid artery. AJNR Am J Neuroradiol 7:937–942
Berenstein A, Choi IS, Kupersmith M, Flamm E, Kricheff II, Madrid MM (1989a) Complications of endovascular embolization in 202 patients with cerebral AVMs. AJNR 10:876
Berenstein AB, Krall R, Choi IS (1989b) Embolization with n-butyl-cyanoacrylate in management of CNS lesions (a). AJNR Am J Neuroradiol 10:883
Berenstein A, Wisoff J, Epstein F et al (1989c) Endovascular embolization and surgery in the management of vein of Galen malformations. In: Marlin A (ed) Concepts in pediatric neurosurgery. Karger, Basel

Berenstein A, Choi IS, Neophitydes A, Benjamin V (1990) Endovascular treatment of spinal cord arteriovenous malformations (SCAVMs). AJNR 10:898
Berg NO (1950) Tumors arising from the tympanic gland (glomus jugularis) and their differential diagnosis. Acta Pathol Microbiol Scand 27:194–221
Berger MS, Wilson CB (1984) Intracranial dissecting aneurysms of the posterior circulation. Report of six cases and review of the literature. J Neurosurg 61:882–894
Bergeron P, Chambran P, Benichou H et al (1996) Recurrent carotid disease: will stents be an alternative to surgery? J Endovasc Surg 3:76–79
Bergstrand A, Hook O, Lidvall H (1963) Vertebral hemangiomas compressing the spinal cord. Acta Neurol Scand 39:59
Bergstrand H, Olivecrona H, Tonnis W (1936) Gefäßmißbildungen und Gefäßgeschwülste des Gehirns. Thieme, Leipzig
Berry RG, Alpers BS, White JC (1966) Angiomas. In: Millikan CH (ed) Cerebrovascular disease. Williams and Wilkins, Baltimore
Besznyak I, Markos G (1961) Chemodectoma malignum. Zentralbl Allg Pathol 102: 298–305
Bettmann M, Katzen B, Whisnant J, Brant-Zawadzki M (1998) Carotid stenting and angioplasty: a statement for healthcare professionals from the councils on cardiovascular radiology, stroke, cardio-thoracic and vascular surgery, epidemiology and prevention, and clinical cardiology, American Heart Association. Stroke 29:336–338
Bhattacharya J, Luo CB, Suh DC, Alvarez H, Rodesch G, Lasjaunias P (2001) Wyburn-Mason or Bonnet-Dechaume-Blanc as cerebrofacial arteriovenous metameric syndromes (CAMS) Intervent Neuroradiol 7:5–17
Bickerstaff ER (1964) Etiology of acute hemiplegia in childhood. Br J Med II:82–87
Bicknell JM, Carlow TJ, Kornfeld M, Stouring J, Turner P (1978) Familial cavernous angiomas. Arch Neurol 35:746–749
Biesecker JL, Marcove RC, Huvos AG et al (1970) Aneurysmal bone cysts. A clinicopathologic study of 66 cases. Cancer 26:615–625
Binder B, Eng GD, Milhorat TH et al (1982) Spinal arteriovenous malformations in an infant: unusual symptomatology and pathology. Dev Med Child Neurol 24:380–385
Biondi A, Merland JJ, Reizine D, Aymard A, Hodes J, Lecoz P, Rey A (1990) Embolization with particles in thoracic intramedullary arteriovenous malformations: long-term angiographic and clinical results. Radiology 177:651–658
Biondi A, Clemenceau S, Dormont D, Deladoeuille M, Riccciardi GK, Mokhtari K, Sichez JP, Marsault C (2002) Intracranial extra-axial cavernous hemangiomas: tumors or vascular malformations? J Neuroradiol 29, 91–104
Bitoh S, Hasegawa H, Fujiwara M, Nakata M (1980) Traumatic arteriovenous fistula between the middle meningeal artery and cortical vein. Surg Neurol 14:355–358
Bjorkesten G, Halonen V (1965) Incidence of intracranial vascular lesions in patients with subarachnoid hemorrhage investigated by four-vessel angiography. J Neurosurg 23:29–32
Blanc R, Weill A, Piotin M, Ross I, Moret J (2001) Delayed stroke secondary to increasing mass effect after endovascular treatment of giant aneurysm by parent vessel occlusion. AJNR Am J Neuroradiol 22:1841–1843
Blasi RD, Lasjaunias P (1997) Endovascular treatment of a ruptured intracranial arterial aneurysm in a 12-year-old child with recessive polycystic kidney disease. Intervent Neuroradiol 3:333–336
Block P (1994) Restenosis after percutaneous transluminal coronary angioplasty – anatomic and pathophysiological mechanisms: strategies for prevention. Circulation 81:IV2–IV4
Blum U, Krumme B, Fluegel P, Gabelmann A (1997) Treatment of ostial renal-artery stenoses with vascular endoprostheses after unsuccessful balloon angioplasty. N Engl J Med 336:459–465
Boatmann KK, Bradford VA (1958) Excision of internal carotid artery aneurysm during pregnancy employing hypothermia and vascular shunt. Ann Surg 148:271–275
Bock R, Gray-Weale A, Mock P et al (1993) The natural history of asymptomatic carotid artery disease. J Vasc Surg 17:160–171
Bogousslavsky J, Barnett H, Fox A, Hachinski V (1986) Atherosclerotic disease of the middle cerebral artery. Stroke 17:1112–1120

Bogousslavsky J, Regli F, Van Melle G et al (1988) Migraine stroke. Neurology 38: 223–227
Bohmfalk GL, Story JL, Wissinger JP, Brown WE (1978) Bacterial intracranial aneurysms. J Neurosurg 48:369–382
Boissel J (1996) Is thrombolytic therapy beneficial in acute stroke patients? Eur Heart J 17:1773–1774
Boldrey E, Maas L, Miller E (1957) Role of atlantoid compression in etiology of internal carotid thrombosis. J Neurosurg 13:127–139
Bollaert P, Bracard S, Boulanger T, Picard L (1995) Early local intra-arterial thrombolysis for severe middle cerebral artery stroke. Cerebrovasc Dis 5:292–296
Bombeli T, Schwartz B, Harlan J (1998) Adhesion of activated platelets to endothelial cells: evidence for a GPIIbIIIa-dependent bridging mechanism and novel roles for endothelial intercellular adhesion molecule 1 (ICAM-1), (alpha)v(beta)3 integrin, and GPIb(alpha). J Exp Med 187:329–339
Bonakdarpour A, Levy WM, Aegerter E (1978) Primary and secondary aneurysmal bone cyst: a radiological study of 75 cases. Radiology 126:75–82
Bonnet P, Dechaume J, Blanc E (1937) L'anévrysme cirsoïde de la réfine (anévrysme racemeux) ses relations avec l'anévrysme cirsoïde de la face et avec l'anévrysme cirsoïde du cerveau. J Med Lyon 18:165–178
Bonstelle CT, Kori SH, Rekate H (1983) Intracarotid chemotherapy of glioblastoma after intended blood–brain barrier disruption. AJNR Am J Neuroradiol 4:810
Bontozoglou N, Spanos H, Lasjaunias P, Zarifis G (1994) Three-dimensional display of the orifice of intracranial aneurysms: a new potential application for magnetic resonance angiography. Neuroradiology 36:346–349
Borden J, Wu JK, Shucart WA (1995) A proposed classification for spinal and cranial dural arteriovenous fistulous malformations and implications for treatment. J Neurosurg 82:166–179
Bostrom K, Lliequist B (1967) Primary dissecting aneurysm of the extracranial part of the internal carotid and vertebral arteries. Neurology 17:179–186
Bougousslavsky J, Gates P, Fox A, Barnett H (1986) Bilateral occlusion of vertebral artery: clinical patterns and long-term prognosis. Neurology 36:1309–1315
Bousser M (1999) Cerebral venous thrombosis: nothing, heparin or local thrombolysis? Stroke 1999 30:481–483
Bousser M (2000) Cerebral venous thrombosis: diagnosis and management. J Neurol 247:252–258
Bousser M, Mas J (1988) Epidémiologie des accidents vasculaires cérébraux du sujet jeune. Presse Med 17:143–145
Bousser M, Chiras J, Bories J, Castaigne P (1985) Cerebral venous thrombosis: a review of 38 cases. Stroke 16:199–213
Bove E, Fry W, Gross W, Stanley J (1979) Hypotension and hypertension as consequences of baroreceptor dysfunction following carotid endarterectomy. Surgery 85:633–637
Boysen G, Overgaard K (1995) Thrombolysis in ischaemic stroke: how far from a clinical breakthrough? J Intern Med 237:95–103
Bracard S, Picard L, Marchal J, Ducrocq X (1990) Role of angioplasty in the treatment of symptomatic vascular spasm occurring in the post-operative course of intracranial ruptured aneurysms. J Neuroradiol 17:6–19
Bradac GB, Simon RS, Schramm J (1977) Cervical epidural AVM – report of a case of uncommon location. Neuroradiology 14:97–100
Brandt T, Pessin M, Kwan E, Caplan L (1995) Survival with basilar artery occlusion. Cerebrovasc Dis 5:182–187
Brandt T, von Kummer R, Muller-Kuppers M, Hacke W (1996) Thrombolytic therapy of acute basilar artery occlusion: variables affecting recanalization and outcome. Stroke 27:875–881
Branston NM (1995) The physiology of the cerebrovascular parasympathetic innervation. Br J Neurosurg 9:319–329
Brassier G, Morandi X, Mercier PH,Velut S (1994) The posterior part of the arterial circle of Willis. Caudal division of the embryonic internal carotid artery. Riv Neuroradiol 7 [Suppl 4]:85–89

Brem S (1976) The role of vascular proliferation in the growth of brain tumors. Clin Neurosurg 33:440–453
Bret P, Salzmann M, Bascoulergue Y, Guyotat J (1994) Dural arteriovenous fistula of the posterior fossa draining into the spinal medullary veins. Neurosurgery 35: 965–968
Brilstra EH, Hop JW, Rinkel GJE (1997) Quality of life after perimesencephalic haemorrhage. J Neurol Neurosurg Psychiatry 63:382–384
Brilstra EH, Rinkel GJE, van der Graaf Y, van Rooij WJJ, Algra A (1999) Treatment of intracranial aneurysms by embolization with coils a systematic review. Stroke 30:470–476
Brion S, Netsky MG, Zimmerman HM (1952) Vascular malformations of the spinal cord. Arch Neurol Psychiatr 68:339–361
Brody WR, Angell WW, Kosek JC (1972) Histologic fate of the venous coronary artery by-pass in dogs. Am J Pathol 66:222–229
Brook-Carter PT, Peral B, Ward CJ, Thompson P, Hughes J et al (1994) Deletion of the TSC2 and PKD1 genes associated with severe infantile polycystic kidney disease: a contiguous gene syndrome. Nature Genet 8:328–332
Brothers M, Holgate R (1990) Intracranial angioplasty for treatment of vasospasm after subarachnoid hemorrhage: technique and modifications of improve branch access. AJNR 11:239–247
Brott T, Adams H, Olinger C et al (1989) Measurement of acute cerebral infarction: a clinical examination scale. Stroke 1989 20:864–870
Brott T, Haley E, Levy D et al (1992) Urgent therapy for stroke, part I: pilot study of tissue plasminogen activator administered within 90 minutes. Stroke 2:632–640
Brown J, Coyne T, Hurlbert R, Fehlings M, Ter Brugge K (1993) Deep cerebral system thrombosis. Neurosurgery 33:911–913
Brown RD, Wiebers DO, Forbes G, O'Fallon WM, Piepgras DG, Marsh R, Maciunas RJ (1988) The natural history of unruptured intracranial arteriovenous malformations. J Neurosurg 68:352–357Brown R, Wiebers DO, Forbes GS (1990) Unruptured intracranial aneurysms and arteriovenous malformations. Frequency of intracranial hemorrhage and relationship of lesions. J Neurosurg 73:859–863
Browne TR, Adams RD, Robertson GH (1976) Hemangioblastomas of the spinal cord. Arch Neurol 33:435–441
Brownlee RD, Tranmer BI, Sevick RJ et al (1995) Spontaneous thrombosis of an unruptured anterior communicating artery aneurysm. Stroke 26:1945–1949
Brucker A, Vollert-Rogenhofer H, Wagner M (1998) Heparin treatment in acute cerebral sinus venous thrombosis: a retrospective clinical and MR analysis of 42 cases. Cerebrovasc Dis 8:331–337
Bruggen ACV, Dippel DWJ, Habbema JDF, Mooij JJA (1996) Acoustic detection of intracranial aneurysms: a decision analysis. Acta Neurochir 138:1148–1156
Brugières P, Castrec-Carpo A, Heran F, Goujon C, Gaston A, Marsault C (1989) Magnetic resonance imaging in the exploration of dissection of the internal carotid artery. J Neuroradiol 16:1–10
Brunereau L, Gobin YP, Meder JF, Cognard C, Tubiana JM, Merland JJ (1996) Intracranial dural arteriovenous fistulas with spinal venous drainage: relation between clinical presentation and angiographic findings. AJNR 17:1549–1554
Buchta K, Sands J, Rosenkrantz H, Roche WD (1982) Early mechanism of action of arterially infused alcohol in renal devitalization. Radiology 145:45–48
Buckingham RA, Aimi K, Perrelli SC (1959) Multicentric origin of glomus jugulare tumors. Arch Otolaryngol 70:94–97
Buckwalter JA, Sasaki CT, Virapongse C, Kier EL, Bauman N (1983) Pulsatile tinnitus arising from jugular megabulb deformity: a treatment rationale. Laryngoscope 93:1534–1539
Buonaguidi B, Cvanapicci R, Mimassin N, Ferdeghini M (1984) Intrasellar cavernous hemangiomas. Neurosurgery 14:732–734
Burton C, Johnston J (1970) Multiple cerebral aneurysm and cardiac myxoma. N Engl J Med 282:35–36
Buxton JT Jr, Stevenson TB, Stallworth JM (1964) Arteriosclerotic aneurysm of extracranial internal carotid artery treated by excision and primary reanastomosis under controlled hypertension. Ann Surg 159:222–226

Byrne JV, Molyneux AJ (1999) Five-years experience in using coil embolization for ruptured intracranial aneurysms: outcomes and incidences of late rebleeding. J Neurosurg 90:656–663
Cahan LD, Higashida RD, Halbach VV, Hieshima GB (1987) Variants of radiculomeningeal vascular malformations of the spine. J Neurosurg 66:333–337
Calcaterra TC, Rich R, Ward PW (1974) Neurilemmona of the sphenoid sinus. Arch Otolaryng 100:385–386
Caldas JGMP, Cavalheiro S, Nalli DR, Frudit ME, Puglia P (1998) Endovascular treatment of intravenous carotid aneurysm with hyperprolactinaemia. Intervent Neuroradiol 4:253–256
Campiche R, Oberson R (1972) Syndrome d'émaciation provoqué par un méningiome du tubercule stellaire. Oto Neuro Ophthalmol 44:353–358
Campos C, Churojana A, Rodesch G, Alvarez H, Lasjaunias P (1998a) Basilar tip aneurysm and basilar tip anatomy. Intervent Neuroradiol 4:121–125
Campos C, Churojana A, Rodesch G, Alvarez H, Lasjaunias P (1998b) Multiple intracranial arterial aneurysms: a congenital metameric disease? Intervent Neuroradiol 4:293–299
Cantasdemir M, Kantarci F, Mihmanli I, Numan F (2002) Embolization of profunda femoris artery branch pseudoaneurysms with ethylene vinyl alcohol copolymer (onyx). J Vasc Interv Radiol 13:725–728
Capan LM, Labdizabal S, Sinha K, Ashok U et al (1983) Acute pulmonary embolism during therapeutic arterial embolization with silicone fluids. Anesthesiology 58:569–571
Caplan L (1991) Migraine and vertebrobasilar ischaemia. Neurology 41:55–61
Caplan L, Mohr J, Kistler J, Koroshetz W (1997) Should thrombolytic therapy be the first-line treatment for acute ischemic stroke? Thrombolysis–not a panacea for ischemic stroke. New Engl J Med 337:1309–1310
Caplan L, Gorelick P, Heir D (1986) Race, sex and cerebrovascular disease: a review. Stroke 17:648–655
CAPRIE Steering Committee (1996) A randomized, blinded, trial of clopidogrel versus aspirin in patients at risk of ischaemic events. Lancet 348:1329–1339
Carmeliet P (2000) Mechanisms of angiogenesis and arteriogenesis. Nat Med 6: 389–395
Caroscio JT, Brannan T, Budabin M, Huang YP, Yahr MD (1980) Subarachnoid hemorrhage secondary to spinal arteriovenous malformation and aneurysm. Report of a case and review of the literature. Arch Neurol 37:101–103
Carpenter G, Schwartz H, Walker AE (1943) Neurogenic polycythaemia. Ann Intern Med 19:470
Carr S, Farb A, Pearce W et al (1996) Atherosclerotic plaque rupture in symptomatic carotid artery stenosis. J Vasc Surg 23:755–766
Carter A, Laird JR (1996) Experimental results with endovascular irradiation via a radioactive stent. Int J Radiat Oncol Biol Phys 36:797–803
Carter LP, Gumerlock MK (1995) Steal and cerebral arteriovenous malformations. Stroke 26: 2371–2372
Casasco A, Houdart E, Merland JJ (1992) Embolization of spinal vascular malformations Neuroimaging Clin N Am 2:337–358
Casasco A, Herbreteau E, George E, Tran Ba Huy P, Deffresne D, Merland JJ (1994) Devascularization of craniofacial tumors by percutaneous tumor puncture. AJNR Am J Neuroradiol 15:1233–1239
Casasco A, Houdart E, Biondi A, Jhaveri H, Herbreteau D, Aymard A, Merland JJ (1999) Major complications of percutaneous embolization of skull-base tumors. AJNR Am J Neuroradiol 20:179–181
Castaigne P, Bories J, Brunet P, Merland JJ, Meininger V (1976) Les fistules artério-veineuses méningés pures à drainage veineux cortical. Rev Neurol 132:169–181
Casto L, Caverni L, Camerlingo M, Censori B (1996) Intra-arterial thrombolysis in acute ischaemic stroke: experience with a superselective catheter embedded in the clot. J Neurol Neurosurg Psychiatry 60:667–670
Castro E, Fortea F, Villoria F et al (1999) Treatment of a giant aneurysm of the right middle cerebral artery with GDCs after extracranial to intracranial bypass. Intervent Neuroradiol 5:51–56

CAVATAS (1996) Major ongoing stroke trials: carotid and vertebral artery transluminal angioplasty study (CAVATAS). Stroke 27:358
Cersoli M, Campanile S, Campanile A, Amore A (1989) Unusual findings in Sturge-Weber syndrome. AJNR 10:S85
Chaloupka JC, Gobin YP, Guglielmi G, Steichen JD, Vinuela F (1995) Two concurrent spinal dural arteriovenous fistulae in a patient with rapidly progressive myelopathy. Angiology 46:251–257
Chaloupka J, Huddle J, Alderman J, Fink S, Hammond R, Vintners H (1999a) A reexamination of the angiotoxicity of superselective injection of DMSO in the swine rete embolization model. AJNR 20:401–410
Chaloupka J, Sundeep M, Huddle D (1999b) Use of mechanical thrombolysis via microballoon percutaneous transluminal angioplasty for the treatment of acute dural sinus thrombosis: case presentation and technical report. Neurosurgery 45:650–657
Chang S, Steinberg G, Rosario M, Crowley R, Hevner R (1997) Mixed arteriovenous malformation and capillary telangiectasia: a rare subset of mixed vascular malformations. J Neurosurg 86: 699–703
Chang SC, Schi YM (1984) Neurilemmoma of the vagus nerve. A case report and brief literature review. Laryngoscope 94:946–949
Chapman AB, Rubinstein D, Hughes R, Stears JC, Earnest MP, Johnson AM, Gabow PA, Kaehny WD (1992) Intracranial aneurysms in autosomal dominant polycystic kidney disease [see comments]. N Engl J Med 327:916–920
Chaudhary MY, Sachved VP, Cho SH, Weitzner I, Puljic S, Huang YP (1982) Dural arteriovenous malformation of the major venous sinuses: an acquired lesion. AJNR 3:3–19
Chaudary RR (1987) Sturge Weber syndrome with extensive intracranial calcifications contralateral to the bulk of the facial nevus, normal intelligence, and absent seizure disorder. AJNR 8:736
Chauveau D, Pirson Y, Verellen-Dumoulin C, Macnicol A, Gonzalo A, Grunfeld JP (1994) Intracranial aneurysms in autosomal dominant polycystic disease. Kidney Int 45:1140–1146
Chen H, Chopp M, Zhang R, Bodzin G, Chen Q (1994) Anti-CD11b monoclonal antibody reduces ischemic cell damage after transient focal cerebral ischemia in rat. Ann Neurol. 35:458–463
Chen YL, Luo CB, Hsu SW, Rodesch G, Lasjaunias P (2001) Tuberous sclerosis complex with an unruptured intracranial aneurysm: manifestations of continuous gene syndrome. Intervent Neuroradiol 3
Chimowitz M, Kokkinos J, Strong J et al (1995) The Warfarin-Aspirin Symptomatic Intracranial Disease Study. Neurology 45:1488–1493
Chiras J, Depriester C, Weill A, Sola-Martinez MT, Deramond H (1997) Percutaneous vertebral surgery. Technics and indications. J Neuroradiol 24:45–59
Choi I, Berenstein A, Ransohoff J, Foo S, Kricheff I (1984) Intra-arterial infusion of BCNU and Cis-platinum (a). AJNR Am J Neuroradiol 5:665
Choi IS, Berenstein A (1988a) Surgical neuroangiography of the spine and spinal cord. Imaging in neuroradiology, part II. Radiol Clin North Am 26:1131–1141
Choi IS, Berenstein A (1988b) Spinal angiography and embolization for spinal tumors. In: Schmidek D, Sundaresan T, Schiller A, Rosenthal P (eds) Tumors of the spine. Grune and Stratton, New York
Choi IS, Berenstein A, Flamm E (1988c) Superselective catheterization and embolization of cerebral AVMs. In: Pluching F, Broggi G (eds) Advanced technology in neurosurgery. Springer, Berlin Heidelberg New York, pp 183–192
Choi NW, Schuman LM, Gullen WH (1970) Epidemiology of primary central nervous system neoplasms in Minnesota. Am J Epidemiol 91:238–259
Choi NW, Schuman LM, Gullen WH (1970) Epidemiology of primary central nervous system neoplasms. II. Case-control study. Am J Epidemiol 91:467–485
Chopko B, Kerber C, Wong W, Georgy B (2000) Transcatheter snare removal of acute middle cerebral artery thromboembolism: technical case report. Neurosurgery 46:1529–1531
Chopp M, Zhang R, Chen H, Li Y (1994) Postischemic administration of an anti-Mac-1 antibody reduces ischemic cell damage after transient middle cerebral artery occlusion in rats. Stroke 25:869–876

Choudhri T, Hoh B, Zerwes H, Prestigiacomo C (1998) Reduced microvascular thrombosis and improved outcome in acute murine stroke by inhibiting GP IIb/IIIa receptor-mediated platelet aggregation. J Clin Invest 102:1301–1310
Choy DSJ, Ascher P, Lammer J, Rothman L, Snowdon J (1986) Percutaneous laser catheter recanalization of carotid arteries in seven cadavers and one patient. AJNR Am J Neuroradiol 7:1050
Christiansen TA, Duvall AJ, Rosenberg Z, Carley RB (1974) Juvenile nasopharyngeal angiofibroma. Trans Am Acad Opthalmol Otolaryngol 78:140–147
Churojana A, Chawalparit O, Chiewwit P, Suthisak S (2001) Spontaneous occlusion of a bilateral post-traumatic carotid cavernous fistula. Intervent Neuroradiol 7:245–252
Cifarelli F, Sadiq S (1971) Bilateral cervical carotid aneurysms treated by resection and replacement grafts. Report of a case. Arch Surg 102:74–75
Clare CE, Barrow DL (1992) Infectious intracranial annulares. Neurosurg Clin North Am 3:551–565
Clark JV (1970) Familial occurrence of cavernous angiomata of the brain. J Neurol Neurosurg Psychiatry 33:871–876
Clark W, Madden K, Rothlein R, Zivin JA (1991) Reduction of central nervous system ischemic injury in rabbits using leukocyte adhesion antibody treatment. Stroke 22:877–883
Clough JR, Price CHG (1973) Aneurysmal bone cyst: pathogenesis and long-term results of treatment. Clin Orthop 97:52–63
Clouston J, Numaguchi Y, Zoarski G et al (1995) Intraarterial papaverine infusion for cerebral vasospasm after subarachnoid hemorrhage. AJNR Am J Neuroradiol 16: 27–38
Cogen P, Stein BM (1983) Spinal cord arteriovenous malformations with significant intramedullary components. J Neurosurg 59:471–478
Cognard C, Gobin YP, Pierot L, Bailly AL, Houdart E, Casasco A, Chiras J, Merland JJ (1995) Cerebral dural arteriovenous fistulas: clinical and angiographic correlation with a revised classification of venous drainage. Radiology 194:671–680
Cognard C, Sernaan H, Bakchine S, Miaux Y, Thibault S, Martinez MTS, Chiras J (1995) Paraspinal arteriovenous fistula with perimedullary venous drainage. AJNR Am J Neuroradiol 16:2044–2048
Cognard C, Houdart E, Casasco A, Gabrillargues J, Chiras J, Merland JJ (1997) Long-term changes in intracranial dural arteriovenous fistulae leading to worsening in the type of venous drainage. Neuroradiology 39:59–66
Cognard C, Weil A, Castaings L, Rey A, Moret J (1998) Intracranial berry aneurysms: angiographic and clinical results after endovascular treatment. Radiology 206: 499–510
Cole IE (1982) Haemangioendothelioma of the head and neck. J Laryng Otol 96: 545–558
Coller B (1955) The role of platelets in arterial thrombosis and the rationale for blockade of platelet GP IIb/IIIa receptors as antithrombotic therapy. Eur Heart J 16 [Suppl L]:11–15
Coller B (1978) GPIIb/IIIa antagonists: pathophysiologic and therapeutic insights from studies of c7E3 Fab. Thromb Haemost 78
Collice M, D'Aliberti G, Arena O, Solaini C, Fontana R, Talamonti G (2000) Surgical treatment of intracranial dural arteriovenous fistulae: role of venous drainage. Neurosurgery 47:56–67
Collins R, Peto R, Flather M, Parish S (1995) ISIS 4: a randomised factorial trial assessing oral captopril, oral mononitrate, and iv magnesium sulphate in 58,050 patients with suspected myocardial infarction. Lancet 345:669–685
Compagno J, Hyams VJ (1976) Hemangiopericytoma like intranasal tumors Am J Clin Path 65:428–432
Conley JJ, Clairmont AA (1977) Intramuscular hemangioma of the masseter muscle. Case report. Plast Reconstr Surg 60:121–125
Connolly ES Jr, Zubay JP, McCormick PC (1998) The posterior approach to a series of glomus (type II) intramedullary spinal cord arteriovenous malformations Neurosurgery 42:774–786
Connors J, Wojak J (1999a) Interventional neuroradiology strategies and practical techniques. W.B. Saunders Co., Philadelphia

Connors J, Wojak J (1999b) Percutaneous transluminal angioplasty for intracranial atherosclerotic lesions: evolution of technique and short-term results. J Neurosurg 91:415–423
Constantino A, Vitners HV (1986) A pathogenic correlate of the "steal" phenomenon in a patient with cerebral arteriovenous malformation. Stroke 17:103–106
Cosgrove GR, Bertrand G, Fontaine S, Robitaille Y, Melanson D (1988) Cavernous angiomas of the spinal cord. J Neurosurg 68:31–36
Coubes P, Humbert CV, Rodesch G, Lasjaunias P, Echenne B, Frerebeau P (1996) Total endovascular occlusion of a giant direct arteriovenous fistula in the posterior fossa in a case of Rendu-Osler-Weber disease. Childs Nerv Syst 12:785–788
Couly G, Coltey P, Eichmann A, Le Douarin NM (1995)The angiogenic potentials of the cephalic mesoderm and the origin of brain and head blood vessels Mech Dev 53:97–112
Courtheoux P, Alachkar F, Casasco A (1985) Chimioembolisation des métastases du rachis lombaire. J Neuroradiol 12:151–162
Courville CB (1945) Pathology of the nervous system, 2nd edn. Pacific Press, Mountain View
Cox RH, Fisher GM (1978) Effects of sex hormones on the passive mechanical properties of rat carotid artery. Blood vessels 15:266–276
Craig W, McK, Wagener HP, Kernohan JW (1941) Lindau-von Hippel disease. Arch Neurol Psychiat 46:36
Cramer F, Kinsey WH (1952) The cerebellar hemangioblastoma: a review of 53 cases. Arch Neurol Psychiatr 67:237
Crawford JV, Russell DS (1956) Cryptic arteriovenous and venous hamartomas of the brain. J Neurol Neurosurg Psychiatry 19:1–11
Crawford PM, West CR, Chadwick DW, Shaw MDM (1986) Arteriovenous malformations of the brain: natural history in unoperated patients. J Neurol Neurosurg Psychiatry 49:1–10
Crawford RA, Gregory PC, Griffiths IA (1980) The response of feline spinal pial arterioles to norepinephrine. J Neurosurg 52:60–63
Crevel HV, Habbema JDF, Braakman R (1986) Decision analysis of the management of incidental intracranial saccular aneurysms. Neurology 36:1335–1339
Crompton MR (1966) Mechanism of growth and rupture in cerebral berry aneurysms. Br Med J 1:1138–1142
Cromwell LD, Harris AB (1980) Treatment of cerebral arteriovenous malformations. A combined neurosurgical and neuroradiological approach. J Neurosurg 52:705–708
Cromwell LD, Kerber C (1980) Modification of cyanoacrylate for therapeutic embolization: preliminary experience. AJNR 1:113
Cronqvist S, Granholm I, Lundstrom NR (1972) Hydrocephalus and congestive heart failure caused by intracranial arteriovenous malformations in infants. J Neurosurg 36:249–254
Cromwell LD, Kerber C (1979) Modification of cyanoacrylate for therapeutic embolization: preliminary experience. Am J Roentgenol 132:799–801
Crouse SK, Berg BO (1972) Intracranial meningiomas in childhood adolescence. Neurology (Minneapolis) 22:135–141
Cummings BJ (1980) Relative risk factors in the treatment of juvenile nasopharyngeal angiofibroma. Head Neck Surg 3:21–26
Cummings BJ, Blend R, Fitzpatrick P, Clark R, Harwood A, Keane T, Beale F, Garrett P, Payne D, Rider W (1984) Primary radiation therapy for juvenile nasopharyngeal angiofibroma. Laryngoscope 94:1599–1605
Cunha E, Sa MJ, Stein BM, Solomon RA, McCormick PC (1992) The treatment of associated intracranial aneurysms and arteriovenous malformations. J Neurosurg 77:853–859
Currier J, Faxon D (1995) Restenosis after percutaneous transluminal coronary angioplasty: have we been aiming at the wrong target? J Am Coll Cardiol 25:516–520
Cushing H, Eisenhardt L (1938) The meningiomas. Charles C. Thomas, Springfield, Ill
Cytel Software (1995) Statxat 3 for Windows: User Manual. Cytel Software Corporation, Boston

Dalkara T, Morikawa H, Moskowitz M, Panahian N (1994) Blood flow-dependent functional recovery in a rat model of cerebral ischemia. Am J Physiol 267: H678–H683
Dalkara T, Moskowitz M (1997) The role of nitric oxide in cerebral ischemia. In: Welch K, Caplan L, Reis D, Siesjo B, Weir B (eds) Primer on cerebrovascular diseases. Academic Press, San Diego, pp 96–98
Damon E, Kelsay, Paulo Robeiro (1996) Aortic coarctation with two intercostal aneurysm, appearing radiographically as a subclavian aneurysm. Angiology 47: 103–106
Dandy WE (1928) Arteriovenous aneurysm of the brain. Arch Surg 17:190–243
David CA, Vishteh AG, Spetzler RF et al (1999) Late angiographic follow-up review of surgically treated aneurysms. J Neurosurg 91:396–401
David M (1982) Les fistules artério-veineuses epiduro-meningées à drainage veineux médullaire. Revue de 28 cas. Thesis, Paris
Davies M (1990) A macro and micro view of coronary vascular insult in ischemic heart disease. Circulation 82 [Suppl II]:II38–II46
Davies M (1994) Pathology of arterial thrombosis. Br Med Bull 50:789–802
Davies M, Hagen P (1994) Pathobiology of intimal hyperplasia. Br J Surg 81:1254–1269
Davies M, Richardson P, Woolf N (1993) Risk of thrombosis in human atherosclerotic plaques: role of extracellular liquid, macrophage and smooth muscle content. Br Heart J 69:377–381
Davies M, Ter Brugge KG, Willinsky R, Coyne T, Saleh J, Wallace MC (1996) The validity of classification for the clinical presentation of intracranial dural arteriovenous fistulas. J Neurosurg 85:830–837
Davies MA, Saleh J, Ter Brugge KG, Willinsky R, Wallace MC (1997a) The natural history and management of intracranial dural arteriovenous fitulae. Part I: Benign lesions. Intervent Neuroradiol 3:295–302
Davies MA, Ter Brugge KG, Willinsky R, Wallace MC (1997b) The natural history and management of intracranial dural arteriovenous fistulae. Part II: Aggressive lesions. Intervent Neuroradiol 3:303–311
Davis J, Zimmerman R (1983) Injury of the carotid and vertebral arteries. Neuroradiology 25:55–69
Dawson TM, Dawson VL, Snyder SH (1992) A novel neuronal messenger molecule in brain: the free radical, nitric oxide [see comments]. Ann Neurol 32:297–311
Dawson TM, Snyder SH (1994) Gases as biological messengers: nitric oxide and carbon monoxide in the brain. J Neurosci 14:5147–159
Day AL, Rhoton AL (1982) Aneurysms and arteriovenous fistulae of the intracavernous carotid artery and its branches. In: Youmans JR (ed) Neurological Surgery, Saunders, Philadelphia
De Bakey M (1996) Carotid endarterectomy revisited. J Endovasc Surg 3(1):4
De Blasi R, Lasjaunias P, Rodesch G, Alvarez H (1997) Endovascular treatment of a ruptured intracranial arterial aneurysm in a 12-year old child with recessive polycystic kidney disease. Intervent Neuroradiol:3:333–336
De Bruyn S, Stam J (1999) Randomized, placebo-controlled trial of anticoagulant treatment with low-molecular-weight heparin for cerebral sinus thrombosis. Stroke 30:484–488
De Merritt JS, Pile-Spellman J, Mast H, Moohan N, Lu DC, Young WL, Hacein-Bey L, Mohr JP, Stein BM (1995) Outcome analysis of preoperative embolization with n-butyl cyanoacrylate in cerebral arteriovenous malformations. AJNR Am J Neuroradiol 16:1801–1807
De Veber G, Andrew M, Adams C (2001) Cerebral sinovenous thrombosis in children. N Engl J Med 435:417–423
De Visser M, Rosendaal F, Bertina R (1999) A reduced sensitivity for activated protein C in the absence of factor V Leiden increases the risk of venous thrombosis. Blood 93:1271–1276
Deans W, Bloch S, Leibrock L, Berman B, Skultety F (1982) Arteriovenous fistula in patients with neurofibromatosis. Radiology 144:103–107
Debrun G, Lacour P, Caron JP et al (1975a) Inflatable and released balloon technique. Experimental in dog – application in men. Neuroradiology 9:267–271

Debrun G, Lacour P, Caron JP, Hurth M et al (1975b) Traitement des fistules arterioveineuses et d'anevrysmes par ballon gonflable et largable. Nouv Press Med 4:2315–2318
Debrun G, Lacour P, Carson JP et al (1978) Detachable balloon and calibrated leak balloon technique in the treatment of cerebrovascular lesions. J Neurosurg 49: 635–649
Debrun G, Fox A, Drake C et al (1981) Giant unclippable aneurysms: treatment with detachable balloons. AJNR Am J Neuroradiol 2:167–173
Debrun GM, Aletich VA, Kehrli P, Misra M, Ausman JI, Charbel FT (1998) Selection of cerebral aneurysms for treatment using Guglielmi detachable coils: the preliminary University of Illinois at Chicago experience. Neurosurgery 43:1281–1295
Deen HG, Scheithauer BW, Ebersold MJ (1982) Clinical and pathological study of meningiomas in the first two decades of life. J Neurosurg 56:317–322
Defreyne L, Achten R, Vandekerckhove T, Kunnen M (1999) Rupture of a cervical spinal cord arteriovenous malformation: a rare complication of endovascular therapy. Eur Radiol 9:734–737
Del Zoppo G, Garcia J (1995) PMN leukocyte adhesion in cerebrovascular ischemia. In: Granger D, Schmid-Schonbein G (eds) Physiology and pathophysiology of leukocyte adhesion. Oxford Press, New York, pp 408–433
Del Zoppo G, Ferbert A, Otis S, Bruckmann H et al (1988) Local intra-arterial fibrinolytic therapy in acute carotid territory stroke: a pilot study. Stroke 19:307–313
Del Zoppo G, Schmid-Schonbein G, Mori E, Copeland B, Chang C-M (1991) Polymorphonuclear leukocytes occlude capillaries following middle cerebral artery occlusion and reperfusion in baboons. Stroke 22:1276–1283
Del Zoppo G, Poeck K, Pessin M et al (1992) Recombinant tissue plasminogen activator in acute thrombotic and embolic stroke. Ann Neurol 32:78–86
Del Zoppo G, Higashida R, Furlan A et al (1998) PROACT: a phase II randomized trial of recombinant pro-urokinase b direct arterial delivery in acute middle cerebral artery stroke. Stroke 29:4–11
Delarue J, Paillas J, Payen J, Burgeat M (1956) Les fibromes naso-pharyngiens: étude anatomopathologique. Semaine Hop 32:3801–3809
Dennis M, Bamford J, Sandercock P, Warlow C (1990) Prognosis of transient ischemic attacks in the Oxfordshire Community Stroke Project. Stroke 21:848–853
Denny-Brown D (1966) Pathophysiology of focal cerebral ischemia. Research Publications – Association for Research in Nervous and Mental Disease 41:196–204
Deruty R, Mottolese C, Soustiel JF, Pelissou-Guyotat I (1990) Association of cerebral arteriovenous malformation and cerebral aneurysm. Diagnosis and management. Acta Neurochir 107:133–139
Deshpande DH, Vidyasagar C (1980) Histology of the persistent embryonic veins in arteriovenous malformations of brain. Acta Neurochir 53:227–236
Detweiler PW, Porter RW, Spetzler RF (1999) Spinal arteriovenous malformations Neurosurg Clin N Am 10:89–100
Detwiler P, Porter R, Zabramski J, Spetzler R (1997) De novo formation of a central nervous system cavernous malformation: implications for predicting risk of hemorrhage. J Neurosurg 87:629–632
Deutsch G (1983) Blood flow changes in arteriovenous malformation during behavioral activation. Ann Neurol 13:38–43
Di Chiro G (1957) Combined retino-cerebellar angiomatosis and deep cervical angiomas: case report. J Neurosurg 14:658–687
Di Chiro G, Doppman JG (1969) Differential angiographic features of hemangioblastomas and arteriovenous malformations of the spinal cord. Radiology 93:25–30
Di Chiro G, Doppman JL (1970) Endocranial drainage of spinal cord veins. Radiology 95:555–560
Di Chiro G, Wener L (1973) Angiography of the spinal cord. A review of contemporary techniques and applications. J Neurosurg 39:1–29
Di Chiro G, Doppman JL, Ommaya AK (1967) Selective arteriography of arteriovenous aneurysms of the spinal cord. Radiology 88:1065–1077
Di Chiro G, Timmins E, Jones A, Johnston G (1974) Radionuclide scanning and microangiography of evolving and completed brain infarction. A correlative study in monkeys. Neurology 24:418–423

Di Rocco C, Iannelli A, Leone G, Moschini M, Valori V (1981) Heparinurokinase treatment in aseptic dural sinus thrombosis. Arch Neurol 38:431–435
Dias MS, Sekhar LN (1990) Intracranial hemorrhage from aneurysms and arteriovenous malformations during pregnancy and the puerperium. Neurosurgery 27:855–866
Diaz J, Schiffman J, Urban E, Maccario M (1992) Superior sagittal sinus thrombosis and pulmonary embolism: a syndrome rediscovered. Acta Neurol Scand 86: 390–396
Diethrich E, Ndiaye M, Reid D (1996) Stenting in the carotid artery: initial experience in 110 patients. J Endovasc Surg 3:42–62
Dilenge D, Heon M, Metzger J (1973) Selective spinal angiography in multiple CNS lesions. J Can Assoc Radiol 24:178–183
Dion JE, Frazee J, Jordan S, Kar S, Vinuela F, Rand R, Corday E (1989) Rescue of ischemic brain by selective venous retroperfusion of arterial blood. AJNR Am J Neuroradiol 10:871
Dippel DWJ, ter Berg JWM, Habbema JDF (1992) Screening for unruptured familial intracranial aneurysms. A decision analysis. Acta Neurol Scand 86:381–389
Djindjian M, Djindjian R, Hurth M et al (1977) Spinal cord arteriovenous malformations and the Klippel-Trenaunay-Weber syndrome. Surg Neurol 8:229–237
Djindjian R (1962) Spinal cord hemangioblastomas and von Hippel-Lindau's disease. Rev Neurol 124:707–717
Djindjian R (1969) Arteriography of the spinal cord. Roentgenology 107:461–478
Djindjian R (1975) Embolization of angiomas of the spinal cord. Surg Neurol 4:411–420
Djindjian R (1976) Le traitement chirurgical des angiomes intramédullaires. Thesis, Paris
Djindjian R (1978) Clinical symptomatology and natural history of arteriovenous malformations of the spinal cord – a study of the clinical aspects and prognosis, based on 150 cases. In: Pia HW, Djindjian R (eds) Spinal angiomas: advances in diagnosis and therapy. Springer, Berlin Heidelberg New York
Djindjian R, Faure C (1965) L'aortographie dans les angiomes médullaires. La radiographie des formations intra-rachidiennes. Masson, Paris
Djindjian R, Merland JJ (1978) Superselective arteriography of the external carotid artery. Springer, Berlin Heidelberg New York
Djindjian R, Dumesnil M, Faure C, Lefebre J, Leveque P (1962) Etude angiographique d'un angiome intra-rachidien. Rev Neurol 106:278–285
Djindjian R, Cophignon J, Comoy J, Rey J, Houdart R (1968) Polymorphisme neuroradiologique des fistules carotido-caverneuses. Neurochirurgie 14:881–890
Djindjian R, Houdart R, Hurth M (1969a) Les angiomes de la moelle. Sandoz, Paris
Djindjian R, Hurth M, Houdart R (1969b) Angiomes médullaires, dysplasies vasculaires segmentaires ou généralisées et phacomatoses. Rev Neurol (Paris) 121: 190–211
Djindjian R, Hurth M, Houdart R (1970a) L'angiographie de la moelle épinière. Masson, Paris
Djindjian R, Hurth M, Thurel CL (1970b) Cervicocranial phlebography of angiomas of the spinal cord. Neuroradiology 1:42–46
Djindjian R, Houdart R, Cophignon J, Hurth M (1971a) Premiers essais d'embolisation par voie fémorale dans un cas d'angiome médullaire et dans un cas d'angiome alimenté par la carotide externe. Rev Neurol 125:119–130
Djindjian R, Hurth M, Houdart R (1971b) Angiomes médullaires, dysplasies vasculaires segmentaires ou généralisées et phacomatoses. Rev Neurol 124:121–142
Djindjian R, Manelfe C, Picard L (1973) Fistules artérioveineuses carotide externe-vinus caverneux; étude angiographique à propos de 6 observations et revue de la littérature. Neurochirurgie 19:91–110
Djindjian R, Houdart R, Hurth M, Cophignon J, Rey A, Thurel C (1975) Embolisation dans les angiomes de la moelle. J Neuroradiol 2:73–172
Djindjian R, Merland JJ, Djindjian M, Stoeter P (1981) Angiography of spinal column and spinal cord tumors. Neuroradiological atlas. Thieme, New York
Do HM, Jensen ME, Cloft HJ, Kallmes DF, Dion JE (1999) Dural arteriovenous fistula of the cervical spine presenting with subarachnoid hemorrhage. AJNR Am J Neuroradiol 20:348–350

Dobbelaere P, Jomin M, Clarisse J, Laine E (1979) Intérêt pronostique de l'étude du drainage veineux des anévrysmes artérioveineux cérébraux. Neurochirurgie 25:178–184
Donnell MW, Meyer GA, Donegan WI (1979) Estrogen-receptor protein in intracranial meningiomas. J Neurosurg 50:499–502
Doppman JL (1980a) The treatment of hyperparathyroidism by transcatheter techniques. Cardiovasc Intervent Radiol 3:268–281
Doppman JL (1980b) The localization and treatment of parathyroid adenomas by angiographic techniques. Ann Radiol 23:253–258
Doppman JL (1971) The nidus concept of spinal cord arteriovenous malformations. A surgical recommendation based upon angiographic observations. Br J Radiol 44:758–763
Doppman JL, Di Chiro G (1965) Subtraction angiography of spinal cord vascular malformations. Report of a case. J Neurosurg 23:440–443
Doppman JL, Di Chiro G (1976) Paraspinal muscle infarction. A painful complication of lumbar artery embolization associated with pathognomonic radiographic and laboratory findings. Radiology 119:609–613
Doppman JL, Di Chiro G, Glancy DL (1968a) Collateral circulation through dilated spinal cord arteries in aortic coarctation and extraspinal arteriovenous shunts. An arteriographic study. Clin Radiol 20:192–197
Doppman JL, Di Chiro G, Ommaya AK (1968b) Obliteration of spinal cord arteriovenous malformation by percutaneous embolization (letter to editor). Lancet 1:577
Doppman J, Dedrick R, Shook D, Lutz R, Goldstein S, Blacklock J (1986) Glioblastoma: catheter techniques for isolated chemotherapy perfusion. Radiology 159: 477–483
Doppman JL, Di Chiro G, Ommaya AK (1971a) Percutaneous embolization of spinal cord arteriovenous malformations. J Neurosurg 34:48–55
Doppman JL, Zapol W, Pierce J (1971b) Transcatheter embolization with a silicone rubber preparation. Experimental observations. Invest Radiol 6:304–309
Doppman JL, di Chiro G, Dwyer AJ, Frank JL, Oldfield EH (1987) Magnetic resonance imaging of spinal arteriovenous malformations. J Neurosurg 66:830–834
Dormont D, Assouline E, Gelbert F, Helias A, Halimi P, Chiras J, Bories J, Doyon D, Merland JJ (1987) MRI study of spinal arteriovenous malformations. J Neuroradiol 14:351–364
Dorros G (1998a) Stent deployment resolves a petrous carotid artery angioplasty dissection. AJNR Am J Neuroradiol 19: 392–394
Dorros G (1998b) Stent-supported carotid angioplasty. Circulation 98:927–930
Dotter C (1969) Transluminally-placed coilspring endarterial tube grafts: long-term patency in canine popliteal artery. Invest Radiol 4:327–332
Dotter C, Buschman P, McKinney M, Rosch J (1983) Transluminal expandable nitinol coil stent grafting: preliminary report. Radiology 147:259–260
Doyon D, Metzger J (1973) Malformations vasculaires duremeriennes sustentorielles. Acta Radiol 13:792–800
Drake CG (1979a) Cerebral arteriovenous malformations: considerations for an experience with surgical treatment in 166 cases. Clin Neurosurg 26:145–208
Drake CG (1979b) Giant intracranial aneurysms: experience with surgical treatment in 174 patients. Clin Neurosurg 26:12–95
Drake CG, Peerless SJ (1997) Giant fusiform intracranial aneurysms: review of 120 patients treated surgically from 1965 to 1992. J Neurosurg 87:1041–162
Drouet L (1980) Oestrogènes, androgènes et vaisseaux. Quot Med [Suppl 2] 150:16–31
Du Boulay G, Darling M (1975) Autoregulation in external carotid artery branches in the baboon. Neuroradiology 9:129–132
Dubovsky J, Zabramski JM, Kurth J, Spetzler RF, Rich SS, Orr HT, Weber JL (1995) A gene responsible for cavernous malformations of the brain maps to chromosome 7q. Hum Mol Genet 4:453–458
Dubrovsky T, Curless R, Scott G et al (1998) Cerebral aneurysmal arteriopathy in childhoo AIDS. Neurology 51:560–565
Duchen L (1992) General pathology of neurons and neuralgia. In: Adams J, Duchen L (eds) Greenfield's neuropathology. Oxford Press, New York, pp 153–268

Duckwiler GR, Dion JE, Vinuela F, Martin N, Jabour B, Bentson J (1990) Intravascular microcatheter pressure monitoring: experimental results and early clinical evaluation. AJNR Am J Neuroradiol 11:169–175
Ducreux D, Oppenheim C, Vandamme X (2001) Diffusion-weighted imaging patterns of brain damage associated with cerebral venous thrombosis. AJNR Am J Neuroradiol 22:261–268
Duerig T, Pelton A, Stockel D (1996) The utility of superelasticity in medicine. Biomed Mater Eng 6:255–266
Duffau H, Lopes M, Janosevic V, Sichez JP, Faillot T, Capelle L, Ismail M, Bitar A, Arthus F, Fohanno D (1999) Early rebleeding from intracranial dural arteriovenous fistulas. J Neurosurg 90:78–84
Duker J, Sivalingam A, Brown G, Reber R (1991) A prospective study of acute central retinal artery obstruction: the incidence of secondary ocular neovascularization. Arch Ophthalmol 47:690–703
Dunlop DAB, Papapoulos SE, Lodge RW, Fulton AJ, Kendall BE, O'Riordan JLH (1980) Parathyroid venous sampling: anatomic considerations and results in 95 patients with primary hyperparathyroidism. Brit J of Radiol 53:1183–1191
Duong DH, Young WL, Vang MC, Sciacca RR, Mast H, Koennecke HC, Hartmann A, Joshi S, Mohr JP, Pile-Spellman J (1998) Feeding artery pressure and venous drainage pattern are primary determinants of hemorrhage from cerebral arteriovenous malformations. Stroke 29:1167–1176
Duplay J, Cossa P, Marchal E (1957) Anevrismes multiples de la carotide interne dans son segment exocranien et dans son segment endocranien. Presse Med 65:143–144
Dusser A, Boyer-Neumann C, Wolf M (1988) Temporary protein C deficiency associated with cerebral arterial thrombosis in childhood. J Pediatr 113:849–852
Dutton J, Isherwood I (1970) Iatrogenic vertebral arteriovenous fistulae Neurochirurgia 13:49–60
Duvernoy HM, Delon S, Vannson JL (1981) Cortical blood vessels of the human brain. Brain Res Bull 7:519–579
Dyker A, Lees K (1998) Duration of neuroprotective treatment for ischemic stroke. Stroke 29:535–542
Dyken M, Pokra S (1984) The performance of endarterectomy for diseases of the extracranial arteries of the head. Stroke 15:948–956
Dyken M, Barnett H, Easton J, Fields W (1992) Low-dose aspirin and stroke. "It ain't necessarily so". Stroke 23:1395–1399
Earle KM, Richany SF (1969) Meningiomas. A study of the histology, incidence, and biologic behavior of 243 cases from the Frazier-Grant collection of brain tumors. Med Ann D C 38:353–358
Eckberg D, Cavanaugh M, Mark A, Abboud F (1975) A simplified neck suction device for activation of carotid baroreceptors. J Lab Clin Med 85:167–173
ECST ECSTG (1991) MRC European carotid surgery trial: interim results for symptomatic patients with severe (70–99%) or with mild (0–29%) carotid stenosis. Lancet 337:1235–1243
ECST ECSTCG (1996) Endarterectomy for moderate symptomatic carotid stenosis: interim results from the MRC European Carotid Surgery Trial. Lancet 347:1591–1593
Edelsohn L, Caplan L, Rosenbaum A (1972) Familial aneurysms and infundibular widening. Neurology 22:1056–1060
Edner G (1991) One -session operation via bilateral craniotomies for multiple aneurysms after subarachnoid hemorrhage. Br J Neurosurg 5.55–60
Edner G, Feuerberg I (1984) Optic glioma, neurofibromatosis and ruptured aneurysm. Case report. OPMEAR 29:14–15
Edwards W, Mulherin JJ (1980) The surgical approach to significant stenosis of vertebral and subclavian arteries. Surgery 87:20–28
Ehni G, Barrett JH (1960) Hemorrhage from ear due to aneurysm of internal carotid artery. N Engl J Med 262:1323–1325
Ehrenfeld WK, Hays RJ (1972) False aneurysms after carotid endarterectomy Arch Surg 104:288–291
Ehrenfeld WK, Wylie EJ (1974) Fibromuscular dysplasia of the internal carotid artery. Surgical management. Arch Surg 109:676–681

Eichhorn J, Sima D, Thiele B, Lindschau C (1996) Anti-endothelial cell antibodies in Takayasu arteritis. Circulation 94:2396–2401
Einhaupl K, Villringer A, Meister W, Mehraein S (1991) Heparin treatment in sinus venous thrombosis. Lancet 338:597–600
Eisenman JI, Alekoubides A, Priba MH (1972) Spontaneous thrombosis of vascular malformations of the brain. Acta Radiol Diagn (Stockh) 13:77–85
Ekseth K, Bostrom S, Vegfors M (1998) Reversibility of severe sagittal sinus thrombosis with open surgical thrombectomy combined with local infusion of tissue plasminogen activator: technical case report. Neurosurgery 43:960–965
El Gohary M, Tomita T, Guitierrez FA, McLone DG (1987) Angiographically occult vascular malformations in childhood. Neurosurgery 20:759–766
Elders RA (cited by Zak) (1962) Paraganglioma. Een overzicht en een besspreking van 92 Nederlandse patienten. Thesis, University of Groningen
Eliasziw M, Streifler J, Fox A et al (1994) Significance of plaque ulceration in symptomatic patients with highgrade carotid stenosis. Stroke 25:304–308
Ellman BA, Parkhill BJ, Curry III TS, Marcus PB, Peters PC (1981) Ablation of renal tumors with absolute ethanol: a new technique. Radiology 141:619–626
Ellman BA, Parkhill BJ, Marcus PB (1984) Renal ablation with absolute ethanol: mechanism of action. Invest Radiol 19:416–422
Emery DJ, Willinsky R, Burrows P, Armstrong D, Montanera W, Ter Brugge K (1998) Paediatric spinal arteriovenous malformations: angioarchitecture and endovascular treatment. Interv Neuroradiol 4:127–139
Endo S, Nishijima M, Nomura H, Takaku A, Okada E (1993) A pathological study of intracranial posterior circulation dissecting aneurysms with subarachnoid hemorrhage: report of three autopsied cases and review of the literature. Neurosurgery 33: 732–744
Endo S, Kuwayama N, Hirashima Y, Akai T, Nishijima M, Takaku A (1998) Results of urgent thrombolysis in patients with major stroke and atherothrombotic occlusion of the cervical internal carotid artery. AJNR Am J Neuroradiol 19:1169–1175
Enzinger FM, Smith BH (1976) Hemangiopericytoma. An analysis of 106 cases. Human Pathol 7:61–82
EPILOG Investigators (1997) Platelet glycoprotein IIb/IIIa receptor blockade and low-dose heparin during percutaneous coronary revascularization. N Engl J Med 336:1689–1696
EPISTENT Investigators (1998) Randomized placebo-controlled and balloon-angioplasty-controlled trial to assess safety of coronary stenting with use of platelet glycoprotein-IIb/IIIa blockade. Lancet 352:87–92
Erickson D, Kudva YC, Ebersold MJ, Thompson GB, Grant CS, van Heerden JA, Young WF (2001) Benign paragangliomas: clinical presentation and treatment outcomes in 236 patients. J Clin Endocrinol Metab 86:5210–5216
Eskridge JM, Shaw DWW, Scott JS (1991) Preoperative embolization of hemangioblastomas. AJNR (in press)
Eskridge J, Newell D, Winn HR (1994) Endovascular treatment of vasospasm. Neurosurg Clin North Amer 5:437–447
Eskridge J, McAuliffe W, Song J et al (1998) Balloon angioplasty for the treatment of vasospasm: results of first 50 cases. Neurosurgery 44:975–979
Etchevers HC (2001) The cephalic neural crest provides pericytes and smooth muscle cells to all blood vessels of the face and forebrain. Development 128:1059–1068
Evans MC, Linton RA, Cameron IR (1977) The effect of local changes in calcium concentration on hypothalamic blood flow in the anesthetized rabbit. Acta Neurol Scand Suppl 64:388–389
Ewing JA, Shively EH (1981) Angiofibroma: a rare case in an elderly female. Otolaryngol Head Neck Surg 89:602–603
Falk E (1991) Coronary thrombosis: pathogenesis and clinical manifestations. Am J Cardiol 68:28B–35B
Falk E, Shah P, Fuster V (1996) Pathogenesis of plaque disruption. In: Fuster V, Ross R, Topol E (eds) Atherosclerosis and coronary artery disease. Lippincott-Raven, Philadelphia, pp 492–510
Faraci FM, Brian JE Jr (1994) Nitric oxide and the cerebral circulation. Stroke 25: 692–703

Farb RI, McGregor C, Kim JK, Laliberte M, Derbyshire JA, Willinsky RA, Cooper PW, Westman DG, Cheung G, Schwartz ML, Stainsby JA, Wright GA (2001) Intracranial arteriovenous malformations: real-time autotriggered elliptic centric-ordered 3D gadolinium-enhanced MR angiography: initial assessment. Radiology 220:244–251

Farb RI, Kim JK, Willinsky RA, Montanera W, TerBrugge KG, Derbyshire JA, van Dijk JM, Wright GA (2002a) Spinal dural arteriovenous fistula localization with a technique of first-pass gadolinium-enhanced MR angiography: initial experience. Radiology 222:843–850

Farb R, Scott JN, Willinsky RA, Montanera WJ, Wright GA, ter Brugge KG (2003) Gadolinium enhanced venography of the intracranial venous system using an auto-triggerered elliptical centric ordered (ATECO) sequence. Radiology 226: 203–209

Faria MA, Fleischer AS (1980) Dual cerebral and meningeal supply to giant arteriovenous malformations of the posterior cerebral hemisphere. J Neurosurg 52: 153–161

Farr HW, Gray GF, Vrana M, Panio M (1973) Extracranial meningioma. J Surg Oncol 5:411–420

Farrior JB, Hyams VJ, Benke RH (1980) Carcinoid apudoma arising in a glomus jugulare tumor: review of endocrine activity in glomus jugulare tumors. Laryngoscope 90:110–118

Faught W, van Bemmelen P, Mattos M et al (1993) Presentation and natural history of internal carotid artery occlusion. J Vasc Surg 18:512–524

Fehlings MG, Tucker WS (1988) Cavernous hemangioma of Meckel's cave. J Neurosurg 68:645–647

Feigin VL, Anderson CS, Andersen NE, Broad JB, Pledger MJ, Bonita R (2001) Is there a temporal pattern in occurrence of subarachnoid hemorrhage in the southern hemisphere? Pooled data from 3 large, population-based incidence studies in Australia, 1981 to 1997. Stroke 32(3):613–619

Fein JM, Flamm E (1979) Planned intracranial revascularization before proximal ligation for traumatic aneurysm. Neurosurgery 5:254–258

Feinberg DA, Dacey RG Jr, Jonhston SC, Zhao S, Dudley RA, Berman MF, Gress DR (2001) Treatment of unruptured cerebral aneurysms in California. Stroke 32:597–605

Feldman R, Trigg L, Gaudier J, Galat J (1996) Use of coronary Palmaz-Schatz stent in the percutaneous treatment of an intracranial carotid artery stenosis. Cathet Cardiovasc Diagn 84:883–887

Feng L, Yu-Hai B (1994) Myelopathy and multiple aneurysms associated with aortic arch interruption: case report. J Neurosurg 35:310–313

Feng L, Bao Y, Zhang H, Wang D (1999) Chinese experience in endovascular management of spinal cord vascular malformations. Intervent Neuroradiol 5:109–126

Fenyes G, Kepes J (1956) Über das gemeinsame Vorkommen von Meningeomen und Geschwulsten anderen Typs im Gehirn. Zentralbl Neurochir 16:251–260

Ferber L, Lampe I (1942) Hemangiomas of vertebral associated with compression of the cord. Response to radiation therapy. Arch Neurol Psychiatry 47:19–29

Ferlito A, Pesavento G, Recher G, Nicolai P, Narne S, Polidoro F (1984) Assessment and treatment of neurogenic and non-neurogenic tumors of the parapharyngeal space. Head Neck Surg 7:32–43

Fernand M, Reizine D, Melki JP (1987) Long-term follow-up of 43 pure dural arteriovenous fistulae (AVF) of the lateral sinus. Neuroradiology 29:348–353

Ferrante L, Celli P, Fraioli B, Santoro A (1984) Haemangioblastomas of the posterior cranial fossa. Acta Neurochir (Wien) 71:283–294

Fessler R, Ringer A, Qureshi A, Guterman L, Hopkins L (2000) Intracranial stent placement to trap an excluded coil during endovascular aneurysm treatment: technical note. Neurosurgery 46:248–253

Feuerstein G, Miller A (1997) Vasoactive mediators of cerebral vessels. In: Welch K, Caplan L, Reis D, Siesjo B, Weir B (eds) Primer on cerebrovascular diseases. Academic Press, San Diego, pp 8–13

Figlos J, CervosNavarro J et al (1988) Microthrombi in the development of ischemic irreversible brain infarct. In: Cervos-Navarro J, Ferszt R (eds) Stroke and microcirculation. Raven Press, New York

Fincher EF (1951) Arteriovenous fistula between the middle meningeal artery and the greater petrosal sinus. Case report. Ann Surg 133:886–888
Finney LA, David NJ (1964) Aneurysm of extracranial internal carotid artery; report of case and discussion. Neurology (Minneap.) 14:376–379
Fisch U (1982) Infratemporal fossa approach for glomus tumors of the temporal bone. Ann Otol Rhin Laryng 91:474–479
Fisch U, Fagan P, Valavanis A (1984) The infratemporal fossa approach for the lateral skull base. Otolaryngol Clin North Am 17:513–552
Fischell T, Carter A, Laird J (1996) The beta-particle-emitting radioisotope stent (isostent) animal studies and planned clinical trials. Am J Cardiol 78:45–50
Fischer WS (1989) Decision analysis: a tool of the future: an application to unruptured arteriovenous malformations. Neurosurgery 24:129–136
Fischman D, Leon M, Baim D, Schatz R (1994) A randomized comparison of coronary stent placement and balloon angioplasty in treatment of coronary artery disease. N Engl J Med 331:496–501
Fisher CM, Kistler JP, Davis JM (1980) Relation of cerebral vasospasm to subarachnoid hemorrhage visualized by CT scanning. Neurosurgery 6:1–9
Fitch W, MacKenzie E, Harper A (1975) Effects of decreasing arterial blood pressure on cerebral blood flow in the baboon. Influence of the sympathetic nervous system. Circ Res 37:550–557
Fitzgerald G, Patrono C (1998) Antiplatelet drugs. In: Verstraete M, Fuster V, Topol E (eds) Cardiovascular thrombosis. Lippincott Raven, Philadelphia, pp 121–140
Fitzpatrick PJ, Rider WD (1973) The radiotherapy of nasopharyngeal angiofibroma. Radiology 109:171–178
Fletcher AP, Alkjaersig N, Lewis N, Tulevski V et al (1976) A pilot study of urokinase therapy in cerebral infarction. Stroke 7:135–142
Flood LM, Kemink JL (1984) Surgery in lesions of the petrous apex. Otolaryngol Clin North Am 17: 565–575
Fog M (1937) Cerebral circulation: the reaction of the pail arteries to a fall in blood pressure. Arch Neurol Psychiatry 37:351–364
Foix CH, Alajouanine TH (1926) La myélite nécrotique subaiguë. Myélite centrale angio-hypertrophique à évolution progressive. Paraplégie amyotrophique lentement ascendante, d'abord spasmodique, puis flasque, s'accompagnant de dissociation albumino-cytologique. Rev Neurol 33:1–42
Folkman J (1975) Tumor angiogenesis: a possible control point in tumor growth. Ann Intern Med 82:96–100
Folkman J (1986) How is blood vessel growth regulated in normal and neoplastic tissue? Cancer Res 46:467–473
Folkman J (1995) Clinical applications of research on angiogenesis. N Engl J Med 333:1757–1763
Folpe AL, Fanburgh-Smith JC, Miettinen M, Weiss SW(2001) Atypical and malignant glomus tumors: analysis of 52 cases, with a proposal for the reclassification of glomus tumors. Am J Surg Pathol 25:1–12
Fontaine S, Melanson D, Cosgrove R, Bertrand G (1988) Cavernous hemangiomas of the spinal cord: MR imaging. Radiology 166:839–841
Foo S, Choi I, Berenstein A, Wise A, Ransohoff J (1986) Supraophthalmic intracarotid infusion of BCNU for malignant glioma. Neurology 11:1437–1444
Foote RA, Reagan TJ, Saudok BA (1978) Cerebral arterial lesions resulting from inflammatory emboli. Stroke 9:498–503
Forbes G, Nichols DA, Jack CR, Ilstrup DM et al (1988) Complications of spinal cord arteriography: prospective assessment of risk for diagnostic procedures. Radiology 169:479–484
Forbes H, Cobb S (1938) Vasomotor controls of cerebral vessels. Brain 61:221–233
Forbes K, Pipe J, Heiserman J (2001) Evidence for cytotoxic edema in the pathogenesis of cerebral venous infarction. AJNR Am J Neuroradiol 22:450–455
Forbus WD (1930) On the origin of miliary aneurysms of the superficial cerebral artery. Bull Johns Hopkins Hosp 47:239–284
Forster DMC, Steiner L, Hakanson S (1972) Arteriovenous malformations of the brain. A long-term clinical study. J Neurosurg 37:562–570

Fournier D, Ter Brugge K, Rodesch G, Lasjaunias P (1990) Revascularization of brain arteriovenous malformations after embolization with bucrylate. Neuroradiology 32: 497–501
Fournier D, Ter Brugge KG, Willinsky R, Lasjaunias P, Montanera W (1991) Endovascular treatment of intracerebral arteriovenous malformations: experience in 49 cases. J Neurosurg 75:228–233
Fox AJ, Drake CG (1987) Aneurysm neck remnant following balloon embolization (letter). J Neurosurg 67:321–322
Fox AJ, Vinuela F, Pelz DM et al (1987) Use of detachable balloons for proximal artery occlusion in the treatment of unclippable cerebral aneurysms. J Neurosurg 66: 40–46
Fox JL (1982) Familial intracranial aneurysms. J Neurosurg 57:416–417
Frackowiak RS, Jones T, Lenzi GL, Heather JD (1980) Regional cerebral oxygen utilization and blood flow in normal man using oxygen-15 and positron emission tomography. Acta Neurol Scand 62:336–344
Fraser GR (1971) Congenital internal carotid–internal jugular fistula (letter). J Pediatr 79:343–344
Fredricks H, Kievit J, van Baalen J, van Bockel J (1998) Carotid recurrent stenosis and risk of ipsilateral stroke: a systematic review of the literature. Stroke 129:244– 250
Frey J, Muro G, McDougall C, Dean B, Jahnke H (1999) Cerebral venous thrombosis: combined intrathrombus rtpa and intravenous heparin. Stroke 30:489–494
Friede RL, Schachenmayr W (1978) The origin of subdural neomembranes. Am J Pathol 92:69–84
Friedmann I, Osborn DA (1976) Systemic pathology, vol 1, 2nd edn. Churchill Livingstone, Edinburgh, pp 228–230
Fu YS, Perzin KH (1974) Nonepithelial tumors of the nasal cavity, paranasal sinuses, and nasopharynx: a clinicopathologic study I. General features and vascular tumors. Cancer 33:1275–1287
Fujiwara S, Hachisuga S, Numaguchi Y (1980) Intracranial hypoglossal neurinoma: report of a case. Neuroradiology 20:87–90
Fukuoka S, Suematsu K, Fujiwara H et al (1984) Completely thrombosed giant aneurysm of the angular artery. Surg Neurol 22:145–148
Fukushima T, Hamano K et al (1989) A case of multiple arteriovenous malformations and diffuse venous abnormalities with facial port-wine stain. Child's Nerv Syst 5:114–117
Fults D, Kelly DL (1984) Natural history of arteriovenous malformations of the brain: a clinical study. Neurosurgery 15:658–662
Furlan A, Kanoti G (1997) When is thrombolysis justified in patients with acute ischemic stroke? A bioethical perspective. Stroke 28:214–218
Fuse A, Rodesch G, Alvare HZ, Lasjaunias P (2000) Endovascular management of intradural berry aneurysms. Review of 203 consecutive patients managed between 1993 and morphological and clinical results at mid-term follow-up. Intervent Neuroradiol 6:27–39
Fuster V (1994) Mechanisms leading to myocardial infarction: insights from studies of vascular biology. Circulation 90:2126–2146
Fuster V, Badimon L, Badimon J et al (1992) The pathogenesis of coronary artery disease and the acute coronary syndromes. N Engl J Med 326:310–318
Gaillard J, Haguenauer JP, Romanet P, Dubreuil C, Dumolard F (1978) Evolution insolite de deux chémotectomes tympano-jugulaires. J Oto-Rhino-Laryng 27:553–556
Galibert P, Deramond H, Rosat P, Le Gars D (1987) Preliminary note on the treatment of vertebral angioma by percutaneous acrylic vertebroplasty. Neurochirurgie 33: 166–168
Garcia CA, Dulcey S, Dulcey J (1979) Ruptured aneurysm of the spinal artery of Adamkiewicz during pregnancy. Neurology (NY) 29:394–398
Garcia J, Liu K, Ho K (1995) Neuronal necrosis after middle cerebral artery occlusion in Wistar rats progresses at different time intervals in the caudoputamen and the cortex. Stroke 26:636–643
Garcia JC, Roach S, McLean WT (1981) Recurrent thrombotic deterioration in the Sturge-Weber syndrome. Childs Brain 8:427–433

Garcia-Monaco R, Alvarez H, Goulao Z, Pruvost Ph, Lasjaunias P (1990a) Posterior fossa arteriovenous malformations. Angioarchitecture in relation to their hemorrhagic episodes. Neuroradiology 31:471–475

Garcia-Monaco R, Alvarez H, Lasjaunias P (1990b) Utilization of the mini-torquer in cerebral arteriovenous malformations of the newborn and infant. Diagn Int Radiol 2:123–124

Garcia-Monaco R, Rodesch G, Alvarez H, Iizuka Y, Hui F, Lasjaunias P (1993) Pseudoaneurysms within ruptured intracranial arteriovenous malformations: diagnosis and early endovascular management. AJNR 14:315–321

Garcia-Monaco R, Taylor W, Rodesch G, Alvarez H, Burrows P, Coubes P, Lasjaunias P (1995) Pial arteriovenous fistula in children as revealing manifestation of Rendu-Osler-Weber disease. Neuroradiology 37:60–64

Gardiner HM, Celermajer DS, Sorensen KE, Georgeakoupolos D, Robinson J, Thomas O, Deanfield JE (1994) Arterial reactivity is significantly impaired in normotensive young adults after successful repair of aortic coarctation in childhood. Circulation 89:1745–1750

Garretson HD (1985) Intracranial arteriovenous malformations. In: Wilkins RH, Rengachary SS (eds) Neurosurgery. McGraw-Hill, New York, pp 1448–1457

Gaupp J (1988) Casuistische Beiträge zur pathologischen Anatomie des Rückenmarks und seiner Häute. Beitr Pathol Anat 2:510–524

Geachan NE, Lambert J, Micheau C, Richard JM (1983) Synovialome malin du larynx. Ann Oto-Laryng 100:61–65

Gelber BR, Sundt TM Jr (1980) Treatment of intracavernous and giant carotid aneurysms by combined internal carotid ligation and extra to intracerebral bypass. J Neurosurg 52:1–10

Gelbert F, Riche MC, Reizine D, Merland JJ, Cormeir JM (1988) Direct arteriovenous fistula of the external carotid artery. Treatment with detachable balloon. Ann Vasc Surg 2:358–361

Gentili F, Schwartz M, Ter Brugge KG, Wallace MC, Willinsky RW, Young C (1992) A multidisciplinary approach to the treatment of brain vascular malformations. In: Symon L (ed) Advances in technical standards in neurosurgery, vol 19. Springer, Berlin Heidelberg New York, pp 179–207

Geoffray A, Lee YY, Jings BS, Wallace S (1984) Extracranial meningiomas of the head and neck. AJNR 5:599–604

George B, Zerah M, Mourier KL et al (1989) Ruptured intracranial aneurysms. The influence of sex and fibromuscular dysplasia upon prognosis. Acta Neurochirurg 97:26–30

Gerber S, Dormont D, Sahel M et al (1994) Complete spontaneous thrombosis of a giant intracranial aneurysm. Neuroradiology 36:316–317

Geremia G, Haklin M, Brennecke L (1994) Embolization of experimentally created aneurysms with intravascular stent devices. Am J Neuroradiol 15:1223–1231

Gianotta S, McGillicuddy JE, Kindt GW (1979) Gradual carotid artery occlusion in the treatment of inaccessible internal carotid artery aneurysm. Neurosurgery 5:417–421

Gibbon JRP, Brookes JPCM (1967) Phaechromocytoma associated with multiple neurofibromatosis and aneurysm of the circle of Willis. Brit J Clin Pract 21:360–362

Gibbons GH, Dzau VJ (1994) The emergent concept of vascular remodeling N Engl J Med 20:1431–1438

Gibson JB, Taylor AR, Richardson AE (1959) Congenital arteriovenous fistula with an aneurysm of the great cerebral vein and hydrocephalus treated surgically. J Neurol Neurosurg Psychiatry 22:224–228

Gijn JV, Bromberg JEC, Lindsay KW, Hasan D, Vermeulen M (1994) Definition of initial grading, specific events, and overall outcome in patients with aneurysmal subarachnoid hemorrhag – a survey. Stroke 25:1623–1627

Gilbertson JR, Miller GM, Goldman MS, Marsh WR (1995) Spinal dural arteriovenous fistulas: MR and myelographic findings. AJNR Am J Neuroradiol 16: 2049–2057

Gillilan LA. General principles of the arterial blood vessel patterns to the brain. Trans Am Neurol Assoc 82:65

Gillilian LA (1970) Veins of the spinal cord. Anatomic details: suggested clinical applications. Neurology 20:860–868
Ginzburg B, Montanera W, Tyndel F, Griesman J, McLennan M, Ter Brugge K, Willinsky RA (1992) Diagnosis of von Hippel-Lindau Disease in a patient with blindness resulting from bilateral optic nerve hemangioblastomas. AJR 159:403–405
Giombini S, Morello G (1978) Cavernous angiomas of the brain. Account of fourteen personal cases and review of the literature. Acta Neurochir (Wien) 40:61–82
Girevendulis AK, Lipper MH, Kishore PRS, Vines FS, Greenfeild LJ (1980) Congenital arteriovenous fistula of the external carotid artery. South Med J 73:1549–1550
Girgis IH, Fahmy SA (1973) Nasopharyngeal fibroma: its histopathological nature. J Laryngol 87:1107–1123
Glagov S, Weisenberg E, Zarins C, Stankunavicius R, Kolettis G (1987) Compensatory enlargement of human atherosclerotic coronary arteries. N Engl J Med 316:1371–1375
Glasgov S, Zarins C, Giddens D et al (1988) Mechanical factors in the pathogenesis, localization and evolution of atherosclerotic plaques. Diseases of the arterial wall. Springer, Berlin Heidelberg New York, pp 217–239
Glass TA, Hennessey PM, Pazdera L, Chang HM, Wityk RJ, Dewitt LD, Pessin MS, Caplan LR (2002) Outcome at 30 days in the New England Medical Center Posterior Circulation Registry. Arch Neurol 59: 359–360
Glasscock ME, Smith PG, Schwaber MK, Nissen AJ et al. (1984) Clinical aspects of osseous hemangiomas of the skull base. Laryngoscope 94:869–873
Glenner GC, Grimley PM (1974) Tumors of the extra-adrenal paranglion system (including chemoreceptors). Atlas of tumor pathology, 2nd series, fasc 9. Armed Forces Institute of Pathology, Washington DC
Gobin YP, Laurent A, Merienne L, Schlienger M, Aymard A, Houdart E, Casasco A, Lefkopoulos D, George B, Merland JJ (1996) Treatment of brain arteriovenous malformations by embolization and radiosurgery. J Neurosurg 85: 19–28
Gold D (1977) Retinal arterial occlusion. Am Acad Ophthalmol Otolaryngol 83:392–406
Gold RE, Grace DM (1975) Gelfoam embolization of the left gastric artery for bleeding ulcers. Experimental considerations. Radiology 116:575–580
Goldberg RA, Goldey SH, Duckwiler G, Vinuela F (1996) Management of cavernous sinus-dural fistulas. Indications and techniques for primary embolization via the superior ophthalmic vein. Arch Ophthalmol 114:707–714
Goldenberg RR, Campbell CJ, Bonfiglio M (1970) Giant cell tumor of bone. An analysis of two hundred and eighteen cases. J Bone Joint Surg 52A:619
Goldstein L, Moore W, Robertson J et al (1997) Complication rates for carotid endarterectomy. A call to action. Stroke 28:889–890
Gomori JM, Dermer R, Shifrin E (1983) Aneurysm of the lingual artery. Neuroradiology 25:111–112
Goncalves CG, Briant TDR (1978) Radiologic findings in nasopharyngeal angiofibromas. J Can Assoc Radiol 29:209–215
Gonner F, Remonda L, Mattle H, Sturzenegger M (1998) Local Intra-arterial thrombolysis in acute ischemic stroke. Stroke 29:1894–1900
Gordon DH, Levin DC (1976) Treatment of angiographically produced cord seizures by infra-arterial diazepam. Cathet Cardiovas Diagn 6:297–300
Gore J, Dalen J (1996) Cardiovascular disease. JAMA 275:1797–1798
Gorelick P, Caplan L, Hier D et al (1984) Clinical and angiographic comparison of asymptomatic occlusive cerebrovascular disease. Neurology 35:54–59
Gotlieb A, Langille B (1996) The role of rheology in atherosclerotic coronary artery disease. In: Fuster V, Ross R, Topol EJ (eds) Atherosclerosis and coronary artery disease. Lippincott-Raven, Philadelphia, pp 595–606
Gotman I (1997) Characteristics of metals used in implants. J Endourol 11:383–389
Goto K (1988) Cerebral and cranial artery navigation without using leak balloon – new combination of low-friction high-torque guide wire and thin supple catheter. AJNR Am J Neuroradiol 9:1040
Goto K, Halbach VV, Hardin CW (1988) Permanent inflation of detachable balloons with low viscosity hydrophilic polymerizing system. Radiology 169:787–790

Gough RCP, Lamiell JM, Hsia YE (1984) Secretion and linkage analysis from Von Hippel Lindau Disease among 220 descendants from kindred. Am J Hum Genet 36: 131–142
Goyal M, Ter Brugge KG, Farb R (1999a) Endovascular retrograde cortical venous approach to disconnect retrograde leptomeningeal venous reflux in a patient with dural AVF. Intervent Neuroradiol 5:195–198
Goyal M, Willinsky R, Montanera W, Ter Brugge K (1999b) Spontaneous vertebrovertebral arteriovenous fistulae. Clinical features, angioarchitecture and management of twelve patients. Intervent Neuroradiol 5:219–224
Graf CJ (1965) Spontaneous carotid cavernous fistula: Ehlers Danlos syndrome and related conditions. Arch Neurol 13:262–272
Graf CJ, Perret GE, Torner JC (1983) Bleeding from cerebral arteriovenous malformations as part of their natural history. J Neurosurg 58:331–337
Graham D (1992) Hypoxia and vascular disorders. In: Adams J, Duchen L (eds) Greenfield's neuropathology. Oxford Press, New York, pp 153–268
Graham JJ, Yang WC (1984) Vertebral hemangioma with compression fracture and paraparesis treated with preoperative embolization and vertebral resection. Spine 9:97–101
Grand C, Bank WO, Baleriaux D, Matos C, Dewitte O, Brotchi J, Delcour C (1993) Gadolinium-enhanced MR in the evaluation of preoperative meningioma embolization. AJNR Am J Neuroradiol 14:583–586
Graves VB, Partington CR, Rufenacht DA et al (1989) Platinum coil placement with Tracker 18 catheter. Observation in dog carotid model (a). AJNR Am J Neuroradiol10:876
Graves VB, Partington CR, Rufenacht DA, Strother CM (1990) Treatment of carotid artery aneurysm with platinum coils: an experimental study in dogs. AJNR Am J Neuroradiol 11:249–252
Graves V, Rappe A, Strother C et al (1993) An endovascular retrieving device for the use in small vessels. AJNR Am J Neuroradiol 14:804–808
Grayston J, Holbrook T, Hoyt D et al (1995) Chlamydia pneumonia (TWAR) in atherosclerosis of the carotid artery. Circulation 92:3397–3400
Green JF, Fitzwater JE, Burgess J (1974) Arterial lesions associated with neurofibromatosis. Am J Pathol 62:481–487
Greenberg MS. Handbook of neurosurgery, 4th edn, vol II. pp 835–836
Gregarius FK, Weingarten SM (1970) The natural history of vascular malformation of the spinal cord with a presentation of two cases and a review of the literature. Bull Los Angeles Neurol Soc 35:25–33
Griffin MD, Torres VE, Grande JP, Kumar R (1997) Vascular expression of polycystin. J Am Soc Nephrol 8:616–626
Griffiths PD, Blaser S, Armstrong D, Chuang S, Humphreys RP, Harwood-Nash D (1998) Cerebellar arteriovenous malformations in children. Neuroradiology 40:324–331
Grisoli F, Vincentelli F, Fuchs S, Baldinin M, Raybaud C, Leclerc TA, Vigouroux RP (1984) Surgical treatment of tentorial arteriovenous malformations draining into the subarachnoid space. J Neurosurg 60:1059–1066
Grote E, Voigt K (1999) Clinical syndromes, natural history and pathophysiology of vascular lesions of the spinal cord. Neurosurg Clin N Am 10:17–45
Grotta J (1997) Elective stenting of extracranial carotid arteries. Circulation 95:303–305
Groubi M, Dalal I, Nisbet-Brown E et al (1998) Cerebral vasculitis associated with chronic mucocutaneous candidiasis. J Pediatr 133:571–574
Groves H, Kinlough-Rathbone R, Richardson M et al (1979) Platelet interaction with damaged rabbit aorta. Lab Invest 40:194–200
Grube E, Gerkens U, Rowold S et al (2001) Inhibition of in-stent restenosis by the qanam drug eluting polymer stent: two year follow-up. J Am Coll Cardiol 37 [Suppl A]:19
Gruber A, Mazal P, Bavinski G, Killer M, Budka H, Richling B (1996) Repermeation of partially embolized cerebral arteriovenous malformations: a clinical, radiologic and histologic study. AJNR Am J Neuroradiol 17: 1323–1331
Gruber A, Killer M, Bavinzski G et al (1999) Clinical and angiographical results of endosaccular coiling treatment of giant and very large intracranial aneurysms: a 7-year single-center experience. Neurosurgery 45:793–804

Gruber A, Bavinzski G, Killer M, Richling B (2000a) Preoperative embolization of hypervascular skull base tumors. Minim Invasive Neurosurg 43:62–71
Gruber A, Killer M, Mazal P, Bavinzski G, Richling B (2000b) Preoperative embolization of intracranial meningiomas: a 17-year single-centre experience. Minim Invasive Neurosurg 43:18–29
Gruentzig A, Hopff M (1974) Perkutane rekanalization chromischer arteriller verschloss mit eineur neuen dilatatiouscatheter: Modification der Dotter-Technik. Deutsch Med Wochenscriff 99
Gruszkiewicz J, Doron Y, Peyser E et al (1982) Aneurysmal bone cyst of spine. Acta Neurochir (Wien) 66:109–121
Guegen B, Merland JJ, Riche MC, Rey A (1987) Vascular malformations of the spinal cord: Intrathecal perimedullary arteriovenous fistulas fed by medullary arteries. Neurology 37:969–979
Gugliemi G, Vinuela F, Sepetka I et al (1991a) Electrothrombosis of saccular aneurysms via endovascular approach. Part 1: electrochemical basis, technique and experimental results. J Neurosurg 75:1–7
Gugliemi G, Vinuela F, Dion J et al (1991b) Electrothrombosis of saccular aneurysms via endovascular approach. Part 2: preliminary clinical experience. J Neurosurg 75:8–14
Guidetti B, Fortuna A (1967) Surgical treatment of intramedullary hemangioblastoma of the spinal cord. Report of six cases. J Neurosurg 27:530–540
Guillain G, Bertrand I, Lereboullet J (1932) Hemangioblastomes du système nerveux central à localisations multiples. Rev Neurol 47:432–441
Guillon B, Levy C, Bousser M (1998) Internal carotid artery dissection: an update. J Neurol Sci 153:146–158
Gunel M, Awad I, Finberg K, Steinberg G, Craig HD, Cepeda O, Nelson-Williams C, Lifton R (1996) Genetic heterogeneity of inherited cerebral cavernous malformation. Neurosurgery 38:1265–1271
Guo WY, Pan DHC, Wu HM, Chung WY, Shiau CY, Wang LW, Chiou HJ, Yen MY, Teng MMH (1998) Radiosurgery as a treatment alternative for dural arteriovenous fistulas of the cavernous sinus. Am J Neuroradiol 19:1081–1087
Gurian J, Martin N, King W (1995) Neurosurgical management of cerebral aneurysms following unsuccessful or incomplete embolisation. J Neurosurg 83:843–853
Guttmacher AE, Marchuk DA, White RIJ (1995) Hereditary hemorrhagic telangiectasia. N Engl J Med 333:918–924
Haar F, Patterson RH Jr (1972) Surgery for metastatic intracranial neoplasm. Cancer 30:1241–1245
Habbema JDF, Bossuyt PMM, Dippel DWJ, Marshall S, Hilden J (1990) Analysing clinical decision analyses. Stat Med 9:1229–1242
Hacke W, Zeumer H, Berg-Dammer E (1983) Monitoring of hemispheric and brainstem functions with neurophysiological methods during interventional neuroradiology. Am J Neuroradiol 4:382–384
Hacke W, Zeumer H, Ferbert A, Bruckmann H (1988) Intra-arterial thrombolytic therapy improves outcome in patients with acute vertebrobasilar occlusive disease. Stroke 19:1216–1222
Hacke W, Kaste M, Fieschi Cea, for the ECASS Study Group (1995) Intravenous thrombolysis with recombinant tissue plasminogen activator for acute hemispheric stroke: the European Cooperative Acute Stroke Study (ECASS). JAMA 274:1017–1025
Hacke W, Toni D, Steiner T et al (1997) Rt-PA in acute ischemic stroke: results from the ECASS three-hour cohort. Stroke 28:272
Hackney DB, Lesnick JE, Zimmerman RA et al (1986) MR identification of bleeding site in subarachnoid hemorrhage with multiple intracranial aneurysms. J Comput Assist Tomogry 10:878–880
Halasz NA, Kennady JC (1964) Excision of arteriosclerotic aneurysm of cervical internal carotid artery. J. Neurosurg 21:352–357
Halbach VV, Higashida RT, Hieshima GB et al (1987) Normal perfusion pressure breakthrough occurring during treatment of carotid and vertebral fistulas. AJNR 8:751–756

Halbach VV, Higashida RT, Heishima GB, Hardin CW (1988a) Arteriovenous fistula of the internal maxillary artery: treatment with transarterial embolization. Radiology 168:443–445
Halbach VV, Higashida RT, Heishima GB, Harding CW (1988b) Transvenous embolization of direct carotid–cavernous fistula. AJNR Am J Neuroradiol 9:741–747
Halbach VV, Higashida RT, Hieshima GB, Harding CW, Dowd CF, Barnwell SL (1989) Transarterial occlusion of solitary intracerebral arteriovenous fistulas. AJNR 10:747
Haley E, Levy D, Brott T et al (1992) Urgent therapy for stroke. Part II: pilot study of tissue plasminogen activator administered 91–180 minutes from onset. Stroke 23:641–645
Hall WA, Oldfield EH, Doppman JL (1989) Recanalization of spinal cord arteriovenous malformations following embolization. J Neurosurg 70:714–720
Halsted WS (1919) Congenital arteriovenous and lymphaticovenous fistula – unique clinical and experimental observations
Hamby WB (1966) Carotid cavernous fistulas. Charles C. Thomas Springfield, IL
Han SS, Love MB, Simeone FA (1987) Diagnosis and treatment of a lumbar extradural arteriovenous malformation. AJNR Am J Neuroradiol 8:1129–1130
Hanieh A, Blumbergs PC, Carney PG (1981) Multiple cerebral arteriovenous malformations associated with soft-tissue vascular malformations: case report. J Neurosurg 54:670–672
Hankey G (1999) Stroke: how large a public health problem, and how can the neurologist help? Arch Neurol 56:748–754
Hardwig P, Robertson DM (1984) Von Hippel-Lindau disease: a familial, often lethal, multisystem phakomatosis. Opthalmology 91:263–270
Harkins JC, Reed RJ (1969) Tumors of the peripheral nervous system. In: Atlas of tumor pathology, fasc 3. Armed Forces Institute of Pathology, Washington DC
Harris GY, Jzkobiec FA (1979) Cavernous hemangiomas of the orbit. J Neurosurg 51:219–228
Harrison DFN (1954) Two cases of bleeding from ear from carotid aneurysm. Guy's Hosp Rep 103:207–212
Harrison K (1974) Glomus jugulare tumors: their clinical behavior and management. Proc Roy Soc Med 67: 264–267
Harrison THM, Odom GL, Kunkle EC (1963) Internal carotid artery aneurysm arising in carotid canal. Arch Neurol Chicago 8:328–331
Hart R, Harrison M (1996) Aspirin wars: the optimal dose of aspirin to prevent stroke. Stroke 27:585–587
Hartman A, Mast H, Mohr JP, Koennecke HC, Osipov A, Pile-Spellman J, Duong DH, Young W (1998) Morbidity of intracranial hemorrhage in patients with cerebral arteriovenous malformations. Stroke 29:931–934
Hasegawa S, Hamada JI, Morioka M, Kai Y, Takaki S, Ushio Y (1999) Multiple cerebral arteriovenous malformations (AVMs) associated with spinal AVM Acta Neurochir (Wien) 141:315–319
Hash CJ, Grossman CB, Shenkin HA (1975) Concurrent intracranial and spinal cord arteriovenous malformations. Case report. J Neurosurg 43:104–107
Hashima SM, Asakura T, Koichi U, Kadota K, Awa H, Kusumoto K, Yamashita K (1985) Angiographically occult arteriovenous malformations. Surg Neurol 23:431–439
Hashimoto I (1977) Familial intracranial aneurysms and cerebral vascular anomalies. J Neurosurg 46:419–427
Hassler W (1986) Hemodynamic aspects of cerebral angiomas. Acta Neurochir Suppl (Wien) 37:1–6
Hasso A, Lasjaunias P, Thompson JR, Hinshaw DB Jr (1979) Venous occlusions of the cavernous area. A complication of crushing fractures of the sphenoid bone. Radiology 132:375–379
Hawe A, Svien JH, Ellis EH, Layton D, Baker HL (1972) The surgical treatment of vascular anomalies of the spinal cord. Surg Gynecol Obstet 135:369–372
Hay MC, Paterson D, Taylor TKF (1978) Aneurysmal bone cysts of the spine. J Bone Joint Surg Br 60:406–411
Hayashi S, Arimoto T, Itakura T, Fujii T, Nishiguchi T, Komai N (1981) The association of intracranial aneurysms and arteriovenous malformations in the brain. Case report. J Neurosurg 55:971–975

Hayes GJ (1963) External carotid cavernous sinus fistulas. J Neurosurg 20:692–700
Hayman LA, Evans RA, Ferell RE, Fahr LM, Ostrom P, Riccocdi VM (1982) Familial cavernous angiomas. Natural history and genetic study over a 5-year period. Am J Med Genet 11:147–160
Hayward E, Whitewell H, Paul KS, Barnes DM (1983) Steroid receptors in human meningioma (abstract) J Steroid Biochem 19 [Suppl]:164
Hebold O (1985) Aneurysmen der kleinsten Rückenmarksgefäße. Arch Psychiatr Nervenkr 16:813–873
Heckster REM, Luvendijk W, Tan TI (1972) Spinal cord compression caused by vertebral hemangioma relieved by percutaneous catheter embolization. Neuroradiology 3:160–164
Heiskanen O (1981) Risk of bleeding from unruptured aneurysms in cases with multiple intracranial aneurysms. J Neurosurg 55:524–526
Heiss W (1983) Flow thresholds of functional and morphological damage of brain tissue. Stroke 14:329–331
Heiss W, Huber M, Fink G, Herholz K, Pietrzyk U, Wagner R (1992) Progressive derangement of periinfarct viable tissue in ischemic stroke. J Cereb Blood Flow Metab 12:193–203
Heistad D, Marcus M, Abboud F (1978) Role of large arteries in regulation of cerebral blood flow in dogs. J Clin Invest 62:761–768
Helle TL, Conley FK (1980) Hemorrhage associated with meningioma: a case report and review of the literature. J Neurol Neurosurg Psychiat 43:725–729
Henderson JW, Schneider RC (1959) The ocular findings in carotid-cavernous fistula in a series of 17 cases. Am J Ophthal 48:585–597
Henderson JW, Campbell RJ (1977) Primary intraorbital meningioma with intraocular extension. May Clin Proc 52:504–508
Hennerici M, Hulsbomer H, Hefter H et al (1987) Natural history of asymptomatic extracranial arterial disease: results of a long-term prospective study. Brain 110: 777–791
Henry M, Amor M, Henry I et al (1997) Endovascular treatment of atherosclerotic internal carotid artery stenosis. J Endovasc Surg 4 [Suppl I]:1–14
Henry M, Amor M, Masson I, Henry I (1998) Angioplasty and stenting of the extracranial carotid arteries. J Endovasc Surg 15:293–304
Heros R (1986) Lateral suboccipital approach for vertebral and vertebrobasilar artery lesions. J Neurosurg 64:559–562
Heros R, Zervas N, Varsos V (1983) Cerebral vasospasm after subarachnoid hemorrhage: an update. Ann Neurol 16:599–608
Heros RC, Debrun GM, Ojemann RG et al (1986) Direct spinal arteriovenous fistula: a new type of spinal AVM. J Neurosurg 64:134–139
Heros RC, Korosue K (1989) Hemodilution for cerebral ischemia. Stroke 20:423–427
Herrmann CL (1999) Surgical management of intramedullary hemangioblastoma of the spinal cord. Acta Neurochir 141:333–339
Hertzanu Y, Mendelsohn DB, Kassner G, Hockman M (1982) Haemangiopericytoma of the larynx. Brit J Radiol 55:870–873
Hiatt B, Ikeno F, Yeung A, Carter A (2002) Drug-eluting stents for the prevention of restenosis: in quest for the Holy Grail. Cather Cardiovasc Interv 55:409–417
Hickey R, Albin MS, Bunegin L, Gelineau J (1986) Autoregulation of spinal cord blood flow: is the cord a microcosm of the brain? Stroke 17:1183–1190
Hida K, Iwasaki Y, Goto K, Miyasaka K, Abe H (1999) Results of the surgical treatment of perimedullary arteriovenous fistula with special reference to embolization J Neurosurg 90:198–205
Hieshima GB, Higashida RT (1987) Aneurysm neck remnant following balloon embolization (letter). J Neurosurg 67:322–323
Hieshima GB, Grinnell VS, Mehringer CM (1981) A detachable balloon for therapeutic transcatheter occlusions. Radiology 138:227–228
Hieshima GB, Higishida RT, Wapenski J et al (1986) Balloon embolization of large distal basilar artery aneurysms. J Neurosurg 65:413–416
Hieshima GB, Higishita RT, Wapenski J et al (1987) Intravascular balloon embolization of large midbasilar artery aneurysms: case report. J Neurosurg 66:124–127

Higashida R, Halbach V, Cahan L, Brant-Zawadzki MB (1989a) Transluminal angioplasty for treatment of intracranial arterial vasospasm. J Neurosurg 71:648–653

Higashida RT, Halbach VV, Cahan DL, Hieshima GB, Konishi Y (1989b) Detachable balloon embolization therapy of posterior circulation intracranial aneurysms. J Neurosurg 71:512–519

Higashida R, Helmer E, Halbach V, Hieshima G (1989c) Direct thrombolytic therapy for superior sagittal sinus thrombosis. AJNR Am J Neuroradiol 10:S4–S6

Higashida RT, Halbach VV, Barnwell SL, Dowd C, Dormandy B, Bell J, Hieshima GB (1990a) Treatment of intracranial aneurysms with preservation of parent vessel: results of percutaneous balloon embolization in 84 patients. AJNR Am J Neuroradiol 11:633–640

Higashida R, Halbach V, Dormandy B, Bell J (1990b) New microballoon device for transluminal angioplasty of intracranial arterial vasospasm. AJNR Am J Neuroradiol 11:233–238

Higashida RT, Halbach VV, Dormandy B, Bell J, Hieshima GB (1990c) Endovascular treatment of intracranial aneurysms with a new silicone microballoon device: technical considerations and indications for therapy. Radiology 174:687–691

Higashida RT, Halbach VV, Dowd C, Barnwell SL, Dormandy B, Bell J, Hieshima GB (1990d) Endovascular detachable balloon embolization therapy of cavernous carotid artery aneurysms: results in 87 cases. J Neurosurg 72:857–863

Higashida R, Smith W, Gress D et al (1997) Intravascular stent and endovascular coil placement for a ruptured fusiform aneurysm of the basilar artery. J Neurosurg 87:944–949

Hilal SK, Michelson WJ (1975) Therapeutic percutaneous embolization for extraaxial vascular lesions of head, neck and spine. J Neurosurg 43:275–287

Hilal SK, Sane P, Michelson WJ, Kossein A (1978) The embolization of vascular malformations of the spinal cord with low-viscosity silicone rubber. Neuroradiology 16:430–433

Hilal SK, Khandji AG, Chi TL, Stein BM, Bello JA, Silver AJ (1988) Synthetic fiber-coated platinum coils successfully used for endovascular treatment of arteriovenous malformations and direct arteriofistulas of CNS. AJNR Am J Neuroradiol 9:1030

Hillis AE, Anderson N, Sampath P, Rigamonti D (2000) Cognitive impairments after surgical repair of ruptured and unruptured aneurysms. J Neurol Neurosurg Psychiatry 69:608–615

Hino A, Fujimoto M, Iwamoto Y et al (2000) False localization of rupture site in patients with multiple cerebral aneurysms and subarachnoid hemorrhage. Neurosurgery 46:825–830

Hino H, Maruyama H, Inomata H (1989) A case of spinal artery aneurysm presenting with transverse myelopathy associated with coarctation of aorta. Rinsho Shinkeigaku 29:1009–1012

Hiranandani LH, Melgeri RD, Juveker RV (1967) Angiofibroma of the ethmoidal sinus in female. J Laryngol Otol 81:935–939

Hite SJ, Grooves RA, Sharkey PC (1966) Superficial temporal artery aneurysms. Neurology 16:1044–1046

Hobson R, Weiss D, Fields WS et al (1993) Efficacy of carotid endarterectomy for asymptomatic carotid stenosis. N Engl Med 328:221–227

Hodgson TJ, Carol T, Jellinked DA (1998) Subarachnoid hemorrhage due to late recurrence of a previously unruptured aneurysm after complete endovascular occlusion. AJNR Am J Neuroradiol 19:1939–1941

Hoefnagel D, Wegner W (1961) Vertebral hemangioma with spinal cord compression. Am J Dis Child 102:96–100

Hoff JT, Ray BS (1968) Cerebral hemangioblastoma occurring in a patient with von Hippel-Lindau disease. Case report. J Neurosurg 28:365–368

Hoffman JH, Mohr G, Kusunoki T (1976) Multiple arteriovenous malformations of spinal cord and brain in a child. Case report. Childs Brain 2:317–324

Hofmeister C, Stapf C, Hartmann A, Sciacca R, Mansmann U, Ter Brugge K, Lasjaunias P (2000) Epidemiological, clinical and morphological characteristics of 1289 patients with cerebral arteriovenous malformation. Stroke 31:1307–1310

Hogemann KE, Gustafson G, Bjorlin G (1961) Ivalon surgical sponge used as temporary cover of experimental skin defects in rats. A preliminary report. Acta Chir Scand 121:83–89
Holder C, Bell A, Lundell A, Ulmer J, Glazier S (1997) Isolated straight sinus and deep cerebral venous thrombosis: successful treatment with local infusion of urokinase. J Neurosurg 86:704–707
Hommel M, Boissel J, Cornu C et al, for the MAST Study Group (1995) Termination of trial of streptokinase in severe acute ischaemic stroke. Lancet 345:57
Hook O, Johanson C (1988) Intracranial arteriovenous aneurysms. A follow-up study with particular attention to their growth. Arch Neurol Psychiatry 80:39–54
Hora JF, Brown AK (1962) Paranasal juvenile angiofibroma. Arch Ontolaryngol 76:457–459
Hormia M, Koskinen O (1969) Metastasizing nasopharyngeal angiofibroma. Arch Oto Laryng 89:107–110
Horowitz M, Purdy P (2000) The use of stents in the management of neurovascular disease: a review of historical and present status. Neurosurgery 46:1335–1343
Horowitz M, Purdy P, Unwin H et al (1995) Treatment of dural sinus thrombosis using selective catheterization and urokinase. Ann Neurol 38:58–67
Horowitz M, Purdy P, Kopitnik T, Dutton K, Samson D (1999) Aneurysm retreatment after Guglielmi detachable coil and nondetachable coil embolization: Report of nine cases and review of the literature. Neurosurgery 44:712–720
Horton JA, Dawson RC (1988) Retinal wada test. AJNR Am J Neuroradiol 9:1167
Horton WA, Wong V, Eldridge R (1976) Von Hippel-Lindau disease. Arch Intern Med 135:769–777
Hosobuchi Y (1975) Electrothrombosis of carotid-cavernous fistula. J Neurosurg 42:76–85
Houdart R, Djindjian R (1974) Hemangioblastomes du cervelet de la moelle, du tronc cérébral et maladie de von Hippel-Lindau. J Med Leysin 55:773
Houdart R, Djindjian R, Hurth M (1966) Vascular malformations of the spinal cord. J Neurosurg 2:583–594
Houdart R, Rey A, Djindjian M, Djindjian R (1978) Arteriovenous malformations of the cord (spinal cord angiomas). In: Carrera P (ed) Neurological surgery, international congress series. Excerpta Medica, Amsterdam, pp 194–202
House WP, Glassock ME (1968) Glomus tympanicum tumors. Arch Oto Laryngol 87:550–554
Houser OW, Baker HL (1968) Fibromuscular dysplasia and other uncommon disease of the cervical carotid artery: angiographic aspects. Amer J Roentgenol 104:201–212
Houser OW, Baker HL, Rhoton AL, Okazaki H (1972) Intracranial dural arteriovenous malformations. Radiology 1105:55–64
Hsu S, Rodesch G, Luo C, Chen Y, Alvarez H, Lasjaunias P (2002) Concomitant conus medullaris arteriovenous malformation and sacral dural arteriovenous fistula of the filum terminale. Intervent Neuroradiol 8:47–53
Hubert P, Choux M, Houtteville JP (1989) Cavernomes cérébraux de l'enfant et du nourrisson. Neurochirurgie 35:104–140
Huffmann BC, Spetger U, Reinges M, Bertalanffy H, Thron A, Gilsbach JM (1998) Treatment strategies and results in spinal vascular malformations. Neurol Med Chir (Tokyo) 38 [Suppl]:231–237
Hui F, Trosselo MP, Meisel HJ, Alvarez H, Sequeira E, Lasjaunias P (1994) Paraspinal arteriovenous shunts in children. Neuroradiology 36:69–73
Hunt WE, Hess RM (1968) Surgical risk as related to time of intervention in the repair of intracranial aneurysms. J Neurosurg 28:14–20
Hurn P, Traystman R (1997) Overview of cerebrovascular hemodynamics. In: Welch K, Caplan L, Reis D, Siesjo B, Weir B (eds) Primer on cerebrovascular diseases. Academic Press, San Diego, pp 42–44
Hurst RW, Choi IS, Persky M (1992) Mycotic aneurysms of intracavernous carotid artery: a case report and review of the literature. Surg Neurol 37:142–146
Hurst RW, Kenyon LC, Lavi E, Raps EC, Marcotte P (1995) Spinal dural arteriovenous fistula: the pathology of venous hypertensive myelopathy. Neurology 45:1309–1313

Hurst R, Bagley L, Galetta S, Glosser G, Lieberman A, Trojanowski J, Sinson G, Stecker M, Zager E, Raps E, Flamm E (1998) Dementia resulting from dural arteriovenous fistulas: the pathologic findings of venous hypertensive encephalopathy. AJNR Am J Neuroradiol 19:1267–1273

Hurth M, Andre JM, Djindjian R, Escourolle R, Houdart R, Roirier J, Rey A (1975a) Les hemangioblastomes intrarachidiens. Neurochirurgie 21[Suppl]:1

Hurth M, Djindjian B, Houdart D, Rey A, Djindjian M (1976) Les angiomes de la moelle. Prog Neurol Surg

Hurth M, Djindjian R, Houdart R, Rey A (1975b) Hemangioblastomes intra-rachidiens. Neurochirurgie 21:1–140

Hurth M, Houdart R, Djindjian R, Rey A, Djindjian M (1978) Arteriovenous malformations of the spinal cord. Clinical, anatomic and therapeutic considerations. A series of 150 cases. Prog Neurol Surg 9:238–266

Huston J, Tores VE, Sullivan PP, Offord KP, Wiebers DO (1993) Value of magnetic resonance angiography for the detection of intracranial aneurysms in autosomal dominant polycystic kidney disease. J Am Soc Nephrol 3:1871–1877

Huston J 3rd, Nichols DA, Leutmer PH et al (1994) Blinded prospective evaluation of sensitivity of MR angiography to known intracranial aneurysms: importance of aneurysm size. AJNR Am J Neuroradiol 15:1607–1614

Hutchings M, Weller RO (1986) Anatomical relationships of the pia mater to cerebral blood vessels in man. J Neurosurg 65: 316–325

Hütter BO, Gilsbach JM (1993) Which neuropsychological deficits are hidden behind a good outcome (GOS=1) after aneurysmal subarachnoid hemorrhage? Neurosurgery 33:999–1006

Hwang GJ, Berenstein A, Niimi Y, Setton A, Pryor J, Baltsavias G, Albert R, Hartman J (2000) The accuracy of plain skull x-ray examination as a predictor of recanalization following Guglielmi detachable coil embolisation in the treatment of cerebral aneurysm. Intervent Neuroradiol 6:195–202

Hyman MH, Whittemore VH (2000) National Institutes of Health Consensus Conference: tuberous sclerosis complex. Arch Neurol 57:662–665

Hynes R (1992) Integrins: versatility, modulation and signaling in cell adhesion. Cell 69:11–25

Iadocola C, Pelligrino D, Moskowitz M, Lassen N (1994) Nitric oxide synthase inhibition and cerebrovascular regulation. J Cereb Blood Flow Metab 14:175–192

Iizuka Y, Rodesch G et al (1992) Multiple cerebral arteriovenous shunts in children: report of 13 cases. Child's Nerv Syst 8:437–444

Imparato A (1985) Vertebral arterial reconstruction: a nineteen-year experience. J Vasc Surg 2:626–634

International Study of Unruptured Intracranial Aneurysms Investigators (1998) Unruptured intracranial aneurysms: risk of rupture and risks of surgical intervention. N Engl J Med 339:1725–1733

Ip J, Fuster V, Badimon L, Badimon J (1990) Syndromes of accelerated atherosclerosis: role of vascular injury and smooth muscle cell proliferation. J Am Coll Cardiol 15:1667–1687

Iplikcioglu AC, Benli K, Bertan V, Ruacan S (1986) Cystic cavernous hemangioma of the cerebellopontine angle: case report. Neurosurgery 19:641–642

Ishikawa K (1988) Diagnostic approach and proposed criteria for the clinical diagnosis of Takayasu's arteriopathy. J Am Coll Cardiol 12:964–972

Ishikawa T, Nakamura N, Houkin K, Nomura M (2003) Pathological consideration of a "blister–like" aneurysm at the superior wall of the internal carotid artery: case report. Neurosurgery, 40 2:403–406

Ito J, Imamura H, Kobayashi K, Tsuchida T, Sato S (1983) Dural arteriovenous malformations of the base of the anterior cranial fossa. Neuroradiology 24:149–154

Itzchak Y, Katznelson D, Boichis H et al (1974) Angiographic features of arterial lesions in neurofibromatosis. AJR 122:643–647

Iwama T, Andoh T, Iwata T, Hirata T, Yamada H (1990) Dissecting and fusiform aneurysms of vertebro-basilar system: MR imaging. Neuroradiology 32:272–279

Iwasa H, Indei I, Sato F (1983) Intraventricular cavernous hemangioma. Case report. J Neurosurg 59:153–157

Iyer S, Roubin G, Yadav J, Diethrich E (1996) Angioplasty and stenting for extracranial carotid stenosis: multicenter experience. Circulation 94:1–58
Iyer S, Roubin G, Yadav J, Vitek J (1997) Elective stenting of the extracranial carotid arteries. Circulation 95:376–381
Izukawa D, Lach B, Benoit B (1987) Intravascular papillary endothelial hyperplasia in intracranial cavernous hemangioma. Neurosurgery 21:939–941
Jaaskelainen J, Servo A, Haltia M (1985) Intracranial hemangiopericytoma. Surg Neurol 23:227–241
Jafar JJ, Johns MM, Mullan SF (1986) Effects of mannitol on cerebral blood flow. J Neurosurg 64:754–759
Jafar JJ, Davis AJ, Berenstein A, Choi IS, Kupersmith MJ (1993) The effect of embolization with N-butyl cyanoacrylate prior to surgical resection of cerebral arteriovenous malformations. J Neurosurg 78: 60–69
Jafek BW, Nahum AM, Butler RM, Ward PH (1973) Surgical treatment of juvenile nasopharyngeal angiofibroma. Laryngoscope 83:707–720
Jaff M (1998) The natural history of extracranial carotid atherosclerosis. In: Henry M, Amor M, Theron J, Roubin G (eds) Carotid angioplasty and stenting. pp 47–50
Jaffee HL, Lichtenstein L, Portis RB (1940) Giant cell tumor of bone. Its pathological appearance, grading, supposed variants and treatment. Arch Pathol 30:993
Jahan R, Murayama Y, Gobin YP, Duckwiler GR, Vinters HV, Vinueala F (2001) Embolization of arteriovenous malformation with Onyx: clinicopathological experience in 23 patients. Neurosurgery 48: 984–995; discussion 995–997
Jamieson KG (1965) Vertebral arteriovenous fistula caused by angiographic needle: report of one case. J Neurosurg 23:620–621
Jane JA, Kassell NF, Torner JC et al (1985) The natural history of aneurysms and arteriovenous malformations. J Neurosurg 62:321–323
Jansen O, von Kummer R, Forsting M, Hacke W, Sartor K (1995) Thrombolytic therapy in acute occlusion of the intracranial internal carotid artery bifurcation. Am J Neuroradiol 16:1977–1986
Jarus-Dziedzic K, Zub W, Wronski J, Juniewicz H, Kasper E (2000) The relationship between cerebral blood flow velocities an the amount of blood clots in computed tomography after subarachnoid haemorrhage. Acta Neurochir 142:309–318
Jayakrishnan VK, Rodesch G, Alvarez H, Lasjaunias P (2001) A case of multiple intracranial aneurysms with unruptured associated aneurysms and newly developed ruptured aneurysms. Intervent Neuroradiol 7:259–262
Jefferson G (1938) Sacular aneurysms of the internal carotid artery in the cavernous sinus. Br J Surg 26:267–302
Jellinger K (1966) Zur Orthologie und Pathologie der Rückenmarksdurchblutung. Springer, Berlin Heidelberg New York
Jellinger K (1972) Circulation disorders of the spinal cord. Acta Neurochir (Wien) 26:327–337
Jellinger K (1978) Pathology of spinal vascular malformations and vascular tumors. In: Pia HW, Djindjian R (eds) Spinal angiomas: advances in diagnosis and therapy. Springer, Berlin Heidelberg New York
Jellinger K (1986) Vascular malformations of the ventral nervous system: a morphological overview. Neurosurg Rev 9:177–216
Jellinger K, Slowik F (1975) Histologic subtypes and prognostic problems in meningiomas. J Neurol 208:279–298
Jellinger K, Minauf M, Garzuly F, Neumayer E (1968) Angiodysgenetische nekrotisierende. Myelopathie. Arch Psychiatr Nervenkr 211:377–404
Jennett B, Bond M (1975) Assessment of outcome after severe brain damage: a practical scale. Lancet 1:480–484
Jensen ME, Evan AJ, Mathis JM, Kallmes DF, Cloft HJ, Dion JE (1997) Percutaneous polymethacrylate vertebroplasty in the treatment of osteoporotic vertebral body compression fractures: technical aspects. AJNR Am J Neuroradiol: 18:1897–1904
Jiarakongmun P, Chewit P, Pongpech S, Lasjaunias P (2002) Anterior spinal artery aneurysm associated with coarctation of aorta: a case report and review of the literature. Intervent Neuroradiol

Jimenez JL, Lasjqunias P, Terbrugge K (1989) The transcerebral veins: normal and nonpathologic angiographic aspects. Surg Radiol Anat 11:63–72
Jiminez F, Goree J (1969) Traumatic arteriovenous fistula of the superficial temporal artery. Radiology 106:279–281
John ER, Chabot RJ, Prichep LS, Ransohoff J, Epstein F, Berenstein A (1989) Realtime intraoperative monitoring during neurosurgical and neuroradiological procedures. J Clin Neurophysiol 6:125–158
Johns ME, McLeod RM, Cantrell RW (1980) Estrogen receptors in nasopharyngeal angiofibromas. Laryngoscope 90:630–634
Johnson B, Verlato F, Bergelin R et al (1995) Clinical outcome in patients with mild and moderate carotid artery stenosis. J Vasc Surg 21:120–126
Johnson CE, Russel EJ, Huckman MS (1990) Resolution of spinal epidural vascular pseudotumor following balloon occlusion of a postoperative vertebral arteriovenous fistula. Neuroradiology 31:529–532
Johnston SC, Dudley RA, Gress DR, Ono L (1999) Surgical and endovascular treatment of unruptured cerebral aneurysms at university hospitals. Neurology 52:1700–1805
Johnston S, Gress D, Browner W, Sidney S (2000) Short-term prognosis after emergency department diagnosis of TIA. JAMA 284:2901–2906
Johnston SC, Higashida R, Barrow D et al (2002) Recommendations for endovascular treatment of intracranial aneurysms. A statement for healthcare professional from the Committee on Cerebrovascular Imaging of the American Heart Association Council on Cardiovascular Radiology Stroke 33:2536–2544
Jomin M, Lesoin F, Lozes G (1985) Prognosis for arteriovenous malformations of the brain in adults based on 150 cases. Surg Neurol 23:362–366
Jonasson L, Holm J, Skalli O, Bondjers G, Hansson G (1986) Regional accumulations of T cells, macrophages, and smooth muscle cells in the human atherosclerotic plaque. 6:131–138
Jones T, Morawetz R, Crowell R, Marcoux F, FitzGibbon S (1981) Thresholds of focal cerebral ischemia in awake monkeys. J Neurosurg 54:773–782
Jordan J, Marks M, Lane B, Steinberg G (1996) Cost-effectiveness of endovascular therapy in the surgical management of cerebral arteriovenous malformations. AJNR Am J Neuroradiol 17: 247–254
Jungreis CA (1991) Skull-base tumors: ethanol embolization of the cavernous carotid artery. Radiology 181:741–743
Jungreis CA, Horton JA (1989) Pressure changes in arterial feeder to cerebral AVM as guide to monitoring therapeutic embolization. AJNR 10:1057
Jungreis C, Wechsler L, Horton J (1989) Intracranial thrombolysis via a catheter embedded in the clot. Stroke 20:1578–1580
Juvela S (1996) Prevalence of risk factors in spontaneous intracerebral hemorrhage and aneurysmal subarachnoid hemorrhage. Arch Neurol 53:734–740
Juvela S (2000) Risk factors for multiple intracranial aneurysms. Stroke 31:392–397
Juvela S, Hillbom M, Numminen H, Koskinen P (1993a) Cigarette smoking and alcohol consumption as risk factors for aneurysmal subarachnoid hemorrhage. Stroke 24:639–646
Juvela S, Porras M, Heiskanen O (1993b) Natural history of unruptured intracranial aneurysms: a long-term follow-up study. J Neurosurg 79:174–182
Juvela S, Porras M, Poussa K (1998) Natural history of unruptured intracranial aneurysms: probability of and risk factors for aneurysm rupture. J Neurosurg 93:379–387
Juvela S, Porras M, Poussa K (2000) Natural history of unruptured intracranial aneurysms: probability of and risk factors for aneurysm rupture. J Neurosurg 93:379–387
Juvela S, Poussa K, Porras M (2001) Factors affecting formation and growth of intracranial aneurysms: a long-term follow-up study. Stroke 32:485–491
Kaarlainen H, Koskimies O, Norio R (1998) Dominant and recessive polycystic kidney disease in children: evaluation of clinical features and laboratory data. Pediatr Nephrol 2:296–302
Kai Y, Hamada J, Morioka M, Yano S, Todaka T, Ushio Y (2002) Appropriate interval between embolization and surgery in patients with meningioma. AJNR Am J Neuroradiol 23:139–142

Kaji T, Hama Y, Iwasaki Y, Kyoto Y, Kusano S (1999) Preoperative embolization of meningiomas with pial supply: successful treatment of two cases. Surg Neurol 52:270–273
Kaku Y, Yonekawa Y, Tsukahara T, Kazekawa K (1992) Superselective intra-arterial infusion of papaverine for treatment of cerebral vasospasm after subarachnoid hemorrhage. J Neurosurg 77:842–847
Kallmes DF, Evans AJ, Kaptain GJ, Mathis JM, Jensen ME, Jane JA, Dion JE (1997) Hemorrhagic complications in embolization of a meningioma: case report and review of the literature. Neuroradiology 39:877–880
Kamijyo Y, Garcia J, Cooper J (1977) Temporary regional cerebral ischemia in the cat. A model of hemorrhagic and subcortical infarction. J Meuropathol Exp Neurol 36:338–350
Kanaan I, Lasjaunias P, Coates R (1995) The spectrum of intracranial aneurysms in pediatrics. Minim Invas Neurosurg 38:1–9
Kandel EI, Filatov YM (1966) Clinical picture and surgical treatment of meningiomas of the lateral ventricle. In: Devet AC (ed) Proceedings of the Third International Congress of Neurological Surgery. Copenhagen, 1965, Excerpta Medica, Amsterdam, pp , 719–723
Kaplan B, Brint S, Tanabe J, Jacewicz M, Wang X (1991) Temporal thresholds for neocortical infarction in rats subjected to reversible focal cerebral ischemia. Stroke 22:1032–1039
Kaplan G, Roswit B, Krueger EG (1952) Results of radiation therapy in vascular anomalies of the central nervous system. Radiology 25:555–558
Kappetein AP, Gittenberger-de Groot AC, Zwinderman AH, Rohmer J, Poelmann RE, Huysmans HA (1991) The neural crest as a possible pathogenetic factor in coarctation of the aorta and bicuspid aortic valve. J Thorac Cardiovasc Surg 102:830–836
Karlsson B, Lindquist C, Steiner L (1997) Prediction of obliteration after gamma knife surgery for cerebral arteriovenous malformations. Neurosurgery 40:425–431
Karp LA, Zimmerman LE, Borit A, Spencer W (1974) Primary intraorbital meningiomas. Arch Ophthalmol 91:24–28
Kasarkis EJ, Tibbs PA, Lee C (1988) Cerebellar hemangioblastoma symptomatic during pregnancy. Neurosurgery 22:770–772
Kassell N, Helm G, Simmons N et al (1992) Treatment of cerebral vasospasm with intra-arterial papaverine. J Neurosurg 77:848–852
Kataoka K, Taneda M (1984) Angiographic disappearance of multiple dural arteriovenous malformations. J Neurosurg 60:1275–1278
Kato T, Nimoto R (1978) Microencapsulation of mitomycin C for infra-arterial infusion chemotherapy. Proc Jpn Aclad 54:413–417
Kato Y, Sano H., Iritani K, Shankar K, Ninomiya T, Kanno I., Kuroda M, Abe M (1997) Clinical study of 16 fully grown cerebral aneurysms. Minim Invas Neurosurg 40151
Kaufman HH, Ommaya AK, di Chiro et al (1970) Compression vs steal. The pathogenesis of symptoms in arteriovenous malformations of the spinal cord. Arch Neurol 23:173–178
Kawamura S, Yoshida T, Nonoyama Y (1999) Ruptured anterior spinal artery aneurysm: a case report. Surg Neurol 51:608–612
Kayama T, Suzuki S, Sakurai Y, Nagayama T, Ogawa A, Yoshimoto T (1986) A case of Moyamoya disease accompanied by an arteriovenous malformation. Neurosurgery 18:465–468
Kelly J (1985) In: Kandel E, Schwartz J (eds) Principles in neural science. Elsevier, New York, pp 187–195
Kendall B (1983) Results of treatment of arteriovenous fistulae with the Debrun technique. AJNR Am J Neuroradiol 4:405–408
Kendall B (1986) Spinal angiography iohexol. Neuroradiology 28:72–73
Kendall BE, Logue L (1977) Spinal epidural angiomatous malformation draining into intrathecal veins. Neuroradiology 13:181–189
Kendall BE, Russell J (1966) Haemangioblastomas of the spinal cord. Br J Radiol 39:817–823

Kepes JJ (1982) Meningiomas. Biology, pathology, and differential diagnosis. Masson, Chicago
Kerber C (1975) Intracranial cyanoacrylate: a new catheter therapy for arteriovenous malformation. Invest Radiol 10:536–538
Kerber CW (1976) A new system of catheter occlusive therapy. Invest Radiol 11:370
Kerber CW (1980) Flow controlled therapeutic embolization: a physiologic and safe technique. Am J Roentgenol 134:557–561
Kerber C, Wong W, Howell S, Hanchett K, Robbins K (1998) An organ-preserving selective arterial chemotherapy strategy for head and neck cancer. AJNR Am J Neuroradiol 19:935–941
Kerber CW, Heilman CB (1984) Flow in experimental berry aneurysms: method and model. AJNR Am J Neuroradiol 4:378
Kerber CW, Newton TH (1973) The macro and microvasculature of the dura mater. Neuroradiology 6:175–179
Kerber CW, Cromwell LD, Sheptak PE (1978) Intra-arterial cyanoacrylate: an adjunct in the treatment of spinal/paraspinal arteriovenous malformations. Am J Roentgenol 103:99–103
Kerber CW, Cromwell LD, Zanetti PH (1985) Experimental carotid aneurysms: part 2. Endovascular treatment with cyanoacrylate. Neursurgery 16:13–17
Kerr G, Hallahan C, Giordano J, Leavitt R (1994) Takayasu arteritis. Ann Intern Med 120:919–929
Kety S, Schmidt C (1948) The effects of altered arterial tensions of carbon dioxide and oxygen on cerebral blood flow and cerebral oxygen consumption of normal young men. J Clin Invest 27:484–492
Khalifa MC, Bassyouni A (1981) Nasal schwannoma. J Laryngol Otol 95:503–507
Khan MT, Mc Kinstry CS, Bell KE et al (1990) Serpentine aneurysm of the posterior circulation: report of two cases. Br J Neurosurg 4:217–233
Kikuchi T, Strother CM, Boyar M (1987) New catheter for endovascular interventional procedures. Radiology 165:870–871
Kilian H (1951) Aneurysmen des branchiocephalen Stromgelueetes und weitere Erfahrungen mit der Mediatinotomia Sternoclavicularis. Arch Klin Chir 269:200–214
Kim SJ, Choi IS (2000) Midterm outcome of partially thrombosed intracranial aneurysms treated with Guglielmi detachable coils. Intervent Neuroradiol 6:13–25
Kim S, Suh J (1997) Direct endovascular thrombolytic therapy for dural sinus thrombosis: Infusion of alteplase. AJNR Am J Neuroradiol 18:639–645
Kinney TD, Fitzgerald PJ (1947) Lindau-von Hippel disease with hemangioblastoma of the spinal cord and syringomyelia. Arch Pathol 43:439
Kirino T (1982) Delayed neuronal death in the gerbil hippocampus following ischemia. Brain Res 237:57–69
Kissel P, Dureux JB (1972) Cutaneo-meningo-spinal angiomatosis or syndrome de Cobb. In: Vinken PJ, Bruyn GW (eds) The phakomatoses. Handbook of clinical neurology, vol 14. Elsevier, Amsterdam
Kitanaka C, Sasaki T, Eguchi T, Teraoka A, Nakan M, Hoya H (1994) Intracranial vertebral artery dissections: clinical, radiological features, and surgical considerations. Neurosurgery 34:620–627
Kjellberg RM, Hanamura T, Davis KR et al (1983) Bragg peak proton beam therapy for arteriovenous malformations of the brain. N Engl J Med 309:269–274
Klatzo I (1967) Presidential address. Neuropathological aspects of brain edema. J Neuropathol Exp Neurol 26:1–14
Klein JP, Moeschberger ML (1997) Survival analysis: techniques for censored and truncated data. Springer, Berlin Heidelberg New York
Kleihues P, Burger PC, Scheithauer BW (1993) Histological classification of CNS tumours. In: Sobin LH (ed) Histological typing of tumours of the central nervous system, 2nd edn. Springer, Berlin Heidelberg New York
Klippel M, Trenaunay C: (1900) Du naevus variqueux ostéohypertrophique. Arch Gen Med 77:641–672
Kobayashi H, Kawano H, Ito H, Hayashi M, Yamamoto S (1984) Hemangiomas calcificans in the fourth ventricle. Neurosurgery 14:737–739
Kocher O, Huttner I, Gabbiani G (1988) Atherosclerosis: cellular aspects. Diseases of the arterial wall. Springer, Berlin Heidelberg New York, pp 166–183

Koeppen AH, Barron KD, Cox JF (1974) Foix-Alajouanine syndrome. Acta Neuropathol (Berl) 29:187–197
Koh W, Mayberg M, Chambers J et al (1996) The potential role of external beam radiation in preventing restenosis after coronary angioplasty. Int J Radiat Oncol Biol Phys 36:829–834
Kojima M, Nagasawa S, Lee YE, Takeichi Y, Tsuda E, Mabuchi N (1998) Asymptomatic familial cerebral aneurysms. Neurosurgery 43 4:776–781
Kollar C, Parker G, Johnston I (2001) Endovascular treatment of cranial venous sinus obstruction resulting in pseudotumor syndrome. Report of three cases. J Neurosurg 94:646–651
Kominami S, Y Liu, H Alvarez, G Rodesch, P Coubes, P Lasjaunias (1996) A case of vertebrovertebral arteriovenous fistula presenting with subarachnoid haemorrhage. A case report. Intervent Neuroradiol 2:229–233
Kon H, Ezura R, Takahashi A, Yoshimoto T (1997) Giant multilocular fusiform aneurysm of the posterior cerebral artery. Intervent Neuroradiol 3:319–324
Konan AV, Raymond J, Roy D (1999) Transarterial embolization of aneurysms associated with spinal cord arteriovenous malformations. Report of four cases J Neurosurg [Suppl 1] 90:148–154
Kondor T, Tamaki N, Takeda N, Suyama T et al (1988) Fatal intracranial hemorrhage after balloon occlusion of an extracranial vertebral arteriovenous fistula. J Neurosurg 69:945–948
Kondziolka D, Nixon B, Lasjaunias P, Tucker W, Ter Brugge K, Spiegel S (1988) Cerebral arteriovenous malformations with associated arterial aneurysms: hemodynamic and therapeutic considerations. Can J Neurol Sci 15:130–134
Konishi K, Maemura E, Yokata H et al (1988) Treatment of cerebral vasospasm with dilation balloon catheter: basic study of percutaneous transluminal angioplasty. In: Wilkens RH(ed) Cerebral vasospasm. Raven, New York, pp 509–511
Kontos HA, Wei EP, Navari RM, Levasseur JE, Rosenblum WI, Patterson JL Jr (1978) Responses of cerebral arteries and arterioles to acute hypotension and hypertension. Am J Physiol 234:H371–H83
Koo AH, Newton TH (1972) Pseudoxanthoma elasticum associated with carotid rete mirabile. Am J Roentgenol Radium Ther Nucl Med 116:16–22
Korsgaard O, Lindholm J, Rasmussen P (1976) Endocrine function in patients with suprasellar and hypothalamic tumors. Acta Endocrinol 83:1–8
Kosary IA, Braham J, Shacked I et al (1977) Spinal epidural hematoma due to hemangioma of vertebra. Surg Neurol 7:61–62
Kosnick EJ, Hunt WE, Miller CA (1974) Dural arteriovenous malformations. J Neurosurg 40:322–329
Koulouris S, Rizzoli HV (1981) Coexisting intracranial aneurysms and arteriovenous malformation: case report. Neurosurgery 8:219–222
Koussa A, Chiras J, Poirier B, Carpena JP, Bories J (1985) Aspect tomodensitométrique et angiographique des angiomes veineux du cerveau. A propos de 15 cas. Neurochirurgie 31:161–168
Kramer W (1969) Hyperplasie fibromusculaire et anévrisme extracranien de la carotide interne avec syndrome parapharyngien typique. Rev Neurol (Paris) 120: 239–244
Krayenbuhl HA (1977) Angiographic contribution to the problem of enlargement of cerebral arteriovenous malformations. Acta Neurochir (Wien) 36:215–242
Krayenbuhl H, Siebenmann R (1965) Small vascular malformations as a cause of primary intracerebral hemorrhage. J Neurosurg 22:7–20
Krayenbuhl H, Yasargil M (1968) Cerebral angiography. Butterworths, London
Krayenbuhl H, Yasargil MG (1972) Klinik der Gefasmisbildungen und gefasfisteln. In: Ganshirt E (ed) Der Hirnkreislauf. Thieme, Stuttgart, pp 465–511
Krenchel NJ (1961) Intracranial racemose angiomas. A clinical study. Universitetsforlaget, Aarhus
Kricheff II, Berenstein A (1979) Simplified solid particle embolization with a new introducer. Radiology 131:794–795
Kricheff II, Madayag M, Braunstein P (1972) Transfemoral catheter embolization of cerebral and posterior fossa arteriovenous malformations. Radiology 103:107–111

Krieger AJ (1972) A vascular malformation of the spinal cord in association of cauda equina ependymoma. Vasc Surg 6:167–172
Kuether T, Nesbit G, Barnwell S (1998) Clinical and angiographic outcomes, with treatment data, for patients with cerebral aneurysms treated with Guglielmi detachable coils: a single-centre experience. Neurosurgery 43:1016–1025
Kumagami H (1993) Sex hormones in juvenile nasopharyngeal angiofibroma tissue. Auris Nasus Larynx: 20:131–135
Kupersmith MJ, Berenstein A, Choi IS et al (1984) Percutaneous transvascular treatment of giant carotid aneurysms: neurophthalmic findings. Neurology 34:328–335
Kupersmith M, Berenstein A, Flamm E et al (1986) Neuroophthalmologic abnormalities and intravascular therapy of traumatic carotid cavernous fistulas. Ophthalmology 93:906–912
Kupersmith MJ (1993) Neurovascular neuro-ophthalmology. Springer, New York
Kupersmith MJ, Berenstein A, Choi IS et al (1984) Percutaneous transvascular treatment of giant carotid aneurysms: neurophthalmic findings. Neurology 34:328–335
Kupersmith M, Hurst R, Berenstein A et al (1992) The benign course of cavernous carotid artery aneurysms. J Neurosurg 77:690–693
Kure K, Park Y, Kim T et al (1989) Immunohistochemical localization of an HIV epitope in cerebral aneurysmal arteriopathy in pediatric acquired immunodeficiency syndrome (AIDS). Pediatr Pathol 9:655–667
Kurita H, Ueki K, Shin M, Kawamoto S, Sasaki T, Tago M, Kirino T (2000) Headache in patients with radiosurgically treated occipital arteriovenous malformations. J Neurosurg 93:224–228
Kushner J, Alexander E Jr (1970) Partial spontaneous regressive arteriovenous malformation. Case report with angiographic evidence. J Neurosurg 32:360–366
Kuss JJ, Karli A, Fischbach M, Lutz JD, Dietemann JL, Eisenmann B, Keiny R, Levy JM (1979) Congenital carotid to jugular aneurysm [French]. Arch Fr Pediatr 36:502–507
Kwiatkowski T, Libman R, Frankel M, Tilley B, Morgenstern L (1999) Effects of tissue plasminogen activator for acute ischemic stroke at one year. National Institute of Neurological Disorders and Stroke Recombinant Tissue Plasminogen Activator Stroke Study Group. New Engl J Med 340:1781–1787
Laccourreye H, Beutter P, Brasnu D, Lacau-Saint-Guily J, Candauz P, Laval-Jeantet M, Buy JN (1983) Intérêt de la tomodensitométrie dans les tumeurs du pharyngo-larynx. Ann Oto-Laryng 100:341–345
Lack EE, Cubilla AL, Woodruff JM, Farr HW (1977) Paragangliomas of the head and neck region. A clinical study of 69 patients. Cancer 39:397–409
Laine E, Galibert P, Lopez C, Delahouse J, Delandtsheer JM, Christiaens JL (1963) Anévrysmes artérioveineux intra-duraux (développés dans l'épaisseur de la duremère) de la fosse postérieure. Neurochirurgie 9:147–158
Laine E, Jomin M, Clarisse J, Combelles G (1981) Les malformations artérioveineuses cérébrales profondes. Classification topographique. Possibilités thérapeutiques à propos de 46 observations. Neurochirurgie 27:147–160
Lamas E, Lobato RD, Esparza J, Escudero L (1977) Dural posterior fossa AVM producing raised sagittal sinus pressure. J Neurosurg 46:804–809
Lang C, Jacobi G, Kreuz W et al (1992) Rapid development of giant aneurysm at the base of brain in an 8-year-old boy with perinatal HIV infection. Acta Histochem Suppl 42:83–90
Lange R, Willard J, Hillis L (1993) Restenosis: the Achilles heel of coronary angioplasty. Am J Med Sci 306:265–275
Langer D, Lasner T, Hurst R, Flamm E, Zager E, King J (1998) Hypertension, small size, and deep venous drainage are associated with risk of hemorrhagic presentation of cerebral arteriovenous malformations. Neurosurgery 42:481–489
Langsfeld M, Gray-Weale A, Lusby R (1989) The role of plaque morphology and diameter reduction in the development of new symptoms in asymptomatic carotid arteries. J Vasc Surg 9:548–557
Lansky LL, Maxwell JA (1975) Mycotic aneurysms of the internal carotid artery in an unusual intracranial location. Dev Med Child Neurol 17:79–88

Lantos G, Fein JM, Knep S (1984) Cortical artery aneurysm formation after extracranial to intracranial bypass surgery. J Neurosurg 60:636–639
Larson J, Ball W, Bove K, Crone K, Tew J (1998) Formation of intracerebral cavernous malformations after radiation treatment for central nervous system neoplasia in children. J Neurosurg 88:51–56
Lasjaunias P (1986) The external carotid artery: functional anatomy. In: Taveras JM, Ferruci JT (eds) Radiology. Lippincott, Philadelphia
Lasjaunias P (1997a) Angioarchitecture and natural history of dural arteriovenous shunts. Intervent Neuroradiol 3:313–317
Lasjaunias P (1997b) A revised concept of the congenital nature of cerebral arteriovenous malformations. Intervent Neuroradiol 3:275–281
Lasjaunias P (1997c) Arterial aneurysms. In: Lasjaunias P (ed) Vascular diseases in neonates, infants, and children. Springer, Berlin Heidelberg New York, pp 373–393
Lasjaunias P (1997d) Vascular diseases in neonates, infants and children. Springer, Berlin, Heidelberg New York
Lasjaunias P (1999) From aneurysms to aneurysmal vasculopathies. Interventional Neuroradiology 5:105–108
Lasjaunias P (2000a) From aneurysm to aneurysmal vasculopathies. Operative techniques. Neurosurgery.3:160–165
Lasjaunias P (2000b) Segmental identity and vulnerability in cerebral arteries. Intervent Neuroradiol 6:113–124
Lasjaunias P, Doyon D (1978) The ascending pharyngeal artery and the blood supply of the lower cranial nerves. J Neuroradiol 5:287–301
Lasjaunias P, Picard L, Manelfe C, Moret J, Doyon D (1980) Angiofibrome nasopharyngien : revue de 53 cas avec embolisation. Place de l'angiographie préthérapeutique, hypothèses physio-pathogéniques. J Neuroradiol 7:73–95
Lasjaunias P, Halimi PH, Lopez-Ibor L, Sichez JP, Hurth M, De Tribolet N (1984) Traitement endovasculaire des malformations vasculaires durales (MVD) pures "spontanées". Revue de 23 cas explorés et traités entre mai 1980 et octobre 1983. Neurochirurgie 30:207–223
Lasjaunias P, Burrows P, Planet C (1986a) Developmental venous anomalies: the so-called venous angiomas. Neurosurg Rev 9:233–244
Lasjaunias P, Ming C, Terbrugge K, Tolia A, Hurth M, Bernstein M (1986b) Neurological manifestations of intracranial dural arteriovenous malformations. J Neurosurg 64:724–730
Lasjaunias P, Piske R, Terbrugge K, Willinsky R (1988) Cerebral arteriovenous malformations and associated arterial aneurysms. Acta Neurochir (Wien) 91:29–36
Lasjaunias P, Ter Brugge K, Rodesch G, Willinsky R, Burrows P, Pruvost P (1989) Vraies et fausses lésions veineuses cérébrales. Pseudo-angiomes veineux et hémangiomes caverneux. Neurochirurgie 35:132–139
Lasjaunias P, Campi A, Rodesch G, Alvarez H, Kanaan I, Taylor W (1997) Aneurysmal disease in children. Review of 20 cases with intracranial arterial localisations Intervent Neuroradiol 3:215–229
Lasjaunias P, Maillot C Ter Brugge K (2000a) Pial relations with spinal cord veins explain MRI occult spinal AV shunts. Intervent Neuroradiol 6:333–336
Lasjaunias P, Rodesch G, Alvarez H (2000b) Concepts in endovascular interventional neuroradiology. In: Crockard A, Hayward R, Hoff J (eds) Neurosurgery. The scientific basis of clinical practice, vol 2, 3rd edn. Blackwell Science, pp 727–753
Lasjaunias P, Berenstein A, Ter Brugge K (2001) Spine and spinal cord arteries and veins. In: Surgical neuroangiography. Clinical vascular anatomy and variations, vol 1, 2nd edn. Springer, Berlin Heidelberg New York, pp 73–164
Lasjuanias P, Berenstein A, Ter Brugge K (2001) Surgical neuroangiography: clinical vascular anatomy and variations, vol 1, 2nd edn. Springer, Berlin Heidelberg New York
Lassen N (1982) Incomplete cerebral infarction-focal incomplete ischemic tissue necrosis not leading to emollision. Stroke 1982 13:522–523
Latchaw RE, Gold LH (1979) Polyvinyl foam embolization of vascular and neoplastic lesions of the head, neck and spine. Radiology 131:669–679
Laughlin S, Ter Brugge K, Willinsky RA et al (1997) Endovascular management of paedriatic intracranial aneurysms. Intervent Neuroradiol 3:205–215

Launay M, Chiras J, Bories J (1979) Angiography of the spinal cord: venous phase. J Neuroradiol 6:287–315
Lawson W, Reino AJ (1997) Isolated sphenoid sinus disease. An analysis of 132 cases. Laryngoscope 107:1590–1595
Lazinski D, Willinsky RA, Ter Brugge K, Montanera W (2000) Dissecting aneurysms of the posterior cerebral artery: angioarchitecture and a review of the literature. Neuroradiology 42:128–133
Lazorthes G (1978) Arteriovenous malformations of the spinal cord: a critical review. In: Carrera P (ed) Neurological surgery, international congress series. Excerpta Medica, Amsterdam, pp 210–211
Le B, Hemo I, Keshet E (1998)
Leber KA, Klein E, Trummer M, Eder HG (1998) Intracranial aneurysms: a review of endovascular and surgical treatment in 248 patients. Minim Invas Neurosurg 41:81–85
Lee DS, Kobrine A (1983) Neurogenic pulmonary edema associated with ruptured spinal cord arteriovenous malformation. Neurosurgery 12:691–693
Lee KC, Joo JY, Lee KS (1996) False localization of rupture by computed tomography in bilateral internal carotid artery aneurysms. Surg Neurol 45:435–441
Lee R, Libby P (1997) The unstable atheroma. Arterioscler Thromb Vasc Biol 17: 1859–1867
Lee S, Kim B, Ter Brugge K (2002a) Clinical presentation, imaging and treatment of cerebral venous thrombosis (CVT). Intervent Neuroradiol 8:5–14
Lee SK, Vilela P, Willinsky RA, Ter Brugge KG (2002b) Spontaneous regression of cerebral arteriovenous malformations: clinical and angiographic analysis with review of the literature. Diagn Neuroradiol 44:11–16.
Lee S, Willinsky R, Ter Brugge K (2002c) Dural sinus thrombosis complicated with heparin-induced thrombocytopenia and thrombosis (HITT). Intervent Neuroradiol 8:77–80
Lees F (1962) The migrainous symptoms of cerebral angiomata. J Neurol Neurosurg Psychiatry 25:45–50
Lefkovits J, Plow E, Topol E (1995) Platelet glycoprotein IIb/IIIa receptors in cardiovascular medicine. N Engl J Med 332:1553–1559
Lehmann RAW, Hayes GJ (1966) Toxicity of alkyl 2-cyanoacrylates. I. Peripheral nerve. Arch Surg 93:441–446
Lehmann RAW, Hayes GJ (1967) The toxicity of alkyl 2-cyanoacrylate tissue adhesive: brain and blood vessels. Surgery 61:915–922Lejeune JP (1997) Les anévrysmes intracraniens familiaux. Revue de la littérature. Neurochirurgie 43:292–298
Lejeune JP, Combelles G, Christiaens JL (1969) Formes familiales des cavernomes. Neurochirurgie 35:111–112
Lejeune JP, Combelles G, Christiaens JL (1989) Familial forms of cavernomas Neurochirurgie 35:111–112
Lempert T, Malek A, Halbach V et al (2000) Endovascular treatment of ruptured posterior circulation cerebral aneurysms. Clinical and Angiographic Outcomes. Stroke 31:100–110
Lenthall RK, Cinalli G., Rodesch G, Lasjaunias P (1999) Endovascular management of a traumatic basilar tip aneurysm following endoscopic ventriculostomy in a child. Intervent Neuroradiol 5:57–60
Leo JS, Lin JP, Kircheff II (1979) Pseudoaneurysm formation secondary to spontaneous thrombosis of a massive cerebral arteriovenous malformation. Neuroradiology 17:115–119
Leroy D, Dompmartin A, Houtteville JP et al (1989) Aneurysm associated with chronic mucocutaneous candidiasis during long-term therapy with ketoconazole. Dermatologica 178:43–46
Lester J (1966) Arteriovenous fistula after percutaneous vertebral angiography. Acta Radiol (Diagn) 5:337–340
Levine OS, Jameson AG, Nelhaus G (1962) Cardiac complications of cerebral arteriovenous fistulas in infancy. Pediatrics 30:563–575
Levy D (1998) Endovascular treatment of carotid artery occlusion in progressive stroke syndromes: technical note. Neurosurgery 42:186–193

Levy D, Brott T, Haley EJ et al (1994) Factors related to intracranial hematoma formation in patients receiving tissue-type plasminogen activator for acute ischemic stroke. Stroke 25:291–297
Levy E, Firlik A, Wisniewski S, Rubin G (1999) Factors affecting survival rates for acute vertebrobasilar artery occlusions treated with intra-arterial thrombolytic therapy: a meta-analytical approach. Neurosurgery 45:539–548
Levy LM, di Chiro G, Brooks RA, Dwyer AJ, Wenen L, Frank J (1988) Spinal cord artifacts from truncation errors during MR imaging. Radiology 166:479–483
Leys D, Pruvo J, Godefroy O, Rondepierre P (1992) Prevalence and significance of hyperdense middle cerebral artery in acute stroke. Stroke 23:317–324
Li ZB, Zhao H, Zhang S (1988) Giant serpentine intracranial aneurysm. A case report. Chin Med J (Engl) 101:55–57
Libby P, Ross R (1996) Cytokines and growth regulatory molecules. In: Fuster V, Ross R, Topol E (eds) Atherosclerosis and coronary artery disease. Lippincott-Raven, Philadelphia, pp 585–594
Lichtenstein L (1950) Aneurysmal bone cyst. A pathological entity commonly mistaken for giant-cell tumor and occasionally for hemangioma and osteogenic carcinoma. Cancer 3:279–289
Lichtenstein L (1972) Bone tumors, 4th edn. Mosby, St Louis
Lin M, Almus-Jacobs F, Chen H et al (1997) Shear stress induction of the tissue factor gene. J Clin Invest 99:737–744
Lindau A (1926) Cysts in the cerebellum: structure, pathogenesis, and relations to angiomatosis of the retina. Acta Pathol Microbiol Scand [Suppl]1:1–128
Lindborn A, Soderberg G, Spjut JH, Sunnquist O (1961) Angiography of aneurysmal bone cyst. Acta Radiol (Stockh) 55:12
Lindegaard KJ, Bakke SJ, Grolimund P, Aaslid R, Huber P, Nornes H (1985) Assessment of intracranial hemodynamics in carotid artery disease by transcranial Doppler ultrasound. J Neurosurg 63:890
Lindsay KW, Teasdale G, Knill-Jones RP, Murray L (1982) Observer variability in grading patients with subarachnoid hemorrhage. J Neurosurg 56:628–633
Link J, Fayerabend B, Grabener M, Linstedt U (1996) Dacron covered stent-grafts for the percutaneous treatment of carotid artery aneurysms: effectiveness and biocompatibility – Experimental study in swine. Radiology 200:397–401
Linn FHH, Rinkel GJE, Algra,A, van Gijn J (1996) The incidence of subarachnoid haemorrhage – role of region, year, and rate of computed tomography a meta-analysis. Stroke 27:625–629
Lipton RB, Nerger AR, Lesser ML, Lantos G, Portenoy RK (1987) Lobar us thalamic and basal ganglion hemorrhage: clinical and radiographic features. J Neurol 234: 86–90
Liscak R, Vladyka V, Wowra B, Kemeny A, Forster D, Burzaco JA, Martinez R, Eustacchio S, Pendl G, Regis J, Pellet W (1999) Gamma knife radiosurgery of the glomus jugulare tumour-early multicentre experience. Acta Neurochir (Wien); 141:1141–1146
Liu A (1999) Long-term outcomes after carotid artery stent placement for treatment of carotid artery dissection. Neurosurgery 45:1368–1374
Liu A, Paulsen R, Marcellus M, Steinberg G (1999) Long-term outcomes after carotid stent placement for treatment of carotid artery dissection. Neurosurgery 45:1368–1374
Lloyd GA (1982) Primary orbital meningioma: a review of 41 patients investigated radiologically. Clin Radiol 33:181–187
Lloyd G, Howard D, Phelps P, Cheesman A (1999) Juvenile angiofibroma: the lessons of 20 years of modern imaging. J Laryngol Otol: 113:127–134
Locksley HB (1966) Report on the cooperative study of intracranial aneurysms and subarachnoid haemorrhage. Section V, Part I. Natural history of subarachnoid haemorrhage, intracranial aneurysms and arteriovenous malformations. Based on 6368 cases in the cooperative study. J Neurosurg 25:219–239
Lombardi G, Migliavacca F (1959) Angiomas of the spinal cord. Br J Radiol 32: 810–814
Longa L, Scolari F, Brusco A et al (1997) A large TSC2 and PKD1 gene deletion is associated with renal and extra renal signs of autosomal dominant polycystic kidney disease. Nephrol Dial Transplant 12:1900–1907

Longstreth WT, Nelson LM, Koepsell TD, van Belle G (1992) Cigarette smoking, alcohol use, and subarachnoid hemorrhage. Stroke 23:1242–1249
Lopez DA, Silvers DN, Hellwig EB (1974) Cutaneous meningiomas – a clinicopathologic study. Cancer 34:728–744
Lord JW, Stone PW, Cloutheir WA et al (1958) Major blood vessel injury during elective surgery. Arch Surg 77:282–288
Louvel A, Abelanet R (1979) Anatomie pathologique des polunéoplasies endocraniennes. Ann Med Interne 12:583–589
Lozano AM, Leblanc R (1987) Familial intracranial aneurysms. J Neurosurg 66: 522–528
Lozano AM, Leblanc R (1992) Cerebral aneurysms and polycystic kidney disease: a critical review. Can J Neurol Sci 19:222–227
Lucas C, Zabramski J, Spetzler R, Jacobowitz R (1997) Treatment of intracranial dural arteriovenous malformations: a meta-analysis from the english language literature. Neurosurgery 40:1119–1132
Lucas RB (1976) Pathology of tumors of the oral tissues. Churchill Livingstone, Edinburgh
Luessenhop AJ, Velasquez AC (1964) Observation on the tolerance of the intracranial arteries to catheterization. J Neurosurg 21:85–91
Luessenhop AJ, Gennarelli TA (1977) Anatomical grading of supratentorial arteriovenous malformations for deforming operability. Neurosurgery 1:30–35
Luessenhop AJ, Rosa L (1984) Cerebral arteriovenous malformations. Indications for and results of surgery, and the role of intravascular techniques. J Neurosurg 60:14–22
Luessenhop AJ, Gibbs M, Velasquez AC (1962) Cerebrovascular response to emboli. Observations in patients with arteriovenous malformations. Arch Neurol 7:264–274
Luizy F (1998) Lesion of carotid artery. echo-doppler.transcranial doppler. In: Henry M, Amor M, Theron J, Roubin G (eds) Carotid angioplasty and stenting. pp 73–80
Lum C, Ter Brugge KG (2002) Intervention in vascular lesions of the vertebrae. Semin Intervent Radiol19:245–255
MacPherson P (1991) The value of pre-operative embolization of meningioma estimated subjectively and objectively. Neuroradiology 33:334–337
MacPherson RI (1980) Aneurysmal bone cyst of spine diagnosed by cutaneous opacification. J Can Assoc Radiol 31:210–212
Madan M, Kereiakes D, Rund M et al (1997) Abciximab readministration for coronary interventions: is it safe? (abstract]). Circulation 96 [Suppl I]:162
Maddison FE (1970) Arteriographic evaluation of carotid artery surgery. AJR 109: 121–126
Madoule PH, Trampont PH, Doyon D et al (1981) Expérimentation chez le chien de micro-billes utisasbles en angiographie therapeutique. J Radiol 62:457–462
Maeder P, Gudinchet R, Meuli R, de Tribolet N (1998) Development of a cavernous malformation of the brain. AJNR Am J Neuroradiol 19:1141–1145
Mahagne MH, Rogopoulos A, Paquis P, Guilham D, Lonjon M, Grellier P, Chatel M (1992) Intracranial dural arteriovenous fistula with spinal venous drainage. Rev Neurol 148:789–792
Mahaley MS Jr, Brooks WH, Roszman TL et al (1977) Immunobiology of primary intracranial tumors. Part I: studies of the cellular and humoral general immune competence of brain tumor patients. J Neurosurg 46:467–476
Mahe E, Poncet P, Basset JM, Le Doussal V (1983) Tumeurs bénignes rares des fosses nasales et des sinus de la face (schwannomes bénins, fibromyxome). Ann Otolaryng 100:347–351
Maher CO, Piepgras DG, Brown RD, Friedman JA, Pollock BE (2001) Cerebrovascular manifestations in 321 cases of hereditary hemorrhagic telangiectasia. Stroke 32:877–882
Maillot C (1996) Eloquent pictures: "linea splendens." Intervent Neuroradiol 2:287
Malek A, Higashida R, Balousek P et al (1999) Endovascular recanalization with balloon angioplasty and stenting of an occluded occipital sinus for treatment of intracranial venous hypertension: technical case report. Neurosurgery 44:896–901

Malik GM, Pearce JE, Ausman JL, Mehta B (1984) Dural arteriovenous malformations and intracranial hemorrhage. Neurosurgery 15:332–339
Malis LI (1982a) Arteriovenous malformations of the brain. In: Youmans JR (ed) Neurological surgery, vol 3. Saunders, Philadelphia, pp 1786–1806
Malis L (1982b) Arteriovenous malformations of the spinal cord. In: Youmans JR (ed) Neurological surgery, vol 3. WB Saunders Co, Philadelphia, pp 1850–1874
Malisch T, Guglielmi G, Vinuela F et al (1997) Intracranial aneurysms treated with the Guglielmi detachable coil: midterm clinical results in a consecutive series of 100 patients. J Neurosurg 87:176–183
Manabe H., Oda N, Ishii M, Ishii A (1991) The posterior inferior cerebellar artery originating from the internal carotid artery, associated with multiple aneurysms. Neuroradiology 33:513–515
Mandzia JL, Ter Brugge K, Faughnan ME, Hyland RH (1999) Spinal cord arteriovenous malformations in two patients with hereditary hemorrhagic telangiectasia Childs Nerv Syst 15:80–83
Manelfe C, Berenstein A (1980) Treatment of carotid cavernous fistulas by venous approach. J Neuroradiol 7:13–19
Manelfe C, Lazorthes G, Roulleau J (1972) Artères de la dure-mère rachidienne chez l'homme. Acta Radiol 13:829–841
Manelfe C, Clarisse J, Fredy D et al (1974) Dysplasies fibromusculaires des artères cervico-cephalique. J Neuroradiol 1:149–231
Manelfe C, Espagno B, Guiraud M et al (1975) Therapeutic embolization of craniocerebral tumors. J Neuroradiol 2:257–274
Manelfe C, Guiraud B, David J, Eymeri JC, Tremoulet M, Espagno J, Rascol A, Geraud J (1975) Embolization by catheterization of intracranial meningiomas. Rev Neurol (Paris) 128:339–351
Manjo G, Joris I (1994) Cells, tissues and disease. Oxford: Blackwell Science, pp 655–660
Manzione J, Newman G, Shapiro A, Santo-Ocampo R (2000) Diffusion-and perfusion-weighted MR imaging of dural sinus thrombosis. AJNR Am J Neuroradiol 21:68–73
Marc JA, Takei Y, Schechter MM et al (1975) Intracranial hemangiopericytomas: angiography, pathology and differential diagnosis. AJR 125:823–832
Marchuk DA, Gallione CJ, Morrison LA, Clericuzio CL, Hart BL, Louis DN, Guesella JF, Davis LE, Prenger VL (1995) A locus for cerebral cavernous malformations maps to chromosome 7q in two families. Genomics 28:311–314
Marcus A (1996) Platelet activation. In: Fuster V, Ross R, Topol E (eds) Atherosclerosis and coronary artery disease. Lippincott Raven, Philadelphia, pp 607–637
Margolis G, Odom G, Woodhall B (1961) Further experiences with small vascular malformations as a cause of massive intracerebral bleeding. J Neuropathol Exp Neurol 20:161–167
Margolis MT, Stein RL, Newton TH (1972) Extracranial aneurysms of the internal carotid artery. Neuroradiology 4:78–89
Margulies D, Hestrin M, Lemus J, Bjerke H (1993) Bradycardia following carotid endarterectomy. Am Surg 59:578–581
Markert JM, Chandler WF, Deveikis JP, Ross DA (1996) Use of the extreme lateral approach in the surgical treatment of an intradural ventral cervical spinal cord vascular malformation: technical case report. Neurosurgery 38:412–415
Markham JW (1969) Spontaneous arteriovenous fistula of the vertebral artery and veins. Case report. J Neurosurg 31:220–223
Marks MP, Lange B, Steinberg GK, Snipes GJ (1992) Intranidal aneurysms in cerebral arteriovenous malformations evaluation and endovascular treatment. Radiology 183:355–360
Marks M, Dake M, Steinberg G, Norbash A (1994) Stent placement for arterial and venous cerebrovascular disease: preliminary experience. Radiology 191:441–446
Marks PV, Brookes GB (1983) Malignant paraganglioma of the larynx. J Laryng and Otol 97:1183–1188
Marsh WR (1999) Vascular lesions of the spinal cord: history and classification. Neurosurg Clin N Am 10:1–8

Marsot-Dupuch K, Riachi S, Berthet K, Azizi L (2000) Anévrisme infectieux de la carotide intracaverneuse. J Radiol 81:891–898
Martin D, Rodesch G, Alvarez H, Lasjaunias P (1996) Preliminary results of embolisation of nonsurgical intracranial aneurysms with GD coils: the 1st year of their use. Neuroradiology 38: S142–S150
Martin H, Ehrlich HE, Abels JC (1948) Juvenile nasopharyngeal angiofibroma. Ann Surg 127:513–536
Martin NA, Khanna RK, Batzdorf U (1995) Posterolateral cervical or thoracic approach with spinal cord rotation for vascular malformations or tumors of the ventrolateral spinal cord. J Neurosurg 83:254–261
Martinelli I, Mannucci P, De Stefano V et al (1998a) Different risks of thrombosis in four coagulation defects associated with inherited thrombophilia: a study of 150 families. Blood 92:2353–2358
Martinelli I, Sacchi E, Landi G, Taioli E, Duca F, Mannucci P (1998b) High risk of cerebral-vein thrombosis in carriers of a prothombin-gene mutation and in users of oral contraceptives. New Engl J Med 338:1793–1797
Martyn C, Gale C, Jespersen S et al (1998) Impaired fetal growth and atherosclerosis of carotid and peripheral arteries. Lancet 352:173–178
Marzewski D, Furlan A, St. Louis P et al (1982) Intracranial internal carotid artery stenosis: long-term prognosis. Stroke 13:821–824
Masaryk TJ, Ross JS, Modic MT, Ruff R, Selman WR, Ratcheson RA (1987) Radiculomeningeal vascular malformations of the spine: MR imaging. Radiology 164: 845–849
Mascalchi M, Ferrito G, Quilici N, Mangiafico S, Cosottini M, Cellerini M, Politi LS, Guerrini L, Bartolozzi C, Villari N (2001) Spinal vascular malformations: MR angiography after treatment. Radiology. 2001;219: 346–353
Massoud T, Turjman F, Ji C, Vinuela F (1995) Endovascular treatment of fusiform aneurysms with stents and coils: technical feasibility in a swine model. Am J Neuroradiol 16:1953–1963
Mast H, Mohr JP, Thompson JLP, Osipov A, Trocio SH, Mayer S (1995) Transcranial Doppler ultrasonography in cerebral arteriovenous malformations: diagnostic sensitivity and association of flow velocity with spontaneous hemorrhage and focal neurological deficit. Stroke 26:1024–1027
Mast H, Young WL, Koennecke HC, Sciacca RR, Osipov A, Pile-Spellman J, Hacein-Bey L, Duong H, Stein BM, Mohr JP (1997) Risk of spontaneous haemorrhage after diagnosis of cerebral arteriovenous malformation. Lancet 350 (9084):1065–1068
Mathias KD (1999) Angioplasty and stenting for carotid lesions: an argument for. Adv Surg 32:225–243
Mathur A, Dorros G, Iyer S, Vitek J (1997) Palmaz stent compression in patients following carotid artery stenting. Cathet Cardiovasc Diagn 41:137–140
Matsubara S, Manzia J, Ter Brugge K, Willinsky R, Montanera W, Faughnan M (2000) Angiographic and clinical characteristics of patients with cerebral arteriovenous malformations associated with hereditary hemorrhage telangiectasia. AJNR Am J Neuroradiol 21:1016–1020
Matsumaru Y, Pongpech S, Laothamas J, Alvarez H, Rodesch G, Lasjaunias P (1999) Multifocal and metameric spinal cord arteriovenous malformations: review of 19 cases. Interv Neuroradiol 5:27–34
Matsumura A, Tsuboi K, Hyodo A, Yoshizawa K, Nose T (1986) Lumbosacral extradural spinal arteriovenous malformation with blood supply from branches of internal iliac arteries. Neurochirurgia 29:235–237
Matsunaga N, Hayashi K, Sakamoto I, Ogawa Y (1997) Takayasu arteritis: protean radiologic manifestations and diagnosis. Radiographics 17:579–594
Maurice M, Milad M (1981) Pathogenesis of juvenile nasopharyngeal fibroma (a new concept). J Laryng Otol 95:1121–1126
Mawad M. Endovascular treatment of cerebral aneurysms with liquid polymer. Working Group in Interventional Neuroradiology. Val d'Isère, France
Mawad M, Klucznik R (1995) Giant serpentine aneurysms: radiographic features and endovascular treatment. AJNR Am J Neuroradiol 16:1053–1060
Mawad ME, Hilal SK, Michelson WJ et al (1984) Occlusive disease associated with cerebral arteriovenous malformations. Radiology 153:401–408

Mawad M, Cekirge S, Ciceri E, Saatci I (2002) Endovascular treatment of giant and large intracranial aneurysms by using a combination of stent placement and liquid polymer injection. Neurosurgery 96:474–482
Mayberg M, Wilson S, Yatsu F et al (1991) Carotid endarterectomy and prevention of cerebral ischemia in symptomatic carotid stenosis. JAMA 266:3289–3294
Mazighi M, Porter P, Alvarez H, Rodesch G, Meisel J, Brock M, Lasjaunias P (2000) Associated cerebral and spinal AVM in an infant and in an adult. Report of 2 cases treated by endovascular approach. Interv Neruroradiol 6:31–326
Mazza C, Scienza R, Dalla Bernardin B, Beltramello A, Bontempini L, Dapian R (1989) Malformations caverneuses cérébrales (cavernomes) de l'enfant. Neurochirurgie 35:106–108
Mazzei TS, Mazzei CM, Sonener A (1976) Hypocalcemia y tetania en el meningioma. Desaparicion despues de su extirpacion. Sindrome paraneoplasico. Rev Clin Esp 141:183–186
Mazziotta J, Cohen M, Toga A (1997) The measurement of cerebral blood flow and metabolism in human subjects. In: Welch K, Caplan L, Reis D, Siesjo B, Weir B (eds) Primer on cerebrovascular diseases. Academic Press, San Diego, pp 38–41
McAllister KA, Grogg KM, Johnson DW (1994) Endoglin, a TGF-β binding protein of endothelial cells, is the gene for hereditary hemorrhagic telangiectasia type 1. Nat Genet 8(4):345–351
McAllister VL, Kendall BE, Bull JWD (1975) Symptomatic vertebral haemangiomas. Brain 98:71–80
McCaffrey TV, Meyer FB, Michels VV, Piepgras DG, Marion MS (1994) Familial paragangliomas of the head and neck. Arch Otolaryngol Head Neck Surg 120:1211–1126
Mc Cormick WF, Rosenfield DB (1973) Massive brain hemorrhage. A review of 144 cases and an examination of their causes. Stroke 4:946–954
McCormick P, Spetzler R, Bailes J, Zabramski J (1992) Thromboendarterectomy of the symptomatic occluded internal carotid artery. J Neurosurg 76:752–758
McDowell HA (1971) Postarteriographic arteriovenous fistula of the cervical vertebral artery. South Med J 64:119–120
McKenzie I (1953) The clinical presentation of the cerebral angioma. A review of 50 cases. Brain 76:184–214
McKissock W, Richardson A, Walsh L et al (1964) Multiple intracranial aneurysms. Lancet 1:623–626
McLaughlin M, Kondziolka D, Flickinger J, Lunsford S, Lunsford D (1998) The prospective natural history of cerebral venous malformations. Neurosurgery 43: 195–201
McMahon J, Dorsch N (1999) Subarachnoid haemorrhage of unknown aetiology: what next? Crit Rev Neurosurg 9:47–155
McMillan D (1985) Blood flow and the localization of atherosclerotic plaques. Stroke 16:582–587
Meder JF, Devaux B, Merland JJ, Fredy D (1995) Spontaneous disappearance of a spinal dural arteriovenous fistula. AJNR Am J Neuroradiol 16: 2058–2062
Meguro T, Nakashima H, Kawada S, Tokunaga K (2000) Effect of external stenting and systemic hypertension on intimal hyperplasia in rat vein grafts. Neurosurgery 46:963–970
Meier P, Zierler K (1954) On the theory of the indicator-dilution method for measurement of blood flow and volume. J Applied Physiol 6:731–744
Meisel HJ, Lasjaunias P, Brock M (1996a) Modern management of spinal and spinal cord vascular lesions Minim. Invas Neurosurg 38:138–145
Meisel HJ, Lasjaunias P, Brock M (1996b) Multiple arteriovenous malformations of the spinal cord in an adolescent: case report. Neuroradiology 38:490–493
Meisel HJ, Mansmann U, Alvarez H, Rodesch G, Brock M, Lasjaunias P (2000) Cerebral arteriovenous malformation and associated aneurysms: analysis of 305 cases from a series of 662 patients. Neurosurgery 46:793–802
Meisel HJ, Mansmann U, Alvarex H, Rodesch G, Brock M, Lasjaunias P (2002) Effect of partial targeted NBCA embolization in brain AVM. Acta Neuochurgica Acta Neuochurgica 144:879–888
Meissner I, Whisnant J, Garraway W (1988) Hypertension management and stroke recurrence in a community (Rochester Minnesota, 1950–1979). Stroke 19:459–463

Melki JP, Riche MC, Reizine D, Assouline E, Aymard A, Merland JJ (1986) Simultaneous bifemoral retrograde arteriography under pressure. First stage in angiographic exploration of the spine and spinal cord. J Neuroradiol 13:62–70
Melon C (1964) Physiopathologie générale de la muqueuse nasale. Acta Oto Rhino Laryng Belgica 18:219–279
Melot GH, Jeanmart L, Brihaye J et al (1966) Atypies arterielles cervicales infantiles. J Belge Radiol 49:229–233
Mendelsohn F, Weissman N, Lederman R, Crowley J et al (1998) Acute hemodynamic changes during carotid artery stenting. Am J Cardiol 82:1077–1081
Mericle R, Lanzino G, Wakhloo A et al (1998) Stenting and secondary coiling of intracranial internal carotid artery aneurysm: Technical case report. Neurosurgery 43:1229–1234
Mericle R, Kim S, Lanzino G, Lopes D (1999) Carotid artery angioplasty and use of stents in high risk patients with contralateral occlusions. J Neurosurg 90:1031–1036
Merland JJ, Chiras J (1979) Données de l'artériographie médullaire dans le cadre des paraplégies et quadriplégies traumatiques. Chirurgie 105:154–160
Merland JJ, Reizine D (1987) Treatment of arteriovenous spinal cord malformations. Semin Intervent Radiol 4:281–290
Merland JJ, Thiebot J, Tubiana JM, Brault B, Bories J (1976) Tumeurs bénignes des os et artériographie. Apport de l'artériographie superselective. A propos de 22 cas. J Radiol Electrol Med Nucl 57:630
Merland JJ, Riche MC, Chiras J (1980a) Les fistules artérioveineuses intracanalaires extra-médullaires à drainage veineux médullaire. J Neuroradiol 7:221–230
Merland JJ, Riche MC, Chiras J (1980b) Intraspinal extramedullary arteriovenous fistulae draining into the medullary veins. J Neuroradiol 7:271–320
Merland JJ, Reizine D, Laurent A, Khayata M, Casasco A, Aymard A, Gobin YP (1992) Embolization of spinal cord vascular lesions. In: Vinuela F, Van Halbach V, Dion J (eds) Interventional neuroradiology, endovascular therapy of the central nervous system. Raven Press, New York, pp 153–165
Mettinger KL (1982) Fibromuscular dysplasia and the Brain. II. Current concept of the disease. Stroke 13:53–56
Mettinger KL, Ericson K (1982) Fibromuscular dysplasia and the brain. Observations on angiographic, clinical and genetic characteristics. Stroke 13:46–52
Meyer F, Piepgras D, Sandok B et al (1986) Emergency carotid endarterectomy for patients with acute carotid occlusion and profound neurological deficits. Ann Surg 203:82–89
Meyer FB, Sundt TM et al (1989) Cerebral aneurysms in childhood and adolescence. J Neurosurg 70:420–425
Meyer F, Piepgras D, Fode N (1994) Surgical treatment of recurrent carotid artery stenosis. J Neurosurg 80:781–787
Meziti L, Iffenecker C, Fuerxer F, Benoudiba F, Comoy J, Lacroix C, Doyon D (1998) Pseudoneurinome du XII par transformation fibreuse spontanée d'un anévrysme de l'artère vertébrale. J. Neuroradiol. 25 307–311
Micheli F, Schteinschnaider A, Plaghos LL et al (1989) Bacterial cavernous sinus aneurysm treated by detachable balloon technique. Stroke 20:1751–1754
Michelsen JJ, New PFJ (1969) Brain tumor and pregnancy. J Neurol Neurosurg Psychiatry 32:305–307
Miller D, Bell A (1987) Cerebral blood flow: variations with perfusion, pressure and metabolism. In: Wood J (ed) Cerebral blood flow. McGraw-Hill, New York, pp 119–130
Miller JD, Jawad K, Jennett B (1977a) Safety of carotid ligation and its role in the management of intracranial aneurysms. J Neurol Neurosurg Psychiatry 40: 64–72
Miller JDR, Grace MG, Russell DB, Zacks DJ (1977b) Complications of cerebral angiography and pneumography. Radiology 124:741–744
Minakawa T, Tanaka R, Koike T, Takeuchi S, Sasaki O (1989) Angiographic follow-up study of vertebral arteriovenous malformations with reference to their enlargement and regression. Neurosurgery 24:64–74
Mirrizi PC (1935) Tumeur du corpuscule carotidien. Presse Med 43:1804–1907

Mishkin MM, Baum S, Ng L et al (1972) Cerebrospinal fluid iodine levels after uncomplicated and complicated angiography (abstract). Invest Radiol 7:439
Miyamoto S, Kikuchi H, Karasawa J, Ikota T, Hagata I (1983) Spinal cord arteriovenous malformations associated with spinal aneurysms. Neurosurgery 13:577–580
Miyasaka K, Takei H, Nomura M, Sugimoto S, Aida T, Abe H, Tsuru M (1980) Computerized tomography findings in aural arteriovenous malformations. J Neurosurg 53:698–702
Miyasaka K, Wolpert SM, Prager RJ (1982) The association of cerebral aneurysms, infundibula and intracranial arteriovenous malformations. Stroke 13:196–203
Miyasaka Y, Kurata A, Tanaka R et al (1997) Mass effect caused by clinically unruptured cerebral arteriovenous malformations. Neurosurgery 41:1060–1063
Miyazaki S, Kamata K, Yamaura A (1981) Multiple aneurysms of the vertebrobasilar system associated with fenestration of the vertebral artery. Surg Neurol 15:192–195
Mizoi K, Suzuki J, Yoshimoto T (1989) Surgical treatment of multiple aneurysms. Acta Neurochir (Wien) 96:8–14
Mizutani T, Tanaka H, Aruga T (1992) Multiple arteriovenous malformations located in the cerebellum, posterior fossa, spinal cord, dura, and scalp with associated port-wine stain and supratentorial venous anomaly. Neurosurgery 31:137–140; discussion 140–131
Mizutani T, Miki Y, Kojima H et al (1999) Proposed classification of nonatherosclerotic cerebral fusiform and dissecting aneurysms. Neurosurgery 45:253–259
Modan B, Baidatz D, Mart H et al (1974) Radiation induced head and neck tumours. Lancet 1:277–279
Modan B, Wagener D (1992) Some epidemiological aspects of stroke: mortality/morbidity trends, age, sex, race, socioeconomic status. Stroke 23:1230–1236
Modesti LM, Binet EF, Collins GH (1976) Meningiomas causing spontaneous intracranial hematomas. J Neurosurg 45:437–441
Moes P, Maillot C (1981) Les veines superficielles de la moelle épinière chez l'homme. Arch Anat Histol Embryol Norm Exp 64:5–110
Moffat DB (1961) The development of the posterior cerebral artery. J Anat 95:485–496
Mohr JP (1984) Neurological manifestations and factors related to therapeutic decisions. In: Wilson CB, Stein BM (eds) Intracranial arteriovenous malformations. Williams and Wilkins, Baltimore, pp 12–23
Mohr J, Orgogozo J, Harrison M, Hennerici M (1994) Meta-analysis of oral nimodipine trials in acute ischaemic stroke. Cerebrovasc Dis 4:197–203
Mokri B, Houser O, Sundt T (1977) Idiopathic regressing arteriopathy. Ann Neurol 2:466–472
Molyneux A (2002) International Subarachnoid Aneurysms Trial (ISAT) of neurosurgical clipping versus endovascular coiling in 2143 patients with ruptured intracranial aneurysms: a randomised trial. Lancet 360:1267–1274
Molyneux AJ, Coley SC (2000) Embolization of spinal cord arteriovenous malformations with an ethylene vinyl alcohol copolymer dissolved in dimethyl sulfoxide (Onyx liquid embolic system). Report of two cases. J Neurosurg 93: 304–308
Moncada S, Pamer R, Higgs E (1991) Nitric oxide: physiology, pathophysiology and pharmacology. Pharmacol Rev 43:109–142
Mondy J, Lindner V, Miyashiro J, Berk B, Dean R, Geary R (1997) Platelet-derived growth factor ligand and receptor expression in response to altered blood flow in vivo. Circ Res 81:320–327
Monsein LH, Debrun GM, Chazaly JR (1990) Hydroxyethyl methacrylate and latex balloons. AJNR Am J Neuroradiol 11:663–664
Monsein L, Debrun G, Miller N, Nauta H, Chazaly J (1991)Treatment of dural carotid-cavernous fistulas via the superior ophthalmic vein. AJNR 12:435–439
Montanera W, Marotta T, Ter Brugge KG, Lasjaunias P, Willinsky R, Wallace MC (1990) Cerebral arteriovenous malformations associated with moyamoya phenomenon. AJNR 11:1153–1156
Moody DM, Ghatak NR, Kelly DL (1976) Extensive calcification in a tumor of the glomus jugulare. Neuroradiology 12:131–135
Moody RA, Poppen JL (1970) Arteriovenous malformations. J Neurosurg 23:503–511
Mooij JJA (2001) Grading and decision making in (aneurysmal) subarachnoid haemorrhage. Intervent Neuroradiol 7:283–289

Moore MT (1954) The fate of clinically unrecognized intracranial meningiomas. Neurology (Minneapolis) 4:837–856
Moore W, Barnett H, Beebe H et al (1995) Guidelines for carotid enterectomy: a multidisciplinary consensus statement from the Ad Hoc Committee, American Heart Association. Stroke 26:188–201
Morello G, Borghi GP (1973) Cerebral angiomas. A report of 154 personal cases and a comparison between the results of surgical excision and conservative management. Acta Neurochir (Wien) 28:135–155
Moret J, Lasjaunias P, Doyon D (1979) Occipital approach for treatment of arteriovenous malformations of the vertebral artery by balloon occlusion. Neuroradiology 17:269–273
Moret J, Lasjaunias P (1986b) Vascular architecture of tympano-jugular glomus tumor. In: Vignaud J, Jardin C, Rosen L (eds) The ear. Masson, Paris, pp 289–303
Moret J, Cognard C, Weil A et al (1997) The "remodeling" technique in the treatment of wide neck intracranial aneurysms. Intervent Neuroradiol 3:21–35
Morgan MK, Johnston IH, De Silva M (1985) Treatment of ophthalmofacial-hypothalamic arteriovenous malformations (Bonnet-Dechaume-Blanc syndrome). J Neurosurg 63:794–796
Morgan MK, Chaseling R, Johnston I, de Silva M (1986) Spinal arteriovenous malformation presenting at birth: case report. Neurosurgery 19:637–640
Morgan MK, Johnston I, Besser M, Baines D (1987) Cerebral arteriovenous malformations, steal and the hypertensive breakthrough threshold. J Neurosurg 66: 563–567
Morgan MK, Marsh WR (1989) Management of spinal dural arteriovenous malformations. J Neurosurg 70:832–836
Mori E, Yoneda Y, Tabuchi M et al (1992) Intravenous recombinant tissue plasminogen activator in acute carotid artery territory stroke. Neurology 42:976 –982
Moriarity J, Wetzel M, Clatterbuck R, Javedan S, Sheppard JM, Hoenig-Rigamonti K, Crone N, Breiter S, Lee R, Rigamonti D (1999) The natural history of cavernous malformations: a prospective study of 68 patients. Neurosurgery 44:1166–1173
Moriwaki R, Noda M, Yajima M, Sharma B (1997) Clinical manifestations of Takayasu arteritis in India and Japan: new classification of angiographic findings. Angiology 48:369–379
Morley TP, Barr HWK (1969) Giant intracranial aneurysms. Diagnosis, course and management. Clin Neurosurg 16:73–94
Morris G (1969) Delayed perforation of the internal carotid artery by an ingested foreign body. Br J Surg 56:711–712
Morris PP, Branden G (1999) Neurointerventional experience with an arteriotomy suture device. AJNR 20: 1706–1709
Morris P, Martin E, Regan J, Braden G (1999) Intracranial deployment of coronary stents for symptomatic atherosclerotic disease. Am J Neuroradiol 20:1688–1694
Moscow NP, Newton HN (1975) Angiographic features of hypervascular neurinomas of the head and neck. Radiology 114:635–640
Moskowitz MA, Coughlin SR (1981) Clinical applications of prostaglandins and their inhibitors. Stroke 12:882–886
Moss JG, Sellar RJ, Hadley DM (1989) Intracerebral and spinal vascular malformation in a patient without hereditary haemmorhagic telangiectasia. Neuroradiology 31:280–281
Moufarrij N, Little J, Furlan A, Leatherman J, Williams G (1986) Basilar and distal vertebral artery stenosis: long-term follow-up. Stroke 17:938–942
Moulin T, Cattin F, Crepin-Leblond T et al (1996) Early CT signs in acute middle cerebral artery infarction: predictive value for subsequent infarct locations and outcome. Neurology 47:366–375
Mourier KL, Gobin YP, George B, Lot G, Merland JJ (1993) Intradural perimedullary arteriovenous fistulae: results of surgical and endovascular treatment in a series of 35 cases Neurosurgery 32:885–891
Muir K, Lees K (1995a) A randomized, double-blind, placebo controlled trial of intravenous magnesium sulphate in acute stroke. Stroke 26:1183–1188
Muir K, Lees K (1995b) Clinical experience with excitatory amino acid antagonist drugs. Stroke 26:503–513

Muir K, Lees K (1995c) Dose ranging study of magnesium sulphate after acute stroke. Eur J Neurol 2 [Suppl 2]:7–8
Mujica RH, Rosenblat AM, Luessenhop AJ (1981) Subarachnoid hemorrhage secondary to an aneurysm of the ascending pharyngeal artery case report. J Neurosurg 54:818–820
Mullan S, Brown FD, Patrona WJ (1979) Hyperemic and ischemic problems of surgical treatment of arteriovenous malformations. J Neurosurg 51:757–764
Müller-Forell W, Bohl J (1999) Psychic stress as a trigger of the spontaneous development and rupture of an aneurysm? A case report. Intervent Neuroradiol 5:179–186
Multicentre Acute Stroke Trial–Italy (MAST-I) Group (1995) Randomized controlled trial of streptokinase, aspirin, and combination of both in treatment of acute ischaemic stroke. Lancet 346:1509–1514
Muraszko K, Wang HH, Pelton G, Stein BM (1970) A study of the reactivity of feeding vessels to arteriovenous malformations: correlation with clinical outcome. Neurosurgery 26:190–199
Murayama Y, Vinuela F, Zenteno M et al (1997) Nonadhesive liquid embolic agent for neuroendovascular applications: experimental studies and preliminary clinical utilization in brain arteriovenous malformations. Intervent Neuroradiol 3S:101
Murayama Y, Vinuela F, Ulhoa A, Akiba Y, Duckwiler GR, Gobin YP, Vinters HV, Greff RJ (1998) Nonadhesive liquid embolic agent for cerebral arteriovenous malformations: preliminary histopathological studies in swine rete mirabile. Neurosurgery 43:198–206
Murayama Y, Vinuela F, Duckwiler GR, Gobin YP, Guglielmi G (1999) Embolization of incidental cerebral aneurysms by using the Guglielmi detachable coil system. J Neurosurg 90:207–214
Murayama Y, Vinuela F, Tateshima S, Vinuela FJ, Akib Y (2000) Endovascular treatment of experimental aneurysms by use of a combination of liquid embolic agents and protective devices. AJNR Am J Neuroradiol 21:1726–1735
Murayama Y, Vinuela F, Teteshima S et al (2001) Bioabsorbable polymeric material coils for embolization of intracranial aneurysms: a preliminary experimental study. J Neurosurg 94:454–463
Murray RO, Jacobson HG (1977) Radiology of skeletal disorders, 2nd edn. Churchill Livingston, New York
Muuronen A (1984) Outcome of surgical treatment of 110 patients with transient ischemic attack. Stroke 15:959–964
Nagahiro S, Goto S, Yoshioka, Ushio Y (1993) Dissecting aneurysm of posterior inferior cerebellar artery: case report. Neurosurgery 33 4:730–744
Nagahiro S, Hamada JI, Sakamoto Y, Ushio Y (1997) Follow-up evaluation of dissecting aneurysms of the vertebrobasilar circulation by using gadolinium-enhanced magnetic resonance imaging. J Neurosurg 87:385–390
Nagashima C, Miyoshi A, Nagashima R, Ogawa M, Enomoto K, Watabe T (1996) Spinal giant intradural perimedullary arteriovenous fistula: clinical and neuroradiological study in one case with review of the literature. Surg Neurol 45:524–531
Nagel T, Resnick N, Atkinson W, Dewey C, Gimbrone M (1994) Shear stress selectively upregulates intercellular adhesion molecule-1 expression in cultured human vascular endothelial cells. J Clin Invest 94:885–891
Nakahara I, Taki W, Kikuchi H, Sakai N, Isaka F, Oowaki H, Kondo A, Iwasaki K, Nishi S (1999) Endovascular treatment of aneurysms on the feeding arteries of intracranial arteriovenous malformations. Neuroradiology 41: 60–66
Nakajima F, Shibahara N et al (2000) Intracranial aneurysms and autosomal dominant polycystic kidney disease: follow-up study by magnetic resonance angiography. J Urol 164:311–313
Nakashima Y, Raines E, Plump A, Breslow J, Ross R (1998) Upregulation of VCAM-1 and ICAM-1 at atherosclerosis-prone sites on the endothelium in the ApoE-deficient mouse. Arterioscler Thromb Vasc Biol 18:842–851
Nakstad P, Hald JK, Bakke SJ (1993) Multiple spinal arteriovenous fistulas in Klippel-Trenaunay-Weber syndrome treated with platinum coils. Neuroradiology 35: 163–165

Napoli C, D'Armiento F, Mancini F et al (1997) Fatty streak formation occurs in human fetal aortas and is greatly enhanced by maternal hypercholesterolemia: intimal accumulation of low density lipoprotein and its oxidation precede monocyte recruitment into early atherosclerotic lesions. J Clin Invest 100:2680–2690

National Institute of Neurological Disorders and Stroke rt-PA Stroke Study Group (NINCDS) (1995) Tissue plasminogen activator for acute ischemic stroke. N Engl J Med 333:1581–1587

Naylor A, Bolia A, Abbott R, Pye I (1998) Randomized study of carotid angioplasty and stenting versus carotid endarterectomy: a stopped trial. J Vasc Surg 28: 326–334

Neel HB, Whicker JH, Devine KD, Weiland LH (1973) Juvenile angiofibromas: review of 120 cases. Am J Surg 126:547–556

Nehls DG, Pittman HW (1982) Spontaneous regression of arteriovenous malformations. Neurosurgery 11:776–780

Nehls DG, Flom RA, Carter LP, Spetzler RF (1985) Multiple intracranial aneurysms: determining the site of rupture. J Neurosurg 63:342–348

Nelson D, Mahru M (1963) Death following digital carotid artery occlusion. Arch Neurol 8:640–643

Nelson PK, Setton A, Choi IS, Ransohoff J, Berenstein A (1994) Current status of interventional neuroradiology in the management of meningiomas. Neurosurg Clin N Am 5:235–259

Nesbit G, Clark W, O'Neill O, Barnwell S (1996) Intracranial intraarterial thrombolysis facilitated by microcatheter navigation through an occluded cervical internal carotid artery. J Neurosurgery 84:387–392

Netterville JL, Jackson CG, Miller FR, Wanamaker JR, Glasscock ME (1998) Vagal paraganglioma: a review of 46 patients treated during a 20-year period. Arch Otolaryngol Head Neck Surg; 124:1133–1140

Neuwelt E, Glasberg M, Frenkel E, Barnett P (1983) Neurotoxicity of chemotherapeutic agents after blood–brain barrier modification. Neuropathological studies. Ann Neurol 14:316–324

New P, Momose K (1969) Traumatic dissection of the internal carotid artery at the atlanto-axial level secondary to nonpenetrating injury. Radiology 93:41–49

Newell D, Eskridge J, Mayberg M, Grady M (1989) Angioplasty for the treatment of symptomatic vasospasm following subarachnoid hemorrhage. J Neurosurg 71:654–660

Newman MJD (1959) Racemose angioma of the spinal cord. Q J Med 28:97–108

Newton TH, Adams J (1968) Angiographic demonstrated and non-surgical embolization of a spinal cord angioma. Radiology 91:873–876

Newton TH, Cronqvist S (1969) Involvement of dural arteries in intracranial arteriovenous malformations. Radiology 93:1071–1078

Newton TH, Hoyt WF (1970) Dural arteriovenous shunts in the region of the cavernous sinus. Neuroradiology 1:71–78

Newton TH, Weidner W, Greitz T (1968) Dural arteriovenous malformations in the posterior fossa. Radiology 90:27–32

Nibbelink DW, Peters BH, McCormich WF (1969) On the association of pheochromocytoma and cerebellar hemangioblastoma. Neurology 19:455–460

Nicholas D, Weller R (1988) The fine anatomy of the human spinal meninges. A light and scanning electron microscopic study. J Neurosurg 69:276–282

Nicol AAM (1957) Lindau's disease in five generations. Ann Hum Genet 22:7–15

Nicola N, Lins E (1987) Vertebral hemangioma: retrograde embolization – stabilization with methyl methacrylate. Surg Neurol 27:481–486

Nimii Y, Berenstein A (1999) Endovascular treatment of spinal arteriovenous malformations Neurosurg Clin N Am 10:47–71

Niimi Y, Berenstein A, Setton A et al (1996) Occlusion of the internal carotid artery based on a simple tolerance test. Intervent Neuroradiol 2:289–296

Niimi Y, Berenstein A, Setton A, Neophytides A (1997) Embolization of spinal dural arteriovenous fistulae: results and follow-up. Neurosurgery. 40:675–682

Nimii Y, Ito U, Tone O, Yoshida K, Sato S, Berenstein A (1998) Multiple spinal perimedullary arteriovenous fistulae associated with the Parkes-Weber Syndrome. A case. Intervent Neuroradiol 4:151–157

Nimii Y, Berenstein A, Setton A, Prior J (2000) Endovascular treatment of spinal cord ateriovenous malformations (abstract). Sixth International Workshop on Cerebrovascular Surgery, Seoul, Korea, June 4–7, 2000
Nishioka H (1966) Results of the treatment of intracranial aneurysms by occlusion of the carotid artery in the nerve. J Neurosurg 25:600–687
Nishizaki T, Tamaki N, Matsumoto S, Fujita S (1986) Consideration of the operative indications for posterior fossa venous angiomas. Surg Neurol 25:441–445
Noel de Tilly L, Willinsky R, Ter Brugge K, Montanera W, Marotta T, Wallace C (1992) Cerebral AVMs causing pistaxis. AJNR 13:333–334
Nora JD, Hallett J, O'Brien PC, Naessens JM, Cherry KJ Jr, Pairolero(1988) Surgical resection of carotid body tumors: long-term survival, recurrence, and metastasis. Mayo Clin Proc 63:348–352
Norlen G (1949) Arteriovenous aneurysms of the brain: report of 10 cases of total removal of the lesion. J Neurosurg 6:475–494
Nornes H, Grip A (1980) Hemodynamic aspects of cerebral arteriovenous malformations. J Neurosurg 53:456–464
Nornes H, Grip A, Wikeby P (1979a) Intraoperative evaluation of cerebral hemodynamics using direction Doppler technique, part 1: arteriovenous malformations. J Neurosurg 50:145–151
Nornes H, Lundar T, Wikeby P (1979b) Cerebral arteriovenous malformations: results of microsurgical management. Acta Neurochir (Wien) 50:243–257
Norrgard O, Angquist KA, Fodstand H, Forsell A, Lindberg M (1987) Intracranial aneurysms and heredity. Neurosurgery 20:236–239
Norris J, Zhu C, Bornstein N, Chambers B (1991) Vascular risks of asymptomatic carotid stenosis. Stroke 22:1485–1490
North American Symptomatic Carotid Endarterectomy Trial Collaborators (1991) Beneficial effect of carotid endarterectomy in symptomatic patients with high-grade carotid stenosis. N Engl J Med 1991 325:445–453
Notelet L, Houtteville JP, Khoury S, Lechevalier B, Chapon F (1997) Proliferating cell nuclear antigen (PCNA) in cerebral cavernomas: an immunocytochemical study of 42 cases. Surg Neurol 47:364–370
Novak Z, Coldwell D, Brega K (2000) Selective infusion of urokinase and thrombectomy in the treatment of acute cerebral sinus thrombosis. AJNR Am J Neuroradiol 21:143–145
Noyek AM, Greyson ND, Steinhart MI, Kassel EE, Shulman HS, Rothberg R, Goldfinger M, Miskin M, Freeman JL (1983) Thyroid tumor imaging. Arch Otolaryng 109:205–224
Numaguchi Y, Kishikawa T, Fukui M, Sawada K, Kitamura K, Matsuura K, Russel WJ (1979) Prolonged injection angiography for diagnosis intracranial cavernous hemangiomas. Radiology 131:137–138
Nusbaum A, Som P, Dubois P, Silvers A (1998) Isolated vagal nerve palsy associated with a dissection of the extracranial internal carotid artery. Am J Neuroradiol 19:1845–1847
Nussbaum E, Heros R, Madison M, Awasthi D, Truwit C (1998) The pathogenesis of arteriovenous malformations: insights provided by a case of multiple arteriovenous malformations developing in relation to a developmental venous anomaly. Neurosurgery 43:347–352
Obley DL, Winzelberg GG, Qjarmolowski CR, Hydovitz JD, Danowski TS, Wholey MH (1984) Parathyroid adenomas studied by digital substraction angiography. Radiology 153:449–451
Obrador S, Soto M, Sileva J (1975) Clinical syndromes of arteriovenous malformations of the transverse sigmoid sinus. J Neurol Neurosurg Psy 38:436–451
O'Callaghan FJ, Osborne JP (2000) Advances in the understanding of tuberous sclerosis (general and specialist paediatrics: recent advances). Arch Dis Child 83:140–142
Oesterle S, Baim D, Hayasse M et al (1998) A coaxial catheter system for prevention of distal embolization. JACC 31:236
Ogura JH (1978) Glomus jugulare and vagale. Ann Otol Rhinol Laryngol 87:622–629
Oguz K, Firat M, Cila A (2001) Fusiform aneurysms detected 5 years after removal of an atrial myxoma. Neuroradiology 43:990–992

Ohata K, Takami T, El-Naggar A, Morino M, Nishio A, Inoue Y, Hakuba A (1999) Posterior approach for cervical intramedullary arteriovenous malformation with diffuse type nidus. Report of 3 cases. J Neurosurg [Suppl 1]91:105–111

Ohki T, Veith FJ (2001) Carotid artery stenting: utility of cerebral protection devices. J Invasive Cardiol 13:47–55

Ohki T, Marin M, Lyon R et al (1998) Ex-vivo human carotid artery bifurcation stenting: correlation of lesion characteristics with embolic potential. J Vasc Surg 27:463–471

Ohman E, Kleiman N, Gacioch G et al, for the IMPACT-AMI Investigators (1997) Combined accelerated tissue-plasminogen activator and platelet glycoprotein IIb/IIIa integrin receptor blockade with Integrilin in acute myocardial infarction: results of a randomized, placebo-controlled, dose-ranging trial. Circulation 95:846–854

Ojemann RG (1982) Surgical management of bacterial intracranial aneurysms. In: Schmideck HH, Sweet WH (eds) Operative neurosurgical techniques, indications, methods, and results, vol 2. Grune & Stratton, New York, pp 923–940

Oka H, Kurata A, Kawano N, Saegusa H, Kobayashi I, Ohmomo T, Miyasaka Y, Fujii K (1998) Preoperative superselective embolization of skull-base meningiomas: indications and limitations. J Neurooncol 40:67–71

Okamoto S, Handa H, Hashimoto N (1984) Location of intracranial aneurysms associated with cerebral arteriovenous malformations: statistical analysis. Surg Neurol 22:335–340

Oldfield EH, Dedrick RL, Chatterji DC et al (1985) Arterial drug infusion with extracorporeal removal. II Internal carotid BCNU in the rhesus monkey. Cancer Treat Rep 69:293–303

Oldfield EH, di Chiro G, Quindlen EA, Reith KG, Doppman JL (1989) Successful treatment of a group of spinal cord arteriovenous malformations by interruption of dural fistula. J Neurosurg 59:1019–1030

Olivecrona H (1957) The cerebellar angioreticulomas. J Neurosurg 9:317–330

Oller DW, Gee W, Kingsley JR (1976) Treatment of high extracranial internal carotid artery aneurysms. Ann Surg 42:311–315

Olutola PS, Eliam M, Molot M, Talalla A (1983) Spontaneous regression of a aural arteriovenous malformation. Neurosurgery 12:687–690

O'Mahony D (1995) Pathophysiology of carotid sinus hypersensitivity in elderly patients. Lancet 346:950–952

Ommaya AK (1985) Spinal arteriovenous malformations. Neurosurgery 22:1495–1499

Ommaya AK, di Chiro G, Doppman J (1969) Ligation of arterial supply in the treatment of spinal cord arteriovenous malformations. J Neurosurg 30:679–692

Omojola MF, Fox AJ, Vinuela F et al (1985) Stenosis of afferent vessels of intracranial arteriovenous malformations. AJNR 6:791–793

Ondra SL, Troupp H, George ED, Schwab K (1990) The natural history of symptomatic arteriovenous malformations of the brain: a 24-year follow up assessment. J Neurosurg 73:387–391

Oostergard JR, Voldby B (1983) Intracranial arterial aneurysms in children and adolescents. J Neurosurg 48:832–837

O'Reilly GV, Kleefield J, Svendsen PA, Serur JR (1984) Fabrication of microballoons for interventional neuroradiology: preliminary report. AJNR Am J Neuroradiol 5:625

O'Reilly GV, Kleefield J, Klein LA, Blume HW, Dubuisson D, Cosgrove GR (1989) Embolization of solitary spinal metastases from renal cell carcinoma: alternative therapy for spinal cord or nerve root compression. Surg Neurol 31:268–271

Osborn DA (1959) So-called juvenile angiofibroma of nasopharynx. J Laryngol Otol 73:295–316

Osborn DA, Sokolovski A (1965) Juvenile angiofibroma in a female. Arch Otolaryng 82:629–632

Oshiro EM, Walter KA, Piantadosi S, Witham TF, Tamargo RJ (1997) A new subarachnoid hemorrhage grading system based on the Glasgow Coma Scale: a comparison with the Hunt and Hess and World Federation of Neurological Surgeons scales in a clinical series. Neurosurgery 41:140–148

Osler WA (1901) A family form of recurring epistaxis associated with multiple telangiectasia of the skin and mucuous membranes. Johns Hopkins Hosp Bull 12:33–337
Ostergaard JR (1989) Risk factors in intracranial saccular aneurysms. Aspects on the formation and rupture of aneurysms, and development of cerebral vasospasm. Acta Neurol Scand 80:81–98
Ostergaard JR (1991) Aetiology of intracranial saccular aneurysms in childhood. Br J Neurosurg 5:575–580
Ostergaard JR, Hog E (1985) Incidence of multiple intracranial aneurysms. Influence of arterial hypertension and gender. J Neurosurg 63:49–55
Otten P, Pizzolato GP, Rilliet B, Berney J (1989) A propos de 131 cas d'angiomes caverneux (cavernomes) du S.N.C. repérés par l'analyse rétrospective de 24 535 autopsies. Neurochirurgie 35:82–83
Overgaard K, Sereghy T, Boysen G, Pedersen H, Diemer N (1993) Reduction of infarct volume by thrombolysis with rt-PA in an embolic rat stroke model. Scand J Clin Lab Invest 53:383–393
Padolecchia R, Puglioli M, Ragone M, Romani A (1999) Superselective intraarterial fibrinolysis in central retinal artery occlusion. Am J Neuroradiol 20:565–567
Padovani R, Tognetti F, Proietti D et al (1982) Extrathecal cavernous hemangioma. Surg Neurol 18:463–465
Paige ML, Hemmati M (1977) Spinal cord compression by vertebral hemangioma. Pediatr Radiol 6:43–45
Pakarinen S (1967) Incidence, aetiology, and prognosis of primary SAH: a study based in 589 cases diagnosed in a defined urban population during a defined period. Acta Neurol Scand 43 [Suppl 29]:1–128
Papatheodorou CA, Gross SW, Hollin S (1961) Small arteriovenous malformations of the brain. Arch Neurol 5:666–672
PARADIGM Investigators (1998) Combining thrombolysis with the platelet glycoprotein IIb/IIIa inhibitor lamifiban: results of the Platelet Aggregation Receptor Antagonist Dose Investigation and Reperfusion Gain in Myocardial Infarction (PARADIGM) trial. J Am Coll Cardiol 32:2003–2010
Paris J, Guelfucci B, Moulin G, Zanaret M, Triglia JM (2001) Diagnosis and treatment of juvenile nasopharyngeal angiofibroma. Eur Arch Otorhinolaryngol: 258:120–124
Park TS, Cail WS, Delashaw JB, Kattwinkel J (1986) Spinal cord arteriovenous malformation in a neonate. Case report. J Neurosurg 64:322–324
Park YD, Belman AL, Kim TS et al (1990) Stroke in pediatric acquired immunodeficiency syndrome Ann Neurol 28:303–311
Parkes-Weber F (1918) Haemangiectatic hypertrophy of limbs congenital phlebarteriectasis and so-called congenital varicose. Br J Child Dis 15:13–23
Parkinson D (1973) Carotid cavernous fistula: direct repair with preservation of the carotid artery. Technical note. J Neurosurg 38:99–106
Parkinson D, Bachers G (1980) Arteriovenous malformations. Summary of 100 consecutive supratentorial cases. J Neurosurg 53:285–299
Parkinson D, West M (1977) Spontaneous subarachnoid hemorrhage first from an intracranial and then from a spinal arteriovenous malformation. Case report. J Neurosurg 47:965–968
Pascual-Castroviejo I, Pascual JI, Blazquez MG, Lopez Martin V (1977) Spontaneous occlusion of an intracranial arteriovenous malformation. Childs Brain 3:169–179
Paterson JH, McKissock W (1956) A clinical survey of intracranial angiomas with special reference to their mode of progression and surgical treatment: a report of 110 cases. Brain 79:233–266
Patra P, Raffi F, Delajartre AY (1986) Anévrismes infectieux artériels. Aspects anatomocliniques et chirurgicaux: à propos de 12 observations. J Chir 123:655–662
Patterson J, Grabois M (1986) Locked-in syndrome: our view of 139 cases. Stroke 17:758–764
Pearse AGE (1977) The diffuse neuroendocrine system and the apud concept: related "endocrine" peptides in brain, intestine, pituitary, placenta, and anuran cutaneous glands. Med Biol 55:115–125

Pecker J, Bonnal J, Javalet A (1965) Deux nouveaux cas d'anévrismes artérioveineux intraduraux de la fosse postérieure alimentés par la carotide externe. Neurochirurgie 11:327–332
Pedroza A, Dujovny M, Ausman J et al (1986) Microvascular anatomy of the interpeduncular fossa. J Neurosurgery 64:484–493
Peeters FL, Kroger R (1979) Dural and direct cavernous sinus fistulas. AJR Am J Roentgenol 132:599–606
Pellettieri L (1980) Surgical versus conservative treatment of intracranial arteriovenous malformations: a study in surgical decision making. Acta Neurochir Suppl (Wien) 29:1–86
Pepin M, Schwarze U, Superti-Furga A, Byers P (2000) Clinical and genetic features of Ehlers-Danlos syndrome type IV, the vascular type. New Engl J Med 342:673–680
Perret G, Nishioka H (1966) Report on the cooperative study of intracranial aneurysms and subarachnoid hemorrhage. Section VI. Arteriovenous malformations. An analysis of 545 cases of cranio-cerebral arteriovenous malformations and fistulae reported to the cooperative study. J Neurosurg 25:467–490
Pertuiset B, Ancri D, Arthuis F, Basset JY, Fusciaradi J, Nakano H (1985) Shunt-induced haemodynamic disturbances in supratentorial arteriovenous malformations. J Neuroradiol 12:165–178
Pesavento G, Ferlito A (1982) Hemangiopericytoma of the larynx. A clinicopathological study with review of the literature. J Laryng Otol 96:1065–1073
Pessin M, del Zoppo G, Furlan A (1995) Thrombolytic treatment in acute stroke, review and update on selective topics, cerebrovascular diseases. 19th Princeton Stroke Conference, Boston, Mass, Butterwood-Heinemann
Petito C, Pulsinelli W (1984) Delayed neuronal recovery and neuronal death in rat hippocampus following severe cerebral ischemia: possible relationship to abnormalities in neuronal processes. J Cereb Blood Flow Metab 4:194–205
Pettet JR, Woolner LB, Judd ES (1937) Carotid body tumors of the carotid body. Review of 159 histologically verified cases. Report of case. West J Surg 45:42–46
Phatouros C, Higashida R, Malek A, Meyers P (2000) Endovascular stenting for carotid artery stenosis: preliminary experience using the shape-memory-alloy-recoverable-technology (SMART) stent. Am J Neuroradiol 21:732–738
Philippet P, Blanche S, Sebag G et al (1994) Stroke and cerebral infarcts in children infected with human immunodeficiency virus. Arch Pediatr Adolesc Med 148: 965–970
Pia HW (1978) Classification of aneurysms of the internal carotid system. Acta Neurochir (Wien) 40:5–31
Pia HW, Djindjian R (eds) (1978) Spinal angiomas. Springer, Berlin Heidelberg New York
Pia HW, Vogelsang H (1965) Diagnose und Therapie spinaler Angiome. Dtsch Z: Nervenheilkd 187:74–96
Pia HW, Langmaid C, Zierski J (1979) Cerebral aneurysms. Advances in diagnosis and therapy.Springer, Berlin Heidelberg New York
Picard L, Moret J, Lepoire J (1984a) Endovascular treatment of intracerebral arteriovenous angiomas. J Neuroradiol 11:9–28
Picard L, Moret J, Lepoire J (1984b) Traitement endovasculaire des angiomes artérioveineux intra-cérébraux. Technique, indications, résultats. J Neuroradiology 11: 9–28
Pickering J, Weir L, Jekanowski J, Kearney M, Isner J (1993) Proliferative activity in peripheral and coronary atherosclerotic plaque among patients undergoing percutaneous revascularization. J Clin Invest 91:1469–1480
Piepgras DG, Sundt TM, Ragoowansi AT, Stevens AL (1993) Seizure outcome in patients with surgically treated cerebral arteriovenous malformations. J Neurosurg 78:5–11
Pierot L, Boulin A, Castaings L et al (1997) The endovascular approach in the management of patients with multiple intracranial aneurysms. Neuroradiology 39: 361–366
Pierot L, Vlachopoulos T, Attal N, Martin N, Bert S, Chiras J (1993) Double spinal dural arteriovenous fistulas: report of 2 cases. AJNR Am J Neuroradiol 14: 1109–1112

Pile-Spellman JMD, Baker KF, Lisczak TM, Sandrew BB et al (1986) High-flow angiopathy: cerebral blood vessel changes in experimental chronic arteriovenous fistula. AJNR 7:811–815
Pile-Spellman J, Berenstein A, Bun T (1987) Angioplasty of canine cerebral vessels (abstract). AJNR Am J Neuroradiol 8:938
Pinto R, Kircheff II, Butler A et al (1979) Correlation of computed tomographic angiographic and neuropathological changes in giant cerebral aneurysms. Radiology 132:85–92
Pirouzmand F, Wallace C, Willinsky R (1997) Spinal epidural arteriovenous fistula with intramedullary reflux. J Neurosurg 87:633–635
Pirson Y, Chauveau D (1996) Intracranial aneurysms in autosomal polycystic kidney disease. In: Watson ML, TorresVE (eds) Polycystic kidney disease. Oxford University Press, Oxford, pp 530
Pirson Y, Chauveau D, van Gijn J (1996) Subarachnoid haemorrhage in ADPKD patients: how to recognize and how to manage? Nephrol Dial Transplant 11: 1236–1238
Pirson Y, Chauveau D, Watson ML, Zeier M, Breuning MH (1997) La polykystose autosomique dominante: progrès cliniques et génétiques. Medecine/Sciences 13:37
Piske R, Lasjaunias P (1988) Extrasinusal dural arteriovenous malformations. Report of three cases. Neuroradiology 30:426–432
Piske R, Darwich R, Campos C, Fonseca N, Oliveira E, Souza A (1998) Spontaneous resolution of a ruptured dissecting PICA aneurysm. Intervent Neuroradiol 4:287–292
Pletcher JD, Newton TH, Dedo HH, Norman D (1975) Preoperative embolization of juvenile angiofibromas of the nasopharynx. Ann Otol Rhinol Laryngol 84: 740–746
Plow E, McEver R, Coller B, Woods VJ, Marguerie G, Ginsberg M (1985) Related binding mechanisms for fibrinogen, fibronectin, von Willebrand factor, and thrombospondin on thrombin-stimulated human platelets. Blood 66:724–727
Plow E, Marguerie G, Ginsberg M (1987) Fibrinogen, fibrinogen receptors, and the peptides that inhibit these interactions. Biochem Pharmacol 36:4035–4040
Poisson M, Magdelenat H, Foncini JF et al (1980) Récepteurs d'estrogènes et de progestérone dans les méningiomes. Etude de 22 cas. Rev Neurol (Paris) 136:193–203
Pollock B, Flickinger J, Lunsford D, Bissonette D, Kondziolka D (1996) Hemorrhage risk after stereotactic radiosurgery of cerebral arteriovenous malformations. Neurosurgery 38:652–661
Pollock B, Flickinger J, Lunsford D, Maitz A, Kondziolka D (1998) Factors associated with successful arteriovenous malformation radiosurgery. Neurosurgery 42: 1239–1247
Pomposelli FB, Lamparello PJ, Riles TS, Craighead CC, Giangola G, Imparato AM (1988) Intracranial hemorrhage after carotid endarterectomy. J Vasc Surg 7: 248–255
Pool JL, Potts DG (1965) Aneurysms and arteriovenous anomalies of the brain: diagnosis and treatment. Harper and Row, New York
Poole-Wilson PA, Langer GA (1975) Effect of pH on ionic exchange and function in rat and rabbit myocardium. Am J Physiol 229:570–581
Poolos PN Jr, White RJ (1980) Aneurysmal bone cyst of the cervical spine: a twelve-year follow-up after surgical treatment. Surg Neurol 14:259–262
Pope FM (1975) Historical evidence for the genetic heterogeneity of pseudoxanthoma elasticum. Br J Dermatol 92:493–509
Porter P, Ter Brugge K, Stefani MA, Kerr RG, Montanera W, Willinsky RA, Wallace C (1997a) A prospective study assessing the risk factors for hemorrhage from arteriovenous malformations. Intervent Neuroradiol 3 [Suppl 1]:96
Porter P, Willinsky R, Harper W, Wallace MC (1997b) Cerebral cavernous malformations: natural history and prognosis after clinical deterioration with or without hemorrhage. J Neurosurg 87:190–197
Porter P, Ter Brugge K, Willinsky RA, Kerr RG, Montanera W, Stefania MA, Wallace C (1998) Failure of partial therapy to reduce the risk of hemorrhage from arteriovenous malformations. J Neurosurg 88:188A

Porter PJ, Mazighi M, Rodesch G, Alvarez H, Aghakhani N, David P, Lasjaunias P (2001) Endovascular and surgical management of multiple intradural aneurysms: review of 122 patients managed between 1993 and 1999. Interv Neuroradiol 7:291

Pouyanne H, Leran P, Got M, Voinessen A, Leger H (1951) Kyste aneuvrysmal monstrueux de l'atlas et de l'axis. Etude angiographique. Neurochirurgie 7:132

Powers AD, Smith RR (1990) Hyperperfusion syndrome after carotid endarterectomy. Transcranial Doppler evaluation. Neurosurgery 26:59–60

Pozzati E, Padovani R, Fabizi A, Sabattini L, Gaist G (1991) Benign arterial dissections of the posterior circulation. J Neurosurg 75:69–72

Pozzati E, Giangaspero F, Marliani F, Acciarri N (1996) Occult cerebrovascular malformations after irradiation. Neurosurgery 39:677–684

Prabhakar S, Sawhney IM, Chopra JS, Kak VK, Banerjee AK (1984) Hemibase syndrome: an unusual presentation of intracranial paraganglioma. Surg Neurol 22: 39–42

Pribil S, Boone SC, Waley R (1983) Obstructive hydrocephalus at the anterior third ventricle caused by dilated veins from an arteriovenous malformation. Surg Neurol 20:487–492

Price DL, Harris JL, New PFJ, Cantu RC (1970) Cardiac myxoma. A clinico-pathologic and angiographic study. Arch Neurol 23:558–567

Price HI, Batznitzky S (1985) Computed tomographic findings in benign diseases of the vertebral column. CRC Crit Rev Diagn Imaging 24:39–89

Probst FP (1980) Vascular morphology and angiographic flow patterns in Sturge-Weber angiomatosis: facts, thoughts and suggestions. Neuroradiology 20:73–78

Pudenz RH, Odom FL (1942) Meningocerebral adhesions. An experimental study of human amniotic membrane, amnioplastin, beef allantoic membrane, cargile membrane, tantalum foil, and polyvinyl alcohol foam. Surgery 12:318–344

Pulsinelli W (1997) Selective neuronal vulnerability and infarction in cerebrovascular disease. In: Welch K, Caplan L, Reis D, Siesjo B, Weir B (eds) Primer on cerebrovascular diseases. Academic Press, San Diego, 104–107

Pulsinelli W, Brierley J, Plum F (1982) Temporal profile of neuronal damage in a model of transient forebrain ischemia. Ann Neurol 11:491–498

Purdon Martin J, Sheehan HL (1941) Primary thrombosis of the cerebral veins (following childbirth) BMJ 1:349–356

Putman C, Chaloupka J, Fulbright R, Awad I, White R, Fayad P (1998) Exceptional multiplicity of cerebral arteriovenous malformations associated with hereditary telangiectasia (Osler-Weber-Rendu Syndrome). AJNR Am J Neuroradiol 19:477–484

Quint DJ, Spickler EM (1997) Magnetic resonance demonstration of vertebral artery dissection: report of two cases. J Neurosurg 72:964–967

Quisling RG, Mickley JP et al. (1984) Histopathologic analysis of intra-arterial polyvinyl alcohol microemboli in rats cerebral cortex. AJNR Am J Neuroradiol 5:101–104

Qureshi AI, Suarez JI, Parekh PD et al (1998) Risk factors for multiple intracranial aneurysms. Neurosurgery 43:22–27

Qureshi A, Luft A, Lopes D, Lanzino G (1999) Postoperative hypotension after carotid angioplasty and stenting: report of three cases. Neurosurgery 44:1320–1324

Qureshi AI, Mohammad Y, Yahia AM et al (2000a) Ischemic events associated with unruptured intracranial aneurysms: multicenter clinical study and review of the literature. Neurosurgery 46:282–289

Qureshi A, Suri M, Khan J, Fessler R, Guterman L, Hopkins L (2000b) Abciximab as an adjunct to high-risk carotid or vertebrobasilar angioplasty: preliminary experience. Neurosurgery 46:1316–1324

Raaymakers D (1999) Risks and benefits of screening for intracranial aneurysms in first degree relative of patients with sporadic SAH. New Engl J Med 341:1344–1350

Raaymakers THWM, Rinkel GJE, Limburg M, Algra A (1998) Mortality and morbidity of surgery for unruptured intracranial aneurysms a meta-analysis. Stroke 29:1531–1538

Raines E, Rosenfeld M, Ross R (1996) The role of macrophages. In: Fuster V, Ross R, Topol E (eds) Atherosclerosis and coronary artery disease. Lippincott-Raven, Philadelphia, pp 539–555

Raithel D (1996) Recurrent carotid disease: optimum technique for redo surgery. J Endovasc Surg 3:69–75
Ramsay G (1998) DNA chips: state-of-the-art. Nat Biotechnol 16:40–44
Rand CW (1957) Two cerebral complications of pregnancy: brain tumor, and spontaneous subarachnoid hemorrhage. Clin Neurolosurg 3:104–141
Rand RM, Rand DW (1970) Intraspinal tumors of childhood. Vascular anomalies of the spinal cord. Thomas, Springfield, pp 281–284
Ranson J, Imparato A, Clauss R, Reed G (1969) Factors in the mortality and morbidity associated with surgical treatment of cerebrovascular insufficiency. Circulation 39:I269–I274
RANTTAS Investigators(1997) A randomized trial of tirilazad mesylate in patients with acute stroke (RANTTAS). Stroke 27:1453–1458
Rao VRK, Mandalam KR, Gupta AK, Kumar S, Joseph S (1989) Dissolution of isobutyl-2-cyanoacrylate on long-term follow-up. AJNR Am J Neuroradiol 10:135
Raper A, Kontos H, Patterson J (1971) Response of Pial precapillary vessels to changes in arterial carbon dioxide tension. Circ Res 28:518–523
Raphael HA, Bernatz PE, Spittell JA Jr et al (1963) Cervical carotid aneurysms: treatment by excision and restoration of arterial continuity. Am J Surg 105:771–778
Raps EI, Rogers S, Galetta et al (1998) The clinical spectrum of unruptured intracranial aneurysms. Arch Neurol 50:265–268
Raymond J, Roy D, Bojanowski M, Moumdyian R, L'Esperance G (1997) Endovascular treatment of acutely ruptured and unruptured aneurysms of the basilar bifurcation. J Neurosurg 86:211–219
Reddy K, West M et al (1987) Multiple intracerebral arteriovenous malformations: a case report and a literature review. Surg Neurol 27:495–499
Reddy KA, Mendelhall WM, Amdur RJ, Stringer SP, Cassisi NJ (2001) Long-term results of radiation therapy for juvenile nasopharyngeal angiofibroma. Am J Otolaryngol 22:172–175
Redekop G, Ter Brugge KG, Montanera W, Willinsky R (1998) Arterial aneurysms associated with cerebral arteriovenous malformations: classifications, incidence, and risk of hemorrhage. J Neurosurg 89:539–546
Reese AB (1976) Tumors of the eye, 3rd ed. Harper and Row, Hagerstown Md
Reinhoff WF (1924) Congenital arteriovenous fistula. An embryological study with the report of a case. Bull Johns Hopkins Hosp 35:271–284
Reivich M, Holling HE, Robert B, Toole JF (1961) Reversal of blood flow through the vertebral artery and its effect on cerebral circulation. N Engl J Med 265:878–885
Reizine D, Merland JJ, Birkur P, Leban M, Riche MC (1985) Treatment of spontaneous intraparotid direct arteriovenous fistulae using a detachable balloon technique. J Neuroradiol 12:35–43
Rengachary SS, Derek A (1993) Spinal arterial aneurysm: case report. J Neurosurg 33:125–130
Resnick N, Collins T, Atkinson W, Bonthron D, Dewey C, Gimbrone M (1993) Platelet-derived growth factor B chain promoter contains a cis-acting fluid shear-stress-responsive element. Proc Natl Acad Sci U S A 90:4591–4595
Reyes S (2000) Dissecting intracranial aneurysm of the left vertebral artery. Intervent Neuroradiol 6:349–351
Ribes F. Des recherches faites sur la phlébite. Rev Med 1825:3
Rice HE, Arbabi S, Kremer R, Needle D, Johansen K (1997) Ruptured Salmonella mycotic aneurysm of the extracranial carotid artery. Ann Chir Vasc 11:416–419
Rich NM, Baugh JH, Hughes CW (1970) Acute arterial injuries in Vietnam: 1000 cases. J Trauma 10:35–369
Riche MC, Melki JP, Merland JJ (1983a) The current state of embolization of spinal cord vascular malformations via the anterior spinal artery. AJNR Am J Neuroradiol 4:378–381
Riche MC, Melki JP, Merland JJ (1983b) Embolization of spinal cord arteriovenous malformations via the anterior spinal artery AJNR Am J Neuroradiol 4:378–381

Riche MC, Scialfa G, Gueguen B, Merland JJ (1983c) Giant extramedullary arteriovenous fistula supplied by the anterior spinal artery: treatment by detachable balloons AJNR Am J Neuroradiol 4:391–394
Ricolfi F, Gobin YP, Aymard A, Brunelle F, Gaston A, Merland JJ (1997) Giant perimedullary arteriovenous fistulas of the spine: clinical and radiologic features and endovascular treatment AJNR Am J Neuroradiol 18:677–687
Riles T, Kopeman I, Imparato A (1979) Myocardial infarction following carotid endarterectomy: a review of 683 operations. Surgery 85:249–252
Rinne JK, Hernesniemi JA (1993) De novo aneurysms: special multiple intracranial aneurysms. Neurosurgery 33:981–985
Rinne J, Hernesniemi J, Puranen M et al (1994) Multiple intracranial aneurysms in a defined population: prospective angiographic and clinical study. Neurosurgery 35:803–808
Rinne J, Hernesniemi J, Niskanen M et al (1995) Management outcome for multiple intracranial aneurysms. Neurosurgery 36:31–38
Rinne J, Hernesniemi J, Niskanen M, Vapalahti M (1996) Analysis of 561 patients with 690 middle cerebral artery aneurysms: anatomic and clinical features as correlated to management outcome. Neurosurgery 38:2–11
Risau W (1997) Mechanisms of angiogenesis. Nature 386:671–674
Risau W, Flamme I (1995) Vasculogenesis. Annu Rev Cell Dev Biol 11:73–91
Rob R (1954) Arterial aneurysms. Ann Roy Coll Surg Eng 14:35–49
Robbin M, Lockhart M, Weber T et al (1997) Carotid artery stents: early and intermediate follow-up with Doppler US. Radiology 205:749–756
Robbins SL, Cotran RS (1979) Pathologic basis of disease, 2nd ed. Saunders, Philadelphia, p 165
Roberson GH, Price AC, Davis JM, Gulati A (1979) Therapeutic embolization of juvenile angiofibroma. AJR Am J Roentgenol 133:657–663
Robinson RG (1965) Aspects of the natural history of cerebellar haemangioblastomas. Acta Neurol Scand 41:372–380
Rockman C, Riles T, Lamparello P et al (1997) Natural history and management of the asymptomatic, moderately stenotic internal carotid artery. J Vasc Surg 25:423–431
Rodesch G, Pongpech S, Alvarez H, Zerah M, Hurth M, Sebire G, Lasjaunias P (1995) Spinal cord arteriovenous malformations in the pediatric population (children below 15 years of age). The place of endovascular management. Interv Neuroradiol 1:29–42
Rodesch G, Alvarez H, Chaskis C, Peeters J, Lasjaunias P (1996a) Clinical manifestations in paraspinal arteriovenous malformations: spinal cord symptoms, pathophysiology and treatment objectives. Int J Neuroradiol 2:430–436
Rodesch G, Hurth M, Alvarez H, Lasjaunias P (1996b) Shunts artério-veineux spinaux: l'expérience de Bicêtre (1982–1995). Rachis, 8:271–278
Rodesch G, Hurth M, Alvarez H, Lasjaunias P (1996c) Spinal arteriovenous shunts: the Bicêtre experience. Rachis8:271–278
Rodesch G, Hurth M, Alvarez H, Lasjaunias P (1997) Embolization of spinal cord arteriovenous malformations with glue through the anterior spinal axis. Review of 20 cases. Interv Neuroradiol 3:131–143
Rodesch G, Hurth M, Alvarez H, Tadie M, Lasjaunias P (2002) Classification of spinal cord arteriovenous shunts: proposal for a reappraisal–the Bicêtre experience with 155 consecutive patients treated between 1981 and 1999. Neurosurgery 51:374–379; discussion 379–380
Roman G, Fischer M, Perl DP et al (1978) Neurological manifestations of hereditary hemorrhagic telangiectasia (Rendu-Osler-Weber disease). Report of 2 cases and review of the literature. Ann Neurol 4:130–144
Romodanov AP, Shchegelov VI (1979) Endovascular method of excluding from the circulation saccular cerebral arterial aneurysms, leaving intact vessels patent. Acta Neurochir (Wien) 28:312–315
Romodanov AP, Shchegelov VI (1982) Intravascular occlusion of a saccular aneurysm of the cerebral arteries by use of a detachable balloon catheter. In: Krayenbuhl H (ed) Advances in technical standards in neurosurgery. Springer, Berlin Heidelberg New York, pp 25–49

Ronkainen A, Hernesniemi, Ryynanen M (1993) Familial subarachnoid hemorrhage in east Finland, 1977–1990. Neurosurgery 33:787–795
Ronkainen A, Miettinen H, Karkola K, Papinaho S, Vanninen R, Puranen M, Hernesniemi J (1998) Risk of harboring an unruptured intracranial aneurysm. Stroke 29:359–36
Rosenblum BR, Bonner RF, Oldfield EH (1987a) Intraoperative measurement of cortical blood flow adjacent to cerebral AVM using laser Doppler velocimetry. J Neurosurg 66:396–399
Rosenblum B, Oldfield EH, Doppman JL, di Chiro G (1987b) Spinal arteriovenous malformations: a comparison of dural arteriovenous fistulas and intradural AVM's in 81 patients. J Neurosurg 67:795–802
Rosendaal F (1997) Thrombosis in the young: epidemiology and risk factors: a focus on venous thrombosis. Thromb Haemost 78:1–6
Rosenow J, Rawanduzy A, Weitzner I Jr, Couldwell WT (2000) Type IV spinal arteriovenous malformation in association with familial pulmonary vascular malformations: case report. Neurosurgery 46:1240–1245
Rosenwasser H (1958) Metastasis from glomus jugulare tumors. Arch Otolaryng 67: 197–203
Rosenwasser H (1968) Monograph on glomus jugulare tumors. Arch Otolaryng 88: 29–66
Rosenwasser H (1974) Glomus jugulare tumors. Proc Roy Soc Med 67:259–264
Ross JS, Masaryk TJ, Modic MT, Carter JR, Mapstone T, Dengel F (1987) Vertebral hemangiomas: MR imaging. Radiology 165:155–159
Ross JS, Masaryk TJ, Modic MT et al (1990) Intracranial aneurysms: evaluation by MR angiography. AJNR Am J Neuroradiol 11:449–455
Ross R (1981) Atherosclerosis – a problem of the biology of arterial wall cells and their interactions with blood components. Arteriosclerosis 1:293–311
Ross R (1986) The pathogenesis of atherosclerosis – an update. N Engl J Med 314: 488–500
Ross R (1992) Atherosclerosis. In: McGee JD, Isaacson P, Wright N (eds) Oxford textbook of pathology, vol 2a. Oxford University Press, Oxford, pp 798–822
Ross R (1993a) Atherosclerosis: a defense mechanism gone awry. Am J Pathol 143: 987–1002
Ross R (1993b) The pathogenesis of atherosclerosis: a perspective for the 1990s. Nature 362:801–809
Ross R (1999) Mechanisms of disease: atherosclerosis – an inflammatory disease. New Engl J Med 340:115–116
Ross R, Glomset J (1973) Atherosclerosis and the arterial smooth muscle cell: proliferation of smooth muscle is a key event in the genesis of the lesions of atherosclerosis. Science 180:1332–1339
Ross R, Glomset J (1976) The pathogenesis of atherosclerosis. New Engl J Med 295: 369–377; discussion,420–425
Rothwell P, Slattery J, Warlow C (1996) A systematic comparison of the risks of stroke and death due to carotid endarterectomy for symptomatic and asymptomatic stenosis. Stroke)27:266–269
Roubin G, Yadav J, Iyer S, Vitek J (1996) Carotid stent-supported angioplasty: a neurovascular intervention to prevent stroke. Am J Cardiol 78:8–12
Roy D, Raymond J (1997) The role of transvenous embolization in the treatment of intracranial dural arteriovenous fistulas. Neurosurgery 40:1133–1144
Rubi F (1945) Neurofibromatose et lesions vasculaires. Schweiz Med Wochenschr 75:463–465
Rubinstein LJ (1972) Tumors of the central nervous system. Atlas of tumor pathology, 2nd series, fasc 8. Armed Forces Institute of Pathology, Washington DC
Rubinstein LJ (1981) Tumors of the central nervous system, vol 6. Armed Forces Institute of Pathology, Washington DC, pp 235–256
Rufenacht D, Merland JJ (1986a) A polyethylene microcatheter with a latex balloon as an implant for permanent vascular occlusions. A way for the treatment of distal intracranial or intraspinal large AV fistulas or aneurysms. In: Valk J (ed) Neuroradiology. Elsevier, Amsterdam

Rufenacht D, Merland JJ (1986b) Detachable latex balloon with valve-mechanism for the permanent occlusion of large brain AV fistulas of cerebral arteries. In: Valk J (ed) Neuroradiology. Elsevier, Amsterdam
Rufenacht D, Merland JJ (1986c) Modifications of a supple catheter avoiding the need of a balloon for flow-guidance. In: Valk J (ed) Neuroradiology. Excerpta Medica, Amsterdam, pp 311–314
Rufenacht D, Merland JJ (1986d) More precision in superselective angiography: flow independent guidance of soft catheters. AJNR Am J Neuroradiol 8:959
Ruggieri PM, Poulos N, Marsaryk TJ et al (1994) Occult intracranial aneurysms in polycystic kidney disease: screening with MR angiography. Radiology 191:33–39
Rushton AR (1980) The genetics of fibromuscular dysplasia. Arch Intern Med 140: 233–236
Russell DS (1954) The pathology of spontaneous intracranial hemorrhage. Proc R Soc Med 47:689–693
Russell DS, Rubinstein LJ (1971) Pathology of tumours of the nervous system, 3rd edn. Arnold, London
Russell EJ, Berenstein A (1981) Meningeal collateralization to normal cerebral vessels associated with intracerebral arteriovenous malformations: a functional angiographic study. Radiology 139:617–622
Russell DR, Rubinstein LJ (1989) Pathology of tumours of the nervous system, 5th edn. Williams and Wilkens, Philadelphia
Rutka JT, Zawadski MB, Wilson CB, Rosenblum ML (1988) Familial cavernous malformation. Diagnostic potential of magnetic resonance imaging. Surg Neurol 29:467–474
Sacco R, Wolf P, Kannel W et al (1982) Survival and recurrence following stroke: the Framingham study. Stroke 13:290–295
Sacco RL, Wolf MA, Bharucha NE, Meeks SL, Kannel WB, Charette LJ, McNamara PM, Palmer EP, D'Agostino R (1984) Subarachnoid and intracerebral hemorrhage: natural history, prognosis, and precursive factors in the Framingham Study. Neurology 34:847–854
Sachs E (1977) Diagnosis and treatment of brain tumors and care of the neurosurgical patient. J Neuroradiol 4:385–398
Sadato A, Taki W, Ikada Y et al (1994) Experimental study and clinical use of poly (vinyl acetate) emulsion as liquid embolization material. Neuroradiology 36:634–641
Sahs AL, Perret GE, Locksley HB (1969) Intracranial aneurysms and subarachnoid hemorrhage: a cooperative study. Lippincot, Philadelphia
Saito Y, Kobayashi N (1981) Cerebral venous angiomas clinical evaluation and possible etiology. Radiology 139:87–94
Sakaki T, Tominaga M, Miyamoto K et al (1993) Clinical studies of de novo aneurysms. Neurosurgery 32:512–517
Sakata Y, Higashi K, Aoki H (1998) Simultaneous occurrence of intracranial aneurysms and arteriovenous malformation. Arch Jpn Chir 37:242–247
Sala F, Nimii Y, Krzan MJ, Berenstein A, Deletis V (1999) Embolization of a spinal arteriovenous malformation: correlation between motor evoked potentials and angiographic findings: technical case report. Neurosurgery 45:932–938
Saldana MJ, Salem LE, Travezan R (1973) High altitude hypoxia and chemodectomas. Human Pathol 4:251–263
Samy LL, Hashem M (1962) Nonchromaffin paraganglioma of the ear with a report of six cases with abnormal features. J Laryngol Otol 76:499–534
Sang H, Kerber C (1983) Ventricular obstruction secondary to vascular malformations. Neurosurgery 5:572–574
Sano K, Jimbo M, Saito I et al (1966) Artificial embolization with liquid plastic. Neurol Med Chir (Tokyo) 8:198–201
Sano K, Jimbo M, Saito I (1975) Artificial embolization of inoperable angiomas with polymerizing substance. In: Pia HW, Glaeve et al (eds) Cerebral angiomas: advances in diagnosis and therapy. Springer, Berlin Heidelberg New York, pp 222–229
Sanoudos GM, Ramp J, Imparato I (1973) Internal carotid aneurysms. Am Surg 39: 118

Sasaki O, Ogawa H, Koike T, Koizumi T, Tanaka R (1991) A clinico-pathological study of dissecting aneurysms of the intracranial vertebral artery. J Neurosurg 75:874–882
Sasaki O, Takeuchi S, Koike T, Koizumi T (1995) Fibrinolytic therapy for acute embolic stroke: intravenous, intracarotid and intra-arterial local approaches. Neurosurgery 36:246 –253
Sato S, Suzuki J (1975) Ultrastructural observations of the capsule of chronic subdural hematoma in various clinical stages. J Neurosurg 43:569–578
Sato O, Tamura A, Sano K (1975) Brain tumors of early infants. Childs Brain 1:121–125
Sato Y, Waziri M, Smith W, Frey E, Yuh WTC, Hanson J, Franken EA (1988) Hippel-Lindau disease: MR imaging. Radiology 166:241–246
Satoh A, Nakamura H, Odaki M, Kobayashi S, Kageyama Y, Fukuda K, Watanabe Y, Shinohara Y (1993) High risk aneurysm of the internal carotid artery: dorsal IC aneurysms. Surg Cereb Stroke 121:467–472
Satomi J, van Dijk M, Ter Brugge K, Willinsky RA, Wallace C (2002) Benign cranial dural arteriovenous fistulas: natural history and proposed management. J Neurosurg 97:767–770
Sattler CH (1920) Beitrag zur Kenntnis des pulsierenden Exophthalmus. Augenh 43:534–552
Saylor WR, Saylor DC (1974) Vascular lesions of neurofibromatosis. Angiology 25:510–519
Scarff TB, Reigel DH (1979) Arteriovenous malformations of the spinal cord in children. Childs Brain 5:341–351
Scarrow A, Williams R, Jungreis C, Yonas H, Scarrow M (1999) Removal of a thrombus from the sigmoid and transverse sinuses with a rheolytic thrombectomy. AJNR Am J Neuroradiol 20:1467–1469
Schaller C, Schramm J (1997) Microsurgical results for small arteriovenous malformations accessible for radiosurgical or embolization treatment. Neurosurgery 40:664–674
Schechter DC (1979) Cervical carotid arteries. N Y State J Med 79:892–901Schievink WI (1997) Intracranial aneurysms. New Engl J Med 336:28–40
Schievink WI (2001) Spontaneous dissection of the carotid and vertebral arteries. New Engl J Med 344:898–905
Schievink WI, Limburg M, Dreissen JJ, Peeters FL, ter Berg HW (1991) Screening for unruptured familial intracranial aneurysms: subarachnoid hemorrhage 2 years after angiography negative for aneurysms. Neurosurgery 29:434–437; discussion 437–438
Schievink WI, Torres VE, Piepgras DG, Wiebers DO (1992) Saccular intracranial aneurysms in autosomal dominant polycystic kidney disease. J Am Soc Nephrol 3:88–95
Schievink W, Mokri B, Whisnant J (1993) Internal carotid artery dissection in a community: Rochester, Minnesota, 1987. Stroke 24:1678–1680
Schievink WI, Michels VV, Piepgras DG (1994a) Neurovascular manifestations of heritable connective tissue disorders. A review. Stroke 25:889–903
Schievink W, Mokri B, O'Fallon W (1994b) Recurrent spontaneous cervical-artery dissection. N Engl J Med 330:393–397
Schievink W, Prakash U, Piepgras D, Mokri B (1994c) Alpha 1-antitrypsin deficiency in intracranial aneurysms and cervical artery dissection. Lancet 343:452–453
Schievink WI, Schaid DJ, Rogers HM, Piepgras DG, Michels VV (1994d) On the inheritance of intracranial aneurysms. Stroke 25:2028–2037
Schievink WI, Mokri B, Piepgras D, Gittenberger-de Groot AC (1996) Intracranial aneurysms and cervicocephalic arterial dissections associated with congenital heart disease. Neurosurgery 39:685–690
Schiff M (1959) Juvenile nasopharyngeal angiofibroma: a theory of pathogenesis. Laryngoscope 69:981–1016
Schiffer J, Bibi C, Avidan D (1984) Cerebral arteriovenous malformation: papilledema as a presenting sign. Surg Neurol 22:524–526
Schlachter LB, Fleischer AS et al (1980) Multifocal intracranial arteriovenous malformations. Neurosurgery 7:440–444

Schlienger M, Atlan D, Lefkopoulos D, Merienne L, Touboul E, Missir O, Nataf F, Mammar H, Platoni K, Grandjean P, Foulquier JN, Huart J, Oppenheim C, Meder JF, Houdart E, Merland JJ (2000) Linac radiosurgery for cerebral arteriovenous malformations: results in 169 patients. Int J Radiation Oncol Biol Phys 46:1135–1142

Schmidt D, Schumacher M, Wakhloo A (1992) Microcatheter urokinase infusion in central retinal artery occlusion. Am J Ophthalmol 113:429–434

Schmorl G, Junghanne H (1971) The human spine in health and disease, 2nd edn. Grune & Stratton, New York

Schnee CL, Flamm ES (1997) Unusual aneurysms. Neuroimaging Clin North Am 7:803–818

Schnegg JF, Gomez F, LeMarchand-Beraud T, Tribolet N (1981) Presence of sex steroid hormone receptors in meningioma tissue. The unique association between meningiomas and breast cancer. Surg Neurol 15:415–418

Schoenberg BS, Christine BW, Whisnant JP (1975) Nervous system neoplasms and primary malignancies of other sites. Neurology (Minneapolis) 25:705–712

Scholz W, Wechsler W (1959) Ein weiterer Beitrag zur angiodysgenetischen nekrotisierenden Myelopathie (Foix-Alajouaninische Krankheit). Arch Psychiatr Nervenkr 199:609–629

Schroth G, Haldemann AR, Mariani L, Remonda L, Raveh J (1996) Preoperative embolization of paragangliomas and angiofibromas. Measurement of intratumoral arteriovenous shunts. Arch Otolaryngol Head Neck Surg 122:1320–1325

Schubiger O, Valavanis A, Hayek J (1980) Computed tomography in cerebral aneurysms with special emphasis on giant intracranial aneurysms with special emphasis on giant intracranial aneurysms. J Comput Assist Tomogr 4:24–32

Schubiger O, Valavanis A, Wichmann W (1987) Growth-mechanism of giant intracranial aneurysms: demonstration by CT and MR imaging. Neuroradiology 29: 266–277

Schumacher M, Schmidt D, Wakhloo A (1993) Intra-arterial fibrinolytic therapy in central retinal artery occlusion. Neuroradiology 35:600–605

Scialfa G, Valsecchi F, Tonon C (1979) Treatment of external carotid arteriovenous fistula with detachable balloon. Neuroradiolgy 17:265–267

Scialfa G, Valsecchi F, Scotti G (1983) Treatment of vascular lesions with balloon catheters. AJNR Am J Neuroradiol 4:395–398

Scott BB, McGillicuddy JE, Seeger JF, Kindt GW, Giannotta SL (1978) Vascular dynamics of an experimental cerebral arteriovenous shunt in the primate. Surg Neurol 10:34–38

Scott JA, Berenstein A, Blumenthal D (1986) Use of the activated coagulation time as a measure of anticoagulation during interventional procedures. Radiology 158: 849–850

Scott J, Pascuzzi R, Hall P, Becker G (1988) Treatment of dural sinus thrombosis with local urokinase infusion. Case Report. J Neurosurg 68:284–287

Second International Study of Infarct Survival Collaborative Group (ISIS-2) (1988) Randomized trial of intravenous streptokinase, oral aspirin, both, or neither among 17,187 cases of suspected acute myocardial infarction. Lancet 2:349–360

Sedat J, Alvarez H, Rodesch G, Lasjaunias P (1999a) Multifocal cerebral fusiform aneurysms in children with immune deficiencies. Report of four cases. Intervent Neuroradiol 5:151–156

Sedat J, Kominami S, Siriwimonmas S, Pongpech S, Suthipongchai S, Alvarez H (1999b) Extracavernous arteriovenous fistulae. Report of five cases. Interv Neuroradiol 5:235–243

Sedzimir CB, Robinston J (1973) Intracranial hemorrhage in children and adolescents. J Neurosurg 38:269

Segal HD, McLaurin RL (1977) Giant serpentine aneurysm. Report of two cases. J Neurosurg 46:115–120

Seidenwurm D, Hyman A, Kowalski H, Berenstein A (1991) Vein of Galen malformation correlation of arteriography, magnetic resonance imaging and computed tomography. AJNR 12:347–354

Sekhar LN, Heros RC (1981) Origin, growth and rupture of saccular aneurysms: a review. Neurosurgery 8:248–260

Sekhon L, Morgan M, Sorby W et al (1998) Combined endovascular stent implantation and endosaccular coil placement for the treatment of a wide-necked vertebral artery aneurysm: technical case report. Neurosurgery 43:380–384
Seligsohn U, Lubetsky A (2001) Genetic susceptibility to venous thrombosis. New Engl J Med 344:1222–1231
Sellier N, Chiras J, Benhamou M, Bories J (1983) Spontaneous dissection of the internal carotid artery. Clinical, radiological and evolutive features. A study of 46 cases. J Neuroradiol 10:243–259
Serbinenko FA (1974) Balloon catheterization and occlusion of major cerebral vessels. J Neurosurg 41:125–145
Serruys P, de Jaegere P, Kiemeneij F, Macaya C (1994) A comparison of balloon expandable stent implantation with balloon angioplasty in the treatment of coronary artery disease. N Engl J Med 331:489–495
Serze S, Hurth M, Djindjian R, Kahn MF, Hubault A, Dryll A (1966) A propos d'un cas d'angiomatose métamerique cutanéo-vertébro-médullaire. Rev Rhum 9:455–460
Shah SS, Zimmerman RA, Rorke LB et al (1996) Cerebrovascular complications of HIV in children. AJNR Am J Neuroradiol 17:1913–1917
Shalon D, Smith S, Brown P (1996) A DNA microarray system for analyzing complex DNA samples using two-color fluorescent probe hybridization. Genome Res 6:639–645
Sharbrough FW, Messick MJ Jr, Sundt TM Jr (1973) Correlation of continous electroencephalograms with cerebral blood flow measurements during carotid endartarectomy. Stroke 4:674–683
Sharma PD, Johnson AP, Whitton AC (1984) Radiotherapy for jugulo-tympanic paragangliomas (glomus jugulare tumors) J Laryng Otol 98:621–629
Shawl F (1998) Technical considerations and results. Indian Heart J 50:138–144
Shchegelov VI (1989) Endovascular occlusion of saccular intracranial aneurysms: results in 617 patients, Proceedings of the 27th annual meeting of the American Society of Neuroradiology, pp 19–24
Shea PC Jr, Glass LF, Reid WA, Harland A (1955) Anastomosis of common and internal carotid arteries following excision of mycotic aneurysm. Surgery 37:829–832
Shenkin HA, Spitz EB, Grant FC et al (1948) Physiologic studies of arteriovenous anomalies of the brain. J Neurosurg 5:165–172
Shi Y, Chen X (1986) A proposed scheme for grading intracranial arteriovenous malformations. J Neurosurg 65:484–489
Shinoda S, Murata H, Waga S, Kojima T (1998) Bilateral spontaneous dissection of the posteroinferior cerebellar arteries: case report. Neurosurgery 43:357–359
Shiromura Y, Hukuda S, Mizuno S (1968) Experimental study of ischemic damage to the cervical spinal cord. J Neurosurg 28:565–581
Siegel G, Jaeger R, Nolte J (1974) Ionic concentrations and membrane potential in cerebral and extracerebral arteries. In: Cervos-Navarro J, de Gruyter W (eds) Pathology of cerebral microcirculation. Berlin, pp 96–120
Siesjo BK (1984) Cerebral circulation and metabolism. J Neurosurg 60:883–908
Simard JM, Garcia-Bengochea F, Balliner WE, Mickle JP, Quisling RG (1986) Cavernous angioma: a review of 126 collected and 12 new clinical cases. Neurosurgery 18:162–172
Simionescu N, Vasile E, Lupu F, Popescu G (1986) Prelesional events in atherogenesis: accumulation of extracellular cholesterol-rich liposomes in the arterial intima and cardiac valves of the hyperlipidemic rabbit. Am J Pathol 123:109–125
Simmonds N (1962) Embolus of central retinal artery: successfully treated by paracentesis. Am J Ophthalmol 54:1129–1130
Skizora I, Guterman LR, Standard SC, Wakhloo AK, Hopkins LN (1996) Endovascular treatment of experimental aneurysms with liquid polymers: the protective potential of stents. Neurosurgery 38: 339–347
Skultety FM (1968) Meningioma simulating ruptured aneurysm. Case report. J Neurosurg 28:380–382
Smith DR, Donat JF (1981) Giant arteriovenous malformation of the vein of Galen: total surgical removal. Neurosurgery 8:378–382
Smith ME, Barth PG et al (1981) Congenital multiple angiomatosis with brain involvement. Childs Brain 8:461–467

Smith T, Higashida R, Barnwell S et al (1994) Treatment of dural sinus thrombosis by urokinase infusion. AJNR Am J Neuroradiol 15:801–807
Snowdon JA (1974) Cerebral aneurysm, renal cysts and hamartomas in a case of tuberous sclerosis. Br J Urol 46:583
Söderman M, Moersdorf M, Lysdahl M, Mendel L (1997) Otorrhagia from the "aberrant internal carotid" artery in the middle ear. Surgical and endovascular aspect. Intervent Neuroradiol 3:231–238
Soffer D, Pittaluga S, Feiner M et al (1983) Intracranial meningiomas following low-dose irradiation to the head. J Neurosurg 59:1048–1053
Solander S, Ulhoa A, Vinuela F et al (1999) Endovascular management of multiple intracranial aneurysms by using Guglielmi detachable coils. J Neurosurg 90:857–864
Som PM, Cohen BA, Scher M, Choi IS, Bryan NR (1982) The angiomatous polyp and the angiofibroma: two different lesions. Radiology 144:329–334
Somach FM, Shenkin HA (1966) Angiographic end-results of carotid ligation in the treatment of carotid aneurysm. J Neurosurg 24:966–974
Somasundar P, Krouse R, Hostetter R, Vaughan R, Covey T (2000) Paragangliomas – a decade of clinical experience. J Surg Oncol 74:286–290
Song JK, Gobin YP, Duckwiler GR, Murayama Y, Frazee JG, Martin NA, Vinuela F (2001a) N-butyl 2-cyanoacrylate embolization of spinal dural arteriovenous fistulae. AJNR Am J Neuroradiol 22:40–47
Song JK, Vinuela F, Gobin YP, Duckwiler GR, Murayama Y, Kureshi I, Frazee JG, Martin NA (2001b) Surgical and endovascular treatment of spinal dural arteriovenous fistulas: long-term disability assessment and prognostic factors. J Neurosurg 94 [Suppl]:199–204
Sousa J, Costa M, Abizaid A et al (2001) Lack of neointimal proliferation after implantation of sirolimus-coated stents in human coronary arteries: a quantitative coronary angioplasty and three-dimensional intravascular ultrasound study. Circulation 103:192–195
Spearman M, Jungreis C, Wechsler L (1995) Angioplasty of the occluded internal carotid artery. Am J Neuroradiol 16:1791–1796
Spearman M, Jungreis C, Wehner J, Gerszten P, Welch W (1997) Endovascular thrombolysis in deep cerebral venous thrombosis. AJNR 18:502–506
Spector FJ, Maisel RH, Ogura JH (1973) Glomus tumors in the middle ear. I. An analysis of 46 patients. Laryngoscope 83:1652–1672
Spence AM, Rubinstein LJ (1975) Cerebellar capillary hemangioblastomas: its histogenesis studied by organ culture and electron microscopy. Cancer 35:326–341
Spetzler RF, Martin NA (1986) A proposed grading system for arteriovenous malformations. J Neurosurg 65:476–483
Spetzler RF, Selman WR (1984) Pathophysiology of cerebral ischemia accompanying arteriovenous malformations. In: Wilson CB, Stein BM (eds) Intracranial arteriovenous malformations. Williams and Wilkins, Baltimore, pp 24–31
Spetzler RF, Wilson CB (1975) Enlargement of an arteriovenous malformation documented by angiography. J Neurosurg 43:767–769
Spetzler RF, Wilson CB, Weinstein P, Mehdorn M, Townsend J, Telles D (1978) Normal perfusion pressure breakthrough theory. Clin Neurosurg 25:651–672
Spetzler R, Hadley M, Martin N, Hopkins L (1987a) Vertebrobasilar insufficiency. Part 1: microsurgical treatment of extracranial vertebrobasilar disease. J Neurosurg 66:648–661
Spetzler RF, Martin RNA, Carter LP, Flam RA, Raudzens PA et al (1987b) Surgical management of large AVMs by staged embolization and operative excision. J Neurosurg 67:17–28
Spetzler RF, Zabramski JM, Flom RA (1989) Management of juvenile spinal AVMs by embolization and operative excision. J Neurosurg 70:628–632
Spetzler RF, Hargraves RW, McCormick PW, Zabramski JM, Flom RA, Zimmerman RS (1992) Relationship of perfusion pressure and size to risk of hemorrhage from arteriovenous malformations. J Neurosurg 76:918–923
Spetzler et al (2002) Modified classification of spinal cord lesion. J Neurosurg 96 (Suppl 2):145–156
Squire I, Lees K, Pryse-Phillips W, Kertesz A, Bamford J (1995) The effects of lifarizine in acute cerebral infarction: a pilot safety study. Cerebrovasc Dis 6:156–160

Stary H (1996) The histological classification of atherosclerotic lesions in human coronary arteries. In: Fuster V, Ross R, Topol E (eds) Atherosclerosis and coronary artery disease. Lippincott-Raven, Philadelphia, pp 463–474
Stary H, Chandler A, Glagov S et al (1994) A definition of initial, fatty streak, and intermediate lesions of atherosclerosis: a report from the Committee on Vascular Lesions of the Council on Arteriosclerosis, American Heart Association. Circulation 89:2462–2478
Steel TR, Botterill P, Sheehy JP (1994) Paraganglioma of the cauda equina with associated syringomyelia: case report. Surg Neurol: 42:489–493
Stefani MA, Porter PJ, Ter Brugge KG, Montanera W, Willinsky RA, Wallace MC (2002) Large and deep brain arteriovenous malformations are associated with risk of future hemorrhage. Stroke 33:1220–1224
Stehbens WE (1963) Histopathology of cerebral aneurysms. Arch Neurol 8:272–285
Stehbens WE (1972) Pathology of the cerebral blood vessels. Mosby, St. Louis, pp 351–470
Stehbens WE (1975) Ultrastructure of aneurysms. Arch Neurol 32:798–807
Stehbens WE (1989) Etiology of intracranial berry aneurysms. J Neurosurg 70: 823–831
Stehbens W (1995) Cerebrovascular disease. In: Stehbens W, Lie J (eds) Vascular pathology. Chapman and Hall, London, pp 437–485
Steiger HJ, Markwalder RV, Reulen HJ (1989) Y a-t-il une relation entre manifestation clinique et l'image pathologique des cavernomes cérébraux? Neurochirurgie 35:84–88
Stein BM (1979) Arteriovenous malformations of the brain and spinal cord. In: Hoff J (ed) Practice of surgery. Harper and Row, Hagerstown, pp 1–40
Stein BM (1985) Comment. Neurosurgery 16:303
Stein BM, Wolpert SM (1980) Arteriovenous malformations of the brain. I. Current concepts and treatment. Arch Neurol 37:1–5
Steinberg G, Fabrikant J, Marks M, Levy R, Frankel K, Philips M, Shuer L, Silverberg G (1990) Stereotactic heavy-charged-particle Bragg-peak radiation for intracranial arteriovenous malformations. N Engl J Med 323:96–101
Steinberg G, Drake C, Peerless S (1993) Deliberate basilar or vertebral artery occlusion in the treatment of intracranial aneurysms. J Neurosurg 79:161–173
Steinberg G, Perez-Pinzon M, Maier C, Sun G (1994) CGS-19755: correlation of in vitro neuroprotection, protection against experimental ischemia and CSF levels in cerebrovascular surgery patients, 5th International Symposium on Pharmacology of Cerebral Ischemia, Marburg, Germany
Steinmeier R, Schramm J, Muller HG, Fahlbusch R (1989) Evaluation of prognostic factors in cerebral arteriovenous malformations. Neurosurgery 24:193–200
Sterpetti A, Schults R, Feldhaus R et al (1988) Ultrasonographic features of carotid plaque and the risk of subsequent neurologic deficits. Stroke 19:652–660
Stevens JM, Ruiz JS, Kendall BE (1983a) Observation on peritumoral oedema in meningioma. Part I. Distribution, spread and resolution of vasogenic oedema seen on computed tomography. Neuroradiology 25:71–80
Stevens JM, Ruiz JS, Kendall BE (1983b) Observations on peritumoral oedema in meningioma. Part II. Mechanisms of oedema production. Neuroradiology 25: 125–131
Stewart P (1997) Glial-Vascular relations. In: Welch K, Caplan L, Reis D, Siesjo B, Weir B (eds) Primer on cerebrovascular diseases. Academic Press, San Diego, pp 17–21
Stimac GK, Solomon MA, Newton TH (1986) CT and MR of angiomatous malformations of the choroid plexus in patients with Sturge-Weber disease. AJNR 7:623–627
Stoane L, Allen JH, Collin HA (1996) Radiologic observations in cerebral embolization from left heart myxoma. Radiology 87:262–266
Stock JL, Krudy AG, Doppman JL et al (1981) Parathyroid imaging after intraarterial injections of (75 SE) selenomethionine. J Clin Endocr Met 52:835–839
Stone JL, Crowell RM et al (1983) Bilateral parietal arteriovenous malformations: report of a case. Neurosurgery 5:587–592
Stoodley M, Thompson R, Mitchell R, Marks M (2000) Neurosurgical and neuroendovascular management of Takayasu's arteritis. Neurosurgery 46:841–852

Strand T, Asplund K, Eriksson S, Hagg E, Lithner F, Wester P (1984) A randomized controlled trial of hemodilution therapy in acute ischemic stroke. Stroke 15:980–989

Strandgaard S, MacKenzie ET, Sengupta D, Rowan JO, Lassen NA, Harper AM (1974) Upper limit of autoregulation of cerebral blood flow in the baboon. Circ Res 34:435–440

Strandgaard S, Jones JV, MacKenzie ET, Harper AM (1975) Upper limit of cerebral blood flow autoregulation in experimental renovascular hypertension in the baboon. Circ Res 37:164–167

Strauss M (1983) Long-term complications or radiotherapy confronting the head and neck surgeon. Laryngoscope 93:310–313

Strauss M, Nicholas GG, Abt AB, Harrison TS, Seaton JF (1983) Malignant catecholamine-secreting carotid body paraganglioma. Otolaryng Head Neck Surg 91:315–321

Strenger L (1966) Neurological deficits following therapeutic collapse of intracavernous carotid aneurysm. J Neurosurg 25:215–218

Strong J (1992) Atherosclerotic lesions, natural history, risk factors, and topography. Arch Pathol Lab Med 116:1268–1275

Stroobandt G, Harmant-van Ruckevorsel K, Mathurin P, De Nijs C, De Ville de Goyet J (1986) Hydrocephalie externe et interne par malformation artério-veineuse chez un nourrisson. Neurochirurgie 32:81–85

Strother CM, Kikuchi Y, Graves VM, Eldivik P, Partington C (1988) Observation on thrombus formation, structure and evolution in intracranial aneurysms treated by balloon occlusion. AJNR Am J Neuroradiol 9:1008

Strother CM, Eldevik P, Kikuchi Y, Graves V, Partington C, Merlis A (1989a) Thrombus formation and structure and evolution of mass effect in intracranial aneurysms treated by balloon embolization: emphasis on MR findings. AJNR Am J Neuroradiol 10:787

Strother CM, Lunde S, Graves V, Toutant S, Hieshima GB (1989b) Large paraophthalmic aneurysm rupture following endovascular treatment. J Neurosurg 71: 777–780

Sturge WA (1879) A case of partial epilepsy, apparently due to a lesion of one of the vaso-motor centers of the brain. Trans Clin Soc London 12:162–167

Sturzenegger M, Mattle H, Rivoir A, Barmgartner R (1995) Ultrasound findings in carotid artery dissection: analysis of 43 patients. Neurology 45:691–698

Sukoff MH, Barth B, Moran T (1972) Spontaneous occlusion of a massive arteriovenous malformation. Case report. Neuroradiology 4:121–123

Sundaresan N, Galicich J, Lane J et al (1985) Treatment of neoplastic epidural cord compression by vertebral body resection and stabilization. J Neurosurg 63:676–684

Sundaresan N, Scher H, DiGiacinto G et al (1986) Surgical treatment of spinal cord compression in kidney cancer. J Clin Oncol 4:1851–1856

Sundt TM, Piepgras DG (1983) The surgical approach to arteriovenous malformations of the lateral and sigmoid aural sinuses. J Neurosurg 59:32–39

Sundt TM, Sharbrough FW, Piepgras DO, Kearns TP et al (1981) Correlation of cerebral blood flow and electroencephalographic changes during carotid endarterectomy – with results of surgery and hemodynamics of cerebral ischemia. Mayo Clin Proc 56:533–543

Sutherland GR, King M, Drake CG, Peerless SJ, Vezina WC (1988) Platelet aggregation within cerebral arteriovenous malformations. J Neurosurg 68:198–204

Suwanwela C, Suwanvela N, Charuchinda S (1972) Intracranial mycotic aneurysms of extravascular origin. J Neurosurg 36:552–559

Suzuki J (1986) Moyamoya disease. Springer, Berlin Heidelberg, New York

Suzuki J, Ohara H (1978) Clinicopathological study of cerebral aneurysms. Origin, rupture, repair and growth. J Neurosurg 48:505–514

Suzuki J, Yoshimoto T (1979) Distribution of cerebral aneurysms. In: Pia HW, Langmain C, Zierski J (eds) Cerebral aneurysms: advances in diagnosis and therapy, 1st edn. Springer, Berlin Heidelberg New York, pp 127–133

Swift DM, Solomon RA (1992) Unruptured aneurysms and postoperative volume expansion. J Neurosurg 77:908–910

Symon L (1969) The concept of intracerebral steal. Int Anesth Clin 7:597–615
Symon L, Pasztor E, Branston N (1974) The distribution and density of reduced cerebral blood flow following acute middle cerebral artery occlusion: an experimental study by the technique of hydrogen clearance in baboons. Stroke 5:355–364
Symon L, Kuyama H, Kendall B (1984) Dural arteriovenous malformations of the spine: clinical features and surgical results in 55 cases. J Neurosurg 60:238–247
Szikora I, Guterman L, Wells K, Hopkins L (1994) Combined use of stents and coils to treat experimental wide necked carotid aneurysms: Preliminary result. Am J Neuroradiol 15:1091–1102
Tada T, Sugita K, Kobayashi S et al (1986) Supra- and infratentorial arteriovenous malformations with an aneurysmal dilatation: a case report. Neurosurgery 5:831–834
Tadie M, Hemet J, Freger P, Clavier E et al (1985) Morphological and functional anatomy of spinal cord veins. J Neuroradiol 12:3–10
Tagaki K, Tamura A, Nakagomi T, Nakayama H, Gotoh O, Kawai K, Taneda M, Yasui N, Hadeishi H, Sano K (1999) How should a subarachnoid hemorrhage grading scale be determined? A combinatorial approach based solely on the Glasgow Coma Scale. J Neurosurg 90:680–687
Tagle P, Huete I, Mendez J, Del Villard S (1986) Intracranial cavernous angiomas: presentation and management. J Neurosurg 64:720–723
Takano K, Sadoshima S, Ibayashi S, Ichiya Y (1993) Altered cerebral hemodynamics and metabolism in Takayasu's arteritis with neurological deficits. Stroke 24: 1501–1506
Takenaka K, Sakai H, Yamakawa H, Yoshimura SI, Kumagai M, Yamakawa H, Nakashima S, Nozawa Y, Sakai N (1999) Polymorphism of the endoglin gene in patients with intracranial saccular aneurysms. J Neurosurg 90:935–938
Takeuchi S, Kikuchi H, Karasawa J, Naruo Y et al (1987) Cerebral hemodynamics in arteriovenous malformations: evaluation by single-photon emission CT. AJNR 8:193–197
Taki W, Handa H, Yamagata S et al (1979) Balloon embolization of giant aneurysms using a newly developed catheter. Surg Neurol 12:363–365
Taki W, Handa H, Yamagata S et al (1980a) Radiopaque solidifying liquid for releasable balloon techniques. Technical note. Surg Neurol 13:140–142
Taki W, Handa H, Yamagata S (1980b) The released balloon technique with aggravated high frequency electrical current. Surg Neurol 13:405–408
Taki, W, Yonekawa Y, Iwata H, Uno A, Yamashita K, Amemiya H (1990) A new liquid material for embolization of arteriovenous malformations. AJNR Am J Neuroradiol 11:163–168
Taki W, Nishi S, Yamashita K, Sadatoh A, Nakahara I, Kikuchi H, Iwata H (1992) Selection and combination of various endovascular techniques in the treatment of giant aneurysms. J Neurosurg 77: 37–42
Tamaki N, Fujita K, Yamashita H (1971) Multiple arteriovenous malformations involving the scalp, dura, retina, cerebrum and posterior fossa: cases report. J Neurosurg 34:95–98
Tamiya T, Ono Y, Matsumoto K, Ohmoto T (2001) Peritumoral brain edema in intracranial meningiomas: effects of radiological and histological factors. Neurosurg 49:1046–1051
Tampieri D, Le Blanc R, Ter Brugge K (1993) Preoperative embolization of brain and spinal hemangioblastomas. Neurosurgery 33:502–505
Tan CB, Rodesch G, Lasjaunias P (2001) Growth and spontaneous regression of a middle cerebral artery aneurysm after surgical clipping. InterventNeuroradiol 7:147–151
Tanaka K, Waga S, Kojima T, Furuno M, Kubo Y, Murata H (1989) Spinal dural arteriovenous malformation: report of an unusual case. Neurosurgery 24:915–918
Tanaka Y, Furuse M, Iwasa H, Masazawa T, Saito K, Sato F, Mizuno Y (1986) Lobar intracerebral hemorrhage: etiology and a long-term follow-up study of 32 patients. Stroke 17:51–57
Tapia Acuna R (1965) The nasopharyngeal fibroma and its treatment. Arch Otolaryng 64:451–455
Taptas JN (1961) Intracranial meningioma in a four-month-old infant simulating subdural hematoma. J Neurosurg 18:120–121

Tardif J, Cote G, Lesperance J et al (1997) Probucol and multivitamins in the prevention of restenosis after coronary angioplasty. New Engl J Med 337:365–372
Tarlov IM (1947) Spinal extradural hemangioblastoma roentgenographically visualized with Diodrast at operation and successfully removed. Radiology 49:717–723
Tazelear HD, Locke TJ, Mc Gregor CJA (1992) Pathology of surgically excised primary cardiac tumors. Mayo Clin Proc 67:957–965
Tcheng J, Kereiakes D, George B et al (1998) Safety of readministration of abciximab: interim results of the ReoPro Readministration Registry (abstract). J Am Coll Cardiol 31:55A
Teal JS, Bergeron RT, Rumbaugh CL et al (1972) Aneurysms of the cervical portion of the internal carotid artery associated with neck trauma. Radiology 105:353–358
Teng MMH, Guo WY, Huang CI, Wu CC, Chang T (1988) Occlusions of arteriovenous malformations of the cavernous sinus via the superior ophthalmic vein. AJNR 9:539–546
Ter Berg H, Dippel D, Limburg M, Schievink W, van Gijn J (1992) Familial intracranial aneurysms. A review. Stroke 23:1024–1030
Ter Brugge K, Scotti G, Ethier R, Melancon D, Tchang S, Milner C (1977) Computed tomography in intracranial arteriovenous malformations. Radiology 122:703–705
Terada T, Kikuchi H, Karasawa J, Nagata I (1984) Intracerebral arteriovenous malformations fed by the anterior ethmoidal artery: case report. Neurosurgery 14:578–582
Terada T, Okuno T, Moriwaki H, Nakai E, Komai N (1985) Chronic encapsulated intracerebral hematoma during infancy: case report. Neurosurgery 16:833–835
Therkelsen J (1958) Angioma racemosum venosum medullae spinalis. Acta Psychiatr Neurol Scand 33:219–231
Theron J, Dorros G (1996)A rationale for endovascular therapy with balloon occlusion during extracranial atherosclerotic carotid artery stenosis. J Intervent Cardiol 9:209–213
Theron J, Lasjaunias P (1976) Participation of the external and internal carotid arteries in the blood supply of acoustic neurinomas. Radiology 118:83–88
Theron J, Newton TH, Hoyt WF (1974) Unilateral retinocephalic vascular malformations. Neuroradiology 7:185–196
Theron J, Cosgrove R, Melanson D, Ethier R (1986) Spinal arteriovenous malformations: advances in therapeutic embolization. Radiology 158:163–169
Theron J, Courtheoux P, Cassco A et al (1989) Local intraarterial fibrinolysis in the carotid territory. AJNR Am J Neuroradiol 10:753
Theron J, Courtheoux P, Alachkar F, Bouvard G, Maiza D (1990) New triple coaxial catheter system for carotid angioplasty with cerebral protection. AJNR American J Neuroradiol 11:869–874
Theron J, Alachkar F, Maiza D (1992) Dynamic digitized cerebral parenchymography. Neuroradiology 34:361–366
Theron J, Coskun O, Huet H, Oliveira G (1996a) Local intraarterial thrombolysis in the carotid territory. Intervent Neuroradiol 2:111–126
Theron J, Payelle G, Coskun O, Huet H (1996b) Carotid artery stenosis: treatment with protected balloon angioplasty and stent placement. Radiology 201:627–636
Theron J, Coskun O, Huet H, Oliveira G, Toulas P (1998) Local intraarterial thrombolysis in the carotid territory. In: Henry M, Amor M, Theron J, Roubin G (eds) Carotid angioplasty and stenting. pp 301–312
Thiebot J, Claviere TM, Freger P, Dundelot J, Benozio M (1986) Multiple intrathecal extramedullary arteriovenous fistulae draining freely into the spinal veins. J Neuroradiol 13:173–180
Thomas D (1997) Basilar thrombosis. In: Welch K, Caplan L, Reis D, Siesjo B, Weir B (eds) Primer on cerebrovascular diseases. Academic Press, San Diego, pp 96–98
Thomas D, Crockard A (1985) Cerebral metabolism and blood flow. In: Crockard A, Hayward R, Hoff J (eds) Neurosurgery: The scientific basis of the clinical practice. Blackwell Scientific, Oxford, pp 223–239
Thomas DJ (1982) Whole blood viscosity and cerebral blood flow. Stroke 13:285–287
Thomas HG, Dolman CL, Berry K (1981) Malignant meningioma: clinical and pathological features. J Neurosurg 55:929–934

Thompson J (1986) Don't throw out the baby with the bath water: a perspective on carotid endarterectomy. J Vasc Surg 4:543
Thompson R, Steinberg G, Levy R, Marks M (1998) The management of patients with arteriovenous malformations and associated intracranial aneurysm. Neurosurgery 43:202–212
Thron A (1988) Vascular anatomy of the spinal cord. Neuroradiological investigations and clinical syndromes. Springer, Berlin Heidelberg New York
Tikkakoski T, Luotonen J, Leinonen S, Siniluoto T, Heikkila O, Paivansalo M, Hyrynkangas K (1997) Preoperative embolization in the management of neck paragangliomas. Laryngoscope: 107:821–826
Tillman BP, Dahlin DC, Lipscomb PR et al (1968) Aneurysmal bone cyst: an analysis of ninety-five cases. Proc Staff Meet Mayo Clin 43:478–495
Tindall G, Kapp J, Odom G (1966) The use of tantalum dust as an adjunct in the postoperative management of subdural hematomas. J Neurosurg
Tobin WD, Layton DD (1976) The diagnosis and natural history of spinal cord arteriovenous malformations. Mayo Clin Proc 51:637–646
Toda N, Okamura T, Miyazaki M (1985) Heterogeneity in the response to vasoconstrictors of isolated dog proximal and distal middle cerebral arteries. Eur J Pharmacol 106:291–296
Tomlinson FH, Rufenacht DA, Sundt TM Jr, Nichols DA, Fode NC (1993) Arteriovenous fistulas of the brain and the spinal cord [see comments]. J Neurosurg 79:16–27
Tomsick T, Brott T, Barsan W, Broderick J (1996) Prognostic value of the hyperdense middle cerebral artery sign and stroke scale score before ultraearly thrombolytic therapy. Am J Neuroradiol 17:79–85
Tonn JC, Hoffmann O, Hofmann E et al (1999) "De novo" formation of intracranial aneurysms: who is at risk? Neuroradiology 41:674–679
Tonnis W (1936) Aneurysma arteriovenosum. In: Bergstrand H, Olivecrona H, Tönnis E (eds) Gefäßmißbildungen und Gefäßgeschwülste des Gehirns. Thieme, Leipzig, pp 88–134
Toppozada H, Michaels L, Toppozada M, El-Ghazzawi E, Talaat A, Elwany S (1981) The human nasal mucosa in the menstrual cycle. J Laryng Otol 95:1237–1247
Toppozada H, Michaels L, Toppozada M, El-Ghazzawi E, Talaat A, Elwany S (1982) The human respiratory nasal mucosa in pregnancy. An electron microscopic and histochemical study. J Laryng Otol 96:613–626
Torma T (1957) Malignant tumors of the spinal extradural space: a study based on 250 histologically verified cases. Acta Chir Scand [Suppl] 225:1–176
Touho H, Monobe T, Ohnishi H, Karasawa J (1995) Treatment of type II perimedullary arteriovenous fistulas by intraoperative transvenous embolization: case report. Surg Neurol 43:491–496
Toya S, Shiobara R, Izumi J, Shinomiya Y, Shiga H, Kimura C (1981) Spontaneous carotid-cavernous fistula during pregnancy or in the postpartum stage. J Neurosurg 54:252–256
Tranbahuy P, Borsik M, Herman P, Wassef M, Casasco A (1994) Direct intratumoral embolization of juvenile angiofibroma. Am J Otolaryngol 15:429–435
Treil J, Morel C, Bonafe A, Manelfe C (1977) Traumatic rupture of the middle meningeal artery. Angiographic appearance. A review of 30 cases. J Neuroradiol 4:399–414
Tsai FY, Hieshima GB, Mehringer CM, Grinnell V, Pribram HW (1983) Delayed effects in the treatment of carotid-cavernous fistulas. AJNR Am J Neuroradiol 4:357–361
Tsai F, Higashida R, Matovich V, Alfieri K (1992) Acute thrombosis of the intracranial dural sinus: direct thrombolytic treatment. AJNR Am J Neuroradiol 13:1137–1141
Tsai F, Wang A, Matovich V et al (1995) MR staging of acute dural sinus thrombosis: correlation with venous pressure measurements and implications for treatment and prognosis. AJNR Am J Neuroradiol 16:1021–1029
Tsurushima H, Meguro K, Matsumara A, Narushima K, Nakada Y, Nose T (1995) Multiple arteriovenous malformations of spinal cord and brain in a child. Pediatr Neurosurg 23:166–170
Turjman F, Massoud T, Vinuela F, Sayre J Guglielmi G, Duckwiler G (1994) Aneurysms related to cerebral arteriovenous malformations: superselective angiographic assessment in 58 patients. AJNR Am J Neuroradiol 15:1601–1605

Turner DM, Kassell NF, Sasaki T, Comair YG, Beck DO, Boarini DJ (1984) High dose naloxone produces cerebral vasodilation. Neurosurgery 15:192–197
Turney T, Garraway W, Whisnant J (1984) The natural history of hemispheric and brainstem infarction in Rochester, Minnesota. Stroke 15:790–794
Tymianski M, Willinsky RA, Tator C, Mikulis D, Ter Brugge K, Markson L (1994) Embolization with temporary balloon occlusion of the internal carotid artery and in vivo proton spectroscopy improves radical removal of petrous-tentorial meningioma. Neurosurgery 35:974–977
Ueda S, Saito A, Inomori S et al (1987) Cavernous angioma of the cauda equina producing subarachnoid hemorrhage. Case report. J Neurosurg 66:134–136
Ueda T, Hatakeyama T, Kumon Y et al (1994) Evaluation of risk of hemorrhagic transformation in local intra-arterial thrombolysis in acute ischemic stroke by initial SPECT. Stroke 25:298–303
Ueda T, Hatekeyama T, Kohno K, Kumon Y, Sakaki S (1997) Endovascular treatment for acute thrombotic occlusion of the middle cerebral artery: local intra-arterial thrombolysis combined with percutaneous transluminal angioplasty. Neuroradiology 39:99–104
Uflaker R, De Lima S, Ribas GC (1983) Carotid-cavernous fistula: embolisation through the superior ophthalmic vein approach. Radiology 159:175–179
Ulrich P, Perneczky P, Muacevic A (1997) Surgical strategy in cases of multiple aneurysms (German). Zentralblatt fur Neurochirurgie 58:163–170
Umemura K, Wada K, Uematsu T, Nakashima M (1993) Evaluation of the combination of a tissue-type plasminogen activator, SUN9216, and a thromboxane A2 receptor antagonist, vapiprost, in a rat middle cerebral artery thrombosis model. Stroke 24:1077–1081
Ungkanont K, Byers RM, Weber RS, Callender DL, Wolf PF, Goepfert H (1996) Juvenile nasopharyngeal angiofibroma: an update of therapeutic management. Head Neck 18:60–66
Uranishi R, Nakase H, Sakaki T (1999) Expression of angiogenic growth factors in dural arteriovenous fistula. J. Neurosurg 91: 781–786
Urtasun F, Biondi A, Casaco A, Houdart E, Caputo N, Aymard A, Merland JJ (1996) Cerebral dural arteriovenous fistulas: percutaneous transvenous embolization. Radiology 199:209–217
Vajda J (1992) Multiple intracranial aneurysms: a high-risk condition. Acta Neurochir (Wien) 118:59–75
Valavanis A, Wellauer J, Yasargyl AG (1983) The radiological diagnosis of cerebral venous angioma. Cerebral angiography and computed tomography. Neuroradiology 24:193–199
Valavanis A, Yasargil MG (1998) The endovascular treatment of brain arteriovenous malformations. Adv Tech Stand Neurosurg 24:131–214
Van de Werf AJ (1964) Sur un cas d'anévrisme artérioveineux intradural bilatéral de la fosse postérieure chez un enfant. Neurochirurgie 10:140–144
Van den Berg R, Rodesch G, Lasjaunias P (2002) Management of paragangliomas. Clinical and angiographic aspects. Intervent Neuroradiol 8: 127–134
Van der Wal A, Das P, Bentz van de Berg D, van der Loos C, Becker A (1989) Atherosclerotic lesions in humans: in situ immunophenotypic analysis suggesting an immune mediated response. Lab Invest 61:166–170
Van Dijk MA, Chang PC, Peters DJ, Bruening MH (1995) Intracranial aneurysms in polycystic kidney disease linked to chromosome 4. J Am Soc Nephrol 6:1670–1673
Van Dijk M, Ter Brugge K, Willinsky RA, Wallace C (2002a) Multiplicity of dural arteriovenous fistulas. J Neurosurg 96:76–78
Van Dijk M, Ter Brugge K, Willinsky RA, Wallace C (2002b) The clinical course of cranial dural AV fistulas with long-term persistent cortical venous reflux. Stroke 33:1233–1236
Van Dijk M, TerBrugge K, Willinsky RA, Farb RI, Wallace MC (2002) Multidisciplinary management of spinal dural arteriovenous fistulas: clinical presentation and long-term follow-up in 49 patients. Stroke 33:1578–1583
Van Halbach V, Higashida R, Dowd C et al (1993) Treatment of giant intradural (perimedullary) arteriovenous fistulas. Neurosurgery 33:972–980

Van Rooij WJ, Tijssen CC (1999) One stage endovascular treatment of multiple intracranial aneurysms. J Neurol Neurosurg Psychiatry 66:112
Van Swieten JC, Koudstaal PJ, Visser MC, Schouten HJA, van Gijn J (1988) Interobserver agreement for the assessment of handicap in stroke patients. Stroke 19:604–607
Vandenbroucke J, Koster T, Briet E, Reitsma P (1994) Increased risk of venous thrombosis in oral-contraceptive users who are carriers of factor V Leiden mutation. Lancet 344:1453–1457
Vandenbroucke J, Rosing J, Bloemenkamp K et al (2001) Oral contraceptives and the risk of venous thrombosis. N Engl J Med 344:1527–1534
Vander Ark G, Kempe L, Kobrine A (1972) Classification of internal carotid aneurysms as a basis for surgical approach. Neurochirurgia 15:81–85
Vega Molina J, Chiras J, Poirier B, Bories J (1985) Dysplasie fibro-musculaire de l'artère vertébrale (aspect angiographique). A propos de 85 cas. Neuroradiology 12:123–134
Verbiest H (1951) L'anévrisme artérioveineux intradural. Rev Neurol 85:189–199
Verstraete M (1991) Risk factors, interventions and therapeutic agents in the prevention of atherosclerosis-related ischaemic diseases. Drugs 42 [Suppl 5]:22–38
Verstraete M, Collen D (1986) Thrombolytic therapy in the eighties. Blood 67: 1529–1541
Vidyasagar C (1979) Persistent embryonic veins in arteriovenous malformations of the posterior fossa. Acta Neurochir (Wien) 48:67–82
Vilela P, Willinsky RA, Ter Brugge KG (2001a) Dural arteriovenous fistula associated with neoplastic dural sinus thrombosis: two cases. Neuroradiology 43:816–820
Vilela P, Willinsky R, Ter Brugge K (2001b) Treatment of intracranial venous occlusive disease with sigmoid sinus angioplasty and stent placement in a case of infantile multifocal arteriovenous shunts. Intervent Neuroradiolo 7:51–60
Vincent FM (1981) Anterior spinal artery aneurysm presenting as a subarachnoid hemorrhage. Stroke 12:230–232
Vines F, Davis D (1971) Clinical radiological correlation in cerebral venous occlusive disease. Radiology 98:9–22
Vinters HV (1985) The hystotoxicity of cyanoactrylate. Neuroradiology 27:279–291
Vinters HV, Debrun G, Kaufmann JCE et al (1981) Pathology of arteriovenous malformations embolized with isobutyl-2-cyanoacrylate. J Neurosurg 55:819–825
Vinuela F, Drake CG, Fox AJ et al (1982) Giant intracranial varices secondary to high-flow arteriovenous fistulae. J Neurosurg 66:198–203
Vinuela F, Dion JE, Duckwiler G, Martin NA, Lylyk P, Fox A, Pelz D, Drake CG, Girvin JJ, Debrun G (1991) Combined endovascular embolization and surgery in the management of cerebral arteriovenous malformations: experience with 101 cases. J Neurosurg 75:856–864
Vinuela F, Duckwiler D, Mawad M (1997) Guglielmi detachable coil embolisation of acute intracranial aneurysms: perioperative anatomical and clinical outcome in 403 patients. J Neurosurg 86:475–482
Vlodaver Z (1971) Pathologic changes in aortic coronary arterial saphenous vein grafts. Circulation 44:719–728
Vocgeli E, Fuchs WA (1976) Arteriography in bone tumors. Br J Radiol 49:407
Vodoff MV, Gilbert B, Le Breton F, Rodesch G, Laroche C, Lagarrigue JF, De Lumley L, Lasjaunias P (2001) Paraplégie et malformation artérioveineuse médullaire. Place de la chirurgie, de la corticothérapie et de l'embolisation. Arch Pédiatr 8:608–610
Voigt K, Lumper A (1976) Röntgenologische Direktdarstellung von Wirbelhaemangiomen durch die intraossare Angiographie. In: Schiefer W, Wieck HH (eds) Spinale raumfordernde Prozesse. Perimed, Erlangen
Von Kummer R, Meyding-Lamade U, Forsting M, Rosin L, Rieke K (1994) Sensitivity and prognostic value of early CT in occlusion of the middle cerebral artery trunk. Am J Neuroradiol 15:9–15
Vorchheimer D, Badimon J, Fuster V (1999) Platelet glycoprotein IIb/IIIa receptor antagonists in cardiovascular disease. JAMA 281:1407–1414
Wada JT, Rasmussen L (1972) Intracarotid injection of sodium Amytal for the lateralization of cerebral speech dominance. J Neurosurg 17:266–282

Wada JT, Rasmussen S (1960) Intracarotid injection of sodium amytal for the lateralization of cerebral speech dominance. J Neurosurg 17:266–282
Wahlgren N, MacMahon D, De Keyser J et al, for the INWEST Study Group (1994) Intravenous Nimodipine West European Stroke Trial (INWEST) of nimodipine in the treatment of acute ischaemic stroke. Cerebrovasc Dis 2:204–210
Wakhloo A, Schellhammer F, de Vries J, Habersroh J (1994) Self-expanding and balloon expandable stents in the treatment of carotid aneurysms: an experimental study in a canine model. Am J Neuroradiol 15:493–502
Wakhloo AK, Juengling FD, Van Velthoven V, Schumacher M, Hennig J, Schwechheimer K (1993) Extended preoperative polyvinyl alcohol microembolization of intracranial meningiomas: assessment of two embolization techniques. AJNR Am J Neuroradiol 14: 571–582
Waldmann TA, Levin EH, Baldwin M (1961) The association of polycythemia with a cerebellar hemangioblastoma. The production of an erythropoiesis stimulating factor by the tumor. Am J Med 31:318–324
Waldman SR, Levine HL, Astor F, Wood BG, Weinstein M, Tucker HM (1981) Surgical experience with nasopharyngeal angiofibroma. Arch Otolaryngol 107:677–682
Walike JW, MacKay B (1970) Nasopharyngeal angiofibroma: light and electron microscopic changes after stilbesterol therapy. Laryngoscope 80:1109–1127
Wallace R, Flom R, Khayata M, Dean B, McKenzie J, Rand J, Obuchowksi N, Zepp R, Zabramski J, Spetzler R (1995) The safety and effectiveness of brain arteriovenous malformation embolization using acrylic and particles: the experiences of a single institution. Neurosurgery 37:606–618
Walsh FB, King AB (1942) Ocular sign of intracranial saccular aneurysms: experimental work on collateral circulation through the ophthalmic artery. Arch Ophthalmol 27:1–33
Walters B, Ojemann R, Heros R (1987) Emergency carotid endarterectomy. J Neurosurg 66:817–823
Waltimo O (1973b) The relationship of size, density and localization of intracranial arteriovenous malformations to the type of initial symptom. J Neurol Sci 19:13–19
Wang AM, Morries JH, Fisher EG, Peterson R, Lin JCT (1988) Cavernous hemangioma of the thoracic spinal cord. Neuroradiology 30:261–264
Wardlaw J, Warlow C, Counsell C (1997) Systemic review of evidence on thrombolytic therapy for acute ischaemic stroke. Lancet 350:607–614
Ward PH, Thompson R, Calcaterra T, Kadin MR (1974) Juvenile angiofibroma: a more rational approach based upon clinical and experimental evidence. Laryngoscope 84 :2181–2194
Watanabe A, Takahara Y, Ibuchi Y, Mizukami K (1984) Two cases of aural arteriovenous malformation occurring after intracranial surgery. Neuroradiology 26:375–380
Weber FP (1922) Right-sided hemi-hypertrophy resulting from right-sided congenital spastic hemiplegia, with a morbid condition of the left side of the brain, revealed by radiograms. J Neurol Psychopathol 3:134–139
Weber J, Lovblad K, Remonda L et al (1997) Intraarterial fibrinolysis in central retinal artery occlusion. Neuroradiology 39:S43
Weir B (1987) Aneurysms affecting the central nervous system. Williams & Wilkins, Baltimore
Weir B, MacDonald RL (1996) Aneurysms and subarachnoid hemorrhage. In: Wilkins RH, Rengachary SS (eds) Neurosurgery, vol 2, 2nd edn. McGraw-Hill, New York, pp 2191–2213
Wester P, Asplund K, Eriksson S, Hagg E (1984) Infusion of magnesium in patients with acute brain infarction. Acta Neurol Scand 70:143
Westphal M, Koch C (1999) Management of spinal dural arteriovenous fistulae using an interdisciplinary neuroradiological/neurosurgical approach: experience with 47 cases. Neurosurgery 45:451–457
Weyand RD, MacCarthy CS, Wilson RB (1951) The effect or pregnancy on intracranial meningiomas occurring around the optic chiasm. Clin North Am 31:1225–1233
Whelan A, Watson M, Porter F, Steiner R (1995) Klippel-Trenaunay-Weber syndrome associated with a 5:11 balanced translocation. Am J Med Genet 59:492–494

Wemple JB, Smith GW (1966) Extracranial carotid aneurysm: report of four cases. J Neurosurg 24:667–671
Whisnant J, Cartlidge N, Elveback L (1978) Carotid and vertebral-basilar transient ischemic attacks: effect of anticoagulants, hypertension, and cardiac disorders on survival and stroke occurrence–a population study. Ann Neurol 3:107–115
White RI, Strandbert JV, Gross GS et al (1977) Therapeutic embolization with long-term occluding agents and their affects on embolized tissues. Radiology 125:677–687
Whittle IR, Dorsch NW, Besser M (1982) Spontaneous thrombosis in giant intracranial aneurysms. J Neurol Neurosurg Psychiatry 45:1040–1047
WHO/ISFC (1997) Study of pathological determinants of atherosclerosis in youth (PBDAY Study), WHO, CVC97
Wholey M, Eles G (1998) Clinical experience in cervical carotid artery stent placement. Carotid Neurovasc Intervent 1:2–9
Wholey MH, Wholey M, Bergeron P, Diethrich E et al (1998) Current global status of carotid artery stent placement. Cathet Cardiovasc Diagn 44:1–6
Wiebers DO, Whisnant JP, Sundt TM Jr et al (1987) The significance of unruptured intracranial saccular aneurysms. J Neurosurg 66:23–29
Wikholm G (1995) Occlusion of cerebral arteriovenous malformation with N-butyl cyano-acrylate is permanent. AJNR 16:479–482
Wilenzt J, Sanborn T, Haudenschild C et al (1987) Platelet accumulation in experimental angioplasty: time course and relation to vascular injury. Circulation 75:636–642
Williams K, Tabas L (1995) The response-to-retention hypothesis of early atherogenesis. Arteriolscl Thromb Vasc Biol 15:551–561
Willinsky RA (1999) Detachable coils to treat intracranial aneurysms. Can Med Ass J 161:1136
Willinsky R, Lasjaunias P, Pruvost P, Boucherat M (1987) Petrous internal carotid aneurysm causing epistaxis: balloon embolization with preservation of the parent vessel. Neuroradiology 29:570–572
Willinsky R, Lasjaunias P, Ter Brugge K, Pruvost P (1988a) Brain arteriovenous malformations: analysis of the angioarchitecture in relationship to hemorrhage. J Neuroradiol 15:225–237
Willinsky R, Lasjaunias P, Comoy J, Pruvost P (1988b) Cerebral microarteriovenous malformations (mAVMs). Review of 13 cases. Acta Neurochir (Wien) 91:37–41
Willinsky R, Lasjaunias P, Ter Brugge K, Burrows P (1990a) Multiple cerebral arteriovenous malformations. Review of our experience from 203 patients with cerebral vascular lesions. Neuroradiology 32:207–210
Willinsky R, Lasjaunias P, Ter Brugge KN, Hurth M (1990b) Angiography in the investigation of spinal dural arteriovenous fistula. A protocol with application of the venous phase. Neuroradiology 32:114–116
Willinsky R, Ter Brugge K, Lasjaunias P, Montanera W (1990c) The variable presentations of craniocervical and cervical dural arteriovenous malformations. Surg Neurol 34:118–123
Willinsky R, Ter Brugge KG, Montanera W, Wallace C, Gentilli F (1993) Spinal epidural arteriovenous fistulas: arterial and venous approaches to embolization. AJNR Am J Neuroradiol 14:812–817
Willinsky R, Ter Brugge K, Montanera W, Mikuls D, Wallace MC (1994) Venous congestion: an MR finding in dural arteriovenous malformations with cortical venous drainage. AJNR Am J Neuroradiol 15:1501–1507
Willinsky R, Harper W, Wallace M, Kucharczyk W, Montanera W, Mikulis D, Ter Brugge K (1996) Follow-up MR of intracranial cavernomas, the relationship between haemorrhagic events and morphology. Intervent Neuroradiol 2:127–135
Willinsky R, Goyal M, Ter Brugge K, Montanera W (1999) Tortuous, engorged pial veins in intracranial dural arteriovenous fistulas: correlations with presentation, location and MR findings in 122 patients. AJNR Am J Neuroradiol 20: 1031–103
Willinsky R, Goyal M, Ter Brugge K, Montanera W, Wallce MC, Tymianski M (2001) Embolization of small (<3 cm) brain arteriovenous malformations. Correlation of angiographic results to a proposed angioarchitecture grading system. Intervent Neuroradiol 7:19–27

Willis AG, Birrell JH (1955) The structure of a carotid body tumor. Acta Anat (Basel) 25:220–265
Wilson AJ, Ratliff JL, Lagios MD et al (1979) Mediastinal meningioma. Am J Surg Pathol 3:557–562
Wilson CB, U HS, Dominique J (1979) Microsurgical treatment of intracranial vascular malformations. J Neurosurg 51:446–454
Wilson FM, Jaspan T, Holland IM (1989) Multiple cerebral aneurysms: a reappraisal. Neuroradiology 31:232–236
Wilson JR, Jordon PH Jr (1961) Excision of an internal carotid aneurysm: restitution of continuity by substitution of external for internal carotid artery. Ann Surg 154:45–47
Wilson WB, Gordon M, Lehman RA (1979) Meningiomas confined to the optic canal and foramina. Surg Neurol 12:21–28
Winn HR, Richardson AE, Jane JA (1977) The long-term prognosis in untreated cerebral aneurysms. I. The incidence of late hemorrhage in cerebral aneurysm: A 10-year evaluation of 364 patients. Ann Neurol 1:358–370
Winn HR, Almaani WS, Berga SL et al (1983) The long-term outcome in patients with multiple aneurysms: incidence of late hemorrhage and implications for treatment of incidental aneurysms. J Neurosurg 59:642–651
Winslow N (1926) Extracranial aneurysms of internal carotid artery: history and analysis of cases registered to Aug. 1, 1925. Arch Surg 13:689–729
Wolpert S, Bruckmann H, Greenlee R, Wechsler L, Pessin M, del Zoppo G (1993) Neuroradiologic evaluation of patients with acute stroke treated with recombinant tissue plasminogen activator. Am J Neuroradiol 14:3–13
Wolpert SM. The trigeminal artery and associated aneurysms. Neurology 16:610–614
Wolpert SM, Stein BM (1975) Catheter embolization of intracranial arteriovenous malformations as an aid to surgical excision. Neuroradiology 10:73–85
Wolverson MK, Sundaram M, Eddelston B, Prendergast J (1981) Diagnosis of parathyroid adenoma by computed tomography. J Comput Ass Tomogr 5:818–826
Wong J, Findlay J, Suarez-Almazor M (1997) Hemodynamic instability after carotid endarterectomy: risk factors and associations with operative complications. Neurosurgery 41:35–43
Wood E, Correll J (1969) Atheromatous ulceration in major neck vessels as a cause of cerebral embolism. Acta Radiol (Diagn) 9:520–536
Wood EH (1964) Angiographic identification of the ruptured lesion in patient with multiple cerebral aneurysms. J Neurosurg 21:182–198
Wood JH (1987) Cerebral blood flow. Physiologic and clinical aspects. McGraw-Hill, New York
Wood MW, White RJ, Kernohan JW (1957) One hundred intracranial meningiomas found incidentally at necropsy. J Neuropathol Exp Neurol 16:337–340
Work WP, Hybels RL (1974) A study of tumors of the parapharyngeal space. Laryngoscope 84:1748–1755
Wortzman G (1963) Traumatic pseudoaneurysms of the superficial temporal artery. Radiology 80:444–446
Wosnessenski WP (1923) Geschwulst der Carotisdrüse. Medizinskaja Myssl 2:732–739
Wu Z, Zhang Y,Wang C, Yang X, Li Y (2000) Treatment of carotid-cavernous fistula. Intervent Neuroradiol 6:277–289
Wyburn-Mason R (1943a) Arteriovenous aneurysm of midbrain and retina, facial naevi and mental changes. Brain 66:163–203
Wyburn-Mason R (1943b) The vascular abnormalities and tumours of the spinal cord and its membranes. Kimpton, London
Wychulis AR, Beahrs OH, Bernatz PE (1964) Aneurysms of internal carotid artery treated by excision and anastomosis to external carotid artery. Arch Surg (Chicago) 88:803–806
Yadav J, Roubin G, King P, Iyer S (1996) Angioplasty and stenting for restenosis after carotid endarterectomy: initial experience. Stroke 27:2075–2079
Yadav J, Roubin G, Iyer S et al (1997) Elective stenting of the extracranial carotid arteries. Circulation 95:376–381

Yakes W, Rossi P, Odink H (1996) How I do it. Arteriovenous malformation management. Cardiovasc Intervent Radiol 19:65–71
Yakes W, Krauth L, Ecklund J et al (1997) Ethanol endovascular management of brain arteriovenous malformations: initial results. Neurosurgery 40:1145–1154
Yamada S (1982) Arteriovenous malformations in the functional area: surgical treatment and regional cerebral blood flow. Neurol Res 4:283–322
Yamada S, Cojocaru T (1987) Arteriovenous malformations. In: Wood JH (ed) Cerebral blood flow. Physiologic and clinical aspects. McGraw-Hill, New York, pp 580–590
Yamada S, Kindt G, Youman J (1967) Carotid artery occlusion due to nonpenetrating injury. J Trauma 7:333–342
Yamakawa Y, Kinoshita K, Fukui M et al (1980) Radiosensitive meningioma. Surg Neurol 13:471–475
Yamasaki T, Handa H, Yamashita J, Moritake K, Nagasawa S (1984) Intracranial cavernous angiomas angiographically mimicking venous angioma in an infant. Surg Neurol 22:461–466
Yamashita K, Kashiwagi S, Kato S, Takasago T, Ito h (1997) Cerebral aneurysms in the elderly in Yamaguchi, Japan. Analysis of the Yamaguchi Data Bank of Cerebral Aneurysm from 1985 to 1995. Stroke 28(10):1926–1931
Yamashita K, Kashiwagi S, Suzuki M (2000) The Yamaguchi data bank of cerebral aneurysms: incidence rate and management outcome for ruptured and unruptured cerebral aneurysms in Yamaguchi, Japan since 1995. Stroke 31:2788
Yamaura A, Watanabe Y, Saeki N (1990) Dissecting aneurysms of the intracranial vertebral artery. J Neurosurg 72:183–188
Yang PJ, Halbach VV, Higshida RT, Hieshima GB (1988) Platinum wire: a new transvascular embolic agent. AJNR Am J Neuroradiol 9:547–550
Yasargil MG (1976) Intradural spinal arteriovenous malformations. In: Vinken PJ, Bruyn GB (eds) Handbook of clinical neurology. Elsevier/North Holland, Amsterdam
Yasargil MG (1978) Operative treatment of spinal angioblastomas. In: Pia HW, Djindjian H (eds) Spinal angiomas: advances in diagnosis and therapy. Springer, Berlin Heidelberg New York
Yasargil MG (1984) Clinical considerations, surgery of the intracranial aneurysms and results, vols. 1 and 2. Microneurosurgery. Thieme Verlag, Stuttgart
Yasargil MG (1987a) Microneurosurgery, vol 3a. Thieme, New York
Yasargil MG (1987b) Microsurgery, vol 4. Thieme, New York
Yasargil MG (1987c) Pathologic considerations. In: Yasargil MG (ed) Microneurosurgery, AVM of the brain: history, embryology, pathologic considerations, hemodynamics, diagnostic studies, microsurgical anatomy, vol 3A. Thieme, New York, pp 49–211
Yasargil MG, DeLong WB, Guarnaschelli JJ (1975) Complete microsurgical excision of cervical extramedullary vascular malformation. Surg Neurol 4:211–224
Yasargil MG, Antic J, Laciga R et al (1976) Arteriovenous malformations of the vein of Galen. Microsurgical treatment. Surg Neurol 16:195–200
Yasargil MG, Symon L, Teddy PG (1984) Arteriovenous malformations of the spinal cord. In: Symon L (ed) Advances and technical standards in neurosurgery. Springer, Wien, pp 61–102
Yasui N, Magarisawa S, Suzuki A et al (1996) Subarachnoid hemorrhage caused by previously diagnosed, previously unruptured intracranial aneurysms: a retrospective analysis of 25 cases. Neurosurgery 39:1096–1101
Yatsu FM, Pettigrew LC, Grotta JC (1987) Medical therapies for acute ischemic stroke. In: Wood JH (ed) Cerebral blood flow. Physiologic and clinical aspects. McGraw-Hill, New York, pp 603–612
Yoichi A, Murayama Y, Vinuela F, Lefkowitz MA, Duckwiler GR, Gobin YP (1999) Balloon-assisted Guglielmi detachable coiling of wide-necked aneurysms. Part I. Experimental evaluation. Neurosurgery 45:519–530
Yonas H, Agamanolis D, Takaoka Y, White RJ (1977) Dissecting intracranial aneurysms. Surg Neurol 8:407–415
Yonas H, Patre S, White RJ (1980) Anterior spinal artery aneurysm. Case report. J Neurosurg 53:570–573
Yong-Zhong G, van Alphen HA (1990) Pathogenesis and histopathology of saccular aneurysms: review of the literature. Neurol Res 12:249–255

Young AE (1988) Combined vascular malformations. In: Mulliken J, Young A (eds) Vascular birthmarks. Hemangiomas and malformations. WB Saunders Company Philadelphia, pp 246–274
Young B (1979) Hydrocephalus and elevated intracranial venous pressure. Case report. Childs Brain 5:73–80
Young N (1941) Bleeding from ear as sign of leakage aneurysm of extracranial portion of internal carotid artery. J Laryng 56:35–64
Young W, Berenstein A (1984) Somatosensory evoked potential monitoring of intraoperative procedures. J Neurosurg 60:777–785
Young W, Berenstein A (1985) Somatosensory evoked potential monitoring of intraoperative procedures. Spinal cord monitoring. Springer, Berlin Heidelberg New York, pp 197–203
Young W, Pile-Spellman J, Prohovnik I, Kader A, Stein B (1994) Evidence for adaptive autoregulatory displacement in hypotensive cortical territories adjacent to arteriovenous malformations. Neurosurgery 34:601–611
Zachrisson BF (1976) Thyroid arteriography. Acta Radiol Suppl 350:1–112
Zak FG, Lawson W (1982) The paraganglionic chemoreceptor system. Physiology, pathology and clinical medicine. Springer, New York
Zakka KA, Summerer RW, Yee RD et al (1979) Optociliary veins in a primary optic nerve sheath meningioma. Am J Ophthalmol 87:91–95
Zanetti PH, Sherman FE (1972) Experimental evaluation of a tissue adhesive as an agent for the treatment of aneurysms and arteriovenous anomalies. J Neurosurg 36:72–79
Zang KD, Singer H (1967) Chromosomal constitution of meningiomas. Nature 216:84–85
Zarins C (1996) Carotid endarterectomy: the gold standard. J Endovasc Surg 3:10–15
Zellem RT, Buchheit WA (1985) Multiple intracranial arteriovenous malformations: case report. Neurosurgery 17:88–93
Zerah M, Garcia-Monaco R, Rodesch G, Ter Brugge K, Tardieu M, De Victor D, Lasjaunias P (1992) Hydrodynamics in vein of Galen malformation. Childs Nerv Syst 8:1–7
Zeumer H, Hacke W, Ringelstein EB (1983) Local intraarterial thrombolysis in vertebrobasilar thromboembolic disease. AJNR Am J Neuroradiol 4:401–404
Zeumer H, Hundgen R, Ferbert A, Ringelstein EB (1984) Local intraarterial fibrinolytic therapy in inaccessible internal carotid occlusion. Neuroradiology 26: 315–317
Zeumer H, Bruckmann H, Adelt D, Hacke W, Ringelstein EB (1985) Balloon embolization in the treatment of basilar aneurysms. Acta Neurochir (Wien) 78:136–141
Zeumer H, Freitag H, Knospe V (1992) Intravascular thrombolysis in central nervous system cerebrovascular disease. Neuroimaging Clinics of North America. Intervent Neuroradiol 2:359–369
Zeumer H, Freitag H, Zanella F, Thie A (1993) Local intra-arterial fibrinolytic therapy in patients with stroke: urokinase versus recombinant tissue plasminogen activator (rt-PA). Neuroradiology 35:159–162
Zubkov Y, Nikoforov B, Shustin V (1984) Balloon catheter technique for dilatation of constricted cerebral arteries after aneurysmal SAH. Acta Neurochir (Wien) 70:65–79

Subject Index for Volumes 2.1 and 2.2

A
abciximab 36, 38
acetylcholine 13
acrylate 973, 977, 991, 993, 1059, 1059–1074
– carciogenesis 1063
– catheter withdrawal 1069
– continuous column 1069
– cyanoacrylate 1025
– flow-control 1069
– HEMA (hydroxy-methylmethacrylate) 1144
– histoacryl 1060
– histotoxicity 1060–1063
– IBCA (isobutyl homologue isobutyl-2-cyanoacrylate) 1059
– in situ injection 1069
– injection 1063–1066
– mutagenecity 1063
– NBCA (N-butyl-cyanoacrylate) 332, 946, 1059, 1063, 1140
– octacyanoacrylate 1055, 1059
ACT (activation coagulation time) 923
activated clotting time 38
activated coagulation monitoring 924, 925
Aculynker 1175
adenoma, parathyroid 269
adenosine 14
adenosine diphosphate 14
adenosine receptor antagonists 35
adrenal carcinoma 271
Agility, guidewire 965
AIDS 509
amaurosis fugax 74, 406, 407
amines 12
amobarbital 925–929, 1125
amytal 1125
anastomosis
– intrinsic venous 795
– protection 1101
anastomotic system, intrinsic longitudinal 777
anatomy, venous MRI 141
anesthesia 919–929
– general 919, 920
– input and output monitoring 921
– local 920
– neuroleptic 920
aneurysm
– age 380–382
– anatomy, single/mirror/twin saccular arterial aneurysm 442–453
– arteriovenous malformation 708–715
– – spinal cord 786–794
– associated post-traumatic 59
– associated with proliferative diseases 523, 524
– atherosclerotic 398
– bleeding rate 451
– blister 482–486
– classification 374, 375
– clonal mutation/clonal phenotype 379
– coarctation of the aorta 524–527
– congenital 377
– congenital heart disorders 524–527
– de novo 547, 548
– dissecting (*see also* dissection) 60, 333, 454–477, 1027, 1046
– dolichoectatic type 479, 481–483
– dysplastic 401, 653, 789
– embryological origin 377–380
– extradural 382–430, 1020
– – external carotid artery 425–431
– – – facial artery, false 427
– – – internal maxillary artery 425
– – – superficial temporal 425
– – internal carotid artery 382–384
– – – blunt trauma 389–393
– – – cavernous segment 401–407
– – – cervical 384, 385
– – – clinical presentation 408–415
– – – developmental 385–387
– – – dissection, spontaneous 394–398
– – – mycotic 398, 421
– – – occlusion 417–420
– – – penetrating trauma 387–389
– – – petrous 399–401
– – vertebral 420–425
– familial forms 366
– – nonsyndromic familial 438–440
– false 135, 278, 550, 790, 799, 1109
– fenestration 1016
– flow-related 333, 376, 429, 514–517, 646–653, 787
– fusiform 478, 484, 497
– hypophysial 998
– incidence 366
– intercostal 526
– intradural 431–453
– – giant saccular 478–486
– – – with thrombosis 486–497
– – giant nonsaccular 478–486, 497, 498
– – immunological 509–513
– – infectious 502–509
– – inflammatory diseases 513
– – traumatic 518–522
– location 451, 515
– male-to-female ratio 375
– megadolicho artery 498–500
– mesencephalic region 450
– mid-basilar 1049
– middle cerebral artery 135
– mirror 448, 449, 453, 555, 556
– – giant 500
– morbidity 367, 538, 547
– mortality 367, 538, 547
– multiple 453
– – giant 500
– mycotic 398, 421, 502–509
– origin 378
– phylogenetic age 376
– physiopathogenesis 371–374
– preexisting 279
– prevalence 366
– prosencephalic region 450
– proximal, shape 515
– pseudoaneurysm 347, 389, 421, 653, 662, 776
– regrowth 554, 559
– rhombencephalic region 450
– risk 371–374
– rupture 1141, 1142
– saccular

aneurysm
– saccular multiple 440–442, 442
– – single 453
– segmental vulnerability 375–377
– serpentine arterial 498–500
– shrinkage 560
– sphenoid sinus 322
– thrombosis 470
– topography 372
– traumatic 283, 360, 973, 1046
– treatment 527–563
– – balloon remodeling 1031–1037
– – coil 1030
– – combined endovascular treatment 1147, 1148
– – deconstructive operation 1020–1028
– – endovascular treatment
– – – literature review 530, 531
– – – results 538–549
– – EVAL 1083–1089
– – giant arterial aneurysm 560–564
– – method 532–538
– – multiple arterial aneurysms 549–560
– – postembolization care 1128, 1129
– – reconstructive operation 1030
– – sclerotherapy 1074–1083
– – second intervention 529
– – *Trispan* 1039–1043
– – two-microcatheter technique 1039, 1040
– unrupted 380, 545
– – natural history 546
– venous 790
– wide-neck 1031
angiofibroma, juvenile
– angiography 211–214
– clinical findings 210
– CT examination 211
– development, global hypothesis 207–210
– embolization 214
– – technical aspects 221–223
– epidemiology 205
– extension
– – intracranial, false 213
– – intracranial, true 211–213
– – pattern 202
– invasion, pattern 203
– macroscopic pathology 201–204
– microscopic pathology 204, 205
– MRI examination 211
– nasal mucosa 206
– natural history 211
– pathophysiology 206–210
– radiation therapy 221
– sex hormons 206
– therapeutic findings 214–221
– tumor recurrence 223
angiogenesis 378, 756
angiography, angiographic evaluation 41–44
– carotid 84
– catheter, 3-D selective 85
– cerebral 100–103
– computer tomographic (CTA) 78–80, 99, 100
– follow-up angiography 535
– MRA (magnetic resonance angiography) 80–83, 100, 535
angiopathy, high-flow 786
angioplasty 53, 90–98, 116–135
– balloon (*see there*)
– techniques 1152–1181
– – intervention 1154–1163
– – postdeployment 1173
– – predilatation 1164
– – premedication 1153, 1154
– – vasoactive medication 1154
– and stenting (CAS) 92
angioseal 933
angiotensin II 14
anterior horn syndrome 839
antibiotics 505
anticoagulation 104, 804, 845, 1132, 1133
anticonvulsants 918, 919
antiedema 1134, 1135
antiphospholipid antibody syndrome 141
antiplatelets 34, 398, 475, 919, 1128, 1132
α_1-antitrypsin deficiency 58
aorta
– abdominal 23
– coarctation 786
aortic arch study 41, 42
aortitis syndrome 526
apoptosis 378
Aquaphor 1130
arterial stenosis 524
arteriopathy, idiopathic regressing 57, 58
arteriotomy sites 929–933
– closure device 932, 933
– introducer sheath 930
arteritis, *Takayasu* 115, 116
aspirin 34, 35, 39, 419, 495, 1153
astrocyte 3
atheroma, aortic arch 99
atherosclerosis 23–29, 73
– accelerated 97
– atherogenesis, mechanisms 24–27
– carotid 29
– epidemiology 23
– introduction 23
– middle cerebral artery 44
– pathogenesis 24
ATP 8
atropine 917, 1152, 1154
Attracter 18 1052
austenite phase 1170
autoregulation, cerebral 5–7, 22, 40
– breakthrough 6
Avatine 1077
azygos vein 739

B
balloon angioplasty 36, 53, 57, 62, 68, 80, 95
– guidewire through balloon technique 123, 124
– *Higashida* balloon catheter 119
– latex balloon 122–124
– over-the-guidewire balloon tip catheter 125
– over-the-guidewire *Dotter* technique 125
– silicone balloon 119–121
– vasospasm, indications and results 128–133
barbiturates 1135
baroreceptor 1152
Barthel Index 150–152
basilar artery
– thrombosis 110–114
– unfused 447
BAVM (*see* malformation, arteriovenous)
Berenstein
– double lumen occlusive balloon catheter 944
– liquid coil (BLC) 993, 995
– variable stiffness 934
bicuspid aortic valve 524
bifemoral approach 1030
biopsy, epistaxis 359
biorheological factors 1133, 1134
blebs 482, 484, 542
blindness, transient monocular 74
blister 482–486
blood flow, cerebral (*see* CBF)
blood pressure 433
blood-brain barrier 3, 4, 10
blunt trauma 389–393
bone
– cyst, aneurysmal 890–892
– erosion 410, 414, 755
brachial nerve, deficit 805
brachiocephalic vessel 106
– totally occluded 1176–1178
brachytherapy, endovascular 1019
bradykinin 13
breast carcinoma 155, 272

bruit
– carotid 73
– dural arteriovenous shunt 581, 582
– traumatic arteriovenous fistula 299, 300
– vertebro-vertebral arteriovenous fistula 751
bypass 102, 105, 1020, 1027, 1029

C
Ca^{2+} channel blocker 918, 921
calcification 1163
– arteriovenous malformation 676, 677
– mural 472, 500
calcitonin gene-related peptide 13
calcium channel antagonist 21, 1135
calibrated leak technique 119–127, 130, 959, 961
candida albicans 509
candidosis, chronic mucocutaneous 509
capilarectasia 472
capilary 3
CAPTURE 38
carbon dioxide reactivity 9
carbon monoxide 14
cardiac overload 739
carotid artery 931
– extracranial, stenosis
– – asymptomatic 86–89
– – imaging 75–84
– – natural history 73–75
– – symptomatic 86
– – treatment 84, 85
– internal
– – aneurysm, extradural (*see there*)
– – dissection 57–67
– – ligation 418
– – occlusion 48, 52–57, 417, 418
– – – intravenous thrombolysis 56
– – – revascularization 55
– – – tolerance test occlussion 418–420
– – stenosis, above carotid bulb 68, 69
– petrous 103
– physiology 1096
carotid bulb 1153
carotid trapping 389
catheter, balloon 53
– angioplasty 958–961
– balloon-tip 1031
– *Berenstein* variable stiffness 934
– detachable 955–958, 1006
– double-lumen 924, 943–949
– – *Berenstein* 944
– – *Comodor* 125, 950
– – modified 950
– *Envoy 5-F* 935
– flow control 942, 943
– *Fogarty* 280
– *Flowrider* 1091
– guiding catheter 933, 935
– *Headway* catheter 935
– *Hieshima Apollo* 958, 959
– *Higashida* balloon catheter 119, 953
– *Lasjaunias 4-F* catheter 986
– latex balloon 122–124, 325, 957, 958
– – *Debrun* 957, 958, 960, 1144
– – gold valve balloon 957
– – *O'Reilly* 958
– microcatheter (*see there*)
– *Mini-Torquer* 936, 942, 943
– silastic 958
– silicone balloon 119–121, 326
– single-lumen 950–955
– – *Endeavor* 952
– – *Equinox* 125, 956, 959, 1034, 1085
– – *Hyperglide* 956
– – *Sentry* 125, 955, 958, 1034
– – *Stealth* 125, 950, 952, 958
– stent delivery 962–964
– tolerance testing 314, 942, 943, 1020, 1029, 1030
– withdrawal 1069, 1111
catheterization, distal 1106, 1107
caudal fusion 444
CAVATAS 93
cavernoma 587, 687–690
– classification 687
– de novo 688
– familial 688
– multiple 689
CBF (cerebral blood flow) 4, 5, 27
– metabolism 8
– regional (rCBF) 10
CBV (cerebral blood volume) 7
cerebral arteriovenous malformation (*see also* shunt)
– angioarchitecture 631–634
– aneurysms (*see there*)
– arteries 634
– brain function 678, 679
– calcifications 676, 677
– cavernoma 687–690
– choroid plexus 629–631
– classification 614, 615
– – principles 612–614
– cryptic 690
– CSF changes 676
– DAVS (*see* arteriovenous shunt, dural)
– deep-seated 629
– dural supply 642–644
– fistula (*see there*)
– headache 681–683, 704, 707
– hemangioma, cavernous 686, 687
– hemorrhage 677, 678, 703, 704
– incidence 609–612
– lesions, reach the cortex 626
– management/treatment 695–735
– – age 700, 701
– – combined endovascular treatment 1147, 1150
– – embolization
– – – contraindications 732–734
– – – curative 720–727
– – – emergency 732
– – – intraoperative 729
– – – palliative 720
– – – partial (targeted) 716–720
– – – postembolization care 1128
– – – presurgical 728, 729
– – – prior to radiosurgery 729–731
– – – results 734, 735
– – – staging 732
– – indications 696–699
– – lifestyle/occupation 701
– – location/size 708
– – sex 701
– – strategy 715, 716
– – symptoms 703–708
– maxillofacial 1083
– microarteriovenous 655, 656, 940
– multiple 618–625
– natural history 677
– neurological deficit 708
– nidus 794–801
– – angioarchitecture 654, 655
– – intranidal ectasias 659–664
– – size change 656–659
– occult 690
– paravertebral 862
– pregnancy 683, 684
– rupture 1137–1141
– seizures 679, 680, 704
– stenotic changes 638–642
– thrombosis 669
– topographic analysis 625, 626
– unclassified 624, 625
– variations, arterial 644–646
– vasospasm 642
– veins 668
– – developmental anomalies 685
– – variations 668–675, 684
cerebral artery, middle (MCA)
– hyperdense sign 60
– stroke 44, 45
cerebral-facial syndromes 621–624
chemoembolization 877–880, 1094

chemotherapy 1093, 1094
– intra-arterial infusion 1093, 1094
chiasmatic ectasia 336
Chlamydia pneumoniae 24
chromosome
– chromosome 4 431, 432
– chromosome 9 436
– chromosome 16 431, 436
– chromosome 17 435
cigarette smoking 440
cisplatinum 1094
clipping 131
clival artery, lateral 569
clopidogrel 35
closed-cell design 1164
closure device 923, 1129
CMV (cytomegalovirus) 512
coagulation profile 99
coagulopathy 357
coarctation, aorta, aneurysm 524–527
coaxial assembly system 1155
Cobb syndrome 755, 773
coil
– *Cordis 3-D* 1000, 1012, 1013
– 3-D shape memory 1000
– detachable 981, 1030
– – *Cook* 1012, 1013
– – *Guglielmi* 528, 998–1002
– – radioactive 1019
– fiber 746, 980
– fixation 1053
– GDC, bioabsorbable polymeric 1012, 1016
– *Gianturco* coils 980
– glue, combination 991
– *Hilal* coil 987
– hydrocoil 1012, 1014
– liquid 980, 981, 1066
– – *Berenstein* 993, 995, 1118, 1119
– microcoils 986, 1025
– *Micrus* 1010, 1011
– pusher 987
– retrieval 1051
– stretch-resistant 1000–1002
– stretching 1045
– ultrasoft 1000
COL5A1/COL5A2 gene 434
collagen disease 739
collateral circulation 101, 314
combined endovascular treatment
– aneurysm therapy 1147
– brain arteriovenous malformation 1147
– occlusive/hemorrhagic vascular disease 1147
Comodor double-lumen balloon-tip catheter 125, 950
compaction 537, 562, 1035, 1039, 1049, 1090
complications, embolization 1129–1146
connective tissue disorder 396
contiguous gene syndrome 436, 437
contraceptives, oral 136
contrast material, extravasation 359, 361, 1136, 1139
conus medularis 839
Cook detachable coil 1012, 1013
Cordis 3-D coil 1000, 1012, 1013
Corinthian stent 1171
cortical artery, occlusion 54
corticosteroids 918, 1096, 1129
costocervical artery 747
coumadin 39
cranial nerve
– deficit 1129
– dysfunction 285, 298–300
– paralysis 476
– symptoms 580, 581
cranial sinus 739
craniofacial tumor 270–275
CREST (carotid revascularization endarterectomy versus stenting trial) 93
CT (computed tomography) 30
CTA (computer tomographic angiography) 78–80, 99, 100
cutaneous discoloration 756
cyanoacrylate 1025
cyst
– liver 437
– renal 433
cytokinase 10
cytotoxics 1059

D

DAVS (dural arteriovenous shunt) 565–607
– associated conditions 590–593
– cavernous sinus 603, 996
– classification 570, 575–579
– cranial fossa, anterior 589, 602
– cranial nerve symptoms 580, 581
– clinical presentation 579–593
– neurological deficits
– – focal 582–585
– – global 585–587
– foramen magnum 583, 589, 603
– historical review 566–569
– hormonal influence 587, 588
– intracranial hemorrhage 587
– multiplicity 590–593
– natural history 594–596
– pathophysiology 570, 571
– pretherapeutic evaluation 598
– sagital sinus, superior 602
– symptoms, progression 596–598
– tentorium 602
– therapy
– – embolization 983
– – – complications 606
– – – results 606
– – – timing 605, 606
– – indications/strategy 598–602
– – surgery 607
– – technical aspects 605
– – topographic considerations 602–605
– tinnitus and objective bruits 581, 582
– torcular 583
– transverse sinus 582, 603
Debrun catheter 957, 958, 960, 1144
deconstructive operation 1002, 1020–1028
– middle cerebral artery aneurysm 1023
– vertebrobasilar junction aneurysm 1020
degeneration, neuronal 20
– anterograde 21
– axon (*Wallerian*) 21
– retrograde 21
delta sign 138
dextran 1133
dialysis, peritoneal 433
diastolic fraction 514
DIC (dissemianted intravascular coagulation) 406
diplopia 298, 405
diseases (*see* syndromes)
dissection 106
– carotid 57–67, 1159
– – iatrogenic 65
– – spontaneous 394
– catheter 1159
– complications 477
– fusiform 456, 467, 468
– healing, spontaneous 468
– intracranial iatrogenic 1179
– intradural artery 454–477
– multifocality 469
– mural diseases 477
– process 478
– subacute 472
– subadventitial 391
– subintimal 454
– vertebral artery 83
DMSO (dimethyl sulfoxide solvent) 1083
dopamine 12, 1154
Doppler
– color-flow 76
– transcranial 76, 99
double lumen 393, 395
drainage
– bilateral 289
– external ventricular (EVD) 1141

– venous, thrombosed 793
drug treatment 97
dual therapy 34
duplex scan 76
duplex ultrasonography, carotid 74
dural venous plexus 572, 573
DWI (diffusion-weighted imaging) 70–72, 81, 100

E
echocardiography, transesophageal 99
ECST 86, 87
ectasia, segmental 481
edema, brain 1134
edematous reaction 490
EEG 918
Ehlers-Danlos syndrome 57, 279, 280, 297, 387, 434, 435, 743
eicosanoids 13
elastica lamina, internal (IEL) 456, 479
electrical current 998
electrolysis 998, 1039
embolic agents
– absorbable materials 970–973
– coils (*see there*)
– liquid 977
– nonabsorbable particulate materials 974–979
– particulate agents 969, 970
embolism
– cardiogenic 99
– pulmonary 138
embolization
– fluid 1050
– – liquids 1055
– – nonabsorbables 1059–1089
– – silicone fluid 947, 1059
– partial targeted 788, 792
– palliative 835
embospheres 977–979
endarterectomy, carotid (CEA) 86–89, 92, 105, 1153
– restenosis 89, 93–97
Endeavor catheter 952
endocarditis, subacute bacterial 503
endoluminal clot 392, 422, 423, 490, 543
endoscopy, virtual 534
endothelial cells 26, 51
– origin 452
endothelial dysfunction 24
endothelin 14
endothelium 10, 25, 94
Envoy 5-F 935
ephedrine 923
EPIC 97
epidural lake 751
epidural venous plexus, transvenous occlusion 749
epistaxis 303, 306, 354–359, 409, 426, 674
– biopsy 359
– coagulopathy 357
– emergency treatment 322
– spontaneous 357
– traumatic 362, 363
– tumoral 357–359
EPISTENT 37
eptifibatide 36
Equinox catheter 125, 956, 959, 1034, 1085
equipment, angiographic 917
esthesioneuroblastoma 199, 200
esthesioneuroepithelioma 224
ethanol 977
Ethiodol 1063, 1077, 1093
– ethanol-*Ethiodol* mixture 1079
ethmoidal artery, anterior/posterior 567
ethyl cellulose 1094
ethylic alcohol 1074–1083
– arterial system, injection 1075, 1076
– arteriovenous malformation, injection 1080–1083
– ethanol-*Ethiodol* mixture 1079
– venous malformation, injection 1076–1080
EVAL (ethylene-vinyl alcohol copolymer) 1059, 1083, 1084
EVOH (*see Onyx*)
Ewing's sarcoma 875
Excelsior 10 microcatheter 938
exophthalmos 285, 409
extravasation, contrast material 359, 361, 1136, 1139

F
facial nerve, monitoring 925, 926
Fahraeus-Lindqvist effect 8
false sac 517
female gender 440
FGF (fibroblast growth factor) 25
fibrinogen 35
fibrinolysis 67
fibromuscular dysplasia (FMD) 57, 338, 438, 743
– cervical 415–417
fibrous cap 26
filum terminale lesion 767, 789
Fisher's grading 369
fistula, arteriovenous
– carotid cavernous 520
– filum 774, 802
– high-flow 337, 778, 791, 991, 1066, 1119, 1124
– – congenital 945
– iatrogenic 341
– microarteriovenous 801
– parachordal
– – ascending pharyngeal-internal jugular (hypoglossal) 743
– – clinical manifestation 739
– – direct 784
– – general remarks 738–740
– – maxilla artery-to-vein (stapedial) 743
– – paraspinal 752–758
– – throacolumbar paraspinal 755
– – vertebro-vertebral (proatlantal and intersegmental, VVAVF) 743–752
– spinal dural (*see* SDAVF)
– tentorial dural 761
– traumatic 277–363
– – carotid cavernous 522
– – common carotid 342
– – external carotid 342–353
– – extracavernous 334–338
– – malignant 354
– – middle meningeal 345
– – scalp 343
– – traumatic carotid cavernous fistula (*see* TCCF)
– – vertebral 338–341
flow
– arrest 946, 1111
– bidirectional, *figure* 1100
– control 1097–1128
– – cerebral circulation 1104, 1105
– – cortical level 1110
– – craniofacial area 1097
– – distal catheterization 1106, 1107
– – dural surface 1104
– – intralesional 1101, 1102
– – surgical 1104
– modifications 954
– reversal 948, 1064, 1099, 1101, 1108–1110
– – occlusive balloon 1102–1104
flow-directed navigation 937
Flowrider 1091
flushing solutions 1095, 1096
Fogarty balloon 280
follow-up 1146
foramen lacerum 401
foramen rotundum, artery 569
fracture
– optic canal 297
– pelvis 284
– skull base 279
functional
– evaluation 925
– investigation 946
fusiform ectasia 422

G
galactorrhea 413
gastrointestinal rupture 435
GDC coil 528, 998–1002
– bioabsorbable polymeric Matrix 1012, 1016
Gelfoam 839
– gelatin sponge 970, 971
– particles 973
– powder 948, 971–973, 1077, 1098, 1102
geniculate body network 495
Gerolakos and Nicolaides classification 78
GFX II 1171–1173
giant cell tumors 893–895
Gianturco coils 980
Glasgow Coma Scale 369
Glasgow Outcome Scale 147, 369, 535
glaucoma 285
– secondary 293
glial cells 19
glossopharyngeal nerve 1152
glucose 8, 18
glue 758
glycoprotein IIb/IIIa receptor 27
– antagonists 35–39, 1055
– safety 38, 39
gold valve balloon 957
guanylyl cyclase 9
Guard-Wire system 1175
Guglielmi detachable coils (GDC) 528, 998–1002
– bioabsorbable polymeric matrix 1012, 1016
– *Vortex* 1002, 1004
guidewires 965–969, 1158–1163
– microguidewires 965–969
– monorail 967
gunshot wound 279, 338, 387, 426

H
head injury 470
headache 681–683, 704, 707, 1129
Headway
– catheter 935
– valve 1031, 1095
heart disease 75
– congenital, aneurysm 524–527
hemangioblastoma, spinal cord 898–900
hemangioendothelioma 1073
hemangioma
– bony 265
– cavernous 686, 687
– vertebral 883–890
– – associated lesions 888
– – embolization 889, 890
– – MRI 884
– – pretherapeutic evaluation 888, 889
– – spinal angiography 884
hemangiopericytoma 165, 166, 1099
hematocrit 1133
hematoma
– extradural 425
– fresh 489
– mural 392, 457
– spinal epidural 421
– subdural 832
hematomyelia 519, 805, 826, 828, 829, 1120
– morbidity 828
hemodilution 1133
hemodynamic
– insufficiency 112
– stress 514
hemorrhage 973
– aneurysm (*see* subarachnoid)
– arteriovenous malformation 677, 678, 703, 704
– epidural 832
– generalities 1135–1137
– intracranial 587
– intradural 278
– intraventricular 740
– postembolization 1138
– recurrent 841
– spinal 778, 825–828
– subadventitial 454
– subarachnoid (SAH) 116, 289, 740, 752, 826
– tongue 352
hemorrhagic conversion 111, 114, 139
hemorrhagic vascular disease, combined endovascular treatment 1147
heparin 398, 843, 1153
– adjunctive 37, 38
– low-molecular-weight (LMWH) 143
heparinization 534, 923, 924, 1128
hepatic failure 433
hepatitis B 511
herpes virus 24
HHT1 (hereditary hemorrhagic teleangiectasias) 618–621, 794, 812, 822
Hieshima Apollo catheter 958, 959
Higashida balloon catheter 119, 953
Hilal coil 987
histamine 12
histoacryl 1060
HITS (high-intensity transient signals) 77
HIV 504, 510, 512
HMCAS (hyperdense middle cerebral artery sign) 47
homocysteine 24
Horner's syndrome 396, 401, 417
Hunt and Hess Classification 148, 368
hydrophilic coating 939
5-hydroxytryptamine (5-HT) 12
hypercapnia 9
hypercholesterolemia 23
Hyperglide catheter 956
hypernephroma, metastatic 881
hyperplasia, intimal 89, 93–97, 1170
hyperprolactinemia 413
hypertension 58
– venous 804
hypocapnia 9
hypophyseal portal system 337
hypotension 921, 922
– systemic 1111
hypotube 1174
HZV (herpes zoster virus) 512

I
IBCA (isobutyl homologue isobutyl-2-cyanoacrylate) 1059
ICP (intracranial pressure) 5
immunoallergic mechanism 505
In Time 1052, 1053
infarction
– atheroembolic 30
– embolic 83
– incomplet 18
inferolateral trunk 567
integrin uperfamily 35
intimal tear 391
iodized oil 1093
iophendylate 1093
ischemia, cerebral 51
– cell change 19
– depolarization 19
– focal 18
– global 18
– hemodynamic effects 21
– necrosis 19
– neuronal metabolism 17
– nitrous oxide 21, 22
ischemic stroke, arterial
– acute 31
– age 15
– angiographic evaluation 41–44
– causes 16
– cryptogenic 99
– definition 14–16
– incidence 15
– middle cerebral artery 44, 45, 51
– neuroimaging 30, 31
– neuronal metabolism 17, 18
– neuronal vulnerability, selective 18–21

– North America 15
– posterior circulation 98–109
– presentation 74
– race 15
– risk factors 16, 74
– treatment 31–73
– – medical therapy 1130, 1131
ischemic syndrome, crescendo 51
isovolemia 1133

J
J-curve 966, 1036
jugular puncture 930

K
Karnofsky score 369, 535, 829
Kassel Bach syndrome 1073
kinking, carotid 942
Klippel-Trénaunay syndrome 766, 767, 771, 820

L
laceration, external carotid 347
laryngeal malignancy 429
Lasjaunias 4-F catheter 986
LDL (low-density lipoprotein) 24
leak, calibrated 952, 953
lenticulostriate artery 51, 54
lesion, intermediate 25
leukotriene 13
LIAT (local intra-arterial thrombolytic therapie) 45–52, 110, 1131
ligation
– endovascular 1105, 1110
– intradural 843
– proximal 314
lipid mediators 13
Lipiodol 1063, 1093
liver
– cyst 436
– fibrosis 432
locked-in state 112
lupus syndrome 513
lymphoproliferative disease, X-chromosome-linked 513

M
macrophage 25
magnesium 41
malformation
– arteriovenous
– – cerebral (*see there*)
– – spinal cord (*see there*)
– venous 1081
Mani 1155
Marfan syndrome 57, 435, 437
Marlin 1052
martensite phase 1170
matrix coil (polyglycolic/poly-L-lactid acid copolymer) 1012
maxillary trauma 425
maxillofacial trauma 457
McCune Albright syndrome 522
medullary syndrome 466
menigiomatosis, menigeal 166
meningioangiomatosis 166
meningioma 427
– angiographic investigation 184–186
– angioplastic 165, 166
– association with other tumors 155
– cavernous sinus, involving 178
– children 156
– chromosomal patterns 156
– clinical presentation 166–169
– CT-scanning 181, 182
– differential diagnosis 187
– embolization, technical aspects 189–192
– – complications 196–198
– – pre- and postembolization medical management 194
– epidural 177
– etiology 157, 158
– extracranial 224
– familial occurrence 157
– gelfoam powder 972
– growth and spread 162
– incidence 154, 155
– intracranial vascular involvement 179, 180
– malignant 162–164
– MRI-Scanning 182–184
– oncogenic viruses 158–161
– operation, time 196
– orbit 177, 178
– origin 154
– pathology 161, 162
– peritumoral edema 181
– pial supply 194
– pretherapeutic evaluation 181
– recurrent 192–194
– sex hormone receptors 156
– sites 169–177
– spinal cord 910
– therapeutic strategy and clinical objectives 187–189
– tumor extension, extracranial 192
– unusual sites 179
menstruation 831, 832
MEP (motor-evoked potential) 925, 928, 1032, 1124
metalloproteinase 14, 28
metamere 379
metameric artery 738
metameric syndrome, spinal arteriovenous (*see* SAMS) 764, 766, 770, 813–821
metaraminol 1154
metastases, vertebral 895
metastatic disease 524
methylene blue 929
metrizamide powder 1077
microcapsules, time-released 1094
microcatheter 934, 936
– calibrated leak 119–127, 130, 959, 961
– *Excelsior* 10 938
– flow-guided 937, 939
– over-the guidewire 937
– *Rebar* 938, 1085
– two-microcatheter technique 1039, 1040
– variable-stiffness 936, 937
– wire-braided 938
microcirculation agents 1132
microcoils 986, 1025
microemboli 77
microseal adapter 1174
microtrauma, tentorium 518
Micrus coil 1010, 1011
Mini-Torquer 936, 942, 943
miscellaneous 1094–1096
mitochondria 19
Mönckeberg disease 23
monorail 1164
Moret's technique 1032
MRI (magnetic resonance imaging) 30
– angiography (MRA) 80–83, 100, 535
– diffusion-weighted (DWI)/perfusion-weighted (PWI) 70–72, 81
MRV (magnetic resonance venography) 142
muscle atrophy 832
mutation 374
– germinal 380
– somatic 380
mycobacterium 512
myelomere 767
– topography, *figure* 778
myelopathy 760
– cervical 761
myoamoya phenomenon 638
myxoma, atrial 523

N
naloxone 1132
nasal mucosa, physiology 206, 207
NASCET 84, 86–88
NBCA (N-butyl-cyanoacrylate) 332, 946, 1059, 1063, 1140
– *Trufil* 1060

neck
– bridging 1039
– protection 1030, 1031
necrosis, ischemic 19, 971, 972
– coagulative 20
– focal 26
– generalized neuronal 20
– skin 1130
nerve root compression 751
neurinoma 199
neuroblastoma 224
neurofibromatosis 57, 297, 338, 739, 743, 748
– type I 421, 424, 435, 436
– type II 436
Neuroform, stent 963, 1171
neurological deficits 708, 1129
– focal 582–585
– global 585–587
neuronal vulnerability, selective 18–21
neuro-ophtalmic abnormalities 299
neuropeptide Y 14
neuroprotective agents 39, 40
– binding properties 41
– pharmacological properties 40, 41
neutrophil 23
nidus 794–801
– angioarchitecture 654, 655
– intramedullary 763
– intranidal ectasias 659–664
– size change 656–659
NIH Stroke Scale 148–150
nitinol 962, 963, 1168–1170
nitric oxide synthase (NOS) 9
– isoforms 10
nitroglycerin 133–135, 921, 1031, 1032, 1089, 1146
nitroprusside drip 921
nitrous oxide (NO_2) 21, 22, 920
– cerebral circulation 9, 10
NMDA (*N*-methyl-D-aspartate) 18
norepinephrine 12
notochord 738
nucleus tractus solitarius 1152
NYU introducer 974

O
O'Reilly catheter 958
occipital artery 567
occlusion
– deconstructive 1005
– test 328, 1029
octacyanoacrylate 1055, 1059
OER (oxygen extraction ratio) 17
Ohm's law 4
Onyx (EVOH) 946, 1055, 1059, 1084–1091, 1149
– aneurysm treatment 1084–1089
– arteriovenous malformation treatment 1089–1091
opacifying agents 1092, 1093
open-cell design 1164
ophtalmoplegia 409
– acute 403
optic atrophy 409
orbit, menigioma 177, 178
orbital injury 279
osteoblastoma 878
osteodural-venous complex 571, 572
osteomyelitis 421
oxygen 8
– reactivity 9

P
pacemaker 1154
packing 540
PAF (platelet-activating factor) 13
pain
– dorsal 819
– facial 751
Palmaz, stent 1153
Pantopaque 1093
papaverine 131, 133, 135, 1160
paraganglioma 224, 227, 228
– angiographic protocol 252
– associated lesions 246
– cervical 238–243, 257–260
– classification 235, 237
– differential diagnosis 246–250
– embolization 261
– – complications 264
– – technical aspects 261–263
– embryology 228–230
– epidemiology 230–232
– familial distribution 231
– jugular 238
– laryngeal 244
– malignant 231
– multicentric 231
– natural history 235, 236
– orbital 245
– pathology 232, 233
– pharyngeal 265
– pretherapeutic evaluation 250–259
– radiotherapy 260, 261
– secretory 245, 246
– spinal cord 909–911
– temporal 252–257
– thyroidal 265
– tympanic 236–238
– vagal 241
– vascular architecture 233–235
Parkes-Weber syndrome 766, 820, 821
partial repair 466
patient preparation 917–919
patterning 378
PDGF (platelet derived growth factor) 25, 376
PDK1/PDK2 431
pentoxifylline 1134
penumbra, ischemic 17
peptide 13
perclose 932
perfusion
– misery 22
– reserve 17
pericallosal arch 495
pericytes 3, 376
peritoneal dialysis 433
PET (positron emission tomography) 30, 31
petrous lesion 68
pH 8, 9
PHACE syndrome 399, 400
phagocytosis 4
pharyngeal artery, ascending
– carotid branch 567
– neuromenigeal division 569
physiology, cerebrovascular 3–14
pial network 797
PICA (posterior inferior cerebellar artery), dissection 463
plaque
– complicated 28, 29
– fatty 28
– fibrous 28
– morphology 77
– – *Gerolakos and Nicolaides* classification 78
– ulceration 75
plasma 1133
plasmocytoma 875, 880
platelets 26, 27
Plavix 1153
Poiseuille, equation 5, 8
polyarteriitis nodosa 385
polycystic kidney disease 431–433, 436
– children 375
polycystin 431
polyglycolic/poly-L-lactid acid copolymer 1012
polyvinyl alcohol foam (PVA) 839, 974–977, 1063, 1123
– ethanol combination 977
postembolization care
– cerebral arteriovenous malformation 1128
– head and neck 1128
– intradural aneurysm 1128, 1129
– spinal arteriovenous malformation 1129
pouch, venous 755

pregnancy 136, 787, 831
preoperative medication 917, 918
pressure
– arterial, mean 5
– cerebral perfusion pressure 5
– intracranial (ICP) 5
– venous 5
prism therapy 298
PROACT II (prolyse in acute cerebral thromboembolism trial II) 46, 47
proatlantal artery 740
probucol 97
procollagen
– type III 396, 434
– type V 396
proptosis 299
prostacyclin (PGI_2) 13
prostaglandines 12, 13
protamine sulfate 923
protection/protecting
– agents 1134
– distal cerebral 1173–1175
– mechanical 1099
protein C 136
protein S 136
provocative testing, cranial nerve 1129
pseudoaneurysm 347, 389, 653, 662, 776
pseudonidus 813
pseudoxanthoma elasticum (PXE) 385, 437
PT (prothrombin time) 38, 923
PTT (partial thromboplastin time) 38, 923
puerperium 136
pulmonic valve stenosis 524
pupillary abnormality 409
purine nucleotide 14
Purkinje cells 19
PVA (polyvinyl alcohol foam) suspension 839, 974–977, 1063, 1123
PWI (perfusion-weighted imaging) 70–72, 81

R
radiation 97
– beta radiation 1019
radical, free 41
radicular vein 739
radiosensitizer 916
Radius, stent 964
Rankin Scale, modified 148
reanastomosis 930
Rebar microcatheter 938, 1085
rebleed 539
recanalization 45, 494, 975, 977, 979, 1063, 1119, 1131, 1132
reconstructive operation 1030
remodeling 25, 374, 376, 955, 1031–1037
– *Moret's* technique 1032
– technique 534
renal artery stenosis 435
renal function 433
Rendu-Osler-Weber disease 739, 766
ReoPro 36
reperfusion, cerebral 19
– injury 22, 23, 39, 41
resistance, vascular 6
– segmental 6
restenosis 89, 93–97
retinal artery, central, occlusion 67, 68
Retriever 1052
revascularisation 42, 52, 55, 62, 105–109, 923, 931, 1143, 1144, 1162
– complications 1178, 1179
– emergency 65
– mechanical 1176
Robin Hood effect 1132
r-TPA (recombined tissue plasminogen activator) 31–33, 67, 144, 1131
r-UK (recombined urokinase) 46, 60, 144, 961, 1131
rupture, vessel 1137

S
sacral artery, lateral 752
salmonella 505
SAMS (spinal arteriovenous metameric syndrome) 764, 766, 770, 813–821
SCAVM (spinal cord arteriovenous malformation) 760–773
– aggravating factors 831, 832
– angioarchitecture 775, 829, 830
– angiography 809810
– arterial aneurysm 786–794
– arterial features 775–784
– associated malformations 822–825
– bifocal 763
– classification 767–773
– clinical aspects 825–832
– clinical assessment 808
– CSF pulsation artifact 809
– CT 808
– embolization 1116, 1117
– hemodynamics 810, 811
– incidence 769, 814
– intradural fistula 811, 812
– MRI 808
– multifocal 815
– myelography 808
– natural history 760, 825
– nidus (*see there*)
– postembolization care 1129
– prognosis 830
– retromedullary 806
– thrombosis, spontaneous 843, 844, 847
– treatment
– – complications 840–842
– – indications 833–839
– – medical therapy 843–847
– – radiotherapy 843
– – results 839, 840
– – surgery 842, 843
– veins 802–807
– – thrombosis 803
sclerosis, medial
– calcified 23
– cystic 57
sclerotherapy 1074–1083
SDAVF (spinal dural arteriovenous fistula) 849–872
– age distribution 849
– clinical presentation 858, 859
– embolization 1125–1128
– – indication 867
– – results 871
– – technique 867–869
– imaging 859–867
– location 863
– macro 812, 813
– macroscopic apearance 851–853
– micro 812
– microscopic apearance 853, 854
– pathology 850, 851
– pathophysiology 854–858
– sacrum 778
– surgery 871, 872
security point 928
segmental vulnerability 492
seizure 918
– outcome 919
sella turcica 410
Sentry catheter 125, 955, 958, 1034
SEP (somatosensory-evoked potential) 809, 840, 925, 928, 1124
Serbinenko 955
serotonin 12
sex hormons 206, 207
shear stress 514
shunt, arteriovenous (*see also* malformation)
– dural (*see* DAVS)
– epidural 861
– filum terminale 797
– general appearance 615–618
– radicular 766
silicone
– fluid 947, 1059
– spheres 977
Silvadene 1130

Silverspeed, guidewire 965
size-to-neck ratio 532
size-to-parent-artery-diameter ratio 532
Sjögren's syndrome 513
skin
– discoloration 817, 1092
– vascular malformation 814
SMART 1165
smoking 440
smooth muscle 26, 27
– proliferation 97
snare, microvena 1051, 1052
Sorcerer, guidewire 965
sphenoid
– bone 408
– sinus 305, 509
spinal artery, anterior, pial branches 798, 799
spinal cord
– aneurysmal bone cyst 890–892
– angiographic protocol 875, 876
– angiography 874, 875
– arteriovenous malformation (*see* SCAVM)
– catheterization, distal 1116
– collateral circulation 1114
– embolization 876–883
– – arteriovenous malformation 1116, 1117
– – cervical tumors 877
– – chemoembolization 877–880
– – flow control 1117–1120
– – intralesional 880
– – thoracic/lumbar/sacral tumors 877
– endovascular treatment, technical aspects 1113, 1114
– giant cell tumors 893–895
– hemangioblastoma 898–900
– – pretherapeutic evaluation 904–906
– – treatment 906–909
– hemangioma, vertebral 883–890
– malignant tumors 895–897
– – embolization 897
– meningioma 910
– metastases 895
– monitoring 1124, 1125
– paraganglioma 909–911
– pathological changes 854
– vascular lesion 758–760
– *von Hippel-Lindau* disease 900–904
steal
– arterial 300, 754
– intracerebral 9
– subclavian 105, 1176
Stealth catheter 125, 950, 952, 958
stenosis, arterial 1143–1146
– carotid 16, 99
stent 36, 57, 62, 69
– balloon-expandable 59, 106, 962, 1161, 1164, 1165, 1171, 1180, 1181
– coating 97
– collapsed 1178
– construction design 1164
– covered 962
– delivery catheter 962–965
– metal alloys 1164
– nitinol 962, 963, 1168–1170
– protection 1045
– retrieval 1179–1181
– selection 1164–1168
– self-expandable 59, 962, 1160, 1164, 1169, 1170
stenting 90–98, 104
– hemodynamic disturbances 1152, 1153
– techniques 1152–1181
– – intervention 1154–1163
– – premedication 1153, 1154
– – vasoactive medication 1154
stopcocks 1095
streaks, fatty 23, 24, 27, 28
streptokinase 33
stroke 421, 495, 1129
– children 422
– deep-seated 460
– embolic 477
– ischemic (*see there*)
stroke center 71
stroke emergency team 70, 71
Sturge-Weber syndrome 691–694, 812
subclavian artery 105
– revascularisation 42
subclavian steal syndrome 105, 1179
subintimal trauma 392
substance P 12, 13
sump effect 747
superelasticity 1170
surface
– abluminal 4
– rendering 532, 533, 541
swelling
– postembolization 1060
– postoperative 1130
Symbiot, stent 964
Symphony 1165
syndromes/diseases (names only)
– *Bourneville* disease 436, 437
– *Cobb* syndrome 755, 773
– *Ehlers-Danlos* syndrome 57, 279, 280, 297, 387, 434, 435, 743
– *Horner's* syndrome 396, 401, 417
– *Kassel Bach* syndrome 1073
– *Klippel-Trénaunay* syndrome 766, 767, 771, 820
– *Marfan* syndrome 57, 435, 437
– *McCune Albright* syndrome 522
– *Mönckeberg* disease 23
– Moyamoya disease 438
– *Paget's* disease 427
– *Parkes-Weber* syndrome 766, 820, 821
– *Rendu-Osler-Weber* disease 739, 766
– *Sjögren's* syndrome 513
– *Sturge-Weber* syndrome 691–694, 814
– *von Hippel-Lindau* disease 900–904
– *von Willebrand's* disease 750
syphillis 454
syringes 1094

T
Takayasu's arteritis 115, 116
tandem lesion 68, 69
tantalum powder 947, 1063, 1084, 1092, 1093
TCCF (traumatic carotid cavernous fistula)
– clinical aspects 285–306
– – associated traumatic lesions 302–305
– – ophtalmological symptoms 293–298
– etiology/epidemiology 279–284, 297
– location 308–313
– pretherapeutic evaluation 306–320
– therapy
– – embolization 321, 322
– – – balloon selection 325–330
– – – inferior petrosal approach 332
– – – postembolization care 333
– – – retrograde ophthalmic vein catheterization 332
– – – venous approach 330
– – emergency treatment 322–324
– – manual compression 332
– – NBCA 332
– – surgical approach 324, 325
– venous drainage 314
teleangiectasias, hereditary hemorrhagic (HHT1) 618–621, 794, 812, 822
tentorium, microtrauma 518
Terumo, guidewire 965
TGFβ1 (tissue growth factor β1) 376
thalassemia, heterozygotic α 522
thrombin 36
thrombocytopenia 38, 144

thromboembolism 110
thromboendarterectomy 54
thrombolysis/thrombolytic therapy 32, 33, 39, 53, 144
– local intra-arterial thrombolytic therapie (LIAT) 110, 1131
– – anterior circulation 45–52
thrombolytics 1055
thrombosis
– aneurysm 470
– arteriovenous malformation 669
– basilar artery 110–114
– cerebral venous (*see* venous occlusive disease)
– cortical vein 139
– spontaneous 791
– superior sagital sinus 138, 140, 147
– traumatic 278
– venous 752
thromboxane A_2 (TXA_2) 13, 27, 34, 35
thrombus 479, 494
thyroid carcinoma 273
thyrolaryngeal tumors 265–270
TIA (transient ischemic attack) 14, 44, 73, 74
– posterior circulation 99
ticlopidine hydrochloride 35, 37, 1153
TIMI (thrombolysis in myocardial infarction) 46, 47
tinnitus 581, 582
– pulsatile 285
tirilazad 41
tirofiban 36
tissue plasminogen activator, recombined (r-TPA) 31–33, 67, 144, 1131
tolerance test 314, 942, 943, 1020, 1029, 1030
tongue hemorrhage 352
torticollis, painfull 751
tracheostomy 920
transdural veins 573–575
Transent platinum, guidewire 966
transitory deficits 840
transmedullary
– supply 795
– vein 796
transphenoidal surgery 279, 403, 404
transposition, great arteries 524
transvenous approach 756
tray container 1095
tricuspid atresia 524
trigeminal artery 103
trigger 374
Trispan 1039–1043
tropoelastin 396, 435
Trufil 1060
truncus arteriosus 524
tuberous sclerosis 436, 437
tubular design 1164
Tuohy-Borst 1095
– Y-adapter 944, 960
twin, homocygotic 452
two-arteriotomy-site 1178

U
ultrasound, carotid 75–78, 98
– double enhanced 77
– hemodynamic assessment 77
urokinase, recombined (r-UK) 46, 60, 144, 961, 1131

V
VA (veterans Administration) 87
Valsalva maneuver 814, 831, 920, 922
vasa vasorum 94, 96, 376, 398, 459, 489, 494
vascular insufficiency, cerebral
– management 104–109
– pretherapeutic evaluation 99–103
vascular lesion
– limb 820
– pelvic 821
vascular phenotypic vulnerability, variability 374
vascular system, sex hormons 207
vasculitis 83
vasculogenesis 23
vasculopathy, mural 371
vasoactive substances 11
vasopressin 14
vasoseal 932
vasospasm 117–135, 952, 959, 1031, 1146
– angioplasty, indications and results 128–133
– arteriovenous malformation 642
– chemical treatment 133–135
VCAM-1 (vascular endothelial molecule) 26
venography, magnetic resonance (MRV) 142
venous nerve, perispinal network 807
venous occlusive disease
– clinical presentation 137, 138
– combined endovascular treatment 1147
– etiology 135, 136
– imaging 138–143
– incidence 136, 137
– natural history 137, 138
– risk factors 136
– treatment 143–147
ventriculostomy 456
vertebral artery
– dissection 83
– duplicated 447
– fenestration 447
– occlusion 107
vertebrobasilar insufficiency 98, 425, 751
vertebroplasty, percutaneous 897
vessel wall, proliferative disease 490
vidian canal 401
viscosity, blood 8, 1133
vision loss 66
visual loss 299, 302, 304, 405
vitamin E 41
Vitek 1155
volume rendering 532, 533, 541
volume, cerebral blood (CBV) 7
von Hippel-Lindau disease 900–904
von Willebrand's disease 750
vulnerability, segmental 492
VVAVF (vertebro-vertebral arterio-venous fistula, proatlantal and intersegmental) 743–751
– clinical findings 751, 752

W
Wada test 928
Wallerian degeneration 21
Wallstent 1046, 1165, 1167, 1169
warfarin 398
WFNS gerading scale 368
Willis, circle 1108, 1109
wisdom tooth extraction 362
Wyburn-Mason 758

X
xylocaine 927, 929, 1125

Y
Y hemostatic valve 1031, 1095
Yasargil, grading system 368

Z
Zubkov's technique 117, 118

Manufacturers

AVE/Medtronic
Minneapolis, MN 55432, USA

Beiersdorf Inc.
187 Danbury Road, Wilton, CT 06897, USA

Biosphere Medical
1050 Hingham Street, Rockland, MA 02370, USA

Boston Scientific
One SciMed Place, Maple Grove, MN 55311-1566, USA

Cook Inc.
PO Box 489, Bloomington, IN 47402, USA

Cordis Endovascular
14000 NW 57th Court, Miami Lakes, FL 33014, USA

Ethicon Inc.
Somerville, NJ 08876, USA

Lilly Research Laboratories
Lilly Corporate Center, Indianapolis, IN 46285, USA

Medtronic
3576 Unocal Place, Santa Rosa, CA 95403, USA

Microtherapeutics Inc.
2 Goodyear, Irvine, CA 92618, USA

Microvena
1861 Buerkle Road, White Bear Lake, MN 55110-5246, USA

Microvention
72 Argonaut, Aliso Viejo, CA 92656, USA

Micrus Corporation
495 Clyde Avenue, Mountain View, CA 94043, USA

Monarch Pharmaceuticals
335 Beecham Street, Bristol, TN 37620, USA

Savage Labs
Melville, NY 11747, USA

Provasis Therapeutics Inc.
9275 Sky Park Ct., Ste. 125, San Diego, CA 92123, USA